Scientific and Technical Aerospace Reports

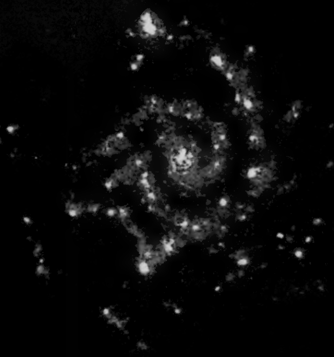

An Abstract Journal

Volume 32, Number 4
April 1994
N94-17678 to N94-19799

The NASA STI Program ... in Profile

Since its founding, NASA has been dedicated to the advancement of aeronautics and space science. The NASA Scientific and Technical Information (STI) Program plays a key part in helping NASA maintain this important role.

The NASA STI Program provides access to the NASA STI Database, the largest collection of aeronautical and space science STI in the world. The Program is also NASA's institutional mechanism for disseminating the results of its research and development activities.

Specialized services that help round out the Program's diverse offerings include creating custom thesauri, translating material to or from 34 foreign languages, building customized databases, organizing and publishing research results ... even providing videos.

For more information about the NASA STI Program, you can:

- **Phone** the NASA Access Help Desk at (301) 621-0390
- **Fax** your question to the NASA Access Help Desk at (301) 621-0134
- **E-mail** your question via the **Internet** to help@sti.nasa.gov
- **Write** to:

NASA Access Help Desk
NASA Center for AeroSpace Information
800 Elkridge Landing Road
Linthicum Heights, MD 21090-2934

Scientific and Technical Aerospace Reports

STAR

Scientific and Technical Aerospace Reports (STAR), is published each month as a major product of the NASA Scientific and Technical Information (STI) Program.

Inside this issue you will find:

- **Front Matter** containing a typical citation and abstract sample explaining the standard format, including codes for ordering reports
- **An Abstract Section** containing citations and abstracts of reports and publications that provide comprehensive coverage of worldwide aerospace-related topics including aeronautics and space science technology. *STAR* lists published and publicly available reports entered into the NASA STI Database during the four weeks preceding publication of this issue. These citations and abstracts are listed by subject categories.
- **An Index Section**
    - Subject
    - Personal author
    - Corporate source
    - Contract number
    - Report number
- **An Appendix** containing a guide for ordering cited reports, registering with the NASA STI Program, and using the available products and services. Additionally, price schedules, phone numbers, and addresses are included in this information packed section.

NASA also sponsors the companion journal, *NASA Open Volumes on Aerospace (NOVA),* which lists abstracts of the open literature on aerospace subjects available worldwide. *NOVA* is for internal NASA use only, available from the NASA Center for AeroSpace Information (CASI).

Entries found in *STAR* are available through the NASA online retrieval service, RECON, and through DIALOG as the Aerospace Database.

The NASA STI Program gathers information through national and international agreements and exchanges and makes this information available to the NASA community and to the public in many forms through various outlets.

For additional information on the NASA STI Program, call the NASA Access Help Desk at (301) 621-0390, or write to:

NASA Center for AeroSpace Information
800 Elkridge Landing Road
Linthicum Heights, Maryland 21090-2934

US ISSN 0036-8741

This publication was prepared by the NASA Center for AeroSpace Information,
800 Elkridge Landing Road, Linthicum Heights, MD 21090-2934, (301) 621-0390.

Volume 32 Number 4 / April 1994

TABLE OF CONTENTS

AERONAUTICS For related information see also *Astronautics.*

01 AERONAUTICS (GENERAL) 1305

02 AERODYNAMICS 1311
Includes aerodynamics of bodies, combinations, wings, rotors, and control surfaces; and internal flow in ducts and turbomachinery. For related information see also *34 Fluid Mechanics and Heat Transfer.*

03 AIR TRANSPORTATION AND SAFETY 1315
Includes passenger and cargo air transport operations; and aircraft accidents. For related information see also *16 Space Transportation* and *85 Urban Technology and Transportation.*

04 AIRCRAFT COMMUNICATIONS AND NAVIGATION 1316
Includes digital and voice communication with aircraft; air navigation systems (satellite and ground based); and air traffic control. For related information see also *17 Space Communications, Spacecraft Communications, Command and Tracking* and *32 Communications and Radar.*

05 AIRCRAFT DESIGN, TESTING AND PERFORMANCE 1317
Includes aircraft simulation technology. For related information see also *18 Spacecraft Design, Testing and Performance* and *39 Structural Mechanics.* For land transportation vehicles see *85 Urban Technology and Transportation.*

06 AIRCRAFT INSTRUMENTATION 1320
Includes cockpit and cabin display devices; and flight instruments. For related information see also *19 Spacecraft Instrumentation* and *35 Instrumentation and Photography.*

07 AIRCRAFT PROPULSION AND POWER 1320
Includes prime propulsion systems and systems components, e.g., gas turbine engines and compressors; and onboard auxiliary power plants for aircraft. For related information see also *20 Spacecraft Propulsion and Power, 28 Propellants and Fuels,* and *44 Energy Production and Conversion.*

08 AIRCRAFT STABILITY AND CONTROL 1321
Includes aircraft handling qualities; piloting; flight controls; and autopilots. For related information see also *05 Aircraft Design, Testing and Performance.*

09 RESEARCH AND SUPPORT FACILITIES (AIR) 1322
Includes airports, hangars and runways; aircraft repair and overhaul facilities; wind tunnels; shock tubes; and aircraft engine test stands. For related information see also *14 Ground Support Systems and Facilities (Space).*

ASTRONAUTICS For related information see also *Aeronautics.*

12 ASTRONAUTICS (GENERAL) 1323
For extraterrestrial exploration see *91 Lunar and Planetary Exploration.*

13 ASTRODYNAMICS 1331
Includes powered and free-flight trajectories; and orbital and launching dynamics.

14 GROUND SUPPORT SYSTEMS AND FACILITIES (SPACE) .... N.A.
Includes launch complexes, research and production facilities; ground support equipment, e.g., mobile transporters; and simulators. For related information see also *09 Research and Support Facilities (Air).*

15 LAUNCH VEHICLES AND SPACE VEHICLES 1331
Includes boosters; operating problems of launch/space vehicle systems; and reusable vehicles. For related information see also *20 Spacecraft Propulsion and Power.*

16 SPACE TRANSPORTATION 1332
Includes passenger and cargo space transportation, e.g., shuttle operations; and space rescue techniques. For related information see also *03 Air Transportation and Safety* and *18 Spacecraft Design, Testing and Performance.* For space suits see *54 Man/System Technology and Life Support.*

17 SPACE COMMUNICATIONS, SPACECRAFT COMMUNICATIONS, COMMAND AND TRACKING....1333
Includes telemetry; space communications networks; astronavigation and guidance; and radio blackout. For related information see also *04 Aircraft Communications and Navigation* and *32 Communications and Radar.*

N.A.—No abstracts were assigned to this category for this issue.

18 SPACECRAFT DESIGN, TESTING AND PERFORMANCE **1333**
Includes satellites; space platforms; space stations; spacecraft systems and components such as thermal and environmental controls; and attitude controls. For life support systems see *54 Man/System Technology and Life Support.* For related information see also *05 Aircraft Design, Testing and Performance, 39 Structural Mechanics*, and *16 Space Transportation.*

19 SPACECRAFT INSTRUMENTATION **1337**
For related information see also *06 Aircraft Instrumentation* and *35 Instrumentation and Photography.*

20 SPACECRAFT PROPULSION AND POWER **1337**
Includes main propulsion systems and components, e.g., rocket engines; and spacecraft auxiliary power sources. For related information see also *07 Aircraft Propulsion and Power, 28 Propellants and Fuels, 44 Energy Production and Conversion*, and *15 Launch Vehicles and Space Vehicles.*

CHEMISTRY AND MATERIALS

23 CHEMISTRY AND MATERIALS (GENERAL) **1338**

24 COMPOSITE MATERIALS **1339**
Includes physical, chemical, and mechanical properties of laminates and other composite materials. For ceramic materials see *27 Nonmetallic Materials.*

25 INORGANIC AND PHYSICAL CHEMISTRY **1345**
Includes chemical analysis, e.g., chromatography; combustion theory; electrochemistry; and photochemistry. For related information see also *77 Thermodynamics and Statistical Physics.*

26 METALLIC MATERIALS **1355**
Includes physical, chemical, and mechanical properties of metals, e.g., corrosion; and metallurgy.

27 NONMETALLIC MATERIALS **1367**
Includes physical, chemical, and mechanical properties of plastics, elastomers, lubricants, polymers, textiles, adhesives, and ceramic materials. For composite materials see *24 Composite Materials.*

28 PROPELLANTS AND FUELS **1376**
Includes rocket propellants, igniters and oxidizers; their storage and handling procedures; and aircraft fuels. For related information see also *07 Aircraft Propulsion and Power, 20 Spacecraft Propulsion and Power*, and *44 Energy Production and Conversion.*

29 MATERIALS PROCESSING **1379**
Includes space-based development of products and processes for commercial application. For biological materials see *55 Space Biology:*

ENGINEERING For related information see also *Physics.*

31 ENGINEERING (GENERAL) **1379**
Includes vacuum technology; control engineering; display engineering; cryogenics; and fire prevention.

32 COMMUNICATIONS AND RADAR **1382**
Includes radar; land and global communications; communications theory; and optical communications. For related information see also *04 Aircraft Communications and Navigation* and *17 Space Communications, Spacecraft Communications, Command and Tracking.* For search and rescue see *03 Air Transportation and Safety,* and *16 Space Transportation.*

33 ELECTRONICS AND ELECTRICAL ENGINEERING **1394**
Includes test equipment and maintainability; components, e.g., tunnel diodes and transistors; microminiaturization; and integrated circuitry. For related information see also *60 Computer Operations and Hardware* and *76 Solid-State Physics.*

34 FLUID MECHANICS AND HEAT TRANSFER **1408**
Includes boundary layers; hydrodynamics; fluidics; mass transfer and ablation cooling. For related information see also *02 Aerodynamics* and *77 Thermodynamics and Statistical Physics.*

35 INSTRUMENTATION AND PHOTOGRAPHY **1423**
Includes remote sensors; measuring instruments and gauges; detectors; cameras and photographic supplies; and holography. For aerial photography see *43 Earth Resources and Remote Sensing.* For related information see also *06 Aircraft Instrumentation* and *19 Spacecraft Instrumentation.*

36 LASERS AND MASERS **1434**
Includes parametric amplifiers. For related information see also *76 Solid-State Physics.*

37 MECHANICAL ENGINEERING 1443
Includes auxiliary systems (nonpower); machine elements and processes; and mechanical equipment.

38 QUALITY ASSURANCE AND RELIABILITY 1447
Includes product sampling procedures and techniques; and quality control.

39 STRUCTURAL MECHANICS 1448
Includes structural element design and weight analysis; fatigue; and thermal stress. For applications see *05 Aircraft Design, Testing and Performance* and *18 Spacecraft Design, Testing and Performance.*

GEOSCIENCES For related information see also *Space Sciences.*

42 GEOSCIENCES (GENERAL) 1461

43 EARTH RESOURCES AND REMOTE SENSING 1461
Includes remote sensing of earth resources by aircraft and spacecraft; photogrammetry; and aerial photography. For instrumentation see *35 Instrumentation and Photography.*

44 ENERGY PRODUCTION AND CONVERSION 1464
Includes specific energy conversion systems, e.g., fuel cells; global sources of energy; geophysical conversion; and windpower. For related information see also *07 Aircraft Propulsion and Power, 20 Spacecraft Propulsion and Power,* and *28 Propellants and Fuels.*

45 ENVIRONMENT POLLUTION 1470
Includes atmospheric, noise, thermal, and water pollution.

46 GEOPHYSICS 1480
Includes aeronomy; upper and lower atmosphere studies; ionospheric and magnetospheric physics; and geomagnetism. For space radiation see *93 Space Radiation.*

47 METEOROLOGY AND CLIMATOLOGY 1488
Includes weather forecasting and modification.

48 OCEANOGRAPHY 1495
Includes biological, dynamic, and physical oceanography; and marine resources. For related information see also *43 Earth Resources and Remote Sensing.*

LIFE SCIENCES

51 LIFE SCIENCES (GENERAL) 1501

52 AEROSPACE MEDICINE 1504
Includes physiological factors; biological effects of radiation; and effects of weightlessness on man and animals.

53 BEHAVIORAL SCIENCES 1508
Includes psychological factors; individual and group behavior; crew training and evaluation; and psychiatric research.

54 MAN/SYSTEM TECHNOLOGY AND LIFE SUPPORT 1511
Includes human engineering; biotechnology; and space suits and protective clothing. For related information see also *16 Space Transportation.*

55 SPACE BIOLOGY .... N.A.
Includes exobiology; planetary biology; and extraterrestrial life.

MATHEMATICAL AND COMPUTER SCIENCES

59 MATHEMATICAL AND COMPUTER SCIENCES (GENERAL) 1514

60 COMPUTER OPERATIONS AND HARDWARE 1514
Includes hardware for computer graphics, firmware, and data processing. For components see *33 Electronics and Electrical Engineering.*

61 COMPUTER PROGRAMMING AND SOFTWARE 1516
Includes computer programs, routines, algorithms, and specific applications, e.g., CAD/CAM.

62 COMPUTER SYSTEMS 1533
Includes computer networks and special application computer systems.

63 CYBERNETICS **1539**
Includes feedback and control theory, artificial intelligence, robotics and expert systems. For related information see also *54 Man/System Technology and Life Support.*

64 NUMERICAL ANALYSIS **1545**
Includes iteration, difference equations, and numerical approximation.

65 STATISTICS AND PROBABILITY **1556**
Includes data sampling and smoothing; Monte Carlo method; and stochastic processes.

66 SYSTEMS ANALYSIS **1560**
Includes mathematical modeling; network analysis; and operations research.

67 THEORETICAL MATHEMATICS **1561**
Includes topology and number theory.

PHYSICS For related information see also *Engineering.*

70 PHYSICS (GENERAL) **1561**
For precision time and time interval (PTTI) see *35 Instrumentation and Photography*; for geophysics, astrophysics or solar physics see *46 Geophysics, 90 Astrophysics*, or *92 Solar Physics.*

71 ACOUSTICS **1562**
Includes sound generation, transmission, and attenuation. For noise pollution see *45 Environment Pollution.*

72 ATOMIC AND MOLECULAR PHYSICS **1564**
Includes atomic structure, electron properties, and molecular spectra.

73 NUCLEAR AND HIGH-ENERGY PHYSICS **1573**
Includes elementary and nuclear particles; and reactor theory. For space radiation see *93 Space Radiation.*

74 OPTICS **1576**
Includes light phenomena and optical devices. For lasers see *36 Lasers and Masers.*

75 PLASMA PHYSICS **1581**
Includes magnetohydrodynamics and plasma fusion. For ionospheric plasmas see *46 Geophysics.* For space plasmas see *90 Astrophysics.*

76 SOLID-STATE PHYSICS **1592**
Includes superconductivity. For related information see also *33 Electronics and Electrical Engineering* and *36 Lasers and Masers.*

77 THERMODYNAMICS AND STATISTICAL PHYSICS **1606**
Includes quantum mechanics; theoretical physics; and Bose and Fermi statistics. For related information see also *25 Inorganic and Physical Chemistry* and *34 Fluid Mechanics and Heat Transfer.*

SOCIAL SCIENCES

80 SOCIAL SCIENCES (GENERAL) **1610**
Includes educational matters.

81 ADMINISTRATION AND MANAGEMENT **1610**
Includes management planning and research.

82 DOCUMENTATION AND INFORMATION SCIENCE **1612**
Includes information management; information storage and retrieval technology; technical writing; graphic arts; and micrography. For computer documentation see *61 Computer Programming and Software.*

83 ECONOMICS AND COST ANALYSIS .... **N.A.**
Includes cost effectiveness studies.

84 LAW, POLITICAL SCIENCE AND SPACE POLICY **1620**
Includes NASA appropriation hearings; aviation law; space law and policy; international law; international cooperation; and patent policy.

85 URBAN TECHNOLOGY AND TRANSPORTATION **1620**
Includes applications of space technology to urban problems; technology transfer; technology assessment; and surface and mass transportation. For related information see *03 Air Transportation and Safety, 16 Space Transportation,* and *44 Energy Production and Conversion.*

SPACE SCIENCES For related information see also *Geosciences.*

88 SPACE SCIENCES (GENERAL) 1620

89 ASTRONOMY 1621
Includes radio, gamma-ray, and infrared astronomy; and astrometry.

90 ASTROPHYSICS 1624
Includes cosmology; celestial mechanics; space plasmas; and interstellar and interplanetary gases and dust. For related information see also *75 Plasma Physics.*

91 LUNAR AND PLANETARY EXPLORATION 1628
Includes planetology; and manned and unmanned flights. For spacecraft design or space stations see *18 Spacecraft Design, Testing and Performance.*

92 SOLAR PHYSICS 1629
Includes solar activity, solar flares, solar radiation and sunspots. For related information see also *93 Space Radiation.*

93 SPACE RADIATION 1630
Includes cosmic radiation; and inner and outer earth's radiation belts. For biological effects of radiation see *52 Aerospace Medicine.* For theory see *73 Nuclear and High-Energy Physics.*

GENERAL

Includes aeronautical, astronautical, and space science related histories, biographies, and pertinent reports too broad for categorization; histories or broad overviews of NASA programs.

99 GENERAL 1631

SUBJECT INDEX I-1

PERSONAL AUTHOR INDEX I-153

CORPORATE SOURCE INDEX I-171

CONTRACT NUMBER INDEX I-197

REPORT NUMBER INDEX I-203

APPENDIX A-1

TYPICAL CITATION AND ABSTRACT

NASA SPONSORED
ON MICROFICHE
↓↓

ACCESSION NUMBER → **N94-12270*#** United Technologies Corp., West Palm Beach, FL. Pratt and Whitney. ← **CORPORATE SOURCE**
TITLE → **ADVANCED CONTROL FOR AIRBREATHING ENGINES, VOLUME 1: PRATT AND WHITNEY**
AUTHOR → J. A. Ralph Jul. 1993 83 p ← **PUBLICATION DATE**
CONTRACT OR GRANT → (Contract NAS3-25952; RTOP 505-62-61)
REPORT NUMBERS → (NASA-CR-189203; E-8006; NAS 1.26:189203) Avail: CASI HC A05/MF A01 ← **AVAILABILITY SOURCE AND PRICE CODE**

The application of advanced control concepts to air breathing engines may yield significant improvements in aircraft/engine performance and operability. Screening studies of advanced control concepts for air breathing engines were conducted by three major domestic aircraft engine manufacturers to determine the potential impact of concepts on turbine engine performance and operability. The purpose of the studies was to identify concepts which offered high potential yet may incur high research and development risk. A target suite of proposed advanced control concepts was formulated and evaluated in a two phase study to quantify each concept's impact on desired engine characteristics. To aid in the evaluation specific aircraft/engine combinations were considered: a Military High Performance Fighter mission, a High Speed Civil Transport mission, and a Civil Tiltrotor mission. Each of the advanced control concepts considered in the study are defined and described. The concept potential impact on engine performance was determined. Relevant figures of merit on which to evaluate the concepts are determined. Finally, the concepts are ranked with respect to the target aircraft/engine missions. A final report describing the screening studies was prepared by each engine manufacturer. Volume 1 of these reports describes the studies performed by Pratt & Whitney. Author (revised)

VOLUME 32 NUMBER 4 / April 1994

Scientific and Technical Aerospace Reports

A Monthly Publication of the National Aeronautics and Space Administration

01 AERONAUTICS (GENERAL)

N94-18279 General Accounting Office, Washington, DC. National Security and International Affairs Div.
NAVAL AVIATION: CONSIDER ALL ALTERNATIVES BEFORE PROCEEDING WITH THE F/A-18E/F
Aug. 1993 12 p Limited Reproducibility: More than 20% of this document may be affected by microfiche quality
(AD-A269302; GAO/NSIAD-93-144) Avail: CASI HC A03

This report discusses the Navy's decision to develop the F/A-18E/F aircraft. The General Accounting Office believes the results of the examination should be fully considered in the ongoing review of the type and mix of fixed-wing tactical aircraft that will be required for future conflicts. Derived from text

N94-18415# Advisory Group for Aerospace Research and Development, Neuilly-Sur-Seine (France). Fluid Dynamics Panel.
HIGH-LIFT SYSTEM AERODYNAMICS [L'AERODYNAMIQUE DES SYSTEMES HYPERSUSTENTATEURS]
Sep. 1993 494 p The 71st Symposium held in Banff, Alberta, 5-8 Oct. 1992
(AGARD-CP-515; ISBN-92-835-0715-0) Copyright Avail: CASI HC A21/MF A04

This report includes the 32 technical papers developed for the High-Lift System Aerodynamics Symposium along with an edited transcript of the Round Table Discussion and a Symposium Evaluation Report. The symposium objectives were to address (1) how the most appropriate high-lift system can be selected; (2) how an efficient design can be produced; and (3) the experimental and analysis techniques which are necessary to explore and enhance the performance of a high-lift system. Thus, although the aerodynamics of high-lift systems was the dominant theme, the very pertinent aspects of weight, simplicity, reliability, and structural and mechanical integrity were an integral part of the Symposium, and were treated in the papers presented. In this sense, this Symposium has attempted to take a broader view of the high-lift system than has been taken by similar conferences in the past. For individual titles, see N94-18416 through N94-18447.

N94-18416# Defence Research Agency, Farnborough (England). Low Speed Aerodynamics Div.
WHERE IS HIGH-LIFT TODAY? A REVIEW OF PAST UK RESEARCH PROGRAMMES
D. S. Woodward and D. E. Lean *In* AGARD, High-Lift System Aerodynamics Sep. 1993 45 p (For primary document see N94-18415 04-01)
Copyright Avail: CASI HC A03/MF A04

Some of the history of the development of slotted high-lift systems is reviewed in this paper. In particular, the National High Lift Programme run in the UK during the 1970's is reviewed in some detail. In addition, the research program in high lift since the completion of the National High Lift Programme is described qualitatively and references given. The contents cover techniques of high lift testing, results of positional optimization of slats and flaps, the derivation of a simple prediction method suitable for use with a project optimization method, and the description, with results, of a method for interpreting aerodynamic and weight data on high lift systems in the context of a complete aircraft. Author (revised)

N94-18417# Middle East Technical Univ., Ankara (Turkey). Dept. of Aeronautical Engineering.
EXPERIMENTAL INVESTIGATION OF FLOW AROUND A MULTIELEMENT AIRFOIL c02
Nafiz Alemdaroglu *In* AGARD, High-Lift System Aerodynamics Sep. 1993 19 p (For primary document see N94-18415 04-01)
Copyright Avail: CASI HC A03/MF A04

This paper presents the results of experimental investigations performed around a multielement airfoil and gives detailed information about the flow in and around the flap-well and slat cavity regions. Measurements are made using pitot probes, hotwire anemometer and laser Doppler velocimeter at a Reynolds number of 0.5 and 0.8x10(exp 6). The results obtained show the complex nature of the shear flows investigated and put into evidence the necessity of accurate modeling of these flows by numerical methods. Author (revised)

N94-18418# Politecnico di Milano (Italy). Dipt. di Ingegneria Aerospaziale.
A DESIGN PROCEDURE FOR SLOTTED FLAPS c05
Sergio DePonte, Alessandro Cella, and Mario Marcazzan *In* AGARD, High-Lift System Aerodynamics Sep. 1993 6 p Sponsored in part by CNR (For primary document see N94-18415 04-01)
Copyright Avail: CASI HC A02/MF A04

In the design of slotted flaps it is attempted to avoid a reacceleration between the trailing edge of an upstream element of the system and the peak velocity of the downstream element, to reach the maximum lift. It is proved that it is possible by means of a numerical procedure based on a vortex distribution. The resulting shapes are then discussed with reference to the application to a real design. Author

N94-18419# Dornier Luftfahrt G.m.b.H., Friedrichshafen (Germany).
CALCULATION OF MAXIMUM AND HIGH LIFT CHARACTERISTICS OF MULTI ELEMENT AEROFOILS c02
Willy Fritz *In* AGARD, High-Lift System Aerodynamics Sep. 1993 12 p (For primary document see N94-18415 04-01)
Copyright Avail: CASI HC A03/MF A04

The flow field around multi-element aerofoil sections possesses a high degree of complexity. Due to the strong interactions between wakes from the upstream elements and the upper surface boundary layers developing on the downstream elements, there are thick viscous layers present over the upper surface of the trailing edge flap. Large regions of separated flow can be present, even for conditions well below maximum lift. Finally, the flow around the leading edge slat can become locally supersonic, even for low freestream Mach numbers, due to the large suction levels induced in this region. The viscous-inviscid interaction methods, which are most widely in use for the prediction of multi-element aerofoil flows, are computationally very efficient, but unable to describe many of the complex flow features present. A more complete description of the physical phenomena can be achieved only by methods based on a solution of the Reynolds-averaged Navier-Stokes equations, in conjunction with a suitable turbulence model. The generation of a suitable computational grid then becomes a major problem. Within the present work, a method to generate suitable block structured grids around multi-element aerofoils has been developed. The Dornier 2-D block structured Navier-Stokes solver has been extended for grids with arbitrary block structure. After very encouraging results for a two-element high lift system at low angles of attack, in this work the method was applied for realistic two- and three-element high lift systems at high angles of attack. Derived from text

N94-18420# Technische Univ., Berlin (Germany). Inst. fuer Luft- und Raumfahrt.

NAVIER-STOKES COMPUTATIONS OF TURBULENT FLOW AROUND HIGH-LIFT CONFIGURATIONS **c02**

P. Bartsch, W. Nitsche, and M. Britsch *In* AGARD, High-Lift System Aerodynamics Sep. 1993 10 p (For primary document see N94-18415 04-01)

Copyright Avail: CASI HC A02/MF A04

This paper presents Navier-Stokes calculations of the turbulent flow around two different high-lift configurations, for which experimental data exist. In the calculations, the flow field is considered as of steady-state and two-dimensional. Because of the low Mach numbers, the fluid is treated as incompressible. The solution procedure uses a finite volume method in order to solve the Reynolds-averaged Navier-Stokes equations. The effects of turbulence on the mean flow field are described by the k-epsilon turbulence model. The computational mesh is systematically refined in order to assess numerical solution errors. The results presented in this paper include surface pressure distributions as well as mean velocities and turbulence quantities. If possible, the calculations are compared to experimental data. Author

N94-18421*# National Aeronautics and Space Administration. Ames Research Center, Moffett Field, CA.

EFFICIENT SIMULATION OF INCOMPRESSIBLE VISCOUS FLOW OVER MULTI-ELEMENT AIRFOILS **c02**

Stuart E. Rogers, N. Lyn Wiltberger, and Dochan Kwak *In* AGARD, High-Lift System Aerodynamics Sep. 1993 9 p (For primary document see N94-18415 04-01)

Copyright Avail: CASI HC A02/MF A04

The incompressible, viscous, turbulent flow over single and multi-element airfoils is numerically simulated in an efficient manner by solving the incompressible Navier-Stokes equations. The solution algorithm employs the method of pseudo compressibility and utilizes an upwind differencing scheme for the convective fluxes, and an implicit line-relaxation scheme. The motivation for this work includes interest in studying high-lift take-off and landing configurations of various aircraft. In particular, accurate computation of lift and drag at various angles of attack up to stall is desired. Two different turbulence models are tested in computing the flow over an NACA 4412 airfoil; an accurate prediction of stall is obtained. The approach used for multi-element airfoils involves the use of multiple zones of structured grids fitted to each element. Two different approaches are compared; a patched system of grids, and an overlaid Chimera system of grids. Computational results are presented for two-element, three-element, and four-element airfoil configurations. Excellent agreement with experimental surface pressure coefficients is seen. The code converges in less than 200 iterations, requiring on the order of one minute of CPU time on a CRAY YMP per element in the airfoil configuration. Author (revised)

N94-18422*# McDonnell Aircraft Co., Saint Louis, MO.

NAVIER-STOKES CALCULATIONS ON MULTI-ELEMENT AIRFOILS USING A CHIMERA-BASED SOLVER **c02**

Donald W. Jasper, Shreekant Agrawal, and Brian A. Robinson *In* AGARD, High-Lift System Aerodynamics Sep. 1993 11 p Sponsored by NASA. Ames Research Center and Cray Research, Inc. (For primary document see N94-18415 04-01)

Copyright Avail: CASI HC A03/MF A04

A study of Navier-Stokes calculations of flows about multielement airfoils using a chimera grid approach is presented. The chimera approach utilizes structured, overlapped grids which allow great flexibility of grid arrangement and simplifies grid generation. Calculations are made for two-, three-, and four-element airfoils, and modeling of the effect of gap distance between elements is demonstrated for a two element case. Solutions are obtained using the thin-layer form of the Reynolds averaged Navier-Stokes equations with turbulence closure provided by the Baldwin-Lomax algebraic model or the Baldwin-Barth one equation model. The Baldwin-Barth turbulence model is shown to provide better agreement with experimental data and to dramatically improve convergence rates for some cases. Recently developed, improved farfield boundary conditions are incorporated into the solver for greater efficiency. Computed results show good comparison with experimental data which include aerodynamic forces, surface pressures, and boundary layer velocity profiles. Author

N94-18423# Toronto Univ., Downsview (Ontario). Inst. for Aerospace Studies.

NUMERICAL SOLUTION OF THE NAVIER-STOKES EQUATIONS FOR HIGH-LIFT CONFIGURATIONS ON STRUCTURED COMPOSITE GRIDS **c02**

T. E. Nelson, D. W. Zingg, and G. W. Johnston *In* AGARD, High-Lift System Aerodynamics Sep. 1993 14 p (For primary document see N94-18415 04-01)

Copyright Avail: CASI HC A03/MF A04

A numerical method is presented for the solution of the compressible Reynolds-averaged, thin-layer Navier-Stokes equations on structured composite grids as applied to high-lift configurations. The method is an adaptation of an implicit approximate factorization algorithm for block structured composite grids. Interfaces between blocks are treated by overlapping the grids and taking one layer of points from neighboring blocks. Turbulence is treated using the Baldwin-Barth one-equation turbulence model. High-lift applications presented for comparison with wind tunnel data include: a NACA 4412 airfoil with NACA 4415 flap, a GA(W)-1 airfoil with a 29 percent chord flap at 30 degree flap angle and two gap settings, and a GA(W)-1 airfoil with 15 percent chord slat and 29 percent chord flap. Good agreement with experimental data is obtained for cases with fully attached flow or small regions of separated flow. For cases with extensive regions of flow separation, the thickness and extent of the separated regions are underpredicted. Author

N94-18424*# National Aeronautics and Space Administration. Langley Research Center, Hampton, VA.

HIGH REYNOLDS NUMBER CONFIGURATION DEVELOPMENT OF A HIGH-LIFT AIRFOIL **c02**

Walter O. Valarezo (Douglas Aircraft Co., Inc., Long Beach, CA.), Chet J. Dominik (Douglas Aircraft Co., Inc., Long Beach, CA.), Robert J. McGhee, and Wesley L. Goodman *In* AGARD, High-Lift System Aerodynamics Sep. 1993 8 p (For primary document see N94-18415 04-01)

Copyright Avail: CASI HC A02/MF A04

An experimental program has been conducted to assess performance of a transport multielement airfoil at flight Reynolds numbers. The studies were performed at chord Reynolds numbers as high as 16 million in the NASA Langley Low Turbulence Pressure Tunnel. Sidewall boundary-layer control to enforce flow two dimensionality was provided via an endplate suction system. The basic airfoil was an 11.55 percent thick supercritical airfoil representative of the stall critical station of a new-generation transport aircraft wing. The multielement airfoil was configured as a three-element airfoil with slat and flap chord ratios of 14.48 percent and 30 percent respectively. Testing focused on the development of landing configurations with high maximum lift capability and the assessment of Reynolds and Mach number effects. Also assessed were high-lift performance effects due to devices such as drooped spoilers and trailing-edge wedges. The present experimental studies revealed significant effects on high-lift airfoil performance due to Reynolds and Mach number variations and favorable lift increments at approach angles of attack due to the use of drooped spoilers or trailing-edge wedges. However, no substantial improvements in maximum lift capability were identified. A recently developed high performance single-segment flap was also tested and results indicated considerable improvements in lift and drag performance over existing airfoils. Additionally, it was found that this new flap shape at its optimum rigging was less sensitive to Reynolds number variations than previous designs. Author

N94-18425# Office National d'Etudes et de Recherches Aerospatiales, Paris (France).

A VISCOUS-INVISCID SOLVER FOR HIGH-LIFT INCOMPRESSIBLE FLOWS OVER MULTI-ELEMENT AIRFOILS AT DEEP SEPARATION CONDITIONS [UNE METHODE D'INTERACTION VISQUEUX NON-VISQUEUX POUR ECOULEMENTS INCOMPRESSIBLES HYPERSUSTENTES SUR PROFILS MULTI-CORPS EN REGIME DE DECOLLEMENT PROFOND] **c02**

J. C. LeBalleur and M. Neron *In* AGARD, High-Lift System Aerodynamics Sep. 1993 12 p In FRENCH (For primary document see N94-18415 04-01)

Copyright Avail: CASI HC A03/MF A04

A viscous-inviscid interaction numerical method for incompressible flows over multi-element airfoils, which is an extension of the numerical method previously suggested for compressible attached or separated or even stalled flows over airfoils, is presented. The robust algorithms of the method are capable now to converge well for attached flows or massively separated flows, such as induced by slope discontinuities of airfoils or slats, or such as induced by stall. The viscous-inviscid approach introduces a self-adaptative viscous grid in both normal and streamwise directions along the displacement surfaces, with everywhere a streamwise grid-resolution of the same order as the separating boundary layer thicknesses, even at slat apexes, which is believed to eliminate any aleatory effect of numerical viscosity. The method is validated with respect to ONERA experiments, on the three-element RA16SC1 high-lift device, with the severe AMD slat-geometry. A realistic non-uniqueness of the separated flow solutions has been exhibited by the calculation method. A satisfactory agreement between theory and experiment is obtained, with the suggested 2-equation turbulence model. Author (revised)

N94-18426# National Aerospace Lab., Amsterdam (Netherlands).

HIGH-LIFT SYSTEM ANALYSIS METHOD USING UNSTRUCTURED MESHES **c02**

K. deCock *In* AGARD, High-Lift System Aerodynamics Sep. 1993 20 p (For primary document see N94-18415 04-01)

Copyright Avail: CASI HC A03/MF A04

A 2D high-lift configuration analysis method is described. The flow model used is based on the Euler equations, discretized on unstructured meshes. The generation of the unstructured meshes is based on the principle of successive grid adaptation with respect to the geometry. This approach makes later extension towards fully integrated grid adaptation with respect to the solution straightforward. The main characteristics of the Euler solver are upwind flux-difference splitting of the convective part of the Euler equations (second-order accurate discretization in space) and four stage Runge Kutta local time stepping. Results obtained with this analysis method are shown for the NACA0012 airfoil and three-element airfoils. Conclusions are drawn. Author

N94-18427# Manchester Coll. of Science and Technology (England). Dept. of Mechanical Engineering.

PREDICTION OF THE HIGH-LIFT PERFORMANCE OF MULTI-ELEMENT AEROFOILS USING AN UNSTRUCTURED NAVIER-STOKES SOLVER **c02**

Leslie J. Johnston and Luca Stolcis *In* AGARD, High-Lift System Aerodynamics Sep. 1993 18 p (For primary document see N94-18415 04-01)

(Grant CEC-SC1/900369)

Copyright Avail: CASI HC A03/MF A04

A detailed description is presented of a computational method to predict the aerodynamic performance of mechanical high-lift systems. The Reynolds-averaged Navier-Stokes equations applicable to compressible, two-dimensional mean flow are solved using a cell-centered, finite-volume spatial discretization and an explicit multi-stage to time march to steady-state solutions. The governing mean-flow equations are solved in conjunction with a two-equation, high-Reynolds number k-epsilon turbulence model, this level of turbulence model sophistication being considered as the minimum required to enable an adequate resolution of the complex flow physics. The geometric complexity associated with practical multi-element airfoil configurations is addressed by adopting unconstructed computational grids. Results for the RAE 2822 transonic single-airfoil section are presented, comparing two near-wall treatments for the turbulence-transport equations. Thereafter, a detailed evaluation is presented of the predictive capability of the method, in its current form, by comparison with experimental data for the low-speed, high-lift NLR 7301 airfoil/trailing-edge flap configuration. Results are also presented for the SKF 1.1 airfoil/manoeuver flap configuration over a range of transonic flow conditions, from fully-subcritical flow to supercritical flow with shock-induced separation. The level of agreement between predictions and experiment is encouraging for the cases considered. However, it is concluded that improved modeling of the complex flow physics is required, with the lack of response of the current k-epsilon turbulence model to streamline curvature being a significant limitation on quantitative accuracy around maximum lift conditions. Similarly, procedures to automatically adapt the computational grid to the flow solution would improve predictions over the extended range of conditions associated with the practical operation of a mechanical high-lift system. Author (revised)

N94-18428# Deutsche Forschungsanstalt fuer Luft- und Raumfahrt, Brunswick (Germany). Inst. for Design Aerodynamics.

NUMERICAL CALCULATIONS OF HIGH LIFT FLOWS USING STRUCTURED AND UNSTRUCTURED METHODS **c02**

R. Bailey, J. M. A. Longo, R. Radespiel, A. Ronzheimer, A. Demier, N. Kroll, and C.-C. Rossow *In* AGARD, High-Lift System Aerodynamics Sep. 1993 13 p (For primary document see N94-18415 04-01)

Copyright Avail: CASI HC A03/MF A04

At the DLR Institute for Design Aerodynamics current research in the area of high lift aerodynamics is directed towards the development of a computational analysis capability for high lift systems. The Navier-Stokes equations are solved with a multigrid method based on central spatial differencing and Runge-Kutta time stepping. Two particular problems are addressed in this paper. The first concerns the calculation of maximum lift for a single airfoil and a clean wing configuration. The accuracy of the basic structured flow solver is investigated by comparing the results with experimental data for two test problems and several flow conditions. Emphasis is placed on the sensitivity of the computed solution associated with turbulence modeling. The second aspect dealt with in the present paper concerns the extension of the numerical method to multi-element airfoils. Both, the block-structured and the unstructured grid approach are investigated in order to explore their specific merits and limitations. Detailed comparisons of the structured and unstructured approach are presented for low Reynolds number laminar viscous flows around a single airfoil, and for the inviscid flow around a multi-element airfoil. Author

N94-18429# Grumman Aerospace Corp., Bethpage, NY.

NAVIER-STOKES SIMULATION OF FLOW FIELD AROUND A BLOWN-FLAP HIGH-LIFT SYSTEM **c02**

R. Chow, K. Chu, and G. Carpenter *In* AGARD, High-Lift System Aerodynamics Sep. 1993 10 p (For primary document see N94-18415 04-01)

Copyright Avail: CASI HC A02/MF A04

Solution of the Reynolds averaged Navier-Stokes equations is obtained to simulate the flow field around a 13 percent thickness supercritical airfoil slat/blown-flap high-lift system. A stacked-C mesh topology is used in conjunction with the slat and the flap trailing edge streamlines and adapted to accurately locate the strong viscous flow regions. A previously modified PARC2D implicit ADI solver is employed whereby the multiply connected boundary value problem can be treated with a single computation zone. A modeled injection boundary condition was demonstrated to connect transient flap wake vortices downstream of the computational domain. The converged surface pressures and the values of the lift coefficient are compared with the wind tunnel data at M(infinity) = 0.17, Re = 3.4 M for momentum injection coefficients of C(mu) = 0.01 and C(mu) = 0.04, respectively. Author (revised)

N94-18430# Office National d'Etudes et de Recherches Aerospatiales, Paris (France).

THE GARTEUR HIGH LIFT RESEARCH PROGRAMME **c02**

J. J. Thibert *In* AGARD, High-Lift System Aerodynamics Sep. 1993 21 p (For primary document see N94-18415 04-01)

Copyright Avail: CASI HC A03/MF A04

An extensive European wind tunnel research program on high lift systems has been carried out in the past few years within the framework of a GARTEUR Action Group. To provide a relevant and realistic case, permission was given by British Aerospace to use a section from the A-310 wing from which a 2D airfoil could be derived. A Deutsche Airbus 3D half model of the A-310 aircraft has been used for the 3D test and an airfoil representative of the 59 percent span section has been used for the 2D test. The wind tunnel test program carried out in the major European low speed wind tunnels (ONERA F1 in France, NLR HST and LST in Netherlands, RAE 5 m in UK) was complemented by a full scale flight test supported by Airbus Industries. A wide range of Reynolds numbers and Mach numbers has been covered by the test and a very comprehensive, well integrated and accurate body of data has been generated by this research program. After presenting GARTEUR the paper deals with the Reynolds number and the Mach number effects as well as the correlations between 2D and 3D data and between wind tunnel and flight test results. Author

N94-18431# Defence Research Agency, Farnborough (England).
AN EXPERIMENTAL INVESTIGATION OF THE OPTIMUM SLAT SETTING ON A COMBAT AIRCRAFT MODEL c05
I. R. M. Moir *In* AGARD, High-Lift System Aerodynamics Sep. 1993 16 p (For primary document see N94-18415 04-01)
Copyright Avail: CASI HC A03/MF A04

Tests have been carried out, on a combat aircraft model with high-lift devices, in the DRA Farnborough 5-meter pressurized low-speed wind tunnel. The deflection angle and position of a leading-edge slat were varied and optimum settings established. The separate effects of Reynolds number and Mach number on overall lift coefficient and on the optimum slat setting were investigated. The results show that optimum performance is achieved at a very high slat deflection angle and the performance is strongly influenced by compressibility effects. Author

N94-18432# Defence Research Agency, Farnborough (England).
AN EXPERIMENTAL INVESTIGATION OF ATTACHMENT-LINE TRANSITION ON THE SLAT OF A COMBAT AIRCRAFT MODEL c05
B. C. Hardy *In* AGARD, High-Lift System Aerodynamics Sep. 1993 11 p (For primary document see N94-18415 04-01)
Copyright Avail: CASI HC A03/MF A04

An experimental investigation into scale effect at low speed and high lift has been carried out in the DRA 5-m, pressurized wind tunnel on a subsonic strike-fighter model equipped with slotted high-lift devices. The attachment-line boundary layer on the leading-edge slat was found to be turbulent on the outboard part of the wing near maximum lift for a range of unit Reynolds number. An adverse Reynolds number effect on maximum lift was measured which correlated quite well with the onset of attachment-line transition. The conditions for onset of transition were not consistent with the assumption of gross contamination by the fuselage boundary layer, the attachment-line boundary layer remaining laminar on the inboard slat to more than double the expected free-stream Reynolds number. It is suggested that this result is due to spanwise variation in attachment-line position, which results in suppression of the disturbances emanating from the root region of the high-lift wing. It is concluded that attachment-line transition is a potentially significant factor in wind tunnel testing of high-lift wings equipped with leading-edge slats. Author

N94-18433# Boeing Commercial Airplane Co., Seattle, WA.
VISCOUS PHENOMENA AFFECTING HIGH-LIFT SYSTEMS AND SUGGESTIONS FOR FUTURE CFD DEVELOPMENT c02
P. T. Meredith *In* AGARD, High-Lift System Aerodynamics Sep. 1993 8 p (For primary document see N94-18415 04-01)
Copyright Avail: CASI HC A02/MF A04

This paper describes a number of viscous phenomena which affect the aerodynamic performance of high-lift systems typical of commercial jet transports. The nature of these phenomena suggest a course of action regarding the continuing development of computational fluid dynamics (CFD): in addition to the ongoing work of grid generation and algorithm development, increased attention to fundamental fluid mechanics is called for. Author

N94-18434# Defence Research Agency, Farnborough (England).
A STUDY OF THE USE OF HALF-MODELS IN HIGH-LIFT WIND-TUNNEL TESTING c02
P. B. Earnshaw, A. R. Green, B. C. Hardy, and A. H. Jelly *In* AGARD, High-Lift System Aerodynamics Sep. 1993 9 p (For primary document see N94-18415 04-01)
Copyright Avail: CASI HC A02/MF A04

An experimental investigation into the use of half-model testing techniques specifically aimed at high-lift testing has been carried out in the 5 Metre Pressurized Wind Tunnel at the DRA, Farnborough. The aim of the program was to provide an assessment of the extent to which the measured characteristics of a high-lift model might be compromised by, in particular, the existence of a boundary layer on the reflection plane and how any penalties might be minimized. The results suggest that, provided care is taken with experimental technique, good agreement is possible on stall incidence as well as the absolute values of lift, drag and pitching moment. Author

N94-18435*# National Aeronautics and Space Administration. Langley Research Center, Hampton, VA.
IN-FLIGHT PRESSURE DISTRIBUTIONS AND SKIN-FRICTION MEASUREMENTS ON A SUBSONIC TRANSPORT HIGH-LIFT WING SECTION c02
Long P. Yip, Paul M. H. W. Vijgen (High Technology Corp., Hampton, VA.), Jay D. Hardin (Lockheed Engineering and Sciences Co., Hampton, VA.), and C. P. vanDam (California Univ., Davis.) *In* AGARD, High-Lift System Aerodynamics Sep. 1993 19 p (For primary document see N94-18415 04-01)
(Contracts NAS1-19299; NAS1-19000; NCC1-163)
Copyright Avail: CASI HC A03/MF A04

Flight experiments are being conducted as part of a multiphased subsonic transport high-lift research program for correlation with wind-tunnel and computational results. The NASA Langley Transport Systems Research Vehicle (B737-100 aircraft) is used to obtain in-flight flow characteristics at full-scale Reynolds numbers to contribute to the understanding of 3-D high-lift, multi-element flows including attachment-line transition and relaminarization, confluent boundary-layer development, and flow separation characteristics. Flight test results of pressure distributions and skin friction measurements were obtained for a full-chord wing section including the slat, main-wing, and triple-slotted, Fowler flap elements. Test conditions included a range of flap deflections, chord Reynolds numbers (10 to 21 million), and Mach numbers (0.16 to 0.40). Pressure distributions were obtained at 144 chordwise locations of a wing section (53-percent wing span) using thin pressure belts over the slat, main-wing, and flap elements. Flow characteristics observed in the chordwise pressure distributions included leading-edge regions of high subsonic flows, leading-edge attachment-line locations, slat and main-wing cove-flow separation and reattachment, and trailing-edge flap separation. In addition to the pressure distributions, limited skin-friction measurements were made using Preston-tube probes. Preston-tube measurements on the slat upper surface suggested relaminarization of the turbulent flow introduced by the pressure belt on the slat leading-edge surface when the slat attachment line was laminar. Computational analysis of the in-flight pressure measurements using two-dimensional, viscous multielement methods modified with simple-sweep theory showed reasonable agreement. However, overprediction of the pressures on the flap elements suggests a need for better detailed measurements and improved modeling of confluent boundary layers as well as inclusion of three-dimensional viscous effects in the analysis. Author

N94-18436# Wright Lab., Wright-Patterson AFB, OH.
HIGH LIFT AND THE FORWARD SWEPT WING c05
Lawrence A. Walchli *In* AGARD, High-Lift System Aerodynamics Sep. 1993 9 p (For primary document see N94-18415 04-01)
Copyright Avail: CASI HC A02/MF A04

A broad overview of the X-29 Forward Swept Wing (FSW) Technology Demonstrator Program traces the aircraft's history from design through flight test. Brief descriptions of the aircraft and its flight control system provide insight for evaluating this unique vehicle. Wind tunnel design data substantiate theory and highlight potential solutions to a more 'missionized' aircraft. Flight test results validate the X-29's wind tunnel data base and provide for piloted simulation of possible improvements for the specific X-29 technologies. Author

N94-18437# Institut fuer Theoretische Stroemungsmechanik, Goettingen (Germany).
A FAST COMPUTING METHOD FOR THE FLOW OVER HIGH-LIFT WINGS c02
K. Jacob *In* AGARD, High-Lift System Aerodynamics Sep. 1993 12 p (For primary document see N94-18415 04-01)
Copyright Avail: CASI HC A03/MF A04

A quasi 3-dimensional method for analyzing the viscous steady subsonic flow over wings with flaps for high lift is briefly presented. The total iterative procedure combines a 3-dimensional inviscid lifting surface theory with a 2-dimensional surface-singularity method for analyzing multi-element airfoils in a curved basic flow field. This method also includes boundary layer calculations and a model for rear separation. Also, small compressibility effects are accounted for by simple corrections, and ground effects are included by means of the reflected image technique. First attempts to validate the method by a few theory-experiment comparisons are reported.

The results are encouraging but more experimental data are needed for a thorough validation. The computing time requirements of the method are modest. Author

N94-18438# California State Univ., Long Beach. Dept. of Aerospace Engineering.

CALCULATION OF MULTIELEMENT AIRFOILS AND WINGS AT HIGH LIFT c02

Tuncer Cebeci *In* AGARD, High-Lift System Aerodynamics Sep. 1993 15 p (For primary document see N94-18415 04-01)

Copyright Avail: CASI HC A03/MF A04

A calculation method based on an interactive boundary-layer approach to multi-element airfoils and wings is described. For two-dimensional flows, the method is applied to three types of airfoil configurations with and without flap wells in order to demonstrate its applicability and accuracy to general high-lift configurations. This method, extensively tested for single airfoils as a function of shape, angle of attack, and Reynolds number, is shown here to apply equally well to multi-element airfoils. The calculation method is also applied to a wing and wing/flap configuration in order to demonstrate its promise for addressing three-dimensional flows. Preliminary results indicate that with further development, the method, as for multi-element airfoils, will also become a practical, accurate and efficient tool for multi-element wings. Author

N94-18439# Politecnico di Milano (Italy). Dipt. di Ingegneria Aerospaziale.

WAKE STRUCTURE AND AERODYNAMIC BEHAVIOR OF HIGH LIFT AIRCRAFT CONFIGURATIONS DURING UNSTEADY MANEUVERS IN GROUND EFFECT c02

A. Baron and M. Boffadossi *In* AGARD, High-Lift System Aerodynamics Sep. 1993 15 p (For primary document see N94-18415 04-01)

Copyright Avail: CASI HC A03/MF A04

A nonlinear unsteady vortex lattice scheme is used and flight dynamics equations are solved in order to predict the structure of the wakes and the instantaneous distribution of the aerodynamic loads on high-lift aircraft configurations, during general unsteady take-off maneuvers in ground effect. The numerical scheme here presented can treat an arbitrary number of mutually interfering lifting and moving control surfaces having arbitrary planform and camber. Wakes can be released in the flowfield from any of the sharp edges of the lifting surfaces, depending on their planform, aspect ratio and angle of attack, while the effects of the fuselage are ignored in the present formulation. Turbulent diffusion of the cores of the Rankine vortex filaments is regarded as a preeminent factor in a correct simulation of the development of unsteady interfering wakes. A vortex core diffusion model is used capable to deal even with the severe roll-up of the mutually interfering wakes developing close and impinging on the ground. Typical applications of the unsteady vortex lattice scheme are presented, aimed at illustrating the capabilities of the code. Author

N94-18440# Office National d'Etudes et de Recherches Aerospatiales, Paris (France).

VISCOUS-INVISCID CALCULATION OF HIGH-LIFT SEPARATED COMPRESSIBLE FLOWS OVER AIRFOILS AND WINGS [CALCUL PAR INTERACTION VISQUEUX NON-VISQUEUX DES ECOULEMENTS COMPRESSIBLES FORTEMENT DECOLLES AUX GRANDES PORTANCES SUR PROFILS D'AILES ET VOILURES] c02

J. C. LeBalleur *In* AGARD, High-Lift System Aerodynamics Sep. 1993 18 p In FRENCH Sponsored by Ministry of Defence (For primary document see N94-18415 04-01)

Copyright Avail: CASI HC A03/MF A04

The viscous-inviscid interaction transonic numerical method previously defined by the author for computing attached or separated flows over airfoils, including the deeply stalled flows, is extended into a new three-dimensional method for strongly separated flows over wings at high-lift and compressible speeds. The numerical nonlinearly implicit boundary layer technique (direct/inverse), the turbulent models, the grid generation and grid-adaption, the coupling and wake-equilibration algorithms, the inviscid full-potential schemes, are extended in three dimension, with approximation on the viscous equations (2.75D-local). New theoretical results are given on the singularities and characteristic cones of the fully three-dimensional boundary layer in inverse mode. A new 'Massive-separation 2.75D' extension of the 'Semi-inverse' algorithm of Le Balleur for coupling is given and detailed, together with its stability theory. Results are shown for 2D-stall, and for 3D separated flows over rectangular or swept wings, with satisfactory agreement between theory and experiment. A self-adaptation technique of the grid to the viscous effects is displayed. The results demonstrate that the viscous-inviscid interaction methods give a full access to the calculation of three-dimensional separation. Author (revised)

N94-18441# Fokker B.V., Schipol-Oost (Netherlands).

FORTY YEARS OF HIGH-LIFT R/D: AN AIRCRAFT MANUFACTURER'S EXPERIENCE

E. Obert *In* AGARD, High-Lift System Aerodynamics Sep. 1993 28 p (For primary document see N94-18415 04-01)

Copyright Avail: CASI HC A03/MF A04

In the course of four decades a large amount of high-lift applied research and development has taken place at the Fokker Company. In the fifties and sixties the F-27 and the F-28 were developed. In the eighties these aircraft were developed further into the Fokker 50 and Fokker 100. In the seventies an extensive R&D program was performed in preparation of a possible successor to the F-28 leading to the F-29 project study. In each case two- and three-dimensional wind tunnel models were investigated in numerous configurations. In the last decade these investigations have increasingly been preceded by theoretical investigations. Where data are available comparisons have been made with flight test data. Of each development program a detailed account is presented. Particular attention is paid to Reynolds-number effects and the interconnection between the high-speed cruise and low-speed high-lift design requirements. Author

N94-18442# Aerospatiale, Toulouse (France). Div. Avions.

HIGH-LIFT RESEARCH: APPLICATION TO THE DESIGN OF THE ATR72 FLAP c05

P. Capbern *In* AGARD, High-Lift System Aerodynamics Sep. 1993 10 p (For primary document see N94-18415 04-01)

Copyright Avail: CASI HC A02/MF A04

Due to slightly reduced Clmax objectives in landing configuration for the ATR72, compared to the ATR42, the high-lift system of the ATR72 is made up of a single dropped hinge flap, whereas the ATR42 was equipped with a double slotted vane type flap. Elimination of the vane has had a beneficial effect in greatly simplifying the high-lift system for the ATR72. This simplification has been achieved while ensuring that Clmax levels are maintained or improved at same flap deflection (up to the value required for landing), and take-off L/D ratio is improved, which has a direct repercussion on operational performance, such as minimum runway lengths and maximum take-off weight. This aerodynamic performance has been achieved thanks to the systematic introduction, since 1985, of numerical methods in the design phase, in addition to the empirical and experimental methods used almost exclusively until then. The ATR72 flap is indeed the first to be essentially designed with numerical methods at Aerospatiale. Beside this, more severe new regulations for turboprop A/C, leading to a restriction in the use of large flap deflections for the ATR42, the effect of the elimination of the vane on Clmax has been numerically investigated for this A/C. This study having shown promising results, some wind-tunnel and flight test verifications were conducted which confirmed the reliability of the numerical tools. The development of new design and analysis methods has been pursued; it has involved, on one hand, an extension of their field of use and the quality of the modeling, and, on the other, a reduction in the design cycle time. The objective was twofold: better optimization of high-lift systems, and, above all, an appreciable reduction in the associated design costs. Author

N94-18443# Short Bros. and Harland Ltd., Belfast (Northern Ireland). Aerodynamics Dept.

THE AERO-MECHANICAL DESIGN OF A NOVEL FOWLER FLAP MECHANISM c05

J. R. Mathews *In* AGARD, High-Lift System Aerodynamics Sep. 1993 9 p (For primary document see N94-18415 04-01)

Copyright Avail: CASI HC A02/MF A04

The flow around a 2-dimensional wing and flap is reviewed using inviscid and viscous computational fluid dynamic techniques. In particular, the effect of flap gap is explored. The results indicate that for optimum aerodynamic performance at low flap angles, flap gaps in the region of 2 to 3 percent are required. A novel 4-bar Fowler flap mechanism is described which is shown to give these required gaps for flap angles greater than 3 degrees.

Such a mechanism can be readily optimized for minimum flap overlap at specified take-off flap settings. A comparison of a track and roller arrangement with the 4-bar mechanism indicates significant advantages for the latter. Author

N94-18444# Boeing Defense and Space Group, Seattle, WA.
DESIGN, DEVELOPMENT, AND FLIGHT EVALUATION OF THE BOEING YC-14 USB POWERED LIFT AIRCRAFT c05
Ted C. Nark *In* AGARD, High-Lift System Aerodynamics Sep. 1993 17 p (For primary document see N94-18415 04-01)
Copyright Avail: CASI HC A03/MF A04

The Boeing YC-14 was designed to perform a 400nm mission carrying a 26000 lb payload and land in 2000 feet on a semi-prepared landing strip. The high-lift system was one that had never been flown before; a upper surface blowing (USB) concept utilizing the 'Coanda' effect. The take-off and landing performance estimates developed from wind tunnel data were completely substantiated in the flight test program. The critical issue of continuing either a landing or takeoff after the loss of one of the two CF6 engines was also proven in the flight test program. The design details behind the performance of the YC-14 are discussed and some of the performance features of the airplane are explained. Author (revised)

N94-18445# Deutsche Airbus G.m.b.H., Bremen (Germany). Aerodynamics Dept.
HIGH-LIFT DESIGN FOR LARGE CIVIL AIRCRAFT c05
A. Flaig and R. Hilbig *In* AGARD, High-Lift System Aerodynamics Sep. 1993 12 p (For primary document see N94-18415 04-01)
Copyright Avail: CASI HC A03/MF A04

A general reflection of the high-lift system design process is given in the first part of the presentation. First the objectives and constraints are reflected which drive the high-lift design for civil transport aircraft. Further information is given on the applied theoretical methods and the Deutsche Airbus wind-tunnel strategy. An example of the high-lift system design process is given in the second part of the presentation. This deals with the conversion of a single-slotted Fowler flap to a part span double slotted flap, a high-lift system which was developed by Deutsche Airbus for the A-321. Author (revised)

N94-18446# De Havilland Aircraft Co. of Canada Ltd., Downsview (Ontario). Technology and Research.
HIGH LIFT SYSTEMS FOR TRANSPORT AIRCRAFT WITH ADVANCED AIRFOILS c05
B. Eggleston and R. J. D. Poole *In* AGARD, High-Lift System Aerodynamics Sep. 1993 13 p Sponsored in part by National Research Council of Canada (For primary document see N94-18415 04-01)
Copyright Avail: CASI HC A03/MF A04

This paper describes an on-going program of R&D into the development of high lift systems for future propeller driven regional transport aircraft. The work includes tests of two-dimensional airfoils and flaps, while half models are used for wing integration development. Comparisons are made between earlier commuter airfoil designs and advanced supercritical airfoils capable of NLF (natural laminar flow), using single and double-slotted flap systems in both cases. The advanced airfoils were also tested with a leading edge slat. Some effects of Reynolds number on lift characteristics are reviewed which show airfoils without leading edge slats were more sensitive at the scale of the half model used and that higher Reynolds numbers may be required. The advanced airfoils stalled at lower incidences than the commuter airfoils which are much thicker and better tailored to high lift performance. Advanced airfoils will likely require an additional flap segment to achieve similar lift to commuter airfoils. Leading edge slats gave large increases in maximum lift coefficients (up to 30 percent), which would allow substantial increases in wing loading if needed for the future. The half model development has entailed work on improving the sealing of the fuselage to the tunnel wall to minimize leakage. The paper provides some details of such work on high lift models and also on models used for cruise drag investigations. Author

N94-18447# Alenia Aeronautica, Naples (Italy). Flight Technology.
CHOICE AND OPTIMIZATION OF A HIGH-LIFT SYSTEM FOR AN ADVANCED AMPHIBIOUS AIRCRAFT c05
M. A. Averardo, M. deLeo, and V. Russo *In* AGARD, High-Lift System Aerodynamics Sep. 1993 13 p (For primary document see N94-18415 04-01)
Copyright Avail: CASI HC A03/MF A04

The design history of a flap system for an advanced amphibious aircraft is presented in this paper. All the most significant phases of the 2D theoretical studies and the experimental 2D and 3D investigations which have allowed to achieve the final geometry of the high-lift device will be described and, hence, the design criteria, the methods of analysis, the choices will be pointed out. Starting from the preliminary design of several flap systems, the development of this project needed a great deal of numerical studies and wind-tunnel tests in order to select, step by step, the most efficient geometries and to optimize the flap configurations. So, different technical aspects involved with these activities will be discussed: the choice of the flap types to be investigated, related to the special aerodynamic requirements of an amphibious aircraft and to the needs of other design areas (structure, weight, production); the geometrical elements effecting the aerodynamic performance of a high-lift device; general problems connected with theoretical and experimental studies of multi-body systems. Author (revised)

N94-18937* National Aeronautics and Space Administration, Washington, DC.
AERONAUTICAL ENGINEERING: A CONTINUING BIBLIOGRAPHY WITH INDEXES (SUPPLEMENT 297)
Nov. 1993 231 p
(NASA-SP-7037(297); NAS 1.21:7037(297)) Avail: CASI HC A11

This bibliography lists 825 reports, articles, and other documents introduced into the NASA scientific and technical information system in Nov. 1993. Subject coverage includes: design, construction and testing of aircraft and aircraft engines; aircraft components, equipment, and systems; ground support systems; and theoretical and applied aspects of aerodynamics and general fluid dynamics. CASI

N94-19070* National Aeronautics and Space Administration, Washington, DC.
AERONAUTICAL ENGINEERING: A CONTINUING BIBLIOGRAPHY WITH INDEXES (SUPPLEMENT 296)
Oct. 1993 172 p
(NASA-SP-7037(296); NAS 1.21:7037(296)) Avail: CASI HC A08

This bibliography lists 592 reports, articles, and other documents introduced into the NASA scientific and technical information system in Oct. 1993. Subject coverage includes: design, construction and testing of aircraft and aircraft engines; aircraft components, equipment, and systems; ground support systems; and theoretical and applied aspects of aerodynamics and general fluid dynamics. Author

N94-19383# Messerschmitt-Boelkow-Blohm G.m.b.H., Munich (Germany).
[RESEARCH AND DESIGN ACTIVITIES AND THE ECONOMIC BALANCE OF MBB] Annual Report, FY 1991 [DAS GESCHAEFTSJAHR 1991]
1991 40 p In GERMAN
(ETN-93-94909) Avail: CASI HC A03/MF A01

Research and design activities and economic balance of the company in 1991 are presented. The integration process of MBB into Deutsche Aerospace was continued in 1991. The French company Aerospatiale and MBB decided to collaborate in a new company christened Eurocopter in order to design and develop helicopters such as the Tiger. The Tornado production program was carried out and 35 aircraft were supplied to the German Air Force in Jan. 1992. The fan ranger program, which is based on the collaboration with Rockwell to JPATS (Joint Primary Aircraft Training System) program of U.S. Air Force and Navy, was started. The second test flight of X-31A, which is a program of cooperation with Rockwell for maneuverability studies, was successful. Space programs such as Eutelsat and ASTRO-SPAS satellites, and the Huygens probe, and defense programs were carried out following the predicted plan. ESA

02 AERODYNAMICS

Includes aerodynamics of bodies, combinations, wings, rotors, and control surfaces; and internal flow in ducts and turbomachinery.

For related information see also *34 Fluid Mechanics and Heat Transfer.*

N94-17721 Aeronautical Research Inst. of Sweden, Stockholm. Aerodynamics Dept.

WBNGRID, A PROGRAM FOR GENERATION OF C-H AND C-O TOPOLOGY GRIDS AROUND WING/BODY/NACELLE CONFIGURATIONS: USER'S GUIDE

Sven G. Hedman and Lars G. Tysell Jan. 1993 91 p Sponsored by Foersvarets Materialverk, Stockholm, Sweden, and National Board for Industrial and Technical Development, Sweden Limited Reproducibility: More than 20% of this document may be affected by microfiche quality

(FFA-TN-1992-09; ETN-93-94856) Avail: Issuing Activity (European Space Agency (ESA))

The principles of WBNGRID, a computer program for generation of C-H or C-O topology grids for the discretization of flow fields around configurations consisting of a wing alone or a wing with a fuselage and/or a nacelle, are described. WBNGRID is a development from an earlier grid generation progam MATGRID for wing fuselage combinations. In case the configuration contains a nacelle the grid is divided into two blocks. It is thought that primarily the grids will be used together with the full potential flow solver WBNFLOW which is a two block extension from the one block solver MATRICS (Multicomponent Aircraft Transonic Inviscid Computation System). The files required, some parameters, how to modify the input, and how to run the program are described. An example is also included as a test case. ESA

N94-17722 Aeronautical Research Inst. of Sweden, Stockholm.

A STUDY OF THE INFLUENCE OF A DELTA WING GEOMETRY ON THE INDUCED DRAG AT TRANSONIC SPEED (M=0.55) AND HIGH ANGLES OF ATTACK

Georg Drougge Feb. 1993 23 p Limited Reproducibility: More than 20% of this document may be affected by microfiche quality

(Contracts FMV-82260-91-087-073-001; FMV-82260-92-060-073-001)

(FFA-TN-1992-14; ETN-93-94857) Avail: CASI HC A03

An investigation which concerns mainly the effect of variation of the leading edge geometry and droop for a delta wing with given planform is reported. The lift and the induced drag at M = 0.55 at high angles of attack are calculated with a Euler code. It is found that with the leading edge drooping angle increasing over the span and with the nose radius increasing from 0.1% at the root to 0.7% at the tip it was possible to obtain attached flow over the wing for alpha = 17 deg and alpha = 18 deg. This resulted in very high efficiency factors which means low induced drag which in turn, improves the maneuver performance. The effect of viscosity not included in the Euler equations is discussed. ESA

N94-17919# Aeronautical Research Inst. of Sweden, Stockholm.

CFD INVESTIGATIONS OF THE HYPERSONIC DOUBLE DELTA WING GRETA: SANGER PROJECT NO. 3.2

Stefan Wallin and Tor-Arne Groenland 31 Mar. 1993 40 p Sponsored by Swedish Board for Space Activities, Solna

(FFA-TN-1992-42; ETN-93-94860) Avail: CASI HC A03/MF A01

The flow field over the double delta wing Greta with neutral flaps, was computed by solving the inviscid Euler equations and the laminar and turbulent Navier-Stokes equations at two Mach numbers, Mach 4 and 7. The Euler computations were made at three different angles of attack, alpha equals +10 deg, 0 deg, and -10 deg, while the Navier Stokes computations were made only at alpha equals +10 deg. The Computational Fluid Dynamics (CFD) were compared to measurements of the integrated forces and oil flow patterns. The flow field over the Greta vehicle is quite complex and is dominated by a strong bow shock and a strong primary vortex in the leeward side of the wing. At the high Mach number a cross flow shock is observed. The inviscid results show one strong vortex in the leeward side while the laminar results shows additional secondary vortices that introduce a couple of separation and reattachment lines. The turbulent flow solutions show a more viscous behavior, with thicker boundary layers and less distinct vortices and separation lines. The oil flow pattern from the wind tunnel experiments looks like something between the laminar and turbulent results. There is a reason to believe that the computational meshes have to be refined to get more accurate turbulent results. ESA

N94-17957# Institut National de Recherche d'Informatique et d'Automatique, Valbonne (France). Programme 6: Calcul Scientifique, Modelisation et Logiciels Numeriques.

SYNTHESIS OF THE WORKSHOP ON HYPERSONIC FLOWS FOR REENTRY PROBLEMS

Remi Abgrall, Jean-Antoine Desideri, Michel Mallet (Dassault-Breguet Aviation, Saint Cloud, France.), Jacques Periaux (Dassault-Breguet Aviation, Saint Cloud, France.), Pierre Perrier (Dassault-Breguet Aviation, Saint Cloud, France.), and Bruno Stoufflet (Dassault-Breguet Aviation, Saint Cloud, France.) Jun. 1992 85 p Workshop held in Antibes, France, Jan. 1990 and Apr. 1991

(INRIA-RR-1721; ETN-93-94431) Avail: CASI HC A05/MF A01

The organization of a workshop open to the international scientific community on hypersonic flows for reentry problems is addressed. This workshop was focused on the issues of validation of numerical methodologies for the computation of high Mach number flows, and gathered experts in scientific computing, fluid mechanics and experimentalists associated with the research and development Hermes program. This report presents a general synthesis of the motivations for this initiative, the development of the meetings, and the main conclusions drawn. ESA

N94-18275# Sandia National Labs., Albuquerque, NM.

ERROR PROPAGATION EQUATIONS AND TABLES FOR ESTIMATING THE UNCERTAINTY IN HIGH-SPEED WIND TUNNEL TEST RESULTS

E. L. Clark Aug. 1993 100 p

(Contract DE-AC04-76DP-00789)

(DE93-018685; SAND-93-0208) Avail: CASI HC A05/MF A02

Error propagation equations, based on the Taylor series model, are derived for the nondimensional ratios and coefficients most often encountered in high-speed wind tunnel testing. These include pressure ratio and coefficient, static force and moment coefficients, dynamic stability coefficients, calibration Mach number, and Reynolds number. The error equations contain partial derivatives, denoted as sensitivity coefficients, which define the influence of free-stream Mach number, M(infinity), on various aerodynamic ratios. To facilitate use of the error equations, sensitivity coefficients are derived and evaluated for nine fundamental aerodynamic ratios, most of which relate free-stream test conditions (pressure, temperature, density, or velocity) to a reference condition. Tables of the ratios, R, absolute sensitivity coefficients, (partial derivative)R/(partial derivative)M(infinity), and relative sensitivity coefficients, (M(infinity)/R) ((partial derivative)R/(partial derivative)M(infinity)), are provided as functions of M(infinity). DOE

N94-18402# Naval Postgraduate School, Monterey, CA.

A COMPUTATIONAL AND EXPERIMENTAL INVESTIGATION OF INCOMPRESSIBLE OSCILLATORY AIRFOIL FLOW AND FLUTTER PROBLEMS M.S. Thesis

Peter J. Riester Jun. 1993 158 p

(AD-A268748) Avail: CASI HC A08/MF A02

In this thesis several incompressible oscillatory flow and flutter problems were investigated. First, a previously developed unsteady panel code was modified so that systematic comparisons with Theodorsen's classical theory could be accomplished. It was found that the panel code is in excellent agreement with the Theodorsen results. Second, the panel code was applied to the analysis of bending-torsion flutter. Again, general agreement with Theodorsen's flutter predictions was obtained. In the experimental part of the thesis, two flow visualization experiments were performed. First, the vortical flow patterns generated by an airfoil executing harmonic plunge oscillations were visualized. In the second experiment, the interference effects between a stationary airfoil and a small vane executing plunge oscillations were explored. DTIC

N94-18413# Maryland Univ., College Park. Dept. of Aerospace Engineering.

AERODYNAMIC CHARACTERISTICS OF A HELICOPTER ROTOR AIRFOIL AS AFFECTED BY SIMULATED BALLISTIC DAMAGE Final Report, Apr. - Dec. 1992

J. G. Leishman Sep. 1993 60 p
(Contract DAAD05-92-C-0114; DA Proj. 1L1-62618-AH-80)
(AD-A269206; ARL-CR-66) Avail: CASI HC A04/MF A01

Tests were made in a two-dimensional insert at the University of Maryland's Glenn L. Martin subsonic wind tunnel to examine the effects of simulated ballistic damage on the aerodynamic characteristics of a UH-60A Black Hawk helicopter main rotor blade section. Tests were conducted on the undamaged blade section, and on the same section with simulated ballistic damage comprising a circular hole with a surrounding portion of the skin removed, exposing the internal honeycomb structure. The structural lift, drag, and pitching moment were measured at small increments in angle of attack up through stall at Reynolds numbers of 10(exp 6) and 2 x 10(exp 6). In addition, tests were conducted over a full 360-degree range in angle of attack for a Reynolds number of 10(exp 6). The measurements were complemented by mini-tuft flow visualization on the upper wing section, particularly near the hole. DTIC

N94-18571 Naval Postgraduate School, Monterey, CA.
TWO-DIMENSIONAL BOUNDARY SURFACES FOR AXI-SYMMETRIC EXTERNAL TRANSONIC FLOWS M.S. Thesis
Waleed Isa Al-hashel Mar. 1993 69 p Limited Reproducibility: More than 20% of this document may be affected by microfiche quality
(AD-A269678) Avail: Issuing Activity (Defense Technical Information Center (DTIC))

Investigation of two-dimensional transonic flows is extended to axisymmetric problems. This is of considerable practical interest, for example, with regard to missiles or aircraft engines which approximate much more closely bodies of revolution than two-dimensional bodies. The main concern with axisymmetric flows lies not only with the complexity of the governing nonlinear partial differential equation which is mixed of elliptic-hyperbolic type but also with the lack of a general method for accurately solving this type of equation. We solve the nonlinear transonic equation using the separation of variables technique, which yields two nonlinear ordinary differential equations. The x-dependence can be integrated numerically, and the solution for the r-dependence can be obtained using the expansion method originated by Van Dyke. This works well with only three terms in the expansion. The sonic solution of these equations is obtained analytically since both equations are simple enough to be integrated for this case (M(sub infinity) = 1.0) The small parameter (1-M(sub infinity)(exp 2)) plays an important role in specifying the shape of the boundary surfaces for external axisymmetric steady flow of interest for design. A Navier-Stokes solver was used to compute the inviscid flow to confirm our results in the region over the surface where the small perturbations apply. DTIC

N94-18964* National Aeronautics and Space Administration, Washington, DC.
AIRFLOW RESEARCH (Videotape)
Dec. 1985 Videotape: 3 min. 5 sec. playing time, in color, with sound
(NASA-TM-109372; NONP-VT-94-198219) Avail: CASI VHS A01/BETA A22

This is an overview of research being done in laminar flow at Ames Dryden Flight Research Center and Langley Research Center. Airflow research at Ames Dryden has resulted in a special wing covering that will artificially induce laminar flow on the wing surface; this specially adapted wing is shown being tested in different flying conditions. This video also features research done at Langley in producing a chemical covering for wings that will make visible natural laminar flow and turbulent airflow patterns as they occur. Langley researchers explain possible use of this technology in supersonic flight. CASI

N94-19119*# National Aeronautics and Space Administration. Ames Research Center, Moffett Field, CA.
INTERFEROMETRIC INVESTIGATIONS OF COMPRESSIBLE DYNAMIC STALL OVER A TRANSIENTLY PITCHING AIRFOIL
M. S. Chandrasekhara (Naval Postgraduate School, Monterey, CA.), L. W. Carr, and M. C. Wilder (MCAT Inst., San Jose, CA.) 14 Jan. 1993 18 p Presented at the 31st Aerospace Sciences Meeting and Exhibit, Reno, NV, 11-14 Jan. 1993; sponsored by AIAA See also A93-22628
(Contracts MIPR-92-0004; ARO-MIPR-130-92)
(NASA-TM-109380; AIAA Paper 93-0211; AD-268794; NAS 1.15:109380) Avail: CASI HC A03/MF A01

The dynamic stall flow field over NACA 0012 airfoil pitching transiently from 0 - 60 at a constant rate under compressible flow conditions has been studied using the real-time technique of point diffraction interferometry. This investigation using nonintrusive diagnostics provides a quantitative description of the overall flow field, including the finer details of dynamic stall vortex formation, growth and the concomitant changes in the pressure distribution. Analysis of several hundred interferograms obtained for a range of flow conditions shows that the peak leading edge suction pressure coefficient that stall is nearly constant for a given free stream Mach number at all nondimensional pitch rates. Also, this value is below that seen in steady flow at static stall for the same Mach number, indicating that dynamic effects significantly effect the separation behavior. Further, for a given Mach number, the dynamic stall vortex seems to form rapidly at nearly the same angle of attack for all pitch rates studied. As the vortex is shed, it induces an anti-clockwise trailing edge vortex, which grows in a manner similar to that of a starting vortex. The measured peak suction pressure coefficient drops as the free stream Mach number increases. For free stream Mach numbers above 0.4, small multiple shocks appear near the leading edge. DTIC

N94-19388*# North Carolina State Univ., Raleigh. Dept. of Mechanical and Aerospace Engineering.
SEMI-SPAN MODEL TESTING IN THE NATIONAL TRANSONIC FACILITY Annual Status Report
Ndaona Chokani and William E. Milholen, II Oct. 1993 16 p
(Contract NCC1-169)
(NASA-CR-194479; NAS 1.26:194479) Avail: CASI HC A03/MF A01

A semi-span testing technique has been proposed for the NASA Langley Research Center's National Transonic Facility (NTF). Semi-span testing has several advantages including (1) larger model size, giving increased Reynolds number capability; (2) improved model fidelity, allowing ease of flap and slat positioning which ultimately improves data quality; and (3) reduced construction costs compared with a full-span model. In addition, the increased model size inherently allows for increased model strength, reducing aeroelastic effects at the high dynamic pressure levels necessary to simulate flight Reynolds numbers. The Energy Efficient Transport (EET) full-span model has been modified to become the EET semi-span model. The full-span EET model was tested extensively at both NASA LRC and NASA Ames Research Center. The available full-span data will be useful in validating the semi-span test strategy in the NTF. In spite of the advantages discussed above, the use of a semi-span model does introduce additional challenges which must be addressed in the testing procedure. To minimize the influence of the sidewall boundary layer on the flow over the semi-span model, the model must be off-set from the sidewall. The objective is to remove the semi-span model from the sidewall boundary layer by use of a stand-off geometry. When this is done however, the symmetry along the centerline of the full-span model is lost when the semi-span model is mounted on the wind tunnel sidewall. In addition, the large semi-span model will impose a significant pressure loading on the sidewall boundary layer, which may cause separation. Even under flow conditions where the sidewall boundary layer remains attached, the sidewall boundary layer may adversely effect the flow over the semi-span model. Also, the increased model size and sidewall mounting requires a modified wall correction strategy. With these issues in mind, the semi-span model has been well instrumented with surface pressure taps to obtain data on the expected complex flow field in the near wall region. This status report summarizes the progress to date on developing the semi-span geometry definition suitable for generating structured grids for the computational research. In addition, the progress on evaluating three state-of-the-art Navier-Stokes codes is presented. Derived from text

N94-19433*# California Polytechnic State Univ., San Luis Obispo. Aeronautical Engineering Dept.
NUMERICAL PREDICTION OF TRANSITION OF THE F-16 WING AT SUPERSONIC SPEEDS Final Report
Russell M. Cummings and Joseph A. Garcia Sep. 1993 52 p
(Contract NCC2-754; NGT-70228)
(NASA-CR-194407; NAS 1.26:194407) Avail: CASI HC A04/MF A01

A parametric study is being conducted as an effort to numerically predict the extent of natural laminar flow (NLF) on finite swept wings at supersonic speeds. This study is one aspect of a High Speed Research Program (HSRP) to gain an understanding of the technical requirements for high-speed aircraft flight. The parameters that are being addressed in

this study are Reynolds number, angle of attack, and leading-edge wing sweep. These parameters were analyzed through the use of an advanced Computational Fluid Dynamics (CFD) flow solver, specifically the ARC 3-D Compressible Navier-Stokes (CNS) flow solver. From the CNS code, pressure coefficients (Cp) are obtained for the various cases. These Cp's are then used to compute the boundary-layer profiles through the use of the 'Kaups and Cebeci' compressible 2-D boundary layer code. Finally, the boundary-layer parameters are processed into a 3-D compressible boundary layer stability code (COSAL) to predict transition. The parametric study then consisted of four geometries which addressed the effects of sweep, and three angles of attack from zero to ten degrees to yield a total of 12 cases. The above process was substantially automated through a procedure that was developed by the work conducted under this study. This automation procedure then yields a 3-D graphical measure of the extent of laminar flow by predicting the transition location of laminar to turbulent flow.
Derived from text

N94-19484*# National Aeronautics and Space Administration. Lewis Research Center, Cleveland, OH.
SUPERSONIC JETS FROM BEVELLED RECTANGULAR NOZZLES
Edward J. Rice and Ganesh Raman (Sverdrup Technology, Inc., Brook Park, OH.) Nov. 1993 9 p Proposed for presentation at the Winter Annual Meeting of the ASME Symposium on Flow Acoustics Interaction and Fluid Control, New Orleans, LA, 28 Nov. - 3 Dec. 1993; sponsored by ASME
(Contract NAS3-25266; RTOP 537-02-22)
(NASA-TM-106403; E-8239; NAS 1.15:106403; Rept-93-WA/NCA-26)
Avail: CASI HC A02/MF A01

The influence of nozzle exit geometry on jet mixing and noise production was studied experimentally for a series of rectangular nozzles operating at supersonic jet velocities. Both converging (C) and converging-diverging (C-D) nozzles were built with asymmetrical (single bevel) and symmetrical (double bevel) exit chambers and with conventional straight exits for comparison. About a four decibel reduction of peak mixing noise was observed for the double bevelled C-D nozzle operated at design pressure ratio. All bevelled geometries provided screech noise reduction for under-expanded jets and an upstream mixing noise directivity shift which would be beneficial for improved acoustic treatment performance of a shrouded system. Author

N94-19524 Institut Franco-Allemand de Recherches, Saint-Louis (France).
NUMERICAL INVESTIGATION OF THE INCOMPRESSIBLE FLOW AROUND A WING WITH A FIXED SPOILER [NUMERISCHE UNTERSUCHUNG DER INKOMPRESSIBLEN STROEMUNG UM EINEN TRAGFLUEGEL MIT FESTEM SPOILER]
W. Czichowsky 20 Aug. 1991 99 p In GERMAN
(ISL-R-109/91; ETN-93-95121) Copyright Avail: Issuing Activity (Fachinformationszentrum Karlsruhe, 7514 Eggenstein-Leopoldshafen 2, Germany)

A differential method for the numerical solution of Navier-Stokes equations for calculation of time dependent incompressible flow around a wing is presented. The method was based on Chaplygin equation and vortex transport equation with the psi-omega formalism. A coordinates system, numerically established and body fitted, was chosen. The solution of finite stream equations was iteratively obtained for each time step with the successive overrelaxation method. The flow around a wing without incidence, with a spoiler with an angle of 40 deg, and without a spoiler was analyzed. Numerical results give flow structure, pressure distribution, and force coefficients as a function of time for Reynolds numbers equal to 100, 500, 1000, and 5000. ESA

N94-19621*# Old Dominion Univ., Norfolk, VA. Dept. of Aerospace Engineering.
NAVIER-STOKES, DYNAMICS AND AEROELASTIC COMPUTATIONS FOR VORTICAL FLOWS, BUFFET AND FLUTTER APPLICATIONS
Progress Report, 1 Oct. 1992 - 30 Sep. 1993
Osama A. Kandil Sep. 1993 75 p
(Grant NAG1-648)
(NASA-CR-194520; NAS 1.26:194520) Avail: CASI HC A04/MF A01

Research on Navier-Stokes, dynamics, and aeroelastic computations for vortical flows, buffet, and flutter applications was performed. Progress during the period from 1 Oct. 1992 to 30 Sep. 1993 is included. Papers on the following topics are included: vertical tail buffet in vortex breakdown flows; simulation of tail buffet using delta wing-vertical tail configuration; shock-vortex interaction over a 65-degree delta wing in transonic flow; supersonic vortex breakdown over a delta wing in transonic flow; and prediction and control of slender wing rock. CASI

N94-19667# Technische Univ., Delft (Netherlands). Faculty of Aerospace Engineering.
ADAS IMPLEMENTATION OF A PANEL METHOD FOR THE PREDICTION OF AERODYNAMIC LOADS
P. M. Heyma Jun. 1993 57 p Original contains color illustrations
(LR-723; ETN-93-95027) Avail: CASI HC A04/MF A01

New developments and extensions to the Aircraft Design and Analysis System (ADAS) are discussed. ADAS semi automatically generates a finite element model suitable for structural analysis and optimization. Major structural components can be defined. The aircraft loads are determined by aerodynamic forces. For aerodynamic loads, a simplified lift distribution was used. To improve the prediction of the aerodynamic loads, the panelcode O215 is implemented. This panel method computes the potential flow around complex arbitrary configurations. The program requires a quadrilateral panel surface discritization. The same ADAS finite element model was used for the structural as well as the aerodynamic calculations. The panel program O215, the coordinate system setup, the panel partitioning, the way lifting parts are modeled and the system of integral equations are reported. The ADAS Finite Element (FE)-model and the usefulness of the structural mesh for aerodynamic calculations are discussed. The use of a structural mesh for aerodynamic calculations is validated. New subprograms added to the ADAS system are described and some results for a typical transport aircraft are presented. ESA

N94-18417# Middle East Technical Univ., Ankara (Turkey). Dept. of Aeronautical Engineering.
EXPERIMENTAL INVESTIGATION OF FLOW AROUND A MULTIELEMENT AIRFOIL
Nafiz Alemdaroglu *In* AGARD, High-Lift System Aerodynamics Sep. 1993 19 p (For primary document see N94-18415 04-01)
Copyright Avail: CASI HC A03/MF A04

N94-18419# Dornier Luftfahrt G.m.b.H., Friedrichshafen (Germany).
CALCULATION OF MAXIMUM AND HIGH LIFT CHARACTERISTICS OF MULTI ELEMENT AEROFOILS
Willy Fritz *In* AGARD, High-Lift System Aerodynamics Sep. 1993 12 p (For primary document see N94-18415 04-01)
Copyright Avail: CASI HC A03/MF A04

N94-18420# Technische Univ., Berlin (Germany). Inst. fuer Luft- und Raumfahrt.
NAVIER-STOKES COMPUTATIONS OF TURBULENT FLOW AROUND HIGH-LIFT CONFIGURATIONS
P. Bartsch, W. Nitsche, and M. Britsch *In* AGARD, High-Lift System Aerodynamics Sep. 1993 10 p (For primary document see N94-18415 04-01)
Copyright Avail: CASI HC A02/MF A04

N94-18421*# National Aeronautics and Space Administration. Ames Research Center, Moffett Field, CA.
EFFICIENT SIMULATION OF INCOMPRESSIBLE VISCOUS FLOW OVER MULTI-ELEMENT AIRFOILS
Stuart E. Rogers, N. Lyn Wiltberger, and Dochan Kwak *In* AGARD, High-Lift System Aerodynamics Sep. 1993 9 p (For primary document see N94-18415 04-01)
Copyright Avail: CASI HC A02/MF A04

N94-18422*# McDonnell Aircraft Co., Saint Louis, MO.
NAVIER-STOKES CALCULATIONS ON MULTI-ELEMENT AIRFOILS USING A CHIMERA-BASED SOLVER
Donald W. Jasper, Shreekant Agrawal, and Brian A. Robinson *In* AGARD, High-Lift System Aerodynamics Sep. 1993 11 p Sponsored by NASA. Ames Research Center and Cray Research, Inc. (For primary document see N94-18415 04-01)
Copyright Avail: CASI HC A03/MF A04

N94-18423# Toronto Univ., Downsview (Ontario). Inst. for Aerospace Studies.
NUMERICAL SOLUTION OF THE NAVIER-STOKES EQUATIONS FOR HIGH-LIFT CONFIGURATIONS ON STRUCTURED COMPOSITE GRIDS
T. E. Nelson, D. W. Zingg, and G. W. Johnston *In* AGARD, High-Lift System Aerodynamics Sep. 1993 14 p (For primary document see N94-18415 04-01)
Copyright Avail: CASI HC A03/MF A04

N94-18424*# National Aeronautics and Space Administration. Langley Research Center, Hampton, VA.
HIGH REYNOLDS NUMBER CONFIGURATION DEVELOPMENT OF A HIGH-LIFT AIRFOIL
Walter O. Valarezo (Douglas Aircraft Co., Inc., Long Beach, CA.), Chet J. Dominik (Douglas Aircraft Co., Inc., Long Beach, CA.), Robert J. McGhee, and Wesley L. Goodman *In* AGARD, High-Lift System Aerodynamics Sep. 1993 8 p (For primary document see N94-18415 04-01)
Copyright Avail: CASI HC A02/MF A04

N94-18425# Office National d'Etudes et de Recherches Aerospatiales, Paris (France).
A VISCOUS-INVISCID SOLVER FOR HIGH-LIFT INCOMPRESSIBLE FLOWS OVER MULTI-ELEMENT AIRFOILS AT DEEP SEPARATION CONDITIONS [UNE METHODE D'INTERACTION VISQUEUX NON-VISQUEUX POUR ECOULEMENTS INCOMPRESSIBLES HYPERSUSTENTES SUR PROFILS MULTI-CORPS EN REGIME DE DECOLLEMENT PROFOND]
J. C. LeBalleur and M. Neron *In* AGARD, High-Lift System Aerodynamics Sep. 1993 12 p In FRENCH (For primary document see N94-18415 04-01)
Copyright Avail: CASI HC A03/MF A04

N94-18426# National Aerospace Lab., Amsterdam (Netherlands).
HIGH-LIFT SYSTEM ANALYSIS METHOD USING UNSTRUCTURED MESHES
K. deCock *In* AGARD, High-Lift System Aerodynamics Sep. 1993 20 p (For primary document see N94-18415 04-01)
Copyright Avail: CASI HC A03/MF A04

N94-18427# Manchester Coll. of Science and Technology (England). Dept. of Mechanical Engineering.
PREDICTION OF THE HIGH-LIFT PERFORMANCE OF MULTI-ELEMENT AEROFOILS USING AN UNSTRUCTURED NAVIER-STOKES SOLVER
Leslie J. Johnston and Luca Stolcis *In* AGARD, High-Lift System Aerodynamics Sep. 1993 18 p (For primary document see N94-18415 04-01)
(Grant CEC-SC1/900369)
Copyright Avail: CASI HC A03/MF A04

N94-18428# Deutsche Forschungsanstalt fuer Luft- und Raumfahrt, Brunswick (Germany). Inst. for Design Aerodynamics.
NUMERICAL CALCULATIONS OF HIGH LIFT FLOWS USING STRUCTURED AND UNSTRUCTURED METHODS
R. Bailey, J. M. A. Longo, R. Radespiel, A. Ronzheimer, A. Demier, N. Kroll, and C.-C. Rossow *In* AGARD, High-Lift System Aerodynamics Sep. 1993 13 p (For primary document see N94-18415 04-01)
Copyright Avail: CASI HC A03/MF A04

N94-18429# Grumman Aerospace Corp., Bethpage, NY.
NAVIER-STOKES SIMULATION OF FLOW FIELD AROUND A BLOWN-FLAP HIGH-LIFT SYSTEM
R. Chow, K. Chu, and G. Carpenter *In* AGARD, High-Lift System Aerodynamics Sep. 1993 10 p (For primary document see N94-18415 04-01)
Copyright Avail: CASI HC A02/MF A04

N94-18430# Office National d'Etudes et de Recherches Aerospatiales, Paris (France).
THE GARTEUR HIGH LIFT RESEARCH PROGRAMME
J. J. Thibert *In* AGARD, High-Lift System Aerodynamics Sep. 1993 21 p (For primary document see N94-18415 04-01)
Copyright Avail: CASI HC A03/MF A04

N94-18433# Boeing Commercial Airplane Co., Seattle, WA.
VISCOUS PHENOMENA AFFECTING HIGH-LIFT SYSTEMS AND SUGGESTIONS FOR FUTURE CFD DEVELOPMENT
P. T. Meredith *In* AGARD, High-Lift System Aerodynamics Sep. 1993 8 p (For primary document see N94-18415 04-01)
Copyright Avail: CASI HC A02/MF A04

N94-18434# Defence Research Agency, Farnborough (England).
A STUDY OF THE USE OF HALF-MODELS IN HIGH-LIFT WIND-TUNNEL TESTING
P. B. Earnshaw, A. R. Green, B. C. Hardy, and A. H. Jelly *In* AGARD, High-Lift System Aerodynamics Sep. 1993 9 p (For primary document see N94-18415 04-01)
Copyright Avail: CASI HC A02/MF A04

N94-18435*# National Aeronautics and Space Administration. Langley Research Center, Hampton, VA.
IN-FLIGHT PRESSURE DISTRIBUTIONS AND SKIN-FRICTION MEASUREMENTS ON A SUBSONIC TRANSPORT HIGH-LIFT WING SECTION
Long P. Yip, Paul M. H. W. Vijgen (High Technology Corp., Hampton, VA.), Jay D. Hardin (Lockheed Engineering and Sciences Co., Hampton, VA.), and C. P. vanDam (California Univ., Davis.) *In* AGARD, High-Lift System Aerodynamics Sep. 1993 19 p (For primary document see N94-18415 04-01)
(Contracts NAS1-19299; NAS1-19000; NCC1-163)
Copyright Avail: CASI HC A03/MF A04

N94-18437# Institut fuer Theoretische Stroemungsmechanik, Goettingen (Germany).
A FAST COMPUTING METHOD FOR THE FLOW OVER HIGH-LIFT WINGS
K. Jacob *In* AGARD, High-Lift System Aerodynamics Sep. 1993 12 p (For primary document see N94-18415 04-01)
Copyright Avail: CASI HC A03/MF A04

N94-18438# California State Univ., Long Beach. Dept. of Aerospace Engineering.
CALCULATION OF MULTIELEMENT AIRFOILS AND WINGS AT HIGH LIFT
Tuncer Cebeci *In* AGARD, High-Lift System Aerodynamics Sep. 1993 15 p (For primary document see N94-18415 04-01)
Copyright Avail: CASI HC A03/MF A04

N94-18439# Politecnico di Milano (Italy). Dipt. di Ingegneria Aerospaziale.
WAKE STRUCTURE AND AERODYNAMIC BEHAVIOR OF HIGH LIFT AIRCRAFT CONFIGURATIONS DURING UNSTEADY MANEUVERS IN GROUND EFFECT
A. Baron and M. Boffadossi *In* AGARD, High-Lift System Aerodynamics Sep. 1993 15 p (For primary document see N94-18415 04-01)
Copyright Avail: CASI HC A03/MF A04

N94-18440# Office National d'Etudes et de Recherches Aerospatiales, Paris (France).
VISCOUS-INVISCID CALCULATION OF HIGH-LIFT SEPARATED COMPRESSIBLE FLOWS OVER AIRFOILS AND WINGS [CALCUL PAR INTERACTION VISQUEUX NON-VISQUEUX DES ECOULEMENTS COMPRESSIBLES FORTEMENT DECOLLES AUX GRANDES PORTANCES SUR PROFILS D'AILES ET VOILURES]
J. C. LeBalleur *In* AGARD, High-Lift System Aerodynamics Sep. 1993 18 p In FRENCH Sponsored by Ministry of Defence (For primary document see N94-18415 04-01)
Copyright Avail: CASI HC A03/MF A04

N94-18553*# National Aeronautics and Space Administration. Lewis Research Center, Cleveland, OH.
A COMPARATIVE STUDY OF TURBULENCE MODELS IN PREDICTING HYPERSONIC INLET FLOWS
Kamlesh Kapoor *In its* Workshop on Computational Turbulence Modeling 1993 9 p (For primary document see N94-18545 04-34)
Avail: CASI HC A02/MF A04

03 AIR TRANSPORTATION AND SAFETY

Includes passenger and cargo air transport operations; and aircraft accidents.

For related information see also *16 Space Transportation* and *85 Urban Technology and Transportation.*

N94-17733 National Aerospace Lab., Amsterdam (Netherlands). Flight Div.
FEASIBILITY OF A WIND-ELLIPSE CRITERION IN A VORTEX ADVISORY SYSTEM FOR SCHIPHOL AIRPORT
F. R. Polak 7 Oct. 1991 24 p Presented at FAA International Wake Vortex Symposium, 29-31 Oct. 1991 Limited Reproducibility: More than 20% of this document may be affected by microfiche quality
(NLR-TP-91384-U; ETN-93-94782) Avail: Issuing Activity (European Space Agency (ESA))

The feasibility of a wind-ellipse criterion in a possible future Vortex Advisory System (VAS) for Schiphol Airport (the Netherlands), based on an extensive data collection and analysis concerning 11 months in 1980 and 1981, is investigated. A VAS must enable air traffic control to determine in real time whether or not the large separations during the approach of smaller aircraft behind heavy aircraft have to be applied. A VAS in its simplest form will show the air traffic controller, by means of a red/green indicator, whether the wind vector is inside the ellipse (red light) or outside the ellipse (green light). ESA

N94-18490 Federal Aviation Administration, Washington, DC.
AIRPORT ACTIVITY STATISTICS OF CERTIFICATED ROUTE AIR CARRIERS, 1992 Report, period ending 31 Dec. 1992
31 Dec. 1992 373 p Limited Reproducibility: More than 20% of this document may be affected by microfiche quality
(AD-A269042; FAA-APO-93-8) Avail: CASI HC A16

There are some major changes in this publication due to the new T-100 data collection system for U.S. air carriers which began 1 Jan. 1990. The format has been changed to comply with the regulations of 14 CFR 241.19.6 that restrict public disclosure of T-100 detail and summary international data. Non-U.S. airport data does not appear. Data is no longer broken out by domestic or international operations at airports, only system operations are shown. This edition presents the volume of revenue passenger, freight, and mail traffic handled by the nation's large certificated air carriers at each airport served by these scheduled airlines during the 12 months ending 31 Dec. 1992. In addition, a presentation of aircraft departures is shown including detail by aircraft type for total departures performed in scheduled, nonscheduled, and all services. Large certificated air carriers hold Certificates of Public Convenience and Necessity issued by the Department of Transportation (DOT) authorizing the performance of air transportation. Large certificated air carriers operate aircraft with seating capacity of more than 60 seats or a maximum payload capacity of more than 18,000 pounds. Data for charter only, commuter, intra-state, and foreign-flag air carriers are not included in this publication. DTIC

N94-18822# Applied Research Associates, Inc., Lakewood, CO.
AIRCRAFT FIRE SENTRY. VOLUME 1: SUMMARY Final Report, 17 Aug. 1990 - 17 Aug. 1992
R. M. Mugele, P. T. Dzwilewski, and J. T. Cilke Jan. 1993 61 p
(Contract F08635-88-C-0067)
(AD-A270087; AFCESA/ESL-TR-92-63-Vol-1) Avail: CASI HC A04/MF A01

This report summarizes the development of an Aircraft Fire Sentry (AFS) system. The AFS is designed to automatically detect a fire in the cargo bay of large cargo aircraft, provide an audio and visual alarm locally, and remotely notify the nearest fire department by radio frequency link. The basic design philosophy in developing the AFS was to use commercially available fire detection hardware and radio transmitters/receivers. The finished assembly is to be lightweight and portable. The AFS is to be deployed onboard parked aircraft and left to sense fire stimulus for up to 60 continuous hours in the self-powered mode. A prototype model was designed, built, and tested for performance and reliability. DTIC

N94-18823# Applied Research Associates, Inc., Lakewood, CO.
AIRCRAFT FIRE SENTRY. VOLUME 2: APPENDICES A, B, C AND D Final Report, 17 Aug. 1990 - 17 Aug. 1992
R. M. Mugele, P. T. Dzwilewski, and J. T. Cilke Jan. 1993 380 p
(Contract F08635-88-C-0067)
(AD-A270088; AFCESA/ESL-TR-92-63-Vol-2) Avail: CASI HC A17/MF A03

This report summarizes the development of an Aircraft Fire Sentry (AFS) system. The AFS is designed to automatically detect a fire in the cargo bay of large cargo aircraft, provide an audio and visual alarm locally, and remotely notify the nearest fire department by radio frequency link. The basic design philosophy in developing the AFS was to use commercially available fire detection hardware and radio transmitters/receivers. The finished assembly is to be lightweight and portable. The AFS is to be deployed onboard parked aircraft and left to sense fire stimulus for up to 60 continuous hours in the self-powered mode. A prototype model was designed, built, and tested for performance and reliability. DTIC

N94-18844*# Computer Technology Associates, Inc., Pleasantville, NJ.
DENVER TMA ASSESSMENT
Kelly Harwood and Beverly Sanford Oct. 1993 79 p
(Contract DTFA03-89-C-00023)
(NASA-CR-4554; A-94009; NAS 1.26:4554) Avail: CASI HC A05/MF A01

This report describes the assessment of the Traffic Management Advisor (TMA) conducted at the Denver Center and TRACON, January 11-February 5, 1993. The assessment addressed the effectiveness of TMA for supporting various traffic management activities. At the Center, traffic management coordinators (TMC's) shadowed traffic operations, using TMA to make metering time and internal release decisions. At the TRACON, TMC's accessed TMA in an advisory mode for different planning activities such as staffing, distributing the traffic load, and changing the airport acceptance rate. These different opportunities for assessing TMA provide insight into TMA as a potential communication aid and planning tool. Findings from this assessment indicate that TMA can be used to support traffic management planning and decisions. TMC's at the center were able to use information provided by TMA to determine metering times as well as internal release times. At the TRACON, TMA supported decisions on airport configuration, airport acceptance rate, load distribution, proactive coordination with the center, and staffing. While findings of TMA use are generally positive, it must be kept in mind that this assessment is a snapshot in time. Not all TMA capabilities were assessed, nor were TMC's fully trained and knowledgeable on all features. Feature use will continue to evolve and strategies emerge as the TMC's gain experience with TMA over a variety of traffic situations and their understanding of TMA capabilities broadens with continued training. Author

N94-18852*# Microwave Monolithics, Inc., Simi Valley, CA.
HIGH EFFICIENCY LOW COST MONOLITHIC MODULE FOR SARSAT DISTRESS BEACONS
Wendell C. Petersen and Daniel P. Siu 29 Oct. 1992 26 p
(Contract NAS3-25712; SBIR-14.03-6642)
(NASA-CR-194234; NAS 1.26:194234) Avail: CASI HC A03/MF A01

The program objectives were to develop a highly efficient, low cost RF module for SARSAT beacons; achieve significantly lower battery current drain, amount of heat generated, and size of battery required; utilize MMIC technology to improve efficiency, reliability, packaging, and cost; and provide a technology database for GaAs based UHF RF circuit architectures. Presented in viewgraph form are functional block diagrams of the SARSAT distress beacon and beacon RF module as well as performance goals, schematic diagrams, predicted performances, and measured performances for the phase modulator and power amplifier. CASI

N94-19352# National Transportation Safety Board, Washington, DC.
AIRCRAFT ACCIDENT REPORT: MIDAIR COLLISION, MITSUBISHI MU-2B-60, N74FB, AND PIPER PA-32-301, N82419, GREENWOOD MUNICIPAL AIRPORT, GREENWOOD, INDIANA, 11 SEPTEMBER 1992
13 Sep. 1993 84 p
(PB93-910406; NTSB/AAR-93/05) Avail: CASI HC A05/MF A01

The midair collision of an MU-2 aircraft with a PA-32 aircraft about 2 miles northeast of the Greenwood Municipal Airport, Greenwood, Indiana, on 11 Sep. 1992 is explained. Safety issues focused on the deficiencies in the see-and-avoid concept as a primary means of collision avoidance, and the failure of pilots to fully utilize the air traffic control system by obtaining instrument flight rules clearances before takeoff. Recommendations concerning these issues were made to the Federal Aviation Administration, the National Business Aircraft Association, the National Association of Flight Instructors, the Experimental Aircraft Association, and the Aircraft Owners and Pilots Association. Author (revised)

N94-19661# Massachusetts Inst. of Tech., Lexington.
ESTIMATION OF WAKE VORTEX ADVECTION AND DECAY USING METEOROLOGICAL SENSORS AND AIRCRAFT DATA
Kethryn M. Butler 28 Sep. 1993 35 p
(Contract DTFA01-91-Z-02036)
(AD-A270763; ATC-201; DOT/FAA/RD-93/16) Avail: CASI HC A03/MF A01

The lift-generated wake vortices trailing behind an aircraft present a danger to aircraft following the same or nearby path. The degree of hazard to the following aircraft depends on the nature of the wake encountered in its flight path and on the ability of the aircraft to counter its effects. This report describes the current state of understanding of the factors that influence the motion and dissipation of wake vortices. The relationships of these factors to parameters that are measurable through meteorological sensors and from a priori knowledge of the vortex generating aircraft characteristics are discussed as an aid to structuring development plans for the creation of wake vortex advisory products by the Integrated Terminal Weather System (ITWS) and by special wake vortex sensors. DTIC

04 AIRCRAFT COMMUNICATIONS AND NAVIGATION

Includes digital and voice communication with aircraft; air navigation systems (satellite and ground based); and air traffic control.

For related information see also *17 Space Communications, Spacecraft Communications, Command and Tracking* and *Communications and Radar.*

N94-17921# Deutsche Forschungsanstalt fuer Luft- und Raumfahrt, Goettingen (Germany). Abt. Systemtechnik und Navigation.
ON THE USE OF DIFFERENTIAL GPS FOR AUTOMATIC APPROACH AND LANDING OF SPACE AND AIRCRAFT
Yusuke Suzuki (National Space Development Agency, Tokyo, Japan.) Sep. 1992 43 p
(DLR-Mitt-93-05; ETN-93-94867) Avail: CASI HC A03/MF A01

The integration of an Inertial Navigation System (INS) with Differential Global Positioning System (DGPS) is investigated with the aim of meeting the critical requirement for the automatic landing of aircraft and recoverable spacecraft according to ICAO, CAT 3 (vertical position accuracy of 0.6 meters (2 sigma)). In a first Kalman filter of the reference system on ground and of the system on board the pseudoranges, ionospheric effects and phase ambiguities are estimated. In a second Kalman filter the pseudorange compensation data and receiver clock errors are estimated on ground and the position, velocity, attitude, and heading and receiver clock errors are estimated on board. Experiments were performed based on GPS receivers SEL GLOBOS 2000 and a simulated INS. The results show that this system can meet the above mentioned requirements. Recommendations for the system improvement are included. ESA

N94-18146# Deutsche Forschungsanstalt fuer Luft- und Raumfahrt, Brunswick (Germany). Abt. fuer Systemtechnik und Navigation.
ABOUT THE ACCURACY OF AN IMAGE-BASED NAVIGATION SYSTEM DURING THE RUNWAY APPROACH [ANALYSE DES FEHLERVERHALTENS EINER LUFTBILD-STUETZUNG IM LANDEANFLUG]
Hans-Ullrich Doehler Jan. 1993 35 p In GERMAN
(DLR-Mitt-93-01; ETN-93-94866) Avail: CASI HC A03/MF A01

Flight tests with trajectory measurements in the vicinity of an airport in a runway referenced coordinate system, such as flight inspection systems for testing landing aids in civil airports are considered. Position measurement procedures extracting the position information from images recorded on board the aircraft are studied. To estimate the accuracy of the achieved position data, a simulation of such a system is presented. Under the assumption of different kinds of error sources, regarded as system constraints, the overall position error was numerically determined. ESA

N94-18336# Federal Aviation Administration, Washington, DC. Office of Aviation Policy and Plans.
TERMINAL AREA FORECASTS, FY 1993-2005
Jul. 1993 583 p
(AD-A269855; FAA-APO-93-9) Avail: CASI HC A25/MF A06

This report contains forecasts of aviation activity of 873 airports in the United States for fiscal years 1993-2005. These include 401 airports with FAA air traffic control towers and radar approach control services and 27 FAA contract towers. For each airport, detailed forecasts are made for the four major users of the air traffic system: air carriers, air taxi/commuters, general aviation, and military. Summary tables contain national, FAA regional, and state aviation data and other airport specific-highlights. The forecasts have been prepared to meet the budget and planning needs of the FAA and to provide airport-specific information that can be used by state and local aviation authorities, the aviation industry, and the general public. DTIC

N94-18384 Mitre Corp., Bedford, MA.
VHF AIR/GROUND COMMUNICATIONS FOR AIR TRAFFIC CONTROL. VOLUME 1: A DECISION TREE APPROACH TO SYSTEM INNOVATIONS
Cheng-Hong Chen, James W. Howland, Robert I. Millar, Brian E. White, and Warren J. Wilson Jul. 1993 46 p Limited Reproducibility: More than 20% of this document may be affected by microfiche quality
(Contract DTFA01-93-C-0001)
(AD-A268485; MTR-M-93B0000096-Vol-1) Avail: Issuing Activity (Defense Technical Information Center (DTIC))

Improvements to VHF air/ground communications for civil aviation in the 118-137 MHz aeronautical mobile frequency band are systematically explored by means of a decision tree approach. Seven individual papers analyze in detail the operational and technical factors involved in making these improvements. Basic tradeoffs between analog and digital modulation are discussed to frame the problem. Near-term improvements utilizing various analog modulations with closer channel spacing are first reviewed. Then far-term improvements employing a wide range of digital modulation and coding techniques are considered. Multiplexing methods - frequency, time, and code division - are discussed in detail. Methods for random access to a shared communications channel are compared, with emphasis upon real-time operations for air traffic control. Volume I provides an executive summary of this work, while Volume II presents the technical details. DTIC

N94-18728# Federal Aviation Administration, Atlantic City, NJ. Technical Center.
VMC LEFT TURN CURVED APPROACHES, TEST RESULTS Technical Note, Sep. 1989 - Jul. 1990
Rosanne M. Weiss Jul. 1993 45 p
(AD-A269476; DOT/FAA/CT-TN92/46) Avail: CASI HC A03/MF A01

Flight tests were conducted at the Federal Aviation Administration (FAA) Technical Center in 1989 and 1990 to aid in answering questions concerning curved approaches to a heliport under visual meteorological conditions (VMC). These questions include protected airspace within the curved segment of the approach, the most feasible angle of turn and minimum final approach segment. The FAA's Sikorsky S-76 and UH-1H were used for these tests. Data were collected from approaches using turn angles of 45-, 90-, and 180-degrees, each with three different final segments, 800, 1200, and 1600 feet (ft). Due to airspace restrictions at the time of these tests, left turns to final were flown. All maneuvers were tracked by ground-based tracking systems. This report documents the results of these flights. The test procedures, evaluation methodology, and technical and operational issues are described. Analysis of pilot performance as well as pilot subjective input are provided. Conclusions are presented that address the airspace, turn angle, and final segment issues. The results will be considered in future modifications of the FAA Heliport Design Advisory Circular, AC 150/5390-2. All appendixes can be found in Research Directorate for Aviation Technology Division Report DOT/FAA/CT-ACD33093/6. DTIC

N94-19300# Oak Ridge National Lab., TN.
ROBOT NAVIGATION IN UNKNOWN TERRAINS: INTRODUCTORY SURVEY OF NON-HEURISTIC ALGORITHMS
N. S. V. Rao, S. Kareti (Old Dominion Univ., Norfolk, VA.), Weimin Shi

(Old Dominion Univ., Norfolk, VA.), and S. S. Iyengar (Louisiana State Univ., Baton Rouge.) Jul. 1993 58 p
(Contract DE-AC05-84OR-21400)
(DE93-019221; ORNL/TM-12410) Avail: CASI HC A04/MF A01

A formal framework for navigating a robot in a geometric terrain through an unknown set of obstacles is considered. Here the terrain model is not known a priori, but the robot is equipped with a sensor system (vision or touch) employed for the purpose of navigation. The focus is restricted to the non-heuristic algorithms which can be theoretically shown to be correct within a given framework of models for the robot, terrain, and sensor system. These formulations, although abstract and simplified compared to real-life scenarios, provide foundations for practical systems by highlighting the underlying critical issues. First, the authors consider the algorithms that are shown to navigate correctly without much consideration given to the performance parameters, such as distance traversed. Second, they consider non-heuristic algorithms that guarantee bounds on the distance traversed or the ratio of the distance traversed to the shortest path length (computed if the terrain model is known). Then they consider the navigation of robots with very limited computational capabilities such as finite automata. DOE

N94-19572# Naval Surface Warfare Center, Dahlgren, VA.
ABSOLUTE POSITIONING BY COLLECTING GLOBAL POSITIONING SYSTEM (GPS) DATA ALONG SHORT BASELINES Final Report
Bruce R. Hermann and Alan G. Evans Sep. 1993 34 p
(AD-A271324; NSWCDD/TR-93/309) Avail: CASI HC A03/MF A01

This report addresses the problem of determining absolute positions (longitude and latitude) from Global Positioning System (GPS) data in the presence of Selective Availability (SA). The SA-epsilon effect can be avoided if one can wait until corrected or post-fitted satellite ephemerides and clock estimates become available. However, the SA-dither effect cannot easily be eliminated from the ranging data in the field. This report considers both problems and suggests methods that have the potential to allow absolute position solutions to be obtained even with dither corrupting the satellite data. The requirements and practicality of each are reviewed. DTIC

05 AIRCRAFT DESIGN, TESTING AND PERFORMANCE

Includes aircraft simulation technology.

For related information see also *18 Spacecraft Design, Testing and Performance* and *39 Structural Mechanics.*For land transportation vehicles see *85 Urban Technology and Transportation.*

N94-17704 Department of the Navy, Washington, DC.
LIFT ENHANCEMENT DEVICE Patent
Samuel Greenhalgh, inventor (to Navy) 13 Jul. 1993 10 p Filed 30 Jan. 1992
(AD-D015868; US-Patent-5,226,618; US-Patent-Appl-SN-830206) Avail: CASI HC A02/MF A01

A lift enhancing device for an inextensible, membraneous wing is disclosed. The device comprises the 'forced' reattachment of a section of the trailing edge back to the trailing edge so that a warp is introduced therein. The section is reattached with flexible tape to allow oscillation of the section, and increased lift from the wing, at prescribed airspeeds. DTIC

N94-17734 National Aerospace Lab., Amsterdam (Netherlands). Flight Simulation Div.
TAKE-OFF PERFORMANCE MONITORING SYSTEM ALGORITHM AND DISPLAY DEVELOPMENT
Sjack J. L. H. Verspay 15 Nov. 1991 13 p Presented at AIAA Atmospheric Flight Mechanics Conference, New Orleans, MA, 12-14 Aug. 1991 Sponsored by Netherlands Agency for Aerospace Programs, Delft Limited Reproducibility: More than 20% of this document may be affected by microfiche quality
(NLR-TP-91395-U; ETN-93-94783) Avail: CASI HC A03

As part of a study into the potential safety benefit of a Take Off Performance Monitoring (TOPM) system the development of the algorithms and displays needed for such a system are presented. The predictive algorithms make use of a first order correction polynome which is shown to be capable of predicting performance better than a zero order correction. Three displays for three different types of TOPM, which represent different levels of sophistication, are presented. ESA

N94-17826# Defence Research Agency, Bedford (England).
COMPARISON BETWEEN SWEPT AND DELTA CANARDS ON A MODEL OF A COMBAT AIRCRAFT
D. G. Mabey and C. R. Pyne Feb. 1993 36 p
(AD-A269561; DRA-TM-AP-23; DRIC-BR-318039) Avail: CASI HC A03/MF A01

The aerodynamic characteristics of a low speed half model of a typical combat aircraft configuration fitted with a 65 deg delta canard planform are compared with those for the same model fitted with 44.3 deg swept canard. Both canards had an RAE 104 aerofoil section. The tests were made in the DRA 13 ft x 9 ft Wind Tunnel on a large model of the DRA High Incidence Research Model (HIRM 1), modified to represent the Experimental Aircraft (EAP) configuration. For a 15% smaller planform area, the delta canard gives higher lift and comparable pitching moments for trimming. For canard and wing buffeting the differences are small. Overall, these low speed measurements suggest that delta canards with round leading edges have significant advantages over swept canards for future combat aircraft. DTIC

N94-18227# Notre Dame Univ., IN. Dept. of Aerospace and Mechanical Engineering.
PRELIMINARY STRUCTURAL DESIGN: DEFINING THE DESIGN SPACE Final Report, Sep. 1989 - Dec. 1992
Stephen M. Batill and Richard A. Swift Feb. 1993 156 p
(Contract F33615-89-C-3208)
(AD-A268898; WL-TR-93-3004) Avail: CASI HC A08/MF A02

A series of studies were performed to evaluate the application of finite element-based analysis and optimization methods to the preliminary design of lightweight, aerospace structures. Either the internal structural arrangement or the structural materials were used as the design variables in each concept study. The concepts considered ranged from truss structures such as a helicopter tail-boom or complex space truss to a series of semi-monocoque lifting surfaces. Both static and dynamic constraints were used in the design of these concepts. Multidisciplinary optimization and analysis procedures were used to develop detailed information from finite element models for each structural concept. From this detailed design data, neural network representations of the design space were developed for the particular problem. The neural networks were then coupled with either simulated annealing or numerical search optimization techniques to identify improved design concepts. DTIC

N94-18315 Aeronautical Research Labs., Melbourne (Australia).
APPLICATION OF THE A* ALGORITHM TO AIRCRAFT TRAJECTORY GENERATION
M. E. Halpern Jul. 1993 27 p Limited Reproducibility: More than 20% of this document may be affected by microfiche quality
(AD-A268728; ARL-TR-20; DODA-AR-007-078) Avail: CASI HC A03

Work carried out on the development of concepts for an automated trajectory generator for military aircraft is described. The system uses the A* optimization algorithm to design a ground track which represents an optimal tradeoff between a short path and a path over low terrain. This is achieved by minimizing a cost function which is user selectable. This work incorporates path segments consisting of circular arcs, the design of an appropriate cost function and heuristics, as well as the inclusion of threats. Measures taken to improve the computational speed of the system are also described. Some examples of trajectories generated by the system are presented. DTIC

N94-18577 KSA Technology, Columbus, OH.
LIFT AND PITCHING MOMENT INDUCED ON JET STOVL AIRCRAFT HOVERING IN GROUND EFFECT Final Report
Richard E. Kuhn and Vearl R. Stewart Jun. 1993 593 p Limited Reproducibility: More than 20% of this document may be affected by microfiche quality
(Contract F33615-89-C-3611)
(AD-A269700; KSA-92-2; WL-TR-93-3044) Avail: CASI HC A25

The data obtained during an investigation of the effects of crossflow on the suckdown and fountain effects induced by various arrangements of vertically impinging jets are presented in this report. The jet arrangements included circular and rectangular jets in various single, dual, and triple jet configurations. The tests were conducted in the 14 by 22 foot tunnel at the NASA LaRC. Tests covered a range of heights above the ground, nozzle pressure ratios, and forward velocities. DTIC

N94-18733# KSA Technology, Columbus, OH.

LIFT AND PITCHING MOMENT INDUCED ON JET STOVL AIRCRAFT BY THE GROUND VORTEX Final Report, May 1990 - 1993

Richard E. Kuhn and Vearl R. Stewart Jun. 1993 106 p

(Contract F33615-89-C-3611)

(AD-A269816; KSA-92-1; WL-TR-93-30445) Avail: CASI HC A06/MF A02

The data obtained during an investigation of the effects of the ground vortex on a generic wing-body configuration are presented in this report. Circular, rectangular, and thrust reverser jets were tested. The tests were conducted in the 14 by 22 foot tunnel at the NASA Langley Research Center. The tests covered a range of heights above the ground, forward velocities, and ground belt speeds. DTIC

N94-18779# Wright Lab., Wright-Patterson AFB, OH.

PROCEDURES AND DESIGN DATA FOR THE FORMULATION OF AIRCRAFT CONFIGURATIONS Final Report, Jan. 1992 - Jun. 1993

Thomas R. Sieron, Dudley Fields, A. W. Baldwin, and David W. Adamczak Aug. 1993 153 p

(AD-A270150; WL-TR-93-3068) Avail: CASI HC A08/MF A02

This report contains design data and rapid analysis methods to assist in establishing an initial aircraft configuration to begin the conceptual design process. It is based on an array of data acquired over many years for fighter, bomber, and transport aircraft. The data is compiled to estimate the gross take-off weight and physical size of a representative configuration for various range, payload, and speed requirements. Other data and procedures are included to define the general dimensions of the fuselage, wing, vertical, and horizontal stabilizers. Aerodynamic methods and data are provided to rapidly estimate the drag and lift characteristics at subsonic, transonic, and supersonic speeds for this class of aircraft. Performance data has been assembled to show the impact of range, payload, speed, maneuverability, take-off and landing requirements on the physical and geometric characteristics of these configurations. A sample problem is presented to illustrate the use of this design data in formulating an aircraft configuration. DTIC

N94-18789# Federal Aviation Administration, Atlantic City, NJ. Technical Center.

VERTICAL DROP TEST OF A METRO 3 AIRCRAFT Final Report, Apr. 1991 - Apr. 1992

Robert J. McGuire, William J. Nissley, and James E. Newcomb Jun. 1993 80 p

(AD-A270032; DOT/FAA/CT-93/1) Avail: CASI HC A05/MF A01

A commuter category Fairchild Metro 3 fuselage and wingbox assembly was subjected to a vertical impact test at the Federal Aviation Administration (FAA) Technical Center, Atlantic City International Airport, NJ. The purpose of the test was to measure the structural response of the fuselage, floor, cabin furnishings (including standard and modified seats), and anthropomorphic dummies. The test was conducted to simulate the potentially survivable impact conditions of an actual crash. The airframe was dropped from 11.2 feet and impacted at a velocity of 26.32 feet per second (ft/sec). The test weight simulated an airplane configuration that was approximately 1,450 pounds less than the maximum zero fuel weight (13,100 pounds) of the airplane with a 14,100-pound maximum takeoff weight. Acceleration, load, and deflection data were collected throughout the test. Instrumentation were located on the fuselage, floor, seats, and within the 'crash test dummies.' The vertical impact test resulted in peak accelerations of gravity (g) ranging from 40g to 60g throughout the airframe. DTIC

N94-18795# Air Force Inst. of Tech., Wright-Patterson AFB, OH.

FLIGHT TEST TECHNIQUES FOR AIRCRAFT PARAMETER ESTIMATION IN GROUND EFFECT M.S. Thesis

James M. Clark 1993 146 p

(AD-A270058; AFIT/CI/CIA-93-145) Avail: CASI HC A07/MF A02

The effect of ground proximity on the performance and handling of an aircraft has received extensive study, particularly in the wind tunnel. Previous research, however, provides few consistent quantitative conclusions regarding ground effect, and flight test methods for directly measuring ground effect are needed. This effort identifies flight test maneuvers suitable for measuring aircraft stability and control parameters in ground effect, using simulated response data and pEst, a parameter estimation program developed at NASA-Dryden. This study also considers the effects of instrument precision, system sampling rate, instrument bias, and response noise. Five simple longitudinal and eleven lateral-directional maneuvers that allow accurate parameter estimation, keep the aircraft in ground effect, and do not result in responses that are unsafe in ground proximity are identified. The longitudinal maneuvers provide accurate lift and moment parameters, and the lateral-directional analysis estimates all fifteen lateral-directional derivatives of interest within ten percent of their simulated values. DTIC

N94-18962* National Aeronautics and Space Administration, Washington, DC.

X-29: RESEARCH AIRCRAFT (Videotape)

Jan. 1991 Videotape: 2 min. 35 sec. playing time, in color, with sound

(NASA-TM-109370; NONP-VT-94-198217) Avail: CASI VHS A01/BETA A22

A preliminary look at the Ames Dryden Flight Research Center in the context of the X-29 aircraft is provided. The uses of the X-29's 30 deg forward swept wing are examined. The video highlights the historical development of the forward swept wing, and its unique blend of speed, agility, and slow flight potential. The central optimization of the wing, the forward canard, and the rear flaps by an onboard flight computer is also described. CASI

N94-19448*# Kansas Univ. Center for Research, Inc., Lawrence. Flight Research Lab.

AN INVESTIGATION OF FIGHTER AIRCRAFT AGILITY Final Technical Report, 1 Jan. 1989 - 31 Dec. 1993

John Valasek and David R. Downing 5 Nov. 1993 263 p

(Contract NCC2-588)

(NASA-CR-194608; NAS 1.26:194608; KU-FRL-831-7) Avail: CASI HC A12/MF A03

This report attempts to unify in a single document the results of a series of studies on fighter aircraft agility funded by the NASA Ames Research Center, Dryden Flight Research Facility and conducted at the University of Kansas Flight Research Laboratory during the period January 1989 through December 1993. New metrics proposed by pilots and the research community to assess fighter aircraft agility are collected and analyzed. The report develops a framework for understanding the context into which the various proposed fighter agility metrics fit in terms of application and testing. Since new metrics continue to be proposed, this report does not claim to contain every proposed fighter agility metric. Flight test procedures, test constraints, and related criteria are developed. Instrumentation required to quantify agility via flight test is considered, as is the sensitivity of the candidate metrics to deviations from nominal pilot command inputs, which is studied in detail. Instead of supplying specific, detailed conclusions about the relevance or utility of one candidate metric versus another, the authors have attempted to provide sufficient data and analyses for readers to formulate their own conclusions. Readers are therefore ultimately responsible for judging exactly which metrics are 'best' for their particular needs. Additionally, it is not the intent of the authors to suggest combat tactics or other actual operational uses of the results and data in this report. This has been left up to the user community. Twenty of the candidate agility metrics were selected for evaluation with high fidelity, nonlinear, non real-time flight simulation computer programs of the F-5A Freedom Fighter, F-16A Fighting Falcon, F-18A Hornet, and X-29A. The information and data presented on the 20 candidate metrics which were evaluated will assist interested readers in conducting their own extensive investigations. The report provides a definition and analysis of each metric; details of how to test and measure the metric, including any special data reduction requirements; typical values for the metric obtained using one or more aircraft types; and a sensitivity analysis if applicable. The report is organized as follows. The first chapter in the report presents a historical review of air combat trends which demonstrate the need for agility metrics in assessing the combat performance of fighter aircraft in a modern, all-aspect missile environment. The second chapter presents a framework for classifying each candidate metric according to time scale (transient, functional, instantaneous), further subdivided by axis (pitch, lateral, axial). The report is then broadly divided into two parts, with the transient agility metrics (pitch lateral, axial) covered in chapters three, four, and five, and the functional agility metrics covered in chapter six. Conclusions, recommendations, and an extensive reference list and biography are also included. Five appendices contain a comprehensive list of the definitions of all the candidate metrics; a description of the aircraft models and flight simulation programs used for testing the metrics; several relations and concepts which are fundamental to the study of lateral agility; an in-depth analysis of the axial agility metrics; and a derivation of the relations for the instantaneous agility and their approximations. Author (revised)

N94-19496# Messerschmitt-Boelkow-Blohm G.m.b.H., Munich (Germany). Hubschrauber und Flugzeuge.

NEW AIRCRAFT MATERIALS AND STRUCTURES [NEUE FLUGWERKSTOFFE UND BAUWEISEN]

Juergen Klenner, Johann Krammer, Hans Lonsinger, and Josef Vilsmeier 28 Aug. 1992 41 p In GERMAN Submitted for publication Original contains color illustrations

(MBB-LME-202-S-PUB-502-A; ETN-93-95093) Copyright Avail: CASI HC A03/MF A01

The features of fiber composite materials employed in military aircraft design are reviewed. Fiber reinforced plastics are made with duromer matrices, such as polyester, epoxy, bismaleimide, and polyimide, or thermoplastic matrices, such as polyether ether ketone, polypropylene sulfide, and polyether imide. Carbon fibers were differentiated as high strain, intermediate modulus, and high modulus fibers. Mechanical properties of prepregs and laminates are described. The way in which fiber reinforced composites are fitted to aircraft structure weight minimization is ascertained. The use of the NASTRAN (NASA Structural Analysis) program to calculate aircraft structures with the finite element method is depicted. The importance of multidisciplinary optimization (flight controls, aerodynamics, and flight mechanics) in aircraft design is outlined. Manufacturing processes for composites production, such as tape steering, hot forming, net molding, and co-curing are reviewed. Methods for nondestructive inspection of aircraft materials, such as ultrasonic evaluation, holography, and thermography, are depicted. Carbon fiber composites are concluded to be particularly interesting for aircraft development because of their properties of mechanical strength, repairability, and maintainability. ESA

N94-19500# Messerschmitt-Boelkow-Blohm G.m.b.H., Munich (Germany). Militaerflugzeuge.

THREE DIMENSIONAL NETWORK GENERATION AND EULER CALCULATION FOR A WING FUSELAGE CANARD CONFIGURATION Thesis - Tech. Univ. Munich [DREIDIMENSIONALE NETZGENERIERUNG UND EULERRECHNUNG FUER FLUEGEL-RUMPF-CANARD KONFIGURATION]

Oliver Vogelgesang Dec. 1992 92 p In GERMAN Original contains color illustrations

(MBB-LME-211-S-PUB-511-A; ETN-93-95095) Copyright Avail: CASI HC A05/MF A01

A vortex flow model, based on a computer aided design surface model of a body with a curve and surface representation, is developed. After establishing the topology (location and order of blocks in space), each block was described with six simple three dimensional areas and the corresponding block edges. Geometrical data were fed in VDA-FS (German acronym for Union of Automobile Industry - interface) format by the Dogrid surface net generator. All blocks were connected into a calculation domain in order to perform Euler calculations for delta wing configurations with and without canard. Euler equations in a conservative form were solved with a finite volume scheme; a biased upwind difference scheme of Godunov type was used for the fluxes in the cell boundaries and the Newton method supplied a time implicit solution. The front edge vortex on the main wing was accurately obtained and the predicted interferences of both vortex systems of canard and main wing could be attested. ESA

N94-19781 Army Research Lab., Aberdeen Proving Ground, MD.

BLADE AND HUB LOADS OF BALLISTICALLY DAMAGED HELICOPTER ROTORS Final Report, Apr. 1992 - May 1993

Ki C. Kim Oct. 1993 44 p Limited Reproducibility: More than 20% of this document may be affected by microfiche quality

(AD-A270663; ARL-TR-235) Avail: CASI HC A03

The effects of (simulated) ballistic damage on helicopter rotor blade response and rotor hub loads are investigated. A finite element formulation based on Hamilton's principle is used for structural analysis, and aerodynamic loads are calculated using quasisteady aerodynamic theory. Each blade is as being composed of elastic beams undergoing flap bending, lag bending, elastic twist, and axial deflections. Dynamic responses of multi-blade rotor systems are calculated from nonlinear periodic normal mode equations using a finite element in time scheme. Results are calculated for the SA349/2 Gazelle helicopter for both undamaged and damaged blade configurations. Blade damage effects are determined in terms of blade mode shapes and frequencies, aeroelastic response, and rotor hub loads. Blade dissimilarity due to ballistic damage can induce a luge 1/rev vibratory component on the rotor hub. DTIC

N94-19796# Technische Univ., Delft (Netherlands). Faculty of Aerospace Engineering.

NOISE MEASUREMENTS ON TWO TYPES OF AIRPLANES USED FOR SPRAYING IN AGRICULTURE [GELUIDSMETINGEN AAN TWEE TYPEN LANDBOUW-SPROEIVLIEGTUIGEN]

D. M. VanPaassen and G. J. J. Ruijgrok Dec. 1992 19 p In DUTCH (LR-706; ETN-93-94423) Avail: CASI HC A03/MF A01

The flyover noise of two types of propeller driven, single engined airplanes, used for agricultural purposes, was measured. The flyovers were conducted at two different altitudes over the microphone position. The flight runs were further divided into two flight profiles. The first profile required the aircraft to perform a standard climb-out after takeoff using the power setting and air speed for maximum climb rate. The second profile contained the execution of level flights at constant (normal) cruising speed and cruising power. The different noise levels are listed. ESA

N94-18240# Office National d'Etudes et de Recherches Aerospatiales, Paris (France).

NON-LINEAR FLIGHT DYNAMICS

P. Guicheteau *In* AGARD, Non Linear Dynamics and Chaos Jun. 1993 13 p Sponsored in part by Services Techniques des Programmes Aeronatiques (For primary document see N94-18236 04-77) Copyright Avail: CASI HC A03/MF A02

N94-18418# Politecnico di Milano (Italy). Dipt. di Ingegneria Aerospaziale.

A DESIGN PROCEDURE FOR SLOTTED FLAPS

Sergio DePonte, Alessandro Cella, and Mario Marcazzan *In* AGARD, High-Lift System Aerodynamics Sep. 1993 6 p Sponsored in part by CNR (For primary document see N94-18415 04-01) Copyright Avail: CASI HC A02/MF A04

N94-18431# Defence Research Agency, Farnborough (England).

AN EXPERIMENTAL INVESTIGATION OF THE OPTIMUM SLAT SETTING ON A COMBAT AIRCRAFT MODEL

I. R. M. Moir *In* AGARD, High-Lift System Aerodynamics Sep. 1993 16 p (For primary document see N94-18415 04-01) Copyright Avail: CASI HC A03/MF A04

N94-18432# Defence Research Agency, Farnborough (England).

AN EXPERIMENTAL INVESTIGATION OF ATTACHMENT-LINE TRANSITION ON THE SLAT OF A COMBAT AIRCRAFT MODEL

B. C. Hardy *In* AGARD, High-Lift System Aerodynamics Sep. 1993 11 p (For primary document see N94-18415 04-01) Copyright Avail: CASI HC A03/MF A04

N94-18436# Wright Lab., Wright-Patterson AFB, OH.

HIGH LIFT AND THE FORWARD SWEPT WING

Lawrence A. Walchli *In* AGARD, High-Lift System Aerodynamics Sep. 1993 9 p (For primary document see N94-18415 04-01) Copyright Avail: CASI HC A02/MF A04

N94-18442# Aerospatiale, Toulouse (France). Div. Avions.
HIGH-LIFT RESEARCH: APPLICATION TO THE DESIGN OF THE ATR72 FLAP
P. Capbern *In* AGARD, High-Lift System Aerodynamics Sep. 1993 10 p (For primary document see N94-18415 04-01)
Copyright Avail: CASI HC A02/MF A04

N94-18443# Short Bros. and Harland Ltd., Belfast (Northern Ireland). Aerodynamics Dept.
THE AERO-MECHANICAL DESIGN OF A NOVEL FOWLER FLAP MECHANISM
J. R. Mathews *In* AGARD, High-Lift System Aerodynamics Sep. 1993 9 p (For primary document see N94-18415 04-01)
Copyright Avail: CASI HC A02/MF A04

N94-18444# Boeing Defense and Space Group, Seattle, WA.
DESIGN, DEVELOPMENT, AND FLIGHT EVALUATION OF THE BOEING YC-14 USB POWERED LIFT AIRCRAFT
Ted C. Nark *In* AGARD, High-Lift System Aerodynamics Sep. 1993 17 p (For primary document see N94-18415 04-01)
Copyright Avail: CASI HC A03/MF A04

N94-18445# Deutsche Airbus G.m.b.H., Bremen (Germany). Aerodynamics Dept.
HIGH-LIFT DESIGN FOR LARGE CIVIL AIRCRAFT
A. Flaig and R. Hilbig *In* AGARD, High-Lift System Aerodynamics Sep. 1993 12 p (For primary document see N94-18415 04-01)
Copyright Avail: CASI HC A03/MF A04

N94-18446# De Havilland Aircraft Co. of Canada Ltd., Downsview (Ontario). Technology and Research.
HIGH LIFT SYSTEMS FOR TRANSPORT AIRCRAFT WITH ADVANCED AIRFOILS
B. Eggleston and R. J. D. Poole *In* AGARD, High-Lift System Aerodynamics Sep. 1993 13 p Sponsored in part by National Research Council of Canada (For primary document see N94-18415 04-01)
Copyright Avail: CASI HC A03/MF A04

N94-18447# Alenia Aeronautica, Naples (Italy). Flight Technology.
CHOICE AND OPTIMIZATION OF A HIGH-LIFT SYSTEM FOR AN ADVANCED AMPHIBIOUS AIRCRAFT
M. A. Averardo, M. deLeo, and V. Russo *In* AGARD, High-Lift System Aerodynamics Sep. 1993 13 p (For primary document see N94-18415 04-01)
Copyright Avail: CASI HC A03/MF A04

06 AIRCRAFT INSTRUMENTATION

Includes cockpit and cabin display devices; and flight instruments.

For related information see also *19 Spacecraft Instrumentation* and *35 Instrumentation and Photography.*

N94-18536# Naval Postgraduate School, Monterey, CA.
PRELIMINARY DESIGN OF A WATER COOLED AVIONICS COOLING RACK M.S. Thesis
Colleen L. Ellis 25 Mar. 1993 47 p
(AD-A268826) Avail: CASI HC A03/MF A01

Military electronics are frequently operated in excessively confined spaces aboard ships and aircraft. This limited space impacts significantly on the space available for cooling equipment. The optimal solution is the development of one universal, modular rack for shipboard and aviation use. With a modular design, upgrades to equipment could also be accompanied by an upgrade to the cooling rack itself with very little additional cost or difficulty. A water cooled avionics rack can provide sufficient cooling for any piece or combination of avionics equipment if enough water flow paths are used, the water is at the appropriate temperature, and the water is properly distributed within the passages. To determine if the cooling medium, water, is properly distributed within a modular cooling rack, an analysis of the flow and pressure distribution of the coolant is required. This thesis presents a computer code that has been developed as an initial step in the total design of a modular cooling rack for avionics equipment. In itself, the code details a specific design technique and allows for the determination of whether a proposed configuration, including source location, characteristics of the cooling water, and the size and shape of the proposed flow passages will indeed provide a proper distribution of the coolant. DTIC

N94-18658# Naval Air Warfare Center, Indianapolis, IN. Aircraft Div.
EMBEDDED COMPUTER PERFORMANCE MEASUREMENT (ECPM). ADVANCED AVIONICS SUBSYSTEMS AND TECHNOLOGY MULTIPROCESSOR ECPM SOFTWARE DOCUMENTATION Final Report, Oct. 1990 - Jun. 1993
Diane Kohalmi, John Newport, Chuck Roark, Diane Paul, and Dave Struble Jun. 1993 118 p
(AD-A269921) Avail: CASI HC A06/MF A02

The report consists of software documentation for a new computer performance measurement tool written in Ada. The tool is designed for easy portability between computer systems. Included are a MIL-STD-1553B Interface Definition, a DoD-STD-2167 Systems Requirements Specification, and a DoD-STD-2167 Interface Requirements Specification. DTIC

07 AIRCRAFT PROPULSION AND POWER

Includes prime propulsion systems and systems components, e.g., gas turbine engines and compressors; and onboard auxilliary power plants for aircraft.

For related information see also *20 Spacecraft Propulsion and Power, 28 Propellants and Fuels,* and *44 Energy Production and Conversion.*

N94-18333 Analytic Sciences Corp., Midwest City, OK.
THE J85 COST/BENEFIT ENGINE STUDY Final Report
Lawrence E. Machado, John M. Pfalz, and Paul R. Wetzel 28 May 1993 53 p Limited Reproducibility: More than 20% of this document may be affected by microfiche quality
(Contract F33657-92-D-2055)
(AD-A269280) Avail: CASI HC A04

This report documents the results of an independent evaluation of J85 maintenance practices and the data reporting system used for parts life tracking (PLT) of selected life limited components. A major requirement of the study was to quantify the costs/benefits associated with using the D042 Comprehensive Engine Management System (CEMS) for J85 PLT versus the system now in use. The techniques and methodologies used in the analysis are compatible with the philosophy of Reliability-Centered Maintenance (RCM). DTIC

N94-18748 Army Research Lab., Aberdeen Proving Ground, MD.
NUMERICAL SIMULATION OF FLUID DYNAMICS AND COMBUSTION FOR RAM ACCELERATOR PROJECTILE/OBTURATOR INTERACTION Final Report, Jan. - Dec. 1992
Michael J. Nusca Sep. 1993 44 p Limited Reproducibility: More than 20% of this document may be affected by microfiche quality
(AD-A269715; ARL-TR-198) Avail: CASI HC A03

Computational fluid dynamics solutions of the Navier-Stokes equations have been applied to both nonreacting and reacting in-bore flowfields for a ram accelerator projectile launch system. In this system, a projectile is injected at supersonic velocity into a stationary tube filled with a pressurized mixture of hydrocarbon, oxidizer, and inert gases. After ignition, the shock system generated by the projectile can result in sustained combustion around and aft of the projectile. This energy release process, which travels with the projectile, also generates high pressures and imparts thrust to the projectile. Experimental observations indicate that the porous obturator may play a significant role in the initiation of combustion after projectile injection. Numerical simulations have been used to investigate the role of the obturator in both the 38mm and 120mm (bore diameter) systems. DTIC

N94-18907 Wright Lab., Wright-Patterson AFB, OH.
VANE OPTIMIZATION FOR MAXIMUM EFFICIENCY USING DESIGN OF EXPERIMENTS (DOX) Final Report, Apr. 1992 - Mar. 1993
Paul T. Kerney Mar. 1993 47 p Limited Reproducibility: More than

20% of this document may be affected by microfiche quality
(AF Proj. 681B)
(AD-A270270; WL-TR-93-2055) Avail: CASI HC A03

Optimization of vane and bleed settings in a multistage axial compressor undergoing development can be a difficult, time-consuming, and expensive process. This project optimized seven variable vanes and one variable bleed on the five-stage Pratt & Whitney XTC66 compressor at the aerodynamic design point (ADP) for maximum efficiency using Design of Experiments (DOX). The DOX are statistical methods for changing process inputs in a systematic way, and analyzing the resulting outputs in order to improve a response to an acceptable or optimum value, find a less expensive design, material, or method providing equivalent results, or understand process sensitivities. Along with developing a model for maximum efficiency, the project also developed models for predicting pressure ratio and mass flow. Results show the number of Steady State Data Points (SSDP's) to be reduced, as well as, the total test time without sacrificing data integrity.
DTIC

N94-19353*# National Aeronautics and Space Administration. Lewis Research Center, Cleveland, OH.
OVERVIEW OF STOVL AIRCRAFT PROPULSION RESEARCH OFFTAKES AND VERTICAL LIFT SYSTEMS
Thomas J. Biesiadny, Jack G. McArdle, and Barbara S. Esker Dec. 1993 14 p Presented at the International Powered Lift Conference, Santa Clara, CA, 1-3 Dec. 1993; sponsored by AIAA
(RTOP 505-68-32)
(NASA-TM-106387; E-8207; NAS 1.15:106387; AIAA Paper 93-4865)
Avail: CASI HC A03/MF A01

The overall Short Takeoff and Vertical Landing (STOVL) Aircraft Propulsion Research program includes key technologies involving offtake systems, vertical lift systems, hot gas ingestion, STOVL augmentors, and integrated flight propulsion controls. A part of the NASA Lewis work involving STOVL aircraft propulsion systems is presented with the emphasis on component-level experiments and analysis related to offtakes and vertical lift systems.
Author (revised)

08 AIRCRAFT STABILITY AND CONTROL

Includes aircraft handling qualities; piloting; flight controls; and autopilots.

For related information see also *05 Aircraft Design, Testing and Performance.*

N94-18401# Naval Postgraduate School, Monterey, CA.
AN APPLICATION OF PARAMETER ESTIMATION TO THE STABILITY AND CONTROL OF THE BQM-147 UNMANNED AERIAL VEHICLE M.S. Thesis
Patrick J. Quinn Jun. 1993 132 p
(AD-A268741) Avail: CASI HC A07/MF A02

Parameter estimation methods were used to obtain estimates of stability and control derivatives for the Marine Corps BQM-147 Unmanned Air Vehicle. The results from a simple, PC-based linear model and those from a more robust nonlinear model, pEst, were compared. A Cramer-Rao bound was used to assess the accuracy of the estimates for both methods. The bounds were high for both the longitudinal case and the lateral-directional case due to the limited maneuvers tested, high levels of noise in the same general frequency range as the control input, and the lack of body-angle data. The linear model failed to provide estimates for the lateral-directional case. Though the results may be used as starting points for a dynamic model of the aircraft, it is recommended that the flight test procedures be modified to address the issues raised concerning noise, recorded signals, and the need for repeated maneuvers.
DTIC

N94-18541# Naval Postgraduate School, Monterey, CA.
CLOSE-COUPLED OSCILLATING CANARD EFFECTS ON POST-STALL LIFT ENHANCEMENT M.S. Thesis
Douglas G. McBane Jun. 1993 97 p
(AD-A268938) Avail: CASI HC A05/MF A02

The effects of an oscillating close-coupled canard on the canard/wing vortex interaction for increased lift enhancement were studied. Two test conditions were studied: the first with a model angle of attack of 22 deg and the second of 34 deg. The canard was positioned at three mean deflection angles equal to 4, 7, and 10 deg for the model angle of attack of 22 deg and -4, -7, and -10 deg for the model angle of attack of 34 deg. At each of the canard mean deflection angles, the canard was oscillated with amplitudes of +/- 5 deg and +/- 10 deg with reduced frequencies ranging from 0.046 to 0.232. Because of the small effects noted which were of the order of accuracy of the balance, only general trends are discussed. The trends indicate that for this particular model configuration and geometry, lift was decreased slightly with increasing canard frequency and amplitude. No lift-enhancement benefits were revealed during the study.
DTIC

N94-19316*# National Aeronautics and Space Administration. Langley Research Center, Hampton, VA.
ISAC: A TOOL FOR AEROSERVOELASTIC MODELING AND ANALYSIS
William M. Adams, Jr. and Sherwood Tiffany Hoadley Dec. 1993 12 p
See also A93-33974
(RTOP 505-64-52-03)
(NASA-TM-109031; NAS 1.15:109031) Avail: CASI HC A03/MF A01

The capabilities of the Interaction of Structures, Aerodynamics, and Controls (ISAC) system of program modules is discussed. The major modeling, analysis, and data management components of ISAC are identified. Equations of motion are displayed for a Laplace-domain representation of the unsteady aerodynamic forces. Options for approximating a frequency-domain representation of unsteady aerodynamic forces with rational functions of the Laplace variable are shown. Linear time invariant state-space equations of motion that result are discussed. Model generation and analyses of stability and dynamic response characteristics are shown for an aeroelastic vehicle which illustrates some of the capabilities of ISAC as a modeling and analysis tool for aeroelastic applications.
Author (revised)

N94-19615# Technische Univ., Delft (Netherlands). Faculty of Aerospace Engineering.
THE DYNAMIC STABILITY OF THE HELICOPTER
H. Wittenberg Apr. 1993 116 p
(LR-772; ISBN-9-06-275887-8; ETN-93-95031) Copyright Avail: CASI HC A06/MF A02

The longitudinal and lateral dynamic stability of conventional helicopters with one main rotor and tail rotor are analyzed. The analysis is similar as for fixed wing aircraft and based on linearized equations of motion. For the hovering flight the stability derivatives are derived for rotors with central unconstrained and constraint flapping hinges. The latter type simulates rotors with flapping hinge off set or hingeless rotors. The helicopter has a longitudinal and lateral unstable oscillatory mode in hovering flight. It is found that for highly constrained flapping hinges the lateral oscillatory mode can be slightly damped. The qualitative analysis of the dynamic stability in forward flight based on the root locus method of Evans is presented. It is shown that for helicopters with horizontal tail the longitudinal characteristics at moderate and high speeds are the same as for fixed wing aircraft. The short period motion and phugoid motion are damped and the helicopter is dynamically stable. The same observation applies to the lateral dynamic stability. The roll and Dutch roll modes are damped, but the spiral mode can be damped or undamped, depending on the contribution of the tailrotor in the stability derivatives.
ESA

N94-19711 Technische Univ., Brunswick (Germany). Inst. fuer Regelungstechnik.
A LEARNING AUTOPILOT FOR AUTOMATICALLY CONTROLLED ROBUST REGULATION Ph.D. Thesis [EIN LERNENDER AUTOPILOT MIT SELBSTEINSTELLENDER ROBUSTER REGELUNG]
Kai Schulz 1992 140 p In GERMAN Limited Reproducibility: More than 20% of this document may be affected by microfiche quality
(ETN-93-95075) Avail: CASI HC A07

The motion control of vehicles in three dimensional space is investigated. Particular consideration is given to the improvement of trajectory accuracy, taking into account model uncertainties. The physical model parameters were estimated with an offline identification process. A two step procedure, based on the equation error and least squares methods, was chosen for the following reasons: it is unsensitive to noncorrelated perturbations; it is independent of convergence behavior; and it produces parameters for continuous models, in combination with state variable filters. The structure of the controller was realized with the H(infinity) norm in order to suppress the dependence on boundary conditions such as limit frequencies of actuators and sensors. A forward control concept is proposed which allows the strong interactions between the motion degrees of freedom to be compensated. Simulation results of ship steering are presented for validation of the autopilot system. ESA

09 RESEARCH AND SUPPORT FACILITIES (AIR)

Includes airports, hangars and runways; aircraft repair and overhaul facilities; wind tunnels; shock tubes; and aircraft engine test stands. For related information see also *14 Ground Support Systems and Facilities (Space).*

N94-17735 Norwegian Defence Research Establishment, Kjeller.
SAFETY-ROUTINES AND GUIDELINES FOR WORK IN THE CLEAN ROOM AT THE EPITEK-LABORATORY, KJELLER (NORWAY) [SIKKERHETSRUTINER OG RETNINGSLINJER FOR ARBEID I RENROMMET, EPITEK-LABORATORIET, KJELLER]
Dag Willy Minsaas 28 Jan. 1993 15 p In NORWEGIAN Limited Reproducibility: More than 20% of this document may be affected by microfiche quality
(FFI-93/7012; ETN-93-94888) Avail: CASI HC A03

Guidelines for work in clean room are given. These guidelines aim to reduce the risk of accidents; in the case of an accident, to reduce injuries on human beings and damage to equipment; and to maintain the clean room standard. Procedures to be followed when an alarm is released, and where safety equipment, exits and fire fighting equipment are located, are explained. Some general advice about first aid (for example in the case of spill of chemicals etc.) and what to do in the case of an accident is given. Advice and rules on clean room behavior are given. ESA

N94-18123# Deutsche Forschungsanstalt fuer Luft- und Raumfahrt, Cologne (Germany). Hauptabt. Verkehrsforschung.
TRANSPORT POLICY OPTIONS FOR REDUCING NOISE AT AIRPORTS; HAMBURG AIRPORT TAKEN AS AN EXAMPLE [VERKEHRSPOLITISCHE OPTIONEN ZUR LAERMREDUKTION AN FLUGHAEFEN DARGESTELLT AM BEISPIEL DES FLUGHAFENS HAMBURG]
Stefan Beyhoff, Hansjochen Ehmer, Horst Focke, and Volker Warlitzer Dec. 1992 279 p In GERMAN
(DLR-FB-92-40; ETN-93-94872) Avail CASI HC A13/MF A03

The air transport demand of scheduled and charter traffic in the northern part of Germany is studied. Based on a detailed analysis of passenger transport demand by size and structure and the assignment to the airports Hamburg and Hannover a forecast of the demand by region and of passenger emplanement and aircraft movements by airport for the year 2000 was made. Measures of transport policy for reducing noise emissions at Hamburg airport are presented. Detailed descriptions of the measures like noise contingents, differentiation of fees, restrictions or bans of certain aircraft or segments of demand, cooperation between airports, and influencing the model split between air and rail transport are given. It is concluded that in the long run larger conforming measures like noise contingents are more efficient as compared with administrative measures. ESA

N94-18324# Aeronautical Research Labs., Melbourne (Australia).
A WIND TUNNEL MODEL CONTROL SURFACE ACTUATOR INTERFACE
S. A. Kent Jun. 1993 45 p
(AD-A268729; ARL-TN-13; DODA-AR-006-658) Avail: CASI HC A03/MF A01

A microprocessor controlled system is described for the remote positioning of flight control surfaces on a wind tunnel aircraft model. The system utilizes DC micromotors and Linear Variable Displacement Transducers (LVDTs) for driving force and accurate position feedback. The Actuator Module was developed primarily for use with a 1/9th scale F/A-18 model to collect data for the International Follow On Structural Test Program (IFOSTP). DTIC

N94-18330# Florida Univ., Eglin AFB.
INTERFEROMETER STATIONS AT THE AIR FORCE AEROBALLISTIC RESEARCH FACILITY Final Report, Aug. 1988 - Dec. 1990
R. C. Anderson and J. E. Milton Jul. 1993 41 p
(Contract F08635-88-C-0160)
(AD-A268776; WL-TR-92-7035) Avail: CASI HC A03/MF A01

Two interferometer stations were installed in the Eglin AFB ballistic range--a holographic and a common path interferometer. The latter was used in both dark central ground and field absorption modes. A theoretical development given for the common path instrument predicts an improved type of phase contrast interferometer with a half wave shifting filter instead of the quarter wave used in the past. Experimentally measured interferograms were found to be in good agreement with synthetic interferograms calculated with data from a Navier-Stokes Computational Fluid Dynamics (CFD) code. DTIC

N94-18890# Los Alamos National Lab., NM.
FOIL SUPPORT STRUCTURE FOR LARGE ELECTRON GUNS
J. P. Brucker and E. A. Rose 1993 5 p Presented at the 9th IEEE Pulsed Power Conference, Albuquerque, NM, 21-23 Jun. 1993
(Contract W-7405-eng-36)
(DE93-018478; LA-UR-93-2623; CONF-930616-18) Avail: CASI HC A01/MF A01

This paper describes a novel support structure for a vacuum diode used to pump a gaseous laser with an electron beam. Conventional support structures are designed to hold a foil flat and rigid. This new structure takes advantage of the significantly greater strength of metals in pure tension, utilizing curved shapes for both foil and support structure. The shape of the foil is comparable to the skin of a balloon, and the shape of the support structures is comparable to the cables of a suspension bridge. This design allows a significant reduction in foil thickness and support structure mass resulting in a lower electron-beam loss between diode and laser gas. In addition, the foil is pre-formed in the support structure at pressures higher than operating pressure. Therefore, the foil is operated far from the yield point. Increased reliability is anticipated. DOE

N94-18953* National Aeronautics and Space Administration. Marshall Space Flight Center, Huntsville, AL.
TECHNOLOGY TEST BED (Videotape)
Aug. 1988 Videotape: 1 min. 30 sec. playing time, in color, with sound
(NASA-TM-109354; NONP-VT-94-198201) Avail: CASI VHS A01/BETA A22

This video details the renewed use of the massive rocket propulsion test stand at Marshall Space Flight Center, first used to test Saturn 5 rockets during the Apollo Program. The test stand can incorporate over 600 sensors during test firings of the Space Shuttle's main engines, which will result in increased safety and reliability, and reduced production costs. CASI

N94-18963* National Aeronautics and Space Administration, Washington, DC.
THE WORLD'S LARGEST WIND TUNNEL (Videotape)
Oct. 1987 Videotape: 2 min. 47 sec. playing time, in color, with sound
(NASA-TM-109371; NONP-VT-94-198218) Avail: CASI VHS A01/BETA A22

NASA's National Full Scale Aerodynamics Complex, which houses two of the world's largest wind tunnels and has been used for testing experimental aircraft since 1944, is presented. This video highlights the structure and instrumentation of the 40 x 80 foot and 80 x 120 foot wind tunnels and documents their use in testing full scale aircraft, NASA's Space Shuttle and the XV-15 Tiltrotor aircraft. CASI

N94-19332# Swedish Inst. for Materials Testing, Boras.
CONSTRUCTION AND EVALUATION OF AN ENVIRONMENTAL CHAMBER FOR CALIBRATION OF TEMPERATURE AND PRESSURE SENSORS FOR LASER INTERFEROMETERS EMPERATURE AND PRESSURE SENSORS FOR LASER INTERFEROMETERS) [KONSTRUKTION OCH UTVAERDERING AV EN MILJOEKAMMARE FOER KALIBRERING AV TEMPERATUR OCH TRYCKGIVARE TILL LASER INTERFEROMETRAR]
N. Bratt and N. Johansson 1993 63 p In SWAHILI
(PB93-197838; SP-RAPP-1993:05) Avail: CASI HC A04/MF A01

To be able to calculate the wavelength of the light used in laser interferometer measurements the temperature and the pressure must be known. Therefore the laser interferometers are equipped with temperature and pressure sensors. To be able to calibrate these sensors a chamber with adjustable temperature in the interval 15-25 C and adjustable pressure in the interval 920-1050 mbar has been constructed and evaluated. The temperature of the chamber is regulated by means of an electrical PD-regulator, where the desired temperature is set manually. The air pressure of the chamber is regulated with manual valves and a vacuum pump with one blow and one suck side. The temperature in the environmental chamber is measured with Pt-100 sensors, which are connected to a temperature instrument and the absolute air pressure is measured with a digital barometer. NTIS

N94-19372# Technische Univ., Delft (Netherlands). Faculty of Aerospace Engineering.
SURVEY ON THE APPLICATION OF A 3D GENERAL PURPOSE WIND-TUNNEL RESEARCH MODEL
M. J. Pagen Mar. 1993 49 p
(LR-713; ETN-93-95024) Avail: CASI HC A03/MF A01

A general purpose wind tunnel research model, which is the major element of a proposed aerodynamic design research program, is described. As a first stage in the design of the model a study was conducted to determine the aspects of interest of aircraft configuration research. This has brought out that attention in configuration aerodynamics is directed to the aerodynamic integration of highly loaded propellers, and the performance evaluation of multi wings. The model is designed in assembly kit form so that various configurations can be composed, including two and three surface arrangements of which the lifting surfaces can have different settings. The propulsion system can be mounted in various fashions. Systematic component buildup tests were performed starting from a baseline fuselage to identify aerodynamic contributions of individual airframe components, and aerodynamic interference effects. The same configurations were used to establish the effects of propeller slipstream on the flow field around the model. ESA

N94-19581 Range Commanders Council, White Sands Missile Range, NM. Range Safety Group.
RANGE SAFETY TRANSPONDER CATALOG
Sep. 1993 249 p Supersedes RSG-308-84, dated Mar. 1984, AD-A140095 Limited Reproducibility: More than 20% of this document may be affected by microfiche quality
(AD-A270882; RSG-308-93; RSG-308-84) Avail: CASI HC A11

This catalog provides reference information on radar tracking transponders used to support range-safety functions at the DOD and NASA test ranges and facilities. The information is taken from manufacturer supplied specifications and is provided as reference material only. DTIC

12 ASTRONAUTICS (GENERAL)

For extraterrestrial exploration see *91 Lunar and Planetary Exploration.*

N94-18849*# National Aeronautics and Space Administration. Marshall Space Flight Center, Huntsville, AL.
SPACELAB 3
[1984] 36 p
(NASA-TM-108750; NAS 1.15:108750) Avail: CASI HC A03/MF A01

The primary purpose of the Spacelab 3 mission is to conduct materials science experiments in a stable low-gravity environment. In addition, the crew will do research in life sciences, fluid mechanics, atmospheric science, and astronomy. Spacelab 3 and a mission scenario are described. Mission development and management and the crew are described. Summaries of the scientific investigations are also included. CASI

N94-18979* National Aeronautics and Space Administration, Washington, DC.
APOLLO 11: 20TH ANNIVERSARY (Videotape)
Jul. 1989 Videotape: 3 min. 27 sec. playing time, in color, with sound
(NASA-TM-109364; NONP-VT-94-198211) Avail: CASI VHS A01/BETA A22

The Apollo 11 Mission which culminated in the first manned lunar landing on July 20, 1969 is recounted. Historical footage of preparation, takeoff, stage separation, the Eagle Lunar Lander, and the moon walk accompany astronauts Michael Collins, Buzz Aldrin, and Neal Armstrong giving their recollections of the mission are shown. CASI

N94-18981* National Aeronautics and Space Administration, Washington, DC.
SPACE EXPLORATION INITIATIVE (Videotape)
Jul. 1990 Videotape: 3 min. 17 sec. playing time, in color, with sound
(NASA-TM-109366; NONP-VT-94-198213) Avail: CASI VHS A01/BETA A22

An overview of President Bush's Space Exploration Initiative (SEI) and it's three main components, Space Station Freedom, a Permanent Lunar Base, and a Manned Mission to Mars is provided. Computer simulations of the Space Station Freedom and Permanent Lunar Base are shown, and an animated sequence describes a Mars mission where heavy lift vehicle will bring components of a Mars Spacecraft into orbit, where it will be put together by astronauts using a robotic arm. The Mars spacecraft is shown orbiting Mars and discharging a lander to the surface, carrying human explorers. The video also details the SEI's Outreach Program, designed to garner interest in and ideas for Space Exploration. CASI

N94-19146# Joint Publications Research Service, Arlington, VA.
JPRS REPORT: SCIENCE AND TECHNOLOGY. CENTRAL EURASIA: SPACE
27 Aug. 1993 40 p Transl. into ENGLISH from various Russian articles
(JPRS-USP-93-004) Avail: CASI HC A03/MF A01

Reports on the following are included: optimum spatial entry of space vehicle into geostationary orbit from artificial earth satellite orbit; the lunar hydrogen problem; Martian gravity field; mineralogical and velocity section of Martian crust; methods for identifying Martian rocks using data from instrument package carried aboard 'Mars-94' and 'Mars-96' spacecraft; determining dynamic characteristics of elastic moduli of spacecraft using data from frequency tests of their elements; analysis of optimality of two-impulse rendezvous trajectories for two vehicles in circular orbit; algorithm for nonautonomous terminal control of space glider with guidance to radio beacon; constructing trajectories of geocentric propulsion of spacecraft with solar sail; use of indirect data for monitoring periods of electrification disturbances of high-orbit satellites; early work on tether systems for spacecraft artificial gravity; processing of 'Okean' spacecraft data for classification of vegetation of boreal forests; evaluation of accuracy in monitoring orbit of satellite of 'meteor- 3' series using system for predicting motion of artificial earth satellites of international 'radiation-balance' project; determining spatial resolution of multiband scanning devices from results of control surveys; and status of Russia's environmental satellite programs. CASI

N94-19162*# National Aeronautics and Space Administration. Goddard Space Flight Center, Greenbelt, MD.
THE 1993 SHUTTLE SMALL PAYLOADS SYMPOSIUM
Lawrence R. Thomas, ed. and Frances L. Mosier, ed. (Interstel, Inc., Beltsville, MD.) Oct. 1993 194 p Conference held in Annapolis, MD, 4-7 Oct. 1993
(NASA-CP-3233; Rept-93B00119; NAS 1.55:3233) Avail: CASI HC A09/MF A03

The 1993 Shuttle Small Payloads Symposium is a combined symposia of the Get Away Special (GAS), Hitchhiker, and Complex Autonomous Payloads (CAP) programs, and is proposed to continue as an annual conference. The focus of this conference is to educate potential Space Shuttle Payload Bay users as to the types of carrier systems provided and for current users to share experiment concepts. For individual titles, see N94-19163 through N94-19185.

N94-19163*# Utah Univ., Salt Lake City.
CHARACTERIZATION OF FLUID PHYSICS EFFECTS ON CARDIOVASCULAR RESPONSE TO MICROGRAVITY (G-572) c52
George M. Pantalos, M. Keith Sharp, Stewart J. Woodruff, Richard D. Lorange, Thomas E. Bennett (Bellarmine-Ursuline Coll., Louisville, KY.), Jan J. Sojka (Utah State Univ., Logan.), and Mark W. Lemon (Utah State Univ., Logan.) *In* NASA. Goddard Space Flight Center, The 1993 Shuttle

Small Payloads Symposium Oct. 1993 p 1-10 (For primary document see N94-19162 04-12)
Avail: CASI HC A02/MF A03

The recognition and understanding of cardiovascular adaptation to spaceflight has experienced substantial advancement in the last several years. In-flight echocardiographic measurements of astronaut cardiac function on the Space Shuttle have documented a 15 percent reduction in both left ventricular volume index and stroke volume with a compensatory increase in heart rate to maintain cardiac output. To date, the reduced cardiac size and stroke volume have been presumed to be the consequence of the reduction in circulating fluid volume following diuresis and other physiological processes to reduce blood volume within a few days after orbital insertion. However, no specific mechanism for the reduced stroke volume has been elucidated. The following investigation proposes the use of a hydraulic model of the cardiovascular system to examine the possibility that the observed reduction in stroke volume may, in part, be related to fluid physics effects on heart function. The automated model is being prepared to fly as a GAS payload. The experimental apparatus consists of a pneumatically actuated, elliptical artificial ventricle connected to a closed-loop, hydraulic circuit with compliance and resistance elements to create physiologic pressure and flow conditions. The ventricle is instrumented with high-fidelity, acceleration-insensitive, catheter-tip pressure transducers (Millar Instruments) in the apex and base to determine the instantaneous ventricular pressures and (delta)P(sub LV) across the left ventricle (LVP(sub apex)-LVP(sub base). The ventricle is also instrumented with a flow probe and pressure transducers immediately upstream of the inflow valve and downstream of the outflow valve. The experiment will be microprocessor controlled with analog signals stored on the FM data tape recorder. By varying the circulating fluid volume, ventricular function can be determined for varying preload pressures with fixed afterload pressure. Pilot experiments on board the NASA KC-135 aircraft have demonstrated proof-of-concept and provided early support for the proposed hypothesis. A review of the pilot experiments and developmental progress on the GAS version of this experiment will be presented. Author

N94-19164*# Air Force Systems Command, Vandenberg AFB, CA. Space Information Labs.
CALIFORNIA STUDENT GET AWAY SPECIAL PAYLOAD GAS-450
Glen Ray, Edmund Burke, and Marty Waldman *In* NASA. Goddard Space Flight Center, The 1993 Shuttle Small Payloads Symposium Oct. 1993 p 11-23 (For primary document see N94-19162 04-12)
Avail: CASI HC A03/MF A03

The California Student Get Away Special Payload GAS-450, recently went into orbit on the STS-57 Mission, Space Shuttle, Endeavour, 21 June 1993, 6:14 AM and landed on the 29 June 1993 at Kennedy Space Center (KSC). Fifty students from 13 California Central Coast Schools and one in San Francisco designed and built 13 active experiments (6 modules) for this mission. Preliminary analysis of our completely reusable payload bus system indicated that the structure, power system, microprocessor, and sensor systems in each experiment module worked flawlessly. The experiments themselves performed exceptionally well with a 60 percent success ratio. The students are thoroughly documenting their own experiments and results via a standard research paper guideline generated by the GAS-450 technical staff. Lessons learned (program management and technical) are documented at the end of the paper. If any other organization needs payload/experiment development or NASA documentation assistance, then please contact us. We can help make your idea a space tested reality. Three years of intense effort culminated on 3 February 1993, the GSFC field operations team at Kennedy Space Center performed the final pressure decay and electrical tests upon the fully integrated GAS-450 flight canister. Subsequently, the payload was integrated with its parent GAS Bridge Assembly in mid-February and the bridge was transferred to the KSC orbiter team in late February 1993. The STS-57 mission originally scheduled to launch on the 29 April 1993 slipped until 21 June 1993. Our Payload shared the cargo bay with ten other GAS Canisters, the EUREKA experiment, the SHOOT experiment, and the SPACEHAB-1 module. The SIL technical staff retrieved the GAS-450 payload after flight from the NASA Spin Test Facility at KSC and shipped it back to California on the 22 July 1993 for student analysis at Allan Hancock College this summer. Author (revised)

N94-19165*# National Aeronautics and Space Administration. Goddard Space Flight Center, Greenbelt, MD.
NEW ROOM TEMPERATURE HIGH RESOLUTION SOLID-STATE DETECTOR (CdZnTe) FOR HARD X RAYS AND GAMMA RAYS **c72**
AmyElizabeth C. Stewart (Maryland Univ., College Park.) and Upendra D. Desai *In its* The 1993 Shuttle Small Payloads Symposium Oct. 1993 p 25-31 (For primary document see N94-19162 04-12)
Avail: CASI HC A02/MF A03

The new CdZnTe high 'Z' material represents a significant improvement in detectors for high energy photons. With the thicknesses available, photons up to 100 keV can be efficiently detected. This material has a wide band gap of 1.5 - 2.2 eV which allows it to operate at room temperature while providing high spectral resolution. Results of resolution evaluations are presented. This detector can be used for high resolution spectral measurements of photons in x-ray and gamma-ray astronomy, offering a significant reduction in the weight, power, and volume of the detector system compared to more conventional detector types such as scintillation counters. In addition, the detector will have the simplicity and reliability of solid-state construction. The CdZnTe detector, as a new development, has not yet been evaluated in space. The Get Away Special program can provide this opportunity. Author (revised)

N94-19166*# National Aeronautics and Space Administration. Goddard Space Flight Center, Greenbelt, MD.
TELESCOPE FOR X RAY AND GAMMA RAY STUDIES IN ASTROPHYSICS **c89**
W. D. Weaver (Arkansas State Univ., State University.) and Upendra D. Desai *In its* The 1993 Shuttle Small Payloads Symposium Oct. 1993 p 33-36 (For primary document see N94-19162 04-12)
Avail: CASI HC A01/MF A03

Imaging of x-rays has been achieved by various methods in astrophysics, nuclear physics, medicine, and material science. A new method for imaging x-ray and gamma-ray sources avoids the limitations of previously used imaging devices. Images are formed in optical wavelengths by using mirrors or lenses to reflect and refract the incoming photons. High energy x-ray and gamma-ray photons cannot be reflected except at grazing angles and pass through lenses without being refracted. Therefore, different methods must be used to image x-ray and gamma-ray sources. Techniques using total absorption, or shadow casting, can provide images in x-rays and gamma-rays. This new method uses a coder made of a pair of Fresnel zone plates and a detector consisting of a matrix of CsI scintillators and photodiodes. The Fresnel zone plates produce Moire patterns when illuminated by an off-axis source. These Moire patterns are deconvolved using a stepped sine wave fitting or an inverse Fourier transform. This type of coder provides the capability of an instantaneous image with sub-arcminute resolution while using a detector with only a coarse position-sensitivity. A matrix of the CsI/photodiode detector elements provides the necessary coarse position-sensitivity. The CsI/photodiode detector also allows good energy resolution. This imaging system provides advantages over previously used imaging devices in both performance and efficiency. Author (revised)

N94-19167*# Swedish Space Corp., Solna.
MUZO FLIGHT EXPERIENCE WITH THE PROGRAMMABLE MULTIZONE FURNACE **c29**
Christian Lockowandt and Kenneth Loth *In* NASA. Goddard Space Flight Center, The 1993 Shuttle Small Payloads Symposium Oct. 1993 p 37-45 (For primary document see N94-19162 04-12)
Avail: CASI HC A02/MF A03

The Multi-Zone (MUZO) furnace has been developed for growing germanium (Ge) crystals under microgravity in a Get Away Special (GAS) payload. The MUZO furnace was launched with STS-47 Endeavour in September 1992. The payload worked as planned during the flight and a Ge sample was successfully processed. The experiment has given valuable scientific information. The design and functionality of the payload together with flight experience is reported. Author (revised)

N94-19168*# California Inst. of Tech., Pasadena.
THE GAMCIT GAMMA RAY BURST DETECTOR **c93**
Benjamin J. McCall, John M. Grunsfeld, Srdjan D. Sobajic, Chinley Leonard Chang, David M. Krum, Albert Ratner, and Jennifer E. Trittschuh *In* NASA. Goddard Space Flight Center, The 1993 Shuttle Small Payloads

Symposium Oct. 1993 p 47-56 (For primary document see N94-19162 04-12)
Avail: CASI HC A02/MF A03

The GAMCIT payload is a Get-Away-Special payload designed to search for high-energy gamma-ray bursts and any associated optical transients. This paper presents details on the design of the GAMCIT payload, in the areas of battery selection, power processing, electronics design, gamma-ray detection systems, and the optical imaging of the transients. The paper discusses the progress of the construction, testing, and specific design details of the payload. In addition, this paper discusses the unique challenges involved in bringing this payload to completion, as the project has been designed, constructed, and managed entirely by undergraduate students. Our experience will certainly be valuable to other student groups interested in taking on a challenging project such as a Get-Away-Special payload. Author

N94-19169*# Hancock (Thomas), Huntsville, AL.
STATIC COMPUTER MEMORY INTEGRITY TESTING (SCMIT): AN EXPERIMENT FLOWN ON STS-40 AS PART OF GAS PAYLOAD G-616 **c60**
Thomas Hancock *In* NASA. Goddard Space Flight Center, The 1993 Shuttle Small Payloads Symposium Oct. 1993 p 57-62 (For primary document see N94-19162 04-12)
Avail: CASI HC A02/MF A03

This experiment investigated the integrity of static computer memory (floppy disk media) when exposed to the environment of low earth orbit. The experiment attempted to record soft-event upsets (bit-flips) in static computer memory. Typical conditions that exist in low earth orbit that may cause soft-event upsets include: cosmic rays, low level background radiation, charged fields, static charges, and the earth's magnetic field. Over the years several spacecraft have been affected by soft-event upsets (bit-flips), and these events have caused a loss of data or affected spacecraft guidance and control. This paper describes a commercial spin-off that is being developed from the experiment. Author

N94-19170*# Bristol Aerospace Ltd., Winnipeg (Manitoba).
THE FIRST FLIGHT OF THE QUESTS GAS PAYLOAD G-521
Darrin Gates *In* NASA. Goddard Space Flight Center, The 1993 Shuttle Small Payloads Symposium Oct. 1993 p 63-71 (For primary document see N94-19162 04-12)
Avail: CASI HC A02/MF A03

An overview of all of the phases of the QUESTS Get Away Special project is presented. Details from the early phases of the project--design, manufacture, and testing--to the first flight results are provided. The handling of safety issues, payload capabilities, the experiment complement, payload integration, and de-integration and interfacing with NASA is also discussed. Author

N94-19171*# Evolving Technologies Corp., New York, NY.
VPU(TM) DEMONSTRATION MISSION VICINITY PROCESSOR UNIT(TM) OVERVIEW **c60**
Loren Abdulezer *In* NASA. Goddard Space Flight Center, The 1993 Shuttle Small Payloads Symposium Oct. 1993 p 73-74 (For primary document see N94-19162 04-12)
Avail: CASI HC A01/MF A03

Evolving Technologies Corporation is designing a new type of computer called a Vicinity Processor Unit (VPU). The VPU is designed to monitor and control payloads using an operating system, control process and software environment that specifically takes into account the time delay associated with remotely controlling and monitoring a group of payloads in real time. This is a fundamentally different way of computing which has vast scientific implications for the design and implementation of data processing systems for future space flight missions. As a demonstration mission, the VPU is expected to be flown aboard the Space Shuttle (Payload Identification No. G-700) as a part of NASA's Small Self-Contained Payloads (SSCP) Program. We believe this mission can greatly facilitate the development and validation of technology which may prove to be mission critical for many future space flight missions. Author (revised)

N94-19172*# European Space Agency. European Space Research and Technology Center, ESTEC, Noordwijk (Netherlands).
ATTITUDE SENSOR PACKAGE **c19**
R. Aceti, M. Trischberger, P. J. Underwood, A. Pomilia (Officine Galileo S.p.A., Florence, Italy.), M. Cosi (Officine Galileo S.p.A., Florence, Italy.), and F. Boldrini (Officine Galileo S.p.A., Florence, Italy.) *In* NASA. Goddard Space Flight Center, The 1993 Shuttle Small Payloads Symposium Oct. 1993 p 75-85 (For primary document see N94-19162 04-12)
Avail: CASI HC A03/MF A03

This paper describes the design, construction, testing, and successful flight of the Attitude Sensor Package. The payload was assembled on a standard HITCHHIKER experiment mounting plate, and made extensive use of the carrier's power and data handling capabilities. The side mounted HITCHHIKER version was chosen, since this configuration provided the best viewing conditions for the instruments. The combustion was successfully flown on board Space Shuttle Columbia (STS-52), in October 1992. The payload was one of the 14 experiments of the In-Orbit Technology Demonstration Program (Phase 1) of the European Space Agency. Author

N94-19173*# Tennessee Univ., Tullahoma. Center for Space Transportation and Applied Research.
SPACE APPLICATIONS INDUSTRIAL LASER SYSTEM (SAILS) **c36**
T. D. McCay, J. B. Bible, and R. E. Mueller *In* NASA. Goddard Space Flight Center, The 1993 Shuttle Small Payloads Symposium Oct. 1993 p 87-95 Prepared in cooperation with Tennessee Univ. Space Inst., Tullahoma (For primary document see N94-19162 04-12)
(Grant NAGw-1195)
Avail: CASI HC A02/MF A03

A program is underway to develop a YAG laser based materials processing workstation to fly in the cargo bay of the Space Shuttle. This workstation, called Space Applications Industrial Laser System (SAILS), will be capable of cutting and welding steel, aluminum, and Inconel alloys of the type planned for use in constructing the Space Station Freedom. As well as demonstrating the ability of a YAG laser to perform remote (fiber-optic delivered) repair and fabrication operations in space, fundamental data will be collected on these interactions for comparison with terrestrial data and models. The flight system, scheduled to fly in 1996, will be constructed as three modules using standard Get-Away-Special (GAS) canisters. The first module holds the laser head and cooling system, while the second contains a high peak power electrical supply. The third module houses the materials processing workstation and the command and data acquisition subsystems. The laser head and workstation cansisters are linked by a fiber-optic cable to transmit the laser light. The team assembled to carry out this project includes Lumonics Industrial Products (laser), Tennessee Technological University (structural analysis and fabrication), Auburn University Center for Space Power (electrical engineering), University of Waterloo (low-g laser process consulting), and CSTAR/UTSI (data acquisition, control, software, integration, experiment design). This report describes the SAILS program and highlights recent activities undertaken at CSTAR. Author

N94-19174*# Naval Research Lab., Washington, DC. Center for Space Research.
A HIGH RESOLUTION ULTRAVIOLET SHUTTLE GLOW SPECTROGRAPH **c19**
George R. Carruthers *In* NASA. Goddard Space Flight Center, The 1993 Shuttle Small Payloads Symposium Oct. 1993 p 97-105 (For primary document see N94-19162 04-12)
Avail: CASI HC A02/MF A03

The High Resolution Shuttle Glow Spectrograph-B (HRSGS-B) is a small payload being developed by the Naval Research Laboratory. It is intended for study of shuttle surface glow in the 180-400 nm near- and middle-ultraviolet wavelength range, with a spectral resolution of 0.2 nm. It will search for, among other possible features, the band systems of excited NO which result from surface-catalyzed combination of N and O. It may also detect O2 Hertzberg bands and N2 Vegard-Kaplan bands resulting from surface recombination. This wavelength range also includes possible N2+ and OH emissions. The HRSGS-B will be housed in a Get Away Special canister, mounted in the shuttle orbiter payload bay, and will observe the glow on the tail of the orbiter. Author

N94-19175*# Case Western Reserve Univ., Cleveland, OH. Center on the Commercial Development of Space.
MATERIALS FLIGHT EXPERIMENT CARRIER CAPABILITY AND FUTURE FLIGHT EXPERIMENTS ON HITCHHIKER-M CARRIER PROGRAM
D. Davis *In* NASA. Goddard Space Flight Center, The 1993 Shuttle Small Payloads Symposium Oct. 1993 p 107-113 (For primary document see N94-19162 04-12)
Avail: CASI HC A02/MF A03

The CMSS has designed, fabricated, and qualified a unique Materials FLight EXperiment (MFLEX) carrier. The MFLEX is a reusable materials experiment carrier designed to support a wide array of sensors that measure synergistic effects on candidate space materials in Low Earth Orbit (LEO). The MFLEX can be integrated on a variety of launch vehicles/carriers and multiple units can be networked to optimize the surface area of carriers such as the Hitchhiker-M currently being built by the Goddard Space Flight Center (GSFC). Author

N94-19176*# Case Western Reserve Univ., Cleveland, OH. Center on the Commercial Development of Space Programs.
LIMITED DURATION OF CANDIDATE MATERIALS EXPOSURE EXPERIMENT (LDCE): A COMPLEX AUTONOMOUS PAYLOAD (CAP) USING A GET AWAY SPECIAL (GAS) CANISTER c25
D. Davis *In* NASA. Goddard Space Flight Center, The 1993 Shuttle Small Payloads Symposium Oct. 1993 p 115-124 (For primary document see N94-19162 04-12)
Avail: CASI HC A02/MF A03

CMSS has designed, fabricated, qualified and flown the LDCE payload as a cost effective space flight hardware to conduct exposure of materials to the space environment. The hardware has been qualified for 10 missions, utilizing a GAS Canister, supplied by Goddard Space Flight Center. Results of the first series of LDCE experiments have shown that the hardware performed as expected. Author

N94-19177*# National Aeronautics and Space Administration. John F. Kennedy Space Center, Cocoa Beach, FL.
KENNEDY SPACE CENTER PROCESSING OF SHUTTLE SMALL PAYLOADS
Michael E. Haddad *In* NASA. Goddard Space Flight Center, The 1993 Shuttle Small Payloads Symposium Oct. 1993 p 125-144 (For primary document see N94-19162 04-12)
Avail: CASI HC A03/MF A03

There are many steps involved in preparing a payload for a mission into space on the Space Shuttle. Operations at the John F. Kennedy Space Center (KSC) are the last of those steps for the hardware before the payload is launched. To assure a successful and efficient KSC processing flow, a great deal of planning between the Robert H. Goddard Space Flight Center (GSFC) and KSC personnel is required before the payload arrives at KSC. After arrival, pre-flight operations occur between payload personnel, GSFC personnel, and KSC personnel for integration of the payload into its carrier (if required), in preparation for installation into a Orbiter. Once installed into an Orbiter, final test(s), checkout, and close-out of the payload is performed by GSFC and KSC personnel before launch. Mission support varies depending on the payload flying, but once the mission is complete and the Orbiter has returned to KSC, post-flight operations begin. This usually involves a reverse flow of the pre-flight operations. KSC operations conclude when the payload, its ground support equipment (GSE), and personnel depart KSC. A list of lessons learned is generated at the end of each payload flow, to avoid repeating the same mistakes (if any) for the next payload or for multiple repeat flights of the same payload. Always monitored are planned changes that may affect the payloads, GSE, KSC facilities, payload personnel, GSFC personnel, and/or KSC personnel. Author

N94-19178*# Trieste Univ. (Italy). Dept. of Astronomy.
UVSTAR: AN IMAGING SPECTROGRAPH WITH TELESCOPE FOR THE SHUTTLE HITCHHIKER-M PLATFORM c89
Roberto Stalio, Bill R. Sandel (Arizona Univ., Tucson.), and A. Lyle Broadfoot (Arizona Univ., Tucson.) *In* NASA. Goddard Space Flight Center, The 1993 Shuttle Small Payloads Symposium Oct. 1993 p 145-152 (For primary document see N94-19162 04-12)
Avail: CASI HC A02/MF A03

UVSTAR is an EUV spectral imager intended as a facility instrument devoted to solar system and astronomy studies. It covers the wavelength range of 500 to 1250 A, with sufficient spectral resolution to separate emission lines and to form spectrally resolved images of extended plasma sources. Targets include the Io plasma torus at Jupiter, hot stars, planetary nebulae and bright galaxies. UVSTAR consists of a pair of telescopes and concave grating spectrographs that cover the overlapping spectral ranges of 500-900 and 850-1250 A. The telescopes use two 30 cm diameter off-axis paraboloids having focal length of 1.5 m. An image of the target is formed at the entrance slits of the two concave grating spectrographs. The gratings provide dispersion and re-image the slits at the detectors, intensified CCD's. The readout format of the detectors can be chosen by computer, and three slit widths are selectable to adapt the instrument to specific tasks. UVSTAR has internal gimbals which allow rotation of plus or minus 3 deg about each of two axes. Dedicated finding and tracking telescopes will acquire and track the target after rough pointing is achieved by orienting the Orbiter. Responsibilities for implementation and utilization of UVSTAR are shared by groups in Italy and the U.S. UVSTAR is scheduled for flight in early 1995, timed for an opportunity to observe the Jovian system. Author

N94-19179*# Trieste Univ. (Italy).
THE STAR IDENTIFICATION, POINTING AND TRACKING SYSTEM OF UVSTAR, AN ATTACHED PAYLOAD INSTRUMENT SYSTEM FOR THE SHUTTLE HITCHHIKER-M PLATFORM c19
Francesco DeCarlo, Roberto Stalio, Paolo Trampus, A. Lyle Broadfoot (Arizona Univ., Tucson.), Bill R. Sandel (Arizona Univ., Tucson.), and Giovanni Sicuranza *In* NASA. Goddard Space Flight Center, The 1993 Shuttle Small Payloads Symposium Oct. 1993 p 153-167 (For primary document see N94-19162 04-12)
Avail: CASI HC A03/MF A03

We describe an algorithm for star identification and pointing/tracking of a spaceborne electro-optical system and simulation analyses to test the algorithm. The algorithm will be implemented in the guiding system of UVSTAR, a spectrographic telescope for observations of astronomical and planetary sources operating in the 500-1250 A waveband at approximately 1 A resolution. The experiment is an attached payload and will fly as a Hitchhiker-M payload on the Shuttle. UVSTAR includes capabilities for independent target acquisition and tracking. The spectrograph package has internal gimbals that allow angular movement of plus or minus 3 deg from the central position. Rotation about the azimuth axis (parallel to the Shuttle z axis) and elevation axis (parallel to the Shuttle x axis) will actively position the field of view to center the target of interest in the fields of the spectrographs. The algorithm is based on an on-board catalog of stars. To identify star fields, the algorithm compares the positions of stars recorded by the guiding imager to positions computed from the on-board catalog. When the field has been identified, its position within the guiding imager field of view can be used to compute the pointing corrections necessary to point to a target of interest. In tracking mode, the software uses the past history to predict the quasi-periodic attitude control motions of the shuttle and sends pointing commands to cancel the motion and stabilize UVSTAR on the target. The guiding imager (guider) will have an 80-mm focal length and f/1.4 optics giving a field of view of 6 deg x 4.5 deg using a 385 x 288 pixel intensified CCD. It will be capable of providing high accuracy (better than 2 arc-sec) attitude determination from coarse (6 deg x 4.5 deg) initial knowledge of the pointing direction; and of pointing toward the target. It will also be capable of tracking at the same high accuracy with a processing time of less than a few hundredths of a second. Author

N94-19180*# Anser Analytic Services, Inc., Arlington, VA.
UTILIZATION OF SHUTTLE SMALL PAYLOAD ACCOMMODATIONS IN THE DOD SPACE TEST PROGRAM
Thomas Hagler and Eva Czajkowski *In* NASA. Goddard Space Flight Center, The 1993 Shuttle Small Payloads Symposium Oct. 1993 p 169-177 (For primary document see N94-19162 04-12)
(Contract F49620-91-C-0031)
Avail: CASI HC A02/MF A03

Over the past 27 years, the U.S. Air Force, as executive agent for the Department of Defense (DOD) Space Test Program, has flown approximately 325 space experiments for the Army, Navy, Air Force, and other DOD agencies. These experiments have made significant contributions to the improvement of military technology and operations. Flight of Space Test Program experiments has been carried out utilizing free flyer spacecraft, the Space Shuttle crew cabin, and the Space Shuttle cargo bay. This paper will concentrate on those experiments which have been flown by the NASA Space Shuttle small payload flight systems, e.g., GAS, uprated GAS (CAP), and Hitchhiker flight systems. Discussions of Space Test Program experiments flown by Space Shuttle small payloads flight systems will include the experiment objectives, the accommodations and services provided by the flight systems, experiment results, and lessons learned from the planning and conduct of the flight. Particular emphasis will be placed on those experiments which required and were provided with a new and unique capability by the small payloads flight systems. These capabilities include the first use of the GAS opening lid, the first use of the GAS payload ejection capability, and the first use of the Hitchhiker cross bay carrier. Author

N94-19181*# Simpson Weather Associates, Inc., Charlottesville, VA.
SPNDL: A CONCEPT FOR A SMALL SATELLITE DOPPLER LIDAR WIND SOUNDER **c47**
G. D. Emmitt and M. M. Sokoloski (Science and Technology Corp., Washington, DC.) *In* NASA. Goddard Space Flight Center, The 1993 Shuttle Small Payloads Symposium Oct. 1993 p 179-191 (For primary document see N94-19162 04-12)
Avail: CASI HC A03/MF A03

Given current resources and the technical challenges in developing a full coverage space-based Doppler lidar wind measuring system such as LAWS (Laser Atmospheric Wind Sounder), it is not likely that the science community will have data streams with which to work before the end of this decade. Currently, a 'fast track' demonstration mission is being seriously considered by several U.S. agencies. Such a mission would have as its primary objectives the demonstration of coherent Doppler lidar technology in space and the delivery of wind observations for science algorithm evaluation and development. However, for such a mission to be achieved at modest costs and within a short time frame, deviations from the full system design are required. Simulation models have been developed over the last decade to aide in the design of Doppler lidar missions and to provide simulated data for use in wind computation algorithm development. SWA has used both models to examine some options that might be cost-effective for a demonstration mission. Over the past few months, Simpson Weather Associates has been studying SPNDL (Spinning Platform with a Non-rotating telescope Doppler Lidar), a new concept for Doppler lidar wind observations from space. Science and Technology Corporation has an interest in participating in an engineering and shuttle accommodation study for SPNDL. Author

N94-19182*# Earth News, Titusville, FL.
YOUR GAS EXPERIMENT AND THE MEDIA OR WHY DOES THAT OTHER CAN GET ALL OF THE PUBLICITY? Abstract Only
Philip Chien *In* NASA. Goddard Space Flight Center, The 1993 Shuttle Small Payloads Symposium Oct. 1993 p 193 (For primary document see N94-19162 04-12)
Avail: CASI HC A01/MF A03

NASA has flown almost 100 Get Away Special (GAS) cans. Only a few of them are remembered by the general public, including the 'snowflakes in space' from STS-6, 'ants in space' from STS-7, and CanDO from STS-57. Why do some GAS cans get all of the publicity, while others are barely mentioned in press conferences, press kits, and on NASA Select during the mission? How can you make sure your GAS can gets as much attention as the others on your flight? And why is it important for you to make sure the public finds out about your activities? Writer Philip Chien has covered the space program since 1983, and is a regular participant in GAS press conferences. This paper will use STS-57 as a case study showing why some GAS cans got more publicity than others. The paper will offer advice for upcoming GAS payloads and how to prepare your press kits and other handouts. Author

N94-19183*# Rockwell International Corp., Cocoa Beach, FL. Space Systems Div.
ISOBUS: A NEW VERSATILE SPACECRAFT PLATFORM USING SHUTTLE SMALL PAYLOADS **c18**
David Tamir, Rex W. Ridenoure (Jet Propulsion Lab., California Inst. of Tech., Pasadena.), and R. Gilbert Moore (Utah State Univ., Logan.) *In* NASA. Goddard Space Flight Center, The 1993 Shuttle Small Payloads Symposium Oct. 1993 p 195-198 (For primary document see N94-19162 04-12)
Avail: CASI HC A01/MF A03

The new NASA credo of 'faster, better, cheaper' calls for a new generation of smaller and less complex spacecraft. In response to this challenge, many new spacecraft concepts have been generated within NASA, industry, and academia. The JPL, Rockwell International Space Systems Division, and The Space Dynamics Laboratory (SDL)/Utah State University (USU) are jointly examining one such new spacecraft concept, hereafter termed ISOBUS, which is derived from recent research and development work in isogrid structures based on a six-sided hexagon shaped structure. Two prototypical products from SDL/USU's work are ISOSPACEPACK and ISOSAT. These hexagon shaped elements serve as building blocks for the ISOBUS spacecraft concept. Various aspects of the ISOBUS concept are discussed. Derived from text

N94-19184*# Harris Corp., Melbourne, FL.
RADIATION HARDENED MICROPROCESSOR FOR SMALL PAYLOADS Abstract Only **c60**
Ravi Shah *In* NASA. Goddard Space Flight Center, The 1993 Shuttle Small Payloads Symposium Oct. 1993 p 199 (For primary document see N94-19162 04-12)
(Contract N00014-91-C-2005)
Avail: CASI HC A01/MF A03

The RH-3000 program is developing a rad-hard space qualified 32-bit MIPS R-3000 RISC processor under the Naval Research Lab sponsorship. In addition, under IR&D Harris is developing RHC-3000 for embedded control applications where low cost and radiation tolerance are primary concerns. The development program leverages heavily from commercial development of the MIPS R-3000. The commercial R-3000 has a large installed user base and several foundry partners are currently producing a wide variety of R-3000 derivative products. One of the MIPS derivative products, the LR33000 from LSI Logic, was used as the basis for the design of the RH-3000 chipset. The RH-3000 chipset consists of three core chips and two support chips. The core chips include the CPU, which is the R-3000 integer unit and the FPA/MD chip pair, which performs the R-3010 floating point functions. The two support whips contain all the support functions required for fault tolerance support, real-time support, memory management, timers, and other functions. The Harris development effort had first passed silicon success in June, 1992 with the first rad-hard 32-bit RH-3000 CPU chip. The CPU device is 30 kgates, has a 508 mil by 503 mil die size and is fabricated at Harris Semiconductor on the rad-hard CMOS Silicon on Sapphire (SOS) process. The CPU device successfully passed tesing against 600,000 test vectors derived directly on the LSI/MIPS test suite and has been operational as a single board computer running C code for the past year. In addition, the RH-3000 program has developed the methodology for converting commercially developed designs utilizing logic synthesis techniques based on a combination of VHDK and schematic data bases. Author

N94-19185*# National Aeronautics and Space Administration. Goddard Space Flight Center, Greenbelt, MD.
SUPERFLUID HELIUM ON-ORBIT TRANSFER (SHOOT) FLIGHT DEMONSTRATION
Peter Shirron, Michael DiPirro, Jim Tuttle, Steve Volz, and Neal Barthelme *In its* The 1993 Shuttle Small Payloads Symposium Oct. 1993 p 201 (For primary document see N94-19162 04-12)
Avail: CASI HC A01/MF A03

The Superfluid Helium On-Orbit Transfer (SHOOT) Flight Demonstration was an attached Shuttle payload mounted on a Hitchhiker cross-bay carrier which flew on STS-57 in June of 1993. SHOOT successfully demonstrated the handling and transfer of superfluid helium between two containers, called dewars, in low gravity. SHOOT was a class C payload and for the STS-57 mission was termed a complex secondary payload. The primaries were the retrieval of the EURECA carrier and a collection of modular experiments contained in SPACEHAB. Because the liquid helium was continuously boiling off, SHOOT's activities were scheduled for the first three days of the mission, concurrent with some SPACEHAB experiments, but well before the EURECA retrieval. Control of the SHOOT experiment was highly interactive and originated primarily from the Goddard Payload Operations and Control Center (POCC). Transfer and calibration activities required continuous command windows of up to 50 minutes duration and up to 80 minutes out of each orbit. Occasionally the crew controlled the experiment using the Payload General Support Computer (PGSC) when near-real time control and monitoring was required. SHOOT also placed considerable demands on the orbiter, including a pitch rotation of 3 deg./sec for 15 minutes, and translational burns using both the aft and forward RCS jets to generate accelerations up to 7 milli-g. The basis for these and other requirements are discussed. Interacion with the crew and timing of crew activity during the mission will be detailed. The processing flow of SHOOT at KSC is described with emphasis on the tradeoffs for vertical, as opposed to horizontal, installation in the orbiter. Finally, some lessons learned are presented that are relevant to future cryogenic and Hitchhiker payloads. Author (revised)

N94-19622# European Space Agency, Paris (France).
CLUSTER: MISSION, PAYLOAD, AND SUPPORTING ACTIVITIES
W. R. Burke, ed. Noordwijk, Netherlands Mar. 1993 293 p Original contains color illustrations
(ESA-SP-1159; ISBN-9-29-092073-4; ETN-93-94863) Copyright Avail: CASI HC A13/MF A03; ESA, EPD, ESTEC, Noordwijk, Netherlands, HC

The Cluster mission, which will study the three dimensional dynamic behavior of small scale structures in the Earth's plasma environment, is addressed. Descriptions of the eleven instruments, the spacecraft design, the ground segment, the scientific operations planned by ESOC for the Joint Science Operations Center, and the Cluster science data system are described. To achieve the scientific goals of the mission, attempts were made from the very beginning to cooperate with the plasma simulations community and with the ground observations community. The activities of these two communities in support of Cluster are described. Two candidate orbits for Cluster are discussed. For individual titles, see N94-19623 through N94-19641.

N94-19623# Centre National de la Recherche Scientifique, Orleans (France).
THE WAVE EXPERIMENT CONSORTIUM
F. Lefeuvre, A. Roux (Centre National d'Etudes des Telecommunications, Issy-les-Moulineaux, France.), B. delaPorte (Centre National d'Etudes des Telecommunications, Issy-les-Moulineaux, France.), C. Dunford (Sheffield Univ., England.), L. J. C. Woolliscroft (Sheffield Univ., England.), P. N. H. Davies (Sussex Univ., Brighton, England.), S. J. Davis (Sussex Univ., Brighton, England.), and M. P. Gough (Sussex Univ., Brighton, England.) *In* ESA, Cluster: Mission, Payload, and Supporting Activities Mar. 1993 p 5-15 (For primary document see N94-19622 04-12)
Copyright Avail: CASI HC A02/MF A03; ESA, EPD, ESTEC, Noordwijk, Netherlands, HC

In order to get the maximum scientific return from available spacecraft resources, the wave experimenters on Cluster established the Wave Experiment Consortium (WEC), the scientific objectives of which are described, together with its capability to achieve them in the course of the mission. Their aims include the characterization of plasma waves and turbulence, and the assessment of their role in the 'anomalous' behavior of critical layers. The five experiments and the interfaces between them are shown in a general block diagram. The need for technical coordination led to the formation of a Wave Experiment Consortium Technical Coordination Office (WECTCO), the tasks of which are described. The planned modes of operation of the WEC experiments are described. ESA

N94-19624*# National Aeronautics and Space Administration. Goddard Space Flight Center, Greenbelt, MD.
THE SPHERICAL PROBE ELECTRIC FIELD AND WAVE EXPERIMENT FOR THE CLUSTER MISSION
G. Gustafsson (Swedish Inst. of Space Physics, Uppsala.), R. Bostroem (Swedish Inst. of Space Physics, Uppsala.), B. Holback (Swedish Inst. of Space Physics, Uppsala.), G. Holmgren (Swedish Inst. of Space Physics, Uppsala.), K. Stasiewicz (Swedish Inst. of Space Physics, Uppsala.), T. Aggson, R. Pfaff, L. P. Block (Royal Inst. of Tech., Stockholm, Sweden.), C.-G. Faelthammar (Royal Inst. of Tech., Stockholm, Sweden.), and P.-A. Lindqvist (Royal Inst. of Tech., Stockholm, Sweden.) et al *In* ESA, Cluster: Mission, Payload, and Supporting Activities Mar. 1993 p 17-31 (For primary document see N94-19622 04-12)
Copyright Avail: CASI HC A03/MF A03; ESA, EPD, ESTEC, Noordwijk, Netherlands, HC

The Electric Field and Wave experiment (EFW) on Cluster, which is designed to measure the electric field and density fluctuations with sampling rates, on some occasions, up to 36,000 samples/s in two channels, is decribed. Langmuir sweeps can also be made to determine the electron density and temperature. Among the more interesting objectives of the experiment is to study nonlinear processes that result in acceleration of plasma. Large scale phenomena where all four spacecraft are needed are also studied. ESA

N94-19625# Centre National d'Etudes des Telecommunications, Issy-les-Moulineaux (France).
STAFF (SPATIO-TEMPORAL ANALYSIS OF FIELD FLUCTUATIONS) EXPERIMENT FOR THE CLUSTER MISSION
N. Cornilleau-Wehrlin, P. Chauveau, A. Meyer, J. M. Nappa, S. Perraut, L. Rezeau, P. Robert, A. Roux, M. Belkacemi (Observatoire de Paris-Meudon, France.), and Y. deConchy (Observatoire de Paris-Meudon, France.) et al *In* ESA, Cluster: Mission, Payload, and Supporting Activities Mar. 1993 p 33-48 Original contains color illustrations (For primary document see N94-19622 04-12)
Copyright Avail: CASI HC A03/MF A03; ESA, EPD, ESTEC, Noordwijk, Netherlands, HC

A technical description of the Spatio Temporal Analysis of Field Fluctuations (STAFF) experiment, which is to be implemented on the four Cluster spacecraft and which consists of a triaxial search coil magnetometer to measure the magnetic components of electromagnetic fluctuations (up to 4 kHz) and of a spectrum analyzer to perform on board each satellite the auto and cross correlation coefficients of the spectral matrix, using three magnetic and two electric components of the waves, is given. Details of the instrument's various inflight operational modes are also given. The magnetic waveform up to either 10 or 180 Hz is also transmitted. STAFF is one of the five complementary experiments which form the Wave Experiment Consortium (WEC). Some of the scientific objectives are discussed, the main one being the study of the electromagnetic fluctuations in the key regions of solar wind/magnetosphere interaction. Some of the methods by which the wave data characteristics are determined are mentioned. ESA

N94-19626# Centre National de la Recherche Scientifique, Orleans (France).
WHISPER: A SOUNDER AND HIGH-FREQUENCY WAVE ANALYSER EXPERIMENT
P. M. E. Decreau, P. Fergeau, M. Leveque, P. Martin, O. Randriamboarison, F. X. Sene, J. G. Trotignon, P. Canu (Centre National d'Etudes des Telecommunications, Issy-les-Moulineaux, France.), H. deFeraudy (Centre National d'Etudes des Telecommunications, Issy-les-Moulineaux, France.), and A. Bahnsen (Danish Space Research Inst., Lyngby.) et al *In* ESA, Cluster: Mission, Payload, and Supporting Activities Mar. 1993 p 49-67 (For primary document see N94-19622 04-12)
Copyright Avail: CASI HC A03/MF A03; ESA, EPD, ESTEC, Noordwijk, Netherlands, HC

The WHISPER (Waves of High frequency and Sounder for Probing Electron density by Relaxation) experiment, whose primary objective is the accurate measurement of the total plasma density within the range from 0.2 to 80 cu cm, is presented. The WHISPER experiment is included in the payload of Cluster. The measurement of the plasma density is achieved by means of a resonance sounding technique which has proved successful in ionospheric dense plasma as well as in dilute space plasmas. The relaxation sounder can also be used as a natural wave receiver and then fulfils the second objective of WHISPER: to provide a continuous survey of one electric component of plasma waves in the frequency range from 4 to 80 kHz with a resolution of about 300 Hz at best. ESA

N94-19627# Iowa Univ., Iowa City. Dept. of Physics and Astronomy.
THE WIDEBAND PLASMA WAVE INVESTIGATION
D. A. Gurnett, R. L. Huff, and D. L. Kirchner *In* ESA, Cluster: Mission, Payload, and Supporting Activities Mar. 1993 p 69-79 Original contains color illustrations (For primary document see N94-19622 04-12)
Copyright Avail: CASI HC A02/MF A03; ESA, EPD, ESTEC, Noordwijk, Netherlands, HC

The Cluster Wideband (WBD) Plasma Wave investigation which is designed to provide high resolution frequency/time spectra of plasma waves in the Earth's magnetosphere is reported. Wideband measurements are important for identifying and studying plasma emissions that have very complex frequency/time characteristics. As part of the Wave Experiment Consortium (WEC), the WBD instrument provides measurements of both electric and magnetic fields in selected frequency bands from 25 Hz to 577 kHz. Continuous waveforms are digitized, formatted, and transferred to the spacecraft telemetry system using either a 220 kbit/s real time mode or a 73 kbit/s burst mode. The real time data require direct acquisition by a NASA Deep Space Network (DSN) receiving station, and the burst mode data are stored on the spacecraft tape recorder for later playback. On the ground the waveforms are Fourier transformed to provide high resolution frequency/time spectrograms. The WBD measurements complement those of the other WEC instruments and also provide unique new capabilities such as very long baseline interferometry. ESA

N94-19628# Sheffield Univ. (England).

IMPLEMENTATION OF THE DIGITAL WAVE-PROCESSING EXPERIMENT

L. J. C. Woolliscroft, H. Saint C. Alleyne, C. M. Dunford, A. Sumner, J. A. Thompson, K. H. Yearby, S. Chapman (Sussex Univ., Brighton, England.), M. P. Gough (Sussex Univ., Brighton, England.), N. Cornilleau-Wehrlin (Centre National d'Etudes des Telecommunications, Issy-les-Moulineaux, France.), and A. Roux (Centre National d'Etudes des Telecommunications, Issy-les-Moulineaux, France.) et al *In* ESA, Cluster: Mission, Payload, and Supporting Activities Mar. 1993 p 81-94 Sponsored by British National Space Centre (For primary document see N94-19622 04-12)

Copyright Avail: CASI HC A03/MF A03; ESA, EPD, ESTEC, Noordwijk, Netherlands, HC

The implementation of the Digital Wave Processing (DWP) experiment, which will be flown on the four ESA/NASA Cluster satellites as a component of the Wave Experiment Consortium (WEC), is reported. The wide variety of geophysical plasmas that will be investigated by the Cluster mission contain waves with a frequency range from DC to over 100 kHz with both magnetic and electric components. The characteristic duration of these waves extends from a few milliseconds to minutes and a dynamic range of over 90 dB is desired. All of these factors make it essential that the onboard control system for the WEC instruments be flexible so as to make effective use of the limited spacecraft resources of power and telemetry information bandwith. The processing system within the DWP instrument will also perform particle and wave/particle correlations in order to permit the direct study of wave/particle interactions. The DWP instrument employs a novel architecture based on the use of transputers with parallel processing and reallocatable tasks to provide a high reliability system. ESA

N94-19629*# National Aeronautics and Space Administration. Goddard Space Flight Center, Greenbelt, MD.

THE CLUSTER MAGNETIC FIELD INVESTIGATION: SCIENTIFIC OBJECTIVES AND INSTRUMENTATION

A. Balogh (Imperial Coll. of Science and Technology, London, England.), S. W. H. Cowley (Imperial Coll. of Science and Technology, London, England.), M. W. Dunlop (Imperial Coll. of Science and Technology, London, England.), D. J. Southwood (Imperial Coll. of Science and Technology, London, England.), J. G. Thomlinson (Imperial Coll. of Science and Technology, London, England.), K. H. Glassmeier (Technische Univ., Brunswick, Germany.), G. Musmann (Technische Univ., Brunswick, Germany.), H. Luehr (Technische Univ., Brunswick, Germany.), M. H. Acuna, and D. H. Fairfield et al *In* ESA, Cluster: Mission, Payload, and Supporting Activities Mar. 1993 p 95-114 Sponsored by Science Research Council; Deutsche Agentur fuer Raumfahrtangelegenheite G.m.b.H.; and Oesterreichische Akademie der Wissenschaften Original contains color illustrations (For primary document see N94-19622 04-12)

Copyright Avail: CASI HC A03/MF A03; ESA, EPD, ESTEC, Noordwijk, Netherlands, HC

The Cluster magnetic field investigation is presented. Cluster represents a qualitatively new type of space mission which will provide, for the first time, a three dimensional view of small scale plasma processes and structures in the different regions in and around the Earth's magnetosphere. Concepts of data analysis needed to interpret the four spacecraft magnetic field data in terms of magnetospheric processes and structures are outlined. The instrument itself, a vital component of the scientific payload, follows a long tradition of fluxgate magnetometers on space missions, yet represents an evolution in terms of built in functions and reliability. A detailed description of the instrument is given with emphasis on those aspects that are unique to the mission. ESA

N94-19630# Max-Planck-Inst. fuer Extraterrestrische Physik, Garching (Germany).

THE ELECTRON DRIFT INSTRUMENT FOR CLUSTER c19

G. Paschmann, F. Melzner, G. Haerendel, O. H. Bauer, W. Baumjohann, N. Sckopke, R. Treumann, C. E. McIlwain (California Univ., San Diego, La Jolla.), W. Fillius (California Univ., San Diego, La Jolla.), and E. C. Whipple (California Univ., San Diego, La Jolla.) et al *In* ESA, Cluster: Mission, Payload, and Supporting Activities Mar. 1993 p 115-132 (For primary document see N94-19622 04-12)

Copyright Avail: CASI HC A03/MF A03; ESA, EPD, ESTEC, Noordwijk, Netherlands, HC

The scientific objectives, the experimental method, and the technical realization of the various elements of the Electron Drift Instrument (EDI) for the Cluster mission are reported. The EDI measures the drift of a weak beam of test electrons that, when emitted in certain directions, return to the spacecraft after one gyration. This drift is related to the electric field and the gradient in the magnetic field, and these quantities can, by the use of different electron energies, be determined separately. As a by product, the magnetic field strength is also measured. ESA

N94-19631# Centre d'Etude Spatiale des Rayonnements, Toulouse (France).

THE CLUSTER ION SPECTROSCOPY EXPERIMENT

H. Reme, J. M. Bosqued, J. A. Sauvaud, A. Cros, J. Dandouras, C. Aoustin, C. Martz, J. L. Medale, J. Rouzaud, and E. Moebius (New Hampshire Univ., Durham.) et al *In* ESA, Cluster: Mission, Payload, and Supporting Activities Mar. 1993 p 133-161 Original contains color illustrations (For primary document see N94-19622 04-12)

Copyright Avail: CASI HC A03/MF A03; ESA, EPD, ESTEC, Noordwijk, Netherlands, HC

The Cluster Ion Spectrometry (CIS) experiment on board the four Cluster spacecraft and which consists of a comprehensive ionic plasma spectrometry package capable of obtaining full three dimensional ion distributions with high time resolution (in one spacecraft spin) and mass per charge resolution is presented. The broad scientific objectives and the wide dynamic range cannot be covered with a single instrument. Consequently, the CIS experiment comprises two different instruments, a Hot Ion Analyzer (HIA) and a time of flight ion Composition and Distribution Function (CODIF) analyzer. These sensors are controlled by a dual processor based Data Processing System (DPS), which permits extensive onboard processing. Both instruments use symmetrical top hat analyzers which provide a continuous, uniform, and well characterized phase-space coverage. The CODIF determines the distributions of the major ion species with energies from spacecraft potential to 40 keV/e with an angular resolution of 22.5 by 10.25 deg and with two different sensitivities. The HIA does not provide mass measurements, but extends the dynamic range to the highest ion fluxes, and has the necessary angular resolution capability (5.6 by 5.6 deg) for ion beam and solar wind measurements. ESA

N94-19632# Mullard Space Science Lab., Dorking (England).

PEACE: A PLASMA ELECTRON AND CURRENT EXPERIMENT

A. D. Johnstone, C. Alsop, P. J. Carter, A. J. Coates, A. J. Coker, R. A. Gowen, B. K. Hancock, T. E. Kennedy, P. H. Sheather, and R. D. Woodliffe et al *In* ESA, Cluster: Mission, Payload, and Supporting Activities Mar. 1993 p 163-184 (For primary document see N94-19622 04-12)

Copyright Avail: CASI HC A03/MF A03; ESA, EPD, ESTEC, Noordwijk, Netherlands, HC

An electron analyzer to measure the three dimensional velocity distribution of electrons on the multispacecraft Cluster mission is described, and the steps taken to meet the special requirements imposed by the novel character of the mission are explained. The onboard data processing unit is described and the telemetry outputs are addressed. The mass, power consumption, and calibration of the equipment is addressed. ESA

N94-19633*# Max-Planck-Inst. fuer Aeronomie, Katlenburg-Lindau (Germany).

RAPID: THE IMAGING ENERGETIC PARTICLE SPECTROMETER ON CLUSTER c19

B. Wilken, W. Guettler, A. Korth, S. Livi, W. Weiss, F. Gliem (Technische Univ., Brunswick, Germany.), A. Muellers (Technische Univ., Brunswick, Germany.), R. Rathje (Technische Univ., Brunswick, Germany.), T. A. Fritz (Los Alamos National Lab., NM.), and J. F. Fennell (Aerospace Corp., Los Angeles, CA.) et al *In* ESA, Cluster: Mission, Payload, and Supporting Activities Mar. 1993 p 185-217 Sponsored by Deutsche Agentuer fuer Raumfahrtangelegenheite G.m.b.H.; Science Research Council; and Norweigian Research Council for Science and Humanities Original contains color illustrations (For primary document see N94-19622 04-12)
(NASA Order S-47197-E)
Copyright Avail: CASI HC A03/MF A03; ESA, EPD, ESTEC, Noordwijk, Netherlands, HC

The RAPID spectrometer for the Cluster mission, an advanced particle detector for the analysis of suprathermal plasma distributions in the energy range from 20 to 400 keV and from 2 keV/nuc to 1500 keV for electrons and ions, respectively, is presented. Novel detector concepts in combination with pinhole acceptance permit the measurement of angular distributions over a range of 180 deg in polar angle for either species. The detection principle for the ionic component is based on a two dimensional analysis of a particle's velocity and energy. Electrons are identified by the well known energy range relationship. The detection techniques are described and selected areas in geospace are used to highlight the scientific objectives of this investigation. ESA

N94-19634# Institut fuer Weltraumforschung, Graz (Austria).
ACTIVE SPACECRAFT POTENTIAL CONTROL: AN ION EMITTER EXPERIMENT FOR CLUSTER **c19**
W. Riedler, K. Torkar, F. Ruedenauer (Oesterreichisches Forschungszentrum Seibersdorf G.m.b.H., Vienna.), M. Fehringer (Oesterreichisches Forschungszentrum Seibersdorf G.m.b.H., Vienna.), W. Steiger (Oesterreichisches Forschungszentrum Seibersdorf G.m.b.H., Vienna.), A. Pedersen (European Space Agency. European Space Research and Technology Center, ESTEC, Noordwijk, Netherlands.), R. J. L. Grard (European Space Agency. European Space Research and Technology Center, ESTEC, Noordwijk, Netherlands.), R. Schmidt (European Space Agency. European Space Research and Technology Center, ESTEC, Noordwijk, Netherlands.), B. T. Narheim (Norwegian Defence Research Establishment, Kjeller.), and J. Troeim (Norwegian Defence Research Establishment, Kjeller.) et al *In* ESA, Cluster: Mission, Payload, and Supporting Activities Mar. 1993 p 219-234 Original contains color illustrations (For primary document see N94-19622 04-12)
Copyright Avail: CASI HC A03/MF A03; ESA, EPD, ESTEC, Noordwijk, Netherlands, HC

The design of the Active Spacecraft Potential Control (ASPOC) instrument on the Cluster spacecraft is presented with focus on the ion emitters. The ion emitters are of the liquid metal ion source type and are used for charge neutralization. The emitters will produce indium ions at approximately 6 KeV. The ion current will be adjusted in a feedback loop with instruments measuring the spacecraft potential. A stand alone mode is seen as a backup. The operating principle of the ASPOC is field evaporation of indium in the apex field of a needle. The advantages are low power consumption, compactness, and high mass efficiency. ESA

N94-19635# European Space Agency. European Space Research and Technology Center, ESTEC, Noordwijk (Netherlands).
THE CLUSTER SPACECRAFT **c18**
J. Credland and G. Lehn (Dornier System G.m.b.H., Friedrichshafen, Germany.) *In its* Cluster: Mission, Payload, and Supporting Activities Mar. 1993 p 235-250 Original contains color illustrations (For primary document see N94-19622 04-12)
Copyright Avail: CASI HC A03/MF A03; ESA, EPD, ESTEC, Noordwijk, Netherlands, HC

An overview of the Cluster mission and system design is given. The spacecraft design and performance characteristics are addressed. The program for Cluster, which is based on a development philosophy incorporating six spacecraft models (one structural model, one engineering model and four flight spacecraft) is addressed. The Cluster mission is a 'first' for the ESA in that it requires the delivery of four identical spacecraft for simultaneous launch on a single launch vehicle. This series production of spacecraft to meet a unique launch opportunity has never before been attempted and represents a serious challenge to ESA, industry and the experimenters. The mission relies on the four spacecraft being placed in near identical eccentric polar orbits with a tetrahedal configuration achieved at the cusp region of the magnetosphere. The launch vehicle chosen for the mission is the first Ariane 5 qualification flight in late 1995 and the launch opportunity is offered under the APEX Program. ESA

N94-19636# European Space Agency. European Space Operations Center, Darmstadt (Germany). Mission Operations Dept.
CLUSTER GROUND SEGMENT AND MISSION OPERATIONS
S. J. Dodsworth and M. Warhaut *In its* Cluster: Mission, Payload, and Supporting Activities Mar. 1993 p 251-258 Original contains color illustrations (For primary document see N94-19622 04-12)
Copyright Avail: CASI HC A02/MF A03; ESA, EPD, ESTEC, Noordwijk, Netherlands, HC

The Cluster ground segment and mission operations, which were designed to permit the transfer of the four spacecraft into the required mission orbit in such a way that they will form a tetrahedral configuration with predefined separation distances when crossing the regions of scientific interest, is presented. The spatial configuration will be adjusted for different phases of the mission. Scientific mission planning inputs and command requests originating from the Principal Investigators (PI's) are considered. The scientific data will be distributed to the scientific community on a hard raw data medium, though PI's will in addition have access to quick look data via an electronic network. ESA

N94-19637# European Space Agency. European Space Operations Center, Darmstadt (Germany). Mission Operations Dept.
THE CLUSTER ORBIT AND MISSION SCENARIO
J. Rodriguez-Canabal, M. Warhaut, R. Schmidt (European Space Agency. European Space Research and Technology Center, ESTEC, Noordwijk, Netherlands.), and M. Bello-Mora (Grupo de Mecanica del Vuelo S.A., Madrid, Spain.) *In its* Cluster: Mission, Payload, and Supporting Activities Mar. 1993 p 259-278 Original contains color illustrations (For primary document see N94-19622 04-12)
Copyright Avail: CASI HC A03/MF A03; ESA, EPD, ESTEC, Noordwijk, Netherlands, HC

The selection of Cluster's operational orbit and its relation with new magnetic field models is reviewed, and the optimization of a multiple maneuver control strategy to achieve the required three dimensional spacecraft configuration is analyzed. The Cluster mission is based on four almost identical spacecraft placed into orbits that take them through the regions of scientific interest of geomagnetic space. The orbits were selected so as to ensure coverage of the northern polar cusp region and the geotail, and to optimize the coverage of the magnetopause, the bow shock and the solar wind. The four Cluster spacecraft will be controlled in such a way that, at selected points of their orbits, they will achieve a configuration in which each spacecraft is at the vertex of a tetrahedron with the required interspacecraft distances. The design of the orbit of each spacecraft depends on the position and structure of certain regions of the magnetic field of the Earth perturbed by the Sun. The characteristics of these regions depend on the position of the Earth's magnetic dipole with respect to the Sun and on the Sun's activity. Their motion is, therefore, unpredictable. ESA

N94-19638# European Space Agency. European Space Research and Technology Center, ESTEC, Noordwijk (Netherlands). Space Science Dept.
THE CLUSTER SCIENCE DATA SYSTEM: A DISTRIBUTED SYSTEM TO SERVE A WIDE INTERNATIONAL COMMUNITY **c82**
R. Schmidt and L. J. C. Woolliscroft (Sheffield Univ., England.) *In its* Cluster: Mission, Payload, and Supporting Activities Mar. 1993 p 279-290 (For primary document see N94-19622 04-12)
Copyright Avail: CASI HC A03/MF A03; ESA, EPD, ESTEC, Noordwijk, Netherlands, HC

The distributed science data system attached to Cluster and ESA/NASA four spacecraft mission, designed to permit the study of plasma processes in three dimensions using the combined data from eleven instruments on each spacecraft, is addressed. A wide scientific community that will wish to use Cluster data will have differing data rights, experience and means of access. Users will include those working primarily with other data sets, and the use of more than one set of data is essential to the mission. The community includes people belonging to some twenty nations. The Cluster Science Data System (CSDS) is distributed across seven national data centers in Europe, one in the U.S., and possibly one in China. ESANET

will be used to interconnect the data centers and the spacecraft Operations Control Centre at European Space Operations Centre, Darmstadt. The European Space Information System (ESIS) will provide the user interface.
ESA

N94-19639# Rutherford Appleton Lab., Chilton (England). Space Science Dept.
THE CLUSTER JOINT SCIENCE OPERATIONS CENTRE c14
E. Dunford, P. Vaughan, E. Golton, and T. Dimbylow *In* ESA, Cluster: Mission, Payload, and Supporting Activities Mar. 1993 p 291-297 (For primary document see N94-19622 04-12)
Copyright Avail: CASI HC A02/MF A03; ESA, EPD, ESTEC, Noordwijk, Netherlands, HC

The role that the Cluster Joint Science Operations Center (JSOC) will play in the scientific operations of the Cluster mission is described. This includes the coordination of operations and commanding of the Cluster payload and the dissemination of science planning data to the community. A description of the JSOC design concepts and organization is given.
ESA

N94-19640# Swedish Inst. of Space Physics, Uppsala.
CO-ORDINATION OF GROUND-BASED OBSERVATIONS WITH CLUSTER
H. Opgenoorth *In* ESA, Cluster: Mission, Payload, and Supporting Activities Mar. 1993 p 299-305 (For primary document see N94-19622 04-12)
Copyright Avail: CASI HC A02/MF A03; ESA, EPD, ESTEC, Noordwijk, Netherlands, HC

The prime scientific topics for the planned Cluster/ground based coodination are identified and the main advantages of using coordinated observations from Cluster and ground based instruments are addressed. Some of the instruments that are expected to participate in the Cluster/ground based coordination are listed. The preparation of reduced ground based data sets in the form of indices, summary data sets, and refined high resolution data is addressed. The establishment of a common data base is considered. Interface with other satellite missions or coordinated ground based activities is discussed.
ESA

N94-19641# Centre National d'Etudes des Telecommunications, Issy-les-Moulineaux (France).
EUROPEAN NETWORK FOR THE NUMERICAL SIMULATION OF SPACE PLASMAS c14
G. Chanteur and A. Roux *In* ESA, Cluster: Mission, Payload, and Supporting Activities Mar. 1993 p 307-317 (For primary document see N94-19622 04-12)
Copyright Avail: CASI HC A02/MF A03; ESA, EPD, ESTEC, Noordwijk, Netherlands, HC

The European Numerical Simulation Network (ENSN), which is comprised of ten European groups experienced in working on the numerical simulation of space plasmas, is addressed. The network aims at providing theoretical support in the preparation of ESA's Cluster mission. The following ENSN tasks which have been identified as essential are discussed: the setting up of thematic working groups to direct specific efforts on the prime objectives of the Cluster mission; the development of new numerical simulation codes with emphasis on the tools that will be necessary to investigate the physics of the boundary layers that are the prime scientific targets of Cluster; the sharing of the development of the visualization software necessary for the display of numerical simulation results on work stations; the development of software models of Cluster instruments and the implementation of these software models into numerical simulations runs.
ESA

13 ASTRODYNAMICS

Includes powered and free-flight trajectories; and orbital and launching dynamics.

N94-19366*# Applied Research, Inc., Huntsville, AL.
AUTOMATED RENDEZVOUS AND CAPTURE DEMONSTRATION STUDY Final Report
11 Jun. 1993 18 p
(Contract NAS8-39211)
(NASA-CR-192587; NAS 1.26:192587) Avail: CASI HC A03/MF A01

This study was instituted to assist NASA and MSFC in the development of ground and flight options to demonstrate the capability of Automated Rendezvous and Capture (AR&C). Study goals placed emphasis on low cost approaches and the need to be responsive to newly developing programs and studies such as Space Station Freedom and the Cargo Transfer Vehicle. This study provides an assessment of vehicle options and AR&C requirements to assist in the meaningful development of an AR&C capability. This report documents study activities performed at Applied Research, Inc. (ARI) between 1 Apr. 1992 and May 1993.
Author (revised)

14 GROUND SUPPORT SYSTEMS AND FACILITIES (SPACE)

Includes launch complexes, research and production facilities; ground support equipment, e.g., mobile transporters; and simulators.

For related information see also *09 Research and Support Facilities (Air).*

N94-19639# Rutherford Appleton Lab., Chilton (England). Space Science Dept.
THE CLUSTER JOINT SCIENCE OPERATIONS CENTRE
E. Dunford, P. Vaughan, E. Golton, and T. Dimbylow *In* ESA, Cluster: Mission, Payload, and Supporting Activities Mar. 1993 p 291-297 (For primary document see N94-19622 04-12)
Copyright Avail: CASI HC A02/MF A03; ESA, EPD, ESTEC, Noordwijk, Netherlands, HC

N94-19641# Centre National d'Etudes des Telecommunications, Issy-les-Moulineaux (France).
EUROPEAN NETWORK FOR THE NUMERICAL SIMULATION OF SPACE PLASMAS
G. Chanteur and A. Roux *In* ESA, Cluster: Mission, Payload, and Supporting Activities Mar. 1993 p 307-317 (For primary document see N94-19622 04-12)
Copyright Avail: CASI HC A02/MF A03; ESA, EPD, ESTEC, Noordwijk, Netherlands, HC

15 LAUNCH VEHICLES AND SPACE VEHICLES

Includes boosters; operating problems of launch/space vehicle systems; and reusable vehicles.

For related information see also *20 Spacecraft Propulsion and Power.*

N94-18411# RAND Corp., Santa Monica, CA.
AN EVOLUTIONARY APPROACH TO SPACE LAUNCH COMMERCIALIZATION
Brian G. Chow 1993 134 p
(Contract MDA903-90-C-0004)
(AD-A269861) Avail: CASI HC A07/MF A02

The findings and recommendations of this study fall into two groups: Department of Defense (DoD) space launch procurement and DoD steps to strengthen U.S. launch competitiveness. Our analytic results support the choices that the Air Force and the Navy have made since 1985 in the methods of procuring launch services and in the degree of government oversight stipulated in these launch contracts. We further found that the Air Force's upcoming Medium Launch Vehicle-3 (MLV-3) procurement is DoD's most suitable major program to be procured with commercial practices over the next ten years. We recommend that the MLV-3 Request For Proposal (RFP) include commercial launches as an option and that the Air Force consider this option. To help strengthen launch competitiveness, we recommend that DoD concentrate its new launcher development on the most commercially relevant (MCR) range, which is the capability to lift 10,000 to 50,000 lbs of payload into low earth orbits (LEO's).
DTIC

N94-18760 Air Force Inst. of Tech., Wright-Patterson AFB, OH. Foreign Aerospace Science and Technology Center.
DYNAMIC RESPONSE ANALYSIS OF COMPOSITE STRUCTURAL MEMBERS DURING MISSILE LAUNCH
Lianzhu He and Peiling Zhao 14 Sep. 1993 12 p Transl. into ENGLISH from Hangkong Xuebao (Aeronautics), China, v. 13, no. 8 Aug. 1992 p 448-451 Limited Reproducibility: More than 20% of this document may be affected by microfiche quality
(AD-A270023; FASTC-ID(RS)T-0201-93) Avail: CASI HC A03

By analyzing the dynamic characteristics and the dynamic response of composite structural members of aircraft wings, the article presents the methods and steps for computational analysis, as well as further processing of the analytical results, in addition to suggestions for design improvements. It was found that improved lamina design can eliminate design weakness since local vibration phenomena were discovered in the prototype design when the dynamic characteristics of structural members were analyzed. By comparing three computational missile launch variants for outboard wing, mid-wing, and inner-wing, the values of the dynamic response in the most serious situation are given. Finally, the dynamic strength is determined. DTIC

16 SPACE TRANSPORTATION

Includes passenger and cargo space transportation, e.g., shuttle operations; and space rescue techniques.

For related information see also *03 Air Transportation and Safety* and *18 Spacecraft Design, Testing and Performance.* For space suits see *54 Man/System Technology and Life Support.*

N94-18321 Naval Surface Warfare Center, Dahlgren, VA.
NSWCWODET PARTICIPATION IN SPACE SHUTTLE MISSION STS-46
John V. Foltz 20 Jul. 1993 24 p Limited Reproducibility: More than 20% of this document may be affected by microfiche quality
(AD-A268875; NSWCDD/TR-92/472) Avail: CASI HC A03

NSWCWODET submitted 27 specimens for space flight STS-46 exposure on the space shuttle. The sample set included various carbide, oxide, and phosphate coatings which are being developed to protect space structural and thermal management components from the atomic oxygen present in low earth orbits; structural carbon-carbon composite material; and a space mirror made of foam metal matrix composite. At this writing, the samples returned from the orbital exposure are being analyzed to determine the degree of reactivity with the space environment. DTIC

N94-18669*# National Aeronautics and Space Administration. Lyndon B. Johnson Space Center, Houston, TX.
HUMAN TRANSPORTATION SYSTEM (HTS) STUDY: EXECUTIVE SUMMARY
N. Lance, M. S. Geyer, and M. T. Gaunce Oct. 1993 82 p
(RTOP 906-11-01-01)
(NASA-TM-104780; S-740; NAS 1.15:104780) Avail: CASI HC A05/MF A01

Work completed under the Human Transportation System Study is summarized. This study was conducted by the New Initiatives Office at JSC with the technical support of Boeing, General Dynamics, Lockheed, McDonnell-Douglas, Martin Marietta, and Rockwell. The study was designed to generate information on determining the appropriate path to follow for new system development to meet the Nation's space transportation needs. The study evaluates 18 transportation architecture options using a parametric set of mission requirements. These options include use of current systems as well as proposed systems to assess the impact of various considerations, such as the cost of alternate access, or the benefit of separating people and cargo. The architecture options are compared to each other with six measurable evaluation criteria or attributes. They are the following: funding profile, human safety, probability of mission success, architecture cost risk, launch schedule confidence, and environmental impact. Values for these attributes are presented for the architecture options, with pertinent conclusions and recommendations. Author (revised)

N94-18670*# National Aeronautics and Space Administration. Lyndon B. Johnson Space Center, Houston, TX.
HUMAN TRANSPORTATION SYSTEM (HTS) STUDY, VOLUME 1 Final Report
N. Lance, M. S. Geyer, and M. T. Gaunce Oct. 1993 427 p
(RTOP 906-11-01-01)
(NASA-TM-104779; S-739-Vol-1; NAS 1.15:104779) Avail: CASI HC A19/MF A04

Work completed under the Human Transportation System Study is summarized. This study was conducted by the New Initiatives Office at JSC with the technical support of Boeing, General Dynamics, Lockheed, McDonnell-Douglas, Martin Marietta, and Rockwell. The study was designed to generate information on determining the appropriate path to follow for new system development to meet the Nation's space transportation needs. The study evaluates 18 transportation architecture options using a parametric set of mission requirements. These options include use of current systems as well as proposed systems to assess the impact of various considerations, such as the cost of alternate access, or the benefit of separating people and cargo. The architecture options are compared to each other with six measurable evaluation criteria or attributes. They are the following: funding profile, human safety, probability of mission success, architecture cost risk, launch schedule confidence, and environmental impact. Values for these attributes are presented for the architecture options, with pertinent conclusions and recommendations. Author (revised)

N94-18820*# Boeing Defense and Space Group, Huntsville, AL.
SPACE TRANSFER CONCEPTS AND ANALYSES FOR EXPLORATION MISSIONS Final Report
Sep. 1993 21 p
(Contract NAS8-37857)
(NASA-CR-193876; NAS 1.26:193876) Avail: CASI HC A03/MF A01

The current technical effort is part of the fourth phase of a broad-scoped and systematic study of space transfer concepts for human lunar and Mars missions. The study addresses the costs of the First Lunar Outpost habitat and alternatives to this habitat. Author

N94-18920* National Aeronautics and Space Administration, Washington, DC.
ROBOTICS (Videotape)
Aug. 1985 Videotape: 2 min. 51 sec. playing time, in color, with sound
(NASA-TM-109351; NONP-VT-94-198198) Avail: CASI VHS A01/BETA A22

An overview of research being done into the use of robotic devices in space by MSFC is discussed. The video includes footage and explanations of robots being used to blast layers of thermal coating from the Space Shuttle's external tanks, the Shuttle's Remote Manipulator Arm, and animations of an Orbiting Maneuvering Vehicle to retrieve and repair satellites. CASI

N94-18954* National Aeronautics and Space Administration. Marshall Space Flight Center, Huntsville, AL.
SHUTTLE-C, THE FUTURE IS NOW (Videotape)
Feb. 1989 Videotape: 7 min. 12 sec. playing time, in color, with sound
(NASA-TM-109355; NONP-VT-94-198202) Avail: CASI VHS A01/BETA A22

This video details plans for Shuttle-C, an unmanned heavy launch vehicle to carry payloads into orbit. Computer animations depict the Shuttle-C, which uses the same recoverable external boosters, external fuel tank and main orbiter engines as the existing Space Shuttles, through liftoff and entry into orbit, where it progressively jettisons the cargo shroud, external fuel tank, and nose shroud. The video also shows computer simulations of a remotely controlled orbital maneuvering vehicle positioning preassembled components of a Space Station and delivering planetary probes and lunar exploration materials to orbit. CASI

N94-18955* National Aeronautics and Space Administration, Washington, DC.
RETURN TO SPACE (Videotape)
Aug. 1989 Videotape: 14 min. 30 sec. playing time, in color, with sound
(NASA-TM-109356; NONP-VT-94-198203) Avail: CASI VHS A01/BETA A22

This video documents the preparations for Shuttle Flight STS-26 with

Shuttle Discovery, NASA's return to manned space flight after the Challenger disaster. Footage and descriptions document such changes to the new Shuttle as new joints, improved insulation, and added O-rings to the solid rocket boosters; new safety hardware and procedures such as parachute and sidewire evacuations during liftoff, and new pressure suits; modified landing gear, brakes, and nose wheel steering, as well as a modified landing runway. Also profiled are the 5 member crew of all veteran Shuttle astronauts, the TDRS 3 Satellite to be released from the cargo bay in orbit, and 11 commercial and student experiments to be performed during the mission. CASI

N94-19071* National Aeronautics and Space Administration. Marshall Space Flight Center, Huntsville, AL.
PATHFINDER: SHUTTLE EXHIBIT (Videotape)
Aug. 1988 Videotape: 1 min. 46 sec. playing time, in color, with sound
(NASA-TM-109357; NONP-VT-94-198204) Avail: CASI VHS A01/BETA A22

This video introduces the Pathfinder Shuttle Exhibit, a joint project between the Marshall Space Flight Center and the State of Alabama's Space and Rocket Center in Huntsville. The exhibit features a never flown Shuttle vehicle, Pathfinder, that was used in early ground tests in the Shuttle Program, as well as an actual external fuel tank and set of booster rockets. The video includes footage of actual launches, the Pathfinder Shuttle Exhibit, and shots of the Space Camp at Alabama's Space and Rocket Center. CASI

N94-19765 Naval Academy, Annapolis, MD.
A STEREOSCOPIC VISION SYSTEM WITH APPLICATIONS TO AUTOMATED DOCKING AND TRACKING Trident Scholar Project Report No. 201
Michael M. Hsu 17 May 1993 80 p Limited Reproducibility: More than 20% of this document may be affected by microfiche quality
(AD-A270754) Avail: CASI HC A05

A current project of great importance to the National Aeronautics and Space Administration is the development of an automated docking and tracking system to facilitate autonomous operations in space. Such a system would have to be able to determine the relative positions, velocities, and orientations of a multitude of bodies. A stereoscopic vision system was developed to implement an automated docking solution. This system used artificial neural networks to identity beacons or fixed points on the objects to be tracked. Specifically, this research sought to solve the problems inherent in the planned 1995 docking of the U.S. Space Shuttle to the former Soviet Space Station Mir. In addition to the basics of an optical ranging and object-recognition system, a simple user interface for operation monitoring was designed. Specifically, the coordinates of the Space Station, shuttle waypoints, and smooth trajectory position, velocity, and acceleration information were calculated and displayed. A mock docking was also simulated, with the vision system providing the range and orientation data. By placing the vision system at known coordinates and checking its computed trajectory, the accuracy of the algorithms and given hardware were checked. DTIC

17 SPACE COMM., SPACECRAFT COMM., COMMAND & TRACKING

Includes telemetry; space communications networks; astronavigation and guidance; and radio blackout.

For related information see also *04 Aircraft Communications and Navigation* and *32 Communications and Radar.*

N94-19313*# National Aeronautics and Space Administration. Lewis Research Center, Cleveland, OH.
MULTICHANNEL ERROR CORRECTION CODE DECODER
Paul K. Wagner (Sverdrup Technology, Inc., Brook Park, OH.) and William D. Ivancic Dec. 1993 11 p Proposed for presentation at the 15th International Communication Satellite Systems Conference, San Diego, CA, 28 Feb. - 3 Mar. 1994; sponsored by AIAA
(RTOP 506-72-21)
(NASA-TM-106331; E-8092; NAS 1.15:106331; AIAA Paper 94-1025)
Avail: CASI HC A03/MF A01

A brief overview of a processing satellite for a mesh very-small-aperture (VSAT) communications network is provided. The multichannel error correction code (ECC) decoder system, the uplink signal generation and link simulation equipment, and the time-shared decoder are described. The testing is discussed. Applications of the time-shared decoder are recommended. Author (revised)

18 SPACECRAFT DESIGN, TESTING AND PERFORMANCE

Includes satellites; space platforms; space stations; spacecraft systems and components such as thermal and environmental controls; and attitude controls.

For life support systems see *54 Man/System Technology and Life Support.* For related information see also *05 Aircraft Design, Testing and Performance, 39 Structural Mechanics,* and *16 Space Transportation.*

N94-17765*# National Aeronautics and Space Administration. Langley Research Center, Hampton, VA.
PACKAGING, DEPLOYMENT, AND PANEL DESIGN CONCEPTS FOR A TRUSS-STIFFENED 7-PANEL PRECISION DEPLOYABLE REFLECTOR WITH FEED BOOM
Walter L. Heard, Jr., Timothy J. Collins, James W. Dyess, Scott Kenner, and Harold G. Bush Nov. 1993 33 p
(RTOP 506-43-41-02)
(NASA-TM-109000; NAS 1.15:109000) Avail: CASI HC A03/MF A01

A concept is presented for achieving a remotely deployable truss-stiffened reflector consisting of seven integrated sandwich panels that form the reflective surface, and an integrated feed boom. The concept has potential for meeting aperture size and surface precision requirements for some high-frequency microwave remote sensing applications. The packaged reflector/feed boom configuration is a self-contained unit that can be conveniently attached to a spacecraft bus. The package has a cylindrical envelope compatible with typical launch vehicle shrouds. Dynamic behavior of a deployed configuration having a 216-inch focal length and consisting of 80-inch-diameter, two-inch-thick panels is examined through finite-element analysis. Results show that the feed boom and spacecraft bus can have a large impact on the fundamental frequency of the deployed configuration. Two candidate rib-stiffened sandwich panel configurations for this application are described, and analytical results for panel mass and stiffness are presented. Results show that the addition of only a few rib stiffeners, if sufficiently deep, can efficiently improve sandwich panel stiffness. Author

N94-17782# Lawrence Livermore National Lab., CA.
PREDICTED STRUCTURAL RESPONSE OF THE LIGHTWEIGHT-INTERCEPTOR TECHNOLOGY DEMONSTRATION VEHICLE
D. J. Trummer and S. M. Bahowick 1 Nov. 1992 64 p
(Contract W-7405-eng-48)
(DE93-014676; UCRL-ID-112131) Avail: CASI HC A04/MF A01 (US Sales Only)

The Advanced Implementation Technology Program (AIT) at Lawrence Livermore National Laboratory has been participating in the development of a lightweight-interceptor technology demonstration vehicle. This vehicle, commonly referred to as a probe, is a small spacecraft that is self-contained, lightweight, and highly maneuverable. The probe contains a guidance and control system that requires complete information on the dynamic response of the probe during operation. A finite element model of the probe was generated to provide information on the dynamic response of the probe when subjected to launch and operational loads. In order to validate the analytical results, a mass mockup of the probe was constructed and an experimental modal survey was performed to determine the natural frequencies, mode shapes, and damping values for each natural mode of the mockup. The results of the modal survey were then compared with the finite element model, and the necessary changes were incorporated into the finite element model. The validated finite element model could then be used to study the impact of structural or loading changes on probe mechanical vibration modes and sensor deflections. DOE

N94-18149 Naval Research Lab., Washington, DC.
UVPI IMAGING FROM THE LACE SATELLITE: THE NIHKA ROCKET PLUME Interim Report
H. W. Smathers, D. M. Horan, J. G. Cardon, E. R. Malaret, and J. E. Brandenburg 12 Jul. 1993 92 p Limited Reproducibility: More than 20% of this document may be affected by microfiche quality
(AD-A268456; NRL/FR/8121-93-9537) Avail: Issuing Activity (Defense Technical Information Center (DTIC))

The Nihka flight was the first demonstration of the ability of the Ultraviolet Plume Instrument (UVPI), carried abroad the LACE (Low-power Atmospheric Compensation Experiment) satellite, to observe missiles in flight above the atmosphere. The UVPI is a small, plume-tracking instrument flown on the Naval Research Laboratory's LACE satellite, which was launched on 14 Feb. 1990. The Nihka was launched from the Wallops Island Launch Facility in Virginia to coincide with a LACE pass. The two cameras of the UVPI were used to observe the Nihka in the ultraviolet. These cameras were a tracker camera, viewing over a relatively wide field and broad spectrum, and a plume camera that has a narrow field of view (0.180 deg by 0. 135 deg) and can observe sources through any of four filters. A three-stage sounding rocket (called Black Brant X) was used for the test. The third stage, or Nihka, reached 190 km altitude and was successfully detected and tracked by the UVPI from a range of 448 to 463 km. The Nihka plume was successfully tracked for 3.23 seconds; 91 images of plume data (each 1/30th of a second) were acquired by using the first plume-camera filter in the 235 to 350 nm range. DTIC

N94-18264 Keo Consultants, Brookline, MA.
SPACE DEBRIS DETECTION Final Report, 7 Mar. 1991 - 6 Nov. 1992
Robert H. Eather 23 Dec. 1992 40 p Limited Reproducibility: More than 20% of this document may be affected by microfiche quality
(Contract F19628-91-C-0054)
(AD-A269254; PL-TR-93-2058) Avail: CASI HC A03

A feasibility study on the possibility of detecting less than or = 10 cm space debris using a large-aperture ground-based telescope (with an intensified CCD detector) was completed, showing that detection should be possible. A detector system was designed and built, and installed on the 2.54 m WRDC telescope at Wright Patterson AFB. Bad seeing conditions in the Dayton area prevented the expected debris detection. Subsequently, a small 40 cm telescope was built and operated from the Haystack Observatory (Groton, MA). Known objects were used to test pointing and acquisition procedures, and the system was then shipped to Rattlesnake Observatory (Richland, WA) for participation in the ODERAC's debris calibration experiment from the Space Shuttle. This experiment failed, and our instrument has been stored at Rattlesnake in anticipation of a new ODERAC's flight in late 1993. DTIC

N94-18408# Space and Missile Systems Organization, Los Angeles Air Force Station, CA.
CONTACT: AN AIR FORCE TECHNICAL REPORT ON MILITARY SATELLITE CONTROL TECHNOLOGY Final Report, Jan. - Jun. 1993
Christopher K. Weakley 9 Jul. 1993 52 p
(AD-A269375) Avail: CASI HC A04/MF A01

This technical report focuses on Military Satellite Control Technologies and their application to the Air Force Satellite Control Network (AFSCN). This report is a compilation of articles that provide an overview of the AFSCN and the Advanced Technology Program, and discusses relevant technical issues and developments applicable to the AFSCN. Among the topics covered are articles on Future Technology Projections; Future AFSCN Topologies; Modeling of the AFSCN; Wide Area Communications Technology Evolution; Automating AFSCN Resource Scheduling; Health & Status Monitoring at Remote Tracking Stations; Software Metrics and Tools for Measuring AFSCN Software Performance; Human-Computer Interface Working Group; Trusted Systems Workshop; and the University Technical Interaction Program. In addition, Key Technology Area points of contact are listed in the report. DTIC

N94-18470# Naval Postgraduate School, Monterey, CA.
PARALLELIZATION OF THE AIR FORCE SPACE COMMAND (AFSPACECOM) SATELLITE MOTION MODELS M.S. Thesis
Sara R. Ostrom Mar. 1993 93 p
(AD-A269327) Avail: CASI HC A05/MF A01

The Air Force Space Command (AFSPACECOM) uses an analytic satellite motion model based on the Brouwer theory, referred to as SGP4, for near-earth objects, and another satellite motion model based on the work of Hujsak, referred to as SDP4, for deep-space objects. These models assist in tracking over 7000 objects around the Earth each day. Original satellite motion model used by the AFSPACECOM based on the work of Kozai and Brouwer, known as the Simplified General Perturbations model or SGP, is an analytic model still being used at several sites. Based on the increasing number of space objects that require tracking and the desire for accuracy, there is a growing need to reduce computation time in implementing satellite motion models. Parallel computing offers one method to achieve this objective. This thesis investigates the parallel computing potential of SGP, SGP4, and SDP4 using the Intel iPSC/2 hypercube multicomputer. This thesis chooses a parallel algorithm and applies it to SGP, SGP4, and SDP4 for implementation on the hypercube, and reports on the potential reduction in computer time by first considering only the calculational portion of the algorithm and then including the effects of the reading and writing portions. DTIC

N94-18718# Phillips Lab., Kirtland AFB, NM.
CONSTANT-THRUST ORBIT-RAISING TRANSFER CHARTS Final Report, Aug. 1992 - May 1993
Salvatore Alfano and James D. Thorne Jul. 1993 23 p
(AF Proj. 2181)
(AD-A269088; AD-E201589; PL-TR-93-1010) Avail: CASI HC A03/MF A01

This report outlines a method to generate minimum-fuel trajectories between coplanar circular orbits for a vehicle with constant thrust. The rocket equation models the effects of continuous fuel expenditure while also serving to recast the solution in terms of accumulated velocity change. These orbit-raising solutions are globally mapped with no restrictions on initial thrust magnitude, intermediate eccentricity, or number of revolutions of the central body. Several examples are presented to verify the transfer charts and familiarize the reader with their use. These charts are useful tools for mission planners and satellite designers to assess preliminary fuel requirements for constant-thrust systems or to compare different propulsion technologies. DTIC

N94-18921* National Aeronautics and Space Administration, Washington, DC.
LDEF UPDATE (Videotape)
Oct. 1990 Videotape: 3 min. 17 sec. playing time, in color, with sound
(NASA-TM-109352; NONP-VT-94-198199) Avail: CASI VHS A01/BETA A22

This video explores the research being done on the Long Duration Exposure Facility (LDEF), a satellite carrying 57 experiments designed to study the effects of the space environment, which had been in orbit for almost 6 years, and was retrieved and brought back to Earth by the Space Shuttle Astronauts. The video shows scenes of the retrieval of LDEF, as well as scenes of ongoing research into the data returned with the satellite from experiments on external coating, contamination of optical materials by thermal control paint, the effects of cosmic rays on different materials, and the effect of the space environment on 12 million tomato seeds that have since been planted. CASI

N94-18922* National Aeronautics and Space Administration, Washington, DC.
DESIGNING SPACE STATION (Videotape)
Oct. 1986 Videotape: 3 min. 23 sec. playing time, in color, with sound
(NASA-TM-109353; NONP-VT-94-198200) Avail: CASI VHS A01/BETA A22

An overview of preparations for the construction of Space Station Freedom (SSF) is presented. The video includes footage of astronauts testing materials for erectable structures in space both in the Shuttle bay while in orbit and in a neutral buoyancy tank at McDonald Douglas' Underwater Test Facility. Also shown are footage of robot systems that will assist the astronauts in building SSF, a computer simulation of an Orbiting Maneuvering Vehicle, solar dynamic mirrors that will power SSF, and mockups of the living quarters of the SSF. CASI

N94-18942# Lawrence Livermore National Lab., CA.
DYNAMIC CHARACTERIZATION OF A LIGHTWEIGHT, HIGHLY MANEUVERABLE SPACECRAFT USING MODAL AND FINITE ELEMENT ANALYSES
P. A. Manning, R. B. Burdick, and T. G. Woehrle Nov. 1992 10 p Presented at the 11th International Modal Analysis Conference, Kissimmee, FL, 1-4 Feb. 1993
(Contract W-7405-eng-48)
(DE93-018095; UCRL-JC-110987; CONF-930241-2) Avail: CASI HC A02/MF A01

The Lawrence Livermore National Laboratory is engaged in a technology development project which includes designing a lightweight, autonomous, highly maneuverable space vehicle, commonly referred to as a probe. The current probe design includes a guidance and control system that requires complete information on the dynamic response of the probe during operation. A finite element model of the probe was constructed to provide analytical information on the dynamic response to specific operational inputs. In order to verify the assumptions made in the model, a mass mock-up of the probe was constructed at LLNL and an experimental modal survey was performed to determine the frequencies, damping values and deflection shapes for each natural mode of the mock-up. The experimental modal parameters were compared with the parameters obtained through modal analysis of the finite element model to provide a measure of the correlation between the model and the actual structure. This report describes the experimental modal testing and analysis of the mass mock-up and compares the experimental results with the finite element results. DOE

N94-18965* National Aeronautics and Space Administration. Goddard Space Flight Center, Greenbelt, MD.
TDRS PRESS RELEASE (Videotape)
Oct. 1988 Videotape: 7 min. playing time, in color, with sound
(NASA-TM-109373; NONP-VT-94-198220) Avail: CASI VHS A01/BETA A22

This material is released to both local and national broadcast media showing the Tracking and Data Relay Satellite (TDRS). The tape has split audio to facilitate ease of customizing for individual broadcast formats. CASI

N94-19275# Lawrence Livermore National Lab., CA.
MODIL CRYOCOOLER PRODUCIBILITY DEMONSTRATION PROJECT RESULTS
G. E. Cruz and R. M. Franks Apr. 1993 10 p Presented at the Society of Photo-Optical Instrumentation Engineers OE/Aerospace Science and Sensing Meeting, Orlando, FL, 11-16 Apr. 1993
(Contract W-7405-eng-48)
(DE93-017981; UCRL-JC-112216; CONF-930445-21) Avail: CASI HC A02/MF A01

The production of large quantities of spacecraft needed by SDIO will require a cultural change in design and production practices. Low rates of production and the need for exceedingly high reliability has driven the industry to custom designed, hand crafted, and exhaustively tested satellites. These factors have mitigated against employing design and manufacturing cost reduction methods commonly used in tactical missile production. Additional challenges to achieving production efficiencies are presented by the SDI spacecraft mission requirement. IR sensor systems, for example, are comprised of subassemblies and components that require the design, manufacture, and maintenance of ultra-precision tolerances over challenging operational lifetimes. These IR sensors demand the use of reliable, closed loop, cryogenic refrigerators or active cryocoolers to meet stringent system acquisition and pointing requirements. The authors summarize some spacecraft cryocooler requirements and discuss observations regarding industry's current production capabilities of cryocoolers. The results of the Lawrence Livermore National Laboratory (LLNL) Spacecraft Fabrication and Test (SF&T) MODIL's Phase I producibility demonstration project is presented. DOE

N94-19371*# Colorado Univ., Boulder. Center for Space Construction.
[ACTIVITIES OF THE CENTER FOR SPACE CONSTRUCTION] Annual Report, 1 October 1992 - 30 Sep. 1993
1 Oct. 1993 88 p
(Grant NAGw-1388)
(NASA-CR-193717; NAS 1.26:193717) Avail: CASI HC A05/MF A01

The Center for Space Construction (CSC) at the University of Colorado at Boulder is one of eight University Space Engineering Research Centers established by NASA in 1988. The mission of the center is to conduct research into space technology and to directly contribute to space engineering education. The center reports to the Department of Aerospace Engineering Sciences and resides in the College of Engineering and Applied Science. The college has a long and successful track record of cultivating multi-disciplinary research and education programs. The Center for Space Construction is prominent evidence of this record. At the inception of CSC, the center was primarily founded on the need for research on in-space construction of large space systems like space stations and interplanetary space vehicles. The scope of CSC's research has now evolved to include the design and construction of all spacecraft, large and small. Within this broadened scope, our research projects seek to impact the underlying technological basis for such spacecraft as remote sensing satellites, communication satellites, and other special purpose spacecraft, as well as the technological basis for large space platforms. The center's research focuses on three areas: spacecraft structures, spacecraft operations and control, and regolith and surface systems. In the area of spacecraft structures, our current emphasis is on concepts and modeling of deployable structures, analysis of inflatable structures, structural damage detection algorithms, and composite materials for lightweight structures. In the area of spacecraft operations and control, we are continuing our previous efforts in process control of in-orbit structural assembly. In addition, we have begun two new efforts in formal approach to spacecraft flight software systems design and adaptive attitude control systems. In the area of regolith and surface systems, we are continuing the work of characterizing the physical properties of lunar regolith, and we are at work on a project on path planning for planetary surface rovers. Author (revised)

N94-19614# Technische Univ., Delft (Netherlands). Faculty of Aerospace Engineering.
START USER MANUAL VERSION 2.1
E. Mooij Jul. 1993 119 p
(LR-726; ETN-93-95030) Avail: CASI HC A06/MF A02

The Simulation Tool for Atmospheric Reentry Trajectories (START) version 2.1 is presented. The software is capable of doing six degrees of freedom reentry simulations, starting with a deorbit burn maneuver in orbit. After the atmospheric entry, the descent under a parachute can be simulated as well. Central bodies included are: Earth, the Moon, Mars and Titan. The program was equipped with a menu oriented user interface, giving full access to the input data. The manual is focused on how to use the software. Before discussing the capabilities of START, a short overview of START and some general remarks on the user interface are given. ESA

N94-19787# Naval Research Lab., Washington, DC.
UVPI IMAGING FROM THE LACE SATELLITE: THE STRYPI ROCKET PLUME Interim Report
H. W. Smathers, D. M. Horan, J. G. Cardon, E. R. Malaret, and M. Singh 17 Sep. 1993 268 p
(AD-A270967; NRL/FR/8121-93-9526) Avail: CASI HC A12/MF A03

The Ultraviolet Plume Instrument (UVPI) is a small plume-tracking instrument that was flown on the Naval Research Laboratory's Low-power Atmospheric Compensation Experiment (LACE) satellite. The UVPI plume camera has a narrow field of view (0.180 deg by 0.135 deg), and it observes sources through any of four filters with passbands of 195 to 295 nm, 220 to 320 nm, 235 to 350 nm, and 300 to 320 nm. The Strypi rocket was launched from Hawaii on 18 Feb. 1991. The second (Antares) and the third (Star 27) stages reached 110 km altitude and were successfully detected and tracked by the UVPI from a range of 450 to 550 km. The spectral radiance and spectral radiant intensities of the missile plumes were extracted from these images for the four passbands. DTIC

N94-19183*# Rockwell International Corp., Cocoa Beach, FL. Space Systems Div.
ISOBUS: A NEW VERSATILE SPACECRAFT PLATFORM USING SHUTTLE SMALL PAYLOADS
David Tamir, Rex W. Ridenoure (Jet Propulsion Lab., California Inst. of Tech., Pasadena.), and R. Gilbert Moore (Utah State Univ., Logan.) *In* NASA. Goddard Space Flight Center, The 1993 Shuttle Small Payloads Symposium Oct. 1993 p 195-198 (For primary document see N94-19162

04-12)
Avail: CASI HC A01/MF A03

N94-19635# European Space Agency. European Space Research and Technology Center, ESTEC, Noordwijk (Netherlands).
THE CLUSTER SPACECRAFT
J. Credland and G. Lehn (Dornier System G.m.b.H., Friedrichshafen, Germany.) *In its* Cluster: Mission, Payload, and Supporting Activities Mar. 1993 p 235-250 Original contains color illustrations (For primary document see N94-19622 04-12)
Copyright Avail: CASI HC A03/MF A03; ESA, EPD, ESTEC, Noordwijk, Netherlands, HC

19 SPACECRAFT INSTRUMENTATION

For related information see also *06 Aircraft Instrumentation* and *35 Instrumentation and Photography.*

N94-18956* National Aeronautics and Space Administration. Marshall Space Flight Center, Huntsville, AL.
ASTRO-1 TO EXPLORE INVISIBLE UNIVERSE (Videotape)
Nov. 1989 Videotape: 3 min. 55 sec. playing time, in color, with sound (NASA-TM-109360; NONP-VT-94-198207) Avail: CASI VHS A01/BETA A22

This video explains the ASTRO 1 observatory and its ten day mission aboard SpaceLab on NASA's Space Shuttle, which Marshall Space Flight Center (MSFC) and Goddard Space Flight Center (GSFC) astronomers will use to study distant stars, supernovae, and black holes. The observatory contains ultraviolet and x ray telescopes that will capture images earth-bound observatories can't, due to interference from the earth's atmosphere. The video contains footage of the instrument being loaded on the shuttle, animations of anticipated images to be captured, and scenes of the SpaceLab Control Center at MSFC. CASI

N94-18338*# Johns Hopkins Univ., Laurel, MD. Applied Physics Lab.
EXPERIENCE WITH CUSTOM PROCESSORS IN SPACE FLIGHT APPLICATIONS
M. E. Fraeman, J. R. Hayes, D. A. Lohr, B. W. Ballard, R. L. Williams, and R. M. Henshaw *In* Idaho Univ., The 1991 3rd NASA Symposium on VLSI Design 1991 13 p (For primary document see N94-18337 04-33)
Avail: CASI HC A03/MF A04

N94-19172*# European Space Agency. European Space Research and Technology Center, ESTEC, Noordwijk (Netherlands).
ATTITUDE SENSOR PACKAGE
R. Aceti, M. Trischberger, P. J. Underwood, A. Pomilia (Officine Galileo S.p.A., Florence, Italy.), M. Cosi (Officine Galileo S.p.A., Florence, Italy.), and F. Boldrini (Officine Galileo S.p.A., Florence, Italy.) *In* NASA. Goddard Space Flight Center, The 1993 Shuttle Small Payloads Symposium Oct. 1993 p 75-85 (For primary document see N94-19162 04-12)
Avail: CASI HC A03/MF A03

N94-19174*# Naval Research Lab., Washington, DC. Center for Space Research.
A HIGH RESOLUTION ULTRAVIOLET SHUTTLE GLOW SPECTROGRAPH
George R. Carruthers *In* NASA. Goddard Space Flight Center, The 1993 Shuttle Small Payloads Symposium Oct. 1993 p 97-105 (For primary document see N94-19162 04-12)
Avail: CASI HC A02/MF A03

N94-19179*# Trieste Univ. (Italy).
THE STAR IDENTIFICATION, POINTING AND TRACKING SYSTEM OF UVSTAR, AN ATTACHED PAYLOAD INSTRUMENT SYSTEM FOR THE SHUTTLE HITCHHIKER-M PLATFORM
Francesco DeCarlo, Roberto Stalio, Paolo Trampus, A. Lyle Broadfoot (Arizona Univ., Tucson.), Bill R. Sandel (Arizona Univ., Tucson.), and Giovanni Sicuranza *In* NASA. Goddard Space Flight Center, The 1993 Shuttle Small Payloads Symposium Oct. 1993 p 153-167 (For primary document see N94-19162 04-12)
Avail: CASI HC A03/MF A03

N94-19630# Max-Planck-Inst. fuer Extraterrestrische Physik, Garching (Germany).
THE ELECTRON DRIFT INSTRUMENT FOR CLUSTER
G. Paschmann, F. Melzner, G. Haerendel, O. H. Bauer, W. Baumjohann, N. Sckopke, R. Treumann, C. E. McIlwain (California Univ., San Diego, La Jolla.), W. Fillius (California Univ., San Diego, La Jolla.), and E. C. Whipple (California Univ., San Diego, La Jolla.) et al *In* ESA, Cluster: Mission, Payload, and Supporting Activities Mar. 1993 p 115-132 (For primary document see N94-19622 04-12)
Copyright Avail: CASI HC A03/MF A03; ESA, EPD, ESTEC, Noordwijk, Netherlands, HC

N94-19633*# Max-Planck-Inst. fuer Aeronomie, Katlenburg-Lindau (Germany).
RAPID: THE IMAGING ENERGETIC PARTICLE SPECTROMETER ON CLUSTER
B. Wilken, W. Guettler, A. Korth, S. Livi, W. Weiss, F. Gliem (Technische Univ., Brunswick, Germany.), A. Muellers (Technische Univ., Brunswick, Germany.), R. Rathje (Technische Univ., Brunswick, Germany.), T. A. Fritz (Los Alamos National Lab., NM.), and J. F. Fennell (Aerospace Corp., Los Angeles, CA.) et al *In* ESA, Cluster: Mission, Payload, and Supporting Activities Mar. 1993 p 185-217 Sponsored by Deutsche Agentuer fuer Raumfahrtangelegenheite G.m.b.H.; Science Research Council; and Norweigian Research Council for Science and Humanities Original contains color illustrations (For primary document see N94-19622 04-12)
(NASA Order S-47197-E)
Copyright Avail: CASI HC A03/MF A03; ESA, EPD, ESTEC, Noordwijk, Netherlands, HC

N94-19634# Institut fuer Weltraumforschung, Graz (Austria).
ACTIVE SPACECRAFT POTENTIAL CONTROL: AN ION EMITTER EXPERIMENT FOR CLUSTER
W. Riedler, K. Torkar, F. Ruedenauer (Oesterreichisches Forschungszentrum Seibersdorf G.m.b.H., Vienna.), M. Fehringer (Oesterreichisches Forschungszentrum Seibersdorf G.m.b.H., Vienna.), W. Steiger (Oesterreichisches Forschungszentrum Seibersdorf G.m.b.H., Vienna.), A. Pedersen (European Space Agency. European Space Research and Technology Center, ESTEC, Noordwijk, Netherlands.), R. J. L. Grard (European Space Agency. European Space Research and Technology Center, ESTEC, Noordwijk, Netherlands.), R. Schmidt (European Space Agency. European Space Research and Technology Center, ESTEC, Noordwijk, Netherlands.), B. T. Narheim (Norwegian Defence Research Establishment, Kjeller.), and J. Troeim (Norwegian Defence Research Establishment, Kjeller.) et al *In* ESA, Cluster: Mission, Payload, and Supporting Activities Mar. 1993 p 219-234 Original contains color illustrations (For primary document see N94-19622 04-12)
Copyright Avail: CASI HC A03/MF A03; ESA, EPD, ESTEC, Noordwijk, Netherlands, HC

20 SPACECRAFT PROPULSION AND POWER

Includes main propulsion systems and components, e.g., rocket engines; and spacecraft auxilliary power sources.

For related information see also *07 Aircraft Propulsion and Power, 28 Propellants and Fuels, 44 Energy Production and Conversion,* and *15 Launch Vehicles and Space Vehicles.*

N94-17856*# National Aeronautics and Space Administration. Lewis Research Center, Cleveland, OH.
LOW POWER ARCJET SYSTEM SPACECRAFT IMPACTS
Eric J. Pencil, Charles J. Sarmiento, D. A. Lichtin (Martin Marietta Astro Space, Princeton, NJ.), J. W. Palchefsky (Martin Marietta Astro Space, Princeton, NJ.), and A. L. Bogorad (Martin Marietta Astro Space, Princeton, NJ.) Jun. 1993 33 p Presented at the 29th Joint Propulsion Conference and Exhibit, Monterey, CA, 28-30 Jun. 1993; sponsored by AIAA, SAE, ASME, and ASEE See also A93-50157
(RTOP 506-42-31)

(NASA-TM-106307; E-8048; NAS 1.15:106307; AIAA Paper 93-2392)
Avail: CASI HC A03/MF A01

Application of electrothermal arcjets on communications satellites requires assessment of integration concerns identified by the user community. Perceived risks include plume contamination of spacecraft materials, induced arcing or electrostatic discharges between differentially charged spacecraft surfaces, and conducted and radiated electromagnetic interference (EMI) for both steady state and transient conditions. A Space Act agreement between Martin Marietta Astro Space, the Rocket Research Company, and NASA's Lewis Research Center was established to experimentally examine these issues. Spacecraft materials were exposed to an arcjet plume for 40 hours, representing 40 weeks of actual spacecraft life, and contamination was characterized by changes in surface properties. With the exception of the change in emittance of one sample, all measurable changes in surface properties resulted in acceptable end of life characteristics. Charged spacecraft samples were benignly and consistently reduced to ground potential during exposure to the powered arcjet plume, suggesting that the arcjet could act as a charge control device on spacecraft. Steady state EMI signatures obtained using two different power processing units were similar to emissions measured in a previous test. Emissions measured in UHF, S, C, Ku and Ka bands obtained a null result which verified previous work in the UHF, S, and C bands. Characteristics of conducted and radiated transient emissions appear within standard spacecraft susceptibility criteria. Author

N94-17863# EG and G Energy Measurements, Inc., Idaho Falls.
MISSION NEEDS AND SYSTEM COMMONALITY FOR SPACE NUCLEAR POWER AND PROPULSION
David Buden, Anthony Zuppero, and Lawrence Redd (Department of Energy, Idaho Falls, ID.) 1993 7 p Presented at the 28th Intersociety Energy Conversion Engineering Conference, Atlanta, GA, 8-13 Aug. 1993
(Contract DE-AC07-76ID-01570)
(DE93-016557; EGG-M-93191; CONF-930804-11) Avail: CASI HC A02/MF A01

Nuclear power enables or significantly enhances a variety of space missions, whether near-Earth or for solar system exploration, lunar-Mars exploration, or recovery of near-Earth resources. Performance optimizations for individual missions lead to a large number of power and propulsion systems to be developed. However, the realities of the budget and schedules indicate that the number of nuclear systems that will be developed are limited. One needs to seek the 'minimum requirements' to do a job rather than the last ounce of performance, and areas of commonality. To develop a minimum number of systems to meet the overall DoD, NASA, and commercial needs, the broad spectrum of requirements has been examined along with cost drivers. DOE

N94-17879 Ballistic Missile Defense Program Office, Washington, DC.
SINGLE STAGE ROCKET TECHNOLOGY (SSRT) DC-X TEST PROGRAM ENVIRONMENTAL ASSESSMENT Final Report
Jun. 1992 105 p Limited Reproducibility: More than 20% of this document may be affected by microfiche quality
(AD-A265940) Avail: Issuing Activity (Defense Technical Information Center (DTIC))

This document presents an assessment of the potential environmental consequences of the development and subsequent validation of the signal stage rocket technology (SSRT) using a subscale vehicle that is capable of vertical takeoff and landing. Findings from the assessment determined no significant impact will result from conducting the SSRT program. DTIC

N94-17884# Brookhaven National Lab., Upton, NY.
KINETIC: A SYSTEM CODE FOR ANALYZING NUCLEAR THERMAL PROPULSION ROCKET ENGINE TRANSIENTS
E. Schmidt, O. Lazareth, and H. Ludewig 1993 6 p Presented at the 10th Symposium on Space Nuclear Power and Propulsion, Albuquerque, NM, 10-14 Jan. 1993
(Contract DE-AC02-76CH-00016)
(DE93-016825; BNL-48699; CONF-930103-41) Avail: CASI HC A02/MF A01

A system code suitable for analyzing Nuclear Thermal Propulsion (NTP) rocket engines is described in this paper. The code consists of a point reactor model and nodes to describe the fluid dynamics and heat transfer mechanism. Feedback from the fuel coolant, moderator and reflector are allowed for, and the control of the reactor is by motion of control elements (drums or rods). The worth of the control clement and feedback coefficients are predetermined. Separate models for the turbo-pump assembly (TPA) and nozzle are also included. The model to be described in this paper is specific for the Particle Bed Reactor (PBR). An illustrative problem is solved. This problem consists of a PBR operating in a blowdown mode. DOE

N94-17908# Argonne National Lab., IL.
CRITICAL TECHNOLOGIES FOR REACTORS USED IN NUCLEAR ELECTRIC PROPULSION
S. K. Bhattacharyya 1993 5 p Presented at the American Nuclear Society Annual Meeting, San Diego, CA, 20-24 Jun. 1993
(Contract W-31-109-eng-38)
(DE93-017685; ANL/EP/CP-80316; CONF-930601-25) Avail: CASI HC A01/MF A01

Nuclear electric propulsion (NEP) systems are expected to play a significant role in the exploration and exploitation of space. Unlike nuclear thermal propulsion (NTP) systems, NEP systems include electric power generation and conditioning units that in turn are used to drive electric thrusters. These thrusters accelerate subatomic particles to produce thrust. This document provides a quick overview of the technological development needs of NEP systems. Derived from text

N94-18202# Naval Postgraduate School, Monterey, CA.
ADAPTATIONS TO MICROPEP AND ROCKET TO ALLOW PERFORMANCE EVALUATION OF MULTIPLE GRAIN AND/OR AIRBREATHING MOTORS M.S. Thesis
Aaron M. McAtee Jun. 1993 57 p
(AD-A268798) Avail: CASI HC A04/MF A01

Adaptations to two existing rocket motor performance computer programs were made. MICROPEP, a FORTRAN program developed by the Naval Air Warfare Center Weapons Division, China Lake, California to evaluate theoretical performance of various propellants in rocket motors, was modified to allow calculation of the effects of non-ideal expansion and mixed shifting equilibrium-frozen composition nozzle flow on performance. In addition, the ability to handle vitiated air heaters, to calculate combustion chamber Mach number, and to calculate stagnation pressure for airbreathing engines was incorporated. ROCKET, an internal ballistics program written by the Lockheed Corporation and modified by the Naval Air Warfare Center Weapons Division, was updated to purge the program of unused code and allow input of performance losses in both the combustor and nozzle flows. DTIC

N94-18574 Naval Research Lab., Washington, DC.
ULTRAVIOLET PLUME INSTRUMENT CALIBRATION AND SENSOR ASSESSMENT Interim Report
E. R. Malaret, J. G. Cardon, L. Perez, H. W. Smathers, and D. M. Horan 1 Sep. 1993 116 p Limited Reproducibility: More than 20% of this document may be affected by microfiche quality
(AD-A269687; NRL/FR/8105-93-9564) Avail: CASI HC A06

The Ultraviolet Plume Instrument (UVPI) is a calibrated, plume-tracking instrument flown on the Naval Research Laboratory's Low-power Atmospheric Compensation Experiment (LACE) satellite. The UVPI's primary mission was to collect images of rocket plumes in the ultraviolet wavelengths. The purpose of this report is to describe the procedures followed in calibrating the UVPI, to present final instrument response functions for use in subsequent data reduction and analysis, and to provide conversion constants useful for revising data values contained on delivered data tapes and in completed rocket plume reports. DTIC

N94-18830# Sandia National Labs., Albuquerque, NM.
SOME PARAMETRIC FLOW ANALYSES OF A PARTICLE BED FUEL ELEMENT
D. Dobranich May 1993 126 p
(Contract DE-AC04-76DP-00789)
(DE93-018440; SAND-93-0529) Avail: CASI HC A07/MF A02

Parametric calculations are performed, using the SAFSIM computer program, to investigate the fluid mechanics and heat transfer performance of a particle bed fuel element. Both steady-state and transient calculations are included, addressing such issues as flow stability, reduced thrust operation, transpiration drag, coolant conductivity enhancement, flow maldistributions, decay heat removal, flow perturbations, and pulse cooling.

The calculations demonstrate the dependence of the predicted results on the modeling assumptions and thus provide guidance as to where further experimental and computational investigations are needed. The calculations also demonstrate that both flow instability and flow maldistribution in the fuel element are important phenomena. Furthermore, results are encouraging that geometric design changes to the element can significantly reduce problems related to these phenomena, allowing improved performance over a wide range of element power densities and flow rates. Such design changes will help to maximize the operational efficiency of space propulsion reactors employing particle bed fuel element technology. Finally, the results demonstrate that SAFSIM is a valuable engineering tool for performing quick and inexpensive parametric simulations addressing complex flow problems. DOE

N94-19128# New Mexico Univ., Albuquerque. Dept. of Chemical and Nuclear Engineering.
SHRINKAGE VOID FORMATION AND ITS EFFECT ON FREEZE AND THAW PROCESSES OF LITHIUM AND LITHIUM-FLUORIDE FOR SPACE APPLICATIONS
Jae-Young Yang and M. S. El-Genk 10 Jul. 1991 6 p Prepared for LANL, NM
(Contract W-7405-eng-36)
(DE93-019303; LA-Sub-93-216) Avail: CASI HC A02/MF A01 (US Sales Only)

The effects of shrinkage void forming during freezing of lithium and lithium-fluoride on subsequent thaw processes are investigated using a numerical scheme that is based on a single (solid/liquid) cell approach. Results show that a void forming at the wall appreciably reduces the solid-liquid interface velocity, during both freeze and thaw, and causes a substantial rise in the wall temperature during thaw. However, in the case of Li, the maximum wall temperature was much lower than the melting temperature of PWC-11, which is used as the structure material in the SP-100 system. Hence, it is concluded that a formation of hot spots is unlikely during the startup or restart of the SP-100 system. DOE

N94-19438*# Alabama Univ., Tuscaloosa. Dept. of Mechanical Engineering.
ANALYSIS OF FILM COOLING IN ROCKET NOZZLES Final Report
Keith A. Woodbury Sep. 1993 49 p Original contains color illustrations
(Grant NAG8-212)
(NASA-CR-194674; NAS 1.26:194674; BER-596-37) Avail: CASI HC A03/MF A01; 2 functional color pages

This report summarizes the findings on the NASA contract NAG8-212, Task No. 3. The overall project consists of three tasks, all of which have been successfully completed. In addition, some supporting supplemental work, not required by the contract, has been performed and is documented herein. Task 1 involved the modification of the wall functions in the code FDNS (Finite Difference Navier-Stokes) to use a Reynolds Analogy-based method. This task was completed in August, 1992. Task 2 involved the verification of the code against experimentally available data. The data chosen for comparison was from an experiment involving the injection of helium from a wall jet. Results obtained in completing this task also show the sensitivity of the FDNS code to unknown conditions at the injection slot. This task was completed in September, 1992. Task 3 required the computation of the flow of hot exhaust gases through the P&W 40K subscale nozzle. Computations were performed both with and without film coolant injection. This task was completed in July, 1993. The FDNS program tends to overpredict heat fluxes, but, with suitable modeling of backside cooling, may give reasonable wall temperature predictions. For film cooling in the P&W 40K calorimeter subscale nozzle, the average wall temperature is reduced from 1750R to about 1050R by the film cooling. The average wall heat flux is reduced by a factor of 3. Author (revised)

N94-19516# European Space Agency. European Space Research and Technology Center, ESTEC, Noordwijk (Netherlands). Power and Energy Conversion Div.
RATIONALE FOR THE POWER STANDARD
Nov. 1992 72 p
(ESA-PSS-02-10-Vol-2-Issue-1; ETN-93-94882) Copyright Avail: CASI HC A04/MF A01

The Power Standard defines the requirements on electrical power systems to be applied by contractors and subcontractors to ESA spacecraft and associated equipment or payloads. The Power Standard consists of two volumes, which support two guideline specifications. This document, volume 2, a reference document, is called the Power standard Rationale (PR); it serves as a guide for volume 1 by explaining the rationale of the requirements specified in volume 1. Volume 1, the standard itself, is called Power Standard (PS). The guidelines for the establishment of a power supply subsystem specification and the guidelines for the establishment of an electrical unit specification are given. ESA

N94-19706*# Alabama Univ., Huntsville.
FNAS/SUMMER FACULTY FELLOWSHIP RESEARCH CONTINUATION PROGRAM. TASK 6: INTEGRATED MODEL DEVELOPMENT FOR LIQUID FUELED ROCKET PROPULSION SYSTEMS. TASK 9: ASPECTS OF MODEL-BASED ROCKET ENGINE CONDITION MONITORING AND CONTROL Semiannual Report
L. Michael Santi (Christian Brothers Coll., Memphis, TN.) and Arthur J. Helmicki (Cincinnati Univ., OH.) 27 Oct. 1993 112 p
(Grant NAG8-212)
(NASA-CR-194574; NAS 1.26:194574) Avail: CASI HC A06/MF A02

The objective of Phase I of this research effort was to develop an advanced mathematical-empirical model of SSME steady-state performance. Task 6 of Phase I is to develop component specific modification strategy for baseline case influence coefficient matrices. This report describes the background of SSME performance characteristics and provides a description of the control variable basis of three different gains models. The procedure used to establish influence coefficients for each of these three models is also described. Gains model analysis results are compared to Rocketdyne's power balance model (PBM). Derived from text

23 CHEMISTRY AND MATERIALS (GENERAL)

N94-18314 New Orleans Univ., LA. Dept. of Chemistry.
DENSE ENERGETIC COMPOUNDS OF C, H, N, AND O ATOMS. 3: 5-(4-NITRO-(1,2,5) OXADIAZOLYL)-5H-(1,2,3) TRIAZOLO (4,5-C)(1,2,5) OXADIAZOLE
Ananthakrishnan Gunasekaran and Joseph H. Boyer 21 Jul. 1993 11 p Limited Reproducibility: More than 20% of this document may be affected by microfiche quality
(Contract N00014-90-J-1661)
(AD-A268715; TR-52) Avail: Issuing Activity (Defense Technical Information Center (DTIC))

Diazidoazofurazan 8 was obtained from the bis-diazonium salt of diaminoazofurazan 7 by treatment with sodium azide and underwent thermolysis to 5-(4-azido- (1,2,5) oxadiazolyl) -5H- (1,2,3) triazolo (4,5,-c) (1,2,5) oxadiazole 5. The corresponding amine 13 was obtained from the azide 5 by reduction with stannous chloride and was oxidized by ammonium persulfate to 5-(4 nitro-(1,2,5)oxadizolyl) -5H- (1,2,3)triazolo(4,5,-c) (1,2,5)oxadiazole 1. The azide 5 was converted to phosphinimine 9 in a reaction with triphenylphospine. DTIC

N94-18703 Royal Society, London (England).
ROYAL SOCIETY OF CHEMISTRY, HETEROCYCLIC CHEMISTRY GROUP, LAKELAND HETEROCYCLIC SYMPOSIUM
10 May 1993 35 p The 11th Symposium held in Grasmere, England, 6-10 May 1993 Limited Reproducibility: More than 20% of this document may be affected by microfiche quality
(Contract DAJA45-93-M-0328)
(AD-A270374; R/D-7107-CH-02) Avail: CASI HC A03

Partial contents: Chiral Dihydropyridones as Synthetic Intermediates; Stereocontrol using Dithiane Oxide Building Blocks; Rearrangements of Isoxazoles; Reissert Compound Studies with Pyridine; Friedel's Folly Revisited - A Great New Approach to Pyridines, Quinolines, etc; New Stereoselective Methods for O-Heterocyclic Synthesis; The Versatility of Microbial Oxidation of Aromatic Compounds in the Synthesis of Heterocyclic Natural Products; Sequential Transformations in Organic Synthesis - A Synthetic Strategy with a Future; The Design and Synthesis of Selective Protein Kinase C Inhibitors; and Isocondensed Heteroaromatic Pyrroles -

Syntheses, and Applications in the Syntheses of Natural Products and Conducting Polymers. DTIC

N94-18833# Joint Publications Research Service, Arlington, VA.
JPRS REPORT: SCIENCE AND TECHNOLOGY. CENTRAL EURASIA: MATERIALS SCIENCE
5 Mar. 1993 80 p Transl. into ENGLISH from various Russian articles
(JPRS-UMS-93-002) Avail: CASI HC A05/MF A01

Articles cover the following topics: aluminum-based composite alloys; analytical techniques for predicting elastic properties of three-dimensional reinforced composites; stability of composite materials with interlaminar cracks; characteristics of strain gauge measurements on composites; corrosion cracking of high-strength steels in neutral media; experimental methods and devices for studying metal fracture toughness; effect of structural state on fatigue crack nucleation mechanism and growth kinetics in aluminum and magnesium alloys; and the effect of structural state of TiN coats on their strength. CASI

N94-19117# Oak Ridge National Lab., TN.
[RESEARCH PROGRAM ACTIVITIES OF THE ORNL ANALYTICAL CHEMISTRY DIVISION] Annual Progress Report, period ending 31 Dec. 1992
W. D. Shults Apr. 1993 255 p
(Contract DE-AC05-84OR-21400)
(DE93-017938; ORNL-6749) Avail: CASI HC A12/MF A03

This report is divided into: Analytical spectroscopy (optical spectroscopy, organic mass spectrometry, inorganic mass spectrometry, secondary ion mass spectrometry), inorganic and radiochemistry (transuranium and activation analysis, low-level radiochemical analysis, inorganic analysis, radioactive materials analysis, special projects), organic chemistry (organic spectroscopy, separations and synthesis, special projects, organic analysis, ORNL/UT research program), operations (quality assurance/quality control, environmental protection, safety, analytical improvement, training, radiation control), education programs, supplementary activities, and presentation of research results. Tables are included for articles reviewed or refereed for periodicals, analytical service work, division manpower and financial summary, and organization chart; a glossary is also included. DOE

24 COMPOSITE MATERIALS

Includes physical, chemical, and mechanical properties of laminates and other composite materials.

For ceramic materials see *27 Nonmetallic Materials.*

N94-17766*# Old Dominion Univ., Norfolk, VA. Inst. for Computational and Applied Mechanics.
ANALYSIS OF PULTRUSION PROCESSING FOR LONG FIBER REINFORCED THERMOPLASTIC COMPOSITE SYSTEM
W. Tso, T. H. Hou, and S. N. Tiwari Nov. 1993 82 p
(Grant NAG1-363)
(NASA-CR-194504; NAS 1.26:194504; ODU/ICAM-93-103) Avail: CASI HC A05/MF A01

Pultrusion is one of the composite processing technology, commonly recognized as a simple and cost-effective means for the manufacturing of fiber-reinforced, resin matrix composite parts with different regular geometries. Previously, because the majority of the pultruded composite parts were made of thermosetting resin matrix, emphasis of the analysis on the process has been on the conservation of energy from various sources, such as heat conduction and the curing kinetics of the resin system. Analysis on the flow aspect of the process was almost absent in the literature for thermosetting process. With the increasing uses of thermoplastic materials, it is desirable to obtain the detailed velocity and pressure profiles inside the pultrusion die. Using a modified Darcy's law for flow through porous media, closed form analytical solutions for the velocity and pressure distributions inside the pultrusion die are obtained for the first time. This enables us to estimate the magnitude of viscous dissipation and it's effects on the pultruded parts. Pulling forces refined in the pultrusion processing are also analyzed. The analytical model derived in this study can be used to advance our knowledge and control of the pultrusion process for fiber reinforced thermoplastic composite parts. Author

N94-17846# Oak Ridge National Lab., TN.
METAL-NANOCLUSTER COMPOSITES MADE BY ION IMPLANTATION: A NOVEL THIRD-ORDER NONLINEAR MATERIAL
R. F. Haglund, Jr., L. Yang, R. H. Magruder, III, K. Becker, J. E. Wittig, C. W. White, R. A. Zhur, L. Yang, R. Dorsinville, and R. Alfano Mar. 1993 13 p Presented at the OE/LASE 1993 International Society for Optical Engineering Conference, Los Angeles, CA, 16-23 Jan. 1993
(Contract DE-AC05-84OR-21400)
(DE93-015908; CONF-930159-38) Avail: CASI HC A03/MF A01

We describe our recent studies of metal-insulator nanocluster composites made by ion implantation in such substrates as glass and sapphire. The metal clusters have diameters ranging from 3 to 30 nm. The composites exhibit an electronic nonlinear optical response which is fast on the picosecond time scale. In addition to possibilities for technological application, these materials also offer a way of studying unusual properties of composite materials, such as the quantum confinement of conduction-band electrons and the transverse relaxation time T(sub 2) as a function of cluster size. DOE

N94-17958# Technical Research Centre of Finland, Espoo. Metals Lab.
THE CALCULATION METHODS OF A CRACKED PLASTIC COMPOSITE LAMINATE: A LITERATURE SURVEY [SAEROELLISEN MUOVIKOMPOSIITTILAMINAATIN LUJUUDEN LASKENTAMENETELMAET. KIRJALLISUUSTUTKIMUS]
Heikki Keinaenen May 1992 56 p In FINNISH Sponsored by Technical Research Centre of Finland, Espoo
(VTT-TIED-1362; ISBN-951-38-4175-8; ETN-93-94478) Copyright Avail: CASI HC A04/MF A01

The full potential of composite materials has not yet been realized. This is due to lack of fundamental understanding and a lack of confidence in material behavior, particularly for primary structural applications. Innovative design tools are required to make more efficient use of composites for future primary structural components. This is an essential goal for industry to ensure competitive position in the next generation of advanced structures and components. The objective of this literature study is to examine the analytical and numerical predictive methods for the strength of a cracked fiber reinforced plastic composite. Especially, methods based on fracture mechanics are studied. Due to the fracture behavior of composites the problem is very complicated. Most of the work reported in literature has been done to assess the effect of delaminations on the behavior of a fiber reinforced composite. This creates the basis for the more general predictive methods for strength and lifetime. Also, some similarity can be seen with the analyses of glued joints. The special techniques required to numerically determine the effect of a delamination on the strength of a fiber reinforced composite laminate are also discussed. ESA

N94-17971 Aeronautical Research Inst. of Sweden, Stockholm.
IMPACT RESPONSE OF COMPOSITE LAMINATES: A GUIDE TO CLOSED FORM SOLUTIONS
Robin Olsson Jan. 1993 106 p Sponsored by Foersvarets Materialverk, Stockholm, Sweden Limited Reproducibility: More than 20% of this document may be affected by microfiche quality
(FFA-TN-1992-33; ETN-93-94859) Avail: CASI HC A06

A guide to the use of available closed form solutions for the analysis of the impact response of laminated composite plates is presented. Responses mainly governed by wave propagation and by conditions of fixed boundaries are discussed and criteria are given for determining the type of response to be considered. Contact conditions and their influence on the type of response are dicussed. Methods to analyze the large local stresses close to the point of impact are described and applied to predict initiation and size of damage observed in a number of published experimental studies. More special topics such as sandwich plates, dynamical material data, and a number of application examples of impacts occurring in practice are also covered. ESA

N94-18074 Department of the Navy, Washington, DC.
PROCESS FOR PREPARING THERMOPLASTIC COMPOSITES Patent
Roland C. Cochran, inventor (to Navy) and Edwin L. Rosenzweig, inventor (to Navy) 17 Aug. 1993 11 p Filed 2 Mar. 1992
(AD-D015864; US-Patent-5,236,646; US-Patent-Appl-SN-844276) Avail: CASI HC A02/MF A01

This invention relates to a process for preparing thermoplastic composites, i.e., laminates from a plurality of individual plies of thermoplastic resin prepregs. The prepregs are formed into composites under two substantially concentric vacuum chambers. High temperatures and low consolidating pressures are applied against the prepregs in an inner vacuum chamber while a lower vacuum is drawn from the rigid outer chamber to remove the volatiles and consolidate the prepregs. DTIC

N94-18087# Oak Ridge National Lab., TN.
LIGHTWEIGHT MATERIALS FOR TRANSPORTATION: PROGRAM PLAN
1993 107 p
(Contract DE-AC05-84OR-21400)
(DE93-017381; ORNL/ATD-75) Avail: CASI HC A06/MF A02

This program plan has been prepared by the Office of Transportation Materials in response to a request by the House Committee on Appropriations. It recognizes that a significant commitment to long-term, stable materials research and development (R&D) is required to realize the benefits of lighter weight vehicles, including economic, environmental, and energy related benefits. Extensive input was obtained from the major US automakers and from representative materials and component suppliers. Considerable interaction with the key members of the US Automotive Materials Partnership (USAMP) has ensured consistency of technical direction. The program will support R&D activity at industrial sites through competitively bid subcontracts with cost sharing anticipated at 30-50%, with the higher amounts in process scale-up and manufacturing technology development. The recommended LWM Program will enable industry to develop necessary technology by utilizing their capabilities as well as accessing supporting technology at national laboratories, universities, and ongoing program activity at NASA, DoD, DOT, NIST, etc., and thereby leverage industry resources through integrated team approaches. Many individual program efforts are currently in place that address small portions of the overall needs of the LWM Program, both within DOE and in other agencies. Cognizance of these and overall integration of research activities are planned as significant program management tasks. Because of the international nature of the automobile business, benchmarking of foreign technology and tracking of worldwide developments are also key program elements. DOE

N94-18113# Lawrence Livermore National Lab., CA.
SAND CONTACT IN DYNA3D
R. G. Whirley and B. E. Engelmann 25 Aug. 1992 15 p Presented at the DYNA3D User's Group Conference, Manchester, England, 22-23 Sep. 1992
(Contract W-7405-eng-48)
(DE93-016451; UCRL-JC-111560; CONF-9209372-1) Avail: CASI HC A03/MF A01

This paper describes some recent developments in adaptive contact algorithms for the transient analysis of penetration and material failure in DYNA3D. A failure criterion is defined for volumes of potentially failing material on each side of a contact surface. As material within an element fails, the element is deleted from the calculation, and the contact surface is adaptively redefined to include the newly exposed outer material boundary. This algorithm admits arbitrary combinations of shell and solid elements to allow modeling of composite or honeycomb structures. The algorithms and their efficiency are illustrated with several DYNA3D simulations, and results are compared with experimental data. DOE

N94-18122# Deutsche Forschungsanstalt fuer Luft- und Raumfahrt, Cologne (Germany). Abt. Werkstoffmechanik.
STRENGTH OPTIMIZATION OF C/Al METAL MATRIX COMPOSITES PRODUCED FROM PREPREGS Ph.D. Thesis - Duisburg Univ. [FESTIGKEITSOPTIMIERUNG AUS PREPREGS HERGESTELLTER KOHLENSTOFFASERVERSTAERKTER ALUMINIUMMATRIX-VERBUNDWERKSTOFFE]
Jean-Jacques Masson Dec. 1992 110 p In GERMAN
(DLR-FB-92-39; ETN-93-94871) Avail: CASI HC A06/MF A02

Long fiber reinforced C/Al composites manufactured from prepregs are considered. The consolidation of the composite material was performed by hot pressing in vacuum. It is found that the formation of aluminum-carbide crystals at the fiber/matrix interface during composite processing is detrimental to fiber strength. In order to determine the degradation of fiber strength, single Al coated fibers were tested after annealing treatments corresponding to normal processing conditions. The strength distributions could not well be described by the Weibull theory and a new model was applied, which is based on a description of the populations of defects in a fiber. On the basis of the results of the fiber investigations, strength of the composite was optimized by choosing appropriate processing parameters. A model is presented to predict composite strength from strength distributions obtained from single fibers. The four parameters of elasticity of unidirectional laminates could be estimated on the basis of simple micromechanical models. ESA

N94-18180# National Inst. of Standards and Technology, Gaithersburg, MD.
EQUIPMENT FOR INVESTIGATION OF CRYOGENIC COMPACTION OF NANOSIZE SILICON NITRIDE POWDERS
Wei Chen, G. J. Piermarini, S. J. Dapkunas, S. G. Malghan, and A. Pechenik (Air Force Office of Scientific Research, Bolling AFB, Washington, DC.) 1992 10 p
(Contract DE-AI05-92OR-22041)
(DE93-018740; DOE/OR-22041/1) Avail: CASI HC A02/MF A01

A system for studies of time-dependent compaction of nanosize silicon nitride powders under various atmospheres at 77 to 1000 K is described. The system incorporates a screw-driven press (10 ton capacity) with a piston-cylinder type die and can produce cylindrical powder compacts, 3 mm dia and about 1 mm thick, using pressures up to 3 GPa. The system is computer-controlled and permits accurate measurements of the sample volume, and, after appropriate calibration, can determine the rate and degree of densification of the compacting powder as pressure is applied. Frictional forces between the piston and the die are measured during the compaction process. For calibration of the system, powders with known volume-change accompanied by phase transition under pressure were studied, and good agreement with published results was demonstrated. Several Si3N4 samples were compacted and sintered at 1300 to 1600 C. Max random packing density of 64% was obtained using liquid nitrogen lubricant at pressure less than 2.5 GPa. Both green samples and samples sintered at temperatures to 1500 C were transparent. DOE

N94-18201 Naval Command, Control and Ocean Surveillance Center, San Diego, CA. RDT and E Div.
EVALUATION OF THE PRODUCTION-GRADE CLASS 4 FLEXTENSIONAL TRANSDUCER SHELL Final Report
J. D. Maltby Apr. 1993 47 p Limited Reproducibility: More than 20% of this document may be affected by microfiche quality
(AD-A268796; NCCOSC-TR-1604) Avail: CASI HC A03

This report evaluates physical characteristics and mechanical properties of the production-grade composite Class 4 flextensional transducer shell produced by Brunswick Defense. The void content was very low; the average was less than 0.5%. The fiber distribution was very uniform throughout the shell; the average fiber volume was 52%. Interlaminar shear strength averaged 11.4 ksi. The shear modulus was very nonlinear. Its initial value was 0.52 Mpsi. Through-the-thickness strength averaged 6.7 ksi in tension and 24.4 ksi in compression. Through-the-thickness test results revealed a nonlinear modulus in compression and a fairly linear modulus in tension. DTIC

N94-18205 Drexel Univ., Philadelphia, PA.
A COMPREHENSIVE STUDY OF MATRIX FRACTURE MECHANISMS IN FIBER-REINFORCED CERAMIC MATRIX COMPOSITES Final Technical Report, 15 Feb. 1990 - 30 Apr. 1993
A. S. Wang and M. W. Barsoum 30 Jun. 1993 79 p Limited Reproducibility: More than 20% of this document may be affected by microfiche quality
(Grant AF-AFOSR-0172-90)
(AD-A268809; AFOSR-93-0664TR) Avail: CASI HC A05

This final technical report summarizes the activities, accomplishment, and research results obtained under the research grant AFOSR-90-0712, which covered the period from 15 Feb. 1990 to 30 Apr. 1993. The main objective of the research is to study the physical mechanisms of matrix microcracking which constitutes the fundamental cause for the toughness and strength properties in fiber-reinforced ceramic-matrix composites. Major results summarized in this report include the following: (1) fabrication of the test specimens with controlled microstructural variables; (2) laboratory tests of matrix microcracking with in-situ and real-time monitoring; and (3) formulation of a simulation model and modeling results. A list of publications that have resulted from this research is included in this report. DTIC

N94-18327# Aeronautical Research Labs., Melbourne (Australia).
MATHEMATICAL MODELLING OF BONDED FIBRE-COMPOSITE REPAIRS TO AIRCRAFT
P. D. Chalkley May 1993 35 p
(AD-A268732; ARL-RR-7; DODA-AR-008-365) Avail: CASI HC A03/MF A01

Bonded fibre-composite doublers are increasingly being used to reinforce and/or repair damaged or underdesigned metallic aircraft structure. This trend will continue as the average age of Australian civilian and military aircraft increases. Two mathematical models of the stress state in bonded doublers are presented in this report: the end-tapered double-lap joint and the stepped double-lap joint. The mathematical development of the two models is detailed and the fidelity of the predicted stress states compared with that obtained from finite element analyses and experiment. DTIC

N94-18450 California Univ., Santa Barbara. Dept. of Materials.
COMPOSITES: MATERIALS OF THE FUTURE Final Report, 1 Jan. 1992 - 30 Apr. 1993
A. G. Evans 31 Oct. 1992 7 p Limited Reproducibility: More than 20% of this document may be affected by microfiche quality
(Contract N00014-92-J-1652)
(AD-A268945) Avail: Issuing Activity (Defense Technical Information Center (DTIC))

A diverse group from Europe and the U.S. were brought together to address broad aspects of composite systems, ranging from processing to design and including novel concepts. One objective was to compare and contrast approaches used for polymer-based systems with those for metal and ceramic systems. Another was to assess opportunities for new initiatives. A third was to explore concurrent engineering issues. Various generalizations can be made based on the presentations and discussions on the following: delamination and large scale bridging, remaining life, deformation and creep, crack growth micromeasurements, and novel approaches. DTIC

N94-18544# Air Force Inst. of Tech., Wright-Patterson AFB, OH. Foreign Aerospace Science and Technology Center.
CARBON/CARBON COMPOSITES COATED WITH SiC BY CHEMICAL VAPOR DEPOSITION
Sun Shoujin, Liu Wenchuan, and Li Minjun 14 Sep. 1993 20 p
(AD-A269934; FASTC-ID(RS)T-0222-93) Avail: CASI HC A03/MF A01

Oxidation-resistant carbon/carbon (C/C) composites were fabricated by chemical vapor deposition (CVD) of SiC on the surface of C/C composites; the latter were densified in preforms of carbon cloth lay-up by chemical vapor infiltration (CVI) of carbon. The mechanical properties, thermal properties, and the oxidation resistant properties in air of the material are studied. Author (DTIC)

N94-18572 Phillips Lab., Edwards AFB, CA.
PROCESS RELATIONSHIP AS INFLUENCED BY CARBONIZATION RATE Extended Abstract
Kristen M. Kliner, David P. Anderson, and Timothy D. Naughton Jun. 1993 5 p Limited Reproducibility: More than 20% of this document may be affected by microfiche quality
(AF Proj. 2864)
(AD-A269680) Avail: Issuing Activity (Defense Technical Information Center (DTIC))

The typical process cycle for a carbon-carbon composite begins with an organic matrix impregnated fibrous preform cured according to conventional composite practices (e.g., lay-up, bagging and autoclave cure; hot pressing; etc.). This cured composite is then subjected to a pyrolysis cycle in the absence of oxygen which results in the carbonization of the matrix. Carbonization cycles are carried out to temperatures of 650-800 C for several hours or even days. During these cycles as much as 50% of the matrix mix can be volatilized with simultaneous shrinkage and microcracking. The resultant porous, low density carbonaceous solid is usually densified by additional matrix impregnation and heat treatment steps. The extreme length of the carbonization process is due to the heating cycle development methodology. The development of the material properties was not understood, so to keep catastrophic defects from occurring, the heating cycle was made very low. To intelligently control the process, the materials process/property relationship must be understood. In this study the relationship between heating rate and physical development of the carbonization of a phenolic preform was investigated. DTIC

N94-18630 Virginia Polytechnic Inst. and State Univ., Blacksburg.
THE 6TH JAPAN-U.S. CONFERENCE ON COMPOSITE MATERIALS Final Report, 1 Sep. 1991 - 31 Aug. 1992
K. L. Reifsnider Mar. 1993 877 p Conference held in Orlando, FL, 22-24 Jun. 1992 Limited Reproducibility: More than 20% of this document may be affected by microfiche quality
(Grant AF-AFOSR-0330-91)
(AD-A268535; AFOSR-93-0620TR) Avail: CASI HC A99

This conference has achieved its goal of updating the research and development community about recent advances in the area of modern composite materials, and about interactions and opportunities associated with US-Japan Cooperation. The conference was organized and administered by the US-Japan Council for Composite Materials, with financial backing from the Virginia Institute for Materials Systems, which is part of Virginia Tech. Cooperating organizations include the American Society for Composites, American Society of Mechanical Engineers, Ohio Aeronautics Institute, and the Society of Engineering Mechanics. The scope of the Conference included all types of high performance composite systems, interfaces and interphases, high temperature materials, smart materials and structures, fracture, fatigue, and damage analysis. Specific topic areas include: Materials System Design, Manufacturing and Processing. Fabrication of Components, Interfaces and Interphases, Woven and n-Dimensional Materials, High Temperature Materials, Stress Analysis and Micromechanics. The conference lasted for three days with 120 papers presented (40 from Japan and 80 from the US). The papers presented at the conference were relevant for the current Air Force technology thrusts such as the Integrated High Performance Turbine Engine Program and the National Aerospace Plane. DTIC

N94-18636 Texas Univ., Austin.
DEVELOPING AND UNDERSTANDING THE HIGH TEMPERATURE BEHAVIOR OF NIOBIUM ALUMINIDES AND NIOBIUM ALUMINIDE COMPOSITES Final Report, 1 Dec. 1989 - 31 May 1993
Juan M. Sanchez Jun. 1993 30 p Limited Reproducibility: More than 20% of this document may be affected by microfiche quality
(Grant AF-AFOSR-0070-90)
(AD-A268874; AFOSR-93-0627TR) Avail: CASI HC A03

The present three year study has sought to understand the potential for, and limitations to, development of high temperature structural materials based on niobium aluminide and transition metal beryllide intermetallic compounds. Beginning with a broad examination of some important properties, this project has identified promising areas for research and culminates with significant additions to the body of knowledge on both of these classes of materials. During the first two years of this program, significant effort was concentrated on securing a source and establishing processing routes for the materials under consideration. This was necessarily accompanied by the development and use of scoping techniques for initial characterization of the candidate materials and processes. Such techniques need to be rapid and informative tests which are forgiving of sample imperfections, so that a few parameters of interest of a large number of sample materials can be easily compared. In this study the techniques based upon high temperature micro-indentation were chosen to rank the various static and time-dependent mechanical properties, and scanning electron microscopy (SEM) with energy dispersive spectroscopy (EDS) was used for microstructural and chemical evaluation. DTIC

N94-18692# Rockwell International Science Center, Thousand Oaks, CA.
FATIGUE RESISTANT Ti3Al COMPOSITES Final Report, 28 Sep. 1990 - 27 Sep. 1992
D. B. Marshall, M. C. Shaw, M. R. James, J. Graves, and W. L. Morris Jan. 1993 93 p
(Contract F33615-90-C-5928)
(AD-A270305; SC71034.FRD; WL-TR-93-4034) Avail: CASI HC A05/MF A01

Measurements of interfacial properties and residual stresses in Ti3 Al/SiC composites with and without ductile Ag/Ta layers are presented as the first step in determining the role of the ductile layers in the fatigue of these composites. In the composite without ductile layers, debonding and fiber sliding occurred along the interface between the outer surface of the fiber and the layer of reaction products. In the composite with Ag/Ta layers, debonding and sliding occurred within the SCS-6 layers that form the outer part of the fiber, with a higher frictional stress resisting sliding (100 MPa c.f. 66 MPa). Fatigue crack growth measurements indicated only minor differences in growth rates in the two composites in a given environment, but both composites exhibited much larger growth rates in air than in vacuum. High resolution crack opening displacement measurements are used to assess relative bridging effects. To avoid the limitation imposed by the presence of weak SCS-6 layers on the SiC fibers, a composite composed of sapphire fibers in matrix of Ti3Al with an interfacial layer of Ta was fabricated. In situ observations during transverse loading indicated that the interfacial bonding was sufficiently strong that interfacial debonding or plasticity did not affect transverse properties. DTIC

N94-18700# Air Force Inst. of Tech., Wright-Patterson AFB, OH.
DEVELOPMENT OF A FINITE ELEMENT METHOD PROGRAM FOR THE ANALYSIS OF LAMINATED COMPOSITE PLATES USING FIRST-ORDER SHEAR DEFORMATION THEORY M.S. Thesis
Brett A. Pauer Aug. 1993 137 p
(AD-A270318; AFIT/CI/CIA-93-146) Avail: CASI HC A07/MF A02

A finite element computer program for determining the deflection and stresses in general laminated composite plates was developed. The program is based on first-order shear deformation theory of laminated plates with small deflections. The program includes the flexibility to impose general boundary conditions, has three different quadrilateral elements, and is able to analyze both static and dynamic plate problems. The program code tested favorably against results from other analytical methods and literature sources. The results from this program demonstrate the need to include shear deformation in the analysis of composite plates. DTIC

N94-18702# Naval Surface Warfare Center, Bethesda, MD. Survivability Structures and Materials Directorate.
MECHANICAL PROPERTIES AND IMPACT DAMAGE RESISTANCE OF COMPOSITES FABRICATED BY LOW COST, VACUUM ASSISTED, RESIN TRANSFER MOLDING
Thomas Juska, J. S. Mayes, and William H. Seemann, III Aug. 1993 64 p
(AD-A270361; CDNSWC/SSM-64-93/04) Avail: CASI HC A04/MF A01

Fabric-reinforced laminates made by SCRIMP (Seemann Composites Resin Infusion Molding Process) were tested in compression, tension, flexure, short beam shear, and impact. A global study of the properties of SCRIMP panels was the goal of this program. Four vinyl esters, one polyester, and two epoxies were tested, as were seven different styles of E-glass fabric. The properties of E-glass fabrics were compared with those of carbon, Kevlar, and Spectra fabrics, and with the hybrids E-glass:carbon, E-glass:Kevlar, and E-glass:Spectra. Composite properties increased with resin modulus, provided the resin failure strain was above a critical (undetermined) minimum value. Light woven roving and textile fabrics had somewhat better properties than coarser woven rovings, and glass was the overall best performer based on cost, strength, and impact resistance. An E-glass:Kevlar hybrid was identified which had significant weight savings but comparable properties to E-glass. DTIC

N94-18704# Colorado School of Mines, Golden. Center for Welding and Joining Research.
WETTABILITY AND REACTION KINETICS IN METAL MATRIX COMPOSITES Annual Report
Glen R. Edwards and David L. Olson Aug. 1993 59 p
(Contract N00014-92-J-1389)
(AD-A270377; MT-CWR-093-019) Avail: CASI HC A04/MF A01

Research accomplishment during the last academic year are in two related areas: (1) further applications of the thermodynamic model developed in the previous years, and (2) kinetic studies in alumina/reactive metal systems. The ongoing projects are adaptations of the research findings from the previous years, aimed at improving the wettability at an aluminum/alumina interface and understanding the nature of the oxide barrier formed at the ceramic/liquid aluminum interface. DTIC

N94-18715 National Academy of Sciences - National Research Council, Washington, DC.
SOLID STATE SCIENCES COMMITTEE FORUM Final Report, 1 Aug. 1992 - 31 Jul. 1993
Ronald Taylor Aug. 1993 12 p Limited Reproducibility: More than 20% of this document may be affected by microfiche quality
(Contract F49620-92-J-0455)
(AD-A270454; AFOSR-93-0740TR) Avail: CASI HC A03/MF A01

The theme of the Forum was the Advanced Materials and Processing Program (AMPP) and the Restructuring of Materials Science and Technology in the U.S. The session topics included: implementing and building on government-industry partnership programs via a technology policy; a perspective on AMPP from the federal agencies; the integration of science, engineering, and societal needs in materials; and challenges for materials in the 21st century. Derived from text

N94-18720# Materials Research Society, Pittsburg, PA.
JOINING AND ADHESION OF ADVANCED INORGANIC MATERIALS SYMPOSIUM
A. H. Carim (Pennsylvania State Univ., University Park.), D. S. Schwartz (McDonnell-Douglas Corp., Saint Louis, MO.), and R. S. Silberglitt (FM Technologies, Inc., Fairfax, VA.) 14 Apr. 1993 248 p Symposium held in San Francisco, CA, 12-14 Apr. 1993
(Contract N00014-93-I-0299)
(AD-A269748) Avail: CASI HC A11/MF A03

This volume is a record of the first Joining and Adhesion of Advanced Inorganic Materials Symposium, held on April 12-14 at the 1993 MRS Spring Meeting in San Francisco, California. We brought together for this symposium an international group of researchers working in every aspect of materials joining and adhesion, from fundamental theoretical aspects of adhesion to joining techniques being applied in the commercial world. Adhesion of thin films and coatings was discussed at the atomic/electronic level, as well as on the practical level of coatings for wear resistance. Joining of a broad range of materials was discussed, including ceramics and ceramic matrix composites, metals and metal matrix composites, and semiconductors. A variety of novel joining techniques were described, many of which are destined to become commercially important technologies in the near future. DTIC

N94-18756 Army Research Lab., White Sands Missle Range, NM.
OPTICAL PROPERTIES OF REDISPERSED IRON FIBERS MEASURED AT 94 GHz Final Report
C. W. Bruce, A. V. Jelinek, and P. A. Silva Aug. 1993 23 p Limited Reproducibility: More than 20% of this document may be affected by microfiche quality
(AD-A269739; ARL-TR-59) Avail: CASI HC A03

Millimeter wavelength attenuative properties of iron fibers produced by the high temperature reduction of iron carbonyl were measured in both controlled and field environments. Aerosol morphology was evaluated statistically for the controlled studies, and results were used as a basis for calculations of the absorption efficiency. Scattering efficiency for such small diameter fibers can be assumed to be a negligible proportion of the net attenuation. Reasonable agreement between measurements and theory is indicated. Efficiencies remain relatively high for visible wavelengths. DTIC

N94-18757 Army Research Lab., White Sands Missle Range, NM.
EFFICIENCY OF FIBER DISPERSION Final Report
C. W. Bruce, Mike J. Thurston, and A. V. Jelinek Jul. 1993 25 p Limited Reproducibility: More than 20% of this document may be affected by microfiche quality
(AD-A269740; ARL-TR-56) Avail: CASI HC A03

Net efficiencies for the dissemination of graphitic fibers are determined for two continuous processes (fibers cut as part of the dispersion process or precut). In both cases an extensive grid of passive dosimetric samplers inset with a coarser grid of time resolved aerosol density samplers provided an absolute time average dosage profile, which was integrated over space to give the total effective airborne aerosol mass. The efficiency is expressed as a ratio of the airborne mass to the total mass dispersed from the bulk. For lower dosages corresponding to a dispersed mass of less than 1 lb, use of the passive, high spatial resolution grid gave efficiencies at about the 50-percent level with no large deviations from the mean. At larger dosages, for which the total mass dispersed ranged from about 1 lb to about 50 lb, only the values obtained using coarser grid (3 x 3 instruments) were valid. In the latter case the variation in efficiency was much larger, but the average indicates at least the same level of efficiency. Dispersion rates varied from 1 lb/minute to 10 lb/minute. DTIC

N94-18761# Oak Ridge Y-12 Plant, TN.

NONDESTRUCTIVE INSPECTION OF GRAPHITE-EPOXY LAMINATES FOR HEAT DAMAGE USING DRIFT AND LPF SPECTROSCOPIES

G. L. Aowell, N. R. Smyrl, C. J. Janke (Oak Ridge National Lab., TN.), E. A. Wachter (Oak Ridge National Lab., TN.), W. G. Fisher, J. Lucania (Harrick Scientific, Inc., Ossining, NY.), M. Milosevic (Spectra-Tech, Inc., Stamford, CT.), and G. Auth (MIDAC Corp., Cosa Mesa, CA.) 3 Jun. 1993 18 p Presented at the Conference on Characterization and NDE of Heat Damage in Graphite Epoxy Composites, Austin, TX, 27-28 Apr. 1993

(Contract DE-AC05-84OS-21400)

(DE93-017228; Y/DZ-1008/R1; CONF-9304170-1) Avail: CASI HC A03/MF A01

The effect of heat damage on polymer matrix composites (PMC) used in aircraft structures presents a unique problem for nondestructive testing (ND) in that damage may result as a combination of thermally cycling the PMC above the glass transition temperature of the polymer and oxidative degradation of the polymer or the polymer-fiber interface. The usual techniques for the detection of voids and flaws by radiographic, ultrasonic, and thermal imaging techniques play an important role in this ND problem. However, heat damage may result in loss of strength in these materials without producing physical flaws (cracks and delaminations) big enough to be detected. Diffuse reflectance Fourier transform infrared (DRIFT) and laser pumped fluorescence (LPF) measurements previously obtained on IM6/3501-6 laminate panels were re-evaluated to improve these techniques for the nondestructive inspection of aircraft. A more robust algorithm for relating flexural strength to changes in DRIFT spectra related to oxidation is presented and used to interpret previously reported evacuable cell DRIFT measurements. Recent advances in DRIFT technology are described which include an evacuable cell with a hemispherical window for oxidation kinetics studies, and the development of a portable DRIFT spectrometer that was used to make measurements on an aircraft. The use of a 633-nm helium-neon laser for LPF is reported as a means for rapidly relating both fluorescence intensity and spectral distribution to flexural strength. DOE

N94-18763# Brookhaven National Lab., Upton, NY.

MECHANICAL-PROPERTY CHANGES OF STRUCTURAL COMPOSITE MATERIALS AFTER LOW-TEMPERATURE PROTON IRRADIATION: IMPLICATIONS FOR USE IN SSC MAGNET SYSTEMS

J. Morena (Ace, Inc., Stuart, FL.), C. L. Snead, Jr., C. Czajkowski (Superconducting Super Collider Lab., Dallas, TX.), and J. Skaritka (Superconducting Super Collider Lab., Dallas, TX.) 1993 4 p Presented at the 5th Annual International Industrial Symposium on the Super Collider and Exhibition, San Francisco, CA, 6-8 May 1993

(Contract DE-AC02-76CH-00016)

(DE93-016735; BNL-49067; CONF-930537-84) Avail: CASI HC A01/MF A01

Longterm physical, mechanical, electrical, and other properties of advanced composites, plastics, and other polymer materials are greatly affected by high-energy proton, neutron, electron, and gamma radiation. The effects of high-energy particles on materials is a critical design parameter to consider when choosing polymeric structural, nonstructural, and elastomeric matrix resin systems. Polymer materials used for filled resins, laminates, seals, gaskets, coatings, insulation, and other nonmetallic components must be chosen carefully, and reference data viewed with caution. Most reference data collected in the high-energy physics community to date reflects material property degradation using other than proton irradiations. In most instances, the data were collected for room-temperature irradiations, not 4.2 K or other cryogenic temperatures, and at doses less than 10(exp 8)-10(exp 9) Rad. An energetic proton and the accompanying spallation-product particles provide good simulation fidelity to the expected radiation fields predicted for the cold-mass regions of the SSC magnets, especially the corrector magnets. Results are presented for some structural composite materials which were part of a larger irradiation-characterization of polymeric materials for SSC applications. DOE

N94-18869 Phillips Lab., Kirtland AFB, NM.

CHARACTERIZATION OF VAPOR PLUME SPECIES AND DEPOSITION RESIDUES RESULTING FROM PULSED LASER ABLATION OF A GRAPHITE/EPOXY COMPOSITE Final Report, Jun. 1992 - Jan. 1993

Robert E. Roybal, Charles J. Miglionico, Charles Stein, Larry E. Murr (Texas Univ., El Paso.), and Kenneth A. Lincoln (Eloret Corp., Moffett Field, CA.) Aug. 1993 30 p Limited Reproducibility: More than 20% of this document may be affected by microfiche quality

(AD-A270101; AD-E201625; PL-TR-92-1075) Avail: CASI HC A03

A modified time-of-flight mass spectrometer (TOFMS) fitted with a special collection stage for carbon-coated transmission electron microscope specimen grids is used to monitor laser-pulse ablation products from graphite/epoxy composite targets. Scanning electron microscopy observations show ablation damage to consist of matrix pyrolysis, fiber fracture, and spallation of fragments which include elemental hydrogen, carbon epoxide, and acetylene groups. Transmission electron microscope examination of specimen grids showed a variety of crystals and polycrystalline hexagonal graphites having a wide range of shapes including spheres and faceted polyhedra and platelets, textured flake structures, and microrosettes. These observations lend some credibility to a model for laser-shock and pyrolysis effects which creates molecular plume fragments and deposition fragments of hexagonal graphite. DTIC

N94-18914# Ames Lab., IA.

A NUMERICAL ANALYSIS OF CRACK GROWTH IN BRITTLE MICROCRACKING COMPOSITES

S. B. Biner 1993 23 p Presented at the Mechanism and Mechanics of Composite Fracture Meeting, Pittsburgh, PA, 17-21 Oct. 1993

(Contract W-7405-eng-82)

(DE93-011562; IS-M-747; CONF-931078-1) Avail: CASI HC A03/MF A01

A set of numerical analyses of crack growth was performed to elucidate the mechanism of microcracking on the observed fracture behavior of brittle solids and composites. The random nucleation, orientation and size effects of discrete microcracks and resulting interactions are fully accounted for in a hybrid finite element model. The results indicate that the energy expenditure due the microcrack nucleation seems not to contribute significantly to the resistance to crack growth. The main controlling parameter appears to be elastic interaction of the microcracks with the main crack in the absence of a reinforcing phase; therefore, the microcrack density plays an important role. In the case of the composites, the interaction of the main crack with the stress fields of the reinforcing phase, rather than interaction of microcracks, is the controlling parameter for the resistance to the crack growth even in the presence of a large population of microcracks. It will be also shown that the crack branching and crack kinking can readily develop as a result of microcracking. DOE

N94-19281# Instituut TNO voor Bouwmaterialen en Bouwconstructies, Delft (Netherlands).

COMPUTATIONAL MECHANICS OF COMPOSITE MATERIALS

A. C. W. M. Vrouwenvelder 1992 72 p Prepared in cooperation with Technische Univ., Delft, Netherlands

(PB93-195782) Avail: CASI HC A04/MF A01

In the first article of the issue fiber-reinforced concrete is described using a homogenization procedure and the resulting model is applied in a non-linear finite element analysis of a beam loaded by impact. The next level of refinement is the meso-level. At such a scale damage mechanics is commonly used as a vehicle for modelling the degradation processes that take place in the solid. The second article of the issue outlines a model that is rather typical for these approaches. In this case the numerical application will be for a polymer-based composite, but the ideas underlying the approach may be used for any composite material. The latter statement also holds true for the last article, where a micromechanics analysis is carried out of a carbon fiber-reinforced silicium carbide matrix and in which delamination in a chip is simulated. NTIS

N94-19335# Pacific Northwest Lab., Richland, WA.

SUBCRITICAL CRACK GROWTH IN CONTINUOUS-FIBER REINFORCED CERAMIC COMPOSITES

C. H. Henager, Jr. and R. H. Jones Jun. 1993 13 p Presented at the 95th Annual Meeting of the American Ceramic Society, Cincinnati, OH, 18-22 Apr. 1993

(Contract DE-AC06-76RL-01830)
(DE93-018784; PNL-SA-22777; CONF-930438-28) Avail: CASI HC A03/MF A01

Time-dependent crack growth measurements of ceramic composites in varying PO2 environments were conducted on materials consisting of chemical vapor infiltration (CVI) SiC reinforced with Nicalon fibers having C- and BN-interfaces. Crack velocities are determined as a function of applied stress intensity and time for varying O2 levels. Results are presented for crack growth in pure Ar and in Ar plus 2000-, 5000-, 10,000-, and 20,000-ppM O2 atmospheres at 1100 C. A 2D micromechanics model is used to represent the time-dependence of observed fiber bridging events and is able to rationalize the observed phenomena. DOE

N94-19391# Admiralty Research Establishment, Gosport (England).
LOW FREQUENCY ACOUSTICS OF LAMINATED COMPOSITE AXISYMMETRIC STRUCTURES
J. H. James Feb. 1993 31 p
(DRA-TM(USGR)-93302; BR316760; ETN-93-94969) Copyright Avail: CASI HC A03/MF A01

A theory of low frequency sound radiation from and scattering by finite axisymmetric laminated composites is given. The structure is modeled by conical shell finite elements or axisymmetric solid finite elements. The surrounding fluid is modeled by the Helmholtz integral equation. Excitations are a time harmonic mechanical force at a selected node or a plane wave at arbitrary incidence. Degrees of freedom other than those 'normal' to the structure's exterior surface are removed by receptance coupling methods. ESA

N94-19551# Argonne National Lab., IL.
THERMAL WAVE IMAGE PROCESSING FOR CHARACTERIZATION OF SUBSURFACE OF FLAWS IN MATERIALS
K. Gopalan and N. Gopalsami 1993 16 p Presented at the 36th Midwest Symposium on Circuits and Systems, Detroit, MI, 16-18 Aug. 1993
(Contract W-31-109-eng-38)
(DE93-019024; ANL/ET/CP-78721; CONF-930854-1) Avail: CASI HC A03/MF A01

Infrared images resulting from back-scattered thermal waves in composite materials are corrupted by instrument noise and sample heat-spread function. This paper demonstrates that homomorphic deconvolution and 'demultiplication' result in enhanced image quality for characterization of subsurface flaws in Kevlar and graphic composites. The choice of processing depends on the material characteristics and the extent of noise in the original image. DOE

N94-19576 Army Armament Research, Development and Engineering Center, Picatinny Arsenal, NJ.
RECENT ADVANCES IN HIGH DENSITY TUNGSTEN COMPOSITE PROCESSING
Sheldon Cytron Oct. 1993 21 p Limited Reproducibility: More than 20% of this document may be affected by microfiche quality
(AD-A270764; ARAED-TR-93007) Avail: CASI HC A03

Conventional liquid phase sintering has been the mainstay for processing tungsten alloy composites for the past several decades. New application demands being placed on these high density composites have resulted in the emergence of new processing approaches aimed at developing a new generation of high density tungsten composite materials. Recent investigative studies into rapid solidification technology, solid state sintering, mechanical alloying, and explosive compaction are reported here to highlight these recent processing trends. DTIC

N94-19662# Naval Academy, Annapolis, MD.
DELAMINATION IN COMPOSITE MATERIALS AS OBSERVED USING AN OPTICAL FIBER STRAIN GAGE
Glen E. Sabin 17 May 1993 66 p
(AD-A270803; USNA-TSPR-209) Avail: CASI HC A04/MF A01

Composite materials are used extensively in the air and space industries, where materials of high strength and light weight are required. Unlike metals, these materials often give little or no warning before failing - a potentially fatal characteristic for structural members in aircraft. A common mode of failure in composites is delamination, in which the layers of the material separate from each other. Delamination can be caused by impact, longitudinal shear stress between the layers, or transverse tensile stress across the layers. Optical fibers embedded in the composite material provide a means of monitoring the strains which lead to such failures. This project involves the use of an optical fiber strain gage in the configuration of a Michelson interferometer to study a composite sample that experiences transverse tensile stress resulting in delamination. The transverse tensile stress is produced by straightening out an already curved specimen of composite material. The output signal of the interferometer represents the integrated strain over the length of the optical fibers. By embedding the fibers in a composite specimen, the strain experienced in the material can be measured. This signal is recorded on a common audio tape, transferred to a computer, and analyzed quantitatively. DTIC

N94-19666# Technische Univ., Delft (Netherlands). Faculty of Aerospace Engineering.
RESIDUAL STRENGTH PREDICTIONS FOR FIBRE METAL LAMINATES: THE R-CURVES APPROACH
C. A. J. R. Vermeeren Apr. 1993 97 p Sponsored by Structural Laminates Co.
(LR-717; ETN-93-95025) Avail: CASI HC A05/MF A02

The purpose of this study is to investigate whether the R curve method is applicable for the prediction of the residual strength of unstiffened GLARE 2, GLARE 3, GLARE 4 and ARALL 2 laminates. Comparisons were made with 2024-T3 aluminum alloy. The R curve determination practice itself is discussed with respect to its applicability on fiber metal laminates. Center Cracked Tension (CCT) specimens were tested after which it was found that an invariant R curve could be generated for each investigated laminate. Plastic zone sizes of the reference material 2024-T3 aluminum alloy are well predicted by the Irwin plastic zone size correction. In spite of the fact that the plastic zone size in ARALL 2 and GLARE 2 is not entirely equal to the plastic zone size correction used in the R curve method, also for these materials a more or less invariant R curve could be found. Mathematical expressions for R curves of fiber metal laminates are given with which predictions can be made for specimens of an arbitrary width and initial crack size. ESA

N94-19720# Washington Univ., Seattle. Dept. of Mechanical Engineering.
DAMAGE ACCUMULATION IN ADVANCED METAL MATRIX COMPOSITES UNDER THERMAL CYCLING/CREEP LOADINGS Annual Technical Report, 15 Jul. 1992 - 14 Jul. 1993
M. Taya, M. S. Lui, W. D. Armstrong, and M. L. Dunn 1 Sep. 1993 25 p
(Contract F49620-92-J-0367)
(AD-A271207; AFOSR-93-0784TR) Avail: CASI HC A03/MF A01

Both experimental and analytical studies were conducted during the first year with the aim of identifying the damage accumulation process in a metal matrix Composite (MMC) subjected to combined creep and thermal cycling loadings. The main achievements in the experimental study are: completion of a new thermal cycler with constant stress loading capability, preliminary data of dimensional change of SiCp/6061 Al matrix composite and R-Curve behavior of PSZ-SS/PSZ composite – PSZ laminate. Whereas the first year analytical study includes construction of dislocation Punching model from ceramic/metal interfaces, a construction of analytical modeling of creep strain of a MMC subjected to either creep loading or combined creep/thermal cycling loading where the debonding of the matrix-fiber interface is accounted for. Three-parameter Weibull function is employed in the model to simulate the distribution of the actual interfacial strength. DTIC

N94-19744# Minnesota Univ., Minneapolis. Dept. of Chemical Engineering and Materials Science.
MICROSTRUCTURE AND TEXTURE CONTROL OF FATIGUE IN HYDROGEN AND MARINE ENVIRONMENTS Fiscal Year Letter, 1 Oct. 1992 - 30 Sep. 1993
William W. Gerberich 30 Sep. 1993 7 p
(Contract N00014-89-J-1726)
(AD-A271277) Avail: CASI HC A02/MF A01

It is currently not understood how the anisotropic elastic, plastic, and fracture characteristics interact with environment to limit fatigue life in a corrosive medium. This program examines how texture and anisotropic slip character interact with environment in two general classes of BCC iron base and HCP titanium base alloy systems. Selected area electron channeling, transmission electron microscopy, atomic force microscopy, and fracture micromechanic methods are combined to evaluate microstructural effects on environmentally-induced fatigue initiation and growth. In addition, as it is essential to understand the transition from small crack to long crack behavior, additional threshold studies on both Fe-Si and HSLA polycrystals need to be accomplished. In this way, the various stages of nucleation and growth may be combined together for life prediction. The objective is to provide a partial basis for alloy and materials processing design against fatigue in a marine environment. DTIC

N94-19746# Massachusetts Inst. of Tech., Cambridge. Research Lab. of Electronics.
NANOFABRICATION BY FOCUSED ION BEAM Final Report, 1 May 1992 - 31 Aug. 1993
John Melngailis and Dimitri A. Antoniadis 28 Sep. 1993 10 p
(Contract DAAL03-92-G-0217)
(AD-A271290; ARO-29631.2-EL) Avail: CASI HC A02/MF A01

Nanometer scale patterning is one of the keys to advances in electronic devices. At present most patterning is done by a multistep lithography process: resist is exposed and developed and the uncovered surface is altered. The focused ion beam may offer simplification of this multistep process. A surface film may be made to grow or dissolve where it has been irradiated. This can be viewed as a new (inorganic) resist process, but in some cases the patterned film may be the desired final structure on the substrate. The problem is that, although examples of such ion sensitive films have been found, they suffer from some drawbacks such as low sensitivity, or poor resolution. One of the aims of the work was to seek new and useful processes and materials. Another direct patterning technique, more ideally suited for ion beams, is direct maskless implantation of dopants in semiconductors. One of the limits of resolution of this technique is the lateral straggle of ions as they penetrate into the substrate. This has important bearing on the ability to fabricate the confined carrier structures in semiconductors needed in the study of quantum effect devices. The other object of the work was to characterize this straggle and to apply focused ion beam implantation to the fabrication of confined carrier structures, in particular the in-plane-gate field effect transistor. The final report provides a summary of the most important results. DTIC

N94-19776# Minnesota Univ., Minneapolis. Dept. of Chemical Engineering and Material Science.
MICROMECHANICS OF INTERFACES IN METAL MATRIX COMPOSITES Fiscal Year 1993 Letter, 1 Oct. 1992 - 30 Sep. 1993
William W. Gerberich 30 Sep. 1993 6 p
(Contract N00014-92-J-1962)
(AD-A271012) Avail: CASI HC A02/MF A01

Defining the role of the interface is critical to understanding mechanical properties of metal matrix composite (MMC) materials. Measurements of interfacial fracture toughness are being conducted to aid in the development of MMC's. The scientific research goals are to develop a better understanding of how nonlinear behavior in the metal matrix and chemical bonding or frictional effects at the bi-material interface combine to provide the interfacial fracture toughness. To accomplish that a number of spectroscopies including Rutherford Backscattering Spectroscopy (RBS) and several fracture mechanics approaches including fiber push-out are being employed. These will provide feedback to current processing conditions utilized in MMC's. The practical application is to assist 3M in the Model Factory program. DTIC

25 INORGANIC AND PHYSICAL CHEMISTRY

Includes chemical analysis, e.g., chromatography; combustion theory; electrochemistry; and photochemistry.

For related information see also *77 Thermodynamics and Statistical Physics.*.

N94-17691 International Atomic Energy Agency, Vienna (Austria).
DEVELOPMENT AND EVALUATION OF ALTERNATIVE RADIOANALYTICAL METHODS, INCLUDING MASS SPECTROMETRY FOR MARINE MATERIALS
Jan. 1993 90 p Presented at the Advisory Group Meeting on Development and Evaluation of Alternative Radioanalytical Methods, Including Mass Spectrometry for Marine Materials, Monaco, 6-9 Jun. 1989 Limited Reproducibility: More than 20% of this document may be affected by microfiche quality
(DE93-625117; IAEA-TECDOC-683; CONF-8906428) Avail: CASI HC A05 (US Sales Only)

One, if not the most important, aspect of environmental protection against radioactive contamination is the ability to measure accurately low-levels of radionuclides present in the environment. This is particularly true of the marine environment where improved and more rapid methods of analysis are required to identify the source and radiological impact of anthropogenic inputs to the oceans. More sensitive and rapid analytical methods with smaller analytical errors are required to study the behavior of different radionuclides in the marine environment. Some of these radionuclides serve as useful research tracers that aid in understanding many complex oceanographic processes. With the ever-increasing demand for more accurate data, the IAEA considered it necessary to convene an Advisory Group Meeting to identify those long-lived radionuclides that may be measured by alternative techniques and discuss and evaluate the sensitivity of the analytical methods. The meeting was held at the IAEA Marine Environment Laboratory in Monaco from 6 to 9 June 1989 and was attended by 6 invited participants and several observers. This report from the meeting is divided into two parts. The first contains 5 contributing chapters. In these chapters, the authors have endeavored to explain the principles of each measurement technique, the strengths and weakness of the method as applied to marine sciences, comparative costs and sensitivities, future developments, and topics of interest to the Agency. The reviews and sensitivities were prepared exclusively by the participants on the basis of their own experience and knowledge of the existing literature. The second part of this report is the appendices section in which can be found tables of radionuclides considered in this report and a comparison of sensitivities for different methods of detection. DOE

N94-17808# Texas Univ., Austin.
CATALYTIC HYDROCARBON REACTIONS OVER SUPPORTED METALS
J. G. Ekerdt 29 Mar. 1993 3 p
(Contract DE-FG05-86ER-13604)
(DE93-018168; DOE/ER-13604/22) Avail: CASI HC A01/MF A01

During the past year we have completed our characterization of the factors that control the structure of fully oxidized W and Mo on silica and have established that support hydroxyl groups play a central role in dispersing and attaching cations to the support oxide. Work with M(sub 2)(CO)(sub 4)Cp(sub 2)(M(sub 2)=MoMo, WW, MoW) system has been very encouraging and continues to support the notion that it may be possible to control the structure of adsorbed catalysts (in this case generate metal dimers) by use of organometallic precursors. Techniques are being developed necessary to employ XPS as a means to characterize the attachment process and the oxidation state of the cations after various thermal and photolytic reduction steps. DOE

N94-17820# Sandia National Labs., Albuquerque, NM.
FINITE ELEMENT MODELING OF EVAPORATION AND CONDENSATION DURING SOL-GEL FILM AND FIBER FORMATION
P. R. Schunk, A. J. Hurd, C. J. Brinker, and R. R. Rao 1993 11 p
Presented at the 8th International Conference on Finite Elements in Fluids: New Trends and Applications, Barcelona, Spain, 20-24 Sep. 1993
(Contract DE-AC04-76DP-00789)
(DE93-017655; SAND-92-2701C; CONF-9309156-1) Avail: CASI HC A03/MF A01

Free surfaces, multicomponent phase change, volume expansion and compression, and surface tension gradients make for challenging application of the finite element method to sol-gel (ceramic) film and fiber formation. The microstructure of the final product is largely controlled by the competition between the drying, curing, and underlying fluid mechanics of formation. Sol-gel materials are peculiar because they often contain more than one solvent, each solvent differing in volatility and surface tension. Hence, nonuniform evaporation can produce surface tension gradients that dramatically change the meniscus shape. These processes are complicated further by a volume change that accompanies evaporation and condensation, making for shock-like discontinuities in concentration and velocity at the free surface. Computer-aided predictions of film formation by dip coating and of fiber spinning are made for alcohol-water mixtures with one non-volatile species. The Navier-Stokes system is augmented with two convective-diffusion equations to track the concentration of alcohol and water, and an energy equation to monitor temperature changes. The equations are solved in both phases by discretizing them first with the Galerkin/finite element method. The resulting non-linear algebraic equation set is solved with Newton's method. The subdomaining technique is based on elliptic grid generation and is designed to parameterize the moving meniscus. Special treatment of the functional representations of velocity and concentration within the elements lining the free surface are made to accommodate the volume change that accompanies mass exchange between phases. DOE

N94-17900 National Physical Lab., Teddington (England). Materials Metrology Div.
GUIDELINES FOR THE EXPRESSION OF UNCERTAINTIES IN SURFACE CHEMICAL ANALYSIS BY AUGER ELECTRON SPECTROSCOPY (AES) AND X RAY PHOTOELECTRON SPECTROSCOPY (XPS)
P. J. Cumpson and M. P. Seah Apr. 1993 16 p Sponsored by Dept. of Trade and Industry, London, England
(NPL-DMM(A)-99; ETN-93-94884) Copyright Avail: National Physical Laboratory, Teddington, Middlesex, TW11 0LW, United Kingdom

Guidelines for the statements of uncertainty that accompany analytical results from AES (Auger Electron Spectroscopy) and XPS (X-ray Photoelectron) are presented. Recent recommendations are put into context for these spectroscopies to ensure that results are accompanied by the most relevant uncertainty values. A mathematical description of quantification is given and the statement of uncertainties is described. ESA

N94-17973# Technical Research Centre of Finland, Espoo. Food Research Lab.
FT-NIR SPECTROSCOPY IN QUANTITATIVE AND QUALITATIVE MEASUREMENTS OF CEREAL PRODUCTS [FT-NIR-SPEKTROSKOPIA VILJATUOTTEIDEN PITOISUUS- JA LAATUMITTAUKSESSA]
Jaana Sorvaniemi, Arvo Kinnunen, and Yrjoe Maelkki Feb. 1992 82 p In FINNISH Sponsored by Technical Research Centre of Finland, Espoo; Technology Development Centre, Finland; and Finnish Industry
(VTT-TIED-1331; ISBN-951-38-4144-8; ETN-93-94472) Copyright Avail: CASI HC A05/MF A01

The theoretical basis of IR/NIR spectroscopy and equipment techniques are addressed. In the NIR range the most important molecular groups in foodstuffs are the C-H, the O-H and the N-H groups. Equipment technology is divided into that of filtering, dispersive and Fourier Transformation (FT) equipment. Filtering equipment measures 6 to 20 narrow ranges of the spectrum. Of these, two to four ranges are used to determine a given component. With dispersive and FT spectrometers either the whole NIR range or the greater part of it is measured. In the analysis either a few spectral points or a few spectral ranges are used in the calculations, which are done using multivariate regression. The advantages of FT-IR/NIR equipment when compared to dispersive equipment are shown and the sample techniques of FT-IR/NIR equipment with samples in various states are studied. The areas of application for IR/NIR technology cover grain, meat and dairy products, pharmaceutical and technochemical products as well as packaging materials. The most important areas of application have thus far been grain or grain based products. The most important goal of the study was to determine the possibility of measuring quality factors using the fast IR/NIR technique. Another goal was to determine which one of the analyzed variables, had the greatest impact on the specific volume and on the aging process of bread. Here, instead of NIR data, measurements from the samples, determined by chemical and physical means, were used. The information gained can be used in planning the baking process. The problem of determining the baking properties of wheat was chosen as test case. The impact of variates measured, on the volume and hardness of bread, were studied using templates deviced with the aid of the UNSCRAMBLER program. Here, instead of NIR spectra, results of grain analysis were used. Virtually all measured characteristics affected the volume of bread, but aging showed no correlation. This range gave no suggestions for practical process planning, as a sufficiently reliable forecast of bread volume would have required more than ten measurements of the grain variates. A study was also undertaken to determine the possibility of replacing malt analysis with NIR techniques. In studies on barley malt, spectral measurements were made from pulverized malts, but part of the analysis dealt with the proper-results because of the insufficient accuracy of the detector in use at the time. ESA

N94-17987# Oak Ridge Y-12 Plant, TN.
SUMMARY REPORT FOR SUPERCRITICAL CARBON DIOXIDE EXTRACTION AND CARBONIZATION OF RESORCINOL-FORMALDEHYDE (RF) FOAMS
R. F. Simandl, D. N. Robinson, and J. D. Brown Mar. 1993 14 p
(Contract DE-AC05-84OS-21400)
(DE93-016924; Y-2461) Avail: CASI HC A03/MF A01

Emulsion-derived resorcinol-formaldehyde (RF) foams supplied by Sandia National Laboratories-California (SNL-California), were successfully extracted at the Oak Ridge Y-12 Plant using supercritical carbon dioxide. One half of the resulting foams were carbonized. Careful study of the extraction process has yielded a predictive model for supercritical extraction of thin RF foams and has resulted in the optimization of the extraction process. Extraction times and costs were minimized. After the initial solvent exchange step, solvents were supercritically extracted from the RF gels in less than 24 h at a cost of less than $0.01 of CO2 per gram of solvent extracted. DOE

N94-17997# Sandia National Labs., Livermore, CA.
EXCHANGE FRONT STABILITY IN PACKED-COLUMN CHROMATOGRAPHY
S. K. Griffiths and R. H. Nilson (Maxwell Labs., Inc., La Jolla, CA.) Apr. 1993 27 p
(Contract DE-AC04-76DR-00789)
(DE93-017526; SAND-93-8503) Avail: CASI HC A03/MF A01

Exchange front deformation in gas-phase chromatography may sometimes impair column performance. Such deformation can arise from column heterogeneities or from the unstable growth of small disturbances inherently present in the flow field. Here we examine the fundamental stability of a planar traveling exchange front subject to a small sinusoidal perturbation in the front position. The analysis includes the disparity between fluid and front velocities characteristic of exchange chromatography, as well as the distinction between fluid velocities ahead of and behind the front resulting from the net sorption of gases. Fluid compressibility is also considered. Disturbance growth rates are computed as a function of the wavelength, fluid viscosity ratio, and normalized front and fluid velocities over a wide range of each parameter. We find that growth rates increase with increasing viscosity ratio, decreasing wavelength, and increasing normalized front and fluid velocities. Conditions of neutral stability are also determined and indicate that fluid compressibility and net desorption tend to destabilize the exchange front. Sample calculations are presented for the problem of hydrogen isotope exchange in a column of palladium powder. DOE

N94-18048# Westinghouse Savannah River Co., Aiken, SC.
STRUCTURAL STABILITY OF 1100 C HEATED Pd/k DURING ABSORPTION CYCLING IN PROTIUM
I. A. Fisher 12 Mar. 1993 8 p
(Contract DE-AC09-89SR-18035)
(DE93-016270; WSRC-RP-93-401) Avail: CASI HC A02/MF A01

Pd/k is a hydride forming packing material which is used in the Thermal Cycling Absorption Process (TCAP). Palladium is supported on kieselguhr to create a packing material which will provide adequate void space to prevent excessive pressure drops and flow restrictions. The use of unsupported palladium would result in blockage of columns and clogging of filters due to the small particle size of unsupported palladium hydride powder. During pilot scale demonstrations, it was noted that the Pd/k packing material had degraded causing severe flow restrictions within the TCAP column. A solution to the problem involved the heating of Pd/k at 1,100 C to strengthen the packing material, and render it more resistant to breakdown. The 1,100 C heated Pd/k has been shown to be more resistant to mechanical breakdown than the Pd/k prior to heat treatment. Two primary modes of Pd/k particle degradation have been identified: mechanical breakdown caused by particle fluidization and degradation caused by absorption/desorption cycling. Absorption/desorption cycling causes the palladium particles within the packing to expanded and contract upon formation and decomposition of the hydride, respectively. This expansion and contraction causes large localized stresses within the packing material, which if these stresses can not be accommodated within the packing will cause the material to crack and degrade. The purpose of this report is to document the results of the absorption/desorption cycling of 1,100 C heated Pd/k and compare these results to the results obtained from the absorption/desorption cycling of Pd/k which had not been heated at 1,100 C. DOE

N94-18059# Stanford Research Inst., Menlo Park, CA.
X RAY ABSORPTION SPECTROSCOPIC STUDIES OF THE ACTIVE SITES OF NICKEL- AND COPPER-CONTAINING METALLOPROTEINS Ph.D. Thesis
G. O. Tan Jun. 1993 248 p
(Contract DE-AC03-76SF-00515)
(DE93-017142; SU-SLAC-420; SLAC/SSRL-0037; SSRL-M-420) Avail: CASI HC A11/MF A03

X-ray absorption spectroscopy (XAS) is a useful tool for obtaining structural and chemical information about the active sites of metalloproteins and metalloenzymes. Information may be obtained from both the edge region and the extended X-ray absorption fine structure (EXAFS) or post-edge region of the K-edge X-ray absorption spectrum of a metal center in a compound. The edge contains information about the valence electronic structure of the atom that absorbs the X-rays. It is possible in some systems to infer the redox state of the metal atom in question, as well as the geometry and nature of ligands connected to it, from the features in the edge in a straightforward manner. The EXAFS modulations, being produced by the backscattering of the ejected photoelectron from the atoms surrounding the metal atom, provide, when analyzed, information about the number and type of neighboring atoms and the distances at which they occur. In this thesis, analysis of both the edge and EXAFS regions has been used to gain information about the active sites of various metalloproteins. The metalloproteins studied were plastocyanin (Pc), laccase, and nickel carbon monoxide dehydrogenase (Ni CODH). Studies of Cu(I)-imidazole compounds, related to the protein hemocyanin, are also reported here. DOE

N94-18081# Research Inst. of National Defence, Linkoeping (Sweden).
SPECTRAL RADIANCE MEASUREMENTS ON A BLUFF BODY STABILIZED FLAME: CHARACTERIZATION OF THE IR SIGNATURE
C. Nelsson Dec. 1992 29 p
(PB93-195899; FOA-30694-8.3,3.1) Avail: CASI HC A03/MF A01

Spectral radiance measurements have been performed with an FTIR spectrometer on a bluff body stabilized flame. As a complement, time resolved broad band radiance measurements were made with a radiometer. Spectra with a resolution of 1/cm were obtained in the wavelength region 0.7 - 13 micrometers showing strong band emissions from H2O and CO2. The time resolved measurements showed radiance variations up to 1 kHz. Comparisons between the FTIR and radiometer results were in good agreement. The data will be used in future flame modeling work. NTIS

N94-18092# Lawrence Livermore National Lab., CA.
FEEST: A METHOD FOR TABULATING EQUATION OF STATE AND OPACITY TABLES
R. H. White Mar. 1993 13 p
(Contract W-7405-eng-48)
(DE93-017965; UCRL-ID-113714) Avail: CASI HC A03/MF A01

The tabulation of equations of state presently used by codes which carry temperature and density as independent variables, provides separate tables for pressure (P) and specific internal energy ((var epsilon)) as functions of the temperature (T) and density ((rho)). Both P and (var epsilon) are determined by bi-quadratic interpolation in tables of P and (var epsilon) values arranged on a rectangular grid in the T-(rho) plane. The system was designed for use on the 709-7094 generation of computers and has been used, essentially unmodified, for approximately twenty years. It has long been recognized that this 'Bi-quadratic Tabulation' system has several drawbacks. In this paper, the authors describe the Free Energy Equations of State Tabulation (FEEST) scheme which is intended to replace the presently used Bi-Quadratic Tabulation. The Bi-quadratic Tabulation, now used, treats opacities ((kappa)) in the same way as P and (var epsilon) expect that (1/T) replaces T as one of the interpolation variables. Since (kappa) may vary inversely with a high (3 to 8) power of T and since bi-quadratic interpolation in (1/T) includes terms only up to T(-2), opacity tables have been large and difficult to produce. DOE

N94-18185 Woods Hole Oceanographic Inst., MA. Dept. of Biology.
MODIFIED AEQUORIN SHOWS INCREASED BIOLUMINESCENCE ACTIVITY Final Report, 15 Mar. 1990 - 31 Jul. 1992
Douglas C. Prasher 18 Aug. 1993 10 p Limited Reproducibility: More than 20% of this document may be affected by poor print and microfiche quality
(Contract N00014-90-J-1704)
(AD-A268774) Avail: Issuing Activity (Defense Technical Information Center (DTIC))

Aequorin belongs to a unique class of photoproteins that emit light upon the binding of certain metals, calcium being the principal intracellular activator. This 'reporting function' of the metal-binding is instantaneous and is very easy to quantitate experimentally. The objective of the project was to develop a variety of recombinant forms of aequorin so they can be employed as metal biosensors. Three calcium-binding sites of aequorin were modified to examine their roles in the calcium-dependent luminescence as well as potentially binding other metal ions. Aequorins having Site 2 substitutions unexpectedly produce more light than wild-type aequorin. DTIC

N94-18193# California Univ., Berkeley. Lawrence Berkeley Lab.
FUNDAMENTAL STUDIES OF THE MECHANISM OF CATALYTIC REACTIONS WITH CATALYSTS EFFECTIVE IN THE GASIFICATION OF CARBON SOLIDS AND THE OXIDATIVE COUPLING OF METHANE
H. Heinemann, G. A. Somorjai, and D. L. Perry Sep. 1992 17 p
(Contract DE-AC03-76SF-00098)
(DE93-015262; LBL-32857) Avail: CASI HC A03/MF A01

Work will continue on the oxidative coupling reaction of methane over ternary oxide catalysts to produce C(sub 2), C(sub 3) and C(sub 4) hydrocarbons and particularly Olefins with high selectivity. The work which has shown that close to 100% selectivity can be obtained has received wide attention and has resulted in collaborative efforts with industry (CRADA) towards the development of a commercial process. An immediate purpose of additional work is to increase the conversion without diminishing the extremely high selectivity of the reaction and also to permit operation at higher space velocity to reduce equipment size. The mechanism of this reaction is not understood and much additional work is needed to explain the role of carbon formation and of water as intermediates in the reaction and to investigate whether carbon oxides are intermediates. It has been found that oxides other than calcium-nickel-potassium oxides can be useful catalysts for this reaction in the presence of steam and at relatively low temperatures and long contact times. Better definition of the class of binary metal oxides is required and better catalyst characterization is needed to ensure reproducibility of catalyst preparation and operational results. Pretreatment of the catalyst should be shortened and higher space velocities must be obtained. Close collaboration with Orion ACT is required to advance the project toward the pilot plant stage. In the area of coal and char catalytic steam gasification, the large volume of data obtained at atmospheric pressure will be extended to operations at higher pressures. DOE

N94-18194# California Univ., Berkeley. Lawrence Berkeley Lab.
CONVERSION OF ETHANE AND OF PROPANE TO HIGHER OLEFIN HYDROCARBONS
H. Heinemann and G. A. Somorjai Sep. 1992 25 p
(Contract DE-AC03-76SF-00098)
(DE93-015282; LBL-32858) Avail: CASI HC A03/MF A01

It has become apparent during the past few months that results obtained in the oxidative coupling of methane cannot be extended to ethane and propane. Good selectivities and yields for the oxydehydrogenation to olefins can be obtained but production of higher hydrocarbons is small. The present report summarizes results of experiments using zeolite based catalysts and compares these with basic oxide catalysts. The oxydehydrogenation of ethane over zeolite based catalysts (H+-, Na+-, Ni2+-, Pt2+-, Ga3+-, and (V)-ZSM-5) and oxide catalysts (Li/MgO, Ca-Ni-K) was studied in the temperature range 450-600 C. Selectivity to olefins close to 80% was achieved at 550 C. Basic (Na-ZSM-5) and neutral (V-ZSM-5) zeolite catalysts were shown to be more active and selective for the oxydehydrogenation of ethane than oxide catalysts. DOE

N94-18209# North Carolina State Univ., Raleigh.
SYNTHESIS OF HIGHER ALCOHOLS FROM CARBON MONOXIDE AND HYDROGEN IN A SLURRY REACTOR Ph.D. Thesis

M. S. McCutchen 28 Aug. 1992 113 p
(Contract DE-AC22-90PC-90043)
(DE93-015086; DOE/PC-90043/T9) Avail: CASI HC A06/MF A02

Higher, i.e. C(sub 2+), alcohols are desired as gasoline additives, feedstocks for producing ethers and as alternative fuels for automobiles. In all cases, the backbone branching of an alcohol improves octane rating, which is essential for good engine performance. These types of branched, higher alcohols are the desired products for a process converting synthesis gas, a CO and H2 mixture, often generated from coal gasification. Based on this premise, promoted ZnCr oxide catalysts appear to be as one of the best avenues for further investigation. Once this investigation is complete, a natural extension is to replace the Cr in the ZnCr oxide catalyst with Mo and W, both in the same elemental triad with Cr. Mo has already been shown as an active HAS catalyst, both on a SiO2 support and in the MoS2 form. The three catalyst combinations, ZnMo, ZnW, and MnCr oxides will be tested in the stirred autoclave system. However, if none of the three indicate any comparable activity and/or selectivity toward higher alcohols as compared with other HAS catalysts, then an investigation of the effects of Cs promotion on the ZnCr oxide methanol catalysts will be executed. DOE

N94-18221# Northwestern Univ., Evanston, IL. Dept. of Chemistry.
EXPERIMENTAL AND THEORETICAL INVESTIGATION OF SURFACE CHEMISTRY INDUCED BY DIRECT AND INDIRECT ELECTRONIC EXCITATION Final Report, 30 Sep. 1991 - 31 Mar. 1993
Peter C. Stair and Eric Weitz Jul. 1993 16 p
(Grant AF-AFOSR-0377-91)
(AD-A268846; AFOSR-93-0655TR) Avail: CASI HC A03/MF A01

There is now a considerable body of work concerned with the UV photochemistry of molecules adsorbed on well characterized metal and to a lesser extent, semiconductor and insulator surfaces. Several detailed review articles have already appeared on this subject. It has become clear that the photochemistry of monolayer adsorbates on surfaces is strongly influenced by a competition between promotion of the molecule to an excited state and quenching of that excited state. Excitation can be driven either by adsorbate or substrate photon absorption, and depending upon the excited state lifetime, a variety of relaxation mechanisms (quenching), may be important. These include radiative processes (fluorescence and phosphorescence), non-radiative processes (energy transfer to the surface or neighboring molecules via excitation of plasmons, phonons, or creation of electron-hole pairs), and chemical reaction. As a result, extensive modification of photochemical behavior has been observed for an adsorbate molecule with respect to its gas phase counterpart. DTIC

N94-18249# Argonne National Lab., IL.
ULTRASONIC PROCESS FOR DESTRUCTION OF CHLORINATED ORGANIC COMPOUNDS IN AQUEOUS SOLUTION
Jiann M. Wu and Hann S. Huang 1993 15 p Presented at the 1993 Chinese American Academic and Professional Convention, Chicago, IL, 2-5 Jul. 1993
(Contract W-31-109-eng-38)
(DE93-015551; ANL/ES/CP-79581; CONF-930796-1) Avail: CASI HC A03/MF A01

Laboratory investigations of the ultrasonic process for destruction of low concentrations of carbon tetrachloride (CCl4) into nonhazardous end products were carried out in a bench-scale batch reactor, equipped with a 600-W ultrasonic power supply. Process parameters studied included irradiation time, concentration, steady-state operating temperature, pH, and the intensity of applied ultrasonic-wave energy. High destruction efficiencies of greater than 99% were achieved through this process, and the irradiation time and the intensity of applied energy were identified to be the most important process parameters. The irradiation time required for a given degree of destruction decreased with increasing intensity of the applied ultrasonic energy. In addition, a detailed chemical reaction mechanism for the destruction of CCl4 in water was formulated. The agreement between the model and experimental results is generally good. DOE

N94-18255# California Inst. of Tech., Pasadena. Dept. of Chemistry.
APPLICATIONS OF SCANNING TUNNELING MICROSCOPY TO ELECTROCHEMISTRY
Nathan S. Lewis 26 Aug. 1993 3 p
(Contract N00014-92-J-1183)
(AD-A269129) Avail: CASI HC A01/MF A01

Our research during the last contract period involved an evaluation of the efficacy of using partially insulated STM tips as ultramicroelectrodes in studies of heterogeneous electron transfer. We initially fabricated these electrodes to serve as tips for imaging surfaces in solutions that contain significant concentrations of electroactive species. The tips that we have prepared (by partially coating etched Pt wire with molten glass) can have diameters as small as a few nanometers, and, by the nature of their small size, are useful in examining fundamental quantities such as the heterogeneous electron transfer rate constant for redox species. DTIC

N94-18256# Colorado State Univ., Fort Collins. Dept. of Biochemistry.
PROTON TRANSFER DYNAMICS AND CLUSTER ION FRAGMENTATION IN PHENOL/AMMONIA CLUSTERS Technical Report
M. Hineman, D. F. Kelley, and E. R. Bernstein 24 Aug. 1993 21 p
(Contract N00014-89-J-1237)
(AD-A269133; TR-86) Avail: CASI HC A03/MF A01

Excited-state proton transfer dynamics are reported for the phenol(NH3)n cluster system. Excited state proton transfer is shown to occur for this system by isotopic substitution of the hydroxyl proton and ammonia protons. The observed dynamics slow from 80 ps to 600 ps upon cluster deuteration. The effects of cluster vibrational energy and ammonia concentration in the expansion gas are also studied. The results of these experiments are compared with a previous study which used a single excitation energy and varied ionization energy. Our experiments indicate that a significant amount of cluster ion fragmentation occurs for this system and caution must be exercised in assigning the decays observed in a given ion mass channel to a particular parent cluster. Due to the difficulties of associating a given decay curve with a cluster of particular mass, a previously proposed model of proton transfer in isolated clusters which details the effect of cluster vibrational energy on the proton transfer rate, cannot be applied to the phenol/ammonia system. DTIC

N94-18257# Princeton Univ., NJ. Dept. of Mechanical and Aerospace Engineering.
STUDIES ON HIGH PRESSURE AND UNSTEADY FLAME PHENOMENA: REVISION Annual Report, 15 Apr. 1992 - 14 Apr. 1993
C. K. Law 4 Jun. 1993 139 p
(Contract F49620-92-J-0227)
(AD-A269138; AFOSR-93-0672TR) Avail: CASI HC A07/MF A02

The objective of the present program is to study the structure and response of steady and unsteady laminar premixed and nonpremixed flames in reduced and elevated pressure environments through (1) non-intrusive experimentation, (2) computational simulation using detailed flame and kinetic codes, and (3) asymptotic analysis with reduced kinetic mechanisms. During the reporting period, progress has been made in the following projects: (1) a theoretical and experimental study of unsteady diffusion flames; (2) a computational and experimental study of methane/air flames at elevated pressures; (3) an asymptotic analysis of the structure of methane/air premixed flames with reduced chemistry; (4) an asymptotic analysis of the extinction of laminar premixed flames with volumetric heat loss and chain mechanisms; and (5) asymptotic analyses of ignition in the supersonic laminar flat-plate boundary layer and mixing layer. A total of five reprints are appended. DTIC

N94-18389# Pennsylvania State Univ., University Park.
COMBUSTION INSTABILITY PHENOMENA OF IMPORTANCE TO LIQUID PROPELLANT ENGINES Annual Report, 1 Jul. 1992 - 30 Jun. 1993
Robert J. Santoro and William E. Anderson 31 Jul. 1993 23 p
(Grant AF-AFOSR-0336-91)
(AD-A268800; AFOSR-93-0667TR) Avail: CASI HC A03/MF A01

A study examining impinging liquid jets has been underway to determine physical mechanisms responsible for combustion instabilities in liquid bi-propellant rocket engines. Primary atomization has been identified as an important process. Measurements of atomization length, wave structure, and drop size and velocity distribution were made under various ambient conditions. Test parameters included geometric effects and flow effects. It was observed that pre-impingement jet conditions, specifically whether they were laminar or turbulent, had the major effect on primary atomization. Comparison of the measurements with results from a two-dimensional linear aerodynamic stability model of a thinning, viscous sheet were made. Measured turbulent impinging jet characteristics were contrary to model predictions; the structure of waves generated near the point of jet impingement were dependent primarily on jet diameter and independent of jet velocity. It has been postulated that these impact waves are related to pressure and momentum fluctuations near the impingement region and control the eventual disintegration of the liquid sheet into ligaments. Examination of the temporal characteristics of primary atomization (ligament shedding frequency) strongly suggests that the periodic nature of primary atomization is a key process in combustion instability. DTIC

N94-18395# University of Southern California, Los Angeles. Dept. of Chemistry.
AN AB INITIO STUDY OF THE WEAKLY BONDED CO-Cl2 COMPLEX Final Report, Mar. 1992 - Mar. 1993
Steven W. Bunte, Cary F. Chabalowski, Curt Wittig, and Robert A. Beaudet Aug. 1993 25 p
(Contract DE-FG03-89ER-04053; DA Proj. 1L1-61102-AH-43)
(AD-A269000; ARL-TR-178) Avail: CASI HC A03/MF A01

Ab initio structure and vibrational frequency calculations have been performed on the weakly bonded CO-Cl2 complex at the SCF and MP2 levels of approximation. Minima were found for the two linear structures, specifically CO-Cl2 and OC-Cl2, with the latter being slightly more stable than the former. In addition, minima were found for two nonlinear structures--one T-shaped and the other essentially parallel. In the T-shaped structure, the oxygen is very weakly bonded to the chlorines (C(sub 2v) symmetry). The parallel isomer is slightly lower in energy than the T-shaped structure; however, both of the nonlinear isomers are less stable than either of the linear isomers. The calculated properties of the OC-Cl2 isomers are in excellent agreement with the experimental results reported earlier, lending further support to the conclusion that the structure of the experimentally observed isomer is OC-Cl2 rather than CO-Cl2. DTIC

N94-18456 Army Research Lab., Aberdeen Proving Ground, MD.
FLAME STRUCTURE STUDIES OF A LEAN 20-TORR H2/N2O/Ar FLAME EMPLOYING MOLECULAR BEAM MASS SPECTROMETRY Final Report, 3 Aug. - 2 Nov. 1992
David C. Dayton and Rosario C. Sausa Aug. 1993 29 p Limited Reproducibility: More than 20% of this document may be affected by microfiche quality
(DA Proj. 1L1-61102-AH-43)
(AD-A268889; ARL-TR-183) Avail: Issuing Activity (Defense Technical Information Center (DTIC))

In this report, we present the results of our continued experimental efforts to investigate the structure of low-pressure, burner-stabilized H2/N2O/Ar flames. Coated Pt/Pt-Rh(10%) thermocouples and molecular beam sampling followed by quadrupole mass spectrometric detection (MB/MS) were employed to obtain temperature and species mole fraction profiles, respectively, in a fuel lean (Phi=0.64), 20-torr H2/N2O/Ar flame. Species profiles of H2, N2O, N2, H2O, NO, O2, H, O, and OH are compared to profiles generated using a detailed flame kinetic model. This provides a stringent test of the detailed chemical flame model and chemical mechanism for the H2/N2O/Ar system which is presently being developed at the U.S. Army Research Laboratory to enhance the understanding of nitramine propellant combustion and decomposition. DTIC

N94-18532# SRI International Corp., Menlo Park, CA.
NOVEL CATALYSTS FOR METHANE ACTIVATION
A. S. Hirschon, R. Malhotra, and R. B. Wilson Jul. 1993 16 p
(Contract DE-AC22-92PC-92112)
(DE93-040630; DOE/PC-92112/T2) Avail: CASI HC A03/MF A01

The objectives of this project are to test novel fullerene based catalysts for application in methane activation. Fullerenes are a recently discovered allotrope of carbon that have been found to possess unusual properties, some of which may be ideal for methane conversion to higher hydrocarbons. The project is divided into three technical tasks. Task 1 deals with the synthesis and characterization of the fullerenes and fullerene soots, Task 2 with the testing of the catalysts, and Task 3 with the evaluation of the results and technical reporting requirements. This quarter we prepared fullerene soot and conducted experiments to determined its reactivity towards methane, hydrogen, and ethylene. Soot containing approximately 12-14 wt % fullerenes was prepared by the discharge method of Haufler et al. SRI is in the process of developing methodology to produce large scale amounts of fullerenes and fullerene based materials and is working with a private company to that end. In order to provide a background of fullerene soot and describe some of these methods we have included Appendix A. We conducted some preliminary experiments in order to determine the temperature regime at which fullerene based soot would begin to be active for methane activation. We also were interested to determine if the soot would interact with methane or any of the product gases to undergo hydrogenation or methanation reactions. DOE

N94-18736 California Univ., Irvine. Dept. of Mechanical and Aerospace Engineering.
METAL SLURRY DROPLET AND SPRAY COMBUSTION Final Report, 1 Oct. 1988 - 30 Sep. 1992
W. A. Sirignano and R. Bhatia 15 Sep. 1993 219 p Limited Reproducibility: More than 20% of this document may be affected by microfiche quality
(Contract N00014-89-J-1135)
(AD-A269648) Avail: CASI HC A10

Analytical and numerical studies on n-octane and aluminum metal slurry droplet combustion and metal slurry spray combustion are discussed. Two limiting isolated droplet configurations are studied: one with a large metal particle enveloped by a liquid hydrocarbon and another with many fine metal particles inside a liquid drop. Vaporization models for isolated slurry droplets are formulated which can be used in spray combustion calculations. An analytical model describes the combustion of aluminum particles in air. The particle transient heating, the phase-equilibrium conditions of the vapor and condensed products are analyzed. Mass and energy interactions between the slurry droplets and gas flow are studied in an idealized configuration consisting of parallel droplet streams. Without forced convection and preheat of the ambient air to temperatures near the aluminum oxide melting point, the flame does not possess sufficient energy to ignite the metal. Ignition times for the metal particle depend on the solid mass loading and can be several times larger than the liquid fuel burnout time. With many fine metal particles which are initially uniformly distributed in a liquid fuel droplet, depending on the shell characteristics, different modes of liquid vaporization from the droplet can occur. At different combustor locations, interacting and distinct premixed and diffusion type reaction zones are present. The heating and burning times of the metal agglomerate are much larger than the liquid fuel vaporization times and increase with increasing metal particle size and metal loading of the droplets. DTIC

N94-18776# Illinois Univ., Urbana. Dept. of Aeronautical and Astronautical Engineering.
MATHEMATICAL PROBLEMS IN COMBUSTION Final Report, 1 May 1990 - 30 Apr. 1993
John Buckmaster 30 Apr. 1993 9 p
(Grant AF-AFOSR-0220-90)
(AD-A270147; AFOSR-93-0699TR) Avail: CASI HC A02/MF A01

Flame-balls are stationary spherical premixed flames observed in certain near-limit mixtures. Sufficiently large flame-balls are subject to a three-dimensional instability which defines a maximum mixture strength for which steady flame-balls can exist. The researchers studied the dynamics of flame-balls in the neighborhood of the neutral stability point and show that there is a transcritical bifurcation and that the dynamics are governed by a fifth-order system of nonlinear ordinary differential equations. The late time behavior of the solution of these equations corresponds either to a stationary sphere (stable solution) or a growing prolate spheroid. Prolate spheroids are observed experimentally, and the relationship between the experimental observations and the theoretical predictions. DTIC

N94-18785 Yale Univ., New Haven, CT. Dept. of Chemical Engineering.
TRANSPORT PHENOMENA AND INTERFACIAL KINETICS IN MULTIPHASE COMBUSTION SYSTEMS Annual Technical Report, 15 Feb. 1992 - 14 Feb. 1993
Daniel E. Rosner Aug. 1993 57 p Limited Reproducibility: More than 20% of this document may be affected by microfiche quality
(Grant AF-AFOSR-0170-91)
(AD-A270202; AFOSR-93-0712TR) Avail: CASI HC A04

This annual technical report summarizes Yale High Temperature Chemical Reaction Engineering Laboratory research activities (under Grant AFOSR 91-0170) for the one-year period ending 14 February 1993. Among our research results described in detail in the cited references, perhaps the most noteworthy are the development/reporting of: rational methods to predict the accessible surface area of aggregated 'soot' particles in high pressure combustion gases; experimental inference of particle thermophoretic diffusivities for titania aggregates in laminar counterflow laminar diffusion flames; consequences of particle thermophoresis for flame radiation, flame synthesis, and particle-based diagnostics; and quantitative methods for predicting/correlating the effects vapor phase chemical reactions on the rate and quality of vapor-deposited metal oxide thin films. DTIC

N94-18799 Puerto Rico Univ., Rio Piedras. Dept. of Chemistry.
PHOTODISSOCIATION STUDIES OF POLYATOMIC FREE RADICALS Final Report, 1 Jun. 1989 - 30 Sep. 1992
Brad R. Weiner Aug. 1993 152 p Limited Reproducibility: More than 20% of this document may be affected by microfiche quality
(Contract F49620-89-C-0070)
(AD-A270084; AFOSR-93-0703TR) Avail: CASI HC A08

An experimental program in gas phase polyatomic photochemistry and photophysics has been extablished in the Department of Chemistry at the University of Puerto Rico. Real time dynamics of sulfur monoxide photoelimination reactions have been studied by laser induced fluorescence spectroscopy of the nascent SO fragment on the B(sup 3)(Sigma(exp -) - X(sup 3)(Sigma(exp -)) transition in the region of 237-295 nm. The group of molecules under investigation are Sulfur dioxide (SO2), dimethyl sulfoxide ((CH3)2SO), and the thionyl halides (SOX2; where X = F, Cl, or Br). In all of these experiments, the parent molecule is irradiated with an excimer laser (either 193 or 248 nm) and the energy disposal into the nascent SO photofragment is determined and used as a mechanistic probe. The experiments indicate that several of these parent molecules undergo three body dissociations. A second set of experiments measures kinetic decay constants of the C2H3O, both in the ground state and in the excited state. The temperature (295-374 K) and pressure (2.5-100 torr) dependencies for the rate constant of the C2H3O + NO2 reaction have been measured by laser flash photolysis/laser induced fluorescence kinetic spectroscopy. The temperature dependent reaction for the decay of C2H3O in the presence of NO2 is characterized over the measured region by the rate expression, k(sub 2) = (1.48 +/- 0.70) x 1O(exp -11)exp(80.7 +/- 23.4K/T)cu cm/molecule-s. Fluorescence decay rates were determined in the presence to ten collision partners: He, Ar, N2, O2, CO, H2, HCl, CO2, C2H4, and CH3OCH = CH2. The measured electronic quenching cross-sections vary from 0.01 - 66.5 sq A. A vibrational level dependence was found for the radiative lifetimes. DTIC

N94-18895# Trane Co., LaCrosse, WI.
COMPATIBILITY OF REFRIGERANTS AND LUBRICANTS WITH MOTOR MATERIALS, VOLUME 1 Final Report
Robert Doerr and Stephen Kujak May 1993 154 p
(Contract DE-FG02-91CE-23810)
(DE93-040216; DOE/CE-23810/13-Vol-1) Avail: CASI HC A08/MF A02

This volume contains the abstract, scope, discussion of results, charts of motor material compatibility, test procedures, material identifications, and 84 pages of data summary tables. Compatibility test results for 11 pure refrigerants and 17 refrigerant-lubricant combinations with 24 motor materials are included. The greatest effect on the motor materials was caused by adsorption followed by desorption of refrigerants at higher temperatures. High internal pressure of the adsorbed refrigerants and their tendency to evolve from the materials resulted in blisters, cracks, internal bubbles in the varnish, and delamination or bubbles in the sheet insulations. The second effect was extraction or dissolution of materials that lead to embrittlement of some sheet insulations. HCFC-22 and HCFC-22/mineral oil had the most deleterious effects; the materials are expected to be reliable when used with most of the new refrigerants and lubricants. DOE

N94-18896# Trane Co., LaCrosse, WI.
COMPATIBILITY OF REFRIGERANTS AND LUBRICANTS WITH MOTOR MATERIALS, VOLUME 2
Robert Doerr and Stephen Kujak May 1993 254 p
(Contract DE-FG02-91CE-23810)
(DE93-040217; DOE/CE-23810/13-Vol-2) Avail: CASI HC A12/MF A03

This volume contains all the recorded measurements from the tests on the motor materials after exposures to the 11 pure refrigerants and to nitrogen at 60, 90, and 121 C. DOE

N94-18977# Imagination Resources, Inc., Dublin, OH.
MEASUREMENT OF VISCOSITY, DENSITY, AND GAS SOLUBILITY OF REFRIGERANT BLENDS IN SELECTED SYNTHETIC LUBRICANTS
R. C. Cavestri Jul. 1993 40 p
(Contract DE-FG02-91CE-23810)
(DE93-040221; DOE/CE-23810/20C) Avail: CASI HC A03/MF A01

Liquid/liquid miscibilities of four different 32 ISO VG polyoresters and one alkylbenzene at three concentrations has been determined with five refrigerant blends, one blend comprising HC-290. A vapor lubricant equilibrium (VLE) viscosity reduction of 32 ISO VG mineral oil with HCFC-22 has been completed. Composite Viscosity reduction information by the fractionate components from R-502 in 32 ISO VG mineral oil has been obtained from -10 C (14 F) to 125 C (257 F) isotherms. DOE

N94-18987# Lawrence Livermore National Lab., CA.
NUMERICAL SIMULATION OF TURBULENT MIXING AND COMBUSTION NEAR THE INLET OF A BURNER
L. D. Cloutman Feb. 1993 27 p
(Contract W-7405-eng-48)
(DE93-017960; UCRL-ID-112943) Avail: CASI HC A03/MF A01

The COYOTE computer program was used to simulate the flow field and turbulent mixing near the fuel and air inlets in a simplified burner that was proposed for experimental study at the Combustion Laboratory at the University of California at Irvine. Four cases are presented, with and without chemical reactions, with two different outflow boundary conditions, and with two different swirl numbers. These preliminary results demonstrate the ability of COYOTE to simulate burners, and they illustrate some limitations and requirements of such modeling. DOE

N94-19017# North Carolina Univ., Charlotte. Dept. of Chemistry.
OLIGOMER AND MIXED-METAL COMPOUNDS, POTENTIAL MULTIELECTRON TRANSFER CATALYSTS
D. P. Rillema 1993 21 p
(Contract DE-FG05-84ER-13263)
(DE93-019592; DOE/ER-13263/T1) Avail: CASI HC A03/MF A01

Physical, photophysical, and photochemical properties of Ru(2), Re(1), Pt(2), and Cu(2) monometallic complexes and of Ru(2)-Ru(2), Ru(2)-Co(3), Ru(2)-Re(1) bimetallic complexes were investigated. In an application, Pt and Au working electrodes were modified with the hydrogel kappa-carrageenan (anionic polysaccharide from seaweed), which was cured on the electrode surface with Ru(2) trisbipyridine and methyl viologen. Max photocurrent obtained was 12 micro-A-sq cm. DOE

N94-19097# California Univ., Berkeley. Lawrence Berkeley Lab.
CHEMICAL DYNAMICS IN TIME AND ENERGY SPACE Ph.D. Thesis
J. D. Myers Apr. 1993 233 p
(Contract DE-AC03-76SF-00098)
(DE93-018595; LBL-34091) Avail: CASI HC A11/MF A03

The development of a versatile picosecond ultraviolet/vacuum ultraviolet temporal spectrometer and its potential use for measuring internal energy redistribution in isolated molecules are described in detail. A detailed description of the double-pass Nd:YAG amplifier and the dye amplifiers is given with the pulse energies achieved in the visible, ultraviolet, and vacuum ultraviolet. The amplified visible pulses are shown to be of sub-picosecond duration and near transform limited. The instrument's temporal response ((le)10 ps) is derived from an instrument limited measurement of the dissociation lifetime of methyl iodide at 266 nm. The methyl iodide experiment is used to discuss the various sources of noise and background signals that are intrinsic to this type of experiment. Non-time-resolved experiments measuring the branching ratio and kinetic energy distributions of products from the 193 nm photodissociation of cyclopentadiene and thiophene are presented. These studies were done using the molecular beam Photofragment Translational Spectroscopy (PTS) technique. The results from the cyclopentadiene experiment confirm that H atom elimination to yield the cyclopentadienyl radical is the dominant dissociation channel. A barrier of (ge)5 kcal/mol can be understood in terms of the delocalization of the radical electron of the cyclopentadienyl fragment. A concerted elimination yielding cyclopropene and acetylene was also observed and is proposed to occur via a bicyclo-(2.1.0)pent-2-ene intermediate. Two other channels, yielding acetylene plus the CH2CHCH triplet carbene, and CH2 plus 1-buten-3-yne, are postulated to occur via ring opening. The implications of the experimental results for bulk thermal oxidation and pyrolysis models

are discussed. The thiophene experiment shows six competing dissociation channels. The postulated intermediates for the various thiophene dissociation channels include bicyclo, ring opened, and possibly ring contracted forms.
DOE

N94-19110# Air Force Inst. of Tech., Wright-Patterson AFB, OH. Foreign Aerospace Science and Technology Center.

SOME SUPERHIGH-FREQUENCY AND MAGNETIC PROPERTIES OF CHEMICALLY PRECIPITATED FILMS

L. V. Kirenskiy, N. S. Chistyakov, L. A. Chekanova, B. P. Tushkov, and G. I. Fish 2 Jun. 1993 12 p Transl. into ENGLISH from Fizika Magnitnikh Plenok (USSR), no. 3, 1970 12 p

(AD-A266195; FASTC-IR(RS)T-0300-93) Avail: CASI HC A03/MF A01

Magnetic films obtained by the method of chemical deposition have, in recent years, attracted the attention of researchers due to their interesting properties, the comparatively simple technology of deposition, and some possibilities for their practical utilization. For the purpose of obtaining additional information about the physical properties of chemically precipitated films and searching for the possibilities of their practical utilization in superhigh-frequency technology, we investigated Co-p magnetic films in the range of the super high frequencies (f = 9000 MHz). The fundamental, superhigh-frequency parameters of films (width and intensity of the line of ferromagnetic resonance, the components of complex shf susceptibility, etc.) were investigated on a standard shf spectrometer with the recording of differential curves of resonance absorption. Measurement of components of complex shf susceptibility was conducted on a setup described in detail earlier. The processes of quasi-static magnetic reversal were also studied. The structural properties of films were investigated by the method of X-ray diffraction analysis. Chemical analysis was conducted by the calorimetric method.
DTIC

N94-19118# Oak Ridge National Lab., TN.

DENSITIES AND VISCOSITIES OF TERNARY AMMONIA/WATER FLUIDS

R. H. Reiner and A. Zaltash Mar. 1993 16 p Presented at the Annual Winter Meeting of the ASME, New Orleans, LA, 28 Nov. - 3 Dec. 1993

(Contract DE-AC05-84OR-21400)

(DE93-015966; CONF-931121-9) Avail: CASI HC A03/MF A01

The densities, viscosities, and boiling points (at barometric pressure) of solutions formed by inorganic salts dissolved in an ammonia/water (NH3/H2O) solvent have been measured. These ternary solutions of ammonia/water/dissolved salt are being investigated to reduce rectification requirements and to expand the temperature range of ammonia/water in advanced absorption cycles. Densities and viscosities of these fluids were measured over the temperature range of 283.15 to 343.15 K (10.0 to 70.0 C). Observed densities and viscosities were expressed as empirical functions of temperature by means of the least-squares method. The dynamic viscosities of ternary fluids were found to be three to seven times greater than those of the binary system of NH3/H2O, which implies that a substantial decrease in the film heat and mass transfer coefficient is possible. However, because this quantitative linkage is not well understood, direct measurements of heat and mass transfer rates in a minisorber are recommended and planned.
DOE

N94-19132# Lehigh Univ., Bethlehem, PA.

SELECTIVE METHANE OXIDATION OVER PROMOTED OXIDE CATALYSTS

K. Klier, R. G. Herman, J. Sarkany, and Q. Sun Mar. 1993 19 p

(Contract DE-FG21-92MC-29228)

(DE93-040002; DOE/MC-29228/3407) Avail: CASI HC A03/MF A01

Sulfate anion was used to modify the surface basicity of 1 wt% Sr/La2O3, and catalytic tests were carried out to probe the selective oxidation of methane to C2 coupling products over these catalysts. Over a range of reaction temperatures of 500-700 C, most of the catalytic tests were carried out with a 1 wt% SO4 (sup 2-)/1 wt% Sr/La2O3 with a CH4 /air = 1/1 reactant mixture at 1 atm and with a gas hourly space velocity (GHSV) = 70,000 (ell)/kg catal/hr. The sulfated catalyst showed the largest improved catalytic effect at 500 C. Compared to the activity of the nonsulfated Sr/La2O3, the sulfated catalyst resulted in enhancement of the methane conversion, the C2 selectivity, and the yield of C2 products. In situ laser Raman spectroscopy was used to characterize the surface of sulfated and nonsulfated catalysts. Preliminary results indicate that the sulfate anion preferentially bonded to the Sr rather than to the La ions. The promoting effect of the acidic sulfate on the catalytic activity of basic Sr/La2O3 seems to be due to the inhibition of carbonate formation on the surface Sr ions.
DOE

N94-19134# National Inst. of Standards and Technology, Gaithersburg, MD. Thermophysics Div.

THERMOPHYSICAL PROPERTIES

R. F. Kayser Apr. 1993 237 p

(Contract DE-FG02-91CE-23810)

(DE93-040219; DOE/CE-23810/16) Avail: CASI HC A11/MF A03

Numerous fluids have been identified as promising alternative refrigerants, but much of the information needed to predict their behavior as pure fluids and as components in mixtures does not exist. In particular, reliable thermophysical properties data and models are needed to predict the performance of the new refrigerants in heating and cooling equipment and to design and optimize equipment to be reliable and energy efficient. The objective of this fifteen-month project has been to provide highly accurate, selected thermophysical properties data for Refrigerants 32, 123, 124, and 125, and to use these data to fit equations of state and transport property models. The new data have filled gaps in the existing data sets and resolved problems and uncertainties that existed in and between the data sets.
DOE

N94-19136# Dayton Univ. Research Inst., OH.

ACCELERATED SCREENING METHODS FOR DETERMINING CHEMICAL AND THERMAL STABILITY OF REFRIGERANT-LUBRICANT MIXTURES. PART 1: METHOD ASSESSMENT

R. Kauffman Apr. 1993 33 p

(Contract DE-FG02-91CE-23810)

(DE93-040215; DOE/CE-23810/10-Pt-1) Avail: CASI HC A03/MF A01

This report presents results of a literature search performed to identify analytical techniques suitable for accelerated screening of chemical and thermal stabilities of different refrigerant/lubricant combinations. Search focused on three areas: Chemical stability data of HFC-134a and other non-chlorine containing refrigerant candidates; chemical stability data of CFC-12, HCFC-22, and other chlorine containing refrigerants; and accelerated thermal analytical techniques. Literature was catalogued and an abstract was written for each journal article or technical report. Several thermal analytical techniques were identified as candidates for development into accelerated screening tests. They are easy to operate, are common to most laboratories, and are expected to produce refrigerant/lubricant stability evaluations which agree with the current stability test ANSI/ASHRAE (American National Standards Institute/American Society of Heating, Refrigerating, and Air-Conditioning Engineers) Standard 97-1989, 'Sealed Glass Tube Method to Test the Chemical Stability of Material for Use Within Refrigerant Systems.' Initial results of one accelerated thermal analytical candidate, DTA, are presented for CFC-12/mineral oil and HCFC-22/mineral oil combinations. Also described is research which will be performed in Part 2 to optimize the selected candidate.
DOE

N94-19150# Lehigh Univ., Bethlehem, PA. Center for Surface Studies.

SELECTIVE METHANE OXIDATION OVER PROMOTED OXIDE CATALYSTS

K. Klier, R. G. Herman, J. Sarkany, and Q. Sun Jun. 1993 23 p

(Contract DE-FG21-92MC-29228)

(DE93-040001; DOE/MC-29228/3408) Avail: CASI HC A03/MF A01

A 1 wt% SO4(sup 2(minus))/1 wt% Sr/La2O3 catalyst has been shown by us to be one of the most active catalyst for the oxidative coupling of CH4 to C2 hydrocarbons. One of the by-products is CO2 and this is a potential strong poison for the formation of C2 (sup +) products. Hence, various pretreatments of this catalyst were studied in terms of effect on the catalytic performance. Before the reaction was carried out at 500 or 550 C, the catalyst was pretreated in flowing air or He at 500, 700, or 800 C. Relative to the 500 C treatment, the pretreatment in air at 700 C only slightly decreased the C2 (sup +) selectivity while the CO(x) selectivity increased. This effect was larger when the pretreatment was carried out at 800 C. It was observed that the deactivation effect was slightly smaller when the pretreatments were carried out in He instead of air. For both air and He, the CH4, conversion and the C2 % yield showed more or less parallel changes (small decreases) with increasing pretreatment temperature. After a standard pretreatment (air, 500 C, 1 hr), the reaction temperature was increased stepwise from 500 to 700 C and then lowered to 550 (or 500 C). It was observed that the catalytic performance showed deactivation towards the C2 (sup +) products. Decreasing stepwise the total flow rate (GHSV) of the reacting gas mixture (CH4)/air = 1/1) from 70,175 to 5,388 (ell)/kg catal/hr at a reaction temperature of 550 C caused large changes in both the activity and selectivity. After going back at 550 C to the original GHSV = 70,175 (ell)/kg catal/hr, the temperature was increased stepwise up to 600 C. Up to 580 C, the catalytic activity and selectivity did not change very much. DOE

N94-19191# Trane Co., LaCrosse, WI.
COMPATIBILITY OF REFRIGERANTS AND LUBRICANTS WITH MOTOR MATERIALS, VOLUME 3
R. Doerr and S. Kujak May 1993 349 p
(Contract DE-FG02-91CE-23810)
(DE93-040218; DOE/CE-23810/13-Vol-3) Avail: CASI HC A15/MF A03

This volume contains all the recorded measurements from the tests on the motor materials after exposure to the 17 refrigerant-lubricants combinations and to nitrogen at 126 or 127 C. DOE

N94-19192# California Univ., Berkeley. Lawrence Berkeley Lab.
CURRENT-POTENTIAL CHARACTERISTICS OF ELECTROCHEMICAL SYSTEMS Ph.D. Thesis
V. S. Battaglia Jul. 1993 210 p
(Contract DE-AC03-76SF-00098)
(DE93-040303; LBL-34386) Avail: CASI HC A10/MF A03

This dissertation contains investigations in three distinct areas. Chapters 1 and 2 provide an analysis of the effects of electromagnetic phenomena during the initial stages of cell discharge. Chapter 1 includes the solution to Maxwell's equations for the penetration of the axial component of an electric field into an infinitely long cylindrical conductor. Chapter 2 contains the analysis of the conductor included in a radial circuit. Chapter 3 provides a complete description of the equations that describe the growth of an oxide film. A finite difference program was written to solve the equations. The system investigated is the iron/iron oxide in a basic, aqueous solution. Chapters 4 and 5 include the experimental attempts for replacing formaldehyde with an innocuous reducing agent for electroless deposition. In chapter 4, current-versus-voltage curves are provided for a sodium thiosulfate bath in the presence of a copper disk electrode. Also provided are the cathodic polarization curves of a copper/EDTA bath in the presence of a copper electrode. Chapter 5 contains the experimental results of work done with sodium hypophosphite as a reducing agent. Mixed-potential-versus-time curves for solutions containing various combinations of copper sulfate, nickel chloride, and hypophosphite in the presence of a palladium disk electrode provide an indication of the reducing power of the solutions. DOE

N94-19239# Oak Ridge National Lab., TN.
ATOMIC RESOLUTION ELECTRON ENERGY LOSS SPECTROSCOPY IN THE SCANNING TRANSMISSION ELECTRON MICROSCOPE
N. D. Browning, M. F. Chisholm, and S. J. Pennycook 1993 3 p
Presented at the 6th Analytical Electron Microcopy (AEM) Workshop, Los Angeles, CA, 11-16 Jul. 1993
(Contract DE-AC05-84OR-21400)
(DE93-015334; CONF-930755-3) Avail: CASI HC A01/MF A01

Electron energy loss spectroscopy (EELS) in the scanning transmission electron microscope (STEM) is an invaluable tool for the microanalysis of materials, providing information on both compositional and electronic structure fluctuations on the sub-nanometer scale. To utilize fully the high resolution potential of the energy loss signal, it is essential to have a reference high-resolution image showing the atomic structure in the region of study. The recently developed high-resolution Z-contrast imaging technique for the STEM, provides an intuitive reference image of the atomic structure that, as both imaging and microanalysis can be performed simultaneously, can be conveniently used to position the electron probe over individual atomic columns. The spatial resolution of both the image and the energy loss spectrum can be identical, and in principle limited only by the probe size of the microscope. Therefore, for the 2.2 A probe size of the VG HB501 UX dedicated STEM, there exists the ability to be able to resolve individual atomic columns or planes. DOE

N94-19240# Los Alamos National Lab., NM.
KINETIC STUDIES OF ELECTROCHEMICAL GENERATION OF Ag(II) ION AND CATALYTIC OXIDATION OF SELECTED ORGANICS
C. Zawodzinski, W. H. Smith, and K. R. Martinez 1993 8 p Presented at the 183rd Electrochemical Society Meeting, Honolulu, HI, 16-21 May 1993
(Contract W-7405-eng-36)
(DE93-016601; LA-UR-93-2196; CONF-930571-24) Avail: CASI HC A02/MF A01

The goal of this research is to develop a method to treat mixed hazardous wastes containing selected organic compounds and heavy metals, including actinide elements. One approach is to destroy the organic compounds via electrochemical oxidation to carbon dioxide, then recover the metal contaminants through normally accepted procedures such as ion exchange, precipitation, etc. The authors have chosen to study the electrochemical oxidation of a simple alcohol, iso-propanol. Much of the recent work reported involved the use of an electron transfer mediator, usually the silver(1)/(2) redox couple. This involved direct electrochemical generation of the mediator at the anode of a divided cell followed by homogeneous reaction of the mediator with the organic compound. In this study the authors have sought to compare the mediated reaction with direct electrochemical oxidation of the organic. In addition to silver(1)/(2), they also looked at the cobalt(2)/(3) redox couple. In the higher oxidation state, both of these metal ions readily hydrolyze in aqueous solution to ultimately form insoluble oxide. The study concluded that in a 6M nitric acid solution at room temperature, iso-propanol can be oxidized to carbon dioxide and acetic acid. Acetic acid is a stable intermediate and resists further oxidation. The presence of Co(3) enhances the rate or efficiency of the reaction. DOE

N94-19266# Lawrence Livermore National Lab., CA.
PENETROMETER COMPATIBLE, FIBER-OPTIC SENSOR FOR CONTINUOUS MONITORING OF CHLORINATED HYDROCARBONS: FIELD TEST RESULTS
F. P. Milanovich, S. B. Brown, and B. W. Colston, Jr. Apr. 1993 7 p Presented at the Chemical Sensor Symposium, Honolulu, HI, 16-21 May 1993
(Contract W-7405-eng-48)
(DE93-017974; UCRL-JC-112182; CONF-9305124-3) Avail: CASI HC A02/MF A01

We have developed and field tested a fiber optic chemical sensor for use in environmental monitoring and remediation. The principle of detection is colorimetric and is based on an irreversible chemical reaction between a specific reagent and the target compound. The formation of reaction products are monitored remotely with optical fibers. Successive or on-demand measurements are made possible with a reagent reservoir and a miniature pumping system. The sensor has been evaluated against gas chromatography standards and has demonstrated accuracy and sensitivity sufficient for the environmental monitoring of the contaminants triceoroethlyene (TCE) and chloroform. The sensor system can be used for bench-top analyses or for in-situ measurements such as groundwater and vadose monitoring wells or in penetrometry mediated placements. DOE

N94-19304# California Univ., Berkeley. Lawrence Berkeley Lab.
UNIMOLECULAR PHOTODISSOCIATION DYNAMICS OF KETENE (CH2CO): THE SINGLET/TRIPLET BRANCHING RATIO AND EXPERIMENTAL OBSERVATION OF THE VIBRATIONAL LEVEL THRESHOLDS OF THE TRANSITION-STATE Ph.D. Thesis
S. K. Kim May 1993 202 p
(Contract DE-AC03-76SF-00098)
(DE93-019252; LBL-34251) Avail: CASI HC A10/MF A03

The rotational distributions of CO products from the dissociation of ketene at photolysis energies 10 cm(exp -1) below and 56, 110, 200, 325, 425, 1,107, 1,435, 1,720, and 2,500 cm(exp -1) above the singlet threshold, are measured in a supersonic free jet of ketene. The CO(v'') = 0 rotational distributions at 56, 110, 200, 325, and 425 cm(exp -1) are bimodal. The peaks at low J's, which are due to CO from the singlet channel, show that the product rotational distribution of CO product from ketene dissociation on the singlet surface is well described by phase space theory (PST). For CO(v'') = 0 rotational distributions at higher excess energies, the singlet and triplet contributions are not clearly resolved, and the singlet/triplet branching ratios are estimated by assuming that PST accurately predicts the CO rotational distribution from the singlet channel and that the distribution from the triplet channel changes little from that at 10 cm(exp -1) below the singlet threshold. At 2,500 cm(exp -1) excess energy, the CO(v'') = 1 rotational distribution is obtained, and the ratio of CO(v'') = 1 to CO(v'') = 0 products for the singlet channel is close to the variational RRKM calculation, 0.038, and the separate statistical ensembles (SSE) prediction, 0.041, but much greater than the PST prediction, 0.016. Rate constants for the dissociation of ketene (CH2CO) and deuterated ketene (CD2CO) have been measured at the threshold for the production of the CH(D2) and CO. Sharp peaks observed in photofragment excitation (PHOFEX) spectra probing CO (v = 0, J = 2) product are identified with the C-C-O bending mode of the transition state. RRKM calculations are carried out for two limiting cases for the dynamics of K-mixing in highly vibrationally excited reactant states. DOE

N94-19367*# Carnegie-Mellon Univ., Pittsburgh, PA. Dept. of Chemical Engineering.
ELECTROKINETIC TRANSPORT OF HETEROGENEOUS PARTICLES IN SUSPENSIONS Status Report, 1 Jan. - 31 Dec. 1993
John L. Anderson 1 Oct. 1993 3 p
(Grant NAG8-964)
(NASA-CR-194478; NAS 1.26:194478) Avail: CASI HC A01/MF A01

The focus of research over the past nine months had been on a theory for the electrophoresis of slender particles and on trajectory analysis of colloidal doublets rotating in electric fields. Brief summaries of the research are given. Derived from text

N94-19376# Ecole Centrale de Lyon (France). Lab. de Mecanique des Fluides et d'Acoustique.
EXPERIMENTAL STUDY OF FLAME FRONT INTERACTIONS Ph.D. Thesis [ETUDE EXPERIMENTALE DE L'INTERACTION DE FRONTS DE FLAMMES]
Didier Larrauri 1991 114 p In FRENCH
(ECL-91-40; ETN-93-94586) Avail: CASI HC A06/MF A02

The flame front interaction is characterized by measuring the temperature, the hydrogen concentration, and the flame velocity and applying tomography for flow visualizations. Particular attention is given to flow velocity measurements which give information on the dynamics of processes. The purpose of the investigation is to study the coalescence of flame fronts at the flow between two flames. Data was acquired under three combustion conditions: laminar flames; flame and vortice interactions, where the vortices were generated by a von Karman device placed between the two flames; and the flame fronts are disturbed by a turbulent flow due to a grid. The results show that the interaction between two flames can be detected not only by changes of flame behavior, but also by flow changes in the region between the two flames. ESA

N94-19406# Ecole Centrale de Lyon (France). Dept. de Physiochimie des Materiaux.
CONSTRUCTION OF A SCANNING TUNNELING MICROSCOPE IN LIQUID MEDIA: STUDIES OF THE PREPARATION OF THE GRAPHITE SURFACE AND THE CHEMICAL CLEANING OF INDIUM PHOSPHIDE Ph.D. Thesis [REALISATION D'UN MICROSCOPE A EFFET TUNNEL EN MILIEU LIQUIDE. ETUDES DE LA FONCTIONNALISATION DE LA SURFACE GRAPHITIQUE ET DU DECAPAGE CHIMIQUE DU PHOSPHURE D'INDIUM]
Magali Phaner 1992 170 p In FRENCH
(ECL-92-25; ETN-93-94589) Avail: CASI HC A08/MF A02

The principle of the Scanning Tunneling Microscope (STM) and the exploitation of images with different representations and the problems of theoretical interpretation are presented. The realization of the microscope is described. The scanning tunneling microscope is a precision device sensitive to a large range of perturbations. Different perturbations are studied and the retained alternatives are presented. The liquid environment adds some instrumental constraints with the need of a tree electrodes cell and a potentiostat. Two studies realized with this apparatus are presented. The first one concerns the deposition of palladium particles by chemical way on HOPG (Highly Oriented Pyrolitic Graphite) in order to study catalysts. A special study is made on the graphite surface at atomical scale after the oxidation phase. The images show a modification of the atomic network attributed to the presence of organic groups. Some reactive sites are then created in the graphitic surface and are used for the palladium complexes fixation. The second experiment consists in the observation of the InP(n) surface in diluted acid solution. The surface is prepared by a mechanochemical polish. The liquid is used in that case to protect the surface from an oxidation. The preliminary study is the first one made in InP in liquids. It shows a relief constituted by some tenths of nanometers high hillocks. ESA

N94-19456 Institut d'Aeronomie Spatiale de Belgique, Brussels.
ULTRAVIOLET ABSORPTION CROSS-SECTIONS OF SOME CARBONYL COMPOUNDS AND THEIR TEMPERATURE DEPENDENCE
D. Gillotay, P. C. Simon, and L. Dierickx 1993 18 p Presented at Quadrennial Ozone Symposium, Charlottesville, VA, 4-13 Jun. 1992 Submitted for publication
(Aeronautica-Acta-A-368-1993; ETN-93-94960) Copyright Avail: Issuing Activity (Institut d'Aeronomie Spatiale de Belgique, 3 Avenue Circulaire, B-1180 Brussels, Belgium)

Ultraviolet absorption cross section of phosgene (CCl2O), trichloroacetylchloride (CCl3-CClO), and trichloroacetaldehyde (CCl3-CHO) were measured between 170 and 320 nm for temperature ranging from 210 to 295 K with a classical double beam equipment. The data are compared with other available determinations performed at room temperature. Photodissociation coefficients are estimated and their temperature dependence is discussed. Impact of the photodissociation on the total atmospheric destruction of these compounds is illustrated. ESA

N94-19459 Institut d'Aeronomie Spatiale de Belgique, Brussels.
TEMPERATURE DEPENDENCE OF ULTRAVIOLET ABSORPTION CROSS-SECTIONS OF ALTERNATIVE HYDROCHLOROFLUOROCARBONS
D. Gillotay, P. C. Simon, and L. Dierickx 1993 22 p Presented at Quadrennial Ozone Symposium, Charlottesville, VA, 4-13 Jun. 1992 Submitted for publication
(Aeronautica-Acta-A-369-1993; ETN-93-94961) Copyright Avail: Issuing Activity (Institut d'Aeronomie Spatiale de Belgique, 3 Avenue Circulaire, B-1180 Brussels, Belgium)

Ultraviolet absorption cross section of six alternative hydrochlorofluorocarbons (HCFC-21, HCFC-22, HCFC-123, HCFC-124, HCFC-141b and HCFC-142b) and of one alternative hydrobromofluorocarbon (Halon-22b1) were measured between 170 and 260 nm for temperature ranging from 210 to 295K. The data are compared with other available determinations performed at room temperature, and their temperature dependence is discussed. Photodissociation coefficients are estimated and their temperature dependence is discussed. Impact of the photodissociation on the total atmospheric destruction of these compounds is illustrated. ESA

N94-19538# California Univ., Berkeley. Lawrence Berkeley Lab.
METALLIZATION AND CHARGE-TRANSFER GAP CLOSURE OF TRANSITION-METAL IODIDES UNDER PRESSURE Ph.D. Thesis
A. Li-Chung Chen May 1993 105 p
(Contract DE-AC03-76SF-00098)
(DE93-040301; LBL-34400) Avail: CASI HC A06/MF A02

It is shown with resistivity and near-IR absorption measurements that NiI2, CoI2, and FeI2 metallize under pressure by closure of the charge-transfer energy gap at pressures of 17, 10, and 23 GPa, respectively, which is close to the antiferromagnetic-diamagnetic transition in NiI2 and CoI2. Thus, the magnetic transitions probably are caused by the metallization; in NiI2 and CoI2, the insulator-metal transitions are first order. Moessbauer and XRD data were also collected. DOE

N94-19552# Argonne National Lab., IL.
ADSORPTION ANALYSIS OF AMMONIA IN AN AQUEOUS SOLUTION
B. Arman and C. B. Panchal 1993 7 p Presented at the 28th Intersociety Energy Conversion Engineering Conference, Atlanta, GA, 8-13 Aug. 1993
(Contract W-31-109-eng-38)
(DE93-019512; ANL/ES/CP-80045; CONF-930804-15) Avail: CASI HC A02/MF A01

An analysis is carried out to determine the effects of the diffusional resistance on the rate of the adsorption of ammonia in an aqueous solution. A performance prediction model is developed to calculate the local rate of heat and mass transfer, including physical and thermodynamic property calculations of the mixture. An algorithm is developed for calculating the interfacial conditions. The local heat- and mass-transfer calculation is then incorporated into the performance prediction method for adsorption for a given geometry. DOE

N94-19653# California Univ., Berkeley. Lawrence Berkeley Lab.
ELECTROCATALYSTS FOR OXYGEN ELECTRODES
E. Yeager (Case Western Reserve Univ., Cleveland, OH.) Feb. 1993 62 p
(Contract DE-AC03-76SF-00098)
(DE93-040446; LBL-33814) Avail: CASI HC A04/MF A01

The object of this project was to understand factors controlling the activity of O_2 reduction and generation electrocatalysts in order to attain higher activity and longer-term stability. Two broad classes of catalysts were developed: transition metal macrocycles in monomeric and polymeric forms, and transition metal oxides including perovskites and pyrochlores. DOE

N94-19660# Massachusetts Inst. of Tech., Cambridge.
CONTROL OF CATALYTIC HYDROTREATING SELECTIVITY WITH AMMONIA
C. N. Satterfield and S. Gultekin 1993 6 p
(Contract DE-FG22-89PC-89775)
(DE93-041223; DOE/PC-89775/13) Avail: CASI HC A02/MF A01

We have chosen the following as our standard reaction conditions: T = 3600, total pressure about 6.9 MPa, partial pressure of PBz = 24.4 kPa, partial pressure of H_2S = 13.3 kPa, partial pressure of NH_3 = 13.3 kPa, and space-time = 200 h. g. cat/mol PBz. The carrier liquid is hexadecane ($C_{16}H_{34}$). As before, the H_2S and NH_3 are generated in situ by hydrogenation of 1-dodecane thiol and n-propyl amine, respectively, added to the C16 feed. The activity of the fresh catalyst dropped to a steady state level after about 120 hours on stream following which four runs were carried out at p.p. NH_3 values of 0, 13.3, 24.4, and 48.8 kPa, respectively. For each NH_3 p.p., space-times were varied at the following levels: 50, 100, 200, 400, and 600. Analyses were made for propylcyclohexene (C(sub A)), propylcyclohexane (C(sub B)), and benzene (C(sub D)). No other products were found in any significant amounts. The ratio C(sub B)/C(sub D) is a measure of the activity for ring hydrogenation relative to hydrocracking. The data are shown in four tables that follow. The results will be analyzed kinetically in the next quarter. However, the following generalizations are evident: NH_3 significantly reduces the activity of the catalyst for both types of reaction; and the activity for hydrocracking is reduced more than that for ring hydrogenation, a favorable result, but the effect is not large at the conditions studied thus far. The effect is most evident at low NH_3 concentrations. DOE

N94-19728# California Univ., Santa Barbara. Dept. of Chemistry.
HIGH RESOLUTION TRANSMISSION ELECTRON MICROSCOPY OF MESOPOROUS MCM-41 TYPE MATERIALS Technical Report, 1 Jun. 1993 - 31 May 1994
V. Alfredsson, M. Keung, A. Monnier, G. Stucky, and K. Unger 30 Sep. 1993 7 p
(Contract N00014-90-J-1159)
(AD-A271271) Avail: CASI HC A02/MF A01

The mesoporous silica based materials invented by scientists of the Mobil Corporation have attracted considerable interest since the first scientific publications appeared in 1992. Recently a detailed mechanism was suggested how these materials can be formed via a layered intermediate. Although already in the first publications transmission electron micrographs have been published, it is yet not clear whether the pore shape is hexagonal or round. A model describing the intensities of the X-ray diffraction patterns is favoring a hexagonal pore shape. This was, however, not confirmed by other techniques. Here we present for the first time a direct observation of the transition between the layered and the hexagonal phase which also allows to discriminate between two possible mechanisms for this transformation, as well as direct evidence of the hexagonal pore shape. DTIC

N94-19755 Rome Lab., Griffiss AFB, NY.
THE APPLICATION OF JET SPRAY AND ION BEAM CONTAMINATION REMOVAL TECHNIQUES TO SAMPLES FROM THE LDEF SPACECRAFT Report, Jun. - Sep. 1992
S. P. Hotaling Jun. 1993 47 p Limited Reproducibility: More than 20% of this document may be affected by microfiche quality
(AD-A270973; RL-TR-93-109) Avail: CASI HC A03

Two samples from LDEF experiment M10003-4 were analyzed for molecular and particulate contamination prior to and following treatment with advanced satellite contamination removal techniques (CO_2 Gas/Solid Jet Spray and Oxygen Ion Beam). The pre- and post-cleaning measurements and analyses are presented. The Jet Spray removed particulates in seconds. The low energy reactive oxygen ion beam removed 5000 angstroms of photopolymerized hydrocarbon contamination in less than 1 hour. Spectroscopic analytical techniques were applied to the analysis of cleaning efficiency including: Fourier transform infrared, auger, x-ray photo emission, energy dispersive x-ray, and ultraviolet/visible. The results of this work suggest that the contamination was due to spacecraft self contamination enhanced by atomic oxygen plasma dynamics and solar UV radiation. These results also suggest the efficacy for the Jet Spray and Ion Beam contamination control technologies for spacecraft optical surfaces. DTIC

N94-19778 Rolls-Royce, Inc., Atlanta, GA.
COLLABORATIVE RESEARCH ON COMBUSTION DIAGNOSTICS AND MODELING BETWEEN ROLLS-ROYCE, INC. AND THE UNITED STATES AIR FORCE WRIGHT LABORATORY Interim Report, 1 May 1990 - 30 Nov. 1992
A. Rose Jan. 1993 119 p Limited Reproducibility: More than 20% of this document may be affected by microfiche quality
(Contract F33615-90-C-2092)
(AD-A270660; WL-TR-93-2061) Avail: Issuing Activity (Defense Technical Information Center (DTIC))

Diagnostic techniques are employed to investigate flows typical of a gas turbine combustor with the aim of furthering the understanding of the complex physical and chemical processes involved and using this understanding in validating and developing combustion Computational Fluid Dynamic (CFD) codes. Detailed measurements of velocities and Reynolds stresses have been made with a Laser Doppler Velocimeter (LDV) in an axisymmetric combustor with a strongly swirling, isothermal, turbulent flow. Anomalies identified in the initial measurements were attributed to LDV signal noise problems caused by reflections off the internal combustor walls. Future LDV measurements will be taken along a vertical diameter within the combustor to minimize these noise problems. Comparisons of the isothermal measurements with CFD predictions are presented and discussed. Both a Reynolds Stress Transport Model (RSTM) and a k epsilon turbulence model have been employed. The RSTM outperforms the k - epsilon model for this strongly swirling flow. Although the bar-(v'w') shear stress could not be measured with the current combustor configuration, the results from the modeling illustrate the important role played by the bar-(v'w') shear stress in defining the nature of the swirling flow. A new Rolls-Royce designed and manufactured water-cooled combustor, with enhanced optical access will permit the simultaneous measurement of all velocity components and all Reynolds stresses. Details of this new test section are presented. DTIC

N94-19176*# Case Western Reserve Univ., Cleveland, OH. Center on the Commercial Development of Space Programs.
LIMITED DURATION OF CANDIDATE MATERIALS EXPOSURE EXPERIMENT (LDCE): A COMPLEX AUTONOMOUS PAYLOAD (CAP) USING A GET AWAY SPECIAL (GAS) CANISTER
D. Davis *In* NASA. Goddard Space Flight Center, The 1993 Shuttle Small Payloads Symposium Oct. 1993 p 115-124 (For primary document see N94-19162 04-12)
Avail: CASI HC A02/MF A03

26 METALLIC MATERIALS

Includes physical, chemical, and mechanical properties of metals, e.g., corrosion; and metallurgy.

N94-17679 China Nuclear Information Centre, Beijing.
THE EFFECT OF SURFACE TREATMENT AND GASEOUS RUST PROTECTION PAPER ON THE ATMOSPHERIC CORROSION STABILITY OF ALUMINIUM ALLOY
Guizhong Gao (Beijing Inst. of Nuclear Engineering, China.) Mar. 1992 Limited Reproducibility: More than 20% of this document may be affected by microfiche quality
(DE93-623326; CNIC-00601; BINE-0017) Avail: Issuing Activity (Department of Energy (DOE)) (US Sales Only)

The experimental results of atmospheric corrosion of 166 aluminum alloy of Al-Mg-Si-Cu system and 167 aluminum alloy of Al-Mg-Si-Cu-Fe-Ni system for different surface treatment and different wrapping papers used are introduced. The results show: (1) The composition of aluminum alloy has some effect on the performance of atmospheric corrosion stability and the local corrosion depth for 167 aluminum alloy specimen is considerable. (2) After 8 years storage, the 167 aluminum alloy tubular specimen, which was treated with surface treatment in deionized water at 100 to approx 230 deg C, has no spot of atmospheric corrosion found. (3) Within the test period, the performance of atmospheric corrosion stability by sulphuric-acid anodization film is remarkable. (4) The No. 19 gaseous rust protection paper has no effect of atmospheric corrosion stability on the 166 and 167 aluminum alloys which were treated with quenching and natural ageing method. DOE

N94-17692 Gosudarstvennyi Komitet po Ispolzovaniyu Atomnoi Energii, Obninsk (USSR).
EFFECT OF OXYGEN CONCENTRATION AND ORDERING ON VANADIUM-OXYGEN ALLOY VIBRATIONAL SPECTRA
V. V. Sumin, S. A. Danilkin, and V. P. Minaev 1991 22 p Limited Reproducibility: More than 20% of this document may be affected by microfiche quality
(DE93-627003; FEI-2173) Avail: CASI HC A03 (US Sales Only)

The calculations of disordered interstitial solid solution vanadium - oxygen vibrational spectra are presented. The qualitative description of vanadium atom spectrum deformation caused by oxygen was obtained in frame of virtual crystal approximation. The interatomic vanadium - oxygen potential is presented. The oxygen atoms vibrational spectra for different oxygen contents were calculated using the computer simulation method. The concentration dependence of oxygen vibrational band widths and the oxygen atoms ordering effects are discussed. DOE

N94-17711# Lawrence Livermore National Lab., CA.
MODELING MICROSTRUCTURAL EVOLUTION AND THE MECHANICAL RESPONSE OF SUPERPLASTIC MATERIALS
D. R. Lesuer, C. K. Syn, K. L. Cadwell, and C. S. Preuss 11 Jan. 1993 16 p Presented at the Fall Meeting of the Metallurgical Society and American Institute of Metallurgical and Petroleum Engineers, Chicago, IL, 1-5 Nov. 1992
(Contract W-7405-eng-48)
(DE93-014417; UCRL-JC-110128; CONF-921109-5) Avail: CASI HC A03/MF A01

A model was developed that accounts for grain growth during superplastic flow and its subsequent influence on stress-strain-strain rate behavior. These studies are experimentally based and have involved two different types of superplastic materials - a quasi-single phase metal (Coronze 638) and a microduplex metal (ultrahigh-carbon steel - UHCS). In both materials the kinetics of strain-enhanced grain growth were studied as a function of strain, strain rate, and temperature. An equation for the rate of grain growth was developed that incorporates the influence of temperature. The evolution of the grain size distribution during superplastic deformation was also investigated. Our model integrates grain growth laws derived from these studies with two mechanism based, rate dependent constitutive laws to predict the stress-strain-strain rate behavior of materials during superplastic deformation. The influence of grain size distribution and its evolution with strain and strain rate on the stress-strain-strain rate behavior was represented through the use of distributed parameters. The model can capture the stress-strain-strain rate behavior over a wide range of strains and strain rates with a single set of parameters. Many subtle features of the mechanical response of these materials can be adequately predicted. DOE

N94-17752# Oak Ridge National Lab., TN.
METALS 2000
S. W. Allison, L. C. Rogers, G. Slaughter, F. D. Boensch, R. O. Claus, and M. deVries May 1993 213 p
(Contract DE-AC05-84OR-21400)
(DE93-016761; ORNL/ATD-73) Avail: CASI HC A10/MF A03

This strategic planning exercise identified and characterized new and emerging advanced metallic technologies in the context of the drastic changes in global politics and decreasing fiscal resources. In consideration of a hierarchy of technology thrusts stated by various Department of Defense (DOD) spokesmen, and the need to find new and creative ways to acquire and organize programs within an evolving Wright Laboratory, five major candidate programs identified are C-17 Flap, Transport Fuselage, Mach 5 Aircraft, Fighter Structures, and Missile Structures. These results were formed by extensive discussion with selected major contractors and other experts, and a survey of advanced metallic structure materials. Candidate structural applications with detailed metal structure descriptions bracket a wide variety of uses which warrant consideration for the suggested programs. An analysis on implementing smart skins and structures concepts is given from a metal structures perspective. DOE

N94-17757# Oak Ridge National Lab., TN.
ALLOY DEVELOPMENT OF FeAl ALUMINIDE ALLOYS FOR STRUCTURAL USE IN CORROSIVE ENVIRONMENTS
C. T. Liu, V. K. Sikka, and C. G. McKamey Feb. 1993 68 p
(Contract DE-AC05-84OR-21400)
(DE93-015100; ORNL/TM-12199) Avail: CASI HC A04/MF A01

Objectives include adequate ductilities (greater than 10%) at ambient temperature, high-temperature strength better than stainless steels (types 304 and 316), and fabricability and weldability by conventional techniques (gas tungsten arc). The alloys should be capable of being corrosion resistant in molten nitrate salts with rates lower than other iron-base structural alloys and coating materials (such as Fe-Cr-Al alloys). Such corrosion rates should be less than 0.3 mm per year. The FeAl aluminide containing 35.8 at. % Al was selected as base composition. Preliminary studies indicate that additions of B and Zr, increase the room-temperature ductility of FeAl. Further alloying with 0.2% Mo, and/or 5% Cr, improves the creep. Our preliminary alloying effort has led to identification of the following aluminide composition with promising properties: Fe - (35 +/- 2)Al - (0.3 +/- 0.2)Mo - (0.2 +/- 0.15)Zr - (0.3 +/- 0.2)B up to 5Cr, at. %. However, this composition is likely to be modified in future work to improve the weldability of the alloy. The FeAl alloy FA-362 (Fe-35.8% Al-0.2% Mo-0.05% Zr-0.24% B) produced by hot extrusion at 900 C showed a tensile ductility of more than 10% at room temperature and a creep rupture life longer than unalloyed FeAl by more than an order of magnitude at 593 C at 138 MPa. Melting and processing of scaled-up heats of selected FeAl alloys are described. Forging, extruding, and hot-rolling processes for the scale-up heats are also described. DOE

N94-17767# Concurrent Technologies Corp., Johnstown, PA.
ATLAS OF FORMABILITY: ULTIMET Final Report, 28 Dec. 1992 - 24 Mar. 1993
24 Mar. 1993 65 p
(Contract N00140-88-C-RC21)
(AD-A268352) Avail: CASI HC A04/MF A01

In this investigation, flow behavior of Ultimet alloy was studied by conducting compression tests over a wide range of temperatures (950-1200 C) and strain rates (0.001-20/s). The true stress-true strain flow curves are presented for each test condition. Constitutive relations were determined from the flow behavior, and a dynamic material modeling was performed on this material. Thus, the optimum processing condition in terms of temperature and strain rate was identified as 1012 C and 0.001/s for this alloy. Workability of the material as a function of strain rate and temperature was also determined. Microstructural changes during high temperature deformation were characterized, and selective micrographs are presented together with corresponding flow curves. Dynamic recrystallization and grain growth occurred during high temperature deformation in some test conditions.

This report supplies ample mechanical and microstructural data on Ultimet alloy for engineers in the field of metalworking process design. DTIC

N94-17768# Concurrent Technologies Corp., Johnstown, PA.
ATLAS OF FORMABILITY: HAYNES 556 Final Report, 31 Oct. 1992 - 29 Jan. 1993
Prabir K. Chaudhury and Dan Zhao 29 Jan. 1993 69 p
(Contract N00140-88-C-RC21)
(AD-A268354) Avail: CASI HC A04/MF A01

In this investigation, flow behavior of Haynes 556 alloy was studied by conducting compression tests over a wide range of temperatures (950 - 1200 C) and strain rates (0.001 - 20 /s). The true stress-true strain flow curves are presented for each test conditions. Constitutive relations were determined from the flow behavior, and a dynamic material modeling was performed on this alloy. Thus, the optimum processing condition in terms of temperature and strain rate was identified as 1125 C and 0.001 /s for this alloy. Microstructural changes during high temperature deformation were also characterized, and selective micrographs are presented together with corresponding flow curves. Dynamic recrystallization and grain growth occurred during high temperature deformation over the range of temperatures tested. This report supplies ample mechanical property and microstructure data on Haynes 556 alloy for mechanical and materials engineers in the field of metalworking process design. The data presented here are also very helpful in finite element analysis of metalworking processes. DTIC

N94-17769 Concurrent Technologies Corp., Johnstown, PA.
ATLAS OF FORMABILITY: HAYNES 188 Final Report, 30 Nov. 1992 - 28 Feb. 1993
Prabir K. Chaudhury and Dan Zhao 28 Feb. 1993 69 p Limited Reproducibility: More than 20% of this document may be affected by microfiche quality
(Contract N00140-88-C-RC21)
(AD-A268355) Avail: CASI HC A04

In this investigation, flow behavior of Haynes 188 alloy was studied by conducting compression tests over a wide range of temperatures (950 - 1200 C) and strain rates (0.001 - 20 /s). The true stress-true strain flow curves are presented for each test condition. Constitutive relations were determined from the flow behavior, and a dynamic material modeling was performed on this alloy. Thus, the optimum processing condition in terms of temperature and strain rate was identified as 1100 C and 0.001/s for this alloy. Microstructural changes during high temperature deformation were also characterized, and selective micrographs are presented together with corresponding flow curves. Dynamic recrystallization and grain growth occurred during high temperature deformation over the range of temperatures tested. This report supplies ample mechanical and microstructural data on Haynes 188 alloy for engineers in the field of metalworking process design. The data presented here are also very helpful in finite element analysis of metalworking processes. DTIC

N94-17772# Concurrent Technologies Corp., Johnstown, PA.
ATLAS OF FORMABILITY: NICKELVAC K-500 Final Report, 31 Jul. - 31 Oct. 1992
Prabir K. Chaudhury and Dan Zhao 31 Oct. 1992 78 p
(Contract N00140-88-C-RC21)
(AD-A268351) Avail: CASI HC A05/MF A01

In this investigation, flow behavior of Nickelvac K-500 alloy was studied by conducting compression tests over a wide range of temperatures and strain rates. Constitutive relations were determined from the flow behavior, and dynamic material modeling was conducted on this alloy. Thus, the optimum processing condition in terms of temperature and strain rate was identified. Microstructural changes during high temperature deformation were also characterized. DTIC

N94-17788# Concurrent Technologies Corp., Johnstown, PA.
ATLAS OF FORMABILITY: HAYNES 230 Final Report, 30 May - 30 Aug. 1992
Prabir Chaudhury and Dan Zhao 30 Aug. 1992 69 p
(Contract N00140-88-C-RC21)
(AD-A268325) Avail: CASI HC A04/MF A01

In this investigation, flow behavior of Haynes 230 alloy was studied by conducting compression tests over a wide range of temperatures and stain rates. Constitutive relations were determined from the flow behavior, and a dynamic material modeling was performed on this alloy. Thus, the optimum processing condition in terms of temperature and during high temperature deformation were also characterized. DTIC

N94-17789# Concurrent Technologies Corp., Johnstown, PA.
ATLAS OF FORMABILITY: INCONEL 718 Final Report, 30 Apr. - 31 Jul. 1992
Prabir K. Chaudhury and Dan Zhao 31 Jul. 1992 36 p
(Contract N00140-88-C-RC21)
(AD-A268350) Avail: CASI HC A03/MF A01

In this investigation, flow behavior of Inconel 718 alloy was studied by conducting compression tests over a wide range of temperatures and strain rates. Constitutive relations were determined from the flow behavior, and a dynamic material modeling was conducted on this alloy. Thus, the optimum processing condition in terms of temperature and strain rate was identified. Microstructural changes during high temperature deformation were also characterized. DTIC

N94-17791# Oak Ridge National Lab., TN.
ASSESSMENT OF AN IMPROVED MULTIAXIAL STRENGTH THEORY BASED ON CREEP-RUPTURE DATA FOR INCONEL 600
R. L. Huddleston 1993 11 p Presented at the Pressure Vessels and Piping Conference, Denver, CO, 25-29 Jul. 1993
(Contract DE-AC05-84OR-21400)
(DE93-015929; CONF-930702-44) Avail: CASI HC A03/MF A01

A new multiaxial strength theory incorporating three independent stress parameters was developed and reported by the author in 1984. It was formally incorporated into ASME Code Case N47-29 in 1990. The new theory provided significantly more accurate stress-rupture life predictions than obtained using the classical theories of von Mises, Tresca, and Rankins (maximum principal stress), for Types 304 and 316 stainless steel tested at 593 and 600 C respectively under different biaxial stress states. Additional results for Inconel 600 specimens tested at 816 C under tension-tension and tension-compression stress states are presented in this paper and show a factor of approximately 2.4 reduction in the scatter of predicted versus observed lives as compared to the classical theories of von Mises and Tresca and a factor of about 5 as compared to the Rankins theory. A key feature of the theory, which incorporates the maximum deviatoric stress, the first invariant of the stress tensor, and the second invariant of the deviatoric stress tensor, is its ability to distinguish between life under tensile versus compressive stress states. DOE

N94-17796 Concurrent Technologies Corp., Johnstown, PA.
ATLAS OF FORMABILITY: HASTELLOY C-22 Final Report, 30 Jun. - 30 Sep. 1992
Prabir Chaudhury and Dan Zhao 30 Sep. 1992 68 p Limited Reproducibility: More than 20% of this document may be affected by microfiche quality
(Contract N00140-88-C-RC21)
(AD-A268324) Avail: Issuing Activity (Defense Technical Information Center (DTIC))

In this investigation, flow behavior of Hastelloy C-22 was studied by conducting compression tests at various temperatures and strain rates. Constitutive relations were determined from the flow behavior, and a dynamic material modeling for this alloy was performed. Thus, the optimum processing condition in terms of temperature and strain rate was determined. Microstructural changes during high temperature deformation were also characterized to aid process design engineers to select processing conditions in terms of resulting microstructure. DTIC

N94-17801# Concurrent Technologies Corp., Johnstown, PA.
ATLAS OF FORMABILITY: PERMALLOY - 80 FLOW STRESS CURVES Final Report, 30 Nov. 1992 - 25 Feb. 1993
Howard A. Kuhn 25 Feb. 1993 22 p
(Contract N00140-88-C-RC21)
(AD-A268263) Avail: CASI HC A03/MF A01

In this investigation, flow behavior of Permalloy - 80 alloy was studied by conducting compression tests over a wide range of temperatures (1112 - 2192 F) at high strain rates (1-10/s). The true stress-true strain flow curves are presented for each test condition. This report supplies ample mechanical property data on Permalloy - 80 alloy for mechanical and materials engineers in the field of metalworking process design. The data presented here are also very helpful in finite element analysis of metalworking processes. DTIC

N94-17802# Concurrent Technologies Corp., Johnstown, PA.
ATLAS OF FORMABILITY: NICKELVAC C-276 Final Report, 30 Sep. - 31 Nov. 1992
Prabir K. Chaudhury and Dan Zhao 30 Nov. 1992 69 p
(Contract N00140-88-C-RC21)
(AD-A268264) Avail: CASI HC A04/MF A01

In this investigation, flow behavior of Nickelvac C-276 alloy was studied by conducting compression tests over a wide range of temperatures (950 - 1200 C) and strain rates (0.001 - 20/s). The true stress strain flow curves are presented for each test condition. Constitutive relations were determined from the flow behavior, and a dynamic material modeling was performed on this alloy. Thus, the optimum processing condition in terms of temperature and strain rate was identified as 1075 C and 0.001/s for this alloy. Microstructural changes during high temperature deformation were also characterized, and selective micrographs are presented together with corresponding flow curves. Dynamic recrystallization and grain growth occurred during high temperature deformation over the range of temperatures tested. The recrystallization is complete at 1050 C and 0.001/s. This report supplies ample mechanical property and microstructure data on Nickelvac C-276 alloy for engineers in the field of metalworking process design. The data presented here are also essential in finite element analysis of metalworking processes. DTIC

N94-17803 Concurrent Technologies Corp., Johnstown, PA.
ATLAS OF FORMABILITY: Ti-6Al-4V ELI Final Report, 31 Jul. - 31 Oct. 1992
Prabir Chaudhury and Dan Zhao 31 Oct. 1992 56 p Limited Reproducibility: More than 20% of this document may be affected by poor print and microfiche quality
(Contract N00140-88-C-RC21)
(AD-A268300) Avail: Issuing Activity (Defense Technical Information Center (DTIC))

In this investigation, flow behavior of Ti-6Al-4V ELI alloy was studied by conducting compression tests over a wide range of temperatures and strain rates. Constitutive relations were determined from the flow behavior, and a dynamic material modeling was conducted on this alloy. Thus, the optimum processing condition in terms of temperature and strain rate was identified. Microstructural changes during high temperature deformation were also characterized. DTIC

N94-17804# Concurrent Technologies Corp., Johnstown, PA.
ATLAS OF FORMABILITY: ALLVAC 718 Final Report, 30 Sep. - 31 Dec. 1992
Prabir K. Chaudhury and Dan Zhao 31 Dec. 1992 70 p
(Contract N00140-88-C-RC21)
(AD-A268304) Avail: CASI HC A04/MF A01

In this investigation, flow behavior of Allvac 718 alloy was studied by conducting compression tests over a wide range of temperatures (850 - 1150 C) and strain rates (0.001 - 20/s). The true stress-true strain flow curves are presented for each test condition. Constitutive relations were determined from the flow behavior, and a dynamic material modeling was performed on this alloy. Thus, the optimum processing condition in ten-ns of temperature and strain rate was identified as 1025 C and 0.001/s for this alloy. Microstructural changes during high temperature deformation were also characterized, and selective micrographs are presented together with corresponding flow curves. Dynamic recrystallization and grain growth occurred during high temperature deformation over the range of temperatures tested. The recrystallization is complete at 1000 C and 0.001/ s. This report supplies ample mechanical property and microstructure data on Allvac 718 alloy for engineers in the field of metalworking process design. The data presented here are also very helpful in finite element analysis of metalworking processes. DTIC

N94-17819# Sandia National Labs., Albuquerque, NM.
A NEW MULTIPHASE EQUATION OF STATE FOR IRON
G. I. Kerley 1993 4 p Presented at the 14th International Conference of the International Association for the Advancement of High Pressure Science and Technology, Colorado Springs, CO, 27 Jun. - 2 Jul. 1993
(Contract DE-AC04-76DP-00789)
(DE93-017629; SAND-93-1455C; CONF-930676-6) Avail: CASI HC A01/MF A01

The PANDA code was used to develop an equation of state (EOS) for iron. Separate EOS tables were constructed for four solid phases and the fluid phase. The phase diagram and multiphase EOS table were then computed using the free energies. Results are in good agreement with thermophysical, static compression, phase boundary, and shock-wave measurements. Predicted pressures for the shock-induced epsilon-gamma and gamma-liquid transitions agree with those determined from sound speed measurements. Predicted melting temperatures fall in between two recent sets of experimental data which sharply disagree with one another. DOE

N94-17859# Oak Ridge National Lab., TN.
TECHNIQUE TO ELIMINATE HELIUM INDUCED WELD CRACKING IN STAINLESS STEELS
Chin-An Wang, B. A. Chin, and M. L. Grossbeck 1992 10 p Presented at the 16th Annual Symposium of American Society of Testing and Materials on Effects of Radiation on Materials, Denver, CO, 21-25 Jun. 1992
(Contracts DE-AC05-84OR-21400; DE-FG05-91ER-54134)
(DE93-015982; CONF-920673-20) Avail: CASI HC A02/MF A01

Experiments have shown that Type 316 stainless steel is susceptible to heat-affected-zone (HAZ) cracking upon cooling when welded using the gas tungsten arc (GTA) process under lateral constraint. The cracking has been hypothesized to be caused by stress-assisted helium bubble growth and rupture at grain boundaries. This study utilized an experimental welding setup which enabled different compressive stresses to be applied to the plates during welding. Autogenous GTA welds were produced in Type 316 stainless steel doped with 256 appm helium. The application of a compressive stress, 55 Mpa, during welding suppressed the previously observed catastrophic cracking. Detailed examinations conducted after welding showed a dramatic change in helium bubble morphology. Grain boundary bubble growth along directions parallel to the weld was suppressed. Results suggest that stress-modified welding techniques may be used to suppress or eliminate helium-induced cracking during joining of irradiated materials. DOE

N94-17860# Lawrence Livermore National Lab., CA.
SUPERHARDNESS EFFECT IN Au/Ni MULTILAYERS
A. F. Jankowski Mar. 1993 24 p Presented at the 1st International Symposium on Metallic Multilayers, Kyoto, Japan, 1-5 Mar. 1993
(Contract W-7405-eng-48)
(DE93-016444; UCRL-JC-112831; CONF-9303193-1) Avail: CASI HC A03/MF A01

The presence of an enhanced hardness, that is a 'superhardness effect', is found as a behavior parallel to the supermodulus effect in Au/Ni multilayer structures. The submicron thick Au/Ni coatings are prepared by magnetron sputter deposition. A microindenter is used to measure load as a function of indentation depth. An increase in hardness is measured as the Au/Ni layer pair spacing decreases. A local maximum in hardness occurs for samples with layer pairs consisting of 4-6 atomic planes of each metal component. DOE

N94-17862# Sandia National Labs., Albuquerque, NM. Center for Solder Science and Technology.
DEVELOPMENT OF ALTERNATIVES TO LEAD-BEARING SOLDERS
Paul T. Vianco 1993 17 p Presented at the Surface Mount Technical Association International Conference, San Jose, CA, 31 Aug. - 2 Sep. 1993 Prepared in cooperation with National Center for Mfg. Sciences, Ann Arbor, MI
(Contract DE-AC04-76DP-00789)
(DE93-016509; SAND-93-0225C; CONF-9308126-1) Avail: CASI HC A03/MF A01

Soldering technology using tin-lead alloys has had a significant role in the packaging of highly functional, low cost electronic devices. The elimination of lead from all manufactured products, whether through legislation or tax incentives, will impact the electronics community which uses lead-containing solders. In response to these proposed measures, the National Center for Manufacturing Sciences has established a multi-year program involving participants from industry, academia, and the national laboratories with the objective to identify potential replacements for lead-bearing solders. Selection of candidate alloys is based upon the analysis of materials properties, manufacturability, and modeling codes for reliability prediction as well as toxicological properties and resource availability data developed in the program. DOE

N94-17875# Los Alamos National Lab., NM.
MECHANICAL PROPERTIES OF EXCIMER LASER MODIFIED TITANIUM SURFACES
T. R. Jervis, T. G. Zocco, K. M. Hubbard, and M. Nastasi 1993 6 p Presented at the MRS Symposium on Thin Films, Stresses and Mechanical Properties, Pittsburgh, PA, 12-16 Apr. 1993
(Contract W-7405-eng-36)
(DE93-012663; LA-UR-93-1201; CONF-9304136-1) Avail: CASI HC A02/MF A01

Excimer laser processing enables both thermally-driven transformations and the incorporation of solutes into the surface of materials through melting and diffusional mixing. We have examined the effect of excimer laser processing on the microstructure and surface mechanical properties of titanium alloys. Changes in the surface hardness due to laser processing were studied using a Nanoindenter (trademark). Alloying experiments using both mixing of evaporated surface layers of boron and laser gas alloying in air and in nitrogen all result in changes in the surface hardness of the material. Alloying with boron results in an amorphous surface which is somewhat harder than the as polished surface. Laser processing in air and pure nitrogen results in incorporation of oxygen and nitrogen and the development of fine (approximately 50 nm) precipitates of TiO and TiN respectively. Substantial increases in surface hardness result due to solution and precipitation mechanisms. The effects of alloying on the surface hardness of the materials will be discussed in terms of the concentration of the solute and microstructures observed. DOE

N94-17915# Oak Ridge National Lab., TN.
HELIUM-INDUCED WELD DEGRADATION OF HT-9 STEEL
Chin-An Wang (Auburn Univ., AL.), B. A. Chin (Auburn Univ., AL.), Hua T. Lin, and M. L. Grossbeck 1992 15 p Presented at the 16th Annual ASTM Symposium on Effects of Radiation on Materials, Denver, CO, 21-25 Jun. 1992
(Contracts DE-AC05-84OR-21400; DE-FG05-86ER-52139; DE-AC05-76OR-00033)
(DE93-015981; CONF-920673-21) Avail: CASI HC A03/MF A01

Helium-bearing Sandvik HT-9 ferritic steel was tested for weldability to simulate the welding of structural components of a fusion reactor after irradiation. Helium was introduced into HT-9 steel to 0.3 and 1 atomic parts per million (appm) by tritium doping and decay. Autogenous single pass full penetration welds were produced using the gas tungsten arc (GTA) welding process under laterally constrained conditions. Macroscopic examination showed no sign of any weld defect in HT-9 steel containing 0.3 appm helium. However, intergranular micro cracks were observed in the HAZ of HT-9 steel containing 1 appm helium. The microcracking was attributed to helium bubble growth at grain boundaries under the influence of high stresses and temperatures that were present during welding. Mechanical test results showed that both yield strength (YS) and ultimate tensile strength (UTS) decreased with increasing temperature, while the total elongation increased with increasing temperature for all control and helium-bearing HT-9 steels. DOE

N94-17947# Brookhaven National Lab., Upton, NY.
PHASE SEPARATION AND ORDERING PROCESS IN Al-Li ALLOYS STUDIED BY SMALL-ANGLE NEUTRON SCATTERING AND NEUTRON DIFFRACTION
M. Furusaka, S. I. Fujikawa (Tohoku Univ., Sendai, Japan.), and J. M. Tranquada 1993 6 p Presented at the International Symposium on Advanced Nuclear Energy Research-Neutrons as Microscopic Probes, Mito Ibaraki, Japan, 10-12 Mar. 1993
(Contract DE-AC02-76CH-00016)
(DE93-016750; BNL-49081; CONF-9303190-2) Avail: CASI HC A02/MF A01

To study phase separation kinetics of Al-9.5at.%Li polycrystalline alloys in which precipitates have ordered Al3Li ((delta)(prime)) structure, profile analysis of small-angle neutron scattering and superlattice reflections (100) and (110) were done. A small-angle scattering instrument and a triple-axis spectrometer in elastic mode were used in the measurements. Strong texture was observed in the reflections. Therefore, measurements were done using the crystal orientation where the intensity of the reflection was at the maximum. Profiles of small-angle scattering and superlattice reflections were almost identical at higher momentum transfer side. At lower momentum transfer side, small-angle scattering showed interference effects, but superlattice reflection did not show any sign of interference. Integrated intensities of superlattice reflections were obtained and compared with small-angle scattering intensity. The order parameter was not saturated in the (delta)(prime) precipitates at the early stage of the phase separation process. DOE

N94-18003# Sandia National Labs., Albuquerque, NM.
EMBRITTLEMENT OF SURFACE MOUNT SOLDER JOINTS BY HOT SOLDER-DIPPED, GOLD-PLATED LEADS
P. T. Vianco 1993 45 p Presented at the Surface Mount Technical Association International Conference, San Jose, CA, 31 Aug. - 2 Sep. 1993
(Contract DE-AC04-76DP-00789)
(DE93-017659; SAND-93-0082C; CONF-9308126-3) Avail: CASI HC A03/MF A01

The detachment of beam-leaded transistors from several surface mount circuit boards following modest thermal cycling was examined. Microstructural analysis of the package leads and bonding pads from the failed units indicated that gold embrittlement was responsible for a loss of solder joint mechanical integrity that caused detachment of transistors from the circuit boards. An analysis of the hot dipping process used to remove gold from the leads prior to assembly demonstrated that the gold, although dissolved from the lead, remained in the nearby solder and was subsequently retained in the coating formed on the lead upon withdrawal from the bath. This scenario allowed gold to enter the circuit board solder joints. It was hypothesized, and later confirmed by experimental trials, that increasing the number of dips prevented gold from entering the solder coatings. DOE

N94-18100# Sandia National Labs., Albuquerque, NM.
EFFECT OF PHASE CHANGE IN A DEBRIS CLOUD ON A BACKWALL STRUCTURE
L. N. Kmetyk, L. C. Chhabildas, M. B. Boslough, and R. J. Lawrence 1993 4 p Presented at the 14th International Conference of the International Association for the Advancement of High Pressure Science and Technology, Colorado Springs, CO, 27 Jun. - 2 Jul. 1993
(Contract DE-AC04-76DP-00789)
(DE93-017506; SAND-93-0390C; CONF-930676-8) Avail: CASI HC A01/MF A01

The physical state of a debris cloud generated upon impact of a thin flier plate with a thin bumper depends on the impact velocity. At impact velocities of 10km/s, the debris cloud is expected to be primarily molten with some vapor present. A series of calculations using the finite-difference code CTH has been used to evaluate the effect of phase change (i.e., higher concentrations of vapor) in debris clouds and their subsequent impact on a backwall structure. In these calculations, the higher concentrations of vapor is achieved by increasing the initial temperature of the impactor and the bumper material while keeping the same impact velocity. The nature of the interaction of the debris cloud and the subsequent loading on the backwall depends on its thermophysical state. This interaction (with a backwall) can cause either spallation, rupture, or simply bulging of the backwall structure. These results will be discussed and compared with an impact experiment performed at (approximately)10km/s on the Sandia hypervelocity launcher. In the experiment, the debris cloud was generated by the impact of a titanium plate with a titanium bumper. DOE

N94-18111# Lawrence Livermore National Lab., CA.
RECENT STUDIES OF SHORT-RANGE ORDER IN ALLOYS: THE COWLEY THEORY REVISITED
L. Reinhard and S. C. Moss (Houston Univ., TX.) Feb. 1993 34 p Presented at the John M. Crowley Symposium on Ultramicroscopy, Scottsdale, AZ, 5-8 Jan. 1993
(Contract W-7405-eng-48)
(DE93-016416; UCRL-JC-112438; CONF-9301114-2) Avail: CASI HC A03/MF A01

We present comparisons of various statistical theories for effective pair interactions (EPI) in alloys. We then evaluate these EPI's using the following methods: Cowley theory; the Krivoglaz-Clapp-Moss (KCM)

approximation; the (gamma)-expansion method (GEM) of Tokar, Masanskii, and coworkers; and the exact inverse Monte Carlo (IMC) method, introduced by Gerold and Kern. Via a series of model calculations on a hypothetical bcc alloy with a single nearest-neighbor interaction, we show that the Cowley theory is successful in evaluating the EPI's in more dilute alloys but tends to overestimate the magnitude of the nearest neighbor energy at higher concentrations, whereas the KCM expression becomes increasingly inaccurate at lower concentrations. In general, however, the approximate mean field theories are most accurate at higher concentrations and higher temperatures. Recent studies of short-range order in single crystals are discussed in which these EPI's have been evaluated using the IMC, KCM, GEM, and Cowley theories. Examples include the bcc alloy Fe(0.53)Cr(0.47) and the fcc alloys Cu(3)Au, Cu(0.69)Zn(0.31), and Ni(0.89)BgCr(0.11). In all cases the approximate expressions do quite well, especially the GEM.
DOE

N94-18114# Los Alamos National Lab., NM.
A REVIEW OF THE STAGES OF WORK HARDENING
A. D. Rollett and U. F. Kocks 1993 19 p Presented at the Dislocations 1993, Assois, France, 1-9 Apr. 1993
(Contract W-7405-eng-48)
(DE93-016456; LA-UR-93-2339; CONF-9304166-1) Avail: CASI HC A03/MF A01

Stages of work hardening are reviewed with emphasis on links between each stage. Simple quantitative descriptions are given for each stage. Similarities between stage 1, easy glide, and stage 4, large strain hardening, are pointed out both in terms of magnitude of the hardening rate and of the underlying mechanism of dislocation debris accumulation. Stage 2 is described as an athermal hardening stage that occurs when statistical variations in the dislocation 'forest' lead to geometrical storage of dislocations. The steadily decreasing hardening rate observed in stage 3 is characterized by the increasing rate of loss of dislocation density due to dynamic recovery. Stage 3 appears to have an asymptote to a saturation stress which is determined by the characteristics of the dislocation tangles, or cell walls. The imperfect nature of the dynamic recovery process, however, leads to the accumulation of dislocation debris and this, by analogy with stage 1, causes the apparent saturation stress to rise, thus causing stage 4.
DOE

N94-18127# Sandia National Labs., Albuquerque, NM.
WETTING BEHAVIOR OF ALTERNATIVE SOLDER ALLOYS
F. M. Hosking, P. T. Vianco, C. L. Hernandez, and J. A. Rejent 1993 8 p Presented at the Static Memory Interface Conference, San Jose, CA, 1 Sep. 1993
(Contract DE-AC04-76DP-00789)
(DE93-016730; SAND-93-1063C; CONF-9309195-1) Avail: CASI HC A02/MF A01

Recent economic and environmental issues have stimulated interest in solder alloys other than the traditional Sn-Pb eutectic or near eutectic composition. Preliminary evaluations suggest that several of these alloys approach the baseline properties (wetting, mechanical, thermal, and electrical) of the Sn-Pb solders. Final alloy acceptance will require major revisions to existing industrial and military soldering specifications. Bulk alloy and solder joint properties are consequently being investigated to validate their producibility and reliability. The work reported in this paper examines the wetting behavior of several of the more promising commercial alloys on copper substrates. Solder wettability was determined by the meniscometer and wetting balance techniques. The wetting results suggest that several of the alternative solders would satisfy pretinning and surface mount soldering applications. Their use on plated through hole technology might be more difficult since the alloys generally did not spread or flow as well as the 60Sn-40Pb solder.
DOE

N94-18182# Dartmouth Coll., Hanover, NH.
THE HALL-PETCH RELATIONSHIP AND MECHANISMS OF FRACTURE IN B2 COMPOUNDS
I. Baker 30 Dec. 1992 13 p
(Contract DE-FG02-87ER-45311)
(DE93-018887; DOE/ER-45311/T2) Avail: CASI HC A03/MF A01

A study was initiated in 1987 to examine structure and properties of grain boundaries in the B2 ordered alloys FeAl and NiAl. This project continued from 1990, with initial emphasis on CoAl, FeCo, and CuZn, but with continued work on FeAl and NiAl. Effect of alloy composition on structure/chemistry and properties of grain boundaries were examined by measuring yield strength vs grain size, measuring grain boundary composition using a scanning Auger electron microprobe, examining dislocation/grain boundary interactions during in-situ straining in transition electron microscopy (TEM), and determining fracture modes and assessing strain extent at fracture surfaces using selected area channeling patterns. Progress during the last 3 years is reviewed.
DOE

N94-18218 Joint Inst. for Nuclear Research, Dubna (USSR). Lab. of High Energy.
DEEP ION IMPLANTATION INTO MANGANIN TO MODIFY ITS PRESSURE AND ELECTROTHERMOCHARACTERISTICS
R. Wisniewski and B. Slowinski 1992 7 p Limited Reproducibility: More than 20% of this document may be affected by microfiche quality
(DE93-630229; JINR-E-14-92-178) Avail: CASI HC A02 (US Sales Only)

On the grounds of previously obtained experimental data concerning the high energy ((approx)1 MeV/u) Ar and Xe ions implantation into manganin, two suggestions to create the manganin based systems having improved pressure and electro-thermocharacteristics are put forward. The first way is to fabricate a multilayer system with the resultant plateau of the temperature dependence of the relative resistance much broader than the initial one. The second way comes to the formation of some manganin based self compensating structure.
DOE

N94-18245# Oak Ridge National Lab., TN.
EFFECTS OF IRRADIATION TEMPERATURE ON EMBRITTLEMENT OF NUCLEAR PRESSURE VESSEL STEELS
F. M. Haggag 1992 15 p Presented at the 16th Annual Symposium of the ASTM on Effects of Radiation and Materials, Denver, CO, 21-25 Jun. 1993
(Contract DE-AC05-84OR-21400)
(DE93-015428; CONF-920673-18) Avail: CASI HC A03/MF A01

The effects of neutron irradiation on the steel reactor vessel for the modular high-temperature gas-cooled reactor (MHTGR) are being investigated, primarily because the operating temperatures are low (121-288 C (250-550 F)) compared to those for commercial light-water reactors (LWR's) (approximately 288 C (550 F)). The need for design data on the reference temperature (RT(sub NDT)) shift necessitated the irradiation at different temperatures of A 533 grade B class 1 plates, A 508 class 3 forging, and welds used for the vessel shell, vessel closure head, and vessel flange. This paper presents regular- and mini-tensile, Automated Ball Indentation (ABI), and Charpy V-notch (CVN) impact test results from five irradiation capsules of this program.
DOE

N94-18306 Army Research Lab., Watertown, MA. Materials Directorate.
ENVIRONMENTAL EFFECTS ON INTERMETALLIC COMPOUNDS: A GUIDE TO THE LITERATURE Final Report
Saul Isserow Aug. 1993 24 p Limited Reproducibility: More than 20% of this document may be affected by microfiche quality
(AD-A269587; ARL-MR-112) Avail: Issuing Activity (Defense Technical Information Center (DTIC))

This report is a guide to the literature on environmental effects on intermetallic compounds, primarily the aluminides of nickel, titanium, iron, and niobium. The guide relies heavily upon the proceedings of recent conferences. Brief technical discussions introduce the various topics and lead to specific sources of information. Various relevant review articles are also listed.
DTIC

N94-18322 Minerals, Metals and Materials Society, Warrendale, PA.
DIFFUSION IN ORDERED ALLOYS
B. Fultz, R. W. Cahn, and D. Gupta 4 Nov. 1992 272 p Symposium held in Chicago, IL, 3-4 Nov. 1992 Limited Reproducibility: More than 20% of this document may be affected by microfiche quality
(Contract N00014-92-J-1921)
(AD-A268232) Avail: Issuing Activity (Defense Technical Information Center (DTIC))

Diffusion in ordered binary alloys has been treated using the pair-approximation of the Path Probability Method (PPM) based on an atomistic model. The effect of the atomic interaction on the ordering behavior and its influence on transport properties have been clarified. Compositional dependences of both the intrinsic diffusion and interdiffusion coefficients, correlation factor, and thermodynamic factor agree very well with results from Monte Carlo simulations. The calculated properties also show qualitative agreement with the experimental data on diffusivity, activity, and creep in an NiAl system. DTIC

N94-18325# Aeronautical Research Labs., Melbourne (Australia).
A BENCHMARK BENDING TEST OF A THICK SPECIMEN. PART 1: EXPERIMENTS
J. M. Finney and E. Kowal Jun. 1993 44 p
(AD-A268730; ARL-RR-6-Pt-1; DODA-AR-008-363-Pt-1) Avail: CASI HC A03/MF A01

An experiment has been undertaken to provide benchmark data for validating methods of calculating the plastic behavior of metals. In this experiment a 30 mm square-test-section specimen of 7050-T7451 aluminum alloy has been loaded in four-point bending, and the surface distortions of all four faces have been measured with the aid of a square grid pattern imposed on the surfaces before deformation. This part of the Report describes the experimental details and gives the results of the material property tests, thus providing sufficient information for the prediction of surface displacements. Part II of the Report gives the measured displacements with which predictions may be compared. DTIC

N94-18386# California Inst. of Tech., Pasadena. Div. of Engineering and Applied Science.
CONTINUUM MODELING OF MATERIALS THAT CAN UNDERGO MARTENSITIC PHASE TRANSITIONS
Jim M. Restuccio Jun. 1993 48 p
(Contract N00014-90-J-1871)
(AD-A268767; TR-12) Avail: CASI HC A03/MF A01

In this paper, a continuum model for materials that can undergo martensitic phase transformations is developed and applied to the study of several problems that involve such transformations. Among other things, the continuum model that is developed provides the correct material symmetry group for each phase of the material, and results in the corresponding boundary value problem being in a form that permit direct linearization, while still retaining finite shape deformations for the martensite phases. All of the problems that this continuum model is applied to in this paper deal with the issue of which phase or which variant of martensite is preferred during the growth process when a boundary traction is applied. Among these problems are the case of a uniaxial tensile traction applied to a cylindrical body and the case of a hydrostatic pressure applied to a material that has a finite shape deformation with an infinitesimal dilatation. DTIC

N94-18398# California Univ., Berkeley. Lawrence Berkeley Lab.
THE LOW-TEMPERATURE SPECIFIC HEAT OF CeCu2Ge2 AT 0 AND 9.5 kbar
R. A. Fisher, J. P. Emerson, N. E. Phillips, R. Caspary (Technische Hochschule, Darmstadt, Germany.), and F. Steglich (Technische Hochschule, Darmstadt, Germany.) Apr. 1993 6 p Presented at the Conference of the International Union of Pure and Applied Physics on Low Temperature Physics (LT 20), Eugene, OR, 1-11 Aug. 1993
(Contract DE-AC03-76SF-00098)
(DE93-014914; LBL-34028; CONF-930801-4) Avail: CASI HC A02/MF A01

The compound CeCu2Ge2 is isostructural with CeCu2Si2, the first heavy-fermion superconductor. Although CeCu2Ge2 is not superconducting at zero pressure (P), it is superconducting for P greater than 70 kbar. Previous specific-heat (C) measurements for P = 0, 0.05 less than or equal to T less than or equal to 30 K, and magentic fields (H) to 8T, showed antiferromagnetic ordering at T(sub N) = 4.2 K and an anomaly in C at 0.45 K and H = 0 that was interpreted as a maximum in gamma(T). The anomaly was supressed, but not shifted in temperature, with increasing H and disappeared at H = 8T. This paper reports new data for C, 0.35 less than or equal to T less than or equal to 20 K, and P = 0. Additionally, data obtained at 9.5 kbar, the first for P not equal to 0, are reported. The P = 0 data are in excellent agreement with the earlier work suggesting that the featrures observed are intrinsic properties and not subject to the uncertainties related to sample dependence that are associated with some heavy-fermion compounds. DOE

N94-18501# Los Alamos National Lab., NM.
CALCULATION OF THE LiF-CeF3-BeF2 AND LiF-PuF3-BeF2 TERNARY PHASE DIAGRAMS
R. N. R. Mulford Jul. 1993 24 p
(Contract W-7405-eng-36)
(DE93-017437; LA-12569) Avail: CASI HC A03/MF A01

The LiF-CeF3-BeF2 and LiF-PuF3-BeF2 ternary phase diagrams were calculated from optimized binary diagrams using computer programs developed by Lukas and coworkers. The approximate overall diagrams were calculated without the use of ternary interaction terms, but inclusion of ternary terms was necessary to reproduce the experimental data for solubilities of CeF3 and PuF3 which are considerably less soluble in LiF-BeF2 liquid than predicted without ternary interaction terms. DOE

N94-18542# Army Armament Research, Development and Engineering Center, Watervliet, NY.
MECHANISM-DEPENDENT FRACTAL CHARACTER OF FRACTURE SURFACES IN HIGH STRENGTH AND TOUGHNESS ASTM A723 STEELS Final Report
Peter McAnulty, L. V. Meisel, and P. J. Cote Jun. 1993 12 p
(AD-A268956; ARCCB-TR-93024) Avail: CASI HC A03/MF A01

The fractal character of fracture surfaces of thick-walled pressure vessels produced in the final fast fracture that terminates low cycle fatigue tests is compared with that of fracture surfaces produced in Charpy impact tests in samples of the same high strength and toughness steel (ASTM A723) alloy. Slit island analysis yielded fractal dimensions near 1.25 for the Charpy specimens, which is typical of high strength steel alloys previously studied, however, extremely high fractal dimensions near 1.40 were determined for the low cycle fatigue specimens. The distributions of island and lake areas and of island and lake perimeters on random sections exhibit hyperbolic distributions analogous to those found for geographic islands and lakes. DTIC

N94-18660# Dayton Univ., OH. Research Inst.
IMPLEMENTATION OF A NONISOTHERMAL UNIFIED INELASTIC-STRAIN THEORY INTO ADINA6.0 FOR A TITANIUM ALLOY: USER GUIDE Interim Report, Jan. - Dec. 1992
Joseph L. Kroupa and Richard W. Neu Jan. 1993 91 p
(Contract F33615-91-C-5606)
(AD-A269927; WL-TR-93-4005) Avail: CASI HC A05/MF A01

Simulations with many modern aerospace materials require realistic mechanical response models for use in isothermal and nonisothermal applications. One such model is a unified inelastic-strain theory which has been applied to capture the strain-rate sensitivity and time dependent behavior of the titanium alloy Timetal 21S (formerly B21S). The Bodner-Partom form of unified theory satisfactorily describes the B21S stress-strain response for a range of temperatures from 23 deg C and 815 deg C and strain rate from 10 3/S to 1.X10-7/S. Practical use of the theory in finite element applications depends on advanced numerical algorithms that rapidly solve the inherently 'stiff' constitutive equations. Special 'user-defined' subroutines provide the framework for the incorporation of these numerical algorithms into ADINA6.0, a general purpose finite element package. This user-guide contains a brief overview of the theory, the B21S material parameters, subroutine structure, variable nomenclature, and numerical algorithms. Test cases are described to illustrate the numerical integration schemes and provide guidance for error management. The appendices contain hard-copies of the subroutines for two- and three-dimensional elements. DTIC

N94-18687# Cornell Univ., Ithaca, NY. Dept. of Chemistry.
POTENTIAL DEPENDENT STRUCTURAL CHANGES OF UNDERPOTENTIALLY DEPOSITED COPPER ON AN IODINE TREATED PLATINUM SURFACE DETERMINED IN SITU BY SURFACE EXAFS AND ITS POLARIZATION DEPENDENCE
G. M. Bommarito, D. Acevedo, J. F. Rodriguez, and H. D. Abruna 25 Aug. 1993 60 p
(Contract N00014-84-K-0656)
(AD-A269890; TR-33) Avail: CASI HC A04/MF A01

An in situ structural investigation of the underpotential deposition of copper on an iodine covered platinum surface (Pt/C layered synthetic microstructure (LSM) with Pt as the outermost layer) has been carried out using surface EXAFS (extended x-ray absorption fine structure) and its polarization dependence. The effects of rinsing the electrode with pure supporting electrolyte have also been investigated. At an applied potential of +0.20 V (corresponding to half a monolayer of electrodeposited copper) there are two in-plane Cu-Cu distances: 2.56+/-0.05A and 4.21+/-0.05A. This suggests a coexistence between a close-packed phase with a more open phase. It is likely that the open phase is stabilized by repulsive interactions between partially charged copper atoms, as well as by the presence of the strongly adsorbed iodine layer. At +0.10V (corresponding to a full monolayer of electrodeposited copper) there is only one Cu-Cu distance of 2.56+/-0.05A. Combining in-plane (delta polarization) and monolayer coverage, the copper UPD layer is incommensurate with respect to the platinum surface. The iodine ad-layer rides the electrodeposited copper forming a 3x3 unit cell. This interfacial structure is not altered upon rinsing with pure supporting electrolyte. DTIC

N94-18735# Army Armament Research, Development and Engineering Center, Watervliet, NY. Benet Lab.
SELF-ORGANIZED CRITICALITY AND THE BARKHAUSEN EFFECT IN AMORPHOUS AND POLYCRYSTALLINE METALS Final Report
Paul J. Cote and Lawrence V. Meisel Jul. 1993 12 p
(AD-A269817; ARCCB-TR-93027) Avail: CASI HC A03/MF A01

An investigation of the possibility that the Barkhausen effect in amorphous and polycrystalline ferromagnets is an example of self-organized criticality is described. Since the theory of self-organized criticality was introduced by Bak, Tang, and Weisenfeld to explain the behavior of spatially extended, dissipative dynamical systems, the Barkhausen effect is a natural candidate for such a description. The data are consistent with self-organized critical behavior: the power spectral densities depend on frequency f as 1/f(exp 2) and the distribution of pulse energies are well described by a power law analogous to the Gutenberg-Richter law for earthquakes. Alternative explanations for power-law dependences are also presented. DTIC

N94-18742 California Univ., Los Angeles. Dept. of Materials Science and Engineering.
DEVELOPMENT OF THE MICROSTRUCTURE BASED STOCHASTIC LIFE PREDICTION MODEL Progress Report
Marek A. Przystupa, Jimin Zhang, and Annetta J. Luevano Aug. 1993 112 p Limited Reproducibility: More than 20% of this document may be affected by microfiche quality
(Contract N00014-91-J-1299)
(AD-A269742) Avail: CASI HC A06

The objective of the fatigue life prediction program at UCLA is as follows: (1) to ascertain microstructural features relevant to fatigue in aluminum 7050 alloys and develop quantitative methods for their characterizations; (2) to characterize initial microstructures and accumulation of microstructural damage during fatigue of 7050-T7451 plate alloys; and (3) to formulate and test scaling relationships and models relating relevant microstructural features to fatigue damage in aluminum 7050 alloys. Emphasis during the reporting period were on the completion of the metallographic and fractographic examinations of the high and low porosity 7050-T7451 commercial 6 in. plate alloys. Obtained results include quantification of the through thickness gradients of grain structures and volume fractions and size distributions of the constituent particles, pores, and precipitates. To our knowledge this is the most complete set of microstructural data on the 7050-T7451 commercial plate alloys. Characterizations of the fracture surfaces and microstructures of fatigued samples are in progress. Up to date results include data on the change of surface roughness and fractal dimension with fatigue crack length and preliminary information about microstructural features on the crack path. Modeling has been focused on the predictions of the size distributions of the fatigue crack initiating pores and on the incorporation of the microstructural variables into existing fatigue life prediction models. DTIC

N94-18788 Virginia Univ., Charlottesville. Dept. of Materials Science and Engineering.
FUNDAMENTAL CONCEPTS RELATING LOCAL ATOMIC ARRANGEMENTS, DEFORMATION, AND FRACTURE OF INTERMETALLIC ALLOYS Final Report, 2 Jan. 1990 - 1 Jan. 1993
J. A. Wert Jun. 1993 171 p Limited Reproducibility: More than 20% of this document may be affected by microfiche quality
(Grant AF-AFOSR-0143-90)
(AD-A268745; UVA/525725/MSE93/101; AFOSR-93-0654TR) Avail: CASI HC A08

This final contract report describes research activities on two topics of fundamental importance for application of intermetallic alloys as elevated temperature engineering materials: brittle fracture and creep resistance. On the topic of brittle fracture, the process of crack tip plasticity has been investigated by extending the Rice-Thomson model to treat the case of crack tip emission of dissociated superlattice dislocations that commonly occur in intermetallic alloys. The model shows that superlattice dislocation emission from crack tips can be inhibited in intermetallic alloys, and predicts the occurrence of cleavage fracture in particular intermetallic alloys. The fracture mode predictions can be compared with experimentally observed fracture modes; such comparisons for intermetallic alloys with the L12 and B2 crystal structures show that the model predictions match the experimental observations for every intermetallic alloy where sufficient data are available to perform the model calculations (about 25 alloys in all). A novel result of the dislocation emission modeling work is the finding that the antiphase boundary energy plays a central role in determining whether a particular intermetallic alloy will exhibit cleavage fracture or not. DTIC

N94-18802# Los Alamos National Lab., NM.
DISLOCATION-DRAG CONTRIBUTION TO HIGH-RATE PLASTIC DEFORMATION IN SHOCK-LOADED TANTALUM
D. L. Tonks, R. S. Hixson, J. N. Johnson, and G. T. Gray, III 1993 10 p Presented at the 14th International Conference of the International Association for the Advancement of High Pressure Science and Technology, Colorado Springs, CO, 27 Jun. - 2 Jul. 1993
(Contract W-7405-eng-36)
(DE93-018286; LA-UR-93-2799; CONF-930676-29) Avail: CASI HC A02/MF A01

Time-resolved plastic waves in plate-impact experiments give information on relations between applied shear stress and plastic strain rate at low plastic strain. This information is different from that obtained at intermediate strain rates using Hopkinson bar techniques because the material deformation state is driven briefly into the regime dominated by dislocation drag. Two VISAR records of particle velocity at the tantalum/sapphire (window) interface are obtained for symmetric impact producing peak in-situ longitudinal stresses of 75 and 111 kbar. Rise-times of plastic waves are about 100 and 50 ns, respectively, with peak strain rates of about 2 to 8.5 x 10(exp 5)/s, respectively, as determined by weak-shock analysis. These data show a much stronger dependence of plastic strain rate on applied shear stress than predicted by linear viscous drag models in combination with thermal activation through a large Peierls barrier. The data also show complex evolution of the mobile dislocation density during early stages of high-rate plastic flow. This measurement and corresponding analysis aid significantly in establishing the fundamental picture of dynamic deformation of metals and the evolution of the internal material state at early times following shock compression. DOE

N94-18806# Massachusetts Inst. of Tech., Cambridge.
DEFORMATION MECHANISMS IN A LAVES PHASE
Yaping Liu, S. M. Allen, and J. D. Livingston 1992 6 p Presented at the High-Temperature Ordered Intermetallic Alloys V, Boston, MA, 30 Nov. - 3 Dec. 1992
(Contract DE-FG02-90ER-45426)
(DE93-018331; CONF-9211205-3) Avail: CASI HC A02/MF A01

The stress-induced phase transformation between C36 and C15 structures in Fe2Zr is studied by electron microscopy. Nucleus of transformation is believed to be pre-existing C15 layers in C36 particles. Microstructural evidence for three mechanisms of growth of a new phase were found: fault accumulation and rearrangement; moving of individual partial dislocations between two phases; and the migration of microscopic ledges composed of a series of Shockley partials between C36 and C15. Plastic deformation by slip on non-basal planes of C36 caused by indentation is studied. DOE

N94-18807# Massachusetts Inst. of Tech., Cambridge.
MORPHOLOGY, DEFORMATION, AND DEFECT STRUCTURES OF TiCr2 IN Ti-Cr ALLOYS
K. C. Chen, S. M. Allen, and J. D. Livingston 1992 6 p Presented at the High-Temperature Ordered Intermetallic Alloys V, Boston, MA, 30 Nov.

- 3 Dec. 1992
(Contract DE-FG02-90ER-45426)
(DE93-018332; CONF-9211205-4) Avail: CASI HC A02/MF A01

The morphologies and defect structures of TiCr2 in several Ti-Cr alloys have been examined by optical metallography, x-ray diffraction, and transmission electron microscopy (TEM) in order to explore the room-temperature deformability of the Laves phase TiCr2. The morphology of the Laves phase was found to be dependent upon alloy composition and annealing temperature. Samples deformed by compression have also been studied using TEM. Comparisons of microstructures before and after deformation suggest an increase in twin, stacking fault, and dislocation density within the Laves phase, indicating some but not extensive room-temperature deformability. DOE

N94-18809# Los Alamos National Lab., NM.
EFFECTS OF SHOCK LOADING ON A SOLID-SOLUTION STRENGTHENED SUPERALLOY
K. S. Vecchio and G. T. Gray, III 1993 5 p Presented at the 14th International Conference of the International Association for the Advancement of High Pressure Science and Technology, Colorado Springs, CO, 27 Jun. - 2 Jul. 1993
(Contract W-7405-eng-36)
(DE93-018345; LA-UR-93-2290; CONF-930676-17) Avail: CASI HC A01/MF A01

Ni-based HAYNES(reg sign) 230(trademark) ALLOY has been studied to determine the effect of shock loading on post-shock quasistatic and dynamic mechanical response and microstructural evolution. Compression properties of this material was studied in both the as-received and shock-loaded conditions at strain rates from 10(exp -3)/s to 3000/s and 77 and 293K. Damage evolution was documented via TEM and correlated with observed mechanical response. Changes in deformation mechanisms and second phase distributions resulting from shock pre-straining and subsequent testing are correlated with changes in strain hardening behavior. Comparison of these results with shock loading results on pure Ni revealed distinct differences in strengthening and defect storage mechanisms. DOE

N94-18917# EG and G Rocky Flats, Inc., Golden, CO.
EFFECT OF INTERNAL HEATING DURING HOT COMPRESSION TESTING ON THE STRESS-STRAIN BEHAVIOR AND HOT WORKING CHARACTERISTICS OF ALLOY 304L
M. C. Mataya and V. E. Sackschewsky 1993 80 p Presented at the Fall Meeting of the Minerals, Metals and Materials Society: Physical Metallurgy and Materials in Conjunction with Materials Week and the Materials Applications and Services Exposition, Pittsburgh, PA, 17-21 Oct. 1993
(Contract DE-AC34-90DP-62349)
(DE93-012701; RFP-4739; CONF-931009-1) Avail: CASI HC A05/MF A01

Temperature change from conversion of deformation to internal heat, and its effect on stress-strain behavior of alloy 304L was investigated by initially isothermal (temperature of specimen, compression dies, environment equilibrated at initiation of test) uniaxial compression. Strain rate was varied 0.01 s(sup (minus)1) to 1 s(sup (minus)1) (thermal state of specimen varied from nearly isothermal to nearly adiabatic). Specimens were deformed at 750 to 1150 to a strain of 1. Change in temperature with strain was calculated via finite element analysis from measured stress-strain data and predictions were confirmed with thermocouples to verify the model. Temperature increased nearly linearly at the highest strain rate, consistent with temperature rise being a linear function of strain (adiabatic). As strain rate was lowered, heat transfer from superheated specimen to cooler dies caused sample temperature to increase and then decrease with strain as the sample thinned and specimen-die contact area increased. As-measured stress was corrected. Resulting isothermal flow curves were compared to predictions of a simplified method suggested by Thomas and Shrinivasan and differences are discussed. Strain rate sensitivity, activation energy for deformation, and flow curve peak associated with onset of dynamic recrystallization were determined from both as-measured and isothermal stress-strain data and found to vary widely. The impact of utilizing as-measured stress-strain data, not corrected for internal heating, on results of a number of published investigations is discussed. DOE

N94-18919# Sandia National Labs., Albuquerque, NM.
DYNAMICAL BEHAVIOR OF TANTALUM
M. D. Furnish, L. C. Chhabildas, and D. J. Steinberg (Lawrence Livermore National Lab., CA.) 1993 3 p Presented at the 14th International Conference of the International Association for the Advancement of High Pressure Science and Technology, Colorado Springs, CO, 27 Jun. - 2 Jul. 1993
(Contract DE-AC04-76DP-00789)
(DE93-017877; SAND-93-0427C; CONF-930676-10) Avail: CASI HC A01/MF A01

The authors have performed four dynamic impact tests on tantalum to determine its high-pressure yield and viscoelastic properties. Their experiments used compressed gas gun techniques to produce a combination of shocks, reshocks, and releases over the pressure range 0-12 GPa in samples 5.0 and 7.3 mm thick. Profiles were recorded using VISAR (velocity interferometry) techniques. Elastic precursors suggest a yield strength of 0.95 GPa, which is somewhat above literature values. As with other metals, release waves do not show a perfect elastic-plastic behavior, indicating a slight Baushinger effect. Lagrangian sound velocities for singly shocked states are consistent with earlier results (about 4.5 km/sec). DOE

N94-18923 BDM International, Inc., McLean, VA.
THE INTELLIGENT PROCESSING OF MATERIALS Final Technical Report, 24 Jan. 1986 - 14 Nov. 1991
Brian G. Kushner 19 Aug. 1993 55 p Limited Reproducibility: More than 20% of this document may be affected by microfiche quality
(Contract F49620-86-C-0036; ARPA Order 5636; AF Proj. 5636)
(AD-A269250; AFOSR-93-0673TR) Avail: CASI HC A04

This report covers progress in novel concepts for the development and implementation of intelligent processing of materials (IPM) in the production of advanced materials, with special emphasis on defense applications. IPM is inherently a multidisciplinary effort, combining the latest in materials processing knowledge in the form of process models; novel, in-situ process sensors; and emerging control theory for adaptive control of highly nonlinear processes. The concepts reported below have been studied to assess their value in streamlining the development of new methods for establishing regions of process variable space which are inherently stable, thereby reducing the laborious and experimentally intensive task of process design for production of advanced materials, and to a distributed simulation environment known as the Virtual Factory for rapid prototyping of intelligent control systems, which was originally developed in a parallel research project sponsored by ARPA through NIST. Finally, these new techniques, concepts, and capabilities have been applied to the processing of advanced materials for military applications, including near net shape forming of titanium alloy powders to form shaped parts representative of gas turbine engine components and the growth of single crystal infrared detector materials based upon cadmium zinc telluride, which is the substrated material for infrared focal plane arrays. These efforts have been conducted by BDM scientists and engineers, in conjunction with leading university research from MIT and the University of California, Santa Barbara (UCSB). DTIC

N94-18938# Oak Ridge National Lab., TN.
DEVELOPMENT OF DUCTILE Fe3Al-BASED ALUMINIDES
C. G. McKamey, V. K. Sikka, and G. M. Goodwin 1993 10 p Presented at the 7th Annual Conference on Fossil Energy Materials, Oak Ridge, TN, 11-13 May 1993
(Contract DE-AC05-84OR-21400)
(DE93-017865; CONF-9305135-8) Avail: CASI HC A02/MF A01

Iron aluminides based on Fe3Al are of interest because of their excellent oxidation and corrosion resistance, especially in sulfur-bearing atmospheres. Work at ORNL has centered on developing Fe3Al-based alloys with improved ambient temperature ductilities and increased strengths at temperatures of 600-700 C. Ambient temperature brittleness in this system is not 'inherent,' but is caused by atomic hydrogen which is produced by an environmental reaction between aluminum in the alloy and water vapor in the atmosphere. Great strides have been made in understanding this embrittlement phenomenon, and the production of alloys with room temperature ductilities of over 10% and tensile yield strengths at 600 C of as high as 500 MPa is now possible through modifications in alloy composition and control of thermomechanical processing techniques. Creep rupture lifes of over 200 h at 593 C (1100 F) and 207 MPa (30 ksi) can also be produced through control of alloy composition and microstructure. This paper summarizes our present efforts to improve the tensile and creep rupture properties and gives the status of efforts to commercialize Fe3Al-based alloy compositions. DOE

N94-18939# Lawrence Livermore National Lab., CA.
ELECTRON IMPACT EXCITATION OF COPPER ATOMS
B. J. Stumpf (Idaho Univ., Moscow.) 1993 13 p
(Contract W-7405-eng-48)
(DE93-017995; UCRL-CR-113452) Avail: CASI HC A03/MF A01

The optical excitation function method has been used in a crossed atom and electron beam arrangement to measure the electron impact cross section of the copper 4(sup 2)P to 4(sup 2)S resonance lines (324.8, 327.4 nm) from threshold (3.8 eV) to 8 eV. Relative experimental cross section data are normalized at an energy of 1000 eV with respect to first Born theory that includes the 4(sup 2)S to 4(sup 2)P resonance transition with an oscillator strength of 0.652 and cascading from the (3d(sup 10)nd)(sup 2)D states with n = 4, ...10. The measured Cu 4(sup 2)S(sup 4) to 4(sup 2)P cross section is compared with recent theoretical calculations in close-coupling approximation. Very good agreement is found with the ten-state close-coupling theory of Scheibner. DOE

N94-18940# Westinghouse Electric Corp., West Mifflin, PA. Atomic Power Lab.
ENVIRONMENTAL DEGRADATION OF ALLOY 600 AND WELDED FILLER METAL EN82 IN AN ELEVATED TEMPERATURE AQUEOUS ENVIRONMENT
G. L. Webb 1993 8 p Presented at the 6th International Symposium on Environmental Degradation of Materials in Nuclear Power Systems: Water Reactors, San Diego, CA, 3-5 Aug. 1993
(Contract DE-AC11-89PN-38014)
(DE93-018049; WAPD-T-2989; CONF-930825-4) Avail: CASI HC A02/MF A01

The stress corrosion cracking (SCC) behavior of Alloy 600 and welded nickel base filler metal EN82 in high temperature water was investigated. A regression model was developed to show the effects of stress and temperature on SCC initiation for Alloy 600 tubing. An activation energy of 50.6 kcal/mole and a stress exponent of -5.7, applicable to these heats of low temperature mill annealed tubing, were determined from the regression analysis. Data are also presented on the SCC behavior of other classes of materials, including low temperature thermally treated tubing, hot worked and annealed ring forgings, and EN82 weld metal in relation to the tubing data. DOE

N94-18952# Research Inst. of National Defence, Stockholm (Sweden). Dept. of Weapon Systems, Effects and Protection.
INTELLIGENT MATERIALS SYSTEMS AND STRUCTURES. PART 4: THE INFLUENCE OF THERMOMECHANICAL LOADING ON THE LIFE OF SHAPE MEMORY ALLOYS [INTELLIGENTA MATERIALSYSSTEM OCH STRUKTURER. DEL 4: INVERKAN AV TERMOMEKANISK BELASTNING PA MINNESMETALLERS LIVSLANGD]
S. Tiensuu Mar. 1993 37 p In SWAHILI See also PB92-219195
(PB93-195923; FOA-C-20923-8.4-Pt-4) Avail: CASI HC A03/MF A01

The report begins with a short presentation of the shape memory alloy phenomenon, including its history and terminology. After introductory comments the investigation of a NiTi wire is described. To study fatigue and changes in properties during thermomechanical loading, measurements of strain and cycles to failure were measured as a function of stress. This entailed construction of an experimental apparatus, which is described. Other properties, including transformation temperatures, electrical resistivity and microstructure were measured before and after fatigue testing to further investigate the influence of thermomechanical loads on a shape memory alloy. NTIS

N94-18975# Oak Ridge National Lab., TN.
TENSILE PROPERTIES OF AS-CAST IRON-ALUMINIDE ALLOYS
S. Viswanathan, P. J. Maziasz, V. K. Sikka, and C. G. McKamey 1993 10 p Presented at the 7th Annual Conference on Fossil Energy Materials, Oak Ridge, TN, 11-13 May 1993
(Contract DE-AC05-84OR-21400)
(DE93-017852; CONF-9305135-7) Avail: CASI HC A02/MF A01

Room-temperature tensile properties of as-cast Fe3Al, Fe3Al with chromium, and Fe3Al-based FA-129 alloy are investigated. Tensile properties were obtained in the as-cast condition and after homogenization at 700, 900, and 1200 C. Transmission electron microscopy (TEM) was used to characterize ordered phases, and optical metallography and scanning electron microscopy (SEM) were used to characterize the microstructure and fracture morphology. The results indicate that the low ductility of as-cast Fe3Al-based alloys may be related to the relatively large grain size in the cast condition, the low dislocation density in as-cast samples, and the presence of the D0(sub 3) ordered phase. Homogenized samples of FA-129 alloy exhibited almost twice the ductility of the as-cast condition. Microstructural characterization of the homogenized samples and comparison of the as-cast and homogenized microstructures may provide a clue to the poor ductility in the as-cast state. DOE

N94-19019# Marquette Univ., Milwaukee, WI. Dept. of Chemistry.
RESONANCE RAMAN AND PHOTOPHYSICAL STUDIES OF TRANSITION METAL COMPLEXES IN SOLUTION AND ENTRAPPED IN ZEOLITES
J. R. Kincaid 1993 11 p
(Contract DE-FG02-86ER-13619)
(DE93-019892; DOE/ER-13619/7) Avail: CASI HC A03/MF A01

A study of the effects of entrapment of ruthenium(2)-polypyridyl complexes within the supercages of Y-zeolite is discussed. Results of initial studies document alterations in photophysical properties of entrapped complexes and provide insight into the factors responsible for these changes. A second major activity was to undertake an investigation of the feasibility of entrapment of metallophthalocyanines within the Y-zeolite supercages. The initial problems with the preparative methodology used for these systems have been overcome and several systems have now been prepared and purified for projected photoredox studies. A third major objective was to develop and utilize a sound interpretive framework for resonance Raman (RR) and time-resolved RR (TR(sup 3)) methods for investigating subtle perturbations in ground- and (sup 3)MLCT-state electronic structure which might be induced by substituent or environmentally-induced asymmetry, effects which could possibly lead to critical functional alterations. DOE

N94-19021# Rensselaer Polytechnic Inst., Troy, NY.
THE EFFECTS OF RADIOLYSIS ON THE CORROSION AND STRESS CORROSION BEHAVIOR OF 316 STAINLESS STEELS
D. J. Duquette and D. Steiner 1993 14 p
(Contract DE-FG02-89ER-52161)
(DE93-019933; DOE/ER-52161/5) Avail: CASI HC A03/MF A01

This program is focused on the corrosion, stress corrosion, and corrosion fatigue behavior of Type 316 stainless steel (316SS) at 50, 90, and 130 C in high-purity water. Irradiated solution tests are performed using high-energy photon radiation. Purpose of this work is to determine the effects of radiolysis products on the environmental stability of 316SS in support of the ITER first wall/shield/blanket design. Preliminary results suggest that irradiation of pure water at 50 C results in a shift in the electrochemical potential for 316SS of approximately 100mV in the active direction and nearly an order of magnitude increase in the passive current density as compared to non-irradiated conditions. This proposal outlines a three-year program to develop corrosion design criteria for the use of 316SS in an ITER environment. DOE

N94-19028# Los Alamos National Lab., NM.
BERYLLIUM PROCESSING TECHNOLOGY REVIEW FOR APPLICATIONS IN PLASMA-FACING COMPONENTS
R. G. Castro, L. A. Jacobson, and P. W. Stanek Jul. 1993 27 p
(Contract W-7405-eng-36)
(DE93-018396; LA-12545-MS) Avail: CASI HC A03/MF A01

Materials research and development activities for the International Thermonuclear Experimental Reactor (ITER), i.e., the next generation fusion reactor, are investigating beryllium as the first-wall containment material for the reactor. Important in the selection of beryllium is the ability to process, fabricate and repair beryllium first-wall components using existing technologies. Two issues that will need to be addressed during the engineering design activity will be the bonding of beryllium tiles in high-heat-flux areas of the reactor, and the in situ repair of damaged beryllium tiles. The following review summarizes the current technology associated with welding and joining of beryllium to itself and other materials, and the state-of-the-art in plasma-spray technology as an in situ repair technique for damaged beryllium tiles. In addition, a review of the current status of beryllium technology in the former Soviet Union is also included. DOE

N94-19032# Michigan Univ., Ann Arbor.
A FREE ENERGY SIMULATION METHOD BASED STUDY OF INTERFACIAL SEGREGATION
D. J. Srolovitz 18 May 1993 2 p
(Contract DE-FG02-88ER-45367)
(DE93-019462; DOE/ER-45367/5) Avail: CASI HC A01/MF A01

Binary alloys were investigated. Segregation to and thermodynamics of twist grain boundaries in Cu-Ni were studied. Segregation to and order-disorder phase transitions at grain boundaries in ordered Ni3(-x)Al(1+x) were also investigated. Order-disorder transitions at and segregation to the (001), (011), and (111) surfaces in Pd-Cu, Pd-Ag, and Pd-Au alloys were investigated. The (001) surface in Cu-rich alloys undergoes a surface phase transition from disordered to ordered surface phase upon cooling from high temperature, similar to the (001) surface transition in Ni-rich Pt-Ni alloys. Segregation and ordering appear to be correlated. The free energy minimization method was also used to calculate the heat of formation and lattice parameter of Ag-Cu metastable phases. Results of free energy minimization for free energy and entropy of Si agree with experiment and quasiharmonic calculations. DOE

N94-19043# Pacific Northwest Lab., Richland, WA.
HIGH DOSE EFFECTS IN NEUTRON IRRADIATED FACE-CENTERED CUBIC METALS
F. A. Garner and M. B. Toloczko (California Univ., Santa Barbara.) Jun. 1993 47 p Presented at the Time Dependence of Radiation Damage Accumulation and Its Impact on Material Properties, Montreau (Switzerland), 14-21 Oct. 1993
(Contract DE-AC06-76RL-01830)
(DE93-017671; PNL-SA-21235; CONF-9310133-1) Avail: CASI HC A03/MF A01

During neutron irradiation, most face-centered cubic metals and alloys develop saturation or quasi-steady state microstructures. This, in turn, leads to saturation levels in mechanical properties and quasi-steady state rates of swelling and creep deformation. Swelling initially plays only a small role in determining these saturation states, but as swelling rises to higher levels, it exerts strong feedback on the microstructure and its response to environmental variables. The influence of swelling, either directly or indirectly via second order mechanisms, such as elemental segregation to void surfaces, eventually causes major changes, not only in irradiation creep and mechanical properties, but also on swelling itself. The feedback effects of swelling on irradiation creep are particularly complex and lead to problems in applying creep data derived from highly pressurized creep tubes to low stress situations, such as fuel pins in liquid metal reactors. DOE

N94-19044# Argonne National Lab., IL.
MODELING OF THE FORMATION OF MICROPOROSITY IN ALLOYS
F. C. Chang and H. L. Tsai (Missouri Univ., Rolla.) 1993 6 p Presented at the 1993 Chinese American Academic and Professional Convention, Chicago, IL, 2-5 Jul. 1993
(Contract W-31-109-eng-38)
(DE93-017733; ANL/ET/CP-78882; CONF-930796-3) Avail: CASI HC A02/MF A01

A complete mathematical model, consisting of a continuum model and a gas evolution model, was established for the prediction of shrinkage- and gas-caused porosity in castings. The model allows simultaneous calculation of transient temperature, velocity, pressure, and porosity distributions in a solidifying casting. Fluid flow caused by both natural convection and solidification contraction, as well as change of global domain due to shrinkage, were considered. A parametric study was performed to investigate the effects of various solidification variables in the formation of microporosity, including the use of chilling, initial gas content, characteristics of heat transfer between the casting and the mold, casting size, and riser height. It was found that a low initial gas content in the molten metal and casting conditions that facilitate solidification-rate decrease the formation of microporosity. The calculated porosity distribution in 1% Cr-steel alloys compares favorably with published experimental data. DOE

N94-19080# Sandia National Labs., Albuquerque, NM.
BINDING OF COPPER TO NANOCAVITY SURFACES IN SILICON
S. M. Myers, D. M. Follstaedt, and D. M. Bishop 1993 10 p Presented at the 17th International Conference on Defects in Semiconductors, Gmunden, Austria, 18-23 Jul. 1993
(Contract DE-AC04-76DP-00789)
(DE93-019073; SAND-93-0244C; CONF-9307124-1) Avail: CASI HC A02/MF A01

We demonstrate that nanometer-scale voids within Si, formed by He ion implantation and annealing, trap Cu atoms with a binding energy of 2.2 +/- 0.2 eV relative to solution. This trapping saturates at a level consistent with monolayer coverage of the cavity walls, and it is ascribed to the reaction of Cu with Si dangling bonds on the internal surfaces. Our experiments also confirm the previously reported solution enthalpy of Cu in Si relative to precipitated Cu3Si, 1.7 eV, so that the binding at cavity traps is stronger. It is proposed that nanocavities may provide superior gettering of metallic impurities in Si. DOE

N94-19100# Sandia National Labs., Albuquerque, NM.
METALLURGICAL EVALUATION OF SRAM 2/SRAM A PROGRAM MER BASE PLATES
B. K. Damkroger, M. C. Maguire, and C. V. Robino May 1993 65 p
(Contract DE-AC04-76DP-00789)
(DE93-018689; SAND-93-0763) Avail: CASI HC A04/MF A01

Ten MC4073/4369 programmer base plates were analyzed. This component, a programmer base plate for the SRAM II (and later the SRAM A), is specified as a Grade C quality casting made of aluminum Alloy A356, heat treated to the T6 condition. A concern was expressed regarding the choice of an A356 casting for this application, given the complexity and severity of the loading environment. Preliminary tests and analyses suggested that the design was adequate, but noted the uncertainty involved in a number of their underlying assumptions. The uncertainty was compounded by the discovery that the casting used in the original series of mechanical tests failed. In this investigation, several production castings were examined and found to be of a quality superior to that required under current specifications. Their defect content and microstructure were studied and compared with published data to establish a mechanical property data base. The data base was supplemented with a series of X-direction static tests, which characterized the loading environment and measured the overall casting performance. It was found that the mechanical properties of the supplied castings were adequate for the anticipated X-direction loading environment, but the component is not over-designed. The established data base further indicates that a reduction in casting quality to the allowable level could result in failure of the component. Recommendations were made including (1) change the component specification to require higher casting quality in highly stressed areas, (2) supplement the inspection procedures to ensure adequate quality in critical regions, (3) alter the component design to reduce the stress levels in the mounting feet, (4) substitute a modified A356 alloy to improve the mechanical properties and their consistency, and (5) more thoroughly establish a data base for the mechanical property consequences of levels and configurations of casting defects. DOE

N94-19203# Oak Ridge National Lab., TN.
PREDICTION OF NON-EQUILIBRIUM SOLIDIFICATION MODES IN AUSTENITIC STAINLESS STEEL LASER WELDS
J. M. Vitek and S. A. David 1993 37 p Presented at the Annual Meeting of the Metallurgical Society, Denver, CO, 21-25 Feb. 1993
(Contract DE-AC05-84OR-21400)
(DE93-018457; CONF-930202-11) Avail: CASI HC A03/MF A01

A primary austenitic, non-equilibrium mode of solidification can be induced in many 300 series austenitic stainless steels by laser welding and other rapid solidification techniques. The change in solidification mode can often result in a fully austenitic microstructure compared to the two phase ferrite plus austenite microstructure that is commonly found after primary ferrite solidification. A predictive capability for the solidification mode under rapid solidification conditions such as laser welding is needed since the microstructure and properties are closely related to solidification behavior. Conventional constitutional diagrams do not predict with any reliability the change to non-equilibrium austenitic solidification mode. Several means that have been attempted to predict the solidification behavior under extreme conditions are reviewed. The Cr(sub EQ)/Ni(sub EQ) ratio is shown to be unreliable, at least with the equivalence factors commonly used. Theoretical calculations of growth rate competition between ferrite and austenite solidification show promise, but some ambiguity results from inaccuracy in thermophysical material parameters. Use of calculated thermodynamic parameters such as equilibrium and non-equilibrium liquidus and solidus temperatures also shows some promise. However, this approach is not completely satisfactory and reliable either. It is concluded that a reliable and accurate method for predicting the tendency of austenitic stainless steels to solidify in the non-equilibrium mode is not yet available. DOE

N94-19263# Lawrence Livermore National Lab., CA.
MOLECULAR DYNAMICS MODELING OF THE MECHANICAL BEHAVIOR OF METALLIC MULTILAYERS
J. Belak and D. B. Boercker Apr. 1993 7 p Presented at the 205th American Chemical Society National Meeting, Denver, CO, 28 Mar. - 2 Apr. 1993
(Contract W-7405-eng-48)
(DE93-017972; UCRL-JC-112347; CONF-930304-31) Avail: CASI HC A02/MF A01

Constant-stress molecular dynamics simulations are used to study the mechanical properties of equal concentration Cu-Ni (111) metallic multilayers of repeat lengths 0.4-0.5 nm. Uniaxial stress is applied along the close-packed and perpendicular to the close-packed directions within the (111) plane. The observed elastic moduli do not display a supermodulus effect as observed in experimental bulge tests for the biaxial modulus. However, both the average interlayer spacing and the out-of-plane Poisson ratio display anomalous effects for multilayer repeat lengths below about two nanometers. DOE

N94-19274# Oak Ridge National Lab., TN.
LOW-ALUMINUM-CONTENT IRON-ALUMINUM ALLOYS
V. K. Sikka, R. H. Baldwin, and C. R. Howell 1993 12 p Presented at the 7th Annual Conference on Fossil Energy Materials, Oak Ridge, TN, 11-13 May 1993
(Contract DE-AC05-84OR-21400)
(DE93-017862; CONF-9305135-9) Avail: CASI HC A03/MF A01

The low room-temperature ductility of Fe3Al-based alloys is associated with their environmental embrittlement. Reducing the aluminum level from 29 to 16 at. % has been found to be an effective method in essentially eliminating the environmental embrittlement effect and increasing the room-temperature ductility value to over 25%. This paper will present data on alloy compositions, melting, casting and processing methods, and mechanical properties. Plans for future work on these alloys will also be described. DOE

N94-19280# Lawrence Livermore National Lab., CA.
THE EFFECT OF COMPOSITION ON THE MECHANISM OF CONTINUOUS RECRYSTALLIZATION AND SUPERPLASTIC RESPONSE OF ALUMINUM-SCANDIUM ALLOYS Ph.D. Thesis
E. L. Bradley, III May 1993 102 p
(Contract DE-AC03-76SF-00098)
(DE93-018594; LBL-34291) Avail: CASI HC A06/MF A02

Continuous recrystallization (CRX) seems to be fundamental in Al-Sc because it occurs irrespective of solute composition. It appears to be due to a combination of subgrain coalescence at low strains and incorporation of additional dislocations generated during grain boundary sliding at higher strains when the misorientation has increased sufficiently. Alloying additives such as Mg and Li are more important with respect to deformation after CRX is completed. Mg, and to a lesser extent Li, affect the max m-values (strain-rate sensitivities) in Al-Sc by changing the melting points (mp). Max m-values correlate inversely with mp so that the alloy with the greatest Mg had the highest m-values and lowest mp; the stress is raised at which power-law creep and breakdown occurs. The power-law breakdown at much lower stresses in Al-0.5Sc and Al-1.2Li-0.5Sc causes the m-value to decrease more rapidly with strain rate. Al alloys for commercial superplastic applications should contain elements that raise the power-law strength so that the m-values are maximized while preserving the post-formed mechanical properties. DOE

N94-19282# California Univ., Berkeley. Lawrence Berkeley Lab.
THE MICROSTRUCTURAL MECHANISM OF ELECTROMIGRATION FAILURE IN NARROW INTERCONNECTS OF Al ALLOYS Ph.D. Thesis
Choongun Kim Apr. 1993 203 p
(Contract DE-AC03-76SF-00098)
(DE93-018598; LBL-34189) Avail: CASI HC A10/MF A03

This thesis reports a study of the mechanism of electromigration failure in Al-2Cu-1Si thin-film conducting lines on Si. Samples were patterned from 0.5 micron thick vapor-deposited films with various mean grain sizes (G). The samples had line widths (W) of 1.3, 2, 4 and 6 microns. The lines were aged at various conditions to change the Cu-precipitate distribution and were tested to failure at T = 225 C and j = 2.5 x 10(exp 6) A/sq cm. Some samples were tested over a range of substrate temperatures, current densities, and current reversal times. Aging produces an initially dense distribution of metastable theta' (Al2Cu; coherent) in the grain interiors, with stable theta (Al2Cu; incoherent) at the grain boundaries. The intragranular theta' is gradually absorbed into the grain boundary precipitates. In the wide lines, the mean time to failure increases slowly and monotonically with pre-aging time and current reversal time. The failure mode is the formation and coalescence of voids that form on grain boundaries with an apparent activation energy of 0.65 eV. In the narrow lines, the lines failed by a transgranular-slit mechanism with an activation energy near 0.93 eV. The distribution of the polygranular segments and the kinetics of failure varies with the linewidths. Failure occurs after Cu has been swept from the grains that fail. Pre-aging the line to create a more stable distribution of Cu significantly increases the time to failure. When the density of intragranular theta-phase precipitates is maximized, the transgranular-slit failure mechanism is suppressed, and the bamboo grain fails by diffuse thinning to rupture. The results from the current reversal test indicate that the time to sweep Cu in the polygranular segments is longer for longer polygranular segments. Thus the time to first failure in an array of lines is much longer than predicted by a log-normal fit to the distribution of failure times. DOE

N94-19374# Technical Research Centre of Finland, Espoo. Metals Lab.
THE APPLICATIONS OF MODIFIED METALS IN THE CONSTRUCTION INDUSTRY [MODIFIOITUJEN METALLIEN KAEYTTOESOVELLUTUKSET RAKENNUSTEOLLISUUDESSA]
Jaakko Salmi, Paavo Hassinen, and Pertti Auerkari Feb. 1992 45 p In FINNISH Sponsored by Technical Research Centre of Finland, Espoo
(VTT-TIED-1329; ISBN-951-38-4142-1; ETN-93-94471) Copyright Avail: CASI HC A03/MF A01

The properties of metal matrix composites, bimetals and memory metals are presented and applications in construction industry are discussed. Bimetals are already widely used in thermal switches and relays as well as in components in measuring instruments which react to temperature changes. Memory metals are used in various pipe and electrical connectors and in control devices for ventilation windows and air conditioners. Most applications of metal matrix composites have been in space, aircraft and defense industries. However, now the prices of the materials are falling, while their use is growing and extending, and finding applications in other branches too is becoming feasible. The applications presented are not ready products, though they could give useful indications for applications where the properties of traditional materials are inadequate. ESA

N94-19400# Ecole Centrale de Lyon (France). Dept. de Mecanique des Solides.
FORMULATION AND IDENTIFICATION OF THE ANISOTROPIC LAWS FOR THIN SHEETS DRAWING Ph.D. Thesis [FORMULATION ET IDENTIFICATION DE LOIS DE COMPORTEMENT ANISOTROPES POUR TOLES MINCES EN EMBOUTISSAGE]
Abdelkrim Benchouikh 1992 149 p In FRENCH
(ECL-92-55; ETN-93-94600) Avail: CASI HC A07/MF A02

Work done to formulate the realistic models for the numerical simulation of deep drawing is reported. These models must be mechanically consistent and sufficiently simple in their formulation and identification. This work is developed within the framework of rigid plasticity in plasma stress, which is a suitable approximation for sheet metal forming. Three classes of models were developed taking into account the initial anisotropy of the material together with isotropic hardening. Attention is restricted to the transverse isotropic case. This work was done as a part of a joint project on constitutive equation for deep drawing. The first class of models is relatively classic and permits the correct description of some radial stress paths taking into account the anisotropy coefficient, by using a non-associated flow rule. The principal contribution consists in developing an identification strategy and together with the appropriate numerical schemes starting from existing experiments results. The second class of models allows modification of the description of some experimental results and specially the plane traction by introducing new internal variables hardening more or less related to the microstructural (mean free path). For the description of subsequent behavior following a change in the loading trajectory (complex loading), a model which uses an internal tensorial variable was developed. The third class of models is based on the utilization of a nonquadratic criterium. A general methodology of representation of plane stress isotropic and transversly isotropic criteria was developed. The application of this representation to a nonquadratic criterium and a nonassociated flow rule allows the construction of models which give a good description of radial loading and anisotropy. ESA

N94-19436# Ecole Centrale de Lyon (France). Dept. Materiaux-Mecanique Physique.
NI-AL2O3 SOLID STATE BINDING: ELABORATION, STATE OF THERMAL CONSTRAINTS, MECHANICAL BEHAVIOR Ph.D. Thesis [LES LIAISONS NI-AL2O3 A L'ETAT SOLIDE: ELABORATION, ETAT DES CONTRAINTES THERMIQUES, COMPORTEMENT MECANIQUE]
Pierre Lourdin 1992 161 p In FRENCH
(ECL-92-31; ETN-93-94591) Avail: CASI HC A08/MF A02

Nickel-alumina chemical bindings are prepared by thermal compression in the solid state and submitted to tensile and four point flexion tests. Several physical-chemical mechanisms to explain bindings are considered. The quality of the contact between the two materials depends on the plastic strain of the metal. The formation of an interface is associated with the behavior of secondary phases found in ceramics. Recent developments of brittle two phase materials allowed to characterize the interface's fracture energy, which was found to be 40 J sq m. The feasibility and the mechanical resistance of a metal/ceramic assembly depend on the thermal stresses state. The available models are not satisfactory, and a new model to describe the thermal stress level is proposed. It takes into account the speed of cooling and describes quite accurately the stress state after creep tests. ESA

N94-19546# Massachusetts Inst. of Tech., Cambridge. Plasma Fusion Center.
INCOLOY 908 DATABASE REPORT: ON PROCESS-STRUCTURE-PROPERTY RELATIONSHIP
L. S. Toma, I. S. Hwang, and M. M. Steeves May 1993 39 p
(Contract DE-FC02-93ER-54186)
(DE93-017616; DOE/ER-54186/T1; PFC/RR-93-2) Avail: CASI HC A03/MF A01

Incoloy 908 is a nickel-iron base superalloy with a coefficient of expansion (COE) and mechanical properties that have been optimized for use in Nb3Sn superconducting magnets. It has been proposed for use as a conduit material for the International Thermonuclear Experimental Reactor (ITER) magnets. The relationship between manufacturing processes, microstructures, and mechanical properties of Incoloy 908 are characterized in support of the magnet fabrication and quality control. This report presents microhardness, microstructure, and yield and ultimate tensile strengths as functions of thermomechanical process variables including heat treatment, annealing, and cold work for laboratory prepared Incoloy 908 specimens. Empirical correlations have been developed for the microhardness at room temperature and tensile strength at room temperature and at 4K. These results may be used for manufacturing quality control or for design. DOE

N94-19594# Missouri Univ., Rolla.
USE OF SHAPE MEMORY ALLOYS IN THE ROBUST CONTROL OF SMART STRUCTURES Final Report, Feb. 1990 - Jun. 1993
Vittal S. Rao, Thomas J. OKeefe, and Leslie R. Koval Aug. 1993 134 p
(Contract DAAL03-90-G-0053)
(AD-A270827; ARO-27686.11-EG-SM) Avail: CASI HC A07/MF A02

This report details an integrated interdisciplinary approach for designing and implementing robust controllers on smart structures. The application of shape memory alloy materials as actuators and sensors in the active control of smart structures has been investigated. A process was developed for the electrodeposition of In-Tl alloys in a composition range where this system exhibits the shape memory effect. Cu-Zn, Au-Ca, and In-Cd alloy films were produced using the electrolytic techniques and their shape memory properties evaluated. To demonstrate some of the capabilities of smart structures and to determine the limitations imposed by hardware realizations, we have designed and fabricated experimental test articles incorporating flexible structures with SMA actuators, strain gauge sensors, signal processing circuits and digital controllers. Structural identification techniques have been employed in determining mathematical models of test articles from experimental data. A modified robust control design methodology was developed to accommodate the limited control force provided by the SMA actuators. The robustness properties of closed loop structural systems were verified experimentally. Adaptive control methods were implemented. Neural network based identification and control algorithms were developed. DTIC

N94-19673# Wyman-Gordon Co., Worcester, MA.
DEVELOPMENT AND CHARACTERIZATION OF ADIABATIC SHEAR PRONE TUNGSTEN HEAVY ALLOYS Final Report, 1 Oct. 1991 - 31 Jan. 1993
Aniimesh Bose, James Lankford, Jr., and Herve Couque Jul. 1993 81 p
(Contract DAAL04-91-C-0065)
(AD-A270477; SwRI-06-4601; ARL-CR-60) Avail: CASI HC A05/MF A01

Depleted uranium (DU) is currently the top-performing kinetic energy penetrator, followed closely (but not matched) by several tungsten heavy alloy variants. Because of the adverse environmental impact associated with DU, it is extremely desirable to determine a means of upgrading the ballistic performance of heavy alloys to a level at least comparable to that of DU. It is thought that the reason for the improved ballistic performance of DU-0.75 Ti alloy is embedded in its ability to self sharpen during armor penetration, and it is further postulated that this self-sharpening ability is due to the susceptibility of DU to adiabatic shear during penetration events. The contrasting inability of current tungsten heavy alloys to localize shear during penetration causes mushrooming at the head of the projectile, thus, decreasing the depth of penetration. Consequently, there is a great urgency to develop new tungsten alloys that will exhibit localized, unstable shear failure, and associated self sharpening during armor penetration. DTIC

N94-19733# Oak Ridge National Lab., TN.
COMMERCIALIZATION EFFORT IN SUPPORT OF ELECTROSLAG-CASTING TECHNOLOGY
V. K. Sikka Jun. 1993 37 p
(Contract DE-AC05-84OR-21400)
(DE93-017988; ORNL/TM-12341) Avail: CASI HC A03/MF A01

This report summarizes the results of an effort to revive interest in the electroslag casting (ESC) of components in the United States. The ESC process is an extension of a well established electroslag-remelting (ESR) process. Both processes use the electrode of a material that is continuously melted and cast in a water-cooled copper mold. For simple shapes, the mold can be movable, allowing the continuous casting of long lengths. In an effort to revive U.S. industries' interest in ESC, the following approaches were taken: U.S. industries with prior experience in ESC or currently operating an ESR unit were contacted, followed up with telephone conversation, and/or sent copies of prior published reports on the topic, and, in some cases, personal visits were made; with two companies, a potential interest in ESC was worked out by initially conducting ESR; and to further strengthen the industrial interest, the newly developed iron-aluminide alloy, FA-129, was chosen as the material of choice for this study. The two industrial companies that worked with ORNL were Special Metals Corporation (New Hartford, New York) and Precision Rolled Products, Inc. (PRP, Florham Park, New Jersey). Even with its advantages, a survey of the industry indicated that ESC technology has a very limited chance of advancement in the United States. However, the processing of rounds and slabs by the ESR process is a well established commercial technology and will continue to expand. DOE

N94-19775# Memry Technologies, Inc., Norwalk, CT.
DAMPING IN FERROUS SHAPE MEMORY ALLOYS Final Report
L. M. Schetky, M. H. Wu, C. Y. Lei, C. M. Wayman, and M. Wuttig Aug. 1993 64 p
(Contract N00014-90-C-0076)
(AD-A271009) Avail: CASI HC A04/MF A01

The damping properties of Fe-Mn-Si, Fe-Ni-Co-Ti, and Fe-Al-C alloy systems were examined by DMTA (Dynamic Mechanical Thermal Analyzer) and oscillation methods. The martensite transformations and microstructures were studied and examined by transition electron microscopy (TEM), resistivity, and DSC. High damping was found in Fe-Mn-Si and Fe-Ni-Co-Ti alloys with microstructures containing glissile inter-variant martensite interfaces, while those with sessile inter-variant martensite interfaces exhibit lower damping. The general agreement between the damping peaks and transformation temperatures further confirms the close relations between high damping and shape memory behavior. DTIC

N94-18008# ASULAB S.A., Neuchatel (Switzerland). Lab. de Recherches du Groupe SMH.
ACCELERATED TESTS ON THE TARNISH RESISTANCE OF GOLD ALLOYS [TESTS ACCELERES DE LA RESISTANCE AU TERNISSEMENT DES ALLIAGES D'OR]
Jean-Paul Randin, Jean-Pierre Renaud (CCF S.A., La Chaux-de-Fonds, Switzerland.), and Pierre Ramoni (Metaux Precieux S.A. Metalor, Nauchatel, Switzerland.) *In* Societe Suisse de Chronometrie, Proceedings of the 4th European Congress on Chronometry 1992 p 17-20 In FRENCH (For primary document see N94-18006 04-35)
Copyright Avail: CASI HC A01/MF A02

N94-18009# Centre Technique de l'Industrie Horlogere, Besancon (France).
EVALUATION OF THE NICKEL RELEASE BY HOROLOGICAL PRODUCTS [EVALUATION DE LA LIBERATION DE NICKEL PAR LES PRODUITS HORLOGERS]
Jean Picaut *In* Societe Suisse de Chronometrie, Proceedings of the 4th European Congress on Chronometry 1992 p 21-23 In FRENCH (For primary document see N94-18006 04-35)
Copyright Avail: CASI HC A01/MF A02

N94-18011# Stuttgart Univ. (Germany). Inst. fuer Zeitmesstechnik, Fein- und Mikrotechnik.
SPUTTERED TIN COATINGS IN PLASTIC [GESPUTTERTE TIN-SCHICHTEN AUF KUNSTSTOFFEN]
Benedikt Martin and Jutta Martin *In* Societe Suisse de Chronometrie, Proceedings of the 4th European Congress on Chronometry 1992 p 29-32 In GERMAN (For primary document see N94-18006 04-35)
Copyright Avail: CASI HC A01/MF A02

N94-18012# Metaux Precieux S.A. Metalor, Nauchatel (Switzerland).
GOLD-COPPER-ZINC COATINGS AS AN ALTERNATIVE TO GOLD-COPPER-CADMIUM [DEPOTS OR-CUIVRE-ZINC COMME ALTERNATIVE A OR-CUIVRE-CADMIUM]
Pierre-Andre Aeby and Paul Bagnoud *In* Societe Suisse de Chronometrie, Proceedings of the 4th European Congress on Chronometry 1992 p 33-37 In FRENCH (For primary document see N94-18006 04-35)
Copyright Avail: CASI HC A01/MF A02

27 NONMETALLIC MATERIALS

Includes physical, chemical, and mechanical properties of plastics, elastomers, lubricants, polymers, textiles, adhesives, and ceramic materials.

For composite materials see *24 Composite Materials.*

N94-17678# Pennsylvania State Univ., University Park. Dept. of Physics.
VIBRATIONAL AND ELECTRONIC PROPERTIES OF CLUSTERS AND ULTRATHIN FILMS
J. S. Lannin 1993 8 p
(Contract DE-FG02-84ER-45095)
(DE93-012291; DOE/ER-45095/7) Avail: CASI HC A02/MF A01

This covers approximately 26 months of research. In addition to clusters and thin films, studies of bulk fullerene and amorphous carbon are also reported. Results and activities are reported under the headings: structure of C60, dynamics of C60, Raman scattering of fullerene-based systems, B1 clusters, and amorphous carbon structure. DOE

N94-17706 Department of the Navy, Washington, DC.
POLARIZED THIN FILMS FROM DYE-SUBSTITUTED POLYMERS CONTAINING HYDROPHOBICALLY TERMINATED STILBAZOLIUM RADICALS Patent
Robert C. Hall, inventor (to Navy), Geoffrey A. Lindsay, inventor (to Navy), and James M. Hoover, inventor (to Navy) 6 Jul. 1993 9 p Filed 5 Oct. 1990
(AD-D015873; US-Patent-5,225,285; US-Patent-Appl-SN-623865) Avail: CASI HC A02/MF A01

Comb-shaped polymers, comprised of hydrophilic backbones and dye-containing, hydrophobic side chains are fabricated into multilayered, polarized, noncentro-symmetric, thin films by means of Langmuir-Blodgett processing techniques. These films exhibit harmonic, generated by shining a laser through the film, increases quadratically with the number of layers of polymeric dye in the film. DTIC

N94-17719 Department of the Navy, Washington, DC.
POLYURETHANE SELF-PRIMING TOPCOATS Patent
Charles R. Hegedus, inventor (to Navy), Donald J. Hirst, inventor (to Navy), and Anthony T. Eng, inventor (to Navy) 17 Aug. 1993 6 p Filed 20 Dec. 1991
(AD-D015870; US-Patent-Appl-SN-701406; US-Patent-Class-524-204)
Avail: CASI HC A02/MF A01

A corrosion-resistant coating which can be applied directly to a surface as a self-priming topcoat comprising a polyurethane binder and a combination of pigments consisting essentially of an alkaline earth metal phosphosilicate, zinc salts of benzoic acids, and an alkaline earth metal phosphate such as zinc-barium phosphate is described. In addition, the coating contains up to about 35 parts by weight of a titanium dioxide pigment and up to about 3.0 parts by weight of an oil soluble surface active agent and up to about 50 parts by weight of at least one organic solvent. DTIC

N94-17847# Oak Ridge National Lab., TN.
SCREENING ANALYSIS FOR CHLORINE-FREE ALTERNATIVE REFRIGERANTS TO REPLACE R-22 IN AIR CONDITIONING APPLICATIONS
S. K. Fischer and J. R. Sand 1993 17 p Presented at the 1993 American Society of Heating, Refrigerating and Air-Conditioning Engineers Summer Meeting, Denver, CO, 26-30 Jun. 1993
(Contract DE-AC05-84OR-21400)
(DE93-015920; CONF-930675-5) Avail: CASI HC A03/MF A01

The potential health and environmental effects of the depletion of stratospheric ozone from refrigerants containing chlorine have resulted in international treaties, laws, and non-binding agreements to phase-out and eliminate many common refrigerants. R-22 is one of these compounds. A study was conducted to evaluate the potential of twenty-two chlorine-free compounds in refrigerant mixtures of up to three components as substitutes for R-22. The selection or screening of blends was based on vapor compression cycle COP at the 95 F (35 C) cooling condition, the volumetric cooling capacity of the blend, evaporator and condenser temperature glides, and the 'estimated' flammability of the blend. Promising results were obtained for nine ternary blends containing E-125 and eleven ternary blends that exclude E-125. Recommendations are made to obtain further experimental data on E-125 since the mixtures with the best performance contain that compound. Results from this study will be used in an in-depth follow-on analysis. DOE

N94-17878# Missouri Univ., Rolla. Dept. of Chemistry.
NMR STUDIES OF ENRICHED SPECIES AT INTERFACES Interim Technical Report, Jun. 1992 - May 1993
Frank D. Blum 1 May 1993 30 p
(Contract N00014-91-J-1274)
(AD-A264703; UMR-FDB-30) Avail: CASI HC A03/MF A01

A review of the use of NMR at interfaces of solid surfaces is made. Special attention is focussed on the use of H-2, C-13, and N-15 isotopes in studies of polymers and silane surfaces active agents on solid surfaces. DTIC

N94-17881# Oak Ridge National Lab., TN.
SUMMARY OF WORK ON COATINGS AND CLADDINGS FOR FOSSIL ENERGY APPLICATIONS

R. W. Swindeman May 1993 25 p
(Contract DE-AC05-84OR-21400)
(DE93-017005; ORNL/TM-12367) Avail: CASI HC A03/MF A01

A summary of efforts to examine coatings and cladding materials for high-strength austenitic steels is provided. Chromized coatings on 17-14CuMo stainless steel and a modified type 316 (HT-UPS) stainless steel were investigated. Claddings included alloy 671, 690, and an iron-aluminide intermetallic alloy. Structural alloys that were clad included type 304 stainless steel, modified type 316 stainless steel, and modified alloy 800H. The capability of producing co-extruded tubing of the experimental alloys was demonstrated. DOE

N94-17905# Department of the Navy, Washington, DC.
PROCESS FOR APPLYING HIGH APPLICATION-TEMPERATURE COATING TO HEAT-SENSITIVE ALUMINUM ALLOYS Patent Application
James R. Quartarone, inventor (to Navy), William M. Cicchelli, inventor (to Navy), Kenneth E. Barthelemy, inventor (to Navy), and George V. Morris, inventor (to Navy) 29 Mar. 1993 21 p
(AD-D015823; US-Patent-Appl-SN-038369) Avail: CASI HC A02/MF A01

A process is provided for coating a given surface of a heat sensitive metal article (e.g., thermally massive aluminum) with a high cure temperature coating forming powder. A first oven heating step elevates the metal article's temperature to a predetermined preheat cycle high limit of heat load temperature. After a first predetermined period of time, the metal alloy article is withdrawn from the oven. A high cure temperature coating forming powder is then sprayed onto the given surface of the metal article. The spraying, comprising first and second spray sequences, is initiated essentially immediately after withdrawal of the metal article from the oven. Author (DTIC)

N94-17946# Oak Ridge National Lab., TN.
EXCIMER LASER INDUCED PERMANENT ELECTRICAL CONDUCTIVITY AND NANOSTRUCTURES IN POLYMERS
H. M. Phillips, T. Feurer, S. P. LeBlanc, D. L. Callahan (Rice Univ., Houston, TX.), R. Sauerbrey, and J. Bentley 1993 13 p Presented at the OE/LASE 1993 International Society for Optical Engineering Conference, Los Angeles, CA, 16-23 Jan. 1993 Prepared in cooperation with Oak Ridge Inst. for Science and Education, TN
(Contracts DE-AC05-84OR-21400; DE-AC05-76OR-00033)
(DE93-015965; CONF-930159-39) Avail: CASI HC A03/MF A01

The electrical conductivity of high temperature polymers (i.e. polyimide) has been changed permanently from 10(sup (minus)17) (Omega)(sup (minus)1) cm(sup (minus)1) to 10 (Omega)(sup (minus)1) cm(sup (minus)1) by KrF (248 nm) excimer laser irradiation. The conduction mechanism is found to be phonon assisted variable range hopping between small ((approximately)10 nm) carbon rich clusters that form a macroscopic percolation cluster. Using a holographic technique, periodic line structures with periods ranging from 166 nm to 950 nm have been produced in polyimide by direct ablation with a KrF excimer laser. Taking advantage of the large nonlinearity in the laser ablation process, linewidths ranging from 30 nm to several hundred nm could be obtained. This technique was combined with the ability to induce electrical conductivity in polyimide to produce an array of 500 nm wide electrically conducting wires. The conductivity of these wires was similar to that found in macroscopic regions of laser induced conductivity. DOE

N94-17982# Department of the Navy, Washington, DC.
POLYMERIZABLE LIPIDS IN THE DEVELOPMENT OF CONTROLLED RELEASE CARRIERS Patent Application
Alok Singh, inventor (to Navy) and Joel M. Schnur, inventor (to Navy) 23 Feb. 1993 24 p
(AD-D015789; US-Patent-Appl-SN-023834) Avail: CASI HC A03/MF A01

The present invention provides novel polymerizable lipids and mixtures thereof with non-polymerizable lipids and methods for the controlled release of encapsulated materials using stabilized or polymerized vesicles. Release is induced by pH, ions, temperature, light or other changes in the environment. Time release mechanisms are also employed. Applications of the present invention especially include encapsulation of enzymes and their subsequent sustained release for degradation of environmental pollutants, encapsulation of fluorescent markers for use in sensor systems, and encapsulation and release of fragrant molecules in detergents. DTIC

N94-18075*# National Aeronautics and Space Administration. Langley Research Center, Hampton, VA.
EFFECT OF TEMPERATURE AND O-RING GLAND FINISH ON SEALING ABILITY OF VITON V747-75
Cynthia L. Lach Nov. 1993 15 p
(RTOP 505-63-50-02)
(NASA-TP-3391; L-17214; NAS 1.60:3391) Avail: CASI HC A03/MF A01

As a part of the redesign project of the Space Shuttle solid rocket motor (SRM) following the Challenger accident, the field joint was redesigned to minimize the relative joint motion caused by internal motor pressurization during ignition. The O-ring seals and glands for the field joint were designed both to accommodate structural deflections and to promote pressure-assisted sealing. Tests were conducted in various face seal fixtures to evaluate the ability of Viton V747-75 O-rings to seal for a range of temperatures and surface finishes of the redesigned O-ring gland. The effect of surface finish on the sealing performance and wear characteristics of the O-rings was evaluated during simulated launch conditions that included low-frequency vibrations, gap openings, and rapid pressurizations. The effect of contamination on the sealing performance was also investigated. The O-rings sealed throughout the 75 deg F leak check test and for the seal tests from 50 deg F to 120 deg F for the range of surface finishes investigated. Although abrasions were found in the O-rings from pressurization against the rougher finishes, these abrasions were not detrimental to sealing. Below 50 deg F, Viton V747-75 O-rings were insufficiently resilient to track the test gap opening. Author (revised)

N94-18096# Los Alamos National Lab., NM.
MOLECULAR COMPOSITES FROM LIQUID CRYSTALLINE POLYMERS AND LIQUID CRYSTALLINE THERMOSETS
B. C. Benicewicz, E. P. Douglas, and R. P. Hjelm, Jr. 1993 9 p Presented at the International Workshop on Liquid Crystalline Polymers, Capri, Italy, 1-4 Jun. 1993
(Contracts W-7405-eng-36; W-31-109-eng-38)
(DE93-016608; LA-UR-93-2169; CONF-9306187-1) Avail: CASI HC A02/MF A01

We propose a new approach to molecular composites. This approach uses a mixture of a liquid crystalline polymer and a liquid crystalline thermoset to enhance the miscibility. Preliminary neutron scattering data is presented on a system of short and long rod aromatic amides. The data is interpreted using the interpenetrating phase model of Debye and Bueche. The analysis indicates that the scattering is consistent with this model and shows a characteristic length scale in the range of 70 to 80 A. The intensity of the scattering is lower than calculated for the strong segregation limit, suggesting that there is some intermixing of the components. DOE

N94-18098# Argonne National Lab., IL.
ELASTIC PROPERTIES OF A POLYIMIDE FILM DETERMINED BY BRILLOUIN SCATTERING AND MECHANICAL TECHNIQUES
R. S. Kumar (Amoco Oil Co., Naperville, IL.), I. K. Schuller (California Univ., San Diego, La Jolla.), S. S. Kumar, A. Fartash, and M. Grimsditch Jun. 1993 8 p Presented at the Spring Meeting of the Materials Research Society, San Francisco, CA, 12-16 Apr. 1993
(Contract W-31-109-eng-38)
(DE93-017404; ANL/MSD/CP-80248; CONF-930405-31) Avail: CASI HC A02/MF A01

We discuss here the complete determination of the elastic properties of a polyimide film using two experimental techniques. One technique employs the polymer film as a vibrating membrane and allows a direct determination of the 'macroscopic' biaxial modulus. Brillouin scattering, which measures the elastic properties on an (approximately) 100(mu) scale, allows for a complete characterization of the elastic behavior. Results obtained by the two techniques are in agreement within reported error bars. DOE

N94-18110 Battelle Columbus Labs., OH.
STUDIES OF DYNAMIC CONTACT OF CERAMICS AND ALLOYS FOR ADVANCED HEAT ENGINES
P. A. Gaydos and K. F. Dufrane Jun. 1993 63 p Prepared for ORNL,

TN Limited Reproducibility: More than 20% of this document may be affected by microfiche quality
(Contract DE-AC05-84OR-21400)
(DE93-016366; ORNL/Sub-84-00216/2) Avail: CASI HC A04

Advanced materials and coatings for low heat rejection engines have been investigated for almost a decade. Much of the work has concentrated on the critical wear interface between the piston ring and cylinder liner. Simplified bench tests have identified families of coatings with high temperature wear performance that could meet or exceed that of conventional engine materials at today's operating temperatures. More recently, engine manufacturers have begun to optimize material combinations and manufacturing processes so that the materials not only have promising friction and wear performance but are practical replacements for current materials from a materials and manufacturing cost standpoint. In this study, the advanced materials supplied by major diesel engine manufacturers were evaluated in an experimental apparatus that simulates many of the in-cylinder conditions of a low heat rejection diesel engine. Results include ring wear factors and average dynamic friction coefficients measured at intervals during the test. These results are compared with other advanced materials tested in the past as well as the baseline wear of current engines. Both fabricated specimens and sections of actual ring and cylinder liners were used in the testing. Observations and relative friction and wear performance of the individual materials are provided. DOE

N94-18112# Lawrence Livermore National Lab., CA.
REMOTE CURE MONITORING OF POLYMERIC RESINS BY LASER RAMAN SPECTROSCOPY
K. C. Hong, T. M. Vess, R. E. Lyon (Federal Aviation Administration, Atlantic City, NJ.), and M. L. Myrick (South Carolina Univ., Columbia.) May 1993 11 p Presented at the 38th International Society for the Advancement of Material and Process Engineering (SAMPE) Symposium and Exhibition, Anaheim, CA, 10-13 May 1993
(Contract W-7405-eng-48)
(DE93-016445; UCRL-JC-112824; CONF-9305232-1) Avail: CASI HC A03/MF A01

The validity of using Raman spectroscopy to monitor the cure chemistries of amine-cured epoxy is demonstrated by correlating NIR absorbance measurements with Raman measurements for a concentration series of bisphenol-A diglycidylether in its own reaction product with diethylamine. The intensity of a normalized Raman peak at 1240 cm(exp -1), assigned to the epoxide functionality, was found to be linearly related to the concentration of epoxide groups in the resin mixtures. Also, it is shown that the Ciba-Geigy Matrimid 5292 system can be monitored by ex-situ FT-Raman spectroscopy by observing changes in the carbonyl stretching (1773 cm(exp -1)) or the C=C stretching of maleimide (1587 cm(exp -1)) during the cure reaction. DOE

N94-18163# Cornell Univ., Ithaca, NY.
CERAMIC FILMS AND INTERFACES: CHEMICAL AND MECHANICAL PROPERTIES
R. Raj Jun. 1993 6 p
(Contract DE-FG02-87ER-45303)
(DE93-018416; DOE/ER-45303/3) Avail: CASI HC A02/MF A01

Results are reported in two areas: (1) understanding the mechanism of superplasticity in those that show unusual resistance to intergranular cavitation, and (2) understanding the growth of heteroepitaxial films of oxides by chemical vapor deposition (CVD) (NiO, TiO_2). DOE

N94-18166# Argonne National Lab., IL.
DEVELOPMENT AND APPLICATION OF LOCAL 3-D X RAY CT RECONSTRUCTION SOFTWARE FOR IMAGING CRITICAL REGIONS IN LARGE CERAMIC TURBINE ROTORS
E. A. Sivers, D. L. Holloway, W. A. Ellingson, and J. Ling (Academia Sinica, Shanghai, China.) 1992 9 p Presented at the Review of Progress in Quantitative Nondestructive Evaluation (NDE), La Jolla, CA, 19-24 Jul. 1992
(Contract W-31-109-eng-38)
(DE93-015159; ANL/MCT/CP-76064; CONF-920799-8) Avail: CASI HC A02/MF A01

Current 3-D X ray CT imaging technology is limited in some cases by the size and sensitivity of the x ray detector. This limitation can be overcome to some degree by the use of region-of-interest (ROI) reconstruction software when only part of a larger object need be examined. However, images produced from ROI data often exhibit severe density shading if they are reconstructed by unaltered 3-D X ray CT algorithms (called Global methods). These density artifacts can be so severe that low-contrast features are hidden. Time-consuming methods introduced previously to remedy these artifacts require specialized processing to replace or approximate the missing data outside the desired volume. Although these methods are required for true densitometry measurements, in many nondestructive tests (NDT) applications only the detection of internal features or relative density variations is required. In such cases, the use of Local (or Lamda) X ray CT, which produces an 'edge-enhanced' reconstruction and requires only minor modifications of the standard 3-D X ray CT algorithm, is recommended. Since the primary difference between Global and Local CT concerns the design of the convolution filter, two versions of a Local CT filter are discussed. These two filters are used in a Local CT implementation to reconstruct 3D X ray CT data. For comparison, Global CT using the Shepp-Logan variation of the fan-beam convolution filter is used to reconstruct the same data. This comparison shows the relative merits of Local and Global CT for fairly noisy scans of large, green Si_3N_4 pressure-slip-cast parts. The Feldkamp modification of fan-beam CT reconstruction is used in the reconstructions. In each case, real-number, reconstructed images are scaled linearly to optimize the available grey-scale levels in the images presented. DOE

N94-18188# California Univ., Santa Barbara. Dept. of Materials.
METAL/CERAMIC INTERFACES: RELATIONSHIPS BETWEEN STRUCTURE AND CHEMISTRY Final Report, 15 Mar. 1989 - 15 Mar. 1992
M. Ruhle 31 Dec. 1992 83 p
(Contract N00014-89-J-1764)
(AD-A268792) Avail: CASI HC A05/MF A01

Studies have been conducted on interfaces between Al_2O_3 and three different metals: Nb, Pd, and Ni. The objectives have been to establish orientation relationships and to understand the atomistic structure along the interface. In the case of Ni, the formation of a spinel reaction product has also been explored. For Nb/Al_2O_3, it has been found that the orientation relationships and the atomic arrangements depend on the temperature at which the interface was formed. Those formed at high temperature by diffusion bonding have (110) planes in the Nb parallel to the interface. There are also misfit dislocations which 'stand-off' the interface. Conversely, interfaces formed at lower temperatures by molecular beam epitaxy have (111) planes in the Nb parallel to the interface. Moreover, the misfit dislocations are located at the interface itself. The differences are attributed to diffusional effects, such as dislocation climb, that can occur at the higher temperatures. DTIC

N94-18220# Japan Atomic Energy Research Inst., Tokyo.
STUDY ON RADIATION-INDUCED DETERIORATION OF GREASE AT HIGH TEMPERATURE, 3
Kazuo Arakawa (Japan Atomic Energy Research Inst., Takasaki.), Tuneo Sasuga (Japan Atomic Energy Research Inst., Takasaki.), Tadao Seguchi (Japan Atomic Energy Research Inst., Takasaki.), Takao Soda, Hiroshi Nakanishi, Tamio Akada, Tetsuya Yagi, and Miyuki Hagiwara Nov. 1992 38 p In JAPANESE
(DE93-788368; JAERI-M-92-176) Avail: CASI HC A03/MF A01

Radiation-thermal resistant greases were developed, using pentaphenyl ether (5P4E) and mono-alkyltetraphenyl ether (R-4P) for base oil and bentonite (B) for thickeners. The radiation-thermal resistance of the greases were evaluated by measuring changes in penetration, oil separation, weight loss (amount of volatilized and/or evaporated base oil), and molecular weight of base oil after irradiation with (gamma)-rays at high temperatures (125, 150, 175 and 200 C). The greases showed excellent stability against both radiation and high temperature, and was found usable under the condition up to 4 MGy at 150 C. DOE

N94-18233# Pacific Northwest Lab., Richland, WA.
STUDIES OF INTERACTIONS BETWEEN CONDUCTING POLYMER AND ORGANIC VAPORS: APPLICATIONS TO CHEMICAL SENSING
M. Josowicz, P. Topart, and R. Cabala May 1993 3 p Presented at the 183rd Electrochemical Society Meeting, Honolulu, HI, 16-21 May 1993
(Contract DE-AC06-76RL-01830)

(DE93-015694; PNL-SA-21801; CONF-930571-19) Avail: CASI HC A01/MF A01

In order to understand the physicochemical mechanism involved in the organic semiconductor charge-transfer processes occurring upon doping of the films with vapor molecules different experimental approaches must be taken. The effect of vapor diffusion into the electrochemically deposited poly(pyrrole), PP and poly(N-vinylcarbazole), PNVCz, films was investigated by monitoring the mass change of the exposed polymer, absorbance changes in the absorption spectra, and the work function change due to the modulation of the Fermi level in the material. An important step in that investigation was to establish the link between the distribution of the active dopant within the surface and the bulk of the material. DOE

N94-18280# Burns (Jay) Scientific Consultants, North Indiatlantic, FL.

ANOMALOUS DIELECTRIC PROPERTIES OF CARBON-BLACK FILLED ELASTOMERS Final Report

Jay Burns 15 Jul. 1993 50 p
(Contract N62190-91-M-0526)
(AD-A269378; NRL-MR-7304) Avail: CASI HC A03/MF A01

Dielectric measurements covering nearly ten decades in frequency are given for a series of neoprene elastomers containing various amounts of conductive carbon black filler. The influence of the conductive filler upon the dielectric properties of the elastomers is treated by an extension of the Maxwell-Wagner-Sillars effect to account for slow tunneling and hopping modes of conduction within the elastomer. Effects upon dielectric response due to clustering and agglomeration of carbon particles are discussed together with some of the problems associated with application of dielectric measurements to obtain information about the internal structure of inhomogeneous materials. DTIC

N94-18282# Dayton Univ., OH. Research Inst.

STUDIES ON GEL ELECTROLYTE BASED ON NITRILE-BUTADIENE COPOLYMERS Final Report, 1 Nov. 1991 - 30 Nov. 1992

A. K. Sircar, B. Kumar, S. M. Linden, and P. T. Weissman Jun. 1993 81 p
(Contract F33615-90-C-2036)
(AD-A269450; WL-TR-93-2083) Avail: CASI HC A05/MF A01

This study is concerned with the preparation of a hybrid electrolyte, suitable for solid-polymer batteries. Based on the study of ionic conductivity in the presence of LiBF4 of a number of nitrile-butadiene copolymers (NBR), hydrogenated NBR (HNBR) was selected as the host polymer. DC conductivity studies with three different lithium salts in different plasticizers showed the highest conductivity for LiBF4. Conductivity of LiBF4 in different plasticizers decreases in the order DMF greater than DMAC greater than Gamma butyrolactone greater than NMP greater than PC=gamma-valerolactone greater than glymes. NMP was chosen as the plasticizer for hybrid films based on its moderate conductivity, low vapor pressure, and low freezing point. DTIC

N94-18403# California Univ., Santa Barbara. Dept. of Physics.

MORPHOLOGY OF POLYMERIZED MEMBRANES ON AN AMORPHOUS SUBSTRATE AT MOLECULAR RESOLUTION BY AFM Technical Report, 1 Jan. - 31 Dec. 1993

M. Radmacher, B. M. Goettgens, R. W. Tillmann, H. G. Hansma, and P. K. Hansma 15 Sep. 1993 13 p
(Contract N00014-92-J-1260)
(AD-A268760; TR-4-ONR) Avail: CASI HC A03/MF A01

The morphology of lipid membranes on solid supports was studied by micro-fluorescence film-balance technique and atomic force microscopy. The potential of AFM to visualize defects in lipid bilayers was demonstrated. The structure of polymerized membranes of the two lipids 10, 12-penta cosadiynoic acid (PC) and dimethyl bis(penta cosadiynoyl oxyethyl) ammonium bromide (BRONCO) was investigated with AFM. In both cases molecular resolution was achieved using amorphous silicon oxide as substrate. PC showed a highly regular packing of the hydrocarbon chains whereas in the case of the BRONCO film, which was polymerized in the high temperature phase, the positional correlation was only local. DTIC

N94-18448 Office of Naval Research European Office, FPO New York, NY.

AGEING IN PROCESSED POLYMERS: PROGRAMME, SUMMARY, AND ABSTRACTS DISCUSSION MEETING Final Report

1993 28 p Meeting held in Birmingham, England, 5-7 May 1993
Limited Reproducibility: More than 20% of this document may be affected by microfiche quality
(AD-A268931) Avail: CASI HC A03

The manufacture of almost any plastic article involves some form of quenching as occurs, for example, in extrusion or injection molding. The primary intention is to extract the product from, say, a mold as quickly as possible in order to maximize productivity. This, unfortunately, cannot be equated with the structural stability of the workpiece and so the properties of the formed component may subsequently change (i.e. age) as it slowly relaxes to a more stable state. Such a process is purely physical in origin and may be reversed on heating: it must be distinguished from the more familiar chemical effects which are generally irreversible and are associated with decreases in molar mass. 'Physical aging' was not a serious problem when polymers were used only for low grade applications (although even here it contributed to the 'cheap and nasty' image that is still widespread for plastics - a simple example is the warping of an article that was well formed initially). Now that plastic componeents are increasingly designed for use in demanding situations it becomes essential for the manufacturer to have the ability to forecast long-term changes (particulary in the dimensional, mechanical and thermal properties of the processed component). This, in turn, implies the existence of simple and rapid tests that are able to define the condition of an aged component at some time after its fabrication. DTIC

N94-18477# Sandia National Labs., Albuquerque, NM.

SOLDERABILITY PERSERVATIVE COATINGS: ELECTROLESS TIN VERSUS ORGANIC AZOLES

I. Artaki (Bell Telephone Labs., Inc., Princeton, NJ.), U. Ray (Bell Telephone Labs., Inc., Princeton, NJ.), A. M. Jackson (Bell Telephone Labs., Inc., Princeton, NJ.), H. M. Gordon (Bell Telephone Labs., Inc., Princeton, NJ.), and P. T. Vianco 1993 14 p Presented at the Surface Mount Technical Association International Conference, San Jose, CA, 31 Aug. - 2 Sep. 1993
(Contract DE-AC04-76DP-00789)
(DE93-017634; SAND-93-1414C; CONF-9308126-2) Avail: CASI HC A03/MF A01

This paper compares the solderability performance and corrosions ion protection effectiveness of electroless tin coatings versus organic azole films after exposure to a series of humidity and thermal (lead-free solders) cycling conditions. The solderability of immersion tin is directly related to the tin oxide growth on the surface and is not affected by the formation of Sn-Cu intermetallic phases as long as the intermetallic phase is protected by a Sn layer. For a nominal tin thickness of 60 micro-inches, the typical thermal excursions associated with assembly are not sufficient to cause the intermetallic phase to consume the entire tin layer. Exposure to humidity at moderate to elevated temperatures promotes heavy tin oxide formation which leads to solderability loss. In contrast, thin azole films are more robust to humidity exposure; however, upon heating in the presence of oxygen, they decompose and lead to severe solderability degradation. Evaluations of lead-free solder pastes for surface mount assembly applications indicate that immersion tin significantly improves the spreading of Sn:Ag and Sn:Bi alloys as compared to azole surface finishes. DOE

N94-18515 Nebraska Univ., Lincoln. Dept. of Chemistry.

RELAXATION OF POLAR ORIENTATIONAL ORDER IN NONLINEAR OPTICAL POLYMERS BY SECOND HARMONIC GENERATION

C. H. Wang, H. W. Guan, and S. H. Gu 24 Aug. 1993 22 p Sponsored by ONR Limited Reproducibility: More than 20% of this document may be affected by microfiche quality
(AD-A269059) Avail: CASI HC A03

An investigation of the decay of the second harmonic generation (SHG) signals from a main chain accordion and a guest/host nonlinear optical (NLO) polymer has been carried out. The shape of the decay of the SHG signal from the main chain polymer is stretched exponential with the width parameter, beta, increasing with increasing temperature. The increase in beta indicates a narrowing of the distribution of relaxation times. On the other hand, the SHG decay signal from the guest/host system is found to be better described by the sum of two single exponential functions with the first short time component affected strongly by the surface change effect and the second slow component associated with the relaxation of the macroscopic polarization. The time constant of the slow component is found to be successively increasing with the poling-decay cycle and it reaches a steady state value after several cycles. The relaxation time lengthening effect is obtained both above and below T(sub g); however, the effect rapidly diminishes as the temperature is increased above T(sub g). The temperature dependence of the steady state relaxation time is not Arrhenius; the Vogel-Fulcher-Tamann equation gives a satisfactory fit to the temperature dependence data. DTIC

N94-18519# Sandia National Labs., Albuquerque, NM.
PHOTO-INDUCED AND ELECTROOPTIC PROPERTIES OF (Pb,La)(Zr,Ti)O3 FILMS
D. Dimos, W. L. Warren, and B. A. Tuttle 1993 12 p Presented at the Spring Meeting of the Materials Research Society, San Francisco, CA, 12-16 Apr. 1993
(Contract DE-AC04-76DP-00789)
(DE93-017496; SAND-93-0541C; CONF-930405-33) Avail: CASI HC A03/MF A01

Photo-induced changes in the hysteresis behavior of sol-gel derived Pb(Zr,Ti)O3 (PZT) and (Pb,La)(Zr,Ti)O3 (PLZT) films have been characterized. Film photosensitivity has been evaluated with respect to magnitude of effects, time response and spectral dependence. Photo-induced hysteresis changes exhibit a stretched-exponential time dependence, which implies a dispersive mechanism. The spectral dependence is strongly peaked at the band edge (approximately 3.4 eV), which indicates that generation of electron-hole pairs in the material is critical. The photo-induced hysteresis changes are reproducible and stable, which indicates that the controlling charge traps are stable. However, improvements in film photosensitivity will be required to develop these materials for optical memory applications. DOE

N94-18529# Department of the Navy, Washington, DC.
AN ULTRAVIOLET FARADAY ROTATOR GLASS Patent Application
James L. Dexter, inventor (to Navy), David G. Cooper, inventor (to Navy), and Douglas H. Blackburn, inventor (to Navy) 29 Apr. 1993 26 p
(AD-D015879; US-Patent-Appl-SN-053287) Avail: CASI HC A03/MF A01

A Faraday rotator glass composition based on a fluoride glass, phosphate glass, fluorophosphate glass or a mixture there of is doped with a lanthanide in concentration sufficient to provide a Verdet constant above at least 2870 deg/Tesla-meter (1 MIN/CM-Oe) x (1.667 x 10 (exp 4) = 1 deg/Tesla-meter and optical transmission above at least 50 percent in a 25mm thick polished glass sample at least at one wavelength in the 200 to 400 nm wavelength region. The faraday rotator glass also includes monovolent non-lanthanide cations such as Na, Li, K or mixtures there of in a concentration sufficient to provide a Verdet constant above at least 2870 deg/Telsa-meter and optical transmission above at least 50 percent in a 25mm thick polished glass sample at least at one wave-length in the 200 to 400 nm wave-length region. The Faraday rotator glass further includes a concentration of divalent or trivalent non-lanthanide cations such as Mg, Be, Ca, Al or mixtures thereof sufficient to provide surface flatness of at least 1/10 of the operating wavelength at 632.8 nm. DTIC

N94-18691 Missouri Univ., Rolla.
PRESSURELESS DENSIFICATION OF CERAMIC MATRIX COMPOSITES Final Report, Mar. 1990 - May 1993
M. N. Rahaman, L. R. Dharani, and R. E. Moore 31 Jul. 1993 265 p Limited Reproducibility: More than 20% of this document may be affected by microfiche quality
(Grant AF-AFOSR-0267-90)
(AD-A269137) Avail: CASI HC A12

The project produced a remarkable improvement in our understanding of how ceramic matrix composites densify and how they may be persuaded to reach high density by pressureless sintering. The key factors which hinder the sintering of ceramic matrix composites were determined and an innovative processing method for alleviating the sintering difficulties was developed. The method involves coating the reinforcement phase with a cladding of the matrix by chemical precipitation. The research formed the first reported study in which polycrystalline ceramic matrix composites containing an appreciable volume fraction of a reinforcement phase (up to 35 vol% particles or 25 vol% whiskers) were sintered to full density. The room temperature mechanical properties of the composites fabricated by pressureless sintering of coated powders were significantly better than those for similar composites fabricated from mechanically mixed powders. Pressureless sintering of a ceramic matrix with rigid inclusions was analyzed by a viscoelastic finite element method. The effects of inclusion volume fraction, inclusion shape, inclusion interactions, and matrix packing were considered. The model predictions showed good agreement with the experimental data. Considerable potential exists for the application of the experimental and theoretical procedures developed in the project. DTIC

N94-18713# Texas Christian Univ., Fort Worth.
HYDROLYSIS REACTION AND POSITRONIUM DECAY IN SILICA GELS Final Report, 1991 - 1993
T. W. Zerda 23 Aug. 1993 18 p
(Grant AF-AFOSR-0165-90)
(AD-A270028; AFOSR-93-0709TR) Avail: CASI HC A03/MF A01

Positronium decay was used to measure pore size distribution in porous sol-gel glass. It was also used to determine the population of surface strained rings at various stages of firing and drying procedures. Rotational and translational diffusion of molecular liquids, semiconductor clusters, and fullerenes was investigated. Preferential adsorption, surface interactions, and their effects on electronic transitions, vibrational relaxation, rotational, and translational motion were discussed. Computer simulations for molecular motion of SF 6 and cyclohexane inside small pores were run as a function of temperature and pressure. Results were compared with experimental data. Experimental evidence for the pentavalent transitions state for TMOS and TEOS hydrolysis reactions were provided. DTIC

N94-18740# California Inst. of Tech., Pasadena. Div. of Engineering and Applied Science.
SCALING LAWS FOR DIAMOND CHEMICAL VAPOR DEPOSITION. 2: ATOMIC HYDROGEN TRANSPORT
D. G. Goodwin 15 Sep. 1993 33 p
(AD-A269842) Avail: CASI HC A03/MF A01

Scaling relations are developed to allow estimation of the atomic hydrogen concentration at the substrate during diamond chemical vapor deposition for both diffusion-dominated and convection-dominated reactors. In the convection-dominated case, it is shown that there exists an optimal Mach number which maximizes the H concentration delivered to the substrate. In addition, when homogeneous recombination is taken into account, there exists an optimal operating pressure. This analysis shows that a sonic flow of highly dissociated hydrogen at a pressure near atmospheric is optimal for rapid growth of high-quality diamond. DTIC

N94-18746# Department of the Navy, Washington, DC.
DIAMOND BRAZED TO A METAL Patent Application
Thomas P. Thorpe, inventor (to Navy) and Leo A. Snail, inventor (to Navy) 30 Jul. 1993 24 p
(AD-D015877; US-Patent-Appl-SN-099640) Avail: CASI HC A03/MF A01

A unitary article that is solid at a temperature in excess of about 1100 C and which includes a diamond, a metal, and a brazing material brazing the diamond and the metal is described. The brazing material includes a metal carbide adhering to the diamond and a platinum family metal or nickel adhering to the metal. The platinum family metal has dissolved therein carbide forming metal and contains particles of metal carbide. The article is made by depositing a platinum family metal or nickel on a metal melting above the melting point of the platinum family metal or nickel, depositing a carbide forming metal which is soluble in molten platinum family metal or nickel, heating the assembly until platinum family metal or nickel is in a molten state, and cooling the molten platinum family metal or nickel to a solid state. Author (DTIC)

N94-18750# Purdue Univ., West Lafayette, IN. Ceramics Information Analysis Center.
BIBLIOGRAPHY ON CERAMIC MATRIX COMPOSITES AND REINFORCING WHISKERS, PLATELETS, AND FIBERS, 1970-1990 Special Report
Jill Larsen, Christopher D. Carpenter, and Said K. El-Rahaiby Aug. 1993 218 p
(Contract DLA900-90-D-0304)
(AD-A270139; CIAC-SR-2) Avail: CASI HC A10/MF A03

This report contains bibliographic information on pertinent documents dealing with ceramic matrix composites (CMC's) and reinforcing whiskers,

platelets, and fibers in the period 1970 to 1990. The report is organized into three broad categories. The first category presents bibliographies on the processing methods and properties of various types of reinforcements. The second category constitutes the bulk of the report. This section is divided into seven parts, each being concerned with a particular type of ceramic matrix material, such as borides, carbides, nitrides, oxides, glasses, and glass-ceramics. Within each matrix material, there are further categories sorted by the reinforcement used, e.g., fibers, whiskers, platelets, particulates, etc. The final section of the report contains bibliographies of articles discussing the theories of reinforcement, processing, testing and test methods, as well as certain applications for ceramic matrix composites.
DTIC

N94-18792# Fraunhofer Inst. fuer Werkstoffmechanik, Freiburg (Germany).
EXPERIMENTAL INVESTIGATION OF WAVE AND FRACTURE PHENOMENA IN IMPACTED CERAMICS: EXPERIMENTS ON SAPPHIRE Final Report
S. Winkler May 1993 80 p
(Contract DAJA45-90-C-0053)
(AD-A270040; IWM-T-8/93; R/D-6472-MS-01) Avail: CASI HC A05/MF A01

Experiments have been performed in order to investigate the behavior of monocrystalline sapphire under impact loading. Tile shaped samples were hit edge-on by spherical or flat steel impactors. The generation of pressure waves and disintegration effect were observed by a Cranz-Schardin high speed camera. The results are compared with earlier ones obtained with glass and alumina as target material. A terminal crack velocity was not found. Crack velocities exceeding the Rayleigh wave speed have been measured. Similar as with glass, nucleations of cracks in the field between the primary wave front and the front of the disintegration area form a damage velocity which can approach the longitudinal wave speed. Usually, cracks did not follow crystal planes; the influence of the crystal structure does not seem to be a strong one.
DTIC

N94-18891# Pennsylvania Univ., Philadelphia.
MOLECULAR AND POLYMERIC CERAMIC PRECURSORS
Larry G. Sneddon May 1993 13 p
(Contract DE-FG02-87ER-13732)
(DE93-040364; DOE/ER-13732/7) Avail: CASI HC A03/MF A01

The development of new methods for the production of complex materials is one of the most important problems in modern solid state chemistry and materials science. This project is attempting to apply the synthetic principles which have evolved in inorganic and organometallic chemistry to the production of technologically important non-oxide ceramics, such as boron nitride, boron carbide, and metal borides. Our recent work has now resulted in the production of new polymer systems, including poly(B-vinylborazine), polyvinylpentaborane, and polyborazylene, that have proven to be high yield precursors to boron-based ceramic materials. Current work is now directed toward the synthesis of new types of molecular and polymeric boron-containing species and an exploration of the solid state properties of the ceramics that have been produced in these studies.
DOE

N94-18932# Argonne National Lab., IL.
QUANTIFICATION OF VOLUME FLAW SIZES IN CERAMICS BY IMAGE PROCESSING OF 3D X RAY TOMOGRAPHIC DATA SETS
M. C. Stinson (University of Central Michigan, Mount Pleasant.), D. A. Holloway, and W. A. Ellingson Jan. 1993 12 p Presented at the 17th Annual Conference on Composites and Advanced Ceramics, Cocoa Beach, FL, 11-15 Jan. 1993
(Contract W-31-109-eng-38)
(DE93-018573; ANL/ET/CP-77180; CONF-930164-13) Avail: CASI HC A03/MF A01

This paper introduces a technique to quantify internal flaws in a ceramic body. The approach uses data images obtained from 3D x-ray computed tomography. An approach called guided segmentation uses image processing methods applied to a series of the data images to quantify the flaw volumes. The techniques is tested on synthesized data for spheres. The technique is than applied to real images of known size to examine its use.
DOE

N94-18946# Oak Ridge National Lab., TN.
SURVEY OF CERAMIC MACHINING IN JAPAN
B. P. Bandyopadhyay and P. J. Blau Jul. 1993 27 p
(Contract DE-AC05-84OR-21400)
(DE93-018277; ORNL/M-2881) Avail: CASI HC A03/MF A01

This report is a compilation of four subcontract reports provided by B. P. Bandyopadhyay who, while a visiting professor at Toyohashi University in Japan, conducted a survey of ceramic machining technology in that country from January 1 through December 31, 1992. Various aspects of machining technology were surveyed: types of parts being produced, types of ceramic materials being used, the nature of current ceramic machining research and development, and types of machine tools. The four separate reports compiled here were originally provided in a narrative, chronological form, and some of the information has been reorganized into topical areas for this compilation. This report is organized into three sections: The first describes ten ceramic machining research and development organizations and provides a reference list of their current technical publications; the second, two major trade shows; and the third, several other products and commercial developments noted during the course of Bandyopadhyay's stay in Japan. An Appendix lists key individuals who are currently conducting ceramic machining research in Japan.
DOE

N94-19052 Helsinki Univ. of Technology, Espoo (Finland).
POLYMER TECHNOLOGY PUBLICATION. SERIES NO. 14, 1993
1993 70 p See also PB93-195972 through PB93-195998 Limited Reproducibility: More than 20% of this document may be affected by microfiche quality
(PB93-195964; ISBN-951-22-1384-2) Avail: CASI HC A04

Contents: Mechanical and Dynamic-Mechanical Properties of PP/LCP Blends in the Flow and Transversal Direction; The Effect of Viscosity Ratio on the Formation of Fibrous Morphology in LCP Blends; Mixing and Dispersion of Multiphase Polymer Melts.
NTIS

N94-19059# Sandia National Labs., Albuquerque, NM.
A CONSTITUTIVE THEORY FOR RIGID POLYURETHANE FOAM
M. K. Neilsen, R. D. Krieg (Tennessee Univ., Knoxville.), and H. L. Schreyer (New Mexico Univ., Albuquerque.) 1992 18 p Presented at the Annual Winter Meeting of the ASME, New Orleans, LA, 28 Nov. - 3 Dec. 1993
(Contract DE-AC04-76DP-00789)
(DE93-011596; SAND-92-2487C; CONF-931121-4) Avail: CASI HC A03/MF A01

Rigid, closed-cell, polyurethane foam consists of interconnected polyurethane plates which form cells. When this foam is compressed, it exhibits an initial elastic regime which is followed by a plateau regime in which the load required to compress the foam remains nearly constant. In the plateau regime, cell walls are damaged and large permanent volume changes are generated. As additional load is applied, cell walls are compressed against neighboring cell walls, and the stiffness of the foam increases and approaches a value equal to that of solid polyurethane. When the foam is loaded in tension, the cell walls are damaged and the foam fractures. A constitutive theory for rigid polyurethane foam has been developed. This theory is based on a decomposition of the foam into two parts: a skeleton and a nonlinear elastic continuum in parallel. The skeleton accounts for the foam behavior in the elastic and plateau regimes and is described using a coupled plasticity with continuum damage theory. The nonlinear elastic continuum accounts for the lock-up of the foam due to internal gas pressure and cell wall interactions. This new constitutive theory has been implemented in both static and dynamic finite element codes. Numerical simulations performed using the new constitutive theory are presented.
DOE

N94-19202# Los Alamos National Lab., NM.
ELASTIC PROPERTIES OF AMORPHOUS THIN FILMS STUDIED BY RAYLEIGH WAVES
R. B. Schwarz and J. B. Rubin 1993 13 p Presented at the 8th International Conference on Rapidly Quenched and Metastable Materials, Sendai, Japan, 22-27 Aug. 1993
(Contract W-7405-eng-36)
(DE93-018375; LA-UR-93-2499; CONF-9308140-2) Avail: CASI HC A03/MF A01

Physical vapor deposition in ultra-high vacuum was used to co-deposit nickel and zirconium onto quartz single crystals and grow amorphous Ni(sub 1-x)Zr(sub x) (0.1 less than x less than 0.87) thin films. A high-resolution surface acoustic wave technique was developed for in situ measurement of film shear moduli. The modulus has narrow maxima at x = 0.17, 0.22, 0.43, 0.5, 0.63, and 0.72, reflecting short-range ordering and formation of aggregates in amorphous phase. It is proposed that the aggregates correspond to polytetrahedral atom arrangements limited in size by geometrical frustration. DOE

N94-19271# Sandia National Labs., Albuquerque, NM.
SHOCK COMPRESSION PROPERTIES OF SILICON CARBIDE
D. E. Grady and M. E. Kipp Jul. 1993 47 p
(Contract DE-AC04-76DP-00789)
(DE93-019927; SAND-92-1832) Avail: CASI HC A03/MF A01

An investigation of the shock compression and release properties of silicon carbide ceramic has been performed. A series of planar impact experiments has been completed in which stationary target discs of ceramic were struck by plates of either similar ceramic or other appropriate material at velocities up to 2.2 km/s with a propellant gun facility. The particle velocity history at the interface between the back of the target ceramic and a lithium-fluoride window material was measured with laser velocity interferometry (VISAR). Impact stresses achieved in these experiments range between about 10 and 50 GPa. Numerical solutions and analytic methods were used to determine the dynamic compression and release stress-strain behavior of the ceramic. Further analysis of the data was performed to determine dynamic strength and compressibility properties of silicon carbide. DOE

N94-19308# Sandia National Labs., Albuquerque, NM.
REDUCING INADVERTENT ALLOYING OF METAL/CERAMIC BRAZES
J. J. Stephens and P. F. Hlava 1992 27 p Presented at the Minerals and Materials Metals Society Meeting on Low Thermal Expansion Alloys and Composites, Chicago, IL, 1-5 Nov. 1993
(Contract DE-AC04-76DP-00789)
(DE93-009842; SAND-92-0535C; CONF-931154-1) Avail: CASI HC A03/MF A01

Inadvertent alloying of Cu braze metal can compromise metal/ceramic seals. Electron microprobe analyses have quantified alloying of Cu brazes in metal/ceramic feedthroughs. Pin material and processing parameters above 1084C both affect alloying levels. Using either Kovar or Ni-plated 316L stainless steel pins limits alloying compared to Palco pins. Minimizing the time during which the braze is molten also avoids excessive alloying. The original thickness of the Ni plating on the Mo-Mn metallization of the ceramic also influences the alloying content of these brazes. Metal/ceramic brazes made with long brazing cycles, Mo-Mn metallization, and Kovar components grow a layer of intermetallic Mo6(Fe(3.5)CO(3.5))7 on the metallization. Layer thicknesses observed do not appear to compromise joint integrity. Ni additions of approximately 10 and 20 wt.% to Cu apparently increases the stress required to maintain creep rates required for stress relaxation during cooldown. Relative to unalloyed Cu, this strengthening effect tends to increase as temperature is decreased. DOE

N94-19321# Argonne National Lab., IL.
THE DIRECT SYNTHESIS OF ORGANIC AND ORGANOMETALLIC-CONTAINING MICA-TYPE ALUMINOSILICATES
K. A. Carrado and A. Awaluddin 1993 10 p Presented at the 206th American Chemical Society National Meeting, Chicago, IL, 22-27 Aug. 1993
(Contract W-31-109-eng-38)
(DE93-019001; ANL/CHM/CP-79161; CONF-930802-6) Avail: CASI HC A02/MF A01

Layer-silicate clay structures can provide supramolecular organization for catalysis, chiral reactions, colloid science, and electron transfer. The authors have successfully modified the experimental preparations of several different layer silicates in order to incorporate a wide variety of organic and organometallic molecules in the clay galleries. Synthesis and physical characterization of these materials are described and compared to ion-exchanged natural clay analogs. In addition, the photophysical properties of organometallic Ru(II) complexes incorporated by direct hydrothermal crystallization into synthetic clays were measured. DOE

N94-19338# Sandia National Labs., Albuquerque, NM.
IMPACT STRENGTH AND INDENTATION HARDNESS OF HIGH-STRENGTH CERAMICS
D. E. Grady 1993 12 p Presented at the 14th International Conference of the International Association for the Advancement of High Pressure Science and Technology, Colorado Springs, CO, 27 Jun. - 2 Jul. 1993
(Contract DE-AC04-76DP-00789)
(DE93-018833; SAND-93-0388C; CONF-930676-27) Avail: CASI HC A03/MF A01

Hugoniot elastic limit and indentation hardness data are provided for selected high-strength ceramics AlN, Al2O3, B4C, SiC, TiB, and Zr2. Degree of correlation of the strength data by the two test methods is examined. The influence of the reformation mechanism on strength measurement, including rate sensitivity, size scale, and confining pressure is discussed. DOE

N94-19402*# Alabama Agricultural and Mechanical Coll., Normal. Office of Research and Development.
FEASIBILITY STUDY: MONODISPERSE POLYMER PARTICLES CONTAINING LASER-EXCITABLE DYES Final Report
Putcha Venkateswarlu, K. X. He, and A. Sharma 15 Nov. 1993 28 p
(Grant NAG8-907)
(NASA-CR-194280; NAS 1.26:194280) Avail: CASI HC A03/MF A01

The optical properties associated with small particles, which include aerosols, hydrosols and solid microspheres have an impact on several areas of science and engineering. Since the advent of high-speed computers and lasers, the interaction of light with matter in the form of small particles with a discontinuous optical boundary relative to the surroundings has been much better understood. Various nonlinear optical effects have been observed involving interaction of a laser beam with both solid microspheres and liquid microdroplets. These include observation of second and third harmonic generation, four wave mixing, optical visibility, two photon absorption, observation of stimulated emission and lasing, and Stimulated Raman Scattering. Many of these effects are observed with laser intensities which are orders of magnitude less than that required by threshold condition for interactions in macroscopic bulk medium. The primary reason for this is twofold. The front surface of the microsphere acts as a thick lens to enhance the internal intensity of the input laser radiation, and the spherical shape of the droplet acts as an optical cavity to provide feedback at specific wavelengths corresponding to the whispering gallery modes or the morphology dependent resonances (MDR's). The most interesting and significant recent finding in this field is undoubtedly the existence of resonance peaks in linear and nonlinear optical spectra. Such resonance peaks are only dependent on the particle morphology, which means the size, shape and refractive index of the particle. Because of the simultaneous presence of these resonances, they have been referred to by many names, including structural resonances, whispering modes or whispering gallery modes, creeping waves, circumferential waves, surfaces modes, and virtual modes. All of these names refer to the same phenomena, i.e. morphology dependent resonances (MDR's) which has already been described and predicted precisely by electromagnetic theory and Loentz-Mie theory since 1908. MDR's can become important when the particle size (radius a) approaches and exceeds the wavelength of the electromagnetic wave (lambda) and the refractive index of the particle is greater than that of the surrounding medium. Such resonances are easiest to observe from a single particle with high symmetry, such as a sphere, spheroid, or cylinder. MDR's correspond to solutions of the characteristic equations of the electromagnetic fields in the presence of a sphere. Derived from text

N94-19405# Ecole Centrale de Lyon (France). Lab. de Materiaux-Mecanique Physique.
PHYSICO CHEMICAL AND MECHANIC APPROACH OF LUBRICATING PROPERTIES OF GRAPHITE + ADDITIVE POWDERS Ph.D. Thesis [APPROCHE PHYSICO-CHIMIQUE ET MECANIQUE DES PROPRIETES LUBRIFIANTES DE POUDRES GRAPHITES + ADDITIFS]
Cecile Langlade 1993 179 p In FRENCH
(ECL-93-02; ETN-93-94896) Avail: CASI HC A09/MF A02

The lubricating property mechanisms of graphite are investigated by macroscopic and microscopic approaches. The physical and tribological properties of graphite are reviewed. Two additives are selected: NA2S2O3 and Na2MoO4. The development of transfer films on metal surfaces is studied. The coefficient of friction is calculated. X-rays diffraction, Raman spectrocopy, electron spectroscopy for chemical analysis, and transmission electron microscopy techniques were used. The results showed that transfer films were developed on a metal surface only in the case of graphite plus additive mixtures. The development of films is observed to occur by successive steps. The growth layer, which develops over the germination layer, has a nanocrystalline structure. ESA

N94-19532# Metals Information Analysis Center, West Lafayette, IN.
BIBLIOGRAPHY ON SILICIDES Special Report
B. F. Gilp, P. D. Desai, and C. Y. Ho Jul. 1993 391 p
(Contract DLA900-90-D-0305)
(AD-A270516; MIAC-3) Avail: CASI HC A17/MF A04

This report is an annotated bibliography of over 750 documents on silicides. Documents published from 1952 to early 1993 are covered. Bibliographic information is organized in alphabetical order by silicide type, i.e. chromium silicides, cobalt silicides, etc. Within each chapter information is reported for specific silicides. A miscellaneous section contains silicides which are neither specifically identified nor warrant a separate section. Chapters are also included for commercially designated silicides and for those silicides which are neither properly identified nor have enough data to warrant a separate chapter. Each section is complete and self contained for efficient use. DTIC

N94-19561# Oak Ridge National Lab., TN.
CERAMIC TECHNOLOGY PROJECT DATA BASE Summary Report, Sep. 1992
B. L. P. Keyes Jun. 1993 171 p
(Contract DE-AC05-84OR-21400)
(DE93-019360; ORNL/M-2775) Avail: CASI HC A08/MF A02

Data presented in this report represent an intense effort to improve processing methods, testing methods, and general mechanical properties (rupture modulus, tensile, creep, stress-rupture, dynamic and cyclic fatigue, and fracture toughness) of candidate ceramics for use in advanced heat engines. This work was performed by many facilities and represents only a small part of the data generated by the Ceramic Technology Project (CTP) since 1986. Materials discussed include GTE PY6, GN-10, NT-154, NT-164, SN-260, SN-251, SN-252, AY6, and silicon nitride combined with rare-earth oxides, Y-TZP, ZTA, NC-433, NT-230, Hexoloy SA, MgO-PSZ-to-MgO-PSZ joints, MgO-PSZ-to-cast iron, and a few whisker/fiber-reinforced ceramics. Information in this report was taken from the project's semiannual and bimonthly progress reports and from final reports summarizing the results of individual studies. Test results are presented in tabular form and in graphs. All data, including test rig descriptions and material characterizations, are stored in the CTP data base and are available to all project participants on request. The objective of this report is to make available the test results from these studies but not to draw conclusions from those data. DOE

N94-19574 California Univ., Los Angeles. Dept. of Chemistry and Biochemistry.
PHYSICAL CHEMICAL STUDIES OF CONDUCTING POLYMERS FUNDAMENTAL AND APPLIED Final Report, 15 Aug. 1989 - 14 Apr. 1993
Howard Reiss 20 Aug. 1993 10 p Limited Reproducibility: More than 20% of this document may be affected by microfiche quality
(Grant AF-AFOSR-0425-89)
(AD-A270728; AFOSR-93-0768TR) Avail: CASI HC A02

Reversible electroactive doping of conducting polymers was studied with a view toward the determination of important electroactive mechanisms in the polymers. Also, the transport of solutes in polymer films was investigated. Research eventually focused on polyaniline where various modified Donnan phenomena were investigated both by means of theory and experiment. Films formed from proton doped emeraldine base proved to be a remarkably efficient gas selective membrane. The mechanism of this process was studied, also by means of theory and experiment. Proton doped polyaniline may be the most universal membrane for gas separations, and possibly the most important technological fallout of basic research on conducting polymers. Besides a number of publications in scientific journals, a patent has been granted to the use of doped conducting polymer films for separation. DTIC

N94-19577 Hughes Research Labs., Malibu, CA.
ELECTRO-OPTIC BEAM STEERING USING NON-LINEAR ORGANIC MATERIALS Final Report, 15 Aug. 1991 - 31 Mar. 1993
R. A. Forber, A. Au, and U. Efron Aug. 1993 19 p Limited Reproducibility: More than 20% of this document may be affected by microfiche quality
(Contract F49620-91-C-0068)
(AD-A270809; HAC/REF-J3338; AFOSR-93-0756TR) Avail: CASI HC A03

This report summarizes Hughes Research Laboratories efforts on evaluation of nonlinear optical polymer materials supplied by State University of New York (SUNY), Buffalo, for potential application to the Hughes electro-optic beam deflector device. Evaluations include electro-optic coefficient, response time, transmission, and resistivity. Electro-optic coefficient measurements were made at 633 nm using a simple reflection technique. The samples measured in the range of 1-2.5 pm/V, which is too low to be of practical use in the Hughes beam deflector device. DTIC

N94-19585# Texas Univ., Austin. Dept. of Chemical Engineering.
BIENZYME SENSORS BASED ON ELECTRICALLY WIRED PEROXIDASE Technical Report No. 7, Oct. 1992 - Oct. 1993
T. J. Ohara, M. S. Vreeke, F. Battaglini, and A. Heller 8 Oct. 1993 4 p
(Contract N00014-91-J-1656)
(AD-A271364) Avail: CASI HC A01/MF A01

Single layer and bilayer bienzyme electrodes based on the combination of a 3-dimensional redox epoxy network that electrically connects redox centers of bound horseradish peroxidase (HRP) to electrodes with a hydrogen peroxide generating enzyme, the redox centers of which are not connected to the redox epoxy network, are described. In the single layer electrodes, H2O2 generated by the first enzyme oxidizes the second enzyme HRP, which oxidizes the redox polymer network, that is electrochemically reduced at 0mV (SCE). When the redox centers of the H2O2 generating enzyme are also electrically connected to the redox epoxy network, the substrate reduced redox centers are oxidized by the redox polymer network, thus lowering the cathodic current. Such attenuation is avoided in bilayer electrodes, where the H2O2 producing enzyme and the redox-epoxy-HRP network are not electrically connected. The single-layer bienzyme electrodes extend the range of amperometric biosensors based on directly redox-epoxy wired enzymes to enzymes that are difficult to electrically connect to redox polymer networks and whose preferred or only co-substrate is oxygen. For a difficult to wire enzyme, choline oxidase, the cathodic current density in the single-layer peroxidase and choline oxidase containing electrode is 80 micro A/sq cm at 10 mM choline concentration, while the anodic current density of the directly wired enzyme is only 5 micro-A/sq cm. Alcohol oxidase is an enzyme that could not be electrically connected to the HRP wiring 3-dimensional redox epoxy network. The anodic current density of its redox epoxy wired electrodes is close to nil, while the cathodic current density, observed in alcohol oxidase and wired peroxidase containing single layer electrodes at 10 mM ethanol is 5 micro-A/sq cm. DTIC

N94-19586# Massachusetts Univ., Lowell.
MICROBIAL DEGRADATION OF POLY-B-ESTERS: A MECHANISTIC STUDY, CELLULOSE ACETATE BIODEGRADABILITY Final Report, 1 May 1990 - 31 Jul. 1993
Richard A. Gross 30 Aug. 1993 8 p
(Contract DAAL03-92-G-0111)
(AD-A271368; ARO-27314.6-LS) Avail: CASI HC A02/MF A01

In this Final Report, work carried out under ARO grant C-DAAL03-G-0111 is described. The investigations performed include the following: (1) isolation, purification, and characterization of a poly(3-hydroxybutyrate) depolymerase enzyme from Penicillium funiculosum, (2) determination that the depolymerase is a serine esterase, (3) study of the effect of polymer stereochemistry and crystalline order in a semi-crystalline polymer film substrate on enzyme specificity and activity, (3) isolation, purification, and characterization of cellulose acetate degrading microorganisms, and (4) determination of the biodegradability of cellulose acetate with degrees of substitution up to 2.5 under aerobic thermophilic conditions. DTIC

N94-19600# Pennsylvania State Univ., University Park. Materials Research Lab.
ADVANCED CIVIL ENGINEERING MATERIALS BASED ON INORGANIC POLYMERS Final Report, 1 Oct. 1989 - 28 Feb. 1993

Paul W. Brown 29 Apr. 1993 166 p
(Grant AF-AFOSR-0405-89)
(AD-A270837; AFOSR-93-0785TR) Avail: CASI HC A08/MF A02

The present program was undertaken to evaluate cement chemistries more suitable for macrodefect-free cement materials. Therefore, the thrust of this work is oriented to the chemistry of advanced cements. Two strategies are being employed. The first is to modify conventional high alumina and portland cements to develop advanced properties. Such properties in this context include improvement in moisture sensitivity and extension of useful service range to temperatures higher than those tolerated by conventional organic polymers. The second strategy is to evaluate novel chemistries. This has included forming alkali zirconium phosphates at low temperature. This class of materials exhibits zero thermal expansion, is stable to high temperature, and therefore may be useful in aerospace applications where dimensional stability is important. DTIC

N94-19611 Technische Univ., Berlin (Germany). Fachbereich Physik.
STRUCTURE AND PROPERTIES OF POLYCARBONATE ALLOYS Ph.D. Thesis [STRUKTUR UND EIGENSCHAFTEN VON POLYCARBONAT-LEGIERUNGEN]
Guenter Dieter Butzbach 1991 112 p In GERMAN Limited Reproducibility: More than 20% of this document may be affected by microfiche quality
(ETN-93-95071) Avail: CASI HC A06

Influence of adhesion between polymer alloy phase boundaries and of polymer morphology on material structure and properties is investigated. Mixtures of polystyrol and polymethyl methacrylate with polycarbonate were considered as model systems. Differential calorimetry was used for evaluation of glass transition temperature of both mixtures. Raster and transmission electron microscopy experiments show the existence of a two phase structure in both mixtures. Traction and torsion tests were performed in order to obtain modulus of elasticity and mechanical strength values. It is examined how alloy properties can be estimated from pure polymer properties; the Kerner theory was used which allows mechanical and thermal properties of a polymer mixture to be calculated from corresponding values of the homopolymer. Comparisons between experimental and theoretical results show low discrepancies of the relaxation behavior, due to the partial miscibility. Monophased and two phase polymethyl methacrylate and polycarbonate systems are studied as a function of temperature, in order to show that at 170K suppression of beta relaxation and strong ductility drop reduction occur. ESA

N94-19651# Brookhaven National Lab., Upton, NY.
TESTING OF PROTECTIVE COATINGS IN HYDROGEN
P. E. Vanier, R. Barletta, J. Adams, and J. Svandrlik Jul. 1993 12 p
(Contract DE-AC02-76CH-00016)
(DE93-040326; BNL-49386) Avail: CASI HC A03/MF A01

A series of tests of protective coatings on carbon-carbon substrates were performed. The tests involved exposure of the coated material to hydrogen at high temperatures, the examination of the coatings by scanning electron microscopy, and the measurement of weight losses. The coatings included Re, TaHfC, TaC, and NbC, with thicknesses of the order of 20-60 microns. DOE

N94-19740# Florida Univ., Gainesville. Dept. of Chemistry.
POLYMER FILMS WITH ENHANCED DIELECTRIC PROPERTIES Final Report, 11 Jun. 1990 - 30 Jun. 1993
John R. Reynolds 26 Jul. 1993 11 p
(Contract DAAL03-90-G-0149)
(AD-A271148; ARO-27808.4-CH) Avail: CASI HC A03/MF A01

A program has been completed utilizing copolymerization and polymer blending methods to prepare polymer films with useful dielectric properties. A scaled-up procedure for the synthesis of a-fluoro acrylonitrile and ethyl-a-fluoroacrylate has been developed. These monomers have been polymerized using free-radical methods and the polymer structures have been fully characterized. Both polymers are atactic. Films of poly(a-fluoro acrylonitrile) exhibit a dielectric constant at 8.9 while films of poly(ethyl-a- fluoroacrylate) have a dielectric constant of 4.0 (50 Hz). Blends of poly(vinylidene fluoride or trifluoroethylene) with poly(methyl methacrylate) have been shown to be miscible over a wide phase composition. At 80% fluorocopolymer the blend exhibits a dielectric constant at 7. DTIC

N94-19742# California Univ., Santa Barbara. Dept. of Chemistry.
COOPERATIVE FORMATION OF INORGANIC-ORGANIC INTERFACES IN THE SYNTHESIS OF SILICATE MESOSTRUCTURES
A. Monnier, F. Schuth, Q. Huo, D. Kumar, and D. Margolese 3 Sep. 1993 26 p
(Contract N00014-90-J-1159)
(AD-A271196) Avail: CASI HC A03/MF A01

A model is presented to explain the formation and morphologies of surfactant-silicate mesostructures. Three processes are identified: multidentate binding of silicate oligomers to the cationic surfactant; preferential silicate polymerization in the interface region; and charge density matching between the surfactant and the silicate. The model explains present experimental data, including the transformation between lamellar and hexagonal mesophases, and provides a guide for predicting conditions favoring the formation of lamellar, hexagonal or cubic mesostructures. The model Q230 proposed by Mariani et al. satisfactorily fits the X-ray data collected on the cubic mesostructure material. This model suggests that the silicate polymer forms a unique infinite silicate sheet sitting on the gyroid minimal surface and separating the surfactant molecules into two disconnected volumes. DTIC

N94-19758# Materials Research Society, Pittsburg, PA.
MAGNETIC ULTRATHIN FILMS: MULTILAYERS AND SURFACES, INTERFACES, AND CHARACTERIZATION, VOLUME 313
B. T. Jonker, Scott A. Chambers, R. F. Farrow, C. Chappert, and R. Clarke Apr. 1993 880 p Symposium held in San Francisco, CA, 12-16 Apr. 1993
(Contracts N00014-93-1-0472; N00014-93-1-0365)
(AD-A271402) Avail: CASI HC A99/MF A10

The contents of the document are broken down into the following topics: giant magnetoresistance in multilayers - role of interface structure; giant magnetoresistance in alloys - a simple route to magnetic devices; interlayer coupling; giant magnetoresistance in multilayers; structure and magnetism; giant magnetoresistance in low fields - multilayers and spin valves; magnetism and structure in ultrathin films; surface magnetism; magnetic bilayers, trilayers, and multilayers; magnetic anisotropy; magneto-optics; theories and spin polarized spectroscopies; applications of synchrotron radiation techniques to magnetic materials; structural and interfacial characterization; nanostructural characterization; and magnetism in multilayers - structure and properties. DTIC

N94-18010# Stuttgart Univ. (Germany). Inst. fuer Feinwerk- und Zeitmesstechnik.
TITANIUM CARBON-HYDROGEN LAYERS ON DECORATIVE SURFACES [TITAN-KOHLENWASSERSTOFF-SCHICHTEN ZUR DEKORATIVEN OBERFLAECHENVEREDELUNG]
Bernd Bader and Klaus Scheerer (Stuttgart Univ., Germany.) *In* Societe Suisse de Chronometrie, Proceedings of the 4th European Congress on Chronometry 1992 p 25-28 In GERMAN (For primary document see N94-18006 04-35)
Copyright Avail: CASI HC A01/MF A02

N94-18013# Scientific Research Inst. of Instrument Automation, Moscow (USSR).
THE PERSPECTIVES IN APPLICATION OF HOT CASTING TECHNOLOGY FOR CERAMIC PARTS OF TIMEKEEPING DEVICES
O. G. Andreyeva, P. O. Gribovsky, G. B. Kartashov, and N. A. Romanova *In* Societe Suisse de Chronometrie, Proceedings of the 4th European Congress on Chronometry 1992 p 39-41 (For primary document see N94-18006 04-35)
Copyright Avail: CASI HC A01/MF A02

28 PROPELLANTS AND FUELS

Includes rocket propellants, igniters, and oxidizers; their storage and handling procedures; and aircraft fuels.

For related information see also *07 Aircraft Propulsion and Power, 20 Spacecraft Propulsion and Power,* and *44 Energy Production and Conversion.*

N94-17751# Los Alamos National Lab., NM.
DIRECT MONTE CARLO SIMULATION OF THE CHEMICAL EQUILIBRIUM COMPOSITION OF DETONATION PRODUCTS
M. S. Shaw 1993 17 p Presented at the 10th Detonation Symposium, Boston, MA, 12-16 Jul. 1993
(Contract W-7405-eng-36)
(DE93-014559; LA-UR-93-1815; CONF-930713-13) Avail: CASI HC A03/MF A01

A new Monte Carlo simulation method has been developed by the author which gives the equilibrium chemical composition of a molecular fluid directly. The usual NPT ensemble (isothermal-isobaric) is implemented with N being the number of atoms instead of molecules. Changes in chemical composition are treated as correlated spatial moves of atoms. Given the interaction potentials between molecular products, 'exact' EOS points including the equilibrium chemical composition can be determined from the simulations. This method is applied to detonation products at conditions in the region near the Chapman-Jouget state. For the example of NO, it is shown that the CJ detonation velocity can be determined to a few meters per second. A rather small change in cross potentials is shown to shift the chemical equilibrium and the CJ conditions significantly. DOE

N94-17813# Los Alamos National Lab., NM.
DETONATION REACTION STEPS FROZEN BY FREE EXPANSION AND ANALYZED BY MASS SPECTROMETRY
N. R. Greiner, H. A. Fry, N. C. Blais, and R. P. Engelke 1993 6 p Presented at the 10th Detonation Symposium, Boston, MA, 12-16 Jul. 1993
(Contract W-7405-eng-36)
(DE93-012734; LA-UR-93-1545; CONF-930713-7) Avail: CASI HC A02/MF A01

Detonation reactions in small pellets of explosive are frozen by free expansion into a large vacuum chamber and analyzed by time-of-flight mass spectrometry. Sensitive explosives like PETN, RDX, and HMX show rapidly evolving reaction zones and mostly simple products like H_2O, CO, N_2, and CO_2. Less sensitive explosives like TATB, HNS, and TNT show slower evolution of the reaction zone, and more complex products in addition to the simple ones seen in PETN. Isotopic substitution shows that the more complex products contain moderate amounts of NH_3, HCN, NO, HNCO, and NO_2. Other observations include the following: polymerization of aromatic explosive molecules, adducts to the explosive molecules, and explosive molecules with functional groups missing. The more complex products are reservoirs of unreleased energy that may affect performance. DOE

N94-17840# Naval Surface Warfare Center, Silver Spring, MD.
ALUMINUM POWDER/WATER REACTION IGNITED BY ELECTRICAL PULSED POWER Final Report, Oct. 1990 - Apr. 1992
W. M. Lee 12 Aug. 1993 33 p
(AD-A269223; NSWCDD/TR-93/108) Avail: CASI HC A03/MF A01

The effectiveness of the electrical pulsed power technique in driving aluminum-water reactions has been studied. The reactant was prepared by mixing, in the stoichiometric ratio, fine aluminum powder (the fuel) and water (the oxidizer). The electrical energy was delivered to the reactant through an ignition wire embedded in it. The primary objective of the study was to maximize the energy efficiency, which is defined as the ratio of the chemical energy output from the reaction to the electrical energy input. The energy efficiency depends critically on the electrical circuit parameters, physical parameters of the metal fuel powder, and geometrical arrangements of the reactant. Under an optimized set of experimental variables, the energy efficiency exceeds 100. DTIC

N94-18045# Midwest Research Inst., Golden, CO. National Renewable Energy Lab.
FIFTEENTH SYMPOSIUM ON BIOTECHNOLOGY FOR FUELS AND CHEMICALS: PROGRAM AND ABSTRACTS
1993 139 p Symposium held in Colorado Springs, CO, 10-14 May 1993
(Contract DE-AC02-83CH-10093)
(DE93-010005; NREL/CP-420-5466; CONF-9305238) Avail: CASI HC A07/MF A02

This collection contains 173 abstracts from presented papers and poster sessions. The five sessions of the conference were on the subjects of: (1) Thermal, Chemical, and Biological Processing, (2) Applied Biological Research, (3) Bioprocessing Research, (4) Process Economics and Commercialization, and (5) Environmental Biotechnology. Examples of specific topics in the first session include the kinetics of ripening cheese, microbial liquefaction of lignite, and wheat as a feedstock for fuel ethanol. Typical topics in the second session were synergism studies of bacterial and fungal celluloses, conversion of inulin from jerusalem artichokes to sorbitol and ethanol by saccharomyces cerevisiae, and microbial conversion of high rank coals to methane. The third session entertained topics such as hydrodynamic modeling of a liquid fluidized bed bioreactor for coal biosolubilization, aqueous biphasic systems for biological particle partitioning, and arabinose utilization by xylose-fermenting yeast and fungi. The fourth session included such topics as silage processing of forage biomass to alcohol fuels, economics of molasses to ethanol in India, and production of lactic acid from renewable resources. the final session contained papers on such subjects as bioluminescent detection of contaminants in soils, characterization of petroleum contaminated soils in coral atolls in the south Pacific, and landfill management for methane generation and emission control. DOE

N94-18095# Lawrence Livermore National Lab., CA.
MODELING SHOCK INITIATION IN COMPOSITION B
M. J. Murphy, E. L. Lee, A. M. Weston (KMI Energy, Livermore, CA.), and A. E. Williams (Naval Research Lab., Washington, DC.) May 1993 8 p Presented at the 10th Detonation Symposium, Boston, MA, 12-16 Jul. 1993
(Contract W-7405-eng-48)
(DE93-016544; UCRL-JC-111975; CONF-930713-19) Avail: CASI HC A02/MF A01

A hydrodynamic modeling study of the shock initiation behavior of the Composition B explosive was performed using the 'Ignition and Growth of Reaction in High Explosive' model developed at the Lawrence Livermore National Laboratory. The HE (heterogeneous explosives) responses were computed using the CALE and DYNA2D hydrocodes and then compared to experimental results. The data from several standard shock initiation and HE performance experiments were used to determine the parameters required for the model. Simulations of the wedge tests (pop plots) and failure diameter tests were found to be sufficient for defining the ignition and growth parameters used in the two term version of the computational model. These coefficients were then applied in the response analysis of several Composition B impact initiation experiments. A description of the methodology used to determine the coefficients and the resulting range of useful application of the ignition and growth of reaction model is described. DOE

N94-18203# Materials Research Labs., Ascot Vale (Australia).
SOME PROBLEMS IN THE RHEOLOGICAL CHARACTERISATION OF COMPOSITE ROCKET PROPELLANTS
R. C. Warren Jun. 1993 25 p
(AD-A268806; MRL-TN-642; DODA-AR-008-271) Avail: CASI HC A03/MF A01

Apparent viscosities of a composite propellant analogue were measured with both rotary and extrusion instruments. A Haake Viscometer in the Couette configuration was used with 2 gap widths and also with a profiled cup and rotor. An extrusion rheometer was fitted with a slit die and measurements were made at 2 slit thicknesses. The flow was found to be time dependent, and there was apparent slip at the wall. It is suggested that the cause of this behaviour is filler particle migration in the non-uniform stress fields. The filler migration is assumed to cause a layer of binder to develop at the walls confining the flow, and this layer would lubricate the flow of the bulk of the material causing an apparent slip. The effect of the

slip is to reduce the apparent viscosity of the material, which also appears to be affected by ageing of the samples under ambient conditions for several days. Particle sizes of the solid ingredients were also measured.
DTIC

N94-18489 University of Eastern Kentucky, Richmond. Dept. of Chemistry.
ANALYSIS OF DEPOSIT PRECURSORS IN JET FUELS USING FOURIER TRANSFORM INFRARED SPECTROSCOPY Interim Report, Apr. - Aug. 1991
William Schulz and David B. Shehee Jan. 1993 53 p Limited Reproducibility: More than 20% of this document may be affected by microfiche quality
(Contract F33615-87-C-2714)
(AD-A269035; WL-TR-93-2015) Avail: Issuing Activity (Defense Technical Information Center (DTIC))

Thermal oxidation products from jet fuels will be formed in the presence of fuel and oxygen at elevated temperatures. Development of fuels that will not form solid residues depends on the development of a method to analyze the rate of oxidation of fuels. Gravimetric determination of fuel residues was imprecise and time consuming. Gas Chromatography-Mass Spectrometry (GC-MS) of oxidation products yields a great deal of fundamental information but is too specific to be used as a rapid method for determining the rate of oxidation. Fourier Transform Infrared (FTIR) Spectrometry is non-specific and gives integrated signals for classes of oxidation products that will give rapid analytical results for rates of oxidation as well as the ability to study the effectiveness of chemical additives.
DTIC

N94-18491 Thiokol Corp., Brigham City, UT.
STRAINED RING ENERGETIC BINDERS Final Report, Nov. 1990 - Aug. 1993
L. F. Cannizzo, R. H. Grubbs, M. A. Hillmyer, and J. P. Schaller 27 Aug. 1993 35 p Limited Reproducibility: More than 20% of this document may be affected by microfiche quality
(Contract N00014-90-C-0263)
(AD-A269056) Avail: CASI HC A03

The use of thermoplastic elastomers (TPE's) containing strained hydrocarbon rings as energetic propellant binders is an attractive approach to increasing the performance of highly oxidized propellant formulations which currently use HTPB as a binder. The recently reported strained-ring elastomeric polymer polybenzvalene (PBV), produced by ring-opening metathesis polymerization (ROMP), is an example of a strained ring polymer. However, PBV is thermally unstable (T(sub onset) = 77 C, T(sub max)= 137 C) and deflagrates under severe mechanical stretching. In this program several areas were investigated. First, studies to attempt the thermal stabilization of PBV were undertaken. One approach was the partial reduction of the double bonds present in PBV which gave only small increases in thermal stability (Delta T(sub max) = 9 C). The second approach was the addition of radical traps to PBV which, again, gave only small increases in thermal stability (delta T(sub max) = 8 C). The second area investigated a different strained ring polymer, polyhomobenzvalene (PHBV). PHBV was not found to have the mechanical instability problems of PBV, but was still thermally unstable (T(sub onset) = 66 C, T(sub max) = 109 C). The last area studied was the application of acyclic olefins as chain-transfer agents during polymer formation which produced difunctional hydroxytelechelic polymers of cyclooctene and cyclooctadiene (as model systems) with good control of molecular weight.
DTIC

N94-18617# Midwest Research Inst., Golden, CO. National Renewable Energy Lab.
EVALUATION OF AFTERMARKET LPG CONVERSION KITS IN LIGHT-DUTY VEHICLE APPLICATIONS
E. A. Bass (Southwest Research Inst., San Antonio, TX.) Jun. 1993 155 p
(Contract DE-AC02-83CH-10093)
(DE93-010035; NREL/TP-421-5462) Avail: CASI HC A08/MF A02

SwRI was contracted by NREL to evaluate three LPG conversion kits on a Chevrolet Lumina. The objective of the project was to measure the Federal Test Procedure (FTP) emissions and fuel economy of these kits, and compare their performance to gasoline-fueled operation and to each other. Varying LPG fuel blends allowed a preliminary look at the potential for fuel system disturbance. The project required kit installation and adjustment according to manufacturer's instructions. A limited amount of trouble diagnosis was also performed on the fuel systems. A simultaneous contract from the Texas Railroad Commission, in cooperation with NREL, provided funds for additional testing with market fuels (HD5 propane and industry average gasoline) and hydrocarbon (HC) emissions speciation to determine the ozone-forming potential of LPG HC emissions. This report documents the procurement, installation, and testing of these LPG conversion kits.
DOE

N94-18708 Army Armament Research, Development and Engineering Center, Picatinny Arsenal, NJ.
MOLECULAR STRUCTURE OF LOW TEMPERATURE FORM OF TRIAMINOGUANIDINIUM NITRATE (TAGN)
A. J. Bracuti Sep. 1993 23 p Limited Reproducibility: More than 20% of this document may be affected by microfiche quality
(AD-A270409; ARAED-TR-93012) Avail: CASI HC A03

A rigid-body motion study of triaminoguanidinium nitrate (TAGN) was initiated originally in order to determine if nitrate ion libration might be responsible for the TAGN fast burning rate. A low temperature polymorph of TAGN was discovered by this laboratory during the course of this rigid-body motion study. Continuation of this libration study in the lower temperature regime, however, necessitated understanding the molecular structure of the low temperature form of TAGN. To do this a signal-crystal x-ray diffraction structure determination of the low temperature form was undertaken. The crystal structure was determined including space group, lattice parameters, atomic coordinates and temperature factors, hydrogen bonding, and density.
DTIC

N94-18758 Aerospace Corp., El Segundo, CA. Engineering and Technology Group.
NEW TEST METHOD TO DETERMINE MODULUS OF ELASTICITY OF ROCKET GRAIN MATERIAL Technical Report
Dick J. Chang, Rolf W. Gross, and Farzad Baban 15 Jan. 1993 20 p Limited Reproducibility: More than 20% of this document may be affected by microfiche quality
(Contract F04701-88-C-0089)
(AD-A269758; TR-93(3935)-5) Avail: CASI HC A03

A new testing technique was demonstrated for measuring the modulus of elasticity of low-modulus materials such as rocket propellant grains. The technique described herein offers substantial advantages over the dog bone testing method. The testing procedure is less complicated, and data reduction is simpler. More importantly, a biaxial stress field can be established in the test specimen to simulate conditions encountered during pressurization of a nonlinear and viscoelastic material (e.g., propellant used in solid rocket motors). For metals or linearly elastic materials, dog bone testing may be considered a viable technique through which material properties such as the modulus of elasticity can be extracted accurately. However, for highly filled materials or propellants that exhibit nonlinear and viscoelastic behavior, results obtained through the uniaxial stress data of dog bone tests do not provide material characteristics under biaxial strain conditions. Lack of such material properties will be detrimental to the ability in evaluating and predicting the integrity of the components.
DTIC

N94-18893# Lawrence Livermore National Lab., CA.
LX-17 CHEMICAL KINETIC MATERIAL MODEL FOR CHEMICAL TOPAZ2D
J. T. Hendricks Feb. 1993 51 p
(Contract W-7405-eng-48)
(DE93-014363; UCRL-ID-113563) Avail: CASI HC A04/MF A01 (US Sales Only)

A chemical reaction kinetic material model for Chemical TOPAZ2D has been developed for modeling burning of LX-17 high explosive. The model was developed to predict warhead thermal response when subjected to fuel and/or propellant fires. Prior to this work, material models have been unavailable for Chemical TOPAZ2D to accurately predict the thermal response of burning LX-17. Numerical results compared to George Bloom's experimental test in 1983 indicate that the burn rate and burn temperature can be simulated with excellent correlation when using, the present LX-17 material model. Numerical modeling, also have insight to the shape of the burn front and the thermal propagation. Observations indicate that a higher burn rate resulted from the experimental test over the adiabatic burn rate of LX-17. This effect was due to the thermal diffusion down the outer stainless steel can wall resulting in LX-17 preignition. The burn rate of LX-17 from George Bloom's experiment was recorded as 3.7-3.9 mm/min. Using the LX-17 material model, a one-dimensional numerical simulation indicates that the adiabatic burn rate is 2.2 mm/min. Since the burning of LX-17 within a weapon is closer to an adiabatic burn, the lower estimate for burn rate shows an enhancement in thermal protection. DOE

N94-18913# Battelle Columbus Labs., OH.
DATA COLLECTION PLAN FOR PHASE 2 ALTERNATIVE FUELS BUS DATA COLLECTION PROGRAM
T. Krenelka Jul. 1993 34 p Prepared for Midwest Research Inst., Golden, CO
(Contract DE-AC02-83CH-10093)
(DE93-010047; NREL/TP-421-5264) Avail: CASI HC A03/MF A01

This document constitutes the plan for collecting and reporting data associated with a special set of transit bus demonstrations to be conducted under the Urban Bus Program of the Alternative Motor Fuels Act (AMFA) of 1988. This program, called the Phase 2 Bus Data Collection Program, serves as an adjunct to the Phase 1 Bus Data Collection Program, collecting detailed data on just a few buses to augment and enhance the Phase 1 data in fulfilling the urban bus requirements of AMFA. Demonstrations will be conducted at a few transit system locations throughout the US and will use alternative fuels and associated technologies to reduce undesirable transit bus exhaust emissions. Several organizations will be involved in the data collection; NREL will manage the program, analyze and store vehicle data, and make these data available through the Alternative Fuels Data Center. This information will enable transit agencies, equipment manufacturers, fuel suppliers, and government policy makers to make informed decisions about buying and using alternative fuels. DOE

N94-19042# Sandia National Labs., Albuquerque, NM.
THE MINIMUM DETECTION LIMITS OF RDX AND TNT DEPOSITED ON VARIOUS SURFACES AS DETERMINED BY ION MOBILITY SPECTROSCOPY
P. Rodacy Aug. 1993 27 p
(Contract DE-AC04-76DP-00789)
(DE93-018521; SAND-92-0229) Avail: CASI HC A03/MF A01

An ion mobility spectrometer (IMS) was used to determine the detection limits of RDX and TNT on six different substrates. The preparation of the explosive deposits on the surfaces is examined as well as effects due to the size, uniformity, method of application, and time that a deposit has been on a surface. Sampling methods are discussed along with effects of the surface topology. The transfer of explosives from a hand to a surface and methods to reduce the detection limits are presented. DOE

N94-19242# Lawrence Livermore National Lab., CA.
THE USE OF POST DETONATION ANALYSIS OF STABLE ISOTOPE RATIOS TO DETERMINE THE TYPE AND PRODUCTION PROCESS OF THE EXPLOSIVE INVOLVED
R. R. McGuire, C. A. Velsko, C. G. Lee, and E. Raber Mar. 1993 18 p
(Contract W-7405-eng-48)
(DE93-018497; UCRL-ID-113275) Avail: CASI HC A03/MF A01

The detonation of a series of explosives was performed in a controlled manner to collect the resulting, solid residue or soot. This residue was examined to determine the ratios of the stable carbon, hydrogen, and nitrogen isotopes. The goal of the experiment was to determine if these ratios could be used to indicate, from the post detonation residues, the type and origin of the detonated explosive. The ratios of the stated stable isotopes in the undetonated explosive were also determined. Despite some reservations in the quality of the data resulting from contamination by nonexplosive components, certain trends can be discerned. (1) Carbon isotopes allow aromatic explosives to be distinguished from nonaromatic explosives. This trend seems to carry through the detonation so that the distinction might be made after the fact. (2) The amination process for TATB can be detected through the hydrogen and, to some extent, the nitrogen isotope ratios. Unfortunately, the data are not sufficiently good to determine if this differential carries through the detonation. (3) The relative magnitude and sign of the nitrogen isotope ratio seems to carry through the detonation: some exchange with atmospheric nitrogen is probable. Even though this set of experiments must also be viewed as preliminary, there is a definite indication that certain qualitative characteristics of explosives can be detected after the detonation. This 'signature' could have application to both intelligence and counter terrorism. DOE

N94-19445 Prins Maurits Lab. TNO, Rijswijk (Netherlands).
ROUND ROBIN EXPERIMENTS ON THE EXPLOSIVE COMPONENTS WATER GAP TEST (ECWGT) Final Report
E. G. deJong Jan. 1993 26 p Sponsored by DMKL, The Hague, Netherlands
(Contract A84/KL/147)
(PML-1992-69; TD92-2413; ETN-93-94934) Copyright Avail: Issuing Activity (TNO Prins Maurits Laboratory, P.O. Box 45, 2280 AA Rijswijk, Netherlands)

Experiments carried out on the explosive components water gap test are reported. This is an accurate test to establish the sensitivity of explosive components and boosters meant for uninterrupted use in explosive trains. The explosive component (acceptor) is glued on the witness rod. The witness rod slides through the locating plug which has an extra hole of 2 mm diameter for water filling purposes. The donor charge is glued in the other end of the tube. To ensure a watertight closure, and to allow a secure fit for the detonator, another locating plug is glued under the donor charge and the tube. The distance between the top of the donor charge and the bottom of the explosive component is filled with demineralized water. The length of the water gap is inversely proportional to the pressure applied on the component. A number 8 detonator is placed just before firing, and the entire test set-up is placed on an assembly holder covered with a cardboard plate with a hole to allow a close fit on the detonator holder. Detailed drawings of the items are given. The results obtained with the leads immersed approximately 2 mm in the water give a higher 'NO GO' level than when the water surface just touches the bottom of the lead. ESA

N94-19494*# Alabama Univ., Huntsville. Center for Automation and Robotics.
MATERIALS CHARACTERIZATION OF PROPELLANTS USING ULTRASONICS Final Report
Gary L. Workman and David Jones 31 Oct. 1993 17 p
(Contract NAS8-38609)
(NASA-CR-193877; NAS 1.26:193877) Avail: CASI HC A03/MF A01

Propellant characteristics for solid rocket motors were not completely determined for its use as a processing variable in today's production facilities. A major effort to determine propellant characteristics obtainable through ultrasonic measurement techniques was performed in this task. The information obtained was then used to determine the uniformity of manufacturing methods and/or the ability to determine non-uniformity in processes. Author (revised)

N94-19674# Army Research Lab., Aberdeen Proving Ground, MD.
MECHANICAL RESPONSE COMPARISON OF GUN PROPELLANTS EVALUATED UNDER EQUIVALENT TIME-TEMPERATURE CONDITIONS Final Report, Sep. - Nov. 1992
Robert J. Lieb and Michael G. Leadore Sep. 1993 24 p
(DA Proj. 1L1-61102-AH-43)
(AD-A270479; ARL-TR-228) Avail: CASI HC A03/MF A01

Compressive stress relaxation measurements were performed for single- (M14), double- (JA2), and triple-base (M30) propellants, as well as a nitramine composite (M43) gun propellant. This was done to evaluate the response of gun propellants at higher rates than can be easily reached within the laboratory by calculating time-temperature shift factors from these relaxation curves. However, in order to apply these shift parameters to high rate events to predict propellant mechanical response and damage, a link must be established between predicted equivalent response and the actual mechanical and failure behavior observed for these propellants. The mechanical response of these four propellants was characterized at strain rates, which spanned four orders of magnitude, and at the corresponding shifted temperatures. Test results show that the mechanical response for a given propellant type under each of these temperature-rate conditions was the same in the strain domain for which the relaxation shift factors were measured. In addition, the failure response for a given propellant type also proved to be nearly identical at strain levels outside the domain of the stress relaxation tests. These observations permit greater confidence to be placed in the prediction of mechanical and failure response for gun propellants undergoing deformation in strain rate regime the current range of laboratory measurement. DTIC

29 MATERIALS PROCESSING

Includes space-based development of products and processes for commercial applications.

For biological materials see *55 Space Biology.*

N94-17763*# Colorado Univ., Boulder. Dept. of Chemical Engineering.
MODELING AND NEW EQUIPMENT DEFINITION FOR THE VIBRATION ISOLATION BOX EQUIPMENT SYSTEM Progress Report
Robert L. Sani 1993 11 p
(Grant NAG3-1410)
(NASA-CR-193185; NAS 1.26:193185; CU-153-6505) Avail: CASI HC A03/MF A01

Our MSAD-funded research project is to provide numerical modeling support for the VIBES (Vibration Isolation Box Experiment System) which is an IML2 flight experiment being built by the Japanese research team of Dr. H. Azuma of the Japanese National Aerospace Laboratory. During this reporting period, the following have been accomplished: A semi-consistent mass finite element projection algorithm for 2D and 3D Boussinesq flows has been implemented on Sun, HP And Cray Platforms. The algorithm has better phase speed accuracy than similar finite difference or lumped mass finite element algorithms, an attribute which is essential for addressing realistic g-jitter effects as well as convectively-dominated transient systems. The projection algorithm has been benchmarked against solutions generated via the commercial code FIDAP. The algorithm appears to be accurate as well as computationally efficient. Optimization and potential parallelization studies are underway. Our implementation to date has focused on execution of the basic algorithm with at most a concern for vectorization. The initial time-varying gravity Boussinesq flow simulation is being set up. The mesh is being designed and the input file is being generated. Some preliminary 'small mesh' cases will be attempted on our HP9000/735 while our request to MSAD for supercomputing resources is being addressed. The Japanese research team for VIBES was visited, the current set up and status of the physical experiment was obtained and ongoing E-Mail communication link was established. Derived from text

N94-18840*# Alabama Univ., Huntsville.
CONSORTIUM FOR MATERIALS DEVELOPMENT IN SPACE Annual Technical Report
1993 8 p
(Grant NAGw-812)
(NASA-CR-194411; NAS 1.26:194411) Avail: CASI HC A02/MF A01

During fiscal 1993, the Consortium for Materials Development in Space (CMDS) maintained the organizational structure and project orientation established in prior years. The commercial objectives are improved materials, biomedical applications, and infrastructure and support hardware. Projects include nonlinear optical materials; space materials (specifically polymer foam/films, atomic oxygen and high temperature superconductors); alloyed and blended materials: sintered and alloyed materials; polymer and carbonate blends; electrodeposition; organic separation; materials dispersion and biodynamics; space carriers: Consort, COMET support, Spacehab utilization; and flight services: accelerometers, CMIX, USEC, ORSEP, and Space Experiment Facility (SEF). Derived from text

N94-19489# Universitaet der Bundeswehr Muenchen, Neubiberg (Germany). Inst. fuer Luft- und Raumfahrttechnik.
AXIAL RESPONSE OF DIFFERENTLY EXCITED ANCHORED VISCOUS LIQUID BRIDGES IN ZERO-GRAVITY
Helmut F. Bauer 1990 59 p
(LRT-WE-9-FB-1-1992; ETN-93-95087) Avail: CASI HC A04/MF A01

A cylindrical liquid column with anchored edges at the rim of circular upper and lower discs and consisting of incompressible and viscous liquid, is subjected to different axial excitations, such as one sided or counter directional excitations. The response of the free liquid surface and the velocity and pressure distribution were determined. The response of the free liquid surface was evaluated numerically. ESA

N94-19491 Universitaet der Bundeswehr Muenchen, Neubiberg (Germany). Inst. fuer Raumfahrttechnik.
FREE FALL LIQUID COLUMN DYNAMICS IN A DROPTOWER
Helmut F. Bauer 1992 21 p Limited Reproducibility: More than 20% of this document may be affected by microfiche quality
(LRT-WE-9-FB-6-1992; ETN-93-95091) Avail: CASI HC A03

The vibrational behavior of a circular cylindrical liquid column is investigated. Before release in a drop tower, the initial condition is an amphora type equilibrium geometry. The problem presents a free vibration case with given initial conditions. The analysis of such a system for frictionless and viscous liquid with slipping and anchored contact line is presented. ESA

N94-19492# Universitaet der Bundeswehr Muenchen, Neubiberg (Germany). Inst. fuer Raumfahrttechnik.
TRANSIENT RESPONSE OF A VISCOUS AND ANCHORED LIQUID BRIDGE TO AN AXIAL PULSE
Helmut F. Bauer 1992 35 p
(LRT-WE-9-FB-7-1992; ETN-93-95092) Avail: CASI HC A03/MF A01

The response of a liquid column to an axial pulse disturbance of the form z(bar)(sub zero) e(exp -alpha x t), exhibiting a sudden rise at the time t = 0 and decaying from there on, was investigated for a viscous anchored-edge liquid column of finite length. The increasing decay magnitude of the pulse shows a strong decay response, that is shorter response times, and increasing free surface displacements. The increase of the surface tension parameter (sigma x a)/(rho x nu(exp 2)) yields to heavily decreasing free surface response. It was found that the response is larger for larger aspect ratios of the liquid bridge. ESA

N94-19167*# Swedish Space Corp., Solna.
MUZO FLIGHT EXPERIENCE WITH THE PROGRAMMABLE MULTIZONE FURNACE
Christian Lockowandt and Kenneth Loth *In* NASA. Goddard Space Flight Center, The 1993 Shuttle Small Payloads Symposium Oct. 1993 p 37-45 (For primary document see N94-19162 04-12)
Avail: CASI HC A02/MF A03

31 ENGINEERING (GENERAL)

Includes vacuum technology; control engineering; display engineering; cryogenics; and fire prevention.

N94-17725# Los Alamos National Lab., NM.
MALONE REFRIGERATION
G. W. Swift 1993 6 p Presented at the Oak Ridge National Laboratory (ORNL) Refrigeration and Air Conditioning Technology Workshop, Breckenridge, CO, 23-25 Jun. 1993
(Contract W-7405-eng-36)
(DE93-014468; LA-UR-93-1890; CONF-9306166-1) Avail: CASI HC A02/MF A01

Malone refrigeration is the use of a liquid near its critical points without evaporations as working fluid in a regenerative or recuperative refrigeration cycle such as the Stirling and Brayton cycles. It's potential advantages include compactness, efficiency, an environmentally benign working fluid, and reasonable cost. One Malone refrigerator has been built and studied; two more are under construction. Malone refrigeration is such a new, relatively unexplored technology that the potential for inventions leading to improvements in efficiency and simplicity is very high. DOE

N94-18147 Phillips Lab., Kirtland AFB, NM.
THE 7TH INTERNATIONAL CRYOCOOLER CONFERENCE Final Report
Apr. 1993 268 p Conference held in Sante Fe, NM, 17-19 Nov. 1992
Limited Reproducibility: More than 20% of this document may be affected by microfiche quality
(AF Proj. 1105)
(AD-A268451; AD-E201519; PL-CP-93-1001-Pt-4) Avail: Issuing Activity (Defense Technical Information Center (DTIC))

The partial contents of this document include the following: SDIO and Air Force Cryocooler Technology Developments at USAF Phillips Laboratory; JPL Cryocooler Development and Test Program Overview; Development and Demonstration of a Diaphragm Stirling 65 K Standard Spacecraft

Cryocooler; Stirling Space Cooler; Thermal, Vibration, and Reliability Test Results for a Balanced 80 K Cryocooler; Spacecraft Cooler Characterization; Performance of a Long Life Reverse Brayton Cryocooler; SDI Cryocooler Producibility Program; Miniature Pulse Tube Cooler; Flow Patterns Intrinsic to the Pulse Tube Refrigerator; Experimental Investigation of the Regenerative Magnetic Refrigerator Operating Between 4.2 K and 1.8 K; A 4 K Gifford-McMahon Refrigerator for Radio Astronomy; A Stirling Cycle Cryocooler for 4 K Applications; Regenerator Performance and Refrigeration Mechanism for 4 K GM Refrigerator Using Rare Earth Compound Regenerator Materials; Superfluid Stirling Refrigerator with a Counterflow Regenerator; Graded and Nongraded Regenerator Performance; Evolution of the 10 K Periodic Sorption Refrigerator Concept; Development of a Periodic 10 K Sorption Cryocooler; Assessment of a Hydrogen Joule-Thomson Expander and Vanadium Hydride Sorption Beds for 20 K Cryocoolers; Design of a Metal Hydride Sorption Cryocooler System; Linear Compressor for JT Cryocooler; JT Cryostat with Liquid-Solid Cryogen Reservoir; Design of A Metal Hydride Sorption Cryocooler System; Linear Compressor for JT Cooler; and Phase Equilibria in Cryogenic Mixtures.
DTIC

N94-18710# Lawrence Livermore National Lab., CA.
AEROSOL FILTRATION WITH STEEL FIBER FILTERS
W. Bergman, K. Wilson, G. Larsen, and R. Lopez Apr. 1993 9 p Presented at the American Filtration Society Seminar and Expo Annual Meeting, Chicago, IL, 3-6 May 1993
(Contract W-7405-eng-48)
(DE93-016990; UCRL-JC-113854; CONF-9305166-3) Avail: CASI HC A02/MF A01

An experimental study has been conducted of aerosol penetration through a new high efficiency steel fiber filter and filter media that was developed in cooperation with Pall Corporation. Previous studies have shown that sintered steel fiber media have significant improvements in higher filter efficiency and lower pressure drop than the previous steel filter technology based on sintered powder metal media. In the present study, measurements were made of the penetration of dioctyl sebacate (DOS) aerosols through flat sheet samples, pleated cartridge filters, and a 1000 cfm filter having 64 cartridges housed in a 2 x 2 x 1 ft. frame. The steel fiber media used in our study consists of 2 micron diameter stainless steel (316 L) fibers sintered together into sheets.
DOE

N94-18818# Los Alamos National Lab., NM.
REGENERATOR OPTIMIZATION FOR STIRLING CYCLE REFRIGERATION
S. A. Colgate and A. G. Petschek (New Mexico Inst. of Mining and Technology, Socorro.) 1993 47 p Presented at the International Cryogenic Engineering and Material Conference, Albuquerque, NM, 12-16 Jul. 1993
(Contract W-7405-eng-36)
(DE93-018468; LA-UR-93-2656; CONF-930703-15) Avail: CASI HC A03/MF A01

A cryogenic regenerator for a Stirling cycle is designed using fractional loss or entropy gain as the criterion of performance. The gas losses are treated separately from heat storage medium losses. For the optimum channel flow nonturbulent design, the maximization of heat transfer from the gas to the wall and the minimization of entropy production by friction leads to a gas flow velocity criterion of sound speed times loss fraction. This velocity with a given frequency leads to a Stirling cycle dead volume ratio and consequently a channel of specified length and width. The thermal properties of the channel wall must then accommodate this cyclic heat flow without substantially increasing the loss fraction. It is found that stainless steel or plastics are adequate for 30 to 300 K, but that the lower temperature stages of 4 to 30 K require either a special lead alloy of moderate conductivity or a segmented anisotropic construction of alternate highly conducting lead layers and alternate insulating glass or epoxy fiber glass spacers. An overall efficiency of (congruent) 50% of Carnot is predicted at a frequency of 30 Hz and a pressure of one atmosphere.
DOE

N94-19254 Technische Univ., Delft (Netherlands). Faculty of Civil Engineering.
RESEARCH ACTIVITIES, FACULTY OF CIVIL ENGINEERING, DELFT UNIVERSITY OF TECHNOLOGY, 1990 - 1991
1991 252 p See also PB91-137497 Limited Reproducibility: More than 20% of this document may be affected by microfiche quality
(PB93-195022) Avail: CASI HC A12

In the report on research activities, the research work of the Structural Mechanics and Computer Integrated Construction Division is summarized under five main headings: computational mechanics; dynamics; computational concrete mechanics; risk, reliability, and integrity; and computer integrated construction.
NTIS

N94-19322# Instituut TNO voor Bouwmaterialen en Bouwconstructies, Delft (Netherlands).
MICROSTRUCTURE OF THE INTERFACIAL ZONE AROUND AGGREGATE PARTICLES IN CONCRETE
J. A. Larbi 1993 72 p See also PB93-179240 Prepared in cooperation with Technische Univ., Delft, Netherlands
(PB93-195790) Avail: CASI HC A04/MF A01

The study is aimed at examining the microstructural characteristics of the interfacial region around aggregate particles in concrete and exploring the influence of this interfacial zone on some of the properties of concrete such as the compressive strength, the water transport capacity, and the diffusion of ions into concretes prepared with and without mineral additives.
NTIS

N94-19373# Technical Research Centre of Finland, Espoo. Structural Engineering Lab.
THE FIRE RESISTANCE OF PROFILED THIN STEEL SHEET STRUCTURES [OHUTLEVYRAKENTEIDEN PALONKESTO: RAKENTEIDEN ANALYSOINTI TIETOKONEELLA. OHJELMAT JA MENETELMAET]
Tapio Leino, Pekka Salmi, and Jukki Myllymaeki Jan. 1992 116 p In FINNISH
(VTT-TIED-1320; ISBN-951-38-4053-0; ETN-93-94469) Copyright Avail: CASI HC A06/MF A02

Research to compare different methods of calculating the fire resistance of thin profiled metal sheet structures and to find out about any possible computer programs developed for this purpose is presented. The fire-technical material properties of thin profiled metal sheets and some special fire-technical features concerning the structures made with the thin profiled metal sheets are presented. The loads and their combinations which should be considered in case of the fire are also explained. Some analysis results are presented to give an idea about the changes of stresses and the support reactions acting at the connections of the thin metal sheet structures in the fire situation. All the analysis results were compared (when possible) with the fire test results. Some analysis tools (computer programs) were developed for calculating the fire resistance of structures. The accuracy of the analysis results depend greatly on the available material property values used in the models. The analysis tools are utilized at the design phase of the structure (or new products) to minimize the number of fire tests needed.
ESA

N94-19423*# Alabama Univ., Huntsville. Materials Processing Lab.
MELT SPINNING STUDY Final Report
Gary L. Workman and Thomas Rathz 19 Apr. 1993 15 p
(Contract NAS8-38609)
(NASA-CR-193823; NAS 1.26:193823) Avail: CASI HC A03/MF A01

Containerless processing of materials provides an excellent opportunity to study nucleation phenomena and produce unique materials, primarily through the formation of metastable phases and deep undercoolings. Deep undercoolings can be readily achieved in falling drops of molten material. Extended solute solubilities and greatly refined microstructures can also be obtained in containerless processing experiments. The Drop Tube Facility at Marshall Space Flight Center has played an important role in enhancing that area of research. Previous experiments performed in the Drop Tube with refractory metals has shown very interesting microstructural changes associated with deep undercoolings. It is apparent also that the microstructure of the deep undercooled species may be changing due to the release of the latent heat of fusion during recalescence. For scientific purposes, it is important to be able to differentiate between the microstructures of the two types of metallic species. A review of the literature shows that although significant advances have been made with respect to the engineering aspects of rapid solidification phenomena, there is still much to be learned in terms of understanding the basic phenomena.

The two major ways in which rapid solidification processing provides improved structures and hence improved properties are: (1) production of refined structures such as fine dendrites and eutectics, and (2) production of new alloy compositions, microstructures, and phases through extended solid solubility, new phase reaction sequences, and the formation of metallic-glass microstructures. The objective of this work has been to determine the optimal methodology required to extract this excess energy without affecting the thermo-physical parameters of the under-cooled melt. In normal containerless processing experiments recalescence occurs as the melt returns toward the melting point in order to solidify. A new type of experiment is sought in which the resultant microstructure of the undercooled species is frozen in without going through the melting point regime and subsequent near equilibrium solidification of the remaining liquid. This experimental approach entails the design of an appropriate melt spinning system which is compatible with Drop Tube operations and processing constraints. That work is the goal of this study. Derived from text

N94-19480# Sandia National Labs., Albuquerque, NM.
MANUFACTURING TECHNOLOGY
J. A. Leonard, ed., H. L. Floyd, ed., B. Goetsch, ed., and L. Doran, ed. Aug. 1993 8 p
(Contract DE-AC04-76DP-00789)
(DE93-019580; SAND-93-1672) Avail: CASI HC A02/MF A01

This bulletin depicts current research on manufacturing technology at Sandia laboratories. An automated, adaptive process removes grit overspray from jet engine turbine blades. Advanced electronic ceramics are chemically prepared from solution for use in high-voltage varistors. A selective laser sintering process automates wax casting pattern fabrication. Numerical modeling improves the performance of a photoresist stripper (a simulation on a Cray supercomputer reveals the path of a uniform plasma). Improved mathematical models will help make the dream of low-cost ceramic composites come true. DOE

N94-19539# Lawrence Livermore National Lab., CA.
TEMPERATURE OF AIRCRAFT CARGO FLAME EXPOSURE DURING ACCIDENTS INVOLVING FUEL SPILLS
J. A. Mansfield Jan. 1993 299 p
(Contract W-7405-eng-48)
(DE93-019633; UCRL-CR-114509; DDV-93-0004) Avail: CASI HC A13/MF A03

This report describes an evaluation of flame exposure temperatures of weapons contained in alert (parked) bombers due to accidents that involve aircraft fuel fires. The evaluation includes two types of accident: collisions into an alert aircraft by an aircraft that is on landing or take-off; and engine start accidents. Both the B-1B and B-52 alert aircraft are included in the evaluation. DOE

N94-19540# Superconducting Super Collider Lab., Dallas, TX.
DESIGN VERIFICATION AND ACCEPTANCE TESTS OF THE ASST-A HELIUM REFRIGERATION SYSTEM
V. Ganni and T. V. V. R. Apparao Jul. 1993 12 p Presented at the International Cryogenic Engineering and Material Conference, Albuquerque, NM, 12-16 Jul. 1993
(Contract DE-AC35-89ER-40486)
(DE93-019746; SSCL-Preprint-488; CONF-930703-27) Avail: CASI HC A03/MF A01

Three similar helium refrigerator systems have been installed at the Superconducting Super Collider Laboratory (SSCL) N15 site: the ASST-A system, which will be used for the accelerator system's full cell string test; the N15-B system, which will be used for string testing in the tunnel; and a third plant, dedicated to magnet testing at the Magnet Testing Laboratory. The ASST-A and N15-B systems will ultimately be a part of the collider's N15 sector station equipment. Each of these three systems has many subsystems, but the design basis for the main refrigerator is the same. Each system has a guaranteed capacity of 2000 W of refrigeration and 20 g/s liquefaction at 4.5 K. The testing and design verification of the ASST-A refrigeration system consisted of parametric tests on the compressors and the total system. A summary of the initial performance test data is given in this paper. The tests were conducted for two cases: (1) all four compressors were operating; and (2) only one compressor in each stage was operating. In each case, tests were conducted in three modes of operation described later on. The process design basis supplied by the manufacturers and used in the design of the main components--the compressor and expanders and heat exchangers for the coldbox--were used to reduce the actual test data using process simulation methodology. In addition, the test results and the process design submitted by the manufacturer were analyzed using exergy analysis. This paper presents both the process and the exergy analyses of the manufacturer's design and the actual test data for Case 1. The process analyses are presented in the form of T-S diagrams. The results of the energy analyses comparing the exergy losses of each component and the total system for the manufacturer's design and the test data are presented. DOE

N94-19544# Lawrence Livermore National Lab., CA.
PRECISION MACHINING AND POLISHING OF SCINTILLATING CRYSTALS FOR LARGE CALORIMETERS AND HODOSCOPES
C. R. Wuest and B. A. Fuchs May 1993 6 p Presented at the 5th Annual International Industrial Symposium on the Super Collider and Exhibition, San Francisco, CA, 6-8 May 1993
(Contract W-7405-eng-48)
(DE93-018663; UCRL-JC-114014; CONF-930537-94) Avail: CASI HC A02/MF A01

New machining and polishing techniques have been developed for large barium fluoride scintillating crystals that provide crystalline surfaces without sub-surface damage or deformation as verified by Atomic Force Microscopy (AFM) and Rutherford Back-Scattering (RBS) analyses. Surface roughness of about 10-20 angstroms and sub-micron mechanical tolerances have been demonstrated on large crystal samples. Mass production techniques have also been developed for machining and polishing up to five 50 cm long crystals at one time. We present this technology along with surface studies of barium fluoride crystals polished with this technique. This technology is applicable for a number of new crystal detectors including the Barium Fluoride Electromagnetic Calorimeter at SSC, the Crystal Clear Collaboration's cerium fluoride calorimeter at LHC, and the KTeV and PHENIX scintillating hodoscopes at Fermilab and RHIC, respectively. Lawrence Livermore National Laboratory (LLNL) has an active program of study on barium fluoride scintillating crystals for the Barium Fluoride Electromagnetic Calorimeter Collaboration and cerium fluoride and lead fluoride for the Crystal Clear Collaboration. This program has resulted in a number of significant improvements in the mechanical processing, polishing, and coating of fluoride crystals. Techniques have been developed using diamond-loaded pitch lapping that can produce 15 A RMS surface finishes over large areas. Also, special polishing fixtures have been designed based on mounting technology developed for the 1.1 m diameter optics used in LLNL's Nova Laser. These fixtures allow as many as five 25-50 cm long crystals to be polished and lapped at the same time with tolerances satisfying the stringent requirements of crystal calorimeters. We also discuss results on coating barium fluoride with UV reflective layers of magnesium fluoride and aluminum. DOE

N94-19650# Technische Univ., Berlin (Germany). Fachbereich Physikalische Ingenieurwissenschaften.
MEASURING METHODS FOR EVALUATION OF DYNAMIC TYRE PROPERTIES Ph.D. Thesis [MESSTECHNISCHE METHODEN ZUR BEWERTUNG DYNAMISCHER REIFENEIGENSCHAFTEN]
Klaus Kmoch 1992 288 p In GERMAN
(ETN-93-95054) Avail: CASI HC A13/MF A03

Extensive measuring methods for macroscopic assessment of tire properties, based on classical mechanics and dynamics, are presented. Theoretical results and measurements were included in an expert system, where the pneumatic tire is represented as a wheel with particular elastic properties. For geometry measurement of the tire surface, a laser scanner test bed was used. The tire was excited with a shaker in order to obtain acceleration signals and for estimating global parameters such as stiffness, damping, and nonlinearity influence, which is found to increase with excitation force. Tire dynamic behavior was examined by low velocities with microscopy and infrared thermography, in order to quantify temperature augmentation and tangential and normal forces in the contact area; the slip stick oscillations were recorded on microphones. A drum test bed was used for studying tire behavior at high velocities and the tire vehicle interaction was established with acceleration measurements; nonuniformity influence on rolling stability was ascertained. The results were compared with data from theoretical models, which are pinpoint mass systems or multiple bodies problems. ESA

32 COMMUNICATIONS AND RADAR

Includes radar; land and global communications; communications theory; and optical communications.

For related information see also *04 Aircraft Communications and Navigation* and *17 Space Communications, Spacecraft Communications, Command and Tracking.* For search and rescue see *03 Air Transportation and Safety,* and *16 Space Transportation.*

N94-17695 Oak Ridge National Lab., TN.
ARC DETECTION AND PROTECTION IN HIGH-POWER ANTENNA SYSTEMS
J. B. O. Caughman and D. J. Hoffman 1993 5 p Presented at the 10th Topical Conference on Radio Frequency Power in Plasmas, Boston, MA, 1-3 Apr. 1993 Limited Reproducibility: More than 20% of this document may be affected by microfiche quality
(Contract DE-AC05-84OR-21400)
(DE93-013272; CONF-9304112-6) Avail: CASI HC A01

In an effort to establish a criteria for determining the presence of an arc in an antenna system, the change in the input reflection coefficient caused by an arc of arbitrary impedance and location has been calculated for two representative antenna systems. The antenna systems that have been studied are a resonant double loop antenna system (Tore Supra, TFTR) and a coupled four-strap antenna system (D3-D). The amount of power that is coupled into an arc as a function of the reflection coefficient and arc impedance has been calculated. Results of the calculation have shown that up to fifty percent of the forward power can be coupled to an arc, when the measured reflection coefficient is 0.5 and up to ten percent of the forward power can be coupled to an arc when the reflection coefficient is 0.1, depending on the impedance and location of the arc and the particular antenna system. The calculations have shown that changes in the magnitude of the reflection coefficient caused by an arc are often accompanied by changes in voltage ratios on the same current strap or between different straps and by changes in the phase angles of the voltages and/or the reflection coefficient. Recommendations for the use of voltage magnitude and phase detectors as a diagnostic for arc detection and protection are made. DOE

N94-17806# Sandia National Labs., Albuquerque, NM.
PVDF MEASUREMENT OF SOFT X RAY INDUCED SHOCK AND FILTER DEBRIS IMPULSE
D. E. Johnson (Ktech Corp., Albuquerque, NM.), L. M. Lee (Ktech Corp., Albuquerque, NM.), M. A. Hedemann, and F. Bauer (Institut Franco-Allemand de Recherches, Saint-Louis, France.) 1993 4 p Presented at the 14th International Conference of the International Association for the Advancement of High Pressure Science and Technology, Colorado Springs, CO, 27 Jun. - 2 Jul. 1993
(Contract DE-AC04-76DP-00789)
(DE93-017633; SAND-93-1539C; CONF-930676-4) Avail: CASI HC A01/MF A01

PVDF piezoelectric polymer shock stress sensors have been used to measure the shock and impulse generated by soft X-rays and by filter debris in the SATURN Plasma Radiation Source at Sandia National Laboratories, NM. SATURN was used to generate 30 to 40 kJ, 20-ns duration, line radiation at 2 to 3 keV. Fluence on samples was nominally 40, 200, and 400 kJ/m(sup 2) (1, 5, and 10 cal/cm(sup 2)). Measurements of X-ray induced material shock response exposing both aluminum and PMMA acrylic samples agree well with companion measurements made with single crystal X-cut quartz gauges. Time-of-flight, stress, and impulse produced by Kimfol (polycarbonate/aluminum) filter debris were also measured with the PVDF gauges. DOE

N94-17844 Defense Nuclear Agency, Washington, DC.
RADIO WAVE PROPAGATION IN STRUCTURED IONIZATION FOR SATELLITE AND RADAR APPLICATIONS
Leon A. Wittwer 1 Aug. 1993 83 p Limited Reproducibility: More than 20% of this document may be affected by microfiche quality
(AD-A268457; DNA-IR-93-35) Avail: Issuing Activity (Defense Technical Information Center (DTIC))

This report is an extension to DNA 5304D and DNA-IR-82-02 which presented the radio propagation algorithms recommended for use by DNA to calculate the properties of scintillated signals. This report covers effects related to antennas and extends the formalism to cover two component power spectra of plasma fluctuations. In addition, an improved representation of the total electron content power spectrum is included to support space radar and similar applications. Appendix E contains SUBROUTINE PROP which implements the radio propagation models. DTIC

N94-17861# Sandia National Labs., Albuquerque, NM.
FLIGHT DEMONSTRATION OF IMAGE FIX-TAKING WITH SAR
Richard Gibbs (Draper, Charles Stark Lab., Inc., Cambridge, MA.), Matthew Bottkol (Draper, Charles Stark Lab., Inc., Cambridge, MA.), and Todd Owen 11 Jun. 1993 6 p Presented at the 49th Inst. of Navigation Annual Meeting, Cambridge, MA, 21-23 Jun. 1993
(Contract DE-AC04-76DP-00789)
(DE93-016499; SAND-93-0779C; CONF-9306185-1) Avail: CASI HC A02/MF A01

Airborne synthetic aperture radar (SAR) uses coherent radar processing techniques to image ground reflectors. After processing, range and Doppler can be associated with any feature of interest in the final image. The location of any imaged feature can be estimated using a Kalman filter to combine these data with GPS and INS navigation data. This paper reports on the results of a flight demonstration of such a system, using an airborne SAR developed at Sandia. Collected data consisted of multiple SAR images containing surveyed reflectors, GPS/INS output taken aboard the aircraft, and GPS output recorded at surveyed ground stations. These data were post-processed at Sandia and at Draper Laboratory to obtain a navigation solution based on differential GPS and to demonstrate SAR fix-taking performance. This study successfully demonstrates accuracy of about one meter for fixing the position of a point imaged with SAR from an airborne platform. Because differential GPS was used, the navigation error was of about the same magnitude as the SAR range measurement error. Consequently, the measurements served primarily to fix the SAR image rather than to update the navigator. DOE

N94-17902# Department of the Navy, Washington, DC.
SUPPRESSION OF BACKSCATTER AND STRAY REFLECTION INDUCED PHASE NOISE IN MICHELSON INTERFEROMETERS Patent Application
Alan D. Kersey, inventor (to Navy), M. J. Marrone, inventor (to Navy), C. A. Villarruel, inventor (to Navy), Clay Kirkendall, inventor (to Navy), and Anthony Dandridge, inventor (to Navy) 30 Apr. 1993 28 p
(AD-D015809; US-Patent-Appl-SN-056019) Avail: CASI HC A03/MF A01

An optical system, including a reflectometric interferometer such as of the Michelson type, and method of reducing phase noise in such systems uses an uni-directional optical isolator in at least one of two optical links, such as optical fibers, to prevent propagation of backscattered radiation or radiation which may be backscattered in respective ones of the two optical links in order to limit the introduction of phase noise when the optical lengths and/or illumination coherence length is made long. The uni-directional isolation is preferably done with polarization independent isolators comprising a Faraday rotator between two prisms. If the uni-directional isolators are placed adjacent the interferometer, the length of optical leads or links to and from the interferometer can be increased up to several kilometers in length without any significant increase in phase noise over the noise levels present in the interferometer alone. DTIC

N94-17909# Lawrence Livermore National Lab., CA.
VARIABLE TIME-STEP INTEGRATION FOR INTENSE FIELD EFFECTS
C. Cerjan and R. Kosloff (Hebrew Univ., Jerusalem, Israel.) Oct. 1992 7 p Presented at the NATO Advanced Research Workshop on Time Dependent Quantum Molecular Dynamics; Experiments and Theory, Snowbird, UT, 30 Mar. - 3 Apr. 1992
(Contract W-7405-eng-48)
(DE93-013296; UCRL-JC-112157; CONF-9203238-3) Avail: CASI HC A02/MF A01

In many physically interesting problems with explicit time dependence, it is advantageous to directly solve the time-dependent Schroedinger equation. For example, the interaction of a particle with a time-dependent dissipative bath, such as a solid, would find its most natural interpretation with an explicit solution, compared to say a high order perturbative decomposition. Furthermore, the time-dependent formulation more closely resembles most experimental investigations which typically prepare an initial wavepacket with a specified temporal and spatial spread. Given the desirability of using a time-dependent formulation, the question of numerical efficiency will inevitably arise when detailed calculations are attempted. Strictly numerical attempts to solve the Schroedinger equation can be broadly classified as either time-independent or time-dependant methods. The former category typically expands the solution in an appropriate set of convenient basis functions and then solves the associated energy characteristic value problem. The difficult part of these calculations is usually the evaluation of potential matrix elements over the chosen basis set. The second category typically uses a spatial grid and an approximation to the temporal evolution operator to generate a pointwise solution to the Hamiltonian operator. This class of methods does not require potential matrix evaluations, but defers the difficulties to the representation of the Laplacian operator. It is not possible in general to simultaneously have diagonal matrix representations for both the kinetic and potential energy contributions to the Hamiltonian operator. Thus any numerical method must confront a more or less difficult calculational problem for either contribution. DOE

N94-17932 Politecnico di Milano (Italy). Dipt. di Elettronica e Informazione.

AUTOMATIC TUNING OF AN INTEGRAL FUZZY CONTROLLER

Riccardo Scattolini and Nicola Schiavoni 1993 18 p Sponsored in part by Ministry of University and Scientific Research and Technology, Italy, and CNR

(Rept-93-006; ETN-93-94513) Avail: Politecnico di Milano, Piazza Leonardo da Vinci 32, 20133 Milan, Italy

An empirical method for the automatic tuning of integral type fuzzy controller, where the regulator 'gain' is made to depend on the actual values of the error and the error variation, both appropriately normalized, is presented. The design technique is based upon the assumption that an approximate first order plus delay plant model, derived from the open loop step response, is available. The input membership functions as well as the values of the members of the output fuzzy set depend on the model characteristics. A number of simulation results are reported to witness the potentialities of the proposed approach. Some implementation considerations and comparisons with standard PI control are given. ESA

N94-17935 Politecnico di Milano (Italy). Dipt. di Elettronica e Informazione.

NEURAL NETWORKS TO CLASSIFY SPEAKER INDEPENDENT ISOLATED WORDS RECORDED IN RADIO CAR ENVIRONMENTS

C. Alippi (University Coll., London, England.), M. Simeoni, and V. Torri Feb. 1993 21 p

(Rept-93-013; ETN-93-94517) Avail: Politecnico di Milano, Piazza Leonardo da Vinci 32, 20133 Milan, Italy

Many applications, in particular the ones requiring nonlinear signal processing, have proved Artificial Neural Networks (ANN's) to be invaluable tools for model free estimation. The classifying abilities of ANN's are addressed by testing their performance in a speaker independent word recognition application. A real world case requiring implementation of compact integrated devices is taken into account: the classification of isolated words in radio car environment. A multispeaker database of isolated words was recorded in different environments. Data were first processed to determinate the boundaries of each word and then to extract speech features, the latter accomplished by using cepstral coefficient representation, log area ratios and filters bank techniques. Multilayered perceptron and adaptive vector quantization neural paradigms were tested to find a reasonable compromise between performances and network simplicity, fundamental requirement for the implementation of compact real time running neural devices. ESA

N94-17952 International Centre for Theoretical Physics, Trieste (Italy).

GAUGE UNIFICATION OF FUNDAMENTAL FORCES: THE STORY OF SUCCESS

R. B. Misra and S. M. W. Ahmad Jan. 1993 13 p Limited Reproducibility: More than 20% of this document may be affected by microfiche quality

(DE93-624813; IC-93/12) Avail: CASI HC A03 (US Sales Only)

Historical aspects concerning the gauge unification of fundamental forces are briefly reviewed. DOE

N94-17994# Lawrence Livermore National Lab., CA.

SECURING ELECTRONIC MAIL: THE RISKS AND FUTURE OF ELECTRONIC MAIL

S. A. Weeber Mar. 1993 16 p Presented at the 15th Computer Security Group Training Conference: Mission Possible - Connected and Protected, Albuquerque, NM, 3-6 May 1993

(Contract W-7405-eng-48)

(DE93-017187; UCRL-JC-113355; CONF-9305151-8) Avail: CASI HC A03/MF A01

The network explosion of the past decade has significantly affected how many of us conduct our day to day work. We increasingly rely on network services such as electronic mail, file transfer, and network newsgroups to collect and distribute information. Unfortunately, few of the network services in use today were designed with the security issues of large heterogeneous networks in mind. In particular, electronic mail, although heavily relied upon, is notoriously insecure. Messages can be forged, snooped, and even altered by users with only a moderate level of system proficiency. The level of trust that can be assigned at present to these services needs to be carefully considered. In the past few years, standards and tools have begun to appear addressing the security concerns of electronic mail. Principal among these are RFC's 1421, 1422, 1423, and 1424, which propose Internet standards in the areas of message encipherment, key management, and algorithms for privacy enhanced mail (PEM). Additionally, three PEM systems, offering varying levels of compliance with the PEM RFC's, have also recently emerged: PGP, RIPEM, and TIS/PEM. This paper addresses the motivations and requirements for more secure electronic mail, and evaluates the suitability of the currently available PEM systems. DOE

N94-18055# California Univ., Berkeley. Lawrence Berkeley Lab.

ADVANCES AND APPLICATIONS OF ABCI

Y. H. Chin May 1993 3 p Presented at the International Particle Accelerator Conference, Washington, DC, 17-20 May 1993

(Contract DE-AC03-76SF-00098)

(DE93-016971; LBL-33268; ESG-220; CONF-930511-222) Avail: CASI HC A01/MF A01

ABCI (Azimuthal Beam Cavity Interaction) is a computer program which solves the Maxwell equations directly in the time domain when a Gaussian beam goes through an axi-symmetrical structure on or off axis. Many new features have been implemented in the new version of ABCI (presently version 6.6), including the 'moving mesh' and Napoly's method of calculation of wake potentials. The mesh is now generated only for the part of the structure inside a window and moves together with the window frame. This moving mesh option reduces the number of mesh points considerably, and very fine meshes can be used. Napoly's integration method makes it possible to compute wake potentials in a structure such as a collimator, where parts of the cavity material are at smaller radii than that of the beam pipes, in such a way that the contribution from the beam pipes vanishes. For the monopole wake potential, ABCI can be applied even to structures with unequal beam pipe radii. Furthermore, the radial mesh size can be varied over the structure, permitting use a fine mesh only where actually needed. With these improvements, the program allows computation of wake fields for structures far too complicated for older codes. Plots of a cavity shape and wake potentials can be obtained in the form of a Top Drawer file. The program can also calculate and plot the impedance of a structure and/or the distribution of the deposited energy as a function of the frequency from Fourier transforms of wake potentials. Its usefulness is illustrated by showing some numerical examples. DOE

N94-18070 Physics and Electronics Lab. TNO, The Hague (Netherlands).

C-BAND PARC MANUAL Final Report

J. S. Groot May 1992 26 p

(FEL-92-B159; TD92-1443; ETN-93-94523) Copyright Avail: TNO Physics and Electronics Laboratory, P.O. Box 96864, 2509 JG The Hague, Netherlands

Measurement results of radar cross section, crosstalk level, etc., of a C band Polarimetric Active Radar Calibrator (PARC), which is used to calibrate air and spaceborne radars commonly used in remote sensing, are reported. The results are used to infer guidelines for the use of this PARC. The PARC consists of a high gain amplifier connected between two linearly polarized horn antennas. ESA

N94-18071# Deutsche Forschungsanstalt fuer Luft- und Raumfahrt, Oberpfaffenhofen (Germany). Abt. Hochfrequenzphysik.

THE ACCURACY OF MONOSTATIC AND BISTATIC RADAR IMAGING BY RANGE-DOPPLER-PROCESSING WITH AND WITHOUT MOTION COMPENSATION Ph.D. Thesis - Wuppertal Univ. [ZUR FOKUSSIERTEN ZWEIDIMENSIONALEN ABBILDUNG AUS MONOSTATISCHEN UND BISTATISCHEN RANGE-DOPPLER-MESSUNGEN MIT EINEM KOHAERENTEN KURZPULSRADAR MIT FEST EINSTELLBAREN RANGE-GATES IM ZENTIMETER-WELLENBEREICH]

Michael Kleintz Feb. 1993 208 p In GERMAN Original contains color illustrations

(DLR-FB-93-07; ETN-93-94876) Avail: CASI HC A10/MF A03

Two dimensional range Doppler imaging of flat rotating targets is discussed. The theory of imaging was extended to an arbitrary bistatic geometry by means of a linear transform of the far field focused range and doppler shift to the horizontal cartesian coordinates of the turntable. From the properties of the unfocused point spread function the algorithms of focusing in Doppler and were derived. The boundaries of validity of the point scatter model were shown by a simple example of wandering glint points. Simulations (mono and bistatic) as well as measurements (monostatic) in order to confirm theoretical results are shown. ESA

N94-18116# Helsinki Univ. of Technology, Espoo (Finland). Electromagnetics Lab.

WAVEGUIDE AND RESONATOR PERTURBATION TECHNIQUES FOR MEASURING CHIRALITY AND NON-RECIPROCITY OF BIISOTROPIC MATERIALS

S. A. Tretyakov and A. J. Viitanen Feb. 1993 13 p

(PB93-187243; ISBN-951-22-1411-3) Avail: CASI HC A03/MF A01

Waveguide and resonator measurement techniques for determining electromagnetic parameters of general biisotropic, or non-reciprocal chiral, materials are considered. The biisotropic materials are the most general linear isotropic media. The constitutive relations of these materials are governed by four complex material parameters. The perturbation techniques for measuring the materials through the change in the propagation constant of waveguide modes and the shift in resonance frequency for resonators are considered. To measure these parameters a method using waveguides or cavity resonators with two degenerated modes is proposed. NTIS

N94-18186# California Univ., Berkeley. Center for Pure and Applied Mathematics.

TOMOGRAPHIC MATHEMATICAL IDEAS APPLIED TO RADAR DETECTION Final Report, 1 Sep. 1989 - 31 Oct. 1992

F. A. Grunbaum 31 Oct. 1992 4 p

(Contract F49620-89-C-0107)

(AD-A268789; AFOSR-93-0624TR) Avail: CASI HC A01/MF A01

The researchers undertook an examination of many of the mathematical issues that are well understood in the case of the medical application of these tomographic ideas (i.e. x-ray scanners) but have not yet been explored in the arena of radar imaging. Among the issues concentrated on were the following: (1) an understanding of the way in which data might be collected in radar; (2) the proper interpretation of these data as projections of a two dimensional distribution in range-Doppler space; (3) a careful study of the effect that 'ellipsoidal integrals' or even simpler 'strip integrals' will have on an algorithm that is supposed to work with 'line integrals;' and (4) a study of the effect that an increase of 'lateral sampling per one dimensional projection' will have on the final reconstructions. This issue is well understood in the medical application and it serves to determine the number of detectors to be used, but has to be reexamined and reinterpreted in the radar context, a study of the competing methods to obtain range-Doppler images. These include Synthetic Aperture Radar and are based on the relative motion of the object vis-a-vis the radar. DTIC

N94-18187# Ohio State Univ., Columbus. Electroscience Lab.

WIDEBAND ELECTROMAGNETIC SCATTERING/ANALYSIS PROGRAM: FAR ZONE ELECTROMAGNETIC SCATTERING FROM COMPLEX SHAPES USING GEOMETRICAL THEORY OF DIFFRACTION Interim Report, 1 May 1991 - 31 Dec. 1992

N. Akhter and R. J. Marhefka Dec. 1992 193 p

(AF Proj. 7622)

(AD-A268790; Rept-724733-1; WL-TR-93-1030) Avail: CASI HC A09/MF A03

Backscatter and bistatic scattering in the far zone using the uniform theory of diffraction (UTD) from shapes which require second and higher order interactions to get an accurate solution over a wide range of angles is considered. One of the simplest of these shapes is the two-dimensional dihedral. The solution contains interactions of up to third order, which provide excellent results for the dihedrals of 60 deg or greater and for sizes larger than one wavelength in extent. The dihedral solution is modified for curvature and caustic corrections to get results for the top-hat, bruderhedral, and bi-cone. Another extension to the dihedral is the parallel plate cavity and the circular cavity. First and second order caustic corrections for the donut are included. Also, the result of the dihedral is modified to get results for the multi-joined cylinders made of PVC pipes filled with absorber. Analytical results are validated against method of moments or measurements. DTIC

N94-18210# Lawrence Livermore National Lab., CA.

RESPONSE OF TRANSMISSION LINE SYSTEMS TO PULSE EXCITATION BY RADIATION AND INJECTION METHODS

J. SooHoo and M. Bland Jul. 1992 6 p Presented at the 1993 HEART Conference, Orlando, FL, 1-5 Feb. 1993

(Contract W-7405-eng-48)

(DE93-015112; UCRL-JC-111481; CONF-9302120-2) Avail: CASI HC A02/MF A01

Calculated currents and voltages in a transmission line system induced by two different methods of pulse excitation are presented and compared. The two methods under consideration are the radiation and injection methods. Calculations indicate that, for a given set of transmission line parameters and a pulse waveform, these methods generally induce significantly different current and voltage distributions. It also suggests that in general the response of transmission line systems to pulse excitation is sensitive to the incident and polarization angles of the radiation, as well as to the point of injection on the line. While response of transmission line systems to monochromatic-wave excitation is fairly well understood, response to pulse excitation by either the radiation or the injection method had not been sufficiently analyzed and compared in the past. The purpose here is to present a comparison of the currents and voltages that the two methods of excitation would induce in a transmission line system. Mathematically, such a system can be characterized by a set of transmission line equations with source terms proportional to the source pulse of excitation. The currents and voltages then can be calculated by solving the system of equations numerically. In what follows we present calculations for two source pulses, one of which is about 5 nanoseconds in duration and the other about 250 nanoseconds. Both pulses are of the double-exponential form. These two particular pulses were so used in the calculations because they are good approximations to the type of electromagnetic pulses of current interest. DOE

N94-18216# Naval Command, Control and Ocean Surveillance Center, San Diego, CA.

INTENTIONALLY SHORT RANGE COMMUNICATIONS (ISRC) Final Report

J. Yen, P. Poirier, M. E. OBrien, and L. Gibeson May 1993 115 p

(AD-A268788; NRAD-TR-1600) Avail: CASI HC A06/MF A02

This document details the feasibility studies conducted for the Intentionally Short Range Communications (ISRC) project. The short-range limitation arises from the need for low probability of intercept (LPI), low probability of detection (LPD) communication links. The detection of an undecipherable transmission would still provide an enemy with information regarding transmitter location. The technologies being studied are ultraviolet (UV) lamps, UV lasers, infrared (IR) lasers, millimeter waves (MMW), and direct sequence spread spectrum. DTIC

N94-18228# Coast Guard Research and Development Center, Groton, CT.

AN/APS-137 FORWARD LOOKING AIRBORNE RADAR (FLAR) EVALUATION SPRING 1992 EXPERIMENT Interim Report, May 1991 - Jan. 1993

R. Q. Robe, K. OBrien, and D. L. Raunig Jan. 1993 65 p

(AD-A268899; CGR/DC-08/93) Avail: CASI HC A04/MF A01

During Apr. 1992, the U.S. Coast Guard R&D Center conducted an experiment to determine the sweep width for the AN/APS-137 Forward Looking Airborne Radar (FLAR) when searching for 4-, 6-, and 10-person life rafts. A total of 507 target detection opportunities were generated for life-raft targets. The experiment was conducted in the coastal waters off the west coast of Florida from Wacussa Bay to Gasparilla Island. Radar searches to collect data used unalerted sensor operators and standard search patterns. Aircraft and target positions were recorded using a Differential Global Positioning System (DGPS). Target detections were recorded by observers on board the aircraft, and environmental conditions were recorded by observers on the workboats. In addition, two MINIMET (TM) environmental buoys recorded the sea and wind conditions in the search area. Environmental conditions represented in the data set included 1.6 to 3.6 foot significant wave heights and 2.9 to 13.0 knot winds. DTIC

N94-18232# Sandia National Labs., Albuquerque, NM.
THE SPATIAL VARIANCE OF IONOSPHERICALLY-INDUCED PHASE ERRORS IN SAR IMAGERY
W. D. Brown and G. D. Cable 1993 9 p Presented at the 7th International Ionospheric Effects Symposium, Alexandria, VA, 4-6 May 1993
(Contract DE-AC04-76DP-00789)
(DE93-015643; SAND-93-0976C; CONF-9305217-1) Avail: CASI HC A02/MF A01

Images taken with a synthetic aperture radar (SAR) on an airplane were distorted with phase errors generated by a computer program that simulates the propagation of radar waves through the disturbed ionosphere. The simulation is for an orbiting SAR imaging a scene on the ground. Both the spatially-invariant (decorrelation length projected onto the ground much larger than the scene size) and spatially-variant (decorrelation length much smaller than the scene size) cases are described. The spatially-invariant phase errors can be removed using several different algorithms. Problems and strategies in restoring SAR images distorted with spatially-variant phase errors are discussed. DOE

N94-18260# Range Commanders Council, White Sands Missile Range, NM. Inter-Range Inst. Ation Group.
MISSILE ANTENNA PATTERN COORDINATE SYSTEM AND DATA FORMATS
Aug. 1993 49 p Supersedes ETMWG-253-65, AD-A637189
(AD-A269153; IRIG-STANDARD-253-93; ETMWG-253-65) Avail: CASI HC A03/MF A01

Antenna performance data pertains to missile, space, and aerodynamic vehicles' transmitting or receiving antennas used with range data collection, missile trajectory measurements, impact predictions, communications, or flight termination systems. As used in this document, the terms missile space vehicle, airborne, and aerodynamic vehicle are synonymous. This standard is intended to cover antennas for telemetry, pulsed radar beacons, continuous wave (CW) transponders, communication transmitters and receivers, command control/flight termination, receivers/decoders, pseudo random noise (PRN) ranging systems, and the Global Positioning System. DTIC

N94-18287# Aerospace Corp., El Segundo, CA.
BROADBAND RF SPECTRUM FROM ELECTROSTATIC DISCHARGES ON SPACECRAFT
Harry C. Koons and Thomas S. Chin 1 May 1993 12 p
(Contract F04701-88-C-0089)
(AD-A269543; TR-93(3940)-6; SMC-TR-93-47) Avail: CASI HC A03/MF A01

Electromagnetic interference from discharges on spacecraft subject to the charging environment near geosynchronous orbit may interfere with communication systems on the spacecraft. New measurements of the RF spectrum from the Kapton blanket from the backside of the MILSTAR spacecraft's flexible substrate solar array (FSSA) are compared with other space and laboratory data so that they will be more readily available for the analysis of spacecraft systems. The data may be used to estimate the effects of EMI from discharges on spacecraft systems operating in the frequency range from 100 kHz to 10 GHz. DTIC

N94-18288# Massachusetts Inst. of Tech., Cambridge. Plasma Fusion Center.
STUDIES OF ENHANCED RADAR BACKSCATTER Annual Report, 15 Jun. 1992 - 14 Jun. 1993
Min-Chang Lee 14 Jun. 1993 18 p
(Contract F49620-92-J-0297)
(AD-A269544; AFOSR-93-0690TR) Avail: CASI HC A03/MF A01

Since 1 October 1991, experimental and theoretical research has been conducted aimed at investigating ionospheric plasma disturbances which can significantly affect radio wave propagation from satellite communications systems. The efforts have developed a theory to explain reflectivity of radio waves from lightning induced plasmas. In addition, the research has focused on enhanced radar backscatter, source mechanisms for generating symmetric lower hybrid sidebands in the upper ionosphere, and the characteristics of the HF enhanced plasma lines. DTIC

N94-18291 Naval Research Lab., Washington, DC.
RADARC HF IONOSPHERIC PREDICTION PROGRAM FOR OTH RADAR Memorandum Report
D. L. Lucas, G. S. Prinson, J. M. Headrick, and J. F. Thomason 3 Sep. 1993 235 p Limited Reproducibility: More than 20% of this document may be affected by microfiche quality
(AD-A269557; NRL/MR/5309-93-7316) Avail: CASI HC A11

A model for predicting the performance of an over-the-horizon high frequency (HF) radar is described. The program can also be used for management of an existing radar or for HF broadcasting assessment. When the radar parameters, such as power, antenna, and frequency are given, the program predicts the signal-to-noise, ground clutter-to-noise, ionospheric spread Doppler clutter-to-noise, and received power as a function of range from the radar site. The report is intended to provide the reader with a general description of the prediction model and to show those mathematics and procedures which are upgraded from NRL Report 2226. The procedures should provide the OTH radar engineers with information to execute the program for studies or evaluation of existing or planned radars. DTIC

N94-18301# Aerospace Corp., El Segundo, CA. Engineering and Technology Group.
A RFI MEASUREMENT SYSTEM FOR FIELD SITES
R. B. Dybdal, G. M. Shaw, and T. T. Mori 1 Sep. 1993 35 p
(Contract F04701-88-C-0089)
(AD-A269340; TR-92(2930)-5; SMC-TR-93-46) Avail: CASI HC A03/MF A01

A compact system has been developed for performing RFI measurements at remote sites. This system covers a 0.5- to 18-GHz frequency range. The system's sensitivity meets or exceeds the sensitivity of a ground terminal when the interfering signals arrive through its wide-angle sidelobes. This sensitivity is achieved with a commercial spectrum analyzer and a specially designed preamplifier system. In addition, a combination of passive bandpass filtering and tuned band-reject filtering preserves the system's linearity when operating, in the presence of strong signals. Example measurements illustrate the operation of this RFI measurement system. DTIC

N94-18404# Vermont Univ., Burlington. Dept. of Mathematics and Statistics.
THE ASYMPTOTIC THEORY OF THE REFLECTION AND TRANSMISSION OF A PULSED ELECTROMAGNETIC BEAM FIELD AT A PLANAR INTERFACE SEPARATING TWO DISPERSIVE MEDIA Final Report, 1 Apr. 1992 - 31 Mar. 1993
Kurt Oughston 21 Mar. 1993 3 p
(Contract F49620-92-J-0206)
(AD-A269033; AFOSR-93-0623TR) Avail: CASI HC A01/MF A01

The long term research goal is to develop a rigorous analytic formulation and, based upon this, a uniform asymptotic description of pulsed electromagnetic beam-field propagation, reflection, and transmission phenomena in causally dispersive dielectric and conducting media. Emphasis has been placed first on a formulation that is rigorously derived from the macroscopic Maxwell's equations with constitutive relations that are appropriate for a homogeneous, isotropic, nonhysteretic, locally linear, and temporally dispersive medium, followed by the development and application of the required uniform asymptotic expansion techniques necessary to yield a completely continuous description of the space-time evolution of the pulsed beam-field at large propagation distances from the input plane. DTIC

N94-18449 Naval Postgraduate School, Monterey, CA.
SPECIFICATION AND ANALYSIS OF A HIGH SPEED TRANSPORT PROTOCOL M.S. Thesis
Huseyin A. Tipici Jun. 1993 95 p Limited Reproducibility: More than 20% of this document may be affected by microfiche quality
(AD-A268941) Avail: CASI HC A05

While networks have been getting faster, perceived throughput at the application has not always increased accordingly and the bottleneck has moved to the communications processing part of the system. The issues that cause the performance bottlenecks in the current transport protocols are discussed in this thesis, and a further study on a high speed transport protocol which tries to overcome these difficulties with some unique features is presented. By using the Systems of Communicating Machines (SCM) model as a framework, a refined and improved version of the formal protocol specification is built over the previous work, and it is analyzed to verify that the protocol is free from logical errors such as deadlock, unspecified reception, unexecuted transitions and blocking loops. The analysis is conducted in two phases which consists of the application of the associated system state analysis and the simulation of the protocol using the programming language ADA. The thesis also presents the difficulties encountered during the course of the analysis, and suggests possible solutions to some of the problems. DTIC

N94-18454 Army Research Lab., White Sands Missle Range, NM.
DISPERSION EFFECTS ON MILLIMETER WAVELENGTH ATTENUATION EFFICIENCIES FOR A VARIETY OF FIBERS Final Report
C. W. Bruce, A. V. Jelinek, E. Crosby, R. Haloren, and J. Hale Aug. 1993 23 p Limited Reproducibility: More than 20% of this document may be affected by microfiche quality
(AD-A268992; ARL-TR-58) Avail: CASI HC A03

Results of several field experiments have been used to determine extinction efficiencies primarily of graphitic fibers and to relate these efficiencies to length distributions. Of the three dispersion techniques employed, two were driven by constant air pressure and the third dispersed fibers by explosive force. Generally, the latter significantly altered the distribution. When a significant proportion of the fibers was fragmented to lengths shorter than a half wavelength, the efficiency decreased notably. Extinction efficiencies for almost all the explosively dispersed clouds were in this category. For frequencies of 35 GHz and lower, efficiencies for explosive dissemination typically were reduced by factors of 2 to 4. Efficiencies at 94 GHz were much less affected because the ratio of particle length to wavelength remained, on the average, higher than one-half. In contrast, length distributions for fibers cut from spools and immediately disseminated by constant air flow almost always sharply peaked near the cut length and had efficiencies near to that calculated for the cut length. Calculations and measurements are in agreement on this issue. DTIC

N94-18469# Kent State Univ., OH. Dept. of Physics.
THEORY OF ELECTROMAGNETIC WAVES PROPAGATING IN NONLINEAR ANISOTROPIC OPTICAL MATERIALS Final Technical Report, 15 Mar. 1991 - 30 Jun. 1993
David S. Moroi 30 Jun. 1993 60 p
(Grant AF-AFOSR-0202-91)
(AD-A269305; AFOSR-93-0678TR) Avail: CASI HC A04/MF A01

Method of multiple scales is used to calculate the electromagnetic fields for first and second harmonics, in first two orders of small parameter expansion, which satisfy the nonlinear coupled wave equations in a chi(2) medium. The results contain no secular terms nor ill-behaved terms. The fields obtained in lowest order calculations are the same as those in slowly varying amplitude approximation. The secular terms and ill-behaved terms resulted in the previous calculations are carefully removed in consistent with this method. We have shown that the first order correction to the electromagnetic field in each harmonic in slowly varying amplitude approximation is down by a factor of 10(exp -5) compared with the leading term. In other words, slowly varying amplitude approximation itself is proven to be a very good approximation. We have estimated the angular deviation of light propagation direction from a straight line in a chi(2) medium which is roughly in a range of 0.2 - 0.6 for an incident laser of intensity 6kW/sq cm. We have obtained the exact coupled differential equations for the amplitudes of the lth confined TE and TM modes for both first and second harmonics in a nonlinear slab waveguide. They become slightly simplified in slowly varying amplitude approximation but still too complicated to be tractable. For a special case of a nonlinear slab waveguide made of material with bar-42m crystalline symmetry, these equations are further simplified. For the case of perfect phase matching or very small phase mismatch and of other specific conditions being met, the equations are reduced to the well-known coupled differential equations which have the solutions given by Jacobian elliptic functions. DTIC

N94-18473 IIT Research Inst., Chicago, IL.
COMPILATION OF 1992 ANNUAL REPORTS OF THE NAVY ELF COMMUNICATIONS SYSTEM ECOLOGICAL MONITORING PROGRAM, VOLUME 1 Annual Report, Jan. - Dec. 1992
J. E. Zapotosky Aug. 1993 428 p Limited Reproducibility: More than 20% of this document may be affected by microfiche quality
(Contract N00039-93-C-0001)
(AD-A269569; IITRI-D06205-2-Vol-1) Avail: CASI HC A19

During 1992, the U.S. Navy continued to conduct a program to monitor flora, fauna, and their ecological relationships for possible effects from electromagnetic (EM) fields produced by the Navy's Extremely Low Frequency (ELF) Communications System. Physiological, developmental, behavioral, and ecological variables for dominant biota in upland and riverine habitats near the Naval Radio Transmitting Facility at Republic, Michigan (NRTF-Republic) have been monitored since 1982. The NRTF-Republic was intermittently energized at low amperages beginning in early 1986. Electric current and periods of energization were then gradually increased until 1989, when the transmitter became a fully operational facility. A split-plot or blocked strategy was used to examine biological variables for possible effects from EM exposure. Reports compiled in this document present the progress of these studies through 1992. It is anticipated that data will continue to be collected through 1993. Final results and conclusions are expected after all data have been analyzed in 1994. Investigators for similar studies completed in Wisconsin concluded that there were no EM bioeffects from intermittent or full operation of the transmitter in that state. DTIC

N94-18495# Mitre Corp., Bedford, MA.
VHF AIR/GROUND COMMUNICATIONS FOR AIR TRAFFIC CONTROL: A DECISION TREE APPROACH TO SYSTEM INNOVATIONS, VOLUME 2
Cheng-Hong Chen, James W. Howland, Robert I. Millar, Brian E. White, and Warren J. Wilson Jul. 1993 275 p
(Contract DTFA01-93-C-0001)
(AD-A268632; MTR-M-93B0000096-Vol-2) Avail: CASI HC A12/MF A03

Improvements to VHF air/ground communications for civil aviation in the 188-137 MHz aeronautical mobile frequency band are systematically explored by means of a decision tree approach. Seven individual papers analyze in detail the operational anitechnical factors involved in making these improvements. Basic tradeoffs between analog and digital modulation are discussed to frame the problem. Near-term improvements utilizing various analog modulations with closer channel spacing are first reviewed. Then far-term improvements employing a wide range of digital modulation and coding techniques are considered. Multiplexing methods - frequency, time, and code division - are discussed in detail. Methods for random access to a shared communications channel are compared, with emphasis upon real-time operation for air traffic control. Volume 1 provides an executive summary of this work, while Volume 2 presents the technical details. DTIC

N94-18503# Brookhaven National Lab., Upton, NY.
SIMULATION OF EMITTANCE DILUTION IN ELECTRON STORAGE RING FROM COMPTON BACKSCATTERING
L. N. Blumberg and E. Blum 1993 3 p Presented at the International Particle Accelerator Conference, Washington, DC, 17-20 May 1993
(Contract DE-AC02-76CH-00016)
(DE93-017611; BNL-49166; CONF-930511-302) Avail: CASI HC A01/MF A01

A Monte-Carlo simulation of Compton backscattered kappa(sub L) = 3.2-micron photons from an IR-FEL on 75-MeV electrons in a storage ring yields an RMS electron energy spread of delta(sub E) = 11.9-keV for a sample of 10(exp 7) single scattering events. Electrons are sampled from a beam of natural energy spread sigma(sub E) = 5.6-keV and damped transverse angle spreads sigma(sub x)(prime) = .041-mrad and sigma(sub y)(prime) = .052-mrad (100%) coupling, scaled from the 200-MeV BNL

XLS compact storage ring. The Compton-scattered x-rays are generated from an integral of the CM Klein-Nishina cross-section transformed to the lab. A tracking calculation has also been performed in 6-dimensional phase space. Initial electron coordinates are selected randomly from a Gaussian distribution of RMS spreads sigma(sub xo) = .102-mm, sigma(sub x(prime)o) = .041-mrad, sigma(sub yo) = .018-mm, sigma(sub y(prime)o) = .052-mrad, sigma(sub (phi)o) = 22-mrad and sigma(sub Eo) = 6-keV. A sample of 10000 electrons were each following for 40000 turns around the ring through an RF cavity of f(sub RF) = 211.54-MHz and peak voltage V(sub m)=300-keV. Preliminary results indicate that the resulting energy distribution is quite broad with an RMS width of delta(sub E) = 124-keV. The transverse widths are only slightly increased from their original values, i.e. delta(sub x) = .106-mm and delta(sub x)(prime) = .043 mrad. The scaled energy spread of delta(sub E) approximately = 360-keV for approximately 350,000 turns desired in a 10-msec x-ray angiography exposure is well within the RF bucket used here; even V(sub m) less than 50-kV is adequate. Further, the electron energy spread adds a negligible RMS x-ray energy spread of delta(sub Ex) = .32-keV. The electron energy damping time of tau(sub E) = 379-msec at 75-MeV in an XLS-type ring allows for damping this induced spread and top-off of the ring between heart cycles. DOE

N94-18510# Schwartz Electro-Optics, Inc., Orlando, FL.
LASER IMAGING RADAR SYSTEM Final Report, Aug. 1989 - Apr. 1993
Steven P. Yun and Robert A. Olson Sep. 1993 63 p
(Contract F08635-90-C-0050)
(AD-A270436; WL-TR-93-7032) Avail: CASI HC A04/MF A01

The simplicity, compactness, and reasonable cost of direct detection diode-laser range finders provide incentive for their use in laser imaging radar systems (LIRS). Efforts have been made to increase range performance of a diode-laser range finder by means of narrow bandwidth operation. This involved narrowing the line width of the diode laser via a narrow bandwidth filter in an external cavity so that it was compatible with a 5 A receiver filter. The narrow bandwidth of the receiver filter limited the amount of solar background radiation incident upon the receiver, thereby increasing the signal-to-noise ratio and thus maximizing the range capability. The study comprised the development and testing of a line-narrowed single-element diode-laser range finder, an analysis of multi-element diode-laser ranger finder, an analysis of multi-element diode-laser geometries, and an experimental evaluation of diode-laser collimation by means of a cylindrical microlens. DTIC

N94-18512# Army Communications-Electronics Command, Fort Monmouth, NJ.
ELECTROMAGNETIC ENVIRONMENTAL EFFECTS COMPENDIUM
Kenneth H. Brockel, David Cofield, William DeAllaume, Lanny Gorr, and Paul A. Major Aug. 1993 107 p
(AD-A270441; CECOM-TR-93-5) Avail: CASI HC A06/MF A02

This report summarizes the electromagnetic environmental effects (E3) program of the U.S. Army Communications-Electronics Command (CECOM). The report includes background information on CECOM's role in the Army E3 program, presents the approach used to identify the electromagnetic environment, summarizes E3 criteria (i.e., the CECOM model electromagnetic environment), and provides a sample E3 assessment. The report also discusses electromagnetic trends and their implications. DTIC

N94-18513 Air Force Inst. of Tech., Wright-Patterson AFB, OH.
APPLICATION OF FOURIER-BASED FEATURES FOR CLASSIFICATION OF SYNTHETIC APERTURE RADAR IMAGERY M.S. Thesis
David G. Ehrhard 14 Sep. 1992 95 p Limited Reproducibility: More than 20% of this document may be affected by microfiche quality
(AD-A270450; AFIT/CI/CIA-93-108) Avail: CASI HC A05

A method for segmenting synthetic aperture radar (SAR) images has been developed to operate primarily in the frequency domain. It is based on and was tested against a similar method which involves isolating information of the frequency-domain image that defines unique textural features within a class. The comparison involved classifying four simple vegetation SAR scenes with both segmentation methods. A statistical test was then performed against the null hypothesis that the new textural segmentation method is as accurate or more accurate than the original method based on random pixel classification results. All tests concluded that the texture extraction methods are not statistically different. Both methods were implemented on a mainframe computer and are computationally intensive, but the new method may be implemented optically more easily. DTIC

N94-18525# Lowell Univ., MA. Center for Atmospheric Research.
MODELING A YAGI ARRAY ANTENNA FOR VHF RADAR USE
Jens C. Ostergaard 14 Jul. 1993 20 p
(Contract F19628-90-K-0039)
(AD-A268973; PL-TR-93-2152; SR-5) Avail: CASI HC A03/MF A01

This report details the results of modeling of an array of 4 Yagi antennas used with a 49.92 MHz radar. Each of the Yagi antennas has 6 elements and is optimized for narrow bandwidth and high gain. The model includes free space patterns and boresight patterns over uneven terrain. DTIC

N94-18601# Wright Lab., Eglin AFB, FL.
MILLIMETER WAVE REFLECTIVITY MEASUREMENT SYSTEM Final Report, Oct. 1991 - Jan. 1993
Keith D. Trott and John R. Walker, Jr. Sep. 1993 22 p
(AF Proj. 2068)
(AD-A270008; WL-TR-93-7027) Avail: CASI HC A03/MF A01

The RF Technology Section of WL/MNGS is developing an in-house capability for modeling and measurement of target scattering and material characteristics at millimeter wave (MMW) frequencies. The goal of the modeling effort is to understand the basic mechanisms that contribute to the target scattering (coated and uncoated) at MMW frequencies. The measurement effort is two-fold: verify theoretical models (target and materials); and assess the effectiveness of actualcountermeasures. The MMW Reflectivity Measurement System (MRMS) is capable of bistatic swept frequency measurements for copolarized (COPOL) transmit and receive signals, and it gives a quick-look capability useful in evaluating countermeasures. The primary goal is the understanding of the various mechanisms that contribute to the scattering in order to develop the algorithms and technology necessary to exploit these effects and improve seeker guidance techniques. This paper discusses the current hardware configuration and planned upgrades and outlines the modeling effort. Examples of the MRMS measurements are compared to theoretical predictions. DTIC

N94-18666# Rome Lab., Hanscom AFB, MA.
STATISTICAL DESCRIPTION OF THE BISTATIC RADAR CROSS SECTION DISTRIBUTIONS FOR A RIGHT CIRCULAR CYLINDER Report, Jan. 1991 - Apr. 1992
Richard L. Wittschen Jun. 1993 47 p
(AF Proj. 4600)
(AD-A270001; RL-TR-92-159) Avail: CASI HC A03/MF A01

Detection probabilities for monostatic and bistatic radars are compared by computer simulation. The computer generated radar cross section (RCS) of a long thin cylinder is utilized in the computation of detection probabilities for both the monostatic and bistatic configurations. The statistics of the RCS distributions are used to determine the best characterizing function for the cylinder data. It is shown that the beta distribution provides the most accurate description of the cylinder RCS for both configurations. The beta distribution is used as the fluctuation model for the RCS of the cylinder and in the determination of the probability of detection. Comparison of detection probabilities shows that the detection probabilities for large angle bistatic cases are greater than for the monostatic case. DTIC

N94-18721 Delta Information Systems, Inc., Horsham, PA.
COLOR TEST CHART FOR FACSIMILE Final Report
Aug. 1992 22 p Limited Reproducibility: More than 20% of this document may be affected by microfiche quality
(Contract DCA100-91-C-0031)
(AD-A269754; NCS-TIB-92-10) Avail: CASI HC A03

The CCITT has standardized Group 4 facsimile, and has reached agreement on adding higher resolutions to 400 pels per inch to Group 3 facsimile. In order to measure and verify the quality of transmission for Group 4 apparatus and the advanced resolution Group 3 apparatus, it is necessary to have a standard test chart. The purpose of this project was to complete and obtain reproducible masters and evaluation prints of the printed color chart, and to define the layout and content of the photographically reproduced chart. This report is comprised of four sections. Section 1 provides a brief description of the objective of the study and an outline of the contents of this report. Section 2 discusses the steps taken to produce the final version of the color chart. Section 3 contains the description of the color chart and a guide to its use. Section 4 is a summary of the work performed. DTIC

N94-18722 Naval Research Lab., Washington, DC.
MORPHOLOGY AND CHARACTERISTICS OF DISTURBED HF SKYWAVE CHANNELS Interim Report
Leonard S. Wagner 3 Sep. 1993 15 p Limited Reproducibility: More than 20% of this document may be affected by microfiche quality
(AD-A269755; NRL/MR/5554-93-7389) Avail: CASI HC A03

The normal HF skywave channel is one in which propagation via ionospheric reflection predominates. A disturbed HF skywave channel is defined to be one in which ionospheric scatter plays a significant, often dominant, role in point-to-point radiowave propagation. From a communications perspective, a disturbed channel is one which exhibits reduced signal level in combination with the extensive delay and Doppler spread. Channels which are regularly disturbed include the trans-equatorial, trans-polar and trans-auroral channels. This report covers a number of topics including: (1) measurements that have contributed to our knowledge about the structure and behavior of disturbed channels, (2) solar-terrestrial control factors (e.g., diurnal, seasonal, solar cycle, and geomagnetic), (3) irregularity source regions and current theories of irregularity generation processes, and (4) sample data, available from channel probes, for each of the disturbed channels. DTIC

N94-18741# IIT Research Inst., Chicago, IL.
COMPILATION OF 1992 ANNUAL REPORTS OF THE NAVY ELF COMMUNICATIONS SYSTEM ECOLOGICAL MONITORING PROGRAM. VOLUME 3: TABS G - I Annual Report, Jan. - Dec. 1992
J. E. Zapotosky Aug. 1993 440 p
(Contract N00039-93-C-0001)
(AD-A269727; IITRI-TR-D06205-2-Vol-3) Avail: CASI HC A19/MF A04

During 1992, the U.S. Navy continued to conduct a program to monitor flora, fauna, and their ecological relationships for possible effects from electromagnetic (EM) fields produced by the Navy's Extremely Low Frequency (ELF) Communications System. Physiological, developmental, behavioral, and ecological variables for dominant biota in upland and riverine habitats near the Naval Radio Transmitting Facility at Republic, Michigan (NRTF-Republic) have been monitored since 1982. The NRTF-Republic was intermittently energized at low amperages beginning in early 1986. Electric current and periods of energization were then gradually increased until 1989, when the transmitter became a fully operational facility. A split-plot or blocked strategy was used to examine biological variables for possible effects from EM exposure. Reports compiled in this document present the progress of these studies through 1992. It is anticipated that data will continue to be collected through 1993. Final results and conclusions are expected after all data have been analyzed in 1994. Investigators for similar studies completed in Wisconsin concluded that there were no EM bioeffects from intermittent or full operation of the transmitter in that state. DTIC

N94-18751 IIT Research Inst., Chicago, IL.
COMPILATION OF 1992 ANNUAL REPORTS OF THE NAVY ELF COMMUNICATIONS SYSTEM ECOLOGICAL MONITORING PROGRAM, VOLUME 2 Annual Report, Jan. - Dec. 1992
J. E. Zapotosky Aug. 1993 440 p Limited Reproducibility: More than 20% of this document may be affected by microfiche quality
(Contract N00039-93-C-0001)
(AD-A269726; IITRI-TR-D06205-2-Vol-2) Avail: CASI HC A19

During 1992, the U.S. Navy continued to conduct a program to monitor flora, fauna, and their ecological relationships for possible effects from electromagnetic (EM) fields produced by the Navy's Extremely Low Frequency (ELF) Communications System. Physiological, developmental, behavioral, and ecological variables for dominant biota in upland and riverine habitats near the Naval Radio Transmitting Facility at Republic, Michigan (NRTF-Republic) have been monitored since 1982. The NRTF-Republic was intermittently energized at low amperages beginning in early 1986. Electric current and periods of energization were then gradually increased until 1989, when the transmitter became a fully operational facility. A split-plot or blocked strategy was used to examine biological variables for possible effects from EM exposure. Reports compiled in this document present the progress of these studies through 1992. It is anticipated that data will continue to be collected through 1993. Final results and conclusions are expected after all data have been analyzed in 1994. Investigators for similar studies completed in Wisconsin concluded that there were no EM bioeffects from intermittent or full operation of the transmitter in that state. DTIC

N94-18769 Army Construction Engineering Research Lab., Champaign, IL.
EFFECTS OF HARMONICS ON EMI/RFI FILTERS OPERATING UNDER NONLINEAR LOADING CONDITIONS Final Report
Steve J. Briggs, Michael S. Kim, and Franklin H. Holcomb May 1993 41 p Limited Reproducibility: More than 20% of this document may be affected by microfiche quality
(AD-A269559; CERL-TR-FE-93/22) Avail: CASI HC A03

Electromagnetic interference/radio frequency interference (EMI/RFI) power-line filters are widely used in the Army for filtering unwanted signals on power lines serving sensitive equipment, particularly computers and communication gear. Typically, these loads are highly nonlinear and cause severe harmonic loading on the filters. Harmonics cause filter failure and shortened filter lifetimes. The objective of this research was to quantify the effects of harmonics and nonlinear loads on EMI/RFI filters and to recommend a derating factor for EMI/RFI filters in nonlinear load applications. EMI/RFI filters were purchased and placed in an experimental apparatus with a known source of harmonics. The filters were instrumented and temperature data was recorded. A mathematical model of the filters was developed and simulations were performed to predict filter failure. The results of the research indicate that filter ampacity should be derated by 50 percent for filters that are being specified for nonlinear loading applications. DTIC

N94-18777# Army Engineer Waterways Experiment Station, Vicksburg, MS. Environmental Lab.
ENVIRONMENTAL CHARACTERIZATION FOR TARGET ACQUISITION. REPORT 3: NEW CONCEPTS FOR EVALUATING LOW-GRAZING ANGLE RADAR MEASUREMENTS
John O. Curtis and Bruce M. Sabol Jun. 1993 249 p
(AD-A269956; WES/TR/EL-93-9) Avail: CASI HC A11/MF A03

In an attempt to develop a scene characterization methodology for long-range (2 to 7 km), low-grazing angle (less than 10 deg or .17 radians) active millimeter wave radar systems, a two-fold approach is taken. First, slant range versus azimuth maps of radar backscatter measurements are filtered to collect statistics on the occurrence of target-like features and to relate those signatures to natural terrain conditions. Second, a prediction of radar return from the terrain is modeled by a point light source at the radar location and the assumption of Lambertian scattering from the terrain facets. Model predictions are combined with overlays of vegetation at each test site and compared qualitatively with the measured data to assess the impact of terrain conditions on backscatter response. These approaches are applied to a set of test site K(a)-band radar measurements made at Fort Hunter Liggett during the winter of 1988. DTIC

N94-18782 Kings Coll., London (England). Dept. of Physics.
NUMERICAL MODELLING OF FRINGING FIELDS AND THEIR USE FOR COMPLEX PERMITTIVITY MEASUREMENTS AT HIGH FREQUENCIES Final Report, Feb. 1992 - Jan. 1993
Camelia Gabriel Mar. 1993 28 p Limited Reproducibility: More than 20% of this document may be affected by microfiche quality
(Grant AF-AFOSR-0122-91)
(AD-A270198; AFOSR-93-0706TR) Avail: CASI HC A03

A technique was developed to measure the complex permittivity of materials using an open-ended coaxial probe in contact with a semi-infinite sample. It is based on a rigorous theoretical formulation of the admittance of the probe and was tested by measurements on standard solutions at frequencies of up to 20 GHz. The technique was further used to perform measurements on aqueous ionic solutions. The data were analyzed and used to develop models to predict the dielectric parameters of NaCl and KCl solutions at a given temperature as a function of concentration with the concentration range extending from pure water to saturated salt solutions. The theoretical study and techniques were adapted to the measurement of thin samples in contact with the probe provided they are backed by a metallic plane. The success and range of applicability of the thin sample technique was tested with measurements on standard solutions. Expressions were derived for the electric field in the medium terminating the probe. These expressions were used to determine the pattern of power deposition in the medium terminating the probe. Examples are given to illustrate this statement. DTIC

N94-18801 Mitre Corp., Bedford, MA.
INTRODUCTION TO WAVELETS
Pankaj N. Topiwala and David Colella Jul. 1993 100 p Limited Reproducibility: More than 20% of this document may be affected by microfiche quality
(AD-A268465; M93B0000076) Avail: CASI HC A05

This half-day course on wavelets is intended to be a general introduction to this exciting new topic in signal processing. Wavelets have been proven effective for a number of signal processing tasks, including compression and edge and transient detection. The computational complexity of a wavelet decomposition is O(N), versus O(N log N) for the FFT, making it very competitive. In addition, it has several specific advantages over the FFT in many applications. Two of these applications will be discussed in this course: transient detection and image compression. Wavelets have been applied for a wide variety of tasks, and MITRE has been involved in wavelet research for a number of years, leading to over thirty publications. This course was developed in conjunction with W090 and W096 staff (who ran a successful 3-day wavelet course in Washington), and taught in Bedford by P. Topiwala. This introductory course will be followed by a second course covering the wavelet research and applications currently being developed at MITRE. DTIC

N94-18811 Massachusetts Inst. of Tech., Cambridge. Research Lab. of Electronics.
NUMERICAL AND SYMBOLIC SIGNAL REPRESENTATION AND PROCESSING Final Report, 1 Apr. 1989 - 30 Sep. 1993
Alan V. Oppenheim 30 Sep. 1993 11 p Limited Reproducibility: More than 20% of this document may be affected by microfiche quality
(Contract N00014-89-J-1489)
(AD-A270271) Avail: Issuing Activity (Defense Technical Information Center (DTIC))

This is the final report summarizing the efforts performed under the grant Numerical and Symbolic Signal Representation and Processing. The format of the report is a comprehensive list of theses, conference presentations, journal articles, and patent disclosures that have been supported either in full or in part by the grant. Copies of the full texts have been sent to the program manager as they were written. DTIC

N94-18897# Toledo Univ., OH. Dept. of Electrical Engineering.
A PARALLEL AND PIPELINED ARCHITECTURE FOR ESTIMATION OF DIRECTION OF ARRIVAL USING A BILINEAR TRANSFORMATION METHOD, VOLUME 3 Final Report
M. M. Jamali, S. C. Kwatra, and Ravindranath Suria Aug. 1993 161 p
(Contract N00014-91-J-1011)
(AD-A270137; DSPH-3-Vol-3) Avail: CASI HC A08/MF A02

High resolution direction-of-arrival (DOA) estimation is important in many sensor systems. It is based on the processing of the received signal and extracting the desired parameters of the DOA of plane waves. The estimation of angle of arrivals of multiple broadband sources has been carried out in a variety of ways over the past few years. In this research an algorithm for broadband DOA estimation using a simple bilinear transformation matrix is investigated and a parallel and pipelined architecture is developed. When compared to other coherent approaches, this algorithm has the advantages of being non-iterative and does not require any initial estimates of the angles of arrival and all angles are computed from a single step of coherent subspace calculations. Hence it is a very suitable algorithm for computation of DOA using dedicated hardware. The advances in the area of Very Large Scale Integration (VLSI) have made it possible to design special purpose hardware which has the advantage of very high speed and overall lower system cost when compared to a system which runs off a general purpose computer. DTIC

N94-18950# Research Inst. of National Defence, Linkoeping (Sweden).
SOLUTION OF THE POISSON EQUATION WITH APPLICATION TO RADAR IMAGING
L. E. Andersson, T. Elfving, and R. Karlsson Nov. 1992 35 p See also PB93-168094
(PB93-195865; FOA-C-30683-3.3) Avail: CASI HC A03/MF A01

In a radar imaging process (the so called CARABAS project) using broad-band, low-frequency waves, the authors encounter the problem of solving Poisson's equation over a very large rectangular grid, typically 5000 x 20000 pixels. In addition, no information about boundary values is available. In order to select suitable solutions the authors solve the Poisson equation under the side condition that some criterion function, usually a Sobolev norm, should be minimized. In some cases this problem may be reformulated as a boundary value problem for the biharmonic equation. Numerical techniques are investigated for this problem. The authors also include the results of some numerical experiments. NTIS

N94-18951# Research Inst. of National Defence, Linkoeping (Sweden).
POLARIMETRIC STATISTICS OF ELECTROMAGNETIC WAVES SCATTERED BY DISTRIBUTED TARGETS
S. Axelsson Jan. 1993 132 p See also AD-A193667
(PB93-195907; FOA-C-30656-3.3) Avail: CASI HC A07/MF A02

The variances and correlation coefficients of the instantaneous scattering matrix of the target and the scattered wave are studied first. The probability density functions of the envelopes and the phase difference of the polarization components are analyzed as well. Then the corresponding statistical analysis is applied to the Stokes vector, which can be expressed in terms of the rotation angle and the ellipticity angle of the polarization ellipse. These angles also describe the projection of the Stokes vector on the Poincare sphere. Analytical expressions are derived for the probability density functions of these angles and the mapping of the Stokes vector on the Poincare sphere. Methods of classifying polarimetric radar data and the estimation of optimal polarizations in order to maximize the received power or contrast ratio are also discussed. In the last part of the report, scatter models are analyzed for rough surfaces, clouds of chaff, and man-made targets such as bridges, ships, and vehicles. The target model includes both one-bounce and two-bounce scattering. Finally, a Monte-Carlo model is studied for predictions of the polarization components of the scattered wave when the correlation matrix of the target is known and can be used as input data to the model. NTIS

N94-19009# Arizona State Univ., Tempe.
APPLICATION OF WAVELET TRANSFORM TECHNIQUES TO SPREAD SPECTRUM DEMODULATION AND JAMMING Final Technical Report, 1 Nov. 1990 - 31 Dec. 1992
Douglas Cochran 26 Feb. 1993 33 p
(Grant AF-AFOSR-0081-91)
(AD-A267389; AFOSR-93-0562TR) Avail: CASI HC A03/MF A01

This project has investigated the application of wavelet methods in spread spectrum communications. Use of the wavelet transform as an alternative to the short-time Fourier and quadratic time-frequency transforms for measuring critical parameters of intercepted slow frequency hopping communication signals has been explored. Direct application of the wavelet transform was found to not offer performance advantages over the Fourieer transform in this application. However, use of the wavelet transform in conjunction with Fourier methods provided an efficient hybrid framework for precise measurement of hopping times and frequencies. A new approach to multiple-access spread spectrum communications was also developed in this project. This approach employs orthogonal wavelets as symbols for encoding digital communication signals. Several users can transmit simultaneously in the same medium using channels defined by wavelet scale in much the same way that channels are defined by frequency in traditional frequency division multiple access. Appropriate choices of wavelet symbols make the transmitted signals robust with respect to detection and jamming. DTIC

N94-19053# California Univ., Berkeley. Lawrence Berkeley Lab.
THREE DIMENSIONAL MULTIPOLE DECOMPOSITION OF FIELDS
K. Hahn May 1993 5 p Presented at the International Particle Accelerator Conference, Washington, DC, 17-20 May 1993
(Contract DE-AC03-76SF-00098)
(DE93-018530; LBL-33286; HIFAN-571; CONF-930511-322) Avail: CASI HC A01/MF A01

A new method to generate the general multipole representation of the three dimensional static field, electric or magnetic, is obtained via a scalar potential evaluated from the arbitrary specified source. As an application of this formulation, a previously described 3-D electric field decomposition method has been further generalized to the magnetic field. DOE

N94-19114# Lawrence Livermore National Lab., CA.
MOMENTS OF AMBIENT DOPPLER SPECTRA
S. K. Lehman 23 Mar. 1993 17 p
(Contract W-7405-eng-48)
(DE93-017948; UCRL-ID-113761) Avail: CASI HC A03/MF A01

The author studied the first four moments (center of mass, standard deviation, skew, and kurtosis) of the Doppler spectra in ambient regions of LLNL-Hughes real aperture radar data collected during WCSEX91-92. The goal was to correlate trends in the moments with wind velocity and direction. Although the center of mass appears to increase when the wind is blowing into the radar antenna, no other conclusions have been drawn from the higher order moments. DOE

N94-19230# Universiteit Twente, Enschede (Netherlands). Tele-Informatics and Open Systems Group.
A HIGHLY CONCURRENT MEDIUM ACCESS CONTROL STRATEGY FOR HIGH SPEED MULTIWAVELENGTH NETWORKS USING TRANSCEIVERS WITH LIMITED TUNABILITY
J. H. Laarhuis and A. M. J. Koonen 1993 10 p
(Memo-INF-93-07; TIOS-93-04; ETN-93-94681) Copyright Avail: CASI HC A02/MF A01

High speed multichannel interconnection MAN's (Metropolitan Area Networks) with medium access control mechanisms based on a fixed assignment are considered. A medium access control strategy which accounts for the limited tunability of lasers and filters is proposed. Network performance is achieved by creating disjunct subnetworks in a wavelengtth basis, and reconfiguring them on a time basis. ESA

N94-19267# Universiteit Twente, Enschede (Netherlands). Dept. of Computer Science.
SPECIFYING AND PROVING COMMUNICATION CLOSEDNESS IN PROTOCOLS
Wil Janssen and Job Zwiers Apr. 1993 31 p Presented at the 13th IFIP Symposium on Protocol Specification, Testing and Verification, Liege, Belgium, 25-28 May 1993 Sponsored in part by Commission of the European Communities
(Memo-INF-93-23; ETN-93-94695) Copyright Avail: CASI HC A03/MF A01

The principle of communication closed layers by Elrad and Francez was shown to be very useful in the design of distributed protocols and algorithms. An investigation of the communication closed layers principle as an 'algebraic law' with 'syntactic' side conditions is presented. Although these side conditions seem to put limits to the applicability, it is shown that by means of multiplexing and data refinement techniques the scope of the law can be enlarged to numerous examples, including the derivation of a Two Phase Commit protocol and the Gallagher, Humblet, and Spira algorithm for minimum weight spanning trees. The relation to more general formulations of the principle of communication closed layers by means of temporal logics and the relation between partial order temporal logics and our process language are also discussed. ESA

N94-19306# Lawrence Livermore National Lab., CA.
A PROGRAM FOR PASSIVELY TRACKING A TARGET USING AN ARRAY OF SENSORS
M. R. Buhl Jan. 1993 73 p
(Contract W-7405-eng-48)
(DE93-019554; UCRL-ID-114259) Avail: CASI HC A04/MF A01

The problem of passively tracking a moving signal source has importance in a variety of applications such as radar, sonar, seismology, and radio astronomy. In many applications, only limited information is available about the signal source. It will be assumed here that only the signals which are detected by the sensors and the velocity of the source signal are known. The objective of this document is to present a program which passively tracks a target using an array of sensors. This program is available in MATLAB, version 3.5. The algorithm which is implemented consists of three main parts: time delay estimation, passive localization, and data post processing. Each of these parts are discussed, and the mathematical foundation for their solution given. Following this, the organization of the program is presented, and an example of its usage is given. DOE

N94-19416 Max-Planck-Inst. fuer Physik und Astrophysik, Garching (Germany). Inst. fuer Extraterrestrische Physik.
BROADBAND IF MATCHING FOR QUASIOPTICAL MIXERS
A. I. Harris, K. F. Schuster, and L. J. Tacconi Jan. 1993 17 p
Submitted for publication
(MPE-Preprint-240; ETN-93-94920) Copyright Avail: Issuing Activity (Max-Planck-Institut fuer Physik und Astrophysik, Giessenbachstrasse, 8046 Garching, Munich, Germany)

The need to drive symmetric quasioptical antennas in a symmetric way to maintain clean antenna patterns recognized by all is discussed. The advantages of bringing out the IF in a symmetric (balanced) way as well are reported. The main difference in IF circuits between waveguide and open structure mixers is that the quasioptical mixers are usually also open at IF wavelengths, so IF currents can flow on the outside of the mixer mounting structures. These surface currents and their associated resonances were measured on a scale model of our mixer block for a 690 GHz SIS mixer. Bringing the IF off the mixer with a balanced circuit solves the surface current problems, yielding a broad bandwidth with predictable impedances. An octave bandwidth IF matching circuit for open structure mixers that incorporates a commercial 180 degree hybrid at cryogenic temperatures was tested. It was found that surface currents are not significant for corner cube mixers because they generate their own balancing currents. ESA

N94-19447 Physics and Electronics Lab. TNO, The Hague (Netherlands).
THE SPLIT-STEP ALGORITHM FOR MICROWAVE PROPAGATION MODELING ABOVE A CONDUCTING SURFACE Final Report
M. H. Vogel Feb. 1993 31 p Sponsored by Royal Netherlands Navy, The Hague, Netherlands
(Contract A92/KM/662)
(FEL-92-A430; TD-92-3675; ETN-93-94945) Copyright Avail: Issuing Activity (TNO Physics and Electronics Laboratory, P.O. Box 96864, 2509 JG The Hague, Netherlands)

Microwave propagation in the troposphere is largely dependent on the variation of the air's refractive index with altitude. For a radar system, this strongly affects the probability of detection of a given target. Relevant equations for microwave propagation in a maritime environment are derived and their implementation in a computer code is outlined. Some results of the code are presented. In the implementation of the equation in the computer code, it is assumed that the sea surface is a good conductor and is not very rough. A critical factor in the code is the construction of an absorbing boundary. When the absorption is either too strong or too weak, the results will be in error. A comparison of the results of the code with the PCPEM (personal computer parabolic equation method) microwave propagation calculation program shows good agreement. For higher evaporation ducts there may be discrepancies between the codes. The propagation factor at a certain distance may vary strongly with altitude, and deep nulls may exist, which makes the results of the codes extremely sensitive to the exact receiver height that is chosen. ESA

N94-19449 Physics and Electronics Lab. TNO, The Hague (Netherlands).
A COMPARISON BETWEEN SEVERAL COMPUTER CODES FOR CALCULATIONS ON MICROWAVE PROPAGATION Final Report
M. H. Vogel Mar. 1993 19 p Sponsored by Royal Netherlands Navy, The Hague, Netherlands
(Contract A90/KM/666)
(FEL-92-A435; TD-92-3677; ETN-93-94946) Copyright Avail: Issuing Activity (TNO Physics and Electronics Laboratory, P.O. Box 96864, 2509 JG The Hague, Netherlands)

Microwave propagation in the troposphere is largely dependent on the variation of the air's refractive index with altitude. For a radar system, this strongly affects the probability of detection of a given target. Six computer codes for calculations on microwave propagation are compared. The advantages and disadvantages of each code when used in a maritime environment are discussed. The analyzed codes are: PCPEM (Personal Computer Parabolic Equation Method), EMPE (Electromagnetic Parabolic Equation), RPO (Radio Physical Optics), IREPS (Integrated-Refractive Effects Prediction System), EREPS (Engineers' Refraction Effects Prediction System), and MPPM (Microwave Propagation Prediction Model). ESA

N94-19542# Coleman Research Corp., Orlando, FL.
EARTH PENETRATION RADAR IMAGING SYSTEM (EPRIS)
Aug. 1993 83 p
(Contract DE-AI01-92EW-50616)
(DE93-019890; DOE/EW-50616/T13) Avail: CASI HC A05/MF A01
(US Sales Only)

The Earth Penetration Radar Imaging System (EPRIS) has been developed and has the capability to detect and locate buried mines, buried ordnance delivered by precision munitions, buried drums, buried waste/contaminants, and geological structures/features. The detected objects or features are mapped in three dimensions with high resolution. This information is then available for integration into a site characterization study. The EPRIS is a significant improvement in non-intrusive sensing and imaging capability. This phase of the EPRIS development has been extremely successful. Coleman Research Corporation (CRC) has implemented significant advances in technology into the EPRIS equipment. The frequency stepped radar sensor design has a very wide dynamic signal range and improved sensitivity over currently available equipment. The two- and three-dimensional image processing algorithms allow high-resolution placement and sizing of buried objects and/or features. The discussions related to the analog-to-digital converter and the spiral antenna, define the source of the dynamic range capability realized by EPRIS. The processing for this new radar makes use of unique synthetic aperature imaging (SAI) algorithms developed by CRC for frequency stepped radar systems. The SAI algorithms are necessary to obtain excellent spatial resolution on objects buried up to seven meters. The sensor signal processing represents a significant improvement in imaging systems. The CRC test facility permitted tests on objects buried up to 2.44 meters. DOE

N94-19582# Naval Surface Warfare Center, Dahlgren, VA.
TRACKING WITH TIME-DELAYED DATA IN MULTISENSOR SYSTEMS Final Report
Richard D. Hilton, David A. Martin, and William D. Blair Aug. 1993 56 p
(AD-A271334; NSWCDD/TR-93/351) Avail: CASI HC A04/MF A01

When techniques for target tracking are expanded to make use of multiple sensors in a multiplatform system, the possibility of time delayed data becomes a reality. When a discrete-time Kalman filter is applied and some of the data entering the filter are delayed, proper processing of these late data is a necessity for obtaining an optimal estimate of a target's state. If this problem is not given special care, the quality of the state estimates can be degraded relative to that quality provided by a single sensor. A negative-time update technique is developed using the criteria of minimum mean-square error (MMSE) under the constraint that only the results of the most recent update are saved. The performance of the MMSE technique is compared to that of the ad hoc approach employed in the Cooperative Engagement Capabilities (CEC) system for processing data from multiple platforms. It was discovered that the MMSE technique is a stable solution to the negative-time update problem, while the CEC technique was found to be less than desirable when used with filters designed for tracking highly maneuvering targets at relatively low data rates. The MMSE negative-time update technique was found to be a superior alternative to the existing CEC negative-time update technique. DTIC

N94-19587# Kaman Sciences Corp., Utica, NY.
GENERALIZED MULTICHANNEL SIGNAL DETECTION Final Report, Nov. 1992 - Nov. 1993
Robert L. Vienneau, David Dekkers, and Sue Eilers Jul. 1993 41 p
(Contract F30602-92-C-0033)
(AD-A271385; RL-TR-93-154) Avail: CASI HC A03/MF A01

The Multichannel Signal Processing Simulation System (MSPSS) provides the following: a synthesis procedure for simulating multichannel Autoregressive (AR) processes in which intertemporal and interchannel correlations are controlled by specifying signal characteristics such as the one-lag temporal and cross-channel correlation parameters; a capability for analyzing the performance of various multichannel estimation algorithms; and a multichannel signal detection algorithm, based on a generalized likelihood ratio using an innovations approach. Under this effort the MSPSS was enhanced to provide synthesis and analysis of more general processes including multipath and feedback processes, non-Gaussian Spherically Invariant Random Processes, and processes with non-constrained quadrature components. DTIC

N94-19617# Kernforschungszentrum G.m.b.H., Karlsruhe (Germany). Projekt Kernfusion.
EXPERIMENTAL AND THEORETICAL INVESTIGATION OF BROADBAND HIGH-POWER WINDOWS FOR MILLIMETER WAVES Thesis - Karlsruhe Univ. [EXPERIMENTELLE UND THEORETISCHE UNTERSUCHUNG BREITBANDIGER HOCHLEISTUNGSFENSTER FUER MILLIMETERWELLEN]
U. Ambrosy Feb. 1993 85 p In GERMAN
(KfK-5157; ETN-93-95079) Copyright Avail: CASI HC A05/MF A01

Transmission windows guaranteeing a reliable vacuum air seal for extraction of high power millimeter waves from a vacuum tube oscillator (for example a gyrotron) and for coupling of the wave into an applicator vessel (for example a nuclear fusion reactor) are addressed. The windows used so far usually consist of plane disks of low loss dielectric material mounted perpendicularly to the direction of wave propagation. Since only waves in a narrow frequency range can penetrate this type of window this is only useful for monofrequent systems. For frequency variable systems, using for example step tunable gyrotrons, cyclotron autoresonance masers, or free electron masers as a source, special windows are required, that can transmit a relatively large frequency range (greater than or equal to +/- 5). Different broadband window types are developed and further investigated. The main point of the work is the realization of the required frequency dependences. For the construction of the different test windows materials are used that are suitable for transmission of high power waves. ESA

N94-19646 Technische Univ., Berlin (Germany). Fachbereich Elektrotechnik.
TRANSIENT SKIN EFFECT IN A MASSIVE CYLINDER BY ECCENTRIC LOCATION OF EXCITING CONDUCTION BANDS Ph.D. Thesis [TRANSIENTER SKINEFFEKT IN EINEM MASSIVEN ZYLINDER BEI EXZENTRISCHER LAGE DER ERREGENDEN LEITERSCHLEIFE]
Ulrich Goelz 1993 98 p In GERMAN Limited Reproducibility: More than 20% of this document may be affected by microfiche quality
(ETN-93-95048) Avail: CASI HC A05

The transient skin effect in a massive conductive cylinder, located in the field of an eccentrically layered, thin conduction band, is calculated. It was assumed, that field distribution, for any profile of the excitation current, can be calculated provided the solution of the switching process in the folding integral is known. Since the vectorial field equation of the vector potential A cannot be separated in cylindrical coordinates because of the eccentricity, it was necessary to use a superordered vector potential P for the solution of the three dimensional boundary value problem; the vectorial skin effect equation of the vector potential A was reduced to two scalar skin effect equations for two potentials P(w1) and P(w2) so that the field in the cylinder was decomposed into two components. The magnetic field in nonconducting, current free, outspace was described by the superordered scalar potential P(wa). The boundary conditions at the cylinder wall were written as two independent eigenvalues equations. For validation of the calculation, the method was successfully applied to the particular case of a rotation symmetric conduction band. ESA

N94-19676# Mitre Corp., Bedford, MA.
SYSTEMS ENGINEERING FOR AIR FORCE C3I SYSTEMS
John H. Monahan 1993 212 p
(AD-A270482; M-93-B0000032) Avail: CASI HC A10/MF A03

Each day, sophisticated information systems provide the U.S. with crucial capabilities both to understand the world situation and to react effectively as required by our nation's decision makers. These systems attest to the success of the cooperative efforts of government and industry. Over the last 35 years, to help provide those capabilities, The MITRE Corporation has been privileged to fulfill the role of systems engineer on more than 100 different command, control, communications, and intelligence (C3I) systems for the Air Force and other elements of the Department of Defense (DOD). A long history of successful performance in this broad role provides MITRE with detailed knowledge of the systems' operational capabilities and needs, proficiency in their systems engineering, and a C3I-related corporate memory unmatched by any other organization. That background is the foundation of this book on systems engineering at MITRE. DTIC

N94-19680# New Mexico State Univ., Las Cruces. Physical Science Lab.

SYSTOLIC DESIGN WITH ASYNCHRONOUS CONTROLS FOR DIGITAL-SIGNAL PROCESSING Final Report, 8 Aug. 1991 - 15 Jul. 1993

Kamran Reihani 15 Jul. 1993 34 p
(Contract DAAL03-90-G-0211)
(AD-A270976; PSL-93/49; ARO-28176.9-MA-SAH) Avail: CASI HC A03/MF A01

The research sponsored by this grant is focused on the development of a theoretical and technological basis for designing efficient systolic arrays for digital-signal processing algorithms. The major contributions of the research are the following: data reduction techniques via the utilization of algorithm properties; conversion of sequential input signal into input blocks by means of a spiral systolic mesh that is suitable for parallel processing and that is flexible for enabling various array dimensions; and devising a hybrid of SA and data-flow approach, making data streams independent of computations executed in each processor, thus reducing waiting time. The communication (PE) protocols resolve the data-flow conflicts created by the merging of the spiral and asynchronous systolic array architecture. DTIC

N94-19718# Case Western Reserve Univ., Cleveland, OH.

COMPARATIVE EVALUATION OF KIRCHHOFF, PERTURBATION, AND FULL WAVE METHODS FOR ROUGH SURFACE SCATTERING Final Report, May 1990 - Jun. 1993

R. E. Collin 13 Aug. 1993 16 p
(Contract DAAL03-90-G-0122)
(AD-A271198; ARO-27911.4-GS) Avail: CASI HC A03/MF A01

This report summarizes the principal results in three areas of investigation. The first is a new full wave method that takes two dimensional surface roughness into account and does not use the telegraphist's equations. The second study concerns scattering from a rough surface when the incident field is a Gaussian beam. The third is a summary of the difficulties inherent in Bahar's extended full wave theory on which the prediction of enhanced backscatter was based. It was found that enhanced backscatter occurred only because of the invalid assumption that the heights and slopes were uncorrelated. DTIC

N94-19724# Pennsylvania State Univ., University Park. Dept. of Computer Science.

SIGNAL PROCESSING ALGORITHMS FOR HETEROGENEOUS ARCHITECTURES Final Report, 1 Jan. 1987 - 31 Oct. 1991

Mary J. Irwin and Robert M. Owens 1 Aug. 1993 34 p
(Contract DAAL03-87-K-0118)
(AD-A271248; ARO-23908.24-EL) Avail: CASI HC A03/MF A01

As stated in our proposal, our research goal was to derive architectures which preserve the VLSI implementation advantages of regular meshes while still obtaining sufficient increases in performance and/or decreases in size and cost. Our problem domain was signal and image processing applications which require either significant computational resources or which must be solved in real time. Our research has been successful in that we have derived a number of such architectures for important problem areas in image and signal processing. These architectures are outlined in more detail in the final report. We even successfully prototyped one of our architectures, the Arithmetic Cube, which involved both VLSI chip and PCB board design and fabrication. The Arithmetic Cube directly solves both the discrete Fourier transform and cyclic convolution. In parallel with our architecture work, we also investigated algorithms which map efficiently onto the various derived architectures and which take advantage of their particular architectural aspects. DTIC

N94-19736# Stanford Univ., CA. Information Systems Lab.

ALGORITHMS AND ARCHITECTURES FOR HIGH SPEED SIGNAL PROCESSING Final Report, 1 May 1990 - 30 Apr. 1993

Thomas Kailath and Arogyaswami Paulraj 31 Jul. 1993 18 p
(Contract DAAL03-90-G-0108)
(AD-A271000; ARO-28060.25-MA) Avail: CASI HC A03/MF A01

This document discusses issues related to designing configurable and fault-tolerant processor arrays such that even if some processors are faulty, a fault free array can be constructed using the healthy processors. The general models that have been explored consist of a set of identical processors embedded in a flexible interconnection structure that is configured in the form of a rectangular grid. In particular, models were studied that use multiple tracks along every grid line. Efficient scheduling algorithms were also developed for such processor arrays in the presence of communication delays. Also discussed are aspects of antenna array processing relating to methods for dealing with unknown or partially known noise field and the array manifold. DTIC

N94-19737# Michigan Univ., Ann Arbor. Dept. of Electrical Engineering and Computer Science.

CONGESTION/FLOW CONTROL AND ROUTING IN DATA NETWORKS: A CONTROL-THEORETIC APPROACH Final Report, 1 Apr. 1990 - 31 Mar. 1993

Semyon M. Meerkov and Lotfi Benmohamed 25 Jun. 1993 75 p
(Contract DAAL03-90-G-0094)
(AD-A271121; ARO-27834.1-EL) Avail: CASI HC A04/MF A01

In this project, a novel architecture for congestion control in store-and-forward networks has been developed and design techniques for congestion controllers have been derived. In the framework of this architecture, each switching node is equipped with a congestion controller which calculates the throttled source admission rates using only local information available at the node. Each source receives the throttled admission rates and responds by transmitting with the lowest one. The design methodology developed in this project leads to the choice of the controller gains that ensure a stable congestion-free behavior of the network. No similar results are available in the current literature. DTIC

N94-19738# Johns Hopkins Univ., Baltimore, MD. Dept. of Electrical and Computer Engineering.

COMMUNICATION IN THE PRESENCE OF UNKNOWN INTERFERENCE Final Report, 1 Jul. 1989 - 30 Apr. 1993

Brian L. Hughes 21 Jun. 1993 7 p
(Contract DAAL03-89-K-0130)
(AD-A271146; ARO-27028.6-EL) Avail: CASI HC A02/MF A01

A brief summary is presented of results obtained during the final period (1 July 1992 to 30 April 1993) under Grant DAAL03-89-K-0130 sponsored by the Army Research Laboratory and the Army Research Office. This report complements earlier reports which summarized the first three years of research under this grant. The research covers list decoding for jammed channels, multiple-access channels with jamming, random-access for channels with large propagation delays, and coding for multiple-access channels. DTIC

N94-19748 Naval Research Lab., Washington, DC.

TEMPLATE BASED LOW DATA RATE SPEECH ENCODER Interim Report

Lawrence Fransen 30 Sep. 1993 15 p Limited Reproducibility: More than 20% of this document may be affected by microfiche quality
(AD-A270900; NRL/MR/5531-93-7371) Avail: Issuing Activity (Defense Technical Information Center (DTIC))

The 2400-b/s linear predictive coder (LPC) is currently being widely deployed to support tactical voice communication over narrowband channels. However, there is a need for lower-data-rate voice encoders for special applications: improved performance in high bit-error conditions, low-probability-of-intercept (LPI) voice communication, and narrowband integrated voice/data systems. An 800-b/s voice encoding algorithm is presented which is an extension of the 2400-b/s LPC. To construct template tables, speech samples of 420 speakers uttering 8 sentences each were excerpted from the Texas Instrument - Massachusetts Institute of Technology (TIMIT) Acoustic-Phonetic Speech Data Base. Speech intelligibility of the 800-b/s voice encoding algorithm measured by the diagnostic rhyme test (DRT) is 91.5 for three male speakers. This score compares favorably with the 2400-b/s LPC of a few years ago. DTIC

N94-19749 SRI International Corp., Menlo Park, CA.

A REAL-TIME SPOKEN-LANGUAGE SYSTEM FOR INTERACTIVE PROBLEM-SOLVING, COMBINING LINGUISTIC AND STATISTICAL TECHNOLOGY FOR IMPROVED SPOKEN LANGUAGE UNDERSTANDING Annual Report, 1 Oct. 1992 - 30 Sep. 1993

Robert C. Moore and Michael H. Cohen 30 Sep. 1993 8 p Limited Reproducibility: More than 20% of this document may be affected by

microfiche quality
(Contracts N00014-90-C-0085; N00014-93-C-0142)
(AD-A270901) Avail: CASI HC A02

Under this effort, SRI has developed spoken-language technology for interactive problem solving, featuring real-time performance for up to several thousand word vocabularies, high semantic accuracy, habitability within the domain, and robustness to many sources of variability. Although the technology is suitable for many applications, efforts to date have focused on developing an Air Travel Information System (ATIS) prototype application. SRI's ATIS system has been evaluated in four ARPA benchmark evaluations, and has consistently been at or near the top in performance. These achievements are the result of SRI's technical progress in speech recognition, natural-language processing, and speech and natural-language integration. DTIC

N94-19752 Harris Corp., Rochester, NY. RF Communications Div.
IMPROVED HF DATA NETWORK SIMULATOR, VOLUME 1 Final Technical Report, Sep. 1989 - Oct. 1992
Marvin C. Baker Jul. 1993 178 p Limited Reproducibility: More than 20% of this document may be affected by microfiche quality
(Contract F30602-89-C-0136)
(AD-A270953; RL-TR-93-139-Vol-1) Avail: CASI HC A09

This effort advances the state-of-the-art in networking for both data/voice communications in the HF (2-30 MHZ) band. This is contained in a PC portable simulation called the Improved HF Data Network Simulator (INS). INS algorithms emphasize a decentralized, distributed architecture and interoperability for both military and civilian air-land-sea mobile users. Up to 100 users are contained in up to 10 nets that make up one network. The intended radii for the nets/network are 400 and 4000 miles, respectively. Technical issues addressed are improved HF networking, LQA techniques, LPD/LPE waveforms for OPSEC, and frequency hop (FH) frequency management. The INS provides the means for configuring a network to any user's protocols/architectures with node, path, and network results available over the 24 hour time period of the propagation model (IONCAP). To receive the INS, you must complete a statement of terms and conditions for release of USAF owned developed software. Contact the RL program manager to obtain this. A Phase 2 effort entitled Adaptive Network Controller (ANC) will put the phase 1 algorithms into use on real-time over-the-air HF networks to demonstrate the improvement in HF communications. DTIC

N94-19753 Harris Corp., Rochester, NY. RF Communications Div.
IMPROVED HF DATA NETWORK SIMULATOR, SOFTWARE USER'S MANUAL, VOLUME 2 Final Technical Report, Sep. 1989 - Oct. 1992
Marvin C. Baker Jul. 1993 48 p Limited Reproducibility: More than 20% of this document may be affected by microfiche quality
(Contract F30602-89-C-0136)
(AD-A270954; RL-TR-93-139-Vol-2) Avail: CASI HC A03

This effort advances the state-of-the-art in networking for both data/voice communications in the HF (2-30 MHZ) band. This is contained in a PC portable simulation called the Improved HP Data Network Simulator (INS). INS algorithms emphasize a decentralized, distributed architecture and interoperability for both military and civilian air-land-sea mobile users. Up to 100 users are contained in up to 10 nets that make up one network. The intended radii for the nets/network are 400 and 4000 miles, respectively. Technical issues addressed are improved HF networking, LQA techniques, LPD/LPE waveforms for OPSEC, and frequency hop (FH) frequency management. The INS provides the means for configuring a network to any user's protocols/architectures with node, path, and network results available over the 24 hour time period of the propagation model (IONCAP). To receive the INS, you must complete a statement of terms and conditions for release of USAF owned developed software. Contact the RL program manager to obtain this. A phase 2 effort entitled Adaptive Network Controller (ANC) will put the phase 1 algorithms into use on real-time over-the-air HF networks to demonstrate the improvement in HF communications. DTIC

N94-19779 Naval Research Lab., Washington, DC.
CONTROL OF INTEGRATED VOICE/DATA MULTI-HOP RADIO NETWORKS VIA REDUCED-LOAD APPROXIMATIONS Interim Report, Dec. 1991 - Dec. 1992
Evaggelos Geraniotis and Ie-Hong Lin 30 Sep. 1993 171 p Limited Reproducibility: More than 20% of this document may be affected by microfiche quality
(NR Proj. RR0-1509)
(AD-A270661; NRL/MR/5520-93-7390) Avail: Issuing Activity (Defense Technical Information Center (DTIC))

In this report we develop reduced-load approximation techniques based on the stochastic knapsack and the Pascal distribution, which enable the computationally efficient and accurate evaluation of the probability of voice blocking, the probability of data queueing, and the average data delay in integrated voice/data multi-hop radio networks. Monte-Carlo summation techniques are also used to verify the accuracy of the approximations. The reduced-load approximations exhibit excellent to very satisfactory accuracy for the entire range of network and traffic parameters of interest, while the computational effort necessary for their evaluation is substantially lower than that of the exact expressions (which is prohibitive for multi-hop radio networks of even moderate size). They are also used successfully to approximate the derivatives (sensitivities) of the above performance measures with respect to network and traffic parameters. These approximations are applicable to single-rate and multi-rate voice models, as well as to models with voice activity and silence periods. Besides the accurate and time-efficient performance evaluation of integrated voice/data multi-hop radio networks, the computational efficiency and the accuracy of these approximations enables their use for control and optimization purposes. DTIC

N94-19793# ITT Aerospace/Optical Div., Fort Wayne, IN.
METEOR BURST COMMUNICATIONS IMPROVEMENT STUDY Final Report, Jan. 1989 - Oct. 1992
David Peterson Jul. 1993 158 p
(Contract F30602-89-C-0024)
(AD-A270866; ITT-A/CD-33433A007; RL-TR-93-134) Avail: CASI HC A08/MF A02

Two identical Meteor Burst Radio Terminals were developed, fabricated, and delivered to the Air Force. Each is controlled by a PC computer in a menu driven manner. The mode of operation is full duplex. The RF frequency range is 40 to 60 MHz with tuning increments of 25 KHz. Data rates are 4, 8, 16, 32, 64, 128, 256, and 512 kbps. Modulation is coherent Binary Phase Shift Keying (BPSK) and incoherent Differential Phase Shift Keying (DPSK). Protocol includes Automatic Repeat Request (ARQ) with source and destination addressing, message number, start of message, and end of message. Messages are packetized, and Reed Solomon (R-S) coding is an option. The ARQ is under the control of a Cyclic Redundancy Check Code (CRCC) which detects binary errors within each packet. The terminal is intended to increase meteor trail availability and data throughput by several orders of magnitude--by operating with new antennas that provide much higher gains without sacrificing meteor trail acquisition performance. DTIC

N94-19798 Physics and Electronics Lab. TNO, The Hague (Netherlands).
AUTOMATED PROCESSING OF MILITARY MESSAGES ACCORDING TO ADatP-3 Final Report [GEAUTOMATISEERDE VERWERKING VAN MILITAIRE BERICHTEN VOLGENS ADATP-3]
M. deNiet and R. A. Nissink Jun. 1992 86 p In DUTCH
(Contract A91/KL/645)
(FEL-92-A044; TD-92-0812; ETN-93-94524) Copyright Avail: Issuing Activity (TNO Physics and Electronics Laboratory, P.O. Box 96864, 2509 JG The Hague, Netherlands)

The automated support during the drafting of outgoing messages and the processing of incoming messages formatted according to the military message system ADatP-3 was studied in order to increase the quality of the information service by an upgrading of message processing capabilities. The ADatP-3 message structure was analyzed. The advantages and disadvantages of ADatP-3 are discussed. The problems are not insurmountable. The message processing functionality, some existing message handling systems, and an automated message handling system are being developed. ESA

N94-18351*# Stanford Univ., CA. Dept. of Electrical Engineering.
LOW POWER SIGNAL PROCESSING RESEARCH AT STANFORD
J. Burr, P. R. Williamson, and A. Peterson *In* Idaho Univ., The 1991 3rd NASA Symposium on VLSI Design 1991 13 p (For primary document see N94-18337 04-33)
(Grants NAGw-1910; NAGw-419)
Avail: CASI HC A03/MF A04

33 ELECTRONICS AND ELECTRICAL ENGINEERING

Includes test equipment and maintainability; components, e.g., tunnel diodes and transistors; microminiaturization; and integrated circuitry.

For related information see also *60 Computer Operations and Hardware* and *76 Solid-State Physics.*

N94-17703 Department of the Navy, Washington, DC.
PRECISION DIGITALLY-CONTROLLED VARIABLE ATTENUATION CIRCUIT Patent
Kenneth L. Atwood, inventor (to Navy), Hyun S. Kim, inventor (to Navy), and Kang M. Lee, inventor (to Navy) 4 May 1993 9 p Filed 1 Nov. 1991
(AD-D015862; US-Patent-5,208,842; US-Patent-Appl-SN-786665) Avail: CASI HC A02/MF A01

A precise digitally-controlled variable attenuation circuit for adjusting the attenuation of a signal in an external circuit includes a signal magnitude detector, a resistance adjustment control, and a resistance divider network. The signal magnitude detector has lower and upper threshold limits representing a desired range of attenuation and is operable to receive and compare a control signal with the lower and upper threshold limits, and, in response thereto, produce either a first signal if the control signal is less than the lower threshold limit or a second signal if the control signal is greater than the upper threshold limit. The adjustment control is capable of receiving the first and second signals and is operable to produce either a digital count-down signal in response to the first signal or a digital count-up signal in response to the second signal. The resistance divider network has a fixed resistance and a digitally-adjustable device with a variable resistance. DTIC

N94-17707 Department of the Navy, Washington, DC.
EXTENDING BANDWIDTH OF OPTICAL EMITTERS USING ACTIVE MATCHING TECHNIQUE Patent
Vladimir Gershman, inventor (to Navy), Afshin S. Daryoush, inventor (to Navy), and Warren A. Rosen, inventor (to Navy) 25 May 1993 14 p Filed 13 Sep. 1991
(AD-D015875; US-Patent-5,214,525; US-Patent-Appl-SN-759296; US-Patent-Class-359-180) Avail: CASI HC A02/MF A01

An optical transmitter particularly suited for high frequency applications is disclosed. The optical transmitter successfully operates in harsh environments such as those found in avionic applications. The optical transmitter employs an LED as a light source which cooperates with an active bandpass amplifier to provide a relatively wide bandwidth from about 250 MHz to about at least 1.35 GHz. The bandpass amplifier is selected to have a slope characteristic which is complementary to a roll-off characteristic of the LED and compensates for the high frequency loss of the LED. The slope characteristic of the bandpass amplifier predominates at the high frequencies of the response of the optical transmitter, whereas the frequency response of the LED dominates at the lower frequencies of the response. DTIC

N94-17718 Department of the Navy, Washington, DC.
MIXED POLYMER ELECTROLYTE AND MIXED POLYMER ELECTROLYTE BATTERY Patent
Kuzhikalail M. Abraham, inventor (to Navy) and Mohamed Alamgir, inventor (to Navy) 24 Nov. 1993 9 p Filed 28 Mar. 1991
(AD-D015856; US-Patent-5,166,009; US-Patent-Appl-SN-676507) Avail: CASI HC A02/MF A01

A mixed polymer electrolyte and a solid rechargeable battery which uses a solid mixed polymer electrolyte of polybis (methoxyethoxyethoxide) phosphazene is described. DTIC

N94-17750 Argonne National Lab., IL.
THE ANL ELECTRIC VEHICLE BATTERY R&D PROGRAM FOR DOE-EHP
15 Jun. 1993 10 p Limited Reproducibility: More than 20% of this document may be affected by microfiche quality
(Contract W-31-109-eng-38)
(DE93-017414; ANL/CMT/RP-80217) Avail: CASI HC A02

The Electrochemical Technology Program at Argonne National Laboratory (ANL) provides technical and programmatic support to DOE's Electric and Hybrid Propulsion Division (DOE-EHP). The goal of DOE-EHP is to advance promising electric-vehicle (EV) propulsion technologies to levels where industry will continue their commercial development and thereby significantly reduce air pollution and petroleum consumption due to the transportation sector of the economy. In support of this goal, ANL provides research, development, testing/evaluation, post-test analysis, modeling, and project management on advanced battery technologies for DOE-EHP. The battery-related activities undertaken during the period of 1 Jan. 1993 through 31 Mar. 1993 are summarized. The objective, background, technical progress, and status are described for each task. The work is organized into the following task areas: Project Management; Sodium/Metal Chloride R&D; and Microreference Electrodes for Lithium/Polymer Batteries. DOE

N94-17755# Lawrence Livermore National Lab., CA.
DESIGN AND TEST OF A LOW JITTER METAL TO METAL CONTACT SOLID DIELECTRIC SWITCH Ph.D. Thesis
E. E. Domning 1 Mar. 1993 81 p
(Contract W-7405-eng-48)
(DE93-016957; UCRL-LR-112757) Avail: CASI HC A05/MF A01

A low jitter metal to metal contact solid dielectric switch was designed and tested. A metal to metal contact solid dielectric switch with a jitter of less than 25 ns is required for the 150 kJ experiment. Since this is one fourth the 100 ns jitter reported using exploding bridge foil (EBF) triggers, experiments to optimize this trigger were performed. A jitter of 25 ns was achieved using the EBF trigger and it was also achieved using a new type of trigger called the magnetic push trigger. This trigger uses the magnetic force between the two plates of a parallel plate transmission line to push the dielectric. It was found to be better than the EBF trigger because it was easier to design, easier to implement, and did less damage to switch components. DOE

N94-17770# Lawrence Livermore National Lab., CA.
MECHANICALLY REFUELABLE ZINC/AIR ELECTRIC VEHICLE CELLS
J. Noring, S. Gordon, A. Maimoni, M. Spragge, and J. F. Cooper Dec. 1992 4 p Presented at the 183rd Electromechanical Society Meeting, Honolulu, HI, 16-21 May 1993
(Contract W-7405-eng-48)
(DE93-016446; UCRL-JC-112422; CONF-930571-22) Avail: CASI HC A01/MF A01

Refuelable zinc/air batteries have long been considered for motive as well as stationary power because of a combination of high specific energy, low initial cost, and the possibility of mechanical recharge by electrolyte exchange and additions of metallic zinc. In this context, advanced slurry batteries, stationary packed bed cells, and batteries offering replaceable cassettes have been reported recently. The authors are developing self-feeding, particulate-zinc/air batteries for electric vehicle applications. Emissionless vehicle legislation in California motivated efforts to consider a new approach to providing an electric vehicle with long range (400 km), rapid refueling (10 minutes) and highway safe acceleration - factors which define the essential functions of common automobiles. Such an electric vehicle would not compete with emerging secondary battery vehicles in specialized applications (commuting vehicles, delivery trucks). Rather, different markets would be sought where long range or rapid range extension are important. Examples are: taxis, continuous-duty fork-lift trucks and shuttle busses, and general purpose automobiles having modest acceleration capabilities. In the long range, a mature fleet would best use regional plants to efficiently recover zinc from battery reaction products. One option would be to use chemical/thermal reduction to recover the zinc. The work described focuses on development of battery configurations which efficiently and completely consume zinc particles, without clogging or changing discharge characteristics. DOE

N94-17780# Sandia National Labs., Albuquerque, NM.
A RADIAL TRANSMISSION LINE MATERIAL MEASUREMENT APPARATUS
L. K. Warne, R. D. Moyer, T. E. Koontz, and M. E. Morris May 1993 186 p
(Contract DE-AC04-76DP-00789)
(DE93-018508; SAND-92-2788) Avail: CASI HC A09/MF A02

A radial transmission line material measurement sample apparatus (sample holder, offset short standards, measurement software, and instrumentation) is described which has been proposed, analyzed, designed, constructed, and tested. The purpose of the apparatus is to obtain accurate surface impedance measurements of lossy, possibly anisotropic, samples at low and intermediate frequencies (vhf and low uhf). The samples typically take the form of sections of the material coatings on conducting objects. Such measurements provide the key input data for predictive numerical scattering codes. Prediction of the sample surface impedance from the coaxial input impedance measurement is carried out by two techniques. The first is an analytical model for the coaxial-to-radial transmission line junction. The second is an empirical determination of the bilinear transformation model of the junction by the measurement of three full standards. The standards take the form of three offset shorts (and an additional lossy Salisbury load), which have also been constructed. The accuracy achievable with the device appears to be near one percent. DOE

N94-17783# Sandia National Labs., Albuquerque, NM.

ANALYSIS OF HIGH CONTACT RESISTANCES ASSOCIATED WITH HERMETIC AND LIGHTNING ARRESTOR CONNECTORS

M. J. Craig Apr. 1993 33 p
(Contract DE-AC04-76DP-00789)
(DE93-014850; SAND-92-2259) Avail: CASI HC A03/MF A01

Contact resistances of greater than 40 milliohms have been associated with hermetic connectors and lightning arrestor connectors (LAC) during routine testing. Empirical analysis demonstrated that the platings could be damaged within several mating cycles. The oxides that formed upon the exposed copper alloy had no significant impact upon contact resistance when the mated contacts were stationary, but effectively disrupted continuity when the mating interfaces were translated. The stiffness of the pin contact was determined to be about five times greater than the socket contact. As the pin contact engages the socket, therefore, the socket spring member deflects and the pin does not deflect. Hence, the pin contact could easily remain centered within the socket cavity in a mated condition, contacting the hemispherical spring at a localized point. Thus the only avenue for electrical conduction is between two contacting curved surfaces -- the pin surface and the socket contact dimple surface. This scenario, coupled with the presence of corrosion products at the contacting interface, presents the opportunity for high contact resistances. DOE

N94-17849# Lawrence Livermore National Lab., CA.

THE AEROCAPACITOR: A CARBON AEROGEL BASED SUPERCAPACITOR

S. T. Mayer, R. W. Pekala, and J. L. Kaschmitter Dec. 1992 22 p
Presented at the 2nd International Seminar on Double Layer-Capacitors and Similar Energy Storage Devices, Deerfield, FL, 7-9 Dec. 1992
(Contract W-7405-eng-48)
(DE93-016537; UCRL-JC-112652; CONF-921232-2) Avail: CASI HC A03/MF A01

During the 1980's, a wide variety of carbon foams, formed by the pyrolysis of polymeric foams, were developed at several Department of Energy Laboratories. These foams are known for their monolithic structure and the ability to tailor their critical parameters (e.g. porosity, density). Lawrence Livermore National Laboratory (LLNL) exclusively developed a unique type of carbon foam, known as carbon aerogels. Carbon aerogels are a special class of open-cell foams with (1) homogeneous ultrafine particle and pore size, (2) very large useful surface area per unit volume, and (3) monolithic structure, that yields (4) excellent electrical conductivity due to the intimate connection of the particles. We have applied carbon aerogels to make an 'Aerocapacitor'; a high power- and energy-density electrochemical double layer capacitor (EDLC) that uses carbon aerogels as electrodes. Carbon aerogel surface areas range from about 100 to 700 m(sup 2)/cc (as measured by BET analysis), with bulk densities of 0.05 to 1.0 g/cm(sup 3) and their morphology allows stored energy to be released rapidly, resulting in high power-densities. DOE

N94-17872 Lawrence Livermore National Lab., CA.

HEAT LOAD ANALYSIS ON THE CABLE-IN-CONDUIT WITH CENTRAL CORE CONDUCTOR FOR THE TF COIL REBUT LAYER DESIGN

A. E. Long (Massachusetts Inst. of Tech., Cambridge.) 23 Sep. 1992 37 p Limited Reproducibility: More than 20% of this document may be affected by microfiche quality
(Contract W-7405-eng-48)
(DE93-013783; UCRL-ID-111589) Avail: CASI HC A03

The current Rebut Layer Design for the ITER TF coil calls for a cable-in-conduit with central core conductor, representing a break from the conventional configuration. In an effort to find the maximum heat load which this conductor can sustain without instigating quench, a model was developed to characterize the heat transfer behavior of the core. This model approximates the superconducting strands as double-sided fins exposed to two separate, parallel liquid helium flows. The model successfully predicts a reasonable value of maximum heat load, and yields results that compare well with a preliminary, computational analysis. The double-sided fin model also provides information on how such geometric parameters as core-to-cable space area ratio and strand winding angle can be adjusted to improve the heat transfer performance of the conductor. Experimental verification of the model is needed to insure compatibility with actual designs. DOE

N94-17882 Lawrence Livermore National Lab., CA.

AEROGELS FOR MICROELECTRONIC APPLICATIONS: FAST, INEXPENSIVE, AND LIGHT AS AIR

R. J. Contolini, L. W. Hrubesh, and A. F. Bernhardt 25 Mar. 1993 4 p
Presented at the NCAIM Workshop, Albuquerque, NM, 30-31 Mar. 1993
Limited Reproducibility: More than 20% of this document may be affected by microfiche quality
(Contract W-7405-eng-48)
(DE93-017170; UCRL-JC-113650; CONF-9303198-3) Avail: CASI HC A01

Silica aerogel consists of bonded silicon and oxygen joined into log strands, which are randomly linked together with pockets of air between them. Discovered in the 1930s, the material was thought to have little use outside of theoretical science. However, with the advent of greatly improved processing techniques, such as those developed at Lawrence Livermore National Laboratory, aerogels are on the verge of commercialization. This document describes the need for aerogels in the high-speed microelectronics industry, and state of the art processing techniques. Collaboration is welcomed in the endeavor. DOE

N94-17903 Department of the Navy, Washington, DC.

PLASMA KLYSTRON AMPLIFIER Patent Application

Han S. Uhm, inventor (to Navy) 20 May 1993 17 p Limited Reproducibility: More than 20% of this document may be affected by poor print and microfiche quality
(AD-D015819; US-Patent-Appl-SN-064321) Avail: Issuing Activity (Defense Technical Information Center (DTIC))

A body of dense plasma is established within a short drift tube of a klystron amplifier between input and output resonator cavities thereof to support current modulation of microwave energy by interaction with an electron beam propagated through the drift tube. The plasma is confined to a column radially spaced from the electron beam for two-stream interaction enabling enhancement of current modulation under simultaneous high-power and high frequency operation. DTIC

N94-17920# Deutsche Forschungsanstalt fuer Luft- und Raumfahrt, Brunswick (Germany). Abt. fuer Messtechnik und Sensoren.

DEVELOPMENT AND TEST OF READOUT ELECTRONICS FOR OPTICAL QUADRATURE SIGNALS [ENTWICKLUNG UND TEST EINER AUSWERTEELEKTRONIK FUER OPTISCHE QUADRATURSIGNALE]

Walter Schmidt, Hans Naumann, and Dieter Albrecht Dec. 1992 46 p
In GERMAN
(DLR-Mitt-92-11; ETN-93-94865) Avail: CASI HC A03/MF A01; DLR, Wissenschaftliches Berichtswesen, Postfach 90 60 58, 5000 Cologne 90, Germany, HC

A fast, high resolution, electronic processing and readout unit for phase shifted optical signals, especially from two beam interferometers is described. Over two decades of amplitude and from DC up to several MHz, it produces digital pulses and analog linearized signals between these pulses. The phase difference between the signals was also measured with high resolution. Half automatic signal offset adjustment was done with the first signals received. ESA

N94-17991# Lawrence Livermore National Lab., CA.
LIMITATIONS ON THE FIDELITY OF 100 fs PULSES PRODUCED BY CHIRPED PULSE AMPLIFICATION
W. E. White, F. G. Patterson, L. D. VanWoerkom, D. F. Price, and R. L. Shepherd May 1993 6 p Presented at the Society of Photo-Optical Instrumentational Engineers Meeting, Las Vegas, NV, 6-23 Jan. 1993
(Contract W-7405-eng-48)
(DE93-017167; UCRL-JC-113138; CONF-930192-2) Avail: CASI HC A02/MF A01

A system for continuously variable independent tuning of the higher order frequency dependent phase of ultrashort laser pulses was developed. This technique relies on geometric aberrations that arise from adjustments to the relative alignment of the elements of an air spaced doublet lens in systems such as a diffraction grating stretcher in which the spectral components of the optical pulses are spatially dispersed. Modeling results are compared to experimental measurements for a nonoptimized pulse stretcher/compressor combination showing the higher order phase aberrations that limit the performance of a chirped pulse amplification system. Numerical results are presented indicating these higher order phase terms can be compensated by a properly adjusted air spaced doublet design within the pulse stretcher. DOE

N94-18062 Department of the Navy, Washington, DC.
OPTICALLY CONTROLLED ACTIVE IMPEDANCE ELEMENT AND FILTERS EMPLOYING THE SAME Patent
William D. Jemison, inventor (to Navy) and Peter R. Herczfeld, inventor (to Navy) 20 Jul. 1993 11 p Filed 11 Dec. 1992
(AD-D015863; US-Patent-5,229,665; US-Patent-Appl-SN-989295) Avail: CASI HC A02/MF A01

An optically controlled active impedance element particularly suited to serve as a tuneable inductive element for a microwave oscillator is disclosed. The optically controlled active inductive element is comprised of a circuit arrangement, preferably consisting of MESFET devices which exhibit a composite inductive characteristic, and whose inductance may be determined and controlled by direct illumination impinging on the MESFET's. The optically controlled active inductive element lends itself to being adapted to monolithic microwave integrated circuit (MMIC) applications and may find use in a wide variety of microwave circuits. Also disclosed is an embodiment which uses the optical controlled active impedance element, in a prescribed manner, to serve as a tuneable capacitor for use in various microwave circuits. DTIC

N94-18091# Helsinki Univ. of Technology, Espoo (Finland). Circuit Theory Lab.
APLAC: AN OBJECT-ORIENTED ANALOG CIRCUIT SIMULATOR AND DESIGN TOOL. 6.1 REFERENCE MANUAL
M. Valtonen, H. Jokinen, A. Kankkunen, K. Mannersalo, and R. Niutanen 1992 497 p See also PB93-187201 and PB92-134246 Prepared in cooperation with Nokia Research Center, Espoo, Finland
(PB93-187193; ISBN-951-22-1344-3) Copyright Avail: CASI HC A21/MF A04

The report serves as the reference manual for the Analysis Program for Linear Active Circuits (APLAC), version 6.1. The main goal of APLAC is to give the user full freedom in solving his/her problems without the restrictions of conventional simulators. The sixth generation of APLAC was created having improved convergence algorithms for DC, transient, and harmonic analyses and improved menu-driven actions. In addition, convolution technique was implemented enabling the use of frequency-dependent components in the transient analysis of nonlinear circuits. NTIS

N94-18135 Argonne National Lab., IL.
PERFORMANCE EVALUATIONS OF DEMOUNTABLE ELECTRICAL CONNECTIONS
R. C. Niemann, Y. S. Cha, J. R. Hull, W. E. Buckles (Superconductivity, Inc., Madison, WI.), and M. A. Daugherty (Superconductivity, Inc., Madison, WI.) 1993 9 p Presented at the International Cryogenic Engineering Conference and International Cryogenic Materials Conference, Albuquerque, NM, 12-16 Jul. 1993 Limited Reproducibility: More than 20% of this document may be affected by poor print
(Contract W-31-109-eng-38)
(DE93-017399; ANL/ET/CP-78473; CONF-930703-6) Avail: Issuing Activity (Department of Energy (DOE))

Electrical conductors operating in cryogenic environments can require demountable connections along their lengths. The connections must have low resistance and high reliability and should allow ready assembly and disassembly. In this work, the performance of two types of connections has been evaluated. The first connection type is a clamped surface-to-surface joint. The second connection type is a screwed joint that incorporates male and female machine-thread components. The connections for copper conductors have been evaluated experimentally at 77 K. Experimental variables included thread surface treatment and assembly methods. The results of the evaluations are presented. DOE

N94-18278# Illinois Univ., Urbana. Dept. of General Engineering.
OPTIMAL DESIGN OF BINARY PHASE-ONLY FILTERS USING GENETIC ALGORITHMS Final Report, Feb. 1992 - Feb. 1993
Kalyanmoy Deb Aug. 1993 55 p
(Contract F08630-92-K-0017)
(AD-A268737; WL-TR-93-7017) Avail: CASI HC A04/MF A01

The genetic algorithm is a mathematical optimization technique which has generally been applied to one-dimensional problems. In this work, the genetic algorithm was applied to a two-dimensional problem--the construction of binary phase-only spatial filters for optical pattern recognition. Spatial filters that are invariant to range and aspect changes are required for robust pattern recognition. Construction of invariant filters is an optimization problem where the correlation is the objective function for the genetic algorithm. Results are presented for correlation of a genetic algorithm-constructed filter with a multiple aspect angle target set. Filters using a hill-climber algorithm were also constructed and tested. DTIC

N94-18284# Hughes Aircraft Co., Torrance, CA. Electron Dynamics Div.
RF VACUUM MICROELECTRONICS Quarterly Technical Report, 1 Apr. - 30 Jun. 1993
David S. Komm 30 Jun. 1993 8 p
(Contract MDA972-92-C-0034)
(AD-A269454) Avail: CASI HC A02/MF A01

Both masks have been procured and used to fabricate devices. There was no design and procurement activity during this period. Processing was completed in this quarter. One lot of four wafers was processed, two of the wafers in the lot were of sufficient quality to test in vacuum. Test results were mixed, and the devices operated to higher breakdown potentials but emission current levels were not greatly increased. A number of in-situ gas and plasma exposure measurements were performed. A complete description of the test results is given. The first two wafers of a 4 wafer matrix were completed in this quarter. This experiment was basically designed to test and verify some of the early conclusions. The variables under consideration were the following: the dielectric thickness at two levels (5000 A and 10,000 A); the thickness of the gate meal (at two levels); and the aperture size of the emitters. DTIC

N94-18293# Microelectronics Center of North Carolina, Research Triangle Park.
FIELD EMITTER ARRAY RF AMPLIFIER DEVELOPMENT PROJECT, PHASE 1, OPTION 1 Quarterly Technical Report No. 7, 16 Apr. - 15 Jul. 1993
Gary E. McGuire 15 Jul. 1993 43 p
(Contract MDA972-91-C-0028)
(AD-A268687) Avail: CASI HC A03/MF A01

Key ideas include development of field emitter arrays with a cutoff frequency above 1 GHz, total current greater than 5 mA, and 5 A/sq cm current density with the gate electrode potential less than 250V. These characteristics are to be demonstrated for a lifetime of greater than 1 hour. We reduce capacitance and increase transconductance of field emitter arrays to improve frequency response. We focus on development of tall emitter columns to minimize capacitance and evaluate low work function materials and metals as emitter surface coatings, reduce gate dimensions, and improve tip sharpening to increase transconductance. Test methods are examined to permit characterization of more devices per test cycle. DTIC

N94-18311# Morehead State Univ., KY.
WORKSHOP ON MULTIFACTOR AGING MECHANISMS AND MODELS Final Report
V. K. Agarwal 22 Oct. 1992 31 p Workshop held in Victoria, BC, Canada, 22 Oct. 1992
(Contract N00014-92-J-1922)
(AD-A268668) Avail: CASI HC A03/MF A01

There have been considerable efforts to understand the aging and failure mechanisms of insulation in electrical systems. However, progress has been slow because of the complex nature of the subject particularly when dealing with multiple stresses e.g. electrical, thermal, mechanical, radiation, humidity and other environmental factors. When an insulating material is exposed to just one stress factor e.g. electric field, one must devise test(s) which are not only economically efficient and practical but which take into account the nature of electric field (ac, dc and pulsed), duration and level or field strength, and field configurations. Any additional stress factor(s) make the matrix of measurements and the understanding of resulting degradation processes more complex, time consuming and expensive. DTIC

N94-18312# Stanford Univ., CA. Dept. of Electrical Engineering.
SUPERCONDUCTING/SEMICONDUCTING HYBRIDS AND ADVANCE MEMORY CONCEPTS FOR SUPERCONDUCTING ELECTRONICS Technical Performance Report
M. R. Beasley and M. Horowitz 30 Jul. 1993 5 p
(Contract N00014-92-J-1886)
(AD-A268679) Avail: CASI HC A01/MF A01

The goal of this program is to explore advanced alternatives to the standard approaches to memory in Josephson junction digital electronics. The work includes the physics, circuits and systems aspects of the problem. It is widely recognized that memory is the weak suit of digital superconductive electronics. There are several problems. They are hard to build, particularly at high densities. Their speed is being challenged by leading edge semiconductor memories, albeit at the expense of high power dissipation. They are susceptible to trapped flux, which is both random in space and likely varying in time. All the current approaches to memory are based on the concept of storage of magnetic flux in a superconducting ring first proposed over 25 years ago by Anacker. Basically, there have been no new ideas in superconductive memory since that time. DTIC

N94-18318 Texas Technological Univ., Lubbock. Dept. of Electrical Engineering.
HIGH-POWER MICROWAVE BREAKDOWN OF DIELECTRIC INTERFACES Final Technical Report, 15 May 1991 - 14 May 1993
M. Kristiansen, L. Hatfield, and Mark Crawford 15 Jul. 1993 19 p
Limited Reproducibility: More than 20% of this document may be affected by microfiche quality
(Grant AF-AFOSR-0260-91)
(AD-A268844; AFOSR-93-0661TR) Avail: Issuing Activity (Defense Technical Information Center (DTIC))

This is the final technical report for AFOSR Grant No. 91-0260, that began in May 1991 and concluded two years later on 15 May 1993. The first objective of this project was to study the electrical breakdown, due to microwaves, which occurs on the surface of vacuum/atmosphere interfaces. This part of the contract was continuing work started on AFOSR Grant No. 88-102. The second objective of the project was to begin the development of a coaxial vircator. Most of the breakdown results were reported in the previous annual technical report and will only be mentioned briefly. One particular window was tested during the last year of the contract and its results will be detailed in this report. Extensive simulations have been conducted on the coaxial vircator geometry with surprising results. AH of the results from the coaxial vircator simulations are given in this report. DTIC

N94-18337*# Idaho Univ., Moscow. NASA Space Engineering Research Center.
THE 1991 3RD NASA SYMPOSIUM ON VLSI DESIGN
Gary K. Maki 1991 492 p Symposium held in Moscow, ID, 30-31 Oct. 1991 Sponsored in part by IEEE
(Grant NAGw-3293)
(NASA-CR-194589; NAS 1.26:194589) Avail: CASI HC A21/MF A04

Papers from the symposium are presented from the following sessions: (1) featured presentations 1; (2) very large scale integration (VLSI) circuit design; (3) VLSI architecture 1; (4) featured presentations 2; (5) neural networks; (6) VLSI architectures 2; (7) featured presentations 3; (8) verification 1; (9) analog design; (10) verification 2; (11) design innovations 1; (12) asynchronous design; and (13) design innovations 2. For individual titles, see N94-18338 through N94-18381.

N94-18338*# Johns Hopkins Univ., Laurel, MD. Applied Physics Lab.
EXPERIENCE WITH CUSTOM PROCESSORS IN SPACE FLIGHT APPLICATIONS c19
M. E. Fraeman, J. R. Hayes, D. A. Lohr, B. W. Ballard, R. L. Williams, and R. M. Henshaw *In* Idaho Univ., The 1991 3rd NASA Symposium on VLSI Design 1991 13 p (For primary document see N94-18337 04-33)
Avail: CASI HC A03/MF A04

The Applied Physics Laboratory (APL) has developed a magnetometer instrument for a swedish satellite named Freja with launch scheduled for August 1992 on a Chinese Long March rocket. The magnetometer controller utilized a custom microprocessor designed at APL with the Genesil silicon compiler. The processor evolved from our experience with an older bit-slice design and two prior single chip efforts. The architecture of our microprocessor greatly lowered software development costs because it was optimized to provide an interactive and extensible programming environment hosted by the target hardware. Radiation tolerance of the microprocessor was also tested and was adequate for Freja's mission – 20 kRad(Si) total dose and very infrequent latch-up and single event upset events. Author (revised)

N94-18339*# Calgary Univ. (Alberta). Electrical Engineering Dept.
NEW DYNAMIC FET LOGIC AND SERIAL MEMORY CIRCUITS FOR VLSI GaAs TECHNOLOGY
A. G. Eldin *In* Idaho Univ., The 1991 3rd NASA Symposium on VLSI Design 1991 9 p (For primary document see N94-18337 04-33)
Avail: CASI HC A02/MF A04

The complexity of GaAs field effect transistor (FET) very large scale integration (VLSI) circuits is limited by the maximum power dissipation while the uniformity of the device parameters determines the functional yield. In this work, digital GaAs FET circuits are presented that eliminate the DC power dissipation and reduce the area to 50% of that of the conventional static circuits. Its larger tolerance to device parameter variations results in higher functional yield. Author (revised)

N94-18340*# Idaho Univ., Moscow. NASA Space Engineering Research Center.
AUTOMATED ILA DESIGN FOR SYNCHRONOUS SEQUENTIAL CIRCUITS
M. N. Liu, K. Z. Liu, G. K. Maki, and S. R. Whitaker *In its* The 1991 3rd NASA Symposium on VLSI Design 1991 12 p (For primary document see N94-18337 04-33)
Avail: CASI HC A03/MF A04

An iterative logic array (ILA) architecture for synchronous sequential circuits is presented. This technique utilizes linear algebra to produce the design equations. The ILA realization of synchronous sequential logic can be fully automated with a computer program. A programmable design procedure is proposed to fullfill the design task and layout generation. A software algorithm in the C language has been developed and tested to generate 1 micron CMOS layouts using the Hewlett-Packard FUNGEN module generator shell. Author (revised)

N94-18341*# University of Western Australia, Nedlands. Dept. of Computer Science.
SINGLE PHASE DYNAMIC CMOS PLA USING CHARGE SHARING TECHNIQUE
Y. B. Dhong and C. P. Tsang *In* Idaho Univ., The 1991 3rd NASA Symposium on VLSI Design 1991 12 p (For primary document see N94-18337 04-33)
Avail: CASI HC A03/MF A04

A single phase dynamic CMOS NOR-NOR programmable logic array (PLA) using triggered decoders and charge sharing techniques for high speed and low power is presented. By using the triggered decoder technique, the ground switches are eliminated, thereby, making this new design much faster and lower power dissipation than conventional PLA's. By using the charge-sharing technique in a dynamic CMOS NOR structure, a cascading AND gate can be implemented. The proposed PLA's are presented with a delay-time of 15.95 and 18.05 nsec, respectively, which compare with a conventional single phase PLA with 35.5 nsec delay-time. For a typical example of PLA like the Signetics 82S100 with 16 inputs, 48 input minterms (m) and 8 output minterms (n), the 2-SOP PLA using the triggered 2-bit decoder is 2.23 times faster and has 2.1 times less power dissipation than the conventional PLA. These results are simulated using maximum drain current of 600 micro-A, gate length of 2.0 micron, V sub DD of 5 V, the capacitance of an input miniterm of 1600 fF, and the capacitance of an output minterm of 1500 fF. Author (revised)

N94-18342*# Idaho Univ., Moscow. NASA Space Engineering Research Center.
AN SEU IMMUNE LOGIC FAMILY
J. Canaris *In its* The 1991 3rd NASA Symposium on VLSI Design 1991 11 p (For primary document see N94-18337 04-33)
(Grant NAGw-1406)
Avail: CASI HC A03/MF A04

A new logic family, which is immune to single event upsets, is described. Members of the logic family are capable of recovery, regardless of the shape of the upsetting event. Glitch propagation from an upset node is also blocked. Logic diagrams for an Inverter, Nor, Nand, and Complex Gates are provided. The logic family can be implemented in a standard, commercial CMOS process with no additional masks. DC, transient, static power, upset recovery and layout characteristics of the new family, based on a commercial 1 micron CMOS N-Well process, are described. Author (revised)

N94-18343*# Idaho Univ., Moscow. NASA Space Engineering Research Center.
CELLULAR LOGIC ARRAY FOR COMPUTATION OF SQUARES
M. Shamanna, S. Whitaker, and J. Canaris *In its* The 1991 3rd NASA Symposium on VLSI Design 1991 7 p (For primary document see N94-18337 04-33)
(Grant NAGw-1406)
Avail: CASI HC A02/MF A04

A cellular logic array is described for squaring binary numbers. This array offers a significant increase in speed, with a relatively small hardware overhead. This improvement is a result of novel implementation of the formula (x + y)exp 2 = x(exp 2) + y(exp 2) + 2(x)(y). These results can also be incorporated in the existing arrays achieving considerable hardware reduction. Author (revised)

N94-18344*# Idaho Univ., Moscow. NASA Space Engineering Research Center.
FAULT TOLERANT SEQUENTIAL CIRCUITS USING SEQUENCE INVARIANT STATE MACHINES
M. Alahmad and S. Whitaker *In its* The 1991 3rd NASA Symposium on VLSI Design 1991 12 p (For primary document see N94-18337 04-33)
Avail: CASI HC A03/MF A04

The idea of introducing redundancy to improve the reliability of digital systems originates from papers published in the 1950's. Since then, redundancy has been recognized as a realistic means for constructing reliable systems. A method using redundancy to reconfigure the Sequency Invariant State Machine (SISM) to achieve fault tolerance is introduced. This new architecture is most useful in space applications, where recovery rather than replacement of faulty modules is the only means of maintenance. Author (revised)

N94-18345*# Superconducting Super Collider Lab., Dallas, TX.
VLSI ARCHITECTURES FOR GEOMETRICAL MAPPING PROBLEMS IN HIGH-DEFINITION IMAGE PROCESSING
K. Kim and J. Lee (Houston Univ., TX.) *In* Idaho Univ., The 1991 3rd NASA Symposium on VLSI Design 1991 8 p (For primary document see N94-18337 04-33)
Avail: CASI HC A02/MF A04

This paper explores a VLSI architecture for geometrical mapping address computation. The geometric transformation is discussed in the context of plane projective geometry, which invokes a set of basic transformations to be implemented for the general image processing. The homogeneous and 2-dimensional cartesian coordinates are employed to represent the transformations, each of which is implemented via an augmented CORDIC as a processing element. A specific scheme for a processor, which utilizes full-pipelining at the macro-level and parallel constant-factor-redundant arithmetic and full-pipelining at the micro-level, is assessed to produce a single VLSI chip for HDTV applications using state-of-art MOS technology. Author (revised)

N94-18346*# Idaho Univ., Moscow. Dept. of Electrical Engineering.
PERFORMANCE OF DEFECT-TOLERANT SET-ASSOCIATIVE CACHE MEMORIES
J. F. Frenzel *In its* The 1991 3rd NASA Symposium on VLSI Design 1991 9 p (For primary document see N94-18337 04-33)
(Grant NAGw-1406)
Avail: CASI HC A02/MF A04

The increased use of on-chip cache memories has led researchers to investigate their performance in the presence of manufacturing defects. Several techniques for yield improvement are discussed and results are presented which indicate that set-associativity may be used to provide defect tolerance as well as improve the cache performance. Tradeoffs between several cache organizations and replacement strategies are investigated and it is shown that token-based replacement may be a suitable alternative to the widely-used LRU strategy. Author (revised)

N94-18347*# Hewlett-Packard Co., Corvallis, OR.
SPROC: A MULTIPLE-PROCESSOR DSP IC
R. Davis *In* Idaho Univ., The 1991 3rd NASA Symposium on VLSI Design 1991 10 p (For primary document see N94-18337 04-33)
Avail: CASI HC A02/MF A04

A large, single-chip, multiple-processor, digital signal processing (DSP) integrated circuit (IC) fabricated in HP-Cmos34 is presented. The innovative architecture is best suited for analog and real-time systems characterized by both parallel signal data flows and concurrent logic processing. The IC is supported by a powerful development system that transforms graphical signal flow graphs into production-ready systems in minutes. Automatic compiler partitioning of tasks among four on-chip processors gives the IC the signal processing power of several conventional DSP chips. Author (revised)

N94-18348*# Idaho Univ., Moscow. NASA Space Engineering Research Center.
AN EXTENDED REED SOLOMON DECODER DESIGN
J. Chen, P. Owsley (Advanced Hardware Architectures, Moscow, ID.), and J. Purviance *In its* The 1991 3rd NASA Symposium on VLSI Design 1991 9 p (For primary document see N94-18337 04-33)
Avail: CASI HC A02/MF A04

It has previously been shown that the Reed-Solomon (RS) codes can correct errors beyond the Singleton and Rieger Bounds with an arbitrarily small probability of a miscorrect. That is, an (n,k) RS code can correct more than (n-k)/2 errors. An implementation of such an RS decoder is presented in this paper. An existing RS decoder, the AHA4010, is utilized in this work. This decoder is especially useful for errors which are patterned with a long burst plus some random errors. Author (revised)

N94-18349*# Idaho Univ., Moscow. NASA Space Engineering Research Center.
AN IMPROVED DISTRIBUTED ARITHMETIC ARCHITECTURE
X. Guo and D. W. Lynn *In its* The 1991 3rd NASA Symposium on VLSI Design 1991 13 p (For primary document see N94-18337 04-33)
(Grant NAGw-1406)
Avail: CASI HC A03/MF A04

Speed requirements have been, and will continue to be, a major consideration in the design of hardware to implement digital signal processing functions like digital filters and transforms like the DFT and DCT. The conventional approach is to increase speed by adding hardware and increasing chip area. The real challenge is to save chip area while still maintaining high speed performance. The approach we propose is based on the distributed arithmetic implementation (DA) of digital filters. The improvement is based on two observations. Firstly, a single memory element can replace several identical memory elements in a fully parallel DA implementation. Secondly, truncation or rounding may be introduced into the computation at strategic points without increasing error unduly. Both of these approaches can be used to attain area savings without impairing speed of operation. Author (revised)

N94-18350*# Lawrence Livermore National Lab., CA.
AN ANALOG RETINA MODEL FOR DETECTING DIM MOVING OBJECTS AGAINST A BRIGHT MOVING BACKGROUND **c61**
R. M. Searfus, M. E. Colvin, F. H. Eeckman, J. L. Teeters, and T. S. Axelrod *In* Idaho Univ., The 1991 3rd NASA Symposium on VLSI Design 1991 12 p (For primary document see N94-18337 04-33)
(Contract W-7405-eng-48)
Avail: CASI HC A03/MF A04

We are interested in applications that require the ability to track a dim target against a bright, moving background. Since the target signal will be less than or comparable to the variations in the background signal intensity, sophisticated techniques must be employed to detect the target. We present an analog retina model that adapts to the motion of the background in order to enhance targets that have a velocity difference with respect to the background. Computer simulation results and our preliminary concept of an analog 'Z' focal plane implementation are also presented. Author (revised)

N94-18351*# Stanford Univ., CA. Dept. of Electrical Engineering.
LOW POWER SIGNAL PROCESSING RESEARCH AT STANFORD **c32**
J. Burr, P. R. Williamson, and A. Peterson *In* Idaho Univ., The 1991 3rd NASA Symposium on VLSI Design 1991 13 p (For primary document see N94-18337 04-33)
(Grants NAGw-1910; NAGw-419)
Avail: CASI HC A03/MF A04

This paper gives an overview of the research being conducted at Stanford University's Space, Telecommunications, and Radioscience Laboratory in the area of low energy computation. It discusses the work we are doing in large scale digital VLSI neural networks, interleaved processor and pipelined memory architectures, energy estimation and optimization, multichip module packaging, and low voltage digital logic. Author (revised)

N94-18352*# United Technologies Corp., Colorado Springs, CO.
TECHNOLOGY, DESIGN, SIMULATION, AND EVALUATION FOR SEP-HARDENED CIRCUITS
J. R. Adams, D. Allred, M. Barry, P. Rudeck, R. Woodruff, J. Hoekstra, and H. Gardner *In* Idaho Univ., The 1991 3rd NASA Symposium on VLSI Design 1991 11 p (For primary document see N94-18337 04-33)
Avail: CASI HC A03/MF A04

This paper describes the technology, design, simulation, and evaluation for improvement of the Single Event Phenomena (SEP) hardness of gate-array and SRAM cells. Through the use of design and processing techniques, it is possible to achieve an SEP error rate less than 1.0 x 10(exp -10) errors/bit-day for a 9O percent worst-case geosynchronous orbit environment. Author (revised)

N94-18353*# Washington State Univ., Pullman. School of Electrical Engineering and Computer Science.
PULSE-FIRING WINNER-TAKE-ALL NETWORKS **c63**
Jack L. Meador *In* Idaho Univ., The 1991 3rd NASA Symposium on VLSI Design 1991 10 p (For primary document see N94-18337 04-33)
Avail: CASI HC A02/MF A04

Winner-take-all (WTA) neural networks using pulse-firing processing elements are introduced. In the pulse-firing WTA (PWTA) networks described, input and activation signal shunting is controlled by one shared lateral inhibition signal. This organization yields an O(n) area complexity that is convenient for integrated circuit implementation. Appropriately specified network parameters allow for the accurate continuous evaluation of inputs using a signal representation compatible with established pulse-firing neural network implementations. Author

N94-18354*# Idaho Univ., Moscow. Dept. of Electrical Engineering and Microelectronics Research Center.
TRAINING PRODUCT UNIT NEURAL NETWORKS WITH GENETIC ALGORITHMS **c63**
D. J. Janson, J. F. Frenzel, and D. C. Thelen *In its* The 1991 3rd NASA Symposium on VLSI Design 1991 8 p (For primary document see N94-18337 04-33)
Avail: CASI HC A02/MF A04

The training of product neural networks using genetic algorithms is discussed. Two unusual neural network techniques are combined; product units are employed instead of the traditional summing units and genetic algorithms train the network rather than backpropagation. As an example, a neural netork is trained to calculate the optimum width of transistors in a CMOS switch. It is shown how local minima affect the performance of a genetic algorithm, and one method of overcoming this is presented. Author (revised)

N94-18355*# Montana State Univ., Bozeman. Dept. of Electrical Engineering.
VLSI SYNTHESIS OF DIGITAL APPLICATION SPECIFIC NEURAL NETWORKS **c63**
Grant Beagles and Kel Winters (Advanced Hardware Architectures, Moscow, ID.) *In* Idaho Univ., The 1991 3rd NASA Symposium on VLSI Design 1991 10 p (For primary document see N94-18337 04-33)
Avail: CASI HC A02/MF A04

Neural networks tend to fall into two general categories: (1) software simulations, or (2) custom hardware that must be trained. The scope of this project is the merger of these two classifications into a system whereby a software model of a network is trained to perform a specific task and the results used to synthesize a standard cell realization of the network using automated tools. Author (revised)

N94-18356*# Washington State Univ., Pullman. School of Electrical Engineering and Computer Science.
MEASUREMENT SELECTION FOR PARAMETRIC IC FAULT DIAGNOSIS
A. Wu and J. Meador *In* Idaho Univ., The 1991 3rd NASA Symposium on VLSI Design 1991 12 p Sponsored by NSF-UIC CDADIC Project 90-1 (For primary document see N94-18337 04-33)
Avail: CASI HC A03/MF A04

Experimental results obtained with the use of measurement reduction for statistical IC fault diagnosis are described. The reduction method used involves data pre-processing in a fashion consistent with a specific definition of parametric faults. The effects of this preprocessing are examined. Author (revised)

N94-18357*# Idaho Univ., Moscow. NASA Space Engineering Research Center.
FUZZY CONTROL OF MAGNETIC BEARINGS **c37**
J. J. Feeley, G. M. Niederauer, and D. J. Ahlstrom *In its* The 1991 3rd NASA Symposium on VLSI Design 1991 14 p (For primary document see N94-18337 04-33)
Avail: CASI HC A03/MF A04

The use of an adaptive fuzzy control algorithm implemented on a VLSI chip for the control of a magnetic bearing was considered. The architecture of the adaptive fuzzy controller is similar to that of a neural network. The performance of the fuzzy controller is compared to that of a conventional controller by computer simulation. Author (revised)

N94-18358*# Houston Univ., TX. Dept. of Electrical Engineering.
DIRECT KINEMATICS SOLUTION ARCHITECTURES FOR INDUSTRIAL ROBOT MANIPULATORS: BIT-SERIAL VERSUS PARALLEL **c37**
J. Lee and K. Kim (Superconducting Super Collider Lab., Dallas, TX.) *In* Idaho Univ., The 1991 3rd NASA Symposium on VLSI Design 1991 10 p (For primary document see N94-18337 04-33)
Avail: CASI HC A02/MF A04

A Very Large Scale Integration (VLSI) architecture for robot direct kinematic computation suitable for industrial robot manipulators was investigated. The Denavit-Hartenberg transformations are reviewed to exploit a proper processing element, namely an augmented CORDIC. Specifically, two distinct implementations are elaborated on, such as the bit-serial and parallel. Performance of each scheme is analyzed with respect to the time to compute one location of the end-effector of a 6-links manipulator, and the number of transistors required. Author (revised)

N94-18359*# Idaho Univ., Moscow. Space Engineering Research Center.
SIMPLIFIED MICROPROCESSOR DESIGN FOR VLSI CONTROL APPLICATIONS c60
K. Cameron *In its* The 1991 3rd NASA Symposium on VLSI Design 1991 9 p (For primary document see N94-18337 04-33)
Avail: CASI HC A02/MF A04

A design technique for microprocessors combining the simplicity of reduced instruction set computers (RISC's) with the richer instruction sets of complex instruction set computers (CISC's) is presented. They utilize the pipelined instruction decode and datapaths common to RISC's. Instruction invariant data processing sequences which transparently support complex addressing modes permit the formulation of simple control circuitry. Compact implementations are possible since neither complicated controllers nor large register sets are required. Author (revised)

N94-18360*# Idaho Univ., Moscow. Space Engineering Research Center.
A MODIFIED RECONFIGURABLE DATA PATH PROCESSOR c60
G. Ganesh, S. Whitaker, and G. Maki *In its* The 1991 3rd NASA Symposium on VLSI Design 1991 10 p (For primary document see N94-18337 04-33)
(Grants NAGw-1406; NAG5-1043)
Avail: CASI HC A02/MF A04

High throughput is an overriding factor dictating system performance. A configurable data processor is presented which can be modified to optimize performance for a wide class of problems. The new processor is specifically designed for arbitrary data path operations and can be dynamically reconfigured. Author (revised)

N94-18361*# Hewlett-Packard Co., Corvallis, OR. Northwest IC Div.
SYSTOLIC ARRAY IC FOR GENETIC COMPUTATION
D. Anderson *In* Idaho Univ., The 1991 3rd NASA Symposium on VLSI Design 1991 5 p (For primary document see N94-18337 04-33)
Avail: CASI HC A01/MF A04

Measuring similarities between large sequences of genetic information is a formidable task requiring enormous amounts of computer time. Geneticists claim that nearly two months of CRAY-2 time are required to run a single comparison of the known database against the new bases that will be found this year, and more than a CRAY-2 year for next year's genetic discoveries, and so on. The DNA IC, designed at HP-ICBD in cooperation with the California Institute of Technology and the Jet Propulsion Laboratory, is being implemented in order to move the task of genetic comparison onto workstations and personal computers, while vastly improving performance. The chip is a systolic (pumped) array comprised of 16 processors, control logic, and global RAM, totaling 400,000 FETS. At 12 MHz, each chip performs 2.7 billion 16 bit operations per second. Using 35 of these chips in series on one PC board (performing nearly 100 billion operations per second), a sequence of 560 bases can be compared against the eventual total genome of 3 billion bases, in minutes--on a personal computer. While the designed purpose of the DNA chip is for genetic research, other disciplines requiring similarity measurements between strings of 7 bit encoded data could make use of this chip as well. Cryptography and speech recognition are two examples. A mix of full custom design and standard cells, in CMOS34, were used to achieve these goals. Innovative test methods were developed to enhance controllability and observability in the array. This paper describes these techniques as well as the chip's functionality. This chip was designed in the 1989-90 timeframe. Derived from text

N94-18362*# Stanford Univ., CA. Computer Systems Lab.
HIGH-PERFORMANCE MULTIPROCESSOR ARCHITECTURE FOR A 3-D LATTICE GAS MODEL c60
F. Lee, M. Flynn, and M. Morf *In* Idaho Univ., The 1991 3rd NASA Symposium on VLSI Design 1991 14 p (For primary document see N94-18337 04-33)
(Grant NAGw-419)
Avail: CASI HC A03/MF A04

The lattice gas method has recently emerged as a promising discrete particle simulation method in areas such as fluid dynamics. We present a very high-performance scalable multiprocessor architecture, called ALGE, proposed for the simulation of a realistic 3-D lattice gas model, Henon's 24-bit FCHC isometric model. Each of these VLSI processors is as powerful as a CRAY-2 for this application. ALGE is scalable in the sense that it achieves linear speedup for both fixed and increasing problem sizes with more processors. The core computation of a lattice gas model consists of many repetitions of two alternating phases: particle collision and propagation. Functional decomposition by symmetry group and virtual move are the respective keys to efficient implementation of collision and propagation. Author

N94-18363*# Idaho Univ., Moscow. Dept. of Computer Science.
VERIFICATION OF VLSI DESIGNS
P. J. Windley *In its* The 1991 3rd NASA Symposium on VLSI Design 1991 14 p (For primary document see N94-18337 04-33)
Avail: CASI HC A03/MF A04

In this paper we explore the specification and verification of VLSI designs. The paper focuses on abstract specification and verification of functionality using mathematical logic as opposed to low-level boolean equivalence verification such as that done using BDD's and Model Checking. Specification and verification, sometimes called formal methods, is one tool for increasing computer dependability in the face of an exponentially increasing testing effort. Author

N94-18364*# Montreal Univ. (Quebec). Dept. of Electrical and Computer Engineering.
A NEW VARIABLE TESTABILITY MEASURE
M. Jamoussi, B. Kaminska, and D. Mukhedkar *In* Idaho Univ., The 1991 3rd NASA Symposium on VLSI Design 1991 8 p (For primary document see N94-18337 04-33)
Avail: CASI HC A02/MF A04

In this paper, we propose a new Variable Testability Measure (VTM) for implementing testability at the high-level synthesis stage of the design process of integrated circuits. This new approach, based on binary decision diagrams, representing fully functional blocks of a circuit, and on their cyclomatic testability measures. It manipulates dataflow blocks to predict whether the circuit is testable and the vector set required to test it. Author

N94-18365*# Concordia Univ., Montreal (Quebec). Dept. of Computer Science.
CONTROLLING STATE EXPLOSION DURING AUTOMATIC VERIFICATION OF DELAY-INSENSITIVE AND DELAY-CONSTRAINED VLSI SYSTEMS USING THE POM VERIFIER
D. Probst and L. Jensen *In* Idaho Univ., The 1991 3rd NASA Symposium on VLSI Design 1991 8 p (For primary document see N94-18337 04-33)
(Grants A3363; MEF0040121)
Avail: CASI HC A02/MF A04

Delay-insensitive VLSI systems have a certain appeal on the ground due to difficulties with clocks; they are even more attractive in space. We answer the question, is it possible to control state explosion arising from various sources during automatic verification (model checking) of delay-insensitive systems? State explosion due to concurrency is handled by introducing a partial-order representation for systems, and defining system correctness as a simple relation between two partial orders on the same set of system events (a graph problem). State explosion due to nondeterminism (chiefly arbitration) is handled when the system to be verified has a clean, finite recurrence structure. Backwards branching is a further optimization. The heart of this approach is the ability, during model checking, to discover a compact finite presentation of the verified system without prior composition of system components. The fully-implemented POM verification system has polynomial space and time performance on traditional asynchronous-circuit benchmarks that are exponential in space and time for other verification systems. We also sketch the generalization of this approach to handle delay-constrained VLSI systems. Author

N94-18366*# California Univ., Davis. Div. of Computer Science.
FORMAL VERIFICATION OF AN MMU AND MMU CACHE c60
E. T. Schubert *In* Idaho Univ., The 1991 3rd NASA Symposium on VLSI Design 1991 12 p (For primary document see N94-18337 04-33)
Avail: CASI HC A03/MF A04

We describe the formal verification of a hardware subsystem consisting of a memory management unit and a cache. These devices are verified independently and then shown to interact correctly when composed. The MMU authorizes memory requests and translates virtual addresses to real addresses. The cache improves performance by maintaining a LRU (least recently used) list from the memory resident segment table. Author

N94-18367*# British Columbia Univ., Vancouver. Dept. of Computer Science.

FORMAL HARDWARE VERIFICATION OF DIGITAL CIRCUITS

J. Joyce and C.-J. Seger *In* Idaho Univ., The 1991 3rd NASA Symposium on VLSI Design 1991 11 p Sponsored in part by NSERC (For primary document see N94-18337 04-33)

Avail: CASI HC A03/MF A04

The use of formal methods to verify the correctness of digital circuits is less constrained by the growing complexity of digital circuits than conventional methods based on exhaustive simulation. This paper briefly outlines three main approaches to formal hardware verification: symbolic simulation, state machine analysis, and theorem-proving. Author

N94-18368*# Washington State Univ., Pullman. School of Electrical Engineering and Computer Scienece.

HIGH ACCURACY SWITCHED-CURRENT CIRCUITS USING AN IMPROVED DYNAMIC MIRROR

G. Zweigle and T. Fiez *In* Idaho Univ., The 1991 3rd NASA Symposium on VLSI Design 1991 10 p Sponsored in part by NSF (For primary document see N94-18337 04-33)

Avail: CASI HC A02/MF A04

The switched-current technique, a recently developed circuit approach to analog signal processing, has emerged as an alternative/compliment to the well established switched-capacitor circuit technique. High speed switched-current circuits offer potential cost and power savings over slower switched-capacitor circuits. Accuracy improvements are a primary concern at this stage in the development of the switched-current technique. Use of the dynamic current mirror has produced circuits that are insensitive to transistor matching errors. The dynamic current mirror has been limited by other sources of error including clock-feedthrough and voltage transient errors. In this paper we present an improved switched-current building block using the dynamic current mirror. Utilizing current feedback the errors due to current imbalance in the dynamic current mirror are reduced. Simulations indicate that this feedback can reduce total harmonic distortion by as much as 9 dB. Additionally, we have developed a clock-feedthrough reduction scheme for which simulations reveal a potential 10 dB total harmonic distortion improvement. The clock-feedthrough reduction scheme also significantly reduces offset errors and allows for cancellation with a constant current source. Experimental results confirm the simulated improvements. Author (revised)

N94-18369*# Idaho Univ., Moscow. NASA Space Engineering Research Center.

A TUNABLE CMOS CONSTANT CURRENT SOURCE

D. Thelen *In its* The 1991 3rd NASA Symposium on VLSI Design 1991 9 p (For primary document see N94-18337 04-33)

Avail: CASI HC A02/MF A04

A constant current source has been designed which makes use of on chip electrically erasable memory to adjust the magnitude and temperature coefficient of the output current. The current source includes a voltage reference based on the difference between enhancement and depletion transistor threshold voltages. Accuracy is +/- 3% over the full range of power supply, process variations, and temperature using eight bits for tuning. Author

N94-18370*# Idaho Univ., Moscow. NASA Space Engineering Research Center.

DC AND SMALL-SIGNAL PHYSICAL MODELS FOR THE AlGaAs/GaAs HIGH ELECTRON MOBILITY TRANSISTOR

J. C. Sarker and J. E. Purviance *In its* The 1991 3rd NASA Symposium on VLSI Design 1991 15 p (For primary document see N94-18337 04-33)

(Grant NAG5-1043)

Avail: CASI HC A03/MF A04

Analytical and numerical models are developed for the microwave small-signal performance, such as transconductance, gate-to-source capacitance, current gain cut-off frequency and the optimum cut-off frequency of the AlGaAs/GaAs High Electron Mobility Transistor (HEMT), in both normal and compressed transconductance regions. The validated I-V characteristics and the small-signal performances of four HeMT's are presented. Author

N94-18371*# Idaho Univ., Moscow. Dept. of Computer Science.

FORMAL SPECIFICATION OF A HIGH SPEED CMOS CORRELATOR

P. J. Windley *In its* The 1991 3rd NASA Symposium on VLSI Design 1991 8 p (For primary document see N94-18337 04-33)

(Grant NAGw-1406)

Avail: CASI HC A02/MF A04

The formal specification of a high speed CMOS correlator is presented. The specification gives the high-level behavior of the correlator and provides a clear, unambiguous description of the high-level architecture of the device. Author

N94-18372*# Idaho Univ., Moscow. NASA Space Engineering Research Center.

A VERIFICATION LOGIC REPRESENTATION OF INDETERMINISTIC SIGNAL STATES

J. W. Gambles and P. J. Windley *In its* The 1991 3rd NASA Symposium on VLSI Design 1991 21 p (For primary document see N94-18337 04-33)

Avail: CASI HC A03/MF A04

The integration of modern CAD tools with formal verification environments require translation from hardware description language to verification logic. A signal representation including both unknown state and a degree of strength indeterminacy is essential for the correct modeling of many VLSI circuit designs. A higher-order logic theory of indeterministic logic signals is presented. Author

N94-18373*# Stanford Univ., CA. Dept. of Electrical Engineering.

ULTRA LOW POWER CMOS TECHNOLOGY

J. Burr and A. Peterson *In* Idaho Univ., The 1991 3rd NASA Symposium on VLSI Design 1991 12 p (For primary document see N94-18337 04-33)

(Grants NAGw-1910; NAGw-419)

Avail: CASI HC A03/MF A04

This paper discusses the motivation, opportunities, and problems associated with implementing digital logic at very low voltages, including the challenge of making use of the available real estate in 3D multichip modules, energy requirements of very large neural networks, energy optimization metrics and their impact on system design, modeling problems, circuit design constraints, possible fabrication process modifications to improve performance, and barriers to practical implementation. Author

N94-18374*# Idaho Univ., Moscow. Dept. of Electrical Engineering.

PARALLEL OPTIMIZATION ALGORITHMS AND THEIR IMPLEMENTATION IN VLSI DESIGN c61

G. Lee and J. J. Feeley *In its* The 1991 3rd NASA Symposium on VLSI Design 1991 12 p (For primary document see N94-18337 04-33)

Avail: CASI HC A03/MF A04

Two new parallel optimization algorithms based on the simplex method are described. They may be executed by a SIMD parallel processor architecture and be implemented in VLSI design. Several VLSI design implementations are introduced. An application example is reported to demonstrate that the algorithms are effective. Author

N94-18375*# Portland State Univ., OR. Dept. of Electrical Engineering.

CANONICAL MULTI-VALUED INPUT REED-MULLER TREES AND FORMS c61

M. A. Perkowski and P. D. Johnson *In* Idaho Univ., The 1991 3rd NASA Symposium on VLSI Design 1991 13 p Sponsored in part by NSF (For primary document see N94-18337 04-33)

Avail: CASI HC A03/MF A04

There is recently an increased interest in logic synthesis using EXOR gates. The paper introduces the fundamental concept of Orthogonal Expansion, which generalizes the ring form of the Shannon expansion to the logic with multiple-valued (mv) inputs. Based on this concept we are able to define a family of canonical tree circuits. Such circuits can be considered for binary and multiple-valued input cases. They can be multi-level (trees and DAG's) or flattened to two-level AND-EXOR circuits. Input decoders similar to those used in Sum of Products (SOP) PLA's are used in realizations of multiple-valued input functions. In the case of the binary logic the family of flattened AND-EXOR circuits includes several forms discussed by Davio and Green. For the case of the logic with multiple-valued inputs, the family of the flattened mv AND-EXOR circuits includes three expansions known from literature and two new expansions. Author

N94-18376*# Idaho Univ., Moscow. NASA Space Engineering Research Center.

ASYNCHRONOUS SEQUENTIAL CIRCUIT DESIGN USING PASS TRANSISTOR ITERATIVE LOGIC ARRAYS

M. N. Liu, G. K. Maki, and S. R. Whitaker *In its* The 1991 3rd NASA Symposium on VLSI Design 1991 14 p (For primary document see N94-18337 04-33)

Avail: CASI HC A03/MF A04

The iterative logic array (ILA) is introduced as a new architecture for asynchronous sequential circuits. This is the first ILA architecture for sequential circuits reported in the literature. The ILA architecture produces a very regular circuit structure. Moreover, it is immune to both 1-1 and 0-0 crossovers and is free of hazards. This paper also presents a new critical race free STT state assignment which produces a simple form of design equations that greatly simplifies the ILA realizations. Author

N94-18377*# Idaho Univ., Moscow. NASA Space Engineering Research Center.

PULSE MODE VLSI ASYNCHRONOUS CIRCUITS

Q. Chen and G. Maki *In its* The 1991 3rd NASA Symposium on VLSI Design 1991 11 p (For primary document see N94-18337 04-33)

Avail: CASI HC A03/MF A04

A new basic VLSI circuit element is presented that can be used to realize pulse mode asynchronous sequential circuits. A synthesis procedure is developed along with an unconventional state assignment procedure. Level input asynchronous sequential circuits can be realized by converting a regular flow table into a differential mode flow table, thereby allowing the new synthesis technique to be general. The new circuits tolerate 1-1 crossovers. This circuit also provides a means for state sequence detection and real time fault detection. Author

N94-18378*# Idaho Univ., Moscow. NASA Space Engineering Research Center.

IMPROVED SELF ARBITRATED VLSI ASYNCHRONOUS CIRCUITS

P. Winterrowd *In its* The 1991 3rd NASA Symposium on VLSI Design 1991 10 p (For primary document see N94-18337 04-33)

Avail: CASI HC A02/MF A04

This paper introduces an improved method for designing the class of CMOS VLSI asynchronous sequential circuits introduced in the paper by Sterling R. Whitaker and Gary K. Maki, 'Self Arbitrated VLSI Asynchronous Circuits.' Of main interest here is the simple design by inspection rules that arise from these circuits. This paper presents a variation on these circuits which reduces the number of transistors required.
Author (revised)

N94-18379*# Madras Univ. (India). Coll. of Engineering.

A SPECIAL PURPOSE SILICON COMPILER FOR DESIGNING SUPERCOMPUTING VLSI SYSTEMS **c60**

N. Venkateswaran, P. Murugavel, V. Kamakoti, M. J. ShankarRaman, S. Rangarajan, M. Mallikarjun, B. Karthikeyan, T. S. Prabhakar, V. Satish, and P. R. Venkatasubramaniam et al *In* Idaho Univ., The 1991 3rd NASA Symposium on VLSI Design 1991 15 p (For primary document see N94-18337 04-33)

Avail: CASI HC A03/MF A04

Design of general/special purpose supercomputing VLSI systems for numeric algorithm execution involves tackling two important aspects, namely their computational and communication complexities. Development of software tools for designing such systems itself becomes complex. Hence a novel design methodology has to be developed. For designing such complex systems a special purpose silicon compiler is needed in which: the computational and communicational structures of different numeric algorithms should be taken into account to simplify the silicon compiler design, the approach is macrocell based, and the software tools at different levels (algorithm down to the VLSI circuit layout) should get integrated. In this paper a special purpose silicon (SPS) compiler based on PACUBE macrocell VLSI arrays for designing supercomputing VLSI systems is presented. It is shown that turn-around time and silicon real estate get reduced over the silicon compilers based on PLA's, SLA's, and gate arrays. The first two silicon compiler characteristics mentioned above enable the SPS compiler to perform systolic mapping (at the macrocell level) of algorithms whose computational structures are of GIPOP (generalized inner product outer product) form. Direct systolic mapping on PLA's, SLA's, and gate arrays is very difficult as they are micro-cell based. A novel GIPOP processor is under development using this special purpose silicon compiler. Author (revised)

N94-18380*# Old Dominion Univ., Hampton, VA. Dept. of Computer science.

A FAST ADAPTIVE CONVEX HULL ALGORITHM ON TWO-DIMENSIONAL PROCESSOR ARRAYS WITH A RECONFIGURABLE BUS SYSTEM **c61**

S. Olariu, J. Schwing, and J. Zhang *In* Idaho Univ., The 1991 3rd NASA Symposium on VLSI Design 1991 9 p (For primary document see N94-18337 04-33)

(Contract NCC1-99; NSF CCR-89-09996)

Avail: CASI HC A02/MF A04

A bus system that can change dynamically to suit computational needs is referred to as reconfigurable. We present a fast adaptive convex hull algorithm on a two-dimensional processor array with a reconfigurable bus system (2-D PARBS, for short). Specifically, we show that computing the convex hull of a planar set of n points taken O(log n/log m) time on a 2-D PARBS of size mn x n with 3 less than or equal to m less than or equal to n. Our result implies that the convex hull of n points in the plane can be computed in O(1) time in a 2-D PARBS of size n(exp 1.5) x n.
Author (revised)

N94-18381*# Idaho Univ., Moscow. NASA Space Engineering Research Center.

VHDL SIMULATION WITH ACCESS TO TRANSISTOR MODELS

J. Gibson *In its* The 1991 3rd NASA Symposium on VLSI Design 1991 5 p (For primary document see N94-18337 04-33)

Avail: CASI HC A01/MF A04

Hardware description languages such as VHDL have evolved to aid in the design of systems with large numbers of elements and a wide range of electronic and logical abstractions. For high performance circuits, behavioral models may not be able to efficiently include enough detail to give designers confidence in a simulation's accuracy. One option is to provide a link between the VHDL environment and a transistor level simulation environment. The coupling of the Vantage Analysis Systems VHDL simulator and the NOVA simulator provides the combination of VHDL modeling and transistor modeling. Author

N94-18390 Massachusetts Inst. of Tech., Cambridge. National Magnet Lab.

SYNTHESIS AND STUDY OF HIGH-T(SUB c) SUPERCONDUCTING ELECTRONIC MATERIALS Final Technical Report, 1 Apr. 1989 - 31 Dec. 1992

Paul M. Tedrow 30 Jul. 1993 11 p Limited Reproducibility: More than 20% of this document may be affected by microfiche quality

(Grant AF-AFOSR-0130-90)

(AD-A268851; AFOSR-93-0658TR) Avail: CASI HC A03

The research program described here was designed to contribute to the evaluation of high T(sub c) superconducting materials for usefulness in electronic circuitry. The experimental techniques emphasized in this plan included electron tunneling and the use of intense magnetic fields to obtain information about the electronic properties of thin films of these materials. The superconductors studied included BiSrCaCuO, NdCeCuO, and BaKBiO. Thin films were formed by pulsed laser ablation, magnetron sputtering, and molecular beam epitaxy. In addition to obtaining electronic transport and tunneling data on these materials, a technique was found to make high-quality superconductor-insulator-superconductor tunnel junctions using artificial grain boundaries. This technique is the only one thus far discovered for making all-thin-film quasiparticle tunnel junctions reliably from high T(sub c) materials. DTIC

N94-18400 Iowa Univ., Iowa City.

ON TIMING FAULTS IN DIGITAL LOGIC CIRCUITS Final Report

Sudhakar M. Reddy 9 Aug. 1993 12 p Limited Reproducibility: More than 20% of this document may be affected by microfiche quality
(Contract N00014-90-J-1793)
(AD-A268714) Avail: CASI HC A03

To insure correct operation of digital logic circuits one must ascertain that the circuits perform functionally correct operations, at desired speeds or clock rates. Extensive research has been expended to derive procedures to ascertain the correct functional behavior of logic circuits. For example, procedures to detect line stuck-at faults and other logic faults help identify faulty circuits that do not perform correct functional operations. Relatively much less effort has been expended to derive procedures to ascertain correct operations by digital logic circuit at desired clock rates. Circuit failures causing malfunctions while operating at desired clock rates, but may not at other clock rates, are modeled to test logic circuits to detect and locate delay faults and to develop methods to design logic circuits that are easily testable for delay faults. DTIC

N94-18452 Phillips Lab., Kirtland AFB, NM.
THE GYROTRON BACKWARD-WAVE-OSCILLATOR EXPERIMENT Final Progress Report, Oct. 1991 - Sep. 1992
T. A. Spencer, C. E. Davis, M. J. Arman, and K. J. Hendricks Jul. 1993 47 p Limited Reproducibility: More than 20% of this document may be affected by microfiche quality
(AF Proj. 2301)
(AD-A268982; AD-E201588; PL-TR-93-1011) Avail: CASI HC A03

Experimental and theoretical analyses, including particle-in-cell computer code simulations, are presented for the Gyrotron Backward Wave oscillator (Gyro-BWO) highpower microwave device. The Gyro-BWO has been designed, constructed, and initially tested as a frequency tunable device. The design has concentrated on a TE01, 4- to 6- GHz annular beam device. The annular beam is produced by the RAMBO pulser, which has a diode voltage of -300 to -800 kV and diode current of 1 to 20 kA. Initial results have shown that the device is operating in the backward wave mode. Initial results have also demonstrated that the device is magnetically tunable; that is, the frequency is tunable by adjusting the magnetic field. A Vlasov-type antenna is used for the extraction of the microwave signal on the diode end of the experiment, with initial power extraction of up to 2 MW. DTIC

N94-18471# Army Lab. Command, Fort Monmouth, NJ. Electronics Technology and Devices Lab.
LOW-NOISE OSCILLATORS FOR AIRBORNE RADAR APPLICATIONS, REVISION 1 Technical Report
Raymond L. Filler and John R. Vig Aug. 1993 20 p
(DA Proj. 1L1-62705-AH-94)
(AD-A269372; SLCET-TR-91-26-REV-1) Avail: CASI HC A03/MF A01

Vibration-induced phase noise can change the probability of detection of moving-target indicator (MTI) radar from near-100 percent to zero. Oscillators that are capable of meeting the requirements of MTI radar systems in a quiet environment are readily available. In the vibrating environments of airborne platforms, however, the phase noise of oscillators degrades very significantly. For example, a 10-MHz crystal oscillator may have a phase noise of -140 dBc/Hz, 100 Hz from the carrier. Assuming a typical one part per billion per g acceleration sensitivity, this phase noise degrades to -93 dBc/Hz under a 0.1 sq g/Hz random vibration at 100 Hz away from the carrier. If there is a 1g sinusoidal vibration at 100 Hz, there will be a pair of -86 dBc spectral lines superimposed on the signal. Of course, upon multiplication to 10 GHz, the phase noise increases by at least another 60 dB. This report reviews the causes and effects of acceleration sensitivity of bulkwave quartz crystal resonators, and the methods that reduce or compensate for that sensitivity. Most of what is discussed is equally relevant to surface acoustic wave (SAW), shallow bulk acoustic wave (SBAW), dielectric resonator-oscillators (DRO), and other types of oscillators. DTIC

N94-18638 California Univ., Berkeley. Electronics Research Lab.
JOINT SERVICES ELECTRONICS PROGRAM Final Report, 6 Jun. 1990 - 5 Jun. 1993
Jeffrey Bokor and Michael A. Lieberman 31 Jul. 1993 17 p Limited Reproducibility: More than 20% of this document may be affected by microfiche quality
(Contract F49620-90-C-0029)
(AD-A269383; UCB/ERL-90/4; AFOSR-93-0676TR) Avail: CASI HC A03

This report summarizes the research activity supported by the Joint Services Electronics Program at the Electronics Research Laboratory for the period June 1990 to June 1993. It includes the Director's overview, a listing of principal investigators, degrees awarded to students, and a list of publications and presentations. The research was organized into three themes during this period: Quantum Electronic Devices, Semiconductor Electronic Devices, and Neural Networks and Applications. Significant advances were made in all three areas. Under Quantum Electronic Devices considerable progress was made in overcoming the difficulties of realizing surface emitting optoelectronic devices. The novel growth technique of phase-locked epitaxy was developed which allowed for the improvement in the control of layer thicknesses and improved performance of lasers. Under Semiconductor Electronic Devices, success was achieved in the deep sub-micron MOSFET program. Careful analysis of the fundamental issues that limit the continuation of the miniaturization of transistors has been an ongoing activity in this program. In the Neural Network and Applications Area, a prominent feature of the program has been the integration between theory and hardware. Revolutionary new architectures and algorithms for neural networks were investigated and tested on real-world applications, with particular attention given to applications of specific DOD interest. DTIC

N94-18639# Georgia Tech Research Inst., Atlanta. Inst. of Technology.
FIELD EMISSION CATHODE AND VACUUM MICROELECTRONIC MICROWAVE AMPLIFIER DEVELOPMENT Technical Progress Report, 1 Jul. 1992 - 31 Mar. 1993
Wayne L. Ohlinger and D. N. Hill 31 Mar. 1993 55 p
(Contract MDA972-91-C-0034)
(AD-A269526) Avail: CASI HC A04/MF A01

The objective of this report is to summarize progress, indicate problem areas that have been addressed, outline plans for future work, and to discuss, in a realistic manner, the likelihood that the proposed work will be completed in a reasonable time frame. Although we knew that the growth of the ZrO2 (center dot) Y2O3-W (ZYW) composite was far from an exact science, we felt that we could build on prior work in this area and make rapid progress toward solving some problems. However, a few of these problems, particularly that of banding in the structure (discontinuities in the growth of the tungsten fibers) proved to be more recalcitrant than expected. Nevertheless, an adequate amount of material with continuous fiber growth has now been made to fabricate a sufficient supply of samples to complete the proposed work. The composite growth work is discussed. Etching of the composites also proved more difficult than anticipated. Plasma etching was investigated, which may eventually provide better, and more uniform, pin tip geometries than were ever available with the chemical etches. LVFE structure development is recounted. Most of the work on emission testing has been associated with the set-up of a vacuum test station, design and assembly of a test vehicle, and collection of the associated electrical equipment needed for both the CW and RF electrical tests of the field emission cathodes. DTIC

N94-18667# Raytheon Co., Lexington, MA. Research Div.
RF VACUUM MICROELECTRONICS
16 Sep. 1993 6 p
(Contract MDA972-91-C-0032; ARPA Order 8162)
(AD-A270003; RAY/RD/S-4922) Avail: CASI HC A02/MF A01

This document reports progress on the following: (1) Stress in evaporated and sputtered moly metalization reduced; (2) Two chips evaluated at moderate current levels (6 devices/chip) and coated with 200 A of silicon and zirconium carbide respectively; (3) High frequency alumina redesigned; and (4) Masks for optical lithography for low resolution steps obtained for increased throughput. DTIC

N94-18695 University of Southern California, Marina del Rey. Information Sciences Inst.
ARPA/CSTO RAPID VLSI IMPLEMENTATION Final Technical Report, 28 Sep. 1987 - 30 Sep. 1991
Cesar A. Pina Jul. 1993 144 p Limited Reproducibility: More than 20% of this document may be affected by microfiche quality
(Contract F29601-87-C-0069; ARPA Order 6132)
(AD-A269170) Avail: CASI HC A07

The task objective was to provide rapid access to cost effective, state-of-the-art U.S. microelectronics industry fabrication technology for DoD customers and the educational community. This access was provided through the establishment of a prototyping service for use by the DARPA and NSF research communities which offered access to a variety of technologies unobtainable from a single fabrication source. The Defense Advanced Research Projects Agency (DARPA) had the goal of providing state-of-the-art VLSI fabrication services and electronic systems assembly technology to DoD customers and the educational community to ensure that DoD has access to low-cost, advanced electronic assemblies and to ensure that the country's newly emerging engineers will be able to support military needs in the area of electronics. The first task was to provide VLSI fabrication to DoD and DARPA supported contractors who have need of custom chips and assemblies. The second task was to provide this same technology to NSF-sponsored activities, under DARPA guidance. DTIC

N94-18701# Wright State Univ., Dayton, OH. Dept. of Electrical Engineering.

DESIGN AND SIMULATION OF A GALLIUM-ARSENIDE SECOND ORDER SIGMA-DELTA ANALOG TO DIGITAL CONVERTER Final Report, 4 Jan. - 16 Aug. 1993

Raymond E. Siferd and Eric W. Mahurin 16 Aug. 1993 64 p
(Contract F33615-92-C-1056)
(AD-A269494; WL-TR-93-5028) Avail: CASI HC A04/MF A01

In this report, the design and simulation of a sigma-delta analog-digital converter is presented. The key to sigma-delta conversion is trading off time resolution for amplitude resolution. In this report, second-order converters are used which allows the amplitude resolution to increase several times faster than the time resolution decreases. The sigma-delta modulator contains two basic components--an analog sigma-delta modulator and a digital low-pass filter. The modulator generates a stream of bits representing the analog input. The low-pass filter takes out the high frequency variations in this bit stream and generates a stream of multi-bit words. The report shows the designs and simulations of two different second-order sigma-delta modulators. Both of these circuits use Gallium-Arsenide MESFET technology to achieve an oversampled clock rate of 512-MHz. The first modulator contains unique integrators based on the square law of field effect transistors (FET's). The second modulator contains integrators using single-stage op-amps, current sources, and current sinks. Both modulators contain a unique clocking scheme that allows the continuous-time integrators to be insensitive to the delay of the quantizers. DTIC

N94-18706 California Univ., Los Angeles.

VLSI FOR HIGH-SPEED DIGITAL SIGNAL PROCESSING Report, 1 Oct. 1992 - 30 Sep. 1993

Alan N. Willson, Jr. 30 Sep. 1993 13 p Limited Reproducibility: More than 20% of this document may be affected by microfiche quality
(Contract N00014-91-J-1852)
(AD-A270406) Avail: CASI HC A03

During the past quarter we have completed the testing of our recently fabricated single-processor IC. This is the last preliminary chip we intend to fabricate before fabricating our full five-processor ring IC. Its primary purpose is to verify that all aspects of our ALU, program and coefficient RAM's, and Register Blocks are functioning correctly. The chip provides for 11-bit input and output data with 16-bit internal data and 11-bit coefficients (stored in on-chip memory). The chip also has an 8-bit microprocessor bus interface for loading programs and coefficients. The IC contains 25,000 transistors and occupies an area of 14.8 mm squared (3.7 mm by 4.0 mm including pads) in 1.2 micron CMOS technology. DTIC

N94-18709 California Univ., Los Angeles.

PROGRAMMABLE LINEAR PHASE DIGITAL FILTERS Report, 1 Oct. 1992 - 30 Sep. 1993

Alan N. Willson, Jr. 30 Sep. 1993 4 p Limited Reproducibility: More than 20% of this document may be affected by microfiche quality
(Contract N00014-93-I-1019)
(AD-A270413) Avail: CASI HC A01

This AASERT grant has only been in effect for one month. During this period, however, one paper has been submitted for publication in the IEEE Transactions on Signal Processing. The paper describes a technique using Jacobian elliptic functions which, by removing a previous method's double zero constraint, yields improved designs of linear phase IIR filters. DTIC

N94-18749 Army Research Lab., Adelphi, MD.

FABRICATION PROCESS FOR CANTILEVER BEAM MICROMECHANICAL SWITCHES Final Report, Jul. 1985 - Dec. 1989

Timothy J. Mermagen and Bernard J. Rod Aug. 1993 22 p Limited Reproducibility: More than 20% of this document may be affected by microfiche quality
(AD-A269716; ARL-MR-96) Avail: CASI HC A03

This report presents a detailed process description for fabrication of a micromechanical accelerometer sensor switch. The switch consists of a metallic cantilever beam structure that is defined with silicon micromachining processing technology. The beam is made up of a gold-nickel-gold trimetallic structure, which is anchored at one end to a silicon substrate; the process was designed to be compatible with current integrated circuit technology used in industry. DTIC

N94-18805# Los Alamos National Lab., NM.

HIGH PRESSURE METALLIZATION OF MOTT INSULATORS: MAGNETIC, STRUCTURAL AND ELECTRONIC PROPERTIES

M. P. Pasternak, G. Hearne, E. Sterer (Tel-Aviv Univ., Israel.), R. D. Taylor, and R. Jeanloz (California Univ., Berkeley.) 20 Jul. 1993 8 p Presented at the 14th International Conference of the International Association for the Advancement of High Pressure Science and Technology, Colorado Springs, CO, 27 Jun. - 2 Jul. 1993
(Contract W-7405-eng-36)
(DE93-018295; LA-UR-93-2692; CONF-930676-30) Avail: CASI HC A02/MF A01

High pressure studies of the insulator-metal transition in the (TM)I(sub 2) (TM = V, Fe, Co, and Ni) compounds are described. Those divalent transition-metal iodides are structurally isomorphous and classified as Mott Insulators. Resistivity, X-ray diffraction, and Moessbauer Spectroscopy were employed to investigate the electronic, structural, and magnetic properties as a function of pressure both on the highly correlated and on the metallic regimes. DOE

N94-18827# Sandia National Labs., Albuquerque, NM.

THE LEVER OSCILLATOR FOR USE IN HIGH RESISTANCE RESONATOR APPLICATIONS

K. O. Wessendorf 1993 7 p Presented at the 1993 IEEE Frequency Control Symposium, Salt Lake City, UT, 2-4 Jun. 1993
(Contract DE-AC04-76DP-00789)
(DE93-017652; SAND-93-0145C; CONF-9306205-1) Avail: CASI HC A02/MF A01

The Lever oscillator has been specifically designed for use with quartz resonator sensors. The use of quartz resonators as sensors is of particular interest and depending on the sensing environment, e.g., liquid, the oscillator design is both critical and difficult due to the wide dynamic range of resonator resistance possible due to damping of the resonator. Standard oscillator designs do not work well as sensor oscillators. An oscillator design will be presented that allows both frequency and loss (R(sub m)) of the resonator to be determined over a wide dynamic range of resonator loss. The Lever oscillator uses negative feedback in a differential amplifier configuration to actively and variably divide (or leverage) the resonator impedance such that the oscillator can maintain the phase and gain of the loop over a wide range of resonator resistance. DOE

N94-18872# Phillips Lab., Kirtland AFB, NM.

NOVEL ELECTRON BEAM CATHODE Final Report, 20 Jan. 1992 - 20 Apr. 1993

K. J. Hendricks, D. E. Voss, E. Garate, R. McWilliams, and T. A. Spencer Jul. 1993 12 p
(AD-A270106; AD-E201616; PL-TR-93-1024) Avail: CASI HC A03/MF A01

Experiments have been conducted during the past year to develop an electron beam cathode which is capable of producing a moderate perveance beam for several microsecond pulse lengths and is not susceptible to diode closure. The requirements, successfully met by this salt-based cold emission cathode, include operating in modest vacuums of 10-5 Torr, voltages less than or equal 160 kV, and the ability to generate solid or annular cross section space-charge-limited electron beams. Data on the operating performance of this salt cathode and streak photographs showing the uniformity of the emission of the electron beam are presented.

Comparisons of this salt cathode will be made with other electron beam cathode materials. DTIC

N94-18909 Optical Society of America, Washington, DC.

ULTRAFAST ELECTRONICS AND OPTOELECTRONICS: SUMMARIES OF PAPERS. TECHNICAL DIGEST CONFERENCE EDITION Final Report

Jarus W. Quinn Jan. 1993 213 p Meeting held in San Francisco, CA, 25-27 Jan. 1993 Limited Reproducibility: More than 20% of this document may be affected by microfiche quality
(AF Proj. 2301)
(AD-A269233; AFOSR-93-0640TR) Avail: CASI HC A10

The symposium was held on the following topics: advanced solid state lasers, compact blue-green lasers, integrated photonics research, nonlinear guide-wave optics, optical amplifiers and their applications, optical design for photonics, photonics in switching, quantum optoelectronics, short-wavelength -- physics with intense laser pulses, soft x-ray protection lithography, ultrafast electronics and optoelectronics, optical computing, and spatial light modulators. DTIC

N94-18928# Sandia National Labs., Albuquerque, NM.

ENVIRONMENTALLY ASSISTED CRACKING OF NICKEL ANODE SUBSTRATES IN LI/SOCI2 CELLS: AN ENGINEERING APPROACH

W. R. Cieslak, D. E. Weigand, and R. G. Buchheit 1993 2 p Presented at the 184th Meeting of the Electrochemical Society, New Orleans, LA, 10-15 Oct. 1993
(Contract DE-AC04-76DP-00789)
(DE93-015130; SAND-93-1083C; CONF-931024-1) Avail: CASI HC A01/MF A01

Intergranular environmentally assisted cracking (EAC) of Ni anode substrates is likely to occur in a large proportion of Li/SOCl2 cells, but it is not generally detected because in the majority of cases it does not lead to catatrophic failure. However, EAC could become a problem for applications requiring continuous power with high reliability for 10-15 years. In the present work, we determine why simple galvanic couple constant-strain tests do not produce cracking and introduce a constant strain test that does produce cracking. The objective of this investigation is to determine the stress threshold for cracking as a function of Ni composition and microstructure. DOE

N94-18941# Lawrence Livermore National Lab., CA.

INTEGRATED CIRCUITS: RESISTLESS PROCESSING SIMPLIFIES PRODUCTION AND CUTS COSTS

K. Weiner 25 Mar. 1993 4 p Presented at the National Center for Advanced Information Components Manufacturing Workshop, Albuquerque, NM, 30-31 Mar. 1993
(Contract W-7405-eng-48)
(DE93-018069; UCRL-JC-113651; CONF-9303198-4) Avail: CASI HC A01/MF A01

Reducing the complexity and cost of producing deep-submicrometer integrated circuits (IC's) will soon be possible using a revolutionary approach being developed at the Lawrence Livermore National Laboratory (LLNL). Resistless Projection Doping (RPD) will eliminate the need for photoresist processing during the impurity doping step. This single innovation will reduce the doping sequence from 13 steps to 1 and eliminate the need for five pieces of capital equipment costing more than $5 million. The overall cost of high-volume wafer fabrication will be reduced by more than 10 percent. In addition, the LLNL RPD machine is compact and modular, minimizing facilities costs when compared to today's industry-standard doping equipment. These physical characteristics of the machine also allow the RPD process to be easily incorporated into single-wafer, 'cluster' processing tools. When integrated with existing deposition, etching, and annealing steps and developing lithography techniques, the LLNL doping process completes the technology set required to produce a flexible fabrication facility of the future. At one-fifth the cost of current mega-fabrication facilities, the availability of these compact, low-volume, smart factories will give US manufacturers a substantial competitive advantage in the world-wide marketplace for high-value custom and semi-custom integrated circuits. DOE

N94-19035# Sandia National Labs., Albuquerque, NM.

CONCEPTUAL DESIGN OF A SODIUM SULFUR CELL FOR US ELECTRIC VAN BATTERIES

Peter J. Binden (Beta Power, Inc., Wayne, PA.) May 1993 52 p
(Contract DE-AC04-76DP-00789)
(DE93-018683; SAND-92-7331) Avail: CASI HC A04/MF A01

A conceptual design of an advanced sodium/sulfur cell for US electric-van applications has been completed. The important design factors included specific physical and electrical requirements, service life, manufacturability, thermal management, and safety. The capacity of this cell is approximately the same as that for the PB cell being developed by Silent Power Limited (10 Ah). The new cell offers a 50% improvement in energy capacity and nearly a 100% improvement in peak power over the existing PB cells. A battery constructed with such cells would significantly exceed the USABC's mid-term performance specifications. In addition, a similar cell and battery design effort was completed for an advanced passenger car application. A battery using the van cell would have nearly 3 times the energy compared to lead-acid batteries, yet weigh 40% less; a present-day battery using a cell specifically designed for this car would provide 50% more energy in a package 60% smaller and 50% lighter. DOE

N94-19079# Sandia National Labs., Albuquerque, NM.

SUPERCONDUCTING FLUX FLOW DEVICES, DIGITAL CIRCUITS AND MEMORIES

J. S. Martens (Conductus, Inc., Sunnyvale, CA.), M. E. Johansson (Conductus, Inc., Sunnyvale, CA.), A. Pance (Conductus, Inc., Sunnyvale, CA.), V. M. Hietalia, J. R. Wendt, G. A. Vawter, T. A. Plut, C. P. Tigges, M. P. Siegal, and S. Y. Hou (Bell Telephone Labs., Inc., Murray Hill, NJ.) 1993 9 p Presented at the 183rd Electrochemical Society Meeting, Honolulu, HI, 16-21 May 1993
(Contracts DE-AC04-76DP-00789; N00014-91-F-0055)
(DE93-019072; SAND-92-2257C; CONF-930571-26) Avail: CASI HC A02/MF A01

Flux flow based devices have advanced to the point where real digital circuits can be considered that have attractive speed and power properties. An ECL-like logic family has been developed with sub-10 ps gate delays with fan-outs of 5 or more. Adders with 25 ps delays and 30 nW static power dissipation have also been demonstrated. These logic families enable a hybrid memory concept with extremely low power needs and access times of a few hundred ps. DOE

N94-19112# Sandia National Labs., Albuquerque, NM.

SILICON MCM SUBSTRATES FOR INTEGRATION OF 3-5 PHOTONIC DEVICES AND CMOS IC'S

P. Seigal, R. Carson, R. Flores, and B. Rose 1993 10 p Presented at the International Workshop on Optoelectronic Packaging Science, Santa Barbara, CA, 28 Jul. 1993
(Contract DE-AC04-76DP-00789)
(DE93-017894; SAND-93-1773C; CONF-9307112-1-Vugraphs) Avail: CASI HC A02/MF A01

The progress made in advanced packaging development at Sandia National Laboratories for integration of 3-5 photonic devices and CMOS IC's on Silicon MCM substrates for planar aid stacked applications will be reported. Studies to characterize precision alignment techniques using solder attach materials compatible with both silicon IC's and 3-5 devices will be discussed. Examples of the use of back-side alignment and IR through-wafer inspection will be shown along with the extra processing steps that are used. Under bump metallurgy considerations are also addressed. DOE

N94-19292# Stockholm Univ. (Sweden). Dept. of Physics.

A PROGRAMMABLE SYSTOLIC TRIGGER PROCESSOR FOR FERA-BUS DATA

G. Appelquist, B. Hovander, B. Sellden, and C. Bohm Sep. 1992 16 p
(USIP-92-04; ETN-93-94847) Avail: CASI HC A03/MF A01

A generic CAMAC based trigger processor module for fast processing of large amounts of Analog to Digital Converter (ADC) data was designed. This module was realized using complex programmable gate arrays. The gate arrays were connected to memories and multipliers in such a way that different gate array configurations can cover a wide range of module applications. Using this module, it is possible to construct complex trigger processors. The module uses both the fast ECL FERA bus and the CAMAC bus for inputs and outputs. The latter is used for set up and control but may also be used for data output. Large numbers of ADC's can be served by a hierarchical arrangement of trigger processor modules which process ADC data with pipeline arithmetics and produce the final result at the apex of the pyramid. The trigger decision is transmitted to the data acquisition system via a logic signal while numeric results may be extracted by the CAMAC controller. The trigger processor was developed for the proposed neutral particle search. It was designed to serve as a second level trigger processor. It was required to correct all ADC raw data for efficiency and pedestal, calculate the total calorimeter energy, obtain the optimal time of flight data, and calculate the particle mass. A suitable mass cut would then deliver the trigger decision. ESA

N94-19297# Ecole Centrale de Lyon (France). Centre de Genie Electrique de Lyon.

CONTRIBUTION TO THE STUDY OF THE ADDITIONAL LOSSES IN COIL ELEMENTS USED IN STATIC CONVERTERS Ph.D. Thesis [CONTRIBUTION A L'ETUDE DES PERTES SUPPLEMENTAIRES DANS LES ELEMENTS BOBINES UTILISES DANS LES CONVERTISSEURS STATIQUES]

Mohamed Ould-Khouna 1992 124 p In FRENCH
(ECL-92-60; ETN-93-94892) Avail: CASI HC A06/MF A02

The objective is to explain the physical mechanisms responsible for losses. Theoretical models to be used as base data for optimizing such constraints in static converters are developed. Frequencies from a few Hz to tens of kHz within a power range from a few kVA to tens of kVA are considered. Emphasis is placed on currents induced in conductors, in particular their distribution in the different coils constituting a winding. The study is carried out using flexible electromagnetic models which facilitate the analysis of the influence of main parameters on the secondary losses. They are then subjected to experimental measurements and numerical simulations using finite elements method. ESA

N94-19310# Brookhaven National Lab., Upton, NY.

RF PHASE STABILIZATION FOR RF PHOTOCATHODE GUN THROUGH ELECTRO-OPTICAL MONITORING

K. P. Leung, L. H. Yu, and I. Ben-Zvi 1993 5 p Presented at the Annual Meeting of the Society of Photo-Optical Instrumentation Engineers (SPIE), San Diego, CA, 11-16 Jul. 1993
(Contract DE-AC02-76CH-00016)
(DE93-019059; BNL-49276; CONF-930722-20) Avail: CASI HC A01/MF A01

An electro-optical technique is being developed at the Brookhaven National Laboratory (BNL) Accelerator Test Facility (ATF) to monitor and control the phase of the photocathode laser beam with respect to the RF drive field for the RF photocathode gun. This technique utilizes the RF field induced birefringence which is probed by the photocathode laser beam. A proof-of-principle experiment is described which was performed using the ATF RF photocathode gun injection system for the linac. DOE

N94-19387# Technische Univ., Berlin (Germany). Fachbereich Elektrotechnik.

IMPEDENCE CALCULATION WITH RECURSIVE FOLDING Ph.D. Thesis [IMPEDANZBERECHNUNG MIT HILFE DER REKURSIVEN FALTUNG]

Klemens Ahrens 1993 142 p In GERMAN
(ETN-93-95049) Avail: CASI HC A07/MF A02

A method, based on the folding integral for solving the first order differential equation which mathematically describes the short circuit path, is presented. The distance to the short circuit location could be calculated with only two scan values, when no light arc errors and no compensation processes, due to band capacities, occur. It is noticed that the evaluation of input and output quantities always gives the same weight function for a time invariant linear system; this property allows the solution to be not influenced by the overoscillations of the active network. Earth capacities of the short circuited transmission line or light arc faults were taken into account through calculations performed with the error quadratic sum as optimization criterion. This structure of the distance protection algorithm allows the most important perturbation sources on the travelling waves to be considered. The recursive folding was compared with other usual algorithms in terms of secondary lines perturbation, digital processing, calculation time needs and filter properties; it is concluded that the method is fast and evolutive. ESA

N94-19390# Technische Univ., Berlin (Germany). Fachbereich Elektrotechnik.

COMPARATIVE EXAMINATIONS OF SEVERAL FIELD ORIENTED POSITION CONTROL STRUCTURES FOR ASYNCHRONOUS SERVOMOTORS WITH A MULTITRANSPUTER SYSTEM Ph.D. Thesis [VERGLEICHENDE UNTERSUCHUNGEN VON UNTERSCHIEDLICHEN FELDORIENTIERTEN LAGEREGLERSTRUKTUREN FUER ASYNCHRON-SERVOMOTOREN MIT EINEM MULTI-TRANSPUTER-SYSTEM]

Stefan Beierke 1993 153 p In GERMAN
(ETN-93-95051) Avail: CASI HC A08/MF A02

The design and the realization of a universal development platform and the identification and the adaption of the electrical motor parameters are investigated. The asynchronous machine was mathematically described and field oriented model was decoupled and linearized. Short circuit current and transient response of the asynchronous machine were determined. A multitransputer development platform was realized; characterized by high flexibility, good extension possibilities, and high calculation power. Three position regulation structures for field oriented control of squirrel cage asynchronous machines were experimentally confronted: cascade, state, and cascade state controls. Practical examinations of cascade regulation show the influence of control cycle time and scan ratio of control lines on drive behavior of the regulation system. A parameter sensitivity analysis was carried out in order to determine the influence of stator inductivity, inertia momentum, and rotor time constant, which was adapted with an online identification process based on reactive power balance. Simulations of dynamic control behavior show cascade state control as the best. ESA

N94-19490# Institut National des Sciences Appliquees de Lyon, Villeurbanne (France). Lab. de Genie Electrique et de Ferroelectricite.

MODELING AND CHARACTERIZATION OF MECHANOELECTRIC CONVERSION PIEZOELECTRIC GENERATORS THROUGH DYNAMICAL OR QUASI STATIC UNIAXIAL STRESS Ph.D. Thesis [MODELISATION ET CARACTERISATION DES GENERATEURS PIEZOELECTRIQUES DE CONVERSION MECANOELECTRIQUE PAR COMPRESSION UNIAXIALE DYNAMIQUE OU QUASI-STATIQUE]

Christian Garabedian 1992 276 p In FRENCH
(ISAL-92-0097; ETN-93-95013) Avail: CASI HC A13/MF A03

Mechanoelectric conversion is recalled and a means of determining electrical parameters is considered in order to characterize the piezoelectric element under dynamic stress. The incoherence between the values of low level coefficients and those calculated from experiments led to the proposal of a more complex model whose equivalent schema take into account the mechanical and dielectrical losses in the material and the mechanical environment in which the piezoelement is found. This model permitted, with the aid of simulation software, the characterization of ceramic under high level mechanical solicitation, in dynamic stress and to calculate the nonlinearities. The analysis of the slow stress is carried out. The bringing into evidence of the residual field in the piezoelectric element enabled the redefinition of the electric energy value delivered in a line of sparks on a relaxation-stress cycle, and the definition for a given composition, of the optimal interelectrode distance. The two modes of conversion were compared and the formulation to obtain the maximal electric energy is determined. ESA

N94-19501# Institut National Polytechnique, Grenoble (France). Techniques de l'Informatique, des Mathematiques, de la Microelectronique et de la Microscopie Quant.

SILICON COMPILATION: FROM THE CIRCUIT TO THE SYSTEM Ph.D. Thesis [COMPILATION DE SILICIUM: DU CIRCUIT AU SYSTEME]

Keven OBrien 1993 196 p In FRENCH
(ETN-93-95010) Avail: CASI HC A09/MF A03

The methodology used for the compilation of silicon from a behavioral level to a system level is presented. The aim was to link the heretofore unrelated areas of high level synthesis and system level design. This link will play an important role in the development of future design automation tools as it will allow hardware/software co-designs to be synthesized. A design methodology that alllows, through the use of an intermediate representation, SOLAR, a System level Design Language (SDL), to be combined with a Hardware Description Language (VHDL) is presented. Two main steps are required in order to transform this specification into a synthesizable one. Firstly, a system level synthesis step including partitioning and communication synthesis is required in order to split the model into a set of interconnected subsystems, each of which will be processed by a high level synthesis tool. For this latter step AMICAL is used and this allows powerful scheduling techniques to be used, that accept very abstract descriptions of control flow dominated circuits as input, and interconnected RTL blocks that may feed existing logic-level synthesis tools to be generated. ESA

N94-19553# Argonne National Lab., IL.
DIMENSIONAL CROSSOVER IN THE TORQUE IN A LAYERED SUPERCONDUCTOR
R. A. Klemm Apr. 1993 3 p Presented at the Conference of the International Union of Pure and Applied Physics on Low Temperature Physics (LT 20), Eugene, OR, 1-11 Aug. 1993
(Contract W-31-109-eng-38)
(DE93-019544; ANL/MSD/CP-79555; CONF-930801-11) Avail: CASI HC A01/MF A01

The procedure of Bulaevski, Ledvij, and Kogan for evaluating the line energy of single, straight vortex in the Lawrence-Doniach model in the linearized phase-only approximation is modified to take accurate account of the vortex core cross-sections. Dimensional crossover effects are found to be pronounced, with oscillations in the regular dependence of the torque for theta approximately = pi/2 and T approximately = T* less than Tc. DOE

N94-19584# California Univ., Los Angeles. School of Engineering and Applied Science.
QUASI-OPTICAL TRANSPONDER USING FET'S AND PATCH ANTENNAS
Kimin Cha and Tatsuo Itoh 30 Jul. 1993 52 p
(Contract DAAH04-93-G-0068)
(AD-A271339; UCLA-Eng-93-48; ARO-30921.9-EL) Avail: CASI HC A04/MF A01

Quasi-optical planar transponder that integrates a self-oscillating mixer, an IF amplifier and two patch antennas, one for receiving RF signal (14GHz) and another for transmitting amplified IF signal (8GHz) is presented. The prototype circuit is designed in microstrip structure and fabricated on a single substrate. As an active source, GaAs FET is selected. Self-oscillating (6GHz) mixer with patch antenna in receiver front end is developed based on quasi-optical technique. To obtain enough power level of IF signal before it is transmitted, the amplifier is designed with bandpass filter which blocks undesirable mixing products except 8GHz. This prototype of transponder, which is compact and self-contained unit as a single entity has many applications in microwave and millimeter-wave area. DTIC

N94-19642*# Auburn Univ., AL.
DESIGN OF POWER ELECTRONICS FOR TVC EMA SYSTEMS Final Report
R. Mark Nelms 30 Aug. 1993 62 p
(Contract NAS8-39131)
(NASA-CR-193839; NAS 1.26:193839) Avail: CASI HC A04/MF A01

The Composite Development Division of the Propulsion Laboratory at Marshall Space Flight Center (MSFC) is currently developing a class of electromechanical actuators (EMA's) for use in space transportation applications such as thrust vector control (TVC) and propellant control valves (PCV). These high power servomechanisms will require rugged, reliable, and compact power electronic modules capable of modulating several hundred amperes of current at up to 270 volts. MSFC has selected the brushless dc motor for implementation in EMA's. This report presents the results of an investigation into the applicability of two new technologies, MOS-controlled thyristors (MCT's) and pulse density modulation (PDM), to the control of brushless dc motors in EMA systems. MCT's are new power semiconductor devices, which combine the high voltage and current capabilities of conventional thyristors and the low gate drive requirements of metal oxide semiconductor field effect transistors (MOSFET's). The commanded signals in a PDM system are synthesized using a series of sinusoidal pulses instead of a series of square pulses as in a pulse width modulation (PWM) system. A resonant dc link inverter is employed to generate the sinusoidal pulses in the PDM system. This inverter permits zero-voltage switching of all semiconductors which reduces switching losses and switching stresses. The objectives of this project are to develop and validate an analytical model of the MCT device when used in high power motor control applications and to design, fabricate, and test a prototype electronic circuit employing both MCT and PDM technology for controlling a brushless dc motor. Derived from text

N94-19643*# Wisconsin Univ., Madison. Dept. of Electrical and Computer Engineering.
HIGH TEMPERATURE CO-AXIAL WINDING TRANSFORMERS Final Interim Report, May 1992 - Feb. 1993
Deepakraj M. Divan and Donald W. Novotny 1993 57 p
(Contract NCC3-261)
(NASA-CR-194580; NAS 1.26:194580) Avail: CASI HC A04/MF A01

The analysis and design of co-axial winding transformers is presented. The design equations are derived and the different design approaches are discussed. One of the most important features of co-axial winding transformers is the fact that the leakage inductance is well controlled and can be made low. This is not the case in conventional winding transformers. In addition, the power density of co-axial winding transformers is higher than conventional ones. Hence, using co-axial winding transformers in a certain converter topology improves the power density of the converter. The design methodology used in meeting the proposed specifications of the co-axial winding transformer specifications are presented and discussed. The final transformer design was constructed in the lab. Co-axial winding transformers proved to be a good choice for high power density and high frequency applications. They have a more predictable performance compared with conventional transformers. In addition, the leakage inductance of the transformer can be controlled easily to suit a specific application. For space applications, one major concern is the extraction of heat from power apparatus to prevent excessive heating and hence damaging of these units. Because of the vacuum environment, the only way to extract heat is by using a cold plate. One advantage of co-axial winding transformers is that the surface area available to extract heat from is very large compared to conventional transformers. This stems from the unique structure of the co-axial transformer where the whole core surface area is exposed and can be utilized for cooling effectively. This is a crucial issue here since most of the losses are core losses. Derived from text

N94-19665# Bell Communications Research, Inc., Livingston, NJ.
VLSI IMPLEMENTATION OF NEUROMORPHIC LEARNING NETWORKS Final Report, 1 Aug. 1990 - 31 Mar. 1993
Joshua Alspector 31 Mar. 1993 9 p
(Contract F49620-90-C-0042; DARPA Order 7013)
(AD-A270825; AFOSR-93-0754TR) Avail: CASI HC A02/MF A01

The researchers have shown how to rigorously derive deterministic systems from stochastic ones in the Boltzmann machine framework that they are using for their implementations. They have further shown how to search for new learning algorithms suitable for VLSI implementation using a genetic algorithm approach. They have analyzed the effect of precision constraints such as is found in hardware implementations on the learning and generalization abilities of neural networks. They have studied the learning behavior of neural networks under conditions where they can or cannot classify perfectly. DTIC

N94-19722# Ohio State Univ., Columbus. Dept. of Mechanical Engineering.
MICROTRIBOLOGY OF MAGNETIC MEDIA
Bharat Bhushan, Vilas N. Koinkar, and Ju-Ai Ruan 1 Oct. 1993 46 p Revised
(Contract N00014-93-I-0067)
(AD-A271209) Avail: CASI HC A03/MF A01

Scanning tunneling microscopy (STM), atomic force microscopy (AFM), and the modification of AFM's (such as friction force microscopy (FFM)) are becoming increasingly important in the understanding of fundamental mechanisms of friction, wear and lubrication and in studying the interfacial phenomena in micro- and nanostructures used in magnetic storage devices and micro-electromechanical systems (MEMS). In the paper, we describe modified AFM and FFM techniques and present data microtribological studies of magnetic media-magnetic tapes and disks. Local variation in microscale friction is found to correspond to the local slope suggesting that ratchet mechanism is responsible for this variation. Wear rates for magnetic tapes are approximately constant for various loads and test duration. However, for the magnetic disks, the wear of the diamondlike carbon overcoat is catastrophic. Evolution of the wear has also been studied using AFM. AFM has been modified for nanoindentation hardness measurements. We have shown that hardness of ultra thin films can be measured using AFM. AFM has also shown to be useful for nanofabrication. DTIC

N94-19751 Dayton Univ., OH. Dept. of Electrical Engineering.
ELECTRO-OPTICS DISPLAY RESEARCH, TEST, AND EVALUATION LABORATORY PROGRAM Final Report, Sep. 1987 - Jun. 1993
Mohammad A. Karim and Donald L. Moon 29 Jun. 1993 61 p Limited Reproducibility: More than 20% of this document may be affected by microfiche quality
(Contract DAAL03-87-K-0121)
(AD-A270947; ARO-25557.10-EL) Avail: CASI HC A04

The goal of the research effort is to analyze and develop a model to characterize overall electro-optical display systems of particular interest to U.S. Army Center for Night Vision and Electro-Optics at Ft. Belvoir, Virginia. The main thrust of the research reported herein is to implement accepted standards for evaluating displays, take an active role in forming new measurement standards, and provide unbiased evaluation of displays in use or contemplated for military missions. Measurement parameters include display brightness, contrast, resolution, chromatic range, frequency response, angular field-of-view, reliability, and sensitivity to environment. Another important facet of this research is to determine image dynamics involving the response time between sensor input and the reaction of the observer for influencing what display improvements, such as variable acuity displays, color, contrast, or brightness lead to significant improvement in performance. DTIC

N94-19756# Biotronics Technologies, Inc., Waukesha, WI.
TRANSCUTANEOUS ANALYTE MEASURING METHODS (TAMM) Quarterly Progress Report No. 7, Apr. - Sep. 1993
Kenneth J. Schlager 4 Oct. 1993 21 p
(Contract N00014-91-C-0190)
(AD-A271387) Avail: CASI HC A03/MF A01

This document contains a comprehensive status report on the TAMM Phase II SBIR project at Biotronics Technologies. It is important to understand at this stage of TAMM development the strengths and weaknesses of current instrumentation and the design approach to overcoming current shortcomings. Optimism of Biotronics remains high. Even though the low signal-to-noise ratio (SNR) of TAMM I instrumentation (the BI-800 Array Analyzer) made signal processing difficult and limited measurement accuracy, encouraging test results were still achieved, especially on the last 73 patients tested in Milwaukee. DTIC

N94-19759# Department of the Navy, Washington, DC.
TRANSDUCERS AND METHOD FOR MAKING SAME Patent Application
Manfred Kahn, inventor (to Navy) and C. Kim, inventor (to Navy) 9 Jun. 1993 28 p
(AD-D015949; US-Patent-Appl-SN-076135; Navy-Case-74904) Avail: CASI HC A03/MF A01

The invention pertains generally to transducers and more particularly to transducers which convert hydrostatic or acoustic pressure into electrical signals. Elongated electrically nonconducting transducer preforms are made from a stiff resin. The preforms have grooves in their upper and lower surfaces. Transducer elements may be formed from staked preforms whereby grooves in their upper and lower surfaces form compartments between adjoining stacked preforms. PZT rods are disposed in the grooves disposed on the upper surface of each stacked preform, and a soft resin surrounds the rods and fills the compartment. The method for making the transducer assembly includes the steps of loading by gravity the rods into the upper grooves of the preforms; stacking the loaded preforms so that upper grooves in the lower preform communicate with lower grooves in the upper preform, thus forming cavities; flowing a soft resin around the rods; and curing the soft resin. DTIC

N94-19763# Department of the Navy, Washington, DC.
POLARIZED OPTICAL EMISSION DUE TO DECAY OR RECOMBINATION OF SPIN-POLARIZED INJECTED CARRIERS Patent Application
Berend T. Jonker, inventor (to Navy) 29 Jun. 1993 16 p
(AD-D015907; US-Patent-Appl-SN-083231; Navy-Case-74741) Avail: CASI HC A03/MF A01

A device for producing circularly polarized optical emission includes a light emitting semiconductor heterostructure, further including at least one semiconducting layer; a ferromagnetic contact having a magnetic moment, in electrical contact with a layer of the semiconductor heterostructure; and a contact electrically connected to a different region of the semiconductor heterostructure. This light emitting semiconductor heterostructure may be a light emitting diode (LED), or some other structure. The ferromagnetic contact injects spin polarized carriers (electrons or holes) into the semiconducting device, which recombine with their opposing carriers to produce circularly polarized light. A process for producing circularly polarized optical emission includes applying a bias across a light emitting semiconductor heterostructure having a contact with a net magnetic moment, thereby injecting spin polarized carriers into the light emitting semiconductor heterostructure. DTIC

N94-18015# Centre Technique de l'Industrie Horlogere, Besancon (France).
PIEZO-ELECTRIC MOTOR: PERSPECTIVES AND MINIATURIZATION [MOTEUR PIEZO-ELECTRIQUE: PERSPECTIVES DE MINIATURISATION]
Roland Duffait and Patrice Minotti (Paris Univ., Besancon, France.) *In* Societe Suisse de Chronometrie, Proceedings of the 4th European Congress on Chronometry 1992 p 49-52 In FRENCH (For primary document see N94-18006 04-35)
Copyright Avail: CASI HC A01/MF A02

N94-18017# Centre Technique de l'Industrie Horlogere, Besancon (France).
SILICON MICRO-ACTUATOR [MICROTRANSLATEUR SILICIUM]
Pascal Blind *In* Societe Suisse de Chronometrie, Proceedings of the 4th European Congress on Chronometry 1992 p 57-60 In FRENCH Sponsored by Ministere de la Recherche (For primary document see N94-18006 04-35)
Copyright Avail: CASI HC A01/MF A02

N94-18022# ETA S.A., Grenchen (Switzerland).
ELECTRIC MEASUREMENT OF LAVET MOTORS [MESURE ELECTRIQUE DES MOTEURS LAVET]
Christian Peclat, Daho Taghezout, and Yves Guerin *In* Societe Suisse de Chronometrie, Proceedings of the 4th European Congress on Chronometry 1992 p 77-80 In FRENCH (For primary document see N94-18006 04-35)
Copyright Avail: CASI HC A01/MF A02

N94-18023# Scientific Research Inst. of Instrument Automation, Moscow (USSR).
CONTROL OF TORQUE IN STEPPING MOTORS OF QUARTZ WATCHES AND CLOCKS
Alexander Ketsaris *In* Societe Suisse de Chronometrie, Proceedings of the 4th European Congress on Chronometry 1992 p 81-83 (For primary document see N94-18006 04-35)
Copyright Avail: CASI HC A01/MF A02

N94-18033# Swiss Center for Electronics and Microtechnology, Inc., Neuchatel.
EVALUATION OF THE CONSUMPTION OF ELECTRONIC CLOCKS [BILAN DE CONSOMMATION DE MONTRES ELECTRONIQUES]
V. vonKaenel and C. Piguet *In* Societe Suisse de Chronometrie, Proceedings of the 4th European Congress on Chronometry 1992 p 127-13 In FRENCH (For primary document see N94-18006 04-35)
Copyright Avail: CASI HC A01/MF A02

34 FLUID MECHANICS AND HEAT TRANSFER

Includes boundary layers; hydrodynamics; fluidics; mass transfer; and ablation cooling.

For related information see also *02 Aerodynamics* and *77 Thermodynamics and Statistical Physics.*

N94-17728# Los Alamos National Lab., NM.
UNDERSTANDING CURVED DETONATION WAVES

B. G. Bukiet (New Jersey Inst. of Tech., Newark.), K. S. Lackner, and R. Menikoff 1993 9 p Presented at the 10th Detonation Symposium, Boston, MA, 12-16 Jul. 1993
(Contract W-7405-eng-36)
(DE93-014581; LA-UR-93-1723; CONF-930713-15) Avail: CASI HC A02/MF A01

The reaction zone of a detonation wave is very small compared to the dynamic length scale for a typical application. Consequently, it is impractical for numerical calculations to fully resolve the reaction zone. A non-zero reaction zone width is critical to describe curved detonation waves because it affects the wave speed. The curvature effect is the result of an interaction between the rate of energy release and geometric source terms within the reaction zone. When the reaction zone width is determined by the computational cell size rather than the physical scale, the numerics introduces an artificial curvature effect which frequently dominates the physical effect and leads to mesh dependence of simulations. Modified Hugoniot jump conditions are derived which characterize the curvature effect. They express the conservation laws and are not sensitive to the detailed reaction dynamics but instead depend only on the reaction zone width, and averages of pressure and of mass, momentum and energy densities. DOE

N94-17901# Von Karman Inst. for Fluid Dynamics, Rhode-Saint-Genese (Belgium).

RECIRCULATION IN FORWARD ROLL COATING

P. J. Wicks and J.-M. Buchlin Dec. 1992 35 p
(VKI-TM-48; ETN-93-94840) Avail: CASI HC A03/MF A01

A prediction for the onset of recirculating flow in symmetric forward roll coating, as the capillary number is decreased, is made using an approximate analytic technique based on a model by Pitts and Greiller. Recirculating flow is predicted to exist when the capillary number is below about 0.62. Streamline patterns and contour plots of the pressure distribution predicted by the model are provided. An explanation for the existence of recirculation at low capillary number is suggested. The structure of the recirculating flow on symmetric and asymmetric forward coating is discussed. It is claimed, on grounds of structural stability, that in the asymmetric case there is a wedge of fluid which starts off near one of the cylinders, but then passes backwards between the two recirculation zones before joining the film attached to the other cylinder. ESA

N94-18004# Argonne National Lab., IL.

FIN-EFFICIENCY CALCULATION FOR CONDENSATION IN THE PRESENCE OF NONCONDENSABLE GASES

C. B. Panchal 1993 11 p Presented at the Condensation and Condenser Design Conference, St. Augustine, FL, 7-12 Mar. 1993
(Contract W-31-109-eng-38)
(DE93-017684; ANL/ES/CP-80354; CONF-9303200-2) Avail: CASI HC A03/MF A01

Plate-fin heat exchangers are being considered for many condenser applications. They are commonly used for the gas-separation process because they can provide a high thermal performance to obtain a low mean-temperature difference, essential for the gas-separation process. Plate-fin heat exchangers are also considered for the heat-pump system using nonazeotropic refrigerant mixtures. The brazed plate-fin condenser was considered to be a leading candidate for the Ocean Thermal Energy Conversion (OTEC) system, where high-performance heat exchangers are essential for maintaining a low mean-temperature difference. Calculation of the fin efficiency is difficult for condensation in the presence of noncondensable gases due to the spatial variation of the interfacial temperature. An analysis was carried out to develop a simplified method to calculate the fin efficiency for condensation of a vapor in the presence of noncondensable gases. The analysis includes the variation in the interfacial temperature along the fin surface. Appropriate assumptions are made to simplify the coupled heat-conduction equation in the fin and the heat/mass fluxes at the interface. The resulting expression for the fin efficiency includes mass-flux parameters, and it is similar to the common expression used for single-phase flow. DOE

N94-18076# Deutsche Forschungsanstalt fuer Luft- und Raumfahrt, Brunswick (Germany). Abt. Antriebsintegration.

INVESTIGATION OF A MATRIX-MODEL FOR THE ARTIFICIAL DISSIPATION IN A CELL VERTEX FINITE VOLUME SCHEME FOR SOLVING THE NAVIER-STOKES EQUATIONS Thesis - Tech. Univ. Brunswick [UNTERSUCHUNG EINER MATRIX-DISSIPATION IN EINEM ZELLENECKPUNKT-FINITE-VOLUMEN-SCHEMA ZUR LOESUNG DER NAVIER-STOKES-GLEICHUNGEN]

Olaf Brodersen Jun. 1992 100 p In GERMAN
(DLR-FB-92-33; ETN-93-94869) Avail: CASI HC A05/MF A02

A matrix dissipation model is evaluated for the numerical solution of the Navier-Stokes equations. The numerical approach, a finite volume scheme with central differencing, was outlined and the necessity of artificially added dissipation was shown. The design of the dissipation term for modeling an upwind scheme is described for the one dimensional linear wave equation. Following this approach results in time consuming matrix multiplications for two dimensional and three dimensional cases. Because of a new splitting technique of the matrices found in the literature, it is now possible to use this dissipation model in a more efficient way. The basic effects were analyzed for viscous flow around the RAE 2822 airfoil. The results show a higher resolution of shocks and the boundary layer. Thus, it is possible to use coarser meshes so that CPU (Central Processing Unit) time is reduced by about a factor of three. ESA

N94-18124 Deutsche Forschungsanstalt fuer Luft- und Raumfahrt, Goettingen (Germany). Inst. fuer Experimentelle Stroemungsmechanik.

ON MEMORY EFFECTS IN TURBULENCE Thesis - Goettingen Univ. [UEBER GEDAECHTNISEFFEKTE IN DER TURBULENZ]

Stefan Woppowa Feb. 1993 48 p In GERMAN Limited Reproducibility: More than 20% of this document may be affected by microfiche quality
(DLR-FB-93-03; ETN-93-94873) Avail: CASI HC A03

A Reynolds stress closure scheme which takes into account memory effects in turbulent shear flows is tested against data for fully developed turbulent rotating channel flow. In the rotating cases the zone where memory effects are essential contains the region of negative turbulence production and overshoots the edge of the latter to the stable side of the channel. In this region the relationship between local Reynolds stress and mean velocity field is not of local nature. The comparison between calculated and experimental mean velocity profiles leads to satisfactory agreement. The field equations for highly accelerated two-dimensional turbulent boundary layers were substantiated by the method of matched asymptotic expansions. ESA

N94-18248# Argonne National Lab., IL.

FLUID-STRUCTURE-INTERACTION ANALYSES OF REACTOR VESSEL USING IMPROVED HYBRID LAGRANGIAN EULERIAN CODE ALICE-II

C. Y. Wang 1993 38 p Presented at the Pressure Vessels and Piping Conference, Denver, CO, 25-29 Jul. 1993
(Contract W-31-109-eng-38)
(DE93-015536; ANL/RE/CP-77653; CONF-930702-34) Avail: CASI HC A03/MF A01

This paper describes fluid-structure-interaction and structure response analyses of a reactor vessel subjected to loadings associated with postulated accidents, using the hybrid Lagrangian-Eulerian code ALICE-II. This code has been improved recently to accommodate many features associated with innovative designs of reactor vessels. Calculational capabilities have been developed to treat water in the reactor cavity outside the vessel, internal shield structures and internal thin shells. The objective of the present analyses is to study the cover response and potential for missile generation in response to a fuel-coolant interaction in the core region. Three calculations were performed using the cover weight as a parameter. To study the effect of the cavity water, vessel response calculations for both wet- and dry-cavity designs are compared. Results indicate that for all cases studied and for the design parameters assumed, the calculated cover displacements are all smaller than the bolts' ultimate displacement and no missile generation of the closure head is predicted. Also, solutions reveal that the cavity water of the wet-cavity design plays an important role of restraining the downward displacement of the bottom head. Based on these studies, the analyses predict that the structure integrity is maintained throughout the postulated accident for the wet-cavity design. DOE

N94-18270# Los Alamos National Lab., NM.
ADVANCED IN MACROSTATISTICAL HYDRODYNAMICS
Alan L. Graham, Nicholas Tetlow, James R. Abbott, Lisa A. Mondy (Sandia National Labs., Albuquerque, NM.), and Howard Brenner (Massachusetts Inst. of Tech., Cambridge.) 1993 17 p Presented at the Advances in Structures Heterogenous Continua, Moscow, Russia, 22-27 Aug. 1993
(Contracts W-7405-eng-36; DE-AC04-76DP-00789)
(DE93-018479; LA-UR-93-2612; CONF-9308141-1) Avail: CASI HC A03/MF A01

An overview is presented of research that focuses on slow flows of suspensions in which colloidal and inertial effects are negligibly small (macrostatistical hydrodynamics). First, we describe nuclear magnetic resonance imaging experiments to quantitatively measure particle migration occurring in concentrated suspensions undergoing a flow with a nonuniform shear rate. These experiments address the issue of how the flow field affects the microstructure of suspensions. In order to understand the local viscosity in a suspension with such a flow-induced, spatially varying concentration, one must know how the viscosity of a homogeneous suspension depends on such variables as solids concentration and particle orientation. We suggest the technique of falling ball viscometry, using small balls, as a method to determine the effective viscosity of a suspension without affecting the original microstructure significantly. We also describe data from experiments in which the detailed fluctuations of a falling ball's velocity indicate the noncontinuum nature of the suspension and may lead to more insights into the effects of suspension microstructure on macroscopic properties. Finally, we briefly describe other experiments that can be performed in quiescent suspensions (in contrast to the use of conventional shear rotational viscometers) in order to learn more about the microstructure and boundary effects in concentrated suspensions. DOE

N94-18326# Aeronautical Research Labs., Melbourne (Australia).
APPLICATIONS OF THE PROGRAM UIFLOW-2D TO THE NUMERICAL SIMULATION OF AXISYMMETRIC FLOWS
D. Davis and E. Brizuela Jun. 1993 27 p
(AD-A268731; ARL-TN-38; DODA-AR-008-338) Avail: CASI HC A03/MF A01

The computer program UIFLOW-2D has been applied to the numerical simulation of turbulent axisymmetric flows. In a preliminary test of the performance of the program it has been used to simulate four different types of flows, isothermal and reactive, with and without swirl. Numerical results are discussed and compared with published experimental data. Recommendations are made for future development and application to gas turbine combustors. DTIC

N94-18385 Wisconsin Univ., Madison. Center for Mathematical Sciences.
WAVE STRUCTURE INDUCED BY FLUID DYNAMIC LIMITS IN THE BROADWELL MODEL Technical Summary Report
Athanasios E. Tzavaras Jul. 1993 44 p Sponored in part by NSF and ONR Limited Reproducibility: More than 20% of this document may be affected by microfiche quality
(AD-A268512; CMS-TSR-94-2) Avail: CASI HC A03

Consider the fluid dynamic limit problem for the Broadwell system of the kinetic theory of gases, for Riemann, Maxwellian initial data. The formal limit is the Riemann problem for a pair of conservation laws and is invariant under dilations of coordinates. The approach of self-similar fluid dynamic limits consists in replacing the mean free path in the Broadwell model so that the resulting problem preserves the invariance under dilations. The limiting procedure was justified by Slemrod and Tzavaras. Here, we study the structure of the emerging solutions. We show that they consist of two wave fans separated by a constant state. Each wave fan is associated with one of the characteristic fields and is either a rarefaction wave or a shock wave. The shocks satisfy the Lax shock conditions and have the internal structure of a Broadwell shock profile. DTIC

N94-18391 Army Research Lab., Aberdeen Proving Ground, MD.
PARABOLIZED NAVIER-STOKES COMPUTATION OF SURFACE HEAT TRANSFER CHARACTERISTICS FOR SUPERSONIC AND HYPERSONIC KE PROJECTILES Final Report, Sep. 1991 - Apr. 1993
Bernard J. Guidos and Paul Weinacht Aug. 1993 52 p See also BRL-IMR-970, Apr. 1992 Limited Reproducibility: More than 20% of this document may be affected by microfiche quality
(AD-A268858; ARL-TR-191; BRL-IMR-970) Avail: Issuing Activity (Defense Technical Information Center (DTIC))

Perfect gas heat transfer characteristics are presented for two existing supersonic finned kinetic energy (KE) projectiles (M735 and M829) and for a conceptual hypersonic KE projectile configuration. The hypersonic configuration is obtained by replacing the fins of the M829 with a conical flare of varying sweep angle. A three-dimensional, viscous, parabolized Navier-Stokes (PNS) computational technique is used to compute the perfect gas adiabatic wall temperatures and heat transfer rates in the velocity range 1.3 km/sec to 4 km/sec (Mach number range about 4 to 12). The heat transfer characteristics provide a necessary boundary condition for subsequent heat conduction computations, which simulate the transient in-flight thermal response of projectile configurations. DTIC

N94-18472# California Inst. of Tech., Pasadena. Graduate Aeronautical Labs.
CHEMICAL REACTIONS IN TURBULENT MIXING FLOWS Annual Technical Report, 1 Jun. 1992 - 31 May 1993
Paul E. Dimotakis and Anthony Leonard 15 Jul. 1993 135 p
(Contract F49620-92-J-0290)
(AD-A269377; AFOSR-93-0679TR) Avail: CASI HC A07/MF A02

In the course of this research we have conducted investigations of turbulent mixing, chemical reaction, and combustion processes in turbulent, subsonic, and supersonic flows. The program was comprised of several parts: an experimental effort, a theoretical and numerical simulation effort, and a development of instrumentation and diagnostics; an upgrade of flow and combustion facilities; and the development of data-acquisition sub-systems. We have carried out a series of theoretical and experimental studies of turbulent mixing in two well-defined, fundamentally important flow fields: free-shear layers and axisymmetric jets. To elucidate molecular transport effects, experiments and theory have dealt with both reacting and non-reacting flows of liquids and gases in fully-developed turbulent flows. A criterion for fully-developed turbulence was recently developed. The computational studies are, at present, focused at fundamental formulation and implementation issues pertaining to the simulation of both compressible and incompressible flows characterized by strong fronts, such as shock waves and flames. In our diagnostic development efforts we have improved the signal-to-noise ratio of flow images, in both gas- and liquid-phase flows, as well as continued with the development of data-acquisition electronics to meet very high-speed, high-volume data requirements; the acquisition of single, or pairs, of two-dimensional images in rapid succession; and the acquisition of data from arrays of supersonic flow sensors. DTIC

N94-18545*# National Aeronautics and Space Administration. Lewis Research Center, Cleveland, OH.
WORKSHOP ON COMPUTATIONAL TURBULENCE MODELING
1993 405 p Workshop held in Cleveland, OH, 15-16 Sep. 1993
(NASA-TM-109266; NAS 1.15:109266) Avail: CASI HC A18/MF A04

This document contains presentations given at Workshop on Computational Turbulence Modeling held 15-16 Sep. 1993. The purpose of the meeting was to discuss the current status and future development of turbulence modeling in computational fluid dynamics for aerospace propulsion systems. Papers cover the following topics: turbulence modeling activities at the Center for Modeling of Turbulence and Transition (CMOTT); heat transfer and turbomachinery flow physics; aerothermochemistry and computational methods for space systems; computational fluid dynamics and the k-epsilon turbulence model; propulsion systems; and inlet, duct, and nozzle flow. For individual titles, see N94-18546 through N94-18556.

N94-18546*# National Aeronautics and Space Administration. Lewis Research Center, Cleveland, OH.
RESEARCH ACTIVITIES AT THE CENTER FOR MODELING OF TURBULENCE AND TRANSITION
Tsan-Hsing Shih *In its* Workshop on Computational Turbulence Modeling 1993 21 p (For primary document see N94-18545 04-34)
Avail: CASI HC A03/MF A04

The main research activities at the Center for Modeling of Turbulence and Transition (CMOTT) are described. The research objective of CMOTT is to improve and/or develop turbulence and transition models for propulsion systems. The flows of interest in propulsion systems can be both compressible and incompressible, three dimensional, bounded by complex wall geometries, chemically reacting, and involve 'bypass' transition. The most relevant turbulence and transition models for the above flows are one- and two-equation eddy viscosity models, Reynolds stress algebraic- and transport-equation models, pdf models, and multiple-scale models. All these models are classified as one-point closure schemes since only one-point (in time and space) turbulent correlations, such as second moments (Reynolds stresses and turbulent heat fluxes) and third moments, are involved. In computational fluid dynamics, all turbulent quantities are one-point correlations. Therefore, the study of one-point turbulent closure schemes is the focus of our turbulence research. However, other research, such as the renormalization group theory, the direct interaction approximation method, and numerical simulations are also pursued to support the development of turbulence modeling. Author (revised)

N94-18547*# National Aeronautics and Space Administration. Lewis Research Center, Cleveland, OH.
RESEARCH ON TWO EQUATION MODELS
Z. Yang *In its* Workshop on Computational Turbulence Modeling 1993 10 p (For primary document see N94-18545 04-34)
Avail: CASI HC A02/MF A04

The k-epsilon model is the most widely used turbulence model in engineering calculations. However, the model has several deficiencies that need to be fixed. This document presents improvements to the capabilities of the k-epsilon model in the following areas: a Galilean and tensorial invariant k-epsilon model for near wall turbulence; a new set of wall functions for attached flows; a new model equation for the dissipation rate, which has a better theoretical basis, contains the contribution of flow inhomogeneity, and captures the effect of the pressure gradient accurately; and a better model for bypass transition due to freestream turbulence. Derived from text

N94-18548*# National Aeronautics and Space Administration. Lewis Research Center, Cleveland, OH.
ASSESSMENT AND DEVELOPMENT OF SECOND ORDER TURBULENCE MODELS
Aamir Shabbir *In its* Workshop on Computational Turbulence Modeling 1993 14 p (For primary document see N94-18545 04-34)
Avail: CASI HC A03/MF A04

Second order turbulence models describe the effect of mean flow and external agencies (such as buoyancy) on the evolution of turbulence. Therefore, in principle, these models give a more accurate description of complicated flow fields (e.g. flows with large anisotropy in turbulence, such as near the leading edge of a turbine blade) than the two equation models. The objectives of this document are to assess the performance of the various second order turbulence models in benchmark flows and to seek improvements where necessary in models for the pressure correlation term in the scalar flux equation and for the scalar dissipation equation. Derived from text

N94-18549*# Toledo Univ., OH.
A COUPLED IMPLICIT SOLUTION METHOD FOR TURBULENT SPRAY COMBUSTION IN PROPULSION SYSTEMS
K.-H. Chen and J.-S. Shuen (Sverdrup Technology, Inc., Cleveland, OH.) *In* NASA. Lewis Research Center, Workshop on Computational Turbulence Modeling 1993 16 p (For primary document see N94-18545 04-34)
Avail: CASI HC A03/MF A04

Many reacting flows in propulsion devices cannot be efficiently calculated by modern compressible flow CFD algorithms. Most low-speed reacting flow codes based on TEACH-type technologies are inefficient and lack robustness for complex flows. Tremendous progress has been made in high-speed compressible flow CFD in the past two decades; extending its application range to low-speed regimes is highly desirable. The objectives of this document is to present an efficient and robust algorithm for multi-phase chemically reacting flows at all speeds, with emphasis on low Mach number flows, and to calculate turbulent spray combustion flow in a gas turbine combustor. Derived from text

N94-18550*# National Aeronautics and Space Administration. Lewis Research Center, Cleveland, OH.
NUMERICAL INVESTIGATION OF COMPLEX, TRANSITIONAL, AND CHEMICALLY REACTING FLOWS
S.-W. Kim *In its* Workshop on Computational Turbulence Modeling 1993 15 p (For primary document see N94-18545 04-34)
Avail: CASI HC A03/MF A04

This document is divided into two parts. Part A, on turbulent transport of chemical species in compressible reacting flows, includes the following topics: mixing of chemical species in reacting flows; chemically reacting turbulent flows; turbulent mixing of chemical species in reacting flows, which includes large eddy mixing, turbulent mixing, and molecular mixing; multiple time scale turbulence equations; species conservation equations for reacting flows; and a finite volume numerical method. Part B, on unsteady transitional flows over forced oscillatory surfaces, discusses unsteady transitional flow equations with moving boundaries and the application of the finite volume numerical solution method. CASI

N94-18551*# Sverdrup Technology, Inc., Cleveland, OH. Internal Fluid Mechanics Div.
ANALYSIS OF SUPERSONIC FLOWS USING k-EPSILON MODEL AND THE RPLUS CODE: PROGRESS TOWARDS HIGH SPEED COMBUSTOR ANALYSIS
J. Lee *In* NASA. Lewis Research Center, Workshop on Computational Turbulence Modeling 1993 11 p (For primary document see N94-18545 04-34)
Avail: CASI HC A03/MF A04

The problem of interest here is the analysis of chemically reacting flow inside of supersonic ramjet combustors. Two key parameters need to be determined: mixing/combustion efficiency and kinetic energy efficiency. In order to determine these parameters, several potential loss mechanisms must be modeled correctly, including mixing, shear, turbulence, vorticity, shock waves, heat transfer, fuel injector drag, poor wall pressure integral, and chemical dissociation. This document discusses k-epsilon turbulence models for use in the RPLUS code for numerical modeling of combustor flow fields. CASI

N94-18552*# National Aeronautics and Space Administration. Lewis Research Center, Cleveland, OH.
COMPUTATIONAL AERO-ACOUSTICS AS A BRANCH OF TURBULENCE RESEARCH
Reda R. Mankbadi *In its* Workshop on Computational Turbulence Modeling 1993 10 p (For primary document see N94-18545 04-34)
Avail: CASI HC A02/MF A04

Computational aero-acoustics (CAA) is concerned with calculations of the aerodynamically generated sound source and its propagation. This paper presents a background to CAA, prediction of the time-dependent sound source using large-eddy simulations, and sound propagation to the far-field. Derived from text

N94-18553*# National Aeronautics and Space Administration. Lewis Research Center, Cleveland, OH.
A COMPARATIVE STUDY OF TURBULENCE MODELS IN PREDICTING HYPERSONIC INLET FLOWS c02
Kamlesh Kapoor *In its* Workshop on Computational Turbulence Modeling 1993 9 p (For primary document see N94-18545 04-34)
Avail: CASI HC A02/MF A04

A computational study has been conducted to evaluate the performance of various turbulence models. The NASA P8 inlet, which represents cruise condition of a typical hypersonic air-breathing vehicle, was selected as a test case for the study; the PARC2D code, which solves the full two dimensional Reynolds-averaged Navier-Stokes equations, was used. Results are presented for a total of six versions of zero- and two-equation turbulence models. Zero-equation models tested are the Baldwin-Lomax model, the Thomas model, and a combination of the two. Two-equation models tested are low-Reynolds number models (the Chien model and the Speziale model) and a high-Reynolds number model (the Launder and Spalding model). Derived from text

N94-18554*# National Aeronautics and Space Administration. Lewis Research Center, Cleveland, OH.
AN ALGEBRAIC TURBULENCE MODEL FOR TURBOMACHINERY
Rodrick V. Chima *In its* Workshop on Computational Turbulence Modeling 1993 14 p (For primary document see N94-18545 04-34)
Avail: CASI HC A03/MF A04

This paper presents a description and verification of RVC3D (rotor viscous code 3-D) which provides a Euler or Navier-Stokes analysis for steady three dimensional flows in turbomachinery. A motivation for this analysis is the calculation of turbine endwall heat transfer. Features of the turbulence model code include thin-layer formulation, Baldwin-Lomax or Cebeci-Smith turbulence models, node-centered finite difference formulation, and explicit four-stage Runge-Kutta time marching scheme. Results for flat plate, annular turbine cascade, turbine endwall heat transfer, and supersonic compressor blade test cases are presented. CASI

N94-18555*# National Aeronautics and Space Administration. Lewis Research Center, Cleveland, OH.

TURBULENCE MODELING IN AIRCRAFT ICING

Mark G. Potapczuk *In its* Workshop on Computational Turbulence Modeling 1993 11 p (For primary document see N94-18545 04-34)
Avail: CASI HC A03/MF A04

The Icing and Cryogenic Technology Branch develops computational tools which predict ice growth on aircraft surfaces and uses existing CFD technology to evaluate the aerodynamic changes associated with such accretions. Surface roughness, transition location, and laminar, transition, or turbulent convective heat transfer all influence the ice growth process on aircraft surfaces. Turbulence modeling is a critical element within the computational tools used for both ice shape prediction and for performance degradation evaluation. Author

N94-18556*# National Aeronautics and Space Administration. Lewis Research Center, Cleveland, OH.

SEVERAL EXAMPLES WHERE TURBULENCE MODELS FAIL IN INLET FLOW FIELD ANALYSIS

Bernhard H. Anderson *In its* Workshop on Computational Turbulence Modeling 1993 22 p (For primary document see N94-18545 04-34)
Avail: CASI HC A03/MF A04

Computational uncertainties in turbulence modeling for three dimensional inlet flow fields include flows approaching separation, strength of secondary flow field, three dimensional flow predictions of vortex liftoff, and influence of vortex-boundary layer interactions; computational uncertainties in vortex generator modeling include representation of generator vorticity field and the relationship between generator and vorticity field. The objectives of the inlet flow field studies presented in this document are to advance the understanding, prediction, and control of intake distortion and to study the basic interactions that influence this design problem. Derived from text

N94-18557# Von Karman Inst. for Fluid Dynamics, Rhode-Saint-Genese (Belgium).

COMPUTATIONAL FLUID DYNAMICS

1993 587 p Lecture series held in Rhode-Saint-Genese, Belgium, 15-19 Mar. 1993
(VKI-LS-1993-04; ETN-93-94445) Copyright Avail: CASI HC A25/MF A06

The aim was to provide in-depth presentations on well established methods and on recent advances in the field of numerical flow simulation. The space discretizations studied were finite volume, finite element, and spectral methods. Applications were covered in the fields of incompressible flow and aerodynamics. The theory of hyperbolic conservation laws is given, including a comparison of the currently used high resolution Total Variation Diminishing (TVD) finite volume schemes. The finite volume line was elaborated in separate lectures on Essentially Non Oscillatory (ENO) schemes including application to unstructured grids. Alternative discretizations which received equal attention were variational methods such as the finite element method, and spectral methods. Next to the basic discretizations, attention was given to the time integration methods for unsteady flows and to the iterative solution methods for steady state computations. For individual titles, see N94-18558 through N94-18568.

N94-18558# Houston Univ., TX. Dept. of Mathematics.

HIGH ORDER NON-OSCILLATORY SCHEMES FOR THE COMPRESSIBLE EULER EQUATIONS

Richard Sanders *In* VKI, Computational Fluid Dynamics 1993 31 p (For primary document see N94-18557 04-34)
Copyright Avail: CASI HC A03/MF A06

Some of the basic ideas used today to numerically simulate high speed compressible fluid flow are reviewed. Some of the mathematical facts that are known about first order hyperbolic partial differential equations are listed. Remarks and examples are given to highlight questions concerning existence, uniqueness, and stability of solutions to the scalar equation. Differences between the scalar equation and the system of equations, as well as gaps in the mathematical theory are discussed. The Riemann problem, approximate Riemann problem solvers, and numerical flux functions that can be derived from approximate Riemann problem solvers are discussed. The first order Godunov method is developed and modified to include a number of higher order extensions. One dimensional variation stability is discussed for the scalar version of these extensions. A notion of accuracy that differs from the usual notion of pointwise accuracy is included. The finite volume method and a weakness of its quasi one dimensional version are considered. A two dimensional supersonic nozzle is numerically simulated. ESA

N94-18559# Houston Univ., TX. Dept. of Mathematics.

A MULTIGRID ACCELERATION TECHNIQUE FOR COMPUTING STEADY SOLUTIONS TO THE EQUATIONS OF COMPRESSIBLE FLOW

Richard Sanders *In* VKI, Computational Fluid Dynamics 1993 22 p (For primary document see N94-18557 04-34)
Copyright Avail: CASI HC A03/MF A06

The role that multigrid techniques play in solving the challenging problem of finding steady state solutions to the compressible Euler equations is discussed. The multigrid approach is a powerful tool for rapidly computing solutions to large linear and nonlinear systems of equations. Most notably is its application to finding solutions of elliptic boundary value problems. The rate of convergence offered by conventional iterative techniques is illustrated by solving a finite difference scheme. A two dimensional scalar model problem is discussed. ESA

N94-18560*# National Aeronautics and Space Administration. Lyndon B. Johnson Space Center, Houston, TX.

COMPUTATIONAL TECHNIQUES FOR HIGH-SPEED FLOWS WITH VISCOUS AND CHEMICAL EFFECTS

C. P. Li *In* VKI, Computational Fluid Dynamics 1993 73 p (For primary document see N94-18557 04-34)
Copyright Avail: CASI HC A04/MF A06

Algorithms for solving the Euler and the Navier-Stokes equations in conjunction with chemical kinetic equations are presented. The convective flux is estimated from a quasi one dimensional interpolation procedure. Shock, contact, and expansion waves and thermochemical nonequilibrium phenomena are captured by the Lax-Friedrichs technique. Relaxation techniques were developed to enhance their effectiveness in dealing with spatial and temporal stiffness associated with the physical problems. Both explicit and implicit smoothers were implemented into the standard multigrid time stepping method. Unsteady and steady scalar problems are discussed. A perfect gas and equilibrium air shock tube problem is investigated. Numerical schemes and techniques are compared for the problems of shock and boundary layer interaction and three dimensional viscous, nonequilibrium flow encompassing an aerobrake. The results are comparable in accuracy against other high order non-oscillatory techniques. The multigrid methods are assessed using a Mach 8 flow over a complete planar body, a sphere, and a blunt delta wing at 20 deg incidence. Applying an implicit multigrid method on a nested grid of 128 by 64 nodes the reduction factor is 0.25. The central processing unit reduction factor is 2.2 after both the single and multigrid Runge-Kutta solutions converged to machine zero on a grid of 37 by 41 by 73 nodes. ESA

N94-18561# Institut National de Recherche d'Informatique et d'Automatique, Valbonne (France).

ENO SCHEMES ON UNSTRUCTURED MESHES

R. Abgrall and F. C. Lafon (Commissariat a l'Energie Atomique, Villeneuve-Saint-Georges, France.) *In* VKI, Computational Fluid Dynamics 1993 60 p (For primary document see N94-18557 04-34)
Copyright Avail: CASI HC A04/MF A06

The class of the Essentially Non Oscillatory (ENO) schemes is presented. The purpose is to provide a description of the basic ideas of ENO methods and to show how it is possible to adapt them on general geometries. The basic idea of ENO schemes is to use a Lagrange type interpolation with an adapted stencil: when a discontinuity is detected, the procedure looks for the region around this discontinuity where the function is the smoothest. The principle of finite volume schemes is reviewed. The reconstruction step, the evolution step, and the projection step are shown. Before the reconstruction step, several Runge-Kutta methods are given. The 'classical' methods that are applied to real valued functions are presented. Some pathologies of ENO reconstruction procedures and how to cure the problems are discussed. ESA

N94-18562# Centre Europeen Recherche et de Formation Advance en Calcul Scientific, Toulouse (France).

MULTIDIMENSIONAL WAVE DECOMPOSITIONS FOR THE EULER EQUATIONS

Michael A. Rudgyard *In* VKI, Computational Fluid Dynamics 1993 29 p (For primary document see N94-18557 04-34)

Copyright Avail: CASI HC A03/MF A06

The aim is to present an overview of wave modeling and its application to the two dimensional Euler equations. Both new and existing models are discussed. Some basic issues relating to the use of multidimensional upwinding applied to the Euler equations are summarized. This includes a description of a positive nonlinear advection scheme using a cell vertex, or 'fluctuation splitting.' A conservative linearization for Euler equations is presented. Concerning wave modeling, directional splitting approach, fine wave model, Roe's model, Parpia's five wave model, and flow wave models are summarized. The models of multidimensional upwinding give solutions that rival the accuracy of classical total variation diminishing schemes applied to simple test problems. The techniques are still in their infancy and are not yet robust enough to be used in an industrial environment. Nonetheless, the initial evidence is promising enough for us to continue research in this area. ESA

N94-18563# Centre Europeen Recherche et de Formation Advance en Calcul Scientific, Toulouse (France).

CELL VERTEX METHODS FOR STEADY INVISCID FLOW

Michael A. Rudgyard *In* VKI, Computational Fluid Dynamics 1993 51 p (For primary document see N94-18557 04-34)

Copyright Avail: CASI HC A04/MF A06

The development of cell vertex methods and their application to the equations of steady, inviscid, compressible flow are described. The aim is to serve as an overview of cell vertex techniques in general and as an introduction to the lectures on 'fluctuation splitting' and multidimensional upwinding. Both theoretical and practical aspects of the cell vertex method are discussed. In particular, aspects of the residual distribution are focused upon. The importance of some basic issues is highlighted by examining simple model problems in one and two dimensions. Examples of the application of these ideas to real flow problems are included. ESA

N94-18564# Von Karman Inst. for Fluid Dynamics, Rhode-Saint-Genese (Belgium).

COMPACT ADVECTION SCHEMES ON UNSTRUCTURED GRIDS

H. Deconinck, Robert Struijs, G. Bourgois, and Philip L. Roe (Michigan Univ., Ann Arbor.) *In its* Computational Fluid Dynamics 1993 81 p (For primary document see N94-18557 04-34)

Copyright Avail: CASI HC A05/MF A06

The status of compact cell vertex advection schemes for scalar conservation laws, discretized on unstructured grids composed of triangles of tetrahedra is described. The concepts of fluctuation splitting schemes in one, two, and three dimensions are discussed. Attention is given to a careful definition of upwind concepts in three dimensions and to design criteria to be satisfied by the advection schemes. It is shown that linearity preservation and positivity are incompatible for linear schemes generalizing well known results on structured grids. Two classes of linear schemes, one satisfying positivity at the price of first order accuracy and one satisfying linearity preservation with the price of spurious oscillations near discontinuities, are discussed. Nonlinear schemes which do satisfy positivity and linearity preservation are described. These schemes are compared with least squares Galerkin finite element schemes. A numerical accuracy study of the different schemes is added. A study of the shock capturing properties for the monotone higher order schemes is given. The performance of the different schemes is compared for different testcases among which scalar advection of a discontinuity and a nonlinear conservation law with shock. ESA

N94-18565*# California Univ., Davis. Dept. of Mechanical, Aeronautical and Materials Engineering.

VARIATIONAL APPROACHES TO CFD: APPLICATIONS TO POTENTIAL EULER AND NAVIER-STOKES EQUATIONS

M. Hafez *In* VKI, Computational Fluid Dynamics 1993 152 p Sponsored by NASA. Ames Research Center (For primary document see N94-18557 04-34)

Copyright Avail: CASI HC A08/MF A06

Flow simulations based on variational techniques are discussed. Variational techniques are applied for the problem formulation, for the construction of discrete schemes, and for the solution procedures. Inviscid transonic flows, as well as viscous incompressible and compressible flows, are analyzed by several methods. Variational techniques to solve the discrete systems of equations are well known. The most popular one is the conjugate gradient method. Extensions to nonsymmetric and nonpositive definite systems were under investigation for the last two decades. Variational techniques were used for convergence acceleration of iterative procedures. Some of these ideas based on recent work are examined. The lectures are organized in three parts including numerical simulation of inviscid as well as viscous incompressible and compressible flows. ESA

N94-18566# Paris VI Univ. (France).

INTRODUCTION TO SPECTRAL METHODS: APPLICATION TO THE STOKES PROBLEM

Y. Maday *In* VKI, Computational Fluid Dynamics 1993 26 p (For primary document see N94-18557 04-34)

Copyright Avail: CASI HC A03/MF A06

Basic features of spectral methods, their numerical analysis, the spectral element method in curved geometries, the Stokes problem, and an extension to more complex situations such as nonhomogenous Dirichlet and Neumann boundary conditions are introduced. Spectral methods are used to approximate the solution of partial differential equations. The discrete functions are polynomials, the degree of which, denoted N, is the discretization parameter so that the convergence is achieved by letting N go to infinity. The general strategy involves a weighted residual technique or a collocation technique in order to define the discrete solution. Spectral methods are used when the domain where the solution is defined is a square or a rectangle in two dimensions, or when it is a cube or a rectangle parallelogram in three dimensions. In the case where the domain is more complex, a domain decomposition is required to use spectral type methods. Spectral element methods combine the rapid convergence rate of the plain spectral methods with the generality of finite element techniques. By construction, the spectral element methods are applicable to many complex geometries and also to many equations. ESA

N94-18567# Paris VI Univ. (France).

INTRODUCTION TO SPECTRAL METHODS FOR HYPERBOLIC SYSTEM OF CONSERVATION LAWS

Y. Maday *In* VKI, Computational Fluid Dynamics 1993 12 p (For primary document see N94-18557 04-34)

Copyright Avail: CASI HC A03/MF A06

Spectral type approximations follow the same global rule and the approximation of discontinuous functions by these methods is only very slowly convergent and, apparently, not better than the finite order methods. Actually there are global oscillations everywhere on the domain of computation even if the solution is discontinuous at one point and regular everywhere else. A method to compute accurately the first Legendre coefficients of the discontinuous solution of some hyperbolic conservation law is presented. Particular attention is given to spectral viscosity approximation. Theoretical and numerical results are provided. ESA

N94-18568# Katholieke Univ. te Leuven (Belgium). Dept. of Computer Science.

DISTRIBUTED MEMORY PARALLEL COMPUTERS AND COMPUTATIONAL FLUID DYNAMICS

D. Roose and R. VanDriessche *In* VKI, Computational Fluid Dynamics 1993 44 p (For primary document see N94-18557 04-34)

Copyright Avail: CASI HC A03/MF A06

A tutorial on aspects of parallel computing that are important for the development of efficient parallel algorithms and software for Computational Fluid Dynamics (CFD) is presented. Some important concepts concerning distributed memory parallel computers and parallel algorithms and the parallelization of CFD algorithms on structured grids are given. Many techniques used in CFD are shown to be suited for parallelization. The minimization of work load imbalance and communication and the expectation of a general high speedup and parallel efficiency are outlined. Some methods for partitioning and mapping unstructured grids are described. These methods range from simple heuristics to global optimization methods. Methods that show a good tradeoff between execution time and quality of the result, such as inertial recursive bisection and eigenvector recursive bisection, are considered. ESA

N94-18578# Von Karman Inst. for Fluid Dynamics, Rhode-Saint-Genese (Belgium).

INTRODUCTION TO THE MODELING OF TURBULENCE

1993 518 p Lecture series held in Rhode-Saint-Genese, Belgium, 8-11 Feb. 1993
(VKI-LS-1993-02; ETN-93-94447) Copyright Avail: CASI HC A22/MF A04

The purpose is to provide an introduction to the fundamental physical principles of turbulence and of its modeling and to make a survey of the models currently available and of their domain of application. Emphasis is given to those models which can be considered ready for application to a range of problems of practical interest and to recent advances in second moment closures. Fields of advanced turbulence modeling such as large eddy simulation and compressible flow turbulence are discussed. For individual titles, see N94-18579 through N94-18597.

N94-18579# Manchester Univ. (England).

AN INTRODUCTION TO THE MODELLING OF TURBULENCE

B. E. Launder *In* VKI, Introduction to the Modeling of Turbulence 1993 16 p (For primary document see N94-18578 04-34)
Copyright Avail: CASI HC A03/MF A04

Turbulent flow models are reviewed. A turbulent flow can be obtained under the following conditions: at moderate Reynolds numbers the restraining effects of viscosity are too weak to prevent small, random disturbances in a shear flow from amplifying; the disturbances grow, become nonlinear and interact with neighboring disturbances; this mutual interaction leads to a tangling of vorticity filaments; the flow reaches a chaotic, nonrepeating form describable only in statistical terms. Direct numerical simulations of turbulent shear flows, based on time dependent Navier-Stokes equations, are discussed. Mathematical and physical statements on forming turbulent transport equations are summarized. Velocity distribution and heat and mass transports in turbulent flows are overviewed. ESA

N94-18580# Manchester Univ. (England).

AN INTRODUCTION TO SECOND MOMENT CLOSURE

B. E. Launder *In* VKI, Introduction to the Modeling of Turbulence 1993 13 p (For primary document see N94-18578 04-34)
Copyright Avail: CASI HC A03/MF A04

Second moment closures of either differential or algebraic type equations to describe two dimensional, thin shear flows are introduced. They give more accurate solutions than eddy-viscosity scheme equations. The Reynolds stress transport and the scalar flux equations are obtained. Pressure fluctuations in shear turbulence are discussed. The physical characteristics of phi(sub ij) products, that promote an evolution of turbulence towards isotropy, are listed. The return to isotropy models and the problem of coordinate rotation are considered. The formulations of wall effects and the gradient diffusion hypothesis are summarized. The weakness of the algebraic second moment model is stressed. The analysis shows that differential second moment closures are needed to describe swirling flows and that the epsilon-equation and phi(sub ij) models need extensive testing before being incorporated into general purpose software. ESA

N94-18581# Manchester Univ. (England).

MODELLING FORCE-FIELD EFFECTS ON TURBULENCE

B. E. Launder *In* VKI, Introduction to the Modeling of Turbulence 1993 11 p (For primary document see N94-18578 04-34)
Copyright Avail: CASI HC A03/MF A04

The effects involving fluctuating force fields in the instantaneous momentum equations, which give rise to source or sink terms in the stress and heat flux equations, are investigated. In particular, the following effects are discussed: direct and indirect effects of body forces in second moment equations; buoyancy effects on the epsilon equation and on stress transport; and secondary generation effects in plumes. The analysis shows that when force fields modify turbulence structure directly, second moment closure is needed to capture effects. Moreover, in highly stable flows it may be important to include buoyant effects on triple moments. The basic model developed for shear flows without force fields extrapolates well to buoyant and swirling flows. However, if buoyant and shear generation of k are equally effective in modifying epsilon, c(sub epsilon 1) needs to be reduced. ESA

N94-18582# Manchester Univ. (England).

A NEW FORM OF SECOND-MOMENT CLOSURE

B. E. Launder *In* VKI, Introduction to the Modeling of Turbulence 1993 16 p (For primary document see N94-18578 04-34)
Copyright Avail: CASI HC A03/MF A04

The purpose of this study is: to introduce the stress invariants and their characteristics; to discuss the models of pressure interactions for phi(sub ij) and phi(sub i phi); to consider new forms of the dissipation rate equations; and to compare the model's performance in a selection of flows with simpler formulations. The study is motivated by the fact that: the basic model does rather poorly in free shear flows; wrong dependence of effective turbulent Prandtl number on strain rate; and that thermal dynamic time scale ratio is not constant. Direct data simulation suggests that even when the right effect is achieved it may be for the wrong reasons. ESA

N94-18583# Manchester Univ. (England).

AN INTRODUCTION TO SINGLE-POINT CLOSURE METHODOLOGY

B. E. Launder *In* VKI, Introduction to the Modeling of Turbulence 1993 90 p (For primary document see N94-18578 04-34)
Copyright Avail: CASI HC A05/MF A04

Several principles of mathematical physics leading to turbulence modeling approaches are reviewed. The purpose is to simulate processes not exactly determinable at second moment level in terms of mean turbulence properties. The Reynolds number hypothesis, the dissipative correlations, and nondispersive pressure interactions are overviewed. The strategy to take into account mean strain contributions and the effect of force fields is presented. The importance of near wall flow pressure reflections on the pressure-strain correlation is underlined and low Reynolds number turbulence near walls is discussed. The Eddy viscosity models are discussed. ESA

N94-18584# Manchester Univ. (England).

SECOND-MOMENT CLOSURE: PRESENT... AND FUTURE? Abstract Only

B. E. Launder *In* VKI, Introduction to the Modeling of Turbulence 1993 2 p Repr. from Int. J. Heat and Fluid Flow, v. 10, no. 4, Dec. 1989 p 282 (For primary document see N94-18578 04-34)
Copyright Avail: CASI HC A01/MF A04

The present position of second moment closure and the possible directions for future development are discussed. It is argued that a simple form of second moment treatment, widely used for computing industrial flows, gives demonstrably superior predictive accuracy than any eddy viscosity model. Schemes now in the final phases of development, that exactly satisfy various limiting constraints, are presented. The introduction of a further second rank tensor into the closure is considered. The split spectrum approach may be attractive for certain flows with unusual spectral distributions of energy. The introduction of a second scale related equation is arguably a more sensible approach since the extra computational cost is small while the added flexibility could bring significant benefits in modeling turbulence far from equilibrium. ESA

N94-18585# Manchester Univ. (England). Dept. of Mechanical Engineering.

CONTRIBUTION TO THE MODELLING OF NEAR-WALL TURBULENCE Abstract Only

B. E. Launder and D. P. Tselepidakis *In* VKI, Introduction to the Modeling of Turbulence 1993 2 p Also presented at the 8th International Symposium on Turbulent Shear Flows, Munich, Germany, 9-11 Sep. 1991 (For primary document see N94-18578 04-34)
Copyright Avail: CASI HC A01/MF A04

The modeling, within the framework of second moment closure, of the turbulent stress field in the wall adjacent sublayer is discussed. Particular attention is given to handling wall proximity effects on the pressure strain and stress dissipation processes. The resultant model is compared with

the direct numerical simulations of plane channel flow and shows close agreement of the Reynolds stress profiles at two Reynolds numbers.
ESA

N94-18586# Manchester Univ. (England).

TWO-EQUATION MODELS FOR HIGH-REYNOLDS-NUMBER FLOW

M. A. Leschziner and B. E. Launder *In* VKI, Introduction to the Modeling of Turbulence 1993 16 p (For primary document see N94-18578 04-34)

Copyright Avail: CASI HC A03/MF A04

The advantages and disadvantages of one equation model are reviewed. The k-epsilon turbulence model is introduced. Two equation models allow much wider range of turbulent flows to be predicted than one equation variants. The k-epsilon turbulence model is the most popular two equation model: it forms a good compromise between generality and economy of use for many engineering problems. Often complex engineering flows can be modeled to acceptable accuracy with such schemes. The k approximately equal to epsilon model has a number of weaknesses related to curvature, adverse pressure gradient, and flow geometry. Corrections proposed are not generally applicable.
ESA

N94-18587# Manchester Univ. (England).

TWO-EQUATION MODELS FOR LOW-REYNOLDS-NUMBER VARIANTS

M. A. Leschziner and B. E. Launder *In* VKI, Introduction to the Modeling of Turbulence 1993 13 p (For primary document see N94-18578 04-34)

Copyright Avail: CASI HC A03/MF A04

A low Reynolds flow or flow region is one in which the large scale turbulent motion is affected by fluid viscosity. Some of the essential physics of turbulent flow are applied to the near wall sublayer flow. Representative forms of low Reynolds number two equation models are presented. Applications of the models to strongly nonequilibrium flows are shown. Weaknesses and approaches to their cure are indicated. The study shows that: the best models of this type are successful in predicting laminarization and related phenomena; the effects of curvature can only be roughly accounted for by the usual epsilon correction. Only the k-epsilon model was tested in separated flows; the Yap correction is useful but not fully satisfactory; direct simulation data would be helpful in refining the epsilon equation.
ESA

N94-18588# Manchester Univ. (England).

INCLUSION OF SECOND-MOMENT CLOSURES INTO FINITE-VOLUME SOLVERS

M. A. Leschziner *In* VKI, Introduction to the Modeling of Turbulence 1993 11 p (For primary document see N94-18578 04-34)

Copyright Avail: CASI HC A03/MF A04

Second moment closure equations are summarized. The main steps in finite volume discretization are indicated and destabilizing mechanisms are identified. The commonly used algorithmic techniques are outlined. The numerical stability for algebraic and differential closure forms are enhanced. Near wall treatment of second moment equations are described. The study shows that in order to use second moment closure for complex flows, special stabilization practices are needed. These include the use of apparent viscosity terms and careful distinction between negative and positive source terms to improve diagonal dominance. Further measures such as different types of underrelaxation techniques are needed, particularly in strongly swirling flow.
ESA

N94-18589# Manchester Univ. (England).

NUMERICAL IMPLEMENTATION AND PERFORMANCE OF REYNOLDS-STRESS CLOSURES IN FINITE-VOLUME COMPUTATIONS OF RECIRCULATING AND STRONGLY SWIRLING FLOWS

M. A. Leschziner *In* VKI, Introduction to the Modeling of Turbulence 1993 69 p Sponsored in part by United Kingdom Science and Engineering Research Council; Rolls Royce Ltd.; Ministry of Defence, London, England; British Aerospace; and Nielson Engineering and Research, Inc. (For primary document see N94-18578 04-34)

Copyright Avail: CASI HC A04/MF A04

Recent progress made in computing complex recirculating and strongly swirling flows with Reynolds stress closures and nondiffusive discretization within the finite volume framework are outlined. The results reported illustrate that stress closures provide a superior representation of turbulent transport processes to that returned by the Boussinesq viscosity model. This applies both to mean flow and turbulence features. In the case of plane flows, stress closures are especially appropriate and beneficial when the flow is dominated by a recirculation zone 'driven' by a shear layer in which curvature attenuates turbulent transport, especially if this shear layer is adjacent to a wall. In swirling flows, the algebraic representation of stress transport is deficient and must be avoided.
ESA

N94-18590# Manchester Univ. (England).

APPLICATION OF SECOND-MOMENT CLOSURE IN COMPLEX FLOWS

M. A. Leschziner *In* VKI, Introduction to the Modeling of Turbulence 1993 26 p (For primary document see N94-18578 04-34)

Copyright Avail: CASI HC A03/MF A04

Application examples of differential and algebraic second moment closure equations are given. Comments on boundary conditions at fluid inlet and outlet, and walls and symmetry lines are included. The results show that stress models do not perform consistently well, but are virtually always superior to eddy viscosity models, particularly in flows with large recirculation regions and most strongly swirling flows. These advantages appear to extend to three dimensional and transonic flows. The sources of defects are often difficult to identify. Stress transport is influential in axisymmetric flows, particularly with swirl. Only stress models are capable of capturing the main features of strongly swirling confined flows which become 'subcritical' due to severe curvature induced reduction in mixing.
ESA

N94-18591# Manchester Univ. (England).

MODELLING ENGINEERING FLOWS WITH REYNOLDS STRESS TURBULENCE CLOSURE Abstract Only

M. A. Leschziner *In* VKI, Introduction to the Modeling of Turbulence 1993 2 p Repr. from J. of Wind Engineering and Industrial Aerodynamics, v. 35, 1990 p 21-47 (For primary document see N94-18578 04-34)

Copyright Avail: CASI HC A01/MF A04

A Reynolds stress model consists of differential or algebraic equations each governing the balance between generation, dissipation, redistribution, and transport of a related Reynolds stress. The second moment closure combines the above stress equations with additional transport equations for heat or scalar fluxes. The potential advantages of using such closures in preference to eddy viscosity models in the presence of recirculation, swirl, and buoyancy are considered. Some basic forms of Reynolds stress closure are introduced, and their numerical implementation is outlined. Results of computations of complex flow types are presented. Improvements appear to be rooted in the ability of the closures to mimic the strong response of the turbulence structure to streamline curvature.
ESA

N94-18592# Manchester Univ. (England).

TURBULENCE MODELLING CHALLENGES POSED BY COMPLEX FLOWS Abstract Only

M. A. Leschziner *In* VKI, Introduction to the Modeling of Turbulence 1993 2 p Presented also at ROOMVENT, Lyngby, Denmark, Sep. 1992 (For primary document see N94-18578 04-34)

Copyright Avail: CASI HC A01/MF A04

Influential issues pertaining to the computational modeling of multidimensional, separated, turbulent flow are discussed. The modeling implications of a range of distinct physical flow characteristics are considered. Issues addressed include the interaction between turbulence, streamline curvature, buoyancy and normal strain, and the relevance of adverse pressure gradient, acceleration, separation and three dimensionality. Attention is focused on modern approaches to turbulence modeling, based on second moment closure and including adaptations to low Reynolds number regions. Established model variants are introduced, recent developments are reviewed and application examples included.
ESA

N94-18593# Karlsruhe Univ. (Germany).

EXAMPLES OF TURBULENCE MODEL APPLICATIONS

W. Rodi *In* VKI, Introduction to the Modeling of Turbulence 1993 53 p (For primary document see N94-18578 04-34)

Copyright Avail: CASI HC A04/MF A04

Commonly used turbulent models and flow situations of practical relevance are described. Examples of model calculations are presented for a wide range of flows from different areas of engineering. The results are compared with experimental data. Attention is focused on the application of eddy viscosity models, particularly the k-epsilon model. Results obtained with other models are included for comparison, and the relative performance of the different models is discussed. ESA

N94-18594# Deutsche Forschungsanstalt fuer Luft- und Raumfahrt, Oberpfaffenhofen (Germany). Inst. fuer Physik der Atmosphaere.
DIRECT AND LARGE EDDY SIMULATION OF TURBULENCE: SUMMARY OF THE STATE OF THE ART 1993
U. Schumann *In* VKI, Introduction to the Modeling of Turbulence 1993 61 p (For primary document see N94-18578 04-34)
Copyright Avail: CASI HC A04/MF A04

The basic approach used to simulate turbulence either directly or in terms of the large eddies is described. Both methods can be applied for: basic studies of the turbulent motion; generation of reference data for calibration of models; and analysis of turbulence under extreme forcing. The properties of turbulence are summarized. The direct numerical simulation approach is applied to solve turbulent diffusion in stratified homogeneous turbulent flows. A large eddy simulation method computes the three dimensional time dependent details of large eddies, using a simple subgrid scale model for the effects of small eddies in large eddies. ESA

N94-18595# Deutsche Forschungsanstalt fuer Luft- und Raumfahrt, Oberpfaffenhofen (Germany).
LARGE-EDDY SIMULATION OF TURBULENT DIFFUSION IN STABLY STRATIFIED SHEAR FLOW Abstract Only
H.-J. Kaltenbach, U. Schumann, and T. Gerz *In* VKI, Introduction to the Modeling of Turbulence 1993 2 p Submitted for publication (For primary document see N94-18578 04-34)
Copyright Avail: CASI HC A01/MF A04

By means of large eddy simulation, homogeneous turbulence is simulated for neutrally and stably stratified shear flow at gradient Richardson numbers between zero and one. The turbulent transport of three passive species which have uniform gradients in either vertical, downstream, or cross stream direction are investigated. The results are compared with previous measurements. The computed and measured flow properties agree with each other generally within the scatter of the measurements. At strong stratification, the Froude number becomes the relevant flow controlling parameter. Stable stratification suppresses vertical overturning mixing when the inverse Froude number exceeds a critical value. The turbulent diffusivity tensor is anisotropic and asymmetric. However, only the vertical and the cross stream diagonal component are of practical importance in shear flows. The vertical diffusion coefficient is much smaller than the cross stream one in strong stratification. This anisotropy is stronger than predicted by previous second order closure models. Downstream and cross stream diffusion follows classical mixing length models. ESA

N94-18596# Deutsche Forschungsanstalt fuer Luft- und Raumfahrt, Oberpfaffenhofen (Germany). Atmospheric Physics Inst.
NUMERICAL SIMULATION OF TURBULENT CONVECTIVE FLOW OVER WAVY TERRAIN
A. Doernbrack and U. Schumann *In* VKI, Introduction to the Modeling of Turbulence 1993 44 p Submitted for publication (For primary document see N94-18578 04-34)
Copyright Avail: CASI HC A03/MF A04

By means of large eddy simulation the convective boundary layer is investigated for flows over wavy terrain. The lower surface height varies sinusoidally in the downstream direction while remaining constant in the other. Several cases are considered with amplitude delta up to 0.15 H and wavelength lambda of H to 8 H, where H is the mean fluid layer height. At the lower surface the vertical heat flux is prescribed to be constant and the momentum flux is determined locally from the Monin-Obukhov relationship with a roughness length z(sub 0) = 0.0001 H. The mean wind is varied in between zero and 5 w, where w is the convective velocity scale. Weak mean wind destroys regular spatial structures induced by the surface undulation at zero mean wind. The surface heating suppresses mean flow recirculation regions even for steep surface waves. Short surface waves cause strong drag due to hydrostatic and dynamic pressure forces in addition to frictional drag. The pressure drag increases slowly with the mean velocity, and strongly with delta/H. The turbulence variances increase mainly in the lower half of the mixed layer for U/w greater than 2. ESA

N94-18597# Rouen Univ. (France).
TURBULENCE MODELING FOR COMPRESSIBLE FLOWS AND IMPLEMENTATION IN NAVIER-STOKES SOLVERS
D. Vandromme *In* VKI, Introduction to the Modeling of Turbulence 1993 65 p (For primary document see N94-18578 04-34)
Copyright Avail: CASI HC A04/MF A04

A survey on turbulence modeling problems is given. For a given problem, several ways to solve it along with the advantages and the drawbacks attached to the mode of solution, are presented. Focus is given to the treatment of compressible turbulent flows, or in a wider sense, to turbulent flows in which variable density effects exist. ESA

N94-18642# Pennsylvania State Univ., University Park. Applied Research Lab.
CALCULATION OF TURBULENT BOUNDARY LAYER WALL PRESSURE SPECTRA
D. E. Capone and G. C. Lauchle Aug. 1993 78 p
(AD-A269549; PSU/ARL-TR-93-10) Avail: CASI HC A05/MF A01

This study is an investigation into the suitability of various wavevector-frequency models of turbulent boundary layer wall pressure fluctuations for the prediction of experimental measurements of turbulent boundary layer wall pressure spectra. Three separate models of the wavevector-frequency spectrum proposed by D. M. Chase in 1980 and 1987 are evaluated. The wavevector-frequency spectral models are integrated numerically using a formulation for the point wall pressure spectrum (based on the work of Uberoi and Kovasznay). The representation of the wall pressure spectrum used accounts for the effect of a finite sized transducer on the measured wall pressure spectrum. By accounting for the area averaging effect of finite sized transducers on the measured turbulent boundary layer wall pressure spectra, it was possible to use Chase's rigorous formulations for the wavevector-frequency spectrum instead of the point pressure spectrum representations which assume an infinitely small measurement sensor. Results from the numerical integrations are compared to recent experimental data to determine which model of the wavevector-frequency spectrum most accurately predicts measured turbulent boundary layer wall pressure spectra. Data from experiments using fluids with a wide range of physical properties (air, water, and glycerine) are used for comparison purposes. Using the selected model, new empirical constants are established for use in the model for each fluid under consideration. Justification for use of the new empirical constants is given, and current limitations of the wavevector-frequency models are discussed. DTIC

N94-18671# Science Applications International Corp., McLean, VA.
UUGM CODE DEVELOPMENT Final Report, 1 Dec. 1991 - 31 Mar. 1993
S. Eidelman 26 Jul. 1993 693 p
(Contract F49620-89-C-0087; DARPA Order 6775)
(AD-A269945; SAIC-93/1152; AFOSR-93-0702TR) Avail: CASI HC A99/MF A06

The primary objective of SAIC was to develop an unstructured grid algorithm and code that dynamically adapts to the computed solution of the time dependent Euler equations of gasdynamics in two and three spatial dimensions. Important requirements that were imposed on the algorithm were: robustness, accuracy, efficiency, flexibility, and adaptability. The main research and code development effort was focused on achieving these objectives; extensive testing and code validation effort was undertaken to demonstrate the code's performance for realistic CFD problems. The method is accurate in all flow regimes from subsonic to hypersonic. The main achievement was the development of the AUGUST code (adaptive unstructured grid upwind second order for triangles). AUGUST is implemented for solution of Euler's equations on dynamically adaptive triangular or tetrahedral grids. The code fully implements the second-order Godunov method, allowing accurate and robust numerical solution of Euler equations of gas dynamics. A new method was developed for direct dynamic grid refinement (DDR). The AUGUST code was also implemented for multiphase, multicomponent flows. A combined structured/unstructured version of the AUGUST code was also developed. The AUGUST code was extensively validated for a wide range of problems and has proven to be a robust tool. DTIC

N94-18672# Army Engineer Waterways Experiment Station, Vicksburg, MS. Hydraulics Lab.
STREMR: NUMERICAL MODEL FOR DEPTH-AVERAGED INCOMPRESSIBLE FLOW Final Report
Bernard Roberts Sep. 1993 183 p
(AD-A269949; WES/TR/HL-REMR-HY-11) Avail: CASI HC A09/MF A02

The STREMR computer code is a two-dimensional model for depth-averaged incompressible flow. It accommodates irregular boundaries and nonuniform bathymetry, and it includes empirical corrections for turbulence and secondary flow. Although STREMR uses a rigid-lid surface approximation, the resulting pressure is equivalent to the displacement of a free surface. Thus, the code can be used to model free-surface flow wherever the local Froude number is 0.5 or less. STREMR uses a finite-volume scheme to discretize and solve the governing equations for primary flow, secondary flow, and turbulence energy and dissipation rate. The turbulence equations are taken from the standard k-Epsilon turbulence model, and the equation for secondary flow is developed herein. Appendices to this report summarize the principal equations, as well as the procedures used for their discrete solution. DTIC

N94-18739# Wright Lab., Wright-Patterson AFB, OH.
COMPUTATIONAL FLUID DYNAMICS (CFD) RESEARCH BRANCH TECHNICAL BRIEFS Final Report, May 1992 - 1993
Don W. Kinsey 9 Jun. 1993 31 p
(AF Proj. 2404)
(AD-A269698; WL-TR-93-3047) Avail: CASI HC A03/MF A01

This report consists of brief technical descriptions and one or more pictures of charts depicting research conducted in-house during the past year. The briefs are designed to provide enough information to clearly define the task, but are short enough to hold the reader's interest. Where applicable, a reference for more detailed information is provided. The research covers a wide spectrum of work; from grid generation to flow solvers, to post-processors; and from incompressible to hypersonic speeds. DTIC

N94-18755 Army Engineer Waterways Experiment Station, Vicksburg, MS. Hydraulics Lab.
A FINITE ELEMENT SCHEME FOR SHOCK CAPTURING Final Report
R. C. Berger Aug. 1993 63 p Limited Reproducibility: More than 20% of this document may be affected by microfiche quality
(AD-A270182; WES/TR/HL-93-12) Avail: CASI HC A04

The representation of hydraulic jumps or shocks in compressible fluids is a difficult task for numerical models. These models require more smoothness than the analytic solution contains. For this reason, these models are plagued with oscillations. The most widespread method is to smear the solution in the vicinity of the shock, giving up 0(1) errors, but restricting the error to the neighborhood of the jump or shock. This technique is called shock-capturing. In this report, a method to capture hydraulic jumps formed by the shallow-water equations in a finite element model is demonstrated. The model itself is two-dimensional. The method it relies upon is a Petrov-Galerkin approach in which the degree of upstream bias in the test function is based upon the characteristics of the convection matrix. Furthermore, in order to restrict the shock capturing to the vicinity of the jump, a method of jump detection is implemented which depends on the variation of mechanical energy within an element. The veracity of the model is tested by comparison of the predicted jump speed and magnitude with analytic and flume results. A comparison is also made to a flume case of steady-state supercritical lateral transition. DTIC

N94-18780 Colorado State Univ., Fort Collins.
CENTRIFUGE MODELING OF EXPLOSION-INDUCED CRATERS IN UNSATURATED SAND Final Report, May - Aug. 1991
K. C. Brownell and W. A. Charlie Nov. 1992 236 p Limited Reproducibility: More than 20% of this document may be affected by microfiche quality
(Contract F08635-90-C-0306)
(AD-A270194; AFCESA/ESL-TR-92-46) Avail: CASI HC A11

Craters, induced by explosive detonations, were modeled in dry and partially saturated sand in a geotechnical centrifuge. The apparent dimensions of the explosion-induced craters are analyzed as dimensional terms and dimensionless pi terms. Analysis of dimensional terms through a comparison of yield exponents shows that the scaling laws for apparent crater dimensions are the same for dry and partially saturated sand. Analysis of the dimensionless pi terms derived by Schmidt and Holsapple for buried charges, shows apparent crater volume (pi sub 1 = Pi exp v) and depth (Pi sub 1 = Pi sub d) do not follow the same scaling laws in partially saturated sand. Normalized (divided by the cube root of the charge mass) apparent crater diameter and depth data fit the best-fit prediction curves for sand derived by the U.S. Army Engineer Waterways Experiment Station. However, the apparent crater diameter data do not fall within the range from dry to wet sand predicted by the Air Force Protective Construction Design Manual. Scaled apparent crater dimensions of crater volume, radius, and depth increase at a point between 0 and 20 percent compaction saturation. Between 20 to 70 percent, the influence of compaction saturation on apparent crater dimensions appears to remain constant. DTIC

N94-18796# Air Force Inst. of Tech., Wright-Patterson AFB, OH.
CORRELATION OF INCOMING BOUNDARY LAYER PITOT PRESSURE FLUCTUATIONS WITH THE UNSTEADINESS OF FIN-INDUCED SHOCK WAVE TURBULENT BOUNDARY LAYER INTERACTIONS M.S. Thesis
Scott R. Nowlin Dec. 1993 155 p
(AD-A270059; AFIT/CI/CIA-93-143) Avail: CASI HC A08/MF A02

This study focuses on the effects of boundary layer pitot pressure fluctuations on fin-induced separation shock unsteadiness. Experiments performed in two phases under adiabatic wall conditions in a Mach 5 wind tunnel used high frequency-response transducers to measure fluctuating pressures in a turbulent boundary layer and a separated flow induced by a hemi-cylindrical unswept fin. Phase 1 results indicate that the turbulent boundary layer/freestream interface pitot pressure fluctuation frequency levels do not correlate with the sharp fin-induced shock wave turbulent boundary layer interaction aperiodic separation shock motion frequencies. In Phase 2, correlations between fluctuations in incoming boundary layer pitot pressures, intermittent region wall pressures, separation shock dynamics, and fin leading edge pressures show contributions from fluctuations at both low frequencies (approximately 500 Hz)--their source is not well understood--and high frequencies, driven by incoming turbulence. DTIC

N94-18831# Los Alamos National Lab., NM.
DEVELOPMENT OF A CRYOGENIC HEAT PIPE
F. C. Prenger, W. F. Stewart, and J. E. Runyan 1993 11 p Presented at the International Cryogenic Engineering Conference and International Cryogenic Materials Conference, Albuquerque, NM, 12-16 Jul. 1993
(Contract W-7405-eng-36)
(DE93-018448; LA-UR-93-2515; CONF-930703-13) Avail: CASI HC A03/MF A01

Heat pipe operating characteristics can be used to advantage in cryogenic systems. Diode operation of the heat pipe, the ability to conduct heat in one direction only, is useful in protecting the heat load if the heat sink temperature rises above the load temperature. Because of this, the heat pipe can be made to act as a thermal switch. A screened-wick, inverted-artery, cryogenic heat pipe was designed, fabricated, and tested. The tests were first conducted with hydrogen and then with oxygen as the working fluid. Heat pipe performance limits were measured as a function of operating temperature, and startup from both the supercritical and the frozen state was demonstrated. The heat pipe was designed to operate as a thermal diode, and transient tests were used to determine the turndown ratio. The heat pipe test results were correlated with the Los Alamos heat pipe computer code and good agreement was obtained between the predicted and measured performance. The heat pipe was developed for spacecraft sensor cooling applications. Test results show significant performance advantages over solid conductors. DOE

N94-18843*# Ecodynamics Research Associates, Inc., Denver, CO.
MULTIGRID METHODS FOR FLOW TRANSITION IN THREE-DIMENSIONAL BOUNDARY LAYERS WITH SURFACE ROUGHNESS Final Report
Chaoqun Liu, Zhining Liu, and Steve McCormick Washington Sep. 1993 148 p
(Contract NAS1-19312; RTOP 505-59-50-01)
(NASA-CR-4540; NAS 1.26:4540) Avail: CASI HC A07/MF A02

The efficient multilevel adaptive method has been successfully applied to perform direct numerical simulations (DNS) of flow transition in 3-D channels and 3-D boundary layers with 2-D and 3-D isolated and distributed roughness in a curvilinear coordinate system. A fourth-order finite difference technique on stretched and staggered grids, a fully-implicit time marching scheme, a semi-coarsening multigrid method associated with line distributive relaxation scheme, and an improved outflow boundary-condition treatment, which needs only a very short buffer domain to damp all order-one wave reflections, are developed. These approaches make the multigrid DNS code very accurate and efficient. This allows us not only to be able to do spatial DNS for the 3-D channel and flat plate at low computational costs, but also to do spatial DNS for transition in the 3-D boundary layer with 3-D single and multiple roughness elements, which would have extremely high computational costs with conventional methods. Numerical results show good agreement with the linear stability theory, the secondary instability theory, and a number of laboratory experiments. The contribution of isolated and distributed roughness to transition is analyzed. Author (revised)

N94-18867# Clemson Univ., SC. Dept. of Mechanical Engineering.
EXPERIMENTAL INVESTIGATION OF TURBULENT PRANDTL NUMBER AND REYNOLDS ANALOGY IN TRANSITIONAL AND POST-TRANSITIONAL BOUNDARY LAYERS Final Report
Ting Wang Jul. 1993 62 p
(Contract N00014-89-J-3105)
(AD-A270092) Avail: CASI HC A04/MF A01

The effects of elevated free-stream turbulence and streamwise acceleration on flow and thermal structures in transitional boundary layers have been investigated experimentally on a heated flat plate. The effects on the turbulent Prandtl number and Reynolds analogy were included in this study. The free-stream turbulence levels ranged from 0.5 to 7%, and the acceleration strengths, based on K, ranged from 0.39x10 to the minus 6th power to 4.1x10 to the minus 6th power. A three-wire probe was used to measure the detailed momentum and thermal boundary layer structures, including the streamwise and cross-stream velocity fluctuations, the temperature fluctuation, the Reynolds stresses, the Reynolds heat fluxes, the eddy viscosity, the turbulent thermal diffusivity and the turbulent Prandtl number. The results show that elevated free-stream turbulence values result in an earlier onset of transition and reduced length of transition, whereas streamwise acceleration delays the onset of transition and lengthens the transition region, even at elevated FSTI. Compared to streamwise acceleration, FSTI is the more dominant factor on flow and thermal structure in transitional boundary layers; however, streamwise acceleration significantly reduces the turbulent spot formation rate. DTIC

N94-18870 California Univ., Berkeley. Seismographic Station.
WAVE PROPAGATION NEAR EXPLOSIVE SOURCES
Lane R. Johnson 20 May 1993 32 p Limited Reproducibility: More than 20% of this document may be affected by microfiche quality
(Contract F19628-90-K-0055)
(AD-A270102; PL-TR-93-2118; AD-E201621) Avail: CASI HC A03

A basic goal of seismic yield estimation is to understand the relationship between the yield of an explosion and the amplitude of seismic waves radiated into the far field. Of particular interest in this relationship is the role played by material properties in the vicinity of the source. This study is an attempt to investigate this problem through the use of an equivalent elastic treatment for the region between the original cavity radius and the elastic radius. Equations are developed which allow the material properties to be modified as a function of the level of stress, and a propagator method is presented which solves the elastodynamic equations for a visco-elastic material with properties that vary as a function of radial distance from the explosive source. The relations between parameters measures in laboratory tests and the material properties required in wave propagation problems are also reviewed. While this approach is only an approximation to calculations with hydrodynamic and equation-of-state codes, it has the advantage of providing simple analytic results in which the role of various model parameters is easily investigated. DTIC

N94-18878 Lawrence Livermore National Lab., CA.
HEMP 3D: A FINITE DIFFERENCE PROGRAM FOR CALCULATING ELASTIC-PLASTIC FLOW, APPENDIX B
Mark L. Wilkins 26 May 1993 65 p Sponsored by DARPA Limited Reproducibility: More than 20% of this document may be affected by microfiche quality
(AD-A269171; UCRL-ID-114993-App-B) Avail: CASI HC A04

The HEMP 3D program can be used to solve problems in solid mechanics involving dynamic plasticity and time dependent material behavior and problems in gas dynamics. The equations of motion, the conservation equations, and the constitutive relations listed below are solved by finite difference methods following the format of the HEMP computer simulation program formulated in two space dimensions and time. DTIC

N94-18888# Lawrence Livermore National Lab., CA.
FLOW VOLUMES FOR INTERACTIVE VECTOR FIELD VISUALIZATION
N. Max, B. Becker, and R. Crawfis Apr. 1993 7 p Presented at the Visualization 1993, San Jose, CA, 25-29 Oct. 1993
(Contract W-7405-eng-48)
(DE93-017102; UCRL-JC-113625; CONF-931080-2) Avail: CASI HC A02/MF A01

Flow volumes are the volumetric equivalent of stream lines. They provide more information about the vector field being visualized than do stream lines or ribbons. Presented is an efficient method for producing flow volumes, composed of transparently rendered tetrahedra, for use in an interactive system. The problems of rendering, subdivision, sorting, rendering artifacts, and user interaction are dealt with. DOE

N94-18906# Naval Undersea Warfare Center, Newport, RI.
RELATION BETWEEN THE FLUCTUATING WALL PRESSURE AND THE TURBULENT STRUCTURE OF A BOUNDARY LAYER ON A CYLINDER IN AXIAL FLOW Ph.D. Thesis - Northwestern Univ., 1992
Stephen R. Snarski 12 Aug. 1993 245 p
(Contract N00014-89-J-1439)
(AD-A270242; NUWC-NPT-TR-10223) Avail: CASI HC A11/MF A03

The turbulent flow structures responsible for the fluctuating wall pressure in the turbulent boundary layer on a cylinder in axial flow (delta/a = 5.04, Re(sub theta) = 2870) have been investigated. Simultaneous measurements of the fluctuating wall pressure and turbulent streamwise velocities have been performed throughout a large volume of the boundary layer (y(sup +) = 14 to y/delta = 1.91, 0 less than or equal to x/delta less than or equal to 1.52, azimuthal angle phi = 0 deg, 20 deg, 40 deg) with a subminiature electret microphone (d(sup +) = 25.9) and hotwire velocity probe (1(sup +) = 18.5). Pressure-velocity cross-spectra and cross-correlation measurements indicate that two primary groups of pressure fluctuations exist in the cylindrical boundary layer: (1) small-scale, high-frequency disturbances concentrated close to the wall associated with the burst-sweep cycle; and (2) large-scale, low-frequency disturbances extending from the wall to the turbulent/potential-flow interface that are consistent with a large spanwise-oriented 'vortex' in close contact with and inclined to the wall. DTIC

N94-18918# Sandia National Labs., Albuquerque, NM.
VISUALIZATION FOR APPLICATIONS IN SHOCK PHYSICS
C. J. Pavlakos and D. L. Campbell 1993 4 p Presented at the Visualization 1993, San Jose, CA, 25-29 Oct. 1993
(Contract DE-AC04-76DP-00789)
(DE93-012849; SAND-93-0916C; CONF-931080-1) Avail: CASI HC A01/MF A01

This case study presents work being done to provide visualization capabilities for a family of codes at Sandia in the area of shock physics. The codes, CTH and Parallel CTH, are running in traditional supercomputing as well as massively parallel environments. These are Eulerian codes which produce data on structured grids. Data sets can be large, so managing large data is a priority. A supercomputing-based distributed visualization environment has been implemented to support such applications. This environment, which is based in New Mexico, is also accessible from our branch site in California via a long haul FDDI/ATM link. Functionality includes the ability to track ongoing simulations. A custom visualization file has been developed to provide efficient, interactive access to result data. Visualization capabilities are based on the commercially available AVS software. A few example results are presented, along with a brief discussion of future work. DOE

N94-18995# Lawrence Livermore National Lab., CA.
THERMAL STRESSES IN THE MICROCHANNEL HEATSINK COOLED BY LIQUID NITROGEN
R. A. Riddle 30 Jun. 1993 17 p Presented at the Annual Meeting of the Society of Photo-Optical Instrumentation Engineers (SPIE), San Diego, CA, 11-16 Jul. 1993

(Contract W-7405-eng-48)
(DE93-018660; UCRL-JC-114422; CONF-930722-15) Avail: CASI HC A03/MF A01

Microchannel heatsinks represent a highly efficient and compact method of heat removal in high heat flux components. Excellent thermal performance of a silicon microchannel heatsink has been demonstrated using liquid nitrogen as the coolant. For the heating of a 1 square centimeter area, at a heat dissipation of 500 W, a typical silicon heatsink cooled by liquid nitrogen has a thermal resistance of 0.046 sq cm K/W. The actual heatsink structure in this case is only 0.1 cm high. Silicon, although it has excellent thermal properties at liquid nitrogen temperatures, may fracture with very little plastic deformation due to mechanical and thermal stresses. Because the fracture strength of silicon depends on the presence of small defects, the strength of the heatsink structures must be addressed to insure highly reliable heatsink devices. Microchannel heatsink reliability can be affected by thermal stresses that arise due to temperature gradients between the base and fin and along the film length. These stresses are combined with the bonding stresses that arise in attaching components at elevated temperatures to the silicon heatsink and then cooling the structure to the cryogenic operating temperatures. These bonding stresses are potentially large because of the differences in the values of the coefficients of thermal expansion in silicon heatsink material, and the attached component materials. The stress results are shown for a 17:1 aspect ratio heatsink cooled in liquid nitrogen. The temperature gradients are a result of a surface heat flux of 1.3 kW/sq cm, approximating the heat dissipation of an RF power chip. The chip is connected to an aluminum nitride substrate, then the chip and substrate module are attached to the heatsink at a bonding temperature of 600 K, as for a gold tin eutectic bond. The stresses are shown to be within the allowables of the materials involved. DOE

N94-19025# Los Alamos National Lab., NM.
THE APPLICATION OF FRONT TRACKING TO THE SIMULATION OF SHOCK REFRACTIONS AND SHOCK ACCELERATED INTERFACE MIXING
D. H. Sharp (Department of Energy, Washington, DC.), John W. Grove (State Univ. of New York, Stony Brook.), Yumin Yang (Department of Energy, Washington, DC.), Brian Boston (Department of Energy, Washington, DC.), R. Holmes (Department of Energy, Washington, DC.), and Qiang Zhang (Department of Energy, Washington, DC.) 1993 11 p Presented at the 4th International Workshop on the Physics of Compressible Turbulent Mixing, Cambridge, United Kingdom, 29 Mar. - 1 Apr. 1993
(Contracts W-7405-eng-36; DE-FG02-90ER-25084; DAAL03-92-G-0185; DAAL03-91-C-0027; NSF DMS 92-01581; NSF DMS 90-57429)
(DE93-018342; LA-UR-93-2335; CONF-9303126-7) Avail: CASI HC A03/MF A01

The mixing behavior of two or more fluids plays an important role in a number of physical processes and technological applications. The authors consider two basic types of mechanical (i.e., non-diffusive) fluid mixing. If a heavy fluid is suspended above a lighter fluid in the presence of a gravitational field, small perturbations at the fluid interface will grow. This process is known as the Rayleigh-Taylor instability. One can visualize this instability in terms of bubbles of the light fluid rising into the heavy fluid, and fingers (spikes) of the heavy fluid falling into the light fluid. A similar process, called the Richtmyer-Meshkov instability occurs when an interface is accelerated by a shock wave. These instabilities have several common features. Indeed, Richtmyer's approach to understanding the shock induced instability was to view that process as resulting from an acceleration of the two fluids by a strong gravitational field acting for a short time. Here, the authors report new results on the Rayleigh-Taylor and Richtmyer-Meshkov instabilities. Highlights include calculations of Richtmyer-Meshkov instabilities in curved geometries without grid orientation effects, improved agreement between computations and experiments in the case of Richtmyer-Meshkov instabilities at a plane interface, and a demonstration of an increase in the Rayleigh-Taylor mixing layer growth rate with increasing compressibility, along with a loss of universality of this growth rate. The principal computational tool used in obtaining these results was a code based on the front tracking method. DOE

N94-19027# Los Alamos National Lab., NM.
IMPLEMENTATION OF THE TURN FUNCTION METHOD IN KIVA-F90
P. J. ORourke and M. S. Fairfield Aug. 1993 34 p
(Contract W-7405-eng-36)
(DE93-018394; LA-12536-MS) Avail: CASI HC A03/MF A01

We document the implementation of the Turn Function Method (TFM) in KIVA-F90, a version of the KIVA computer program written in the FORTRAN 90 programming language that is used on some massively parallel computers. TFM solves both linear momentum and vorticity equations in numerical calculations of compressible fluid flow. Solving a vorticity equation allows vorticity to be both conserved and transported more accurately than is possible in traditional methods for computing compressible flow. To calculate the convective transport of vorticity more accurately, we have also implemented an improved method for the rezone phase of the KIVA computational cycle. This first implementation of TFM in a three-dimensional hydrodynamics code involved some modification of the original method and some novel numerical difference approximations. In particular, we used a penalty method to keep the divergence of the computed vorticity field close to zero. Also, difference operators are defined in such a way that the finite difference analog of divergence of curl of u = 0 is exactly satisfied. Three example problems presented in this report show the greater accuracy that can be gained when TFM is used for calculations of flows with rotational motion, as well as the added computational costs incurred. Use of the method can increase by 60% the computational times of the Euler equation solver in KIVA-F90. Although TFM sometimes does degrade accuracy in calculations that have large vorticity gradients, generally the calculations show beneficial effects of TFM on accuracy. We will continue to evaluate the costs and benefits of TFM in future KIVA-F90 calculations. DOE

N94-19058# Sandia National Labs., Albuquerque, NM.
NUMERICAL SOLUTIONS FOR A FLOW WITH MIXED CONVECTION IN A VERTICAL GEOMETRY
J. R. Torczynski 1993 37 p Presented at the Annual Winter Meeting of the ASME, New Orleans, LA, 28 Nov. - 3 Dec. 1993
(Contract DE-AC04-76DP-00789)
(DE93-011592; SAND-93-0186C; CONF-931121-5) Avail: CASI HC A03/MF A01

The K-12 Aerospace Heat Transfer Committee of the American Society of Mechanical Engineers recently specified a computational benchmark problem involving steady incompressible laminar flow with mixed convection using the Boussinesq approximation in a two-dimensional backstep geometry. FIDAP v6.0 (Fluid Dynamics International) and NEKTON v2.85 (Nektonics, Fluent) are capable of simulating situations with this type of coupled fluid flow and heat transfer. FIDAP uses conventional finite elements and has both steady and transient solvers, whereas NEKTON uses spectral elements with a transient solver (for large problems). Numerical solutions to the benchmark problem are obtained with both of these codes, and grid-refinement studies are performed to verify that grid-independence is achieved. The grid-independent solutions from both codes are found to be in excellent agreement with each other and with results in the archival literature regarding velocity and temperature profiles and the locations of separation and reattachment points. DOE

N94-19068# Research Inst. of National Defence, Stockholm (Sweden). Dept. of Weapon Systems, Effects and Protection.
AIR BLAST MEASUREMENTS AT 20 AND 40 km DISTANCE FROM DETONATING 10 AND 20 TON HIGH EXPLOSIVE CHARGES [LJUDTRYCKSMATNINGAR VID ALVDALENS SKJUTFALT: SPRANGNING AV 10 OCH 20 TON LADDNINGAR]
T. Eriksson, B. Selin, and I. Aseborn Feb. 1993 74 p In SWAHILI
(PB93-195949; FOA-C-20922-2.3) Avail: CASI HC A04/MF A01

Air blast overpressure measurements have been made at 20 and 40 km distance from the detonation of 10 and 20 ton high explosive charges at Alvdalen Shooting Range in Sweden. Temperatures and wind velocities were also measured. Simple rules were set up and methods elaborated to avoid complaints, and damage to buildings outside the Alvdalen Shooting Range. NTIS

N94-19087# Technische Univ., Delft (Netherlands). Faculty of Technical Mathematics and Informatics.
TIME DOMAIN CALCULATIONS OF THE SECOND-ORDER DRIFT FORCE ON A FLOATING TWO-DIMENSIONAL OBJECT IN CURRENT AND WAVES

H. J. Prins and A. J. Hermans 1993 21 p
(Rept-93-13; ETN-93-94640) Avail: CASI HC A03/MF A01

The influence of a current on the horizontal drift force is studied for a horizontal cylinder of infinite length. A theory which is correct up to second order in the current velocity is developed. It is shown that especially for higher velocities these second order terms become very important. A numerical algorithm which solves the time dependent equations and is stable for all current velocities is found. A computer program is developed and very encouraging results are found for the added mass and damping coefficients and the drift force. ESA

N94-19139# Technische Univ., Delft (Netherlands). Faculty of Technical Mathematics and Informatics.
SIMILARITY SOLUTIONS FOR GRAVITY-DOMINATED SPREADING OF A LENS OF ORGANIC CONTAMINANT
Clarence A. Miller (Rice Univ., Houston, TX.) and Cornelis J. vanDuijn 1993 23 p Sponsored in part by Kerr (Robert S.) Environmental Research Lab., Ada, OK
(Rept-93-24; ETN-93-94651) Copyright Avail: CASI HC A03/MF A01

Similarity solutions for gravity dominated spreading at the water table of a lens of organic liquid largely immiscible with water are developed. Different solutions deal with different mechanisms by which the lens volume decreases with time: dissolution or evaporation, trapping as water invades the region beneath the central part of the lens, and uniform degradation. In the last case, the solution is a special case of the Barenblatt-Pattle solution. The same is true for the limiting case of a lens of constant volume. In all cases information is presented on variation of lens radius and thickness with time. All solutions except that involving trapping can be carried over with minor modifications to the case of a lens simultaneously spreading and translating along a slightly inclined water table. ESA

N94-19144# Technische Univ., Delft (Netherlands). Faculty of Technical Mathematics and Informatics.
MULTIGRID FOR A GROUNDWATER FLOW PROBLEM
J. Molenaar 1993 15 p
(Rept-93-29; ETN-93-94656) Copyright Avail: CASI HC A03/MF A01

The stationary, two dimensional, gravity driven flow of fresh and salt water in a horizontal aquifer is studied. A mathematical model for the problem which is based on the introduction of a stream function is presented. A finite volume discretization is proposed and a multigrid algorithm for the iterative solution of the resulting system of nonlinear equations is developed. If the difference in specific weight of the salt and fresh water is ignored the problem reduces to a Dirichlet problem, and an efficient Jacobi type smoother for the standard five-point discretization of the Laplace operator is proposed. Some results from numerical experiments are presented. ESA

N94-19345# Sandia National Labs., Albuquerque, NM.
A SIMPLE DESCRIPTION OF FLOW INSTABILITY WITH APPLICATION TO A PACKED BED
D. Dobranich 1993 8 p Presented at the 10th Symposium on Space Nuclear Power and Propulsion, Albuquerque, NM, 10-14 Jan. 1993
(Contract DE-AC04-76DP-00789)
(DE93-017492; SAND-93-1263C; CONF-930103-43) Avail: CASI HC A02/MF A01

A simplified explanation for gas flow instability in parallel heated channels is presented with specific applications to channels containing packed beds of power-producing particles. The explanation captures the basic governing physics of the viscosity-driven instability and hopefully removes some of the misconceptions surrounding this issue. Simple illustrative calculations, steady-state and transient, using the SAFSIM computer program are included in the explanation. The explanation points out that flow instability is common to any and all gas flow systems with parallel heated channels, that the addition of flow resistance to the entrance of a channel mitigates flow instability, and that instabilities do not occur instantaneously. DOE

N94-19356# Max-Planck-Inst. fuer Stroemungsforschung, Goettingen (Germany).
THE EFFECT OF FINE SURFACE RIBLETS ON THE FLOW AROUND AN INCLINED AXIALLY SYMMETRICAL BODY [ZUR WIRKUNG FEINER OBERFLAECHENRILLEN AUF DIE UMSTROEMUNG EINES ANGESTELLTEN ROTATIONSKOERPERS]
Michael Schneider 1993 78 p In GERMAN
(MPIS-105/1993; ETN-93-94838) Avail: CASI HC A05/MF A01

The dependence of the friction drag of a body of revolution (axially symmetric body) on the body surface structure and on the angle beta between the body axis and the flow direction is investigated. The experiments were performed in a water tunnel with flow velocities from U(sub infinity) = 0.5 to 5.5 m/s. The surface of the test body was covered either with smooth film or with different V groved riblet films with the riblet direction parallel to the body axis. The angle of the incidence beta varied between beta = 0 and 7 degrees. The experiments show that over a wide range of Reynolds number and for all angles of incidence investigated the friction drag with riblet film is smaller than with the smooth reference film. Drag reductions of about 10% were measured. The results indicate that riblet film can have a favorable influence on the three dimensional boundary layer occurring on an inclined axially symmetric body. The trend of the experimental data indicates that this favorable effect will continue to occur at angles greater than 7 degrees. ESA

N94-19365 Grenoble-1 Univ. (France). Lab. de Modelisation et du Calcul.
ON THE NUMERICAL APPROXIMATION OF NONLINEAR HYPERBOLIC PROBLEMS: APPLICATION TO THE DYNAMICS OF COMPRESSIBLE GAS Ph.D. Thesis [SUR LA THEORIE ET L'APPROXIMATION NUMERIQUE DES PROBLEMES HYPERBOLIQUES NON LINEAIRES: APPLICATION A LA DYNAMIQUE DES GAZ COMPRESSIBLES]
Saad Benharbit 1992 162 p In FRENCH Limited Reproducibility: More than 20% of this document may be affected by microfiche quality
(ETN-93-95020) Avail: CASI HC A08

Theoretical and approximation problems involving the theory of gas dynamics are discussed. The mathematical model used to represent these physical phenomena is the system of Euler conservation laws equations. Numerical approximation of the solutions were obtained by boundary value problems. The numerical solution results are based on the finite volume method which is the most currently applied to conservation laws. The boundary value problem convergence was obtained by the finite volume method, and by using the uniqueness solutions of the conservation law equations. ESA

N94-19381# Ecole Centrale de Lyon (France).
THEORETICAL STUDY AND MODELLING OF HOMOGENEOUS TURBULENCE UNDER ROTATION FOR IMPLANTATION IN A CODE FOR SOLVING NAVIER-STOKES EQUATIONS Ph.D. Thesis [ETUDE THEORIQUE DE LA TURBULENCE HOMOGENE SOUMISE A DES EFFETS DE ROTATION ET MODELISATION EN VUE DE L'IMPLANTATION AU SEIN D'UN CODE RESOLVANT LES EQUATIONS DE NAVIER-STOKES]
Jean-Louis Lubrano 1993 135 p In FRENCH Sponsored by FIRTECH Original contains color illustrations
(ECL-93-05; ETN-93-94897) Avail: CASI HC A07/MF A02

An approach to investigate the effect of Coriolis forces in homogeneous turbulence during rotation is presented. The spectral tensor equation was solved in the spectral space. The direction of the energy field can be characterized by its polarization component. An extension of homogeneous turbulence model under strain is proposed. The results showed that the equation second order terms should be developed, however an approach based on the spectral theory was chosen. The model consists of splitting the classic deviator a(sub i, j) into two components, which correspond to directional dependence and tensor polarization in Fourier space. ESA

N94-19398# Ecole Centrale de Lyon (France). Lab. de Mecanique des Fluides et d'Acoustique.
SIMULATION OF THREE DIMENSIONAL UNSTEADY VISCOUS FLOWS IN TURBOMACHINES Ph.D. Thesis [SIMULATION DES ECOULEMENTS TRIDIMENSIONNELS, INSTATIONNAIRES ET VISQUEUX EN TURBOMACHINES]
Najat Benbouta 1992 227 p In FRENCH Original contains color illustrations
(ECL-92-15; ETN-93-94588) Avail: CASI HC A11/MF A03

The method used to compute the conservative Navier-Stokes equations is implicit in time and makes no use of factorization in space. It is based on the 'Delta' formulation of Pade. This method is implemented in terms of curvilinear coordinates, which allows for a better description of the flow behavior in complex geometry; this permits better treatment of the boundary conditions. A finite volume formulation was chosen. For the spatial differences, an upwind scheme is used. This scheme is implemented with the flux vector splitting technique of Van Leer. The spatial derivatives of splitted fluxes (backward and forward) were approximated as a flux balance in the control volume, using a MUSCL (Monotone Upstream Centered Schemes of Conservation Laws) method. The viscous terms are approximated by classical second order centered differences. The iterative Gauss-Seidel's method while convergence was accelerated with the MMPE (Modified Minimal Polyomial Extrapolation) method and a particular storage of matrix was adapted. A modular approach is presented which permits the use of different numerical schemes in time and space as well as the performance of calculations which are steady or not, viscous or non-viscous, and two or three dimensional. The model was validated for one and two dimensional configurations, varying from incompressible to transonic, and for three dimensional configurations. ESA

N94-19399# Ecole Centrale de Lyon (France). Lab. de Mecanique des Fluides et d'Acoustique.

NUMERICAL SIMULATIONS OF TURBULENT BUOYANT FLOWS BY FINITE ELEMENT METHOD: APPLICATION TO THE STUDY OF STRONGLY HEATED OR COOLED STRATIFIED FLOW Ph.D. Thesis [SIMULATION NUMERIQUE DES ECOULEMENTS TURBULENTS DILATABLES AVEC LA METHODE DES ELEMENTS FINIS: APPLICATION A L'ETUDE DES ECOULEMENTS STRATIFIES FORTEMENT CHAUFFES OU REFROIDIS]

Abdeljalil Laassibi 1992 284 p In FRENCH Original contains color illustrations
(ECL-92-28; ETN-93-94590) Avail: CASI HC A13/MF A03

The mass conservation equation, the momentum and the energy equation are statistically described. The problems of parameters closure due to compression effects are discussed. The volume mass fluctuations are analyzed by numerical approximations. Two models which describe the interaction of volume mass fluctuations and the mean pressure gradient are given. The inadequacy of the classical K-epsilon model, based on scalars which do not represent anisotropy, is demonstrated. A new model that takes into account the anisotropy effect of gravity on turbulence is proposed. The model is applied to hot jets in a steady atmosphere and to the study of the behavior of thermal and kinetic atmosphere layers. ESA

N94-19461# Ecole Centrale de Lyon (France).

CONTRIBUTION TO THE STUDY OF A SYMMETRIC FILM FLOW (WITH OR WITHOUT TENSIO-ACTIVE ELEMENTS) Ph.D. Thesis [CONTRIBUTION A L'ETUDE DE L'ECOULEMENT D'UN RIDEAU SYMETRIQUE (AVEC OU SANS TENSIO-ACTIFS)]

Daniel Barthod 1993 191 p In FRENCH Sponsored in part by Kodak-Pathe, France, and ANRT Original contains color illustrations
(ECL-93-13; ETN-93-94899) Avail: CASI HC A09/MF A02

The purpose of the study was to develop a one dimensional model to describe as accurately as possible the symmetric flow film. The physical bases of capillarity phenomena are reviewed. The effect of tensio-active elements on the film configuration and on the surface energy gradients is investigated. The phenomena controlling the motion of tensio-active molecules in the bulk and on the surface are studied. The isothermal stationary liquid flow is modeled in the symmetric film configuration. A method of mobile grids associated with the finite volume method is applied to solve a two dimensional film flow system. ESA

N94-19493*# Stanford Univ., CA. Dept. of Aeronautics and Astronautics.

RESEARCH AND TRAINING ACTIVITIES OF THE JOINT INSTITUTE FOR AERONAUTICS AND ACOUSTICS Progress Report, Oct. 1992 - Sep. 1993

L. Roberts Dec. 1993 26 p
(Contract NCC2-55)
(NASA-CR-194742; NAS 1.26:194742) Avail: CASI HC A03/MF A01

During the period October 1992 to September 1993 progress was made on each of the following tasks: (1) experimental studies of free shear flows; (2) analysis of conical flow; (3) experimental and theoretical studies of vortex flows; and (4) aircraft attitude control using active flow control devices. The details of this work was discussed with the technical and management staff at Ames Research Center. Author (revised)

N94-19495# Institut National Polytechnique, Toulouse (France). Inst. de Mecanique des Fluides.

STUDY AND MODELING OF COMPRESSIBLE FLOWS OF FLAPPER NOZZLE TYPE POTENTIOMETRIC SYSTEMS Ph.D. Thesis [ETUDE ET MODELISATION EN ECOULEMENTS COMPRESSIBLES DES SYSTEMES POTENTIOMETRIQUES DE TYPE BUSE-PALETTE]

Stephane Colin 1992 278 p In FRENCH Sponsored by FIRTECH
(ETN-93-95012) Avail: CASI HC A13/MF A03

Static and dynamic behavior of flapper nozzle is predicted by a fully theoretical method. The compressibility of the flow and the nozzle geometry are taken into account. Instabilities due to fluid structure interactions are examined and some new realizations (in particular a flapper nozzle with linear characteristic) are presented. ESA

N94-19497# Messerschmitt-Boelkow-Blohm G.m.b.H., Munich (Germany). Militaerflugzeuge.

NUMERICAL SIMULATION OF VISCOUS FLOWS IN CHEMICAL NONEQUILIBRIUM Thesis - Tech. Univ. Munich [RECHNERISCHE SIMULATION REIBUNGSBEHAFTETER STROEMUNGEN IM CHEMISCHEN NICHTGLEICHGEWICHT]

C. Mundt Oct. 1992 127 p In GERMAN
(MBB-LME-211-S-PUB-506; ETN-93-95094) Copyright Avail: CASI HC A07/MF A02

A process for numerical simulation of viscous, chemically reacting hypersonic flows is developed. The flow was divided into an inviscid part, which was calculated with a Euler process, and a viscous part, simulated with a boundary layer process of second order. The method is proved to be useful for reentry trajectories because boundary layer equations can be solved with a space marching process with low calculation costs. Boundary layer equations were derived from Navier-Stokes equations and written in a local monocline coordinates system; conditions and models of statistical thermodynamics, chemical properties, and transport coefficients such as viscosity, heat capacity, and diffusion coefficients were used for the equation closure. The resulting system and Euler equations were solved with a difference process and the coupling of both systems is discussed. The method was successfully applied to the three dimensional flow around the Hermes forebody. ESA

N94-19502# Institut National Polytechnique, Toulouse (France). Inst. de Mecanique des Fluides.

MATHEMATICAL MODELING OF THE FREE SURFACE HYDRODYNAMIC AND OF TRANSPORT IN SUSPENSIONS OF NON COHESIVE SEDIMENTS: AID TO THE INTERPRETATION OF SPATIAL IMAGES Ph.D. Thesis [MODELISATION MATHEMATIQUE DE L'HYDRODYNAMIQUE A SURFACE LIBRE ET DU TRANSPORT EN SUSPENSION DE SEDIMENTS NON COHESIFS. AIDE A L'INTERPRETATION D'IMAGES SPATIALES]

Sylvain Ouillon 1993 307 p In FRENCH
(ETN-93-95011) Avail: CASI HC A14/MF A03

Coupling between space imaging and digital simulation to study the sediment transfer in local aquatic areas is still recent. The development and the numerical statement of mathematical models for free surface hydrodynamics and Suspended Sediment (SS) transport is dealt with. The solid transport phenomena, the capabilities to couple space imaging and digital models at local scales are reviewed. The one Dimensional (1D), 2D and 3D mathematical models, are presented. Their enhancements on a finite element code, MEFAME (1D and 2DH), and on a finite volume code, PHOENICS, follow. The 2DH and 1D models are applied on the Gambia estuary. Maps of instant and residual velocities and maps of concentrations are analyzed with information arising from SPOT image treatments. The developments of two original numerical modules in the 3D Navier-Stokes solver is then focused upon: the first deals with the free surface consideration and its semi implicit transient calculation in a fixed grid mesh, the second deals with the 3D SS transfer. Some 3D test cases relating to the flow around a groyne and to the sediment transfer in open channel flows under equilibrium and nonequilibrium conditions are presented and analyzed. ESA

N94-19509# Max-Planck-Inst. fuer Stroemungsforschung, Goettingen (Germany).

FILM CONDENSATION IN A SHOCK WAVE Thesis
[FILMKONDENSATION IM STOSSROHR]

Thomas Teske Sep. 1992 152 p In GERMAN
(MPIS-22/1992; ETN-93-95102) Avail: CASI HC A08/MF A02

Interferometric thickness measurements on n-heptane film condensation in a shock tube are carried out for investigation of the dynamical and thermodynamic processes involved in fuel condensation on the walls of engines and for determination of the time dependence of film thickness on the side and end walls of the tube as a function of gas initial state. Some theoretical results about condensation and supersaturation are discussed such as the Stefan problem and the solution given by Neumann. Transition state is described assuming one dimensional flow, thermally ideal gas, and constant physical properties of film and wall. The homogeneous nucleation in the boundary layer is neglected and thermal conductivity and shear viscosity are presumed to be linear in temperature. The interference of light beams reflected from both sides of the liquid film is used for the optical measurement. The resulting thickness is calculated from intensities of reflected or transmitted light. Time scales results are found to be higher than the time from fuel injection until auto-ignition. ESA

N94-19510# Max-Planck-Inst. fuer Stroemungsforschung, Goettingen (Germany).

TWO-DIMENSIONAL TURBULENT NONSTATIONARY SUPERFLUID COUNTERFLOWS: NUMERICAL SIMULATIONS, QUALITATIVE EFFECTS

W. Fiszdon (Polish Academy of Sciences, Warsaw.), J. Piechna (Warsaw Technical Univ., Poland.), and G. Stamm Oct. 1992 80 p
(MPIS-23/1992; ETN-93-95103) Avail: CASI HC A05/MF A01

Numerical simulations of simple cases of plane and axisymmetric two dimensional turbulent nonstationary superfluid counterflows were performed. The purpose was to obtain qualitative information on their structure. A closer picture of the real flows and help in assessing the limitation of the often used one dimensional treatment of real superfluid flows are expected. The influence of the boundary layer appears to be rather small, leading to the curvature of temperature shocks in straight channels and to a not strictly top hat distribution of flow parameters in a cross section of the tube. Discontinuities in the channel shape lead to nonstationary nonlocal flow perturbations inside the channel. Local flow parameters may be affected by multi-dimensional flow effects. ESA

N94-19515# Lawrence Livermore National Lab., CA.

VELOCITY MEASUREMENTS IN A BOUNDARY LAYER WITH A DENSITY GRADIENT

P. Neuwald (Ernst-Mach-Inst., Freiburg, Germany.), H. Reichenbach (Ernst-Mach-Inst., Freiburg, Germany.), and A. L. Kuhl Nov. 1992 18 p
(Contract W-7405-eng-48)
(DE93-019627; UCRL-CR-113904) Avail: CASI HC A03/MF A01

A number of experiments were performed at the EMI shock tube facility on shock waves propagating in a stratified atmosphere with density gradient modelled by air layered above Freon (C Cl2 F2). This report presents streamwise velocity data for the flow behind the shock front. Additional information from measurements of overpressure history and shadowgraphs of the flow will be presented in a future EMI-report. DOE

N94-19520# Max-Planck-Inst. fuer Stroemungsforschung, Goettingen (Germany).

STABILITY MEASUREMENTS OF RAYLEIGH-BENARD CONVECTION NEAR THE CRITICAL STATE USING A SPECTRAL MODEL Thesis
[STABILITAETSUNTERSUCHUNGEN DER RAYLEIGH-BENARD-KONVEKTION IN DER NAEHE DES KRITISCHEN ZUSTANDS MIT HILFE EINES SPEKTRALMODELLS]

Ralph Nolte Jul. 1992 83 p In GERMAN Sponsored by Studienstiftung des Deutschen Volkes
(MPIS-15/1992; ETN-93-95100) Avail: CASI HC A05/MF A01

Hydrostatic stability of a horizontal fluid layer heated from below is lost if the temperature gradient exceeds a critical value. The onset of convection in a fluid near its gas liquid critical point is investigated theoretically. Hydrostatic density and temperature profiles were computed numerically. The orders of magnitude of the terms occurring in the dynamical equations were estimated, showing that due to the divergence of the compressibility in the critical region pressure terms neglected in the Boussinesq approximation have to be retained. A Galerkin method was applied to the two dimensional problem, and a low order truncation which far from the critical point reduces to the familiar Lorenz equations was analyzed. According to this model the critical Rayleigh number decreases to a finite value while the corresponding horizontal wavenumber increases as the system approaches the critical state. ESA

N94-19525# Max-Planck-Inst. fuer Stroemungsforschung, Goettingen (Germany).

THEORETICAL EXAMINATION OF THE FLOW AROUND A CYLINDER WITH A LOW DIMENSIONAL GALERKIN PROCESS Thesis
[THEORETISCHE UNTERSUCHUNG DER ZYLINDERUMSTROEMUNG MIT EINEM NIEDRIGDIMENSIONALEN GALERKIN-VERFAHREN]

Bernd R. Noack Nov. 1992 112 p In GERMAN
(MPIS-25/1992; ETN-93-95105) Avail: CASI HC A06/MF A02

A low dimensional Galerkin method with less than 200 global modes is presented for the three dimensional, incompressible, viscous flow around a circular cylinder. In particular, important mathematical and physical aspects for the construction of successful Galerkin methods for wake flows are systematically investigated for the ,cylinder wake. With this method, the steady, periodic, and turbulent wakes were computed for Reynolds numbers up to 300. Furthermore, the first global, non-parallel, three dimensional stability analysis of the steady and periodic solution is presented. This stability investigation explains the experimental observation of large scale three dimensional structures in the laminar wake and the formation of small scale, in spanwise direction, periodical structures in the turbulent wake. ESA

N94-19568# Lawrence Livermore National Lab., CA.

LOCALLY ADAPTIVE REMESHING SCHEME FOR CALCULATING FLUID INSTABILITIES

G. D. Kramer, W. P. Crowley, and V. C. Rupert Jul. 1993 7 p
Presented at the 19th International Symposium on Shock Waves, Marseille, France, 26-30 Jul. 1993
(Contract W-7405-eng-48)
(DE93-019577; UCRL-JC-114801; CONF-930788-5) Avail: CASI HC A02/MF A01

LAM is a two dimensional Eulerian hydro-code with local adaption that uses a Van Leer limiter, artificial viscosity, and a staggered mesh. It differs from the Godonov schemes used elsewhere, but this formulation makes it easier to add additional physics to the code. Two distinct advantages of the present code are a conformal quadrilateral mesh option and a grow capability. The code is presently being extended to three dimensions. DOE

N94-19569# Naval Postgraduate School, Monterey, CA.

AN INVESTIGATION OF LOW MARANGONI NUMBER FLUID FLOW IN A COLD CORNER M.S. Thesis

Michael R. Huber Jun. 1993 91 p
(AD-A271317) Avail: CASI HC A05/MF A01

A large pool of liquid with a horizontal free surface is bounded on one side by a vertical solid wall. The wall is maintained at a cold temperature to a depth of unity, with a warmer temperature below that point. The fluid surface is assumed adiabatic, and average surface tension forces keep the surface flat. Surface tension is assumed to be a decreasing function of temperature, so that the surface thermal gradient associated with the temperature variations drives flow toward the corner. This problem is examined numerically for different Marangoni numbers ranging from 1 to 300 using a Green's function approximation method for viscous case (in the limit as the Reynolds number approaches zero). DTIC

N94-19598# Massachusetts Inst. of Tech., Cambridge. Artificial Intelligence Lab.

AUTOMATED QUALITATIVE MODELING OF DYNAMIC PHYSICAL SYSTEMS

Jonathan Amsterdam Jan. 1993 115 p
(Contract N00014-91-J-4038)
(AD-A270835; AI-TR-1412) Avail: CASI HC A06/MF A02

This report describes MM, a computer program that can model a variety of mechanical and fluid systems. It addresses several issues: What is the appropriate input to the modeling process? How should the search for models be organized? What evidence can be brought to bear to constrain the task? MM takes as input both a description of the structure of the system to be modeled and a trace of the system's behavior. The structure can be represented by 2D line drawings augmented with some additional information, or by component types and their interconnections, or both. The behavior trace provides the program with qualitative information about the behavior that the user wishes to capture with a model. DTIC

N94-19604# Los Alamos National Lab., NM.
GROUP-INVARIANT SOLUTIONS OF HYDRODYNAMICS AND RADIATION HYDRODYNAMICS
S. V. Coggeshall 1993 9 p Presented at the Conference on the Engineering Applications of Computational Fluid Dynamics, London, England, 7-8 Sep. 1993
(Contract W-7405-eng-36)
(DE93-018373; LA-UR-93-2505; CONF-930978-1) Avail: CASI HC A02/MF A01

Using the property of invariance under Lie groups of transformations, the equations of hydrodynamics are transformed from partial differential equations to ordinary differential equations for which special analytic solutions can be found. These particular solutions can be used for the following: (1) numerical benchmarks; (2) the basis for analytic models; and (3) insight into more general solutions. Additionally, group transformations can be used to construct new solutions from existing ones. A space-time projective group is used to generate complicated solutions from simpler solutions. Discussion of these procedures is presented along with examples of analytic solutions of 1-, 2-, and 3-D hydrodynamics. DOE

N94-19645 Technische Univ., Delft (Netherlands). Faculty of Technical Mathematics and Informatics.
VISUALIZATION OF TURBULENT FLOW WITH PARTICLES
Andrea J. S. Hin and Frits H. Post 1993 15 p Sponsored in part by Delft Hydraulics Lab. Limited Reproducibility: More than 20% of this document may be affected by microfiche quality
(Rept-93-31; ETN-93-94658) Copyright Avail: CASI HC A03

A method for visualization of three dimensional turbulent flow using particle motion animation is presented. The method is based on Reynolds decomposition of a turbulent flow field into a convective and a turbulent motion. At each step of particle path generation, a stochastic perturbation is added, resulting in random walk motions of particles. A physical relation is established between the perturbations and the eddy diffusivity, which is calculated in a turbulent flow simulation. The flow data used is a steady mean velocity field, and an eddy diffusivity field. The erratic particle motions are more than just a visual effect, but represent a real physical phenomenon. An implementation of the method is described, and an example of a turbulent channel flow is given, which clearly shows the random particle motions in their context of general fluid motion patterns. ESA

N94-19668# Technische Univ., Delft (Netherlands). High Speed Aerodynamics Lab.
A REVIEW OF HOT-WIRE TECHNIQUE IN COMPRESSIBLE FLOWS
F. Motallebi Jun. 1993 72 p Sponsored by the International Office, and Tech. Univ. Delft, Netherlands
(LR-724; ETN-93-95028) Avail: CASI HC A04/MF A01

The use of hot wire anemometer for obtaining turbulence data in compressible flows is reviewed. Based on the existing experimental results, the methods of extracting different turbulent quantities from the output signal of the hot wire anemometer in a given flow environment are described and evaluated. Comparison between the results obtained with the laser Doppler velocimeter and the hot wire anemometer shows that the latter should still be considered as one of the main tools for turbulence research in compressible non-separated turbulent flows not only for its comparable accuracy but also for its much lower cost and ease of operation as compared with the optical methods. ESA

N94-19730 Stuttgart Univ. (Germany). Inst. fuer Hydraulische Stroemungsmaschinen.
EXAMINATIONS OF THE FRICTION BEHAVIOR IN NONSTATIONARY FLOW PROCESSES IN PIPES Ph.D. Thesis [UNTERSUCHUNG DES REIBUNGSVERHALTENS BEI INSTATIONAEREN STROEMUNGSVORGAEGEN IN ROHRLEITUNGEN]
Peter Eichinger 1992 153 p In GERMAN Sponsored by DFG Limited Reproducibility: More than 20% of this document may be affected by microfiche quality
(Mitt-7; ISBN-3-98-021306-4; ETN-93-95074) Avail: CASI HC A08

A calculation procedure is presented in order to use an improved unsteady friction term. The method of characteristics for the water hammer calculation along the pipe axis and a finite difference calculation of the unsteady radial velocity distribution were combined. Various turbulence models, which are used for the calculation of the velocity distribution along the radius for laminar and turbulent flow, were considered. The turbulence models are as follows: the Prandtl mixture length model; a one equation model in which kinetic turbulent energy is calculated with a transport equation; and the k-epsilon model. The procedure was validated with experimental results of fluctuating single pressure peaks and with examples from the literature. ESA

N94-19774# Stanford Univ., CA. Dept. of Aeronautics and Astronautics.
THE EFFECTS OF INITIAL CONDITIONS ON THE 3-D TOPOLOGY OF TEMPORALLY EVOLVING WAKES (ARI ON 3-D BLUFF BODY WAKES) Final Report
Brian J. Cantwell 27 Sep. 1993 10 p
(Contract N00014-90-J-1976)
(AD-A271008) Avail: CASI HC A02/MF A01

A three year study of the effect of initial conditions on the topology and fine scale structure of temporally evolving wakes was completed. Early in the project new topological analysis tools were developed and used to analyze available simulations of the plane mixing layer. During the course of these preliminary studies it was found that certain geometrical features of the fine scale motions in the mixing layer were very similar to those seen in simulations of forced isotropic turbulence. As a consequence, a two-track approach to the work was adopted; one track was to gather together simulation data on as wide a variety of shear flows as possible with the objective of identifying universal feature of the fine scale structure. The second track was to carry out a new direct simulation of the plane wake in which systematic variations of the initial conditions were used to identify structural features of the developed flow which depend on initial conditions. The fundamental questions addressed were: what features of the fine scale motions in turbulent flow are universal, what features are not, and, in the case of the plane wake, what information about the near wake survives far downstream? DTIC

35 INSTRUMENTATION AND PHOTOGRAPHY

Includes remote sensors; measuring instruments and gages; detectors; cameras and photographic supplies; and holography.

For aerial photography see *43 Earth Resources and Remote Sensing.* For related information see also *06 Aircraft Instrumentation,* and *19 Spacecraft Instrumentation.*

N94-17700# Sandia National Labs., Albuquerque, NM.
PORTABLE, SOLID STATE, FIBER OPTIC COUPLED DOPPLER INTERFEROMETER SYSTEM FOR DETONATION AND SHOCK DIAGNOSTICS
K. J. Fleming and O. B. Crump 1993 7 p Presented at the 10th Detonation Symposium, Boston, MA, 12-16 Jul. 1993
(Contract DE-AC04-76DP-00789)
(DE93-013917; SAND-92-2117C; CONF-930713-16) Avail: CASI HC A02/MF A01

VISAR (Velocity Interferometer System for Any Reflector) is a specialized Doppler interferometer system that is gaining world-wide acceptance as the standard for shock phenomena analysis. The VISAR's large power and cooling requirements, and the sensitive and complex nature of the interferometer cavity, has restricted the traditional system to the laboratory. This paper describes the new portable VISAR, its peripheral sensors, and the role it played in optically measuring ground shock of an underground nuclear detonation (UGT). The Solid State VISAR uses a prototype diode pumped ND:YAG laser and solid state detectors that provide a suitcase-size system with low power requirements. A special window and sensor was developed for fiber optic coupling (1 kilometer long) to the VISAR. The system has proven itself as a reliable, easy-to-use instrument that is capable of field test use and rapid data reduction employing only a personal computer (PC). DOE

N94-17717 Department of the Navy, Washington, DC.
FRICTION DRIVE POSITION TRANSDUCER Patent
Ronald E. Waclawik, inventor (to Navy), James L. Cayer, inventor (to Navy), and Kenneth M. Lapointe, inventor (to Navy) 22 Jun. 1993 8 p Filed 28 Oct. 1991
(AD-D015851; US-Patent-5,220,731; US-Patent-Appl-SN-783660; US-Patent-Class-33-773) Avail: CASI HC A02/MF A01

A spring force loaded contact wheel mounted in a stationary position relative to a reciprocating shaft is disclosed. The apparatus of the present invention includes a tensioning assembly for maintaining absolute contact between the contact wheel and the reciprocating shaft wherein the tensioning assembly urges the contact wheel against the shaft to maintain contact there between so that the wheel turn as the shaft is linearly displaced. A rotary encoding device is coupled to the wheel for translating the angular and rotational movement thereof into an electronic signal for providing linear displacement information and derivative data with respect to displacement of the shaft. Absolute friction contact and cooperative interaction between the shaft and the contact wheel is further enhanced in the preferred embodiment by advantageously selecting the type of surface finish and the amount of surface area of the contact wheel relative to the surface condition of the shaft as well as by reducing the moment of inertia of the contact wheel. DTIC

N94-17778# Oak Ridge National Lab., TN.
SOLID-STATE, RESISTIVE HYDROGEN SENSORS FOR SAFETY MONITORING
B. S. Hoffheins, R. J. Lauf, P. H. Fleming, and S. E. Nave (Westinghouse Savannah River Co., Aiken, SC.) 1993 16 p Presented at the 3rd International Joint ISA POWID/EPRI Controls and Instrumentation Conference, Phoenix, AZ, 7-9 Jun. 1993
(Contracts DE-AC05-84OR-21400; DE-AC09-89SR-18035)
(DE93-017769; CONF-930672-1) Avail: CASI HC A03/MF A01

Solid-state, resistive hydrogen sensors have been designed and fabricated at Oak Ridge National Laboratory. Sensor response has been successfully tested with H2 gas in argon and air under ambient temperature and pressure, while immersed in transformer oil at temperatures between 25 and 90 C, and under site-specific conditions at Westinghouse Savannah River Co. Current versions of the sensors (25 x 25 x 0.6 mm) are small enough to be incorporated into hand-held leak detectors or distributed sensor systems for safety monitoring throughout a large area. Another foreseeable application is in electrical power transformers where the buildup of hydrogen gas accompanies oil breakdown. The use of these sensors to monitor transformer oil changes could help predict and prevent catastrophic failure. DOE

N94-17904# Department of the Navy, Washington, DC.
FLUID DYNAMOMETER HAVING FLUID CHARACTERISTIC POWER ABSORPTION ADJUSTMENT CAPABILITY Patent Application
James R. Quararone, inventor (to Navy) 29 Mar. 1993 18 p
(AD-D015820; US-Patent-Appl-SN-037880) Avail: CASI HC A02/MF A01

A fluid dynamometer is provided for absorbing a range of power output produced by an engine's rotating shaft. Power absorbing characteristics are controlled by adjusting the fluid media characteristics in terms of its temperature and/or its density and viscosity. A tank, containing an energy or power absorbing fluid, receives the rotating shaft. One or more disks, submerged in the fluid and coaxially mounted on the rotating shaft for rotating therewith, cooperate with the fluid to absorb power from the rotating shaft. The disk(s) are sized so that a first specified amount of power from the rotating shaft is absorbed at a calibration temperature of the fluid. Heating and cooling units are provided to respectively heat and cool the fluid. A controller energizes the heating and cooling units in a cooperative fashion to adjust and maintain the fluid at a predetermined temperature value for power absorption at a second specified amount of power produced by the rotating shaft. A fluid composition exchanger may also be provided to alter the power absorbing characteristics by altering the fluid's composition. DTIC

N94-17999# Sandia National Labs., Albuquerque, NM.
CHARACTERISTICS AND PULSED RADIATION RESPONSE OF NON-IDEAL QUARTZ SHOCK STRESS GAUGES
R. P. Reed and J. I. Greenwoll 1993 4 p Presented at the 14th International Conference of the International Association for the Advancement of High Pressure Science and Technology, Colorado Springs, CO, 27 Jun. - 2 Jul. 1993
(Contract DE-AC04-76DP-00789)
(DE93-017628; SAND-93-0376C; CONF-930676-7) Avail: CASI HC A01/MF A01

This cautionary paper reminds users of quartz shock stress gauges that sensors that ignore the design rules of the 'Sandia quartz gauge' may produce substantial and unrecognized deviations from normal sensitivity, waveform distortion, and anomalous conduction. Each deviant design must be extensively characterized. The consequence of non-standard gauge designs, like the 'shorted quartz gauge' designs, are given for prompt response to pulsed radiation while stressed. DOE

N94-18006# Societe Suisse de Chronometrie, Neuchatel.
PROCEEDINGS OF THE 4TH EUROPEAN CONGRESS ON CHRONOMETRY [ACTES DU 4EME CONGRES EUROPEEN DE CHRONOMETRIE]
1992 160 p In ENGLISH; FRENCH; and GERMAN Congress held in Lausanne, Switzerland, 29-30 Oct. 1992
(ETN-93-94633) Copyright Avail: CASI HC A08/MF A02

The main topics were as follows: timing systems and components, accelerated life tests on material resistance, nickel toxicity, thin protective coatings, hot casting technology for ceramics, electrostatic micromotors, piezoelectric motors, miniaturization, phase coded signal processing algorithms, computerized simulation of clock operations, torque control of stepping motors, marine chronometry, clock repairing, perpetual motion clock, gear train behavior, reliability tests, low power consumption circuits, design supporting system, atomic standards development, a new concept for the divers watch, an analog quartz clock, and a multifunction chronometer. For individual titles, see N94-18007 through N94-18044.

N94-18007# Musee International d'Horologerie, La Chaux-de-Fonds (Switzerland). Inst. l'Homme et le Temps.
THE CLOCKS AND THE PERCEPTION OF TIME IN THE 18TH CENTURY SOCIETY [L'HORLOGE ET LA PERCEPTION DU TEMPS DANS LA SOCIETE URBAINE DU 18EME SCIECLE]
Catherine Cardinal *In* Societe Suisse de Chronometrie, Proceedings of the 4th European Congress on Chronometry 1992 p 11-13 In FRENCH (For primary document see N94-18006 04-35)
Copyright Avail: CASI HC A01/MF A02

The ownership of clocks and watches became widespread in 18th century society, particularly amongst the wealthy classes. They liked the decorative appearance, practical advantages, and social prestige which those objects conferred. The use of 'mechanized' time in the towns supplanted the age old reliance on time as dictated by nature and the Church. New temporal reference points gave the day its rhythm. Data from that era (correspondence, memoirs, newspapers, engravings, and paintings) make it possible to catch a glimpse of the influence of clocks on the perception of time. From the beginning of the 'mechanized time' era, efforts to improve the accuracy and the technical performance of mechanisms were made. The importance of such a precise time measurement in every day life is considered. ESA

N94-18008# ASULAB S.A., Neuchatel (Switzerland). Lab. de Recherches du Groupe SMH.
ACCELERATED TESTS ON THE TARNISH RESISTANCE OF GOLD ALLOYS [TESTS ACCELERES DE LA RESISTANCE AU TERNISSEMENT DES ALLIAGES D'OR] **c26**
Jean-Paul Randin, Jean-Pierre Renaud (CCF S.A., La Chaux-de-Fonds, Switzerland.), and Pierre Ramoni (Metaux Precieux S.A. Metalor, Nauchatel, Switzerland.) *In* Societe Suisse de Chronometrie, Proceedings of the 4th European Congress on Chronometry 1992 p 17-20 In FRENCH (For primary document see N94-18006 04-35)
Copyright Avail: CASI HC A01/MF A02

Three tarnish testing procedures were applied to four gold alloys widely used in decorative applications. A liquid based method known as the Tuccillo-Lielsen test, where samples are alternatively immersed in an aqueous sulphide solution, was used. In the gaseous phase, the alloys were exposed to thioacetamide and flower of sulphur vapors. The tarnished samples were characterized by calorimetric measurements. The results showed that the tarnishing aspect encountered can be reproduced. The liquid based test was faster (3 hours) than those in the gaseous phase (5 days) but it is difficult to apply to any forms of finished products. Poor reproducibility and reliability was obtained by the thioacetamide test results. In addition, the color changes after 5 days exposure at ambient temperature were small and thioacetamide is a carcinogen. It is proposed to replace the thioacetamide tests by the flower of sulphur test. ESA

N94-18009# Centre Technique de l'Industrie Horlogere, Besancon (France).
EVALUATION OF THE NICKEL RELEASE BY HOROLOGICAL PRODUCTS [EVALUATION DE LA LIBERATION DE NICKEL PAR LES PRODUITS HORLOGERS] **c26**
Jean Picaut *In* Societe Suisse de Chronometrie, Proceedings of the 4th European Congress on Chronometry 1992 p 21-23 In FRENCH (For primary document see N94-18006 04-35)
Copyright Avail: CASI HC A01/MF A02

Nickel and nickel alloys are often used by watch makers, and several watch parts can release nickel. Coming from the substrate or from the coatings, nickel reaches the skin. Nickel is by far the most common cause of contact allergy. Sensitization can be obtained by prolonged and close contact with the skin. Different methods can be used to determine the nickel content of watch parts. The relationship between the analysis results and dermatisis risk is under investigation. ESA

N94-18010# Stuttgart Univ. (Germany). Inst. fuer Feinwerk- und Zeitmesstechnik.
TITANIUM CARBON-HYDROGEN LAYERS ON DECORATIVE SURFACES [TITAN-KOHLENWASSERSTOFF-SCHICHTEN ZUR DEKORATIVEN OBERFLAECHENVEREDELUNG] **c27**
Bernd Bader and Klaus Scheerer (Stuttgart Univ., Germany.) *In* Societe Suisse de Chronometrie, Proceedings of the 4th European Congress on Chronometry 1992 p 25-28 In GERMAN (For primary document see N94-18006 04-35)
Copyright Avail: CASI HC A01/MF A02

Brass is covered with titanium-carbon:hydrogen layers using the technique of reactive radio frequency magnetron plasma deposition in an atmosphere enriched by methane. The deposited films exhibited special properties: high hardness, low friction coefficient, high scratch resistance, and good adhesion. These products are suitable for tribological purposes in situations where lubrication with grease is not possible. The variation of the methane flow rate can change the optical properties: from a bright silver-grey at low rates to a dark anthrazite at relatively high methane flow rates. The deposited Ti-C:H films are also suitable for scratch resistive and decorative surface protection in commodity utensils. ESA

N94-18011# Stuttgart Univ. (Germany). Inst. fuer Zeitmesstechnik, Fein- und Mikrotechnik.
SPUTTERED TIN COATINGS IN PLASTIC [GESPUTTERTE TIN-SCHICHTEN AUF KUNSTSTOFFEN] **c26**
Benedikt Martin and Jutta Martin *In* Societe Suisse de Chronometrie, Proceedings of the 4th European Congress on Chronometry 1992 p 29-32 In GERMAN (For primary document see N94-18006 04-35)
Copyright Avail: CASI HC A01/MF A02

Sputtering processes enable the use of materials combined with precisely tailored properties to generate hard and decorative coatings in different substrate materials. Thin films of titanium nitride can be deposited onto polymer substrates by reactive high frequency sputtering. Among the polymers successfully coated were polyvinyl chlorides and fluorides. In comparison to the coating process of metallic substrates, the specimen surface temperature of the polymers has to be kept low. The intrinsic stress of the thin films can be reduced by choosing a suitable working gas pressure as well as interrupting the coating procedure several times. The use of chromium interlayers enabled TiN films to be produced with a thickness of about 1 to 2 microns with good adhesion properties in the polymer substrates. The decorative requirements were found to be very similar to films in metallic specimens. ESA

N94-18012# Metaux Precieux S.A. Metalor, Nauchatel (Switzerland).
GOLD-COPPER-ZINC COATINGS AS AN ALTERNATIVE TO GOLD-COPPER-CADMIUM [DEPOTS OR-CUIVRE-ZINC COMME ALTERNATIVE A OR-CUIVRE-CADMIUM] **c26**
Pierre-Andre Aeby and Paul Bagnoud *In* Societe Suisse de Chronometrie, Proceedings of the 4th European Congress on Chronometry 1992 p 33-37 In FRENCH (For primary document see N94-18006 04-35)
Copyright Avail: CASI HC A01/MF A02

Gold-copper-cadmium (AuCuCd) coatings were commonly used for decorative purposes. Now gold-copper-zinc (AuCuZn) is used for watch and jewellery applications. A review of the art is given. The properties of both types of deposits are compared. The progress in achieving a sucessful process is discussed. An advantage of AuCuZn deposits is in preventing any anxiety from the consumers' side and to offer an alternative in the case of the banning of cadmium in some countries. ESA

N94-18013# Scientific Research Inst. of Instrument Automation, Moscow (USSR).
THE PERSPECTIVES IN APPLICATION OF HOT CASTING TECHNOLOGY FOR CERAMIC PARTS OF TIMEKEEPING DEVICES **c27**
O. G. Andreyeva, P. O. Gribovsky, G. B. Kartashov, and N. A. Romanova *In* Societe Suisse de Chronometrie, Proceedings of the 4th European Congress on Chronometry 1992 p 39-41 (For primary document see N94-18006 04-35)
Copyright Avail: CASI HC A01/MF A02

The results of research concerning the oxide ceramics for timekeeping devices parts are presented. Physical and mechanical characteristics and tribotechnical parameters are defined. Questions of peculiarities in the design of time keeping devices movement parts are considered. Special attention is given to hot casting technology and properties of ceramic materials. ESA

N94-18014# ASULAB S.A., Neuchatel (Switzerland). Lab. de Recherche du Groupe SMH.
ELECTROSTATIC MICROMETERS: RECENT DEVELOPMENTS AND PERSPECTIVES OF USES IN CLOCK AND WATCH MAKING [MICROMOTEURS ELECTROSTATIQUES: DEVELOPPEMENTS RECENTS ET PERSPECTIVES D'UTILISATION EN HORLOGERIE]
Etienne Bornand, Lionel Paratte (Neuchatel Univ., Switzerland.), Georges-Andre Racine (Neuchatel Univ., Switzerland.), and Nico deRooij (Neuchatel Univ., Switzerland.) *In* Societe Suisse de Chronometrie, Proceedings of the 4th European Congress on Chronometry 1992 p 45-48 In FRENCH Sponsored by Comission pour l'Encouragement de la Recherche Scientifique (For primary document see N94-18006 04-35)
Copyright Avail: CASI HC A01/MF A02

The characteristics of construction and operation of electrostatic micromotors built by silicon surface micromachining are summarized. Two particular realizations, the comb and the wobble micromotors, are presented. Their torques are larger than those of other silicon micromotors. Their characteristics are compared with the one's of a watch motor (Lavet motor). The investigation shows that questions on their lifetime, on their mechanical outputs, and on their closures remain to be solved. ESA

N94-18015# Centre Technique de l'Industrie Horlogere, Besancon (France).
PIEZO-ELECTRIC MOTOR: PERSPECTIVES AND MINIATURIZATION [MOTEUR PIEZO-ELECTRIQUE: PERSPECTIVES DE MINIATURISATION] **c33**
Roland Duffait and Patrice Minotti (Paris Univ., Besancon, France.) *In* Societe Suisse de Chronometrie, Proceedings of the 4th European Congress on Chronometry 1992 p 49-52 In FRENCH (For primary document see N94-18006 04-35)
Copyright Avail: CASI HC A01/MF A02

Traveling wave piezoelectric motors work much better than conventional electromagnetic motors (high torque/mass ratio, high hold torque). Results of investigations on piezoelectric motors are presented. The miniaturization possibilities and the different applications in microtechnics and horology are discussed. The design and the results of the first prototype of a travelling wave micromotor are included. Some technological innovations, for which patents are presently requested, are underlined. ESA

N94-18016# Seiko Instruments, Inc., Matsudo (Japan).
DEVELOPMENT OF ULTRASONIC MOTOR AND APPLICATION TO SILENT ALARM ANALOG QUARTZ WATCH
Masao Kasuga, Takashi Satoh, Jun Hirotomi, and Masayuki Kawata *In*

Societe Suisse de Chronometrie, Proceedings of the 4th European Congress on Chronometry 1992 p 53-56 (For primary document see N94-18006 04-35)
Copyright Avail: CASI HC A01/MF A02

An ultrasonic motor was developed for use in new generation watches and portable information devices. This motor shows promise as a new principle actuator. Measuring 10 mm in diameter and 4.5 mm thick, this ultrasonic motor is the world's smallest for practical use. Powered by a single lithium coin battery, this motor is expected to be applied to a broad range of miniature devices, including watches. The structure of the motor makes it possible to reduce its size and drive frequency. This motor was used to incorporate a silent alarm into an analog quartz watch. Unlike conventional electronic alarm watches, an eccentric weight rotates intermittently at high speed generating gentle vibration which notifies the wearer. The silent alarm analog quartz watch which incorporates the new ultrasonic motor, as well as the influence of design parameters on the performance of the ultrasonic motor, are described. ESA

N94-18017# Centre Technique de l'Industrie Horlogere, Besancon (France).
SILICON MICRO-ACTUATOR [MICROTRANSLATEUR SILICIUM] c33
Pascal Blind *In* Societe Suisse de Chronometrie, Proceedings of the 4th European Congress on Chronometry 1992 p 57-60 In FRENCH Sponsored by Ministere de la Recherche (For primary document see N94-18006 04-35)
Copyright Avail: CASI HC A01/MF A02

An electrostatic linear actuator without friction is studied. A process of chemical etching of silicon is used. The manufacturing method consists of selective etching of the substrate following the patterns designed by the photolithographic mask-film. The orientation of the crystal planes modifies the etching used. Mechanical tests were performed and strain-stress behavior was analyzed. ESA

N94-18018# Scientific Research Inst. of Instrument Automation, Moscow (USSR).
THE OPTIMAL NUMERICAL ALGORITHM FOR PROCESSING OF PHASE CODED TIME SIGNALS FOR RADIO-CLOCKS c61
Boris Rudyakov and Gennady Chvilyov *In* Societe Suisse de Chronometrie, Proceedings of the 4th European Congress on Chronometry 1992 p 61-63 (For primary document see N94-18006 04-35)
Copyright Avail: CASI HC A01/MF A02

Methods of complete numerical processing of phase coded signals (applied to radio clocks), which are performed with the use of microcomputer, are discussed. In contrast to reference coded time signals emitted by European transmitters, time signals of Russian radio stations are coded by phase and thus create certain problems in realization of algorithms for their processing in radio clocks. The computation for noise immunity of the algorithms in use are presented. ESA

N94-18019# Stuttgart Univ. (Germany). Inst. fuer Feinwerk- und Zeitmesstechnik.
SIMULATION OF A QUARTZ-CLOCKWORK [SIMULATION AN QUARZGROSSUHRWERKEN] c61
Uwe Thissen *In* Societe Suisse de Chronometrie, Proceedings of the 4th European Congress on Chronometry 1992 p 67-70 In GERMAN (For primary document see N94-18006 04-35)
Copyright Avail: CASI HC A01/MF A02

A model of a quartz controlled clockwork, which simulated both the electrical and the kinematical behavior of a driving system for any control voltage, is presented. The driving system consists of the step motor and the gearing with two transmissions. The model calculates the resulting impact pulses within the bearings of every single cogwheel as a measure for the initiated working noise. The model allows the simulation of the work behavior for free defined, regulated control voltages according to a given regulation criterion. The basic temporal interdependencies of the essential system quantities and the elaboration of the criteria for a regulated disconnection are described. It is shown, that only a suitable combination of the selected control voltage and the regulated disconnection can lead to an acceptable noise reduction of more than 10 dB. ESA

N94-18020# Hahn-Schickard-Inst. fuer Mikro- und Informationstechnik, Villingen-Schwenningen (Germany).
PROCESS AND QUALITY ON-LINE CONTROL IN LASER WELDING [PROZESSUEBERWACHUNG UND ON-LINE QUALITAETSKONTROLLE BEIM LASERPUNKTSCHWEISSEN] c37
Mani Alavi *In* Societe Suisse de Chronometrie, Proceedings of the 4th European Congress on Chronometry 1992 p 71-72 In GERMAN (For primary document see N94-18006 04-35)
Copyright Avail: CASI HC A01/MF A02

The interaction between the laser beam and the metal during laser welding generates optical and acoustic emissions which are characteristic of the welding process and of materials. The relation between these signals and the laser beam parameters as well as the weld quality was investigated. The results were used to develop an equipment on-line monitoring the Nd:YAG laser welding. ESA

N94-18021# Stuttgart Univ. (Germany). Inst. fuer Zeitmesstechnik, Fein- und Mikrotechnik.
SIMULATION OF QUARTZ RESONATORS [SIMULATIONEN AN SCHWINGQUARZEN] c76
M. Weinmann, R. Radius, and R. Mohr *In* Societe Suisse de Chronometrie, Proceedings of the 4th European Congress on Chronometry 1992 p 73-76 In GERMAN (For primary document see N94-18006 04-35)
Copyright Avail: CASI HC A01/MF A02

Quartz resonators are suitable as novel sensor elements in the field of profilometry and three dimensional measurement techniques. This application requires a tailoring of the oscillator circuit which is performed by a network analysis program. The equivalent network parameters are computed by a finite element analysis. The mechanical loading of the quartz is modeled by a viscous damping approach. ESA

N94-18022# ETA S.A., Grenchen (Switzerland).
ELECTRIC MEASUREMENT OF LAVET MOTORS [MESURE ELECTRIQUE DES MOTEURS LAVET] c33
Christian Peclat, Daho Taghezout, and Yves Guerin *In* Societe Suisse de Chronometrie, Proceedings of the 4th European Congress on Chronometry 1992 p 77-80 In FRENCH (For primary document see N94-18006 04-35)
Copyright Avail: CASI HC A01/MF A02

The performance of an electrical measurement system for Lavet type motors is discussed. This system measures all motor parameters by phase current analysis, without particular support or external measurement device. The most important results are current consumption, limit voltages, coupling factor, holding torque, rubbing torques and generated torque. The system can be applied to the motor pulse width optimization. The program can be used for measuring the movement gear and for checking magnetical properties of coil cores. ESA

N94-18023# Scientific Research Inst. of Instrument Automation, Moscow (USSR).
CONTROL OF TORQUE IN STEPPING MOTORS OF QUARTZ WATCHES AND CLOCKS c33
Alexander Ketsaris *In* Societe Suisse de Chronometrie, Proceedings of the 4th European Congress on Chronometry 1992 p 81-83 (For primary document see N94-18006 04-35)
Copyright Avail: CASI HC A01/MF A02

The method for control (test) of torque in stepping motors on the basis of analysis of current curve in motor winding is presented. The use of reduction gear and gram gauge is not required. It is characterized by labor input and minimal control time, below 3 s with sufficient precision control. The acquisition of the control data can be performed either by the numerical value of the torque or by the two position indication 'standard-brack'. The first variant should be followed by a laboratory analysis while the second variant is acceptable for a workshop control. ESA

N94-18024# Chronometer Prufstelle Stralsung, Greifswald (Germany).
ABOUT TIME [GEDANKEN UBER DIE ZEIT]
Hans Vilkner *In* Societe Suisse de Chronometrie, Proceedings of the 4th European Congress on Chronometry 1992 p 87-88 In GERMAN (For primary document see N94-18006 04-35)
Copyright Avail: CASI HC A01/MF A02

Concepts and principles involving time perception and measurement are discussed. The meaning of time measurement on Earth and on other planets is considered. The analysis shows that several standards can be used for time measurements, such as the speed of light and atomic oscillations. Some properties inherent to time perception are discussed, in particular: velocity, direction, behavior in magnetic field, future and past. ESA

N94-18025# Musee International d'Horologerie, La Chaux-de-Fonds (Switzerland). Inst. l'Homme et le Temps.
MARINE CHRONOMETRY IN THE NEUCHATEL MOUNTAINS (SWITZERLAND) [LA CHRONOMETRIE DE MARINE DANS LES MONTAGNES NEUCHATELOISES]
Estelle Fallet *In* Societe Suisse de Chronometrie, Proceedings of the 4th European Congress on Chronometry 1992 p 89-94 In FRENCH (For primary document see N94-18006 04-35)
Copyright Avail: CASI HC A02/MF A02

The history and evolution of the Swiss marine chronometer industry are summarized. From the 18th century onwards, Neuchatel watchmakers strove to develop precision horology. First J. F. Houriet and later S. Mairet, L. Richard, W. Dubois and H. Grandjean introduced the marine chronometer in the Neuchatel mountains. Precision having become a necessity for the industry, they helped achive this by means of a complex system for the distribution and maintenance of exact time, which allowed optimal adjustment. These men of vision called for the building of a cantonal observatory and strove to have their art practiced in modern watchmaking schools. Under the guidance first of Ulysse and then of Paul David Nardin, the manufacture of marine chronometers began in Le Locle in 1876. In La Chaux-de-Fonds at the beginning of the 20th century, Paul Ditisheim built a number of improved marine, ship and pocket chronometers. Together with scientists and watchmakers, the chronometer makers perfected the regulating parts of the timekeepers and solved the problems of adjustment caused by the various external influences. The manufacturers, the watchmakers at their branches, the timers and the Neuchatel business all contributed to strengthening the position of the products of their region in the world market. ESA

N94-18026# Musee International d'Horologerie, La Chaux-de-Fonds (Switzerland). Inst. l'Homme et le Temps.
RESTORATION OF AN 18TH CENTURY ENGLISH CLOCK [RESTAURATION D'UNE HORLOGE ANGLAISE DU 18TH SIECLE]
Daniel Curtit and Jean-Michel Piguet *In* Societe Suisse de Chronometrie, Proceedings of the 4th European Congress on Chronometry 1992 p 95-97 In FRENCH (For primary document see N94-18006 04-35)
Copyright Avail: CASI HC A01/MF A02

The background knowledge and the steps required to repair ancient clocks and watches are described. The restoration of old clocks and watches involves the problem of making them work. The wear that results from years of use and the fact that parts are lost or broken leads the restorer to replace certain component parts of the watch or clock. The parts are made in such a way that they fit in with the appearance of the object. This work requires the watchmaker/restorer to have a thorough knowledge of all the mechanisms used in watchmaking and knowhow which covers the whole field, from watches to monumental clocks. An example of a restoration carried out on a Bracket clock is given. ESA

N94-18027# Musee International d'Horologerie, La Chaux-de-Fonds (Switzerland). Inst. l'Homme et le Temps.
THE MYSTERY OF THE PERPETUAL MOTION CLOCK OF GEISER AND SON [LE MYSTERE DE L'HORLOGE A MOUVEMENT DIT PERPETUEL DE GEISER ET FILS]
Jean-Michel Piguet *In* Societe Suisse de Chronometrie, Proceedings of the 4th European Congress on Chronometry 1992 p 99-102 In FRENCH (For primary document see N94-18006 04-35)
Copyright Avail: CASI HC A01/MF A02

A description of the operation and mechanisms of a so called perpetual motion clock is given. At the end of the 18th and beginning of the 19th century, the achievement of perpetual motion was one of the Neuchatel clockmakers' great interests. Some watchmakers presented scientists and the public with constructions which, at first sight, seemed to have solved the problem. In 1815 a really interesting clock mechanism invented by Jean Geiser and his son was presented in Neuchatel. ESA

N94-18028# Citizen Watch Co. Ltd., Tanashi (Japan).
GEAR TRAIN BEHAVIOR ANALYZER USING LASER BEAM SCANNING FOR WATCH MOVEMENT c37
Toshio Ohmori, Hiroshi Yanagawa, Makoto Ohmuro, and Hiroo Fujita *In* Societe Suisse de Chronometrie, Proceedings of the 4th European Congress on Chronometry 1992 p 105-10 (For primary document see N94-18006 04-35)
Copyright Avail: CASI HC A01/MF A02

The method and technology to analyze the train wheel behavior of a watch using a laser beam are described. Progress in automatic assembly of analog watch movement is considered. After assembling, however, the train wheel behavior is manually inspected, and automation is desired. A laser beam scanning method was developed to analyze wheel behavior. The system comprises a beam control unit in which an acoustic optical element is used, a signal processing unit, and a personal computer. In this system, the teeth of train wheels running at high speed and from the background of the teeth is continuously analyzed to permit time series understanding of the quantity and direction of wheel rotation. The dynamic train wheel behavior of the movement can be analyzed in detail. The configuration and measuring method are described in detail, and the result of the behavior analysis is touched upon. ESA

N94-18029# Ecole d'Ingenieurs du Canton de Neuchatel (Switzerland).
UNIVERSAL MEASUREMENT DEVICE FOR ELECTRONIC WATCHES AND SMALL CLOCKS [APPAREIL UNIVERSEL DE MESURES POUR MONTRES ET PENDULETTES ELECTRONIQUES]
Michel Vermot *In* Societe Suisse de Chronometrie, Proceedings of the 4th European Congress on Chronometry 1992 p 109-11 In FRENCH (For primary document see N94-18006 04-35)
Copyright Avail: CASI HC A01/MF A02

The project and the device set up for performing automatic measurements are described. The system development involved: a specially designed acquisition card, a standard personal computer and specific management programs. It is designed as laboratory equipment and is able to perform most of measurements required by electronic watchmaking industry such as current/consumption measurements, frequency, torque, motor pulses generation. Versions meeting specific production testing needs at reasonable costs can be developed. For after sale servicing, it is possible to deliver a diskette giving all parameters needed for a specific movement, avoiding changes in hardware. ESA

N94-18030# CCF S.A., La Chaux-de-Fonds (Switzerland).
RELIABILITY CONTROL FOR WRIST WATCHES AND THEIR CASEMENTS [CONTROLES DE FIABILITE DE LA MONTRE ET DE SON HABILLEMENT]
Jean-Claude Schneider *In* Societe Suisse de Chronometrie, Proceedings of the 4th European Congress on Chronometry 1992 p 113-11 In FRENCH (For primary document see N94-18006 04-35)
Copyright Avail: CASI HC A01/MF A02

The reliability tests developed for controlling wrist watch movements and their casements are summarized. For controlling the watch movements, ageing accelerated tests and impact tests were performed. Testing the performance of a wrist watch casement is of great importance: since it is this which is initially attacked by the environment. The casement is submitted to impact, fatigue, vibration, and corrosion tests. The waterproof capabilities and ageing behavior of the casements are examined. ESA

N94-18031# Mutron S.A., Boudry (Switzerland).
MUTROMETRE: CONSTRUCTION FOR FAST WATER PROOF MEASUREMENTS UNDER LOW PRESSURE AND AIR SUPPRESSION [MUTROMETRE: CONSTRUCTION POUR LA MESURE RAPIDE DE L'ETANCHEITE EN DEPRESSION ET SUPPRESSION D'AIR]
Roger Wellinger *In* Societe Suisse de Chronometrie, Proceedings of the 4th European Congress on Chronometry 1992 p 117-12 In FRENCH (For primary document see N94-18006 04-35)
Copyright Avail: CASI HC A01/MF A02

The mutrometer which repidly detects leaks and measures leak rates at a precision better than +/- 1 microg/air/min is described. It was found that some leaks are nonlinear, one way only. This implies that tests based on retrodiffusion do not detect or only partially detect one way leaks. Underwater tests may hide leaks, whether a detergent is addded or not. Tests to search for different type of leaks are described. The design of a mutrometer to test for leaks slightly above or below atmospheric pressure, then extreme pressures up to 60 bar to determine the validity of such tests is presented. ESA

N94-18032# Swiss Center for Electronics and Microtechnology, Inc., Neuchatel.
TECHNIQUES FOR LOW CONSUMPTION CIRCUITS [TECHNIQUES DE CONCEPTION DE CIRCUITS A BASSE CONSOMMATION]
C. Piguet, V. vonKaenel, J.-M. Masgonty, J.-F. Perotto, and R. Klootsema *In* Societe Suisse de Chronometrie, Proceedings of the 4th European Congress on Chronometry 1992 p 123-12 In FRENCH (For primary document see N94-18006 04-35)
Copyright Avail: CASI HC A01/MF A02

Several techniques used for designing integrated circuits are summarized. These techniques are currently applied and of major importance in the electric clock and watch industry. It is shown that these techniques must be applied at all the steps of integrated circuit production: from the architecture layouts to the putting together stage. The results show that energy consumption is related to the number of components in a circuit: few elements is equal to low consumption. Moreover, a low number of components reduce the risk of imperfections. ESA

N94-18033# Swiss Center for Electronics and Microtechnology, Inc., Neuchatel.
EVALUATION OF THE CONSUMPTION OF ELECTRONIC CLOCKS [BILAN DE CONSOMMATION DE MONTRES ELECTRONIQUES] **c33**
V. vonKaenel and C. Piguet *In* Societe Suisse de Chronometrie, Proceedings of the 4th European Congress on Chronometry 1992 p 127-13 In FRENCH (For primary document see N94-18006 04-35)
Copyright Avail: CASI HC A01/MF A02

Two power consumption analyses of electronic watches and future trends are presented. The analysis of the distribution of power consumption enables the parts that mainly determine battery life to be localized. It is important to notice that the stepper motor used to drive the hands of a watch already consumes as much as the quartz oscillator at 32 kHz and the dividers. The self discharge of the battery is almost equal to the consumption of the electronic circuits. The processor architecture and the basic cells originate from knowhow in very low power cicuits. Since the microprocessor in a watch is only active during a small period of battery life, the average power consumption of the microprocessor accounts for only a few percent of the total power dissipation. ESA

N94-18034# EUROSIL G.m.b.H., Eching (Germany).
NEW CURRENT REDUCTION SYSTEM FOR WATCHES WITH INTEGRATED CURRENT REGULATION MOTORS [NEUE STROMSPARANDE SYSTEME FUER INTEGRIERTE KLEINUHRENSCHALTKREISE MIT MOTORSTROMREGELUNG]
Stephan Lehmann *In* Societe Suisse de Chronometrie, Proceedings of the 4th European Congress on Chronometry 1992 p 131-13 In GERMAN (For primary document see N94-18006 04-35)
Copyright Avail: CASI HC A01/MF A02

An optimized system, comprising watch motor and an Integrated Current (IC) with motor current regulation enables a reduction of the system current (IC and motor) up to 50% when compared to a solution with no motor current regulation. This leads to a significantly longer battery life, or alternatively permits the development of even flatter modules, and reduces the noise level. This kind of system improvement is not only applicable to watches, but also to clocks (IC with motor current regulation). However only watch applications are considered. In order to cover the complete spectrum of application areas, two algorithms are offered for motor current regulation. These can for example supply the means to system optimization for 1.5 V and 3 V applications. ESA

N94-18035# Valtronic S.A., Les Charbonnieres (Switzerland).
SOME VARIATION IN THE MOVEMENT BASE OF THE ETA 251 SERIES [QUELQUES VARIATIONS SUR LA BASE DES MOUVEMENTS ETA DE LA SERIE 251]
Jean-Claude Berney *In* Societe Suisse de Chronometrie, Proceedings of the 4th European Congress on Chronometry 1992 p 135-13 In FRENCH (For primary document see N94-18006 04-35)
Copyright Avail: CASI HC A01/MF A02

Different functional applications can be obtained by parameter changes in the electronic module of an ETA 251. The motions of an ETA 251 are controlled by a stepping micromotor and a microprocessor. New functions can be introduced by programming new algorithms without touching the mechanical parts. The following application examples are given: yachting function, golf counter, Moon phase changes. ESA

N94-18036# Citizen Watch Co. Ltd., Tanashi (Japan).
TOOTH FORM DESIGN SUPPORTING SYSTEM IN MODULE DESIGN
Junji Nagasawa, Ryou Namiki, Souichi Tanaka, and Shigeru Aoyama *In* Societe Suisse de Chronometrie, Proceedings of the 4th European Congress on Chronometry 1992 p 141-14 (For primary document see N94-18006 04-35)
Copyright Avail: CASI HC A01/MF A02

A lot of time was spent in designing the tooth form because there was no Computer Aided Design (CAD) system suitable for designing the tooth form of gears. A CAD system to support the tooth form design to promote efficiency of the tooth form design of gears for a wristwatch was developed. This system can perform calculation of torque transmission factor of gears, automatic drawing of tooth form drawing, and engagement simulation, and by utilizing this system the tooth form can be designed in less than one fourth of the time required by the conventional method. The characteristics of the system used to calculate the torque transmission factor of a pair of gears are summarized and the displayed results are shown. ESA

N94-18037# Citizen Watch Co. Ltd., Tanashi (Japan).
AUTOMATIC SOLDERING FOR WATCH CIRCUIT COMPONENTS **c37**
Tohru Furuyama, Toshio Furutani, and Mikio Takemoto *In* Societe Suisse de Chronometrie, Proceedings of the 4th European Congress on Chronometry 1992 p 145-14 (For primary document see N94-18006 04-35)
Copyright Avail: CASI HC A01/MF A02

Automatic welding systems for watch circuits were developed to automate large variety small quantity production processes. The aim of the development was achieved by solving problems involving prevention of solder ball generation and development of a new heating method for components with low heat resistance, and development of a system that permits production of various watch circuits operations. As a result, it was possible to produce systems for stable soldering and switchover production of a variety of watch circuits with reduced switchover time. ESA

N94-18038# Observatoire Cantonal, Neuchatel (Switzerland).
DEVELOPMENT OF ATOMIC STANDARDS AT THE NEUCHATEL OBSERVATORY [DEVELOPPEMENT D'ETALONS ATOMIQUES A L'OBSERVATOIRE CANTONAL DE NEUCHATEL] **c72**
Pierre Thomann *In* Societe Suisse de Chronometrie, Proceedings of the 4th European Congress on Chronometry 1992 p 151-15 In FRENCH Sponsored by ESTEC; Fonds National Suisse pour la Recherche Scientifique; and Office Suisse de Metrologie (For primary document see N94-18006 04-35)
Copyright Avail: CASI HC A01/MF A02

The development of atomic frequency standards under way at the Observatory of Neuchatel concerns three projects: miniaturized rubidium standard for space applications, hydrogen masers for radioastronomy and for space research, and work on laser cooling of cesium atoms. The characteristics of standards already built or under development are reviewed. Some results are discussed. ESA

N94-18039# ETA S.A., Grenchen (Switzerland). Fabrique d'Ebauches.
SWATCH PAGER
Pierre-Andre Meister and Viron Teodoridis *In* Societe Suisse de Chronometrie, Proceedings of the 4th European Congress on Chronometry 1992 p 155-15 In FRENCH (For primary document see N94-18006 04-35)
Copyright Avail: CASI HC A01/MF A02

The telecommunication network applying the Swatch Pager is described. The Swatch Pager is a wrist watch with embedded radio receiver able to alert the bearer with the incoming tone or numeric message. The message is sent through the telephone line by dialling the number of each pager. In Switzerland, the Post-Office Telecommunications and Telegraph company are the network operator for this wide paging system, named Appel local B. The network is developed through the whole country covering 90% of the population. ESA

N94-18040# Epson Corp., Suwa (Japan).
A STUDY OF THE AUTOMATIC GENERATING SYSTEM. 3: IMPROVEMENT OF THE TOTAL SYSTEM PERFORMANCE
Shouichi Nagao, Naoaki Yakusawa, and Motomu Hayakawa *In* Societe Suisse de Chronometrie, Proceedings of the 4th European Congress on Chronometry 1992 p 159-16 (For primary document see N94-18006 04-35)
Copyright Avail: CASI HC A01/MF A02

The power generating performance of Automatic Generating System (AGS) watches mounted with small generators designed to generate power by arms motion is investigated. Since arm movements function as the energy source, the amount of power generated when watches are worn varies for person to person. The required power generating performance also varies depending on the watch wearers. Since the power generating performance represents the balance between the generated power volume and the power volume consumed by the driving of watch mechanisms, it is essential to study both phases of increase in generating volumes and reduction of consumption volumes when attempting to improve power generating performance. The results of a simulation study of watch wearing and the results of experiments and analyses conducted for improving power generating performance are presented. ESA

N94-18041# Epson Corp., Suwa (Japan).
DEVELOPMENT OF A NEW CONCEPT DIVER'S WATCH
Takeo Tsunoda and Hitomi Aizawa *In* Societe Suisse de Chronometrie, Proceedings of the 4th European Congress on Chronometry 1992 p 165-16 (For primary document see N94-18006 04-35)
Copyright Avail: CASI HC A01/MF A02

The 'Scuba Master' diver's watch represents a new concept. It was developed and announced in 1990. This watch automatically displays information necessary for safe scuba diving and records diving data. The watch was well accepted by divers all over the world. Safe diving techniques were investigated. This led to the need for developing a highly accurate, highly reliable depth measurement system. The functions and features of 'Scuba Masters' are described. The way to make the depth measurement system highly accurate and highly reliable is explained. ESA

N94-18042# ETA S.A., Grenchen (Switzerland). Fabrique d'Ebauches.
QUARTZ ANALOG WATCH WITH PERPETUAL CALENDAR [MONTRE A QUARTZ ANALOGIQUE AVEC QUANTIEME PERPETUEL]
Eric Favre, Pierre Schmidli, and Bruno Erni *In* Societe Suisse de Chronometrie, Proceedings of the 4th European Congress on Chronometry 1992 p 169-17 In FRENCH (For primary document see N94-18006 04-35)
Copyright Avail: CASI HC A01/MF A02

The Caliber ETA 252.411 with perpetual calendar, which is similar in dimensions and display to classic quartz watch movements, is described. The main characteristics are: the date display in the window is always correct (until 28 Feb. 2100); the change of time zones is operated without losing minute and second by means of a date correction at each midnight passage; and the use of nonvolatile memories for information concerning the perpetual calendar allows an easy time resetting after change of battery. ESA

N94-18043# Citizen Watch Co. Ltd., Tanashi (Japan).
DEVELOPMENT OF ANALOG WATCH WITH MINUTE REPEATER
Tomio Okigami, Shigeru Aoyama, Takashi Osa, Kiyotaka Igarashi, and Tomomi Ikegami *In* Societe Suisse de Chronometrie, Proceedings of the 4th European Congress on Chronometry 1992 p 173-17 (For primary document see N94-18006 04-35)
Copyright Avail: CASI HC A01/MF A02

A complementary metal oxide semiconductor with large scale integration was developed for an electronic minute repeater. It is equipped with the synthetic struck sound circuit to generate natural struck sound necessary for the minute repeater. This circuit consists of an envelope curve drawing circuit, frequency mixer, polyphonic mixer, and booster circuit made by using analog circuit technology. This large scale integration is a single chip microcomputer with motor drivers and input ports in addition to the synthetic struck sound circuit, and it is possible to make an electronic system of minute repeater at a very low cost in comparison with the conventional type. ESA

N94-18044# Conseilray S.A., La Chaux-de-Fonds (Switzerland).
MULTIFUNCTION CHRONOGRAPH MOVEMENT USING A MODULAR STRUCTURE MULTIMOTOR [MOUVEMENT CHRONOGRAPHE MULTIFONCTION MULTIMOTEUR A STRUCTURE MODULAIRE]
Michiel Groothuis *In* Societe Suisse de Chronometrie, Proceedings of the 4th European Congress on Chronometry 1992 p 177-18 In FRENCH (For primary document see N94-18006 04-35)
Copyright Avail: CASI HC A01/MF A02

A multifunction chronograph movement, using motor modules assembled on metal or plastic housing is described. The advantages of chronographs where the start/stop/split/lap functions are generated by electronic systems are summarized. The absence of mechanical functions improves reliability and reduces production and servicing costs. Technological developments allowed the production of high quality systems with large movement integration. ESA

N94-18102# Sandia National Labs., Albuquerque, NM.
APPLICATION OF PIEZOELECTRIC STRESS GAUGES TO THE MEASUREMENT OF FAST-RISE-TIME MULTIMEGAMPERE ELECTRIC CURRENTS
D. L. Hanson, R. B. Spielman, J. F. Seamen, and K. W. Struve (Mission Research Corp., Albuquerque, NM.) 1993 20 p Presented at the 14th International Conference of the International Association for the Advancement of High Pressure Science and Technology, Colorado Springs, CO, 27 Jun. - 2 Jul. 1993
(Contract DE-AC04-76DP-00789)
(DE93-017625; SAND-93-0425C; CONF-930676-3) Avail: CASI HC A03/MF A01

Modeling of load behavior in Z-pinch plasma radiation sources driven by high current generators requires accurate measurement of fast-rise-time multimegampere electrical currents close to the load. Using a novel application of high pressure technology, we have demonstrated that fast-response piezoelectric stress transducers can measure such currents under conditions of extremely high current density, induced electric fields, and bremsstrahlung radiation where conventional current diagnostics fail. Large signal, nanosecond-time-resolution lithium niobate piezoelectric stress gauges are employed to directly measure the magnetic pressure B(sup 2)/2(mu)(sub 0) = (mu)(sub 0)I(sup 2)/8(pi)(sup 2)r(sup 2) generated at radius r by a current I flowing in a radial transmission line near the load of a pulsed power current source. With a current diagnostic consisting of a pure tungsten electrode on a Y-cut lithium niobate stress gauge, current densities up to 1/2(pi)cr = 78MA/m can be measured before the electrode yield strength and piezoelectric operating stress limit are exceeded. Based on this work, we have developed a compact modular current probe for use on the high current (20-25 MA) DECADE simulator being constructed for the Defense Nuclear Agency. We also describe recent work extending this measurement technique to higher current densities (125 MA/m) using a copper-sapphire electrode impedance stack on an X-cut quartz piezoelectric element. DOE

N94-18207# Mississippi State Univ., Mississippi State. Diagnostic Instrumentation and Analysis Lab.
DEVELOPMENT OF A MULTI-POINT TWO-COLOR PYROMETER FOR TUBE AND WALL TEMPERATURE AND EMISSIVITY MEASUREMENT AT THE CFFF
R. D. Benton and P. R. Jang 1993 5 p Presented at the 31st Symposium on Engineering Aspects of Magnetohydrodynamics, Whitefish, MT, 29 Jun. - 1 Jul. 1993
(Contract DE-AC02-80ET-15601)
(DE93-014716; CONF-930626-1) Avail: CASI HC A01/MF A01

The Diagnostic Instrumentation and Analysis Laboratory (DIAL) has been actively engaged in developing and applying advanced optical diagnostic techniques and instrumentation systems to high temperature coal-fired gas streams for over a decade. DIAL's systems have been used primarily in support of the US Department of Energy's (DOE) magnetohydrodynamic (MHD) research program. One of the earliest diagnostic systems developed by DIAL was a two color pyrometer (TCP). The TCP is used to measure surface temperature and emissivity. This system has been used extensively to make measurements in support of the national MHD program. In this system, two commercial single-color pyrometers and a microprocessor system were used to form a TCP to make accurate measurements of surfaces of unknown emissivity and temperature. This paper describes an improvement in the DIAL TCP which provides for near simultaneous multipoint measurements, reduced dependence on electronic circuits, and a greatly improved data display system. Commercial two-color pyrometer systems are not suitable for our work because they do not provide for emissivity measurement. The emissivity measurement provides insight into changes in surface characteristics and is an important consideration in our work. A second and important reason for our development of this system is the need to make simultaneous measurements at widely separated points. Finally, the data measured by this system is stored on magnetic media and can be correlated with other measurements on the system, e.g. furnace, under study. DOE

N94-18235# Lawrence Livermore National Lab., CA.
HIGH SPEED 512X512 CAMERA SYSTEM
A. Conder Jul. 1992 13 p
(Contract W-7405-eng-48)
(DE93-015671; UCRL-ID-111216) Avail: CASI HC A03/MF A01

Lawrence Livermore National Laboratory has been involved in the design of high speed solid state camera systems for over a decade. The latest camera system designed by the laboratory utilizes the CCD-13 multiport 512 x 5l2 CCD array, manufactured by English Electric Valve. Simultaneous readout from each port at a 20 MHz pixel rate allows this camera system to achieve up to 500 frames per second. A first generation camera system was designed by LLNL to provide data on the CCD-13, and as proof of principle for the camera system electronics. The results of the tests involving this camera will be presented in this report. A second generation camera system has been designed which incorporates the knowledge gained from these tests, and is currently being manufactured. This system should be available for testing in September '92. DOE

N94-18299 Army Research Lab., Fort Monmouth, NJ.
MILITARY APPLICATIONS OF HIGH-ACCURACY FREQUENCY STANDARDS AND CLOCKS
John R. Vig Aug. 1993 22 p Limited Reproducibility: More than 20% of this document may be affected by microfiche quality
(AD-A269303; ARL-TR-68) Avail: CASI HC A03

Frequency control and timing devices are essential components in modern military electronics systems. Reviewed in this paper are the applications of these devices, and the manner in which the stability and accuracy of these devices impact the performance of military communication, navigation, surveillance, electronic warfare, missile guidance, and identification-friend-or-foe systems. DTIC

N94-18406# Naval Postgraduate School, Monterey, CA.
DEVELOPMENTAL TESTING OF A PROTOTYPE ALL-REFLECTION MICHELSON INTERFEROMETER M.S. Thesis
Allan D. Risley, Jr. Jun. 1993 48 p
(AD-A269064) Avail: CASI HC A03/MF A01

A prototype all-reflective Michelson interferometer is tested using visible laser, sodium, and mercury light sources. The design uses an off-axis parabolic mirror for collimation, a plane diffraction grating, and two plane mirrors to divide and recombine incident light. Interference fringes were seen using the laser light source, but instrument performance with other sources was unreliable as a result of difficulties in constructing the instrument with enough mechanical precision. A method of using a full-size template to position the instrument's optical elements was discovered, and the efficacy of an image intensifier/photodiode array combination for use as a detector was verified. The feasibility of the interferometer design was verified by the observation of interference fringes using mercury 5461 A light. A practical instrument would be compact, light weight, and require no moving parts. DTIC

N94-18481# Argonne National Lab., IL.
PERFORMANCE OF THE AMORPHOUS MATERIALS DIFFRACTOMETER GLAD AT IPNS
A. J. G. Ellison, K. J. Volin, D. L. Price, and R. K. Crawford 1993 10 p Presented at the 12th International Collaboration of Advanced Neutron Sources Meeting (ICANS), Abingdon, England, 24-28 May 1993
(Contract W-31-109-eng-38)
(DE93-017746; ANL/MSD/CP-79154; CONF-9305177-8) Avail: CASI HC A02/MF A01

The Glass, Liquids, and Amorphous Materials Diffractometer (GLAD) at IPNS has now been commissioned and the first scientific measurements have been performed. Details of the performance of this instrument including background, calibration, resolution, data rate, data quality, and data reduction and analysis are discussed. DOE

N94-18530# Department of the Navy, Washington, DC.
HIGH SPATIAL RESOLUTION, RANGE GATED, UNDERWATER IMAGING METHOD AND APPARATUS Patent Application
Edgar A. McLean, inventor (to Navy) 30 Jun. 1993 22 p
(AD-D015882; US-Patent-Appl-SN-083580) Avail: CASI HC A02/MF A01

This patent application discloses a method and apparatus for imaging objects in turbid mediums, such as water, the invention using a laser pulse, a detector of the reflected laser pulse, and a shutter on the detector. The shutter is kept closed except at the excepted return time of the laser pulse from the reflected object to be detected and identified at which time the shutter is opened to permit the detector to receive the reflected laser pulse. Typically, laser pulses with widths of about 100 to about 500 psecs are used. In addition, typical shutter times or gate width of about 100 to about 500 psecs are also used. Gate widths on the order of 120 psecs are preferred. The detector or GOI camera is shielded from spurious signals, most notably, scattered laser light from the turbid medium. DTIC

N94-18537# Naval Command, Control and Ocean Surveillance Center, San Diego, CA. RDT and E Div.
RESIDUAL STRAIN MEASUREMENT ON THE PRODUCTION-GRADE CLASS 4 FLEXTENSIONAL TRANSDUCER SHELL Final Report
J. D. Maltby Apr. 1993 23 p
(AD-A268828; NRAD-TR-1603) Avail: CASI HC A03/MF A01

This document reports on the task of empirically determining the residual strain state of a production-grade flextensional transducer shell. DTIC

N94-18569 Colorado Univ., Boulder. Dept. of Astrophysical Science.
COMPETITIVE DYNAMICS AND SELF-ORGANIZATION IN PHOTOREFRACTIVE SYSTEMS Final Report, Jun. 1992 - Jun. 1993
Dana Z. Anderson 1 Sep. 1993 20 p Limited Reproducibility: More than 20% of this document may be affected by microfiche quality
(Contract N00014-91-J-1212)
(AD-A269663) Avail: CASI HC A03

Information can be manipulated and processed by a nonlinear dynamical system. This work investigates the properties of such nonlinear optical systems based upon real-time holographic materials known as photorefractive media. Our goal is to understand how and when a dynamical system can self-organize, or learn on its own to process information in a useful way. We have demonstrated systems, for example, that can separate multiple fiber optic communication channels or learn to classify incoming images. We have discovered that such self-organizing systems will exhibit a phase transition with the information content of the input as the critical parameter. The phase transitions are analogous to those common to thermodynamic systems. In order to better provide an analytical basis of treatment of our systems we have developed various analytical tools, in particular, stability analysis tools. We have also looked at the photorefractive version of well known nonlinear dynamical problems such as the formation of hexagonal patterns in pumped photorefractive media. DTIC

N94-18643# Von Karman Inst. for Fluid Dynamics, Rhode-Saint-Genese (Belgium).
MEASUREMENT TECHNIQUES
1993 532 p Lecture series held in Rhode-Saint-Genese, Belgium, 19-23 Apr. 1993 Original contains color illustrations
(VKI-LS-1993-05; ETN-93-94628) Copyright Avail: CASI HC A23/MF A04

General concepts widely applicable in experimental techniques are provided. Focus is on general data acquisition principles and treatment as an example of widely used techniques for different kinds of measurements: pressure measurements, infrared thermography and liquid crystal techniques; all of them can be characterized as nonintrusive. The lectures on pressure measurements deal with techniques, such as pressure sensitive paints and laser induced luminescence. The physical properties on which the techniques are based are explained and possible applications are illustrated with test cases. The two other techniques are devoted to temperature and heat transfer measurements. The physics of each is discussed in an introductory lecture on Infrared Thermography (IT) and Liquid Crystals (LC). The emphasis is placed on IT. The application domain and limitations of IT and LC are discussed and illustrated. For individual titles, see N94-18644 through N94-18654.

N94-18644# Oxford Univ. (England). Dept. of Engineering Science.
DATA ACQUISITION IN AERODYNAMIC RESEARCH
R. W. Ainsworth *In* VKI, Measurement Techniques 1993 78 p (For primary document see N94-18643 04-35)
Copyright Avail: CASI HC A05/MF A04

Data acquisition, related to aerodynamic flows is discussed. Typical transducers used in aerodynamic research, how they are constructed, their excitation and response through any conditioning electronics to the equipment used to record their output are discussed. Those discussed include response transducers for pressure measurement, hot wire anemometers and thin film sensors. With the rapid and continuing reduction in the cost of computing power, there is a continuing emphasis on the digital manipulation of output signals (digital signal processing) involving much use of frequency time transformations, Fourier analysis and correlation functions. The basics of all the technology encompassed in data acquisition are introduced and examples of how the technology is used at the forefront of current research in aerodynamics are given. Examples are in general confined to the field of turbomachinery. ESA

N94-18645# Oxford Univ. (England). Dept. of Engineering Science.
RECENT DEVELOPMENTS IN FAST RESPONSE AERODYNAMIC PROBE TECHNOLOGY
R. W. Ainsworth *In* VKI, Measurement Techniques 1993 23 p (For primary document see N94-18643 04-35)
Copyright Avail: CASI HC A03/MF A04

The design and construction of fast response probes pertinent to use in aerodynamic research is discussed. The recent progress in the area of fast response aerodynamic probes, increasingly being used as an alternative to hot wire anemometers, is reviewed. Focus is on semiconductor pressure sensing. Data which helps to assess and optimize the geometry of these probes is given. Future research directions are described. ESA

N94-18646# Institut de Mecanique des Fluides de Lille (France).
STATIC PRESSURE MEASUREMENTS FOR NEAR ISENTROPIC FLOWS USING LASER INDUCED IODINE FLUORESCENCE
F. Lemoine and B. Leporcq *In* VKI, Measurement Techniques 1993 28 p (For primary document see N94-18643 04-35)
Copyright Avail: CASI HC A03/MF A04

A simple adaptation of pressure measurement using Laser induced Iodine Fluorescence (LIF), which allows the approximate determination of the pressure in isentropic or near isentropic flows using a simple experimental set up, is considered. Pressure measurement using LIF was demonstrated on a free jet issuing from an underexpanded axisymmetric nozzle. A broadband multimode laser at the wavelength of 514.5 nm was used. Nonintrusive experimental measurement techniques are required for experimental validation of calculation models in the field of fluid mechanics, especially for three dimensional flows. ESA

N94-18647# McDonnell-Douglas Astronautics Co., Saint Louis, MO.
PRESSURE SENSITIVE PAINT TECHNIQUE
R. C. Crites *In* VKI, Measurement Techniques 1993 70 p Original contains color illustrations (For primary document see N94-18643 04-35)
Copyright Avail: CASI HC A04/MF A04

The basic concepts and some of the more important engineering details of an optical pressure measurement, which is based on the fact that some compounds emit light when excited by a suitable light source (photoluminescence) are discussed. The intensity of the emitted light is inversely related to the partial pressure of oxygen and is of longer wavelength than the excitation light. This phenomena can be incorporated into a pressure measurement system. An oxygen quenched photoluminescent compound is mixed with an oxygen permeable binder to form a Pressure Sensitive Paint (PSP). This paint is applied to an aircraft model and excited with a proper light source. The light source must be filtered so that it emits no light in the luminescence band. A high resolution video camera views the model through a filter that removes all light except that emitted by the paint. The distribution of pressure over the model is computed from the measured distribution of light intensity; that is, the brighter a point in the image, the lower the pressure. The specification of a typical PSP system, current research in the area, and the future potential of the technique are discussed. ESA

N94-18648# Office National d'Etudes et de Recherches Aerospatiales, Paris (France).
FUNDAMENTALS OF INFRARED THERMOGRAPHY
D. L. Balageas *In* VKI, Measurement Techniques 1993 26 p Original contains color illustrations (For primary document see N94-18643 04-35)
Copyright Avail: CASI HC A03/MF A04

The fundamentals of infrared thermography are discussed. The principles of infrared radiometry are outlined and a general description of infrared scanners and their characteristic parameters is given. The principle of quantitative thermometry by infrared thermography is outlined and certain problems and solutions of this method are considered: imager related problems; problems related to the object being studied; problems related to the optical path between the object and the imager; and acquisition and data processing problems. ESA

N94-18649# Office National d'Etudes et de Recherches Aerospatiales, Paris (France).
APPLICATION OF INFRARED THERMOGRAPHY IN FLUID MECHANICS
D. L. Balageas and A.-M. Bouchardy *In* VKI, Measurement Techniques 1993 42 p Original contains color illustrations (For primary document see N94-18643 04-35)
Copyright Avail: CASI HC A03/MF A04

The history of infrared thermography in fluid mechanics is outlined and special problems related to infrared thermography in wind tunnels are addressed: IR windows; distance between model and camera; model emissivity/conductivity problems; short duration tests. The use of passive and active thermography to image the space distribution of the convective heat transfer at the wall of the model, in view of detecting the transition location, or of determining the convective fluxes (heat flux metrology) is discussed. The detection of transition is discussed and various other flow features detection (shock waves, separation, reattachment, vortices) are considered. ESA

N94-18650# Office National d'Etudes et de Recherches Aerospatiales, Paris (France).
HEAT TRANSFER QUANTITATIVE CHARACTERIZATION: PASSIVE AND ACTIVE METHODS
D. L. Balageas *In* VKI, Measurement Techniques 1993 32 p Original contains color illustrations (For primary document see N94-18643 04-35)
Copyright Avail: CASI HC A03/MF A04

Two ways of determining the convective fluxes from the nonsteady temperatures are discussed: the passive method of classical thermography, in which the heating due to convection alone is used; and the active method of stimulated thermography in which the heat transfer coefficients are found directly from the heating due to a source of radiation, which is added to the convection for very brief intervals. The various algorithms used for identification of the heat transfer coefficient are presented together with some experimental results. For heat transfer identification, monodimensional models are used in both the passive and active modes. Moreover, considering the fact that supersonic or hypersonic flows are being dealt with, it is assumed that the linearized transfer coefficient corresponding to the radiative transfers between the model and the wind tunnel wall is negligible compared with the convective transfer coefficient. ESA

N94-18651# Office National d'Etudes et de Recherches Aerospatiales, Paris (France).
PERSPECTIVE AND FUTURE POSSIBILITIES
A.-M. Bouchardy and D. L. Balageas *In* VKI, Measurement Techniques 1993 24 p (For primary document see N94-18643 04-35)
Copyright Avail: CASI HC A03/MF A04

Future possibilities of infrared thermography are considered: staring array cameras for high thermal, temporal and spatial resolution imagery; infrared thermography for cryogenic wind tunnel; and photothermal cameras. The infrared array detectors are faster and faster and use a greater number of elements: HgCdTe, PtSi and InSb. Noise and sensitivity, the principle parameters characterizing the infrared camera, are discussed. ESA

N94-18652# Naples Univ. (Italy).
INFRARED THERMOGRAPHY
G. M. Carlomagno *In* VKI, Measurement Techniques 1993 114 p Original contains color illustrations (For primary document see N94-18643 04-35)
Copyright Avail: CASI HC A06/MF A04

With regard to infrared thermography, problems connected with signal acquisition and limitations, both from the sensor and the camera points of view, are addressed together with a critical analysis of the main parameters characterizing the performance of the sensor and of the Infrared Scanning Radiometer (IRSR). In particular, the formulation of a cascade model for the evaluation of the actual System Transfer Function (STF) of a sampled IR imaging system coupled to a heat transfer sensor is discussed. Significant results referring to flow visualizations and heat transfer measurements performed with an IRSR in a number of applications are also presented. ESA

N94-18653# Oxford Univ. (England).
LIQUID CRYSTAL HEAT TRANSFER MEASUREMENTS
P. T. Ireland, Z. Wang, and T. V. Jones *In* VKI, Measurement Techniques 1993 48 p Original contains color illustrations (For primary document see N94-18643 04-35)
Copyright Avail: CASI HC A03/MF A04

General aspects of temperature measurement using liquid crystals are considered. Methods of visualizing flow fields using thermal tracing and of measuring the heat transfer coefficient h under a uniform heat flux are discussed. The transient heat transfer method is covered and compared to the uniform heat flux technique. A hybrid method for visualizing turbulent spots is introduced. Optical data acquisition and processing aspects are discussed. ESA

N94-18654# Von Karman Inst. for Fluid Dynamics, Rhode-Saint-Genese (Belgium).
THE APPLICATION OF LIQUID CRYSTAL TECHNIQUES TO DETERMINE HEAT TRANSFER RATES
G. Rau, J. Vanhalst, and T. Arts *In its* Measurement Techniques 1993 40 p (For primary document see N94-18643 04-35)
Copyright Avail: CASI HC A03/MF A04

Different methods using liquid crystals to determine surface temperature are listed. These methods depend on the unique characteristic of cholesteric and chiral nematic liquid crystals to change color with variation of temperature. An explanation of 'color' is given. There is a direct relation between the temperature and the maximum intensity wavelength scattered by the liquid crystal layer. This expression leads directly to the spectral distribution of light and the basic optical properties of liquid crystals which are reviewed. Early methods used the human eye as measurement instrument, while later developed methods went over to cameras taking color pictures and video recordings. It is clear that neither photographic nor video cameras were developed for making accurate heat transfer measurements. They try to reproduce the human color perception as close as possible, and for their application in heat transfer measurement chains basic considerations about their recording technique have to be made. Other color influencing parameters which can deteriorate the measurements are considered. A narrow bandpass filter method is described. The application to a practical case and the difficulties in calculating the heat transfer coefficients are discussed. ESA

N94-18681# Naval Research Lab., Washington, DC.
EFFICIENT SIMULATION OF DEDS BY MEANS OF STANDARD CLOCK TECHNIQUES: QUEUEING AND INTEGRATED RADIO NETWORK EXAMPLES Interim Report, Jun. 1992 - Jun. 1993
Jeffrey E. Wieselthier, Craig M. Barnhart, and Anthony Ephremides 7 Sep. 1993 57 p
(AD-A269878; NRL/MR/5521-93-7392) Avail: CASI HC A04/MF A01

We discuss the application of the Standard Clock (SC) approach to the simulation of several examples of discrete event dynamic systems (DEDS), and demonstrate the improved efficiency that can be achieved by using this approach. In SC simulation, a common clock (event time, event type) sequence is used by a large number of simulations running in parallel, thereby resulting in a significant decrease in the most costly aspect of the simulation process, namely the generation of events. In studies of the M/M/1/K queue, we quantify the time spent in the various aspects of the simulation, and compare predicted performance improvement with that which is actually measured. This approach scales well when applied to larger problems, including queueing networks and multihop radio networks. We develop a SC simulation model for a multihop, integrated voice/data radio network, and demonstrate its use for the determination of admission control policies. Ordinal optimization techniques are shown to provide good, although not optimal, control policies on the basis of short simulation runs. DTIC

N94-18731# Department of the Navy, Washington, DC.
PHOTODETECTOR ARRAY HAVING HIGH PIXEL DENSITY Patent Application
Carmen I. Huber, inventor (to Navy), Tito E. Huber, inventor (to Navy), Tak-Kin Chu, inventor (to Navy), and Nicholas Caviris, inventor (to Navy) 18 Jun. 1993 10 p
(AD-D015859; US-Patent-Appl-SN-077806) Avail: CASI HC A02/MF A01

Photoconductive semiconductor material is injected into narrow and closely spaced cylindrical channels in an insulating matrix plate to form pixel elements of a high resolution photodetector array. A transparent conductive layer is deposited on one surface of the photoconductor array while light reflecting pads are formed on the elements at the opposite surface. Subsequently, a layer of light modulating material and a transparent conductive layer are deposited on the opposite surface to obtain a high resolution spatial light modulator. DTIC

N94-18828# Los Alamos National Lab., NM.
AN RS-170 TO 700 FRAME PER SECOND CCD CAMERA
K. L. Albright, N. S. P. King, G. J. Yates, T. E. McDonald, and B. T. Turko 1993 9 p Presented at the Annual Meeting of the Society of Photo-Optical Instrumentation Engineers, San Diego, CA, 11-16 Jul. 1993
(Contract W-7405-eng-36)
(DE93-018367; LA-UR-93-2544; CONF-930722-17) Avail: CASI HC A02/MF A01

A versatile new camera, the Los Alamos National Laboratory (LANL) model GY6, is described. It operates at a wide variety of frame rates, from RS-170 to 700 frames per second. The camera operates as an NTSC compatible black and white camera when operating at RS-170 rates. When used for variable high-frame rates, a simple substitution is made of the RS-170 sync/clock generator circuit card with a high speed emitter-coupled logic (ECL) circuit card. DOE

N94-18846# Stockholm Univ. (Sweden). Dept. of Physics.
CONVERSION OF ADC PULSE HEIGHTS INTO MIP UNITS: NUMASS TEST DATA, SEPTEMBER 1991
Q.-P. Zhang Apr. 1993 21 p
(USIP-93-03; ETN-93-94851) Avail: CASI HC A03/MF A01

Analog to Digital Converter (ADC) calibration is an important part of the data analysis in particle physics. Data analysis of ADC pulse heights is based on a physical unit which is called MIP (most probable energy loss of Minimum Ionization Particles). The ADC calibration work for the Sep. 1991 NUMASS test data, which were produced at Centre d'Etudes et Recherche Nucleaire (CERN) at the Super Proton Synchrotron (SPS) facility is described. The NUMASS (renamed to NEWMASS) experiment was a proposal to search for neutral strange matter in heavy ion collisions. The Vavilov function is used to fit the energy loss distributions of minimum ionizing particles traversing the time of flight scintillators embedded in the uranium scintillator calorimeter. It is assumed that the energy loss distribution is the same for identical scintillators and the value at the peak of these distributions is used. ESA

N94-18875# RADEX, Inc., Bedford, MA.
ASPECTS OF THE CALIBRATION AND PROCESSING OF THE CRRES FLUXGATE MAGNETOMETER DATA Scientific Report No. 1
W. J. McNeil 21 May 1993 62 p
(Contract F19628-93-C-0023)
(AD-A270127; RXR-930501; PL-TR-93-2124; AD-E201614) Avail: CASI HC A04/MF A01

The report describes algorithms for on-orbit calibration and processing of the Fluxgate Magnetometer data from the Combined Release and Radiation Effects Satellite. The calibration problem is parameterized in a completely general treatment in terms of instrument alignment and magnetometer offsets and gains. Fits to the data from the spinning satellite are used to derive all but two of the parameters needed for despinning. Data taken during precession maneuvers and attitude data is used to derive these remaining two. The report includes a discussion of anomalies in the instrument and includes a description of the data products. DTIC

N94-19000# Pacific Northwest Lab., Richland, WA.
OPERATIONAL PARAMETERS OF AN OPTO-ELECTRONIC NEURAL NETWORK EMPLOYING FIXED PLANAR HOLOGRAPHIC INTERCONNECTS
P. E. Keller and A. F. Gmitro (Arizona Univ., Tucson.) Jul. 1993 5 p
Presented at the World Congress on Neural Networks, Portland, OR, 11-15 Jul. 1993
(Contract DE-AC06-76RL-01830)
(DE93-018795; PNL-SA-21852; CONF-930741-4) Avail: CASI HC A01/MF A01

A prototype neutral network system of multifaceted, planar interconnection holograms and opto-electronic neurons is analyzed. This analysis shows that a hologram fabricated with electron-beam lithography has the capacity to connect 6700 neuron outputs to 6700 neuron inputs, and that, the encoded synaptic weights have a precision of approximately 5 bits. Higher interconnection densities can be achieved by accepting a lower synaptic weight accuracy. For systems employing laser diodes at the outputs of the neurons, processing rates in the range of 45 to 720 trillion connections per second can potentially be achieved. DOE

N94-19004# Lawrence Livermore National Lab., CA.
RADIATION INDUCED DARKENING OF THE OPTICAL ELEMENTS IN THE STARTRACKER CAMERA
R. H. White and G. R. Wirtenson Mar. 1993 29 p
(Contract W-7405-eng-48)
(DE93-018907; UCRL-ID-113713) Avail: CASI HC A03/MF A01

Optical glass flats that closely simulate the elements used in the Startracker lens designs were exposed to doses of ionizing radiation ranging from 0.44 to 1300 krad. Photometer traces determined the transmittance of the samples as a function of both wavelength and dose for wavelengths in the range 300 to 1200 nm. Cerium stabilized glasses used in the radiation stabilized Startracker system showed only a small amount of darkening for doses up to and exceeding 1 Mrad. Glasses used in the unstabilized Startracker design showed significant darkening to visible and ultra-violet spectra for doses as low as 5 krad. Plots of transmittance versus wavelength for various doses are given for each of the Startracker optical elements. Radiation induced absorption parameters that determine the radiation induced absorption coefficient are tabulated and plotted versus wavelength. DOE

N94-19041# Westinghouse Hanford Co., Richland, WA.
INTEGRATED TEST PLAN FOR THE DEMONSTRATION OF A COMMERCIAL FOURIER TRANSFORM INFRARED INSTRUMENT
K. J. Koegler 1993 8 p
(Contract DE-AC06-87RL-10930)
(DE93-018518; WHC-SD-EN-TP-030) Avail: CASI HC A02/MF A01

This integrated test plan describes the use of a commercial Fourier Transform Infrared instrument for measuring carbon tetrachloride concentrations. The Fourier Transform Infrared will measure CCL4 concentrations in a line of sight path average mode in mass per cubic meter as a function of time. Demonstration of this device will be conducted at the 200 West Area Carbon Tetrachloride Expedited Response Action (ERA) site. The goal of this test is to demonstrate the usefulness of a long path Fourier Transform Infrared instrument in determining CCL4 fluxes from the soil in the 200 area adjacent to disposal cribs where high soil fluxes are believed to exist. The instrument will be set up such that it can have a clear line of site path to its reflector and this line of site will be as near to the Z-9 fence as possible and have a path length as long as possible. DOE

N94-19054# SRI International Corp., Menlo Park, CA.
NOVEL MASS SPECTROMETRIC INSTRUMENT FOR GASEOUS AND PARTICULATE CHARACTERIZATION AND MONITORING
M. J. Coggiola Apr. 1993 15 p
(Contract DE-AC21-92MC-29116)
(DE93-019992; DOE/MC-29116/3406) Avail: CASI HC A03/MF A01

SRI International will develop a unique new instrument that will be capable of providing real-time (less than one minute), quantitative, chemical characterization of gaseous and particulate pollutants generated from DOE waste cleanup activities. The instrument will be capable of detecting and identifying volatile organic compounds, polynuclear aromatic hydrocarbons, heavy metals, and transuranic species released during waste cleanup activities. The instrument will be unique in its ability to detect and quantify in real-time these diverse pollutants in both vapor and particulate form. The instrument to be developed under this program will consist of several major components: an isokinetic sampler capable of operating over a wide range of temperatures (up to 500 K) and flow rates; a high pressure to low pressure transition and sampling region that efficiently separates particles from vapor-phase components for separate, parallel analyses; two small mass spectrometers, one optimized for organic analysis using a unique field ionization source and one optimized for particulate characterization using thermal pyrolysis and electron-impact ionization (EI); and a powerful personal computer for control and data acquisition. DOE

N94-19111# Sandia National Labs., Albuquerque, NM.
EXPERIMENTS AND ANALYSIS OF LATERAL PIEZORESISTANCE GAUGES
M. K. W. Wong 1993 5 p Presented at the 14th International Conference of the International Association for the Advancement of High Pressure Science and Technology, Colorado Springs, CO, 27 Jun. - 2 Jul. 1993
(Contract DE-AC04-76DP-00789)
(DE93-017874; SAND-93-0882C; CONF-930676-13) Avail: CASI HC A01/MF A01

The response of lateral piezoresistance gauges to shock wave uniaxial strain loading has been examined in a combined experimental and calculational effort. Plate impact experiments provided lateral gauge data which were analyzed using quasi-static and dynamic inclusion analyses. Experimental data showed that the response of the lateral gauge output depended upon the matrix material and gauge emplacement method. The calculations indicated that these differences were due to complex gauge-matrix interactions. These interactions were influenced by the stress and strain distributions in and around the gauge, plasticity effects, properties of the gauge and matrix materials, and emplacement conditions. DOE

N94-19135# Minnesota Univ., Minneapolis. Dept. of Mecahnical Engineering.
SUBSTRATE TEMPERATURE MEASUREMENT AND CONTROL DURING THERMAL PLASMA CVD
Q. D. Zhuang, H. Guo, Q. Y. Han, J. V. R. Heberlein, and E. Pfender 1993 29 p
(Contract DE-FG02-85ER-13433)
(DE93-040305; DOE/ER-13433/5) Avail: CASI HC A03/MF A01

A technique is proposed for substrate temperature control, with emphasis on temperature uniformity across substrate. The technique includes a substrate holder design employing non-uniform water cooling and a means of substrate attachment featured by controlled thermal contact resistance for a given heat flux distribution from the plasma. The technique was applied to deposit diamond films over a 5 cm diameter area in a DC thermal plasma reactor, and proved adequate. Performance of single-color (0.655 (mu)m) and two-color (2.1 and 2.4 (mu)m) pyrometers were evaluated against DC thermal plasma radiation. It was found that both line and continuum emission of plasma jets caused large errors in temperature measurement of the single-color pyrometer. The two-color pyrometer, however, is shown to be less sensitive to the plasma radiation. The way the substrate temperature was controlled and monitored in this study is in general applicable to other TPCVD processes where intense local heating and a bright plasma background exist. DOE

N94-19243# Sandia National Labs., Albuquerque, NM.
DEVELOPMENT OF A QUARTZ DIGITAL ACCELEROMETER FOR ENVIRONMENTAL SENSING AND NAVIGATION APPLICATIONS
W. J. Kass and P. T. Vianco Mar. 1993 138 p
(Contract DE-AC04-76DP-00789)
(DE93-018503; SAND-92-2844) Avail: CASI HC A07/MF A02

A quartz digital accelerometer has been developed which uses double ended tuning forks as the active sensing elements. The authors have demonstrated the ability of this accelerometer to be capable of acceleration measurements between (+/-)150 G with (+/-)0.5 G accuracy. They have further refined the original design and assembly processes to produce accelerometers with less than 1m G stability in inertial measurement applications. This report covers the development, design, processing, assembly, and testing of these devices. DOE

N94-19314*# Sverdrup Technology, Inc., Brook Park, OH.
HIGH TEMPERATURE STRAIN MEASUREMENT WITH A RESISTANCE STRAIN GAGE Final Report
Jih-Fen Lei, Ed Fichtel (Pratt and Whitney Aircraft Group, West Palm Beach, FL.), and Amos McDaniel (Pratt and Whitney Aircraft Group, West Palm Beach, FL.) Dec. 1993 7 p Presented at the SEM Fall Conference and Exhibit: Structural Testing Technology at High Temperature-2, Ojai, CA, 8-10 Nov. 1993
(Contract NAS3-25266; RTOP 505-62-5B)
(NASA-CR-194441; E-8300; NAS 1.26:194441) Avail: CASI HC A02/MF A01

A PdCr based electrical resistance strain gage was demonstrated in the laboratory to be a viable sensor candidate for static strain measurement at high temperatures. However, difficulties were encountered while transferring the sensor to field applications. This paper is therefore prepared for recognition and resolution of the problems likely to be encountered with PdCr strain gages in field applications. Errors caused by the measurement system, installation technique and lead wire attachment are discussed. The limitations and some considerations related to the temperature compensation technique used for this gage are also addressed. Author (revised)

N94-19414# Ecole Centrale de Lyon (France). Lab. de Technologies Magnetiques.
CONTRIBUTION TO THE TRIBOLOGICAL STUDY OF MAGNETIC-TAPE HEAD CONTACT Ph.D. Thesis [CONTRIBUTION A L'ETUDE TRIBOLOGIQUE DU CONTACT TETE MAGNETIQUE-BANDE]
Nicolas Blanchard 1992 159 p In FRENCH Original contains color illustrations
(ECL-92-57; ETN-93-94601) Avail: CASI HC A08/MF A02

A study which investigated the possibility of protecting magnetic tape heads from wear with a thin layer of hard material is reported. The material chosen was hydrogenated amorphous carbon for its hardness and because it is possible to deposit very thin layers in the cold. In order to understand better the wear, the interface between the magnetic tape and a solid was studied. The constraints of magnetic recording are exposed, and the rubbing conditions in a helicoidal recorder are described using simple models. The interaction between the head and the tape is examined, and the influence on the contact of Van De Waals forces and of the damping is estimated. The origin of wear is then looked into. The interaction between the tape and the head through the intermediate of the pigment is modeled integrating the tape deformations which leads to a definition of a new contact plasticity index which takes account of the appearance of wearing. ESA

N94-19659 Laboratoire d'Automatique et d'Analyse des Systemes, Toulouse (France). Groupe Micro-Structures et Micro-Systemes Integres.
SIMULATION OF THE BEHAVIOR OF MICRO-ELECTRONIC CAPACITIVE PRESSURE SENSORS Ph.D. Thesis - Inst. National des Sciences Appliquees, Toulouse [SIMULATION DU COMPORTEMENT DES CAPTEURS DE PRESSION CAPACITIFS MICROELECTRONIQUES]
Pierre-Nicolas Ratier 1993 144 p In FRENCH Limited Reproducibility: More than 20% of this document may be affected by microfiche quality
(LAAS-93190; ETN-93-95014) Avail: CASI HC A07

The numerical simulation of the response of microelectronic capacitive pressure sensors is studied. Response curves for classical capacitive sensors are provided. Modifications brought about by the superposition of an electrostatic pressure on a constant pressure are examined and sensors of more complex structures are analyzed. The case where the sensor deformable armature has non-uniform thickness is treated. The influence of the variation of thickness upon the sensor response is shown. The analysis of polygonal shaped sensors is also presented and followed by two applications aimed at extending the pressure range. The behavior of sensors when subjected to contact is studied: the resulting curves are obtained with significant improvements. The modeling of capacitive sensors by using the nonlinear plate theory of von Karman is proposed. In fact the use of von Karman theory becomes unavoidable as soon as the plate deflection is of the order of its thickness. Therefore, the models employed involve linear and nonlinear equations and systems of partial differential equations in two dimensional spatial domains. The discretization of these equations is carried out by the general method of finite differences. To solve the resulting equations iterative methods such as the conjugate gradient algorithm and the Newton-Raphson algorithm are used. An interactive software for the discretization of stationary linear and nonlinear partial differential equations was developed. An outline of a methodology for curvilinear finite difference method and its application to the study of flexed plates are provided. ESA

N94-19791# Rome Lab., Griffiss AFB, NY.
THE PERFORMANCE AND SURVIVABILITY OF DICHROMATED POLY (VINYL ALCOHOL) HOLOGRAMS FOR SPACE BASED PHOTONIC APPLICATIONS Final Report, Nov. 1991 - Mar. 1992
Steven P. Hotaling, Gurusamy Manivannan, Rupak Changkakoti, and Roger A. Lessard Jul. 1993 18 p
(AD-A270974; RL-TR-93-131) Avail: CASI HC A03/MF A01

The results of an experiment which subjected high diffraction efficiency holograms (average: 40%, max. = 58%) written into DCPVA (dichromated polyvinyl alcohol) photopolymer thin films to the combination of ionizing radiation, temperature, and atomic oxygen are presented. This simulated to some extent, the synergistic effects of the LEO (Low Earth Orbital) environment. Remarkably, diffraction efficiency was not found to be significantly degraded in these experiments. A regression model for gamma ray radiation induced degradation in DCPVA holograms is presented. DTIC

N94-19797 Physics and Electronics Lab. TNO, The Hague (Netherlands).
FEASIBILITY STUDY FOR A MEASURING SYSTEM VELOCITY PROJECTILE Final Report [VOORONDERZOEK MEETUITRUSTING SNELHEID PROJECTIEL]
J. vanderHaven, N. deJager, and H. C. A. Romijn Jun. 1992 31 p In DUTCH
(Contract A87/KL/055)
(FEL-91-A368; TD-91-3972; ETN-93-94522) Copyright Avail: Issuing Activity (TNO Physics and Electronics Laboratory, P.O. Box 96864, 2509 JG The Hague, Netherlands)

A feasibility study of a possible setup for measuring the external ballistic speed of large caliber projectiles was performed leading to a conceptual design. The measuring system uses semiconductor optoelectrical detectors. These detectors are shown to have a lower signal to noise ratio than photomultipliers used in separate photocell units. The detection correlation method and the measuring system are described. The most important computer programs are explained. The optimization of the signal to noise ratio of the detection system and the application of detection correlation techniques provide a high sensitivity of the velocity measuring system. ESA

36 LASERS AND MASERS

Includes parametric amplifiers.
For related information see also *76 Solid-State Physics.*

N94-17709# Los Alamos National Lab., NM.
MEASURING EMITTANCE USING BEAM POSITION MONITORS
S. Russell and B. Carlsten 1993 8 p Presented at the International Particle Accelerator Conference, Washington, DC, 17-20 May 1993
(Contract W-7405-eng-36)
(DE93-014470; LA-UR-93-1880; CONF-930511-48) Avail: CASI HC A02/MF A01

The Los Alamos Advanced Free Electron Laser uses a high charge (greater than 1 nC), low emittance (normalized rms emittance less than 5(pi) mm mrad) photoinjector driven accelerator. The high brightness achieved is due, in large part, to the rapid acceleration of the electrons to relativistic velocities. As a result, the beam does not have time to thermalize its distribution and its universe profile is, in general, non-Gaussian. This, coupled with the very high brightness, makes it difficult to measure the transverse emittance. Techniques used must be able to withstand the rigors of very intense electron beams and not be reliant on Gaussian assumptions. Beam position monitors are ideal for this. They are not susceptible to beam damage, and it has been shown previously that they can be used to measure the transverse emittance of a beam with a Gaussian profile. However, this Gaussian restriction is not necessary and, in fact, a transverse emittance measurement using beam position monitors is independent of the beam's distribution. DOE

N94-17723# Lawrence Livermore National Lab., CA.
THE COPPER-PUMPED DYE LASER SYSTEM AT LAWRENCE LIVERMORE NATIONAL LABORATORY
R. P. Hackel and B. E. Warner 12 Jan. 1993 13 p Presented at the OE/LASE 1993: International Society for Optical Engineering (SPIE) Conference, Los Angeles, CA, 16-23 Jan. 1993
(Contract W-7405-eng-48)
(DE93-014429; UCRL-JC-111378; CONF-930159-35) Avail: CASI HC A03/MF A01

The Atomic Vapor Isotope Separation (AVLIS) Program has developed a high-average-power, pulsed, tunable, visible laser system. Testing of this hardware is in progress at industrial scales. The copper-dye Laser system is prototypical of a basic module of a uranium-AVLIS plant. The laser demonstration facility (LDF) system consists of copper vapor lasers arranged in oscillator-amplifier chains providing optical pump power to dye-laser master oscillator-power-amplifier chains. This system is capable of thousands of watts (average) tunable between 550 and 650 mm. The copper laser system consists of 12 chains operating continuously. The copper lasers operate at nominally 4.4 kHz, with 50 ns pulse widths and produce 20 W at near the diffraction limit from oscillators and greater than 250 W from each amplifier. Chains consist of an oscillator and three amplifiers and produce greater than 750 W average, with availabilities greater than 95% (i.e. greater than 8300 h/y). The total copper laser system power averages approximately 9000 W and has operated at over 10,000 W for extended intervals. The 12 copper laser beams are multiplexed and delivered to the dye laser system where they pump multiple dye laser chains. Each dye chain consists of a master oscillator and three or four power amplifiers. The master oscillator operates at nominally 100 mW with a 50 MHz single mode bandwidth. Sustained dye chain powers are up to 1400 W with dye conversion efficiency greater than 50%, ASE content less than 5%, and wavefront quality correctable to less than (lambda)/10 RMS, using deformable mirrors. The dye laser system is capable of repetition rates which are multiples of 4.4 kHz, up to 26 kHz. DOE

N94-17724# Los Alamos National Lab., NM.
EXPERIMENTS IN SIDEBAND SUPPRESSION ON THE LOS ALAMOS NATIONAL LABORATORY FREE-ELECTRON LASER
C. J. White (Mission Research Corp., Albuquerque, NM.), M. R. Coyle (Mission Research Corp., Albuquerque, NM.), A. H. Paxton (Mission Research Corp., Albuquerque, NM.), P. G. OShea, S. C. Bender, D. A. Byrd, D. W. Feldman, J. C. Goldstein, T. J. Zaugg, and E. J. Pitcher 1993 17 p Presented at the OE/LASE 1993: International Society for Optical Engineering (SPIE) Conference, Los Angeles, CA, 16-23 Jan. 1993
(Contract W-7405-eng-36)
(DE93-014466; LA-UR-93-1895; CONF-930159-31) Avail: CASI HC A03/MF A01

Two versions of the 'Phase-Step Mirror' (PSM), a novel optical component that prevents the formation of sidebands in a Free-Electron Laser (FEL) were tested on the Los Alamos National Laboratory (LANL) APEX FEL. Sideband suppression and frequency control with high extraction efficiency and single line, transform limited operation were demonstrated. The results of our LANL experiments and computer simulations showed that for very high gain applications, the first-order sideband is completely suppressed, but the laser gain is so strong that on about pass 300 the sideband at the second-order or next free spectral range of the PSM appears. This second-order sideband may be suppressed by designing a PSM with grooves having two alternating depths, one chosen to suppress the first-order sideband, and the other, the second-order sideband. DOE

N94-17759# Lawrence Livermore National Lab., CA.
SAFETY APPROACHES FOR HIGH POWER MODULAR LASER OPERATION
R. T. Handren Mar. 1993 6 p Presented at the International Laser Safety Conference on Non-Beam Hazards, Cincinnati, OH, 1-4 Dec. 1992
(Contract W-7405-eng-48)
(DE93-017213; UCRL-JC-111934; CONF-921233-3) Avail: CASI HC A02/MF A01

Approximately 20 years ago, a program was initiated at the Lawrence Livermore National Laboratory (LLNL) to study the feasibility of using lasers to separate isotopes of uranium and other materials. Of particular interest was the development of a uranium enrichment method for the production of commercial nuclear power reactor fuel to replace current more expensive methods. The Uranium Atomic Vapor Laser Isotope Separation (U-AVLIS) Program progressed to the point where a plant-scale facility to demonstrate commercial feasibility was built and is being tested. The U-AVLIS Program uses copper vapor lasers which pump frequency selective dye lasers to photoionize uranium vapor produced by an electron beam. The selectively ionized isotopes are electrostatically collected. The copper lasers are arranged in oscillator/amplifier chains. The current configuration consists of 12 chains, each with a nominal output of 800 W for a system output in excess of 9 kW. The system requirements are for continuous operation (24 h a day, 7 days a week) and high availability. To meet these requirements, the lasers are designed in a modular form allowing for rapid change-out of the lasers requiring maintenance. Since beginning operation in early 1985, the copper lasers have accumulated over 2 million unit hours at a greater than 90% availability. The dye laser system provides approximately 2.5 kW average power in the visible wavelength range. This large-scale laser system has many safety considerations, including high-power laser beams, high voltage, and large quantities (approximately 3000 gal) of ethanol dye solutions. The Laboratory's safety policy requires that safety controls be designed into any process, equipment, or apparatus in the form of engineering controls. Administrative controls further reduce the risk to an acceptable level. Selected examples of engineering and administrative controls currently being used in the U-AVLIS Program are described. DOE

N94-17771 International Centre for Theoretical Physics, Trieste (Italy).
CO2 LASER WITH MODULATED LOSSES: THEORETICAL MODELS AND EXPERIMENTS IN THE CHAOTIC REGIME
C. L. PandoL, R. Meucci (Istituto Nazionale di Ottica, Florence, Italy.), M. Ciofini (Istituto Nazionale di Ottica, Florence, Italy.), and F. T. Arecchi (Istituto Nazionale di Ottica, Florence, Italy.) Apr. 1993 33 p Limited Reproducibility: More than 20% of this document may be affected by microfiche quality
(DE93-624901; IC-93/62) Avail: CASI HC A03 (US Sales Only)

We compare two different theoretical models for a CO2 laser, namely the two-and four-level model, and show that the second one traces with much better accuracy the experimental behavior in the case of a chaotic dynamics due to time modulation of the cavity losses. Even though the two-level model provides a qualitative explanation of the chaotic dynamics, only the four-level one assures a quantitative fitting. We also show that, at the onset of chaos, the chaotic dynamics is low dimensional and can be described in terms of a noninvertible unidimensional map. DOE

N94-17855# Lawrence Livermore National Lab., CA.
OBSERVATIONS OF MeV ELECTRONS AND SCATTERED LIGHT FROM INTENSE, SUBPICOSECOND LASER-PLASMA INTERACTIONS
C. Darrow, S. Lane, D. Klem, and M. D. Perry 17 Feb. 1993 6 p Presented at the OE/LASE 1993: International Society for Optical Engineering (SPIE) Conference, Los Angeles, CA, 16-23 Jan. 1993
(Contract W-7405-eng-48)
(DE93-017153; UCRL-JC-111151; CONF-930159-47) Avail: CASI HC A02/MF A01

In this paper the authors present work in progress in their experimental investigation of the coupling of intense, subpicosecond laser pulses with plasmas performed on solid targets. (This situation is to be contrasted with the interaction of intense laser fields with solid-density matter. A subject which has generated considerable interest in the last several years.) The characterization of the energy distribution of energetic electrons which escape a solid target irradiated by an intense laser is discussed. The authors have also performed experiments to study the excitation of parametric instabilities near the quarter-critical layer and second-harmonic generation near the critical layer in the plasma. They discuss some preliminary scattered light spectroscopy measurements. DOE

N94-17865# Los Alamos National Lab., NM.
DESIGNS FOR OPTICAL COMPONENTS RELATED TO THE LOS ALAMOS FREE-ELECTRON LASER
Donald A. Byrd and S. C. Bender 1993 12 p Presented at the Annual Meeting of the Society of Photo-Optical Instrumentation Engineers, San Diego, CA, 11-16 Jul. 1993
(Contract W-7405-eng-36)
(DE93-016617; LA-UR-93-2136; CONF-930722-5) Avail: CASI HC A03/MF A01

Several optomechanical tasks for the Los Alamos National Laboratory's (LANL) Free-Electron Laser (FEL) were set by the envisioned project goals as early as 1988. Unfortunately, the FEL project has been set aside due to funding constraints. The tasks reported here required extensive modeling for final adaptability into the FEL environment. The systems to be described are best identified as a Brewster attenuation device, an optical mode relay lens system, a spectral harmonics band-filtering system, a 25-nm micropulse spectrometer system, a 12.5-nm micropulse spectrometer system, a 0.6-nm micropulse spectrometer system, and a reflective mode profile rotator. The Brewster attenuation device was successfully used inside the FEL resonator. The optical mode relay lens system, spectral harmonics band filtering system, and reflective mode profile rotator were completed but never used. The 25-nm micropulse spectrometer was optically and mechanically completed, but the detector electronics were never finished. The 12.5- and 0.6-nm micropulse spectrometers were never assembled, due to hardware that was common to the 25-nm system. These systems will be described in the order listed above. The nominal wavelength of operation for the listed systems is 3.0 micron, except for the harmonics filtering which works on the subharmonics of 3.0 micron. All of these systems were operated remotely due to the harsh radioactive/x-ray optical environment during FEL operation. DOE

N94-17868 Lawrence Livermore National Lab., CA.
X-RAY LASER OSCILLATOR-AMPLIFIER EXPERIMENTS
G. M. Shimkaveg, M. R. Carter, B. K. F. Young, R. S. Walling, A. L. Osterheld, J. E. Trebes, R. A. London, R. P. Ratowsky, R. E. Stewart, and R. S. Craxton (Rochester Univ., NY.) 19 Mar. 1993 8 p Presented at the 1992 International Conference on Lasers, Houston, TX, 7-11 Dec. 1992 Limited Reproducibility: More than 20% of this document may be affected by microfiche quality
(Contract W-7405-eng-48)
(DE93-017165; UCRL-JC-110927; CONF-921256-6) Avail: CASI HC A02

We present results from experiments directed toward increasing the degree of transverse coherence in x-ray laser beams. We have concentrated on the neon-like yttrium (Z=39) collisionally-pumped x-ray laser as the test system for these studies because of its unique combination of brightness, monochromaticity, and high-reflectivity optics availability. Attempts at improving laser performance using proximate feedback optics failed. Modest success has been found to date in "double foil" experiments, involving two x-ray lasers spatially separated by 29 cm and shot sequentially in an 'oscillator-amplifier' configuration. DOE

N94-17869# California Univ., Berkeley. Lawrence Berkeley Lab.
THREE-DIMENSIONAL SIMULATION ANALYSIS OF THE FIRST SECTIONS OF A STANDING-WAVE FREE-ELECTRON LASER TWO-BEAM ACCELERATOR
Changbiao Wang and A. M. Sessler May 1993 3 p Presented at the International Particle Accelerator Conference, Washington, DC, 17-20 May 1993
(Contract DE-AC03-76SF-00098)
(DE93-016977; LBL-33256; CONF-930511-228) Avail: CASI HC A01/MF A01

A 3-D, time-dependent code is used to simulate an array of standing-wave free-electron lasers (SWFEL's) in the two-beam accelerator. It is shown that for an array of SWFEL's with 9 cavities and a 100.6-ns, 0.5-kA, 7.98-MeV electron beam prebunched at 17.1 GHz, an averaged energy output of 14.7J/m can be obtained with a fluctuation of less than 11%. DOE

N94-17883 Fermi National Accelerator Lab., Batavia, IL.
PULSED LASER FOR TESTING SILICON STRIP DETECTORS
M. Vaz, S. Cihangir, and P. Rapidis Jul. 1993 16 p Limited Reproducibility: More than 20% of this document may be affected by microfiche quality
(Contract DE-AC02-76CH-03000)
(DE93-017816; FNAL-TM-1849) Avail: CASI HC A03

This DO Note describes a pulsed LASER setup for testing silicon strip detectors at the Silicon Detector Facility (SiDet) of Fermilab supporting the related projects and, in particular, the DO Silicon Tracker Upgrade. It will be used in the measurements of the efficiency of individual strips and their coupling. The LASER wavelength is 1060 nm, at which the absorption length in silicon is about 2 mm. The LASER setup is capable of producing light pulses with rise time of less than 1 ns, allowing the measurement of charge pulse shaping at individual strips and their capacitive couplings. Due to the high power output of the LASER, safety considerations are included. Also discussed are precautions for the safety of the LASER itself, and how to limit the light to an area smaller than 50 micrometers of diameter. DOE

N94-17954 International Centre for Theoretical Physics, Trieste (Italy).
HOMOCLINIC CRISES IN A MODEL FOR THE CO2 LASER
C. L. PandoL and H. A. Cerdeira Apr. 1993 18 p Limited Reproducibility: More than 20% of this document may be affected by microfiche quality
(DE93-624900; IC-93/61) Avail: CASI HC A03 (US Sales Only)

We show that the four-level model for the CO2 laser with modulated losses predicts a critical exponent close to 1/2 for the characteristic times in two homoclinic crises. In the five-dimensional Poincare map corresponding to this model, a sequential horseshoe formation due to the period three unstable orbit takes place after a region of multistability. DOE

N94-17996# Lawrence Livermore National Lab., CA.
DYNAMICS OF SHORT-PULSE EXCITATION, IONIZATION AND HARMONIC CONVERSION
K. C. Kulander, K. J. Schafer, and J. L. Krause Jan. 1993 16 p Presented at the NATO Workshop, Han-Sur-Lesse, Belgium, 8-14 Jan. 1993
(Contract W-7405-eng-48)
(DE93-017220; UCRL-JC-112686; CONF-9301119-1) Avail: CASI HC A03/MF A01

In this paper we discuss recent calculations for xenon in pulsed laser fields which illustrate the multiphoton processes. In these calculations we have employed a single-active-electron (SAE) model which explicitly follows the separate time evolution of each of the valence electrons in the frozen, mean-field of the remaining, unexcited electrons, the nucleus and the laser field. This model works well for the rare gas atoms, at least partially because the neglected double or higher excitations involve states well above the ionization threshold. In the next section we give a brief description of the SAE model, emphasizing in particular the development of ion-core specific effective potentials. We present ionization, photoelectron and photoemission rates for xenon at 1.06 (mu)m and compare them to recent experimental results in the third section. We show that harmonics and ATI although related are not identical. The electron energy distributions do not show the cutoff observed in harmonics. After describing the quantum mechanical results and comparing them to recent experiments, we will present a simple two-step, quasi-classical model which explains these differences and which gives a more complete understanding of the dynamics of non-perturbative excitation. DOE

N94-17998# Brookhaven National Lab., Upton, NY.
A SUPERCONDUCTING SHORT PERIOD UNDULATOR FOR A HARMONIC GENERATION FEL EXPERIMENT
G. Ingold, L. Solomon, I. Ben-Zvi, S. Krinsky, D. Li, D. Lynch, J. Sheehan, M. Woodle, X. Z. Qiu, and L. H. Yu et al 1993 4 p Presented at the International Particle Accelerator Conference, Washington, DC, 17-20 May 1993
(Contract DE-AC02-76CH-00016)
(DE93-017581; BNL-49144; CONF-930511-250) Avail: CASI HC A01/MF A01

A three stage superconducting (SC) undulator for a high gain harmonic generation (HGE) FEL experiment in the infrared is under construction at the NSLS in collaboration with Grumman Corporation. A novel undulator technology suitable for short period (6-40mm) undulators will be employed for all three stages, the modulator, the dispersive section and the radiator. The undulator triples the frequency of a 10.4(mu)m CO2 seed laser. So far a 27 period (one third of the final radiator) prototype radiator has been designed, built and tested. DOE

N94-18060# Allied-Signal Aerospace Co., Kansas City, MO.
LASER INDUCED DAMAGE TESTING: EQUIPMENT AND TECHNIQUES
G. L. Morelli Jul. 1993 32 p
(Contract DE-AC04-76DP-00613)
(DE93-017143; KCP-613-5080) Avail: CASI HC A03/MF A01

A laser damage test station was designed and built at the AlliedSignal Inc., Kansas City Division (KCD). The purpose of this effort was to establish the capability for testing polished optical fibers for high energy laser transmission to support the Direct Optical Initiation (DOI), optical firing-set program. A single shot, conditioned threshold type laser damage test was implemented. A flashlamp pumped, multimode, Q-switched, Nd:YAG laser was utilized as the test source. The test laser's operational parameters were extensively characterized. The pulse width, beam divergence, and polarization state of the laser were all held constant throughout the tests. A single plano-convex lens was utilized to focus the laser beam energy into the optical fibers. A focusing geometry was utilized which avoided bulk damage and minimized damage at the fiber's core/cladding interface. A special holding fixture was fabricated, which minimized the mechanical stresses on the fiber during testing. Several uncoated, step-index, multimode, optical fibers were damage tested to verify the functionality of the test station. The fibers all had a 400 micron diameter core of pure fused silica, a 440 micron diameter fluorine doped fused silica cladding, and a 15 micron thick polyimide buffer layer. The fibers were tested up to a fluence level greater than 55.7 J/cm(exp 2) or until damage was observed. Cleaning, inspection, and testing procedures were developed and documented. DOE

N94-18061# Deutsche Forschungsanstalt fuer Luft- und Raumfahrt, Stuttgart (Germany). Inst. fuer Technische Physik.
ELECTRICALLY EXCITED CO-LASERS WITH GAS DYNAMIC COOLING Ph.D. Thesis - Stuttgart Univ. [ELEKTRISCH ANGEREGTE CO-LASER MIT GASDYNAMISCHER KUEHLUNG]
Hartwig vonBuelow Jan. 1993 157 p In GERMAN
(DLR-FB-93-08; ETN-93-94877) Avail: CASI HC A08/MF A02

Scaling laws for gas dynamically cooled CO lasers, which are excited by an electric discharge in the subsonic flow, are derived from the results of experimental investigations. These experiments concern the excitation of the laser-gas mixture by a DC or RF discharge, the gas dynamic cooling of the excited gas in a supersonic nozzle, the extraction of laser power in the supersonic gas flow, and the laser beam quality. Based on the experimental results, gas dynamically cooled CO lasers with a closed gas cycle were developed, using either a DC or RF excitation technique. The performance of these laser systems were investigated and proposals were given for lasers in the multi kW range. Using the results of a literature survey and a system analysis, a comparison was for CO lasers with different cooling techniques. ESA

N94-18083# Lawrence Livermore National Lab., CA.
ULTRA-SHALLOW BOX-LIKE PROFILES FABRICATED BY PULSED UV-LASER DOPING PROCESS
E. Ishida, T. W. Sigmon (Stanford Univ., CA.), and K. H. Weiner 23 Mar. 1993 9 p Presented at the 2nd International Workshop on the Measurement and Characterization of Ultra-Shallow Doping Profiles in Semiconductors, Triangle Park, NC, 23-25 Mar. 1993
(Contract W-7405-eng-48)
(DE93-017221; UCRL-JC-113469; CONF-9303196-1) Avail: CASI HC A02/MF A01

Ultra-shallow, box-like impurity profiles are produced using gas immersion laser doping (GILD) and then analyzed by spreading resistance profilometry (SRP) and secondary ion mass spectrometry (SIMS) to determine the impurity distribution. At high concentrations, the profiles obtained by SRP exhibit the expected box-like shape over the entire range of junction depths: The measured concentration within the junction region is uniform while the dopant gradient at the junction exceeds 0.5 decades/nm. In comparison, the same profiles analyzed by SIMS show a broader transition at the metallurgical junction. Caused by knock-ons and ion mixing during the sputtering process, this inaccuracy is reduced, but not eliminated by lowering the acceleration energy of the primary Cs(+) ion beam. At lower concentrations (less than 10(exp 19)/cm(exp 3)), profiles analyzed by SRP exhibit shallower junctions than expected. Electrical measurements of diodes and Hall structures show that high-quality, ultra-shallow n(sup +)p, np and pn are fabricated with good dose control using GILD. For complete characterization of GILD, accurate measurement of both chemical and electrically-active dopant profiles are required. At present, neither SIMS nor SRP provides an entirely accurate impurity profile. DOE

N94-18093# Lawrence Livermore National Lab., CA.
LASER MATERIALS PROCESSING APPLICATIONS AT LAWRENCE LIVERMORE NATIONAL LABORATORY
R. S. Hargrove, E. P. Dragon, R. P. Hackel, D. D. Kautz, and B. E. Warner 25 Feb. 1993 12 p Presented at the OE/LASE 1993: International SPIE Conference, Los Angeles, CA, 16-23 Jan. 1993
(Contract W-7405-eng-48)
(DE93-017976; UCRL-JC-113221; CONF-930159-52) Avail: CASI HC A03/MF A01

High power and high radiance laser technologies developed at Lawrence Livermore National Laboratory (LLNL) such as copper-vapor lasers, solid-state slab lasers, dye lasers, harmonic wavelength conversion of these lasers, and fiber optic delivery systems show great promise for material processing tasks. Evaluation of models suggests significant potential for tenfold increases in welding, cutting, and drilling performance, as well as capability for applications in emerging technologies such as micromachining, surface treatment, and stereolithography. The goals of this program are to develop low-cost, reliable and maintainable industrial laser systems. Chains of copper lasers currently operate at more than 1.5 kW output and achieve mean time between failures of more than 1,000 hours. The beam quality of copper vapor lasers is approximately three times the diffraction limit. Dye lasers have near diffraction limited beam quality at greater than 1.0 kW. diode laser pumped, Nd:YAG slab lasers are also being developed at LLNL. Current designs achieve powers of greater than 1.0 kW and projected beam quality is in the two to five times diffraction limited range. Results from cutting and drilling studies in titanium and stainless steel alloys show that cuts and holes with extremely fine features can be made with dye and copper-vapor lasers. High radiance beams produce low distortion and small heat-affected zones. The authors have accomplished very high aspect ratio holes in drilling tests (greater than 60:1) and features with micron scale (5-50 (mu)m) sizes. Other, traditionally more difficult, materials such as copper, aluminum and ceramics will soon be studied in detail. DOE

N94-18131# Lawrence Livermore National Lab., CA.
DEVELOPMENT OF SHORT PULSE SOFT X RAY LASERS
L. B. DaSilva, B. J. MacGowan, J. A. Koch, S. Mrowka, D. L. Matthews, D. Eder, and R. London Feb. 1993 7 p Presented at the OE/LASE 1993 International Society for Optical Engineering (SPIE) Conference, Los Angeles, CA, 16-23 Jan. 1993
(Contract W-7405-eng-48)
(DE93-017150; UCRL-JC-113179; CONF-930159-48) Avail: CASI HC A02/MF A01

X-ray lasers with pulse durations shorter than 20 ps allow the possibility of imaging laser produced plasmas with micron resolution. In addition, the high peak brightness of these new sources will allow us to study nonlinear optics in the xuv region. In this paper we will describe our efforts to produce collisionally pumped short pulse x-ray lasers. Initial results, which have produced approximately 45 ps (FWHM) x-ray lasers, using a double pulse irradiation technique, are presented along with a discussion of the prospects for reducing the pulse width. DOE

N94-18134# Lawrence Livermore National Lab., CA.
DESIGN OF A TUNABLE 4-MW FREE ELECTRON MASER FOR HEATING FUSION PLASMAS
M. Caplan, G. Kamin, C. C. Shang, and W. Lindquist Sep. 1993 5 p Presented at the 18th Annual International Conference on Infrared and Millimeter Waves, Colchester, England, 6-10 Sep. 1993
(Contract W-7405-eng-48)
(DE93-017172; UCRL-JC-114531; CONF-9309124-1) Avail: CASI HC A01/MF A01

There is an ongoing program at the FOM institute, The Netherlands, to develop a 1-MW, long-pulse, 200-GHz Free Electron Maser (FEM) using a DC accelerator system with depressed collector. We present an extrapolation of this design to more than 4-MW of output microwave power in order to reduce the cost per kW and increase the power per module in a plasma heating system. DOE

N94-18160 Japan Atomic Energy Research Inst., Tokyo.
FEL EXPERIMENT WITH A FOCUSING WIGGLER
Takayuki Kobayashi (Saitama Univ., Urawa, Japan.), Mayuko Takahashi (Saitama Univ., Urawa, Japan.), Sunao Kawasaki (Saitama Univ., Urawa, Japan.), Keishi Sakamoto, Akihiko Watanabe, S. Musyoki, Hiroshi Ishizuka, Takashi Nagashima, and Makoto Shiho Aug. 1992 74 p In JAPANESE Limited Reproducibility: More than 20% of this document may be affected by poor print
(DE93-788586; JAERI-M-92-109) Avail: Issuing Activity (Department of Energy (DOE))

The FEL experiment in the Raman region was carried out using a focusing planar wiggler on the LAX-1 (Large current Accelerator Experiment). The energy of the electron beam is approximately 1 MeV. A beam transport ratio of more than 75% was attained. In the amplification experiment, the spatial growth ratio of 56 dB/m and the output power of more than 5 MW was obtained. DOE

N94-18161 Japan Atomic Energy Research Inst., Tokyo.
DYNAMIC BEHAVIORS OF FRAGMENTS EJECTED FROM THE SURFACE OF CARBON MATERIALS BY LASER ABLATION
Osamu Yoda (Japan Atomic Energy Research Inst., Takasaki.), Atsumi Miyashita (Japan Atomic Energy Research Inst., Takasaki.), Takasumi Ohyanagi, and Kouichi Murakami Oct. 1992 35 p Limited Reproducibility: More than 20% of this document may be affected by poor print
(DE93-788620; JAERI-M-92-173) Avail: Issuing Activity (Department of Energy (DOE))

A time-resolved X-ray absorption spectroscopy apparatus on the laboratory scale has been set-up by utilizing laser plasmas as an X-ray source. One of the major goals for this apparatus is to observe X-ray absorption fine structures (XAFS) of various materials during materials processing in an energy region between 100 eV and 3 keV. For this purpose, we have provided two sets of optical and detecting systems. The most intense X-rays are generated from Au plasma and the intensity reaches as high as 10(exp 16) photons/pulse in 2(pi) steradian in the energy region below 300 eV. The energy resolution of the spectrometer (Delta)E/E has been determined to be 5(10)(exp -3). The dynamic behavior of fragments ejected from the surface by laser ablation has been observed for a carbon rod and a pellet of C60 powder. Dominant fragments removed from the carbon rod have been found to be clusters, neutral atoms and ions. Maximum velocities of ejected clusters and atoms have been estimated to be less than 1.4 (10)(exp 4) m/s and more than 2(10)(exp 4) m/s, respectively. C60 molecules have been removed from the pellet surface without decomposition by mild laser ablation. X-ray photoelectron measurements suggest that some reorganization has occurred on the surface of the ablated C60 pellet. A periodic structure has been discovered on the laser ablated C60 pellet, and the spacing of that periodic structure is explained by the surface scattering model. DOE

N94-18250# New Mexico Univ., Albuquerque. Center for Advanced Studies.
TUNABLE SYNCHRONOUSLY PUMPED INTRACAVITY TWO-STAGE OPTICAL FREQUENCY UPCONVERSION Final Report, May - Oct. 1992
Gerald T. Moore Jun. 1993 10 p
(Contract F29601-92-C-0022)
(AD-A269105; PL-TN-93-1025) Avail: CASI HC A02/MF A01

Optical parametric oscillation (OPO) with intracavity sum-frequency generation (SFG) of the signal and pump has been studied theoretically and numerically, using the CW plane wave theory as well as a numerical code developed to simulate either synchronously pumped pulse propagation or walk-off effects in one transverse dimension. The configuration where the SFG crystal precedes the OPO crystal in the cavity gives stable high-efficiency conversion over a larger range of pump intensity, as well as lower power loading on the OPO crystal. About 85 percent conversion efficiency from 1.064 microns to 589 nm is predicted at pump intensities up to 9 MW/sq cm for a device using AgGaS2 and KTP crystals. Also, the angular distribution of parametric fluorescence from AgGaS2 has been calculated in good agreement with measurements made at the Phillips Laboratory. DTIC

N94-18258# Emory Univ., Atlanta, GA. Dept. of Chemistry.
NITRIDATION OF GaAs(100) BY LASER-INDUCED DECOMPOSITION OF HN3 Technical Report
Y. Bu and M. C. Lin 1993 10 p
(Contract N00014-89-J-1235)
(AD-A269147; TR-21-ONR) Avail: CASI HC A02/MF A01

GaAs can be readily nitridated at low temperatures by photolysis of adsorbed HN3 at 308 nm. The annealing of the exposed and photolyzed samples at 450 K, GaN, AsN and bridged AsNGa species were detected by HREELS and XPS. Further annealing at 780 K caused the desorption of most AsN species while GaN and AsNGa nitrides remained on the surface. DTIC

N94-18460 Naval Research Lab., Washington, DC.
NONLINEAR THOMSON SCATTERING OF INTENSE LASER PULSE FROM BEAMS AND PLASMAS Memorandum Report
Eric Esarey, Sally K. Ride, and Phillip Sprangle 23 Aug. 1993 55 p Limited Reproducibility: More than 20% of this document may be affected by microfiche quality
(AD-A269556; NRL/MR/6790-93-7365) Avail: CASI HC A04

A Comprehensive theory is developed to describe the nonlinear Thomson scattering of intense laser fields from beams and plasmas. This theory is valid for linearly or circularly polarized incident laser fields of arbitrary intensities and for electrons of arbitrary energies. Explicit expressions for the intensity distributions of the scattered radiation are calculated and numerically evaluated. The space-charge electrostatic potential, which is important in high density plasmas and prevents the axial drift of electrons, is included self-consistently. Various properties of the scattered radiation are examined, including the linewidth, angular distribution, and the behavior of the radiation spectra at ultrahigh intensities. Non-ideal effects, such as electron energy spread and beam emittance, are discussed. A laser synchrotron source (LSS), based on nonlinear Thomson scattering, may provide a practical method for generating tunable, near monochromatic, well collimated, short pulse x-rays in a compact, relatively inexpensive source. Two examples of possible LSS configurations are presented: an electron beam LSS generating hard (30 keV, 0.4 A) x-rays; and a plasma LSS generating soft (0.3 keV, 40 A) x-rays. These LSS configurations are capable of generating ultrashort (approximately 1 ps) x-ray pulses with high peak flux (greater than 10(exp 21) photons/s) and brightness (greater than 10(exp 19) photons/s-sq mm-sq mrad 0.1% BW). DTIC

N94-18492 Optical Society of America, Washington, DC.
ADVANCED SOLID-STATE LASERS/COMPACT BLUE-GREEN LASERS. 1993 TECHNICAL DIGEST SERIES. VOLUME 2: ORGANIZATION OF THE 1993 PHOTONICS SCIENCE TOPICAL MEETINGS Final Report
Jarus W. Quinn 4 Feb. 1993 531 p Meetings held in New Orleans, LA, 1-4 Feb. 1993 Limited Reproducibility: More than 20% of this document may be affected by microfiche quality
(Contract F49620-93-1-0181)
(AD-A269058; AFOSR-93-0645TR-Vol-2) Avail: CASI HC A23

The following symposia were held: Advanced Solid State Lasers; Compact Blue-Green Lasers; Integrated Photonics Research; Nonlinear Guide-Wave Optics; Optical Amplifiers and Their Applications; Optical Design for Photonics, Photonics in Switching; Quantum Optoelectronics; Short wavelength--Physics With Intense Laser Pulses; Soft X-Ray Protection Lithography; Ultrafast Electronics and Optoelectronics; Optical Computing; and Spatial Light Modulators. DTIC

N94-18504# Brookhaven National Lab., Upton, NY.
MAGNETIC FIELD MEASUREMENTS OF A SUPERCONDUCTING UNDULATOR FOR A HARMONIC GENERATION FEL EXPERIMENT AT THE NSLS
L. Solomon, G. Ingold, I. Ben-Zvi, S. Krinsky, L. H. Yu, W. Sampson, and K. Robins 1993 4 p Presented at the International Particle Accelerator Conference, Washington, DC, 17-20 May 1993
(Contract DE-AC02-76CH-00016)
(DE93-017621; BNL-49153; CONF-930511-272) Avail: CASI HC A01/MF A01

An 18 mm period, 0.54 Tesla, 8 mm gap superconducting undulator with both horizontal and vertical focusing has been built and tested. This magnet, which is fabricated in 25 cm length sections, is being tested for use in the radiator section (total magnet length of 1.5 m) of the Harmonic

Generation Free Electron Laser experiment at the National Synchrotron Light Source - Accelerator Test Facility at Brookhaven National Lab., in collaboration with Grumman Corp. The measurement system is outlined, sources and estimates of errors are described, and some magnetic field data are presented and discussed. DOE

N94-18522# Sandia National Labs., Albuquerque, NM.
NEW APPLICATIONS FOR HIGH AVERAGE POWER BEAMS
E. L. Neau, B. N. Turman, and E. L. Patterson 1993 4 p Presented at the 9th IEEE Pulsed Power Conference, Albuquerque, NM, 21-23 Jun. 1993
(Contract DE-AC04-76DP-00789)
(DE93-018845; SAND-93-0183C; CONF-930616-21) Avail: CASI HC A01/MF A01

The technology base formed by the development of high peak power simulators, laser drivers, FEL's, and ICF drivers from the early 60's through the late 80's is being extended to high average power short-pulse machines with the capabilities of supporting new types of manufacturing processes and performing new roles in environmental cleanup applications. This paper discusses a process for identifying and developing possible commercial applications, specifically those requiring very high average power levels of hundreds of kilowatts to perhaps megawatts. The authors discuss specific technology requirements and give examples of application development efforts. The application development work is directed at areas that can possibly benefit from the high specific energies attainable with short pulse machines. DOE

N94-18576 Naval Research Lab., Washington, DC.
DESIGNS FOR A 10.6 MICROMETER ELECTROMAGNETIC WIGGLER FREE-ELECTRON LASER (FEL)
Arne W. Fliflet and Wallace M. Manheimer 30 Aug. 1993 32 p Limited Reproducibility: More than 20% of this document may be affected by microfiche quality
(AD-A269695; NRL/MR/6793--93-7373) Avail: Issuing Activity (Defense Technical Information Center (DTIC))

The possibility of developing gyrotron-powered electromagnetic wiggler free-electron laser (FEL) oscillators is of considerable interest for reducing the electron energy required for operation in the infrared spectrum. This memorandum considers the design of a 10.6 micron electromagnetic wiggler FEL experiment based on the University of California at Santa Barbara (UCSB) 6 MeV electrostatic accelerator. Both waveguide and quasioptical wiggler resonator configurations are considered. A prescription for optimizing the gain of a waveguide electromagnetic wiggler FEL is derived and the nonlinear regime is treated by relating the electromagnetic wiggler FEL equations-of-motion to the Universal normalized FEL equations. Point designs are given showing accelerator, gyrotron, and output parameters for 10.6 micron Proof-of-Principle FEL experiments based on both waveguide gyrotron and quasioptical gyrotron wigglers. Designs are given for both 5 A and 2 A FEL electron beam currents. DTIC

N94-18614# Air Force Inst. of Tech., Wright-Patterson AFB, OH. Foreign Aerospace Science and Technology Center.
SINGLE-TRANSVERSE-MODE, NARROW-BANDWIDTH PULSED TUNABLE DYE LASER WITH HOLLOW CIRCULAR INTRACAVITY DIELECTRIC WAVEGUIDE
Zhengguo Lu and Jianying Zhou 14 Sep. 1993 14 p Transl. into ENGLISH from Guangxue Xuebao, China, v. 2, no. 9, 1991 p 844-847
(AD-A270022; FASTC-ID(RS)T-0198-93) Avail: CASI HC A03/MF A01

This paper presents a tunable, narrow-bandwidth pulsed dye laser with hollow circular intracavity waveguide and grazing-incidence grating. The experimental results show that the laser system can have an output with a single transverse mode, a narrow bandwidth, and that is highly-efficient. The paper analyzes the design mechanism of the system. DTIC

N94-18656# Pittsburgh Univ., PA.
PHASE CONJUGATION AND BEAM COMBINATION USING STIMULATED BRILLOUIN SCATTERING Final Report, 21 Apr. 1989 - 31 Jan. 1992
Joel Falk and Morton Kanefsky Jul. 1993 30 p
(Contract F29601-89-K-0019)
(AD-A269899; AD-E201594; PL-TR-93-1007) Avail: CASI HC A03/MF A01

This report summarizes work performed on the use of stimulated Brillouin scattering for phase conjugation and beam combination. The mutual coherence between two stimulated Brillouin signals produced by two, partially overlapped pumped beams is studied both experimentally and theoretically. In addition, the transient buildup of a phase conjugate Stokes beam is described using a zero-order numerical solution to the governing equations. DTIC

N94-18674# Air Force Inst. of Tech., Wright-Patterson AFB, OH. Foreign Aerospace Science and Technology Center.
THE EFFICIENCY OF CONTINUOUS OUTPUT OF SOME TITANIUM-DOPED GEM-CRYSTAL LASERS HAS EXCEEDED 1 W
8 Sep. 1993 6 p Transl. into ENGLISH from Zhongguo Jigung, China, v. 19, no. 6, 1992 p 447
(AD-A269953; FASTC-ID(RS)T-0041-93) Avail: CASI HC A02/MF A01

By use of the induced furnace up-pumping method (IFUS) developed by the authors, a new technique enables the growth of a titanium-doped gem crystal which can emit pulses in the forward as well as in the backward direction in the preparation of a continuous laser beam transmission. Since December of 1991 after it first appeared in China, the continuous transmission of a titanium crystal laser with hydrogen ion laser-pumping has reached a laser output efficiency of 303 mW and the threshold efficiency of 1.5 W. Recently, the crystalline mass grown has made another step forward to form a continuously lasing apparatus which acquired new progress in the output efficiency and resonance-harmonization capability. DTIC

N94-18724# Oak Ridge National Lab., TN.
IMAGING AND BLACKBODY EMISSION SPECTRA OF HOT PARTICULATES GENERATED DURING LASER ABLATION
D. B. Geohegan 19 Apr. 1993 9 p Presented at the 2nd International Conference on Laser Ablation: Mechanisms and Applications, Knoxville, TN, 19-22 Apr. 1993
(Contract DE-AC05-84OR-21400)
(DE93-015818; CONF-9304144-7) Avail: CASI HC A02/MF A01

Blackbody emission from particulates generated during KrF-laser ablation of Y(1)Ba(2)Cu(3)O(7-x) (YBCO) and BN has been recorded for the first time by sensitive photography and emission spectroscopy in order to study the velocity, temperature and cooling of the ejecta. The techniques of fast, intensified-CCD photography and emission spectroscopy with photon-counting sensitivity are described as diagnostics for particulate generation and temperature measurement for a wide variety of materials used for pulsed laser deposition. Time-of-flight velocities inferred from the two techniques indicate velocities (v approximately (0.45-1.2) x 10(sup 4) cm s(sup -1)) comparable to those measured for the large particles which often accompany the pulsed laser deposition (PLD) process. Gated photon counting is employed to obtain temporally resolved spectra of this weak emission. The spectral shape is characteristic of blackbody emission. The spectra shift to longer wavelengths as the particles cool during flight in vacuum. Estimates of the temperature of the particles are made based on the emissivity of a perfect blackbody and range from 2200 K to 3200 K for both BN and YBCO when irradiated at Phi(sub 248) = 3.5 J cm(sup -2) and 1.5 J cm(sup -2), respectively. The temperature decrease of the particles in vacuum is compared to a radiative cooling model which gives estimates of the initial surface temperature and radii of the particles. DOE

N94-18737 Maryland Univ., College Park. Lab for Plasma Research.
INTERACTION OF INTENSE LASERS AND RELATIVISTIC ELECTRON BEAMS WITH SOLIDS, GASES AND PLASMAS Progress Report, Jan. - 30 Jun. 1993
Edward Ott, C. S. Liu, and V. L. Grantstein Jun. 1993 20 p Limited Reproducibility: More than 20% of this document may be affected by microfiche quality
(Contract N00014-90-K-2010)
(AD-A269655) Avail: CASI HC A03

The focus of the Maryland Program is to establish strong experimental and theoretical support for ongoing programs at NRL. Areas of research which are of mutual interest are pursued by members of the University of Maryland faculty in collaboration with their counterparts at NRL. The proposal encompasses basically three broad areas of research activities. The first area deals with excimer laser technology and the interaction of high power lasers with matter (gases, solids, and plasma). The second area of mutual

interest involves diagnostics of intense relativistic electron beams and study of their propagation and interaction with a background gas. The nonlinear temporal dynamics in neural networks is the third area for collaboration.
DTIC

N94-18747# Department of the Navy, Washington, DC.
TUNABLE YTTERBIUM-DOPED SOLID STATE LASER Patent Application
John M. McMahon, inventor (to Navy), Leon Esterowitz, inventor (to Navy), and Robert C. Stoneman, inventor (to Navy) 30 Jul. 1993 14 p
(AD-D015878; US-Patent-Appl-SN-099638) Avail: CASI HC A03/MF A01

A tunable ytterbium-doped solid-state laser has a laser cavity defined by a pair of mirrors, a laser medium positioned in this cavity, means for pumping the laser medium, and means for tuning the output of this laser medium to a selected wavelength within a wavelength range. The laser medium has a host material doped with enough ytterbium ions to produce a longitudinal mode laser emission when the laser medium is pumped. In a most preferred embodiment, the laser emission is frequency-doubled and tuned to a wavelength corresponding to a Fraunhoffer line in the solar spectrum.
Author (DTIC)

N94-18771# Naval Research Lab., Washington, DC.
A TUNABLE COMPACT HIGH POWER FAR-INFRARED GRATING FREE-ELECTRON LASER Interim Report
B. Hafizi, P. Sprangle, and A. Fisher 13 Sep. 1993 34 p
(AD-A269875; NRL/MR/6790-93-7384) Avail: CASI HC A03/MF A01

The linear and nonlinear operation of a multiwave grating free-electron laser is described. The radiation is generated by the passage of an annular electron beam through a coaxial waveguide with the central conductor being in the form of a corrugated cylinder. The model includes the effects of self-field forces, beam emittance and gyromotion of electrons in a guide magnetic field. The efficiency is determined by numerical simulation and compared with analytical estimates. A compact source that is tunable in the band 35-55 micron with output in the kilowatt range is shown to be feasible.
DTIC

N94-18834*# Massachusetts Univ., Amherst. Dept. of Electrical and Computer Engineering.
DIRECT SOLAR PUMPING OF SEMICONDUCTOR LASERS: A FEASIBILITY STUDY Final Report
Neal G. Anderson 30 Apr. 1992 9 p
(Grant NAG1-1148)
(NASA-CR-193760; NAS 1.26:193760) Avail: CASI HC A02/MF A01

This report describes results of NASA Grant NAG-1-1148, entitled Direct Solar Pumping of Semiconductor Lasers: A Feasibility Study. The goals of this study were to provide a preliminary assessment of the feasibility of pumping semiconductor lasers in space with directly focused sunlight and to identify semiconductor laser structures expected to operate at the lowest possible focusing intensities. It should be emphasized that the structures under consideration would provide direct optical-to-optical conversion of sunlight into laser light in a single crystal, in contrast to a configuration consisting of a solar cell or storage battery electrically pumping a current injection laser. With external modulation, such lasers could perhaps be efficient sources for intersatellite communications. We proposed specifically to develop a theoretical model of semiconductor quantum-well lasers photopumped by a broadband source, test it against existing experimental data where possible, and apply it to estimating solar pumping requirements and identifying optimum structures for operation at low pump intensities. These tasks have been accomplished, as described in this report of our completed project. The report is organized as follows: Some general considerations relevant to the solar-pumped semiconductor laser problem are discussed in Section 2, and the types of structures chosen for specific investigation are described. The details of the laser model we developed for this work are then outlined in Section 3. In Section 4, results of our study are presented, including designs for optimum lattice-matched and strained-layer solar-pumped quantum-well lasers and threshold pumping estimates for these structures. It was hoped at the outset of this work that structures could be identified which could be expected to operate continuously at solar photoexcitation intensities of several thousand suns, and this indeed turned out to be the case as described in this section. Our project is summarized in Section 5, and information on publications resulting from this work is provided in Section 6.
Derived from text

N94-18880 Texas Univ. at Dallas, Richardson. Center for Quantum Electronics.
PROOF OF THE FEASIBILITY OF COHERENT AND INCOHERENT SCHEMES FOR PUMPING A GAMMA RAY LASER Final Report, 24 Dec. 1989 - 31 May 1993
C. B. Collins 31 Aug. 1993 218 p Limited Reproducibility: More than 20% of this document may be affected by microfiche quality
(Contract N00014-90-K-2001)
(AD-A269173; GRL/9301) Avail: CASI HC A10

The most productive approaches to the problem of the gamma-ray laser have focused upon upconversion techniques in which metastable nuclei are pumped with long wavelength radiation. At the nuclear level, the storage of energy can approach tera-Joules (10(exp 12)J) per liter for thousands of years. However, any plan to use such a resource for a gamma-ray laser poses problems of a broad interdisciplinary nature requiring the fusion of concepts taken from relatively unrelated fields of physics. Our research group has described several means through which this energy might be coupled to radiation fields with cross sections for stimulated emission that could reach 10(exp -17)sq cm. Such a stimulated release could lead to output powers as great as 3 x 1021 Watts/liter. Since 1978, we have pursued an approach for the upconversion of longer wavelength radiation incident upon isomeric nuclear populations that can avoid many of the difficulties encountered with traditional concepts of single photon pumping. Experiments have confirmed the general theory and have indicated that a gamma-ray laser is feasible if the right combination of energy levels and branching ratios exists in some real material. Of the 1,886 distinguishable nuclear materials, the present state-of-the-art has been adequate to identify 29 first-class candidates, but further evaluation cannot proceed without remeasurements of nuclear properties with higher precision.
DTIC

N94-18889# Lawrence Livermore National Lab., CA.
MULTI-TERRAWATT, 100 FSEC LASER SYSTEM USING FLASHLAMP-PUMPED, DYE-CONVERTED Ti:SAPPHIRE AS AN AMPLIFIER
W. E. White, D. H. Reitize, D. F. Price, R. L. Shepherd, J. D. Bonlie, J. R. Hunter, F. G. Patterson, and D. L. Perressini (Union Carbide Corp., Washougal, WA.) 14 Apr. 1993 5 p Presented at the Quantum Electronics and Laser Science Conference, Baltimore, MD, 2-7 May 1993
(Contract W-7405-eng-48)
(DE93-017190; UCRL-JC-113579; CONF-930586-6) Avail: CASI HC A01/MF A01

We report on amplification of 100 fsec laser pulses to 250 mJ using flashlamp-pumped, dye converted Ti:Sapphire. The resulting 5 Hz beam is focused to irradiances in excess of 5 x 10(exp 18) W/cm(exp 2).
DOE

N94-18900# State Univ. of New York, Stony Brook.
ADVANCES IN LASER COOLING Final Technical Report, 1 Aug. 1991 - 31 Jul. 1993
Harold J. Metcalf 15 Sep. 1993 113 p
(Grant AF-AFOSR-0305-91)
(AD-A270152; AFOSR-93-0745TR) Avail: CASI HC A06/MF A02

Topics include beam profile flattening, quantum calculations, simplest laser cooling system, bichromatic cooling, quantum effects in helium cooling, and isotropic light cooling.
DTIC

N94-18912 University of Central Florida, Orlando.
FINAL CONSTRUCTION AND OPERATION OF A CONTINUOUS FAR-INFRARED FREE-ELECTRON LASER FOR SCIENTIFIC APPLICATIONS Annual Progress Report, 1 Aug. 1992 - 31 Jul. 1993
Luis R. Elias 31 Jul. 1993 2 p Limited Reproducibility: More than 20% of this document may be affected by microfiche quality
(Contract N00014-92-J-4088)
(AD-A269248) Avail: CASI HC A01

This report finalizes the construction of a compact, high-power, continuous wave, free-electron laser (CW FEL) for the far-infrared (FIR) region and utilizes the FEL for scientific applications. The laser will initially put out 600 watts of average power with an expected 10(exp -8) fractional linewidth.
DTIC

N94-18974# Southeastern Univ. Research Association, Newport News, VA.

LASER POWERED BEAM CONDITIONER FOR FREE-ELECTRON LASERS AND SYNCHROTRONS

H. Liu, G. R. Neil, C. Sinclair, and B. Yunn Jun. 1993 5 p Presented at the International Particle Accelerator Conference, Washington, DC, 17-20 May 1993
(Contract DE-AC05-84ER-40150)
(DE93-017821; DOE/ER-40150/227; CEBAF-PR-93-030; CONF-930511-316) Avail: CASI HC A01/MF A01

A new method of using an additional laser for electron beam conditioning in free-electron lasers (FEL's) and synchrotrons is proposed. Theoretical analysis and calculations are presented, showing that the axial energy spread of electrons due to their betatron motion in undulators can be dramatically reduced by interacting with a quasi-TEM(sub 10) Gaussian mode optical beam. It is required that the electrons be prebunched over half an optical cycle in advance. DOE

N94-19030# California Univ., Berkeley. Lawrence Berkeley Lab.

COHERENCE AND LINEWIDTH STUDIES OF A 4-nm HIGH POWER FEL

W. M. Fawley, A. M. Sessler, and E. T. Scharlemann (Lawrence Livermore National Lab., CA.) May 1993 5 p Presented at the International Particle Accelerator Conference, Washington, DC, 17-20 May 1993
(Contract DE-AC03-76SF-00098)
(DE93-018533; LBL-33285; HIFAN-570; CONF-930511-323) Avail: CASI HC A01/MF A01

Recently the SSRL/SLAC and its collaborators elsewhere have considered the merits of a 2 to 4-nm high power FEL utilizing the SLAC linac electron beam. The FEL would be a single pass amplifier excited by spontaneous emission rather than an oscillator, in order to eliminate the need for a soft X-ray resonant cavity. We have used GINGER, a multifrequency 2D FEL simulation code, to study the expected linewidth and coherence properties of the FEL, in both the exponential and saturated gain regimes. We present results concerning the effective shot noise input power and mode shape, the expected subpercent output line widths, photon flux, and the field temporal and spatial correlation functions. We also discuss the effects of tapering the wiggler upon the output power and line width. DOE

N94-19251# Lawrence Livermore National Lab., CA.

LASER GUIDE STAR MEASUREMENTS AT LAWRENCE LIVERMORE NATIONAL LABORATORY

H. Friedman, K. Avicola, H. Bissinger, J. Brase, J. Duff, D. Gavel, J. Horton, C. Max, S. Olivier, and D. Rapp et al Feb. 1993 16 p Presented at the Society for Photo-Optical Instrumentation Engineers (SPIE) International Conference, Albuquerque, NM, 31 Jan. - 4 Feb. 1993
(Contract W-7405-eng-48)
(DE93-018081; UCRL-JC-113177; CONF-930171-4) Avail: CASI HC A03/MF A01

Recent studies from the Laser Guide Star Project at Lawrence Livermore National Laboratory are presented. Photometry of the return signal has shown that the photon return is approximately 10 photons/sq cm/ms at the pupil of the receiving telescope in agreement with a detailed model of the sodium interaction. Wavefronts of the laser guide star have also been measured with a Shack-Hartmann technique and power spectra have been shown to agree with those of nearby natural stars. Plans for closed loop demonstrations using the laser guide star at LLNL and nearby Lick Observatory are discussed. DOE

N94-19294# Lawrence Livermore National Lab., CA.

CUTTING AND DRILLING STUDIES USING HIGH POWER VISIBLE LASERS

D. D. Kautz, E. P. Dragon, M. E. Werve, R. S. Hargrove, and B. E. Warner 27 May 1993 10 p Presented at the 1992 International Conference on Lasers, Houston, TX, 7-11 Dec. 1992
(Contract W-7405-eng-48)
(DE93-019149; UCRL-JC-111666; CONF-921256-7) Avail: CASI HC A02/MF A01

High power and radiance laser technologies developed at Lawrence Livermore National Laboratory such as copper-vapor and dye lasers show great promise for material processing tasks. Evaluation of models suggests significant increases in welding, cutting, and drilling capabilities, as well as applications in emerging technologies such as micromachining, surface treatment, and stereolithography. Copper lasers currently operate at 1.8 kW output at approximately three times the diffraction limit and achieve mean time between failures of more than 1,000 hours. Dye lasers have near diffraction limited beam quality at greater than 1.0 kW. Results from cutting and drilling studies in titanium and stainless steel alloys show that cuts and holes with extremely fine features can be made with dye and copper-vapor lasers. High radiance beams produce low distortion and small heat-affected zones. The authors have accomplished very high aspect ratios (less than 60:1) and features with micron scale (5-50 microns) sizes. The paper gives a description of the equipment, discusses cutting theory, and gives experimental results of cutting and drilling studies on Ti-6Al-4V and 304 stainless steel. DOE

N94-19307# Texas Univ., Austin. Center for Electromechanics.

PULSED POWER SUPPLY FOR NOVA UPGRADE

J. L. Bacon, J. P. Kajs, A. Walls, W. F. Weldon, and R. C. Zowarka 1992 106 p Prepared for LLNL, CA
(Contract W-7405-eng-48)
(DE93-019626; UCRL-CR-112610) Avail: CASI HC A06/MF A02

This report describes work carried out at the Center for Electromechanics at The University of Texas at Austin (CEM-UT). A baseline design of the Nova Upgrade has been completed by Lawrence Livermore National Laboratory. The Nova Upgrade is an 18 beamline Nd:glass laser design utilizing fully relayed 4 x 4 30 cm aperture segmented optical components. The laser thus consists of 288 independent beamlets nominally producing 1.5 to 2.0 MJ of 0.35 micron light in a 3 to 5 ns pulse. The laser design is extremely flexible and will allow a wide range of pulses to irradiate ICF targets. This facility will demonstrate ignition/gain and the scientific feasibility of ICF for energy and defense applications. The pulsed power requirements for the Nova Upgrade are given. CEM-UT was contracted to study and develop a design for a homopolar generator/inductor (HPG/inductor) opening switch system which would satisfy the pulsed power supply requirements of the Nova Upgrade. The Nd:glass laser amplifiers used in the Nova Upgrade will be powered by light from xenon flashlamps. The pulsed power supply for the Nova Upgrade powers the xenon flashlamps. This design and study was for a power supply to drive flashlamps. DOE

N94-19369*# Columbia Univ., New York, NY. Dept. of Physics.

TETRAVALENT CHROMIUM (Cr(4+)) AS LASER-ACTIVE ION FOR TUNABLE SOLID-STATE LASERS Semiannual Progress Report, 31 Oct. 1991 - 31 Mar. 1992

A. Seas, V. Petricevic, and Robert R. Alfano 1992 10 p
(Grant NAG1-1346)
(NASA-CR-194529; NAS 1.26:194529) Avail: CASI HC A02/MF A01

During 10/31/91 - 3/31/92, the following summarizes are major accomplishments: (1) numerical modeling of the four mirror astigmatically compensated, Z-fold cavity was performed; and (2) the simulation revealed several design parameters to be used for the construction of a femtosecond forsterite laser. Derived from text

N94-19394*# City Coll. of the City Univ. of New York, NY. Dept. of Physics.

TETRAVALENT CHROMIUM (Cr(4+)) AS LASER-ACTIVE ION FOR TUNABLE SOLID-STATE LASERS Semiannual Progress Report, 31 Oct. 1992 - 31 Mar. 1993

A. Seas, V. Petricevic, and Robert R. Alfano 1993 7 p
(Grant NAG1-1346)
(NASA-CR-194528; NAS 1.26:194528) Avail: CASI HC A02/MF A01

During 10/31/92 - 3/31/93, the following summarizes our major accomplishments: (1) the self-mode-locked operation of the Cr:forsterite laser was achieved; (2) synchronous pumping was used to mode lock the forsterite laser resulting in picosecond pulses, which in turn provided the starting mechanism for self-mode-locking; and (3) the pulses generated had a FWHW of 105 fs and were tunable between 1230 - 1270 nm. Derived from text

N94-19426 Physics and Electronics Lab. TNO, The Hague (Netherlands).

FIRST AND SECOND ORDER STOKES GENERATION BY SRS IN METHANE: INFLUENCE OF REP-RATE, BEAM QUALITY AND ASTIGMATISM Final Report

F. J. M. vanPutten, J. C. vandenHeuvel, and R. J. L. Lerou Sep. 1992 39 p
(FEL-92-A125; TD-92-1754; ETN-93-94943) Copyright Avail: Issuing Activity (TNO Physics and Electronics Laboratory, P.O. Box 96864, 2509 JG The Hague, Netherlands)

Experiments to obtain a high efficiency for conversion of 1064 nm to eye safe 1543 nm radiation by Stimulated Raman Scattering (SRS) in methane were performed. A first order Stokes photon conversion efficiency of about 75% is obtained for an input energy of 280 mJ, using combinations of cylindrical lenses for focusing. The highest obtainable efficiency appears to be limited by generation of second order Stokes radiation, at a wavelength of 2805 nm. The energy of the second order Stokes component could be increased to 17.9 mJ. Without circulation of the gas in the Raman cell, thermal blooming effects decreased the efficiency and caused deflection of the beam at pulse repetition rates above 3 Hz. With a gas circulating device, a high efficiency up to 10 Hz was maintained. Threshold and beam profile measurements are included. Beam profile measurements showed that the laser beam can be regarded as 'near Gaussian and diffraction limited' only when the smallest available 1.5 mm diaphragm is placed in the laser cavity. With larger laser diaphragms the parameter describing the quality of the laser beam must be taken into account. The influence of the beam quality is included in the numerical model and was confirmed by the experimental results. ESA

N94-19554# Lawrence Livermore National Lab., CA.
LEGACY OF THE X RAY LASER PROGRAM
J. Nilsen Aug. 1993 12 p
(Contract W-7405-eng-48)
(DE93-019550; UCRL-LR-114552) Avail: CASI HC A03/MF A01

The X-Ray Laser Program has evolved from a design effort focusing on developing a Strategic Defense Initiative weapon that protects against Soviet ICBM's to a scientific project that is producing new technologies for industrial and medical research. While the great technical successes and failures of the x-ray laser itself cannot be discussed, this article presents the many significant achievements made as part of the x-ray laser effort that are now being used for other applications at LLNL. DOE

N94-19563# Sandia National Labs., Albuquerque, NM.
SPECTRALLY AND TEMPORALLY RESOLVED LASER EMISSION FROM VERTICAL CAVITY SURFACE EMITTING LASERS
M. Sinclair, P. L. Gourley, T. M. Brennan, and B. E. Hammons 1992 8 p Presented at the Quantum Electronics and Laser Science Conference, Baltimore, MD, 2-7 May 1993
(Contract DE-AC04-76DP-00789)
(DE93-019410; SAND-92-2759C; CONF-930586-7) Avail: CASI HC A02/MF A01

We have measured the laser emission spectra of several vertical cavity surface emitting lasers following pulsed laser excitation, with a time resolution of less than 1 ps. Correlations between the observed pulse widths and cavity lifetimes were observed. DOE

N94-19647 Technische Univ., Berlin (Germany). Fachbereich fuer Elektrotechnik.
EXPERIMENTAL EXAMINATIONS OF SEMICONDUCTOR LASER AMPLIFIERS FOR OPTICAL COMMUNICATION TECHNOLOGY Ph.D. Thesis [EXPERIMENTELLE UNTERSUCHUNGEN AN HALBLEITERLASERVERSTAERKERN FUER DIE OPTISCHE NACHRICHTENTECHNIK]
Reinhold Ludwig 1993 217 p In GERMAN Limited Reproducibility: More than 20% of this document may be affected by microfiche quality
(ETN-93-95050) Avail: CASI HC A10

Properties of SLA (Semiconductor Laser Amplifier), which are particularly interesting for application to linear repeaters in coherent multichannel systems, are studied and design rules for future optimized amplifier structure are deduced. Laser diode antireflection was examined and reflection factor was measured. Low signal properties were discussed considering injection current, wavelengths, temperature and polarization. The coupling between amplifiers and glass fibers was examined. The utilization of cascade amplifiers as linear repeaters in multichannel heterodyne systems and television distribution systems was investigatied. The following results are obtained: measurement and calculation of the paradiaphony between two signals radiated in a SLA; multichannel data transfer through a SLA; polarization independent amplification with SLA configurations; measurement of the frequency dependence of four wave mixing sidelines in a SLA; measurement of the system degradation through echoes in a bidirectional SLA chain; data transmission with frequency conversion and calculation of multichannel transmission systems with cascade SLA, taking into account saturation, signal to noise ratio, bandwidth reduction and echo. ESA

N94-19658# Retina Foundation, Boston, MA. Eye Research Inst.
CENTER-OF-EXCELLENCE: MICROLASER MICROSCOPE
R. H. Webb 1993 13 p
(Contract DE-FG02-91ER-61229)
(DE93-040688; DOE/ER-61229/2) Avail: CASI HC A03/MF A01

This Center-of-Excellence grant has supported the development of an imaging system based on microlaser arrays. In the second year of the grant, we dealt with the slow delivery of new microlaser arrays by developing a new approach to the idea of all-solid-state confocal microscopy. One solution was moderately successful, and the other has produced the first microscope that is electronically switchable from confocal to non-confocal. We think this may be a useful alternative to the final design. This report thus discloses patentable material. We describe first the central Microlaser Microscope project, then we will touch briefly on the other projects of the Center. The publications are primarily those of the smaller projects, though no longer exclusively so. The appendix includes some of the publications. DOE

N94-19729# Massachusetts Inst. of Tech., Cambridge. Research Lab. of Electronics.
COMPACT FREE ELECTRON LASERS FOR MEDICAL APPLICATIONS Annual Report, 30 Sep. 1992 - 29 Sep. 1993
George Bekefi 14 Oct. 1993 11 p
(Contract N00014-90-J-4130)
(AD-A271272) Avail: CASI HC A03/MF A01

The MIT Microwiggler has been deployed at Brookhaven National Laboratory's Accelerator Test Facility (ATF). We have begun experiments to produce visible light from the ATF's 50 MeV electron beam. This report describes the visible light experiments now in progress, as well as the efforts leading to the commencement of these experiments: we doubled the repetition rate of the Microwiggler system while preserving very high field precision and introducing wiggler entrance and exit tapering, and installed the Microwiggler on the ATF beamline. Derived from text

N94-19770 Naval Postgraduate School, Monterey, CA. Dept. of Physics.
A STUDY OF THE AMPLIFICATION OF LASER AND VLF WAVES USING A SIMPLE PENDULUM MODEL Ph.D. Thesis
Keith A. Sturgess Jun. 1993 103 p Limited Reproducibility: More than 20% of this document may be affected by microfiche quality
(AD-A270857) Avail: CASI HC A06

The Lorentz force equation governing the interaction between radiation and charged particles in the presence of a static magnetic field can be reduced to the form of the simple pendulum equation, when applied to the Free Electron Laser (FEL) and to the amplification of whistler waves in the magnetosphere. The first topic in this thesis is the start-up of an FEL with a compact design having a small, spatial undulator period, many periods, and a small undulator field strength. Under these conditions, the number of photons spontaneously emitted into the resonator mode each pass is so small that a classical field cannot be established. Quantum fluctuations affect the wave-particle interaction and therefore diminish weak field gain. An FEL start-up condition, several orders of magnitude more restrictive than determined by quantum recoil alone, is derived from the photon rate equation. The next topic is the evolution of a weak, classical radiation field driven by a long electron pulse. DTIC

N94-19788# SRI International Corp., Menlo Park, CA.
NOVEL NONLINEAR LASER DIAGNOSTIC TECHNIQUES Final Report, 1 Jun. 1990 - 31 Jul. 1993
Gregory W. Faris, Jay B. Jeffries, and David L. Huestis Jul. 1993 162 p
(Contract F49620-90-C-0044)
(AD-A270968; SRI-MP-93-137; AFOSR-93-0755TR) Avail: CASI HC A08/MF A02

Research on laser-based diagnostic techniques in two areas is described: (1) extension of laser-based diagnostics to shorter wavelengths for two-photon detection of atomic ions and other detection techniques requiring high powers in the VUV and (2) investigation of quantitative concentration, temperature, and velocity measurements using two-photon-excited amplified spontaneous emission (ASE) of atomic oxygen and hydrogen. For the first task, a broadly tunable high power VUV source based on two-photon-resonant difference frequency mixing in hydrogen and krypton gas was developed. Up to 65 mJ at 133 nm was generated and wavelengths as short as 122 nm were produced. This radiation was applied to multiphoton spectroscopy at VUV wavelengths below 150 nm, including two-photon-excited fluorescence in neon at 133 nm. Research on Task 2 included demonstration measurements of the bandwidth of ASE signals from both oxygen and hydrogen atoms in low-pressure flames. A model of the ASE signal shows gas temperature determination from ASE bandwidth measurements is possible. Gain on a cw diode probe laser from two-photon-excited oxygen atoms was demonstrated in low-pressure flames; from such direct gain measurements, quantitative atom concentration measurements are feasible. DTIC

N94-19173*# Tennessee Univ., Tullahoma. Center for Space Transportation and Applied Research.
SPACE APPLICATIONS INDUSTRIAL LASER SYSTEM (SAILS)
T. D. McCay, J. B. Bible, and R. E. Mueller *In* NASA. Goddard Space Flight Center, The 1993 Shuttle Small Payloads Symposium Oct. 1993 p 87-95 Prepared in cooperation with Tennessee Univ. Space Inst., Tullahoma (For primary document see N94-19162 04-12)
(Grant NAGw-1195)
Avail: CASI HC A02/MF A03

37 MECHANICAL ENGINEERING

Includes auxiliary systems (nonpower); machine elements and processes; and mechanical equipment.

N94-17705 *Department of the Navy, Washington, DC.*
ELECTRICALLY CONTROLLED LIQUID-CRYSTAL HEAT VALVE Patent
Rand R. Biggers, inventor (to Navy), Jeff W. Rish, III, inventor (to Navy), Girardeau L. Henderson, inventor (to Navy), Chuong N. Pham, inventor (to Navy), and Robert R. Fuller, inventor (to Navy) 29 Jun. 1993 16 p Filed 26 May 1992
(AD-D015872; US-Patent-5,222,548; US-Patent-Appl-SN-888096) Avail: CASI HC A02/MF A01

An improved electrically controlled thermotropic liquid-crystal heat valve to control the flow of heat between two bodies of different temperatures by interposing there between a fluid layer of liquid-crystal material having a nematic temperature range that includes the temperature of both bodies. This type of heat valve has particular application to any free-swimming divers' diving garments, to provide some thermal protection against the cold ambient water. The heat valve uses stable liquid-crystal materials encapsulated in a sealed environment, with the valves' electrodes being shielded and not in direct electrical contact with the liquid-crystal material. This arrangement essentially completely eliminates the electrochemical effects which can otherwise degrade the liquid-crystal materials, so that the liquid crystal may function for a very long time. The valve is electrically controlled between the respective two different modes of its open and closed conditions, the open mode occurring when a low frequency AC field is applied to one of the liquid crystal materials; and the closed mode occurring when a high frequency field is applied to effect reorientation of the molecules of the liquid crystal materials in a direction perpendicular to the applied AC field, precluding establishment of convective flow cells, thereby retarding the transfer of heat. DTIC

N94-17730 Ohio State Univ., Columbus.
INTERDISCIPLINARY RESEARCH ON WEAR OF MATERIALS Final Report, 1 Oct. 1991 - 20 Sep. 1992
D. A. Rigney 28 Jul. 1993 12 p Limited Reproducibility: More than 20% of this document may be affected by microfiche quality
(Contract N00014-89-J-1234)
(AD-A268190) Avail: Issuing Activity (Defense Technical Information Center (DTIC))

This interdisciplinary research was designed to provide complementary information on materials subjected to lubricated and unlubricated sliding contact. With the aid of changes in test environment, surface activation, ion implantation, electron microscopy, diffraction analysis, surface analysis (Auger and laser Raman), and fracture mechanics, basic mechanisms of wear are being related to plastic flow, stress intensity, and surface chemistry. The three main thrusts have been lubricated sliding, unlubricated sliding, and fracture considerations. DTIC

N94-17761# Westinghouse Savannah River Co., Aiken, SC.
MICROSTRUCTURAL ANALYSIS OF SOLID-STATE RESISTANCE WELDS
W. R. Kanne, Jr. 1993 14 p Presented at the DOE Workshop: Sedimentary Systems, Aqueous and Organic Geochemistry, Berkeley, CA, 15-16 Jul. 1993
(Contract DE-AC09-89SR-18035)
(DE93-017295; WSRC-MS-93-008; CONF-9307107-1) Avail: CASI HC A03/MF A01

No melting is present in solid-state welds and the microstructure is therefore very different from the solidification structures found in fusion welds. Improved properties of the weld result from the solid-state metallurgical structure. Solid-state resistance welding therefore has advantages compared to fusion welding processes. Different types of solid-state resistance welds were developed for several unique applications ranging from small tube closure welds to vessel fabrication welds. Solid-state resistance upset welds have a hot worked microstructure, usually with recrystallization near the mating surfaces. Quality of the weld can be related to the metallographic appearance of the bond line at the mating surfaces. Impurities such as oxidation effect both the appearance of the bond line and weld quality. Microstructural examination of flow lines can provide a remarkably clear picture of the deformation pattern, or upsetting, that occurs during welding. Unusual effects such as multiple interfaces can be clearly seen from microstructural examination. Hardness traverses across metallographic sections are used to relate weld area strength to microstructural characteristics. Solid-state weld and heat-affected zone strengths were compared to base metal and to fusion weld strengths using hardness data. DOE

N94-17785# Argonne National Lab., IL.
CORROBORATION OF MAGNETIC FORCES IN US MAGLEV DESIGN
H. Coffey, J. He, and Z. Wang 1993 6 p Presented at the 12th International Conference on Magnetically Levitated Systems and Linear Drives, Argonne, IL, 19-21 May 1993
(Contract W-31-109-eng-38)
(DE93-014918; ANL/ES/CP-79714; CONF-930550-4) Avail: CASI HC A02/MF A01

Four System Concept Definition (SCD) contractors to the National Maglev Initiative (NMI) developed conceptual designs of maglev systems in 1991-1992. The objective of the work reported here was to perform independent calculations of the magnetic forces and fields of these four systems to assess the 'reasonableness' of the results presented to the government. Commercial computer software was used for computing forces in the system employing nonlinear ferromagnetic materials and for some calculations of induced eddy current effects in finite-sized systems. Other cases required the use of models developed at ANL and verified by experiment, or in a few cases, new computer programs that have not been validated by experiment. The magnetic forces calculated by the contractors were found to be credible in every case evaluated. The stray fields were also found to be in reasonable agreement with those calculated by the contractors, but, for lack of space, are not reported here. DOE

N94-17937 Politecnico di Milano (Italy). Dipt. di Elettronica e Informazione.
JOINT STIFFNESS ESTIMATION BASED ON FORCE SENSOR MEASUREMENTS IN INDUSTRIAL MANIPULATORS
Gianni Ferretti, Claudio Maffezzoni, Gianantonio Magnani, and Paolo Rocco 1992 31 p
(Rept-92-053; ETN-93-94505) Avail: Politecnico di Milano, Piazza Leonardo Da Vinci 32, 20133 Milan, Italy

The problem of estimating the stiffness constants of the joints in industrial manipulators is addressed. The model of the robot constrained by a rigid environment is shown to yield a simple relationship between variations of the motor coordinates and the forces arising at the contact with the environment. By exploiting the measurements of the motor positions sensors and of a force sensor located at the end effector, two methods are proposed to simply compute good estimates of the stiffness constants. Experiments were made on the industrial robot SMART and the results are given and discussed. ESA

N94-17940 Politecnico di Milano (Italy). Dipt. di Elettronica e Informazione.
EFFICIENT DYNAMIC MODELING OF MANIPULATORS CONTAINING CLOSED KINEMATIC LOOPS
Gianni Ferretti and Paolo Rocco 1992 34 p
(Rept-92-083; ETN-93-94509) Avail: Politecnico di Milano, Piazza Leonardo da Vinci 32, 20133 Milan, Italy

An approach to efficiently solve the forward dynamics problem for manipulators containing closed chains is proposed. The two main distinctive features of this approach are: the dynamics of the equivalent open loop tree structures (any closed loop can be in general modeled by imposing some additional kinematic constraints to a suitable tree structure) is computed through an efficient Newton Euler formulation; the constraint equations relative to the most commonly adopted closed chains in industrial manipulators are explicitly solved, thus, overcoming the redundancy of Lagrange's multipliers method while avoiding the inefficiency due to a numerical solution of the implicit constraint equations. The constraint equations considered for an explicit solution are those imposed by articulated gear mechanisms and planar closed chains (pantograph type structures). Articulated gear mechanisms are actually used in all industrial robots to transmit motion from actuators to links, while planar closed chains are usefully employed to increase the stiffness of the manipulators and their load capacity, as well to reduce the kinematic coupling of joint axes. The accuracy and the efficiency of the proposed approach are shown through a simulation test. ESA

N94-17963# Centre de Recherches Scientifiques et Techniques de l'Industrie des Fabrications Metalliques, Brussels (Belgium). Section Construction Mecanique.
MEASURING MACHINES FOR DIGITALIZING AND MEASURING COMPLEX SURFACES, MODELS AND MATRICES [MACHINES DE MESURE POUR DIGITALISER ET MESURER DES SURFACES COMPLEXES, MODELES ET MATRICES]
Geert Vandenhoudt Nov. 1992 11 p In FRENCH Sponsored by Regions Wallonne, Brussels, Belgium
(CRIF-MC-97; ETN-93-94442) Copyright Avail: CASI HC A03/MF A01

Complex surfaces digitalization and measuring techniques are overviewed. The measurement of complex surfaces is a very important chapter in technology of three dimensional measurements. The difficulties come from the fact that the surface to be digitalized has a mathematically unmodeled geometry. The choice of the measuring machine, the measurement strategy and the degree of integration with a computer assisted design system determine the possibilities and the user friendly qualities of this measuring technique. ESA

N94-17964# Centre de Recherches Scientifiques et Techniques de l'Industrie des Fabrications Metalliques, Brussels (Belgium). Section Construction Mecanique.
PRESENT EVOLUTION OF TOOLS MANAGEMENT [EVOLUTION ACTUELLE DANS LA GESTION D'OUTILS]
Frank VanderStede Dec. 1992 60 p In FRENCH Sponsored by Regions Wallonne, Brussels, Belgium, and Institut pour l'Encouragement de la Recherche Scientifique dans l'Industrie et l'Agriculture, Brussels, Belgium
(CRIF-MC-102; ETN-93-94443) Copyright Avail: CASI HC A04/MF A01

Several aspects of tool management which need special attention when planning the acquisition of a tool management system are presented. Functionalities of available systems and the successive steps to be considered before application to industrial uses are analyzed. An example is tool management applied to an industrial machining sector. The advantages and disadvantages of different approaches concerning hard and soft materials are summarized. The way followed by the tools from their arrival until they reach the machines and the role of the tool management system at each step are described. The costs due to the implementation of a tool management systems are evaluated. Some available systems are described. ESA

N94-17974# Technical Research Centre of Finland, Espoo. Heating and Ventilation Lab.
AN EMULATOR FOR TESTING HVAC-CONTROL AND ENERGY MANAGEMENT SYSTEMS [LVI-SAEAETOE- JA ENERGIAJAERJESTELMIEN KOESTUS- JA TESTAUSLAITTEISTO (EMULAATTORI). LAITETEKNINEN KUVAUS]
Paeivi Laitila, Satu Kaerki, Kalevi Piira, Katri Katajisto, and Reijo Kohonen Feb. 1992 66 p In FINNISH Sponsored by Kauppa-ja Teollisuusministerio, Helsinki, Finland
(VTT-TIED-1337; ISBN-951-38-4150-2; ETN-93-94473) Copyright Avail: CASI HC A04/MF A01

A technical description of an emulator for control and energy systems is presented. The emulator is made up of both physical components and numerical models programmed for a computer. In the emulator, the building and its internal and external heart and moisture loads are numerical models in all cases, if they are included in the system under study. The emulator can be used to study control equipment and energy management systems as well as other devices such as heat producing equipment. This is facilitated by the emulator's physical test equipment, which comprises an exchangeable heat producing device, two separate cooling water systems and their heat exchangers, and the mains water supply. At the heart of the emulator's ADP hardware are two microcomputers linked by an Ethernet line. The TRNSYS simulation software has been installed in one of the microcomputers, and the GENESIS process control program in the other. GENESIS is not needed for running the emulation. The process interface equipment and simulation software are connected to one another via their RS-232 serial ports. The performance functionality of the emulator was tested by investigating the control of an air conditioning system with a commercial controller (substation). ESA

N94-18159 Japan Atomic Energy Research Inst., Tokyo.
A SURVEY ON TECHNICAL PROBLEMS IN DESIGNING HIGH-SPEED ROTORS WITH DEVELOPING MATERIALS
Tetsuya Abe (Japan Atomic Energy Research Inst., Naka.), Yoshio Murakami (Japan Atomic Energy Research Inst., Naka.), Takeo Hirabayashi, Harushige Ohsawa, Kazuo Hikida, Shigeyuki Shiraishi, and Satoshi Hata Jun. 1992 60 p In JAPANESE Limited Reproducibility: More than 20% of this document may be affected by poor print
(DE93-788519; JAERI-M-92-092) Avail: Issuing Activity (Department of Energy (DOE))

A survey was made on technical problems and limitations in designing high-speed rotors of turbo vacuum pumps using developing materials (fine ceramics, new composite materials, etc.) as well as conventional metals. Based on the surveyed results, the applicability of the developing materials to rotors has been evaluated assuming their use in large-size pumps for fusion reactors. DOE

N94-18266 Wright Lab., Wright-Patterson AFB, OH.
A FINITE STRAIN RING DYNAMICAL MODEL FOR PNEUMATIC TIRES Final Report, May 1992 - May 1993
Ned J. Lindsley Aug. 1993 104 p Limited Reproducibility: More than 20% of this document may be affected by microfiche quality
(AD-A269286; WL-TR-93-3089) Avail: CASI HC A06

In this report, using the most general 'plane sections remain plane' rod theory and the continuum mechanics approach, the exact strain expressions for a shearable, extensible ring are derived. These expressions are nonlinear in terms of both the displacements and the geometry of the ring and are Taylor series approximated after their derivation. A linear viscoelastic stress-strain relationship is assumed. The radial stress is considered negligible. The model includes extension of the neutral axis, transverse shear deformation, and the full complement of inertial forces created by rotation of the ring. A pretensioning force due to pressurizing the tire is included. The tire sidewall (viscoelastic foundation) is considered to act in a completely radial direction. The equations of motion are developed from the free body and inertial force diagrams of a differential element. The membrane forces and bending moment are then substituted to yield three nonlinear equations of motion. The equations of motion are then put into matrix form with the linear and nonlinear portions separated. Chapters 3 and 4 study linear wave propagation, while Chapter 5 provides verifying comparison examples with existing finite element codes, as well as a numerical example for the KC-135 transport aircraft tire. DTIC

N94-18307# Northeast Sustainable Energy Association, Greenfield, MA.
S/EV 1992: SOLAR AND ELECTRIC VEHICLES. VOLUME 1: PROCEEDINGS
1992 247 p Presented at the S/EV 1992: Solar/Electric Vehicle Symposium: Transportation Alternatives, Boston, MA, 9-10 Oct. 1992
(Contracts DE-FG41-92R1-10445; W-31-109-eng-38)
(DE93-015762; CONF-9210362-Vol-1) Avail: CASI HC A11/MF A03

These proceedings include the morning plenary sessions and then sessions on each of the following topics: Electric Vehicle (EV) fundamentals, advanced EV's, photovoltaics, policy, and fleets. Many individual topics are considered to include: EV races, environmental benefits, demonstration programs, lightweight composite materials, advanced components, and electric batteries. DOE

N94-18465# Massachusetts Inst. of Tech., Cambridge. Dept. of Ocean Engineering.
THERMAL INSULATION OF WET SHIELDED METAL ARC WELDS M.S. Thesis
Patrick J. Keenan Jun. 1993 80 p
(Contract N00123-89-G-0580)
(AD-A268697) Avail: CASI HC A05/MF A01

Computational and experimental studies were performed to determine the effect of static thermal insulation on the quality of wet shielded metal arc welds (SMAW). A commercially available heat flow and fluid dynamics spectral-element computer program was used to model a wet SMAW and to determine the potential effect on the weld cooling rate of placing thermal insulation adjacent to the weld line. Experimental manual welds were made on a low carbon equivalent (0.285) mild steel and on a higher carbon equivalent (0.410) high tensile strength steel, using woven fabrics of alumina-boria-silica fibers to insulate the surface of the plate being welded. The effect of the insulation on weld quality was evaluated through the use of post-weld Rockwell Scale hardness measurements on the surface of the weld heat affected zones (HAZ's) and by visual inspection of sectioned welds at 10 X magnification. The computational simulation demonstrated a 150% increase in surface HAZ peak temperature and a significant decrease in weld cooling rate with respect to uninsulated welds, for welds in which ideal insulation had been placed on the base plate surface adjacent to the weld line. Experimental mild steel welds showed a reduction in surface HAZ hardness attributable to insulation at a 77% significance level. A visual comparison of the cross-sections of two welds made in 0.410 carbon equivalent steel-with approximately equivalent heat input-revealed underbead cracking in the uninsulated weld but not in the insulated weld. DTIC

N94-18634# Massachusetts Inst. of Tech., Cambridge. Dept. of Ocean Engineering.
DESIGN CONSIDERATIONS FOR REMOTELY OPERATED WELDING IN SPACE: TASK DEFINITION AND VISUAL WELD MONITORING EXPERIMENT M.S. Thesis
Charles M. Reynerson May 1993 245 p
(Contract N00123-89-G-0580)
(AD-A268752) Avail: CASI HC A11/MF A03

This thesis explores the concept of welding in a space environment with the use of automation. Since the amount of time astronauts can work outside a spacecraft is limited, future construction and repair tasks will likely be assisted by automation. It is also likely that remote space welding will be needed for the construction of large-scale space structures in earth orbit as well as for lunar and Martian ground-based structures. Due to the complex nature of the tasks to be accomplished, the equipment will probably not be fully autonomous but instead supervised by a human operator. The welding fabrication problem in space is examined in a broad sense including some of the considerations for designing a human supervisory remote welding system. The history of space welding processes is examined, as well as current research in the field. A task definition and functional analysis is provided to assist future designers in outlining typical operational sequences for such a remote welding system. Such analysis is important when deciding whether the human operator should perform certain tasks or if the operator should supervise the automated system while it performs the tasks. DTIC

N94-18778 Army Aeromedical Research Lab., Fort Rucker, AL.
LABORATORY TEST AND EVALUATION REPORT OF THE ESSEX MODEL 60C-0037-2 MOLECULAR SIEVE OXYGEN GENERATING SYSTEM Final Report
Brendan E. Squire, James E. Bruckart, Martin Quattlebaum, and Leslie W. Johnston Jun. 1993 58 p Limited Reproducibility: More than 20% of this document may be affected by microfiche quality
(AD-A269967; USAARL-93-23) Avail: CASI HC A04

The Essex Model 60C-0037-2 Molecular Sieve Oxygen Generating System was tested for environmental and electromagnetic interference/compatibility under the U.S. Army Program for Testing and Evaluation of Equipment for Aeromedical Operations. The tests were conducted using current military and industrial standards and procedures for environmental tests and electromagnetic interference/compatibility and human factors. The Essex Model 60C-0037-2 performed properly in the test environments. The oxygen concentration produced by the unit depends on the compressed air pressure, oxygen flow, and vent pressure. A separate oxygen concentration analyzer would be required to determine the oxygen concentration for patient use. The unit produces a significant amount of noise while operating. DTIC

N94-18813# Air Force Inst. of Tech., Wright-Patterson AFB, OH.
COOPERATIVE CONTROL OF MULTIPLE SPACE MANIPULATORS Ph.D. Thesis
Gary E. Yale Sep. 1993 181 p
(AD-A270291; AFIT/CI/CIA-93-20D) Avail: CASI HC A09/MF A02

This research concerns the development of cooperative control of two spacecraft mounted two-link manipulators as they reposition a common payload. Lagrangian formulation is used to determine the system equations of motion. Lyapunov stability theory is used to develop the cooperative control by using a reference trajectory and reference actuator torques. Polynomial curves represent potential reference trajectories. Numerical methods select specific reference trajectories to minimize the disturbance torque transmitted to the spacecraft during the payload repositioning maneuver. The reference actuator torques are selected to minimize weighted norms of the torques. Analytical and experimental models of planar motion are used to study the performance of different cooperative controllers. The fifth order polynomial reference trajectory leads to superior performance in terms of spacecraft attitude accuracy, actuator torque magnitude, payload repositioning accuracy, and maneuver time. The higher order polynomial reference trajectory results in only minor improvement in performance. The experimental results verify the concept of cooperative control. DTIC

N94-18976# Oak Ridge National Lab., TN.
MODELING OF SINGLE-CRYSTAL LASER-WELD MICROSTRUCTURES
J. M. Vitek, T. Zacharia, S. A. David, L. A. Boatner, and M. Rappaz 1993 18 p Presented at the Annual Meeting of the Minerals, Metals and Materials Society, Denver, CO, 21-25 Feb. 1993
(Contract DE-AC05-84OR-21400)
(DE93-017853; CONF-9302103-3) Avail: CASI HC A03/MF A01

A heat and fluid-flow model has been used to calculate the weld-pool size and shape for a high-speed, single-pass, autogenous laser weld as a function of time. Based on the calculated weld-pool shape, and with the use of a geometric model relating the dendritic growth to the weld-pool shape, the dendritic growth pattern was calculated for a single-crystal laser weld with an (001) surface that was welded along the (100) direction. The calculated results were compared to an actual experimental laser weld of an Fe-15Cr-15Ni alloy for the same orientation and weld direction. Agreement was obtained between the calculations and the experimental observations and the experimental dendritic growth pattern was accurately reproduced. DOE

N94-19047# Oak Ridge National Lab., TN.
EFFECTS OF IRRADIATION TEMPERATURE ON CHARPY AND TENSILE PROPERTIES OF HIGH-COPPER, LOW UPPER-SHELF, SUBMERGED-ARC WELDS
R. K. Nanstad and R. G. Berggren 1992 30 p Presented at the 16th Annual Symposium of American Society of Testing and Materials on Effects of Radiation on Materials, Denver, CO, 21-25 Jun. 1992
(Contract DE-AC05-84OR-21400)
(DE93-017858; CONF-920673-23) Avail: CASI HC A03/MF A01

This paper presents analyses of the Charpy impact and tensile test data, including adjustments for irradiation temperature and fluence normalization which make possible comparison of the irradiation sensitivity of the different welds. Analyses revealed dependence of yield and ultimate strength on irradiation temperature -0.8 MPA/C, respectively. Similarly, the Charpy impact energy changes due to irradiation temperature were -0.5 C/C for transition shift and -0.05 J/C for upper-shelf energy decrease. After adjustment to an irradiation temperature of 288 C and normalization to a fluence of 8 x 10(exp 18) neutrons/cm(exp 2) percentage increases in yield strength due to irradiation ranged from about 21 to 35% while those for ultimate strength ranged from about 13 to 20%. The Charpy transition temperature shifts ranged from 59 to 123 C while the postirradiation upper-shelf energies ranged from 58 to 79 J. DOE

N94-19291# Oak Ridge National Lab., TN.

ANALYTICAL AND EXPERIMENTAL EVALUATION OF JOINING SILICON NITRIDE TO METAL AND SILICON CARBIDE TO METAL FOR ADVANCED HEAT ENGINE APPLICATIONS

S. Kang, J. H. Selverian, D. ONeil, H. Kim, and K. Kim May 1993 169 p Prepared in cooperation with GTE Labs, Inc., Waltham, MA
(Contract DE-AC05-84OR-21400)
(DE93-018128; ORNL/Sub-90-SB047/2) Avail: CASI HC A08/MF A02

This report summarizes the results of Phase 2 of 'Analytical and Experimental Evaluation of Joining Silicon Nitride to Metal and Silicon Carbide to Metal for Advanced Heat Engine Applications.' A general methodology was developed to optimize the joint geometry and material systems for 650 C applications. Failure criteria were derived to predict the fracture of the braze and ceramic. Extensive finite element analyses (FEA) were performed to examine various joint geometries and to evaluate the affect of different interlayers on the residual stress state. Also, material systems composed of coating materials, interlayers, and braze alloys were developed for the program based on the chemical stability and strength of the joints during processing and service. The FEA results were compared with experiments using two methods: (1) an idealized strength relationship of the ceramic; and (2) a probabilistic analysis of the ceramic strength (NASA CARES). The results showed that the measured strength of the joint reached 30-80% of the strength predicted by FEA. Also, potential high-temperature braze alloys were developed and evaluated for the high-temperature application of ceramic-metal joints. DOE

N94-19318*# National Aeronautics and Space Administration. Lewis Research Center, Cleveland, OH.

GEAR SOUND LEVELS WITH VARIOUS TOOTH CONTACT RATIOS AND FORMS

Joseph W. Lenski, Jr. (Boeing Helicopter Co., Philadelphia, PA.), Robert H. Spencer (Boeing Helicopter Co., Philadelphia, PA.), Raymond J. Drago (Boeing Helicopter Co., Philadelphia, PA.), Mark J. Valco (Army Research Lab., Cleveland, OH.), and Fred B. Oswald Dec. 1993 17 p Presented at the Rotary Wing Propulsion Specialists Meeting, Williamsburg, VA, 25-28 Oct. 1993; sponsored by the American Helicopter Society and at the American Gear Manufacturer's Association Fall Technical Meeting, Detroit, MI, 14-15 Oct. 1993
(DA Proj. 1L1-62211-A-47-A; RTOP 505-62-10)
(NASA-TM-106432; E-8274; NAS 1.15:106432; USARL-MR-122) Avail: CASI HC A03/MF A01

The real noise reduction benefits which may be obtained through the use of one gear tooth form as compared to another is an important design parameter for any geared system, especially for helicopters in which both weight and reliability are very important factors. The design and testing of nine sets of gears which are as identical as possible except for their basic tooth geometry are described. Noise measurements were made at various combinations of load and speed for each gear set so that direct comparisons could be made. The resultant data was analyzed so that valid conclusions could be drawn and interpreted for design use. Author (revised)

N94-19334# Westinghouse Savannah River Co., Aiken, SC.

OVERLAY WELDING IRRADIATED STAINLESS STEEL

W. R. Kanne, G. T. Chandler, D. Z. Nelson, and E. A. Franco-Ferreira 1993 14 p Presented at the 6th International Conference on Fusion Reactor Materials, Stresa, Italy, 27 Sep. - 1 Oct. 1993
(Contract DE-AC09-89SR-18035)
(DE93-018767; WSRC-MS-93-091; CONF-930928-1) Avail: CASI HC A03/MF A01

An overlay technique developed for welding irradiated stainless steel may be important for repair or modification of fusion reactor materials. Helium, present due to (n,alpha) reactions, is known to cause cracking using conventional welding methods. Stainless steel impregnated with 3 to 220 appm helium by decay of tritium was used to develop a welding process that could be used for repair. The result was a gas metal arc weld overlay technique with low-heat input and low-penetration into the helium-containing material. Extensive metallurgical and mechanical testing of this technique demonstrated substantial reduction of helium embrittlement damage. The overlay technique was applied to irradiated 304 stainless steel containing 10 appm helium. Surface cracking, present in conventional welds made on the same steel at lower helium concentrations, was eliminated. Underbead cracking, although greater than for tritium charged and aged material, was minimal compared to conventional welding methods. DOE

N94-19547# Sandia National Labs., Albuquerque, NM.

SIX DEGREE OF FREEDOM FINE MOTION POSITIONING STAGE BASED ON MAGNETIC LEVITATION

R. W. Arling and S. M. Kohler 1993 12 p Presented at the 2nd International Symposium on Magnetic Suspension Technology, Seattle, WA, 11-13 Aug. 1993
(Contract DE-AC04-76DP-00789)
(DE93-017651; SAND-93-1597C; CONF-930840-1) Avail: CASI HC A03/MF A01

The design of a magnetically suspended six degree of freedom positioning system capable of nanometer positioning is presented. The sample holder is controlled in six degrees of freedom (DOF) over 300 micrometers of travel in the X, Y, and Z directions. A design and control summary and test results indicating stability and power dissipation are included in the paper. The system is vacuum compatible, uses commercially available materials, and requires minimal assembly and setup. DOE

N94-19678# American Society of Mechanical Engineers, New York, NY.

ATOMIC-SCALE FRICTION MEASUREMENTS USING FRICTION FORCE MICROSCOPY. PART 1: GENERAL PRINCIPLES AND NEW MEASUREMENT TECHNIQUES

Ju-Ai Ruan and Bharat Bhushan 15 Jun. 1993 11 p
(AD-A270749) Avail: CASI HC A03/MF A01

Friction force measurements using modified atomic force microscopy, called here Friction Force Microscopy (FFM), are becoming increasingly important in the understanding of fundamental mechanisms of friction, wear, and lubrication, and to study interfacial phenomena in micro- and nanostructures used in magnetic storage systems and Micro-electromechanical Systems (MEMS). FFM's can be used to study engineering surfaces in dry or wet conditions. A review of existing designs of FFM's and methods of friction force measurements is presented. In terms of friction force measurements, there are important issues related to the basic operation and calibration of these instruments which have not been fully studied. A new method of measuring friction force using a commercial FFM and a calibration procedure for conversion of measured data to normal and friction forces are presented. Microscale friction data of selected materials are presented and discussed in light of macrofriction measurements. DTIC

N94-19754 Carnegie-Mellon Univ., Pittsburgh, PA. Dept. of Chemical Engineering.

SURFACE SPECIES IN TRIBOLOGY Final Report, 15 Apr. 1989 - 14 Sep. 1993

Andrew J. Gellman 14 Sep. 1993 18 p Limited Reproducibility: More than 20% of this document may be affected by microfiche quality
(Grant AF-AFOSR-0278-89)
(AD-A270970; AFOSR-93-0752TR) Avail: CASI HC A03

The global aims of this research program have been to understand the surface chemistry of materials having important applications in tribology and to understand the influence of adsorbate structure on the frictional properties of metal-metal interfaces. The materials chosen for study have been those used as boundary layer additives to lubricant mixtures. Boundary layer additives are usually amphiphilic species present in low concentrations in lubricant fluids whose role is to form surfactant-like monolayers on metal surfaces. These monolayers form the last barrier to metal-metal contact when two surfaces are in contact under sufficiently high loads that all the fluid lubricant has been squeezed out of the contact region. For the most part, our work has concentrated on the fluorinated alcohols, acids, and fluorinated alkyl groups on metal surfaces. In addition, we have begun the study of fluorinated ether surface chemistry. DTIC

N94-19767 Ohio State Univ., Columbus. Dept. of Mechanical Engineering.
ATOMIC-SCALE FRICTION MEASUREMENTS USING FRICTION FORCE MICROSCOPY. PART 2: APPLICATION TO MAGNETIC MEDIA
Bharat Bhushan and Ju-Ai Ruan Oct. 1993 8 p Limited Reproducibility: More than 20% of this document may be affected by microfiche quality
(AD-A270759) Avail: CASI HC A02

Atomic Force/Friction Force Microscopes (AFM/FFM) were used to study tribological properties of metal-particle tapes with two roughnesses, Co gamma Fe_2O_3 tapes (unwiped and wiped), and unlubricated and lubricated thin-film magnetic rigid disks (as-polished and standard textured). Nanoindentation studies showed that the hardness of the tapes through the magnetic coating is not uniform. These results are consistent with the fact that the tape surface is a composite and is not homogeneous. Nanoscratch experiments performed on magnetic tapes using silicon nitride tips revealed that deformation and displacement of tape surface material occurred after one pass under light loads. A comparison between friction force profiles and the corresponding surface roughness profiles of all samples tested shows a poor correlation between localized values of friction and surface roughness. DTIC

N94-19784# Ohio State Univ., Columbus. Computer Microtribology and Contamination Lab.
TRIBOLOGICAL STUDIES OF SILICON FOR MAGNETIC RECORDING APPLICATIONS (INVITED)
Bharat Bhushan and Vilas N. Koinkar 5 Oct. 1993 24 p
(AD-A270878) Avail: CASI HC A03/MF A01

Read-write sliders made of silicon using integrated-circuit technology offer advantages of low-cost and high volume production. In the present study our objective is to investigate whether the friction and wear performance of bare silicon is adequate for disk drive application or whether certain coatings/treatments are necessary for low friction and wear. Macrotribological experiments have been performed with various pin/slider materials and magnetic disks in a modified disk drive. Microtribological studies have also been conducted on silicon using a friction force microscope. Based on macrotests, we found that the friction and wear performance of bare silicon is not adequate. With single and polycrystalline silicon, transfer of amorphous carbon from the disk to the pin/slider and oxidation-enhanced fracture of pin/slider material followed by oxidation of the transfer coating is responsible for degradation of the sliding interface and consequent friction increase in ambient air. With dry-oxidized or PECVD-SiO_2-coated silicon, no significant friction increase or interfacial degradation was observed in ambient air. In the absence of an oxidizing environment (in dry nitrogen), the coefficient of friction decreased from 0.2 to 0.05 following amorphous carbon transfer for the materials tested. Nanoscratching/nanowear and nanoindentation studies also indicate that coated silicon is superior to bare silicon. DTIC

N94-18020# Hahn-Schickard-Inst. fuer Mikro- und Informationstechnik, Villingen-Schwenningen (Germany).
PROCESS AND QUALITY ON-LINE CONTROL IN LASER WELDING [PROZESSUEBERWACHUNG UND ON-LINE QUALITAETSKONTROLLE BEIM LASERPUNKTSCHWEISSEN]
Mani Alavi *In* Societe Suisse de Chronometrie, Proceedings of the 4th European Congress on Chronometry 1992 p 71-72 In GERMAN (For primary document see N94-18006 04-35)
Copyright Avail: CASI HC A01/MF A02

N94-18028# Citizen Watch Co. Ltd., Tanashi (Japan).
GEAR TRAIN BEHAVIOR ANALYZER USING LASER BEAM SCANNING FOR WATCH MOVEMENT
Toshio Ohmori, Hiroshi Yanagawa, Makoto Ohmuro, and Hiroo Fujita *In* Societe Suisse de Chronometrie, Proceedings of the 4th European Congress on Chronometry 1992 p 105-10 (For primary document see N94-18006 04-35)
Copyright Avail: CASI HC A01/MF A02

N94-18037# Citizen Watch Co. Ltd., Tanashi (Japan).
AUTOMATIC SOLDERING FOR WATCH CIRCUIT COMPONENTS
Tohru Furuyama, Toshio Furutani, and Mikio Takemoto *In* Societe Suisse de Chronometrie, Proceedings of the 4th European Congress on Chronometry 1992 p 145-14 (For primary document see N94-18006 04-35)
Copyright Avail: CASI HC A01/MF A02

N94-18357*# Idaho Univ., Moscow. NASA Space Engineering Research Center.
FUZZY CONTROL OF MAGNETIC BEARINGS
J. J. Feeley, G. M. Niederauer, and D. J. Ahlstrom *In its* The 1991 3rd NASA Symposium on VLSI Design 1991 14 p (For primary document see N94-18337 04-33)
Avail: CASI HC A03/MF A04

N94-18358*# Houston Univ., TX. Dept. of Electrical Engineering.
DIRECT KINEMATICS SOLUTION ARCHITECTURES FOR INDUSTRIAL ROBOT MANIPULATORS: BIT-SERIAL VERSUS PARALLEL
J. Lee and K. Kim (Superconducting Super Collider Lab., Dallas, TX.) *In* Idaho Univ., The 1991 3rd NASA Symposium on VLSI Design 1991 10 p (For primary document see N94-18337 04-33)
Avail: CASI HC A02/MF A04

38 QUALITY ASSURANCE AND RELIABILITY

Includes product sampling procedures and techniques; and quality control.

N94-18128# Sandia National Labs., Albuquerque, NM.
THE APPLICATION OF NONDESTRUCTIVE TECHNIQUES TO THE TESTING OF A WIND TURBINE BLADE
H. J. Sutherland and W. Musial (Midwest Research Inst., Golden, CO.) 1993 8 p Presented at the Windpower 1993, San Francisco, CA, 12-16 Jul. 1993
(Contract DE-AC04-76DP-00789)
(DE93-016731; SAND-93-0251C; CONF-930726-1) Avail: CASI HC A02/MF A01

NonDestructive Testing (NDT) is commonly used to monitor structures before, during, and after testing. This paper reports on the use of two NDT techniques to monitor the behavior of a typical wind turbine blade during a quasi-static test-to-failure. The test used a three-point spanwise load distribution to load a 7.9-m blade to failure. The two NDT techniques used were acoustic emission and coherent optical. The former monitors the acoustic energy produced by the blade as it is loaded. The latter uses electronic shearography to measure the differences in surface displacements between two load states with an accuracy of a few microns. Typical results are presented to demonstrate the ability of these two techniques to locate and monitor both high damage regions and flaws in the blade structure. Further, this experiment highlights the limitations in the techniques that must be addressed before one or both can be transferred, with a high probability of success, to the inspection and monitoring of turbine blades during the manufacturing process and under normal operating conditions. DOE

N94-18225 Vanderbilt Univ., Nashville, TN. Dept. of Physics and Astronomy.
HIGH RESOLUTION SQUID MAGNETOMETRY FOR NON-DESTRUCTIVE EVALUATION Final Report, 1 Sep. 1987 - 30 Apr. 1993
John P. Wikswo 30 Apr. 1993 30 p Limited Reproducibility: More than 20% of this document may be affected by microfiche quality
(Grant AF-AFOSR-0337-87)
(AD-A268884; AFOSR-93-0659TR) Avail: Issuing Activity (Defense Technical Information Center (DTIC))

Superconducting QUantum Interference Device (SQUID) magnetometers offer promise as multi-mode instruments capable of obtaining high resolution images of extremely low frequency injected currents or eddy currents, and they can be configured to image the magnetic susceptibility of titanium, aluminum, and nonmetallic composites. While high resolution SQUID magnetometers will generally be noisier than conventional SQUID's, the small coils and reduced coil-to-source spacing more than compensate to provide low-noise, high-resolution images. The high spatial resolution which can be obtained with SQUID magnetometers, the unparalleled sensitivity of SQUID's at low frequencies, the ability to measure weak perturbations in strong applied magnetic fields, and the ability to discriminate against external sources of noise should make SQUID magnetometers well suited for NDE of deep flaws in aluminum and titanium aerostructures. To explore SQUID NDE, we have developed research facilities that include the high-resolution MicroSQUID magnetometer, a magnetic shield, a scanning stage, and a computer-based control and data acquisition system. Using this instrumentation, we have imaged magnetic fields produced by sources as varied as intrinsic currents due to corrosion or Johnson noise, remanent magnetization from ferromagnetic contamination, flaw-induced perturbations in either injected current or eddy currents induced by an AC field, Johnson noise currents in a copper ring, persistent currents in high transition-temperature superconductors, distributions of dia- or paramagnetism in an AC or DC magnetic field, and surface flaws decorated with a paramagnetic tracer. DTIC

N94-19189# Westinghouse Savannah River Co., Aiken, SC.
ULTRASONIC TECHNIQUE FOR INSPECTION OF GPHS CAPSULE GIRTH WELD INTEGRITY
Arnost Placr May 1993 18 p
(Contract DE-AC09-89SR-18035)
(DE93-040072; WSRC-TR-93-299) Avail: CASI HC A03/MF A01

An innovative nondestructive examination (NDE) technique for the inspection of integrity of General Purpose Heat Source (GPHS) capsule girth welds was developed employing a Lamb wave as the mode of the sound propagation. Reliability of the Lamb wave technique was tested on GPHS capsules using plutonium pallet simulators. All ten capsules, which were previously rejected, passed ultrasonic (UT) inspection using the Lamb wave technique. DOE

N94-19252# Lawrence Livermore National Lab., CA.
THREE DIMENSIONAL ULTRASONIC IMAGING: AN AGING AIRCRAFT NONDESTRUCTIVE INSPECTION TOOL
G. H. Thomas, S. Benson, and S. Crawford Jul. 1993 10 p Presented at the Annual Meeting of the Society of Photo-Optical Instrumentation Engineers, San Diego, CA, 11-16 Jul. 1993
(Contract W-7405-eng-48)
(DE93-018068; UCRL-JC-112604; CONF-930722-14) Avail: CASI HC A02/MF A01

Ultrasonic nondestructive evaluation is a valuable technique for finding defects in aircraft structures. It can detect unbonds, corrosion damage, and cracks in various aircraft components. Ultrasonic nondestructive evaluation techniques interrogate materials with high frequency acoustic energy. A piezoelectric transducer generates acoustic energy and converts returned acoustic energy into electrical signals which can be processed to identify the reflector. The acoustic energy propagates through the component and is reflected by abrupt changes in modulus and/or density that can be caused by a defect. Ultrasonic nondestructive evaluation typically provides a two dimensional image of internal defects. These images are either a planar view (C-scan) or a cross-sectional view (B-scan) of the component. The planar view is generated by raster scanning an ultrasonic transducer over the area of interest and capturing the peak amplitude of internal reflections. Depth information is generally ignored. The cross-sectional view is generated by scanning the transducer along a line and capturing the amplitude and time of flight for each internal reflection. The amplitude and time of flight information is converted into an image of the cross section of the component. By fusing the C-scan information with the B-scan information a three dimensional image of the internal structure of the component can be produced. The three dimensional image can be manipulated by rotating and slicing to produce the optimal view of the internal structure. Visualizing defects in three dimensions aids the interpretation of the severity of defects and helps confirm the need to repair or replace components. DOE

N94-19336# Pacific Northwest Lab., Richland, WA.
QUALITY, MANAGEMENT, AND THE INTERPLAY OF SELF-ASSESSMENT, PROCESS ASSESSMENTS, AND PERFORMANCE-BASED OBSERVATIONS
D. J. Willett Apr. 1993 11 p Presented at the 4th Conduct of Operations Workshop: The Key to Continued Success, Tampa, FL, 4-6 May 1993
(Contract DE-AC06-76RL-01830)
(DE93-018787; PNL-SA-22371; CONF-930538-4) Avail: CASI HC A03/MF A01

In this document, the author presents his observations on the topic of quality assurance (QA). Traditionally the focus of quality management has been on QA organizations, manuals, procedures, audits, and assessments; quality was measured by the degree of conformance to specifications or standards. Today quality is defined as satisfying user needs and is measured by user satisfaction. The author proposes that quality is the responsibility of line organizations and staff and not the responsibility of the QA group. This work outlines an effective Conduct of Operations program. The author concludes his observations with a discussion of how quality is analogous to leadership. DOE

N94-19766 Naval Academy, Annapolis, MD.
APPLICATIONS OF NEURAL NETWORKS IN FAULT DETECTION OF ROTATING MACHINERY Trident Scholar Project Report No. 205
William O. Nash, Jr. 17 May 1993 52 p Limited Reproducibility: More than 20% of this document may be affected by microfiche quality
(AD-A270755) Avail: CASI HC A04

The purpose of this research was to design a neural network based fault diagnosis system that is capable of detecting and classifying incipient faults in rotating machinery. A neural network is essentially a pattern recognition system which produces a mapping from a set of input data to a set of output data. Neural networks are unique in that this mapping is created autonomously, based on a learning algorithm that the user specifies. In this research, the mapping is from a set of measured parameters (e.g., vibration spectrum) of the rotating machinery to a classification of the system's condition (e.g., worn bearings). Limited success has been achieved in this area over the past decade. Research to date indicates that neural networks have the ability to recognize faults in machinery. This research focused on the following objectives: (1) creating a system that can recognize basic fault conditions based on the fault's vibration signature; (2) improving the ability of the neural network to recognize transient conditions as normal rather than classify them as faults; (3) examining the effect that disturbances have on the neural network's output; and (4) developing a system that will enable detection of faults which are not included in the training set. DTIC

39 STRUCTURAL MECHANICS

Includes structural element design and weight analysis; fatigue; and thermal stress.

For applications see *05 Aircraft Design, Testing and Performance* and *18 Spacecraft Design, Testing and Performance.*

N94-17814# Rensselaer Polytechnic Inst., Troy, NY.
INELASTIC DEFORMATION AND DAMAGE AT HIGH TEMPERATURE
E. Krempl 1993 4 p
(Contract DE-FG02-86ER-13566)
(DE93-018155; DOE/ER-13566/6) Avail: CASI HC A01/MF A01

Combined experimental and theoretical investigations into the inelastic deformation and damage behavior of engineering alloys at elevated temperatures are being pursued. Modeling of effects of recovery of state observed in modified 9Cr-lMo steel has been completed. Finite deformation formulations of viscoplasticity theory based on overstress (VBO) include a modified growth law for the equilibrium stress and a rationale for choosing objective derivatives of stress-like state variables. Numerical simulations are in progress. Seven biaxial low-cycle fatigue tests at 538 C have been completed with the reversing DC potential drop apparatus attached. A new method of data analysis and smoothing was developed which showed a significant increase in voltage drop in the area of crack formation. Correlation with solutions of Laplace's Equation for a semi-elliptical crack showed similar shapes for the voltage drop. DOE

N94-17827*# Computer Software Management and Information Center, Athens, GA.
THE TWENTY-FIRST NASTRAN (R) USERS' COLLOQUIUM
Washington NASA Sep. 1993 186 p Colloquium held in Tampa, FL, 26-30 Apr. 1993 Sponsored by NASA, Washington
(NASA-CP-3203; NAS 1.55:3203) Avail: CASI HC A09/MF A02

This publication contains the proceedings of the Twenty-First NASTRAN Users' Colloquium held in Tampa, FL, April 26 through April 30, 1993. It provides some comprehensive general papers on the application of finite elements in engineering, comparisons with other approaches, unique applications, pre-and postprocessing with other auxiliary programs and new methods of analysis with NASTRAN. For individual titles, see N94-17828 through N94-17839.

N94-17828*# Thoroughbred CAE Software, Louisville, KY.
IMPLEMENTATION OF MIXED FORMULATION ELEMENTS IN PC/NASTRAN
Harry G. Schaeffer *In* COSMIC, The Twenty-First NASTRAN (R) Users' Colloquium Sep. 1993 p 1-7 Prepared in cooperation with Louisville Univ., KY (For primary document see N94-17827 04-39)
Avail: CASI HC A02/MF A02

The purpose of this paper is to describe the implementation and use of a consistent family of two and three dimensional elements in NASTRAN. The elements which are based on a mixed formulation include a replacement of the original NASTRAN shear element and the addition of triangular quadrilateral shell elements and tetrahedral, pentahedral and hexahedral solid elements. These elements support all static loads including temperature gradient and pressure load. The mass matrix is also generated to support all dynamic rigid formats. Author

N94-17829*# McDonnell-Douglas Aerospace, Huntsville, AL.
IMPROVED OMIT SET DISPLACEMENT RECOVERIES IN DYNAMIC ANALYSIS
Tom Allen, Greg Cook, and Bill Walls *In* COSMIC, The Twenty-First NASTRAN (R) Users' Colloquium Sep. 1993 p 8-16 (For primary document see N94-17827 04-39)
Avail: CASI HC A02/MF A02

Two related methods for improving the dependent (OMIT set) displacements after performing a Guyan reduction are presented. The theoretical bases for the methods are derived. The NASTRAN DMAP ALTERs used to implement the methods in a NASTRAN execution are described. Data are presented that verify the methods and the NASTRAN DMAP ALTERs. Author

N94-17830*# Chrysler Technologies Airborne Systems, Inc., Waco, TX.
MODELLING CHAOTIC VIBRATIONS USING NASTRAN
T. J. Sheerer *In* COSMIC, The Twenty-First NASTRAN (R) Users' Colloquium Sep. 1993 p 17-40 (For primary document see N94-17827 04-39)
Avail: CASI HC A03/MF A02

Due to the unavailability and, later, prohibitive cost of the computational power required, many phenomena in nonlinear dynamic systems have in the past been addressed in terms of linear systems. Linear systems respond to periodic inputs with periodic outputs, and may be characterized in the time domain or in the frequency domain as convenient. Reduction to the frequency domain is frequently desireable to reduce the amount of computation required for solution. Nonlinear systems are only soluble in the time domain, and may exhibit a time history which is extremely sensitive to initial conditions. Such systems are termed chaotic. Dynamic buckling, aeroelasticity, fatigue analysis, control systems and electromechanical actuators are among the areas where chaotic vibrations have been observed. Direct transient analysis over a long time period presents a ready means of simulating the behavior of self-excited or externally excited nonlinear systems for a range of experimental parameters, either to characterize chaotic behavior for development of load spectra, or to define its envelope and preclude its occurrence. Author

N94-17831*# Martin Marietta Corp., Orlando, FL. Computer Aided Analysis Group.
FEM/SINDA: COMBINING THE STRENGTHS OF NASTRAN, SINDA, I-DEAS, AND PATRAN FOR THERMAL AND STRUCTURAL ANALYSIS
P. Richard Zarda, Ted Anderson, and Fred Baum *In* COSMIC, The Twenty-First NASTRAN (R) Users' Colloquium Sep. 1993 p 41-59 (For primary document see N94-17827 04-39)
Avail: CASI HC A03/MF A02

This paper describes the interface/integration between FEM/SINDA, a general purpose geometry driven thermal analysis code, and the FEM software: I-DEAS, PATRAN, and NASTRAN. FEM/SINDA brings together the advantages of the finite element method to model arbitrary geometry and anisotropic materials and SINDA's finite difference capability to model thermal properties, loads, and boundary conditions that vary with time or temperature. I-DEAS and PATRAN thermal entities are directly supported since FEM/SINDA uses the nodes of the FEM model as the point at which the temperature is determined. Output from FEM/SINDA (as well as the FEM/SINDA input deck) can be used directly by NASTRAN for structural analysis. Author

N94-17832*# Butler Analyses, Towson, MD.
GENERALIZED SEISMIC ANALYSIS **c46**
Thomas G. Butler *In* COSMIC, The Twenty-First NASTRAN (R) Users' Colloquium Sep. 1993 p 60-72 (For primary document see N94-17827 04-39)
Avail: CASI HC A03/MF A02

There is a constant need to be able to solve for enforced motion of structures. Spacecraft need to be qualified for acceleration inputs. Truck cargoes need to be safeguarded from road mishaps. Office buildings need to withstand earthquake shocks. Marine machinery needs to be able to withstand hull shocks. All of these kinds of enforced motions are being grouped together under the heading of seismic inputs. Attempts have been made to cope with this problem over the years and they usually have ended up with some limiting or compromise conditions. The crudest approach was to limit the problem to acceleration occurring only at a base of a structure, constrained to be rigid. The analyst would assign arbitrarily outsized masses to base points. He would then calculate the magnitude of force to apply to the base mass (or masses) in order to produce the specified acceleration. He would of necessity have to sacrifice the determination of stresses in the vicinity of the base, because of the artificial nature of the input forces. The author followed the lead of John M. Biggs by using relative coordinates for a rigid base in a 1975 paper, and again in a 1981 paper . This method of relative coordinates was extended and made operational as DMAP ALTER packets to rigid formats 9, 10, 11, and 12 under contract N60921-82-C-0128. This method was presented at the twelfth NASTRAN Colloquium. Another analyst in the field developed a method that computed the forces from enforced motion then applied them as a forcing to the remaining unknowns after the knowns were partitioned off. The method was translated into DMAP ALTER's but was never made operational. All of this activity jelled into the current effort. Much thought was invested in working out ways to unshakle the analysis of enforced motions from the limitations that persisted. Derived from text

N94-17833*# General Electric Co., Houston, TX. Government Services.
A NONITERATIVE IMPROVEMENT OF GUYAN REDUCTION
N. Ganesan *In* COSMIC, The Twenty-First NASTRAN (R) Users' Colloquium Sep. 1993 p 73-80 (For primary document see N94-17827 04-39)
Avail: CASI HC A02/MF A02

In determining the natural modes and frequencies of a linear elastic structure, Guyan reduction is often used to reduce the size of the mass and stiffness matrices and the solution of the reduced system is obtained first. The reduced system modes are then expanded to the size of the original system by using a static transformation linking the retained degrees of freedom to the omitted degrees of freedom. In the present paper, the transformation matrix of Guyan reduction is modified to include additional terms from a series accounting for the inertial effects. However, the inertial terms are dependent on the unknown frequencies. A practical approximation is employed to compute the inertial terms without any iteration. This new transformation is implemented in NASTRAN using a DMAP sequence alter. Numerical examples using a cantilever beam illustrate the necessary condition for allowing a large number of additional terms in the proposed series correction of Guyan reduction. A practical example of a large model of the Plasma Motor Generator module to be flown on a Delta launch vehicle is also presented. Author

N94-17834*# Wright Lab., Wright-Patterson AFB, OH.
DESIGN OPTIMIZATION STUDIES USING COSMIC NASTRAN
Stephen M. Pitrof, G. Bharatram, and Vipperla B. Venkayya *In* COSMIC, The Twenty-First NASTRAN (R) Users' Colloquium Sep. 1993 p 81-98 (For primary document see N94-17827 04-39)
Avail: CASI HC A03/MF A02

The purpose of this study is to create, test and document a procedure to integrate mathematical optimization algorithms with COSMIC NASTRAN. This procedure is very important to structural design engineers who wish to capitalize on optimization methods to ensure that their design is optimized for its intended application. The OPTNAST computer program was created to link NASTRAN and design optimization codes into one package. This implementation was tested using two truss structure models and optimizing their designs for minimum weight, subject to multiple loading conditions and displacement and stress constraints. However, the process is generalized so that an engineer could design other types of elements by adding to or modifying some parts of the code. Author

N94-17835*# Rockwell International Corp., Downey, CA.
THE ROLE OF NASTRAN IN THE PRELIMINARY DESIGN CYCLE
H. R. Grooms and V. J. Baipsys *In* COSMIC, The Twenty-First NASTRAN (R) Users' Colloquium Sep. 1993 p 99-110 (For primary document see N94-17827 04-39)
Avail: CASI HC A03/MF A02

This paper explains how NASTRAN can be utilized advantageously in the preliminary design cycle. The initial portion of the preliminary design process lends itself to programs that can produce multiple configurations or variations on a particular design with minimal cost or effort. The latter portion of the process encompasses refining the design and adding more detailed analyses (particularly for other disciplines). A method for quickly generating balanced spacecraft loading conditions for use in preliminary design and analysis also is explained. The following additional sections are included: Background, Symbols, Analytical Process, Aerodynamic Load Distributions, NASTRAN Applications, Conclusion and References. Author

N94-17836*# General Electric Co., Houston, TX. Government Services.
A METHODOLOGY TO MODEL PHYSICAL CONTACT BETWEEN STRUCTURAL COMPONENTS IN NASTRAN
Annappa A. Prabhu *In* COSMIC, The Twenty-First NASTRAN (R) Users' Colloquium Sep. 1993 p 113-125 (For primary document see N94-17827 04-39)
Avail: CASI HC A03/MF A02

Two components of a structure which are located side by side, will come in contact by certain force and will transfer the compressive force along the contact area. If the force acts in the opposite direction, the elements will separate and no force will be transferred. If this contact is modeled, the load path will be correctly represented, and the load redistribution results in more realistic stresses in the structure. This is accomplished by using different sets of rigid elements for different loading conditions, or by creating multipoint constraint sets. Comparison of these two procedures is presented for a 4 panel unit (PU) stowage drawer installed in an experiment rack in the Spacelab Life Sciences (SLS-2) payload. Author

N94-17837*# Wright Lab., Wright-Patterson AFB, OH.
BENCHMARKING THE QUAD4/TRIA3 ELEMENT
Stephen M. Pitrof and Vipperla B. Venkayya *In* COSMIC, The Twenty-First NASTRAN (R) Users' Colloquium Sep. 1993 p 126-141 (For primary document see N94-17827 04-39)
Avail: CASI HC A03/MF A02

The QUAD4 and TRIA3 elements are the primary plate/shell elements in NASTRAN. These elements enable the user to analyze thin plate/shell structures for membrane, bending and shear phenomena. They are also very new elements in the NASTRAN library. These elements are extremely versatile and constitute a substantially enhanced analysis capability in NASTRAN. However, with the versatility comes the burden of understanding a myriad of modeling implications and their effect on accuracy and analysis quality. The validity of many aspects of these elements were established through a series of benchmark problem results and comparison with those available in the literature and obtained from other programs like MSC/NASTRAN and CSAR/NASTRAN. Never-the-less such a comparison is never complete because of the new and creative use of these elements in complex modeling situations. One of the important features of QUAD4 and TRIA3 elements is the offset capability which allows the midsurface of the plate to be noncoincident with the surface of the grid points. None of the previous elements, with the exception of bar (beam), has this capability. The offset capability played a crucial role in the design of QUAD4 and TRIA3 elements. It allowed modeling layered composites, laminated plates and sandwich plates with the metal and composite face sheets. Even though the basic implementation of the offset capability is found to be sound in the previous applications, there is some uncertainty in relatively simple applications. The main purpose of this paper is to test the integrity of the offset capability and provide guidelines for its effective use. For the purpose of simplicity, references in this paper to the QUAD4 element will also include the TRIA3 element. Derived from text

N94-17838*# Wright Lab., Wright-Patterson AFB, OH.
EIGENVALUE ROUTINES IN NASTRAN: A COMPARISON WITH THE BLOCK LANCZOS METHOD
V. A. Tischler and Vipperla B. Venkayya *In* COSMIC, The Twenty-First NASTRAN (R) Users' Colloquium Sep. 1993 p 142-174 (For primary document see N94-17827 04-39)
Avail: CASI HC A03/MF A02

The NASA STRuctural ANalysis (NASTRAN) program is one of the most extensively used engineering applications software in the world. It contains a wealth of matrix operations and numerical solution techniques, and they were used to construct efficient eigenvalue routines. The purpose of this paper is to examine the current eigenvalue routines in NASTRAN and to make efficiency comparisons with a more recent implementation of the Block Lanczos algorithm by Boeing Computer Services (BCS). This eigenvalue routine is now available in the BCS mathematics library as well as in several commercial versions of NASTRAN. In addition, CRAY maintains a modified version of this routine on their network. Several example problems, with a varying number of degrees of freedom, were selected primarily for efficiency bench-marking. Accuracy is not an issue, because they all gave comparable results. The Block Lanczos algorithm was found to be extremely efficient, in particular, for very large size problems. Author

N94-17839*# McDonnell-Douglas Space Systems Co., Huntsville, AL.
AUTOMATIC A-SET SELECTION FOR DYNAMICS ANALYSIS
Tom Allen *In* COSMIC, The Twenty-First NASTRAN (R) Users' Colloquium Sep. 1993 p 175-181 (For primary document see N94-17827 04-39)
Avail: CASI HC A02/MF A02

A method for selecting optimum NASTRAN analysis set degrees of freedom for the dynamic eigenvalue problem is described. Theoretical development of the Guyan reduction procedure on which the method is based is first summarized. The algorithm used to select the analysis set degrees of freedom is then developed. Two example problems are provided to demonstrate the accuracy of the algorithm. Author

N94-17848# Oak Ridge National Lab., TN.
CHARPY IMPACT TOUGHNESS OF MARTENSITIC STEELS IRRADIATED IN FFTF: EFFECT OF HEAT TREATMENT
R. L. Klueh and D. J. Alexander 1992 16 p Presented at the 16th Annual Symposium of the ASTM on Effects of Radiation on Materials, Denver, CO, 21-25 Jun. 1993
(Contract DE-AC05-84OR-21400)
(DE93-015960; CONF-920673-22) Avail: CASI HC A03/MF A01

Charpy tests were made on plates of 9Cr-1MoVNb and 12Cr-1MoVW steels given four different normalizing-and-tempering treatments. One-third-size Charpy specimens from each steel were irradiated to 7.4 - 8 (times) 10(sup 26) n/m(sup 2) (about 34 - 37 dpa) at 420 C in the Materials Open Test Assembly of the Fast Flux Test Facility. Specimens were also thermally aged to 20000 h at 400 C to determine the effect of aging during irradiation. Previous work on these steels irradiated to 4 - 5 dpa at 365 C in MOTA were reexamined in light of the new results. The tests indicated that prior austenite grain size, which was varied by different normalizing treatments, had an effect on impact behavior of the 9Cr-1MoVNb but not on the 12Cr-1MoVW. Tempering treatment had relatively little effect on the shift in DBTT for both steels. Conclusions are presented on how heat treatment can be used to optimize properties. DOE

N94-17864# Los Alamos National Lab., NM.

MEASUREMENT AND ANALYSIS OF THREE 1.5-GPa SHOCK-WAVE PROFILES IN COPPER

R. H. Warnes and D. L. Tonks 1993 5 p Presented at the 14th International Conference on High Pressure Science and Technology and 1993 Technical Meeting of the Topical Group on Shock Compression of Condensed Matter, Colorodo Springs, CO, 28 Jun. - 3 Jul. 1993
(Contract W-7405-eng-36)
(DE93-016559; LA-UR-93-2276; CONF-9306167-10) Avail: CASI HC A01/MF A01

Three wave-profile experiments were performed on OFE fully annealed (600 C for one hour) copper using a 101.6 mm diameter gas gun at impact velocities of 86 m/s. A symmetric impact produced a 1.5 GPa shock wave in the target. A sapphire window was bonded to the front (non-impact) face of the target, and a four-detector push-pull velocity interferometer (VISAR) measured the velocity of the copper/sapphire interface. The impactor thickness (4 mm) was the same in all experiments; the target thicknesses were 10, 20, and 30 mm. The stresses and strains, including the deviatoric stresses and strains, have been extracted from these data using a quasi-Lagrangian analysis. (The waves are not steady.) The use of three separate shots in Lagrangian analysis yields only approximate results for the deviatoric stresses; but the results for the normal stresses, and for the strains, are fairly accurate. Even though the strain rates fall in the Hopkinson bar regime, the mechanism of dislocation motion appears to be dislocation drag, as is the case for stronger shock waves in Cu. DOE

N94-17899 National Physical Lab., Teddington (England). Materials Metrology Div.

A PRELIMINARY MODEL FOR CRACK-TIP HYDROGEN TRANSPORT

A. Turnbull, D. H. Ferriss, and H. Anzai Mar. 1993 48 p Sponsored by Dept. of Trade and Industry, London, England
(NPL-DMM(A)-84; ETN-93-94883) Copyright Avail: National Physical Laboratory, Teddington, Middlesex, TW11 0LW, United Kingdom

A preliminary analysis of the hydrogen concentration distribution at the tip of a crack as a basis for a more rigorous model leading to prediction of crack growth kinetics was carried out. The distinctive features are the use of a boundary fitted coordinate method for the numerical analysis and the adoption of flux boundary conditions at the crack tip and crack walls. At this stage of development, simple analytical expressions for the stress state were employed. Using limiting cases, the boundary fitted coordinate method was shown to give results comparable with boundary integral and finite element methods. Comparison of predictions of the hydrogen distribution at the crack tip from constant concentration and flux boundary conditions indicates that the latter should be adopted for application to low alloy steels, but equivalent results can be obtained for face centred cubic lattices because of the much lower lattice diffusivity. ESA

N94-17906# Los Alamos National Lab., NM.

IMPACT MODELING WITH SMOOTH PARTICLE HYDRODYNAMICS

R. F. Stellingwerf and C. A. Wingate 1993 13 p Presented at the Smooth Particle Hydrodynamics in Astrophysics OAT Workshop, Trieste, Italy, 6 Jul. 1993
(Contract W-7405-eng-36)
(DE93-016561; LA-UR-93-2256; CONF-9307102-1) Avail: CASI HC A03/MF A01

Smooth Particle Hydrodynamics (SPH) can be used to model hypervelocity impact phenomena via the addition of a strength of materials treatment. SPH is the only technique that can model such problems efficiently due to the combination of three dimensional geometry, large translations of material, large deformations, and large void fractions for most problems of interest. This makes SPH an ideal candidate for modeling of asteroid impact, spacecraft shield modeling, and planetary accretion. In this paper we describe the derivation of the strength equations in SPH, show several basic code tests, and present several impact test cases with experimental comparisons. DOE

N94-17913# Oak Ridge National Lab., TN.

INTERPRETATION OF WARM PRESTRESS-INDUCED FRACTURE TOUGHNESS BASED ON CRACK-TIP CONSTRAINT

D. K. M. Shum 1993 18 p Presented at the 25th National Symposium on Fracture Mechanics, Bethlehem, PA, 29 Jun. - 1 Jul. 1993
(Contract DE-AC05-84OR-21400)
(DE93-015967; CONF-930695-1) Avail: CASI HC A03/MF A01

This study explores the possibility of using J-Q-related crack-tip constraint concepts to provide a basis for both the interpretation of warm prestress (WPS)-induced fracture toughness and their transferability to structural applications. A finite-element boundary-layer formulation based on small-scale yielding (SSY), remote mode I K-dominant assumptions is adopted. Effects of WPS-induced crack-tip constraint are quantified in terms of deviation in either the opening-mode or the mean stress component of the WPS crack-tip fields relative to the reference K-dominant SSY state associated with monotonic-loading conditions. Over the range of WPS load-paths considered the WPS-induced crack-tip constraint closely resembles a spatially varying hydrostatic stress field. Interpretation and transferability of WPS fracture toughness under SSY conditions are specified in terms of the unload and reload ratio. DOE

N94-17918# Ecole Centrale de Lyon (France). Lab. de Technologie des Surfaces.

EXPERIMENTAL CONTRIBUTION TO THE CONTACT BETWEEN TWO BODIES AND THE EFFECT OF ROUGHNESS Ph.D. Thesis [CONTRIBUTION EXPERIMENTALE AU CONTACT ENTRE DEUX CORPS ET INFLUENCE DE LA RUGOSITE]

Alexandre Guinet 1991 130 p In FRENCH
(ECL-91-41; ETN-93-94587) Avail: CASI HC A07/MF A02

Some of the methods applied to measure surface topogaphy and the parameters which characterize the surface states at a microscopic scale are presented. These parameters are measured by statistical analysis and filtering techniques. Fractal geometry is applied to describe the surface mathematically. Rheological parameters and principles used in surface technologies are reviewed. In order to characterize the surface roughness, under given tangential forces and displacements, a sclerometric experiment was carried out. The Coulomb friction coefficient is shown to be affected by the surface anisotropy. Rough surfaces with cracks are modeled and validated. The model is applied to rough surfaces and the valleys are modeled by a notch on a thin plate. A film critical thickness, under which no crack propagation is possible, is defined. ESA

N94-17929 National Physical Lab., Teddington (England). Materials Metrology Div.

RATIO OF SPECIMEN THICKNESS TO DETECTION AREA FOR RELIABLE HYDROGEN PERMEATION MEASUREMENT

R. B. Hutchings, D. H. Ferriss, and A. Turnbull Jun. 1993 13 p
(NPL-DMM(A)-103; ETN-93-94886) Copyright Avail: National Physical Laboratory, Teddington, Middlesex, TW11 0LW, United Kingdom

Two dimensional diffusion of hydrogen atoms in a membrane was analyzed. The hydrogen atoms are assumed to be generated in a circular area on one side of the membrane and detected in a circular region on the opposite side. The average flux on the detection side was calculated as a function of membrane thickness and detection area and compared with the prediction from the conventional one dimensional solution. The applicability of the latter increases with decreasing thickness to detection area ratio. Recommendations are given for reliable utilization of the one dimensional analysis. ESA

N94-17931 Prins Maurits Lab. TNO, Rijswijk (Netherlands).

INSTRUMENTED EXPERIMENTS ABOARD THE FRIGATE WOLF. WOLF 2: MEASUREMENT RESULTS OF THE 5.5 kg TNT IN THE CREW AFT SLEEPING COMPARTMENT Final Report

T. L. A. Verhagen and R. M. vandeKasteele Aug. 1992 68 p Original contains color illustrations
(Contract A88/KM/419)
(PML-1992-12; TD91-2526; ETN-93-94521) Copyright Avail: TNO Prins Maurits Laboratory, P.O. Box 45, 2280 AA Rijswijk, Netherlands

Within the framework of the research into the vulnerability of ships, an experimental investigation took place in 1989 aboard the frigate 'Wolf.' The recordings of an instrumented experiment in the crew aft sleeping compartment are presented. During this experiment, a nonfragmenting charge of 5.5 kg TNT was initiated. Preceding the 5.5 kg TNT experiment, a 2 kg TNT experiment was performed on the same day. Later that day the 15 kg TNT experiment took place. Reparation/modification of the instrumentation was not possible. The settings of the instrumentation equipment were based on the expected extreme responses of the 15 kg TNT experiment later that day which had, however, an influence on the signal to noise ratio. The blast measurements seem to have recorded correctly. The quasi static pressure in the experiment compartment as well as in the adjacent compartments showed classical behavior. The strain measurements seemed to be good, although some of them malfunctioned after a period of time. ESA

N94-17941 Prins Maurits Lab. TNO, Rijswijk (Netherlands).
SCALING LAWS FOR DIFFRACTION LOADING BY AIR BLAST Final Report
E. A. Bakkum Jun. 1992 32 p Sponsored by TNO Defence Research, Delft, Netherlands
(PML-1991-54; TD91-2834; ETN-93-94520) Copyright Avail: TNO Prins Maurits Laboratory, P.O. Box 45, 2280 AA Rijswijk, Netherlands

An approximate scaling law for complex blast loadings was constructed. This blast loading together with the structural response is used to assess the damage, which is done to structures by an explosion. The blast loading in a model of a shelter was studied in the 40 by 40 sq cm blast simulator. The density distribution around the model was determined by means of flow visualization with a shearing interferometer. An approximate scaling law, which eliminates the dependency on the shock strength is proposed for the time behavior of the blast loading. The scaling law is confirmed by measurement of the density at various locations in the model for shock strengths of 6.5 kPa and 33.2 kPa. ESA

N94-17959# Technical Research Centre of Finland, Espoo. Metals Lab.
THE RESPECTIVENESS OF RESPONSE IN A BAR UNDER STATIC AND TRANSIENT LOADS [STAATTISEN JA TRANSIENTIN KUORMAN VASTEEN VERRANNOLLISUUS SAUVASSA]
Timo Kujala Jun. 1992 21 p In FINNISH
(VTT-TIED-1377; ISBN-951-38-4190-1; ETN-93-94479) Copyright Avail: CASI HC A03/MF A01

When responses of structures under impact load (in this case transient load) are evaluated pure statical analyses give too small values of displacements and stresses. In simple structures, under transient load, the displacements and stresses can be analyzed with analytical and numerical methods. In more complicated structures the Finite Element Method (FEM) will offer the way to solution. To verify different methods to analyze displacements and stresses of the bar caused by statical and transient loads, the Duhamel's integral and FEM were used. When solving Duhamel's integral Simpson's rule and superposition of eigenmodes were used at the same time. The direct time integration and superposition of eigenmodes were used separately for FEM analysis. In both FEM methods, the consistent mass matrix were used. Also, the suitability of numerical methods in doing 'impact' analyses were researched. In superposition of eigenvalues, the highest acceptable frequency determines the length of the time increment. Depending on the complexity of the structure, the choice of optimal element type and element mesh for an accurate solution might be difficult. Because in real structures any kind of elements have to be used, the bar was modeled by ten three dimensional solid elements. There were no remarkable differences between displacements and stresses caused by static and transient loads. ESA

N94-17970# Aeronautical Research Inst. of Sweden, Stockholm.
SPECTRUM FATIGUE TESTING OF T-SHAPED TENSION CLIPS
Bjoern Palmberg and Bengt Wallstenius Dec. 1992 37 p
(Contract FMV/FFL-82250-90-276-16-001)
(FFA-TN-1992-22; ETN-93-94858) Avail: CASI HC A03/MF A01

An investigation of strain distributions during static loading and crack propagation and fatigue lives under spectrum loading of T-shaped tension clips was carried out. Three slightly different, with respect to geometry, T shaped tension clips made of aluminum alloy 7010-T73651 were studied. The type 1 and 4 test specimens were different only with respect to the web thickness of the clamping end. The type 1 and 2 test specimens were different with repect to milled flat circular countersink around the holes in the type 2 specimens and with respect to the radius between the web and foot. The spectrum fatigue loading consisted of a load sequence representative for the wing root, lower side, of a fighter aircraft. Tests were made at two different load levels for each specimen type. The strain measurements show that the countersink in the type 2 specimens increases the stresses in the fatigue critical region. This is also manifested in the spectrum fatigue life results, where type 2 specimens show the shortest fatigue lives. The strain measurements show that the torque used for the bolts in joining two test specimens or one test specimen and a dummy has a rather large impact on the strain in the fatigue region. The strains decrease with increasing torque. The spectrum fatigue loading resulted in approximately an equal number of flights to obtain a 10.0 mm crack for specimens of type 1 and 4. This suggests that the type 1 configuration is superior since the web thickness is smaller for this type as compared to the type 4 specimens. In other words, the type 4 specimens have an unnecessary oversize of the clamping end web thickness. ESA

N94-17995# Sandia National Labs., Albuquerque, NM.
MICROSTRUCTURALLY BASED THERMOMECHANICAL FATIGUE LIFETIME MODEL OF SOLDER JOINTS FOR ELECTRONIC APPLICATIONS
D. R. Frear, M. M. Rashid, and S. N. Burchett 1993 12 p Presented at the ASME Design Technical Conference, Albuquerque, NM, 9-19 Sep. 1993
(Contract DE-AC04-76DP-00789)
(DE93-016508; SAND-93-1181C; CONF-9309175-1) Avail: CASI HC A03/MF A01

We present a new methodology for predicting the fatigue life of solder joints for electronics applications. This approach involves integration of experimental and computational techniques. The first stage involves correlating the manufacturing and processing parameters with the starting microstructure of the solder joint. The second stage involves a series of experiments that characterize the evolution of the microstructure during thermal cycling. The third stage consists of a computer modeling and simulation effort that utilizes the starting microstructure and experimental data to produce a reliability prediction of the solder joint. This approach is an improvement over current methodologies because it incorporates the microstructure and properties of the solder directly into the model and allows these properties to evolve as the microstructure changes during fatigue. DOE

N94-18049# Lawrence Livermore National Lab., CA.
NUMERICAL INTEGRATION OF STRUCTURAL ELEMENTS IN NIKE3D AND DYNA3D
B. N. Maker, R. G. Whirley, and B. E. Engelmann Aug. 1992 12 p
(Contract W-7405-eng-48)
(DE93-016325; UCRL-ID-111476) Avail: CASI HC A03/MF A01

The beam and shell elements found in many linear elastic finite element codes accept integrated cross sectional properties as input, and produce solutions using classical beam and shell theory. These theories are built upon the equation of resultant forces and moments with integrals of assumed stress distributions over the cross section. In contrast, the structural elements in NIKE3D and DYNA3D are formulated to represent nonlinear geometric and material behavior. Thus stress distributions may not necessarily be representable by simple functions of cross section variables. In NIKE3D and DYNA3D, the Hughes-Liu beam element and all shell elements accommodate these more general stress distributions by computing stresses at various points in the cross section. The integration of stresses within each element is then performed numerically, using a variety of methods. This report describes these numerical integration procedures in detail, and highlights their application to engineering problems. Several other features of the structural elements are also described, including force and moment resultants, user-defined reference surfaces, and user-defined integration rules. Finally, the shear correction factor is described in a section which relates results from NIKE3D and DYNA3D to those obtained from classical beam theory. DOE

N94-18079 Technische Univ., Delft (Netherlands). Faculty of Civil Engineering.
COMPUTATIONAL STRATEGIES FOR COMPOSITE STRUCTURES Thesis
J. C. J. Schellekens 1993 169 p
(PB93-195097; ISBN-90-9005673-4) Avail: CASI HC A08/MF A02

In the thesis the numerical tools are developed that can be applied to the analysis of composite structures at micro, meso, and macro-level. The study can be divided into three different parts: formulation of finite elements, constitutive modeling, and solution techniques. The proper combination of these numerical/mechanical aspects is essential for the accurate prediction of the nonlinear structural behavior of composites in the pre-failure and the post-failure regime. With respect to the description of structural failure the authors distinguish between discrete and continuous modeling of fracture. In the latter approach the fractured medium is considered as a continuum, whereas in a discrete description geometric discontinuities are introduced in the model once material failure occurs. NTIS

N94-18084# General Electric Co., Schenectady, NY.
FACTORS WHICH AFFECT FATIGUE STRENGTH OF FASTENERS
G. W. Skochko and T. P. Herrmann Nov. 1992 19 p
(DE93-017272; MAO-PR-92-01) Avail: CASI HC A03/MF A01

Axial load cycling fatigue tests of threaded fasteners are useful in determining fastener fatigue failure or design properties. By using appropriate design factors between the failure and design fatigue strengths, such tests are used to establish fatigue failure and design parameters of fasteners for axial and bending cyclic load conditions. This paper reviews the factors which influence the fatigue strength of low alloy steel threaded fasteners, identifies those most significant to fatigue strength, and provides design guidelines based on the direct evaluation of fatigue tests of threaded fasteners. Influences on fatigue strength of thread manufacturing process (machining and rolling of threads), effect of fastener membrane and bending stresses, thread root radii, fastener sizes, fastener tensile strength, stress relaxation, mean stress, and test temperature are discussed. DOE

N94-18108# Lawrence Livermore National Lab., CA.
DEVELOPMENT AND APPLICATION OF SPECIALLY-FOCUSED ULTRASONIC TRANSDUCERS TO LOCATION AND SIZING OF DEFECTS IN 75 mm- TO 127 mm-THICK AUSTENITIC STAINLESS STEEL WELD METALS
E. N. C. Dalder, S. Benson, B. J. McKinley, and T. Carodiskey Aug. 1992 36 p Presented at the 2nd Symposium on Cyclic Deformation, Fracture, and Nondestructive Evaluation of Advanced Materials, Miami, FL, 16-17 Nov. 1992
(Contract W-7405-eng-48)
(DE93-015975; UCRL-JC-111577; CONF-9211134-2) Avail: CASI HC A03/MF A01

Special ultrasonic transducer (UT) parts, capable of focusing incident signals within a 25 mm x 25 mm x 25 mm volume in an austenitic stainless weld metal at depths that varied from 25 mm to 127 mm, were developed and demonstrated to be capable of detecting a defect with cross section equivalent to that of a 4.76 mm-dia flat-bottom hole. Defect length sizing could be accomplished to +/- 50% for 100% of the time and to +/- 25% on selected defect types as follows: porosity groups, 100%; cracks, 67%; combined slag and porosity, 60%; and linear slag indications, 59%. Extensive linear elastic-fracture mechanics analyses were performed to establish allowable defect sizes at functions of stress based on a cyclic-life criterion of 10(exp 3) full power cycles of the MFTF-B magnet system. These defect sizes were used to determine which UT indicating were to be removed and repaired and which were to be retained and their recorded sizes and locations. DOE

N94-18246# Oak Ridge National Lab., TN.
A PROBABILITY METHOD OF FRACTURE MECHANICS ANALYSIS FOR HFIR VESSEL
Shih-Jung Chang 1993 33 p Presented at the Pressure Vessels and Piping Conference, Denver, CO, 25-29 Jul. 1993
(Contract DE-AC05-84OR-21400)
(DE93-015510; CONF-930702-42) Avail: CASI HC A03/MF A01

A preliminary estimate is made on the dynamic strength of the HFIR pressure vessel to resist internal explosive pulses of hypothetical accidents. The effect of fluid-structure interaction and radiation embrittlement are both taken into consideration. The pressure pulse is applied at the center of the fluid volume enclosed within the vessel. The vessel is located within a pool of water. The effect of the pool of water on the vessel response is considered in this calculation. Dynamic stress components at several locations along the vessel wall as functions of time are calculated. The material of the vessel has been assumed to be either elastic or elastic-plastic. The vessel failure is determined both by the location of maximum stress and by the arrival time of the stress-pulse. The capability that the pressure vessel may not break under the hypothetical accident is analyzed by the method of linear elastic fracture mechanics. The possible crack sizes are based on an assumed probability distribution function. Fracture condition under a single crack is estimated first. The probability of vessel fracture with multiple number of cracks is then obtained as a function of the applied hoop stress. The probability of fracture function is assumed to follow a lognormal distribution and the probability of fracture is extended to include different levels of confidence and variability. It, therefore, enables one to estimate the high confidence and low probability fracture capacity of the reactor vessel under a range of accident loading conditions. DOE

N94-18285# Florida Univ., Gainesville. Dept. of Aerospace Engineering Mechanics and Engineering Science.
SEVERAL FUNDAMENTAL ISSUES IN THE MECHANICS OF INELASTIC BEHAVIOR
14 Sep. 1993 4 p
(Contract N00014-87-J-1193)
(AD-A269455) Avail: CASI HC A01/MF A01

This is the final report for the support of research that began in 1987 and continued through to 1993 with a three year no additional cost extension. The International Symposium on Plasticity and its Current Applications was held in Baltimore on 19-23 Jul., and I presented two papers that summarized my endeavor's under ONR sponsorship. One was an extension of my earlier published work (Lee Anniversary Volume) on the microstructural features that control the flow strength of ductile metals and alloys. The other was an explanation of why, in a useful constitutive relation, it is necessary to define a plastic strain rate or increment that is not the rate of change or increment of whatever quantity may appeal to an author as an appropriate measure of finite plastic strain. Such a definition mirrors the accepted and necessary usage in fluid mechanics of the rate of deformation, a quantity which does not integrate over time to the finite deformation of the fluid. DTIC

N94-18328# Washington Univ., Seattle. Coll. of Engineering.
STEEP GEOMETRIC GRATING FOR USE IN MOIRE INTERFEROMETRY
F. X. Wang, G. B. May, and A. S. Kobayashi Jun. 1993 19 p
(Contract N00014-89-J-1276)
(AD-A268759; UWA/DME/TR-93/73) Avail: CASI HC A03/MF A01

The theoretical background and the procedure of executing a new moire interferometry method, which combines the advantages of the geometric moire method with traditional moire interferometry, is reported. The method uses a steep geometric grating of about 40 lines/mm on a mirror finished specimen surface to achieve high contrast moire fringes. A special four beam moire interferometry bench is designed for the low grating frequency used. An application to experimental fracture mechanics analysis is briefly discussed. DTIC

N94-18382# Wright Materials Research, Beavercreek, OH.
ANALYSIS OF BOLTED AND BONDED COMPOSITE Interim Report, May 1991 - Jun. 1992
Seng C. Tan Sep. 1992 190 p Limited Reproducibility: Document partially illegible
(Contract F33615-89-C-5643)
(AD-A267792; UDR-TR-92-120; WL-TR-92-4084) Avail: CASI HC A09/MF A02

In the analysis and design of bonded and bolted composite joints, certain input data are required that are not readily available. Many engineering hours at the depots are expended in obtaining the required information. Even when the data are obtained, the accuracy of it is sometimes questionable. The availability of this information in a computerized database would greatly facilitate composite joint analysis and design. The work described in this report involved an extensive search of the technical literature for adhesive and composite material property data as well as bonded and bolted joint properties. The data collected in the literature search were tabulated into a user friendly format for ready retrieval. The data in this tabulation include, in addition to material properties, discussions of fastener and joint design parameters, loading and environmental effects, and test methods. DTIC

N94-18387# California Inst. of Tech., Pasadena. Div. of Engineering and Applied Science.
THE LONGITUDINAL FREE VIBRATIONS OF A FIXED-FREE TWO-PHASE ELASTIC BAR
Jim M. Restuccio Jun. 1993 30 p

(Contract N00014-90-J-1871)
(AD-A268768; TR-14) Avail: CASI HC A03/MF A01

In this paper, the longitudinal free vibrations of a fixed-free bar are studied. It is assumed that the bar initially consists of two phases, one of which was obtained from the other by a martensitic phase transformation. It is also assumed that both phases of the bar have elastic constitutive behavior. For a bar that consists entirely of one phase that behaves elastically, it is well known that during the free vibrations of the bar the displacement and stress at each point of the bar oscillate as time progresses. If there is damping present, these oscillations will decay and go to zero as time goes to infinity, otherwise their amplitudes will remain constant in time. Considering this, for a bar that initially consists of two different phases that both behave elastically, one might expect that the displacement and stress at each point of the bar will also have oscillatory-type behavior during the free vibrations of the bar. If this is the case, the driving traction at the interface separating the two phases will oscillate. As a result of this, if the nominal phase boundary velocity is related to the driving traction through a kinetic relation that does not have an interval of the driving traction corresponding to a zero nominal phase boundary velocity, the nominal phase boundary velocity will also oscillate. Since energy is dissipated when the phase boundary moves and passes over particles of material of one phase converting them into particles of material of the other phase, one might conclude that the oscillatory-type response of the two-phase bar during the free vibrations of the bar should decay as time increases. This damping behavior of the two-phase bar is discussed. DTIC

N94-18466# Massachusetts Inst. of Tech., Cambridge. Dept. of Ocean Engineering.
INITIATION AND GROWTH OF MICROCRACKS IN HIGH STRENGTH STEEL BUTT WELDS M.S. Thesis
Edward Olsen May 1993 185 p
(Contract N00123-89-G-0580)
(AD-A268751) Avail: CASI HC A09/MF A02

Early tests such as the explosion bulge test created a preference for overmatched welds (welds which are stronger than the base metal) which eventually became codified for many structural applications. While an overmatched system offers advantages such as the shedding of strain to the base plate, it requires the use of expensive fabrication procedures to avoid cracking. Undermatched welding of some high strength steels may offer reductions in welding costs with little sacrifice in weld performance or low cycle fatigue integrity. An experimental study was carried out to observe microcrack initiation and growth of overmatched and undermatched butt welded high strength steel samples using globally elastic low cycle fatigue testing. First, 1 inch thick HY-80 and HY-100 base plates were multipass, spray gas metal arc welded (GMAW) with overmatching and undermatching filler metal using a semiautomatic welding machine. Second, 1/4 inch thick MIL-A-46100 high hardness armor plates (HHA) were manually, two pass spray GMAW welded with two grades of undermatching consumables. Weld reinforcements were removed from all HY specimens and six HHA specimens. All specimens had a crack initiator slit machined in the test section. The specimens were fatigue tested by transverse tensile loading with a 12 to 13 Hz tension-tension profile. The loading range was from 10% to 85% of the tensile strength of the HY steel base plate and HHA weld metal respectively. Crack initiation and propagation was observed in situ using a confocal scanning laser microscope. DTIC

N94-18479# Argonne National Lab., IL.
MECHANICAL PROPERTIES OF FIBER-REINFORCED YBa2Cu3O(x) AND Bi2Sr2CaCu2O(x) BARS
K. C. Goretta, L. J. Martin, D. Singh, R. B. Poeppel, Nan Chen, C. Y. Chu, J. C. Routbort, and R. A. Gleixner (Babcock and Wilcox Co., Alliance, OH.) Jul. 1993 9 p Presented at the International Cryogenic Engineering Conference and International Cryogenic Materials Conference, Albuquerque, NM, 12-16 Jul. 1993
(Contract W-31-109-eng-38)
(DE93-017689; ANL/ET/CP-78558; CONF-930703-10) Avail: CASI HC A02/MF A01

Strength in four-point bending and fracture toughness of YBa2Cu3O(x) (123) and Bi2Sr2CaCu2O(x) (2212) were examined at room temperature. The 123 was reinforced with 15 vol.% Y2BaCuO5 (211) fibers and was processed to 90-91% density by cold pressing and sintering. The 2212 was reinforced with 15 vol.% 2212 fibers and was processed to approximately 90% density by sinter forging. The 123/211 composites had a fracture toughness of 1.9 MPa(m)(exp 0.5), which is 20-30% higher than that of corresponding monoliths, but exhibited no improvement in strength. The strength and fracture toughness of the 2212/2212 composites were 102 MPa and 2.7 MPa(m)(exp 0.5), respectively, which were slight improvements over the monoliths. Transport critical current densities at 77 K were only slightly affected by the fiber additions. DOE

N94-18487# Florida Atlantic Univ., Boca Raton. Center for Applied Stochastics Research.
FUNDAMENTAL RESEARCH IN NONLINEAR RANDOM VIBRATION FOR AEROSPACE APPLICATIONS Final Report, 15 Nov. 1991 - 14 Nov. 1992
Y. K. Lin 11 Jan. 1993 22 p
(Grant AF-AFOSR-0073-91)
(AD-A268929; AFOSR-93-0666TR) Avail: CASI HC A03/MF A01

Response and safety of nonlinear structures under random excitations are investigated. The excitations can be either external, or parametric, or both. Extensions are made along two directions from the earlier works on exact solutions when the excitations are Gaussian white noises: (1) the excitations are impulsive, but non-Gaussian; and (2) the system does not belong to the class of generalized stationary potential, thus, exact solution is not obtainable at the present time. In the first case, the probability density of the structural response is governed by a partial differential equation, with infinite number of terms. A perturbation analysis is devised to obtain approximate solutions. In the second case, a new technique is developed to obtain approximate solutions on the principle of weighted residuals. On the issues of structural safety, two failure modes are investigated: catastrophic failure and fatigue failure. Catastrophic failure occurs when structural response exceeds, for the first time, a critical limit. Fatigue failure is investigated from a fracture mechanics point of view, namely, failure is assumed to occur when a dominant crack is propagated to a critical size. DTIC

N94-18661 Naval Postgraduate School, Monterey, CA. Dept. of Mechanical Engineering.
WAVELET TRANSFORM FOR TIME-FREQUENCY ANALYSIS OF THE VIBRATIONAL SIGNATURE AND ITS APPLICATION
Jae-Jin Jeon and Young S. Shin 17 Aug. 1993 68 p Limited Reproducibility: More than 20% of this document may be affected by microfiche quality
(AD-A269928; NPS-ME-93-004) Avail: CASI HC A04

Wavelet transform is applied to the analysis of vibration signatures in order to verify the ability of the detection of abnormal condition. It can well describe the dynamics of the signal's spectral composition of a non-stationary and stationary signal to be measured and presented in the form of 3-D time-frequency map. Although wavelet has been developed over about ten years in the mathematics and physics, its engineering applications is a first stage. The objective of this report outlines the definition of the wavelet transform and is to discuss the properties of the wavelet transform as new tool for the vibration analysis, and then demonstrates how it may be applied to the machinery condition monitoring. DTIC

N94-18683# California Univ., Los Angeles. Dept. of Materials Science and Engineering.
DEVELOPMENT OF THE MICROSTRUCTURE BASED STOCHASTIC LIFE PREDICTION MODELS
Marek A. Przystupa, Jimin Zhang, and Annetta J. Luevano Sep. 1993 26 p
(Contract N00014-91-J-1299)
(AD-A269880) Avail: CASI HC A03/MF A01

The microstructural features of 7050 T7451 aluminum alloy in the vicinity of fatigue cracks and on the crack path were studied to determine which of them influence fatigue crack propagation. The studies included characterization of the full spectrum of microstructural and fracture surface features starting from the largest ones such as roughness and grain type to the smallest such as second phase particles and dislocations. Of all the features studied, only the second phase particles were shown to have a definite influence by causing crack deflection. The number of particles encountered by the fatigue cracks were significantly higher than the expected average. The fatigue crack path was predominately transgranular and there was no changes in the dislocation and precipitation structures in the crack affected zone. DTIC

N94-18714 California Univ., Los Angeles. Dept. of Materials Science and Engineering.

DEVELOPMENT OF THE MICROSTRUCTURE BASED STOCHASTIC LIFE PREDICTION MODELS Annual Report

M. A. Przystupa and A. K. Vasudevan 1993 4 p Limited Reproducibility: More than 20% of this document may be affected by microfiche quality
(Contract N00014-91-J-1299)
(AD-A270453) Avail: CASI HC A01

This study explores the methods of incorporating material microstructural characteristics into the fatigue life prediction models based on the results of the microstructural characterizations and fatigue testing of aluminum 7050-T7451 plate alloys. The emphases in the microstructural characterization part of the program are on the identification of the fatigue-relevant microstructural features and on the characterizations of the microstructural gradients. The characterizations are carried out using both the standard and novel techniques such as tessellation, fractal and modified linear intercept methods. The key measurement is determination of the size distributions of the fatigue crack initiating flaws -- they are assumed equal to the extreme value distributions of the micropore and/or constituent particle size distributions measured on the metallographic sections. DTIC

N94-18716 Earl and Wright, San Francisco, CA.

FATIGUE TECHNOLOGY ASSESSMENT AND STRATEGIES FOR FATIGUE AVOIDANCE IN MARINE STRUCTURES. APPENDICES Final Report

Cuneyt C. Capanoglu 1993 191 p Limited Reproducibility: More than 20% of this document may be affected by microfiche quality
(Contract DTCG23-88-C-20029)
(AD-A269053; SR-1324-App) Avail: CASI HC A09

This report provides an up-to-date assessment of fatigue technology, directed specifically toward the marine industry. A comprehensive overview of fatigue analysis and design, a global review of fatigue including rules and regulations and current practices, and a fatigue analysis and design criteria are provided as a general guideline to fatigue assessment. A detailed discussion of all fatigue parameters is grouped under three analysis blocks: fatigue stress model, covering environmental forces, structure response and loading, stress response amplitude operations (RAO's) and hot-spot stresses; fatigue stress history model covering long-term distribution of environmental loading; and fatigue resistance of structures and damage assessment methodologies. The analyses and design parameters that affect fatigue assessment are discussed together with uncertainties and research gaps, to provide a basis for developing strategies for fatigue avoidance. Additional in-depth discussions of wave environment, stress concentration factors, etc. are presented in the appendixes. Assessment of fatigue technology, fatigue stress models, fatigue stress history models, fatigue resistance, fatigue parameters, and fatigue avoidance strategies. DTIC

N94-18829# Sandia National Labs., Albuquerque, NM.

THREE-DIMENSIONAL SHOCK WAVE PHYSICS SIMULATIONS WITH MIMD PAGOSA ON MASSIVELY PARALLEL COMPUTERS

D. R. Gardner, C. T. Vaughan, and D. D. Cline (Texas Univ., Austin.) 1992 5 p Presented at the Summer Computer Simulation Conference, Boston, MA, 19-21 Jul. 1993
(Contract DE-AC04-76DP-00789)
(DE93-011682; SAND-92-2825C; CONF-930765-3) Avail: CASI HC A01/MF A01

The numerical modeling of penetrator-armor interactions for design studies requires rapid, detailed, three-dimensional simulation of complex interactions of exotic materials at high speeds and high rates of strain. To perform such simulations, we have developed a multiple-instruction, multiple-data (MIMD) version of the PAGOSA hydrocode. The code includes a variety of models for material strength, fracture, and the detonation of high explosives. We present a typical armor/antiarmor penetration simulation conducted with this code, and measurements of its performance. The scaled speedups for MIMD PAGOSA on the 1024-processor nCUBE 2 parallel computer, measured as the simulation size is increased with the number of processors, reveal that small grind times (computational time per cell per cycle) and parallel scaled efficiencies of 90% can be achieved for realistic problems. This simulation demonstrates that massively parallel hydrocodes can provide rapid, highly-detailed armor/antiarmor simulations. DOE

N94-18864# Alabama Univ., Huntsville. Dept. of Civil and Environmental Engineering.

TOWARD A CHARACTERIZATION OF THE DEBRIS CLOUD CREATED IN A HYPERVELOCITY IMPACT ON A THIN PLATE Final Report, Sep. 1992 - Mar. 1993

William P. Schonberg Aug. 1993 113 p
(Contract F49620-90-C-0076)
(AD-A269190; WL-TR-93-7028) Avail: CASI HC A06/MF A02

Semi-analytical lethality assessment models fall into one of two general categories: discrete particle models and expanding shell models. Discrete particle models account for and track only a small number of solid fragments in a debris cloud generated by a hypervelocity impact. They are best suited for impact scenarios in which melting and/or vaporization of the projectile and target materials do not occur. Expanding shell models assume that all of the debris cloud material is homogeneously distributed over a uniformly expanding spherical shell in those impact scenarios where melting and/or vaporization of the projectile and target materials do occur. A lethality assessment model that considers the creation and subsequent effects of debris clouds containing all three states of matter is needed. This report describes the results of an investigation into the composition of the material in a debris cloud generated by a hypervelocity projectile impact. The work completed represents the first step in a long-term research program whose overall objective is to develop a general model of the response of a target structure to a hypervelocity impact over the 4-16 kilometers per second impact regime. DTIC

N94-19033# Los Alamos National Lab., NM.

SHOCK-LOADING RESPONSE OF ADVANCED MATERIALS

G. T. Gray, III 1993 5 p Presented at the 14th International Conference of the International Association for the Advancement of High Pressure Science and Technology, Colorado Springs, CO, 27 Jun. - 2 Jul. 1993
(Contract W-7405-eng-36)
(DE93-018344; LA-UR-93-2291; CONF-930676-16) Avail: CASI HC A01/MF A01

Advanced materials, such as composites (metal, ceramic, or polymer-matrix), intermetallics, foams (metallic or polymeric-based), laminated materials, and nanostructured materials are receiving increasing attention because their properties can be custom tailored specific applications. The high-rate/impact response of advanced materials is relevant to a broad range of service environments such as the crashworthiness of civilian/military vehicles, foreign-object-damage in aerospace, and light-weight armor. Increased utilization of these material classes under dynamic loading conditions requires an understanding of the relationship between high-rate/shock-wave response as a function of microstructure if we are to develop models to predict material behavior. In this paper, the issues relevant to defect generation, storage, and the underlying physical basis needed in predictive models for several advanced materials are reviewed. DOE

N94-19039# Sandia National Labs., Albuquerque, NM.

A GENERAL-PURPOSE CONTACT DETECTION ALGORITHM FOR NONLINEAR STRUCTURAL ANALYSIS CODES

M. W. Heinstein, S. W. Attaway, J. W. Swegle, and F. J. Mello May 1993 98 p
(Contract DE-AC04-76DP-00789)
(DE93-018507; SAND-92-2141) Avail: CASI HC A05/MF A02

A new contact detection algorithm has been developed to address difficulties associated with the numerical simulation of contact in nonlinear finite element structural analysis codes. Problems including accurate and efficient detection of contact for self-contacting surfaces, tearing and eroding surfaces, and multi-body impact are addressed. The proposed algorithm is portable between dynamic and quasi-static codes and can efficiently model contact between a variety of finite element types including shells, bricks, beams, and particles. The algorithm is composed of a location strategy that uses a global search to decide which slave nodes are in proximity to a master surface and an accurate detailed contact check that uses the projected motions of both master surface and slave node. In this report, currently used contact detection algorithms and their associated difficulties are discussed. Then the proposed algorithm and how it addresses these problems is described. Finally, the capability of the new algorithm is illustrated with several example problems. DOE

N94-19060# Sandia National Labs., Albuquerque, NM.
A PARTICLE METHOD FOR HISTORY-DEPENDENT MATERIALS
Deborah Sulsky (New Mexico Univ., Albuquerque.), Zhen Chen (New Mexico Univ., Albuquerque.), and Howard L. Schreyer (New Mexico Univ., Albuquerque.) Jun. 1993 33 p
(Contracts DE-AC04-76DP-00789)
(DE93-018696; SAND-93-7044) Avail: CASI HC A03/MF A01

A broad class of engineering problems including penetration, impact, and large rotations of solid bodies causes severe numerical problems. For these problems, the constitutive equations are history dependent so material points must be followed; this is difficult to implement in an Eulerian scheme. On the other hand, purely Lagrangian methods typically result in severe mesh distortion and the consequence is ill-conditioning of the element stiffness matrix leading to mesh lockup or entanglement. Remeshing prevents the lockup and tangling but then interpolation must be performed for history dependent variables, a process which can introduce errors. Proposed here is an extension of the particle-in-cell method in which particles are interpreted to be material points that are followed through the complete loading process. A fixed Eulerian grid provides the means for determining a spatial gradient. Because the grid can also be interpreted as an updated Lagrangian frame, the usual convection term in the acceleration associated with Eulerian formulations does not appear. With the use of maps between material points and the grid, the advantages of both Eulerian and Lagrangian schemes are utilized so that mesh tangling is avoided while material variables are tracked through the complete deformation history. Example solutions in two dimensions are given to illustrate the robustness of the proposed convection algorithm and to show that typical elastic behavior can be reproduced. Also, it is shown that impact with no slip is handled without any special algorithm for bodies governed by elasticity and strain hardening plasticity. DOE

N94-19061# Sydney Univ. (Australia). School of Civil and Mining Engineering.
PLASTIC MECHANISM ANALYSIS OF T-JOINTS IN RHS SUBJECT TO COMBINED BENDING AND CONCENTRATED FORCE
X. L. Zhao and G. J. Hancock Feb. 1993 37 p See also PB92-225374, PB93-118784 and PB93-118792
(PB93-195774; R-673) Avail: CASI HC A03/MF A01

Joints can occur in tubular structures where the main member is subjected to a bending moment rather than an axial force, particularly for rigid jointed frames. A model of the strength of T-joints in rectangular hollow sections (RHS) subject to combined bending and concentrated force is developed based on experimental observations of joint tests performed by the authors. NTIS

N94-19078# Sandia National Labs., Albuquerque, NM.
STRESS PULSE PHENOMENA
M. McGlaun 1993 6 p Presented at the Los Alamos Technology Exchange Workshop on Dynamic Response of Materials to Pulsed Heating, Los Alamos, NM, 22-25 Jan. 1993
(Contract DE-AC04-76DP-00789)
(DE93-019064; SAND-93-1661C; CONF-9301125-2) Avail: CASI HC A02/MF A01

This paper is an introductory discussion of stress pulse phenomena in simple solids and fluids. Stress pulse phenomena is a very rich and complex field that has been studied by many scientists and engineers. This paper describes the behavior of stress pulses in idealized materials. Inviscid fluids and simple solids are realistic enough to illustrate the basic behavior of stress pulses. Sections 2 through 8 deal with the behavior of pressure pulses. Pressure is best thought of as the average stress at a point. Section 9 deals with shear stresses which are most important in studying solids. DOE

N94-19095*# Virginia Polytechnic Inst. and State Univ., Blacksburg. Dept. of Engineering Science and Mechanics.
A COMPARATIVE EVALUATION OF IN-PLANE SHEAR TEST METHODS FOR LAMINATED GRAPHITE-EPOXY COMPOSITES Final Report, Sep. 1989 - Dec. 1991
John Morton and Henjen Ho 30 Jun. 1992 6 p
(Grant NAG1-1053)
(NASA-CR-193808; NAS 1.26:193808) Avail: CASI HC A02/MF A01

The objectives were to evaluate popular shear test methods for various forms of graphite-epoxy composite materials and to determine the shear response of graphite-epoxy composites with various forms of fiber architecture. Numerical and full-field experimental stress analyses were performed on four shear test configurations for unidirectional and bidirectional graphite-epoxy laminates to assess the uniformity and purity of the shear stress (strain) fields produced in the specimen test section and to determine the material in-plane shear modulus and shear response. The test methods were the 10 deg off-axis, the +/- 45 deg tension, the Iosipescu V-notch, and a compact U-notch specimen. Specimens were prepared from AS4/3501-6 graphite-epoxy panels, instrumented with conventional strain gage rosettes and with a cross-line moire grating, and loaded in a convenient testing machine. The shear responses obtained for each test method and the two methods of specimen instrumentation were compared. In a second phase of the program the shear responses obtained from Iosipescu V-notch beam specimens were determined for woven fabric geometries of different weave and fiber architectures. Again the responses of specimens obtained from strain gage rosettes and moire interferometry were compared. Additional experiments were performed on a bidirectional cruciform specimen which was also instrumented with strain gages and a moire grating. Author (revised)

N94-19116# California Inst. of Tech., Pasadena. Graduate Aeronautical Labs.
INTERFACIAL CRACKS IN PLATES: A THREE-DIMENSIONAL NUMERICAL INVESTIGATION
Yeong Joo Lee and A. J. Rosakis 1992 44 p Original contains color illustrations
(Contract N00014-90-J-1340; NSF MSS-90-24838)
Avail: CASI HC A03/MF A01; 1 functional color page

The 3-D field at a crack front in a bimaterial interface is investigated in order to identify relevant fracture parameters in thin plate laboratory specimens. Existence of plane stress K-dominance is necessary for the proper analysis of experimental data, which can be obtained directly from the crack tip field by optical methods. The analysis of the 3-D structure of the crack tip field presented here is performed in relation to the three-point bend specimen geometry used in the experiments described in Lee and Rosakis. It is well known that the 3-D field at the vicinity of a crack in a plate composed of a homogeneous material extends over a half plate thickness from the crack front. However, in a bimaterial fracture specimen, in addition to the singular field at the crack tip, mismatch of material properties along the interface induces a 3-D strip along the bimaterial interface ahead of the crack tip. The extent of the 3-D zone and a critical discussion of the zone of K-dominance are presented. The relation-between the stress intensity factors in the remote plane stress K-field and the stress intensity factors inside the near-tip plane strain K-field is also derived by means of a separate boundary-layer type of numerical analysis. Finally, a means of scaling the results obtained by experimentation in thin plate specimens of a specific thickness to plate specimens of any thickness is proposed. Author (revised)

N94-19130# California Inst. of Tech., Pasadena. Graduate Aeronautical Labs.
THE INTERPRETATION OF OPTICAL CAUSTICS IN THE PRESENCE OF DYNAMIC NON-UNIFORM CRACK-TIP MOTION HISTORIES: A STUDY BASED ON A HIGHER ORDER TRANSIENT CRACK-TIP EXPANSION
Cheng Liu, Ares J. Rosakis, and L. B. Freund Nov. 1991 54 p
(Contract N00014-90-J-1340)
(SM91-12) Avail: CASI HC A04/MF A01

The optical method of caustics is re-examined by considering the presence of dynamic nonuniform crack tip motion histories. Based on the higher order transient expansion obtained by Freund and Rosakis (1990, 1991) and Rosakis, Liu, and Freund (1991), in which dynamic transient

effects were included in the near tip deformation field, the exact mapping equations of caustics are derived for nonuniformly propagating cracks. The resulting equations indicate that the classical analysis of caustics based on the assumption of K(sup d)(sub I) dominance, is inadequate to interpret the experimental caustic patterns when dynamic transient effects become significant. In this paper, an explicit relation between the instantaneous value of the dynamic stress intensity factor K(sup d)(sub I)(t) and the geometrical characteristics of the caustic is established. This relation shows that for the case of nonuniformly propagating cracks, the relation between the dynamic stress intensity factor, and the geometrical characteristics of the caustic pattern depends on the crack tip acceleration and on K(sup d)(sub I)(t). It also reduces to the classical relation between K(sup d)(sub I)(t) and the caustic diameter for the case of K(sup d)(sub I)-dominance (when the crack tip fields are well described by the r exp -1/2 singularity in stresses). The Broberg problem is used as an example problem to check the feasibility of analyzing caustics in the presence of higher order transient terms. It is shown the value of the dynamic stress intensity factor obtained by the proposed method agrees remarkably well with the exact analytical value while large errors are introduced when the classical analysis (K(sup d)(sub I)-dominant) of the method of caustics is used.
Author (revised)

N94-19207# Los Alamos National Lab., NM.
SMOOTH PARTICLE HYDRODYNAMICS: THE SPHINX AND SPHC CODES
C. A. Wingate and R. F. Stellingwerf 1993 9 p Presented at the Annual Winter Meeting of the ASME, New Orleans, LA, 28 Nov. - 3 Dec. 1993
(Contract W-7405-eng-36)
(DE93-014358; LA-UR-93-1938; CONF-931121-7) Avail: CASI HC A02/MF A01

Smooth particle hydrodynamics (SPH) is a new computational technique well suited to computation of hypervelocity impact phenomena. This paper reviews the characteristics, philosophy, and a bit of the derivation of the method. As illustrations of the technique, several test case computations and several application computations are shown. DOE

N94-19279# Los Alamos National Lab., NM.
INFLUENCE OF PEAK PRESSURE AND TEMPERATURE ON THE SHOCK-LOADING RESPONSE OF TANTALUM
G. T. Gray, III 1993 5 p Presented at the 14th International Conference of the International Association for the Advancement of High Pressure Science and Technology, Colorado Springs, CO, 27 Jun. - 2 Jul. 1993
(Contract W-7405-eng-36)
(DE93-018561; LA-UR-93-2214; CONF-930676-33) Avail: CASI HC A01/MF A01

While the deformation response of tantalum subjected to high-rate loading has attracted considerable study, few studies have systematically investigated the influence of peak shock pressure and starting temperature on the shock response of tantalum. In this study the deformation behavior of annealed tantalum has been compared to tantalum shock pre-strained to 7 and 15 GPa at 250 C as well as to 7 GPa after first preheating to 200 and 400 C. The reload yield behavior of shock prestrained Ta was found to exhibit no enhanced shock hardening compared to Ta deformed quasi-statically or dynamically to an equivalent strain level. In addition the reload yield behavior of Ta shock prestrained to 7 GPa at 200 or 400 C was found to exhibit increased hardening compared to the shock prestraining at 25 C. The shock-hardening response of Ta is discussed in terms of defect storage and compared to that seen in fcc metals. DOE

N94-19350*# Virginia Polytechnic Inst. and State Univ., Blacksburg. Dept. of Aerospace and Ocean Engineering.
COMPRESSION STRENGTH OF COMPOSITE PRIMARY STRUCTURAL COMPONENTS Semiannual Status Report, 1 May - 31 Oct. 1993
Eric R. Johnson Oct. 1993 23 p
(Grant NAG1-537)
(NASA-CR-194562; NAS 1.26:194562) Avail: CASI HC A03/MF A01

Two projects are summarized. The first project is entitled 'Stiffener Crippling Inititated by Delaminations' and its objective is to develop a computational model of the stiffener specimens that includes the capability to predict the interlaminar stress response at the flange free edge in postbuckling. The second is entitled 'Pressure Pillowing of an Orthogonally Stiffened Cylindrical Shell'. A paper written on this project is included.
Author (revised)

N94-19351*# National Aeronautics and Space Administration. Lewis Research Center, Cleveland, OH.
DESIGN FOR CYCLIC LOADING ENDURANCE OF COMPOSITES
Michael C. Shiao (Sverdrup Technology, Inc., Brook Park, OH.), Pappu L. N. Murthy, Christos C. Chamis, and Leslie D. G. Liaw (Sverdrup Technology, Inc., Brook Park, OH.) Dec. 1993 22 p Presented at the 24th International SAMPE Technical Conference, Toronto, Ontario, 20-22 Oct. 1992; sponsored by the Society for the Advancement of Material and Process Engineering See also A93-53395
(RTOP 510-02-12)
(NASA-TM-106407; E-8244; NAS 1.15:106407) Avail: CASI HC A03/MF A01

The application of the computer code IPACS (Integrated Probabilistic Assessment of Composite Structures) to aircraft wing type structures is described. The code performs a complete probabilistic analysis for composites taking into account the uncertainties in geometry, boundary conditions, material properties, laminate lay-ups, and loads. Results of the analysis are presented in terms of cumulative distribution functions (CDF) and probability density function (PDF) of the fatigue life of a wing type composite structure under different hygrothermal environments subjected to the random pressure. The sensitivity of the fatigue life to a number of critical structural/material variables is also computed from the analysis.
Author (revised)

N94-19358# Aeronautical Research Inst. of Sweden, Stockholm. Structures Dept.
A REVIEW OF AERONAUTICAL FATIGUE INVESTIGATIONS IN SWEDEN DURING THE PERIOD MAY 1991 TO APRIL 1993
Anders F. Blom, ed. May 1993 84 p Presented at the 23rd International Committee on Aeronautical Fatigue Conference, Stockholm, Sweden, 7-8 Jun. 1993 Sponsored by Foersvarets Materialverk, Stockholm, Sweden
(FFA-TN-1993-22; ETN-93-94911) Avail: CASI HC A05/MF A01

The work carried out in Sweden in the area of aeronautical fatigue during the period from May 1991 to Apr. 1993 is reviewed. The review includes basic studies of fatigue development in metals and composites, stress analysis and fracture mechanics, studies of crack propagation and residual strength, testing of joints and full scale structures, and fatigue life predictions. A reference list of relevant papers issued during the period covered by the review is included. ESA

N94-19375# Ecole Centrale de Lyon (France). Lab. de Mecanique des Solides.
CONSTRUCTION OF A TENSION-TORSION ANISOTROPIC BRITTLE DAMAGE ELASTIC MODEL Ph.D. Thesis [CONSTRUCTION D'UN MODELE ELASTIQUE FRAGILE ANISOTROPE ENDOMMAGE EN TRACTION-TORSION]
Mahmoud Ketata 1991 130 p In FRENCH
(ECL-91-27; ETN-93-94585) Avail: CASI HC A07/MF A02

The behavior of concrete can be described in the first approximation by a brittle damaged elastic model. This model presents an induced anisotropy which depends on loading path. A second order symmetric tensor D is used to represent the anisotropic evolution of damage. A model based on effective stresses is applied for a tension-torsion load. Having a symmetric law either in tension and compression leads to consider other forms of effective stresses which contain the sign of principal stresses and another scalar variable of damage d, so that the damage acts differently in tension and in compression loads. ESA

N94-19403# Ecole Centrale de Lyon (France). Dept. de Mecanique des Solides.
TIME DEPENDENT IDENTIFICATION OF NONLINEAR STRUCTURES Ph.D. Thesis [IDENTIFICATION TEMPORELLE DES STRUCTURES NON-LINEAIRES]
Fabrice Thouverez 1992 236 p In FRENCH
(ECL-92-64; ETN-93-94895) Avail: CASI HC A11/MF A03

Methods of nonlinear identification, which are based on nonparametrical technique are discussed. New strategies allowing strong nonlinearities are taken into account in a multidimensional context. The problem of identification is analyzed by the following methods: nonparametrical, Volterra series and the NARMAX (nonlinear autoregressive moving average with exogeneous inputs) method. These methods are applied together with an analytical tool so that they may have an analytical function in the nonlinear phenomens. The possibilities and the limits of every method on numerical examples are shown. The methods are applied to real structures by using nonlinear dampers as well as localized nonlinearities. ESA

N94-19411# Ecole Centrale de Lyon (France). Lab. de Mecanique des Solides.
CONTRIBUTION TO THE IDENTIFICATION OF NONLINEAR BEHAVIOR LAWS IN MATERIAL MECHANICS Ph.D. Thesis [CONTRIBUTION A L'IDENTIFICATION DES LOIS DE COMPORTEMENT NON LINEAIRES EN MECANIQUE DES MATERIAUX]
Bachir Lamani 1992 200 p In FRENCH
(ECL-92-36; ETN-93-94593) Avail: CASI HC A09/MF A03

Tools specific to the identification of nonlinear behavior are considered taking the following into account: identification is an essential step in the development of a constitutive model; in view of the model's structure, this step remains often empirical. A parameter, which is essential to the modeling, the elasticity limit, is identified. With this in view the use of the Houg transform, a method stemming from picture processing techniques, is suggested. The identification of component functions is then taken into account. For this, traditional optimization methods are used. Several applications which were carried out from examples on the plasticity of metals and soils are presented. Forming problems are identified. These applications enable the different methods used to be assessed. ESA

N94-19444 Prins Maurits Lab. TNO, Rijswijk (Netherlands).
SIMULATION OF THE IMPACT OF A PLASTIC FLYER ON AN ALUMINUM BLOCK USING THE HYDROCODE AUTODYNE Final Report
H. J. Verbeek Sep. 1992 24 p Sponsored by DMKL, The Hague, Netherlands Original contains color illustrations
(Contract A84/KL/147)
(PML-1992-26; TD-92-1518; ETN-93-94933) Copyright Avail: Issuing Activity (TNO Prins Maurits Laboratory, P.O. Box 45, 2280 AA Rijswijk, Netherlands)

A mega ampere pulse was built to accelerate thin plastic flyers which are subsequently impacted on different target materials. To reach a better understanding of the shape and time development of the shock pulses generated in the target material, a computer simulation of this situation was carried out, using the hydrocode Autodyn. The set up and results of the simulation and an evaluation of the results and analysis of the consequences for the experiments are described. ESA

N94-19460# Ecole Centrale de Lyon (France). Lab. de Mecanique des Solides.
REANALYSIS OF STRUCTURE MODELS Ph.D. Thesis [RECALAGE DES MODELES DE BATIMENT]
Bambang Supriyadi 1993 169 p In FRENCH
(ECL-93-07; ETN-93-94898) Avail: CASI HC A08/MF A02

The purpose of the study is to develop a software to optimize structural models and describe as accurately as possible real structures. A method, named sensibility method, which allows estimating the structure's dynamical behavior sensibility to changes is applied. The first and second derivatives of eigenfrequencies and the first derivative of eigenvectors are calculated. The models chosen to describe the dynamic-characteristics are based on the modeling of three dimensional structural beams. Efforts were made to determine the equivalent real characteristics of those structures. The analysis shows that the vibrational behavior of the model is relatively far from the behavior of real structures. ESA

N94-19465*# National Aeronautics and Space Administration. Langley Research Center, Hampton, VA.
COMPUTATIONAL METHODS FOR CRASHWORTHINESS
Ahmed K. Noor, comp. (Virginia Univ., Hampton.) and Huey D. Carden, comp. Washington Aug. 1993 261 p Workshop held in Hampton, VA, 2-3 Sep. 1992; cosponsored by Virginia Univ.
(RTOP 505-63-50-09)
(NASA-CP-3223; L-17284; NAS 1.55:3223) Avail: CASI HC A12/MF A03

Presentations and discussions from the joint UVA/NASA Workshop on Computational Methods for Crashworthiness held at Langley Research Center on 2-3 Sep. 1992 are included. The presentations addressed activities in the area of impact dynamics. Workshop attendees represented NASA, the Army and Air Force, the Lawrence Livermore and Sandia National Laboratories, the aircraft and automotive industries, and academia. The workshop objectives were to assess the state-of-technology in the numerical simulation of crash and to provide guidelines for future research. For individual titles, see N94-19466 through N94-19476.

N94-19466*# Northwestern Univ., Evanston, IL. Dept. of Civil Engineering.
ADAPTIVE METHODS FOR NONLINEAR STRUCTURAL DYNAMICS AND CRASHWORTHINESS ANALYSIS
Ted Belytschko *In* NASA. Langley Research Center, Computational Methods for Crashworthiness Aug. 1993 p 7-35 (For primary document see N94-19465 04-39)
Avail: CASI HC A03/MF A03

The objective is to describe three research thrusts in crashworthiness analysis: adaptivity; mixed time integration, or subcycling, in which different timesteps are used for different parts of the mesh in explicit methods; and methods for contact-impact which are highly vectorizable. The techniques are being developed to improve the accuracy of calculations, ease-of-use of crashworthiness programs, and the speed of calculations. The latter is still of importance because crashworthiness calculations are often made with models of 20,000 to 50,000 elements using explicit time integration and require on the order of 20 to 100 hours on current supercomputers. The methodologies are briefly reviewed and then some example calculations employing these methods are described. The methods are also of value to other nonlinear transient computations. Author (revised)

N94-19467*# National Aeronautics and Space Administration. Langley Research Center, Hampton, VA.
COMPOSITE IMPACT DYNAMICS RESEARCH AT NASA LARC: A REVIEW
Huey D. Carden *In its* Computational Methods for Crashworthiness Aug. 1993 p 37-64 (For primary document see N94-19465 04-39)
Avail: CASI HC A03/MF A03

The Landing and Impact Dynamics Branch of NASA Langley Research Center has been involved in impact dynamics research since the early 1970's. For the first ten years, the emphasis of the research was on metal aircraft structures in both the General Aviation Crash Dynamics Program and the Controlled Impact Demonstration (CID) Program, a transport aircraft program culminating in the controlled crash test of a Boeing 720 aircraft in 1984. Subsequent to the transport work, the emphasis has been on composite structures with efforts directed at understanding the behavior, responses, failure mechanisms, and general loads associated with the composite material systems under crash type loadings. Considerable work has been conducted to address the energy absorption characteristics and it indicates that composites can absorb as much if not considerably more energy than comparable aluminum structures. However, due to their brittle nature, attention must be given to proper geometry and designs to take advantage of the good energy absorbing properties while providing desired structural integrity. Achieving the desired new designs often requires an understanding of how more conventional designs behave under crash type loadings. The purpose is to present a review of the composite impact dynamics research being conducted at NASA Langley Research Center. Examples are presented of experimental and analytical data to illustrate the activities in the four program elements of the composite research.
Author (revised)

N94-19468*# Grumman Aerospace Corp., Bethpage, NY. Research Dept.
IMPACT ANALYSIS OF COMPOSITE AIRCRAFT STRUCTURES
Allan B. Pifko and Alan S. Kushner (State Univ. of New York, Stony Brook.) *In* NASA. Langley Research Center, Computational Methods for Crashworthiness Aug. 1993 p 65-94 (For primary document see N94-19465 04-39)
Avail: CASI HC A03/MF A03

The impact analysis of composite aircraft structures is discussed. Topics discussed include: background remarks on aircraft crashworthiness; comments on modeling strategies for crashworthiness simulation; initial study of simulation of progressive failure of an aircraft component constructed of composite material; and research direction in composite characterization for impact analysis. CASI

N94-19469*# Army Aviation Systems Command, Fort Eustis, VA. Aviation Applied Technology Directorate.
DEVELOPMENT AND USE OF COMPUTATIONAL TECHNIQUES IN ARMY AVIATION RESEARCH AND DEVELOPMENT PROGRAMS FOR CRASH RESISTANT HELICOPTER TECHNOLOGY
LeRoy T. Burrows *In* NASA. Langley Research Center, Computational Methods for Crashworthiness Aug. 1993 p 95-104 (For primary document see N94-19465 04-39)
Avail: CASI HC A02/MF A03

During the 1960's over 30 full-scale aircraft crash tests were conducted by the Flight Safety Foundation under contract to the Aviation Applied Technology Directorate (AATD) of the U.S. Army Aviation Systems Command (AVSCOM). The purpose of these tests were to conduct crash injury investigations that would provide a basis for the formulation of sound crash resistance design criteria for light fixed-wing and rotary wing aircraft. This resulted in the Crash Survival Design Criteria Designer's Guide which was first published in 1967 and has been revised numerous times, the last being in 1989. Full-scale aircraft crash testing is an expensive way to investigate structural deformations of occupied spaces and to determine the decelerative loadings experienced by occupants in a crash. This gave initial impetus to the U.S. Army to develop analytical methods to predict the dynamic response of aircraft structures in a crash. It was believed that such analytical tools could be very useful in the preliminary design stage of a new helicopter system which is required to demonstrate a level of crash resistance and had to be more cost effective than full-scale crash tests or numerous component design support tests. From an economic point of view, it is more efficient to optimize for the incorporation of crash resistance features early in the design stage. However, during preliminary design it is doubtful if sufficient design details, which influence the exact plastic deformation shape of structural elements, will be available. The availability of simple procedures to predict energy absorption and load-deformation characteristics will allow the designer to initiate valuable cost, weight, and geometry tradeoff studies. The development of these procedures will require some testing of typical specimens. This testing should, as a minimum, verify the validity of proposed procedures for providing pertinent nonlinear load-deformation data. It was hoped that through the use of these analytical models, the designer could optimize aircraft design for crash resistance from both a weight and cost increment standpoint, thus enhancing the acceptance of the design criteria for crash resistance. Author (revised)

N94-19470*# Wright Lab., Wright-Patterson AFB, OH. Aircrew Enclosures Group.
EXPLICIT SOLUTION TECHNIQUES FOR IMPACT WITH CONTACT CONSTRAINTS
Robert E. McCarty *In* NASA. Langley Research Center, Computational Methods for Crashworthiness Aug. 1993 p 105-123 (For primary document see N94-19465 04-39)
Avail: CASI HC A03/MF A03

Modern military aircraft transparency systems, windshields and canopies, are complex systems which must meet a large and rapidly growing number of requirements. Many of these transparency system requirements are conflicting, presenting difficult balances which must be achieved. One example of a challenging requirements balance or trade is shaping for stealth versus aircrew vision. The large number of requirements involved may be grouped in a variety of areas including man-machine interface; structural integration with the airframe; combat hazards; environmental exposures; and supportability. Some individual requirements by themselves pose very difficult, severely nonlinear analysis problems. One such complex problem is that associated with the dynamic structural response resulting from high energy bird impact. An improved analytical capability for soft-body impact simulation was developed. Author (revised)

N94-19471*# Ford Motor Co., Dearborn, MI.
NUMERICAL SIMULATION OF VEHICLE CRASHWORTHINESS AND OCCUPANT PROTECTION
Nripen K. Saha *In* NASA. Langley Research Center, Computational Methods for Crashworthiness Aug. 1993 p 125-139 (For primary document see N94-19465 04-39)
Avail: CASI HC A03/MF A03

Numerical simulation of vehicle crashworthiness and occupant protection are addressed. The vehicle crashworthiness design objectives are to design the vehicle structure for optimum impact energy absorption, and to design the restraint system (seatbelts, airbags, bolsters, etc.) for optimum occupant protection. The following approaches are taken; a major part of the impact energy is to be absorbed by the vehicle structure; the restraint components will provide protection against the remaining crash energy; certain vehicle components are designed to deform under specific types and speeds of impact in a desired mode for sound energy management; structural components such as front side rails, rear rails, door structure and pillars undergo large amounts of deformation; and with properly designed geometry and material these components assist in mitigating the effects of impact. Author (revised)

N94-19472*# General Motors Corp., Warren, MI. Engineering Mechanics Dept.
DIRECTIONS FOR COMPUTATIONAL MECHANICS IN AUTOMOTIVE CRASHWORTHINESS
James A. Bennett and T. B. Khalil *In* NASA. Langley Research Center, Computational Methods for Crashworthiness Aug. 1993 p 141-154 (For primary document see N94-19465 04-39)
Avail: CASI HC A03/MF A03

The automotive industry has used computational methods for crashworthiness since the early 1970's. These methods have ranged from simple lumped parameter models to full finite element models. The emergence of the full finite element models in the mid 1980's has significantly altered the research direction. However, there remains a need for both simple, rapid modeling methods and complex detailed methods. Some directions for continuing research are discussed. Author (revised)

N94-19473*# Virginia Univ., Charlottesville. Dept. of Mechanical and Aerospace Engineering.
EFFICIENCY AND BIOFIDELITY OF OCCUPANT SIMULATIONS c54
Walter D. Pilkey *In* NASA. Langley Research Center, Computational Methods for Crashworthiness Aug. 1993 p 155-163 (For primary document see N94-19465 04-39)
Avail: CASI HC A02/MF A03

Efficiency and biofidelity of occupant simulations are addressed. Topics covered include: R (ratio of rebound energy to initial energy) and G (ratio of permanent deformation to maximum deformation) parameters: ATB simulator unloading behavior; motion of sphere relative to vehicle after vehicle decelerates; sphere for belt restraint; sphere data for wall impact; head acceleration vs. belt slack x-direction (measured); and head acceleration vs. belt slack x-direction (simulated). CASI

N94-19474*# Key Associates, Albuquerque, NM.
CURRENT CAPABILITIES FOR SIMULATING THE EXTREME DISTORTION OF THIN STRUCTURES SUBJECTED TO SEVERE IMPACTS
Samuel W. Key *In* NASA. Langley Research Center, Computational Methods for Crashworthiness Aug. 1993 p 165-184 (For primary document see N94-19465 04-39)
Avail: CASI HC A03/MF A03

The explicit transient dynamics technology in use today for simulating the impact and subsequent transient dynamic response of a structure has its origins in the 'hydrocodes' dating back to the late 1940's. The growth in capability in explicit transient dynamics technology parallels the growth in speed and size of digital computers. Computer software for simulating the explicit transient dynamic response of a structure is characterized by algorithms that use a large number of small steps. In explicit transient dynamics software there is a significant emphasis on speed and simplicity. The finite element technology used to generate the spatial discretization of a structure is based on a compromise between completeness of the representation for the physical processes modelled and speed in execution. That is, since it is expected in every calculation that the deformation will be finite and the material will be strained beyond the elastic range, the geometry and the associated gradient operators must be reconstructed, as well as complex stress-strain models evaluated at every time step. As a result, finite elements derived for explicit transient dynamics software use the simplest and barest constructions possible for computational efficiency while retaining an essential representation of the physical behavior. The best example of this technology is the four-node bending quadrilateral derived by Belytschko, Lin and Tsay. Today, the speed, memory capacity and availability of computer hardware allows a number of the previously used algorithms to be 'improved.' That is, it is possible with today's computing hardware to modify many of the standard algorithms to improve their representation of the physical process at the expense of added complexity and computational effort. The purpose is to review a number of these algorithms and identify the improvements possible. In many instances, both the older, faster version of the algorithm and the improved and somewhat slower version of the algorithm are found implemented together in software. Specifically, the following seven algorithmic items are examined: the invariant time derivatives of stress used in material models expressed in rate form; incremental objectivity and strain used in the numerical integration of the material models; the use of one-point element integration versus mean quadrature; shell elements used to represent the behavior of thin structural components; beam elements based on stress-resultant plasticity versus cross-section integration; the fidelity of elastic-plastic material models in their representation of ductile metals; and the use of Courant subcycling to reduce computational effort. Author (revised)

N94-19475*# Lawrence Livermore National Lab., CA. Methods Development Group.
CRASHDYNAMICS WITH DYNA3D: CAPABILITIES AND RESEARCH DIRECTIONS
Robert G. Whirley and Bruce E. Engelmann *In* NASA. Langley Research Center, Computational Methods for Crashworthiness Aug. 1993 p 185-205 (For primary document see N94-19465 04-39)
(Contract W-7405-eng-48)
Avail: CASI HC A03/MF A03

The application of the explicit nonlinear finite element analysis code DYNA3D to crashworthiness problems is discussed. Emphasized in the first part of this work are the most important capabilities of an explicit code for crashworthiness analyses. The areas with significant research promise for the computational simulation of crash events are then addressed. Author (revised)

N94-19476*# Sandia National Labs., Albuquerque, NM.
TRANSIENT DYNAMICS CAPABILITY AT SANDIA NATIONAL LABORATORIES
Steven W. Attaway, Johnny H. Biffle, G. D. Sjaardema, M. W. Heinstein, and L. A. Schoof *In* NASA. Langley Research Center, Computational Methods for Crashworthiness Aug. 1993 p 207-249 (For primary document see N94-19465 04-39)
Avail: CASI HC A03/MF A03

A brief overview of the transient dynamics capabilities at Sandia National Laboratories, with an emphasis on recent new developments and current research is presented. In addition, the Sandia National Laboratories (SNL) Engineering Analysis Code Access System (SEACAS), which is a collection of structural and thermal codes and utilities used by analysts at SNL, is described. The SEACAS system includes pre- and post-processing codes, analysis codes, database translation codes, support libraries, Unix shell scripts for execution, and an installation system. SEACAS is used at SNL on a daily basis as a production, research, and development system for the engineering analysts and code developers. Over the past year, approximately 190 days of CPU time were used by SEACAS codes on jobs running from a few seconds up to two and one-half days of CPU time. SEACAS is running on several different systems at SNL including Cray Unicos, Hewlett Packard PH-UX, Digital Equipment Ultrix, and Sun SunOS. An overview of SEACAS, including a short description of the codes in the system, are presented. Abstracts and references for the codes are listed at the end of the report. Author (revised)

N94-19543# Lawrence Livermore National Lab., CA.
THE INFLUENCE OF THE TARGET STRENGTH MODEL ON COMPUTED PERFORATION
J. E. Reaugh Jun. 1993 6 p Presented at the 14th International Conference of the International Association for the Advancement of High Pressure Science and Technology, Colorado Springs, CO, 27 Jun. - 2 Jul. 1993
(Contract W-7405-eng-48)
(DE93-018659; UCRL-JC-113151; CONF-930676-32) Avail: CASI HC A02/MF A01

The authors used an axisymmetric, two-dimensional Eulerian computer simulation program to simulate the penetration of a tungsten rod, with length to diameter ratio $L/D = 10$, into a thick steel target and the same rod into finite steel plates of thicknesses between 0.9 and 1.3 L. They compare the perforation limit with the semi-infinite penetration depth at the same velocity (the excess thickness) when the model for target strength is constant yield stress and when the model incorporates work hardening and thermal softening. The authors also compare their computed results with available experimental results, which show an excess thickness of about 1 rod diameter. DOE

N94-19603# Los Alamos National Lab., NM.
SIMULATION OF DYNAMIC MATERIAL RESPONSE WITH THE PAGOSA CODE
K. S. Holian and T. F. Adams 1993 5 p Presented at the Annual Winter Meeting of the ASME, New Orleans, LA, 28 Nov. - 3 Dec. 1993
(Contract W-7405-eng-36)
(DE93-018285; LA-UR-93-2802; CONF-931121-13) Avail: CASI HC A01/MF A01

The 3D Eulerian PAGOSA hydrocode is being run on the massively parallel Connection Machine (CM) to simulate the response of materials to dynamic loading, such as by high explosives or high velocity impact. The code has a variety of equation of state forms, plastic yield models, and fracture and fragmentation models. The numerical algorithms in PAGOSA and the implementation of material models are discussed briefly. DOE

N94-19606# Edgewood Arsenal, Aberdeen Proving Ground, MD. Research Development and Engineering Center.
SHELL DESIGNS Final Report, Jun. 1991 - Jul. 1992
Ronald B. Crosier Aug. 1993 22 p
(AD-A270656; ERDEC-TR-104) Avail: CASI HC A03/MF A01

The shell designs consist of two series of related designs (the uniform shell designs and the simplicial shell designs) that are used for fitting second-order response surfaces over spherical regions. The shell designs for two, four, six, and eight factors require fewer experimental runs than the central composite designs or the Box-Behnken designs, but they have not been used much because of their unequal treatment of the design factors. Rotations of the shell designs that provide an equal treatment of the factors are given. The rotated uniform shell designs have seven levels of each factor with the exception of the three-factor design (three levels) and the eight-factor design (five levels). An orthogonal blocking scheme is given for the uniform shell designs with an even number of factors. The simplicial shell designs have nine levels, except for the two-factor and seven-factor designs, which have seven levels, and the three-factor design, which has five levels but is singular. The simplicial shell designs have an orthogonal blocking scheme for any number of factors. DTIC

N94-19648# Technische Univ., Berlin (Germany). Inst. fuer Mechanik.
DEVELOPMENT OF ENGINEERING MODELS FOR CALCULATION OF FAILURE LOADS AND DEFECT STATES OF STEEL CONCRETE BEAMS AND PLATES Ph.D. Thesis [ERWEITERUNG VON INGENIEURMODELLEN ZUR BERECHNUNG VON BRUCHLASTEN UND VERSAGENSZUSTAENDEN VON STAHLBETONBALKEN UND -PLATTEN]
Christian Enderle 1992 134 p In GERMAN
(ETN-93-95052) Avail: CASI HC A07/MF A02

A model for shear behavior of reinforced concrete beams is formulated and extended to spatial punching problem. The main theories of shear behavior and calculations based on the finite-element method are presented. A model, which takes into account crack bank dovetailing, was developed for depicting shear behavior of concrete slabs with an optimization of elastic potential. The model is shown to allow the maximal transverse force in failure state to be estimated and the failure cause of a beam to be determined. Principles of calculation of reinforced concrete plates and theories of punching behavior with concentrated single loads were summarized, considering ideally elastic or plastic materials. The model of a plane slab was extended to the calculation of beam on a spatial assembly of slabs and slices. ESA

N94-19669 Technische Univ., Delft (Netherlands). Structures and Materials Lab.

FATIGUE CRACK INITIATION IN RIVETED LAP JOINTS AND IN PRESSURIZED FUSELAGES

Richard P. G. Mueller Jun. 1993 27 p Presented at the SAMPE European Conference, Birmingham, England, 19-21 Oct. 1993 Limited Reproducibility: More than 20% of this document may be affected by microfiche quality

(LR-725; ETN-93-95029) Avail: CASI HC A03

Riveted joints in pressurized fuselages are exposed to severe fatigue loading. The study was carried out to increase fundamental understanding of the behavior of riveted fuselage joints. Areas of interest include rivet flexibility, load transfer, residual stress distribution, fatigue crack location, secondary bending and inter-sheet friction. These aspects depend on the squeezing force used to drive the rivet. Flat uniaxially loaded riveted lap joint specimens show longer fatigue lives than curved riveted panels loaded by internal pressure in a barrel test setup. Strain gauge measurements on a barrel test setup show more severe loading of the non-countersunk inner sheet compared to the countersunk outer sheet. Finite element calculations gave insight to the improved fatigue crack initiation performance for increased sqeezing force and to the crack initiation location. The early crack initiation at the edges of flat riveted lap joint panels is explained. ESA

42 GEOSCIENCES (GENERAL)

N94-17893# State Univ. of New York, Albany.

GEOGRAPHY AND METEOROLOGICAL STUDIES IN THE FAR EAST

M. R. Riches 10 Aug. 1992 20 p

(Contract DE-FG02-92ER-61369)

(DE93-013563; DOE/FTR-93013563) Avail: CASI HC A03/MF A01 (US Sales Only)

This trip diary reports the details of travel to China. The traveler attended a variety of meetings in addition to the International Workshop on Climate Variabilities and the Fourth International Summer Colloquium and International Symposium for Young Scientists on Climate, Environment and Geophysical Fluid Dynamics. Also included is the discussions on the joint research on the greenhouse effect. DOE

N94-19209# Joint Publications Research Service, Arlington, VA.

JPRS REPORT: SCIENCE AND TECHNOLOGY. CENTRAL EURASIA: EARTH SCIENCES

1 Sep. 1993 16 p Transl. into ENGLISH from various Russian articles

(JPRS-UES-93-004) Avail: CASI HC A03/MF A01

Papers on the following topics are included: plate tectonics hypothesis: progress or regression in geology; long-range weather forecasts; integral characteristics of the echo signal in aerospace laser sounding of sea water through an agitated surface; structure of database of space and hydrometeorological observations of mesoscale tropical disturbances; and formation of acid aerosol trails in atmosphere behind solid-propellant rockets. CASI

43 EARTH RESOURCES AND REMOTE SENSING

Includes remote sensing of earth resources by aircraft and spacecraft; photogrammetry; and aerial photography.

For instrumentation see *35 Instrumentation and Photography.*

N94-17851# Edgerton, Germeshausen and Grier, Inc., Idaho Falls, ID.

RAPID GEOPHYSICAL SURVEYOR

L. G. Roybal, G. S. Carpenter, and N. E. Josten 1993 16 p Presented at the SAGEEP 1993: Symposium on the Application of Geophysics To Environmental and Engineering Problems, San Diego, CA, 18-21 Apr. 1993

(Contract DE-AC07-76ID-01570)

(DE93-016637; EGG-M-92598; CONF-9304109-5) Avail: CASI HC A03/MF A01

The Rapid Geophysical Surveyor (RGS) is a system designed to rapidly and economically collect closely-spaced geophysical data used for characterization of Department of Energy (DOE) waste sites. Geophysical surveys of waste sites are an important first step in the remediation and closure of these sites; especially older sites where historical records are inaccurate and survey benchmarks have changed due to refinements in coordinate controls and datum changes. Closely-spaced data are required to adequately differentiate pits, trenches, and soil vault rows whose edges may be only a few feet from each other. A prototype vehicle designed to collect magnetic field data was built at the Idaho National Engineering Laboratory (INEL) during the summer of 1992. The RGS was one of several projects funded by the Buried Waste Integrated Demonstration (BWID) program. This vehicle was demonstrated at the Subsurface Disposal Area (SDA) within the Radioactive Waste Management Complex (RWMC) on the INEL in Sep. of 1992. Magnetic data were collected over two areas in the SDA, with a total survey area of about 1.7 acres. Data were collected at a nominal density of 2 1/2 inches along survey lines spaced 1 foot apart. Over 350,000 data points were collected over a 6 day period corresponding to about 185 man-days using conventional ground survey techniques. This report documents the design and demonstration of the RGS concept including the presentation of magnetic data collected at the SDA. The surveys were able to show pit and trench boundaries and determine details of their spatial orientation never before achieved. DOE

N94-18063# Institute of Oceanographic Sciences, Wormley (England). Deacon Lab.

CTD AND XBT DATA COLLECTED ON ERS-1 VALIDATION CRUISE RRS CHARLES DARWIN CRUISE 62A, ICELAND-FAEROES REGION

R. T. Tokmakian, A. I. Morrison, S. G. Alderson, and M. A. Srokosz 1992 83 p

(IOS-294-1992; ETN-93-94557) Avail: CASI HC A05/MF A01

The hydrographic data set from the RRS Charles Darwin Cruise 62A, 6-26 Sep. 1991, whose objective was to evaluate the data from the sensors onboard the ESA ERS-1 satellite against in situ measurements, is described. The data set was collected in the region from 60 to 64 deg north and from 3 to 7 deg west. The region is to the north of the Faeroes. Two Conductivity/ Temperature/ Depth (CTD) and XBT surveys were conducted along two ERS-1 ground tracks, an ascending track and a descending track, forming a triangular survey region. The bottom corner of the survey is the point at which the two satellite tracks cross. XBT drops were conducted between the CTD stations. The collection, calibration, and processing of the CTD and XBT data are reported. Temperature, conductivity, and pressure were measured for each CTD station. A total number of 27 profiles are presented. Profile plots and listings are included for each CTD station. Both CTD and XBT contour plots are shown for each leg of the two surveys. ESA

N94-18107# Pacific Northwest Lab., Richland, WA.

APPLICATION OF ARC/INFO TO REGIONAL SCALE HYDROGEOLOGIC MODELING

S. K. Wurstner, G. McWethy, J. L. Devary, and M. G. Foley May 1993 10 p Presented at the 13th ESRI Annual Users Conference, Palm Springs, CA, 24-28 May 1993

(Contract DE-AC06-76RL-01830)

(DE93-015673; PNL-SA-22530; CONF-9305220-1) Avail: CASI HC A02/MF A01

A Geographic Information System (GIS) can be a useful tool in data preparation for groundwater flow modeling, especially when studying large regional systems. ARC/INFO is being used in conjunction with GRASS to support data preparation for input to the CFEST (Coupled Fluid, Energy, and Solute Transport) groundwater modeling code. Simulations will be performed with CFEST to model three-dimensional, regional, groundwater flow in the West Siberian Basin. DOE

N94-18137 Institute of Oceanographic Sciences, Wormley (England). Deacon Lab.

RADIOSONDE DATA COLLECTED ON THE ERS-1 VALIDATION CRUISE RRS CHARLES DARWIN CRUISE 62A, ICELAND FAEROES REGION

T. N. Forrester and T. H. Guymer 1992 82 p Limited Reproducibility: More than 20% of this document may be affected by microfiche quality

(IOS-297-1992; ETN-93-94560) Avail: CASI HC A05

Radiosonde measurements made during Sep. 1991 in a survey region to the north east of the Faeroe Islands, during the ERS-1 validation cruise, are reported. A total of 35 radiosondes were launched (two per day). Data from 34 ascents processed between values of pressure at the surface and at 200 mb (approximately 11.8 km high) are presented. Atmospheric temperature and relative humidity were observed and potential temperature and specific humidity were calculated from these observations. ESA

N94-18309 Army Topographic Engineering Center, Fort Belvoir, VA.
DIRECTIONAL REGIONS IN GEOGRAPHIC INFORMATION SYSTEMS (GIS)
Douglass R. Caldwell and Linda H. Graff 3 Aug. 1993 10 p Limited Reproducibility: More than 20% of this document may be affected by microfiche quality
(AD-A268536; TEC-R-196) Avail: Issuing Activity (Defense Technical Information Center (DTIC))

While direction is fundamental to geography, the implementation of directional functions in Geographical Information Systems (GIS) is limited. The focus paper is the extension of direction-related concepts through the definition of directional regions, such as the area north of Washington DC. Directional regions are constructed from combinations of six elements: the feature, the reference, an orientation, a viewspan, a viewfield and a region of interest. This approach allows users to create new area features which can be incorporated in a GIS. These features are a valuable tool for geographical analysis, since they further constrain reasoning on a data set. DTIC

N94-18631# Titan Spectron Div., Tustin, CA.
SUPER-RESOLUTION OF MULTI-PIXEL AND SUB-PIXEL IMAGES FOR THE SDI Final Report
8 Jun. 1993 160 p Also included with AD-M000266
(Contract N00014-90-C-0173)
(AD-A268537; Rept-93-2881-06) Avail: CASI HC A08/MF A02

The recent profound shift in the global balance of power in favor of the United States of America has had major repercussions on Strategic Defense Initiative (SDI) planning. In particular, the focus has shifted from the provision of protection for the United States against a massive raid, involving possibly thousands of reentry vehicles, to defense against a much more limited attack which could now, however, be launched from any part of the world. Additionally, the United States is seeking to protect its forces and allies overseas, and in the task of missile detection and tracking, allowance must now be made for trajectories which can begin and end in almost any inhabited area of the globe. Thus SDI demands on surveillance technology have been significantly expanded. Space-based imaging systems will play a vital role in the surveillance task. In this report a description is first given of a typical scenario. The potential imaging problems are then examined, the mathematical background is discussed, and the innovative algorithms which have been developed for correcting and enhancing the performance of the imaging sensor are described. DTIC

N94-18677 Naval Research Lab., Bay Saint Louis, MS.
THE NAVY TESSELLATED SPHEROID MAP PROJECTION SYSTEM: A COMPREHENSIVE DEFINITION Final Report
Maura C. Lohrenz, Michael E. Trenchard, Stephanie A. Myrick, Perry B. Wischow, and Lancelot M. Riedlinger 11 Aug. 1993 30 p Limited Reproducibility: More than 20% of this document may be affected by microfiche quality
(AD-A269989; NRL/FR/7441-92-9408) Avail: CASI HC A03

This report describes a map projection model, called the Tessellated Spheroid (TS), which provides a seamless, global framework in which to store scanned chart data and, potentially, other types of spatial data as well. The Compressed Aeronautical Chart (CAC) is being developed at the Naval Research Laboratory in direct support of tactical Navy and Marine Corps aircraft mission planning systems and digital moving map systems. Aircraft programs that currently utilize the CAC database include the AV-8B Harrier, F/A-18 Hornet, and V-22 Osprey. There has been recent interest in using the TS system to store datasets other than CAC: the newly formed A-X program (which replaced the A-12 program) is interested in storing the Defense Mapping Agency Digital Landmass System data in the TS model; and other programs have shown interest in storing scanned nautical charts and satellite imagery in the TS system and, possibly, compressing that data in the same manner in which the CAC data is compressed. Following a detailed description of the TS model, this report discusses certain issues that must be addressed before the TS model can be applied to databases other than the original CAC. The most pressing issue relates to geographic scale. The CAC database includes six scale-models of chart data: 1:50k (k = thousand), 1:100k, 1:250k, 1:500k, 1:1M (M = million), and 1:2M. All TS parameters are based on the 1:2M scale-model, and any additional scales that are to utilize TS must be an integral divisor of 2,000,000. In addition, the TS segment file naming convention currently stipulates a maximum of 9000 TS segment rows, but scales that are larger than approximately 1:50k have more than 9000 rows. DTIC

N94-18679# Naval Research Lab., Bay Saint Louis, MS.
COLOR PALETTE CONSIDERATIONS FOR DIGITAL MAP DISPLAYS Final Report
Michael E. Trenchard, Maura C. Lohrenz, Stacen Tyskiewicz, and Henry Rosche, III 3 Aug. 1993 17 p
(AD-A269991; NRL/FR/7441-92-9415) Avail: CASI HC A03/MF A01

The Map Data Formatting Facility is creating a library of Compressed Aeronautical Chart (CAC) data on a compact disk (CD) media in support of mission planning systems and airborne digital moving-map systems for military aircraft. The CAC library is generated by transforming the Defense Mapping Agency's Equal Arc-Second Raster Chart (ARC) Digitized Raster Graphics data from the ARC projection system into the Navy-specified tessellated spheroid projection system. The data are then color and spatially compressed using a technique known as vector quantization. This report discusses the method by which a standard set of thirty 8-bit color palettes, which are used for the color-compression portion of CAC generation, are built. Briefly, color compression is achieved by reducing the amount of color information from 24 bits per pixel to 8 bits per pixel via a color look-up table. A CAC color palette, which contains 256 entries (including 16 that are reserved for vector graphic overlays), is used to define the color look-up table. In addition, the color palette is written onto the final CAC CD-ROM for decompression operations. Since a single color palette will be used to color compress ARC digitized raster graphics data for one-fifth of the world at a given scale, prudent color selection is vital. DTIC

N94-18729 Massachusetts Inst. of Tech., Lexington.
PROCEEDINGS OF THE 11TH SPACE SURVEILLANCE WORKSHOP
R. W. Miller and R Sridharan 1 Apr. 1993 140 p Workshop held in Lexington, MA, 30 Mar. - 1 Apr. 1993 Limited Reproducibility: More than 20% of this document may be affected by microfiche quality
(Contract F19628-90-C-0002)
(AD-A269477; STK-206-Vol-2; ESC-TR-93-249-Vol-2) Avail: CASI HC A07

The eleventh Annual Space Surveillance Workshop hosted by MIT Lincoln Laboratory was held 30-31 March and 1 April 1993. The purpose of the series of workshops is to provide a forum for the presentation and discussion of space surveillance issues. This Proceedings documents most of the presentations from this workshop. The papers contained were reproduced directly from copies supplied by their authors (with minor mechanical changes where necessary). It is hoped that this publication will enhance the utility of the workshop. DTIC

N94-18753 Naval Postgraduate School, Monterey, CA.
RESOLUTION IN RADAR MAPPING M.S. Thesis
Michael D. Anderson Mar. 1993 90 p Limited Reproducibility: More than 20% of this document may be affected by microfiche quality
(AD-A269730) Avail: CASI HC A05

Signal processing has led to great performance gains in radar mapping. The most critical feature of these systems is cell size, which determines resolution. Cell size is defined by range resolution and azimuth resolution. Range resolution is improved through pulse compression. Phase of frequency modulation of a waveform yields increased bandwidth and shorter effective pulse width without reducing total signal energy. Several families of codes are investigated emphasizing matched filter output and doppler tolerance. Azimuth resolution is improved through beam sharpening. Several beam sharpening techniques are illustrated with radar images provided by Hughes Aircraft. Range bin output plots demonstrate the effectiveness of these techniques. With these techniques, 'near-SAR' quality output can be obtained from real beam mapping radars allowing the real-time and all aspect capabilities of real beam systems to be more fully employed in tactical missions. DTIC

N94-18800# Defence Research Establishment Valcartier (Quebec).
ANALYTIC APPROXIMATIONS OF AN INTEGRAL IN REMOTE SENSING
G. R. Fournier and B. T. Evans Sep. 1993 31 p
(AD-A270085; DREV-R-4724/93) Avail: CASI HC A03/MF A01

Approximate analytic solutions to the integrated bistatic signal from Gaussian distributed scatterers in an absorbing medium are derived. Some solutions are useful over limited ranges of the parameters, and others are globally more valid. The former are simpler than the latter. The error behaviors of each solution is thoroughly discussed. DTIC

N94-19003# Lawrence Livermore National Lab., CA.
PROTOCOL FOR COMPUTATION OF SURFACE BOUNDARY LAYER PARAMETERS USED TO DETERMINE SOIL MOISTURE FLUX FROM METEOROLOGICAL DATA COLLECTED AT LLNL, 1992-1993
F. Gouveia Mar. 1993 22 p
(Contract W-7405-eng-48)
(DE93-018906; UCRL-ID-113516) Avail: CASI HC A03/MF A01

Starting May 1992, meteorological data is continuously collected for Environmental Restoration Division (ERD) at the LLNL weather-tower site. Mounted on a 2-meter mast are sensors for air temperature, wind speed and direction, relative humidity, net radiation flux, and ground heat flux. The height of the sensors and the sensor accuracies are listed. These sensors are sampled every second, and 15-minute averages are saved by the data logger for retrieval. Average and standard deviation (sigma(sub theta)) of wind direction are computed by the Campbell logger using polar coordinates. This report describes the reduction of continuously monitored data from 15-minute averages to hourly averages. The bulk of this report is dedicated to describing the computation of parameters that characterize the surface boundary layer. The ultimate goal is to provide estimates of the amount of evaporation of water from the surface. DOE

N94-19384# Remote Sensing Technology Center, Tokyo (Japan).
DEVELOPMENT OF ISY DATA SET, PART 2 [ISY DETA SETTO NO SEIBI]
National Space Development Agency 31 Mar. 1993 27 p In JAPANESE
(NASDA-CNT-930006-Pt-2; JTN-93-80460) Avail: CASI HC A03/MF A01

This report describes the study for the data set preparation of the sea surface temperature (SST) and the polar region ice zone, and the data set preparation algorithms developed for ISY (International Space Year) activities. Preparation process of the SST data set (including the VTIR (visible and thermal infrared radiometer) data set, comparison of the data by different kinds of sensors and production of marginal data set, production of data set for evaluating the algorithm, and evaluation of the algorithms) and the polar region ice zone data set (including superposition of the MSR (microwave scanning radiometer) and VTIR images, MESSR (multispectral electronic self-scanning radiometer) and VTIR images, production of MSR mosaic images, superposition of MSR and MSS (multi-spectral scanner) images, study on superposition of MESSR and SAR (synthetic aperture radar) images, and auxiliary information overlays), and the development of algorithms for polar region ice zone data set (including the development of the algorithm for the MOS-1 (Marine Observation Satellite-1) data set, comparison evaluation of MSR data set and MSS data, and study on integrated use of SAR data and visible and near infrared data) are outlined. Author (NASDA)

N94-19430*# Colorado Univ., Boulder. Cooperative Inst. for Research in Environmental Sciences.
GRAVITY AND THE GEOID IN THE NEPAL HIMALAYA Final Technical Report, 1 Jul. 1991 - 30 Jun. 1992
Roger Bilham 1992 35 p
(Grant NAGw-2704)
(NASA-CR-194166; NAS 1.26:194166) Avail: CASI HC A03/MF A01

Materials within the Himalaya are rising due to convergence between India and Asia. If the rate of erosion is comparable to the rate of uplift the mean surface elevation will remain constant. Any slight imbalance in these two processes will lead to growth or attrition of the Himalaya. The process of uplift of materials within the Himalaya coupled with surface erosion is similar to the advance of a glacier into a region of melting. If the melting rate exceeds the rate of downhill motion of the glacier then the terminus of the glacier will receed up-valley despite the downhill motion of the bulk of the glacier. Thus although buried rocks, minerals and surface control points in the Himalaya are undoubtably rising, the growth or collapse of the Himalaya depends on the erosion rate which is invisible to geodetic measurements. Erosion rates are currently estimated from suspended sediment loads in rivers in the Himalaya. These typically underestimate the real erosion rate since bed-load is not measured during times of heavy flood, and it is difficult to integrate widely varying suspended load measurements over many years. An alternative way to measure erosion rate is to measure the rate of change of gravity in a region of uplift. If a control point moves vertically it should be accompanied by a reduction in gravity as the point moves away from the Earth's center of mass. There is a difference in the change of gravity between uplift with and without erosion corresponding to the difference between the free-air gradient and the gradient in the acceleration due to gravity caused by a corresponding thickness of rock. Essentially gravity should change precisely in accord with a change in elevation of the point in a free-air gradient if erosion equals uplift rate. We were funded by NASA to undertake a measurement of absolute gravity simultaneously with measurements of GPS height within the Himalaya. Since both absolute gravity and time are known in an absolute sense to 1 part in 10(exp 10) it is possible to estimate gravity with a precision of 0.1 mu gal. Known systematic errors reduce the measurement to an absolute uncertainty of 6 mu gal. The free air gradient at the point of measurement is typically about 3 mu gals/cm. At Simikot where our experiment was conducted we determined a vertical gravity gradient of 4.4 mu gals/cm. Derived from text

N94-19435# World Meteorological Organization, Geneva (Switzerland). World Climate Applications and Services Programme.
A SURVEY OF CURRENT APPROACHES TO MODELLING OF HYDROLOGICAL TIME-SERIES WITH RESPECT TO CLIMATE VARIABILITY AND CHANGE
George S. Cavadias Nov. 1992 51 p
(WMO/TD-534; WCASP-23) Avail: CASI HC A04/MF A01; print copy available at WMO, Geneva, Switzerland

The purpose of this report is to continue the implementation of project A2 of the World Climate Programme entitled 'Analyzing Long Time Series of Hydrological Data with Respect to Climate Variability and Change'. WMO is responsible for the implementation of this project. During the earlier stages of the project, member countries were invited to submit long hydrological time series. These were then forwarded by WMO to the data base of GRDC in Koblenz. Concurrently, WMO published Report No. WMO/TD No. 224 (WCAP-3) which contains a number of tests useful for analyzing time series for the purpose of detecting changes in their structure as well as a computer program for their application. The time series submitted to GRDC were used by Dr. H. Mitosek to test the hypothesis of no change in their means and variances and the results of this study show that, for a substantial number of the series tested, the above hypothesis was rejected. The further development of project A2 must be in the direction of a quantification of the location, form and magnitude of the changes in the structure of these series and of linking these changes to causative factors related to changes of climatic conditions. The quantification of the impacts of climatic change on the hydrologic conditions of river basins can be achieved by the formulation and estimation of mathematical models of two main types: (1) univariate models of meteorological and hydrological time series and (2) multivariate models which, in addition to flows, take into account the inputs of the basin system coming from the atmosphere, e.g. temperature and precipitation. The purpose of this report is twofold: to present a survey of the current literature on univariate and multivariate models taking into account the effects of climatic change on the hydrology of basins and to formulate a number of questions and point out possible directions for further research into this important problem. Derived from text

N94-19672# Army Cold Regions Research and Engineering Lab., Hanover, NH.
FOOTPRINT SIZE OF A HELICOPTER-BORNE ELECTROMAGNETIC INDUCTION SOUNDING SYSTEM VERSUS ANTENNA ALTITUDE
Austin Kovacs, J. S. Holladay, and Clyde J. Bergeron, Jr. Jul. 1993 19 p
(Contract N68452-86-MP-6003)
(AD-A270468; CRREL-93-12) Avail: CASI HC A03/MF A01

Helicopter-towed electromagnetic induction sounding systems were recently used for the remote measurement of sea-ice thickness and shallow sea bathymetry. An inherent aspect of this sensing technology is the large area, the footprint, over which an individual sounding is made. An overview of previous footprint size assessments is given and new footprint size estimates determined from sea ice survey data and analytical calculations are presented. All footprint determinations were found to be in reasonable agreement. For a vertical coaxial coil antenna arrangement the apparent footprint diameter was found to be about 1.25 times the antenna height above the conductive surface, and for a horizontal coplanar coil configuration the ratio is about 3.75 times the antenna height. DTIC

N94-19681*# Massachusetts Inst. of Tech., Cambridge. Research Lab. of Electronics.

REMOTE SENSING OF EARTH TERRAIN Progress Report, Jan. - 30 Jun. 1993

J. A. Kong 1993 17 p
(Grant NAGw-1617)
(NASA-CR-194598; NAS 1.26:194598) Avail: CASI HC A03/MF A01

Progress report on remote sensing of Earth terrain covering the period from Jan. to June 1993 is presented. Areas of research include: radiative transfer model for active and passive remote sensing of vegetation canopy; polarimetric thermal emission from rough ocean surfaces; polarimetric passive remote sensing of ocean wind vectors; polarimetric thermal emission from periodic water surfaces; layer model with tandom spheriodal scatterers for remote sensing of vegetation canopy; application of theoretical models to active and passive remote sensing of saline ice; radiative transfer theory for polarimetric remote sensing of pine forest; scattering of electromagnetic waves from a dense medium consisting of correlated mie scatterers with size distributions and applications to dry snow; variance of phase fluctuations of waves propagating through a random medium; polarimetric signatures of a canopy of dielectric cylinders based on first and second order vector radiative transfer theory; branching model for vegetation; polarimetric passive remote sensing of periodic surfaces; composite volume and surface scattering model; and radar image classification. CASI

44 ENERGY PRODUCTION AND CONVERSION

Includes specific energy conversion systems, e.g., fuel cells; global sources of energy; geophysical conversion; and windpower.

For related information see also *07 Aircraft Propulsion and Power, 20 Spacecraft Propulsion and Power,* and *28 Propellants and Fuels.*

N94-17712# Brookhaven National Lab., Upton, NY.

SUNRAYCE 1993: WORKING SAFELY WITH LEAD-ACID BATTERIES AND PHOTOVOLTAIC POWER SYSTEMS

M. P. DePhillips, P. D. Moskowitz, and V. M. Fthenakis 3 Nov. 1992 13 p
(Contract DE-AC02-76CH-00016)
(DE93-016553; BNL-48416) Avail: CASI HC A03/MF A01

The US Department of Energy (DOE) is sponsoring SUNRAYCE 93 to advance tile technology and use of photovoltaics and electric vehicles. Participants will use cars powered by photovoltaic modules and lead-acid storage batteries. This brochure, prepared for students and faculty participating in this race, outlines the health hazards presented by these electrical systems and gives guidance on strategies for their safe usage. At the outset, it should be noted that working with photovoltaic systems and batteries requires electric vehicle drivers and technicians to have 'hands-on' contact with the car on a daily basis. It is important that no one work near a photovoltaic energy system or battery, either in a vehicle or on the bench, unless they familiarize themselves with the components in use and know and observe safe work practices including the safety precautions described in the manuals provided by the various equipment vendors and this document. DOE

N94-17731# Astropower, Inc., Newark, DE.

DEVELOPMENT OF LARGE-AREA MONOLITHICALLY INTEGRATED SILICON-FILM PHOTOVOLTAIC MODULES

J. A. Rand, J. E. Cotter, A. E. Ingram, T. R. Ruffins, K. P. Shreve, R. B. Hall, and A. M. Barnett Jun. 1993 22 p Prepared for Midwest Research Inst., Golden, CO
(Contract DE-AC02-83CH-10093)
(DE93-010037; NREL/TP-413-5581) Avail: CASI HC A03/MF A01

This report describes work to develop Silicon-Film (trademark) Product 3 into a low-cost, stable solar cell for large-scale terrestrial power applications. The Product 3 structure is a thin (less than 100 micron) polycrystalline layer of silicon on a durable, insulating, ceramic substrate. The insulating substrate allows the silicon layer to be isolated and metallized to form a monolithically interconnected array of solar cells. High efficiency is achievable with the use of light trapping and a passivated back surface. The long-term goal for the product is a 1200 sq cm, 18%-efficient, monolithic array. The short-term objectives are to improve material quality and to fabricate 100 sq cm monolithically interconnected solar cell arrays. Low minority-carrier diffusion length in the silicon film and series resistance in the interconnected device structure are presently limiting device performance. Material quality is continually improving through reduced impurity contamination. Metallization schemes, such as a solder-dipped interconnection process, have been developed that will allow low-cost production processing and minimize R(sub s) effects. Test data for a nine-cell device (16 sq cm) indicated a V(sub oc) of 3.72 V. These first-reported monolithically interconnected multicrystalline silicon-on-ceramic devices show low shunt conductance (less than 0.1 mA/sq cm) due to limited conduction through the ceramic and no process-related metallization shunts. DOE

N94-17781# National Inst. of Standards and Technology, Gaithersburg, MD.

PULSE RADIOLYTIC STUDIES OF ELECTRON TRANSFER PROCESSES AND APPLICATIONS TO SOLAR PHOTOCHEMISTRY

P. Neta 1 Apr. 1993 22 p
(Contract DE-AI05-83ER-13108)
(DE93-018715; DOE/ER-13108/T8) Avail: CASI HC A03/MF A01

Electron transfer and other reactions of various short-lived intermediates have been studied by pulse radiolysis and laser flash photolysis. Highlights of results during the past year are summarized under two main sections: metalloporphyrin electron transfer and associated reactions, and solvent effects on reactions of inorganic radicals and organic peroxyl radicals. DOE

N94-17787# Sandia National Labs., Albuquerque, NM.

SIMPLIFIED PROCESSING FOR 23 PERCENT-EFFICIENT SILICON CONCENTRATOR SOLAR CELLS

D. S. Ruby, P. A. Basore, M. E. Buck, J. M. Gee, W. K. Schubert, and H. L. Tardy 1992 6 p Presented at the 23rd Institute of Electrical and Electronics Engineers (IEEE) Photovoltaic Specialists Conference, Louisville, KY, 10-14 May 1993
(Contract DE-AC04-76DP-00789)
(DE93-015018; SAND-92-2808C; CONF-930540-4) Avail: CASI HC A02/MF A01

We have developed a three-photomask process that requires only a single furnace step above 800 C to fabricate silicon concentrator cells with efficiencies approaching 23% on float-zone (FZ) Si and, for the first time, an efficiency of 20% on solar-grade Czochralski (Cz) Si. Until now, high-efficiency silicon concentrator cells that have demonstrated conversion efficiencies greater than 22% have used FZ silicon and required multiple dopant diffusions and several high-temperature furnace steps. These complexities increase processing costs and preclude the use of lower cost Cz silicon, which is easily degraded by repeated high-temperature cycling. Our simplified processing schedule retains most of the benefit available from high-performance cell designs while holding down processing costs, and it makes the use of lower cost Cz Si a viable option. The incorporation of a better optimized antireflection coating and a lower recombination back-surface field are projected to increase this performance even further. DOE

N94-17798# Sandia National Labs., Albuquerque, NM.

PERFORMANCE MAPPING OF THE STM4-120 KINEMATIC STIRLING ENGINE USING A STATISTICAL DESIGN OF EXPERIMENTS METHOD

M. A. Powell and K. S. Rawlinson 1992 6 p Presented at the 28th Intersociety Energy Conversion Engineering Conference, Atlanta, GA, 8-13 Aug. 1993

(Contract DE-AC04-76DP-00789)
(DE93-015132; SAND-92-2869C; CONF-930804-6) Avail: CASI HC A02/MF A01

A kinetic Stirling cycle engine, the Stirling Thermal Motors (STM) STM4-120, was tested at the Sandia National Laboratories Engine Test Facility (ETF) from March 1989-August 1992. Sandia is interested in determining this engine's potential for solar-thermal-electric applications. The last round of testing was conducted from July-August 1992 using Sandia-designed gas-fired heat pipe evaporators as the heat input system to the engine. The STM4-120 was performance mapped over a range of sodium vapor temperatures, cooling water temperatures, and cycle pressures. The resulting shaft power output levels ranged from 5-9 kW. The engine demonstrated high conversion efficiency (24-31%) even though the power output level was less than 40% of the rated output of 25 kW. The engine had been previously derated from 25 kW to 10 kW shaft power due to mechanical limitations that were identified by STM during parallel testing at their facility in Ann Arbor, MI. A statistical method was used to design the experiment, to choose the experimental points, and to generate correlation equations describing the engine performance given the operating parameters. The testing was truncated due to a failure of the heat pipe system caused by entrainment of liquid sodium in the condenser section of the heat pipes. Enough data was gathered to generate the correlations and to demonstrate the experimental technique. The correlation is accurate in the experimental space and is simple enough for use in hand calculations and spreadsheet-based system models. Use of this method can simplify the construction of accurate performance and economic models of systems in which the engine is a component. The purpose of this paper is to present the method used to design the experiments and to analyze the performance data. DOE

N94-17853# Lawrence Livermore National Lab., CA.
REGENERATIVE FUEL CELLS FOR HIGH ALTITUDE LONG ENDURANCE SOLAR POWERED AIRCRAFT
F. Mitlitsky, N. J. Colella, B. Myers, and C. J. Anderson (AeroVironment, Inc., Monrovia, CA.) 2 Jun. 1993 8 p Presented at the 28th Intersociety Energy Conversion Engineering Conference, Atlanta, GA, 8-13 Aug. 1993
(Contract W-7405-eng-48)
(DE93-016991; UCRL-JC-113485; CONF-930804-12) Avail: CASI HC A02/MF A01

High Altitude Long Endurance (HALE) unmanned missions appear to be feasible using a lightweight, high efficiency, span-loaded, Solar Powered Aircraft (SPA) which includes a Regenerative Fuel Cell (RFC) system and novel tankage for energy storage. An existing flightworthy electric powered flying wing design was modified to incorporate present and near-term technologies in energy storage, power electronics, aerodynamics, and guidance and control in order to substantiate feasibility. The design philosophy was to work with vendors to identify affordable near-term technological opportunities that could be applied to existing designs in order to reduce weight, increase reliability, and maintain adequate efficiency of components for delivery within 18 months. The energy storage subsystem for a HALE SPA is a key driver for the entire vehicle because it can represent up to half of the vehicle weight and most missions of interest require the specific energy to be considerably higher than 200 W-hr/kg for many cycles. This stringent specific energy requirement precludes the use of rechargeable batteries or flywheels and suggests examination of various RFC designs. An RFC system using lightweight tankage, a single fuel cell (FC) stack, and a single electrolyzer (EC) stack separated by the length of a spar segment (up to 39 ft), has specific energy of approximately 300 W-hr/kg with 45% efficiency, which is adequate for HALE SPA requirements. However, this design has complexity and weight penalties associated with thermal management, electrical wiring, plumbing, and structural weight. A more elegant solution is to use unitized RFC stacks (reversible stacks that act as both FC's and EC's) because these systems have superior specific energy, scale to smaller systems more favorably, and have intrinsically simpler thermal management. DOE

N94-17888# Midwest Research Inst., Golden, CO. National Renewable Energy Lab.
THE VALUE OF WINDPOWER: AN INVESTIGATION USING A QUALIFIED PRODUCTION COST MODEL
M. R. Milligan and A. H. Miller Jul. 1993 10 p Presented at the Windpower 1993, San Francisco, CA, 12-16 Jul. 1993
(Contract DE-AC02-83CH-10093)
(DE93-010043; NREL/TP-441-5730; CONF-930726-2) Avail: CASI HC A02/MF A01

As part of the US Department of Energy's Wind Energy Program at the National Renewable Energy Laboratory, we are using the Environmental Defense Fund's Electric Utility Financial & Production Cost Model (Elfin) as a tool to determine the value of wind energy to specific utilities. The cases we have developed exercise a number of options in the way in which wind energy is treated: as a load modifier (negative load); as a quick-start supply-side resource with hourly varying output; and probabilistically, using time-varying Weibull distributions. By using two wind speed distributions, two different wind turbines, and two different utilities, we show what the wind turbine cost/kW might be that results in a positive value of wind energy for these utilities. DOE

N94-18001# Sandia National Labs., Albuquerque, NM.
FAROW: A TOOL FOR FATIGUE AND RELIABILITY OF WIND TURBINES
P. S. Veers, C. H. Lange (Stanford Univ., CA.), and S. R. Winterstein (Stanford Univ., CA.) 1993 9 p Presented at the Windpower 1993 Conference, San Francisco, CA, 12-16 Jul. 1993
(Contract DE-AC04-76DP-00789)
(DE93-017639; SAND-93-0424C; CONF-930726-3) Avail: CASI HC A02/MF A01

FAROW is a computer program that evaluates the fatigue and reliability of wind turbine components using structural reliability methods. A deterministic fatigue life formulation is based on functional forms of three basic parts of wind turbine fatigue calculation: (1) the loading environment, (2) the gross level of structural response given the load environment, and (3) the local failure criterion given both load environment and gross stress response. The calculated lifetime is compared with a user specific target lifetime to assess probabilities of premature failure. The parameters of the functional forms can be defined as either constants or random variables. The reliability analysis uses the deterministic lifetime calculation as the limit state function of a FORM/SORM (first and second order reliability methods) calculation based on techniques developed by Rackwitz. Besides probability of premature failure, FAROW calculates the mean lifetime, the relative importance of each of the random variables, and the sensitivity of the results to all of the input parameters, both constant inputs and the parameters that define the random variable inputs. The ability to check the probability of failure with Monte Carlo simulation is included as an option. DOE

N94-18089 Deutsche Forschungsanstalt fuer Luft- und Raumfahrt, Cologne (Germany). Hauptabt. Managementdienste-Energietechnik.
DEVELOPMENT OF A SELECTIVE VOLUMETRIC RECEIVER FOR CENTRAL RECEIVER SYSTEMS: INVESTIGATION OF PARAMETERS AND EXERGETIC EVALUATION Ph.D. Thesis - Ruhr Univ. [ENTWICKLUNG EINES SELEKTIVEN VOLUMETRISCHEN RECEIVERS FUER SOLARTURMKRAFTWERKE: PARAMETER-UNTERSUCHUNGEN UND EXERGETISCHE BEWERTUNG]
Robert Pitz-Paal Jan. 1993 162 p In GERMAN Limited Reproducibility: More than 20% of this document may be affected by microfiche quality
(DLR-FB-93-05; ETN-93-94875) Avail: CASI HC A08

A concept of a staggered selective volumetric receiver for central receiver systems is proposed. A physical model was developed which is able to calculate the temperature distribution within the receiver parallel to the flow direction. Solar and thermal radiation were taken into account as a function of the wavelength as well as for convective heat transfer and heat conduction in the absorber walls. A variation of geometrical parameters, physical properties and running conditions shows important trends of the thermal behavior of the receiver which was rated by an exergetic efficiency. It was ascertained that the calculations offer a high potential for the exergetic efficiency of this receiver type, if an appropriate selection of the cutoff wavelength describing the selective absorption is performed. A general idealized behavior of physical absorber properties as well as the combination of Si-SiC ceramic and fused silica as absorber material were investigated in detail. A comprehensive estimation of the accuraccy of the code and the chosen assumptions was performed. ESA

N94-18103 Department of Energy, Washington, DC. Office of the Deputy Assistant Secretary for Advanced Research and Special Technologies.
FUEL CELL SYSTEMS PROGRAM PLAN, FISCAL YEAR 1993
1993 43 p Limited Reproducibility: More than 20% of this document may be affected by microfiche quality
(DE93-017828; DOE/FE-0280) Avail: CASI HC A03

DOE Office of Fossil Energy (OoFE) is participating with private sector in developing molten carbon fuel cell (MCFC) and advanced concepts including solid oxide fuel cell for application in utility/commercial/industrial sectors. Phosphoric acid fuel cell (PAFC) development was sponsored by OoFE and is now being commercialized. In 1993 DOD is undertaking use and demonstration of PAFC and other fuel cells. DOE Office of Conservation and Renewable Energy is sponsoring fuel cell development for propulsion. The Conservation program is focused on polymer electrolyte or proton exchange membrane fuel cells, although they also are implementing a demonstration program for PAFC buses. DOE fuel cell research, development and demonstration efforts are also supported by private sector funding. This Plan describes the fuel cell activities of the Office of Fossil Energy. DOE

N94-18109# Department of Energy, Washington, DC. Assistant Secretary for Energy Efficiency and Renewable Energy.
SAFEGUARDING OUR ENERGY FUTURE
1993 22 p
(DE93-016001; DOE/FE-0398) Avail: CASI HC A03/MF A01

Throughout the past several years, states have been receiving settlement monies distributed from escrow accounts maintained by the Department of Energy and various courts. These monies are paid by oil companies for alleged violations of the petroleum pricing regulations of the 1970's. These funds, commonly referred to as Petroleum Violation Escrow (PVE) or Oil Overcharge funds, have been an important tool in supporting energy efficiency programs and technologies at the state level. The aim of this publication is to highlight some of the many interesting, replicable projects funded with PVE monies and to serve as a resource for successful, energy efficiency programs in planning, technology application, and education. By capturing a number of these innovative state-level programs, this document will expand the information network on renewable energy and energy efficiency and serve as a point of departure for others pursuing similar goals. Projects referenced throughout this publication reflect some of the program areas in which the Department of Energy takes an active interest and fall into the following categories: (1) alternative fuels; (2) industrial efficiency and waste minimization; (3) electric power production from renewable resources; (4) building efficiency; (5) integrated resource planning; and (6) energy education. DOE

N94-18208# Sandia National Labs., Albuquerque, NM.
FIRST ON-SUN TEST OF NaK POOL-BOILER SOLAR RECEIVER
J. B. Moreno, C. E. Andraka, T. A. Moss, P. G. Cordeiro, V. E. Dudley, and K. S. Rawlinson 1993 9 p Presented at the 28th International Energy Conservation Engineering Conference, Atlanta, GA, 8-13 Aug. 1993
(Contract DE-AC04-76DP-00789)
(DE93-015003; SAND-93-1207C; CONF-930804-5) Avail: CASI HC A02/MF A01

During 1989-1990, a refluxing liquid-metal pool-boiler solar receiver designed for dish/Stirling application at 75 kW(sub t) throughput was successfully demonstrated at Sandia National Laboratories. Significant features of this receiver included (1) boiling sodium as the heat transfer medium, and (2) electric-discharge-machined (EDM) cavities as artificial nucleation sites to stabilize boiling. Following this first demonstration, a second-generation pool-boiler receiver that brings the concept closer to commercialization has been designed, constructed, and successfully tested. For long life, the new receiver is built from Haynes Alloy 230. For increased safety factors against film boiling and flooding, the absorber area and vapor-flow passages have been enlarged. To eliminate the need for trace heating, sodium has been replaced by the sodium-potassium alloy NaK-78. To reduce manufacturing costs, the receiver has a powdered-metal coating instead of EDM cavities for stabilization of boiling. To control incipient-boiling superheats, especially during hot restarts, it contains a small amount of xenon. In this paper, we present the receiver design and report the results of on-sun tests using a nominal 75 kW(sub t) test-bed concentrator to characterize boiling stability, hot-restart behavior, and thermal efficiency at temperatures up to 750 C. We also report briefly on late results from an advanced-concepts pool-boiler receiver. DOE

N94-18247# Oak Ridge National Lab., TN.
PHOTOBIOTECHNOLOGY: APPLICATION OF PHOTOSYNTHESIS TO THE PRODUCTION OF RENEWABLE FUELS AND CHEMICALS
E. Greenbaum 1993 16 p Presented at the 2nd International Conference on Solar Energy Storage and Applied Photochemistry, Cairo, Egypt, 6-11 Jan. 1993
(Contract DE-AC05-84OR-21400)
(DE93-015522; CONF-930105-1) Avail: CASI HC A03/MF A01

Sustained hydrogen photoevolution from Chlamydomonas reinhardtii and C. moewusii was measured under an anoxic, CO2-containing atmosphere. It has been discovered that light intensity and temperature influence the partitioning of reductant between the hydrogen photoevolution pathway and the Calvin cycle. Under low incident light intensity (1-3 W m(sup -2)) or low temperature (approx. 0 C), the flow of photosynthetic reductant to the Calvin cycle was reduced, and reductant was partitioned to the hydrogen pathway as evidenced by sustained H2 photoevolution. Under saturating light (25 W m(sup -2)) and moderate temperature 20 plus/minus 5 C, the Calvin cycle became the absolute sink for reductant with the exception of a burst of H2 occurring at light on. A novel photobiophysical phenomenon was observed in isolated spinach chloroplasts that were metalized by precipitating colloidal platinum onto the surface of the thylakoid membranes. A two-point irradiation and detection system was constructed in which a continuous beam helium-neon laser (lambda = 632.8 nm) was used to irradiate the platinized chloroplasts at varying perpendicular distances from a single linear platinum electrode in pressure contact with the platinized chloroplasts. No external voltage bias was applied to the system. The key objective of the experiments reported in this report was to measure the relative photoconductivity of the chloroplast-metal composite matrix. DOE

N94-18276# Pacific Northwest Lab., Richland, WA.
ANALYSIS OF SUPERCONDUCTING MAGNETIC ENERGY STORAGE APPLICATIONS AT A PROPOSED WIND FARM SITE NEAR BROWNING, MONTANA
K. L. Gaustad and J. G. DeSteese Jul. 1993 8 p Presented at the Windpower 1992, Seattle, WA, 19-23 Oct. 1992
(Contract DE-AC06-76RL-01830)
(DE93-018793; PNL-SA-22609; CONF-921049-10) Avail: CASI HC A02/MF A01

A computer program was developed to analyze the viability of integrating superconducting magnetic energy storage (SMES) with proposed wind farm scenarios at a site near Browning, Montana. The program simulated an hour-by-hour account of the charge/discharge history of a SMES unit for a representative wind-speed year. Effects of power output, storage capacity, and power conditioning capability on SMES performance characteristics were analyzed on a seasonal, diurnal, and hourly basis. The SMES unit was assumed to be charged during periods when power output of the wind resource exceeded its average value. Energy was discharged from the SMES unit into the grid during periods of low wind speed to compensate for below-average output of the wind resource. The option of using SMES to provide power continuity for a wind farm supplemented by combustion turbines was also investigated. Levelizing the annual output of large wind energy systems operating in the Blackfeet area of Montana was found to require a storage capacity too large to be economically viable. However, it appears that intermediate-sized SMES economically levelize the wind energy output on a seasonal basis. DOE

N94-18335# Sandia National Labs., Albuquerque, NM.
PHOTOVOLTAIC CONCENTRATOR INITIATIVE: CONCENTRATOR CELL DEVELOPMENT
J. H. Wohlgemuth and S. Narayanan (Solarex Corp., Frederick, MD.) May 1993 37 p
(Contract DE-AC04-76DP-00789)
(DE93-018505; SAND-92-7007) Avail: CASI HC A03/MF A01

This project involves the development of a large-area, low-cost, high-efficiency concentrator solar cell for use in the Entech 22-sun linear-focus Fresnel lens concentrator system. The buried contact solar cell developed at the University of New South Wales was selected for this project. Both Entech and the University of New South Wales are subcontractors. This annual report presents the program efforts from November 1990 through December 1991, including the design of the cell, development of a baseline cell process, and presentation of the results of preliminary cell processing. Important results include a cell designed for operation in a real concentrator system and substitution of mechanical grooving for the previously utilized laser scribing. DOE

N94-18409# Sandia National Labs., Albuquerque, NM.
HIGH-EFFICIENCY SILICON CONCENTRATOR CELL COMMERCIALIZATION
R. A. Sinton and R. M. Swanson (SunPower, Inc., Sunnyvale, CA.) May 1993 59 p
(Contract DE-AC04-76DP-00789)
(DE93-018491; SAND-93-7055) Avail: CASI HC A04/MF A01

This report summarizes the first phase of a forty-one month program to develop a commercial, high-efficiency concentrator solar cell and facility for manufacturing it. The period covered is November 1, 1990 to December 31, 1991. This is a joint program between the Electric Power Research Institute (EPRI) and Sandia National Laboratories. During the first year of the program, SunPower accomplished the following major objectives: (1) a new solar cell fabrication facility, which is called the Cell Pilot Line (CPL), (2) a baseline concentrator cell process has been developed, and (3) a cell testing facility has been completed. Initial cell efficiencies are about 23% for the baseline process. The long-range goal is to improve this efficiency to 27%. DOE

N94-18475# Department of Energy, Washington, DC. Assistant Secretary for Fossil Energy.
REPORT TO CONGRESS: COMPREHENSIVE PROGRAM PLAN FOR ADVANCED TURBINE SYSTEMS
Jul. 1993 51 p
(DE93-016718; DOE/FE-0279) Avail: CASI HC A04/MF A01

Consistent with the Department of Energy (DOE) mission, the Advanced Turbine Systems (ATS) Program will develop more efficient gas turbine systems for both utility and industrial electric power generation (including cogeneration). The program will develop base-load power systems for commercial offering in the year 2000. Although the target fuel is natural gas, the ATS will be adaptable to coal and biomass firing. All ATS will exhibit these characteristics: Ultra-high efficiency utility systems: 60 percent (lower heating value basis); industrial systems--15 percent improvement over today's best gas turbine systems; Environmental superiority (reduced nitrogen oxides (NO(x)), carbon dioxide (CO2), carbon monoxide (CO), and unburned hydrocarbons (UHC)); and cost competitiveness (10 percent lower cost of electricity). This Program Plan was requested in the House, Senate, and Conference Reports on the FY 1993 Interior and Related Agencies Appropriations Act, Public Law 102--381, and is consistent with the Energy Policy Act of 1992, which (in Section 2112) identifies work for improving gas turbines. This plan outlines the 8-year ATS Program and discusses rationale and planning. Total Program costs are estimated to be $700 million, consisting of an approximate $450 million government share, and an approximate $250 million cost-share by industrial participants. DOE

N94-18478# Oak Ridge National Lab., TN.
WORKSHOP ON INNOVATION IN MATERIALS PROCESSING AND MANUFACTURE: EXPLORATORY CONCEPTS FOR ENERGY APPLICATIONS
L. L. Horton, comp. Jun. 1993 69 p Workshop held in Oak Ridge, TN, 11-12 Mar. 1993
(Contract DE-AC05-84OR-21400)
(DE93-017674; ORNL-6760) Avail: CASI HC A04/MF A01

The goal of the workshop was to bring together industrial, academic, and DOE Laboratory personnel to discuss and identify potential areas for which creative, innovative, and/or multidisciplinary solutions could result in major payoffs for the nation's energy economy, DOE, and industry. The topics emphasized in these discussions were: surfaces and interfacial processing technologies, biomolecular materials, powder/precursor technologies, magnetic materials, nanoscale materials, novel ceramics and composites, novel intermetallics and alloys, environmentally benign materials, and energy efficiency. The workshop had a 2-day format. On the first day, there was an introductory session that summarized future directions within DOE's basic and materials technology programs, and the national studies on manufacturing and materials science and engineering. The balance of the workshop was devoted to brainstorming sessions by seven working groups. During the first working group session, the entire group was divided to discuss topics on: challenges for hostile environments, novel materials in transportation technologies, novel nanoscale materials, and opportunities in biomolecular materials. For the second session, the entire group (except for the working group on biomolecular materials) was reconfigured into new working groups on: alternative pathways to energy efficiency, environmentally benign materials and processes, and waste treatment and reduction: a basic sciences approach. This report contains separate reports from each of the seven working groups. DOE

N94-18483# Spire Corp., Bedford, MA.
GALLIUM ARSENIDE-BASED TERNARY COMPOUNDS AND MULTI-BAND-GAP SOLAR CELL RESEARCH
S. Vernon Jul. 1993 168 p Prepared for Midwest Research Inst., Golden, CO
(Contract DE-AC02-83CH-10093)
(DE93-010049; NREL/TP-451-5354) Avail: CASI HC A08/MF A02

This report describes work to achieve a high-efficiency, low-cost solar cell. The basic approach to the problem is centered upon the heteroepitaxial growth of a III-V compound material onto a single-crystal silicon wafer. The growth technique employed throughout this work is metal-organic chemical vapor deposition. The silicon wafer may serve as a mechanical substrate and ohmic contact for a single-junction device, or it may contain a p-n junction of its own and form the bottom cell of a two-junction tandem solar cell structure. The III-V material for the single-junction case is GaAs, and for the two-junction case it is either GaAlAs or GaAsP, either material having the proper composition to yield a band gap of approximately 1.7 eV. Results achieved in this contract include (1) a 17.6%-efficient GaAs-on-Si solar cell; (2) an 18.5%-efficient GaAs-on-Si concentrator solar cell at 400 suns; (3) a 24.8%-efficient GaAs-on-GaAs solar cell; (4) a 28.7%-efficient GaAs-on-GaAs concentrator solar cell at 200 suns; (5) the measurement of the effects of dislocation density and emitter doping on GaAs cells; and (6) improvements in the growth process to achieve reproducible thin AlGaAs window layers with low recombination velocities and environmental stability. DOE

N94-18518# United Solar Systems Corp., Troy, MI.
RESEARCH ON STABLE, HIGH-EFFICIENCY AMORPHOUS SILICON MULTIJUNCTION MODULES
S. Guha Jul. 1993 64 p Prepared for Midwest Research Inst., Golden, CO
(Contract DE-AC02-83CH-10093)
(DE93-010046; NREL/TP-411-5654) Avail: CASI HC A04/MF A01

This report describes the progress made during Phase 2 of the R&D program to obtain high-efficiency amorphous alloy multijunction PV (photovoltaic) modules. The highlight of the work includes: (1) demonstration of world-record small-area efficiency of 11.2% after one-sun light-soaking at 50 C for 600 h using a dual band gap, double-junction structure; and (2) demonstration of initial module efficiency of 10.6% over 0.09-m(exp 2) (1-ft(exp 2)) area using the same double-junction approach. In addition, fundamental studies on material properties and cell performance have shown an interesting correlation between microstructure in the material and cell efficiency both in the initial and light-degraded conditions. DOE

N94-18520# Sandia National Labs., Albuquerque, NM.
TESTING AND EVALUATION OF LARGE-AREA HELIOSTATS FOR SOLAR THERMAL APPLICATIONS
J. W. Strachan and R. M. Houser Feb. 1993 61 p
(Contract DE-AC04-76DP-00789)
(DE93-018509; SAND-92-1381) Avail: CASI HC A04/MF A01

Two heliostats representing the state-of-the-art in glass-metal designs for central receiver (and photovoltaic tracking) applications were tested and evaluated at the National Solar Thermal Test Facility in Albuquerque, New Mexico from 1986 to 1992. These heliostats have collection areas of 148 and 200 m(exp 2) and represent low-cost designs for heliostats that employ glass-metal mirrors. The evaluation encompassed the performance and operational characteristics of the heliostats, and examined heliostat beam quality, the effect of elevated winds on beam quality, heliostat drives and controls, mirror module reflectance and durability, and the overall operational and maintenance characteristics of the two heliostats. A comprehensive presentation of the results of these and other tests is presented. The results are prefaced by a review of the development (in the United States) of heliostat technology. DOE

N94-18821*# Rockwell International Corp., Canoga Park, CA. Rocketdyne Div.
POTASSIUM-RANKINE POWER CONVERSION SUBSYSTEM MODELING FOR NUCLEAR ELECTRIC PROPULSION
Gregory A. Johnson Sep. 1993 128 p
(Contract NAS3-25808; RTOP 593-72-00)
(NASA-CR-191134; NAS 1.26:191134) Avail: CASI HC A07/MF A02

A potassium-Rankine power conversion system model was developed under Contract No. NAS3-25808 for the NASA-LeRC. This model predicts potassium-Rankine performance for turbine inlet temperatures (TIT) from 1200 - 1600 K, TIT to condenser temperature ratios from 1.25-1.6, power levels from 100 to 10,000 kWe, and lifetimes from 2-10 years. The model is for a Rankine cycle with reheat for turbine stage moisture control. The model assumes heat is supplied from a lithium heat transport loop. The model does not include a heat source or a condenser/heat rejection system model. These must be supplied by the user. Author

N94-18925# Morgantown Technology Center, WV.
MOLTEN CARBONATE FUEL CELL NETWORKS: PRINCIPLES, ANALYSIS, AND PERFORMANCE
J. G. Wimer and M. C. Williams Jan. 1993 44 p
(DE93-000281; DOE/METC-93-4112) Avail: CASI HC A03/MF A01

The chemical reactions in an internally reforming molten carbonate fuel cell (IRMCFC) are described and combined into the overall IRMCFC reaction. Thermodynamic and electrochemical principles are discussed, and structure and operation of fuel cell stacks are explained. In networking, multiple fuel cell stacks are arranged so that reactant streams are fed and recycled through stacks in series for higher reactant utilization and increased system efficiency. Advantages and performance of networked and conventional systems are compared, using ASPEN simulations. The concept of networking can be applied to any electrochemical membrane, such as that developed for hot gas cleanup in future power plants. DOE

N94-18944# Midwest Research Inst., Golden, CO. National Renewable Energy Lab.
POLYCRYSTALLINE THIN-FILM CADMIUM TELLURIDE SOLAR CELLS FABRICATED BY ELECTRODEPOSITION
J. U. Trefny, T. E. Furtak, N. Wada, D. L. Williamson, and D. Kim Aug. 1993 42 p
(Contract DE-AC02-83CH-10093)
(DE93-018201; NREL/TP-451-5652) Avail: CASI HC A03/MF A01

This report describes progress during the first year of a 3-year program at Colorado School of Mines, based upon earlier studies performed by Ametek Corporation, to develop specific layers of the Ametek n-i-p structure as well as additional studies of several transparent conducting oxides. Thin films of ZnO and ZnO:Al were deposited under various conditions. For the n-layer of the Ametek structure, a dip-coating method was developed for the deposition of CdS films. The authors also present data on the characterization of these films by X-ray diffraction, Raman spectroscopy, scanning tunneling microscopy, small-angle X-ray scattering, and other techniques. They made progress in the electrodeposition of the CdTe i-layer of the Ametek structure. They developed appropriate electrochemical baths and are beginning to understand the role of the many experimental parameters that must be controlled to obtain high-quality films of this material. They explored the possibility of using an electrochemical process for fabricating the ZnTe p-layer. Some preliminary success was achieved, and this step will be pursued in the next phase. Finally, they fabricated a number of 'dot' solar cells with the structure glass/SnO2/CdS/CdTe/Au. Several cells with efficiencies in the range of 5%-6% were obtained, and they are confident, given recent progress, that cells with efficiencies in excess of 10% will be achieved in the near future. DOE

N94-18986# Oak Ridge National Lab., TN.
ENERGY EFFICIENCY AND RENEWABLE ENERGY PROGRAM
K. H. Vaughan Jun. 1993 151 p
(Contract DE-AC05-84OR-21400)
(DE93-017936; ORNL/CON-368) Avail: CASI HC A08/MF A02

The bibliography contains listings of publicly available reports, journal articles, and published conference papers sponsored by the DOE Office of Energy Efficiency and Renewable Energy and published between 1987 and mid-1993. The topics of the bibliography include: analysis and evaluation; building equipment research; building thermal envelope systems and materials; district heating; residential and commercial conservation program; weatherization assistance program; existing buildings research program; ceramic technology project; alternative fuels and propulsion technology; microemulsion fuels; industrial chemical heat pumps; materials for advanced industrial heat exchangers; advanced industrial materials; tribology; energy-related inventions program; electric energy systems; superconducting technology program for electric energy systems; thermal energy storage; biofuels feedstock development; biotechnology; continuous chromatography in multicomponent separations; sensors for electrolytic cells; hydropower environmental mitigation; environmental control technology; and continuous fiber ceramic composite technology. DOE

N94-19014# Sandia National Labs., Albuquerque, NM.
TEHACHAPI SOLAR THERMAL SYSTEM Annual Report No. 1
A. Rosenthal (Southwest Technology Development Inst., Las Cruces, NM.) May 1993 60 p
(Contract DE-AC04-76DP-00789)
(DE93-018443; SAND-93-7000) Avail: CASI HC A04/MF A01

The staff of the Southwest Technology Development Institute (SWTDI), in conjunction with the staff of Industrial Solar Technology (IST), have analyzed the performance, operation, and maintenance of a large solar process heat system in use at the 5,000 inmate California Correctional Institution (CCI) in Tehachapi, CA. This report summarizes the key design features of the solar plant, its construction and maintenance histories through the end of 1991, and the performance data collected at the plant by a dedicated on-site data acquisition system (DAS). DOE

N94-19015# Sandia National Labs., Albuquerque, NM.
SILICON CONCENTRATOR SOLAR CELL RESEARCH
M. A. Green (New South Wales Univ., Kensington, Australia.), J. Zhao (New South Wales Univ., Kensington, Australia.), A. Wang (New South Wales Univ., Kensington, Australia.), X. Dai (New South Wales Univ., Kensington, Australia.), A. Milne (New South Wales Univ., Kensington, Australia.), S. Cai (New South Wales Univ., Kensington, Australia.), A. Aberle (New South Wales Univ., Kensington, Australia.), and S. R. Wenham (New South Wales Univ., Kensington, Australia.) Jun. 1993 35 p
(Contract DE-AC04-76DP-00789)
(DE93-018489; SAND-93-7049) Avail: CASI HC A03/MF A01

This report describes work conducted between December 1990 and May 1992 continuing research on silicon concentrator solar cells. The objectives of the work were to improve the performance of high-efficiency cells upon p-type substrates, to investigate the ultraviolet stability of such cells, to develop concentrator cells based on n-type substrates, and to transfer technology to appropriate commercial environments. Key results include the identification of contact resistance between boron-defused areas and rear aluminum as the source of anomalously large series resistance in both p- and n-type cells. A major achievement of the present project was the successful transfer of cell technology to both Applied Solar Energy Corporation and Solarex Corporation. DOE

N94-19016# Sandia National Labs., Albuquerque, NM.
DEFECT BEHAVIOR OF POLYCRYSTALLINE SOLAR CELL SILICON
D. K. Schroder (Arizona State Univ., Tempe.), S. H. Park (Arizona State Univ., Tempe.), I. G. Hwang (Arizona State Univ., Tempe.), J. B. Mohr (Arizona State Univ., Tempe.), and M. P. Hanly (Arizona State Univ., Tempe.) May 1993 83 p
(Contract DE-AC04-76DP-00789)
(DE93-018490; SAND-93-7051) Avail: CASI HC A05/MF A01

The major objective of this study, conducted from October 1988 to September 1991, was to gain an understanding of the behavior of impurities in polycrystalline silicon and the influence of these impurities on solar cell efficiency. The authors studied edge-defined film-fed growth (EFG) and cast poly-Si materials and solar cells. With EFG Si they concentrated on chromium-doped materials and cells to determine the role of Cr on solar cell performance. Cast poly-Si samples were not deliberately contaminated. Samples were characterized by cell efficiency, current-voltage, deep-level transient spectroscopy (DLTS), surface photovoltage (SPV), open-circuit voltage decay, secondary ion mass spectrometry, and Fourier transform infrared spectroscopy measurements. They find that Cr forms Cr-B pairs with boron at room temperature and these pairs dissociate into Cr(i)(sup +) and B(sup -) during anneals at 210 degrees C for 10 min. Following the anneal, Cr-B pairs reform at room temperature with a time constant of 230 h. Chromium forms CrSi2 precipitates in heavily contaminated regions and they find evidence of CrSi2 gettering, but a lack of chromium segregation or precipitation to grain boundaries and dislocations. Cr-B pairs have well defined DLTS peaks. However, DLTS spectra of other defects are not well defined, giving broad peaks indicative of defects with a range of energy levels in the band gap. In some high-stress, low-efficiency cast poly-Si they detect SiC precipitates, but not in low-stress, high-efficiency samples. SPV measurements result in nonlinear SPV curves in some materials that are likely due to varying optical absorption coefficients due to locally varying stress in the material. DOE

N94-19036# Sandia National Labs., Albuquerque, NM.
OPTIMIZING WIND TURBINE CONTROL SYSTEM PARAMETERS
Larry L. Schluter and William A. Vachon (Vachon, William A. and Associates, Inc., Manchester, MA.) 1993 8 p Presented at the Windpower 1993 Conference, San Francisco, CA, 12-16 Jul. 1993
(Contract DE-AC04-76DP-00789)
(DE93-018861; SAND-93-0391C; CONF-930726-5) Avail: CASI HC A02/MF A01

The impending expiration of the levelized period in the Interim Standard Offer Number 4 (ISO4) utility contracts for purchasing wind-generated power in California mandates, more than ever, that windplants be operated in a cost-effective manner. Operating plans and approaches are needed that maximize the net revenue from wind parks--after accounting for operation and maintenance costs. This paper describes a design tool that makes it possible to tailor a control system of a wind turbine (WT) to maximize energy production while minimizing the financial consequences of fatigue damage to key structural components. Plans for code enhancements to include expert systems and fuzzy logic are discussed, and typical results are presented in which the code is applied to study the controls of a generic Danish 15-m horizontal axis wind turbine (HAWT). DOE

N94-19040# Sandia National Labs., Albuquerque, NM.
BENCH-SCALE SCREENING TESTS FOR A BOILING SODIUM-POTASSIUM ALLOY SOLAR RECEIVER
J. B. Moreno and T. A. Moss Jun. 1993 71 p
(Contract DE-AC04-76DP-00789)
(DE93-018512; SAND-92-2253) Avail: CASI HC A04/MF A01

Bench-scale tests were carried out in support of the design of a second-generation 75-kW(sub t) reflux pool-boiler solar receiver. The receiver will be made from Haynes Alloy 230 and will contain the sodium-potassium alloy NaK-78. The bench-scale tests used quartz lamp heated boilers to screen candidate boiling stabilization materials and methods at temperatures up to 750 degree C. Candidates that provided stable boiling were tested for hot-restart behavior. Poor stability was obtained with single 1/4-inch diameter patches of powdered metal hot press sintered onto the wetted side of the heat-input area. Laser-drilled and electric discharge machined cavities in the heated surface also performed poorly. Small additions of xenon, and heated-surface tilt out of the vertical, dramatically improved poor boiling stability; additions of helium or oxygen did not. The most stable boiling was obtained when the entire heat-input area was covered by a powdered-metal coating. The effect of heated-area size was assessed for one coating: at low incident fluxes, when even this coating performed poorly, increasing the heated-area size markedly improved boiling stability. Good hot-restart behavior was not observed with any candidate, although results were significantly better with added xenon in a boiler shortened from 3 to 2 feet. In addition to the screening tests, flash-radiography imaging of metal-vapor bubbles during boiling was attempted. Contrary to the Cole-Rohsenow correlation, these bubble-size estimates did not vary with pressure; instead they were constant, consistent with the only other alkali metal measurements, but about 1/2 their size. DOE

N94-19098# California Univ., Berkeley. Lawrence Berkeley Lab.
ENERGY CONVERSION AND STORAGE PROGRAM Annual Report, 1992
E. J. Cairns Jun. 1993 24 p
(Contract DE-AC03-76SF-00098)
(DE93-018602; LBL-33444) Avail: CASI HC A03/MF A01

This report is the 1992 annual progress report for the Energy Conversion and Storage Program, a part of the Energy and Environment Division of the Lawrence Berkeley Laboratory. Work described falls into three broad areas: electrochemistry; chemical applications; and materials applications. The Energy Conversion and Storage Program applies principles of chemistry and materials science to solve problems in several areas: (1) production of new synthetic fuels, (2) development of high-performance rechargeable batteries and fuel cells, (3) development of advanced thermochemical processes for energy conversion, (4) characterization of complex chemical processes and chemical species, and (5) study and application of novel materials for energy conversion and transmission. Projects focus on transport-process principles, chemical kinetics, thermodynamics, separation processes, organic and physical chemistry, novel materials, and advanced methods of analysis. Electrochemistry research aims to develop advanced power systems for electric vehicle and stationary energy storage applications. Chemical applications research includes topics such as separations, catalysis, fuels, and chemical analyses. Included in this program area are projects to develop improved, energy-efficient methods for processing product and waste streams from synfuel plants, coal gasifiers, and biomass conversion processes. Materials applications research includes evaluation of the properties of advanced materials, as well as development of novel preparation techniques. For example, techniques such as sputtering, laser ablation, and poised laser deposition are being used to produce high-temperature superconducting films. DOE

N94-19109# Sandia National Labs., Albuquerque, NM.
THE CAESAR PROJECT: EXPERIMENTAL AND MODELING INVESTIGATIONS OF METHANE REFORMING IN A CATALYTICALLY ENHANCED SOLAR ABSORPTION RECEIVER ON A PARABOLIC DISH
J. F. Muir, R. E. Hogan, Jr., R. D. Skocypec, and R. Buck (Deutsche Forschungsanstalt fuer Luft- und Raumfahrt, Stuttgart, Germany.) Jul. 1993 136 p
(Contract DE-AC04-76DP-00789)
(DE93-040203; SAND-92-2131) Avail: CASI HC A07/MF A02

A joint US/Federal Republic of Germany (FRG) project has successfully tested a unique solar-driven chemical reactor in the Catalytically Enhanced Solar Absorption Receiver (CAESAR) experiment. The CAESAR test was a proof-of-concept demonstration of carbon-dioxide reforming of methane in a commercial-scale, solar, volumetric receiver/reactor on a parabolic dish concentrator. The CAESAR design, test facility and instrumentation, thermal and chemical tests, and analysis of test results are presented in detail. Numerical models for the absorber and the receiver are developed and predicted performance is compared with test data. Post test analyses to assess the structural condition of the absorber and the effectiveness of the rhodium catalyst are presented. Unresolved technical issues are identified and future development efforts are recommended. DOE

N94-19346# Department of Energy, Washington, DC. Office of Assistant Secretary for Conservation and Renewable Energy.
NATIONAL PROGRAM PLAN FUEL CELLS IN TRANSPORTATION
Feb. 1993 30 p
(Contract W-31-109-eng-38)
(DE93-017557; DOE/CH-93019) Avail: CASI HC A03/MF A01

Fuel cells are being developed for application in the transportation sector because they will convert hydrogen to electric power at high efficiencies with virtually no detrimental environmental impact. To realize these energy, environmental, and economic benefits, developers of FCV's need to (1) reduce the size and weight of current designs, (2) develop fuel cell propulsion systems with rapid start-up and greater load-following capability, (3) reduce system cost and/or improve performance, and (4) utilize alternative fuels to a large extent. This Plan addresses the FCV-related requirements of the Energy Act, describing a development program for light- and heavy-duty propulsion systems, a basic R&D program on fuel cell technology that is separate from, but feeds into, the system development activities, and supporting analyses. Implementation of the Program Plan by means of industry/government alliances will accelerate the commercialization of FCV's. In the long term, the successful deployment of large numbers of FCV's promises to eliminate the transportation sector as a major contributor to the nation's environmental problems. DOE

N94-19654 Technische Univ., Berlin (Germany). Fachbereich Physik.
EXAMINATION OF CHARGE CARRIERS DYNAMICS IN SILICON AND SILICON SOLAR CELLS WITH PHOTOINDUCED LASER BEAM DEFLECTION Ph.D. Thesis [UNTERSUCHUNG DER LADUNGSTRAEGERDYNAMIK IN SILIZIUM UND SILIZIUMSOLARZELLEN MIT PHOTOINDUZIERTER LASERSTRAHLABLENKUNG]
Paul Grunow 1993 151 p In GERMAN Limited Reproducibility: More than 20% of this document may be affected by microfiche quality
(ETN-93-95060) Avail: CASI HC A08

Photovoltaic solar cells are examined with photothermal deflection spectroscopy in a semiconductor. At solar cells with crystalline silicon basis, the concurrent recombination channels for recombination at the surface, in the space charge zone and in basis volume could be differentiated in closed and opened circuits from the laser signal course, as a function of polarization voltage and auxiliary exposure. The recombination in volume is described by minority carriers injection in solar cell basis volume and the recombination at the boundary surface is depicted with thermoionic emission of majority carriers above the barrier. Both currents show an exponential dependence on polarization voltage. The injection current in the space surface zone was obtained by solving the equation diffusion at the surface and both recombination currents were taken into account as boundary conditions for solving temperature distribution. The influence of the nonexposed side in charge carrier distribution was calculated and experimentally assessed with thickness dependent measurement at a silicon slice; it is found that heat flow from exposed surface in volume is limited by the nonexposed side so that the signal is saturated in the thermally dominated area of low modulation frequencies. ESA

N94-19760# Research Triangle Inst., Research Triangle Park, NC.
AMORPHOUS SILICON BATCH PROCESS COST ANALYSIS
R. A. Whisnant and C. Sherring Aug. 1993 94 p Prepared in cooperation with Midwest Research Inst., Golden, CO
(Contract DE-AC02-83CH-10093)
(DE93-018203; NREL/TP-411-5644) Avail: CASI HC A05/MF A01

This report describes the development of baseline manufacturing cost data to assist photovoltaic manufacturing technology (PVMaT) monitoring teams in assessing current and future subcontracts, with an emphasis on commercialization and production. A process for the manufacture of a single-junction, large-area, a-Si module was modeled using an existing Research Triangle Institute (RTI) computer model. The model estimates a required, or break-even, price for the module based on its production process and the financial structure of the company operating the process. Sufficient detail on cost drivers is presented so the relationship of the process features and business characteristics can be related to the estimated required price. DOE

45 ENVIRONMENT POLLUTION

Includes atmospheric, noise, thermal, and water pollution.

N94-17710# Colorado State Univ., Fort Collins. Dept. of Atmospheric Science.
MONITORING THE RESPONSE OF THE UPPER TROPOSPHERE/LOWER STRATOSPHERE TO A GREENHOUSE GAS SCENARIO
J. M. Davis and S. K. Cox 15 Dec. 1992 22 p
(Contract DE-FG02-90ER-60970)
(DE93-014509; DOE/ER-60970/T1) Avail: CASI HC A03/MF A01

During the past two years a system has been under development to contribute to this monitoring process by making measurement of the downwelling infrared radiance field at moderate spectral resolution. Sensitivity of the measurements to the presence of cirrus cloudiness, and effective particle size in cirrus clouds has been demonstrated. Sensitivity of the measurements to concentration of CO2 and to the gross temperature structure of a 2CO2 atmosphere have been modeled, and measurements have been made at various locations to provide a data base for further system evaluation. A temperature retrieval algorithm has been acquired and examined concerning its potential for monitoring temperature and gaseous concentration profiles. A continued research program is described herein that may be divided into three parts. First, continued system development must be pursued. This includes continued attention to the absolute accuracy of the measurements, and implementation of the Path Characterization Algorithm (retrieval code). Second, the value of long term deployment of the system at a site of considerable elevation is necessary. Third, inclusion of a solar transmission capability at moderate resolution is proposed. DOE

N94-17749# Pacific Northwest Lab., Richland, WA.
VISIBILITY IMPAIRMENT ASSESSMENT: IMPORTANCE OF USING THEORETICALLY DERIVED OPTICAL CHARACTERIZATIONS
P. Middleton, D. Hopkins, E. Trexler, and N. Laulainen Jun. 1993 11 p Presented at the 86th Annual Meeting and Exhibition of the AWMA, Denver, CO, 13-18 Jun. 1993
(Contract DE-AC06-76RL-01830)
(DE93-017147; PNL-SA-21568; CONF-930647-5) Avail: CASI HC A03/MF A01

The 1990 federal amendments to the National Clean Air Act identified improvement of visibility as an important national goal. To help accomplish this goal, a national assessment of visibility impairment is being conducted for the US Department of Energy. The assessment examines the nature and extent of improvements in visual air quality that could result from major energy policy changes. Specifically, it is designed to assess the impact of SO2, NO(x), and VOC emission changes on visibility throughout the United States. A major objective of the ongoing work is to develop credible assessments that can be easily and meaningfully communicated to decision makers as well as to the scientific community. The overall assessment concept is outlined schematically. The visibility impairment assessment produces visibility patterns for a year at selected representative sites as a function of emissions and meteorological conditions. Annual cycles of visibility are generated from carefully selected observational and model data. The initial studies focus on individual sites and observation data. Later stages will employ more regional analyses with the help of more comprehensive modeling, tools. Results as well as a discussion of the implications for future characterizations at different locations through the US are discussed. DOE

N94-17762*# Nebraska Univ., Lincoln. Dept. of Agricultural Meteorology.
BIOPHYSICAL CHARACTERIZATION AND SURFACE RADIATION BALANCE Final Report, 15 Sep. 1991 - 14 Sep. 1993
Elizabeth A. Walter-Shea, Blaine L. Blad, Mark A. Mesarch, Cynthia J. Hays, and Patrick J. Starks 14 Sep. 1993 97 p
(Grant NAG5-1762)
(NASA-CR-194659; NAS 1.26:194659) Avail: CASI HC A05/MF A02

The Kursk 1991 Experiment (KUREX-91) was conducted as one of a suite of international studies to develop capabilities to monitor global change. The studies were designed specifically to understand the earth's land-surface vegetation and atmospheric boundary layer interaction. An intensive field campaign was conducted at a site near Kursk, Russia during the month of July in 1991 by a team of international scientists to aid in the understanding of land-surface-atmosphere interactions in an agricultural/grassland setting. We were one of several teams of scientists participating at KUREX-91 at the Streletskaya Steppe Researve near Kursk, Russia. The main goals of our research were to: (1) characterize biophysical properties of the prairie vegetation; and (2) to characterize radiation regime through measurements and from estimates derived from canopy bidirectional reflectance data. Four objectives were defined to achieve these goals: (1) determine dependence of leaf optical properties on leaf water potential of some dominant species in discrete wavebands in the visible, near-infrared, and mid-infrared (spanning 0.4-2.3 microns range); (2) characterize the effective leaf area index (LAI) and leaf angle distribution of prairie vegetation; (3) characterize the radiation regime of the prairie vegetation through measures of the radiation balance components; and (4) examine, develop, and test methods for estimating albedo, APAR, and LAI from canopy bidirectional reflectance data. Papers which were the result of the research efforts are included. Author (revised)

N94-17773# Oak Ridge National Lab., TN.
AIR POLLUTION EFFECTS FIELD RESEARCH FACILITY. 3: UV-B EXPOSURE AND MONITORING SYSTEM
J. A. McEvers, M. S. Hileman, and N. T. Edwards Mar. 1993 119 p

(Contract DE-AC05-84OR-21400)
(DE93-013098; ORNL/TM-11607) Avail: CASI HC A06/MF A02

The Oak Ridge National Laboratory Outdoor UltraViolet-B (UV-B) Exposure and Monitoring Facility was developed in 1980 to provide well-controlled and -monitored exposure of specific terrestrial plant. species to elevated levels of ultraviolet (UV) radiation. The introduction of various anthropogenic agents into the earth's stratosphere has resulted in a decrease in the volume of ozone (O3) present here. The decrease in O3 has resulted in an increase in the level of UV radiation reaching thee earth's surface. Of particular interest is the level of UV-B, because it has the most detrimental effect on living tissue. A thorough understanding of the effects of elevated levels of UV-B on living tissue is critical to the formulation of economic policy regarding production of such agents and alternative strategies. The UV region of interest is referred to as UV-B and corresponds to radiation with a wavelength of 290 to 320 nm. Design, operation, and performance of the automated generation, exposure, and monitoring system are described. The system has proved to be reliable and easy to maintain and operate, and it provides significant flexibility in exposure programs. The system software is described, and detailed listings are provided. The ability to expose plants to controlled set point percentages of UV-B above the ambient level was developed. DOE

N94-17774# Oak Ridge National Lab., TN. Carbon Dioxide Information Analysis Center.

CARBON DIOXIDE INFORMATION ANALYSIS CENTER: FY 1992 ACTIVITIES

R. M. Cushman and F. W. Stoss Mar. 1993 87 p
(Contract DE-AC05-84OR-21400)
(DE93-013845; ORNL/CDIAC-58; ESDC-3984) Avail: CASI HC A05/MF A01

During the course of a fiscal year, Oak Ridge National Laboratory's Carbon Dioxide Information Analysis Center (CDIAC) distributes thousands of specialty publications-numeric data packages (NDPs), computer model packages (CMPs), technical reports, public communication publications, newsletters, article reprints, and reference books-in response to requests for information related to global environmental issues, primarily those pertaining to climate change. CDIACs staff also provides technical responses to specific inquiries related to carbon dioxide (CO2), other trace gases, and climate. Hundreds of referrals to other researchers, policy analysts, information specialists, or organizations are also facilitated by CDIAC's staff. This report provides an account of the activities accomplished by CDIAC during the period October 1, 1991 to September 30, 1992. An organizational overview of CDIAC and its staff is supplemented by a detailed description of inquiries received and CDIAC's response to those inquiries. As analysis and description of the preparation and distribution of numeric data packages, computer model packages, technical reports, newsletters, fact sheets, specialty publications, and reprints is provided. Comments and descriptions of CDIAC's information management systems, professional networking, and special bilateral agreements are also described. DOE

N94-17777# Argonne National Lab., IL.

TITLE 1 IMPLEMENTATION: STATUS REPORT ON NONATTAINMENT AREAS

L. D. Kenkeremath and T. C. Snyder Jan. 1993 99 p
(Contract W-31-109-eng-38)
(DE93-017677; ANL/EAIS/TM-98) Avail: CASI HC A05/MF A02

Key provisions of Title 1 of the Clean Air Act Amendments of 1990 (CAAA) focus on bringing cities and other areas into attainment of the National Ambient Air Quality Standards for ozone, carbon monoxide (CO), and fine particulates (PM-10). The CAAA's new classification scheme for pollutant nonattainment areas is based on the relative severity of pollution in these areas and determines the stringency of control measures and the dates by which attainment of the standards will be required. The US Environmental Protection Agency's (EPA's) final rule on air quality designations and classifications, published in late 1991, shows that ozone pollution remains a persistent problem; the number of counties that fail to meet the ozone standard has sharply increased since 1987. In contrast, incidence of PM-10 pollution has decreased; many counties have achieved the PM-10 standard since 1987. Nationwide, the number of CO nonattainment areas has increased, though not dramatically. Many of the new Title 1 requirements focus on the role of nitrogen oxides (NO(x)) in the formation of ground-level ozone. In ozone nonattainment areas and ozone transport regions, Title 1 generally requires major sources of NO(x) to have the same control measures as those that apply to major sources of volatile organic compounds (VOCs). This requirement compels state regulators to adopt an integrated VOC/NO(x) control strategy. The NO(x) emission standards proposed by state regulators are considerably more stringent than those given in federal guidelines. Both the EPA and the states plan to allow the use of multifacility emissions averaging in state NO(x) control strategies, thereby, providing industry flexibility. Proposed federal Economic Incentive Program (EIP) rules would also allow sources in states with approved EIPs to use mobile source emission reduction credits to meet certain stationary source emission reduction requirements. DOE

N94-17790# Oak Ridge National Lab., TN.

ASSESSING IMPACTS OF CLIMATE CHANGE ON FORESTS: THE STATE OF BIOLOGICAL MODELING

V. H. Dale and H. M. Rauscher Apr. 1993 49 p Presented at the Workshop on Integrated Assessments of the Impacts of Climate Change on Natural Resources, San Diego, CA, 28 Feb. - 4 Mar. 1993
(Contract DE-AC05-84OR-21400)
(DE93-015916; CONF-9302127-1) Avail: CASI HC A03/MF A01

Models that address the impacts to forests of climate change are reviewed by four levels of biological organization: global, regional or landscape, community, and tree. The models are compared as to their ability to assess changes in greenhouse gas flux, land use, maps of forest type or species composition, forest resource productivity, forest health, biodiversity, and wildlife habitat. No one model can address all of these impacts, but landscape transition models and regional vegetation and land-use models consider the largest number of impacts. Developing landscape vegetation dynamics models of functional groups is suggested as a means to integrate the theory of both landscape ecology and individual tree responses to climate change. Risk assessment methodologies can be adapted to deal with the impacts of climate change at various spatial and temporal scales. Four areas of research development are identified: (1) linking socioeconomic and ecologic models, (2) interfacing forest models at different scales, (3) obtaining data on susceptibility of trees and forest to changes in climate and disturbance regimes, and (4) relating information from different scales. DOE

N94-17821# Pacific Northwest Lab., Richland, WA.

THE CARBON DIOXIDE EMISSIONS GAME: PLAYING THE NET

K. R. Richards, J. A. Edmonds, D. H. Rosenthal, and M. Wise Jun. 1993 14 p Presented at the Carbon Sinks Workshop for the Interagency National Action Plan Development Process, Washington, DC, 10-11 Jun. 1993
(Contract DE-AC06-76RL-01830)
(DE93-017670; PNL-SA-22658; CONF-9306214-1) Avail: CASI HC A03/MF A01

Concern about rising concentrations of carbon dioxide in the earth's atmosphere has led to calls for the United States and other countries to reduce carbon emissions. These concerns resulted in the signing of the Framework Convention on Climate Change at the United Nations Conference on the Environment and Development in Rio de Janeiro in June 1992. The Framework calls for nations to develop action plans for limiting emissions of carbon and other greenhouse gases. In December 1992, in accordance with the Framework, the US Government released for public comment its National Action Plan for Global Climate Change (US Department of State, 1992). The Action Plan detailed steps for reducing carbon emissions by 93 to 130 million metric tons (MMT) by 2000. Some of the steps included in the Action Plan were reforming regulations, setting energy standards, promoting research and development of new energy technologies, expanding the use of alternative-fueled vehicles, and planting trees to sequester carbon. This paper explores the economic implications of implementing a much larger tree-planting program than the one presented in the Action Plan. Whereas the Action Plan estimated that 5 to 9 MMT of carbon (MMTC) could be sequestered in 2000 (with perhaps threefold increases in sequestration in later years when trees are growing the fastest), the program being considered in this analysis annually sequesters as much as 231 MMTC during its peak years. Our analysis focuses on how much the costs of stabilizing US carbon emissions at 1990 levels are reduced when economic criteria alone determine the number of trees that will be used. Our results show that when the focus is shifted from stabilization of gross emissions to net emissions the cost reductions are dramatic, about 20 to 80 percent depending on the assumed cost of trees. Political and institutional obstacles to the formation of such a cost effective response are explored in the conclusions. DOE

N94-17852# Brookhaven National Lab., Upton, NY.

COST EFFECTIVE ENERGY STRATEGIES FOR THE REDUCTION OF CO2 EMISSIONS IN THE UNITED STATES: COUNTRY REPORT FOR ETSAP ANNEX 4

S. C. Morris, J. L. W. Marcuse, and G. Goldstein Feb. 1993 36 p
(Contract DE-AC02-76CH-00016)
(DE93-016842; BNL-48961) Avail: CASI HC A03/MF A01

The energy system of the United States of America was analyzed using MARKAL. The time period of the study was 1990-2030. Projected energy demands over this period for a Reference Scenario were largely modeled after the US Energy Information Administration's 1992 Annual Energy Outlook for 1990-2010 and from the National Energy Strategy for the period 2010-2030. Expectations of maximum growth rates of conservation and renewable energy technologies were based on the same sources. Reductions in CO2 emissions were achieved by setting absolute constraints on total emissions levels by year and by carbon taxes. A 10% reduction in CO2 emissions was near the limit of technical feasibility for this scenario. This resulted in an overall cost increase of $1.1 trillion present value, but marginal costs on CO2 emissions reductions ranged up to $3300/ton. Over 70% of the CO2 emissions reduction occurred in electrical generation, partly resulting from decreases in demand for electricity. Additional scenarios were run for conditions of low economic growth and with the addition of carbon sequestering technologies. DOE

N94-17890# Argonne National Lab., IL. Environmental Assessment and Information Sciences Div.

A BAYESIAN APPROACH TO CONTAMINANT PLUME DELINEATION

R. L. Johnson 1993 10 p Presented at the 1993 Groundwater Modeling Conference, Boulder, CO, 6-12 Jun. 1993
(Contract W-31-109-eng-38)
(DE93-012909; ANL/EAIS/CP-79173; CONF-9306158-2) Avail: CASI HC A02/MF A01

Fundamental to accurate modeling of groundwater contaminant transport is an understanding of the initial extent of contamination. The initial location of contamination must typically be inferred from relatively little 'hard' sampling data, and related 'soft' information. A combination of Bayesian analysis and spatial statistics is used to generate initial estimates of contamination based both on 'soft' information (i.e., prior modeling results, past experience, etc.) and 'hard' data (i.e., sampling results). A Beta distribution is used to represent the probability that contamination is present at any grid node. For every node, prior Beta probability density functions are revised into posterior distributions as additional data become available. The result is a node by node probabilistic representation of plume extent that can be updated as new information is generated, that indicates where additional sampling would have the greatest impact on the uncertainty associated with plume extent, and that can serve as the basis for Monte Carlo analysis of contaminant transport. This approach is demonstrated with information from a subsurface chromium plume beneath the chemical waste landfill at Sandia National Laboratory, Albuquerque, New Mexico. DOE

N94-17891# Argonne National Lab., IL. Environmental Assessment and Information Sciences Div.

SETTING THE GLOBAL THERMOSTAT WITH AN EXHAUSTIBLE TRADEABLE PERMIT SYSTEM

R. G. Kosobud (Illinois Univ., Chicago.), K. G. Quinn (Illinois Univ., Chicago.), D. W. South, and T. A. Daly 1993 20 p Presented at the 4th International Conference on the Scientific and Policy Issues Facing All Governments, Chicago, IL, 5-8 Apr. 1993
(Contract W-31-109-eng-38)
(DE93-012911; ANL/EAIS/CP-79424; CONF-930415-1) Avail: CASI HC A03/MF A01

The global warming policy debate has centered largely on near-term objectives such as freezing 1990 CO2 emissions without regard to long-run implications. A policy of freezing CO2 emissions is shown to slow but not halt global warming, while requiring expensive near-term adjustments. If the long-run temperature change outcome of the freeze policy is set as the goal of a more graduated control policy, one which allows the market to determine annual emissions, a more cost-effective solution is obtained that reduces the negative adjustment effects on the energy and other affected industries. The most cost-effective emissions time path of a graduated control policy could be achieved by an evaporative marketable CO2 emissions permit system. This paper provides a preliminary examination of an evaporative permit system used to achieve long-run stabilization of greenhouse-induced temperature change. DOE

N94-17910# Oak Ridge National Lab., TN.

PRACTICAL REPORTING TIMES FOR ENVIRONMENTAL SAMPLES

C. K. Bayne, D. D. Schmoyer, and R. A. Jenkins Feb. 1993 50 p
(Contract DE-AC05-84OR-21400)
(DE93-013461; ORNL/TM-12316) Avail: CASI HC A03/MF A01

Pre-analytical holding times for environmental samples are specified because chemical and physical characteristics may change between sampling and chemical analysis. For example, the Federal Register prescribes a pre-analytical holding time of 14 days for volatile organic compounds in soil stored at 4 C. The American Society for Testing Materials (ASTM) uses a more technical definition that the pre-analytical holding time is the day when the analyte concentration for an environmental sample falls below the lower 99% confidence interval on the analyte concentration at day zero. This study reviews various holding time definitions and suggest a new pre-analytical holding time approach using acceptable error rates for measuring an environmental analyte. This practical reporting time (PRT) approach has been applied to nineteen volatile organic compounds and four explosives in three environmental soil samples. A PRT nomograph of error rates has been developed to estimate the consequences of missing a pre-analytical holding time. This nomograph can be applied to a large class of analytes with concentrations that decay linearly or exponentially with time regardless of sample matrices and storage conditions. DOE

N94-17985# Nevada Univ., Reno. Atmospheric Sciences Center.

CLOUD CCN FEEDBACK

J. G. Hudson 1992 4 p Presented at the 11th International Conference on Clouds and Precipitation, Montreal, Quebec, 17-21 Aug. 1992
(Contract DE-FG08-90ER-61012)
(DE93-016878; CONF-920881-4) Avail: CASI HC A01/MF A01

Cloud microphysics affects cloud albedo precipitation efficiency and the extent of cloud feedback in response to global warming. Compared to other cloud parameters, microphysics is unique in its large range of variability and the fact that much of the variability is anthropogenic. Probably the most important determinant of cloud microphysics is the spectra of cloud condensation nuclei (CCN) which display considerable variability and have a large anthropogenic component. When analyzed in combination three field observation projects display the interrelationship between CCN and cloud microphysics. CCN were measured with the Desert Research Institute (DRI) instantaneous CCN spectrometer. Cloud microphysical measurements were obtained with the National Center for Atmospheric Research Lockheed Electra. Since CCN and cloud microphysics each affect the other, a positive feedback mechanism can result. DOE

N94-17986# Nevada Univ., Reno. Desert Research Inst.

SHIP-PRODUCED CLOUD LINE OF 13 JULY 1991

E. E. Hindman, W. M. Porch, J. G. Hudson, and P. A. Durkee 1992 5 p Presented at the 11th International Conference on Clouds and Precipitation, Montreal, Quebec, 17-21 Aug. 1992
(Contract DE-FG08-90ER-61012)
(DE93-016879; CONF-920881-3) Avail: CASI HC A01/MF A01

Steaming ships can produce long linear cloud lines in regions of fog and broken stratus as well as in marine stratus layers. The lines are not always detected in 0.63 micron satellite images, but are often detected in the corresponding 3.7 microns images because the lines contain smaller and more numerous droplets than the stratus in which they are embedded as deduced by Coakley, et al. and measured by Radke, et al. They postulate cloud condensation nuclei (CCN) from steaming ships produced the more numerous and, hence, smaller cloud droplets. The ship-produced clouds are not always detected in 0.63 microns images because this wavelength is not as sensitive to changes in droplet size as is 3.7 microns. On 13 July 1991 a dramatic, ship-produced cloud line formed offshore of Baja California. Satellite images of the line and corresponding photographs from the R/V EGABRAG III which passed under the line are presented. The images and photos reveal the structure of the line. The EGABRAG was a source of CCN but did not produce a cloud line; they attempt to explain this important finding. DOE

N94-18005# Lawrence Livermore National Lab., CA.
STATISTICAL INTERCOMPARISON OF GLOBAL CLIMATE MODELS: A COMMON PRINCIPAL COMPONENT APPROACH WITH APPLICATION TO GCM DATA
S. K. Sengupta and J. S. Boyle May 1993 37 p
(Contract W-7405-eng-48)
(DE93-017951; UCRL-ID-114222) Avail: CASI HC A03/MF A01

Variables describing atmospheric circulation and other climate parameters derived from various GCM's and obtained from observations can be represented on a spatio-temporal grid (lattice) structure. The primary objective of this paper is to explore existing as well as some new statistical methods to analyze such data structures for the purpose of model diagnostics and intercomparison from a statistical perspective. Among the several statistical methods considered here, a new method based on common principal components appears most promising for the purpose of intercomparison of spatio-temporal data structures arising in the task of model/model and model/data intercomparison. A complete strategy for such an intercomparison is outlined. The strategy includes two steps. First, the commonality of spatial structures in two (or more) fields is captured in the common principal vectors. Second, the corresponding principal components obtained as time series are then compared on the basis of similarities in their temporal evolution. DOE

N94-18050# California Univ., Berkeley. Lawrence Berkeley Lab. Energy and Environment Div.
ENERGY EFFICIENCY AND THE ENVIRONMENT: INNOVATIVE WAYS TO IMPROVE AIR QUALITY IN THE LOS ANGELES BASIN
R. Ritschard Feb. 1993 46 p Presented at the 89th Annual Meeting of Association of American Geographers, Atlanta, GA, 6-10 Apr. 1993
(Contract DE-AC03-76SF-00098)
(DE93-016964; LBL-33725; CONF-9304172-1) Avail: CASI HC A03/MF A01

This paper focuses on novel, innovative approaches for reducing or delaying the production of photochemical smog in the Los Angeles Basin. These approaches include modifying the surface characteristics of the basin by increasing surface albedo and an extensive tree-planting program. The changes in surface conditions are designed to reduce the basin air temperatures, especially during the summer months, which will result in two possible effects. First, a decrease in temperature would lead to a reduction in energy use with an associated decline in emissions of nitrogen oxides (NO(x)) and a lowering of evaporative emission of reactive organic gases. Reductions in these smog precursors could improve the air quality of the basin without imposing additional emissions regulations. The second effect is associated with the possible causal relationship between air temperature and smog formation (i.e., lower temperatures and lower incidence of smog). Since this approach to mitigating air emissions is broad, the studies to date have concentrated on how changes in surface characteristics affect the meteorological conditions of the basin and on how these meteorological changes subsequently affect smog production. A geographic information system database of key surface characteristics (i.e., vegetative cover, albedo, moisture availability, and roughness) was compiled, and these characteristics were evaluated using prognostic meteorological models. The results of two- and three-dimensional meteorological simulations will be presented and discussed in this paper. DOE

N94-18101 Princeton Univ., NJ. Plasma Physics Lab.
REMOVING CFC'S FROM THE ATMOSPHERE WITH LASERS: A SECOND LOOK
T. H. Stix Jul. 1993 36 p Presented at the 20th IEEE International Conference on Plasma Sciences, Vancouver, British Columbia, 7-9 Jun. 1993 Limited Reproducibility: More than 20% of this document may be affected by microfiche quality
(Contract DE-AC02-76CH-03073)
(DE93-017516; PPL-2923; CONF-930652-1) Avail: CASI HC A03

An option to both mitigate greenhouse warming and to help preserve the ozone layer could be to remove chlorofluorocarbons (CFC's) from their principal reservoir, the troposphere. But due to the extremely low atmospheric concentration of the CFC's (less than one part per billion by volume), such a process must be enormously selective to be cost-effective. It was suggested in 1989 that vast arrays of extremely powerful infrared lasers might be used to break up tropospheric CFC's via multiphoton dissociation (MPD). Computer calculations making use of an extensive atmospheric-gas infrared cross-section database suggest that -- at carefully chosen wavelengths -- 90% transmission over 50-kilometer paths would be possible through dry atmospheres. Still, a factor of 10 or 20 greater efficiency for the laser-CFC dissociation process is needed to bring the projected costs down to where the plan would merit serious consideration. The likeliest possibility for improvement appears to be to 'chirp' the infrared laser frequency, that is, lowering its frequency during each pulse so as to remain in resonance -- as long as possible -- with the anharmonic vibrations of the CFC molecules. What is needed is a factor of 10 or more decrease below the laser-beam fluence now thought to be required for CFC infrared multiphoton dissociation. Specifically, one would look to achieve CFC NTD with an infrared fluence of 0.1 to 0.2 joules per cm(sup 2). This goal may not be reachable, but laboratory experiments using presently available apparatus and techniques could explore this intriguing question. Following a summary of present knowledge concerning ozone depletion, this paper discusses the process of multiphoton dissociation and ways, including laser chirping, by which the MPD efficiency might be enhanced. DOE

N94-18139# National Defence Research Establishment, Umea (Sweden). NBC Defence Dept.
CONDENSED GASES UNDER WINTER CONDITIONS: A STUDY FOR THE RESCUE SERVICES [KONDENSERADE GASER UNDER VINTERFOERHAELLANDEN: EN FOERSTUDIE FOER RAEDDNINGSTJAENSTEN]
Stellan Winter and Per Olof Granbom Dec. 1992 47 p In SWEDISH
Sponsored by National Rescue Services Board, Sweden
(FOA-C-40305-4.5; ETN-93-94491) Avail: CASI HC A03/MF A01

The behavior of spills of condensed gases under Winter conditions was studied using literature data. It was found that the liquids easily penetrate a snow layer and spread along the bottom of the snow cover. On flat ice the liquids may spread until the liquid film is only 0.5 mm thick. The study indicates that snow might give rise to considerable and fast evaporation of liquids having a low boiling point. Experiments are proposed to investigate the fraction of evaporation of chlorine, ammonia and sulphur dioxide when they are spilled onto snow at various topographic conditions. Experiments are also suggested to study how vapors of propane or butane burn in snow. For ammonia, ethylene oxide and sulphuric acid special experiments are recommended to find out how water solubility affects evaporation, pool spreading and state of aggregation. ESA

N94-18167# Oak Ridge National Lab., TN.
METADATA COMPILED AND DISTRIBUTED BY THE CARBON DIOXIDE INFORMATION ANALYSIS CENTER FOR GLOBAL CLIMATE CHANGE AND GREENHOUSE GAS-RELATED DATA BASES
T. A. Boden 1992 8 p Presented at the Scientific Data Management Workshop 1992, Salt Lake City, UT, 3-5 Nov. 1992
(Contract DE-AC05-84OR-21400)
(DE93-015338; CONF-9211115-3) Avail: CASI HC A02/MF A01

The Carbon Dioxide Information Analysis Center (CDIAC) compiles and provides information to help international researchers, policymakers, and educators evaluate complex environmental issues associated with elevated levels of atmospheric carbon dioxide (CO2) and other trace gases, including potential climate change. CDIAC is located within the Environmental Sciences Division of Oak Ridge National Laboratory (ORNL) in Oak Ridge, Tennessee and is line funded by the U.S. Department of Energy's (DOE) Global Change Research Program (GCRP). CDIAC is an information analysis center (IAC). In operation since 1982, CDIAC identifies sources of primary data at national and international levels; obtains, archives, evaluates, and distributes data and computer models; fully documents select data sets and computer models and offers them as numeric data packages (NDP's) and computer model packages (CMP's); distributes data and computer models on a variety of magnetic and electronic medias including 9-track magnetic tapes, IBM-formatted floppy diskettes, CD-ROM, and over Internet, Omnet, and Bitnet electronic networks; develops derived, often multidisciplinary data products useful for carbon cycle and climate-change research; distributes reports pertinent to greenhouse effect and climate change issues; produces the newsletter, CDIAC Communications; and in general acts as the information focus for the GCRP's research projects. Since its inception, CDIAC has responded to thousands of requests for information, and since 1985 has distributed more than 70,000 reports, NDP's and CMP's to 97 countries worldwide. DOE

N94-18183# Arizona Univ., Tucson. Inst. of Atmospheric Physics.
THE LAND COMPONENT OF THE GLOBAL CLIMATE SYSTEM WITH ADEQUATE SPATIAL RESOLUTION
R. E. Dickinson 1 Mar. 1993 4 p
(Contract DE-FG02-91ER-61216)
(DE93-018951; DOE/ER-61216/2) Avail: CASI HC A01/MF A01

The overall import of this project was to support and focus collaboration between the University of Arizona and NCAR (and when appropriate DOE staff) towards achieving a state of the art land surface model available for CHAAMP and more general community use along with NCAR's CCM2 climate model. The goals of this program over a three year period are: to upgrade the BATS1e code to current programming standards as implemented in CCM2; and to document and design the next generation of this code; to reprogram BATS1e to carry out its integration over land in efficient vector loops and interface this code to CCM2; to formulate and implement CCM2 schemes to provide statistically prescribed distributions of precipitation, radiation and sub-scale cloudiness; and to perform sensitivity studies with the BATS1e scheme implemented in CCM2; and to develop graphical visualization procedures for scientific evaluation of the fine mesh output. Progress to date includes the following: the BATS code is being implemented in CCM2; statistics at the T-42 model resolution were developed; monthly average patterns of gauge precipitation, along with intensities and frequency of occurrence were mapped; PC hardware and software support was increased, and a geographic information system was used to support fine mesh data visualization. DOE

N94-18499# Argonne National Lab., IL.
ON-LINE MONITORING OF INCINERATOR EMISSIONS
Zhuo-Xiong Mao, J. C. Demirgian, and E. Hwang 1993 22 p Presented at the 12th Annual International Symposium on Thermal Treatment Technologies - Incineration Conference, Knoxville, TN, 3-7 May 1993
(Contract W-31-109-eng-38)
(DE93-017406; ANL/CMT-ACL/CP-77718; CONF-930572-8) Avail: CASI HC A03/MF A01

As part of efforts to develop an on-line emissions monitor to detect specific organic compounds for incinerators, the authors tested a Fourier transform infrared spectrometer (FTIR) coupled with a long-path cell (LPC). A mixture of toluene, chlorobenzene, 1,1,1-trichloroethane, and trichloroethylene with elemental ratio C:H:Cl = 3:3.1:0.9 was incinerated in a methane/air flame. The effluent was continuously passed through a heated long-path cell. Eleven target compounds were simultaneously analyzed: methane, toluene, chlorobenzene, 1,1,1-trichloroethane, trichloroethylene, benzene, ethylene, hydrogen chloride, carbon monoxide, carbon dioxide, and water. During the testing, the incinerator temperature and the excess air ratio were deliberately changed to simulate both complete and incomplete combustion conditions in the incinerator. Test results indicate that the FTIR/LPC system can successfully follow concentration changes in the emissions that are associated with the change in the incinerator operations. In addition to carbon monoxide, methane, ethylene, and benzene have been found to be major products of incomplete combustion of the mixture. In this paper, the authors also discuss problems related to obtaining representative calibration standards and to developing adequate methods for continuous monitoring of emissions. DOE

N94-18502# Argonne National Lab., IL.
A COMPARISON OF WET AND DRY SCRUBBING SYSTEMS FOR CONTROL OF METALS AND DIOXIN/FURAN EMISSIONS FROM INCINERATORS
P. S. Farber and H. S. Huang 1993 13 p Presented at the Spring National Meeting of the American Inst. of Chemical Engineers, Houston, TX, 28 Mar. - 1 Apr. 1993
(Contract W-31-109-eng-38)
(DE93-017446; ANL/ES/CP-80079; CONF-930364-6) Avail: CASI HC A03/MF A01

In Europe and the United States, both wet and dry (including semidry) scrubbing systems are being used for control of emissions from all types of waste incinerators. In terms of the effectiveness of controlling particulates and acid gases, both types of scrubbing systems are capable of meeting US Environmental Protection Agency and European Community limits. Two of the more difficult emissions requirements for an incinerator air-pollution-control system to meet are the metals and the dioxin/furan limits. The dioxin/furan emissions requirement is especially stringent, calling for levels below 1 ng (10(exp -9)) per cubic meter toxic equivalency. The differences between wet and dry scrubbing systems are discussed in this paper, as well as the advantages and disadvantages of each in its application to the control of emissions from incinerators. Particular attention will be paid to control of metals and dioxin/furan emissions and to the sampling and analysis techniques used to measure these emissions. Toxic equivalency factors are explained, and in particular, the international toxic equivalency factor proposed as the US and European standard is discussed. This paper will also address some of the techniques being employed to minimize the emissions of toxic compounds and discuss the use of combined wet and dry scrubbing systems for increased assurance of compliance. DOE

N94-18521# Sandia National Labs., Albuquerque, NM.
CHARACTERIZATION OF THE FACILITY FOR ATMOSPHERIC CORROSION TESTING (FACT) AT SANDIA
C. J. Greenholt, N. R. Sorensen, G. A. Poulter, and T. R. Guilinger Jun. 1993 24 p
(Contract DE-AC04-76DP-00789)
(DE93-018510; SAND-92-1864) Avail: CASI HC A03/MF A01

The capability to perform atmospheric corrosion testing of materials and components now exists at Sandia resulting from the installation of a system called the Facility for Atmospheric Corrosion Testing (FACT). This report details the design, equipment, operation, maintenance, and future modifications of the system. This report also presents some representative data acquired from testing copper in environments generated by the FACT. DOE

N94-18523# Oak Ridge National Lab., TN.
THE URBAN PERSPECTIVES OF ACID RAIN
B. E. Tonn Jun. 1993 123 p Presented at the Urban Perspective of Acid Rain, Raleigh, NC, 23-24 Sep. 1992
(Contract DE-AC05-84OR-21400)
(DE93-018881; ORNL/M-2936-Summ; CONF-9209381-Summ) Avail: CASI HC A06/MF A02

This report documents discussions held during a workshop an Urban Perspective of Acid Rain. The workshop was sponsored by the Office of the Director, National Acid Precipitation Assessment Program (NAPAP). NAPAP anticipates giving increased emphasis to the benefits in urban areas of emissions reductions. The goal of this informal, exploratory workshop was to serve as a first step towards identifying pollutant monitoring, and research and assessment needs to help answer, from an urban perspective, the two key questions posed to NAPAP by Congress: (1) what are the costs, benefits, and effectiveness of the acid rain control program, and (2) what reductions in deposition, rates are needed in order to prevent adverse effects? The workshop addressed research activities needed to respond to these questions. The discussions focused, sequentially, on data needs, data and model availability, and data and modeling gaps. The discussions concentrated on four areas of effects: human health, materials, urban forests, and visibility. DOE

N94-18688# Phillips Lab., Hanscom AFB, MA.
A REVIEW AND EVALUATION OF THE ADAM 2.1 DISPERSION MODEL Final Report, Oct. 1991 - Sep. 1992
Bruce A. Kunkel 1 Oct. 1992 68 p
(AD-A269896; AD-E201605; PL-TR-92-2245; ERP-1109) Avail: CASI HC A04/MF A01

ADAM 2.1 is a heavy gas, gaussian puff dispersion model which predicts the hazard area resulting from the release of a toxic chemical. The model takes into account: (1) the chemical reaction, if any, that takes place when the chemical is released to the atmosphere; (2) the gravitational slumping due to the high density of the cloud (due to aerosol presence, temperature or molecular weight); and, (3) the dispersion due to atmospheric turbulence. Sixteen different source types are modeled including instantaneous and continuous releases, pressurized liquid and gas releases, and non-pressurized liquid releases, cryogenic and non-cryogenic liquid releases, and diked and undiked releases. The chemical data base contains data on eight chemicals -- ammonia, chlorine, fluorine, hydrogen fluoride, hydrogen sulfide, nitrogen tetroxide, phosgene, and sulfur dioxide. This report gives a general review of the model structure and its performance capabilities. A more detailed discussion of the model physics can be obtained from two earlier contractor reports. Model results are compared with the AFTOX dispersion model results and with field data. DTIC

N94-18775 Army Cold Regions Research and Engineering Lab., Hanover, NH.
INTERNATIONAL SYMPOSIUM ON THE ECOLOGICAL EFFECTS OF ARCTIC AIRBORNE CONTAMINANTS Abstracts Only
S. J. Christie, J. M. Martin, and J. E. Mello 8 Oct. 1993 152 p
Symposium held in Reykjavik, Iceland, 4-8 Oct. 1993 Limited Reproducibility: More than 20% of this document may be affected by microfiche quality
(AD-A269955; CRREL-SR-93-23) Avail: CASI HC A08

This volume contains abstracts submitted to the symposium and accepted prior to July 1, 1993. The Steering Committee has decided to publish all accepted abstracts in a gesture to improve communications and awareness among all arctic researchers. This book is organized by session. Each session's abstracts are presented alphabetically by first author. The index in the back lists all authors and identifies the pages on which each author's abstracts are printed. Sessions cover the following topics: pathways of contaminants to the arctic biosphere, distribution of contaminants in the arctic biosphere, human health issues, arctic ecosystem responses to atmospheric contaminants, contaminant relationship to climate change, and information gaps and research needs. CASI

N94-18817# Sandia National Labs., Albuquerque, NM.
EFFECTS OF THE MOUNT PINATUBO ERUPTION ON SOLAR INSOLATION: FOUR CASE STUDIES
A. L. Rosenthal and J. M. Robert (New Mexico State Univ., Las Cruces.) May 1993 60 p
(Contract DE-AC04-76DP-00789)
(DE93-018454; SAND-93-7031) Avail: CASI HC A04/MF A01

The Southwest Technology Development Institute staff analyzed solar insolation data from four sites recorded during the years 1990 through 1992. Analyses were performed to identify and quantify the effects on insolation caused by the eruption of Mount Pinatubo in the Philippines on 15-16 June 1991. The four monitoring stations that supplied the raw data for this report were: The Southwest Region Experiment Station in Las Cruces, New Mexico; The Solar Radiation Research Laboratory at the National Renewable Energy Laboratory in Golden, Colorado; The Solar Insolation Monitor Program Station operated by the Pacific Gas and Electric Company in Carrisa Plains, California; and The Solar Insolation Monitor Station at Sandia National Laboratories in Albuquerque, New Mexico. Data from each of the sites were recorded by dedicated datalogging equipment. Every effort was made to prevent data acquisition system problems (e.g., drift of the datalogger clock) from influencing the accuracy of the results. DOE

N94-18832# Oak Ridge National Lab., TN. Carbon Dioxide Information Analysis Center.
CDIAC CATALOG OF NUMERIC DATA AND COMPUTER MODEL PACKAGES
T. A. Boden, F. M. OHara, Jr., and F. W. Stoss May 1993 84 p
(Contract DE-AC05-84OR-21400)
(DE93-017675; ORNL/CDIAC-62) Avail: CASI HC A05/MF A01

The Carbon Dioxide Information Analysis Center acquires, quality-assures, and distributes to the scientific community numeric data packages (NDP's) and computer model packages (CMP's) dealing with topics related to atmospheric trace-gas concentrations and global climate change. These packages include data on historic and present atmospheric CO2 and CH4 concentrations, historic and present oceanic CO2 concentrations, historic weather and climate around the world, sea-level rise, storm occurrences, volcanic dust in the atmosphere, sources of atmospheric CO2, plants' response to elevated CO2 levels, sunspot occurrences, and many other indicators of, contributors to, or components of climate change. This catalog describes the packages presently offered by CDIAC, reviews the processes used by CDIAC to assure the quality of the data contained in these packages, notes the media on which each package is available, describes the documentation that accompanies each package, and provides ordering information. Numeric data are available in the printed NDP's and CMP's, in CD-ROM format, and from an anonymous FTP area via Internet. All CDIAC information products are available at no cost. DOE

N94-18835# Department of Energy, Washington, DC.
ENVIRONMENTAL RESTORATION AND WASTE MANAGEMENT FIVE-YEAR PLAN, FISCAL YEARS 1994-1998. VOLUME 3: PUBLIC CONCERNS
Aug. 1993 125 p
(DOE/S-00097P-Vol-3) Avail: CASI HC A06/MF A02

This document is the third and final volume of the Department of Energy (DOE) Environmental Restoration and Waste Management Five-Year Plan for Fiscal Years (FY) 1994-1998. The Five-Year Plan is the primary planning document for DOE environmental restoration and waste management activities. This document reflects increased stakeholder involvement and the continuing dialogue between DOE and those who are interested in, and affected by, the activities of the Office of Environmental Restoration and Waste Management (EM). It is designed to respond to public concerns regarding Volumes 1 and 2 of the the preliminary Five-Year Plan. The document is divided into the following sections: plan organization and structure; public participation and education; funding and budget issues; planning and management issues; regulatory compliance; waste management; environmental restoration; technology development; transportation; facility transition and management; and site-specific issues. Author (revised)

N94-18881 Corps of Engineers, Washington, DC.
ECOLOGICAL AND ENVIRONMENTAL IMPACTS OF CONSTRUCTION IN THE COASTAL ZONE Report, 1987 - 1991
E. O. Gangstad 15 Sep. 1992 11 p Limited Reproducibility: More than 20% of this document may be affected by microfiche quality
(AD-A269196; OCE/NRM/93-3) Avail: CASI HC A03

Engineering works have been developed to alter the coastline to suit man's desires. However, imperfect knowledge of the nature of the forces acting in the coastal zone and their effects has resulted in unexpected or undesirable effects. Frequently such alterations create substantial conflicts between uses. For instance, use of the waters for waste disposal, resulting in pollution, directly conflicts with recreational and fishing uses. The filling of wetlands for use in residential, industrial, or port construction conflicts with wildlife and estuarine preservation, recreational uses, and fishing interests. DTIC

N94-18885 Corps of Engineers, Washington, DC.
THE ECOLOGICAL AND ENVIRONMENTAL IMPACTS OF MANMADE MARSHES Final Report, 1988 - 1993
E. O. Gangstad 1993 9 p Limited Reproducibility: More than 20% of this document may be affected by microfiche quality
(AD-A269213; OCE/NRM/93-2) Avail: CASI HC A02

The U.S. Corps of Army Engineers has been charged by the Congress of the United States with the responsibility for construction and maintenance of shipping channels throughout the country. During the past 200 years it has created over 25,000 miles of channels and has developed over 100 commercial ports and harbors as well as over 4,000 small boat harbors. Each year the Corps of Engineers removes over 350 million cubic yards of dredged materials from the navigation channels. One particularly fruitful area of research is the Corps' attempt to create new marshes with dredged material. DTIC

N94-18949# Rijksinstituut voor Volksgezondheid en Milieuhygieene, Bilthoven (Netherlands).
LAND-USE RELATED SOURCES OF CO2, CH4 AND N2O: CURRENT GLOBAL EMISSIONS AND PROJECTIONS FOR THE PERIOD 1990-2100
A. F. Bouwman, G. J. VanDenBorn, and R. J. Swart May 1992 106 p
See also PB92-209097
(PB93-194819; RIVM-222901004) Avail: CASI HC A06/MF A02

The report presents part of the results of a study carried out by the RIVM for the ESCAPE project 'Development of a Framework for the Evaluation of Policy Options to Deal with the Greenhouse Effect'. The report describes a preliminary study carried out to provide a basis for the development of the IMAGE Land Use Model. The main purpose of the study is to assess the relations existing between various land use changes and agricultural processes, to outline the trade-offs between the different policy options, and to evaluate the impact of different strategies to control emissions related to land use. The results for 1990 have been used to calibrate the model for the base year. The projections presented in the report have been used to test the scenarios developed with the IMAGE Land Use Model. NTIS

N94-18960* National Aeronautics and Space Administration, Washington, DC.
OZONE HOLE (Videotape)
Feb. 1988 Videotape: 3 min. 15 sec. playing time, in color, with sound
(NASA-TM-109368; NONP-VT-94-198215) Avail: CASI VHS A01/BETA A22

The first segment of this video gives an overview of the Ozone Hole Airborne Arctic Stratospheric Expedition, an international effort using balloon payloads, ground based instruments, and airborne instruments to study ozone depletion and the hole in the ozone over Antarctica which occurs every spring. False color imagery taken from NASA's Nimbus 7 satellite which documents daily changes in ozone is also shown. The second segment of this video shows actual take-off and flight footage of the two aircraft used in the experiment: the DC-8 Flying Laboratory and the high flying ER-2. CASI

N94-18967* National Aeronautics and Space Administration. Goddard Space Flight Center, Greenbelt, MD.
OCTOBER 1979-1989 SOUTHERN HEMISPHERE TOTAL OZONE AS SEEN BY TOMS (Videotape)
Nov. 1989 Videotape: 7 min. 20 sec. playing time, in color, with sound
(NASA-TM-109375; NONP-VT-94-198222) Avail: CASI VHS A01/BETA A22

This is raw video from space taken by the Total Ozone Mapping Satellite (TOMS). CASI

N94-19038# Lawrence Livermore National Lab., CA.
INCLUSION OF A THREE-DIMENSIONAL WASHOUT COEFFICIENT IN ADPIC
E. Naeslund and H. Holmstroem May 1993 20 p
(Contract W-7405-eng-48)
(DE93-018499; UCRL-ID-114054) Avail: CASI HC A03/MF A01

In ADPIC, the deposition emerging from washout has thus far been modelled rather crudely, since the only option has been to turn the rain on and off at different times. This kind of modelling is particularly unsatisfactory when ADPIC is used to model continuous releases over long periods of time. The assumption of simultaneous rain throughout such a large plume is simply not true. In this report a modified version of ADPIC with a three-dimensional (3-D) washout coefficient is presented. The effect of space variable precipitation is examined via two separate releases that are simulated for a period of 48 hours: one continuous 'Chernobyl-like source' release and one instantaneous 'nuclear explosion-like' release. Simulations with both the new and old formulation are made and the resulting deposition patterns are compared. DOE

N94-19045# Argonne National Lab., IL. Environmental Research Div.
ORGANIC CARBONYL COMPOUNDS IN ALBUQUERQUE, NEW MEXICO, AIR: A PRELIMINARY STUDY OF THE EFFECTS OF OXYGENATED FUEL USE
Carl J. Popp (New Mexico Inst. of Mining and Technology, Socorro.), Lin Zhang (New Mexico Inst. of Mining and Technology, Socorro.), and Jeffrey S. Gaffney Jun. 1993 32 p Presented at the Symposium on Alternative Fuels and the Environment, Ann Arbor, MI, 28 Mar. - 2 Apr. 1993
(Contract W-31-109-eng-38)
(DE93-017748; ANL/ER/CP-80321; CONF-9303207-1) Avail: CASI HC A03/MF A01

A suite of inorganic and organic species were analyzed for four 2-4 day time periods over a year in Albuquerque, New Mexico to determine baseline conditions for organic pollutants under the current air pollution control parameters. Concentrations of low molecular weight carbonyl compounds were relatively high compared with areas such as Los Angeles. Formic acid concentrations in air samples were significant even in winter. In addition, ratios of peroxypropionyl nitrate to peroxyacyetyl nitrate are higher than expected and may be related to the use of oxygenated fuels which are used to mitigate CO concentrations. The number of CO violations in Albuquerque has decreased steadily since 1982 and the downward trend has continued since 1989 when oxygenated fuel use was mandated. It is, therefore, difficult to correlate the drop in CO violations directly to the use of oxygenated fuels when such factors as fleet turnover, woodburning controls, emissions testing and meteorological conditions also may be playing significant roles. More detailed studies are needed to determine the specific relationship between the use of oxygenated fuels and the air quality in Albuquerque, New Mexico and similar urban areas in the western United States. DOE

N94-19064# Clarkson Univ., Potsdam, NY. Dept. of Civil and Environmental Engineering.
OIL SPREADING IN SURFACE WATERS WITH AN ICE COVER
P. D. Yapa, S. A. Weerasuriya, D. P. Belaskas, and T. Chowdhury Feb. 1993 96 p Sponsored by Geological Survey, Reston, VA
(Contracts DI-14-08-0001-G-1915; USGS-G-1915)
(PB93-190767; REPT-93-3; USGS/G-1915) Avail: CASI HC A05/MF A01

A study of oil spreading in surface waters in the presence of a floating ice cover is presented. The ice can be solid or fragmented. Both axi-symmetrical and uni-directional spreading are studied. The report describes the analytical and numerical model development, the experimental set-up, results from the laboratory experiments, and their comparison with the derived theory and the numerical simulation. To analyze the spreading of oil under solid ice, new equations are derived. These equations consider gravity (buoyancy) - inertia phase, gravity (buoyancy) - viscous phase, and the termination of spreading during the buoyancy - surface tension phase. The derivation considers both the constant discharge mode and the constant volume mode. Therefore, a complete description of the spreading phenomena from the time of initial spill to termination of spreading is presented. The emphasis of the study is on the dominant spreading mechanism for oil under ice, which is the buoyancy-viscous phase. NTIS

N94-19065# National Oceanic and Atmospheric Administration, Research Triangle Park, NC. Atmospheric Sciences Modeling Div.
SPATIOTEMPORAL VARIABILITY OF NON-URBAN OZONE CONCENTRATIONS OVER THE EASTERN UNITED STATES AND ITS POTENTIAL REPLICATION BY SATELLITE DATA
B. K. Eder (Environmental Protection Agency, Research Triangle Park, NC.), S. K. LeDuc (Environmental Protection Agency, Research Triangle Park, NC.), and L. E. Truppi (Environmental Protection Agency, Research Triangle Park, NC.) 1993 28 p
(PB93-191328; EPA/600/A-93/079) Avail: CASI HC A03/MF A01

The spatial and temporal variability of the maximum 24 hourly surface ozone concentrations over the eastern United States was examined for the period 1985-1990 using Rotated Principal Component Analysis (RPCA). This led to the delineation of six contiguous subregions, each of which displayed statistically unique ozone characteristics. Examination of the time series associated with the Subregions revealed that the Great Lakes and Mid-Atlantic Subregions tend to contain a stronger seasonal cycle, with maximum concentrations occurring during the last week in June and the first week in July, respectively. The strength of this seasonality is weakened for the Northeast and South Subregions and the timing of its maximum delayed, until the end of July and the first of August, respectively. The Southwest Subregion experiences a greatly diminished seasonality, with maximum concentrations delayed until the middle of August. The seasonality found in the Florida Subregion is unique in both its strength and timing, as the highest concentrations consistently occur during the months of April and May. The time series were then deseasonalized and autocorrelations and spectral density estimates calculated, revealing that persistence is much more prevalent in the Florida, South and Southwest Subregions and less prevalent in the Northeast, Great Lakes and Mid-Atlantic Subregions. NTIS

N94-19104# Los Alamos National Lab., NM.
KINETICS PROGRAMS FOR SIMULATION OF TROPOSPHERIC PHOTOCHEMISTRY ON THE GLOBAL SCALE
S. Elliott, C. Y. J. Kao, R. P. Turco, and X. P. Zhao Aug. 1993 55 p
(Contract W-7405-eng-36)
(DE93-019035; LA-12539-MS) Avail: CASI HC A04/MF A01

The study of tropospheric kinetics underlies global change because key greenhouse gases are photochemically active. Modeling of tropospheric chemistry on a global scale is essential because some indirect greenhouse gases are short-lived and interact in a non-linear fashion. It is also extremely challenging, however; the global change grid is extensive in both the physical and temporal domains, and critical lower atmospheric species include the organics and their oxidized derivatives, which are numerous. Several types of optimization may be incorporated into kinetics modules to enhance their ability to simulate the complete lower atmospheric gas phase chemical system. (1) The photochemical integrator can be accelerated by avoiding matrix and iterative solutions and by establishing families. Accuracy and mass conservation are sacrificed in the absence of iteration, but atom balancing is restorable post hoc. (2) Chemistry can be arranged upon the massive grid to exploit parallel processing, and solutions to its continuity equations can be automated to permit experimentation with species and reaction lists or family definitions. Costs in programming effort will be incurred in these cases. (3) Complex hydrocarbon decay sequences can be streamlined either through structural lumping methods descended from smog investigations, which require considerable calibration, or by defining surrogates for classes of compounds, with a loss in constituent detail. From among the available options, the most advantageous permutations will vary with the specific nature of any eventual global scale study, and there is likely to be demand for many approaches. Tracer transport codes serve as a foundation upon which tropospheric chemistry packages will be tested. Encroachment of the NO(x) sphere of influence upon tropical rain forests and the upper free troposphere are two examples of specific problems to which full three-dimensional chemical simulations might be applied.

DOE

N94-19105# California Univ., Berkeley. Lawrence Berkeley Lab.
ENVIRONMENTAL RESEARCH PROGRAM
Jul. 1993 22 p
(Contract DE-AC03-76SF-00098)
(DE93-019101; LBL-33445) Avail: CASI HC A03/MF A01

The objective of the Environmental Research Program is to contribute to the understanding of the formation, mitigation, transport, transformation, and ecological effects of energy-related pollutants on the environment. The program is multidisciplinary and includes fundamental and applied research in chemistry, physics, biology, engineering, and ecology. The program undertakes research and development in efficient and environmentally benign combustion, pollution abatement and destruction, and novel methods of detection and analysis of criteria and non-criteria pollutants. This diverse group investigates combustion, atmospheric processes, flue-gas chemistry, and ecological systems. DOE

N94-19231*# North Carolina State Univ., Raleigh. Dept. of Marine, Earth and Atmospheric Sciences.
CARBON ISOTOPE BIOGEOCHEMISTRY OF METHANE FROM ANOXIC SEDIMENTS Final Technical Report
Neal E. Blair 8 Nov. 1993 166 p
(Grant NAGw-838)
(NASA-CR-194620; NAS 1.26:194620) Avail: CASI HC A08/MF A02

The isotopic composition of naturally occurring methane was used to constrain the tropospheric budget of that radiatively active gas. Numerous studies have shown that the isotopic composition is not constant, even for a specific source, and may vary temporally and spatially. The objective was to develop a process-level model that reproduced the seasonal variations in the C-13/C-12 composition of methane observed at the coastal site, Cape Lookout Bight, NC. Details of the mass balance are provided. Experiments and models designed to determine what factors incluence C-13/C-12 ratio of dissolved CO2 are reported. All the factors described were combined in a model that faithfully reproduces the seasonal C-13/C-12 variations observed at Cape Lookout. The model is described. For individual titles, see N94-19232 through N94-19235.

N94-19232*# North Carolina State Univ., Raleigh.
A CARBON ISOTOPE MASS BALANCE FOR AN ANOXIC MARINE SEDIMENT: ISOTOPIC SIGNATURES OF DIAGENESIS
Susan E. Boehme *In its* Carbon Isotope Biogeochemistry of Methane from Anoxic Sediments 8 Nov. 1993 50 p (For primary document see N94-19231 04-45)
Avail: CASI HC A03/MF A02

A carbon isotope mass balance was determined for the sediments of Cape Lookout Bight, NC to constrain the carbon budgets published previously. The diffusive, ebullitive and burial fluxes of sigma CO2 and CH4, as well as the carbon isotope signatures of these fluxes, were measured. The flux-weighted isotopic signature of the remineralized carbon (-18.9 plus or minus 2.7 per mil) agreed with the isotopic composition of the remineralized organic carbon determined from the particulate organic carbon (POC) delta(C-13) profiles (-19.2 plus or minus 0.2), verifying the flux and isotopic signature estimates. The measured delta(C-13) values of the sigma CO2 and CH4 diffusive fluxes were significantly different from those calculated from porewater gradients. The differences appear to be influenced by methane oxidation at the sediment-water interface, although other potential processes cannot be excluded. The isotope mass balance provides important information concerning the locations of potential diagenetic isotope effects. Specifically, the absence of downcore change in the delta(C-13) value of the POC fraction and the identical isotopic composition of the POC and the products of remineralization indicate that no isotopic fractionation is expressed during the initial breakdown of the POC, despite its isotopically heterogeneous composition. Author (revised)

N94-19233*# North Carolina State Univ., Raleigh.
THE CARBON ISOTOPE BIOGEOCHEMISTRY OF (EPSILON)CO2 PRODUCTION IN A METHANOGENIC MARINE SEDIMENT
Susan E. Boehme *In its* Carbon Isotope Biogeochemistry of Methane from Anoxic Sediments 8 Nov. 1993 46 p (For primary document see N94-19231 04-45)
Avail: CASI HC A03/MF A02

To investigate the relationship between sigma(CO2) delta(C-13) values and rates of the dominant remineralization processes at the organic-rich field site of Cape Lookout Bight, NC, the isotopic composition of porewater sigma(CO2) was measured on a seasonal basis. The sigma(CO2) delta(C-13) values varies seasonally in response to changes in rates of sulfate reduction and methanogenesis, the dominant remineralization processes at this site. A tube incubation experiment was also performed to determine the isotopic signature of the sigma(CO2) produced by sulfate reduction and methanogenesis. The delta(C-13) of the sigma(CO2) produced in the sulfate reduction zone determined from the tube incubation was -14.3 plus or minus 1.9, a value enriched in C-13 relative to the labile organic fraction. The C-13-enrichment may be caused by low rates of methanogenesis occurring in the sulfate reduction zone. The delta(C-13) of the sigma(CO2) produced in the methanogenic zone was estimated to be +44 per mil, whereas the co-produced methane was -65 per mil. The fractionation factor for CO2 reduction was calculated to be 1.055, a value in agreement with previous estimates at this site. The measured concentration and delta(C-13) of the sigma(CO2) at Cape Lookout was closely reproduced by a diagenetic model using the measured rates of sulfate reduction and sigma(CO2) production, and the isotopic signature of the sigma(CO2) production in the two biogeochemical zones. Author (revised)

N94-19234*# North Carolina State Univ., Raleigh.
THE CARBON ISOTOPE BIOGEOCHEMISTRY OF METHANE PRODUCTION IN ANOXIC SEDIMENTS. 1: FIELD OBSERVATIONS
Neal E. Blair, Susan E. Boehme, and W. Dale Carter, Jr. *In its* Carbon Isotope Biogeochemistry of Methane from Anoxic Sediments 8 Nov. 1993 33 p (For primary document see N94-19231 04-45)
Avail: CASI HC A03/MF A02

The natural abundance C-13/C-12 ratio of methane from anoxic marine and freshwater sediments in temperate climates varies seasonally. Carbon isotopic measurements of the methanogenic precursors, acetate and dissolved inorganic carbon, from the marine sediments of Cape Lookout Bight, North Carolina were used to determine the sources of the seasonal variations at that site. Movement of the methanogenic zone over an isotopic gradient within the dissolved CO2 pool appears to be the dominant control of the methane C-13/C-12 ratio from February to June. The onset of acetoclastic methane-production is a second important controlling process during mid-summer. An apparent temperature dependence on the fractionation factor for CO2-reduction may have a significant influence on the isotopic composition of methane throughout the year. Author (revised)

N94-19235*# North Carolina State Univ., Raleigh.
FACTORS THAT CONTROL THE STABLE CARBON ISOTOPIC COMPOSITION OF METHANE PRODUCED IN AN ANOXIC MARINE SEDIMENT
M. J. Alperin (North Carolina Univ., Chapel Hill.), Neal E. Blair, D. B. Albert (North Carolina Univ., Chapel Hill.), T. M. Hoehler (North Carolina Univ., Chapel Hill.), and C. S. Martens (North Carolina Univ., Chapel Hill.) *In its*

Carbon Isotope Biogeochemistry of Methane from Anoxic Sediments 8 Nov. 1993 21 p Repr. from Global Biogeochemical Cycles, v. 6, no. 3, Sep. 1992 p 271-291 (For primary document see N94-19231 04-45)
Avail: CASI HC A03/MF A02

The carbon isotopic composition of methane produced in anoxic marine sediment is controlled by four factors: (1) the pathway of methane formation, (2) the isotopic composition of the methanogenic precursors, (3) the isotope fractionation factors for methane production, and (4) the isotope fractionation associated with methane oxidation. The importance of each factor was evaluated by monitoring stable carbon isotope ratios in methane produced by a sediment microcosm. Methane did not accumulate during the initial 42-day period when sediment contained sulfate, indicating little methane production from 'noncompetitive' substrates. Following sulfate depletion, methane accumulation proceeded in three distinct phases. First, CO_2 reduction was the dominant methanogenic pathway and the isotopic composition of the methane produced ranged from -80 to -94 per thousand. The acetate concentration increased during this phase, suggesting that acetoclastic methanogenic bacteria were unable to keep pace with acetate production. Second, acetate fermentation became the dominant methanogenic pathway as bacteria responded to elevated acetate concentrations. The methane produced during this phase was progressively enriched in C-13, reaching a maximum delta(C-13) value of -42 per thousand. Third, the acetate pool experienced a precipitous decline from greater than 5 mM to less than 20 micro-M and methane production was again dominated by CO_2 reduction. The delta(C-13) of methane produced during this final phase ranged from -46 to -58 per thousand. Methane oxidation concurrent with methane production was detected throughout the period of methane accumulation, at rates equivalent to 1 to 8 percent of the gross methane production rate. Thus methane oxidation was too slow to have significantly modified the isotopic signature of methane. A comparison of microcosm and field data suggests that similar microbial interactions may control seasonal variability in the isotopic composition of methane emitted from undisturbed Cape Lookout Bight sediment. Author (revised)

N94-19241# Argonne National Lab., IL.
ADVANCES IN PASSIVE-REMOTE AND EXTRACTIVE FOURIER TRANSFORM INFRARED SYSTEMS
J. C. Demirgian, C. Hammer, E. Hwang, and Zhuo-Xiong Mao 1993 16 p Presented at the 12th Annual International Symposium on Thermal Treatment Technologies - Incineration Conference, Knoxville, TN, 3-7 May 1993
(Contract W-31-109-eng-38)
(DE93-017402; ANL/CMT/CP-79698; CONF-930572-9) Avail: CASI HC A03/MF A01

The Clean Air Act of 1990 requires the monitoring of air toxics including those from incinerator emissions. Continuous emission monitors (CEM) would demonstrate the safety of incinerators and address public concern about emissions of hazardous organic compounds. Fourier transform infrared (FTIR) spectroscopy can provide the technology for continuous emission monitoring of stacks. Stack effluent can be extracted and analyzed in under one minute with conventional FTIR spectrometers. Passive-remote FTIR spectrometers can detect certain emission gases over 1 km away from a stack. The authors will discuss advances in both extractive and passive-remote FTIR technology. Extractive systems are being tested with EPA protocols, which will soon replace periodic testing methods. Standard operating procedures for extractive systems are being developed and tested. Passive-remote FTIR spectrometers have the advantage of not requiring an extracted sample; however, they have less sensitivity. The authors have evaluated the ability of commercially available systems to detect fugitive plumes and to monitor carbon monoxide at a coal-fired power plant. DOE

N94-19272# Los Alamos National Lab., NM.
THE MEXICO CITY 1991 LIDAR MEASUREMENTS CAMPAIGN Final Report
C. R. Quick, Jr., F. L. Archuleta, D. E. Hof, R. R. Karl, Jr., J. J. Tiee, W. E. Eichinger, D. B. Holtkamp, and L. L. Tellier 1993 171 p
(Contract W-7405-eng-36)
(DE93-019960; LA-UR-93-2921) Avail: CASI HC A08/MF A02

Over the last two decades, Mexico City, like many large industrial and populous urban areas, has developed a serious air pollution problem, especially during the winter months when there are frequent temperature inversions and weak winds. The deterioration in air quality is the result of several factors. The basin within which Mexico City lies is Mexico's center of political, administrative, and economic activity, generating 34% of the gross domestic product and 42% of the industrial revenue and supporting a population which is rapidly approaching the 20 million mark. The basin is surrounded by mountains on three sides which inhibit rapid dispersal of pollutants. Emissions from the transportation fleet (more than 3 million vehicles) are one of the primary pollution sources and are mostly uncontrolled. Catalytic converters are just now being introduced into the fleet. The Mexico City Air Quality Research Initiative is an international collaborative project between the Los Alamos National Laboratory and the Mexican Petroleum Institute dedicated to the investigation of the air quality problem in Mexico City. The main objective of the project is to identify and assess the cost and benefits of major options being proposed to improve the air quality. DOE

N94-19303# California Univ., Berkeley. Lawrence Berkeley Lab.
CROSSED MOLECULAR BEAM STUDIES OF ATMOSPHERIC CHEMICAL REACTION DYNAMICS Ph.D. Thesis
Jing-Song Zhang Apr. 1993 223 p
(Contract DE-AC03-76SF-00098)
(DE93-019246; LBL-34297) Avail: CASI HC A10/MF A03

The dynamics of several elementary chemical reactions that are important in atmospheric chemistry are investigated. The reactive scattering of ground state chlorine or bromine atoms with ozone molecules and ground state chlorine atoms with nitrogen dioxide molecules is studied using a crossed molecular beam apparatus with a rotatable mass spectrometer detector. The $Cl + O_3$ yields $ClO + O_2$ reaction has been studied at four collision energies ranging from 6 kcal/mole to 32 kcal/mole. The derived product center-of-mass angular and translational energy distributions show that the reaction has a direct reaction mechanism and that there is a strong repulsion on the exit channel. The ClO product is sideways and forward scattered with respect to the Cl atom, and the translational energy release is large. The Cl atom is most likely to attack the terminal oxygen atom of the ozone molecule. The $Br + O_3$ yields ClO $+ O_2$ reaction has been studied at five collision energies ranging from 5 kcal/mole to 26 kcal/mole. The derived product center-of-mass angular and translational energy distributions are quite similar to those in the $Cl + O_3$ reaction. The $Br + O_3$ reaction has a direct reaction mechanism similar to that of the $Cl + O_3$ reaction. The electronic structure of the ozone molecule seems to play the central role in determining the reaction mechanism in atomic radical reactions with the ozone molecule. The $Cl + NO_2$ yields $ClO + NO$ reaction has been studied at three collision energies ranging from 10.6 kcal/mole to 22.4 kcal/mole. The center-of-mass angular distribution has some forward-backward symmetry, and the product translational energy release is quite large. The reaction proceeds through a short-lived complex whose lifetime is less than one rotational period. The experimental results seem to show that the Cl atom mainly attacks the oxygen atom instead of the nitrogen atom of the NO_2 molecule. DOE

N94-19305# EIC, Inc., Norwood, MA.
FIBER OPTIC RAMAN SPECTROGRAPH FOR IN SITU ENVIRONMENTAL MONITORING
M. M. Carrabba Nov. 1992 35 p Prepared for ANL, IL
(Contract W-31-109-eng-38)
(DE93-019466; DOE/CH-9205) Avail: CASI HC A03/MF A01

This report discusses the development and testing of a small laboratory prototype field Raman spectrometer which can be used with a fiber optic sampling probe incorporating substrates tailored for surface enhanced Raman spectroscopy (SERS) for low level detection of chemical species. The report also discusses demonstration of apparatus for both laboratory and field environmental samples typical of DOE environmental restoration sites. Preliminary results establish a new technique which can be used in the field to identify and profile in situ a wide variety of pollutants at the action levels required for remediation. DOE

N94-19319# Pacific Northwest Lab., Richland, WA.
VALUATION OF TEMPORARY AND FUTURE GREENHOUSE GAS REDUCTIONS
K. R. Richards Jun. 1993 45 p Presented at the Carbon Sinks Workshop for the Interagency National Action Plan Development Process,

Washington, DC, 10-11 Jun. 1993
(Contract DE-AC06-76RL-01830)
(DE93-018876; PNL-SA-22659; CONF-9306214-2) Avail: CASI HC A03/MF A01

The potential of augmented carbon sinks to decrease atmospheric levels of carbon dioxide has proved attractive to many government policy makers, politicians and industry representatives. Consequently, several proposals for new laws, both domestic and international, have recognized the CO2 emitters who are encouraged or required to reduce levels of emissions should also be allowed to offset their emissions by sequestering carbon in forest stands. This idea is described. DOE

N94-19379# Stockholm Univ. (Sweden). Dept. of Meteorology.
THE GLOBAL ATMOSPHERIC SULFUR CYCLE: AN EVALUATION OF MODEL PREDICTIONS AND OBSERVATIONS
J. Langner (Swedish Meteorological and Hydrological Inst., Norkoeping.), T. S. Bates (National Oceanic and Atmospheric Administration, Seattle, WA.), R. J. Charlson (Washington Univ., Seattle.), A. D. Clarke (Hawaii Univ., Manoa.), P. A. Durkee (Naval Postgraduate School, Monterey, CA.), J. Gras (Commonwealth Scientific and Industrial Research Organization, Mordialoc, Australia.), J. Heintzenberg, D. J. Hofmann (National Oceanic and Atmospheric Administration, Boulder, CO.), B. Huebert (Rhode Island Univ., Narragansett.), and C. Leck et al May 1993 32 p Workshop held in Stockholm, Sweden, 17-21 Jun. 1991 Prepared in cooperation with International Meteorological Inst., Stockholm, Sweden
(CM-81; ETN-93-94910) Avail: CASI HC A03/MF A01

Results from a workshop which compared dimethyl sulfide (DMS), SO2 and sulfate aerosol with the predictions of the global tropospheric sulfur model developed within the European research project GLOMAC (Global Modeling of Atmospheric Chemistry) are presented. The exercise had two primary aims: validating the model and evaluating the usefulness of experiments for refining this and other models. The comparisons indicate several areas where the model has to be improved. In particular, improvements in both emission estimates and description of chemical processes are necessary in order to improve the simulation of seasonal variability. Furthermore, the calculated non-sea-salt-sulfate concentrations in the upper troposphere are much higher than the very few available observations. If available concentrations are representative, the treatment of volcanic emissions and vertical transport may have to be improved. On the measurement side the following points are made: the estimates of the emission of DMS from the oceans have to be improved. Further measurements are necessary in order to better characterize the concentration of non-sea-salt sulfate in the free troposphere. The importance of sampling more than one sulfur species at the same location is stressed. ESA

N94-19507# Kernforschungszentrum G.m.b.H., Karlsruhe (Germany). Inst. fuer Meteorologie und Klimaforschung.
SUITABILITY OF INFRARED SPECTROSCOPY FOR REMOTE SENSING OF TROPOSPHERIC TRACE GASES Thesis - Karlsruhe Univ. [EIGNUNG DER INFRAROTSPEKTROSKOPIE ZUR FERNERKUNDUNG TROPOSPHAERISCHER SPURENGASE]
Gerald Wetzel Mar. 1993 121 p In GERMAN
(KfK-5183; ETN-93-95083) Copyright Avail: CASI HC A06/MF A02

Synthetic radiance spectra in the mid-infrared of the electromagnetic spectrum were calculated at a spectral resolution of about 0.1 cm for various observation geometries. Separability of the lines was studied for a number of trace gases, such as water vapor, ozone, carbon monoxide, methane, nitrous oxide, nitrogen oxides, sulfur dioxide, fluorochlorocarbons, etc. Separation of the spectral lines was complicated by the high water vapor absorption and pressure broadening of the lines in the troposphere. The separated spectral features of the individual gases were investigated with regard to their sensitivity to changes of the respective trace gas concentrations and to errors on the temperature profile and surface temperature. The effect of calibration errors and spectral noise on the spectra and on the accuracy of the trace concentrations to be determined were estimated, as was the influence of unprecise spectroscopic data. To determine the atmospheric layers most contributing to the radiance signal, contribution functions were calculated. The influence of cirrus clouds on the IR spectra was investigated. To avoid errors when determining the integral gas mass, this influence depending both on the thickness and the height of the clouds must be taken into account in the evaluation of the spectra. Horizontal sounding measurements from satellites serve to determine trace gas concentrations in the stratosphere and the upper troposphere with a good vertical, but a limited horizontal, resolution over large altitude ranges with an accuracy of 10 to 20. Horizontal soundings of the troposphere are much more obstructed by the presence of clouds than nadir soundings. ESA

N94-19518 Institut d'Aeronomie Spatiale de Belgique, Brussels.
GLOBAL THREE DIMENSIONAL MODEL OF TROPOSPHERIC TRACE GASES CHEMISTRY AND TRANSPORT Ph.D. Thesis - Univ. Libre, Brussels [MODELISATION TRI-DIMENSIONNELLE GLOBALE DE LA CHIMIE ET DU TRANSPORT DES GAZ EN TRACE DANS LA TROPOSPHERE]
Jean-Francois Mueller 1993 216 p In FRENCH Sponsored by National Foundation for Scientific Research, Belgium
(Aeronautica-Acta-A-370-1993; ETN-93-94962) Copyright Avail: Issuing Activity (Institut d'Aeronomie Spatiale de Belgique, 3 Avenue Circulaire, B-1180 Brussels, Belgium)

The Images model, a numerical chemistry/transport model of tropospheric trace gases is presented. The three dimensional distributions of about 40 chemical species are calculated, with focus on the key compounds governing the oxidation capacity of the atmosphere, ozone and hydroxl. Images is a powerful tool to study the possible perturbations of the oxidation capacity of the atmosphere. The model domain is the global troposphere and the lower stratosphere below 50 mbars. Tropospheric chemistry is discussed. The chemical degradation of several important organic species is studied. A simplified chemical scheme is proposed and used in the global model. Images is used to study present day and preindustrial chemistry of the troposphere. The results agree with available experimental data. The possible causes of the increase of atmospheric concentrations of methane and ozone are discussed. The results show that the mean hydroxyl concentration did not change very much since the preindustrial era. Ozone increased rapidly at the vicinity of the Earth surface. The tropospheric ozone burden increased by about a quarter. ESA

N94-19521 Institut d'Aeronomie Spatiale de Belgique, Brussels.
INFRARED CROSS SECTIONS AND GLOBAL WARMING POTENTIALS OF 10 ALTERNATIVE HYDROHALOCARBONS
C. Clerbaux (Brussels Univ., Belgium.), R. Colin (Brussels Univ., Belgium.), P. C. Simon, and C. Granier (National Center for Atmospheric Research, Boulder, CO.) 1993 32 p Submitted for publication Sponsored in part by Belgian State Prime Minister's Service-Science Policy Office, Brussels, Belgium
(Contract GAS-Res-Inst-5090-254-1993)
(Aeronautica-Acta-A-371-1993; ETN-93-94963) Copyright Avail: Issuing Activity (Institut d'Aeronomie Spatiale de Belgique, 3 Avenue Circulaire, B-1180 Brussels, Belgium)

Absorption cross sections were obtained in the infrared atmospheric window, between 600 and 1500/cm, for 10 alternative hydrohalocarbons: HCFC-22, HCFC-123, HCFC-124, HCFC-141b, HCFC-142b, HCFC-225ca, HCFC-225cb, HFC-125, HFC-134a, and HFC-152a. The measurements were made at three temperatures (287K, 270K and 253K) with a Fourier transform spectrometer operating at 0.03/cm apodized resolution. Integrated cross sections were introduced into a two dimensional radiative chemical dynamical model in order to calculate the global warming potential of each gas. ESA

N94-19575 Washington Univ., Seattle. Dept. of Atmospheric Sciences.
AIRBORNE STUDIES OF OCEAN-PARTICLE-CLOUD INTERACTIONS IN THE ARCTIC Final Report, 1 Oct. 1991 - 30 Sep. 1993
Peter V. Hobbs 30 Sep. 1993 7 p Limited Reproducibility: More than 20% of this document may be affected by microfiche quality
(Contract N00014-92-J-1191)
(AD-A270752) Avail: CASI HC A02

The specific tasks of this grant were to operate the University of Washington's Convair C-131A research aircraft in the Arctic in support of LeadEx, to analyze data collected aboard the aircraft, and to provide this data to other LeadEX investigators. The Convair C-131A made 18 flights totaling 70 hours over the ice pack north of Deadhorse, Alaska, in April 1992. Data was collected on: (1) Particles and gases in the air; (2) The radiative properties of the ice surface, leads and ice crystal clouds; (3)

Various methods for the remote detection of leads and surface temperatures; and (4) Heat fluxes from leads. DTIC

N94-19732# Lawrence Livermore National Lab., CA.

APPLICATION OF AN ATMOSPHERIC DISPERSION MODEL TO SIMULATED POLLUTANT RELEASES IN THE COLORADO FRONT RANGE

R. Lange May 1993 6 p Presented at the Topical Meeting on Environmental Transport and Dosimetry, Charleston, SC, 31 Aug. - 3 Sep. 1993

(Contract W-7405-eng-48)

(DE93-017118; UCRL-JC-114098; CONF-930810-5) Avail: CASI HC A02/MF A01

The 1991 ASCOT (Atmospheric Studies in Complex Terrain) field study in the vicinity of the Department of Energy's Rocky Flats Plant, Colorado, was conducted to study the local and regional circulations and their interactions with synoptic flows over the complex terrain of the Rocky Mountains Colorado Front range. The study was combined with the Rocky Flats Winter Validation Study (WVS) which had similar objectives. Tracer plumes were released as part of this field campaign over the period of February 3-19, 1991 from the Rocky Flats Plant. Twelve intensive experiments, centered around eleven-hour long surface releases of sulfur hexafloride (SF6) tracer material, were conducted by teams from a number of national laboratories, government agencies, and private contractors. One-hourly averaged tracer concentrations were collected from approximately 170 surface samplers deployed along two concentric circles at a radius of 8 km and 16 km from the release location. The concentration patterns resulting from the transport and turbulent diffusion of the SF6 traces plumes within the atmospheric boundary layer during two night-time, one morning transition, and one day-time period were simulated for this paper. The scenarios selected represent the first-choice of all twelve experiments to be addressed, based on the quality and completeness of the collected data base and the presence of the desired meteorological conditions. DOE

46 GEOPHYSICS

Includes aeronomy; upper and lower atmosphere studies; ionospheric and magnetospheric physics; and geomagnetism.

For space radiation see 93 Space Radiation.

N94-17682# International Centre for Theoretical Physics, Trieste (Italy).

ON A CONFORMAL PERFECT FLUID IN THE CLASSICAL VACUUM

H. Culetu Feb. 1993 8 p

(DE93-624797; IC-93/23) Avail: CASI HC A02/MF A01 (US Sales Only)

A possible existence of a conformal perfect fluid in the classical vacuum is investigated. It is shown, contrary to Madsen's opinion, that the scalar field stress tensor acquires a perfect fluid form even with a nonminimal coupling (xi = 1/6) in the Einstein Lagrangian, provided the geometry is the Lorentzian analogue of the Euclidean Hawking wormhole. In addition, our T(sub (mu)(nu)) equals (up to a constant factor) the vacuum expectation value of the Fulling stress tensor for a massless scalar field and Visser's one concerning transversible wormholes. On the other side of the light cone, there is a coordinate system (the dimensionally reduced Witten bubble) where the stress tensor becomes diagonal. DOE

N94-17720 Swedish Inst. of Space Physics, Kiruna.

PROBLEMS RELATED TO STIMULATED ELECTROMAGNETIC EMISSIONS, STRONG TURBULENCE AND IONOSPHERIC MODIFICATION Ph.D. Thesis - Uppsala Univ.

Simon Goodman May 1993 94 p Limited Reproducibility: More than 20% of this document may be affected by microfiche quality

(IRF-SR-212; ETN-93-94855) Copyright Avail: CASI HC A05

Optical pumping of the ionospheric plasma by high frequency radio waves produces a state of turbulence. Several consequences of the pumping are considered. At reflection altitude the plasma is thought to be dominated by parametric instabilities and strong turbulence; these are both encapsulated in the so called Zakharov equations. The Zakharov equations are derived and generalized from kinetic theory. Limits of validity, corrections to the ion sound speed, effective ponderomotive force, nonlinear damping, and other generalizations are included. As an example of the difference a kinetic approach makes, the threshold for parametric instabilities is seen to be lowered in a kinetic plasma. Mostly relevant to the upper hybrid layer is the recent discovery in the pumping experiments of Stimulated Electromagnetic Emissions (SEE). In particular one feature of SEE which occurs around the cyclotron harmonics and depends on density striations is investigated. The observed frequency of emission, dependency on striations, time evolution, and cutoff frequency below which the feature does occur are explained. Two theoretical approaches are taken. The first is a parametric three wave decay instability followed by a nonlinear mixing to produce SEE. Thresholds for the instability are well within experimental capacity. The second, less orthodox, approach, is a finite amplitude model. The finite amplitude model goes beyond the traditional parametric approach by being able to predict radiated power output. Miscellaneous aspects of a turbulent ionosphere are also examined. The dependency of the scattering cross section of a turbulent plasma upon higher order perturbations is considered. In a turbulent plasma, density gradients steeper than charateristic plasma scales may develop. The case of calculating the dielectric permittivity for a linear gradient of arbitary steepness is considered. ESA

N94-17898# California Univ., Berkeley. Lawrence Berkeley Lab.

HETEROGENEOUS SLIP AND RUPTURE MODELS OF THE SAN ANDREAS FAULT ZONE BASED UPON THREE-DIMENSIONAL EARTHQUAKE TOMOGRAPHY Ph.D. Thesis

W. Foxall Nov. 1992 178 p

(Contract DE-AC03-76SF-00098)

(DE93-015037; LBL-33984) Avail: CASI HC A09/MF A02

Crystal fault zones exhibit spatially heterogeneous slip behavior at all scales, slip being partitioned between stable frictional sliding, or fault creep, and unstable earthquake rupture. An understanding the mechanisms underlying slip segmentation is fundamental to research into fault dynamics and the physics of earthquake generation. This thesis investigates the influence that large-scale along-strike heterogeneity in fault zone lithology has on slip segmentation. Large-scale transitions from the stable block sliding of the Central 4D Creeping Section of the San Andreas fault to the locked 1906 and 1857 earthquake segments takes place along the Loma Prieta and Parkfield sections of the fault, respectively, the transitions being accomplished in part by the generation of earthquakes in the magnitude range 6 (Parkfield) to 7 (Loma Prieta). Information on sub-surface lithology interpreted from the Loma Prieta and Parkfield three-dimensional crustal velocity models computed by Michelini (1991) is integrated with information on slip behavior provided by the distributions of earthquakes located using the three-dimensional models and by surface creep data to study the relationships between large-scale lithological heterogeneity and slip segmentation along these two sections of the fault zone. DOE

N94-18088# Deutsche Forschungsanstalt fuer Luft- und Raumfahrt, Berlin (Germany). Abt. Sensordatennutzung.

APPLICATION OF FRACTAL METHODS TO ESTIMATE THE AEROSOL-OPTICAL DEPTH FOR ATMOSPHERIC CORRECTION OF HIGH RESOLUTION SATELLITE DATA Ph.D. Thesis - Freie Univ. [ANWENDUNG FRAKTALER METHODEN ZUR ABSCHAETZUNG DER AEROSOL-OPTISCHEN TIEFE FUER DIE ATMOSPHAERENKORREKTUR RAEUMLICH HOCHAUFGELOESTER SATELLITENDATEN]

Carmen Tornow Jan. 1993 96 p In GERMAN Original contains color illustrations

(DLR-FB-93-04; ETN-93-94874) Avail: CASI HC A05/MF A02

The development and the application of an atmospheric correction method for remotely sensed images of land surfaces with high spatial resolution are presented. An approximate solution of radiative transfer including non Lambertian reflection from the ground and the phenomenon of adjacency effect is presented. The atmosphere was a one layer model containing three different types of aerosol (urban, rural, maritime) which can be bailed out alternatively. The aerosol-optical depth and the single scattering albedo were taken to adapt the model to the actual state of the atmosphere. The validity of the approximative solution and the atmospheric model was checked using LOWTRAN calculations of global irradiance and diffuse transmission. The disagreement between the LOWTRAN data and those computed with the presented model is very low (lower than 5 percent). A strategy to estimate the optical depth from image data is developed using the influence of aerosol to the variability of the measured data. As a necessary reference value the variability of the ground reflectance which can be derived using structure measures with global transformation invariance was considered. They were computed by means of fractal geometry but they were not generalized dimensions due to the arbitrarity of covering a set containing many but a finite number of points. The application of the atmospheric correction model to TM (Thematic Mapper) satellite data shows good agreement between ground measurements and the results of an alternative algorithm for all TM channels of the solar spectrum except for channel 1. ESA

N94-18142 Royal Netherlands Meteorological Inst., De Bilt.
THE EARTH RADIATION BUDGET EXPERIMENT: OVERVIEW OF DATA-PROCESSING AND ERROR SOURCES
Arnout J. Feijt 1992 37 p
(Contract NOP-8520587)
(KNMI-TR-146; ISBN-90-369-2024-8; ETN-93-94531; PB93-191898)
Copyright Avail: Royal Netherlands Meteorological Institute, P.O. Box 201, 3730 AE De Bilt, Wilhelminalaan 10, Netherlands

The data processing and error sources of the Earth Radiation Budget Experiment (ERBE), which provides global information on the radiation properties of the Earth's atmosphere and surface, are addressed. The data processing scheme, which is used to convert raw radiometer counts into values for radiant exitance at the top of the atmosphere, is described and error sources are evaluated. When possible, the magnitude of the errors is estimated. This is proven difficult, because the errors depend on surface characteristics, atmospheric conditions, latitude, solar zenith angle, and the viewing geometry. Most scanner measurements were processed and validated. When using monthly mean scanner values one should be aware that specific regions may show considerable biased values of the radiant existance. The standard deviation in the regional monthly mean values is of the order of 5 W/sq m. Instantaneous scanner values should be used with caution, because errors in the radiant existance values for shortwave radiation in the order of 45 W/sq m are no exception. The error is highly dependent on viewing geometry, atmospheric conditions, and latitude. Nonscanner data are not fully validated yet. Probably the errors will exceed those of the scanner. ESA

N94-18229# Naval Postgraduate School, Monterey, CA.
CALIBRATION OF A HIGH FREQUENCY MONOSTATIC ACOUSTIC ECHOSOUNDER M.S. Thesis
David R. Cherry 17 Jun. 1993 56 p
(AD-A268901) Avail: CASI HC A04/MF A01

Atmospheric turbulence degrades a coherent laser beam when it propagates through the atmosphere. Measurements of the distribution of atmospheric turbulence provide insight into the underlying mechanisms that produce optical turbulence and suggest possible means to overcome or circumvent the effects of such turbulence. A variety of acoustic, optical, and thermal probe instruments provide measurements of atmospheric turbulence. Of these, the acoustic echosounder can measure atmospheric density and velocity irregularities. During the course of previous work, questions arose concerning the calibration of the NPS echosounder. The echosounder appears to detect a higher level of atmospheric turbulence than do other instruments used at the same altitude. This resulting overestimation of atmospheric turbulence could significantly influence programs such as the Advanced Electro-Optic Site (AEOS), a proposed 4 m telescope to be built in Hawaii. This thesis will attempt to identify key components contributing to the sounder calibration including the transducer transmit and receive efficiencies as well as their dependence on pressure and atmospheric density. Additionally a modified acoustic echosounder equation will be developed which more accurately profiles the atmospheric turbulence measured by such a sounder. DTIC

N94-18297 Science Applications International Corp., Arlington, VA. Center for Seismic Studies.
CONSTRUCTING A REFERENCE EVENT LIST FOR ARCESS Special Technical Report
Florence Riviere-Barbier 25 Aug. 1993 215 p Limited Reproducibility: More than 20% of this document may be affected by microfiche quality
(Contract F29601-92-C-0005)
(AD-A269288; SAIC/CSS-STR-C93-03) Avail: CASI HC A10

A cluster analysis method has been applied to a data set consisting of thousands of events recorded at ARCESS. Northern Scandinavia has been divided into smaller areas in which seismic events were organized into groups of similar events. The locations of these groups have been compared with known mine locations in Northern Scandinavia. Many of these groups have been associated with these mines. For comparison purposes, reference events were defined for each group. DTIC

N94-18451 Mission Research Corp., Nashua, NH.
UPPER ATMOSPHERIC EFFECTS OF THE HF ACTIVE AURORAL RESEARCH PROGRAM IONOSPHERIC RESEARCH INSTRUMENT (HAARP IRI) Scientific Report No. 2
V. Eccles and R. Armstrong May 1993 19 p Limited Reproducibility: More than 20% of this document may be affected by microfiche quality
(Contract F19628-90-C-0118)
(AD-A268948; PL-TR-93-21502) Avail: Issuing Activity (Defense Technical Information Center (DTIC))

The earth's ozone layer occurs in the stratosphere, primarily between 10 and 30 miles altitude. The amount of ozone, O, present is the result of a balance between production and destruction processes. Experiments have shown that natural processes such as auroras create molecules that destroy O. One family of such molecules is called 'odd nitrogen' of which nitric oxide (NO) is an example. Because the HAARP (HF Active Auroral Research Program) facility is designed to mimic and investigate certain natural processes, a study of possible effects of HAARP on the ozone layer was conducted. The study used a detailed model of the thermal and chemical effects of the high power HF beam, which interacts with free electrons in the upper atmosphere above 50 miles altitude. It was found only a small fraction of the beam energy goes into the production of odd nitrogen molecules, whereas odd nitrogen is efficiently produced by auroras. Since the total energy emitted by HAARP in the year is some 200,000 times less than the energy deposited in the upper atmosphere by auroras, the study demonstrates that HAARP HF beam experiments will cause no measurable depletion of the earth's ozone layer. DTIC

N94-18467# Arkansas Univ., Pine Bluff. Space and Environment Studies Lab.
GLOBAL ZONES OF PARTICLE PRECIPITATION AS OBSERVED EXOS-C Final Annual Report, 31 Jul. 1989 - 30 Jun. 1993
31 Jul. 1993 28 p
(Contract F49620-89-C-0071)
(AD-A268758; SESC-USPB-02-93; AFOSR-93-0669TR) Avail: CASI HC A03/MF A01

A study of the precipitation of protons (0.64 - 35 MeV) and electrons (0.19 - 3.2 MeV) in the northern auroral zone based on the observations of EXOS-C satellite during 1994-86 reveal that the global peak flux profile follows the global minimum magnetic field profile with a full-width-at-half-maximum (FWFM) of approx 7 deg for the proton zone and approximately 5 deg for the electron zone. Maximum particle flux occurs in the longitude range of 36 deg-72 deg, and minimum in 216 deg-252 deg. Both the kinds of fluxes show the altitude dependence with the electron flux having pronounced exponential dependence. The instrument (S-1 telescope) response function correlates very well with the angle-chi between the telescope axis and the local magnetic field direction. The particle flux depends on chi in the same way as the particle pitch angle distribution sin(sup n)alpha. It is found that the variation of flux with L depends on the angle chi. Both these types of flux varies with the local time having peak values at early morning hours. A study of the monthly variation shows that fluxes of both protons and electrons show significantly relative variation and also a periodicity of maximum and minimum. This long-term variation is thought to be related with magnetospheric conditions. DTIC

N94-18485# Southern Methodist Univ., Dallas, TX. Dept. of Geological Sciences.
HIGH RESOLUTION GEOLOGICAL SITE CHARACTERIZATION UTILIZING GROUND MOTION DATA Final Report, 1 Nov. 1988 - 31 Jan. 1993
Mike Craven and Brian W. Stump 9 Jul. 1993 235 p
(Grant AF-AFOSR-0176-89)
(AD-A268926; SMU-G-11; AFOSR-93-0652TR) Avail: CASI HC A11/MF A03

Experimentally produced surface waves at high frequencies (5-50 Hz) and short source-receiver distances (5-100 m) are utilized in the determination of shallow shear structures in geological materials. This procedure is shown to provide a high resolution picture of these shallow materials which may be of interest to the engineering and environmental community. Love waves are generated by the Sh source, SWIG, developed under this contract. Rayleigh waves are produced by the commercially available Betsy Seisgun. Group velocity determination includes multiple filter analysis with the application of narrow band Gaussian filters to the data and determination of the peaks in the resulting amplitude envelopes. Phase velocities are determined from the array data using the p-omega technique. Dispersion data is inverted to refine the velocity estimates and produce an attenuation model. DTIC

N94-18610*# Alabama Univ., Huntsville. Dept. of Chemistry.
CRRES EXPERIMENTS, DATA COLLECTION, ANALYSIS AND PUBLICATION Final Report, 20 Aug. - 20 Oct. 1992
George P. Miller 20 Oct. 1992 16 p
(Contract NAS8-38609)
(NASA-CR-192419; NAS 1.26:192419) Avail: CASI HC A03/MF A01

The tasks undertaken to be performed under this contract included the continued coordination and documentation of the CRRES program and the development of an archive that details the experimental results obtained by the CRRES Program. Details of the work undertaken and results achieved are summarized in the following sections. Author

N94-18622# Belgian Royal Observatory, Brussels.
[BELGIAN ROYAL OBSERVATORY COMMUNICATIONS, SERIES A, NO. 104, GEOPHYSICS SERIES NO. 175] [OBSERVATORIE ROYAL DE BELGIQUE COMMUNICATIONS, SERIES A, NO. 104, SERIE GEOPHYSIQUE NO. 175]
Dec. 1990 69 p Repr. from Annales de la Societe Geologique de Belgique, v. 112, no. 2, 1989 In FRENCH
(Communications-Ser-A-104; Ser-Geophys-175; ETN-93-94626) Avail: CASI HC A04/MF A01

The following reports are presented: historical seismicity of Hainault, Flanders and Artois (Belgium, France); current seismic activity in Belgium; macroseismic study of the Dour (Belgium) earthquakes; the contribution of gravimetry to tectonics; positioning possibilities from space; and instrumentation of the Royal Observatory of Belgium. For individual titles, see N94-18623 through N94-18628.

N94-18623# Belgian Royal Observatory, Brussels.
HISTORICAL SEISMICITY OF HAINAUT, FLANDERS AND ARTOIS [LA SEISMICITE HISTORIQUE DU HAINAUT, DE LA FLANDRE ET DE L'ARTOIS]
Pierre Alexandre *In its* Belgian Royal Observatory Communications, Series A, No. 104, Geophysics Series No. 175 Dec. 1990 15 p Repr. from Annales de la Societe Geologique de Belgique, v. 112, no. 2, 1989 p 329-343 In FRENCH (For primary document see N94-18622 04-46)
Avail: CASI HC A03/MF A01

The historical seismicity of Hainaut, Flanders and Artois (Belgium, France) was only known to the present day by incomplete compilations without critical value. A revision of sources and a new survey of texts connected with past earthquakes has enabled the elimination of seismic faults (about fifteen from 330 to 1671, and specially the so called disaster of 1317 in eastern Flanders) and the proposal of a more correct localization for the earthquakes of 1000, 1081, and 1095. On the other hand, a new catalog of the earthquakes occurring from 700 to 1800 in the investigated area was elaborated. With the help of copious documentation, it was possible to make a more detailed study of the three great earthquakes of 1382, 1449, and 1580, which affected both England and the Continent. ESA

N94-18624# Belgian Royal Observatory, Brussels. Centre de Geophysique Interne.
CURRENT (1985-1988) SEISMIC ACTIVITY IN BELGIUM: COMPARISON WITH HISTORICAL AND INSTRUMENTAL SEISMIC DATA Seismotectonic Analysis [L'ACTIVITE SEISMIQUE ACTUELLE (1985-1988) EN BELGIQUE. COMPARAISON AVEC LES DONNEES DE SEISMICITE HISTORIQUE ET INSTRUMENTALE: ANALYSE SEISMOTECTONIQUE]
T. Camelbeeck *In its* Belgian Royal Observatory Communications, Series A, No. 104, Geophysics Series No. 175 Dec. 1990 19 p Repr. from Annales de la Societe Geologique de Belgique, v. 112, no. 2, 1989 p 347-365 In FRENCH (For primary document see N94-18622 04-46)
Avail: CASI HC A03/MF A01

Reliable information concerning the historical and instrumental seismicity in Belgium is discussed in comparison with the more recent data of microseismicity. The Brabant Massif and the north of France are characterized by an important historical seismicity. Since the Middle Ages, four earthquakes caused considerable concern in that region. The actual seismic activity is not well known due to the lack of seismological stations. It is thus impossible to base the tectonic pattern on seismological data. The seismic activity in Hainaut was analyzed with the data of the seismic sequence near Dour in 1987 and the reexamination of the bigger earthquakes having occurred since 1965. The seismogenic layer is limited to the 8 first km of the crust. The occurrence under the form of swarms or sequences is an evidence of strong fracturation. The fault-plane solution of the Dour earthquake in 1987 indicates an almost north-south extension at this place of the Mons Basin. The focal mechanisms of 5 earthquakes in the center region shows a north-west south-east oriented maximal horizontal compressive stress. This information is in agreement with the dextral strike-slip of the 'shear zone of north-Artois' made conspicuous by geology. Important information about the seismotectonics in the eastern part of Belgium is given by the study of the actual microseismicity with a dense network of seismological stations. The fault-plane solution of the Malmedy (12 May 1985, M (sub L) = 2.5) earthquake indicates a south-west north-east extension along a fault of rhenish orientation. This is a favorable argument to the hypothesis of the prolongation across the Ardennes of the quaternary faults of the lower Rhine embayment. The analysis of the Bilzen (16 Jul. 1985, M(sub L) = 3.0), Gulpen (17 Oct. 1988, M(sub L) = 3.5), and Sprimont (27 Dec. 1988, M(sub L) = 3.6) earthquakes supplies new information on the complex tectonics of the Liege region. ESA

N94-18625# Liege Univ. (Belgium). Service de Geomorphologie et de Geologie du Quaternaire.
MACROSEISMIC STUDY OF THE DOUR (BELGIUM) EARTHQUAKES OF 22 MARCH 1987 AND OF GULPEN (BELGIUM) 17 OCTOBER 1988 [L'ETUDE MACROSEISMIQUE DES SEISMES DE DOUR DU 22 MARS 1987 ET DE GULPEN DU 17 OCTOBRE 1988]
M. Francois, T. Camelbeeck (Belgian Royal Observatory, Brussels.), and A. Chiapparo (Belgian Royal Observatory, Brussels.) *In* Belgian Royal Observatory, Belgian Royal Observatory Communications, Series A, No. 104, Geophysics Series No. 175 Dec. 1990 8 p Repr. from Annales de la Societe Geologique de Belgique, v. 112, no. 2, 1989 p 393-400 In FRENCH (For primary document see N94-18622 04-46)
Avail: CASI HC A02/MF A01

Following the earthquakes of Dour (Belgium) (22 Mar. 1987) and of Gulpen (17 Oct. 1988) macroseismic inquiry was made simultaneously by the Royal Observatory of Belgium and the geomorphological section of the Liege University. The procedures that were used for the two kinds of inquiry are presented. For seismological stations in the perceptibility zone, measured ground motions are compared with observed macroseismic intensity. ESA

N94-18626# Belgian Royal Observatory, Brussels. Centre de Geophysique Interne.
WHAT CAN GRAVIMETRY CONTRIBUTE TO RECENT AND CURRENT TECTONICS IN BELGIUM? [QUEL PEUT ETRE L'APPORT DE LA GRAVIMETRIE A LA TECTONIQUE RECENTE ET ACTUELLE EN BELGIQUE?]
C. Poitevin *In its* Belgian Royal Observatory Communications, Series A, No. 104, Geophysics Series No. 175 Dec. 1990 14 p Repr. from Annales de la Societe Geologique de Belgique, v. 112, no. 2, 1989 p 407-420 In FRENCH (For primary document see N94-18622 04-46)
Avail: CASI HC A03/MF A01

Possible gravimetric contributions at the Belgian scale are considered in the context of recent technical evolutions and data availability. The first question is as follows: can we reasonably suspect in Belgium some secular variations of gravity or rapid variations of pre- or post seismic origin? We can believe that if these phenomena exist, their amplitudes are such that they are not detectable by the conventional methods of field gravimetry, even if the precision of these techniques has dramatically increased in the last few years. Other instruments, for example absolute and superconducting gravimeters, seem much more adequate for this kind of investigation. The

second question is as follows: for which purpose can gravimetry be useful in the future (except of course for geophysical interpretation)? The answer is contained in a quite old geodetic concept: the geoid. The techniques of satellite positioning have become so accurate that we can presently level with the precision of a few cm over distances of 20 km or more. This enables us to discover crustal movements on a relatively large scale. The relation between satellite height determination and precise levelling requires knowledge about the conventional reference surface, the 'geoid,' with the same accuracy. At this moment only gravimetry is able to objectively produce such a surface. A summary of the data available in Belgium and those needed in order to reach the level of precision required is presented.
ESA

N94-18627# Belgian Royal Observatory, Brussels.

CURRENT POSITIONING POSSIBILITIES BY SPATIAL TECHNIQUES AND THE ROYAL OSERVATORY OF BELGIUM PROGRAM [LES POSSIBILITES ACTUELLES DE POSITIONNEMENT PAR LES TECHNIQUES SPATIALES ET LE PROGRAMME DE L'OBSERVATOIRE ROYAL DE BELGIQUE]

P. Paquet *In its* Belgian Royal Observatory Communications, Series A, No. 104, Geophysics Series No. 175 Dec. 1990 6 p Repr. from Annales de la Societe Geologique de Belgique, v. 112, no. 2, 1989 p 453-458 In FRENCH (For primary document see N94-18622 04-46)
Avail: CASI HC A02/MF A01

Since 1972, the Royal Observatory of Belgium has been involved in a space geodetic program aiming to determine the Earth's rotational parameters and the geocentric coordinates of terrestrial sites. With respect to the center of mass of the Earth, the cartesian coordinates are currently determined with a precision close to 10 to 20 cm; between terrestrial sites this method does not improve the precision of relative positioning and is more or less not useful for geodynamics studies on regional scales. Since 1983, new satellites have been progressively launched and will form the Global Positioning System (GPS); in its final issue, expected for 1991-1992, it will be composed of at least 18 satellites. For several years, experiences have demonstrated the capability of this new system to obtain precision close to the centimeter level over distances extended till 30 km. For larger distances, the precision decreases as a consequence of the perturbations of the ionosphere on the radio signal propagation and the lack of accuracy of the orbit determination; however, recent technological improvements of the ground receivers indicate that a precision of a few units of 10(exp -8) power are obtainable; that is equivalent to one centimeter over 1000 km. The Royal Observatory of Belgium has just acquired two receivers with, in a first phase, the following objectives: integration of the fundamental Belgian geodetic mark in the international networks; between two Belgian sites development of a calibration basis with systematic measurements between the two stations; and participation in geophysical programs such as regular controls of seismological stations and first order gravimetric network. ESA

N94-18628# Belgian Royal Observatory, Brussels.

INSTRUMENTATION DEVELOPED AT THE ROYAL OBSERVATORY OF BELGIUM FOR MEASURING SLOW DISPLACEMENTS OF THE EARTH [INSTRUMENTATIONS DEVELOPPEES A L'OBSERVATOIRE ROYAL DE BELGIQUE POUR LA MESURE DE DEFORMATIONS LENTES DU SOL]

M. vanRuymbeke *In its* Belgian Royal Observatory Communications, Series A, No. 104, Geophysics Series No. 175 Dec. 1990 6 p Repr. from Annales de la Societe Geologique de Belgique, v. 112, no. 2, 1989 p 459-464 In FRENCH (For primary document see N94-18622 04-46)
Avail: CASI HC A02/MF A01

A review of the gravimeters, clinometers, extensometers, capacitative sensors, and high resolution thermometers is presented. The geophysical instruments were originally built with mechanical and electrical transducers. The precision was limited, and only large signals were observed. The introduction of electronics for transducers, amplifiers, filters, recorders, time signals, and data processing has improved the possibilities. For very small displacements, capacitative transducers are used. The feedback systems with digital filter improve tidal registrations. It is important to measure the temperature and atmospheric pressure influences. ESA

N94-18655# Northwest Research Associates, Inc., Bellevue, WA.

AN INVESTIGATION OF METHODS FOR UPDATING IONOSPHERIC SCINTILLATION MODELS USING TOPSIDE IN-SITU PLASMA DENSITY MEASUREMENTS Final Report, 1 May 1990 - 30 Apr. 1993

James A. Secan 1 May 1993 110 p
(Contract F19628-90-C-0072)
(AD-A269872; NWRA-CR-93-R096; PL-TR-93-2122) Avail: CASI HC A06/MF A02

Modern military communication, navigation, and surveillance systems depend on reliable, noise free transionospheric radio-frequency channels and can be severely impacted by small-scale electron-density irregularities in the ionosphere. This report summarizes the results of a three year investigation into the methods for updating ionospheric scintillation models using observations of ionospheric plasma-density irregularities measured by the DMSP Scintillation Meter (SM) sensor. Results are reported from the analysis of data from a campaign conducted in January 1990 near Tromso, Norway, in which near coincident in-situ plasma-density and transionospheric scintillation measurements were made. Estimates for the level of intensity and phase scintillation on a transionospheric UBF radio link in the early-evening auroral zone were calculated from DMSP SM data and compared to the levels actually observed. Results are also presented from a comparison with scintillation observations made with a coincident DNA Polar BEAR satellite pass. DTIC

N94-18690# Virginia Polytechnic Inst. and State Univ., Blacksburg. Dept. of Geological Sciences.

A COMPARISON OF SINGLE-STATION BACKAZIMUTH ESTIMATES WITH REGIONAL EVENT LOCATIONS IN THE CENTRAL APPALACHIANS

Martin C. Chapman, Shaosong Huang, and J. A. Snoke 30 Jun. 1993 52 p
(Contract F19628-92-K-0029)
(AD-A269897; AD-E201600; PL-TR-93-2126; SR-1) Avail: CASI HC A04/MF A01

The study examines the accuracy of single-station backazimuth measurements from polarization analysis of near regional P wave arrivals. The data set consists of 37 signals from mining explosions in the distance range 100 to 300 km, recorded at station BLA, Blacksburg, Virginia. The station-source backazimuth estimates derived from the three-component station are compared with results derived from independent information, primarily from regional network epicenter locations. For signal/noise ratios in excess of 2.0, the mean backazimuth error of the single-station estimate is 6 degrees (for sources in the northwest quadrant) and the standard deviation is 21 degrees. Generally, only the initial (1 second or less) portion of the P wave arrival is polarized in the source-station azimuth. Off-azimuth arrivals consisting of converted and scattered energy appear early in the P coda. Emergent P wave arrivals from the delay-fired explosions, combined with steep apparent angles of incidence (averaging 22 degrees) complicate the single-station, three-component location problem. DTIC

N94-18712# Naval Command, Control and Ocean Surveillance Center, San Diego, CA. RDT and E Div.

WORK PLAN FOR THE MARINE AEROSOL PROPERTIES AND THE THERMAL IMAGER PERFORMANCE TRIAL (MAPTIP)

D. R. Jensen, G. DeLeeuw, and A. M. VanEjik Sep. 1993 112 p
(AD-A270026; NRAD/TD-2573) Avail: CASI HC A06/MF A02

Atmospheric aerosol and infrared sea and terrain background models are of special importance for the assessment of the performance of electro-optical (EO) systems. The degradation of the radiance contrast between a target and its natural background, as viewed by an infrared sensor, is determined by the constituents of the intervening atmosphere that absorb and scatter the radiation. The assessment, therefore, depends upon the accuracy of the atmospheric models being used in the propagation prediction codes. The performance of the electro-optical systems is further degraded by turbulence and refractivity effects, causing blurring, scintillation, beam wander, mirages, etc. In thermal imagers, these effects may result in image distortion, contrast reduction, and other detection problems.
DTIC

N94-18717# California Univ., San Diego, La Jolla. Inst. of Geophysics and Planetary Physics.

THE USE OF VELOCITY SPECTRA FOR STACKING RECEIVER FUNCTIONS WITH APPLICATION TO IRIS/IDA STATIONS OBNINSK (OBN) AND ARTI (ARU), RUSSIA Final Report, 1 Dec. 1991 - 30 Oct. 1992

H. Gurrola, J. B. Minster, T. Owens (South Carolina Univ., Columbia.), and

H. Given 30 Oct. 1992 58 p
(Contract F19628-90-K-0045)
(AD-A269087; PL-TR-93-2069) Avail: CASI HC A04/MF A01

To improve signal to noise ratio (SNR), it is typical to stack receiver functions calculated from events at similar distances and back azimuths. We have adapted the velocity spectrum stacking (VSS) technique from reflection seismology to stack data with different ray parameters and improve the SNR. The VSS technique exploits differences in the shapes of the moveout curves of converted phases and reverberations to separate phases and infer velocity structure. By applying conventional receiver function techniques to the IRIS/IDA seismographic station at Obninsk, Russia, we infer a 2 km thick slow velocity surface layer and a 47 km depth to Moho with relatively uncomplicated crustal structure. By comparing VSS computed for OBN and Arti (ARU), Russia with PREM synthetics we have identified Ps phases from the 400 and 670 km discontinuities. We find mantle structure characterized by higher S velocities and deeper discontinuities than PREM. We find no evidence of a 210 km discontinuity beneath either station. VSS comparisons between OBN and ARU imply that the 670 km discontinuity is about 2 km shallower beneath ARU than OBN. DTIC

N94-18725# Westinghouse Savannah River Co., Aiken, SC.
APPLICATIONS OF QUATERNARY STRATIGRAPHIC, SOIL-GEOMORPHIC, AND QUANTITATIVE GEOMORPHIC ANALYSES TO THE EVALUATION OF TECTONIC ACTIVITY AND LANDSCAPE EVOLUTION IN THE UPPER COASTAL PLAIN, SOUTH CAROLINA
Kathryn L. Hanson (Geomatrix Consultants, San Francisco, CA.), Thomas F. Bullard (Geomatrix Consultants, San Francisco, CA.), Mark W. deWit (Geomatrix Consultants, San Francisco, CA.), and Alice L. Stieve 1993 18 p Presented at the 4th Energy Natural Phenomena Hazards Mitigation Conference, Atlanta, GA, 19-22 Oct. 1993
(Contract DE-AC09-89SR-18035)
(DE93-016269; WSRC-MS-93-361; CONF-9310102-1) Avail: CASI HC A03/MF A01

Geomorphic analyses combined with mapping of fluvial terraces and upland geomorphic surfaces provide new approaches and data for evaluating the Quaternary activity of post-Cretaceous faults that are recognized in subsurface data at the Savannah River Site in the Upper Coastal Plain of southwestern South Carolina. Analyses of longitudinal stream and terrace profiles, regional slope maps, and drainage basin morphometry indicate long-term uplift and southeast tilt of the site region. Preliminary results of drainage basin characterization suggests an apparent rejuvenation of drainages along the trace of the Pen Branch fault (a Tertiary reactivated reverse fault that initiated as a basin-margin normal fault along the northern boundary of the Triassic Dunbarton Basin). This apparent rejuvenation of drainages may be the result of nontectonic geomorphic processes or local tectonic uplift and tilting within a framework of regional uplift. DOE

N94-18838*# Colorado Univ., Boulder.
[RESEARCH ON EARTH'S ROTATION AND THE EFFECT OF ATMOSPHERIC PRESSURE ON VERTICAL DEFORMATION AND SEA LEVEL VARIABILITY] Final Report
John Wahr 18 Mar. 1993 4 p
(Grant NAG5-485)
(NASA-CR-194300; NAS 1.26:194300) Avail: CASI HC A01/MF A01

The work done under NASA grant NAG5-485 included modelling the deformation of the earth caused by variations in atmospheric pressure. The amount of deformation near coasts is sensitive to the nature of the oceanic response to the pressure. The PSMSL (Permanent Service for Mean Sea Level) data suggest the response is inverted barometer at periods greater than a couple months. Green's functions were constructed to describe the perturbation of the geoid caused by atmospheric and oceanic loading and by the accompanying load-induced deformation. It was found that perturbation of up to 2 cm are possible. Ice mass balance data was used for continental glaciers to look at the glacial contributions to time-dependent changes in polar motion, the lod, the earth's gravitational field, the position of the earth's center-of-mass, and global sea level. It was found that there can be lateral, non-hydrostatic structure inside the fluid core caused by gravitational forcing from the mantle, from the inner core, or from topography at the core/mantle or inner core/outer core boundaries. The nutational and tidal response of a non-hydrostatic earth with a solid inner core was modeled. Monthly, global tide gauge data from PSMSL was used to look at the 18.6-year ocean tide, the 14-month pole tide, the oceanic response to pressure, the linear trend and inter-annual variability in the earth's gravity field, the global sea level rise, and the effects of post glacial rebound. The effects of mantle anelasticity on nutations, earth tides, and tidal variation in the lod was modeled. Results of this model can be used with Crustal Dynamics observations to look at the anelastic dissipation and dispersion at tidal periods. The effects of surface topography on various components of crustal deformation was also modeled, and numerical models were developed of post glacial rebound. Derived from text

N94-18853*# Scripps Institution of Oceanography, La Jolla, CA. Inst. of Geophysics and Planetary Physics.
CONTRIBUTIONS FROM GEOMAGNETIC INVERSE THEORY TO THE STUDY OF HYDROMAGNETIC CONDITIONS NEAR THE CORE-MANTLE BOUNDARY Final Report
George E. Backus 18 Nov. 1991 4 p
(Grant NAG5-818)
(NASA-CR-194303; NAS 1.26:194303) Avail: CASI HC A01/MF A01

The Final Report on contributions from geomagnetic inverse theory to the study of hydromagnetic conditions near the core-mantle boundary (CMB) is presented. The original proposal was to study five questions concerning what the surface and satellite magnetic data imply about hydromagnetic and electromagnetic conditions near the CMB. The five questions are: (1) what do the surface and satellite data imply about the geomagnetic field B near the surface of the earth; (2) how does one extrapolate B down through the conducting mantle to the CMB; (3) if B on the CMB is visible, how accurately does it satisfy the frozen-flux approximation; (4) if frozen flux is a good approximation on the CMB, what can be inferred about the fluid velocity v in the upper core; and (5) if v at the CMB is visible, does it suggest any dynamical properties of the core, such as vertical advection, Alfven-inertial waves, link instabilities, or mantle effects. A summary of the research is provided. Derived from text

N94-18854# Indian Inst. of Geomagnetism, Bombay.
ACTIVITIES OF THE INDIAN INSTITUTE OF GEOMAGNETISM Annual Report, 1991 - 1992
1992 51 p Original contains color illustrations
Avail: CASI HC A04/MF A01

The Indian Institute of Geomagnetism in Bombay Annual Report for 1991 to 1992 is presented. Major scientific activities are described. These activities include studies on: electrojet current system; ionospheric scintillation; airglow observations; geomagnetic pulsations; electromagnetic induction; magnetic anomalies; and geomagnetic field. CASI

N94-18868# State Univ. of New York, Binghamton. Dept. of Geological Science and Environmental Studies.
SURFACE WAVE GROUP VELOCITY TOMOGRAPHY OF EAST ASIA, PART 1 Final Report, 1 Feb. 1992 - 1 Feb. 1993
Francis T. Wu 25 Jul. 1993 48 p
(Contract F19628-90-K-0042)
(AD-A270100; PL-TR-93-2102-Pt-1; AD-E201598) Avail: CASI HC A03/MF A01

Group velocities of both Rayleigh and Love waves are used in a tomographic inversion to obtain group velocity maps of East Asia (60 deg E-140 deg E and 20 deg N-50 deg N). The period range studied is 30-70 seconds. For periods longer than 40 seconds, a high group velocity gradient clearly exists along longitude 105 deg E; the velocities are noticeably higher east of this longitude than west of this longitude. The Tibetan Plateau appears as a prominent low velocity (about 15%) structure in this area; central Tibet appears as the area with the lowest velocity. The North China Plain is an area of high velocities, probably as a result of thin crust. The variability of deep crustal and upper mantle structures underneath the different tectonic provinces in the study can clearly be seen. In a separate study, using the dataset above and that from the former Soviet Union, we have derived the Rayleigh tomographic images of a larger area (40 deg E-160 deg E and 20 deg N-70 deg N). While the Tibetan plateau still remains to be the most prominent low velocity features, two other features are also clear, a very high velocity Siberian platform and a high velocity ridge extending from Lake Baikal to Central Mongolia. These studies are useful in delineating tectonics. DTIC

N94-18873# State Univ. of New York, Binghamton. Dept. of Geological Science and Environmental Studies.
ANALYSIS OF REGIONAL BODYWAVE PHASES FROM EARTHQUAKES IN WESTERN CHINA, PART 2 Final Report, 1 Aug. 1991 - 1 Feb. 1993
Jeffrey S. Barker 17 Jun. 1993 54 p
(Contract F19628-90-K-0042)
(AD-A270125; PL-TR-93-2102-Pt-2; AD-E201606) Avail: CASI HC A04/MF A01

Broadband regional bodywave data have been collected and modeled for three profiles of earthquakes recorded at CDSN station WMQ in western China. The first profile is from earthquakes located to the southwest, within the Tienshan and Tarim basin. The second is from earthquakes to the NNE across the Altai mountains and the western tip of Mongolia and into Siberia. The third profile is from earthquakes to the SSE, some near the Lop Nor test site, and others from the Altyn Tagh and Qaidam Basin. Plane-layered velocity structure models were determined for each profile, and synthetic seismograms were computed using a frequency-wavenumber integration technique. For each earthquake, an appropriate source mechanism is assumed, and synthetic seismograms are computed for source depths of 10, 20 and 30 km. The modeling demonstrates that regional P(sub n)-P(sub pg) wavetrains result from the interference of several phases. Since some of these depart the source upward and other depart downward, this interference is sensitive to source depth and source mechanism. Therefore, as long as accurate synthetic seismograms can be computed, modeling these phases can serve as a powerful discriminant of earthquakes and explosions. DTIC

N94-18874# Lockheed Missiles and Space Co., Palo Alto, CA. Space Sciences Lab.
PENETRATING RADIATION ENVIRONMENT AND EFFECTS STUDY Scientific Report No. 1
H. D. Voss, W. L. Imhof, J. Mobilia, and E. E. Gaines 15 Jun. 1993 82 p
(Contract F19628-90-C-0103)
(AD-A270126; PL-TR-93-2147; AD-E201608) Avail: CASI HC A05/MF A01

This report summarizes some of the PREE achievements to date on data acquired from the Lockheed IMS-HI and SEP instruments on the CRRES satellite. The primary objectives of the PREE research are to: (1) inter-calibrate the ONR 307 instruments; (2) develop algorithms and software for understanding and modeling the radiation belts; (3) develop key parameters; and, (4) study the dynamic radiation belt variations in the slot region and the outer belt. The new IMS-HI instrument performed well during the CRRES mission and has been inter-calibrated with the IMS-LO, SEP and EPAS instruments. Much progress has been made in the development of key algorithms and software for mapping the electron, ion, and neutral flux. Energetic neutrals from the ring current have been observed directly and are an important low altitude and low latitude ionization source. Surveys of the medium energy (20-1000 keV) ion and neutral database indicate a sharp edge to the ring current flux which is not apparent in previous studies. The neutral flux is linked strongly with the low altitude edge of the ring current. To properly map the radiation belts and select key parameters a simple physical model was developed for the response of the magnetosphere to magnetic storms. The CRRES data indicate that the radiation belts including the inner belt are strongly modified during a sudden commencement (SC) on the order of several minutes. This momentary compression results in a net acceleration and transport of particles to low L in violation of the third invariant. For the 24 March 1991 magnetic storm the magnetopause is inferred to have penetrated to L approximately 3.0 resulting in the possible establishment of the 'new inner belt'. DTIC

N94-18894# Los Alamos National Lab., NM.
GEOTHERMAL ACTIVITY NEAR CLEARLAKE, CALIFORNIA
K. L. Burns and R. M. Potter 1993 8 p Presented at the Annual Meeting of the Geothermal Resources Council, San Francisco, CA, 10-13 Oct. 1993
(Contract W-7405-eng-36)
(DE93-016627; LA-UR-93-2073; CONF-931042-2) Avail: CASI HC A02/MF A01

Geothermal activity in the region of high heat flow near the city of Clearlake includes hot springs, fumeroles, vents, and areas of hydrothermal alteration. Onshore, the location is controlled by Quaternary longitudinal NNW-trending faults of the San Andreas systems, and the transverse Burns Valley fault. Offshore, an additional control is arcuate graben-forming faults. The city is bracketed by three hydrothermal 'hot spots,' which are Sulphur Bank hot spring, resurgences in Burns Valley, and the Oak Cove hot spot. All three are associated with sharp 'spikes' in the isotherms and locally enhanced heat flow. DOE

N94-18899# California Inst. of Tech., Pasadena. Seismological Lab.
SHOCK PROPAGATION IN CRUSTAL ROCK Annual Report, 1 Jul. 1992 - 30 Jun. 1993
William W. Anderson and Thomas J. Ahrens 8 Sep. 1993 9 p
(Contract F49620-92-J-0402)
(AD-A270148; CIT-64649; AFOSR-93-0741TR) Avail: CASI HC A02/MF A01

The shock Hugoniot and adiabatic release curves of sedimentary rocks display a range of different behaviors that affect the decay of shock waves propagating away from a confined source. Many of the minerals making up sandstones, shales, and limestones undergo phase transitions when shocked to pressures of interest to studies of coupling of energy from explosive sources into far field seismic waves. Both sandstones and limestones have been observed to exhibit elastic precursors and multiple wave behavior at shock velocities up to 3.7 km/s and 5.7 km/s, respectively Ahrens and Gregson, 1964. Hysteresis in the shock-release paths of materials results in irreversible energy deposition, thus depriving the shock wave of energy required to drive its propagation and resulting in a more rapid decay and less efficient coupling to far field waves than expected from geometrical effects alone. Thus, data constraining this behavior in rocks are essential for determining the cavity volumes for various degrees of decoupling for different lithologies. The behavior of most sedimentary rocks during adiabatic release has not been experimentally investigated to a significant extent. Our objective was to obtain experimental data for shock and release behaviors of elastic and carbonate sedimentary rocks and use those data along with data from other sources, to develop a theoretical model of the hysteretic shock-release paths of these rocks. We use this model to constrain the energy deposited irreversibly in these rocks by the passage of shock and release waves. The release model we use is a modification of that used by Sekine et al. 1993, submitted for granite. DTIC

N94-18929# California Univ., Berkeley. Lawrence Berkeley Lab.
EXTENSIONS OF 2D GRAVITY
A. Sevrin Jun. 1993 14 p Presented at the Journees Relativistes Conference, Brussels, Belgium, 5-7 Apr. 1993
(Contract DE-AC03-76SF-00098)
(DE93-018525; LBL-34240; UCB-PTH-93/21; CONF-9304184-1) Avail: CASI HC A03/MF A01

After reviewing some aspects of gravity in two dimensions, I show that non-trivial embeddings of sl(2) in a semi-simple (super) Lie algebra give rise to a very large class of extensions of 2D gravity. The induced action is constructed as a gauged WZW model and an exact expression for the effective action is given. DOE

N94-19001# Sandia National Labs., Albuquerque, NM.
USING COMPUTERIZED TOMOGRAPHY TO DETERMINE IONOSPHERIC STRUCTURES
C. N. Vittitoe Aug. 1993 44 p
(Contract DE-AC04-76DP-00789)
(DE93-018903; SAND-93-1388) Avail: CASI HC A03/MF A01

Properties of the ionosphere are reviewed along with its correlations with other geophysical phenomena and with applications of ionospheric studies to communication, navigation, and surveillance systems. Computer tomography is identified as a method to determine the detailed, three-dimensional distribution of electron density within the ionosphere. Several tomography methods are described with a basic approach illustrated by an example. Limitations are identified. DOE

N94-19002# Sandia National Labs., Albuquerque, NM.
USING COMPUTERIZED TOMOGRAPHY TO DETERMINE IONOSPHERIC STRUCTURES
C. N. Vittitoe Aug. 1993 41 p

(Contract DE-AC04-76DP-00789)
(DE93-018904; SAND-93-1389) Avail: CASI HC A03/MF A01

A method is presented to unfold the two-dimensional vertical structure in electron density by using data on the total electron content for a series of paths through the ionosphere. The method uses a set of orthonormal basis functions to represent the vertical structure and takes advantage of curved paths and the eikonical equation to reduce the number of iterations required for a solution. Curved paths allow a more thorough probing of the ionosphere with a given set of transmitter and receiver positions. The approach can be directly extended to more complex geometries. DOE

N94-19008# Boston Univ., MA. Center for Space Physics.
THE EFFECTS OF MAGNETIC STORM PHASES ON F-LAYER IRREGULARITIES FROM AURORAL TO EQUATORIAL LATITUDES Quarterly Report, 1 Apr. - 30 Jun. 1993
Jules Aarons and Michael Mendillo 30 Jun. 1993 2 p
(Contract N00014-89-J-1754)
(AD-A267388) Avail: CASI HC A01/MF A01

We continued with the comparison of scintillation and total electron content (TEC) data from a chain of stations in the Pacific. The study compares TEC and scintillation data for the following station locations: Manila, the Philippines; Palehua, Hawaii; Lunping, Taiwan; and Osan, Korea. Three of the stations, Manila, Lunping, and Osan, are spaced along a narrow range of longitudes. For some periods in 1980 and 1981, all the data are available. The data set for June and July 1980 and 1981 have been reduced and are being studied. The data present many problems. It was assumed than an equatorial plume extending well over 1500 km in altitude would be effective in the anomaly region 15 to 20 deg from the equator. What is puzzling is that there are effects (scintillations and fluctuations in Faraday rotation) that appear over several hours with no activity reported from the site near the magnetic equator (Manila). This might be due to the high electron content in the Osan region plus the sensitivity of its propagation angle. Further studies are needed to resolve this issue. DTIC

N94-19018# West Virginia Univ., Morgantown. Coll. of Engineering.
GROUND MOVEMENTS ASSOCIATED WITH GAS HYDRATE PRODUCTION
H. J. Siriwardane 1992 17 p
(Contract DE-FG21-91MC-28080)
(DE93-019887; DOE/MC-28080/3381) Avail: CASI HC A03/MF A01

The grantee will evaluate the influence of hydrate production on ground subsidence near the wellbore and the surface. The objective of this research will be achieved by using computer simulations of what is expected in a hydrate reservoir during the production stage as reported by hydrate production models and available data. The model will be based on theories of continuum mechanics, thermomechanics of hydrate production, principles of rock mechanics and geomechanics, and special features of geomaterials under cold temperatures such as those found in permafrost regions. The research work involved in the proposed investigation will be divided into three major tasks: (1) Mechanics of subsidence in permafrost regions; (2) modeling of subsidence; and (3) parametric studies. Progress reports are presented for tasks 1 and 2. DOE

N94-19081# Technische Univ., Delft (Netherlands). Faculty of Technical Mathematics and Informatics.
FAST ITERATIVE SOLUTION OF SPARSELY SAMPLED SEISMIC INVERSE PROBLEMS
Agur G. J. Sevink and Gerard C. Herman 1993 12 p
(Rept-93-16; ETN-93-94643) Copyright Avail: CASI HC A03/MF A01

A paper showing how the convergence of iterative scattering methods is accelerated significantly by using (asymptotic) Born inversion as a preconditioner is presented. The scattering of acoustic waves by an inhomogeneous ideal fluid occupying a bounded two dimensional subdomain is considered. So far, the method has only been evaluated for constant background models. ESA

N94-19140# Technische Univ., Delft (Netherlands). Faculty of Technical Mathematics and Informatics.
INVERSE SCATTERING OF SURFACE WAVES: A NEW LOOK AT SURFACE CONSISTENCY
Bastian Blonk and Gerard C. Herman 1993 35 p Presented at the 62nd Annual SEG Meeting, New Orleans, LA, Oct. 1992 Sponsored in part by Netherlands Technology Foundation, and Shell Research
(Rept-93-25; ETN-93-94652) Copyright Avail: CASI HC A03/MF A01

A method for removing near surface scattered noise from seismic data is presented. Starting from an appropriately chosen background model, a surface consistent impedance scattering model is determined using linearized elastodynamic inverse scattering theory. This scattering model does not necessarily equal the actual scatterer distribution, but it enables the near surface scattered part of the data to be approximately calculated. The method honors at least some of the complexity of the near surface scattering process and can be applied in cases where traditional methods, like wavenumber frequency filtering techniques and methods for static corrections, are ineffective. From a number of tests on synthetic data, it is concluded that the method is rather robust; its main sensitivity is due to errors in the determination of the background Rayleigh wave velocity. ESA

N94-19237*# Iowa State Univ. of Science and Technology, Ames.
ANALYSIS OF SATELLITE-DERIVED OZONE AND WATER VAPOR MEASUREMENTS Final Report, 15 Jul. 1988 - 30 Sep. 1992
John L. Stanford 30 Sep. 1992 2 p
(Grant NAG5-1060)
(NASA-CR-193810; NAS 1.26:193810) Avail: CASI HC A01/MF A01

Research under this grant has involved analyses of satellite-derived measurements of water vapor and total ozone. Upper tropospheric water vapor data from the Nimbus 7 temperature-humidity infrared radiometer (THIR) 6.7 micron channel were analyzed by Fourier transformation to provide wavenumber spectra for a case of an upper level system over Europe. The power law spectrum for horizontal scales from 60 to several hundred km suggests that when convective cloud energy sources are not present, the enstrophy-cascading process (with variance proportional to the minus three power of wavenumber) may hold to much smaller scales than previously thought. Several investigations of the middle atmosphere (stratosphere and mesosphere) were also conducted. Slow atmospheric oscillations with periods of 1-2 months were investigated in total ozone measurements and in ionospheric data. Using one-point correlation maps and total ozone mapping spectrometer (TOMS) data, strong statistical evidence was found for the planetary-scale oscillations at these periods. A dipole-like pattern in the tropical equatorial Indian ocean-western Pacific region was documented, along with wavetrain-like patterns emanating into the extratropics. While attempting to follow the oscillations upward above stratosphere, oscillations were studied in ionospheric data (D-region radio wave absorption, in the upper mesosphere, around 80-90 km altitude). Cross-spectral analyses with solar flux data revealed that much of the observed 1-2 month variance in the ionospheric D-region was well correlated to solar variations. Further research has involved investigations of the photochemical lifetime of greenhouse gases methane and nitrous oxide. Using Nimbus 7 satellite data, a new analysis technique was employed to determine the lifetime of these gases in situ in the upper stratosphere. The lifetimes are found to be in good agreement with theoretical estimates. Author (revised)

N94-19255 International Centre for Theoretical Physics, Trieste (Italy).
A PHYSICAL MODEL FOR ONE-DIMENSION AND TIME-DEPENDENT IONOSPHERE. PART 1: DESCRIPTION OF THE MODEL
Shun-Rong Zhang, S. M. Radicella, Xin-Yu Huang, and Yuan-Zhi Su Mar. 1993 10 p Limited Reproducibility: More than 20% of this document may be affected by microfiche quality
(DE93-627958; IC-93/45-Pt-1) Avail: CASI HC A02 (US Sales Only)

On the basis of continuity and momentum equations for the ionospheric F region, a time-dependent and one-dimension model for O(sup +), N2(sup +), O2(sup +), and NO(sup +), taking into account photoionization production, 10 recombination reactions, thermospheric wind and electromagnetic drifts, have been derived. The bottom side boundary is set to be dominated by photo-chemical reactions, meanwhile, the top side can be influenced by other processes. Electron density, especially foF(sub 2), or flux can be given as input. The present model can be used for the investigation of the influence of different parameters on the ionospheric processes, such as neutral wind, solar radiation flux, electromagnetic forces, and others. Part 1 gives the description of the model. Numerical results and its physical discussions will be addressed in the next paper. DOE

N94-19380# Ecole Centrale de Lyon (France). Dept. de Mecanique des Solides.
NUMERICAL ANALYSIS OF PRESSURE METER TESTS: APPLICATION OF PARAMETER IDENTIFICATION OF SOILS BEHAVIOR Ph.D. Thesis [ANALYSE NUMERIQUE DE L'ESSAI PRESSIOMETRIQUE: APPLICATION A L'IDENTIFICATION DE PARAMETRES DE COMPORTEMENT DES SOLS]
Ramdane Bahar 1992 222 p In FRENCH
(ECL-92-52; ETN-93-94893) Avail: CASI HC A10/MF A03

The results of pressure meter tests to define constants of constitutive models for soils using nonviscous models and viscous models are analyzed. An equation defining the problem of the expansion of the pressure meter probe considering the assumption of plane strain is presented. Phenomena for the identification procedure are numerically analyzed using the nonviscous model. The model parameter identification procedure is presented using the results of pressure meter tests. To take into account the creep phenomena of soils, a nonlinear viscoelastic rheological model is proposed. This approach is used to identify the constants of the Pithiviers limestone of the site of Saint Laurent des Eaux and the pasty chalk of Nogent sur Seine (France). Two examples of the use of this procedure are presented and compared to forecasts and in situ measurements. ESA

N94-19397*# Columbia Univ. Teachers Coll., New York, NY. Center for the Study of Global Habitability.
A NEW APPROACH TO THE STUDY OF THE TURBULENCE LAYER Final Technical Report, 1 Oct. 1991 - 31 Oct. 1993
Ruth A. Levenson 18 Oct. 1993 4 p
(Contract NCC5-45)
(NASA-CR-194546; NAS 1.26:194546) Avail: CASI HC A01/MF A01

Turbulent thermal convection is of considerable importance in fluid dynamical transport phenomena occurring, for example, in the planetary boundary layer of the Earth, the interiors of stars, and accretion disks. In particular, during a significant portion of the evolutionary phase of many stars having convectively unstable cores or outer envelopes, a substantial fraction of energy is transported from the central layers to the outer layers by thermal convection. Moreover, as much of the interior of a star is in highly turbulent motion, a complete theory of stellar structure and evolution requires the explicit consideration of turbulence in order to have expressions for the turbulent quantities arising in the stellar structure equations, and particularly, the turbulent fluxes that appear in the total flux conservation equation, such as the convective flux, kinetic energy flux, etc. A reliable quantification of these fluxes continues to present a challenge in astrophysical fluid dynamics, primarily because astrophysical turbulence is almost always fully-developed and nearly inviscid, and therefore governed by strong nonlinear interactions that distribute the energy among a very wide spectrum of eddies with scales ranging from the characteristic dimension of the flow to those sufficiently small to be affected by viscous dissipation. Furthermore, astrophysical flows are invariably compressible, anisotropic, and inhomogeneous, which requires the consideration of the dynamics of longitudinal modes and their interaction with the transverse modes, as well as complicated boundary conditions. In order to reach a compromise between analytical and numerical tractability and the basic physics of turbulent convection, we have constructed a model of stationary turbulent convection that yields various turbulence statistics, including the convective flux, that are required in stellar evolution models. Author (revised)

N94-19428*# Cornell Univ., Ithaca, NY. Dept. of Geological Sciences.
ANALYSIS OF REGIONAL DEFORMATION AND STRAIN ACCUMULATION DATA ADJACENT TO THE SAN ANDREAS FAULT Final Technical Report, 1 Nov. 1986 - 31 Dec. 1991
Donald L. Turcotte 31 Dec. 1991 12 p
(Grant NAG5-860)
(NASA-CR-194072; NAS 1.26:194072) Avail: CASI HC A03/MF A01

A new approach to the understanding of crustal deformation was developed under this grant. This approach combined aspects of fractals, chaos, and self-organized criticality to provide a comprehensive theory for deformation on distributed faults. It is hypothesized that crustal deformation is an example of comminution: Deformation takes place on a fractal distribution of faults resulting in a fractal distribution of seismicity. Our primary effort under this grant was devoted to developing an understanding of distributed deformation in the continental crust. An initial effort was carried out on the fractal clustering of earthquakes in time. It was shown that earthquakes do not obey random Poisson statistics, but can be approximated in many cases by coupled, scale-invariant fractal statistics. We applied our approach to the statistics of earthquakes in the New Hebrides region of the southwest Pacific because of the very high level of seismicity there. This work was written up and published in the Bulletin of the Seismological Society of America. This approach was also applied to the statistics of the seismicity on the San Andreas fault system. Derived from text

N94-19432*# Massachusetts Inst. of Tech., Cambridge. Dept. of Earth, Atmospheric, and Planetary Sciences.
THE INTERPRETATION OF CRUSTAL DYNAMICS DATA IN TERMS OF PLATE MOTIONS AND REGIONAL DEFORMATION NEAR PLATE BOUNDARIES Final Technical Report, 22 Sep. 1986 - 31 Dec. 1991
Sean C. Solomon 1991 9 p
(Grant NAG5-814)
(NASA-CR-194302; NAS 1.26:194302) Avail: CASI HC A02/MF A01

During our participation in the NASA Crustal Dynamics Project under NASA contract NAS-27339 and grant NAG5-814 for the period 1982-1991, we published or submitted for publication 30 research papers and 52 abstracts of presentations at scientific meetings. In addition, five M.I.T. Ph.D. students (Eric Bergman, Steven Bratt, Dan Davis, Jeanne Sauber, Anne Sheehan) were supported wholly or in part by this project during their thesis research. Highlights of our research progress during this period include the following: application of geodetic data to determine rates of strain in the Mojave block and in central California and to clarify the relation of such strain to the San Andreas fault and Pacific-North American plate motions; application of geodetic data to infer post seismic deformation associated with large earthquakes in the Imperial Valley, Hebgen Lake, Argentina, and Chile; determination of the state of stress in oceanic lithosphere from a systematic study of the centroid depths and source mechanisms of oceanic intraplate earthquakes; development of models for the state of stress in young oceanic regions arising from the differential cooling of the lithosphere; determination of the depth extent and rupture characteristics of oceanic transform earthquakes; improved determination of earthquake slip vectors in the Gulf of California, an important data set for the estimation of Pacific-North American plate motions; development of models for the state of stress and mechanics of fold-and-thrust belts and accretionary wedges; development of procedures to invert geoid height, residual bathymetry, and differential body wave travel time residuals for lateral variations in the characteristic temperature and bulk composition of the oceanic upper mantle; and initial GPS measurements of crustal deformation associated with the Imperial-Cerro Prieto fault system in southern California and northern Mexico. Full descriptions of the research conducted on these topics may be found in the Semi-Annual status Reports submitted regularly to NASA over the course of this project and in the publications listed. Derived from text

N94-19477# Brookhaven National Lab., Upton, NY.
HELIUM ISOTOPIC ABUNDANCE VARIATION IN NATURE
N. E. Holden 1993 9 p Presented at the 37th International Union of Pure and Applied Chemistry Meeting, Lisbon, Portugal, 5-12 Aug. 1993
(Contract DE-AC02-76CH-00016)
(DE93-019050; BNL-49331; CONF-9308148-6) Avail: CASI HC A02/MF A01

The isotopic abundance of helium in nature has been reviewed. This atomic weight value is based on the value of helium in the atmosphere, which is invariant around the world and up to a distance of 100,000 feet. Helium does vary in natural gas, volcanic rocks and gases, ocean floor sediments, waters of various types, and in radioactive minerals and ores due to (alpha) particle decay of radioactive nuclides. DOE

N94-19529# Army Cold Regions Research and Engineering Lab., Hanover, NH.
PROCEEDINGS: INTERNATIONAL SYMPOSIUM ON THERMAL ENGINEERING AND SCIENCE FOR COLD REGIONS
V. J. Lunardini and S. L. Bowen 1993 363 p The Fourth Symposium held in Hanover, NH, 28 Sep. - 1 Oct. 1993
(AD-A270636; CRREL-SR-93-22) Avail: CASI HC A16/MF A03

This document contains a collection of papers from the Fourth International Symposium on Thermal Engineering and Science for Cold

Regions. Topics covered include: some topics on melting heat transfer problems; osmotic model of ice segregation; thermosyphon applications in cold regions; an analytic study of liquid solidification in low Peclet number forced flows inside a parallel plate channel concerning axial heat conduction; freezing within laminar fast-growing thermally developing region of a uniform heat flux cooled parallel plate duct; the morphology of ice layers in curved rectangular channels; effect of heat conductor plates on ice formation near a wall; freezing characteristics of water flow in a horizontal cooled tube with the separated region; stability of thick ice formation in pipes; experiments and analysis of pipe freezing; experimental study of freezing of water in a closed circular tube with pressure increasing; and effects of a porous medium in a flow passage with miter bend. DTIC

N94-19644 Technische Univ., Delft (Netherlands). Faculty of Technical Mathematics and Informatics.
AN ITERATIVE INVERSE SCATTERING METHOD FOR THE REMOVAL OF SCATTERED SURFACE WAVES
Bastian Blonk and Gerard C. Herman 1993 18 p Sponsored in part by Netherlands Technology Foundation and Shell Research Ltd. Limited Reproducibility: More than 20% of this document may be affected by microfiche quality
(Rept-93-18; ETN-93-94645) Copyright Avail: CASI HC A03

An iterative method for removing near surface scattered noise from seismic data is presented. It is applied to large scale models and appears to be rather robust, except for the fact that a rather accurate knowledge of the Rayleigh wave velocity is required. The formulation of the method, however, offers possibilities for estimating this velocity with sufficient accuracy. ESA

N94-17832*# Butler Analyses, Towson, MD.
GENERALIZED SEISMIC ANALYSIS
Thomas G. Butler *In* COSMIC, The Twenty-First NASTRAN (R) Users' Colloquium Sep. 1993 p 60-72 (For primary document see N94-17827 04-39)
Avail: CASI HC A03/MF A02

47 METEOROLOGY AND CLIMATOLOGY

Includes weather forecasting and modification.

N94-17715# Los Alamos National Lab., NM.
SURFACE FLUXES IMPORTANT TO CLOUD DEVELOPMENT
F. J. Barnes, W. Porch, and K. E. Kunkel (Illinois State Water Survey, Champaign.) 1993 5 p Presented at the 3rd ARM Science Team Meeting, Norman, OK, 1-5 Mar. 1993
(Contract W-7405-eng-36)
(DE93-016633; LA-UR-93-1990; CONF-9303122-4) Avail: CASI HC A01/MF A01

To address some of the issues in scaling and averaging of measurements, collaborative field campaigns were conducted in June 1991 and 1992 by the DOE laboratories funded under the ARM program. We selected a site in Boardman, OR, with two distinct regions where the sensible and latent heat fluxes would differ sharply and where each region was sufficiently extensive for full development of boundary layers and for utilizing aircraft-mounted instrument systems. Measurements were clustered along a 16-km transect across adjoining irrigated farmland and semi-arid rangeland regions that allowed the collaborating teams to conduct a variety of studies relating to overall goals. The Los Alamos team efforts were focused on assessing the effects of different surface characteristics on fluxes of heat and water vapor. DOE

N94-17758# Lawrence Livermore National Lab., CA.
A TECHNIQUE FOR MEASURING WINDS IN THE LOWER ATMOSPHERE USING INCOHERENT DOPPLER LIDAR
D. H. DeSlover, D. R. Slaughter, W. M. Tulloch, and W. E. White 14 Apr. 1993 7 p Presented at the Optical Society of America Meeting on Optical Remote Sensing of the Atmosphere, Salt Lake City, UT, 8-12 Mar. 1993
(Contract W-7405-eng-48)
(DE93-017163; UCRL-JC-113310; CONF-930346-3) Avail: CASI HC A02/MF A01

Wind speed is useful from a meteorological standpoint, in atmospheric modeling, and assessment of trace gas dispersal. A continuing effort is involved in improving the sensitivity of such measurements, and is exemplified by the literature. The Mobile Atmospheric Research Laboratory (MARL) at Lawrence Livermore National Laboratory (LLNL) is currently developing a method to improve the sensitivity of wind sounding in the lower through middle atmosphere using a pair of Fabry-Perot interferometers in parallel. This technique, first described by Chanin, for the middle atmosphere using Doppler Rayleigh lidar, can be applied to the lower atmosphere where Mie (aerosol) backscatter is strong. Elastic events, inherent in both Rayleigh and Mie backscatter, dominate the return signal throughout the atmosphere. Both are susceptible to local wind vectors; which will Doppler shift the laser frequency proportional to the wind velocity. A pair of Fabry-Perot interferometers, tuned to either side of the laser frequency, will provide necessary data to determine the shift in frequency of the backscattered signal. Spectral drift and jitter of the laser and a lack of data points to determine the wind vector place limits on the sensitivity of the system. A method to minimize each of these is presented. DOE

N94-17895# Pacific Northwest Lab., Richland, WA.
A REVIEW OF WIND FIELD MODELS FOR ATMOSPHERIC TRANSPORT
J. V. Ramsdell, Jr. and E. D. Skyllingstad Jun. 1993 56 p
(Contract DE-AC06-76RL-01830)
(DE93-016085; PNWD-2148-HEDR) Avail: CASI HC A04/MF A01

The primary objective of the Hanford Environmental Dose Reconstruction (HEDR) Project is to estimate the radiation dose that individuals could have received as a result of emissions since 1944 from the US Department of Energy's (DOE) Hanford Site near Richland, Washington. The HEDR Project is developing a computer code to estimate these doses and their uncertainties. The code, known as the HEDR Integrated Code (HEDRIC), consists of four separate component codes. One of the component codes, called the Regional Atmospheric Transport Code for Hanford Emission Tracking (RATCHET), combines meteorological and release data to estimate time-integrated air concentrations and surface contamination at specific locations in the vicinity of the Hanford Site. The RATCHET domain covers approximately 75,000 square miles, extending from the crest of the Cascade Mountains on the west to the eastern edge of the Idaho panhandle and from central Oregon on the south to the Canadian border. This letter report explains the procedures in RATCHET that transform observed wind data into the wind fields used in atmospheric transport calculations. It also describes and evaluates alternative procedures not selected for use in RATCHET. DOE

N94-17924 Royal Netherlands Meteorological Inst., De Bilt.
VERIFICATION OF 3I RETRIEVALS VIS-A-VIS RADIOSONDE OBSERVATIONS
G. J. Prangsma 1993 39 p
(KNMI-TR-150; ISBN-90-369-2031-0; ETN-93-94535) Copyright Avail: Royal Netherlands Meteorological Institute, P.O. Box 201, 3730 AE De Bilt, Wilhelminalaan 10, Netherlands

A set of Tiros Operational Vertical Sounder (TOVS) observations from 58 NOAA-11 orbits in the period 14 Sep. to 3 Oct. 1992 over Europe were processed with the 3I system. The resulting retrievals were compared with collocated radiosondes extracted from the operational database for the same period. The collocation criteria (less than 3 hours time difference and a maximum distance of 50 km) resulted in a statistical dataset with about 100 or more items in each of the considered sub cases: clear-cloudy, day-night, and their combinations. Apart from results for the layer mean virtual temperatures, statistics for the stability index and for the total water vapor content were obtained. Error correlation matrices for the thickness errors in the various layers were computed. ESA

N94-17942# Lawrence Livermore National Lab., CA.
MIXTURE DISTRIBUTIONS IN CLIMATOLOGICAL RESEARCH
S. L. Grotch Dec. 1992 8 p Presented at the 17th Annual Climate Diagnostics Conference, Norman, OK, 19-23 Oct. 1992
(Contract W-7405-eng-48)
(DE93-014125; UCRL-JC-111263; CONF-9210334-3) Avail: CASI HC A02/MF A01

Mixture distributions have had a long history in statistics where the central problem has been the decomposition of multiple distributions into their component parts and the estimation of the parameters of these sub-distributions. Here, in the climatological context however, the nature of these complex distributions is examined, without any attempt to decompose them, examining not only data distributions for a range of climatological variables, but their anomaly distributions as well. Histograms are easily generated, providing a rich visual display for intercomparison purposes. They serve to readily flag suspect or unusual data and can be suggestive of underlying mechanism. They can provide information which can be of considerable value for extreme value studies. Finally, an enormously rich statistical literature exists on the nature of distributions, physical processes leading to their development, and techniques for parameter estimation. Of particular relevance to model/data intercomparisons, there exist a broad range of tools for addressing the fundamental question: 'are two distributions statistically the same?'. DOE

N94-18046# Midwest Research Inst., Golden, CO. National Renewable Energy Lab.

DEFINING THE NORMAL TURBINE INFLOW WITHIN A WIND PARK ENVIRONMENT

N. D. Kelley Jun. 1993 12 p Presented at the IEA Expert Meeting 24: Wind Conditions for Wind Turbine Design, Roskilde, Denmark, 29-30 Apr. 1993
(Contract DE-AC02-83CH-10093)
(DE93-010032; NREL/TP-442-5619; CONF-9304177-1) Avail: CASI HC A03/MF A01

This brief paper discusses factors that must be considered when defining the 'normal' (as opposed to 'extreme') loading conditions seen in wind turbines operating within a wind park environment. The author defines the 'normal' conditions to include fatigue damage accumulation as a result of: (1) start/stop cycles, (2) emergency shutdowns, and (3) the turbulence environment associated with site and turbine location. He also interprets 'extreme' loading conditions to include those events that can challenge the survivability of the turbine. DOE

N94-18052# Pacific Northwest Lab., Richland, WA.

BOUNDARY LAYER HEAT BUDGETS FROM WIND PROFILER/RASS DATA: A FEASIBILITY STUDY

M. Furger and C. D. Whiteman Mar. 1993 4 p Presented at the 3rd ARM Science Team Meeting, Norman, OK, 1-5 Mar. 1993
(Contract DE-AC06-76RL-01830)
(DE93-013187; PNL-SA-21918; CONF-9303122-3) Avail: CASI HC A01/MF A01

Radar wind profilers (WP) and radio-acoustic sounding systems (RASS) are now available commercially and offer the promise of improving our knowledge of processes in the lower atmosphere on scales that were until now unresolved spatially and/or temporally. Plans to install a network of boundary layer WP/RASSes are now under discussion in the US Department of Energy's ARM (Atmospheric Radiation Measurement) program and in other national programs and may be realized within two or three years. The new devices raise the prospect of gaining better insight into planetary boundary layer processes. With this background in mind we re-evaluate some classical methods for the calculation of kinematic and dynamic quantities using measurements from these new remote sensing devices. DOE

N94-18053# Lawrence Livermore National Lab., CA.

EFFECT OF SPATIAL RESOLUTION ON THE SIMULATION OF REGIONAL PRECIPITATION IN CHINA IN A GLOBAL CLIMATE MODEL

G. L. Potter, K. R. Sperber, J. S. Boyle, and S. Hameed Sep. 1992 5 p Presented at the 73rd American Meteorological Society Meeting, Anaheim, CA, 17-22 Jan. 1992
(Contracts W-7405-eng-48; DE-FG02-85ER-60314)
(DE93-013433; UCRL-JC-111835; CONF-9201148-2) Avail: CASI HC A01/MF A01

In order to evaluate the consequences of climate change for agriculture and the economy we need to develop climate models capable of correctly simulating regional precipitation patterns. The deficiency of global climate models in the simulation of orographic precipitation may be related to the crudeness of model topography. Inadequacies in the parameterizations of physical processes cause additional errors in the calculation of orographic as well as frontal precipitation. In this study, we have investigated the role of model resolution in simulating the geographical distribution of precipitation over China. Comparisons are made between observations and the calculated precipitation fields in a seasonal run with climatological sea surface temperatures. This study describes results for June and July from 12 month simulations of the ECMWF model at the following four resolutions: T21 (5(times)5 degree), T42 (3(times)3 degree), T63 (2(times)2 degree) and T106 (1(times)1 degree). A description of this model is given by Simmons et. al. (1988). The various resolutions of the ECMWF model are virtually identical with the exception of the gravity wave drag (Palmer et al. 1986), vertical diffusion coefficients and orography. The T21 resolution lacks gravity wave drag completely. DOE

N94-18126# National Oceanic and Atmospheric Administration, Boulder, CO. Climate Monitoring Lab.

ANALYSIS OF METEOROLOGICAL CONDITIONS DURING AGASP-4: 30 MARCH - 23 APRIL 1992

G. A. Herbert, P. J. Sheridan (Colorado Univ., Boulder.), R. C. Schnell, M. Z. Bieniulis (Colorado Univ., Boulder.), and B. A. Bodhaine Apr. 1993 123 p See also PB88-164140
(PB93-190205; NOAA-TM-ERL-CMDL-5) Avail: CASI HC A06/MF A02

The fourth Arctic Gas and Aerosol Sampling Program (AGASP-IV) was conducted over Alaska and the Beaufort Sea during March and April 1992. The NOAA WP-3D aircraft made nine flights. On the first eight flights special aerosol and gas sampling instrumentation was installed, and extensive time was spent over the pack ice. Measurements of wind, pressure, temperature, relative humidity, ozone, and condensation nucleus (CN) concentration were used to identify the air mass type, recent origin, and existence of pollution-derived aerosols, i.e., haze. While small patches of elevated CN concentrations and higher aerosol scattering coefficients were observed, significantly large regions, of the type found in previous AGASP missions, were not observed during the series. On most flights the CN concentrations in the troposphere were representative of 'clean' background conditions at this latitude. Significant concentrations of CN (CN greater than 7000/cm(exp 3)) found above the tropopause on three flights indicated the presence of volcanic aerosol probably from the Pinatubo volcanic plume at high latitudes. In four instances low ozone concentrations suggest the destruction of ozone in the surface layer. NTIS

N94-18132# Lawrence Livermore National Lab., CA.

A MOBILE REMOTE SENSING LABORATORY FOR WATER VAPOR, TRACE GAS, AEROSOL, AND WIND SPEED MEASUREMENTS

D. Slaughter, W. White, W. Tulloch, and D. DeSlover 19 Mar. 1993 7 p Presented at the Optical Society of America Meeting on Optical Remote Sensing of the Atmosphere, Salt Lake City, UT, 8-12 Mar. 1993
(Contract W-7405-eng-48)
(DE93-017158; UCRL-JC-113269; CONF-930346-2) Avail: CASI HC A02/MF A01

The Lawrence Livermore National Laboratory has developed a mobile field laboratory for remote measurement of atmospheric processes and observables that are important in global climate change, dispersal of hazardous materials, and atmospheric pollution. Specific observables of interest are water vapor, trace gases, aerosol size and density, wind, and temperature. The goal is to study atmospheric processes continuously for extended periods in remote field locations. This laboratory has just reached field ready status with sensors for aerosol and trace gas measurement based on established techniques. A development program is underway to enhance the sensor suite with several new techniques and instruments that are expected to significantly extend the state of the art in remote trace gas analysis. The new sensors will be incorporated into the lab during the next two years. DOE

N94-18143 Royal Netherlands Meteorological Inst., De Bilt.

ON THE CONSTRUCTION OF A REGIONAL ATMOSPHERIC CLIMATE MODEL

Jens Hesselbjerg Christensen (Danish Meteorological Inst., Copenhagen.) and Erik vanMeijgaard 1992 33 p
(KNMI-TR-147; ISBN-90-369-2026-4; ETN-93-94532; PB93-191880)
Copyright Avail: Royal Netherlands Meteorological Institute, P.O. Box 201, 3730 AE De Bilt, Wilhelminalaan 10, Netherlands

A regional atmospheric climate model which combines the physical parametrization package of a general circulation or climate model (ECHAM) and the dynamics package of the Nordic/Dutch/Irish High Resolution Limited Area Model (HIRLAM) was developed. The objectives of the project are formulated, and the developing strategy is described in some detail mainly as a guidance for the potential user with a limited knowledge of either of the two models. Furthermore, the necessary changes applied to both model packages in order to obtain a working code are described. Preliminary results of the very first experiments are presented and discussed. ESA

N94-18206# Naval Postgraduate School, Monterey, CA.
SPECTRAL ANALYSIS OF SYNOPTIC TIME SCALE DISTURBANCES OVER THE TROPICAL EASTERN PACIFIC DURING SUMMER 1989, 1990 AND 1991 M.S. Thesis
William C. Swett 25 Mar. 1993 93 p
(AD-A268821) Avail: CASI HC A05/MF A01

In this study we used data analyzed by the Navy Operational Global Analysis and Prediction System (NOGAPS) to study the 4-10 day disturbances over the eastern tropical Pacific. The period of study is May - Sep. of 1989, 1990 and 1991. Spectral and cross-spectral analyses were used to determine the structure of the disturbances. The results show zonal wavelengths of 3000 to 8000 kilometers and a tendency for northeast-southwest tilt in the meridional direction. The most active year appears to be 1991, with the highest relative variance in the 4-10 day window and the highest coherence between parameters. The vertical tilt was found to be westward with height above 300-400 hpa in 1989 and above 200 hpa in 1990 and 1991. This interannual variation was consistent with the change in vertical shear of the mean zonal wind. Below 400 hpa in 1989 and 200 hpa in 1990 and 1991, the vertical tilt was eastward with height. The thermal structure was consistent with the hydrostatic relationship in all three years. The waves transport heat poleward above 200 hpa and equatorward below 200 hpa. DTIC

N94-18265# Wisconsin Univ., Madison.
RAPID OCEANIC CYCLOGENESIS STUDIES Technical Report
Patricia M. Pauley 30 Aug. 1993 132 p
(Contract N00014-88-K-0021)
(AD-A269258) Avail: CASI HC A07/MF A02

The effect of resolution on the depiction of central sea-level pressure for an intense oceanic extratropical cyclone is examined through a one-dimensional Fourier analysis. Profiles of sea-level pressure were manually interpolated along the latitude passing through the storm center from two subjective analyses and the 00, 24, and 48 h Nested Grid Model (NGM) forecasts, all valid at 0000 UTC 5 January 1989. At this time, the Experiment on Rapidly Intensifying Cyclones over the Atlantic (ERICA) Intensive Observing Period 4 (IOP-4) cyclone attained its maximum intensity, with a central pressure of 936 mb at 41 deg N 58 deg W. DTIC

N94-18281# Air Force Environmental Technical Applications Center, Scott AFB, IL.
CLOUDIEST YEAR STUDY: AN ANALYSIS OF THE 3DNEPH AND RTNEPH DATABASES
Billy D. Banter Apr. 1993 25 p
(AD-A269403; USAFETAC/PR-93/004) Avail: CASI HC A03/MF A01

Described are techniques used to analyze total cloud cover values from the USAF Environmental Technical Applications Center's nephanalysis databases: 3DNEPH and RTNEPH. The object of the study was to determine if total global cloud cover differed significantly on a year-to-year basis. Contoured global maps in an appendix show the results. DTIC

N94-18300# Naval Postgraduate School, Monterey, CA.
THREE-DIMENSIONAL CLOUD VISUALIZATION BASED ON SATELLITE IMAGERY M.S. Thesis
Kevin L. Stone Dec. 1992 73 p
(AD-A269318) Avail: CASI HC A04/MF A01

This thesis presents three dimensional visualizations of cloud scenes created with scientific visualization software implemented on high-performance graphics workstations. Cloud scenes are constructed for four separate cases, consisting of low stratus clouds off the California coast, stratus over the Great Plains, convective cumulus over the Gulf Coast region and Hurricane Andrew as it crossed southern Florida. The user interacts with the cloud scenes, on the computer screen, allowing the clouds to be studied from different perspectives. Procedures have been modified to integrate satellite information with sounding data to construct cloud tops. Techniques have been developed to integrate gridded surface observations with topography data to construct cloud bases with varying heights. Cloud bases determined in this manner are a more realistic representation than previous methods of using a constant height for all cloud bases in the cloud scene. DTIC

N94-18303 Air Force Environmental Technical Applications Center, Scott AFB, IL.
STATION CLIMATIC SUMMARIES: NORTH AMERICA. VOLUME 1: THE CONTIGUOUS UNITED STATES
Feb. 1993 600 p Limited Reproducibility: More than 20% of this document may be affected by microfiche quality
(AD-A269567; USAFETAC/DS-93/031-1) Avail: CASI HC A25

A collection of summarized monthly and annual climatic data for specific locations in North America is presented. Summarized climatological elements are: percent frequency of occurrence of ceiling and visibility; means, extremes, and number of days with specified values of temperature, precipitation, and snowfall; means of relative humidity, vapor pressure, dew point, pressure altitude, and cloud cover; prevailing wind direction, with mean and extreme speeds; and number of days with thunderstorms and fog. DTIC

N94-18486# Northwest Research Associates, Inc., Bellevue, WA.
INTERNAL INSTABILITY OF NONPARALLEL FLOW ON AN EQUATORIAL BETA-PLANE Annual Report, 15 May 1992 - 14 May 1993
Timothy J. Dunkerton 14 Jun. 1993 54 p
(Contract F49620-92-C-0033)
(AD-A268927; NWRA-CR-93-R103; AFOSR-93-0670TR) Avail: CASI HC A04/MF A01

A simple theoretical model was developed to investigate the inertial instability of zonally nonuniform, nonparallel flow near the equator. The basic state was independent of height and time but included cross-equatorial shear with longitudinal variation, as observed in the tropical mesosphere and elsewhere. Numerical solutions were obtained for the most unstable modes. It is shown that, in addition to previously known 'global' (symmetric and nonsymmetric) modes of inertial instability, there exist 'local' modes within regions of anomalous potential vorticity. The local mode has properties similar to those of 'absolute' instability of nonparallel flow as discussed elsewhere in fluid dynamics. DTIC

N94-18514 Pennsylvania State Univ., University Park. Dept. of Meteorology.
THE VERTICAL DISTRIBUTION OF HEATING IN THE TROPICAL ATMOSPHERE Annual Report No. 2
William M. Frank and John L. McBride 28 Sep. 1993 12 p Limited Reproducibility: More than 20% of this document may be affected by microfiche quality
(Contract N00014-92-J-1069)
(AD-A270452) Avail: CASI HC A03/MF A01

The project has three major research goals: (1) Assist the planning of TOGA COARE; (2) Participate in the TOGA COARE field program; and (3) Carry out a research program using the TOGA COARE data set to examine the mean properties and vertical heating profiles of mesoscale and larger scale phenomena in the COARE region. The work will focus on exploring relationships between tropical weather systems in this region and larger scale forcing, and determining processes that affect the vertical structure of the tropical atmosphere. DTIC

N94-18573 Air Weather Service, Scott AFB, IL.
NEW TECHNIQUES FOR CONTRAIL FORECASTING Technical Report
Jeffrey L. Peters Aug. 1993 37 p Limited Reproducibility: More than 20% of this document may be affected by microfiche quality
(AD-A269686; AWS/TR-93/001) Avail: Issuing Activity (Defense Technical Information Center (DTIC))

This report documents the results of a study requested by the Strategic Air Command Deputy Chief of Staff for Operations (SAC/DO) to update previous contrail forecasting research done by Herbert Appleman for HQ Air Weather Service in 1953. Advancements in aircraft power plants, especially the development of bypass turbofan engines, made the new study necessary. This attempt to update and improve current contrail forecasting methods was performed by the SAC Directorate of Weather (SAC/DOW). It describes the development of new contrail forecast algorithms for several types of engines used in high-flying aircraft. It also provides contrail forecasting rules that correlate synoptic-scale upward vertical motion with contrail formation. The results indicate significant improvement in contrail forecasting accuracy over the Appleman technique now in use at the Air Force Global Weather Central. DTIC

N94-18599# Army Research Lab., Adelphi, MD.

SOME POTENTIAL ERRORS IN SATELLITE WIND ESTIMATES USING THE GEOSTROPHIC APPROXIMATION AND THE THERMAL WIND Final Report

James Cogan Jun. 1993 35 p
(AD-A269784; ARL-MR-36) Avail: CASI HC A03/MF A01

Current and planned passive sensors on meteorological satellites measure radiances that are converted directly into temperature and humidity soundings. In turn, wind velocity is derived from the temperature soundings and other derived variables (for example, geopotential heights). Current operational methods involve either the geostrophic wind or the thermal wind approximation. This report presents some information and sample calculations on the types of errors that may be expected when either approximation is used to estimate the actual wind from data gathered by passive satellite sensors. The assumption is that no additional data are available (that is, only satellite sounding data from sensors of the type found on present day environmental satellites). This report does not treat the improvements that should occur when data from other sources of data (for example, radar profilers, ground-based radiometers, unmanned aerial vehicles) are combined with the satellite data. DTIC

N94-18602*# Wisconsin Univ., Madison. Cooperative Inst. for Meteorological Satellite Studies.

MICROWAVE (SSM/I) ESTIMATES OF THE PRECIPITATION RATE TO IMPROVE NUMERICAL ATMOSPHERIC MODEL FORECASTS Final Report

William H. Raymond and William S. Olson 1990 189 p
(Grant NAGw-1855)
(NASA-CR-193566; NAS 1.26:193566) Avail: CASI HC A09/MF A02

Delay in the spin-up of precipitation early in numerical atmospheric forecasts is a deficiency correctable by diabatic initialization combined with diabatic forcing. For either to be effective requires some knowledge of the magnitude and vertical placement of the latent heating fields. Until recently the best source of cloud and rain water data was the remotely sensed vertical integrated precipitation rate or liquid water content. Vertical placement of the condensation remains unknown. Some information about the vertical distribution of the heating rates and precipitating liquid water and ice can be obtained from retrieval techniques that use a physical model of precipitating clouds to refine and improve the interpretation of the remotely sensed data. A description of this procedure and an examination of its 3-D liquid water products, along with improved modeling methods that enhance or speed-up storm development is discussed. For individual titles, see N94-18603 through N94-18608.

N94-18603*# Wisconsin Univ., Madison. Cooperative Inst. for Meteorological Satellite Studies.

DIABATIC FORCING AND INITIALIZATION WITH ASSIMILATION OF CLOUD AND RAIN WATER IN A FORECAST MODEL: METHODOLOGY

William H. Raymond, William S. Olson, and Geary Callan (National Environmental Satellite Service, Madison, WI.) *In its* Microwave (SSM/I) Estimates of the Precipitation Rate to Improve Numerical Atmospheric Model Forecasts 1990 69 p Submitted for publication (For primary document see N94-18602 04-47)
(Grants NAGw-1855; NSF ATM-89-20508)
Avail: CASI HC A04/MF A02

The focus of this part of the investigation is to find one or more general modeling techniques that will help reduce the time taken by numerical forecast models to initiate or spin-up precipitation processes and enhance storm intensity. If the conventional data base could explain the atmospheric mesoscale flow in detail, then much of our problem would be eliminated. But the data base is primarily synoptic scale, requiring that a solution must be sought either in nonconventional data, in methods to initialize mesoscale circulations, or in ways of retaining between forecasts the model generated mesoscale dynamics and precipitation fields. All three methods are investigated. The initialization and assimilation of explicit cloud and rainwater quantities computed from conservation equations in a mesoscale regional model are examined. The physical processes include condensation, evaporation, autoconversion, accretion, and the removal of rainwater by fallout. The question of how to initialize the explicit liquid water calculations in numerical models and how to retain information about precipitation processes during the 4-D assimilation cycle are important issues that are addressed. The explicit cloud calculations were purposely kept simple so that different initialization techniques can be easily and economically tested. Precipitation spin-up processes associated with three different types of weather phenomena are examined. Our findings show that diabatic initialization, or diabatic initialization in combination with a new diabatic forcing procedure, work effectively to enhance the spin-up of precipitation in a mesoscale numerical weather prediction forecast. Also, the retention of cloud and rain water during the analysis phase of the 4-D data assimilation procedure is shown to be valuable. Without detailed observations, the vertical placement of the diabatic heating remains a critical problem. Author (revised)

N94-18604*# Wisconsin Univ., Madison. Cooperative Inst. for Meteorological Satellite Studies.

PHYSICAL RETRIEVAL OF PRECIPITATION WATER CONTENTS FROM SPECIAL SENSOR MICROWAVE/IMAGER (SSM/I) DATA. PART 1: A CLOUD ENSEMBLE/RADIATIVE PARAMETERIZATION FOR SENSOR RESPONSE (REPORT VERSION)

William S. Olson and William H. Raymond *In its* Microwave (SSM/I) Estimates of the Precipitation Rate to Improve Numerical Atmospheric Model Forecasts 1990 34 p Submitted for publication (For primary document see N94-18602 04-47)
(Grants NAGw-1855; NSF ATM-89-20508)
Avail: CASI HC A03/MF A02

The physical retrieval of geophysical parameters based upon remotely sensed data requires a sensor response model which relates the upwelling radiances that the sensor observes to the parameters to be retrieved. In the retrieval of precipitation water contents from satellite passive microwave observations, the sensor response model has two basic components. First, a description of the radiative transfer of microwaves through a precipitating atmosphere must be considered, because it is necessary to establish the physical relationship between precipitation water content and upwelling microwave brightness temperature. Also the spatial response of the satellite microwave sensor (or antenna pattern) must be included in the description of sensor response, since precipitation and the associated brightness temperature field can vary over a typical microwave sensor resolution footprint. A 'population' of convective cells, as well as stratiform clouds, are simulated using a computationally-efficient multi-cylinder cloud model. Ensembles of clouds selected at random from the population, distributed over a 25 km x 25 km model domain, serve as the basis for radiative transfer calculations of upwelling brightness temperatures at the SSM/I frequencies. Sensor spatial response is treated explicitly by convolving the upwelling brightness temperature by the domain-integrated SSM/I antenna patterns. The sensor response model is utilized in precipitation water content retrievals. Author (revised)

N94-18605*# Wisconsin Univ., Madison. Cooperative Inst. for Meteorological Satellite Studies.

PHYSICAL RETRIEVAL OF PRECIPITATION WATER CONTENTS FROM SPECIAL SENSOR MICROWAVE/IMAGER (SSM/I) DATA. PART 2: RETRIEVAL METHOD AND APPLICATIONS (REPORT VERSION)

William S. Olson *In its* Microwave (SSM/I) Estimates of the Precipitation Rate to Improve Numerical Atmospheric Model Forecasts 1990 24 p Submitted for publication (For primary document see N94-18602 04-47)
(Grant NAGw-1855)
Avail: CASI HC A03/MF A02

A physical retrieval method for estimating precipitating water distributions and other geophysical parameters based upon measurements from the DMSP-F8 SSM/I is developed. Three unique features of the retrieval method are (1) sensor antenna patterns are explicitly included to accommodate varying channel resolution; (2) precipitation-brightness temperature relationships are quantified using the cloud ensemble/radiative parameterization; and (3) spatial constraints are imposed for certain background parameters, such as humidity, which vary more slowly in the horizontal than the cloud and precipitation water contents. The general framework of the method will facilitate the incorporation of measurements from the SSMJT, SSM/T-2 and geostationary infrared measurements, as well as information from conventional sources (e.g., radiosondes) or numerical forecast model fields. Author

N94-18606*# Wisconsin Univ., Madison. Cooperative Inst. for Meteorological Satellite Studies.

FORECAST MODEL APPLICATIONS OF RETRIEVED THREE DIMENSIONAL LIQUID WATER FIELDS

William H. Raymond and William S. Olson *In its* Microwave (SSM/I) Estimates of the Precipitation Rate to Improve Numerical Atmospheric Model Forecasts 1990 28 p Submitted for publication (For primary document see N94-18602 04-47)
(Grants NAGw-1855; NSF ATM-89-20508)
Avail: CASI HC A03/MF A02

Forecasts are made for tropical storm Emily using heating rates derived from the SSM/I physical retrievals described in chapters 2 and 3. Average values of the latent heating rates from the convective and stratiform cloud simulations, used in the physical retrieval, are obtained for individual 1.1 km thick vertical layers. Then, the layer-mean latent heating rates are regressed against the slant path-integrated liquid and ice precipitation water contents to determine the best fit two parameter regression coefficients for each layer. The regression formulae and retrieved precipitation water contents are utilized to infer the vertical distribution of heating rates for forecast model applications. In the forecast model, diabatic temperature contributions are calculated and used in a diabatic initialization, or in a diabatic initialization combined with a diabatic forcing procedure. Our forecasts show that the time needed to spin-up precipitation processes in tropical storm Emily is greatly accelerated through the application of the data. Author

N94-18607*# Wisconsin Univ., Madison. Cooperative Inst. for Meteorological Satellite Studies.

MOIST WIND RELATIONSHIPS

William H. Raymond *In its* Microwave (SSM/I) Estimates of the Precipitation Rate to Improve Numerical Atmospheric Model Forecasts 1990 12 p (For primary document see N94-18602 04-47)
(Grants NAGw-1855; NSF ATM-89-20508)
Avail: CASI HC A03/MF A02

The equations describing the temporal and spatial behavior of the kinematic moisture and heat flux are described. In these nonlinear equations, the contribution by diabatic processes to the large-scale flux is composed of two parts. One part is associated with a Rayleigh damping term while the other arises from temporal and spatial changes in the pressure gradient term. It was found that the influence of diabatic processes on large-scale moisture fluxes depends greatly on the degree of balance between forcing and damping terms in the governing kinematic flux equations. The existence of a near balance requires a reduction in the large-scale horizontal geostrophic wind speed. Based on an examination of the moisture flux equations, it is argued that reductions in the large-scale horizontal wind speed observed within major cumulus cloud systems help conserve large-scale moisture fluxes. The deviation of the wind from geostrophic conditions is easily estimated for a near balanced state. This wind modification induces secondary vertical circulations that contribute to convergence, creating or supporting long-lived mesoscale flows. We believe this process to be a major supporter of the mesoscale circulations observed in severe storms and squall lines. In the tropics the wind modification has an antitriptic relationship. These diagnostic findings suggest possible modifications to the wind field in the application of a cumulus parameterization, and may be important in diabatic initialization of numerical weather prediction models. Author (revised)

N94-18608*# Wisconsin Univ., Madison. Cooperative Inst. for Meteorological Satellite Studies.

INITIALIZATION AND ASSIMILATION OF CLOUD AND RAINWATER IN A REGIONAL MODEL

William H. Raymond and William S. Olson *In its* Microwave (SSM/I) Estimates of the Precipitation Rate to Improve Numerical Atmospheric Model Forecasts 1990 13 p (For primary document see N94-18602 04-47)
Avail: CASI HC A03/MF A02

The initialization and assimilation of cloud and rainwater quantities in a mesoscale regional model was examined. Forecasts of explicit cloud and rainwater are made using conservation equations. The physical processes include condensation, evaporation, autoconversion, accretion, and the removal of rainwater by fallout. These physical processes, some of which are parameterized, represent source and sink in terms in the conservation equations. The question of how to initialize the explicit liquid water calculations in numerical models and how to retain information about precipitation processes during the 4-D assimilation cycle are important issues that are addressed. Author (revised)

N94-18637# Atmospheric and Environmental Research, Inc., Cambridge, MA.

SERCAA CLOUD ANALYSIS INTEGRATION: DESIGN CONCEPTS AND INTERACTION WITH CLOUD FORECAST MODELS Technical Report

Thomas M. Hamil and Ross Hoffman 16 Apr. 1993 60 p
(Contract F19628-92-C-0149)
(AD-A269104; PL-TR-93-2100; SR-1) Avail: CASI HC A04/MF A01

A new cloud analysis model to eventually replace the Real-Time Nephanalysis operating at the Air Force Global Weather Central is being prototyped. This new cloud analysis model will process multisource satellite data, geostationary and polar-orbiting, civilian and military. The output will be used primarily to initialize cloud forecast models but may be used also for climate research and other applications. This report reviews the customer requirements for cloud analysis data, the existing and future cloud forecast algorithms, and how the new cloud analysis model can integrate the multisource satellite data into one coherent analysis useful to all users. The likely approach for this 'analysis integration' will be to blend optimum interpolation techniques, common in numerical weather analysis, with a knowledge base commonly used in artificial intelligence. DTIC

N94-18675# Air Force Inst. of Tech., Wright-Patterson AFB, OH. Foreign Aerospace Science and Technology Center.

THE ACTIVITIES OF EQUATORIAL ANTICYCLONES OF THE WESTERN PACIFIC AND THE SOUTH CHINA SEA AND THEIR EFFECTS ON THE TRACKS OF TYPHOON MOVEMENT

Cheng-Lan Bao, Rong-Mao Wei, and Chang-Hua Huang 8 Sep. 1993 21 p Transl. into ENGLISH from Daqi Kexue, China, v. 3, no. 2, 1979 p 141-149
(AD-A269954; FASTC-ID(RS)T-0096-93) Avail: CASI HC A03/MF A01

This paper carries out a preliminary investigation and analysis of the activities of equatorial anticyclones over the western Pacific and South China Sea. They occur on average eight times a year and are mostly concentrated during the months of June-September. An equatorial anticyclone is a tropical weather system of meteorological magnitude of 1,000 - 2,000 km. It can continue on for a few days. It is a kind of a warm and high pressure system, and is often related to a fair weather system. The equatorial anticyclone clearly has an effect on the development of the typhoon genesis and the track of its movement. Once a deep, thick, and strong equatorial anticyclone appears to the south of a typhoon, the typhoon often seems to search for its path. However, the actual track of the typhoon is determined by the high pressure cooperative activities of the equatorial anticyclone and subtropics. This paper also presents several typhoon tracks for analyses. DTIC

N94-18684 Massachusetts Inst. of Tech., Lexington.

INTEGRATED TERMINAL WEATHER SYSTEM (ITWS) Annual Report, 1992

James E. Evans 7 Sep. 1993 104 p Limited Reproducibility: More than 20% of this document may be affected by microfiche quality
(Contract F19628-90-C-0002)
(AD-A269884; ATC-203; DOT/FAA/RD-93/27) Avail: CASI HC A06

Hazardous weather in the terminal area is the major cause of aviation system delays as well as a principal cause of air carrier accidents. Several systems presently under development will provide significant increases in terminal safety. However, these systems will not make a major impact on weather-induced delays in the terminal area, meet a number of the safety needs (such as information to support ground deicing decisions), or reduce the workload of the terminal controller. The Integrated Terminal Weather System (ITWS) will provide improved aviation weather information in the allocated TRACON area (up to 50 nmi from the airport) by integrating data and products from various Federal Aviation Administration (FAA) and National Weather Service (NWS) sensors and weather information systems. The data from these sources will be combined to provide a unified set of safety and planning weather products for pilots, controllers, and terminal area traffic managers. By using data from multiple sensors, ITWS can generate important new products where no individual sensor alone could generate a single, reliable product. In other instances, use of data from several sources can compensate for erroneous data from one sensor and thus improve the overall integrity of existing products. Major objectives of the ITWS program are to increase the effective airport acceptance rate in adverse weather by providing information to support terminal automation systems, better terminal route planning, and wake vortex advisory services, and to reduce the need for controllers to communicate weather information to pilots via VHF voice. DTIC

N94-18732# Air Force Environmental Technical Applications Center, Scott AFB, IL.
STATION CLIMATIC SUMMARIES, NORTH AMERICA. VOLUME 2: ALASKA, CANADA AND GREENLAND
Feb. 1993 258 p
(AD-A269793; USAFETAC/DS-93/031-2) Avail: CASI HC A12/MF A03

A collection of summarized monthly and annual climatic data for specific locations in North America is presented. Summarized climatological elements are: percent frequency of occurrence of ceiling and visibility; means, extremes, and number of days with specified values of temperature, precipitation, and snowfall; means of relative humidity, vapor pressure, dew point, pressure altitude, and cloud cover; prevailing wind direction, with mean and extreme speeds; and number of days with thunderstorms and fog. DTIC

N94-18781# Army Missile Command, Redstone Arsenal, AL. Weapons Science Directorate.
SOLAR RADIATION IN SAUDI ARABIA Final Technical Report, Mar. - Dec. 1992
Dorathy A. Stewart, Helmut P. Dudel, and Larry J. Levitt Jun. 1993 58 p
(AD-A269970; AD-E952102; AMSMI/TR-RD-WS-93-6) Avail: CASI HC A04/MF A01

Original solar irradiance data were obtained from the U.S. Air Force Environmental Technical Applications Center. These data were based on a model which used standard meteorological data and an albedo supplied by us. A procedure was developed to interpolate missing solar irradiances, and serially complete sets of hourly total solar irradiances were established for the three Saudi Arabian stations Riyadh, Dhahran, and Quisumah for the period January 1981 through July 1990. Tables of maximum, minimum, and mean daily totals; mean hourly values; and frequency distributions for noon are included. Comparison of monthly means and extremes with published data did not produce conclusive results. Considerable disagreement exists among published amounts of solar radiation reaching the surface in this region. The solar irradiance estimates in this report agree with the highest published values and should be considered upper limits. DTIC

N94-18812 Air Force Inst. of Tech., Wright-Patterson AFB, OH.
AN INVESTIGATION OF WARM-CLOUD MICROPHYSICS USING A MULTI-COMPONENT CLOUD MODEL: INTERACTIVE EFFECTS OF THE AEROSOL SPECTRUM M.S. Thesis
Stephen G. Zahn Dec. 1993 118 p Limited Reproducibility: More than 20% of this document may be affected by microfiche quality
(AD-A270273; AFIT/CI/CIA-93-140) Avail: CASI HC A06

Clouds, especially low, warm, boundary-layer clouds, play an important role in regulating the earth's climate due to their significant contribution to the global albedo. The radiative effects of individual clouds are controlled largely by cloud microstructure which is itself sensitive to the concentration and spectral distribution of the atmospheric aerosol. Increases in aerosol particle concentrations from anthropogenic activity could result in increased cloud albedo and global cloudiness, increasing the amount of reflected solar radiation. However, the effects of increased aerosol particle concentrations could be offset by the presence of giant or ultragiant aerosol particles. A one-dimensional, multi-component microphysical cloud model has been used to demonstrate the effects of aerosol particle spectral variations on the microstructure of warm clouds. Simulations performed with this model demonstrate that the introduction of increased concentrations of giant aerosol particles has a destabilizing effect on the cloud microstructure. Also, it is shown that warm-cloud microphysical processes modify the aerosol particle spectrum favoring the generation of the largest sized particles via the collision-coalescence process. These simulations provide further evidence that the effect of aerosol particles on cloud microstructure must be addressed when considering global climate forecasts. DTIC

N94-18871# Phillips Lab., Hanscom AFB, MA.
CONVECTION ALGORITHMS FOR MAGNETOSPHERIC PARTICLES Interim Report
Kevin J. Kerns 10 Aug. 1993 42 p
(AF Proj. 7601)
(AD-A270103; PL-TR-93-2183; ERP-1127) Avail: CASI HC A03/MF A01

This report documents in detail the implementation of the convection model used for the research by Kerns, Hardy, and Gussenhoven titled 'Modelling of Convection Boundaries Seen by CRRES in 120 eV to 28 keV Particles.' This research is to be published in the Journal of Geophysical Research, Space Physics in 1993. The convection model assumes an Earth centered dipole magnetic field with equipotential field lines and a static cross tail electric field. Convection results from EXB drifts and magnetic field gradient and curvature drifts. Algorithms are provided to calculate drift paths of particles as well as to calculate the energy range of particles at a specified position that are on open drift paths to the magnetospheric tail. The algorithms presented in this document are optimized to converge to a solution quickly for any particle energy, position, and equatorial pitch angle. These algorithms are implemented in the CRRES survey software called SHOWLEPA.EXE which was used in support of the research. DTIC

N94-18883 Air Force Environmental Technical Applications Center, Scott AFB, IL.
EASTERN EUROPE: A CLIMATOLOGICAL STUDY
Kathleen M. Traxler, Richard D. Arnold, John W. Louer, III, Michael T. Gifford, and Kenneth R. Gibson Jul. 1993 379 p Limited Reproducibility: More than 20% of this document may be affected by microfiche quality
(AD-A269200; USAFETAC/TN-93/004) Avail: CASI HC A17

This document presents a climatological study of Eastern Europe, a region that comprises Poland, the Czech Republic, Slovakia, Hungary, Romania, the former Yugoslavia, Albania, Greece, Latvia, Lithuania, Estonia, Belarus, Moldova, Ukraine, Azerbaijan, Armenia, Georgia, Turkey west of the Sea of Marmara, and also Russia, Kazakhstan, Uzbekistan, and Turkmenistan west of 60 deg E, including Novaya Zemyla. For this study, the entire region is divided into eight zones of climatic commonality. After describing the general geography of Eastern Europe, the study discusses major meteorological features of the entire region. Geography and the major climatic controls for each of the eight climatic commonality zones are then described. Finally, each season is defined and discussed in considerable detail, to include typical weather, clouds, visibility, winds, precipitation, temperature, and weather hazards. DTIC

N94-19051# Pacific Northwest Lab., Richland, WA.
SEASONAL VARIABILITY OF WIND ELECTRIC POTENTIAL IN THE US
M. N. Schwartz, D. L. Elliott, and G. L. Gower Jul. 1993 8 p Presented at the Windpower 1993, San Francisco, CA, 12-16 Jul. 1993
(Contract DE-AC06-76RL-01830)
(DE93-018182; PNL-SA-22090; CONF-930726-4) Avail: CASI HC A02/MF A01

Seasonal wind electric potential has been estimated for the contiguous United States based on the methods previously used to estimate the annual average wind electric potential. National maps show estimates of the seasonal wind electric potential averaged over the state as a whole, and gridded maps show the distribution of the seasonal wind electric potential within a state. The seasons of winter and spring have highest wind electric potential for most windy areas in the United States. Summer is the season with the least potential for most of the contiguous United States. Wind electric potential patterns in autumn generally resemble the annual average potential map. Excellent matches between seasonal wind electric potential and electric energy use occur during winter for the northern parts of the nation. California has a good match between summer wind potential and electric use. DOE

N94-19127# Pacific Northwest Lab., Richland, WA.
PANTEX PLANT METEOROLOGICAL MONITORING PROGRAM

S. F. Snyder Jul. 1993 34 p
(Contract DE-AC06-76RL-01830)
(DE93-018495; PNL-8744) Avail: CASI HC A03/MF A01

The current meteorological monitoring program of the US Department of Energy's Pantex Plant, Amarillo, Texas, is described in detail. Instrumentation, meteorological data collection and management, and program management are reviewed. In addition, primary contacts are noted for instrumentation, calibration, data processing, and alternative databases. The quality assurance steps implemented during each portion of the meteorological monitoring program are also indicated. DOE

N94-19298# Lawrence Livermore National Lab., CA.

TOWARD A HIGH PERFORMANCE DISTRIBUTED MEMORY CLIMATE MODEL

M. F. Wehner, J. J. Ambrosiano, J. C. Brown, W. P. Dannevik, P. G. Eltgroth, A. A. Mirin, J. D. Farrara (California Univ., Los Angeles.), C. C. Ma (California Univ., Los Angeles.), C. R. Mechoso (California Univ., Los Angeles.), and J. A. Spahr (California Univ., Los Angeles.) 15 Feb. 1993 14 p Presented at the 2nd International Symposium on High-Performance Distributed Computing, Spokane, WA, 20-23 Jul. 1993
(Contract W-7405-eng-48)
(DE93-019156; UCRL-JC-113039; CONF-9307111-2) Avail: CASI HC A03/MF A01

As part of a long range plan to develop a comprehensive climate systems modeling capability, the authors have taken the Atmospheric General Circulation Model originally developed by Arakawa and collaborators at UCLA and have recast it in a portable, parallel form. The code uses an explicit time-advance procedure on a staggered three-dimensional Eulerian mesh. The authors have implemented a two-dimensional latitude/longitude domain decomposition message passing strategy. Both dynamic memory management and interprocessor communication are handled with macro constructs that are preprocessed prior to compilation. The code can be moved about a variety of platforms, including massively parallel processors, workstation clusters, and vector processors, with a mere change of three parameters. Performance on the various platforms as well as issues associated with coupling different models for major components of the climate system are discussed. DOE

N94-19312# World Meteorological Organization, Geneva (Switzerland). World Climate Data and Monitoring Programme.

REPORT OF THE EXPERTS MEETING ON REFERENCE CLIMATOLOGICAL STATIONS (RCS) AND NATIONAL CLIMATE DATA CATALOGUES (NCC)

Jan. 1993 97 p Meeting held in Offenbach am Main, Germany, 25-27 Aug. 1992
(WMO-TD-535; WCDMP-23) Avail: CASI HC A05/MF A02; print copy available at WMO, Geneva, Switzerland

The Experts Meeting concerned Reference Climatological Stations and National Climate Data Catalogs within the framework of the World Climate Data and Monitoring Program (WCDMP). The meeting was held at the main building of Deutscher Wetterdienst (DWD) in Offenbach am Main, Germany during the period 25 to 27 August 1992 and was hosted by the CCl rapporteur on INFOCLIMA, Mr. Volker Vent-Schmidt. Author (revised)

N94-19503# Technische Univ., Hanover (Germany). Inst. fuer Meteorologie und Klimatologie.

SHAPE OF WIND GUSTS AT A 130m TOWER AT WILHELMSHAVEN (GERMANY) [BESTIMMUNG VON BOEEN GEMESSEN AN EINEM 130M-MAST BEI WILHELMSHAVEN]

G. Tetzlaff, K.-J. Schreiber, M. Kotzian, J. Rissmann, and E. Hollwurtel 1992 208 p In GERMAN
(Contract BMFT-0328787A)
(Ber-Band-B3; ISBN-3-92-362422-0; ETN-93-95096) Avail: CASI HC A10/MF A03

A tower equipped with wind sensors at different levels above the ground is described. The tower had a triangular cross section with a side length of 1 m; the length of the sensor carrying booms was slightly more than 3 m, thus minimizing the wake effects of the main body of the tower. The main sensors were three component propeller anemometers, tilted at an angle of 45 degrees into the main wind direction to avoid the stagnation sector of a vertically oriented propeller. Cup anemometers, wind vanes, and radiation shielded thermometers were installed. The data of the propeller anemometers were sampled at a rate of about 3 Hz. They served for online calculation of several coproducts as a basis for the computation of fluxes and stresses. The data of all sensors were processed into one hour average values of wind data and several derived quantities. Gusts were sampled by event triggering. The event trigger was set if a certain threshold was exceeded, either in the horizontal or vertical windspeed change. The main interest was concentrated on large gusts of more than 60 m vertical extension and with large changes of the wind speed, both horizontally and vertically. Closer analysis of these gusts gave shape and spatial distribution of the windspeed changes. A gust of more than 60 m size and more than 10 m/s(exp 2) wind speed change does occur with a probability of about 2 such events per year. ESA

N94-19616# Kernforschungszentrum G.m.b.H., Karlsruhe (Germany). Energie- und Stoffumsetzungen in der Umwelt.

INVESTIGATIONS OF A COHERENT VECTOR RADAR TECHNIQUE FOR THE OBSERVATION OF THE ATMOSPHERE NEAR 10 GHz Thesis - Karlsruhe Univ. [UNTERSUCHUNGEN EINES KOHAERENTEN VEKTORIELLEN RADARVERFAHRENS ZUR BEOBACHTUNG DER ATMOSPHAERE BEI 10 GHZ]

D. Graebe Dec. 1992 65 p In GERMAN
(KfK-5068; ETN-93-95078) Copyright Avail: CASI HC A04/MF A01

A radar measurement system built on the basis of a vector network analyzer and its capability are examined. The main feature of this system is the measurement technique, where the received signal is analyzed for magnitude and phase. The subsequent fast Fourier transformation provides the representation of the radar echo over the delay time. To characterize the system parameters a reference line was set up to a mast at a distance of approximately 700 m. First measurements show that static targets with small radar cross sections are detectable. For typically weather phenomena like clouds and rain the resolution limit are shown. Consequences for the design of future measurement systems are described. ESA

N94-19698 Royal Netherlands Meteorological Inst., De Bilt.

REPORTS OF THE 1992 SYNOPTIC SYMPOSIUM [HET SYNOPTISCH SYMPOSIUM 1992: DE VERSLAGEN]

H. G. Theihzen, ed. 1993 72 p In DUTCH Symposium held in 1992
(KNMI-TR-151; ISBN-9-03-692032-9; ETN-93-94536) Copyright Avail: Issuing Activity (Royal Netherlands Meteorological Inst., Postbus 201, 3730 AE De Bilt, Wilhelminalaan 10, Netherlands)

The meteorological model HIRLAM, the WAQUA/CSM-16 water level forecasting model, and the wave forecasting model NEDWAM are presented. The Organized Track System for the optimization of airways is presented. The treatment of calamities by the Royal Dutch Meteorological Institute is outlined. The Interactive Production Line for the introduction of innovative projects is presented. For individual titles, see N94-19699 through N94-19704.

N94-19699 Royal Netherlands Meteorological Inst., De Bilt.

HIRLAM [HIRLAM]

Gerard Cats, Toon Moene, Ben Wichers Schreur, Sylvia Barlag, Cisco deBruijn, Bert Holtslag, and Wim deRooy *In its* Reports of the 1992 Synoptic Symposium 1993 p 1-18 In DUTCH (For primary document see N94-19698 04-47)
Copyright Avail: Issuing Activity (Royal Netherlands Meteorological Inst., Postbus 201, 3730 AE De Bilt, Wilhelminalaan 10, Netherlands)

The model HIRLAM, a meteorological component of the Automatic Production Line (APL), which has a forecast period of between 24 and 36 hours, is presented. The emphasis of the discussion is on the aspects which are important for the operational system. The model and its implementation in the KNMI (Royal Dutch Meteorological Institute) are described. ESA

N94-19700 Royal Netherlands Meteorological Inst., De Bilt.

THE WAQUA/CSM-16 MODEL [HET WAQUA/CSM-16 MODEL]

Hans deVries *In its* Reports of the 1992 Synoptic Symposium 1993 p 19-31 In DUTCH (For primary document see N94-19698 04-47)
Copyright Avail: Issuing Activity (Royal Netherlands Meteorological Inst., Postbus 201, 3730 AE De Bilt, Wilhelminalaan 10, Netherlands)

The WAQUA/CSM-16 model for the forecasting of water levels at the Dutch coast is presented. The WAQUA system solves the nonlinear shallow water equations and calculates the astronomical tide as well as the meteorological effect on water levels and currents. The CSM-16 model covers the whole continental shelf. The parameters' topography and surface roughness are adjusted to represent the astronomical tide as well as possible. The wind drag coefficient is also treated as a parameter. A data assimilation scheme using a Kalman filter was introduced to compensate information errors. Suggestions for further developments are given. ESA

N94-19701 Royal Netherlands Meteorological Inst., De Bilt.
THE WAVE FORECASTING MODEL NEDWAM [GOLFVERWACHTINGSMODEL NEDWAM]
Evert Bouws *In its* Reports of the 1992 Synoptic Symposium 1993 p 32-43 In DUTCH (For primary document see N94-19698 04-47)
Copyright Avail: Issuing Activity (Royal Netherlands Meteorological Inst., Postbus 201, 3730 AE De Bilt, Wilhelminalaan 10, Netherlands)

The wave forecasting model NEDWAM, which is one of the modules of the Automatic Production Line (APL), is described. The operational characteristics of NEDWAM are outlined. A wave data assimilation scheme is being introduced, as well as an extension of the forecasting period to 96 hours. The effect of the wind fields provided by atmospheric models on the quality of wave forecasting is discussed. ESA

N94-19702 Royal Netherlands Meteorological Inst., De Bilt.
ORGANIZED TRACK SYSTEM: AIR WAYS ABOVE THE OCEAN [ORGANIZED TRACK SYSTEM, LUCHTWEGEN OVER DE OCEAAN]
G. R. daGraca *In its* Reports of the 1992 Synoptic Symposium 1993 p 44-53 In DUTCH (For primary document see N94-19698 04-47)
Copyright Avail: Issuing Activity (Royal Netherlands Meteorological Inst., Postbus 201, 3730 AE De Bilt, Wilhelminalaan 10, Netherlands)

The Organized Track System (OTS) for the optimization of airways above the Atlantic Ocean is presented. OTS determines an optimal set of air routes at both sides of the ocean by taking into account wind and temperature data and air traffic particularities. There is no radar escort, and aircraft have to fulfill the minimum navigation performance specifications. The interpretation of jet stream forecasting is discussed with a view to fuel consumption. ESA

N94-19703 Royal Netherlands Meteorological Inst., De Bilt.
CALAMITY WEATHER: ENVIRONMENTAL CALAMITIES AND METEOROLOGY [RAMPENWEER, OVER MILIEU CALAMITEITEN EN METEOROLOGIE]
Frank Kroonenberg *In its* Reports of the 1992 Synoptic Symposium 1993 p 54-59 In DUTCH (For primary document see N94-19698 04-47)
Copyright Avail: Issuing Activity (Royal Netherlands Meteorological Inst., Postbus 201, 3730 AE De Bilt, Wilhelminalaan 10, Netherlands)

The treatment of calamities by the KNMI (Royal Netherlands Meteorological Institute) is outlined. The KNMI is confronted with three types of calamities: calamities caused by meteorological circumstances; industrial calamities, the effects of which on public health are determined by meteorology; and other calamities for which meteorological circumstances in principle do not play a role. The calamity coordinator mainly has to deal with the second type of calamity. The demand from society and the societal relevance of the KNMI are growing. The meteorological aids at the disposal of the calamity meteorologist are outlined. ESA

N94-19704 Royal Netherlands Meteorological Inst., De Bilt.
INTERACTIVE PRODUCTION LINE (IPL) [INTERACTIEVE PRODUCTIE LIJN]
Dick Blaauboer *In its* Reports of the 1992 Synoptic Symposium 1993 p 60-68 In DUTCH (For primary document see N94-19698 04-47)
Copyright Avail: Issuing Activity (Royal Netherlands Meteorological Inst., Postbus 201, 3730 AE De Bilt, Wilhelminalaan 10, Netherlands)

The Master plan IPL for the introduction of innovative projects in the framework of the interactive production line at the KNMI (Royal Dutch Meteorological Institute) is presented. IPL contains all the processes in which the meteorologist is actively involved and in which expertise is combined with automatically produced forecasts. The availability of a large number of data and a number of aids are characteristic for interactive production processes. ESA

N94-19705# World Meteorological Organization, Geneva (Switzerland). World Climate Data and Monitoring Programme.
REPORT OF THE SECOND CLICOM EXPERTS MEETING
1992 101 p Meeting held in Washington, DC, 18-22 May 1992
(WCDMP-19; WMO-TD-511) Avail: CASI HC A06/MF A02; print copy available at WMO, Geneva, Switzerland

The Second CLICOM Experts Meeting was held in the headquarters of the National Weather Service in Silver Spring, MD, from 18-22 May, 1992. There were 16 experts in attendance from all the WMO Regions. The main issues of the meeting were to review the status of the CLICOM Project, discuss the issues related to new CLICOM software, and make recommendations for the future. Issues relating to the CLICOM software included installation and upgrade, data exchange, quality control, data archiving, local area networking, memory management, maintenance, and training. Derived from text

N94-19181*# Simpson Weather Associates, Inc., Charlottesville, VA.
SPNDL: A CONCEPT FOR A SMALL SATELLITE DOPPLER LIDAR WIND SOUNDER
G. D. Emmitt and M. M. Sokoloski (Science and Technology Corp., Washington, DC.) *In* NASA. Goddard Space Flight Center, The 1993 Shuttle Small Payloads Symposium Oct. 1993 p 179-191 (For primary document see N94-19162 04-12)
Avail: CASI HC A03/MF A03

48 OCEANOGRAPHY

Includes biological, dynamic, and physical oceanography; and marine resources.

For related information see also *43 Earth Resources and Remote Sensing.*

N94-17779# Lawrence Livermore National Lab., CA.
A ONE DIMENSIONAL NUMERICAL MODEL, WITH AN APPLICATION TO THE VERTICAL DISTRIBUTION OF DISSOLVED OXYGEN IN THE OCEAN
D. E. Eliason May 1993 25 p
(Contract W-7405-eng-48)
(DE93-018481; UCRL-MA-114027) Avail: CASI HC A03/MF A01

This manual describes the one dimensional model M1D, and its application to the vertical distribution of dissolved oxygen in the ocean. Section 2 describes the partial differential equation upon which the model is based, and the required boundary conditions. Section 3 gives the finite difference equations used to approximate the partial differential equations, and the scheme used for their solution. In Section 4, a linear stability analysis of the finite difference equations is given. Section 5 describes the program M1D that implements the solution of the finite difference equations. The program description is done from a programmer's point of view, especially with regard to parameters that control the simulation, location of variables on the grid, and the output file. A flow chart of the solution algorithm is also provided in this section. Section 6 presents some results of using the model to simulate the vertical distribution of oxygen in the ocean. Comparisons of model results to an analytical solution and to measured data from the North Eastern Tropical Pacific are given in this section. Finally, a summary and conclusions are presented in Section 7. DOE

N94-17822# Miami Univ., FL. Div. of Applied Marine Physics.
DESIGN OF A GENERAL PURPOSE AND AUTONOMOUS TRANSMITTER AND RECEIVER SYSTEM FOR UNDERWATER ACOUSTIC EXPERIMENTS AT SEA Final Report, 1 Oct. 1988 - 30 Sep. 1992
Hien Nguyen, Harry Deferrari, and Neil Williams 31 Aug. 1993 43 p
(Contract N00014-89-J-1356)
(AD-A269268) Avail: CASI HC A03/MF A01

A versatile multi-frequency, multi-purpose acoustic transmitter and receiver system has been developed and used to measure low frequency acoustic backscatter from the ocean wave surface. The instrumentation is general purpose in that all signal and sample parameters are selected by software and a variety of transmission, scattering, and reverberation experiments are possible without hardware modification. The system is

battery-powered and self-contained for remote and unattended operation for periods of months, depending upon the experimental parameters that affect power and tape consumption. The main features of the system are: a high powered broadband set of acoustic sources-with center frequencies of 100, 200, 400, and 800 Hz; programmable output signal types; a 64 element vertical hydrophone array; twenty gigabytes of data storage capacity; dynamically-tuneable band pass filters and variable sampling rates, high power microprocessors for in-situ signal processing; and independent subsystems for recording mooring depth and inclination. The system has been used in surface backscattering experiments at sea and results that demonstrate the capability of the system are presented and discussed.
DTIC

N94-17923 Royal Netherlands Meteorological Inst., De Bilt.
THE PERFORMANCE OF DRAG RELATIONS IN THE WAQUA STORM SURGE MODEL
J. R. N. Onvlee Jan. 1993 30 p
(Contract MAST-0050-C(PROFILE))
(KNMI-TR-149; ISBN-90-369-2030-2; ETN-93-94534) Copyright Avail: Royal Netherlands Meteorological Institute, P.O. Box 201, 3730 AE De Bilt, Wilhelminalaan 10, Netherlands

In most storm surge models, a drag relation is applied which parametrizes the wind induced surface stress in terms of wind velocity alone. In the WAQUA/CSM-16 model, used to predict water elevations along the Dutch North Sea coast, the wind stress was modeled until recently by the linear drag relation of Smith and Banke (1975). A number of alternatives to this relation have been suggested. For two of these, a piecewise continuous function provided by the Tidal Waters Division of Rijkswaterstaat and a Charnock drag formulation, the performance within the WAQUA system was evaluated and compared to that of the Smith and Banke function. Fore and hindcast analyses were made for all three drag relations for several periods of various types of weather, including four recent storms. Both the Charnock and Rijkswaterstaat drag relations represent a significant improvement over the Smith and Banke drag coefficient, particularly in the prediction and reconstruction of powerful surges during storm conditions. The Charnock and Rijkswaterstaat functions yield similar results for all weather types, the Charnock coefficient on average resulting in a slightly better agreement with observed surge levels; the standard deviation of the model errors is significantly smaller for the Charnock function. On the basis of these observations it is recommended that the Charnock drag formulation be implemented in the operational WAQUA system in the near future.
ESA

N94-18064# Institute of Oceanographic Sciences, Wormley (England). Deacon Lab.
SEASOAR AND CTD SECTIONS ACROSS THE ICELAND-FAEROES FRONT AND FAEROE SHETLAND CHANNEL, AUGUST 1990
J. T. Aleen, J. F. Read, S. G. Alderson, and H. Desai 1992 121 p
(IOS-295-1992; ETN-93-94558) Avail: CASI HC A06/MF A02

In Aug. 1990, RRS Charles Darwin Cruise 51 made two Conductivity/ Temperature/ Depth (CTD) and four SeaSoar sections across the inflow to the GIN Seas in addition to one large scale SeaSoar survey of the Iceland-Faeroes front, and three repeat fine scale SeaSoar surveys of a selected region of the front. Sections of temperature, salinity, and derived parameters including sound speed are presented. The data provide detailed information to identify water mass characteristics and indicate their relative locations. In addition, the SeaSoar surveys of the Iceland-Faeroes front present a time sequence in which the generation and development of meanders and eddies may be observed.
ESA

N94-18065# Institute of Oceanographic Sciences, Wormley (England). Deacon Lab.
CTD OXYGEN, TRACER AND NUTRIENT DATA FROM RRS CHARLES DARWIN CRUISES 58/59 IN THE NE ATLANTIC AS PART OF VIVALDI 1991
G. Griffiths, S. Cunningham, M. Griffiths, R. T. Pollard, H. Leach, S. Holley, R. Paylor, T. W. N. Haine, A. Rios, and S. G. Alderson et al 1992 49 p
(IOS-296-1992; ETN-93-94559) Avail: CASI HC A03/MF A01

CTD (Conducting/ Temperature/ Depth) and sample data recorded on Cruises 58 and 59 of RRS Charles Darwin are reported. The cruises were a trial of the Vivaldi concept of seasonal surveys of the north east Atlantic. The concept uses a combination of deep CTD stations spaced at 300 km with SeaSoar tows between to map the ocean over a wide area with high resolution in the upper layers where seasonal changes are important. Vivaldi forms part of the U.K. contributions to the World Ocean Circulation Experiment. Forty deep CTD stations were occupied using CTD with an oxygen sensor and a 24 bottle rosette sampler. A transmissometer and a fluorometer were also mounted on the package. Water samples were analyzed for dissolved oxygen, salinity, nitrate, silicate phosphate, chlorofluorocarbons (CFC-11, CFC-12 and CFC-113), chlorophyll-a, and, on Cruise 58, for alkanity and pH. Contoured sections of the CTD and water sample measurements are shown, with listings of all sample data and listings at selected depths of standard variables from the CTD stations. Instrument calibrations are also reported and the quality of data is discussed.
ESA

N94-18066# Institute of Oceanographic Sciences, Wormley (England). Deacon Lab.
SEASOAR CTD, FLUORESCENCE AND SCALAR IRRADIANCE DATA FROM RRS CHARLES DARWIN CRUISES 58/59, NE ATLANTIC, VIVALDI 1991
S. A. Cunningham, M. J. Griffiths, S. G. Alderson, G. Griffiths, R. T. Pollard, J. C. Donlan, P. Lancaster, H. Leach, R. K. Lowry, and M. W. Stirling et al 1992 46 p
(IOS-299-1992; ETN-93-94562) Avail: CASI HC A03/MF A01

SeaSoar data from RRS Charles Darwin Cruise 58 and 59 (24 Apr. - 9 Jun. 1991) are reported. Data were collected on the northeast Atlantic between 39 to 54 deg north, 11 to 34 deg west. With the aid of a new winch, SeaSoar undulated between the surface and 500 m every 2.5 km, measuring Conductivity/ Temperature/ Depth (CTD) data with a double conductivity cell CTD unit. Chlorophyll 'a' and scalar irradiance were also measured. Six meridional legs, four degrees apart, were surveyed. The western four legs were 1500 km long and the others 900 km and 600 km. The legs were surveyed in three degree sections between full depth CTD casts. The meridional legs were joined by seven zonal sections. Processing and calibration of the data are described and the data are presented as contoured sections. Variables contoured against pressure are potential temperature, salinity, sigma0, sound velocity, scalar irradiance, and cholorophyll. Temperature and salinity are also contoured against sigma0. The aims of Vivaldi are to calculate seasonal upper ocean heat and fresh water budgets, map isopycnic potential vorticity variations from the subtropical gyre to the subpolar gyre, map interannual changes in the properties of water masses formed by deep convection, calculate statistics of upper ocean parameters and air sea fluxes, and to investigate the role of eddies.
ESA

N94-18215 Army Engineer Waterways Experiment Station, Vicksburg, MS.
TECHNOLOGIES FOR ASSESSING THE GEOLOGIC AND GEOMORPHIC HISTORY OF COASTS Final Report
Andrew Morang, Joann Mossa, and Robert J. Larson Mar. 1993 175 p
Limited Reproducibility: More than 20% of this document may be affected by microfiche quality
(AD-A268780; CERC-93-5) Avail: CASI HC A08

The geologic and geomorphic history of coastal areas can be assessed using a four-part process: thorough examination of technical literature and existing data from various archives; field data collection and observation; laboratory examination of samples collected in the field; and office interpretation of all project data, both newly collected and historic. It is vital that existing sources of data be evaluated before field studies are undertaken to prevent duplicating efforts and to guide the optimum sampling scheme. Field studies must be designed to answer basic questions about the study area: What physical processes affect the region? Does the underlying geology have a major influence? How has man modified or damaged the local environment? How much data can we afford to collect? Do we have the knowledge, ability, managerial skill, or money to properly analyze the data we want to collect at the project site? Is it more important to conduct a long-term sampling program or a shorter, more intensive program? Coastal scientists must be aware of how historic data were collected and what assumptions and procedures were used by the original field technicians and analysts. The quality of historic data may vary from excellent to worse than useless. The use of instruments in the coastal zone is far from straightforward; incorrect use of instruments may lead to erroneous results because the wrong parameters may be monitored. Coastal engineers are urged to consult specialists in the field to help plan and conduct field studies. The analysis of contemporary coastal data is difficult and also requires the skills of specialists with experience in the particular types of instruments and methods that have been used. DTIC

N94-18230# North Carolina Univ., Chapel Hill. Marine Sciences.
SYNOPTIC OCEAN PREDICTION EXPERIMENT. EN216 CTD SECTION DATA REPORT Summary Report, 29 Aug. - 1 Sep. 1990
Dana K. Savidge, Thomas J. Shay, and John M. Bane, Jr. Mar. 1993 21 p
(Contracts N00014-90-J-1596; N00014-90-J-1568; NSF OCE-87-17141; NSF OCE-87-17144)
(AD-A268903; CMS-93-1) Avail: CASI HC A03/MF A01

A CTD section was taken across the Gulf Stream during late Aug. 1990, approximately 100 km downstream from Cape Hatteras. The work was done from the R/V Endeavor during the third leg of cruise EN216, which was part of the Synoptic Ocean Prediction (SYNOP) program. The section consisted of 12 stations located along a line from 34 deg 50 min N, 73 deg 10 min W to 35 deg 57.23 min N, 74 deg 43.14 min W, spaced 8 to 30 km apart. The Seabird Sealogger utilized was equipped with conductivity, temperature, pressure, and oxygen sensors. Nominal drop speed was 0.5-1.0 m/s, with a sampling rate of 1 Hz. This report discusses the acquisition and processing of the CTD data obtained along this section. In addition, plots of potential temperature vs. salinity, salinity vs. pressure, potential temperature vs. pressure, and oxygen vs. pressure are shown for each station. Vertical sections of salinity, potential temperature, density, and oxygen are also presented. DTIC

N94-18277# Environmental Research Inst. of Michigan, Ann Arbor.
ARCTIC ICE STUDIES Final Report, Dec. 1982 - Jun. 1991
R. A. Shuchman, R. G. Onstott, and C. C. Wackerman Feb. 1993 327 p
(Contract N00014-81-C-0295)
(AD-A268608; ERIM-154600-63-F) Avail: CASI HC A15/MF A03

This report consists of a collection of journal articles and conference proceedings covering a decade of research into synthetic aperture radar (SAR) remote sensing of the Arctic regions. Four main areas are covered: (1) Data collections and SAR imaging generation; (2) Geophysical parameter estimation; (3) Sensor intercomparison; and (4) Algorithm development. DTIC

N94-18329# Materials Research Labs., Ascot Vale (Australia).
AN ATLAS OF BATHY-THERMOGRAPH TEMPERATURE CROSS-SECTIONS FOR CORAL AND TASMAN SEA TRANSECTS FROM 1960 TO 1987
L. J. Hamilton Apr. 1993 32 p
(AD-A268775; MRL-TN-620; DODA-AR-008-219) Avail: CASI HC A03/MF A01

An atlas of 190 temperature cross-sections is presented for the Tasman and Coral Seas for 1960 to 1987. The sections were constructed from bathy-thermograph (BT) temperature profiles obtained by ships on routes between Australia, New Zealand, and Fiji in the region 20-50 S, 150-180 E. About 150 sections lie on six major routes, e.g. 50 sections are available from Sydney to New Zealand along 34 S, and 40 sections from Sydney to Fiji. Depth of sections is nominally 450 m. The sections provide the background for an examination of Tasman and Coral Sea surface flow and temperature structure presented elsewhere. Data were obtained from the Australian Oceanographic Data Center. DTIC

N94-18393# University of Southern Mississippi, Long Beach.
COASTAL OCEAN MODELING WORKSHOP
Scott Dinnel, Kenneth Matulewski, and Robert Williems Jun. 1993 123 p Workshop held in Long Beach, MS, 23-24 Mar. 1993
(AD-A268955; TR-2/93) Avail: CASI HC A06/MF A02

The recent changes in global politics that we all have experienced have also led to a rethinking of naval strategy. This strategy has been summarized in the White Paper '...From the Sea'. The primary message of this new policy is that the Navy will refocus from deep water operations to coastal and over-the-shore operations. The goal of the Coastal Ocean Modeling Workshop is to review ongoing work in light of this changing strategy and to recommend a program that is responsive to these changes. In doing so, the aim is to assure that the objectives of the Navy Ocean Modeling and Prediction Program are in line with Navy/Marine Corps operational needs for environmental products and that modeling efforts yield products that are optimized for rapid implementation into operational environments. DTIC

N94-18414 Coastal Engineering Research Center, Vicksburg, MS.
WIND PRODUCTS FOR USE IN COASTAL WAVE AND SURGE MODELS Final Report
Zeki Demirbilek, Steven M. Bratos, and Edward F. Thompson Aug. 1993 136 p Limited Reproducibility: More than 20% of this document may be affected by microfiche quality
(AD-A269753; CERC-MP-93-7) Avail: CASI HC A07

Winds over the ocean surface are the essential driving force in creating waves. Winds also have important effects on currents and nearshore water levels. Wind information is often used within the Corps of Engineers (CE) as input to numerical models of waves, storm surges, and circulation. The National Oceanic and Atmospheric Administration (NOAA) and the U.S. Navy routinely produce global wind information. Recent advances in atmospheric modeling capabilities and operational numerical models, particularly within the Navy, have made available new and improved products applicable to CE hydrodynamic modeling. Available products from NOAA and the Navy are described including both climatological archives and real time forecasting products. Interfaces to assist CE users in obtaining and using the Navy products are presented. Sources of surface wind (10-m elevation) information of greatest potential value for CE modeling are evaluated using the wave model WISWAVE and NOAA National Data Buoy Center measurements along the U.S. Atlantic coast. Necessary tools are provided and recommendations are given for further evaluation and use of Navy wind information in future modeling efforts. DTIC

N94-18455# Coastal Engineering Research Center, Vicksburg, MS.
ADCIRC: AN ADVANCED THREE-DIMENSIONAL CIRCULATION MODEL FOR SHELVES, COASTS, AND ESTUARIES. REPORT 3: DEVELOPMENT OF A TIDAL CONSTITUENT DATABASE FOR THE WESTERN NORTH ATLANTIC AND GULF OF MEXICO
J. J. Westerink (Notre Dame Univ., IN.), R. A. Luettich, Jr. (North Carolina Univ., Chapel Hill.), and Norman Scheffner Jun. 1993 151 p
(AD-A268685; CERC-TR-92-6) Avail: CASI HC A08/MF A02

This report describes the application of model ADCIRC-2DDI, a two-dimensional, depth-integrated, finite-element-based hydrodynamic circulation code, to the western North Atlantic, Gulf of Mexico, and Caribbean Sea in order to develop a tidal constituent database. Issues that are emphasized in the development of the Western North Atlantic Tidal (WNAT) model include the definition of hydrodynamically simple open ocean boundaries; the use of large domains; the importance of a high degree of grid resolution in coastal regions; and the use of finite element meshes with highly varying nodal densities in order to minimize the size of the discrete problem. The development of an optimal graded finite element mesh is based on regular and graded grid convergence studies using an M2 tidal forcing function on the boundary and within the domain. The optimal graded mesh is then forced for eight diurnal and semidiurnal astronomical tidal constituents (K1, O1, Pl, Ql, M2, S2, N2, and K2) on the open ocean boundary by coupling to Schwiderski's global model results as well as within the interior domain using a tidal potential forcing function. The structure of the various tides is examined and results are compared to field data at 77 stations. DTIC

N94-18494# Brookhaven National Lab., Upton, NY.
OVERVIEW OF PHYSICAL OCEANOGRAPHIC MEASUREMENTS TAKEN DURING THE MOUNT MITCHELL CRUISE TO ROPME SEA AREA
R. M. Reynolds 31 Mar. 1993 61 p Presented at the 1st Scientific Workshop on Results of the R/V Mount Mitchell Cruise, Kuwait City, Kuwait, 24-28 Jan. 1993
(Contract DE-AC05-84OR-21400)
(DE93-018460; BNL-49194; CONF-9301123-1) Avail: CASI HC A04/MF A01

The ROPME Sea Area (RSA) is one of the most important commercial waterways in the world. However, the number of direct oceanographic observations is small. An international program to study the effect of the Iraqi oil spill on the environment was sponsored by the ROPME, the

Intergovernmental Oceanographic Commission, and the National Oceanic and Atmospheric Administration (NOAA). DOE

N94-18600# Woods Hole Oceanographic Inst., MA.
THREE-DIMENSIONAL HIGH-RESOLUTION SEISMIC PROFILING ON THE NEW JERSEY OUTER CONTINENTAL SHELF Final Technical Report
John D. Milliman 1993 2 p
(Contract N00014-89-K-0148)
(AD-A269835) Avail: CASI HC A01/MF A01

Previous work using the Huntec Deep-Towed Seismic (DTS) system off New Jersey (1987) identified a thick sequence of late Pleistocene sediments on the outer continental shelf. It was suggested that these sediments were deposited by several major melt events during the late Wisconsin glaciation. The physical nature of the sediments, their stratigraphic relation with acoustic stratigraphy and the fine-scale variations of both reflectors and topographic character, however, can be defined only through sediment coring and closely spaced high-resolution profiling. The purpose of this project was to obtain a series of vibrocores to determine the stratigraphic and sedimentologic character of the sediments and to obtain digital data that would allow us to gain a three-dimensional understanding of the shallow structure on the sedimentary sequences in the area. DTIC

N94-18662 Scripps Institution of Oceanography, La Jolla, CA. Marine Physical Lab.
PROCESSING AND ANALYSIS OF SeaMARC 2 DATA: FIEBERLING GUYOT; RAW PHASE EXPERIMENT IN NORWEGIAN-GREENLAND SEA Final Report, 1 Oct. 1990 - 30 Sep. 1992
C. DeMoustier and P. F. Lonsdale Apr. 1993 6 p Limited Reproducibility: More than 20% of this document may be affected by microfiche quality
(Contract N00014-91-J-1073)
(AD-A269930; MPL-U-16/93) Avail: CASI HC A02

The objectives of this work were to devise processing techniques for acoustic measurements made with bathymetric sidescan sonar systems and to apply them to data collected with the SeaMARC II system. The main goals were to provide end-users with co-registered acoustic imagery and bathymetry displayed in a geographic reference frame with a minimum of artifacts and with improved contrast or feature definition, while retaining as much as possible the relative acoustic backscatter contrast due to the geology of the area. DTIC

N94-18663# Scripps Institution of Oceanography, La Jolla, CA. Marine Physical Lab.
CONSTRAINTS ON CRUSTAL STRUCTURE FROM LONG PERIOD PRESSURE AND DISPLACEMENT MEASUREMENTS ON THE DEEP SEAFLOOR Final Report, 1 Oct. 1990 - 30 Sep. 1992
Spahr C. Webb Apr. 1993 8 p
(Contract N00014-91-J-1088)
(AD-A269931; MPL-U-22/93) Avail: CASI HC A02/MF A01

Accurate estimates of seafloor shear and compressional velocities are essential for modelling long range acoustic propagation within the ocean. Compressional wave velocities have been measured using seismic refraction techniques for decades, however shallow seafloor structure is poorly resolved with sources and receivers located near the sea surface. Shear velocity is poorly known at all depths; since the ocean does not support shear propagation, only converted waves are observable at the sea surface. At MPL we have developed instrumentation capable of measuring the very small seafloor deformations resulting from very low frequency surface gravity waves (infragravity waves). By measuring a number of sites we will study the elastic changes associated with aging of the oceanic crust. We investigated the inverse problem associated with this technique which allows a quantitative connection between measured seafloor transfer functions and the elastic properties of the shallow crust. DTIC

N94-18665# University of Southern Mississippi, Bay Saint Louis. Center for Ocean and Atmospheric Modeling.
PREPARATION OF DATA ASSIMILATION AND MODEL EVALUATION EXPERIMENT DATA SETS
C. A. Lai and Wen Qian Aug. 1993 145 p
(Contract N00014-92-J-4112)
(AD-A269996; TR-1/94) Avail: CASI HC A07/MF A02

The goal of DAMEE is briefly stated because it provides the rationale for the experiment plan which decides the data need for the four phases of the experiment. The preparation of the DAMEE data set consisted of a series of processes: (1) collection of observational data; (2) analysis and interpretation; (3) interpolation, using the Optimum Thermal Interpolation System (OTIS) package; (4) quality control and re-analysis; and (5) data archiving and software documentation. The data products from these processes included a time series of 3-D fields of temperature and salinity, 2-D fields of surface dynamic height, 2-D bogus information of the Gulf Stream and rings system and XBT profiles. To date, they are the most detailed and high-quality data for mesoscale modeling, data assimilation, and forecasting research. Feedback from ocean modeling groups who tested them were incorporated into the refinement of data. It is intended to make this data set easy to access. An ideal way is to put it into a few CD-ROM's. Suggestions for DAMEE data usage include the following: (1) ocean modeling and data assimilation; (2) diagnosis and theoretical studies; and (3) comparisons with locally detailed observations, such as those in the SYNOP project to guide field programs. DTIC

N94-18685# Florida Inst. of Tech., Melbourne.
FULL BOLTZMANN DISCRETE SPECTRAL WAVE MODEL, IMPLEMENTATION AND NONDIMENSIONAL TESTS Final Report
Donald T. Resio Aug. 1993 52 p
(AD-A269885; CERC-93-1) Avail: CASI HC A04/MF A01

A full Boltzmann integration scheme is implemented within a functioning discrete spectral wave model. Preliminary testing (academic) is presented and compared to alternate solution methods. It is found that third-generation models depend on a detailed balance among source terms, and it is important that these source terms be specified accurately. In the present state of the art, information on all of the source terms does not appear to be sufficient to permit definitive estimates of all source terms in the detailed balance evaluations. Older means of estimating the nonlinear wave-wave interaction (Sn1) are much less accurate than the full Boltzmann method. Even the Discrete Interaction Approximation (WAMDIG 1988) representation for Sn1, used in the only documented third-generation wave model (WAM), is shown incapable of providing an accurate estimate of Sn1. The full Boltzmann model should provide an improved method to investigate several important wave generation and decay situations. The WAM source terms are inconsistent with observed wave-growth laws and equilibrium-range behavior from the Joint North Sea Wave Project (Hasselmann et al. 1973). New source terms postulated in this report provide a very good match to the JONSWAP wave growth rates and equilibrium-range behavior. The present version of the full Boltzmann model should be regarded as a research tool. It is a very new model and, as such, will need to undergo considerable additional testing over several years before it could be considered as a viable option for an operational model. DTIC

N94-18723# Coastal Engineering Research Center, Vicksburg, MS.
DYNLET1 MODEL FORMULATION AND USER'S GUIDE Final Report
Mary A. Cialone and Michael Amein (Civil Analysis Group, Inc., Raleigh, NC.) Aug. 1993 62 p
(AD-A269843; CERC-93-3) Avail: CASI HC A04/MF A01

A state-of-the-art design-level model for predicting tide-dominated velocities and water level fluctuations at an inlet and interior back-bay system and detailed instruction in use of the model are presented. The model solves the full one-dimensional (1-D) shallow-water equations employing an implicit finite-difference technique. The model is named DYNLET1, reflecting the fact that it is a 1-D model of the dynamic (time-dependent) behavior of the tidal flow at inlets. The DYNLET1 numerical model was originally developed by Dr. Michael Amein, Civil Analysis Group, Inc., Raleigh, North Carolina, under contract to the U.S. Army Engineer Waterways Experiment Station (WES) Coastal Engineering Research Center (CERC). The model is capable of simulating 1-D fluid flow from the ocean through a tidal inlet, into back-bay regions, and up tributaries. An important feature of the model is the ability to represent an accurate flow distribution across any cross section, given the inherent limitations of a 1-D model. DYNLET1 has a rigorous theoretical foundation, is numerically implemented in a sound manner, and is capable of describing realistic situations. It provides detailed velocity information across the inlet channels, is able to describe multi-channel inlets, and importantly, is easy to operate on a personal computer. The model can be used for design-level studies for most inlets by providing reliable and accurate answers while requiring minimal modeling expertise, data entry, and numerical grid generation. DTIC

N94-18727# Naval Research Lab., Bay Saint Louis, MS.
ATLAS OF SSM/I SATELLITE ICE CONCENTRATION INTERPOLATED TO OPERATIONAL ICE MODEL DOMAINS OF THE ARCTIC FOR 1992 Final Report
G. N. Lundeen, R. H. Preller, P. G. Posey, and A. Cheng Sep. 1993 320 p
(AD-A270306; NRL/MR/7322-93-7064) Avail: CASI HC A14/MF A03

The Navy's Polar Ice Prediction System, which is run daily at the Fleet Numerical Oceanography Center (FNOC), is initialized once a week from ice concentration data derived by the Navy/National Oceanic and Atmospheric Administration Joint Ice Center. Ice concentration data, derived by applying the U.S. Navy's algorithm to the Defense Meteorological Satellite Program Special Sensor Microwave Imager (SSI) data, have been collected from FNOC on a daily basis and archived at the Naval Research Laboratory. These data were interpolated to the operational ice model grids for possible use as real-time daily update to the operational forecast systems. Collection of data with coverage from the Pole southward to 400 N latitude allows for the observation of ice concentrations for the entire Arctic region and surrounding coastal seas. SSM/I ice concentration data from 1992 are presented for each available day and on each of the operational model grids. DTIC

N94-18819*# Saint Vincent Coll., Latrobe, PA.
MODIFICATIONS OF AIRBORNE OCEANOGRAPHIC LIDAR FOR THE LONG RANGE P-3 MISSIONS Final Report, 1 Mar. 1992 - 30 Sep. 1993
Richard E. Berry 1993 4 p
(Grant NAG5-689)
(NASA-CR-194682; NAS 1.26:194682) Avail: CASI HC A01/MF A01

This has been an extraordinary series of Airborne Oceanographic Lidar (AOL) missions. The AOL was flown over the North Pole on three low altitude sea ice mapping flights. These flights were followed by six Joint Global Ocean Flux Study (JGOFS) flights based from Hawaii and Christmas Island to measure chlorophyll along the equator. On return to the west coast, there were several terrain mapping flights in Nevada and Arizona. This was followed by mapping of the Greenland ice cap from the airport at Sondresstrom Greenland. This research proposal was developed to support the AOL instrumentation research that prepares the AOL for each science mission. Saint Vincent College physics professor, Dr. Richard Berry, is engaged in LIDAR instrumentation research to improve the AOL. Dr. Berry's participation in the AOL mission was to implement the instrumentation modifications that optimized data acquisition. Derived from text

N94-18903 Naval Research Lab., Bay Saint Louis, MS.
ESTIMATING THE OCEANIC SOUND SPEED ENVIRONMENTAL FOR LONG-RANGE ACOUSTIC PROPAGATION Final Report
Janice D. Boyd Aug. 1993 91 p Limited Reproducibility: More than 20% of this document may be affected by microfiche quality
(AD-A270231; NRL/MR/7332-93-7068) Avail: CASI HC A05

The High Gain Initiative (HGI) Program was established in 1987 as a focused Block Program of the office of Naval Technology (now part of the Office of Naval Research). One of its objectives was to investigate the oceanic environment and its effects on long-range sound transmission. One potential important factor was identified as imprecise knowledge of the oceanic sound speed field. Substantial Program resources were therefore invested in devising and executing sound speed measurement programs for two major field experiments, VAST (Various Acoustic Systems Tests) and MDA (Multi-Dimensional Array), which took place in 1989 in the Northeast Pacific and in 1991 in the western Subtropical Atlantic, respectively. This document reviews available oceanic sound speed measurement techniques, describes the combinations of techniques and strategies that made up each experiment's measurement plan, summarizes the results and the sound speed environment during each experiment, and evaluates what the work has revealed to date about sound speed uncertainties and long-range sound transmission. DTIC

N94-18910 Defence Research Establishment Atlantic, Dartmouth (Nova Scotia).
BACKSCATTER.FOR: A PROGRAM TO CALCULATE THE BACKSCATTERING STRENGTH OF AN INHOMOGENEOUS SEABED
Aug. 1993 23 p Limited Reproducibility: More than 20% of this document may be affected by microfiche quality
(AD-A269235; DREA-TC-93/306) Avail: CASI HC A03

The author has previously reported on a theoretical model for acoustic backscattering from an inhomogeneous volume beneath a smooth water/sediment interface. In spite of the good agreement between model and data obtained by the author, the model's complexity somewhat undermines its usefulness to other users. To alleviate this drawback, a user's manual for the FORTRAN 77 code developed by the author to evaluate the model is presented in this paper. To assist potential users of the software, the interpretation of the model in terms of the FORTRAN 77 code employed is explained and a sample run is presented. DTIC

N94-19063# National Oceanic and Atmospheric Administration, Seattle, WA. Pacific Marine Environmental Lab.
METHOD FOR EXTRACTING TIDAL AND INERTIAL MOTION FROM ARGOS ICE BUOYS APPLIED TO THE BARENTS SEA DURING CEAREX
P. Turet (Washington Univ., Seattle.), C. H. Pease, R. S. Pritchard (IceCasting, Inc., Seattle, WA.), and J. E. Overland Apr. 1993 69 p
(PB93-190213; NOAA-TM-ERL-PMEL-99) Avail: CASI HC A04/MF A01

A harmonic analysis of tidal and inertial motion was applied to observations of position of ARGOS buoys deployed on drifting multiyear sea ice in the Eastern Arctic-Barents Sea during CEAREX (1988-89). An ARGOS positioning-data screening protocol was developed and constructed using a constrained least squares algorithm for separate estimation of tidal and inertial currents. The analysis provided estimates of individual tidal components at 15-day intervals along the sea ice buoy drift tracks. The technique shows a reasonable qualitative distinction in current components at nearby semi-diurnal frequencies. Estimates of errors due to sampling and collinearity are derived directly from model statistics. Estimates of velocity produced from the unequally time-based data are then used for interpolation to a regular time grid for spectral analysis. Computed velocities (up to 70 cm/s for M(2) tidal motion over Spitsbergen Bank southeast of Svalbard) are in close agreement with the regional tidal model of Gjevik, et al. (1990, 1993). NTIS

N94-19580 Massachusetts Inst. of Tech., Cambridge. Dept. of Ocean Engineering.
ACOUSTIC TRAVEL TIME PERTURBATIONS DUE TO AN INTERNAL TIDE AND INTERNAL WAVE FIELD IN THE BARENTS SEA M.S. Thesis
Douglas S. Ray Aug. 1993 73 p Limited Reproducibility: More than 20% of this document may be affected by microfiche quality
(Contract N00123-89-G-0580)
(AD-A270879) Avail: CASI HC A04

Travel time perturbations of adiabatic normal modes due to an internal tide and internal mode field in the Barents Sea are examined. A formalism for the travel time perturbation due to a change in sound speed is presented. Internal tide and internal wave amplitude spectra are calculated from Brancker temperature loggers which were deployed on moorings in the Barents Sea during the August 1992 Barents Sea Polar Front Experiment. In particular, the first three internal wave mode amplitudes are estimated from the four Brancker temperature loggers on the southwest mooring of the array. Modal perturbations in acoustic pulse travel time and the travel time covariance are calculated and compared for consistency to a simple ray model. These perturbations are small for the modal arrivals that the vertical acoustic array which was deployed is expected to resolve. The third internal wave mode has the largest impact on the acoustic arrivals, per unit amplitude, but the first internal wave mode dominates the scattering due to having a much larger amplitude overall. DTIC

N94-19609# Naval Research Lab., Washington, DC.
MODELING OF CURRENT FEATURES IN GULF STREAM SAR IMAGERY Interim Report
Robert W. Jansen, Scott R. Chubb, Robert A. Fusina, and Gasper R. Valenzuela 13 Sep. 1993 57 p
(AD-A270734; NRL/MR/7234-93-7401) Avail: CASI HC A04/MF A01

The theoretical formulation, numerical implementation, and testing of NRL's recently developed time-dependent ocean wave model (NTOW) is described. The propagation of the wave field is computed via the action density conservation equation for general time varying currents, winds, and bathymetry. The NTOW model is used to predict wave-current interaction effects in a region of strong surface convergence near the edge of the Gulf Stream off Cape Hatteras. The computed wave field is used in conjunction with a composite scattering radar model to derive radar imagery. Our radar predictions are compared with real aperture radar data collected during the NRL high-resolution remote sensing experiment. DTIC

N94-19727# Woods Hole Oceanographic Inst., MA.
ANALYSIS OF DATA FROM COLUMBIA POINT ARENA OCEAN-BOTTOM SEISMIC STATION (OBSS) Final Technical Report
G. M. Purdy and G. H. Sutton 1993 9 p
(Contract N00014-90-J-1916)
(AD-A271263) Avail: CASI HC A02/MF A01

This research was the continuation and conclusion of research conducted through FY 89 by G. H. Sutton and others at Rondout Associates, Inc., Stone Ridge, NY and was part of the ULF/VLF ARI to understand the ambient acoustic/seismic noisefield in the ocean as a function of location and time in the ULF (0.001 to 1Hz) and VLF (1 to 50 Hz) frequency band. The objectives of this Grant were to analyze and interpret data from the Columbia Point Arena ocean bottom seismic station (OBSS); to compare the data with available source information; and to compare the OBSS data with concurrent data from continental arrays. DTIC

N94-19743# Massachusetts Univ., Amherst. Dept. of Electrical and Computer Engineering.
THEORETICAL AND EXPERIMENTAL RESEARCH ON COHERENT MICROWAVE BACKSCATTER FROM THE OCEAN Final Report
Robert E. McIntosh 1993 6 p
(Contract N00014-88-K-0443)
(AD-A271276) Avail: CASI HC A02/MF A01

The goal of this document is the development of frequency and polarization diverse radars to measure coherent backscatter of microwave signals from the ocean surface to better understand the effects of surface motion on synthetic aperture radar (SAR) images. DTIC

N94-19745# Naval Research Lab., Bay Saint Louis, MS.
FAULTED STRUCTURE OF THE BOTTOM SIMULATING REFLECTOR ON THE BLAKE RIDGE, WESTERN NORTH ATLANTIC Final Report
M. M. Rowe and J. F. Gettrust Sep. 1993 5 p Repr. from Geology, v. 21, Sep. 1993 p 833-836
(AD-A271289; NRL/JA/7321-93-0008) Avail: CASI HC A01/MF A01

High-resolution multichannel seismic data collected from the Blake Ridge in the western North Atlantic by the Naval Research Laboratory's Deep Towed Acoustics/Geophysics System (DTAGS) show that the bottom simulating reflector (BSR) in this area is the reflection from the interface between an approximately 440-m-thick section of hydrate bearing sediment overlying an approximately 5-m-thick layer of methane gas-rich sediment. The high resolution attainable by the deep-tow seismic system reveals normal fault offsets of approximately 20 m in the BSR. These growth faults may provide a path for vertical migration of methane initially concentrated beneath the hydrate-bearing sediment, enabling hydrate to form throughout sediment above the BSR. Because the BSR represents a methane gas/methane hydrate phase boundary rather than a lithologic or diagenetic horizon, the observed off-set of the BSR itself reflects discontinuities in the pressure-temperature field across the fault zones where they intersect the BSR. DTIC

N94-19747 Woods Hole Oceanographic Inst., MA.
SEISMIC STUDIES OF THE GEOLOGIC STRUCTURE AND PHYSICAL PROPERTIES OF THE SEABED Final Report
John I. Ewing 4 Oct. 1993 4 p Limited Reproducibility: More than 20% of this document may be affected by microfiche quality
(Contract N00014-90-J-1817)
(AD-A270895) Avail: CASI HC A01

The purpose of these studies are the following: to determine the physical parameters that most affect low frequency acoustic propagation in shallow water areas where elastic and acoustics waves interact intimately; to develop instrumentation, field procedures, and data inversion methods for accurate measurement of shear wave speed and attenuation as functions of frequency, depth, and locations in the seabed; and to determine the effects of anisotropy and other inhomogeneities created by sedimentary processes. DTIC

N94-19762 Naval Command, Control and Ocean Surveillance Center, San Diego, CA.
MARINE-MODIFIED LOWTRAN: THE CONTRIBUTION OF SUN GLINT Final Technical Report
C. R. Zeisse Jun. 1993 48 p Limited Reproducibility: More than 20% of this document may be affected by microfiche quality
(AD-A269547; NRAD-TR-1611) Avail: CASI HC A03

Sun glint was added to the Atmospheric Transmittance/Radiance Computer Code LOWTRAN 6 in order to provide a more realistic representation of the infrared marine environment. The modified model's results were compared with infrared data that were taken at 3-5 microns over the open ocean during different solar elevations and wind speed conditions. A significant glint contribution was obtained at 1450 PDT on 10 October 1991. At this time, a close match between the shape of the predicted and observed radiance values in the sky and sea was noted. The absolute value of the predicted and observed radiances differed, however, by a large constant with an equivalent blackbody temperature of approximately 5 C. It was speculated that the origin of this additional radiance may be multiple scattering of solar radiation. DTIC

N94-19785# Naval Undersea Warfare Center, Newport, RI.
A REGISTER OF UNDERWATER ACOUSTIC TEST FACILITIES IN THE US, CANADA, AND THE UNITED KINGDOM
C. A. Ledoux 1 Apr. 1993 61 p
(AD-A270884; NUWC-NPt-TD-10184) Avail: CASI HC A04/MF A01

This document provides a register of underwater acoustic facilities in the United States, Canada, and the United Kingdom. The data included in the register were derived from information received from 25 of the 57 organizations contacted. An active search of the United Kingdom facilities was not conducted because those organizations were previously listed in a register of Western Europe facilities. DTIC

N94-19786# Naval Research Lab., Washington, DC.
MEASUREMENTS OF OCEAN SURFACE AND BOTTOM BACKSCATTERING STRENGTHS IN THE NORTHWESTERN ATLANTIC OCEAN Final Report
Nolan R. Davis, Joseph Jeffrey, and Fred T. Erskine 8 Oct. 1993 59 p
(DA Proj. R03-5-B-03)
(AD-A270893; NRL/FR/7142-93-9570) Avail: CASI HC A04/MF A01

Experimental measurements of ocean surface and bottom backscattering strengths were carried out in the northwestern Atlantic Ocean during Jul. and Aug. 1990. The experiment used ship and air deployed explosive charges to provide ensonification of the ocean surface and bottom over a range of low frequencies up to 1 kHz. Overall, the surface backscatter results agreed well with the Ogden-Erskine curves, matching the predicted dependence on wind speed, grazing angle, and frequency. At two sites northeast of the Grand Banks, the surface backscattering strengths appeared to be dominated by volume backscattering caused by fish. The bottom backscattering strengths were observed to have considerable variation in level (up to 17 dB) between different sites. As a function of grazing angle, most of the bottom backscattering strength curves paralleled the Mackenzie curve for the grazing angles between 30 and 50 deg. A moderate frequency dependence of approximately 3 dB was observed. Comparisons of the bottom backscattering strengths with the Damuth 3.5 kHz echo-character province types yielded no consistent correlations. Comparisons with archival results for the same region yielded general agreement within 6 dB. Comparison of the ship-based and airborne techniques yielded comparable backscattering strengths to within 5 dB. DTIC

N94-19792# Woods Hole Oceanographic Inst., MA.
A LABORATORY MODEL OF A COOLED CONTINENTAL SHELF
J. A. Whitehead and Robert E. Frazel Jun. 1993 40 p
(Contract N00014-89-J-1037)
(AD-A270862; WHOI-93-22) Avail: CASI HC A03/MF A01

A laboratory model of wintertime cooling over a continental shelf has a water surface cooled by air in an annular rotating tank. A flat shallow outer 'continental shelf' region is next to a conical 'continental slope' bottom and a flat 'deep ocean' center. The shelf flow consists of cellular convection cells descending into a region with very complicated baroclinic eddies. Extremely pronounced fronts are found at the shelf break and over the slope. Associated with these are sizable geostrophic currents along the shelf and over shelf break contours. Eddies are particularly energetic there. The cooling rate is compared with temperature difference between 'continental shelf' and 'deep ocean'. Scaling considerations produce an empirical best fit formula for temperature difference as a function of cooling rate. This produces a relatively straight regression line over a wide range of rotation rates, shelf depths, and cooling rates. If this formula is valid for the ocean, water over continental shelves will be much colder due to constraints imposed by rotation of the earth than if the fluid were not rotating. DTIC

51 LIFE SCIENCES (GENERAL)

N94-17729 Texas Univ. Health Science Center, San Antonio.
CELLULAR AND MOLECULAR LEVEL RESPONSES AFTER RADIOFREQUENCY RADIATION EXPOSURE, ALONE OR IN COMBINATION WITH X RAYS OR CHEMICALS Annual Technical Report, 1 Apr. 1992 - 31 Mar. 1993
Martin L. Meltz 27 Jul. 1992 94 p Limited Reproducibility: More than 20% of this document may be affected by microfiche quality
(Grant AF-AFOSR-0206-91)
(AD-A268189; K-GAUO-00-030-102; AFOSR-93-0586TR) Avail: Issuing Activity (Defense Technical Information Center (DTIC))

The focus of the second years' activities has been to establish, for the human 244B human lymphoblastoid cell line, selected biological effects of standard dose rate ionizing radiation (over the same low total dose range as to be used for combined microwave/ionizing radiation experiments) and hyperthermia (at the same temperature as will be used in the combined studies). The endpoints which have been examined, and for which alterations have been observed after either ionizing radiation exposure or heat treatment (for different times and temperatures), include cell proliferation and viability, cell cycle distribution, cell surface membrane markers, stress protein synthesis, DNA binding protein induction (NF-kB), and proto-oncogene induction. The observation of the two latter endpoints, at low doses, was unexpected. An interaction of ionizing radiation and hyperthermia, reducing stress protein synthesis, was also unexpected. Of the final 10 surface markers examined, 4 have been identified for their potential use in detecting either ionizing radiation or hyperthermia effects. DTIC

N94-17889# Brookhaven National Lab., Upton, NY.
IN VIVO ANIMAL MODELS OF BODY COMPOSITION IN AGING
S. Yasumura, K. Jones, P. Spanne, G. Schidlovsky, and L. Wielopolski 1992 7 p Presented at the Aging and Body Composition: Technological Advances and Physiological Interrelationships, Anaheim, CA, 7 Apr. 1992
(Contract DE-AC02-76CH-00016)
(DE93-012527; BNL-48787; CONF-9204244-1) Avail: CASI HC A02/MF A01

We developed several techniques that provide data on body elemental composition from in vivo measurements in rats. These methods include total body potassium by whole-body counting of endogenous K-40; total body calcium (TBCa), sodium, and chloride by in vivo neutron activation analysis; and total body phosphorus (TBP) and nitrogen (TBN) by photon activation analysis. These elements provide information on total body fat, total body protein, and skeletal mass. Measurements were made in 6-, 12- and 24-month-old rats. TBN increased slightly between 6 and 12 months but was significantly lower by 24 months, indicating a substantial loss in total body protein. Working at the National Synchrotron Light Source, we studied rat femurs by computed microtomography (CMT) and the elemental profile of the femur cortex by synchrotron-radiation induced X-ray emission (SRIXE). Although there were no significant changes in TBCa and TBP, indices of skeletal mass, CMT revealed a marked increase in the size and number of cavities in the endosteal region of the femur cortex with increasing age. The SRIXE analysis of this cortical bone revealed a parallel decrease in the endosteal Ca/P ratio. Thus, there are major alterations in bone morphology and regional elemental composition despite only modest changes in total skeletal mass. DOE

N94-18051# Pacific Northwest Lab., Richland, WA.
IMPROVING THE BIODEGRADATIVE CAPACITY OF SUBSURFACE BACTERIA
M. F. Romine and F. J. Brockman Apr. 1993 16 p Presented at the 2nd International Symposium In Situ and On-Site Bioreclamation, San Diego, CA, 5-8 Apr. 1993
(Contract DE-AC06-76RL-01830)
(DE93-013171; PNL-SA-21765; CONF-930482-7) Avail: CASI HC A03/MF A01

The continual release of large volumes of synthetic materials into the environment by agricultural and industrial sources over the last few decades has resulted in pollution of the subsurface environment. Cleanup has been difficult because of the relative inaccessibility of the contaminants caused by their wide dispersal in the deep subsurface, often at low concentrations and in large volumes. As a possible solution for these problems, interest in the introduction of biodegradative bacteria for in situ remediation of these sites has increased greatly in recent years (Timmis et al. 1988). Selection of biodegradative microbes to apply in such cleanup is limited to those strains that can survive among the native bacterial and predator community members at the particular pH, temperature, and moisture status of the site (Alexander, 1984). The use of microorganisms isolated from subsurface environments would be advantageous because the organisms are already adapted to the subsurface conditions. The options are further narrowed to strains that are able to degrade the contaminant rapidly, even in the presence of highly recalcitrant anthropogenic waste mixtures, and in conditions that do not require addition of further toxic compounds for the expression of the biodegradative capacity (Sayler et al. 1990). These obstacles can be overcome by placing the genes of well-characterized biodegradative enzymes under the control of promoters that can be regulated by inexpensive and nontoxic external factors and then moving the new genetic constructs into diverse groups of subsurface microbes. The objective of this research is to test this hypothesis by comparing expression of two different toluene biodegradative enzymatic pathways from two different regulatable promoters in a variety of subsurface isolates. DOE

N94-18231# Tennessee Univ., Memphis. Dept. of Anatomy and Neurobiology.
SOMATOSENSORY RESPONSIVENESS IN BEHAVING MONKEYS AND HUMAN SUBJECTS Annual Report, 1 Jul. 1992 - 30 Jun. 1993
Randall J. Nelson 31 Jul. 1993 18 p
(Grant AF-AFOSR-0333-91)
(AD-A268924; AFOSR-93-0671TR) Avail: CASI HC A03/MF A01

Three research goals were accomplished during this second year. First, analysis of data indicated that sensory responsiveness of primary somatosensory (SI) cortical neurons that respond to vibratory go-cues for wrist movement with the greatest fidelity have their activity modulated just prior to movement onset. This observation fits with the hypothesis that prior to active movement, sensory inputs that are no longer behaviorally relevant are gated so as not to interfere with monitoring movement parameters by the primate CNS. Second, the preliminary results from the recordings from 249 task related sensorimotor cortical neurons indicate that when behavioral conditions become suddenly unpredictable, responsiveness to peripheral sensory and centrally-generated inputs is increased. This is tentatively being viewed as a release from the tonic attenuation that probably occurs during the performance of stereotypic behaviors. Finally, preliminary findings suggest that human subjects can alter wrist movements toward a positional target if vibratory abort-cues are presented early enough. Correct alterations in movement become more likely with increased practice. Final performance and the time necessary to achieve it range on the order of 4-6 days. DTIC

N94-18242# Oak Ridge National Lab., TN.
MATRIX- AND SUBSTRATE-ASSISTED LASER DESORPTION FOR FAST DNA SEQUENCING
C. H. Chen, S. L. Allman, K. Tang, and R. B. Jones 1993 8 p Presented at the OE/LASE 1993 International Society for Optical Engineering (SPIE) Conference, Los Angeles, CA, 16-23 Jan. 1993
(Contract DE-AC05-84OR-21400)
(DE93-015332; CONF-930159-37) Avail: CASI HC A02/MF A01

Tremendous effort has been put to achieving fast sequencing of DNA due to the potential great applications in biological and medical research. Current DNA sequencing methods were developed by Sanger and Maxam-Gilbert. Both radioactive methods and fluorescent dye labeling methods for DNA sequencing require the use of the time-consuming gel electrophoresis method. It is desirable to consider a time-of-flight mass spectrometer approach to DNA sequencing since the time needed for separation of DNA segments in a mass spectrometer is a few microseconds instead of a few hours in gel electrophoresis. However, there are two major difficulties: developing a reliable method to deliver these nonvolatile biopolymers to the mass spectrometer's ionization zone, and achieving ion production without significant fragmentation in either the desorption or ionization steps. Electrospray and laser-desorption ionization have been considered to have good potential for overcoming these difficulties. Large polypeptide molecules can be put into the gas phase and ionized by a laser in the presence of excessive amounts of nicotinic acid molecules serving as a matrix, a method called the matrix-assisted laser desorption/ionization (MALDI). Matrix-assisted UV desorption and ionization has also been applied to DNA segments; however, the success has been limited to very small segments. MALDI has been used here for detecting medium sizes of oligomers. Fast sequencing of DNA by laser mass spectrometry can possibly be achieved by discovering new matrices for efficient production of parent ions of large oligomers. Another approach is to achieve efficient post-ionization after the desorption. The first step has been taken, the success may not be very far away. DOE

N94-18305 Hawaii Univ., Manoa.

PHOTOSYNTHETIC RESPONSES TO THE ENVIRONMENT, VOLUME 8 Final Report

Harry Y. Yamamoto and Celia M. Smith 27 Aug. 1992 263 p Presented at the Proceedings Symposium, Manoa, HI, 24-27 Aug. 1992 Limited Reproducibility: More than 20% of this document may be affected by microfiche quality
(Contract N00014-92-J-1523)
(AD-A269584) Avail: CASI HC A12

Certain fundamental differences separate marine, aquatic, and terrestrial plants as obviously as the difference in physical factors among their habitats. Yet at the core of their responses to environmental factors, photosynthesis ties these entities together in ways not typically seen in scientific meetings or collaboration among researchers. It was our optimistic intent in organizing this meeting 'Photosynthetic Responses to the Environment' to try to bridge these diverse groups of plant life and scientists by bringing together leaders, researchers, and young scientists for three days of in-depth discussions that could refresh us with new appreciation, new ideas, and new colleagues. DTIC

N94-18476# Argonne National Lab., IL.

THE c-JUN GENE EXPRESSION IN HUMAN CELLS EXPOSED TO EITHER IONIZING RADIATION OR HYDROGEN PEROXIDE

F. R. Collart, M. Horio, and E. Huberman Jun. 1993 6 p Presented at the International Seminar on Molecular Mechanisms in Radiation Mutagenesis and Carcinogenesis, Doorwerth, Netherlands, 19-22 Apr. 1993
(Contract W-31-109-eng-38)
(DE93-017436; ANL/CBM/CP-80231; CONF-930454-3) Avail: CASI HC A02/MF A01

We investigated the role of reactive oxygen intermediates (ROI's) and protein kinase C (PKC) in radiation- and H2O2-evoked c-jun gene expression in human HL-205 cells. This induction of c-jun gene expression could be prevented by pretreatment of the cells with Nacetylcysteine (an antioxidant) or H7 (a PKC and PKA inhibitor) but not by HA1004, a PKA inhibitor, suggesting a role for ROIs and PKC in mediating c-jun gene expression. We also investigated potential differences in c-jun gene expression in a panel of normal and tumor cells untreated or treated with ionizing radiation or H2O2. Treatment with radiation or H2O2 produced a varied response, from some reduction to an increase of more than an order of magnitude in the steady-state level of c-jun mRNA. These data indicate that although induction of c-jun may be a common response to ionizing radiation and H2O2, this response was reduced or absent in some cell types. DOE

N94-18924# Michigan State Univ., East Lansing. Dept. of Pediatrics/Human Development.

THE ROLE OF CHEMICAL INHIBITION OF GAP JUNCTIONAL INTERCELLULAR COMMUNICATION IN TOXICOLOGY Annual Report, 15 May 1992 - 14 May 1993

James E. Trosko and Burra V. Madhukar 19 May 1993 15 p
(Contract F49620-92-J-0293; AF Proj. 2312)
(AD-A269251; AFOSR-93-0675TR) Avail: CASI HC A03/MF A01

Progress during this past grant period has continued to mount, with new findings, new techniques to achieve our aims and objectives, and new support for our original working hypothesis that chemical modulation of gap junctional intercellular communication (GJIC) is involved in multiple formats of toxicity. We now have evidence on how certain tumor promoting chemicals, neurotoxicants, reproductive toxicants, teratogens, or immunotoxicants can affect GJIC at either the transcriptional, translational, or posttranslational levels. Using cells mutated for altered GJIC; transfected with various oncogenes; or treated with different kinds of chemical toxicants, We have now elucidated the different mechanisms by which GJIC can be effected. This new mechanistic understanding should contribute to a more biologically-based risk assessment model and an understanding of how epigenetic toxicants work. DTIC

N94-19210*# National Aeronautics and Space Administration, Washington, DC.

SPACE LIFE SCIENCES RESEARCH: THE IMPORTANCE OF LONG-TERM SPACE EXPERIMENTS

Oct. 1993 43 p Prepared in cooperation with George Washington Univ., Washington, DC
(NASA-TM-4502; NAS 1.15:4502) Avail: CASI HC A03/MF A01

This report focuses on the scientific importance of long-term space experiments for the advancement of biological science and the benefit of humankind. It includes a collection of papers that explore the scientific potential provided by the capability to manipulate organisms by removing a force that has been instrumental in the evolution and development of all organisms. Further, it provides the scientific justification for why the long-term space exposure that can be provided by a space station is essential to conduct significant research. For individual titles, see N94-19211 through N94-19217.

N94-19211*# National Aeronautics and Space Administration, Washington, DC.

THE RATIONALE FOR FUNDAMENTAL RESEARCH IN SPACE BIOLOGY: INTRODUCTION AND BACKGROUND

Thora W. Halstead and Robert W. Krauss *In its* Space Life Sciences Research: The Importance of Long-Term Space Experiments Oct. 1993 p 1-2 (For primary document see N94-19210 04-51)
Avail: CASI HC A01/MF A01

With the construction of Space Station Freedom, NASA will have available a new platform for experiments in space that promises many advantages over those already flown. Biologists are poised to take advantage of the greater space, the increased power, and especially the long duration of the station for a cascade of innovative experiments in fundamental science that are long overdue. The unique space environment will provide new dimensions for approaching some of the most challenging problems still facing modern biology. Solutions to basic questions about living systems, which may now be grown through many generations in space, will not only explain abnormalities already observed there, but will add to our understanding of how life functions on Earth. Much will be learned about evolution that has built us the way we are, but also about what it has in store for the Earth's species in the future. NASA must not lose this opportunity to contribute to the welfare of the peoples of the Earth while at the same time create knowledge that will enable human exploration of space in the decades ahead. Author

N94-19212*# National Aeronautics and Space Administration. Ames Research Center, Moffett Field, CA.

OPPORTUNITIES AND QUESTIONS FOR THE FUNDAMENTAL BIOLOGICAL SCIENCES IN SPACE

Joseph C. Sharp and Joan Vernikos *In* NASA. Headquarters, Space Life Sciences Research: The Importance of Long-Term Space Experiments Oct. 1993 p 3-6 (For primary document see N94-19210 04-51)
Avail: CASI HC A01/MF A01

With the advent of sophisticated space facilities we discuss the overall nature of some biological questions that can be addressed. We point out the need for broad participation by the biological community, the necessary facilities, and some unique requirements. Author

N94-19213*# National Aeronautics and Space Administration, Washington, DC.

SPACE RESEARCH WITH INTACT ORGANISMS: THE ROLE OF SPACE STATION FREEDOM

Robert W. Phillips and Francis J. Haddy (Uniformed Services Univ. of the

Health Sciences, Bethesda, MD.) *In its* Space Life Sciences Research: The Importance of Long-Term Space Experiments Oct. 1993 p 7-12 (For primary document see N94-19210 04-51)
Avail: CASI HC A02/MF A01

The study of intact organisms has provided biologists with a good working knowledge of most of the common organisms that have evolved in the 1 g environment of Earth. Reasonably accurate predictions can be made about organismal responses to most stimuli on Earth. To extend this knowledge to life without gravity, we must have access to the space environment for prolonged periods. Space Station Freedom will provide a facility with which to begin this type of research. Spaceflight research to date has been limited to relatively short-term exposures that have been informative but incomplete. This paper provides a brief background of known changes that have occurred in intact organisms in the space environment and proposes the kinds of experiments that are needed to expand our knowledge of life on Earth and in space. Author

N94-19214*# Arizona Univ., Tucson. Dept. of Biochemistry.
SPACE RESEARCH ON ORGANS AND TISSUES
Marc E. Tischler and Emily Morey-Holton (National Aeronautics and Space Administration. Ames Research Center, Moffett Field, CA.) *In* NASA. Headquarters, Space Life Sciences Research: The Importance of Long-Term Space Experiments Washington Oct. 1993 p 13-20 (For primary document see N94-19210 04-51)
Avail: CASI HC A02/MF A01

Studies in space on various physiological systems have and will continue to provide valuable information on how they adapt to reduced gravitational conditions, and how living in a 1 g (gravity) environment has guided their development. Muscle and bone are the most notable tissues that respond to unweighting caused by lack of gravity. The function of specific muscles and bones relates directly to mechanical loading, so that removal of 'normal forces' in space, or in bedridden patients, causes dramatic loss of tissue mass. The cardiovascular system is also markedly affected by reduced gravity. Adaptation includes decreased blood flow to the lower extremities, thus decreasing the heart output requirement. Return to 1 g is associated with a period of reconditioning due to the deconditioning that occurs in space. Changes in the cardiovascular system are also related to responses of the kidney and certain endocrine (hormone-producing) organs. Changes in respiratory function may also occur, suggesting an effect on the lungs, though this adaptation is poorly understood. The neurovestibular system, including the brain and organs of the inner ear, must adapt to the disorientation caused by lack of gravity. Preliminary findings have been reported for liver. Additionally, endocrine organs responsible for release of hormones such as insulin, growth hormone, glucocorticoids, and thyroid hormone may respond to spaceflight. Author

N94-19215*# Kansas State Univ., Manhattan. Div. of Biology.
A SCIENTIFIC ROLE FOR SPACE STATION FREEDOM: RESEARCH AT THE CELLULAR LEVEL
Terry C. Johnson and John N. Brady (National Cancer Inst., Bethesda, MD.) *In* NASA. Headquarters, Space Life Sciences Research: The Importance of Long-Term Space Experiments Washington Oct. 1993 p 21-29 (For primary document see N94-19210 04-51)
(Grants NAGw-1197; NAGw-2328)
Avail: CASI HC A02/MF A01

The scientific importance of Space Station Freedom is discussed in light of the valuable information that can be gained in cellular and developmental biology with regard to the microgravity environment on the cellular cytoskeleton, cellular responses to extracellular signal molecules, morphology, events associated with cell division, and cellular physiology. Examples of studies in basic cell biology, as well as their potential importance to concerns for future enabling strategies, are presented. Author

N94-19216*# Washington State Univ., Pullman. Inst. of Biological Chemistry.
MICROGRAVITY RESEARCH IN PLANT BIOLOGICAL SYSTEMS: REALIZING THE POTENTIAL OF MOLECULAR BIOLOGY
Norman G. Lewis and Clarence A. Ryan *In* NASA. Headquarters, Space Life Sciences Research: The Importance of Long-Term Space Experiments Washington Oct. 1993 p 31-34 (For primary document see N94-19210 04-51)
Avail: CASI HC A01/MF A01

The sole all-pervasive feature of the environment that has helped shape, through evolution, all life on Earth is gravity. The near weightlessness of the Space Station Freedom space environment allows gravitational effects to be essentially uncoupled, thus providing an unprecedented opportunity to manipulate, systematically dissect, study, and exploit the role of gravity in the growth and development of all life forms. New and exciting opportunities are now available to utilize molecular biological and biochemical approaches to study the effects of microgravity on living organisms. By careful experimentation, we can determine how gravity perception occurs, how the resulting signals are produced and transduced, and how or if tissue-specific differences in gene expression occur. Microgravity research can provide unique new approaches to further our basic understanding of development and metabolic processes of cells and organisms, and to further the application of this new knowledge for the betterment of humankind. Author

N94-19217*# North Carolina State Univ., Raleigh. Dept. of Animal Science.
LIFE: ORIGIN AND EVOLUTION ON EARTH--HOW CAN WE ESCAPE?
Clement L. Markert and Abraham D. Krikorian (State Univ. of New York, Stony Brook.) *In* NASA. Headquarters, Space Life Sciences Research: The Importance of Long-Term Space Experiments Washington Oct. 1993 p 35-39 (For primary document see N94-19210 04-51)
Avail: CASI HC A01/MF A01

Exploitation of gene regulation rather than the creation of new genes has been predominantly responsible for the evolutionary advances in animals and plants that are widely recognized today. Until very recently it was not possible to examine life in the absence of gravity. We can now imagine forms of life in the universe adapting to circumstances different from those found on Earth. Our own life forms would surely become different in time if they were transferred to other planets with different conditions, including much lower or higher gravity. Author

N94-19341# Oak Ridge National Lab., TN.
EFFECT OF EMP FIELDS ON CELL MEMBRANE POTENTIALS
P. C. Gailey and C. E. Easterly 1993 2 p Presented at the Nuclear Science Symposium, San Francisco, CA, 2-5 Nov. 1993
(Contract DE-AC05-84OR-21400)
(DE93-015819; CONF-931107-3) Avail: CASI HC A01/MF A01

A simple model is presented for cell membrane potentials induced during exposure to electromagnetic pulse (EMP). Using calculated values of internal electric field strength induced during EMP exposure, the model predicts that cell membrane potentials of about 100 mV may be induced for time frames on the order of 10 ns. Possible biological effects of these potentials including electroporation are discussed. DOE

N94-19757 Biological Components Corp., Menlo Park, CA.
PHOTOSYNTHETIC REACTION CENTERS AS ACTIVE MOLECULAR ELECTRONIC COMPONENTS, PHASE 1 Final Report, 15 Jan. - 14 Jul. 1993
Albert F. Lawrence 13 Aug. 1993 51 p Limited Reproducibility: More than 20% of this document may be affected by microfiche quality
(Contract DAAH04-93-C-0003)
(AD-A271388; ARO-30818.1-CH-SBI-Phase-1) Avail: CASI HC A04

The aim of this project is the development of reaction centers from photosynthetic bacteria for use in molecule-based components and devices. Reaction centers (RC's) exhibit a highly efficient, rapid, long-distance photoinduced charge separation under a wide variety of conditions. The reaction center has electronic properties which are far superior, more flexible, and much less expensive to produce than any known synthetic donor/acceptor system. During the course of this project the author developed strategies for the attachment of reaction centers to electrode surfaces, and demonstrated the first steps in this process. The approach employed molecular modeling, site-directed mutagenesis, and the attachment of dye molecules to a particular RC site. Correlated developments include refinement and simplification of the process for preparing reaction centers, studies of materials issues, studies of device concepts, and transfer of RC preparation techniques to Biological Components Corporation. DTIC

N94-19789# Wright State Univ., Dayton, OH. Dept. of Chemistry.
A STUDY OF THE EFFECT OF HYDROCARBON STRUCTURE ON THE INDUCTION OF MALE RAT NEPHROPATHY AND METABOLIC STRUCTURE Final Report, 1 Jun. 1989 - 31 Aug. 1993
M. P. Serve 31 Aug. 1993 64 p
(Grant AF-AFOSR-0396-89)
(AD-A270969; AFOSR-93-0751TR) Avail: CASI HC A04/MF A01

Certain hydrocarbons were shown to cause nephrotoxicity in male rats. Since many of the hydrocarbons have a branched alkyl side chain, several isomers of octane including 2,5-dimethylhexane, 2-methylheptane, 3-methylheptane, and 4-methylheptane were evaluated on their ability to induce the nephrotoxicity. Since the above hydrocarbons are components of fuels and solvents, an investigation into their pathways of metabolism was undertaken in order to see if a pattern of biotransformation could be deduced and determined if potentially harmful metabolites were produced. Male 344 Fischer rats were dosed intragastrically with the above hydrocarbons over a 14 day period. When compared with rats, the order of mephrotoxicity was determined. DTIC

52 AEROSPACE MEDICINE

Includes physiological factors; biological effects of radiation; and effects of weightlessness on man and animals.

N94-17699# Oak Ridge National Lab., TN.
NUCLEAR MEDICINE PROGRAM Quarterly Progress Report, period ending 31 Mar. 1993
F. F. Knapp, Jr., K. R. Ambrose, A. L. Beets, A. P. Callahan, D. W. McPherson, S. Mirzadeh, and C. R. Lambert Apr. 1993 13 p
(Contract DE-AC05-84OR-21400)
(DE93-013896; ORNL/TM-12343) Avail: CASI HC A03/MF A01

We have explored the possibility of measuring urinary radioactivity as an index of pancreatic lipase activity after oral administration of a new triglyceride containing a radioactive iodine-1 25-labeled fatty acid moiety. The new agent, 1,2-dipalmitoyl- 3(15- (p-iodophenyl) pentandecan-1-oyl)-racglycerol (1,2-Pal-3-IPPA), was prepared by the thallation-iodide displacement method. Following oral gavage of the radioiodinated triglyceride to rats, about 30% of the administered activity was excreted in 24 hours in the urine. In normal human controls a higher urinary excretion (of about 75%) was observed. In this report, we describe an evaluation of the metabolites excreted in the urine and the chemical species stored in adipose from rats. The urine activity co-chromatographed with hippuric acid by TLC indicating conjugation of the IPPA metabolites. Release of the acidic components from the conjugated excretory products by acid hydrolysis of the urine provided the radioactive acidic IPPA metabolites. Analysis of the Folch extracts of fat samples from rats demonstrated that the radioactive components co-chromatographed in the triglyceride region. Recent studies in patients with compromised pancreatic exocrine function have demonstrated significantly decreased 24 hr. urinary excretion of about 25%, following oral administration of (1-131)- 1,2-Pal-3-IPPA. Thus, urine analysis after oral administration of (1-131)- 1,2-Pal-3-IPPA may be a simple, non-invasive tool for the clinical evaluation of various diseases involving dietary fat digestion. DOE

N94-17823# Defence and Civil Inst. of Environmental Medicine, Downsview (Ontario). Inst. of Environmental Medicine.
EFFECTS OF A HIGH-ENERGY FOOD SUPPLEMENT ON COLD-INDUCED THERMOGENESIS
A. L. Vallerand and I. Jacobs Aug. 1993 29 p
(AD-A269301; DCIEM-93-36) Avail: CASI HC A03/MF A01

In previous studies, we have not been able to confirm the theory that energy substrate mobilization is a limiting factor for cold-induced thermogenesis (M) in humans. One possible explanation for the conflicting results is that the dose of energy substrates may not have been optimal. The goal of this study was to determine whether the ingestion of a high-energy food supplement (710 kcal or 2,970 kJ; Ensure Pulse) in the cold could alter: (1) M, (2) heat balance (min by min determination of heat debt (S) where S = M - heat losses, (3) rectal (T sub re) and (4) mean skin temperatures (T sub sk), (5) rates of substrate oxidation, and (6) plasma levels of substrates and hormones, taken as indices of substrate mobilization. Seven healthy males were subjected to two semi-nude cold exposure tests (3h at 7 C, 1 m/.s wind, fasting, tests performed 1 wk apart). The ingestion of a high-energy supplement did not influence either T sub re, T sub sk, m, or S in comparison to the placebo test in the same subjects. This absence of changes was observed even though the supplement elevated carbohydrate mobilization and oxidation (P less than 0.05), albeit at the expense of lipid mobilization and oxidation (P less than 0.05). The present results demonstrate that the ingestion of a food supplement that enhances energy substrate mobilization and oxidation does not alter cold thermogenesis, heat debt or body temperatures in humans, under normal conditions. DTIC

N94-17824# Army Aeromedical Research Lab., Fort Rucker, AL.
USING CONTROLLED DAYLIGHT EXPOSURE AND SLEEP TIMING IN THE PREVENTION OF SHIFT LAG DURING NIGHT OPERATIONS Technical Report
Carlos A. Comperatore Jun. 1993 37 p
(AD-A269304; USAARL-93-25) Avail: CASI HC A03/MF A01

In the Army aviation community, a significant component of combat and training missions is night operations. Mission requirements often necessitate an initial shift from daytime to nighttime duty hours within 24 to 48 hours. Rapid shifts from daytime to nighttime work, and nighttime to daytime sleep usually result in loss of sleep, degradation of alertness, increased fatigue, and reduced work effectiveness. These symptoms are referred to as 'shift-lag' because the body's physiological adjustment lags behind the rapid shift to the new work schedule. Research on shiftwork provides a variety of approaches to avoid the deterioration of performance and health of shiftworkers. Shift-lag prevention plans may consider the speed of shiftwork rotation, the duration of each shift, age of workers, physical strength associated with work demands, diet, timing of sleep, and in some cases, the use of drugs to induce sleep and attempt to resynchronize the body's internal biological clock. However, the use of controlled timing of daylight exposure and of sleep schedules are of overriding importance. In the Army aviation context, consequences of shifts to nocturnal work schedules without the implementation of a shift-lag prevention plan have been recently documented. This work reviews the mechanism of biological timing in humans, the role of environmental lighting, and specifically identifies methods of preventing sleep loss and fatigue during the transition from daytime to nighttime duty hours. DTIC

N94-17966 Institute for Perception RVO-TNO, Soesterberg (Netherlands). Work Environment Group.
SYNCHRONISATION OF COLD INDUCED VASODILATION AT VARIOUS LOCATIONS OF ONE HAND Final Report
H. A. M. Daanen and W. A. Lotens 6 Jul. 1992 22 p Sponsored by TNO Defence Research, Delft, Netherlands
(IZF-1992-B3; TD92-0258; ETN-93-94526) Copyright Avail: TNO Institute for Perception, Kampweg 5, 3769 ZG Soesterberg, Netherlands

The amount of correspondence between the Cold Induced Vasodilation (CIVD) responses in several sites of the left hand is quantified by the Pearson Correlation Coefficient (PCC) of the local skin temperatures. A PCC of zero means that all registrations are independent, indicating a purely local mechanism. A PCC approaching 1 indicates an increasing central component. Twelve subjects immersed their left hands in a calorimeter water bath of 5 C. All PCC's of the fingers and the ventral and dorsal side of the hand were calculated. A period of 30 minutes was analyzed, starting 10 minutes after immersion. The PCC was higher for neighboring fingers (PCC = 0.67) than for fingers separated by other fingers (PCC = 0.48). For neighboring fingers those mainly innervated by the same somatic nerve (ring-little and index-middle finger) had a higher PCC (PCC = 0.80) than for the fingers with more separate innervation (PCC = 0.55). The PCC between the two locations on the hands and the fingers were insignificant. It is concluded that the CIVD of the fingers shows so much correspondence that a central component is clearly presented. From the difference in PCC between neighboring and other fingers it can be seen that local mechanisms also determine the CIVD characteristics. Theories based on nervous involvement are supported by the finding that shared somatic innervation enhances the PCC. ESA

N94-18080 Technische Univ., Delft (Netherlands).
CONTROL OF SHOULDER MUSCLES DURING GOAL DIRECTED MOVEMENTS

R. Happee 1992 190 p
(PB93-195139; ISBN-90-370-0077-0) Copyright Avail: CASI HC A09/MF A02

The control of shoulder muscles during goal directed movements has been studied experimentally and by simulations. Muscular activity was assessed experimentally by measuring electromyographic (EMG) activity. In the EMG of maximally fast movements, triphasic activity comparable to activity reported in other joints was found. The agonist activity in the first phase causes acceleration of the limb. The antagonist activity in the second phase serves to decelerate the limb. In a simulation study it was shown that the third phase contributes to a time optimal movement. The role of the third phase is shown to be related to muscle dynamics. A model has been developed which gives an accurate description of movement kinematics and which is based on interpretable parameters. Four parameters describe the timing of a triphasic muscular input and a fifth parameter describes neuromuscular dynamics. The parameters provide a means to compare the shape of movement traces under different experimental conditions. After scaling towards the movement velocity, these parameters revealed a significant dependence on the movement direction and the maximum velocity obtained by the subjects. NTIS

N94-18190 California Univ., Berkeley. School of Optometry.
FY 1991 AASERT: SPATIO-TEMPORAL MAKING IN HUMAN VISION AND ITS APPLICATION TO IMAGE CODING Annual Report, 15 Jun. 1992 - 14 Jun. 1993
Stanley A. Klein Jul. 1993 4 p Limited Reproducibility: More than 20% of this document may be affected by microfiche quality
(Contract F49620-92-J-0359)
(AD-A268795; AFOSR-93-0635TR) Avail: CASI HC A01

We measured the temporal dynamics of relative motion judgement. Two lines or dots oscillated either in the same phase of motion, or in 180 phase relative to each other. Subjects were required to discriminate between the two kinds of motion. The dots either oscillated vertically or horizontally. The former case produced oscillating orientation and the later case produced oscillating separation. The temporal frequency of oscillation was varied (presented at OSA-1992). In experiments with lines, the separation of the lines was varied while the distance of the lines from the fovea was held constant. The discriminability of two different phases of relative motion was measured and compared to the detectability of these motions. The physchometric transducer functions were measured and plotted. DTIC

N94-18226 Naval Biodynamics Lab., New Orleans, LA.
BIBLIOGRAPHY OF SCIENTIFIC PUBLICATIONS OF THE NAVAL BIODYNAMICS LABORATORY, 1980 - 1992
Jul. 1993 33 p Limited Reproducibility: More than 20% of this document may be affected by microfiche quality
(AD-A268886; NBDL-93R001) Avail: Issuing Activity (Defense Technical Information Center (DTIC))

This report lists all research reports, special reports, monographs, technical memoranda, joint reports, research information bulletin, journal articles, and conference proceedings published by the Naval Biodynamics Laboratory between Jan. 1980 and Dec. 1992 DTIC

N94-18289# Army Aeromedical Research Lab., Fort Rucker, AL.
US ARMY AVIATION EPIDEMIOLOGY DATA REGISTER: PREVALENCE OF REFRACTIVE ERROR AMONG US AIRCREW MEMBERS Final Report
Kevin T. Mason, S. C. Shannon, and Robert H. Schrimsher Jun. 1993 30 p
(DA Proj. 3M1-62787-A-879)
(AD-A269550; USAARL-93-24) Avail: CASI HC A03/MF A01

The U.S. Army aviation branch is making final funding and planning decisions on the fielding of a contact lens program for Army aircrew members. This report stratifies the prevalence of refractive error by aviation duty position, service component, and rank. There is an increasing prevalence of refractive error in the higher ranking aircrew members, paralleling increasing age with rank promotion. Comparing service components, the prevalence is higher in the reserve component and civilian forces than active duty forces. Within the aviator service component cohorts, there has been a significant upward trend in the annual period prevalence of refractive error from 1986 through 1992, especially in the Army Reserve and National Guard cohorts. This upward trend may be related to the observed upward trend in the average age of Army aircrew members as a group from 1986 through 1990. DTIC

N94-18294# Food and Drug Administration, Rockville, MD. Center for Devices and Radiological Health.
A STUDY OF THE EFFECTS OF HIGH POWER PULSED 2450 MHZ MICROWAVES, ELF MODULATED MICROWAVES, AND ELF FIELDS ON HUMAN LYMPHOCYTES AND SELECTED CELL LINES Final Report, 1 Sep. 1991 - 31 Dec. 1992
Mays L. Swicord 27 Jan. 1993 98 p
(AD-A269070) Avail: CASI HC A05/MF A02

The Center for Devices and Radiological Health of the Food and Drug Administration has performed research over the past two years with financial support from the Walter Reed Army Institute of Research. This research has addressed three tasks which are described in the report. DTIC

N94-18392 Geo-Centers, Inc., Frederick, MD.
REVIEW OF SHORT-TERM, HIGH-LEVEL EXPOSURE TO METALS: ANTIMONY, BARIUM, AND CADMIUM Technical Report, Sep. 1992 - Jun. 1993
James C. Eaton 16 Jun. 1993 25 p Limited Reproducibility: More than 20% of this document may be affected by microfiche quality
(Contract DAMD17-93-C-3006; DA Proj. 3M1-62787-A-878)
(AD-A268896; USABRDL-TR-9303) Avail: Issuing Activity (Defense Technical Information Center (DTIC))

The adverse health effects of inhaling the metals antimony, barium, and cadmium which are components of exhaust from military weapons systems have been reviewed. The metals antimony and cadmium are suspected carcinogens. In addition, cadmium at chronic low level has been implicated in kidney dysfunction. There are no documented exposures of Army personnel to the high levels that would result in severe acute effects. Since the chronic effects of these three metals are cumulative, the 8-hour time-weighted average exposure is the proper mechanism for regulating episodic short-term exposures to them at moderately high levels. The report recommends that the Army adhere to the established Federal workplace exposure limits for the three metals and that exposure to antimony and cadmium, the two metals with demonstrated carcinogenic activity, be reduced to a level as low as is reasonably achievable. DTIC

N94-18407 California Univ., Irvine. Center for the Neurobiology of Learning and Memory.
[THE IDENTIFICATION OF THE COMPUTATIONAL SIGNIFICANCE OF KEY NEUROBIOLOGICAL CHARACTERISTICS FOUND IN A NUMBER OF TELENCEPHALIC BRAIN REGIONS] Final Technical Report
Gary Lynch and Richard Granger 1993 7 p Limited Reproducibility: More than 20% of this document may be affected by microfiche quality
(Contract N00014-89-J-3179)
(AD-A269374) Avail: CASI HC A02

The funded research has had as its primary goal the identification of the computational significance of key neurobiological characteristics found in a number of telencephalic brain regions. Recent findings have identified novel, computationally valuable algorithms derived from simulation and analysis of specific brain networks, including the olfactory system and the hippocampus as well as auditory neocortex. Analysis has shown that, as might be expected from networks faced with demanding signal-processing tasks under limited-resource situations, these brain-based algorithms have very efficient time and space complexity characteristics and are directly applicable to signal processing tasks of known difficulty, including processing of complex time-varying signals such as speech and sonar. DTIC

N94-18538# Colorado State Univ., Fort Collins. Dept. of Anatomy and Neurobiology.
INTRACELLULAR PHYSIOLOGY OF THE RAT SUPRACHIASMATIC NUCLEUS: ELECTRICAL PROPERTIES, NEUROTRANSMISSION AND EFFECTS OF NEUROMODULATORS Final Report, 15 Jul. 1992 - 14 Jul. 1993
F. E. Dudek 30 Apr. 1993 13 p
(Contract F49620-92-J-0417)
(AD-A268829) Avail: CASI HC A03/MF A01

Knowledge of the neuronal membrane properties and synaptic physiology of the suprachiasmatic nucleus (SCN) is critical for an understanding of the cellular basis of circadian rhythms in mammals. The hypothalamic slice preparation from rodents and a combination of electrophysiological techniques (i.e., extracellular single- and multiple-unit recording, intracellular recording, and whole-cell patch clamp) were used to study the following: (1) the role of excitatory and inhibitory amino acids (i.e., glutamate and GABA) in synaptic transmission; (2) the membrane properties of SCN neurons; and (3) the mechanisms of neuronal synchronization. Antagonists for N-methyl-D-aspartate (NMDA) and non-NMDA receptors blocked excitatory postsynaptic potentials (EPSPs) evoked by stimulation of the optic nerve other sites when SCN cells were depolarized or at rest, respectively. Bicuculline blocked inhibitory postsynaptic potentials (IPSP's) that were evoked by local stimulation or that occurred spontaneously. The IPSP reversal potential was near the Cl(-) equilibrium potential and was shifted to depolarized levels by raising intracellular Cl(-). Thus, glutamate and GABA appear to mediate fast excitatory inhibitory synaptic transmission in the SCN. Some SCN neurons, but not all of them, have low-threshold Ca(2+) spikes and time-dependent inward rectification, thus indicating that the electrical properties of SCN neurons are not homogenous. Neurons with a firing rate greater than 6 Hz had a regular pattern, and neurons with a rate less than 4 Hz had an irregular pattern; since both the firing rate and pattern could be modified with injected currents, SCN neurons with different firing patterns are unlikely to represent distinct classes of cells. DTIC

N94-18598 Louisiana State Univ., New Orleans. Medical Center.
METABOLIC CHANGES AND HEMODYNAMIC DYSFUNCTION FOLLOWING HYPOTHERMIC SHOCK Final Technical Report
Harvey I. Miller 30 Jun. 1993 20 p Limited Reproducibility: More than 20% of this document may be affected by microfiche quality
(Contract N00014-89-J-3124)
(AD-A269780; WES/TR/HL-93-10) Avail: CASI HC A03

The results of the metabolic studies suggest that while there are very large increases in circulating catecholamines, the catecholamines were less sensitive in the hypothermic animals after rewarm. Heart rate was elevated almost immediately upon immersion in cold water and did not fall until 2 minutes after immersion. When the BT returned to normal (0 time) so did the heart rate, even though the catecholamine levels were very high. It would appear that the adrenergic receptors are down-regulated and seemed less sensitive. This may be the reason for lack of elevation of the FFA. However another explanation maybe the 'Adipose Tissue Electronic Blanket Theory'. The changes we observed in the metabolic samples (FFA, glucose and lactate) are related to the elevation of NorEpi. When the energy bearing metabolites cannot be mobilized by catecholamines due to down-regulation and, the futile cycle of triglycerides within the adipose tissue does not produce the heat required, then the organism can no longer thermoregulate appropriately. DTIC

N94-18632 Minnesota Univ., Duluth.
EVALUATION OF PHYSIOLOGICAL AND PSYCHOLOGICAL IMPAIRMENT OF HUMAN PERFORMANCE IN COLD STRESSED SUBJECTS Final Report, 9 May 1988 - 8 May 1992
Lorentz E. Wittmers and Richard Hoffman 5 Jun. 1993 183 p Limited Reproducibility: More than 20% of this document may be affected by microfiche quality
(Contract DAMD17-88-C-8054; DA Proj. 3O1-62787-A-879)
(AD-A268637) Avail: CASI HC A09

The effects of 2 shiver suppression techniques on performance of military relevant motor tasks, body heat conservation, and metabolic functions during cold exposure were investigated using a repeated measures MANOVA design. Nine male volunteers, 24.3 + or - 0.8 yr, were exposed for 3 hours to 3 conditions: (1) warm W = 21 deg C air; (2) Cold C = -7 deg C air; and (3) Shiver suppression (SS)= -7 deg C air with shiver suppression techniques (breath holding and voluntary relaxation) applied. Motor speed and accuracy tasks included rifle and pistol shooting and reloading, magazine reloading. Rectal temperature decreased more during SS than in W or C. Skin temperatures and temperature perceptions in C and SS declined more than W, but were similar to each other. Heart rate decreased in W and increased in C and SS. Performance on motor tasks showed decrement's with both C and SS. Decrements in rifle reloading and pistol reloading were less in SS than in C. Decrements in rifle and pistol shooting performance were greater in SS than in C. Decrements in magazine loading were not significantly different in SS and C. In conclusion, SS caused a decline in core temperature, and an improvement in cold exposure performance in simple repetative motor tasks involving little concentration, but a decrement in performance in tasks which required more mental concentration. DTIC

N94-18793 Naval Command, Control and Ocean Surveillance Center, San Diego, CA. RDT and E Div.
COUPLED NEURAL-DENDRITIC PROCESSES: COOPERATIVE STOCHASTIC EFFECTS AND THE ANALYSIS OF SPIKE TRAINS
A. R. Bulsara and A. J. Maren May 1993 14 p Limited Reproducibility: More than 20% of this document may be affected by microfiche quality
(AD-A270041) Avail: CASI HC A03

We can create a richer and more neurophysiologically realistic model of neural activity in the brain by developing a model of neural-dendritic coupling, one which expressly accounts for the way in which the many afferent connections into the neural body influence the somatic membrane potential. Such a model would begin to fill the need within the Artificial Neural Network community for neural models which go beyond the current weighted sum paradigm for artificial neuron connectivity. Although such models have use in engineering applications, there are many aspects of biological neural-dendritic organization which could enrich artificial neural networks. Moving from simple axonal connection weight neural models to neural-dendritic models with a richer structure will allow investigation of both events at the neural level (e.g., inter-spike interval histograms and stochastic resonance) and also potentially at the neural systems level. This will also introduce the possibility of introducing cross-scale interactions into artificial neural systems. DTIC

N94-18862*# Massachusetts Inst. of Tech., Cambridge. Dept. of Brain and Cognitive Services.
STRATEGIES FOR ENHANCING CATECHOLAMINE-MEDIATED NEUROTRANSMISSION Final Technical Report
Richard J. Wurtman 22 Sep. 1992 4 p
(Grant NAG2-210)
(NASA-CR-193807; NAS 1.26:193807) Avail: CASI HC A01/MF A01

Major findings made during this project period included the following observations: changes in tyrosine availability do affect brain dopamine release, as assessed by in vivo microdialysis, but that neuronal feedback mechanisms limit the durations of this effect except when dopaminergic neurotransmission has been deficient; the circulating hormone TRH markedly stimulates brain dopamine release, an effect probably mediated by its diketopiperazine metabolite; the amount of circulating L-dopa which enters the brain is both enhanced by carbohydrate consumption and suppressed by protein intake (both nutritional effects can be damaging, inasmuch as a sudden rush of L-dopa into the brain can facilitate dyskinesias, while the inhibition of brain L-dopa uptake by proteins suppresses its conversion to brain dopamine; an appropriate mixture of dietary proteins and carbohydrates can obviate both effects); serotonin release from superfused hypothalamic slices is a linear function of available tryptophan levels throughout the normal dynamic range; the daily rhythm in plasma melatonin levels is abnormal both in the sudden infant death syndrome and in women with secondary amenorrhea; tyrosine can potentiate the anorectic effects of widely-used sympathomimetic drugs; newly-described COMT inhibitors can enhance brain dopamine release in vivo; and a cell culture system, based on Y-79 (retinoblast) cells, exists in which melatonin reliably suppresses dopamine release. Author (revised)

N94-18911 State Univ. of New York, Plattsburgh. Auditory Research Lab.
THE EFFECTS OF REVERBERANT IMPULSE NOISE (BLAST WAVES) ON HEARING: PARAMETRIC STUDIES Midterm Report, 9 Sep. 1991 - 8 Mar. 1993
Roger P. Hamernik 16 Jun. 1993 93 p Limited Reproducibility: More than 20% of this document may be affected by microfiche quality
(Contract DAMD17-91-C-1113)
(AD-A269242) Avail: CASI HC A05

This research is directed at studying the effects on the auditory system of exposure to high levels of reverberant impulse noise using an animal (chinchilla) model. The blast waves were generated by a three inch diameter shock tube (source III), which produced wave signatures having spectral energy concentrated in the 12 kHz region. The waves were discharged into a reverberant chamber within which animals were individually exposed.

Animals were exposed to either 150, 155, or 160 dB peak SPL impulses. The number of impulses presented at each intensity was 1, 10, or 100, with repetition rates fixed at 1 impulse/sec. This parametric design yielded 9 groups of animals. There were 15 animals in each group. Brainstem evoked potentials were used to estimate temporary and permanent threshold shifts and conventional surface preparations of the cochlea were used to quantitatively assess sensory cell loss. This midterm report presents the audiometric data and a portion of the histological data for the 136 animals that completed the exposure protocol. The audiometric and available histological data showed that damage to the auditory system systematically increased as the energy of the exposure was increased through manipulation of number of presentations or peak SPL. DTIC

N94-18936* National Aeronautics and Space Administration, Washington, DC.
AEROSPACE MEDICINE AND BIOLOGY: A CONTINUING BIBLIOGRAPHY WITH INDEXES (SUPPLEMENT 382)
Dec. 1993 51 p
(NASA-SP-7011(382); NAS 1.21:7011(382)) Avail: CASI HC A04

This bibliography lists 119 reports, articles, and other documents recently introduced into the NASA Scientific and Technical Information System. Subject coverage includes the following: aerospace medicine and physiology, life support systems and man/system technology, protective clothing, exobiology and extraterrestrial life, planetary biology, and flight crew behavior and performance. Author

N94-19069* National Aeronautics and Space Administration, Washington, DC.
AEROSPACE MEDICINE AND BIOLOGY: A CONTINUING BIBLIOGRAPHY WITH INDEXES (SUPPLEMENT 381)
Nov. 1993 46 p
(NASA-SP-7011(381); NAS 1.21:7011(381)) Avail: CASI HC A03

This bibliography lists 89 reports, articles and other documents introduced into the NASA Scientific and Technical Information System during Nov. 1993. Subject coverage includes: aerospace medicine and physiology, life support systems and man/system technology, protective clothing, exobiology and extraterrestrial life, planetary biology, and flight crew behavior and performance. Author

N94-19523 Institut d'Aeronomie Spatiale de Belgique, Brussels.
THE BRAIN ELECTRICAL ACTIVITY IN DIFFERENT G SITUATIONS
K. deMetz (Antwerp Univ., Belgium.), O. Quadens (Antwerp Univ., Belgium.), and M. DeGraeve 1993 19 p Submitted for publication Sponsored in part by National Foundation for Scientific Research, Belgium
(Aeronautica-Acta-A-372-1993; ETN-93-94964) Copyright Avail: Issuing Activity (Institut d'Aeronomie Spatiale de Belgique, 3 Avenue Circulaire, B-1180 Brussels, Belgium)

The electrical activity of the brain was recorded during parabolic flights in trained astronauts and nontrained volunteers. It was quantified with the fast Fourier transform method. The electrical activity of the brain analyses evidenced more asymmetry between the two brain hemispheres in the subject who suffered from motion sickness than in the others. A first attempt was made to calculate the dimensionality of 'chaotic attractors' in the electrical activity of the brain patterns as a function of the different g-epochs of 1 parabola. This method allows us to discriminate between deterministic and stochastic events and to indicate trends. Preliminary results are given. ESA

N94-19593 East Carolina Univ., Greenville, NC.
EVALUATION OF DRIED STORAGE OF PLATELETS FOR TRANSFUSION: PHYSIOLOGIC INTEGRITY AND HEMOSTATIC FUNCTIONALITY Triannual Report No. 2
Arthur P. Bode 8 Oct. 1993 6 p Limited Reproducibility: More than 20% of this document may be affected by microfiche quality
(Contract N00014-92-J-1244)
(AD-A270756) Avail: CASI HC A02

The meeting consisted of a review of all project findings to date (1989-present) to evaluate the prospects of commercialization of dried human platelets for transfusion. Data was presented to show the typical yields, retention of platelet integrity and function, and possible in vivo application. The discussion that proceeded was generally very favorable and supported a progression toward GMP/GLP large-scale production of pharmaceutical grade human platelet preparations as a next step. We view this outcome as a validation of our efforts. DTIC

N94-19608# Naval Health Research Center, San Diego, CA.
A COMPARISON OF POLYGRAPHIC AND ACTIGRAPHIC MONITORING OF SLEEP USING A 5-CHANNEL PROGRAMMABLE-SENSITIVITY ACTIGRAPH Final Report, 15 Nov 1990 - 14 Nov. 1992
Timothy F. Elsmore and Paul Naitoh 30 Nov. 1992 62 p
(Contract MIPR-91MM1505)
(AD-A270731) Avail: CASI HC A04/MF A01

The purpose of this project was to investigate the utility of a new device, the AMA-32 actigraph, for monitoring the general activity of human subjects both during sleep and wake. In the first phase of the project, a software program for the analysis of AMA-32 data files was developed. In the second phase, the effects of frequency passband and threshold settings of the AMA-32 amplifier were examined in a 96-hour study. It was concluded that discrimination of sleep from wake was best with the 2-3 Hz passband, which emulates earlier-generation actigraphs, and that existing algorithms for automatic sleep scoring of actigraphs are not applicable to actigraph data collected with non-traditional analog amplifier characteristics. Additional studies are needed to further explore the utility of the additional features offered by the AMA-32. DTIC

N94-19675# Naval Medical Research Inst., Bethesda, MD.
CEREBRAL ISCHEMIA AND REPERFUSION INJURY: A BRIEF REVIEW Technical Report, Dec. 1992 - May 1993
J. S. Colton and S. L. Pocotte Jul. 1993 31 p
(DA Proj. MR0-4101)
(AD-A270480; NMRI-93-55) Avail: CASI HC A03/MF A01

Cerebral injury, whether due to cardiac arrest, stroke, air embolism, head trauma, asphyxiation or cerebral edema, is a major medical challenge. The understanding of the basic physiology and biochemistry of brain damage helps lay a foundation for informed diagnosis and treatment, as well as the development of future intervention and treatment strategies. It is hoped that the review provides a useful collection of facts and concepts that can be integrated into a working understanding of brain injury induced by a compromised oxygen supply. This review is the result of an extensive literature search and compilation of information on ischemia and reperfusion injury. This information was used, in part, for the preparation and construction of a research preproposal on the same subject matter. DTIC

N94-19783# California Univ., San Diego, La Jolla. Dept. of Psychiatry.
EXTRATHALAMIC MODULATION OF CORTICAL FUNCTION Final Technical Report, 1 Jul. 1990 - 30 Jun. 1993
Stephen L. Foote and Jaime A. Pineda 15 Sep. 1993 12 p
(Grant AF-AFOSR-0325-90)
(AD-A270869; AFOSR-93-0784TR) Avail: CASI HC A03/MF A01

The overall goal of the proposed study is to characterize the effects of noradrenergic (NA) afferents on cortical information processing. Our previous studies indicate that the primate locus coeruleus (LC) system, originating in the pontine brainstem, innervates the neocortex more densely than previously thought, exhibiting highly specific patterns in terms of the regional and laminar distribution of its axons across the neocortex. Previous neurophysiological observations suggest that this highly divergent system imposes state-related modulatory effects on thalamo-cortical and cortico-cortical systems. For example, we have shown that primate LC-NA neurons are more active during waking than sleep and exhibit bursts of activity during increases in attentiveness. We have also previously demonstrated that the microiontophoretic application of NA to monkey auditory cortex neurons increases the selectiveness of their responses to auditory stimuli. DTIC

N94-19163*# Utah Univ., Salt Lake City.
CHARACTERIZATION OF FLUID PHYSICS EFFECTS ON CARDIOVASCULAR RESPONSE TO MICROGRAVITY (G-572)
George M. Pantalos, M. Keith Sharp, Stewart J. Woodruff, Richard D. Lorange, Thomas E. Bennett (Bellarmine-Ursuline Coll., Louisville, KY.), Jan J. Sojka (Utah State Univ., Logan.), and Mark W. Lemon (Utah State Univ., Logan.) *In* NASA. Goddard Space Flight Center, The 1993 Shuttle Small Payloads Symposium Oct. 1993 p 1-10 (For primary document

see N94-19162 04-12)
Avail: CASI HC A02/MF A03

53 BEHAVIORAL SCIENCES

Includes psychological factors; individual and group behavior; crew training and evaluation; and psychiatric research.

N94-17967 Institute for Perception RVO-TNO, Soesterberg (Netherlands). Skilled Behavior Group.
A METHOD FOR COGNITIVE TASK ANALYSIS Final Report
A. M. Schaafstal and J. M. C. Schraagen 24 Jul. 1992 39 p Sponsored by TNO Defence Research, Delft, Netherlands
(IZF-1992-B5; TD92-2278; ETN-93-94527) Copyright Avail: TNO Institute for Perception, Kampweg 5, 3769 ZG Soesterberg, Netherlands

A method for cognitive task analysis based on the notion of 'generic tasks' is described. The method distinguishes three layers of analysis. At the first layer, the task structure, top level goals of a certain task that have to be fulfilled during task execution are identified. The task structure may also be viewed as the global strategy to carry out the task. At the second layer of analysis, the local strategies (procedures) are identified by means of which values are obtained for goals in the task structure. The third layer of analysis consists of a description of the underlying domain knowledge. The potentialities of the task model in predicting and diagnosing human cognitive behavior are discussed, and implications of the model for applied areas such as the development of knowledge based systems and training, are considered. ESA

N94-18121# Amsterdam Univ. (Netherlands).
LOCALIZATION OF FIGURE BACKGROUND SEGREGATION MECHANISMS IN PRIMATE VISUAL CORTEX Ph.D. Thesis
V. A. F. Lamme 20 Oct. 1992 182 p
(PB93-187961) Avail: CASI HC A09/MF A02

Contents of the document include the following: an introduction to anatomical organization of primary visual cortex, orientation selectivity, direction selectivity, and image segmentation; rationale and methods; equivalent dipole localization of texture segregation mechanisms in man and monkey; intracortical organization of texture segregation processing; and intracortical organization of motion defined image segmentation processing. NTIS

N94-18292# Johns Hopkins Univ., Baltimore, MD. Dept. of Psychology.
STOCHASTIC MODELS OF ATTENTION AND SEARCH Annual Report, 1 Mar. 1992 - 28 Feb. 1993
Steven Yantis 28 Feb. 1993 15 p
(Contract F49620-92-J-0186)
(AD-A268622; AFOSR-93-0629TR) Avail: CASI HC A03/MF A01

Four lines of experimentation have been carried out. In the first set of experiments, we have tested and rejected a two-process model of visual attention allocation. The PI has proposed an alternative perceptual sampling model and performed stochastic simulations of the model to show that it can account for certain aspects of human performance in cued visual search tasks. In the second and third set of experiments, the PI has found that a common mechanism may underlie the perception of bistable apparent motion and the capture of visual attention in certain visual search tasks. In particular, the appearance of a new perceptual object in the visual field captures attention and this may influence how object identity is assigned in apparent motion perception. In the final set of experiments, the PI has examined the possible influence of factors influencing figural identity on the perception of bistable apparent motion. Preliminary results suggest that grouping by spatial proximity can modulate the assignment of motion correspondence in apparent motion perception. DTIC

N94-18304 California Univ., Los Angeles.
CORTICAL SUBSTRATE OF HAPTIC REPRESENTATION Final Report
24 Aug. 1993 9 p Limited Reproducibility: More than 20% of this document may be affected by microfiche quality
(Contract N00014-89-J-1805)
(AD-A269583) Avail: CASI HC A02

The focus of the research has been on the role and mechanisms of memory in motor control. Based on experience and data from primates, computational models of short-term active memory have been developed. Such models may have technological interest and applications because this kind of memory is an essential feature of any motor control system, biological or mechanical. It appears that the neurally based and neurally testable modeling of the function of memory networks is unique among ONR-sponsored programs. Laboratory research led to the discovery of memory cells in the cerebral cortex of the monkey. Over a period of several years, extensive studies of neuronal activity and reversible cryogenic inactivation in monkeys performing memory tasks have provided theoretical framework of perceptual memory. Within that framework, memory cells are the constituents of widely distributed cortical networks which, by mechanisms yet unknown, are activated above certain thresholds and kept active, for seconds or minutes, to retain information for prospective motor action. DTIC

N94-18313 Minnesota Univ., Minneapolis. Dept. of Psychology.
PSYCHOPHYSICAL ANALYSES OF PERCEPTUAL REPRESENTATIONS Annual Report, 15 Apr. 1992 - 14 Apr. 1993
Irving Biederman 16 Jul. 1993 12 p Limited Reproducibility: More than 20% of this document may be affected by microfiche quality
(Grant AF-AFOSR-0274-90)
(AD-A268711; AFOSR-93-0626TR) Avail: Issuing Activity (Defense Technical Information Center (DTIC))

Research during the year has been divided between studies at USC (Biederman and students) and Minnesota. Our research continues to focus on linking early sensory representations to higher-level perceptual representations. For this reason, we refer to our Center informally as the 'Middle Kingdom'. Studies outlined below have examined the sensory/perceptual 'middle ground' in object recognition, depth perception, reading acuity, and auditory perception. Several of our studies have used ideal-observer analysis. The ideal-observer approach provides a means for quantifying the information available to perception and for evaluating the effectiveness with which humans use that information. DTIC

N94-18657# Rice Univ., Houston, TX. Dept. of Psychology.
COMPARING PERFORMANCE ON IMPLICIT MEMORY TESTS Annual Technical Report, 1 Aug. 1992 - 31 Jul. 1993
Henry Roediger, III 1 Sep. 1993 11 p
(Contract F49620-92-J-0437)
(AD-A269900; AFOSR-93-0714TR) Avail: CASI HC A03/MF A01

During the past year grant related work has begun on five major projects and a similar number of projects less directly related to the original proposal, but still germane to it. Most of these concern the relation between measures of explicit and implicit memory performance, fulfilling the stated aims of the proposal. To cite some of our major findings during the first year of work, we have found that (1) priming on perceptual implicit memory tests can be boosted by imagery; (2) distinctive events that have powerful effects on explicit tests have little or no effect on perceptual priming; (3) a direct comparison of two methods for telling whether implicit memory tests are contaminated by conscious recollection both reveal that the tests are not contaminated, and (4) we have obtained some puzzling results (unlike those described above) which seem to indicate that repetition effects on implicit memory tests are more complicated than we had previously expected. Because we have just completed 12 months of a 36-month grant, some of the projects have not yet been completed. However, even after this first year, we plan to submit four papers on this work within the next few months. Most of the research conducted under the auspices of the grant has been at Armstrong Laboratories at Brooks AFB in San Antonio. This summer we have completed several pilot projects that will launch us on our second year's work at Armstrong Laboratories. Altogether, we tested some thirteen hundred subjects during the past year at Armstrong Laboratories, as well as several hundred more at Rice University, on these various projects. We believe we are making good progress toward our goals of the original proposal. DTIC

N94-18682# California Univ., Berkeley. Dept. of Psychology.
VISUAL PERCEPTION OF FEATURES AND OBJECTS Annual Report, 15 Mar. 1992 - 28 Feb. 1993
Anne Treisman 19 Mar. 1993 14 p
(Grant AF-AFOSR-0370-90)
(AD-A269879; AFOSR-93-0713TR) Avail: CASI HC A03/MF A01

This period of grant support was used to continue experiments on the

preattentive processing of features, focusing on the role of attention in the integration of information across opposite directions of contrast. While unicontrast dots can be integrated in parallel across space and time to give rise to preattentive perception of either orientation or motion, attention seems to be required when the dots are of opposite contrast, consistent with the predictions of feature integration theory. A new method of dissociating preattentive and attentive processing through selective adaptation was explored. The second main area of research concerned perception and visual memory for novel objects, using priming tasks to discover the nature of the representations formed either automatically or with attention. We discovered a surprising combination of plasticity and persistence in implicit memory: Unattended novel patterns apparently leave memory traces that are formed in a single presentation but persist across at least 200 intervening trials with other similar patterns. Yet no conscious explicit memory is available even immediately after the presentation.
DTIC

N94-18686# Naval Weapons Center, China Lake, CA.
OPERATOR PERFORMANCE IN PATTERN MATCHING AS A FUNCTION OF REFERENCE MATERIAL STRUCTURE Summary Report, FY 1992 and 1993
Marion P. Kibbe and Jan S. Stiff Sep. 1993 31 p
(AD-A269889; NAWCWPNS-TP-8145) Avail: CASI HC A03/MF A01

This report describes the results of two experiments that examine operator accuracies and response times to recognize matches and mismatches between line drawings and photographs. The line drawings used in the experiments were generated by the procedures used in the Land-Attack Multi-sensor Correlation (LMC), which is a targeting system under development at China Lake. The experiments varied the number of pixels in the line drawings, the manner in which the pixels were varied, and the kind of premission experience the operators had with the imagery. In addition, the performance results were used to demonstrate an approach that might be used to set a criterion score for calling out a match by the LMC.
DTIC

N94-18744 Air Force Systems Command, Wright-Patterson AFB, OH. Armstrong Lab.
PUTTING KNOWLEDGE TO USE: THE ACQUISITION AND TRANSFER OF KNOWLEDGE IN SITUATED PROBLEM SOLVING ENVIRONMENTS Final Report, Jan. 1989 - Dec. 1992
Michael D. McNeese Jan. 1993 137 p Limited Reproducibility: More than 20% of this document may be affected by microfiche quality
(AF Proj. 7184)
(AD-A269746; AL/CF-TR-1993-0052) Avail: CASI HC A07

Within the areas of cooperative learning and group problem solving there has been great emphasis placed on the benefits of 'two heads being greater than one.' However, within each of these areas there is a lack of focus placed upon understanding naturalistic problems, the roles of metacognitive and perceptual expertise in collaboration, and the influence such factors have on transfer and use of knowledge from one situation to another. A research program is described which uses the Jasper series (a laser-disc based experimental macrocontext) to address these inadequacies and to investigate group-to-individual transfer in cooperative learning. The question asked is: 'What are the conditions in group collaboration which lead to a group member's use of knowledge as an individual?' Multiple statistical analyses were performed on various study components to clarify the relationships among individual and cooperative learning, collective induction, and the role of perceptual experience. Results highlight the different roles of perceptual context and collective induction in the knowledge acquisition/transfer process. Interpretation of the findings is given by proposing a situated cognition approach to problem solving. Finally, applications of the research suggest new forms of intelligent tutoring systems.
DTIC

N94-19348 Katholieke Univ., Nijmegen (Netherlands). Inst. for Cognition and Information.
SERIAL PATTERN COMPLEXITY: IRREGULARITY AND HIERARCHY
P. A. vanderHelm, R. J. vanLier, and E. L. J. Leeuwenberg 1993 47 p See also PB85-200574 and PB88-209911 Limited Reproducibility: More than 20% of this document may be affected by microfiche quality
(PB93-191914; Rept-91-NICI-05) Avail: CASI HC A03

In perception research, various models have been designed for the encoding of e.g. visual patterns, in order to predict the human interpretation of such patterns. Each of these encoding models provides a few coding rules to obtain codes of a pattern, each code expressing regularity and hierarchy in that pattern. Some of these models employ the minimum principle which states that the human interpretation of a pattern is reflected by the simplest code of that pattern. That is, the simplest code according to a given complexity metric. The authors propose a new complexity metric. The metric is based on a formal analysis of the concept of regularity. Some conclusions of the analysis are sketched. The new metric accounts for the amounts of irregularity and hierarchy as represented in a code of a pattern, such that these two amounts can be added to determine the complexity of a code.
NTIS

N94-19419 Institute for Perception RVO-TNO, Soesterberg (Netherlands). Skills Group.
STIMULUS-DRIVEN CAPTURE AND ATTENTIONAL SET: SELECTIVE SEARCH FOR COLOR AND VISUAL ABRUPT ONSETS Final Report
J. Theeuwes 25 Sep. 1992 22 p Sponsored by TNO Defence Research, Delft, Netherlands
(IZF-1992-B-9; TD-92-2292; ETN-93-94926) Copyright Avail: Issuing Activity (TNO Institute for Perception, Kampweg 5, 3769 DE Soesterberg, Netherlands)

Recent evidence suggests that the occurrence of attentional capture is contingent on the attentional control setting induced by the task demands. The experiments on which these conclusions are based can be criticized for several reasons: the contingent capture hypothesis was tested by means of two visual search tasks in which subjects searched multielement displays in which a color singleton and onset singleton were simultaneously present. When subjects had to search for a color singleton, on some trials another location contained an irrelevant onset. When subjects had to search for an onset singleton, on some trials another location contained an irrelevant color singleton. Both experiments show that the contingent capture hypothesis does not hold: attention was captured by the most salient singleton. The results suggest a stimulus driven model of performance on which selection is completely determined by the properties of the objects present in the visual field.
ESA

N94-19420 Institute for Perception RVO-TNO, Soesterberg (Netherlands). Skilled Behavior Group.
EFFECTS OF PRACTICE IN SELECTING AND EXECUTING KEYPRESSING SEQUENCES Final Report
W. B. Verwey 7 Oct. 1992 38 p Sponsored by TNO Defence Research, Delft, Netherlands
(IZF-1992-B-10; TD-92-2293; ETN-93-94927) Copyright Avail: Issuing Activity (TNO Institute for Perception, Kampweg 5, 3769 DE Soesterberg, Netherlands)

Three experiments that aimed at examining the effects of practice in a sequential keypressing task are described: in the first experiment a two choice sequence production task was practiced extensively. The second experiment assessed the effect of this practice on the production of a series of slightly changed sequences. In the third experiment a four choice reaction task was performed which included the practiced pair of sequences as well as a new pair in order to assess the effects of frequency of occurrence of each pair and their mutual similarity in terms of length and spatial layout. The results are used for the development of two sequence execution mechanisms. One allows programming to continue while the earlier keypresses in the sequence are already executed. The other allows unpacking of individual motor elements from a short term motor buffer during execution of the preceding keypresses. Practice with consistent stimulus sequence mappings made performance less sensitive to the presence of similar sequences than practice with varied mappings which suggests that stimulus sequence associations develop with consistent stimulus sequence mapping.
ESA

N94-19422 Institute for Perception RVO-TNO, Soesterberg (Netherlands). Skilled Behavior Group.
A FORTHCOMING KEY PRESS CAN BE SELECTED WHILE EARLIER ONES ARE EXECUTED Final Report
W. B. Verwey 20 Jan. 1993 24 p Sponsored by TNO Defence Research, Delft, Netherlands
(IZF-1993-B-2; TD-92-3202; ETN-93-94929) Copyright Avail: Issuing

Activity (TNO Institute for Perception, Kampweg 5, 3769 DE Soesterberg, Netherlands)

The issue of selecting a response while executing earlier response movements is addressed. Although there is the general notion that this may be possible, there is no conclusive evidence on whether it can occur without interference. A direct test of whether concurrent response selection and execution of previous resonses develops with practice was carried out by having subjects press a number of keys, determined in advance, prior to pressing a stimulus dependent key. Response selection demands were varied by utilizing spatially compatible and incompatible stimulus response mappings the demands of which are known not to diminish much with practice. The results show that the longer time needed to select an incompatible response vanishes almost entirely when the stimulus dependent response is preceded by two and four predetermined key presses. The conclusion is drawn that response selection can concur with the execution of movement sequences without interference. ESA

N94-19439 Institute for Perception RVO-TNO, Soesterberg (Netherlands). Work Environment Group.

PILOT STUDIES ON OBJECT MOTION PERCEPTION DURING LINEAR SELF-MOTION AFTER LONG DURATION CENTRIFUGATION OF HUMAN SUBJECTS Final Report

A. H. Wertheim 1 Feb. 1993 33 p Sponsored by TNO Defence Research, Delft, Netherlands

(IZF-1993-B-3; TD-92-3203; ETN-93-94930) Copyright Avail: Issuing Activity (TNO Institute for Perception, Kampweg 5, 3769 DE Soesterberg, Netherlands)

Four experiments are reported. They were carried out to investigate whether a particular experimental paradigm to investigate the effects of long duration centrifugation of human subjects could be used and optimized. The method involved the psychophysical measurement of visual thresholds for perceiving object motion during self motion on a linear track sled. The experiments were of a preliminary nature and definite conclusions as to their theoretical interpretation can not be drawn. Two hypotheses can be underlined: according to the first hypothesis, long duration centrifugation affects the way in which visual information interacts with otolith reactivity; according to the second hypothesis, subjects who rely largely on visual information for a correct percept of egomotion are more susceptible to centrifuge induced sickness than others. ESA

N94-19440 Institute for Perception RVO-TNO, Soesterberg (Netherlands). Information Processing Group.

COGNITIVE ABILITY AND WHOLE-BODY ROTATION Final Report

L. C. Boer 3 Mar. 1993 25 p Sponsored by TNO Defence Research, Delft, Netherlands

(IZF-1993-B-4; TD93-0371; ETN-93-94931) Copyright Avail: Issuing Activity (TNO Institute for Perception, Kampweg 5, 3769 DE Soesterberg, Netherlands)

A series of studies examining how whole body rotation affects cognitive processing is summarized, and a new experiment is described. The main question was whether rotations of the body capture attention and reduce cognitive processing capacity. An additional question was whether the attention caught is resource specific, that is, whether particular cognitive capacities are more affected than others. Previous experiments revealed that cognitive processing comes to a complete standstill while body rotations are made actively on a swivel chair. The duration of the suspension depended on the nature of the cognitive task, suggesting resource specificity. In the present experiment a rotating chair was used on which subjects were rotated while performing on spatial and nonspatial tasks. Performance losses were small and limited to the spatial task. The conclusion based on the whole series of experiments is that body rotations capture general as well as specific processing capacity, but that the amount of capacity caught is small, or the duration of capacity capture is short. Large attention capture is expected only if subjects execute the rotations actively. The striking similarity with the effects of eye movements on cognitive processing suggests that the active search for new information in the visual environment is the real reason why whole body rotation can be so disturbing. ESA

N94-19443 Institute for Perception RVO-TNO, Soesterberg (Netherlands). Skilled Behavior Group.

EFFECTS OF LOCATION CUING ON REDUNDANT TARGET PROCESSING Final Report

J. Theeuwes 6 Jan. 1993 14 p Sponsored by TNO Defence Research, Delft, Netherlands

(IZF-1993-B-1; TD-92-3197; ETN-93-94932) Copyright Avail: Issuing Activity (TNO Institute for Perception, Kampweg 5, 3769 DE Soesterberg, Netherlands)

Redundancy gain is discussed. It is observed that subjects respond faster to simultaneously presented redundant targets than to single targets. This finding is usually interpreted as evidence for parallel, self terminating, unlimited capacity processing. It is claimed that the reaction time advantage with redundant targets is simply due to spatial uncertainty under single target conditions. The present study tested this hypothesis. Subjects responded when one, two or three letter E's were presented, and refrained from responding when one, two or three letter F's were presented. On half of the trials, location uncertainty was eliminated by presenting a line segment at one of the locations of the subsequently appearing target letters. The results reject the alternative spatial uncertainty explanation: even when the location of the impending target is cued in advance, there is no attenuation of the redundancy gain. ESA

N94-19649# Technische Univ., Berlin (Germany). Fachbereich Verkehrswesen.

MODELING OF DRIVER BEHAVIOR: INFORMATION PERCEPTION, RULE AND CONTROL STRATEGIES IN EXPERIMENTS AND SIMULATIONS Ph.D. Thesis [MODELLIERUNG DES FAHRERVERHALTENS: INFORMATIONSAUFNAHME, REGEL- UND STEUERSTRATEGIEN IN EXPERIMENT UND SIMULATION]

Mihaela Neculau 1992 112 p In GERMAN

(ETN-93-95053) Avail: CASI HC A06/MF A02

For modeling several aspects of driver behavior, such as controllability and information processing, driver, vehicle, and environment are included in a system. The optimal control model was used as the theoretical basis. A vehicle model is developed, which involves longitudinal and transverse dynamics; nonlinear characteristics line for the motor moment and dynamic wheel loading were assumed; peripheral forces were separately calculated for rolling and braking. The street contour was represented in fixed coordinates with a parameter dependent curvature variation. The driver was assumed to have an internal model of the effects of his actions and to be able to estimate distances and relative angle variations; he must have a spatial representation of observed objects location and their relative position. Modern cognitive psychology theories were used for describing information subjective interpretation and its consequences on information processing modeling. Measured data used for model validation were extracted from tests of rally driver performances. It is concluded that the model is a powerful simulation tool for engineers, as far as it allows standard maneuvers to be represented. ESA

N94-19677# Battelle Memorial Inst., Columbus, OH.

INTEGRATED MEASUREMENT OF CREW RESOURCE MANAGEMENT AND TECHNICAL FLYING SKILLS Final Report, Feb. 1992 - May 1993

George L. Keampf and David W. Klinger Aug. 1993 114 p

(AD-A270512; DOT/FAA/RD-93/26; DOT-VNTSC-FAA-93-6) Avail: CASI HC A06/MF A02

The findings of a study designed with the objectives to produce a prototype performance measurement instrument (PMI) that integrates the assessment of Crew Resource Management (CRM) and technical flying skills and to investigate the suitability of the Critical Decision Method (CDM) for eliciting expert information concerning performance measurement are presented. The work was funded by the FAA in support of the Advanced Qualification Program (AQP) and conducted in cooperation with a major U.S. carrier. The researchers used CDM to identify critical components of performance assessment for specific flight tasks and developed a prototype PMI. The instrument contains two sections for each task. One section allows an evaluator to record significant pilot and crew behaviors observed; the second section allows the evaluator to provide a subjective assessment of pilot and crew proficiency. The researchers pretested the instrument and made revisions based on recommendations from experienced instructors. The researchers then evaluated the PMI with eight instructors observing a total of 16 different flight crews in recurrent training, performing a standard Line Oriented Flight Training (LOFT) scenario in a flight simulator. The instructors reliably and accurately employed the PMI to assess performance of the crew and the individual pilot. The authors recommended that AQP developers use Cognitive Task Analysis (CTA) techniques to develop training programs for cognitive and team tasks. DTIC

54 MAN/SYSTEM TECHNOLOGY AND LIFE SUPPORT

Includes human engineering; biotechnology; and space suits and protective clothing.

For related information see also *16 Space Transportation.*

N94-17841# Technical Research Associates, Salt Lake City, UT.
MAGNETOSTRICTIVE ACTUATORS FOR HUMAN SENSORY FEEDBACK Final Report, Jul. 1992 - Jan. 1993
Owen D. Brimhall, Daniel Knowlton, and Howard R. Curtin Feb. 1993 37 p
(Contract F41624-92-C-6005)
(AD-A269266; AL/CF-TR-1993-0074) Avail: CASI HC A03/MF A01

The development of actuators with enhanced capabilities is critical to the achievement of sensory feedback systems for intuitive, real time human operation of telerobotic systems. The objective of this research project was to demonstrate feasibility of new actuators using active materials which will enhance the capabilities of dexterous, exoskeletal feedback systems for telerobotic applications. In phase 1, feasibility of several novel Terfenol-D magnetostrictive actuators were demonstrated. Several prototype actuators were fabricated and tested, including resistive single axis brakes, resistive multiaxis (ball) brake joints, and linear motors. The new actuators are relatively efficient, responsive, small and exert high forces. The actuators provide proportional forces and are easily interfaced with digital electronics. Several of the actuators were integrated into a simple demonstration board. Phase 2 will pursue advanced development of proportional force resistive brake actuators and active linear motion actuators. DTIC

N94-18244# Oak Ridge National Lab., TN.
HUMAN RELIABILITY ANALYSIS APPLICATION GUIDE
May 1993 107 p
(Contract DE-AC05-84OR-21400)
(DE93-015361; ES/CSET-16) Avail: CASI HC A06/MF A02

Martin Marietta Energy Systems, Inc., (MMES) is engaged in a phased program to update the MMES safety documentation for the existing DOE facilities it manages. This guidance for Human Reliability Analysis (HRA) is intended for use in probabilistic safety analysis of DOE facilities. It is intended to supplement the Facility Safety Evaluation Application Guide, CSET-10, (July 1991), and subsequent revisions. The primary intended use of the guidance is to support accident analysis in Phase 2 of the Energy Systems Safety Analysis Report Update Program (SARUP). However, the guidance can be used for any safety analysis that needs human reliability analysis. The human reliability analysis methods covered by 'how-to' sections of the guide are direct application of or adaptations of methods developed for Probabilistic Risk Assessments (PRA) of nuclear power plants. The adaptations of these methods were designed to make the methods more suitable to DOE non-reactor applications. The methods have been adapted for use by the personnel who will perform the accident analysis task. This has been done by furnishing guidance intended for accident analysts who are experienced in human reliability analysis and by providing various methods of several levels of complexity and sophistication that lend themselves to a graded approach. The methods also lend themselves to progressive, iterative refinement so that the more burdensome versions of the methods may be reserved for use only when the importance to safety of the human reliability issues clearly warrants the time and effort. The recommended techniques build upon logic models of the human interactions with the facility that contribute to accident sequences. The recommended techniques employ assessments of a catalog of Performance Shaping Factors (PSF's) that influence the reliability of operating crews in carrying out their activities. DOE

N94-18296# Army Aeromedical Research Lab., Fort Rucker, AL.
ANALYSIS OF SEATING AND RESTRAINT LIMITATIONS RESTRICTING TOTAL BODY WEIGHT FOR AIRCREW AND PASSENGERS ON US ARMY HELICOPTERS
James E. Bruckhart, Joseph R. Licina, Samuel G. Shannon, and Joseph L. Haley Jul. 1993 23 p
(DA Proj. 3M1-62787-A-878)
(AD-A269117; USAARL-93-26) Avail: CASI HC A03/MF A01

Aviation Life Support Equipment (ALSE) and crashworthy seating protect the crew and passengers in military aircraft. If the user exceeds the design weight or size range for personal protective equipment, it may not function properly. The distribution and changes in body weight and relevant anthropometric measures were evaluated for soldier and aviator groups. Current ALSE and aircraft restraints were surveyed to determine the largest available sizes. Each aircraft seat was evaluated to determine the crash strength and maximum allowable weight for a given crash pulse. The 99th percentile male soldier and aviator weigh 237.5 and 228.2 pounds, respectively. The average body weight increases with age for the male aviator population. The largest available flight suit (size 48L), SRU-21/P survival vest, and webbing restraints accommodate a 47-inch waist circumference. DTIC

N94-18394# Air Force Occupational Measurement Center, Randolph AFB, TX.
AIRCREW LIFE SUPPORT, AFSC 122X0(1T1X1) Occupational Survey Report
Aug. 1993 75 p
(AD-A268998; AFPT-90-122-956) Avail: CASI HC A04/MF A01

As described in the AFR 39-1 Specialty Descriptions for AFSC 12210/30/50, 3- and 5-skill level, members are responsible for inspecting and maintaining aircrew life support and aircrew chemical defense equipment; inspecting, maintaining, installing, and removing life support equipment on aircraft; issuing, fitting, and adjusting aircrew life upport and chemical defense equipment; assisting aircrews to don, doff, and preflight pressure suits, antiexposure suits, and aircrew chemical defense equipment; conducting aircrew chemical defense decontamination and shelter processing; and instructing aircrews on purpose, operation, care, and use of equipment as well as chemical decontamination, bail out, and ejection procedures. DTIC

N94-18412# Air Force Flight Test Center, Edwards AFB, CA.
REVISION AND VERIFICATION OF A SEVEN-POINT WORKLOAD ESTIMATE SCALE Technical Information Manual, Jan. - Jun. 1992
Lawrence L. Ames and Edward J. George Jul. 1993 35 p
(AD-A269194; AFFTC-TIM-93-01) Avail: CASI HC A03/MF A01

This technical information memorandum presents the results of an AFFTC effort to revise and verify the technical characteristics of a seven-point workload estimate scale. The original scale was the School of Aerospace Medicine (SAM) Form 202. From the results of the revision effort, it was concluded that the AFFTC revised workload estimate scale would be suitable for flight test applications. DTIC

N94-18484*# Lockheed Missiles and Space Co., Sunnyvale, CA.
LUNAR BASE CONTROLLED ECOLOGICAL LIFE SUPPORT SYSTEM (LCELSS): PRELIMINARY CONCEPTUAL DESIGN STUDY Final Report
Steven H. Schwartzkopf 30 Apr. 1991 207 p
(Contract NAS9-18069)
(NASA-CR-188479; NAS 1.26:188479; LMSC-F280196) Avail: CASI HC A10/MF A03

The objective of this study was to develop a conceptual design for a self-sufficient LCELSS. The mission need is for a CELSS with a capacity to supply the life support needs for a nominal crew of 30, and a capability for accommodating a range of crew sizes from 4 to 100 people. The work performed in this study was nominally divided into two parts. In the first part, relevant literature was assembled and reviewed. This review identified LCELSS performance requirements and the constraints and advantages confronting the design. It also collected information on the environment of the lunar surface and identified candidate technologies for the life support subsystems and the systems with which the LCELSS interfaced. Information on the operation and performance of these technologies was collected, along with concepts of how they might be incorporated into the LCELSS conceptual design. The data collected on these technologies was stored for incorporation into the study database. Also during part one, the study database structure was formulated and implemented, and an overall systems engineering methodology was developed for carrying out the study. Author

N94-18673# Air Force Inst. of Tech., Wright-Patterson AFB, OH. Foreign Aerospace Science and Technology Center.

RESEARCH ON MAN-MACHINE PRODUCTIVITY IN AVIATION AT HUMAN ENGINEERING INSTITUTE OF HANGZHOU UNIVERSITY

Wenxiong Jin, Zuxiang Zhu, and Jian Wang 6 Aug. 1993 14 p Transl. into ENGLISH from Guoji Hangkong, China, no. 4, 1991 p 55-57
(AD-A269952; FASTC-ID(RS)T-0851-92) Avail: CASI HC A03/MF A01

The Human Engineering Research Institute of Hangzhou University is a scientific research organization engaged in research on the interdiscipline between psychology and technology. In recent years, ergonomic research on the fundamental theories and applications of man-machine productivity--regarding aircraft instrumentation lighting, displays, and controls; warning signals; computer terminal displays; human reliability; human body measurements; as well as management and decision making--was carried on. DTIC

N94-18730# Department of the Navy, Washington, DC.

CONDUCTIVE GARMENTS TO PREVENT RADIO-FREQUENCY (RF) BURNS Patent Application

Richard G. Olsen, inventor (to Navy) 14 Jun. 1993 13 p
(AD-D015832; US-Patent-Appl-SN-076062) Avail: CASI HC A02/MF A01

This invention relates to protective garments to prevent radio-frequency (RF) burns. More particularly, this invention relates to conductive gloves, socks and other clothing that dissipate RF charges and thereby prevent RF burns. DTIC

N94-18754 Human Resources Research Organization, Alexandria, VA.

BUILDING A JOINT-SERVICE CLASSIFICATION RESEARCH ROADMAP: CRITERION-RELATED ISSUES Final Report, Jan. 1992 - Apr. 1993

Deirdre J. Knapp and John P. Campbell Jul. 1993 98 p Limited Reproducibility: More than 20% of this document may be affected by microfiche quality
(Contract F33615-91-C-0015)
(AD-A269735; AL/HR-TP-1993-0028) Avail: CASI HC A05

The Air Force Armstrong Laboratory, the Army Research Institute, the Navy Personnel Research and Development Center, and the Center for Naval Analyses are committed to enhancing the overall efficiency of the Services' selection and classification research agenda. This means reducing redundancy of research efforts across Services and improving inter-Service research planning, while ensuring that each Service's priority needs are served. The Roadmap project is composed of six tasks. The first task identified classification research objectives. Tasks 2 through 5 consist of reviews of specific predictor, job analytic, criterion, and methodological needs of each of the methods and issues as they relate to the selection and classification research objectives outlined in Task 1 of the Roadmap project. DTIC

N94-18765# Logistics Management Engineering, Inc., Warminster, PA. Systems Engineering Group.

ARMY COCKPIT DELETHALIZATION PROGRAM (CDP) Final Report, Oct. 1989 - Dec. 1992

Ricky L. Greth, Mark S. Pfaff, and W. B. Shope Aug. 1993 75 p
(Contract DAAJ02-89-C-0017)
(AD-A268990; CDP-871-041-A005; USAATCOM-TR-93-D-2) Avail: CASI HC A04/MF A01

Injury data indicate that secondary cockpit strikes to the head and upper torso account for approximately two-thirds of all major and fatal injuries in potentially survivable Army helicopter mishaps. A two-year program of research, biodynamic simulation, detail design, test, and evaluation was performed to examine the head/upper torso strike problem and demonstrate potential solutions. This report describes the investigation and conceptual process leading to the development of crew protection designs, including an advanced harness geometry, a harness tensioner/retractor, and a harness mounted airbag that could be candidates for current as well as year 2000+ helicopter or light aircraft applications. The protective concepts were evaluated in a series of computer simulations and in 15 dynamic tests on a horizontal accelerator using a replication of an advanced attack helicopter crewstation interior with a stroking crewseat. Overall effectiveness and physiological compatibility of the protective concepts were evaluated under varying crash pulses and impact orientations. Results show significant improvement in reduction of head displacement and linear acceleration, torso displacement, inertia reel strap payout, and neck torque compared to a baseline conventional restraint. DTIC

N94-18774# Naval Research Lab., Washington, DC.

A USER TASK ANALYSIS FOR COMMAND AND CONTROL SYSTEMS AND ITS USE IN HUMAN-COMPUTER INTERACTION RESEARCH Interim Report, 1 Oct. 1992 - 30 Jun. 1993

Deborah Hix 3 Sep. 1993 33 p
(AD-A269877; NRL/MR/5530-93-7397) Avail: CASI HC A03/MF A01

The Advanced Interfaces Section of the Human-Computer Interaction (HCI) Laboratory at the Naval Research Laboratory (NRL) is engaged in creating and evaluating interactive computer systems that address the unique issues encountered in developing innovative, high performance human-computer interfaces. A goal of this project is to build a testbed based on Naval command and control (C2) systems as a vehicle for this research. Previous work at the HCI Lab has developed new interaction techniques-ways of using physical input and output devices to perform tasks in a human-computer interface. We now wish to transition into more realistic Naval-related applications for new techniques, in particular, command and control systems. This report discusses a user task analysis performed for interactive computer-based C2 systems; this task analysis is a basis for developing and evaluating new interaction techniques. As a result of this task analysis, appropriate user tasks for incorporation into the command-and-control-like testbed will be identified. The testbed will also incorporate some of the new interaction techniques, and will be used for empirical evaluation of these techniques in human-computer interfaces. DTIC

N94-18882 Army Research Inst. of Environmental Medicine, Natick, MA.

ROAD MARCH PERFORMANCE OF SPECIAL OPERATIONS SOLDIERS CARRYING VARIOUS LOADS AND LOAD DISTRIBUTIONS

Joseph Knapik, Richard Johnson, Philip Ang, Herbert Meiselman, and Carolyn Bensel 1993 144 p Limited Reproducibility: More than 20% of this document may be affected by microfiche quality
(AD-A269198; USARIEM-T-14-93) Avail: CASI HC A07

This study examined the influence of load and load distribution on road march performance. Subjects were 21 Special Forces Soldiers who performed six individual road marches carrying three loads (34, 48, and 61 kg) and two pack systems (ALICE pack and an experimental double-pack). All marches were 20 km in length and soldiers were asked to complete the distance as rapidly as possible. Heart rates were monitored continuously during the march. Before and after each march, soldiers completed questionnaires and performed a series of tasks to evaluate cognitive ability and performance on typical soldier tasks. At the end of each march soldiers' feet were examined for injuries. Results indicated that march times increased as loads increased and march times were faster with the ALICE pack than with the double-pack. Heart rate while marching was lower for double-pack even after adjustment for march time suggesting a lower energy expenditure. The double-pack resulted in less low back discomfort and a lower incidence of blisters at the highest load but also resulted in more discomfort in the neck and hips and more heat illness symptoms. Neither load nor load distribution affected soldiers' cognitive ability or performance on marksmanship tasks, grenade throw, leg strength, hand-grip strength, or obstacle course. On the other hand, the march itself (independent of load and load distribution) resulted in decrements in marksmanship ability (vertical shot group dispersion), leg strength, and time to complete the obstacle course. DTIC

N94-18886 Maryland Univ., College Park. Office of Research Administration and Advancement.

INTERDISCIPLINARY TRAINING IN LIFE SCIENCE (FY 1991 ASSERT) Annual Report, 1 Jun. 1992 - 31 May 1993

Robert M. Steinman 4 Aug. 1993 4 p Limited Reproducibility: More than 20% of this document may be affected by microfiche quality
(Contract F49620-92-J-0260)
(AD-A269220; AFOSR-93-0677TR) Avail: CASI HC A01

This grant supports the interdisciplinary training (psychology, neuroscience, and computer science) of an advanced graduate student (Julie Epelboim), who is earning a Ph.D. in Psychology by participating as a graduate Research Assistant on AFOSR Grant 91-0124, entitled Coordinated action in 3-D Space. Her doctoral thesis will be derived from problems investigated in this parent grant which has two main thrusts. First, it tests alternative hypotheses about the mechanism that controls the gaze-shifts associated with arm motions, when an unrestrained, seated subject manipulates objects within arms's reach. The second thrust is to study the speed and accuracy of visually-guided hand movements and the correlation of these performance measures with binocular gaze-errors. Advancing knowledge in this rather technical interdisciplinary research area requires developing expertise in the areas included in Epelboim's AASSERT training program, which has been designed so as to contribute to the goals of the parent grant and at the same time prepare her for a productive career as a research scientist during the next 3 or 4 decades. DTIC

N94-18935# California Univ., Berkeley. Lawrence Berkeley Lab.
INDOOR ENVIRONMENT PROGRAM
J. M. Daisey Jun. 1993 34 p
(Contract DE-AC03-76SF-00098)
(DE93-018601; LBL-33442) Avail: CASI HC A03/MF A01

This paper reports progress during the year 1992 in the Indoor Environment Program in the Energy and Environment Division of Lawrence Berkeley Laboratory. Studies in the following areas are reported: energy performance and ventilation in buildings; physical and chemical characterization of indoor air pollutants; indoor radon; indoor air quality; exposure to indoor air pollutants; and risk analysis. Pollutants of particular interest include: radon; volatile, semi-volatile and particulate organic compounds; and combustion emissions including environmental tobacco smoke, carbon monoxide, and nitrogen oxides. DOE

N94-18992# Federal Aviation Administration, Atlantic City, NJ. Technical Center.
THE FAA TECHNICAL CENTER HUMAN FACTORS LABORATORY INFORMATION GUIDE
Vincent J. Lasewicz, Jr. and Mark W. Smolensky Apr. 1993 16 p
(AD-A269343; DOT/FAA/CT-TN93/15) Avail: CASI HC A03/MF A01

This information guide provides an overview of the capabilities of the FAA Technical Center's Human Factors Laboratory (HFL) and how those capabilities are being used to support research critical to the development and implementation of the National Airspace System (NAS). The HFL was officially opened and dedicated on November 2, 1992. This unique state-of-the-art facility is the only one of its kind in the FAA. It is important that the information about this facility is made available not only to FAA organizations, but academic and private sector organizations as well. This information guide specifically provides the reader with background on why the facility was developed, an in-depth overview of its unique design capabilities, a description of the type of work the HFL will be engaged in, and a representative sampling of the directions and goals of the HFL. DTIC

N94-19349*# Houston Univ., Clear Lake, TX. Research Inst. for Computing and Information Systems.
ADVANCED SOFTWARE DEVELOPMENT WORKSTATION: OBJECT-ORIENTED METHODOLOGIES AND APPLICATIONS FOR FLIGHT PLANNING AND MISSION OPERATIONS
Michel Izygon 30 Jun. 1993 8 p
(Contract NCC9-16; RICIS Proj. SR-02)
(NASA-CR-193706; NAS 1.26:193706) Avail: CASI HC A02/MF A01

The work accomplished during the past nine months in order to help three different organizations involved in Flight Planning and in Mission Operations systems, to transition to Object-Oriented Technology, by adopting one of the currently most widely used Object-Oriented analysis and Design Methodology is summarized. Author (revised)

N94-19442# European Space Agency. European Space Research and Technology Center, ESTEC, Noordwijk (Netherlands). Thermal Control and Life Support Div.
ENVIRONMENTAL CONTROL AND LIFE SUPPORT
Dec. 1992 63 p
(ESA-PSS-03-40-Issue-1; ETN-93-94880) Avail: CASI HC A04/MF A01

Top level definitions applicable to Environmental Control and Life Support (ECLS) terminology are presented. A breakdown of the functional requirements of ECLS subsystems, and guidelines to the ECLS design philosophy on atmosphere, water, food, hygiene and waste are given. The report constitutes a framework which should support the documentation of ECLS specifications for manned space projects. All designers are encouraged to use its terminology, the ECLS funcional breakdown, and the given symbols. Appendices detail the ECLS specification tree, symbols, a verification method for the requirements, related documents, and acronyms and definitions. The report is not applicable for spacesuits and payloads. ESA

N94-19531# Kent State Univ., OH.
A MULTIVARIATE ANTHROPOMETRIC METHOD FOR CREW STATION DESIGN Final Report, Jan. 1989 - Jan. 1993
Gregory F. Zehner, Richard S. Meindl, and Jeffrey A. Hudson Mar. 1993 41 p
(Contract F33615-85-C-0541)
(AD-A270652; AL-TR-1993-0054) Avail: CASI HC A03/MF A01

Body size accommodation in USAF cockpits is still a significant problem despite all the years of experience and the many aircraft designs that have been developed. Adequate reach to controls, body clearances (particularly during escape), and vision (internal and external) are all functions of pilot body size and position in the cockpit. One of the roots of this problem is the way cockpit accommodation is specified and tested. For many years the percentile pilot has been used. This paper describes the errors inherent in the percentile man approach and presents a multivariate alternative for describing the body size variability existing in a given flying population. A number of body size representative cases are calculated which, when used properly in specifying, designing, and testing new aircraft, should ensure the desired level of accommodation. The approach can be adapted to provide anthropometric descriptions of body size variability for a great many designs or for computer models of the human body by altering the measurements of interest and/or selecting different data sets describing the anthropometry of a user population. DTIC

N94-19570# Anthropology Research Project, Yellow Springs, OH.
HUMAN INTEGRATION EVALUATION OF THREE HELMET SYSTEMS Interim Report, Sep. 1991 - Nov. 1992
Sherri U. Blackwell and Kathleen M. Robinette Mar. 1993 108 p
(Contract F33615-89-C-0572)
(AD-A271320; AL-TR-1993-0028) Avail: CASI HC A06/MF A02

As protective equipment becomes more complex, more sophisticated tests of fit and function must be designed to determine and assess the effects of interactions between the user and various elements of the equipment. Among the newest protective ensembles available on the market are helmets with built-in Night Vision Goggles (WG's) or Helmet Mounted Displays (HMD's). A program called the Interim-Night Integrated Goggle and Head Tracking System (I-NIGHTS) was established to examine such helmets. Under this program, a series of fit and performance tests of three helmet systems was done. This report documents the fit, or human integration, evaluation designed to determine how well each helmet accommodated test subjects for comfort, stability, and optical placement. The test method used was the first to examine these three elements simultaneously as well as the first to include the measurement of head contour and three-dimensional placement of key human features. Results were intended to be used to better understand the fit related effects on later performance testing of subjects in a centrifuge, on a drop tower, and under actual flying conditions. Recommendations were made regarding design features which appear to be most effective for accommodating people. DTIC

N94-19764 Massachusetts Inst. of Tech., Cambridge. Research Lab. of Electronics.
HUMAN-MACHINE INTERFACES Final Report, 1 Mar. 1990 - 31 Jul. 1993
Nathaniel Durlach 31 Jul. 1993 26 p Limited Reproducibility: More than 20% of this document may be affected by microfiche quality
(Grant AF-AFOSR-0200-90)
(AD-A270730; AFOSR-93-0769TR) Avail: CASI HC A03

The normal human auditory system suffers from many deficiencies in its ability to localize sound sources in space. Not only is it generally poor at determining the elevation and distance of a sound source, but in certain cases it is relatively poor at determining the azimuth of the source. The research discussed in this report is concerned with the development and evaluation of systems that result in improved localization, i.e., in supernormal auditory localization, by altering the localization cues that are available to the listener. Although such enhanced performance should be of value in essentially all systems that make use of auditory localization for conveying information to the human user, the application area of primary interest in this proposal is that of human-machine interfaces for teleoperator and virtual systems. In general, localization performance can be summarized in terms of (1) resolution and (2) response bias. Resolution refers to the ability to detect small changes in the spatial position of a sound source and to separate out multiple sources located at different positions, as well as to the amount of information transfer that can be achieved in the identification of source position. Response bias refers to the average differences between perceived source position (as measured by the mean of the listener's objective responses) and the actual source position. DTIC

N94-19773# Midwest Systems Research, Inc., Dayton, OH.
FAA AIRBORNE DATA LINK HUMAN FACTORS RESEARCH PLAN Technical Note, Oct. 1991 - 1992
Albert J. Rehmann, Michael C. Reynolds, and Mark E. Neumeier Jul. 1993 54 p
(AD-A271006; DOT/FAA/CT-TN93/5) Avail: CASI HC A04/MF A01

A five-year plan to perform research of human factors issues and topics related to Data Link implementations in general aviation and transport category aircraft is presented. Elements such as resource allocation and management and coordinated cooperative research efforts are considered to be critical and are carefully developed. DTIC

N94-19473*# Virginia Univ., Charlottesville. Dept. of Mechanical and Aerospace Engineering.
EFFICIENCY AND BIOFIDELITY OF OCCUPANT SIMULATIONS
Walter D. Pilkey *In* NASA. Langley Research Center, Computational Methods for Crashworthiness Aug. 1993 p 155-163 (For primary document see N94-19465 04-39)
Avail: CASI HC A02/MF A03

55 SPACE BIOLOGY

Includes exobiology; planetary biology; and extraterrestrial life.

No abstracts in this category.

59 MATHEMATICAL AND COMPUTER SCIENCES (GENERAL)

N94-19478# National Academy of Sciences - National Research Council, Washington, DC. Commission on Physical Sciences, Mathematics, and Applications.
MATHEMATICAL SCIENCES, TECHNOLOGY, AND ECONOMIC COMPETITIVENESS
James G. Glimm, ed. 1991 118 p Sponsored in part by AFOSR, ARO, DOE, NSF, National Security Agency, and ONR
(LC-91-60253; ISBN-0-309-04483-9) Avail: CASI HC A06/MF A02

The fundamental importance of mathematics to the U.S. technology base, to the ongoing development of advanced technology, and, indirectly, to U.S. competitiveness is well known in scientific circles. However, the declining number of U.S. high school students who decide to seek a career in science or engineering is an important indication that many people do not appreciate how central the mathematical sciences have become to our technological enterprise. The National Research Council's Board on Mathematical Sciences prepared this report to underscore the importance of supporting mathematics instruction at all levels, from kindergarten through graduate school, to prepare our youth for successful careers in science and engineering. To trace the impact of mathematics on U.S. technology necessarily involves making choices. The examples are intended to illustrate the widespread use of mathematical reasoning. The board focused primarily on the use of such reasoning by mathematical scientists themselves, as defined by their professional training, departmental or professional affiliation, or funding resources. Also included in this discussion are examples of the cross-disciplinary impacts of mathematical scientists working with members of other disciplines. A few examples were drawn from the mathematically oriented portions of related disciplines such as engineering and computer science. Derived from text

60 COMPUTER OPERATIONS AND HARDWARE

Includes hardware for computer graphics, firmware, and data processing.

For components see *33 Electronics and Electrical Engineering.*

N94-17799# California Univ., Berkeley. Lawrence Berkeley Lab.
RESQme STUDIES FOR SDC REGIONAL COMPUTING CENTERS
C. T. Day Feb. 1993 35 p
(Contract DE-AC03-76SF-00098)
(DE93-015230; LBL-33540) Avail: CASI HC A03/MF A01

The Technical Design Report for the SDC proposes a model for offline computing which includes a computing center at the SSCL, containing all of the physics data, together with a number of regional computing centers around the world. These regional centers would contain subsets of the data, and would support the daily work of most physicists. For large or unusual requests, where the data are not held at the regional center, the requests would automatically be forwarded to the SSCL. It is assumed that the 'closeness' of the regional centers and their reduced demand from fewer users would result in improved system performance. Such a system is too complex to model analytically; simulation is the only viable approach. However, Monte Carlo models built from scratch for complicated systems are very difficult to maintain and hard to modify. Fortunately, we have obtained from IBM a modeling framework, RESQme, explicitly designed for building statistical models of computer systems. This note describes a first pass at modeling the proposed offline system. DOE

N94-17877# Army Research Lab., Aberdeen Proving Ground, MD.
INTRODUCTORY USER'S GUIDE TO THE ARL SUPERCOMPUTER FACILITY AT ABERDEEN PROVING GROUND Final Report
Claude J. Lapointe, Richard Angelini, Lee A. Brainard, Denice Brown, John Cole, Monte Coleman, Phillip Dykstra, Carol Ellis, Gary Kuehl, and Deborah L. Thompson et al Jun. 1993 168 p
(AD-A265204; ARL-TR-150) Avail: CASI HC A08/MF A02

The purpose of this report is to provide an introductory user's guide to many of the computers, operating systems, utilities, and software packages available at the US Army Research Laboratory Supercomputer Facility located at Aberdeen Proving Ground, MD, together with the facilities normal operating procedures. DTIC

N94-18317# Carnegie-Mellon Univ., Pittsburgh, PA. Dept. of Computer Science.
WHY ARE HUMAN-COMPUTER INTERFACES DIFFICULT TO DESIGN AND IMPLEMENT?
Brad A. Myers Jul. 1993 17 p
(Contract F33615-90-C-1465; ARPA Order 7597)
(AD-A268843; CMU-CS-93-183) Avail: CASI HC A03/MF A01

It is well known that designing and implementing a human-computer interface is a difficult and time-consuming task. However, there is little discussion of why this is true. Should we expect that a new method is around the corner that will make the design easier? Will the next generation of user interface toolkits make the implementation trivial? No. This article discusses reasons why user interface design and implementation are inherently difficult tasks and will remain so for the foreseeable future. DTIC

N94-18961* National Aeronautics and Space Administration, Washington, DC.
THE WORLD'S MOST POWERFUL COMPUTER (Videotape)
Oct. 1986 Videotape: 2 min. 42 sec. playing time, in color, with sound
(NASA-TM-109369; NONP-VT-94-198216) Avail: CASI VHS A01/BETA A22

The use of the Cray 2 supercomputer, the fastest computer in the world, at ARC is detailed. The Cray 2 can perform 250 million calculations per second and has 10 times the memory of any other computer. Ames researchers are shown creating computer simulations of aircraft airflow, waterflow around a submarine, and fuel flow inside of the Space Shuttle's engines. The video also details the Cray 2's use in calculating airflow around the Shuttle and its external rockets during liftoff for the first time and in the development of the National Aero Space Plane. CASI

N94-19295# Stockholm Univ. (Sweden). Dept. of Physics.
FASTBUS SIMULATION MODELS IN VHDL
G. Appelquist Nov. 1992 10 p
(USIP-92-07; ETN-93-94849) Avail: CASI HC A02/MF A01

Four hardware simulation models implementing the FASTBUS protocol are described. The models are written in the Very High Speed Integrated Circuit Hardware Description Language (VHDL) to obtain portability, that is, without being constrained to any specific simulator. They include two complete FASTBUS devices, a full duplex segment interconnect, and ancillary logic for the segment.Master and slave models using a high level interface to describe FASTBUS operations are presented. With these models, different configurations of FASTBUS systems can be evaluated and the FASTBUS transactions of new devices can be verified. ESA

N94-19401# National Academy of Sciences - National Research Council, Washington, DC.
COMPUTING PROFESSIONALS: CHANGING NEEDS FOR THE 1990'S
1993 152 p
(Contract N00014-87-J-1110; NSF CDA-91-21558)
(B-030; ISBN-0-309-04790-0; LC-92-85596) Copyright Avail: CASI HC A08/MF A02

To better understand trends in the supply of and demand for computing professionals, the Computer Science and Telecommunications Board (CSTB) and the Office of Scientific and Engineering Personnel (OSEP) of the National Research Council convened an exploratory workshop. Understandably, given the complexity of the issues, the limited time available to workshop participants to address them, and the restricted attendance at the workshop, not all viewpoints were addressed; those addressed were not examined in equal depth; and it was not possible for participants to reach strong conclusions and to formulate detailed recommendations. Moreover, the views, requirements, and concerns of participants from academic computer science and engineering clearly differed from those of participants based in industry and government. Nonetheless, a number of notable findings emerged. This report summarizes the discussions at that workshop and the further deliberations of the steering committee that organized it. Derived from text

N94-19535# Sandia National Labs., Albuquerque, NM.
OPTOELECTRONIC PACKAGING: A REVIEW
R. F. Carson 1993 17 p Presented at the Annual Winter Meeting of the ASME, New Orleans, LA, 28 Nov. - 3 Dec. 1993
(Contract DE-AC04-76DP-00789)
(DE93-040059; SAND-93-1990C; CONF-931121-20) Avail: CASI HC A03/MF A01

Optoelectronics and photonics hold great potential for high data-rate communication and computing. Their wide use in computing applications was limited first by device technologies and now suffers due to the need for high-precision, mass-produced packaging. The use of photons as a medium of communication and control implies a unique set of packaging constraints that was not present in traditional telecommunications applications. The state-of-the-art in optoelectronic packaging is now driven by microelectric techniques that have potential for low cost and high volume manufacturing. DOE

N94-19591 Carnegie-Mellon Univ., Pittsburgh, PA. Dept. of Computer Science.
SERVICE WITHOUT SERVERS
Chris Maeda and Brian N. Bershad Aug. 1993 7 p Limited Reproducibility: More than 20% of this document may be affected by microfiche quality
(Contract MDA972-90-C-0035; ARPA Order 7330)
(AD-A270612; CMU-CS-93-144) Avail: CASI HC A02

We propose a new style of operating system architecture appropriate for microkernel-based operating systems: services are implemented as a combination of shared libraries and dedicated server processes. Shared libraries implement performance critical portions of each system service, while dedicated servers implement the parts of each service that do not require high performance or that are difficult to implement in an application. Our initial experiments show that this approach to operating system structure can yield performance that is comparable to monolithic kernel systems while retaining all the modularity advantages of microkernel technology. Since services reside in libraries, an application is free to use the library that is most appropriate. This approach can even yield better performance than monolithic kernel systems by allowing the shared libraries to be closely coupled with the applications, thereby exploiting application-specific knowledge in policy decisions. DTIC

N94-19799# Nationaal Inst. voor Kernfysica en Hoge Energiefysica, Amsterdam (Netherlands).
THE UNIVERSAL BitBus NODE [DE UNIVERSELE BITBUS NODE]
J. T. VanEs and G. Luigjes 1993 36 p In DUTCH
(DIGEL-1993-1; ETN-93-94622) Avail: CASI HC A03/MF A01

The hardware and software of the universal BitBus Module (MUTAD 910705) are described. This module or node was developed to fulfill the need of a small and simple microcontroller with sufficient analog and digital inputs/outputs. The BitBus network consists of a master node and one or several slave nodes. The master node is generally integrated in a host computer environment. The module consists of two prints. The first contains the BitBus microcontroller with ROM (Read Only Memory), RAM (Random Access Memory), and BitBus interface. The second print contains the analog and digital inputs and outputs. ESA

N94-18359*# Idaho Univ., Moscow. Space Engineering Research Center.
SIMPLIFIED MICROPROCESSOR DESIGN FOR VLSI CONTROL APPLICATIONS
K. Cameron *In its* The 1991 3rd NASA Symposium on VLSI Design 1991 9 p (For primary document see N94-18337 04-33)
Avail: CASI HC A02/MF A04

N94-18360*# Idaho Univ., Moscow. Space Engineering Research Center.
A MODIFIED RECONFIGURABLE DATA PATH PROCESSOR
G. Ganesh, S. Whitaker, and G. Maki *In its* The 1991 3rd NASA Symposium on VLSI Design 1991 10 p (For primary document see N94-18337 04-33)
(Grants NAGw-1406; NAG5-1043)
Avail: CASI HC A02/MF A04

N94-18362*# Stanford Univ., CA. Computer Systems Lab.
HIGH-PERFORMANCE MULTIPROCESSOR ARCHITECTURE FOR A 3-D LATTICE GAS MODEL
F. Lee, M. Flynn, and M. Morf *In* Idaho Univ., The 1991 3rd NASA Symposium on VLSI Design 1991 14 p (For primary document see N94-18337 04-33)
(Grant NAGw-419)
Avail: CASI HC A03/MF A04

N94-18366*# California Univ., Davis. Div. of Computer Science.
FORMAL VERIFICATION OF AN MMU AND MMU CACHE
E. T. Schubert *In* Idaho Univ., The 1991 3rd NASA Symposium on VLSI Design 1991 12 p (For primary document see N94-18337 04-33)
Avail: CASI HC A03/MF A04

N94-18379*# Madras Univ. (India). Coll. of Engineering.
A SPECIAL PURPOSE SILICON COMPILER FOR DESIGNING SUPERCOMPUTING VLSI SYSTEMS
N. Venkateswaran, P. Murugavel, V. Kamakoti, M. J. ShankarRaman, S. Rangarajan, M. Mallikarjun, B. Karthikeyan, T. S. Prabhakar, V. Satish, and P. R. Venkatasubramaniam et al *In* Idaho Univ., The 1991 3rd NASA Symposium on VLSI Design 1991 15 p (For primary document see N94-18337 04-33)
Avail: CASI HC A03/MF A04

N94-19169*# Hancock (Thomas), Huntsville, AL.
STATIC COMPUTER MEMORY INTEGRITY TESTING (SCMIT): AN EXPERIMENT FLOWN ON STS-40 AS PART OF GAS PAYLOAD G-616
Thomas Hancock *In* NASA. Goddard Space Flight Center, The 1993

Shuttle Small Payloads Symposium Oct. 1993 p 57-62 (For primary document see N94-19162 04-12)
Avail: CASI HC A02/MF A03

N94-19171*# Evolving Technologies Corp., New York, NY.
VPU(TM) DEMONSTRATION MISSION VICINITY PROCESSOR UNIT(TM) OVERVIEW
Loren Abdulezer *In* NASA. Goddard Space Flight Center, The 1993 Shuttle Small Payloads Symposium Oct. 1993 p 73-74 (For primary document see N94-19162 04-12)
Avail: CASI HC A01/MF A03

N94-19184*# Harris Corp., Melbourne, FL.
RADIATION HARDENED MICROPROCESSOR FOR SMALL PAYLOADS Abstract Only
Ravi Shah *In* NASA. Goddard Space Flight Center, The 1993 Shuttle Small Payloads Symposium Oct. 1993 p 199 (For primary document see N94-19162 04-12)
(Contract N00014-91-C-2005)
Avail: CASI HC A01/MF A03

61 COMPUTER PROGRAMMING AND SOFTWARE

Includes computer programs, routines, alogorithms, and specific applications, e.g., CAD/CAM.

N94-17701# Stanford Univ., CA. Systems Optimization Lab.
PLANNING UNDER UNCERTAINTY SOLVING LARGE-SCALE STOCHASTIC LINEAR PROGRAMS
G. Infanger (Technische Univ., Vienna, Austria.) Dec. 1992 116 p
(Contract DE-FG03-92ER-25116)
(DE93-013920; SU-SOL-92-8) Avail: CASI HC A06/MF A02

For many practical problems, solutions obtained from deterministic models are unsatisfactory because they fail to hedge against certain contingencies that may occur in the future. Stochastic models address this shortcoming, but up until recently seemed to be intractable due to their size. Recent advances both in solution algorithms and in computer technology now allow us to solve important and general classes of practical stochastic problems. We show how large-scale stochastic linear programs can be efficiently solved by combining classical decomposition and Monte Carlo (importance) sampling techniques. We discuss the methodology for solving two-stage stochastic linear programs with recourse, present numerical results of large problems with numerous stochastic parameters, show how to efficiently implement the methodology on a parallel multi-computer, and derive the theory for solving a general class of multi-stage problems with dependency of the stochastic parameters within a stage and between different stages. DOE

N94-17732# University of Southern California, Marina del Rey.
EMPLOYING KNOWLEDGE RESOURCES IN A NEW TEXT PLANNER ARCHITECTURE Research Report
Eduard Hovy, Julia Lavid, Elisabeth A. Maier, Vibhu O. Mittal, and Cecile L. Paris Apr. 1993 16 p
(Contract DABT63-91-C-0025)
(AD-A269669; ISI/RR-93-328) Avail: CASI HC A03/MF A01

We describe in this paper a new text planner that has been designed to address several problems we had encountered in previous systems. Motivating factors include a clearer and more explicit separation of the declarative and procedural knowledge used in a text generation systems as well as the identification of the distinct types of knowledge necessary to generate coherent discourse, such as communicative goals, text types, schemas, discourse structure relations, and theme development patterns. This knowledge is encoded as separate resources and integrated under a flexible planning process that draws from appropriate resources whatever knowledge is needed to construct a text. We describe the resources and the planning process and illustrate the ideas with an example. DTIC

N94-17740# Lawrence Livermore National Lab., CA.
AN EFFICIENT IMPLEMENTATION OF ERROR-VALUED SEMANTICS ON IMPERATIVE MACHINES Ph.D. Thesis
P. J. Miller Apr. 1993 122 p
(Contract W-7405-eng-48)
(DE93-014658; UCRL-LR-113559) Avail: CASI HC A06/MF A02

Error values must be implemented efficiently if they are to be useful for exception handling. Error values support implicit parallelism because they do not require explicit control flow primitives. Naive implementations test for error input values at each operation and propagate them to the outputs. Such an implementation is expensive on von Neumann style, imperative machines because the test-and-propagation overhead is more expensive than the actual computation. When run-time errors do not occur, any test-and-propagate work is wasted. However, it cannot generally be known at run-time whether or not a computation will generate errors. The challenge for the compiler is to preserve the error test-and-propagate semantics at a cost no higher than that of simple error detection. The dissertation presents a code space partitioning model for implementing error-valued semantics, which will be shown to work well on von Neumann architectures. Computation begins in a fast, error-free partition, and moves to a slower, safer, test-and-propagate partition when errors occur. The technique combines the speed of the error detect-and-halt model with the utility of the test-and-propagate model. If no errors occur, then the computation completes as fast as it would in error-detect only code. Additionally, for applicative languages, isolated blocks with errors can compute in the error-possible partition while other blocks can compute in the faster, error-testing free partition. The dissertation also presents a prototype compiler that uses the partitioning method to compile THISAL (a powerful subset of SISAL) programs. DOE

N94-17786# Sandia National Labs., Albuquerque, NM.
PROPOSAL FOR A NUMERICAL ARRAY LIBRARY
K. G. Budge 24 May 1993 37 p Presented at the American National Standards Institute and International Standards Organization Joint Meeting, Munich, Germany, 12-16 Jul. 1993 Revised
(Contract DE-AC04-76DP-00789)
(DE93-015017; SAND-93-1349C; CONF-930792-1) Avail: CASI HC A03/MF A01

One of the most widely recognized inadequacies of C is its low-level treatment of arrays. Arrays are not first-class objects in C; an array name in an expression almost always decays into a pointer to the underlying type. This is unfortunate, especially since an increasing number of high-performance computers are optimized for calculations involving arrays of numbers. On such machines, double (square brackets) may be regarded as an intrinsic data type comparable to double or int and quite distinct from double. This weakness of C is acknowledged in the ARM where it is suggested that the inadequacies of the C array can be overcome in C++ by wrapping it in a class that supplies dynamic memory management, bounds checking, operator syntax, and other useful features. Such 'smart arrays' can in fact supply the same functionality as the first-class arrays found in other high-level, general-purpose programming languages. Unfortunately, they are expensive in both time and memory and make poor use of advanced floating-point architectures. Is there a better solution? The most obvious solution is to make arrays first-class objects and add the functionality mentioned. However, this would destroy C compatibility and significantly alter the C++ language. Major conflicts with existing practice would seem inevitable. I propose instead that numerical array classes be adopted as part of the C++ standard library. These classes will have the functionality appropriate for the intrinsic arrays found on most high-performance computers, and the compilers written for these computers will be free to implement them as built-in classes. On other platforms, these classes may be defined normally, and will provide users with basic array functionality without imposing an excessive burden on the implementor. DOE

N94-17800# California Univ., Berkeley. Lawrence Berkeley Lab.
A MODIFIED DIRECT PRECONDITIONER FOR INDEFINITE SYMMETRIC TOEPLITZ SYSTEMS
P. Concus and P. Saylor (Illinois Univ., Urbana.) Nov. 1992 15 p
(Contract DE-AC03-76SF-00098)
(DE93-015234; LBL-33167; UIUCDCS-R-92-1782) Avail: CASI HC A03/MF A01

A modification is presented of the classical O(n(sup 2)) algorithm of Trench for the direct solution of Toeplitz systems of equations. The Trench algorithm can be guaranteed to be stable only for matrices that are (symmetric) positive definite; it is generally unstable otherwise. The modification permits extension of the algorithm to compute an approximate inverse in the indefinite symmetric case, for which the unmodified algorithm breaks down when principal submatrices are singular. As a preconditioner, this approximate inverse has an advantage that only matrix-vector multiplications are required for the solution of a linear system, without forward and backward solves. The approximate inverse so obtained can be sufficiently accurate, moreover, that, when it is used as a preconditioner for the applications investigated, subsequent iteration may not even be necessary. Numerical results are given for several test matrices. The perturbation to the original matrix that defines the modification is related to a perturbation in a quantity generated in the Trench algorithm; the associated stability of the Trench algorithm is discussed. DOE

N94-17812# Los Alamos National Lab., NM.
THERMODYNAMICS OF COMPUTATION AND INFORMATION DISTANCE
C. H. Bennett, P. Gacs, M. Li, P. M. B. Vitanyi, and W. H. Zurek 12 Mar. 1993 21 p Presented at the Symposium on Theory of Computation, San Diego, CA, 7-11 Jun. 1993
(Contract W-7405-eng-36)
(DE93-012730; LA-UR-93-1569; CONF-9306155-1) Avail: CASI HC A03/MF A01

Applying the tools of algorithmic information theory, we compare several candidates for an asymptotically machine-independent. absolute measure of the informational or 'cognitive' distance between discrete objects x and y. The maximum of the conditional Kolmogorov complexities max(K(yz) K(my)), is shown to be optimal, in the sense of being minimal within an additive constant among semicomputable, symmetric, positive semidefinite functions of z and y satisfying a reasonable normalization condition and obeying the triangle intequality. The optimal metric, in turn, differs by at most an additive logarithmic term from the size of the smallest program for a universal reversible computer to transform x into y. This program functions in a 'catalytic" capacity, being retained in the computer before, during, and after the computation. Similarly, the sum of the conditional complexities. K(yx) + K(xy), is shown to be equal within a logarithmic term to the minimal amount Of information flowing out and in during a reversible computation in which the program is not retained. Finally. using the physical theory of reversible computation, it is shown that the simple difference K(x) - K(y) is an appropriate (i.e., universal, antisymmetric, and transitive) measure of the amount of thermodynamic work required to transform string x into string y by the most efficient process. DOE

N94-17867 Lawrence Livermore National Lab., CA.
AN OBJECT-ORIENTED ENVIRONMENT FOR COMPUTER VISION AND PATTERN RECOGNITION
J. E. Hernandez Dec. 1992 6 p Limited Reproducibility: More than 20% of this document may be affected by microfiche quality
(Contract W-7405-eng-48)
(DE93-017098; UCRL-ID-112584) Avail: CASI HC A02

Vision is a flexible and extensible object-oriented programming environment for prototyping solutions to problems requiring computer vision and pattern recognition techniques. Vision integrates signal/image processing, statistical pattern recognition, neural networks, low and mid level computer vision, and graphics into a cohesive framework useful for a wide variety of applications at Lawrence Livermore National Laboratory. DOE

N94-17911# Lawrence Livermore National Lab., CA.
VERIFICATION OF VALISYS CAD BASED CMM SOFTWARE AT LLNL
R. N. Frank 12 Nov. 1992 8 p Presented at the 75th Interagency Mechanical Operations Group Measurement Technology Subgroup Meeting, Livemore, CA, 12 Nov. 1992
(Contract W-7405-eng-48)
(DE93-013854; UCRL-JC-112020; CONF-9211237-1) Avail: CASI HC A02/MF A01 (US Sales Only)

This data was compiled as a first step in the quality assurance process for the VALISYS CMM programming and analysis system. The Nuclear Weapons Complex Coordinate Measuring Machine Test Artifact No. NWC101-3 was chosen as a test standard for two reasons. First, this same part had been measured previously on the LEITZ CMM at LLNL and sufficient data had been obtained for a direct comparison. Secondly, the LEITZ machines throughout the NWC performed exceptionally well in the actual DOE NWC study, thereby validating the LEITZ data as a reasonable standard. The LEITZ machine has a volumetric accuracy of 1.8 microns (70 mu(double prime)) as determined with a 450 mm MOORE step gage. This CORDAX data was measured on a Sheffield Cordax Apollo RS-50 DCC CMM, serial number A-0485-0989, between October 30 and November 4, 1992. The CORDAX is fitted with a RENISHAW PH-10 probe head and TP2 SW probe. The VALISYS system was used to facilitate the measurement and analysis of the part on the CORDAX CMM. VALISYS, running on a DEC platform, McDonnell Douglas UNIGRAPHICS CAD/CAM system, was used to create inspection tool (probing) paths and control the CMM through an interface with the Hewlett-Packard Model 310, Series 9000 computer running the Sheffield FLB3 software. VALISYS was then used to analyze the data and report the results. The CORDAX machine has an average volumetric accuracy of 9.6 microns in a (partial) 700 mm spherical envelope as determined through use of the Renishaw Machine Checking Gauge. DOE

N94-17914# Lawrence Livermore National Lab., CA.
SX USER'S MANUAL FOR SX, VERSION 2.0
S. A. Brown and D. Braddy Jan. 1993 70 p
(Contract W-7405-eng-48)
(DE93-015971; UCRL-MA-112315) Avail: CASI HC A04/MF A01

Scheme is a lexically scoped, properly tail recursive dialect of the LISP programming language. The PACT implementation is described abstractly in Abelson and Sussman's book, Structure and Interpretation of Computer Programs. It features all of the 'essential procedures' described in the 'Revised Report on Scheme' which defines the standard for Scheme. In PACT, Scheme is implemented as a library; however, a small driver delivers a stand alone Scheme interpreter. The PACT implementation features a reference counting incremental garbage collector. This distributes the overhead of memory management throughout the running of Scheme code. It also tends to keep Scheme from trying to grab the entire machine on which it is running which some garbage collection schemes will attempt to do. SX is perhaps the ultimate PACT statement. It is simply Scheme plus the other parts of PACT. A more precise way to describe it is as a dialect of LISP with extensions for PGS, PDB, PDBX, PML, and PANACEA. What this yields is an interpretive language whose primitive procedures span the functionality of all of PACT. Like the Scheme implementation which it extends, SX provides both a library and a stand alone application. The stand alone interpreter is the engine behind applications such as PDBView and PDBDiff. The SX library is the heart of TRANSL, a tool to translate data files from one database format to another. The modularization and layering make it possible to use the PACT components like building blocks. In addition, SX contains functionality which is the generalization of that found in ULTRA II. This means that as the development of SX proceeds, an SX driven application will be able to,perform arbitrary dimensional presentation, analysis, and manipulation tasks. Because of the fundamental unity of these two PACT parts, they are documented in a single manual. The first part will cover the standard Scheme functionality and the second part will discuss the SX extensions. DOE

N94-17917 National Physical Lab., Teddington (England). Information Technology and Computing Div.
POSTSCRIPT: A STUDY IN CONFORMITY
B. A. Wichmann Apr. 1993 49 p
(NPL-DITC-214/93; ETN-93-94958) Copyright Avail: National Physical Laboratory, Teddington, Middlesex, TW11 0LW, United Kingdom

The support given to standardized programming languages by means of validation suites is well understood. Although such suites are expensive to produce, suppliers and users can exploit them to ensure compilers conform to the standard. Less quantifiable aspects of compilers, such as 'quality' or 'user friendliness' could be left to market forces to resolve. The purpose of part of the current research program is to report how the methods adopted for compilers could be adapted to other areas. This report applies such methods to PostScript as a case study. ESA

N94-17926 Politecnico di Milano (Italy). Dipt. di Elettronica e Informazione.

MULTISTACK LANGUAGES AND GRAMMARS

Alessandra Cherubini, Luca Breveglieri, Claudio Citrini, and Stefano CrespiReghizzi Apr. 1993 39 p Sponsored in part by Ministry of University and Scientific Research and Technology and Commission of the European Communities

(Rept-93-016; ETN-93-94570) Avail: Issuing Activity (Politecnico di Milano, Piazza Leonardo da Vinci 32, 20133 Milan, Italy)

A superfamily of context free formal languages is recognized by automata with a finite, ordered set of pushdown stacks. This n-stack machine can write in any stack, but it cannot read from a stack unless all preceding ones are empty. The languages are generated by n-depth grammars which differ from context free ones by having a n-tuple of strings on the right hand side of a production. A practical example is procedural nesting in Ada. This family enjoys several useful properties of context free languages (semilinearity, closure with respect to intersection with regular sets, etc.) and especially the Chomsky Schutzenberger homomorphic characterization (using a generalized Dyck language) and an iteration lemma. The latter allows to prove that n depth languages form an infinite hierarchical with respect to n. ESA

N94-17927 Politecnico di Milano (Italy). Dipt. di Elettronica e Informazione.

SHOP PROBLEMS WITH TWO MACHINES AND TIME LAGS

Mauro DellAmico 1993 30 p Sponsored in part by Ministry of Public Education and Ministry of University and Scientific Research and Technology

(Rept-93-020; ETN-93-94571) Avail: Issuing Activity (Politecnico di Milano, Piazza Leonardo da Vinci 32, 30133 Milan, Italy)

Job-Shop and Flow-Shop scheduling problems with two machines are addressed having no more than two operations per job and Time Lags, that is, a minimum time interval between the completion time of the first operation and the starting time of the second one. Complexity results for the preemptive and non preemptive cases are given and the relations between the two problems are studied. For the Flow-Shop problem, lower bounds and upper bounds are given and a Tabu Search algorithm is defined. Extensive computational results prove the effectiveness of the proposed bounds. ESA

N94-17930 National Physical Lab., Teddington (England). Information Technology and Computing Div.

STRATEGIES FOR TESTING FORM ASSESSMENT SOFTWARE

M. G. Cox and A. B. Forbes Dec. 1992 29 p Sponsored by Dept. of Trade and Industry, London, England

(NPL-DITC-211/92; ETN-93-94887) Copyright Avail: National Physical Laboratory, Teddington, Middlesex, TW11 0LW, United Kingdom

Methods for generating test data sets and reference results which can be used to test assessment software employed in coordinate metrology for finding least squares best fit curves and surfaces to data are described. The methods do not rely on the use of reference software but instead exploit known mathematical properties which hold at the solution of the data approximation problem. The methods are flexible, straightforward to implement, and should be of value in designing conformance testing procedures. The methods are illustrated for the problem of finding the least squares best fit circle to data. ESA

N94-17943# Sandia National Labs., Albuquerque, NM.

CURRENT DEVELOPMENT IN SELECTED STRESS AND THERMAL ANALYSIS SOFTWARE INTERFACES WITH PRO-ENGINEER

J. Schulze 1993 25 p Presented at the Pro-users Meeting, Orlando, FL, 9 Jun. 1993

(Contract DE-AC04-76DP-00789)

(DE93-014935; SAND-93-1327C; CONF-9306173-1) Avail: CASI HC A03/MF A01

Ever since PRO-ENGINEER has become a dominating CAD package available to the public, some of us have been saying, 'Gee, if only I could export my geometry to a stress analysis program without having to recreate any of the details already created, wouldn't that be spectacular?' Well, much to the credit of the major stress and thermal analysis software vendors, some of them have been listening to design engineers like me badger them to furnish a seamless interface between PRO and their stress analysis programs. The down side of this problem is the fact that a lot of problems still exist with most of the vendors and their interfaces. I want to discuss the interfaces that I feel are currently 'State of the Art', and how they are developing and the future for finally arriving at a transparent procedure that an engineer at a workstation can utilize in his or her design process. In years past, engineers would develop a design and changes would evolve based on intuition, or somebody else's critical evaluation. Then the design would be forwarded to the production group, or the stress analysis group for further evaluation and analysis. Maybe data from a preliminary prototype would be collected and an evaluation report made. All of this took time and increased the cost of the item to be manufactured. Today, the engineer must assume responsibility for design and functional capability early on in the design process, if for no other reason than costs associated with diverse channels of critiquing. For that reason, one place to enhance the design process is to have the ability to do preliminary stress and thermal analysis during the initial design phase. This is both cost and time effective. But, as I am sure you are aware, this has been easier said than done. DOE

N94-17944# Sandia National Labs., Albuquerque, NM.

INTERACTIVE COLLABORATIVE ENVIRONMENTS (ICE) IN THE DESIGN TO MANUFACTURING PROCESS

M. R. Ashby, N. G. Rackley, M. Asher, and K. Musgrave Apr. 1993 11 p Presented at the 1993 American Telephone and Telegraph Design for X Conference, Albuquerque, NM, 12-13 May 1993

(Contract DE-AC04-76DP-00789)

(DE93-014994; SAND-93-1278C; CONF-9305170-3) Avail: CASI HC A03/MF A01

Interactive Collaborative Environments (ICE) technologies allow teams at separate locations to work concurrently on joint problem solving. Examples of ICE use include engineers simultaneously viewing and manipulating the same CAD application to discuss design/production changes and trade-offs. This concept was demonstrated in March of 1992 between AT&T, Shreveport Works and Holmdel. In May 1992, Sandia National Laboratories demonstrated a platform independent version of application sharing code using the workstations and application software available at AT&T, Shreveport Works. AT&T and Sandia are currently negotiating future work agreements. In addition, Sandia has provided demonstrations and created pilot project links for internal Sandia use, and for communication with other facilities, e.g. Los Alamos National Laboratories and Sandia, California location. ICE can also be used to link up suppliers and customers, even in different companies. Anywhere team members are separated geographically, or even between building and facilities at a particular site, ICE can improve remote problem solving, cutting down on delays and miscommunication fiascoes. DOE

N94-17960 Politecnico di Milano (Italy). Dipt. di Elettronica e Informazione.

AN ANALYTICAL APPROACH TO ERROR LOCALIZATION BY USING INFORMATION DERIVED FROM ERROR SIGNATURE

Serge Demidenko (Akademiya Nauk BSSR, Minsk.) and Vincenzo Piuri 1993 18 p Sponsored by CNR and Politecnico di Milano

(Rept-93-023; ETN-93-94573) Avail: Issuing Activity (Politecnico di Milano, Piazza Leonardo da Vinci 32, 20133 Milan, Italy)

Signature registers are widely used in digital circuit diagnostics to compress the output sequences of the circuit under test. Compression essentially reduces the volume of diagnostic data: diagnosis of the faulty circuits is simplified since a fault is detected whenever the signature generated by testing does not match the reference value corresponding to fault free circuit. When an incorrect signature is observed, it is often desirable to identify, within the stream being compressed, the bit locations which caused the incorrect signature. An approach to localize the erroneous bits by using information contained in the error signature is presented. The analytical solution for the most general case is derived for any capacity of the signature register, for any feedback structure, for any number of channels, and for any length of the sequences being compressed. ESA

N94-17965 Physics and Electronics Lab. TNO, The Hague (Netherlands).

THE FIRST INTERNATIONAL CONFERENCE ON PCTE

J. W. L. J. Mager and W. Treurniet May 1992 60 p Conference held in The Hague, Netherlands, 25-27 Sep. 1991 Sponsored by Royal Netherlands Navy

(Contract A87/K/102)
(FEL-92-A134; TD92-1448; ETN-93-94525) Copyright Avail: TNO Physics and Electronics Laboratory, P.O. Box 96864, 2509 JG The Hague, Netherlands

Presentations given at the 1991 Portable Common Tool Environment (PCTE) conference are reported. PCTE is a set of software services reported to build Integrated Project Support Environment (IPSE). The PCTE services support the integration and portability of tools. Amongst the topics discussed are the following: organizations behind PCTE, industrial PCTE strategy; the Software Technology for Adaptable, Reliable Systems (STARS), and PCTE; user requirements for control in large scale IPSE, the Computer Aided Software Engineering (CASE) Data Interchange Format (CDIF) standards; PCTE training; tools for PCTE environments; and tool integration. ESA

N94-17975 Politecnico di Milano (Italy). Dipt. di Elettronica.

A GEOMETRIC ALGORITHM FOR THE EUCLIDEAN 1-CENTER PROBLEM

Giovanni Righini Jan. 1993 30 p
(Rept-93-001; ETN-93-94510) Avail: Politecnico di Milano, Piazza Leonardo da Vinci 32, 20133 Milan, Italy

An algorithm for the euclidean 1-center problem is presented. The algorithm applies both to the weighted and to the unweighted versions. The algorithm is exact and finite. Its time complexity is conjectured to be linear in the number of points. ESA

N94-17977# Institut National Polytechnique, Grenoble (France). Lab. d'Informatique Fondamentale et d'Intelligence Artificielle.

ANALYSIS, REPRESENTATION AND PROCESSING OF THE INSTRUMENTAL GESTURE: APPLICATION TO KEYBOARD INSTRUMENTS Ph.D. Thesis [ANALYSE, REPRESENTATION ET TRAITEMENT DU GESTE INSTRUMENTAL: APPLICATION AUX INSTRUMENTS A CLAVIER]

Christophe Ramstein 1991 213 p In FRENCH
(ETN-93-94402) Avail: CASI HC A10/MF A03

In the scope of studies involving computer assisted music, the gesture is described and stored as an assembly of sampled signals. The aim of the study is to design and construct a gesture editor to analyze, to represent and to process the stored gesture data. The study is also aimed towards the real time control of sound synthesis processing by stimulation of instrumental mechanisms and the study of its relationship with music. The representations of the instrumental gesture which are pertinent to a composer and well adapted to the informatic constraints are developed. The processing of the instrumental gesture organizes it under different logic at each representation level. Examples for testing and validating the results are proposed. ESA

N94-17978# Grenoble-1 Univ. (France). Lab. de Genie Informatique.

OBJECT-ORIENTED EXTENSION OF A RELATIONAL DBMS Ph.D. Thesis [EXTENSION ORIENTEE OBJET D'UN SGBN RELATIONNEL]

Francois Exertier 1991 159 p In FRENCH
(ETN-93-94403) Avail: CASI HC A08/MF A02

The objective is the specification and development of a Relational Database Management System (RDBMS) which incoporates 'object' technology and concepts. The principle of the approach is to extend relational domains with Abstract Data Types (ADT) and consists of loosely coupling object concepts and mechanisms to the relational model and system. The data model and the features of the extension are defined. The concept of ADT is introduced in order to express new domains: an ADT specifies a data structure together with a set of methods which constitutes its manipulation interface. A simple inheritance mechanism is provided. Constructors are supplied to define the data structure of a type, introducing the notion of comiex object. The concept of sharing, based on object identity, is an important contribution of this work. The language which materializes the model is a SQL extension, named ESQL; methods are presently written using a C extension. The realization of such a system consists of the implementation of different components providing the object support and in the integration of these components to an existing RDBMS kernel. There are three main modules. The type manager is a part of a relational catalogue manager which handles ADT definitions. The method manager provides different functions like compilation and execution. The object manager supplies object storage and manipulation capabilities. ESA

N94-18002# Sandia National Labs., Albuquerque, NM.

AN OVERVIEW OF THE SAFSIM COMPUTER PROGRAM

D. Dobranich 1993 6 p Presented at the 10th Symposium on Space Nuclear Power and Propulsion, Albuquerque, NM, 10-14 Jan. 1993
(Contract DE-AC04-76DP-00789)
(DE93-017657; SAND-93-1215C; CONF-930103-42) Avail: CASI HC A02/MF A01

SAFSIM (System Analysis Flow SIMulator) is a FORTRAN computer program that provides engineering simulations of user-specified flow networks at the system level. It includes fluid mechanics, heat transfer, and reactor dynamics capabilities. SAFSIM provides sufficient versatility to allow the simulation of almost any flow system, from a backyard sprinkler system to a clustered nuclear reactor propulsion system. In addition to versatility, speed and robustness are primary goals of SAFSIM development. The current capabilities of SAFSIM are summarized and some sample applications are presented. It is applied here to a nuclear thermal propulsion system and nuclear rocket engine test facility. DOE

N94-18072# Lawrence Livermore National Lab., CA.

HIGH PERFORMANCE FORTRAN: AN OVERVIEW

M. E. Zosel 23 Dec. 1992 7 p Presented at the IEE COMPON Spring Meeting, San Francisco, CA, 22-26 Feb. 1993
(Contract W-7405-eng-48)
(DE93-017181; UCRL-JC-112573; CONF-9302135-1) Avail: CASI HC A02/MF A01

The purpose of this paper is to give an overview of the work of the High Performance Fortran Forum (HPFF). This group of industry, academic, and user representatives has been meeting to define a set of extensions for Fortran dedicated to the special problems posed by very high performance computers, especially the new generation of parallel computers. The paper describes the HPFF effort and its goals and gives a brief description of the functionality of High Performance Fortran (HPF). DOE

N94-18086# Los Alamos National Lab., NM.

SOFTWARE TOOLKIT FOR ANALYSIS RESEARCH (STAR)

T. Burr, J. E. Doak, B. Hoffbauer, J. A. Howell, P. M. Kelly, L. McGavran, R. Pitts, J. M. Prommel, T. R. Thomas, and R. B. Strittmatter et al Aug. 1993 102 p
(Contract W-7405-eng-36)
(DE93-017368; LA-12617-MS) Avail: CASI HC A06/MF A02

The authors discuss the development of a Software Toolkit for Analysis Research (STAR) that will facilitate the development and interchange of algorithms for locating phenomena of interest in large quantities of data. Using this toolkit, researchers will be able to ascertain which existing techniques are the most promising, develop new and possibly more effective methods, and add/delete algorithms without major re-design work. This report describes the components of STAR, how these components will work together, and the algorithms with which they currently have expertise. Some modules or components of STAR will preprocess incoming data; some will select which information is appropriate for a particular application; some will analyze data to uncover items of significance; and others will assess the effectiveness of the various components. Some of the specific techniques employed by the various modules will be feature selection algorithms, machine learning algorithms, a purely statistical model, and expert system methodologies. DOE

N94-18097# Los Alamos National Lab., NM.

A TIME-FREQUENCY SMOOTHING ALGORITHM FOR CYCLIC SPECTRAL ANALYSIS

R. S. Roberts 13 Aug. 1992 11 p Presented at the Workshop on Cyclostationary Signals, Yountville, CA, Apr. 1993
(Contract W-7405-eng-36)
(DE93-016634; LA-UR-93-1984; CONF-9304167-1) Avail: CASI HC A03/MF A01

A hybrid smoothing algorithm is described that smooths first in time and then in frequency. The time-frequency smoothing algorithm is designed to compute estimates of the cyclic (cross) spectrum along lines of constant cycle frequency. A variation on the algorithm, one that incorporates the One Bit Spectral Correlation Algorithm (OBSCA), is also described. A simulation study is presented that evaluates the algorithms. DOE

N94-18117# Helsinki Univ. of Technology, Espoo (Finland). Dept. of Computer Science.
CUT AND PASTE BASED MODELING WITH BOUNDARY FEATURES
M. Ranta (Tokyo Univ., Japan.), M. Inui (Tokyo Univ., Japan.), F. Kimura (Tokyo Univ., Japan.), and M. Mantylae 1993 22 p
(PB93-187250; ISBN-951-22-1282-X) Avail: CASI HC A03/MF A01

The paper proposes a boundary feature approach that allows the user to define new features according to useful portions of previous design solutions. The approach is based on boundary manipulation operations that provide facilities for attaching and detaching boundary portions. A cut and paste style is introduced for the user interaction with boundary feature models. A small prototype system has been implemented in order to experience the suggested approach. NTIS

N94-18118# Helsinki Univ. of Technology, Espoo (Finland). Digital Systems Lab.
WEAKENED NEGATIVE INTROSPECTION IN AUTOEPISTEMIC REASONING
T. Janhunen Feb. 1993 89 p
(PB93-187375; ISBN-951-22-1407-5) Avail: CASI HC A05/MF A01

A new weakened scheme for negative introspection in autoepistemic reasoning is proposed. The scheme is formulated proof-theoretically in terms of enumerations of formulae. The resulting sets of conclusions based on the negative introspection principle, cautious autoepistemic expansions, generalize Moore style stable expansions such that every set of premises has a cautious expansion. A finitary characterization is developed for cautious expansions. The elimination of weakly grounded cautious expansions yields a subclass of cautious expansions: the N-grounded cautious expansions. The least N-grounded cautious expansion is shown to be unique and the intersection of all N-grounded cautious expansions. This is in contrast with Moore style stable expansions. The least N-grounded cautious expansion can be constructed iteratively as the least fixed point of a monotonic operator. A comparison is made with some other schemes of weakened negative introspection. The given set of examples demonstrates that the proposed negative introspection principle is stronger than that of the well-founded semantics. NTIS

N94-18130# Lawrence Livermore National Lab., CA.
TEXTURE SPLATS FOR 3D VECTOR AND SCALAR FIELD VISUALIZATION
R. A. Crawfis and N. Max Apr. 1993 9 p Presented at the Visualization 1993, San Jose, CA, 25-29 Oct. 1993
(Contract W-7405-eng-48)
(DE93-017104; UCRL-JC-113626; CONF-931080-3) Avail: CASI HC A02/MF A01

Volume Visualization is becoming an important tool for understanding large 3D datasets. A popular technique for volume rendering is known as splatting. In light of the new hardware architectures offering substantial improvements in the performance of rendering texture mapped objects, we present textured splats. An ideal reconstruction function for 3D signals is developed which can be used as a texture map for a splat. Extensions to the basic splatting technique are then developed to additionally represent vector fields. DOE

N94-18133# Lawrence Livermore National Lab., CA.
AN EVOLVING INFRASTRUCTURE FOR SCIENTIFIC COMPUTING AND THE INTEGRATION OF NEW GRAPHICS TECHNOLOGY
K. W. Fong Feb. 1993 8 p Presented at the 14th Annual Conference of the National Computer Graphics Association, Philadelphia, PA, 26-29 Apr. 1993
(Contract W-7405-eng-48)
(DE93-017164; UCRL-JC-113274; CONF-9304176-1) Avail: CASI HC A02/MF A01

The National Energy Research Supercomputer Center (NERSC) at the Lawrence Livermore National Laboratory is currently pursuing several projects to implement and integrate new hardware and software technologies. While each of these projects ought to be and is in fact individually justifiable, there is an appealing metaphor for viewing them collectively which provides a simple and memorable way to understand the future direction not only of supercomputing services but of computer centers in general. Once this general direction is understood, it becomes clearer what future computer graphics technologies would be possible and desirable, at least within the context of large scale scientific computing. DOE

N94-18136 Politecnico di Milano (Italy). Dipt. di Elettronica e Informazione.
NAVIGATION IN HYPERMEDIA APPLICATIONS: MODELLING AND SEMANTICS
Franco Garzotto, Luca Mainetti, and Paolo Paolini May 1993 35 p
Sponsored in part by Commission of the European Communities
(Rept-93-034; ETN-93-94580) Avail: Issuing Activity (Politecnico di Milano, Piazza Leonardo da Vinci 32, 20133 Milan, Italy)

'Navigation' or 'browsing' is an important way of accessing information for a large class of applications: hypermedia, object oriented data bases, and multimedia data bases. In most systems today, the support for navigation is (still) very primitive. A variety of sophisticated navigation patterns, some of which involve integration with query mechanisms, are presented and their static and run time models are described. It is pointed out that the definition of an adequate browsing semantics requires a model for information and link structures which is more complex than the models commonly found in hypermedia or data bases. These concepts are illustrated by examples taken from a real life application for banking activities. ESA

N94-18138 Politecnico di Milano (Italy). Dipt. di Elettronica e Informazione.
EXACT COST FLOW PROBLEMS IN ACYCLIC NETWORKS
Vincenzo Caglioti and Marco Trubian 1993 11 p Sponsored in part by Ministry of University and Scientific Research and Technology
(Rept-93-030; ETN-93-94578) Avail: Issuing Activity (Politecnico di Milano, Piazza Leonardo da Vinci 32, 30133 Milan, Italy)

The NP-complete problem of finding a flow of cost equal to a given integer value (an exact-cost flow) in acyclic networks is addressed. This problem is reduced to the Exact weight Perfect Matching Problem on a bipartite graph (XPMB). The existence XPMB problem can be solved by a random pseudo-polynomial algorithm. A new constructive procedure for the XPMB problem is proposed, to be applied once the existence is given, whose time complexity is O(mT(sub TM)), where T(sub PM) indicates the time required for the randomized existence procedure, and m indicates the number of arcs in the bipartite graph. ESA

N94-18145 Politecnico di Milano (Italy). Dipt. di Elettronica e Informazione.
ANNEALING ALGORITHMS FOR MULTIRESOURCE ABSOLUTE LOCATION PROBLEMS ON GRAPH
Giovanni Righini Apr. 1993 15 p Sponsored in part by Ministry of University and Scientific Research and Technology
(Rept-93-028; ETN-93-94577) Avail: Issuing Activity (Politecnico di Milano, Piazza Leonardo da Vinci 32, 20133 Milan, Italy)

A methodology is presented for applying annealing techniques to multisource absolute location problems on graphs. Two kinds of objective-functions are considered: barycenters and centers. Starting from the classical iterative algorithm 'cluster and locate', robust and distributed algorithms are developed, relying upon the relaxation of the integrality constraints on allocation variables. Experimental results are reported. ESA

N94-18251# Naval Air Warfare Center, Warminster, PA. Aircraft Div.
REFERENCE MODEL FOR PROJECT SUPPORT ENVIRONMENTS, VERSION 1.0 Final Report
P. Oberndorf, A. Brown, D. Carney, and M. Zelkowitz 28 Feb. 1993 130 p
(AF Proj. X19-76)
(AD-A269110; NAWCADWAR-93023-70) Avail: CASI HC A07/MF A02

This report documents a reference model that describes the full scope of functionality that is expected of a Project Support Environment (PSE). The scope includes support for System Engineering, Software Engineering, and Life-Cycle Process Engineering as well as the infrastructure services required to support these. The first three chapters contain a general description of the model. The remaining chapters provide detail of individual aspects of the model. DTIC

N94-18259# Texas A&M Univ., College Station.
SYNTHESIS TECHNIQUES AND ANALYSIS TOOL FOR ON-CHIP FAULT-TOLERANCE Final Report
Dhiraj K. Pradham 1993 17 p
(Contract N00014-91-J-1404)
(AD-A269148) Avail: CASI HC A03/MF A01

This report summarizes significant research on a broad range of issues related to fault-tolerant design both at the chip and system level. First discussed is an integrated approach, currently under development for integrating concurrent checking with BIST. The goal here is to generate synthesis tools to develop low cost fault-tolerant VLSI chip design tools that are both easy to test as well as being robust against operational errors. Section 2 reviews REACT, a tool currently under development for fault-tolerant architecture characterization. Finally, Section 3 presents on-going research on the development of novel fault-tolerant architectures. DTIC

N94-18271# Los Alamos National Lab., NM.
A RATIONAL DESIGN CHANGE METHODOLOGY BASED ON EXPERIMENTAL AND ANALYTICAL MODAL ANALYSIS
D. J. Weinacht and J. G. Bennett 1993 11 p Presented at the 11th International Invitational Symposium on the Unification of Analytical, Computational, and Experimental Solution Methodologies, Danvers, MA, 18-20 Aug. 1993
(Contract W-7405-eng-36)
(DE93-018537; LA-UR-93-2611; CONF-9308138-1) Avail: CASI HC A03/MF A01

A design methodology that integrates analytical modeling and experimental characterization is presented. This methodology represents a powerful tool for making rational design decisions and changes. An example of its implementation in the design, analysis, and testing of a precisions machine tool support structure is given. DOE

N94-18290* University of Southern California, Marina del Rey. Information Sciences Inst.
INTELLIGENT HELP FACILITIES: GENERATING NATURAL LANGUAGE DESCRIPTIONS WITH EXAMPLES Research Report
Vibhu O. Mittal and Cecile Paris Apr. 1993 9 p Limited Reproducibility: More than 20% of this document may be affected by microfiche quality
(Contracts NCC2-250; DABT63-91-C-0025; NSF ISI-90-03087)
(AD-A269555; ISI/RR-93-334) Avail: CASI HC A02

On-line help facilities are essential in any complex system, especially for introductory or naive users. Previous studies have highlighted the need for appropriate examples along with the description. This paper describes a help/documentation facility built within an explanation framework that plans the presentation of text and examples using techniques in natural language generation. The paper shows how text and examples can influence each other and enumerates some of the other issues that arise in planning such presentations. DTIC

N94-18308 California State Univ., Stanislaus. Dept. of Computer Science.
TEACHING A COMPUTER SIMULATION COURSE WITH Ada Final Report
Edward L. Lamie May 1993 129 p Limited Reproducibility: More than 20% of this document may be affected by microfiche quality
(Contract MDA972-92-J-1019)
(AD-A267901) Avail: Issuing Activity (Defense Technical Information Center (DTIC))

The purpose of this project was to develop a nucleus of routines, along with accompanying documentation, for use in software engineering courses in discrete-event system simulation. The system is called SIMPACK, after the main package that contains most of the simulation modules. SIMPACK was developed on an MS DOS computer using Meridian Ada, version 4.1.1. In addition to documentation, a floppy disk is included which contains all the Ada routines used, a compiled version of the system, and a template system to create data files for use by SIMPACK. DTIC

N94-18453 Carnegie-Mellon Univ., Pittsburgh, PA. Dept. of Computer Science.
THE CMU MASTERS IN SOFTWARE ENGINEERING CORE CURRICULUM
David Garlan, Alan Brown, Daniel Jackson, Jim Tomayko, and Jeannette Wing 6 Aug. 1993 20 p Limited Reproducibility: More than 20% of this document may be affected by microfiche quality
(AD-A268983; CMU-CS-93-180) Avail: CASI HC A03

Since 1989 Carnegie Mellon University has offered an academic program leading to a professional Master of Software Engineering (MSE) degree. The objective of the MSE program is to develop technical leaders in industrial software engineering. Students entering the program have at least two years industrial experience, and normally complete the program in sixteen months of full-time study. The MSE program is centered on a Software Development Studio, supported by a Core Curriculum and a set of elective tracks. These components occupy approximately 40%, 30%, and 30% (respectively) of a student's time in the program. In the Software Development Studio students plan and implement a significant software project for an external client over the full duration of the program. Students work in a team environment under the guidance of faculty advisors to analyze a problem, plan a software development project, execute a solution, and evaluate their work. The studio is similar to the design studios that characterize architectural degree programs. The MSE Core Curriculum develops foundational skills in the fundamentals of software engineering, with an emphasis on design, analysis, and management of large-scale software systems. DTIC

N94-18458 Massachusetts Inst. of Tech., Cambridge. School of Management.
SOFTWARE RELIABILITY: ESTIMATION AND PREDICTION Final Report, 1 May 1989 - 31 Dec. 1992
Gordon Kaufman 31 Dec. 1992 18 p Limited Reproducibility: More than 20% of this document may be affected by microfiche quality
(Grant AF-AFOSR-0371-89)
(AD-A268895; AFOSR-93-0657TR) Avail: Issuing Activity (Defense Technical Information Center (DTIC))

The principal purpose of this research was to provide new tools for measuring probabilities of failure free operation of software systems and to develop methods for predictions of software reliability. Links are established between stochastic models of fault occurrence suggested by Scholtz (1985) and Miller (1986) and an important class of finite population sampling models called 'successive sampling' in the sample survey literature. Successive sampling consists of sampling a finite population of objects, each with an assigned magnitude, proportional to magnitude and without replacement. Recognition of linkages between Schoz and Miller's 'Exponential Order Statistics Models' and successive sampling allows application of an emerging body of research on methods of estimation for successive sampling models to software reliability estimation. DTIC

N94-18543# Office of Naval Research, Arlington, VA.
NAVAL RESEARCH REVIEWS. MIXING ENHANCEMENT FOR AIR-BREATHING PROPULSION. NON-AXISYMMETRIC JETS INCREASE MIXING, VOLUME 44 AND VOLUME 45
1993 31 p
(AD-A268966) Avail: CASI HC A03/MF A01

The Navy's need for faster, smaller computers has inspired research on the use of more than two levels of logic in computer circuits. This paper focusses on work at NPS in multiple-valued logic. It discusses the development of multiple-valued programmable logic arrays (MVL-PLA), as well as computer-aided design tools for MVL-PLA's. DTIC

N94-18659# Carnegie-Mellon Univ., Pittsburgh, PA. Software Engineering Inst.
A CASE STUDY IN SOFTWARE MAINTENANCE Final Technical Report
Susan Dart, Alan M. Christie, and Alan W. Brown Jul. 1993 55 p
(Contract F19628-90-C-0003)
(AD-A269923; CMU/SEI-93-TR-08; ESC-TR-93-185) Avail: CASI HC A04/MF A01

In an effort to find out more about the tools, procedures, and techniques project personnel use in their work, the Computer-Aided Software Engineering (CASE) Environments Project interviewed personnel in eight software maintenance projects within an agency of the U.S/government. These interviews highlighted problems that we believe are typical of many software maintenance organizations (i.e., the need for more effective software maintenance tools, lack of communication between individuals working on similar projects, low status of maintenance personnel, and lack of a design-for-maintenance philosophy during the software development phase). This report highlights the findings of these interviews, provides our analysis of the findings, and makes recommendations directed at the agency for improvement in the areas of tools, people, and process. We believe that what we observed is very typical of the state of the practice in these areas and as such that this report and its recommendations are applicable to other large or small software maintenance projects. DTIC

N94-18680 University of Southern California, Marina del Rey. Information Sciences Inst.
GENERATING OBJECT DESCRIPTIONS: INTERGRATING EXAMPLES WITH TEXT Research Report
Vibhu O. Mittal and Cecile Paris Jan. 1993 11 p Limited Reproducibility: More than 20% of this document may be affected by microfiche quality
(Contract DABT63-91-C-0025)
(AD-A269992; ISI/RR-93-327) Avail: CASI HC A03

Descriptions of complex concepts often use examples for illustrating various points. This paper discusses the issues that arise in generating complex descriptions in tutorial contexts. Although some tutorial systems have used examples in explanation, they have rarely been considered as an integral part of the complete explanation; they have usually been merely supportive devices and inserted in the explanations without any representation in the system of how the examples relate to and complement the textual explanations that accompany the examples. This can lead to presentations that are at best, weakly coherent, and at worst, confusing and mis-leading for the learner. In this paper, we consider the generation of examples as an integral part of the overall process of generation resulting in examples and text that are smoothly integrated and complement each other. We address the requirements of a system capable of this and present a framework in which it is possible to generate examples as an integral part of a description. DTIC

N94-18696# Carnegie-Mellon Univ., Pittsburgh, PA. Dept. of Computer Science.
EFFICIENT TRANSPARENT OPTIMISTIC ROLLBACK RECOVERY FOR DISTRIBUTED APPLICATION PROGRAMS
David B. Johnson Mar. 1993 20 p
(Contract MDA972-90-C-0035; ARPA Order 7330)
(AD-A268981; CMU-CS-93-127) Avail: CASI HC A03/MF A01

Existing rollback-recovery methods using consistent checkpointing may cause high overhead for applications that frequently send output to the 'outside world,' since a new consistent checkpoint must be written before the output can be committed, whereas existing methods using optimistic message logging may cause large delays in committing output, since processes may buffer received messages arbitrarily long before logging and may also delay propagating knowledge of their logging or checkpointing progress to other processes. This paper describes a new transparent rollback-recovery method that adds very little overhead to distributed application programs and efficiently supports the quick commit of all output to the outside world. Each process can independently choose at any time either to use checkpointing alone (as in consistent checkpointing) or to use optimistic message logging. The system is based on a new commit algorithm that requires communication with and information about the minimum number of other processes in the system and supports the recovery of both deterministic and nondeterministic processes. DTIC

N94-18698# Carnegie-Mellon Univ., Pittsburgh, PA. Dept. of Computer Science.
PORTABLE PARALLEL RAY TRACING ALGORITHMS
Michael J. Garland May 1993 20 p
(AD-A268984; CMU-CS-93-176) Avail: CASI HC A03/MF A01

For a variety of reasons, realistic computer rendering is an important technology; it creates a wide range of new possibilities for effectively communicating information. The crucial goal is to provide realistic images in a short period of time. Ray tracing is a powerful technique for rendering. It is conceptually simple, and it can produce effects beyond the capability of some other more traditional methods. Unfortunately, ray tracing is rather expensive by comparison. This project is aimed at producing a reasonably fast and efficient ray tracer based on parallel ray tracing algorithms. The code is written in NESL, a data-parallel language developed by Guy Blelloch. It is supported on Cray Y-MP, Connection Machine CNI-2, and serial workstation platforms. DTIC

N94-18726# West Virginia Univ., Morgantown. Dept. of Electrical Engineering.
THE DEVELOPMENT OF A COURSE SEQUENCE IN REAL-TIME SYSTEMS DESIGN Final Report
H. H. Ammar Aug. 1993 219 p
(Contract MDA972-92-J-1022)
(AD-A269459) Avail: CASI HC A10/MF A03

This project deals with the development of a senior level course sequence in software intensive real-time systems. The sequence consists of a course in real-time software development, referred to in this report as the software course, followed by a course in hardware development and hardware-software interfacing, referred to in the sequel as the hardware course. The objective of the course sequence is to fill a demand in industry for real-time software engineers. It is aimed at preparing Computer Engineering students with a solid background in both software development and hardware design for an engineering industrial career in real-time systems development. The course sequence emphasizes practical standards, techniques, and tools for system development. Few universities include real-time systems development in their undergraduate Computer Engineering or Computer Science curriculum, forcing engineers to learn real-time methodology on-the-job. Real-time applications are increasing in complexity. Real-time designs have several performance as well as functional constraints, they have longer design cycles and larger project teams. They require more intricate real-time design work such as hardware interfacing, and often use multiprocessors in distributed environments. The growing complexity of real-time designs makes it difficult for an engineer to learn about real-time methodology on-the-job. DTIC

N94-18786 Naval Postgraduate School, Monterey, CA.
COMPUTER-AIDED PROTOTYPING SYSTEM (CAPS) WITHIN THE SOFTWARE ACQUISITION PROCESS. A CASE STUDY M.S. Thesis
Mary K. Ellis Jun. 1993 114 p Limited Reproducibility: More than 20% of this document may be affected by microfiche quality
(AD-A268705) Avail: Issuing Activity (Defense Technical Information Center (DTIC))

This thesis provides a case study which examines the benefits derived from the practice of computer-aided prototyping within the software acquisition process. An experimental prototyping system currently in research is the Computer Aided Prototyping System (CAPS), managed under the Computer Science department of the Naval Post Graduate School, Monterey, California. This thesis determines the qualitative value which may be realized by applying the Computer-Aided Prototyping System (CAPS) to the initial stages of the acquisition process for a software system on the scale of a prototype model, then projecting the results to a real-time distributed computer system. As a prelude to this analysis, information is presented concerning how the acquisition process is currently managed within DoD and what role prototyping plays within that process. An introduction to the CAPS is then given, along with a description of its capabilities obtained through personal examination of the system. Following this walkthrough of the CAPS, software acquisition is discussed further, including an analysis of its major obstacles and where a CAPS could best be used within the acquisition cycle. This thesis concludes with a cost analysis and results from a comparison of performing a requirements analysis and feasibility study with and without a CAPS. DTIC

N94-18794 National Inst. of Standards and Technology, Gaithersburg, MD.
INITIAL GRAPHICS EXCHANGE SPECIFICATION (IGES)
30 Nov. 1992 11 p Limited Reproducibility: More than 20% of this document may be affected by microfiche quality
(AD-A270049; NIST-FIPS-PUB-177) Avail: CASI HC A03

This publication announces the adoption of American National Standard Digital Representation for Communication of Product Definition Data, ASME/ANSI Y14.26M-1989, as a Federal Information Processing Standard (FIPS). ASME/ANSI Y14.26M-1989, more commonly known as the Initial Graphics Exchange Specification (IGES), specifies file structure and syntactical definition, and defines the representation of geometric, topological, and nongeometric product definition data. ASME/ANSI Y14.26M-1989 establishes information structures for the digital representation and communication of product definition data. Use of this standard permits the compatible exchange of product definition data used by various computer-aided design and computer-aided manufacturing (CAD/CAM) systems. DTIC

N94-18879 Stanford Univ., CA. Dept. of Aeronautics and Astronautics.
CONTROLSHELL: A REAL-TIME SOFTWARE FRAMEWORK Quarterly Progress Report, Oct. - Dec. 1992
J. C. Latombe, R. H. Cannon, Jr., and S. A. Schneider 3 Sep. 1993 41 p Limited Reproducibility: More than 20% of this document may be affected by microfiche quality
(Contract N00014-92-J-1809)
(AD-A269172) Avail: CASI HC A03

We are creating a new paradigm for building and maintaining complex real-time software systems for the control of moving mechanical systems. This objective is being met through the simultaneous development of both a powerful software environment and cogent motion planning and control capabilities. Our research concentrates on three key areas: (1) Building an innovative, powerful real-time software framework; (2) Implementing new distributed control architectures for intelligent mechanical systems; and (3) Developing distribution architectures and new algorithms for the computationally hard motion planning and direction problem. Perhaps more importantly, we are working on the vertical integration of these technologies into a powerful, working system. It is only through this coordinated, cooperative approach that a truly revolutionary, usable architecture can result. DTIC

N94-18901 Yale Univ., New Haven, CT. Dept. of Computer Science.
STATISTICAL LEARNING THEORY AND ALGORITHMS Final Report, 15 Feb. 1992 - 14 Feb. 1993
John Moody 14 Feb. 1993 2 p Limited Reproducibility: More than 20% of this document may be affected by microfiche quality
(Contract F49620-92-J-0143)
(AD-A270209; AFOSR-93-0701TR) Avail: CASI HC A01

This project addressed three fundamental areas in statistical learning theory and algorithms: (1) a practical and theoretically sound method for estimating generalization performance of nonlinear learning systems (Generalized Prediction Error (GPE)); (2) a more powerful and efficient class of network architectures (Parameterized Projection Pursuit Regression (P(3)R) Networks); and (3) faster real-time learning methods based on asymptotically optimal stochastic gradient search. Three papers were published under this grant. Additionally, a graduate student finished his Ph.D. by researching the topic of 'Networks with Learned Unit Response Functions.' DTIC

N94-18905 Air Force Inst. of Tech., Wright-Patterson AFB, OH.
A TEACHING TOOL FOR LINEAR PROGRAMMING M.S. Thesis
Wendy Cook 1 Jul. 1993 55 p Limited Reproducibility: More than 20% of this document may be affected by microfiche quality
(AD-A270240) Avail: CASI HC A04

This paper discusses several main concepts in linear programming. The purpose of this paper is to supplement the textbook teaching of these concepts to further the students' understanding. These main concepts include bases, extreme points, the simplex algorithm, and sensitivity analysis. Before any of these concepts are discussed, a necessary review of linear algebra is done. The ideas presented here should give the professor additional knowledge about how to successfully teach the students these concepts. Computer programs are developed in MOR/ML in order to aid in these discussions. MOR/ML is a computer programming language which has the syntax necessary to facilitate these concepts. MOR/ML is a set structured language which allows for the programming of matrices and sets. This structure makes it possible to formulate the programs dealing with linear programming. DTIC

N94-18926# Sandia National Labs., Albuquerque, NM.
ADAPTIVE PATH PLANNING: ALGORITHM AND ANALYSIS
Pang C. Chen 1993 10 p Presented at the 6th International Symposium of Robotics Research, Pittsburgh, PA, 2 Oct. 1993
(Contract DE-AC04-76DP-00789)
(DE93-008348; SAND-93-0242C; CONF-931055-1) Avail: CASI HC A02/MF A01

Path planning has to be fast to support real-time robot programming. Unfortunately, current planning techniques are still too slow to be effective, as they often require several minutes, if not hours of computation. To alleviate this problem, we present a learning algorithm that uses past experience to enhance future performance. The algorithm relies on an existing path planner to provide solutions to difficult tasks. From these solutions, an evolving sparse network of useful subgoals is learned to support faster planning. The algorithm is suitable for both stationary and incrementally-changing environments. To analyze our algorithm, we use a previously developed stochastic model that quantifies experience utility. Using this model, we characterize the situations in which the adaptive planner is useful, and provide quantitative bounds to predict its behavior. The results are demonstrated with problems in manipulator planning. Our algorithm and analysis are sufficiently general that they may also be applied to task planning or other planning domains in which experience is useful. DOE

N94-18943# Lawrence Livermore National Lab., CA.
AUTOMATED ASSISTANCE FOR DETECTING MALICIOUS CODE
R. Crawford, P. Kerchen, K. Levitt, R. Olsson, M. Archer, and M. Casillas 18 Jun. 1993 14 p
(Contract W-7405-eng-48)
(DE93-018106; UCRL-JC-113874) Avail: CASI HC A03/MF A01

This paper gives an update on the continuing work on the Malicious Code Testbed (MCT). The MCT is a semi-automated tool, operating in a simulated, cleanroom environment, that is capable of detecting many types of malicious code, such as viruses, Trojan horses, and time/logic bombs. The MCT allows security analysts to check a program before installation, thereby avoiding any damage a malicious program might inflict. DOE

N94-18989# Oak Ridge National Lab., TN.
SOFTWARE DISTRIBUTION USING XNETLIB
J. J. Dongarra, T. H. Rowan, and R. C. Wade Jun. 1993 15 p
(Contract DE-AC05-84OR-21400)
(DE93-018278; ORNL/TM-12318) Avail: CASI HC A03/MF A01

Xnetlib is a new tool for software distribution. Whereas its predecessor netlib uses e-mail as the user interface to its large collection of public-domain mathematical software, xnetlib uses an X Window interface and socket-based communication. Xnetlib makes it easy to search through a large distributed collection of software and to retrieve requested software in seconds. DOE

N94-19005# Westinghouse Savannah River Co., Aiken, SC.
FINITE DIFFERENCE PROGRAM FOR CALCULATING HYDRIDE BED WALL TEMPERATURE PROFILES
J. E. Klein 29 Oct. 1992 45 p
(Contract DE-AC09-89SR-18035)
(DE93-019272; WSRC-TR-92-501) Avail: CASI HC A03/MF A01

A QuickBASIC finite difference program was written for calculating one dimensional temperature profiles in up to two media with flat, cylindrical, or spherical geometries. The development of the program was motivated by the need to calculate maximum temperature differences across the walls of the Tritium metal hydrides beds for thermal fatigue analysis. The purpose of this report is to document the equations and the computer program used to calculate transient wall temperatures in stainless steel hydride vessels. The development of the computer code was motivated by the need to calculate maximum temperature differences across the walls of the hydrides beds in the Tritium Facility for thermal fatigue analysis. DOE

N94-19006# Sandia National Labs., Albuquerque, NM.
MOTOROLA MC68040 HIGH-SPEED DESIGN USING ALTERA EPM5000 ERASABLE PROGRAMMABLE LOGIC DEVICES
Hui-Chien Shen and S. M. Becker 1993 4 p Presented at the 1993 IEEE International ASIC Conference and Exhibit, Rochester, NY, 27 Sep. 1993
(Contract DE-AC04-76DP-00789)
(DE93-017635; SAND-93-1598C; CONF-9309201-1) Avail: CASI HC A01/MF A01

Many designs use EPLD's (Erasable Programmable Logic Devices) to implement control logic and state machines. If the design is slow, timing through the EPLD is not crucial so designers often treat the device as a black box. In high speed designs, timing through the EPLD is critical. In these cases, a thorough understanding of the device architecture is necessary. This paper discusses lessons learned in the implementation of a high-speed design using the Altera EPM5130. DOE

N94-19024# Colorado Univ., Boulder. Dept. of Computer Science.
A PROGRAMMING PARADIGM FOR DISTRIBUTED-MEMORY COMPUTERS
S. Crivelli and E. R. Jessup 30 Dec. 1992 4 p Presented at the 6th Society for Industrial and Applied Mathematics Conference on Parallel Processing for Scientific Computing, Norfolk, VA, 21-24 Mar. 1993
(Contract DE-FG02-92ER-25122)
(DE93-018336; DOE/ER-25122/5; CONF-930331-13) Avail: CASI HC A01/MF A01

One of the problems that arises in programming a multicomputer is the effective partitioning of the work into tasks and the assigning of those tasks to the processors. We will present a programming paradigm as a method of structuring the algorithms, allowing us to identify and separate programming phases. This paradigm allows us to develop a general software tool for dynamically allocating work to the processors while hiding many details of load balancing. Our paradigm consists of four phases: partitioning the work, mapping the tasks into the processors connected by some virtual topology, running the application program, and embedding the virtual architecture into the actual machine. The paradigm applies to diverse problems and to a variety of multiprocessors without significant reprograming. We will use the multisection method for computing eigenvalues to show how this tool works. DOE

N94-19048# Lawrence Livermore National Lab., CA.
CAVEMAN: CONFIGURATION AND VERSION MANAGEMENT
K. M. Dyer 12 Mar. 1993 164 p
(Contract W-7405-eng-48)
(DE93-018066; UCRL-MA-113603) Avail: CASI HC A08/MF A02

The mission of the CAVEMAN project is to provide the tools for large code systems so that those who work on them can perform source control and configuration control on UNIX-based file servers, rather than the LC Crays. An outside product called the Concurrent Versions System (CVS) has been chosen as the underlying source control system. It is a freeware program that runs on most UNIX stations. To quote from the CVS man page: CVS is a front end to the RCS revision control system which extends the notion of revision control from a collection of files in a single directory to a hierarchical collection of directories consisting of revision controlled files. These directories and files can be combined together to form a software release. CVS provides the functions necessary to manage these software releases and to control the concurrent editing of source files among multiple software developers. While CVS may be run directly, there are several tasks in the LLNL environment that it seemed either safer or easier to automate. CAVEMAN provides the needed functionality, generally in the form of wrappers to CVS. DOE

N94-19062# Vrije Univ., Amsterdam (Netherlands). Faculteit der Wiskunde en Informatica.
ASYNCHRONOUS RENDEZVOUS IN THE PRESENCE OF BACKTRACKING
A. Elieans and E. P. deVink Jun. 1992 29 p See also PB89-182828 and PB89-205256
(PB93-197739; IR-291) Avail: CASI HC A03/MF A01

The distributed logic programming language DLP extends Prolog with constructs for parallel object oriented programming. Its distinguishing feature is an asynchronous rendezvous that allows distributed backtracking over the solutions resulting from a method call. The paper studies the rendezvous mechanism of DLP. An abstract, uninterpreted language called Beta embodying the control flow skeleton of DLP is introduced and serves as a vehicle to clarify the asynchronous aspects of the rendezvous in the presence of backtracking. Both a transition system based operational semantics and a metric denotational semantics for Beta are presented. The notion of a resumption (an action that is delivered as the result of a method call) is proposed to describe the communication taking place between processes engaged in a rendezvous, and makes a remarkably smooth comparison possible of the two types of models. NTIS

N94-19066# Technische Univ., Eindhoven (Netherlands). Dept. of Mathematics and Computing Science.
USEFUL LAMBDA NOTATION
R. Nederpelt and F. Kamareddine 1992 26 p
(PB93-191856; Computing-Science-Notes-92/22) Copyright Avail: CASI HC A03/MF A01

Lambda Calculus is fundamental for the foundation of Logic, Mathematics, Computer and Cognitive Science. This makes it indispensable to formalize the Lambda Calculus in a way which avoids most of the complications associated with, among others, substitution, variable renaming, the search of bound and free occurrences of variables. Combinatory Logic could be seen as an attempt to do so, but is not as intuitive as the lambda calculus. This paper provides a new formulation of the lambda calculus. Such a formulation is shown to be useful for term and variable manipulation and for locating the type of a term. This will have advantages on all areas of the lambda calculus including substitution (global and local), unification and typing. NTIS

N94-19076# Oak Ridge National Lab., TN.
COORDINATION OF SOFTWARE-DEVELOPMENT ACTIVITIES AMONG SITES THAT ARE GEOGRAPHICALLY SEPARATED
L. F. Truett, J. P. Loftis, P. C. Shipe, E. Z. Faby, and J. W. Grubb 29 Jun. 1993 7 p Presented at the 1993 Seventeenth Annual International Computer Software and Applications Conference, Phoenix, AZ, 3-5 Nov. 1993
(Contract DE-AC05-84OR-21400)
(DE93-019201; CONF-931148-2) Avail: CASI HC A02/MF A01

The Department of Defense is sponsoring development of a centralized, integrated database, which will be a repository international surface cargo movement data. Scheduled for implementation surface in early 1994, the system will include a relational database management system, processing modules, and complex communication components. Four geographically separated sites are involved with development. Design and development of a major computer system is never simple, but when design and development occur at multiple sites, the problems are compounded, especially when the timeframe for project completion is extremely tight. Issues such as identical developmental platforms and communications strategies must be addressed. A design plan must be strictly followed to ensure consistency and to coordinate integration of modules developed at different sites. DOE

N94-19084# Technische Univ., Delft (Netherlands). Faculty of Technical Mathematics and Informatics.
NEW INSIGHTS IN GMRES-LIKE METHODS WITH VARIABLE PRECONDITIONERS
Kees Vuik 1993 20 p
(Rept-93-10; ETN-93-94637) Copyright Avail: CASI HC A03/MF A01

GMRES (Generalized Minimal Residual Algorithms) methods with variable preconditioners are addressed. Two recently proposed methods, FGMRES and GMRESR, for the iterative solution of sparse linear systems with an unsymmetric nonsingular matrix, are compared. Both methods compute minimal residual approximations using preconditioners, which may be different from step to step. The insights resulting from this comparison lead to better variants of both methods. ESA

N94-19089# Technische Univ., Delft (Netherlands). Faculty of Technical Mathematics and Informatics.
THE THEORY OF LINEAR PROGRAMMING: SKEW SYMMETRIC SELF-DUAL PROBLEMS AND THE CENTRAL PATH
B. Jansen, C. Roos, and T. Terlaky 1993 15 p Sponsored in part by Shell Research
(Contracts OTKA-2116; NWO-611-304-028)
(Rept-93-15; ETN-93-94642) Copyright Avail: CASI HC A03/MF A01

The literature in the field of interior point methods for linear programming has been almost exclusively algorithm oriented. Recently Guler, Roos, Terlaky and Vial presented a complete duality theory for linear programming based on the interior point approach. A more simple approach which is based on an embedding of the primal problem and its dual into a skew symmetric self dual problem is presented. This embedding is essentially due to Ye, Todd and Mizuno. First, a skew symmetric self dual linear program is considered. The strong duality theorem is shown to trivially hold in this case. Then, using the logarithmic barrier problem and the central path, the existence of a strictly complementary optimal solution is proved. Using the embedding just described, the strong duality theorem and the existence of strictly complementary optimal solutions for general linear programming problems are easily obtained. ESA

N94-19102# Sandia National Labs., Albuquerque, NM.
GENSHELL: A GENESIS DATABASE 2D TO 3D SHELL TRANSFORMATION PROGRAM
G. D. Sjaardema Jul. 1993 37 p
(Contract DE-AC04-76DP-00789)
(DE93-018694; SAND-93-1373) Avail: CASI HC A03/MF A01

GENSHELL is a three-dimensional shell mesh generation program. The three-dimensional shell mesh is generated by mapping a two-dimensional quadrilateral mesh into three dimensions according to one of several types of transformations: translation, mapping onto a spherical, ellipsoidal, or cylindrical surface, and mapping onto a user-defined spline surface. The generated three-dimensional mesh can then be reoriented by offsetting, reflecting about an axis, revolving about an axis, and scaling the coordinates. GENSHELL can be used to mesh complex three-dimensional geometries composed of several sections when the sections can be defined in terms of transformations of two-dimensional geometries. The code GJOIN is then used to join the separate sections into a single body. GENSHELL updates the EXODUS quality assurance and information records to help track the codes and files used to generate the mesh. GENSHELL reads and writes two-dimensional and three-dimensional mesh databases in the GENESIS database format; therefore, it is compatible with the preprocessing, postprocessing, and analysis codes in the Sandia National Laboratories Engineering Analysis Code Access System (SEACAS). DOE

N94-19124# Sandia National Labs., Albuquerque, NM.
THE EFFECTS OF INITIAL CONDITIONS AND CONTROL TIME ON OPTIMAL ACTUATOR PLACEMENT BY WAY OF A MAX-MIN GENETIC ALGORITHM
J. Redmond and G. Parker 1993 11 p Presented at the Annual Winter Meeting of the ASME, New Orleans, LA, 28-Nov. - 3 Dec. 1993
(Contract DE-AC04-76DP-00789)
(DE93-017640; SAND-93-1495C; CONF-931121-12) Avail: CASI HC A03/MF A01

This paper examines the role of the control objective and the control time in determining fuel-optimal actuator placement for structural vibration suppression. A general theory is developed that can be easily extended to include alternative performance metrics such as energy and time-optimal control. The performance metric defines a convex admissible control set which leads to a max-min optimization problem expressing optimal location as a function of initial conditions and control time. A solution procedure based on a nested Genetic Algorithm is presented and applied to an example problem. Results indicate that the optimal locations vary widely as a function of control time and initial conditions. DOE

N94-19143# Technische Univ., Delft (Netherlands). Faculty of Technical Mathematics and Informatics.
INTERIOR-POINT METHODOLOGY FOR LINEAR PROGRAMMING: DUALITY, SENSITIVITY ANALYSIS AND COMPUTATIONAL ASPECTS
B. Jansen, C. Roos, T. Terlaky, and J.-P. Vial (Geneva Univ., Switzerland.) 1993 55 p Sponsored in part by Shell Research
(Contracts OTKA-2116; NWO-611-304-028; FNSRS-12-34002.92)
(Rept-93-28; ETN-93-94655) Copyright Avail: CASI HC A04/MF A01

The interior point methodology is used to cover the main issues in linear programming: duality theory, parametric and sensitivity analysis, and algorithmic and computational aspects. The aim is to provide a global view on the subject matter. Various major facets of the theory are gathered. Only one specific algorithm is presented with its convergence analysis. ESA

N94-19145# Stockholm Univ. (Sweden). Dept. of Physics.
EXANA: A PROGRAM FOR ANALYSING EXTENDED ENERGY LOSS FINE STRUCTURES, EXELFS SPECTRA
M. A. Tafreshi, C. Bohm, and S. Csillag Sep. 1992 25 p
(USIP-92-01; ETN-93-94844) Avail: CASI HC A03/MF A01

A users guide and reference manual for EXANA is presented. It is an IBM or IBM compatible personal computer based program used for analyzing extended fine structures occurring on the high energy side of the ionization edges. The radial distance function obtained from this analysis contains information about the number, distance, and type of the nearby atoms, as well as the inelastic mean free path and disorder in distances from the center atom to the atoms in an atomic shell around it. The program can be made available on request. ESA

N94-19154# Technische Univ., Delft (Netherlands). Faculty of Technical Mathematics and Informatics.
ON THE CONVERGENCE OF AN UNFEASIBLE PRIMAL-DUAL INTERIOR-POINT METHOD FOR CONVEX PROGRAMMING
Kurt M. Anstreicher (Iowa Univ., Iowa City.) and Jean-Philippe Vial (Geneva Univ., Switzerland.) 1993 18 p Sponsored in part by Tech. Univ., Delft, Netherlands
(Grant FNSRS-12-24434.89)
(Rept-93-34; ETN-93-94661) Copyright Avail: CASI HC A03/MF A01

The unfeasible primal dual algorithm for smooth convex programming recently introduced by Vial is considered. It is shown under mild assumptions, that a SUMT (Sequential Unconstrained Minimization Technique) or 'long step path following' version of the algorithm is globally convergent. The steplength on each iteration is based on a merit function which is a modification of the potential function proposed by Vial. ESA

N94-19155# Technische Univ., Delft (Netherlands). Faculty of Technical Mathematics and Informatics.
CONTENT BASED-GRID NODE SELECTION FOR VECTOR FIELD VISUALIZATION
Theo vanWalsum 1993 14 p
(Rept-93-35; ETN-93-94662) Copyright Avail: CASI HC A03/MF A01

Data selection techniques are indispensable for exploration of large scientific datasets. A technique for content-based data selection is presented. This technique uses a selection expression, an expression consisting of conditions on data values. To select a set of grid nodes of a data set, the expression is evaluated for each grid node. The selected set of grid nodes can be visualized directly; it can be also be used for further exploration of the dataset. ESA

N94-19156# Technische Univ., Delft (Netherlands). Faculty of Technical Mathematics and Informatics.
A POLYNOMIAL PRIMAL-DUAL DIKIN-TYPE ALGORITHM FOR LINEAR PROGRAMMING
B. Jansen, C. Roos, and T. Terlaky 1993 25 p Sponsored in part by Shell Research
(Contracts OTKA-2116; NWO-611-304-028)
(Rept-93-36; ETN-93-94663) Copyright Avail: CASI HC A03/MF A01

A primal dual affine scaling method for linear programming is presented. The method yields a strictly complementary optimal solution pair, and also allows a polynomial time convergence proof. The search direction is obtained by using the original idea of Dikin, namely by minimizing the objective function (which is the duality gap in the primal dual case), over some suitable ellipsoid. This gives rise to completely new primal dual affine scaling directions, having no obvious relation with the search directions proposed in the literature so far. The new directions guarantee a significant decrease in the duality gap in each iteration, and at the same time they drive the iterates to the central path. In the analysis of the algorithm, a barrier function which is the natural primal dual generalization of Karmakar's potential function is used. The iteration bound is O(nL), which is a factor O(L) better than the iteration bound of an earlier primal dual affine scaling method (Monteiro, Adler and Resende). ESA

N94-19186# Fermi National Accelerator Lab., Batavia, IL.
A MULTI-THREAD APPROACH TO COALESCING SMALL TRANSFERS GENERATED BY PORTABLE TOOL SETS
M. Fischler and M. Uchima Apr. 1993 23 p Presented at the Supercomputing Conference on High Performance Computing and Communications, Portland, OR, 15-19 Nov. 1993
(Contract DE-AC02-76CH-03000)
(DE93-012128; FNAL/C-93/076; CONF-931115-1) Avail: CASI HC A03/MF A01

An approach to providing scientific users with the means to code complex algorithms in a natural way is to provide portable tool sets implementing the concepts of each scientific field. These tool sets facilitate implementation on massively parallel systems, but often tend toward large numbers of small inter-CPU data transfers which adversely impact efficiency. We present techniques for mitigating this effect without affecting the way the user sees the tools. Efficiency improvements obtained by transfer coalescing via 'multi-threading' are studied in the context of Lattice Gauge Theory computations. DOE

N94-19196# Universiteit Twente, Enschede (Netherlands). Tele-Informatics and Open Systems Group.

REDUCING EXTENDED TRANSITION SYSTEMS

Henk Eertink, Pim Kars, and Henk Wennink 22 Jan. 1993 16 p
(Memo-INF-93-09; TIOS-93-06; ETN-93-94683) Copyright Avail: CASI HC A03/MF A01

A tool that can be used to reduce the number of states and transitions in an extended finite state machine derived from a LOTOS (Language of Temporal Ordering Specification) specification, in which both transitions and states are parameterized with values and predicates over these values, is presented. The algorithms used in the tool are derived from standard weak bisimulation laws and from optimization techniques used in regular programming languages, and can be seen as a first step towards model checking and verification techniques for arbitrary LOTOS specifications. The implementation of the tool was done in C, and it encompasses an X11 based user interface. ESA

N94-19200# Universiteit Twente, Enschede (Netherlands). Dept. of Computer Science.

MODELLING SOFTWARE FOR STRUCTURE METRICS

P. M. vandenBroek and K. G. vandenBerg Feb. 1993 21 p
(Memo-INF-93-13; ETN-93-94687) Copyright Avail: CASI HC A03/MF A01

In the approach to structural software metrics which has become standard nowadays, software is modeled by means of flowgraphs. A tacit assumption in this approach is that the structure of a program is reflected by the structure of the flowgraph. However, this assumption is not always true. An introduction of structure graphs for the modeling of software is presented. Structure graphs can, just as flowgraphs, be uniquely decomposed into a hierarchy of indecomposable prime structures. It is shown how programs in an imperative language can be modeled by means of structure graphs in such a way that the structure of a program is always reflected by the structure of the corresponding structure graph. A prototype implementation for the mapping of programs of a small example language to structure graphs, and for the decomposition of structure graphs into a hierarchy of indecomposable structure graphs, is given. ESA

N94-19205# Los Alamos National Lab., NM.

A PARALLEL HASHED OCT-TREE N-BODY ALGORITHM

M. S. Warren and J. K. Salmon 29 Mar. 1993 22 p Presented at the Supercomputing Conference on High Performance Computing and Communications, Portland, OR, 15-19 Nov. 1993
(Contract W-7405-eng-36)
(DE93-012654; LA-UR-93-1244; CONF-931115-3) Avail: CASI HC A03/MF A01

The authors report on an efficient adaptive N-body method which was recently designed and implemented. The algorithm computes the forces on an arbitrary distribution of bodies in a time which scales as N log N with particle number. The accuracy of the force calculations is analytically bounded and can be adjusted via a user defined parameter between a few percent relative accuracy, down to machine arithmetic accuracy. Instead of using pointers to indicate the topology of the tree, each possible cell is identified with a key. The mapping of keys into memory locations is achieved via a hash table. This allows the access of data in an efficient manner across multiple processors using a virtual shared memory model. Performance of the parallel program is measured on the 512 processor Intel Touchstone Delta system. The authors also comment on a number of wide-ranging applications which can benefit from application of this type of algorithm. DOE

N94-19220# Universiteit Twente, Enschede (Netherlands). Dept. of Computer Science.

ABSTRACTING INTER-OBJECT COMMUNICATIONS USING COMPOSITION FILTERS

Mehmet Aksit, Ken Wakita (Tokyo Inst. of Tech., Japan.), Jan Bosch, Lodewijk Bergmans, and Akinori Yonezawa (Tokyo Univ., Japan.) Dec. 1992 24 p
(Memo-INF-92-78; ETN-93-94669) Copyright Avail: CASI HC A03/MF A01

One of the major obstacles in object oriented modeling is due to the lack of abstraction mechanisms for object interactions. The message passing model of conventional object oriented languages is considered as being too low level because it can only specify communications that involve two partner objects at a time and its semantics cannot be extended easily. The so called 'composition filters' approach 'modularly' extends the basic object model by introducing 'input' and 'output composition filters' that affect the received and sent messages respectively. This mechanism enables software engineers to abstract communications among objects into a first class object called 'Abstract Communication Type' (ACT). ACT's make it easier to enforce the invariant behavior among objects, to reduce the complexity of programs by hiding the interaction details, to improve reusability through the application of object oriented principles to ACT classes, and to enhance the expression power of the object oriented model. ESA

N94-19221# Universiteit Twente, Enschede (Netherlands). Dept. of Computer Science.

DATATYPELOG: A DEDUCTIVE OBJECT ORIENTED QUERY LANGUAGE

Rene Bal Dec. 1992 57 p
(Memo-INF-92-79; ETN-93-94670) Copyright Avail: CASI HC A04/MF A01

Object oriented systems have complex objects which are structured in a class hierarchy. Now that these systems have become more prevalent, there is a need for a well founded powerful query language. In the case of the relational model there exists such a language, Datalog. Datalog uses a logical programming style of expressing deductions concerning the contents of the database. However this could not be used for object oriented databases because it is untyped and it is unable to deal with complex objects and inheritance. A definition of DataTypeLog (DTL), which is an extension of Datalog with typing, complex objects, sets, and method calls, is presented. DTL is able to deal with inheritance and complex objects. Furthermore the concepts used in the theory of logical language are extended in order to define the semantics and the resolution of DTL programs. ESA

N94-19222# Universiteit Twente, Enschede (Netherlands). Dept. of Computer Science.

THE TM TYPING RULES

Rene Bal, Herman Balsters, and Rolf A. deBy Dec. 1992 12 p
(Memo-INF-92-80; ETN-93-94671) Copyright Avail: CASI HC A03/MF A01

Twente-Milano (TM) is a high level specification language for object oriented database schemas. Originally, TM was conceived of as a sugared layer on top of its formal counterpart, the formal language FM. The FM language consists of a typed lambda calculus employing a notion of subtyping and is based on the well known ideas of Cardelli-Wegner type theory. New aspects of FM are the incorporation of a full first order typed logic and a complete theory of object oriented set constructions. The formal meaning of a TM specification is given by its translation to FM, and the same applies to typing rules in TM. It is, however, possible to also give a type theory for the TM language itself; this typing of TM expressions should of course be consistent with the typing of the corresponding expressions in the FM counterparts of the translation. It is shown that such a typing of TM expressions is possible, hence yielding an independent type theory for the TM language. ESA

N94-19224# Universiteit Twente, Enschede (Netherlands). Dept. of Computer Science.

ATTRIBUTE EVALUATION DURING GENERALIZED PARSING

Paul OudeLuttighuis and Klaas Sikkel Dec. 1992 98 p
(Memo-INF-92-85; ETN-93-94673) Copyright Avail: CASI HC A05/MF A02

A thorough discussion of generalized parsing with simultaneous attribute evaluation is presented. Parsers and combined parser evaluators are presented for the LL(0), LR(0), and SKLR(0) strategies, the last one being an intermediate strategy between the first two. Syntactic as well as semantic nondeterminism is handled by processing all alternatives simultaneously. Attribute evaluation during SKLR(0) and LR(0) parsing is accompanied by serious complications. Existing techniques can be viewed as special deterministic implementational variants of the nondeterministic specifications as presented. ESA

N94-19225# Universiteit Twente, Enschede (Netherlands). Dept. of Computer Science.

COMPUTER-ASSISTED INSTRUCTION AND NATURAL LANGUAGE SYSTEMS

M. Offereins Dec. 1992 28 p
(Memo-INF-92-86; ETN-93-94674) Copyright Avail: CASI HC A03/MF A01

An overview of the use of natural language in Computer Assisted Instruction (CAI) systems is given. CAI systems are viewed as computer applications in which the computer is used as a tutor. They provide instruction in a particular knowledge domain. CAI systems have traditionally been based on the use of static and predifined knowledge sources, like problem descriptions together with possible answers, errors, and feedback messages. More intelligent CAI systems use AI techniques to let the program itself reason about the user's progress in learning, and they create a more dynamic learning environment. In both approaches, the interface environment is essential as a means through which knowledge is communicated to the learner. The development of an intelligent CAI system is dependent on the development of an intelligent interface environment. Different types of CAI systems are distinguished as well as different types of communication styles. It turns out that communication is hardly based on natural language processing techniques, as these cause a lot of overhead. But, a special purpose Natural Language system can be developed and built into the interface environment of a CAI system, as the communication language for the instruction, or into a CAI system for learning a particular language skill. Furthermore, a general purpose Natural Language system can be developed and built into a CAI system for Language Learning. Different research applications in Computer Assisted Language Learning (CALL) and in instructional Natural Language Interfaces are discussed. The conclusions and recommendations show that there is still a huge research gap that needs to be filled in when talking about the communication of knowledge and the use of natural language processing techniques in CAI systems. ESA

N94-19227# Universiteit Twente, Enschede (Netherlands). Tele-Informatics and Open Systems Group.

GOAL-DRIVEN LOTOS EXECUTION

Ed Brinksma and Henk Eertink 1993 28 p
(Memo-INF-93-04; TIOS-93-02; ETN-93-94678) Copyright Avail: CASI HC A03/MF A01

An algorithm for the guided simulation of LOTOS (Language of Temporal Ordering Specification) specifications is presented. Based on the selection of a behavior expression occurrence contained in a LOTOS specification the algorithm determines a reduced inference system that calculates, if it exists, the shortest path from the initial state of the specification behavior to an 'active' context of the selected expression, that is, one in which it can execute (some of) its actions. Thus each selected occurrence gives rise to a corresponding filter over the usual action inference system of LOTOS. These filters are constructed using only static information of the LOTOS specification: the position of the selected behavior expression occurrence. Constructing and applying such filters for goal driven LOTOS execution has a better performance with respect to both speed and memory than full simulation using standard tree walking algorithms. This LOTOS execution model is especially useful for the experimental validation of process algebraic specifications and test (preamble) derivation from specifications. ESA

N94-19229# Universiteit Twente, Enschede (Netherlands). Dept. of Computer Science.

THE TM MANUAL VERSION 1.3 WORKING DOCUMENT

Rolf A. deBy, Herman Balsters, and Chris C. deVreeze Dec. 1992 36 p
(Memo-INF-93-06; ETN-93-94680) Copyright Avail: CASI HC A03/MF A01

TM (Twente Milano) is a high level specification language for object oriented database schemas. TM is based on a variant of Cardelli-Wegner type theory employing a notion of subtyping to describe a framework of inheritance. The TM language is meant as a user language, which means that the language should be able to be learnt and applied in a more or less easy manner, and without necessarily getting involved with formal semantics. A paper aimed at providing the essentials of the TM language without appealing to formal semantics is presented. The TM language is described by using syntax diagrams accompanied by informal explanations. Various example specifications are offered and some semantical issues are discussed. ESA

N94-19238# Lawrence Livermore National Lab., CA.

AN INNOVATIVE NEURAL MANUFACTURING CONCEPT

Chi Yung Fu 25 Mar. 1993 4 p Presented at the NCAICM Workshop, Albuquerque, NM, 30-31 Mar. 1993
(Contract W-7405-eng-48)
(DE93-017212; UCRL-JC-113619; CONF-9303198-2) Avail: CASI HC A01/MF A01

Researchers at Lawrence Livermore National Laboratory are developing a neural network system to provide intelligence for real-time, in-situ process monitoring, adaptive control, metrology, and equipment diagnostics. They call the applications of neural networks and other human-like intelligence to manufacturing 'neural manufacturing.' Performance, cost, and space requirements must be considered for implementing a neural network controller in a manufacturing environment. They are currently developing a 96-neuron cascadeable neural network VLSI chip for their process monitor/control system. This chip is expected to run at 12 billion interconnects per second and cost only a few hundred dollars. DOE

N94-19245# Sandia National Labs., Albuquerque, NM.

HOW TO APPLY THE IEEE STANDARDS TO SOFTWARE TESTING

J. Klamerus and J. Weeks Jun. 1993 19 p
(Contract DE-AC04-76DP-00789)
(DE93-018514; SAND-92-2521) Avail: CASI HC A03/MF A01

Testing is an important part of the software application development process. To achieve quality software deliverables and to avoid costly redevelopment of program code or repair of bad data, testing must be performed throughout the software development life cycle. This paper discusses a software engineering process to produce a software test plan based upon the IEEE (Institute of Electrical and Electronics Engineers) Software Engineering Standards Collection guidelines and corporate guidelines. Demonstrated examples of the software testing process involving interactive graphical user interface software and standard ASCII forms-based text are provided. Sandia National Laboratories has a Software Quality Assurance Department which provides corporate guidelines, in addition to recommending the use of IEEE processes. Both corporate guidelines and a specific subset of the IEEE guidelines were applied to the software development projects discussed herein. The rationale for applying a specific subset of the IEEE guidelines for each of the software development projects will be given. The development of the test procedures in the INGRES/WINDOWS 4GL environment (graphical user interface) as well as in the INGRES/ABF environment (Applications-By-Forms, ASCII Text) are presented and contrasted. The documentation of the testing process and results are explained. DOE

N94-19261# Universiteit Twente, Enschede (Netherlands). Tele-Informatics and Open Systems Group.

ADVANCES IN ARCHITECTURAL CONCEPTS TO SUPPORT DISTRIBUTED SYSTEMS DESIGN

Luis FerreiraPires, Chris A. Vissers, and Marten vanSinderen 6 Apr. 1993 29 p
(Memo-INF-93-17; TIOS-93-09; ETN-93-94690) Copyright Avail: CASI HC A03/MF A01

Some architectural concepts for distributed systems design are presented and discussed. These concepts are derived from an analysis of limitations of some currently available standard design languages. It is concluded that language design should be based upon the careful consideration of architectural concepts. This paper aims at supporting designers by presenting a methodological design framework in which they can reason about the design and implementation of distributed systems. The paper is also meant for language developers and formalists by presenting a collection of architectural concepts which deserve consideration for formal support. ESA

N94-19262# Universiteit Twente, Enschede (Netherlands). Dept. of Computer Science.

STOCHASTIC GRAMMARS: THEORY AND APPLICATIONS

Rieks opdenAkker Apr. 1993 21 p
(Memo-INF-93-19; ETN-93-94692) Copyright Avail: CASI HC A03/MF A01

An investigation of stochastic grammars and stochastic languages is presented. Their use as a formal model to describe statistical aspects of sentences in natural languages is discussed. Weakly restricted stochastic context free grammars are introduced and compared with the classical model of stochastic grammars. It is argued that a restricted stochastic grammar is a better model for ordering the structures of ambiguous sentences than the usual (unrestricted) stochastic grammars. The notion of consistency for these grammars is defined. Problems concerning parameters inference and stochastic parsing are stated. Several problems concerning inference of stochastic grammars and grammar classification are posed. ESA

N94-19276# Lawrence Livermore National Lab., CA.

VOLUME RENDERING OF 3D SCALAR AND VECTOR FIELDS AT LAWRENCE LIVERMORE NATIONAL LABORATORY

R. Crawfis, N. Max, B. Becker, and B. Cabral Apr. 1993 11 p Presented at the Supercomputing Conference on High Performance Computing and Communications, Portland, OR, 15-19 Nov. 1993
(Contract W-7405-eng-48)
(DE93-018000; UCRL-JC-113639; CONF-931115-9) Avail: CASI HC A03/MF A01

Simulation of complex three dimensional phenomena data sets which are hard to comprehend using conventional two-dimensionally oriented visualization tools is discussed. One way to overcome this limitation is to employ various volume visualization techniques. While early volume visualization techniques worked well on simple scalar volumes they failed to exploit frame buffer hardware capabilities and handle higher order data such as vector field. Work at Lawrence Livermore National Laboratory has centered on developing new techniques and extending existing techniques. DOE

N94-19330 Technische Univ., Eindhoven (Netherlands). Dept. of Mathematics and Computing Science.

USING GEOMETRIC TECHNIQUES TO IMPROVE DYNAMIC PROGRAMMING ALGORITHMS FOR THE ECONOMIC LOT-SIZING PROBLEM AND EXTENSIONS

C. P. M. VanHoesel, A. P. M. Wagelmans, and B. Moerman Nov. 1992 40 p See also N92-29819 Limited Reproducibility: More than 20% of this document may be affected by microfiche quality
(PB93-197556; MEMO-COSOR-92-45) Avail: CASI HC A03

The paper discusses two basic geometric techniques that can be used to speed up certain types of dynamic programs. The authors first present the algorithms in a general form, and then they show how these techniques can be applied to the economic lot-sizing problem and extensions. Furthermore, it is illustrated that the geometric techniques can be used to give elegant and insightful proofs of structural results, like Wagner and Whitin's planning horizon theorem. Finally, the authors present results of computational experiments in which new algorithms for the economic lot-sizing problem are compared with each other, as well as with other algorithms from the literature. NTIS

N94-19333# Swedish Inst. for Materials Testing, Boras. Fysik och Eleknik.

SOFTWARE QUALITY IN TEST AND MEASURMENT EQUIPMENT [PROGRAMVARUKVALITET I MAET-OCH PROVUTRUSTNING]

J. Jacobson, G. Kjell, P. Lau, I. Thoren, and J. Tunare 1993 71 p In SWAHILI
(PB93-197846; SP-RAPP-1993:08) Avail: CASI HC A04/MF A01

The report is the result of work carried out to establish common recommendations for software used in test and measurement equipment. The different steps of the software development model are discussed. Recommendations are given for specification, programming, validation, administration, documentation, back-up and maintenance. Some application examples are given in the appendices. NTIS

N94-19344# Sandia National Labs., Albuquerque, NM.

REFINING A TRIANGULATION OF A PLANAR STRAIGHT-LINE GRAPH TO ELIMINATE LARGE ANGLES

S. A. Mitchell 13 May 1993 22 p Presented at the 34th Meeting of the IEEE Foundation of Computer Science, Palo Alto, CA, 3-5 Nov. 1993
(Contract DE-AC04-76DP-00789)
(DE93-016510; SAND-93-1392C; CONF-931167-1-Extd-Abst) Avail: CASI HC A03/MF A01

Triangulations without large angles have a number of applications in numerical analysis and computer graphics. In particular, the convergence of a finite element calculation depends on the largest angle of the triangulation. Also, the running time of a finite element calculation is dependent on the triangulation size, so having a triangulation with few Steiner points is also important. Bern, Dobkin and Eppstein pose as an open problem the existence of an algorithm to triangulate a planar straight-line graph (PSLG) without large angles using a polynomial number of Steiner points. We solve this problem by showing that any PSLG with upsilon vertices can be triangulated with no angle larger than 7(pi)/8 by adding O(upsilon(exp 2) log upsilon) Steiner points in O(upsilon(exp 2) log(exp 2) upsilon) time. We first triangulate the PSLG with an arbitrary constrained triangulation and then refine that triangulation by adding additional vertices and edges. Some PSLG's require Omega(upsilon(exp 2)) Steiner points in any triangulation achieving any largest angle bound less than pi. Hence the number of Steiner points added by our algorithm is within a log upsilon factor of worst case optimal. We note that our refinement algorithm works on arbitrary triangulations: Given any triangulation, we show how to refine it so that no angle is larger than 7(pi)/8. Our construction adds O(nm+np log m) vertices and runs in time O((nm+np(log m)) log(m+ p)), where n is the number of edges, m is one plus the number of obtuse angles, and p is one plus the number of holes and interior vertices in the original triangulation. A previously considered problem is refining a constrained triangulation of a simple polygon, where p = 1. For this problem we add O(upsilon(exp 2)) Steiner points, which is within a constant factor of worst case optimal. DOE

N94-19359# Institut National Polytechnique, Grenoble (France). Lab. d'Informatique Fondamentale et d'Intelligence Artificielle.

NEW AUTOMATIC DEDUCTION TECHNIQUES IN FIRST ORDER FINITE AND INFINITE POLYVALENT LOGIC Ph.D. Thesis [NOUVELLES TECHNIQUES DE DEDUCTION AUTOMATIQUE EN LOGIQUES POLYVALENTES FINIES ET INFINIES DU PREMIER ORDRE]

Nicolas Zabel 1993 234 p In FRENCH
(ETN-93-95003) Avail: CASI HC A11/MF A03

Problems of studying polyvalent logic are recalled. A mechanical method of obtaining inference rules for propositional connectors of the tableaux method, from the matrical definition of logic, is elaborated. A similar treatment is done for the inference rules of the quantifiers. The refinement studied is thus a lazy skolemization. It enables unification to be used to calculate the useful instances to construct a closed tableau. Polyvalent logic with gradual equality is proposed, a method of ordered paramodulation resolution. Truth values are provided for lattice or two dimensional lattice structures. The systematic processing of finite logic follows a study of two typical cases of first order infinite polyvalent logic, the Post and Lukasiewicz logic. The link between Hornand Post logic is used to propose the automatization of Post logic based on possible semantic worlds. From this semantic a prefixed tableaux method is defined. To increase the efficiency, constraints resolved in polynomial time on the prefixes, are introduced. ESA

N94-19363 Grenoble-1 Univ. (France). Traitement de l'Information et Modelisation en Biomedecine.

MULTIMODAL IMAGE CORRELATION APPLIED TO COMPUTER AIDED PEDICULAR SCREWING Ph.D. Thesis [MISE EN CORRESPONDANCE D'IMAGES MULTIMODALES APPLIQUEE A LA VISEE PEDICULAIRE ASSISTEE PAR ORDINATEUR]

Bruno Mazier 1992 158 p In FRENCH Limited Reproducibility: More than 20% of this document may be affected by microfiche quality
(ETN-93-95018) Avail: CASI HC A08

Insertion of a screw in the solid zone of the pedicle bone of a lumbar vertebra allows to fix implants that are meant to correct some morphological pathologies of the spinal column. The aim of the Computer Aided Pedicular Screwing (CAPS) is to help surgeons to plan and make this critical task. Its principle is based on the three phases general methodology of image guided operating robot. It consists of rationally and quantitatively linking multimodal imaged information collected before and during the operation. The perception phase consists of acquiring and modeling before and during the operation the imaged information related to the vertebra to be installed. The acquisition always comes after the calibration of the image sensors used. During the decision phase the surgeon uses the former data to plan his operative strategy by simulation of this strategy. The different referentials used are linked by rigid transformations to find again, during the operation, the pre-operation planned strategy. The action phase allows to guide the gesture itself by using more or less robotized guiding systems. ESA

N94-19368 Grenoble-1 Univ. (France). Lab. de Genie Informatique.
MANAGING PERSISTENT OBJECTS: FROM THE PROGRAMMING LANGUAGE TO THE SYSTEM Ph.D. Thesis [GESTION D'OBJETS PERSISTANTS: DU LANGAGE DE PROGRAMMATION AU SYSTEME]
Pascal Dechamboux 1993 168 p In FRENCH Limited Reproducibility: More than 20% of this document may be affected by microfiche quality
(ETN-93-95021) Avail: CASI HC A08

PEPLOM (Persistent Programming Language for Object Management) is described at two levels: model definition and implementation. PEPLOM covers three main issues: safety, efficiency and flexibility of the application schema. It is a language based on the C/C++ language. Covering the combination of databases and programming languages, possible memory models to support various type systems are studied. Existing object oriented database management systems are evaluated and compared at different levels. The problem of programs structuration is solved by introducing types and modules: abstract types organize intentional data definitions while modules organize extensional data definitions. Two phases are required to produce PEPLOM programs. The first phase consists of defining application components. A dictionary, managed by the compiler, incrementally records all these components that compose the schema. It allows transient inconsistencies of this schema. The second phase consists of producing ready to run applications. The produced object code supports the structural and semantic data models and runs on a low level memory manager. The performance observed on the prototype implemented is comparable to that of persistent C++ systems offering less functionality. ESA

N94-19370# Grenoble-1 Univ. (France). Lab. de Genie Informatique.
CONTRIBUTION TO APPLICATIONS SYSTEMS DESIGN MOSAIC METHOD IN THE ARISTOTE PROJECT Ph.D. Thesis [CONTRIBUTION A LA CONCEPTION LOGICIELLE DE SYSTEMES D'APPLICATIONS. LA METHODE MOSAIC DANS LE PROJET ARISTOTE]
Frederic Brissaud 1993 292 p In FRENCH
(ETN-93-95022) Avail: CASI HC A13/MF A03

Object Oriented Data Base Management Systems (OODBMS) integrate object languages concepts and DBMS mechanisms. They are suited to develop applications systems built on persistent data shared by various applications. The actual state of the art, focused on programming, database management and user interfaces, proposes specific techniques well adapted to design parts of these applications. Current methods do not permit complete and detailed design of applications systems, neither do they advise designers in programming application with OODBMS. The MOSAIC method was designed to develop applications systems running on OODBMS. Object oriented decomposition is used. A MOSAIC application has two components: the application body consists of applicative objects, models of real world entities, and the dialog manager consists of interactive objects, models of the man machine dialogs. Applicative objects, persistent or temporary, are both software modules and 'potentially persistent' or temporary data containers. Interactive objects group information and functions are presented to the user. An applications system is composed of an applicative objects base and of applications. The MOSAIC model allows the study of object and application systems according to the structural, functional and dynamic points of view. An O2 programmed example illustrates the MOSAIC method. ESA

N94-19378# Norwegian Defence Research Establishment, Kjeller.
CESAR USER LIBRARY
Halvor Bjordal, Per Atle Vaaland, and Svein-Erik Soegaard 18 Mar. 1993 116 p
(FFI-93/7021; ETN-93-94890) Avail: CASI HC A06/MF A02

Cesar is a powerful vector computer developed for processing of images from Synthetic Aperture Radar (SAR) satellites. It combines parallelism and pipelining on different levels to achieve a programmable 'algorithm processor' for computational intensive vector problems. This is the users interface to the Cesar computer. The library has a C interface, and the library routines are called from a standard C program running on Cesar's host computer. The host is a workstation running the UNIX operating system. Cesar is connected to the host computer by VME bus. The system's block diagram concerning Cesar connected to UNIX workstation is presented. ESA

N94-19382# Loughborough Univ. of Technology (England). Dept. of Mathematical Sciences.
OPTIMAL SAFETY SYSTEM DESIGN USING FAULT TREE ANALYSIS
J. D. Andrews Jun. 1993 32 p
(MATHS-Rept-A-187; ETN-93-94905) Avail: CASI HC A03/MF A01

A design optimization scheme for systems which require a high likelihood of functioning on demand is described. The final design specification is achieved by solving a sequence of optimization problems. Each of these problems is defined by assuming some form of the objective function and specifying a subregion of the design space over which this function will be representative of the system unavailability. An example of a high pressure protection system was used to demonstrate the technique. Design parameters for this system include redundancy levels, the number of elements required for a voting system to function, component selection options and maintenance inspection intervals. Both implicit and explicit contraint forms were used. The implicit constraints require a full system analysis to determine whether the current design is feasible or not. All system assessments were carried out using fault tree analysis. ESA

N94-19396 Grenoble-1 Univ. (France). Techniques de l'Imagerie, de la Modelisation et de la Cognition.
PROGRESS IN EDGE DETECTION
Marc Salotti Apr. 1993 34 p Limited Reproducibility: More than 20% of this document may be affected by microfiche quality
(RR-914-I; ETN-93-95002) Avail: CASI HC A03

A new approach to edge detection for gray level images is presented. The goal of edge detectors as an early stage of a machine vision, just finding relevant discontinuities in images, is defined. A survey of problems encountered in edge detection is presented: problems relative to noise, to specific configurations of gray values and problems relative to our way of working, particularly the methodology used to build an edge detector. A new edge detector that tries to solve the problems previously discussed is presented. It is an edge growing detector based on a powerful information management. The main features are an incremental approach justified by an adequate analysis of the problem 'focusing, exploration of the neighborhood and synthesis', and a cooperation with a region growing technique operating on a small area to compute a relative gradient. The protocol used to build the edge detector is new: no a priori edge model is chosen. The information management provides the main ideas for building the algorithm, then progressive algorithmic improvements are made towards a hypothetical ideal edge model. Some results are presented. ESA

N94-19409# Ecole Centrale de Lyon (France). Lab. de Mecanique des Solides.
CONTRIBUTION TO THE MODELLING AND THE IDENTIFICATION OF NONLINEAR MECHANICAL SYSTEMS Ph.D. Thesis [CONTRIBUTION A LA MODELISATION ET L'IDENTIFICATION DES SYSTEMES MECANIQUES NON-LINEAIRES]
Claude-Henri Lamarque 1992 449 p In FRENCH
(ECL-92-32; ETN-93-94592) Avail: CASI HC A19/MF A04

Tools to model and identify nonlinear mechanical systems are presented. Analytical nonlinearities are considered. Normal form theory brings back again classical results: frequency amplitude relation, resonances, bifurcation results. Classical or generalized nonlinear modes can be easily defined in the case of general finite number of freedom systems or Hamiltonian systems. Computation of periodic solutions is of special importance. The aim is to build nonlinear modes and to give a nonlinear superposition formula. It is shown that such an expression is approached by introducing generalized frequencies, generalized masses, and nonlinear modes. Stability analysis of periodic solutions is carried out by using normal form, or Poincare sections. Continuous systems are discretized. In order to investigate general behavior of nonlinear oscillators, software is developed. Classical quantities such as Lyapunov exponents, Poincare sections, fixed points, (un)stable manifolds, are calculated. Some examples of chaotic behavior are considered. ESA

N94-19412# Loughborough Univ. of Technology (England). Dept. of Mathematical Sciences.
ROBUSTNESS AND EFFICIENCY OF GENERALIZED PREDICTIVE CONTROL ALGORITHMS WITH GUARANTEED STABILITY
J. A. Rossiter and B. Kouvaritakis (Oxford Univ., England.) Jul. 1993 21 p
(MATHS-Rept-A-190; OUEL-1991/93; ETN-93-94908) Avail: CASI HC A03/MF A01

Modifications to the generalized predictive control algorithm which guarantee closed loop stability were proposed in three recent publications. Of these, the first two adopt the same philosophy, namely that of Constraint Receding Horizon Predictive Control (CRHPC), whereas the third adopts a Stable Generalized Predictive Control (SGPC) strategy by first stabilizing, then controlling the plant. The purpose of the study is to examine the relationship between CRHPC and SGPC. It is shown that the two approaches are theoretically equivalent, but it is also shown that CRHPC could be subject to significant numerical instability problems. Two alternative improved implementations of CRHPC are proposed. SGPC is shown to have the advantage both in terms of numerical stability and computational efficiency. ESA

N94-19429*# Virginia Univ., Charlottesville. Dept. of Computer Science.
A RESEARCH PROGRAM IN EMPIRICAL COMPUTER SCIENCE Final Report, 22 Nov. 1989 - 21 Nov. 1990
J. C. Knight Feb. 1991 24 p
(Grant NAG1-1073)
(NASA-CR-194069; NAS 1.26:194069; UVA/528334/CS91/101) Avail: CASI HC A03/MF A01

During the grant reporting period our primary activities have been to begin preparation for the establishment of a research program in experimental computer science. The focus of research in this program will be safety-critical systems. Many questions that arise in the effort to improve software dependability can only be addressed empirically. For example, there is no way to predict the performance of the various proposed approaches to building fault-tolerant software. Performance models, though valuable, are parameterized and cannot be used to make quantitative predictions without experimental determination of underlying distributions. In the past, experimentation has been able to shed some light on the practical benefits and limitations of software fault tolerance. It is common, also, for experimentation to reveal new questions or new aspects of problems that were previously unknown. A good example is the Consistent Comparison Problem that was revealed by experimentation and subsequently studied in depth. The result was a clear understanding of a previously unknown problem with software fault tolerance. The purpose of a research program in empirical computer science is to perform controlled experiments in the area of real-time, embedded control systems. The goal of the various experiments will be to determine better approaches to the construction of the software for computing systems that have to be relied upon. As such it will validate research concepts from other sources, provide new research results, and facilitate the transition of research results from concepts to practical procedures that can be applied with low risk to NASA flight projects. The target of experimentation will be the production software development activities undertaken by any organization prepared to contribute to the research program. Experimental goals, procedures, data analysis and result reporting will be performed for the most part by the University of Virginia. Derived from text

N94-19482# Rochester Univ., NY. Dept. of Computer Science.
BITS AND RELATIVE ORDER FROM RESIDUES, SPACE EFFICIENTLY
Paul F. Dietz, Ioan I. Macarie, and Joel I. Seiferas Oct. 1993 7 p
(TR-464) Avail: CASI HC A02/MF A01

For each k, let P(sub k) be the product of the first k primes, p(sub 1) less than p(sub 2) less than .... less than p(sub k). By the Chinese remainder theorem, each integer in the interval (0, P(sub k)) is determined by its residues modulo these k primes. The problems of space-efficiently computing the bits and the relative order of such numbers from their residues are addressed. Author (revised)

N94-19483# Rochester Univ., NY. Dept. of Computer Science.
FAULT-TOLERANCE AND COMPLEXITY
Lane A. Hemachandra Apr. 1993 17 p Presented at the 20th International Colloquium on Automata, Languages, and Programming, Lund, Sweden, 1993
(Grants NSF CCR-89-57604; NSF INT-91-16781)
(TR-450) Avail: CASI HC A03/MF A01

Robust computation - a radical approach to fault-tolerant database access - was explicitly defined one decade ago, and in the following year this notion was presented at ICALP (International Colloquium on Automata, Languages, and Programming) in Antwerp. A decade's study of robust computation by many researchers determined which problems can be fault-tolerantly solved via access to databases of many strengths. These results are surveyed and some interesting unresolved issues are mentioned. Author (revised)

N94-19488# Institut National Polytechnique, Grenoble (France). Lab. d'Informatique Fondamentale et d'Intelligence Artificielle.
PROBLEM OF CONTROL IN AN INTEGRAL VISION SYSTEM: USE OF A MULTI-AGENT SYSTEM Ph.D. Thesis [PROBLEME DU CONTROLE DANS UN SYSTEME INTEGRE DE VISION: UTILISATION D'UN SYSTEME MULTI-AGENTS]
Olivier Boissier 1993 253 p In FRENCH Sponsored by EEC, and Grenoble-1 Univ., France
(ETN-93-95007) Avail: CASI HC A12/MF A03

Control aspects in an integrated computer vision system are studied. Such a system has an architecture which enables to add or retract dynamically both processing methods and representations schemes according to the type of the scenes to be treated. The control problem was decomposed in four different subproblems concerning the definition of the goal to be satisfied (decision), the selection criteria implied by this goal (adaptation), the action to be executed when applying these criteria (command), and the observations which must be collected for solving the former subproblems. A multi agent approach was adopted in order to design an open and flexible integration scheme. The control problems are represented in this architecture along two dimensions: individual control (internal control of an agent) and social control (interaction control). The control structure within each agent is organized in three different layers, which correspond to the resolution of the decision, adaptation and command problems respectively. The social control restricts the possible interaction and resolution methods which can be used by each of the agents. Protocols define the sequence of interactions between them. These two notions take part into our society model where three different control layers are responsible for solving each of the former control subproblems. The proposed architecture enables the study of control policies for deliberate and reactive behavior. On the other hand, it enables the dynamic integration of reconstruction and recognition processing modes into interaction management policies. The interest of this approach is illustrated by examples from the Vision As Process (VAP) system developed in the framework of the European project BRA3038. ESA

N94-19498# Institut National Polytechnique, Grenoble (France). Lab. Conception de Systemes Integres.
ON-LINE TEST METHODS OF MICROPROCESSOR BASED SYSTEMS Ph.D. Thesis [TEST EN LIGNE DES SYSTEMES A BASE DE MICROPROCESSEUR]
Thierry Michel 1993 271 p In FRENCH
(ETN-93-95008) Avail: CASI HC A12/MF A03

Online test methods using hardware devices dedicated to control flow checking in microprocessor based systems are considered. A compaction scheme (signature analysis) is used to facilitate the verification. Most of the methods proposed up to now require a program modification to force invariant properties (the signature at each point in the flowchart is independent from the previously followed paths). On the contrary, the methods proposed here do not require any modification in the verified program and use a watchdog processor with a local memory to ensure the signature is invariant. Two such methods are presented. The first one can be easily adapted to different microprocessors and is one of the most efficient methods proposed up to now. The second method, derived from the previous one, was proposed in order to reduce the amount of information required for test purpose. This latter method was implemented in a programmable logic controller and its efficiency was evaluated through fault injection experiments. The low overhead induced by the implemented mechanisms leads to envisage the evolution of the prototype towards an industrial product. ESA

N94-19508# Rochester Univ., NY. Dept. of Computer Science.
A TIGHT LOWER BOUND FOR ON-LINE MONOTONIC LIST LABELING
Paul F. Dietz, Joel I. Seiferas, and Ju Zhang Nov. 1993 10 p
(Grant NSF CCR-89-09667)
(TR-478) Avail: CASI HC A02/MF A01

Maintaining a monotonic labeling of an ordered list during the insertion of n items requires Omega(n log(n)) individual relabelings, in the worst case, if the number of usable labels is only polynomial in n. Author (revised)

N94-19517 Institut National Polytechnique, Grenoble (France). Lab. de Modelisation et de Calcul.
CONCEPTION AND ANALYSIS OF NUMERICAL PARALLEL ALGORITHMS: REALIZATION ON THE CONNECTION MACHINE Ph.D. Thesis [CONCEPTION ET ANALYSE D'ALGORITHMES NUMERIQUES PARALLELES: REALISATIONS SUR LA CONNECTION MACHINE]
Denis Delesalle 1993 173 p In FRENCH Limited Reproducibility: More than 20% of this document may be affected by microfiche quality
(ETN-93-95005) Avail: CASI HC A08

The limits of the Single Instruction Multiple Data (SIMD) mode within the frame of linear algebra algorithms using a Connection Machine 2 are presented. In particular, those of data parallelism ('one matrix element per processor') are developed. It is shown how, with new communication routines and a judicious mapping, close to the peak rate performance is obtained. But this method does not work for each algorithm. The BLAS decomposition for massively parallel algorithms is considered. They display the bottleneck in the Conjugate Gradient method. For this case, a solution which consists of a well known old method is proposed. Indeed, although its convergence is slower on sequential, its execution time is better on parallel. Moreover, the matrix structure is an important property. It leads to speed up the computation time and increases the dimension of problem. But the architecture is not yet taking account of it. Permutations and communications they bring about are considered. In the frame of Burg's algorithm, a solution which computes in the same time, the reflection coefficient and those of autocorrelation, is described. ESA

N94-19548# Seattle City Light, WA. Office of Conservation.
RADIOSITY ALGORITHMS USING HIGHER ORDER FINITE ELEMENT METHODS
R. Troutman and N. Max 1 Aug. 1993 6 p Presented at the Siggraph 1993 Special Interest Group on Graphics Conference, Anaheim, CA, 2-6 Aug. 1993
(Contract W-7405-eng-48)
(DE93-018098; UCRL-JC-113527; CONF-930881-4) Avail: CASI HC A02/MF A01

Many of the current radiosity algorithms create a piecewise constant approximation to the actual radiosity. Through interpolation and extrapolation a continuous solution is obtained. An accurate solution is found by increasing the number of patches which describe the scene. This has the effect of increasing the computation time as well as the memory requirements. By using techniques found in the finite element method, we can incorporate an interpolation function directly into our form factor computation. We can then use less elements to achieve a more accurate solution. Two algorithms, derived from the finite element method, are described and analyzed. DOE

N94-19562# Sandia National Labs., Albuquerque, NM.
MIMD MASSIVELY PARALLEL METHODS FOR ENGINEERING AND SCIENCE PROBLEMS
W. J. Camp and S. J. Plimpton 1993 16 p Presented at the 1993 International Simulators Conference on High Performance Computing, Arlington, VA, 29 Mar. - 1 Apr. 1993
(Contract DE-AC04-76DP-00789)
(DE93-019409; SAND-93-0875C; CONF-930372-12) Avail: CASI HC A03/MF A01

MIMD massively parallel computers promise unique power and flexibility for engineering and scientific simulations. We review the development of a number of software methods and algorithms for scientific and engineering problems which are helping to realize that promise. We discuss new domain decomposition, load balancing, data layout, and communications methods applicable to simulations in a broad range of technical field including signal processing, multi-dimensional structural and fluid mechanics, materials science, and chemical and biological systems. DOE

N94-19573 Air Force Inst. of Tech., Wright-Patterson AFB, OH. School of Engineering.
OORA AUTOMATED KNOWLEDGE SYSTEM (OAKS) CODE, APPENDIX C
Nancy L. Crowley Sep. 1993 155 p Limited Reproducibility: More than 20% of this document may be affected by microfiche quality
(AD-A270709; AFIT/EN/TR/93-07-App) Avail: Issuing Activity (Defense Technical Information Center (DTIC))

This technical report is an appendix to AFIT Doctoral Dissertation AFIT/DS/ENG/93-11, On the Automation of Object-Oriented Requirements Analysis, September 1993. The technical report contains the LISP code for the Object-Oriented Requirements Analysis (OORA) Automated Knowledge System (OAKS). DTIC

N94-19590 Naval Air Warfare Center, China Lake, CA. Weapons Div.
REFINEMENT OF UNIT CELL PARAMETERS BY LEAST-SQUARES: COMMENTS ON AN OLD TECHNIQUE AND THE DEVELOPMENT OF A NEW COMPUTER PROGRAM Final Report, May 1992 - Apr. 1993
C. L. Lowe-Ma Sep. 1993 31 p Limited Reproducibility: More than 20% of this document may be affected by microfiche quality
(AD-A270610; NAWC-WPNS-TP-8128) Avail: CASI HC A03

The determination of unit cell parameters from (x-ray) diffraction data is integral to studies to new crystalline materials. The sensitivity of unit cell parameters to microscopic compositional variations leads to their wide use in the characterization of materials with potentially useful optical and/or electronic properties. Consequently, precise (and accurate) cell parameters are needed even for samples in which incorporation of an internal standard is not possible. To eliminate the requirement of an internal standard, a computer program has been developed that explicitly include refinement of possible systematic errors and geometric aberrations along with the refinement of the unit cell parameters. DTIC

N94-19592 Carnegie-Mellon Univ., Pittsburgh, PA. Dept. of Computer Science.
CVL: A C VECTOR LIBRARY MANUAL. VERSION 2
Guy E. Blelloch, Jonathan C. Hardwick, Jay Sipelstein, Siddhartha Chatterjee, and Margaret Reid-Miller Feb. 1993 16 p Limited Reproducibility: More than 20% of this document may be affected by microfiche quality
(Contract F33615-90-C-1465; ARPA Order 7597)
(AD-A270614; CMU-CS-93-114) Avail: Issuing Activity (Defense Technical Information Center (DTIC))

CVL is a library of low-level vector routines callable from C. This library includes a wide variety of vector operations such as elementwise function applications, scans, reductions, and permutations. Most CVL routines are defined for segmented and unsegmented vectors. This paper is intended for CVL users and implementors and assumes familiarity with vector operations and the scan-vector model of parallel computation. DTIC

N94-19619# National Science Foundation, Washington, DC. Center for Telecommunications Research.
PROGRAM DESCRIPTIONS
25 Oct. 1992 36 p
(NSF-92-123) Avail: CASI HC A03/MF A01

Through its Directorate for Engineering (ENG), NSF promotes the progress of engineering and technology, helping the Nation stay in the forefront of technology by giving engineering education and research broad, long-range support. Engineering's mission is carried out through the creative interaction of the following seven divisions: (1) Biological and Critical Systems (BCS); (2) Chemical and Thermal Systems (CTS); (3) Design and Manufacturing Systems (DDM); (4) Electrical and Communications Systems (ECS); (5) Engineering Education and Centers (EEC); (6) Industrial Innovation Interface (III); and (7) Mechanical and Structural Systems (MSS). Each of these divisions are further subdivided into programs which are all described in this document. Derived from text

N94-19652 Technische Univ., Berlin (Germany). Fachbereich Informatik.
TECHNICAL DEVELOPMENT OF A THEORY OF PROGRAMS Ph.D. Thesis [FACHSPRACHLICHE ENTWICKLUNG EINER THEORIE DER PROGRAMME]
Burkhard Messer 1992 352 p In GERMAN Limited Reproducibility: More than 20% of this document may be affected by microfiche quality
(ETN-93-95058) Avail: CASI HC A16

The technical terminology, needed for the formulation of program aspects and the result of programming process, which is produced and modified by means of programming environments, is theoretically investigated. It was ascertained why examinations of the terminology are essential for the research process; a methodological discussion shows that theoretical understanding of computer science is still incomplete for a program theory. The field of a program theory was regarded as a fundamental element of the computer science empirical theory, whose purely scientific and technological character was outlined, and a coarse structure of the network of partial theories was sketched. The reconstruction of core aspects of program theory was based on the idea that program semantics is established through interpretation rules of chemical and physical phenomena. An abstract model, which explains when the 'program' concept can be considered during the software development, was proposed. As a conclusion the interpretation of computer science was discussed in philosophical, technological and ethical terms. ESA

N94-19707# Defense Technical Information Center, Alexandria, VA.
LEARNING ABOUT THE INTERNET BIBLIOGRAPHY AND BEGINNER'S GUIDE
Phyllis L. Ovsiew 16 Aug. 1993 29 p
(AD-A268847) Avail: CASI HC A03/MF A01

This documentation briefly describes and explores the basic functionality of using the Internet computer network for e-mail, ftp (file transfer protocol), and telnet. In addition, once these basics are mastered, the user is provided with a bibliography of sources available both on the Internet as well as traditional print sources. The bibliography is a short list of information resources (beginning and advanced) that will help the network novice become familiar with the Internet. The main focus is on material of use to the beginning networker. DTIC

N94-19712# Grenoble-1 Univ. (France). Lab. de Modelisation et Calcul.
ON THE COMPUTATION OF VERSAL FAMILY OF MATRICES
Laurent Stolovitch 21 May 1992 19 p
(RR-892-M; ETN-93-94983) Avail: CASI HC A03/MF A01

Algorithms for the computation of versal deformations of matrices are presented. A deformation of a matrix A(sub 0) is a holomorphic matrix valued function whose value at a point t(sub 0), a member of C(sup p), is the matrix A(sub 0). The properties of these matrices in a neighborhood of t(sub 0) are studied. It is possible for each value t in this neighborhood to compute the Jordan form as well as the change of basis matrix; but, generally, the result is not analytic. So, a deformation of the matrix A(sub 0) is constructed into which any deformation can be transformed by an invertible deformation of the matrix Id. After introducing the notion of versal deformation, computer algebra algorithms are provided to compute these normal forms. It is shown that a one parameter deformation can be transformed into a simpler form than the general versal deformation. ESA

N94-19713 Centre National d'Etudes Spatiales, Toulouse (France). Direction Centrale de la Qualite.
COMPUTER SECURITY. EVOLUTIONS 1987 TO 1992: TRENDS AND PERSPECTIVES [SURETE DE FONCTIONNEMENT INFORMATIQUE. EVOLUTIONS 1987 - 1992: TENDANCES ET PERSPECTIVES]
B. Courtois (Grenoble-1 Univ., France.), M. C. Gaudel (Paris-Sud Univ., Orsay, France.), J. C. Laprie (Laboratoire d'Automatique et d'Analyse des Systemes, Toulouse, France.), and D. Powell (Laboratoire d'Automatique et d'Analyse des Systemes, Toulouse, France.) Dec. 1992 144 p In FRENCH Limited Reproducibility: More than 20% of this document may be affected by microfiche quality
(RR-905-I; LRI-786; LAAS-92382; ETN-93-95023) Avail: CASI HC A07

A critical analysis of the state of the art evolution of computer security from 1987 to 1992 is given. The basic concepts of computer security are overviewed and an extension to software security is included. Software integrity, confidentiality, and standardization approaches and the impact on object oriented systems are discussed. Recent developments in hardware, in particular those applying computer systems design and integration technologies, are presented. Concerning software, development models and object oriented programming approaches are considered. The constraints of the programming language logic, of PROLOG-3, of formal calculation, and of Ada and C++ on computer security are investigated. The influence of fault tolerance on the development of self testing components and the concept of fault tolerance software are discussed. Validation procedures on fault tolerance concepts are summarized. ESA

N94-19716# General Accounting Office, Washington, DC. Information Management and Technology Div.
SOFTWARE REUSE: MAJOR ISSUES NEED TO BE RESOLVED BEFORE BENEFITS CAN BE ACHIEVED. REPORT TO THE CHAIRMAN, SUBCOMMITTEE ON DEFENSE, COMMITTEE ON APPROPRIATIONS, HOUSE OF REPRESENTATIVES
Jan. 1993 21 p
(GAO/IMTEC-93-16; B-251542) Avail: CASI HC A03/MF A01; also available from GAO, PO Box 6015, Gaithersburg, MD 20877

The Department of Defense (DOD) estimates that expenditures for developing and maintaining software for its weapons, command and control, and other automated information systems currently exceed $24 billion a year. In an attempt to better manage these costs and improve its ability to develop and maintain high-quality software, Defense has initiated a comprehensive effort to incorporate software reuse practices into its software development efforts. Software reuse -- the practice of developing new applications from existing software -- offers the potential to greatly reduce the time, cost and effort needed to develop and maintain high-quality software. This report provides background information on software reuse, including an overview of issues that can inhibit effective software reuse and information on Defense's strategy to implement a department-wide software reuse program. Derived from text

N94-19761*# National Aeronautics and Space Administration. Goddard Space Flight Center, Greenbelt, MD.
SeaTrack: GROUND STATION ORBIT PREDICTION AND PLANNING SOFTWARE FOR SEA-VIEWING SATELLITES
Kenneth S. Lambert (Maryland Univ., College Park.), Watson W. Gregg, Charles M. Hoisington (Science Systems and Applications, Inc., Lanham, MD.), and Frederick S. Patt (General Sciences Corp., Laurel, MD.) Dec. 1993 39 p
(NASA-RP-1331; NAS 1.61:1331; Rept-94B00031) Avail: CASI HC A03/mf A01

An orbit prediction software package (Sea Track) was designed to assist High Resolution Picture Transmission (HRPT) stations in the acquisition of direct broadcast data from sea-viewing spacecraft. Such spacecraft will be common in the near future, with the launch of the Sea viewing Wide Field-of-view Sensor (SeaWiFS) in 1994, along with the continued Advanced Very High Resolution Radiometer (AVHRR) series on NOAA platforms. The Brouwer-Lyddane model was chosen for orbit prediction because it meets the needs of HRPT tracking accuracies, provided orbital elements can be obtained frequently (up to within 1 week). Sea Track requires elements from the U.S. Space Command (NORAD Two-Line Elements) for the satellite's initial position. Updated Two-Line Elements are routinely available from many electronic sources (some are listed in the Appendix). Sea Track is a menu-driven program that allows users to alter input and output formats. The propagation period is entered by a start date and end date with times in either Greenwich Mean Time (GMT) or local time. Antenna pointing information is provided in tabular form and includes azimuth/elevation pointing angles, sub-satellite longitude/latitude, acquisition of signal (AOS), loss of signal (LOS), pass orbit number, and other pertinent pointing information. One version of Sea Track (non-graphical) allows operation under DOS (for IBM-compatible personal computers) and UNIX (for Sun and Silicon Graphics workstations). A second, graphical, version displays orbit tracks, and azimuth-elevation for IBM-compatible PC's, but requires a VGA card and Microsoft FORTRAN. Author (revised)

N94-19782 Air Force Inst. of Tech., Wright-Patterson AFB, OH. School of Engineering.
ON THE AUTOMATION OF OBJECT-ORIENTED REQUIREMENTS ANALYSIS Ph.D. Thesis
Nancy L. Crowley Sep. 1993 281 p Limited Reproducibility: More

than 20% of this document may be affected by microfiche quality
(AD-A270673; AFIT/DS/Eng/93-11) Avail: CASI HC A13

The research investigated the possibility that an object-oriented requirements analysis (OORA) specification model can be represented in a computer system and used as a basis for the elicitation of the information necessary for the development of an object-oriented specification for a particular problem. The proof-of-concept system developed is called the OORA Automated Knowledge System (OAKS). OAKS contains a generic domain model that is modified to satisfy a particular problem in the domain. The core of OAKS is a reusable domain model, which represents a domain of interest. The domain model is used as a basis for user changes that are made to meet specific requirements of a particular problem. The domain model was structured to allow it to be ported to other domains of interest and inserted into the OAKS system. Therefore, OAKS represents an OORA system that can be used in numerous domains to develop an OORA specification for a particular problem. DTIC

N94-18018# Scientific Research Inst. of Instrument Automation, Moscow (USSR).
THE OPTIMAL NUMERICAL ALGORITHM FOR PROCESSING OF PHASE CODED TIME SIGNALS FOR RADIO-CLOCKS
Boris Rudyakov and Gennady Chvilyov *In* Societe Suisse de Chronometrie, Proceedings of the 4th European Congress on Chronometry 1992 p 61-63 (For primary document see N94-18006 04-35)
Copyright Avail: CASI HC A01/MF A02

N94-18019# Stuttgart Univ. (Germany). Inst. fuer Feinwerk- und Zeitmesstechnik.
SIMULATION OF A QUARTZ-CLOCKWORK [SIMULATION AN QUARZGROSSUHRWERKEN]
Uwe Thissen *In* Societe Suisse de Chronometrie, Proceedings of the 4th European Congress on Chronometry 1992 p 67-70 In GERMAN (For primary document see N94-18006 04-35)
Copyright Avail: CASI HC A01/MF A02

N94-18350*# Lawrence Livermore National Lab., CA.
AN ANALOG RETINA MODEL FOR DETECTING DIM MOVING OBJECTS AGAINST A BRIGHT MOVING BACKGROUND
R. M. Searfus, M. E. Colvin, F. H. Eeckman, J. L. Teeters, and T. S. Axelrod *In* Idaho Univ., The 1991 3rd NASA Symposium on VLSI Design 1991 12 p (For primary document see N94-18337 04-33)
(Contract W-7405-eng-48)
Avail: CASI HC A03/MF A04

N94-18374*# Idaho Univ., Moscow. Dept. of Electrical Engineering.
PARALLEL OPTIMIZATION ALGORITHMS AND THEIR IMPLEMENTATION IN VLSI DESIGN
G. Lee and J. J. Feeley *In its* The 1991 3rd NASA Symposium on VLSI Design 1991 12 p (For primary document see N94-18337 04-33)
Avail: CASI HC A03/MF A04

N94-18375*# Portland State Univ., OR. Dept. of Electrical Engineering.
CANONICAL MULTI-VALUED INPUT REED-MULLER TREES AND FORMS
M. A. Perkowski and P. D. Johnson *In* Idaho Univ., The 1991 3rd NASA Symposium on VLSI Design 1991 13 p Sponsored in part by NSF (For primary document see N94-18337 04-33)
Avail: CASI HC A03/MF A04

N94-18380*# Old Dominion Univ., Hampton, VA. Dept. of Computer science.
A FAST ADAPTIVE CONVEX HULL ALGORITHM ON TWO-DIMENSIONAL PROCESSOR ARRAYS WITH A RECONFIGURABLE BUS SYSTEM
S. Olariu, J. Schwing, and J. Zhang *In* Idaho Univ., The 1991 3rd NASA Symposium on VLSI Design 1991 9 p (For primary document see N94-18337 04-33)
(Contract NCC1-99; NSF CCR-89-09996)
Avail: CASI HC A02/MF A04

62 COMPUTER SYSTEMS

Includes computer networks and special application computer systems.

N94-17693 Pacific Northwest Lab., Richland, WA.
PARALLEL INVERSE ITERATION WITH REORTHOGONALIZATION
G. I. Fann and R. J. Littlefield Mar. 1993 5 p Presented at the 6th Society for Industrial and Applied Mathematics (SIAM) Conference on Parallel Processing for Scientific Computing, Norfolk, VA, 21-24 Mar. 1993 Limited Reproducibility: More than 20% of this document may be affected by microfiche quality
(Contract DE-AC06-76RL-01830)
(DE93-012867; PNL-SA-21790; CONF-930331-10) Avail: CASI HC A01

A parallel method for finding the orthogonal eigenvectors of a real symmetric tridiagonal is described. The method uses inverse iteration with repeated Modified Gram-Schmidt (MGS) reorthogonalization of the unconverged iterates for clustered eigenvalues. This approach is more parallelizable than reorthogonalizing against fully converged eigenvectors as is done by LAPACK's current DSTEIN routine. The new method is found to provide accuracy and speed comparable to DSTEIN's and to have good parallel scalability even for matrices with large clusters of eigenvalues. We present empirical results for residual and orthogonality tests plus timings on IBM RS/6000 (sequential) and Intel Touchstone DELTA (parallel) computers. DOE

N94-17976 Institut National Polytechnique, Grenoble (France). Lab. de Genie Informatique.
PARX, KERNEL OF A SYSTEM FOR MASSIVELY PARALLEL COMPUTERS: CONTROL OF COMMUNICATION BETWEEN PROCESSES Ph.D. Thesis [PARX, NOYAU DE SYSTEME POUR LES ORDINATEURS MASSIVEMENT PARALLELES: CONTROLE DE LA COMMUNICATION ENTRE PROCESSUS]
Nestor A. GonzalezValenzuela 1991 236 p In FRENCH Limited Reproducibility: More than 20% of this document may be affected by microfiche quality
(ETN-93-94353) Avail: CASI HC A11

Design aspects involving the application of a communication kernel which is part of PARX (a parallel processing system program for multiprocessors without common memory) are considered. The kernel builds a virtual machine for which the assembly of processors is independent of the underlying interconnection network topology. The state of the art of parallel computers architecture is reviewed. A model and a process for a parallel system kernel are proposed. The model is based on an entity assembly adapted to the process control of parallel programs composed of communicating processes. The communicating process cooperates by message exchanging. The communication control and the synchronism between processes are investigated. ESA

N94-18068 Institut National Polytechnique, Grenoble (France). Lab. de Genie Informatique.
PARX: ARCHITECTURE OF AN OPERATING SYSTEM FOR PARALLEL MACHINES Ph.D. Thesis [PARX: ARCHITECTURE DE NOYAU DE SYSTEME D'EXPLOITATION PARALLELE]
Yves Bertrand LangueTsobgny 1991 174 p In FRENCH Limited Reproducibility: More than 20% of this document may be affected by microfiche quality
(ETN-93-94401) Avail: Issuing Activity (European Space Agency (ESA))

The architecture of the kernel of an operating system for parallel machines is presented. Paradigms for supporting parallel applications at the level of the kernel of an operating system are discussed. Emphasis is given to issues related to process and communication models. The study is based on the following: parallel programming models as defined in progamming langages; and architectures of modern, parallel machines. This two pronged approach allows progress in expressing and actually using parallelism and tendencies and technical improvements in parallel machines technology to be taken into account. The main result is the design of the architecture of an original parallel operating system, PARX, and the design and implementation of a communication kernel for that system. Operating systems can no longer pretend to offer a range of services suitable for all types of applications. As they support a growing spectrum of applications, their functionalities now tend to be split into a kernel called 'micro,' 'light,' and a set of high level servers, which is the approach developed in this investigation. ESA

N94-18482# Oak Ridge National Lab., TN.
THE EVOLUTION OF THE PVM CONCURRENT COMPUTING SYSTEM
G. A. Giest and V. S. Sunderam (Emory Univ., Atlanta, GA.) 1993 10 p Presented at the Institute for Electronic and Electrical Engineers (IEEE) COMPON Spring Meeting, San Francisco, CA, 22-26 Feb. 1993
(Contract DE-AC05-84OR-21400)
(DE93-017764; CONF-9302135-2) Avail: CASI HC A02/MF A01

Concurrent and distributed computing, using portable software systems or environments on general purpose networked computing platforms, has recently gained widespread attention. Many such systems have been developed, and several are in production use. This paper describes the evolution of the PVM system, a software infrastructure for concurrent computing in networked environments. PVM has evolved over the past years; it is currently in use at several hundred institutions worldwide for applications ranging from scientific supercomputing to high performance computations in medicine, discrete mathematics, and databases, and for learning parallel programming. We describe the historical evolution of the PVM system, outline the programming model and supported features, present results gained from its use, list representative applications from a variety of disciplines that PVM has been used for, and comment on future trends and ongoing research projects. DOE

N94-18507 Toledo Univ., OH. Dept. of Electrical Engineering.
DEVELOPMENT OF PARALLEL ARCHITECTURES FOR SENSOR ARRAY PROCESSING, VOLUME 1 Final Report
M. M. Jamali and S. C. Kwatra Aug. 1993 90 p Limited Reproducibility: More than 20% of this document may be affected by microfiche quality
(Contract N00014-91-J-1011)
(AD-A270426; DSPH-3-Vol-1) Avail: CASI HC A05

The high resolution direction-of-arrival (DOA) estimation is important in many sensor systems. It is based on the processing of the received signal and extracting the desired parameters of the DOA of plane waves. Many approaches have been used for the purpose of implementing the function required for the DOA estimation. The Multiple Signal Classification (MUSIC) and the Estimation of Signal Parameters by Rotational Invariance techniques (ESPRIT) algorithms are two novel approaches used recently to provide asymptotically unbiased and efficient estimates of the DOA. They are believed to be promising and appropriate for hardware implementation for real time applications. They estimate the so called signal subspace from the array measurements. The parameters of interest (i.e. determining of the DOA) are then estimated from the intersection between the array manifold and the estimated subspace. DTIC

N94-18508 Toledo Univ., OH. Dept. of Electrical Engineering.
DEVELOPMENT OF PARALLEL ARCHITECTURES FOR SENSOR ARRAY PROCESSING. VOLUME 2: A PARALLEL ARCHITECTURE FOR BROAD-BAND DIRECTION-OF-ARRIVAL ESTIMATION Final Report
M. M. Jamali, S. C. Kwatra, and Raja F. Tabar Aug. 1993 138 p Limited Reproducibility: More than 20% of this document may be affected by microfiche quality
(Contract N00014-91-J-1011)
(AD-A270427; DSPH-3-Vol-2) Avail: CASI HC A07/MF A02

One of today's problems in signal processing is the identification of direction-of-arrival (DOA) for multiple broad-band sources. Many algorithms have been proposed in the literature, however, the algorithms are highly complex and require a lot of computing power. New technologies in the past two decades have decreased the cost of digital hardware, and its speed has increased to such an extent that digital signal processing has replaced a great deal of analog signal processing. This thesis presents a digital-domain parallel-pipelined architecture capable of computing the DOA of multiple broad-band sources in real-time. Broad-Band Signal-Subspace Spatial-Spectrum (BASS-ALE) Estimation algorithm has been selected for DOA estimation and has been simulated and verified through computer software programs. The BASS-ALE algorithm has been modified and parallelized. The parallel algorithm has been mapped on an architecture which is suitable for real-time computation. DTIC

N94-18509# TRW Systems Group, Huntsville, AL. System Development Div.
DISTRIBUTED COMPUTING DESIGN SYSTEM (DCDS) Final Report, 1 Jun. 1990 - 30 Sep. 1993
Jan M. Smedley 30 Sep. 1993 11 p
(Contract DASG60-90-C-0092)
(AD-A270435) Avail: CASI HC A03/MF A01

This report summarizes the activities under the Distributed Computing Design System program. The DCDS program was responsible for the support of the DCDS environment, developed under contract to USASDC. The DCDS environment is an integrated set of tools, languages, and methodologies designed to support the entire life-cycle of system/software development. This LOE contract provided technical assistance, training, distribution, configuration management, sustainment, and enhancement of DCDS. DTIC

N94-18699# Louisiana State Univ., Baton Rouge. Dept. of Computer Science.
A GENERAL THEORY OF SIGNAL INTEGRATION FOR FAULT-TOLERANT DYNAMIC DISTRIBUTED SENSOR NETWORKS Research Summary Report
S. S. Iyengar and B. J. Jones 1 Oct. 1993 8 p
(Contract N00014-91-J-1306)
(AD-A270316) Avail: CASI HC A02/MF A01

The computational issues related to information integration in multisensor systems and distributed sensor networks has become an active area of research. In recent years, a number of significant advances in the field of sensor integration have been made. This interest in the development of Distributed Sensor Networks (DSN's) for information gathering has partly emerged because of the availability of new technology which makes the DSNs economically feasible to implement and the increasing complexity of today's information gathering tasks to which they are applied. From a computational veiwpoint, the efficient extraction of information from noisy and fault signals emanating from many sensors requires the solution of problems related to (1) the architecture and fault-tolerance of the distributed sensor network, (2) the proper synchronisation of sensor signals, (3) the integration of information to keep the communication and the processing requirements small, and (4) the design of efficient computational techniques to abstractly represent and integrate sensor information. DTIC

N94-18767 United Kingdom Atomic Energy Authority, Culham (England). Radio Frequency Effects.
GENERAL GEOMETRY PIC FOR MIMD COMPUTERS Final Report
J. W. Eastwood, W. Arter, and R. W. Hockney Jun. 1993 141 p Limited Reproducibility: More than 20% of this document may be affected by microfiche quality
(Contract F49620-92-C-0035)
(AD-A269085) Avail: Issuing Activity (Defense Technical Information Center (DTIC))

New relativistic PIC algorithms using body fitted for modelling microwave sources in two and three dimensions have been derived. A parallel computer benchmarking program using a multiblock implementation of the two dimensional algorithms has been written. Test computations performed on the IPSC computer at Phillips Laboratory have demonstrated the MIMD computers can be efficiently used to model devices with complex geometry. DTIC

N94-18768 Naval Postgraduate School, Monterey, CA.
IMPLEMENTATION OF ELECTRONIC DATA INTERCHANGE IN THE DEPARTMENT OF DEFENSE: LESSONS LEARNED FROM PRIVATE INDUSTRY M.S. Thesis
Robert B. Turner 1 Jun. 1993 123 p Limited Reproducibility: More than 20% of this document may be affected by microfiche quality
(AD-A269532) Avail: CASI HC A06

The Department of Defense (DoD) has emphasized Electronic Data Interchange (EDI) since 1988 when the Deputy Secretary of Defense issued a policy directive that EDI was to become 'the way of doing business' for DoD in the future. The focus of this research is on how private industry is implementing EDI, and specifically how EDI is being used in the procurement and acquisitions environment. The results from a survey of private industry showed that EDI use will continue to grow in the procurement environment and that most impediments to EDI will be resolved with time and experience;

EDI must be adopted by the critical mass before the full benefits and savings will be recognized by DoD and industry; top level management support and a detailed, well thought out strategic EDI plan are mandatory for successful implementation of EDI; and the transaction sets currently being used by private industry for procurements and acquisitions limit DoD EDI opportunities for large purchases. Recognizing these conclusions, recommendations to DoD are then presented. DTIC

N94-18772# Naval Research Lab., Washington, DC.
CONNECTION MACHINE SOFTWARE CONVERSION OF A NAVY OCEANS MODEL
Paul B. Anderson and Michael A. Young 13 Sep. 1993 12 p
(AD-A269876; NRL/MR/5581-93-7400) Avail: CASI HC A03/MF A01

The instruction of highly parallel machines with peak performance significantly exceeding the Cray machines has sparked interest in running scientific models on these new architectures. This report describes a software conversion, of the Navy model called OCEANS, starting with a Cray Y-MP/8 version in Fortran 77 and ending with a Fortran 90 version for the Connection Machine CM-200. Data mapping, conversion planning, and performance points of view are considered. DTIC

N94-18808# Colorado Univ., Boulder. Dept. of Computer Science.
OPTIMAL EIGENVALUE COMPUTATION ON DISTRIBUTED-MEMORY MIMD MULTIPROCESSORS
S. Crivelli and E. R. Jessup Oct. 1992 20 p Presented at the 6th Society for Industrial and Applied Mathematics Conference on Parallel Processing for Scientific Computing, Norfolk, VA, 21-24 Mar. 1993
(Contracts DE-FG02-92ER-25122; DE-AC05-84OR-21400)
(DE93-018337; DOE/ER-25122/4; CU-CS-617-92; CONF-930331-14)
Avail: CASI HC A03/MF A01

Simon proves that bisection is not the optimal method for computing an eigenvalue on a single vector processor. In this paper, we show that his analysis does not extend in a straightforward way to the computation of an eigenvalue on a distributed-memory MIMD multiprocessor. In particular, we show how the optimal number of sections (and processors) to use for a multisection depends on variables such as the matrix size and certain parameters inherent to the machine. We also show that parallel multisection outperforms the variant of parallel bisection proposed by Swarztrauber or this problem on a distributed-memory MIMD multiprocessor. We present the results of experiments on the 64-processor Intel iPSC/2 hypercube and the 512-processor Intel Touchstone Delta mesh multiprocessor. DOE

N94-18865 Florida Univ., Gainesville. Dept. of Computer and Information Sciences.
SOFTWARE ENGINEERING FOR EFFECTIVE UTILIZATION OF PARALLEL PROCESSING COMPUTING SYSTEM Final Report, May 1991 - Sep. 1992
Stephen S. Yau, Doo-Hwan Bae, Madhan Chidambaram, Gilda Pour, and Venkeepuram R. Satish Jun. 1993 140 p Limited Reproducibility: More than 20% of this document may be affected by microfiche quality
(Contract F30602-91-C-0045)
(AD-A269191; RL-TR-93-113) Avail: CASI HC A07

This effort produced an approach for developing software for parallel processing systems based on the parallel object-oriented functional computational model (PROOF). A benefit of this approach is that it allows the software development to be separated from architecture dependent issues to a great degree. For example, the programmers do not need to be concerned with issues such as synchronization, parallelization, or the topology of the parallel processing system when they address objects in the system. The object-oriented paradigm reflects the parallel structure of the problem space and can represent inherently concurrent behavior. This approach is suitable for MIMD machines and should result in software that is more understandable, modifiable, and portable over a variety of parallel computer architectures. DTIC

N94-18866 Intermetrics, Inc., Cambridge, MA.
CASE STUDIES OF SOFTWARE DEVELOPMENT TOOLS FOR PARALLEL ARCHITECTURES Final Report, Aug. 1990 - Dec. 1992
Chris Garrity, Greg Allen, Ed Chianese, John Reardon, and Larry Shafer Jun. 1993 101 p Limited Reproducibility: More than 20% of this document may be affected by microfiche quality
(Contract F30602-90-C-0023; AF Proj. 5581)
(AD-A269193; RL-TR-93-114) Avail: CASI HC A06

The Parallel Evaluation and Experimentation Platform (PEEP) is the result of an effort at Rome Laboratory to identify the most promising general-purpose software development tools, techniques, and approaches from industry and academia for programming high performance parallel computers to meet the needs of command and control (C2) applications. The PEEP is a prototype platform for evaluating the applicability of results from parallel programming research efforts to improve the productivity of designers and developers. Intermetrics conducted a study of available innovative tools and techniques beginning in early 1990. From the survey, Intermetrics chose candidates for inclusion on a prototype platform and began to install and evaluate the chosen components. With the prototype PEEP, a number of case studies were conducted to develop small parallel programs using the selected tools. The purpose of these case studies was not to advance the state of the art in parallel algorithms, but to exercise the tools collected for the prototype PEEP. This work identified requirements on architectures, life cycle activities, and technologies to support parallel development. DTIC

N94-18930# Los Alamos National Lab., NM.
COMPUTER/INFORMATION SECURITY DESIGN APPROACHES FOR COMPLEX 21/RECONFIGURATION FACILITIES
W. J. Hunteman, N. R. Zack, and C. D. Jaeger (Sandia National Labs., Albuquerque, NM.) 1993 8 p Presented at the 34th Annual Meeting of the Inst. of Nuclear Materials Management, Scottsdale, AZ, 18-21 Jul. 1993
(Contract W-7405-eng-36)
(DE93-018547; LA-UR-93-2585; CONF-930749-39) Avail: CASI HC A02/MF A01

Los Alamos National Laboratory and Sandia National Laboratories have been designated the technical lead laboratories to develop the design of the computer/information security, safeguards, and physical security systems for all of the DOE Complex 21/Reconfiguration facilities. All of the automated information processing systems and networks in these facilities will be required to implement the new DOE orders on computer and information security. The planned approach for a highly integrated information processing capability in each of the facilities will require careful consideration of the requirements in DOE Orders 5639.6 and 1360.2A. The various information protection requirements and user clearances within the facilities will also have a significant effect on the design of the systems and networks. Fulfilling the requirements for proper protection of the information and compliance with DOE orders will be possible because the computer and information security concerns are being incorporated in the early design activities. This paper will discuss the computer and information security addressed in the integrated design effort for the tritium, uranium/lithium, plutonium, plutonium storage, and high explosive/assembly facilities. DOE

N94-19010# Argonne National Lab., IL.
EARLY EXPERIENCES WITH THE IBM SP-1
W. Gropp, ed. Jun. 1993 18 p
(Contract W-31-109-eng-38)
(DE93-018398; ANL/MCS-TM-177) Avail: CASI HC A03/MF A01

The IBM SP-1 is IBM's newest parallel distributed-memory computer. As part of a joint project with IBM, Argonne took delivery of an early system in order to evaluate the software environment and to begin porting programming packages and applications to this machine. This report discusses the results of those early efforts. Despite the newness of the machine and the lack of a fast interprocessor switch (part of the SP-1 but not yet available for the machine), every code that they attempted to port ran on the SP-1 with little or no modification. The report concludes with a discussion of expectations for the fast interconnect. DOE

N94-19046# Argonne National Lab., IL. Mathematics and Computer Science Div.
THE p4 LINDA: A PORTABLE IMPLEMENTATION OF LINDA
Ralph M. Butler (University of North Florida, Jacksonville.), Alan L. Leveton (University of North Florida, Jacksonville.), and Ewing L. Lusk 1993 9 p Presented at the 2nd International Symposium on High-Performance Distributed Computing, Spokane, WA, 20-23 Jul. 1993
(Contract W-31-109-eng-38; NSF CCR-91-21875)

(DE93-017752; ANL/MCS/CP-80307; CONF-9307111) Avail: CASI HC A02/MF A01

Facilities such as interprocess communication and protection of shared resources have been added to operating systems to support multiprogramming and have since been adapted to exploit explicit multiprocessing within the scope of two models: the shared-memory model and the distributed (message-passing) model. When multiprocessors (or networks of heterogeneous processors) are used for explicit parallelism, the difference between these models is exposed to the programmer. The p4 tool set was originally developed to buffer the programmer from synchronization issues while offering an added advantage in portability, however two models are often still needed to develop parallel algorithms. We provide two implementations of Linda in an attempt to support a single high-level programming model on top of the existing paradigms in order to provide a consistent semantics regardless of the underlying model. Linda's fundamental properties associated with generative communication eliminate the distinction between shared and distributed memory. DOE

N94-19115# Lawrence Livermore National Lab., CA.

PERFORMANCE AND SCALABILITY ASPECTS OF DIRECTORY-BASED CACHE COHERENCE IN SHARED-MEMORY MULTIPROCESSORS

S. Picano (Purdue Univ., West Lafayette, IN.), D. G. Meyer (Purdue Univ., West Lafayette, IN.), E. D. Brooks, III, and J. E. Hoag May 1993 6 p Presented at the 22nd Annual International Conference on Parallel Processing, University Park, PA, 16-20 Aug. 1993
(Contract W-7405-eng-48)
(DE93-016442; UCRL-JC-113858; CONF-9308129-1) Avail: CASI HC A02/MF A01

We present a study that accentuates the performance and scalability aspects of directory-based cache coherence in multiprocessor systems. Using a multiprocessor with a software-based coherence scheme, efficient implementations rely heavily on the programmer's ability to explicitly manage the memory system, which is typically handled by hardware support on other bus-based, shared memory multiprocessors. We describe a scalable, shared memory, cache coherent multiprocessor and present simulation results obtained on three parallel programs. This multiprocessor configuration exhibits high performance at no additional parallel programming cost. DOE

N94-19159# Universiteit Twente, Enschede (Netherlands). Dept. of Computer Science.

PEGASUS PROJECT DESCRIPTION

Sape J. Mullender, Ian M. Leslie (Cambridge Univ., England.), and Derek McAuley (Cambridge Univ., England.) Dec. 1992 21 p
(Memo-INF-92-75; Pegasus-Paper-92-1; CCL-TR-284; ETN-93-94666)
Copyright Avail: CASI HC A03/MF A01

The first paper of the Esprit Pegasus project, aimed at the design of an operating systems architecture for scalable distributed multimedia systems and the development of a validating prototype, design, and implementation of a distributed complex object service and a global name service; mechanisms for the creation, communication, and rendering of fully digital multimedia documents in real time and in a distributed fashion (with support for full screen digital motion video and digital high fidelity stereophonic sound); and the design and implementation of an application for the system (a digital television director), is presented. The aims, approach and methods, and potential of the project are outlined, and the objectives, expected results, and exploitation plans are described. ESA

N94-19160# Universiteit Twente, Enschede (Netherlands). Dept. of Computer Science.

PEGASUS: OPERATING SYSTEM SUPPORT FOR DISTRIBUTED MULTIMEDIA SYSTEMS

Ian M. Leslie (Cambridge Univ., England.), Derek McAuley (Cambridge Univ., England.), and Sape J. Mullender Dec. 1992 14 p
(Memo-INF-92-76; Pegasus-Paper-92-2; CCL-TR-282; ETN-93-94667)
Copyright Avail: CASI HC A03/MF A01

The second paper of the Esprit Pegasus project, which is aimed at the design of an operating systems architecture for scalable distributed multimedia systems and the development of a validating prototype design and implementation of a distributed complex object service and a global name service; mechanisms for the creation, communication, and rendering of fully digital multimedia documents in real time and in a distributed fashion; and the design and implementation of an application for the system (a digital television director), is presented. The goals of the project are stated and the plans to set about reaching them are described. ESA

N94-19161# Sandia National Labs., Albuquerque, NM.

A MASSIVELY PARALLEL ADAPTIVE FINITE ELEMENT METHOD WITH DYNAMIC LOAD BALANCING

K. D. Devine, J. E. Flaherty, S. R. Wheat, and A. B. Maccabe (New Mexico Univ., Albuquerque.) 1993 26 p Presented at the Supercomputing Conference on High Performance Computing and Communications, Portland, OR, 15-19 Nov. 1993
(Contract DE-AC04-76DP-00789)
(DE93-012844; SAND-93-0936C; CONF-931115-2) Avail: CASI HC A03/MF A01

We construct massively parallel, adaptive finite element methods for the solution of hyperbolic conservation laws in one and two dimensions. Spatial discretization is performed by a discontinuous Galerkin finite element method using a basis of piecewise Legendre polynomials. Temporal discretization utilizes a Runge-Kutta method. Dissipative fluxes and projection limiting prevent oscillations near solution discontinuities. The resulting method is of high order and may be parallelized efficiently on MIMD computers. We demonstrate parallel efficiency through computations on a 1024-processor nCUBE/2 hypercube. We also present results using adaptive p-refinement to reduce the computational cost of the method. We describe tiling, a dynamic, element-based data migration system. Tiling dynamically maintains global load balance in the adaptive method by overlapping neighborhoods of processors, where each neighborhood performs local load balancing. We demonstrate the effectiveness of the dynamic load balancing with adaptive p-refinement examples. DOE

N94-19188# Sandia National Labs., Albuquerque, NM.

EXPERIENCE IN IMPLEMENTING A PARALLEL FILE SYSTEM

R. Riesen, A. B. Maccabe, and S. R. Wheat Mar. 1993 23 p Presented at the Supercomputing Conference on High Performance Computing and Communications, Portland, OR, 15-19 Nov. 1993
(Contract DE-AC04-76DP-00789)
(DE93-012840; SAND-93-0934C; CONF-931115-4) Avail: CASI HC A03/MF A01

With ever increasing processor and memory speeds, new methods to overcome the 'I/O bottleneck' need to be found. This is especially true for massively parallel computers that need to store and retrieve large amounts of data fast and reliably to fully utilize the available processing power. We have designed and implemented a parallel file system that distributes the work of transferring data to and from mass storage across several I/O nodes and communication channels. The prototype parallel file system makes use of the existing single threaded file system of the Sandia/University of New Mexico Operating System (SUNMOS). SUNMOS is a joint project between Sandia National Laboratory and the University of New Mexico to create a small and efficient OS for Massively Parallel (MP) Multiple Instruction, Multiple Data (MIMD) machines. We chose file striping to interleave files across sixteen disks. By using source-routing of messages, we were able to increase throughput beyond the maximum single channel bandwidth the default routing algorithm of the nCUBE 2 hypercube allows. We describe our implementation, the results of our experiments, and the influence this work has had on the design of the Performance-oriented, User-managed, Messaging Architecture (PUMA) operating system, the successor to SUNMOS. DOE

N94-19197# Universiteit Twente, Enschede (Netherlands). Tele-Informatics and Open Systems Group.

SIMULATION MODELS OF UCN, FDDI-2 AND DQDB

H. L. Pasch 1993 115 p
(Memo-INF-93-10; TIOS-93-07; ETN-93-94684) Copyright Avail: CASI HC A06/MF A02

The simulation models used to compare the performance of UCN with that of FDDI-2 and DQDB in a referenced study on the design and analysis of a load adaptive high speed network are explained. Some general information necessary for understanding the workload and the network models UCN and FDDI-2 is presented and the limited workload model and the extended workload model are explained. These workload models are nearly independent of the network model that is used beneath them;

differences that exist are mentioned. The limited and extended models of UCN and FDDI-2 are discussed. The simulation models (workload model plus network model) are listed. ESA

N94-19198# Universiteit Twente, Enschede (Netherlands). Dept. of Computer Science.

ACOS: A PERFORMANCE BASED APPROACH TO BUILD A PARALLEL COMPLEX OBJECT SERVER

Wouter B. Teeuw, Maarten Klein, and Henk M. Blanken Jan. 1993 29 p Sponsored in part by Netherlands Foundation for Computer Science
(Memo-INF-93-11; ETN-93-94685) Copyright Avail: CASI HC A03/MF A01

The design and implementation of a complex object server for the distributed operating system Amoeba are described. The server is called ACOS (Amoeba Complex Object Server). In order to meet the requirements of non standard, database environments, a complex object server has to provide a high performance. The desire to control the expected performance of ACOS during its design is shown. By using a topdown design/implementation method, in which a simulation model is evolved into a real system by gradual addition of detail, it is required to detect performance bottlenecks in an as early stage as possible. In this way an optimal physical design for ACOS is expected. Measurements with a simple Wisconsin join in the current implementation of ACOS support the strength of the approach. ESA

N94-19206# Sandia National Labs., Albuquerque, NM.

MESSAGE PASSING IN PUMA

Arthur B. Maccabe (New Mexico Univ., Albuquerque.) and Stephen R. Wheat 1993 26 p Presented at the Supercomputing Conference on High Performance Computing and Communications, Portland, OR, 15-19 Nov. 1993
(Contract DE-AC04-76DP-00789)
(DE93-012841; SAND-93-0935C; CONF-931115-5) Avail: CASI HC A03/MF A01

This paper provides an overview of the message passing primitives provided by PUMA (performance-oriented, user-managed messaging architecture). Message passing in PUMA is based on the concept of a portal--an opening in the address space of an application process. Once an application process has established a portal, other processes can write values into the memory associated with the portal using a simple send operation. Because messages are written directly into the address space of the receiving process, there is no need to buffer messages in the PUMA kernel. This simplifies the design of the kernel, increasing its reliability and portability. Moreover, because messages are mapped directly into the address space of the application process, the application can manage the messages that it receives without needing direct support from the kernel. DOE

N94-19219# Universiteit Twente, Enschede (Netherlands). Dept. of Computer Science.

WIDE-ADDRESS SPACES: EXPLORING THE DESIGN SPACE

Alberto Bartoli (Pisa Univ., Italy.), Martijn vanderValk, and Sape J. Mullender Dec. 1992 13 p
(Memo-INF-92-77; Pegasus-Paper-92-3; ETN-93-94668) Copyright Avail: CASI HC A03/MF A01

In a recent issue of Operating System Review, Hayter and McAuley argue that future high performance systems trade a traditonal, bus-based organization for one where all components are linked together by network switches (the Desk Area Network (DAN)). In this issue of Operating System Review, Leslie, McAuley, and Mullender conclude that DAN based architectures allow the exploitation of shared memory on a wider scale than just a single (multi)processor. A study which explores how emerging 64 bit processors can be used to implement shared address spaces spanning multiple machines is presented. The study is the third paper of the Esprit Pegasus project which is aimed at the design of an operating system architecture for scalable distributed multimedia systems. ESA

N94-19223# Universiteit Twente, Enschede (Netherlands). Dept. of Computer Science.

AN ANNOTATED BIBLIOGRAPHY ON PARALLEL PARSING: UPDATED VERSION

Rieks opdenAkker, Henk Alblas, Anton Nijholt, Paul OudeLuttighuis, and Klaas Sikkel Dec. 1992 59 p
(Memo-INF-92-84; ETN-93-94672) Copyright Avail: CASI HC A04/MF A01

An annotated bibliography on parallel parsing and recognition of context free languages, which covers most of the important publications in this area of computer science and natural language processing, is presented. The list of publications is preluded by an introduction which presents an overview of the field. This bibliography is an updated version of the following: Memoranda Informatica 89-67, University of Twente, Enschede, The Netherlands, Dec. 1989. ESA

N94-19249# Sandia National Labs., Albuquerque, NM.

A VISUALIZATION ENVIRONMENT FOR SUPERCOMPUTING-BASED APPLICATIONS IN COMPUTATIONAL MECHANICS

C. J. Pavlakos, L. A. Schoof, and J. F. Mareda 1993 19 p Presented at the Supercomputing Conference on High Performance Computing and Communications, Portland, OR, 15-19 Nov. 1993
(Contract DE-AC04-76DP-00789)
(DE93-015024; SAND-93-0917C; CONF-931115-7) Avail: CASI HC A03/MF A01

In this paper, we characterize a visualization environment that has been designed and prototyped for a large community of scientists and engineers, with an emphasis in superconducting-based computational mechanics. The proposed environment makes use of a visualization server concept to provide effective, interactive visualization to the user's desktop. Benefits of using the visualization server approach are discussed. Some thoughts regarding desirable features for visualization server hardware architectures are also addressed. A brief discussion of the software environment is included. The paper concludes by summarizing certain observations which we have made regarding the implementation of such visualization environments. DOE

N94-19253# Lawrence Livermore National Lab., CA.

VECTORIZED PRESENTATION-LEVEL SERVICES FOR SCIENTIFIC DISTRIBUTED APPLICATIONS

L. C. Stanberry, M. L. Branstetter, and D. M. Nessett Mar. 1993 9 p Presented at the Supercomputing Conference on High Performance Computing and Communications, Portland, OR, 15-19 Nov. 1993
(Contract W-7405-eng-48)
(DE93-018091; UCRL-JC-113319; CONF-931115-10) Avail: CASI HC A02/MF A01

The use of heterogeneous distributed systems is a promising approach to significantly increase computational performance of scientific applications. However, one key to this strategy is to minimize the percentage of time spent by an application moving data between machines. This percentage is composed of two parts: the time to translate data between the formats used on different machines, and the time to move data over the network that interconnects the machines. Previous work suggests that data format conversion activity, generally known as presentation-level services, is by far the more costly of the two. In this paper the authors describe how vectorization can be used to improve presentation-level performance in scientific applications by one or two orders of magnitude over the conventional approach. While others have recognized the advantages of vectorized data format conversion, the authors describe how to automate this process so that an application programmer need not explicitly call vectorization routines. The impact of presentation-level vectorization on software portability, programming efficiency, and protocol standards is explored. Performance results are compared with those of two other popular distributed application programming tools and the lessons learned during the course of the research are summarized. DOE

N94-19264# Universiteit Twente, Enschede (Netherlands). Tele-Informatics and Open Systems Group.

A UNIFIED PERFORMABILITY EVALUATION FRAMEWORK FOR COMPUTER AND COMMUNICATION SYSTEMS

Aad P. A. vanMoorsel and Boudewijn R. Haverkort 1993 21 p Submitted for publication
(Memo-INF-93-21; TIOS-93-12; ETN-93-94693) Copyright Avail: CASI HC A03/MF A01

A unified approach towards model based quantitative evaluation of both computer systems and communication systems is presented. In the area of fault tolerant computer systems, dependability evaluation has been recognized as being a topic of importance, both to judge a system on its merits and to provide trust in the actual dependability of the system. In communication systems, the need for identifying and evaluating quality of service parameters is becoming more and more apparent because of increasing demands on for instance speed and availability. The construction of a framework, the so called performability evaluation framework, within which the quantitative evaluation of both types of systems can be discussed is shown. A general view, a system view, and a modeling view on performability evaluation, leading to a framework which naturally fits known measure definitions, modeling methods, and solution techniques are given. The performability evaluation framework is related with known concepts in both the areas of computer and communication systems. ESA

N94-19296# Universiteit Twente, Enschede (Netherlands). Dept. of Computer Science.
ACTION SYSTEMS AND ACTION REFINEMENT IN THE DEVELOPMENT OF PARALLEL SYSTEMS: AN ALGEBRAIC APPROACH
Wil Janssen, Mannes Poel, and Job Zwiers Feb. 1993 74 p Sponsored in part by Commission of the European Communities
(Memo-INF-93-14; ETN-93-94688) Copyright Avail: CASI HC A04/MF A01

A notion of refinement and several other operators that allow for a compositional algebraic characterization of action systems and serializability in distributed database systems are proposed. A simple design language is introduced and is provided with a semantics essentially based on partial order models. Various algebraic transformation rules are introduced. They are applied in the design process of a simple system, starting from a specification of functional behavior via the intermediate step in the form of a 'true concurrency' based initial design to an actual implementation on a two processor architecture. ESA

N94-19299# Oak Ridge National Lab., TN.
PUMMA: PARALLEL UNIVERSAL MATRIX MULTIPLICATION ALGORITHMS ON DISTRIBUTED MEMORY CONCURRENT COMPUTERS
Jae-Young Choi, D. W. Walker, and J. J. Dongarra (Tennessee Univ., Knoxville.) Aug. 1993 39 p
(Contract DE-AC05-84OR-21400)
(DE93-019163; ORNL/TM-12252) Avail: CASI HC A03/MF A01

This paper describes the Parallel Universal Matrix Multiplication Algorithms (PUMMA) on distributed memory concurrent computers. The PUMMA package includes not only the non-transposed matrix multiplication routine C = A(center dot)B, but also transposed multiplication routines C = A(sup T)(center dot)B, C = A(center dot)B(sup T), and C = A(sup T)(center dot)B(sup T), for a block scattered data distribution. The routines perform efficiently for a wide range of processor configurations and block sizes. The PUMMA provides the same functionality as the Level 3 BLAS routine xGEMM. Details of the parallel implementation of the routines are given, and results are presented for runs on the Intel Touchstone Delta computer. DOE

N94-19512# Rochester Univ., NY. Dept. of Computer Science.
HEAP CONSTRUCTION IN THE PARALLEL COMPARISON TREE MODEL
Paul F. Dietz Feb. 1992 12 p
(Grant NSF CCR-89-09667)
(TR-409) Avail: CASI HC A03/MF A01

I show how to put n values into heap order in O(log log n) time using n/log log n processors in the parallel comparison tree model of computation, and in the Hermitian conjugate of O(alpha(n)) time on n/alpha(n) processors, in the randomized parallel comparison tree model, where alpha(n) is an inverse of Ackerman's function. I prove similar bounds for the related problem of putting n values into a min-max heap. Author (revised)

N94-19514# Institut National Polytechnique, Grenoble (France). Lab. de Genie Informatique.
PROCESS ALLOCATION ON DISTRIBUTED MEMORY PARALLEL ARCHITECTURES Ph.D. Thesis [ALLOCATION DE PROCESSUS SUR LES ARCHITECTURES PARALLELES A MEMOIRE DISTRIBUEE]
El-Ghazali Talbi 1993 197 p In FRENCH
(ETN-93-95004) Avail: CASI HC A09/MF A03

The static allocation problem on a static architecture is considered. An original approach based on genetic algorithms was used to solve this problem. A massively parallel genetic algorithm was proposed, evaluated and integrated in a parallel system. A comparative study with hill climbing algorithms and simulated annealing gives encouraging results in favor of genetic algorithms. In the case of reconfigurable architectures, the allocation goes with the definition of the best configuration adapted to the program. This problem was treated in two steps. In the first one clusters of processes are made to obtain a graph with a number of its nodes equal to the number of processors. This problem may be reduced to a graph partitioning problem. The second step carries out an edge deletion to obtain a graph with a degree inferior to the number of physical links per processor. This problem may be reduced to the maximum c matching of a graph. For dynamic programming models, a dynamic allocation is unavoidable. An algorithm independent of the size and the topology of the network was proposed. The algorithm that is presented is distributed, dynamic, stable, non preemptive and simple. A simulation program to evaluate the algorithm was implemented on a transputer network and preliminary results are presented. ESA

N94-19533# Carnegie-Mellon Univ., Pittsburgh, PA. Dept. of Computer Science.
PROTOCOL SERVICE DECOMPOSITION FOR HIGH-PERFORMANCE NETWORKING
Chris Maeda and Brian N. Bershad Mar. 1993 16 p
(Contract MDA972-90-C-0035; ARPA Order 7330)
(AD-A270613; CMU-CS-93-131) Avail: CASI HC A03/MF A01

In this paper the authors describe a new approach to implementing network protocols that enables the network to have high performance and high flexibility, while retaining complete conformity to existing application programming interfaces. The key insight behind the work is that an application's interface to the network is distinct and separable from its interface to the operating system. The authors have separated these interfaces for two protocol implementations, TCP/IP and UDP/IP, running on the Mach 3.0 operating system and UNIX server. Specifically, library code in the application's address space implements the network protocols and transfers data to and from the network, while an operating system server manages the heavy-weight abstractions that applications use when manipulating the network through operations other than send and receive. On DECstation 5000/200 systems connected by 10Mb/sec Ethernet, this approach to protocol decomposition achieves TCP/IP throughput of 1088 KB/second, which is comparable to that of a high-quality in-kernel TCP/IP implementation, and substantially better than a server-based one. The approach achieves small-packet UDP/IP round trip latencies of 1.23 ms, again comparable to a kernel-based implementation and more than twice as fast as a server-based one. DTIC

N94-19534# Air Force Inst. of Tech., Wright-Patterson AFB, OH. School of Engineering.
A NON-HOMOGENEOUS, SPATIO-TEMPORAL, WAVELET MULTIRESOLUTION ANALYSIS AND ITS APPLICATION TO THE ANALYSIS OF MOTION Ph.D. Thesis
Thomas J. Burns Dec. 1993 183 p
(AD-A270621; AFIT/DS/ENG/93D-12) Avail: CASI HC A09/MF A02

This research presents a multiresolution wavelet analysis tool for analyzing motion in time sequential imagery. A theoretical framework is developed for constructing an L(sub 2)(R(sup 3)) wavelet multiresolution analysis from three non-identical spatial and temporal L(sub 2)(R) wavelet multiresolution analyses. This framework provides the flexibility to tailor the spatio-temporal frequency characteristics of the three dimensional wavelet filter to match the frequency behavior of the analyzed signal. An unconventional, discrete multiresolution wavelet decomposition algorithm is developed which yields a rich set of independent spatio-temporally oriented frequency channels for analyzing the size and speed characteristics of moving objects. Unlike conventional wavelet decomposition methods, this algorithm provides independent zoom-in and zoom-out capability in space and time. Symmetric 3D filters produced by the unconventional decomposition process are combined with the properties of the Hilbert transform to produce a bank of directionally selective wavelet filters. Multiple directionally selective wavelet filters are integrated to form a multiresolution vector wavelet motion sensor capable of unambiguously computing the optical flow of a 3D image sequence. A unique flow restoration methodology is presented which incorporates a modified version of Grossberg's gated dipole filter in a cooperative-competitive flow restoration methodology that reinforces consistent flow behavior and removes flow inconsistencies. Finally, several digital and optical parallel architectures are investigated for their ability to speed up the 3D wavelet decomposition process. DTIC

N94-19588# University of Southern California, Los Angeles. Dept. of Electrical Engineering.
A MULTI-LEVEL DATA-FLOW ARCHITECTURE FOR SIGNAL AND DATA PROCESSING APPLICATIONS
J. L. Gaudiot 2 Sep. 1993 6 p
(Contract DE-FG03-87ER-25043)
(DE93-041272; DOE/ER-25043/T1) Avail: CASI HC A02/MF A01

A grant was awarded to us by the Department of Energy, Office of Energy Research, in May 1987 to support the design and performance analysis of a large grain data-driven multiprocessor system for numerical applications. The basic idea of the work is to apply the data-driven principles of execution at a more appropriate level than conventional 'atomic' instructions. For this purpose, a level such as that of vector operations was under study. This document represents the final report concerning the results of the research supported by this grant. The goals of the project entailed an analysis of Partial Differential Equation solvers in data-driven environments, a preliminary design of our multi-level architecture, an in-depth study of some of the mechanisms of execution, and a design of the software environment. As enumerated in the original proposal, our work has yielded results in three different domains: specifications of the application programs; design of the general concepts of the architecture and simulation; and implementation of a translating environment. We discuss each of the above items and examine specific research results. DOE

N94-19682# Duke Univ., Durham, NC.
IMPLEMENTATION OF PARALLEL ALGORITHMS Quarterly Report, 1 Apr. - 30 Jun. 1993
John H. Reif 30 Jun. 1993 18 p
(Contract N00014-91-J-1985)
(AD-A271035) Avail: CASI HC A03/MF A01

This dissertation develops fast algorithms for solving closest point problems on parallel and vector computers. Algorithms for such problems have applications in many areas including statistical classification, crystallography, data compression, and finite element analysis. We present a simple and flexible programming model for designing and analyzing parallel algorithms. Also, fast parallel algorithms for nearest-neighbor searching and constructing Voronoi diagrams are described. Finally, we demonstrate that the algorithms actually obtain good performance on a wide variety of machine architectures, including the MasPar MP-1, Cray Y-MP, and KSR-1 supercomputers. DTIC

N94-19734# Superconducting Super Collider Lab., Dallas, TX.
DATA-MACHINE INDEPENDENCE (DMI)
M. Botlo, M. Jagielski, L. Miller, and A. Romero May 1993 11 p
(Contract DE-AC35-89ER-40486)
(DE93-018008; SSCL-628) Avail: CASI HC A03/MF A01

A distributed data acquisition system (DAQ) should not restrict the number or type of processors used in a given application. For any software application that must operate on a multi-vendor distributed system, three serious problems have to be addressed regarding data handling: data representation, memory organization, and address alignment. Data representation, memory organization, and address alignment problems are inherent in the various hardware platforms available on the market today. Furthermore, issues such as how to coordinate parallel software efforts on multiple platforms that share data must be resolved. Traditionally such efforts are coordinated through meetings, memos, and documents describing shared data blocks (Data Interface Documents). The traditional approach is risky at best: the frequency of changes demanded by end-users is faster than the rate at which interface documents can be updated. Simple changes in data structures tend to dramatically increase the software development time, as all the tools must be modified to accommodate the changes. In Section 2.0 the authors examine in detail the technical implications for data handling when using distributed applications. In Section 3.0 they compare different approaches in handling the data in distributed environments. The four methods studied are: abstract syntax notation 1 (ASN.1), external data representation (XDR), self describing data format (SDS), and ZEBRA. They compared the four tools with the standard programming method (using 'C'). In Section 4.0 they present conclusions of the test using the four different tools. DOE

N94-19790# Syracuse Univ., NY. Northeast Parallel Architectures Center.
NPAC DISTRIBUTED-PARALLEL SYSTEM FEASIBILITY STUDY Final Report, Sep. 1990 - 1991
Nancy McCracken, Gary Craig, Don Hewitt, and Kanchana Parasuram Aug. 1993 23 p
(Contract F30602-88-D-0025)
(AD-A270972; RL-TR-93-164) Avail: CASI HC A03/MF A01

A distributed-parallel computing testbed, comprised of two shared-memory multiprocessors linked by a wide-area network was established. A missile-tracking simulator application was implemented on this testbed for the purposes of evaluating the feasibility of distributed-parallel computing. Several scenarios were run and performance data collected for each of four computing modes. Preliminary evaluation of the software model and analysis of the scenario performance data are presented. DTIC

63 CYBERNETICS

Includes feedback and control theory, artificial intelligence, robotics and expert systems.

For related information see also *54 Man/System Technology and Life Support.*

N94-17696 Brookhaven National Lab., Upton, NY.
THE DESIGN OF THE MAD DESIGN PROGRAM
J. Niederer 1992 22 p Presented at the Stability of Particle Motion in Storage Rings, Upton, NY, 18-24 Oct. 1992 Limited Reproducibility: More than 20% of this document may be affected by microfiche quality
(Contract DE-AC02-76CH-00016)
(DE93-013343; BNL-48790; CONF-921077-4) Avail: CASI HC A03

The study of long term stability in particle accelerators has long been served by a group of widely circulated computer programs. The progress in these programs has mirrored the growth and versatility in accelerator size, complexity, and purpose, as well as evolving technologies in computing software and hardware. A number of large accelerator projects during the last decade were designed with the aid of physics programs either written for, or tailored for the project at hand, each invariably benefiting from contributions of previous workers. This paper outlines the recent history of an example of an accelerator lattice model tool kit, the Methodical Accelerator Design (MAD) Program, which has tried to knit together this collective wisdom of the accelerator community. The ideas behind the software design of the program itself are traced here; the accelerator physics contents and origins are thoroughly documented elsewhere. These informal notes have a Brookhaven flavor, in part because of early BNL efforts to generalize the ways that technical problems are organized and presented to computers. Some recent BNL applications not covered in the extensive CERN documentation are also included. DOE

N94-17916 Politecnico di Milano (Italy). Dipt. di Elettronica e Informazione.
A STRUCTURED APPROACH FOR MODELING, ANALYZING AND SIMULATING REAL-TIME CONTROL SYSTEMS
Alberto Leva, Eva Locatelli (Master School CEFRIEL, Milan, Italy.), and Riccardo Scattolini 1993 19 p
(Rept-93-044; ETN-93-94901) Avail: Politecnico di Milano, Piazza Leonardo da Vinci 32, 20133 Milan, Italy

A methodology for the development of real time control software is presented. Specifically, this approach can aid the designer in the phase of tailoring a given control scheme on a target hardware/firmware architecture. The methodology is composed of three steps: the overall system, that is the control apparatus and the control software, is modeled with the formalism of Petri Nets; analysis tools are then applied to verify the correctness of the model in terms of absence of deadlocks and fulfilment of time constraints; a simulation environment is described and employed to assess the performance of the design. Focus is on the first and the third items above, since well stated methods and software tools are available for the second one. An application example is reported to illustrate the effectiveness of the proposed approach. ESA

N94-17922 Politecnico di Milano (Italy). Dipt. di Elettronica e Informazione.

ON COMPARISON AND EXTENSIONS OF CONTROL METHODS FOR NARROW-BAND DISTURBANCE REJECTION

Giuseppe DeNicolao (Pavia Univ., Italy.), Fabrizio Lorito, and Silvia Strada 1993 10 p Sponsored in part by CNR, and Ministry of University and Scientific Research and Technology
(Rept-93-015; ETN-93-94519) Avail: Politecnico di Milano, Piazza Leonardo da Vinci 32, 20133 Milan, Italy

Several control methods for the rejection of narrowband disturbances were recently surveyed. In particular, a method, called Disturbance Modeling (DM), which is a Linear Quadratic (LQ) optimization technique hinging on a state space model of the disturbance was introduced. A demonstration that the DM design methodology proposed recently leads to an unsolvable optimizaton problem is presented. It is also suggested how to modify the LQ cost functional in order to obtain an effective DM disturbance rejection scheme. Duality between DM and the approach based on shaped cost functional is discussed. ESA

N94-18125# California Univ., Irvine. Dept. of Civil Engineering.

GENERALIZATION OF OPTIMAL CONTROL THEORY: LINEAR AND NONLINEAR STRUCTURES

J. N. Yang, Z. Li, and S. Vongchavalitkul 2 Nov. 1992 89 p Sponsored by National Center for Earthquake Engineering Research
(Grants NSF BCS-90-25010; NEC-91029)
(PB93-188621; NCEER-92-0026) Avail: CASI HC A05/MF A01

A systematic generalization of the theory of optimal control for seismic-excited linear, nonlinear, and hysteretic structures is presented. The generalized theory includes the effect of actuator dynamics and a penalty on the acceleration response of the structure. The proposed generalized performance index includes the acceleration response so that either a simultaneous reduction of the deformation and acceleration or a trade-off between them can be achieved. Experimental results indicate that a significant contribution to the system time delay comes from the actuator response. In the report, the actuator dynamics is explicitly accounted for in the optimization process so that the gain matrix involves actuator characteristics leading to a better control performance. In Part 1, optimal control theory for linear structures is presented. Numerical simulation results are obtained to demonstrate the advantages of the generalized optimal control theory. In Part 2, an optimal nonlinear control method is proposed for applications to nonlinear and hysteretic structures. NTIS

N94-18189# Wright Lab., Wright-Patterson AFB, OH.

APPLICATION OF THE NETWORK DISCRIMINANT FUNCTION TO LEARNING Interim Report, Jan. - Jun. 1993

Devert Wicker Jun. 1993 33 p
(AD-A268793; WL-TR-93-1086) Avail: CASI HC A03/MF A01

This introduces methods of applying the Network Discriminant Function (NDF) to training and automatic architecture selection of feed-forward multiple layer perceptrons (MLP's) used for Pattern Recognition (PR). Knowledge of the NDF may be used to impact MLP architecture choices. The NDF gives a new insight into MLP performance in that it reflects how well the MLP is clustering the data. If clustering is an intrinsic capability of the MLP which makes it perform well, then the NDF should correlate with other performance measures such as the Sum Squared Error. Architecture choices and training technique need to be selected as to aid the clustering ability of the MLP. The major goals of the research are to establish the NDF as a useful criteria and to compare it to other criteria such as Cascade-Correlation's error correlation. The NDF-Cascade (NDFC) learning architecture and the MLP NDF are proposed, tested, and evaluated. DTIC

N94-18261# Carnegie-Mellon Univ., Pittsburgh, PA. Dept. of Computer Science.

DIALOG-BASED LEARNING (DBL) FOR ADAPTIVE INTERFACE AGENTS AND PROGRAMMING-BY-DEMONSTRATIONS SYSTEMS Research Report

Siegfried Bocionek and Michael Sassin (Massachusetts Inst. of Tech., Cambridge.) Jul. 1993 54 p Sponsored by Siemans AG, Corporate Research and Development, Munich, Germany
(AD-A269154; CMU-CS-93-175) Avail: CASI HC A04/MF A01

Many users of workstation and PC tools often have to perform the same task again and again. For example, a secretary might have to send out a dozen e-mail messages until she finds a free meeting room. Or someone preparing business charts has to draw many special tables with shadowing bars around. Unfortunately, today's macro-facilities of such tools do not support the end user enough in constructing the required automation functions. We propose a mechanism, called dialog-based learning (DBL), that provides the user of software tools exactly with a mechanism to teach new functions or to give hints or additional information to a program on how to perform a task better. Two applications will be considered. The first one is our experimental system RAP, a room reservation apprentice that will eventually overtake a secretary's task to search for a free meeting or lecture room. RAP analyzes the outgoing and incoming e-mail and constructs a finite state machine that can repeat the task of asking all room administrators until a free room is found. The key of RAP's learning is to ask the user for unknown message types (e.g., request, positive answer, etc.) and key-phrases (e.g., 'need a room') and to collect them in a thesaurus. Our second application is a demonstrational graphics editor that allows the user to teach it new functions by giving a few examples. DTIC

N94-18263 Army Missile Command, Redstone Arsenal, AL. Weapons Science Directorate.

FAST-TRAINING ALGORITHM FOR HIDDEN-LAYER FORWARD-FEED NEURAL NETWORKS Summary Report, Mar. 1990 - 1992

Shawn D. Pethel, Charles M. Bowden, and Chi C. Sung Jun. 1993 27 p Limited Reproducibility: More than 20% of this document may be affected by microfiche quality
(AD-A269253; AD-E952096; AMSMI/TR-RD-WS-93-5) Avail: CASI HC A03

A new training algorithm, based on the matrix pseudoinverse method, is shown to train hidden-layer, forward-feed neural networks with high accuracy in a short time for nonlinear time series prediction. The algorithm is applied to chaotic time series generated from the logistics map and the Mackey-Glass delay differential equation and compared to corresponding results generated using a backpropagation training algorithm. We demonstrate orders of magnitude shorter training time and comparable accuracy with the new algorithm and show forecasting and self-generation for these systems. DTIC

N94-18331# Symbus Technology, Inc., Waltham, MA.

AUTONOMOUS NEURAL NETWORK CONTROLLERS FOR ADAPTIVE MATERIAL HANDLING Final Report

James Kottas and Michael Kuperstein 30 Jul. 1993 27 p
(Contract N00014-91-C-0258)
(AD-A268908) Avail: CASI HC A03/MF A01

For robots to be more useful in flexible manufacturing and service applications, the controllers must be able to handle more variable environments. On at least two levels, conventional methods in robot control have problems dealing with high variability. At the current level, conventional dynamic control formulations cannot deal effectively with the highly variable dynamic inertial interactions between multijointed robots and payloads. At the task level, the initial and final positions for materials to be moved may change slightly but unexpectedly. We have developed autonomous neural network controllers that learn from their own experience to deal with environmental variability at these levels. DTIC

N94-18399# SRI International Corp., Menlo Park, CA. Computer Science and Technology Div.

DISTRIBUTED REASONING AND PLANNING Final Report

Kurt G. Konolige 3 Aug. 1993 131 p
(Contract N00014-89-C-0095)
(AD-A268682) Avail: CASI HC A07/MF A02

This document describes research conducted by SRI International on the Office of Naval Research project Distributed Reasoning and Planning. A central focus in artificial intelligence (AI) research is the development of systems that are capable of reasoning about their environments and of planning appropriate courses of action to pursue. Yet for many applications, it is insufficient to rely on a single, autonomous system; instead, a network of physically distributed computer systems must be used. Each of those systems must itself have significant reasoning and planning capabilities, that is, it must be an intelligent agent in its own right. Research in distributed reasoning and planning is concerned with the development of a theoretical framework for designing, building, and managing networks of intelligent agents, which can plan in cooperation with one another to achieve given goals. DTIC

N94-18462 University of Southern California, Marina del Rey. Information Sciences Inst.

ON MASKING EFFECT Research Report

Milind Tambe and Paul S. Rosenbloom Jul. 1993 14 p Limited Reproducibility: More than 20% of this document may be affected by microfiche quality

(Contract N00014-92-K-2015)

(AD-A269593; ISI/RR-93-349) Avail: CASI HC A03

Machine learning approaches to knowledge compilation seek to improve the performance of problem-solvers by storing solutions to previously solved problems in an efficient generalized form. The problem-solver retrieves these learned solutions in appropriate later situations to obtain results more efficiently. However, by relying on its learned knowledge to provide a solution, the problem-solver may miss an alternative solution of higher quality--one that could have been generated using the original (non-learned) problem-solving knowledge. This phenomenon is referred to as the masking effect of learning. In this paper, the authors examine a sequence of possible solutions for the masking effect. Each solution refines and builds on the previous one. The final solution is built on cascaded filters. When learned knowledge is retrieved, these filters alert the system about the inappropriateness of this knowledge so that the system can then derive a better alternative solution. The authors analyze conditions under which this solution will perform better than the others and present experimental data supportive of the analysis. This investigation is based on a simulated robot domain called Ground world. DTIC

N94-18463 University of Southern California, Marina del Rey. Information Sciences Inst.

FLEXIBLE INTEGRATION OF PATH-PLANNING CAPABILITIES Research Report

Iain C. Stobie, Milind Tambe, and Paul S. Rosenbloom Nov. 1992 13 p Limited Reproducibility: More than 20% of this document may be affected by microfiche quality

(Contracts N00014-91-J-1624; DABT63-91-C-0025)

(AD-A269594; ISI/RR-93-348) Avail: Issuing Activity (Defense Technical Information Center (DTIC))

Robots pursuing complex goals must plan paths according to several criteria of quality including shortness, safety, speed, and planning time. Many sources and kinds of knowledge, such as maps, procedures and perception, may be available or required. Both the quality criteria and sources of knowledge may vary widely over time, and in general they will interact. One approach to address this problem is to express all criteria and goals numerically in a single weighted graph, and then to search this graph to determine a path. Since this is problematic with symbolic or uncertain data and interacting criteria, we propose that what is needed instead is an integration of many kinds of planning capabilities. We describe a hybrid approach to integration, based on experiments with building simulated mobile robots using Soar, an integrated problem-solving and learning system. For flexibility, we have implemented a combination of internal planning, reactive capabilities, and specialized tools. We illustrate how these components can complement each other's limitations and produce plans which integrate geometric and task knowledge. DTIC

N94-18474 Naval Command, Control and Ocean Surveillance Center, San Diego, CA. RDT and E Div.

SURVEY OF COLLISION AVOIDANCE AND RANGING SENSORS FOR MOBILE ROBOTS, REVISION 1 Final Report

H. R. Everett, D. E. DeMuth, and E. H. Stitz Dec. 1992 155 p Limited Reproducibility: More than 20% of this document may be affected by microfiche quality

(AD-A269846; NCCOSC/RDT/E-1194-Rev-1) Avail: CASI HC A08/MF A02

The past few years have brought about a tremendous rise in the envisioned potential of robotic systems and a significant increase in the number of proposed applications. In the nonindustrial arena, numerous programs have evolved, each intending to harness some of this promise in hopes of solving some particular application need. Many of these efforts are government sponsored, aimed at the development of systems for fighting fires, handling ammunition, transporting materials, conducting underwater search and inspection operations, and patrolling warehouses and storage areas, etc. Many of the resulting prototypes, which were initially perceived as logical extensions of the traditional industrial robotic scenarios, have met with unexpected difficulty due to an insufficient supporting technology base. This document provides some basic background on the various noncontact distance measurement techniques available, with related discussion of implementation in the acoustical, optical, and electromagnetic portions of the energy spectrum. An overview of candidate systems, both commercially available and under development, is provided, followed by a brief summary of research currently underway in support of the collision avoidance and noncontact ranging needs of a mobile robot. DTIC

N94-18759 University of Southern California, Marina del Rey. Information Sciences Inst.

AUTOMATICALLY GENERATING ABSTRACTIONS FOR PLANNING Research Report

Craig A. Knoblock Jun. 1993 62 p Limited Reproducibility: More than 20% of this document may be affected by microfiche quality

(Contract F30602-91-C-0081)

(AD-A269772; ISI/RR-93-344) Avail: CASI HC A04

This article presents a completely automated approach to generating abstractions for planning. The abstractions are generated using a tractable, domain-independent algorithm whose only input is the definition of a problem to be solved and whose output is an abstraction hierarchy that is tailored to the particular problem. The algorithm generates abstraction hierarchical dropping literals from the original problem definition. It forms abstractions that satisfy the ordered monotonicity property, which guarantees that the structure of an abstract solution is not changed in the process of refining it. The algorithm for generating abstractions is implemented in a system called ALPINE, which generates abstractions for a hierarchial version of the PRODIGY problem solver. The abstractions generated by ALPINE are tested in multiple domains on large problem sets and are shown to produce shorter solutions with significantly less search than planning without using abstraction. DTIC

N94-18773 Naval Research Lab., Washington, DC.

NEUTRAL NETWORKS: AN NRL PERSPECTIVE

Chip Bachmann, Paul Bey, Jeremey Broughton, Victor Chen, and Sheldon Gardner 3 Sep. 1993 72 p Limited Reproducibility: More than 20% of this document may be affected by microfiche quality

(AD-A269122; NRL/MR/1003-93-7396) Avail: Issuing Activity (Defense Technical Information Center (DTIC))

The subject of neural networks is introduced as a brief review and to provide perspective to the subject. A number of programs at the Naval Research Laboratory (NRL) are outlined to describe the general approach used and the anticipated benefits of neural networks. Observations and recommendations concerning the subject are made on the subject. This document serves as a base of information for additional internal discussions concerning opportunities for neural networks within NRL. DTIC

N94-18790# Barron Associates, Inc., Standardsville, VA.

ACTIVE CONTROL OF A MULTIVARIABLE SYSTEM BY WAY OF POLYNOMIAL NEURAL NETWORKS: COMPUTER SIMULATION EVALUATIONS AND LABORATORY EXPERIMENTAL RESULTS Final Technical Report, 15 Apr. 1992 - 31 Mar. 1993

B. E. Parker, Jr., Natalie A. Nigro, and David G. Ward Jun. 1993 116 p

(Contract N00014-89-C-0137)

(AD-A270033; Rept-141-05-FTR) Avail: CASI HC A06/MF A02

The objective of the work described herein was to develop, implement, and demonstrate inductively synthesized active control algorithms that minimize a performance metric that is a function of a signal measured by a sensor external to a multivariable control system. The controller is required to control a (potentially nonlinear) plant when subjected to a broadband (impulsive) disturbance signal. Polynomial neural networks (PNN's) are used to implement the control algorithms. To provide controller/secondary feedback compensation filter parameters for the laboratory experiments, and to provide a benchmark with which to compare the empirical results, computer simulation evaluations were also conducted. The report documents controller designs that achieve up to 24.4 dB error improvement relative to the uncontrolled case. Key differences between the present work and that ongoing elsewhere in active control are as follows: (1) the use of broadband impulsive disturbances, which induce a more complex stochastic control scenario than that of narrowband excitation; and (2) the potential controller structures are adaptive, nonlinear, infinite impulse response PNN's, not traditional linear, finite impulse response filters. The former offer promising new active control approaches for non-Gaussian, as well as Gaussian, signals, and may be used for multiple-input, multiple-output control of unknown plants. DTIC

N94-18887 Massachusetts Univ., Amherst. Dept. of Mechanical Engineering.
KNOWLEDGE SOURCES FOR AN INTELLIGENT MCM ANALYZER Final Technical Report, Jan. 1991 - Jan. 1992
Ian R. Grosse, Prasanna Katragadda, and Anagha Jog Jun. 1993 74 p Limited Reproducibility: More than 20% of this document may be affected by microfiche quality
(Contract F30602-92-C-0010)
(AD-A269224; RL-TR-93-123) Avail: CASI HC A04

This research project resulted in the development of: (1) an intelligent methodology for finite element modeling and analysis of multichip modules (MCM's) for the purpose of rapid mechanical reliability assessment; (2) specific software modules, termed MCM's; and (3) a prototype proof-of-concept computer-based system that integrated these knowledge sources. The approach featured an object-oriented representation of the MCM's and their components. The modeling and analysis methodology itself was represented by the blackboard problem-solving paradigm in which individual experts solve specific tasks involved in finite element modeling and analysis of MCM's and post their results on a common blackboard accessible by the other experts. Several software modules from Sandia National Laboratory were used as well as the contractor developing a three-dimensional thermal analysis finite element code, called FEECAP3D, which includes sophisticated techniques for estimating the finite element discretization error. All of these software codes were integrated into a blackboard-based proof-of-concept computer system called the Intelligent MCM Analyzer (IMCMA). DTIC

N94-18898# Rutgers - The State Univ., New Brunswick, NJ.
CONTROL OF NONLINEAR SYSTEMS Final Report, 1 Aug. 1991 - 30 Sep. 1993
Edwardo Sontag 30 Sep. 1993 6 p
(Grant AF-AFOSR-0346-91)
(AD-A270141; AFOSR-93-0747TR) Avail: CASI HC A02/MF A01

This research by the PI and his graduate students was on: (1) State-Space and I/O systems, (2) Systems with Saturated Control, (3) Discrete-Time Control, (4), Identification of Nonlinear systems and (5) I/O Equations. Twelve papers were published under this grant. DTIC

N94-19007# Sandia National Labs., Albuquerque, NM.
GEOMETRICAL PATTERN LEARNING
P. W. Goldberg Apr. 1993 13 p Presented at the 34th Meeting of the IEEE Foundation of Computer Science, Palo Alto, CA, 3-5 Nov. 1993
(Contract DE-AC04-76DP-00789)
(DE93-017641; SAND-93-1283C; CONF-931167-2-Extd-Abst) Avail: CASI HC A03/MF A01

In this paper, we consider the problem of learning the positions of spheres in metric spaces, given as data randomly drawn points classified according to whether they are internal or external to an unknown sphere. The particular metrics under consideration are geometrical shape metrics, and the results are intended to be applicable to the problem of learning to identify a shape from related shapes classified according to whether they resemble it visually. While it is typically NP-hard to locate a central point for a hypothesis sphere, we find that it is however often possible to obtain a non-spherical hypothesis which can accurately predict whether further random points lie within the unknown sphere. We exhibit algorithms which achieve this, and in the process indicate useful general techniques for computational learning. Finally, we exhibit a natural shape metric and show that it defines a class of spheres not predictable in this sense, subject to standard cryptographic assumptions. DOE

N94-19085# Technische Univ., Delft (Netherlands). Faculty of Technical Mathematics and Informatics.
THE OPTIMAL PROJECTION EQUATIONS FOR FINITE-DIMENSIONAL FIXED-ORDER H2-OPTIMAL CONTROL OF INFINITE-DIMENSIONAL DISCRETE-TIME SYSTEMS
Florin Dan Barb and Willem L. deKoning 1993 22 p
(Rept-93-11; ETN-93-94638) Copyright Avail: CASI HC A03/MF A01

The fixed, finite order H squared optimal control of linear, infinite dimensional discrete time systems is addressed. The set of necessary conditions for the existence of the H squared optimal controller is expressed in terms of four operator equations (two modified Riccati equations and two modified Lyapunov equations) coupled by a projector having the rank given by the dimension of the compensator state. It is shown that, when the order to the compensator is equal to the order of the plant, the four operator equations are decoupled and the infinite dimensional generalization of the finite state space solution to the H squared optimal control problem for time varying systems is obtained. ESA

N94-19091# Technische Univ., Delft (Netherlands). Faculty of Technical Mathematics and Informatics.
DEADBEAT CONTROL BY MEASUREMENT FEEDBACK: A TWO SIDED APPROACH
J. W. vanderWoude 1993 17 p
(Rept-93-20; ETN-93-94647) Copyright Avail: CASI HC A03/MF A01

A linear discrete time system is considered. Focus is on existence and design of a measurmeent feedback compensator such that in the closed loop system any initial state is forced to zero within a prescribed number of time steps. The so called two sided approach is followed and conditions for the existence of a compensator that achieves the required closed loop behavior are derived. With these conditions, an expression for the minimal number of time steps in which any initial state can be forced to zero by means of a measurement feedback compensator is given. A method of computing such a compensator having a reduced order is presented. ESA

N94-19092# Technische Univ., Delft (Netherlands). Faculty of Technical Mathematics and Informatics.
A REFINEMENT FOR NONMONOTONIC LOGIC
G. J. Akkerman 1993 31 p Sponsored by Netherlands Organization for Scientific Research
(Rept-93-21; ETN-93-94648) Copyright Avail: CASI HC A03/MF A01

One approach to refinement of a rule base for a variant of autoepistemic logic is considered. The investigations led to the following results: refinements for modal logics are presented which (together with a decision procedure for implication) could be used to construct learning algorithms for those modal logics; it is argued that no total learning algorithm is known for nonmonotonic logic; a partial learning algorithm for nonmonotonic logic is sketched. ESA

N94-19138# Technische Univ., Delft (Netherlands). Faculty of Technical Mathematics and Informatics.
THE FIXED, FINITE-ORDER L(SUP 2)-OPTIMAL CONTROL OF INFINITE-DIMENSIONAL TIME-VARYING DISCRETE-TIME SYSTEMS
Florin Dan Barb and Willem L. deKoning 1993 27 p
(Rept-93-23; ETN-93-94650) Copyright Avail: CASI HC A03/MF A01

The fixed, finite order l-squared optimal control of linear, infinite dimensional time varying discrete time systems is addressed. The set of necessary conditions for the existence of the l-squared optimal controller is expressed in terms of four operator equations (two modified Riccati equations and two modified Lyapunov equations) coupled by a projector having the rank given by the dimension of the compensator state. It is shown that, when the order of the compensator is equal to the order of the plant, the four operator equations are decoupled, and the infinite dimensional generalization of the solution to the l-squared optimal control problem for time varying discrete systems is obtained. ESA

N94-19142# Technische Univ., Delft (Netherlands). Faculty of Technical Mathematics and Informatics.
THE DIGITAL LINEAR QUADRATIC CONTROL PROBLEM FOR PRITCHARD-SALAMON SYSTEMS
Florin Dan Barb, Willem L. deKoning, and Martin Weiss (Groningen Rijksuniv.,

Netherlands.) 1993 20 p Presented at 2nd European Control Conference, Groningen, Netherlands
(Rept-93-27; ETN-93-94654) Copyright Avail: CASI HC A03/MF A01

The class of time discretized Pritchard-Salamon systems is addressed. It is shown that the digital LQ control problem for Pritchard-Salamon systems is equivalent with a certain discrete time LQ control problem which is solvable under some mild, natural assumptions made on the W and V(sup *) spaces. An example of a spectral Pritchard-Salamon system is considered. ESA

N94-19199# Universiteit Twente, Enschede (Netherlands). Mechatronics Research Center.
MART: AN OVERVIEW OF THE MOBILE AUTONOMOUS ROBOT TWENTE PROJECT
A. J. deGraaf, M. P. Koster, J. M. Nauta, W. Oelen, D. Schipper, and H. G. Tillema, ed. 12 Feb. 1993 47 p
(Memo-INF-93-12; ETN-93-94686) Copyright Avail: CASI HC A03/MF A01

A project to build a mobile autonomous robot system designed to operate in a 'factory of the future' is reviewed. Multiple robots, consisting of a manipulator on top of a vehicle, will drive through an assembly hall to collect components at part supply stations and to assemble (different) products while the vehicle is driving. An overview of many design and implementation aspects is given. These include the mechanical construction of the mobile robot and the part supply station, control of the mobile robot, sensor systems for navigation and calibration, task planning, traffic planning and safe and reliable behavior. The current state of the project including the computer hardware and software necessary to realize the system is described. ESA

N94-19226# Universiteit Twente, Enschede (Netherlands). Tele-Informatics and Open Systems Group.
ON ASYNCHRONOUS TESTING
Louis Verhaard (TFL, Hoersholm, Denmark.), Jan Tretmans, Pim Pars, and Ed Brinksma 1993 27 p Sponsored by part by EEC
(Memo-INF-93-03; TIOS-93-01; ETN-93-94677) Copyright Avail: CASI HC A03/MF A01

A test architecture influences the way a tester communicates with the Implementation Under Test (IUT), in particular, whether communication is synchronous or asynchronous. A study which shows that testers that communicate synchronously with the IUT can detect more differences between different implementations of the same specification than testers that communicate asynchronously is presented. It is shown that test cases derived to be used for synchronous testing give wrong results when used for asynchronous testing. To derive these results, systems are modeled by labeled transition systems. Synchronous communication is modeled by the synchronization operator on labeled transition systems; asynchronous communication is described by a queue operator that models a context consisting of a pair of queues, one for input of messages and one for output. Conformance is studied in the asynchronous context, and a method for test derivation is presented, together with a translation of the derived test cases to TTCN, the standardized test notation. ESA

N94-19286# Technische Univ., Delft (Netherlands). Faculty of Technical Mathematics and Informatics.
DIGITAL CONTROL OF PRITCHARD-SALAMON SYSTEMS
Florin Dan Barb and Willem L. deKoning 1993 25 p
(Rept-93-33; ETN-94660) Copyright Avail: CASI HC A03/MF A01

The digital control problem of Pritchard-Salamon systems, optimal with respect to a quadratic cost function, is addressed. Both digital state feedback and output feedback control problems are investigated. It is shown that the digital control problem can be equivalent with a certain discrete time linear quadratic control problem, and the construction of the optimal control law is based on the solution to classical Riccati equations. ESA

N94-19302# Oak Ridge National Lab., TN.
ANALYSIS AND DESIGN OF ROBUST DECENTRALIZED CONTROLLERS FOR NONLINEAR SYSTEMS
D. A. Schoenwald Jul. 1993 155 p
(Contract DE-AC05-84OR-21400)
(DE93-019224; ORNL/TM-12181) Avail: CASI HC A08/MF A02

Decentralized control strategies for nonlinear systems are achieved via feedback linearization techniques. New results on optimization and parameter robustness of non-linear systems are also developed. In addition, parametric uncertainty in large-scale systems is handled by sensitivity analysis and optimal control methods in a completely decentralized framework. This idea is applied to alleviate uncertainty in friction parameters for the gimbal joints on Space Station Freedom. As an example of decentralized nonlinear control, singular perturbation methods and distributed vibration damping are merged into a control strategy for a two-link flexible manipulator. DOE

N94-19324 Technische Univ., Eindhoven (Netherlands). Dept. of Mathematics and Computing Science.
TANDEM QUEUES WITH DETERMINISTIC SERVICE TIMES
O. J. Boxma and J. A. C. Resing 1992 28 p Prepared in cooperation with Center for Mathematics and Computer Science, Amsterdam, Netherlands Limited Reproducibility: More than 20% of this document may be affected by microfiche quality
(PB93-197465; MEMO-COSOR-92-33) Avail: CASI HC A03

A tandem queueing model is considered for a sequence of multiplexers at the edge of an ATM network. All queues of the tandem queueing model have unit service times. Each successive queue receives the output of the previous queue plus some external arrivals. For the case of two queues in series, the authors study the end-to-end delay of a cell (customer) arriving at the first queue, and the covariance of its delays at both queues. The joint queue length process at all queues is studied in detail for the 2-queue and 3-queue cases, and the authors outline an approach to the case of an arbitrary number of queues in series. NTIS

N94-19326# Technische Univ., Eindhoven (Netherlands). Dept. of Mathematics and Computing Science.
COMPENSATION APPROACH FOR THREE OR MORE DIMENSIONAL RANDOM WALKS
G. J. VanHoutum, I. J. B. F. Adan, J. Wessels, and W. H. M. Zijm 1993 16 p See also PB93-197416
(PB93-197499) Avail: CASI HC A03/MF A01

The authors investigate for which random walks with three or more dimensions the compensation approach can be used to determine the equilibrium distribution. It is shown that the compensation approach is not appropriate for the symmetric shortest queue system with three queues, but for the 2 x 3 buffered switch it is. By using this compensation approach, it is shown that for the 2 x 3 buffered switch, the equilibrium distribution can be expressed as a linear combination of six series of binary trees of product-form (geometric) distributions. NTIS

N94-19328 Technische Univ., Eindhoven (Netherlands). Dept. of Mathematics and Computing Science.
NONLINEAR DISTURBANCE DECOUPLING AND LINEARIZATION: A PARTIAL INTERPRETATION OF INTEGRAL FEEDBACK
H. J. C. Huijberts, H. Nijmeijer, and A. C. Ruiz Oct. 1992 34 p See also N89-23217 and N93-16474 Prepared in cooperation with Technische Univ., Twente, Netherlands Limited Reproducibility: More than 20% of this document may be affected by microfiche quality
(PB93-197515; MEMO-COSOR-92-41) Avail: Issuing Activity (National Technical Information Service (NTIS))

The relation between the solvability of the disturbance decoupling problem for a nonlinear system and its linearization around a working point is investigated. It turns out that generically the solvability of the disturbance decoupling via regular dynamic state feedback is preserved under linearization. The result gives a partial interpretation of introducing integral action in classical PID-control applied to nonlinear systems. The theory is illustrated by means of a worked example. NTIS

N94-19329*# Technische Univ., Eindhoven (Netherlands). Dept. of Mathematics and Computing Science.
DISCRETE-TIME INFINITY CONTROL PROBLEM WITH MEASUREMENT FEEDBACK
A. A. Stoorvogel, A. Saberi, and B. M. Chen Oct. 1992 34 p See also N90-14000, N90-24003 and PB90-253006 Prepared in cooperation with Washington State Univ., Pullman, WA and State Univ. of New York, Stony Brook, NY
(Grant NAG1-1210)

(PB93-197523; MEMO-COSOR-92-42; NASA-CR-194681; NAS 1.26:194681) Avail: CASI HC A03/MF A01

The paper is concerned with the discrete-time H(sub infinity) control problem with measurement feedback. The authors extend previous results by having weaker assumptions on the system parameters. The authors also show explicitly the structure of H(sub infinity) controllers. Finally, they show that it is in certain cases possible, without loss of performance, to reduce the dynamical order of the controllers. NTIS

N94-19360# Laboratoire d'Automatique et d'Analyse des Systemes, Toulouse (France).

CAUSAL REASONING FOR MODEL-BASED PROCESS SUPERVISORY CONTROL Ph.D. Thesis - Inst. National des Sciences Appliquees, Toulouse [RAISONNEMENT CAUSAL POUR LA SUPERVISION DE PROCESSUS BASEE SUR DES MODELES]

Kouamana Bousson 1993 141 p In FRENCH Prepared in cooperation with Centre Hospitalier Univ. Rangueil, Toulouse, France

(LAAS-93241; ETN-93-95015) Avail: CASI HC A07/MF A02

The causal approach is used to model natural and man-made physical systems. Human beings tend to have a causal view of physical phenomena. A reasoning formalism based on the simultaneous use of the concept of causality and first principles is proposed. A process is represented as both a causal network of interacting qualitative automata influencing one another, and analytical equations which are non-causal by nature. A qualitative automaton captures both the dynamics of a process variable and the necessary knowledge to supervise it. To represent the knowledge for the process behavior interpretation, the notion of process pattern is presented. A process pattern is a space subdomain which indicates a significant and stable behavior of the process with regard to the aims of the supervision. The proposed formalism allows us to automate knowledge acquisition about influences, combine influences automatically from the linguistic description of the causal relations among the process variables, predict the behaviors of the process, and to provide a geometric interpretation of the process evolution. The formalism gave rise to a causal engine, implemented in UNIX environment. Causal engines served as a decision support system for the supervisory control of a fedbatch fermentation process for alpha-amylase production. The genericity of this engine makes it possible to be used for gas turbine behavior prediction and diagnosis. ESA

N94-19361# Laboratoire d'Automatique et d'Analyse des Systemes, Toulouse (France).

PHASING STRATEGIES OF THE HERMES TYPE SPACE SHUTTLE: ITS OPTIMIZATION CONSIDERING THE THRUST FAILURES Ph.D. Thesis - Toulouse Univ. [STRATEGIES DE PHASAGE ORBITAL D'UNE NAVETTE SPATIALE DE TYPE HERMES: OPTIMISATION ET PRISE EN COMPTE DES PANNES DES MOTEURS]

Sang Ryool Lee 1993 127 p In FRENCH

(LAAS-93242; ETN-93-95016) Avail: CASI HC A07/MF A02

The space rendezvous problem between a space shuttle and a station is discussed. The orbital phasing consists in reducing initial angular gap and distance between the shuttle and the space station and transferring the shuttle on a near circular target orbit, located a few kilometers below (or above) the space station. Phasing strategies of the Hermes type space shuttle in front of the stochastic aspects are optimized. The performance criterion is to minimize the operational cost. This is a stochastic, nonlinear and mixed variable optimization problem with constraints. Strategies for analyzing the stochastic aspects with different numbers of thrust are described. The developed models permit an analysis of thrust failure problems and also the definition of a robust strategy regarding the stochastic aspects. ESA

N94-19408# Loughborough Univ. of Technology (England). Dept. of Mathematical Sciences.

LEARNING CONTROL OF LARGE-SCALE SYSTEMS

Q. H. Wu Jun. 1993 22 p

(MATHS-Rept-A-186; ETN-93-94904) Avail: CASI HC A03/MF A01

The application of interconnected learning automata to Learning Coordinated Control (LCC) of a large-scale, electrical power system is presented. The interconnected learning automata with variable subsets of control actions are used to optimize parameters of distributed local controllers to improve power system stability based on an integrated performance index. Simulation studies were carried out based on a mathematical model of a four machine power system. Results obtained for simulation studies are presented. The potential application of the method to control a large scale system is shown. ESA

N94-19410# Loughborough Univ. of Technology (England). Dept. of Mathematical Sciences.

NOTES ON MULTI-STEP AHEAD PREDICTION BASED ON THE PRINCIPLE OF CONCATENATION

J. A. Rossiter Jun. 1993 7 p

(MATHS-Rept-A-189; ETN-93-94907) Avail: CASI HC A02/MF A01

A more efficient application of Generalized Predictive Control than that most common in the literature was proposed by other authors. The purpose of the work is to compare that algorithm with two algorithms, already in the literature, and also with the original algorithm and to demonstrate that they all reduce to the same algorithm. The results show that two algorithms are more efficient in the nonadaptive case, and that one algorithm is not efficient in the adaptive case. ESA

N94-19458 Physics and Electronics Lab. TNO, The Hague (Netherlands).

PRACTICAL: PLANNING AND RESOURCE ALLOCATION IN C2-DOMAINS WITH TIME CRITICAL ALGORITHMS Final Report

C. W. dHuy and A. P. Keene Feb. 1993 96 p Sponsored by Ministry of Defence, The Hague, Netherlands

(FEL-93-B029; TD93-0304; ETN-93-94952) Copyright Avail: Issuing Activity (TNO Physics and Electronics Laboratory, P.O. Box 96864, 2509 JG The Hague, Netherlands)

A framework for planning/replanning using a scenario driven approach that centers on methods and techniques for plan generation, plan repair, and replanning with (partial) reuse of the original plan is described. The basis for the framework is a conceptual model of the (re)planning process and a knowledge partitioning that distinguishes between strategic, tactical, causal, and world knowledge. A temporal database management system is used to allow reasoning about the past and present as well as the future. The research culminated in the system PRACTICAL, demonstrating the (re)planning framework and incorporating the demonstrators CALIGULA and ALLOCATOR for resource allocation and scheduling respectively. ESA

N94-19530# Massachusetts Inst. of Tech., Cambridge. Artificial Intelligence Lab.

A METHOD FOR ELIMINATING SKEW INTRODUCED BY NON-UNIFORM BUFFER DELAY AND WIRE LENGTHS IN CLOCK DISTRIBUTION TREES Memorandum Report

Henry M. Wu Apr. 1993 6 p

(Contract N00014-92-J-4097)

(AD-A270649; AIM-1422) Avail: CASI HC A02/MF A01

Non-uniformities in buffer delays and wire lengths introduce skew in clock distribution trees. Previous techniques exist for eliminating skew introduced by each of these causes, not both. This method uses a pair of matched variable delay lines to eliminate skew caused both by differing buffer delays and wire lengths. DTIC

N94-19599# Massachusetts Inst. of Tech., Cambridge. Artificial Intelligence Lab.

EXPLORATIONS OF THE PRACTICAL ISSUES OF LEARNING PREDICTION-CONTROL TASKS USING TEMPORAL DIFFERENCE LEARNING METHODS

Charles L. Isbell Dec. 1992 81 p

(Contracts N00014-89-J-3139; N00014-91-J-4038)

(AD-A270836; AI-TR-1424) Avail: CASI HC A05/MF A01

There has been recent interest in using a class of incremental learning algorithms called temporal difference learning methods to attack problems of prediction. These algorithms have been brought to bear on various prediction problems in the past, but have remained poorly understood. It is the purpose of this thesis to further explore this class of algorithms, particularly the TD (lambda) algorithm. A number of practical issues are raised and discussed from a general theoretical perspective and then explored in the context of several case studies. The thesis presents a framework for viewing these algorithms independent of the particular task at hand and uses this framework to explore not only tasks of prediction, but also prediction tasks that require control, whether complete or partial. This includes applying the TD (Lambda) algorithm to two tasks: learning to play tic-tac-toe from the outcome of self-play and the outcome of play against a perfectly-playing opponent and learning two simple one-dimensional image segmentation tasks. DTIC

N94-19721# Army Armament Research, Development and Engineering Center, Watervliet, NY.
INCREASING MISSION RELIABILITY USING OPEN-LOOP CONTROL Final Report
Ronald L. Racicot Aug. 1993 28 p
(AD-A271208; ARCCB-TR-93030) Avail: CASI HC A03/MF A01

This report proposes to increase the reliability of some single-degree of freedom servo systems by providing a degraded mode of operation in the event of feedback sensor failure. Normally, the system is operated in a closed-loop feedback mode. During normal operation, information is continuously gathered on the disturbing forces encountered and their statistical variations from cycle-to-cycle. This information is used to design an open-loop controller that can take over in the event of sensor malfunction. An ideal closed-loop controller for this purpose is the modified bang-bang controller because the operating cycle for this controller is readily divided into three sections: acceleration, constant velocity, and deceleration. Disturbing forces can be estimated in the three sections. The s-mean and s-variance of the disturbing forces can then be used to design a conservative open-loop cycle. The cycle is conservative in that the target position for open-loop is less than the desired target position by an amount that yields a specified small probability of exceeding the desired target at some specified s-confidence level. The total cycle is then finished using a constant or cyclic motor force or other technique depending on the specific application. We successfully applied the developed techniques to the loading cycle of a large caliber tank ammunition autoloader. DTIC

N94-18241# Air Force Inst. of Tech., Wright-Patterson AFB, OH.
INTRODUCTION TO QUANTITATIVE FEEDBACK THEORY (QFT) TECHNIQUE
Constantine H. Houpis *In* AGARD, Non Linear Dynamics and Chaos Jun. 1993 20 p (For primary document see N94-18236 04-77)
Copyright Avail: CASI HC A03/MF A02

N94-18353*# Washington State Univ., Pullman. School of Electrical Engineering and Computer Science.
PULSE-FIRING WINNER-TAKE-ALL NETWORKS
Jack L. Meador *In* Idaho Univ., The 1991 3rd NASA Symposium on VLSI Design 1991 10 p (For primary document see N94-18337 04-33)
Avail: CASI HC A02/MF A04

N94-18354*# Idaho Univ., Moscow. Dept. of Electrical Engineering and Microelectronics Research Center.
TRAINING PRODUCT UNIT NEURAL NETWORKS WITH GENETIC ALGORITHMS
D. J. Janson, J. F. Frenzel, and D. C. Thelen *In its* The 1991 3rd NASA Symposium on VLSI Design 1991 8 p (For primary document see N94-18337 04-33)
Avail: CASI HC A02/MF A04

N94-18355*# Montana State Univ., Bozeman. Dept. of Electrical Engineering.
VLSI SYNTHESIS OF DIGITAL APPLICATION SPECIFIC NEURAL NETWORKS
Grant Beagles and Kel Winters (Advanced Hardware Architectures, Moscow, ID.) *In* Idaho Univ., The 1991 3rd NASA Symposium on VLSI Design 1991 10 p (For primary document see N94-18337 04-33)
Avail: CASI HC A02/MF A04

64 NUMERICAL ANALYSIS

Includes iteration, difference equations, and numerical approximation.

N94-17680# International Centre for Theoretical Physics, Trieste (Italy).
FUZZY ALMOST LINEAR SPACES
I. Beg, M. Arshad (Quaid-i-Azam Univ., Islamabad, Pakistan.), and M. Shabir (Quaid-i-Azam Univ., Islamabad, Pakistan.) Apr. 1993 13 p
(DE93-624772; IC-93/68) Avail: CASI HC A03/MF A01 (US Sales Only)

Fuzzy almost linear subspaces of an almost linear space are defined and several of their basic properties are studied. DOE

N94-17683# International Centre for Theoretical Physics, Trieste (Italy).
INFINITE GRASSMANNIAN AND MODULI SPACE OF G-BUNDLES
S. Kumar (North Carolina Univ., Chapel Hill.), M. S. Narasimhan, and A. Ramanathan (Tata Inst. of Fundamental Research, Bombay, India.) Mar. 1993 33 p
(DE93-624798; IC-93/28) Avail: CASI HC A03/MF A01 (US Sales Only)

Let C be a smooth irreducible projective curve and G a simply connected simple affine algebraic group of C. We study in this paper the relationship between the space of vacua defined in Conformal Field Theory and the space of sections of a line bundle on the moduli space of G-bundles over C. DOE

N94-17684# International Centre for Theoretical Physics, Trieste (Italy).
(1,1)-GEODESIC MAPS INTO GRASSMANN MANIFOLDS
J. H. Eschenburg (Augsburg Univ., Germany.) and R. Tribuzy Feb. 1993 9 p
(DE93-624799; IC-93/40) Avail: CASI HC A02/MF A01 (US Sales Only)

Nontrivial (1,1)-geodesic immersions in complex and real Grassmannians, even for the limit dimension $m = (p-1)(q-1)+1$ in the case $q = 2$, are constructed. DOE

N94-17685# International Centre for Theoretical Physics, Trieste (Italy).
TENSORIAL STRUCTURE OF A q-DEFORMED sp(4,R) SUPERALGEBRA
A. Georgieva Mar. 1993 16 p
(DE93-624808; IC-93/50) Avail: CASI HC A03/MF A01 (US Sales Only)

A supersymmetric quantum algebra is generated by irreducible tensor operators in respect to the algebra su(sub q)(2). The even generators are realized as tensor products of q-boson creation and annihilation operators, transforming as su(sub q)(2) spinors and acting as odd generators. In this way the transformation properties of all the algebra's generators in respect to the q-deformed algebra of the angular momentum are simultaneously preserved, which is important in view of future applications in physics. In the limit q yields 1, the classical Lie superalgebra sp(4,R) or the osp(1 4) is recovered. DOE

N94-17686# International Centre for Theoretical Physics, Trieste (Italy).
FURTHER ON THE CURRENT ALGEBRA OF WZNW MODELS AT AND AWAY FROM CRITICALITY
M. C. B. Abdalla Apr. 1993 6 p
(DE93-624809; IC-93/70) Avail: CASI HC A02/MF A01 (US Sales Only)

We comment on the off-critical perturbations of WZNW models by a mass term as well as by another descendent operator, when we can compare the results with further algebra obtained from the Dirac quantization of the model, in such a way that a more general class of models be included. We discover, in both cases, hidden Kac-Moody algebras obeyed by some currents in the off-critical case, which in several cases are enough to completely fix the correlation functions. DOE

N94-17793# International Centre for Theoretical Physics, Trieste (Italy).
DIFFERENTIAL GEOMETRY OF CR-SUBMANIFOLDS OF A NORMAL ALMOST PARA CONTACT MANIFOLD
M. H. Shahid Dec. 1992 11 p
(DE93-624764; IC-92/413) Avail: CASI HC A03/MF A01 (US Sales Only)

The aim of this paper is to study the geometry of CR-submanifolds of a normal almost para contact manifold. We discuss the integrability conditions of distributions involved in the definition and geometry of leaves of CR-submanifolds, some results on CR-submanifolds with parallel structures and contact CR-product are also given. DOE

N94-17795# International Centre for Theoretical Physics, Trieste (Italy).
MULTIDIMENSIONAL GEOMETRIC QUANTIZATION AND U(1)-COVERING
Tran Vui Mar. 1993 7 p
(DE93-624770; IC-93/56) Avail: CASI HC A02/MF A01 (US Sales Only)

Our geometric construction of unitary representation is based on the Orbit Method of A.A. Kirillov, and some ideas of Do Ngoc Diep and M. Duflo for constructing the unitary dual of a connected and simple connected Lie group. We lift the character of the stabilizer to U(1)-covering via metaplectic representation. Applying the pairing of vacuum states suggested by P.L. Robinson and J.H. Rawnsley in Lagrangian positive polarizations, we get the following main results: Firstly, in the Bargmann-Segal model we account explicitly the integral kernel of the character. Secondly, we construct the induced unitary representations from a U(1)-admissible K-orbit. Lastly, we prove that the constructed representations coincide with the representations obtained from the multidimensional quantization. DOE

N94-17810 International Centre for Theoretical Physics, Trieste (Italy).
FINITE-DIMENSIONAL SINGLETONS OF THE QUANTUM ANTI DE SITTER ALGEBRA
V. K. Dobrev and P. J. Moylan (Pennsylvania State Univ., Abington.) Mar. 1933 12 p Limited Reproducibility: More than 20% of this document may be affected by microfiche quality
(DE93-624771; IC-93/59) Avail: CASI HC A03 (US Sales Only)

We obtain the positive-energy unitary irreducible representations of the q-deformed anti de Sitter algebra U(sub q)(so(3,2)) by deformation of the classical ones. When the deformation parameter q is N-the root of unity, all these unitary representations become finite-dimensional. Generically, their dimensions are smaller than of the corresponding finite-dimensional non-unitary representation of so(3,2). We discuss in detail the singleton representations, i.e. the Di and Rac. When N is odd the Di has dimension (N(sup 2) - 1)/2 and the Rac has dimension (N(sup 2) + 1)/2, while if N is even both the Di and Rac have dimension N(sup 2)/2. These dimensions are classical only for N = 3 when the Di and Rac are deformations of the two fundamental non-unitary representations of so(3,2). DOE

N94-17811 International Centre for Theoretical Physics, Trieste (Italy).
EXACT SOLUTION OF THE GENERALIZED TIME-DEPENDENT JAYNES-CUMMINGS HAMILTONIAN
J. L. Gruver, J. Aliaga, H. A. Cerdeira, and A. N. Proto Apr. 1993 16 p Limited Reproducibility: More than 20% of this document may be affected by microfiche quality
(DE93-624773; IC-93/76) Avail: Issuing Activity (Department of Energy (DOE)) (US Sales Only)

A time-dependent generalization of the Jaynes-Cummings Hamiltonian is studied using the maximum entropy formalism. The approach, related to a semi-Lie algebra, allows to find three different sets of physical relevant operators which describe the dynamics of the system for any temporal dependence. It is shown how the initial conditions of the operators are determined via the maximum entropy principle density operator, where the inclusion of the temperature turns the description of the problem into a thermodynamical one. The generalized time-independent Jaynes-Cummings Hamiltonian is exactly solved as a particular example. DOE

N94-17815# International Centre for Theoretical Physics, Trieste (Italy).
SOME REMARKS ON INTEGRABLE HAMILTONIAN SYSTEMS WITH TWO DEGREES OF FREEDOM
Nguyen Tien Dung Feb. 1993 27 p
(DE93-624766; IC-93/37) Avail: CASI HC A03/MF A01 (US Sales Only)

In this note, based on examples, we consider some aspects of integrable systems with two degrees of freedom: local and global theory, orbit space, integrable surgery, generalized Delzant spaces, relations with 'pure' symplectic geometry, etc. DOE

N94-17816 International Centre for Theoretical Physics, Trieste (Italy).
ENUMERATIVE GEOMETRY OF DEL PEZZO SURFACES
D. Avritzer Mar. 1993 18 p Limited Reproducibility: More than 20% of this document may be affected by microfiche quality
(DE93-624768; IC-93/53) Avail: CASI HC A03 (US Sales Only)

The number 52 832 040 of elliptic quartic curves of P(sup 3) that meet 16 lines in general position as well as the number 47 867 287 590 090 of Del Pezzo Surfaces in P(sup 4) that meet 26 lines in general position are computed. To this end an explicit description of the Hilbert scheme parameterizing complete intersections of two quadrics in P(sup n) in terms of blowing up of Grassmannians is used. The method applies to the complete intersection of two quadrics in P(sup n), n greater than or equal to 3. DOE

N94-17817 International Centre for Theoretical Physics, Trieste (Italy).
A REDUCTION OF THE GLOBALIZATION AND U(1)-COVERING
Tran Dao Dong Mar. 1993 16 p Limited Reproducibility: More than 20% of this document may be affected by microfiche quality
(DE93-624769; IC-93/55) Avail: CASI HC A03 (US Sales Only)

We suggest a reduction of the globalization and multidimensional quantization to the case of reductive Lie groups by lifting to U(1)-covering. Our construction is connected with M. Duflo's third method for algebraic groups. From a reductive datum of the given real algebraic Lie group we firstly construct geometric complexes with respect to U(1)-covering by using the unipotent positive distributions. Then we describe in terms of local cohomology the maximal globalization of Harish-Chandra modules which correspond to the geometric complexes. DOE

N94-17825# Connecticut Univ., Storrs. Dept. of Mathematics.
MULTIVARIATE WAVELET REPRESENTATIONS AND APPROXIMATIONS Final Report, 1 Jun. 1990 - 31 May 1993
Wolodymyr Madych 31 May 1993 31 p
(Grant AF-AFOSR-0311-90)
(AD-A269350; TR-5; AFOSR-93-0689TR) Avail: CASI HC A03/MF A01

The following work has been completed: The recovery of irregularly samples band-limited functions via tempered splines. Band limited functions can be recovered from their values on certain irregularly distributed discrete sampling sets as the limits of the piecewise polynomial spline interpolants when the order of the splines goes to infinity. This significant extension of the classical case when the sampling set is a lattice which was considered by L. Collatz, W. Quade, I. J. Schoenberg, and others. Orthogonality criteria for compactly supported scaling functions. The question of whether the integer translates of the scaling function constructed from a prescribed scaling sequency in the standard way are mutually orthogonal is quite subtle. The various conditions and the supporting arguments which are currently in the literature are very complicated. DTIC

N94-17885# Sandia National Labs., Albuquerque, NM.
APPLICATIONS OF AN ALGEBRAIC MONGE PROPERTY
W. W. Bein (American Airlines, Inc., Fort Worth, TX.), P. Brucker (Osnabrueck Univ., Germany.), and J. K. Park 1993 5 p Presented at the 3rd Twente Workshop on Graphs and Combinatorial Optimization, Enschede, Netherlands, 2-4 Jun. 1993
(Contract DE-AC04-76DP-00789)
(DE93-016869; SAND-93-1393C; CONF-9306216-1) Avail: CASI HC A01/MF A01

When restricted to cost arrays possessing the sum Monge property, many combinatorial optimization problems with sum objective functions become significantly easier to solve. Examples include the usual sum-objective-function versions of the assignment problem, the transportation problem, the traveling-salesman problem, and several shortest-path problems. Furthermore, the more general algebraic assignment and transportation problems, which are formulated in terms of an ordered commutative semigroup (H, *, (le)), are similarly easier to solve given cost arrays possessing the corresponding algebraic Monge property, which requires that for all i less than k and j less than l, a(i,j) * a(k,l) (le) a(i,l) * a(k,j). In this paper, we show that Monge-array results for two sum-of-edge-costs shortest-path problems can likewise be extended to a general algebraic setting, provided the problems' ordered commutative semigroup (H, *, (le)) satisfies one additional restriction. We also show how our algorithms can be modified to solve certain bottleneck shortest-path problems, even though the ordered commutative semigroup ((Re), max, (le)) naturally associated with bottleneck problems does not satisfy our additional restriction. We also provide improved algorithms for several other bottleneck combinatorial optimization problems whose cost arrays possess the strict bottleneck Monge property. Finally, we show how our bottleneck shortest-path techniques can be used to obtain fast algorithms for a variant of Hirschberg and Larmore's optimal paragraph formation problem, a processor-allocation problem first formulated by Bokhari, and a special case of the bottleneck traveling-salesman problem. DOE

N94-17928 Politecnico di Milano (Italy). Dipt. di Elettronica e Informazione.
AN ANNEALING APPROACH TO MULTI-FACILITY LOCATION PROBLEMS IN EUCLIDEAN SPACES
Francesco Maffioli and Giovanni Righini Mar. 1993 25 p Sponsored in part by Ministry of University and Scientific Research and Technology
(Rept-93-022; ETN-93-94572) Avail: Issuing Activity (Politecnico di Milano, Piazza Leonardo da Vinci 32, 20133 Milan, Italy)

A methodology for applying annealing techniques to multiresource allocation problems in euclidean spaces is presented. Three kinds of locations are considered: medians, barycenters, and centers. For such problems, iterative algorithms were developed in the past; they alternate allocation and location phases until they converge to locally optimal solutions. It is shown how to make such algorithms more robust by the application of annealing techniques. Some experimental results on problems in R squared are summarized to show the usefulness of the approach. ESA

N94-17949 Weizmann Inst. of Science, Rehovoth (Israel).
A ZETA FUNCTION APPROACH TO THE SEMICLASSICAL QUANTIZATION OF MAPS
Uzi Smilansky Nov. 1993 18 p Limited Reproducibility: More than 20% of this document may be affected by microfiche quality
(DE93-624774; WIS-PH-92-90) Avail: CASI HC A03 (US Sales Only)

The quantum analogue of an area preserving map on a compact phase space is a unitary (evolution) operator which can be represented by a matrix of dimension L(proportional to)(Dirac h)(sup -1). The semiclassical theory for spectrum of the evolution operator will be reviewed with special emphasize on developing a dynamical zeta function approach, similar to the one introduced recently for a semiclassical quantization of Hamiltonian systems. DOE

N94-17961 Politecnico di Milano (Italy). Dipt. di Elettronica e Informazione.
HEURISTICS FROM NATURE FOR HARD COMBINATORIAL OPTIMIZATION PROBLEMS
A. Colorni, M. Dorigo, F. Maffioli, V. Maniezzo, Giovanni Righini, and M. Trubian 1993 57 p Sponsored in part by Ministry of University and Scientific Research and Technology and CNR
(Rept-93-025; ETN-93-94574) Avail: Issuing Activity (Politecnico di Milano, Piazza Leonardo da Vinci 32, 20133 Milan, Italy)

An attempt to describe the main characters of nondeterministic heuristic algorithms derived from nature, a border area between operations research and artificial intelligence, with applications to graph optimization problems, is made. Algorithms derive from physics, biology, social sciences, and are obtained by a certain amount of repeated trials, given by one or more 'agents' operating with a mechanism of competition-cooperation, with procedures of learning and modification of their internal model of the environment. Six parts are presented; each of them concerned with a class of heuristics from nature and its application (with a specific software) to an NP hard combinatorial optimization problem. Two general parts, devoted to an introduction of some general concepts of computational complexity and to a brief analysis, with a tentative classification, of heuristics from nature are provided. The following topics are considered: genetic algorithms with timetable problems, simulated annealing with dial-a-ride problems, sampling and clustering with communication spanning tree problems, tabu search with job-shop-scheduling problems, neural nets with p-median problems, and system with quadratic assignment problems. ESA

N94-17962 Politecnico di Milano (Italy). Dipt. di Elettronica e Informazione.
LOCATION OF THE ABSOLUTE BARYCENTER OF A GRAPH
F. Maffioli and Giovanni Righini Mar. 1993 12 p Sponsored in part by Ministry of University and Scientific Research and Technology
(Rept-93-027; ETN-93-94576) Avail: Issuing Activity (Politecnico di Milano, Piazza Leonardo da Vinci 32, 20133 Milan, Italy)

An exact polynomial algorithm is presented for locating the absolute barycenter of a graph. The extension of the algorithm to problems in which a weight is associated with every vertex of the graph is straightforward. ESA

N94-17969# Loughborough Univ. of Technology (England). Dept. of Mathematical Sciences.
FORMAT.M: A USAGE MANUAL. TOWARDS AN EFFICIENT SYMBOLIC-NUMERIC ENVIRONMENT: EXTENDING MATHEMATICA'S FORMAT RULES
Mark Sofroniou May 1993 33 p
(MATHS-Rept-A-185; ETN-93-94556) Avail: CASI HC A03/MF A01

A package which extends Mathematica's built-in formatting rules is presented. Examples of shortcomings of the standard rules where code generated may not be syntactically correct and of appropriate precision are given. These shortcomings and the formatting rules to include as data objects and assignments to expressions are addressed. It is shown that the package may be used to enhance and automate code generation. The result is a symbiosis of symbolic/numeric environments built upon the existing Splice communication process. Some examples from applied numerical mathematics, where the package has been used to establish a generalized formulation to a problem via the use of a template file, are included. ESA

N94-18069# Loughborough Univ. of Technology (England). Dept. of Mathematical Sciences.
AN EXTENSION OF WOLOVICH'S DEFINITION OF EQUIVALENCE OF LINEAR SYSTEMS
N. P. Karampetakis (Aristotle Univ. of Thessaloniki, Greece.), A. C. Pugh, A. I. Vardulakis (Aristotle Univ. of Thessaloniki, Greece.), and G. E. Hayton (Hull Univ., England.) Feb. 1993 21 p Sponsored in part by Greek National Foundation
(MATHS-Rept-A-183; ETN-93-94494) Avail: CASI HC A03/MF A01

Wolovich's classical definition of equivalence for linear systems is extended to the generalized study of linear systems. This new kind of equivalence is an alternative characterization of a notion of equivalence for general dynamical systems. The development is a natural extension of the Wolovich ideas since generalized state space systems are the most simple form of system equations which can simultaneously exhibit finite and infinite frequency behavior. It is shown that this notion of equivalence again implies a number of desirable invariants and reduces to complete system equivalence when both systems are in generalized state space form. It is subsequently shown that this new kind of equivalence is identical to full system equivalence and so has the property of preserving the system's finite and infinite frequency structure. ESA

N94-18077# Technische Univ., Eindhoven (Netherlands). Dept. of Mathematics and Computing Science.
FUNCTIONAL ANALYSIS OF SUBELLIPTIC OPERATORS ON LIE GROUPS
A. F. M. terElst and D. W. Robinson Oct. 1992 27 p See also PB93-194785
(PB93-194793; RANA-92-14) Avail: CASI HC A03/MF A01

Let G be a Lie group with a left Haar measure dg and L the action of G as left translations on Lp(G; dg). Further, let H = dL(C) denote an m-th order subelliptic operator associated with L. The authors establish that for a large family of holomorphic functions f one can use the Cauchy representation to define functions f(H) of the operator H and that these functions are bounded operators if p is a member of (1, infinity). Similar conclusions hold on the spaces formed with respect to right Haar measure, or in any unitary representation. As an application, the authors show that the C(sup n)-subspaces of the left regular representations, or the unitary representations, have natural interpolation properties relative to the complex method. NTIS

N94-18078# Technische Univ., Eindhoven (Netherlands). Dept. of Mathematics and Computing Science.
NUMERICAL METHODS FOR ONE-DIMENSIONAL HYPERBOLIC CONSERVATION LAWS
A. C. Berkenbosch, E. F. Kaasschieter, and J. H. M. tenThijeBoonkkamp Oct. 1992 53 p
(PB93-194801; RANA-92-15) Avail: CASI HC A04/MF A01

The paper contains a survey of some important numerical methods for one-dimensional hyperbolic conservation laws. Weak solutions of hyperbolic conservation laws are introduced and the concept of entropy stability is discussed. Furthermore, the Riemann problem for hyperbolic conservation laws is solved. An introduction to numerical methods is given for which important concepts such as conservativity, stability, and consistency are introduced. Godunov-type methods are elaborated for general systems of hyperbolic conservation laws. Finally, flux limiter methods are developed for the scalar non-linear conservation law. NTIS

N94-18094# Pacific Northwest Lab., Richland, WA.
ADVANCES IN THE IDENTIFICATION OF TRANSFER FUNCTION MODELS USING PRONY ANALYSIS
D. J. Trudnowski, M. K. Donnelly, and J. F. Hauer (Bonneville Power Administration, Portland, OR.) Jun. 1993 3 p Presented at the American Control Conference, San Francisco, CA, 2-4 Jun. 1993
(Contract DE-AC06-76RL-01830)
(DE93-017980; PNL-SA-22018; CONF-930663-3) Avail: CASI HC A01/MF A01

This paper further advances the usefulness and understanding of Prony analysis as a tool for identification of models. The presented results allow more generality in the assumed model formulation. In addition, a comparison is made between Prony analysis and autoregressive moving-average (ARMA) modeling. Special attention is given to system conditions often encountered with power system electromechanical dynamics. DOE

N94-18106 International Centre for Theoretical Physics, Trieste (Italy).
STEEPEST DESCENT METHOD FOR SET-VALUED LOCALLY ACCRETIVE MAPPINGS
C. E. Chidume May 1993 12 p Limited Reproducibility: More than 20% of this document may be affected by microfiche quality
(DE93-628592; IC-93/97) Avail: CASI HC A03 (US Sales Only)

Let E be a real q-uniformly smooth Banach space. Suppose T is a set-valued locally strongly accretive map with open domain D(T) in E and that 0 is an element of Tx has a solution x* in D(T). Then there exists a neighborhood B in D(T) of x* and a real number r(sub 1) greater than 0 such that for any r greater than r(sub 1) and some real sequence (c(sub n)), any initial guess x(sub 1) is an element of B and any single-valued selection T(sub 0) of T, the sequence (x(sub n)) generated from x(sub 1) by x(sub n+1)=x(sub n)-c(sub n)T(sub 0)x(sub n), n (greater than or equal to) 1, remains in D(T) and converges strongly to x* with x(sub n)-x* O(n(sup -(q-1)/)q). A related result deals with iterative approximation of a solution of the equation f is an element of x+Ax when A is a locally accretive map. Our theorems generalize important known results and resolve a problem of interest. DOE

N94-18140# Loughborough Univ. of Technology (England). Dept. of Mathematical Sciences.
ON HIGHER DIMENSIONAL ERMAKOV SYSTEMS: CANONICAL REDUCTIONS
C. Rogers, C. Hoenselaers, and J. R. Ray (Clemson Univ., SC.) Jan. 1993 13 p
(MATHS-Rept-A-182; ETN-93-94493) Avail: CASI HC A03/MF A01

Multiwave solutions to two plus one dimensional Ermakov systems are addressed. The procedure is a development connected with soliton like solutions of nonlinear Klein-Gordon equations. A broad class of multiwave solutions are presented which are appropriate both for a two plus one dimensional Pinnet equation and a two plus one dimensional modulated sine Gordon equation. It is remarked that single wave solutions of a modulated sine Gordon equation were constructed by Ray via an Ermakov system and extended to produce kink solutions. ESA

N94-18169 Joint Inst. for Nuclear Research, Dubna (USSR).
ON PARAGRASSMANN DIFFERENTIAL CALCULUS
A. T. Filippov, A. P. Isaev, and A. B. Kurdikov 1992 19 p Limited Reproducibility: More than 20% of this document may be affected by microfiche quality
(DE93-628594; JINR-E-5-92-392) Avail: CASI HC A03 (US Sales Only)

The paper significantly extends and generalizes our previous paper. Here we discuss explicit general constructions for paragrassmann calculus with one and many variables. For one variable nondegenerate differentiation algebras are identified and shown to be equivalent to the algebra of (p+1)x(p+1) complex matrices. For many variables we give a general construction of the differentiation algebras. Some particular examples are related to the multiparametric quantum deformations of the harmonic oscillators. DOE

N94-18170 International Centre for Theoretical Physics, Trieste (Italy).
UNBOUNDED COMPONENTS IN PARAMETER SPACE OF RATIONAL MAPS
P. M. Makienko May 1993 22 p Limited Reproducibility: More than 20% of this document may be affected by microfiche quality
(DE93-628621; IC-93/84) Avail: CASI HC A03 (US Sales Only)

We apply the pinching construction to the study of boundaries of space of quasi-conformal deformations of rational maps. DOE

N94-18175 Joint Inst. for Nuclear Research, Dubna (USSR).
ASYS: A COMPUTER ALGEBRA PACKAGE FOR ANALYSIS OF NONLINEAR ALGEBRAIC EQUATIONS SYSTEMS
V. P. Gerdt, N. V. Khutornoj, and A. Yu. Zharkov 1992 23 p In RUSSIAN Limited Reproducibility: More than 20% of this document may be affected by microfiche quality
(DE93-629819; JINR-R-11-92-100) Avail: CASI HC A03 (US Sales Only)

A program package ASYS for analysis of nonlinear algebraic equations based on the Groebner basis technique is described. The package is written in REDUCE computer algebra language. It has special facilities to treat polynomial ideals of positive dimension, corresponding to algebraic systems with infinitely many solutions. Such systems can be transformed to an equivalent set of subsystems with reduced number of variables in completely automatic way. It often allows to construct the explicit form of a solution set in many problems of practical importance. Some examples and results of comparison with the standard Reduce package GROEBNER and special-purpose systems FELIX and A1PI are given. DOE

N94-18176 International Centre for Theoretical Physics, Trieste (Italy).
ON A POSSIBLE ALGEBRA MORPHISM OF U(SUB q)(osp1/2) ONTO THE DEFORMED OSCILLATOR ALGEBRA W(SUB q)(N)
T. D. Palev and N. I. Stoilova Mar. 1993 9 p Limited Reproducibility: More than 20% of this document may be affected by microfiche quality
(DE93-629857; IC-93/54) Avail: CASI HC A02 (US Sales Only)

We formulate a conjecture, stating that the algebra of n pairs of deformed Bose creation and annihilation operators is a factor-algebra of U(sub q)(osp(1/2n)), considered as a Hopf algebra, and prove it for n=2 case. To this end we show that for any value of qU(sub q)(osp(1/4)) can be viewed as a superalgebra, freely generated by two pairs B(sub 1)(sup (+-)), B(sub 2)(sup (+-)) of deformed para-Bose operators. We write down all Hopf algebra relations, an analogue of the Cartan-Weyl basis, the 'commutation' relations between the generators and a basis in U(sub q)(osp(1/2n)) entirely in terms of B(sub 1)(sup (+-)), B(sub 2)(sup (+-)). DOE

N94-18195 Joint Inst. for Nuclear Research, Dubna (USSR).
ASYMPTOTIC BEHAVIOUR OF THE SOLUTIONS OF SCHROEDINGER EQUATION WITH IMPULSE EFFECT IN A BANACH SPACE
D. D. Bainov, S. I. Kostadinov, and G. Petrov 1992 12 p Limited Reproducibility: More than 20% of this document may be affected by microfiche quality
(DE93-629865; JINR-E-2-92-274) Avail: CASI HC A03 (US Sales Only)

The asymptotic behavior of the solutions of linear homogeneous differential Schroedinger equation with impulse effect in a Banach space is studied and a dependence between their asymptotic behavior and the spectrum of the linear Hamiltonian operator was found. DOE

N94-18196 Joint Inst. for Nuclear Research, Dubna (USSR).
IMPULSIVE MOVING MIRROR MODEL AND THE STABILITY OF SCHROEDINGER EQUATION WITH IMPULSE EFFECT IN A BANACH SPACE
S. I. Kostadinov and G. Petrov 1992 12 p Limited Reproducibility: More than 20% of this document may be affected by microfiche quality
(DE93-629866; JINR-E-2-92-275) Avail: CASI HC A03 (US Sales Only)

From a special class of systems, a Schroedinger equation with impulse effect in Minkowski space field theory with time dependent boundary conditions, i.e. those of moving mirrors were used. The field theoretical approach for studying the properties of the vacuum starts from an analysis of the behavior of local field quantities in Minkowski space with uniformly moving mirrors. For the impulsive moving mirror model is the real process of interaction between the quantum field and the external mirror a subject to disturbances in its evolution acting in time very short compared with the entire duration of the process. The stability of the solution of the Schroedinger evolution equation for the process in the stability of the vacuum of Casimir is discussed. DOE

N94-18197 Joint Inst. for Nuclear Research, Dubna (USSR).
IMPULSIVE MOVING MIRROR MODEL AND IMPULSIVE DIFFERENTIAL EQUATIONS IN BANACH SPACE
G. Petrov 1992 16 p Limited Reproducibility: More than 20% of this document may be affected by microfiche quality
(DE93-629867; JINR-E-2-92-276) Avail: CASI HC A03 (US Sales Only)

The dependence of vacuum state energy on the distance between the uniformly relatively moving mirrors is used to calculate impulsive differential equations in Banach space. The problem of moving mirrors is formulated, possibly with sudden change of velocity v in t = t(sub n), n = 0, 1, 2,..., upon which quantum fields satisfy Dirichlet boundary conditions, with the associated Casimir effect, in a functional Schroedinger picture. DOE

N94-18198 Joint Inst. for Nuclear Research, Dubna (USSR).
A HYDROGEN ATOM IN THE CURVED SPACE. EXPANSION OVER FREE SOLUTIONS ON THE THREE-DIMENSIONAL SPHERE
S. I. Vinitskij, G. S. Pogosyan, A. N. Sisakyan, T. A. Strizh, and L. G. Mardoyan 1992 23 p Limited Reproducibility: More than 20% of this document may be affected by microfiche quality
(DE93-629868; JINR-R-2-92-302) Avail: CASI HC A03 (US Sales Only)

The Schroedinger wave functions of the hydrogen atom with the harmonic potential are considered. The harmonic potential is the solution of the Laplace equation on the 3-sphere of radius R. For large R the wave functions correspond to the Coulomb wave functions of the hydrogen atom in the flat three-dimensional space. The decompositions of the Schroedinger wave functions in free solutions are constructed and their correspondence with the known expansions of the Coulomb functions over free ones in the three-dimensional space is established. DOE

N94-18200 Joint Inst. for Nuclear Research, Dubna (USSR).
IMPULSIVE MOVING MIRROR MODEL AND THE STABILITY OF LINEAR HOMOGENEOUS DIFFERENTIAL EQUATIONS WITH IMPULSE EFFECT IN A BANACH SPACE
S. I. Kostadinov and G. Petrov 1992 12 p Limited Reproducibility: More than 20% of this document may be affected by microfiche quality
(DE93-629906; JINR-E-2-92-273) Avail: CASI HC A03 (US Sales Only)

From a special class of systems, the linear homogeneous differential equations with impulse effect in Minkowski space field theory with time dependent boundary conditions, i.e. those of moving mirrors were used. The field theoretical approach for studying the properties of the vacuum starts from an analysis of the behavior of local field quantities in Minkowski space with uniformly moving mirrors for the impulsive moving mirror model is the real process of interaction between the quantum field and the external mirror a subject to disturbances in its evolution acting in time very short compared with the entire duration of the process. The stability of the process in the stability of the vacuum state energy. DOE

N94-18697 Maryland Univ., College Park. Inst. for Physical Science and Technology.
VALIDATION OF A-POSTERIORI ERROR ESTIMATORS BY NUMERICAL APPROACH Final Report
I. Babuska, T. Strouboulis (Texas A&M Univ., College Station.), C. S. Upadhyay (Texas A&M Univ., College Station.), S. K. Gangaraj (Texas A&M Univ., College Station.), and K. Copps (Texas A&M Univ., College Station.) Jun. 1993 110 p Limited Reproducibility: More than 20% of this document may be affected by microfiche quality
(Contract N00014-90-J-1030; NSF CCR-88-20279)
(AD-A269493; BN-1151) Avail: CASI HC A06

A numerical methodology which determines the quality (or robustness) of a-posteriori error estimators is described. The methodology accounts precisely for the factors which affect the quality of error estimators for finite-element solutions of linear elliptic problems, namely, the local geometry of the grid and the structure of the solution. The methodology can be employed to check the robustness of any estimator for the complex grids which are used in engineering computations. DTIC

N94-18798# Delaware Univ., Newark. Dept. of Mathematical Sciences.
SPECTRAL ANALYSIS ON THE CANONICAL AUTOREGRESSIVE DECOMPOSITION Final Report, 1 Oct. 1990 - 30 Sep. 1992
Fadil Santosa 30 Sep. 1992 43 p
(Grant AF-AFOSR-0024-91)
(AD-A270083; AFOSR-93-0705TR) Avail: CASI HC A03/MF A01

Time series modeling as the sum of an autoregressive (AR) process and sinusoids is proposed. When the AR model order is infinite, it is called Canonical AutoRegressive Decomposition (CARD) and is equivalent to the Wold decomposition. Maximum likelihood estimation of the sinusoidal and AR parameters is shown to require minimization with respect to only the unknown frequencies. Although the estimation problem is nonlinear in the sinusoidal amplitudes and AR parameters, it was reduced to a linear least squares problem by using a nonlinear parameter transformation. A general class of signals for which such parameter transformations are applicable, thereby reducing estimator complexity drastically, is derived. This class includes sinusoids as well as polynomials and polynomial-times-exponential signals. The ideas are based on the theory of invariant subspaces for linear operators. CARD serves as a powerful modeling tool in signal plus noise settings and therefore finds application in a large variety of statistical signal processing problems. DTIC

N94-18815# Air Force Inst. of Tech., Wright-Patterson AFB, OH.
FUZZY HYPERGRAPHS AND FUZZY INTERSECTION GRAPHS Ph.D. Thesis
William L. Craine Aug. 1993 86 p
(AD-A270303; AFIT/CI/CIA-93-18D) Avail: CASI HC A05/MF A01

We use methods and definitions from fuzzy set theory to generalize results concerning hypergraphs and intersection graphs. For each fuzzy structure defined, we use cut-level sets to define an associated sequence of crisp structures. The primary goal is then to determine what properties of the sequence of crisp structures characterize a given property of the fuzzy structure. In Chapter 2 we pay particular attention to the family of fuzzy transversals of a fuzzy hypergraph. We give an algorithmic method to construct fuzzy transversals. We also generalize the vertex coloring lemma of Berge providing a characterization of the family of all minimal fuzzy transversals of a fuzzy hypergraph. In Chapter 3 we use similar methods to define and characterize the family of vertex colorings of a fuzzy hypergraph. In Chapter 4 we use the max and min operators to define the fuzzy Intersection graph of a family of fuzzy sets. We show that every fuzzy graph without loops is the intersection graph of some family of fuzzy sets. We show that the Gilmore and Hoffman characterization of interval graphs extends naturally to fuzzy interval graphs, but the Fulkerson and Gross characterization does not. DTIC

N94-18863# Stanford Univ., CA. Center for Large Scale Scientific Computation.
3D COMPOSITE GRIDS USING BEZIER CURVES AND SURFACES IN COMPONENT ADAPTIVE METHODS Interim Report, Jul. 1990 - Aug. 1993
Ramana G. Venkata, Steven C. Suhr, Joseph Oliger, and Joel H. Ferziger Aug. 1993 19 p
(Contracts N00014-89-J-1815; N00014-90-J-1344)
(AD-A269188; SU-CLaSSiC-93-32) Avail: CASI HC A03/MF A01

This document discusses the use of component adaptive methods for the solution of time-dependent partial differential equations on complex geometries. After a brief exposition of the system and language requirements for an efficient use of these methods, we describe a grid generation procedure M*E*S*H, built upon Bezier constructs, coupled with a graphical editor VOUS to serve as a visualization platform and a programming language Vorpal designed to facilitate their implementation. We also discuss the interaction of the various components of our system and their interfaces. DTIC

N94-18948# Technische Univ., Eindhoven (Netherlands). Dept. of Mathematics and Computing Science.
L(SUB p)-REGULARITY OF SUBELLIPTIC OPERATORS ON LIE GROUPS
R. J. Burns, A. F. M. terElst, and D. W. Robinson Oct. 1992 27 p
See also PB93-194793
(PB93-194785; RANA-92-13) Avail: CASI HC A03/MF A01

In an earlier paper, Theorem 5.3.I, it was established that the C(sup infinity)-structure of each continuous representation of a Lie group coincides with the C(sup infinity)-structure for each strongly elliptic, or subcoercive, operator, i.e., the C(sup infinity)-elements of the representation are precisely the C(sup infinity)-elements with respect to the subcoercive operator. In the present paper, the authors prove that the differential structure for the left regular representation on the L(sub p)-spaces with respect to the left-, or right-, Haar measure on the Lie group G coincides with the differential structure of each subcoercive operator if p is a member of (1, infinity). NTIS

N94-18991# Technische Univ., Eindhoven (Netherlands). Dept. of Mathmatics and Computing Science.
CATALOGUE OF SIMPLE PERFECT SQUARED SQUARES OF ORDERS 21 THROUGH 25
C. J. Bouwkamp and A. J. W. Duijvestijn Nov. 1992 213 p
(PB93-191971; EUT-92-WSK-03) Avail: CASI HC A10/MF A03

A perfect squared square of order n is a square dissected into a finite number n of squares no two of which are of equal size. It is called compound if it contains a subset of component squares, more than one and less than all, arranged in a rectangle or a sqaure. If it does not contain such subset it is called simple. The very first Simple Perfect Squared Square of this Catalogue was discovered by computer in March, 1978. It has the lowest possible order, n = 21, and it is the only one of that order. Since then, many more of higher order have been found. The Catalogue contains 207 simple perfect squared squares of which 182 were found by Duijvestijn, 13 by Bouwkamp, 5 by Wilson, 3 by Federico, 3 by Skinner, and 1 by Willcocks for the first time. NTIS

N94-19082# Technische Univ., Delft (Netherlands). Faculty of Technical Mathematics and Informatics.
DIFFERENCE EQUATIONS FOR GENERALIZED MEIXNER POLYNOMIALS
Herman Bavinck and Henk vanHaeringen 1993 15 p
(Rept-93-17; ETN-93-94644) Copyright Avail: CASI HC A03/MF A01

A system of polynomials orthogonal with respect to the classical discrete weight function for Meixner polynomials with an extra point mass added at x = 0 is introduced. A difference operator of infinite order is constructed for which these new polynomials are eigenfunctions and a second order difference equation is given with polynomial coefficients, n-dependent and of at most degree 2, which these polynomials satisfy. ESA

N94-19086# Technische Univ., Delft (Netherlands). Faculty of Technical Mathematics and Informatics.
A PRIORI ESTIMATES AND EXISTENCE OF POSITIVE SOLUTIONS OF A SUPERLINEAR POLYHARMONIC EQUATION
Ramon Soranzo 1993 25 p Sponsored in part by Trieste Univ., Italy
(Rept-93-12; ETN-93-94639) Copyright Avail: CASI HC A03/MF A01

Semilinear polyharmonic problems (P) subject to Navier (N) and Dirichlet (D) boundary conditions are considered. Preliminaries and main results of the L(infinity) a priori estimates are given and proofs of a priori bounds for the N and D cases. The existence of positive solutions of (P), (N) and (P), (D) are established by employing a fixed point index theorem for compact maps in a cone. ESA

N94-19088# Technische Univ., Delft (Netherlands). Faculty of Technical Mathematics and Informatics.
DETERMINISTIC GROWTH-DISPERSAL MODELS AND BRANCHING RANDOM WALK
F. M. Dekking 1993 19 p
(Rept-93-14; ETN-93-94641) Copyright Avail: CASI HC A03/MF A01

A study aimed at relating a deterministic growth dispersal model developed by Weinberger to branching random walk so that results from one of these fields will translate to the other is presented. This attempt may be viewed as a discrete version of the well known relation between Fisher equation and branching Brownian motion. ESA

N94-19141# Technische Univ., Delft (Netherlands). Faculty of Technical Mathematics and Informatics.
DECOMPOSITION INVARIANCE OF GENERALIZED STEADY-STATE OF A 1-D DIFFUSION SYSTEM
L. Dekker 1993 12 p
(Rept-93-26; ETN-93-94653) Copyright Avail: CASI HC A03/MF A01

Decomposition invariance of the generalized steady state is elucidated for a 1-D (one dimensional) diffusion system. The boundary conditions are conceived to be corner input signals forcing the so called 'generalized steady state' solution upon the diffusion system. The discussion is based upon the use of the mathematical formulation of this system concept as an infinite series expansion of the derivatives of the corner inputs signals. For large scale systems the 'generalized steady state' is often the main part of the state. Computer simulation of large systems requires partitioning of the definition region into (many) small regions. Then application of the concept generalized steady state only makes sense if the generalized steady state is invariant under spatial decomposition. It is demonstrated that the generalized steady state of a 1-D diffusion system is decomposition invariant by nature. ESA

N94-19153# Technische Univ., Delft (Netherlands). Dept. of Pure Mathematics.
EXISTENCE OF A MAXIMAL SOLUTION FOR QUASIMONOTONE ELLIPTIC SYSTEMS
Enzo Mitidieri (Trieste Univ., Italy.) and Guido Sweers 1993 22 p
(Rept-93-30; ETN-93-94657) Copyright Avail: CASI HC A03/MF A01

Systems of elliptic equations are studied by using a consequence of the maximum principle, namely the 'sub-supersolution method'. Existence of a maximal solution between a subsolution and a supersolution is obtained under the following two conditions: F is a continuous function in the diagonal; F is increasing, not necessarily continuous, for off-diagonal terms (such F are called quasi monotone). ESA

N94-19190# Columbia Univ., New York, NY.
SINGULARITIES AND SYMMETRIES OF NONLINEAR ORDINARY AND PARTIAL DIFFERENTIAL EQUATIONS
C. K. Chu 1993 7 p
(Contract DE-FG02-84ER-13190)
(DE93-040083; DOE/ER-13190/8) Avail: CASI HC A02/MF A01

Real singularities govern self-focusing singularities and current sheet formation. Complex singularities govern integrable properties, nonintegrable properties, intermittency, and front propagation. This project has studied singularities as both fundamental mathematical objects and as the determining mechanism of crucial physical processes. During the past year, progress was made on the following: painleve property and geometry of solvable groups, singularity clustering and psi-lambda series, and current sheet formation in MHD. DOE

N94-19244# International Centre for Theoretical Physics, Trieste (Italy).
A METHOD FOR FINDING THE PERIODIC SOLUTION OF AUTONOMOUS ORDINARY DIFFERENTIAL EQUATIONS
Jin-Jiang Chang Jan. 1993 11 p
(DE93-624725; IC-93/1) Avail: CASI HC A03/MF A01 (US Sales Only)

Using the least square method, the problem for computing periodic solution of autonomous ordinary differential equations has been reduced to a problem of minimization on a normal plane. The conjugate gradient method is used to yield successive initial value, and the Runge-Kutta method is used to solve the initial value problem in the ordinary differential equations. So a new method for this problem is formed. As examples, it is applied to the Brusselator model and Field-Noyes model of Belousov-Zhabotinskii reactions. The numerical results obtained show that this method is very efficient. DOE

N94-19246# International Centre for Theoretical Physics, Trieste (Italy).
A METHOD FOR SOLVING THE KDV EQUATION AND SOME NUMERICAL EXPERIMENTS
Jin-Jiang Chang Jan. 1993 10 p
(DE93-624726; IC-93/2) Avail: CASI HC A02/MF A01 (US Sales Only)

In this paper, by means of difference method for discretization of space partial derivatives of KDV equation, an initial value problem in ordinary differential equations of large dimensions is produced. By using this ordinary differential equations the existence and the uniqueness of the solution of the KDV equation and the conservation of scheme are proved. This ordinary differential equation can be solved by using implicit Runge-Kutta methods, so a new method for finding the numerical solution of the KDV equation is presented. Numerical experiments not only describe in detail the procedure of two solitons collision, soliton reflex and soliton produce, but also show that this method is very effective. DOE

N94-19248# International Centre for Theoretical Physics, Trieste (Italy).
CONTACT 3-MANIFOLDS, INTEGRABLE HAMILTONIAN SYSTEMS AND EXOTIC SYMPLECTIC STRUCTURES IN R(SUP 4)
Tien-Dung Nguyen Feb. 1993 18 p
(DE93-624767; IC-93/38) Avail: CASI HC A03/MF A01 (US Sales Only)

In this note we show a simple relation between contact 3-manifolds, integrable Hamiltonian systems with two degrees of freedom, and symplectic structures in R(sup 4). DOE

N94-19285# Technische Univ., Delft (Netherlands). Faculty of Technical Mathematics and Informatics.
ON POLYNOMIALS ORTHOGONAL WITH RESPECT TO AN INNER PRODUCT INVOLVING DIFFERENCES (THE GENERAL CASE)
Herman Bavinck 1993 14 p
(Rept-93-32; ETN-93-94659) Copyright Avail: CASI HC A03/MF A01

A sequence of monic orthogonal polynomials with respect to an inner product is addressed. An explicit representation for the sequence is derived, and a five term recurrence relation is obtained for them. An analog of the Christoffel-Darboux formula is given and some results on the distribution of the zeros of the sequence are presented. ESA

N94-19301# Oak Ridge National Lab., TN.
ARE BILINEAR QUADRILATERALS BETTER THAN LINEAR TRIANGLES?
E. F. DAzevedo Aug. 1993 31 p
(Contract DE-AC05-84OR-21400)
(DE93-019223; ORNL/TM-12388) Avail: CASI HC A03/MF A01

This paper compares the theoretical effectiveness of bilinear approximation over quadrilaterals with linear approximation over triangles. Anisotropic mesh transformation is used to generate asymptotically optimally efficient meshes for piecewise linear interpolation over triangles and bilinear interpolation over quadrilaterals. The theory and numerical results suggest triangles may have a slight advantage over quadrilaterals for interpolating convex data functions but bilinear approximation may offer a higher order approximation for saddle-shaped functions on a well-designed mesh. This work is a basic study on optimal meshes with the intention of gaining insight into the more complex meshing problems in finite element analysis. DOE

N94-19315*# Institute for Computer Applications in Science and Engineering, Hampton, VA.
PSEUDO-COMPRESSIBILITY METHODS FOR THE INCOMPRESSIBLE FLOW EQUATIONS Final Report
Eli Turkel (National Aeronautics and Space Administration. Langley Research Center, Hampton, VA.) and A. Arnone (Florence Univ., Italy.) Sep. 1993 16 p See also A93-45023 Submitted for publication
(Contracts NAS1-18605; NAS1-19480; RTOP 505-90-52-01)
(NASA-CR-191533; NAS 1.26:191533; ICASE-93-66) Avail: CASI HC A03/MF A01

Preconditioning methods to accelerate convergence to a steady state for the incompressible fluid dynamics equations are considered. The analysis relies on the inviscid equations. The preconditioning consists of a matrix multiplying the time derivatives. Thus the steady state of the preconditioned system is the same as the steady state of the original system. The method is compared to other types of pseudo-compressibility. For finite difference methods preconditioning can change and improve the steady state solutions. An application to viscous flow around a cascade with a non-periodic mesh is presented. Author (revised)

N94-19317*# Institute for Computer Applications in Science and Engineering, Hampton, VA.
ON POSITIVITY PRESERVING FINITE VOLUME SCHEMES FOR COMPRESSIBLE EULER EQUATIONS Final Report
Benoit Perthame (Paris V Univ., France.) and Chi-Wang Shu (Brown Univ., Providence, RI.) Sep. 1993 18 p Submitted for publication
(Contracts NAS1-19480; NAG1-1145; DAAL03-91-G-0123; NSF DMS-92-11820; AF-AFOSR-0090-93; RTOP 505-90-52-01)
(NASA-CR-191534; NAS 1.26:191534; ICASE-93-67) Avail: CASI HC A03/MF A01

Positivity preserving property of first and higher order finite volume schemes for one and two dimensional compressible Euler equations of gas dynamics is considered. A general framework is established which shows the positivity of density and pressure whenever the underlying one dimensional first order building block based on exact or approximate Riemann solver and the reconstruction are both positivity preserving. Appropriate limitation to achieve high order positivity preserving reconstruction is described. Author (revised)

N94-19337# Oak Ridge National Lab., TN.
THE FOURIER ANALYSIS TECHNIQUE AND EPSILON-PSEUDO-EIGENVALUES
J. M. Donato Jul. 1993 23 p
(Contract DE-AC05-84OR-21400)
(DE93-018805; ORNL/TM-12347) Avail: CASI HC A03/MF A01

The spectral radii of iteration matrices and the spectra and condition numbers of preconditioned systems are important in forecasting the convergence rates for iterative methods. Unfortunately, the spectra of iteration matrices or preconditioned systems is rarely easily available. The Fourier analysis technique has been shown to be a useful tool in studying the effectiveness of iterative methods by determining approximate expressions for the eigenvalues or condition numbers of matrix systems. For non-symmetric matrices, the eigenvalues may be highly sensitive to perturbations. The spectral radii of nonsymmetric iteration matrices may not give a numerically realistic indication of the convergence of the iterative method. Trefethen and others have presented a theory on the use of (epsilon)-pseudo-eigenvalues in the study of matrix equations. For Toeplitz matrices, we show that the theory of c-pseudo-eigenvalues includes the Fourier analysis technique as a limiting case. For non-Toeplitz matrices, the relationship is not clear. We shall examine this relationship for non-Toeplitz matrices that arise when studying preconditioned systems for methods applied to a two-dimensional discretized elliptic differential equation. DOE

N94-19342# Los Alamos National Lab., NM.
ASYMPTOTIC DERIVATION OF THE MODIFIED TIME-DEPENDENT SP2 EQUATIONS AND NUMERICAL CALCULATIONS
Uncheol Shin, W. F. Miller, Jr., and J. E. Morel 1993 8 p Presented at the ANS Winter Meeting, San Francisco, CA, 14-19 Nov. 1993
(Contract W-7405-eng-36)
(DE93-016466; LA-UR-93-2301; CONF-931160-6) Avail: CASI HC A02/MF A01

Converting the independent variables of the transport equation to dimensionless parameters, asymptotic analyses can be performed to show that, for an important class of problems, the diffusion equation is an asymptotic limit of the transport equation. A recent paper by Larsen, McGhee, and Morel provides a broadened view of the result discussed above. It deals with the steady-state transport equation and shows that the Simplified Spherical-Harmonics (SP(sub N)) equations are robust high-order asymptotic approximations of the transport equation in a physical regime in which the conventional diffusion equation is the leading-order approximation. According to the reported numerical results for the steady-state cases, for many problems, low-order SP(sub N) equations capture most of the transport corrections to the diffusion approximation. And Larsen shows that, in nearly all cases, the SP(sub 2) results are significantly more accurate than diffusion results in the steady-state problems. DOE

N94-19343# Los Alamos National Lab., NM.
IMPROVED APPROXIMATIONS APPLIED TO THE S(SUB N) EVEN-PARITY EQUATION
Taewan Noh, J. E. Morel, and W. F. Miller, Jr. 1993 6 p Presented at the ANS Winter Meeting, San Francisco, CA, 14-19 Nov. 1993
(Contract W-7405-eng-36)
(DE93-016467; LA-UR-93-2300; CONF-931160-5) Avail: CASI HC A02/MF A01

We have developed various finite element differencing schemes by applying lumping techniques in neutron streaming and removal terms of the S(sub N) even-parity transport equation in two-dimensional x-y geometry. We have derived an analytical form of the even-parity reflective boundary condition, which along with the vacuum boundary condition can be applied directly to solve second-order even-parity boundary value problems. We have also developed a new simplified even-parity equation that is much more computationally efficient than the even-parity equation. The developed schemes are numerically compared with the conventional first-order diamond-differencing (DD) scheme. DOE

N94-19362 Grenoble-1 Univ. (France). Lab. ARTEMIS.
NUMERICAL ANALYSIS OF PROXIMAL METHODS: DECOMPOSITION AND PARALLELIZATION Ph.D. Thesis [ANALYSE NUMERIQUE DES METHODES PROXIMALES: DECOMPOSITION ET PARALLELISATION]
Moulay Es-Said Oualibouch 1992 184 p In FRENCH Limited Reproducibility: More than 20% of this document may be affected by microfiche quality
(ETN-93-95017) Avail: CASI HC A09

A new decomposition method based on the proximal point algorithm is proposed. Its extensions in constrained convex optimization is presented. The numerical sensitivity of these methods with respect to some parameter used to accelerate the convergence is discussed. These methods are applied to several models. The attention is focused on transportation problems in networks and location problems. Numerical results confirm the performances from both sequential and parallel points of view, using the Connection Machine CM-2. ESA

N94-19392# Grenoble-1 Univ. (France). Lab. ARTEMIS.
ON NETWORK REPRESENTATION OF THE SOLUTIONS IN COMBINATORIAL OPTIMIZATION
M. Lomonozov (Ben Gurion Univ. of the Negev, Beersheva, Israel.) and Z. Waksman (Ben Gurion Univ. of the Negev, Beersheva, Israel.) Feb. 1993 24 p
(RR-910-I; ETN-93-94998) Avail: CASI HC A03/MF A01

For a clutter X of subsets of a finite set E, the minimization problem minimize the set of all wx such that x a member of X, with a positive weight function w defined on E is considered. Let X(sub w) denote the solution set of this problem. Clearly, X(sub w) is, in general, weakly structured and hardly observable. It is shown that when X is an upper clutter of A.J. Hoffman, or its blocker, an acyclic digraph with one source and one sink provides a compact data structure extremely helpful in storing, minoring and enumerating X(sub w). ESA

N94-19393# Grenoble-1 Univ. (France). Lab. ARTEMIS.
A PERFECTION-PRESERVING OPERATION
A. Zemirline Feb. 1993 16 p
(RR-911-I; ETN-93-94999) Avail: CASI HC A03/MF A01

A new graph composition, called the g-amalgam, is described, and it is proved that it is perfection preserving. This composition unifies and generalizes operations known to preserve perfection such as join and 2-join, clique identification, amalgam and 2-amalgam, stable set of size 2 identification, connecting clique system operation. It is proved that under some conditions some subclasses of the class of strict quasi parity graphs are stable for the g-amalgam. ESA

N94-19395# Grenoble-1 Univ. (France). Lab. ARTEMIS.
NEIGHBOURHOOD-PERFECT LINE GRAPHS
Jeno Lehel (Hungarian Academy of Sciences, Budapest.) Apr. 1993 13 p
(Contract OTKA-2570)
(RR-915-I; ETN-93-95001) Avail: CASI HC A03/MF A01

It is shown that the line graph of any balanced hypergraph is neighborhood perfect. This results in a hypergraphic extension of a recent theorem saying that the line graphs of bipartite graphs are neighborhood perfect. The note contains also a graphical extension of the same theorem: the characterization of all graphs with neighborhood perfect line graph. The proof relies on a characterization of neighborhood perfect graphs among line graphs in terms of forbidden induced subgraphs. ESA

N94-19407# Ecole Centrale de Lyon (France).
ON THE NUMERICAL ANALYSIS OF NONLINEAR GALERKIN METHODS: SPECTRAL APPROXIMATION AND FINITE ELEMENTS Ph.D. Thesis [SUR L'ANALYSE NUMERIQUE DES METHODES DE GALERKIN NON LINEAIRE: APPROXIMATIONS SPECTRALES ET ELEMENTS FINIS]
Christophe Devulder 1992 113 p In FRENCH
(ETN-93-94900) Avail: CASI HC A06/MF A02

The nonlinear Galerkin methods are numerical schemes adapted to the long thermal integration of dissipative evolution partial differential equations. They consist of looking for approximate solutions lying in nonlinear manifolds that are 'close', in some sense, to the attractor: the Approximate Inertial Manifolds (AIM's). The aim of the work is to derive convergence results and error estimates for these methods. Spectral and finite elements approximations are considered. For the two dimensional Navier-Stokes equations, the convergence of spectral nonlinear Galerkin methods for a large class of AIMs and the corresponding errors are proven. Reaction-diffusion problems, for which AIM's are constructed as graphs of functions over a finite element space, are considered. The associated nonlinear Galerkin methods are studied and error estimates are proved. ESA

N94-19487# Institut National Polytechnique, Grenoble (France).
HIGH PRECISION ON-LINE STANDARD ARITHMETIC OPERATORS: DESIGN AND IMPLEMENTATION Ph.D. Thesis [OPERATEURS ARITHMETIQUES STANDARDS EN-LIGNE A TRES GRANDE PRECISION: CONCEPTION ET IMPLEMENTATION]
Yustina Kusumaputri-Hornik 1993 224 p In FRENCH
(ETN-93-95006) Avail: CASI HC A10/MF A03

The design and implementation of online, very high precision, standard arithmetic operators in Very Large Scale Integration (VLSI) is addressed. An n bits precision operation, using classic number representation, can provoke an addition with a carry which can propagate to n bits. To resolve this problem, an addition without carry propagation, using redundant number representation is presented. It allows the execution of very high precision operations, as the duration of the operation is independent of the length of the operand. The architectures of online standard arithmetic operators using radix-2 redundant number representation are presented. The online operations are executed in series, bit by bit starting at the most significant bit. Because of their architectural characteristics, simplicity, regularity and modularity, these operators can easily be implemented in VLSI. The circuit was realized in 2 micrometer CMOS technology, using full custom cells for most of circuit's blocks, in order to have a high area density. Two Design For Testability (DFT) techniques for the circuit designed are proposed. The first one is 'simple DFT', where the test sequence is in series and the other one is 'enhanced DFT', where the test sequence is in parallel. The latter needs larger area but reduces the time for testing. One of the advantages of an online operation is the reduction of the complexity of processors interconnection to one bit per operand, while the speed can be increased by pipelining successive calculations at the bit level. ESA

N94-19499# Institut National Polytechnique, Grenoble (France).
COMPUTATION OF LARGE NUMBERS AND VLSI: APPLICATION TO GCD, TO STRETCHED GCD AND AT EUCLIDIAN DISTANCE Ph.D. Thesis [CALCUL SUR LES GRANDS NOMBRES ET VLSI: APPLICATION AU PGCD, AU PGCD ETENDU ET A LA DISTANCE EUCLIDIENNE]
Rachid Bouraoui 1993 192 p In FRENCH
(ETN-93-95009) Avail: CASI HC A09/MF A02

The implementation of online arithmetic algorithms was studied. In particular, the design of two Very Large Scale Integration (VLSI) circuits destined for high precision applications is shown. In fact, in numerous fields, such as pseudorandom number generation, cryptography, computer algebra, exact arithmetic, reduction of fractions with infinite precision, modular computing, image processing, etc., classical operators are inefficient. A solution to this type of problem can be provided through online arithmetic by which computations are performed by introducing operands serially digit by digit in a redundant notation. The first circuit presented implements a Greatest Common Divider (GCD) algorithm known as EUCLIDE providing, according to simulations, the best hardware cost/performance compromise. It also provides the Bezout coefficients. This circuit is to be used in order to solve problems related to the classical GCD method found in many applications. A second application shows the possibility of cascading online operators in order to build up new ones. The example reported in this thesis is that of the online computation of the euclidean distance: Z = the square root of (x squared + y squared) used, among other things, in the least square resolution of linear systems. ESA

N94-19522# Max-Planck-Inst. fuer Stroemungsforschung, Goettingen (Germany).

METHODS FOR DESCRIPTION AND CONTROL OF DYNAMICAL SYSTEMS AND THEIR APPLICATION Thesis [METHODEN ZUR BESCHREIBUNG UND STEUERUNG DYNAMISCHER SYSTEME UND DEREN ANWENDUNG]

Frank Ohle Jul. 1992 154 p In GERMAN
(MPIS-17/1992; ETN-93-95101) Avail: CASI HC A08/MF A02

A method to derive an autonomous system of ordinary differential equations from an experimental time series is proposed. The resulting model can describe quantitatively the transient behavior of a system with limit cycle dynamics and is reduced to an evolution equation, the Landau equation, for the amplitude and frequency. In addition, the model was used for a qualitative prediction of the influence of a periodic excitation on the experimental system using the van der Pol transformation and Floquet theory. The instability of the lock in solution, including the Hopf bifurcation, the intermittency scenario, and the period doubling cascade, was considered. The method of reconstructing a differential equation from an experimental time signal was successfully applied to velocity fluctuations of a laminar periodic wake behind a circular cylinder. With the obtained low dimensional model, the response of the vortex sheet to external sinusoidal and square wave signals was predicted and the nonlinear control theory of Huebler and Luescher was applied. Furthermore, by using the Cremers and Huebler approach, a low dimensional model was reconstructed for the regular state of a standard Taylor-Couette system at Re = 120. It can be shown that the model exhibits behavior similar to the experiment. A modeling procedure from which the optimal number of parameters as well as the minimal number of necessary experimental data can be estimated is presented. With this procedure, it is possible to control time dependent dynamical systems without feedback to preselected dynamics. ESA

N94-19556 Technische Univ., Eindhoven (Netherlands). Dept. of Mathematics and Computing Science.

STABILIZATION OF TIME-DELAY SYSTEMS: AN OVERVIEW OF THE ALGEBRAIC APPROACH

L. C. G. J. M. Habets Jun. 1992 120 p See also AD-A152871
Limited Reproducibility: More than 20% of this document may be affected by microfiche quality
(PB93-191989; EUT-92-WSK-02) Avail: CASI HC A06

Time-delay systems can be viewed as a rather simple generalization of classical finite-dimensional linear time-invariant systems. To investigate to what extent the classical theory can be generalized to this class of systems, two approaches are proposed in the literature: the functional analytic and the algebraic approach. In the report, the author gives an overview of the results in the literature on the stabilization problem for time-delay systems using the algebraic approach. In the method, a time-delay system is considered as a linear system over a commutative ring. After a short introduction to the theory of systems over rings, the author investigates how classical methods, such as pole placement by static state feedback, can be used to stabilize a system in the more general class. It turns out that static state feedback is not such a powerful tool to stabilize a time-delay system. Therefore, dynamic feedback is also considered. Moreover Hurwitz sets are introduced to generalize the notion of stability to arbitrary integral domains. In this way one finds necessary and sufficient conditions for the stabilizability by dynamic feedback of a system over an integral domain. NTIS

N94-19557 Technische Univ., Twente (Netherlands). Faculty of Applied Mathematics.

MATHEMATICAL COMMUNICATIONS, VOLUME 27, NUMBERS 1 AND 2, 1992. LIST AND ABSTRACTS OF MEMORANDA PUBLISHED IN THE PERIOD JULY - DECEMBER 1991

1992 22 p See also PB93-110369 Limited Reproducibility: More than 20% of this document may be affected by microfiche quality
(PB93-191997) Avail: Issuing Activity (National Technical Information Service (NTIS))

The Faculty of Applied Mathematics of the University of Twente publishes two series of reports: Memoranda and Mathematical Communications. A Memorandum is a mathematical paper of which at least one of the authors is a staff member or a visiting guest of the faculty. It contains new results in applied mathematics or a survey of some area in applied mathematics. Most of the Memoranda are preprints of papers that the author(s) have submitted or will submit for publication elsewhere. An issue of the Mathematical Communications contains abstracts of the most recent Memoranda. Previously, two issues (one volume) of the Communications were published each year. These issues contain the abstracts of the Memoranda which appeared in the half-year preceding the issue of the Communication. The present volume marks a departure from this arrangement. This volume, Volume 27 (Numbers 1 and 2 combined) contains the abstracts of the Memoranda which appeared from Jul. to Dec. 1991. Future volumes will run concurrently with the period of production of the Memoranda. NTIS

N94-19583# Naval Postgraduate School, Monterey, CA.

NONTRADITIONAL WINDOWS IN SPECTRAL ANALYSIS M.S. Thesis

Ramiro Moreira-Paredes 17 Jun. 1993 128 p
(AD-A271336) Avail: CASI HC A07/MF A02

This thesis studies a new data weighting function, which consists of a complex valued window known as the linear complex valued FM chirp window. This type of window, when used with the Fourier transform, produces a magnitude spectrum which permits identification of single sinusoids and multiple sinusoids which can be separated in frequency by less than one DFT bin. This allows determination of whether or not one or multiple signals are present. The chirp window seems to have better resolution properties than classical windows. When the chirp window is used with a signal that contains a frequency step (i.e., FSK), the resultant spectrum is markedly different for the upward shift and downward shift cases. The work of this thesis consists of replicating the results of J. Griffiths in his paper 'A Novel Window for High Resolution Fourier Transform' to establish the signal to noise ratio dependency of this type of window, and to study its behavior when damped sinusoids are present. Additionally, a review of classical windows and sidelobe behavior is presented. All simulations were performed using MATLAB. DTIC

N94-19605# Technische Univ., Twente (Netherlands). Faculty of Applied Mathematics.

UPDATED CONTRIBUTIONS TO THE TWENTE WORKSHOP OF HAMILTONIAN GRAPH THEORY

H. J. Broersma, Heuvel J. VanDen, and H. J. Veldman Apr. 1992 116 p Workshop held in Enschede, Netherlands, 6-10 Apr. 1992
(PB93-195568; MEMO-1076) Avail: CASI HC A06/MF A02

The Twente Workshop on Hamiltonian Graph Theory was held at the University of Twente from 6-10 Apr. 1992. This volume contains the written contributions of the participants of the workshop and a list of open problems presented at the workshop. The contributions should be considered as discussion papers, not as journal papers. Some of the titles of papers at the workshop include the following: On Hamilton-connectedness of Cayley graphs; On hamiltonian properties of 2-tough graphs; Toughness and the cycle structure of graphs; The Hopping Lemma; Cycles containing all vertices of maximum degree; Long paths and cycles in tough graphs; The complete closure of a graph; Twenty odd statements in Twente; Generalized closures of graphs; and Two problems related to results of Chvatal-Erdos. NTIS

N94-19655# Oak Ridge National Lab., TN.

A COMPARISON OF ITERATIVE METHODS FOR A MODEL COUPLED SYSTEM OF ELLIPTIC EQUATIONS

J. M. Donato Aug. 1993 15 p
(Contract DE-AC05-84OR-21400)
(DE93-040482; ORNL/TM-12447) Avail: CASI HC A03/MF A01

Many interesting areas of current industry work deal with non-linear coupled systems of partial differential equations. We examine iterative methods for the solution of a model two-dimensional coupled system based on a linearized form of the two carrier drift-diffusion equations from semiconductor modeling. Discretizing this model system yields a large non-symmetric indefinite sparse matrix. To solve the model system, various point and block methods, including the hybrid iterative method Alternate Block Factorization (ABF), are applied. We also employ GMRES with various preconditioners, including block and point incomplete LU (ILU) factorizations. The performance of these methods is compared. It is seen that the preferred ordering of the grid variables and the choice of iterative method are dependent upon the magnitudes of the coupling parameters. For this model, ABF is the most robust of the non-accelerated iterative methods. Among the preconditioners employed with GMRES, the blocked 'by grid point' version of both the ILU and MILU preconditioners are the most robust and the most time efficient over the wide range of parameter values tested. This information may aid in the choice of iterative methods and preconditioners for solving more complicated, yet analogous, coupled systems. DOE

N94-19671# Air Force Inst. of Tech., Wright-Patterson AFB, OH. School of Engineering.

EXPONENTIAL CHARACTERISTIC SPATIAL QUADRATURE FOR DISCRETE ORDINATES NEUTRAL PARTICLE TRANSPORT IN TWO-DIMENSIONAL CARTESIAN COORDINATES Ph.D. Thesis

Bryan M. Minor Sep. 1993 183 p
(AD-A270458; AFIT/DS/ENP/93-07) Avail: CASI HC A09/MF A02

The exponential characteristic spatial quadrature for discrete ordinates neutral particle transport with rectangular cells is developed. Numerical problems arising in the derivation required the development of exponential moment functions. These functions are used to remove indeterminant forms which can cause catastrophic cancellations. The EC method is positive and nonlinear. It conserves particles and satisfies first moment balance. Comparisons of the EC method's performance to other methods in optically thin and thick spatial cells were performed. For optically thin cells, the EC method was shown to converge to the correct answer, with third order truncation error in the thin cell limit. In deep penetration problems, the EC method attained its highest computational efficiencies compared to the other methods. For all the deep penetration problems examined, the number of spatial cells required by the EC method to attain a desired accuracy was less than the other methods. DTIC

N94-19683# Universiteit Twente, Enschede (Netherlands). Faculty of Applied Mathematics.

UPDATED CONTRIBUTIONS TO THE TWENTE WORKSHOP ON HAMILTONIAN GRAPH THEORY

H. J. Broersma, ed., J. vandenHeuvel, ed., and H. J. Veldman, ed. Sep. 1992 114 p Workshop held in Enschede, Netherlands, 6-10 Apr. 1992
(Memo-1076; ETN-93-94529; PB93-195568) Avail: CASI HC A06/MF A02

This volume contains discussions of the following subjects: Hamilton connectedness of Cayley graphs; Hamiltonian properties of two tough graphs; toughness and cycle structure of graphs; Hopping Lemma; cycles containing all vertices of maximum degree; long paths and cycle in tough graphs; closure of graphs; odd statements in Twente; generalized closure of graphs; problem related to results of Chvatal-Erdos; circumference of certain families of graphs; Ore type conditions; Hamilton cycles in path-tough graphs; and cubic graphs containing k vertex disjoint subgraphs of given cyclomatic number. For individual titles, see N94-19684 through N94-19697.

N94-19684# Simon Fraser Univ., Burnaby (British Columbia). Dept. of Mathematics and Statistics.

ON HAMILTON-CONNECTEDNESS OF CAYLEY GRAPHS

Brian Alspach *In* Univ. Twente, Updated Contributions to the Twente Workshop on Hamiltonian Graph Theory Sep. 1992 p 7-8 (For primary document see N94-19683 04-64)
Avail: CASI HC A01/MF A02

The question of whether or not every connected Cayley graph has a Hamilton cycle is discussed. A result about Cayley graphs in abelian groups is stated. If a graph X has the property that given any two vertices u and v there is a Hamilton path whose end vertices are u and v, we say X is Hamilton connected. If a bipartite graph X, whose bipartition sets A and B have the same cardinality, has the property that for any vertex u belongs to A and v belongs to B there is a Hamilton path whose end vertices are u and v, we say X is Hamilton-laceable. The following theorem is discussed: let X be a connected Cayley graph of degree at least 3 in an abelian group. If X is bipartite, then X is Hamilton laceable. If X is not bipartite, then X is Hamilton connected. ESA

N94-19685# Stevens Inst. of Tech., Hoboken, NJ. Dept. of Mathematics.

ON HAMILTONIAN PROPERTIES OF 2-TOUGH GRAPHS

D. Bauer, H. J. Broersma (Universiteit Twente, Enschede, Netherlands.), J. vandenHeuvel (Universiteit Twente, Enschede, Netherlands.), and H. J. Veldman (Universiteit Twente, Enschede, Netherlands.) *In* Univ. Twente, Updated Contributions to the Twente Workshop on Hamiltonian Graph Theory Sep. 1992 p 9-13 (For primary document see N94-19683 04-64)
Avail: CASI HC A01/MF A02

A graph, G, is called Hamiltonian if it contains a Hamiltonian cycle (a cycle containing every vertex of G). The graph is called t-tough if the absolute value of S is greater than or equal to (t w(G-S)) for every subset S subset of V(G), with w(G-S) greater than 1. The toughness of G is the maximum value of t for which G is t-tough. The relations between toughness and the existence of Hamiltonian factors or k factors are studied. The following conjectures and theorems are stated: a two-tough graph on at least 3 vertices is Hamitonian; the square of a two-connected graph is Hamiltonian; a four connected line graph is Hamiltonian; a 7 connected line graph is Hamiltonian; and a four-connected K(sub 1,3) free graph is Hamiltonian. ESA

N94-19686# Stevens Inst. of Tech., Hoboken, NJ. Dept. of Mathematics.

TOUGHNESS AND THE CYCLE STRUCTURE OF GRAPHS

D. Bauer and E. Schmeichel (San Jose State Univ., CA.) *In* Univ. Twente, Updated Contributions to the Twente Workshop on Hamiltonian Graph Theory Sep. 1992 p 15-19 (For primary document see N94-19683 04-64)
(Contract MDA904-89-H-2008; NSF DMS-89-04520)
Avail: CASI HC A01/MF A02

The relationship between the toughness of a graph and its cycle structure is discussed. The study was motivated by the conjecture that there exists a constant t(sub zero) such that every t(sub zero)-tough graph is Hamiltonian. The following definitions are explained: the graph G is called t-tough if the absolute value of S is greater than or equal to (tw(G-S)) for every subset S subset of V(G), with W(G-S) greater than 1; the circumference of G is denoted by the length of a longest cycle in G. Directions for future research are given. ESA

N94-19687# Waterloo Univ. (Ontario).

THE HOPPING LEMMA M.S. Thesis

Kerstin Baxter *In* Univ. Twente, Updated Contributions to the Twente Workshop on Hamiltonian Graph Theory Sep. 1992 p 21-48 (For primary document see N94-19683 04-64)
Avail: CASI HC A03/MF A02

The Hopping Lemma is one of the different proof techniques used in graph theory. Used specifically for path and circuit problems, it is based on an iterative definition of sets of vertices in a graph with respect to a chosen circuit or path. Many variants and results based on it were performed. The Lemma and its variants, attempting to show the links between these concepts, are stated and proven. A survey of results proved using the Hopping Lemma or one of its variants is included. ESA

N94-19688# Universiteit Twente, Enschede (Netherlands). Faculty of Applied Mathematics.

CYCLES CONTAINING ALL VERTICES OF MAXIMUM DEGREE

H. J. Broersma, J. vandenHeuvel, H. A. Jung (Technische Univ., Berlin, Germany.), and H. J. Veldman *In its* Updated Contributions to the Twente Workshop on Hamiltonian Graph Theory Sep. 1992 p 49-53 (For primary document see N94-19683 04-64)
Avail: CASI HC A01/MF A02

The maximum degree of a graph is discussed. Let G be a graph and let C be a cycle of G and A and B subsets of V(G). The following definitions are given for a cycle C: A-longest; A-dominating; (A,B)-extendable; A-extendable. A variation of Woodall's Hopping Lemma is presented. It is shown that a Lemma and some of the corollaries presented remain valid if the set A is replaced by a subset S of V(G) - V(C) such that every pair of vertices in the intersection of N(S) and V(C) is joined by a path with all internal vertices in S and at least one internal vertex in A. The results and the open problems are discussed. An extension of Jackson's theorem is presented. ESA

N94-19689# Universiteit Twente, Enschede (Netherlands). Faculty of Applied Mathematics.

LONG PATHS AND CYCLES IN TOUGH GRAPHS

H. J. Broersma, J. vandenHeuvel, H. A. Jung (Technische Univ., Berlin, Germany.), and H. J. Veldman *In its* Updated Contributions to the

Twente Workshop on Hamiltonian Graph Theory Sep. 1992 p 55-60 (For primary document see N94-19683 04-64)
Avail: CASI HC A02/MF A02

The length of longest cycles in t-tough graphs is discussed. The investigation was motivated by the following observation: given a k connected (k greater than or equal to 2) graph on n greater than or equal to 2k vertices, then a longest cycle in that graph has length at least 2k. The results concerning the length of longest cycles and paths in t-tough graphs are given. Bonds with the right order of magnitude for t greater than zero and inferior or equal to 1 are achieved. However, for the length of longest cycles, the right order of magnitude is not known. ESA

N94-19690# Memphis State Univ., TN. Dept. of Mathematical Sciences.
THE COMPLETE CLOSURE OF A GRAPH
Ralph Faudree, Odile Favaron (Paris-Sud Univ., Orsay, France.), Evelyne Flandrin (Paris-Sud Univ., Orsay, France.), and Hao Li (Paris-Sud Univ., Orsay, France.) *In* Univ. Twente, Updated Contributions to the Twente Workshop on Hamiltonian Graph Theory Sep. 1992 p 61-66 Sponsored in part by PRC Mathinfo (For primary document see N94-19683 04-64)
Avail: CASI HC A02/MF A02

The complete closure number cc(G) of a graph G of order n is defined as the greatest integer k less than or equal to 2n - 3 such that the kth Bondy-Chvatal closure Cl sub k (G) is complete. The necessary or sufficient conditions for a graph to have cc(G)=k are given. The complete stability cs(P) of a property P defined in all the graphs of order n is the smallest integer k such that if Cl sub k (G) is complete then G satisfies P. For some properties P, cs(P) is compared with the classical stability s(P) of P and it is shown that cs(P) may be far smaller than s(P). ESA

N94-19691# Umea Univ. (Sweden). Dept. of Mathematics.
TWENTY ODD STATEMENTS IN TWENTE
Roland Haeggkvist *In* Univ. Twente, Updated Contributions to the Twente Workshop on Hamiltonian Graph Theory Sep. 1992 p 67-76 (For primary document see N94-19683 04-64)
Avail: CASI HC A02/MF A02

The work of the mathematician Adrian Bondy is discussed; in particular, the following conjecture: let G be a K connected n order graph for which every independent set of K+1 vertices has degree sum at least n+k(k+1) and let C be a longest cycle in G. Then G-C contains no path length k-1. A theorem that gives a necessary and sufficient condition for a graph with minimum degree at least 8(n-1)/17 to be Hamiltonian is proven. ESA

N94-19692# Academy of Sciences of the Armenian SSR, Erivan. Dept. of Mathematical Cybernetics.
GENERALIZED CLOSURES OF GRAPHS
A. S. Hasratian and N. K. Khachatrian *In* Univ. Twente, Updated Contributions to the Twente Workshop on Hamiltonian Graph Theory Sep. 1992 p 77-83 (For primary document see N94-19683 04-64)
Avail: CASI HC A02/MF A02

The method proposed by Bondy and Chvatal to investigate graphs using closures is summarized. Properties involving a C(sup 2) of a graph are presented. The following definition is given: let the graph H be a supergraph of a graph of G. H is the generalized C(sup 2) closure of G, under given conditions. The following theorem is proved: the graph K(sub n) is the generalized closure of any Fan's graph G on n greater than or equal to 3 vertices. ESA

N94-19693# Academy of Sciences of the Armenian SSR, Erivan. Dept. of Mathematical Cybernetics.
TWO PROBLEMS RELATED TO RESULTS OF CHVATAL-ERDOES
A. S. Hasratian and N. K. Khachatrian *In* Univ. Twente, Updated Contributions to the Twente Workshop on Hamiltonian Graph Theory Sep. 1992 p 85-86 (For primary document see N94-19683 04-64)
Avail: CASI HC A01/MF A02

The following problems are discussed: to find a localization of the conditions alpha (G) less than or equal to k(G) + 1 sufficient for traceability of a graph G; is a connected graph G = (V, E) Hamiltonian if the absolute value of V is greater than or equal to 3 and for each vertex v belonging to V there exists a positive integer n(v) such that alpha (G(sub n(v))(v)) less than or equal to k (G(sub n(v))(v)). ESA

N94-19694# London Univ. (England). Dept. of Mathematical Studies.
CONCERNING THE CIRCUMFERENCE OF CERTAIN FAMILIES OF GRAPHS
Bill Jackson *In* Univ. Twente, Updated Contributions to the Twente Workshop on Hamiltonian Graph Theory Sep. 1992 p 87-94 (For primary document see N94-19683 04-64)
Avail: CASI HC A02/MF A02

Bounds on the circumference of planar graphs, graphs of bounded maximum degree, claw free graphs, and t-tough graphs are discussed. All graphs considered are finite but may contain loops and multiple edges. Let circ(G) denote the circumference of a graph G. For a family of graphs F let f(sub k(n)) = min(braces) circ(G): G pertaining to F, G is k-connected, module of G n(braces). The results and problems concerning the order of magnitude of f(sub k(n)) when F is one of the families of planar graphs of bounded maximum degree, claw free, and t-tough graphs are studied. Proof techniques used in the three connected cases are indicated. ESA

N94-19695# Nihon Univ., Tokyo (Japan). Dept. of Mathematics.
ORE-TYPE CONDITIONS FOR CYCLES THROUGH SPECIFIED VERTICES Abstract Only
Akira Saito *In* Univ. Twente, Updated Contributions to the Twente Workshop on Hamiltonian Graph Theory Sep. 1992 p 95 (For primary document see N94-19683 04-64)
Avail: CASI HC A01/MF A02

The generalization of Hamiltonian cycle is discussed. Ore's theorem states that a graph G of order p is Hamiltonian if deg(sub G)(x) + deg(sub G)(y) is greater than or equal to p for all nonadjacent pairs of vertices x, y of G. If a Hamiltonian cycle is interpreted as a cycle through all vertices of the graph, a similar degree sum condition which assures the existence of a Hamiltonian cycle can be considered. ESA

N94-19696# Technische Hochschule, Aachen (Germany). Lehrstuhl C fuer Mathematik.
HAMILTON CYCLES IN PATH-TOUGH GRAPHS
Ingo Schiermeyer *In* Univ. Twente, Updated Contributions to the Twente Workshop on Hamiltonian Graph Theory Sep. 1992 p 97-99 (For primary document see N94-19683 04-64)
Avail: CASI HC A01/MF A02

Undirected and simple graphs on n greater than or equal to 3 vertices are considered. A graph G is called 1-tough if any proper subset S which is a proper subset of V(G), with w(G-S) greater than or equal to 2, w(G-S) is less than or equal to the absolute value of S. The theorems of Dirac and Ore, which state the sufficient conditions for a graph to have a Hamilton cycle, and the Jung theorem are given. The path toughness of a graph G is defined. Theorems to demonstrate whether a cycle is Hamiltonian or non-Hamiltonian are shown. ESA

N94-19697# Paedagogische Hochschule, Dresden (Germany).
CUBIC GRAPHS CONTAINING k VERTEX-DISJOINT SUBGRAPHS OF GIVEN CYCLOMATIC NUMBER
Heinz-Juergen Voss *In* Univ. Twente, Updated Contributions to the Twente Workshop on Hamiltonian Graph Theory Sep. 1992 p 101-105 (For primary document see N94-19683 04-64)
Avail: CASI HC A01/MF A02

Finite undirected graphs G = (V, E) with vertex set V and edge set E are considered. Loops and multiple edges are allowed. The cardinalities (absolute value of V) and (absolute value of E) are called the order and the size of G. The cyclomatic number z(G) of a graph G is the smallest number of edges such that the deletion of these edges results in a cycle-free graph. A parameter s(G) of graphs G = (V, E), where s(G) = def (absolute value of E) - (absolute value of V) is considered. This parameter is related with the cyclomatic number. If G is connected then s(G) = z(G) - 1, and if G has alpha components then s(G) = z(G) - alpha. ESA

N94-19708 Helsinki Univ. of Technology, Espoo (Finland). Dept. of Computer Science.
FINDING THE STRONG COMPONENTS IN A DIRECTED GRAPH
E. Nuutila and E. Soisalon-Soininen 1993 22 p Limited Reproducibility: More than 20% of this document may be affected by microfiche quality (PB93-187342; TKO-B94) Copyright Avail: Issuing Activity (National Technical Information Service (NTIS))

The document presents two improved versions of Tarjan's algorithm for finding the strongly connected components in a directed graph. The original algorithm can be considered to contain two traversals of the graph. First, a depth-first search traverses all edges of the graph and constructs a depth-first spanning forest. Second, once a root of a strong component is found, all its descendants that are not elements of previously found strong components are marked as elements of this component. The second traversal is implemented by using a pushdown stack, where all nodes are pushed when entered by the depth-first search. The authors' versions of the algorithm minimize the use of the pushdown stack. The first version stores only those nodes that are not roots of strong components. The second version stores only possible roots of nontrivial (containing at least one cycle) components. For graphs that are almost trees or dags these improvements almost completely eliminate the second traversal. NTIS

N94-19731# Grenoble-1 Univ. (France). Lab. de Modelisation et Calcul.
GEOMETRIC CONTACT FOR CURVES AND SURFACES
Marie-Laurence Mazure Jun. 1992 24 p
(RR-893-M; ETN-93-94984) Avail: CASI HC A03/MF A01

The notion of Frenet-contact of order p(F(sup p)) for parametric curves in the real space R(sup d) is defined in a new geometrical way which allows its extension to the case of surfaces. This notion is compared to geometric continuity of order p(G(sup p)). ESA

65 STATISTICS AND PROBABILITY

Includes data sampling and smoothing; Monte Carlo method; and stochastic processes.

N94-17686# California Univ., Berkeley. Lawrence Berkeley Lab.
VORTEX METHODS AND STATISTICS
A. J. Chorin May 1993 47 p Presented at the Les Houches Summer School of Theoretical Physics, Les Houches, France, 28 Jun. - 30 Jul. 1993
(Contract DE-AC03-76SF-00098)
(DE93-016974; LBL-34124; CONF-9306196-1) Avail: CASI HC A03/MF A01

Vortex methods originated from the observation that in incompressible, inviscid, isentropic flow vorticity (or, more accurately, circulation) is a conserved quantity, as can be readily deduced from the absence of tangential stresses. Thus if the vorticity is known at time t = 0, one can deduce the flow at a later time by simply following it around. In this narrow context, a vortex method is a numerical method that makes use of this observation. Even more generally, the analysis of vortex methods leads, to problems that are closely related to problems in quantum physics and field theory, as well as in harmonic analysis. A broad enough definition of vortex methods ends up by encompassing much of science. Even the purely computational aspects of vortex methods encompass a range of ideas for which vorticity may not be the best unifying theme. The author restricts himself in these lectures to a special class of numerical vortex methods, those that are based on a Lagrangian transport of vorticity in hydrodynamics by smoothed particles ('blobs') and those whose understanding contributes to the understanding of blob methods. Vortex methods for inviscid flow lead to systems of ordinary differential equations that can be readily clothed in Hamiltonian form, both in three and two space dimensions, and they can preserve exactly a number of invariants of the Euler equations, including topological invariants. Their viscous versions resemble Langevin equations. As a result, they provide a very useful cartoon of statistical hydrodynamics, i.e., of turbulence, one that can to some extent be analyzed analytically and more importantly, explored numerically, with important implications also for superfluids, superconductors, and even polymers. In the authors view, vortex 'blob' methods provide the most promising path to the understanding of these phenomena. DOE

N94-17938 Politecnico di Milano (Italy). Dipt. di Elettronica e Informazione.
LINEAR PARAMETER IDENTIFICATION METHODS FOR ARMA MODELS WITH PERIODIC COEFFICIENTS
Silvia Strada 1992 13 p Sponsored by Ministry of University and Scientific Research and Technology, Italy
(Rept-92-070; ETN-93-94506) Avail: Politecnico di Milano, Piazza Leonardo da Vinci 32, 20133 Milan, Italy

The class of Periodic AutoRegressive Moving Average (PARMA) models is considered. For the estimation of their coefficients, two different linear and noniterative algorithms are presented. The first one, is order recursive and designed for PAR models identification; the second, valid on more general cases where a moving average part is present, computes the solution in a closed form too. A time series of event related potentials is taken into consideration and analyzed in order to significantly test the developed algorithms. ESA

N94-18073# Lawrence Livermore National Lab., CA.
CRITICALITY BENCHMARK COMPARISONS LEADING TO CROSS-SECTION UPGRADES
H. P. Alesso, C. E. Annese, D. P. Heinrichs, W. R. Lloyd, and E. M. Lent 1 Mar. 1993 14 p Presented at the ANS Topical Meeting on Physics and Methods in Criticality Safety, Nashville, TN, 19-23 Sep. 1993
(Contract W-7405-eng-48)
(DE93-017184; UCRL-JC-112934; CONF-930907-5) Avail: CASI HC A03/MF A01

For several years criticality benchmark calculations with COG have been conducted. COG is a point-wise Monte Carlo code developed at Lawrence Livermore National Laboratory (LLNL). It solves the Boltzmann equation for the transport of neutrons and photons. The principle consideration in developing COG was that the resulting calculation would be as accurate as the point-wise cross-sectional data, since no physics computational approximations were used. The objective of this paper is to report on COG results for criticality benchmark experiments in concert with MCNP comparisons which are resulting in corrections and upgrades to the point-wise ENDL cross-section data libraries. Benchmarking discrepancies reported here indicated difficulties in the Evaluated Nuclear Data Livermore (ENDL) cross-sections for U-238 at thermal neutron energy levels. This led to a re-evaluation and selection of the appropriate cross-section values from several cross-section sets available (ENDL, ENDF/B-V). Further cross-section upgrades are anticipated. DOE

N94-18154 Joint Inst. for Nuclear Research, Dubna (USSR).
PHASE SPACE REPRESENTATIONS AND QUANTUM PROBABILITY THEORY
I. V. Polubarinov 1991 24 p Limited Reproducibility: More than 20% of this document may be affected by microfiche quality
(DE93-629863; JINR-E-2-91-579) Avail: CASI HC A03 (US Sales Only)

Phase space representations are constructed in quantum mechanics of spin 1. In these representations quantum mechanics and quantum probability theory acquire a similarity to the classical ones, however with essential distinctions. In some representations densities are not positive definite, in others densities are positive, but expectation values and other quantities are defined otherwise. For example, in the phase space representations the correlator of components of two spins 1 in the singlet state differs from its possible classical counterpart by extra numerical factors. This leads to the consistent quantum analogs of the Bell inequality. DOE

N94-18397 Air Force Inst. of Tech., Wright-Patterson AFB, OH. School of Engineering.
AN EMPIRICAL EVALUATION OF FIVE CIRCULAR ERROR PROBABLE ESTIMATION TECHNIQUES AND A METHOD FOR IMPROVING THEM
M.S. Thesis
William L. Tongue 10 Mar. 1993 438 p Limited Reproducibility: More than 20% of this document may be affected by microfiche quality
(AD-A266528; AFIT/GST/ENS/93M-13) Avail: Issuing Activity (Defense Technical Information Center (DTIC))

This study compared five CEP estimation techniques under the assumption that the crossrange and downrange miss distances of the sample data follow a bivariate normal distribution. The analysis determined the sensitivities of these models to changes in sample size, bias, correlation, and ellipticity in terms of three measures of effectiveness: Mean relative error (RE), variance of RE, and mean squared error (MSE) of RE. In general, it was found that sample size was the most significant parameter in determining the best CEP method. Mean RE provided a 'strong' distinction between estimators, while variance and MSE provided 'weak' distinctions between estimators. An attempt to improve one of the better estimation techniques using least squares regression proved quite successful. DTIC

N94-18516 Stanford Univ., CA. Dept. of Statistics.
BAYESIAN MODEL CHOICE: ASYMPTOTICS AND EXACT CALCULATIONS
Alan E. Gelfand and D. K. Dey 15 Jun. 1993 21 p Limited Reproducibility: More than 20% of this document may be affected by microfiche quality
(Contract N00014-92-J-1264)
(AD-A269067; SU-TR-470) Avail: CASI HC A03

Model determination is a fundamental data analytic task. Here we consider the problem of choosing amongst a finite (with loss of generality we assume two) set of models. After briefly reviewing classical and Bayesian model choice strategies we present a general predictive density which includes all proposed Bayesian approaches we are aware of. Using Laplace approximations we can conveniently assess and compare asymptotic behavior of these approaches. Concern regarding the accuracy of these approximations for small to moderate sample sizes encourages the use of Monte Carlo techniques to carry out exact calculations. A data set fit with nested nonlinear models enables comparison between proposals and between exact and asymptotic values. DTIC

N94-18517# Stanford Univ., CA. Dept. of Statistics.
EDF TESTS FOR NORMALITY IN LINEAR MODELS AFTER A BOX-COX TRANSFORMATION
Gemai Chen, Richard Lockhart, and Michael A. Stephens 2 Jul. 1993 28 p
(Contract N00014-92-J-1264)
(AD-A269068; SU-TR-472) Avail: CASI HC A03/MF A01

The Box-Cox transformation procedure has been used extensively in data analysis, for example in regression, where the response variable is subjected to a suitable power transformation so that the standard normal-theory linear regression models can be fitted to the transformed values. In this paper, distribution theory is developed for a family of EDF statistics, including the Anderson-Darling statistic A(exp 2) and the Cramer-von Mises statistic W(exp 2), so that these statistics can be used to test for normality in the linear model after applying the Box-Cox transformation. A table of asymptotic critical points is given for A(exp 2) and W(exp 2) and numerical examples are given to illustrate the use of the table. DTIC

N94-18540# Columbia Univ., New York, NY. Radiation Lab.
JSEP FELLOWSHIP: FRACTAL NOISE PROCESSES Final Report, 1 Apr. 1990 - 31 Mar. 1993
Steven B. Lowen, George W. Flynn, and Malvin C. Teich 31 May 1993 6 p
(Grant AF-AFOSR-0250-90)
(AD-A268841; AFOSR-93-0653TR) Avail: CASI HC A02/MF A01

Three fractal stochastic processes were developed and defined. Their statistical properties were derived, and examples were provided. Fractal shot noise (FSN), which is formed when a homogeneous Poisson process is passed through a filter with a power-law decaying impulse response function, was defined. For certain parameters FSN converges to fractional Gaussian noise, while for others it is a Levy-stable random process. The fractal shot-noise-driven Poisson process (FSNDP), formed when FSN becomes the rate function for a second Poisson process, was considered next. The FSNDP is a point process which has a power spectral density inversely proportional to frequency raised to an arbitrary power (between zero and unity) for certain ranges of parameters. Also developed were two fractal renewal processes with power spectral densities similar to that of the FSNDP: a standard renewal process with arbitrary power between zero and unity; and a finite-valued, alternating renewal process where the power extends to two. Several applications of these three processes were examined in detail. DTIC

N94-18640# Wright Research Development Center, Wright-Patterson AFB, OH. Cockpit Integration Directorate.
EFFICIENT DOMAIN-INDEPENDENT EXPERIMENTATION
Yolanda Gil Jan. 1993 11 p
(Contract F33615-90-C-1465)
(AD-A269530; ISI/RR-93-337) Avail: CASI HC A03/MF A01

Planning systems often make the assumption that omniscient world knowledge is available. Our approach makes the more realistic assumption that the initial knowledge about the actions is incomplete, and uses experimentation as a learning mechanism when the missing knowledge causes an execution failure. Previous work on learning by experimentation has not addressed the issue of how to choose good experiments, and much research on learning from failure has relied on background knowledge to build explanations that pinpoint directly the causes of failures. We want to investigate the potential of a system for efficient learning by experimentation without such background knowledge. This paper describes domain-independent heuristics that compare possible hypotheses and choose the ones most likely to cause the failure. These heuristics extract information solely from the domain operators initially available for planning (incapable of producing such explanation) and the planner's experiences in interacting with the environment. Our approach has been implemented in EXPO, a system that uses PRODIGY as a baseline planner and improves its domain knowledge in several domains. The empirical results presented show that EXPO's heuristics dramatically reduce the number of experiments needed to refine incomplete operators. DTIC

N94-18694 Stanford Univ., CA. Dept. of Statistics.
BAYESIAN ANALYSIS OF ARMA PROCESSES: COMPLETE SAMPLING BASED INFERENCE UNDER FULL LIKELIHOODS
John Marriott, N. Ravishanker, and A. E. Gelfand 24 Jun. 1993 36 p Limited Reproducibility: More than 20% of this document may be affected by microfiche quality
(Contract N00014-92-J-1264)
(AD-A269168; SU-TR-471) Avail: CASI HC A03

For a general stationary and invertible ARMA (p,q) process, this document shows how to carry out a fully Bayesian analysis. The approach is through the use of sampling based methods involving three novel aspects. First the constraints on the parameter space arising from the stationarity and invertibility conditions are handled by a convenient reparametrization to all of Euclidean (p+q)-space. Second, required sampling is facilitated by the introduction of latent variables which, though increasing the dimensionality of the problem, greatly simplifies the evaluation of the likelihood. Third, the particular sampling based approach used is a Markov chain Monte Carlo method which is a hybrid of the Gibbs sampler and the Metropolis algorithm. The authors also briefly show how straightforwardly the sampling based approach accommodates missing observations, outlier detection, prediction, and model determination. Finally the approach is illustrated with two examples. DTIC

N94-19011# Argonne National Lab., IL.
A LEAST-SQUARES COMPUTATIONAL TOOL KIT
D. L. Smith Apr. 1993 77 p
(Contract W-31-109-eng-38)
(DE93-018400; ANL/NDM-128) Avail: CASI HC A05/MF A01

The information assembled in this report is intended to offer a useful computational 'tool kit' to individuals who are interested in a variety of practical applications for the least-squares method of parameter estimation. The fundamental principles of Bayesian analysis are outlined first and these are applied to development of both the simple and the generalized least-squares conditions. Formal solutions that satisfy these conditions are given subsequently. Their application to both linear and non-linear problems is described in detail. Numerical procedures required to implement these formal solutions are discussed and two utility computer algorithms are offered for this purpose (codes LSIOD and GLSIOD written in FORTRAN). Some simple, easily understood examples are included to illustrate the use of these algorithms. Several related topics are then addressed, including the generation of covariance matrices, the role of iteration in applications of least-squares procedures, the effects of numerical precision, and an approach that can be pursued in developing data analysis packages that are directed toward special applications. DOE

N94-19090# Technische Univ., Delft (Netherlands). Faculty of Technical Mathematics and Informatics.
EXCURSION THEORY OF A FINITE SET VIA RESOLVENTS
John G. M. Schoenmakers 1993 16 p
(Rept-93-19; ETN-93-94646) Copyright Avail: CASI HC A03/MF A01

Let (Y(sup delta)(sub t)) t greater than or equal to 0 be a strong Markov process with state space S, which is killed when it reaches an element of the finite set A. An extension of Y(sup delta) is a process Y which behaves like Y(sup delta) up to the time that it reaches a point of the set A. In the case where A consists of only one point a, Ito studied an extension Y of Y(sup delta), by using the Poisson point process of excursions of Y from a. He showed that an extension Y of Y(sup delta) is characterized by an entrance law eta, stickiness constant gamma, and a killing constant delta. Rogers derived the characteristics eta, gamma, delta by using only the resolvent of the extension Y. This method is generalized for the case where A is a finite set. ESA

N94-19137# Technische Univ., Delft (Netherlands). Faculty of Technical Mathematics and Informatics.
THE RANK OF THE PRESENT EXCURSION
Carel L. Scheffer 1993 17 p
(Rept-93-22; ETN-93-94649) Copyright Avail: CASI HC A03/MF A01

It is shown that for standard Brownian motion the present excursion from 0 has probability 0.80031 of establishing a record as far as its duration is concerned. This follows from a more general result concerning the rank of an excursion in the point process representation of a renewal process having inter-arrival times, the distribution of which varies regularly at infinity with exponent p 'a member of' open interval -1, 0. Using Palm probabilities for Poisson processes, the generating function of this rank is in fact found explicitly. ESA

N94-19195# Universiteit Twente, Enschede (Netherlands). Tele-Informatics and Open Systems Group.
A SIMPLE CALCULUS OF FINITE PROBABILISTIC PROCESSES
Diego Latella (Consiglio Nazionale delle Ricerche, Pisa, Italy.) 22 Oct. 1992 18 p Sponsored in part by CNR-NATO program
(Memo-INF-93-08; TIOS-93-05; ETN-93-94682) Copyright Avail: CASI HC A03/MF A01

A simple language of finite probabilistic processes is presented. Its formal syntax and interleaving semantics are provided. The relation between the language and a subset of LOTOS (Language of Temporal Ordering Specification) is discussed and it is proven to be 'testing equivalence'. Some examples are given. ESA

N94-19228# Universiteit Twente, Enschede (Netherlands). Tele-Informatics and Open Systems Group.
SPECIFICATION AND VERIFICATION OF A DYNAMIC LEADER ELECTION PROTOCOL IN A BROADCAST NETWORK
Jacob Brunekreef (Amsterdam Univ., Netherlands.), Joost-Pieter Katoen, Ron Koymans (Philips Gloeilampenfabrieken N.V., Eindhoven, Netherlands.), and Sjouke Mauw (Technische Univ., Eindhoven, Netherlands.) 14 Dec. 1992 20 p
(Memo-INF-93-05; TIOS-93-03; ETN-93-94679) Copyright Avail: CASI HC A03/MF A01

Leader election, a well known problem in distributed systems, is addressed. A leader election protocol for a dynamic distributed system (process may join the election spontaneously) with buffered broadcasting as basic interprocess communication means is specified and verified. Existing solutions are mostly restricted to a fixed number of processes and do not exploit broadcast communication. A formal approach to the verification of the leader election protocol is adopted. The requirements are specified in a property oriented way and the protocol is denoted by means of an extended finite state machine. It is proven using linear time temporal logic that the protocol satisfies the requirements. ESA

N94-19265# Universiteit Twente, Enschede (Netherlands). Tele-Informatics and Open Systems Group.
ADAPTIVE UNIFORMIZATION: TECHNICAL DETAILS
Aad P. A. vanMoorsel and William H. Sanders (Arizona Univ., Tucson.) 1993 23 p Sponsored in part by Digital Faculty Program
(Grants NWO-R62-385; NWO-SIR13-1260)
(Memo-INF-93-22; TIOS-93-13; ETN-93-94694) Copyright Avail: CASI HC A03/MF A01

Technical aspects related to adaptive uniformization are discussed. The derivation of the schemes used to compute the jump probabilities are given. Some more detailed results about the complexity of adaptive uniformization are given. The paper is a supplement to a referenced study on adaptive uniformization. ESA

N94-19323 Technische Univ., Delft (Netherlands).
EXCURSIONS OF STOCHASTIC PROCESSES, COX-POINT PROCESSES, ENTRANCE BEHAVIOR AND RESOLVENTS
J. Schoenmakers 1993 122 p Limited Reproducibility: More than 20% of this document may be affected by microfiche quality
(PB93-197291) Avail: CASI HC A06

The central theme in excursion theory is the study of wanderings of a Markov process from a given boundary, along with the behavior of the process in that boundary itself. The chapter headings in the report are as follows: introduction and summary; excursions from a set; point processes; point processes of excursions of a Ray process; construction of a stochastic process from a quasi-Cox process of excursions; theory of marked excursions; and excursion theory of a finite set via resolvents. NTIS

N94-19325 Technische Univ., Eindhoven (Netherlands). Dept. of Mathematics and Computing Science.
BAHADUR-KIEFER THEOREM BEYOND THE LARGEST OBSERVATION
J. H. J. Einmahl 1993 20 p Sponsored by National Science Foundation, Washington, DC Limited Reproducibility: More than 20% of this document may be affected by microfiche quality
(PB93-197473; MEMO-COSOR-92-34) Avail: CASI HC A03

It is shown that under natural extreme-value conditions, a distributional Bahadur-Kiefer theorem holds in a point lying outside the sample. The limiting distribution is degenerate if the extreme-value index is equal to one; the proper refinement for that case is also established. In both cases, the limiting distribution is chi-square with one degree of freedom. NTIS

N94-19327# Technische Univ., Eindhoven (Netherlands). Dept. of Mathematics and Computing Science.
BOUNDS FOR EXPECTED LOSS IN BAYESIAN DECISION THEORY WITH IMPRECISE PRIOR PROBABILITIES
F. P. A. Coolen 1992 36 p See also N92-29897
(PB93-197507; MEMO-COSOR-92-40) Avail: CASI HC A03/MF A01

Classical Bayesian inference uses the expected value of a loss function with regard to a single prior distribution for a parameter to compare decisions, and an optimal decision minimizes the expected loss. Recently interest has grown in generalizations of the framework without specified priors, to allow imprecise prior probabilities. Within the Bayesian context the most promising method seems to be the intervals of measures method. A major problem for the application of this method to decision problems seems to be the amount of calculation required, as for each decision there is no single value for expected loss, but a set of such values corresponding to all possible prior distributions. In the report the determination of lower and upper bounds for such a set of expected loss values with regard to a single decision is discussed, and general results are derived which show that the situation is less severe than would be expected at first sight. A simple algorithm to determine these bounds is described. NTIS

N94-19354# Universiteit Twente, Enschede (Netherlands). Tele-Informatics and Open Systems Group.
A LANGUAGE OF FINITE PROBABILISTIC PROCESSES AND ITS INTERLEAVING SEMANTICS
Rom Langerak and Diego Latella (Consiglio Nazionale delle Ricerche, Pisa, Italy.) 4 Apr. 1993 16 p Sponsored in part by CNR and North Atlantic Treaty Organization
(Memo-Inf-93-24; TIOS-93-14; ETN-93-94696) Copyright Avail: CASI HC A03/MF A01

A simple language of finite probabilistic processes is addressed. Alt is a probabilistic extension to a subset of Basic LOTOS (Language Of Temporal Ordering Specification) including stop, action-prefix, nondeterministic choice and parallel composition. Alt is based on the 'alternating' model of probabilistic processes, which requires that every process must alternate action-steps with probabilistics step, that is, steps in which nothing is done except a probabilistic choice of the next step. This feature of Alt makes the model too much 'clock-synchronous' and, together with the syntactical constraints imposed on the language, results in the presence of a lot of superfluous internal moves. A different algebra, Slip, which overcomes the drawbacks of Alt while still maintaining the correctness relation (that is, testing equivalence) with standard LOTOS is proposed. ESA

N94-19385# Universiteit Twente, Enschede (Netherlands). Tele-Informatics and Open Systems Group.
ADAPTIVE UNIFORMIZATION
Aad P. A. vanMoorsel and William H. Sanders (Arizona Univ., Tucson.) 1992 29 p Submitted for publication Sponsored in part by Digital

Faculty Program
(Grants NWO-R62-385; NWO-SIR13-1260)
(MEMO-INF-92-88; TIOS-92-33; ETN-93-94675) Copyright Avail: CASI HC A03/MF A01

Uniformization has been shown to be, in many cases, a good method to compute transient probabilities of a continuous time Markov chain. However, two elements limit its use: uniformization cannot be used for all desired model classes, for example models with not uniformly bounded transition rates; and uniformization can be computationally very intensive, for instance for stiff models. A study which introduces 'adaptive uniformization', a variation on standard uniformization which can overcome some of these problems, is presented. A formal definition of adaptive uniformization is given, along with a proof that it yields correct results, and examples of its use on simple systems. In particular, it is shown how systems with infinite state spaces and not uniformly bounded transition rates can be solved using the method. Implementation issues related to the use of adaptive uniformization are discussed, together with the complexity of the required computations. In the context of an extended machine repairmen model, a discussion on how stiff problems, for which standard uniformization is very computationally unattractive, can sometimes be solved with less computational effort by adaptive uniformization is given. ESA

N94-19386# Universiteit Twente, Enschede (Netherlands). Tele-Informatics and Open Systems Group.
SENSITIVITY AND UNCERTAINTY ANALYSIS OF MARKOV REWARD MODELS
Boudewijn R. Haverkort and Adrianus M. H. Meeuwissen 8 Jan. 1993 42 p
(MEMO-INF-92-89; TIOS-92-34; ETN-93-94676) Copyright Avail: CASI HC A03/MF A01

Two ways of dealing with uncertain model parameters are addressed: sensitivity analysis and Monte Carlo uncertainty analysis. These two approaches are elaborated in detail in the context of the class of Markov reward models, which are very well suited for system dependability (reliability and availability) and performability analysis. Whereas sensitivity analysis is relatively cheap as compared to a Monte Carlo uncertainty analysis, it only correctly describes the local behavior of the model outcome uncertainty as a result of the model parameter uncertainties. The more expensive Monte Carlo uncertainty analysis provides a more global view. Especially, when the modeled parameters are somehow dependent, sensitivity analysis falls short. From the examples, information derived with 'classical' sensitivity analysis is clearly sometimes overly optimistic as compared to Monte Carlo uncertainty analysis. Therefore, an extension of the classical sensitivity analysis which is still inexpensive to perform and of which the results better conform those of the Monte Carlo uncertainty analysis is presented. The study is useful for reliability, dependability, and system engineers in that it cearly indicates the differences and commonalities between sensitivity analysis and Monte Carlo uncertainty analysis. It also shows how and when sensitivity analysis is a good and cheaper alternative for Monte Carlo uncertainty analysis, when dealing with uncertain model parameters. ESA

N94-19511# Rochester Univ., NY. Dept. of Computer Science.
STATISTICAL PROBABILITIES FOR PLANNING
Nathaniel G. Martin and James F. Allen Nov. 1993 16 p
(Contracts N00014-82-K-0193; F30602-92-C-0010)
(TR-474) Avail: CASI HC A03/MF A01

A formalism, Statistical Event Logic or SEL, that adds statistical reasoning to Allen's planning language, is described. Interval temporal logic supports reasoning about time and events; probability inferred from the planner's experience supports reasoning about incomplete information. Statistical Event Logic can represent knowledge that allows a planner to reason both about choices based on incomplete knowledge and about the future likely to result from these choices. Author (revised)

N94-19549# Lawrence Livermore National Lab., CA.
UNCERTAINTY VERSUS INTERINDIVIDUAL VARIABILITY
K. T. Bogen Apr. 1993 12 p Presented at the EPA Workshop, Charlottesville, VA, 19-21 Apr. 1993
(Contract W-7405-eng-48)
(DE93-018105; UCRL-JC-113547; CONF-9304125-2) Avail: CASI HC A03/MF A01

Distinct treatment of uncertainty and interindividual variability in variates used to model risk ensures that quantitative assessments of these attributes in modeled risk are maximally relevant to potential regulatory concerns. For example, such a distinction is required for quantitative characterization of uncertainty in population risk or in individual risk. Yet, most quantitative uncertainty analyses undertaken as part of environmental health risk assessments have failed to systematically maintain this distinction among modeled distributed input variates, and so have had limited relevance to reasonable concerns that regulators may have about how uncertainty and variability ought to relate to risk acceptability. The distinction is of course impossible if quantitative treatment of distributed input variates is rejected in favor of using single-point estimates due to the perceived impracticality of complex Monte Carlo analyses that might erroneously be thought of as being necessarily involved. Here, some practical methods are presented that facilitate implementation of the analytic framework for uncertainty and variability proposed by Bogen and Spear. Two types of methodology are discussed: one that facilitates the distinction between uncertainty and variability per se, and another that may be used to simplify quantitative analysis of distributed inputs representing either uncertainty or variability. A simple and a complex form for modeled increased risk are presented and then used to illustrate methods facilitating the distinction between uncertainty and variability in reference to characterization of both population and individual risk. Finally, a simple form of discrete probability calculus is proposed as an easily implemented, practical alternative to Monte-Carlo based procedures to quantitative integration of uncertainty and variability in risk assessment. DOE

N94-19555 Leiden Univ. (Netherlands). Div. of Applied Mathematics.
FINDING OPTIMAL POLICIES FOR MARKOV DECISION CHAINS: A UNIFYING FRAMEWORK FOR MEAN-VARIANCE-TRADEOFFS
Y. Huang and L. C. M. Kallenberg 1993 25 p Revised; See also PB93-191948 and PB91-198986 Limited Reproducibility: More than 20% of this document may be affected by microfiche quality
(PB93-191930; TW-92-13) Avail: Issuing Activity (National Technical Information Service (NTIS))

The paper proves constructively the existence of optimal policies for a maximum one-period mean to standard deviation ratio, negative variance with bounded mean, and mean penalized by variance Markov decision chains by reducing them to a related mathematical program. This program entails maximizing (xB/D(xb)) + C(xb) over x in a polytope and with given bounds on xb where C and D are convex and either D is constant or D is positive and nondecreasing, C is nondecreasing, and xB is nonpositive. The program is in turn reduced to maximizing x(B + theta b) over x in the polytope parametrically in theta. Along the way, under the nonnegative initial distribution assumption, the authors generalize the rule of constructing a stationary maximum average reward policy from an extreme optimal solution of the associated linear program. The paper unifies and extends formulations and existence results for problems discussed by other researchers and gives an effective computational procedure to solve them. NTIS

N94-19595# Florida State Univ., Tallahassee.
PROBLEMS IN PROBABILITY, STATISTICS AND RELIABILITY Final Report, 1 May 1990 - 31 Aug. 1993
Jayaram Sethuraman Oct. 1993 16 p
(Contract DAAL03-90-G-0103)
(AD-A270830; ARO-27868.28-MA) Avail: CASI HC A03/MF A01

The final report briefly describes the accomplishments in research during the grant. It gives a list of the technical reports produced, followed by a list of published papers. In a later section it gives a brief summary of the research findings. Most of this research work was also reported at professional meetings. DTIC

N94-19610 Technische Hochschule, Darmstadt (Germany). Fachbereich Mathematik.
PRODUCTION AND TEST OF PSEUDO RANDOM ELEMENTS Ph.D. Thesis [UEBER DAS ERZEUGEN UND TESTEN VON PSEUDOZUFALLSELEMENTEN]
Werner Schindler 1991 174 p In GERMAN Sponsored by Studienstiftung des Deutschen Volkes Limited Reproducibility: More than 20% of this document may be affected by microfiche quality
(ETN-93-95070) Avail: CASI HC A08

The possibility of production of pseudorandom elements on homogeneous spaces, groups and random variables is examined. Theoretical principles, based on simulation concept and algebraic and topological structures, such as Hartmann-Winter and Glivenko-Cantelli lemmas, are presented and the properties of linear congruence factors are described. The case of distributions on a sphere surface is studied and a method is proposed in order to avoid defects due to the transformation which allow simulations to be transferred into a multidimensional space. Quality criteria of standard random numbers are reviewed, verifying the limits of fold method and introducing concepts such as isoperimetric and better quotients and isotropy number. The coupon collector test was applied to Markov dependent pseudorandom numbers, in order to asses their validity. The problem of the simulation on finite dimensional Lie groups is presented. A method for establishing equidistribution on Grassmann random variables is described and the results are successfully applied to the chirotope problem. ESA

N94-19710 Technische Univ., Eindhoven (Netherlands). Dept. of Mathematics and Computer Science.
NON-WELL-FOUNDEDNESS AND TYPE FREENESS CAN UNIFY THE INTERPRETATION OF FUNCTIONAL APPLICATION
F. Kamareddine 1992 25 p Limited Reproducibility: More than 20% of this document may be affected by microfiche quality
(PB93-191849; COMPUTING SCIENCE NOTES-92/21) Copyright Avail: Issuing Activity (National Technical Information Service (NTIS))

The purpose of the paper is to provide a unified interpretation of collective and distributive predication based on an intentional type-free set theory where individuals are non-well-founded sets. The use of type freeness and non-well-foundedness will enable the authors to get all the possible readings of sentences from two simple tables. The notion of internal definability will be fundamental for this uniform interpretation. NTIS

N94-19726# Wisconsin Univ., Madison.
GENERALIZED REGRESSION TREES: FUNCTION ESTIMATION VIA RECURSIVE PARTITIONING AND MAXIMUM LIKELIHOOD
Probal Chudhuri, Wen-Da Lo, Wei-Yin Loh, and Ching-Ching Yang 25 Jul. 1993 29 p
(Contract DAAL03-91-G-0222)
(AD-A271259; ARO-28679.13-MA) Avail: CASI HC A03/MF A01

A method that blends tree-structured nonparametric regression with classical maximum likelihood is used in a generalized regression setting. The function estimates constructed are piecewise polynomials and are produced together with decision trees containing useful information on the regressors. Fitting is carried out by applying maximum likelihood estimation to subsets of the data, where the subsets are selected via recursive partitioning and cross-validation pruning. Examples of Poisson and logistic regression trees are given to illustrate the method applied to count and binary response data. Large-sample properties of the estimates are derived under appropriate regularity conditions. DTIC

N94-19768 Massachusetts Inst. of Tech., Cambridge. Artificial Intelligence Lab.
EQUIVALENCE AND REDUCTION OF HIDDEN MARKOV MODELS
Vijay Balasubramanian Jan. 1993 85 p Limited Reproducibility: More than 20% of this document may be affected by microfiche quality
(Contract N00014-91-J-4038)
(AD-A270762; AI-TR-1370) Avail: CASI HC A05

Hidden Markov Models are one of the most popular and successful techniques used in statistical pattern recognition. However, they are not well understood on a fundamental level. For example, we do not know how to characterize the class of processes that can be well approximated by HMM's. This thesis tries to uncover the source of the intrinsic expressiveness of HMM's by studying when and why two models may represent the same stochastic process. Define two statistical models to be equivalent if they are models of exactly the same process. We use the theorems proved in this thesis to develop polynomial time algorithms to detect equivalence of prior distributions on an HMM, equivalence of HMM's, and equivalence of HMM's with fixed priors. We characterize Hidden Markov Models in terms of equivalence classes whose elements represent exactly the same processes and proceed to describe an algorithm to reduce HMM's to essentially unique and minimal, canonical representations. These canonical forms are essentially 'smallest representatives' of their equivalence classes, and the number of parameters describing them can be considered a representation for the complexity of the stochastic process they model. On the way to developing our reduction algorithm, we define Generalized Markov Models which relax the positivity constraint on HMM parameters. This generalization is derived by taking the view that an interpretation of model parameters as probabilities is less important than a parsimonious representation of stochastic processes. DTIC

66 SYSTEMS ANALYSIS

Includes mathematical modeling; network analysis; and operations research.

N94-18067# Grenoble-1 Univ. (France). Lab. de Genie Informatique.
CONTRIBUTION TO THE ANALYSIS OF TABLEAUS BASED DECISION METHODS Ph.D. Thesis [CONTRIBUTION A L'ANALYSE DE LA METHODE DES TABLEAUX]
Joseph Levy 1991 56 p In FRENCH
(ETN-93-94355) Avail: CASI HC A04/MF A01

Interest in the tableau based decision method stems from the fact that formulas need not be put into some particular form, contrary to the usual methods of automatic demonstration by resolution. The rule for elimination of universal quantifiers (gamma rule) and of existential quantifers (delta rule) were reformulated. The delta time turned out to be insufficiently proved. The subject of the study is the analysis of this rule by means of a presentation of the tableau based decision method as an algorithm of construction of the list of goals to be satisfied. It was possible to accomplish the following: establish that the delta rule is in fact a skolemization for an existential quantifier with a positive occurrence in the goal list considered here as a disjunction of conjunctions; improve the delta rule such that the new function symbol added by the rule has the minimal number of arguments; and describe concisely classes of algorithms of automatic demonstration by tableau based methods for formulas with or without free variables. ESA

N94-18410# District of Columbia Univ., Washington, DC.
SYSTEM DYNAMICS AND COMPUTER MODELING EXPERTISE. A CONCEPTUAL STRUCTURE RESEARCH INQUIRY Final Report, 25 Jan. 1991 - 30 Sep. 1993
Mark E. Siegel 12 Jul. 1993 60 p
(Contract N00014-91-J-1360)
(AD-A269860) Avail: CASI HC A04/MF A01

This research examined the conceptual structures of 22 expert system dynamists from 10 countries in order to investigate the extent to which representations of their knowledge revealed similarities in conceptual structure properties. The results revealed less similarity than has been found in experts from other fields. It was hypothesized that the hetrogeneity of the sample combined with the fact that the field itself is still developing were the major contributing factors that produced the results. The methodology was then employed with graduate students to examine shifts in their conceptual structures as they acquired system dynamics knowledge. The results were reported in an appendix to the main study. DTIC

N94-18990# Leiden Univ. (Netherlands). Div. of Applied Mathematics.
POLLING SYSTEMS: MOMENT STABILITY OF STATION TIMES AND CENTRAL LIMIT THEOREMS
E. Altman (Institut National de Recherche d'Informatique et d'Automatique, Valbonne, France.) and F. Spieksma 20 Oct. 1992 23 p See also N93-16726
(PB93-191955; TW-92-09) Avail: CASI HC A03/MF A01

The station times are an important measure of performance in polling systems, and are often used to determine efficiently other performance measures, such as waiting times. In this paper the authors give sufficient and necessary conditions for the existence of all moments of station times in steady state. Moreover, they show that the transient moments converge geometrically fast. They then address the question of the rate of convergence of the sample averages of functions of the station times. They establish the applicability of central limit theorems (CLT) and the law of iterated logarithm (LIL) for all moments of the station times. In particular, they compute explicitly the constants involved in the CLT and LIL for the cycle durations. NTIS

67 THEORETICAL MATHEMATICS

Includes topology and number theory.

N94-18150 Gosudarstvennyi Komitet po Ispolzovaniyu Atomnoi Energii, Serpukhov (USSR).
ABOUT STRUCTURALLY STABLE GENERATING MECHANISM FOR INVARIANT HYPERBOLIC SETS
S. V. Klimenko and V. V. Smirnova 1991 23 p In RUSSIAN Limited Reproducibility: More than 20% of this document may be affected by microfiche quality
(DE93-629858; IFVE-OMVT-91-131) Avail: CASI HC A03 (US Sales Only)

The given paper describes a generating mechanism for strange invariant sets. A method for finding structurally stable mechanism is presented. Attractors with this mechanism are pointed out. DOE

N94-18151 Gosudarstvennyi Komitet po Ispolzovaniyu Atomnoi Energii, Serpukhov (USSR).
PATH INTEGRALS ON WARPED PRODUCT MANIFOLDS
S. N. Storchak 1991 11 p Limited Reproducibility: More than 20% of this document may be affected by microfiche quality
(DE93-629859; IHEP-OTF-91-190) Avail: CASI HC A03 (US Sales Only)

By reparametrizing the paths in a path integral, set on a warped product manifold, the integral relation between the Green's functions of quantum mechanical problems is derived describing the motion on the manifold as a whole on one of the submanifolds. DOE

N94-18153 Joint Inst. for Nuclear Research, Dubna (USSR).
DEFORMED TRACES AND COVARIANT QUANTUM ALGEBRAS FOR QUANTUM GROUPS GL(SUB qp)(2) AND GL(SUB qp)(1/1)
A. P. Isaev and R. P. Malik 1991 15 p Limited Reproducibility: More than 20% of this document may be affected by microfiche quality
(DE93-629862; JINR-E-2-91-551) Avail: CASI HC A03 (US Sales Only)

The q-deformed traces and orbits for the two parametric quantum groups GL(sub qp)(2) and GP(sub qp)(1/1) are defined which are subsequently used in the construction of q-orbit invariants for these groups. A general qp-(super)-oscillator commutation relations are obtained which remain invariant under the coactions of groups GL(sub qp)(2) and GL(sub qp)(1/1). The GL(sub qp)(2)-covariant deformed algebra is deduced in terms of the bilinears of bosonic qp-oscillators which turns out to be a central extension of the Witten-type deformation of sl(2) algebra. DOE

N94-18155 Joint Inst. for Nuclear Research, Dubna (USSR). Lab. of Theoretical Physics.
IMPULSIVE MOVING MIRROR MODEL IN A SCHROEDINGER PICTURE WITH IMPULSE EFFECT IN A BANACH SPACE
G. Petrov 1992 36 p Limited Reproducibility: More than 20% of this document may be affected by poor print
(DE93-629864; JINR-E-2-92-272) Avail: Issuing Activity (Department of Energy (DOE)) (US Sales Only)

From a special class of systems has been used a Schroedinger equation with impulse effect in Minkowski space field theory with time dependent boundary conditions, i.e. those of moving mirrors. The field theoretical approach for studying the properties of the vacuum starts from an analysis of the behaviour of local field quantities in Minkowski space with uniformly moving mirrors. For the impulsive moving mirror model is the real process of interaction between the quantum field and the external mirror a subject to disturbances in its evolution acting in time very short compared with the entire duration of the process. So the stability of the solution of the Schroedinger evolution equation for the process is the stability of the vacuum of Casimir. The dependence of vacuum state energy on the distance between the uniformly relatively moving mirrors is used to calculate from the impulsive moving model the Schroedinger equation in a Banach space. DOE

N94-18168 Joint Inst. for Nuclear Research, Dubna (USSR).
PARAGRASSMANN ANALYSIS AND QUANTUM GROUPS
A. T. Filippov, A. P. Isaev, and A. B. Kurdikov 1992 16 p Limited Reproducibility: More than 20% of this document may be affected by microfiche quality
(DE93-628593; JINR-E-2-92-171) Avail: CASI HC A03 (US Sales Only)

Paragrassmann algebras with one and many paragrassmann variables are considered from the algebraic point of view without using the Green anzatz. A differential operator with respect to paragrassmann variable and a covariant para-super-derivative are introduced giving a natural generalization of the Grassmann calculus to a paragrassmann one. Deep relations between paragrassmann and quantum groups with deformation parameters being root of unity are established. DOE

N94-18171 International Centre for Theoretical Physics, Trieste (Italy).
A GENERAL SOLUTION OF THE BV-MASTER EQUATION AND BRST FIELD THEORIES
O. F. Dayi May 1993 12 p Limited Reproducibility: More than 20% of this document may be affected by microfiche quality
(DE93-628622; IC-93/94) Avail: CASI HC A03 (US Sales Only)

For a class of first order gauge theories it was shown that the proper solution of the BV-master equation can be obtained straightforwardly. Here we present the general condition which the gauge generators should satisfy to conclude that this construction is relevant. The general procedure is illustrated by its application to the Chern-Simons theory in any odd-dimension. Moreover, it is shown that this formalism is also applicable to BRST field theories, when one replaces the role of the exterior derivative with the BRST charge of first quantization. DOE

N94-19481# Rochester Univ., NY. Dept. of Computer Science.
THE COMPLEXITY OF THE OPTIMAL SPANNING HYPERTREE PROBLEM
Marius Zimand Sep. 1993 19 p
(Grant NSF CCR-89-57604)
(TR-471) Avail: CASI HC A03/MF A01

The notion of h-hypertree was defined previously in order to improve the Bonferroni inequalities. It is proved that the problem of finding the optimal spanning h-hypertree of a complete hypergraph is NP complete, for h is greater than or equal to 3. Moreover, no polynomial time approximate algorithm even with poor approximation ratio seems to exist for this problem. The existence of such an algorithm for the minimum version achieving an approximation ratio of poly(n) implies P = NP, and, for the maximum version, the existence of a quasipolynomial algorithm achieving the ratio 2(sup log(sup epsilon)(n)) implies NP is contained in the set DTIME(n(sup log)(sup O(1))(n)). Author (revised)

70 PHYSICS (GENERAL)

For precision time and time interval (PTTI) see *35 Instrumentation and Photography;* for geophysics, astrophysics or solar physics see *46 Geophysics, 90 Astrophysics,* or *92 Solar Physics.*

N94-17681# International Centre for Theoretical Physics, Trieste (Italy).
ON THE DEBYE-HUCKEL'S THEORY
I. M. Mladenov Mar. 1993 10 p
(DE93-624789; IC-93/57) Avail: CASI HC A02/MF A01 (US Sales Only)

A one-parameter family of perturbed Debye-Huckel's models, all sharing the inherent spherical symmetry of the classical theory, is introduced and solved in a closed form. When the deformation parameter is set equal to zero one regains the Debye-Huckel's model and results. DOE

N94-18177# Ohio State Univ., Columbus. Research Foundation.
THE PHYSICS OF CELLULAR AUTOMATA AND COHERENCE AND CHAOS IN CLASSICAL MANY-BODY DYNAMICAL SYSTEMS
F. Hayot and C. Jayaprakash 1993 5 p
(Contract DE-FG02-88ER-13916)
(DE93-018021; DOE/ER-13916/5) Avail: CASI HC A01/MF A01

Brief summaries are given of work on the following topics: universal properties of the two-dimensional Kuramoto-Sivashinsky (K-S) equation; dynamic scaling in the K-S equation; chaotic interface models of turbulence; self-organized criticality in nonconserving systems; and local dynamics of Josephson junction arrays. DOE

N94-18178# Santa Fe Inst., NM.
THE 1992 ANNUAL REPORT ON SCIENTIFIC PROGRAMS: A BROAD RESEARCH PROGRAM ON THE SCIENCES OF COMPLEXITY

1992 141 p
(Contract DE-FG05-88ER-25054)
(DE93-018151; DOE/ER-25054/T1) Avail: CASI HC A07/MF A02

In 1992 the Santa Fe Institute hosted more than 100 short- and long-term research visitors who conducted a total of 212 person-months of residential research in complex systems. To date this 1992 work has resulted in more than 50 SFI Working Papers and nearly 150 publications in the scientific literature. The Institute's book series in the sciences of complexity continues to grow, now numbering more than 20 volumes. The fifth annual complex systems summer school brought nearly 60 graduate students and postdoctoral fellows to Santa Fe for an intensive introduction to the field. Research on complex systems - the focus of work at SFI - involves an extraordinary range of topics normally studied in seemingly disparate fields. Natural systems displaying complex adaptive behavior range upwards from DNA through cells and evolutionary systems to human societies. Research models exhibiting complex behavior include spin glasses, cellular automata, and genetic algorithms. Some of the major questions facing complex systems researchers are: (1) explaining how complexity arises from the nonlinear interaction of simple components; (2) describing the mechanisms underlying high-level aggregate behavior of complex systems (such as the overt behavior of an organism, the flow of energy in an ecology, and the Gross National Product (GNP) of an economy); and (3) creating a theoretical framework to enable predictions about the likely behavior of such systems in various conditions. DOE

N94-18286# Wisconsin Univ., Madison.
[RESEARCH ACTIVITY ON PARTICLE SPIN SYSTEMS AND RELATED PROBLEMS]
Panagiotis E. Souganidis 20 Sep. 1993 2 p
(Contract N00014-93-1-0015)
(AD-A269456) Avail: CASI HC A01/MF A01

During the period covered by the first year of the award, Souganidis worked on problems related to the following: microscopic models for phase transitions and hydrodynamic limits of spin systems, turbulent premixed combustion, and kinetic formulation for systems of conservation laws. DTIC

N94-18810# Los Alamos National Lab., NM.
TEMPERATURE LOWERING IN CRYOGENIC CHEMICAL-SYNTHESIS TECHNIQUES AND SYSTEM
H. E. Martinez, T. O. Nelson, and L. N. Vikdal 1993 8 p Presented at the International Cryogenic Engineering and Material Conference, Albuquerque, NM, 12-16 Jul. 1993
(Contract W-7405-eng-36)
(DE93-018348; LA-UR-93-2372; CONF-930703-17) Avail: CASI HC A02/MF A01

When evaluating a chemical synthesis process for a reaction that occurs on cryogenically cooled walls, it is sometimes necessary to reduce the wall temperatures to enhance the chemical process. To evaluate the chemical process of lower than atmospheric boiling of liquid nitrogen, we built a system and used it to reduce the temperature of the liquid nitrogen. The technique of lowering the liquid nitrogen temperature by reducing the pressure of the boil-off is established knowledge. This paper presents the engineering aspects of the system, design features, equipment requirements, methods of control, and results of the chemical synthesis. The heat input to the system was approximately 400 watts, which placed a relatively large demand on the pumping system. Our system is a scale-up of the small laboratory experiment, and it provides the information needed to design an effective system. The major problem encountered was the large quantity of liquid escaping the system during the processing, which placed a large gas load on the vacuum system. DOE

N94-18859# Stockholm Univ. (Sweden). Dept. of Meteorology.
ON THE USE OF SEMI-LAGRANGIAN METHODS FOR ACCURATE PREDICTIONS OF GRAVITY WAVES
Gerhard W. Erbes 3 Dec. 1992 44 p Prepared in cooperation with International Meteorological Inst., Stockholm, Sweden
(DM-61; ETN-93-94853) Avail: CASI HC A03/MF A01

A semi-Lagrangian method which accurately predicts the amplitudes and phase speeds of gravity waves when long timesteps are used is presented. The proposed method is applied to the one dimensional, linear shallow water equations and the one dimensional, nonlinear shallow water equations. When using a semi-Lagrangian method on systems of equations containing gravity wave motion it is necessary to focus on some fundamental issues regarding proper implementation. Illustrations of numerical experiments are shown together with conclusions. ESA

71 ACOUSTICS

Includes sound generation, transmission and attenuation.
For noise pollution see *45 Environmental Pollution.*

N94-17873 Lawrence Livermore National Lab., CA.
COMMENTS ON COMPUTATIONAL UNDERWATER ACOUSTICS
G. Hedstrom Apr. 1993 6 p Limited Reproducibility: More than 20% of this document may be affected by microfiche quality
(Contract W-7405-eng-48)
(DE93-013789; UCRL-ID-113953) Avail: CASI HC A02

Two fundamental facts control the choice of computational methods in underwater acoustics. One is that over most of the ocean the sound speed varies much more rapidly with depth than in the horizontal directions. The other is that upon going down from the surface, the sound speed usually decreases to a minimum and then increases from there to the bottom. These properties of the medium imply that the ocean often acts as a waveguide, with energy trapped in a depth-band about the sound-speed minimum. One consequence of these facts is that approximation by normal modes is valid over large regions of the ocean, particularly if correction is made for the slow variation of the modes caused by variation in bottom depth and horizontal variation in sound speed. In portions of the ocean where approximation by normal modes is not valid, we may still often use a paraxial approximation. Paraxial approximations may be used when the wave motion is primarily in a single direction, with slow variation of the signal in directions tangent to the wave front. They are often called 'parabolic' equations in ocean acoustics, but the term 'paraxial' is standard in other branches of physics, including optics and seismology. Finite-difference approximations are also sometimes used in underwater acoustics, but they are much more computationally intensive than normal modes or paraxial approximations. Finite differences are therefore ordinarily used only where these other methods are not valid, such as in shallow water with rapidly varying depth. One could also use finite elements in these instances, but for acoustics problems finite elements are a special class of finite-difference methods. We discuss finite differences only briefly in this report, because they are not generally used in long-range acoustics. DOE

N94-17934 Politecnico di Milano (Italy). Dipt. di Elettronica e Informazione.
ACTIVE CONTROL OF PERIODIC NOISE WITH TIME-VARYING FREQUENCY
Fabrizio Lorito and Marco Campi (Brescia Univ., Italy.) 1993 10 p Sponsored by Ministry of University and Scientific Research and Technolgy, Italy, and CNR
(Rept-93-012; ETN-93-94516) Avail: Politecnico di Milano, Piazza Leonardo da Vinci 32, 20133 Milan, Italy

The basic idea behind Active Noise Control (ANC) is that an acoustic noise field can be canceled by generating a suitable 'anti-noise' field. In most applications, the disturbance is characterized by significant periodic components, whose fundamental frequency omega(sub 0) is not necessarily constant. This happens for example in cars, where the main source of vibration and noise, the fire frequency, is subject to change. The control techniques available in the literature do not seem to be appropriate, since they are usually conceived for constant omega(sub 0) and, when the frequency is variable, the common procedure is simply to substitute omega(sub 0) with omega(t). A 'dead-beat' controller for sinusoidal disturbances with time varying measured frequency is proposed. A correct dynamic model for such a signal is worked out, and, grounded on such a model, the controller is designed and its performances are analyzed both theoretically and in simulation. ESA

N94-18664# Pennsylvania State Univ., University Park. Applied Research Lab.
ACOUSTIC INTENSITY MEASUREMENTS IN THE PRESENCE OF LOW MACH NUMBER FLOW

Toby McNeal and G. C. Lauchle Sep. 1993 110 p
(AD-A269995; ARL/PSU/TR-93-11) Avail: CASI HC A06/MF A02

Acoustic intensity is an important analysis tool since it provides wave propagation directionality along with absolute magnitude, and it can be measured in the near or far field of a source. Acoustic intensity measurements acquired in the presence of a mean flow are susceptible to errors due to the effects of the flow noise on the sensor. To determine if this error could be accurately quantified, intensity measurements were acquired, with the standard two microphone cross spectral technique, in a sound field that contained both mean flow and an independent random broadband noise source. The microphones were flush mounted, at several different separation distances, in the test section of a wind tunnel that provided the desired flow conditions, while a large speaker provided the independent random noise source. The error calculations were based on a technique that had already been derived theoretically and published, but had not been proven experimentally. The experiments performed validate that the error is indeed a bias error and that it can be accurately quantified. In addition, accurate quantification of the error is not limited to one-dimensional sound fields that contain only plane waves, and the method can be easily extended to two or three directions with complex wave propagation. DTIC

N94-18678 Naval Research Lab., Bay Saint Louis, MS.

PARALLEL AND VECTOR ADAPTATIONS OF THE UNDERWATER FINITE ELEMENT PARABOLIC EQUATION MODEL Final Report

Robert A. Zingarelli 18 Aug. 1993 10 p Limited Reproducibility: More than 20% of this document may be affected by microfiche quality
(DA Proj. RJ3-5-O-01)
(AD-A269990; NRL/FR/7181-93-9430) Avail: CASI HC A02

This report describes optimization techniques for several vector and parallel versions of FEPE, a finite element underwater parabolic equation model code. Algorithms are presented for solving linked tridiagonal systems of equations, when the chief computational bottleneck is in FEPE on parallel, massively parallel, and vector machines. Sample execution times for a standard benchmark problem are also given. A broadband version of FEPE, which is highly efficient on vector computers and can be combined with parallel algorithms for even higher performance is presented. DTIC

N94-18734# Department of the Navy, Washington, DC.

MONOLITHIC LOW NOISE PREAMPLIFIER FOR PIEZOELECTRIC SENSORS Patent Application

Timothy B. Straw, inventor (to Navy) 12 Apr. 1993 14 p
(AD-D015860; US-Patent-Appl-SN-045143) Avail: CASI HC A02/MF A01

This patent application discloses a preamplifier for a piezoelectric sensor requiring a high-impedance, low noise interface circuit. The preamplifier is a single, monolithic integrated circuit that can be mounted directly onto or inside a miniature sensor without degrading the sensor's performance. The preamplifier performs signal amplification with a full-differential amplifier that includes common-mode feedback. A pair of feedback capacitors together with the sensor capacitance control the voltage gain of the preamplifier over much of its useful operating range of 100 Hz to 100 kHz. The preamplifier circuit also the feedback resistors that discharge any accumulated DC voltage which might appear on the capacitors. Also the feedback resistors form a high pass filter which rejects low frequency background noise from the sensor. DTIC

N94-19083# Technische Univ., Delft (Netherlands). Faculty of Technical Mathematics and Informatics.

TRANSMISSION OF ACOUSTIC WAVES THROUGH STRONGLY HETEROGENEOUS, TWO-DIMENSIONAL VELOCITY MODELS

Gerard C. Herman 1993 48 p
(Rept-93-09; ETN-93-94636) Copyright Avail: CASI HC A03/MF A01

An explicit expression based on the second order Neumann expansion is derived for computing the gradual evolution of the pulse shape of a scalar seismic wave as it propagates through a medium, the slowness of which varies both horizontally and vertically. In particular, the case is considered where these variations take place on a scale, which is small with respect to the pulse width of the wavefield. The apparent absorption, time delay and dispersion caused by small scale multiple scattering effects are quantified and illustrated by a number of examples. The results indicate that the effects can be significant and should therefore be taken into account in seismic modeling and inversion. For monochromatic plane waves propagating in a particular direction, a medium containing small inhomogeneities can be replaced by a smoother apparent medium. The apparent medium accounts for both first and second order scattering effects, is frequency dependent and also depends on the direction of propagation. With the aid of these smoother apparent media, it can be analyzed how small scale inhomogeneities tend to decrease the temporal and spatial coherence of the wavefield and how they can be incorporated efficiently into forward and inverse wave propagation schemes. ESA

N94-19151# Los Alamos National Lab., NM.

LIQUID SOUND SPEEDS AT PRESSURE FROM THE OPTICAL ANALYZER TECHNIQUE

J. N. Fritz, C. E. Morris, R. S. Hixson, and R. G. McQueen 1993 5 p Presented at the 14th International Conference of the International Association for the Advancement of High Pressure Science and Technology, Colorado Springs, CO, 27 Jun. - 2 Jul. 1993
(Contract W-7405-eng-36)
(DE93-018362; LA-UR-93-2468; CONF-930676-14) Avail: CASI HC A01/MF A01

The optical analyzer technique proved to be a useful means of obtaining wave velocities at high pressures. Stepped wedges of the investigated material emit shock, and later, rarefaction waves into a transparent analyzer covering the material. The time interval between shock and rarefaction plotted versus wedge thickness gives a linear plot whose intercept fixes the target/driver thickness ratio for exact wave overtake, and thus gives a relation between the shock velocity and overtaking wave velocity at pressure. The slope of this line is intimately related to the wave velocity at pressure of the analyzer in front of the wedge. This aspect of the technique has not yet been exploited. The appropriate analysis and some data on bromoform (one of the analyzers used) are presented, and some possible applications of this technique are discussed. DOE

N94-19270# Lawrence Livermore National Lab., CA.

COMMENTS ON COMPUTATIONAL UNDERWATER ACOUSTICS

G. Hedstrom Jul. 1993 13 p Revised
(Contract W-7405-eng-48)
(DE93-019880; UCRL-ID-113953-Rev-1) Avail: CASI HC A03/MF A01

The authors discuss some of the considerations to take into account regarding the choice of methods for computational acoustics. They examine finite differences and finite elements, normal modes, and paraxial (parabolic) approximations. For each of these methods there is a class of problems for which it is well suited. Thus, finite differences and finite elements are best for short-range computations, normal modes are restricted to nearly-stratified media, and paraxial approximations work well when the signal is confined to the underwater sound channel. The authors discuss the reasons behind this state of affairs. They also point out some characteristics of these methods which are important for the numerical applications. It is concluded that the method of normal modes is numerically the most efficient computational method for underwater acoustics when it is a valid approximation. That is, one should use normal modes when the medium is nearly horizontally stratified. Paraxial approximations are very attractive for propagation in an underwater sound channel. They may be modified to incorporate interaction with a solid bottom if the wave speeds in the bottom are close to the speed of sound in water. Thus, an uncompacted solid bottom is not a great difficulty for paraxial approximations. The numerical methods which are most flexible with respect to wide ranges of material properties use finite differences or finite elements, but such methods are only feasible for computation over short distances. DOE

N94-19413# Ecole Centrale de Lyon (France). Lab. de Mecanique des Fluides et d'Acoustique.

NUMERICAL SIMULATION OF ACOUSTIC WAVES PROPAGATION IN TURBULENT MEDIA Ph.D. Thesis [SIMULATION NUMERIQUE DE LA PROPAGATION D'ONDES ACOUSTIQUES EN MILIEU TURBULENT]

Yves Hugon-Jeannin 1992 107 p In FRENCH Original contains color illustrations
(ECL-92-37; ETN-93-94594) Avail: CASI HC A06/MF A02

The propagation of acoustic waves in turbulent media has numerous applications in atmospheric and underwater acoustics. The theory of wave propagation in random media was developed by many authors following a statistical approach. Unfortunately, it is necessary to introduce a hypothesis concerning the correlation of the fluctuation index: the correlation is assumed to be microscopic along the direction of propagation. In order to avoid this assumption, a different approach in which statistical averaging is delayed until the final step is developed. The medium is assumed to have a slow evolution. Each realization is obtained by the superposition of discrete Fourier modes. The amplitude is obtained by the superposition of discrete Fourier modes. The amplitude of these modes is determined by the choice of the power spectrum. The deterministic propagation of acoustic waves is considered in either the geometric or the parabolic approximation through each realization of the modeled turbulent field. The results are then accumulated over an ensemble of realizations to permit the estimation of different statistical quantities. ESA

N94-19715 Max-Planck-Inst. fuer Stroemungsforschung, Goettingen (Germany).
EXAMINATIONS OF CONVERGING CYLINDRICALLY SYMMETRIC SECOND SOUND PROPAGATION IN He2 Thesis [EXPERIMENTE ZUR KONVERGENTEN ZYLINDERSYMMETRISCHEN SECOND-SOUND-AUSBREITUNG IN HE2]
Thomas Olszok May 1992 65 p In GERMAN Limited Reproducibility: More than 20% of this document may be affected by microfiche quality
(MPIS-9/1992; ETN-93-95099) Avail: CASI HC A04

Converging second sound propagation under the influence of the spatial and temporal evolution of the vortex line density is investigated. An axisymmetric flow channel was developed consisting of a circular cylinder (inner diameter 34 mm, outer diameter 40 mm, length 6 mm) whose inner surface is covered by a thin film heater. The ends of the cylinder were closed by two glassplates onto which a bolometer for the temperature measurements and an additional heater to produce (axial running) testpulses are installed. From the damping of these testpulses the temporal and spatial evolution of the vortex line density can be determinated with a time resolution of 300 microseconds. By means of this convergent geometry, it is possible to produce near the focus, spatially separated from the heater surface, high counterflow velocities and thus to observe the increase of the vortex line density in the absence of boundaries. In the case of subcritical heat flux, acoustic wave propagation is found, as predicted by analytical and numerical results. By variation of heat flux, pulse duration, and repetition rate, it is shown that in the case of supercritical heat flux the crucial process of vortex line production is the growth of the remanent vorticity under the influence of the counterflow. There are no hints for any additional vortex line production on the heater surface. It can be concluded from comparison with numerical results that the drift velocity of the vortex tangle must be assumed as equidirectional with the counterflow. ESA

N94-19723# Massachusetts Inst. of Tech., Cambridge.
FORWARD SCATTERING OF A PULSED CONTINUOUS WAVE SIGNAL THROUGH LAMINAR AND TURBULENT THERMAL PLUMES M.S. Thesis
Stephen G. Bowen Sep. 1993 74 p
(Contract N00123-89-G-0580)
(AD-A271210) Avail: CASI HC A04/MF A01

The results of an experiment examining the forward propagation of an acoustic signal through a buoyant plume are discussed. Two distinct testing sights were used. One made use of a small fresh water tank in NUWC to provide a controlled plume. The other used a larger salt water tank at Woods Hole Oceanographic Institute (WHOI) to create a more realistic oceanic model. Using the Born and Rytov approximations, an estimation of the effects of the laminar plume on the propagated signal are shown. As the plume moves from laminar to turbulent, the scintillation index and the Fourier transform of the magnitude square response provide insight into the nature of the transition. Finally, from the turbulent response a model for the scattering function is developed. DTIC

N94-19750 Naval Postgraduate School, Monterey, CA. Dept. of Electrical and Computer Engineering.
ACOUSTIC PROPAGATION MODELING USING MATLAB Interim Report
John P. Powers 1 Sep. 1993 71 p Limited Reproducibility: More than 20% of this document may be affected by microfiche quality
(AD-A270905; NPS-EC-93-014) Avail: CASI HC A04

This report presents a computational technique for the rapid, efficient calculation of fields from transient acoustic sources in linear, isotropic media. The source velocity is separable in space and time. The method uses a spatial impulse response method based on linear systems concepts to express the output in terms of the Green's function of propagation equation and the boundary conditions. The output is expressed as the inverse spatial transform of the product of the transform of the spatial excitation and a time-varying spatial filter that represents propagation. The calculation technique has been implemented in MATLAB and sample cases are presented for the circular and square piston, as well as a Gaussian- and Bessel-weighted spatial excitation. Code for the MATLAB implementation is provided. DTIC

72 ATOMIC AND MOLECULAR PHYSICS

Includes atomic structure, electron properties, and molecular spectra.

N94-17687# International Centre for Theoretical Physics, Trieste (Italy).
ON THE DIFFERENCE CAUSED BY CP VIOLATION IN THE ENERGY SPECTRA OF PIONS IN K(SUP (+-))(YIELDS)(PI)(+-)(PI)(+-)(PI)-+ DECAYS
E. P. Shabalin Mar. 1993 8 p
(DE93-624828; IC-93/58) Avail: CASI HC A02/MF A01 (US Sales Only)

A difference of the slope parameters g(sup +) and g(sup -) describing the energy distributions of odd pions in K(sup (+-)) yields pi(+-)pi(+-)(pi)-+ decays is calculated in the p(sup 4)-approximation of Chiral Theory. The result is (g(sup +) - g(sup -))/(g(sup +) + g(sup -)) = (-1.9(+-)0.8)10(exp -2)s(sub 2)s(sub 3)sin(delta), where s(sub 2), s(sub 3) and delta are the parameters of the Kobayashi-Maskawa matrix. DOE

N94-17738# Edgerton, Germeshausen and Grier, Inc., Idaho Falls, ID.
THE INTENSE SLOW POSITRON SOURCE CONCEPT: A THEORETICAL PERSPECTIVE ON A PROPOSED INEL FACILITY
Henry Makowitz, James D. Abrashoff, William H. Landman, Richard K. Albano, Toshiki Tajima (Texas Univ., Austin.), and James Daniel Larson (Larson, James Daniel, Independence, MO.) 1992 30 p Presented at the 5th International Workshop on Slow-Positron Beam Techniques for Solids and Surfaces, Jackson, WY, 6-10 Aug. 1992
(Contract DE-AC07-76ID-01570)
(DE93-013675; EGG-M-92397; CONF-920829-3) Avail: CASI HC A03/MF A01

An analysis has been performed of the INEL Intense Slow Positron Source (ISPS) concept. The results of the theoretical study are encouraging. A full-scale device with a monoenergetic 5 KeV positron beam of greater than or equal to 10(exp 12) e(+)/s on a less than or equal to 0.03 cm diameter target appears feasible and can be obtained within the existing infrastructure of INEL reactor facilities. A 30.0 cm diameter, large area source dish, moderated at first with thin crystalline W films and later by solid Ne, is proposed as the initial device in order to explore problems with a facility scale system. A demonstration scale beam at greater than or equal to 10(exp 10) slow e(+)/s is proposed using a Co-58 source plated on a 6 cm diameter source dish insert, placed in a 30 cm adapter. DOE

N94-17775# University of Western Michigan, Kalamazoo.
CORRELATED CHARGE-CHANGING ION-ATOM COLLISIONS
J. A. Tanis Feb. 1993 35 p
(Contract DE-FG02-87ER-13778)
(DE93-018717; DOE/ER-13778/6) Avail: CASI HC A03/MF A01

This report summarizes the progress and accomplishments in accelerator atomic physics research supported by DOE grant DE-FG02-87ER13778 from February 16, 1990 through February 15, 1993. This work involves the experimental investigation of atomic interactions in collisions of charged projectiles with neutral targets or electrons, with particular emphasis on two-electron interactions and electron-correlation effects. The processes studied are of interest both from fundamental and applied points of view. In the latter case, results are obtained which are relevant to the understanding of laboratory and astrophysical plasmas, highly-excited (Rydberg) and continuum states of atoms and ions, atomic structure effects, the interaction of ions with surfaces, and the development of heavy-ion storage-rings. The results obtained have provided the basis for several M.A. thesis projects at Western Michigan and several Ph.D. dissertation projects are currently underway. Summaries of work completed and work in progress are given in Section 2. This research has resulted in 26 papers (in print and in press), 12 invited presentations at national and international meetings, and 28 contributed presentations as detailed in Section 3. DOE

N94-17776# Georgia State Univ., Atlanta. Dept. of Physics and Astronomy.
HEAVY ION NUCLEAR PHYSICS RESEARCH
X. T. Liu, G. A. Petitt, and Ziyang Zhang 1992 16 p
(Contract DE-FG05-84ER-40162)
(DE93-018862; DOE/ER-40162/T6) Avail: CASI HC A03/MF A01

We have continued working on essentially the same projects during the period 1991-92 as reported on in our previous progress report. That is, R&D work on a dimuon detector for RHIC and work with the group at LANL on neutron induced fission measurements using the white neutron source at LAMPF. Our work has included participation in the RD-10 experiment at the AGS to study calorimeter/absorber optimization for a RHIC experiment. We have actively participated in the setup of the apparatus, the data-taking, and the subsequent data analysis. We have used the Vax computer system in our department and the eight-processor Silicon Graphics system in the GSU computer center for most of the data analysis work. We have also continued our work on Monte Carlo simulations of various configurations of absorber/calorimeters for detection of electrons and muons in RHIC experiments. We have made increasing use of the Silicon Graphics computer for our work. Each processor has approximately the same power as a Decstation 5000 and we usually have essentially exclusive simultaneous use of three of the processors. We have installed GEANT 315 and PAW on this system. Since our Vaxstation was purchased before DECWINDOWS was a standard part of the Vax software, we have been unable to use the Silicon Graphics computer for doing graphics with PAW and GEANT. We are attempting to solve this problem by installing X-Windows software on our 386SX system which is connected to the campus network. Our work at Los Alamos has consisted of participation in the LAMPF run during the summer of 1991 including constructing and setting up two new neutron detectors for the experiment. These projects are discussed in further detail in this paper. DOE

N94-17797# Lawrence Livermore National Lab., CA.
COMPARISON OF THE MODELING SOLUTIONS WITH THE HYDROGEN DISCHARGE DATA
J. R. Hiskes Nov. 1992 10 p
(Contract W-7405-eng-48)
(DE93-015115; UCRL-JC-112225) Avail: CASI HC A02/MF A01

With the availability of experimental values for H(sub 2) vibrational population distributions up to v=8 and measured distributions up to v=5 with simultaneous measurements of the H(sup (minus)) concentration, it has become possible to test some features of the full-spectrum model of H(sup (minus)) generation. The application of the code developed by Gorse et al. to these discharges by the groups at both Bari and at the Ecole Polytechnique has extended the vibrational distribution calculation to include also the H(sup (minus)) concentration. Comparing the vibrational population calculated by these two groups at the higher levels, where the onset of H(sup (minus)) production occurs, one finds populations for the (upsilon)=5 level that are a factor of eight to ten larger than the experimental values. Since these workers have omitted the role of the H(sub 3)(sup +) ions known to be present in the discharge, the inclusion of the appropriate S-V process should increase the population discrepancies another factor of two or three. This excess population poses something of a dilemma: Since the Bari code simultaneously reproduces the observed H(sup (minus)) concentration but overestimates the vibrational population by a large factor, the standard model of vibrational excitation followed by dissociative attachment is open to question. If measured rather than calculated distributions were used in the H(sup (minus)) calculation, the calculated H(sup (minus)) concentration would presumably be an order-of-magnitude smaller than the observed value. The measured population distributions taken against the background of the modelling solutions would seem to imply alternate sources of H(sup (minus)) production other than dissociative attachment. To examine this problem, we have generated new modelling solutions for comparison with the data of Eenshuistra et al. DOE

N94-17850# Lawrence Livermore National Lab., CA.
SPIN-INTEGRATED AND SPIN-DEPENDENT PHOTOELECTRON DIFFRACTION
S. Y. Tong (Wisconsin Univ., Milwaukee.) Apr. 1993 6 p
(Contract W-7405-eng-48)
(DE93-016546; UCRL-CR-114138) Avail: CASI HC A02/MF A01

This report is the result of a program to develop a spin-polarized multiple scattering algorithm. The author calculates the spin dependent photoelectron diffraction intensities, which allow determination of surface structures in a more sensitive way than conventional photoemission spectra calculations. The code allows the study of magnetic properties of surfaces, such as layer-dependent magnetic moments, surface magnetic anisotropy, and surface exchange and spin-orbit interactions. For scattered electrons the spin-polarizations effects are mainly caused by exchange processes (e.g. ferromagnetic materials) or spin-orbit interactions (heavy atoms) or both (rare earth elements). This program takes both of these effects into account, by starting with the fully relativistic calculation of the single scattering matrix. DOE

N94-17933 Politecnico di Milano (Italy). Dipt. di Elettronica.
ELECTRON MOBILITY IN HIGH RESISTIVITY SILICON
Andrea Castoldi 1993 28 p In ITALIAN
(Rept-93-007; ETN-93-94514) Avail: Politecnico di Milano, Piazza Leonardo da Vinci 32, 20133 Milan, Italy

A method of measuring the properties of electron mobility in high resistivity silicon is presented. The method is based on an original transport scheme formerly applied successfully to a class of radiation indicators, semiconductor derived cameras. The theoretical transport model, governed by Boltzmann equation, is given. ESA

N94-17951 Weizmann Inst. of Science, Rehovoth (Israel).
NEUTRINO MASSES IN SUPERSTRING DERIVED STANDARD-LIKE MODELS
A. E. Faraggi and Edi Haylyo Jan. 1993 16 p Limited Reproducibility: More than 20% of this document may be affected by microfiche quality
(DE93-624802; WIS-PH-93-4) Avail: CASI HC A03 (US Sales Only)

We propose a new scenario in class of superstring derived standard-like models that explains the suppression of the left-handed neutrino masses. Due to nonrenormalizable terms and the breaking of the U(1)(sub Z') symmetry a generalized see-saw mechanism take place. Contrary to the traditional see-saw mechanism in Grand Unified Theories, the see-saw scale and the right-handed neutrino mass scale are suppressed relative to the U(1)(sub Z') breaking scale. DOE

N94-17972# Rome Univ. (Italy). Dipt. di Fisica.
BEAUTY WITHOUT CHARM IN B-MESON DECAYS
G. Martinelli 4 Apr. 1990 8 p
(Preprint-732; ETN-93-94370) Avail: CASI HC A02/MF A01

Experiments evidencing weak decays of beauty mesons without production of particles carrying the charm quantum number are discussed. The establishment of charmless semileptonic decays of B mesons is reported. The value of R = (V(sub ub))/(V(sub cb)) is found to be approximately 0.1--(the precise value depending on the theoretical model used in the analysis)--and definitively different from zero. A further improvement is expected and possibly a confirmation of the present determination of R from the observation of exclusive charmless semileptonic B decays such as B to rho(l)nu or B to pi(l)nu. ESA

N94-17984# Brookhaven National Lab., Upton, NY.
MESON PRODUCTION IN RELATIVISTIC HEAVY-ION COLLISIONS AT AGS ENERGIES
S. G. Steadman 1993 8 p Presented at the 9th Winter Workshop on Nuclear Dynamics, Key West, FL, 30 Jan. - 6 Feb. 1993
(Contract DE-AC02-76CH-00016)
(DE93-016871; BNL-49091; CONF-930197-5) Avail: CASI HC A02/MF A01

Single particle inclusive spectra are presented for pion and kaon production in Si+Au reactions at an incident momentum of 14.6 A GeV/c and Au+Au reactions at an incident momentum of 11.6 A GeV/c. A simple geometric scaling of the pion production for central collisions as A(sub proj)(sup 1/3) and A(sub targ)(sup 2/3) results from the observed production of about one pion per participant. Kaon yields are shown to be proportional to the number of excited participants and consistent with RQMD and ARC calculations. DOE

N94-18085# Brookhaven National Lab., Upton, NY.
FEMTOSECOND FOURIER-TRANSFORM SPECTROSCOPY OF LOW-FREQUENCY INTERMOLECULAR MOTIONS IN WEAKLY INTERACTING LIQUIDS
E. W. Castner, Jr., Y. J. Chang, J. S. Melinger, and D. McMorrow (Naval Research Lab., Washington, DC.) 1993 8 p Presented at the 9th International Conference on Luminescence and Optical Spectroscopy of Condensed Matter, Storrs, CT, 9-13 Aug. 1993
(Contract DE-AC02-76CH-00016)
(DE93-017312; BNL-49195; CONF-930831-1) Avail: CASI HC A02/MF A01

Recent work on the subject of solvation dynamics has concentrated on understanding the ultrafast dynamics of intermolecular interactions in strongly interacting, polar, and hydrogen-bonding solvents. In general, investigations into the effects of solvation dynamics on chemical reactions have concentrated on the highly polar liquids because it is in these solvents that the largest spectroscopic changes with solvent relaxation are observed. In these very polar liquids, however, the intermolecular dynamics are very complex, consisting of contributions from re-orientational diffusion, inertially limited rotations, intermolecular vibrations involving both reorientational (librational) and translational degrees of freedom, and interaction-induced collisional effects. The role of collisional interaction-induced effects in shaping the intermolecular dynamics of molecular liquids has been a subject of considerable discussion. Molecular dynamics simulations have suggested that collisional effects can have a significant role in shaping the femtosecond dynamics and nonlinear-optical properties of molecular liquids. However, for anisotropic molecules, it is difficult to separate experimentally the collisional effects from other phenomena. In this paper the authors examine the intermolecular dynamics of the weakly interacting liquid carbon tetrachloride (CCl4). Because carbon tetrachloride is a spherical top molecule (belonging to the T(sub d) point group), its intermolecular light-scattering spectrum is purely interaction-induced. By studying this purely collision-induced feature in CCl4, the authors hope to gain insight on the lowest-frequency intermolecular vibrational behavior of more complex systems. DOE

N94-18104# Kent State Univ., OH.
HEAVY-ION COLLISIONS AND THE NUCLEAR EQUATION OF STATE
D. Keane 1993 13 p
(Contract DE-FG02-89ER-40531)
(DE93-019263; DOE/ER-40531/4) Avail: CASI HC A03/MF A01

The overall goal of this project is to study nucleus-nucleus collisions experimentally at intermediate and relativistic energies, with emphasis on measurement and interpretation of correlation effects that provide insight into the nuclear phase diagram and the nuclear equation of state. During the course of this reporting period, the PI returned to Kent from a 15-month leave at Lawrence Berkeley Lab, which had been devoted 100% to work on this research project. The EOS Time Projection Chamber at LBL's Bevalac accelerator has continued to be the major focus of research for all of the supported personnel; about a year ago, this detector successfully took data in production mode for the first time, and accumulated in excess of 1000 hours of beam time before the termination of the Bevalac in February 1993. Reduction and analysis of these data is currently our first priority. Effort has also been devoted to the STAR detector at the Relativistic Heavy Ion Collider, in the form of contributions to the Conceptual Design Report, work on HV control hardware and software for use with the STAR Time Projection Chamber, and tracking software development. DOE

N94-18152 Joint Inst. for Nuclear Research, Dubna (USSR). Lab. of Theoretical Physics.
TOROIDAL SOLENOIDS IN THE ELECTROMAGNETIC FIELD AND AHARONOV-CASHER EFFECT
G. N. Afanasev 1991 31 p Limited Reproducibility: More than 20% of this document may be affected by microfiche quality
(DE93-629861; JINR-E-2-91-544) Avail: CASI HC A03 (US Sales Only)

The current toroidal configurations are found which generate gauge nonequivalent vector potentials and correspond to the same quantum scattering of charged particles. The equations for the motion of toroidal moment in the magnetic field are obtained. It is proved the existence of Aharonov-Casher effect for the toroidal solenoids. The relating experiments are proposed. DOE

N94-18158 National Inst. for Fusion Science, Nagoya (Japan).
ELECTRON STRIPPING CROSS SECTIONS FOR LIGHT IMPURITY IONS IN COLLIDING WITH ATOMIC HYDROGENS RELEVANT TO FUSION RESEARCH
H. Tawara Apr. 1992 30 p Limited Reproducibility: More than 20% of this document may be affected by microfiche quality
(DE93-788476; NIFS-Data-17) Avail: CASI HC A03

Electron stripping--ionization--cross sections for impure carbon ions with various charge states in collisions with atomic hydrogens have been surveyed. It has been found that these data are relatively limited both in collision energy and charge state and, in particular, those necessary for high energy neutral beam injection (NBI) heating in fusion plasma research are scarce. Some relevant cross sections for carbon ions, C(sup q+) (q = 0-5) have been estimated, based upon the existing data, empirical behavior, and electron impact ionization data. DOE

N94-18165# Notre Dame Univ., IN.
RESEARCH AT THE NOTRE DAME RADIATION LABORATORY
2 Aug. 1993 33 p
(Contract DE-AC02-76ER-00038)
(DE93-018716; DOE/ER-00038/3626; NDRL-3626; Q-144) Avail: CASI HC A03/MF A01

Forty-four abstracts are presented of research projects in radiation chemistry, photochemistry, and related topics. DOE

N94-18179# Illinois Univ., Urbana.
NUMERICAL METHODS FOR MOLECULAR DYNAMICS
1993 19 p
(Contract DE-FG02-91ER-25099)
(DE93-018321; DOE/ER-25099/2) Avail: CASI HC A03/MF A01

The objective is to find numerical algorithms suitable for large parallel computers that can much more efficiently model the dynamics of macromolecules such as proteins, DNA, and lipids. Emphasis is on the use of integration schemes, notably symplectic schemes, that can use large time steps to produce qualitatively correct simulations for long-time integrations. The goal is to obtain the desired information with the least computational effort, and the methodology is to use mathematical analysis and computational experiments on model problems. The techniques developed are to be tested on realistic molecular models as part of a different, complementary research project involving software development. Among the techniques to be considered, the better known ones are multiple time steps, constraint dynamics, and fast Coulomb solvers. DOE

N94-18199 Gosudarstvennyi Komitet po Ispolzovaniyu Atomnoi Energii, Serpukhov (USSR).
FOUR-FERMION INTERACTIONS
K. G. Klimenko 1992 20 p Limited Reproducibility: More than 20% of this document may be affected by microfiche quality
(DE93-629905; IFVE-OTF-91-181; IHEP-OTF-91-181) Avail: CASI HC A03 (US Sales Only)

The (2+1)-dimensional theory with a four-fermion interaction of a general type was investigated. The conditions obtained specify the possibility for the dynamic generation of the Chern-Simons (CS) term. It was shown that a spontaneous P-parity violation does not always result in the generation of CS terms; there is vacuum in which both the chiral invariance and P-parity are violated; and models with fermion vector-vector couplings are a particular case of the given theory. DOE

N94-18234# Brookhaven National Lab., Upton, NY.
MEASURING THE SEA QUARK POLARIZATION
Y. Makdisi 1993 7 p Presented at the Future Directions in Particle and Nuclear Physics at Multi-GeV Hadron Beam Facilities, Upton, NY, 4-6 Mar. 1993
(Contract DE-AC02-76CH-00016)
(DE93-015792; BNL-49015; CONF-930389-20) Avail: CASI HC A02/MF A01

Spin is a fundamental degree of freedom and measuring the spin structure functions of the nucleon should be a basic endeavor for hadron physics.

Polarization experiments have been the domain of fixed target experiments. Over the years large transverse asymmetries have been observed where the prevailing QCD theories predicted little or no asymmetries, and conversely the latest deep inelastic scattering experiments of polarized leptons from polarized targets point to the possibility that little of the nucleon spin is carried by the valence quarks. The possibility of colliding high luminosity polarized proton beams in the Brookhaven Relativistic Heavy Ion Collider (RHIC) provides a great opportunity to extend these studies and systematically probe the spin dependent parton distributions specially to those reactions that are inaccessible to current experiments. This presentation focuses on the measurement of sea quark and possibly the strange quark polarization utilizing the approved RHIC detectors. DOE

N94-18269# Los Alamos National Lab., NM.
NEUTRINO MASS Status Report
R. G. H. Robertson 1993 20 p Presented at the 14th International Workshop on Weak Interactions and Neutrinos, Seoul, Korea, 19-24 Jul. 1993
(Contract W-7405-eng-36)
(DE93-018467; LA-UR-93-2659; CONF-9307114-1) Avail: CASI HC A03/MF A01

Experimental approaches to neutrino mass include kinematic mass measurements, neutrino oscillation searches at reactors and accelerators, solar neutrinos, atmospheric neutrinos, and single and double beta decay. The solar neutrino results yield fairly strong and consistent indications that neutrino oscillations are occurring. Other evidence for new physics is less consistent and convincing. DOE

N94-18493# Oak Ridge National Lab., TN.
DETECTION OF SINGLE MOLECULES IN MICROSPHERES
M. D. Barnes, W. B. Whitten, J. M. Ramsey, K. C. Ng (California State Univ., Fresno.), and S. Arnold (Polytechnic Univ., Brooklyn, NY.) 1993 8 p Presented at the OE/LASE 1993: International Society for Optical Engineering (SPIE) Conference, Los Angeles, CA, 16-23 Jan. 1993
(Contract DE-AC05-84OR-21400)
(DE93-017776; CONF-930159-53) Avail: CASI HC A02/MF A01

We have investigated the use of micron-sized liquid droplets as sample medium to detect single fluorescent molecules in solution. The use of microdroplets (5-15 micron diameter) offers several powerful advantages over single-molecule detection schemes involving measurements on bulk liquids where the probe volume is defined by the laser beam. In addition, cavity-quantum electrodynamical (QED) effects have been observed which influence both spontaneous emission rates and fluorescence yields of dye molecules in these microspheres. DOE

N94-18526# Phillips Lab., Hanscom AFB, MA.
TEMPERATURE, KINETIC ENERGY, AND ROTATIONAL TEMPERATURE DEPENDENCES FOR THE REACTIONS OF Ar(+)(2)P3/2 WITH O2 AND CO
I. Dotan and A. A. Viggiano 25 Jun. 1993 6 p Repr. from Chemical Physics Letters, v. 209, no. 1/2, 25 Jun. 1993 p 67-71
(AF Proj. 2303)
(AD-A268974; AD-E201577; PL-TR-93-2163) Avail: CASI HC A02/MF A01

Rate constants for the charge transfer reactions of Ar(+)(2P sub 3/2) with O2 and CO have been measured as a function of average center-of-mass kinetic energy (KE(sub cm)) at three temperatures: 93, 300, and 543 K. The rate constants for both reactions were to be slow at room temperature and to decrease with increasing kinetic energy or temperature in good agreement with previous data. No temperature dependence of the rate constants was found at any given (KE(sub cm)) for both reactions, indicating that neither O2 nor CO rotational excitation has much effect on the overall reactivity. The data also indicate that O2 vibrational excitation does not increase the rate constant to the collisional value. DTIC

N94-18533# Northwestern Univ., Evanston, IL. Dept. of Chemistry.
VIBRATIONAL DYNAMICS IN PHOTOINDUCED ELECTRON TRANSFER
K. G. Spears Sep. 1993 3 p
(Contract DE-FG02-91ER-14228)
(DE93-040874; DOE/ER-14228/2) Avail: CASI HC A01/MF A01

The objective is to perform a new type of measurement for optically excited electron transfer processes that can provide unique experimental insight into the molecular mechanism of electron transfer. Measurements of optically excited electron transfer are done with picosecond infrared (IR) absorption spectroscopy to monitor the vibrational motions of the molecules immediately after electron transfer. Theory and experiment suggest that molecular vibrations and distortions are important controlling elements for electron transfer, and direct information has yet to be obtained on these elements of electron transfer mechanisms. The second period of funding has been dedicated to finishing technique development and performing studies of electron transfer in ion pair systems to identify if vibrational dependent electron transfer rates are present in this system. We have succeeded in measuring, for the first time, electron transfer rates as a function of vibrational state in an ion pair complex in solution. In a different area of electron transfer research we have proposed a new mechanism of solvent gated electron transfer. DOE

N94-18534# Boston Univ., MA. Dept. of Physics.
RESEARCH IN PARTICLE PHYSICS
Aug. 1993 150 p
(Contract DE-FG02-91ER-40676)
(DE93-040875; DOE/ER-40676/T1) Avail: CASI HC A07/MF A02

This proposal presents the research accomplishments and ongoing activities of Boston University researchers in high energy physics. Some changes have been made in the structure of the program from the previous arrangement of tasks. Task B, Accelerator Design Physics, is being submitted as a separate proposal for an independent grant; this will be consistent with the nature of the research and the source of funding. We are active in seven principal areas which will be discussed in this report: Colliding Beams - physics of e(sup +)e(sup (minus)) and (bar p)p collisions; MACRO Experiment - search for magnetic monopoles and study of cosmic rays; Proton Decay - search for nucleon instability and study of neutrino interactions; Particle Theory - theoretical high energy particle physics, including two Outstanding Junior Investigator awards; Muon G-2 - measurement of the anomalous magnetic moment of the muon; SSCintcal - calorimetry for the GEM Experiment; and Muon detectors for the GEM Experiment. DOE

N94-18766 Illinois Univ., Urbana. Dept. of Chemistry.
IONIC AND MOLECULAR ENVIRONMENTS IN HETEROGENEOUS ELECTROCATALYSIS: STUDIES BY RADIOACTIVE LABELING AND LEED/AUGER SPECTROSCOPY Final Report, 1 May 1989 - 30 Apr. 1993
Andrzej Wieckowski Jul. 1993 45 p Limited Reproducibility: More than 20% of this document may be affected by microfiche quality
(Grant AF-AFOSR-0368-89)
(AD-A268850; AFOSR-93-0656TR) Avail: CASI HC A03

Adsorption, catalytic activity, and metal deposition at the metal/solution interface have been studied in a coordinated fashion by radiochemistry, ultra-high vacuum spectroscopies of surface science, and electrochemistry. The metal part of the interface was usually a single-crystal of platinum, rhodium, or gold, or an ultra-thin metallic film of either cadmium, copper, or silver obtained via underpotential deposition processes. The adsorbates predominantly included bisulfate, perchlorate, phosphate, acetic acid, and urea. The integrative feature of the adsorbates was their capacity of a reversible adsorption on the platinum electrode. The molecule with which the catalytic rates have been measured was methanol in perchlorate, bisulfate, and phosphate solutions. These studies have focused on effects of anions on the catalytic oxidation of methanol on platinum single crystal electrodes, surface chemistry of the studied adsorbates on the clean and admetal covered electrodes, surface studies of the solid/liquid CO (as the most probable methanol chemisorption product), and phase transitions of urea induced by lateral adsorbate-adsorbate interactions. Two methods for in situ and ex situ electrode characterization, namely the radioactive labeling and the ultra-high vacuum-electrochemistry, have been used and advancements in their performance, or new areas of applications, have been reported. DTIC

N94-18783 Memphis State Univ., TN. Dept. of Chemistry.
NONLINEAR OPTICAL PROPERTIES OF MOLECULES Final Report, Nov. 1989 - Jun. 1993
Henry A. Kurtz 31 Aug. 1993 8 p Limited Reproducibility: More than 20% of this document may be affected by microfiche quality

(Grant AF-AFOSR-0010-90)
(AD-A270199; AFOSR-90-0010TR) Avail: CASI HC A02

Final summary report on calculations of nonlinear optical properties at Memphis State University. Finite-field methods for static values and TDHF methods for frequency dependent quantities are implemented. Results are summarized for polyene oligomers with emphasis on their behavior as the number of subunits is increased. The usefulness of a relationship for the calculation of one type of hyperpolarizability in terms of another is demonstrated by example for the CH2O molecule. Other results on intermolecular effects on hyperpolarizabilities and vibrational contributions are also discussed. DTIC

N94-18784 Rochester Univ., NY.
MOLECULAR NONLINEAR OPTICAL SUSCEPTIBILITIES IN CONDENSED PHASES Final Report, 1 Nov. 1989 - 28 Feb. 1993
Shaul Mukamel 16 Sep. 1993 12 p Limited Reproducibility: More than 20% of this document may be affected by microfiche quality
(Grant AF-AFOSR-0054-90)
(AD-A270200; AFOSR-93-0708TR) Avail: CASI HC A03

A microscopic theory for the nonlinear optical response and susceptibilities of molecular materials with localized and delocalized electronic states (e.g. molecular assemblies, conjugated polymers, aggregates, and monolayers) was developed. The theory, which properly accounts for many-body effects, is based on the derivation of coupled reduced equations of motion for the material variables, which determine the optical response. The present formulation maps the calculation of optical nonlinearities onto solving the dynamics of coupled nonlinear oscillators and overcomes the difficulties associated with the local-field approximation. An operational definition of the nonlinear coherence-size N(c), which controls the cooperative enhancement of the optical response, is developed. A real-space representation of the optical response of conjugated polyenes is developed by using the Wannier representation to derive equations of motion for coupled two-site oscillators representing correlated electron-hole pairs. The resulting elementary excitations are shown to be intermediate between the molecular (Frankel) and the semiconductor (Wannier) excitons, and clearly resemble charge transfer excitons. DTIC

N94-18787 California Univ., Berkeley. Dept. of Chemistry.
THE FOURTEENTH SYMPOSIUM ON MOLECULAR BEAMS Final Report, 1 Apr. 1992 - 31 Mar. 1993
Yuan T. Lee 9 Aug. 1993 493 p Symposium held in Pacific Grove, CA, 7-12 Jun. 1992 Limited Reproducibility: More than 20% of this document may be affected by microfiche quality
(Contract F49620-92-J-0170)
(AD-A268721; AFOSR-93-0630TR) Avail: Issuing Activity (Defense Technical Information Center (DTIC))

The symposium was held on June 7-12, 1992 in Pacific Grove, California. It brought together scientists who work with isolated molecules to share conceptual and practical advances involved with the study of matter in a rarefied, collimated and isolated state represented by the beam. There were 26 invited talks, 25 submitted oral presentations and 78 poster papers in nine sessions on a broad range of topics. The invited talks gave general reviews and reported on recent advances on: the dissociation and predissociation dynamics of large molecular cluster ions and open shell clusters, low energy crossed beam ion-molecule reactions, the hydrogen exchange reaction, new method for manipulating laser cooled atoms, application of laser cooling to the time and frequency domain, molecular probes of quantum clusters, size dependence of elemental clusters, bouncing gases off liquid surfaces, high resolution UV and IR spectroscopy of molecular complexes, reaction dynamics beyond the Born-Oppenheimer approximation, the chemistry of hydrogen in bulk metal, and molecular dissociation on surfaces. The symposium successfully brought together chemists and physicists for a fruitful cross-fertilization of ideas and dissemination of results. The goal of facilitating students and young scientists to attend was fulfilled. There were 64 students and postdoctoral fellows among the 164 attendees. DTIC

N94-18814# California Univ., Santa Barbara. Dept. of Chemistry.
PHOTODISSOCIATION DYNAMICS OF CLUSTER IONS Final Report, 15 Nov. 1991 - 15 Nov. 1992
Michael T. Bowers 6 Aug. 1993 4 p
(Grant AF-AFOSR-0021-92)
(AD-A270296; AFOSR-93-0704TR) Avail: CASI HC A01/MF A01

Progress was made in the following two areas: (1) Photodissociation Dynamics of Small Cluster Ions (work was completed on one system and preliminary work done on several others); and (2) Generation, Structure, and Reactivity of Metallic and Semiconductor Clusters (two papers published and a large amount of preliminary work accomplished). DTIC

N94-18824# Washington Univ., Seattle.
INSTITUTE FOR NUCLEAR THEORY
W. Haxton, G. Bertsch, and E. M. Henley 1993 155 p
(Contract DE-FG06-90ER-40561)
(DE93-017369; DOE/ER-40561/110-INT93) Avail: CASI HC A08/MF A02

This report briefly discusses the following programs of the Institute for Nuclear Theory: fundamental interactions in nuclei; strangeness in hadrons and nuclei; microscopic nuclear structure theory; nuclear physics in atoms and molecules; phenomenology and lattice QCD; and large amplitude collective motion. DOE

N94-18825# Argonne National Lab., IL.
INVERSE NEUTRINOLESS DOUBLE (BETA)-DECAY AT THE NLC?
T. G. Rizzo May 1993 5 p Presented at the International Workshop on Physics and Instrumentation at Future Linear Colliders, Kona, HI, 26-30 Apr. 1993
(Contract W-31-109-eng-38)
(DE93-017397; ANL-HEP-CP-93-24; CONF-930449-1) Avail: CASI HC A01/MF A01

The NLC may allow us to search for the 'inverse' process to neutrinoless double-(beta) decay, e(sup (minus))e(sup (minus)) yields W(sup (minus))W(sup (minus)), which probes the existence of Majorana masses for neutrinos. Expectations for the observation of this process in both the Standard Model and its extension, the Left-Right Symmetric Model, are examined. DOE

N94-18826# Argonne National Lab., IL.
UNITARY (PI)(PI)N MODEL OF N* EXCITATIONS IN (PI)N AND (GAMMA)N REACTIONS
T. S. H. Lee 1993 6 p Presented at the 6th International Workshop on Perspectives in Intermediate Energy Nuclear Physics, Trieste, Italy, 4-7 May 1993
(Contract W-31-109-eng-38)
(DE93-017422; ANL/PHY/CP-80056; CONF-9305241-2) Avail: CASI HC A02/MF A01

A unitary model is presented to describe N* excitations in (pi)N and (gamma)N reactions. Preliminary results of (pi)N scattering in P(sub 11) and P(sub 33) channels are compared with the data. DOE

N94-18837*# Minnesota Univ., Minneapolis.
THE QUANTUM DYNAMICS OF ELECTRONICALLY NONADIABATIC CHEMICAL REACTIONS Final Technical Report
Donald G. Truhlar 9 Apr. 1993 4 p
(Contract NCC2-526)
(NASA-CR-194309; NAS 1.26:194309) Avail: CASI HC A01/MF A01

Considerable progress was achieved on the quantum mechanical treatment of electronically nonadiabatic collisions involving energy transfer and chemical reaction in the collision of an electronically excited atom with a molecule. In the first step, a new diabatic representation for the coupled potential energy surfaces was created. A two-state diabatic representation was developed which was designed to realistically reproduce the two lowest adiabatic states of the valence bond model and also to have the following three desirable features: (1) it is more economical to evaluate; (2) it is more portable; and (3) all spline fits are replaced by analytic functions. The new representation consists of a set of two coupled diabatic potential energy surfaces plus a coupling surface. It is suitable for dynamics calculations on both the electronic quenching and reaction processes in collisions of Na(3p2p) with H2. The new two-state representation was obtained by a three-step process from a modified eight-state diatomics-in-molecules (DIM) representation of Blais. The second step required the development of new dynamical methods. A formalism was developed for treating reactions with very general basis functions including electronically excited states. Our formalism is based on the generalized Newton, scattered wave, and outgoing wave variational principles that were used previously for reactive collisions on a single potential energy surface, and it incorporates three new features: (1) the basis functions include electronic degrees of freedom, as required to treat reactions involving electronic excitation and two or more coupled potential energy surfaces; (2) the primitive electronic basis is assumed to be diabatic, and it is not assumed that it diagonalizes the electronic Hamiltonian even asymptotically; and (3) contracted basis functions for vibrational-rotational-orbital degrees of freedom are included in a very general way, similar to previous prescriptions for locally adiabatic functions in various quantum scattering algorithms. Derived from text

N94-18847# Stockholm Univ. (Sweden). Dept. of Physics.

THE A((2)PI(SUB u))-X((2)PI(SUB g)) SYSTEM OF Br2(+) STUDIED BY VELOCITY MODULATION SPECTROSCOPY

M. Zackrisson Apr. 1993 21 p
(USIP-93-04; ETN-93-94852) Avail: CASI HC A03/MF A01

Observations of 27 bands of the A((2)pi sub u) - X((2)pi sub g) transition recorded in high resolution using the velocity modulation technique are presented. A vibrational and rotational analysis cosrresponding to 79 and 81 mixed isotopic species of Br2(+) and improved molecular constants of the upper and lower states was performed. The results show that the observed bands belong to the A((2)pi sub(u, 1/2)) - X((2)pi sub(g, 1/2)) subsystem and that A prime (sub e) is approximately equal to -710/cm. The analysis removes the anomalous difference in vibrational parameters for omega = 1/2 and 3/2 of the A state found in earlier investigations. ESA

N94-18945# Florida State Univ., Tallahassee. Dept. of Physics.

EXPERIMENTAL CONSEQUENCES OF SUPERSYMMETRY

H. Baer and X. Tata (Hawaii Univ., Honolulu.) 1992 14 p Presented at the 23rd Workshop of the INFN Eloisatron Project Properties of SUSY Particles, Erice, Italy, 28 Sep - 4 Oct. 1992
(Contracts DE-FG05-87ER-40319; DE-AM03-76SF-00235)
(DE93-018270; CONF-9209321-1) Avail: CASI HC A03/MF A01

After a brief review of the assumptions of the Minimal Supersymmetric Model (MSSM) we study the constraints on the masses of various particles as well as on the MSSM Higgs bosons from experiments at the Fermilab Tevatron and at LEP. We also review the range of Higgs boson masses that can be searched for at LEP 200. We then discuss the simulation of supersymmetric particle production at hadron colliders and briefly discuss event generators that we have been using in our analyses. Next, we discuss various signals that can be searched for in the present run of the Tevatron. We conclude with a study of the prospects for the detection of particles as well as MSSM Higgs bosons in experiments at hadron supercolliders, assuming that these are too heavy to be discovered at the Tevatron or at LEP 200. DOE

N94-18973# Fermi National Accelerator Lab., Batavia, IL.

CHARMONIUM PHYSICS FROM (BAR p)p INTERACTIONS

R. Ray Apr. 1993 49 p Presented at the International Conference on Hadron Spectroscopy, College Park, MD, 12-16 Aug. 1992
(Contract DE-AC02-76CH-03000)
(DE93-017809; FNAL/C-93/088; CONF-920847-2) Avail: CASI HC A03/MF A01

Heavy quarkonium is perhaps the best QCD laboratory in existence. Much of what we presently know about the fundamental interactions in nature has resulted from the study of two-body bound states. The hydrogen atom, the deuteron and positronium have provided valuable mechanisms for studying quantum mechanics, the theory of nuclear forces and QED. In the same way, one might hope that the study of two-body bound state systems built from heavy quarks will lead to a detailed understanding of at least some of the fundamental properties of strong interactions. While it is possible to gain some qualitative insights into strong interactions by studying bound states built from light quarks, it is not possible to reach more precise conclusions because of the additional complexities introduced by large relativistic corrections and long range confinement. Charmonium, c(anti c) bound states, has provided us with the first QCD laboratory where the system could be considered to be at least approximately non-relativistic while at the same time lending itself to perturbative calculations. The substantial mass of the charmed quark (m(sub c) approximately 1.5 GeV) corresponds to bound states sufficiently small to begin to probe the asymptotically free component of the strong interaction. The study of c(anti c) as well as b(anti b) bound states has greatly enhanced our understanding of the strong interaction between elementary particles. The scope of this article will be to review what has been learned to date, particularly on the experimental front, as well as to look at what remains to be done. DOE

N94-18985# Sandia National Labs., Albuquerque, NM.

A NUMERICAL STUDY OF HYBRID OPTIMIZATION METHODS FOR THE MOLECULAR CONFORMATION PROBLEMS

J. C. Meza and M. L. Martinez May 1993 26 p
(Contract DE-AC04-76DR-00789)
(DE93-017898; SAND-93-8233) Avail: CASI HC A03/MF A01

An important area of research in computational biochemistry is the design of molecules for specific applications. The design of these molecules depends on the accurate determination of their three-dimensional structure or conformation. Under the assumption that molecules will settle into a configuration for which their energy is at a minimum, this design problem can be formulated as a global optimization problem. The solution of the molecular conformation problem can then be obtained, at least in principle, through any number of optimization algorithms. Unfortunately, it can easily be shown that there exist a large number of local minima for most molecules which makes this an extremely difficult problem for any standard optimization method. In this study, we present results for various optimization algorithms applied to a molecular conformation problem. We include results for genetic algorithms, simulated annealing, direct search methods, and several gradient methods. The major result of this study is that none of these standard methods can be used in isolation to efficiently generate minimum energy configurations. We propose instead several hybrid methods that combine properties of several local optimization algorithms. These hybrid methods have yielded better results on representative test problems than single methods. DOE

N94-18999# University of Western Michigan, Kalamazoo.

SEARCH FOR RESONANT ELECTRON TRANSFER AND DOUBLE EXCITATION IN Kr(SUP 34+) + H2 COLLISIONS

K. E. Zaharakis, R. R. Haar, J. A. Tanis, M. W. Clark (Lawrence Livermore National Lab., CA.), and V. L. Plano (Michigan State Univ., East Lansing.) 1992 4 p Presented at the 6th International Conference on Physics of Highly Charged Ions, Manhattan, KS, 28 Sep. - 2 Oct. 1992
(Contract DE-FG02-87ER-13778)
(DE93-018776; CONF-920948-14) Avail: CASI HC A01/MF A01

Resonant electron transfer and double excitation (RME) is a correlated electron process which is expected to occur in an ion-atom collision when electron capture is accompanied by the simultaneous excitation of two inner-shell electrons. RT2 is similar to resonant transfer excitation (RTE) in which only a single electron is excited. RT2E was investigated experimentally for 38-42 MeV/u Kr34 + H2 collisions by observing x-ray emission associated with single-electron capture. No events associated with Kr K x rays (near 13 keV) were observed; however, events do occur at about twice (greater than 22 keV) the Kr K x-ray energy. Several possible sources of these latter x rays have been considered. DOE

N94-19013# Washington Univ., Seattle. Dept. of Physics.

SSC DETECTOR MUON SUB-SYSTEM BEAM TESTS

R. Downing, S. Errede, A. Gauthier, M. Haney, I. Karliner, T. Liss, T. OHalloran, P. Sheldon, V. Simiatis, and J. Thaler et al 1993 21 p
(Contract DE-FG06-90ER-40541)
(DE93-018415; DOE/ER-40541/1) Avail: CASI HC A03/MF A01

The authors propose to start a test-beam experiment at Fermilab studying the problems associated with tracking extremely high energy muons through absorbers. It is anticipated that in this energy range the observation of the muons will be complicated by associated electromagnetic radiation. Monte Carlo simulations of this background need to be tuned by direct observations. These beam tests are essential to determine important design parameters of a SSC muon detector, such as the choice of the tracking, geometry, hardware triggering schemes, the number of measuring stations, the amount of iron between measuring stations, etc. It is intended that the first phase of this program will begin in November of 1990 utilizing the Tevatron muon beam. The authors plan to measure the multiplicity, direction, and separation of secondary particles associated with the primary muon track as it emerges from an absorber. The second phase of beam test in 1992 or later will be a full scale test for the final design chosen in the muon subsystem proposal. DOE

N94-19029# Yale Univ., New Haven, CT. Dept. of Physics.
TASK A: YALE ACCELERATOR USERS GROUP (YAUG)
R. K. Adair, J. Sandweiss, and M. Schmidt Jul. 1993 47 p
(Contract DE-FG02-92ER-40704)
(DE93-018417; DOE/ER-40704/2-Task-A) Avail: CASI HC A03/MF A01

This report discusses the following topics: Yaug collider detector program; E-791: continued study of heavy flavors at TPL; hadroproduction of charm and beauty; search for composite objects produced in relativistic heavy ion collisions; and high energy physics computer facility. DOE

N94-19096# Argonne National Lab., IL.
EXTRACTION OF Z(PRIME) COUPLING DATA FROM Z(PRIME) (YIELDS) JJ AT THE LHC AND SSC
T. G. Rizzo Jun. 1993 8 p Presented at the Workshop on Physics at Current Accelerators and the Supercollider, Argonne, IL, 2-5 Jun. 1993
(Contract W-31-109-eng-38)
(DE93-018576; ANL-HEP-CP-93-50; CONF-9306176-2) Avail: CASI HC A02/MF A01

A recent analysis has shown that it may be possible at the SSC to extract information about Z(prime) couplings via the decay Z(prime) (yields) jj. This technique was found to be useful for some extended electroweak models provided the Z(prime) is relatively light. In the present paper, the authors generalize this procedure to the LHC and to Z(prime)'s which are more massive than 1 TeV. DOE

N94-19103# Purdue Univ., West Lafayette, IN. Dept. of Physics.
THE STUDY OF THE PHASE STRUCTURE OF HADRONIC MATTER BY SEARCHING FOR THE DECONFINED QUARK-GLUON PHASE TRANSITION USING 2 TeV (BAR-P)-P COLLISIONS, AND BY SEARCHING FOR CRITICAL PHENOMENA IN AN EXCLUSIVE STUDY OF MULTIFRAGMENTATION USING 1 GeV/NUCLEON HEAVY ION COLLISIONS
R. Scharenberg, A. Hirsch, and M. Tincknell 15 Sep. 1993 61 p
(Contract DE-FG02-88ER-40412)
(DE93-018925; DOE/ER-40412/6) Avail: CASI HC A04/MF A01

This report discusses the Fermilab experiment E735 which is dedicated to the search for the quark-gluon plasma from proton-antiproton interactions; multifragmentation using the EOS-TPC; STAR R&D; silicon avalanche diodes as direct time-of-flight detectors; and soft photons at the AGS-E855. DOE

N94-19108# University of Western Michigan, Kalamazoo.
LOW-ENERGY CONTINUUM-ELECTRON EMISSION AT 0 DEGREES FROM O(Q+) + He COLLISIONS
J. A. Tanis, R. R. Haar, D. Schneider (Lawrence Livermore National Lab., CA.), M. W. Clark (Lawrence Livermore National Lab., CA.), M. H. Prior (California Univ., Berkeley. Lawrence Berkeley Lab.), R. D. Dubois (Pacific Northwest Lab., Richland, WA.), and K. Randall (Wesleyan Univ., Middletown, CT.) 1992 5 p Presented at the 6th International Conference on Physics of Highly Charged Ions, Manhattan, KS, 28 Sep. - 2 Oct. 1992 Submitted for publication
(Contract DE-FG02-87ER-13778)
(DE93-018777; CONF-920948-16) Avail: CASI HC A01/MF A01

Low-energy continuum-electron emission along the beam direction, i.e., at 0 degrees, has been investigated for 1.1-6.2 keV/u O(8+) and 2.6 keV/u O(q+) (q = 3, 6, and 8) colliding with He. Spectra were obtained for continuum electrons associated with bound-state capture and with no projectile charge change, respectively. As for previous measurements for 3.75 keV/u O(6+) + He, continuum electrons at 0 degrees were observed only when accompanied by bound-state capture. Cross sections for these continuum electrons are found to be increasing functions of both the projectile energy and the charge state over the ranges investigated. DOE

N94-19120# Los Alamos National Lab., NM.
LAHET CALCULATIONS FOR ACCELERATOR NEUTRON PRODUCTION
R. E. Prael 1993 6 p Presented at the ANS Winter Meeting, San Francisco, CA, 14-19 Nov. 1993
(Contract W-7405-eng-36)
(DE93-016518; LA-UR-93-2429; CONF-931160-4) Avail: CASI HC A02/MF A01

LAHET is a Monte Carlo code for the transport and interaction of nucleons, pions, muons, fight ions, and antinucleons in complex geometry; it is the result of a major effort at Los Alamos National Laboratory to develop a code system based on the LANL version of the HETC Monte Carlo code for the transport of nucleons, pions, and muons, which was originally developed at Oak Ridge National Laboratory. The system of codes based on LAHET is designated as the LAHET Code System (LCS). LAHET, as all the variants of HETC, has been widely used over the years for design of neutron production targets, facility shielding, and experimental analysis. LAHET is now widely used for medical accelerator facility design and application. Particle tracking uses the general geometry model of the LANL MCNP code, and shares the geometry description and input of MCNP, except for lattices and/or repeated structures. HMCNP is a modification of MCNP which accepts an external neutron/photon source created by LAHET. Neutron transport from 20 MeV to thermal and all photon/electron transport is done with HMCNP. DOE

N94-19125# Los Alamos National Lab., NM.
ELECTRON IMPACT POLARIZATION AND CORRELATION PROPERTIES OF THE INERT GASES
G. Csanak, D. C. Cartwright, L. E. Machado (Universidade Federal de Sao Carlos, Brazil.), and G. D. Meneses (Universidade Estadual de Campinas, Brazil.) 1993 29 p Presented at the Polarization and Correlation in Electronic and Atomic Collisions, Bielefeld, Germany, 29-31 Jul. 1993
(Contract W-7405-eng-36)
(DE93-018358; LA-UR-93-2486; CONF-9307116-1) Avail: CASI HC A03/MF A01

For the heavier rare-gas targets, Ne, Ar, Kr, there is now a reasonable amount of experimental electron impact coherence parameter data available for excitation of the lowest J = 1 states. Theoretical results for those rare-gas targets have been restricted to distorted-wave approximation (DWA) type theories. A systemization of the experimental data is presented, and they are compared with available theoretical results. In the case of the heavy rare gases, the experimental and theoretical data available for the three species, Ne, Ar, Kr, are compared in order to identify trends. The experimental data are compared with results from available theories (mainly DWA type), and the importance of spin-orbit coupling effects and 'shell' effects is discussed. A physical picture that is emerging from all collisional data is presented, and future experimental and theoretical activities that will, provide new insight into the physics of these processes are recommended. DOE

N94-19126# Los Alamos National Lab., NM.
T VIOLATING NEUTRON SPIN ROTATION ASYMMETRY
Yasushiro Masuda 1993 9 p Presented at the International Workshop/Time Reversal Invariance and Parity Violation in Neutron Physics, Dubna, Russia, 4-7 May 1993
(Contract W-7405-eng-36)
(DE93-018470; LA-UR-93-2644; CONF-9305235-3) Avail: CASI HC A02/MF A01

A new experiment on T-violation is proposed, where a spin-rotating-neutron transmission through a polarized nuclear target is measured. The method to control the neutron spin is discussed for the new T-violation experiment. The present method has the possibility of providing us with more accurate T-violation information than the neutron EDM measurement. DOE

N94-19129# Oak Ridge National Lab., TN.
COMPUTER CODES FOR CHECKING, PLOTTING AND PROCESSING OF NEUTRON CROSS-SECTION COVARIANCE DATA AND THEIR APPLICATION
Enrico Sartori (Organization for Economic Co-Operation and Development, Paris, France.) and Robert W. Roussin 1992 13 p Presented at the Nuclear Energy Agency Science Committee Specialists Meeting on Evaluation and Processing of Covariance Data, Oak Ridge, TN, 7-9 Oct. 1992
(Contract DE-AC05-84OR-21400)
(DE93-018459; CONF-9210173-7) Avail: CASI HC A03/MF A01

This paper presents a brief review of computer codes concerned with checking, plotting, processing and using of covariances of neutron cross-section data. It concentrates on those available from the computer code information centers of the United States and the OECD/Nuclear Energy Agency. Emphasis will be placed also on codes using covariances for specific applications such as uncertainty analysis, data adjustment and data consistency analysis. Recent evaluations contain neutron cross section covariance information for all isotopes of major importance for technological applications of nuclear energy. It is therefore important that the available software tools needed for taking advantage of this information are widely known as they permit the determination of better safety margins and allow the optimization of more economical designs of nuclear energy systems. DOE

N94-19201# Lawrence Livermore National Lab., CA.
RELATIVISTIC CONFIGURATION INTERACTION CALCULATION OF THE CORRELATION ENERGIES OF HELIUMLIKE IONS
Kwok-Tsang Cheng, Mau Hsiung Chen, and W. R. Johnson Sep. 1993 4 p Presented at the 2nd International Conference on Computational Physics, Beijing, China, 13-17 Sep. 1993
(Contract W-7405-eng-48)
(DE93-018093; UCRL-JC-114326; CONF-9309176-1) Avail: CASI HC A01/MF A01

In this paper, we present a new relativistic configuration interaction (CI) method for atomic structure calculations using finite basis sets constructed from B-spline functions of piecewise polynomials. This method is used to calculate the correlation energies of the low-lying states of two-electron helium-like ions. Our calculations are based on the relativistic no-pair Hamiltonian from quantum electrodynamics (QED). Eigenfunctions of the Hamiltonian are expanded on the basis of two-electron configuration state functions (CSF) constructed from products of one-electron orbitals. Eigenvalues and eigenfuctions of the low-lying two-electron states are then determined by diagonalizing the Hamiltonian matrix as in the usual CI approach. DOE

N94-19204# Ohio State Univ., Columbus. Research Foundation.
REALISTIC THEORIES OF HEAVY ELECTRON AND OTHER STRONGLY CORRELATED MATERIALS
1993 11 p
(Contract DE-FG02-87ER-45326)
(DE93-010350; DOE/ER-45326/T3) Avail: CASI HC A03/MF A01

Research on the following topics is summarized: non-perturbative treatments of multi-channel Kondo models, non-perturbative treatments of multi-band models for the quadrupolar fluctuation model of the cuprates, extension of the two-channel Kondo model to other materials, and treatment of the infinite-dimensional Hubbard model within the non-crossing approximation. Data on the specific heat of Y(0.8)U(0.2)Pd3 and the c-axis susceptibility and specific heat of U in ThRu2Si are shown. DOE

N94-19236*# Columbia Univ., New York, NY.
CALCULATION OF MOLECULAR EXCITATION RATES Final Technical Report, 1 Feb. 1992 - 31 Jan. 1993
George Flynn 31 Jan. 1993 3 p
(Contract NCC5-46)
(NASA-CR-193782; NAS 1.26:193782) Avail: CASI HC A01/MF A01

State-to-state collisional excitation rates for interstellar molecules observed by radio astronomers continue to be required to interpret observed line intensities in terms of local temperatures and densities. A problem of particular interest is collisional excitation of water which is important for modeling the observed interstellar masers. In earlier work supported by a different NASA Grant, excitation of water in collisions with He atoms was studied; after many years of successively more refined calculations that problem now seems to be well understood, and discrepancies with earlier experimental data for related (pressure broadening) phenomena are believed to reflect experimental errors. Because of interstellar abundances, excitation by H2, the dominant interstellar species, is much more important than excitation by He, although it has been argued that rates for excitation by these are similar. Under the current grant theoretical study of this problem has begun which is greatly complicated by the additional degrees of freedom which must be included both in determining the interaction potential and also in the molecular scattering calculation. We have now computed the interaction forces for nearly a thousand molecular geometries and are close to having an acceptable global fit to these points which is necessary for the molecular dynamics calculations. Also, extensive modifications have been made to the molecular scattering code, MOLSCAT. These included coding the rotational basis sets and coupling matrix elements required for collisions of an asymmetric top with a linear rotor. A new method for numerical solution of the coupled equations has been incorporated. Because of the long-ranged nature of the water-hydrogen interaction it is necessary to integrate the equations to rather large intermolecular separations, and the integration methods previously available in MOLSCAT are not ideal for such cases. However, the method used by Alexander in his HIBRIDON code is particularly suited for such cases. We have obtained this code and incorporated that part which solves the coupled differential equations as an option in the MOLSCAT program. Author (revised)

N94-19247# California Univ., Berkeley. Lawrence Berkeley Lab.
THE PAPAGENO PARTONIC MONTE-CARLO PROGRAM
I. Hinchliffe Jul. 1993 10 p Presented at the Workshop on Physics at Current Accelerators and the Supercollider, Argonne, IL, 2-5 Jun. 1993
(Contract DE-AC03-76SF-00098)
(DE93-018524; LBL-34372; CONF-9306176-4) Avail: CASI HC A02/MF A01

This document provides a brief introduction to the PAPAGENO partonic Monte-Carlo event generator. DOE

N94-19257# Cornell Univ., Ithaca, NY.
EXPERIMENTAL STUDY OF INTERACTIONS OF HIGHLY CHARGED IONS WITH ATOMS AT keV ENERGIES
V. O. Kostroun 29 Jan. 1993 30 p
(Contract DE-FG02-86ER-13519)
(DE93-040222; DOE/ER-13519/7) Avail: CASI HC A03/MF A01

The following experiments were done. We measured the absolute total and one- and two- electron transfer cross sections for Ar(sup q+) (8 less than or equal to q less than or equal to 16) on He and H2 at 2.3 qkeV, the angular distributions of the scattered projectiles in Ar(sup 8+,9+) collisions, with Ar and Kr at 2.3 qkeV, the electron emissions in low energy Ar(sup q+) on Ar collisions, the recoil ion charge state distributions in low energy Ar(sup q+) -Ar collisions, the absolute total and one- and two-electron transfer cross sections for Ar(sup 8+) on Ar at 2.3 qkeV, and the absolute total and one- and two-electron transfer cross sections for Ar(sup 8+) on Ar as a function of energy. We also used energy gain spectroscopy to study Ar(sup q+) on Ar collisions at 40 and 30 qeV, and time of flight spectroscopy to investigate ionization and dissociation of CO and N2 in collisions with low energy, highly charged argon ions. In addition, we applied the Goldberger and Watson transition theory to derive transition rates and cross sections for atomic radiative and/or non radiative processes, wrote a computer code TRANSIT which can calculate energies, wave functions and radiative and non radiative rates for atoms and ions. The code is highly modular and can easily be modified to calculate higher order processes. Finally, we have done an Ab-Initio molecular orbital electronic energy level calculation for the (ArAr)(sup 8+) system as a function internuclear separation. DOE

N94-19259# Los Alamos National Lab., NM.
ETA-NUCLEON INTERACTION AND NUCLEAR PRODUCTION OF ETA MESONS
L. C. Liu 1993 15 p Presented at the International Conference on Meson-Nucleus Interactions, Crakow, Poland, 14-19 May 1993
(Contract W-7405-eng-36)
(DE93-018469; LA-UR-93-2652; CONF-9305148-1) Avail: CASI HC A03/MF A01

Eta-nucleon interaction and eta-nucleus dynamics are discussed. The possibility of using eta to probe unnatural-parity nuclear states and to study spin-isospin correlations between two nucleons are demonstrated. DOE

N94-19278# Los Alamos National Lab., NM.
THERMAL NEUTRON MULTIPLICITY MEASUREMENTS USING THE PYROCHEMICAL MULTIPLICITY COUNTER AT LAWRENCE LIVERMORE NATIONAL LABORATORY
D. G. Langner, M. S. Krick, D. R. Parks, and K. S. Hooper (Lawrence Livermore National Lab., CA.) 1993 9 p Presented at the 34th Annual Meeting of the Inst. of Nuclear Materials Management, Scottscale, AZ, 18-21 Jul. 1993

(Contract W-7405-eng-36)
(DE93-018538; LA-UR-93-2610; CONF-930749-45) Avail: CASI HC A02/MF A01

The pyrochemical multiplicity counter designed and built at Los Alamos has been undergoing tests and evaluation at Lawrence Livermore National Laboratory (LLNL). Measurements have been performed using a variety of plutonium oxide and metal materials. The pyrochemical multiplicity counter uses the information contained in the higher moments of the neutron multiplicity distribution to deduce the three unknowns in the assay problem: Pu-240-effective mass, (alpha,n) neutron rate, and self-multiplication. This is an improvement over conventional neutron coincidence counting, which must rely on some estimate of the (alpha,n) neutron rate or self-multiplication to deduce an assay result. Such conventional techniques are generally unsatisfactory for impure materials for which these quantities are unknown. We present the assay results obtained with the pyro-chemical multiplicity counter and discuss the procedures necessary to produce good assay results. Using these procedures, we have obtained assay accuracies of 1%-2% for oxide materials in 1/2 hour measurement times. We also compare these results to those that would have been obtained using conventional neutron assay techniques and discuss the correlations we have observed between assay results and the ratio of total neutron counts in the different rings of the pyrochemical counter. DOE

N94-19283# Lawrence Livermore National Lab., CA.
HARMONIC GENERATION AT HIGH INTENSITIES
K. J. Schafer, J. L. Krause, and K. C. Kulander Jun. 1993 13 p Presented at the North Atlantic Treaty Organization/Advanced Studies Institute Summer School: From Statistical Physics to Statistical Inference and Back, Cargese, France, 31 Aug. - 12 Sep. 1992
(Contract W-7405-eng-48)
(DE93-018632; UCRL-JC-113768; CONF-9208188-2) Avail: CASI HC A03/MF A01

Atomic electrons subject to intense laser fields can absorb many photons leading either to multiphoton ionization or the emission of a single, energetic photon which can be a high multiple of the laser frequency. The latter process, high-order harmonic generation, has been observed experimentally using a range of laser wavelengths and intensities over the past several years. Harmonic generation spectra have a generic form: a steep decline for the low order harmonics, followed by a plateau extending to high harmonic order, and finally, an abrupt cutoff beyond which no harmonics are discernible. During the plateau the harmonic production is a very weak function of the process order. Harmonic generation is a promising source of coherent, tunable radiation in the XUV to soft X-ray range which could have a variety of scientific and possibly technological applications. Its conversion from an interesting multiphoton phenomenon to a useful laboratory radiation source requires a complete understanding of both its microscopic and macroscopic aspects. We present some recent results on the response of single atoms at intensities relevant to the short pulse experiments. The calculations employ time-dependent methods, which we briefly review in the next section. Following that, we discuss the behavior of the harmonics as a function of laser intensity. Two features are notable: the slow scaling of the harmonic intensities with laser intensity, and the rapid variation in the phase of the individual harmonics with respect to harmonic order. We then give a simple empirical formula that predicts the extent of the plateau for a given ionization potential, wavelength, and intensity. DOE

N94-19309# Nevada Univ., Las Vegas.
STUDIES OF CLUSTERS
J. W. Farley 1993 5 p
(Contract DE-FC08-90NV-10872)
(DE93-018961; DOE/NV-10872/T61) Avail: CASI HC A01/MF A01

Positive cluster ions were produced, and the mass spectrum was measured using a radiofrequency quadrupole mass spectrometer. Mass spectra are attached, showing the cluster ions produced using pure ammonia. They have the general formula (NH3)nH(m)(+), where n and m are integers. Peaks with different numbers of hydrogens can barely be resolved. This shows that the ion source can produce cluster ions. The development of sensitive laser techniques is necessary for probing the clusters. During this quarter, a weak diode laser was used to probe a beam of negative molecular ions. The work on the visible absorption spectrum of D(2)O(+) continues, and is now in the analysis phase. The work on the infrared vibrational-rotational spectrum of H(sup 15)NO(-) continues. In the second ion beam machine, a complete reworking of the voltages was completed, and is being reassembled. DOE

N94-19320# Yale Univ., New Haven, CT. Dept. of Physics.
THE ANOMALOUS MAGNETIC MOMENT OF THE MUON
V. W. Hughes, D. H. Brown, R. M. Carey, M. Chertok, M. R. Duckworth, E. S. Hazen, F. Krienen, Z. Liu, J. P. Miller, and J. Ouyang et al 1992 4 p Presented at the 10th International Symposium on High-Energy Spin Physics, Nagoya, Japan, 9-14 Nov. 1992
(Contract DE-FG02-92ER-40704)
(DE93-018932; CONF-921131-14-App-B) Avail: CASI HC A01/MF A01

A new experiments is being developed at Brookhaven National Laboratory to measure the g-2 value of the muon to a precision of 0. 35 ppM, which would improve our present knowledge by a factor of 20. The current scientific motivations, the principle and the status of the experiment are discussed briefly. DOE

N94-19536# Brookhaven National Lab., Upton, NY.
SEARCH FOR TOP QUARK WITH D0 DETECTOR
S. D. Protopopescu 1993 7 p Presented at the 28th Conference on Quantum Chromodynamics and High Energy Hadronic Interactions, Les Arcs, France, 13-27 Mar. 1993
(Contract DE-AC02-76CH-00016)
(DE93-040170; BNL-49360; CONF-930363-7) Avail: CASI HC A02/MF A01

We report preliminary results of a search for the top quark by the D(0) collaboration at the Fermilab Tevatron p(bar-p) collider using a data sample corresponding to an integrated luminosity of about 7.5 pb(exp -1). Events with a high p(sub T) isolated electron and large missing E(sub T) which are candidates for containing W bosons were studied. Only one vent was found having an additional isolated lepton. Combining the ee and e(mu) channels we set a lower limit of 99 GeV/sq c for the top quark mass. DOE

N94-19545# Lawrence Livermore National Lab., CA.
HIGH RATE RESISTIVE PLATE CHAMBERS: AN INEXPENSIVE, FAST, LARGE AREA DETECTOR OF ENERGETIC CHARGED PARTICLES FOR ACCELERATOR AND NON-ACCELERATOR APPLICATIONS
C. R. Wuest, E. Ables, R. M. Bionta, O. Clamp, M. Haro, G. J. Mauger, K. Miller, H. Olson, and P. Ramsey May 1993 4 p Presented at the 5th Annual International Industrial Symposium on the Super Collider and Exhibition, San Francisco, CA, 6-8 May 1993
(Contract W-7405-eng-48)
(DE93-018664; UCRL-JC-114015; CONF-930537-96) Avail: CASI HC A01/MF A01

Resistive Plate Chambers (RPC's) have been used until recently as large detectors of cosmic ray muons. They are now finding use as fast large-area trigger and muon detection systems for different high energy physics detectors such as the L3 Detector at LEP and future detectors to be built at the Superconducting Super Collider (SSC) and at the Large Hadron Collider (LHC) at CERN. RPC systems at these accelerators must operate with high efficiency providing nanosecond timing resolution in particle fluences up to a few tens of kHz/sq cm--with thousands of square meters of active area. RPC's are simple and cheap to construct. The authors report here recent work on RPC's using new materials that exhibit a combination of desirable RPC features such as low bulk resistivity, high dielectric strength, low mass, and low cost. These new materials were originally developed for use in electronics assembly areas and other applications, where static electric charge buildup can damage sensitive electrical systems. DOE

N94-19607# Air Force Inst. of Tech., Wright-Patterson AFB, OH. School of Engineering.
EXCITED ATOMIC BROMINE ENERGY TRANSFER AND QUENCHING MECHANISMS Ph.D. Thesis
Ray O. Johnson Aug. 1993 180 p
(AD-A270672; AFIT/DS/ENP/93-05) Avail: CASI HC A09/MF A02

Pulsed and steady-state photolysis experiments have been conducted to determine the rate coefficients for collisional deactivation of the spin-orbit excited state of atomic bromine, Br((sup 2)P(sub 1/2)). Pulsed lifetime studies for quenching by Br2 and CO2 established absolute rate coefficients at room temperature of k(sub Br2) = 1.2 +/- 0.1 x 10(exp-12) and k(sub CO2) = 1.5 +/0.2 x 10(exp-11) cu cm/molecule-s. Steady-state photolysis methods were used to determine the quenching rates for the rare gases, N2, 02, H2, D2, NO, NO2, N2O, SF6, CF4, CH4, CO, CO2, COS, SO2, H2S, HBr, HC1, and HI relative to that for Br2. Quenching rate temperature dependence was examined for Br2, CO2, N2O, HCl, COS, NO, and NO2 for temperatures from 300 to 420 K. Diffusion and three body effects were examined in order to determine the slowest relative quenching rate measurable by this experimental technique. DTIC

N94-18038# Observatoire Cantonal, Neuchatel (Switzerland).
DEVELOPMENT OF ATOMIC STANDARDS AT THE NEUCHATEL OBSERVATORY [DEVELOPPEMENT D'ETALONS ATOMIQUES A L'OBSERVATOIRE CANTONAL DE NEUCHATEL]
Pierre Thomann *In* Societe Suisse de Chronometrie, Proceedings of the 4th European Congress on Chronometry 1992 p 151-15 In FRENCH Sponsored by ESTEC; Fonds National Suisse pour la Recherche Scientifique; and Office Suisse de Metrologie (For primary document see N94-18006 04-35)
Copyright Avail: CASI HC A01/MF A02

N94-19165*# National Aeronautics and Space Administration. Goddard Space Flight Center, Greenbelt, MD.
NEW ROOM TEMPERATURE HIGH RESOLUTION SOLID-STATE DETECTOR (CdZnTe) FOR HARD X RAYS AND GAMMA RAYS
AmyElizabeth C. Stewart (Maryland Univ., College Park.) and Upendra D. Desai *In its* The 1993 Shuttle Small Payloads Symposium Oct. 1993 p 25-31 (For primary document see N94-19162 04-12)
Avail: CASI HC A02/MF A03

73 NUCLEAR AND HIGH-ENERGY PHYSICS

Includes elementary and nuclear particles; and reactor theory.
For space radiation see *93 Space Radiation.*

N94-17698 Sandia National Labs., Albuquerque, NM.
COMPOUND-LENS INJECTOR FOR A 19-MeV, 700-kA ELECTRON BEAM
T. W. L. Sanford, J. W. Poukey, J. A. Halbleib, and R. C. Mock (Ktech Corp., Albuquerque, NM.) 1992 4 p Presented at the International Particle Accelerator Conference, Washington, DC, 17-20 May 1993 Limited Reproducibility: More than 20% of this document may be affected by microfiche quality
(Contract DE-AC04-76DP-00789)
(DE93-013752; SAND-92-2221C; CONF-930511-3) Avail: CASI HC A01

A robust injector capable of controlling the radius and angle of incidence of the intense, pulsed, annular electron beam extracted from the HERMES-3 accelerator is described. The injector, called the compound lens, uses a tapered anode to control the beam electrostatically, followed by a gas cell with externally applied current to control the beam magnetically. Adjustment of the anode-cathode gap and external current of the injector permits the mean radius and injection angle of the beam to be defined independently of one another. Measurements of these quantities confirm model expectations. The extended planar-anode diode with a thin anode window has been used to inject a 25-ns, 19-MeV, 700-kA, annular electron beam into gas-filled drift cells for beam transport to bremsstrahlung targets located downstream of the HERMES-3 accelerator. By adjusting the anode-cathode (AK) gap of the diode, the radius and angle of incidence of the annular beam at injection can be varied. Here the authors theoretically model and experimentally characterize the electron flow in the compound-lens diode when it is used as a bremsstrahlung source. Results are presented as the AK gap is increased to 40 cm. The model combines the MAGIC code to simulate the time-dependent electron flow in the AK gap and lens with the CYLTRAN code of the ITS system to model window effects and the subsequent transport in the target. DOE

N94-17726# Los Alamos National Lab., NM.
SYNCHROTRON BEAM-LOADING STABILITY WITH A HIGHER RF HARMONIC
Tai-Sen F. Wang 1993 4 p Presented at the International Particle Accelerator Conference, Washington, DC, 17-20 May 1993
(Contract W-7405-eng-36)
(DE93-014549; LA-UR-93-1845; CONF-930511-83) Avail: CASI HC A01/MF A01

This work is an attempt to extend Robinson's stability studies to include a higher RF harmonic. Using an equivalent circuit model, the stability of the 'O-mode' coherent dipole oscillation of bunched beams is studied for synchrotrons or storage rings, with RF systems operated at the fundamental and a higher harmonic, i.e., a 2nd or 3rd harmonic. Analytical expressions of the stability criteria are derived from the linearized circuit equations. Numerical solutions of the fully nonlinear equations are provided to compare with the analytical results. Simple feedback model for stabilization is discussed. DOE

N94-17784# Houston Univ., TX. Dept. of Physics.
DECOHERENCE AND RECOHERENCE OF BEAM IN PHASE SPACE
Jicong Shi and Shoroku Ohnuma 1993 4 p Presented at the International Particle Accelerator Conference, Washington, DC, 17-20 May 1993
(Contract DE-FG05-87ER-40374)
(DE93-014885; DOE/ER-40374/68; CONF-930511-143) Avail: CASI HC A01/MF A01

By use of the particle distribution in phase space, a new approach is introduced to study the decoherence and recoherence of a kicked beam when betatron tunes are far from any resonance. With this method, the decoherence and the recoherence of a beam can be analyzed easily in both 2-dimensional and 4-dimensional cases with any form of the tune spread. The decoherence of a beam initially trapped in a resonance island was also studied. Due to the tune modulation, the separatrix of island develops a chaotic layer and particles within the island can drift out of the island along the layer. Consequently, the beam decoheres gradually. The rate of decoherence is shown to be proportional to the modulation amplitude. As a function of the modulation frequency, it reaches a peak near the tune of trapped particles before decreasing to zero. DOE

N94-17807# Maryland Univ., College Park. Dept. of Physics.
ADVANCED METHODS FOR THE COMPUTATION OF PARTICLE BEAM TRANSPORT AND THE COMPUTATION OF ELECTROMAGNETIC FIELDS AND BEAM-CAVITY INTERACTIONS
A. J. Dragt and R. L. Gluckstern Jun. 1993 20 p
(Contract DE-FG05-92ER-40748)
(DE93-018160; DOE/ER-40748/1) Avail: CASI HC A03/MF A01

The University of Maryland Dynamical Systems and Accelerator Theory Group has been carrying out long-term research work in the general area of Dynamical Systems with a particular emphasis on applications to Accelerator Physics. This work is broadly divided into two tasks: Charged Particle Beam Transport and the Computation of Electromagnetic Fields and Beam-Cavity Interactions. Each of these tasks is described briefly. Work is devoted both to the development of new methods and the application of these methods to problems of current interest in accelerator physics including the theoretical performance of present and proposed high energy machines. In addition to its research effort, the Dynamical Systems and Accelerator Theory Group is actively engaged in the education of students and postdoctoral research associates. DOE

N94-18156 Japan Atomic Energy Research Inst., Tokyo.
REPORT OF THE 1991 WORKSHOP ON PARTICLE-MATERIAL INTERACTIONS FOR FUSION RESEARCH
Nov. 1992 159 p Workshop held in Tokyo, Japan, 12-13 Dec. 1991 Limited Reproducibility: More than 20% of this document may be affected by poor print
(DE93-788393; JAERI-M-92-134) Avail: Issuing Activity (Department of Energy (DOE))

The Annual Workshop on Particle-Material Interactions in the Working Group of the Research Committee on A and M Data was held at the head-quarters of JAERI, Tokyo, on 12-13 Dec. 1991. The purpose of the Workshop was to obtain future prospects for the activities of the Working Group by discussing current states and problems in the research on particle-material interactions relevant to the thermocontrolled fusion. The present report contains 16 papers presented at the Workshop, which are mainly concerned with plasma-facing materials in ITER, radiation damage in carbon materials, trapping, emission and permeation of hydrogen in metals, and heavy ion-solid surface interactions. DOE

N94-18273# Argonne National Lab., IL.
ALTERNATING-PHASE FOCUSING WITH AMPLITUDE MODULATION
L. Sagalovsky and J. R. Delayen 1993 3 p Presented at the International Particle Accelerator Conference, Washington, DC, 17-20 May 1993
(Contract W-31-109-eng-38)
(DE93-018618; ANL/EP/CP-78372; CONF-930511-367) Avail: CASI HC A01/MF A01

We have previously developed a model of alternating-phase focusing (APF) applicable to ion linacs comprised of short independently controlled cavities. The main beam dynamical aspects of APF are adequately described by four parameters: equilibrium synchronous phase, phase modulation amplitude, length of APF period, and incremental energy gain. We report on an extension of the analysis to include simultaneous modulation of the accelerating field amplitude. Two additional parameters are included: relative phase between the amplitude and phase modulation and magnitude of the amplitude modulation. The effects of amplitude modulation on the stable regions and longitudinal acceptance are discussed. DOE

N94-18497# Fermi National Accelerator Lab., Batavia, IL.
COMPARISON OF FERRITE MATERIALS FOR PULSE APPLICATIONS
J. A. Dinkel and C. C. Jensen Jun. 1993 9 p Presented at the 9th IEEE Pulsed Power Conference, Albuquerque, NM, 21-23 Jun. 1993
(Contract DE-AC02-76CH-03000)
(DE93-017224; FNAL/C-93/168; CONF-930616-12) Avail: CASI HC A02/MF A01

Materials are the limiting factor in many pulse power projects. The magnetic materials available from several manufacturers were experimentally compared for their usefulness in high speed magnetic field applications. This particular application is a high speed kicker magnet for manipulation of a charged particle beam. DOE

N94-18845# Stockholm Univ. (Sweden). Dept. of Physics.
A BIT SERIAL FIRST LEVEL CALORIMETER TRIGGER FOR AN LHC DETECTOR
C. Bohm, G. Appelquist, Xing Zhao, N. Yamdagni, and N. Ellis (Birmingham Univ., England.) Nov. 1992 18 p
(USIP-92-08; ETN-93-94850) Avail: CASI HC A03/MF A01

A preliminary design of a compact first level calorimeter trigger, implemented as a farm of bit serial systolic arrays, and for use in a Large Hadron Collider (LHC) detector, is presented. Functionality can be incorporated into the Application Specific Integrated Circuits (ASIC's) that serve as the main processing elements. The trigger processor finds local electromagnetic clusters and evaluates isolation and leakage into the hadron calorimeter to detect electrons, uses cluster finding algorithms to identify jets and missing transverse energy to estimate neutrino energies. It provides means to spatially correlate electron and muon signals. The output is a histogram summarizing the classifications of different signatures detected by the trigger processor. This information serves as decision support for the central first level trigger and delivers region of interest positions to be used by the second level trigger. In its present form the trigger processor relies on optical fibers to transfer its data and provide the fan out needed to supply the ASIC's with their data. ESA

N94-18916# California Univ., Santa Cruz.
EXPERIMENTAL RESEARCH IN HIGH ENERGY PHYSICS Final Technical Progress Report, 1986-1992
1992 14 p
(Contract DE-AT03-86ER-40249)
(DE93-011912; DOE/ER-40249/T1) Avail: CASI HC A03/MF A01

This is the closeout report for DOE supported research in high energy physics for the period 1986-1992, under contract award AT03-86ER40249 at the Santa Cruz Institute for Particle Physics (SCIPP) at U.C. Santa Cruz. The research during this period consisted primarily of the following: (1) Data taking with the MARK II detector at the SLC at SLAC and construction of a silicon vertex detector for the MARK II. This effort included substantial work on commissioning of the SLC accelerator. (2) Preparation of the SLD experiment for the SLC, and initial data taking with this experiment. (3) Participation in the ALEPH physics program at LEP at CERN in Geneva, with an emphasis on its silicon vertex detector. (4) Analysis of data collected with the MARK III experiment at the SPEAR accelerator at SLAC. (5) Electronics development for the leading proton spectrometer for the Zeus experiment at DESY in Hamburg. (6) Design, testing and physics studies for a silicon tracker for the SSC. (7) Theoretical physics program emphasizing phenomenology, Higgs physics, supersymmetry, and some issues in cosmology. DOE

N94-18927# Ames Lab., IA.
INVESTIGATION OF PHYSICAL STRUCTURES AND INTERACTIONS AT HIGH ENERGY
W. E. Anderson, J. M. Hauptman, and J. Qui 31 May 1993 27 p
(Contract DE-FG02-92ER-40730)
(DE93-014444; DOE/ER-40730/1) Avail: CASI HC A03/MF A01

This report contains discussions on the following topics: Experimental program at the Fermilab Tevatron Collider--FNAL E-740; Experimental program at the superconducting super collider: Solenoidal detector collaboration; Computation development program at Iowa State University: Batch after twilight running and parallel processing; Experimental program at the University of Hawaii--Deep underwater muon and neutrino detector; Global analysis of parton distributions; high energy direct photon production; photon fragmentation functions; single transverse-spin asymmetry; associated production of Higgs Boson at collider energies; and Cronin effect in photoproduction and deeply inelastic scattering; and heavy meson production. DOE

N94-18934# Argonne National Lab., IL. Engineering Physics Div.
HALO FORMATION IN MISMATCHED, SPACE-CHARGE-DOMINATED BEAMS
C. L. Bohn and J. R. Delayen 1993 4 p Presented at the International Particle Accelerator Conference, Washington, DC, 17-20 May 1993
(Contract W-31-109-eng-38)
(DE93-018581; ANL/EP/CP-78375; CONF-930511-345) Avail: CASI HC A01/MF A01

A semianalytic formalism was recently developed for investigating the transverse dynamics of a mismatched, space-charge-dominated beam propagating through a focusing channel. It uses the Fokker-Planck equation to account for the rapid evolution of the coarse-grained distribution function in the phase space of a single beam particle. A simple model of dynamical friction and diffusion represents the effects of turbulence resulting from charge redistribution. The initial application was to sheet beams. In this paper, the formalism is generalized to fully two-dimensional beams. DOE

N94-18972# Fermi National Accelerator Lab., Batavia, IL.
EFFECTS OF TRANSVERSE COUPLING ON TRANSVERSE BEAM SIZE, SIMULATION AND MEASUREMENTS
A. M. Halling May 1993 5 p Presented at the International Particle Accelerator Conference, Washington, DC, 17-20 May 1993
(Contract DE-AC02-76CH-03000)
(DE93-017804; FNAL/C-93/125; CONF-930511-311) Avail: CASI HC A01/MF A01

The equations of motion for particles in an accelerator lattice show that a larger physical aperture is required to hold a beam of constant invariant emittance if there is transverse coupling of the tunes. The results of a tracking simulation of particle motion in the Fermilab accumulator ring are discussed, and results are shown from beam tests carried out in the accumulator to demonstrate this effect. DOE

N94-18994# Superconducting Super Collider Lab., Dallas, TX.
LONGITUDINAL BEAM DYNAMICS WITH RF NOISE
H. J. Shih, J. A. Ellison (Texas Univ., Austin.), R. Cogburn (Texas Univ., Austin.), and B. S. Newberger (Texas Univ., Austin.) Jun. 1993 41 p Revised
(Contract DE-AC35-89ER-40486)
(DE93-018649; SSCL-578-Rev-1) Avail: CASI HC A03/MF A01

The Dome-Krinsky-Wang (DKW) diffusion-inaction theory for RF-noise-induced emittance dilution is reviewed and related to recent work on the approximation of stochastic processes by Markov processes. An accurate and efficient numerical procedure is developed to integrate the diffusion equation of the DKW theory. Tracking simulations are undertaken to check the validity of the theory in the parameter range of the Superconducting Super Collider (SSC) and to provide additional information. The study of effects of rf noise is applied to two problems of interest at the SSC: (1) determination of noise tolerance levels in the rf system; and (2) feasibility of beam extraction using crystal channeling. DOE

N94-18996# Lawrence Livermore National Lab., CA.
SPICE MODELING OF A FET-SWITCHED INDUCTION ACCELERATOR CELL
C. W. Ollis, W. R. Cravey, S. A. Hawkins, H. C. Kirbie, and M. A. Newton 11 Jun. 1993 6 p Presented at the 9th IEEE Pulsed Power Conference, Albuquerque, NM, 21-23 Jun. 1993
(Contract W-7405-eng-48)
(DE93-018662; UCRL-JC-112511; CONF-930616-19) Avail: CASI HC A02/MF A01

A PSpice model of an induction accelerator cell switched by field-effect transistors (FET's) has been developed to simulate the modulator's circuit performance and induction core flux behavior. A FET switched induction cell has been built that can generate 4-kV, 1 micro-s pulses at pulse rates exceeding 100 kHz. The circuit architecture provides for core reset between pulses and produces bursts of pulses that are variable in amplitude, pulse width and prf. The transistor switching array, energy storage capacitors, reset circuit, and cell core are all combined into a compact, low-impedance package. This high-prf induction cell is being developed as the accelerating element for a proposed heavy-ion recirculator, which is an arrangement of many small induction cells in a 30 m diameter circle. The recirculator will accept 10-MeV ions from a linear ion accelerator, under development at the Lawrence Berkeley Laboratory, and continue their acceleration to 60-MeV by repeatedly passing the ion beam through the many 5-kV cells. As the ions gain speed, the cell prf must also keep pace by increasing from 70 kHz to 200 kHz. Simple PSpice models have been used to predict B-H loop behavior in the magnetic core and to analyze circuit performance. Simulations of the induction cell will be presented and compared with experimental data. DOE

N94-18997# California Univ., Berkeley. Lawrence Berkeley Lab.
HEAVY ION FUSION INJECTOR PROGRAM
S. Yu, S. Eylon, and W. W. Chupp May 1993 6 p Presented at the International Particle Accelerator Conference, Washington, DC, 17-20 May 1993
(Contract DE-AC03-76SF-00098)
(DE93-018706; LBL-33289; HIFAN-574; CONF-930511-335) Avail: CASI HC A02/MF A01

A program is underway to construct a 2 MV, 800 mA, K(+) injector for heavy ion fusion. The Electrostatic Quadrupole (ESQ) injector configuration consists of a zeolite source, a diode of up to 1 MV, together with several electrostatic quadrupole units to simultaneously focus and accelerate the beam to 2 MV. The key issues of source technology, high voltage breakdown, beam aberrations, and transient effects will be discussed. Results from ongoing experiments and simulations will be presented. DOE

N94-19023# Tufts Univ., Medford, MA.
HIGH ENERGY PHYSICS AT TUFTS UNIVERSITY
15 Jul. 1993 98 p
(Contract DE-FG02-92ER-40702)
(DE93-018299; DOE/ER-40702/4) Avail: CASI HC A05/MF A02

This report discusses the following topics: Fermilab fixed target experiments; Soudan II nucleon decay project; physics at the proton-antiproton collider at (radical)s = 1.8 TeV; the Solenoidal Detector for the supercollider; neutrino telescope proposal; polarization in massive quark and hadron production; production characteristics of top quarks; scattering, spin dependence and mass corrections in Skyrmion models; and computation and networking. DOE

N94-19050# Florida State Univ., Tallahassee. Dept. of Physics.
HIGH ENERGY PHYSICS PROGRAM. TASK A: EXPERIMENT AND THEORY. TASK B: NUMERICAL SIMULATION
1993 90 p
(Contract DE-FG05-87ER-40319)
(DE93-018140; DOE/ER-40319/T3) Avail: CASI HC A05/MF A01

This report discusses research in High Energy Physics at Florida State University. Contained in this paper are: highlights of activities during the past few years; five year summary; fixed target experiments; collider experiments; SSC preparation, detector development and detector construction; computing, networking, and VAX upgrade to ALPHA; and particle theory programs. DOE

N94-19106# Lawrence Livermore National Lab., CA.
CORRECTION OF LONGITUDINAL ERRORS IN ACCELERATORS FOR HEAVY-ION FUSION
W. M. Sharp, D. A. Callahan, J. J. Barnard, A. B. Langdon, and T. J. Fessenden (California Univ., Berkeley. Lawrence Berkeley Lab.) 10 Jun. 1993 5 p Presented at the International Particle Accelerator Conference, Washington, DC, 17-20 May 1993
(Contract W-7405-eng-48)
(DE93-018656; UCRL-JC-112377; CONF-930511-337) Avail: CASI HC A01/MF A01

Longitudinal space-charge waves develop on a heavy-ion inertial-fusion pulse from initial mismatches or from inappropriately timed or shaped accelerating voltages. Without correction, waves moving backward along the beam can grow due to the interaction with their resistively retarded image fields, eventually degrading the longitudinal emittance. A simple correction algorithm that uses a time-dependent axial electric field to reverse the direction of backward-moving waves is presented. The image fields then damp these forward-moving waves. The method is demonstrated by fluid simulations of an idealized inertial-fusion driver, and practical problems in implementing the algorithm are discussed. DOE

N94-19107# Lawrence Livermore National Lab., CA.
SIMULATION OF TRANSIENT EFFECTS IN THE HEAVY ION FUSION INJECTORS
Yu-Jiuan Chen and D. W. Hewett 12 May 1993 5 p Presented at the International Particle Accelerator Conference, Washington, DC, 17-20 May 1993
(Contract W-7405-eng-48)
(DE93-018658; UCRL-JC-112344; CONF-930511-336) Avail: CASI HC A01/MF A01

We have used the 2-D PIC code, GYMNOS, to study the transient behaviors in the Heavy Ion Fusion (HIF) injectors. GYMNOS simulations accurately provide the steady state Child-Langmuir current and the beam transient behavior within a planar diode. The simulations of the LBL HIF ESAC injector experiments agree well with the experimental data and EGUN steady state results. Simulations of the nominal HIF injectors have revealed the need to design the accelerating electrodes carefully to control the ion beam current, particularly the ion loss at the end of the bunch as the extraction voltage is reduced. DOE

N94-19152# California Univ., Berkeley. Lawrence Berkeley Lab.
SIMULATION OF THE ALS LONGITUDINAL MULTIBUNCH FEEDBACK SYSTEM
J. Byrd May 1993 6 p Presented at the International Particle Accelerator Conference, Washington, DC, 17-20 May 1993
(Contract DE-AC03-76SF-00098)
(DE93-019227; LBL-33271; ESG-229; CONF-930511-364) Avail: CASI HC A02/MF A01

Longitudinal coupled bunch growth rates in the Advanced Light Source (ALS), a 1.5 GeV electron storage ring for producing synchrotron radiation, indicate the need for damping via a feedback (FB) system. The design of the system is based on the proposed PEP-II longitudinal FB system which uses a digital filter to provide the required phase and amplitude response. We report the results of a detailed computer simulation of the FB system including single particle longitudinal beam dynamics, measured RF cavity fundamental and higher order modes, and response of major FB components such as the power amplifier and kicker. The simulation addresses issues such as required FB power and gain, noise, digital filter effects, and varying initial bunch conditions. DOE

N94-19287# Northwestern Univ., Evanston, IL.
RESEARCH IN HIGH ENERGY PHYSICS
J. Rosen, M. Block, D. Buchholz, B. Gobbi, H. Schellman, D. Miller, E. Braaten, and R. Oakes Jul. 1993 73 p
(Contract DE-FG02-91ER-40684)
(DE93-018031; DOE/ER-40684/3) Avail: CASI HC A04/MF A01

This report discusses research being conducted in High Energy Physics at Northwestern University. DOE

N94-19558# California Univ., Berkeley. Lawrence Berkeley Lab.
STUDY OF COUPLED-BUNCH COLLECTIVE EFFECTS IN THE ALS
J. M. Byrd and J. N. Corlett May 1993 6 p Presented at the

International Particle Accelerator Conference, Washington, DC, 17-20 May 1993
(Contract DE-AC03-76SF-00098)
(DE93-019236; LBL-33270; ESG-228; CONF-930511-374) Avail: CASI HC A02/MF A01

We present an overview of the calculated longitudinal and transverse coupled-bunch (CB) growth rates using the measured RF cavity higher order mode (HOM) impedance for the Advanced Light Source (ALS), a 1.5 GeV electron storage ring for producing synchrotron radiation. We also describe a visual method of representing the effective beam impedance and corresponding growth rates which is especially useful for understanding the dependence of growth rate on HOM frequency and Q, for determining the requirements of the CB feedback system, and for interpreting measured beam spectra. DOE

N94-19560# California Univ., Berkeley. Lawrence Berkeley Lab.
THE ILSE EXPERIMENTAL PROGRAM
C. M. Celata, R. O. Bangerter, and W. Chupp May 1993 11 p Presented at the International Symposium on Heavy Ion Fusion, Frascati, Italy, 25-28 May 1993
(Contract DE-AC03-76SF-00098)
(DE93-019247; LBL-33800; HIFAN-579; CONF-9305136-11) Avail: CASI HC A03/MF A01

The Heavy Ion Fusion Accelerator Research Program at Lawrence Berkeley Laboratory has proposed building a 10 MeV Induction Linac Systems Experiment, ILSE, to investigate accelerator physics and beam manipulations which are needed or desirable for an induction linac driver. This paper describes the experiments proposed for ILSE: transverse beam combining, drift compression, bending of space-charge-dominated beams, final focus, recirculation, and some studies of beam propagation in the environment of the reactor chamber. DOE

N94-19589# Air Force Inst. of Tech., Wright-Patterson AFB, OH. School of Engineering.
TOTAL HEMISPHERICAL EMITTANCE OF NIOBIUM-1 PERCENT ZIRCONIUM FUEL CLADDING FOR THE SP-100 SPACE REACTOR M.S. Thesis
John E. Thomason, III Dec. 1992 71 p
(AD-A270456; AFIT/GNE/ENP/92D-1) Avail: CASI HC A04/MF A01

Total hemispherical emittance was measured for the SP-100 reactor fuel cladding alloy (Nb-1% Zr). Based on a standard test method (ASTM C 835-82), experiments were conducted on a reference sample of oxidized stainless steel and then on a sample of actual cladding. The sample is heated in a vacuum by passing DC current through it until reaching equilibrium. Measurements are made of the electrical power dissipated in the sample and of the surface temperature. Using the Stefan-Boltzmann Law and some key assumptions concerning conductive and radiative heat transfer, the measured quantities are used to calculate emittance. Calculated values for unoxidized cladding range from 0.159 +/- 5.35% at 913 K to 0.200 +/- 4.51% at 1091 K. The highest value measured after onset of visible oxidation was 0.339 +/- 3.92% at 1269 K. DTIC

74 OPTICS

Includes light phenomena; and optical devices.
For lasers see *36 Lasers and Masers.*

N94-17716 Department of the Navy, Washington, DC.
VARIABLE WIDE BAND FIBER OPTIC DELAY LINE Patent
Gregory H. Ames, inventor (to Navy) 11 May 1993 4 p Filed 29 Jun. 1992
(AD-D015848; US-Patent-5,210,807; US-Patent-Appl-SN-905705) Avail: CASI HC A02/MF A01

Apparatus and method for a variable wide band fiber optic delay line is described. The apparatus comprises components that allow a user to select a delay time of a signal by the use of a wavelength tunable laser. The user selected wavelength determines the length that a light intensity signal corresponding to an electronic signal travels, thereby determining the time of delay. DTIC

N94-17857 Tennessee Univ., Tullahoma. Space inst.
CONSIDERATIONS FOR THE USE OF THE MODIFIED LINE REVERSAL TECHNIQUE FOR GAS TEMPERATURE MEASUREMENT
B. C. Winkleman 1993 16 p Presented at the 31st Symposium on Engineering Aspects of Magnetohydrodynamics, Whitefish, MT, 29 Jun. - 1 Jul. 1993 Limited Reproducibility: More than 20% of this document may be affected by microfiche quality
(Contract DE-AC02-79ET-10815)
(DE93-015752; DOE/ET-10815/219; CONF-930626-9) Avail: CASI HC A03

Several areas related to the successful and accurate application of modified line reversal are discussed. Initially, generalized modified line reversal equations are developed. A review of basic line reversal theory is presented followed by development of correction factors for optical system effects. Image size and their effect on accurate determinations of spectral radiances is discussed. Temperature biases introduced by image vignetting is calculated. Measured image irradiances are given. DOE

N94-17887# Optical Society of America, Washington, DC.
QUANTUM OPTOELECTRONICS TECHNICAL DIGEST, 1993. VOOLUME 8: POSTCONFERENCE EDITION
1993 150 p Presented at the Quantum Optoelectronics Topical Meeting held in Palm Springs, CA, 17-19 Mar. 1993
(AD-A268209) Avail: CASI HC A07/MF A02

This report contains summaries of papers presented at the Quantum Optoelectronics Topical Meeting in March 1993. Topics include microcavity and vertical emitter, modulators, fundamental processes, quantum well lasers, exciton and carrier dynamics, wires and dots, and optics and transport in reduced dimensionality. CASI

N94-18000# Sandia National Labs., Albuquerque, NM.
EXAMINATION OF METRICS AND ASSUMPTIONS USED IN CORRELATION FILTER DESIGN
G. Gheen (Lockheed Missiles and Space Co., Sunnyvale, CA.), F. Dickey, and J. DeLaurentis 1993 12 p Presented at the Annual Meeting of the SPIE, San Diego, CA, 11-16 Jul. 1993
(Contract DE-AC04-76DP-00789)
(DE93-017636; SAND-93-1491C; CONF-930722-8) Avail: CASI HC A03/MF A01

This paper examines some of the metrics that are commonly used to design correlation filters for optical pattern recognition, including: the Fisher ratio, the signal-to-noise ratio, the equal correlation peak (ECP) constraint, and normalized correlation. Attention is given to the underlying assumptions that are required to move from Bayesian decision theory to a particular metric or design principle. Since a Bayes classifier is statistically optimum, this provides a means for assessing the merit of a particular approach. Although the authors only examine a few metrics in this paper, the approach is general and should be useful for assessing the merit and applicability of any of the numerous filter designs that have been proposed in the optical pattern recognition community. DOE

N94-18204# Boeing Defense and Space Group, Seattle, WA.
COHERENT TRANSIENT SYSTEMS EVALUATION Final Report, 1 Sep. 1991 - 7 Jun. 1993
William R. Babbitt 17 Jun. 1993 45 p
(Contract F49620-91-C-0088)
(AD-A268808; AFOSR-93-0649TR) Avail: CASI HC A03/MF A01

This final report of contract F49620-91-C-0088 describes the development of the analytical tools required to evaluate optical coherent transient memory, triple-product correlator, and continuous signal processor systems. One key tool is a coherent transient simulator based on the optical Bloch equations. The coherent transient output signal that results from an arbitrary sequence of pulses, each having an arbitrary amplitude, duration, center frequency, chirp, phase, and timing can be calculated. The simulator was used to study excitation pulse saturation and its effects on the output signal efficiency and fidelity and to study frequency chirped reference pulse saturation. Analytical tools were developed to assess the effects of local heating and spatial crosstalk. A performance evaluation of a coherent transient continuous optical correlator is reported, along with new implementation techniques. The continuous processor's predicted time-bandwidth product, data bandwidth, and pattern storage density are 10000, 5 GHz, and 100000 patterns per square centimeter, respectively. A

proof of concept demonstration of the continuous optical processor was performed in europium doped yttrium silicate in collaboration with IBM Almaden Research Center. Research into divalent ion doped crystals as photon gated materials for coherent transient systems was performed.
DTIC

N94-18217 Gosudarstvennyi Komitet po Ispolzovaniyu Atomnoi Energii, Serpukhov (USSR).
CRYSTAL OPTICS OF HIGH ENERGY GAMMA-BEAMS [KRISTALLOOPTIKA GAMMA-PUCHKOV VYSOKIKH EHNERGIJ]
V. A. Maisheev, V. L. Mikhalev, and A. M. Frolov 1991 30 p In RUSSIAN Limited Reproducibility: More than 20% of this document may be affected by microfiche quality
(DE93-630228; IFVE-OP-91-142) Avail: CASI HC A03 (US Sales Only)

Using the conception of the single crystal as a region of electrical field, generated by spatially ordered atoms, we have determined the tensor of dielectric permeability for greater than or equal to 1 GeV photons in the region of crystal orientation, which corresponds to e (sup +-) pair coherent production. The polarization characteristics of normal EM wave propagation in the crystals were found with the help of this tensor. In particular, it was shown that there exist solutions of a dispersion equation for ellipted polarized waves. Other EM processes in the crystals, in particular, Cherenkov radiation of charged particles, were considered.
DOE

N94-18223 SRI International Corp., Menlo Park, CA.
IR MATERIALS PRODUCIBILITY Quarterly Technical Report No. 4, 1 May - 31 Jul. 1993
A. Sher, M. A. Berding, A. T. Paxton, and M. Muller Aug. 1993 45 p Limited Reproducibility: More than 20% of this document may be affected by microfiche quality
(Contract MDA972-92-C-0053; ARPA Order 8557)
(AD-A268849) Avail: Issuing Activity (Defense Technical Information Center (DTIC))

During this quarter, we completed an important component of our work on the gradient corrections to the defect formation energies. This correction applies to all total energies calculated, including those for defects in HgCeTe, ZnSe, and LiNbO3, and permits us to calculate accurate absolute defect densities. We have developed a preliminary description of the tellurium inclusion formation process in HgCdTe, and proposed a mechanism for the mobility reduction in undoped mercury-annealed LPE material. We have begun the calculation of the lithium vacancy formation energies in LiNbO3. We have continued our work on the impact of dislocations on MCT device properties. We have calculated the electron mobility in Hg(0.22)Cd(0.78)Te by solving the Boltzmann transport equation with Fermi-Dirac statistics and the full band structure, and we have obtained excellent agreement with experiments. The transport-related properties (Hall coefficient, Fermi level, and energy gap) have also been calculated with accurate analytical band structures and Fermi-Dirac statistics, and we find that the results differ appreciably from those using traditional approximations. All of these results are being incorporated into processing strategies to increase yields and performance of devices.
DTIC

N94-18254# Stanford Univ., CA. Dept. of Electrical Engineering.
ADVANCED OPTICAL FIBER COMMUNICATION SYSTEMS Status Report, 1 Mar. - 31 Jul. 1993
Leonid G. Kazovsky 31 Jul. 1993 28 p
(Contract N00014-91-J-1857)
(AD-A269120) Avail: CASI HC A03/MF A01

Our research is focused on three major aspects of advanced optical fiber communication systems: dynamic wavelength division multiplexing (WDM) networks, high dynamic range coherent analog optical links, and fiber nonlinearities. In the area of WDM networks, a prototype high-speed interface board between workstation and WDM network has been designed, implemented, and tested, with a highest data rate so far of 728 Mbps. We also began the theoretical investigation of a system using combined ASK/DPSK modulation formats. The results show the feasibility of using semiconductor lasers with ASK/DPSK combined modulation in future dynamic WDM network. In the area of high dynamic range coherent analog optical links, we completed analyses of the spurious-free dynamic range (SFDR) of coherent amplitude and coherent angle modulated links and compared the results with those for conventional and optically preamplified direct detection links. In the area of fiber nonlinearities, we showed that the pdf of four wave mixing interference is non-Gaussian and analyzed the impact of four wave mixing on the attainable receiver sensitivity of coherent WDM digital systems for both dispersion-shifted and non-dispersion-shifted fiber.
DTIC

N94-18262 Army Missile Command, Redstone Arsenal, AL. Weapons Science Directorate.
EVALUATION OF A LIQUID CRYSTAL SPATIAL LIGHT MODULATOR CAPABLE OF AMPLITUDE- AND PHASE-MODULATING MODES Final Report, 15 Dec. 1992 - 1 Feb. 1993
Tracy D. Hudson Jun. 1993 24 p Limited Reproducibility: More than 20% of this document may be affected by microfiche quality
(AD-A269252; AD-E952072; AMSMI/TR-RD-WS-93-4) Avail: CASI HC A03

An optically-addressed nematic liquid crystal spatial light modulator marketed by Micro-Optics Technologies has been evaluated as an amplitude- and phase-modulating device for optical pattern recognition applications. Experimental results of the device's performance are presented.
DTIC

N94-18283# Optical Society of America, Washington, DC.
SPATIAL LIGHT MODULATORS AND APPLICATIONS: SUMMARIES OF PAPERS PRESENTED AT THE SPATIAL LIGHT MODULATORS AND APPLICATIONS TOPICAL MEETING Final Report
Jarus W. Quinn 17 Mar. 1993 233 p Meeting held in Palm Springs, CA, 15-17 Mar. 1993
(Contract F49620-93-1-0181)
(AD-A269452; AFOSR-93-0647TR) Avail: CASI HC A11/MF A03

The partial contents of this document are as follows: SLM Technologies; Ferroelectric Liquid Crystal SLM's; Smart Pixel SLM's; Poster Session; International Perspective on Liquid Crystal SLM's; Silicon-Addressed Hybrid SLM's; Joint Optical Computing/Photonics in Switching/Spatial Light Modulators (SLM's) Plenary Session; Multiple-Quantum Well SLM Technology; Asymmetric Fabry-Perot MQW Modulators; Optical Interconnects and other SLM Applications; and New Materials.
DTIC

N94-18295# California Univ., Irvine.
MAGNETOSTATIC WAVES-BASED INTEGRATED OPTIC BRAGG CELL MODULES WITH APPLICATIONS TO RF SIGNAL PROCESSING Annual Technical Report No. 3, 1 Jul. 1992 - 30 Jun. 1993
Chen S. Tsai 1993 32 p
(Contract N00014-90-J-4039)
(AD-A269115) Avail: CASI HC A03/MF A01

Two major achievements were made during the third program year (July 1, 1992 to June 30, 1993): First, a complete analysis on ion-milled waveguide lenses in a YIG-GGG layer structure aimed at the key parameters and guidelines for design and fabrication of such waveguide lenses has been carried out. Second, a high-speed wideband integrated magnetooptic (MO) frequency shifter/modulator has been realized, for the first time, using a YIG-GGG tapered waveguide structure.
DTIC

N94-18298 Optical Society of America, Washington, DC.
INTEGRATED PHOTONICS RESEARCH VOLUME 10. CONFERENCE EDITION Final Report
Jarus W. Quinn Mar. 1993 367 p Presented at the Integrated Photonics Research Topical Meeting, Palm Springs, CA, 22-24 Mar. 1993 Limited Reproducibility: More than 20% of this document may be affected by microfiche quality
(Contract F49620-93-1-0181)
(AD-A269298; AFOSR-93-0646TR) Avail: CASI HC A16

The following topics were presented at the symposium: (1) Advanced Solid State Lasers; (2) Compact Blue-Green Lasers; (3) Integrated Photonics Research; (4) Nonlinear Guide-Wave Optics; (5) Optical Amplifiers & Their Applications; (6) Optical Design for Photonics; (7) Photonics in Switching; (8) Quantum Optoelectronics; (9) Shortwavelength: (10) Physics With Intense Laser Pulses; (11) Soft X-Ray Protection Lithography; (12) Ultrafast Electronics & Optoelectronics; (13) Optical Computing; and (14) Spatial Light Modulators.
DTIC

N94-18302 Harris Corp., Melbourne, FL. Government Aerospace Systems Div.
PHOTOREFRACTIVE RECEIVER STUDY Final Report, Sep. 1991 - Dec. 1992

M. R. Lange and D. W. Graves Jun. 1993 60 p Limited Reproducibility: More than 20% of this document may be affected by microfiche quality
(Contract F30602-91-C-0129)
(AD-A269352; RL-TR-93-115) Avail: CASI HC A04

The Photorefractive Receiver Study was a 12 month study into concepts related to the application of photorefractive materials as adaptive beam combining elements for an optical heterodyne receiver. This study concentrates on the behavior of and requirements for the photorefractive element. A set of parameters and approaches for the photorefractive element was selected and a theoretical model constructed to predict performance. An experiment was designed and fabricated to illustrate the dependencies predicted by the theoretical model. All model and experimental results are described and summarized. DTIC

N94-18332# Optical Society of America, Washington, DC.
OPTICAL COMPUTING. ORGANIZATION OF THE 1993 PHOTONICS SCIENCE TOPICAL MEETINGS. TECHNICAL DIGEST SERIES, VOLUME 7 Final Report
Jarus W. Quinn 19 Mar. 1993 347 p Meetings held in Palm Springs, CA, 16-19 Mar. 1993
(Contract F49620-93-1-0181)
(AD-A269025; AFOSR-93-0643TR-Vol-7) Avail: CASI HC A15/MF A03

Contents of the document include the following: joint optical computing/photonics in switching/spatial light modulators plenary session; optical computing posters; wavelength domain processing; parallel systems; optical neural networks; analog optical processing; smart pixels; optical interconnections; digital optical computing; and bit serial optical computing. DTIC

N94-18383 Environmental Research Inst. of Michigan, Ann Arbor. Infrared and Optics Div.
IMAGE RECONSTRUCTION FROM INTERFEROMETER DATA Final Report, Sep. 1990 - Jul. 1992
J. R. Fienup and J. H. Seldin Mar. 1993 38 p Limited Reproducibility: More than 20% of this document may be affected by microfiche quality
(Contract N00014-90-C-0244)
(AD-A268463; ERIM-232800-2-F) Avail: CASI HC A03

In blind tests, we successfully reconstructed images from data simulated to have some of the defects that data coming from the multi-aperture amplitude interferometer (MAAI) at the University of Maryland would have. We also successfully reconstructed good-quality images from phaseless data collected by ERIM's experimental range-angle interferometric imaging system. These successes in reconstructing images with phaseless interferometer data demonstrate the possibility of obtaining fine-resolution images with large, low-cost, light-weight, aberrated optical systems, despite the kinds of noise and other errors that are present in real data. We also showed that it is feasible to insert a beam deviator in the MAAI that would allow us to measure the lower spatial frequencies that are crucial for reconstructing images from low-light-level data. DTIC

N94-18396# Optical Society of America, Washington, DC.
OPTICAL DESIGN FOR PHOTONICS. ORGANIZATION OF THE 1993 PHOTONICS SCIENCE TOPICAL MEETINGS. TECHNICAL DIGEST SERIES, VOLUME 9 Final Report
Jarus W. Quinn 24 Mar. 1993 226 p Meetings held in Palm Springs, CA, 22-24 Mar. 1993
(Contract F49620-93-1-0181)
(AD-A269027; AFOSR-93-0644TR-Vol-9) Avail: CASI HC A11/MF A03

This symposia discussed the following topics: (1) Advanced lasers; (2) Plasma waveguides; (3) Fundamental interactions in atoms/plasmas; (4) Hot electron generation in dense plasmas; (5) Generation and application of short wavelength sources; (6) X-ray lasers; (7) Short pulse x-rays; (8) Propagation effects; (9) Fundamental interactions; and (10) High harmonics. DTIC

N94-18405# Pennsylvania Univ., Philadelphia. Dept. of Materials Science and Engineering.
NOVEL ELECTROCHEMICAL MATERIALS PREPARED BY SOL-GEL CHEMISTRY
Gregory C. Farrington, John O. Thomas (Uppsala Univ., Sweden.), and Stig Friberg (Clarkson Univ., Potsdam, NY.) 31 May 1993 24 p
(Contract N00014-90-J-1156)
(AD-A269060) Avail: CASI HC A03/MF A01

Past efforts in this program have been devoted to exploring the preparation, properties, and structures of various beta alumina compositions in which the mobile sodium ion content was replaced with a variety of divalent and trivalent cations. Though this line of work has produced a great number of new and unusual materials, in particular unusual solid electrolytes and new optical materials, as well as insight into the factors which control fast ion transport in solids, it seemed an appropriate time to move on to another topic. So, over the past year, most of the effort in this program has been devoted to investigations of the use of sol-gel chemistry to produce unusual electrochemical materials, such as solid state ionic conductors, new high rate cathode materials, and unusual organic-inorganic composite materials. DTIC

N94-18457 Rome Lab., Griffiss AFB, NY.
APPLICATIONS OF NONLINEAR OPTIC EFFECTS IN NEW SPECIALTY FIBERS Report, Oct. 1991 - Dec. 1992
Reinhard Erdmann Jun. 1993 36 p Limited Reproducibility: More than 20% of this document may be affected by microfiche quality
(AF Proj. LDFP)
(AD-A268890; RL-TR-93-105) Avail: Issuing Activity (Defense Technical Information Center (DTIC))

Nonlinear Optic effects are in general higher order processes. This dictates relatively weak interaction coefficients, so that the optical field intensity must be greater in order to observe effects. Optical fiber in particular being amorphous hence centro-symmetric, precludes second order effects, so the ones of interest for this study are already third order (X3). Fiber possesses, however, some unique properties which greatly enhance the interaction efficiency, and enable practical applications. The small area confinement (typically less than 50 sq um) over very long interaction lengths permits up to three orders of magnitude increase in efficiency over a free space focus. Brillouin scatter is examined even though it is not noticeable with normal sources, because key new applications require ultra narrow line widths, which are shown to bring the threshold to a disturbingly low value of only several mw. Stimulated Raman effects are examined because of their great versatility in frequency shifting for various practical applications. Fiber amplification is shown to enable fiber lasers with very promising properties; extremely short pulses at very low pump powers, fully integrated with only passive components. Interesting follow-on work is indicated in each of these areas. DTIC

N94-18488 Optical Society of America, Washington, DC.
QUANTUM OPTOELECTRONICS. ORGANIZATION OF THE 1993 PHOTONICS SCIENCE TOPICAL MEETINGS. TECHNICAL DIGEST SERIES, VOLUME 8 Final Report
Jarus W. Quinn 19 Mar. 1993 152 p Meetings held in Palm Springs, CA, 17-19 Mar. 1993 Limited Reproducibility: More than 20% of this document may be affected by microfiche quality
(Contract F49620-93-1-0181)
(AD-A269026; AFOSR-93-0638TR-Vol-8) Avail: CASI HC A08

This symposium covered the following topics: (1) Advanced solid state lasers; (2) Compact blue-green lasers; (3) Integrated photonics research; (4) Nonlinear guide-wave optics; (5) Optical amplifiers and their applications; (6) Optical design for photonics; (7) Photonics in switching; (8) Quantum optoelectronics; (9) Short-wavelength--Physics with intense laser pulses; (10) Soft X-ray protection lithography; (11) Ultrafast electronics and optoelectronics; (12) Optical computing; and (13) Spatial light modulators. DTIC

N94-18528 Optical Society of America, Washington, DC.
PHOTONICS IN SWITCHING: ORGANIZATION OF THE 1993 PHOTONICS SCIENCE TOPICAL MEETINGS. TECHNICAL DIGEST Final Report
Jarus W. Quinn 17 Mar. 1993 240 p Meetings held in Palm Springs, CA, 15-17 Mar. 1993 Limited Reproducibility: More than 20% of this document may be affected by microfiche quality
(Contract F49620-93-1-0181)
(AD-A269024; AFOSR-93-0637TR) Avail: CASI HC A11

The following topics were discussed during this symposium: (1) Advanced solid state lasers; (2) Compact blue-green lasers; (3) Integrated photonics research; (4) Nonlinear guide-wave optics; (5) Optical amplifiers and their applications; (6) Optical design for photonics; (7) Photonics in switching; (8) Quantum optoelectronics; (9) Short-wavelength: Physics with intense laser pulses; (10) Soft X-ray protection lithography; (11) Ultrafast electronics & optoelectronics; (12) Optical computing; and (13) Spatial light modulators. DTIC

N94-18635 Southampton Univ. (England).

METAL FILM SURFACE PLASMON RESONANCE (MFSPR) FIBRE COUPLERS Final Report, 30 Sep. 1990 - 31 Dec. 1992

J. Russell and S. Barcelos Feb. 1993 49 p Limited Reproducibility: More than 20% of this document may be affected by microfiche quality

(Grant AF-AFOSR-0353-90)

(AD-A268871) Avail: CASI HC A03

The project goal was to develop a mode selective coupler, based on long-range surface-plasmons (LRSP's), that provides tunable tapping of individual modes or small groups of modes from a multi-mode fiber carrying several communications channels simultaneously in different areas of its mode spectrum. When a thin metal layer, deposited on a side-polished fiber, supports a LRSP that phase-matches to a fiber mode, resonant tunneling of light from the core into the metal layer can occur; this may then be tapped off through a high index prism (or a second identical fiber) placed against the fiber face, the intervening space being filled with a layer of variable index. Mode selectivity might then be achieved by tuning the index of this layer. In the project, the fiber side-polishing apparatus was designed and built, the polishing procedure perfected, a fully automated computer-driven prism coupler and monochromator set up, and reliable film deposition achieved. The theory of the LRSP modes was fully developed, and a separate field matrix analysis carried out for modelling the behavior of the entire device both for excitation from the prism and the fiber modes. The general conclusion is that the modal selectivity is fundamentally limited by the unavoidable fact that higher order modes (those close to cut-off) couple much more strongly than do lower order modes. The result is that lower order modes cannot be coupled out without a substantial (of order 50% or worse) amount of cross-talk from higher order modes. These observations were confirmed in a number of experiments. DTIC

N94-18668# Rome Lab., Griffiss AFB, NY.

DESIGN AND FABRICATION OF A MULTICHANNEL ADAPTIVE OPTICAL PROCESSOR (MADOP) Report, Feb. 1991 - Sep. 1992

Michael J. Ward, Christopher W. Keefer, and Harold G. Andrews, II Dec. 1992 56 p

(AF Proj. 4600)

(AD-A270004; RL-TR-92-333) Avail: CASI HC A04/MF A01

We designed and built a multichannel adaptive optical processor (MADOP) for the purpose of adaptive cancellation of broadband jamming noise in C-Band antenna arrays. The processor operates at an intermediate frequency (IF) of 80 MHz and is designed to provide greater than 30 dB cancellation of two independent 10 MHz bandwidth noise jammers, where multiple reflections of the jamming energy collected in the sidelobes produce multipath delays of up to 5 micro-sec. The MADOP architecture is portable and designed to function as an on-line 'smart filter' which adaptively cancels broadband noise in the sidelobes. DTIC

N94-18693 Optical Society of America, Washington, DC.

SOFT X RAY PROJECTION LITHOGRAPHY. ORGANIZATION OF THE 1993 PHOTONICS SCIENCE OPTICAL MEETINGS Final Report

Jarus W. Quinn 10 May 1993 180 p Meetings held in Monterey, CA, 10-12 May 1993 Limited Reproducibility: More than 20% of this document may be affected by microfiche quality

(Contract F49620-93-1-0181)

(AD-A269159; AFOSR-93-0641TR) Avail: Issuing Activity (Defense Technical Information Center (DTIC))

The agenda of sessions of this symposium includes: modeling; condenser; multilayer 1; imaging experiments; optical metrology; x-ray metrology; multilayer 2; and alternate strategies. DTIC

N94-18738# Strathclyde Univ., Glasgow (Scotland). Dept. of Electronic and Electrical Engineering.

INVESTIGATION OF A FIBER OPTIC FREQUENCY SHIFTER AND OPTICAL ISOLATOR Final Report, 30 Sep. 1990 - 30 Apr. 1993

Walter Johnstone, Graham Thursby, and Craig Michie 30 Apr. 1993 84 p

(Grant AF-AFOSR-0286-90)

(AD-A269820; EOARD-93-06) Avail: CASI HC A05/MF A01

This report documents a program of investigation of an in-line fiber optic frequency translator and optical isolator on behalf of AFOSR (90-0286). The proposed designs are based on evanescent field coupling from a single mode optical fiber to a multi-mode planar waveguide overlay. The program focused mainly on the development of a particular design of frequency translator and included extensive characterization of fiber optic overlay structures in general. Fabrication of the frequency translator based on bonding lithium niobate to a fiber block and polishing it thin to form the acousto-optic overlay proved to be difficult and yields were low. Several devices were completed but frequency shifting was not observed due to severe attenuation of the surface acoustic waves. On a more positive note the overlay structures demonstrated excellent wavelength selective properties leading to the realization of tunable high resolution (2 nm) dropping filters and band pass filters. Such devices have many applications in communications, sensing, and tuning of fiber lasers. DTIC

N94-18743# Department of the Navy, Washington, DC.

APPARATUS AND METHOD FOR VARYING A BRAGG WAVELENGTH OF A BRAGG GRATING FORMED IN AN OPTICAL FIBER Patent Application

Alan D. Kersey, inventor (to Navy) and C. A. Villarruel, inventor (to Navy) 30 Jun. 1993 32 p

(AD-D015876; US-Patent-Appl-SN-083953) Avail: CASI HC A03/MF A01

An apparatus and method uses a Bragg grating formed in the core of an optical fiber. An element is coupled to the optical fiber and serves to vary a Bragg wavelength (i.e., a wavelength at which reflection occurs) of the Bragg grating by varying a refractive index of the core and/or a cladding of the optical fiber. The element can be an electro-optical element, a magnetooptical element, or a chemo-optical element either sensing or being controllably varied, based on an electric signal, a magnetic signal, or a presence or absence of a chemical, respectively. Alternatively, a dopant, such as a rare-earth ion, can be formed in the core and/or cladding of the optical fiber and irradiated with laser light from a laser pump. A change in absorption spectra from ground state absorption to excited state absorption changes the refractive index of the core and/or cladding so that the Bragg wavelength of the Bragg grating is varied based on an intensity of the laser light. DTIC

N94-18858*# Hughes Danbury Optical Systems, Inc., CT.

IMPACT OF SHORTER WAVELENGTHS ON OPTICAL QUALITY FOR LAWS Final Report

Alan B. Wissinger, Robert J. Noll, James G. Tsacoyeanes, and Jeanette R. Tausanovitch Oct. 1993 35 p Revised

(NASA Order H-20752-D)

(NASA-CR-193873; NAS 1.26:193873; PR-D15-0018-Rev-A) Copyright Avail: CASI HC A03/MF A01

This study explores parametrically as a function of wavelength the degrading effects of several common optical aberrations (defocus, astigmatism, wavefront tilts, etc.), using the heterodyne mixing efficiency factor as the merit function. A 60 cm diameter aperture beam expander with an expansion ratio of 15:1 and a primary mirror focal ratio of f/2 was designed for the study. An HDOS copyrighted analysis program determined the value of merit function for various optical misalignments. With sensitivities provided by the analysis, preliminary error budget and tolerance allocations were made for potential optical wavefront errors and boresight errors during laser shot transit time. These were compared with the baseline l.5 m CO2 LAWS and the optical fabrication state of the art (SOA) as characterized by the Hubble Space Telescope. Reducing wavelength and changing optical design resulted in optical quality tolerances within the SOA both at 2 and 1 micrometers. However, advanced sensing and control devices would be necessary to maintain on-orbit alignment. Optical tolerance for maintaining boresight stability would have to be tightened by a factor of 1.8 for a 2 micrometers system and by 3.6 for a 1 micrometers system relative to the baseline CO2 LAWS. Available SOA components could be used for operation at 2 micrometers but operation at 1 micrometers does not appear feasible. Author

N94-18931# Lawrence Livermore National Lab., CA.
DEVELOPMENT OF ROBUST MULTILAYER OPTICS FOR USE IN HIGH-PEAK POWER RADIATION ENVIRONMENTS
B. J. MacGowan, S. Mrowka, T. W. Barbee, Jr., L. B. DaSilva, D. C. Eder, J. A. Koch, J. A. Turner, and J. H. Underwood 27 Jul. 1993 8 p
Presented at the Spring Meeting of the Materials Research Society, San Francisco, CA, 12-16 Apr. 1993
(Contract W-7405-eng-48)
(DE93-018557; UCRL-JC-113814; CONF-930405-33) Avail: CASI HC A02/MF A01

In many applications, x-ray multilayer mirrors are exposed to high peak fluxes of x-rays with subsequent damage to the mirror. Mirror damage is a particularly severe problem with the use of multilayers as cavity optics for short wavelength x-ray lasers. Intense optical and x-ray radiation, from the x-ray laser plasma amplifier, often damage the multilayer mirror on time scales of hundreds of picoseconds. The phenomenon of multilayer mirror damage by pulsed x-ray emission has been studied using short duration (500 psec) bursts of soft x-rays from a laser produced gold plasma. The results of the experiments will be compared with some simple models and the possibility of increasing the damage thresholds of short wavelength multilayer mirrors will be discussed. DOE

N94-18947# Department of the Navy, Washington, DC.
IMPROVED OPTICAL PSEUDOSPARK SWITCH Patent Application
Michael G. Grothaus, inventor (to Navy), Jack S. Bernardes, inventor (to Navy), and David C. Stoudt, inventor (to Navy) 3 May 1993 12 p
(AD-D015821; US-Patent-Appl-SN-056084) Avail: CASI HC A03/MF A01

Disclosed is a high-voltage, high-current, multichannel, optically-triggered switch with the potential for improved lifetime of operation. Triggering of the switch is accomplished by ultraviolet illumination of multiple cathode apertures via fiber-optic cables. The trigger optics for each channel, being composed of a fiber-optic cable terminated by some collimating optics, are protected from damaging metalization by enclosing them in an angled metal or dielectric tubes in the cathode back-space. The use of collimating optics at the output of the fiber allows the fiber to be recessed inside the shield tube, providing further protection from discharge by-products. DTIC

N94-18970 Sandia National Labs., Albuquerque, NM.
EVALUATION OF FIBER OPTIC PERFORMANCE IN THE ACRR
D. E. Bodette and P. J. Brannon May 1993 50 p Limited Reproducibility: More than 20% of this document may be affected by microfiche quality
(Contract DE-AC04-76DP-00789)
(DE93-018515; SAND-92-1094) Avail: CASI HC A03

Four fluorosilica clad, all silica core fibers with polyamide buffers were examined for radiation-induced, transient absorption in the central cavity of the Annular Core Research Reactor. The reactor operated 24 times in the pulse mode, typically yielding gamma doses of 15 krad(Si) and neutron fluences of 1.4x10(exp 14) nts/cm(sup 2) thermal and 1.0x10(exp 15) nts/cm(sup 2) (fast). The two low-OH fibers absorbed 90% of the light in the 400 to 500 nm region and 30% in the 700 and 800 nm region. The high-OH fibers absorbed 20% in the 400 to 500 nm region and 50% in the 700 to 800 nm region. Saturation of the transient induced absorption was observed in all the fibers. No systematic measurements were taken of long term induced absorption. However, excessive absorption was not a problem in any fibers, even those that received total gamma doses of 5 Mrad(Si). Scintillation in the 680 to 820 mn band was observed. This report documents the data from these experiments. DOE

N94-19113# Sandia National Labs., Albuquerque, NM.
IMAGE BLUR
M. R. Nissen Apr. 1993 16 p
(Contract DE-AC04-76DP-00789)
(DE93-017944; SAND-93-0644) Avail: CASI HC A03/MF A01

The image blur in a photograph is produced by the exposure of a moving object. Knowing the amount of image blur is important for recording useful data. If there is too much blur, it becomes hard to make quantitative measurements. This report discusses image blur, the parameters used to control it, and how to calculate it. DOE

N94-19268# Lawrence Livermore National Lab., CA.
SINGLE SIDED TOMOGRAPHY OF EXTREMELY LARGE DENSE OBJECTS
R. S. Thoe 24 Mar. 1993 14 p Presented at the Society of Photo-Optical Instrumentation Engineers (SPIE) OE/Aerospace Science and Sensing Meeting, Orlando, FL, 11-16 Apr. 1993
(Contract W-7405-eng-48)
(DE93-017993; UCRL-JC-111856; CONF-930445-19) Avail: CASI HC A03/MF A01

One can envision many circumstances where radiography could be valuable but is frustrated by the geometry of the object to be radiographed; for example, extremely large objects, the separation of rocket propellants from the skin of solid fuel rocket motor, the structural integrity of an underground tank or hull of a ship, the location of buried objects, inspection of large castings, etc. The author has been investigating ways to do this type of radiography and as a result has developed a technique which can be used to obtain three dimensional radiographs using Compton scattered radiation from a monochromatic source and a high efficiency, high resolution germanium spectrometer. This paper gives specific details of the reconstruction technique and presents the results of numerous numerical simulations and compares these simulations to spectra obtained in the laboratory. In addition, the author presents the results of calculations made for the development of an alternative single sided radiography technique which will permit inspection of the interior of large objects. As a benchmark, the author seeks to obtain three dimensional images with a resolution of about one cubic centimeter in a concrete cube 30 centimeters on a side. Such a device must use photons of very high energy. For example, 30 cm of concrete represents about 15 mean free paths for photons of 100 keV, whereas at 1 MeV the attenuation is down to about five mean free paths. At these higher energies, Compton scattering becomes much more probable. Although this would appear to be advantageous for single sided imaging techniques, such techniques are hampered by two side effects. In this paper, the results are given of numerous Monte Carlo calculations detailing the extent of the multiple scattering and the feasibility of a variety of imaging schemes is explored. DOE

N94-19424 Physics and Electronics Lab. TNO, The Hague (Netherlands).
DESCRIPTION OF AN INFRARED ZOOMCOLLIMATOR Final Report
A. N. deJong Mar. 1993 15 p Original contains color illustrations
(FEL-93-A034; TD-93-0295; ETN-93-94942) Copyright Avail: Issuing Activity (TNO Physics and Electronics Laboratory, P.O. Box 96864, 2509 JG The Hague, Netherlands)

The performance of thermal imagers is tested by means of test targets, put in the focal plane of a collimator. For Minimum Resolvable Temperature Difference (MRTD) measurements bar targets are used with a certain frequency and variable temperature contrast. The zoomcollimator described provides a variable spatial frequency, which is more comparable to the range variation of a target in the terrain with certain size and temperature contrast. In the focal plane also a line source and a circular source with variable temperature contrast can be used, in order to measure the MRTD. ESA

N94-19455 Physics and Electronics Lab. TNO, The Hague (Netherlands).
APPLICATIONS OF MOTION ESTIMATION IN IMAGE PROCESSING Final Report
W. J. C. Beck Oct. 1992 20 p
(FEL-92-B356; TD92-3314; ETN-93-94949) Copyright Avail: Issuing Activity (TNO Physics and Electronics Laboratory, P.O. Box 96864, 2509 JG The Hague, Netherlands)

Examples of image sequence processing using motion estimation are presented. Results of noise reduction by motion compensated temporal filtering in a noisy image sequence and examples of the detection of moving targets in an air to ground infrared (IR) image sequence are included. The examples show what kind of improvements or detection results can be expected. Noise reduction in a noisy image sequence and some results on IR image sequences are included. The detection of moving objects in image sequences is discussed. These sequences are recorded from a moving platform. The aim is to detect objects moving relative to the moving background. ESA

N94-19578 Massachusetts Inst. of Tech., Cambridge. Research Lab. of Electronics.
OPTICAL FREQUENCY DIVISION USING AN OPTICAL PARAMETRIC OSCILLATOR Final Report, 1 May 1990 - 31 Jul. 1993
Ngai C. Wong 9 Aug. 1993 14 p Limited Reproducibility: More than 20% of this document may be affected by microfiche quality
(Contract DAAL03-90-G-0128)
(AD-A270847) Avail: CASI HC A03

We have pursued a vigorous program of experimental and theoretical research on a novel method of frequency division based on an optical parametric oscillator (OPO). We have successfully demonstrated optical frequency division in a nearly degenerate KTP OPO that is highly efficient and tunable. The difference frequency of the two subharmonic outputs of the OPO was phase locked to a 12-GHz microwave source with a residual phase noise spectral density of 0.3 mrad/VH-z. More recently the use of a THz optical frequency comb permitted the OPO to be phase locked at a difference frequency of 665 GHz. We have studied a number of potential applications including optical frequency counting for frequency standards and multi-THz optical frequency comb generation for optical communications. DTIC

N94-19601# Syracuse Univ., NY. Dept. of Chemistry.
OPTICAL SWITCH EVALUATION SUPPORT Final Report
Joseph Chaiken Jul. 1993 119 p
(Contract F30602-91-D-0001)
(AD-A270948; RL-TR-93-149) Avail: CASI HC A06/MF A02

Extensive testing has been done on nonlinear interface optical switch (NIOS) devices fabricated from laser deposited nonstoichiometric tungsten oxide films. A Fresnel coefficient formalism for evaluating the indices of refraction of the films has been developed. Three cycles of testing involving changing the tungsten-oxygen stoichiometry have not produced extremely large photorefractive effects. It was decided, after using a mathematical model to determine the required incident and reflection angles, to make the next set of NIOS devices from a film deposited on ZnS prisms. ZnS more closely matches the low light intensity index of the films. Preliminary studies of further changes to produce stronger nonlinearity have been performed. Raman spectroscopy showed that these films heated in oxygen organize themselves into octohedra, which are thought to be necessary for the photorefractive effects observed in titanates and niobates. Heating the films in vacuum produces blue films which ESCA shows contain tungsten in the +4 oxidation state. Such electron rich species might be able to provide highly polarizable charge carriers. In addition to use as optical switches, use of these films to make reconfigurable Dammann gratings has been studied. These gratings would allow optical addressing of large size S-SEED arrays. DTIC

N94-19602# Cornell Univ., Ithaca, NY.
EVALUATION OF LASER DIODE BASED OPTICAL SWITCHES FOR OPTICAL PROCESSORS Final Report, Mar. - Dec. 1992
Paul D. Swanson, Michael A. Parker, and Stuart I. Libby Jul. 1993 21 p
(Contract F30602-92-C-0038)
(AD-A270949; RL-TR-93-145) Avail: CASI HC A02/MF A01

Three optical switching elements have been designed, fabricated, and tested for use in an integrated, optical signal processor. The first, an optical NOR logic gate, uses gain quenching as a means of allowing one (or more) light beam(s) to control the output light. This technique, along with the use of a two pad bistable output laser, is used in demonstrating the feasibility of the second device, an all optical RS flip flop. The third device consists of a broad area orthogonal model switching laser, whose corollary outputs correspond to the sign of the voltage difference between its two high impedance electrical inputs. This device also has possible memory applications if bistable mode switching within the broad area laser can be achieved. DTIC

N94-19772# Rochester Univ., NY. Inst. of Optics.
SCHROEDINGER'S HOPE
Carlos Stroud Jul. 1993 11 p
(Contract DAAL03-92-G-0147)
(AD-A270988; ARO-30367.27-PH-URI) Avail: CASI HC A03/MF A01

Recent work at the University of Rochester that was supported by the Army Research Office through the University Research Initiative Program was featured in a recent book Taming the Atom by Hans Christian von Baeyer. An excerpt from that book is presented that shows that the work in Rochester is the realization of Erwin Schroedinger's hope in the earliest days of quantum theory that a solution to his equation could be found in the form of a localized wave packet moving along the elliptical orbit predicted by classical theory. In a series of calculations and experiments the group in Rochester was shown that a short laser pulse can be used to excite such a wave packet state and that as the wave packet moves many times around the orbit it undergoes a complicated time evolution in which it spreads all the way around the orbit, and then repeatedly relocalizes in the form of a single wave packet or a series of identical sub-wave packets equally spaced around the orbit. This work sheds new light on the boundary between microscopic quantum systems and macroscopic classical systems. DTIC

75 PLASMA PHYSICS

Includes magnetohydrodynamics and plasma fusion.

For ionospheric plasmas see *46 Geophysics*. For space plasmas see *90 Astrophysics*.

N94-17688# International Centre for Theoretical Physics, Trieste (Italy).
THE PHASE MIXING OF SHEAR ALFVEN WAVES
C. Uberoi Apr. 1993 7 p
(DE93-624920; IC-93/69) Avail: CASI HC A02/MF A01 (US Sales Only)

The phase mixing of shear Alfven waves is discussed as a current sheets crossover phenomena by using the well-behaved time dependent solution of the Alfven wave equation. This method is a more direct approach than the initial value problem technique to find the collisionless damping time of the surface waves, which as it represents the coherency loss is argued to be the phase mixing time. The phase mixing time obtained by both the methods compares well. The direct method, however, has an advantage that no particular profile for the magnetic field variation need to be chosen and secondly the phase mixing time and the time scale for which the resistivity effects become important can be expressed conveniently in terms of Alfven transit times before crossover. DOE

N94-17689# Ceskoslovenska Akademie Ved, Prague.
TRANSFORMATION OF ENERGY AND MOMENTUM DUE TO LANDAU DAMPING IN SPACE
J. Lacina Aug. 1992 21 p
(DE93-624921; IPPCZ-325) Avail: CASI HC A03/MF A01 (US Sales Only)

General expressions are derived for the time-averaged flow of kinetic energy and of kinetic momentum, valid in the second order approximation. While the time-averaged density of kinetic energy is constant in time, the time-averaged flow of kinetic energy is constant in space. Therefore, no deposition of energy in a plasma occurs, despite the fact that Landau damping in space takes place for stable plasmas. The constant value of the averaged flow of kinetic energy is given by the contribution of the undamped coherent free oscillations, while the spatial damping of the forced oscillations sets off the effect of the phase interference between forced and free oscillations. DOE

N94-17694 Oak Ridge National Lab., TN.
POWER COMPENSATORS FOR PHASED OPERATION OF ANTENNA ARRAYS ON JET AND D3-D
R. H. Goulding, D. J. Hoffman, P. M. Ryan, G. Bosia (Joint European Torus Project, Abingdon, England.), M. Bures (Joint European Torus Project, Abingdon, England.), D. Start (Joint European Torus Project, Abingdon, England.), T. Wade (Joint European Torus Project, Abingdon, England.), C. C. Petty (General Atomic Co., San Diego, CA.), and R. I. Pinsker (General Atomic Co., San Diego, CA.) 1993 4 p Presented at the 10th Topical Conference on Radio Frequency Power in Plasmas, Boston, MA, 1-3 Apr. 1993 Limited Reproducibility: More than 20% of this document may be affected by microfiche quality
(Contract DE-AC05-84OR-21400)
(DE93-013208; CONF-9304112-7) Avail: CASI HC A01

A system has been designed to allow operation of the JET A2 antenna arrays with phasing between elements of other than 0 or pi at increased power. The system uses a hybrid coupler to transfer power in the direction opposite to that occurring at the antenna elements. This results in nearly equal currents and voltages on the feed lines and antenna structures, with nearly equal input powers at the RF generators. The direction and magnitude of the power transfer is controlled by adjustable tuning elements mounted on two of the four coupler ports. Much insight has been gained on optimization of the circuit design to maximize bandwidth (approximately 10 MHz for the present JET design with 20 MHz a possibility) and power-handling capability. The concept has been tested initially on the D3-D tokamak, with a compensator installed in the feed circuit for the four-element FWCD antenna array. In this application it acts to equalize input impedances and will eventually be used to allow operation with multiple transmitters. DOE

N94-17697 Oak Ridge National Lab., TN.
ITER EDA DESIGN CONFINEMENT CAPABILITY
N. A. Uckan 1993 21 p Presented at the International Thermonuclear Experimental Reactor Meeting, Atlanta, GA, 10 Mar. 1993 Limited Reproducibility: More than 20% of this document may be affected by microfiche quality
(Contract DE-AC05-84OR-21400)
(DE93-013729; CONF-9303153-1) Avail: CASI HC A03

Major device parameters for ITER-EDA and CDA are given in this paper. Ignition capability of the EDA (and CDA) operational scenarios is evaluated using both the 1 1/2-D time-dependent transport simulations and 0-D global models under different confinement ((chi((gradient)(T)(sub e)(sub crit)), empirical global energy confinement scalings, chi(empirical), etc.) assumptions. Results from some of these transport simulations and confinement assessments are summarized in and compared with the ITER CDA results. DOE

N94-17702# General Atomic Co., San Diego, CA.
LIMITS ON m = 2, n = 1 ERROR FIELD INDUCED LOCKED MODE INSTABILITY IN TPX WITH TYPICAL SOURCES OF POLOIDAL FIELD COIL ERROR FIELD AND A PROTO TYPE CORRECTION COIL, C-COIL
R. J. LaHaye Dec. 1992 21 p
(Contract DE-AC03-89ER-51114)
(DE93-014408; GA-A-21167) Avail: CASI HC A03/MF A01

Irregularities in the winding or alignment of poloidal or toroidal magnetic field coils in tokamaks produce resonant low m, n = 1 static error fields. Otherwise stable discharges can become nonlinearly unstable, and locked modes can occur with subsequent disruption when subjected to modest m = 2, n = 1 external perturbations. Using both theory and the results of error field/locked mode experiments on DIII-D and other tokamaks, the critical m = 2, n = 1 applied error field for locked mode instability in TPX is calculated for discharges with ohmic, neutral beam, or RF heating. Ohmic discharges are predicted to be most sensitive, but even co-injected neutral beam discharges (at beta(sub N) = 3) in TPX will require keeping the relative 2,1 error field (B(sub r21)/B(sub T)) below 2 x 10(exp -4). The error fields resulting from 'as-built' alignment irregularities of various poloidal field coils are computed. Coils if well-designed must be positioned to within 3 mm with respect to the toroidal field to keep the total 2,1 error field within limits. Failing this, a set of prototype correction coils is analyzed for use in bringing 2,1 error field down to a tolerable level. DOE

N94-17708# Lawrence Livermore National Lab., CA.
ANALYSIS OF NEON SOFT X RAY SPECTRA FROM SHORT-PULSE LASER-PRODUCED PLASMAS
A. C. Abare (Florida Univ., Gainesville.), C. J. Keane, J. K. Crane, L. B. DaSilva, R. W. Lee, M. D. Perry, and R. W. Falcone (California Univ., Berkeley.) Apr. 1993 11 p Presented at the OE/LASE 1993: International Society for Optical Engineering (SPIE) Conference, Los Angeles, CA, 16-23 Jan. 1993
(Contract W-7405-eng-48)
(DE93-014420; UCRL-JC-113498; CONF-930159-36) Avail: CASI HC A03/MF A01

We report preliminary results from the analysis of streaked soft x-ray neon spectra obtained from the interaction of a picosecond Nd:glass laser with a gas jet target. In these experiments streaked spectra show prompt harmonic emission followed by longer time duration soft x-ray line emission. The majority of the line emission observed was found to originate from Li- and Be-like Ne and the major transitions in the observed spectra have been identified. Li-like emission lines were observed to decay faster in time than Be-like transitions, suggesting that recombination is taking place. Line ratios of n = 4-2 and n = 3-2 transitions supported the view that these lines were optically thin and thick, respectively. The time history of Li-like Ne 2p-4d and 2p-3d lines is in good agreement with a simple adiabatic expansion model coupled to a time dependent collisional-radiative code. Further x-ray spectroscopic analysis is underway which is aimed at diagnosing plasma conditions and assessing the potential of this recombining neon plasma as a quasi-steady-state recombination x-ray laser medium. DOE

N94-17713# Los Alamos National Lab., NM.
USING THE TRITIUM PLASMA EXPERIMENT TO EVALUATE ITER PFC SAFETY
Glen R. Longhurst (Edgerton, Germeshausen and Grier, Inc., Idaho Falls, ID.), Robert A. Anderl (Edgerton, Germeshausen and Grier, Inc., Idaho Falls, ID.), John R. Bartlit, Rion A. Causey (Sandia National Labs., Livermore, CA.), and John R. Haines (McDonnell-Douglas Corp., Saint Louis, MO.) 1993 11 p Presented at the International Atomic Energy Agency (IAEA) Technical Committee Meeting on Developments in Fusion Safety, Toronto, Ontario, 7-11 Jun. 1993
(Contracts W-7405-eng-36; DE-AC07-76ID-01570)
(DE93-016614; LA-UR-93-2148; CONF-9306191-1) Avail: CASI HC A03/MF A01

The Tritium Plasma Experiment was assembled at Sandia National Laboratories, Livermore to investigate interactions between dense plasmas at low energies and plasma-facing component materials. This apparatus has the unique capability of replicating plasma conditions in a tokamak divertor with particle flux densities of 2 x 10(exp 19) ions/((sq cm)(s)) and a plasma temperature of about 15 eV using a plasma that includes tritium. With the closure of the Tritium Research Laboratory at Livermore, the experiment was moved to the Tritium Systems Test Assembly facility at Los Alamos National Laboratory. An experimental program has been initiated there using the Tritium Plasma Experiment to examine safety issues related to tritium in plasma-facing components, particularly the ITER divertor. Those issues include tritium retention and release characteristics, tritium permeation rates and transient times to coolant streams, surface modification and erosion by the plasma, the effects of thermal loads and cycling, and particulate production. A considerable lack of data exists in these areas for many of the materials, especially beryllium, being considered for use in ITER. Not only will basic material behavior with respect to safety issues in the divertor environment be examined, but innovative techniques for optimizing performance with respect to tritium safety by material modification and process control will be investigated. Supplementary experiments will be carried out at the Idaho National Engineering Laboratory and Sandia National Laboratory to expand and clarify results obtained on the Tritium Plasma Experiment. DOE

N94-17727# Los Alamos National Lab., NM.
RAPID ANALYSIS OF MIXED WASTE SAMPLES VIA THE OPTICAL EMISSION FROM LASER INITIATED MICROPLASMAS
J. E. Barefield, II, M. D. Ferran, and D. A. Cremers 1993 20 p Presented at the 2nd International Mixed Waste Symposium, Baltimore, MD, 17-20 Aug. 1993
(Contract W-7405-eng-36)
(DE93-014563; LA-UR-93-1795; CONF-930873-16) Avail: CASI HC A03/MF A01

Wavelength resolved optical emission from laser initiated microplasmas in samples containing Pu, Am, Pb, Cr, and Be was used to determine elemental compositions. Traditionally, samples of this type are analyzed by neutron activation, X-ray fluorescence, atomic absorption (AA), inductively coupled plasma - atomic emission spectroscopy (ICP-AES), and inductively coupled plasma mass spectroscopy (ICP-MS). Analysis via the traditional analytical spectroscopic techniques involves extensive sample separation and preparation which results in the generation of significant quantities of additional waste. In the laser based method, little to no sample preparation is required. The method is essentially waste free since only a few micrograms of material is removed from the sample in the generation of the microplasma. Detection limits of the laser based method typically range between subppm to tens of ppM. In this report, the optical emission from samples containing Pu, Am, Pb, Cr, and Be will be discussed. We will also discuss the essential elements of the analysis method. DOE

N94-17739# Oak Ridge Inst. for Science and Education, TN.

MAGNETIC FUSION ENERGY TECHNOLOGY FELLOWSHIP: REPORT ON SURVEY OF INSTITUTIONAL COORDINATORS

Feb. 1993 23 p
(Contract DE-AC05-76OR-00033)
(DE93-014646; DOE/OR-00033/T530) Avail: CASI HC A03/MF A01

In 1980, the Magnetic Fusion Energy Technology (MFET) Fellowship program was established by the US Department of Energy, Office of Fusion Energy, to encourage outstanding students interested in fusion energy technology to continue their education at a qualified graduate school. The basic objective of the MFET Fellowship program is to ensure an adequate supply of scientists in this field by supporting graduate study, training, and research in magnetic fusion energy technology. The program also supports the broader objective of advancing fusion toward the realization of commercially viable energy systems through the research by MFET fellows. The MFET Fellowship program is administered by the Science/Engineering Education Division of Oak Ridge Institute for Science and Education. Guidance for program administration is provided by an academic advisory committee. DOE

N94-17743# Oak Ridge National Lab., TN.

SELF-REGULATED SHEAR FLOW TURBULENCE IN CONFINED PLASMAS

B. A. Carreras, L. A. Charlton, K. Sidikman, P. H. Diamond (California Univ., San Diego, La Jolla.), and L. Garcia (Universidad Complutense, Madrid, Spain.) 1993 4 p Presented at the 20th European Conference on Controlled Fusion and Plasma Physics, Lisbon, Portugal, 26-30 Jul. 1993
(Contract DE-AC05-84OR-21400)
(DE93-015823; CONF-930720-13) Avail: CASI HC A01/MF A01

The need for a radially inhomogenous fluctuation spectrum in a cylindrical plasma has been shown analytically and numerically. For the long wavelength drift wave turbulence model, where a radial inhomogeneity can result from self-binding effects near low-q resonances and edge effects, the calculated Reynolds stress is nonzero only in these spatial regions. In tokamaks, the radial inhomogeneity of the turbulence is particularly important at the plasma edge. Tokamak edge plasmas in OH or L-mode are characterized by large fluctuation levels and strong radial symmetry breaking. Thus, it is clear that edge flows will be regulated by fluctuations. Indeed, the only real question is the mechanism for radial propagation. The possibilities include diamagnetically induced radial wave propagation in the ambient fluctuations, and seed shears and dilatations, which in turn induce radial propagation. The second mechanism is considered in this document. DOE

N94-17753# Texas Univ., Austin.

PROFILE STABILIZATION OF TILT MODE IN A FIELD REVERSED CONFIGURATION

J. W. Cobb, T. Tajima, and D. C. Barnes (Los Alamos National Lab., NM.) Jun. 1993 38 p
(Contract DE-FG05-80ET-53088)
(DE93-016770; DOE/ET-53088/608; IFSR-608) Avail: CASI HC A03/MF A01

The possibility of stabilizing the tilt mode in Field Reversed Configurations without resorting to explicit kinetic effects such as large ion orbits is investigated. Various pressure profiles, P(psi), are chosen, including 'hollow' profiles where current is strongly peaked near the separatrix. Numerical equilibria are used as input for an initial value simulation which uses an extended magnetohydrodynamic (MHD) model that includes viscous and Hall terms. Tilt stability is found for specific hollow profiles when accompanied by high values of separatrix beta, beta(sub sep). The stable profiles also have moderate to large elongation, racetrack separatrix shape, and lower values of 3, average ratio of Larmor radius to device radius. The stability is unaffected by changes in viscosity, but the neglect of the Hall term does cause stable results to become marginal or unstable. Implications for interpretation of recent experiments are discussed. DOE

N94-17809# Old Dominion Univ., Norfolk, VA. Dept. of Electrical and Computer Engineering.

MICROWAVE SCATTERING FROM TAE MODES

L. Vahala 28 Sep. 1992 4 p
(Contract DE-FG05-90ER-54093)
(DE93-018170; DOE/ER-54093/2) Avail: CASI HC A01/MF A01

This is a progress report of calculations involving the effect of magnetic and density fluctuations on both lower hybrid (LH) waves as well as ordinary (O) and extraordinary (X) waves in tokamaks. The fluctuations considered could arise form either drift wave turbulence or TAE models. Derived from text

N94-17854# New York Univ., New York. Courant Inst. of Mathematical Sciences.

PLASMA PROPERTIES RESEARCH: TASK 3

1992 21 p
(Contract DE-FG02-86ER-53223)
(DE93-017087; DOE/ER-53223/207) Avail: CASI HC A03/MF A01

The principal research activities of the Magneto-Fluid Dynamics Division relate to magnetic fusion plasma physics. In addition, there is a modest amount of work in closely related areas including space plasma physics, fluid dynamics, and dynamical systems. Members of the Magneto-Fluid Dynamics Division maintain close contacts with fusion researchers in the US and abroad. Some of the work of the Division is clearly directed towards ITER and TPX, while other problems relate to the broader development of fusion plasma physics and to the support of other issues arising in the many experimental programs. Topics that are discussed in this report are as follows: application of sophisticated statistical techniques to tokamak data reduction, including time series analysis of TFTR fluctuation data and spline analysis of profile data; continuing development of edge plasma and divertor modelling, including initial ergodic divertor studies; analysis of energetic fusion products losses from TFTR plasmas; examination of anomalous transport in dynamical systems induced by chaotic-like Hamiltonian motion; numerical simulation of the development of singular MHD equilibria; exploration of the validity of moment expansions of kinetic equations for weakly collisional systems; studies of RF- and ripple-induced helium ash removal; ballooning mode studies in fluids and rotating stars; and studies in dynamical systems, including explosive instabilities, development of chaos, and motion of collisionless particles in a domain with overlapping islands. DOE

N94-17912# InterScience, Inc., Troy, NY.

LABORATORY MICROFUSION CAPABILITY STUDY

May 1993 208 p
(Contract DE-AC01-91DP-00239)
(DE93-014373; DOE/DP-0017) Avail: CASI HC A10/MF A03

The purpose of this study is to elucidate the issues involved in developing a Laboratory Microfusion Capability (LMC) which is the major objective of the Inertial Confinement Fusion (ICF) program within the purview of the Department of Energy's Defense Programs. The study was initiated to support a number of DOE management needs: to provide insight for the evolution of the ICF program; to afford guidance to the ICF laboratories in planning their research and development programs; to inform Congress and others of the details and implications of the LMC; to identify criteria for selection of a concept for the Laboratory Microfusion Facility; and to develop a coordinated plan for the realization of an LMC. As originally proposed, the LMC study was divided into two phases. The first phase identifies the purpose and potential utility of the LMC, the regime of its performance parameters, driver independent design issues and requirements, its development goals and requirements, and associated technical, management, staffing, environmental, and other developmental and operational issues. The second phase addresses driver-dependent issues such as specific design, range of performance capabilities, and cost. The study includes four driver options: the neodymium-glass solid state laser, the krypton fluoride excimer gas laser, the light-ion accelerator, and the heavy-ion induction linear accelerator. The results of the Phase 2 study are described in the present report. DOE

N94-17945# Texas Univ., Austin. Inst. for Fusion Studies.

FILAMENTARY MAGNETOHYDRODYNAMIC PLASMAS

R. Kinney, T. Tajima, N. Petviashvili, and J. C. McWilliams (National Center for Atmospheric Research, Boulder, CO.) May 1993 57 p
(Contract DE-FG05-80ET-53088)
(DE93-015616; DOE/ET-53088-606; IFSR-606) Avail: CASI HC A04/MF A01

A filamentary construct of magnetohydrodynamical plasma dynamics, based on the Elsasser variables was developed. This approach is modeled after discrete vortex models of hydrodynamical turbulence, which cannot be expected in general to produce results identical to ones based on a Fourier decomposition of the fields. In a highly intermittent plasma, the induction force is small compared to the convective motion, and when this force is neglected, the plasma vortex system is described by a Hamiltonian. For a system with many such vortices we present a statistical treatment of a collection of discrete current-vorticity concentrations. Canonical and microcanonical statistical calculations show that both the vorticity and the current spectra are peaked at long wavelengths, and the expected states revert to known hydrodynamical states as the magnetic field vanishes. These results differ from previous Fourier-based statistical theories, but it is found that when the filament calculation is expanded to include the inductive force, the results approach the Fourier equilibria in the low-temperature limit, and the previous Hamiltonian plasma vortex results in the high-temperature limit. Numerical simulations of a large number of filaments are carried out and support the theory. A three-dimensional vortex model is outlined as well, which is also Hamiltonian when the inductive force is neglected. DOE

N94-17948# Texas Univ., Austin. Inst. for Fusion Studies.
FILAMENTATION, CURRENT PROFILES AND TRANSPORT IN A TOKAMAK
J. B. Taylor Jun. 1993 18 p
(Contract DE-FG05-80ET-53088)
(DE93-016768; DOE/ET-53088/613; IFSR-613) Avail: CASI HC A03/MF A01

A Tokamak with slightly imperfect magnetic surfaces should have a microscopically filamented current structure. If so, its equilibrium has an exact analog in the dynamics of interacting charged rods. Then there will be a natural current-profile, analogous to thermal equilibrium of the rods (and the natural profile can be calculated by conventional statistical mechanics). This would account for the phenomenon of profile consistency or resilience in Tokamaks. In addition to the natural profiles, this filamentary model also predicts an anomalous inward flux of both heat and particles in a Tokamak, as well as an anomalous diffusion. These 'inward-pinch' components are related to the current gradient. DOE

N94-17955 International Centre for Theoretical Physics, Trieste (Italy).
WAKE FIELD IN ELECTRON-POSITRON PLASMAS
K. Avinash and V. I. Berezhiani Mar. 1993 12 p Limited Reproducibility: More than 20% of this document may be affected by microfiche quality
(DE93-624929; IC-93/48) Avail: CASI HC A03 (US Sales Only)

We study the creation of wake field in cold electron positron plasma by electron bunches. In the resulting plasma inhomogeneity we study the propagation of short electromagnetic pulse. It is found that wake fields can change the frequency of the radiation substantially. DOE

N94-17981 Max-Planck-Inst. fuer Plasmaphysik, Munich (Germany).
A FREE BOUNDARY EIGENVAUE PROBLEM
Rita Meyer-Spasche Sep. 1992 17 p
(IPP-6/310; ETN-93-94612) Copyright Avail: Fachinformationszentrum Karslruhe, 7514 Eggenstein-Leopoldschafen 2, Germany

The equilibrium equations for a confined axisymmetric plasma lead to a free boundary problem. A simple model problem is considered. Related equations are known from other applications. If all but one parameter are kept fixed, it is a nonlinear elliptic eigenvalue problem which generalizes a related 'linear' eigenvalue problem. Given a branch of explicitly known solutions, there exist countably infinitely many bifurcation points. This is shown by a perturbation approach and generalizes results by Sijbrand. The structure of the solutions on the bifurcating branches is investigated numerically: their rapid changing near the bifurcation points as well as their asymptotics. The numerical error caused by the free boundary is well understood and was kept small in the investigations. ESA

N94-17983# Texas Univ., Austin. Inst. for Fusion Studies.
TRANSPORT IN THE SELF-ORGANIZED RELAXED STATE OF ION TEMPERATURE GRADIENT INSTABILITY
T. Tajima, M. J. LeBrun, M. G. Gray, J. Y. Kim, W. Horton, V. Wong, M. Kotschenreuther, and Y. Kishimoto (Japan Atomic Energy Research Inst., Ibaraki.) Jun. 1993 23 p
(Contract DE-FG05-80ET-53088)
(DE93-016769; DOE/ET-53088/612; IFSR-612) Avail: CASI HC A03/MF A01

The anomalous heat conduction in a tokamak plasma is investigated analytically and computationally. Our toroidal particle simulation shows a new emerging physical picture that the toroidal plasma exhibits marked properties distinct from a cylindrical plasma: (1) the development of radially extended potential streamers localized to the outside of the torus; (2) more robust ion temperature gradient instability; (3) radially constant eigenfrequency; (4) global temperature relaxation; and (5) radially increasing heat conductivity chi(sub i). These results are analyzed by linear and quasilinear kinetic theory. A relaxation theory based on the reductive perturbation theory in the quasilinear equation is developed. The theory constrains the thermal flux so that chi(sub i) increases radially. The Bohm-like scaling is found in connection with the radially extended mode structure. DOE

N94-17988# Lawrence Livermore National Lab., CA.
EVALUATION OF MATERIALS PROPOSED FOR THE CONSTRUCTION OF THE PLASMA ELECTRODE POCKELS CELL (PEPC) ON BEAMLET
D. Roberts, C. Robb, J. DeYoreo, and J. Atherton Nov. 1992 26 p
(Contract W-7405-eng-48)
(DE93-016952; UCRL-ID-112219) Avail: CASI HC A03/MF A01

The proposed upgrade of the NOVA laser system at Lawrence Livermore National Laboratory employs a multipass architecture that requires an optical switch to emit the laser light at the appropriate fluence. This Pockels cell-based optical switch does not use traditional ring or thin-film electrodes because of the large aperture and high fluence of the laser system. Rather, it uses a plasma electrode Pockels cell with a KD*P crystal as the electro-optical medium. A discharge plasma is formed on each side of the electro-optic crystal and high voltage is applied across the crystal through the plasma electrode to initiate optical switching. In October 1991 we began evaluating materials suggested for the large aperture plasma electrode optical switch. Previous experiments suggested that switching performance could be significantly affected by the deterioration of cell materials. The final prototype switch tested used polyethylene for the switch body, Mykroy for the mid-plane and a silicone vulcanite to encapsulate the KD*P crystal. The encapsulant easily compensated for the effect of assembling the optical switch and no strain-induced birefringence in the crystal after encapsulation was measured. Oxygen was eventually added to the plasma to react with the sputtered carbon from the cathode and produce a gaseous effluent. As an added benefit, the production of ozone absorbed most of the ultraviolet radiation affecting the encapsulant. All the materials tested decomposed and produced volatiles, although no change in the damage threshold of exposed optical surfaces tested to date was seen. An evaluation of the recommended materials for major cell components using published manufacturers data, experimental results from our Material Evaluation Apparatus, and outgassing performance and sputtering data produced at the Laboratory's Vacuum Process Lab is presented. DOE

N94-17990# Lawrence Livermore National Lab., CA.
CONFIGURATION INTERACTION IN LTE SPECTRA OF HEAVY ELEMENTS
A. Bar-Shalom, J. Oreg (Negev Univ., Beersheva, Israel.), and W. Goldstein Nov. 1992 26 p Presented at the Radiative Properties of Hot Dense Matter Conference, Santa Barbara, CA, 2-6 Nov. 1992
(Contract W-7405-eng-48)
(DE93-017166; UCRL-JC-113642; CONF-9211211-3) Avail: CASI HC A03/MF A01

A method for including the effects of configuration interaction (CI) between relativistic subconfigurations of an electron configuration in the calculation of emission and absorption spectra of plasmas in local thermodynamic equilibrium (LTE) is presented. Analytical expressions for the correction to the intensities, owing to CI, of an unresolved transition array (UTA) and of a supertransition array (STA) are obtained when the correction is small compared to the spin-orbit splitting, bypassing the need to diagonalize energy matrices. These expressions serve as working formulas in the STA model and, in addition, reveal a priori the conditions under which CI effects are significant. Examples of the effect are presented. DOE

N94-17993# Lawrence Livermore National Lab., CA.
PRODUCTION OF DENSE VAPOR TARGETS FOR LASER-PLASMA INTERACTION STUDIES WITH INTENSE, ULTRA-SHORT PULSES
P. R. Bolton, D. C. Eder, G. Guethlein, R. E. Stewart, and P. E. Young 19 Mar. 1993 14 p Presented at the OE/LASE 1993: International

Society for Optical Engineering Conference, Los Angeles, CA, 16-23 Jan. 1993
(Contract W-7405-eng-48)
(DE93-017175; UCRL-JC-113302; CONF-930159-46) Avail: CASI HC A03/MF A01

The technique of laser-induced ablation of thin films from glass slide substrates has been investigated as a candidate vapor target production method for studies of both tunneling-driven x-ray/xuv recombination lasers and relativistic propagation using intense, ultra-short laser pulses. It is shown by simultaneous two-wavelength interferometry that particle densities of order 10(exp 19)/cm(exp 3) are readily achieved and that some intrinsic ionization accompanies the plume formation. Absorption measurements with both 100 picosecond and 125 femtosecond pulses are consistent with observed edge velocities near 10(exp 6) cm/sec. The level of ionization driven by the intense 125 femtosecond laser pulse has been coarsely estimated. Averaged estimates from spectral blue shifting of spectra transmitted through the plume are consistently lower than those obtained from evaluation of saturation intensity thresholds based on the sequential nonresonant optical field ionization (OFI) process. DOE

N94-18056# General Atomic Co., San Diego, CA.
ANALYSIS OF THE ITER H-MODE CONFINEMENT DATABASE
D. P. Schissel, O. Kardaun, F. Ryter, and U. Stroth May 1993 4 p Presented at the 20th European Conference on Controlled Fusion and Plasma Physics, Lisbon, Portugal, 26-30 Jul. 1993 Submitted for publication
(Contract DE-AC03-89ER-51114)
(DE93-016984; GA-A-21310; CONF-930720-16) Avail: CASI HC A01/MF A01

In order to predict the global energy confinement time in the next generation of large tokamaks it is essential to have data from machines of different sizes and operating parameter regimes. This data can also be used to construct dimensionless scalings and thereby attempt to differentiate between Bohm and gyro-Bohm based transport models. Previously, at the request of the ITER project, H-mode global confinement data was assembled from six machines, ASDEX, DIII-D, JET, JFT-2M, PBX-M, and PDX, into a single database. This collaboration has continued with the initial database being expanded by extending the plasma parameter space as well as by improving the precision of some of the relevant calculated plasma parameters. This paper summarizes work that has been performed on the newest version (ITERH.DB2) of the confinement database. DOE

N94-18057# General Atomic Co., San Diego, CA.
COUPLED MHD AND TRANSPORT ANALYSIS OF IMPROVED CONFINEMENT D3-D DISCHARGES
H. St.John, J. R. Ferron, L. L. Lao, T. H. Osborne, S. J. Thompson, and D. Wroblewski (California Univ., Livermore. Lawrence Livermore Lab.) May 1993 4 p Presented at the 20th European Conference on Controlled Fusion and Plasma Physics, Lisbon, Portugal, 26-30 Jul. 1993 Submitted for publication
(Contracts DE-AC03-89ER-51114; W-7405-eng-48)
(DE93-016985; GA-A-21309; CONF-930720-15) Avail: CASI HC A01/MF A01

Transiently high internal inductance discharges are used to check the validity of evolvement of current profiles obtained with the MHD/transport coupled scheme presented below. Both a current ramp and an elongation ramp discharge are examined. To simulate energy confinement the Rebut-Lallia-Watkins model is used for the current ramp discharge. In our simulation of experimental discharges external circuit behavior is accounted for by using measured, time dependent flux loops, magnetic probes, field shaping, and ohmic coil currents. The small effect of eddy currents in the plasma vessel are neglected. We use measured, time dependent electron and ion temperature profiles, electron density, Z(sub eff), toroidal rotation, and radiated power profiles to constrain our analyses. For the RLW simulation measured values of T(sub e) and T(sub i) at the plasma edge are used as boundary conditions in the electron and ion energy equations. DOE

N94-18058# General Atomic Co., San Diego, CA.
DEPENDENCE OF HELIUM TRANSPORT ON PLASMA CURRENT AND ELM FREQUENCY IN H-MODE DISCHARGES IN D3-D
M. R. Wade (Oak Ridge Inst. for Science and Education, TN.), D. L. Hillis (Oak Ridge National Lab., TN.), J. T. Hogan (Oak Ridge National Lab., TN.), D. F. Finkenthal (California Univ., Berkeley.), W. P. West, and K. Burrell May 1993 4 p Presented at the 20th European Conference on Controlled Fusion and Plasma Physics, Lisbon, Portugal, 26-30 Jul. 1993 Submitted for publication
(Contracts DE-AC03-89ER-51114; DE-AC05-84OR-21400; DE-FG03-89ER-51116)
(DE93-016986; GA-A-21305; CONF-930720-14) Avail: CASI HC A01/MF A01

The removal of helium (He) ash from the plasma core with high efficiency to prevent dilution of the D-T fuel mixture is of utmost importance for future fusion devices, such as the International Thermonuclear Experimental Reactor (ITER). A variety of measurements in L-mode conditions have shown that the intrinsic level of helium transport from the core to the edge may be sufficient to prevent sufficient dilution (i.e., tau(sub He) /tau(sub E) less than 5). Preliminary measurements in biased-induced, limited H-mode discharges in TEXTOR suggest that the intrinsic helium transport properties may not be as favorable. If this trend is shown also in diverted H-mode plasmas, then scenarios based on ELMing H-modes would be less desirable. To further establish the database on helium transport in H-mode conditions, recent studies on the DIII-D tokamak have focused on determining helium transport properties in H-mode conditions and the dependence of these properties on plasma current and ELM frequency. DOE

N94-18082# Lawrence Livermore National Lab., CA.
CHARACTERIZATION OF SHORT PULSE LASER-PRODUCED PLASMAS AT THE LAWRENCE LIVERMORE NATIONAL LABORATORY ULTRA SHORT-PULSE LASER
R. Shepherd, D. Price, W. White, A. Osterheld, R. Walling, W. Goldstein, R. Stewart, and S. Gordan 14 Jul. 1993 6 p Presented at the OE/LASE 1993 International Society for Optical Engineering (SPIE) Conference, Los Angeles, CA, 16-23 Jan. 1993
(Contract W-7405-eng-48)
(DE93-017191; UCRL-JC-113645; CONF-930159-52) Avail: CASI HC A02/MF A01

The K-shell emission from porous aluminum targets is used to infer the density and temperature of plasmas created with 800 nm and 400 nm, 140 fs laser light. The laser beam is focused to a minimum spot size of 5 micron with 800 nm light and 3 micron with 400 nm light, producing a normal incidence peak intensity of 10(exp 18) Watts/cm(exp 2). A new 800 fs x-ray streak camera is used to study the broadband x-ray emission. The time resolved and time integrated x-ray emission implies substantial differences between the porous target and the flat target temperature. DOE

N94-18115# Lawrence Livermore National Lab., CA.
ABSORPTION AND X RAY MEASUREMENTS FROM ULTRA-INTENSE LASER-PLASMA INTERACTIONS
D. E. Klem, C. Darrow, S. Lane, and M. D. Perry 1 Mar. 1993 6 p Presented at the OE/LASE 1993: International Society for Optical Engineering (SPIE) Conference, Los Angeles, CA, 16-23 Jan. 1993
(Contract W-7405-eng-48)
(DE93-016538; UCRL-JC-112950; CONF-930159-50) Avail: CASI HC A02/MF A01

The interaction of subpicosecond 1.06 mm laser light at intensities up to 10(exp 18) W/sq cm with dense performed plasmas is investigated by measurements of the absorption of the laser light in the plasma and by measurements of the production of bremsstrahlung x-rays. Absorption measurements are made by collecting the scattered light in an Ulbricht sphere. Light scattered in the backward and specular directions is collected separately. Measurements are presented for both high and low Z targets. X-ray production is measured using a nine channel filter/scintillator spectrometer. DOE

N94-18129# Lawrence Livermore National Lab., CA.
TIME-RESOLVED PROBING OF ELECTRON THERMAL CONDUCTION IN FEMTOSECOND-LASER-PULSE-PRODUCED PLASMAS
B. T. V. Vue (California Univ., Berkeley. Lawrence Berkeley Lab.), A. Szoke, and O. L. Landen Jun. 1993 6 p Presented at the 2nd International Conference on Laser Ablation: Mechanisms and Applications, Knoxville, TN, 19-22 Apr. 1993
(Contract W-7405-eng-48)

(DE93-016996; UCRL-JC-113165; CONF-9304144-10) Avail: CASI HC A02/MF A01

We present time-resolved measurements of reflectivity, transmissivity, and frequency shifts of probe light interacting with the rear of a disk-like plasma produced by irradiation of a transparent solid target with 0.1ps FWHM laser pulses at peak intensity 5(10)(exp 14) W/sq cm. Experimental results show a large increase in reflection revealing rapid formation of a steep gradient and overdense surface plasma layer during the first picosecond after irradiation. Frequency shifts due to a moving ionization created by thermal conduction into the solid target are recorded. Calculations using a nonlinear thermal heat wave model show good agreement with the measured frequency shifts, further confining the strong thermal transport effect. DOE

N94-18148 Naval Research Lab., Washington, DC.

ENHANCED ACCELERATION IN A SELF-MODULATED-LASER WAKEFIELD ACCELERATOR Interim Report

J. Krall, A. Ting, E. Esarey, and P. Sprangle 15 Jul. 1993 21 p Limited Reproducibility: More than 20% of this document may be affected by microfiche quality

(AD-A268452; NRL/MR/6790-93-7348) Avail: CASI HC A03

A new configuration of the laser wakefield accelerator is proposed in which enhanced acceleration is achieved via resonant self-modulation of the laser pulse. This requires laser power in excess of the critical power for relativistic guiding and a plasma wavelength that is short compared to the laser pulse-length. Relativistic and density wake effects strongly modulate the laser pulse at the plasma wavelength. This resonantly excites the plasma wave and leads to enhanced acceleration. DTIC

N94-18157 Japan Atomic Energy Research Inst., Tokyo.

AEOLUS-IT MHD SIMULATION CODE BASED ON A TOROIDALLY INCOMPRESSIBLE PLASMA MODEL

Gen-ichi Kurita, Masafumi Azumi, and Tatsuoki Takeda Feb. 1993 57 p Limited Reproducibility: More than 20% of this document may be affected by microfiche quality

(DE93-788461; JAERI-M-93-004) Avail: CASI HC A04

A three dimensional toroidal MHD code, AEOLUS-IT, has been developed, on the basis of the new reduced set of resistive MHD equations with the assumption of toroidal incompressibility instead of the tokamak ordering in the conventional reduced set of resistive MHD equations. The code can carry out an overall MHD calculation with the effect of finite plasma resistivity--linear and nonlinear, of low aspect ratio, and low-q tokamak because the basic equations include the ideal m = 1 mode. The implicit time integration scheme for the linear term of the perturbation is employed dividing the variables into the equilibrium and perturbation parts. The huge CPU time due to solution of the large matrix can be reduced by the high efficiency of vectorialization. The linear calculations, an eigenvalue problem, show the linear growth rates of an ideal m = 1 mode and show the comparison of the growth rates between cylindrical and toroidal configurations of a low-q tokamak. The linear calculations and nonlinear simulations of resistive ballooning modes are carried out and the results are in good agreement with those obtained by the toroidal MHD code, AEOLUS-RT, using the conventional reduced MHD equations. The linear and nonlinear calculations of tearing modes for the numerical equilibrium are also carried out, and approximately the same results are obtained as the one obtained using the analytical equilibrium of approximately the same parameters. DOE

N94-18172 International Centre for Theoretical Physics, Trieste (Italy).

RESONANT ABSORPTION OF ALFVEN WAVES NEAR A NEUTRAL POINT

C. Uberoi May 1993 10 p Limited Reproducibility: More than 20% of this document may be affected by microfiche quality

(DE93-628761; IC-93/89) Avail: CASI HC A02 (US Sales Only)

The resonant absorption of Alfven waves at the neutral point is discussed by using the existing mathematical theories of the Alfven wave equation both for ideal and resistive plasmas. It is found that in the case of ideal system the resonant phenomena of Alfven waves does not show any different behaviour near a finite or a zero singular point. In case of resistive plasma initially the evolution of the system in time proceeds without any difference from the ideal system till time t (less than or equal to) t(sub n). When t is greater than t(sub h), the high frequency surface waves are resonantly mode converted to the resistivity modified shear Alfven wave at non-zero singular points but at the neutral point the zero-frequency surface waves which are symmetrical surface modes of the structured neutral layer couple to the tearing mode of instability of the layer. The importance of this study to the energy balance in tearing modes and the association of surface waves to driven magnetic reconnection is also pointed out. DOE

N94-18212# Japan Atomic Energy Research Inst., Tokyo.

USER'S MANUAL OF TOKAMAK SIMULATION CODE

Yukiharu Nakamura, Tooru Nishino, Toshihide Tsunematsu, and Masayoshi Sugihara Dec. 1992 80 p

(DE93-788388; JAERI-M-92-189) Avail: CASI HC A05/MF A01

The user's manual for the Tokamak Simulation Code (TSC), which simulates the time-evolutional process of deformable motion of an axisymmetric toroidal plasma, is summarized. For use on the JAERI computer system, the TSC is linked with the data management system GAEA. This manual is concerned with the procedure for the input and output by using the GAEA system. Model equations for axisymmetric motion, an outline of the code system, and an optimal method for the well converged solution are also described. DOE

N94-18213# Nagoya Univ. (Japan). Plasma Science Center.

PLASMA PRODUCTION BY HELICON WAVES

T. Shoji, Y. Sakawa, S. Nakazawa, K. Kadota, and T. Sato Nov. 1992 26 p

(DE93-788396; PSC-27) Avail: CASI HC A03/MF A01

Recent works on high density plasma production using m = +1 and -1 helicon waves are reviewed. The characteristics of cylindrical helicon waves including effects of a vacuum space between the plasma and the conducting wall and of a nonuniform density profile are presented. The m = +1 and -1 helicon modes are excited separately by a helical antenna and dependencies of plasma density and antenna loading resistance on RF power are shown to be different for these modes. DOE

N94-18214 Japan Atomic Energy Research Inst., Tokyo.

ACTIVE NEUTRAL PARTICLE DIAGNOSTICS FOR HIGH TEMPERATURE PLASMA

Kenji Tobita Jan. 1993 113 p Limited Reproducibility: More than 20% of this document may be affected by microfiche quality

(DE93-788457; JAERI-M-92-214) Avail: CASI HC A06

This paper describes experimental studies related to active neutral particle diagnostics in the JT-60 tokamak. Detection efficiencies of a micro-channel plate (MCP), which has been widely used in plasma diagnostics, were determined for ions and neutrals. Multi-step processes for a neutral beam are predicted to enhance the beam stopping cross section in a plasma. In order to confirm the predictions, shine-through for a hydrogen and for a helium beam was measured in the JT-60 ohmic plasmas. The measurements for a hydrogen beam resulted in the cross sectional enhancement in the beam stopping. The same experiment using a helium beam indicated that the cross sectional enhancement for helium was much smaller than that for hydrogen at almost the same plasma parameters. Ion temperature diagnostics using active beam scattering were developed in a data processing technique, in consideration of the device function of a neutral particle analyzer and in estimation of the effect of beam ion component. Fundamental experiments for detecting helium ions in a plasma were performed using the two-electron transfer reaction between a helium atomic beam and helium ions, and the energy distribution and the density of the helium ions were determined. These experiments demonstrated the promise of the two-electron transfer reaction as an alpha ash detection in a burning plasma. A parasitic neutral efflux accompanied by active beam injection was investigated. DOE

N94-18272# Argonne National Lab., IL.

STUDY OF MULTI-PHASE FLOW CHARACTERISTICS IN AN MHD POWER TRAIN

S. L. Chang, S. A. Lottes, J. X. Bouillard, and M. Petrick 1993 13 p Presented at the 31st Symposium on Engineering Aspects of Magnetohydrodynamics, Whitefish, MT, 29 Jun. - 1 Jul. 1993

(Contract W-31-109-eng-38)

(DE93-018570; ANL/ES/CP-79722; CONF-930626-13) Avail: CASI HC A03/MF A01

Computer simulation was used to predict two-phase flow processes in the CDIF MHD power train system. The predictions were used to evaluate the effects of operating and design parameters on the performance of the system and a parametric evaluation provides information to enhance the performance of the system. Major components of the system under investigation are the two-stage combustor, the converging/diverging nozzle, the supersonic MHD channel, and the diffuser. Flow in each component was simulated using a computer code. Integrating the computer codes, the two-phase flow processes in the system was calculated. Recently, the computer codes were used to investigate problems of nozzle erosion and the non-uniform iron oxide coverage on the cathode wall in the channel. A limited parametric study was conducted. The results indicated that (1) among the three nozzle geometries under investigation a no. 5 nozzle has the smoothest flow development in the nozzle and has the lowest droplet deposition on wall, and (2) smaller particle size and lower injection velocity tend to disperse the iron oxide particles more uniformly in the nozzle.
DOE

N94-18274# Lawrence Livermore National Lab., CA.
HYDRODYNAMIC INSTABILITY MODELING FOR ICF
S. W. Haan 31 Mar. 1993 8 p Presented at the 4th International Workshop on the Physics of Compressible Turbulent Mixing, Cambridge, England, 29 Mar. - 1 Apr. 1993
(Contract W-7405-eng-48)
(DE93-018634; UCRL-JC-112167; CONF-9303126-8) Avail: CASI HC A02/MF A01

The intent of this paper is to review how instability growth is modeled in ICF targets, and to identify the principal issues. Most of the material has been published previously, but is not familiar to a wide audience. Hydrodynamic instabilities are a key issue in ICF. Along with laser-plasma instabilities, they determine the regime in which ignition is possible. At higher laser energies, the same issues determine the achievable gain. Quantitative predictions are of the utmost importance to planning the ICF program, as well as to understanding current Nova results. The key fact that underlies all this work is the stabilization of short wavelengths. DOE

N94-18505# Lawrence Livermore National Lab., CA.
NONPARAXIAL MHD STABILIZERS FOR AN AXISYMMETRIC MAGNETIC MIRROR
Dmitri Ryutov (Institute of Nuclear Physics, Novosibirsk, USSR.) Dec. 1992 3 p
(Contract W-7405-eng-48)
(DE93-017996; UCRL-CR-112568) Avail: CASI HC A01/MF A01

This report details the theoretical and experimental activity performed this month. The analysis of the MHD stability of flute perturbations in axisymmetric nonparaxial mirrors has been started. The preliminary screening has been completed of the possible candidates for a stabilizer. The experimental portion of the work commenced with preparations for experiments on the plasma equilibrium response to an externally applied small magnetic field in the MHD-anchor region. A brief discussion of the results of the preliminary experiments is provided. Plans for future studies are described. DOE

N94-18524# Texas Univ., Austin. Inst. for Fusion Studies.
ION MOBILITY AND TRANSPORT BARRIERS IN THE TOKAMAK PLASMAS
H. Xiao, R. D. Hazeltine, P. M. Valanju, and Y.-Z. Zhang (International Centre for Theoretical Physics, Trieste, Italy.) Jun. 1993 13 p
(Contract DE-FG05-80ET-53088)
(DE93-040320; DOE/ET-53088/609; IFSR-609) Avail: CASI HC A03/MF A01

The character of charged particle motion in an axisymmetric toroidal system with a constant radial electric field is investigated both analytically and numerically. Ion radial mobility caused by the combined effects of the radial electric field and charge exchange is found. A simple moment argument in the banana regime matches the simulation results well. Relation of present work and high confinement (H-mode) experiment is also discussed. DOE

N94-18803# Los Alamos National Lab., NM.
PARAMETRIC ANALYSIS OF THE ARIES-3D-He-3 TOKAMAK REACTOR
C. G. Bathke, K. A. Werley, R. L. Miller, R. A. Krakowski, and J. F. Santarius (Wisconsin Univ., Madison.) 1993 7 p Presented at the He-3 and Fusion Power Symposium, Madison, WI, 18-22 Jul. 1993
(Contract W-7405-eng-36)
(DE93-018293; LA-UR-93-2700; CONF-9307125-1) Avail: CASI HC A02/MF A01

The multi-institutional ARIES study has completed a series of conceptual designs of tokamak fusion reactors that varies the assumed advances in technology and physics. The ARIES-3 design uses a D-He-3 fuel cycle and requires significant advances in physics to enhance economic attractiveness. The optimal design was characterized through systems analysis for eventual conceptual engineering design. Results from the systems analysis are summarized, and a comparison with the other ARIES designs is included. DOE

N94-18860# Swedish Inst. of Space Physics, Kiruna.
PHASE-SPACE DESCRIPTION OF PLASMA WAVES: LINEAR AND NONLINEAR THEORY
Thomas Biro (Umea Univ., Sweden.) Nov. 1992 35 p
(IRF-SR-211; ETN-93-94854) Avail: CASI HC A03/MF A01

A (r,k) phase description of waves in plasmas is developed by introducing Gaussian window functions to separate short scale oscillations from long scale modulations of the wave fields and variations in the plasma parameters. To obtain a wave equation that unambiguously separates conservative dynamics from dissipation also in an inhomogeneous and time varying background plasma, the proper form of the current response function, is discussed. On the analogy of the particle distribution function f(v,r,t), a wave density N(k,r,t) is introduced on phase space. This function is proven to satisfy a simple continuity equation. Dissipation is also included, and this allows the damping or growth of wave density along rays to be described. Problems involving geometric optics of continuous media often appear simpler when viewed in phase space, since the flow of N in phase space is incompressible. Within the phase space representation, a very general formula for the second order nonlinear current is obtained in terms of the vector potential. This formula is a convenient starting point for studies of coherent as well as turbulent nonlinear processes. Kinetic equations for weakly inhomogeneous and turbulent plasmas are derived, including the effects of inhomogeneous turbulence, wave convection and refraction. ESA

N94-18861*# National Aeronautics and Space Administration. Lewis Research Center, Cleveland, OH.
PLASMA CONTACTOR DEVELOPMENT FOR SPACE STATION
Michael J. Patterson, John A. Hamley, Charles J. Sarmiento, David H. Manzella (Sverdrup Technology, Inc., Brook Park, OH.), Timothy Sarver-Verhey (Sverdrup Technology, Inc., Brook Park, OH.), George C. Soulas (Sverdrup Technology, Inc., Brook Park, OH.), and Amy Nelson (Purdue Univ., West Lafayette, IN.) Dec. 1993 31 p Presented at the 23rd International Electric Propulsion Conference, Seattle, WA, 13-16 Sep. 1993; sponsored by AIAA, AIDAA, DGLR, and JSASS
(Contract NAS3-25266; RTOP 474-46-10)
(NASA-TM-106425; IEPC-93-246; E-8267; NAS 1.15:106425) Avail: CASI HC A03/MF A01

Plasma contactors have been baselined for the Space Station (SS) to control the electrical potentials of surfaces to eliminate/mitigate damaging interactions with the space environment. The system represents a dual-use technology which is a direct outgrowth of the NASA electric propulsion program and, in particular, the technology development effort on ion thrustor systems. The plasma contactor subsystems include the plasma contactor unit, a power electronics unit, and an expellant management unit. Under this pre-flight development program these will all be brought to breadboard or engineering model status. Development efforts for the plasma contactor include optimizing the design and configuration of the contactor, validating its required lifetime, and characterizing the contactor plume and electromagnetic interference. The plasma contactor unit design selected for the SS is an enclosed keeper, xenon hollow cathode plasma source. This paper discusses the test results and development status of the plasma contactor unit subsystem for the SS. Author (revised)

N94-18892# TRW Systems Group, Redondo Beach, CA. Applied Technology Div.

MHD TECHNOLOGY TRANSFER, INTEGRATION AND REVIEW COMMITTEE

Feb. 1993 136 p
(Contract DE-AC22-87PC-90274)
(DE93-040519; DOE/PC-90274/T23; MHD-ITC-93-017) Avail: CASI HC A07/MF A02

This seventh semi-annual status report of the MHD Technology Transfer, Integration, and Review Committee (TTIRC) summarizes activities of the TTIRC during the period April 1991 through September 1991. It includes a summary and minutes of the General Committee meeting, progress summaries of ongoing POC contracts, discussions pertaining to technical integration issues in the POC program, and planned activities for the next six months. The meeting included test plan with western coal, seed regeneration economics, power management for the integrated topping cycle, and status of the Clean Coal Technology Proposal activities. Appendices cover CDIF operations HRSR development, CFFF operations, etc. DOE

N94-18902 Massachusetts Inst. of Tech., Cambridge. Center for Space Research.

CENTER OF EXCELLENCE IN THEORETICAL GEOPLASMA RESEARCH

Tom Chang 31 Aug. 1993 67 p Limited Reproducibility: More than 20% of this document may be affected by microfiche quality
(Grant AF-AFOSR-0085-90)
(AD-A270210; AFOSR-93-0748TR) Avail: CASI HC A04

The Center for Theoretical Geoplasma Physics was established at MIT in 1986 through an AFOSR University Research Initiative grant. The goal of the Center since its inception has been to develop and maintain a program of excellence in interdisciplinary geoplasma research involving the mutual interaction of ionospheric scientists, aeronomists, plasma physicists, and numerical analysts. During the past six years, members of the center have made germinal contributions to a number of definitive research findings in the fundamental understanding of ionospheric turbulence, particle acceleration, and the phenomenon of coupling between the ionosphere and magnetosphere. Some of the results of these research activities have already found practical applications toward the mission of the Air Force by scientists at the Geophysics Directorate of the Phillips Laboratory, particularly those affiliated with the research group headed by Dr. J.R. Jasperse of the Ionospheric Effects Branch. Theoretical geoplasma physics, URI Program. DTIC

N94-18971# Argonne National Lab., IL.

THERMAL ANALYSIS OF COATINGS AND SUBSTRATE MATERIALS DURING A DISRUPTION IN FUSION REACTORS

A. Hassanein Jun. 1993 8 p Presented at the Annual Meeting of the Society of Photo-Optical Instrumentation Engineers, San Diego, CA, 11-16 Jul. 1993
(Contract W-31-109-eng-38)
(DE93-017688; ANL/EP/CP-78902; CONF-930722-9) Avail: CASI HC A02/MF A01

In a tokamak fusion reactor, the frequency of occurrence and the severity of a plasma disruption event will determine the lifetime of the plasma facing components. Disruptions are plasma instabilities which result in rapid loss of confinement and termination of plasma current. Intense energy fluxes to components like the rust wall and the divertor plate are expected during the disruptions. This high energy deposition in short times may cause severe surface erosion of these components resulting from melting and vaporization. Coatings and tile materials are proposed to protect and maintain the integrity of the underneath, structural materials from both erosion losses as well as from high thermal stresses encountered during a disruption. The coating thickness should be large enough to withstand both erosion losses and to reduce the temperature rise in the substrate structural material. The coating thickness should be minimized to enhance the structural integrity, to reduce potential problems from radioactivity, and to minimize materials cost. Tile materials such as graphite and coating materials such as beryllium and tungsten on structural materials like copper, steel, and vanadium are analyzed and compared as potential diverter and first wall design options. The effect of the sprayed coating properties during the disruption is investigated. Porous sprayed material may be found to protect the structure better than condensed phase properties. The minimum coating thickness required to protect the structural material during disruption is discussed. The impact of self shielding effect by the eroded material on the response of both the type/coating and the substrate is discussed. DOE

N94-18978# TRW Systems Group, Redondo Beach, CA. Applied Technology Div.

MHD INTEGRATED TOPPING CYCLE PROJECT

Apr. 1993 55 p
(Contract DE-AC22-87PC-90274)
(DE93-040520; DOE/PC-90274/T22; MHD-ITC-93-040) Avail: CASI HC A04/MF A01

Combustor spare and contingency hardware was shipped to the CDIF. Manufacture of spare and replacement hardware for the IA4 channel and diffuser continued. Fabrication of a modified/spare channel inlet frame which enables iron oxide injection. The cathode power cabinets and associated control system were successfully tested at Westinghouse and met all design requirements. The cathode system was delivered to the CDIF and installed in the current consolidation building. With the delivery of tills component, all prototypical power train components have been delivered to the CDIF. The hot-fire checkout of the channel subsystem and the design verification test series of the integrated power train were completed. A total of 29 tests were performed accumulating 120 thermal and 52 electrical hours. The test series demonstrated the adequacy of the overall cooling of the channel subsystem and provided an initial evaluation of the integrated combustor and channel performance in terms of operating conditions, power output, conductivity, heat loss, slagging behavior, and gas-side wear characteristics. During the test series localized wear in the supersonic nozzle was observed on the right sidewall. Cause of wear is being investigated. At conclusion of DVT test series, the channel was removed for inspection. DOE

N94-18988# Georgia Inst. of Tech., Atlanta.

VISCOSITY IN THE EDGE OF TOKAMAK PLASMAS

W. M. Stacey May 1993 35 p
(Contract DE-FG05-87ER-52141)
(DE93-018039; GTFR-108) Avail: CASI HC A03/MF A01

A fluid representation of viscosity has been incorporated into a set of fluid equations that are maximally ordered in the 'short radial gradient scale length' (srgsl) ordering that is appropriate for the edge of tokamak plasmas. The srgsl ordering raises viscous drifts and other viscous terms to leading order and fundamentally alters the character of the fluid equations. A leasing order viscous drift is identified. Viscous-driven radial particle and energy fluxes in the scrape-off layer and divertor channel are estimated to have an order unity effect in reducing radial peaking of energy fluxes transported along the field lines to divertor collector plates. DOE

N94-19012# Department of Energy, Washington, DC. Office of Energy Research.

REVIEW COMMITTEE REPORT ON THE CONCEPTUAL DESIGN OF THE TOKAMAK PHYSICS EXPERIMENT

Apr. 1993 198 p
(DE93-018408; DOE/ER-0592) Avail: CASI HC A09/MF A03

This report discusses the following topics on the conceptual design of the Tokamak Physics Experiment: role and mission of TPX; overview of design; physics design assessment; engineering design assessment; evaluation of cost, schedule, and management plans; and environment safety and health. DOE

N94-19034# Lawrence Livermore National Lab., CA.

OVERVIEW OF WARP: A PARTICLE CODE FOR HEAVY ION FUSION

Alex Friedman, David P. Grote, Debra A. Callahan, A. Bruce Langdon, and Irving Haber (Naval Research Lab., Washington, DC.) 22 Feb. 1993 12 p Presented at the Computational Accelerator Physics Conference, Pleasanton, CA, 22-26 Feb. 1993
(Contracts W-7405-eng-48; DE-AI05-92ER-54177; DE-AI05-83ER-40112)
(DE93-018637; UCRL-JC-112246; CONF-930269-17) Avail: CASI HC A03/MF A01

The beams in a heavy ion beam driven inertial fusion (HIF) accelerator must be focused onto small spots at the fusion target, and so preservation of beam quality is crucial. The nonlinear self-fields of these space-charge-dominated beams can lead to emittance growth; thus, a self-consistent field description is necessary. We have developed a multi-dimensional discrete-particle simulation code, WARP, and are using it to study the behavior of HIF beams. The code's 3D package combines features of an accelerator code and a particle-in-cell plasma simulation, and can efficiently track beams through many lattice elements and around bends. We have used the code to understand the physics of aggressive drift-compression in the MBE-4 experiment at Lawrence Berkeley Laboratory (LBL). We have applied it to LBL's planned ILSE experiments, to various 'recirculator' configurations, and to the study of equilibria and equilibration processes. Applications of the 3D package to ESQ injectors, and of the r, z package to longitudinal stability in driver beams, are discussed in related papers. DOE

N94-19037# Akademiya Nauk SSSR, Novosibirsk. Budker Inst. of Nuclear Physics.

GENERALIZED ENERGY PRINCIPLE FOR FLUTE PERTURBATIONS IN AXISYMMETRIC MIRROR MACHINES

I. M. Lansky and D. D. Ryutov 20 Jan. 1993 20 p
(Contract W-7405-eng-48)
(DE93-019399; UCRL-CR-113135) Avail: CASI HC A03/MF A01

Axial symmetry is a very desirable property of the mirror devices both for fusion and neutron source applications. The main obstacle to be circumvented in the development of such systems, is the flute instability of axisymmetric mirrors. In recent years, there appeared a number of proposals devoted to the stabilization of the flute perturbations in the framework of axisymmetric magnetic configurations, which are based on the combining of the MHD unstable central cell with various types of end-cell stabilizers. In the present paper, we concentrate ourselves just on this scheme, including long solenoid with a uniform field, conjugated with the end stabilizing anchor, intended to provide MHD stability of the system as a whole. The attractive feature of such a configuration is that it allows to exploit finite larmor radius (FLR) effects for the stabilization of the flute perturbations. As is well known, FLR effects, being strong, stabilize all flute modes, except the one with azimuthal number $m = 1$, corresponding to the 'rigid' displacement of the plasma column (the 'global' mode). Consequently, in the conditions when FLR effects dominate, the anchor has to stabilize the 'global' mode only. Bearing in mind a favorable influence of FLR effects, we don't restrict our paper by discussion of only 'global' mode stability and consider a general case of an arbitrary azimuthal mode. DOE

N94-19055 TRW Space Technology Labs., Redondo Beach, CA. Applied Technology Div.

MHD INTEGRATED TOPPING CYCLE PROJECT

Apr. 1993 54 p Limited Reproducibility: More than 20% of this document may be affected by microfiche quality
(Contract DE-AC22-87PC-90274)
(DE93-040521; DOE/PC-90274/T21; MHD-ITC-92-236) Avail: CASI HC A04

Manufacture, assembly, and checkout of combustion subsystem hardware was completed and the hardware was delivered to CDIF along with the water electrical isolators. A successful nozzle proof test was concluded; its purpose was to evaluate adequacy of the nozzle structure and sealing of sidewall-to-electrode wall joints, water tubes, and stud and wire penetrations at operating pressure. Design modifications to spare channel inlet frame were made to enable iron oxide injection. Results of tests in the CDIF 1A1 channel which compared effect of different cathode wall iron oxide injection locations indicated that injection through the side port may be more effective, particularly if one of the two ports becomes clogged. Design confirmation testing of a pneumatically driven ram to clear a plugged iron oxide injector tip was performed. Manufacture of spare and replacement parts for 1A4 channel and diffuser was begun. Construction of the cathode power cabinets and associated control system was completed. Hot-fire checkout series was completed for the combustion subsystem; 16.8 thermal hours were accumulated during seven tests. This test series demonstrated adequacy of overall cooling of combustion subsystem and provided an initial evaluation of heat losses and slagging characteristics. Several major facility activities at the CDIF were accomplished including installation and testing of new iron oxide pumps, initial on-line checkout of coal feed system modifications, modification of seed system including replacement of silo rotary feeder, installation of new filter receiver on the silo, conversion of fly ash bin to dust collector, removal of all of the electrical wiring (used for 1A1 channel) between the channel and HVR in order to install 1A4 wiring, and installation of the 1A4 channel. DOE

N94-19073# Lawrence Livermore National Lab., CA.

LOWER HYBRID COUNTER CURRENT DRIVE FOR EDGE CURRENT DENSITY MODIFICATION IN D3-D

M. E. Fenstermacher, W. M. Nevins, M. Porkolab (Massachusetts Inst. of Tech., Cambridge.), P. T. Bonoli (Massachusetts Inst. of Tech., Cambridge.), and R. W. Harvey (General Atomic Co., San Diego, CA.) Jul. 1993 6 p
Presented at the 10th Topical Conference on Radio Frequency Power in Plasmas, Boston, MA, 1-3 Apr. 1993
(Contracts W-7405-eng-48; DE-AC03-89ER-53277)
(DE93-019157; UCRL-JC-113264; CONF-9304112-23) Avail: CASI HC A02/MF A01

Each of the Advanced Tokamak operating modes in DIII-D is thought to have a distinctive current density profile. So far these modes have only been achieved transiently through experiments which ramp the plasma current and shape. Extension of these modes to steady state requires non-inductive current profile control, e.g. with lower hybrid current drive (LHCD). Calculations of LHCD have been done for DIII-D using the ACCOME and CQL3D codes, showing that counter driven current at the plasma edge can cancel some of the undesirable edge bootstrap current and potentially extend the VH-mode. Results are presented for scenarios using 2.45 GHz LH waves launched from both the midplane and off-axis ports. The sensitivity of the results to injected power, n(sub e) and T(sub e), and launched wave spectrum is also shown. DOE

N94-19074# Lawrence Livermore National Lab., CA.

EXPERIMENTS ON NONLINEAR ABSORPTION OF ECH WAVES IN MTX AND A COMPARISON WITH THEORY

B. W. Stallard, S. L. Allen, J. A. Byers, T. A. Casper, B. I. Cohen, R. H. Cohen, C. J. Lasnier, M. E. Fenstermacher, J. H. Foote, and E. B. Hooper et al Jul. 1993 11 p Presented at the 10th Topical Conference on Radio Frequency Power in Plasmas, Boston, MA, 1-3 Apr. 1993
(Contract W-7405-eng-48)
(DE93-019158; UCRL-JC-113265; CONF-9304112-22) Avail: CASI HC A03/MF A01

Intense pulse electron cyclotron heating (ECH) experiments have been carried out on the MTX tokamak. RF pulses at 140 GHz, peak power of 1-2 GW, and 25 ns pulse length were generated by the ETA-III/IMP FEL and transported quasi-optically to MTX for o-mode launch. Because of the intense RF electric fields (approximately 250 keV/cm), reduction of plasma absorption by nonlinear effects were expected and several RF beam geometries (k(sub parallel) gradient) were investigated to study their effect on the absorption. As predicted by theory, measurements of beam transmission showed increases compared to low power (2 kW). For these experiments x-ray, ECE, and Thomson diagnostics showed evidence for localized absorption at the cyclotron resonance and hot electron production. A comparison of these results with the orbit following code ORPAT is presented. DOE

N94-19133# Fusion Physics and Technologies, Torrance, CA.

ADVANCED FUSION DIAGNOSTICS

K. G. Moses 14 Jul. 1993 25 p
(Contract DE-FG03-90ER-54089)
(DE93-040085; DOE/ER-54089/2) Avail: CASI HC A03/MF A01

Key among various issues of ignited plasmas is understanding the physics of energy transfer between thermal plasma particles and magnetically confined, highly energetic charged ions in a tokamak device. The superthermal particles are products of fusion reactions. The efficiency of energy transfer by collisions, from charged fusion products (e.g., (alpha)-particles) to plasma ions, grossly determines whether or not plasma conditions are self-sustaining without recourse to auxiliary heating. Furthermore, should energy transfer efficiency be poor, and substantial auxiliary heating power is required to maintain reacting conditions within the plasma, economics may preclude commercial viability of fusion reactors. The required charged fusion product information is contained in the energy distribution function of these particles. Knowledge of temporal variations of the superthermal particle energy distribution function could be used by a fusion reactor control system to balance plasma conditions between thermal runaway and a modicum of fusion product energy transfer. Therefore, diagnostics providing data on the dynamical transfer of alpha-particle and other charged fusion product energy to the plasma ions are essential elements for a fusion reactor control system to insure that proper plasma conditions are maintained. The objective of this work is to assess if spectral analysis of RF radiation emitted by charged fusion products confined in a magnetized plasma, called ion cyclotron emission (ICE), can reveal the vital data of the distribution function of the superthermal particles. DOE

N94-19193# Texas Univ., Austin. Inst. for Fusion Studies.
FINITE BETA PLASMA EQUILIBRIUM IN TOROIDALLY LINKED MIRRORS
V. I. Ilgisonis, H. L. Berk, and V. P. Pastukhov Jul. 1993 36 p
(Contract DE-FG05-80ET-53088)
(DE93-040318; DOE/ET-53088/616; IFSR-616) Avail: CASI HC A03/MF A01

The problem of finite pressure plasma equilibrium in a system with closed magnetic field lines consisting of quadrupole mirrors linked by simple toroidal cells with elliptical cross-sections is analyzed. An appropriate analytical procedure is developed. The procedure uses conformal mapping techniques. This enables one to obtain the magnetic field structure for the free boundary equilibrium problem. This method has general applicability for finding analytic solutions of the two-dimensional Dirichlet problem outside of an arbitrary closed contour. Using this method, the deformations of the plasma equilibrium configuration due to finite plasma pressure in the toroidal cell are calculated analytically to the second order in lambda-expansion, where lambdais approximately equal to beta/(epsilon)E, beta is the ratio of plasma pressure to the magnetic field pressure, epsilon is the inverse aspect ratio and E is the ellipticity of the plasma cross-section. The outer displacement of the plasma column is shown to depend nonlinearly on the increase of plasma pressure and does not prevent the achievement of substantial beta approximately equal to 10% in the toroidal cells. DOE

N94-19194# Texas Univ., Austin. Inst. for Fusion Studies.
ON NEUTRAL PLASMA OSCILLATIONS
B. A. Shadwick and P. J. Morrison Jun. 1993 15 p
(Contract DE-FG05-80ET-53088)
(DE93-040319; DOE/ET-53088/546; IFSR-546) Avail: CASI HC A03/MF A01

We examine the conditions for the existence of spectrally stable neutral modes in a Vlasov-Poisson plasma and show that for stable equilibria of systems that have unbounded spatial domain, the only possible neutral modes are those with phase velocities that correspond to stationary inflection points of the equilibrium distribution function. It is seen that these neutral modes can possess positive or negative free energy. DOE

N94-19269 Lawrence Livermore National Lab., CA.
THERMO-HYDRAULIC ANALYSIS OF SUPERCONDUCTING TOROIDAL-FIELD MAGNETS FOR THE TOKAMAK PHYSICS EXPERIMENT
R. L. Wong, J. P. Zbasnik, and W. V. Hassenzahl Jul. 1993 10 p Presented at the International Cryogenic Engineering Conference and International Cryogenic Materials Conference, Albuquerque, NM, 12-16 Jul. 1993 Limited Reproducibility: More than 20% of this document may be affected by microfiche quality
(Contract W-7405-eng-48)
(DE93-018096; UCRL-JC-112762; CONF-930703-12) Avail: CASI HC A02

The superconducting magnets in fusion reactors are subjected to pulsed, nuclear, and resistive heating. The thermo-hydraulic response of the helium forced-flow cooled conductors to the various heat sources is critical to magnet design and performance. Recently developed computer codes allow accurate modeling of conductor response and have been used as an aid to design of the toroidal field (TF) magnets for the Tokamak Physics Experiment (TPX). We present results of design studies that determine the trade-off between double- and single-pancake helium flow configurations, the minimum-temperature margin, and the stability against rapid heat input. The results guide the choice and design of the liquid helium refrigerator. DOE

N94-19273# Oak Ridge National Lab., TN.
ICRF DIRECT ELECTRON HEATING EXPERIMENTS IN TFTR
M. Murakami, E. F. Jaeger, D. A. Rasmussen, D. B. Batchelor, C. E. Bush, R. C. Goldfinger, D. J. Hoffman, E. Fredrickson (Princeton Univ., NJ.), J. R. Wilson (Princeton Univ., NJ.), and M. C. Zarnstorff (Princeton Univ., NJ.) et al 1993 5 p Presented at the 20th European Conference on Controlled Fusion and Plasma Physics, Lisbon, Portugal, 26-30 Jul. 1993
(Contracts DE-AC05-84OR-21400; DE-AC02-76CH-03073)
(DE93-017857; CONF-930720-17) Avail: CASI HC A01/MF A01

Direct electron damping of the fast wave is a prerequisite to a viable current drive scenario for future steady-state tokamaks. It is also an attractive heating alternative to the standard ion resonance heating methods for DT experiments on TFTR because it does not require the addition of non-reactive ion species and avoids minority ion tails during studies of alpha-particle effects. The absence of minority ions in direct electron heating (DEH) also allows the use of RF power modulation to determine power deposition profiles and to carry out modulation transport studies to characterize electron transport in supershot plasmas, as described in this paper. DOE

N94-19289# Lawrence Livermore National Lab., CA.
ELECTRON CYCLOTRON RESONANCE HEATING IN THE MICROWAVE TOKAMAK EXPERIMENT
S. L. Allen, T. A. Casper, M. E. Fenstermacher, J. H. Foote, E. B. Hooper, K. Hoshino, C. J. Lasnier, P. Lopez, M. A. Makowski, and M. M. Marinak et al Sep. 1992 12 p Presented at the 14th International Conference on Plasma Physics and Controlled Nuclear Fusion Research, Wurzburg, Germany, 30 Sep. - 7 Oct. 1992
(Contract W-7405-eng-48)
(DE93-018083; UCRL-JC-109884; CONF-920913-32; IAEA-CN-56/E-1-4) Avail: CASI HC A03/MF A01

This paper presents the results from a series of Electron Cyclotron Resonance Heating (ECRH) experiments on the Microwave Tokamak Experiment (MTX). On-axis heating at B(sub T) = 5T (f(sub ce) = 140 GHz) has been performed at electron densities up to cutoff. We have used both a long-pulse gyrotron (approximately 200 kW, approximately 0.1s) and a pulsed Free Electron Laser (FEL) as microwave sources. Gyrotron experiments with power densities corresponding to 4 MW m(exp -3) are presented. A far infrared (FIR) polarimeter measured peaking of plasma current profiles in some discharges during the ECRH pulse. During high-power single-pulse FEL experiments, single-pass microwave transmission measurements show nonlinear effects (i.e., higher transmission than predicted by linear theory). A corrugated-wall duct was used in the tokamak port to increase the gradient of the parallel refractive index n(sub parallel) of the incident wave, and increased absorption was observed. Evidence of electron tail heating during FEL pulses was observed on soft x-ray and ECE diagnostics. These results are in agreement with predictions of nonlinear theory; extrapolation of this theory to reactor-like conditions indicates efficient absorption and heating. A Laser Assisted Particle Probe Spectroscopy (LAPPS) diagnostic provided estimates of the vacuum electric field of the FEL which were consistent with the measured power. Multiple pulse operation of the ETA-2 accelerator for the FEL has also been demonstrated indicating the feasibility of high-average power FEL operation. DOE

N94-19290# Lawrence Livermore National Lab., CA.
RADIATIVE DIVERTOR MODELING STUDIES
M. E. Rensink, S. L. Allen, D. N. Hill, T. B. Kaiser, and T. D. Rognlien May 1993 7 p Presented at the 20th European Conference on Controlled Fusion and Plasma Physics, Lisbon, Portugal, 26-30 Jul. 1993
(Contract W-7405-eng-48)
(DE93-018092; UCRL-JC-113033; CONF-930720-18) Avail: CASI HC A02/MF A01

A two-dimensional fluid code called UEDGE is used to simulate the edge plasma in tokamak divertors and to evaluate methods for reducing the heat load on divertor plates by radiating some of the power before it reaches the plates. UEDGE is a fully-implicit code. For these studies, UEDGE uses a banded matrix solver and a fixed-fraction impurity model. Work is presently underway to include a memory-efficient iterative solver and a model of impurity transport. Simulations of the proposed TPX device show that a few percent nitrogen concentration in the scrape-off layer can radiate up to 80% of the divertor power, thus reducing the peak heat flux and electron temperature at the divertor plate to acceptable values. A comparison of the neutral gas distribution from UEDGE with results from the DEGAS Monte Carlo neutrals code confirms the validity of our fluid neutrals model. DOE

N94-19311# Lawrence Livermore National Lab., CA.
BEHAVIOR OF THE PARTICLE TRANSPORT COEFFICIENTS NEAR THE DENSITY LIMIT IN MTX Ph.D. Thesis
M. M. Marinak Apr. 1993 202 p
(Contract W-7405-eng-48)
(DE93-019108; UCRL-LR-113984) Avail: CASI HC A10/MF A03

The perturbed particle transport coefficients were determined for a range of plasma conditions in the Alcator C tokamak, a component of the Microwave Tokamak Experiment (MTX), from analysis of density perturbations created in gas modulation experiments. Density measurements from a 15 chord far-infrared interferometer were sufficiently detailed to allow radial profiles of the transport coefficients to be resolved. Gas modulation experiments were carried out on plasmas over a range of relatively low currents and a wide variety of line-averaged densities including values near the Greenwald density limit. With this technique the perturbed diffusion coefficient D and the perturbed convection velocity V can be determined simultaneously. Measured profiles of D rise toward the outside of the plasma column in a manner generally similar to those determined previously for (chi)(sub e,HP) from sawtooth heat pulse propagation. Values of D are typically smaller than those of (chi)(sub e,HP) given for the same line-averaged densities by a factor of 2 - 5. Diffusion coefficients from a series of discharges at constant current showed little variation with density through most of the saturated ohmic confinement regime. At the Greenwald density limit threshold, a dramatic increase occurred in both the perturbed convective and diffusive transport coefficients in the outer region of the plasma. The increases were most pronounced at the outermost range of the radii where coefficients were determined (r/a = 0.8), but were apparent over a region which extended well into the plasma interior. Density profiles maintained a similar shape near the density limit, congruous with the similar behavior of the transport coefficients. No dramatic deterioration was evident in the global energy confinement. DOE

N94-19364# Grenoble-1 Univ. (France).
MODELIZATION, NUMERICAL SIMULATION AND OPTIMAL CONTROL OF NET TOKAMAK PLASMA CONFIGURATION EVOLUTION FOR THE FUTURE GENERATION OF FUSION REACTORS Ph.D. Thesis [MODELISATION, SIMULATION NUMERIQUE ET CONTROLE OPTIMAL DE L'EVOLUTION DE LA CONFIGURATION DU PLASMA POUR LE TOKAMAK NET ET POUR LA GENERATION FUTURE DE REACTEURS DE FUSION]
Fabienne Bourbon 1993 142 p In FRENCH
(ETN-93-95019) Avail: CASI HC A07/MF A02

Partial differential equations describing a tokamak plasma are presented. The plasma stability is calculated by applying finite element method and Newton algorithm. Particular attention is given to the stability control. It consists of calculating the required tokamak circuit currents to produce a precise plasma configuration. The optimal configuration is calculated by means of a Lagrangian and a gradient combined algorithm. A model describing the plasma configuration during a discharge is developed. Newton algorithm and numerical simulations are applied. The laws describing the evolution of currents and voltages in the tokamak's circuits were developed. ESA

N94-19441*# Hampton Univ., VA. Dept. of Physics.
PLASMA-PUFF INITIATION OF HIGH COULOMB TRANSFER SWITCHES Final Technical Report, 1 Mar. 1989 - 30 Jun. 1993
D. D. Venable and K. S. Han 1993 33 p
(Grant NAG1-970)
(NASA-CR-193186; NAS 1.26:193186) Avail: CASI HC A03/MF A01

The plasma-puff triggering mechanism based on a hypocycloidal pinch geometry was investigated to determine the optimal operating conditions for an azimuthally uniform surface flashover which initiates plasma-puff under wide ranges of fill gas pressures of Ar, He and N2. The optimal fill gas pressures for the azimuthally uniform plasma-puff were about 120 mTorr less than P(opt) less than 450 Torr for He and N2. For Argon 120 mTorr less than P(opt) less than 5 Torr for argon. The inverse pinch switch was triggered with the plasma-puff and the switching capability under various electrical parameters and working gas pressures of Ar, He and N2 was determined. It was also shown that the azimuthally uniform switching discharges were dependent on the type of fill gas and its fill pressure. A new concept of plasma-focus driven plasma-puff was also discussed in comparison with hypocycloidal pinch plasma-puff triggering. The main discharge of the inverse pinch switch with the plasma-focus driven plasma-puff trigger is found to be more azimuthally uniform than that with the hypocycloidal pinch plasma-puff trigger in a gas pressure region between 80 mTorr and 1 Torr. In order to assess the effects of plasma current density on material erosion of electrodes, emissions from both an inverse-pinch plasma switch (INPIStron) and from a spark gap switch under test were studied with an optical multichannel analyzer (OMA). The color temperature of the argon plasma was approximately 4,000 K which corresponded with the peak continuum emission near 750 nm. There are the strong line emissions of argon in the 650 - 800 nm range and a lack of line emissions of copper and other solid material used in the switch. This indicates that the plasma current density during closing is low and the hot spot or hot filament in the switch is negligible. This result also indicates considerable reduction of line emission with the INPIStron switch over that of a spark-gap switch. However, a strong carbon line emission exists due to vaporization of the plastic insulator used. In order to reduce the vaporization of the insulator, the plexiglass insulating material of INPIStron was replaced with Z-9 material. A comparative study of the INPIStron and a spark gap also reveals that the INPIStron, with a low impedance of Z equals 9 ohms, can transfer a high voltage pulse with a superior pulse-shape fidelity over that of a spark gap with Z equals 100 ohms.
Author (revised)

N94-19479# California Univ., Berkeley. Lawrence Berkeley Lab.
INDUCTION ACCELERATOR DEVELOPMENT FOR HEAVY ION FUSION
L. L. Reginato May 1993 18 p Presented at the International Symposium on Heavy Ion Fusion, Frascati, Italy, 25-28 May 1993
(Contract DE-AC03-76SF-00098)
(DE93-019228; LBL-33805; HIFAN-584; CONF-9305136-8) Avail: CASI HC A03/MF A01

For approximately a decade, the Heavy Ion Fusion Accelerator Research (HIFAR) group at LBL has been exploring the use of induction accelerators with multiple beams as the driver for inertial fusion targets. Scaled experiments have investigated the transport of space charge dominated beams (SBTE) and current amplification and transverse emittance control in induction linacs (MBE-4) with very encouraging results. In order to study many of the beam manipulations required by a driver and to further develop economically competitive technology, a proposal has been made in partnership with LLNL to build a 10 MeV accelerator and to conduct a series of experiments collectively called the Induction Linac System Experiments (ILSE). The major components critical to the ILSE accelerator are currently under development. We have constructed a full scale induction module, and we have tested a number of amorphous magnetic materials developed by Allied Signal to establish an overall optimal design. The electric and magnetic quadrupoles critical to the transport and focusing of heavy ion beams are also under development. The hardware is intended to be economically competitive for a driver without sacrificing any of the physics or performance requirements. This paper will concentrate on the recent developments and tests of the major components required by the ILSE accelerator. DOE

N94-19559# California Univ., Berkeley. Lawrence Berkeley Lab.
TRANSVERSE BEAM COMBINER FOR ILSE
K. Hahn, C. Celata, A. Faltens, D. Judd, P. Seidl, and E. Lee May 1993 11 p Presented at the International Symposium on Heavy Ion Fusion, Frascati, Italy, 25-28 May 1993
(Contract DE-AC03-76SF-00098)
(DE93-019239; LBL-33803; HIFAN-582; CONF-9305136-7) Avail: CASI HC A03/MF A01

Previous Heavy Ion Fusion driver system studies suggest that transverse beam combining significantly reduces driver cost. In a combiner, several beams are brought together to a common transport channel which accommodates the increased line charge density. Combining intense beams increases the transverse emittance mainly due to the heating of the beam by space charge forces as the non-uniform original beam configuration becomes more uniform. The combiner itself introduces additional aberrations, which are small for the present design. Those aberrations are due to the reduced available space for the focusing electrodes and reduced clearance from the beamlets to the surrounding electrodes, thereby generating field aberrations and larger image forces. These aberrations can also lead to particle loss. We have studied a particular design of the proposed Induction Linac System Experiment (ILSE) combiner which is a first-order achromat that tolerates a rather large fractional head-to-tail momentum tilt of +/- 10%. Using a 2-D particle-in-cell code we have found that approximately 7% of particles are lost in the combiner. The emittance growth after the combiner is large enough so that the emittance growth due to combiner aberrations is unimportant. The scaled projection to a driver shows the growth is small enough to be tolerated. At present, methods of improving combiner design to reduce particle loss and to minimize emittance growth are being studied. DOE

N94-19613 Technische Hochschule, Darmstadt (Germany). Inst. fuer Angewandte Physik.
MODELLING IDEAL GAS FLUORIDES LASER PLASMAS Ph.D. Thesis [MODELLIERUNG VON EDELGASFLUORID-LASERPLASMEN]
Karin Stein 1991 169 p In GERMAN Sponsored by BMFT Limited Reproducibility: More than 20% of this document may be affected by microfiche quality
(ETN-93-95073) Avail: CASI HC A08

A model of spatially homogeneous ideal gas fluorides discharges is developed for estimation of charge carrier densities, electron energies and drift, and their time dependence is a function of gas composition, partial pressure, geometry and electrical input data. The calculations were based on the Boltzmann equation and the transport equation with the density, impulsion and energy of the electron gas. The equations of the discharge model were analytically evaluated, using a Maxwell distribution for the electron velocity. The electron collision frequencies were assumed to be time dependent so that the operating voltage could be directly calculated from gas composition. Measurements were performed with KrF and ArF laser systems. A KrF laser gas discharge was simulated with helium and neon as buffer gases and it is noticed that velocity distribution of helium systems is dominated by elastic electron/helium interaction and is similar to a Maxwell distribution. ESA

N94-19656# Wisconsin Univ., Madison. Dept. of Physics.
THEORETICAL STUDIES OF TURBULENCE AND ANOMALOUS TRANSPORT IN TOROIDAL CONFINEMENT DEVICES
P. W. Terry 1993 10 p
(Contract DE-FG02-89ER-53291)
(DE93-040684; DOE/ER-53291/4) Avail: CASI HC A02/MF A01

The research performed under this grant has focused on key issues with respect to turbulence and transport in toroidal confinement devices. Progress and publications in these areas are summarized in this report. This work includes the following: analytical and numerical studies of spectral energy transfer and the saturation dynamics and transport of dissipative and collisionless trapped electron turbulence, the role of flow curvature in L-H mode transition physics, fully nonlinear calculations of the anomalous particle transport from the ion mixing mode, and the development of a theory for the drift wave frequency spectrum. Novel aspects of this work include an elucidation of the role of nonlinear frequency shifts in producing nonstationary saturated states, an identification of reverse and non-conserved flows in Hasegawa-Mima turbulence, and a description of the way incoherent emission affects the frequency of turbulent fluctuations. DOE

76 SOLID-STATE PHYSICS

Includes superconductivity.
For related information, see also *33 Electronics and Electrical Engineering* and *36 Lasers and Masers*.

N94-17690 International Centre for Theoretical Physics, Trieste (Italy).
ON RELATION BETWEEN BERRY PHASE AND ONE-DIMENSIONAL MODELS WITH LONG-RANGE 1/r(SUP 2)-INTERACTION
S. A. Bulgadaev Feb. 1993 14 p Limited Reproducibility: More than 20% of this document may be affected by microfiche quality
(DE93-624967; IC-92/142) Avail: CASI HC A03 (US Sales Only)

It is shown, that the effective action of Berry phase type is connected with some one-dimensional models with long-range 1/r(sup 2)-interaction. In particular, the Caldeira-Leggett action for Josephson junction with dissipation and classical spin systems are related with local effective action of holomorphic Berry phase type through the Hilbert reduction. Some consequences of this relation are discussed, including conformal symmetry of Caldeira-Leggett action and a possibility of exact solution of these models. DOE

N94-17714# Los Alamos National Lab., NM.
LECTURES OF FERMI LIQUID THEORY
K. S. Bedell 1993 40 p Presented at the Australian Summer School on Many Body Physics, Canberra, Australia, 11-22 Jan. 1993
(Contract W-7405-eng-36)
(DE93-016630; LA-UR-93-2029; CONF-9301117-1) Avail: CASI HC A03/MF A01

The Fermi liquid theory was first introduced by Landau in 1956 to provide a theoretical basis for the properties of strongly correlated Fermi systems. This theory has proven to be crucial for our understanding of a broad range of materials. These include liquid He-3, He-3/He-4 mixtures, simple metals, heavy-fermions, and nuclear matter to name a few. In the high temperature superconductors, questions have been raised regarding the applicability of Fermi liquid theory to the normal state behavior of these materials. This issue is not addressed in these lectures. The focus will be to summarize the foundations of this theory and to explore the consequences. In the absence of reading the original materials that this work draws upon, the lectures should provide the essentials of a mini-course in Fermi liquid theory. DOE

N94-17741# California Univ., Berkeley. Lawrence Berkeley Lab.
REORIENTATION OF MISFIT DISLOCATIONS DURING ANNEALING IN InGaAs/GaAs(001) INTERFACES
Y. Chen, Z. Liliental-Weber, J. Washburn, J. F. Klem (Sandia National Labs., Albuquerque, NM.), and J. Y. Tsao (Sandia National Labs., Albuquerque, NM.) Apr. 1993 6 p Presented at the Spring Meeting of the Materials Research Society, San Francisco, CA, 12-16 Apr. 1993
(Contracts DE-AC03-76SF-00098; DE-AC04-76DP-00789)
(DE93-015046; LBL-34070; CONF-930405-19) Avail: CASI HC A02/MF A01

Transmission electron microscopy is applied to investigate the effect of post-annealing on misfit dislocations in an In(0.2)Ga(0.8)As/ GaAs(001) heterostructure. An orthogonal array of 60 degree dislocations along (110) and (1(bar-1)0) directions was observed in the interfaces of the samples grown by MBE at 520 C. When the as-grown samples were annealed at temperatures ranging from 600 to 800 C, the 60 degree dislocations were gradually reoriented by dislocation reactions occurring at the 90 degree intersections followed by nonconservative motion driven by dislocation line tension and the residual elastic misfit strain. The final result of this process was a dislocation array lying along (100) and (010) directions. The reoriented u = (100) dislocation has a Burgers vector b = a/2 (101), which is the same as that of 60 degree dislocation, but the edge component of its Burgers vector in the (001) interfacial plane is larger than that of 60 degree dislocation by a factor of square root of 2, resulting in a greater contribution to elastic strain relaxation. This nonconservative reorientation of 60 degree dislocations to form the u=(100) dislocations represents a new strain relaxation mechanism in diamond or zinc blend semiconductor heterostructures. DOE

N94-17742# Sandia National Labs., Albuquerque, NM.
SELECTIVE ELECTROCHEMICAL WAFER THINNING FOR SILICON CHARACTERIZATION
J. W. Medernach, H. J. Stein, and J. O. Stevenson Mar. 1993 24 p
(Contract DE-AC04-76DP-00789)
(DE93-015083; SAND-91-2764) Avail: CASI HC A03/MF A01

A new technique is reported for rapidly determining interstitial oxygen (O(sub i)) in heavily doped n(sup +) and p(sup +) silicon. This technique includes applying a selective electrochemical (SE) thinning process and infrared transmittance to measure the Si-O band on a limited area of a silicon wafer. Oxygen reference material was used to establish a Fourier transform infrared-selective ion mass spectrometry, (FTIR-SIMS) calibration curve for the thinned samples. Internally developed software offers the capability of using different algorithms for calculating O(sub i). The O(sub i) concentrations in Czochralski (CZ) silicon with resistivities as low as 0.009 Ohm cm were determined using the SE technique on bulk and thermally processed silicon. In contrast to mechanical thinning, localized SE area thinning maintains wafer integrity for additional material or device processing. Stress generated during the formation of thick PS layers can exceed the elastic limit of silicon and induce interfacial defects. We identified in n(sup +) silicon a stress-induced dislocation network at 45 degree with a (010) direction for (100) silicon. Orthogonal dislocation networks observed in the (110) direction are identified in boron-doped silicon with concentrations of greater than 3 x 10(exp 17) atoms/cu cm. These dislocation networks show a tendency to agglomerate into bundles as the boron concentration increases. The interfacial defects observed by optical microscopy did not interfere with O(sub i) determination. DOE

N94-17744# Los Alamos National Lab., NM.
MAGNETIC PROPERTIES OF SINGLE-CRYSTALLINE UCu3Al2
H. Nakotte (Amsterdam Univ., Netherlands.), E. Brueck (Amsterdam Univ., Netherlands.), J. H. V. J. Brabers (Amsterdam Univ., Netherlands.), K. Prokes (Amsterdam Univ., Netherlands.), F. R. deBoer (Amsterdam Univ., Netherlands.), V. Sechovsky (Karlova Univ., Prague, Czechoslovakia.), K. H. J. Buschow (Philips Gloeilampenfabrieken N.V., Eindhoven, Netherlands.), A. V. Andreev (Urals A. M. Gorky State Univ., Sverdlovsk, USSR.), R. A. Robinson, and A. Puranto 1993 4 p Presented at the European Magnetic Materials and Applications Conference, Kosice, Czechoslovakia, 24-27 Aug. 1993 Submitted for publication
(Contract W-7405-eng-36)
(DE93-016607; LA-UR-93-2170; CONF-930860-1) Avail: CASI HC A01/MF A01

UCu3Al2 crystallizes in an ordered variant of the hexagonal CaCu5 structure. By neutron powder-diffraction, the U atoms were found to occupy the 1a sites, while the 2c sites are occupied by Cu atoms only and a random occupation of the 3g sites by the remaining Cu and Al is found. The magnetic susceptibility, measured on a single crystal grown by the Czochralski tri-arc technique, is found to be maximal within the hexagonal basal plane with a maximum at about 10 K. For fields applied within the basal plane, the magnetization at 4.2 K exhibits a slight S-shape starting slightly below 15 T. No such anomalies are found for fields applied along the c-axis where the magnetic response is found to be much lower. No additional magnetic peaks, which could be related with long-range antiferromagnetic ordering, were detected in the neutron powder-patterns at low temperatures. DOE

N94-17747# Pacific Northwest Lab., Richland, WA.
OXYGEN REDUCTION AT A STABILIZED ZIRCONIA INTERFACE WITH Y(1-x)Ca(x)MnO3 OR La(1-x)Sr(x)MnO3 CATHODE MATERIALS
G. E. Youngblood, L. R. Pederson, J. L. Bates, and A. S. Rupaal (Washington Univ., Bellingham.) May 1993 14 p Presented at the 183rd Electrochemical Society Meeting, Honolulu, HI, 16-21 May 1993
(Contract DE-AC06-76RL-01830)
(DE93-015681; PNL-SA-21637; CONF-930571-20) Avail: CASI HC A03/MF A01

Impedance spectroscopy, combined with an unbonded interface cell, was used to assess oxygen reduction behavior at interfaces between an yttria-stabilized zirconia electrolyte and perovskite or platinum cathode materials. Intrinsic oxygen reduction specific activities of Y(1-x)Ca(x)MnO(3) (x = 0.5, 0.6, and 0.7) and La(1-x)Sr(x)MnO(3) (x = 0.1 and 0.3) were determined as a function of temperature and oxygen partial pressure, independent of the interface morphology. The overall cathodic interfacial polarization consists of two or more fundamental processes. In the temperature range of 900-1000 C and in air, the operating conditions for a solid oxide fuel cell, charge transfer, and oxygen dissociation processes were approximately equivalent relative to the overall oxygen reduction kinetics. DOE

N94-17748# Joint Inst. for Nuclear Research, Dubna (USSR).
RENORMALIZATIONS IN SUPERSYMMETRIC AND NONSUPERSYMMETRIC NON-ABELIAN CHERN-SIMONS FIELD THEORIES WITH MATTER
L. V. Avdeev, D. I. Kazakov, and I. N. Kondrashuk 1992 27 p
(DE93-626646; JINR-E-2-92-270) Avail: CASI HC A03/MF A01 (US Sales Only)

The renormalization of nonabelian Chern-Simons field theories with matter in (2+1 dimensions) was carried out explicitly. All the renormalization constants are calculated to the leading two-loop order both in terms of component fields and N=1 superfields for the fundamental representation of the SU(n), Sp(n) and SO(n) groups. Renormalization-group fixed points are found, and their stability properties are examined. It is shown that the N=2 supersymmetry is realized as an infrared fixed-point solution, where the ultraviolet divergencies cancel. DOE

N94-17754# Los Alamos National Lab., NM.
POLARON TUNNELING IN HIGH-TEMPERATURE SUPERCONDUCTORS
A. R. Bishop, J. MustredeLeon, and M. I. Salkola 1993 8 p Presented at the NATO Workshop on Nonlinear Coherent Structures in Physics and Biology, Bayreuth, Germany, 1-4 Jun. 1993
(Contract W-7405-eng-36)
(DE93-016880; LA-UR-93-2320; CONF-9306194-1) Avail: CASI HC A02/MF A01

Nonlinear self-trapping effects are frequently proposed in the nonlinear science community -- in contexts from excitons, magnons, and polarons in solid state materials, to molecular crystals and polypeptides, to nonlinear optics. The general phenomena of self-trapping involves the self-consistent response of one field to one or more with which it is coupled, and provides excellent examples of coexisting influences of nonlinearity, lattice discreteness, quantum and thermal fluctuations, disorder, competing timescales, etc. Correspondingly, many approximate analytical and numerical techniques have been used to approach these complex issues. Here we consider a simple copper-oxygen cluster which appears in many high-temperature superconductors, which displays unusual structural and optical behavior, and which we model in terms of 'dynamic polaron tunneling'. We introduce a Peierls-Hubbard model to describe this cluster and use exact diagonalization to evaluate its properties. We emphasize the importance of nonlinear and nonadiabatic aspects of structural measurements, inelastic neutron scattering, and phonon spectroscopy (infrared and Raman). DOE

N94-17760# Oak Ridge National Lab., TN.
CONICAL GEOMETRY FOR SAGITTAL FOCUSING AS APPLIED TO X RAYS FROM SYNCHROTRONS
G. E. Ice and C. J. Sparks Jun. 1993 37 p
(Contract DE-AC05-84OR-21400)
(DE93-017238; ORNL/TM-12327) Avail: CASI HC A03/MF A01

A method for simultaneous focusing and monochromatization of x rays from a fan of radiation having up to 15 mrad divergence in one dimension is described. This geometry is well suited to synchrotron radiation sources at magnifications of one-fifth to two and is efficient for x ray energies between 3 and 40 keV (0.48 and 6.4 fJ). The method uses crystals bent to part of a cone for sagittal focusing and allows for the collection of a larger divergence with less mixing of the horizontal into the vertical divergence than is possible with x ray mirrors. The geometry required to achieve the highest efficiency when a conical crystal follows a flat crystal in a nondispersive two-crystal monochromator is described. At a magnification of one-third, the geometry is identical to a cylindrical focusing design described previously. A simple theoretical calculation is shown to agree well with ray-tracing results. Minimum aberrations are observed at magnifications near one. Applications of the conical focusing geometry to existing and future synchrotron radiation facilities are discussed. DOE

N94-17805# Concurrent Technologies Corp., Johnstown, PA.
ATLAS OF FORMABILITY: WASPALOY Final Report, 30 Apr. - 31 Jul. 1992
Prabir K. Chaudhury and Dan Zhao 31 Jul. 1992 32 p
(Contract N00140-88-C-RC21)
(AD-A268323) Avail: CASI HC A03/MF A01

In this investigation, flow behavior of Waspaloy alloy was studied by conducting compression tests over a wide range of temperatures and strain rates. Constitutive relations were determined from the flow behavior, and a dynamic material modeling was conducted on this alloy. Thus, the optimum processing condition in terms of temperature and strain rate was identified. Microstructural changes during high temperature deformation were also characterized. DTIC

N94-17845# Oak Ridge National Lab., TN.
LATTICE DAMAGE IN ION-IMPLANTED COMPOUND SEMICONDUCTORS AND ITS EFFECT ON ELECTRICAL ACTIVATION
T. E. Haynes, R. Morton (California Univ., San Diego, La Jolla.), and S. S. Lau (California Univ., San Diego, La Jolla.) Apr. 1993 13 p Presented at the Spring Meeting of the Materials Research Society, San Francisco,

CA, 12-16 Apr. 1993
(Contracts DE-AC05-84OR-21400; DE-FG03-84ER-45156)
(DE93-015907; CONF-930405-1) Avail: CASI HC A03/MF A01

In recent years, a number of experimental observations have indicated that interactions between mobile point defects generated during ion implantation play an important role in the damage production in III-V compound semiconductors, and particularly GaAs. This paper reviews a set of such observations based on ion channeling measurements of the lattice damage in GaAs implanted with Si ions. Selected independent observations are also surveyed to illustrate the importance of point-defect interactions. Taken together, these show that at least two contributions to the lattice damage must often be considered: a 'prompt' contribution attributed to direct-impact amorphization, and a 'delayed' contribution attributed to point-defect clustering. New measurements are then described which show the different effects that these two damage components have on the electrical activation in annealed, Si-implanted GaAs. The aim is to indicate the potential to exploit the balance between these two damage contributions in order to improve the electrical performance and reproducibility of ion-implanted and annealed layers. Finally, the applicability of these concepts to other ion species and other compound semiconductors (GaP and InP) is briefly discussed. DOE

N94-17866# Brookhaven National Lab., Upton, NY.
PHASE TRANSITIONS AND NEUTRON SCATTERING
G. Shirane 1993 7 p Presented at the International Symposium on Advanced Nuclear Energy Research-Neutrons as Microscopic Probes, Mito Ibaraki, Japan, 10-12 Mar. 1993
(Contract DE-AC02-76CH-00016)
(DE93-016748; BNL-49092; CONF-9303190-3) Avail: CASI HC A02/MF A01

A review is given of recent advances in neutron scattering studies of solid state physics. The author has selected the study of a structural phase transition as the best example to demonstrate the power of neutron scattering techniques. Since energy analysis is relatively easy, the dynamical aspects of a transition can be elucidated by the neutron probe. He will discuss in some detail current experiments on the 100 K transition in SrTiO3, the crystal which has been the paradigm of neutron studies of phase transitions for many years. This new experiment attempts to clarify the relation between the neutron central peak, observed in energy scans, and the two length scales observed in recent x-ray diffraction studies where only scans in momentum space are possible. DOE

N94-17871# Argonne National Lab., Idaho Falls, ID.
PHENOMENOLOGICAL EXPLANATION OF ELASTIC ANOMALIES IN SUPERLATTICES
M. Grimsditch, E. E. Fullerton, and I. K. Schuller (California Univ., San Diego, La Jolla.) Jun. 1993 10 p Presented at the Spring Meeting of the Materials Research Society, San Francisco, CA, 12-16 Apr. 1993
(Contract W-31-109-eng-38)
(DE93-017475; ANL/MSD/CP-79602; CONF-930405-32) Avail: CASI HC A02/MF A01

The experimental fact that measured elastic and structural properties of superlattices are strongly correlated can be understood on the basis of a simple model based on the packing of hard spheres. The model is consistent with features of many models that have been proposed to explain the supermodulus effect; but contrary to previous explanations, it allows predictions for a given pair of constituents to be made. For an arbitrary pair of elements, it predicts the existence or non-existence of an elastic anomaly, and a rough estimate of its magnitude. DOE

N94-17874# Los Alamos National Lab., NM.
PLASTIC ANISOTROPY IN MoSi2 SINGLE CRYSTALS
T. E. Mitchell and S. A. Maloy 1993 12 p Presented at the Critical Issues in the Development of High Temperature Structural Materials Meeting, Kona, Japan, 8-12 Mar. 1993
(Contract W-7405-eng-36)
(DE93-012650; LA-UR-93-1282; CONF-9303161-1) Avail: CASI HC A03/MF A01

Single crystals of MoSi2 are an order of magnitude stronger when compressed along (001) than along any other orientation. This is because the easy slip systems, (101)(100) and (110)(111), have a zero Schmid factor acting on them so that harder slip systems are forced into operation. We find that (001) crystals compressed at 1000 C yield by slip on (103)(331). TEM shows that the 1/2(331) dislocations tend to decompose into 1/2(111) and (110) dislocations. This decomposition process apparently inhibits the mobility of 1/2(331) dislocations at higher temperatures and another system, (101)(111), becomes operative at 1300 C and above. The (021) crystals have been tested for comparison and are found to yield at much lower stresses on the easy systems. In the design of advanced high temperature structural materials based on MoSi2, the large plastic anisotropy should be used to advantage. DOE

N94-17876# Oregon Univ., Eugene. Dept. of Chemistry.
SURFACE SECOND HARMONIC GENERATION STUDIES OF STEPPED Ag(111) ELECTRODE SURFACES Technical Report, May 1992 - May 1993
K. A. Friedrich and G. L. Richmond 27 May 1993 18 p
(Contract N00014-89-J-1261)
(AD-A265205; TR-3) Avail: CASI HC A03/MF A01

The rotational anisotropy in the optical second harmonic response from flat and stepped Ag electrode surfaces biased in an electrolyte solution have been examined. Compared to the flat Ag(111) surface, the stepped surfaces show a pronounced effect due to the lowering of the surface symmetry. The results are interpreted in terms of a pseudo mirror plante at these steps. DTIC

N94-17896 Lawrence Livermore National Lab., CA.
ANALYSIS OF HgI2 AND PbI2 CRYSTALS AND DETECTORS BY PARTICLE-INDUCED X RAY EMISSION (PIXE) AND ION BACKSCATTERING SPECTROSCOPY (IBS)
G. S. Bench, D. W. Heikkinen, A. J. Antolak (Sandia National Labs., Livermore, CA.), D. H. Morse (Sandia National Labs., Livermore, CA.), A. E. Pontau (Sandia National Labs., Livermore, CA.), R. B. James (Sandia National Labs., Livermore, CA.), D. C. David (Sandia National Labs., Livermore, CA.), A. Burger (Fisk Univ., Nashville, TN.), and L. Vandenberg (EG and G Energy Measurements, Inc., Goleta, CA.) Mar. 1993 11 p Presented at the Spring Meeting of the Materials Research Society, San Francisco, CA, 12-16 Apr. 1993 Limited Reproducibility: More than 20% of this document may be affected by microfiche quality
(Contracts W-7405-eng-48; DE-AC04-76DP-00789)
(DE93-017168; UCRL-JC-113607; CONF-930405-30) Avail: CASI HC A03

The Ion Micro-Analysis Group (IMAG) in Livermore conducts quantitative trace elemental analysis with PIXE and depth profiling with IBS using an MeV ion microbeam. The system has the capability to produce two-dimensional trace element and IBS images. PIXE analyses have been conducted on HgI(sub 2) and PbI(sub 2) crystals and detector materials in order to identify and quantify near surface trace contaminants. IBS measurements have been conducted to investigate elemental depth distributions in various materials. The results of measurements on several different samples are reported and a discussion of factors affecting quantitative in vacuo microanalysis of these materials is presented. DOE

N94-17907# Los Alamos National Lab., NM.
PHASE SEPARATION AND SUPERCONDUCTIVITY IN La2CuO(4 + DELTA): EFFECTS OF OXYGEN DIFFUSION
A. P. Reyes, P. C. Hammel, E. T. Ahrens, J. D. Thompson, P. C. Canfield, Z. Fisk, and J. E. Schirber (Sandia National Labs., Albuquerque, NM.) 1993 10 p Presented at the Conference on Spectroscopies in Novel Superconductors, Santa Fe, NM, 17-19 Mar. 1993
(Contract W-7405-eng-36)
(DE93-016610; LA-UR-93-2162; CONF-930367-7) Avail: CASI HC A02/MF A01

In oxygen-annealed La2CuO(4+delta) (delta approximately 0.03), bulk magnetization measurements show an increase of approximately 4K in the superconducting T(sub c) when the sample is cooled slowly through a narrow temperature range near 195K. At this temperature, La-139 NQR spectra exhibit a concomitant appearance of an anomalous feature associated with the metallic phase whose spectral weight increases with cooling rate. The data suggests a distribution of local structures and annealing-dependent volume fraction on this part of the sample. Interpretation of these results in terms of oxygen diffusion in a phase separated material is considered and a picture consistent with the observed changes in T(sub

c) is obtained. Other possible origins of these anomalies and the role they play in determining the superconducting properties of this system are discussed. DOE

N94-17956# International Centre for Theoretical Physics, Trieste (Italy).
KINETIC GROWTH OF RANDOM-LIKE AND BALLISTIC-LIKE DEPOSITION MODELS
Wei Wang and Hilda A. Cerdeira Mar. 1993 21 p
(DE93-624946; IC-93/42) Avail: CASI HC A03/MF A01 (US Sales Only)

The pattern structure and the scaling behavior of the surface width for two deposition models of two kinds of particles, particle-A with a probability 1-P and particle-C with a probability P, depositing on a (1+1)-dimensional substrate are studied. For model 1, a random-like deposition model, the pattern has a compact structure, and the surface width growth only depends on the time, W approximately t(sup 1/2) for the early stage and W approximately t(sup beta(P)) for the intermediate time where beta is a function of P, as well as W approximately P(sup -gamma) for the later time. For model 2, a ballistic-like deposition model, the pattern and scaling behaviour are similar to the ballistic deposition. The scaling of the surface width is W approximately t(sup beta(P)) for the early stage of growth, and W approximately L(sup alpha) for later stage. The exponent beta is of function of P while alpha is independent of P. DOE

N94-17989# California Univ., Berkeley. Lawrence Berkeley Lab.
INFRARED DETECTION WITH HIGH-(Tc BOLOMETERS AND RESPONSE OF Nb TUNNEL JUNCTIONS TO PICOSECOND VOLTAGE PULSES Ph.D. Thesis
S. Verghese May 1993 103 p
(Contract DE-AC03-76SF-00098)
(DE93-016963; LBL-34171) Avail: CASI HC A06/MF A02

Oxide superconductors with high critical temperature (T(sub c)) make sensitive thermometers for several types of infrared bolometers. Composite bolometers with YBa2Cu3O(7 -delta) thermometers on sapphire substrates which have higher sensitivity than competing thermal detectors which operate at temperatures above 77 K were built. A 1 x 1 mm bolometer with gold black serving as the radiation absorber has useful sensitivity for wavelengths 20-100 microns. A 3 x 3 mm bolometer with a bismuth film as the absorber operates from 20-100 microns. High-(T(sub c)) bolometers which are fabricated with micromachining techniques on membranes of Si or Si3N4 have potential application to large-format arrays which are used for infrared imaging. A nonisothermal high-(T(sub c)) bolometer can be fabricated on a membrane of yttria-stabilized zirconia (YSZ) which is in thermal contact with the heat sink along the perimeter of the membrane. A thermal analysis indicates that the YSZ membrane bolometer can have improved sensitivity compared to the sapphire bolometer for spectrometer applications. The quasiparticle tunneling current in a superconductor-insulator-superconductor (SIS) junction is highly nonlinear in the applied voltage. The first measurement of the linear response of the quasiparticle current in a Nb/AlO(x)/Nb junction over a broad bandwidth from 75-200 GHz was made. Nonlinear measurements made with these pulses may provide information about the quasiparticle lifetime. Preliminary data from such measurements are presented. DOE

N94-17992# Lawrence Livermore National Lab., CA.
HIGH- AND LOW-TEMPERATURE BONDING TECHNIQUES FOR MICROSTRUCTURES
D. R. Ciarlo 22 Jun. 1993 14 p Presented at the 183rd Electrochemical Society Meeting, Honolulu, HI, 16-21 May 1993
(Contract W-7405-eng-48)
(DE93-017173; UCRL-JC-112189; CONF-930571-23) Avail: CASI HC A03/MF A01

The ability to bond together two or more silicon wafers greatly expands the variety and complexity of silicon microstructures that can be designed and fabricated. At LLNL, microstructures have been used for many years as hardware in scientific experiments. The activity has recently been expanded into other areas to include microinstruments for biomedical applications and for chemical analysis. Both high temperature (1100 C) bonding techniques have been used, depending on the application. This paper discusses these applications with emphasis on the most extensive which is the fabrication of microchannel coolers for diode arrays. DOE

N94-18054# California Univ., Berkeley. Lawrence Berkeley Lab.
DEFECTS IN GaAs BULK CRYSTALS AND MULTI-LAYERS CAUSED BY In DIFFUSION
P. Werner, Z. Liliental-Weber, W. Swider, H. Sohn, W. Yau, E. R. Weber, and J. Baranowski (Warsaw Univ., Poland.) Apr. 1993 5 p Presented at the Spring Meeting of the Materials Research Society, San Francisco, CA, 12-16 Apr. 1993
(Contract DE-AC03-76SF-00098)
(DE93-016968; LBL-34143; CONF-930405-29) Avail: CASI HC A01/MF A01

The objective was to study by transmission electron microscopy the lattice defects in GaAs bulk crystals and heterostructures formed by In diffusion. In such samples hints for the existence of superconductivity have been found. Indium was found to move more than 100 micron into bulk GaAs during 1 hour annealing at 550 C (such conditions are typical for molecular beam epitaxy growth on GaAs wafers). This rapid diffusion is accompanied by the creation of dislocation networks and metallic In droplets that show evidence for lattice strain. To study the interaction of In with the GaAs lattice, In/GaAs multi-layers were grown by MBE at about 450 C on a GaAs buffer layer. The interfaces of these structures showed misfit dislocations at islands of InAs besides the presence of lattice strain. Both types of samples showed microwave absorption signals typical for superconductivity. The most likely superconductive phases are small metastable inclusions, probably consisting amorphous Ga or In. DOE

N94-18105# New Energy and Industrial Technology Development Organization, Tokyo (Japan).
FEASIBILITY SURVEY OF THERMOELECTRIC CONVERSION TECHNOLOGY USING SEMICONDUCTORS
Mar. 1993 105 p In JAPANESE
(DE93-520882; NEDO-P-9212) Avail: CASI HC A06/MF A02

The paper takes notice to thermoelectric conversion technology using semiconductors and investigates it in a wide range from high temperature to low temperature to study its feasibility. It is found that in Bi-Te alloy elements applicable to a temperature range of around 200(degree)C, some are over 3.5(times)10(sup -3)K(sup -1) in performance index, and performance of the element can be practically improved in the near future. The thermoelectric power generation system using waste heat from the fuel cell power plant, which is 5-6% in conversion efficiency, can generate output more than 100kW and is expected to improve by approximately 1% in plant overall efficiency. The construction cost, however, is around 1.6-1.9 million yen/kW. The thermoelectric power generation plant which is modeled on No.2 generator of Hatchobaru geothermal power plant can generate electric output of 10-12.5MW, which is smaller than that of the conventional geothermal power generation. The construction cost is around 3.2-4.1 million yen/kW. Even if advantage of the system in running cost is considered, attractive systematization seems to be difficult. DOE

N94-18162# Los Alamos National Lab., NM.
OMEGA PHASE FORMATION IN SHOCK-LOADED ZIRCONIUM
Shihong Song and G. T. Gray, III 1993 5 p Presented at the 14th International Conference of the International Association for the Advancement of High Pressure Science and Technology, Colorado Springs, CO, 27 Jun. - 2 Jul. 1993
(Contract W-7405-eng-36)
(DE93-018343; LA-UR-93-2292; CONF-930676-15) Avail: CASI HC A01/MF A01

A shock recovery experiment and post-shock mechanical measurements were conducted on high-purity Zr. Mechanical properties of the Zr samples before and after the shock loading are compared and discussed in terms of the substructure evolution during the shock loading. Metastable omega-phase was found in the Zr sample following shock-loading to 7 GPa. A new orientation relationship between the alpha and omega phases was derived which does not agree with those previously reported in hydrostatic pressure experiments. A mechanism is proposed for the observed alpha yields omega transformation. DOE

N94-18173 International Centre for Theoretical Physics, Trieste (Italy).
ELECTRON PARAMAGNETIC RESONANCE OF THE ns(SUP 1) CENTERS IN CRYSTALS
S. V. Nistor and I. Ursu May 1993 51 p Limited Reproducibility: More

than 20% of this document may be affected by microfiche quality
(DE93-628793; IC-93/86) Avail: CASI HC A04 (US Sales Only)

The results of the EPR studies concerning the paramagnetic centers with ns(sup 1) (N = n greater than 2) outer electronic configuration contained in crystals are reviewed. Such centers, with (sup 2)S(sub 1/2) ground state, are produced by electron trapping at impurities of the IB and IIB group or by hole trapping at impurities of the IIIB and IV group of elements. The production and structural properties of such centers consisting of ns(sup 1) ions (atoms) at various sites in the crystal lattice with different configurations of neighboring defects are discussed in connection with their EPR characteristics. Tables containing the spin Hamiltonian parameters of all ns(sup 1) centers reported in the literature until the end of year 1992 are given. DOE

N94-18184# Northwestern Univ., Evanston, IL.
STUDY OF MECHANICAL BEHAVIOR AND INTERNAL STRUCTURE OF FERRITIC NANOCRYSTALLINE MATERIAL
J. R. Weertman Mar. 1993 35 p
(Contract DE-FG02-86ER-45229)
(DE93-019264; DOE/ER-45229/33) Avail: CASI HC A03/MF A01

Investigation continued of effect of heat treatment on strength and internal structure of nanocrystalline metals. It is found that low temperature annealing increases the microhardness of nanocrystalline Pd. The anomalous Hall-Petch effect reported in literature is result of strengthening of as-compacted nanocrystalline material by annealing. Tests made up entirely of as-compacted samples or entirely of heat-treated specimens show a normal dependence of strength on grain size. X ray measurements show that short-range strains increase over the same range of annealing temperatures as hardness while long-range strains rapidly drop. SANS measurements of as-compacted and annealed nanocrystalline Pd gave quantitative information on the size and number density of a class of scatterers identified with triple point pores and of a class of larger scatterers interpreted as pores associated with 'missing' grains. A new compaction unit was designed and built that should produce larger samples with greatly reduced flaw content and lowered environmental contamination. DOE

N94-18192# Oak Ridge National Lab., TN.
COMPUTER SIMULATION OF MACROMOLECULAR CRYSTALS AND THEIR DEFECTS
B. Wunderlich, B. G. Sumpter, D. W. Noid, and G. L. Liang 1993 16 p
(Contract DE-AC05-84OR-21400)
(DE93-015213; DOE/OR-21400/T475) Avail: CASI HC A03/MF A01

Computational results on dynamics of polyethylene, are reviewed and connected to experiment. It can be demonstrated that conformational defects can be created at temperatures as much as 100 K below the melting point and that the concentration continues to increase exponentially with temperature, ultimately leading to disordered crystals along the polymer chains (high temperature CONDIS crystals). Although rate of formation of these defects is high, approximately 1 x 10(exp 10) s(sup -1) at 350 K, the defects do not, by themselves, lead at low temperature to lamellar thickening or deformation. Diffusion mechanisms involve coupling of large-amplitude torsional motion with transverse and longitudinal vibrations of the crystal, which lead to formation of dispirations and twists. Such defects can, move towards the end of the crystal, thereby causing a chain diffusion process leading to lamellar thickening and deformation processes. Collective twisting of the chains without major influence of conformational defects leads to hexagonal or pseudo-hexagonal structures of the asymmetric motifs, involving dynamic multidomain arrangements of the chains. The especially efficient molecular dynamics simulation-code produces reasonable agreement with experiment on density, defect concentration, heat capacity, vibrational spectra (including stress-induced frequency shifts), melting temperature, and speed of sound. The simulations produced data on crystals of up to 30,000 atoms for times of up to 100 picoseconds (10(exp -10) s). Total simulation efforts needed 8,000 hours of supercomputer CPU time between 1988 and 1993. DOE

N94-18243# Texas A&M Univ., College Station.
MECHANICAL MODELING OF THE GROWTH OF SALT STRUCTURES Ph.D. Thesis
R. A.M. Alfaro May 1993 217 p
(Contract DE-FG05-87ER-13711)
(DE93-015342; DOE/ER-13711/T3) Avail: CASI HC A10/MF A03

A 2D numerical model for studying the morphology and history of salt structures by way of computer simulations is presented. The model is based on conservation laws for physical systems, a fluid marker equation to keep track of the salt/sediments interface, and two constitutive laws for rocksalt. When buoyancy alone is considered, the fluid-assisted diffusion model predicts evolution of salt structures 2.5 times faster than the power-law creep model. Both rheological laws predict strain rates of the order of 4.0 times 10(exp -15)s(exp -1) for similar structural maturity level of salt structures. Equivalent stresses and viscosities predicted by the fluid-assisted diffusion law are 10(exp 2) times smaller than those predicted by the power-law creep rheology. Use of East Texas Basin sedimentation rates and power-law creep rheology indicate that differential loading is an effective mechanism to induce perturbations that amplify and evolve to mature salt structures, similar to those observed under natural geological conditions. DOE

N94-18316 Aerospace Corp., El Segundo, CA. Technology Operations.
UPDATE ON PARTS SEE SUSCEPTIBILITY FROM HEAVY IONS
D. K. Nickols, L. S. Smith, H. R. Schwartz, G. Soli, and K. Watson 15 Oct. 1992 19 p Limited Reproducibility: More than 20% of this document may be affected by microfiche quality
(Contract F04701-88-C-0089)
(AD-A268735; TR-0091(6940-05)-9; SMC-TR-93-43) Avail: CASI HC A03

Jet Propulsion Laboratory (JPL) and The Aerospace Corporation have collected a fourth set of heavy ion single event effects (SEE) test data since their last joint contributions to IEEE Transactions on Nuclear Science in December 1985, 1987, and 1989. Trends in SEE susceptibility (including soft errors and latchup) for state-of-the-art parts are displayed. DTIC

N94-18320 Rockwell International Science Center, Thousand Oaks, CA. Science Center.
PHOTOREFRACTIVE TUNGSTEN BRONZE CRYSTALS FOR OPTICAL COMPUTING Final Report, 24 Sep. 1990 - 23 Mar. 1993
Ratnakar R. Neurgaonkar 23 Jul. 1993 78 p Limited Reproducibility: More than 20% of this document may be affected by microfiche quality
(Contract F49620-90-C-0089)
(AD-A268859; SC71041; AFOSR-93-0648TR) Avail: Issuing Activity (Defense Technical Information Center (DTIC))

The authors have identified and grown new photorefractive tungsten bronze BSTN and BSKNN single crystals for optical computing applications. These crystals exhibit faster response times than the current best SBN:60 with comparable doping concentrations. At Caltech, holographic fixation has been demonstrated in Rh- and Cr-doped SBN:75 single crystals. Because of such features, various applications in the areas of data storage, optical pattern recognition, and optical computing are emerging for these tungsten bronze crystals. DTIC

N94-18388# California Inst. of Tech., Pasadena. Div. of Engineering and Applied Science.
THE TEMPERATURE AT THE PHASE BOUNDARY DURING QUASI-STATIC MOTIONS OF A TWO-PHASE THERMOELASTIC BAR
Jim M. Restuccio Jun. 1993 26 p
(Contract N00014-90-J-1871)
(AD-A268769; TR-13) Avail: CASI HC A03/MF A01

In this paper, a thermo-mechanical problem involving a finite bar is considered. It is assumed that the bar initially consists of two phases, one of which was obtained from the other by a martensitic phase transformation. It is also assumed that both phases of the bar have thermoelastic constitutive behavior. The two-phase bar is subject to different temperatures at each boundary and to a boundary traction. A quasi-static thermo-mechanical process is considered and the temperature, static equilibrium positions, and quasi-static motions of the phase boundary are studied as the material coefficients, temperature boundary conditions, and end loading are varied. Martensitic phase transformations are diffusionless solid-solid phase transformations which have continuous displacements, with possible discontinuous strains, at their phase boundary. They are also characterized by the parent and product phases having different crystal structures, or at least different crystal orientations, and by the product phase having a shape deformation relative to the undeformed parent phase, which corresponds to an unstressed undeformed state of that product phase. The high-temperature phase of a material that can undergo such a transformation is usually referred to as the austenite phase of the material, and the low-temperature phase that can be created from the austenite by a martensitic phase transformation is usually referred to as the martensite phase of the material. DTIC

N94-18459# North Carolina State Univ., Raleigh. Dept. of Physics.
CHARACTERIZATION OF DIAMOND FILM NUCLEATION AND GROWTH SURFACE Final Report, Apr. 1990 - Aug. 1991
Robert J. Nemanich Sep. 1993 149 p
(Contract N00014-90-J-1707)
(AD-A269400) Avail: CASI HC A07/MF A02

The project has involved advanced studies of diamond nucleation and the diamond growth surface utilizing scanning tunneling microscopy. For diamond growth on Si substrates, diamond nucleation was observed at scratches on the surface. These results were the first reports of nuclei with dimensions less than 100 A. While nucleation was apparently random, many nuclei exhibited growth surfaces which paralleled the substrate. Nuclei which exhibited a nearly hemispherical structure were considered to exhibit 3-dimensional type growth. It was found that both flat or 2 dimensional and three dimensional nucleation were observed on the same sample. Scanning tunneling spectroscopy was applied to the nuclei. It was found that the nuclei exhibited characteristics similar to that expected for diamond. In contrast, the substrate showed an electronic structure similar to graphite, thus indicating that graphitic layers form on the surface prior to nucleation. The interface of a continuous film was examined by etch removal of the Si, and electronic features characteristic of SiC were observed. A detailed analysis of the STS from diamond surfaces indicated Fowler-Nordheim tunneling. The effect indicated that the valence band minimum was essentially coincident with the vacuum level. The results are consistent with a negative electron affinity for diamond. DTIC

N94-18468# Army Research Lab., Aberdeen Proving Ground, MD.
THE EFFECT OF CRYSTALLOGRAPHIC ORIENTATION ON THE PERFORMANCE OF SINGLE CRYSTAL TUNGSTEN SUBSCALE PENETRATORS Final Report, Mar. 1989 - Mar. 1990
W. J. Bruchey, E. J. Horwath, and W. R. Rowe Aug. 1993 36 p
(DA Proj. 1L1-62618-AH-80)
(AD-A268988; ARL-MR-89) Avail: CASI HC A03/MF A01

The performance of tungsten single crystals as kinetic energy penetrator materials was investigated in high length to diameter (L/D) rod geometry at subscale (1/4 geometric scale). (111), (110), and (100) crystal orientations were tested in this 74-g UD - 15 geometry penetrator (6.90-mm dia. x 102.5-mm length). Several 93% tungsten alloy and uranium 3/4 titanium rod geometries were also tested to baseline expected performance of typical penetrator material/geometry combinations. Performance was determined for semi-infinite penetration into rolled homogenous armor (RHA) steel and finite penetration into 76.20-mm RHA steel. Of the orientations tested, the (100) orientation provided the best ballistic results, with performance equal or better than mass and geometric equivalent 93% tungsten alloy rods. The (100) orientation also provided similar performance to the geometric equivalent uranium 3/4 titanium rods. Favorable dislocation motion during the compressive loading of the penetration process to allow penetrator material mass flow away from the penetration interface contribute to the (100) orientation crystal's excellent performance. The net result was less energy expenditure during penetrator flow and, therefore, more energy for deformation of RHA. DTIC

N94-18480# Argonne National Lab., IL.
NANOSTRUCTURED MATERIALS: MIND OVER MATTER
R. W. Siegel May 1993 14 p Presented at the Conference on Nanostructured Materials, Cancun, Mexico, 21-25 Sep. 1992
(Contract W-31-109-eng-38)
(DE93-017690; ANL/MSD/CP-79845; CONF-920947-6) Avail: CASI HC A03/MF A01

Considerable interest is being exhibited in novel, enhanced properties of nanostructured materials. These materials, with constituent phase or grain structures modulated on a length scale less than 100 mn, are now artificially synthesized by a wide variety of physical, chemical, and mechanical methods. Nanostructured material, with modulation dimensionalities of zero (clusters), one (multilayers), two (ultrafine-grained overlayers), and three (nanophase materials) are considered. The basic principles involved in synthesis of these new materials are discussed in terms of the special properties sought using selected examples from particular synthesis and processing methodologies. Some examples of property changes that can result from one of these methods, cluster assembly of nanophase materials, are presented. DOE

N94-18498# Argonne National Lab., IL.
PHOTOEMISSION STUDIES OF Zn, Co, AND Gd SUBSTITUTED YBa2Cu3O(7-DELTA)
Chun Gu, B. W. Veal, and R. Liu Jun. 1993 9 p Presented at the Conference on Spectroscopies in Novel Superconductors, Santa Fe, NM, 17-19 Mar. 1993
(Contract W-31-109-eng-38)
(DE93-017403; ANL/MSD/CP-80258; CONF-930367-8) Avail: CASI HC A02/MF A01

Zn and Co substitute for Cu in YBa2Cu3O(7-delta) at the plane and chain sites, respectively. We report a high resolution angle-resolved photoemission study on Zn and Co substituted YBa2Cu3O(7-delta) single crystals to determine the effects on electronic structure. The valence states near E(sub F) along gamma-S are virtually unaffected by the substitutions for samples that are superconducting. However, the spectral weight near E(sub F) disappears for a higher Co-doped, nonsuperconducting crystal. Results are compared with earlier studies on pure YBa2Cu3O(7-delta) with controlled oxygen stoichiometry. Measurement on Gd-123 crystals with reduced oxygen stoichiometries show gradual reduction of spectral weight for a band along gamma-Y(X), in contrast to the results for the bands along gamma-S. The differences are probably due to a different admix of Cu-O chain and plane characters in these bands. We also measured Gd 4f resonance spectra which exhibit complex structure, indicating the presence of Gd atoms in chemically inequivalent (probably bulk and near surface) sites. DOE

N94-18500# Argonne National Lab., IL.
FABRICATION AND MICROSTRUCTURAL DEVELOPMENT OF Ag-CLAD TlBa2Ca2Cu3O(x) TAPES
A. C. Biondo, M. T. Lanagan, K. C. Goretta, J. Hu, D. J. Miller, C. T. Wu, C. A. Youngdahl, B. Fisher, and R. B. Poeppel Jul. 1993 11 p Presented at the International Cryogenic Engineering Conference and International Cryogenic Materials Conference, Albuquerque, NM, 12-16 Jul. 1993
(Contract W-31-109-eng-38)
(DE93-017407; ANL/ET/CP-78557; CONF-930703-8) Avail: CASI HC A03/MF A01

Three different 1223 powders with varied phase distributions were used to fabricate tapes by the powder-in-tube process. It was found that powders consisting primarily of phase pure 1223 were superior to a phase assemblage of Ca2CuO3, BaCuO2, and Tl2O3 powders. No texturing in the microstructure was observed for any of the annealing times or temperatures. Critical current densities over 5,000 A/cm(exp 2) were measured at 77 K, and J(sub c) degraded as the number of impurity phases increased. Further work will focus on other phase assemblages in the starting powder to determine if grain growth and alignment can be achieved in 1223. DOE

N94-18506# University of Southern California, Los Angeles. Dept. of Materials Science and Engineering.
KINETIC ASPECTS OF LATTICE MISMATCH IN MOLECULAR BEAM EPITAXIAL GROWTH ON PLANAR AND PATTERNED SUBSTRATES Final Report, 1 Feb. 1990 - 31 Mar. 1993
A. Madhukar 31 Mar. 1993 69 p
(Grant AF-AFOSR-0184-90)
(AD-A270424; AFOSR-93-0744TR) Avail: CASI HC A04/MF A01

This final scientific report summarizes the salient accomplishments under the grant AFOSR 90-0184 which include (1) the first demonstration of the realization of 3-dimensionally confined (i.e. quantum box) GaAs structures via a one-step MBE growth on pre-patterned nonplanar GaAs(111)B and GaAs(100) substrates and exhibiting optical activity, (2) the first demonstration of the kinetics of highly strained InGaAs 3D island and defect formation and the potential use of such coherent islands as quantum boxes, (3) introduction of the idea of substrate encoded size-reducing epitaxy (SESRE) that underlies (1) above and provides a means for exploiting (2) for the creation of a regular array of coherent 3D InAs islands as a quantum box array, (4) realization of high quality, highly strained GaAs/InGaAs/AlGaAs single and multiple quantum well structures via RHEED optimized growth kinetics control and their application to high performance resonant tunnelling diodes, doped-channel MISFETs, and asymmetric Fabry-Perot spatial light modulators in a novel inverted cavity geometry, (5) the impact of ex-situ processing steps such as dielectric encapsulation and rapid thermal annealing, and (6) the use of Ga+ focused ion beam for in-situ direct-write patterning of GaAs. DTIC

N94-18511# California Univ., Santa Barbara. Inst. for Polymers and Organic Solids.
MESOEPITAXY: A UNIVERSAL ROUTE TO ORIENTED MATERIALS Final Report, 15 Jun. 1990 - 14 Jun. 1993
Alan J. Heeger and Paul Smith 14 Jun. 1993 85 p
(Grant AF-AFOSR-0283-90)
(AD-A270437; AFOSR-93-0746TR) Avail: CASI HC A05/MF A01

The friction-deposited PTFE layers and their ability to act as orientation inducing substrates were fully characterized. The PTFE layers were studied by optical microscopy, scanning electron microscopy, atomic force microscopy, and by electron diffraction. Both the topology and the molecular structure were determined. The mechanism of mesoepitaxy was explored and clarified in detail through the use of overlayers. The mesoepitaxy technique was expanded from planar surfaces to the internal surfaces of polyethylene oriented by gel processing. There is serious interest by industry in using the PTFE layers for orientation. Areas of specific interest include polarizers for liquid crystal displays, and thin film transistors fabricated from oriented organic semiconductors. UNIAX Corp. (Santa Barbara) has taken an option on exclusive license on the technology and is working with several companies toward development of the technology. DTIC

N94-18527 Colorado Univ., Boulder.
GROWTH OF STRUCTURES FOR INTEGRATED OPTOELECTRONIC DEVICES Final Report, 1 Sep. 1991 - 31 Aug. 1993
Jacques I. Pankove and Moeljanto W. Leksono 31 Aug. 1993 9 p
Limited Reproducibility: More than 20% of this document may be affected by microfiche quality
(Contract N00014-91-J-1749)
(AD-A269014) Avail: CASI HC A02

Low-pressure metalorganic chemical vapor deposition (LPMOCVD) has been used to grow GaAs epitaxially on GaAs substrates by reacting triethylgallium and arsine. Various deposition parameters such as substrate temperature, total pressure, and V/III ratio were varied systematically. Optical and scanning electron microscopy revealed the presence of oval defects. Photoluminescence shows bandgap luminescence at 1.5 eV. Hall effect data indicate that the deposited GaAs is p-type with a carrier concentration of 10(exp 17) /cu cm and a mobility of 275 sq cm/V.s at room temperature. Secondary ion mass spectrometry analysis shows a high concentration of carbon that acts as a shallow acceptor. Raman spectroscopy shows that the ratio of the intensity of the LO to the TO mode is much larger for the deposited GaAs epilayer than for the bare substrate using the same scattering geometry. DTIC

N94-18531# Argonne National Lab., IL.
THE USE OF CHOPPER SPECTROMETERS FOR COLD-TO-EPITHERMAL NEUTRON SCATTERING AT IPNS
C. K. Loong, L. I. Donley, G. E. Ostrowski, R. Kleb, J. P. Hammonds, L. Soderholm, and S. Takahashi 1993 9 p Presented at the 12th International Collaboration of Advanced Neutron Sources Meeting (ICANS), Abingdon, England, 24-28 May 1993
(Contract W-31-109-eng-38)
(DE93-017798; ANL/IPNS/CP-78912; CONF-9305177-10) Avail: CASI HC A02/MF A01

A multi-detector chopper spectrometer enables measurements of the scattering function S(Q,E) to be made over a wide range of momentum and energy transfer (Q,E). The application of pulsed-source chopper spectrometers for inelastic measurements at thermal and epithermal energies (50 meV less than E less than 1000 meV) is well known. Recently at IPNS, we have extended the energy-transfer region down to about 0.5 meV with a resolution of the order of 150 (mu)eV. It is made possible by utilizing the cold-neutron incident spectrum of the 100 K methane moderator in conjunction with a dual beryllium-body rotor system. Neutron incident energies can be changed efficiently over the 4 to 1000 meV region while maintaining an undisturbed sample environment. We describe the operation of the IPNS chopper spectrometers (HRMECS and LRMECS), the instrumental resolution and the background-suppression performance. The capability of measuring inelastic features from 0.5 to 100 meV with an energy resolution of (Delta)E/E(sub 0) = 2.5% is demonstrated by experimental results of crystal-field excitation spectra of a high-T(c) superconductor ErBa2Cu3O7. Preliminary data of quasielastic scattering from a room-temperature molten salt AlCl3-EMIC are presented. DOE

N94-18539# State Univ. of New York, Stony Brook. Dept. of Physics.
TUNNELING SPECTROSCOPY OF ULTRASMALL CLUSTERS AND GRAINS Annual Technical Report, 1 Jul. 1992 - 30 Jun. 1993
K. Likharev Jul. 1993 9 p
(Contract F49620-92-J-0358)
(AD-A268840; AFOSR-93-0634TR) Avail: CASI HC A02/MF A01

This report describes major results obtained during the first year of the three-year research project 'Tunneling Spectroscopy of Ultrasmall Clusters and Grains.' The following topics were covered: (1) New STM/S Concept; (2) Testing the Room Temperature Prototype; and (3) Low-Temperature STM/S. DTIC

N94-18609# Christopher Newport Coll., Newport News, VA.
OPTICAL AND TRANSPORT PROPERTIES OF METALLIC AND SEMICONDUCTOR NANOSTRUCTURES Technical Report, 1 Oct. 1992 - 30 Sep. 1993
Peter A. Knipp 28 Sep. 1993 15 p
(Contract N00014-93-1-0140)
(AD-A270009) Avail: CASI HC A03/MF A01

This technical performance report covers the FY-94 period. The principal investigator studied theoretically the optoelectronic properties of quantum wire and dot systems. These studies included the following: lateral quantization in barrier-modulated wires; optical absorption by dots; and electron-phonon coupling in wells, wires, and dots. DTIC

N94-18616 Arizona State Univ., Tempe. Dept. of Electrical and Computer Engineering.
IN-SITU GROWTH MONITORING OF MOLECULAR BEAM EPITAXY PROCESSES Annual Technical Report, 1 Jul. 1992 - 30 Jun. 1993
George N. Maracas and Guy R. Sohie 3 Sep. 1993 26 p Limited Reproducibility: More than 20% of this document may be affected by microfiche quality
(Contract N00014-92-J-1931)
(AD-A269287; DWA-1808) Avail: CASI HC A03

The strong collaboration between Arizona State University and General Electric Corp. has resulted in a comprehensive program to develop intelligent, in-situ sensors for monitoring and control of semiconductor thin film growth by Molecular Beam Epitaxy (MBE). An intimate collaboration with a commercial MBE manufacturer (DCA Instruments) has resulted in a new ultra-stable substrate manipulator which is compatible with in-situ optical measurements. Another long time collaboration with an ellipsometer manufacturer (Woollam Co.) has generated a new prototype high speed in-situ spectroscopic ellipsometer. Both the manipulator and the ellipsometer have become commercial products. Adaptation of spectroscopic ellipsometry to real time MBE growth monitoring and development of advanced computer algorithms have enabled the tracking of epitaxial layer thickness, temperature and alloy composition. Temperature dependent (from room temperature to 650 deg C) optical constants of GaAs have been measured and verified. Work is continuing on obtaining optical constants for AlGaAs compound semiconductors. DTIC

N94-18633# Rockwell International Science Center, Thousand Oaks, CA.
INTEGRATION OF FERROELECTRIC/SEMICONDUCTOR THIN FILMS FOR SLM AND PHOTOREFRACTIVE APPLICATIONS Final Report, 24 Sep. 1990 - 23 Mar. 1993
R. R. Neurgaonkar 9 Aug. 1993 175 p
(Contract F49620-90-C-0084)
(AD-A268645; SC-71040-FR; AFOSR-93-0650TR) Avail: CASI HC A08/MF A02

This report covers work on the integration of ferroelectric and semiconductor materials for SLM's carried out over the period of September 24, 1990, through March 23, 1993, in the Ferroelectric Materials Department of the Rockwell International Science Center under Contract No. F49620-90-C-0084. During this period, significant progress has been made in the growth of highly grain-oriented perovskite PZT and BaTiO3 thin films on lattice matched SBN, SrTiO3 and MgO substrates. The oriented

PZT films show high polarization in the range of 30 - 38 microcoul/Sq cm, indicating the strong electro-optic effect necessary for photorefractive applications. This report also includes the growth of individual PZT and SBN:75 thin films on semiconducting Si substrates and the successful fabrication of ferroelectric multilayers consisting of alternating PZT and SBN films for spatial light modulators (SLM's). Because excellent quality and optical property PZT, BaTiO3 and multilayer (consisting of PZT and SBN) films are now available, a wide range of optical devices are currently under investigation. Under this program, we are concentrating SLM applications at UCSD using the multilayer stack films; while photorefractive applications are being developed at Rockwell using the grain-oriented PZT and BaTiO3 films deposited on SBN substrates DTIC

N94-18711# Air Force Inst. of Tech., Wright-Patterson AFB, OH. Foreign Aerospace Science and Technology Center.

OPTICAL PROPERTIES OF OXIDE COATINGS PREPARED BY ION-ASSISTED DEPOSITION

Xuefei Tang and Zhengxiu Fang 8 Sep. 1993 19 p Transl. into ENGLISH from High Power Laser and Particle Beams, China, v. 4, no. 2, May 1992 p 245-250
(AD-A270024; FASTC-ID(RS)T-0098-93) Avail: CASI HC A03/MF A01

An investigation was made by changing the preparation parameters, such as different ion species, ion energy, and ion current density, to determine their effects on the refractive indices, absorption, and the laser-induced damage threshold of the coatings of TiO2, ZrO2, and SiO2 whose oxide coatings were prepared by ion-assisted deposition. DTIC

N94-18719# David Sarnoff Research Center, Princeton, NJ.

HIGH PERFORMANCE YBCO FILMS R & D Status Report, 1 May - 31 Jul. 1993

Edgar J. Denlinger, Aly Fathy, David Kalokitis, Valerie Pendrick, and Barry Thaler 31 Jul. 1993 15 p
(Contract N00014-91-C-0216)
(AD-A269090) Avail: CASI HC A03/MF A01

A number of attempts were made to attach a metal handle consisting of Cu/Stainless 409/Cu composite to YBCO using a crystallizing lead-zinc-borate glass as a bonding agent. A strong, well adhering bond was achieved to MgO and SrTiO3 as buffer layers on top of the YBCO. Unfortunately, a substantial portion of the buffer layers and the YBCO appear to have been dissolved by the bonding glass. Experiments with thicker buffer layers and other buffer materials are underway. Initial results with Y2O3 as a buffer layer look very promising. A glass/metal handle attached to a YBCO/Y2O3 layer combination at 460 C showed good adherence and no apparent damage to the YBCO layer. This system is being evaluated further. DTIC

N94-18745# California Inst. of Tech., Pasadena. Div. of Engineering and Applied Science.

SCALING LAWS FOR DIAMOND CHEMICAL VAPOR DEPOSITION. DIAMOND SURFACE CHEMISTRY

David G. Goodwin 15 Sep. 1993 20 p
(AD-A269874) Avail: CASI HC A03/MF A01

A simplified model of the gas-surface chemistry occurring during chemical vapor deposition of diamond thin films is presented. The model results in simple scaling relations, useful for process scale-up and optimization, for growth rate and defect density in terms of the local chemical environment at the substrate. A simple two-parameter expression for growth rate is obtained, which with suitable parameter choices reproduces the results of more detailed mechanisms and experiment over two orders of magnitude in growth rate. The defect formation model suggests that the achievable growth rate at specified defect density scales approximately quadratically with the atomic hydrogen concentration at the substrate. DTIC

N94-18764# Applied Science and Technology, Inc., Woburn, MA.

MATERIALS PROCESSING AND MANUFACTURING TECHNOLOGIES FOR DIAMOND SUBSTRATES MULTICHIP MODULES Technical Report, Apr. - Jun. 1993

Evelio Sevillano 29 Jul. 1993 3 p
(Contract N00014-93-C-2026)
(AD-A268989; DARPA-BAA-92-20) Avail: CASI HC A01/MF A01

We have been able to run diamond chemistry plasmas for only short periods of time, due to the instability of the power supply at higher powers. Under these conditions, we have seen the spectral signature of high growth rate deposition, but were unable to sufficiently heat the substrate nor to hold the discharge stable enough to observe growth. With increased isolation and stable high power operation, we expect to achieve first diamond growth in the near future. An experimental plan to transfer the high growth rate process on 6 diameter substrates will initiate after first growth, and will proceed in parallel with other reactor upgrades. We are continuing to investigate potential improvements in plasma shape. We have already found a significant flattening of the plasma, indicative of higher growth and uniformity, by minor modifications to the chamber cavity scaled from the prototype experiments. As the modeling passes experimental benchmaking, other more significant changes may be incorporated. Other chamber design issues that will be investigated early in these experiments include uniformity of gas delivery, diagnostic window location and orientation, and sufficiency of cooling to the chamber walls. DTIC

N94-18797# North Carolina State Univ., Raleigh. Dept. of Materials Science and Engineering.

GROWTH, CHARACTERIZATION AND DEVICE DEVELOPMENT IN MONOCRYSTALLINE DIAMOND FILMS Quarterly Report, 1 Apr. - 30 Jun. 1993

Robert F. Davis Jun. 1993 27 p
(Contract N00014-90-J-1604)
(AD-A270074) Avail: CASI HC A03/MF A01

A series of computer-based statistical experimental designs have been conducted to determine the optimum conditions for negative bias-enhanced nucleation of diamond. The concentration of CH4 and the effects of pressure and bias voltage on the time for complete coverage of the substrate, film uniformity, and nucleation density were the experimental parameters and the desired results were investigated. Time to complete film formation, uniformity, and nucleation density were all improved with the use of both a negative bias voltage and high CH4 concentrations. Diamond has also been formed on diamond seeds placed on nickel substrates via microwave plasma CVD. The long range nucleation density was low and the formation of clusters of diamond more common. Polycrystalline Si-Ge films have been grown by e-beam deposition on naturally occurring p-type semiconducting diamond C(001) substrates. Room temperature and 300 C 1-5 data show the formation of low-barrier rectifying contacts which exhibit ohmic behavior. Annealing at 850 C under UHV conditions resulted in apparent degradation in the 1-5 characteristics. DTIC

N94-18804# Los Alamos National Lab., NM.

HIGH ENERGY RESOLUTION ARPES MEASUREMENTS OF THE NORMAL AND SUPERCONDUCTING STATES OF Bi2Sr2CaCu2O(8 + DELTA)

D. S. Dessau, D. M. King, and Z. X. Shen (Stanford Univ., CA.) 1993 6 p Presented at the Spring Meeting of the Materials Research Society, San Francisco, CA, 12-16 Apr. 1993
(Contract W-7405-eng-36)
(DE93-018294; LA-UR-93-2693; CONF-930405-34) Avail: CASI HC A02/MF A01

The near-E(sub F) electronic structure and Fermi surface of Bi2212 has been mapped out with ARPES. A key feature of our measured bandstructure is the existence of an extended region of flat CuO22-derived bands at E(sub F). Comparative analysis of this data with that from NdCeCuO and YBCO7 suggests that many of the anomalous (normal) physical properties of Bi2212 and YBCO7 (NdCeCuO) may be related to the existence (absence) of such bands at E(sub F). Superconducting gap anisotropy at least an order of magnitude larger than that of the conventional superconductors has been observed in the a-b plane of Bi2212 in ARPES. For samples with (T(sub c)) of 88 K, the gap size reaches a maximum of approximately 20 MeV along the Cu-O bond direction, and a minimum of much smaller or vanishing magnitude 450 away. The experimental data is discussed within the context of various theoretical models. In particular, a detailed comparison with what is expected from a superconductor with a d(sub x2-y2) order parameter is carried out, yielding a consistent picture. DOE

N94-18816# Pacific Northwest Lab., Richland, WA.

IN SITU OBSERVATION OF RADIATION INDUCED AMORPHIZATION OF CRYSTALS WITH APATITE STRUCTURE

L. M. Wang (New Mexico Univ., Albuquerque.), R. C. Ewing (New Mexico Univ., Albuquerque.), M. Cameron (National Science Foundation, Washington,

DC.), and W. J. Weber (Pacific Northwest Lab., Richland, WA.) Jun. 1993 6 p Presented at the Spring Meeting of the Materials Research Society, San Francisco, CA, 12-16 Apr. 1993
(Contracts DE-AC06-76ER-01830; DE-FG04-84ER-45099)
(DE93-018450; PNL-SA-22730; CONF-930405-35) Avail: CASI HC A02/MF A01

Temperature dependence of amorphization doses for 1.5 MeV Kr ion-irradiated Ca10(PO4)(sub 6)F2 and Ca2La8(SiO4)(sub 6)O2 were studied with in situ transmission electron microscopy. At low temperatures, Ca10(PO4)(sub 6)F2 became amorphized at lower dose than Ca2La8(SiO4)(sub 6)O2. However, the critical amorphization dose increased much more rapidly for the former above 350 K than the latter. At 475 K, Ca10(PO4)(sub 6)F2 required nearly five times of a higher dose to become amorphous than Ca10La8(SiO4)(sub 6)O2. Based on the dose-temperature curves, activation energies for the crystal structure recovery process were determined to be 0.07 eV for Ca10(PO4)(sub 6)F2 and 0.13 eV for Ca2La8(SiO4)(sub 6)O2 respectively. The lower critical amorphization dose and lower activation energy for recovery of Ca10(PO4)(sub 6)F2 are attributed to the weaker P-O bond and the higher fluorine mobility in the structure. DOE

N94-18876 Polytechnic Univ., Brooklyn, NY. Dept. of Physics.
THIN FILM STUDIES OF THE PROXIMITY JOSEPHSON EFFECT Final Technical Report, 15 Apr. 1991 - 14 Apr. 1993
E. L. Wolf Sep. 1993 11 p Limited Reproducibility: More than 20% of this document may be affected by microfiche quality
(Grant AF-AFOSR-0245-91)
(AD-A270129; AFOSR-93-0742TR) Avail: CASI HC A03

The topics of theoretical and experimental interest in this research have been: The Proximity Induced Josephson Effect (PIJE), an effect occurring at a Normal Metal/Superconductor (N/S) interface which displays many of the features of the Josephson effect, the device potential of which has not been at all explored; the design and construction of a cryogenic scanning tunneling microscope capable of operating in ultra high vacuum. The Proximity Induced Josephson Effect (PIJE) has been observed at a Normal Metal/Superconductor (N/S) interfaces in point contact NS systems, and displays features resembling the Josephson effect. In experiments with Nb and Ta probes contacting MO and UBe13 (normal state) surface, the I(V) exhibit a low resistance segment centered at zero bias current resembling a Josephson current with a small series resistance R*, which has been interpreted as a spreading resistance in the normal state electrode. DTIC

N94-18884 California Univ., Los Angeles.
FUNDAMENTAL PROPERTIES AND DEVICE APPLICATIONS OF Ge(x)Si(1-x)/Si SUPERLATTICES (SUPPLEMENTAL) Technical Report, 1 Sep. 1990 - 28 Feb. 1991
Kang L. Wang Jun. 1993 6 p Limited Reproducibility: More than 20% of this document may be affected by microfiche quality
(Contract N00014-90-J-4141)
(AD-A269212) Avail: CASI HC A02

The objectives of this contract is to expand the work on the current ONR supported research in the study of Ge(x)Si(1-x)/Si superlattice and quantum well structures into the electromagnetic wave generation and detection applications. The control parameters such as the band offsets as well as the strain induced critical thickness limitation will be investigated. The band-gap engineered superlattices and quantum structures will be designed for tunable frequency detector applications and studied for their strain induced electrical characteristics. Devices to be considered for this study are based on the concept of the band-gap engineering. In the case of Si-Ge heterosystem, strain induced tunability adds a new degree of freedom on the structure design. The effect of strain on the critical thickness limitation and the band offset is investigated. Resonant tunneling diodes with several different structures, grown at low temperature, are studied by tunneling spectroscopy. DTIC

N94-18904 Harvard Univ., Cambridge, MA. Div. of Applied Sciences.
TUNNELING MICROSCOPY OF SEMICONDUCTORS Final Report, 1 Jul. 1990 - 30 Jun. 1993
S. K. Theiss 31 Aug. 1993 4 p Limited Reproducibility: More than 20% of this document may be affected by microfiche quality
(Grant AF-AFOSR-0248-90)
(AD-A270232; AFOSR-93-0743TR) Avail: CASI HC A01

This is the final report of research activities on Tunneling Microscopy of Semiconductor Surfaces, accomplished during a 3-year JSEP Graduate Fellowship awarded to Silva K. Theiss for work in the Harvard JSEP Laboratory under the guidance of Prof. J. Golovchenko. The work includes the following: construction of a two-tip tunneling microscope, study of low coverage phases of Pb on Si(111), study of surface diffusion of Pb on Ge(111)-c(2x8), and study of Ge growth on Si(111). DTIC

N94-18933# Argonne National Lab., IL.
NEUTRON-INDUCED COLLISION CASCADE MIXING IN Nb/V SUPERLATTICES
Dale E. Alexander, Eric E. Fullerton, P. M. Baldo, C. H. Sowers, and L. E. Rehn Jul. 1993 11 p Presented at the 15th International Conference on Atomic Collision in Solids, London, Canada, 26-30 Jul. 1993
(Contract W-31-109-eng-38)
(DE93-018575; ANL/MSD/CP-79243; CONF-930712-1) Avail: CASI HC A03/MF A01

High-angle X-ray diffraction was used to determine cascade mixing efficiencies, Dt/dpa, in Nb/V superlattices irradiated to small doses (less than 0.26 dpa). Samples were neutron irradiated in the core of the High Flux Beam Reactor at Brookhaven National Laboratory and ion irradiated with 1.5 MeV Ne. No significant differences were observed in cascade mixing efficiencies between the two types of irradiation. Values of Dt/dpa were observed to vary with the modulation wavelength of the superlattice, with thicker wavelength samples yielding values approaching that determined from ion mixing thick Nb/V bilayers (Dt/dpa approximately 110 sq A/dpa). The decrease in mixing efficiency observed at lower wavelengths may be related to an observed structural transition in which the interfaces of the superlattice become coherent. DOE

N94-18968# California Univ., Berkeley. Lawrence Berkeley Lab.
SPECIFIC HEAT OF La(1.875-x)Nd(x)Sr(0.125)C(LC UO4: MAGNETIC AND STRUCTURAL TRANSITIONS
D. A. Wright, R. A. Fisher, N. E. Phillips, M. K. Crawford (Du Pont de Nemours, E. I. and Co., Wilmington, DE.), and E. M. McCarron, III (Du Pont de Nemours, E. I. and Co., Wilmington, DE.) May 1993 6 p Presented at the Conference of the International Union of Pure and Applied Physics on Low Temperature Physics (LT 20), Eugene, OR, 1-11 Aug. 1993
(Contract DE-AC03-76SF-00098)
(DE93-016978; LBL-34030; CONF-930801-6) Avail: CASI HC A02/MF A01

Near 70K (La,Ba)2CuO4 undergoes a structural transition from orthorhombic to tetragonal symmetry (LTO (yields) LTT). Partial substitution of La by Nd produces an additional transition that has been observed in structural studies. The specific heats of La(1.475)Nd(0.4)Sr(0.125)CuO4 and La(1.275)Nd(0.6)Sr(0.125)CuO4 samples exhibit anomalies near 75K, which are associated with these structural transitions, and additional smaller anomalies near 30K, which may be associated with a magnetic transition detected by (mu)SR. DOE

N94-18969# Los Alamos National Lab., NM.
PRESSURE INDUCED METALLIZATION OF THE MOTT INSULATOR 6(SUB 2)
E. Sterer, M. P. Pasternak (Tel-Aviv Univ., Israel.), and R. D. Taylor 20 Jul. 1993 5 p Presented at the 14th International Conference of the International Association for the Advancement of High Pressure Science and Technology, Colorado Springs, CO, 27 Jun. - 2 Jul. 1993
(Contract W-7405-eng-36)
(DE93-018296; LA-UR-93-2690; CONF-930676-31) Avail: CASI HC A01/MF A01

Using diamond anvil cells, (sup 129)I Moessbauer spectroscopy (MS) and resistivity measurements were carried out in the layered antiferromagnet VI(sub 2) at 0-45 GPa and 4-300 K. MS to 15 GPa revealed an impressive increase in Neel temperature and a slight increase in transferred hyperfine field. Pressure behavior of R(P,T), in particular near the metal-insulator pressure P(sub c)=44 GPa, is described. Being the lightest transition metal (TM) in the isostructural (TM)I(sub 2) series, the V(sup 2+) (d(sup 3) configuration) represents a typical candidate for a pure Mott-Hubbard gap closure. Results are compared with the heavy TM diodides such as NiI(sub 2) and CoI(sub 2), where it is expected that the charge transfer regime prevails. DOE

N94-18993 Argonne National Lab., IL.

FABRICATION AND CHARACTERIZATION OF HIGH-T(SUB c) TAPES AND COILS MADE FROM Ag-CLAD Bi-2223 SUPERCONDUCTORS

U. Balachandran, A. N. Iyer, C. A. Youngdahl, L. R. Motowidlo (IGC/Advanced Supercomputers, Inc., Waterbury, CT.), J. G. Hoehn, Jr. (Intermagnetics General Corp., Guilderland, NY.), and P. Haldar (Intermagnetics General Corp., Guilderland, NY.) Jul. 1993 6 p Presented at the 3rd International Conference on Advanced Materials, Tokyo, Japan, 31 Aug. - 4 Sep. 1993 Limited Reproducibility: More than 20% of this document may be affected by microfiche quality
(Contract W-31-109-eng-38)
(DE93-018615; ANL/ET/CP-78928; CONF-9308122-1) Avail: CASI HC A02

Prereacted Pb-doped Bi-Sr-Ca-Cu-O powders were packed into Ag tubes, drawn, rolled, and given intermediate heat treatment to prepare long lengths of Ag-clad Bi-2223 superconductor tapes. With the use of improved process conditions, transport critical current density (J(sub c)) values exceeding 10(exp 5) A/sq cm at 4.2 K and 27 K, and greater than 4 x 10(exp 4) A/sq cm at 77 K, were obtained in zero applied field with short tape samples. Detailed microstructural analysis and J(sub c) measurements in applied fields up to 20 T are reported. Rolled tapes were cut into lengths of up to 10 m, and several such tapes were used in parallel to fabricate small superconducting pancake coils by the 'wind-and-react' technique. Recently, we fabricated a test magnet with six pancake coils, each containing three 10-m lengths of rolled tapes and tested at 4.2, 27, and 77 K as a function of applied fields up to 14.5 T. A maximum generated field of 1.25 T was measured in zero applied field at 4.2 T. Detailed measurements made on the pancake coils and test magnets are reported in this paper. DOE

N94-18998# Oak Ridge National Lab., TN.

GROWTH OF EPITAXIAL SEMICONDUCTOR ALLOYS AND SUPERLATTICES WITH CONTINUOUSLY VARIABLE COMPOSITION BY PULSED-LASER ABLATION

J. W. McCamy (Tennessee Univ., Knoxville.) and D. H. Lowndes 1993 11 p Presented at the 2nd International Conference on Laser Ablation: Mechanisms and Applications, Knoxville, TN, 19-22 Apr. 1993
(Contract DE-AC05-84OR-21400)
(DE93-018726; CONF-9304144-11) Avail: CASI HC A03/MF A01

We describe a new method to grow epitaxial semiconductor alloys with continuously variable composition, while using a single pulsed laser ablation target of fixed composition. Epitaxial ZnSe(1-x)S(x) films with continuously variable sulfur content 'x' were grown by ablating a ZnSe target through low-pressure ambient H2S gas. The sulfur content was easily controlled by varying the H2S partial pressure. The composition of ZnSe(1-x)S(x) films differs by as much as x = 0.52 from the pure ZnSe target. We have used this method to grow heteroepitaxial structures with either continuously graded or periodically repeating, abrupt compositional changes (compositional superlattices). Structures that simultaneously incorporate both types of compositional modulation also have been grown. This development removes the principal barrier to convenient pulsed-laser ablation (PLA) growth of compositionally graded semiconductor thin-film materials, namely that the film and target normally have the same composition. The method appears to have broad application for PLA growth of other compound semiconductor films and heterostructures, as well as for doping individual layers. DOE

N94-19020# Cornell Univ., Ithaca, NY. Dept. of Materials Science and Engineering.

SURFACE PHASES AND THEIR INFLUENCE ON METAL-OXIDE INTERFACES

J. Blakely Jan. 1993 23 p
(Contract DE-FG02-87ER-45328)
(DE93-019931; DOE/ER-45328/7) Avail: CASI HC A03/MF A01

This project is concerned with adsorbed monolayers on metal surfaces and their effects on oxidation kinetics and metal-oxide adhesion; the proposed work is a study of the metallurgy of 2-dimensional systems with emphasis on binary adsorbed layers. Experimental techniques which can be used include electron diffraction, atomic force and tunneling microscopy, environmental SEM, and secondary electron spectroscopies. Our intent is to try to extract information on adsorbate interactions through comparison with model predictions; initially, only simple pair interaction potentials will be used. Atomic steps on single crystal surfaces, which affect the nucleation/growth of overlayers, will be extended to metal oxide systems to form atomic step arrays as preferential sites for surface nucleation of oxides. Adsorbed (or segregated) monolayers at metal/oxide interfaces also affect adhesion and further oxidation. S and O adsorption on Ni and NiFe alloy surfaces were studied and are discussed. DOE

N94-19022# Argonne National Lab., IL. Chemistry and Materials Science Div.

STRUCTURE-PROPERTY RELATIONSHIPS IN RADICAL-CATION (ELECTRON-DONOR MOLECULE) AND ANION-BASED (INCLUDING FULLERIDES) ORGANIC SUPERCONDUCTORS AND THEIR USE IN THE DESIGN OF NEW MATERIALS

Jack M. Williams, K. Douglas Carlson, Aravinda M. Kini, H. Hau Wang, Urs Geiser, John A. Schlueter, Arthur J. Schultz, James E. Schirber (Sandia National Labs., Albuquerque, NM.), Eugene L. Venturini (Sandia National Labs., Albuquerque, NM.), and Donald L. Overmyer (Sandia National Labs., Albuquerque, NM.) 1993 13 p Presented at the NATO Meeting on Materials and Crystallographic Aspects of High T(sub C) Superconductivity, Sicily (Italy), 17-29 May 1993
(Contracts W-31-109-eng-38; DE-AC04-76DP-00789; DE-FG05-86ER-45259)
(DE93-018617; ANL/CHM/CP-79705; CONF-9305269-1) Avail: CASI HC A03/MF A01

The presently known structure-property relations that have been developed for organic superconductors based on the ET molecule (b-phases and k-phases), and the C60-anion-based fullerides, and their use in the structural design of new superconducting materials are discussed. DOE

N94-19031# Purdue Univ., West Lafayette, IN.

GAMMA SCATTERING IN CONDENSED MATTER WITH HIGH INTENSITY MOESSBAUER RADIATION

1993 5 p
(Contract DE-FG02-85ER-45199)
(DE93-019461; DOE/ER-45199/3) Avail: CASI HC A01/MF A01

The first Moessbauer studies of diffusion in liquid state was carried out using (sup 183)Ta ME sources. Liquids studied included pentadecane, polydimethylsiloxane in benzene, and glycercol. Recoilless fractions and Debye-Waller factors were measured. Because of the results of Schecter, we remeasured the ME for dilute tin in lead; no anomalous cutoff was found in the Debye-Waller factor over 4-300 K, and there was a large broadening in the linewidth for 1.6 at.% (50% at 4.5 K). Advances in ME method are described. DOE

N94-19049# Lawrence Livermore National Lab., CA.

SUPERCONDUCTIVITY AND MAGNETISM IN NIOBIUM DOPED YBa2Cu3O7 RELATED HIGH-(Tc) CERAMICS

M. Bennahmias and H. B. Radousky Feb. 1993 21 p Presented at the Annual Meeting of the Minerals, Metals and Materials Society, Denver, CO, 21-25 Feb. 1993
(Contract W-7405-eng-48)
(DE93-018086; UCRL-JC-111591; CONF-9302103-4) Avail: CASI HC A03/MF A01

Magnetic characterization has been performed on the members of the cuprate-niobate RBa2Cu2NbO8 (R = Pr, Nd, and La) series and R(l.5)Ce(0.5)Sr2Cu2N bO10 (R = Pr, Eu, Nd, and Sm) series. The PrBCNO samples show a signature in the magnetization of a magnetic ordering at 12 K. The PrCSCNO sample is non-superconducting and shows two distinct orderings at 17 and 53 K. No such magnetic phase transition is observed down to 2 K in the Nd and La based RBCNO materials or the Nd, Sm, and Eu based RCSCNO materials. Measurements of the lower critical field curve, dc irreversibility line, and critical current densities are reported for each of the superconducting NdCSCNO, SmCSCNO, and EuCSCNO compounds. DOE

N94-19056 State Univ. of New York, Buffalo.

X RAY STUDIES OF MICROSTRUCTURES IN SEMICONDUCTOR AND SUPERCONDUCTING MATERIALS

Y. H. Kao 1993 9 p Limited Reproducibility: More than 20% of this

document may be affected by microfiche quality
(Contract DE-FG02-87ER-45283)
(DE93-040690; DOE/ER-45283/12) Avail: CASI HC A02

A summary of research work performed from Nov. 1, 1986 to Apr. 10, 1993 is presented. Synchrotron x rays were used to probe the short-range-order (SRO) structures in these materials, especially layered semiconductors and high-T(sub c) oxide superconductors. X-ray absorption fine structure spectroscopy, grazing incidence x-ray scattering and fluorescence, and total electron yield as probe for surfaces and interfaces were used. A new soft x-ray detector was developed. DOE

N94-19075# Oak Ridge National Lab., TN.
SURFACE MODIFICATION OF SAPPHIRE FOR IR WINDOW APPLICATION
C. J. McHargue and W. B. Snyder, Jr. 1993 9 p Presented at the Annual Meeting of the Society of Photo-Optical Instrumentation Engineers, San Diego, CA, 11-16 Jul. 1993
(Contract DE-AC05-84OR-21400)
(DE93-019168; CONF-930722-22) Avail: CASI HC A02/MF A01

Two surface modification techniques, a super polish (SP) and ion implantation, were evaluated for improving the mechanical performance of sapphire IR window material. Both techniques increased the average strength as measured by 4-point bend tests and were effective in preventing the propagation of surface flaws. Ion implantation improved the reliability at lower stresses more than the SP. Neither process significantly affected the IR transmission. The SP produced a smoother surface as shown by optical scatter measurements. DOE

N94-19122# Argonne National Lab., IL.
FABRICATION, PROPERTIES, AND MICROSTRUCTURES OF HIGH (Tc) TAPES AND COILS MADE FROM Ag-CLAD Bi-2223 SUPERCONDUCTOR
U. Balachandran, A. N. Iyer, C. A. Youngdahl, L. R. Motowidlo (IGC/Advanced Supercomputers, Inc., Waterbury, CT.), J. G. Hoehn, and P. Haldar (Intermagnetics General Corp., Waterbury, CT.) Jul. 1993 19 p Presented at the International Cryogenic Engineering and Materials Conference, Albuquerque, NM, 12-16 Jul. 1993
(Contract W-31-109-eng-38)
(DE93-017405; ANL/MCT/CP-78646; CONF-930703-7) Avail: CASI HC A03/MF A01

Bi-2223 precursor powders were prepared via a solid-state reaction using carbonates and oxides of Bi, Pb, Sr, Ca, and Cu. Results indicate that an in-situ reaction between constituent phases with the formation of a transient liquid that is consumed during final heat treatment, is essential to obtain increased density with greater connectivity between the 2223 grains. Relative amounts of the constituent phases were adjusted in the powder by varying the calcination conditions, and the powder was then used to fabricate Ag-clad tapes by a powder-in-tube technique. By improving process conditions, transport critical current density (J(sub c)) values greater than 4 (times) 10(exp 4) A/cm(sup 2) at 77 K and 2 (times) 10(exp 5) A/cm(sup 2) at 4.2 and 27 K have been obtained in short tape samples. Long tapes were cut into lengths upto 10 m long and used in parallel to fabricate small superconducting pancake coils. The coils were characterized at 77, 27 and 4.2 K and results are discussed. DOE

N94-19123# Rochester Univ., NY. Lab. for Laser Energetics.
LLE REVIEW Quarterly Report, Jan. - Mar. 1993
D. D. Meyerhofer, ed. 1993 25 p
(Contracts DE-FC03-92SF-19460; DE-FC03-85DP-40200)
(DE93-017618; DOE/DP-40200/251) Avail: CASI HC A03/MF A01

This volume of the LLE Review covers the three-month period January-March 1993. The OMEGA laser facility was decommissioned during this quarter to make room for the OMEGA Upgrade laser facility. The decommissioning is described in this volume. Electron thermal transport in the corona and laser-irradiation uniformity are related issues for direct-drive laser fusion. Thermal transport can affect the laser-irradiation uniformity requirements. The status of Fokker-Planck modeling of electron transport at LLE is reviewed and is followed by a description of a new technique for achieving high laser uniformity using zero-correlation phase masks. The use of fast, optically triggered, superconducting opening switches can, in principle, reduce the peak electrical load requirements of systems like the OMEGA Upgrade. Recent research in this area is described. The last three articles discuss vacuum ultraviolet and x-ray emission from short-pulse, laser-matter interactions. The generation of a high spectral brightness, picosecond K(alpha) source is described. The subsequent articles describe the generation of high-order harmonics of a high-intensity laser system laser system in low- density, laser-atom interactions and the novel gas target used. DOE

N94-19258# Brookhaven National Lab., Upton, NY.
STUDIES OF DEEP LEVELS IN HIGH RESISTIVITY SILICON DETECTORS IRRADIATED BY HIGH FLUENCE FAST NEUTRONS USING A THERMALLY STIMULATED CURRENT SPECTROMETER
Z. Li, H. W. Kraner, W. Chen, R. Beuttenmuller, U. Biggeri, M. Bruzzi, E. Borchi, A. Baldini, and P. Spillantini Apr. 1993 13 p Presented at the Nuclear Science Symposium, San Francisco, CA, 2-5 Nov. 1993
(Contract DE-AC02-76CH-00016)
(DE93-016133; BNL-49017; CONF-931107-2) Avail: CASI HC A03/MF A01

Measurements of deep level spectrum of high resistivity silicon detectors irradiated by high fluence fast neutrons (Phi(sub n): 2 x 10(exp 12) n/cm(exp 2)) have been made using a thermally stimulated current (TSC) spectrometer. It has been found that at least nine new defect levels, with peaking temperature of 19K, 27K, 36K, 44K, 49K, 83K, 93K, 105K, and 120K, begin to appear when Phi(sub n) greater or equal to 1 x 10(exp 13) n/cm(exp 2). All peaks have strong dependences on the filling voltage (V(sub fill), forward bias) or injection current especially for high fluence Phi(sub n) greater or equal to 10(exp 13) n/cm(exp 2) situations. The defect concentration, energy level in the band gap, and cross section of each deep level, totaling at least 13, have been studied systematically and possible identifications of the levels have been discussed. DOE

N94-19277 Melbourne Univ., Parkville (Australia). School of Physics.
PREPARATION AND CHARACTERISATION OF THE COMPOUND Tl(0.65) Bi(0.35) Ca(0.8) Sr(1.7) Cu2 O(y) USING OXALATE COPRECIPITATION AND ANALYTICAL CBED AND AN INITIAL PREPARATION OF Bi2Ca(n-1) Sr2Cu(n) O(4+2n) FOR n=5
P. Goodman, C. Nexhip, T. ODonnell, and P. Miller (Commonwealth Scientific and Industrial Research Organization, Clayton, Australia.) 1992 10 p Limited Reproducibility: More than 20% of this document may be affected by microfiche quality
(DE93-625470; UM-P-92/102) Avail: CASI HC A02 (US Sales Only)

A new superconducting compound of approximate formula Tl(0.65)Bi(0.35) Ca(0.8)Sr(1.7)Cu2O(y) was prepared using oxalate coprecipitation of the Tl-free component followed by reaction with Tl2O3. This compound has orthorhombic symmetry (probable space group P2mm) and a Tc of 87K. A byproduct of this synthesis was the synthesis of a new superconducting compound in the Bi-Ca-Sr-Cu-O series with a c-spacing of 55 Angstroms, and space group A2aa, which requires further evaluation. DOE

N94-19293# Stockholm Univ. (Sweden). Dept. of Physics.
THE d(EXP 3)DELTA-a(EXP 3)DELTA AND b(EXP 3)PHI-a(EXP 3)DELTA SYSTEMS OF ZrS, PART 2: APPENDIX, LIST OF WAVENUMBERS
J. Jonsson and A. G. Taklif Oct. 1992 48 p
(USIP-92-05; ETN-93-94848) Avail: CASI HC A03/MF A01

The wavenumbers of the b(exp 3)phi - a(exp 3)delta and d(exp 3)delta - a(exp 3)delta are given for b-a for the following values--(0,1), (1,2), (2,3), (0,0), (1,0), (2,1), (2,0)--and for d-a for the following values--(0,1), (1,2), (0,0), (1,0), (2,1). The results for J, Q(sub 1), R(sub 1), P(sub 1), Q(sub 2), R(sub 2), and P(sub 2) are given. ESA

N94-19340# Sandia National Labs., Albuquerque, NM.
ROLE OF PRESSURE IN THE STUDY OF FULLERENES
J. E. Schirber, G. A. Samara, B. Morosin, R. Assink, D. Loy, H. Wang, J. Williams, D. Murphy, A. R. Kortan, and M. Rossiensky et al 1993 4 p Presented at the 14th International Conference of the International Association for the Advancement of High Pressure Science and Technology, Colorado Springs, CO, 27 Jun. - 2 Jul. 1993
(Contract DE-AC04-76DP-00789)
(DE93-018839; SAND-93-0743C; CONF-930676-35) Avail: CASI HC A01/MF A01

Although fullerenes and their compounds are very new and exhibit new phenomena, pressure has already been an important factor in the characterization and study of these materials. In order to illustrate this, the authors will review collaborative studies on the following: (1) the effect of pressure on alkali and alkaline earth doped C60 superconductors; (2) the effect of pressure and pressure medium on the ordering temperature of C60; and (3) the role of pressure in the study of the feasibility of using C60 as 'lattice sieves' for separation of gases. DOE

N94-19347# Sandia National Labs., Albuquerque, NM.
EFFECTS OF PRESSURE ON THE ORIENTATIONAL ORDERING AND PHASE TRANSITIONS IN SOLID C(60) AND C(70)
G. A. Samara, L. V. Hansen, B. Morosin, and J. E. Schirber 1993 4 p
Presented at the 14th International Conference of the International Association for the Advancement of High Pressure Science and Technology, Colorado Springs, CO, 27 Jun. - 2 Jul. 1993
(Contract DE-AC04-76DP-00789)
(DE93-018858; SAND-93-0809C; CONF-930676-37) Avail: CASI HC A01/MF A01

The temperature-pressure phase diagrams of solid C(60) and C(70) have been determined and compared. A significant finding is the large influence of interstitial species and of the pressure transmitting medium on the orientational ordering processes. The pressure results reveal different, nearly degenerate configurations in both solids, which are believed to be due to hindered molecular rotations by interstitial species, and possibly different stacking modes in C(70). DOE

N94-19355# Technische Univ., Berlin (Germany). Fachbereich Physik.
OPTICAL FREQUENCY DOUBLING AT ADSORBATES OF SILVER(110) SURFACE Ph.D. Thesis [OPTSICHE FREQUENZVERDOPPLUNG AN ADSORBATEN DER SILBER-(110)-OBERFLAECHE]
Stefan Reiff 1993 163 p In GERMAN
(ETN-93-94837) Avail: CASI HC A08/MF A02

The adsorption of cesium and oxygen on silver (110) surface is investigated, combining second harmonic generation method, diffraction of low energy electrons, and thermodesorption spectrosopy. A macroscopic property so called phi was defined as the difference between the electrochemical potential of electrons in a metallic conductor and the electrostatic potential energy of an electron in vacuum in the neighborhood (a few microns) of the conductor; phi was measured with the Kelvin probe. The real time development of a local cesium induced reconstruction of Ag(110) surface was observed and it is noticed that this phase transformation is activited by an increase of crystal temperature. Oxygen in Ag(110) is shown to produce by adsorption temperatures in the 300 to 500K range an 'added row' reconstruction structure due to a resonance effect. The adsorption of oxygen on cesium coated Ag(110) surface was investigated, in order to obtain the dissociation rate of oxygen molecules with alkali metal atoms. ESA

N94-19357# Ecole Centrale de Lyon (France).
STUDY OF GaAs SUBSTRATES BY AMBIENT TEMPERATURE PHOTOLUMINESCENCE IMAGERY Ph.D. Thesis [ETUDE DES SUBSTRATS DE GAAS PAR L'IMAGERIE DE PHOTOLUMINESCENCE A TEMPERATURE AMBIANTE]
Fara Rahambinintsoa-Krafft 1992 161 p In FRENCH Original contains color illustrations
(ECL-92-61; ETN-93-94894) Avail: CASI HC A08/MF A02

The purpose of the study was to establish correlations between ambient temperature photoluminescence technique and the Diluted Sirtl like with Light (DSL) chemical etching method. The nature of GaAs structural defects was investigated. The application of photoluminescence imagery, at ambient temperature, to GaAs surface treatment studies is discussed. The results show that, for all the GaAs substrates considered, the correlation between photoluminescence images and DSL method exists. The influence of the Arsenic excess distribution on the carrier's lifetime is demonstrated. It is shown that heat treatments under PH3, in the range of 450 to 500C, decrease the surface recombination velocity. X-ray photoelectron spectroscopy analysis showed that the development of passivation GaP films improves surface properties. ESA

N94-19513*# Alabama Univ., Huntsville. Center for Applied Optics.
SYNCHROTRON/CRYSTAL SAMPLE PREPARATION Final Report, 24 Sep. 1992 - 23 Mar. 1993
R. Barry Johnson Jul. 1993 4 p
(Contract NAS8-38609)
(NASA-CR-193837; NAS 1.26:193837) Avail: CASI HC A01/MF A01

The Center for Applied Optics (CAO) of the University of Alabama in Huntsville (UAH) prepared this final report entitled 'Synchrotron/Crystal Sample Preparation' in completion of contract NAS8-38609, Delivery Order No. 53. Hughes Danbury Optical Systems (HDOS) is manufacturing the Advanced X-ray Astrophysics Facility (AXAF) mirrors. These thin-walled, grazing incidence, Wolter Type-1 mirrors, varying in diameter from 1.2 to 0.68 meters, must be ground and polished using state-of-the-art techniques in order to prevent undue stress due to damage or the presence of crystals and inclusions. The effect of crystals on the polishing and grinding process must also be understood. This involves coating special samples of Zerodur and measuring the reflectivity of the coatings in a synchrotron system. In order to gain the understanding needed on the effect of the Zerodur crystals by the grinding and polishing process, UAH prepared glass samples by cutting, grinding, etching, and polishing as required to meet specifications for witness bars for synchrotron measurements and for investigations of crystals embedded in Zerodur. UAH then characterized these samples for subsurface damage and surface roughness and figure. Author (revised)

N94-19541# Brookhaven National Lab., Upton, NY. Dept. of Applied Science.
AN AB INITIO MONTE CARLO STUDY OF LOW ENERGY POSITRON AND ELECTRON IMPLANTATION IN ELEMENTAL METALS AND MULTILAYERS
V. J. Ghosh, M. McKeown, D. O. Welch, and K. G. Lynn 1993 7 p
Presented at the 15th International Conference on Atomic Collision in Solids, London, Canada, 26-30 Jul. 1993
(Contract DE-AC02-76CH-00016)
(DE93-019847; BNL-48823; CONF-930712-4) Avail: CASI HC A02/MF A01

A Monte Carlo code developed at Brookhaven to study positron and electron implantation in solids will be discussed. This code models the trajectories of a large number of positrons or electrons as they move through the material and uses this information to calculate stopping profiles, backscattered fractions, and transmitted fractions. The particle-atom interactions are incorporated via elastic and inelastic scattering cross-sections. The incident particle energies vary from 1 to 10 keV and the simulation stops when the particle energy goes down to 25 eV or if the particle is backscattered. The results of our Monte Carlo simulations of the mean implantation depth and implantation profiles for both semi-infinite metallic elements and multilayers will be discussed. DOE

N94-19550# Argonne National Lab., IL.
THE ELECTROMECHANICAL PROPERTIES OF TETRAGONAL BaTiO3 AND PbTiO3 SINGLE CRYSTALS
Z. Li, C. M. Foster, M. Grimsditch, and S. K. Chan Jul. 1993 7 p
Presented at the 8th International Meeting on Ferroelectricity, Gaithersburg, MD, 8-13 Aug. 1993
(Contract W-31-109-eng-38)
(DE93-019008; ANL/MSD/CP-78507; CONF-930852-2) Avail: CASI HC A02/MF A01

The velocities of propagation for longitudinal and transverse sound waves in various directions have been measured by Brillouin scattering on high-quality mono-domain single crystals of BaTiO3 and PbTiO3. Using these velocities and also the dielectric permittivities measured by the impedance method and by Raman spectroscopy, a complete set of elastic stiffness moduli C(sub ijkl), piezoelectric constants e(sub rij), and dielectric permittivity epsilon(sub ij) has been determined at ambient temperature. Dependence of these electromechanical properties on orientation and frequency is presented for both materials and the physical implications will be discussed. DOE

N94-19564# Brookhaven National Lab., Upton, NY.
THE 1982 TO 1992 DECADE OF RESEARCH ON THE VACUUM ULTRAVIOLET RING AT NATIONAL SYNCHROTRON LIGHT SOURCE
Apr. 1993 8 p
(Contract DE-AC02-76CH-00016)
(DE93-019469; BNL-48805) Avail: CASI HC A02/MF A01

This report discusses highlights of research being conducted at the

National Synchrotron Light Source in physics, chemistry, biology, and x-ray lithography. DOE

N94-19565# Lawrence Livermore National Lab., CA.
FINAL REPORT ON SUBCONTRACT B076260
D. A. Keszler (Oregon State Univ., Corvallis.) 1993 10 p
(Contract W-7405-eng-48)
(DE93-019501; UCRL-CR-103699) Avail: CASI HC A02/MF A01

Work continued on synthesis of borates A6MM'(BO3)6, where A = Sr or Ba, M = lanthanide, Y, Sc, In, or Ca, and M' = heavier lanthanide, Sc, Cr, Mn, Fe, Co, In, Ga, Al, Ru, Rh, Ti, Zr, Hf, or Sn. Their structures are discussed, in particular Sr6HoSc(BO3)6. Other new borates and gallates are being studied. In the fluoride program, single crystals were grown of RbY2ScF10; samples codoped with Cr and Nd ions show only Nd fluorescence when excited by Ar laser. Structures of the laser materials LiCaGaF6, LiSrAlF6, and Sr2ScF7, and fluorescence of the Cr-doped form of the last fluoride were determined. Finally, work on frequency converters include the following: Optical nonlinearities of new borates were calculated. New borates containing Be are being synthesized: SrBe2(BO3)2, BaCuB2O5. Structures of Rb2 Na(NO3)3, RbNO3, and other nitrates will be used to determine the nitrate group's hyperpolarizability coefficient. Work on organic frequency converters covered L-arginine derivatives, lactones, etc. DOE

N94-19566# Argonne National Lab., IL.
CROSSOVER FROM BCS TO BOSE SUPERCONDUCTIVITY: A FUNCTIONAL INTEGRAL APPROACH
M. Randeria, C. A. R. SadeMelo, and J. R. Engelbrecht (Illinois Univ., Urbana.) Apr. 1993 3 p Presented at the Conference of the International Union of Pure and Applied Physics on Low Temperature Physics (LT 20), Eugene, OR, 1-11 Aug. 1993
(Contract W-31-109-eng-38)
(DE93-019503; ANL/MSD/CP-79538; CONF-930801-8) Avail: CASI HC A01/MF A01

We use a functional integral formulation to study the crossover from cooperative Cooper pairing to the formation and condensation of tightly bound pairs in a 3D continuum model of fermions with attractive interactions. The inadequacy of a saddle point approximation with increasing coupling is pointed out, and the importance of temporal (quantum) fluctuations for normal state properties at intermediate and strong coupling is emphasized. In addition to recovering the Nozieres-Schmitt-Pink interpolation scheme for T(sub c), and the Leggett variational results for T = 0, we also present results for evolution of the time-dependent Ginzburg-Landau equation and collective mode spectrum as a function of the coupling. DOE

N94-19567# Argonne National Lab., IL.
NUMERICAL EXPERIMENTS ON THE GINZBURG-LANDAU EQUATIONS
Man Kam Kwong 1992 13 p Presented at the World Congress of Nonlinear Analysts, Melbourne, FL, 19-26 Aug. 1992
(Contract W-31-109-eng-38)
(DE93-019504; ANL/MCS/CP-80513; CONF-920817-1) Avail: CASI HC A03/MF A01

We report on some numerical experiments done on the Ginzburg-Landau equations of the theory of superconductivity. The equations under periodic boundary conditions are solved numerically by using a nonstandard discretization and the sweeping algorithm. The programs, written in MATLAB and FORTRAN, work in an interactive mode and include graphics display. DOE

N94-19579 Ohio State Univ., Columbus. Computer Microbiology and Contamination Lab.
PICOINDENTATION HARDNESS MEASUREMENTS USING ATOMIC FORCE MICROSCOPY
Bharat Bhushan and Vilas N. Koinkar 10 Oct. 1993 11 p Limited Reproducibility: More than 20% of this document may be affected by microfiche quality
(Contract N00014-93-1-0067)
(AD-A270877) Avail: Issuing Activity (Defense Technical Information Center (DTIC))

An atomic force microscope (AFM), with a specially prepared diamond tip, has been modified to measure indentation hardness with an indentation depth as low as 1 nm. This indentation depth is much smaller than the depth of more than 20 nm that have been reported to date. The AFM indentation technique allows the hardness measurements of surface monolayers and ultrathin films in multilayered structures at very shallow depths and low loads. The picoindentation hardness of single crystal silicon are measured using this technique. A subtraction technique is also described which allows the actual hardness measurements of rough surfaces such as magnetic thin film rigid disks. DTIC

N94-19596# Rensselaer Polytechnic Inst., Troy, NY.
IONIZED-CLUSTER BEAM/PARTIALLY IONIZED BEAM DEPOSITION OF ELECTRO-OPTICAL AND NONLINEAR OPTICAL ORGANIC MATERIALS AND DEVICE DEVELOPMENT Final Report, 1 Apr. 1990 - 15 Jul. 1993
Toh-Ming Lu, J. F. McDonald, N. Vlannes, and G. E. Wnek 29 Aug. 1993 21 p
(Contract DAAL03-90-G-0082)
(AD-A270832; ARO-27605.2-MS) Avail: CASI HC A03/MF A01

Our multidisciplinary research efforts over the last few years have been focused on the preparation and characterization of high quality, thermally stable thin film that exhibit high nonlinear optical properties using vacuum vapor deposition and in-situ poling (ionized cluster beam/partially ionized beam (PIB) deposition) techniques. The project's primary accomplishments are the vapor deposition of oriented organic thin films and polymer-chromophore complexes, and the development of novel nonlinear optical materials systems, such as side-chain polymers and particle-polymer complexes. Highlights of the research are as follows: (1) Organic crystals called DAST with the highest known nonlinearity have been grown and characterized; (2) PIB deposited highly transparent MNA films on FM substrates demonstrate a large second harmonic generation (SHG) signal; (3) Vapor deposited chromophore-polymer composite thin films show large EO effect (several pm/V); (4) Seven synthetic diol and triol chromophores developed have been copolymerized into polyurethane cross-linked EO polymer; (5) Vapor deposited polyurethane based side-chain polymeric thin films demonstrate large EO effects with r33 = 5.6 pm/V; (6) Spin-coated BaTiO3/PMMA composite thin films show large electrooptical effect; (7) Two novel techniques, electrooptical characterization and subpicosecond optical rectification, have been implemented. DTIC

N94-19597# Cornell Univ., Ithaca, NY. School of Electrical Engineering.
SUPPRESSED ELECTRON-PHONON SCATTERING IN SUPERLATTICES Final Report
Y.-P. Chen, A. Clark, L. F. Eastman, T. LeTran, and P. Mandeville 23 Aug. 1993 85 p
(Contract DAAL03-90-G-0083)
(AD-A270834; ARO-26755.5-EL) Avail: CASI HC A05/MF A01

This report covers a three-year study of scattering of electrons by phonons in superlattices. The usual bulk polar optical phonons were confined to the quantum wells by the abrupt interfaces with the barriers. In short period superlattices this in turn would be expected to lower the rate of scattering of electrons by these phonons. This study showed that the room temperature mobility was reduced, rather than enhanced as expected from the phonon confinement. Interface phonon scattering was studied to show that it was the cause of the reduced mobility at room temperature. At lower temperatures, such as 77K and lower, the electron mobility measured was higher in the short period superlattice case when the barriers seen by the electrons were A1As. In order to avoid the interface phonon scattering, a graded composition quantum well was used. Devices made from such structures had improved electron mobility, breakdown voltage, and gate leakage. DTIC

N94-19612 Technische Hochschule, Darmstadt (Germany). Fachbereich Physik.
NONLINEAR DYNAMICS AND INSTABILITIES IN FERROMAGNETIC RESONANCE EXPERIMENTS: EXAMINATIONS OF SPHERES FROM YTTRIUM IRON GARNET IN COINCIDENCE AREA OF THE FIRST SUHL INSTABILITIES Ph.D. Thesis [NICHTLINEARE DYNAMIK UND INSTABILITAETEN IN FERROMAGNETISCHEN RESONANZEXPERIMENTEN. UNTERSUCHUNGEN AN KUGELN AUS YTTRIUM-EISENGRANAT IM KOINZIDENZBEREICH DER ERSTEN SUHL-INSTABILITAET]
Garrelt Wiese 1991 108 p In GERMAN Limited Reproducibility: More than 20% of this document may be affected by microfiche quality
(ETN-93-95072) Avail: CASI HC A06

Mechanisms of temperature induced nonlinearities, observed in yttrium iron garnet behavior, such as autooscillations and strong multistability, are explained. Samples were excited by centimeter microwaves, using a spectrometer with a microspool in order to avoid interactions between the resonator and the samples. Measurements were carried out with four different orientations of the sample, relative to the static field; a model for describing the parametrical excitation, using spherical eigenmodes of the sphere instead of spin wave approximation was developed: the modes were classified through a spin quantum number, an effective wave vector and an angle. Nonlinear couplings between the parametrically excited modes were considered, so that the role of indirect resonant excitation of the logwave magnetostatic mode is highlighted. ESA

N94-19664# North Carolina State Univ., Raleigh. Dept. of Materials Science and Engineering.
THE DEPOSITION OF ELECTRO-OPTIC FILMS ON SEMICONDUCTORS Interim Report, 1 Jan. 1992 - 30 Apr. 1993
Angus I. Kingon, Orlando H. Auciello, and Klaus J. Bachmann 8 Oct. 1993 42 p
(Contract N00014-91-J-1307)
(AD-A270823) Avail: CASI HC A03/MF A01

High quality potassium niobate thin films have been grown on magnesium oxide, spinel, potassium tantalate, and sapphire by Ion Beam Sputter Deposition. The effects of substrate preparation, process conditions, and film stoichiometry are being correlated with optical properties. The factors contributing to optical losses is the present focus of our research since low losses are an essential criteria for building device structures. Electro-optic properties of KNbO3 films on MgO are found to be similar to bulk, although the scattering losses are very high for these films. In comparison KNbO3 films grown on KTaO3 exhibit low losses of less than 8 dB, while losses for films on spinel showed to be in between those two. The variety of substrates provide us with differences in lattice mismatch, refractive index mismatch, surface morphologies, and microstructure, all of which influence loss characteristics. DTIC

N94-19679# Ohio State Univ., Columbus. Computer Microbiology and Contamination Lab.
ATOMIC-SCALE FRICTION AND MICROFRICTION OF GRAPHITE AND DIAMOND USING FRICTION FORCE MICROSCOPY
Ju-Ai Ruan and Bharat Bhushan 7 Oct. 1993 39 p
(Contract N00014-93-1-0067)
(AD-A270952) Avail: CASI HC A03/MF A01

Friction of graphite and diamond surfaces against a sharp silicon nitride tip was measured using a friction force microscope (FFM). Atomic-scale friction of a freshly cleaved highly oriented pyrolytic graphite (HOPG) exhibited the same periodicity as that of corresponding topography. However, the peaks in friction and those in corresponding topography profiles were displaced relative to each other. Using Fourier expansion of the interaction potential, the interatomic forces between the FFM tip and graphite surface were calculated. It was shown that the variations in atomic-scale friction and the observed displacement between the peaks in friction and those in corresponding topography can be explained by the variations in interatomic forces in the normal and lateral directions. At large scan sizes (50 nm x 50 nm or larger), the variation of friction for graphite and a single-crystal (IIa) diamond was found to follow the local slope of the sample surface, suggesting that a ratchet mechanism is operative in microscale friction. DTIC

N94-19717# Arizona State Univ., Tempe. Dept. of Electrical and Computer Engineering.
ISOLATION MECHANISMS IN III-V DEVICES Final Report, 15 May 1989 - 15 Nov. 1992
George N. Maracas 17 Aug. 1993 10 p
(Contract DAAL03-89-K-0038)
(AD-A271197; ARO-26686.18-EL) Avail: CASI HC A02/MF A01

This is the final technical report for ARO contract DAAL03-89-K-0038. In the report we describe our progress in the areas of III-V electronic device isolation and how they apply to the phenomena of sidegating and backgating in GaAs based devices. The program evolved into a highly collaborative effort between industry and university with several joint publications resulting. The sidegating/backgating problem in field effect transistors (FET's) has essentially been eliminated by the development of GaAs and other compounds grown at low temperatures by MBE. Research included the developing techniques for synthesis of MBE material at low temperatures (LT), establishment of electrical and optical characterization techniques specifically designed for the study of such materials and the effect of electrical buffer layers made from the LT material on devices. We have made advances in several areas including first realizations of LT GaAs by GSMBE, first realization of LT InP, observation of variable range hopping conductivity in various LT III-V materials, determination of device degradation effects of LT buffer layers and thermal stability of these materials. Additionally we (with MOTOROLA) obtained an enhancement of mobility in two dimensional electron gas structures by separately confining electrons and phonons. DTIC

N94-19719# Princeton Univ., NJ. Dept. of Mathematics.
NUMERICAL MODELLING OF CRYSTAL GROWTH Final Report, Apr. 1990 - 31 Mar. 1993
John Strain 30 Sep. 1992 4 p
(Grant AF-AFOSR-0165-91)
(AD-A271206; AFOSR-93-0786TR) Avail: CASI HC A01/MF A01

A code which solves the two-dimensional Euler equations for inviscid incompressible fluid flow was developed. It is based on (1) adaptive triangulation of initial data, (2) fast summation of the velocity field induced by a piecewise linear vorticity distribution, and (3) Delaunay triangulation of the vortices at each step. The Euler equations were chosen as a model problem for crystal growth because they share the numerical structure of moving points without the added difficulties of finding curvature and normal; instead, the velocity field is simply found from the Biot-Savart law. The code was tested on multiple rotating patches of constant and smooth vorticity. It is second-order in space and fourth-order in time, even on piecewise constant solutions. The errors are much smaller that standard blob-based vortex methods with the same number of degrees of freedom. DTIC

N94-19725# North Carolina State Univ., Raleigh.
SOLID-STATE DYNAMICS IN NOVEL SEMICONDUCTOR NANOSTRUCTURES Final Report, 1 May 1990 - 30 Apr. 1993
Michael A. Stroscio 30 Jun. 1993 8 p
(Contract DAAL03-89-D-0003)
(AD-A271249; ARO-28187.1-EL) Avail: CASI HC A02/MF A01

This research program has focussed on selected aspects of the confinement of optical phonons in structured polar semiconductor structures as well as on the interaction of carriers with phonons in such structures. DTIC

N94-19735# Los Alamos National Lab., NM.
MAGNETIC AND CRYSTALLOGRAPHIC STRUCTURES IN UTX INTERMETALLIC COMPOUNDS
R. A. Robinson, A. C. Lawson, V. Sechovsky (Karlova Univ., Prague, Czechoslovakia.), L. Havela (Karlova Univ., Prague, Czechoslovakia.), Y. Kergadallan (European Atomic Energy Community, Karlsruhe, Germany.), H. Nakotte (Amsterdam Univ., Netherlands.), and F. R. deBoer (European Atomic Energy Community, Karlsruhe, Germany.) 1993 11 p Presented at the Actinides 1993, Santa Fe, NM, 19-24 Sep. 1993
(Contract W-7405-eng-36)
(DE93-018291; LA-UR-93-2739; CONF-930905-1) Avail: CASI HC A03/MF A01

Uranium, along with other actinides and lanthanides, forms a large group of ternary intermetallic compounds of stoichiometry UTX (T = transition metal, X = p-electron metal). These compounds are formed in several structure types and the occurrence and stability of particular structures with respect to the transition metal content suggests reasonable systematics. The authors have also investigated the magnetic structures of selected UTX compounds and it is revealing to relate the crystallographic and magnetic structures, because of the relationship between the magnetic symmetry and that of the U-atom environment produced by the 5f-ligand hybridization, and the consequent anisotropic exchange. Those of ZrNiAl structure type are collinear, with moments along the hexagonal c-axis. In the orthorhombic NiSiTi structure type, the moments are confined to the b-c plane (perpendicular to the uranium chains) and the structures are often incommensurate. In the hexagonal CaIn2 (or GaGeLi) structure type, the magnetic structures form in an orthorhombic cell, and at least in the disordered centric group, again the moments lie perpendicular to the nearest-neighbor uranium spacing. This work presents a phenomenology of trends in UTX ternary compounds. It is shown that there is an apparent strong hybridization parallel to nearest neighbor U-U directions, with ferromagnetic coupling in the same directions. There may be a systematic relationship between the hybridization anisotropy and the magnetic anisotropy, in which the quantization axes are the same and the moments point along directions of relatively weak hybridization. DOE

N94-19739# Texas Univ., Austin. Dept. of Chemistry and Biochemistry.
SINGLE SOURCE PRECURSORS FOR THE OMCVD OF 3/5 COMPOUND SEMICONDUCTORS Final Report, 1 Jan. - 31 May 1993
Richard A. Jones and John G. Ekerdt 31 Jul. 1993 10 p
(Contract DAAL03-89-K-0164)
(AD-A271147; ARO-26748.31-CH) Avail: CASI HC A02/MF A01

The overall goals are to develop the fundamental chemistry of group III and group V compounds in several key areas. The underlying rationale is to ultimately improve on the preparation and properties of important materials used in the semiconductor industries. The research comprises a collaboration between a synthetic inorganic chemist and a chemical engineer. The three main areas are single source precursors for OMCVD of III/V semiconductors; alternative precursors for OMCVD studies, group III or V hydrides; and the organometallic chemistry of bismuth. The first area will employ compounds of the general type (R2M(mu-R'2E))2 (M = Al, Ga, In; E = P, As; R, R' = alkyl, aryl, etc.) and the second will employ similar compounds but with R or R' replaced by the hydride ligand. The paper explores the relationships between precursor structures, mechanisms of decomposition and thin film formation, and the morphological and electrical properties of the grown films. In the third area the document explores the organometallic chemistry of bismuth and compounds which may serve as precursors to important materials such as InBiSb. DTIC

N94-19741# North Carolina Univ., Chapel Hill.
THEORETICAL AND EXPERIMENTAL STUDIES OF QUANTUM WELLS Final Report, 15 Mar. 1990 - 15 Jul. 1993
Raphael Tsu 15 Sep. 1993 12 p
(Contract DAAL03-90-G-0067)
(AD-A271180; ARO-27443.5-EL) Avail: CASI HC A03/MF A01

As the dimension of devices continues to shrink below the mean free path of the electrons, the physics is dominated by the wave nature of the electrons. The transport through a cluster of nanoscale Si-particles in a diode configuration shows discrete steps and peaks in conductance vs voltage at room temperature, attributed to the formation Coulomb blockade, results of Pauli's exclusion principle for the occupation of quantum states in these dots. The extrinsic conduction in these nanoparticles generally disappears due to a significant increase of the binding energy of donors and acceptors because of the decrease of the dielectric screening and the attractive interaction of the quantized electrons with their images at the interface. The disappearance of the extrinsic conduction constitutes a self-limiting factor in the electrochemical etching of porous silicon. DTIC

N94-19769 Northwestern Univ., Evanston, IL.
MOCVD-GROWN InGaAsP HETEROSTRUCTURE DIODE LASERS
M. Razeghi Aug. 1993 19 p Limited Reproducibility: More than 20% of this document may be affected by microfiche quality
(Contract DAAH04-93-G-0044)
(AD-A270848; ARO-31108.1-PH) Avail: CASI HC A03

InGaAsP/InGaP/GaAs compound has been recently proposed to replace AlGaAs/GaAs as advantageous material for high-power laser applications. In this work, we report successful fabrication and study of broad-area double-heterostructure InGaAsP/InGaP laser diodes reproducibly grown by MOCVD. The diodes demonstrated near-100% efficiency of spontaneous radiative recombination in the active region. Threshold current densities of 700 A/sq cm obtained for 900 micron-long cavities were close to the theoretically predicted low limit and lower than respective values experimentally obtained for similar AlGaAs/GaAs diodes. Narrow far-field distribution with FWHM of 28 deg in the direction transverse to p-n junction plane may be of practical interest. Saturation of spontaneous emission above the threshold as well as a flat near field pattern confirm the uniformity of lasing intensity across a 100 micron-wide stripe and the homogeneity of the structures studied. Relatively high internal losses of approximately 40/cm and low differential quantum efficiency of 25% were shown to be inherent for this laser structure design and should be overcome by a combination of the advantages of separate-confinement heterostructures with this laser-quality material. DTIC

N94-19771 General Motors Research Labs., Warren, MI. Physical Chemistry Dept.
PRESSURE AND TEMPERATURE EFFECTS ON THE KINETICS AND QUALITY OF DIAMOND FILMS
Stephen J. Harris and Anita M. Weiner 27 Sep. 1993 36 p Limited Reproducibility: More than 20% of this document may be affected by microfiche quality
(AD-A270876) Avail: CASI HC A03

The first measurements of the effects of pressure on the kinetics and quality of diamond films grown with hot filament chemical vapor deposition are reported. Pressure affects growth kinetics largely because it affects heat transfer between the filament and the substrate and because it affects transport of precursors to the growing surface. H and CH3 concentrations at the growth surfaces are determined with our recombination enthalpy technique combined with appropriate transport analyses. The growth rate rises and then falls with increasing pressure, although there is a saturation in the concentration of CH3 and atomic H at the surface. The fall in-growth rate at higher pressure is explained with our chemical kinetics model as due to an increase in substrate temperature at higher pressures. Since the rate of thermal desorption of the CH3 precursor increases more rapidly with temperature than the competing rate of its incorporation, and since these two rates are comparable, higher substrate temperatures lower incorporation rates, and the growth rate decreases. DTIC

N94-18021# Stuttgart Univ. (Germany). Inst. fuer Zeitmesstechnik, Fein- und Mikrotechnik.
SIMULATION OF QUARTZ RESONATORS [SIMULATIONEN AN SCHWINGQUARZEN]
M. Weinmann, R. Radius, and R. Mohr *In* Societe Suisse de Chronometrie, Proceedings of the 4th European Congress on Chronometry 1992 p 73-76 In GERMAN (For primary document see N94-18006 04-35)
Copyright Avail: CASI HC A01/MF A02

77 THERMODYNAMICS AND STATISTICAL PHYSICS

Includes quantum mechanics; theoretical physics; and Bose and Fermi statistics.

For related information see also *25 Inorganic and Physical Chemistry* and *34 Fluid Mechanics and Heat Transfer.*

N94-17792# International Atomic Energy Agency, Vienna (Austria).
INTERNATIONAL CENTRE FOR THEORETICAL PHYSICS, TRIESTE SCIENTIFIC ACTIVITIES IN 1991
Nov. 1992 110 p
(DE93-624757; IAEA-TECDOC-676) Avail: CASI HC A06/MF A02 (US Sales Only)

The document contains three parts. Part 1 is a general review of the scientific activities of the Center in 1991, including a statistical digest. Part 2 presents the scientific program of the Center in the following fields: Fundamental Physics, Condensed Matter Physics, Mathematics, Physics and Energy, Physics and Environment, Applied Physics, Adriatico Research Conferences, as well as other aspects of the Center activities in 1991. Part 3 lists the publications issued in 1991. DOE

N94-17794# International Centre for Theoretical Physics, Trieste (Italy).
GROUPS ON TRANSFORMATIONS IN FINSLERIAN SPACES
R. B. Misra Jan. 1993 19 p
(DE93-624765; IC-93/11) Avail: CASI HC A03/MF A01 (US Sales Only)

The article first appeared in the Internal Reports of the ICTP in 1981. Since then the topic has attracted a large number of authors and several contributions have been made thereafter. Thus, a previous work of the author is revised and up-dated here including the post-1981 contributions in the field. Infinitesimal transformations defining motions, affine motions, projective motions, conformal transformations and curvature collineations in

various types of Finslerian spaces are discussed here. The notation and symbolism used in the paper is mainly based on the author's works.
DOE

N94-17892# Texas Univ., Austin. Center for Particle Physics.
AVOIDING DEGENERATE COFRAMES IN AN AFFINE GAUGE APPROACH TO QUANTUM GRAVITY
E. W. Mielke, J. D. McCrea, Y. Neeman, and F. W. Hehl Apr. 1993 14 p
(Contract DE-FG03-93ER-40757)
(DE93-013146; DOE/ER-40757/2) Avail: CASI HC A03/MF A01

This report discusses the following concepts on quantum gravity: the affine gauge approach; affine gauge transformations versus active differomorphisms; and affine gauge approach to quantum gravity with topology change. DOE

N94-17950 Weizmann Inst. of Science, Rehovoth (Israel).
GAUGE COUPLING UNIFICATION IN SUPERSTRING DERIVED STANDARD-LIKE MODELS
A. E. Faraggi Nov. 1992 14 p Limited Reproducibility: More than 20% of this document may be affected by microfiche quality
(DE93-624801; WIS-PH-92-17) Avail: Issuing Activity (Department of Energy (DOE)) (US Sales Only)

I discuss gauge coupling unification in a class of superstring standard-like models, which are derived in the free fermionic formulation. Recent calculations indicate that the superstring unification scale is at O(10(sup 18)GeV) while the minimal supersymmetric standard model is consistent with LEP data if the unification scale is at O(10(sup 16))GeV. A generic feature of the superstring standard-like models is the appearance of extra color triplets (D,bar-D) , and electroweak doublets (l,bar-l), in vector-like representations, beyond the supersymmetric standard model. I show that the gauge coupling unification at O(10(sup 18)GeV) in the superstring standard-like models can be consistent with LEP data. I present an explicit standard-like model that can realize superstring gauge coupling unification.
DOE

N94-17953 Weizmann Inst. of Science, Rehovoth (Israel).
CABIBBO MIXING IN SUPERSTRING DERIVED STANDARD-LIKE MODELS
A. E. Faraggi and E. Halyo Jan. 1993 17 p Limited Reproducibility: More than 20% of this document may be affected by microfiche quality
(DE93-624814; WIS-PH-93-3) Avail: Issuing Activity (Department of Energy (DOE)) (US Sales Only)

We examine the problem of generation mixing in realistic superstring derived standard-like models, constructed in the free fermionic formulation. We study the possible sources of family mixing in these models. In a specific model we estimate the Cabibbo angle. We argue that a Cabibbo angle of the correct order of magnitude can be obtained in these models.
DOE

N94-18120# Helsinki Univ. of Technology, Espoo (Finland). Lab. of Thermal Engineering.
THERMODYNAMIC THEORY OF EXERGY ANALYSIS
M. J. Lampinen and M. A. Heikkinen 1993 40 p
(PB93-187847) Avail: CASI HC A03/MF A01

A comprehensive general theory of exergy analysis with several new results is presented. A stationary flow system and its exergy is studied in three cases: there is only one heat input to the system, there are several heat inputs to the system, and also several heat outputs from the system to the surroundings at different temperatures. A relevant reference temperature of the surroundings is derived for each case. The results are applied to mechanical multi-circuit heat pump cycles and to an absorption heat pump. NTIS

N94-18174 International Centre for Theoretical Physics, Trieste (Italy).
ISING MODEL ON TANGLED CHAIN. PART 2: MAGNETIZATION AND SUSCEPTIBILITY
R. Mejdani May 1993 22 p Limited Reproducibility: More than 20% of this document may be affected by microfiche quality
(DE93-628794; IC-93/90) Avail: CASI HC A03 (US Sales Only)

In the preceding paper we have considered an Ising model defined on tangled chain to study the behavior of the free energy and entropy, particularly in the zero-field and zero-temperature limit. In this paper, following the main line and based on some results of the previous work, we shall study in the 'language' of state configurations the behavior of the magnetization and the susceptibility for different conditions of the model, to understand better the competition between the ferromagnetic bonds along the chain and the antiferromagnetic additional bonds across the chain. Particularly interesting is the behavior of the susceptibility in the zero-field and zero-temperature limit. Exact solutions for the magnetization and susceptibility, generated by analytical calculations and iterative algorithms, are described. The additional bonds, introduced as a form of perfectly disorder, indicate a particular effect on the spin correlation. We found that the condition J=-J' between the ferromagnetic interaction J along the chain and the antiferromagnetic interaction J' across the chain is somewhat as a 'transition-region' condition for this behavior. DOE

N94-18211# Japan Atomic Energy Research Inst., Tokyo.
STRUCTURE, THERMODYNAMICS, AND DYNAMICAL PROPERTIES OF SUPERCOOLED LIQUIDS
Shaw Kambayashi Dec. 1992 135 p
(DE93-788387; JAERI-M-92-181) Avail: CASI HC A07/MF A02

The equilibrium properties of supercooled liquids with repulsive soft-sphere potentials, u(r) = (epsilon)(sigma/r)(sup n), have been obtained by solving the integral equation of the theory of liquids and by performing constant-temperature molecular dynamics (MD) simulations. A thermodynamically consistent approximation, proposed recently by Rogers and Young (RY), has been examined for the supercooled soft-sphere fluids. Then, a new approximation for the integral equation, called MHNCS (modified hypernetted-chain integral equation for highly supercooled soft-sphere fluids) approximation, is proposed. The solution of the MHNCS integral equation for highly supercooled liquid states agrees well with the results of computer simulations. The MHNCS integral equation has also been applied for binary soft-sphere mixtures. Dynamical properties of soft-sphere fluids have been investigated by molecular dynamics (MD) simulations. The reduced diffusion constant is found to be insensitive to the choice of the softness of the potential. On the other hand, the spectrum of the velocity autocorrelation function shows a pronounced dependence on the softness of the potential. These significant dynamical properties dependent on the softness parameter (n) are consistent to dynamical behavior observed in liquid alkali metals and liquefied inert gases. The self-part of the density-density autocorrelation function obtained shows a clear nonexponential decay in intermediate time, as the liquid-glass transition is approached. DOE

N94-18236# Advisory Group for Aerospace Research and Development, Neuilly-Sur-Seine (France). Guidance and Control Panel.
NON LINEAR DYNAMICS AND CHAOS [LA DYNAMIQUE NON-LINEAIRE ET LE CHAOS]
Jun. 1993 191 p Lecture series held in Stanford, CA and Sophia Antipolis, France, Jun. 1993
(AGARD-LS-191; ISBN-92-835-0714-2) Copyright Avail: CASI HC A09/MF A02

Many efforts were oriented towards the understanding of the unexpected behavior of systems - linear or non-linear. These could be large (weather systems, biological life) or small (automatic pilot). A new branch of dynamics is now considered; it is called 'chaos'. Some general theories emerged and reconsideration of concepts of non-linear control to determine the stability of such systems is now intensively studied in the scientific community. The following topics are covered: linear (including time varying coefficients equations) vs non-linear systems; types of non-linearity; curved characteristics, jumps, bifurcation; nonlinear dynamics; sensibility to initial conditions and/or uncertainties on the system parameters; robustness; neuronal-type machines; chaos - random process behavior; reversibility; irreversibility; Newtonian mechanics and thermodynamics; fractals; and applications. For individual titles, see N94-18237 through N94-18241.

N94-18237# Nice Univ. (France). Inst. Non-Lineaire.
BIFURCATION THEORY: CHAOS AND PATTERNS
P. Coullet *In* AGARD, Non Linear Dynamics and Chaos Jun. 1993 13 p Sponsored by CNRS and Commission of the European Communities (For primary document see N94-18236 04-77)
Copyright Avail: CASI HC A03/MF A02

The transition towards chaos through the cascade of period doubling bifurcations and the phenomena of symmetry breaking and pattern formation are studied. The qualitative and universal aspects of these phenomena are emphasized. Author (revised)

N94-18238# Office National d'Etudes et de Recherches Aerospatiales, Paris (France).
STABILITY ANALYSIS THROUGH BIFURCATION THEORY, 1
P. Guicheteau *In* AGARD, Non Linear Dynamics and Chaos Jun. 1993 10 p (For primary document see N94-18236 04-77)
Copyright Avail: CASI HC A02/MF A02

This communication is the first part of the three papers which are presented by the author in the same AGARD Lecture Series (LS 191). It aims at the study of asymptotic solutions of non-linear differential equations depending on parameters. The first part is devoted to a brief presentation of the basis of Bifurcation Theory which is limited to the non-linear phenomena observed by the author when he analyzed high performance aircraft behavior. In particular, complex bifurcations and chaotic motions are not treated. Numerical procedures developed to use results from Bifurcation Theory are presented. Then, some remarks are stated to establish a connection between asymptotic and quasi-stationary behavior. Finally, a methodology dedicated to the analysis of non-linear systems is proposed. Author (revised)

N94-18239# Office National d'Etudes et de Recherches Aerospatiales, Paris (France).
STABILITY ANALYSIS THROUGH BIFURCATION THEORY, 2
P. Guicheteau *In* AGARD, Non Linear Dynamics and Chaos Jun. 1993 11 p (For primary document see N94-18236 04-77)
Copyright Avail: CASI HC A03/MF A02

This communication follows a previous communication which was presented in the same Agard Lecture Series (LS 191). In the previous communication, some theoretical foundations of Bifurcation Theory were recalled and a methodology aiming at a systematic prediction of the behavior of non-linear differential equations was presented. This communication mentions some problems which are connected with the introduction of control laws in order to stabilize an unstable dynamic system and presents a brief state of the art related to the determination of the attracting region of a stable equilibrium point. Author (revised)

N94-18240# Office National d'Etudes et de Recherches Aerospatiales, Paris (France).
NON-LINEAR FLIGHT DYNAMICS c05
P. Guicheteau *In* AGARD, Non Linear Dynamics and Chaos Jun. 1993 13 p Sponsored in part by Services Techniques des Programmes Aeronatiques (For primary document see N94-18236 04-77)
Copyright Avail: CASI HC A03/MF A02

In Flight Dynamics, aircraft motion is described by a set of non-linear differential equations, depending on parameters, associating the state vector (angle of attack, sideslip angle, speed, angular rates, etc.) with the control vector (motivators, etc.) through flight dynamics equations, aerodynamic model, and flight control system. Some works which aim at improving the knowledge and the prediction of aircraft behavior, in particular flight phases for which classical linearized analysis of non-linear differential equations is insufficient or not valid, are presented. Author (revised)

N94-18241# Air Force Inst. of Tech., Wright-Patterson AFB, OH.
INTRODUCTION TO QUANTITATIVE FEEDBACK THEORY (QFT) TECHNIQUE c63
Constantine H. Houpis *In* AGARD, Non Linear Dynamics and Chaos Jun. 1993 20 p (For primary document see N94-18236 04-77)
Copyright Avail: CASI HC A03/MF A02

Quantitative Feedback Theory (QFT) has achieved the status as a powerful design technique for the achievement of assigned performance tolerances over specified ranges of plant parameter uncertainties without and with control effector failures. It is a frequency domain design technique utilizing the Nichols chart (NC) to achieve a desired robust design over the specified region of plant parameter uncertainty. An introduction to QFT analog and discrete design techniques is presented for both multiple-input single-output (MISO) and multiple-input multiple-output (MIMO) control systems. QFT computer aided design (CAD) packages are readily available to expedite the design process. The purposes of these lectures are: (1) to provide a basic understanding of QFT, (2) to provide the minimum amount of mathematics necessary to achieve this understanding, (3) to discuss the basic design steps, and (4) to present two practical examples. Author (revised)

N94-18252 Joint Inst. for Nuclear Research, Dubna (USSR). Lab. of Theoretical Physics.
ABOUT SYMMETRY OF THE GRAVITATIONAL ACTION
M. N. Tentyukov 1991 8 p Submitted for publication Limited Reproducibility: More than 20% of this document may be affected by microfiche quality
(DE93-629955; JINR-E-2-91-580) Avail: CASI HC A02 (US Sales Only)

The Einstein equations are investigated by imbedding of the metric tensor to the affinely connected space. It is shown that if using of the Einstein equations, then, despite the action functional invariance being violated with respect to the diffeomorphism group by the background object, a new infinite-parameter invariance appears, i.e., the action invariance can be extended from the group of motions of the background object to any infinite-parameter group. DOE

N94-18253 Joint Inst. for Nuclear Research, Dubna (USSR). Lab. of Computing Techniques and Automation.
THE RISE OF ACCURACY FOR THE MULTICHANNEL SCATTERING PROBLEM SOLVING [POVYSHENIE TOCHNOSTI RESHENIYA MNOGOKANAL'NOJ ZADACHI RASSEYANIYA]
S. I. Vinitskij, I. V. Puzynin, and Yu. S. Smirnov 1992 28 p In RUSSIAN Limited Reproducibility: More than 20% of this document may be affected by microfiche quality
(DE93-630145; JINR-R-11-92-126) Avail: CASI HC A03 (US Sales Only)

The Newton's iterative algorithm for solving the multichannel scattering problem for a system of the Schroedinger radial equations is presented. A discrete approximation of the problem is based on the finite-difference scheme of the n-th order accuracy with respect to a characteristic step h of the quasi-uniform mesh Omega(sub h). The calculations of the wave functions, phase shifts, and cross sections of elastic and inelastic collisions of mesic atoms (d(mu))(sub 1s) and (p(mu))(sub 1s) with nuclei t and p were fulfilled in framework of simple approach of two-level adiabatic approximation for the collision energy values 0.001 eV - 50 eV. As compared with other works more accurate results for the characteristics of the scattering processes (d(mu))(sub 1s)+t and (t(mu))(sub 1s)+d near thresholds in the region 0.001 eV less than or equal to E less than or equal to 0.3 eV were obtained. A correct monotonic behaviour of the partial reaction matrix K(sup 1) elements was achieved for this region of the energy and for values of the total orbital momentum 1 = 0, 1, 2, and 3. DOE

N94-18267 Joint Inst. for Nuclear Research, Dubna (USSR). Lab. of Theoretical Physics.
PHASE STRUCTURE OF (PHI(4))(SUB 3) FIELD THEORY AT FINITE TEMPERATURE
G. V. Efimov and S. N. Nedelko (Tomsk State Univ., USSR.) 1992 23 p Submitted for publication Limited Reproducibility: More than 20% of this document may be affected by microfiche quality
(DE93-629907; JINR-E-2-92-287) Avail: CASI HC A03 (US Sales Only)

Phase structure of phi(sup 4) field theory in the space-time R(sup 3) is investigated at arbitrary coupling constant and temperature. The critical values of the coupling constant and temperature, corresponding to the phase transitions in the system, are calculated by the canonical transformation method within formalism of thermo field dynamics. The Hamiltonians describing the system in each phase are obtained straightforwardly. Comparison with the two-dimensional case shows a crucial influence of higher order renormalization on the phase structure of the model. DOE

N94-18268 Joint Inst. for Nuclear Research, Dubna (USSR). Lab. of High Energy.
ON THE MICHELSON-MORLEY EXPERIMENT [OB OPYTE MAJKEL'SONA-MORLI]
V. N. Streltsov 1991 16 p In RUSSIAN Limited Reproducibility: More than 20% of this document may be affected by microfiche quality
(DE93-629908; JINR-R-2-91-569) Avail: CASI HC A03 (US Sales Only)

The opinion about the important role of the Michelson-Morley experiment in the establishment of the principle of the constancy of the light velocity is expressed. It is noted that Fitzgerald-Lorentz contraction introduced for the explanation of its negative result contradicts the Galilei transformations (and consequently, to ether theory). The theorem is proved that if a length of a moving rod is given by the instantaneous length, the propagation velocity of light along the rod is an inconstant quantity. It is stressed that the using of the radar length for the treatment of Michelson-Morley experiment leads to elongation formula for a longitudinal arm of the interferometer. DOE

N94-18310 Army Research Lab., Aberdeen Proving Ground, MD.
TECHNIQUES FOR THE ESTIMATION OF HEATS OF EXPLOSION (HEX) USING THERMOCHEMICAL CODES Final Report, Sep. 1990 - May 1992
Robert A. Fifer and Jeffrey B. Morris Sep. 1993 48 p Limited Reproducibility: More than 20% of this document may be affected by microfiche quality
(DA Proj. 1L1-61102-AN-43)
(AD-A268584; ARL-TR-195) Avail: CASI HC A03

Procedures are outlined for calculating the heats of explosion (HEX) of neat energetic materials or propellant/explosive formulations using thermochemical codes. The 'exact' method and three approximate techniques are described; the approximate techniques either eliminate the need to sum the internal energies of the predicted products, or eliminate the need to specify a freeze-out temperature. The various techniques are illustrated for HMX and a nitrocellulose/nitroglycerine (NC/NG) mixture. DTIC

N94-18629# California Univ., Berkeley. Lawrence Berkeley Lab.
SPACE AND TIME FROM QUANTUM MECHANICS
G. F. Chew 16 Sep. 1992 7 p
(Contract DE-AC03-76SF-00098)
(DE93-015263; LBL-32852) Avail: CASI HC A02/MF A01

Classical mechanics historically preceded quantum mechanics and thus far has not been displaced from primary status; the path to construction of quantum theory has remained rooted in classical ideas about objective reality within space and time. Use of a less correct theory as underpinning for a more correct theory not only is unaesthetic but has spawned the perplexing and never-resolved puzzle of measurement. A growing number of physicist-philosophers torture themselves these days over the collapse of the quantum-mechanical state vector when measurement is performed. Additionally, the pointlike structure of the spacetime manifold underlying local classical fields has endowed quantum theory with mathematical dilemmas. It has been proposed by Gell-Mann and Hartle that objectively-realistic ideas such as measurement may lack a priori status, the predominantly classical present universe having evolved as a relic of the big bang. Other authors have suggested that spacetime itself need not be a priori but may stem from quantum mechanics. Haag has written recently that spacetime without (quantum) events is probably a meaningless concept. Henry Stapp and I have for several years been exploring a simple quantum system devoid of classical underpinning, even spacetime, but admitting within the Hilbert space a special Lie-group-related category of vector known as a coherent state. Groups unitarily representable in our Hilbert space include the Poincare group, which relates to 3 + 1 spacetime. Coherent states generally are labeled by parameters associated with unitary group representations, and it has long been recognized that when such parameters become large a classical objective interpretation may result. Stapp and I have been attempting to understand space and time via large coherent-state parameters. Six years ago I presented to this gathering a preliminary report on our enterprise; in this paper I provide an update. DOE

N94-18908 Optical Society of America, Washington, DC.
INTEGRATED PHOTONICS RESEARCH: POST-DEADLINE PAPERS Final Report
Jarus W. Quinn Mar. 1993 66 p Meeting held in Palm Springs, CA, 22-24 Mar. 1993 Limited Reproducibility: More than 20% of this document may be affected by microfiche quality
(AF Proj. 2301)
(AD-A269232; AFOSR-93-0646TR) Avail: CASI HC A04

The symposium was held on the following topics: advanced solid state lasers, compact blue-green lasers, integrated photonics research, nonlinear guide-wave optics, optical amplifiers and their applications, optical design for photonics, photonics in switching, quantum optoelectronics, short-wavelength -- physics with intense-laser pulses, soft x-ray protection lithography, ultrafast electronics and optoelectronics, optical computing, and spatial light modulators. DTIC

N94-19121# Argonne National Lab., IL.
THERMODYNAMIC q-DISTRIBUTIONS THAT AREN'T
S. Vokos and C. Zachos 1993 7 p Presented at the 2nd Prague Colloquium on Quantum Groups, Prague, Czech Republic, 24-26 Jun. 1993
(Contracts W-31-109-eng-38; DE-FG06-91ER-40614)
(DE93-017385; ANL-HEP-CP-93-39; CONF-9306203-1) Avail: CASI HC A02/MF A01

Bosonic q-oscillators commute with themselves and so their free distribution is Planckian. In a cavity, their emission and absorption rates may grow or shrink - and even diverge - but they nevertheless balance to yield the Planck distribution via Einstein's equilibrium method, (a careless application of which might produce spurious q-dependent distribution functions). This drives home the point that the black-body energy distribution is not a handle for distinguishing q-excitations from plain oscillators. A maximum cavity size is suggested by the inverse critical frequency of such emission/absorption rates at a given temperature, or a maximum temperature at a given frequency. To remedy fragmentation of opinion on the subject, we provide some discussion, context, and references. DOE

N94-19187# Los Alamos National Lab., NM.
APPLICATION OF DIFFERENTIAL SENSITIVITY THEORY TO CONTINUUM MECHANICS
P. J. Maudlin, R. J. Henninger, and E. N. Harstad 1993 11 p Presented at the Annual Winter Meeting of the ASME, New Orleans, LA, 28 Nov. - 3 Dec. 1993
(Contract W-7405-eng-36)
(DE93-012732; LA-UR-93-1562; CONF-931121-6) Avail: CASI HC A03/MF A01

A sensitivity technique used successfully in the early eighties, called Differential Sensitivity Theory (DST), is applied to a system of time-dependent continuum mechanics equations. DST uses adjoint techniques to determine exact sensitivity derivatives, i.e., if R is a calculational result of interest (response R) and alpha is a calculational input (parameter alpha(sub i) where the subscript is usually not indicated for convenience), then (partial derivative)R/(partial derivative)(alpha)(sub i) is defined as the sensitivity. The advantage of using DST over other sensitivity analysis techniques is mainly economic: for an n-parameter problem all n sensitivities can be obtained by integrating the solutions from only two calculations, a so-called forward (physical) calculation and its corresponding adjoint calculation. This work describes the derivation and solution of the appropriate set of adjoint and sensitivity equations for the ultimate purpose of computing sensitivities for high-rate two dimensional, multi-component, high deformation problems. DOE

N94-19250# Virginia Polytechnic Inst. and State Univ., Blacksburg.
INVESTIGATIONS IN GAUGE THEORIES, TOPOLOGICAL SOLITONS, AND STRING THEORIES
1993 23 p
(Contract DE-AS05-80ER-10713)
(DE93-015029; DOE/ER-10713/T5) Avail: CASI HC A03/MF A01

This is the final report on a supported research project on theoretical particle physics entitled 'Investigations in Gauge Theories, Topological Solitons, and String Theories.' The major theme of particle theory pursued has been within the rubric of the standard model, particularly on the interplay between symmetries and dynamics. Thus, the research has been carried out primarily in the context of gauge with or without chiral fermions and in effective chiral Lagrangian field theories. The topics studied include the physical implications of abelian and non-abelian anomalies on the spectrum and possible dynamical symmetry breaking in a wide range of theories. A wide range of techniques of group theory, differential geometry, and function theory have been applied to probe topological and conformal properties of quantum field theories in two and higher dimensions, the breaking of global chiral symmetries by vector-like gauge theories such as QCD, the phenomenology of a possibly strongly interacting Higgs sector within the minimal standard model, and the relevance of solitonic ideas to non-perturbative phenomena at SSC energies. DOE

N94-19663# Naval Academy, Annapolis, MD.
ESSENTIAL SHIFT: SCIENTIFIC REVOLUTION IN THE 20TH CENTURY
David K. Ismay 17 May 1993 83 p
(AD-A270810; USNA-TSPR-202) Avail: CASI HC A05/MF A01

With the publishing of Sir Isaac Newton's Principia Mathematica in 1687, a scientific paradigm was established that clearly dominated society for two and half centuries. Many historians of science have identified the Copenhagen interpretation of the quantum theory, formulated c.1927, as having completed a scientific revolution that ended the reign of classical Newtonian science. A rival claim to contemporary scientific revolution, however, has been put forward by Ilya Prigogine and the Brussels school of thermodynamics based on Prigogine's work in non-equilibrium thermodynamics. Using the historical consensus model of scientific revolution first articulated by Thomas S. Kuhn in 1962, this analysis examines the extent to which the Copenhagen interpretation of the quantum theory and the work of Ilya Prigogine complete the conceptual, scientific paradigm-shift necessary for a scientific revolution. The resulting historical evidence shows that the Copenhagen interpretation did not complete a paradigm-shift; instead, it was a self-revelation by the scientific community which revealed the essence and fundamental limitations of Newtonian science. Evidence further indicates that the valid claim to scientific revolution in the 20th century lies with the contemporary work of Prigogine and the Brussels school. By abandoning the deterministic, mechanical world-view of the Newtonian paradigm and accepting a new reality of process and irreversible time, Prigogine and his associates have established the foundations for a revolutionary new scientific paradigm. DTIC

N94-19670# Georgia Inst. of Tech., Atlanta. School of Chemical Engineering.
SUPERCRITICAL THERMODYNAMICS OF SULFUR AND NITROGEN SPECIES
C. A. Eckert 1993 12 p
(Contract DE-FG22-91PC-91287)
(DE93-041221; DOE/PC-91287/9) Avail: CASI HC A03/MF A01

Significant opportunity exists for the application of supercritical fluid (SCF) technology to coal processing, both for pretreatment of high sulfur coals, as well as liquefaction and treatment of coal liquids. Supercritical fluids are attractive solvents for a variety of coal processing applications because of their unusual solvating and mass transfer properties. Solubility studies have been carried out for a number of model coal and coal-liquid compounds, primarily in pure supercritical fluids. We are extending this database of model coal compound equilibria using modern techniques that have the advantage of being much more rapid than traditional techniques. Cosolvent effects on solubility are being investigated over a variety of solvent properties. In addition, specific molecular interactions are being investigated through spectroscopic techniques. The resulting data are being used to develop a chemical-physical equation of state (EOS) model of SCF solutions with meaningful parameters. The equation of state will be used to predict solubility behavior, which will permit the design and tailoring of SCF cosolvent systems for specific coal processing applications. DOE

80 SOCIAL SCIENCES (GENERAL)

Includes educational matters.

N94-18982* National Aeronautics and Space Administration. Marshall Space Flight Center, Huntsville, AL.
NATIONAL BOY SCOUT JAMBOREE (Videotape)
Aug. 1989 Videotape: 1 min. 57 sec. playing time, in color, with sound
(NASA-TM-109367; NONP-VT-94-198214) Avail: CASI VHS A01/BETA A22

This video looks at a NASA sponsored exhibit at the National Boy Scout Jamboree in Fredricksburg, VA. Boy Scouts are shown interacting with NASA researchers and astronauts and touring mockups of Space Station Freedom and Apollo 11. NASA's program to encourage the researchers of tomorrow is detailed. CASI

N94-19389# National Science Foundation, Washington, DC. Div. of Science Resources Studies.
UNDERGRADUATE ORIGINS OF RECENT SCIENCE AND ENGINEERING DOCTORATE RECIPIENTS
Susan T. Hill Dec. 1992 54 p
(NSF-92-332) Avail: CASI HC A04/MF A01; SOD HC

Baccalaureate institutions are an essential part of the educational process for persons earning science and engineering (S&E) doctorates. This report summarizes data on the baccalaureate institutions reported by persons completing doctorates from 1985 through 1990. It provides an institutional context for examining this aspect of the education pipeline. Author

N94-19446# National Science Foundation, Washington, DC.
UNDERGRADUATE COURSE AND CURRICULUM DEVELOPMENT PROGRAM AND CALCULUS AND THE BRIDGE TO CALCULUS PROGRAM: 1992 AWARDS
1992 154 p
(NSF-93-24) Avail: CASI HC A08/MF A02

The National Science Foundation's Directorate for Education and Human Resources (EHR) is responsible for providing national leadership, examples of model programs, and support for enhancing the quality of education in science, mathematics, and engineering at all levels of the educational system. Within EHR, the Division of Undergraduate Education (DUE) focuses on ensuring that the best possible undergraduate education is provided to meet the Nation's need for high-quality scientists, engineers, mathematicians, and technologists, dedicated and able teachers of pre-college science and mathematics, and scientifically literate citizens. The Undergraduate Course and Curriculum Development (UCC) Program supports model curriculum reform projects in all disciplines within the Foundation's mission. Initially, the UCC program is concentrating on the crucial lower division and introductory-level courses. The enormous interest from the academic community during the first two years of the comprehensive program clearly reflects a national need and underscores NSF's important leadership role at the undergraduate level. The purpose of the continuing program in 'Curriculum Development in Mathematics: Calculus and the Bridge to Calculus' is to support projects that reform curriculum and instruction in both calculus and the preparation for calculus. Through the Calculus program, NSF has responded to the clear need expressed within the mathematic's community that the teaching of calculus and preparation for calculus must be improved. The projects described in this book were selected for their creativity, scientific and educational quality, and potential for utility at multiple institutions and national impact. We are proud of these projects and hope that they will be of interest to science, mathematics, and engineering faculty at all U.S. colleges and universities. Author (revised)

N94-19485# Rochester Univ., NY. Dept. of Computer science.
FIRST RESULTS WITH UTILE DISTINCTION MEMORY FOR REINFORCEMENT LEARNING
R. Andrew McCallum Dec. 1991 17 p
(Grant NSF IRI-89-03582)
(TR-446) Avail: CASI HC A03/MF A01

A method by which a reinforcement learning agent can solve the incomplete perception problem using memory is presented. The agent uses a Hidden Markov Model (HMM) to represent its internal state space and creates memory capacity by splitting states of the HMM. The key idea is a test to determine when and how a state should be split: the agent only splits a state when the split will help the agent predict utility. Thus the agent can build an internal state space proportionate to the task at hand, not as large as would be required to represent all of its perceivable world. The technique is called UDM, Utile Distinction Memory. Author (revised)

81 ADMINISTRATION AND MANAGEMENT

Includes management planning and research.

N94-17746# University of Southern California, Marina del Rey. Information Sciences Inst.
BIAS IN PLANNING AND EXPLANATION-BASED LEARNING Research Report
Paul S. Rosenbloom, Soowon Lee, and Amy Unruh May 1993 41 p
(Contract N00014-89-K-0155)
(AD-A269608; ISI/RR-93-346) Avail: CASI HC A03/MF A01

Biases enable systems to make decisions in realms where all legitimate sources of knowledge have been exhausted. This article investigates the application of biases to the problem of planning, and how this can indirectly induce effective biases in a learning process that is based on planner's experiences. Experimental results from six biased planners, plus several more complex multimethod planners, indicate complex tradeoffs among planner completeness, planning efficiency, and length. Learning also varies in complex ways among these planners, with one notable result being the ease with which some planners learn rules that can generalize from one object to many: a phenomenon known in machine learning as generalization to N. DTIC

N94-17980# Centre de Recherches Scientifiques et Techniques de l'Industrie des Fabrications Metalliques, Brussels (Belgium). Section Construction Mecanique.

THE MACHINE RECEPTION: A BUSINESS OF EXPERTS [LA RECEPTION DE MACHINES, UNE AFFAIRE DE SPECIALISTES]

Leo Janssen and Geert Vandenhoudt Nov. 1992 20 p In FRENCH Sponsored by Regions Wallonne, Brussels, Belgium, and Institut pour l'Encouragement de la Recherche Scientifique dans l'Industrie et l'Agriculture, Brussels, Belgium

(CRIF-MC-94; ETN-93-94441) Copyright Avail: CASI HC A03/MF A01

The acquisition of an automatic tool machine is quite an important decision to the entreprise, for it determines for several years the type and the accuracy of the tools to be produced. In order to avoid any misunderstandings the tests to be performed and their costs should be inscribed in the contract. An important topic in a contrast is the interpretation of standards, the definition of accuracy criteria and the procedures to be respected from both contractors. It is suggested that different entreprises for machine delivery and machine servicing be chosen. ESA

N94-18090 Defense Advanced Research Projects Agency, Arlington, VA.

WHITE HOUSE TECHNOLOGY REINVESTMENT PROJECT: BRIEFING AND TRANSCRIPTS

1993 313 p See also PB93-169894 Limited Reproducibility: More than 20% of this document may be affected by microfiche quality

(PB93-169829) Avail: CASI HC A14

The book arises from the White House Technology Reinvestment Project (TRP) Briefings given in New York City, Detroit, Orlando, Dallas, and Los Angeles respectively during the week of 12 - 16 April 1993. The TRP is comprised of representatives from the following five agencies: Department of Defense (DOD), National Institute of Standards and Technology (NIST), Department of Energy (DOE), National Aeronautics and Space Administration (NASA), and the National Science Foundation (NSF). Although this is a multi-governmental agency effort, the funding and management of this effort is the responsibility of DOD's Advanced Research Projects Agency (ARPA). The conferences were held to give the TRP representatives the opportunity to discuss and answer questions on both the programmatic and funding aspects of this new national effort called the TRP. The book is comprised of the presentation charts used and transcripts taken during the conferences. The question and answer sessions are included in their entirety, but only the New York City speaker/presenter transcripts are included in the book. NTIS

N94-19131*# National Aeronautics and Space Administration, Washington, DC.

APPLICATION OF NEW TECHNOLOGIES IN THE VIRTUAL LIBRARY: SEMINARS IN TURKEY, PORTUGAL, AND SPAIN

Judy F. Hunter and Gladys A. Cotter Jan. 1994 24 p

(NASA-TM-109718; NAS 1.15:109718) Avail: CASI HC A03/MF A01

This paper focuses on the technologies that are available today to support the concept of a virtual library. The concept of a 'virtual library' or a 'library without walls' is meant to convey the idea that information in any format should be available to the end-user from the desktop as if it were located on the local workstation. Discussed here are the background, trends, technology enablers, end-user requirements, and the NASA Access Mechanism (NAM) system, one example of how it is possible to apply existing technologies to the client server architecture to logically centralize geographically distributed applications and information. Author

N94-19157# Technische Univ., Delft (Netherlands). Faculty of Technical Mathematics and Informatics.

SCALE SENSITIVITY IN THE MULTIPLICATIVE AHP AND SMART

F. A. Lootsma 1993 32 p

(Rept-93-37; ETN-93-94664) Copyright Avail: CASI HC A03/MF A01

A variant of the Analytic Hierarchy Process (AHP) with a one parametric class of geometric scales to quantify human comparative judgement and with a multiplicative structure, logarithmic regression to calculate the impact scores of the alternatives at the first evaluation level, and geometric mean aggregation rule to calculate the final scores at the second level is considered. The rank order of the impact scores and the final scores is demonstrated to be scale independent. The multiplicative AHP is shown to be an exponential version of the Simple Multi Attribute Rating Technique (SMART). In fact, the multiplicative AHP is concerned with ratios of intervals on the dimension of desirability, whereas SMART analyzes differences of the corresponding orders of magnitude. ESA

N94-19158# Technische Univ., Delft (Netherlands). Faculty of Technical Mathematics and Informatics.

CONTEXT-RELATED SCALING OF HUMAN JUDGEMENT IN THE MULTIPLICATIVE AHP, SMART AND ELECTRE

F. A. Lootsma 1993 26 p

(Rept-93-38; ETN-93-94665) Copyright Avail: CASI HC A03/MF A01

Since decisions are invariably made within a given context, relative preferences are modeled as ratios of increments or decrements in an interval on the axis of desirability. The ratio magnitudes are then sorted into a small number of categories, represented by numerical values on a geometric scale. An explanation as to why the Analytic Hierarchy Process (AHP) and the French collection of ELECTRE systems, typically based on pairwise comparison methods, are concerned with category judgement of ratio magnitudes, whereas the Simple Multi Attribute Rating Technique (SMART) essentially uses the orders of magnitude of these ratios, is presented. This phenomenon, well known in psychophysics, provides a common basis for the analysis of the methods in question and for a cross validation of their results. The approach is illustrated throughout via a well known case study, the choice of a location for a nuclear power plant. ESA

N94-19434*# National Aeronautics and Space Administration, Washington, DC.

STRATEGIC PLAN, 1991: A STRATEGY FOR LEADERSHIP IN SPACE THROUGH EXCELLENCE IN SPACE SCIENCE AND APPLICATIONS

1991 68 p

(NASA-TM-109256; NAS 1.15:109256) Avail: CASI HC A04/MF A01

In 1988, the Office of Space Science and Applications (OSSA) developed and published a Strategic Plan for the United States' space science and applications program during the next 5 to 10 years. The Plan presented the proposed OSSA program for the next fiscal year and defined a flexible process that provides the basis for near-term decisions on the allocation of resources and the planning of future efforts. Based on the strategies that have been developed by the advisory committees both of the National Academy of Sciences and of NASA, the Plan balances major, moderate, and small mission initiatives, the utilization of Space Station Freedom, and the requirements for a vital research base. The Plan can be adjusted to accommodate varying budget levels, both those levels that provide opportunities for an expanded science and applications program, and those that constrain growth. SSA's strategic planning is constructed around five actions: establish a set of programmatic themes; establish a set of decision rules; establish a set of priorities for missions and programs within each theme; demonstrate that the strategy can yield a viable program; and check the strategy for consistency with resource constraints. The outcome of this process is a clear, coherent strategy that meets both NASA's and OSSA's goals, that assures realism in long-range planning and advanced technology development, and that provides sufficient resiliency to respond and adapt to both known and unexpected internal and external realities. The OSSA Strategic Plan is revised annually to reflect the approval of new programs, improved understanding of requirements and issues, and any major changes in the circumstances, both within NASA and external to NASA, in which OSSA initiatives are considered. Derived from text

N94-19618# National Science Foundation, Washington, DC.

A FOUNDATION FOR THE 21ST CENTURY: A PROGRESSIVE FRAMEWORK FOR THE NATIONAL SCIENCE FOUNDATION. REPORT OF THE NATIONAL SCIENCE BOARD COMMISSION ON THE FUTURE

OF THE NATIONAL SCIENCE FOUNDATION
20 Nov. 1992 20 p
(NSB-92-196) Avail: CASI HC A03/MF A01

This report of the National Science Board Commission on the future of the National Science Foundation stresses the fundamental importance of continuing the NSF's basic mission of supporting first-rate research, identified and defined by the best researchers within the academic community. At the same time, the commission underscores the importance of supporting key strategic research areas in response to scientific opportunities to meet national goals. Throughout the report, the commission identifies challenging issues that will require NSF attention. These include evolving research fields, interdisciplinary opportunities, increasing dependencies among stages in technology development, grant size, student support, improved science education, knowledge diffusion, and facility needs. The commission strongly recommends that the NSF's responsibilities and opportunities--both present and proposed--and its budgetary needs be examined within the context of a newly conceived Federal R&D budget capable of responding to national needs. To this end, the commission urges that its recommendations be considered by the National Science Board in the context of the board's own responsibility to develop and carry out national policy for science and engineering research and education more broadly. Derived from text

82 DOCUMENTATION AND INFORMATION SCIENCE

Includes information management; information storage and retrieval technology; technical writing; graphic arts; and micrography.

For computer documentation see *61 Computer Programming and Software.*

N94-17737*# National Aeronautics and Space Administration, Washington, DC.
OSSA INFORMATION SYSTEMS PROGRAM Annual Report, 1992
David H. Brown (Center for Space and Advanced Technology, Fairfax, VA.) 1993 30 p
(Contract NASw-4561)
(NASA-TM-108774; NAS 1.15:108774) Avail: CASI HC A03/MF A01

The Office of Space Science and Applications Information Systems Program was established to coordinate and enhance activities that support the processing, analysis, transport, archival, and access of space science data. Within OSSA, the science discipline divisions have the ultimate responsibility for the proper management of the data generated by their missions. The OSSA Information Systems Branch works in concert with the divisions to provide an infrastructure of information system services and expertise in operations, policy, planning, and technology. Discipline specific and infrastructure activities are coordinated through participation in the OSSA Information Systems Management Board. The Information Systems Program is organized into four program areas: scientific computing, networking, data management and archiving, and applied information systems technology. Together, these program areas form a solid technical and policy development base that supports the overall OSSA information systems strategy. The underlying theme of each element is to facilitate science research and ensure the efficient implementation and utilization of OSSA information systems resources. The program activities for this year are discussed. Derived from text

N94-17745# University of Southern California, Marina del Rey. Information Sciences Inst.
EXPECT: INTELLIGENT SUPPORT FOR KNOWLEDGE BASE REFINEMENT Research Report
Cecile L. Paris and Yolanda Gil Jan. 1993 18 p
(Contract DABT63-91-C-0025)
(AD-A269602; ISI/RR-93-339) Avail: CASI HC A03/MF A01

Effective knowledge acquisition amounts to having good sources of expectations that can provide guidance about what knowledge needs to be acquired from users. Current approaches to knowledge acquisition often rely on strong models of the problem-solving method used in the task domain to form expectations. These methods are often implicit in the tool, which is a strong limitation for their use in different domains. Additionally, these tools require an understanding of the method to be used that most experts find difficult to overcome. We present EXPECT, a novel approach to knowledge acquisition based on the EES architecture that forms expectations based on the current knowledge contained in the system about the task, and are not hard-coded in the tool. We show how the explicit representation of domain principles and its relation to compiled procedural knowledge enables a system to form expectations as to what knowledge is missing or incorrect. This capability coupled with a dialogue-based explanation facility makes communication with the knowledge acquisition tool more natural to domain experts. DTIC

N94-17756# General Services Administration, Washington, DC. Office of Management and Budget.
CURRENT INFORMATION TECHNOLOGY RESOURCE REQUIREMENTS OF THE FEDERAL GOVERNMENT: FISCAL YEAR 1994
Nov. 1993 349 p
Avail: CASI HC A15/MF A03

This document is a compilation of Federal agency information technology (IT) acquisition plans for Fiscal Years 1993 through 1998 based on information submitted by the agencies in support of the Budget of the United States Government--Fiscal Year 1994. The report highlights those agencies that proposed significant IT investments in the Fiscal Year 1994 Budget. The report also includes an examination of Federal IT spending trends. Derived from text

N94-17858 Oak Ridge National Lab., TN.
DATA FUSION THROUGH SIMULATED ANNEALING OF REGISTERED RANGE AND REFLECTANCE IMAGES
M. Beckerman and F. J. Sweeney 1993 13 p Presented at the SPIE/OE Aerospace Science and Sensing Meeting, Orlando, FL, 11-16 Apr. 1993 Limited Reproducibility: More than 20% of this document may be affected by microfiche quality
(Contract DE-AC05-84OR-21400)
(DE93-015910; CONF-930445-16) Avail: CASI HC A03

We present results of a study of registered range and reflectance images acquired using a prototype amplitude-modulated CW laser radar. Ranging devices such as laser radars represent new technologies which are being applied in aerospace, nuclear, and other hazardous environments where remote inspections, 3D identifications and measurements are required. However, data acquired using devices of this type may contain non-stationary, signal-dependent noise, range-reflectance crosstalk, and low-reflectance range artifacts. Low level fusion algorithms play an essential role in achieving reliable performace by handling the complex noise, systematic errors, and artifacts. The objective of our study is the development of a stochastic fusion algorithm which takes as its input the registered image pair and produces as its output a reliable description of the underlying physical scene in terms of locally smooth surfaces separated by well-defined depth discontinuities. To construct the algorithm, we model each image as a set of coupled Markov random fields representing pixel and several orders of line processes. Within this framework we impose local smoothness constraints, introducing a simple linearity property in place of the usual sums over clique potentials; fuse the range and reflectance images through line process couplings, and use nonstationary, signal-dependent variances, adaptive thresholding, and a form of Markov natural selection. We show that the resulting algorithm yields reliable results even in worst-case scenarios. DOE

N94-17870# Argonne National Lab., Idaho Falls, ID.
RESTRICTING QUERY RELAXATION THROUGH USER CONSTRAINTS
T. Gaasterland 1993 14 p Presented at the International Conference on Intelligent and Cooperative Information Systems, Rotterdam, Netherlands, 11-14 May 1993
(Contract W-31-109-eng-38)
(DE93-017413; ANL/MCS/CP-80152; CONF-9305242-1) Avail: CASI HC A03/MF A01

This paper describes techniques to restrict and to heuristically control relaxation of deductive database queries. The process of query relaxation provides a user with a means to automatically identify new queries that are related to the user's original query. However, for large databases, many relaxations may be possible. The methods to control and restrict the relaxation process introduced in this paper focus the relaxation process and make it more efficient. User restrictions over the database domain

may be expressed as user constraints. This paper describes how user constraints can restrict relaxed queries. Also, a set of heuristics based on cooperative answering techniques are presented for controlling the relaxation process. Finally, the interaction of the methods for relaxing queries, processing user constraints, and applying the heuristic rules is described.
DOE

N94-17880# EG and G Energy Measurements, Inc., Idaho Falls.
DOCUMENT CONTROL AND CONDUCT OF OPERATIONS
S. K. Collins and F. L. Meltzer 1993 6 p Presented at the 4th Conduct of Operations Workshop: The Key to Continued Success, Tampa, FL, 4-6 May 1993
(Contract DE-AC07-76ID-01570)
(DE93-016555; EGG-M-92690; CONF-930538-3) Avail: CASI HC A02/MF A01

Department of Energy (DOE) Order 5480.19, Conduct of Operations, places stringent requirements on a wide range of activities at DOE facilities. These requirements directly affect personnel at the Advanced Test Reactor (ATR), which is located in the Test Reactor Area of the Idaho National Engineering Laboratory and operated for DOE by EG&G Idaho, Inc. In order for the ATR to comply with 5480.19, the very personality of the reactor facility's document control unit has had to undergo a major change. The Facility and Administrative Support Unit (FAS) is charged with maintenance of ATR's controlled documents - thousands of operating and administrative procedures. Prior to the imposition of 5480.19, FAS was content to operate in a clerical support mode, seldom questioning or seeking to improve. This manner of doing business is inappropriate within the framework of DOE 5480.19 and is also at odds with the approach to Total Quality Management (TQM) promulgated by EG&G Idaho. To comply with the requirements of 5480.19, FAS has actively applied TQM principles, empowered personnel to improve operations through the establishment of a team approach, and begun an automation process that is already paying large dividends in terms of improved procedure accuracy and compliance. A state-of-the-art text retrieval system is already in place. We are vigorously pursuing fully automated document tracking and document management. This paper describes in detail the steps taken to date, the improvements, and the lessons learned. It also discusses plans for the future that will enable FAS to support the ATR in increasing its responsiveness to the Conduct of Operations Order.
DOE

N94-17894# California Univ., Berkeley. Lawrence Berkeley Lab.
INFORMATION TECHNOLOGY RESOURCES ASSESSMENT
S. C. Loken, ed. Jan. 1993 63 p
(Contract DE-AC03-76SF-00098)
(DE93-015276; LBL-33700) Avail: CASI HC A04/MF A01

The emphasis in Information Technology (IT) development has shifted from technology management to information management, and the tools of information management are increasingly at the disposal of end-users, people who deal with information. Moreover, the interactive capabilities of technologies such as hypertext, scientific visualization, virtual reality, video conferencing, and even database management systems have placed in the hands of users a significant amount of discretion over how these resources will be used. The emergence of high-performance networks, as well as network operating systems, improved interoperability, and platform independence of applications will eliminate technical barriers to the use of data, increase the power and range of resources that can be used cooperatively, and open up a wealth of possibilities for new applications. The very scope of these prospects for the immediate future is a problem for the IT planner or administrator. Technology procurement and implementation, integration of new technologies into the existing infrastructure, cost recovery and usage of networks and networked resources, training issues, and security concerns such as data protection and access to experiments are just some of the issues that need to be considered in the emerging IT environment. As managers we must use technology to improve competitiveness. When procuring new systems, we must take advantage of scalable resources. New resources such as distributed file systems can improve access to and efficiency of existing operating systems. In addition, we must assess opportunities to improve information worker productivity and information management through technologies such as distributed computational visualization and teleseminar applications. DOE

N94-17925 National Physical Lab., Teddington (England). Information Technology and Computing Div.
THE STABILITY AND UTILITY OF THE ESPRIT PROJECT, MUSIC, PERFORMANCE-BASED INDICATORS OF USABILITY AND TOOLS: AN EVALUATION OF THE USABILITY OF THE NPL ISDX TELEPHONE SYSTEM
Rosemary Bowden and Jurek Kirakowski (University Coll., Cork, Ireland.) Dec. 1992 53 p
(NPL-DITC-213/92; ETN-93-94546) Copyright Avail: National Physical Laboratory, Teddington, Middlesex, TW11 0LW, United Kingdom

An evaluation to assess and measure the validity and reliability of a set of performance based measures and indicators of usability of information technology based projects is described. The iSDX telephone system was selected as a suitable product to test. The attempts to use some of the features offered by the system were recorded on video. The task goals achieved by each subject during the session were recorded by one analyst who watched the subject and listened to the verbal exchanges. The recorded data was analyzed using the procedures and tools in the MUSiC (Metrics for Usability Standards in Computing) user performance measurement method. The stability of the indicators was tested by evaluating the variance of the results, and the time taken to derive each indicator was recorded to assess the utility of the measurement method. For any size sample of subjects the stability of the metrics can be quoted in terms of confidence intervals about the mean. To obtain a narrow confidence interval with high probability large numbers of subjects may need to be tested and therefore significant time is required to carry out the analysis. However, the mean values of the metrics for carefully selected small groups may be within acceptable confidence intervals particularly if a lower probability level, for example 80 percent, is used. It is up to the promoters of a usability evaluation to decide what is acceptable. The utility of the metrics depends on the circumstances of the evaluation. For a software developer, long analysis periods during development will delay the development cycle thereby affecting the cost of the product. However any assessment of the cost effectiveness of the metrics must include their individual diagnostic value which may compensate for their derivation time. ESA

N94-17936 Politecnico di Milano (Italy). Dipt. di Elettronica e Informazione.
TANGO: A NOTATION FOR DESCRIBING ADVANCED TRANSACTION MODELS
M. Felder Feb. 1993 27 p
(Rept-93-014; ETN-93-94518) Avail: Politecnico di Milano, Piazza Leonardo da Vinci 32, 20133 Milan, Italy

The classical transaction model, that guarantees atomicity, consistency, isolation, and durability of transactions, has proved to be very useful in the development of traditional database applications. However, these properties are not adequate for modeling non traditional applications, such as software engineering environment, CAD (Computer Aided Design), office automation, and cooperative work applications. New transaction models were proposed in order to capture the semantics of nontraditional database applications. These extensions to the traditional transaction model are surveyed and a formal notation, called TANGO, that may be used to describe existing models and, in general, to design nontraditional database applications, involving complex dependencies among transactions, is proposed. TANGO is based on a high level Petri net formalism, and includes a modularization construct that permits to structure a TANGO specification in work units.
ESA

N94-17939 Politecnico di Milano (Italy). Dept. di Elettronica e Informazione.
AN ENVIRONMENT FOR REQUIREMENT REUSE
R. Bellinzona, M. G. Fugini (Pavia Univ., Italy.), and B. Pernici (Udine Univ., Italy.) 16 Dec. 1992 27 p Sponsored in part by EEC, and CNR
(Rept-92-082; ETN-93-94508) Avail: Politecnico di Milano, Piazza Leonardo da Vinci 32, 20133 Milan, Italy

A method and tool for reusing requirement specifications, which are part of a Development Information System, are presented. A centralized repository, named Software Information Base, stores artifacts related to requirements, detailed design and implementation. In particular, it contains information for component reuse, based on development knowledge. Components are formally specified using an object oriented specification model. The same model is used to represent development knowledge.

Focus is on the RECAST (Requirements Composition and Specification Tool) of the Development Information System. The Development Information System and its associated development method are reviewed and the functionalities of RECAST are described: retrieval of specification classes and active assistance in reusing these classes--that is in adapting and composing them into the current requirements. Design guidelines are illustrated; an example of reusable specifications and of their composition with RECAST is given. ESA

N94-17979 Grenoble-1 Univ. (France). Lab. de Genie Informatique.
A MODEL AND AN EXECUTION MECHANISM FOR ACTIVE DATA BASES Ph.D. Thesis [UN MODELE ET UN MECANISME D'EXECUTION POUR LES BASES DE DONNEES ACTIVES]
Maria Francisca GhiraZinhoAntunes 1991 267 p In FRENCH Limited Reproducibility: More than 20% of this document may be affected by microfiche quality
(ETN-93-94404) Avail: CASI HC A12

A model and mechanisms to support the development of active databases are proposed. The model allows an integrated description of static and dynamic aspects. In order to describe the information processing stucture, three concepts are required: focal entity, activity and procedure. The mechanisms and tools applied allow an automatic start of procedures, to control and to follow processing activities. Special attention is given to the mechanism for automatically starting an activity or procedure. The two phases required to establish previous conditions connected to activities and procedures are described. ESA

N94-18099# Argonne National Lab., IL.
USING SEMANTIC INFORMATION FOR PROCESSING NEGATION AND DISJUNCTION IN LOGIC PROGRAMS
T. Gaasterland and J. Lobo (Illinois Univ., Chicago.) 1993 12 p Presented at the 7th International Symposium on Methodologies for Intelligent Systems, Trondheim, Norway, 15-18 Jun. 1993
(Contract W-31-109-eng-38)
(DE93-017412; ANL/MCS/CP-80151; CONF-9306151-1) Avail: CASI HC A03/MF A01

There are many applications in which integrity constraints can play an important role. An example is the semantic query optimization method developed by Chakravarthy, Grant, and Minker for definite deductive databases. They use integrity constraints during query processing to prevent the exploration of search space that is bound to fail. In this paper, the authors generalize the semantic query optimization method to apply to negated atoms. The generalized method is referred to as semantic compilation. They show that semantic compilation provides an alternative search space for negative query literals. They also show how semantic compilation can be used to transform a disjunctive database with or without functions and denial constraints without negation into a new disjunctive database that complies with the integrity constraints. DOE

N94-18119# Helsinki Univ. of Technology, Espoo (Finland). Lab. of Information Processing Science.
EDMS: ENGINEERING DATA MANAGEMENT SYSTEM. USER'S REFERENCE
K. Alho 8 Feb. 1993 67 p
(PB93-187391; TKO-C58) Avail: CASI HC A04/MF A01

The Engineering Data Management System (EDMS) is a database system for the management of technical documents and drawings with attributes, versions, locks, etc. EDMS can be accessed in many ways. The manual describes the graphical user interface implemented with the X Window System and the Motif toolkit under Unix. NTIS

N94-18144 Politecnico di Milano (Italy). Dipt. di Elettronica e Informazione.
BETTER TERMINATION ANALYSIS FOR ACTIVE DATABASES
Elena Baralis (Politecnico di Torino, Italy.), Stefano Ceri, and Jennifer Widom (International Business Machines Corp., San Jose, CA.) 1993 21 p
(Rept-93-026; ETN-93-94575) Avail: Issuing Activity (Politecnico di Milano, Piazza Leonardo da Vinci 32, 20133 Milan, Italy)

An important problem for the usability of active databases is to determine by syntactic analysis whether a given set of rules is guaranteed to terminate. Rule processing in active databases does not terminate when rules activate each other indefinitely. Previous approaches to termination analysis in active databases use very conservative algorithms to determine when rules may activate each other. An algebraic model for a class of active database rules is introduced and a theory by which it can be determined much less conservatively when rules may activate each other is presented. The theory thus forms the basis of better termination analysis for active databases. ESA

N94-18164# Sandia National Labs., Albuquerque, NM.
GREPOS: A GENESIS DATABASE REPOSITIONING PROGRAM
G. D. Sjaardema Jun. 1993 33 p
(Contract DE-AC04-76DP-00789)
(DE93-018517; SAND-90-0566-Rev) Avail: CASI HC A03/MF A01

GREPOS is a mesh utility program that repositions or modifies the configuration of a two-dimensional or three-dimensional mesh. GREPOS can be used to change the orientation and size of a two-dimensional or three-dimensional mesh; change the material block, nodeset, and sideset ID's; or 'explode' the mesh to facilitate viewing of the various parts of the model. GREPOS also updates the EXODUS quality assurance and information records to help track the codes and files used to generate the mesh. GREPOS reads and writes two-dimensional and three-dimensional mesh databases in the GENESIS database format; therefore, it is compatible with the preprocessing, postprocessing, and analysis codes in the Sandia National Laboratories Engineering Analysis Code Access System (SEACAS). DOE

N94-18181# Federal Information Exchange, Inc., Gaithersburg, MD.
FEDIX ON-LINE INFORMATION SERVICE: DESIGN, DEVELOP, TEST, AND IMPLEMENT AN ON-LINE RESEARCH AND EDUCATION INFORMATION SERVICE
J. A. Rodman 1993 51 p
(Contract DE-FG05-89ER-75527)
(DE93-018818; DOE/ER-75527/5) Avail: CASI HC A04/MF A01

Federal Information Exchange, Inc. (FIE) is a diversified information services company that is recognized as the major electronic link between the higher education community and the Federal government in the field of research administration. FIE provides a range of information related services to the government, academic and private sectors, including database management, software development, and technical support. FEDIX is the on-line information service designed, developed, and implemented by FIE to accomplish the following objectives: (1) broaden the participation of the education community in Federal research and education programs by providing free and unrestricted on-line access to information from all participating Federal agencies; and (2) provide the education community with on-line access to a single keyword-searchable system for research and educational funding opportunities at the participating Federal agencies. DOE

N94-18191# Naval Postgraduate School, Monterey, CA.
THE ORGANIZATIONAL PREPARATION OF EXISTING RELATIONAL DATABASES FOR THE INTEGRATION OF EXPERT SYSTEMS M.S. Thesis
Warren W. Snow Jun. 1993 74 p
(AD-A268823) Avail: CASI HC A04/MF A01

This thesis is a management guide for strategically planning a future integration of relational databases and expert systems. It relates best to an organization with large established relational database(s) that is trying to access the changes required to integrate expert systems with those databases. Technical considerations for such a change are discussed, and they include the role of database normalization and the requirement to maintain applications that are independent of the database structure. The organizational considerations of such an integration are examined, and they focus on the people skills required within an organization to develop and maintain database and expert system combinations. Three product categories are established to represent an integrated system, and a commercial off the shelf product from each category is reviewed to illustrate its specific capabilities. The combination of relational databases and expert systems has the potential to deliver information systems of future strategic importance. This thesis serves to assist the information systems management of military organizations in planning the transition to such a system. DTIC

N94-18224 Carnegie-Mellon Univ., Pittsburgh, PA. Dept. of Electrical and Computer Engineering.
OPTICAL ASSOCIATIVE PROCESSORS AND DIRECTED GRAPHS Final Report, Nov. 1992 - Aug. 1993
David Casasent Aug. 1993 189 p Limited Reproducibility: More than 20% of this document may be affected by microfiche quality
(Grant AF-AFOSR-0355-90)
(AD-A268881; AFOSR-93-0660TR) Avail: Issuing Activity (Defense Technical Information Center (DTIC))

The thrust of this research concerns associative processors. Many new aspects exist in this effort: large storage capacity; use of storage density as a measure of efficiency; use of new output recollection vector encoding schemes; general 1:1 and pattern recognition; many:one associative processors; new algorithms and architectures; and applications and laboratory realization. We have devised a new higher-order neutral network concept with increased many:one pattern recognition performance. We have also demonstrated a new technique to improve neural network storage capacity and performance by modeling various nonideal components and accuracy during synthesis. DTIC

N94-18319 Defense Technical Information Center, Alexandria, VA.
DEFENSE TECHNICAL INFORMATION CENTER THESAURUS
John H. Dickert Oct. 1993 589 p See also AD-A226000, DTICH4185.7, Sep. 1990 Limited Reproducibility: More than 20% of this document may be affected by microfiche quality
(AD-A268855; DTIC-TR/93-29) Avail: CASI HC A25

This DTIC Thesaurus provides a basic multidisciplinary subject term vocabulary used by DTIC to index and retrieve scientific and technical information from its various databases and to aid DTIC's users in their information storage and retrieval operations. It includes an alphabetical Posting Term display, a hierarchy display, and a Keyword Out Of Context (KWOC) display. DTIC

N94-18323# Defense Technical Information Center, Alexandria, VA.
HANDBOOK FOR USERS Final Report
Mary J. Brewster and Charles E. Reed Aug. 1993 122 p Supersedes AD-A260738
(AD-A268726; DTIC/TR-93-33; DTIC/TR-93-9; AD-A260738) Avail: CASI HC A06/MF A02

This handbook is your guide to DTIC. It describes DTIC's products and services and provides users step by step instructions for completing all basic DTIC transactions such as registering for general and network services, and ordering and submitting technical reports. To assist the user, it includes examples of the required forms and several appendices containing commonly used abbreviations, telephone numbers and DTIC prices. DTIC

N94-18334# Midwest Research Inst., Golden, CO. National Renewable Energy Lab.
A RUGGED, LOW-COST ADVANCED DATA ACQUISITION SYSTEM FOR FIELD TEST PROJECTS
D. A. Simms and K. L. Cousineau (Zond Systems, Inc., Tehachapi, CA.) Jun. 1993 11 p Presented at the 29th Annual International Telemetering Conference, Las Vegas, NV, 25-28 Oct. 1993
(Contract DE-AC02-83CH-10093)
(DE93-010041; NREL/TP-442-5617; CONF-9310131-1) Avail: CASI HC A03/MF A01

The National Renewable Energy Laboratory (NREL) has teamed up with Zond Systems, Inc., to provide a rugged, low-cost, advanced data-acquisition system (ADAS) for use in field test projects. The ADAS simplifies the process of making accurate measurements on mechanical equipment exposed to harsh environments. It provides synchronized, time-series measurement data from multiple, independent sources. The ADAS is currently being used to acquire data from large wind turbines in operational wind-plant environments. ADAS modules are mounted on rotating blades, turbine towers, nacelles, control modules, meteorological towers, and electrical stations. The ADAS has the potential to meet the testing and monitoring needs of many other technologies as well, including vehicles, heavy equipment, piping and power transmission networks, and building energy systems. DOE

N94-18461 University of Southern California, Marina del Rey. Information Sciences Inst.
RETRIEVING AND INTEGRATING DATA FROM MULTIPLE INFORMATION SOURCES Research Report
Yigal Arens, Chin Y. Chee, Chun-Nan Hsu, and Craig A. Knoblock 30 Apr. 1993 31 p Limited Reproducibility: More than 20% of this document may be affected by microfiche quality
(Contract F30602-91-C-0081)
(AD-A269588; ISI-RR-93-308) Avail: CASI HC A03

With the current explosion of data, retrieving and integrating information from various sources is a critical problem. Work in multi-database systems has begun to address this problem, but it has primarily focused on methods for communicating between databases and requires significant effort for each new database added to the system. This paper describes a more general approach that exploits a semantic model of a problem domain to integrate the information from various information sources. The information sources handled include both databases and knowledge bases, and other information sources could potentially be incorporated into the system. This paper describes how the domain and the information sources are modeled, shows how a query at the domain level is mapped into a set of queries to individual information sources, and presents algorithms for automatically improving the efficiency of queries using knowledge about both the domain and the information sources. This work is implemented in a system called SIMS and has been tested in a transportation planning domain using nine Oracle databases and a LOOM knowledge base. DTIC

N94-18464 University of Southern California, Marina del Rey. Information Sciences Inst.
TOWARDS VERSATILE AND PRACTICAL KNOWLEDGE ACQUISITION Research Report
Yolanda Gil and Cecile L. Paris Jun. 1993 20 p Limited Reproducibility: More than 20% of this document may be affected by microfiche quality
(Contract DABT63-91-C-0025)
(AD-A269596; ISI/RR-93-343) Avail: Issuing Activity (Defense Technical Information Center (DTIC))

Rapid prototyping and tool reusability have pushed knowledge acquisition research to investigate method-specific knowledge acquisition (KA) tools appropriate for predetermined problem-solving methods. We believe that method-dependent KA is not the only approach. The aim of our research is to develop powerful but versatile machine learning mechanisms that can be incorporated into general-purpose but practical knowledge acquisition tools. This paper shows through examples the practical advantages of this approach. In particular, we illustrate how existing knowledge can be used to facilitate KA through analogy mechanisms in a logistics transportation domain and use the same general-purpose mechanism for knowledge acquisition in a different domain through plan generalization. Our hypothetical knowledge acquisition dialogs with a domain expert illustrate which parts of the process are addressed by the human and which parts are automated by the tool, in a synergistic cooperation for knowledge-based extension and refinement. The paper also describes briefly the EXPECT problem-solving architecture and knowledge representation language that facilitate this approach to KA. DTIC

N94-18496# Department of Energy, Washington, DC. Assistant Secretary for Human Resources.
TRENDS IN INFORMATION MANAGEMENT AT DEPARTMENT OF ENERGY HEADQUARTERS
Jun. 1993 55 p
(DE93-017197; DOE-93017197) Avail: CASI HC A04/MF A01

The Trends in Information Resource Management at DOE Headquarters (Trends) is published annually to inform the DOE Headquarters community about changes in the information management environment. The document, in its second year of publication, is becoming more robust as more historical data is available and as the information management environment at Headquarters evolves. One of the purposes of the Trends document is to acquire evidence that Headquarters organizations are assimilating guidance offered in the Emerging Technologies Planning Guide into their IRM strategies. Another purpose is to identify areas of interest and requirements of the Headquarters organizations to direct technology research for future issues of the Guide. These categories have been tentatively established as indicators of the degree of implementation of information management. The main source of data is the Headquarters Organization Plans, which were updated during the long-range update cycle conducted from August to January. Since these plans were published, the Secretary has announced a reorganization of DOE. For the purpose of this document, the information in the various plans is considered to be valid to accomplish the departmental missions. DOE

N94-18535# Naval Postgraduate School, Monterey, CA.
COGNITIVE LIMITATIONS IN COORDINATION IN HIERARCHICAL INFORMATION PROCESSING STRUCTURES M.S. Thesis
Robert R. Armbruster Jun. 1993 126 p
(AD-A268825) Avail: CASI HC A07/MF A02

In Command and Control, the majority of decisions require the fusion of inputs from a number of subordinate decision-makers to arrive at a team decision. Part of the Navy's attempt to address the issue of hierarchical decision making is the Tactical Decision Making Under Stress (TADMUS) program. Under this program, the Coordination in Hierarchical Processing Structures (CHIPS) experiment was conducted at the Naval Postgraduate School during May and Jun. 1993. The CHIPS experiment is described, and data collected during the experiment was used to assess the impact of human cognitive limitations on team performance. Team performance was found to be degraded by increased stress, increased risk, and increased feedback to subordinates in the hierarchy. These effects were found to be due to a reduced ability to distinguish between types of contact, rather than use of a less optimal decision criterion. It was further found that increasing the amount of information available to subordinates increased their ability to distinguish between types of contacts, but not by as much as is theoretically possible. There were also indications that there may be an upper limit on the amount of information that can be successfully integrated by the subordinates, beyond which performance declines rather than improving. DTIC

N94-18570 University of Southern California, Marina del Rey. Information Sciences Inst.
AUTOMATIC DOCUMENTATION GENERATION: THE INTERACTION OF TEXT AND EXAMPLES Research Report
Vibhu O. Mittal and Cecile L. Paris Mar. 1993 6 p Limited Reproducibility: More than 20% of this document may be affected by microfiche quality
(Contract DABT63-91-C-0025)
(AD-A269670; ISI/RR-93-333) Avail: Issuing Activity (Defense Technical Information Center (DTIC))

Good documentation is critical for user acceptance of any system, and empirical studies have shown that examples can greatly increase effectiveness of system documentation. However, studies also show that badly integrated text and examples can be actually detrimental compared to using either text or examples alone. It is thus clear that in order to provide useful documentation automatically, a system must be capable of providing well-integrated examples to illustrate its points. Precious work on example generation has concentrated on the issue of retrieving or constructing examples. In this paper, we look at the integration of text and examples. We identify how text and examples co-constrain each other and show that a system must consider example generation as an integral part of the generation process. Finally, we present such a system together with example. DTIC

N94-18575 Institute for Defense Analyses, Alexandria, VA.
A COMPARISON OF AIR FORCE DATA SYSTEMS Final Report, Jan. - Aug. 1993
Waynard C. Devers, Elizabeth K. Bailey, Lee H. Dymond, William A. Florac, and Stanley A. Horowitz Aug. 1993 244 p Limited Reproducibility: More than 20% of this document may be affected by microfiche quality
(Contract MDA903-89-C-0003)
(AD-A269691; IDA-P-2863; IDA/HQ-93-44150) Avail: Issuing Activity (Defense Technical Information Center (DTIC))

This report evaluates the effectiveness and cost of two alternative Air Force maintenance information systems: CAMS/REMIS and TICARRS. The evaluation considers six dimensions of effectiveness: functionality, scope, operating characteristics, data accuracy and completeness, adaptability, and logistics and operational effectiveness. Each system was found to have shortcomings. CAMS/REMIS suffers from problems in availability, responsiveness, and data integrity, and TICARRS is limited in functionality and scope. IDA considers two alternatives, each one based on one of the systems supporting the entire Air Force. A set of enhancements needed to make the two systems roughly equivalent is provided, along with their costs. The cost analysis includes estimates of the nonrecurring costs to address the system limitations and the recurring costs in system operations and maintenance from FY 1994 through FY 2003. The TICARRS-based alternative is found to be superior in effectiveness but must be expanded in scope and functionality if it is to become the Air Force's standard system. The estimated costs for the TICARRS alternative over the ten-year period are approximately $100 million less (in terms of present value) than the costs for the CAMS/REMIS alternative. DTIC

N94-18641# University of Southern California, Marina del Rey. Information Sciences Inst.
LEARNING DATABASE ABSTRACTIONS FOR QUERY REFORMULATION
Chun-Nan Hsu and Craig A Knoblock 30 Apr. 1993 15 p
(Contract F30602-91-C-0081)
(AD-A269531; ISI-RR-93-309) Avail: CASI HC A03/MF A01

The query reformulation approach takes advantage of the semantic knowledge about the contents of databases for optimization. The basic idea is to use the knowledge to reformulate a query into a less expensive yet equivalent query. Previous work on semantic query optimization has shown the cost reduction that can be achieved by reformulation; we further point out that when applied to distributed multibase queries, the reformulation approach can reduce the cost of moving intermediate data from one site to another. However, a robust and efficient method to discover the required knowledge has not yet been developed. This paper presents an example-guided, data-driven learning approach to acquire the knowledge needed in reformulation. We use example queries to guide the learning to capture the database usage pattern. In contrast to the heuristic-driven approach, the data-driven approach is more likely to learn the required knowledge for the various reformulation needs of the example queries. Since this learning approach minimizes the dependency on the database structure and implementation, it is applicable to heterogeneous multidatabase systems. DTIC

N94-18689# Department of Energy, Washington, DC. Office of Administration and Human Resource Management.
EMERGING TECHNOLOGIES PLANNING GUIDE, 1993 EDITION
Nov. 1992 57 p
(Contract DE-AC01-88MA-33222)
(DE93-017196; DOE/MA-33222/T1) Avail: CASI HC A04/MF A01

Information system technology enhancements during the next five years are expected to provide some of the most significant individual and organization work improvements ever made in the office environment. This guide is an aid to planning these technologies and assessing their roles in improving the effectiveness of Headquarters programs. Their implementation will cost-effectively support Departmental operations and the National Energy Strategy. At the heart of this process is an understanding of the relationship which exists between technology introduction and the planning, budgeting and the acquisition process. The 1993 edition of this guide covers the 1993-1997 time frame. DOE

N94-18707# Energy Information Administration, Washington, DC. Office of Statistical Standards.
DIRECTORY OF ENERGY INFORMATION ADMINISTRATION MODELS 1993
Jul. 1993 137 p
(DE93-016987; DOE/EIA-0293(93)) Avail: CASI HC A07/MF A02

This directory contains descriptions about each model, including the title, acronym, and purpose, followed by more detailed information on characteristics, uses, and requirements. Sources for additional information are identified. Included in this directory are 35 EIA models active as of May 1, 1993. Models that run on personal computers are identified by 'PC' as part of the acronym. EIA is developing new models, a National Energy Modeling System (NEMS), and is making changes to existing models to include new technologies, environmental issues, conservation, and renewables, as well as extend forecast horizon. Other parts of the department are involved in this modeling effort. A fully operational model is planned which will integrate completed segments of NEMS for its first official application--preparation of EIA's Annual Energy Outlook 1994. Abstracts for the new models will be included in next year's version of this directory. DOE

N94-18752# Defense Technical Information Center, Alexandria, VA.
DEPARTMENT OF DEFENSE GATEWAY INFORMATION SYSTEM (DGIS) USERS' GUIDE Final Report
Marie T. OMara Oct. 1993 288 p
(AD-A270140; DTIC-TR-93-26) Avail: CASI HC A13/MF A03

This manual is designed as a reference guide for the users of the Department of Defense Gateway Information System (DGIS). It covers the overview, access, and functionality of the modules featured by the Gateway. The manual is the basis for DTIC's DGIS training course. The manual is organized in modules to facilitate making changes and updates as they occur. DTIC

N94-18770 Anser Analytic Services, Inc., Arlington, VA.
CORPORATE INFORMATION MANAGEMENT (CIM) REPORT ON THE SIMULATION PROCESSES, VERSION 2.0
John Tieso 15 Apr. 1993 73 p Prepared in cooperation with Assistant Secretary of Defense (Communications Command Control and Intelligence), Washington, DC Limited Reproducibility: More than 20% of this document may be affected by microfiche quality
(Contract DAAB07-91-D-B519)
(AD-A269119) Avail: Issuing Activity (Defense Technical Information Center (DTIC))

This report discusses three pilot projects simulating command and control processes. The projects chosen were: Message Processing Center (MPC), Integrated Satellite Control System (ISCS), Theater Missile Defense (TMD). All three projects used the commercial off-the-shelf (COTS) simulation tool, Design/CPN. Design/CPN investigates color petri nets (CPNs) as a mathematical or algorithmic underpinning for analyzing complex information systems and validates claims that Design/CPN could be viewed as an extension of IDEFO activity models. Other tools and algorithms were selectively considered for comparisons. DTIC

N94-18839*# Houston Univ., Clear Lake, TX. Research Inst. for Computing and Information Systems.
NASA ELECTRONIC LIBRARY SYSTEM (NELS) OPTIMIZATION
William L. Pribyl (Datacraft, Inc., Gardena, CA.) Jul. 1993 39 p
(Contract NCC9-16; RICIS Proj. RB-07)
(NASA-CR-193688; NAS 1.26:193688) Avail: CASI HC A03/MF A01

This is a compilation of NELS (NASA Electronic Library System) Optimization progress/problem, interim, and final reports for all phases. The NELS database was examined, particularly in the memory, disk contention, and CPU, to discover bottlenecks. Methods to increase the speed of NELS code were investigated. The tasks included restructuring the existing code to interact with others more effectively. An error reporting code to help detect and remove bugs in the NELS was added. Report writing tools were recommended to integrate with the ASV3 system. The Oracle database management system and tools were to be installed on a Sun workstation, intended for demonstration purposes. CASI

N94-18848# General Accounting Office, Washington, DC. National Security and International Affairs Div.
NASA AERONAUTICS: PROTECTING SENSITIVE TECHNOLOGY. REPORT TO CONGRESSIONAL REQUESTERS
Aug. 1993 16 p
(GAO/NSIAD-93-201) Avail: CASI HC A03/MF A01; GAO, PO Box 6015, Gaithersburg, MD 20877 HC

The National Aeronautics and Space Administration's (NASA) efforts to control the transfer of agency-developed competitively sensitive aeronautics information to U.S. industry's foreign competitors was reviewed. Specifically, areas addressed were: (1) identify how NASA currently controls the disclosure of sensitive information; (2) determine whether NASA has an information control problem; and (3) ascertain what actions, if any, NASA planned to take to improve its information control program. A management review of Ames Research Center and NASA's procedures for handling requests for competitively sensitive information under the Freedom of Information Act was also evaluated. Results are presented.
Derived from text

N94-18983# Energy Information Administration, Washington, DC.
EIA PUBLICATIONS DIRECTORY, 1992
24 Jun. 1993 58 p
(DE93-016833; DOE/EIA-0149(92)) Avail: CASI HC A04/MF A01

This directory contains abstracts and ordering information for EIA publications. The abstracts are arranged by broad subject category such as coal, petroleum, natural gas, and electric power. A comprehensive subject index, a title index, and a report number index are included. Each entry gives the title, report number, publication frequency, date, number of pages, and ordering information. Publication began with the 1979 edition. DOE

N94-18984# Sandia National Labs., Albuquerque, NM.
NETWORKED MS WINDOWS 3.1 BASED CLASSIFIED DOCUMENT CONTROL SYSTEM (CDOCS)
L. M. Desonier 1993 3 p Presented at the 34th Annual Meeting of the Inst. of Nuclear Materials Management, Scottsdale, AZ, 18-21 Jul. 1993
(Contract DE-AC04-76DP-00789)
(DE93-017880; SAND-93-1701C; CONF-930749-16) Avail: CASI HC A01/MF A01

Current classified document management systems require a tremendous amount of space and extensive manpower to account for, inventory, and protect the documents. Comprehensive analysis of current control and accountability procedures reveal the main problem is the actual handling of the paper itself. The purpose of the Networked Microsoft Windows 3.1 based Classified Document Control System (CDOCS) is to eliminate the paper by scanning and storing images of pages on a personal computer using 'write once read mostly' (WORM) high density optical media. By saving images on the computer, not only can manpower and space requirements be reduced, but the chance of compromise is diminished. As an added benefit, the information is now more readily available to the authorized user and is provided to the user at the user's PC. The network target for CDOCS is Microsoft Windows for Workgroups. Thus, the system is also readily applicable to unclassified document imaging uses. DOE

N94-19026# Oak Ridge National Lab., TN.
INVENTORY MANAGEMENT PLAN FOR A RESEARCH AND DEVELOPMENT LOCAL AREA NETWORK
D. Strickler, R. Chester, K. Ingle, P. Payne, J. Rome, and K. Kertis (Tennessee Univ., Knoxville.) Aug. 1993 18 p
(Contract DE-AC05-84OR-21400)
(DE93-018381; ORNL/TM-12408) Avail: CASI HC A03/MF A01

An inventory management plan is presented for the local area network (LAN) for the Security Aspects of Database Management Systems, a Department of Energy (DOE)-sponsored project examining computer and network security in a data management environment. The inventory management plan establishes procedures to ensure that changes in system hardware and software are identified and controlled. Management tools are described, and the roles of the project manager, inventory control manager, and research team members in the implementation of inventory management are defined. DOE

N94-19057# Oak Ridge National Lab., TN.
AN ORACLE CASE HISTORY: EXPERIENCES WITH ORACLE CASE TOOLS
E. Z. Faby, B. R. Hancock (Tennessee Univ., Knoxville.), and L. F. Truett 16 Feb. 1993 15 p Presented at the 17th Annual International Computer Software and Applications Conference, Phoenix, AZ, 3-5 Nov. 1993
(Contract DE-AC05-84OR-21400)
(DE93-010827; CONF-931148-1) Avail: CASI HC A03/MF A01 (US Sales Only)

ORACLE CASE tools were used with limited success during development of a database system for the Army. During project development, the set of tools was used for analysis, design, database implementation, and documentation. The CASE tools provided an acceptable user interface for data entry and data correction; they provided standardized reports and views from which data for customized reports could be extracted. However, they had a number of limitations that significantly increased the effort required to maintain and use the CASE data in each phase of development. In particular, the CASE tools were especially limited in essential functions for modifying the system analysis and design. In addition, a decision was made during system development to change to a different version of the ORACLE Relational Database Management System (RDBMS), thus further reducing the value of the CASE tools. DOE

N94-19067# Vrije Univ., Amsterdam (Netherlands).
AXIOMATIZATION, DECLARATIVE SEMANTICS AND OPERATIONAL SEMANTICS OF PASSIVE AND ACTIVE UPDATES IN LOGIC DATABASES
P. Spruit, R. Wieringa, and J. J. C. Meyer Jun. 1992 71 p
(PB93-195956; IR-294) Avail: CASI HC A04/MF A01

The use of logic in database theory is commonly restricted to the specification of a database state. Reasoning about state changes (the database updates) must then be done outside the logic. The report considers a logic that also takes the updates into account. Taking propositional dynamic logic as a starting point, it defines PDDL: propositional dynamic database logic. The main features of PDDL are: There are two kinds of atomic updates in PDDL, passive and active updates. Passive updates just change the truth value of an atom to true/false and active updates set one atom to true/false and then compute derived updates using a Horn clause program; The declarative semantics for formulas and updates is based on Kripke structures; There is a proof system for PDDL, which is sound and complete for the class of 'full' structures. For non-full structures, the main problem is the axiomatization of successor worlds; There is a Plotkin-style operational semantics for update programs. The operational semantics allows one to compute the result of executing an update in some database state. NTIS

N94-19099# Sandia National Labs., Albuquerque, NM.
DOWNSIZING A DATABASE PLATFORM FOR INCREASED PERFORMANCE AND DECREASED COSTS
M. M. Miller and L. F. Tolendino Jun. 1993 23 p
(Contract DE-AC04-76DP-00789)
(DE93-018687; SAND-93-0587) Avail: CASI HC A03/MF A01

Technological advances in the world of microcomputers have brought forth affordable systems and powerful software that can compete with the more traditional world of minicomputers. This paper describes an effort at Sandia National Laboratories to decrease operational and maintenance costs and increase performance by moving a database system from a minicomputer to a microcomputer. DOE

N94-19101# Sandia National Labs., Albuquerque, NM.
SANDIA EQUATION OF STATE DATA BASE: SESLAN FILE
G. I. Kerley and T. L. Christian-Frear (RE/SPEC, Inc., Albuquerque, NM.) 24 Jun. 1993 57 p
(Contract DE-AC04-76DP-00789)
(DE93-018693; SAND-93-1206) Avail: CASI HC A04/MF A01

Sandia National Laboratories maintains several libraries of equation of state tables, in a modified Sesame format, for use in hydrocode calculations and other applications. This report discusses one of those libraries, the seslan file, which contains 78 tables from the Los Alamos equation of state library. Minor changes have been made to these tables, making them more convenient for code users and reducing numerical difficulties that occasionally arise in hydrocode calculations. DOE

N94-19256*# Stanford Univ., CA. Dept. of Psychology.
[OVERVIEW OF RESEARCH IN PROGRESS AT THE CENTER OF EXCELLENCE] Progress Report, 1 Dec. 1993 - 30 Nov. 1994
Brian A. Wandell 17 Nov. 1993 20 p
(Contract NCC2-307)
(NASA-CR-194329; NAS 1.26:194329) Avail: CASI HC A03/MF A01

The Center of Excellence (COE) was created nine years ago to facilitate active collaboration between the scientists at Ames Research Center and the Stanford Psychology Department. Significant interchange of ideas and personnel continues between Stanford and participating groups at NASA-Ames; the COE serves its function well. This progress report is organized into sections divided by project. Each section contains a list of investigators, a background statement, progress report, and a proposal for work during the coming year. The projects are: Algorithms for development and calibration of visual systems, Visually optimized image compression, Evaluation of advanced piloting displays, Spectral representations of color, Perception of motion in man and machine, Automation and decision making, and Motion information used for navigation and control. Derived from text

N94-19331 Vrije Univ., Amsterdam (Netherlands). Faculteit der Wiskunde en Informatica.
FEASIBILITY STUDY IN LINGUISTICALLY MOTIVATED OBJECT-ORIENTED CONCEPTUAL DESIGN OF INFORMATION SYSTEMS
P. Buitelaar and R. P. VandeRiet Jun. 1992 65 p See also PB91-186494 Limited Reproducibility: More than 20% of this document may be affected by microfiche quality
(PB93-197754; IR-293) Avail: CASI HC A04

In designing information systems words are being used: words with a fixed meaning, such as keywords and words chosen by the designer denoting entities, relationships, attributes, values, actors, messages, etc. Usually these words have a certain meaning and usually their usage is according to that meaning. The paper describes how a Lexicon, containing these words and their meaning, can be used fruitfully in two ways: combined with a CASE tool in interpreting diagrams and in analyzing natural language specifications. NTIS

N94-19377# Federal Aviation Administration, Oklahoma City, OK. Flight Standards Service.
ADVISORY CIRCULAR: INDEX OF ARTICLES (MATERIALS, PARTS, PROCESSES, AND APPLIANCES) CERTIFIED UNDER THE TECHNICAL STANDARD ORDER SYSTEM
Oct. 1993 533 p
(AC-20-36S; ISBN-0-16-042982-X) Avail: CASI HC A23/MF A04

This publication lists those manufacturers who hold a Technical Standard Order (TSO) Authorization or a letter of TSO Design Approval. The requirements for obtaining an authorization or letter are prescribed in Part 21, Subpart O of the Federal Aviation Regulations. The page layout is arranged as follows. Column one lists the specific TSO number. A letter F in this column denotes foreign manufacturers. Column two identifies the person to whom the approval was issued. Column three lists the FAA region which issued the authorization or letter of approval. Column four shows the TSO descriptive title. This title appears one time at the beginning of each group of TSO holders meeting the requirements of a specific TSO. Column five lists the model or part number of the article approved. Author (revised)

N94-19450 Physics and Electronics Lab. TNO, The Hague (Netherlands).
SECURE OPEN SYSTEMS: AN INVESTIGATION OF CURRENT STANDARDISATION EFFORTS FOR SECURITY IN OPEN SYSTEMS Final Report
P. L. Overbeek Jun. 1992 31 p Presented at the 8th International Security Conference and Exhibition, Singapore, 27-29 May 1992
(FEL-92-B225; TD-92-1906; ETN-93-94948) Copyright Avail: Issuing Activity (TNO Physics and Electronics Laboratory, P.O. Box 96864, 2509 JG The Hague, Netherlands)

The achievements of standardization in the area of secure open systems are outlined. Security in open systems is a special problem since each element in an open system must be able to offer security in coordination with other elements. A new view on requirements for security is presented. Security requirements concerning openness, organizational structures, the value of information and services, social structures, and security of the system itself are studied. The results of the investigation of current standardization initiatives in the area of technical security in open systems are presented and main conclusions are given. ESA

N94-19452 Physics and Electronics Lab. TNO, The Hague (Netherlands).
WORKING VISIT TO THE UNIVERSITY OF L'AQUILA, ITALY Final Report
P. J. M. vanOosterom Feb. 1993 53 p
(FEL-93-B020; TD-93-0292; ETN-93-94951) Copyright Avail: Issuing Activity (TNO Physics and Electronics Laboratory, P.O. Box 96864, 2509 JG The Hague, Netherlands)

The working visit to the University of L'Aquila (Italy) during the six week period from 28 Sep. - 7 Nov. 1992 is summarized. The topic of the visit was data modeling and database interaction (querying/browsing) in the context of geographic information systems. The original purpose and agreement are given in this report. The detailed research plan and the day to day accounting of the performed activities are presented. The scientific work of this visit resulted in a paper called 'A Small Set of

Formal Topological Relationships Suitable for End-User Interaction' that is presented in chapter six. ESA

N94-19453 Prins Maurits Lab. TNO, Rijswijk (Netherlands).
EVALUATION OF MASS SPECTRA FOR A VERIFICATION DATABASE Final Report
E. Wils and A. deJong Mar. 1993 62 p Sponsored by DMKL, The Hague, Netherlands
(Contract A93/D/402)
(PML-1993-12; TD92-3702; ETN-93-94939) Copyright Avail: Issuing Activity (TNO Prins Maurits Laboratory, P.O. Box 45, 2280 AA Rijswijk, Netherlands)

The possibility of creating a mass spectral database for verification analysis starting from data already recorded was investigated. Electron impact mass spectra of sixteen compounds submitted by seven laboratories were evaluated. The evaluation was carried out by means of the concept of quality indices used for the quality control of a commercially available database. This concept proved to be insufficient to evaluate and select mass spectra for a verification database. A visual inspection of the mass spectra turned out to be necessary. Based on the hundred spectra studied it was concluded that a database can be established from data submitted by various laboratories. Recommendations for recording, submission and review of spectra are discussed. ESA

N94-19454 Physics and Electronics Lab. TNO, The Hague (Netherlands).
SECURE OPEN SYSTEMS: AN INVESTIGATION Final Report
P. L. Overbeek Dec. 1991 110 p
(FEL-91-B293; TD91-3274; ETN-93-94940) Copyright Avail: Issuing Activity (TNO Physics and Electronics Laboratory, P.O. Box 96864, 2509 JG The Hague, Netherlands)

The achievements of current standardization efforts in the area of secure open systems are outlined. Security in open systems is a special problem since all elements in an open system must be able to offer the required security in coordination with each other. A new view on requirements for security is presented. Security requirements are studied from different angles: security requirements that are specific to open systems, security requirements that stem from organizational considerations, security requirements that reflect the value of information and services for an organization, security requirements that stem from social structures and, security requirements that address the security of the system itself. The results of our investigation of current initiatives in the area of technical security in open systems are presented. ESA

N94-19457 Physics and Electronics Lab. TNO, The Hague (Netherlands).
MODELS AND BUILDING BLOCKS FOR SECURE OPEN SYSTEMS Final Report
P. L. Overbeek Nov. 1992 119 p
(FEL-92-B365; TD92-3313; ETN-93-94950) Copyright Avail: Issuing Activity (TNO Physics and Electronics Laboratory, P.O. Box 96864, 2509 JG The Hague, Netherlands)

Technical security in 'open' systems is discussed. Security in open systems is a special problem since each element in an open system must be able to offer security in coordination with other elements. Concepts found in preceding studies are further developed and new concepts are introduced. The concepts of current international standards are generalized such that they are applicable to open systems. The different concepts are confronted with one another and unified using new models. Models and building blocks to create secure open elements make up a secure open system. The study shows that it is possible to offer security services in open systems that are able to fulfill the majority of today's and tomorrow's requirements for security. The study also shows that there still is a long way to go: standardized interfaces, protocols, and data structures must still be defined. ESA

N94-19571# Naval Surface Warfare Center, Bethesda, MD.
RESULTS OF A JOINT NAVY/AIR FORCE OPERATIONAL TEST TO EVALUATE USAF INTEGRATED MAINTENANCE INFORMATION SYSTEMS (IMIS), INTERACTIVE ELECTRONIC TECHNICAL MANUAL (IETM) TECHNOLOGY APPLIED TO THE F/A-18 AIRCRAFT Final Report, 1 Oct. 1989 - 1 Oct. 1991
Mark T. Kramer, Theodore J. Rainey, and C. Samuel 14 Jun. 1993 151 p
(AD-A271322; CarderockDiv-93/007) Avail: CASI HC A08/MF A02

In a joint effort, the U.S. Navy and Air Force have tested under operational conditions a series of improved techniques developed under the Air Force Integrated Maintenance Information System (IMIS) program for delivering maintenance technical information to squadron technicians. These improvements included use of a portable maintenance aid (PMA) for technical information display. In this test, carried out in an F/A-18 fighter squadron at Marine Corps Air Station, Beaufort, South Carolina each of 16 technicians performed six fault-isolation tasks, three supported by an Interactive Electronic Technical Manual (IETM) displayed on a PMA, and three supported by conventional paper-based work package (WP) technical manual (TM). This report presents a comparison of technician performance supported by the ITEM/PMA combination with performance using conventional paper TM's. The performance data collected during the test showed considerable reduction in performance times for complex multiple fault isolations and maintenance errors, when technicians used the IETM/PMA combination. Also, technician-preference data based on questionnaires showed strong support for virtually all IETM/PMA features. Technicians also made suggestions for improving the IETM and the PMA. DTIC

N94-19709 Technische Univ., Eindhoven (Netherlands). Dept. of Mathematics and Computing Science.
INTEGRITY CHECKING IN DEDUCTIVE DATABASES: AN EXPOSITION
R. R. Seljee 1992 41 p Limited Reproducibility: More than 20% of this document may be affected by microfiche quality
(PB93-191724; COMPUTING SCIENCE NOTES-92/16) Copyright Avail: Issuing Activity (National Technical Information Service (NTIS))

Relational systems are extended in several ways. The author considers extensions with rules and integrity constraints to so-called deductive databases. There are several problems in handling these rules and constraints. One problem is to check, in an efficient way, the integrity of a deductive database when an insertion or deletion is made. There exist several integrity maintenance methods. All these methods avoid a full check of the integrity constraints in order to keep them efficient. Therefore, the database is supposed to be consistent before a transaction is made. The author takes a look at one of the most efficient methods. It determines from the updates, rules, and constraints and without accessing the fact base the so called update constraints which have to be checked in the updated database. Although this method is more efficient than other ones, it is still susceptible to improvement. The goal in the article was to show by some well-chosen examples that in some regards the proposed method is still very inefficient. By these examples it becomes clear where the inefficiencies come from. NTIS

N94-19780 Institute for Defense Analyses, Alexandria, VA.
A COMPARISON AIR FORCE DATA SYSTEMS Final Report, Jul. - Aug. 1993
Waynard C. Devers, Elizabeth K. Bailey, Lee H. Dymond, William A. Florac, and Stanley A. Horowitz Aug. 1993 177 p Limited Reproducibility: More than 20% of this document may be affected by microfiche quality
(Contract MDA903-89-C-0003)
(AD-A270662; IDA-D-1400; IDA/HQ-93-44315; AD-E501701) Avail: CASI HC A09

IDA Paper P-2863 reports on a comparison by IDA of two Air Force maintenance information systems. One of the systems is CAMS/REMIS, which combines the Core Automated Management System (CAMS) with the Reliability and Maintainability Information System (REMIS). The other is the Interim CAMS and REMIS Reporting System (TICARRS). Before Paper P-2863 was released in its final version, IDA gave interested parties the opportunity to comment upon it. This document contains the comments provided to IDA by the Office of the Secretary of Defense, the Air Force, Litton Computer Services, and Dynamics Research Corporation. It also contains IDA's responses to the comments received. DTIC

N94-19795# Technische Univ., Delft (Netherlands). Faculty of Technical Mathematics and Informatics.

SEMANTIC MODELS FOR DISTRIBUTED DATA BASE MANAGEMENT. PART 2: DEVELOPMENT OF AN INTEGRAL META-MODEL FOR DATA MODELING AND DATA BASE MODELING [SEMANTISCHE MODELLEN VOOR GEDISTRIBUEERD DATABASE MANAGEMENT. 2: DE ONTWIKKELING VAN EEN INTEGRAAL METAMODEL VOOR DATAMODELLERING EN DATABASEMODELLERING]

J. A. Bakker 1993 34 p In DUTCH
(Rept-93-08-Pt-2; ETN-93-94303-Pt-2) Copyright Avail: CASI HC A03/MF A01

A metamodel was developed to support a topdown design of data distribution which makes the least possible use of detailed knowledge of location and user frequency of data on different nodes. Semantic concepts for fragmentation, allocation, and local mapping are introduced. The metamodel defines the relation between these concepts. The metamodel makes it possible to decide about data distribution on the basis of reasonable assumptions. The new concepts allow the design of a fragmentation scheme and an allocation scheme based on an existing data model whereby return to a previous phase can be avoided. The use of the new concepts allows automatic control if schemes for distribution fulfill the requirements. ESA

N94-19638# European Space Agency. European Space Research and Technology Center, ESTEC, Noordwijk (Netherlands). Space Science Dept.

THE CLUSTER SCIENCE DATA SYSTEM: A DISTRIBUTED SYSTEM TO SERVE A WIDE INTERNATIONAL COMMUNITY

R. Schmidt and L. J. C. Woolliscroft (Sheffield Univ., England.) *In its* Cluster: Mission, Payload, and Supporting Activities Mar. 1993 p 279-290 (For primary document see N94-19622 04-12)
Copyright Avail: CASI HC A03/MF A03; ESA, EPD, ESTEC, Noordwijk, Netherlands, HC

83 ECONOMICS AND COST ANALYSIS

Includes cost effectiveness studies.

No abstracts in this category.

84 LAW, POLITICAL SCIENCE AND SPACE POLICY

Includes NASA appropriation hearings; aviation law; space law and policy; international law; international cooperation; and patent policy.

N94-18842# Committee on Science, Space and Technology (U.S. House).

THE 1994 NASA AUTHORIZATION, VOLUME 2

Washington GPO 1993 976 p Hearings before the Committee on Science, Space, and Technology, 103rd Congress, 1st Session, No. 41, 20, 27, 29 Apr., 4, 6, 18 May, and 8 Jun. 1993
(GPO-71-510; ISBN-0-16-041532-2) Avail: CASI HC A99/MF A10; Subcommittee on Space Science and Applications, House of Representatives, Washington, DC 20515 HC; SOD HC

Hearings before the Subcommittee on Space of the Committee on Science, Space, and Technology of the House of Representatives is presented. Written testimony, submittals for the record, and responses to written questions are included. Topics concerning NASA 1994 authorization include procurement and management policies, budget projections, program schedules, research and development, and mission safety. CASI

85 URBAN TECHNOLOGY AND TRANSPORTATION

Includes applications of space technology to urban problems; technology transfer; technology assessment; and surface and mass transportation.

For related information see also *03 Air Transportation and Safety, 16 Space Transportation,* and *44 Energy Production and Conversion.*

N94-19777# Software Productivity Consortium, Herndon, VA.

TECHNOLOGY BENEFITS MODEL USER MANUAL, VERSION 01.00.04

Sep. 1993 89 p
(Contract MDA972-92-J-1018)
(AD-A270637; SPC-93111-CMC) Avail: CASI HC A05/MF A01

The Technology Benefits Model tool is a spreadsheet implementation of various models for estimating the effect on the cost of software development due to using some new technology in the software development process. The Technology Benefits Model tool was designed to provide estimates on the impact of one or more technology capabilities on a software development organization. The model provides these estimates for a period of time up to 15 years. The estimates are provided in terms of the impacts on several cost measures, including unit costs, and the total costs to develop a software system of some given size. The tool provides both spreadsheet and graphics capabilities. It requires the use of Microsoft Excel, version 4.0 and can operate on either a Macintosh or an IBM-compatible PC. You can use the Technology Benefits Model tool to help you estimate the potential effect of a technology on the cost of conducting each development activity, such as requirements analysis, preliminary design, or detailed design. The tool will enable you to see the impact of such estimates over a number of years. You can use the Technology Benefits Model tool to estimate the effect on unit labor rate, unit labor cost, product development cost, market cost, and market cost savings due to incorporating some new technologies into the development process. Please be aware that the model implemented in this tool is at an early level of validation. DTIC

88 SPACE SCIENCES (GENERAL)

N94-18851*# National Aeronautics and Space Administration, Washington, DC.

ISTP GLOBAL GEOSPACE SCIENCE. ENERGY TRANSFER IN GEOSPACE

1990 31 p Original contains color illustrations
(NASA-TM-109239; NAS 1.15:109239) Avail: CASI HC A03/MF A01; 25 functional color pages

Solar-terrestrial physics concerns the study of the generation, flow, and dissipation of mass, momentum, and energy between the Sun and the Earth. Mass, momentum, and energy are carried by charged particles that compose the solar wind. When the solar wind reaches the Earth, some solar-wind particles enter the magnetosphere; this coupling between the solar wind and the Earth means that the solar wind can influence the Earth's upper atmosphere. As the first step in addressing the behavior of this solar-terrestrial system, the Global Geospace Science (GGS) Initiative will use the Wind and Polar satellites, provided by NASA, and the Geotail satellite provided by the Japanese Institute of Space and Astronautical Science (ISAS), to perform simultaneous and closely coordinated measurements of the key geospace regions and will add data from equatorial missions. Magnetic field and particle changes that occur when particles are energized during auroral events will be monitored. The intention behind the GGS Initiative is to understand the physical mechanisms and various regions controlling the transport of mass, momentum, and energy in geospace. A summary of the GGS Initiative is presented.

Derived from text

89 ASTRONOMY

Includes radio, gamma-ray, and infrared astronomy, and astrometry.

N94-18141 Max-Planck-Inst. fuer Physik und Astrophysik, Garching (Germany). Inst. fuer Astrophysik.
MAXIMAL HYPERSURFACES IN ASYMPTOTICALLY STATIONARY SPACETIMES
Piotr T. Chrusciel and Robert M. Wald (Chicago Univ., IL.) Dec. 1992 45 p Submitted for publication
(MPA-708; ETN-93-94915) Copyright Avail: Issuing Activity (Max-Planck-Institut fuer Physik und Astrophysik, Karl-Schwarzschild-Strasse 1, 8046 Garching, Germany)

The purpose of the work is to extend the results on the existence of maximal hypersurfaces to encompass some situations considered by other authors. The existence of maximal hypersurface in asymptotically stationary spacetimes is proven. Existence of maximal surface and of foliations by maximal hypersurfaces is proven in two classes of asymptotically flat spacetimes which possess a one parameter group of isometries whose orbits are timelike 'near infinity'. The first class consists of strongly causal asymptotically flat spacetimes which contain no 'blackhole or white hole' (but may contain 'ergoregions' where the Killing orbits fail to be timelike). The second class of space times possess a black hole and a white hole, with the black and white hole horizon intersecting in a compact 2-surface S. ESA

N94-18611*# Washington Univ., Seattle. Dept. of Astronomy.
PULSE-TIMING STUDIES OF X RAY PULSARS Final Technical Report, 1 Jan. 1988 - 31 Dec. 1991
John E. Deeter and Paul E. Boynton 16 Apr. 1992 7 p
(Grant NAG8-695)
(NASA-CR-193778; NAS 1.26:193778) Avail: CASI HC A02/MF A01

The pulse-timing projects supported by NASA Grant NAG8-695 were motivated in large part by our long-standing interest in the physics of rotating neutron stars and particularly the variations in rotation due to internal and external fluctuating torques. For accretion-powered pulsars, observed as compact galactic X-ray sources, our work has been motivated by questions regarding the physics of matter accretion, mass transfer, and mass loss in these X-ray binary systems. For rotation-powered pulsars using X-ray, optical, and radio observations, we have examined the internal structure of neutron stars and mechanisms for secular spin-down. These issues are still central to the continuing process of understanding the complex behavior of these fascinating systems. The work supported by this grant is based mainly on Ginga observations of three pulsating X-ray sources. We observed two of these sources (Her X-1 and SMC X-1) within the framework of a NASA-ISAS program for U.S.-Japan collaborations to obtain and analyze Ginga observations. In addition, we joined with members of the Ginga team to apply our pulse-timing methods to PSR 0540-69 data obtained as a collateral benefit of the regular monitoring by Ginga of SN 1987A. In addition to these Ginga observations, there exist other relevant data on all three of these sources. The direction of our investigations has been affected by the necessity of including these supporting data in our analyses, and setting up the necessary collaborations has sometimes entailed extra work that was not anticipated in our proposals. Indeed, we have often taken the initiative in establishing these joint projects. Author (revised)

N94-18850*# National Aeronautics and Space Administration. Goddard Space Flight Center, Greenbelt, MD.
THE SOLAR OPTICAL TELESCOPE
1990 23 p Original contains color illustrations
(NASA-TM-109240; NAS 1.15:109240) Avail: CASI HC A03/MF A01; 14 functional color pages

Objectives of the Solar Optical Telescope are to study the physics of the Sun on the scale at which many of the important physical processes occur and to attain a resolution of 73km on the Sun or 0.1 arc seconds of angular resolution. Topics discussed in this overview of the Solar Optical Telescope include: why is the Solar Optical Telescope needed; current picture of the Sun's atmosphere and convection zone; scientific problems for the Solar Optical Telescope; a description of the telescope; the facility - science management, contamination control, and accessibility to the instruments; the scientific instruments - a coordinated instrument package for unlocking the Sun's secrets; parameters of the coordinated instrument package; science operations from the Space Shuttle; and the dynamic solar atmosphere. CASI

N94-18855*# Columbia Univ., New York, NY. Dept. of Astronomy and Physics.
ECLIPSING CATACLYSMIC VARIABLES. DEEP ECLIPSES IN H0928+501. YY DRACONIS, THE WHIRLING DERVISH. NEW X RAY PULSAR CANDIDATES FROM HEAO-1 Annual Status Report, 1 Jun. 1992 - 31 May 1993
Joseph Patterson Jun. 1993 19 p
(Grant NAG5-1958)
(NASA-CR-194027; NAS 1.26:194027; CAL-2117) Avail: CASI HC A03/MF A01

The status report covering the period from 1 June 1992 to 31 May 1993 is included. Areas of research include: (1) eclipsing cataclysmic variables; (2) deep eclipses in H0928+501; (3) YY Draconis, the Whirling Dervish; and (4) new x ray pulsar candidates from HEAO-1. CASI

N94-19072* National Aeronautics and Space Administration, Washington, DC.
HUBBLE SPACE TELESCOPE (Videotape)
Feb. 1990 Videotape: 2 min. 28 sec. playing time, in color, with sound
(NASA-TM-109359; NONP-VT-94-198206) Avail: CASI VHS A01/BETA A22

An overview of the mission of the Hubble Space Telescope, a joint project between NASA and the European Space Agency which will be used to study deep space, as well as our solar system is presented. The video contains animations depicting the Hubble Space Telescope in orbit, as well as footage of scientists at the Space Telescope Science Institute making real time observations. The images Hubble acquires will be downloaded into a database that contains images of over 19,000,0000 celestial objects called the Star Catalog. CASI

N94-19288*# Applied Research Corp., Landover, MD.
DETECTION OF ACCRETING GAS TOWARD HD 45677: A NEWLY RECOGNIZED, HERBIG Be PROTO-PLANETARY SYSTEM
C. A. Grady, K. S. Bjorkman (Wisconsin Univ., Madison.), D. Shepherd (Wisconsin Univ., Madison.), R. E. Schulte-Ladbeck (Pittsburgh Univ., PA.), M. R. Perez (Computer Sciences Corp., Greenbelt, MD.), D. deWinter (Astronomical Inst., Amsterdam, Netherlands.), and P. S. The (Astronomical Inst., Amsterdam, Netherlands.) 6 Jul. 1993 14 p
(Contracts NAS5-32059; NASw-4756; NAG5-1783; NAG5-1740)
(NASA-CR-189312; NAS 1.26:189312) Avail: CASI HC A03/MF A01

We report detection of high velocity, accreting gas toward the Be star with IR excess and bipolar nebula, HD 45677. High velocity (+200 to +400 km/s), variable column density gas is visible in all IUE spectra from 1979-1992 in transitions of Si II, C II, Al III, Fe III, Si IV, and C IV. Low-velocity absorption profiles from low oscillator-strength transitions of Si II, Fe II, and Zn II exhibit double-peaked absorption profiles similar to those previously reported in optical spectra of FU Orionis objects. The UV absorption data, together with previously reported analyses of the IR excess and polarization of this object, suggest that HD 45677 is a massive, Herbig Be star with an actively accreting circumstellar, proto-planetary disk. Author

N94-19415 Max-Planck-Inst. fuer Physik und Astrophysik, Garching (Germany). Inst. fuer Extraterrestrische Physik.
THE 0.15 SECONDS NEAR-INFRARED IMAGING OF THE CENTRAL PARSEC OF THE GALAXY
A. Eckart, R. Genzel, R. Hofmann, B. J. Sams, and L. E. Tacconi-Garman Feb. 1993 25 p Submitted for publication Original contains color illustrations
(MPE-Preprint-239; ETN-93-94919) Copyright Avail: Issuing Activity (Max-Planck-Institut fuer Physik und Astrophysik, Giessenbackstrasse, 8046 Garching, Munich, Germany)

Deep 1.6 (H) and 2.2 micrometers (K) images of the central parsec of the Galaxy at a resolution of 0.15 seconds are presented. Most of the flux in earlier seeing limited images comes from about 340 unresolved stellar sources with K magnitudes less than or equal to 14. Most of the fainter stars in the central parsec are likely M rather and K giants. The infrared

Research Satellite (IRS) 16 and 13 complexes are resolved into about 25 and 6 sources, a number of which are probably luminous hot stars. The presence of a blue near infrared object at the position of the compact radio source Sgr A (star) is confirmed. The spatial centroid of the number distribution of compact sources is consistent with the position of Sgr A (star) but not with a position in the IRS 16 complex. The stellar surface density is very well fit by an isothermal cluster model with a core radius of 0.15 +/- 0.05 pc. The central stellar density is a few times 10 to the 7th power of the solar mass/cubed pc. Buildup of massive stars by collisional merging of lower mass stars and collisional disruption of giant atmospheres are very probable processes in the central 0.2 pc. ESA

N94-19417 Max-Planck-Inst. fuer Physik und Astrophysik, Garching (Germany). Inst. fuer Extraterrestrische Physik.
THE MOLECULAR ENVIRONMENT OF S106 IR
J. S. Richer (Cambridge Univ., England.), R. Padman (Cambridge Univ., England.), D. Ward-Thompson (Cambridge Univ., England.), R. E. Hills (Cambridge Univ., England.), and A. I. Harris Jan. 1993 32 p Submitted for publication Sponsored in part by United Kingdom Science and Engineering Research Council, and Cambridge Univ., England
(MPE-Preprint-241; ETN-93-94921) Copyright Avail: Issuing Activity (Max-Planck-Institut fuer Physik und Astrophysik, Giessenbachstrasse, 8046 Garching, Munich, Germany)

Millimeter and submillimeter images of the bipolar nebula S106 are presented. The structure of the circumstellar material around the exciting star S106IR is investigated. The previously unresolved 'dust bar' is seen to break up into a number of sources: there is no evidence for a smooth disc about the star. There is a bright, previously undetected far infrared point source in the dust lane which is not detected at 20 micrometers, suggesting it is an extremely embedded object of moderate luminosity which may be a very young protostellar companion to S106 IR. ESA

N94-19421*# Washington Univ., Seattle.
DETERMINATION OF NITROGEN TO CARBON ABUNDANCE RATIOS FROM TRANSITION LAYER EMISSION LINES Final Report, Sep. 1990 - Aug. 1992
Erika Boehm-Vitense Aug. 1992 10 p
(Grant NAG5-1255)
(NASA-CR-191921; NAS 1.26:191921) Avail: CASI HC A02/MF A01

We have finished studying the nitrogen to carbon abundance ratios for stars with different effective temperatures T(sub eff) and luminosities using transition layer emission lines and using spectra available in the IUE archives. The N/C abundance ratio determinations using transition layer emission lines are as accurate as the photospheric abundance determinations as found by comparison of results obtained by both methods for the same stars. Our measurements confirm photospheric abundance determinations in regions of the HR diagram where they can be obtained. Our studies have extended the temperature range to higher temperatures. They have shown the exact positions in the HR diagram where the mixing due to the outer convection zones reaches deep enough to bring nuclear processed material to the surface. This occurs at effective temperatures which are higher by delta log T(sub eff) approximately 0.04 or roughly 400 K than expected theoretically. Since the depth of the convection zone increases rapidly with decreasing T(sub eff) this may indicate considerable overshoot beyond the lower boundary of the convection zone. Our N/C abundance ratio determinations from transition layer emission lines have confirmed that the actual enrichment observed for some cool giants is larger than expected theoretically, again indicating a larger degree of mixing in several stars either from below or from above. For the supergiants it probably indicates overshoot above the convective core in the progenitor main sequence stars. For the more massive giants this may also be the case, though we did not find a correlation between delta log N/C and the absolute magnitudes, but these are rather uncertain. As byproducts of these studies we also found anomalies in Si/C and N/C abundance ratios for F giants which can be understood as the relict of surface abundance changes for their main sequence progenitors due to diffusion. This anomaly disappears for G giants, for which the depths of the convection zones are apparently deep enough to wipe out these element separations (Bohm-Vitense 1992). Derived from text

N94-19431*# California Univ., Berkeley.
ULTRAVIOLET OBSERVATIONS OF CLUSTERS OF WOLF-RAYET STARS IN THE SBm3 GALAXY NGC 4214 AND ULTRAVIOLET AND OPTICAL OBSERVATIONS OF LINER'S Final Technical Report
Alexei V. Filippenko 1992 4 p
(Grant NAG5-1800)
(NASA-CR-194307; NAS 1.26:194307) Avail: CASI HC A01/MF A01

The purpose of the grant was to obtain and analyze IUE (UV) and ground-based (optical) spectra of the central bar of NGC 4214, which contains several bright H II regions, in order to further explore the properties of the Wolf-Rayet stars in this galaxy. Several spatially distinct regions, with widely different equivalent widths of optical Wolf-Rayet lines, could be sampled by the large IUE entrance aperture. By using newly developed extraction techniques, the spectra of these H II regions could be isolated, and differences in their stellar populations would be systematically studied. Data were obtained with IUE in late February and early March, 1992. Some of the shifts were successful, but a few were not -- apparently the blind offset from the nearby star did not work equally well in all cases. Thus, the signal-to-noise ratio is somewhat lower than we had hoped. This necessitated a more careful extraction of the spectra of individual H II regions from the two-dimensional spectra. (A program that models the point spread function in the spatial direction was used to deblend the distinct H II regions.) The IUE data are currently being analyzed in conjunction with ground-based optical spectra. There appear to be obvious variations in the stellar population over angular scales of only a few arc seconds. The second part of the research performed under this grant was a continuation of a project that uses IUE (UV) and ground-based (optical) spectra to infer the physical conditions in Low-Ionization Nuclear Emission-Line Regions (LINER's). We have obtained spectra of a few key objects that cover a representative range in LINER continuum and emission-line properties. The overall goals are to (1) separate the emission into spatially distinct components, (2) establish whether the observed nuclear ultraviolet continua indicate sufficient photoionizing fluxes to account for the emission lines, (3) determine whether the nuclear emission can be explained by hot stars alone, (4) detect and measure the strengths of UV emission lines, and (5) search for systematic differences in the UV spectra of LINER's whose other properties differ in some respects. Derived from text

N94-19451 Max-Planck-Inst. fuer Physik und Astrophysik, Garching (Germany). Inst. fuer Extraterrestrische Physik.
ROSAT AND OPTICAL OBSERVATIONS OF TWO X-RAY TRANSIENTS: MX 0836-42 AND GS 0834-430
T. Belloni, G. Hasinger, W. Pietsch, S. Mereghetti (Consiglio Nazionale delle Ricerche, Milan, Italy.), G. F. Bignami (Consiglio Nazionale delle Ricerche, Milan, Italy.), and P. Caraveo (Consiglio Nazionale delle Ricerche, Milan, Italy.) Nov. 1992 19 p Submitted for publication
(MPE-Preprint-237; ETN-93-94917) Copyright Avail: Issuing Activity (Max-Planck-Institut fuer Physik und Astrophysik, Giessenbachstrasse, 8046 Garching, Munich, Germany)

Two transient sources were detected in hard X-rays by several instruments at the end of 1990. Both sources were observed with Rosat in the all the sky survey and during the pointing phase. The positive detection of the sources in the Rosat pointing observations made possible to derive accurate positions for both sources. Optical images of the Rosat error boxes obtained with the European Southern Observatory new technology telescope are presented. Pulsations are clearly detected from GS 0834-430 with a period of 12.3203 +/- 0.0015s. The pulse profile is roughly sinusoidal with a 13 percent rms variation. The comparison with hard X-ray data and the possible nature of the sources are discussed. ESA

N94-19462# Max-Planck-Inst. fuer Physik und Astrophysik, Garching (Germany). Ist. fuer Extraterrstrische Physik.
EGRET MISSION AND DATA ANALYSIS
Oct. 1992 10 p Submitted for publication
(MPE-Preprint-223) Avail: CASI HC A02/MF A01

Results of the Energetic Gamma Ray Experiment Telescope (EGRET) observations in the Compton Gamma Ray Observatory are presented. Data acquired on high energy gamma radiation above 30 MeV from the sun is discussed. The gamma radiation in the range around 100MeV was observed for at least 8 hours following the flare. Implications for the storage and release mechanisms of the primary particles with energy of typically a GeV implied by these gamma ray observations are discussed. Preliminary results from two observations of 3C 273 with the EGRET instrument aboard the Compton Observatory are reported. The 3C 273 ($z = 0.158$), an optically very bright quasar is a well known source in all energy regimes ranging from the radio, infrared, optical, and ultraviolet up to the x-rays. For individual titles, see N94-19463 through N94-19464.

N94-19463*# National Aeronautics and Space Administration. Goddard Space Flight Center, Greenbelt, MD.
DETECTION OF A LONG-DURATION SOLAR GAMMA-RAY FLARE ON JUN. 11, 1991 WITH EGRET ON COMPTON-GRO **c93**
G. Kanbach (Max-Planck-Inst. fuer Physik und Astrophysik, Garching, Germany.), D. L. Bertsch, C. E. Fitchel, R. C. Hartman, S. D. Hunter, D. A. Kniffen (Hampden-Sydney Coll., VA.), P. W. Kwok, Y. C. Lin (Stanford Univ., CA.), J. R. Mattox, and H. A. Mayer-Hasslewander (Max-Planck-Inst. fuer Physik und Astrophysik, Garching, Germany.) *In* Max-Planck-Inst. fuer Physik und Astrophysik, EGRET Mission and Data Analysis Oct. 1992 5 p Repr. from Astronomy and Astrophysics Supplement Series, Ser. 1, v. 1-99, no. 2001 See also A93-28958 (For primary document see N94-19462 04-89)
(Grant BMFT-50-QV-90955)
Avail: CASI HC A01/MF A01

On 11 Jun. 1991, the Energetic Gamma Ray Experiment Telescope (EGRET) on the Compton Gamma Ray Observatory (Comption-GRO) observed high energy gamma radiation above 30 MeV from the Sun following an intense flare around 2:00 Universal Time (UT). After the decay of most of the x ray flare, which caused nearly complete deadtime losses in EGRET, high energy emission was registered during the interval from about 3:30 UT to at least 10:30 UT. Gamma rays were detected up to energies above 1 GeV. The solar origin of the emission is assured by the time profile of the gamma ray count rate and by time resolved sky maps, which show a clear maximum at the position of the sun. The gamma ray lightcurve of the flare can be described with two components: a fast decaying emission with an e-folding time constant of about 25 minutes and a slow decay with about 255 minutes. There are indications for a spectral evolution with time, such that the emission below 100 MeV fades away earlier than the 100 to 300 MeV radiation, roughly in the time scale of the fast component. The spectrum of the flare can be fitted with a composite of a proton generated pion neutral spectrum and an electron bremsstrahlung component. The latter can be identified with the fast decaying component of the lightcurve. ESA

N94-19464*# National Aeronautics and Space Administration. Goddard Space Flight Center, Greenbelt, MD.
EGRET OBSERVATIONS OF 3 C 273
C. vonMontigny (Max-Planck-Inst. fuer Physik und Astrophysik, Garching, Germany.), D. L. Bertsch, C. E. Fichtel, R. C. Hartman, S. D. Hunter, G. Kanbach (Max-Planck-Inst. fuer Physik und Astrophysik, Garching, Germany.), D. A. Kniffen (Hampden-Sydney Coll., VA.), P. W. Kwok, Y. C. Lin (Stanford Univ., CA.), and J. R. Mattox *In* Max-Planck-Inst. fuer Physik und Astrophysik, EGRET Mission and Data Analysis Oct. 1992 3 p Repr. from Astronomy and Astrophysics Supplement Series, Ser. 1, v. 1-99, no. 2001 See also A93-28899 (For primary document see N94-19462 04-89)
(Grant BMFT-50-90955)
Avail: CASI HC A01/MF A01

The quasar 3C 273 was detected by the Compton Observatory Satellite (COS-B) in the 1970's. Energetic Gamma Ray Experiment Telescope (EGRET) observations of this sky region in Jun. and Oct. 1991 revealed a flux from 3C 273 lower than that measured by COS-B. The flux observed by EGRET in the June period is approximately 0.0000003/sq cm(exp -2) sec(exp -1) for energies greater than 100 MeV. During the Oct. observation it appears to be even lower. For the first observation a preliminary spectrum was derived which was a photon index of 2.4. ESA

N94-19526 Max-Planck-Inst. fuer Physik und Astrophysik, Garching (Germany). Inst. fuer Extraterrestrische Physik.
[ROSAT AND IRAS OBSERVATIONS]
Sep. 1992 9 p Presented at ESO/EIPC Workshop on Star Forming Galaxies and Their Interstellar Medium, Elba, France, Jun. 1992 Submitted for publication
(MPE-Preprint-231; ETN-93-94614) Copyright Avail: Issuing Activity (Fachinformationszentrum Karlsruhe, 7514 Egeenstein-Leopoldshafen 2, Germany)

Rosat X-ray observations of the 30 Dor giant H2 region and the sample of the Infrared Astronomy Satellite galaxies observed in the Rosat survey are reported. The evaluation of the contribution of the stellar component to X-ray luminosity of the 30 Dor region shows that the presence of a hot interstellar medium is necessary for explaining the total X-ray emission. Concerning starburst or central activity, three issues may be highlighted: the results reveal that such galaxies reach exceptionally high X-ray luminosities; the question on whether the abnormally luminous objects could fit arises; and in order to explain X-ray luminosities for starburst galaxies it is necessary to develop detailed population synthesis models. For individual titles, see N94-19527 through N94-19528.

N94-19527 Max-Planck-Inst. fuer Physik und Astrophysik, Garching (Germany). Inst. fuer Extraterrestrische Physik.
ROSAT X RAY OBSERVATION OF THE 30 DOR GIANT HII REGION
Laura Norci and Hakki B. Oegelman (Wisconsin Univ., Madison.) *In its* ROSAT and IRAS Observations Sep. 1992 3 p (For primary document see N94-19526 04-89)
Copyright Avail: Issuing Activity (Fachinformationszentrum Karlsruhe, 7514 Egeenstein-Leopoldshafen 2, Germany)

A well defined sample of IRAS (Infrared Astronomy Satellite) galaxies were studied from the Rosat All Sky Survey data. Among the detections are Seyfert 2, LINER, and Starburst galaxies with X-ray luminosities more than an order of magnitude higher than observed before. The All Sky Survey carried out with the Rosat satellite offers an opportunity to examine the X-ray characteristics of particular classes of object. A comparison of the infrared and X-ray properties of galaxies is of interest regarding the relative importance of star formation processes and central active nuclei. A statistical investigation of the X-ray emission for IRAS galaxies is reported. Subsequent optical spectroscopy of the most luminous cases reveals that outstanding objects in various categories were detected. ESA

N94-19528 Max-Planck-Inst. fuer Physik und Astrophysik, Garching (Germany). Inst. fuer Extraterrestrische Physik.
IRAS GALAXIES OBSERVED IN THE ROSAT SURVEY: STARBURSTS OR CENTRAL ACTIVITY
E. J. A. Meurs, T. Boller, and M. Dennefeld (Institut d'Astrophysique, Paris, France.) *In its* ROSAT and IRAS Observations Sep. 1992 3 p (For primary document see N94-19526 04-89)
Copyright Avail: Issuing Activity (Fachinformationszentrum Karlsruhe, 7514 Egeenstein-Leopoldshafen 2, Germany)

The Rosat PSPC (Position Sensitive Proportional Counter) pointed observations were used for a morphological and spectral study of the 30 Dor region. 30 Dor region is a high surface brightness giant H2 region located in the Large Magellanic Cloud. Its position in the sky, out of the galactic plane, together with the fact that it is the closest giant extragalactic H2 region renders it an ideal place to study the physics of such a star forming region. A contour map is presented and the contribution of the stellar component of the X-ray luminosity is evaluated. It is important to understand whether the diffuse X-ray emission could be attributed entirely to the stellar population. Otherwise the contribution of a hot interstellar medium would be required. ESA

N94-19657# South African Astronomical Observatory, Cape Town.
THE SOUTH AFRICAN ASTRONOMICAL OBSERVATORY Report for period ending 31 Dec. 1992
1992 49 p
(SAAO-17; ISBN 0-9583227-3-2) Avail: CASI HC A03/MF A01

The South African Astronomical Observatory report for the year ending 31 Dec. 1992 is presented. Areas of research include: galaxies and quasars; Magellanic clouds; galactic structure; star clusters and associations; ground-based observations of celestial x ray sources; pulsating variables; binary star phenomena; stellar astrophysics; photometric standards and photometry; and Sutherland site characteristics. Telescopes and instruments are described. In addition, symposiums, summer school, and other programs are described. CASI

N94-19166*# National Aeronautics and Space Administration. Goddard Space Flight Center, Greenbelt, MD.

TELESCOPE FOR X RAY AND GAMMA RAY STUDIES IN ASTROPHYSICS

W. D. Weaver (Arkansas State Univ., State University.) and Upendra D. Desai *In its* The 1993 Shuttle Small Payloads Symposium Oct. 1993 p 33-36 (For primary document see N94-19162 04-12)
Avail: CASI HC A01/MF A03

N94-19178*# Trieste Univ. (Italy). Dept. of Astronomy.

UVSTAR: AN IMAGING SPECTROGRAPH WITH TELESCOPE FOR THE SHUTTLE HITCHHIKER-M PLATFORM

Roberto Stalio, Bill R. Sandel (Arizona Univ., Tucson.), and A. Lyle Broadfoot (Arizona Univ., Tucson.) *In* NASA. Goddard Space Flight Center, The 1993 Shuttle Small Payloads Symposium Oct. 1993 p 145-152 (For primary document see N94-19162 04-12)
Avail: CASI HC A02/MF A03

90 ASTROPHYSICS

Includes cosmology; celestial mechanics; space plasmas; and interstellar and interplanetary gases and dust.

For related information see also *75 Plasma Physics.*

N94-17736 Max-Planck-Inst. fuer Physik und Astrophysik, Garching (Germany).

UNIFIED NLTE MODEL ATMOSPHERES INCLUDING SPHERICAL EXTENSION AND STELLAR WINDS, 4: IMPROVED LINE TRANSFER AND WIND CONTAMINATION OF H, He PROFILES

F. Sellmaier (Technische Univ., Munich, Germany.), J. Puls (Technische Univ., Munich, Germany.), R. P. Kudritzki (Technische Univ., Munich, Germany.), A. Gabler (Technische Univ., Munich, Germany.), R. Gabler (Technische Univ., Munich, Germany.), and S. A. Voels (Technische Univ., Munich, Germany.) Nov. 1992 16 p Submitted for publication
(MPA-905; ETN-93-94912) Copyright Avail: Issuing Activity (Max-Plank-Institut fuer Physik und Astrophysik, Karl-Schwarzchild-Strasse 1, 8046 Garching, Germany)

The treatment of NLTE (Nonlocal Thermodynamic Equilibrium) multilevel radiative transfer in the presence of sub and supersonic velocity fields of unified model atmospheres is discussed. The solution of the line transfer in the comoving frame is obtained via accelerated lambda iteration. This method yields excellent convergence also in cases, where many strong, intermediate and weak lines have to be treated simultaneously and where other operators failed to achieve convergencve. This algorithm is used to investigate the contamination of photospheric hydrogen and helium absorption lines by emission of the stellar wind. It is found that in the case of early O-supergiants close to the Eddington-limit wind contamination is significant and leads to systematic errors in the determination of stellar parameters, if purely hydrostatic, plane parallel NLTE models are used for the spectral analysis. A specific behavior of the mean line intensity, namely a local minimum around the sonic point, is discussed. ESA

N94-17764*# Sao Paulo Univ. (Brazil). Inst. Astronomico e Geofisico.

DUST IN THE SMALL MAGELLANIC CLOUD Progress Report, 1 Jan. 1992 - 31 Oct. 1993

A. M. Magalhaes 1993 72 p
(Grant NAG5-1463)
(NASA-CR-193344; NAS 1.26:193344) Avail: CASI HC A04/MF A01

Observations of reddened stars in the Small Magellanic Cloud (SMC) indicate that the interstellar grains in that galaxy may show distinct optical properties from those in the Galaxy. In a careful study of three SMC objects, Prevot showed that the UV extinction law in the SMC is almost linear with inverse wavelength and the 2200A feature is generally absent. The first results of a program to determine the wavelength dependence of the interstellar optical polarization in the SMC indicate that highly polarized objects are scarce. Our study has uncovered, however, several objects with optical polarization greater than around 1 percent: AZV 126, AZV 211, AZV 221, AZV 398, and AZV 456. The latter two have already had their UV extinction law determined. Our aim was to obtain International Ultraviolet Explorer (IUE) data and determine the UV extinction law also for AZV 126, AZV 211, and AZV 221. AZV 456, which presents a 'galactic' extinction law, has a 'normal' value for its wavelength of maximum polarization, lmax, while AZV 398, which shows a 'typical' SMC extinction curve, shows a somewhat smaller value for such wavelength. AZV 126, AZV 211, and AZV 221 all present extreme small values of lmax but had not had its extinction curve in the W determined yet. We therefore aimed at ultimately determining the extinction law in the direction of these three objects. Such results, in combination with the optical polarization data, have an important bearing on constraining the composition and size distribution of the interstellar dust in the SMC. In the last report, the images gathered with IUE, their processing, and the extinction curves derived from them were described. Such extinction curves and the theoretical models developed to interpret the SMC extinction and polarization data are discussed. Details are presented in an enclosed preprint. The activities in our ongoing polarimetric program of determining the magnetic field structure of the SMC and the images collected at Cerro Tololo Interamerican Observatory during the period are also briefly described. Other activities are also described. Author (revised)

N94-17843*# Johns Hopkins Univ., Baltimore, MD.

OBSERVATIONS OF COMETS WITH THE IUE Final Report, 1 Jul. 1979 - 30 Sep. 1992

Paul D. Feldman 1992 2 p
(Grant NsG-5393)
(NASA-CR-193652; NAS 1.26:193652) Avail: CASI HC A01/MF A01

Comet Shoemaker-Levey was observed on several dates in June and July 1992. Comparison of the relative brightness of a given emission between IUE and the Hubble Space Telescope (HST) Faint Object Spectrograph apertures provides information about the spatial distribution of the emitting species from which the excitation mechanisms can be inferred. The comparison between the HST and IUE spectra was abetted by the fact that comet Shoemaker-Levy did not show any indication of short-term temporal variability. Comet Swift-Tuttle is a moderately bright periodic comet that shows relatively strong temporal variations on a scale of hours and days. IUE observations of this comet were made in November 1992 and the detected variability was reported on IAU circular 5663. Coordinated ground-based observations led to the first detection of the CI(lambda)9850 transition that complements CI(lambda)1931 observed by the IUE short wavelength spectrograph and provides a means of indirectly determining the CO abundance. Derived from text

N94-17897 Lawrence Livermore National Lab., CA.

EVOLUTION OF r-PROCESS ELEMENTS IN THE HOT SUPERNOVA BUBBLE

G. J. Mathews (California Univ., Livermore.), J. R. Wilson, and S. E. Woosley (California Univ., Santa Cruz.) Feb. 1993 16 p Presented at the Workshop on Nuclear Physics in the Universe, Oak Ridge, TN, 24-26 Sep. 1992 Limited Reproducibility: More than 20% of this document may be affected by microfiche quality
(Contract W-7405-eng-48)
(DE93-017169; UCRL-JC-113173; CONF-9209239-7) Avail: CASI HC A03

We review some of the recent arguments as to why the r-process is thought to be associated with supernovae and how the high-temperature, high-entropy inner region of a core-collapse supernova is an ideal r-process site. We present preliminary extensions of our earlier work on the formation of the high-entropy 'bubble' that describe more accurately its late-time evolution and the ejection of the neutrino-energized wind from the surface of the nascent neutron star. This site leads naturally to a distribution of temperature, density, neutron excess, and entropy for material ejected at different times in the wind as required by Solar abundances. We present simple analytic expressions which approximate these distributions. This site also predicts an amount of reprocess material ejected per event in agreement with simple galactic evolution arguments. However, it is not yet clear whether the entropy in this model is high enough (or the electron fraction is low enough) to produce an optimum fit to the Solar r-process abundance curve and additional mechanisms may be required to increase the entropy per baryon. We conclude with a discussion of nuclear measurements which would help to probe this r-process environment. DOE

N94-18047# Lawrence Livermore National Lab., CA.

SPACE AND TIME AS OUTCOME OF DECOHERENCE IN AN EXPANDING UNIVERSE

G. F. Chew Nov. 1992 10 p
(Contract DE-AC03-76SF-00098)
(DE93-016199; LBL-33027) Avail: CASI HC A02/MF A01

This paper discusses a quantum-cosmological model. The model avoids a priori classical ideas, even spacetime, by invoking a pair of established general principles that relate to each other: (1) Parameter largeness can endow physical approximations with accuracy; and (2) Coherent states labeled by large parameters provide a quantum basis for classical ideas. Generally speaking, the technical term 'coherent state' refers to a special category of Hilbert-space vector that relates to some Lie group unitarily representable within Hilbert space. In the Hilbert space of the quantum-cosmological model discussed, labels on basis vectors lack physical interpretation, but groups unitarily represented include not only the Heisenberg-Weyl group but the Poincare group. Corresponding large-parameter coherent states are interpretable in terms of events and particles: a quantam-based meaning of classical objective reality in 3+1 spacetime is thereby achievable. DOE

N94-18612*# National Aeronautics and Space Administration. Marshall Space Flight Center, Huntsville, AL.
THE EINSTEIN OBSERVATORY CATALOG OF IPC X RAY SOURCES. VOLUME 4E: RIGHT ASCENSION RANGE 08h 00m TO 11h 59m
D. E. Harris (Smithsonian Astrophysical Observatory, Cambridge, MA.), W. Forman (Smithsonian Astrophysical Observatory, Cambridge, MA.), I. M. Gioia (Smithsonian Astrophysical Observatory, Cambridge, MA.), J. A. Hale (Smithsonian Astrophysical Observatory, Cambridge, MA.), F. R. Harnden, Jr. (Smithsonian Astrophysical Observatory, Cambridge, MA.), C. Jones (Smithsonian Astrophysical Observatory, Cambridge, MA.), T. Karakashian (Smithsonian Astrophysical Observatory, Cambridge, MA.), T. Maccacaro (Smithsonian Astrophysical Observatory, Cambridge, MA.), J. D. McSweeney (Smithsonian Astrophysical Observatory, Cambridge, MA.), and F. A. Primini (Smithsonian Astrophysical Observatory, Cambridge, MA.) et al Apr. 1993 537 p The CD-ROM version of the catalog is available from NSSDCA, GSFC/NASA, Code 633, Greenbelt, MD 20771 (request @NSSDCA.GSFC.NASA.GOV)
(Contract NAS8-30751)
(NASA-TM-108401-Vol-4E; NAS 1.15:108401-Vol-4E) Avail: CASI HC A23/MF A04

The Einstein Observatory (HEAO-2, launched November 13, 1978) achieved radically improved sensitivity over previous x-ray missions through the use of focusing optics which simultaneously afforded greatly reduced background and produced true images. During its 2.5-yr mission, the Einstein X-Ray Telescope was pointed toward some 5,000 celestial targets, most of which were detected, and discovered several thousand additional 'serendipitous' sources in the observed fields. This catalog contains contour diagrams and source data, obtained with the imaging proportional counter in the 0.16 to 3.5 keV energy band, and describes methods for recovering upper limits for any sky position within the observed images, The main catalog consists of six volumes (numbered 2 through 7) of right ascension ordered pages, each containing data for one observation. Along with the primary documentaion describing how the catalog was constructed, volume 1 contains a complete source list, results for merged fields, a reference system to published papers, and data useful for calculating upper limits and fluxes. Author (revised)

N94-18613*# National Aeronautics and Space Administration. Marshall Space Flight Center, Huntsville, AL.
THE EINSTEIN OBSERVATORY CATALOG OF IPC X RAY SOURCES. VOLUME 5E: RIGHT ASCENSION RANGE 12h 00m TO 15h 59m
D. E. Harris (Smithsonian Astrophysical Observatory, Cambridge, MA.), W. Forman (Smithsonian Astrophysical Observatory, Cambridge, MA.), I. M. Gioia (Smithsonian Astrophysical Observatory, Cambridge, MA.), J. A. Hale (Smithsonian Astrophysical Observatory, Cambridge, MA.), F. R. Harnden, Jr. (Smithsonian Astrophysical Observatory, Cambridge, MA.), C. Jones (Smithsonian Astrophysical Observatory, Cambridge, MA.), T. Karakashian (Smithsonian Astrophysical Observatory, Cambridge, MA.), T. Maccacaro (Smithsonian Astrophysical Observatory, Cambridge, MA.), J. D. McSweeney (Smithsonian Astrophysical Observatory, Cambridge, MA.), and F. A. Primini (Smithsonian Astrophysical Observatory, Cambridge, MA.) et al Apr. 1993 778 p The CD-ROM version of the catalog is available from NSSDCA, GSFC/NASA, Code 633, Greenbelt, MD 20771 (request @NSSDCA.GSFC.NASA.GOV)
(Contract NAS8-30751)
(NASA-TM-108401-Vol-5E; NAS 1.15:108401-Vol-5E) Avail: CASI HC A99/MF A10

The Einstein Observatory (HEAO-2, launched November 13, 1978) achieved radically improved sensitivity over previous x-ray missions through the use of focusing optics, which simultaneously afforded greatly reduced background and produced true images. During its 2.5-yr mission, the Einstein X-Ray Telescope was pointed toward some 5,000 celestial targets, most of which were detected, and discovered several thousand additional 'serendipitous' sources in the observed fields. This catalog contains contour diagrams and source data, obtained with the imaging proportional counter in the 0.16 to 3.5 keV energy band, and describes methods for recovering upper limits for any sky position within the observed images. The main catalog consists of six volumes (numbered 2 through 7) of right ascension ordered pages, each containing data for one observation. Along with the primary documentation describing how the catalog was constructed, volume 1 contains a complete source list, results for merged fields, a reference system to published papers, and data useful for calculating upper limits and fluxes. Author (revised)

N94-18615*# National Aeronautics and Space Administration. Marshall Space Flight Center, Huntsville, AL.
THE EINSTEIN OBSERVATORY CATALOG OF IPC X RAY SOURCES. VOLUME 6E: RIGHT ASCENSION RANGE 16h 00m TO 19h 59m
D. E. Harris (Smithsonian Astrophysical Observatory, Cambridge, MA.), W. Forman (Smithsonian Astrophysical Observatory, Cambridge, MA.), I. M. Gioia (Smithsonian Astrophysical Observatory, Cambridge, MA.), J. A. Hale (Smithsonian Astrophysical Observatory, Cambridge, MA.), F. R. Harnden, Jr. (Smithsonian Astrophysical Observatory, Cambridge, MA.), C. Jones (Smithsonian Astrophysical Observatory, Cambridge, MA.), T. Karakashian (Smithsonian Astrophysical Observatory, Cambridge, MA.), T. Maccacaro (Smithsonian Astrophysical Observatory, Cambridge, MA.), J. D. McSweeney (Smithsonian Astrophysical Observatory, Cambridge, MA.), and F. A. Primini (Smithsonian Astrophysical Observatory, Cambridge, MA.) et al Apr. 1993 834 p The CD-ROM version of the catalog is available from NSSDCA, GSFC/NASA, Code 633, Greenbelt, MD 20771 (request @NSSDCA.GSFC.NASA.GOV)
(Contract NAS8-30751)
(NASA-TM-108401-Vol-6E; NAS 1.15:108401-Vol-6E) Avail: CASI HC A99/MF A10

The Einstein Observatory (HEAO-2 launched November 13, 1978) achieved radically improved sensitivity over previous x-ray missions through the use of focusing optics, which simultaneously afforded greatly reduced background and produced true images. During its 2.5-yr mission, the Einstein X-Ray Telescope was pointed toward some 5,000 celestial targets, most of which were detected, and discovered several thousand additional 'serendipitous' sources in the observed fields. This catalog contains contour diagrams and source data, obtained with the imaging proportional counter in the 0.16 to 3.5 keV energy band, and describes methods for recovering upper limits for any sky position within the observed images. The main catalog consists of six volumes (numbered 2 through 7) of right ascension ordered pages, each containing data for one observation. Along with the primary documentation describing how the catalog was constructed, volume 1 contains a complete source list, results for merged fields, a reference system to published papers, and data useful for calculating upper limits and fluxes. Author (revised)

N94-18618*# National Aeronautics and Space Administration. Marshall Space Flight Center, Huntsville, AL.
THE EINSTEIN OBSERVATORY CATALOG OF IPC X RAY SOURCES. VOLUME 7E: RIGHT ASCENSION RANGE 20h 00m TO 23h 59m
D. E. Harris (Smithsonian Astrophysical Observatory, Cambridge, MA.), W. Forman (Smithsonian Astrophysical Observatory, Cambridge, MA.), I. M. Gioia (Smithsonian Astrophysical Observatory, Cambridge, MA.), J. A. Hale (Smithsonian Astrophysical Observatory, Cambridge, MA.), F. R. Harnden, Jr. (Smithsonian Astrophysical Observatory, Cambridge, MA.), C. Jones (Smithsonian Astrophysical Observatory, Cambridge, MA.), T. Karakashian (Smithsonian Astrophysical Observatory, Cambridge, MA.), T. Maccacaro (Smithsonian Astrophysical Observatory, Cambridge, MA.), J. D. McSweeney (Smithsonian Astrophysical Observatory, Cambridge, MA.), and F. A. Primini (Smithsonian Astrophysical Observatory, Cambridge, MA.) et al Apr. 1993 519 p The CD-ROM version of the catalog is available from NSSDCA,

GSFC/NASA, Code 633, Greenbelt, MD 20771 (request @NSSDCA.GSFC.NASA.GOV)
(Contract NAS8-30751)
(NASA-TM-108401-Vol-7E; NAS 1.15:108401-Vol-7E) Avail: CASI HC A22/MF A04

The Einstein Observatory (HEAO-2, launched November 13, 1978) achieved radically improved sensitivity over previous x-ray missions through the use of focusing optics which simultaneously afforded greatly reduced background and produced true images. During its 2.5-yr mission, the Einstein X-Ray Telescope was pointed toward some 5,000 celestial targets, most of which were detected, and discovered several thousand additional 'serendipitous' sources in the observed fields. This catalog contains contour diagrams and source data, obtained with the imaging proportional counter in the 0.16 to 3.5 keV energy band, and describes methods for recovering upper limits for any sky position within the observed images. The main catalog consists of six volumes (numbered 2 through 7) of right ascension ordered pages, each containing data for one observation. Along with the primary documentation describing how the catalog was constructed, volume 1 contains a complete source list, results for merged fields, a reference system to published papers, and data useful for calculating upper limits and fluxes. Author (revised)

N94-18619*# National Aeronautics and Space Administration. Marshall Space Flight Center, Huntsville, AL.
THE EINSTEIN OBSERVATORY CATALOG OF IPC X RAY SOURCES. VOLUME 1E: DOCUMENTATION
D. E. Harris (Smithsonian Astrophysical Observatory, Cambridge, MA.), W. Forman (Smithsonian Astrophysical Observatory, Cambridge, MA.), I. M. Gioia (Smithsonian Astrophysical Observatory, Cambridge, MA.), J. A. Hale (Smithsonian Astrophysical Observatory, Cambridge, MA.), F. R. Harnden, Jr. (Smithsonian Astrophysical Observatory, Cambridge, MA.), C. Jones (Smithsonian Astrophysical Observatory, Cambridge, MA.), T. Karakashian (Smithsonian Astrophysical Observatory, Cambridge, MA.), T. Maccacaro (Smithsonian Astrophysical Observatory, Cambridge, MA.), J. D. McSweeney (Smithsonian Astrophysical Observatory, Cambridge, MA.), and F. A. Primini (Smithsonian Astrophysical Observatory, Cambridge, MA.) et al Apr. 1993 517 p The CD-ROM version of the catalog is available from NSSDCA, GSFC/NASA, Code 633, Greenbelt, MD 20771 (request @NSSDCA.GSFC.NASA.GOV)
(Contract NAS8-30751)
(NASA-TM-108401-Vol-1E; NAS 1.15:108401-Vol-1E) Avail: CASI HC A22/MF A04

The Einstein Observatory (HEAO-2, launched November 13, 1978) achieved radically improved sensitivity over previous x-ray missions through the use of focusing optics, which simultaneously afforded greatly reduced background and produced true images. During its 2.5-yr mission, the Einstein X-Ray Telescope was pointed toward some 5,000 celestial targets, most of which were detected, and discovered several thousand additional 'serendipitous' sources in the observed fields. This catalog contains contour diagrams and source data, obtained with the imaging proportional counter in the 0.16 to 3.5 keV energy band, and describes methods for recovering upper limits for any sky position within the observed images. The main catalog consists of six volumes (numbered 2 through 7) of right ascension ordered pages, each containing data for one observation. Along with the primary documentation describing how the catalog was constructed, volume 1 contains a complete source list, results for merged fields, a reference system to published papers, and data useful for calculating upper limits and fluxes. Author (revised)

N94-18620*# National Aeronautics and Space Administration. Marshall Space Flight Center, Huntsville, AL.
THE EINSTEIN OBSERVATORY CATALOG OF IPC X RAY SOURCES. VOLUME 2E: RIGHT ASCENSION RANGE 00h 00m TO 03h 59m
D. E. Harris (Smithsonian Astrophysical Observatory, Cambridge, MA.), W. Forman (Smithsonian Astrophysical Observatory, Cambridge, MA.), I. M. Gioia (Smithsonian Astrophysical Observatory, Cambridge, MA.), J. A. Hale (Smithsonian Astrophysical Observatory, Cambridge, MA.), F. R. Harnden, Jr. (Smithsonian Astrophysical Observatory, Cambridge, MA.), C. Jones (Smithsonian Astrophysical Observatory, Cambridge, MA.), T. Karakashian (Smithsonian Astrophysical Observatory, Cambridge, MA.), T. Maccacaro (Smithsonian Astrophysical Observatory, Cambridge, MA.), J. D. McSweeney (Smithsonian Astrophysical Observatory, Cambridge, MA.), and F. A. Primini (Smithsonian Astrophysical Observatory, Cambridge, MA.) et al Apr. 1993 641 p The CD-ROM version of the catalog is available from NSSDCA, GSFC/NASA, Code 633, Greenbelt, MD 20771 (request @NSSDCA.GSFC.NASA.GOV)
(Contract NAS8-30751)
(NASA-TM-108401-Vol-2E; NAS 1.15:108401-Vol-2E) Avail: CASI HC A99/MF A06

The Einstein Observatory (HEAO-2, launched November 13, 1978) achieved radically improved sensitivity over previous x-ray missions through the use of focusing optics which simultaneously afforded greatly reduced background and produced true images. During its 2.5-yr mission, the Einstein X-Ray Telescope was pointed toward some 5,000 celestial targets, most of which were detected, and discovered several thousand additional 'serendipitous' sources in the observed fields. This catalog contains contour diagrams and source data, obtained with the imaging proportional counter in the 0.16 to 3.5 keV energy band, and describes methods for recovering upper limits for any sky position within the observed images. The main catalog consists of six volumes (numbered 2 through 7) of right ascension ordered pages, each containing data for one observation. Along with the primary documentation describing how the catalog was constructed, volume 1 contains a complete source list, results for merged fields, a reference system to published papers and data useful for calculating upper limits and fluxes. Author (revised)

N94-18621*# National Aeronautics and Space Administration. Marshall Space Flight Center, Huntsville, AL.
THE EINSTEIN OBSERVATORY CATALOG OF IPC X RAY SOURCES. VOLUME 3E: RIGHT ASCENSION RANGE 04h 00m TO 07h 59m
D. E. Harris (Smithsonian Astrophysical Observatory, Cambridge, MA.), W. Forman (Smithsonian Astrophysical Observatory, Cambridge, MA.), I. M. Gioia (Smithsonian Astrophysical Observatory, Cambridge, MA.), J. A. Hale (Smithsonian Astrophysical Observatory, Cambridge, MA.), F. R. Harnden, Jr. (Smithsonian Astrophysical Observatory, Cambridge, MA.), C. Jones (Smithsonian Astrophysical Observatory, Cambridge, MA.), T. Karakashian (Smithsonian Astrophysical Observatory, Cambridge, MA.), T. Maccacaro (Smithsonian Astrophysical Observatory, Cambridge, MA.), J. D. McSweeney (Smithsonian Astrophysical Observatory, Cambridge, MA.), and F. A. Primini (Smithsonian Astrophysical Observatory, Cambridge, MA.) et al Apr. 1993 719 p The CD-ROM version of the catalog is available from NSSDCA, GSFC/NASA, Code 633, Greenbelt, MD 20771 (request @NSSDCA.GSFC.NASA.GOV)
(Contract NAS8-30751)
(NASA-TM-108401-Vol-3E; NAS 1.15:108401-Vol-3E) Avail: CASI HC A99/MF A06

The Einstein Observatory (HEAO-2, launched November 13, 1978) achieved radically improved sensitivity over previous x-ray missions through the use of focusing optics which simultaneously afforded greatly reduced background and produced true images. During its 2.5-yr mission, the Einstein X-Ray Telescope was pointed toward some 5,000 celestial targets, most of which were detected, and discovered several thousand additional 'serendipitous' sources in the observed fields. This catalog contains contour diagrams and source data, obtained with the imaging proportional counter in the 0.16 to 3.5 keV energy band, and describes methods for recovering upper limits for any sky position within the observed images. The main catalog consists of six volumes (numbered 2 through 7) of right ascension ordered pages, each containing data for one observation. Along with the primary documentation describing how the catalog was constructed, volume 1 contains a complete source list, results for merged fields, a reference system to published papers and data useful for calculating upper limits and fluxes. Author (revised)

N94-18841*# State Univ. of New York, Stony Brook. Research Foundation.
WORKING GROUP FOR PLANETARY SYSTEM NOMENCLATURE
28 Sep. 1993 7 p
(Grant NsG-7553)
(NASA-CR-194406; NAS 1.26:194406) Avail: CASI HC A02/MF A01

Most of the activity of the Working Group and Task Group of the IAU during these three years has been centered on the nomenclature of Neptune's satellites and rings as revealed by the Voyager spacecraft. The emphasis is now shifting to Venus, in preparation for the detailed radar mapping of that planet begun by the Magellan spacecraft in August 1990.

Approval has been asked for nomenclature of the Earth's moon, Venus, Mars, and Triton features as well as 4 other Neptune satellites and three Neptune rings. Derived from text

N94-18857# Los Alamos National Lab., NM.
COMPUTATIONAL ASTROPHYSICS: PULSATING STARS
C. G. Davis 1993 10 p Presented at the 2nd International Conference on Computational Physics, Beijing, China, 13-17 Sep. 1993
(Contract W-7405-eng-36)
(DE93-018369; LA-UR-93-2541; CONF-9309176-2) Avail: CASI HC A02/MF A01

The field of computational astrophysics in pulsating star studies has grown considerably since the advent of the computer. Initially calculations were done on the IBM 704 with 32K of memory and now we use the CRAY YMP computers with considerably more memory. Our early studies were for models of pulsating stars using a 1D Lagrangian hydrodynamic code (SPEC) with radiation diffusion. The radiative transfer was treated in the equilibrium diffusion approximation and the hydrodynamics was done utilizing the approximation of artificial viscosity. The early calculations took many hours of 704 CPU time. Early in 1965 we decided to improve on the usual treatment of the radiative transfer used in our codes by utilizing the method of moments, the so-called variable Eddington approximation. In this approximation the material energy field is uncoupled from the radiation energy field and the angular dependence is introduced through the Eddington factor. A multigroup frequency dependent method may also be applied. The Eddington factor is determined by snapshots of the stars structure utilizing a y-line approximation. The full radiative transfer approximation appears necessary in order to understand the light curves for W Virginia stars and may be important for the light curves of RR Lyrae stars. A detailed radiative transfer method does not appear to be necessary for the understanding of Cepheid light curves. A recent improvement to our models for pulsating stars is in the use of an adaptive mesh scheme to resolve the sharp features in the nonlinear hydrodynamic structure. From these improved structures, better analysis of the radius, velocity, and light curves could be obtained. DOE

N94-18877 Air Force Inst. of Tech., Wright-Patterson AFB, OH.
SEARCH FOR LUNAR WATER ICE IN COMETARY IMPACT CRATERS M.S. Thesis
Steve S. Brandt Aug. 1993 64 p Limited Reproducibility: More than 20% of this document may be affected by microfiche quality
(AD-A270130; AFIT/CI/CIA-93-138) Avail: CASI HC A04

The search for water on the moon began with the introduction of the idea of polar cold traps as a region where large deposits of water could be stored. James Arnold (1979) presented this hypothesis after reviewing many methods by which water was delivered to the moon. The principle method is cometary impacts. Carl Sagan and Christopher Chyba (1990) further stated that enough water was delivered to the earth by comets to account for the volume of the terrestrial ocean. We investigate the possibility that large amounts of water are deposited in the floors of cometary impact craters. The impact of a 1-2 km comet brings over 10(15) g of water to the lunar surface. If 1% of the mass survives the impact to be trapped in the crater and 1% of that is retained over the 3-4 billion years required for it to be present today, there will still be a 10(exp 10) g of H2O per impact. With the impact ofa few hundred comets, up to 10(exp 12) g of H2O is trapped in lunar craters. DTIC

N94-19077# Lawrence Livermore National Lab., CA.
INSTITUTE OF GEOPHYSICS AND PLANETARY PHYSICS, 1992
F. J. Ryerson, ed. and C. M. Budwine, ed. 14 Jun. 1993 117 p
(Contract W-7405-eng-48)
(DE93-019209; UCRL-53809-92) Avail: CASI HC A06/MF A02

This report contains brief discussions on topics in the following areas: high-pressure sciences; astrophysics; and geosciences. DOE

N94-19093*# Princeton Univ. Observatory, NJ.
THE UNIVERSE AT MODERATE REDSHIFT Final Report, 1 Mar. 1988 - 28 Feb. 1991
Jeremiah P. Ostriker 1992 10 p
(Grant NAGw-765)
(NASA-CR-193771; NAS 1.26:193771) Avail: CASI HC A02/MF A01

The Final Report on the universe at moderate redshift covering the period from 1 Mar. 1988 to 28 Feb. 1991 is presented. Areas of research included: galaxy formation and large-scale structure; intergalactic medium and background radiation fields; quasar statistics and evolution; and gravitational lenses. CASI

N94-19218*# Illinois Univ., Urbana-Champaign. Dept. of Physics.
IRAS HIGH RESOLUTION STUDIES AND MODELING OF CLOSELY INTERACTING GALAXIES. GALAXY COLLISIONS: INFRARED OBSERVATIONS AND ANALYSIS OF NUMERICAL MODELS. UV SPECTROSCOPY OF MASSIVE YOUNG STELLAR POPULATIONS IN INTERACTING GALAXIES Final Technical Report, 15 Aug. 1989 - 14 Aug. 1991
Susan A. Lamb 30 Sep. 1993 10 p
(Grant NAG5-1241)
(NASA-CR-194483; NAS 1.26:194483) Avail: CASI HC A02/MF A01

The Final Technical Report covering the period from 15 Aug. 1989 to 14 Aug. 1991 is presented. Areas of research included Infrared Astronomy Satellite (IRAS) high resolution studies and modeling of closely interacting galaxies; galaxy collisions: infrared observations and analysis of numerical models; and UV spectroscopy of massive young stellar populations in interacting galaxies. Both observational studies and theoretical modelling of interacting galaxies are covered. As a consequence the report is divided into two parts, one on each aspect of the overall project. CASI

N94-19284# Lawrence Livermore National Lab., CA.
WEAK NEUTRAL CURRENTS AND COLLAPSE INITIATED SUPERNOVA
J. R. Wilson 19 Mar. 1993 9 p Presented at the International Symposium on 30 Years of Neutral Currents, Los Angeles, CA, 3-5 Feb. 1993
(Contract W-7405-eng-48)
(DE93-018652; UCRL-JC-113747; CONF-930293-4) Avail: CASI HC A02/MF A01

Since 1974, the neutrino processes mediated by neutral currents have been a part of supernova (SN) modeling calculations. In this report, only present day SN calculations will be discussed. First, I will give a brief description of the SN computer model and an outline of the explosion process as depicted by that model. Then, I will discuss the role weak neutral current (WNC) processes play in this explosion process. Finally, I will discuss inelastic scattering of tau neutrinos by heavy elements in WNC processes or Earth as a mechanism for measuring the mass of tau neutrino. DOE

N94-19339# Sandia National Labs., Albuquerque, NM.
DYNAMICAL BEHAVIOR OF OCTAHEDRITE FROM THE HENBURY METEORITE
M. D. Furnish, G. T. Gray, III (Los Alamos National Lab., NM.), and J. L. Remo (Quantametrics, Inc., Saint James, NY.) 1993 5 p Presented at the 14th International Conference of the International Association for the Advancement of High Pressure Science and Technology, Colorado Springs, CO, 27 Jun. - 2 Jul. 1993
(Contract DE-AC04-76DP-00789)
(DE93-018834; SAND-93-0457C; CONF-930676-26) Avail: CASI HC A01/MF A01

A suite of dynamic property measurements and characterization studies on an iron-nickel single crystal from the Henbury octahedrite containing Widmanstaetten intergrowths of kamacite and taenite (initial density 7.810) has been performed. These measurements include six impact tests (wave profile compression/release) over the stress range 2-20 GPa, metallography, quasi-static and Hopkinson bar mechanical testing, and ultrasonic mapping and sound velocity measurements. A cryogenic impact test was included to evaluate effects of a brittle/ductile transition which has been reported at 200 K. Temperature sensitivity of the dynamic behavior was measured at high and low strain rates. The impact test results show loading strength (HEL), Hugoniot, and alpha yields epsilon transition signatures to be similar to those for Armco iron and do not show evidence for a ductile-brittle transition at these extremely high strain rates. Metallographic analyses, quasi-static, and Hopkinson bar testing suggest that the material is in a work-hardened state and that kamacite properties dominate the bulk octahedrite properties. DOE

N94-19425*# Colorado Univ., Boulder. Center for Astrophysics and Space Astronomy.
SPECTROPHOTOMETRY OF EMISSION-LINE STARS IN THE MAGELLANIC CLOUDS Final Report
Bruce Bohannan 10 Sep. 1990 4 p
(Grant NAG5-833)
(NASA-CR-194082; NAS 1.26:194082) Avail: CASI HC A01/MF A01

The strong emission lines in the most luminous stars in the Magellanic Clouds indicate that these stars have such strong stellar winds that their photospheres are so masked that optical absorption lines do not provide an accurate measure of photospheric conditions. In the research funded by this grant, temperatures and gravities of emission-line stars both in the Large (LMC) and Small Magellanic Clouds (SMC) have been measured by fitting of continuum ultraviolet-optical fluxes observed with IUE with theoretical model atmospheres. Preliminary results from this work formed a major part of an invited review 'The Distribution of Types of Luminous Blue Variables'. Interpretation of the IUE observations obtained in this grant and archive data were also included in a talk at the First Boulder-Munich Hot Stars Workshop. Final results of these studies are now being completed for publication in refereed journals. Derived from text

N94-19519# Max-Planck-Inst. fuer Physik und Astrophysik, Garching (Germany). Inst. fuer Extraterrestrische Physik.
STRUCTURATION PROCESSES IN PROTOPLANETARY ACCRETION DISKS Ph.D. Thesis - Tuebingen Univ. [STRUKTURIERUNGSPROZESSE IN PROTOPLANETAREN AKKRETIONSSCHEIBEN]
Michael F. Sterzik Feb. 1993 132 p In GERMAN Sponsored by DFG
(MPE-243; ETN-93-95098) Copyright Avail: CASI HC A07/MF A02

The spatial and temporal development of protoplanetary accretion disks is investigated. Flat, homogeneous, mixed gas/dust disks with interstellar elementary frequencies, whose motion is estimated by the gravitation field of the central object, are considered as a starting point. The existence of the turbulent viscosity was assumed with the alpha parameterization for determining spectral energy distribution of radiation emitted at disk surface. Local vertical disk structure was estimated with the approximation of gray atmospheres and allowed the coupled system to be self consistently treated. One dimensional, radial time development calculations show that the radial surface temperature variation due to dust opacity modification is only transient. If preferential particle growth is only considered in main condensation zones, radial development calculations show a strong increase of column thickness in radially limited areas. Two dimensional development calculations were carried out in order to estimate radial and axial structures of protoplanetary accretion disks; a numerical process was introduced in a particle simulation for the treatment of shear viscosity. In a local simulation, a cutting of a viscous Kepler disk was considered and the eigen gravitation was taken into account, so that the ring instability predicted with a linear theory is found. ESA

N94-19794*# Max-Planck-Inst. fuer Physik und Astrophysik, Garching (Germany). Inst. fuer Extraterrestrische Physik.
STELLAR CORONAE AT THE END OF THE MAIN SEQUENCE: A ROSAT SURVEY OF THE LATE M DWARFS
T. A. Fleming, M. S. Giampapa (Joint Inst. for Lab. Astrophysics, Boulder, CO.), J. H. M. M. Schmitt (National Solar Observatory, Tucson, AZ.), and J. A. Bookbinder (Smithsonian Astrophysical Observatory, Cambridge, MA.) Jan. 1993 20 p Submitted for publication
(Grants NAGw-1480; NAGw-112)
(NASA-CR-194700; NAS 1.26:194700; MPE-Preprint-247; ETN-93-94924) Copyright Avail: CASI HC A03/MF A01

X-ray data, both detections and upper limits, from the Rosat all sky survey for most known M dwarfs later than type M5 are presented. Selected Rosat pointed observations of some of these stars are included. These data are compared to similar data for early M dwarfs in an attempt to probe the nature of the magnetic dynamo and coronal heating mechanism for the very late M dwarfs, which are presumably totally convective. The results indicate that late M dwarfs can have coronae which are just as active as those for the early M dwarfs and that coronal heating efficiency for 'saturated' stars does not drop at spectral type M6. ESA

91 LUNAR AND PLANETARY EXPLORATION

Includes planetology; and manned and unmanned flights.
For spacecraft design or space stations see *18 Spacecraft Design, Testing and Performance.*

N94-17842*# Massachusetts Inst. of Tech., Cambridge. Center for Space Research.
DETAILED ANALYSIS OF LOW ENERGY PLASMA DATA UNDER THE VOYAGER URANUS DATA ANALYSIS PROGRAM Final Report, 1 Oct. 1987 - 30 Sep. 1991
Ralph L. McNutt, Jr. (Visidyne, Inc., Burlington, MA.), John W. Belcher, Frances Bagenal, and John D. Richardson 1992 8 p
(Grant NAGw-1209)
(NASA-CR-193668; NAS 1.26:193668) Avail: CASI HC A02/MF A01

Research effort included the PLS data analysis program where modifications to the data fitting procedure and elimination of possible noise and electron contamination were made. The analysis code corrections were used in checking the Neptune data gathered during the Voyager 2 encounter and for analyzing selected plasma spectra from the warm Io torus. A major task accomplished was the summary of Uranus-related research in the U.S. National Report to the International Union of Geodesy and Geophysics for the 1987 - 1990 quadrennium. A limited amount of work was accomplished on assessing the Pedersen conductivity of the ionosphere and comparing it with inferred values from shielding by the Uranian ring current. Under this grant there has been a great deal of effort expended on identifying and classifying plasma waves and oscillations in the magnetosheath and solar wind downstream from Uranus. Large amplitude oscillations in plasma parameters are found in the magnetosheath, with density changes of up to a factor of ten occurring on times scales of minutes. New algorithms developed for analyzing the inbound bow shock crossing of Neptune will probably be applied to a more detailed analysis of the Uranus shock in the near future. Derived from text

N94-18957* National Aeronautics and Space Administration, Washington, DC.
VOYAGER'S LAST ENCOUNTER (Videotape)
Nov. 1989 Videotape: 3 min. 16 sec. playing time, in color, with sound
(NASA-TM-109361; NONP-VT-94-198208) Avail: CASI VHS A01/BETA A22

This video describes Voyager 2's encounter with Neptune. Computer animation and actual data convey Voyager's discoveries such as turbulent storms and dark spots in Neptune's atmosphere, six new moons, Neptune's three rings, and the presence of frozen methane on Triton, as researchers at NASA's Jet Propulsion Laboratory describe Voyager's achievements. CASI

N94-18958* National Aeronautics and Space Administration, Washington, DC.
MAGELLAN, GALILEO, AND ULYSSES (Videotape)
Jan. 1991 Videotape: 4 min. 4 sec. playing time, in color, with sound
(NASA-TM-109362; NONP-VT-94-198209) Avail: CASI VHS A01/BETA A22

A combination of sophisticated computer animation and shuttle footage describe the missions of Ulysses, Galileo, and Magellan satellites to the solar system. Ulysses, launched in October 1990 by the European Space Agency, will study the sun. Galileo, launched in October 1989, will probe the Jovian system by releasing a probe that will descend into Jupiter's atmosphere and by using 12 instruments which will study Jupiter's 16 moons, its atmosphere, and its radiation and magnetic fields. Magellan, released from Space Shuttle Atlantis in May 1989, uses a synthetic aperture radar to probe through Venus' dense atmosphere to map its planetary surface. A computer animation simulates flying over the surface of Venus. CASI

N94-18959* National Aeronautics and Space Administration, Washington, DC.
FUTURE ENERGY SOURCE (Videotape)
Oct. 1990 Videotape: 3 min. 28 sec. playing time, in color, with sound
(NASA-TM-109363; NONP-VT-94-198210) Avail: CASI VHS A01/BETA A22

This video describes the efforts of the Center for the Commercial

Development of Space in Wisconsin to develop a strategy for mining Helium-3, an efficient, environmentally safe alternative to fossil fuels that exists on the moon. Animated sequences depict the equipment that could mine the lunar surface, boil away Helium-3 to be transported back to earth, and return the soil to the moon without destroying the lunar surface. CASI

N94-18966* National Aeronautics and Space Administration. Lewis Research Center, Cleveland, OH.
SPACEWORK 17: O'LEARY'S MARS (Videotape)
May 1988 Videotape: 28 min. 40 sec. playing time, in color, with sound
(NASA-TM-109374; NONP-VT-94-198221) Avail: CASI VHS A01/BETA A22

Brian O'Leary gives his ideas on reaching and exploring Mars. CASI

N94-19094*# Iowa Univ., Iowa City. Dept. of Physics and Astronomy.
PLANETARY PLASMA WAVES
Donald A. Gurnett Jan. 1993 46 p Submitted for publication
(Contract JPL-959193)
(NASA-CR-194295; U-of-Iowa-93-7; NAS 1.26:194295) Avail: CASI HC A03/MF A01

The primary types of plasma waves observed in the vicinity of the planets Venus, Mars, Earth, Jupiter, Saturn, Uranus, and Neptune are described. The observations are organized according to the various types of plasma waves observed, ordered according to decreasing distance from the planet, starting from the sunward side of the planet, and ending in the region near the closest approach. The plasma waves observed include: electron plasma oscillations and ion acoustic waves; trapped continuum radiation; electron cyclotron and upper hybrid waves; whistler-mode emissions; electrostatic ion cyclotron waves; and electromagnetic ion cyclotron waves. Derived from text

N94-19418*# Arizona Univ., Tucson. Dept. of Planetary Sciences.
VENUS LOWER THERMOSPHERE STUDIES Final Technical Report, 1 Oct. 1990 - 31 Dec. 1992
Stephen W. Bougher 31 Dec. 1992 5 p
(Grant NAG2-679)
(NASA-CR-193546; NAS 1.26:193546) Avail: CASI HC A01/MF A01

Studies undertaken in this project have sought to understand lower thermospheric structure and dynamics (less than or equal to 145 km), particularly the processes responsible. This is a region just below the reach of in-situ instruments onboard PVO (Pioneer Venus Orbiter) during the first few diurnal cycles. PVO remote airglow observations (nitric oxide, O2, visible, O 1304A) have been coupled with ground-based observations (CO densities, winds, temperatures, O2 IR nightglow) to address the behavior of lower thermospheric winds and chemistry over 95 to 150 km. This interpretation of PVO and related data is accomplished by using the NCAR Venus thermospheric general circulation model (VTGCM) (Bougher et al., 1988; 1990). This model has been modified over the last two years to improve its ability to calculate O, CO, and O2 densities, temperatures, nightglow, and subsolar-to-antisolar and zonal winds over 95 to 150 km (Bougher and Borucki, 1992). Our VTGCM studies show that: (1) O2 visible and IR nightglow distributions can be used to trace lower thermosphere / upper mesosphere winds over 100-130 km. Typically, weak zonal winds (less than or equal to 25 m/sec) and nightglow maximum patches near 0100 LT prevail. Occasionally, strong zonal winds (30-60 m/sec) and airglow patches peaking near 0300 LT characterize the Venus lower thermosphere. (2) It is clear that the dynamics of the Venus 90-130 km region is highly variable on time scales as short as an hour. This is most likely due to the time variable nature of upward propagating gravity waves, which grow in amplitude and eventually break. The resulting turbulence gives rise to local time variable eddy diffusion and momentum drag, both of which strongly impact global density and nightglow distributions. (3) The oxygen chemistry (O, O2, etc.) over 90-120 km is strongly dependent on HO(x) and CLO(x) tracer species that must be properly included in any coupled chemical dynamical model. (4) The density profiles of light species (O, CO, N, He) are strongly affected by large-scale transport by the winds. Strong eddy diffusion is not a suitable model parameterization for approximating these light species, especially for extrapolation into the region below 140 km where PVO in-situ data is lacking. Instead, the fully coupled chemical dynamical VTGCM model should be used to improve estimates of densities within the VTS3 empirical model (Hedin et al., 1983) below 140 km. Derived from text

92 SOLAR PHYSICS

Includes solar activity, solar flares, solar radiation and sunspots. For related information see *93 Space Radiation.*

N94-18222 Johns Hopkins Univ., Laurel, MD. Applied Physics Lab.
ORIGINS OF SOLAR ACTIVITY. FIRST YEAR REPORT, AASERT GRANT Annual Report, Jun. 1992 - Jun. 1993
David M. Rust 1 Aug. 1993 3 p Limited Reproducibility: More than 20% of this document may be affected by microfiche quality
(Contract F49620-92-C-0284)
(AD-A268848; AFOSR-93-0636TR) Avail: CASI HC A01

This report describes the first year of training and progress of Mr. J.J. Blanchette toward a Ph.D. in Physics, with specialization in Solar Physics. Mr. Blanchette has met all academic requirements in order to proceed with his thesis research. He is a full-time graduate research fellow, and he has gained a good background in solar activity research. He has taken on the task of implementing the focal-plane functions of the Target Selector Telescope of the Flare Genesis Experiment, a balloon-borne telescope for solar activity research. During the report period, Mr. Blanchette presented a description of his work on solar active region NOAA 7260 at the 24th meeting of the Solar Physics Division of the AAS. DTIC

N94-18705# Louisiana State Univ., Baton Rouge. Dept. of Physics and Astronomy.
SOLAR FLARES AND MAGNETOSPHERIC PARTICLES: INVESTIGATIONS BASED UPON THE ONR-602 AND ONR-604 EXPERIMENTS Quarterly Report No. 3
John P. Wefel and T. G. Guzik 3 Sep. 1993 18 p
(Contract N00014-90-J-1466)
(AD-A269495) Avail: CASI HC A03/MF A01

This performance report covers work accomplished under ONR Grant N00014-90-J-1466 related to the radiation environment in near-Earth space. The goal of the research is to measure and describe, quantitatively, the Geospace radiation environment in which men and spacecraft must survive and function. The tools for this investigation are the data returned by the ONR-602 and ONR-604 experiments, both flown under the auspices of ONR and the Air Force Space Test Program, augmented by correlative databases of both space-based and ground-based data. The investigation involves data analysis, modeling and applications to a variety of space equipment and environments. This report builds upon the detailed Technical Report (Fall, 1992) and the previous performance reports. For the current period, the principal effort was in the analysis of the solar energetic particle events that occurred during the CRRES mission, focusing upon the helium component. In addition, we have looked at the galactic quiet-time helium to help determine the modulation level during the CRRES Mission. DTIC

N94-19260# California Univ., Berkeley. Lawrence Berkeley Lab.
THE SUDBURY NEUTRINO OBSERVATORY AND THE SOLAR NEUTRINO PROBLEM
K. T. Lesko Jan. 1993 8 p Presented at the 16th Nuclear Physics Symposium, Oaxtepec, Mexico, 5-8 Jan. 1993
(Contract DE-AC03-76SF-00098)
(DE93-018528; LBL-34241; CONF-930169-3) Avail: CASI HC A02/MF A01

This report discusses experiments at the Sudbury Neutrino Observatory in the area of solar neutrino detection. DOE

N94-19427*# Delaware Univ., Newark. Bartol Research Inst.
RADIAL EVOLUTION OF THE SOLAR WIND TURBULENCE WITH APPLICATION TO CHARGED PARTICLE TRANSPORT Final Technical Report
Charles W. Smith 29 Jul. 1991 6 p
(Grant NAG2-553)
(NASA-CR-194081; NAS 1.26:194081) Avail: CASI HC A02/MF A01

The proposed research efforts funded by the Pioneer-Venus Guest Investigator Grant to the Bartol Research Institute center on a study of the radial and temporal variation of the large-scale interplanetary magnetic field (IMF) and include a study of the radial variation of the observed north-south asymmetry of the IMF spiral based on the previous results of Bieber (1988). The preliminary results of Bieber demonstrated that at Earth orbit there exists an asymmetry between the yearly average winding angles of toward and away sector fields that can be as large as 10 degrees. The Bieber (1988) analysis employed the NSSDC omnitape data set of 1 AU measurements. When the observed asymmetry is related to the state of the solar magnetic dipole, it is possible to conclude that the IMF north of the heliospheric current sheet is more tightly wound than the IMF spiral south of the current sheet. The average difference in the winding angle as measured over a 21 year period spanning 1965 through 1985 was 3.1 degrees + 1.1 degrees. The Bieber analysis was able to rule-out several possible sources for the observed behavior including a possible asymmetry in the solar wind speed or the observed hemispherical dependence of solar rotation. The object of this research was to extend this previous result to include observations within the inner and outer heliosphere, to examine the radial dependence of the reported asymmetry, and to better resolve the possible source of the observations. The Pioneer-Venus Orbiter has proven to be the perfect monitor for the inner heliospheric observations. It has provided 9 years of continuous observations at a fixed heliocentric distance (except for those periods when the spacecraft was within the region of space where the magnetic field is influenced by the presence of the planet). Comparisons between the 1 AU observations recorded on the NSSDC omnitape and the 0.7 AU observations of the Pioneer-Venus Orbiter have greatly improved our understanding of the IMF winding angle asymmetry. Further comparison with outer heliospheric measurements have proven interesting, although less conclusive. Derived from text

93 SPACE RADIATION

Includes cosmic radiation; and inner and outer earth's radiation belts.

For biological effects of radiation see *52 Aerospace Medicine*. For theory see *73 Nuclear and High-Energy Physics*.

N94-17818# Tufts Univ., Medford, MA. Dept. of Physics and Astronomy
INVESTIGATION OF THE RELATIVE ABUNDANCE OF HEAVY VERSUS LIGHT NUCLEI IN PRIMARY COSMIC RAYS USING UNDERGROUND MUON BUNDLES Ph.D. Thesis
N. Sundaralingam Jun. 1993 152 p
(Contract DE-FG02-92ER-40702)
(DE93-017601; DOE/ER-40702/3) Avail: CASI HC A08/MF A02

We study multiple muon events (muon bundles) recorded underground at a depth of 2090 mwe. To penetrate to this depth, the muons must have energies above 0.8 TeV at the Earth's surface; the primary cosmic ray nuclei which give rise to the observed muon bundles have energies at incidence upon the upper atmosphere of 10 to 10(exp 5)TeV. The events are detected using the Soudan 2 experiment's fine grained tracking calorimeter which is surrounded by a 14 m x 10 m x 31 m proportional tube array (the 'active shield'). Muon bundles which have at least one muon traversing the calorimeter, are reconstructed using tracks in the calorimeter together with hit patterns in the proportional tube shield. All ionization pulses are required to be coincident within 3 microseconds. A goal of this study is to investigate the relative nuclear abundances in the primary cosmic radiation around the "knee" region (10(exp 3) - 10(exp 4) TeV) of the incident energy spectrum. Four models for the nuclear composition of cosmic rays are considered: The Linsley model, the Constant Mass Composition model (CMC), the Maryland model, and the Proton-poor model. A Monte Carlo which incorporates one model at a time is used to simulate events which are then reconstructed using the same computer algorithms that are used for the data. Identical cuts and selections are applied to the data and to the simulated events. DOE

N94-18219# National Lab. for High Energy Physics, Tsukuba (Japan).
PROCEEDINGS OF THE 3RD WORKSHOP ON BALLOON-BORNE EXPERIMENTS WITH SUPERCONDUCTING MAGNET SPECTROMETERS
Akira Yamamoto, ed. Apr. 1992 184 p Workshop held in Tsukuba, Japan, 24-25 Feb. 1992
(DE93-788362; KEK-Proc-92-2; CONF-9202174) Avail: CASI HC A09/MF A02 (US Sales Only)

The Third Work Shop on Balloon Borne Experiment with a Superconducting Magnet Spectrometer was held at National Laboratory for High Energy Physics (KEK), Tsukuba, Japan on February 24 - 25, 1992. The main effort for this workshop was focused on the progress of the BESS (Balloon Borne Experiment with a Superconducting Spectrometer) experiment and on the scope for scientific investigation with the BESS detector. The progress was reviewed and further investigation was discussed for the BESS further scientific collaboration among Univ. of Tokyo, Kobe University, KEK, ISAS and NMSU. DOE

N94-18676# Lockheed Missiles and Space Co., Palo Alto, CA. Space Sciences Lab.
THE LET SPECTRUM AND ITS UNCERTAINTY DURING THE CRRES MISSION
D. L. Chenette, T. G. Guzik, and J. P. Wefel 7 May 1993 18 p
(Contract F19628-90-C-0101)
(AD-A269977; AD-E201607; PL-TR-93-2111; SR-2) Avail: CASI HC A03/MF A01

We present LET spectra calculated for the 1990-1991 CRRES mission using the galactic cosmic ray (GCR) and solar energetic particle (SEP) models which were developed for the CRRES/SPACERAD program. We discuss the dependence of the spectra on uncertainties in the galactic cosmic ray and solar energetic particle models and LET calculation methods. Finally, we illustrate the application and significance of these spectra by using them to predict single event upset rates in a sample integrated circuit memory device, a 256 x 4-bit bipolar static RAM device. DTIC

N94-18762# International Centre for Theoretical Physics, Trieste (Italy).
WIDGET: A DATA ACQUISITION SYSTEM FOR A BALLOON BORNE SI PARTICLE CALORIMETER
A. Colavita, F. Aversa, S. Venkataraman, P. Picozza, F. Fratnik (Italian National Inst. of Nuclear Research, Tor Vergata.), and P. Battaiotto (La Plata Univ., Argentina.) Apr. 1993 8 p
(DE93-624668; IC-93/64) Avail: CASI HC A02/MF A01 (US Sales Only)

We describe Widget, a complete data acquisition system (DAS) designed for a balloon-borne calorimeter using silicon strip detectors. The design includes a general purpose CPU as well as five to twenty Digital Signal Processors in order to control the acquisition of the data. This local intelligence also allows the instrument to re-calibrate itself, to perform calculations on the data, and to control the functionality of the instrumentation. The DSP's filter the data to avoid overflowing the radio link to ground. In principle, the system could control the instruments, without direct intervention from the ground, on flights with durations of several days. DOE

N94-18836*# Washington Univ., Seattle. Dept. of Astronomy.
RELATED INVESTIGATIONS ON THE PHYSICS OF HIGH ENERGY EMISSION FROM ACTIVE GALACTIC NUCLEI Final Report, 1 Jul. 1986 - 30 Jun. 1991
Bruce Margon 30 Jun. 1991 4 p
(Grant NAG8-590)
(NASA-CR-193615; NAS 1.26:193615) Avail: CASI HC A01/MF A01

The Final Technical Report on a number of related investigations on the physics of high energy emission from active galactic nuclei, such as Seyfert galaxies and quasi-stellar objects is presented. The chief conclusions of the work are briefly described, and citations to the papers supported by this grant and published in the refereed scientific literature are provided. Areas of research included: 'warm' galaxies observed in x rays; x ray/infrared correlations in galaxies; the contribution of active galaxies to the cosmic x ray background radiation; and an unusual x ray emitting starburst galaxy. Derived from text

N94-19437*# Chicago Univ., IL. Dept. of Geophysical Sciences.
SCIENTIFIC STUDIES IN ASSOCIATION WITH THE SHUTTLE SOLAR BACKSCATTER ULTRAVIOLET (SSBUV) PROJECT Semiannual Progress Report, 1 Jan. - 30 Jun. 1993
John E. Frederick 30 Jun. 1993 52 p
(Grant NAG5-873)
(NASA-CR-193404; NAS 1.26:193404) Avail: CASI HC A04/MF A01

During the past reporting period efforts focused on performing detailed comparisons between measurements made by the SBUV/2 V instruments carried on NOAA-9 and NOAA-11 and the first three flights of the Shuttle Solar Backscatter Ultraviolet (SSBUV) project. The quantities to be compared are the measurables, being the ratio of emergent radiance (I) in the vertical direction to the incoming solar irradiance (F). The backscatter albedo, A(w,j), was defined by: A(w,j) = I(w,j)/F(w,j) where w = 1,2,..., 12 refers to wavelength, and j indicates the instrument and flight on which the data were obtained. The comparisons to be made are NOAA-9 to SSBUV-1, NOAA-11 to SSBUV-2, and NOAA-11 to SSBUV-3. For the comparisons the N-values contained in the data files supplied by GSFC were converted to albedos via: A(w,j) = 10(exp N(w,j)/100). The comparisons described were designed to characterize the differences between the NOAA and SSBUV data sets. Author (revised)

N94-19504# Kernforschungszentrum G.m.b.H., Karlsruhe (Germany). Inst. fuer Kernphysik.

ENERGY LOSS MEASUREMENT OF COSMIC RAY MUONS [MESSUNG DES ENERGIEVERLUSTES VON MYONEN DER KOSMISCHEN STRAHLUNG]

Joseph Unger Feb. 1993 78 p In GERMAN
(KfK-5158; ETN-93-95080) Avail: CASI HC A05/MF A01

Measurements of energy losses of high energy cosmic ray muons in an ionization chamber are presented. The chamber consists of 16 single gap layers, and the liquid tetra methyl silane (TMS) was used as active medium. The absolute energy loss and the relativistic rise were measured and compared with theoretical calculations. The importance of the measurements within the framework of the cosmic ray experiment KASCADE (German acronym for Karlsruhe Shower Core and Array Detector) are discussed, especially with respect to energy calibration of hadrons and high energy muons above 1 TeV. ESA

N94-19505# Kernforschungszentrum G.m.b.H., Karlsruhe (Germany). Inst. fuer Kernphysik.

MEASUREMENT OF THE ENERGY OF HORIZONTAL COSMIC RAY MUONS Thesis - Karlsruhe Univ. [MESSUNG DER ENERGIE VON HORIZONTALEN MYONEN DER KOSMISCHEN STRAHLUNG]

Michael Gettert Mar. 1993 102 p In GERMAN
(KfK-5163; ETN-93-95081) Copyright Avail: CASI HC A06/MF A02

An experiment in which the energy of cosmic ray muons is determined by measuring the electron positron pairs that they radiate off when passing through matter is described. The detector is a stack of lead converters interspersed with ionization chambers for particle detection. The chambers use as active medium the liquid tetra methyl silane (TMS). The radiated quanta initiate electromagnetic cascades in the lead and are recognized due to the characteristic shower development. The energy spectrum of horizontal muons is presented and from this the primary cosmic ray spectrum is deduced. ESA

N94-19506# Kernforschungszentrum G.m.b.H., Karlsruhe (Germany). Inst. fuer Kernphysik.

MEASUREMENTS OF COSMIC RAY MUONS WITH MULTI-WIRE PROPORTIONAL CHAMBERS WITH A PROTOTYPE SETUP FOR KASCADE [MESSUNGEN DER MYONEN DER HOEHENSTRAHLUNG MIT VIELDRAHTPROPORTIONALKAMMERN AN EINEM PROTOTYPAUFBAU FUER KASCADE]

Hermann-Josef Mathes Mar. 1993 77 p In GERMAN
(KfK-5173; ETN-93-95082) Copyright Avail: CASI HC A05/MF A01

The cosmic ray experiment KASCADE (German acronym for Karlsruhe Shower Core and Array Detector) designed for measuring simultaneously the electromagnetic, muonic, and hadronic components of extensive air showers to determine the primary cosmic ray mass composition in the energy range 300 Tev to 100 Btu is described. Beneath the central hadron calorimeter of this experiment, measurements of muons with an energy threshold of 2 GeV are planned. Four large position sensitive multi-wire proportional chambers were brought into operation after the required supply units were installed. This test setup was extended with a trigger system for cosmic ray muons. The trigger allows muon detection efficiencies and the spatial resolution of the chambers to be measured. To enhance the content of multiple track events in the data a trigger system for air showers was required. A small detector array was installed with the possibility to determine roughly the arrival direction of the shower. For that configuration of chambers an algorithm for track reconstruction was developed. It led to satisfying results for single and double track events. It is demonstrated that the determination of hits with only one chamber is influenced by the ambiguities resulting from the chamber layout. In addition this effect is shown to be enhanced by electronic noise and electromagnetic background. An extension with a time measuring system of an accuracy better than 2 ns allowed the arrival times of the muons to be measured for some events. The resulting arrival time distribution could be qualitatively understood. ESA

N94-19714 Max-Planck-Inst. fuer Physik und Astrophysik, Garching (Germany). Inst. fuer Extraterrestrische Physik.

PARTICLE INDUCED BACKGROUND BY ROENTGEN SATELLITES Thesis - Tech. Univ. Munich [TEILCHENINDUZIERTER HINTERGRUND BEI ROENTGENSATELLITEN]

Rudolf Danner 20 Jan. 1993 90 p In GERMAN Limited Reproducibility: More than 20% of this document may be affected by microfiche quality
(MPE-242; ETN-93-95097) Copyright Avail: CASI HC A05

Detailed results concerning a possible particle induced background in highly eccentric orbital trajectories for future X-ray satellite missions using charge coupled device detectors are presented. The different components were characterized and an order of magnitude was given. Several methods were proposed for the reduction of isolated component effects. Existing numerical models of the radiation belt for electrons and protons were examined and assessed. Background events, which are caused by minimal ionizing particles, could be recognized by appropriate discrimination methods, such as neighbor anticoincidence, and were differentiated from X-ray events. Electrons scattered by the mirrors on the detectors are ascertained to strongly contribute to the background, so that some scientific observations can be severely limited or even impossible. An accumulation of background sources by induced radioactivity is found to be negligible in the sensitive energy area of the detector. ESA

N94-19168*# California Inst. of Tech., Pasadena.

THE GAMCIT GAMMA RAY BURST DETECTOR

Benjamin J. McCall, John M. Grunsfeld, Srdjan D. Sobajic, Chinley Leonard Chang, David M. Krum, Albert Ratner, and Jennifer E. Trittschuh *In* NASA. Goddard Space Flight Center, The 1993 Shuttle Small Payloads Symposium Oct. 1993 p 47-56 (For primary document see N94-19162 04-12)
Avail: CASI HC A02/MF A03

N94-19463*# National Aeronautics and Space Administration. Goddard Space Flight Center, Greenbelt, MD.

DETECTION OF A LONG-DURATION SOLAR GAMMA-RAY FLARE ON JUN. 11, 1991 WITH EGRET ON COMPTON-GRO

G. Kanbach (Max-Planck-Inst. fuer Physik und Astrophysik, Garching, Germany.), D. L. Bertsch, C. E. Fitchel, R. C. Hartman, S. D. Hunter, D. A. Kniffen (Hampden-Sydney Coll., VA.), P. W. Kwok, Y. C. Lin (Stanford Univ., CA.), J. R. Mattox, and H. A. Mayer-Hasslewander (Max-Planck-Inst. fuer Physik und Astrophysik, Garching, Germany.) *In* Max-Planck-Inst. fuer Physik und Astrophysik, EGRET Mission and Data Analysis Oct. 1992 5 p Repr. from Astronomy and Astrophysics Supplement Series, Ser. 1, v. 1-99, no. 2001 See also A93-28958 (For primary document see N94-19462 04-89)
(Grant BMFT-50-QV-90955)
Avail: CASI HC A01/MF A01

99 GENERAL

N94-17968# Rutherford High Energy Lab., Chilton (England). Scientific Administration Group.

[ACTIVITIES REPORT OF THE RUTHERFORD APPLETON LABORATORY] Annual Report, 1992

Andy Kurzfeld, ed. and Jacky Hutchinson, ed. 1992 91 p Original contains color illustrations
(ETN-93-94555) Avail: CASI HC A05/MF A01

The annual report of this scientific establishment, whose facilities support work across many fields of science and engineering including physics, chemistry, space, materials, the environment, microelectronics, and information technology, is presented. During 1992 the emphasis of the particle physics department changed from building and commissioning the most challenging detectors ever designed for particle physics research to analyzing the massive volumes of data that they produce. The laboratory's flagship facility, Isis, operated with unprecedented reliability and intensity completing more experiments and serving more users than ever before. The central laser facility's SPRITE laser became the world's brightest ultraviolet laser source opening up exciting new possibilities in areas of physics involving very high electric field interactions with matter. The space science department's work with the Along Track Scanning Radiometer (ATSR), on ESA's ERS-1 satellite, broke new ground in the study of the Earth from space providing unprecendented precision in the determination of the surface temperature of the world's oceans. The instrument worked with perfect reliability and produced images of the Earth of astonishing definition and beauty. In the technology department the Laboratory embarked on a large scale collaboration with industry on high definition lithography. The informatics department attracted funding for a broad portfolio of research projects and played an increasingly important role in the direction and management of ERCIM (European Research Consortium for Informatics and Mathematics). The central computing department entered a new phase with the replacement of the CRAY X-MP which the Laboratory operated for all research councils with a Cray model Y-MP machine with three times the performance of the earlier installation. ESA

N94-18791# California Univ., Santa Barbara. Dept. of Mechanical Engineering.

OFFICE OF NAVAL RESEARCH PUBLICATIONS/PATENTS /PRESENTATIONS/HONORS REPORT, 1 OCTOBER 1992 - 30 SEPTEMBER 1993

Zhigang Suo 30 Sep. 1993 10 p
(Contract N00014-93-1-0110)
(AD-A270037) Avail: CASI HC A02/MF A01

Ferroelectric oxides deform appreciably under an electric field. They are used now as large strain ceramic actuators where a moderate electric voltage can deliver an appreciable mechanical motion. The electrostrictive and piezoelectric strains are incompatible around inhomogeneities, such as electro edge and inclusions. Cracking under electric loading has been identified in recent years. This program seeks to quantify various cracking mechanisms so that future actuator design will have scientific basis. Crack growth under cyclic polarization switching is studied experimentally using a lead lanthanum zirconate-titanate ceramic. We find that the crack growth rate is sensitive to temperature, loading magnitude and frequency. Several mechanisms have been proposed to account for the cyclic crack growth. One such model has been analyzed in detail. More detailed experiments on such cracks are in progress. DTIC

N94-18856# Lawrence Livermore National Lab., CA.

ENGINEERING RESEARCH, DEVELOPMENT AND TECHNOLOGY THRUST AREA REPORT, FY92

R. T. Langland, ed. and C. Minichino, ed. Mar. 1993 252 p
(Contract W-7405-eng-48)
(DE93-016334; UCRL-53868-92) Avail: CASI HC A12/MF A03

The mission of the Engineering Research, Development, and Technology Program at Lawrence Livermore National Laboratory (LLNL) is to develop the technical staff and the technology needed to support current and future LLNL programs. To accomplish this mission, the Engineering Research, Development, and Technology Program has two important goals: (1) to identify key technologies and (2) to conduct high-quality work to enhance our capabilities in these key technologies. To help focus our efforts, we identify technology thrust areas and select technical leaders for each area. The thrust areas are integrated engineering activities and, rather than being based on individual disciplines, they are staffed by personnel from Electronics Engineering, Mechanical Engineering, and other LLNL organizations, as appropriate. The thrust area leaders are expected to establish strong links to LLNL program leaders and to industry; to use outside and inside experts to review the quality and direction of the work; to use university contacts to supplement and complement their efforts; and to be certain that we are not duplicating the work of others. This annual report, organized by thrust area, describes activities conducted within the Program for the fiscal year 1992. Its intent is to provide timely summaries of objectives, theories, methods, and results. The nine thrust areas for this fiscal year are: Computational Electronics and Electromagnetics; Computational Mechanics; Diagnostics and Microelectronics; Emerging Technologies; Fabrication Technology; Materials Science and Engineering; Microwave and Pulsed Power; Nondestructive Evaluation; and Remote Sensing and Imaging, and Signal Engineering. DOE

N94-18915# Department of Energy, Oak Ridge, TN. Office of Scientific and Technical Information.

SUMMARIES OF FY 1993 RESEARCH IN THE CHEMICAL SCIENCES

Aug. 1993 149 p
(DE93-011855; DOE/ER-0144-11) Avail: CASI HC A07/MF A02

The summaries in photochemical and radiation sciences, chemical physics, atomic physics, chemical energy, separations and analysis, heavy element chemistry, chemical engineering sciences, and advanced battery technology are arranged according to national laboratories and offsite institutions. Small business innovation research projects are also listed. Special facilities supported wholly or partly by the Division of Chemical Sciences are described. Indexes are provided for selected topics of general interest, institutions, and investigators. DOE

N94-18980* National Aeronautics and Space Administration, Washington, DC.

LANGLEY'S 50TH YEAR (Videotape)

Oct. 1967 Videotape: 14 min. 30 sec. playing time, in color, with sound
(NASA-TM-109365; NONP-VT-94-198212) Avail: CASI VHS A01/BETA A22

This video gives an historical overview of Langley Research Center's major achievements in aeronautics and astronautics research between the years 1917-1967. Historical footage accompanies explanation of research into wind tunnel, spin tunnel, and hydrodynamic test tanks for studying aircraft airflow, wartime research into overwater combat ditching, diving, and braking, the X series aircraft experiments with supersonic flight, helicopter and vertical Take Off and Landing (VTOL) aircraft, airport landing studies, and early prototypes for the Space Shuttle. CASI

N94-19147# Joint Publications Research Service, Arlington, VA.

JPRS REPORT: CENTRAL EURASIA. AVIATION AND COSMONAUTICS, NO. 1, JANUARY 1993

16 Aug. 1993 24 p Transl. into ENGLISH from various Russian articles
(JPRS-UAC-93-007) Avail: CASI HC A03/MF A01

Papers on the following topics are included: structuring of algorithms for airborne expert systems; and procedures in satellite topography. CASI

N94-19148# Joint Publications Research Service, Arlington, VA.

JPRS REPORT: CENTRAL EURASIA. AVIATION AND COSMONAUTICS, NO. 12, DECEMBER 1992

20 Jul. 1993 26 p Transl. into ENGLISH from various Russian articles
(JPRS-UAC-93-006) Avail: CASI HC A03/MF A01

Papers on the following topics are included: combat pilots helped by 'artificial intelligence'; safety problems in instrument landing explored; theory of more efficient propulsion method explored; and Tu-160, U.S. B-1B features, performance compared. CASI

N94-19149# Joint Publications Research Service, Arlington, VA.

JPRS REPORT: CENTRAL EURASIA. AVIATION AND COSMONAUTICS, NO. 10, OCTOBER 1992

14 May 1993 27 p Transl. into ENGLISH from various Russian articles
(JPRS-UAC-93-004) Avail: CASI HC A03/MF A01

Papers on the following topics are included: launch-complex designer Barmin on past, future of space science; varied nature of satellite ground control operations viewed; and case made for artificial intelligence systems on combat aircraft. CASI

N94-19208# Joint Publications Research Service, Arlington, VA.

JPRS REPORT: CENTRAL EURASIA: AVIATION AND COSMONAUTICS, NO. 11, NOVEMBER 1992

2 Jun. 1993 21 p Transl. into ENGLISH from various Russian articles
(JPRS-UAC-93-005) Avail: CASI HC A03/MF A01

Papers on the following topics are included: continued discussion of artificial intelligence to aid pilots; and importance, ways of maintaining personnel physiological reserves. CASI

N94-19404# European Space Agency, Paris (France). Space Science Dept.

REPORT ON THE ACTIVITIES OF SPACE SCIENCE DEPARTMENT, 1990 - MID 1992

M. C. E. Huber, comp., A. Pedersen, comp., B. G. Taylor, comp., K.-P. Wenzel, comp., and Michael A. Perry, ed. 1993 276 p Original contains color illustrations

(ESA-SP-1161; ISBN-9-29-092081-5; ETN-93-94581) Copyright Avail: CASI HC A13/MF A03

Activities of the ESA space science department during 1990 to mid 1992 in the support of projects and studies covering solar and heliospheric science, planetary and space science, and astrophysics are reported. Within the research area of solar and heliospheric physics the following projects were supported: Ulysses, Soho, Solar Terrestrial Science Program (STSP), Space Physics Analysis Network (SPAN), Polar Platform. Studies supported include PRISMA (Probing Rotation and Interior of Stars: Microvariability and Activity), STEP (Satellite Test of the Equivalence Principle), and SIMURIS (a Solar system and stellar Interferometric Mission for Ultrahigh Resolution Imagery and Spectroscopy). Within the space plasma and planetary physics division projects supported include Giotto extended mission, Cluster, and Huygens/Cassini; studies supported include Rosetta, Marsnet, lunar studies, and optical planetary telescope. Within the astrophysics division projects supported include Exosat, International Ultraviolet Explorer (IUE), Hipparcos, Hubble Space Telescope (HST), Infrared Space Observatory (ISO), and the X-ray Multiple Mirror Telescope (XMM); studies supported include FIRST (Far Infrared and Submillimeter space Telescope), INTEGRAL (International Gamma Ray Astrophysics Laboratory), PRISMA, lunar studies, optical planetary telescope, and the international very long baseline interferometry satellite. ESA

N94-19486*# National Aeronautics and Space Administration. Marshall Space Flight Center, Huntsville, AL.

MARSHALL SPACE FLIGHT CENTER 1989 ANNUAL CHRONOLOGY OF EVENTS

Michael Wright Sep. 1990 68 p

(NASA-TM-109381; NAS 1.15:109381; MHR-19) Avail: CASI HC A04/MF A01

A chronological listing of the major events for the Marshall Space Flight Center for the calendar year 1989 is provided. The MSFC Historian, Management Operations Office, compiled the chronology from various sources and from supplemental information provided by the major MSFC organizations. Author (revised)

N94-19537# Sandia National Labs., Albuquerque, NM.

A SANDIA TECHNOLOGY BULLETIN: TESTING TECHNOLOGY, JULY 1993

1993 12 p

(Contract DE-AC04-76DP-00789)

(DE93-040197; SAND-93-1518) Avail: CASI HC A03/MF A01

Inside this issue, various short articles on current testing technology research at Sandia National Laboratories are presented. The following articles are presented: New techniques of imaging currents in integrated circuits; Geomaterials testing is improved with 'true triaxial' loading under high pressure; Pyroshock simulation tests electronics for space and defense; Insulated cameras get pictures of extremely hot burning fuels; Solar cell testing is improved via spectral response and laser scanning; and Missile launching accomplishments. DOE

N94-19620# National Science Foundation, Washington, DC.

GUIDE TO PROGRAMS, FISCAL YEAR 1993

1993 84 p Supersedes NSF-91-80

(NSF-92-78) Avail: CASI HC A05/MF A01; SOD HC

The Guide to Programs Fiscal Year 1993 for the National Science Foundation (NSF) is presented. The NSF is an independent agency of the Federal Government established in 1950 to promote and advance scientific and engineering progress in the United States. The Foundation does this primarily by sponsoring scientific and engineering research and education. Areas of this research include: biological sciences; computer and information science and engineering; education and human resources engineering; geoscience; mathematical and physical sciences; and social, behavioral, and economic sciences. Derived from text

SUBJECT INDEX

SCIENTIFIC AND TECHNICAL AEROSPACE REPORTS VOLUME 32 NUMBER 4

Typical Subject Index Listing

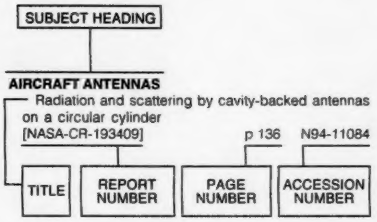

The subject heading is a key to the subject content of the document. Titles, report numbers, and accession numbers of pertinent documents are provided under each subject heading. When the title is insufficiently descriptive of the document content, a title extension is added, separated from the title by three hyphens. The report number helps to indicate the type of document cited (e.g., NASA report, NASA translation, NASA contractor report). The accession number is the number by which the document abstracts are arranged in this journal and by which the document is sold or requested. The page number helps you locate the citation in the abstract section. The titles, with title extensions if present, are arranged under each subject heading in ascending accession number order. The subject headings have been selected from the latest revision of the *NASA Thesaurus*.

A

A-310 AIRCRAFT
The GARTEUR high lift research programme
p 1307 N94-18430

ABERRATION
Limitations on the fidelity of 100 fs pulses produced by chirped pulse amplification
[DE93-017167] p 1396 N94-17991

ABILITIES
A forthcoming key press can be selected while earlier ones are executed
[IZF-1993-B-2] p 1509 N94-19422

ABSORBENTS
Laboratory test and evaluation report of the essex model 60C-0037-2 molecular sieve oxygen generating system
[AD-A269967] p 1445 N94-18778

ABSORPTION
Structural stability of 1100 C heated Pd/k during absorption cycling in protium
[DE93-016270] p 1346 N94-18048

ABSORPTION CROSS SECTIONS
Criticality benchmark comparisons leading to cross-section upgrades
[DE93-017184] p 1556 N94-18073
Ultraviolet absorption cross-sections of some carbonyl compounds and their temperature dependence
[AERONAUTICA-ACTA-A-368-199]
p 1353 N94-19456
Temperature dependence of ultraviolet absorption cross-sections of alternative hydrochlorofluorocarbons
[AERONAUTICA-ACTA-A-369-199]
p 1353 N94-19459
Infrared cross sections and global warming potentials of 10 alternative hydrohalocarbons
[AERONAUTICA-ACTA-A-371-199]
p 1479 N94-19521

ABSORPTION SPECTRA
Configuration interaction in LTE spectra of heavy elements
[DE93-017166] p 1584 N94-17990
X ray absorption spectroscopic studies of the active sites of nickel- and copper-containing metalloproteins
[DE93-017142] p 1347 N94-18059
Apparatus and method for varying a Bragg wavelength of a Bragg grating formed in an optical fiber
[AD-D015876] p 1579 N94-18743
Detection of accreting gas toward HD 45677: A newly recognized, Herbig Be proto-planetary system
[NASA-CR-189312] p 1621 N94-19288
Studies of clusters
[DE93-018961] p 1572 N94-19309
Metallization and charge-transfer gap closure of transition-metal iodides under pressure
[DE93-040301] p 1353 N94-19538

ABSORPTION SPECTROSCOPY
X ray absorption spectroscopic studies of the active sites of nickel- and copper-containing metalloproteins
[DE93-017142] p 1347 N94-18059
Absorption and x ray measurements from ultra-intense laser-plasma interactions
[DE93-016538] p 1585 N94-18115
Dynamic behaviors of fragments ejected from the surface of carbon materials by laser ablation
[DE93-788620] p 1438 N94-18161
Vibrational dynamics in photoinduced electron transfer
[DE93-040874] p 1567 N94-18533
X ray studies of microstructures in semiconductor and superconducting materials
[DE93-040690] p 1601 N94-19056
Metallization and charge-transfer gap closure of transition-metal iodides under pressure
[DE93-040301] p 1353 N94-19538

ABSORPTIVITY
Radiation induced darkening of the optical elements in the Startracker camera
[DE93-018907] p 1433 N94-19004

ABSTRACTS
EIA publications directory, 1992
[DE93-016833] p 1617 N94-18983
Mathematical communications, volume 27, numbers 1 and 2, 1992. List and abstracts of memoranda published in the period July - December 1991
[PB93-191997] p 1553 N94-19557
Updated contributions to the Twente Workshop of Hamiltonian Graph Theory
[PB93-195568] p 1553 N94-19605

ABUNDANCE
Investigation of the relative abundance of heavy versus light nuclei in primary cosmic rays using underground muon bundles
[DE93-017601] p 1630 N94-17818
Helium isotopic abundance variation in nature
[DE93-019050] p 1487 N94-19477

ACCELERATED LIFE TESTS
Accelerated tests on the tarnish resistance of gold alloys p 1367 N94-18008

ACCELEROMETERS
Development of a quartz digital accelerometer for environmental sensing and navigation applications
[DE93-018503] p 1433 N94-19243

ACCEPTABILITY
Design verification and acceptance tests of the ASST-A helium refrigeration system
[DE93-019746] p 1381 N94-19540

ACCESS CONTROL
A highly concurrent medium access control strategy for high speed multiwavelength networks using transceivers with limited tunability
[MEMO-INF-93-07] p 1390 N94-19230

ACCIDENT PREVENTION
SUNRAYCE 1993: Working safely with lead-acid batteries and photovoltaic power systems
[DE93-016553] p 1464 N94-17712
Human reliability analysis application guide
[DE93-015361] p 1511 N94-18244

ACCIDENTS
Fluid-structure-interaction analyses of reactor vessel using improved hybrid Lagrangian Eulerian code ALICE-II
[DE93-015536] p 1409 N94-18248
Calamity weather: Environmental calamities and meteorology p 1495 N94-19703

ACCLIMATIZATION
Space research on organs and tissues
p 1503 N94-19214

ACCRETION DISKS
A new approach to the study of the turbulence layer
[NASA-CR-194546] p 1487 N94-19397
Structuration processes in protoplanetary accretion disks
[MPE-243] p 1628 N94-19519

ACCUMULATORS
SX User's Manual for SX, version 2.0
[DE93-015971] p 1517 N94-17914

ACETATES
Microbial degradation of poly-b-esters: A mechanistic study, cellulose acetate biodegradability
[AD-A271368] p 1374 N94-19586

ACID RAIN
The urban perspectives of acid rain
[DE93-018881] p 1474 N94-18523

ACOUSTIC ATTENUATION
Investigation of a fiber optic frequency shifter and optical isolator
[AD-A269820] p 1579 N94-18738
Acoustic propagation modeling using MATLAB
[AD-A270905] p 1564 N94-19750

ACOUSTIC EMISSION
The application of nondestructive techniques to the testing of a wind turbine blade
[DE93-016731] p 1447 N94-18128

ACOUSTIC IMAGING
Processing and analysis of SeaMARC 2 data: Fieberling guyot; raw phase experiment in Norwegian-Greenland Sea
[AD-A269930] p 1498 N94-18662
Three dimensional ultrasonic imaging: An aging aircraft nondestructive inspection tool
[DE93-018088] p 1448 N94-19252

ACOUSTIC MEASUREMENT
Survey of collision avoidance and ranging sensors for mobile robots, revision 1
[AD-A269846] p 1541 N94-18474
Processing and analysis of SeaMARC 2 data: Fieberling guyot; raw phase experiment in Norwegian-Greenland Sea
[AD-A269930] p 1498 N94-18662
Acoustic intensity measurements in the presence of low Mach number flow
[AD-A269995] p 1562 N94-18664
Estimating the oceanic sound speed environmental for long-range acoustic propagation
[AD-A270231] p 1499 N94-18903
Acoustic travel time perturbations due to an internal tide and internal wave field in the Barents Sea
[AD-A270879] p 1499 N94-19580

ACOUSTIC PROPAGATION
Constraints on crustal structure from long period pressure and displacement measurements on the deep seafloor
[AD-A269931] p 1498 N94-18663
Parallel and vector adaptations of the underwater finite element parabolic equation model
[AD-A269990] p 1563 N94-18678
Estimating the oceanic sound speed environmental for long-range acoustic propagation
[AD-A270231] p 1499 N94-18903
Numerical simulation of acoustic waves propagation in turbulent media
[ECL-92-37] p 1563 N94-19413
Examinations of converging cylindrically symmetric second sound propagation in He2
[MPIS-9/1992] p 1564 N94-19715
Forward scattering of a pulsed continuous wave signal through laminar and turbulent thermal plumes
[AD-A271210] p 1564 N94-19723

Seismic studies of the geologic structure and physical properties of the seabed
[AD-A270895] p 1500 N94-19747
Acoustic propagation modeling using MATLAB
[AD-A270905] p 1564 N94-19750

ACOUSTIC PROPERTIES
A register of underwater acoustic test facilities in the US, Canada, and the United Kingdom
[AD-A270884] p 1500 N94-19785

ACOUSTIC SCATTERING
Design of a general purpose and autonomous transmitter and receiver system for underwater acoustic experiments at sea
[AD-A269268] p 1495 N94-17822
Processing and analysis of SeaMARC 2 data: Fieberling guyot; raw phase experiment in Norwegian-Greenland Sea
[AD-A269930] p 1498 N94-18662
Parallel and vector adaptations of the underwater finite element parabolic equation model
[AD-A269990] p 1563 N94-18678
BACKSCATTER.FOR: A program to calculate the backscattering strength of an inhomogeneous seabed
[AD-A269235] p 1499 N94-18910
Low frequency acoustics of laminated composite axisymmetric structures
[DRA-TM(USGR)-93302] p 1344 N94-19391
Measurements of ocean surface and bottom backscattering strengths in the northwestern Atlantic Ocean
[AD-A270893] p 1500 N94-19786

ACOUSTIC SOUNDING
Boundary layer heat budgets from wind profiler/RASS data: A feasibility study
[DE93-013187] p 1489 N94-18052

ACOUSTIC VELOCITY
Comments on computational underwater acoustics
[DE93-013789] p 1562 N94-17873
Estimating the oceanic sound speed environmental for long-range acoustic propagation
[AD-A270231] p 1499 N94-18903
Transmission of acoustic waves through strongly heterogeneous, two-dimensional velocity models
[REPT-93-09] p 1563 N94-19083
Liquid sound speeds at pressure from the optical analyzer technique
[DE93-018362] p 1563 N94-19151
Comments on computational underwater acoustics
[DE93-019880] p 1563 N94-19270
Acoustic travel time perturbations due to an internal tide and internal wave field in the Barents Sea
[AD-A270879] p 1499 N94-19580
Measurements of ocean surface and bottom backscattering strengths in the northwestern Atlantic Ocean
[AD-A270893] p 1500 N94-19786

ACOUSTO-OPTICS
Investigation of a fiber optic frequency shifter and optical isolator
[AD-A269820] p 1579 N94-18738

ACTINIDE SERIES
Kinetic studies of electrochemical generation of Ag(II) ion and catalytic oxidation of selected organics
[DE93-016601] p 1352 N94-19240

ACTIVATION
Modified aequorin shows increased bioluminescence activity
[AD-A268774] p 1347 N94-18185

ACTIVATION ANALYSIS
In vivo animal models of body composition in aging
[DE93-012527] p 1501 N94-17889

ACTIVATION ENERGY
In situ observation of radiation induced amorphization of crystals with apatite structure
[DE93-018450] p 1599 N94-18816

ACTIVE CONTROL
Active control of periodic noise with time-varying frequency
[REPT-93-012] p 1562 N94-17934
Active control of a multivariable system by way of polynomial neural networks: Computer simulation evaluations and laboratory experimental results
[AD-A270033] p 1541 N94-18790
ISAC: A tool for aeroservoelastic modeling and analysis
[NASA-TM-109031] p 1321 N94-19316

ACTIVE GALACTIC NUCLEI
Related investigations on the physics of high energy emission from active galactic nuclei
[NASA-CR-193615] p 1630 N94-18836

ACTIVITY CYCLES (BIOLOGY)
A comparison of polygraphic and actigraphic monitoring of sleep using a 5-channel programmable-sensitivity actigraph
[AD-A270731] p 1507 N94-19608

ACTUATORS
Magnetostrictive actuators for human sensory feedback
[AD-A269266] p 1511 N94-17841
Silicon micro-actuator p 1408 N94-18017
Generalization of optimal control theory: Linear and nonlinear structures
[PB93-188621] p 1540 N94-18125
A wind tunnel model control surface actuator interface
[AD-A268729] p 1322 N94-18324
Office of Naval Research Publications/Patents /Presentations/Honors report, 1 October 1992 - 30 September 1993
[AD-A270037] p 1632 N94-18791
Cooperative control of multiple space manipulators
[AD-A270291] p 1445 N94-18813
The effects of initial conditions and control time on optimal actuator placement by way of a max-min genetic algorithm
[DE93-017640] p 1525 N94-19124
Six degree of freedom fine motion positioning stage based on magnetic levitation
[DE93-017651] p 1446 N94-19547

ACUITY
Electro-optics display research, test, and evaluation laboratory program
[AD-A270947] p 1408 N94-19751

ADA (PROGRAMMING LANGUAGE)
Teaching a computer simulation course with Ada
[AD-A267901] p 1521 N94-18308

ADAPTATION
Characterization of fluid physics effects on cardiovascular response to microgravity (G-572)
p 1323 N94-19163

ADAPTIVE CONTROL
Autonomous neural network controllers for adaptive material handling
[AD-A268908] p 1540 N94-18331
Fuzzy control of magnetic bearings
p 1399 N94-18357
Comparative examinations of several field oriented position control structures for asynchronous servomotors with a multitransputer system
[ETN-93-95051] p 1406 N94-19390
Notes on multi-step ahead prediction based on the principle of concatenation
[MATHS-REPT-A-189] p 1544 N94-19410
Use of shape memory alloys in the robust control of smart structures
[AD-A270827] p 1366 N94-19594

ADAPTIVE OPTICS
Laser guide star measurements at Lawrence Livermore National Laboratory
[DE93-018081] p 1441 N94-19251

ADDITIVES
Ultra-shallow box-like profiles fabricated by pulsed UV-laser doping process
[DE93-017221] p 1437 N94-18083
Photorefractive tungsten bronze crystals for optical computing
[AD-A268859] p 1596 N94-18320
Analysis of deposit precursors in jet fuels using Fourier transform infrared spectroscopy
[AD-A269035] p 1377 N94-18489
The efficiency of continuous output of some titanium-doped gem-crystal lasers has exceeded 1 W
[AD-A269953] p 1439 N94-18674
Tunable ytterbium-doped solid state laser
[AD-D015878] p 1440 N94-18747
Bench-scale screening tests for a boiling sodium-potassium alloy solar receiver
[DE93-018512] p 1469 N94-19040
Low-aluminum-content iron-aluminum alloys
[DE93-017862] p 1365 N94-19274
The effect of composition on the mechanism of continuous recrystallization and superplastic response of aluminum-scandium alloys
[DE93-018594] p 1365 N94-19280
Microstructure of the interfacial zone around aggregate particles in concrete
[PB93-195790] p 1380 N94-19322
Physico chemical and mechanic approach of lubricating properties of graphite + additive powders
[ECL-93-02] p 1373 N94-19405
Contribution to the study of a symmetric film flow (with or without tensio-active elements)
[ECL-93-13] p 1421 N94-19461

ADHESION
Joining and Adhesion of Advanced Inorganic Materials Symposium
[AD-A269748] p 1342 N94-18720

ADHESIVE BONDING
Mathematical modelling of bonded fibre-composite repairs to aircraft
[AD-A268732] p 1341 N94-18327
Joining and Adhesion of Advanced Inorganic Materials Symposium
[AD-A269748] p 1342 N94-18720

ADHESIVES
Analysis of bolted and bonded composite
[AD-A267792] p 1453 N94-18382

ADIABATIC CONDITIONS
The quantum dynamics of electronically nonadiabatic chemical reactions
[NASA-CR-194309] p 1568 N94-18837

ADIPOSE TISSUES
Nuclear Medicine Program
[DE93-013896] p 1504 N94-17699
In vivo animal models of body composition in aging
[DE93-012527] p 1501 N94-17889
Metabolic changes and hemodynamic dysfunction following hypothermic shock
[AD-A269780] p 1506 N94-18598

ADSORPTION
Experimental and theoretical investigation of surface chemistry induced by direct and indirect electronic excitation
[AD-A268846] p 1348 N94-18221
Nitridation of GaAs(100) by laser-induced decomposition of HN3
[AD-A269147] p 1438 N94-18258
Hydrolysis reaction and positronium decay in silica gels
[AD-A270028] p 1371 N94-18713
Ionic and molecular environments in heterogeneous electrocatalysis: Studies by radioactive labeling and LEED/AUGER spectroscopy
[AD-A268850] p 1567 N94-18766
Surface phases and their influence on metal-oxide interfaces
[DE93-019931] p 1601 N94-19020
Optical frequency doubling at adsorbates of silver(110) surface
[ETN-93-94837] p 1603 N94-19355
Adsorption analysis of ammonia in an aqueous solution
[DE93-019512] p 1353 N94-19552

ADVANCED TEST REACTORS
Document control and conduct of operations
[DE93-016555] p 1613 N94-17880

ADVECTION
Compact advection schemes on unstructured grids
p 1413 N94-18564
Estimation of wake vortex advection and decay using meteorological sensors and aircraft data
[AD-A270763] p 1316 N94-19661

AERIAL EXPLOSIONS
Air blast measurements at 20 and 40 km distance from detonating 10 and 20 ton high explosive charges
[PB93-195949] p 1419 N94-19068

AEROACOUSTICS
Computational aero-acoustics as a branch of turbulence research p 1411 N94-18552
Research and training activities of the Joint Institute for Aeronautics and Acoustics
[NASA-CR-194742] p 1421 N94-19493

AEROBES
Microbial degradation of poly-b-esters: A mechanistic study, cellulose acetate biodegradability
[AD-A271368] p 1374 N94-19586

AERODYNAMIC CHARACTERISTICS
Comparison between swept and delta canards on a model of a combat aircraft
[AD-A269561] p 1317 N94-17826
Non-linear flight dynamics p 1319 N94-18240
Aerodynamic characteristics of a helicopter rotor airfoil as affected by simulated ballistic damage
[AD-A269206] p 1311 N94-18413
Wake structure and aerodynamic behavior of high lift aircraft configurations during unsteady maneuvers in ground effect p 1309 N94-18439

AERODYNAMIC COEFFICIENTS
Error propagation equations and tables for estimating the uncertainty in high-speed wind tunnel test results
[DE93-018685] p 1311 N94-18275
An experimental investigation of the optimum slat setting on a combat aircraft model p 1308 N94-18431

AERODYNAMIC CONFIGURATIONS
A study of the influence of a delta wing geometry on the induced drag at transonic speed (M=0.55) and high angles of attack
[FFA-TN-1992-14] p 1311 N94-17722
High-Lift System Aerodynamics
[AGARD-CP-515] p 1305 N94-18415
Navier-Stokes computations of turbulent flow around high-lift configurations p 1306 N94-18420
Computational Fluid Dynamics (CFD) research branch technical briefs
[AD-A269698] p 1417 N94-18739

Procedures and design data for the formulation of aircraft configurations
[AD-A270150] p 1318 N94-18779
Survey on the application of a 3D general purpose wind-tunnel research model
[LR-713] p 1323 N94-19372
Semi-span model testing in the National Transonic Facility
[NASA-CR-194479] p 1312 N94-19388

AERODYNAMIC DRAG
Aerodynamic characteristics of a helicopter rotor airfoil as affected by simulated ballistic damage
[AD-A269206] p 1311 N94-18413

AERODYNAMIC FORCES
A computational and experimental investigation of incompressible oscillatory airfoil flow and flutter problems
[AD-A268748] p 1311 N94-18402
ISAC: A tool for aeroservoelastic modeling and analysis
[NASA-TM-109031] p 1321 N94-19316

AERODYNAMIC HEATING
Parabolized Navier-Stokes computation of surface heat transfer characteristics for supersonic and hypersonic KE projectiles
[AD-A268858] p 1410 N94-18391

AERODYNAMIC INTERFERENCE
A study of the use of half-models in high-lift wind-tunnel testing p 1308 N94-18434

AERODYNAMIC LOADS
The role of NASTRAN in the preliminary design cycle p 1450 N94-17835
Defining the normal turbine inflow within a wind park environment
[DE93-010032] p 1489 N94-18046
The application of nondestructive techniques to the testing of a wind turbine blade
[DE93-016731] p 1447 N94-18128
Wake structure and aerodynamic behavior of high lift aircraft configurations during unsteady maneuvers in ground effect p 1309 N94-18439
Blade and hub loads of ballistically damaged helicopter rotors
[AD-A270663] p 1319 N94-19781

AERODYNAMIC STALLING
Interferometric investigations of compressible dynamic stall over a transiently pitching airfoil
[NASA-TM-109380] p 1312 N94-19119

AERODYNAMICS
Interferometer stations at the Air Force Aeroballistic Research Facility
[AD-A268776] p 1322 N94-18330
High-Lift System Aerodynamics
[AGARD-CP-515] p 1305 N94-18415
Turbulence modeling in aircraft icing p 1412 N94-18555
Data acquisition in aerodynamic research p 1431 N94-18644
Recent developments in fast response aerodynamic probe technology p 1431 N94-18645
Lift and pitching moment induced on jet STOVL aircraft by the ground vortex
[AD-A269816] p 1318 N94-18733
Aeronautical engineering: A continuing bibliography with indexes (supplement 297)
[NASA-SP-7037(297)] p 1310 N94-18937
The world's largest wind tunnel
[NASA-TM-109371] p 1322 N94-18963
Aeronautical engineering: A continuing bibliography with indexes (supplement 296)
[NASA-SP-7037(296)] p 1310 N94-19070

AEROELASTICITY
Semi-span model testing in the National Transonic Facility
[NASA-CR-194479] p 1312 N94-19388
Blade and hub loads of ballistically damaged helicopter rotors
[AD-A270663] p 1319 N94-19781

AEROGELS
The Aerocapacitor: A carbon aerogel based supercapacitor
[DE93-016537] p 1395 N94-17849
Aerogels for microelectronic applications: Fast, inexpensive, and light as air
[DE93-017170] p 1395 N94-17882

AERONAUTICAL ENGINEERING
Aeronautical engineering: A continuing bibliography with indexes (supplement 297)
[NASA-SP-7037(297)] p 1310 N94-18937
Aeronautical engineering: A continuing bibliography with indexes (supplement 296)
[NASA-SP-7037(296)] p 1310 N94-19070
A review of aeronautical fatigue investigations in Sweden during the period May 1991 to April 1993
[FFA-TN-1993-22] p 1457 N94-19358

AEROSERVOELASTICITY
ISAC: A tool for aeroservoelastic modeling and analysis
[NASA-TM-109031] p 1321 N94-19316

AEROSOLS
Application of fractal methods to estimate the aerosol-optical depth for atmospheric correction of high resolution satellite data
[DLR-FB-93-04] p 1480 N94-18088
Analysis of meteorological conditions during AGASP-4: 30 March - 23 April 1992
[PB93-190205] p 1489 N94-18126
A mobile remote sensing laboratory for water vapor, trace gas, aerosol, and wind speed measurements
[DE93-017158] p 1489 N94-18132
Dispersion effects on millimeter wavelength attenuation efficiencies for a variety of fibers
[AD-A268992] p 1386 N94-18454
Aerosol filtration with steel fiber filters
[DE93-016990] p 1380 N94-18710
Work plan for the Marine Aerosol Properties and the Thermal Imager Performance Trial (MAPTIP)
[AD-A270026] p 1483 N94-18712
Efficiency of fiber dispersion
[AD-A269740] p 1342 N94-18757
An investigation of warm-cloud microphysics using a multi-component cloud model: Interactive effects of the aerosol spectrum
[AD-A270273] p 1493 N94-18812
Effects of the Mount Pinatubo eruption on solar insolation: Four case studies
[DE93-018454] p 1475 N94-18817
The global atmospheric sulfur cycle: An evaluation of model predictions and observations
[CM-81] p 1479 N94-19379

AEROSPACE ENGINEERING
Fundamental research in nonlinear random vibration for aerospace applications
[AD-A268929] p 1454 N94-18487
Interdisciplinary training in life science (FY 1991 ASSERT)
[AD-A269220] p 1512 N94-18886
Research and design activities and the economic balance of MBB
[ETN-93-94909] p 1310 N94-19383

AEROSPACE ENVIRONMENTS
Design considerations for remotely operated welding in space: Task definition and visual weld monitoring experiment
[AD-A268752] p 1445 N94-18634
The rationale for fundamental research in space biology: Introduction and background p 1502 N94-19211
Opportunities and questions for the fundamental biological sciences in space p 1502 N94-19212
Space research with intact organisms: The role of Space Station Freedom p 1502 N94-19213
Space research on organs and tissues p 1503 N94-19214

AEROSPACE MEDICINE
US Army aviation epidemiology data register: Prevalence of refractive error among US aircrew members
[AD-A269550] p 1505 N94-18289
Revision and verification of a seven-point workload estimate scale
[AD-A269194] p 1511 N94-18412
Laboratory test and evaluation report of the essex model 60C-0037-2 molecular sieve oxygen generating system
[AD-A269967] p 1445 N94-18776
Aerospace medicine and biology: A continuing bibliography with indexes (supplement 382)
[NASA-SP-7011(382)] p 1507 N94-18936
Aerospace medicine and biology: A continuing bibliography with indexes (supplement 381)
[NASA-SP-7011(381)] p 1507 N94-19069

AEROSPACE SCIENCES
OSSA Information Systems Program
[NASA-TM-108774] p 1612 N94-17737
Strategic plan, 1991: A strategy for leadership in space through excellence in space science and applications
[NASA-TM-109256] p 1611 N94-19434

AEROSPACE SYSTEMS
Radio wave propagation in structured ionization for satellite and radar applications
[AD-A268457] p 1382 N94-17844

AEROSPACE VEHICLES
Preliminary structural design: Defining the design space
[AD-A268898] p 1317 N94-18227
Fundamental research in nonlinear random vibration for aerospace applications
[AD-A268929] p 1454 N94-18487

AEROTHERMOCHEMISTRY
Workshop on Computational Turbulence Modeling
[NASA-TM-109266] p 1410 N94-18545

AGGREGATES
Microstructure of the interfacial zone around aggregate particles in concrete
[PB93-195790] p 1380 N94-19322

AGING (BIOLOGY)
In vivo animal models of body composition in aging
[DE93-012527] p 1501 N94-17889
The rationale for fundamental research in space biology: Introduction and background p 1502 N94-19211

AGING (MATERIALS)
Reliability control for wrist watches and their casements p 1427 N94-18030
Workshop on multifactor aging mechanisms and models
[AD-A268668] p 1397 N94-18311
Ageing in Processed Polymers: Programme, summary, and abstracts discussion meeting
[AD-A268931] p 1370 N94-18448

AGING (METALLURGY)
Charpy impact toughness of martensitic steels irradiated in FFTF: Effect of heat treatment
[DE93-015960] p 1450 N94-17848

AGRICULTURE
Lunar base Controlled Ecological Life Support System (LCELSS): Preliminary conceptual design study
[NASA-CR-188479] p 1511 N94-18484

AIR BAG RESTRAINT DEVICES
Army Cockpit Delethalization Program (CDP)
[AD-A268990] p 1512 N94-18765
Numerical simulation of vehicle crashworthiness and occupant protection p 1459 N94-19471

AIR BREATHING ENGINES
Adaptations to micropep and rocket to allow performance evaluation of multiple grain and/or airbreathing motors
[AD-A268798] p 1337 N94-18202
Naval research reviews. Mixing enhancement for air-breathing propulsion. Non-axisymmetric jets increase mixing, volume 44 and volume 45
[AD-A268966] p 1521 N94-18543

AIR CONDITIONING EQUIPMENT
An emulator for testing HVAC-control and energy management systems
[VTT-TIED-1337] p 1444 N94-17974

AIR COOLING
A laboratory model of a cooled continental shelf
[AD-A270862] p 1500 N94-19792

AIR CURRENTS
The activities of equatorial anticyclones of the Western Pacific and the South China Sea and their effects on the tracks of typhoon movement
[AD-A269954] p 1492 N94-18675

AIR FILTERS
Aerosol filtration with steel fiber filters
[DE93-016990] p 1380 N94-18710

AIR FLOW
Indoor environment program
[DE93-018601] p 1513 N94-18935
Airflow research
[NASA-TM-109372] p 1312 N94-18964

AIR LAND INTERACTIONS
Biophysical characterization and surface radiation balance
[NASA-CR-194659] p 1470 N94-17762
A survey of current approaches to modelling of hydrological time-series with respect to climate variability and change
[WMO/TD-534] p 1463 N94-19435

AIR MASSES
Analysis of meteorological conditions during AGASP-4: 30 March - 23 April 1992
[PB93-190205] p 1489 N94-18126
The activities of equatorial anticyclones of the Western Pacific and the South China Sea and their effects on the tracks of typhoon movement
[AD-A269954] p 1492 N94-18675

AIR NAVIGATION
Flight demonstration of image fix-taking with SAR
[DE93-016499] p 1382 N94-17861
About the accuracy of an image-based navigation system during the runway approach
[DLR-MITT-93-01] p 1316 N94-18146

AIR POLLUTION
Malone refrigeration
[DE93-014468] p 1379 N94-17725
Visibility impairment assessment: Importance of using theoretically derived optical characterizations
[DE93-017147] p 1470 N94-17749
Air pollution effects field research facility. 3: UV-B exposure and monitoring system
[DE93-013098] p 1470 N94-17773
Carbon Dioxide Information Analysis Center: FY 1992 activities
[DE93-013845] p 1471 N94-17774

Title 1 implementation: Status report on nonattainment areas
[DE93-017677] p 1471 N94-17777
The carbon dioxide emissions game: Playing the net
[DE93-017670] p 1471 N94-17821
Screening analysis for chlorine-free alternative refrigerants to replace R-22 in air conditioning applications
[DE93-015920] p 1367 N94-17847
Energy efficiency and the environment: Innovative ways to improve air quality in the Los Angeles Basin
[DE93-016964] p 1473 N94-18050
Review of short-term, high-level exposure to metals: Antimony, barium, and cadmium
[AD-A268896] p 1505 N94-18392
On-line monitoring of incinerator emissions
[DE93-017406] p 1474 N94-18499
A comparison of wet and dry scrubbing systems for control of metals and dioxin/furan emissions from incinerators
[DE93-017446] p 1474 N94-18502
The urban perspectives of acid rain
[DE93-018881] p 1474 N94-18523
Evaluation of aftermarket LPG conversion kits in light-duty vehicle applications
[DE93-010035] p 1377 N94-18617
International Symposium on the Ecological Effects of Arctic Airborne Contaminants --- abstracts
[AD-A269955] p 1475 N94-18775
CDIAC catalog of numeric data and computer model packages
[DE93-017675] p 1475 N94-18832
Data collection plan for phase 2 Alternative Fuels Bus Data Collection Program
[DE93-010047] p 1378 N94-18913
Land-use related sources of CO2, CH4 and N2O: Current global emissions and projections for the period 1990-2100
[PB93-194819] p 1475 N94-18949
Inclusion of a three-dimensional washout coefficient in ADPIC
[DE93-018499] p 1476 N94-19038
Organic carbonyl compounds in Albuquerque, New Mexico, air: A preliminary study of the effects of oxygenated fuel use
[DE93-017748] p 1476 N94-19045
Spatiotemporal variability of non-urban ozone concentrations over the eastern United States and its potential replication by satellite data
[PB93-191328] p 1476 N94-19065
Advances in passive-remote and extractive Fourier transform infrared systems
[DE93-017402] p 1478 N94-19241
The Mexico City 1991 lidar measurements campaign
[DE93-019960] p 1478 N94-19272
Valuation of temporary and future greenhouse gas reductions
[DE93-018876] p 1478 N94-19319
Application of an atmospheric dispersion model to simulated pollutant releases in the Colorado Front range
[DE93-017118] p 1480 N94-19732

AIR QUALITY
Visibility impairment assessment: Importance of using theoretically derived optical characterizations
[DE93-017147] p 1470 N94-17749
Title 1 implementation: Status report on nonattainment areas
[DE93-017677] p 1471 N94-17777
Energy efficiency and the environment: Innovative ways to improve air quality in the Los Angeles Basin
[DE93-016964] p 1473 N94-18050
The urban perspectives of acid rain
[DE93-018881] p 1474 N94-18523
Indoor environment program
[DE93-018601] p 1513 N94-18935
Organic carbonyl compounds in Albuquerque, New Mexico, air: A preliminary study of the effects of oxygenated fuel use
[DE93-017748] p 1476 N94-19045
Advances in passive-remote and extractive Fourier transform infrared systems
[DE93-017402] p 1478 N94-19241
The Mexico City 1991 lidar measurements campaign
[DE93-019960] p 1478 N94-19272

AIR SAMPLING
Analysis of meteorological conditions during AGASP-4: 30 March - 23 April 1992
[PB93-190205] p 1489 N94-18126
The minimum detection limits of RDX and TNT deposited on various surfaces as determined by ion mobility spectroscopy
[DE93-018521] p 1378 N94-19042
Organic carbonyl compounds in Albuquerque, New Mexico, air: A preliminary study of the effects of oxygenated fuel use
[DE93-017748] p 1476 N94-19045
Novel mass spectrometric instrument for gaseous and particulate characterization and monitoring
[DE93-019992] p 1433 N94-19054

AIR TRAFFIC
Terminal area forecasts, FY 1993-2005
[AD-A269855] p 1316 N94-18336
Integrated Terminal Weather System (ITWS)
[AD-A269884] p 1492 N94-18684
Denver TMA assessment
[NASA-CR-4554] p 1315 N94-18844
Organized track system: Air ways above the ocean
p 1495 N94-19702

AIR TRAFFIC CONTROL
Feasibility of a wind-ellipse criterion in a vortex advisory system for Schiphol Airport
[NLR-TP-91384-U] p 1315 N94-17733
A rugged, low-cost advanced data acquisition system for field test projects
[DE93-010041] p 1615 N94-18334
Terminal area forecasts, FY 1993-2005
[AD-A269855] p 1316 N94-18336
VHF air/ground communications for air traffic control. Volume 1: A decision tree approach to system innovations
[AD-A268485] p 1316 N94-18384
VHF air/ground communications for air traffic control: A decision tree approach to system innovations, volume 2
[AD-A268632] p 1386 N94-18495
Denver TMA assessment
[NASA-CR-4554] p 1315 N94-18844
Aircraft accident report: Midair collision, Mitsubishi MU-2B-60, N74FB, and PIPER PA-32-301, N82419, Greenwood Municipal Airport, Greenwood, Indiana, 11 September 1992
[PB93-910406] p 1315 N94-19352
Estimation of wake vortex advection and decay using meteorological sensors and aircraft data
[AD-A270763] p 1316 N94-19661
Organized track system: Air ways above the ocean
p 1495 N94-19702

AIR TRAFFIC CONTROLLERS (PERSONNEL)
US Army aviation epidemiology data register: Prevalence of refractive error among US aircrew members
[AD-A269550] p 1505 N94-18289
Denver TMA assessment
[NASA-CR-4554] p 1315 N94-18844

AIR TRANSPORTATION
Transport policy options for reducing noise at airports; Hamburg airport taken as an example
[DLR-FB-92-40] p 1322 N94-18123
Airport activity statistics of certificated route air carriers, 1992
[AD-A269042] p 1315 N94-18490
A real-time spoken-language system for interactive problem-solving, combining linguistic and statistical technology for improved spoken language understanding
[AD-A270901] p 1392 N94-19749

AIR WATER INTERACTIONS
The performance of drag relations in the WAQUA storm surge model
[KNMI-TR-149] p 1496 N94-17923
Rapid oceanic cyclogenesis studies
[AD-A269258] p 1490 N94-18265
Airborne studies of ocean-particle-cloud interactions in the Arctic
[AD-A270752] p 1479 N94-19575

AIRBORNE EQUIPMENT
Ozone hole
[NASA-TM-109368] p 1476 N94-18960
Footprint size of a helicopter-borne electromagnetic induction sounding system versus antenna altitude
[AD-A270468] p 1463 N94-19672

AIRBORNE LASERS
Modifications of airborne oceanographic lidar for the long range P-3 missions
[NASA-CR-194682] p 1499 N94-18819

AIRBORNE RADAR
C-band PARC manual
[FEL-92-B159] p 1383 N94-18070
AN/APS-137 Forward Looking Airborne Radar (FLAR) evaluation Spring 1992 experiment
[AD-A268899] p 1384 N94-18228
Low-noise oscillators for airborne radar applications, revision 1
[AD-A269372] p 1403 N94-18471

AIRBORNE/SPACEBORNE COMPUTERS
Experience with custom processors in space flight applications p 1336 N94-18338
X-29: Research aircraft
[NASA-TM-109370] p 1318 N94-18962
VPU(tm) demonstration mission vicinity processor unit(tm) overview p 1325 N94-19171

AIRCRAFT ACCIDENT INVESTIGATION
Aircraft accident report: Midair collision, Mitsubishi MU-2B-60, N74FB, and PIPER PA-32-301, N82419, Greenwood Municipal Airport, Greenwood, Indiana, 11 September 1992
[PB93-910406] p 1315 N94-19352

AIRCRAFT ACCIDENTS
Integrated Terminal Weather System (ITWS)
[AD-A269884] p 1492 N94-18684
Vertical drop test of a Metro 3 aircraft
[AD-A270032] p 1318 N94-18789
Development and use of computational techniques in Army Aviation research and development programs for crash resistant helicopter technology
p 1459 N94-19469
Temperature of aircraft cargo flame exposure during accidents involving fuel spills
[DE93-019633] p 1381 N94-19539

AIRCRAFT APPROACH SPACING
Feasibility of a wind-ellipse criterion in a vortex advisory system for Schiphol Airport
[NLR-TP-91384-U] p 1315 N94-17733

AIRCRAFT COMMUNICATION
VHF air/ground communications for air traffic control: A decision tree approach to system innovations, volume 2
[AD-A268632] p 1386 N94-18495

AIRCRAFT COMPARTMENTS
Army Cockpit Delethalization Program (CDP)
[AD-A268990] p 1512 N94-18765

AIRCRAFT CONFIGURATIONS
Comparison between swept and delta canards on a model of a combat aircraft
[AD-A269561] p 1317 N94-17826
Wake structure and aerodynamic behavior of high lift aircraft configurations during unsteady maneuvers in ground effect p 1309 N94-18439
Procedures and design data for the formulation of aircraft configurations
[AD-A270150] p 1318 N94-18779

AIRCRAFT CONSTRUCTION MATERIALS
Metals 2000
[DE93-016761] p 1355 N94-17752
Advisory circular: Index of articles (materials, parts, processes, and appliances) certified under the technical standard order system
[AC-20-36S] p 1618 N94-19377
New aircraft materials and structures
[MBB-LME-202-S-PUB-502-A] p 1319 N94-19496

AIRCRAFT CONTROL
Research and training activities of the Joint Institute for Aeronautics and Acoustics
[NASA-CR-194742] p 1421 N94-19493

AIRCRAFT DESIGN
Regenerative fuel cells for High Altitude Long Endurance Solar Powered Aircraft
[DE93-016991] p 1465 N94-17853
High-Lift System Aerodynamics
[AGARD-CP-515] p 1305 N94-18415
Where is high-lift today? A review of past UK research programmes p 1305 N94-18416
A design procedure for slotted flaps
p 1305 N94-18418
Forty years of high-lift R/D: An aircraft manufacturer's experience p 1309 N94-18441
High-lift research: Application to the design of the ATR72 flap p 1309 N94-18442
The aero-mechanical design of a novel Fowler flap mechanism p 1309 N94-18443
Design, development, and flight evaluation of the Boeing YC-14 USB powered lift aircraft p 1310 N94-18444
High-lift design for large civil aircraft
p 1310 N94-18445
Choice and optimization of a high-lift system for an advanced amphibious aircraft p 1310 N94-18447
Procedures and design data for the formulation of aircraft configurations
[AD-A270150] p 1318 N94-18779
Survey on the application of a 3D general purpose wind-tunnel research model
[LR-713] p 1323 N94-19372
Research and design activities and the economic balance of MBB
[ETN-93-94909] p 1310 N94-19383
Development and use of computational techniques in Army Aviation research and development programs for crash resistant helicopter technology
p 1459 N94-19469
New aircraft materials and structures
[MBB-LME-202-S-PUB-502-A] p 1319 N94-19496
ADAS implementation of a panel method for the prediction of aerodynamic loads
[LR-723] p 1313 N94-19667

AIRCRAFT ENGINES
Two-dimensional boundary surfaces for axi-symmetric external transonic flows
[AD-A269678] p 1312 N94-18571
Overview of STOVL aircraft propulsion research offtakes and vertical lift systems
[NASA-TM-106387] p 1321 N94-19353
AIRCRAFT EQUIPMENT
Dynamic response analysis of composite structural members during missile launch
[AD-A270023] p 1332 N94-18760
Advisory circular: Index of articles (materials, parts, processes, and appliances) certified under the technical standard order system
[AC-20-36S] p 1618 N94-19377
AIRCRAFT FUELS
Temperature of aircraft cargo flame exposure during accidents involving fuel spills
[DE93-019633] p 1381 N94-19539
AIRCRAFT ICING
Turbulence modeling in aircraft icing
p 1412 N94-18555
AIRCRAFT INDUSTRY
Terminal area forecasts, FY 1993-2005
[AD-A269855] p 1316 N94-18336
Advisory circular: Index of articles (materials, parts, processes, and appliances) certified under the technical standard order system
[AC-20-36S] p 1618 N94-19377
AIRCRAFT INSTRUMENTS
Take-off performance monitoring system algorithm and display development
[NLR-TP-91395-U] p 1317 N94-17734
Research on man-machine productivity in aviation at Human Engineering Institute of Hangzhou University
[AD-A269952] p 1512 N94-18673
JPRS report: Central Eurasia. Aviation and cosmonautics, no. 12, December 1992
[JPRS-UAC-93-006] p 1632 N94-19148
Advisory circular: Index of articles (materials, parts, processes, and appliances) certified under the technical standard order system
[AC-20-36S] p 1618 N94-19377
AIRCRAFT MAINTENANCE
Mathematical modelling of bonded fibre-composite repairs to aircraft
[AD-A268732] p 1341 N94-18327
The J85 cost/benefit engine study
[AD-A269280] p 1320 N94-18333
A comparison of air force data systems
[AD-A269691] p 1616 N94-18575
Three dimensional ultrasonic imaging: An aging aircraft nondestructive inspection tool
[DE93-018088] p 1448 N94-19252
Results of a joint Navy/Air Force operational test to evaluate USAF Integrated Maintenance Information Systems (IMIS), Interactive Electronic Technical Manual (IETM) technology applied to the F/A-18 aircraft
[AD-A271322] p 1619 N94-19571
A comparison Air Force data systems --- Comments on IDA Paper P-2863
[AD-A270662] p 1619 N94-19780
AIRCRAFT MANEUVERS
VMC left turn curved approaches, test results --- (visual meteorological conditions)
[AD-A269476] p 1316 N94-18728
AIRCRAFT MODELS
A wind tunnel model control surface actuator interface
[AD-A268729] p 1322 N94-18324
A study of the use of half-models in high-lift wind-tunnel testing p 1308 N94-18434
High lift systems for transport aircraft with advanced airfoils p 1310 N94-18446
AIRCRAFT NOISE
Transport policy options for reducing noise at airports; Hamburg airport taken as an example
[DLR-FB-92-40] p 1322 N94-18123
Noise measurements on two types of airplanes used for spraying in agriculture
[LR-706] p 1319 N94-19796
AIRCRAFT PERFORMANCE
Take-off performance monitoring system algorithm and display development
[NLR-TP-91395-U] p 1317 N94-17734
High lift and the forward swept wing
p 1308 N94-18436
Design, development, and flight evaluation of the Boeing YC-14 USB powered lift aircraft p 1310 N94-18444
High-lift design for large civil aircraft
p 1310 N94-18445
An investigation of fighter aircraft agility
[NASA-CR-194608] p 1318 N94-19448
AIRCRAFT SAFETY
Army Cockpit Delethalization Program (CDP)
[AD-A268990] p 1512 N94-18765
Aircraft fire sentry. Volume 1: Summary
[AD-A270087] p 1315 N94-18822
Aircraft fire sentry. Volume 2: Appendices A, B, C and D
[AD-A270088] p 1315 N94-18823
AIRCRAFT STABILITY
An application of parameter estimation to the stability and control of the BQM-147 unmanned aerial vehicle
[AD-A268741] p 1321 N94-18401
Flight test techniques for aircraft parameter estimation in ground effect
[AD-A270058] p 1318 N94-18795
AIRCRAFT STRUCTURES
Metals 2000
[DE93-016761] p 1355 N94-17752
High resolution SQUID magnetometry for non-destructive evaluation
[AD-A268884] p 1447 N94-18225
Preliminary structural design: Defining the design space
[AD-A268898] p 1317 N94-18227
Mathematical modelling of bonded fibre-composite repairs to aircraft
[AD-A268732] p 1341 N94-18327
Nondestructive inspection of graphite-epoxy laminates for heat damage using DRIFT and LPF spectroscopies
[DE93-017228] p 1343 N94-18761
Design for cyclic loading endurance of composites
[NASA-TM-106407] p 1457 N94-19351
Impact analysis of composite aircraft structures
p 1458 N94-19468
Development and use of computational techniques in Army Aviation research and development programs for crash resistant helicopter technology
p 1459 N94-19469
AIRCRAFT SURVIVABILITY
Naval aviation: Consider all alternatives before proceeding with the F/A-18E/F
[AD-A269302] p 1305 N94-18279
AIRCRAFT TIRES
A finite strain ring dynamical model for pneumatic tires
[AD-A269286] p 1444 N94-18266
AIRCRAFT WAKES
Feasibility of a wind-ellipse criterion in a vortex advisory system for Schiphol Airport
[NLR-TP-91384-U] p 1315 N94-17733
Estimation of wake vortex advection and decay using meteorological sensors and aircraft data
[AD-A270763] p 1316 N94-19661
AIRFOIL OSCILLATIONS
A computational and experimental investigation of incompressible oscillatory airfoil flow and flutter problems
[AD-A268748] p 1311 N94-18402
AIRFOIL PROFILES
Calculation of maximum and high lift characteristics of multi element aerofoils p 1305 N94-18419
AIRFOILS
A computational and experimental investigation of incompressible oscillatory airfoil flow and flutter problems
[AD-A268748] p 1311 N94-18402
High-Lift System Aerodynamics
[AGARD-CP-515] p 1305 N94-18415
Experimental investigation of flow around a multielement airfoil p 1305 N94-18417
A design procedure for slotted flaps
p 1305 N94-18418
Calculation of maximum and high lift characteristics of multi element aerofoils p 1305 N94-18419
Efficient simulation of incompressible viscous flow over multi-element airfoils p 1306 N94-18421
Navier-Stokes calculations on multi-element airfoils using a chimera-based solver p 1306 N94-18422
Numerical solution of the Navier-Stokes equations for high-lift configurations on structured composite grids
p 1306 N94-18423
High Reynolds number configuration development of a high-lift airfoil p 1306 N94-18424
A viscous-inviscid solver for high-lift incompressible flows over multi-element airfoils at deep separation conditions p 1306 N94-18425
High-lift system analysis method using unstructured meshes p 1307 N94-18426
Prediction of the high-lift performance of multi-element aerofoils using an unstructured Navier-Stokes solver
p 1307 N94-18427
Numerical calculations of high lift flows using structured and unstructured methods p 1307 N94-18428
The GARTEUR high lift research programme
p 1307 N94-18430
Calculation of multielement airfoils and wings at high lift p 1309 N94-18438
Viscous-inviscid calculation of high-lift separated compressible flows over airfoils and wings
p 1309 N94-18440
High lift systems for transport aircraft with advanced airfoils p 1310 N94-18446
Choice and optimization of a high-lift system for an advanced amphibious aircraft p 1310 N94-18447
Turbulence modeling in aircraft icing
p 1412 N94-18555
AIRFRAMES
Vertical drop test of a Metro 3 aircraft
[AD-A270032] p 1318 N94-18789
Explicit solution techniques for impact with contact constraints p 1459 N94-19470
AIRLINE OPERATIONS
Airport activity statistics of certificated route air carriers, 1992
[AD-A269042] p 1315 N94-18490
AIRPORT TOWERS
A rugged, low-cost advanced data acquisition system for field test projects
[DE93-010041] p 1615 N94-18334
AIRPORTS
Transport policy options for reducing noise at airports; Hamburg airport taken as an example
[DLR-FB-92-40] p 1322 N94-18123
Terminal area forecasts, FY 1993-2005
[AD-A269855] p 1316 N94-18336
Airport activity statistics of certificated route air carriers, 1992
[AD-A269042] p 1315 N94-18490
ALBEDO
Cloud CCN feedback
[DE93-016878] p 1472 N94-17985
Energy efficiency and the environment: Innovative ways to improve air quality in the Los Angeles Basin
[DE93-016964] p 1473 N94-18050
An investigation of warm-cloud microphysics using a multi-component cloud model: Interactive effects of the aerosol spectrum
[AD-A270273] p 1493 N94-18812
ALCOHOLS
Synthesis of higher alcohols from carbon monoxide and hydrogen in a slurry reactor
[DE93-015086] p 1347 N94-18209
Kinetic studies of electrochemical generation of Ag(II) ion and catalytic oxidation of selected organics
[DE93-016601] p 1352 N94-19240
ALERTNESS
Using controlled daylight exposure and sleep timing in the prevention of shift lag during night operations
[AD-A269304] p 1504 N94-17824
ALGAE
Photobiotechnology: Application of photosynthesis to the production of renewable fuels and chemicals
[DE93-015522] p 1466 N94-18247
ALGEBRA
Infinite Grassmannian and moduli space of G-bundles
[DE93-624798] p 1545 N94-17683
Tensorial structure of a q-deformed sp(4,R) superalgebra
[DE93-624808] p 1545 N94-17685
Further on the current algebra of WZNW models at and away from criticality
[DE93-624809] p 1545 N94-17686
Paragrassmann analysis and quantum groups
[DE93-628593] p 1561 N94-18168
A teaching tool for linear programming
[AD-A270240] p 1523 N94-18905
A language of finite probabilistic processes and its interleaving semantics
[MEMO-INF-93-24] p 1558 N94-19354
ALGORITHMS
Parallel inverse iteration with reorthogonalization
[DE93-012867] p 1533 N94-17693
Planning under uncertainty solving large-scale stochastic linear programs
[DE93-013920] p 1516 N94-17701
Take-off performance monitoring system algorithm and display development
[NLR-TP-91395-U] p 1317 N94-17734
A modified direct preconditioner for indefinite symmetric Toeplitz systems
[DE93-015234] p 1516 N94-17800
Thermodynamics of computation and information distance
[DE93-012730] p 1517 N94-17812
Heuristics from nature for hard combinatorial optimization problems
[REPT-93-025] p 1547 N94-17961
Location of the absolute barycenter of a graph
[REPT-93-027] p 1547 N94-17962
A geometric algorithm for the Euclidean 1-center problem
[REPT-93-001] p 1519 N94-17975
Proceedings of the 4th European Congress on Chronometry
[ETN-93-94633] p 1424 N94-18006

The optimal numerical algorithm for processing of phase coded time signals for radio-clocks
p 1426 N94-18018
Some variation in the movement base of the ETA 251 series p 1428 N94-18035
Contribution to the analysis of tableaus based decision methods
[ETN-93-94355] p 1560 N94-18067
Software Toolkit for Analysis Research (STAR)
[DE93-017368] p 1519 N94-18086
A time-frequency smoothing algorithm for cyclic spectral analysis
[DE93-016634] p 1519 N94-18097
SAND contact in DYNA3D
[DE93-016451] p 1340 N94-18113
Exact cost flow problems in acyclic networks
[REPT-93-030] p 1520 N94-18138
Annealing algorithms for multiresource absolute location problems on graph
[REPT-93-028] p 1520 N94-18145
Numerical methods for molecular dynamics
[DE93-018321] p 1566 N94-18179
Optical associative processors and directed graphs
[AD-A268881] p 1615 N94-18224
Fast-training algorithm for hidden-layer forward-feed neural networks
[AD-A269253] p 1540 N94-18263
Automated ILA design for synchronous sequential circuits p 1397 N94-18340
Development of parallel architectures for sensor array processing. Volume 2: A parallel architecture for broad-band direction-of-arrival estimation
[AD-A270427] p 1534 N94-18508
ENO schemes on unstructured meshes
p 1412 N94-18561
Distributed memory parallel computers and computational fluid dynamics p 1413 N94-18568
New techniques for contrail forecasting
[AD-A269686] p 1490 N94-18573
Parallel and vector adaptations of the underwater finite element parabolic equation model
[AD-A269990] p 1563 N94-18678
Efficient transparent optimistic rollback recovery for distributed application programs
[AD-A268981] p 1522 N94-18696
Portable parallel ray tracing algorithms
[AD-A268984] p 1522 N94-18698
Active control of a multivariable system by way of polynomial neural networks: Computer simulation evaluations and laboratory experimental results
[AD-A270033] p 1541 N94-18790
Aspects of the calibration and processing of the CRRES fluxgate magnetometer data
[AD-A270127] p 1432 N94-18875
Statistical learning theory and algorithms
[AD-A270209] p 1523 N94-18901
Adaptive path planning: Algorithm and analysis
[DE93-008348] p 1523 N94-18926
A numerical study of hybrid optimization methods for the molecular conformation problems
[DE93-017898] p 1569 N94-18985
Using computerized tomography to determine ionospheric structures
[DE93-018903] p 1485 N94-19001
A least-squares computational tool kit
[DE93-018400] p 1557 N94-19011
A general-purpose contact detection algorithm for nonlinear structural analysis codes
[DE93-018507] p 1455 N94-19039
A particle method for history-dependent materials
[DE93-018696] p 1456 N94-19060
New insights in GMRES-like methods with variable preconditioners
[REPT-93-10] p 1524 N94-19084
Correction of longitudinal errors in accelerators for heavy-ion fusion
[DE93-018656] p 1575 N94-19106
Interior-point methodology for linear programming: Duality, sensitivity analysis and computational aspects
[REPT-93-28] p 1525 N94-19143
On the convergence of an unfeasible primal-dual interior-point method for convex programming
[REPT-93-34] p 1525 N94-19154
A polynomial primal-dual Dikin-type algorithm for linear programming
[REPT-93-36] p 1525 N94-19156
A multi-thread approach to coalescing small transfers generated by portable tool sets
[DE93-012128] p 1525 N94-19186
Experience in implementing a parallel file system
[DE93-012840] p 1536 N94-19188
Reducing extended transition systems
[MEMO-INF-93-09] p 1526 N94-19196
A parallel hashed oct-tree N-body algorithm
[DE93-012654] p 1526 N94-19205
Goal-driven LOTOS execution
[MEMO-INF-93-04] p 1527 N94-19227
Volume rendering of 3D scalar and vector fields at Lawrence Livermore National Laboratory
[DE93-018000] p 1528 N94-19276
PUMMA: Parallel Universal Matrix Multiplication Algorithms on distributed memory concurrent computers
[DE93-019163] p 1538 N94-19299
Robot navigation in unknown terrains: Introductory survey of non-heuristic algorithms
[DE93-019221] p 1316 N94-19300
A program for passively tracking a target using an array of sensors
[DE93-019554] p 1390 N94-19306
Bounds for expected loss in Bayesian decision theory with imprecise prior probabilities
[PB93-197507] p 1558 N94-19327
Using geometric techniques to improve dynamic programming algorithms for the economic lot-sizing problem and extensions
[PB93-197556] p 1528 N94-19330
Numerical analysis of proximal methods: Decomposition and parallelization
[ETN-93-95017] p 1552 N94-19362
Development of ISY data set, part 2
[NASDA-CNT-930006-PT-2] p 1463 N94-19384
Progress in edge detection
[RR-914-I] p 1529 N94-19396
Learning control of large-scale systems
[MATHS-REPT-A-186] p 1544 N94-19408
Notes on multi-step ahead prediction based on the principle of concatenation
[MATHS-REPT-A-189] p 1544 N94-19410
Robustness and efficiency of generalized predictive control algorithms with guaranteed stability
[MATHS-REPT-A-190] p 1530 N94-19412
The split-step algorithm for microwave propagation modeling above a conducting surface
[FEL-92-A430] p 1390 N94-19447
Computation of large numbers and VLSI: Application to GCD, to stretched GCD and at euclidian distance
[ETN-93-95009] p 1552 N94-19499
Heap construction in the parallel comparison tree model
[TR-409] p 1538 N94-19512
Process allocation on distributed memory parallel architectures
[ETN-93-95004] p 1538 N94-19514
Conception and analysis of numerical parallel algorithms: Realization on the Connection Machine
[ETN-93-95005] p 1531 N94-19517
A non-homogeneous, spatio-temporal, wavelet multiresolution analysis and its application to the analysis of motion
[AD-A270621] p 1538 N94-19534
Radiosity algorithms using higher order finite element methods
[DE93-018098] p 1531 N94-19548
Explorations of the practical issues of learning prediction-control tasks using temporal difference learning methods
[AD-A270836] p 1544 N94-19599
Systolic design with asynchronous controls for digital-signal processing
[AD-A270976] p 1392 N94-19680
Implementation of parallel algorithms
[AD-A271035] p 1539 N94-19682
Finding the strong components in a directed graph
[PB93-187342] p 1555 N94-19708
On the computation of versal family of matrices
[RR-892-M] p 1532 N94-19712
Algorithms and architectures for high speed signal processing
[AD-A271000] p 1392 N94-19736

ALIGNMENT
Aspects of the calibration and processing of the CRRES fluxgate magnetometer data
[AD-A270127] p 1432 N94-18875

ALKALI METALS
Structure, thermodynamics, and dynamical properties of supercooled liquids
[DE93-788387] p 1607 N94-18211

ALKALINE EARTH METALS
Polyurethane self-priming topcoats
[AD-D015870] p 1367 N94-17719

ALKENES
Conversion of ethane and of propane to higher olefin hydrocarbons
[DE93-015282] p 1347 N94-18194

ALL-WEATHER AIR NAVIGATION
Integrated Terminal Weather System (ITWS)
[AD-A269884] p 1492 N94-18684

ALLOCATIONS
Process allocation on distributed memory parallel architectures
[ETN-93-95004] p 1538 N94-19514

ALLOYING
Alloy development of FeAl aluminide alloys for structural use in corrosive environments
[DE93-015100] p 1355 N94-17757
Mechanical properties of excimer laser modified titanium surfaces
[DE93-012663] p 1358 N94-17875
The effect of composition on the mechanism of continuous recrystallization and superplastic response of aluminum-scandium alloys
[DE93-018594] p 1365 N94-19280
Reducing inadvertent alloying of metal/ceramic brazes
[DE93-009842] p 1373 N94-19308
Recent advances in high density tungsten composite processing
[AD-A270764] p 1344 N94-19576

ALLOYS
Consortium for materials development in space
[NASA-CR-194411] p 1379 N94-18840

ALPHA PARTICLES
Helium isotopic abundance variation in nature
[DE93-019050] p 1487 N94-19477

ALTERNATING CURRENT
Electrically controlled liquid-crystal heat valve
[AD-D015872] p 1443 N94-17705

ALTERNATING DIRECTION IMPLICIT METHODS
Navier-Stokes simulation of flow field around a blown-flap high-lift system p 1307 N94-18429
An investigation of low Marangoni number fluid flow in a cold corner
[AD-A271317] p 1422 N94-19569

ALUMINATES
Advanced civil engineering materials based on inorganic polymers
[AD-A270837] p 1374 N94-19600

ALUMINIDES
Alloy development of FeAl aluminide alloys for structural use in corrosive environments
[DE93-015100] p 1355 N94-17757
Environmental effects on intermetallic compounds: A guide to the literature
[AD-A269587] p 1359 N94-18306
Developing and understanding the high temperature behavior of niobium aluminides and niobium aluminide composites
[AD-A268874] p 1341 N94-18636
Fatigue resistant Ti3Al composites
[AD-A270305] p 1341 N94-18692
Development of ductile Fe3Al-based aluminides
[DE93-017865] p 1362 N94-18938
Tensile properties of as-cast iron-aluminide alloys
[DE93-017852] p 1363 N94-18975

ALUMINUM
Aluminum powder/water reaction ignited by electrical pulsed power
[AD-A269223] p 1376 N94-17840
Characterization of short pulse laser-produced plasmas at the Lawrence Livermore National Laboratory ultra short-pulse laser
[DE93-017191] p 1585 N94-18082

ALUMINUM ALLOYS
The effect of surface treatment and gaseous rust protection paper on the atmospheric corrosion stability of aluminium alloy
[DE93-623326] p 1355 N94-17679
Magnetic properties of single-crystalline UCu3Al2
[DE93-016607] p 1593 N94-17744
Atlas of formability: Ti-6Al-4V ELI
[AD-A268300] p 1357 N94-17803
Summary of work on coatings and claddings for fossil energy applications
[DE93-017005] p 1367 N94-17881
Process for applying high application-temperature coating to heat-sensitive aluminum alloys
[AD-D015823] p 1368 N94-17905
Phase separation and ordering process in Al-Li alloys studied by small-angle neutron scattering and neutron diffraction
[DE93-016750] p 1358 N94-17947
Effect of phase change in a debris cloud on a backwall structure
[DE93-017506] p 1358 N94-18100
The Hall-Petch relationship and mechanisms of fracture in B2 compounds
[DE93-018887] p 1359 N94-18182
A benchmark bending test of a thick specimen. Part 1: Experiments
[AD-A268730] p 1360 N94-18325
Development of the microstructure based stochastic life prediction models
[AD-A269880] p 1454 N94-18683
Fatigue resistant Ti3Al composites
[AD-A270305] p 1341 N94-18692
Development of the microstructure based stochastic life prediction model
[AD-A269742] p 1361 N94-18742

Development of ductile Fe3Al-based aluminides
[DE93-017865] p 1362 N94-18938

Metallurgical evaluation of SRAM 2/SRAM A program mer base plates
[DE93-018689] p 1364 N94-19100

Low-aluminum-content iron-aluminum alloys
[DE93-017862] p 1365 N94-19274

Commercialization effort in support of electroslag-casting technology
[DE93-017988] p 1366 N94-19733

ALUMINUM GALLIUM ARSENIDE LASERS

MOCVD-grown InGaAsP heterostructure diode lasers
[AD-A270848] p 1606 N94-19769

ALUMINUM GALLIUM ARSENIDES

DC and small-signal physical models for the AlGaAs/GaAs high electron mobility transistor
p 1401 N94-18370

Gallium arsenide-based ternary compounds and multi-band-gap solar cell research
[DE93-010049] p 1467 N94-18483

MOCVD-grown InGaAsP heterostructure diode lasers
[AD-A270848] p 1606 N94-19769

ALUMINUM GRAPHITE COMPOSITES

Strength optimization of C/Al metal matrix composites produced from prepregs
[DLR-FB-92-39] p 1340 N94-18122

ALUMINUM OXIDES

Metal/ceramic interfaces: Relationships between structure and chemistry
[AD-A268792] p 1369 N94-18188

Novel electrochemical materials prepared by sol-gel chemistry
[AD-A269060] p 1578 N94-18405

Pressureless densification of ceramic matrix composites
[AD-A269137] p 1371 N94-18691

Surface modification of sapphire for IR window application
[DE93-019168] p 1602 N94-19075

Ni-Al2O3 solid state binding: Elaboration, state of thermal constraints, mechanical behavior
[ECL-92-31] p 1366 N94-19436

ALUMINUM SILICATES

The direct synthesis of organic and organometallic-containing MICA-type aluminosilicates
[DE93-019001] p 1373 N94-19321

AMBIENCE

Analysis of data from Columbia Point Arena Ocean-Bottom Seismic Station (OBSS)
[AD-A271263] p 1500 N94-19727

A register of underwater acoustic test facilities in the US, Canada, and the United Kingdom
[AD-A270884] p 1500 N94-19785

AMIDES

Molecular composites from liquid crystalline polymers and liquid crystalline thermosets
[DE93-016608] p 1368 N94-18096

AMINO ACIDS

Modified aequorin shows increased bioluminescence activity
[AD-A268774] p 1347 N94-18185

AMMONIA

Condensed gases under winter conditions: A study for the rescue services
[FOA-C-40305-4.5] p 1473 N94-18139

Proton transfer dynamics and cluster ion fragmentation in phenol/ammonia cLusters
[AD-A269133] p 1348 N94-18256

Studies of clusters
[DE93-018961] p 1572 N94-19309

Adsorption analysis of ammonia in an aqueous solution
[DE93-019512] p 1353 N94-19552

Control of catalytic hydrotreating selectivity with ammonia
[DE93-041223] p 1354 N94-19660

AMMONIUM BROMIDES

Morphology of polymerized membranes on an amorphous substrate at molecular resolution by AFM
[AD-A268760] p 1370 N94-18403

AMORPHOUS MATERIALS

Vibrational and electronic properties of clusters and ultrathin films
[DE93-012291] p 1367 N94-17678

Morphology of polymerized membranes on an amorphous substrate at molecular resolution by AFM
[AD-A268760] p 1370 N94-18403

Performance of the Amorphous Materials Diffractometer GLAD at IPNS
[DE93-017746] p 1430 N94-18481

Research on stable, high-efficiency amorphous silicon multijunction modules
[DE93-010046] p 1467 N94-18518

Self-organized criticality and the Barkhausen effect in amorphous and polycrystalline metals
[AD-A269817] p 1361 N94-18735

In situ observation of radiation induced amorphization of crystals with apatite structure
[DE93-018450] p 1599 N94-18816

Elastic properties of amorphous thin films studied by Rayleigh waves
[DE93-018375] p 1372 N94-19202

AMORPHOUS SILICON

Research on stable, high-efficiency amorphous silicon multijunction modules
[DE93-010046] p 1467 N94-18518

Theoretical and experimental studies of quantum wells
[AD-A271180] p 1606 N94-19741

Amorphous silicon batch process cost analysis
[DE93-018203] p 1470 N94-19760

Tribological studies of silicon for magnetic recording applications (Invited)
[AD-A270878] p 1447 N94-19784

AMPHIBIOUS AIRCRAFT

Choice and optimization of a high-lift system for an advanced amphibious aircraft p 1310 N94-18447

AMPLIFICATION

Limitations on the fidelity of 100 fs pulses produced by chirped pulse amplification
[DE93-017167] p 1396 N94-17991

Monolithic low noise preamplifier for piezoelectric sensors
[AD-D015860] p 1563 N94-18734

Multi-terrawatt, 100 fsec laser system using flashlamp-pumped, dye-converted Ti:sapphire as an amplifier
[DE93-017190] p 1440 N94-18889

AMPLITUDE MODULATION

Evaluation of a liquid crystal spatial light modulator capable of amplitude- and phase-modulating modes
[AD-A269252] p 1577 N94-18262

Alternating-phase focusing with amplitude modulation
[DE93-018618] p 1574 N94-18273

VHF air/ground communications for air traffic control. Volume 1: A decision tree approach to system innovations
[AD-A268485] p 1316 N94-18384

ANALOG CIRCUITS

Quartz analog watch with perpetual calendar
p 1429 N94-18042

Development of analog watch with minute repeater
p 1429 N94-18043

APLAC: An object-oriented analog circuit simulator and design tool. 6.1 reference manual
[PB93-187193] p 1396 N94-18091

A tunable CMOS constant current source
p 1401 N94-18369

ANALOG DATA

SPROC: A multiple-processor DSP IC
p 1398 N94-18347

An analog retina model for detecting dim moving objects against a bright moving background
p 1399 N94-18350

Development of parallel architectures for sensor array processing. Volume 2: A parallel architecture for broad-band direction-of-arrival estimation
[AD-A270427] p 1534 N94-18508

The universal BitBus node
[DIGEL-1993-1] p 1515 N94-19799

ANALOG SIMULATION

An analog retina model for detecting dim moving objects against a bright moving background
p 1399 N94-18350

ANALOG TO DIGITAL CONVERTERS

A rugged, low-cost advanced data acquisition system for field test projects
[DE93-010041] p 1615 N94-18334

Design and simulation of a gallium-arsenide second order sigma-delta analog to digital converter
[AD-A269494] p 1404 N94-18701

Conversion of ADC pulse heights into MIP units: NUMASS test data, September 1991
[USIP-93-03] p 1432 N94-18846

A programmable systolic trigger processor for FERA-bus data
[USIP-92-04] p 1405 N94-19292

ANALOGIES

A review of the stages of work hardening
[DE93-016456] p 1359 N94-18114

Towards versatile and practical knowledge acquisition
[AD-A269596] p 1615 N94-18464

ANALYSIS (MATHEMATICS)

ASYS: a computer algebra package for analysis of nonlinear algebraic equations systems
[DE93-629819] p 1548 N94-18175

ANALYTIC FUNCTIONS

Functional analysis of subelliptic operators on lie groups
[PB93-194793] p 1547 N94-18077

ANALYTICAL CHEMISTRY

Research program activities of the ORNL Analytical Chemistry Division
[DE93-017938] p 1339 N94-19117

ANATASE

Dynamical behavior of octahedrite from the Henbury meteorite
[DE93-018834] p 1627 N94-19339

ANDROMEDA GALAXY

Investigation of the relative abundance of heavy versus light nuclei in primary cosmic rays using underground muon bundles
[DE93-017601] p 1630 N94-17818

ANEMOMETERS

Shape of wind gusts at a 130m tower at Wilhelmshaven (Germany)
[BER-BAND-B3] p 1494 N94-19503

ANGLE OF ATTACK

Close-coupled oscillating canard effects on post-stall lift enhancement
[AD-A268938] p 1321 N94-18541

Numerical prediction of transition of the F-16 wing at supersonic speeds
[NASA-CR-194407] p 1312 N94-19433

ANGLES (GEOMETRY)

Refining a triangulation of a planar straight-line graph to eliminate large angles
[DE93-016510] p 1528 N94-19344

ANGULAR DISTRIBUTION

Eta-nucleon interaction and nuclear production of eta mesons
[DE93-018469] p 1571 N94-19259

ANGULAR MOMENTUM

Tensorial structure of a q-deformed sp(4,R) superalgebra
[DE93-624808] p 1545 N94-17685

ANGULAR RESOLUTION

The solar optical telescope
[NASA-TM-109240] p 1621 N94-18850

ANIMALS

Assessing impacts of climate change on forests: The state of biological modeling
[DE93-015916] p 1471 N94-17790

Compilation of 1992 annual reports of the Navy ELF communications system ecological monitoring program, volume 1
[AD-A269569] p 1386 N94-18473

Compilation of 1992 annual reports of the navy ELF communications system ecological monitoring program, volume 2
[AD-A269726] p 1388 N94-18751

ANIONS

Ionic and molecular environments in heterogeneous electrocatalysis: Studies by radioactive labeling and LEED/AUGER spectroscopy
[AD-A268850] p 1567 N94-18766

Oligomer and mixed-metal compounds, potential multielectron transfer catalysts
[DE93-019592] p 1350 N94-19017

ANISOTROPY

Surface second harmonic generation studies of stepped Ag(111) electrode surfaces
[AD-A265205] p 1594 N94-17876

High energy resolution ARPES measurements of the normal and superconducting states of Bi2Sr2CaCu2O(8 + delta)
[DE93-018294] p 1599 N94-18804

Construction of a tension-torsion anisotropic brittle damage elastic model
[ECL-91-27] p 1457 N94-19375

Magnetic and crystallographic structures in UTX intermetallic compounds
[DE93-018291] p 1605 N94-19735

ANNEALING

Reorientation of misfit dislocations during annealing in InGaAs/GaAs(001) interfaces
[DE93-015046] p 1592 N94-17741

An annealing approach to multi-facility location problems in euclidean spaces
[REPT-93-022] p 1547 N94-17928

Annealing algorithms for multiresource absolute location problems on graph
[REPT-93-028] p 1520 N94-18145

Study of mechanical behavior and internal structure of ferritic nanocrystalline material
[DE93-019264] p 1596 N94-18184

Nitridation of GaAs(100) by laser-induced decomposition of HN3
[AD-A269147] p 1438 N94-18258

Fabrication and microstructural development of Ag-clad TlBa2Ca2Cu3O(x) tapes
[DE93-017407] p 1597 N94-18500

Morphology, deformation, and defect structures of TiCr2 in Ti-Cr alloys
[DE93-018332] p 1361 N94-18807

Binding of copper to nanocavity surfaces in silicon
[DE93-019073] p 1364 N94-19080

ANNIHILATION REACTIONS
Tensorial structure of a q-deformed sp(4,R) superalgebra
[DE93-624808] p 1545 N94-17685
On a possible algebra morphism of U(sub q)(osp1/2) onto the deformed oscillator algebra W(sub q)(N)
[DE93-629857] p 1548 N94-18176

ANNUAL VARIATIONS
SeaSoar CTD, fluorescence and scalar irradiance data from RRS Charles Darwin Cruises 58/59, NE Atlantic, Vivaldi 1991
[IOS-299-1992] p 1496 N94-18066
Cloudiest year study: An analysis of the 3DNEPH and RTNEPH databases
[AD-A269403] p 1490 N94-18281
Eastern Europe: A climatological study
[AD-A269200] p 1493 N94-18883
Seasonal variability of wind electric potential in the US
[DE93-018182] p 1493 N94-19051
Spatiotemporal variability of non-urban ozone concentrations over the eastern United States and its potential replication by satellite data
[PB93-191328] p 1476 N94-19065
The carbon isotope biogeochemistry of methane production in anoxic sediments. 1: Field observations
p 1477 N94-19234

ANODES
Compound-lens injector for a 19-MeV, 700-kA electron beam
[DE93-013752] p 1573 N94-17698
Environmentally assisted cracking of nickel anode substrates in Li/SOCl2 cells: An engineering approach
[DE93-015130] p 1405 N94-18928

ANOMALIES
Phenomenological explanation of elastic anomalies in superlattices
[DE93-017475] p 1594 N94-17871

ANTENNA ARRAYS
Power compensators for phased operation of antenna arrays on JET and D3-D
[DE93-013208] p 1581 N94-17694
Development of parallel architectures for sensor array processing, volume 1
[AD-A270426] p 1534 N94-18507
Development of parallel architectures for sensor array processing. Volume 2: A parallel architecture for broad-band direction-of-arrival estimation
[AD-A270427] p 1534 N94-18508
Design and fabrication of a Multichannel Adaptive Optical Processor (MADOP)
[AD-A270004] p 1579 N94-18668
Algorithms and architectures for high speed signal processing
[AD-A271000] p 1392 N94-19736

ANTENNA DESIGN
Arc detection and protection in high-power antenna systems
[DE93-013272] p 1382 N94-17695
Missile antenna pattern coordinate system and data formats
[AD-A269153] p 1385 N94-18260
A RFI measurement system for field sites
[AD-A269340] p 1385 N94-18301

ANTENNA RADIATION PATTERNS
Modeling a Yagi array antenna for VHF radar use
[AD-A268973] p 1387 N94-18525
Physical retrieval of precipitation water contents from Special Sensor Microwave/Imager (SSM/I) data. Part 2: Retrieval method and applications (report version)
p 1491 N94-18605

ANTHROPOMETRY
Analysis of seating and restraint limitations restricting total body weight for aircrew and passengers on US Army helicopters
[AD-A269117] p 1511 N94-18296
A multivariate anthropometric method for crew station design
[AD-A270652] p 1513 N94-19531

ANTICYCLONES
The activities of equatorial anticyclones of the Western Pacific and the South China Sea and their effects on the tracks of typhoon movement
[AD-A269954] p 1492 N94-18675

ANTIFERROMAGNETISM
Ising model on tangled chain. Part 2: Magnetization and susceptibility
[DE93-628794] p 1607 N94-18174
The low-temperature specific heat of CeCu2Ge2 at 0 and 9.5 kbar
[DE93-014914] p 1360 N94-18398

ANTIMISSILE DEFENSE
UVPI imaging from the LACE satellite: The Nihka rocket plume
[AD-A268456] p 1334 N94-18149
Super-resolution of multi-pixel and sub-pixel images for the SDI
[AD-A268537] p 1462 N94-18631
Legacy of the X Ray Laser Program
[DE93-019550] p 1442 N94-19554

ANTIMONY
Review of short-term, high-level exposure to metals: Antimony, barium, and cadmium
[AD-A268896] p 1505 N94-18392

ANTIOXIDANTS
The c-jun gene expression in human cells exposed to either ionizing radiation or hydrogen peroxide
[DE93-017436] p 1502 N94-18476

ANTIPROTONS
Proceedings of the 3rd Workshop on Balloon-Borne Experiments with Superconducting Magnet Spectrometers
[DE93-788362] p 1630 N94-18219
The PAPAGENO Partonic Monte-Carlo Program
[DE93-018524] p 1571 N94-19247

ANTIREFLECTION COATINGS
Simplified processing for 23 percent-efficient silicon concentrator solar cells
[DE93-015018] p 1464 N94-17787
Experimental examinations of semiconductor laser amplifiers for optical communication technology
[ETN-93-95050] p 1442 N94-19647

APEXES
Refining a triangulation of a planar straight-line graph to eliminate large angles
[DE93-016510] p 1528 N94-19344
Cycles containing all vertices of maximum degree
p 1554 N94-19688

APPLICATION SPECIFIC INTEGRATED CIRCUITS
Cellular logic array for computation of squares
p 1398 N94-18343
Verification of VLSI designs p 1400 N94-18363
High accuracy switched-current circuits using an improved dynamic mirror p 1401 N94-18368
Formal specification of a high speed CMOS correlator
p 1401 N94-18371
ARPA/CSTO rapid VLSI implementation
[AD-A269170] p 1403 N94-18695
Signal processing algorithms for heterogeneous architectures
[AD-A271248] p 1392 N94-19724

APPLICATIONS OF MATHEMATICS
Applications of an algebraic Monge property
[DE93-016869] p 1546 N94-17885

APPLICATIONS PROGRAMS (COMPUTERS)
Interactive Collaborative Environments (ICE) in the design to manufacturing process
[DE93-014994] p 1518 N94-17944
Adaptations to micropep and rocket to allow performance evaluation of multiple grain and/or airbreathing motors
[AD-A268798] p 1337 N94-18202
STREMR: Numerical model for depth-averaged incompressible flow
[AD-A269949] p 1417 N94-18672
Efficient transparent optimistic rollback recovery for distributed application programs
[AD-A268981] p 1522 N94-18696
Development of a finite element method program for the analysis of laminated composite plates using first-order shear deformation theory
[AD-A270318] p 1342 N94-18700
BACKSCATTER.FOR: A program to calculate the backscattering strength of an inhomogeneous seabed
[AD-A269235] p 1499 N94-18910
Visualization for applications in shock physics
[DE93-012849] p 1418 N94-18918
Feasibility study in linguistically motivated object-oriented conceptual design of information systems
[PB93-197754] p 1618 N94-19331
START user manual version 2.1
[LR-726] p 1335 N94-19614
The wave forecasting model NEDWAM
p 1495 N94-19701
Report of the Second CLICOM Experts Meeting
[WCDMP-19] p 1495 N94-19705
Improved HF data network simulator, volume 1
[AD-A270953] p 1393 N94-19752
SeaTrack: Ground station orbit prediction and planning software for sea-viewing satellites
[NASA-RP-1331] p 1532 N94-19761
On the automation of object-oriented requirements analysis
[AD-A270673] p 1532 N94-19782

APPROACH
About the accuracy of an image-based navigation system during the runway approach
[DLR-MITT-93-01] p 1316 N94-18146
VMC left turn curved approaches, test results — (visual meteorological conditions)
[AD-A269476] p 1316 N94-18728

APPROACH CONTROL
On the use of differential GPS for automatic approach and landing of space and aircraft
[DLR-MITT-93-05] p 1316 N94-17921

APPROPRIATIONS
Current information technology resource requirements of the federal government: Fiscal year 1994
p 1612 N94-17756
Report to Congress: Comprehensive Program Plan for Advanced Turbine Systems
[DE93-016718] p 1467 N94-18475
The 1994 NASA authorization, volume 2
[GPO-71-510] p 1620 N94-18842

APPROXIMATION
A one dimensional numerical model, with an application to the vertical distribution of dissolved oxygen in the ocean
[DE93-018481] p 1495 N94-17779
Multivariate wavelet representations and approximations
[AD-A269350] p 1546 N94-17825
Recent studies of short-range order in alloys: The Cowley theory revisited
[DE93-016416] p 1358 N94-18111
Full Boltzmann discrete spectral wave model, implementation and nondimensional tests
[AD-A269885] p 1498 N94-18685
Are bilinear quadrilaterals better than linear triangles?
[DE93-019223] p 1551 N94-19301
The complexity of the optimal spanning hypertree problem
[TR-471] p 1561 N94-19481

AQUEOUS SOLUTIONS
Densities and viscosities of ternary ammonia/water fluids
[DE93-015966] p 1351 N94-19118
Current-potential characteristics of electrochemical systems
[DE93-040303] p 1352 N94-19192
Adsorption analysis of ammonia in an aqueous solution
[DE93-019512] p 1353 N94-19552

AQUIFERS
Similarity solutions for gravity-dominated spreading of a lens of organic contaminant
[REPT-93-24] p 1420 N94-19139
Multigrid for a groundwater flow problem
[REPT-93-29] p 1420 N94-19144

ARC DISCHARGES
Low power arcjet system spacecraft impacts
[NASA-TM-106307] p 1336 N94-17856

ARC WELDING
Thermal insulation of wet shielded metal arc welds
[AD-A268697] p 1445 N94-18465
Effects of irradiation temperature on Charpy and tensile properties of high-copper, low upper-shelf, submerged-arc welds
[DE93-017858] p 1445 N94-19047
Overlay welding irradiated stainless steel
[DE93-018767] p 1446 N94-19334

ARCHITECTURE (COMPUTERS)
Employing knowledge resources in a new text planner architecture
[AD-A269669] p 1516 N94-17732
EXPECT: Intelligent support for knowledge base refinement
[AD-A269602] p 1612 N94-17745
RESQme studies for SDC regional computing centers
[DE93-015230] p 1514 N94-17799
Information technology resources assessment
[DE93-015276] p 1613 N94-17894
PARX: Architecture of an operating system for parallel machines
[ETN-93-94401] p 1533 N94-18068
Optical associative processors and directed graphs
[AD-A268881] p 1615 N94-18224
Synthesis techniques and analysis tool for on-chip fault-tolerance
[AD-A269148] p 1521 N94-18259
Performance of defect-tolerant set-associative cache memories p 1398 N94-18346
An improved distributed arithmetic architecture
p 1398 N94-18349
Low power signal processing research at Stanford
p 1393 N94-18351
A modified reconfigurable data path processor
p 1400 N94-18360
High-performance multiprocessor architecture for a 3-D lattice gas model p 1400 N94-18362
Asynchronous sequential circuit design using pass transistor iterative logic arrays p 1402 N94-18376
Improved self arbitrated VLSI asynchronous circuits
p 1402 N94-18378

A special purpose silicon compiler for designing supercomputing VLSI systems p 1402 N94-18379
A fast adaptive convex hull algorithm on two-dimensional processor arrays with a reconfigurable BUS system
p 1402 N94-18380
Development of parallel architectures for sensor array processing, volume 1
[AD-A270426] p 1534 N94-18507
Development of parallel architectures for sensor array processing. Volume 2: A parallel architecture for broad-band direction-of-arrival estimation
[AD-A270427] p 1534 N94-18508
Case studies of software development tools for parallel architectures
[AD-A269193] p 1535 N94-18866
ControlShell: A real-time software framework
[AD-A269172] p 1523 N94-18879
A parallel and pipelined architecture for estimation of direction of arrival using a bilinear transformation method, volume 3
[AD-A270137] p 1389 N94-18897
Visualization for applications in shock physics
[DE93-012849] p 1418 N94-18918
Motorola MC68040 high-speed design using Altera EPM5000 erasable programmable logic devices
[DE93-017635] p 1523 N94-19006
A programming paradigm for distributed-memory computers
[DE93-018336] p 1524 N94-19024
Coordination of software-development activities among sites that are geographically separated
[DE93-019201] p 1524 N94-19076
Advances in architectural concepts to support distributed systems design
[MEMO-INF-93-17] p 1527 N94-19261
FASTBUS simulation models in VHDL
[USIP-92-07] p 1515 N94-19295
A multi-level data-flow architecture for signal and data processing applications
[DE93-041272] p 1539 N94-19588
Service without servers
[AD-A270612] p 1515 N94-19591
CVL: A C vector library manual. Version 2
[AD-A270614] p 1531 N94-19592
The Cluster science data system: A distributed system to serve a wide international community
p 1330 N94-19638
Signal processing algorithms for heterogeneous architectures
[AD-A271248] p 1392 N94-19724
Algorithms and architectures for high speed signal processing
[AD-A271000] p 1392 N94-19736
Congestion/flow control and routing in data networks: A control-theoretic approach
[AD-A271121] p 1392 N94-19737
Improved HF data network simulator, volume 1
[AD-A270953] p 1393 N94-19752

ARCTIC OCEAN
Airborne studies of ocean-particle-cloud interactions in the Arctic
[AD-A270752] p 1479 N94-19575

ARCTIC REGIONS
Analysis of meteorological conditions during AGASP-4: 30 March - 23 April 1992
[PB93-190205] p 1489 N94-18126
Arctic ice studies
[AD-A268608] p 1497 N94-18277
Atlas of SSM/I satellite ice concentration interpolated to operational ice model domains of the Arctic for 1992
[AD-A270306] p 1499 N94-18727
International Symposium on the Ecological Effects of Arctic Airborne Contaminants --- abstracts
[AD-A269955] p 1475 N94-18775
Ozone hole
[NASA-TM-109368] p 1476 N94-18960
Method for extracting tidal and inertial motion from ARGOS ice buoys applied to the Barents Sea during CEAREX
[PB93-190213] p 1499 N94-19063
Airborne studies of ocean-particle-cloud interactions in the Arctic
[AD-A270752] p 1479 N94-19575

ARGON
Experimental study of interactions of highly charged ions with atoms at keV energies
[DE93-040222] p 1571 N94-19257

ARGOS SYSTEM
Method for extracting tidal and inertial motion from ARGOS ice buoys applied to the Barents Sea during CEAREX
[PB93-190213] p 1499 N94-19063

ARITHMETIC
An improved distributed arithmetic architecture
p 1398 N94-18349

ARITHMETIC AND LOGIC UNITS
VLSI for high-speed digital signal processing
[AD-A270406] p 1404 N94-18706

ARMOR
Shock-loading response of advanced materials
[DE93-018344] p 1455 N94-19033
The influence of the target strength model on computed perforation
[DE93-018659] p 1460 N94-19543

ARRAYS
Applications of an algebraic Monge property
[DE93-016869] p 1546 N94-17885

ARRESTERS
Analysis of high contact resistances associated with hermetic and lightning arrestor connectors
[DE93-014850] p 1395 N94-17763

ARTIFICIAL INTELLIGENCE
Weakened negative introspection in autoepistemic reasoning
[PB93-187375] p 1520 N94-18118
Dialog-Based Learning (DBL) for adaptive interface agents and programming-by-demonstrations systems
[AD-A269154] p 1540 N94-18261
Distributed reasoning and planning
[AD-A268682] p 1540 N94-18399
On masking effect
[AD-A269593] p 1541 N94-18462
Flexible integration of path-planning capabilities
[AD-A269594] p 1541 N94-18463
Survey of collision avoidance and ranging sensors for mobile robots, revision 1
[AD-A269846] p 1541 N94-18474
SERCAA cloud analysis integration: Design concepts and interaction with cloud forecast models
[AD-A269104] p 1492 N94-18637
Efficient domain-independent experimentation
[AD-A269530] p 1557 N94-18640
Automatically generating abstractions for planning
[AD-A269772] p 1541 N94-18759
Knowledge sources for an intelligent MCM analyzer
[AD-A269224] p 1542 N94-18887
The intelligent processing of materials
[AD-A269250] p 1362 N94-18923
Geometrical pattern learning
[DE93-017641] p 1542 N94-19007
JPRS report: Central Eurasia. Aviation and cosmonautics, no. 12, December 1992
[JPRS-UAC-93-006] p 1632 N94-19148
JPRS report: Central Eurasia. Aviation and cosmonautics, no. 10, October 1992
[JPRS-UAC-93-004] p 1632 N94-19149
JPRS report: Central Eurasia: Aviation and cosmonautics, no. 11, November 1992
[JPRS-UAC-93-005] p 1632 N94-19208
Computer-assisted instruction and natural language systems
[MEMO-INF-92-86] p 1527 N94-19225
New automatic deduction techniques in first order finite and infinite polyvalent logic
[ETN-93-95003] p 1528 N94-19359
Causal reasoning for model-based process supervisory control
[LAAS-93241] p 1544 N94-19360
PRACTICAL: Planning and resource allocation in C2-domains with time critical algorithms
[FEL-93-B029] p 1544 N94-19458
Automated qualitative modeling of dynamic physical systems
[AD-A270835] p 1422 N94-19598
Explorations of the practical issues of learning prediction-control tasks using temporal difference learning methods
[AD-A270836] p 1544 N94-19599
Equivalence and reduction of hidden Markov models
[AD-A270762] p 1560 N94-19768

ARTIFICIAL SATELLITES
CONTACT: An Air Force technical report on military satellite control technology
[AD-A269375] p 1334 N94-18408
Parallelization of the Air Force Space Command (AFSPACECOM) satellite motion models
[AD-A269327] p 1334 N94-18470
Constant-thrust orbit-raising transfer charts
[AD-A269088] p 1334 N94-18718
JPRS report: Science and technology. Central Eurasia: Space
[JPRS-USP-93-004] p 1323 N94-19146
Absolute positioning by collecting Global Positioning System (GPS) data along short baselines
[AD-A271324] p 1317 N94-19572

ASHES
Effects of the Mount Pinatubo eruption on solar insolation: Four case studies
[DE93-018454] p 1475 N94-18817

ASSAYING
Thermal neutron multiplicity measurements using the pyrochemical multiplicity counter at Lawrence Livermore National Laboratory
[DE93-018538] p 1571 N94-19278

ASSEMBLER ROUTINES
Embedded Computer Performance Measurement (ECPM). Advanced avionics subsystems and technology multiprocessor ECPM software documentation
[AD-A269921] p 1320 N94-18658

ASSEMBLING
Automatic soldering for watch circuit components
p 1428 N94-18037

ASSESSMENTS
Uncertainty versus interindividual variability
[DE93-018105] p 1559 N94-19549

ASSIMILATION
Preparation of data assimilation and model evaluation experiment data sets
[AD-A269996] p 1498 N94-18665

ASSOCIATIVE PROCESSING (COMPUTERS)
Optical associative processors and directed graphs
[AD-A268881] p 1615 N94-18224

ASTRO MISSIONS (STS)
ASTRO-1 to explore invisible universe
[NASA-TM-109360] p 1336 N94-18956

ASTROGRAPHY
The molecular environment of S106 IR
[MPE-PREPRINT-241] p 1622 N94-19417

ASTRONAUTS
Design considerations for remotely operated welding in space: Task definition and visual weld monitoring experiment
[AD-A268752] p 1445 N94-18634
Apollo 11: 20th anniversary
[NASA-TM-109364] p 1323 N94-18979
National Boy Scout Jamboree
[NASA-TM-109367] p 1610 N94-18982

ASTRONOMICAL CATALOGS
The Einstein Observatory catalog of IPC x ray sources. Volume 5E: Right ascension range 12h 00m to 15h 59m
[NASA-TM-108401-VOL-5E] p 1625 N94-18613
The Einstein Observatory catalog of IPC x ray sources. Volume 6E: Right ascension range 16h 00m to 19h 59m
[NASA-TM-108401-VOL-6E] p 1625 N94-18615
The Einstein Observatory catalog of IPC x ray sources. Volume 7E: Right ascension range 20h 00m to 23h 59m
[NASA-TM-108401-VOL-7E] p 1625 N94-18618
The Einstein Observatory catalog of IPC x ray sources. Volume 1E: Documentation
[NASA-TM-108401-VOL-1E] p 1626 N94-18619
The Einstein Observatory catalog of IPC x ray sources. Volume 2E: Right ascension range 00h 00m to 03h 59m
[NASA-TM-108401-VOL-2E] p 1626 N94-18620
The Einstein Observatory catalog of IPC x ray sources. Volume 3E: Right ascension range 04h 00m to 07h 59m
[NASA-TM-108401-VOL-3E] p 1626 N94-18621

ASTRONOMICAL INTERFEROMETRY
Image reconstruction from interferometer data
[AD-A268463] p 1578 N94-18383

ASTRONOMICAL MAPS
Working group for planetary system nomenclature
[NASA-CR-194406] p 1626 N94-18841

ASTRONOMICAL OBSERVATORIES
Space debris detection
[AD-A269254] p 1334 N94-18264
The Sudbury Neutrino Observatory and the solar neutrino problem
[DE93-018528] p 1629 N94-19260
The South African Astronomical Observatory
[SAAO-17] p 1623 N94-19657

ASTRONOMICAL SATELLITES
Particle induced background by Roentgen satellites
[MPE-242] p 1631 N94-19714

ASTRONOMICAL SPECTROSCOPY
The star identification, pointing and tracking system of UVSTAR, an attached payload instrument system for the Shuttle Hitchhiker-M platform p 1326 N94-19179

ASTRONOMY
The South African Astronomical Observatory
[SAAO-17] p 1623 N94-19657

ASTROPHYSICS
Institute of Geophysics and Planetary Physics, 1992
[DE93-019209] p 1627 N94-19077
The South African Astronomical Observatory
[SAAO-17] p 1623 N94-19657

ASYMMETRY
T violating neutron spin rotation asymmetry
[DE93-018470] p 1570 N94-19126

ASYMPTOTIC METHODS
Bayesian model choice: Asymptotics and exact calculations
[AD-A269067] p 1557 N94-18516
Asymptotic derivation of the modified time-dependent SP2 equations and numerical calculations
[DE93-016466] p 1551 N94-19342

ASYMPTOTIC PROPERTIES
Stability analysis through bifurcation theory, 1
p 1608 N94-18238
Stability analysis through bifurcation theory, 2
p 1608 N94-18239
Asymptotic derivation of the modified time-dependent SP2 equations and numerical calculations
[DE93-016466] p 1551 N94-19342

ASYMPTOTIC SERIES
Asymptotic behaviour of the solutions of Schroedinger equation with impulse effect in a Banach space
[DE93-629865] p 1548 N94-18195
Stability analysis through bifurcation theory, 1
p 1608 N94-18238
The asymptotic theory of the reflection and transmission of a pulsed electromagnetic beam field at a planar interface separating two dispersive media
[AD-A269033] p 1385 N94-18404

ASYNCHRONOUS MOTORS
Comparative examinations of several field oriented position control structures for asynchronous servomotors with a multitransputer system
[ETN-93-95051] p 1406 N94-19390

ATLANTIC OCEAN
CTD oxygen, tracer and nutrient data from RRS Charles Darwin Cruises 58/59 in the NE Atlantic as part of Vivaldi 1991
[IOS-296-1992] p 1496 N94-18065
Rapid oceanic cyclogenesis studies
[AD-A269258] p 1490 N94-18265
Wind products for use in coastal wave and surge models
[AD-A269753] p 1497 N94-18414
Organized track system: Air ways above the ocean
p 1495 N94-19702
Measurements of ocean surface and bottom backscattering strengths in the northwestern Atlantic Ocean
[AD-A270893] p 1500 N94-19786

ATMOSPHERIC ATTENUATION
Dispersion effects on millimeter wavelength attenuation efficiencies for a variety of fibers
[AD-A268992] p 1386 N94-18454

ATMOSPHERIC BOUNDARY LAYER
Boundary layer heat budgets from wind profiler/RASS data: A feasibility study
[DE93-013187] p 1489 N94-18052
An investigation of warm-cloud microphysics using a multi-component cloud model: Interactive effects of the aerosol spectrum
[AD-A270273] p 1493 N94-18812
Application of an atmospheric dispersion model to simulated pollutant releases in the Colorado Front range
[DE93-017118] p 1480 N94-19732

ATMOSPHERIC CHEMISTRY
Carbon Dioxide Information Analysis Center: FY 1992 activities
[DE93-013845] p 1471 N94-17774
Characterization of the Facility for Atmospheric Corrosion Testing (FACT) at Sandia
[DE93-018510] p 1474 N94-18521
Organic carbonyl compounds in Albuquerque, New Mexico, air: A preliminary study of the effects of oxygenated fuel use
[DE93-017748] p 1476 N94-19045
Kinetics programs for simulation of tropospheric photochemistry on the global scale
[DE93-019035] p 1476 N94-19104
Environmental Research Program
[DE93-019101] p 1477 N94-19105
Carbon Isotope Biogeochemistry of Methane from Anoxic Sediments
[NASA-CR-194620] p 1477 N94-19231
Analysis of satellite-derived ozone and water vapor measurements
[NASA-CR-193810] p 1486 N94-19237
The Mexico City 1991 lidar measurements campaign
[DE93-019960] p 1478 N94-19272
Crossed molecular beam studies of atmospheric chemical reaction dynamics
[DE93-019246] p 1478 N94-19303
The global atmospheric sulfur cycle: An evaluation of model predictions and observations
[CM-81] p 1479 N94-19379
Global three dimensional model of tropospheric trace gases chemistry and transport
[AERONAUTICA-ACTA-A-370-199]
p 1479 N94-19518
Airborne studies of ocean-particle-cloud interactions in the Arctic
[AD-A270752] p 1479 N94-19575

ATMOSPHERIC CIRCULATION
A review of wind field models for atmospheric transport
[DE93-016085] p 1488 N94-17895
Statistical intercomparison of global climate models: A common principal component approach with application to GCM data
[DE93-017951] p 1473 N94-18005
Effect of spatial resolution on the simulation of regional precipitation in China in a global climate model
[DE93-013433] p 1489 N94-18053
Rapid oceanic cyclogenesis studies
[AD-A269258] p 1490 N94-18265
Three-dimensional cloud visualization based on satellite imagery
[AD-A269318] p 1490 N94-18300
Internal instability of nonparallel flow on an equatorial beta-plane
[AD-A268927] p 1490 N94-18486
Work plan for the Marine Aerosol Properties and the Thermal Imager Performance Trial (MAPTIP)
[AD-A270026] p 1483 N94-18712
Eastern Europe: A climatological study
[AD-A269200] p 1493 N94-18883
Venus lower thermosphere studies
[NASA-CR-193546] p 1629 N94-19418
Application of an atmospheric dispersion model to simulated pollutant releases in the Colorado Front range
[DE93-017118] p 1480 N94-19732

ATMOSPHERIC COMPOSITION
A technique for measuring winds in the lower atmosphere using incoherent Doppler lidar
[DE93-017163] p 1488 N94-17758
Carbon Dioxide Information Analysis Center: FY 1992 activities
[DE93-013845] p 1471 N94-17774
Analysis of meteorological conditions during AGASP-4: 30 March - 23 April 1992
[PB93-190205] p 1489 N94-18126
A mobile remote sensing laboratory for water vapor, trace gas, aerosol, and wind speed measurements
[DE93-017158] p 1489 N94-18132
A review and evaluation of the ADAM 2.1 dispersion model
[AD-A269896] p 1474 N94-18688
CDIAC catalog of numeric data and computer model packages
[DE93-017675] p 1475 N94-18832
Using computerized tomography to determine ionospheric structures
[DE93-018903] p 1485 N94-19001
Spatiotemporal variability of non-urban ozone concentrations over the eastern United States and its potential replication by satellite data
[PB93-191328] p 1476 N94-19065
Valuation of temporary and future greenhouse gas reductions
[DE93-018876] p 1478 N94-19319
The global atmospheric sulfur cycle: An evaluation of model predictions and observations
[CM-81] p 1479 N94-19379
Helium isotopic abundance variation in nature
[DE93-019050] p 1487 N94-19477
Airborne studies of ocean-particle-cloud interactions in the Arctic
[AD-A270752] p 1479 N94-19575

ATMOSPHERIC CORRECTION
Application of fractal methods to estimate the aerosol-optical depth for atmospheric correction of high resolution satellite data
[DLR-FB-93-04] p 1480 N94-18088
The spatial variance of ionospherically-induced phase errors in SAR imagery
[DE93-015643] p 1385 N94-18232

ATMOSPHERIC DENSITY
Calibration of a high frequency monostatic acoustic echosounder
[AD-A268901] p 1481 N94-18229

ATMOSPHERIC EFFECTS
Upper atmospheric effects of the HF Active Auroral Research Program Ionospheric Research Instrument (HAARP IRI)
[AD-A268948] p 1481 N94-18451
Characterization of the Facility for Atmospheric Corrosion Testing (FACT) at Sandia
[DE93-018510] p 1474 N94-18521

ATMOSPHERIC GENERAL CIRCULATION MODELS
A technique for measuring winds in the lower atmosphere using incoherent Doppler lidar
[DE93-017163] p 1488 N94-17758
Toward a high performance distributed memory climate model
[DE93-019156] p 1494 N94-19298

ATMOSPHERIC HEAT BUDGET
Boundary layer heat budgets from wind profiler/RASS data: A feasibility study
[DE93-013187] p 1489 N94-18052

ATMOSPHERIC HEATING
The vertical distribution of heating in the tropical atmosphere
[AD-A270452] p 1490 N94-18514

ATMOSPHERIC IONIZATION
Photodissociation dynamics of cluster ions
[AD-A270296] p 1568 N94-18814

ATMOSPHERIC MODELS
Surface fluxes important to cloud development
[DE93-016633] p 1488 N94-17715
A review of wind field models for atmospheric transport
[DE93-016085] p 1488 N94-17895
The performance of drag relations in the WAQUA storm surge model
[KNMI-TR-149] p 1496 N94-17923
Energy efficiency and the environment: Innovative ways to improve air quality in the Los Angeles Basin
[DE93-016964] p 1473 N94-18050
On the construction of a regional atmospheric climate model
[KNMI-TR-147] p 1489 N94-18143
The land component of the global climate system with adequate spatial resolution
[DE93-018951] p 1474 N94-18183
RADARC HF ionospheric prediction program for OTH radar
[AD-A269557] p 1385 N94-18291
Wind products for use in coastal wave and surge models
[AD-A269753] p 1497 N94-18414
Microwave (SSM/I) Estimates of the Precipitation Rate to Improve Numerical Atmospheric Model Forecasts
[NASA-CR-193566] p 1491 N94-18602
SERCAA cloud analysis integration: Design concepts and interaction with cloud forecast models
[AD-A269104] p 1492 N94-18637
An investigation of methods for updating ionospheric scintillation models using topside in-situ plasma density measurements
[AD-A269872] p 1483 N94-18655
Preparation of data assimilation and model evaluation experiment data sets
[AD-A269996] p 1498 N94-18665
A review and evaluation of the ADAM 2.1 dispersion model
[AD-A269896] p 1474 N94-18688
Work plan for the Marine Aerosol Properties and the Thermal Imager Performance Trial (MAPTIP)
[AD-A270026] p 1483 N94-18712
An investigation of warm-cloud microphysics using a multi-component cloud model: Interactive effects of the aerosol spectrum
[AD-A270273] p 1493 N94-18812
Inclusion of a three-dimensional washout coefficient in ADPIC
[DE93-018499] p 1476 N94-19038
The global atmospheric sulfur cycle: An evaluation of model predictions and observations
[CM-81] p 1479 N94-19379
Global three dimensional model of tropospheric trace gases chemistry and transport
[AERONAUTICA-ACTA-A-370-199]
p 1479 N94-19518
The wave forecasting model NEDWAM
p 1495 N94-19701
Application of an atmospheric dispersion model to simulated pollutant releases in the Colorado Front range
[DE93-017118] p 1480 N94-19732

ATMOSPHERIC MOISTURE
Radiosonde data collected on the ERS-1 validation cruise RRS Charles Darwin Cruise 62A, Iceland Faeroes region
[IOS-297-1992] p 1461 N94-18137
Moist wind relationships p 1492 N94-18607

ATMOSPHERIC PHYSICS
International Centre for Theoretical Physics, Trieste Scientific activities in 1991
[DE93-624757] p 1606 N94-17792
On the construction of a regional atmospheric climate model
[KNMI-TR-147] p 1489 N94-18143
Analysis of satellite-derived ozone and water vapor measurements
[NASA-CR-193810] p 1486 N94-19237

ATMOSPHERIC PRESSURE
Spectral analysis of synoptic time scale disturbances over the tropical eastern Pacific during summer 1989, 1990 and 1991
[AD-A268821] p 1490 N94-18206
Rapid oceanic cyclogenesis studies
[AD-A269258] p 1490 N94-18265
Dispersion effects on millimeter wavelength attenuation efficiencies for a variety of fibers
[AD-A268992] p 1386 N94-18454

Research on Earth's rotation and the effect of atmospheric pressure on vertical deformation and sea level variability
[NASA-CR-194300] p 1484 N94-18838

ATMOSPHERIC SCATTERING

Dispersion effects on millimeter wavelength attenuation efficiencies for a variety of fibers
[AD-A268992] p 1386 N94-18454

A review and evaluation of the ADAM 2.1 dispersion model
[AD-A269896] p 1474 N94-18688

Morphology and characteristics of disturbed HF skywave channels
[AD-A269755] p 1388 N94-18722

Airborne studies of ocean-particle-cloud interactions in the Arctic
[AD-A270752] p 1479 N94-19575

ATMOSPHERIC SOUNDING

Verification of 3I retrievals vis-a-vis radiosonde observations
[KNMI-TR-150] p 1488 N94-17924

Calibration of a high frequency monostatic acoustic echosounder
[AD-A268901] p 1481 N94-18229

Three-dimensional cloud visualization based on satellite imagery
[AD-A269318] p 1490 N94-18300

Some potential errors in satellite wind estimates using the geostrophic approximation and the thermal wind
[AD-A269784] p 1491 N94-18599

Impact of shorter wavelengths on optical quality for laws
[NASA-CR-193873] p 1579 N94-18858

SPNDL: A concept for a small satellite Doppler lidar wind sounder p 1327 N94-19181

JPRS report: Science and technology. Central Eurasia: Earth Sciences
[JPRS-UES-93-004] p 1461 N94-19209

ATMOSPHERIC TEMPERATURE

Monitoring the response of the upper troposphere/lower stratosphere to a greenhouse gas scenario
[DE93-014509] p 1470 N94-17710

Carbon Dioxide Information Analysis Center: FY 1992 activities
[DE93-013845] p 1471 N94-17774

A mobile remote sensing laboratory for water vapor, trace gas, aerosol, and wind speed measurements
[DE93-017158] p 1489 N94-18132

Radiosonde data collected on the ERS-1 validation cruise RRS Charles Darwin Cruise 62A, Iceland Faeroes region
[IOS-297-1992] p 1461 N94-18137

Station climatic summaries: North America. Volume 1: The contiguous United States
[AD-A269567] p 1490 N94-18303

The vertical distribution of heating in the tropical atmosphere
[AD-A270452] p 1490 N94-18514

Some potential errors in satellite wind estimates using the geostrophic approximation and the thermal wind
[AD-A269784] p 1491 N94-18599

Station climatic summaries, North America. Volume 2: Alaska, Canada and Greenland
[AD-A269793] p 1493 N94-18732

ATMOSPHERIC TURBULENCE

Calibration of a high frequency monostatic acoustic echosounder
[AD-A268901] p 1481 N94-18229

A review and evaluation of the ADAM 2.1 dispersion model
[AD-A269896] p 1474 N94-18688

Estimation of wake vortex advection and decay using meteorological sensors and aircraft data
[AD-A270763] p 1316 N94-19661

ATMOSPHERICS

An investigation of warm-cloud microphysics using a multi-component cloud model: Interactive effects of the aerosol spectrum
[AD-A270273] p 1493 N94-18812

ATOM CONCENTRATION

A preliminary model for crack-tip hydrogen transport
[NPL-DMM(A)-84] p 1451 N94-17899

ATOMIC CLOCKS

Development of atomic standards at the Neuchatel Observatory p 1428 N94-18038

Military applications of high-accuracy frequency standards and clocks
[AD-A269303] p 1430 N94-18299

ATOMIC COLLISIONS

Electron stripping cross sections for light impurity ions in colliding with atomic hydrogens relevant to fusion research
[DE93-788476] p 1566 N94-18158

The quantum dynamics of electronically nonadiabatic chemical reactions
[NASA-CR-194309] p 1568 N94-18837

ATOMIC ENERGY LEVELS

Electron impact excitation of copper atoms
[DE93-017995] p 1363 N94-18939

Unimolecular photodissociation dynamics of ketene (CH2CO): The singlet/triplet branching ratio and experimental observation of the vibrational level thresholds of the transition-state
[DE93-019252] p 1352 N94-19304

ATOMIC EXCITATIONS

Comparison of the modeling solutions with the hydrogen discharge data
[DE93-015115] p 1565 N94-17797

Unitary (pi)(pi)N model of N* excitations in (pi)N and (gamma)N reactions
[DE93-017422] p 1568 N94-18826

Electron impact excitation of copper atoms
[DE93-017995] p 1363 N94-18939

Excited atomic bromine energy transfer and quenching mechanisms
[AD-A270672] p 1572 N94-19607

ATOMIC INTERACTIONS

Correlated charge-changing ion-atom collisions
[DE93-018717] p 1564 N94-17775

ATOMIC PHYSICS

Correlated charge-changing ion-atom collisions
[DE93-018717] p 1564 N94-17775

Diffusion in ordered alloys
[AD-A268232] p 1359 N94-18322

Summaries of FY 1993 research in the chemical sciences
[DE93-011855] p 1632 N94-18915

Atomic-scale friction measurements using friction force microscopy. Part 1: General principles and new measurement techniques
[AD-A270749] p 1446 N94-19678

Schroedinger's hope
[AD-A270988] p 1581 N94-19772

ATOMIC STRUCTURE

Correlated charge-changing ion-atom collisions
[DE93-018717] p 1564 N94-17775

Metal/ceramic interfaces: Relationships between structure and chemistry
[AD-A268792] p 1369 N94-18188

Characterization of diamond film nucleation and growth surface
[AD-A269400] p 1597 N94-18459

Scaling laws for diamond chemical vapor deposition. Diamond surface chemistry
[AD-A269874] p 1599 N94-18745

High energy resolution ARPES measurements of the normal and superconducting states of Bi2Sr2CaCu2O(8 + delta)
[DE93-018294] p 1599 N94-18804

Resonance Raman and photophysical studies of transition metal complexes in solution and entrapped in zeolites
[DE93-019892] p 1363 N94-19019

Surface phases and their influence on metal-oxide interfaces
[DE93-019931] p 1601 N94-19020

Relativistic configuration interaction calculation of the correlation energies of heliumlike ions
[DE93-018093] p 1571 N94-19201

Atomic resolution electron energy loss spectroscopy in the scanning transmission electron microscope
[DE93-015334] p 1352 N94-19239

Crossed molecular beam studies of atmospheric chemical reaction dynamics
[DE93-019246] p 1478 N94-19303

Excited atomic bromine energy transfer and quenching mechanisms
[AD-A270672] p 1572 N94-19607

ATOMIC WEIGHTS

Helium isotopic abundance variation in nature
[DE93-019050] p 1487 N94-19477

ATOMIZING

Combustion instability phenomena of importance to liquid propellant engines
[AD-A268800] p 1348 N94-18389

ATOMS

Harmonic generation at high intensities
[DE93-018632] p 1572 N94-19283

ATTENTION

Stimulus-driven capture and attentional set: Selective search for color and visual abrupt onsets
[IZF-1992-B-9] p 1509 N94-19419

Cognitive ability and whole-body rotation
[IZF-1993-B-4] p 1510 N94-19440

ATTENUATORS

Designs for optical components related to the Los Alamos free-electron laser
[DE93-016617] p 1436 N94-17865

ATTITUDE (INCLINATION)

Cooperative control of multiple space manipulators
[AD-A270291] p 1445 N94-18813

ATTITUDE CONTROL

Research and training activities of the Joint Institute for Aeronautics and Acoustics
[NASA-CR-194742] p 1421 N94-19493

ATTITUDE INDICATORS

Attitude sensor package p 1325 N94-19172

AUDIO EQUIPMENT

Design of a general purpose and autonomous transmitter and receiver system for underwater acoustic experiments at sea
[AD-A269268] p 1495 N94-17822

AUDIOMETRY

The effects of reverberant impulse noise (blast waves) on hearing: Parametric studies
[AD-A269242] p 1506 N94-18911

AUDITORY DEFECTS

The effects of reverberant impulse noise (blast waves) on hearing: Parametric studies
[AD-A269242] p 1506 N94-18911

AUDITORY PERCEPTION

Psychophysical analyses of perceptual representations
[AD-A268711] p 1508 N94-18313

Human-machine interfaces
[AD-A270730] p 1513 N94-19764

AUDITORY STIMULI

The effects of reverberant impulse noise (blast waves) on hearing: Parametric studies
[AD-A269242] p 1506 N94-18911

AUGER SPECTROSCOPY

Guidelines for the expression of uncertainties in surface chemical analysis by Auger Electron Spectroscopy (AES) and X ray Photoelectron Spectroscopy (XPS)
[NPL-DMM(A)-99] p 1346 N94-17900

Ionic and molecular environments in heterogeneous electrocatalysis: Studies by radioactive labeling and LEED/AUGER spectroscopy
[AD-A268850] p 1567 N94-18766

AURORAL ZONES

Global zones of particle precipitation as observed EXOS-C
[AD-A268758] p 1481 N94-18467

An investigation of methods for updating ionospheric scintillation models using topside in-situ plasma density measurements
[AD-A269672] p 1483 N94-18655

The effects of magnetic storm phases on f-layer irregularities from auroral to equatorial latitudes
[AD-A267388] p 1486 N94-19008

AURORAS

Upper atmospheric effects of the HF Active Auroral Research Program Ionospheric Research Instrument (HAARP IRI)
[AD-A268948] p 1481 N94-18451

Global zones of particle precipitation as observed EXOS-C
[AD-A268758] p 1481 N94-18467

AUSTENITE

Development and application of specially-focused ultrasonic transducers to location and sizing of defects in 75 mm- to 127 mm-thick austenitic stainless steel weld metals
[DE93-015975] p 1453 N94-18108

AUSTENITIC STAINLESS STEELS

Technique to eliminate helium induced weld cracking in stainless steels
[DE93-015982] p 1357 N94-17859

Summary of work on coatings and claddings for fossil energy applications
[DE93-017005] p 1367 N94-17881

Prediction of non-equilibrium solidification modes in austenitic stainless steel laser welds
[DE93-018457] p 1364 N94-19203

AUTOCORRELATION

Nontraditional windows in spectral analysis
[AD-A271336] p 1553 N94-19583

AUTOMATA THEORY

Multistack languages and grammars
[REPT-93-018] p 1518 N94-17926

The physics of cellular automata and coherence and chaos in classical many-body dynamical systems
[DE93-018021] p 1561 N94-18177

Robot navigation in unknown terrains: Introductory survey of non-heuristic algorithms
[DE93-019221] p 1316 N94-19300

Causal reasoning for model-based process supervisory control
[LAAS-93241] p 1544 N94-19360

Learning control of large-scale systems
[MATHS-REPT-A-186] p 1544 N94-19408

AUTOMATIC CONTROL

Autonomous neural network controllers for adaptive material handling
[AD-A268908] p 1540 N94-18331

Integrated Terminal Weather System (ITWS)
[AD-A269884] p 1492 N94-18684

A learning autopilot for automatically controlled robust regulation
[ETN-93-95075] p 1321 N94-19711
A stereoscopic vision system with applications to automated docking and tracking
[AD-A270754] p 1333 N94-19765

AUTOMATIC FREQUENCY CONTROL
Automatic tuning of an integral fuzzy controller
[REPT-93-006] p 1383 N94-17932

AUTOMATIC GAIN CONTROL
Automatic tuning of an integral fuzzy controller
[REPT-93-006] p 1383 N94-17932

AUTOMATIC LANDING CONTROL
On the use of differential GPS for automatic approach and landing of space and aircraft
[DLR-MITT-93-05] p 1316 N94-17921

AUTOMATIC PILOTS
A learning autopilot for automatically controlled robust regulation
[ETN-93-95075] p 1321 N94-19711

AUTOMATIC REPEAT REQUEST
Meteor burst communications improvement study
[AD-A270866] p 1393 N94-19793

AUTOMATIC TEST EQUIPMENT
Universal measurement device for electronic watches and small clocks p 1427 N94-18029

AUTOMOBILE FUELS
Evaluation of aftermarket LPG conversion kits in light-duty vehicle applications
[DE93-010035] p 1377 N94-18617
Data collection plan for phase 2 Alternative Fuels Bus Data Collection Program
[DE93-010047] p 1378 N94-18913

AUTOMOBILES
Lightweight materials for transportation: Program plan
[DE93-017381] p 1340 N94-18087
Directions for computational mechanics in automotive crashworthiness p 1459 N94-19472
Modeling of driver behavior: Information perception, rule and control strategies in experiments and simulations
[ETN-93-95053] p 1510 N94-19649

AUTOMORPHISMS
Paragrassmann analysis and quantum groups
[DE93-628593] p 1561 N94-18168

AUTONOMOUS NAVIGATION
Geometrical pattern learning
[DE93-017641] p 1542 N94-19007
A stereoscopic vision system with applications to automated docking and tracking
[AD-A270754] p 1333 N94-19765

AUTOREGRESSIVE PROCESSES
Advances in the identification of transfer function models using Prony analysis
[DE93-017980] p 1548 N94-18094
Spectral analysis on the canonical autoregressive decomposition
[AD-A270083] p 1549 N94-18798
Time dependent identification of nonlinear structures
[ECL-92-64] p 1457 N94-19403
Generalized multichannel signal detection
[AD-A271385] p 1391 N94-19587

AVALANCHE DIODES
The study of the phase structure of hadronic matter by searching for the deconfined quark-gluon phase transition using 2 TeV (bar-p)-p collisions, and by searching for critical phenomena in an exclusive study of multifragmentation using 1 GeV/nucleon heavy ion collisions
[DE93-018925] p 1570 N94-19103

AVIATION METEOROLOGY
Integrated Terminal Weather System (ITWS)
[AD-A269884] p 1492 N94-18684

AVIONICS
Preliminary design of a water cooled avionics cooling rack
[AD-A268826] p 1320 N94-18536
FAA airborne data link human factors research plan
[AD-A271006] p 1514 N94-19773

AXIAL FLOW
Relation between the fluctuating wall pressure and the turbulent structure of a boundary layer on a cylinder in axial flow
[AD-A270242] p 1418 N94-18906
Vane optimization for maximum efficiency using Design Of Experiments (DOX)
[AD-A270270] p 1320 N94-18907

AXIAL LOADS
Transient response of a viscous and anchored liquid bridge to an axial pulse
[LRT-WE-9-FB-7-1992] p 1379 N94-19492

AXIAL STRAIN
Experiments and analysis of lateral piezoresistance gauges
[DE93-017874] p 1433 N94-19111
Modeling and characterization of mechanoelectric conversion piezoelectric generators through dynamical or quasi static uniaxial stress
[ISAL-92-0097] p 1406 N94-19490

AXIAL STRESS
Assessment of an improved multiaxial strength theory based on creep-rupture data for Inconel 600
[DE93-015929] p 1356 N94-17791
New test method to determine modulus of elasticity of rocket grain material
[AD-A269758] p 1377 N94-18758

AXISYMMETRIC BODIES
The effect of fine surface riblets on the flow around an inclined axially symmetrical body
[MPIS-105/1993] p 1420 N94-19356

AXISYMMETRIC FLOW
Applications of the program UIFLOW-2D to the numerical simulation of axisymmetric flows
[AD-A268731] p 1410 N94-18326
Two-dimensional boundary surfaces for axi-symmetric external transonic flows
[AD-A269678] p 1312 N94-18571

AXONS
Coupled neural-dendritic processes: Cooperative stochastic effects and the analysis of spike trains
[AD-A270041] p 1506 N94-18793
Extrathalamic modulation of cortical function
[AD-A270869] p 1507 N94-19783

AZIMUTH
A comparison of single-station backazimuth estimates with regional event locations in the Central Appalachians
[AD-A269897] p 1483 N94-18690

AZOLES
Solderability perservative coatings: Electroless tin versus organic azoles
[DE93-017634] p 1370 N94-18477

B

B STARS
Detection of accreting gas toward HD 45677: A newly recognized, Herbig Be proto-planetary system
[NASA-CR-189312] p 1621 N94-19288

B-1 AIRCRAFT
Temperature of aircraft cargo flame exposure during accidents involving fuel spills
[DE93-019633] p 1381 N94-19539

B-52 AIRCRAFT
Temperature of aircraft cargo flame exposure during accidents involving fuel spills
[DE93-019633] p 1381 N94-19539

BACKGROUND NOISE
Chemical dynamics in time and energy space
[DE93-018595] p 1350 N94-19097
Inverse scattering of surface waves: A new look at surface consistency
[REPT-93-25] p 1486 N94-19140

BACKGROUND RADIATION
Particle induced background by Roentgen satellites
[MPE-242] p 1631 N94-19714

BACKSCATTERING
A technique for measuring winds in the lower atmosphere using incoherent Doppler lidar
[DE93-017163] p 1488 N94-17758
Design of a general purpose and autonomous transmitter and receiver system for underwater acoustic experiments at sea
[AD-A269268] p 1495 N94-17822
Analysis of HgI2 and PbI2 crystals and detectors by Particle-Induced X Ray Emission (PIXE) and Ion Backscattering Spectroscopy (IBS)
[DE93-017168] p 1594 N94-17896
Suppression of backscatter and stray reflection induced phase noise in Michelson interferometers
[AD-D015809] p 1382 N94-17902
Wideband electromagnetic scattering/analysis program: Far zone electromagnetic scattering from complex shapes using geometrical theory of diffraction
[AD-A268790] p 1384 N94-18187
Studies of enhanced radar backscatter
[AD-A269544] p 1385 N94-18288
Simulation of emittance dilution in electron storage ring from Compton backscattering
[DE93-017611] p 1386 N94-18503
Environmental characterization for target acquisition. Report 3: New concepts for evaluating low-grazing angle radar measurements
[AD-A269956] p 1388 N94-18777
BACKSCATTER.FOR: A program to calculate the backscattering strength of an inhomogeneous seabed
[AD-A269235] p 1499 N94-18910
Scientific studies in association with the Shuttle Solar Backscatter Ultraviolet (SSBUV) project
[NASA-CR-193404] p 1630 N94-19437
An ab initio Monte Carlo study of low energy positron and electron implantation in elemental metals and multilayers
[DE93-019847] p 1603 N94-19541
Comparative evaluation of Kirchhoff, perturbation, and full wave methods for rough surface scattering
[AD-A271198] p 1392 N94-19718
Theoretical and experimental research on coherent microwave backscatter from the ocean
[AD-A271276] p 1500 N94-19743
Measurements of ocean surface and bottom backscattering strengths in the northwestern Atlantic Ocean
[AD-A270893] p 1500 N94-19786

BACKWARD FACING STEPS
Numerical solutions for a flow with mixed convection in a vertical geometry
[DE93-011592] p 1419 N94-19058

BACKWARD WAVE TUBES
The gyrotron backward-wave-oscillator experiment — final progress report
[AD-A268982] p 1403 N94-18452

BACKWARD WAVES
The gyrotron backward-wave-oscillator experiment — final progress report
[AD-A268982] p 1403 N94-18452

BACTERIA
Improving the biodegradative capacity of subsurface bacteria
[DE93-013171] p 1501 N94-18051
Photosynthetic reaction centers as active molecular electronic components, phase 1
[AD-A271388] p 1503 N94-19757

BAGGAGE
Road march performance of special operations soldiers carrying various loads and load distributions
[AD-A269198] p 1512 N94-18882

BALLISTICS
Adaptations to micropep and rocket to allow performance evaluation of multiple grain and/or airbreathing motors
[AD-A268798] p 1337 N94-18202
Numerical simulation of fluid dynamics and combustion for ram accelerator projectile/obturator interaction
[AD-A269715] p 1320 N94-18748
Development and characterization of adiabatic shear prone tungsten heavy alloys
[AD-A270477] p 1366 N94-19673
Feasibility study for a measuring system velocity projectile
[FEL-91-A368] p 1434 N94-19797

BALLOON-BORNE INSTRUMENTS
Proceedings of the 3rd Workshop on Balloon-Borne Experiments with Superconducting Magnet Spectrometers
[DE93-788362] p 1630 N94-18219
Origins of solar activity. First year report, AASERT grant
[AD-A268848] p 1629 N94-18222
Widget: A data acquisition system for a balloon borne Si particle calorimeter
[DE93-624668] p 1630 N94-18762

BALLOONING MODES
Plasma properties research: Task 3
[DE93-017087] p 1583 N94-17854
AEOLUS-IT MHD simulation code based on a toroidally incompressible plasma model
[DE93-788461] p 1586 N94-18157

BALLOONS
Proceedings of the 3rd Workshop on Balloon-Borne Experiments with Superconducting Magnet Spectrometers
[DE93-788362] p 1630 N94-18219

BANACH SPACE
Functional analysis of subelliptic operators on lie groups
[PB93-194793] p 1547 N94-18077
Steepest descent method for set-valued locally accretive mappings
[DE93-628592] p 1548 N94-18106
Impulsive moving mirror model in a Schroedinger picture with impulse effect in a Banach space
[DE93-629864] p 1561 N94-18155
Asymptotic behaviour of the solutions of Schroedinger equation with impulse effect in a Banach space
[DE93-629865] p 1548 N94-18195
Impulsive moving mirror model and the stability of Schroedinger equation with impulse effect in a Banach space
[DE93-629866] p 1548 N94-18196
Impulsive moving mirror model and impulsive differential equations in Banach space
[DE93-629867] p 1549 N94-18197

Impulsive moving mirror model and the stability of linear homogeneous differential equations with impulse effect in a Banach space
[DE93-629906] p 1549 N94-18200
L(sub p)-regularity of subelliptic operators on Lie groups
[PB93-194785] p 1549 N94-18948

BAND STRUCTURE OF SOLIDS
High energy resolution ARPES measurements of the normal and superconducting states of Bi2Sr2CaCu2O(8 + delta)
[DE93-018294] p 1599 N94-18804
Optical frequency doubling at adsorbates of silver(110) surface
[ETN-93-94837] p 1603 N94-19355

BANDPASS FILTERS
Design of a general purpose and autonomous transmitter and receiver system for underwater acoustic experiments at sea
[AD-A269268] p 1495 N94-17822
Designs for optical components related to the Los Alamos free-electron laser
[DE93-016617] p 1436 N94-17865
Laser imaging radar system
[AD-A270436] p 1387 N94-18510
Quasi-optical transponder using FET's and patch antennas
[AD-A271339] p 1407 N94-19584

BANDWIDTH
Extending bandwidth of optical emitters using active matching technique
[AD-D015875] p 1394 N94-17707
Coherent transient systems evaluation
[AD-A268808] p 1576 N94-18204
Laser imaging radar system
[AD-A270436] p 1387 N94-18510
Modeling a Yagi array antenna for VHF radar use
[AD-A268973] p 1387 N94-18525

BARENTS SEA
Method for extracting tidal and inertial motion from ARGOS ice buoys applied to the Barents Sea during CEAREX
[PB93-190213] p 1499 N94-19063
Acoustic travel time perturbations due to an internal tide and internal wave field in the Barents Sea
[AD-A270879] p 1499 N94-19580

BARIUM
Review of short-term, high-level exposure to metals: Antimony, barium, and cadmium
[AD-A268896] p 1505 N94-18392

BARIUM COMPOUNDS
The electromechanical properties of tetragonal BaTiO3 and PbTiO3 single crystals
[DE93-019008] p 1603 N94-19550

BARIUM FLUORIDES
Precision machining and polishing of scintillating crystals for large calorimeters and hodoscopes
[DE93-018663] p 1381 N94-19544

BARIUM OXIDES
Fabrication and microstructural development of Ag-clad TlBa2Ca2Cu3O(x) tapes
[DE93-017407] p 1597 N94-18500

BARKHAUSEN EFFECT
Self-organized criticality and the Barkhausen effect in amorphous and polycrystalline metals
[AD-A269817] p 1361 N94-18735

BAROCLINITY
A laboratory model of a cooled continental shelf
[AD-A270862] p 1500 N94-19792

BASE FLOW
Multigrid methods for flow transition in three-dimensional boundary layers with surface roughness
[NASA-CR-4540] p 1417 N94-18843

BATHYMETERS
Overview of physical oceanographic measurements taken during the Mount Mitchell cruise to ROPME sea area
[DE93-018460] p 1497 N94-18494
Processing and analysis of SeaMARC 2 data: Fieberling guyot; raw phase experiment in Norwegian-Greenland Sea
[AD-A269930] p 1498 N94-18662
Modifications of airborne oceanographic lidar for the long range P-3 missions
[NASA-CR-194682] p 1499 N94-18819
Modeling of current features in Gulf Stream SAR imagery
[AD-A270734] p 1499 N94-19609

BATHYTHERMOGRAPHS
An atlas of bathy-thermograph temperature cross-sections for Coral and Tasman Sea transects from 1960 to 1987
[AD-A268775] p 1497 N94-18329

BAYES THEOREM
A Bayesian approach to contaminant plume delineation
[DE93-012909] p 1472 N94-17890
Examination of metrics and assumptions used in correlation filter design
[DE93-017636] p 1576 N94-18000
Bayesian model choice: Asymptotics and exact calculations
[AD-A269067] p 1557 N94-18516
Bayesian analysis of ARMA processes: Complete sampling based inference under full likelihoods
[AD-A269168] p 1557 N94-18694
A least-squares computational tool kit
[DE93-018400] p 1557 N94-19011
Bounds for expected loss in Bayesian decision theory with imprecise prior probabilities
[PB93-197507] p 1558 N94-19327

BAYS (STRUCTURAL UNITS)
Aircraft fire sentry. Volume 1: Summary
[AD-A270087] p 1315 N94-18822
Aircraft fire sentry. Volume 2: Appendices A, B, C and D
[AD-A270088] p 1315 N94-18823

BCS THEORY
Crossover from BCS to Bose superconductivity: A functional integral approach
[DE93-019503] p 1604 N94-19566

BEADS
Modeling of single-crystal laser-weld microstructures
[DE93-017853] p 1445 N94-18976

BEAM CURRENTS
Designs for a 10.6 micrometer electromagnetic wiggler Free-Electron Laser (FEL)
[AD-A269695] p 1439 N94-18576
Simulation of transient effects in the heavy ion fusion injectors
[DE93-018658] p 1575 N94-19107

BEAM INJECTION
Compound-lens injector for a 19-MeV, 700-kA electron beam
[DE93-013752] p 1573 N94-17698
FEL experiment with a focusing wiggler
[DE93-788586] p 1438 N94-18160
Heavy Ion Fusion Injector Program
[DE93-018706] p 1575 N94-18997
Simulation of transient effects in the heavy ion fusion injectors
[DE93-018658] p 1575 N94-19107

BEAM INTERACTIONS
Advanced methods for the computation of particle beam transport and the computation of electromagnetic fields and beam-cavity interactions
[DE93-018160] p 1573 N94-17807
Plasma klystron amplifier
[AD-D015819] p 1395 N94-17903
Advances and applications of ABCI
[DE93-016971] p 1383 N94-18055
Laser powered beam conditioner for free-electron lasers and synchrotrons
[DE93-017821] p 1441 N94-18974

BEAMFORMING
The Intense Slow Positron Source concept: A theoretical perspective on a proposed INEL Facility
[DE93-013675] p 1564 N94-17738

BEAMS (RADIATION)
Electro-optic beam steering using non-linear organic materials
[AD-A270809] p 1374 N94-19577

BEAMS (SUPPORTS)
Computational mechanics of composite materials
[PB93-195782] p 1343 N94-19281
Reanalysis of structure models
[ECL-93-07] p 1458 N94-19460
Development of engineering models for calculation of failure loads and defect states of steel concrete beams and plates
[ETN-93-95052] p 1460 N94-19648

BEARING (DIRECTION)
Directional regions in Geographic Information Systems (GIS)
[AD-A268536] p 1462 N94-18309

BEND TESTS
Surface modification of sapphire for IR window application
[DE93-019168] p 1602 N94-19075

BENDING
Benchmarking the QUAD4/TRIA3 element
p 1450 N94-17837
A benchmark bending test of a thick specimen. Part 1: Experiments
[AD-A268730] p 1360 N94-18325
Plastic mechanism analysis of T-joints in RHS subject to combined bending and concentrated force
[PB93-195774] p 1456 N94-19061

BENDING FATIGUE
Defining the normal turbine inflow within a wind park environment
[DE93-010032] p 1489 N94-18046

BENDING MOMENTS
Defining the normal turbine inflow within a wind park environment
[DE93-010032] p 1489 N94-18046
Numerical integration of structural elements in NIKE3D and DYNA3D
[DE93-016325] p 1452 N94-18049

BENZOIC ACID
Polyurethane self-priming topcoats
[AD-D015870] p 1367 N94-17719

BERYLLIUM
Beryllium processing technology review for applications in plasma-facing components
[DE93-018396] p 1363 N94-19028

BERYLLIUM ALLOYS
Developing and understanding the high temperature behavior of niobium aluminides and niobium aluminide composites
[AD-A268874] p 1341 N94-18636

BERYLLIUM FLUORIDES
Calculation of the LiF-CeF3-BeF2 and LiF-PuF3-BeF2 ternary phase diagrams
[DE93-017437] p 1360 N94-18501

BETA PARTICLES
Neutrino mass
[DE93-018467] p 1567 N94-18269
Inverse neutrinoless double (beta)-decay at the NLC?
[DE93-017397] p 1568 N94-18825

BETATRONS
Decoherence and recoherence of beam in phase space
[DE93-014885] p 1573 N94-17784

BIAS
Bias in planning and explanation-based learning
[AD-A269608] p 1610 N94-17746

BIBLIOGRAPHIES
Bibliography of scientific publications of the Naval Biodynamics Laboratory, 1980 - 1992
[AD-A268886] p 1505 N94-18226
Aeronautical engineering: A continuing bibliography with indexes (supplement 297)
[NASA-SP-7037(297)] p 1310 N94-18937
Energy Efficiency and Renewable Energy Program
[DE93-017936] p 1468 N94-18986
Aerospace medicine and biology: A continuing bibliography with indexes (supplement 381)
[NASA-SP-7011(381)] p 1507 N94-19069
Aeronautical engineering: A continuing bibliography with indexes (supplement 296)
[NASA-SP-7037(296)] p 1310 N94-19070
An annotated bibliography on parallel parsing: Updated version
[MEMO-INF-92-84] p 1537 N94-19223
Bibliography on silicides
[AD-A270516] p 1374 N94-19532
Mathematical communications, volume 27, numbers 1 and 2, 1992. List and abstracts of memoranda published in the period July - December 1991
[PB93-191997] p 1553 N94-19557
Learning about the Internet bibliography and beginner's guide
[AD-A268847] p 1532 N94-19707

BIHARMONIC EQUATIONS
Solution of the Poisson equation with application to radar imaging
[PB93-195865] p 1389 N94-18950

BIMETALS
Oligomer and mixed-metal compounds, potential multielectron transfer catalysts
[DE93-019592] p 1350 N94-19017
The applications of modified metals in the construction industry
[VTT-TIED-1329] p 1365 N94-19374

BINARY ALLOYS
Recent studies of short-range order in alloys: The Cowley theory revisited
[DE93-016416] p 1358 N94-18111
Diffusion in ordered alloys
[AD-A268232] p 1359 N94-18322
Deformation mechanisms in a Laves phase
[DE93-018331] p 1361 N94-18806
Morphology, deformation, and defect structures of TiCr2 in Ti-Cr alloys
[DE93-018332] p 1361 N94-18807
Intelligent materials systems and structures. Part 4: The influence of thermomechanical loading on the life of shape memory alloys
[PB93-195923] p 1363 N94-18952
Tensile properties of as-cast iron-aluminide alloys
[DE93-017852] p 1363 N94-18975

A free energy simulation method based study of interfacial segregation
[DE93-019462] p 1364 N94-19032

BINARY DATA
Optimal design of binary phase-only filters using genetic algorithms
[AD-A268737] p 1396 N94-18278
Canonical multi-valued input Reed-Muller trees and forms p 1401 N94-18375

BINARY MIXTURES
Structure, thermodynamics, and dynamical properties of supercooled liquids
[DE93-788387] p 1607 N94-18211

BINARY PHASE SHIFT KEYING
Meteor burst communications improvement study
[AD-A270866] p 1393 N94-19793

BINARY SYSTEMS (MATERIALS)
Effect of oxygen concentration and ordering on vanadium-oxygen alloy vibrational spectra
[DE93-627003] p 1355 N94-17692
The longitudinal free vibrations of a fixed-free two-phase elastic bar
[AD-A268768] p 1453 N94-18387
The temperature at the phase boundary during quasi-static motions of a two-phase thermoelastic bar
[AD-A268769] p 1596 N94-18388
Interfacial cracks in plates: A three-dimensional numerical investigation p 1456 N94-19116

BINDERS (MATERIALS)
Polyurethane self-priming topcoats
[AD-D015870] p 1367 N94-17719
Some problems in the rheological characterisation of composite rocket propellants
[AD-A268806] p 1376 N94-18203

BIOASTRONAUTICS
Characterization of fluid physics effects on cardiovascular response to microgravity (G-572)
p 1323 N94-19163

BIOCHEMISTRY
Fifteenth Symposium on Biotechnology for Fuels and Chemicals: Program and Abstracts
[DE93-010005] p 1376 N94-18045
Photosynthetic responses to the environment, volume 8
[AD-A269584] p 1502 N94-18305
A numerical study of hybrid optimization methods for the molecular conformation problems
[DE93-017896] p 1569 N94-18985

BIOCONVERSION
Fifteenth Symposium on Biotechnology for Fuels and Chemicals: Program and Abstracts
[DE93-010005] p 1376 N94-18045
Photobiotechnology: Application of photosynthesis to the production of renewable fuels and chemicals
[DE93-015522] p 1466 N94-18247
Factors that control the stable carbon isotopic composition of methane produced in an anoxic marine sediment p 1477 N94-19235

BIODEGRADABILITY
Microbial degradation of poly-b-esters: A mechanistic study, cellulose acetate biodegradability
[AD-A271368] p 1374 N94-19586

BIODEGRADATION
Improving the biodegradative capacity of subsurface bacteria
[DE93-013171] p 1501 N94-18051
Microbial degradation of poly-b-esters: A mechanistic study, cellulose acetate biodegradability
[AD-A271368] p 1374 N94-19586

BIODYNAMICS
Control of shoulder muscles during goal directed movements
[PB93-195139] p 1504 N94-18080
Bibliography of scientific publications of the Naval Biodynamics Laboratory, 1980 - 1992
[AD-A268886] p 1505 N94-18226
Army Cockpit Delethalization Program (CDP)
[AD-A268990] p 1512 N94-18765
Consortium for materials development in space
[NASA-CR-194411] p 1379 N94-18840

BIOENGINEERING
Program descriptions
[NSF-92-123] p 1531 N94-19619

BIOGEOCHEMISTRY
Carbon Isotope Biogeochemistry of Methane from Anoxic Sediments
[NASA-CR-194620] p 1477 N94-19231
The carbon isotope biogeochemistry of (epsilon)CO2 production in a methanogenic marine sediment
p 1477 N94-19233
The carbon isotope biogeochemistry of methane production in anoxic sediments. 1: Field observations
p 1477 N94-19234

BIOINSTRUMENTATION
Bienzyme sensors based on electrically wired peroxidase
[AD-A271364] p 1374 N94-19585

BIOLOGICAL EFFECTS
Cellular and molecular level responses after radiofrequency radiation exposure, alone or in combination with x rays or chemicals
[AD-A268189] p 1501 N94-17729
Air pollution effects field research facility. 3: UV-B exposure and monitoring system
[DE93-013098] p 1470 N94-17773
Assessing impacts of climate change on forests: The state of biological modeling
[DE93-015916] p 1471 N94-17790
Compilation of 1992 annual reports of the Navy ELF communications system ecological monitoring program, volume 1
[AD-A269569] p 1386 N94-18473
The c-jun gene expression in human cells exposed to either ionizing radiation or hydrogen peroxide
[DE93-017436] p 1502 N94-18476
Compilation of 1992 annual reports of the navy ELF communications system ecological monitoring program. Volume 3: Tabs G - I
[AD-A269727] p 1388 N94-18741
Compilation of 1992 annual reports of the navy ELF communications system ecological monitoring program, volume 2
[AD-A269726] p 1388 N94-18751
Aerospace medicine and biology: A continuing bibliography with indexes (supplement 382)
[NASA-SP-7011(382)] p 1507 N94-18936
Aerospace medicine and biology: A continuing bibliography with indexes (supplement 381)
[NASA-SP-7011(381)] p 1507 N94-19069
Opportunities and questions for the fundamental biological sciences in space p 1502 N94-19212
Space research with intact organisms: The role of Space Station Freedom p 1502 N94-19213
Effect of EMP fields on cell membrane potentials
[DE93-015819] p 1503 N94-19341

BIOLOGICAL EVOLUTION
Space Life Sciences Research: The Importance of Long-Term Space Experiments
[NASA-TM-4502] p 1502 N94-19210
Opportunities and questions for the fundamental biological sciences in space p 1502 N94-19212
Life: Origin and evolution on Earth--How can we escape? p 1503 N94-19217

BIOLOGICAL MODELS (MATHEMATICS)
Assessing impacts of climate change on forests: The state of biological modeling
[DE93-015916] p 1471 N94-17790
Control of shoulder muscles during goal directed movements
[PB93-195139] p 1504 N94-18080

BIOLOGY
The 1982 to 1992 decade of research on the vacuum ultraviolet ring at National Synchrotron Light Source
[DE93-019469] p 1603 N94-19564

BIOLUMINESCENCE
Modified aequorin shows increased bioluminescence activity
[AD-A268774] p 1347 N94-18185

BIOMASS
Report to Congress: Comprehensive Program Plan for Advanced Turbine Systems
[DE93-016718] p 1467 N94-18475

BIOMASS ENERGY PRODUCTION
Fifteenth Symposium on Biotechnology for Fuels and Chemicals: Program and Abstracts
[DE93-010005] p 1376 N94-18045

BIOPHYSICS
Biophysical characterization and surface radiation balance
[NASA-CR-194659] p 1470 N94-17762

BIOPOLYMERS
Matrix- and substrate-assisted laser desorption for fast DNA sequencing
[DE93-015332] p 1501 N94-18242

BIOPROCESSING
Fifteenth Symposium on Biotechnology for Fuels and Chemicals: Program and Abstracts
[DE93-010005] p 1376 N94-18045

BIOTECHNOLOGY
Fifteenth Symposium on Biotechnology for Fuels and Chemicals: Program and Abstracts
[DE93-010005] p 1376 N94-18045
Multimodal image correlation applied to computer aided pedicular screwing
[ETN-93-95018] p 1528 N94-19363
Photosynthetic reaction centers as active molecular electronic components, phase 1
[AD-A271388] p 1503 N94-19757

BIRD-AIRCRAFT COLLISIONS
Explicit solution techniques for impact with contact constraints p 1459 N94-19470

BIREFRINGENCE
RF phase stabilization for RF photocathode gun through electro-optical monitoring
[DE93-019059] p 1406 N94-19310

BISMUTH COMPOUNDS
Single source precursors for the OMCVD of 3/5 compound semiconductors
[AD-A271147] p 1606 N94-19739

BITS
The universal BitBus node
[DIGEL-1993-1] p 1515 N94-19799

BLACK BODY RADIATION
Imaging and blackbody emission spectra of hot particulates generated during laser ablation
[DE93-015818] p 1439 N94-18724

BLACK HOLES (ASTRONOMY)
Maximal hypersurfaces in asymptotically stationary spacetimes
[MPA-708] p 1621 N94-18141

BLAST LOADS
Instrumented experiments aboard the frigate WOLF. Wolf 2: Measurement results of the 5.5 kg TNT in the crew aft sleeping compartment
[PML-1992-12] p 1451 N94-17931
Scaling laws for diffraction loading by air blast
[PML-1991-54] p 1452 N94-17941
Air blast measurements at 20 and 40 km distance from detonating 10 and 20 ton high explosive charges
[PB93-195949] p 1419 N94-19068

BLOCKING
Structural stability of 1100 C heated Pd/k during absorption cycling in protium
[DE93-016270] p 1346 N94-18048

BLOOD
Evaluation of dried storage of platelets for transfusion: Physiologic integrity and hemostatic functionality
[AD-A270756] p 1507 N94-19593

BLOOD CIRCULATION
Metabolic changes and hemodynamic dysfunction following hypothermic shock
[AD-A269780] p 1506 N94-18598

BLOOD PLASMA
Transcutaneous Analyte Measuring Methods (TAMM)
[AD-A271387] p 1408 N94-19756

BLUFF BODIES
Spectral radiance measurements on a bluff body stabilized flame: Characterization of the IR signature
[PB93-195899] p 1347 N94-18081

BODIES OF REVOLUTION
Two-dimensional boundary surfaces for axi-symmetric external transonic flows
[AD-A269678] p 1312 N94-18571

BODY CENTERED CUBIC LATTICES
Recent studies of short-range order in alloys: The Cowley theory revisited
[DE93-016416] p 1358 N94-18111
Dislocation-drag contribution to high-rate plastic deformation in shock-loaded tantalum
[DE93-018286] p 1361 N94-18802

BODY COMPOSITION (BIOLOGY)
In vivo animal models of body composition in aging
[DE93-012527] p 1501 N94-17889

BODY KINEMATICS
Control of shoulder muscles during goal directed movements
[PB93-195139] p 1504 N94-18080

BODY SIZE (BIOLOGY)
A multivariate anthropometric method for crew station design
[AD-A270652] p 1513 N94-19531

BODY TEMPERATURE
Effects of a high-energy food supplement on cold-induced thermogenesis
[AD-A269301] p 1504 N94-17823
Metabolic changes and hemodynamic dysfunction following hypothermic shock
[AD-A269780] p 1506 N94-18598
Evaluation of physiological and psychological impairment of human performance in cold stressed subjects
[AD-A268637] p 1506 N94-18632

BODY WEIGHT
Analysis of seating and restraint limitations restricting total body weight for aircrew and passengers on US Army helicopters
[AD-A269117] p 1511 N94-18296

BODY-WING AND TAIL CONFIGURATIONS
WBNGRID, a program for generation of C-H and C-O topology grids around wing/body/nacelle configurations: User's guide
[FFA-TN-1992-09] p 1311 N94-17721

Navier-Stokes, dynamics and aeroelastic computations for vortical flows, buffet and flutter applications
[NASA-CR-194520] p 1313 N94-19621

BODY-WING CONFIGURATIONS
Numerical calculations of high lift flows using structured and unstructured methods p 1307 N94-18428

BOEING 720 AIRCRAFT
Composite impact dynamics research at NASA LaRC: A review p 1458 N94-19467

BOILERS
Summary of work on coatings and claddings for fossil energy applications
[DE93-017005] p 1367 N94-17881

BOILING
Temperature lowering in cryogenic chemical-synthesis techniques and system
[DE93-018348] p 1562 N94-18810
Bench-scale screening tests for a boiling sodium-potassium alloy solar receiver
[DE93-018512] p 1469 N94-19040

BOLOMETERS
Infrared detection with high-(Tc bolometers and response of Nb tunnel junctions to picosecond voltage pulses
[DE93-016963] p 1595 N94-17989

BOLTED JOINTS
Analysis of bolted and bonded composite
[AD-A267792] p 1453 N94-18382

BOLTZMANN TRANSPORT EQUATION
Criticality benchmark comparisons leading to cross-section upgrades
[DE93-017184] p 1556 N94-18073
IR materials producibility
[AD-A268849] p 1577 N94-18223
Full Boltzmann discrete spectral wave model, implementation and nondimensional tests
[AD-A269885] p 1498 N94-18685
Modelling ideal gas fluorides laser plasmas
[ETN-93-95073] p 1592 N94-19613

BOLTZMANN-VLASOV EQUATION
On neutral plasma oscillations
[DE93-040319] p 1590 N94-19194

BOMBER AIRCRAFT
Procedures and design data for the formulation of aircraft configurations
[AD-A270150] p 1318 N94-18779

BONDED JOINTS
Mathematical modelling of bonded fibre-composite repairs to aircraft
[AD-A268732] p 1341 N94-18327
Analysis of bolted and bonded composite
[AD-A267792] p 1453 N94-18382
High performance YBCO films
[AD-A269090] p 1599 N94-18719

BONDING
High- and low-temperature bonding techniques for microstructures
[DE93-017173] p 1595 N94-17992
Ising model on tangled chain. Part 2: Magnetization and susceptibility
[DE93-628794] p 1607 N94-18174
Strained ring energetic binders
[AD-A269056] p 1377 N94-18491

BONES
Space research on organs and tissues
p 1503 N94-19214

BOOMS (EQUIPMENT)
Packaging, deployment, and panel design concepts for a truss-stiffened 7-panel precision deployable reflector with feed boom
[NASA-TM-109000] p 1333 N94-17765

BORATES
Final report on subcontract B076260 --- borate synthesis
[DE93-019501] p 1604 N94-19565

BOREHOLES
Ground movements associated with gas hydrate production
[DE93-019887] p 1486 N94-19018

BORESIGHTS
Modeling a Yagi array antenna for VHF radar use
[AD-A268973] p 1387 N94-18525

BORIDES
Molecular and polymeric ceramic precursors
[DE93-040364] p 1372 N94-18891

BORN APPROXIMATION
Fast iterative solution of sparsely sampled seismic inverse problems
[REPT-93-16] p 1486 N94-19081

BORON
Molecular and polymeric ceramic precursors
[DE93-040364] p 1372 N94-18891

BORON CARBIDES
Molecular and polymeric ceramic precursors
[DE93-040364] p 1372 N94-18891

BORON COMPOUNDS
Molecular and polymeric ceramic precursors
[DE93-040364] p 1372 N94-18891

BORON NITRIDES
Molecular and polymeric ceramic precursors
[DE93-040364] p 1372 N94-18891

BOSONS
Experimental consequences of supersymmetry
[DE93-018270] p 1569 N94-18945
Thermodynamic q-distributions that aren't
[DE93-017385] p 1609 N94-19121

BOTANY
Photosynthetic responses to the environment, volume 8
[AD-A269584] p 1502 N94-18305

BOUNDARIES
Cut and paste based modeling with boundary features
[PB93-187250] p 1520 N94-18117
The temperature at the phase boundary during quasi-static motions of a two-phase thermoelastic bar
[AD-A268769] p 1596 N94-18388

BOUNDARY CONDITIONS
Calculation of maximum and high lift characteristics of multi element aerofoils p 1305 N94-18419
Solution of the Poisson equation with application to radar imaging
[PB93-195865] p 1389 N94-18950
Finite difference program for calculating hydride bed wall temperature profiles
[DE93-019272] p 1523 N94-19005
A priori estimates and existence of positive solutions of a superlinear polyharmonic equation
[REPT-93-12] p 1550 N94-19086
Decomposition invariance of generalized steady-state of a 1-D diffusion system
[REPT-93-26] p 1550 N94-19141
A physical model for one-dimension and time-dependent ionosphere. Part 1: Description of the model
[DE93-627958] p 1486 N94-19255
Improved approximations applied to the S(sub N) even-parity equation
[DE93-016467] p 1551 N94-19343
Numerical experiments on the Ginzburg-Landau equations
[DE93-019504] p 1604 N94-19567
Acoustic propagation modeling using MATLAB
[AD-A270905] p 1564 N94-19750

BOUNDARY LAYER CONTROL
Impulsive moving mirror model in a Schroedinger picture with impulse effect in a Banach space
[DE93-629864] p 1561 N94-18155

BOUNDARY LAYER EQUATIONS
Calculation of multielement airfoils and wings at high lift p 1309 N94-18438

BOUNDARY LAYER FLOW
Two-dimensional boundary surfaces for axi-symmetric external transonic flows
[AD-A269678] p 1312 N94-18571
Direct and large eddy simulation of turbulence: Summary of the state of the art 1993 p 1416 N94-18594
Relation between the fluctuating wall pressure and the turbulent structure of a boundary layer on a cylinder in axial flow
[AD-A270242] p 1418 N94-18906
Semi-span model testing in the National Transonic Facility
[NASA-CR-194479] p 1312 N94-19388

BOUNDARY LAYER SEPARATION
Several examples where turbulence models fail in inlet flow field analysis p 1412 N94-18556
Two-dimensional boundary surfaces for axi-symmetric external transonic flows
[AD-A269678] p 1312 N94-18571

BOUNDARY LAYER STABILITY
Two-equation models for high-Reynolds-number flow
p 1415 N94-18586
Two-equation models for low-Reynolds-number variants p 1415 N94-18587
The application of front tracking to the simulation of shock refractions and shock accelerated interface mixing
[DE93-018342] p 1419 N94-19025

BOUNDARY LAYER TRANSITION
An experimental investigation of attachment-line transition on the slat of a combat aircraft model
p 1308 N94-18432
Viscous phenomena affecting high-lift systems and suggestions for future CFD development
p 1308 N94-18433
Research on two equation models
p 1411 N94-18547
Multigrid methods for flow transition in three-dimensional boundary layers with surface roughness
[NASA-CR-4540] p 1417 N94-18843
Experimental investigation of turbulent Prandtl number and Reynolds analogy in transitional and post-transitional boundary layers
[AD-A270092] p 1418 N94-18867
The application of front tracking to the simulation of shock refractions and shock accelerated interface mixing
[DE93-018342] p 1419 N94-19025

BOUNDARY LAYERS
Relation between the fluctuating wall pressure and the turbulent structure of a boundary layer on a cylinder in axial flow
[AD-A270242] p 1418 N94-18906
Protocol for computation of surface boundary layer parameters used to determine soil moisture flux from meteorological data collected at LLNL, 1992-1993
[DE93-018906] p 1463 N94-19003
Velocity measurements in a boundary layer with a density gradient
[DE93-019627] p 1422 N94-19515
Surface species in tribology
[AD-A270970] p 1446 N94-19754

BOUNDARY VALUE PROBLEMS
The phase mixing of shear Alfven waves
[DE93-624920] p 1581 N94-17688
A free boundary eigenvaue problem
[IPP-6/310] p 1584 N94-17981
The longitudinal free vibrations of a fixed-free two-phase elastic bar
[AD-A268768] p 1453 N94-18387
The temperature at the phase boundary during quasi-static motions of a two-phase thermoelastic bar
[AD-A268769] p 1596 N94-18388
A method for finding the periodic solution of autonomous ordinary differential equations
[DE93-624725] p 1550 N94-19244
A method for solving the KDV equation and some numerical experiments
[DE93-624726] p 1550 N94-19246
Improved approximations applied to the S(sub N) even-parity equation
[DE93-016467] p 1551 N94-19343
On the numerical approximation of nonlinear hyperbolic problems: Application to the dynamics of compressible gas
[ETN-93-95020] p 1420 N94-19365
Transient skin effect in a massive cylinder by eccentric location of exciting conduction bands
[ETN-93-95048] p 1391 N94-19646
Numerical modelling of crystal growth
[AD-A271206] p 1605 N94-19719

BOUSSINESQ APPROXIMATION
Modeling and new equipment definition for the vibration isolation box equipment system
[NASA-CR-193185] p 1379 N94-17763
Numerical solutions for a flow with mixed convection in a vertical geometry
[DE93-011592] p 1419 N94-19058

BOX BEAMS
Plastic mechanism analysis of T-joints in RHS subject to combined bending and concentrated force
[PB93-195774] p 1456 N94-19061

BRAGG ANGLE
Apparatus and method for varying a Bragg wavelength of a Bragg grating formed in an optical fiber
[AD-D015876] p 1579 N94-18743

BRAGG CELLS
Magnetostatic waves-based integrated optic bragg cell modules with applications to RF signal processing
[AD-A269115] p 1577 N94-18295

BRAIN
The identification of the computational significance of key neurobiological characteristics found in a number of telencephalic brain regions
[AD-A269374] p 1505 N94-18407
Coupled neural-dendritic processes: Cooperative stochastic effects and the analysis of spike trains
[AD-A270041] p 1506 N94-18793
Strategies for enhancing catecholamine-mediated neurotransmission
[NASA-CR-193807] p 1506 N94-18862
The brain electrical activity in different G situations
[AERONAUTICA-ACTA-A-372-199]
p 1507 N94-19523

BRAIN DAMAGE
Cerebral ischemia and reperfusion injury: A brief review
[AD-A270480] p 1507 N94-19675

BRANCHING (MATHEMATICS)
A free boundary eigenvaue problem
[IPP-6/310] p 1584 N94-17981
Stability analysis through bifurcation theory, 1
p 1608 N94-18238
Stability analysis through bifurcation theory, 2
p 1608 N94-18239
Non-linear flight dynamics p 1319 N94-18240

Deterministic growth-dispersal models and branching random walk
[REPT-93-14] p 1550 N94-19088

BRAZING
Joining and Adhesion of Advanced Inorganic Materials Symposium
[AD-A269748] p 1342 N94-18720
Diamond brazed to a metal
[AD-D015877] p 1371 N94-18746

BREMSSTRAHLUNG
Absorption and x ray measurements from ultra-intense laser-plasma interactions
[DE93-016538] p 1585 N94-18115
Detection of a long-duration solar gamma-ray flare on Jun. 11, 1991 with EGRET on Compton-GRO
p 1623 N94-19463

BRIGHTNESS
Observations of comets with the IUE
[NASA-CR-193652] p 1624 N94-17843
Electro-optics display research, test, and evaluation laboratory program
[AD-A270947] p 1408 N94-19751

BRIGHTNESS TEMPERATURE
Physical retrieval of precipitation water contents from Special Sensor Microwave/Imager (SSM/I) data. Part 1: A cloud ensemble/radiative parameterization for sensor response (report version) p 1491 N94-18604
Physical retrieval of precipitation water contents from Special Sensor Microwave/Imager (SSM/I) data. Part 2: Retrieval method and applications (report version)
p 1491 N94-18605

BRILLOUIN EFFECT
Elastic properties of a polyimide film determined by Brillouin scattering and mechanical techniques
[DE93-017404] p 1368 N94-18098
Applications of nonlinear optic effects in new specialty fibers
[AD-A268890] p 1578 N94-18457
Phase conjugation and beam combination using stimulated brillouin scattering
[AD-A269899] p 1439 N94-18656

BRILLOUIN ZONES
Phase conjugation and beam combination using stimulated brillouin scattering
[AD-A269899] p 1439 N94-18656

BRITTLE MATERIALS
Construction of a tension-torsion anisotropic brittle damage elastic model
[ECL-91-27] p 1457 N94-19375

BRITTLENESS
A numerical analysis of crack growth in brittle microcracking composites
[DE93-011562] p 1343 N94-18914
Dynamical behavior of octahedrite from the Henbury meteorite
[DE93-018834] p 1627 N94-19339

BROADBAND
Wideband electromagnetic scattering/analysis program: Far zone electromagnetic scattering from complex shapes using geometrical theory of diffraction
[AD-A268790] p 1384 N94-18187
Intentionally Short Range Communications (ISRC)
[AD-A268788] p 1384 N94-18216
Development of parallel architectures for sensor array processing. Volume 2: A parallel architecture for broad-band direction-of-arrival estimation
[AD-A270427] p 1534 N94-18508
Parallel and vector adaptations of the underwater finite element parabolic equation model
[AD-A269990] p 1563 N94-18678
Morphology and characteristics of disturbed HF skywave channels
[AD-A269755] p 1388 N94-18722
Broadband IF matching for quasioptical mixers
[MPE-PREPRINT-240] p 1390 N94-19416
Experimental and theoretical investigation of broadband high-power windows for millimeter waves
[KFK-5157] p 1391 N94-19617
The wideband plasma wave investigation
p 1328 N94-19627

BROADBAND AMPLIFIERS
Extending bandwidth of optical emitters using active matching technique
[AD-D015875] p 1394 N94-17707
Experimental examinations of semiconductor laser amplifiers for optical communication technology
[ETN-93-95050] p 1442 N94-19647

BROKEN SYMMETRY
Neutrino masses in superstring derived standard-like models
[DE93-624802] p 1565 N94-17951
T violating neutron spin rotation asymmetry
[DE93-018470] p 1570 N94-19126
Investigations in gauge theories, topological solitons, and string theories
[DE93-015029] p 1609 N94-19250

BROMINE
Excited atomic bromine energy transfer and quenching mechanisms
[AD-A270672] p 1572 N94-19607

BROMINE ISOTOPES
The A((2)pi(sub u))-X((2)pi(sub g)) system of Br2(+) studied by velocity modulation spectroscopy
[USIP-93-04] p 1569 N94-18847

BRONZES
Photorefractive tungsten bronze crystals for optical computing
[AD-A268859] p 1596 N94-18320

BROWNIAN MOVEMENTS
The rank of the present excursion
[REPT-93-22] p 1558 N94-19137

BSCCO SUPERCONDUCTORS
Mechanical properties of fiber-reinforced YBa2Cu3O(x) and Bi2Sr2CaCu2O(x) bars
[DE93-017689] p 1454 N94-18479
Fabrication and characterization of high-T(sub c) tapes and coils made from Ag-clad Bi-2223 superconductors
[DE93-018615] p 1601 N94-18993
Preparation and characterisation of the compound Tl(0.65) Bi(0.35) Ca(0.8) Sr(1.7) Cu2 O(y) using oxalate coprecipitation and analytical CBED and an initial preparation of Bi2Ca(n-1) Sr2Cu(n) O(4+2n) for n=5
[DE93-625470] p 1602 N94-19277

BUBBLES
Technique to eliminate helium induced weld cracking in stainless steels
[DE93-015982] p 1357 N94-17859
Compatibility of refrigerants and lubricants with motor materials, volume 1
[DE93-040216] p 1350 N94-18895

BUFFER STORAGE
Congestion/flow control and routing in data networks: A control-theoretic approach
[AD-A271121] p 1392 N94-19737

BUFFETING
Comparison between swept and delta canards on a model of a combat aircraft
[AD-A269561] p 1317 N94-17826
Navier-Stokes, dynamics and aeroelastic computations for vortical flows, buffet and flutter applications
[NASA-CR-194520] p 1313 N94-19621

BUILDINGS
Indoor environment program
[DE93-018601] p 1513 N94-18935

BUNCHING
Synchrotron beam-loading stability with a higher RF harmonic
[DE93-014549] p 1573 N94-17726
Simulation of the ALS longitudinal multibunch feedback system
[DE93-019227] p 1575 N94-19152

BUOYANCY
Modelling force-field effects on turbulence
p 1414 N94-18581

BUOYS
Method for extracting tidal and inertial motion from ARGOS ice buoys applied to the Barents Sea during CEAREX
[PB93-190213] p 1499 N94-19063

BURNERS
Numerical simulation of turbulent mixing and combustion near the inlet of a burner
[DE93-017960] p 1350 N94-18987

BURNING RATE
Molecular structure of low temperature form of triaminoguanidinium nitrate (TAGN)
[AD-A270409] p 1377 N94-18708
LX-17 chemical kinetic material model for Chemical TOPAZ2D
[DE93-014363] p 1377 N94-18893

BURNS (INJURIES)
Conductive garments to prevent Radio-Frequency (RF) burns
[AD-D015832] p 1512 N94-18730

BUS CONDUCTORS
The universal BitBus node
[DIGEL-1993-1] p 1515 N94-19799

BUTT JOINTS
Initiation and growth of microcracks in high strength steel butt welds
[AD-A268751] p 1454 N94-18466

C

C (PROGRAMMING LANGUAGE)
Proposal for a numerical array library
[DE93-015017] p 1516 N94-17786
Automated ILA design for synchronous sequential circuits p 1397 N94-18340
Managing persistent objects: From the programming language to the system
[ETN-93-95021] p 1529 N94-19368
Cesar user library
[FFI-93/7021] p 1529 N94-19378

C BAND
C-band PARC manual
[FEL-92-B159] p 1383 N94-18070
Design and fabrication of a Multichannel Adaptive Optical Processor (MADOP)
[AD-A270004] p 1579 N94-18668

C-131 AIRCRAFT
Airborne studies of ocean-particle-cloud interactions in the Arctic
[AD-A270752] p 1479 N94-19575

C-135 AIRCRAFT
A finite strain ring dynamical model for pneumatic tires
[AD-A269286] p 1444 N94-18266

CADMIUM
Electron paramagnetic resonance of the ns(sup 1) centers in crystals
[DE93-628793] p 1595 N94-18173
Review of short-term, high-level exposure to metals: Antimony, barium, and cadmium
[AD-A268896] p 1505 N94-18392

CADMIUM ALLOYS
Gold-copper-zinc coatings as an alternative to gold-copper-cadmium p 1367 N94-18012

CADMIUM SULFIDES
Nanostructured materials: Mind over matter
[DE93-017690] p 1597 N94-18480

CADMIUM TELLURIDES
Polycrystalline thin-film cadmium telluride solar cells fabricated by electrodeposition
[DE93-018201] p 1468 N94-18944
New room temperature high resolution solid-state detector (CdZnTe) for hard x rays and gamma rays
p 1324 N94-19165

CALCIUM COMPOUNDS
Advanced civil engineering materials based on inorganic polymers
[AD-A270837] p 1374 N94-19600

CALCIUM OXIDES
Fabrication and microstructural development of Ag-clad TlBa2Ca2Cu3O(x) tapes
[DE93-017407] p 1597 N94-18500

CALCIUM PHOSPHATES
In situ observation of radiation induced amorphization of crystals with apatite structure
[DE93-018450] p 1599 N94-18816

CALCIUM SILICATES
Advanced civil engineering materials based on inorganic polymers
[AD-A270837] p 1374 N94-19600

CALCULUS
A simple calculus of finite probabilistic processes
[MEMO-INF-93-08] p 1558 N94-19195
Development of ISY data set, part 2
[NASDA-CNT-930006-PT-2] p 1463 N94-19384
Undergraduate course and curriculum development program and calculus and the bridge to calculus program: 1992 awards
[NSF-93-24] p 1610 N94-19446

CALENDARS
Quartz analog watch with perpetual calendar
p 1429 N94-18042

CALIBRATING
SeaSoar and CTD sections across the Iceland-Faeroes Front and Faeroe Shetland Channel, August 1990
[IOS-295-1992] p 1496 N94-18064
C-band PARC manual
[FEL-92-B159] p 1383 N94-18070
Calibration of a high frequency monostatic acoustic echosounder
[AD-A268901] p 1481 N94-18229
Space debris detection
[AD-A269254] p 1334 N94-18264
Performance of the Amorphous Materials Diffractometer GLAD at IPNS
[DE93-017746] p 1430 N94-18481
Ultraviolet plume instrument calibration and sensor assessment
[AD-A269687] p 1337 N94-18574
Aspects of the calibration and processing of the CRRES fluxgate magnetometer data
[AD-A270127] p 1432 N94-18875
Construction and evaluation of an environmental chamber for calibration of temperature and pressure sensors for laser interferometers emperature and pressure sensors for laser interferometers)
[PB93-197838] p 1322 N94-19332
Software quality in test and measurment equipment
[PB93-197846] p 1528 N94-19333
Energy loss measurement of cosmic ray muons
[KFK-5158] p 1631 N94-19504

CALIFORNIA
California Student Get Away Special Payload GAS-450
p 1324 N94-19164

CALORIMETERS
Widget: A data acquisition system for a balloon borne Si particle calorimeter
[DE93-624668] p 1630 N94-18762
A bit serial first level calorimeter trigger for an LHC detector
[USIP-92-08] p 1574 N94-18845
Precision machining and polishing of scintillating crystals for large calorimeters and hodoscopes
[DE93-018663] p 1381 N94-19544

CAMERA SHUTTERS
High spatial resolution, range gated, underwater imaging method and apparatus
[AD-D015882] p 1430 N94-18530

CAMERAS
Perspective and future possibilities
p 1431 N94-18651
Radiation induced darkening of the optical elements in the Startracker camera
[DE93-018907] p 1433 N94-19004

CANARD CONFIGURATIONS
Comparison between swept and delta canards on a model of a combat aircraft
[AD-A269561] p 1317 N94-17826
Close-coupled oscillating canard effects on post-stall lift enhancement
[AD-A268938] p 1321 N94-18541
Three dimensional network generation and Euler calculation for a wing fuselage canard configuration
[MBB-LME-211-S-PUB-511-A] p 1319 N94-19500

CANONICAL FORMS
Equivalence and reduction of hidden Markov models
[AD-A270762] p 1560 N94-19768

CANOPIES (VEGETATION)
Remote sensing of Earth terrain
[NASA-CR-194598] p 1464 N94-19681

CANTILEVER BEAMS
Fabrication process for cantilever beam micromechanical switches
[AD-A269716] p 1404 N94-18749

CAPACITANCE
Field emitter array RF amplifier development project, phase 1, option 1
[AD-A268687] p 1396 N94-18293

CAPACITORS
The Aerocapacitor: A carbon aerogel based supercapacitor
[DE93-016537] p 1395 N94-17849
Monolithic low noise preamplifier for piezoelectric sensors
[AD-D015860] p 1563 N94-18734
Spice modeling of a FET-switched induction accelerator cell
[DE93-018662] p 1575 N94-18996

CAPILLARY FLOW
Contribution to the study of a symmetric film flow (with or without tensio-active elements)
[ECL-93-13] p 1421 N94-19461

CARBIDES
Diamond brazed to a metal
[AD-D015877] p 1371 N94-18746

CARBON
Vibrational and electronic properties of clusters and ultrathin films
[DE93-012291] p 1367 N94-17678
The carbon dioxide emissions game: Playing the net
[DE93-017670] p 1471 N94-17821
The Aerocapacitor: A carbon aerogel based supercapacitor
[DE93-016537] p 1395 N94-17849
Electron stripping cross sections for light impurity ions in colliding with atomic hydrogens relevant to fusion research
[DE93-788476] p 1566 N94-18158
Anomalous dielectric properties of carbon-black filled elastomers
[AD-A269378] p 1370 N94-18280
Dense energetic compounds of C, H, N, and O atoms. 3: 5-(4-nitro-(1,2,5) oxadiazolyl)-5H-(1,2,3) triazolo (4,5-c)(1,2,5) oxadiazole
[AD-A268715] p 1338 N94-18314
Novel catalysts for methane activation
[DE93-040630] p 1349 N94-18532
Determination of nitrogen to carbon abundance ratios from transition layer emission lines
[NASA-CR-191921] p 1622 N94-19421
Testing of protective coatings in hydrogen
[DE93-040326] p 1375 N94-19651

CARBON COMPOUNDS
Temperature dependence of ultraviolet absorption cross-sections of alternative hydrochlorofluorocarbons
[AERONAUTICA-ACTA-A-369-199]
p 1353 N94-19459
Infrared cross sections and global warming potentials of 10 alternative hydrohalocarbons
[AERONAUTICA-ACTA-A-371-199]
p 1479 N94-19521

CARBON CYCLE
CDIAC catalog of numeric data and computer model packages
[DE93-017675] p 1475 N94-18832
A carbon isotope mass balance for an anoxic marine sediment: Isotopic signatures of diagenesis
p 1477 N94-19232

CARBON DIOXIDE
Monitoring the response of the upper troposphere/lower stratosphere to a greenhouse gas scenario
[DE93-014509] p 1470 N94-17710
Carbon Dioxide Information Analysis Center: FY 1992 activities
[DE93-013845] p 1471 N94-17774
Assessing impacts of climate change on forests: The state of biological modeling
[DE93-015916] p 1471 N94-17790
The carbon dioxide emissions game: Playing the net
[DE93-017670] p 1471 N94-17821
Cost effective energy strategies for the reduction of CO2 emissions in the United States: Country report for ETSAP Annex 4
[DE93-016842] p 1472 N94-17852
Setting the global thermostat with an exhaustible tradeable permit system
[DE93-012911] p 1472 N94-17891
Summary report for supercritical carbon dioxide extraction and carbonization of Resorcinol-Formaldehyde (RF) foams
[DE93-016924] p 1346 N94-17987
Metadata compiled and distributed by the Carbon Dioxide Information Analysis Center for global climate change and greenhouse gas-related data bases
[DE93-015338] p 1473 N94-18167
CDIAC catalog of numeric data and computer model packages
[DE93-017675] p 1475 N94-18832
Land-use related sources of CO2, CH4 and N2O: Current global emissions and projections for the period 1990-2100
[PB93-194819] p 1475 N94-18949
The CAESAR project: Experimental and modeling investigations of methane reforming in a catalytically enhanced solar absorption receiver on a parabolic dish
[DE93-040203] p 1469 N94-19109
Kinetic studies of electrochemical generation of Ag(II) ion and catalytic oxidation of selected organics
[DE93-016601] p 1352 N94-19240
Valuation of temporary and future greenhouse gas reductions
[DE93-018876] p 1478 N94-19319
Excited atomic bromine energy transfer and quenching mechanisms
[AD-A270672] p 1572 N94-19607

CARBON DIOXIDE CONCENTRATION
Carbon Dioxide Information Analysis Center: FY 1992 activities
[DE93-013845] p 1471 N94-17774
Valuation of temporary and future greenhouse gas reductions
[DE93-018876] p 1478 N94-19319

CARBON DIOXIDE LASERS
CO2 laser with modulated losses: Theoretical models and experiments in the chaotic regime
[DE93-624901] p 1435 N94-17771
Homoclinic crises in a model for the CO2 laser
[DE93-624900] p 1436 N94-17954
A superconducting short period undulator for a harmonic generation FEL experiment
[DE93-017581] p 1436 N94-17998

CARBON DIOXIDE REMOVAL
Valuation of temporary and future greenhouse gas reductions
[DE93-018876] p 1478 N94-19319

CARBON FIBER REINFORCED PLASTICS
New aircraft materials and structures
[MBB-LME-202-S-PUB-502-A] p 1319 N94-19496

CARBON ISOTOPES
The carbon isotope biogeochemistry of methane production in anoxic sediments. 1: Field observations
p 1477 N94-19234

CARBON LASERS
Dynamic behaviors of fragments ejected from the surface of carbon materials by laser ablation
[DE93-788620] p 1438 N94-18161

CARBON MONOXIDE
Title 1 implementation: Status report on nonattainment areas
[DE93-017677] p 1471 N94-17777
Synthesis of higher alcohols from carbon monoxide and hydrogen in a slurry reactor
[DE93-015086] p 1347 N94-18209
An ab initio study of the weakly bonded CO-Cl2 complex
[AD-A269000] p 1349 N94-18395
Temperature, kinetic energy, and rotational temperature dependences for the reactions of Ar(+)(2)P3/2 with O2 and CO
[AD-A268974] p 1567 N94-18526
Organic carbonyl compounds in Albuquerque, New Mexico, air: A preliminary study of the effects of oxygenated fuel use
[DE93-017748] p 1476 N94-19045

CARBON MONOXIDE LASERS
Electrically excited CO-lasers with gas dynamic cooling
[DLR-FB-93-08] p 1437 N94-18061

CARBON STEELS
Thermal insulation of wet shielded metal arc welds
[AD-A268697] p 1445 N94-18465

CARBON TETRACHLORIDE
Femtosecond Fourier-transform spectroscopy of low-frequency intermolecular motions in weakly interacting liquids
[DE93-017312] p 1566 N94-18085
Ultrasonic process for destruction of chlorinated organic compounds in aqueous solution
[DE93-015551] p 1348 N94-18249
Integrated test plan for the demonstration of a commercial Fourier Transform Infrared instrument
[DE93-018518] p 1433 N94-19041

CARBON 12
Carbon Isotope Biogeochemistry of Methane from Anoxic Sediments
[NASA-CR-194620] p 1477 N94-19231

CARBON 13
NMR studies of enriched species at interfaces
[AD-A264703] p 1367 N94-17878
Carbon Isotope Biogeochemistry of Methane from Anoxic Sediments
[NASA-CR-194620] p 1477 N94-19231
A carbon isotope mass balance for an anoxic marine sediment: Isotopic signatures of diagenesis
p 1477 N94-19232
The carbon isotope biogeochemistry of (epsilon)CO2 production in a methanogenic marine sediment
p 1477 N94-19233
Factors that control the stable carbon isotopic composition of methane produced in an anoxic marine sediment p 1477 N94-19235

CARBON-CARBON COMPOSITES
NSWCWODET participation in Space Shuttle mission STS-46
[AD-A268875] p 1332 N94-18321
Carbon/carbon composites coated with SiC by chemical vapor deposition
[AD-A269934] p 1341 N94-18544
Process relationship as influenced by carbonization rate
[AD-A269680] p 1341 N94-18572

CARBONATES
Molten carbonate fuel cell networks: Principles, analysis, and performance
[DE93-000281] p 1468 N94-18925

CARBONIZATION
Summary report for supercritical carbon dioxide extraction and carbonization of Resorcinol-Formaldehyde (RF) foams
[DE93-016924] p 1346 N94-17987
Process relationship as influenced by carbonization rate
[AD-A269680] p 1341 N94-18572

CARBONYL COMPOUNDS
Remote cure monitoring of polymeric resins by laser Raman spectroscopy
[DE93-016445] p 1369 N94-18112
Vibrational dynamics in photoinduced electron transfer
[DE93-040874] p 1567 N94-18533
Optical properties of redispersed iron fibers measured at 94 GHz
[AD-A269739] p 1342 N94-18756
Organic carbonyl compounds in Albuquerque, New Mexico, air: A preliminary study of the effects of oxygenated fuel use
[DE93-017748] p 1476 N94-19045
Ultraviolet absorption cross-sections of some carbonyl compounds and their temperature dependence
[AERONAUTICA-ACTA-A-368-199]
p 1353 N94-19456

CARDIAC OUTPUT
Characterization of fluid physics effects on cardiovascular response to microgravity (G-572)
p 1323 N94-19163

CARDIOVASCULAR SYSTEM
Characterization of fluid physics effects on cardiovascular response to microgravity (G-572)
p 1323 N94-19163

Space research on organs and tissues
p 1503 N94-19214

CARGO
Coordination of software-development activities among sites that are geographically separated
[DE93-019201] p 1524 N94-19076

CARGO AIRCRAFT
Aircraft fire sentry. Volume 1: Summary
[AD-A270087] p 1315 N94-18822
Aircraft fire sentry. Volume 2: Appendices A, B, C and D
[AD-A270088] p 1315 N94-18823

CARRIER DENSITY (SOLID STATE)
Ultra-shallow box-like profiles fabricated by pulsed UV-laser doping process
[DE93-017221] p 1437 N94-18083
Growth of structures for integrated optoelectronic devices
[AD-A269014] p 1598 N94-18527

CARRIER TRANSPORT (SOLID STATE)
Development of large-area monolithically integrated silicon-film photovoltaic modules
[DE93-010037] p 1464 N94-17731

CARTESIAN COORDINATES
Exponential characteristic spatial quadrature for discrete ordinates neutral particle transport in two-dimensional cartesian coordinates
[AD-A270458] p 1554 N94-19671

CASES (CONTAINERS)
Reliability control for wrist watches and their casements p 1427 N94-18030

CAST ALLOYS
Tensile properties of as-cast iron-aluminide alloys
[DE93-017852] p 1363 N94-18975

CASTING
The perspectives in application of hot casting technology for ceramic parts of timekeeping devices
p 1375 N94-18013
Modeling of the formation of microporosity in alloys
[DE93-017733] p 1364 N94-19044
Low-aluminum-content iron-aluminum alloys
[DE93-017862] p 1365 N94-19274
Manufacturing technology
[DE93-019580] p 1381 N94-19480
Commercialization effort in support of electroslag-casting technology
[DE93-017988] p 1366 N94-19733

CASTINGS
Modeling of the formation of microporosity in alloys
[DE93-017733] p 1364 N94-19044
Metallurgical evaluation of SRAM 2/SRAM A program mer base plates
[DE93-018689] p 1364 N94-19100

CATACLYSMIC VARIABLES
Eclipsing cataclysmic variables. Deep eclipses in H0928+501. YY Draconis, the whirling dervish. New x ray pulsar candidates from HEAO-1
[NASA-CR-194027] p 1621 N94-18855

CATALOGS (PUBLICATIONS)
Historical seismicity of Hainaut, Flanders and Artois
p 1482 N94-18623
Catalogue of simple perfect squared squares of orders 21 through 25
[PB93-191971] p 1550 N94-18991
Range safety transponder catalog
[AD-A270882] p 1323 N94-19581

CATALYSIS
Fundamental studies of the mechanism of catalytic reactions with catalysts effective in the gasification of carbon solids and the oxidative coupling of methane
[DE93-015262] p 1347 N94-18193

CATALYSTS
Catalytic hydrocarbon reactions over supported metals
[DE93-018168] p 1345 N94-17808
Fundamental studies of the mechanism of catalytic reactions with catalysts effective in the gasification of carbon solids and the oxidative coupling of methane
[DE93-015262] p 1347 N94-18193
Conversion of ethane and of propane to higher olefin hydrocarbons
[DE93-015282] p 1347 N94-18194
Novel catalysts for methane activation
[DE93-040630] p 1349 N94-18532
Oligomer and mixed-metal compounds, potential multielectron transfer catalysts
[DE93-019592] p 1350 N94-19017
Selective methane oxidation over promoted oxide catalysts
[DE93-040002] p 1351 N94-19132
Selective methane oxidation over promoted oxide catalysts
[DE93-040001] p 1351 N94-19150
Electrocatalysts for oxygen electrodes
[DE93-040446] p 1354 N94-19653
Control of catalytic hydrotreating selectivity with ammonia
[DE93-041223] p 1354 N94-19660

CATALYTIC ACTIVITY
Catalytic hydrocarbon reactions over supported metals
[DE93-018168] p 1345 N94-17808
Ionic and molecular environments in heterogeneous electrocatalysis: Studies by radioactive labeling and LEED/AUGER spectroscopy
[AD-A268850] p 1567 N94-18766
The CAESAR project: Experimental and modeling investigations of methane reforming in a catalytically enhanced solar absorption receiver on a parabolic dish
[DE93-040203] p 1469 N94-19109
Selective methane oxidation over promoted oxide catalysts
[DE93-040002] p 1351 N94-19132
Selective methane oxidation over promoted oxide catalysts
[DE93-040001] p 1351 N94-19150

CATECHOLAMINE
Metabolic changes and hemodynamic dysfunction following hypothermic shock
[AD-A269780] p 1506 N94-18598
Strategies for enhancing catecholamine-mediated neurotransmission
[NASA-CR-193807] p 1506 N94-18862

CATHODES
High-power microwave breakdown of dielectric interfaces
[AD-A268844] p 1397 N94-18318
Field emission cathode and vacuum microelectronic microwave amplifier development
[AD-A269526] p 1403 N94-18639
MHD integrated topping cycle project
[DE93-040520] p 1588 N94-18978

CATHODIC COATINGS
Oxygen reduction at a stabilized zirconia interface with Y(1-x)Ca(x)MnO3 or La(1-x)Sr(x)MnO3 cathode materials
[DE93-015681] p 1593 N94-17747
Novel electrochemical materials prepared by sol-gel chemistry
[AD-A269060] p 1578 N94-18405

CATIONS
Catalytic hydrocarbon reactions over supported metals
[DE93-018168] p 1345 N94-17808
Novel electrochemical materials prepared by sol-gel chemistry
[AD-A269060] p 1578 N94-18405

CAUCHY PROBLEM
Numerical methods for one-dimensional hyperbolic conservation laws
[PB93-194801] p 1547 N94-18078
Impulsive moving mirror model in a Schroedinger picture with impulse effect in a Banach space
[DE93-629864] p 1561 N94-18155

CAVITIES
Experimental investigation of flow around a multielement airfoil p 1305 N94-18417
Binding of copper to nanocavity surfaces in silicon
[DE93-019073] p 1364 N94-19080

CAVITY FLOW
Experimental investigation of flow around a multielement airfoil p 1305 N94-18417

CAVITY RESONATORS
Plasma klystron amplifier
[AD-D015819] p 1395 N94-17903
Homoclinic crises in a model for the CO2 laser
[DE93-624900] p 1436 N94-17954
Waveguide and resonator perturbation techniques for measuring chirality and non-reciprocity of biisotropic materials
[PB93-167243] p 1384 N94-18116
Designs for a 10.6 micrometer electromagnetic wiggler Free-Electron Laser (FEL)
[AD-A269695] p 1439 N94-18576

CEILINGS (METEOROLOGY)
Station climatic summaries: North America. Volume 1: The contiguous United States
[AD-A269567] p 1490 N94-18303
Station climatic summaries, North America. Volume 2: Alaska, Canada and Greenland
[AD-A269793] p 1493 N94-18732

CELL ANODES
Environmentally assisted cracking of nickel anode substrates in Li/SOCl2 cells: An engineering approach
[DE93-015130] p 1405 N94-18928

CELL MEMBRANES (BIOLOGY)
Effect of EMP fields on cell membrane potentials
[DE93-015819] p 1503 N94-19341

CELLS (BIOLOGY)
Cellular and molecular level responses after radiofrequency radistion exposure, alone or in combination with x rays or chemicals
[AD-A268189] p 1501 N94-17729
The c-jun gene expression in human cells exposed to either ionizing radiation or hydrogen peroxide
[DE93-017436] p 1502 N94-18476
The role of chemical inhibition of gap junctional intercellular communication in toxicology
[AD-A269251] p 1502 N94-18924
A scientific role for Space Station Freedom: Research at the cellular level p 1503 N94-19215

CELLULOSE
Microbial degradation of poly-b-esters: A mechanistic study, cellulose acetate biodegradability
[AD-A271368] p 1374 N94-19586

CEMENTS
Microstructure of the interfacial zone around aggregate particles in concrete
[PB93-195790] p 1380 N94-19322
Advanced civil engineering materials based on inorganic polymers
[AD-A270837] p 1374 N94-19600

CENTER OF GRAVITY
Location of the absolute barycenter of a graph
[REPT-93-027] p 1547 N94-17962

CENTER OF MASS
Moments of ambient Doppler spectra
[DE93-017948] p 1390 N94-19114

CENTRAL NERVOUS SYSTEM
Cerebral ischemia and reperfusion injury: A brief review
[AD-A270480] p 1507 N94-19675

CENTRAL PROCESSING UNITS
Performance of defect-tolerant set-associative cache memories p 1398 N94-18346
A modified reconfigurable data path processor
p 1400 N94-18360
Algorithms and architectures for high speed signal processing
[AD-A271000] p 1392 N94-19736

CENTRIFUGES
Centrifuge modeling of explosion-induced craters in unsaturated sand
[AD-A270194] p 1417 N94-18780

CENTRIFUGING
Pilot studies on object motion perception during linear self-motion after long duration centrifugation of human subjects
[IZF-1993-B-3] p 1510 N94-19439

CERAMIC COATINGS
Ni-Al2O3 solid state binding: Elaboration, state of thermal constraints, mechanical behavior
[ECL-92-31] p 1366 N94-19436

CERAMIC FIBERS
Finite element modeling of evaporation and condensation during sol-gel film and fiber formation
[DE93-017655] p 1345 N94-17820

CERAMIC MATRIX COMPOSITES
A comprehensive study of matrix fracture mechanisms in fiber-reinforced ceramic matrix composites
[AD-A268809] p 1340 N94-18205
Pressureless densification of ceramic matrix composites
[AD-A269137] p 1371 N94-18691
Bibliography on ceramic matrix composites and reinforcing whiskers, platelets, and fibers, 1970-1990
[AD-A270139] p 1371 N94-18750
Subcritical crack growth in continuous-fiber reinforced ceramic composites
[DE93-018784] p 1343 N94-19335
Manufacturing technology
[DE93-019580] p 1381 N94-19480

CERAMICS
Development of large-area monolithically integrated silicon-film photovoltaic modules
[DE93-010037] p 1464 N94-17731
The perspectives in application of hot casting technology for ceramic parts of timekeeping devices
p 1375 N94-18013
Studies of dynamic contact of ceramics and alloys for advanced heat engines
[DE93-016366] p 1368 N94-18110
A survey on technical problems in designing high-speed rotors with developing materials
[DE93-788519] p 1444 N94-18159
Ceramic films and interfaces: Chemical and mechanical properties
[DE93-018416] p 1369 N94-18163
Metal/ceramic interfaces: Relationships between structure and chemistry
[AD-A268792] p 1369 N94-18188
Office of Naval Research Publications/Patents /Presentations/Honors report, 1 October 1992 - 30 September 1993
[AD-A270037] p 1632 N94-18791
Experimental investigation of wave and fracture phenomena in impacted ceramics: Experiments on sapphire
[AD-A270040] p 1372 N94-18792

Molecular and polymeric ceramic precursors
[DE93-040364] p 1372 N94-18891
Quantification of volume flaw sizes in ceramics by image processing of 3D x ray tomographic data sets
[DE93-018573] p 1372 N94-18932
Survey of ceramic machining in Japan
[DE93-018277] p 1372 N94-18946
Shock-loading response of advanced materials
[DE93-018344] p 1455 N94-19033
Superconductivity and magnetism in niobium doped YBa2Cu3O7 related high-(Tc) ceramics
[DE93-018086] p 1601 N94-19049
Shock compression properties of silicon carbide
[DE93-019927] p 1373 N94-19271
Analytical and experimental evaluation of joining silicon nitride to metal and silicon carbide to metal for advanced heat engine applications
[DE93-018128] p 1446 N94-19291
Reducing inadvertent alloying of metal/ceramic brazes
[DE93-009842] p 1373 N94-19308
Impact strength and indentation hardness of high-strength ceramics
[DE93-018833] p 1373 N94-19338
Manufacturing technology
[DE93-019580] p 1381 N94-19480
Ceramic technology project data base
[DE93-019360] p 1374 N94-19561

CEREBRAL CORTEX
Localization of figure background segregation mechanisms in primate visual cortex
[PB93-187961] p 1508 N94-18121
Somatosensory responsiveness in behaving monkeys and human subjects
[AD-A268924] p 1501 N94-18231

CEREBRAL VASCULAR ACCIDENTS
Cerebral ischemia and reperfusion injury: A brief review
[AD-A270480] p 1507 N94-19675

CERENKOV RADIATION
Crystal optics of high energy gamma-beams
[DE93-630228] p 1577 N94-18217

CERIUM
The low-temperature specific heat of CeCu2Ge2 at 0 and 9.5 kbar
[DE93-014914] p 1360 N94-18398

CERIUM COMPOUNDS
Calculation of the LiF-CeF3-BeF2 and LiF-PuF3-BeF2 ternary phase diagrams
[DE93-017437] p 1360 N94-18501

CERTIFICATION
Advisory circular: Index of articles (materials, parts, processes, and appliances) certified under the technical standard order system
[AC-20-36S] p 1618 N94-19377

CHANNEL FLOW
On memory effects in turbulence
[DLR-FB-93-03] p 1409 N94-18124
Multigrid methods for flow transition in three-dimensional boundary layers with surface roughness
[NASA-CR-4540] p 1417 N94-18843
MHD integrated topping cycle project
[DE93-040520] p 1588 N94-18978
A simple description of flow instability with application to a packed bed
[DE93-017492] p 1420 N94-19345

CHANNELS (DATA TRANSMISSION)
FASTBUS simulation models in VHDL
[USIP-92-07] p 1515 N94-19295

CHAOS
CO2 laser with modulated losses: Theoretical models and experiments in the chaotic regime
[DE93-624901] p 1435 N94-17771
Modelling chaotic vibrations using NASTRAN
p 1449 N94-17830
Plasma properties research: Task 3
[DE93-017087] p 1583 N94-17854
The physics of cellular automata and coherence and chaos in classical many-body dynamical systems
[DE93-018021] p 1561 N94-18177
Non Linear Dynamics and Chaos
[AGARD-LS-191] p 1607 N94-18236
Bifurcation theory: Chaos and patterns
p 1607 N94-18237

CHARACTERIZATION
High resolution geological site characterization utilizing ground motion data
[AD-A268926] p 1481 N94-18485
Growth, characterization and device development in monocrystalline diamond films
[AD-A270074] p 1599 N94-18797
Role of pressure in the study of fullerenes
[DE93-018839] p 1602 N94-19340
Materials characterization of propellants using ultrasonics
[NASA-CR-193877] p 1378 N94-19494

CHARGE CARRIERS
Examination of charge carriers dynamics in silicon and silicon solar cells with photoinduced laser beam deflection
[ETN-93-95060] p 1470 N94-19654

CHARGE COUPLED DEVICES
High speed 512X512 camera system
[DE93-015871] p 1430 N94-18235
Space debris detection
[AD-A269254] p 1334 N94-18264
An RS-170 to 700 frame per second CCD camera
[DE93-018367] p 1432 N94-18828
The star identification, pointing and tracking system of UVSTAR, an attached payload instrument system for the Shuttle Hitchhiker-M platform p 1326 N94-19179
Center-of-Excellence: Microlaser microscope
[DE93-040688] p 1442 N94-19658
Particle induced background by Roentgen satellites
[MPE-242] p 1631 N94-19714

CHARGE DISTRIBUTION
Cooperative formation of inorganic-organic interfaces in the synthesis of silicate mesostructures
[AD-A271196] p 1375 N94-19742

CHARGE EXCHANGE
Ion mobility and transport barriers in the tokamak plasmas
[DE93-040320] p 1587 N94-18524

CHARGE FLOW DEVICES
A tunable CMOS constant current source
p 1401 N94-18369

CHARGE TRANSFER
Correlated charge-changing ion-atom collisions
[DE93-018717] p 1564 N94-17775
Studies of interactions between conducting polymer and organic vapors: Applications to chemical sensing
[DE93-015694] p 1369 N94-18233
Temperature, kinetic energy, and rotational temperature dependences for the reactions of Ar(+)(2)P3/2 with O2 and CO
[AD-A268974] p 1567 N94-18526
Molecular nonlinear optical susceptibilities in condensed phases
[AD-A270200] p 1568 N94-18784
Pressure induced metallization of the Mott insulator 6(sub 2)
[DE93-018296] p 1600 N94-18969
Metallization and charge-transfer gap closure of transition-metal iodides under pressure
[DE93-040301] p 1353 N94-19538

CHARGED PARTICLES
Advanced methods for the computation of particle beam transport and the computation of electromagnetic fields and beam-cavity interactions
[DE93-018160] p 1573 N94-17807
High rate resistive plate chambers: An inexpensive, fast, large area detector of energetic charged particles for accelerator and non-accelerator applications
[DE93-018664] p 1572 N94-19545

CHARM (PARTICLE PHYSICS)
Beauty without charm in B-meson decays
[PREPRINT-732] p 1565 N94-17972
Charmonium physics from (bar p)p interactions
[DE93-017809] p 1569 N94-18973
Research in high energy physics
[DE93-018031] p 1575 N94-19287

CHARPY IMPACT TEST
Charpy impact toughness of martensitic steels irradiated in FFTF: Effect of heat treatment
[DE93-015960] p 1450 N94-17848
Mechanism-dependent fractal character of fracture surfaces in high strength and toughness ASTM A723 steels
[AD-A268956] p 1360 N94-18542
Effects of irradiation temperature on Charpy and tensile properties of high-copper, low upper-shelf, submerged-arc welds
[DE93-017858] p 1445 N94-19047

CHARTS
Constant-thrust orbit-raising transfer charts
[AD-A269088] p 1334 N94-18718
Color test chart for facsimile
[AD-A269754] p 1387 N94-18721

CHECKOUT
MHD Integrated Topping Cycle Project
[DE93-040521] p 1589 N94-19055

CHEMICAL ANALYSIS
Practical reporting times for environmental samples
[DE93-013461] p 1472 N94-17910
Summaries of FY 1993 research in the chemical sciences
[DE93-011855] p 1632 N94-18915
Research program activities of the ORNL Analytical Chemistry Division
[DE93-017938] p 1339 N94-19117

CHEMICAL BONDS
Novel catalysts for methane activation
[DE93-040630] p 1349 N94-18532

CHEMICAL COMPOSITION
Effect of oxygen concentration and ordering on vanadium-oxygen alloy vibrational spectra
[DE93-627003] p 1355 N94-17692
Direct Monte Carlo simulation of the chemical equilibrium composition of detonation products
[DE93-014559] p 1376 N94-17751
Toward a characterization of the debris cloud created in a hypervelocity impact on a thin plate
[AD-A269190] p 1455 N94-18864
Carbon Isotope Biogeochemistry of Methane from Anoxic Sediments
[NASA-CR-194620] p 1477 N94-19231
A carbon isotope mass balance for an anoxic marine sediment: Isotopic signatures of diagenesis
p 1477 N94-19232

CHEMICAL EFFECTS
Ageing in Processed Polymers: Programme, summary, and abstracts discussion meeting
[AD-A268931] p 1370 N94-18448

CHEMICAL ENERGY
Summaries of FY 1993 research in the chemical sciences
[DE93-011855] p 1632 N94-18915

CHEMICAL ENGINEERING
Summaries of FY 1993 research in the chemical sciences
[DE93-011855] p 1632 N94-18915

CHEMICAL EQUILIBRIUM
Direct Monte Carlo simulation of the chemical equilibrium composition of detonation products
[DE93-014559] p 1376 N94-17751
Metal slurry droplet and spray combustion
[AD-A269648] p 1349 N94-18736
Numerical simulation of viscous flows in chemical nonequilibrium
[MBB-LME-211-S-PUB-506] p 1421 N94-19497

CHEMICAL EXPLOSIONS
Direct Monte Carlo simulation of the chemical equilibrium composition of detonation products
[DE93-014559] p 1376 N94-17751
Detonation reaction steps frozen by free expansion and analyzed by mass spectrometry
[DE93-012734] p 1376 N94-17813
Modeling shock initiation in Composition B
[DE93-016544] p 1376 N94-18095
LX-17 chemical kinetic material model for Chemical TOPAZ2D
[DE93-014363] p 1377 N94-18893
The use of post detonation analysis of stable isotope ratios to determine the type and production process of the explosive involved
[DE93-018497] p 1378 N94-19242

CHEMICAL PROPERTIES
Ceramic films and interfaces: Chemical and mechanical properties
[DE93-018416] p 1369 N94-18163
Advanced civil engineering materials based on inorganic polymers
[AD-A270837] p 1374 N94-19600

CHEMICAL REACTIONS
Detonation reaction steps frozen by free expansion and analyzed by mass spectrometry
[DE93-012734] p 1376 N94-17813
Evaluation of the nickel release by horological products p 1367 N94-18009
Femtosecond Fourier-transform spectroscopy of low-frequency intermolecular motions in weakly interacting liquids
[DE93-017312] p 1566 N94-18085
Metal/ceramic interfaces: Relationships between structure and chemistry
[AD-A268792] p 1369 N94-18188
Ageing in Processed Polymers: Programme, summary, and abstracts discussion meeting
[AD-A268931] p 1370 N94-18448
Chemical reactions in turbulent mixing flows
[AD-A269377] p 1410 N94-18472
Temperature, kinetic energy, and rotational temperature dependences for the reactions of Ar(+)(2)P3/2 with O2 and CO
[AD-A268974] p 1567 N94-18526
Computational techniques for high-speed flows with viscous and chemical effects p 1412 N94-18560
A review and evaluation of the ADAM 2.1 dispersion model
[AD-A269896] p 1474 N94-18688
Royal Society of Chemistry, Heterocyclic Chemistry Group, Lakeland Heterocyclic Symposium
[AD-A270374] p 1338 N94-18703
Wettability and reaction kinetics in metal matrix composites
[AD-A270377] p 1342 N94-18704

Metal slurry droplet and spray combustion
[AD-A269648] p 1349 N94-18736
Scaling laws for diamond chemical vapor deposition. 2: Atomic hydrogen transport
[AD-A269842] p 1371 N94-18740
Scaling laws for diamond chemical vapor deposition. Diamond surface chemistry
[AD-A269874] p 1599 N94-18745
Transport phenomena and interfacial kinetics in multiphase combustion systems
[AD-A270202] p 1349 N94-18785
Temperature lowering in cryogenic chemical-synthesis techniques and system
[DE93-018348] p 1562 N94-18810
The quantum dynamics of electronically nonadiabatic chemical reactions
[NASA-CR-194309] p 1568 N94-18837
The role of chemical inhibition of gap junctional intercellular communication in toxicology
[AD-A269251] p 1502 N94-18924
Molten carbonate fuel cell networks: Principles, analysis, and performance
[DE93-000281] p 1468 N94-18925
Some superhigh-frequency and magnetic properties of chemically precipitated films
[AD-A266195] p 1351 N94-19110
Penetrometer compatible, fiber-optic sensor for continuous monitoring of chlorinated hydrocarbons: Field test results
[DE93-017974] p 1352 N94-19266
Crossed molecular beam studies of atmospheric chemical reaction dynamics
[DE93-019246] p 1478 N94-19303
Experimental study of flame front interactions
[ECL-91-40] p 1353 N94-19376

CHEMICAL REACTORS
Synthesis of higher alcohols from carbon monoxide and hydrogen in a slurry reactor
[DE93-015086] p 1347 N94-18209
Novel catalysts for methane activation
[DE93-040630] p 1349 N94-18532
The CAESAR project: Experimental and modeling investigations of methane reforming in a catalytically enhanced solar absorption receiver on a parabolic dish
[DE93-040203] p 1469 N94-19109

CHEMICAL TESTS
The CAESAR project: Experimental and modeling investigations of methane reforming in a catalytically enhanced solar absorption receiver on a parabolic dish
[DE93-040203] p 1469 N94-19109

CHEMICAL VAPOR INFILTRATION
Carbon/carbon composites coated with SiC by chemical vapor deposition
[AD-A269934] p 1341 N94-18544
Subcritical crack growth in continuous-fiber reinforced ceramic composites
[DE93-018784] p 1343 N94-19335

CHEMICAL WARFARE
Evaluation of mass spectra for a verification database
[PML-1993-12] p 1619 N94-19453

CHEMISTRY
The 1982 to 1992 decade of research on the vacuum ultraviolet ring at National Synchrotron Light Source
[DE93-019469] p 1603 N94-19564

CHILD-LANGMUIR LAW
Simulation of transient effects in the heavy ion fusion injectors
[DE93-018658] p 1575 N94-19107

CHIPS (ELECTRONICS)
Synthesis techniques and analysis tool for on-chip fault-tolerance
[AD-A269148] p 1521 N94-18259
Experience with custom processors in space flight applications p 1336 N94-18338
VLSI architectures for geometrical mapping problems in high-definition image processing
p 1398 N94-18345
SPROC: A multiple-processor DSP IC
p 1398 N94-18347
Systolic array IC for genetic computation
p 1400 N94-18361
Verification of VLSI designs p 1400 N94-18363
RF vacuum microelectronics
[AD-A270003] p 1403 N94-18667
ARPA/CSTO rapid VLSI implementation
[AD-A269170] p 1403 N94-18695
VLSI for high-speed digital signal processing
[AD-A270406] p 1404 N94-18706
Scaling laws for diamond chemical vapor deposition. Diamond surface chemistry
[AD-A269874] p 1599 N94-18745
Knowledge sources for an intelligent MCM analyzer
[AD-A269224] p 1542 N94-18887
Radiation hardened microprocessor for small payloads
p 1327 N94-19184
An innovative neural manufacturing concept
[DE93-017212] p 1527 N94-19238

CHIPS (MEMORY DEVICES)
Ultra low power CMOS technology
p 1401 N94-18373

CHIRAL DYNAMICS
Investigations in gauge theories, topological solitons, and string theories
[DE93-015029] p 1609 N94-19250

CHIRP
Nontraditional windows in spectral analysis
[AD-A271336] p 1553 N94-19583

CHIRP SIGNALS
Limitations on the fidelity of 100 fs pulses produced by chirped pulse amplification
[DE93-017167] p 1396 N94-17991

CHLORINE
Screening analysis for chlorine-free alternative refrigerants to replace R-22 in air conditioning applications
[DE93-015920] p 1367 N94-17847
Condensed gases under winter conditions: A study for the rescue services
[FOA-C-40305-4.5] p 1473 N94-18139
An ab initio study of the weakly bonded CO-Cl2 complex
[AD-A269000] p 1349 N94-18395

CHLOROCARBONS
Ultrasonic process for destruction of chlorinated organic compounds in aqueous solution
[DE93-015551] p 1348 N94-18249

CHLOROFLUOROCARBONS
Removing CFC's from the atmosphere with lasers: A second look
[DE93-017516] p 1473 N94-18101

CHLOROPHYLLS
SeaSoar CTD, fluorescence and scalar irradiance data from RRS Charles Darwin Cruises 58/59, NE Atlantic, Vivaldi 1991
[IOS-299-1992] p 1496 N94-18066

CHLOROPRENE RESINS
Anomalous dielectric properties of carbon-black filled elastomers
[AD-A269378] p 1370 N94-18280

CHOLINE
Bienzyme sensors based on electrically wired peroxidase
[AD-A271364] p 1374 N94-19585

CHROMIUM
Defect behavior of polycrystalline solar cell silicon
[DE93-018490] p 1468 N94-19016
Tetravalent chromium (Cr(4+)) as laser-active ion for tunable solid-state lasers
[NASA-CR-194529] p 1441 N94-19369
Tetravalent chromium (Cr(4+)) as laser-active ion for tunable solid-state lasers
[NASA-CR-194528] p 1441 N94-19394

CHROMIUM ALLOYS
Atlas of formability: Ultimet
[AD-A268352] p 1355 N94-17767
Atlas of formability: HAYNES 556
[AD-A268354] p 1356 N94-17768
Atlas of formability: HAYNES 188
[AD-A268355] p 1356 N94-17769
Atlas of formability: Haynes 230
[AD-A268325] p 1356 N94-17788
Atlas of formability: ALLVAC 718
[AD-A268304] p 1357 N94-17804
Summary of work on coatings and claddings for fossil energy applications
[DE93-017005] p 1367 N94-17881
Bibliography on silicides
[AD-A270516] p 1374 N94-19532
Incology 908 database report: On process-structure-property relationship
[DE93-017616] p 1366 N94-19546

CHROMIUM STEELS
Modeling of the formation of microporosity in alloys
[DE93-017733] p 1364 N94-19044

CHROMOSOMES
Life: Origin and evolution on Earth--How can we escape? p 1503 N94-19217

CHRONOLOGY
Marshall Space Flight Center 1989 annual chronology of events
[NASA-TM-109381] p 1633 N94-19486

CHRONOMETERS
Evaluation of the nickel release by horological products p 1367 N94-18009
Marine chronometry in the Neuchatel mountains (Switzerland) p 1427 N94-18025
Multifunction chronograph movement using a modular structure multimotor p 1429 N94-18044

CIRCADIAN RHYTHMS
Intracellular physiology of the rat suprachiasmatic nucleus: Electrical properties, neurotransmission and effects of neuromodulators
[AD-A268829] p 1505 N94-18538

CIRCUIT PROTECTION
Impedence calculation with recursive folding
[ETN-93-95049] p 1406 N94-19387

CIRCUIT RELIABILITY
Asynchronous sequential circuit design using pass transistor iterative logic arrays p 1402 N94-18376
Pulse mode VLSI asynchronous circuits
p 1402 N94-18377
Improved self arbitrated VLSI asynchronous circuits
p 1402 N94-18378
Algorithms and architectures for high speed signal processing
[AD-A271000] p 1392 N94-19736

CIRCUITS
Precision digitally-controlled variable attenuation circuit
[AD-D015862] p 1394 N94-17703
A method for eliminating skew introduced by non-uniform buffer delay and wire lengths in clock distribution trees
[AD-A270649] p 1544 N94-19530

CIRCULAR CYLINDERS
Statistical description of the bistatic radar cross section distributions for a right circular cylinder
[AD-A270001] p 1387 N94-18666

CIRCULAR ORBITS
Constant-thrust orbit-raising transfer charts
[AD-A269088] p 1334 N94-18718

CIRCULAR POLARIZATION
Polarized optical emission due to decay or recombination of spin-polarized injected carriers
[AD-D015907] p 1408 N94-19763

CIRCUMFERENCES
Concerning the circumference of certain families of graphs p 1555 N94-19694

CIRRUS CLOUDS
Monitoring the response of the upper troposphere/lower stratosphere to a greenhouse gas scenario
[DE93-014509] p 1470 N94-17710
Suitability of infrared spectroscopy for remote sensing of tropospheric trace gases
[KFK-5183] p 1479 N94-19507

CITIES
Title 1 implementation: Status report on nonattainment areas
[DE93-017677] p 1471 N94-17777
The urban perspectives of acid rain
[DE93-018881] p 1474 N94-18523
Organic carbonyl compounds in Albuquerque, New Mexico, air: A preliminary study of the effects of oxygenated fuel use
[DE93-017748] p 1476 N94-19045
The Mexico City 1991 lidar measurements campaign
[DE93-019960] p 1478 N94-19272

CIVIL AVIATION
Airport activity statistics of certificated route air carriers, 1992
[AD-A269042] p 1315 N94-18490
VHF air/ground communications for air traffic control: A decision tree approach to system innovations, volume 2
[AD-A268632] p 1386 N94-18495

CLADDING
Summary of work on coatings and claddings for fossil energy applications
[DE93-017005] p 1367 N94-17881
Total hemispherical emittance of Niobium-1 percent zirconium fuel cladding for the SP-100 space reactor
[AD-A270456] p 1576 N94-19589

CLASSICAL MECHANICS
Space and time from quantum mechanics
[DE93-015263] p 1609 N94-18629

CLASSIFICATIONS
Application of Fourier-based features for classification of synthetic aperture radar imagery
[AD-A270450] p 1387 N94-18513
Building a joint-service classification research roadmap: Criterion-related issues
[AD-A269735] p 1512 N94-18754

CLAYS
The direct synthesis of organic and organometallic-containing MICA-type aluminosilicates
[DE93-019001] p 1373 N94-19321

CLEAN ENERGY
National Program Plan Fuel Cells in Transportation
[DE93-017557] p 1469 N94-19346

CLEAN ROOMS
Safety-routines and guidelines for work in the clean room at the Epitek-Laboratory, Kjeller (Norway)
[FFI-93/7012] p 1322 N94-17735

CLEANERS
A comparison of wet and dry scrubbing systems for control of metals and dioxin/furan emissions from incinerators
[DE93-017446] p 1474 N94-18502
CLEANING
A comparison of wet and dry scrubbing systems for control of metals and dioxin/furan emissions from incinerators
[DE93-017446] p 1474 N94-18502
New applications for high average power beams
[DE93-018845] p 1439 N94-18522
The application of jet spray and ion beam contamination removal techniques to samples from the LDEF spacecraft
[AD-A270973] p 1354 N94-19755
CLEARANCES
Computer/information security design approaches for Complex 21/Reconfiguration facilities
[DE93-018547] p 1535 N94-18930
CLEAVAGE
Fundamental concepts relating local atomic arrangements, deformation, and fracture of intermetallic alloys
[AD-A268745] p 1361 N94-18788
CLIMATE
Carbon Dioxide Information Analysis Center: FY 1992 activities
[DE93-013845] p 1471 N94-17774
Geography and meteorological studies in the Far East
[DE93-013563] p 1461 N94-17893
Mixture distributions in climatological research
[DE93-014125] p 1488 N94-17942
Effect of spatial resolution on the simulation of regional precipitation in China in a global climate model
[DE93-013433] p 1489 N94-18053
On the construction of a regional atmospheric climate model
[KNMI-TR-147] p 1489 N94-18143
SERCAA cloud analysis integration: Design concepts and interaction with cloud forecast models
[AD-A269104] p 1492 N94-18637
CDIAC catalog of numeric data and computer model packages
[DE93-017675] p 1475 N94-18832
Toward a high performance distributed memory climate model
[DE93-019156] p 1494 N94-19298
A survey of current approaches to modelling of hydrological time-series with respect to climate variability and change
[WMO/TD-534] p 1463 N94-19435
CLIMATE CHANGE
Monitoring the response of the upper troposphere/lower stratosphere to a greenhouse gas scenario
[DE93-014509] p 1470 N94-17710
Biophysical characterization and surface radiation balance
[NASA-CR-194659] p 1470 N94-17762
Carbon Dioxide Information Analysis Center: FY 1992 activities
[DE93-013845] p 1471 N94-17774
Assessing impacts of climate change on forests: The state of biological modeling
[DE93-015916] p 1471 N94-17790
The carbon dioxide emissions game: Playing the net
[DE93-017670] p 1471 N94-17821
Geography and meteorological studies in the Far East
[DE93-013563] p 1461 N94-17893
Statistical intercomparison of global climate models: A common principal component approach with application to GCM data
[DE93-017951] p 1473 N94-18005
Effect of spatial resolution on the simulation of regional precipitation in China in a global climate model
[DE93-013433] p 1489 N94-18053
Metadata compiled and distributed by the Carbon Dioxide Information Analysis Center for global climate change and greenhouse gas-related data bases
[DE93-015338] p 1473 N94-18167
International Symposium on the Ecological Effects of Arctic Airborne Contaminants — abstracts
[AD-A269955] p 1475 N94-18775
CDIAC catalog of numeric data and computer model packages
[DE93-017675] p 1475 N94-18832
Toward a high performance distributed memory climate model
[DE93-019156] p 1494 N94-19298
Report of the Experts Meeting on Reference Climatological Stations (RCS) and National Climate Data Catalogues (NCC)
[WMO-TD-535] p 1494 N94-19312
A survey of current approaches to modelling of hydrological time-series with respect to climate variability and change
[WMO/TD-534] p 1463 N94-19435
CLIMATOLOGY
The carbon dioxide emissions game: Playing the net
[DE93-017670] p 1471 N94-17821
Mixture distributions in climatological research
[DE93-014125] p 1488 N94-17942
Statistical intercomparison of global climate models: A common principal component approach with application to GCM data
[DE93-017951] p 1473 N94-18005
A mobile remote sensing laboratory for water vapor, trace gas, aerosol, and wind speed measurements
[DE93-017158] p 1489 N94-18132
Metadata compiled and distributed by the Carbon Dioxide Information Analysis Center for global climate change and greenhouse gas-related data bases
[DE93-015338] p 1473 N94-18167
The land component of the global climate system with adequate spatial resolution
[DE93-018951] p 1474 N94-18183
Rapid oceanic cyclogenesis studies
[AD-A269258] p 1490 N94-18265
Station climatic summaries: North America. Volume 1: The contiguous United States
[AD-A269567] p 1490 N94-18303
Station climatic summaries, North America. Volume 2: Alaska, Canada and Greenland
[AD-A269793] p 1493 N94-18732
Solar radiation in Saudi Arabia
[AD-A269970] p 1493 N94-18781
An investigation of warm-cloud microphysics using a multi-component cloud model: Interactive effects of the aerosol spectrum
[AD-A270273] p 1493 N94-18812
CDIAC catalog of numeric data and computer model packages
[DE93-017675] p 1475 N94-18832
Eastern Europe: A climatological study
[AD-A269200] p 1493 N94-18883
Toward a high performance distributed memory climate model
[DE93-019156] p 1494 N94-19298
HIRLAM p 1494 N94-19699
Report of the Second CLICOM Experts Meeting
[WCDMP-19] p 1495 N94-19705
CLIPS
Spectrum fatigue testing of T-shaped tension clips
[FFA-TN-1992-22] p 1452 N94-17970
CLOCKS
Proceedings of the 4th European Congress on Chronometry
[ETN-93-94633] p 1424 N94-18006
The clocks and the perception of time in the 18th century society p 1424 N94-18007
Electrostatic micrometers: Recent developments and perspectives of uses in clock and watch making
p 1425 N94-18014
Piezo-electric motor: Perspectives and miniaturization
p 1408 N94-18015
Development of ultrasonic motor and application to silent alarm analog quartz watch p 1425 N94-18016
The optimal numerical algorithm for processing of phase coded time signals for radio-clocks
p 1426 N94-18018
Simulation of a quartz-clockwork
p 1426 N94-18019
Control of torque in stepping motors of quartz watches and clocks p 1408 N94-18023
Restoration of an 18th century English clock
p 1427 N94-18026
The mystery of the perpetual motion clock of Geiser and Son p 1427 N94-18027
Gear train behavior analyzer using laser beam scanning for watch movement p 1427 N94-18028
Universal measurement device for electronic watches and small clocks p 1427 N94-18029
Reliability control for wrist watches and their casements p 1427 N94-18030
Mutrometre: Construction for fast water proof measurements under low pressure and air suppression
p 1427 N94-18031
Techniques for low consumption circuits
p 1428 N94-18032
Evaluation of the consumption of electronic clocks
p 1408 N94-18033
New current reduction system for watches with integrated current regulation motors
p 1428 N94-18034
Some variation in the movement base of the ETA 251 series p 1428 N94-18035
Tooth form design supporting system in module design p 1428 N94-18036
Automatic soldering for watch circuit components
p 1428 N94-18037
Swatch Pager p 1428 N94-18039
A study of the automatic generating system. 3: Improvement of the total system performance
p 1429 N94-18040
Development of a new concept diver's watch
p 1429 N94-18041
Quartz analog watch with perpetual calendar
p 1429 N94-18042
Development of analog watch with minute repeater
p 1429 N94-18043
Efficient simulation of DEDS by means of standard clock techniques: Queueing and integrated radio network examples
[AD-A269878] p 1432 N94-18681
Absolute positioning by collecting Global Positioning System (GPS) data along short baselines
[AD-A271324] p 1317 N94-19572
CLOSED ECOLOGICAL SYSTEMS
Lunar base Controlled Ecological Life Support System (LCELSS): Preliminary conceptual design study
[NASA-CR-188479] p 1511 N94-18484
CLOSURE LAW
On memory effects in turbulence
[DLR-FB-93-03] p 1409 N94-18124
Research activities at the Center for Modeling of Turbulence and Transition p 1410 N94-18546
An introduction to second moment closure
p 1414 N94-18580
A new form of second-moment closure
p 1414 N94-18582
An introduction to single-point closure methodology
p 1414 N94-18583
Second-moment closure: Present... and future?
p 1414 N94-18584
Inclusion of second-moment closures into finite-volume solvers p 1415 N94-18588
Numerical implementation and performance of Reynolds-stress closures in finite-volume computations of recirculating and strongly swirling flows
p 1415 N94-18589
Application of second-moment closure in complex flows p 1415 N94-18590
Modelling engineering flows with Reynolds stress turbulence closure p 1415 N94-18591
CLOUD COVER
Monitoring the response of the upper troposphere/lower stratosphere to a greenhouse gas scenario
[DE93-014509] p 1470 N94-17710
Cloudiest year study: An analysis of the 3DNEPH and RTNEPH databases
[AD-A269403] p 1490 N94-18281
Station climatic summaries: North America. Volume 1: The contiguous United States
[AD-A269567] p 1490 N94-18303
Station climatic summaries, North America. Volume 2: Alaska, Canada and Greenland
[AD-A269793] p 1493 N94-18732
An investigation of warm-cloud microphysics using a multi-component cloud model: Interactive effects of the aerosol spectrum
[AD-A270273] p 1493 N94-18812
CLOUD HEIGHT INDICATORS
Three-dimensional cloud visualization based on satellite imagery
[AD-A269318] p 1490 N94-18300
CLOUD PHYSICS
Cloud CCN feedback
[DE93-016878] p 1472 N94-17985
CLOUDS (METEOROLOGY)
Surface fluxes important to cloud development
[DE93-016633] p 1488 N94-17715
Physical retrieval of precipitation water contents from Special Sensor Microwave/Imager (SSM/I) data. Part 1: A cloud ensemble/radiative parameterization for sensor response (report version) p 1491 N94-18604
Initialization and assimilation of cloud and rainwater in a regional model p 1492 N94-18608
SERCAA cloud analysis integration: Design concepts and interaction with cloud forecast models
[AD-A269104] p 1492 N94-18637
An investigation of warm-cloud microphysics using a multi-component cloud model: Interactive effects of the aerosol spectrum
[AD-A270273] p 1493 N94-18812
Investigations of a coherent vector radar technique for the observation of the atmosphere near 10 GHz
[KFK-5068] p 1494 N94-19616
CLUSTER ANALYSIS
Constructing a reference event list for ARCESS
[AD-A269288] p 1481 N94-18297
CLUSTER MISSION
Cluster: Mission, Payload, and Supporting Activities
[ESA-SP-1159] p 1328 N94-19622

The Wave Experiment Consortium
p 1328 N94-19623
The spherical probe Electric Field and Wave Experiment for the Cluster mission p 1328 N94-19624
STAFF (Spatio-Temporal Analysis of Field Fluctuations) experiment for the Cluster mission p 1328 N94-19625
WHISPER: A sounder and high-frequency wave analyser experiment p 1328 N94-19626
The wideband plasma wave investigation
p 1328 N94-19627
Implementation of the digital wave-processing experiment p 1329 N94-19628
The Cluster magnetic field investigation: Scientific objectives and instrumentation p 1329 N94-19629
The Electron Drift Instrument for Cluster
p 1329 N94-19630
The Cluster Ion Spectroscopy experiment
p 1329 N94-19631
PEACE: A Plasma Electron and Current Experiment
p 1329 N94-19632
RAPID: The imaging energetic particle spectrometer on Cluster p 1329 N94-19633
Active spacecraft potential control: An ion emitter experiment for Cluster p 1330 N94-19634
The Cluster spacecraft p 1330 N94-19635
Cluster ground segment and mission operations
p 1330 N94-19636
The Cluster orbit and mission scenario
p 1330 N94-19637
The Cluster science data system: A distributed system to serve a wide international community
p 1330 N94-19638
The Cluster Joint Science Operations Centre
p 1331 N94-19639
Co-ordination of ground-based observations with Cluster p 1331 N94-19640
European network for the numerical simulation of space plasmas p 1331 N94-19641

CLUSTERS
Metal-nanocluster composites made by ion implantation: A novel third-order nonlinear material
[DE93-015908] p 1339 N94-17846
Proton transfer dynamics and cluster ion fragmentation in phenol/ammonia cLusters
[AD-A269133] p 1348 N94-18256
The Fourteenth Symposium on Molecular Beams
[AD-A268721] p 1568 N94-18787
Photodissociation dynamics of cluster ions
[AD-A270296] p 1568 N94-18814

CMOS
Update on parts SEE susceptibility from heavy ions
[AD-A268735] p 1596 N94-18316
Automated ILA design for synchronous sequential circuits p 1397 N94-18340
Single phase dynamic CMOS PLA using charge sharing technique p 1397 N94-18341
An SEU immune logic family p 1398 N94-18342
Training product unit neural networks with genetic algorithms p 1399 N94-18354
High accuracy switched-current circuits using an improved dynamic mirror p 1401 N94-18368
A tunable CMOS constant current source
p 1401 N94-18369
Formal specification of a high speed CMOS correlator
p 1401 N94-18371
Ultra low power CMOS technology
p 1401 N94-18373
VLSI for high-speed digital signal processing
[AD-A270406] p 1404 N94-18706
Silicon MCM substrates for integration of 3-5 photonic devices and CMOS IC's
[DE93-017894] p 1405 N94-19112
Radiation hardened microprocessor for small payloads
p 1327 N94-19184

COAL
Report to Congress: Comprehensive Program Plan for Advanced Turbine Systems
[DE93-016718] p 1467 N94-18475
EIA publications directory, 1992
[DE93-016833] p 1617 N94-18983
Supercritical thermodynamics of sulfur and nitrogen species
[DE93-041221] p 1610 N94-19670

COAL GASIFICATION
Fundamental studies of the mechanism of catalytic reactions with catalysts effective in the gasification of carbon solids and the oxidative coupling of methane
[DE93-015262] p 1347 N94-18193
Synthesis of higher alcohols from carbon monoxide and hydrogen in a slurry reactor
[DE93-015086] p 1347 N94-18209

COAL LIQUEFACTION
Supercritical thermodynamics of sulfur and nitrogen species
[DE93-041221] p 1610 N94-19670

COAL UTILIZATION
MHD Integrated Topping Cycle Project
[DE93-040521] p 1589 N94-19055

COANDA EFFECT
Design, development, and flight evaluation of the Boeing YC-14 USB powered lift aircraft p 1310 N94-18444
Efficiency of fiber dispersion
[AD-A269740] p 1342 N94-18757

COASTAL ECOLOGY
Ecological and environmental impacts of construction in the coastal zone
[AD-A269196] p 1475 N94-18881

COASTAL PLAINS
Applications of Quaternary stratigraphic, soil-geomorphic, and quantitative geomorphic analyses to the evaluation of tectonic activity and landscape evolution in the Upper Coastal Plain, South Carolina
[DE93-016269] p 1484 N94-18725

COASTAL WATER
DYNLET1 model formulation and user's guide
[AD-A269843] p 1498 N94-18723
Ecological and environmental impacts of construction in the coastal zone
[AD-A269196] p 1475 N94-18881

COASTS
Technologies for assessing the geologic and geomorphic history of coasts
[AD-A268780] p 1496 N94-18215
Coastal Ocean Modeling Workshop
[AD-A268955] p 1497 N94-18393
Wind products for use in coastal wave and surge models
[AD-A269753] p 1497 N94-18414
ADCIRC: An advanced three-dimensional circulation model for shelves, coasts, and estuaries. Report 3: Development of a tidal constituent database for the western North Atlantic and Gulf of Mexico
[AD-A268685] p 1497 N94-18455
Ecological and environmental impacts of construction in the coastal zone
[AD-A269196] p 1475 N94-18881
The WAQUA/CSM-16 model p 1494 N94-19700

COATING
Recirculation in forward roll coating
[VKI-TM-48] p 1409 N94-17901
Process for applying high application-temperature coating to heat-sensitive aluminum alloys
[AD-D015823] p 1368 N94-17905
Synchrotron/crystal sample preparation
[NASA-CR-193837] p 1603 N94-19513
Precision machining and polishing of scintillating crystals for large calorimeters and hodoscopes
[DE93-018663] p 1381 N94-19544

COATINGS
Pressureless densification of ceramic matrix composites
[AD-A269137] p 1371 N94-18691
Soft X Ray Projection Lithography. Organization of the 1993 photonics science optical meetings
[AD-A269159] p 1579 N94-18693
Optical properties of oxide coatings prepared by ion-assisted deposition
[AD-A270024] p 1599 N94-18711
Airflow research
[NASA-TM-109372] p 1312 N94-18964
Testing of protective coatings in hydrogen
[DE93-040326] p 1375 N94-19651

COAXIAL CABLES
A radial transmission line material measurement apparatus
[DE93-018508] p 1394 N94-17780

COBALT
Photoemission studies of Zn, Co, and Gd substituted YBa2Cu3O(7-delta)
[DE93-017403] p 1597 N94-18498
Vibrational dynamics in photoinduced electron transfer
[DE93-040874] p 1567 N94-18533

COBALT ALLOYS
Atlas of formability: HAYNES 556
[AD-A268354] p 1356 N94-17768

COCHLEA
The effects of reverberant impulse noise (blast waves) on hearing: Parametric studies
[AD-A269242] p 1506 N94-18911

COCKPITS
Research on man-machine productivity in aviation at Human Engineering Institute of Hangzhou University
[AD-A269952] p 1512 N94-18673
Army Cockpit Delethalization Program (CDP)
[AD-A268990] p 1512 N94-18765
A multivariate anthropometric method for crew station design
[AD-A270652] p 1513 N94-19531

CODE DIVISION MULTIPLEXING
VHF air/ground communications for air traffic control. Volume 1: A decision tree approach to system innovations
[AD-A268485] p 1316 N94-18384

CODERS
Template based low data rate speech encoder
[AD-A270900] p 1392 N94-19748

CODING
FY 1991 AASERT: Spatio-temporal making in human vision and its application to image coding
[AD-A268795] p 1505 N94-18190
Serial pattern complexity: Irregularity and hierarchy
[PB93-191914] p 1509 N94-19348
Communication in the presence of unknown interference
[AD-A271146] p 1392 N94-19738
Template based low data rate speech encoder
[AD-A270900] p 1392 N94-19748

COEFFICIENT OF FRICTION
Studies of dynamic contact of ceramics and alloys for advanced heat engines
[DE93-016366] p 1368 N94-18110
Tribological studies of silicon for magnetic recording applications (Invited)
[AD-A270878] p 1447 N94-19784

COFFIN-MANSON LAW
Microstructure and texture control of fatigue in hydrogen and marine environments
[AD-A271277] p 1344 N94-19744

COGENERATION
Report to Congress: Comprehensive Program Plan for Advanced Turbine Systems
[DE93-016718] p 1467 N94-18475

COGNITION
A method for cognitive task analysis
[IZF-1992-B5] p 1508 N94-17967
Distributed reasoning and planning
[AD-A268682] p 1540 N94-18399
System dynamics and computer modeling expertise. A conceptual structure research inquiry
[AD-A269860] p 1560 N94-18410
Comparing performance on implicit memory tests
[AD-A269900] p 1508 N94-18657
Putting knowledge to use: The acquisition and transfer of knowledge in situated problem solving environments
[AD-A269746] p 1509 N94-18744
Cognitive ability and whole-body rotation
[IZF-1993-B-4] p 1510 N94-19440

COGNITIVE PSYCHOLOGY
A method for cognitive task analysis
[IZF-1992-B5] p 1508 N94-17967
Cognitive limitations in coordination in hierarchical information processing structures
[AD-A268825] p 1616 N94-18535
Visual perception of features and objects
[AD-A269879] p 1508 N94-18682
Modeling of driver behavior: Information perception, rule and control strategies in experiments and simulations
[ETN-93-95053] p 1510 N94-19649

COHERENT ACOUSTIC RADIATION
Computational aero-acoustics as a branch of turbulence research p 1411 N94-18552

COHERENT RADAR
Investigations of a coherent vector radar technique for the observation of the atmosphere near 10 GHz
[KFK-5068] p 1494 N94-19616

COHERENT RADIATION
X-ray laser oscillator-amplifier experiments
[DE93-017165] p 1436 N94-17868
Proof of the feasibility of coherent and incoherent schemes for pumping a gamma ray laser
[AD-A269173] p 1440 N94-18880
Coherence and linewidth studies of a 4-nm high power FEL
[DE93-018533] p 1441 N94-19030

COHERENT SCATTERING
Theoretical and experimental research on coherent microwave backscatter from the ocean
[AD-A271276] p 1500 N94-19743

COLD ACCLIMATIZATION
Effects of a high-energy food supplement on cold-induced thermogenesis
[AD-A269301] p 1504 N94-17823

COLD CATHODES
Novel electron beam cathode
[AD-A270106] p 1404 N94-18872

COLD NEUTRONS
The use of chopper spectrometers for cold-to-epithermal neutron scattering at IPNS
[DE93-017798] p 1598 N94-18531

COLD PLASMAS
Wake field in electron-positron plasmas
[DE93-624929] p 1584 N94-17955

COLD TOLERANCE
Effects of a high-energy food supplement on cold-induced thermogenesis
[AD-A269301] p 1504 N94-17823
Evaluation of physiological and psychological impairment of human performance in cold stressed subjects
[AD-A268637] p 1506 N94-18632
COLLIMATION
Developmental testing of a prototype all-reflection Michelson interferometer
[AD-A269064] p 1430 N94-18406
COLLIMATORS
Advances and applications of ABCI
[DE93-016971] p 1383 N94-18055
Description of an infrared zoomcollimator
[FEL-93-A034] p 1580 N94-19424
COLLISION AVOIDANCE
Survey of collision avoidance and ranging sensors for mobile robots, revision 1
[AD-A269846] p 1541 N94-18474
Aircraft accident report: Midair collision, Mitsubishi MU-2B-60, N74FB, and PIPER PA-32-301, N82419, Greenwood Municipal Airport, Greenwood, Indiana, 11 September 1992
[PB93-910406] p 1315 N94-19352
COLLISIONAL PLASMAS
Transformation of energy and momentum due to Landau damping in space
[DE93-624921] p 1581 N94-17689
COLLISIONS
Low-energy continuum-electron emission at 0 degrees from O(q+) + He collisions
[DE93-018777] p 1570 N94-19108
IRAS high resolution studies and modeling of closely interacting galaxies. Galaxy collisions: Infrared observations and analysis of numerical models. UV spectroscopy of massive young stellar populations in interacting galaxies
[NASA-CR-194483] p 1627 N94-19218
COLLOIDS
Electrokinetic transport of heterogeneous particles in suspensions
[NASA-CR-194478] p 1353 N94-19367
COLOR
Accelerated tests on the tarnish resistance of gold alloys p 1367 N94-18008
Color palette considerations for digital map displays
[AD-A269991] p 1462 N94-18679
Color test chart for facsimile
[AD-A269754] p 1387 N94-18721
Electro-optics display research, test, and evaluation laboratory program
[AD-A270947] p 1408 N94-19751
COLOR CENTERS
Electron paramagnetic resonance of the ns(sup 1) centers in crystals
[DE93-628793] p 1595 N94-18173
COLOR PHOTOGRAPHY
The application of liquid crystal techniques to determine heat transfer rates p 1432 N94-18654
COLOR VISION
Overview of research in progress at the Center of Excellence
[NASA-CR-194329] p 1618 N94-19256
COLORIMETRY
Penetrometer compatible, fiber-optic sensor for continuous monitoring of chlorinated hydrocarbons: Field test results
[DE93-017974] p 1352 N94-19266
COLUMNS (PROCESS ENGINEERING)
Exchange front stability in packed-column chromatography
[DE93-017526] p 1346 N94-17997
COMBINATORIAL ANALYSIS
Applications of an algebraic Monge property
[DE93-016869] p 1546 N94-17885
Heuristics from nature for hard combinatorial optimization problems
[REPT-93-025] p 1547 N94-17961
On network representation of the solutions in combinatorial optimization
[RR-910-I] p 1552 N94-19392
A tight lower bound for on-line monotonic list labeling
[TR-478] p 1531 N94-19508
COMBUSTIBLE FLOW
Transport phenomena and interfacial kinetics in multiphase combustion systems
[AD-A270202] p 1349 N94-18785
COMBUSTION
Techniques for the estimation of Heats of Explosion (HEX) using thermochemical codes
[AD-A268584] p 1609 N94-18310
LX-17 chemical kinetic material model for Chemical TOPAZ2D
[DE93-014363] p 1377 N94-18893
Collaborative research on combustion diagnostics and modeling between Rolls-Royce, Inc. and the United States Air Force Wright Laboratory
[AD-A270660] p 1354 N94-19778
COMBUSTION CHAMBERS
Study of multi-phase flow characteristics in an MHD power train
[DE93-018570] p 1586 N94-18272
Chemical reactions in turbulent mixing flows
[AD-A269377] p 1410 N94-18472
Analysis of supersonic flows using k-epsilon model and the RPLUS code: Progress towards high speed combustor analysis p 1411 N94-18551
Metal slurry droplet and spray combustion
[AD-A269648] p 1349 N94-18736
MHD integrated topping cycle project
[DE93-040520] p 1588 N94-18978
MHD Integrated Topping Cycle Project
[DE93-040521] p 1589 N94-19055
Collaborative research on combustion diagnostics and modeling between Rolls-Royce, Inc. and the United States Air Force Wright Laboratory
[AD-A270660] p 1354 N94-19778
COMBUSTION CHEMISTRY
Research activity on particle spin systems and related problems
[AD-A269456] p 1562 N94-18286
Transport phenomena and interfacial kinetics in multiphase combustion systems
[AD-A270202] p 1349 N94-18785
Collaborative research on combustion diagnostics and modeling between Rolls-Royce, Inc. and the United States Air Force Wright Laboratory
[AD-A270660] p 1354 N94-19778
COMBUSTION PHYSICS
Research activity on particle spin systems and related problems
[AD-A269456] p 1562 N94-18286
Chemical reactions in turbulent mixing flows
[AD-A269377] p 1410 N94-18472
Mathematical problems in combustion
[AD-A270147] p 1349 N94-18776
Environmental Research Program
[DE93-019101] p 1477 N94-19105
Experimental study of flame front interactions
[ECL-91-40] p 1353 N94-19376
A Sandia Technology Bulletin: Testing technology, July 1993
[DE93-040197] p 1633 N94-19537
COMBUSTION PRODUCTS
Direct Monte Carlo simulation of the chemical equilibrium composition of detonation products
[DE93-014559] p 1376 N94-17751
The carbon dioxide emissions game: Playing the net
[DE93-017670] p 1471 N94-17821
Review of short-term, high-level exposure to metals: Antimony, barium, and cadmium
[AD-A268896] p 1505 N94-18392
On-line monitoring of incinerator emissions
[DE93-017406] p 1474 N94-18499
A comparison of wet and dry scrubbing systems for control of metals and dioxin/furan emissions from incinerators
[DE93-017446] p 1474 N94-18502
Evaluation of aftermarket LPG conversion kits in light-duty vehicle applications
[DE93-010035] p 1377 N94-18617
Transport phenomena and interfacial kinetics in multiphase combustion systems
[AD-A270202] p 1349 N94-18785
Indoor environment program
[DE93-018601] p 1513 N94-18935
Organic carbonyl compounds in Albuquerque, New Mexico, air: A preliminary study of the effects of oxygenated fuel use
[DE93-017748] p 1476 N94-19045
Environmental Research Program
[DE93-019101] p 1477 N94-19105
The use of post detonation analysis of stable isotope ratios to determine the type and production process of the explosive involved
[DE93-018497] p 1378 N94-19242
COMBUSTION STABILITY
Combustion instability phenomena of importance to liquid propellant engines
[AD-A268800] p 1348 N94-18389
Mathematical problems in combustion
[AD-A270147] p 1349 N94-18776
COMETS
Observations of comets with the IUE
[NASA-CR-193652] p 1624 N94-17843
COMMAND AND CONTROL
Cognitive limitations in coordination in hierarchical information processing structures
[AD-A268825] p 1616 N94-18535
An investigation of methods for updating ionospheric scintillation models using topside in-situ plasma density measurements
[AD-A269872] p 1483 N94-18655
Corporate Information Management (CIM) report on the simulation processes, version 2.0
[AD-A269119] p 1617 N94-18770
A user task analysis for command and control systems and its use in human-computer interaction research
[AD-A269877] p 1512 N94-18774
Computer-Aided Prototyping System (CAPS) within the software acquisition process. A case study
[AD-A268705] p 1522 N94-18786
Case studies of software development tools for parallel architectures
[AD-A269193] p 1535 N94-18866
Causal reasoning for model-based process supervisory control
[LAAS-93241] p 1544 N94-19360
PRACTICAL: Planning and resource allocation in C2-domains with time critical algorithms
[FEL-93-B029] p 1544 N94-19458
Systems engineering for Air Force C3I systems
[AD-A270482] p 1391 N94-19676
Automated processing of military messages according to ADatP-3
[FEL-92-A044] p 1393 N94-19798
COMMERCE
Implementation of electronic data interchange in the department of defense: Lessons learned from private industry
[AD-A269532] p 1534 N94-18768
COMMERCIAL AIRCRAFT
Airport activity statistics of certificated route air carriers, 1992
[AD-A269042] p 1315 N94-18490
COMMUNICATION
On asynchronous testing
[MEMO-INF-93-03] p 1543 N94-19226
COMMUNICATION EQUIPMENT
VHF air/ground communications for air traffic control: A decision tree approach to system innovations, volume 2
[AD-A268632] p 1386 N94-18495
Coordination of software-development activities among sites that are geographically separated
[DE93-019201] p 1524 N94-19076
COMMUNICATION NETWORKS
Intentionally Short Range Communications (ISRC)
[AD-A268788] p 1384 N94-18216
Specification and analysis of a high speed transport protocol
[AD-A268941] p 1386 N94-18449
Efficient simulation of DEDS by means of standard clock techniques: Queueing and integrated radio network examples
[AD-A269878] p 1432 N94-18681
Simulation models of UCN, FDDI-2 and DQDB
[MEMO-INF-93-10] p 1536 N94-19197
A highly concurrent medium access control strategy for high speed multiwavelength networks using transceivers with limited tunability
[MEMO-INF-93-07] p 1390 N94-19230
Tandem queues with deterministic service times
[PB93-197465] p 1543 N94-19324
Systolic design with asynchronous controls for digital-signal processing
[AD-A270976] p 1392 N94-19680
Improved HF data network simulator, volume 1
[AD-A270953] p 1393 N94-19752
Improved HF data network simulator, software user's manual, volume 2
[AD-A270954] p 1393 N94-19753
Control of integrated voice/data multi-hop radio networks via reduced-load approximations
[AD-A270661] p 1393 N94-19779
COMMUNICATION THEORY
Specifying and proving communication closedness in protocols
[MEMO-INF-93-23] p 1390 N94-19267
Communication in the presence of unknown interference
[AD-A271146] p 1392 N94-19738
COMMUTATION
Applications of an algebraic Monge property
[DE93-016869] p 1546 N94-17885
Deformed traces and covariant quantum algebras for quantum groups GL(sub qp)(2) and GL(sub qp)(1/1)
[DE93-629862] p 1561 N94-18153
Paragrassmann analysis and quantum groups
[DE93-628593] p 1561 N94-18168
On a possible algebra morphism of U(sub q)(osp1/2) onto the deformed oscillator algebra W(sub q)(N)
[DE93-629857] p 1548 N94-18176

COMPACTING
Equipment for investigation of cryogenic compaction of nanosize silicon nitride powders
[DE93-018740] p 1340 N94-18180
COMPARISON
Verification of 3I retrievals vis-a-vis radiosonde observations
[KNMI-TR-150] p 1488 N94-17924
COMPATIBILITY
Compatibility of refrigerants and lubricants with motor materials, volume 1
[DE93-040216] p 1350 N94-18895
Compatibility of refrigerants and lubricants with motor materials, volume 2
[DE93-040217] p 1350 N94-18896
Compatibility of refrigerants and lubricants with motor materials, volume 3
[DE93-040218] p 1352 N94-19191
COMPENSATORS
Power compensators for phased operation of antenna arrays on JET and D3-D
[DE93-013208] p 1581 N94-17694
Deadbeat control by measurement feedback: A two sided approach
[REPT-93-20] p 1542 N94-19091
COMPILERS
PostScript: A study in conformity
[NPL-DITC-214/93] p 1517 N94-17917
High performance Fortran: An overview
[DE93-017181] p 1519 N94-18072
Using semantic information for processing negation and disjunction in logic programs
[DE93-017412] p 1614 N94-18099
A special purpose silicon compiler for designing supercomputing VLSI systems p 1402 N94-18379
COMPLEX COMPOUNDS
An ab initio study of the weakly bonded CO-Cl2 complex
[AD-A269000] p 1349 N94-18395
Resonance Raman and photophysical studies of transition metal complexes in solution and entrapped in zeolites
[DE93-019892] p 1363 N94-19019
COMPLEX SYSTEMS
The 1992 annual report on scientific programs: A broad research program on the sciences of complexity
[DE93-018151] p 1561 N94-18178
Intelligent help facilities: Generating natural language descriptions with examples
[AD-A269555] p 1521 N94-18290
ControlShell: A real-time software framework
[AD-A269172] p 1523 N94-18879
COMPLEXITY
Shop problems with two machines and time lags
[REPT-93-020] p 1518 N94-17927
COMPONENT RELIABILITY
Synthesis techniques and analysis tool for on-chip fault-tolerance
[AD-A269146] p 1521 N94-18259
COMPOSITE MATERIALS
NMR studies of enriched species at interfaces
[AD-A264703] p 1367 N94-17878
The calculation methods of a cracked plastic composite laminate: A literature survey
[VTT-TIED-1362] p 1339 N94-17958
Lightweight materials for transportation: Program plan
[DE93-017381] p 1340 N94-18087
Analysis of bolted and bonded composite
[AD-A267792] p 1453 N94-18382
Composites: Materials of the future
[AD-A268945] p 1341 N94-18450
The 6th Japan-U.S. conference on composite materials
[AD-A268535] p 1341 N94-18630
Solid State Sciences Committee Forum
[AD-A270454] p 1342 N94-18715
High performance YBCO films
[AD-A269090] p 1599 N94-18719
Mechanical-property changes of structural composite materials after low-temperature proton irradiation: Implications for use in SSC magnet systems
[DE93-016735] p 1343 N94-18763
Shock-loading response of advanced materials
[DE93-018344] p 1455 N94-19033
Computational mechanics of composite materials
[PB93-195782] p 1343 N94-19281
Composite impact dynamics research at NASA LaRC: A review p 1458 N94-19467
Impact analysis of composite aircraft structures
p 1458 N94-19468
Thermal wave image processing for characterization of subsurface of flaws in materials
[DE93-019024] p 1344 N94-19551
Ceramic technology project data base
[DE93-019360] p 1374 N94-19561
Recent advances in high density tungsten composite processing
[AD-A270764] p 1344 N94-19576
COMPOSITE PROPELLANTS
Some problems in the rheological characterisation of composite rocket propellants
[AD-A268806] p 1376 N94-18203
COMPOSITE STRUCTURES
Computational strategies for composite structures
[PB93-195097] p 1452 N94-18079
SAND contact in DYNA3D
[DE93-016451] p 1340 N94-18113
Evaluation of the production-grade class 4 flextensional transducer shell
[AD-A268796] p 1340 N94-18201
Analysis of bolted and bonded composite
[AD-A267792] p 1453 N94-18382
Bibliography on ceramic matrix composites and reinforcing whiskers, platelets, and fibers, 1970-1990
[AD-A270139] p 1371 N94-18750
Dynamic response analysis of composite structural members during missile launch
[AD-A270023] p 1332 N94-18760
Mechanical-property changes of structural composite materials after low-temperature proton irradiation: Implications for use in SSC magnet systems
[DE93-016735] p 1343 N94-18763
Computational mechanics of composite materials
[PB93-195782] p 1343 N94-19281
Compression strength of composite primary structural components
[NASA-CR-194562] p 1457 N94-19350
Design for cyclic loading endurance of composites
[NASA-TM-106407] p 1457 N94-19351
Composite impact dynamics research at NASA LaRC: A review p 1458 N94-19467
COMPRESSIBILITY
Effect of internal heating during hot compression testing on the stress-strain behavior and hot working characteristics of alloy 304L
[DE93-012701] p 1362 N94-18917
Shock compression properties of silicon carbide
[DE93-019927] p 1373 N94-19271
Stability measurements of Rayleigh-Benard convection near the critical state using a spectral model
[MPIS-15/1992] p 1422 N94-19520
COMPRESSIBLE BOUNDARY LAYER
Numerical prediction of transition of the F-16 wing at supersonic speeds
[NASA-CR-194407] p 1312 N94-19433
COMPRESSIBLE FLOW
CFD investigations of the hypersonic double delta wing greta: Sanger project no. 3.2
[FFA-TN-1992-42] p 1311 N94-17919
Viscous-inviscid calculation of high-lift separated compressible flows over airfoils and wings
p 1309 N94-18440
A coupled implicit solution method for turbulent spray combustion in propulsion systems p 1411 N94-18549
High order non-oscillatory schemes for the compressible Euler equations p 1412 N94-18558
A multigrid acceleration technique for computing steady solutions to the equations of compressible flow
p 1412 N94-18559
Introduction to the Modeling of Turbulence
[VKI-LS-1993-02] p 1414 N94-18578
Turbulence modeling for compressible flows and implementation in Navier-Stokes solvers
p 1416 N94-18597
A finite element scheme for shock capturing
[AD-A270182] p 1417 N94-18755
On positivity preserving finite volume schemes for compressible Euler equations
[NASA-CR-191534] p 1551 N94-19317
On the numerical approximation of nonlinear hyperbolic problems: Application to the dynamics of compressible gas
[ETN-93-95020] p 1420 N94-19365
Numerical prediction of transition of the F-16 wing at supersonic speeds
[NASA-CR-194407] p 1312 N94-19433
Study and modeling of compressible flows of flapper nozzle type potentiometric systems
[ETN-93-95012] p 1421 N94-19495
A review of hot-wire technique in compressible flows
[LR-724] p 1423 N94-19668
COMPRESSIBLE FLUIDS
A finite element scheme for shock capturing
[AD-A270182] p 1417 N94-18755
COMPRESSION LOADS
Assessment of an improved multiaxial strength theory based on creep-rupture data for Inconel 600
[DE93-015929] p 1356 N94-17791
A methodology to model physical contact between structural components in NASTRAN
p 1450 N94-17836
Technique to eliminate helium induced weld cracking in stainless steels
[DE93-015982] p 1357 N94-17859
The effect of crystallographic orientation on the performance of single crystal tungsten subscale penetrators
[AD-A268988] p 1597 N94-18468
Mechanical response comparison of gun propellants evaluated under equivalent time-temperature conditions
[AD-A270479] p 1378 N94-19674
COMPRESSION TESTS
Atlas of formability: Ultimet
[AD-A268352] p 1355 N94-17767
Atlas of formability: HAYNES 556
[AD-A268354] p 1356 N94-17768
Atlas of formability: HAYNES 188
[AD-A268355] p 1356 N94-17769
Atlas of formability: NICKELVAC K-500
[AD-A268351] p 1356 N94-17772
Atlas of formability: Haynes 230
[AD-A268325] p 1356 N94-17788
Atlas of formability: INCONEL 718
[AD-A268350] p 1356 N94-17789
Atlas of formability: Hastelloy C-22
[AD-A268324] p 1356 N94-17796
Atlas of formability: Permalloy - 80 flow stress curves
[AD-A268263] p 1356 N94-17801
Atlas of formability: Nickelvac C-276
[AD-A268264] p 1357 N94-17802
Atlas of formability: Ti-6Al-4V ELI
[AD-A268300] p 1357 N94-17803
Atlas of formability: ALLVAC 718
[AD-A268304] p 1357 N94-17804
Atlas of formability: Waspaloy
[AD-A268323] p 1593 N94-17805
COMPRESSIVE STRENGTH
Compression strength of composite primary structural components
[NASA-CR-194562] p 1457 N94-19350
COMPRESSORS
The 7th International Cryocooler Conference
[AD-A268451] p 1379 N94-18147
COMPTON EFFECT
Simulation of emittance dilution in electron storage ring from Compton backscattering
[DE93-017611] p 1386 N94-18503
Single sided tomography of extremely large dense objects
[DE93-017993] p 1580 N94-19268
COMPUTATION
An efficient implementation of error-valued semantics on imperative machines
[DE93-014658] p 1516 N94-17740
Thermodynamics of computation and information distance
[DE93-012730] p 1517 N94-17812
Shop problems with two machines and time lags
[REPT-93-020] p 1518 N94-17927
Systolic array IC for genetic computation
p 1400 N94-18361
Optimal eigenvalue computation on distributed-memory MIMD multiprocessors
[DE93-018337] p 1535 N94-18808
Adaptive uniformization: Technical details
[MEMO-INF-93-22] p 1558 N94-19265
Adaptive uniformization
[MEMO-INF-92-88] p 1558 N94-19385
Fault-tolerance and complexity
[TR-450] p 1530 N94-19483
Computation of large numbers and VLSI: Application to GCD, to stretched GCD and at euclidian distance
[ETN-93-95009] p 1552 N94-19499
On the computation of versal family of matrices
[RR-892-M] p 1532 N94-19712
COMPUTATIONAL ASTROPHYSICS
Computational astrophysics: Pulsating stars
[DE93-018369] p 1627 N94-18857
A new approach to the study of the turbulence layer
[NASA-CR-194546] p 1487 N94-19397
COMPUTATIONAL FLUID DYNAMICS
A study of the influence of a delta wing geometry on the induced drag at transonic speed (M=0.55) and high angles of attack
[FFA-TN-1992-14] p 1311 N94-17722
Finite element modeling of evaporation and condensation during sol-gel film and fiber formation
[DE93-017655] p 1345 N94-17820
CFD investigations of the hypersonic double delta wing greta: Sanger project no. 3.2
[FFA-TN-1992-42] p 1311 N94-17919
Synthesis of the Workshop on Hypersonic Flows for Reentry Problems
[INRIA-RR-1721] p 1311 N94-17957

Investigation of a matrix-model for the artificial dissipation in a cell vertex finite volume scheme for solving the Navier-Stokes equations
[DLR-FB-92-33] p 1409 N94-18076
Interferometer stations at the Air Force Aeroballistic Research Facility
[AD-A268776] p 1322 N94-18330
High-performance multiprocessor architecture for a 3-D lattice gas model p 1400 N94-18362
Parabolized Navier-Stokes computation of surface heat transfer characteristics for supersonic and hypersonic KE projectiles
[AD-A268858] p 1410 N94-18391
High-Lift System Aerodynamics
[AGARD-CP-515] p 1305 N94-18415
Calculation of maximum and high lift characteristics of multi element aerofoils p 1305 N94-18419
Navier-Stokes computations of turbulent flow around high-lift configurations p 1306 N94-18420
Efficient simulation of incompressible viscous flow over multi-element airfoils p 1306 N94-18421
Navier-Stokes calculations on multi-element airfoils using a chimera-based solver p 1306 N94-18422
Numerical solution of the Navier-Stokes equations for high-lift configurations on structured composite grids
p 1306 N94-18423
A viscous-inviscid solver for high-lift incompressible flows over multi-element airfoils at deep separation conditions p 1306 N94-18425
High-lift system analysis method using unstructured meshes p 1307 N94-18426
Prediction of the high-lift performance of multi-element aerofoils using an unstructured Navier-Stokes solver
p 1307 N94-18427
Numerical calculations of high lift flows using structured and unstructured methods p 1307 N94-18428
Navier-Stokes simulation of flow field around a blown-flap high-lift system p 1307 N94-18429
Viscous phenomena affecting high-lift systems and suggestions for future CFD development
p 1308 N94-18433
A fast computing method for the flow over high-lift wings p 1308 N94-18437
Calculation of multielement airfoils and wings at high lift p 1309 N94-18438
Wake structure and aerodynamic behavior of high lift aircraft configurations during unsteady maneuvers in ground effect p 1309 N94-18439
Viscous-inviscid calculation of high-lift separated compressible flows over airfoils and wings
p 1309 N94-18440
High-lift research: Application to the design of the ATR72 flap p 1309 N94-18442
The aero-mechanical design of a novel Fowler flap mechanism p 1309 N94-18443
Workshop on Computational Turbulence Modeling
[NASA-TM-109266] p 1410 N94-18545
Research activities at the Center for Modeling of Turbulence and Transition p 1410 N94-18546
Assessment and development of second order turbulence models p 1411 N94-18548
A coupled implicit solution method for turbulent spray combustion in propulsion systems p 1411 N94-18549
Numerical investigation of complex, transitional, and chemically reacting flows p 1411 N94-18550
Analysis of supersonic flows using k-epsilon model and the RPLUS code: Progress towards high speed combustor analysis p 1411 N94-18551
A comparative study of turbulence models in predicting hypersonic inlet flows p 1314 N94-18553
An algebraic turbulence model for turbomachinery
p 1411 N94-18554
Several examples where turbulence models fail in inlet flow field analysis p 1412 N94-18556
Computational Fluid Dynamics
[VKI-LS-1993-04] p 1412 N94-18557
High order non-oscillatory schemes for the compressible Euler equations p 1412 N94-18558
Computational techniques for high-speed flows with viscous and chemical effects p 1412 N94-18560
Multidimensional wave decompositions for the Euler equations p 1413 N94-18562
Cell vertex methods for steady inviscid flow
p 1413 N94-18563
Compact advection schemes on unstructured grids
p 1413 N94-18564
Variational approaches to CFD: Applications to potential Euler and Navier-Stokes equations
p 1413 N94-18565
Introduction to spectral methods for hyperbolic system of conservation laws p 1413 N94-18567
Distributed memory parallel computers and computational fluid dynamics p 1413 N94-18568
Two-equation models for low-Reynolds-number variants p 1415 N94-18587
Inclusion of second-moment closures into finite-volume solvers p 1415 N94-18588
Direct and large eddy simulation of turbulence: Summary of the state of the art 1993 p 1416 N94-18594
Numerical simulation of turbulent convective flow over wavy terrain p 1416 N94-18596
Calculation of turbulent boundary layer wall pressure spectra
[AD-A269549] p 1416 N94-18642
UUGM code development
[AD-A269945] p 1416 N94-18671
STREMR: Numerical model for depth-averaged incompressible flow
[AD-A269949] p 1417 N94-18672
Computational Fluid Dynamics (CFD) research branch technical briefs
[AD-A269698] p 1417 N94-18739
Numerical simulation of fluid dynamics and combustion for ram accelerator projectile/obturator interaction
[AD-A269715] p 1320 N94-18748
Some parametric flow analyses of a particle bed fuel element
[DE93-018440] p 1337 N94-18830
Multigrid methods for flow transition in three-dimensional boundary layers with surface roughness
[NASA-CR-4540] p 1417 N94-18843
Numerical simulation of turbulent mixing and combustion near the inlet of a burner
[DE93-017960] p 1350 N94-18987
Implementation of the turn function method in KIVA-F90
[DE93-018394] p 1419 N94-19027
Numerical solutions for a flow with mixed convection in a vertical geometry
[DE93-011592] p 1419 N94-19058
Multigrid for a groundwater flow problem
[REPT-93-29] p 1420 N94-19144
Content based-grid node selection for vector field visualization
[REPT-93-35] p 1525 N94-19155
Pseudo-compressibility methods for the incompressible flow equations
[NASA-CR-191533] p 1551 N94-19315
On the numerical approximation of nonlinear hyperbolic problems: Application to the dynamics of compressible gas
[ETN-93-95020] p 1420 N94-19365
Theoretical study and modelling of homogeneous turbulence under rotation for implantation in a code for solving Navier-Stokes equations
[ECL-93-05] p 1420 N94-19381
Simulation of three dimensional unsteady viscous flows in turbomachines
[ECL-92-15] p 1420 N94-19398
Numerical simulations of turbulent buoyant flows by finite element method: Application to the study of strongly heated or cooled stratified flow
[ECL-92-28] p 1421 N94-19399
Numerical prediction of transition of the F-16 wing at supersonic speeds
[NASA-CR-194407] p 1312 N94-19433
Analysis of film cooling in rocket nozzles
[NASA-CR-194674] p 1338 N94-19438
Contribution to the study of a symmetric film flow (with or without tensio-active elements)
[ECL-93-13] p 1421 N94-19461
Numerical simulation of viscous flows in chemical nonequilibrium
[MBB-LME-211-S-PUB-506] p 1421 N94-19497
Three dimensional network generation and Euler calculation for a wing fuselage canard configuration
[MBB-LME-211-S-PUB-511-A] p 1319 N94-19500
Two-dimensional turbulent nonstationary superfluid counterflows: Numerical simulations, qualitative effects
[MPIS-23/1992] p 1422 N94-19510
MIMD massively parallel methods for engineering and science problems
[DE93-019409] p 1531 N94-19562
Navier-Stokes, dynamics and aeroelastic computations for vortical flows, buffet and flutter applications
[NASA-CR-194520] p 1313 N94-19621
Collaborative research on combustion diagnostics and modeling between Rolls-Royce, Inc. and the United States Air Force Wright Laboratory
[AD-A270660] p 1354 N94-19778

COMPUTATIONAL GEOMETRY
Using geometric techniques to improve dynamic programming algorithms for the economic lot-sizing problem and extensions
[PB93-197556] p 1528 N94-19330
Geometric contact for curves and surfaces
[RR-893-M] p 1556 N94-19731

COMPUTATIONAL GRIDS
Benchmarking the QUAD4/TRIA3 element
p 1450 N94-17837
Advances and applications of ABCI
[DE93-016971] p 1383 N94-18055
Calculation of maximum and high lift characteristics of multi element aerofoils p 1305 N94-18419
Navier-Stokes calculations on multi-element airfoils using a chimera-based solver p 1306 N94-18422
Numerical solution of the Navier-Stokes equations for high-lift configurations on structured composite grids
p 1306 N94-18423
High-lift system analysis method using unstructured meshes p 1307 N94-18426
Prediction of the high-lift performance of multi-element aerofoils using an unstructured Navier-Stokes solver
p 1307 N94-18427
Numerical calculations of high lift flows using structured and unstructured methods p 1307 N94-18428
Navier-Stokes simulation of flow field around a blown-flap high-lift system p 1307 N94-18429
Several examples where turbulence models fail in inlet flow field analysis p 1412 N94-18556
ENO schemes on unstructured meshes
p 1412 N94-18561
Multidimensional wave decompositions for the Euler equations p 1413 N94-18562
Cell vertex methods for steady inviscid flow
p 1413 N94-18563
Compact advection schemes on unstructured grids
p 1413 N94-18564
Variational approaches to CFD: Applications to potential Euler and Navier-Stokes equations
p 1413 N94-18565
UUGM code development
[AD-A269945] p 1416 N94-18671
3D composite grids using Bezier curves and surfaces in component adaptive methods
[AD-A269188] p 1549 N94-18863
A particle method for history-dependent materials
[DE93-018696] p 1456 N94-19060
Three dimensional network generation and Euler calculation for a wing fuselage canard configuration
[MBB-LME-211-S-PUB-511-A] p 1319 N94-19500

COMPUTER AIDED DESIGN
Verification of VALISYS cad based CMM software at LLNL
[DE93-013854] p 1517 N94-17911
Current development in selected stress and thermal analysis software interfaces with PRO-ENGINEER
[DE93-014935] p 1518 N94-17943
Interactive Collaborative Environments (ICE) in the design to manufacturing process
[DE93-014994] p 1518 N94-17944
The First International Conference on PCTE
[FEL-92-A134] p 1518 N94-17965
Tooth form design supporting system in module design p 1428 N94-18036
APLAC: An object-oriented analog circuit simulator and design tool. 6.1 reference manual
[PB93-187193] p 1396 N94-18091
Cut and paste based modeling with boundary features
[PB93-187250] p 1520 N94-18117
Introduction to Quantitative Feedback Theory (QFT) technique p 1545 N94-18241
A rational design change methodology based on experimental and analytical modal analysis
[DE93-018537] p 1521 N94-18271
Application of the A* algorithm to aircraft trajectory generation
[AD-A268728] p 1317 N94-18315
Distributed Computing Design System (DCDS)
[AD-A270435] p 1534 N94-18509
Naval research reviews. Mixing enhancement for air-breathing propulsion. Non-axisymmetric jets increase mixing, volume 44 and volume 45
[AD-A268966] p 1521 N94-18543
Computer-Aided Prototyping System (CAPS) within the software acquisition process. A case study
[AD-A268705] p 1522 N94-18786
Initial Graphics Exchange Specification (IGES)
[AD-A270049] p 1522 N94-18794
Thermo-hydraulic analysis of superconducting toroidal-field magnets for the Tokamak Physics Experiment
[DE93-018096] p 1590 N94-19269
ISAC: A tool for aeroservoelastic modeling and analysis
[NASA-TM-109031] p 1321 N94-19316
Numerical simulation of vehicle crashworthiness and occupant protection p 1459 N94-19471
ADAS implementation of a panel method for the prediction of aerodynamic loads
[LR-723] p 1313 N94-19667

COMPUTER AIDED MANUFACTURING
Verification of VALISYS cad based CMM software at LLNL
[DE93-013854] p 1517 N94-17911

Initial Graphics Exchange Specification (IGES)
[AD-A270049] p 1522 N94-18794
An innovative neural manufacturing concept
[DE93-017212] p 1527 N94-19238

COMPUTER AIDED TOMOGRAPHY
In vivo animal models of body composition in aging
[DE93-012527] p 1501 N94-17889
Development and application of local 3-D x ray CT reconstruction software for imaging critical regions in large ceramic turbine rotors
[DE93-015159] p 1369 N94-18166
Quantification of volume flaw sizes in ceramics by image processing of 3D x ray tomographic data sets
[DE93-018573] p 1372 N94-18932
Using computerized tomography to determine ionospheric structures
[DE93-018903] p 1485 N94-19001
Using computerized tomography to determine ionospheric structures
[DE93-018904] p 1485 N94-19002

COMPUTER ANIMATION
Shuttle-C, the future is now
[NASA-TM-109355] p 1332 N94-18954

COMPUTER ASSISTED INSTRUCTION
Present evolution of tools management
[CRIF-MC-102] p 1444 N94-17964
Teaching a computer simulation course with Ada
[AD-A267901] p 1521 N94-18308
A teaching tool for linear programming
[AD-A270240] p 1523 N94-18905
Computer-assisted instruction and natural language systems
[MEMO-INF-92-86] p 1527 N94-19225

COMPUTER DESIGN
Performance of defect-tolerant set-associative cache memories p 1398 N94-18346
Verification of VLSI designs p 1400 N94-18363
A new variable testability measure
p 1400 N94-18364
Formal hardware verification of digital circuits
p 1401 N94-18367
Naval research reviews. Mixing enhancement for air-breathing propulsion. Non-axisymmetric jets increase mixing, volume 44 and volume 45
[AD-A268966] p 1521 N94-18543
Systolic design with asynchronous controls for digital-signal processing
[AD-A270976] p 1392 N94-19680
A comparison Air Force data systems — Comments on IDA Paper P-2863
[AD-A270662] p 1619 N94-19780

COMPUTER GRAPHICS
Heavy ion nuclear physics research
[DE93-018862] p 1565 N94-17776
An object-oriented environment for computer vision and pattern recognition
[DE93-017098] p 1517 N94-17867
Texture splats for 3D vector and scalar field visualization
[DE93-017104] p 1520 N94-18130
An evolving infrastructure for scientific computing and the integration of new graphics technology
[DE93-017164] p 1520 N94-18133
Navigation in hypermedia applications: Modelling and semantics
[REPT-93-034] p 1520 N94-18136
GREPOS: A GENESIS database repositioning program
[DE93-018517] p 1614 N94-18164
Three-dimensional cloud visualization based on satellite imagery
[AD-A269318] p 1490 N94-18300
Color palette considerations for digital map displays
[AD-A269991] p 1462 N94-18679
Portable parallel ray tracing algorithms
[AD-A268984] p 1522 N94-18698
Initial Graphics Exchange Specification (IGES)
[AD-A270049] p 1522 N94-18794
Content based-grid node selection for vector field visualization
[REPT-93-35] p 1525 N94-19155
Pegasus project description
[MEMO-INF-92-75] p 1536 N94-19159
Pegasus: Operating system support for distributed multimedia systems
[MEMO-INF-92-76] p 1536 N94-19160
A visualization environment for supercomputing-based applications in computational mechanics
[DE93-015024] p 1537 N94-19249
Numerical experiments on the Ginzburg-Landau equations
[DE93-019504] p 1604 N94-19567

COMPUTER INFORMATION SECURITY
Securing electronic mail: The risks and future of electronic mail
[DE93-017187] p 1383 N94-17994
Computer/information security design approaches for Complex 21/Reconfiguration facilities
[DE93-018547] p 1535 N94-18930
Inventory management plan for a research and development local area network
[DE93-018381] p 1617 N94-19026
The p4 Linda: A portable implementation of Linda
[DE93-017752] p 1535 N94-19046
Secure open systems: An investigation of current standardisation efforts for security in open systems
[FEL-92-B225] p 1618 N94-19450
Secure open systems: An investigation
[FEL-91-B293] p 1619 N94-19454
Models and building blocks for secure open systems
[FEL-92-B365] p 1619 N94-19457
Computer security. Evolutions 1987 to 1992: Trends and perspectives
[RR-905-I] p 1532 N94-19713

COMPUTER NETWORKS
Information technology resources assessment
[DE93-015276] p 1613 N94-17894
Securing electronic mail: The risks and future of electronic mail
[DE93-017187] p 1383 N94-17994
Metadata compiled and distributed by the Carbon Dioxide Information Analysis Center for global climate change and greenhouse gas-related data bases
[DE93-015338] p 1473 N94-18167
Fast-training algorithm for hidden-layer forward-feed neural networks
[AD-A269253] p 1540 N94-18263
Handbook for users
[AD-A268726] p 1615 N94-18323
Distributed reasoning and planning
[AD-A268682] p 1540 N94-18399
Specification and analysis of a high speed transport protocol
[AD-A268941] p 1386 N94-18449
The evolution of the PVM concurrent computing system
[DE93-017764] p 1534 N94-18482
Distributed Computing Design System (DCDS)
[AD-A270435] p 1534 N94-18509
A general theory of signal integration for fault-tolerant dynamic distributed sensor networks
[AD-A270316] p 1534 N94-18699
Implementation of electronic data interchange in the department of defense: Lessons learned from private industry
[AD-A269532] p 1534 N94-18768
Neutral networks: An NRL perspectiva
[AD-A269122] p 1541 N94-18773
Computer/information security design approaches for Complex 21/Reconfiguration facilities
[DE93-018547] p 1535 N94-18930
The p4 Linda: A portable implementation of Linda
[DE93-017752] p 1535 N94-19046
High energy physics program. Task A: Experiment and theory. Task B: Numerical simulation
[DE93-018140] p 1575 N94-19050
Performance and scalability aspects of directory-based cache coherence in shared-memory multiprocessors
[DE93-016442] p 1536 N94-19115
Application of new technologies in the virtual library: Seminars in Turkey, Portugal, and Spain
[NASA-TM-109718] p 1611 N94-19131
Pegasus project description
[MEMO-INF-92-75] p 1536 N94-19159
Pegasus: Operating system support for distributed multimedia systems
[MEMO-INF-92-76] p 1536 N94-19160
Simulation models of UCN, FDDI-2 and DQDB
[MEMO-INF-93-10] p 1536 N94-19197
Wide-address spaces: Exploring the design space
[MEMO-INF-92-77] p 1537 N94-19219
Specification and verification of a dynamic leader election protocol in a broadcast network
[MEMO-INF-93-05] p 1558 N94-19228
A visualization environment for supercomputing-based applications in computational mechanics
[DE93-015024] p 1537 N94-19249
Models and building blocks for secure open systems
[FEL-92-B365] p 1619 N94-19457
Protocol service decomposition for high-performance networking
[AD-A270613] p 1538 N94-19533
Optoelectronic packaging: A review
[DE93-040059] p 1515 N94-19535
Learning about the Internet bibliography and beginner's guide
[AD-A268847] p 1532 N94-19707
Congestion/flow control and routing in data networks: A control-theoretic approach
[AD-A271121] p 1392 N94-19737
Improved HF data network simulator, volume 1
[AD-A270953] p 1393 N94-19752
Improved HF data network simulator, software user's manual, volume 2
[AD-A270954] p 1393 N94-19753
NPAC distributed-parallel system feasibility study
[AD-A270972] p 1539 N94-19790

COMPUTER PROGRAM INTEGRITY
Using semantic information for processing negation and disjunction in logic programs
[DE93-017412] p 1614 N94-18099
Optimal safety system design using fault tree analysis
[MATHS-REPT-A-187] p 1529 N94-19382
A research program in empirical computer science
[NASA-CR-194069] p 1530 N94-19429
Integrity checking in deductive databases: An exposition
[PB93-191724] p 1619 N94-19709
Computer security. Evolutions 1987 to 1992: Trends and perspectives
[RR-905-I] p 1532 N94-19713

COMPUTER PROGRAMMING
SX User's Manual for SX, version 2.0
[DE93-015971] p 1517 N94-17914
Shop problems with two machines and time lags
[REPT-93-020] p 1518 N94-17927
Numerical methods for molecular dynamics
[DE93-018321] p 1566 N94-18179
Dialog-Based Learning (DBL) for adaptive interface agents and programming-by-demonstrations systems
[AD-A269154] p 1540 N94-18261
Teaching a computer simulation course with Ada
[AD-A267901] p 1521 N94-18308
Specification and analysis of a high speed transport protocol
[AD-A268941] p 1386 N94-18449
The CMU masters in software engineering core curriculum
[AD-A268983] p 1521 N94-18453
Distributed Computing Design System (DCDS)
[AD-A270435] p 1534 N94-18509
A case study in software maintenance
[AD-A269923] p 1521 N94-18659
Efficient transparent optimistic rollback recovery for distributed application programs
[AD-A268981] p 1522 N94-18696
The development of a course sequence in real-time systems design
[AD-A269459] p 1522 N94-18726
Connection machine software conversion of a Navy oceans model
[AD-A269876] p 1535 N94-18772
ControlShell: A real-time software framework
[AD-A269172] p 1523 N94-18879
A programming paradigm for distributed-memory computers
[DE93-018336] p 1524 N94-19024
On the convergence of an unfeasible primal-dual interior-point method for convex programming
[REPT-93-34] p 1525 N94-19154
Reducing extended transition systems
[MEMO-INF-93-09] p 1526 N94-19196
How to apply the IEEE standards to software testing
[DE93-018514] p 1527 N94-19245
Vectorized presentation-level services for scientific distributed applications
[DE93-018091] p 1537 N94-19253
Action systems and action refinement in the development of parallel systems: An algebraic approach
[MEMO-INF-93-14] p 1538 N94-19296
Advanced software development workstation: Object-oriented methodologies and applications for flight planning and mission operations
[NASA-CR-193706] p 1513 N94-19349
Computing professionals: Changing needs for the 1990's
[B-030] p 1515 N94-19401
Transient dynamics capability at Sandia National Laboratories p 1460 N94-19476
Technical development of a theory of programs
[ETN-93-95058] p 1532 N94-19652
Implementation of parallel algorithms
[AD-A271035] p 1539 N94-19682
Software reuse: Major issues need to be resolved before benefits can be achieved. Report to the Chairman, Subcommittee on Defense, Committee on Appropriations, House of Representatives
[GAO/IMTEC-93-16] p 1532 N94-19716
Technology benefits model user manual, version 01.00.04
[AD-A270637] p 1620 N94-19777

COMPUTER PROGRAMS
The design of the MAD Design Program
[DE93-013343] p 1539 N94-17696
A one dimensional numerical model, with an application to the vertical distribution of dissolved oxygen in the ocean
[DE93-018481] p 1495 N94-17779

FEM/SINDA: Combining the strengths of NASTRAN, SINDA, I-DEAS, and PATRAN for thermal and structural analysis p 1449 N94-17831

Introductory user's guide to the ARL supercomputer facility at Aberdeen Proving Ground
[AD-A265204] p 1514 N94-17877

SX User's Manual for SX, version 2.0
[DE93-015971] p 1517 N94-17914

Strategies for testing form assessment software
[NPL-DITC-211/92] p 1518 N94-17930

Current development in selected stress and thermal analysis software interfaces with PRO-ENGINEER
[DE93-014935] p 1518 N94-17943

Format.m: A usage manual. Towards an efficient symbolic-numeric environment: Extending Mathematica's format rules
[MATHS-REPT-A-185] p 1547 N94-17969

An emulator for testing HVAC-control and energy management systems
[VTT-TIED-1337] p 1444 N94-17974

FAROW: A tool for fatigue and reliability of wind turbines
[DE93-017639] p 1465 N94-18001

An overview of the SAFSIM computer program
[DE93-017657] p 1519 N94-18002

FEEST: A method for tabulating equation of state and opacity tables
[DE93-017965] p 1347 N94-18092

Using semantic information for processing negation and disjunction in logic programs
[DE93-017412] p 1614 N94-18099

Navigation in hypermedia applications: Modelling and semantics
[REPT-93-034] p 1520 N94-18136

GREPOS: A GENESIS database repositioning program
[DE93-018517] p 1614 N94-18164

ASYS: a computer algebra package for analysis of nonlinear algebraic equations systems
[DE93-629819] p 1548 N94-18175

User's manual of Tokamak Simulation Code
[DE93-788388] p 1586 N94-18212

Study of multi-phase flow characteristics in an MHD power train
[DE93-018570] p 1586 N94-18272

Teaching a computer simulation course with Ada
[AD-A267901] p 1521 N94-18308

Applications of the program UIFLOW-2D to the numerical simulation of axisymmetric flows
[AD-A268731] p 1410 N94-18326

Automated ILA design for synchronous sequential circuits p 1397 N94-18340

Distributed reasoning and planning
[AD-A268682] p 1540 N94-18399

Software reliability: Estimation and prediction
[AD-A268895] p 1521 N94-18458

Parallelization of the Air Force Space Command (AFSPACECOM) satellite motion models
[AD-A269327] p 1334 N94-18470

The evolution of the PVM concurrent computing system
[DE93-017764] p 1534 N94-18482

A case study in software maintenance
[AD-A269923] p 1521 N94-18659

Implementation of a nonisothermal unified inelastic-strain theory into ADINA6.0 for a titanium alloy: User guide
[AD-A269927] p 1360 N94-18660

UUGM code development
[AD-A269945] p 1416 N94-18671

Directory of Energy Information Administration Models 1993
[DE93-016987] p 1616 N94-18707

DYNLET1 model formulation and user's guide
[AD-A269843] p 1498 N94-18723

Automatically generating abstractions for planning
[AD-A269772] p 1541 N94-18759

Connection machine software conversion of a Navy oceans model
[AD-A269876] p 1535 N94-18772

Computer-Aided Prototyping System (CAPS) within the software acquisition process. A case study
[AD-A268705] p 1522 N94-18786

NASA Electronic Library System (NELS) optimization
[NASA-CR-193688] p 1617 N94-18839

Knowledge sources for an intelligent MCM analyzer
[AD-A269224] p 1542 N94-18887

Automated assistance for detecting malicious code
[DE93-018106] p 1523 N94-18943

Software distribution using xnetlib
[DE93-018278] p 1523 N94-18989

Early experiences with the IBM SP-1
[DE93-018398] p 1535 N94-19010

Implementation of the turn function method in KIVA-F90
[DE93-018394] p 1419 N94-19027

Overview of WARP: A particle code for heavy ion fusion
[DE93-018637] p 1588 N94-19034

CAVEMAN: Configuration and version management
[DE93-018066] p 1524 N94-19048

GENSHELL: A genesis database 2D to 3D shell transformation program
[DE93-018694] p 1525 N94-19102

Computer codes for checking, plotting and processing of neutron cross-section covariance data and their application
[DE93-018459] p 1570 N94-19129

Modelling software for structure metrics
[MEMO-INF-93-13] p 1526 N94-19200

How to apply the IEEE standards to software testing
[DE93-018514] p 1527 N94-19245

A program for passively tracking a target using an array of sensors
[DE93-019554] p 1390 N94-19306

Software quality in test and measurment equipment
[PB93-197846] p 1528 N94-19333

The fire resistance of profiled thin steel sheet structures
[VTT-TIED-1320] p 1380 N94-19373

A research program in empirical computer science
[NASA-CR-194069] p 1530 N94-19429

A comparison between several computer codes for calculations on microwave propagation
[FEL-92-A435] p 1390 N94-19449

Transient dynamics capability at Sandia National Laboratories p 1460 N94-19476

OORA Automated Knowledge System (OAKS) code, appendix C
[AD-A270709] p 1531 N94-19573

Refinement of unit cell parameters by least-squares: Comments on an old technique and the development of a new computer program
[AD-A270610] p 1531 N94-19590

CVL: A C vector library manual. Version 2
[AD-A270614] p 1531 N94-19592

Automated qualitative modeling of dynamic physical systems
[AD-A270835] p 1422 N94-19598

Optical switch evaluation support
[AD-A270948] p 1581 N94-19601

Technical development of a theory of programs
[ETN-93-95058] p 1532 N94-19652

Acoustic propagation modeling using MATLAB
[AD-A270905] p 1564 N94-19750

Improved HF data network simulator, software user's manual, volume 2
[AD-A270954] p 1393 N94-19753

Marine-modified LOWTRAN: The contribution of sun glint
[AD-A269547] p 1500 N94-19762

Technology benefits model user manual, version 01.00.04
[AD-A270637] p 1620 N94-19777

A register of underwater acoustic test facilities in the US, Canada, and the United Kingdom
[AD-A270884] p 1500 N94-19785

The universal BitBus node
[DIGEL-1993-1] p 1515 N94-19799

COMPUTER STORAGE DEVICES

New dynamic FET logic and serial memory circuits for VLSI GaAs technology p 1397 N94-18339

An SEU immune logic family p 1398 N94-18342

Photo-induced and electrooptic properties of (Pb,La)(Zr,Ti)O3 films
[DE93-017496] p 1371 N94-18519

Networked MS windows 3.1 based classified document control system (CDOCS)
[DE93-017880] p 1617 N94-18984

Superconducting flux flow devices, digital circuits and memories
[DE93-019072] p 1405 N94-19079

COMPUTER SYSTEMS DESIGN

RESQme studies for SDC regional computing centers
[DE93-015230] p 1514 N94-17799

TANGO: A notation for describing advanced transaction models
[REPT-93-014] p 1613 N94-17936

Object-oriented extension of a relational DBMS
[ETN-93-94403] p 1519 N94-17978

A model and an execution mechanism for active data bases
[ETN-93-94404] p 1614 N94-17979

Better termination analysis for active databases
[REPT-93-026] p 1614 N94-18144

Synthesis techniques and analysis tool for on-chip fault-tolerance
[AD-A269148] p 1521 N94-18259

Systolic array IC for genetic computation
p 1400 N94-18361

High-performance multiprocessor architecture for a 3-D lattice gas model p 1400 N94-18362

A fast adaptive convex hull algorithm on two-dimensional processor arrays with a reconfigurable BUS system
p 1402 N94-18380

Distributed reasoning and planning
[AD-A268682] p 1540 N94-18399

Distributed Computing Design System (DCDS)
[AD-A270435] p 1534 N94-18509

A general theory of signal integration for fault-tolerant dynamic distributed sensor networks
[AD-A270316] p 1534 N94-18699

Task A: Yale Accelerator Users Group (YAUG)
[DE93-018417] p 1570 N94-19029

Coordination of software-development activities among sites that are geographically separated
[DE93-019201] p 1524 N94-19076

ACOS: A performance based approach to build a parallel complex object server
[MEMO-INF-93-11] p 1537 N94-19198

A visualization environment for supercomputing-based applications in computational mechanics
[DE93-015024] p 1537 N94-19249

Contribution to applications systems design MOSAIC method in the Aristote project
[ETN-93-95022] p 1529 N94-19370

Secure open systems: An investigation of current standardisation efforts for security in open systems
[FEL-92-B225] p 1618 N94-19450

Models and building blocks for secure open systems
[FEL-92-B365] p 1619 N94-19457

Problem of control in an integral vision system: Use of a multi-agent system
[ETN-93-95007] p 1530 N94-19488

Silicon compilation: From the circuit to the system
[ETN-93-95010] p 1406 N94-19501

Computer security. Evolutions 1987 to 1992: Trends and perspectives
[RR-905-I] p 1532 N94-19713

COMPUTER SYSTEMS PERFORMANCE

Strategies for testing form assessment software
[NPL-DITC-211/92] p 1518 N94-17930

Embedded Computer Performance Measurement (ECPM). Advanced avionics subsystems and technology multiprocessor ECPM software documentation
[AD-A269921] p 1320 N94-18658

Downsizing a database platform for increased performance and decreased costs
[DE93-018687] p 1618 N94-19099

On asynchronous testing
[MEMO-INF-93-03] p 1543 N94-19226

A unified performability evaluation framework for computer and communication systems
[MEMO-INF-93-21] p 1537 N94-19264

Robot navigation in unknown terrains: Introductory survey of non-heuristic algorithms
[DE93-019221] p 1316 N94-19300

Protocol service decomposition for high-performance networking
[AD-A270613] p 1538 N94-19533

COMPUTER SYSTEMS PROGRAMS

RESQme studies for SDC regional computing centers
[DE93-015230] p 1514 N94-17799

TANGO: A notation for describing advanced transaction models
[REPT-93-014] p 1613 N94-17936

Dialog-Based Learning (DBL) for adaptive interface agents and programming-by-demonstrations systems
[AD-A269154] p 1540 N94-18261

Intelligent help facilities: Generating natural language descriptions with examples
[AD-A269555] p 1521 N94-18290

Development of parallel architectures for sensor array processing, volume 1
[AD-A270426] p 1534 N94-18507

Downsizing a database platform for increased performance and decreased costs
[DE93-018687] p 1618 N94-19099

EXANA: A program for analysing extended energy loss fine structures, EXELFS spectra
[USIP-92-01] p 1525 N94-19145

How to apply the IEEE standards to software testing
[DE93-018514] p 1527 N94-19245

Conception and analysis of numerical parallel algorithms: Realization on the Connection Machine
[ETN-93-95005] p 1531 N94-19517

The universal BitBus node
[DIGEL-1993-1] p 1515 N94-19799

COMPUTER SYSTEMS SIMULATION

Simulation models of UCN, FDDI-2 and DQDB
[MEMO-INF-93-10] p 1536 N94-19197

ACOS: A performance based approach to build a parallel complex object server
[MEMO-INF-93-11] p 1537 N94-19198

Goal-driven LOTOS execution
[MEMO-INF-93-04] p 1527 N94-19227

COMPUTER TECHNIQUES
Analysis, representation and processing of the instrumental gesture: Application to keyboard instruments
[ETN-93-94402] p 1519 N94-17977
A case study in software maintenance
[AD-A269923] p 1521 N94-18659
Computer-Aided Prototyping System (CAPS) within the software acquisition process. A case study
[AD-A268705] p 1522 N94-18786
NASA Electronic Library System (NELS) optimization
[NASA-CR-193688] p 1617 N94-18839
Knowledge sources for an intelligent MCM analyzer
[AD-A269224] p 1542 N94-18887
Networked MS windows 3.1 based classified document control system (CDOCS)
[DE93-017880] p 1617 N94-18984
Multimodal image correlation applied to computer aided pedicular screwing
[ETN-93-95018] p 1528 N94-19363
A research program in empirical computer science
[NASA-CR-194069] p 1530 N94-19429
Improved HF data network simulator, software user's manual, volume 2
[AD-A270954] p 1393 N94-19753
Applications of neural networks in fault detection of rotating machinery
[AD-A270755] p 1448 N94-19766
COMPUTER VIRUSES
Automated assistance for detecting malicious code
[DE93-018106] p 1523 N94-18943
COMPUTER VISION
An object-oriented environment for computer vision and pattern recognition
[DE93-017098] p 1517 N94-17867
Problem of control in an integral vision system: Use of a multi-agent system
[ETN-93-95007] p 1530 N94-19488
COMPUTERIZED SIMULATION
Modeling and new equipment definition for the vibration isolation box equipment system
[NASA-CR-193185] p 1379 N94-17763
Carbon Dioxide Information Analysis Center: FY 1992 activities
[DE93-013845] p 1471 N94-17774
Three-dimensional simulation analysis of the first sections of a standing-wave free-electron laser two-beam accelerator
[DE93-016977] p 1436 N94-17869
An emulator for testing HVAC-control and energy management systems
[VTT-TIED-1337] p 1444 N94-17974
Analysis, representation and processing of the instrumental gesture: Application to keyboard instruments
[ETN-93-94402] p 1519 N94-17977
Simulation of a quartz-clockwork
p 1426 N94-18019
Simulation of quartz resonators p 1426 N94-18021
A study of the automatic generating system. 3: Improvement of the total system performance
p 1429 N94-18040
APLAC: An object-oriented analog circuit simulator and design tool. 6.1 reference manual
[PB93-187193] p 1396 N94-18091
On the construction of a regional atmospheric climate model
[KNMI-TR-147] p 1489 N94-18143
Computer simulation of macromolecular crystals and their defects
[DE93-015213] p 1596 N94-18192
Mechanical modeling of the growth of salt structures
[DE93-015342] p 1596 N94-18243
Fluid-structure-interaction analyses of reactor vessel using improved hybrid Legrangian Eulerian code ALICE-II
[DE93-015536] p 1409 N94-18248
Study of multi-phase flow characteristics in an MHD power train
[DE93-018570] p 1586 N94-18272
Hydrodynamic instability modeling for ICF
[DE93-018634] p 1587 N94-18274
Analysis of superconducting magnetic energy storage applications at a proposed wind farm site near Browning, Montana
[DE93-018793] p 1466 N94-18276
Teaching a computer simulation course with Ada
[AD-A267901] p 1521 N94-18308
Applications of the program UIFLOW-2D to the numerical simulation of axisymmetric flows
[AD-A268731] p 1410 N94-18326
Fuzzy control of magnetic bearings
p 1399 N94-18357
VHDL simulation with access to transistor models
p 1402 N94-18381
System dynamics and computer modeling expertise. A conceptual structure research inquiry
[AD-A269860] p 1560 N94-18410
Numerical simulation of turbulent convective flow over wavy terrain p 1416 N94-18596
Portable parallel ray tracing algorithms
[AD-A268984] p 1522 N94-18698
Directory of Energy Information Administration Models 1993
[DE93-016987] p 1616 N94-18707
Army Cockpit Delethalization Program (CDP)
[AD-A268990] p 1512 N94-18765
Corporate Information Management (CIM) report on the simulation processes, version 2.0
[AD-A269119] p 1617 N94-18770
Active control of a multivariable system by way of polynomial neural networks: Computer simulation evaluations and laboratory experimental results
[AD-A270033] p 1541 N94-18790
Three-dimensional shock wave physics simulations with MIMD PAGOSA on massively parallel computers
[DE93-011682] p 1455 N94-18829
CDIAC catalog of numeric data and computer model packages
[DE93-017675] p 1475 N94-18832
Toward a characterization of the debris cloud created in a hypervelocity impact on a thin plate
[AD-A269190] p 1455 N94-18864
HEMP 3D: A finite difference program for calculating elastic-plastic flow, appendix B
[AD-A269171] p 1418 N94-18878
Visualization for applications in shock physics
[DE93-012849] p 1418 N94-18918
The intelligent processing of materials
[AD-A269250] p 1362 N94-18923
The world's most powerful computer
[NASA-TM-109369] p 1514 N94-18961
Overview of WARP: A particle code for heavy ion fusion
[DE93-018637] p 1588 N94-19034
Kinetics programs for simulation of tropospheric photochemistry on the global scale
[DE93-019035] p 1476 N94-19104
Simulation of the ALS longitudinal multibunch feedback system
[DE93-019227] p 1575 N94-19152
A parallel hashed oct-tree N-body algorithm
[DE93-012654] p 1526 N94-19205
Smooth particle hydrodynamics: The SPHINX and SPHC codes
[DE93-014358] p 1457 N94-19207
A visualization environment for supercomputing-based applications in computational mechanics
[DE93-015024] p 1537 N94-19249
Molecular dynamics modeling of the mechanical behavior of metallic multilayers
[DE93-017972] p 1365 N94-19263
Volume rendering of 3D scalar and vector fields at Lawrence Livermore National Laboratory
[DE93-018000] p 1528 N94-19276
Sensitivity and uncertainty analysis of Markov reward models
[MEMO-INF-92-89] p 1559 N94-19386
Simulation of the impact of a plastic flyer on an aluminum block using the hydrocode AUTODYNE
[PML-1992-26] p 1458 N94-19444
Computational Methods for Crashworthiness
[NASA-CP-3223] p 1458 N94-19465
Development and use of computational techniques in Army Aviation research and development programs for crash resistant helicopter technology
p 1459 N94-19469
Explicit solution techniques for impact with contact constraints p 1459 N94-19470
Numerical simulation of vehicle crashworthiness and occupant protection p 1459 N94-19471
Efficiency and biofidelity of occupant simulations
p 1459 N94-19473
Current capabilities for simulating the extreme distortion of thin structures subjected to severe impacts
p 1459 N94-19474
Crashdynamics with DYNA3D: Capabilities and research directions p 1460 N94-19475
The influence of the target strength model on computed perforation
[DE93-018659] p 1460 N94-19543
Locally adaptive remeshing scheme for calculating fluid instabilities
[DE93-019577] p 1422 N94-19568
Automated qualitative modeling of dynamic physical systems
[AD-A270835] p 1422 N94-19598
START user manual version 2.1
[LR-726] p 1335 N94-19614
European network for the numerical simulation of space plasmas p 1331 N94-19641
Simulation of the behavior of micro-electronic capacitive pressure sensors
[LAAS-93190] p 1434 N94-19659
Systems engineering for Air Force C3I systems
[AD-A270482] p 1391 N94-19676
Improved HF data network simulator, volume 1
[AD-A270953] p 1393 N94-19752
Amorphous silicon batch process cost analysis
[DE93-018203] p 1470 N94-19760
The effects of initial conditions on the 3-D topology of temporally evolving wakes (ARI on 3-D bluff body wakes)
[AD-A271008] p 1423 N94-19774
NPAC distributed-parallel system feasibility study
[AD-A270972] p 1539 N94-19790
COMPUTERS
RESQme studies for SDC regional computing centers
[DE93-015230] p 1514 N94-17799
Technical development of a theory of programs
[ETN-93-95058] p 1532 N94-19652
CONCENTRATION (COMPOSITION)
Practical reporting times for environmental samples
[DE93-013461] p 1472 N94-17910
Scaling laws for diamond chemical vapor deposition. 2: Atomic hydrogen transport
[AD-A269842] p 1371 N94-18740
CONCENTRATORS
Simplified processing for 23 percent-efficient silicon concentrator solar cells
[DE93-015018] p 1464 N94-17787
Photovoltaic concentrator initiative: Concentrator cell development
[DE93-018505] p 1466 N94-18335
High-efficiency silicon concentrator cell commercialization
[DE93-018491] p 1467 N94-18409
Silicon concentrator solar cell research
[DE93-018489] p 1468 N94-19015
The CAESAR project: Experimental and modeling investigations of methane reforming in a catalytically enhanced solar absorption receiver on a parabolic dish
[DE93-040203] p 1469 N94-19109
CONCRETES
Computational mechanics of composite materials
[PB93-195782] p 1343 N94-19281
Microstructure of the interfacial zone around aggregate particles in concrete
[PB93-195790] p 1380 N94-19322
Development of engineering models for calculation of failure loads and defect states of steel concrete beams and plates
[ETN-93-95052] p 1460 N94-19648
CONCURRENT PROCESSING
SPROC: A multiple-processor DSP IC
p 1398 N94-18347
The evolution of the PVM concurrent computing system
[DE93-017764] p 1534 N94-18482
PUMMA: Parallel Universal Matrix Multiplication Algorithms on distributed memory concurrent computers
[DE93-019163] p 1538 N94-19299
CONDENSATES
Molecular nonlinear optical susceptibilities in condensed phases
[AD-A270200] p 1568 N94-18784
CONDENSATION
Finite element modeling of evaporation and condensation during sol-gel film and fiber formation
[DE93-017655] p 1345 N94-17820
CONDENSATION NUCLEI
Cloud CCN feedback
[DE93-016878] p 1472 N94-17985
Ship-produced cloud line of 13 July 1991
[DE93-016879] p 1472 N94-17986
Analysis of meteorological conditions during AGASP-4: 30 March - 23 April 1992
[PB93-190205] p 1489 N94-18126
CONDENSED MATTER PHYSICS
International Centre for Theoretical Physics, Trieste Scientific activities in 1991
[DE93-624757] p 1606 N94-17792
Gamma scattering in condensed matter with high intensity Moessbauer radiation
[DE93-019461] p 1601 N94-19031
CONDENSING
Condensed gases under winter conditions: A study for the rescue services
[FOA-C-40305-4.5] p 1473 N94-18139
Molecular nonlinear optical susceptibilities in condensed phases
[AD-A270200] p 1568 N94-18784
CONDUCTING POLYMERS
Studies of interactions between conducting polymer and organic vapors: Applications to chemical sensing
[DE93-015694] p 1369 N94-18233

Physical chemical studies of conducting polymers fundamental and applied
[AD-A270728] p 1374 N94-19574

CONDUCTION BANDS
Transient skin effect in a massive cylinder by eccentric location of exciting conduction bands
[ETN-93-95048] p 1391 N94-19646

CONDUCTIVE HEAT TRANSFER
Analysis of pultrusion processing for long fiber reinforced thermoplastic composite system
[NASA-CR-194504] p 1339 N94-17766
Transport in the self-organized relaxed state of ion temperature gradient instability
[DE93-016769] p 1584 N94-17983
Fin-efficiency calculation for condensation in the presence of noncondensable gases
[DE93-017684] p 1409 N94-18004
Time-resolved probing of electron thermal conduction in femtosecond-laser-pulse-produced plasmas
[DE93-016996] p 1585 N94-18129
Total hemispherical emittance of Niobium-1 percent zirconium fuel cladding for the SP-100 space reactor
[AD-A270456] p 1576 N94-19589

CONDUCTORS
Heat load analysis on the cable-in-conduit with central core conductor for the TF coil Rebut layer design
[DE93-013783] p 1395 N94-17872
Performance evaluations of demountable electrical connections
[DE93-017399] p 1396 N94-18135
The asymptotic theory of the reflection and transmission of a pulsed electromagnetic beam field at a planar interface separating two dispersive media
[AD-A269033] p 1385 N94-18404
Current-potential characteristics of electrochemical systems
[DE93-040303] p 1352 N94-19192

CONFERENCES
Geography and meteorological studies in the Far East
[DE93-013563] p 1461 N94-17893
The 7th International Cryocooler Conference
[AD-A268451] p 1379 N94-18147
Bibliography of scientific publications of the Naval Biodynamics Laboratory, 1980 - 1992
[AD-A268886] p 1505 N94-18226
Arctic ice studies
[AD-A268608] p 1497 N94-18277
Several fundamental issues in the mechanics of inelastic behavior
[AD-A269455] p 1453 N94-18285
S/EV 1992: Solar and Electric Vehicles. Volume 1: Proceedings
[DE93-015762] p 1445 N94-18307
The 1991 3rd NASA Symposium on VLSI Design
[NASA-CR-194589] p 1397 N94-18337
High-Lift System Aerodynamics
[AGARD-CP-515] p 1305 N94-18415
Report to Congress: Comprehensive Program Plan for Advanced Turbine Systems
[DE93-016718] p 1467 N94-18475
Workshop on Innovation in Materials Processing and Manufacture: Exploratory Concepts for Energy Applications
[DE93-017674] p 1467 N94-18478
Quantum Optoelectronics. Organization of the 1993 photonics science topical meetings. Technical digest series, volume 8
[AD-A269026] p 1578 N94-18488
The LET spectrum and its uncertainty during the CRRES mission
[AD-A269977] p 1630 N94-18676
Royal Society of Chemistry, Heterocyclic Chemistry Group, Lakeland Heterocyclic Symposium
[AD-A270374] p 1338 N94-18703
Proceedings of the 11th Space Surveillance Workshop
[AD-A269477] p 1462 N94-18729
Numerical and symbolic signal representation and processing
[AD-A270271] p 1389 N94-18811
The 1993 Shuttle Small Payloads Symposium
[NASA-CP-3233] p 1323 N94-19162
Updated contributions to the Twente Workshop of Hamiltonian Graph Theory
[PB93-195568] p 1553 N94-19605

CONFIGURATION INTERACTION
Configuration interaction in LTE spectra of heavy elements
[DE93-017166] p 1584 N94-17990
Relativistic configuration interaction calculation of the correlation energies of heliumlike ions
[DE93-018093] p 1571 N94-19201

CONFIGURATION MANAGEMENT
CAVEMAN: Configuration and version management
[DE93-018066] p 1524 N94-19048

CONFINEMENT
ITER EDA design confinement capability
[DE93-013729] p 1582 N94-17697
Analysis of the ITER H-mode confinement database
[DE93-016984] p 1585 N94-18056
Coupled MHD and transport analysis of improved confinement D3-D discharges
[DE93-016985] p 1585 N94-18057
Heavy Ion Fusion Injector Program
[DE93-018706] p 1575 N94-18997
Behavior of the particle transport coefficients near the density limit in MTX
[DE93-019108] p 1591 N94-19311
Theoretical studies of turbulence and anomalous transport in toroidal confinement devices
[DE93-040684] p 1592 N94-19656

CONFORMAL MAPPING
(1,1)-geodesic maps into Grassmann manifolds
[DE93-624799] p 1545 N94-17684
Groups on transformations in Finslerian spaces
[DE93-624765] p 1606 N94-17794
A zeta function approach to the semiclassical quantization of maps
[DE93-624774] p 1547 N94-17949
Steepest descent method for set-valued locally accretive mappings
[DE93-628592] p 1548 N94-18106
Unbounded components in parameter space of rational maps
[DE93-628621] p 1548 N94-18170
Finite beta plasma equilibrium in toroidally linked mirrors
[DE93-040318] p 1590 N94-19193

CONGESTION
Congestion/flow control and routing in data networks: A control-theoretic approach
[AD-A271121] p 1392 N94-19737

CONGRESSIONAL REPORTS
Report to Congress: Comprehensive Program Plan for Advanced Turbine Systems
[DE93-016718] p 1467 N94-18475
The 1994 NASA authorization, volume 2
[GPO-71-510] p 1620 N94-18842

CONICAL FLOW
Research and training activities of the Joint Institute for Aeronautics and Acoustics
[NASA-CR-194742] p 1421 N94-19493

CONJUGATE GRADIENT METHOD
Conception and analysis of numerical parallel algorithms: Realization on the Connection Machine
[ETN-93-95005] p 1531 N94-19517

CONNECTION MACHINE
Connection machine software conversion of a Navy oceans model
[AD-A269876] p 1535 N94-18772
Simulation of dynamic material response with the PAGOSA code
[DE93-018285] p 1460 N94-19603

CONSECUTIVE EVENTS
A forthcoming key press can be selected while earlier ones are executed
[IZF-1993-B-2] p 1509 N94-19422

CONSERVATION
Cost effective energy strategies for the reduction of CO2 emissions in the United States: Country report for ETSAP Annex 4
[DE93-016842] p 1472 N94-17852

CONSERVATION EQUATIONS
A preliminary model for crack-tip hydrogen transport
[NPL-DMM(A)-84] p 1451 N94-17899
A new approach to the study of the turbulence layer
[NASA-CR-194546] p 1487 N94-19397
Modeling of current features in Gulf Stream SAR imagery
[AD-A270734] p 1499 N94-19609

CONSERVATION LAWS
Numerical methods for one-dimensional hyperbolic conservation laws
[PB93-194801] p 1547 N94-18078
Introduction to spectral methods for hyperbolic system of conservation laws p 1413 N94-18567
A massively parallel adaptive finite element method with dynamic load balancing
[DE93-012844] p 1536 N94-19161

CONSISTENCY
Generalized regression trees: Function estimation via recursive partitioning and maximum likelihood
[AD-A271259] p 1560 N94-19726

CONSTITUTIVE EQUATIONS
Implementation of a nonisothermal unified inelastic-strain theory into ADINA6.0 for a titanium alloy: User guide
[AD-A269927] p 1360 N94-18660
A particle method for history-dependent materials
[DE93-018696] p 1456 N94-19080

CONSTRUCTION
Design considerations for remotely operated welding in space: Task definition and visual weld monitoring experiment
[AD-A268752] p 1445 N94-18634

CONSTRUCTION MATERIALS
Development of engineering models for calculation of failure loads and defect states of steel concrete beams and plates
[ETN-93-95052] p 1460 N94-19648

CONTACT DERMATITIS
Evaluation of the nickel release by horological products p 1367 N94-18009

CONTACT LENSES
US Army aviation epidemiology data register: Prevalence of refractive error among US aircrew members
[AD-A269550] p 1505 N94-18289

CONTACT LOADS
A methodology to model physical contact between structural components in NASTRAN
p 1450 N94-17836
A general-purpose contact detection algorithm for nonlinear structural analysis codes
[DE93-018507] p 1455 N94-19039
Surface species in tribology
[AD-A270970] p 1446 N94-19754

CONTACT RESISTANCE
Analysis of high contact resistances associated with hermetic and lightning arrestor connectors
[DE93-014850] p 1395 N94-17783

CONTACTORS
Plasma contactor development for Space Station
[NASA-TM-106425] p 1587 N94-18861

CONTAMINANTS
Title 1 implementation: Status report on nonattainment areas
[DE93-017677] p 1471 N94-17777
Improving the biodegradative capacity of subsurface bacteria
[DE93-013171] p 1501 N94-18051
The urban perspectives of acid rain
[DE93-018881] p 1474 N94-18523
International Symposium on the Ecological Effects of Arctic Airborne Contaminants — abstracts
[AD-A269955] p 1475 N94-18775
Indoor environment program
[DE93-018601] p 1513 N94-18935
Environmental Research Program
[DE93-019101] p 1477 N94-19105
Penetrometer compatible, fiber-optic sensor for continuous monitoring of chlorinated hydrocarbons: Field test results
[DE93-017974] p 1352 N94-19266
The Mexico City 1991 lidar measurements campaign
[DE93-019960] p 1478 N94-19272
Fiber optic Raman spectrograph for in situ environmental monitoring
[DE93-019466] p 1478 N94-19305

CONTAMINATION
A Bayesian approach to contaminant plume delineation
[DE93-012909] p 1472 N94-17890

CONTEXT FREE LANGUAGES
An annotated bibliography on parallel parsing: Updated version
[MEMO-INF-92-84] p 1537 N94-19223

CONTINENTAL SHELVES
ADCIRC: An advanced three-dimensional circulation model for shelves, coasts, and estuaries. Report 3: Development of a tidal constituent database for the western North Atlantic and Gulf of Mexico
[AD-A268685] p 1497 N94-18455
Three-dimensional high-resolution seismic profiling on the New Jersey outer continental shelf
[AD-A269835] p 1498 N94-18600
A laboratory model of a cooled continental shelf
[AD-A270862] p 1500 N94-19792

CONTINUOUS RADIATION
Forward scattering of a pulsed continuous wave signal through laminar and turbulent thermal plumes
[AD-A271210] p 1564 N94-19723

CONTINUOUS WAVE LASERS
Data fusion through simulated annealing of registered range and reflectance images
[DE93-015910] p 1612 N94-17858
Final construction and operation of a continuous far-infrared free-electron laser for scientific applications
[AD-A269248] p 1440 N94-18912
Novel nonlinear laser diagnostic techniques
[AD-A270968] p 1442 N94-19788

CONTINUOUS WAVE RADAR
Investigations of a coherent vector radar technique for the observation of the atmosphere near 10 GHz
[KFK-5068] p 1494 N94-19616

CONTINUUM MECHANICS

Ground movements associated with gas hydrate production [DE93-019887] p 1486 N94-19018

Application of differential sensitivity theory to continuum mechanics [DE93-012732] p 1609 N94-19187

CONTINUUM MODELING

Continuum modeling of materials that can undergo martensitic phase transitions [AD-A268767] p 1360 N94-18386

Modeling of the formation of microporosity in alloys [DE93-017733] p 1364 N94-19044

Crossover from BCS to Bose superconductivity: A functional integral approach [DE93-019503] p 1604 N94-19566

CONTINUUMS

Low-energy continuum-electron emission at 0 degrees from O(q+) + He collisions [DE93-018777] p 1570 N94-19108

CONTOURS

A laboratory model of a cooled continental shelf [AD-A270862] p 1500 N94-19792

CONTRACT MANAGEMENT

The machine reception: A business of experts [CRIF-MC-94] p 1611 N94-17980

CONTRACT NEGOTIATION

The machine reception: A business of experts [CRIF-MC-94] p 1611 N94-17980

CONTRAILS

New techniques for contrail forecasting [AD-A269686] p 1490 N94-18573

CONTROL EQUIPMENT

An emulator for testing HVAC-control and energy management systems [VTT-TIED-1337] p 1444 N94-17974

Universal measurement device for electronic watches and small clocks p 1427 N94-18029

Nonparaxial MHD stabilizers for an axisymmetric magnetic mirror [DE93-017996] p 1587 N94-18505

CONTROL SIMULATION

A one dimensional numerical model, with an application to the vertical distribution of dissolved oxygen in the ocean [DE93-018481] p 1495 N94-17779

CONTROL STABILITY

An application of parameter estimation to the stability and control of the BQM-147 unmanned aerial vehicle [AD-A268741] p 1321 N94-18401

The intelligent processing of materials [AD-A269250] p 1362 N94-18923

Robustness and efficiency of generalized predictive control algorithms with guaranteed stability [MATHS-REPT-A-190] p 1530 N94-19412

Stabilization of time-delay systems: An overview of the algebraic approach [PB93-191989] p 1553 N94-19556

CONTROL SURFACES

A wind tunnel model control surface actuator interface [AD-A268729] p 1322 N94-18324

CONTROL SYSTEMS DESIGN

Introduction to Quantitative Feedback Theory (QFT) technique p 1545 N94-18241

Parallel optimization algorithms and their implementation in VLSI design p 1401 N94-18374

Lunar base Controlled Ecological Life Support System (LCELSS): Preliminary conceptual design study [NASA-CR-188479] p 1511 N94-18484

Denver TMA assessment [NASA-CR-4554] p 1315 N94-18844

Control of nonlinear systems [AD-A270141] p 1542 N94-18898

Motorola MC68040 high-speed design using Altera EPM5000 erasable programmable logic devices [DE93-017635] p 1523 N94-19006

Optimizing wind turbine control system parameters [DE93-018861] p 1469 N94-19036

MART: An overview of the Mobile Autonomous Robot Twente project [MEMO-INF-93-12] p 1543 N94-19199

An innovative neural manufacturing concept [DE93-017212] p 1527 N94-19238

Analysis and design of robust decentralized controllers for nonlinear systems [DE93-019224] p 1543 N94-19302

Problem of control in an integral vision system: Use of a multi-agent system [ETN-93-95007] p 1530 N94-19488

Silicon compilation: From the circuit to the system [ETN-93-95010] p 1406 N94-19501

Use of shape memory alloys in the robust control of smart structures [AD-A270827] p 1366 N94-19594

CONTROL THEORY

On comparison and extensions of control methods for narrow-band disturbance rejection [REPT-93-015] p 1540 N94-17922

Generalization of optimal control theory: Linear and nonlinear structures [PB93-188621] p 1540 N94-18125

Stability analysis through bifurcation theory, 2 p 1608 N94-18239

Introduction to Quantitative Feedback Theory (QFT) technique p 1545 N94-18241

Parallel optimization algorithms and their implementation in VLSI design p 1401 N94-18374

The optimal projection equations for finite-dimensional fixed-order H2-optimal control of infinite-dimensional discrete-time systems [REPT-93-11] p 1542 N94-19085

Deadbeat control by measurement feedback: A two sided approach [REPT-93-20] p 1542 N94-19091

The digital linear quadratic control problem for Pritchard-Salamon systems [REPT-93-27] p 1542 N94-19142

Digital control of Pritchard-Salamon systems [REPT-93-33] p 1543 N94-19286

Discrete-time infinity control problem with measurement feedback [PB93-197523] p 1543 N94-19329

Learning control of large-scale systems [MATHS-REPT-A-186] p 1544 N94-19408

Notes on multi-step ahead prediction based on the principle of concatenation [MATHS-REPT-A-189] p 1544 N94-19410

Problem of control in an integral vision system: Use of a multi-agent system [ETN-93-95007] p 1530 N94-19488

Methods for description and control of dynamical systems and their application [MPIS-17/1992] p 1553 N94-19522

Stabilization of time-delay systems: An overview of the algebraic approach [PB93-191989] p 1553 N94-19556

Mathematical communications, volume 27, numbers 1 and 2, 1992. List and abstracts of memoranda published in the period July - December 1991 [PB93-191997] p 1553 N94-19557

CONTROLLABILITY

An investigation of fighter aircraft agility [NASA-CR-194608] p 1318 N94-19448

CONTROLLERS

Automatic tuning of an integral fuzzy controller [REPT-93-006] p 1383 N94-17932

Autonomous neural network controllers for adaptive material handling [AD-A268908] p 1540 N94-18331

Experience with custom processors in space flight applications p 1336 N94-18338

Simplified microprocessor design for VLSI control applications p 1400 N94-18359

Active control of a multivariable system by way of polynomial neural networks: Computer simulation evaluations and laboratory experimental results [AD-A270033] p 1541 N94-18790

Cooperative control of multiple space manipulators [AD-A270291] p 1445 N94-18813

An innovative neural manufacturing concept [DE93-017212] p 1527 N94-19238

Discrete-time infinity control problem with measurement feedback [PB93-197523] p 1543 N94-19329

Congestion/flow control and routing in data networks: A control-theoretic approach [AD-A271121] p 1392 N94-19737

The universal BitBus node [DIGEL-1993-1] p 1515 N94-19799

CONVECTION

Convection algorithms for magnetospheric particles [AD-A270103] p 1493 N94-18871

Modeling of the formation of microporosity in alloys [DE93-017733] p 1364 N94-19044

Numerical solutions for a flow with mixed convection in a vertical geometry [DE93-011592] p 1419 N94-19058

Proceedings: International Symposium on Thermal Engineering and Science for Cold Regions [AD-A270636] p 1487 N94-19529

CONVECTION CELLS

Physical retrieval of precipitation water contents from Special Sensor Microwave/Imager (SSM/I) data. Part 1: A cloud ensemble/radiative parameterization for sensor response (report version) p 1491 N94-18604

A laboratory model of a cooled continental shelf [AD-A270862] p 1500 N94-19792

CONVECTION-DIFFUSION EQUATION

Asymptotic derivation of the modified time-dependent SP2 equations and numerical calculations [DE93-016466] p 1551 N94-19342

CONVECTIVE FLOW

Numerical simulation of turbulent convective flow over wavy terrain p 1416 N94-18596

CONVECTIVE HEAT TRANSFER

Electrically controlled liquid-crystal heat valve [AD-D015872] p 1443 N94-17705

Turbulence modeling in aircraft icing p 1412 N94-18555

Heat transfer quantitative characterization: Passive and active methods p 1431 N94-18650

Geothermal activity near Clearlake, California [DE93-016627] p 1485 N94-18894

CONVERGENCE

Steepest descent method for set-valued locally accretive mappings [DE93-628592] p 1548 N94-18106

Variational approaches to CFD: Applications to potential Euler and Navier-Stokes equations p 1413 N94-18565

Introduction to spectral methods: Application to the Stokes problem p 1413 N94-18566

On the convergence of an unfeasible primal-dual interior-point method for convex programming [REPT-93-34] p 1525 N94-19154

The Fourier analysis technique and epsilon-pseudo-eigenvalues [DE93-018805] p 1551 N94-19337

Refining a triangulation of a planar straight-line graph to eliminate large angles [DE93-016510] p 1528 N94-19344

CONVERGENT-DIVERGENT NOZZLES

Supersonic jets from bevelled rectangular nozzles [NASA-TM-106403] p 1313 N94-19484

CONVEXITY

On the convergence of an unfeasible primal-dual interior-point method for convex programming [REPT-93-34] p 1525 N94-19154

Are bilinear quadrilaterals better than linear triangles? [DE93-019223] p 1551 N94-19301

COOLING

Screening analysis for chlorine-free alternative refrigerants to replace R-22 in air conditioning applications [DE93-015920] p 1367 N94-17847

Materials processing and manufacturing technologies for diamond substrates multichip modules [AD-A268989] p 1599 N94-18764

Advances in laser cooling [AD-A270152] p 1440 N94-18900

COOLING FINS

Heat load analysis on the cable-in-conduit with central core conductor for the TF coil Rebut layer design [DE93-013783] p 1395 N94-17872

COOLING SYSTEMS

Preliminary design of a water cooled avionics cooling rack [AD-A268826] p 1320 N94-18536

Advances in laser cooling [AD-A270152] p 1440 N94-18900

MHD integrated topping cycle project [DE93-040520] p 1588 N94-18978

MODIL cryocooler producibility demonstration project results [DE93-017981] p 1335 N94-19275

COORDINATE TRANSFORMATIONS

GENSHELL: A genesis database 2D to 3D shell transformation program [DE93-018694] p 1525 N94-19102

COORDINATION

Cognitive limitations in coordination in hierarchical information processing structures [AD-A268825] p 1616 N94-18535

The Cluster Joint Science Operations Centre p 1331 N94-19639

Co-ordination of ground-based observations with Cluster p 1331 N94-19640

COPOLYMERIZATION

Polymer films with enhanced dielectric properties [AD-A271148] p 1375 N94-19740

COPOLYMERS

Molecular and polymeric ceramic precursors [DE93-040364] p 1372 N94-18891

Structure and properties of polycarbonate alloys [ETN-93-95071] p 1375 N94-19611

COPPER

The copper-pumped dye laser system at Lawrence Livermore National Laboratory [DE93-014429] p 1435 N94-17723

Measurement and analysis of three 1.5-GPa shock-wave profiles in copper [DE93-016559] p 1451 N94-17864

X ray absorption spectroscopic studies of the active sites of nickel- and copper-containing metalloproteins
[DE93-017142] p 1347 N94-18059
Characterization of the Facility for Atmospheric Corrosion Testing (FACT) at Sandia
[DE93-018510] p 1474 N94-18521
Potential dependent structural changes of underpotentially deposited copper on an iodine treated platinum surface determined in situ by surface EXAFS and its polarization dependence
[AD-A269890] p 1360 N94-18687
Electron impact excitation of copper atoms
[DE93-017995] p 1363 N94-18939
Effects of irradiation temperature on Charpy and tensile properties of high-copper, low upper-shelf, submerged-arc welds
[DE93-017858] p 1445 N94-19047
Binding of copper to nanocavity surfaces in silicon
[DE93-019073] p 1364 N94-19080
Molecular dynamics modeling of the mechanical behavior of metallic multilayers
[DE93-017972] p 1365 N94-19263
Reducing inadvertent alloying of metal/ceramic brazes
[DE93-009842] p 1373 N94-19308

COPPER ALLOYS
Magnetic properties of single-crystalline UCu3Al2
[DE93-016607] p 1593 N94-17744
Atlas of formability: NICKELVAC K-500
[AD-A268351] p 1356 N94-17772
The low-temperature specific heat of CeCu2Ge2 at 0 and 9.5 kbar
[DE93-014914] p 1360 N94-18398

COPPER OXIDES
Phase separation and superconductivity in La2CuO(4 + delta): Effects of oxygen diffusion
[DE93-016610] p 1594 N94-17907
Fabrication and microstructural development of Ag-clad TlBa2Ca2Cu3O(x) tapes
[DE93-017407] p 1597 N94-18500
Specific heat of La(1.875-x)Nd(x)Sr(0.125)CuO4: Magnetic and structural transitions
[DE93-016978] p 1600 N94-18968

CORE STORAGE
Superconducting/semiconducting hybrids and advance memory concepts for superconducting electronics
[AD-A268679] p 1397 N94-18312

CORNER FLOW
An investigation of low Marangoni number fluid flow in a cold corner
[AD-A271317] p 1422 N94-19569

CORRELATION
Using computerized tomography to determine ionospheric structures
[DE93-018903] p 1485 N94-19001

CORRELATION COEFFICIENTS
Synchronisation of cold induced vasodilation at various locations of one hand
[IZF-1992-B3] p 1504 N94-17966
Polarimetric statistics of electromagnetic waves scattered by distributed targets
[PB93-195907] p 1389 N94-18951

CORRELATORS
Formal specification of a high speed CMOS correlator
p 1401 N94-18371

CORROSION
The effect of surface treatment and gaseous rust protection paper on the atmospheric corrosion stability of aluminium alloy
[DE93-623326] p 1355 N94-17679
Alloy development of FeAl aluminide alloys for structural use in corrosive environments
[DE93-015100] p 1355 N94-17757
Analysis of high contact resistances associated with hermetic and lightning arrestor connectors
[DE93-014850] p 1395 N94-17783
Environmental effects on intermetallic compounds: A guide to the literature
[AD-A269587] p 1359 N94-18306
Characterization of the Facility for Atmospheric Corrosion Testing (FACT) at Sandia
[DE93-018510] p 1474 N94-18521
JPRS report: Science and technology. Central Eurasia: Materials science
[JPRS-UMS-93-002] p 1339 N94-18833
Testing of protective coatings in hydrogen
[DE93-040326] p 1375 N94-19651
Microstructure and texture control of fatigue in hydrogen and marine environments
[AD-A271277] p 1344 N94-19744

CORROSION RESISTANCE
The effect of surface treatment and gaseous rust protection paper on the atmospheric corrosion stability of aluminium alloy
[DE93-623326] p 1355 N94-17679
Polyurethane self-priming topcoats
[AD-D015870] p 1367 N94-17719
Alloy development of FeAl aluminide alloys for structural use in corrosive environments
[DE93-015100] p 1355 N94-17757
Characterization of the Facility for Atmospheric Corrosion Testing (FACT) at Sandia
[DE93-018510] p 1474 N94-18521
The effects of radiolysis on the corrosion and stress corrosion behavior of 316 stainless steels
[DE93-019933] p 1363 N94-19021

CORROSION TESTS
Characterization of the Facility for Atmospheric Corrosion Testing (FACT) at Sandia
[DE93-018510] p 1474 N94-18521

CORTI ORGAN
Extrathalamic modulation of cortical function
[AD-A270869] p 1507 N94-19783

COSMIC DUST
Dust in the Small Magellanic Cloud
[NASA-CR-193344] p 1624 N94-17764

COSMIC RAY SHOWERS
Energy loss measurement of cosmic ray muons
[KFK-5158] p 1631 N94-19504
Measurement of the energy of horizontal cosmic ray muons
[KFK-5163] p 1631 N94-19505
Measurements of cosmic ray muons with multi-wire proportional chambers with a prototype setup for KASCADE
[KFK-5173] p 1631 N94-19506

COSMIC RAYS
Investigation of the relative abundance of heavy versus light nuclei in primary cosmic rays using underground muon bundles
[DE93-017601] p 1630 N94-17818
Proceedings of the 3rd Workshop on Balloon-Borne Experiments with Superconducting Magnet Spectrometers
[DE93-788362] p 1630 N94-18219
Research in particle physics
[DE93-040875] p 1567 N94-18534
Widget: A data acquisition system for a balloon borne Si particle calorimeter
[DE93-624668] p 1630 N94-18762
High rate resistive plate chambers: An inexpensive, fast, large area detector of energetic charged particles for accelerator and non-accelerator applications
[DE93-018664] p 1572 N94-19545

COSMOCHEMISTRY
Investigation of the relative abundance of heavy versus light nuclei in primary cosmic rays using underground muon bundles
[DE93-017601] p 1630 N94-17818

COST ANALYSIS
The carbon dioxide emissions game: Playing the net
[DE93-017670] p 1471 N94-17821
The value of windpower: An investigation using a qualified production cost model
[DE93-010043] p 1465 N94-17888
Feasibility survey of thermoelectric conversion technology using semiconductors
[DE93-520882] p 1595 N94-18105
The J85 cost/benefit engine study
[AD-A269280] p 1320 N94-18333
Report to Congress: Comprehensive Program Plan for Advanced Turbine Systems
[DE93-016718] p 1467 N94-18475
A comparison of air force data systems
[AD-A269691] p 1616 N94-18575
Human Transportation System (HTS) study: Executive summary
[NASA-TM-104780] p 1332 N94-18669
Space transfer concepts and analyses for exploration missions
[NASA-CR-193876] p 1332 N94-18820
Amorphous silicon batch process cost analysis
[DE93-018203] p 1470 N94-19760

COST EFFECTIVENESS
Cost effective energy strategies for the reduction of CO2 emissions in the United States: Country report for ETSAP Annex 4
[DE93-016842] p 1472 N94-17852
Setting the global thermostat with an exhaustible tradeable permit system
[DE93-012911] p 1472 N94-17891
Removing CFC's from the atmosphere with lasers: A second look
[DE93-017516] p 1473 N94-18101
A comparison of air force data systems
[AD-A269691] p 1616 N94-18575
Automated rendezvous and capture demonstration study
[NASA-CR-192587] p 1331 N94-19366

COST ESTIMATES
A comparison of air force data systems
[AD-A269691] p 1616 N94-18575
Technology benefits model user manual, version 01.00.04
[AD-A270637] p 1620 N94-19777

COST REDUCTION
ARPA/CSTO rapid VLSI implementation
[AD-A269170] p 1403 N94-18695
Integrated circuits: Resistless processing simplifies production and cuts costs
[DE93-018069] p 1405 N94-18941
Software reuse: Major issues need to be resolved before benefits can be achieved. Report to the Chairman, Subcommittee on Defense, Committee on Appropriations, House of Representatives
[GAO/IMTEC-93-16] p 1532 N94-19716
Technology benefits model user manual, version 01.00.04
[AD-A270637] p 1620 N94-19777

COSTS
Cost effective energy strategies for the reduction of CO2 emissions in the United States: Country report for ETSAP Annex 4
[DE93-016842] p 1472 N94-17852
Laboratory microfusion capability study
[DE93-014373] p 1583 N94-17912
MODIL cryocooler producibility demonstration project results
[DE93-017981] p 1335 N94-19275
Amorphous silicon batch process cost analysis
[DE93-018203] p 1470 N94-19760

COUETTE FLOW
Methods for description and control of dynamical systems and their application
[MPIS-17/1992] p 1553 N94-19522

COUNTER ROTATION
Two-dimensional turbulent nonstationary superfluid counterflows: Numerical simulations, qualitative effects
[MPIS-23/1992] p 1422 N94-19510

COUNTERFLOW
Two-dimensional turbulent nonstationary superfluid counterflows: Numerical simulations, qualitative effects
[MPIS-23/1992] p 1422 N94-19510

COUNTERMEASURES
Millimeter wave reflectivity measurement system
[AD-A270008] p 1387 N94-18601

COUNTING CIRCUITS
Thermal neutron multiplicity measurements using the pyrochemical multiplicity counter at Lawrence Livermore National Laboratory
[DE93-018538] p 1571 N94-19278

COUPLERS
Metal Film Surface Plasmon Resonance (MFSPR) fibre couplers
[AD-A268871] p 1579 N94-18635

COUPLINGS
Extraction of Z(prime) coupling data from Z(prime) (yields) jj at the LHC and SSC
[DE93-018576] p 1570 N94-19096

COVARIANCE
Data fusion through simulated annealing of registered range and reflectance images
[DE93-015910] p 1612 N94-17858
Computer codes for checking, plotting and processing of neutron cross-section covariance data and their application
[DE93-018459] p 1570 N94-19129
Tandem queues with deterministic service times
[PB93-197465] p 1543 N94-19324
Uncertainty versus interindividual variability
[DE93-018105] p 1559 N94-19549
Acoustic travel time perturbations due to an internal tide and internal wave field in the Barents Sea
[AD-A270879] p 1499 N94-19580

CRACK GEOMETRY
Development of the microstructure based stochastic life prediction models
[AD-A269880] p 1454 N94-18683

CRACK INITIATION
Inelastic deformation and damage at high temperature
[DE93-018155] p 1448 N94-17814
Initiation and growth of microcracks in high strength steel butt welds
[AD-A268751] p 1454 N94-18466
Development of the microstructure based stochastic life prediction models
[AD-A270453] p 1455 N94-18714
Fatigue crack initiation in riveted lap joints and in pressurized fuselages
[LR-725] p 1461 N94-19669

CRACK OPENING DISPLACEMENT
Fatigue resistant Ti3Al composites
[AD-A270305] p 1341 N94-18692

CRACK PROPAGATION
Interpretation of warm prestress-induced fracture toughness based on crack-tip constraint
[DE93-015967] p 1451 N94-17913

Experimental contribution to the contact between two bodies and the effect of roughness [ECL-91-41] p 1451 N94-17918

Spectrum fatigue testing of T-shaped tension clips [FFA-TN-1992-22] p 1452 N94-17970

Steep geometric grating for use in moire interferometry [AD-A268759] p 1453 N94-18328

Composites: Materials of the future [AD-A268945] p 1341 N94-18450

Initiation and growth of microcracks in high strength steel butt welds [AD-A268751] p 1454 N94-18466

Development of the microstructure based stochastic life prediction models [AD-A269880] p 1454 N94-18683

Fatigue resistant Ti3Al composites [AD-A270305] p 1341 N94-18692

Experimental investigation of wave and fracture phenomena in impacted ceramics: Experiments on sapphire [AD-A270040] p 1372 N94-18792

A numerical analysis of crack growth in brittle microcracking composites [DE93-011562] p 1343 N94-18914

The interpretation of optical caustics in the presence of dynamic non-uniform crack-tip motion histories: A study based on a higher order transient crack-tip expansion [SM91-12] p 1456 N94-19130

Subcritical crack growth in continuous-fiber reinforced ceramic composites [DE93-018784] p 1343 N94-19335

Microstructure and texture control of fatigue in hydrogen and marine environments [AD-A271277] p 1344 N94-19744

CRACK TIPS

A preliminary model for crack-tip hydrogen transport [NPL-DMM(A)-84] p 1451 N94-17899

Interpretation of warm prestress-induced fracture toughness based on crack-tip constraint [DE93-015967] p 1451 N94-17913

Interfacial cracks in plates: A three-dimensional numerical investigation p 1456 N94-19116

The interpretation of optical caustics in the presence of dynamic non-uniform crack-tip motion histories: A study based on a higher order transient crack-tip expansion [SM91-12] p 1456 N94-19130

CRACKING (FRACTURING)

Technique to eliminate helium induced weld cracking in stainless steels [DE93-015982] p 1357 N94-17859

Interpretation of warm prestress-induced fracture toughness based on crack-tip constraint [DE93-015967] p 1451 N94-17913

Fundamental concepts relating local atomic arrangements, deformation, and fracture of intermetallic alloys [AD-A268745] p 1361 N94-18788

Office of Naval Research Publications/Patents /Presentations/Honors report, 1 October 1992 - 30 September 1993 [AD-A270037] p 1632 N94-18791

JPRS report: Science and technology. Central Eurasia: Materials science [JPRS-UMS-93-002] p 1339 N94-18833

A numerical analysis of crack growth in brittle microcracking composites [DE93-011562] p 1343 N94-18914

Computational mechanics of composite materials [PB93-195782] p 1343 N94-19281

CRACKS

Inelastic deformation and damage at high temperature [DE93-018155] p 1448 N94-17814

Interpretation of warm prestress-induced fracture toughness based on crack-tip constraint [DE93-015967] p 1451 N94-17913

Development and application of specially-focused ultrasonic transducers to location and sizing of defects in 75 mm- to 127 mm-thick austenitic stainless steel weld metals [DE93-015975] p 1453 N94-18108

Development of the microstructure based stochastic life prediction models [AD-A269880] p 1454 N94-18683

Compatibility of refrigerants and lubricants with motor materials, volume 1 [DE93-040216] p 1350 N94-18895

Interfacial cracks in plates: A three-dimensional numerical investigation p 1456 N94-19116

Subcritical crack growth in continuous-fiber reinforced ceramic composites [DE93-018784] p 1343 N94-19335

CRASH LANDING

Vertical drop test of a Metro 3 aircraft [AD-A270032] p 1318 N94-18789

Composite impact dynamics research at NASA LaRC: A review p 1458 N94-19467

CRASHES

Development and use of computational techniques in Army Aviation research and development programs for crash resistant helicopter technology p 1459 N94-19469

Directions for computational mechanics in automotive crashworthiness p 1459 N94-19472

CRASHWORTHINESS

Analysis of seating and restraint limitations restricting total body weight for aircrew and passengers on US Army helicopters [AD-A269117] p 1511 N94-18296

Vertical drop test of a Metro 3 aircraft [AD-A270032] p 1318 N94-18789

Computational Methods for Crashworthiness [NASA-CP-3223] p 1458 N94-19465

Adaptive methods for nonlinear structural dynamics and crashworthiness analysis p 1458 N94-19466

Impact analysis of composite aircraft structures p 1458 N94-19468

Development and use of computational techniques in Army Aviation research and development programs for crash resistant helicopter technology p 1459 N94-19469

Numerical simulation of vehicle crashworthiness and occupant protection p 1459 N94-19471

Directions for computational mechanics in automotive crashworthiness p 1459 N94-19472

Crashdynamics with DYNA3D: Capabilities and research directions p 1460 N94-19475

CRATERING

Centrifuge modeling of explosion-induced craters in unsaturated sand [AD-A270194] p 1417 N94-18780

CRATERS

Centrifuge modeling of explosion-induced craters in unsaturated sand [AD-A270194] p 1417 N94-18780

CRAY COMPUTERS

Connection machine software conversion of a Navy oceans model [AD-A269876] p 1535 N94-18772

The world's most powerful computer [NASA-TM-109369] p 1514 N94-18961

CREEP PROPERTIES

Alloy development of FeAl aluminide alloys for structural use in corrosive environments [DE93-015100] p 1355 N94-17757

Assessment of an improved multiaxial strength theory based on creep-rupture data for Inconel 600 [DE93-015929] p 1356 N94-17791

Heterogeneous slip and rupture models of the San Andreas fault zone based upon three-dimensional earthquake tomography [DE93-015037] p 1480 N94-17898

Diffusion in ordered alloys [AD-A268232] p 1359 N94-18322

Composites: Materials of the future [AD-A268945] p 1341 N94-18450

Development of ductile Fe3Al-based aluminides [DE93-017865] p 1362 N94-18938

High dose effects in neutron irradiated face-centered cubic metals [DE93-017671] p 1364 N94-19043

The effect of composition on the mechanism of continuous recrystallization and superplastic response of aluminum-scandium alloys [DE93-018594] p 1365 N94-19280

Reducing inadvertent alloying of metal/ceramic brazes [DE93-009842] p 1373 N94-19308

Numerical analysis of pressure meter tests: Application of parameter identification of soils behavior [ECL-92-52] p 1487 N94-19380

Damage accumulation in advanced metal matrix composites under thermal cycling/creep loadings [AD-A271207] p 1344 N94-19720

CREEP RUPTURE STRENGTH

Assessment of an improved multiaxial strength theory based on creep-rupture data for Inconel 600 [DE93-015929] p 1356 N94-17791

CREEP STRENGTH

Fundamental concepts relating local atomic arrangements, deformation, and fracture of intermetallic alloys [AD-A268745] p 1361 N94-18788

Reducing inadvertent alloying of metal/ceramic brazes [DE93-009842] p 1373 N94-19308

Damage accumulation in advanced metal matrix composites under thermal cycling/creep loadings [AD-A271207] p 1344 N94-19720

CREEP TESTS

Damage accumulation in advanced metal matrix composites under thermal cycling/creep loadings [AD-A271207] p 1344 N94-19720

CREW WORKSTATIONS

Army Cockpit Delethalization Program (CDP) [AD-A268990] p 1512 N94-18765

A multivariate anthropometric method for crew station design [AD-A270652] p 1513 N94-19531

CRITERIA

Building a joint-service classification research roadmap: Criterion-related issues [AD-A269735] p 1512 N94-18754

CRITICAL FREQUENCIES

Thermodynamic q-distributions that aren't [DE93-017385] p 1609 N94-19121

CRITICAL TEMPERATURE

Densities and viscosities of ternary ammonia/water fluids [DE93-015966] p 1351 N94-19118

Stability measurements of Rayleigh-Benard convection near the critical state using a spectral model [MPIS-15/1992] p 1422 N94-19520

CROSS CORRELATION

Generalized multichannel signal detection [AD-A271385] p 1391 N94-19587

CROSS FLOW

Lift and pitching moment induced on jet STOVL aircraft hovering in ground effect [AD-A269700] p 1317 N94-18577

CROSSTALK

Data fusion through simulated annealing of registered range and reflectance images [DE93-015910] p 1612 N94-17858

Coherent transient systems evaluation [AD-A268808] p 1576 N94-18204

CRRES (SATELLITE)

CRRES experiments, data collection, analysis and publication [NASA-CR-192419] p 1482 N94-18610

The LET spectrum and its uncertainty during the CRRES mission [AD-A269977] p 1630 N94-18676

Solar flares and magnetospheric particles: Investigations based upon the ONR-602 and ONR-604 experiments [AD-A269495] p 1629 N94-18705

CRUSTAL FRACTURES

Analysis of regional deformation and strain accumulation data adjacent to the San Andreas fault [NASA-CR-194072] p 1487 N94-19428

CRYOGENIC COOLING

Electrically excited CO-lasers with gas dynamic cooling [DLR-FB-93-08] p 1437 N94-18061

MODIL cryocooler producibility demonstration project results [DE93-017981] p 1335 N94-19275

CRYOGENIC EQUIPMENT

Equipment for investigation of cryogenic compaction of nanosize silicon nitride powders [DE93-018740] p 1340 N94-18180

Superfluid Helium On-Orbit Transfer (SHOOT) flight demonstration p 1327 N94-19185

CRYOGENIC TEMPERATURE

Mechanical-property changes of structural composite materials after low-temperature proton irradiation: Implications for use in SSC magnet systems [DE93-016735] p 1343 N94-18763

CRYOGENICS

The 7th International Cryocooler Conference [AD-A268451] p 1379 N94-18147

Equipment for investigation of cryogenic compaction of nanosize silicon nitride powders [DE93-018740] p 1340 N94-18180

Temperature lowering in cryogenic chemical-synthesis techniques and system [DE93-018348] p 1562 N94-18810

Regenerator optimization for Stirling cycle refrigeration [DE93-018468] p 1380 N94-18818

Development of a cryogenic heat pipe [DE93-018448] p 1417 N94-18831

Thin film studies of the proximity Josephson effect [AD-A270129] p 1600 N94-18876

CRYOSTATS

The 7th International Cryocooler Conference [AD-A268451] p 1379 N94-18147

CRYPTOGRAPHY

Securing electronic mail: The risks and future of electronic mail [DE93-017187] p 1383 N94-17994

Geometrical pattern learning [DE93-017641] p 1542 N94-19007

CRYSTAL DEFECTS

Defects in GaAs bulk crystals and multi-layers caused by In diffusion [DE93-016968] p 1595 N94-18054

Electron paramagnetic resonance of the ns(sup 1) centers in crystals [DE93-628793] p 1595 N94-18173

Study of mechanical behavior and internal structure of ferritic nanocrystalline material
[DE93-019264] p 1596 N94-18184
Computer simulation of macromolecular crystals and their defects
[DE93-015213] p 1596 N94-18192
Growth of structures for integrated optoelectronic devices
[AD-A269014] p 1598 N94-18527
Deformation mechanisms in a Laves phase
[DE93-018331] p 1361 N94-18806
Defect behavior of polycrystalline solar cell silicon
[DE93-018490] p 1468 N94-19016
Studies of deep levels in high resistivity silicon detectors irradiated by high fluence fast neutrons using a thermally stimulated current spectrometer
[DE93-016133] p 1602 N94-19258

CRYSTAL DISLOCATIONS
Reorientation of misfit dislocations during annealing in InGaAs/GaAs(001) interfaces
[DE93-015046] p 1592 N94-17741
Selective electrochemical wafer thinning for silicon characterization
[DE93-015083] p 1592 N94-17742
IR materials producibility
[AD-A268849] p 1577 N94-18223

CRYSTAL GROWTH
Kinetic growth of random-like and ballistic-like deposition models
[DE93-624946] p 1595 N94-17956
Photorefractive tungsten bronze crystals for optical computing
[AD-A268859] p 1596 N94-18320
Gallium arsenide-based ternary compounds and multi-band-gap solar cell research
[DE93-010049] p 1467 N94-18483
Scaling laws for diamond chemical vapor deposition. 2: Atomic hydrogen transport
[AD-A269842] p 1371 N94-18740
Materials processing and manufacturing technologies for diamond substrates multichip modules
[AD-A268989] p 1599 N94-18764
MUZO flight experience with the programmable multizone furnace p 1324 N94-19167
Numerical modelling of crystal growth
[AD-A271206] p 1605 N94-19719

CRYSTAL LATTICES
Magnetic properties of single-crystalline UCu3Al2
[DE93-016607] p 1593 N94-17744
Lattice damage in ion-implanted compound semiconductors and its effect on electrical activation
[DE93-015907] p 1593 N94-17845
Defects in GaAs bulk crystals and multi-layers caused by In diffusion
[DE93-016968] p 1595 N94-18054
Kinetic aspects of lattice mismatch in molecular beam epitaxial growth on planar and patterned substrates
[AD-A270424] p 1597 N94-18506
Magnetic and crystallographic structures in UTX intermetallic compounds
[DE93-018291] p 1605 N94-19735

CRYSTAL OPTICS
Crystal optics of high energy gamma-beams
[DE93-630228] p 1577 N94-18217

CRYSTAL OSCILLATORS
Military applications of high-accuracy frequency standards and clocks
[AD-A269303] p 1430 N94-18299
Low-noise oscillators for airborne radar applications, revision 1
[AD-A269372] p 1403 N94-18471

CRYSTAL STRUCTURE
Phenomenological explanation of elastic anomalies in superlattices
[DE93-017475] p 1594 N94-17871
Phase separation and ordering process in Al-Li alloys studied by small-angle neutron scattering and neutron diffraction
[DE93-016750] p 1358 N94-17947
Study of mechanical behavior and internal structure of ferritic nanocrystalline material
[DE93-019264] p 1596 N94-18184
Mesoepitaxy: A universal route to oriented materials
[AD-A270437] p 1598 N94-18511
Molecular structure of low temperature form of triaminoguanidinium nitrate (TAGN)
[AD-A270409] p 1377 N94-18708
Experimental investigation of wave and fracture phenomena in impacted ceramics: Experiments on sapphire
[AD-A270040] p 1372 N94-18792
In situ observation of radiation induced amorphization of crystals with apatite structure
[DE93-018450] p 1599 N94-18816
Specific heat of La(1.875-x)Nd(x)Sr(0.125)CuO4: Magnetic and structural transitions
[DE93-016978] p 1600 N94-18968
The d(exp 3)delta-a(exp 3)delta and b(exp 3)phi-a(exp 3)delta systems of ZrS, Part 2: Appendix, list of wavenumbers
[USIP-92-05] p 1602 N94-19293
Physico chemical and mechanic approach of lubricating properties of graphite + additive powders
[ECL-93-02] p 1373 N94-19405
Precision machining and polishing of scintillating crystals for large calorimeters and hodoscopes
[DE93-018663] p 1381 N94-19544
Final report on subcontract B076260 — borate synthesis
[DE93-019501] p 1604 N94-19565
Refinement of unit cell parameters by least-squares: Comments on an old technique and the development of a new computer program
[AD-A270610] p 1531 N94-19590

CRYSTAL SURFACES
Surface phases and their influence on metal-oxide interfaces
[DE93-019931] p 1601 N94-19020

CRYSTALLINITY
Molecular composites from liquid crystalline polymers and liquid crystalline thermosets
[DE93-016608] p 1368 N94-18096

CRYSTALLIZATION
Elastic properties of amorphous thin films studied by Rayleigh waves
[DE93-018375] p 1372 N94-19202

CRYSTALLOGRAPHY
Omega phase formation in shock-loaded zirconium
[DE93-018343] p 1595 N94-18162
The effect of crystallographic orientation on the performance of single crystal tungsten subscale penetrators
[AD-A268988] p 1597 N94-18468
Implementation of parallel algorithms
[AD-A271035] p 1539 N94-19682

CRYSTALS
Polaron tunneling in high-temperature superconductors
[DE93-016880] p 1593 N94-17754
Analysis of HgI2 and PbI2 crystals and detectors by Particle-Induced X Ray Emission (PIXE) and Ion Backscattering Spectroscopy (IBS)
[DE93-017168] p 1594 N94-17896
Electron paramagnetic resonance of the ns(sup 1) centers in crystals
[DE93-628793] p 1595 N94-18173
Computer simulation of macromolecular crystals and their defects
[DE93-015213] p 1596 N94-18192
Spatial light modulators and applications: Summaries of papers presented at the Spatial Light Modulators and Applications Topical Meeting
[AD-A269452] p 1577 N94-18283
The efficiency of continuous output of some titanium-doped gem-crystal lasers has exceeded 1 W
[AD-A269953] p 1439 N94-18674
In situ observation of radiation induced amorphization of crystals with apatite structure
[DE93-018450] p 1599 N94-18816
Longitudinal beam dynamics with RF noise
[DE93-018649] p 1574 N94-18994
Surface modification of sapphire for IR window application
[DE93-019168] p 1602 N94-19075
Synchrotron/crystal sample preparation
[NASA-CR-193837] p 1603 N94-19513
Precision machining and polishing of scintillating crystals for large calorimeters and hodoscopes
[DE93-018663] p 1381 N94-19544
Refinement of unit cell parameters by least-squares: Comments on an old technique and the development of a new computer program
[AD-A270610] p 1531 N94-19590

CUES
Stochastic models of attention and search
[AD-A268622] p 1508 N94-18292

CUMULUS CLOUDS
Moist wind relationships p 1492 N94-18607

CURING
Remote cure monitoring of polymeric resins by laser Raman spectroscopy
[DE93-016445] p 1369 N94-18112

CURRENT ALGEBRA
Further on the current algebra of WZNW models at and away from criticality
[DE93-624809] p 1545 N94-17686

CURRENT DENSITY
Field emitter array RF amplifier development project, phase 1, option 1
[AD-A268687] p 1396 N94-18293
Optical properties of oxide coatings prepared by ion-assisted deposition
[AD-A270024] p 1599 N94-18711
Superconductivity and magnetism in niobium doped YBa2Cu3O7 related high-(Tc) ceramics
[DE93-018086] p 1601 N94-19049
Lower hybrid counter current drive for edge current density modification in D3-D
[DE93-019157] p 1589 N94-19073
Fabrication, properties, and microstructures of high (Tc) tapes and coils made from Ag-clad Bi-2223 superconductor
[DE93-017405] p 1602 N94-19122
The microstructural mechanism of electromigration failure in narrow interconnects of Al alloys
[DE93-018598] p 1365 N94-19262

CURRENT DISTRIBUTION
Response of transmission line systems to pulse excitation by radiation and injection methods
[DE93-015112] p 1384 N94-18210
Contribution to the study of the additional losses in coil elements used in static converters
[ECL-92-60] p 1406 N94-19297

CURRENT REGULATORS
New current reduction system for watches with integrated current regulation motors
p 1428 N94-18034

CURRENT SHEETS
The phase mixing of shear Alfven waves
[DE93-624920] p 1581 N94-17688

CURVATURE
Understanding curved detonation waves
[DE93-014581] p 1408 N94-17728
Groups on transformations in Finslerian spaces
[DE93-624765] p 1606 N94-17794

CURVE FITTING
Strategies for testing form assessment software
[NPL-DITC-211/92] p 1518 N94-17930

CURVES (GEOMETRY)
Enumerative geometry of Del Pezzo Surfaces
[DE93-624768] p 1546 N94-17816
Geometric contact for curves and surfaces
[RR-893-M] p 1556 N94-19731

CYCLES
Updated Contributions to the Twente Workshop on Hamiltonian Graph Theory
[MEMO-1076] p 1554 N94-19683
Ore-type conditions for cycles through specified vertices p 1555 N94-19695
Hamilton cycles in path-tough graphs
p 1555 N94-19696

CYCLIC ACCELERATORS
Advanced methods for the computation of particle beam transport and the computation of electromagnetic fields and beam-cavity interactions
[DE93-018160] p 1573 N94-17807

CYCLIC LOADS
Factors which affect fatigue strength of fasteners
[DE93-017272] p 1453 N94-18084
Design for cyclic loading endurance of composites
[NASA-TM-106407] p 1457 N94-19351

CYCLOGENESIS
Rapid oceanic cyclogenesis studies
[AD-A269258] p 1490 N94-18265

CYCLONES
Rapid oceanic cyclogenesis studies
[AD-A269258] p 1490 N94-18265

CYCLOTRON RESONANCE
Experiments on nonlinear absorption of ECH waves in MTX and a comparison with theory
[DE93-019158] p 1589 N94-19074
Electron cyclotron resonance heating in the microwave tokamak experiment
[DE93-018083] p 1590 N94-19289

CYCLOTRON RESONANCE DEVICES
The gyrotron backward-wave-oscillator experiment — final progress report
[AD-A268982] p 1403 N94-18452
Designs for a 10.6 micrometer electromagnetic wiggler Free-Electron Laser (FEL)
[AD-A269695] p 1439 N94-18576
Experimental and theoretical investigation of broadband high-power windows for millimeter waves
[KFK-5157] p 1391 N94-19617

CYLINDRICAL BODIES
Recirculation in forward roll coating
[VKI-TM-48] p 1409 N94-17901
Relation between the fluctuating wall pressure and the turbulent structure of a boundary layer on a cylinder in axial flow
[AD-A270242] p 1418 N94-18906
Finite difference program for calculating hydride bed wall temperature profiles
[DE93-019272] p 1523 N94-19005

Current-potential characteristics of electrochemical systems
[DE93-040303] p 1352 N94-19192

Axial response of differently excited anchored viscous liquid bridges in zero-gravity
[LRT-WE-9-FB-1-1992] p 1379 N94-19489

Theoretical examination of the flow around a cylinder with a low dimensional Galerkin process
[MPIS-25/1992] p 1422 N94-19525

Transient skin effect in a massive cylinder by eccentric location of exciting conduction bands
[ETN-93-95048] p 1391 N94-19646

CYLINDRICAL PLASMAS

Transport in the self-organized relaxed state of ion temperature gradient instability
[DE93-016769] p 1584 N94-17983

CYLINDRICAL SHELLS

Compression strength of composite primary structural components
[NASA-CR-194582] p 1457 N94-19350

CYLINDRICAL WAVES

Plasma production by helicon waves
[DE93-788396] p 1586 N94-18213

CYTOLOGY

A scientific role for Space Station Freedom: Research at the cellular level p 1503 N94-19215

D

D REGION

RADARC HF ionospheric prediction program for OTH radar
[AD-A269557] p 1385 N94-18291

Analysis of satellite-derived ozone and water vapor measurements
[NASA-CR-193810] p 1486 N94-19237

DAMAGE

Inelastic deformation and damage at high temperature
[DE93-018155] p 1448 N94-17814

Defining the normal turbine inflow within a wind park environment
[DE93-010032] p 1489 N94-18046

The application of nondestructive techniques to the testing of a wind turbine blade
[DE93-016731] p 1447 N94-18128

Aerodynamic characteristics of a helicopter rotor airfoil as affected by simulated ballistic damage
[AD-A269206] p 1311 N94-18413

Development of the microstructure based stochastic life prediction model
[AD-A269742] p 1361 N94-18742

A constitutive theory for rigid polyurethane foam
[DE93-011596] p 1372 N94-19059

Construction of a tension-torsion anisotropic brittle damage elastic model
[ECL-91-27] p 1457 N94-19375

Synchrotron/crystal sample preparation
[NASA-CR-193837] p 1603 N94-19513

DAMAGE ASSESSMENT

Fatigue technology assessment and strategies for fatigue avoidance in marine structures. Appendices
[AD-A269053] p 1455 N94-18716

Nondestructive inspection of graphite-epoxy laminates for heat damage using DRIFT and LPF spectroscopies
[DE93-017228] p 1343 N94-18761

DAMPING

The phase mixing of shear Alfven waves
[DE93-624920] p 1581 N94-17688

Simulation of the ALS longitudinal multibunch feedback system
[DE93-019227] p 1575 N94-19152

Damping in ferrous shape memory alloys
[AD-A271009] p 1366 N94-19775

DARKENING

Radiation induced darkening of the optical elements in the Startracker camera
[DE93-018907] p 1433 N94-19004

DATA ACQUISITION

CTD and XBT data collected on ERS-1 validation cruise RRS Charles Darwin Cruise 62A, Iceland-Faeroes region
[IOS-294-1992] p 1461 N94-18063

CTD oxygen, tracer and nutrient data from RRS Charles Darwin Cruises 58/59 in the NE Atlantic as part of Vivaldi 1991
[IOS-296-1992] p 1496 N94-18065

Metadata compiled and distributed by the Carbon Dioxide Information Analysis Center for global climate change and greenhouse gas-related data bases
[DE93-015338] p 1473 N94-18167

Technologies for assessing the geologic and geomorphic history of coasts
[AD-A268780] p 1496 N94-18215

Proceedings of the 3rd Workshop on Balloon-Borne Experiments with Superconducting Magnet Spectrometers
[DE93-788362] p 1630 N94-18219

Missile antenna pattern coordinate system and data formats
[AD-A269153] p 1385 N94-18260

A rugged, low-cost advanced data acquisition system for field test projects
[DE93-010041] p 1615 N94-18334

Airport activity statistics of certificated route air carriers, 1992
[AD-A269042] p 1315 N94-18490

CRRES experiments, data collection, analysis and publication
[NASA-CR-192419] p 1482 N94-18610

Measurement Techniques
[VKI-LS-1993-05] p 1430 N94-18643

Data acquisition in aerodynamic research
p 1431 N94-18644

Preparation of data assimilation and model evaluation experiment data sets
[AD-A269996] p 1498 N94-18665

Atlas of SSM/I satellite ice concentration interpolated to operational ice model domains of the Arctic for 1992
[AD-A270306] p 1499 N94-18727

Widget: A data acquisition system for a balloon borne Si particle calorimeter
[DE93-624668] p 1630 N94-18762

Implementation of electronic data interchange in the department of defense: Lessons learned from private industry
[AD-A269532] p 1534 N94-18768

Effects of the Mount Pinatubo eruption on solar insolation: Four case studies
[DE93-018454] p 1475 N94-18817

SSC detector muon sub-system beam tests
[DE93-018415] p 1569 N94-19013

Image blur
[DE93-017944] p 1580 N94-19113

Pantex Plant Meteorological Monitoring Program
[DE93-018495] p 1493 N94-19127

A programmable systolic trigger processor for FERA-bus data
[USIP-92-04] p 1405 N94-19292

FASTBUS simulation models in VHDL
[USIP-92-07] p 1515 N94-19295

Shape of wind gusts at a 130m tower at Wilhelmshaven (Germany)
[BER-BAND-B3] p 1494 N94-19503

A comparison of polygraphic and actigraphic monitoring of sleep using a 5-channel programmable-sensitivity actigraph
[AD-A270731] p 1507 N94-19608

Data-Machine Independence (DMI)
[DE93-018008] p 1539 N94-19734

SeaTrack: Ground station orbit prediction and planning software for sea-viewing satellites
[NASA-RP-1331] p 1532 N94-19761

DATA BASE MANAGEMENT SYSTEMS

OSSA Information Systems Program
[NASA-TM-108774] p 1612 N94-17737

Restricting query relaxation through user constraints
[DE93-017413] p 1612 N94-17870

Information technology resources assessment
[DE93-015276] p 1613 N94-17894

SX User's Manual for SX, version 2.0
[DE93-015971] p 1517 N94-17914

Object-oriented extension of a relational DBMS
[ETN-93-94403] p 1519 N94-17978

A model and an execution mechanism for active data bases
[ETN-93-94404] p 1614 N94-17979

Software Toolkit for Analysis Research (STAR)
[DE93-017368] p 1519 N94-18086

EDMS: Engineering data management system. User's reference
[PB93-187391] p 1614 N94-18119

FEDIX on-line information service: Design, develop, test, and implement an on-line research and education information service
[DE93-018818] p 1614 N94-18181

NASA Electronic Library System (NELS) optimization
[NASA-CR-193688] p 1617 N94-18839

Inventory management plan for a research and development local area network
[DE93-018381] p 1617 N94-19026

An ORACLE CASE history: Experiences with ORACLE CASE tools
[DE93-010827] p 1617 N94-19057

Coordination of software-development activities among sites that are geographically separated
[DE93-019201] p 1524 N94-19076

Downsizing a database platform for increased performance and decreased costs
[DE93-018687] p 1618 N94-19099

Metallurgical evaluation of SRAM 2/SRAM A programmer base plates
[DE93-018689] p 1364 N94-19100

Sandia equation of state data base: Seslan file
[DE93-018693] p 1618 N94-19101

GENSHELL: A genesis database 2D to 3D shell transformation program
[DE93-018694] p 1525 N94-19102

Pantex Plant Meteorological Monitoring Program
[DE93-018495] p 1493 N94-19127

Managing persistent objects: From the programming language to the system
[ETN-93-95021] p 1529 N94-19368

Contribution to applications systems design MOSAIC method in the Aristote project
[ETN-93-95022] p 1529 N94-19370

PRACTICAL: Planning and resource allocation in C2-domains with time critical algorithms
[FEL-93-B029] p 1544 N94-19458

Integrity checking in deductive databases: An exposition
[PB93-191724] p 1619 N94-19709

Semantic models for distributed data base management. Part 2: Development of an integral meta-model for data modeling and data base modeling
[REPT-93-08-PT-2] p 1620 N94-19795

DATA BASES

Restricting query relaxation through user constraints
[DE93-017413] p 1612 N94-17870

SX User's Manual for SX, version 2.0
[DE93-015971] p 1517 N94-17914

Analysis of the ITER H-mode confinement database
[DE93-016984] p 1585 N94-18056

Better termination analysis for active databases
[REPT-93-026] p 1614 N94-18144

GREPOS: A GENESIS database repositioning program
[DE93-018517] p 1614 N94-18164

Metadata compiled and distributed by the Carbon Dioxide Information Analysis Center for global climate change and greenhouse gas-related data bases
[DE93-015338] p 1473 N94-18167

The organizational preparation of existing relational databases for the integration of expert systems
[AD-A268823] p 1614 N94-18191

Arctic ice studies
[AD-A268608] p 1497 N94-18277

Cloudiest year study: An analysis of the 3DNEPH and RTNEPH databases
[AD-A269403] p 1490 N94-18281

Handbook for users
[AD-A268726] p 1615 N94-18323

ADCIRC: An advanced three-dimensional circulation model for shelves, coasts, and estuaries. Report 3: Development of a tidal constituent database for the western North Atlantic and Gulf of Mexico
[AD-A268685] p 1497 N94-18455

Retrieving and integrating data from multiple information sources
[AD-A269588] p 1615 N94-18461

The evolution of the PVM concurrent computing system
[DE93-017764] p 1534 N94-18482

Lunar base Controlled Ecological Life Support System (LCELSS): Preliminary conceptual design study
[NASA-CR-188479] p 1511 N94-18484

Learning database abstractions for query reformulation
[AD-A269531] p 1616 N94-18641

The Navy tessellated spheroid map projection system: A comprehensive definition
[AD-A269989] p 1462 N94-18677

An ORACLE CASE history: Experiences with ORACLE CASE tools
[DE93-010827] p 1617 N94-19057

Axiomatization, declarative semantics and operational semantics of passive and active updates in logic databases
[PB93-195956] p 1618 N94-19067

Coordination of software-development activities among sites that are geographically separated
[DE93-019201] p 1524 N94-19076

Sandia equation of state data base: Seslan file
[DE93-018693] p 1618 N94-19101

GENSHELL: A genesis database 2D to 3D shell transformation program
[DE93-018694] p 1525 N94-19102

Pantex Plant Meteorological Monitoring Program
[DE93-018495] p 1493 N94-19127

ACOS: A performance based approach to build a parallel complex object server
[MEMO-INF-93-11] p 1537 N94-19198

DataTypeLog: A deductive object oriented query language
[MEMO-INF-92-79] p 1526 N94-19221

The TM typing rules
[MEMO-INF-92-80] p 1526 N94-19222
The TM manual version 1.3 working document
[MEMO-INF-93-06] p 1527 N94-19229
Action systems and action refinement in the development of parallel systems: An algebraic approach
[MEMO-INF-93-14] p 1538 N94-19296
A survey of current approaches to modelling of hydrological time-series with respect to climate variability and change
[WMO/TD-534] p 1463 N94-19435
Evaluation of mass spectra for a verification database
[PML-1993-12] p 1619 N94-19453
Fault-tolerance and complexity
[TR-450] p 1530 N94-19483
Incology 908 database report: On process-structure-property relationship
[DE93-017616] p 1366 N94-19546
Ceramic technology project data base
[DE93-019360] p 1374 N94-19561
Absolute positioning by collecting Global Positioning System (GPS) data along short baselines
[AD-A271324] p 1317 N94-19572
Integrity checking in deductive databases: An exposition
[PB93-191724] p 1619 N94-19709
Template based low data rate speech encoder
[AD-A270900] p 1392 N94-19748
A comparison Air Force data systems --- Comments on IDA Paper P-2863
[AD-A270662] p 1619 N94-19780
Semantic models for distributed data base management. Part 2: Development of an integral meta-model for data modeling and data base modeling
[REPT-93-08-PT-2] p 1620 N94-19795

DATA COMPRESSION
An analytical approach to error localization by using information derived from error signature
[REPT-93-023] p 1518 N94-17960
The Navy tessellated spheroid map projection system: A comprehensive definition
[AD-A269989] p 1462 N94-18677
Color palette considerations for digital map displays
[AD-A269991] p 1462 N94-18679
Implementation of parallel algorithms
[AD-A271035] p 1539 N94-19682

DATA CONVERSION ROUTINES
Connection machine software conversion of a Navy oceans model
[AD-A269876] p 1535 N94-18772
Vectorized presentation-level services for scientific distributed applications
[DE93-018091] p 1537 N94-19253

DATA CORRELATION
A Bayesian approach to contaminant plume delineation
[DE93-012909] p 1472 N94-17890

DATA FLOW ANALYSIS
Modelling software for structure metrics
[MEMO-INF-93-13] p 1526 N94-19200
Systolic design with asynchronous controls for digital-signal processing
[AD-A270976] p 1392 N94-19680

DATA INTEGRATION
Data fusion through simulated annealing of registered range and reflectance images
[DE93-015910] p 1612 N94-17858
Retrieving and integrating data from multiple information sources
[AD-A269588] p 1615 N94-18461

DATA LINKS
Intentionally Short Range Communications (ISRC)
[AD-A268788] p 1384 N94-18216
FAA airborne data link human factors research plan
[AD-A271006] p 1514 N94-19773
Control of integrated voice/data multi-hop radio networks via reduced-load approximations
[AD-A270661] p 1393 N94-19779

DATA MANAGEMENT
OSSA Information Systems Program
[NASA-TM-108774] p 1612 N94-17737
EDMS: Engineering data management system. User's reference
[PB93-187391] p 1614 N94-18119
Metadata compiled and distributed by the Carbon Dioxide Information Analysis Center for global climate change and greenhouse gas-related data bases
[DE93-015338] p 1473 N94-18167
User's manual of Tokamak Simulation Code
[DE93-788388] p 1586 N94-18212
Retrieving and integrating data from multiple information sources
[AD-A269588] p 1615 N94-18461
CRRES experiments, data collection, analysis and publication
[NASA-CR-192419] p 1482 N94-18610
CDIAC catalog of numeric data and computer model packages
[DE93-017675] p 1475 N94-18832
Inventory management plan for a research and development local area network
[DE93-018381] p 1617 N94-19026
An ORACLE CASE history: Experiences with ORACLE CASE tools
[DE93-010827] p 1617 N94-19057
Report of the Second CLICOM Experts Meeting
[WCDMP-19] p 1495 N94-19705
Integrity checking in deductive databases: An exposition
[PB93-191724] p 1619 N94-19709
A comparison Air Force data systems --- Comments on IDA Paper P-2863
[AD-A270662] p 1619 N94-19780
Semantic models for distributed data base management. Part 2: Development of an integral meta-model for data modeling and data base modeling
[REPT-93-08-PT-2] p 1620 N94-19795

DATA PROCESSING
Proposal for a numerical array library
[DE93-015017] p 1516 N94-17786
RESQme studies for SDC regional computing centers
[DE93-015230] p 1514 N94-17799
Verification of 3I retrievals vis-a-vis radiosonde observations
[KNMI-TR-150] p 1488 N94-17924
A model and an execution mechanism for active data bases
[ETN-93-94404] p 1614 N94-17979
CTD and XBT data collected on ERS-1 validation cruise RRS Charles Darwin Cruise 62A, Iceland-Faeroes region
[IOS-294-1992] p 1461 N94-18063
SeaSoar and CTD sections across the Iceland-Faeroes Front and Faeroe Shetland Channel, August 1990
[IOS-295-1992] p 1496 N94-18064
CTD oxygen, tracer and nutrient data from RRS Charles Darwin Cruises 58/59 in the NE Atlantic as part of Vivaldi 1991
[IOS-296-1992] p 1496 N94-18065
Software Toolkit for Analysis Research (STAR)
[DE93-017368] p 1519 N94-18086
The Earth radiation budget experiment: Overview of data-processing and error sources
[KNMI-TR-146] p 1481 N94-18142
Performance of the Amorphous Materials Diffractometer GLAD at IPNS
[DE93-017746] p 1430 N94-18481
Overview of physical oceanographic measurements taken during the Mount Mitchell cruise to ROPME sea area
[DE93-018460] p 1497 N94-18494
Cognitive limitations in coordination in hierarchical information processing structures
[AD-A268825] p 1616 N94-18535
SERCAA cloud analysis integration: Design concepts and interaction with cloud forecast models
[AD-A269104] p 1492 N94-18637
Preparation of data assimilation and model evaluation experiment data sets
[AD-A269996] p 1498 N94-18685
Initial Graphics Exchange Specification (IGES)
[AD-A270049] p 1522 N94-18794
A bit serial first level calorimeter trigger for an LHC detector
[USIP-92-08] p 1574 N94-18845
An ORACLE CASE history: Experiences with ORACLE CASE tools
[DE93-010827] p 1617 N94-19057
Pantex Plant Meteorological Monitoring Program
[DE93-018495] p 1493 N94-19127
Volume rendering of 3D scalar and vector fields at Lawrence Livermore National Laboratory
[DE93-018000] p 1528 N94-19276
A program for passively tracking a target using an array of sensors
[DE93-019554] p 1390 N94-19306
New automatic deduction techniques in first order finite and infinite polyvalent logic
[ETN-93-95003] p 1528 N94-19359
Conception and analysis of numerical parallel algorithms: Realization on the Connection Machine
[ETN-93-95005] p 1531 N94-19517
The Cluster magnetic field investigation: Scientific objectives and instrumentation p 1329 N94-19629

DATA PROCESSING EQUIPMENT
VPU(tm) demonstration mission vicinity processor unit(tm) overview p 1325 N94-19171
Implementation of the digital wave-processing experiment p 1329 N94-19628

DATA REDUCTION
A noniterative improvement of Guyan reduction
p 1449 N94-17833
Automatic A-set selection for dynamics analysis
p 1450 N94-17839
Software Toolkit for Analysis Research (STAR)
[DE93-017368] p 1519 N94-18086
Performance of the Amorphous Materials Diffractometer GLAD at IPNS
[DE93-017746] p 1430 N94-18481
CRRES experiments, data collection, analysis and publication
[NASA-CR-192419] p 1482 N94-18610
A least-squares computational tool kit
[DE93-018400] p 1557 N94-19011
Development of ISY data set, part 2
[NASDA-CNT-930006-PT-2] p 1463 N94-19384
Shape of wind gusts at a 130m tower at Wilhelmshaven (Germany)
[BER-BAND-B3] p 1494 N94-19503

DATA RETRIEVAL
Software Toolkit for Analysis Research (STAR)
[DE93-017368] p 1519 N94-18086
Retrieving and integrating data from multiple information sources
[AD-A269588] p 1615 N94-18461
Learning database abstractions for query reformulation
[AD-A269531] p 1616 N94-18641
Software distribution using xnetlib
[DE93-018278] p 1523 N94-18989

DATA STORAGE
Coherent transient systems evaluation
[AD-A268808] p 1576 N94-18204
CRRES experiments, data collection, analysis and publication
[NASA-CR-192419] p 1482 N94-18610
Data-Machine Independence (DMI)
[DE93-018008] p 1539 N94-19734

DATA STRUCTURES
Object-oriented extension of a relational DBMS
[ETN-93-94403] p 1519 N94-17978
High performance Fortran: An overview
[DE93-017181] p 1519 N94-18072
Initial Graphics Exchange Specification (IGES)
[AD-A270049] p 1522 N94-18794
Abstracting inter-object communications using composition filters
[MEMO-INF-92-78] p 1526 N94-19220
Data-Machine Independence (DMI)
[DE93-018008] p 1539 N94-19734

DATA SYSTEMS
Directional regions in Geographic Information Systems (GIS)
[AD-A268536] p 1462 N94-18309
The J85 cost/benefit engine study
[AD-A269280] p 1320 N94-18333
A comparison of air force data systems
[AD-A269691] p 1616 N94-18575
Tracking with time-delayed data in multisensor systems
[AD-A271334] p 1391 N94-19582
Cluster: Mission, Payload, and Supporting Activities
[ESA-SP-1159] p 1328 N94-19622
The Cluster science data system: A distributed system to serve a wide international community
p 1330 N94-19638
A comparison Air Force data systems --- Comments on IDA Paper P-2863
[AD-A270662] p 1619 N94-19780

DATA TRANSFER (COMPUTERS)
Embedded Computer Performance Measurement (ECPM). Advanced avionics subsystems and technology multiprocessor ECPM software documentation
[AD-A269921] p 1320 N94-18658
Implementation of electronic data interchange in the department of defense: Lessons learned from private industry
[AD-A269532] p 1534 N94-18768
Vectorized presentation-level services for scientific distributed applications
[DE93-018091] p 1537 N94-19253
Protocol service decomposition for high-performance networking
[AD-A270613] p 1538 N94-19533
The Cluster science data system: A distributed system to serve a wide international community
p 1330 N94-19638

DATA TRANSMISSION
Data fusion through simulated annealing of registered range and reflectance images
[DE93-015910] p 1612 N94-17858
Securing electronic mail: The risks and future of electronic mail
[DE93-017187] p 1383 N94-17994
A rugged, low-cost advanced data acquisition system for field test projects
[DE93-010041] p 1615 N94-18334

Implementation of electronic data interchange in the department of defense: Lessons learned from private industry
[AD-A269532] p 1534 N94-18768
Message passing in PUMA
[DE93-012841] p 1537 N94-19206
Optoelectronic packaging: A review
[DE93-040059] p 1515 N94-19535
Experimental examinations of semiconductor laser amplifiers for optical communication technology
[ETN-93-95050] p 1442 N94-19647

DEBONDING (MATERIALS)
Fatigue resistant Ti3Al composites
[AD-A270305] p 1341 N94-18692

DEBRIS
Effect of phase change in a debris cloud on a backwall structure
[DE93-017506] p 1358 N94-18100
Toward a characterization of the debris cloud created in a hypervelocity impact on a thin plate
[AD-A269190] p 1455 N94-18864

DEBYE-HUCKEL THEORY
On the Debye-Huckel's theory
[DE93-624789] p 1561 N94-17681

DECISION MAKING
The machine reception: A business of experts
[CRIF-MC-94] p 1611 N94-17980
Contribution to the analysis of tableaus based decision methods
[ETN-93-94355] p 1560 N94-18067
Cognitive limitations in coordination in hierarchical information processing structures
[AD-A268825] p 1616 N94-18535
Scale sensitivity in the multiplicative AHP and SMART
[REPT-93-37] p 1611 N94-19157
Context-related scaling of human judgement in the multiplicative AHP, SMART and ELECTRE
[REPT-93-38] p 1611 N94-19158
Overview of research in progress at the Center of Excellence
[NASA-CR-194329] p 1618 N94-19256
Integrated measurement of crew resource management and technical flying skills
[AD-A270512] p 1510 N94-19677

DECISION THEORY
VHF air/ground communications for air traffic control. Volume 1: A decision tree approach to system innovations
[AD-A268485] p 1316 N94-18384
VHF air/ground communications for air traffic control: A decision tree approach to system innovations, volume 2
[AD-A268632] p 1386 N94-18495
Cognitive limitations in coordination in hierarchical information processing structures
[AD-A268825] p 1616 N94-18535
Scale sensitivity in the multiplicative AHP and SMART
[REPT-93-37] p 1611 N94-19157
Context-related scaling of human judgement in the multiplicative AHP, SMART and ELECTRE
[REPT-93-38] p 1611 N94-19158
Finding optimal policies for Markov decision chains: A unifying framework for mean-variance-tradeoffs
[PB93-191930] p 1559 N94-19555
Generalized regression trees: Function estimation via recursive partitioning and maximum likelihood
[AD-A271259] p 1560 N94-19726

DECISIONS
Scale sensitivity in the multiplicative AHP and SMART
[REPT-93-37] p 1611 N94-19157

DECODERS
Single phase dynamic CMOS PLA using charge sharing technique p 1397 N94-18341
An extended Reed Solomon decoder design
p 1398 N94-18348
Canonical multi-valued input Reed-Muller trees and forms p 1401 N94-18375
Multichannel error correction code decoder
[NASA-TM-106331] p 1333 N94-19313

DECODING
Communication in the presence of unknown interference
[AD-A271146] p 1392 N94-19738

DECOMPOSITION
Ultrasonic process for destruction of chlorinated organic compounds in aqueous solution
[DE93-015551] p 1348 N94-18249
Nitridation of GaAs(100) by laser-induced decomposition of HN3
[AD-A269147] p 1436 N94-18258
Spectral analysis on the canonical autoregressive decomposition
[AD-A270083] p 1549 N94-18798
Single source precursors for the OMCVD of 3/5 compound semiconductors
[AD-A271147] p 1606 N94-19739

DECONTAMINATION
The application of jet spray and ion beam contamination removal techniques to samples from the LDEF spacecraft
[AD-A270973] p 1354 N94-19755

DECOUPLING
Nonlinear disturbance decoupling and linearization: A partial interpretation of integral feedback
[PB93-197515] p 1543 N94-19328

DEEP DRAWING
Formulation and identification of the anisotropic laws for thin sheets drawing
[ECL-92-55] p 1365 N94-19400

DEEP WATER
Coastal Ocean Modeling Workshop
[AD-A268955] p 1497 N94-18393

DEFECTS
Development and application of specially-focused ultrasonic transducers to location and sizing of defects in 75 mm- to 127 mm-thick austenitic stainless steel weld metals
[DE93-015975] p 1453 N94-18108
High resolution SQUID magnetometry for non-destructive evaluation
[AD-A268884] p 1447 N94-18225
Performance of defect-tolerant set-associative cache memories p 1398 N94-18346
Scaling laws for diamond chemical vapor deposition. Diamond surface chemistry
[AD-A269874] p 1599 N94-18745
Morphology, deformation, and defect structures of TiCr2 in Ti-Cr alloys
[DE93-018332] p 1361 N94-18807
Effects of shock loading on a solid-solution strengthened superalloy
[DE93-018345] p 1362 N94-18809
Quantification of volume flaw sizes in ceramics by image processing of 3D x ray tomographic data sets
[DE93-018573] p 1372 N94-18932
Thermal stresses in the microchannel heatsink cooled by liquid nitrogen
[DE93-018660] p 1418 N94-18995
Thermal wave image processing for characterization of subsurface of flaws in materials
[DE93-019024] p 1344 N94-19551

DEFENSE PROGRAM
An evolutionary approach to space launch commercialization
[AD-A269861] p 1331 N94-18411
Department of Defense Gateway Information System (DGIS) users' guide
[AD-A270140] p 1617 N94-18752
Coordination of software-development activities among sites that are geographically separated
[DE93-019201] p 1524 N94-19076
Utilization of Shuttle small payload accommodations in the DOD Space Test Program p 1326 N94-19180

DEFORMATION
Atlas of formability: HAYNES 556
[AD-A268354] p 1356 N94-17768
Atlas of formability: NICKELVAC K-500
[AD-A268351] p 1356 N94-17772
Inelastic deformation and damage at high temperature
[DE93-018155] p 1448 N94-17814
Deformed traces and covariant quantum algebras for quantum groups GL(sub qp)(2) and GL(sub qp)(1/1)
[DE93-629862] p 1561 N94-18153
On a possible algebra morphism of U(sub q)(osp1/2) onto the deformed oscillator algebra W(sub q)(N)
[DE93-629857] p 1548 N94-18176
Composites: Materials of the future
[AD-A268945] p 1341 N94-18450
The effect of crystallographic orientation on the performance of single crystal tungsten subscale penetrators
[AD-A268988] p 1597 N94-18468
Development of a finite element method program for the analysis of laminated composite plates using first-order shear deformation theory
[AD-A270318] p 1342 N94-18700
Deformation mechanisms in a Laves phase
[DE93-018331] p 1361 N94-18806
Morphology, deformation, and defect structures of TiCr2 in Ti-Cr alloys
[DE93-018332] p 1361 N94-18807
Effects of shock loading on a solid-solution strengthened superalloy
[DE93-018345] p 1362 N94-18809
A general-purpose contact detection algorithm for nonlinear structural analysis codes
[DE93-018507] p 1455 N94-19039
Application of differential sensitivity theory to continuum mechanics
[DE93-012732] p 1609 N94-19187
Analysis of regional deformation and strain accumulation data adjacent to the San Andreas fault
[NASA-CR-194072] p 1487 N94-19428
The interpretation of crustal dynamics data in terms of plate motions and regional deformation near plate boundaries
[NASA-CR-194302] p 1487 N94-19432
Simulation of dynamic material response with the PAGOSA code
[DE93-018285] p 1460 N94-19603

DEGRADATION
Structural stability of 1100 C heated Pd/k during absorption cycling in protium
[DE93-016270] p 1346 N94-18048
Environmental degradation of Alloy 600 and welded filler metal EN82 in an elevated temperature aqueous environment
[DE93-018049] p 1363 N94-18940
Microbial degradation of poly-b-esters: A mechanistic study, cellulose acetate biodegradability
[AD-A271368] p 1374 N94-19586

DEGREES OF FREEDOM
Some remarks on integrable Hamiltonian systems with two degrees of freedom
[DE93-624766] p 1546 N94-17815
Automatic A-set selection for dynamics analysis
p 1450 N94-17839
Six degree of freedom fine motion positioning stage based on magnetic levitation
[DE93-017651] p 1446 N94-19547

DEHYDROGENATION
Conversion of ethane and of propane to higher olefin hydrocarbons
[DE93-015282] p 1347 N94-18194

DELAMINATING
Computational strategies for composite structures
[PB93-195097] p 1452 N94-18079
Composites: Materials of the future
[AD-A268945] p 1341 N94-18450
Compression strength of composite primary structural components
[NASA-CR-194562] p 1457 N94-19350
Delamination in composite materials as observed using an optical fiber strain gage
[AD-A270803] p 1344 N94-19662

DELAY
Tandem queues with deterministic service times
[PB93-197465] p 1543 N94-19324

DELAY LINES
Variable wide band fiber optic delay line
[AD-D015848] p 1576 N94-17716
A method for eliminating skew introduced by non-uniform buffer delay and wire lengths in clock distribution trees
[AD-A270649] p 1544 N94-19530

DELTA WINGS
A study of the influence of a delta wing geometry on the induced drag at transonic speed (M=0.55) and high angles of attack
[FFA-TN-1992-14] p 1311 N94-17722
Comparison between swept and delta canards on a model of a combat aircraft
[AD-A269561] p 1317 N94-17826
CFD investigations of the hypersonic double delta wing greta: Sanger project no. 3.2
[FFA-TN-1992-42] p 1311 N94-17919
Three dimensional network generation and Euler calculation for a wing fuselage canard configuration
[MBB-LME-211-S-PUB-511-A] p 1319 N94-19500

DEMODULATION
Application of wavelet transform techniques to spread spectrum demodulation and jamming
[AD-A267389] p 1389 N94-19009

DENSE PLASMAS
Using the Tritium Plasma Experiment to evaluate ITER PFC safety
[DE93-016614] p 1582 N94-17713
Plasma klystron amplifier
[AD-D015819] p 1395 N94-17903
Optical design for photonics. Organization of the 1993 Photonics Science Topical Meetings. Technical digest series, volume 9
[AD-A269027] p 1578 N94-18396

DENSIFICATION
Pressureless densification of ceramic matrix composites
[AD-A269137] p 1371 N94-18691

DENSITY
Velocity measurements in a boundary layer with a density gradient
[DE93-019627] p 1422 N94-19515

DENSITY (MASS/VOLUME)
Densities and viscosities of ternary ammonia/water fluids
[DE93-015966] p 1351 N94-19118

DENSITY DISTRIBUTION
A comparative study of turbulence models in predicting hypersonic inlet flows p 1314 N94-18553
Phase-space description of plasma waves: Linear and nonlinear theory
[IRF-SR-211] p 1587 N94-18860
DENSITY MEASUREMENT
An investigation of methods for updating ionospheric scintillation models using topside in-situ plasma density measurements
[AD-A269872] p 1483 N94-18655
Behavior of the particle transport coefficients near the density limit in MTX
[DE93-019108] p 1591 N94-19311
DEOXYRIBONUCLEIC ACID
Cellular and molecular level responses after radiofrequency radiation exposure, alone or in combination with x rays or chemicals
[AD-A268189] p 1501 N94-17729
Matrix- and substrate-assisted laser desorption for fast DNA sequencing
[DE93-015332] p 1501 N94-18242
DEPLETION
Screening analysis for chlorine-free alternative refrigerants to replace R-22 in air conditioning applications
[DE93-015920] p 1367 N94-17847
DEPOSITION
Kinetic growth of random-like and ballistic-like deposition models
[DE93-624946] p 1595 N94-17956
Nanostructured materials: Mind over matter
[DE93-017690] p 1597 N94-18480
The urban perspectives of acid rain
[DE93-018881] p 1474 N94-18523
Optical properties of oxide coatings prepared by ion-assisted deposition
[AD-A270024] p 1599 N94-18711
Materials processing and manufacturing technologies for diamond substrates multichip modules
[AD-A268989] p 1599 N94-18764
DEPOSITS
Analysis of deposit precursors in jet fuels using Fourier transform infrared spectroscopy
[AD-A269035] p 1377 N94-18489
DEPTH MEASUREMENT
Processing and analysis of SeaMARC 2 data: Fieberling guyot; raw phase experiment in Norwegian-Greenland Sea
[AD-A269930] p 1498 N94-18662
DESIGN ANALYSIS
Design optimization studies using COSMIC NASTRAN
p 1450 N94-17834
Development of a new concept diver's watch
p 1429 N94-18041
Preliminary structural design: Defining the design space
[AD-A268898] p 1317 N94-18227
A rational design change methodology based on experimental and analytical modal analysis
[DE93-018537] p 1521 N94-18271
Verification of VLSI designs p 1400 N94-18363
A new variable testability measure
p 1400 N94-18364
Controlling state explosion during automatic verification of delay-insensitive and delay-constrained VLSI systems using the POM verifier p 1400 N94-18365
Formal verification of an MMU and MMU cache
p 1400 N94-18366
Formal hardware verification of digital circuits
p 1401 N94-18367
Improved self arbitrated VLSI asynchronous circuits
p 1402 N94-18378
Optical design for photonics. Organization of the 1993 Photonics Science Topical Meetings. Technical digest series, volume 9
[AD-A269027] p 1578 N94-18396
The CMU masters in software engineering core curriculum
[AD-A268983] p 1521 N94-18453
Procedures and design data for the formulation of aircraft configurations
[AD-A270150] p 1318 N94-18779
Review Committee report on the conceptual design of the tokamak physics experiment
[DE93-018408] p 1588 N94-19012
Novel mass spectrometric instrument for gaseous and particulate characterization and monitoring
[DE93-019992] p 1433 N94-19054
An ORACLE CASE history: Experiences with ORACLE CASE tools
[DE93-010827] p 1617 N94-19057
Gear sound levels with various tooth contact ratios and forms
[NASA-TM-106432] p 1446 N94-19318
Optimal safety system design using fault tree analysis
[MATHS-REPT-A-187] p 1529 N94-19382
Silicon compilation: From the circuit to the system
[ETN-93-95010] p 1406 N94-19501
Shell designs
[AD-A270656] p 1460 N94-19606
ADAS implementation of a panel method for the prediction of aerodynamic loads
[LR-723] p 1313 N94-19667
DESORPTION
Matrix- and substrate-assisted laser desorption for fast DNA sequencing
[DE93-015332] p 1501 N94-18242
Nitridation of GaAs(100) by laser-induced decomposition of HN3
[AD-A269147] p 1438 N94-18258
DESTRUCTIVE TESTS
Laser induced damage testing: Equipment and techniques
[DE93-017143] p 1437 N94-18060
DETACHMENT
Embrittlement of surface mount solder joints by hot solder-dipped, gold-plated leads
[DE93-017659] p 1358 N94-18003
DETECTION
Space debris detection
[AD-A269254] p 1334 N94-18264
Detection of single molecules in microspheres
[DE93-017776] p 1567 N94-18493
Aircraft fire sentry. Volume 1: Summary
[AD-A270087] p 1315 N94-18822
Aircraft fire sentry. Volume 2: Appendices A, B, C and D
[AD-A270088] p 1315 N94-18823
A general-purpose contact detection algorithm for nonlinear structural analysis codes
[DE93-018507] p 1455 N94-19039
The minimum detection limits of RDX and TNT deposited on various surfaces as determined by ion mobility spectroscopy
[DE93-018521] p 1378 N94-19042
DETERIORATION
Study on radiation-induced deterioration of grease at high temperature, 3
[DE93-788368] p 1369 N94-18220
DETONATION
Direct Monte Carlo simulation of the chemical equilibrium composition of detonation products
[DE93-014559] p 1376 N94-17751
Detonation reaction steps frozen by free expansion and analyzed by mass spectrometry
[DE93-012734] p 1376 N94-17813
Modeling shock initiation in Composition B
[DE93-016544] p 1376 N94-18095
The use of post detonation analysis of stable isotope ratios to determine the type and production process of the explosive involved
[DE93-018497] p 1378 N94-19242
Round robin experiments on the Explosive Components Water Gap Test (ECWGT)
[PML-1992-69] p 1378 N94-19445
DETONATION WAVES
Understanding curved detonation waves
[DE93-014581] p 1408 N94-17728
DEUTERIUM
NMR studies of enriched species at interfaces
[AD-A264703] p 1367 N94-17878
The rise of accuracy for the multichannel scattering problem solving
[DE93-630145] p 1608 N94-18253
DEW POINT
Station climatic summaries: North America. Volume 1: The contiguous United States
[AD-A269567] p 1490 N94-18303
Station climatic summaries, North America. Volume 2: Alaska, Canada and Greenland
[AD-A269793] p 1493 N94-18732
DIAMETERS
The influence of the target strength model on computed perforation
[DE93-018659] p 1460 N94-19543
DIAMOND FILMS
Characterization of diamond film nucleation and growth surface
[AD-A269400] p 1597 N94-18459
Scaling laws for diamond chemical vapor deposition. 2: Atomic hydrogen transport
[AD-A269842] p 1371 N94-18740
Scaling laws for diamond chemical vapor deposition. Diamond surface chemistry
[AD-A269874] p 1599 N94-18745
Growth, characterization and device development in monocrystalline diamond films
[AD-A270074] p 1599 N94-18797
Pressure and temperature effects on the kinetics and quality of diamond films
[AD-A270876] p 1606 N94-19771
DIAMONDS
Characterization of diamond film nucleation and growth surface
[AD-A269400] p 1597 N94-18459
Scaling laws for diamond chemical vapor deposition. Diamond surface chemistry
[AD-A269874] p 1599 N94-18745
Diamond brazed to a metal
[AD-D015877] p 1371 N94-18746
Materials processing and manufacturing technologies for diamond substrates multichip modules
[AD-A268989] p 1599 N94-18764
Growth, characterization and device development in monocrystalline diamond films
[AD-A270074] p 1599 N94-18797
Picoindentation hardness measurements using atomic force microscopy
[AD-A270877] p 1604 N94-19579
Atomic-scale friction and microfriction of graphite and diamond using friction force microscopy
[AD-A270952] p 1605 N94-19679
DIELECTRIC PERMEABILITY
Crystal optics of high energy gamma-beams
[DE93-630228] p 1577 N94-18217
DIELECTRIC PROPERTIES
Design and test of a low jitter metal to metal contact solid dielectric switch
[DE93-016957] p 1394 N94-17755
The Aerocapacitor: A carbon aerogel based supercapacitor
[DE93-016537] p 1395 N94-17849
Aerogels for microelectronic applications: Fast, inexpensive, and light as air
[DE93-017170] p 1395 N94-17882
Anomalous dielectric properties of carbon-black filled elastomers
[AD-A269378] p 1370 N94-18280
Polymer films with enhanced dielectric properties
[AD-A271148] p 1375 N94-19740
DIELECTRICS
Design and test of a low jitter metal to metal contact solid dielectric switch
[DE93-016957] p 1394 N94-17755
Aerogels for microelectronic applications: Fast, inexpensive, and light as air
[DE93-017170] p 1395 N94-17882
Anomalous dielectric properties of carbon-black filled elastomers
[AD-A269378] p 1370 N94-18280
RF vacuum microelectronics
[AD-A269454] p 1396 N94-18284
High-power microwave breakdown of dielectric interfaces
[AD-A268844] p 1397 N94-18318
The asymptotic theory of the reflection and transmission of a pulsed electromagnetic beam field at a planar interface separating two dispersive media
[AD-A269033] p 1385 N94-18404
Single-transverse-mode, narrow-bandwidth pulsed tunable dye laser with hollow circular intracavity dielectric waveguide
[AD-A270022] p 1439 N94-18614
Numerical modelling of fringing fields and their use for complex permittivity measurements at high frequencies
[AD-A270198] p 1388 N94-18782
Experimental and theoretical investigation of broadband high-power windows for millimeter waves
[KFK-5157] p 1391 N94-19617
DIFFERENCE EQUATIONS
Difference equations for generalized Meixner polynomials
[REPT-93-17] p 1550 N94-19082
DIFFERENTIAL CALCULUS
On paragrassmann differential calculus
[DE93-628594] p 1548 N94-18169
DIFFERENTIAL EQUATIONS
Impulsive moving mirror model and impulsive differential equations in Banach space
[DE93-629867] p 1549 N94-18197
A method for finding the periodic solution of autonomous ordinary differential equations
[DE93-624725] p 1550 N94-19244
Methods for description and control of dynamical systems and their application
[MPIS-17/1992] p 1553 N94-19522
DIFFRACTION
Spin-integrated and spin-dependent photoelectron diffraction
[DE93-016546] p 1565 N94-17850
Wideband electromagnetic scattering/analysis program: Far zone electromagnetic scattering from complex shapes using geometrical theory of diffraction
[AD-A268790] p 1384 N94-18187

DIFFRACTOMETERS
Performance of the Amorphous Materials Diffractometer GLAD at IPNS
[DE93-017746] p 1430 N94-18481
DIFFUSION
Using the Tritium Plasma Experiment to evaluate ITER PFC safety
[DE93-016614] p 1582 N94-17713
Diffusion in ordered alloys
[AD-A268232] p 1359 N94-18322
Longitudinal beam dynamics with RF noise
[DE93-018649] p 1574 N94-18994
DIFFUSION COEFFICIENT
Diffusion in ordered alloys
[AD-A268232] p 1359 N94-18322
Behavior of the particle transport coefficients near the density limit in MTX
[DE93-019108] p 1591 N94-19311
DIFFUSION FLAMES
Studies on high pressure and unsteady flame phenomena: Revision
[AD-A269138] p 1348 N94-18257
Transport phenomena and interfacial kinetics in multiphase combustion systems
[AD-A270202] p 1349 N94-18785
DIFFUSION LENGTH
Development of large-area monolithically integrated silicon-film photovoltaic modules
[DE93-010037] p 1464 N94-17731
Defect behavior of polycrystalline solar cell silicon
[DE93-018490] p 1468 N94-19016
DIFFUSION THEORY
Ratio of specimen thickness to detection area for reliable hydrogen permeation measurement
[NPL-DMM(A)-103] p 1451 N94-17929
DIFFUSION WELDING
Joining and Adhesion of Advanced Inorganic Materials Symposium
[AD-A269748] p 1342 N94-18720
DIFFUSIVITY
Diffusion in ordered alloys
[AD-A268232] p 1359 N94-18322
Behavior of the particle transport coefficients near the density limit in MTX
[DE93-019108] p 1591 N94-19311
DIGITAL DATA
Measuring machines for digitalizing and measuring complex surfaces, models and matrices
[CRIF-MC-97] p 1444 N94-17963
The Navy tessellated spheroid map projection system: A comprehensive definition
[AD-A269989] p 1462 N94-18677
Color palette considerations for digital map displays
[AD-A269991] p 1462 N94-18679
The universal BitBus node
[DIGEL-1993-1] p 1515 N94-19799
DIGITAL ELECTRONICS
Magnetostrictive actuators for human sensory feedback
[AD-A269266] p 1511 N94-17841
Superconducting/semiconducting hybrids and advance memory concepts for superconducting electronics
[AD-A268679] p 1397 N94-18312
On timing faults in digital logic circuits
[AD-A268714] p 1402 N94-18400
Superconducting flux flow devices, digital circuits and memories
[DE93-019072] p 1405 N94-19079
Development of a quartz digital accelerometer for environmental sensing and navigation applications
[DE93-018503] p 1433 N94-19243
DIGITAL FILTERS
Examination of metrics and assumptions used in correlation filter design
[DE93-017636] p 1576 N94-18000
An improved distributed arithmetic architecture
p 1398 N94-18349
Programmable linear phase digital filters
[AD-A270413] p 1404 N94-18709
Simulation of the ALS longitudinal multibunch feedback system
[DE93-019227] p 1575 N94-19152
DIGITAL SIMULATION
Numerical modelling of crystal growth
[AD-A271206] p 1605 N94-19719
DIGITAL SYSTEMS
Precision digitally-controlled variable attenuation circuit
[AD-D015862] p 1394 N94-17703
Information technology resources assessment
[DE93-015276] p 1613 N94-17894
Advanced optical fiber communication systems
[AD-A269120] p 1577 N94-18254
Automated ILA design for synchronous sequential circuits p 1397 N94-18340
Single phase dynamic CMOS PLA using charge sharing technique p 1397 N94-18341
An SEU immune logic family p 1398 N94-18342
Fault tolerant sequential circuits using sequence invariant state machines p 1398 N94-18344
VHF air/ground communications for air traffic control: A decision tree approach to system innovations, volume 2
[AD-A268632] p 1386 N94-18495
Color palette considerations for digital map displays
[AD-A269991] p 1462 N94-18679
DIGITAL TECHNIQUES
VHF air/ground communications for air traffic control: A decision tree approach to system innovations, volume 2
[AD-A268632] p 1386 N94-18495
VLSI for high-speed digital signal processing
[AD-A270406] p 1404 N94-18706
Digital control of Pritchard-Salamon systems
[REPT-93-33] p 1543 N94-19286
Implementation of the digital wave-processing experiment p 1329 N94-19628
DIGITAL TRANSDUCERS
Data acquisition in aerodynamic research
p 1431 N94-18644
DIHEDRAL ANGLE
Wideband electromagnetic scattering/analysis program: Far zone electromagnetic scattering from complex shapes using geometrical theory of diffraction
[AD-A268790] p 1384 N94-18187
DILUTION
Simulation of emittance dilution in electron storage ring from Compton backscattering
[DE93-017611] p 1386 N94-18503
DIMENSIONAL ANALYSIS
Multidimensional geometric quantization and U(1)-covering
[DE93-624770] p 1546 N94-17795
DIMENSIONAL MEASUREMENT
Simulation of quartz resonators p 1426 N94-18021
Survey of collision avoidance and ranging sensors for mobile robots, revision 1
[AD-A269846] p 1541 N94-18474
Overview of physical oceanographic measurements taken during the Mount Mitchell cruise to ROPME sea area
[DE93-018460] p 1497 N94-18494
DIODES
Development of a cryogenic heat pipe
[DE93-018448] p 1417 N94-18831
MOCVD-grown InGaAsP heterostructure diode lasers
[AD-A270848] p 1606 N94-19769
DIPPING
Embrittlement of surface mount solder joints by hot solder-dipped, gold-plated leads
[DE93-017659] p 1358 N94-18003
DIRAC EQUATION
Further on the current algebra of WZNW models at and away from criticality
[DE93-624809] p 1545 N94-17686
DIRECT CURRENT
DC and small-signal physical models for the AlGaAs/GaAs high electron mobility transistor
p 1401 N94-18370
DIRICHLET PROBLEM
Impulsive moving mirror model and impulsive differential equations in Banach space
[DE93-629867] p 1549 N94-18197
Finite beta plasma equilibrium in toroidally linked mirrors
[DE93-040318] p 1590 N94-19193
DISCHARGERS
Active spacecraft potential control: An ion emitter experiment for Cluster p 1330 N94-19634
DISCOVERY (ORBITER)
Return to space
[NASA-TM-109356] p 1332 N94-18955
DISCRIMINANT ANALYSIS (STATISTICS)
Application of the network discriminant function to learning
[AD-A268793] p 1540 N94-18189
DISCRIMINATION
Context-related scaling of human judgement in the multiplicative AHP, SMART and ELECTRE
[REPT-93-38] p 1611 N94-19158
DISPLACEMENT
Friction drive position transducer
[AD-D015851] p 1424 N94-17717
A benchmark bending test of a thick specimen. Part 1: Experiments
[AD-A268730] p 1360 N94-18325
Six degree of freedom fine motion positioning stage based on magnetic levitation
[DE93-017651] p 1446 N94-19547
DISPLACEMENT MEASUREMENT
Constraints on crustal structure from long period pressure and displacement measurements on the deep seafloor
[AD-A269931] p 1498 N94-18663
Fatigue resistant Ti3Al composites
[AD-A270305] p 1341 N94-18692
DISPLAY DEVICES
Polaron tunneling in high-temperature superconductors
[DE93-016880] p 1593 N94-17754
Research on man-machine productivity in aviation at Human Engineering Institute of Hangzhou University
[AD-A269952] p 1512 N94-18673
Overview of research in progress at the Center of Excellence
[NASA-CR-194329] p 1618 N94-19256
Results of a joint Navy/Air Force operational test to evaluate USAF Integrated Maintenance Information Systems (IMIS), Interactive Electronic Technical Manual (IETM) technology applied to the F/A-18 aircraft
[AD-A271322] p 1619 N94-19571
Electro-optics display research, test, and evaluation laboratory program
[AD-A270947] p 1408 N94-19751
DISSIPATION
Investigation of a matrix-model for the artificial dissipation in a cell vertex finite volume scheme for solving the Navier-Stokes equations
[DLR-FB-92-33] p 1409 N94-18076
DISSOLVED GASES
A one dimensional numerical model, with an application to the vertical distribution of dissolved oxygen in the ocean
[DE93-018481] p 1495 N94-17779
DISTRIBUTED PARAMETER SYSTEMS
A structured approach for modeling, analyzing and simulating real-time control systems
[REPT-93-044] p 1539 N94-17916
ControlShell: A real-time software framework
[AD-A269172] p 1523 N94-18879
Decomposition invariance of generalized steady-state of a 1-D diffusion system
[REPT-93-26] p 1550 N94-19141
DISTRIBUTED PROCESSING
Information technology resources assessment
[DE93-015276] p 1613 N94-17894
PARX, kernel of a system for massively parallel computers: Control of communication between processes
[ETN-93-94353] p 1533 N94-17976
An evolving infrastructure for scientific computing and the integration of new graphics technology
[DE93-017164] p 1520 N94-18133
The evolution of the PVM concurrent computing system
[DE93-017764] p 1534 N94-18482
Distributed Computing Design System (DCDS)
[AD-A270435] p 1534 N94-18509
Distributed memory parallel computers and computational fluid dynamics p 1413 N94-18568
Efficient transparent optimistic rollback recovery for distributed application programs
[AD-A268981] p 1522 N94-18696
A general theory of signal integration for fault-tolerant dynamic distributed sensor networks
[AD-A270316] p 1534 N94-18699
Computer-Aided Prototyping System (CAPS) within the software acquisition process. A case study
[AD-A268705] p 1522 N94-18786
Optimal eigenvalue computation on distributed-memory MIMD multiprocessors
[DE93-018337] p 1535 N94-18808
The intelligent processing of materials
[AD-A269250] p 1362 N94-18923
A programming paradigm for distributed-memory computers
[DE93-018336] p 1524 N94-19024
Pegasus project description
[MEMO-INF-92-75] p 1536 N94-19159
Pegasus: Operating system support for distributed multimedia systems
[MEMO-INF-92-76] p 1536 N94-19160
Experience in implementing a parallel file system
[DE93-012840] p 1536 N94-19188
ACOS: A performance based approach to build a parallel complex object server
[MEMO-INF-93-11] p 1537 N94-19198
Specification and verification of a dynamic leader election protocol in a broadcast network
[MEMO-INF-93-05] p 1558 N94-19228
Vectorized presentation-level services for scientific distributed applications
[DE93-018091] p 1537 N94-19253

Advances in architectural concepts to support distributed systems design
[MEMO-INF-93-17] p 1527 N94-19261
Toward a high performance distributed memory climate model
[DE93-019156] p 1494 N94-19298
PUMMA: Parallel Universal Matrix Multiplication Algorithms on distributed memory concurrent computers
[DE93-019163] p 1538 N94-19299
Process allocation on distributed memory parallel architectures
[ETN-93-95004] p 1538 N94-19514
The Cluster science data system: A distributed system to serve a wide international community
p 1330 N94-19638
Data-Machine Independence (DMI)
[DE93-018008] p 1539 N94-19734
NPAC distributed-parallel system feasibility study
[AD-A270972] p 1539 N94-19790
Semantic models for distributed data base management. Part 2: Development of an integral meta-model for data modeling and data base modeling
[REPT-93-08-PT-2] p 1620 N94-19795

DISTRIBUTION FUNCTIONS
On polynomials orthogonal with respect to an inner product involving differences (the general case)
[REPT-93-32] p 1551 N94-19285
Bahadur-Kiefer theorem beyond the largest observation
[PB93-197473] p 1558 N94-19325
Production and test of pseudo random elements
[ETN-93-95070] p 1559 N94-19610

DIVERTERS
Radiative divertor modeling studies
[DE93-018092] p 1590 N94-19290

DIVING (UNDERWATER)
Development of a new concept diver's watch
p 1429 N94-18041

DMSP SATELLITES
An investigation of methods for updating ionospheric scintillation models using topside in-situ plasma density measurements
[AD-A269872] p 1483 N94-18655
Atlas of SSM/I satellite ice concentration interpolated to operational ice model domains of the Arctic for 1992
[AD-A270306] p 1499 N94-18727

DOCUMENT STORAGE
EDMS: Engineering data management system. User's reference
[PB93-187391] p 1614 N94-18119
Networked MS windows 3.1 based classified document control system (CDOCS)
[DE93-017880] p 1617 N94-18984

DOCUMENTS
Document control and conduct of operations
[DE93-016555] p 1613 N94-17880
Bibliography of scientific publications of the Naval Biodynamics Laboratory, 1980 - 1992
[AD-A268886] p 1505 N94-18226
CRRES experiments, data collection, analysis and publication
[NASA-CR-192419] p 1482 N94-18610

DOPED CRYSTALS
Selective electrochemical wafer thinning for silicon characterization
[DE93-015083] p 1592 N94-17742
Photoemission studies of Zn, Co, and Gd substituted YBa2Cu3O(7-delta)
[DE93-017403] p 1597 N94-18498
Defect behavior of polycrystalline solar cell silicon
[DE93-018490] p 1468 N94-19016
Superconductivity and magnetism in niobium doped YBa2Cu3O7 related high-(Tc) ceramics
[DE93-018086] p 1601 N94-19049
Role of pressure in the study of fullerenes
[DE93-018839] p 1602 N94-19340
Final report on subcontract B076260 — borate synthesis
[DE93-019501] p 1604 N94-19565
Physical chemical studies of conducting polymers fundamental and applied
[AD-A270728] p 1374 N94-19574

DOPPLER EFFECT
Advances in laser cooling
[AD-A270152] p 1440 N94-18900
Moments of ambient Doppler spectra
[DE93-017948] p 1390 N94-19114

DOPPLER RADAR
The accuracy of monostatic and bistatic radar imaging by range-Doppler-processing with and without motion compensation
[DLR-FB-93-07] p 1384 N94-18071
Impact of shorter wavelengths on optical quality for laws
[NASA-CR-193873] p 1579 N94-18858
SPNDL: A concept for a small satellite Doppler lidar wind sounder p 1327 N94-19181

DOSAGE
Efficiency of fiber dispersion
[AD-A269740] p 1342 N94-18757
In situ observation of radiation induced amorphization of crystals with apatite structure
[DE93-018450] p 1599 N94-18816
Neutron-induced collision cascade mixing in Nb/V superlattices
[DE93-018575] p 1600 N94-18933

DOSIMETERS
Efficiency of fiber dispersion
[AD-A269740] p 1342 N94-18757

DOWNRANGE
An empirical evaluation of five circular error probable estimation techniques and a method for improving them
[AD-A266528] p 1556 N94-18397

DRAG
The performance of drag relations in the WAQUA storm surge model
[KNMI-TR-149] p 1496 N94-17923
High Reynolds number configuration development of a high-lift airfoil p 1306 N94-18424

DRIFT RATE
Time domain calculations of the second-order drift force on a floating two-dimensional object in current and waves
[REPT-93-13] p 1419 N94-19087

DROP TESTS
Vertical drop test of a Metro 3 aircraft
[AD-A270032] p 1318 N94-18789

DROP TOWERS
Free fall liquid column dynamics in a droptower
[LRT-WE-9-FB-6-1992] p 1379 N94-19491

DROPS (LIQUIDS)
Ship-produced cloud line of 13 July 1991
[DE93-016879] p 1472 N94-17986
Detection of single molecules in microspheres
[DE93-017776] p 1567 N94-18493
A coupled implicit solution method for turbulent spray combustion in propulsion systems p 1411 N94-18549
Metal slurry droplet and spray combustion
[AD-A269648] p 1349 N94-18736
Feasibility study: Monodisperse polymer particles containing laser-excitable dyes
[NASA-CR-194280] p 1373 N94-19402

DRYING
A comparison of wet and dry scrubbing systems for control of metals and dioxin/furan emissions from incinerators
[DE93-017446] p 1474 N94-18502
Evaluation of dried storage of platelets for transfusion: Physiologic integrity and hemostatic functionality
[AD-A270756] p 1507 N94-19593

DUALITY THEOREM
The theory of linear programming: Skew symmetric self-dual problems and the central path
[REPT-93-15] p 1524 N94-19089
Interior-point methodology for linear programming: Duality, sensitivity analysis and computational aspects
[REPT-93-28] p 1525 N94-19143
On the convergence of an unfeasible primal-dual interior-point method for convex programming
[REPT-93-34] p 1525 N94-19154
A polynomial primal-dual Dikin-type algorithm for linear programming
[REPT-93-36] p 1525 N94-19156

DUCTILITY
Several fundamental issues in the mechanics of inelastic behavior
[AD-A269455] p 1453 N94-18285
Fatigue resistant Ti3Al composites
[AD-A270305] p 1341 N94-18692
Development of ductile Fe3Al-based aluminides
[DE93-017865] p 1362 N94-18938
Tensile properties of as-cast iron-aluminide alloys
[DE93-017852] p 1363 N94-18975
Low-aluminum-content iron-aluminum alloys
[DE93-017862] p 1365 N94-19274
Dynamical behavior of octahedrite from the Henbury meteorite
[DE93-018834] p 1627 N94-19339

DUMMIES
Vertical drop test of a Metro 3 aircraft
[AD-A270032] p 1318 N94-18789

DUPLEXERS
Meteor burst communications improvement study
[AD-A270866] p 1393 N94-19793

DWARF STARS
Stellar coronae at the end of the main sequence: A Rosat survey of the late M dwarfs
[NASA-CR-194700] p 1628 N94-19794

DYE LASERS
The copper-pumped dye laser system at Lawrence Livermore National Laboratory
[DE93-014429] p 1435 N94-17723
Laser materials processing applications at Lawrence Livermore National Laboratory
[DE93-017976] p 1437 N94-18093
Single-transverse-mode, narrow-bandwidth pulsed tunable dye laser with hollow circular intracavity dielectric waveguide
[AD-A270022] p 1439 N94-18614
Multi-terrawatt, 100 fsec laser system using flashlamp-pumped, dye-converted Ti:sapphire as an amplifier
[DE93-017190] p 1440 N94-18889
Feasibility study: Monodisperse polymer particles containing laser-excitable dyes
[NASA-CR-194280] p 1373 N94-19402

DYES
Polarized thin films from dye-substituted polymers containing hydrophobically terminated stilbazolium radicals
[AD-D015873] p 1367 N94-17706
Detection of single molecules in microspheres
[DE93-017776] p 1567 N94-18493
Vibrational dynamics in photoinduced electron transfer
[DE93-040874] p 1567 N94-18533

DYNAMIC CHARACTERISTICS
Packaging, deployment, and panel design concepts for a truss-stiffened 7-panel precision deployable reflector with feed boom
[NASA-TM-109000] p 1333 N94-17765
The mystery of the perpetual motion clock of Geiser and Son p 1427 N94-18027
Universal measurement device for electronic watches and small clocks p 1427 N94-18029
Dynamic response analysis of composite structural members during missile launch
[AD-A270023] p 1332 N94-18760
A new approach to the study of the turbulence layer
[NASA-CR-194546] p 1487 N94-19397
Reanalysis of structure models
[ECL-93-07] p 1458 N94-19460
Study and modeling of compressible flows of flapper nozzle type potentiometric systems
[ETN-93-95012] p 1421 N94-19495
Measuring methods for evaluation of dynamic tyre properties
[ETN-93-95054] p 1381 N94-19650

DYNAMIC CONTROL
Autonomous neural network controllers for adaptive material handling
[AD-A268908] p 1540 N94-18331
Problem of control in an integral vision system: Use of a multi-agent system
[ETN-93-95007] p 1530 N94-19488

DYNAMIC LOADS
Predicted structural response of the lightweight-interceptor technology demonstration vehicle
[DE93-014676] p 1333 N94-17782
Shock-loading response of advanced materials
[DE93-018344] p 1455 N94-19033
The interpretation of optical caustics in the presence of dynamic non-uniform crack-tip motion histories: A study based on a higher order transient crack-tip expansion
[SM91-12] p 1456 N94-19130
Shock compression properties of silicon carbide
[DE93-019927] p 1373 N94-19271
Impact strength and indentation hardness of high-strength ceramics
[DE93-018833] p 1373 N94-19338
Simulation of dynamic material response with the PAGOSA code
[DE93-018285] p 1460 N94-19603

DYNAMIC MODELS
Joint stiffness estimation based on force sensor measurements in industrial manipulators
[REPT-92-053] p 1443 N94-17937
Efficient dynamic modeling of manipulators containing closed kinematic loops
[REPT-92-083] p 1444 N94-17940
A finite strain ring dynamical model for pneumatic tires
[AD-A269286] p 1444 N94-18266

DYNAMIC PRESSURE
Interferometric investigations of compressible dynamic stall over a transiently pitching airfoil
[NASA-TM-109380] p 1312 N94-19119

DYNAMIC PROGRAMMING
Using geometric techniques to improve dynamic programming algorithms for the economic lot-sizing problem and extensions
[PB93-197556] p 1528 N94-19330
Phasing strategies of the Hermes type space shuttle: Its optimization considering the thrust failures
[LAAS-93242] p 1544 N94-19361

Process allocation on distributed memory parallel architectures
[ETN-93-95004] p 1538 N94-19514
DYNAMIC RANGE
Advanced optical fiber communication systems
[AD-A269120] p 1577 N94-18254
Earth Penetration Radar Imaging System (EPRIS)
[DE93-019890] p 1391 N94-19542
DYNAMIC RESPONSE
Predicted structural response of the lightweight-interceptor technology demonstration vehicle
[DE93-014676] p 1333 N94-17782
The role of NASTRAN in the preliminary design cycle
p 1450 N94-17835
FAROW: A tool for fatigue and reliability of wind turbines
[DE93-017639] p 1465 N94-18001
Generalization of optimal control theory: Linear and nonlinear structures
[PB93-188621] p 1540 N94-18125
Dynamic response analysis of composite structural members during missile launch
[AD-A270023] p 1332 N94-18760
Effects of shock loading on a solid-solution strengthened superalloy
[DE93-018345] p 1362 N94-18809
Dynamic characterization of a lightweight, highly maneuverable spacecraft using modal and finite element analyses
[DE93-018095] p 1335 N94-18942
Shock-loading response of advanced materials
[DE93-018344] p 1455 N94-19033
Free fall liquid column dynamics in a droptower
[LRT-WE-9-FB-6-1992] p 1379 N94-19491
Simulation of dynamic material response with the PAGOSA code
[DE93-018285] p 1460 N94-19603
Blade and hub loads of ballistically damaged helicopter rotors
[AD-A270663] p 1319 N94-19781
DYNAMIC STABILITY
Synchrotron beam-loading stability with a higher RF harmonic
[DE93-014549] p 1573 N94-17726
The Twenty-First NASTRAN (R) Users' Colloquium
[NASA-CP-3203] p 1449 N94-17827
Error propagation equations and tables for estimating the uncertainty in high-speed wind tunnel test results
[DE93-018685] p 1311 N94-18275
DYNAMIC STRUCTURAL ANALYSIS
Improved omit set displacement recoveries in dynamic analysis p 1449 N94-17829
Modelling chaotic vibrations using NASTRAN
p 1449 N94-17830
Generalized seismic analysis p 1449 N94-17832
A noniterative improvement of Guyan reduction
p 1449 N94-17833
A methodology to model physical contact between structural components in NASTRAN
p 1450 N94-17836
Eigenvalue routines in NASTRAN: A comparison with the Block Lanczos method p 1450 N94-17838
Automatic A-set selection for dynamics analysis
p 1450 N94-17839
Dynamic response analysis of composite structural members during missile launch
[AD-A270023] p 1332 N94-18760
A general-purpose contact detection algorithm for nonlinear structural analysis codes
[DE93-018507] p 1455 N94-19039
Reanalysis of structure models
[ECL-93-07] p 1458 N94-19460
Computational Methods for Crashworthiness
[NASA-CP-3223] p 1458 N94-19465
Adaptive methods for nonlinear structural dynamics and crashworthiness analysis p 1458 N94-19466
Composite impact dynamics research at NASA LaRC: A review p 1458 N94-19467
Impact analysis of composite aircraft structures
p 1458 N94-19468
Explicit solution techniques for impact with contact constraints p 1459 N94-19470
Directions for computational mechanics in automotive crashworthiness p 1459 N94-19472
Crashdynamics with DYNA3D: Capabilities and research directions p 1460 N94-19475
Transient dynamics capability at Sandia National Laboratories p 1460 N94-19476
DYNAMIC TESTS
Dynamical behavior of tantalum
[DE93-017877] p 1362 N94-18919
DYNAMICAL SYSTEMS
The Twenty-First NASTRAN (R) Users' Colloquium
[NASA-CP-3203] p 1449 N94-17827
Modelling chaotic vibrations using NASTRAN
p 1449 N94-17830
Plasma properties research: Task 3
[DE93-017087] p 1583 N94-17854
An extension of Wolovich's definition of equivalence of linear systems
[MATHS-REPT-A-183] p 1547 N94-18069
The physics of cellular automata and coherence and chaos in classical many-body dynamical systems
[DE93-018021] p 1561 N94-18177
The 1992 annual report on scientific programs: A broad research program on the sciences of complexity
[DE93-018151] p 1561 N94-18178
Stability analysis through bifurcation theory, 1
p 1608 N94-18238
System dynamics and computer modeling expertise. A conceptual structure research inquiry
[AD-A269860] p 1560 N94-18410
Methods for description and control of dynamical systems and their application
[MPIS-17/1992] p 1553 N94-19522
Automated qualitative modeling of dynamic physical systems
[AD-A270835] p 1422 N94-19598
DYNAMOMETERS
Fluid dynamometer having fluid characteristic power absorption adjustment capability
[AD-D015820] p 1424 N94-17904

E

E GLASS
Mechanical properties and impact damage resistance of composites fabricated by low cost, vacuum assisted, resin transfer molding
[AD-A270361] p 1342 N94-18702
E REGION
RADARC HF ionospheric prediction program for OTH radar
[AD-A269557] p 1385 N94-18291
EARTH ATMOSPHERE
Surface fluxes important to cloud development
[DE93-016633] p 1488 N94-17715
Mixture distributions in climatological research
[DE93-014125] p 1488 N94-17942
Internal instability of nonparallel flow on an equatorial beta-plane
[AD-A268927] p 1490 N94-18486
EARTH CORE
Contributions from geomagnetic inverse theory to the study of hydromagnetic conditions near the core-mantle boundary
[NASA-CR-194303] p 1484 N94-18853
EARTH CRUST
Current (1985-1988) seismic activity in Belgium: Comparison with historical and instrumental seismic data
p 1482 N94-18624
Constraints on crustal structure from long period pressure and displacement measurements on the deep seafloor
[AD-A269931] p 1498 N94-18663
The use of velocity spectra for stacking receiver functions with application to IRIS/IDA stations OBNINSK (OBN) and ARTI (ARU), Russia
[AD-A269087] p 1483 N94-18717
Research on Earth's rotation and the effect of atmospheric pressure on vertical deformation and sea level variability
[NASA-CR-194300] p 1484 N94-18838
Shock propagation in crustal rock
[AD-A270148] p 1485 N94-18899
Analysis of regional deformation and strain accumulation data adjacent to the San Andreas fault
[NASA-CR-194072] p 1487 N94-19428
The interpretation of crustal dynamics data in terms of plate motions and regional deformation near plate boundaries
[NASA-CR-194302] p 1487 N94-19432
EARTH GRAVITATION
What can gravimetry contribute to recent and current tectonics in Belgium? p 1482 N94-18626
Research on Earth's rotation and the effect of atmospheric pressure on vertical deformation and sea level variability
[NASA-CR-194300] p 1484 N94-18838
Gravity and the geoid in the Nepal Himalaya
[NASA-CR-194166] p 1463 N94-19430
EARTH IONOSPHERE
Problems related to stimulated electromagnetic emissions, strong turbulence and ionospheric modification
[IRF-SR-212] p 1480 N94-17720
An investigation of methods for updating ionospheric scintillation models using topside in-situ plasma density measurements
[AD-A269872] p 1483 N94-18655
Using computerized tomography to determine ionospheric structures
[DE93-018903] p 1485 N94-19001
A physical model for one-dimension and time-dependent ionosphere. Part 1: Description of the model
[DE93-627958] p 1486 N94-19255
EARTH MAGNETOSPHERE
Solar flares and magnetospheric particles: Investigations based upon the ONR-602 and ONR-604 experiments
[AD-A269495] p 1629 N94-18705
ISTP Global Geospace Science. Energy transfer in geospace
[NASA-TM-109239] p 1620 N94-18851
Convection algorithms for magnetospheric particles
[AD-A270103] p 1493 N94-18871
The Wave Experiment Consortium
p 1328 N94-19623
The wideband plasma wave investigation
p 1328 N94-19627
EARTH MANTLE
The use of velocity spectra for stacking receiver functions with application to IRIS/IDA stations OBNINSK (OBN) and ARTI (ARU), Russia
[AD-A269087] p 1483 N94-18717
Contributions from geomagnetic inverse theory to the study of hydromagnetic conditions near the core-mantle boundary
[NASA-CR-194303] p 1484 N94-18853
EARTH MOVEMENTS
High resolution geological site characterization utilizing ground motion data
[AD-A268926] p 1481 N94-18485
Macroseismic study of the Dour (Belgium) earthquakes of 22 March 1987 and of Gulpen (Belgium) 17 October 1988 p 1482 N94-18625
Instrumentation developed at the Royal Observatory of Belgium for measuring slow displacements of the Earth
p 1483 N94-18628
Ground movements associated with gas hydrate production
[DE93-019887] p 1486 N94-19018
EARTH ORBITAL ENVIRONMENTS
NSWCWODET participation in Space Shuttle mission STS-46
[AD-A268875] p 1332 N94-18321
Solar flares and magnetospheric particles: Investigations based upon the ONR-602 and ONR-604 experiments
[AD-A269495] p 1629 N94-18705
LDEF update
[NASA-TM-109352] p 1334 N94-18921
Static Computer Memory Integrity Testing (SCMIT): An experiment flown on STS-40 as part of GAS payload G-616 p 1325 N94-19169
Materials flight experiment carrier capability and future flight experiments on Hitchhiker-M carrier program
p 1326 N94-19175
Limited Duration of Candidate Materials Exposure Experiment (LDCE): A Complex Autonomous Payload (CAP) using a Get Away Special (GAS) canister
p 1326 N94-19176
EARTH RADIATION BUDGET
Biophysical characterization and surface radiation balance
[NASA-CR-194659] p 1470 N94-17762
EARTH RADIATION BUDGET EXPERIMENT
The Earth radiation budget experiment: Overview of data-processing and error sources
[KNMI-TR-146] p 1481 N94-18142
EARTH RESOURCES
The ecological and environmental impacts of manmade marshes
[AD-A269213] p 1475 N94-18885
EARTH ROTATION
Research on Earth's rotation and the effect of atmospheric pressure on vertical deformation and sea level variability
[NASA-CR-194300] p 1484 N94-18838
EARTH SCIENCES
JPRS report: Science and technology. Central Eurasia: Earth Sciences
[JPRS-UES-93-004] p 1461 N94-19209
EARTH SURFACE
The land component of the global climate system with adequate spatial resolution
[DE93-018951] p 1474 N94-18183
EARTH TIDES
Instrumentation developed at the Royal Observatory of Belgium for measuring slow displacements of the Earth
p 1483 N94-18628
DYNLET1 model formulation and user's guide
[AD-A269843] p 1498 N94-18723
Acoustic travel time perturbations due to an internal tide and internal wave field in the Barents Sea
[AD-A270879] p 1499 N94-19580

EARTHQUAKE RESISTANT STRUCTURES
Generalization of optimal control theory: Linear and nonlinear structures
[PB93-188621] p 1540 N94-18125
EARTHQUAKES
Heterogeneous slip and rupture models of the San Andreas fault zone based upon three-dimensional earthquake tomography
[DE93-015037] p 1480 N94-17898
Belgian Royal Observatory Communications, Series A, No. 104, Geophysics Series No. 175
[COMMUNICATIONS-SER-A-104] p 1482 N94-18622
Historical seismicity of Hainaut, Flanders and Artois p 1482 N94-18623
Current (1985-1988) seismic activity in Belgium: Comparison with historical and instrumental seismic data p 1482 N94-18624
Macroseismic study of the Dour (Belgium) earthquakes of 22 March 1987 and of Gulpen (Belgium) 17 October 1988 p 1482 N94-18625
Analysis of regional bodywave phases from earthquakes in western China, part 2
[AD-A270125] p 1485 N94-18873
ECHOCARDIOGRAPHY
Characterization of fluid physics effects on cardiovascular response to microgravity (G-572) p 1323 N94-19163
ECOLOGY
Compilation of 1992 annual reports of the Navy ELF communications system ecological monitoring program, volume 1
[AD-A269569] p 1386 N94-18473
Compilation of 1992 annual reports of the navy ELF communications system ecological monitoring program. Volume 3: Tabs G - I
[AD-A269727] p 1388 N94-18741
International Symposium on the Ecological Effects of Arctic Airborne Contaminants — abstracts
[AD-A269955] p 1475 N94-18775
Environmental Research Program
[DE93-019101] p 1477 N94-19105
ECONOMIC ANALYSIS
The carbon dioxide emissions game: Playing the net
[DE93-017670] p 1471 N94-17821
Setting the global thermostat with an exhaustible tradeable permit system
[DE93-012911] p 1472 N94-17891
Parametric analysis of the ARIES-3D-He-3 tokamak reactor
[DE93-018293] p 1587 N94-18803
Using geometric techniques to improve dynamic programming algorithms for the economic lot-sizing problem and extensions
[PB93-197556] p 1528 N94-19330
ECONOMIC FACTORS
Fifteenth Symposium on Biotechnology for Fuels and Chemicals: Program and Abstracts
[DE93-010005] p 1376 N94-18045
ECONOMIC IMPACT
Mathematical sciences, technology, and economic competitiveness
[LC-91-60253] p 1514 N94-19478
ECOSYSTEMS
Development and evaluation of alternative radioanalytical methods, including mass spectrometry for marine materials
[DE93-625117] p 1345 N94-17691
Environmental Research Program
[DE93-019101] p 1477 N94-19105
EDDY CURRENTS
High resolution SQUID magnetometry for non-destructive evaluation
[AD-A268884] p 1447 N94-18225
EDDY VISCOSITY
Research activities at the Center for Modeling of Turbulence and Transition p 1410 N94-18546
Two-equation models for low-Reynolds-number variants p 1415 N94-18587
Direct and large eddy simulation of turbulence: Summary of the state of the art 1993 p 1416 N94-18594
Large-eddy simulation of turbulent diffusion in stably stratified shear flow p 1416 N94-18595
EDGE DETECTION
Progress in edge detection
[RR-914-I] p 1529 N94-19396
EDUCATION
Magnetic Fusion Energy Technology Fellowship: Report on survey of institutional coordinators
[DE93-014646] p 1583 N94-17739
Safeguarding our energy future
[DE93-016001] p 1466 N94-18109
Origins of solar activity. First year report, AASERT grant
[AD-A268848] p 1629 N94-18222
Teaching a computer simulation course with Ada
[AD-A267901] p 1521 N94-18308
The CMU masters in software engineering core curriculum
[AD-A268983] p 1521 N94-18453
The development of a course sequence in real-time systems design
[AD-A269459] p 1522 N94-18726
Interdisciplinary training in life science (FY 1991 ASSERT)
[AD-A269220] p 1512 N94-18886
A teaching tool for linear programming
[AD-A270240] p 1523 N94-18905
California Student Get Away Special Payload GAS-450 p 1324 N94-19164
The GAMCIT gamma ray burst detector p 1324 N94-19168
Undergraduate origins of recent science and engineering doctorate recipients
[NSF-92-332] p 1610 N94-19389
Undergraduate course and curriculum development program and calculus and the bridge to calculus program: 1992 awards
[NSF-93-24] p 1610 N94-19446
Mathematical sciences, technology, and economic competitiveness
[LC-91-60253] p 1514 N94-19478
A foundation for the 21st Century: A progressive framework for the National Science Foundation. Report of the National Science Board Commission on the future of the National Science Foundation
[NSB-92-196] p 1611 N94-19618
Guide to programs, fiscal year 1993
[NSF-92-78] p 1633 N94-19620
EFFERENT NERVOUS SYSTEMS
Coupled neural-dendritic processes: Cooperative stochastic effects and the analysis of spike trains
[AD-A270041] p 1506 N94-18793
EFFICIENCY
Efficiency of fiber dispersion
[AD-A269740] p 1342 N94-18757
EFFLUENTS
Advances in passive-remote and extractive Fourier transform infrared systems
[DE93-017402] p 1478 N94-19241
EIGENVALUES
Parallel inverse iteration with reorthogonalization
[DE93-012867] p 1533 N94-17693
Finite-dimensional singletons of the quantum anti de Sitter algebra
[DE93-624771] p 1546 N94-17810
Improved omit set displacement recoveries in dynamic analysis p 1449 N94-17829
Eigenvalue routines in NASTRAN: A comparison with the Block Lanczos method p 1450 N94-17838
Automatic A-set selection for dynamics analysis p 1450 N94-17839
A free boundary eigenvaue problem
[IPP-6/310] p 1584 N94-17981
Optimal eigenvalue computation on distributed-memory MIMD multiprocessors
[DE93-018337] p 1535 N94-18808
The Fourier analysis technique and epsilon-pseudo-eigenvalues
[DE93-018805] p 1551 N94-19337
EIGENVECTORS
Parallel inverse iteration with reorthogonalization
[DE93-012867] p 1533 N94-17693
Eigenvalue routines in NASTRAN: A comparison with the Block Lanczos method p 1450 N94-17838
EINSTEIN EQUATIONS
About symmetry of the gravitational action
[DE93-629955] p 1608 N94-18252
EJECTA
Imaging and blackbody emission spectra of hot particulates generated during laser ablation
[DE93-015818] p 1439 N94-18724
ELASTIC BARS
The longitudinal free vibrations of a fixed-free two-phase elastic bar
[AD-A268768] p 1453 N94-18387
ELASTIC BENDING
Blade and hub loads of ballistically damaged helicopter rotors
[AD-A270663] p 1319 N94-19781
ELASTIC DEFORMATION
Elastic properties of a polyimide film determined by Brillouin scattering and mechanical techniques
[DE93-017404] p 1368 N94-18098
New test method to determine modulus of elasticity of rocket grain material
[AD-A269758] p 1377 N94-18758
Effect of internal heating during hot compression testing on the stress-strain behavior and hot working characteristics of alloy 304L
[DE93-012701] p 1362 N94-18917
ELASTIC PROPERTIES
Implementation of mixed formulation elements in PC/NASTRAN p 1449 N94-17828
Improved omit set displacement recoveries in dynamic analysis p 1449 N94-17829
Phenomenological explanation of elastic anomalies in superlattices
[DE93-017475] p 1594 N94-17871
Elastic properties of a polyimide film determined by Brillouin scattering and mechanical techniques
[DE93-017404] p 1368 N94-18098
Strength optimization of C/Al metal matrix composites produced from prepregs
[DLR-FB-92-39] p 1340 N94-18122
Several fundamental issues in the mechanics of inelastic behavior
[AD-A269455] p 1453 N94-18285
Continuum modeling of materials that can undergo martensitic phase transitions
[AD-A268767] p 1360 N94-18386
The longitudinal free vibrations of a fixed-free two-phase elastic bar
[AD-A268768] p 1453 N94-18387
Constraints on crustal structure from long period pressure and displacement measurements on the deep seafloor
[AD-A269931] p 1498 N94-18663
JPRS report: Science and technology. Central Eurasia: Materials science
[JPRS-UMS-93-002] p 1339 N94-18833
HEMP 3D: A finite difference program for calculating elastic-plastic flow, appendix B
[AD-A269171] p 1418 N94-18878
A constitutive theory for rigid polyurethane foam
[DE93-011596] p 1372 N94-19059
A particle method for history-dependent materials
[DE93-018696] p 1456 N94-19060
Molecular dynamics modeling of the mechanical behavior of metallic multilayers
[DE93-017972] p 1365 N94-19263
Contribution to the identification of nonlinear behavior laws in material mechanics
[ECL-92-36] p 1458 N94-19411
ELASTIC SCATTERING
The rise of accuracy for the multichannel scattering problem solving
[DE93-630145] p 1608 N94-18253
Unitary (pi)(pi)N model of N* excitations in (pi)N and (gamma)N reactions
[DE93-017422] p 1568 N94-18826
Gamma scattering in condensed matter with high intensity Moessbauer radiation
[DE93-019461] p 1601 N94-19031
ELASTIC WAVES
Experimental investigation of wave and fracture phenomena in impacted ceramics: Experiments on sapphire
[AD-A270040] p 1372 N94-18792
Liquid sound speeds at pressure from the optical analyzer technique
[DE93-018362] p 1563 N94-19151
Seismic studies of the geologic structure and physical properties of the seabed
[AD-A270895] p 1500 N94-19747
ELASTODYNAMICS
Wave propagation near explosive sources
[AD-A270102] p 1418 N94-18870
Inverse scattering of surface waves: A new look at surface consistency
[REPT-93-25] p 1486 N94-19140
ELASTOMERS
Anomalous dielectric properties of carbon-black filled elastomers
[AD-A269378] p 1370 N94-18280
Strained ring energetic binders
[AD-A269056] p 1377 N94-18491
Polymer technology publication. Series no. 14, 1993
[PB93-195984] p 1372 N94-19052
ELASTOPLASTICITY
Measurement and analysis of three 1.5-GPa shock-wave profiles in copper
[DE93-016559] p 1451 N94-17864
ELECTRIC ARCS
Arc detection and protection in high-power antenna systems
[DE93-013272] p 1382 N94-17695
Impedence calculation with recursive folding
[ETN-93-95049] p 1406 N94-19387
ELECTRIC AUTOMOBILES
Mechanically refuelable zinc/air electric vehicle cells
[DE93-016446] p 1394 N94-17770
ELECTRIC BATTERIES
Mixed polymer electrolyte and mixed polymer electrolyte battery
[AD-D015856] p 1394 N94-17718

Evaluation of the consumption of electronic clocks
p 1408 N94-18033
Studies on gel electrolyte based on nitrile-butadiene copolymers
[AD-A269450] p 1370 N94-18282
Environmentally assisted cracking of nickel anode substrates in Li/SOCl2 cells: An engineering approach
[DE93-015130] p 1405 N94-18928
Current-potential characteristics of electrochemical systems
[DE93-040303] p 1352 N94-19192
Rationale for the power standard
[ESA-PSS-02-10-VOL-2-ISSUE-] p 1338 N94-19516

ELECTRIC CHOPPERS
The use of chopper spectrometers for cold-to-epithermal neutron scattering at IPNS
[DE93-017798] p 1598 N94-18531

ELECTRIC CONNECTORS
Analysis of high contact resistances associated with hermetic and lightning arrestor connectors
[DE93-014850] p 1395 N94-17783
Performance evaluations of demountable electrical connections
[DE93-017399] p 1396 N94-18135

ELECTRIC CONTACTS
Design and test of a low jitter metal to metal contact solid dielectric switch
[DE93-016957] p 1394 N94-17755
Analysis of high contact resistances associated with hermetic and lightning arrestor connectors
[DE93-014850] p 1395 N94-17783

ELECTRIC CURRENT
Compound-lens injector for a 19-MeV, 700-kA electron beam
[DE93-013752] p 1573 N94-17698
Application of piezoelectric stress gauges to the measurement of fast-rise-time multimegampere electric currents
[DE93-017625] p 1429 N94-18102
Toroidal solenoids in the electromagnetic field and Aharonov-Casher effect
[DE93-629861] p 1566 N94-18152
Response of transmission line systems to pulse excitation by radiation and injection methods
[DE93-015112] p 1384 N94-18210
A tunable CMOS constant current source
p 1401 N94-18369
Oligomer and mixed-metal compounds, potential multielectron transfer catalysts
[DE93-019592] p 1350 N94-19017

ELECTRIC DISCHARGES
Comparison of the modeling solutions with the hydrogen discharge data
[DE93-015115] p 1565 N94-17797
Coupled MHD and transport analysis of improved confinement D3-D discharges
[DE93-016985] p 1585 N94-18057
Broadband RF spectrum from electrostatic discharges on spacecraft
[AD-A269543] p 1385 N94-18287
Improved optical pseudospark switch
[AD-D015821] p 1580 N94-18947
Modelling ideal gas fluorides laser plasmas
[ETN-93-95073] p 1592 N94-19613

ELECTRIC FIELDS
Electrically controlled liquid-crystal heat valve
[AD-D015872] p 1443 N94-17705
Variable time-step integration for intense field effects
[DE93-013296] p 1382 N94-17909
Crystal optics of high energy gamma-beams
[DE93-630228] p 1577 N94-18217
Relaxation of polar orientational order in nonlinear optical polymers by second harmonic generation
[AD-A269059] p 1370 N94-18515
Numerical modelling of fringing fields and their use for complex permittivity measurements at high frequencies
[AD-A270198] p 1388 N94-18782
Office of Naval Research Publications/Patents /Presentations/Honors report, 1 October 1992 - 30 September 1993
[AD-A270037] p 1632 N94-18791
Convection algorithms for magnetospheric particles
[AD-A270103] p 1493 N94-18871
Three dimensional multipole decomposition of fields
[DE93-018530] p 1389 N94-19053
Correction of longitudinal errors in accelerators for heavy-ion fusion
[DE93-018656] p 1575 N94-19106
Current-potential characteristics of electrochemical systems
[DE93-040303] p 1352 N94-19192
The spherical probe Electric Field and Wave Experiment for the Cluster mission p 1328 N94-19624
The Electron Drift Instrument for Cluster
p 1329 N94-19630

ELECTRIC FILTERS
Effects of harmonics on EMI/RFI filters operating under nonlinear loading conditions
[AD-A269559] p 1388 N94-18769

ELECTRIC GENERATORS
Report to Congress: Comprehensive Program Plan for Advanced Turbine Systems
[DE93-016718] p 1467 N94-18475

ELECTRIC IGNITION
Aluminum powder/water reaction ignited by electrical pulsed power
[AD-A269223] p 1376 N94-17840

ELECTRIC MOTOR VEHICLES
SUNRAYCE 1993: Working safely with lead-acid batteries and photovoltaic power systems
[DE93-016553] p 1464 N94-17712
The ANL electric vehicle battery R&D program for DOE-EHP
[DE93-017414] p 1394 N94-17750
Mechanically refuelable zinc/air electric vehicle cells
[DE93-016446] p 1394 N94-17770
S/EV 1992: Solar and Electric Vehicles. Volume 1: Proceedings
[DE93-015762] p 1445 N94-18307
Conceptual design of a sodium sulfur cell for US electric van batteries
[DE93-018683] p 1405 N94-19035

ELECTRIC MOTORS
Compatibility of refrigerants and lubricants with motor materials, volume 1
[DE93-040216] p 1350 N94-18895
Compatibility of refrigerants and lubricants with motor materials, volume 2
[DE93-040217] p 1350 N94-18896
Compatibility of refrigerants and lubricants with motor materials, volume 3
[DE93-040218] p 1352 N94-19191
Design of power electronics for TVC EMA systems
[NASA-CR-193839] p 1407 N94-19642

ELECTRIC POTENTIAL
A tunable CMOS constant current source
p 1401 N94-18369
Office of Naval Research Publications/Patents /Presentations/Honors report, 1 October 1992 - 30 September 1993
[AD-A270037] p 1632 N94-18791
Plasma contactor development for Space Station
[NASA-TM-106425] p 1587 N94-18861
Correction of longitudinal errors in accelerators for heavy-ion fusion
[DE93-018656] p 1575 N94-19106
Simulation of transient effects in the heavy ion fusion injectors
[DE93-018658] p 1575 N94-19107

ELECTRIC POWER
EIA publications directory, 1992
[DE93-016833] p 1617 N94-18983

ELECTRIC POWER PLANTS
Learning control of large-scale systems
[MATHS-REPT-A-186] p 1544 N94-19408

ELECTRIC POWER SUPPLIES
Design of power electronics for TVC EMA systems
[NASA-CR-193839] p 1407 N94-19642

ELECTRIC POWER TRANSMISSION
Effects of harmonics on EMI/RFI filters operating under nonlinear loading conditions
[AD-A269559] p 1388 N94-18769

ELECTRIC PROPULSION
The ANL electric vehicle battery R&D program for DOE-EHP
[DE93-017414] p 1394 N94-17750
Low power arcjet system spacecraft impacts
[NASA-TM-106307] p 1336 N94-17856
S/EV 1992: Solar and Electric Vehicles. Volume 1: Proceedings
[DE93-015762] p 1445 N94-18307
Constant-thrust orbit-raising transfer charts
[AD-A269088] p 1334 N94-18718

ELECTRIC STIMULI
The brain electrical activity in different G situations
[AERONAUTICA-ACTA-A-372-199]
p 1507 N94-19523

ELECTRIC SWITCHES
Design and test of a low jitter metal to metal contact solid dielectric switch
[DE93-016957] p 1394 N94-17755
Plasma-puff initiation of high Coulomb transfer switches
[NASA-CR-193186] p 1591 N94-19441

ELECTRICAL ENGINEERING
Program descriptions
[NSF-92-123] p 1531 N94-19619

ELECTRICAL FAULTS
High-power microwave breakdown of dielectric interfaces
[AD-A268844] p 1397 N94-18318
On timing faults in digital logic circuits
[AD-A268714] p 1402 N94-18400
Heavy Ion Fusion Injector Program
[DE93-018706] p 1575 N94-18997
Impedence calculation with recursive folding
[ETN-93-95049] p 1406 N94-19387
Results of a joint Navy/Air Force operational test to evaluate USAF Integrated Maintenance Information Systems (IMIS), Interactive Electronic Technical Manual (IETM) technology applied to the F/A-18 aircraft
[AD-A271322] p 1619 N94-19571

ELECTRICAL IMPEDANCE
A radial transmission line material measurement apparatus
[DE93-018508] p 1394 N94-17780
Optically controlled active impedance element and filters employing the same
[AD-D015863] p 1396 N94-18062
Numerical modelling of fringing fields and their use for complex permittivity measurements at high frequencies
[AD-A270198] p 1388 N94-18782

ELECTRICAL INSULATION
Workshop on multifactor aging mechanisms and models
[AD-A268668] p 1397 N94-18311
Compatibility of refrigerants and lubricants with motor materials, volume 1
[DE93-040216] p 1350 N94-18895

ELECTRICAL MEASUREMENT
Electric measurement of Lavet motors
p 1408 N94-18022
Control of torque in stepping motors of quartz watches and clocks p 1408 N94-18023
Numerical modelling of fringing fields and their use for complex permittivity measurements at high frequencies
[AD-A270198] p 1388 N94-18782
Bienzyme sensors based on electrically wired peroxidase
[AD-A271364] p 1374 N94-19585

ELECTRICAL PROPERTIES
Vibrational and electronic properties of clusters and ultrathin films
[DE93-012291] p 1367 N94-17678
Lattice damage in ion-implanted compound semiconductors and its effect on electrical activation
[DE93-015907] p 1593 N94-17845
Ultra-shallow box-like profiles fabricated by pulsed UV-laser doping process
[DE93-017221] p 1437 N94-18083
Performance evaluations of demountable electrical connections
[DE93-017399] p 1396 N94-18135
Photorefractive tungsten bronze crystals for optical computing
[AD-A268859] p 1596 N94-18320
Intracellular physiology of the rat suprachiasmatic nucleus: Electrical properties, neurotransmission and effects of neuromodulators
[AD-A268829] p 1505 N94-18538
Conceptual design of a sodium sulfur cell for US electric van batteries
[DE93-018683] p 1405 N94-19035
Isolation mechanisms in III-V devices
[AD-A271197] p 1605 N94-19717

ELECTRICAL RESISTANCE
Electron mobility in high resistivity silicon
[REPT-93-007] p 1565 N94-17933
Deep ion implantation into manganin to modify its pressure and electrothermocharacteristics
[DE93-630229] p 1359 N94-18218
Theoretical and experimental studies of quantum wells
[AD-A271180] p 1606 N94-19741

ELECTRICAL RESISTIVITY
The Aerocapacitor: A carbon aerogel based supercapacitor
[DE93-016537] p 1395 N94-17849
Excimer laser induced permanent electrical conductivity and nanostructures in polymers
[DE93-015965] p 1368 N94-17946
AEOLUS-IT MHD simulation code based on a toroidally incompressible plasma model
[DE93-788461] p 1586 N94-18157
Resonant absorption of Alfven waves near a neutral point
[DE93-628761] p 1586 N94-18172
High pressure metallization of Mott Insulators: Magnetic, structural and electronic properties
[DE93-018295] p 1404 N94-18805
Pressure induced metallization of the Mott Insulator 6(sub 2)
[DE93-018296] p 1600 N94-18969
Studies of deep levels in high resistivity silicon detectors irradiated by high fluence fast neutrons using a thermally stimulated current spectrometer
[DE93-016133] p 1602 N94-19258

Metallization and charge-transfer gap closure of transition-metal iodides under pressure
[DE93-040301] p 1353 N94-19538
Electro-optic beam steering using non-linear organic materials
[AD-A270809] p 1374 N94-19577

ELECTRO-OPTICAL EFFECT
Photo-induced and electrooptic properties of (Pb,La)(Zr,Ti)O3 films
[DE93-017496] p 1371 N94-18519
Operational parameters of an opto-electronic neural network employing fixed planar holographic interconnects
[DE93-018795] p 1433 N94-19000
RF phase stabilization for RF photocathode gun through electro-optical monitoring
[DE93-019059] p 1406 N94-19310

ELECTRO-OPTICS
Quantum optoelectronics technical digest, 1993. Voolume 8: Postconference edition
[AD-A268209] p 1576 N94-17887
Evaluation of materials proposed for the construction of the Plasma Electrode Pockels Cell (PEPC) on beamlet
[DE93-016952] p 1584 N94-17988
Calibration of a high frequency monostatic acoustic echosounder
[AD-A268901] p 1481 N94-18229
Integrated photonics research volume 10. Conference edition
[AD-A269298] p 1577 N94-18298
Optical computing. Organization of the 1993 Photonics Science Topical Meetings. Technical digest series, volume 7
[AD-A269025] p 1578 N94-18332
Quantum Optoelectronics. Organization of the 1993 photonics science topical meetings. Technical digest series, volume 8
[AD-A269026] p 1578 N94-18488
Advanced Solid-State Lasers/Compact Blue-Green Lasers. 1993 technical digest series. Volume 2: Organization of the 1993 photonics science topical meetings
[AD-A269058] p 1438 N94-18492
Photo-induced and electrooptic properties of (Pb,La)(Zr,Ti)O3 films
[DE93-017496] p 1371 N94-18519
Photonics in Switching: Organization of the 1993 photonics science topical meetings. Technical digest
[AD-A269024] p 1578 N94-18528
Optical and transport properties of metallic and semiconductor nanostructures
[AD-A270009] p 1598 N94-18609
Integration of ferroelectric/semiconductor thin films for SLM and photorefractive applications
[AD-A268645] p 1598 N94-18633
Integrated Photonics Research: Post-deadline papers
[AD-A269232] p 1609 N94-18908
Ultrafast Electronics and Optoelectronics: Summaries of papers. Technical digest conference edition
[AD-A269233] p 1405 N94-18909
The star identification, pointing and tracking system of UVSTAR, an attached payload instrument system for the Shuttle Hitchhiker-M platform p 1326 N94-19179
Optoelectronic packaging: A review
[DE93-040059] p 1515 N94-19535
Electro-optic beam steering using non-linear organic materials
[AD-A270809] p 1374 N94-19577
Ionized-cluster beam/partially ionized beam deposition of electro-optical and nonlinear optical organic materials and device development
[AD-A270832] p 1604 N94-19596
The deposition of electro-optic films on semiconductors
[AD-A270823] p 1605 N94-19664
Electro-optics display research, test, and evaluation laboratory program
[AD-A270947] p 1408 N94-19751

ELECTROCATALYSTS
Ionic and molecular environments in heterogeneous electrocatalysis: Studies by radioactive labeling and LEED/AUGER spectroscopy
[AD-A268850] p 1567 N94-18766
Electrocatalysts for oxygen electrodes
[DE93-040446] p 1354 N94-19653

ELECTROCHEMICAL CORROSION
Workshop on multifactor aging mechanisms and models
[AD-A268668] p 1397 N94-18311

ELECTROCHEMICAL OXIDATION
Kinetic studies of electrochemical generation of Ag(II) ion and catalytic oxidation of selected organics
[DE93-016601] p 1352 N94-19240

ELECTROCHEMISTRY
Applications of scanning tunneling microscopy to electrochemistry
[AD-A269129] p 1348 N94-18255
Novel electrochemical materials prepared by sol-gel chemistry
[AD-A269060] p 1578 N94-18405
Ionic and molecular environments in heterogeneous electrocatalysis: Studies by radioactive labeling and LEED/AUGER spectroscopy
[AD-A268850] p 1567 N94-18766
The effects of radiolysis on the corrosion and stress corrosion behavior of 316 stainless steels
[DE93-019933] p 1363 N94-19021
Energy Conversion and Storage Program
[DE93-018602] p 1469 N94-19098
Current-potential characteristics of electrochemical systems
[DE93-040303] p 1352 N94-19192

ELECTRODEPOSITION
Potential dependent structural changes of underpotentially deposited copper on an iodine treated platinum surface determined in situ by surface EXAFS and its polarization dependence
[AD-A269890] p 1360 N94-18687
Polycrystalline thin-film cadmium telluride solar cells fabricated by electrodeposition
[DE93-018201] p 1468 N94-18944
Use of shape memory alloys in the robust control of smart structures
[AD-A270827] p 1366 N94-19594

ELECTRODES
The Aerocapacitor: A carbon aerogel based supercapacitor
[DE93-016537] p 1395 N94-17849
Surface second harmonic generation studies of stepped Ag(111) electrode surfaces
[AD-A265205] p 1594 N94-17876
Field emitter array RF amplifier development project, phase 1, option 1
[AD-A268687] p 1396 N94-18293
Ionic and molecular environments in heterogeneous electrocatalysis: Studies by radioactive labeling and LEED/AUGER spectroscopy
[AD-A268850] p 1567 N94-18766
Current-potential characteristics of electrochemical systems
[DE93-040303] p 1352 N94-19192
Bienzyme sensors based on electrically wired peroxidase
[AD-A271364] p 1374 N94-19585
Electrocatalysts for oxygen electrodes
[DE93-040446] p 1354 N94-19653
Photosynthetic reaction centers as active molecular electronic components, phase 1
[AD-A271388] p 1503 N94-19757

ELECTROKINETICS
Electrokinetic transport of heterogeneous particles in suspensions
[NASA-CR-194478] p 1353 N94-19367

ELECTROLESS DEPOSITION
Solderability perservative coatings: Electroless tin versus organic azoles
[DE93-017634] p 1370 N94-18477
Current-potential characteristics of electrochemical systems
[DE93-040303] p 1352 N94-19192

ELECTROLYTES
Mechanically refuelable zinc/air electric vehicle cells
[DE93-016446] p 1394 N94-17770
Surface second harmonic generation studies of stepped Ag(111) electrode surfaces
[AD-A265205] p 1594 N94-17876
Studies on gel electrolyte based on nitrile-butadiene copolymers
[AD-A269450] p 1370 N94-18282

ELECTROLYTIC CELLS
Oxygen reduction at a stabilized zirconia interface with Y(1-x)Ca(x)MnO3 or La(1-x)Sr(x)MnO3 cathode materials
[DE93-015681] p 1593 N94-17747
Fuel cell systems program plan, fiscal year 1993
[DE93-017828] p 1466 N94-18103

ELECTROMAGNETIC ABSORPTION
Absorption and x ray measurements from ultra-intense laser-plasma interactions
[DE93-016538] p 1585 N94-18115
Optical and transport properties of metallic and semiconductor nanostructures
[AD-A270009] p 1598 N94-18609

ELECTROMAGNETIC COMPATIBILITY
Electromagnetic environmental effects compendium
[AD-A270441] p 1387 N94-18512
Laboratory test and evaluation report of the essex model 60C-0037-2 molecular sieve oxygen generating system
[AD-A269967] p 1445 N94-18778

ELECTROMAGNETIC FIELDS
Advanced methods for the computation of particle beam transport and the computation of electromagnetic fields and beam-cavity interactions
[DE93-018160] p 1573 N94-17807
Toroidal solenoids in the electromagnetic field and Aharonov-Casher effect
[DE93-629861] p 1566 N94-18152
The asymptotic theory of the reflection and transmission of a pulsed electromagnetic beam field at a planar interface separating two dispersive media
[AD-A269033] p 1385 N94-18404
Theory of electromagnetic waves propagating in nonlinear anisotropic optical materials
[AD-A269305] p 1386 N94-18469
Compilation of 1992 annual reports of the Navy ELF communications system ecological monitoring program, volume 1
[AD-A269569] p 1386 N94-18473
Electromagnetic environmental effects compendium
[AD-A270441] p 1387 N94-18512
Compilation of 1992 annual reports of the navy ELF communications system ecological monitoring program. Volume 3: Tabs G - I
[AD-A269727] p 1388 N94-18741
Compilation of 1992 annual reports of the navy ELF communications system ecological monitoring program, volume 2
[AD-A269726] p 1388 N94-18751

ELECTROMAGNETIC INTERACTIONS
Gauge coupling unification in superstring derived standard-like models
[DE93-624801] p 1607 N94-17950
Gauge unification of fundamental forces: The story of success
[DE93-624813] p 1383 N94-17952
Extraction of Z(prime) coupling data from Z(prime) (yields) jj at the LHC and SSC
[DE93-018576] p 1570 N94-19096

ELECTROMAGNETIC INTERFERENCE
Low power arcjet system spacecraft impacts
[NASA-TM-106307] p 1336 N94-17856
Broadband RF spectrum from electrostatic discharges on spacecraft
[AD-A269543] p 1385 N94-18287
Electromagnetic environmental effects compendium
[AD-A270441] p 1387 N94-18512
Effects of harmonics on EMI/RFI filters operating under nonlinear loading conditions
[AD-A269559] p 1388 N94-18769
Laboratory test and evaluation report of the essex model 60C-0037-2 molecular sieve oxygen generating system
[AD-A269967] p 1445 N94-18778

ELECTROMAGNETIC MEASUREMENT
Survey of collision avoidance and ranging sensors for mobile robots, revision 1
[AD-A269846] p 1541 N94-18474
STAFF (Spatio-Temporal Analysis of Field Fluctuations) experiment for the Cluster mission p 1328 N94-19625

ELECTROMAGNETIC PROPERTIES
Waveguide and resonator perturbation techniques for measuring chirality and non-reciprocity of biisotropic materials
[PB93-187243] p 1384 N94-18116
Electromagnetic environmental effects compendium
[AD-A270441] p 1387 N94-18512

ELECTROMAGNETIC PULSES
PVDF measurement of soft x ray induced shock and filter debris impulse
[DE93-017633] p 1382 N94-17806
Wake field in electron-positron plasmas
[DE93-624929] p 1584 N94-17955
Limitations on the fidelity of 100 fs pulses produced by chirped pulse amplification
[DE93-017167] p 1396 N94-17991
Response of transmission line systems to pulse excitation by radiation and injection methods
[DE93-015112] p 1384 N94-18210
The asymptotic theory of the reflection and transmission of a pulsed electromagnetic beam field at a planar interface separating two dispersive media
[AD-A269033] p 1385 N94-18404
Self-organized criticality and the Barkhausen effect in amorphous and polycrystalline metals
[AD-A269617] p 1361 N94-18735
Effect of EMP fields on cell membrane potentials
[DE93-015819] p 1503 N94-19341

ELECTROMAGNETIC RADIATION
Microwave scattering from TAE modes
[DE93-018170] p 1583 N94-17809
Wake field in electron-positron plasmas
[DE93-624929] p 1584 N94-17955
Crystal optics of high energy gamma-beams
[DE93-630228] p 1577 N94-18217

Theory of electromagnetic waves propagating in nonlinear anisotropic optical materials
[AD-A269305] p 1386 N94-18469
Electromagnetic environmental effects compendium
[AD-A270441] p 1387 N94-18512
Polarimetric statistics of electromagnetic waves scattered by distributed targets
[PB93-195907] p 1389 N94-18951
STAFF (Spatio-Temporal Analysis of Field Fluctuations) experiment for the Cluster mission p 1328 N94-19625

ELECTROMAGNETIC SCATTERING
Wideband electromagnetic scattering/analysis program: Far zone electromagnetic scattering from complex shapes using geometrical theory of diffraction
[AD-A268790] p 1384 N94-18187
Dispersion effects on millimeter wavelength attenuation efficiencies for a variety of fibers
[AD-A268992] p 1386 N94-18454
Solution of the Poisson equation with application to radar imaging
[PB93-195865] p 1389 N94-18950
Polarimetric statistics of electromagnetic waves scattered by distributed targets
[PB93-195907] p 1389 N94-18951
Comparative evaluation of Kirchhoff, perturbation, and full wave methods for rough surface scattering
[AD-A271198] p 1392 N94-19718

ELECTROMAGNETIC SHIELDING
Electromagnetic environmental effects compendium
[AD-A270441] p 1387 N94-18512

ELECTROMAGNETIC WAVE TRANSMISSION
Problems related to stimulated electromagnetic emissions, strong turbulence and ionospheric modification
[IRF-SR-212] p 1480 N94-17720
Optical design for photonics. Organization of the 1993 Photonics Science Topical Meetings. Technical digest series, volume 9
[AD-A269027] p 1578 N94-18396
The asymptotic theory of the reflection and transmission of a pulsed electromagnetic beam field at a planar interface separating two dispersive media
[AD-A269033] p 1385 N94-18404
Theory of electromagnetic waves propagating in nonlinear anisotropic optical materials
[AD-A269305] p 1386 N94-18469
Millimeter wave reflectivity measurement system
[AD-A270008] p 1387 N94-18601
Comparative evaluation of Kirchhoff, perturbation, and full wave methods for rough surface scattering
[AD-A271198] p 1392 N94-19718

ELECTROMAGNETISM
General geometry PIC for MIMD computers
[AD-A269085] p 1534 N94-18767
Engineering research, development and technology thrust area report, FY92
[DE93-016334] p 1632 N94-18856

ELECTROMECHANICAL DEVICES
Atomic-scale friction measurements using friction force microscopy. Part 1: General principles and new measurement techniques
[AD-A270749] p 1446 N94-19678
Microtribology of magnetic media
[AD-A271209] p 1407 N94-19722

ELECTROMECHANICS
Pulsed power supply for Nova Upgrade
[DE93-019626] p 1441 N94-19307
The electromechanical properties of tetragonal BaTiO3 and PbTiO3 single crystals
[DE93-019008] p 1603 N94-19550

ELECTROMIGRATION
The microstructural mechanism of electromigration failure in narrow interconnects of Al alloys
[DE93-018598] p 1365 N94-19282

ELECTROMYOGRAPHY
Control of shoulder muscles during goal directed movements
[PB93-195139] p 1504 N94-18080

ELECTRON ACCELERATORS
Three-dimensional simulation analysis of the first sections of a standing-wave free-electron laser two-beam accelerator
[DE93-016977] p 1436 N94-17869

ELECTRON BEAMS
Compound-lens injector for a 19-MeV, 700-kA electron beam
[DE93-013752] p 1573 N94-17698
Measuring emittance using beam position monitors
[DE93-014470] p 1434 N94-17709
Decoherence and recoherence of beam in phase space
[DE93-014885] p 1573 N94-17784
Three-dimensional simulation analysis of the first sections of a standing-wave free-electron laser two-beam accelerator
[DE93-016977] p 1436 N94-17869
Plasma klystron amplifier
[AD-D015819] p 1395 N94-17903
FEL experiment with a focusing wiggler
[DE93-768586] p 1438 N94-18160
Simulation of emittance dilution in electron storage ring from Compton backscattering
[DE93-017611] p 1386 N94-18503
Designs for a 10.6 micrometer electromagnetic wiggler Free-Electron Laser (FEL)
[AD-A269695] p 1439 N94-18576
A tunable compact high power far-infrared grating free-electron laser
[AD-A269875] p 1440 N94-18771
Novel electron beam cathode
[AD-A270106] p 1404 N94-18872
Foil support structure for large electron guns
[DE93-018478] p 1322 N94-18890
Laser powered beam conditioner for free-electron lasers and synchrotrons
[DE93-017821] p 1441 N94-18974
Coherence and linewidth studies of a 4-nm high power FEL
[DE93-018533] p 1441 N94-19030
The Electron Drift Instrument for Cluster
p 1329 N94-19630
Compact free electron lasers for medical applications
[AD-A271272] p 1442 N94-19729

ELECTRON BUNCHING
Study of coupled-bunch collective effects in the ALS
[DE93-019236] p 1575 N94-19558

ELECTRON CAPTURE
Electron paramagnetic resonance of the ns(sup 1) centers in crystals
[DE93-628793] p 1595 N94-18173
Search for resonant electron transfer and double excitation in Kr(sup 34+) + H2 collisions
[DE93-018776] p 1569 N94-18999

ELECTRON CYCLOTRON HEATING
Experiments on nonlinear absorption of ECH waves in MTX and a comparison with theory
[DE93-019158] p 1589 N94-19074
Electron cyclotron resonance heating in the microwave tokamak experiment
[DE93-018083] p 1590 N94-19289

ELECTRON DENSITY (CONCENTRATION)
Using computerized tomography to determine ionospheric structures
[DE93-018904] p 1485 N94-19002
The effects of magnetic storm phases on f-layer irregularities from auroral to equatorial latitudes
[AD-A267388] p 1486 N94-19008
A physical model for one-dimension and time-dependent ionosphere. Part 1: Description of the model
[DE93-627958] p 1486 N94-19255

ELECTRON DIFFRACTION
Optical frequency doubling at adsorbates of silver(110) surface
[ETN-93-94837] p 1603 N94-19355

ELECTRON EMISSION
RF vacuum microelectronics
[AD-A269454] p 1396 N94-18284
Novel electron beam cathode
[AD-A270106] p 1404 N94-18872
Low-energy continuum-electron emission at 0 degrees from O(q+) + He collisions
[DE93-018777] p 1570 N94-19108
Experimental study of interactions of highly charged ions with atoms at keV energies
[DE93-040222] p 1571 N94-19257

ELECTRON ENERGY
Nonlinear Thomson scattering of intense laser pulse from beams and plasmas
[AD-A269556] p 1438 N94-18460
Simulation of emittance dilution in electron storage ring from Compton backscattering
[DE93-017611] p 1386 N94-18503
Designs for a 10.6 micrometer electromagnetic wiggler Free-Electron Laser (FEL)
[AD-A269695] p 1439 N94-18576
Atomic resolution electron energy loss spectroscopy in the scanning transmission electron microscope
[DE93-015334] p 1352 N94-19239
ICRF direct electron heating experiments in TFTR
[DE93-017657] p 1590 N94-19273
Radiative divertor modeling studies
[DE93-018092] p 1590 N94-19290

ELECTRON GUNS
The Intense Slow Positron Source concept: A theoretical perspective on a proposed INEL Facility
[DE93-013675] p 1564 N94-17738
Foil support structure for large electron guns
[DE93-018478] p 1322 N94-18890
RF phase stabilization for RF photocathode gun through electro-optical monitoring
[DE93-019059] p 1406 N94-19310

ELECTRON IMPACT
Electron impact excitation of copper atoms
[DE93-017995] p 1363 N94-18939
Electron impact polarization and correlation properties of the inert gases
[DE93-018358] p 1570 N94-19125

ELECTRON MICROSCOPES
Tunneling microscopy of semiconductors
[AD-A270232] p 1600 N94-18904
Atomic resolution electron energy loss spectroscopy in the scanning transmission electron microscope
[DE93-015334] p 1352 N94-19239

ELECTRON MICROSCOPY
Construction of a scanning tunneling microscope in liquid media: Studies of the preparation of the graphite surface and the chemical cleaning of indium phosphide
[ECL-92-25] p 1353 N94-19406
A Sandia Technology Bulletin: Testing technology, July 1993
[DE93-040197] p 1633 N94-19537

ELECTRON MOBILITY
Electron mobility in high resistivity silicon
[REPT-93-007] p 1565 N94-17933
IR materials producibility
[AD-A268849] p 1577 N94-18223
Suppressed electron-phonon scattering in superlattices
[AD-A270834] p 1604 N94-19597
Isolation mechanisms in III-V devices
[AD-A271197] p 1605 N94-19717

ELECTRON ORBITALS
Relativistic configuration interaction calculation of the correlation energies of heliumlike ions
[DE93-018093] p 1571 N94-19201

ELECTRON PARAMAGNETIC RESONANCE
Electron paramagnetic resonance of the ns(sup 1) centers in crystals
[DE93-628793] p 1595 N94-18173

ELECTRON PHONON INTERACTIONS
Solid-state dynamics in novel semiconductor nanostructures
[AD-A271249] p 1605 N94-19725

ELECTRON PLASMA
Transformation of energy and momentum due to Landau damping in space
[DE93-624921] p 1581 N94-17689
Optical design for photonics. Organization of the 1993 Photonics Science Topical Meetings. Technical digest series, volume 9
[AD-A269027] p 1578 N94-18396

ELECTRON PROBES
Atomic resolution electron energy loss spectroscopy in the scanning transmission electron microscope
[DE93-015334] p 1352 N94-19239
PEACE: A Plasma Electron and Current Experiment
p 1329 N94-19632

ELECTRON RECOMBINATION
Examination of charge carriers dynamics in silicon and silicon solar cells with photoinduced laser beam deflection
[ETN-93-95060] p 1470 N94-19654

ELECTRON SCATTERING
Compound-lens injector for a 19-MeV, 700-kA electron beam
[DE93-013752] p 1573 N94-17698
Spin-integrated and spin-dependent photoelectron diffraction
[DE93-016546] p 1565 N94-17850
Low-energy continuum-electron emission at 0 degrees from O(q+) + He collisions
[DE93-018777] p 1570 N94-19108
Single sided tomography of extremely large dense objects
[DE93-017993] p 1580 N94-19268
An ab initio Monte Carlo study of low energy positron and electron implantation in elemental metals and multilayers
[DE93-019847] p 1603 N94-19541
Suppressed electron-phonon scattering in superlattices
[AD-A270834] p 1604 N94-19597

ELECTRON SPECTROSCOPY
Guidelines for the expression of uncertainties in surface chemical analysis by Auger Electron Spectroscopy (AES) and X ray Photoelectron Spectroscopy (XPS)
[NPL-DMM(A)-99] p 1346 N94-17900

ELECTRON SPIN
Electron paramagnetic resonance of the ns(sup 1) centers in crystals
[DE93-628793] p 1595 N94-18173

ELECTRON STATES
Characterization of diamond film nucleation and growth surface
[AD-A269400] p 1597 N94-18459

Molecular nonlinear optical susceptibilities in condensed phases
[AD-A270200] p 1568 N94-18784

Electron impact polarization and correlation properties of the inert gases
[DE93-018358] p 1570 N94-19125

Theoretical and experimental studies of quantum wells
[AD-A271180] p 1606 N94-19741

ELECTRON TRANSFER

Pulse radiolytic studies of electron transfer processes and applications to solar photochemistry
[DE93-018715] p 1464 N94-17781

Vibrational dynamics in photoinduced electron transfer
[DE93-040874] p 1567 N94-18533

Search for resonant electron transfer and double excitation in Kr(sup 34+) + H2 collisions
[DE93-018776] p 1569 N94-18999

Oligomer and mixed-metal compounds, potential multielectron transfer catalysts
[DE93-019592] p 1350 N94-19017

Low-energy continuum-electron emission at 0 degrees from O(q+) + He collisions
[DE93-018777] p 1570 N94-19108

LLE Review
[DE93-017618] p 1602 N94-19123

Kinetic studies of electrochemical generation of Ag(II) ion and catalytic oxidation of selected organics
[DE93-016601] p 1352 N94-19240

Experimental study of interactions of highly charged ions with atoms at keV energies
[DE93-040222] p 1571 N94-19257

ICRF direct electron heating experiments in TFTR
[DE93-017857] p 1590 N94-19273

The direct synthesis of organic and organometallic-containing MICA-type aluminosilicates
[DE93-019001] p 1373 N94-19321

ELECTRON TRANSITIONS

Hydrolysis reaction and positronium decay in silica gels
[AD-A270028] p 1371 N94-18713

ELECTRON TUNNELING

Synthesis and study of high-T(sub c) superconducting electronic materials
[AD-A268851] p 1402 N94-18390

Tunneling microscopy of semiconductors
[AD-A270232] p 1600 N94-18904

Construction of a scanning tunneling microscope in liquid media: Studies of the preparation of the graphite surface and the chemical cleaning of indium phosphide
[ECL-92-25] p 1353 N94-19406

ELECTRON-POSITRON PAIRS

Measurement of the energy of horizontal cosmic ray muons
[KFK-5163] p 1631 N94-19505

ELECTRON-POSITRON PLASMAS

Wake field in electron-positron plasmas
[DE93-624929] p 1584 N94-17955

ELECTRONIC COUNTERMEASURES

Electromagnetic environmental effects compendium
[AD-A270441] p 1387 N94-18512

ELECTRONIC EQUIPMENT

A radial transmission line material measurement apparatus
[DE93-018508] p 1394 N94-17780

Microstructurally based thermomechanical fatigue lifetime model of solder joints for electronic applications
[DE93-016508] p 1452 N94-17995

Synthesis techniques and analysis tool for on-chip fault-tolerance
[AD-A269148] p 1521 N94-18259

ELECTRONIC EQUIPMENT TESTS

VLSI for high-speed digital signal processing
[AD-A270406] p 1404 N94-18706

Attitude sensor package p 1325 N94-19172

ELECTRONIC MAIL

Securing electronic mail: The risks and future of electronic mail
[DE93-017187] p 1383 N94-17994

ELECTRONIC PACKAGING

Low power signal processing research at Stanford
p 1393 N94-18351

Silicon MCM substrates for integration of 3-5 photonic devices and CMOS IC's
[DE93-017894] p 1405 N94-19112

Optoelectronic packaging: A review
[DE93-040059] p 1515 N94-19535

ELECTRONIC TRANSDUCERS

Data acquisition in aerodynamic research
p 1431 N94-18644

ELECTRONIC WARFARE

Military applications of high-accuracy frequency standards and clocks
[AD-A269303] p 1430 N94-18299

ELECTRONICS

Results of a joint Navy/Air Force operational test to evaluate USAF Integrated Maintenance Information Systems (IMIS), Interactive Electronic Technical Manual (IETM) technology applied to the F/A-18 aircraft
[AD-A271322] p 1619 N94-19571

ELECTRONS

Compound-lens injector for a 19-MeV, 700-kA electron beam
[DE93-013752] p 1573 N94-17698

Correlated charge-changing ion-atom collisions
[DE93-018717] p 1564 N94-17775

Spin-integrated and spin-dependent photoelectron diffraction
[DE93-016546] p 1565 N94-17850

Observations of MeV electrons and scattered light from intense, subpicosecond laser-plasma interactions
[DE93-017153] p 1435 N94-17855

Variable time-step integration for intense field effects
[DE93-013296] p 1382 N94-17909

Global zones of particle precipitation as observed EXOS-C
[AD-A268758] p 1481 N94-18467

Harmonic generation at high intensities
[DE93-018632] p 1572 N94-19283

An ab initio Monte Carlo study of low energy positron and electron implantation in elemental metals and multilayers
[DE93-019847] p 1603 N94-19541

Suppressed electron-phonon scattering in superlattices
[AD-A270834] p 1604 N94-19597

PEACE: A Plasma Electron and Current Experiment
p 1329 N94-19632

ELECTROPHORESIS

Electrokinetic transport of heterogeneous particles in suspensions
[NASA-CR-194478] p 1353 N94-19367

ELECTROPHYSIOLOGY

Intracellular physiology of the rat suprachiasmatic nucleus: Electrical properties, neurotransmission and effects of neuromodulators
[AD-A268829] p 1505 N94-18538

ELECTROSLAG REFINING

Commercialization effort in support of electroslag-casting technology
[DE93-017988] p 1366 N94-19733

ELECTROSTATIC PROBES

The spherical probe Electric Field and Wave Experiment for the Cluster mission p 1328 N94-19624

ELECTROSTATICS

Electrostatic micrometers: Recent developments and perspectives of uses in clock and watch making
p 1425 N94-18014

Nonlinear Thomson scattering of intense laser pulse from beams and plasmas
[AD-A269556] p 1438 N94-18460

Designs for a 10.6 micrometer electromagnetic wiggler Free-Electron Laser (FEL)
[AD-A269695] p 1439 N94-18576

Heavy Ion Fusion Injector Program
[DE93-018706] p 1575 N94-18997

Three dimensional multipole decomposition of fields
[DE93-018530] p 1389 N94-19053

ELECTROSTRICTION

Office of Naval Research Publications/Patents /Presentations/Honors report, 1 October 1992 - 30 September 1993
[AD-A270037] p 1632 N94-18791

ELEMENTARY EXCITATIONS

Synthesis and study of high-T(sub c) superconducting electronic materials
[AD-A268851] p 1402 N94-18390

Molecular nonlinear optical susceptibilities in condensed phases
[AD-A270200] p 1568 N94-18784

ELEMENTARY PARTICLE INTERACTIONS

The PAPAGENO Partonic Monte-Carlo Program
[DE93-018524] p 1571 N94-19247

ELEVATION

Gravity and the geoid in the Nepal Himalaya
[NASA-CR-194166] p 1463 N94-19430

ELLIPSOMETRY

In-situ growth monitoring of molecular beam epitaxy processes
[AD-A269287] p 1598 N94-18616

ELLIPTIC DIFFERENTIAL EQUATIONS

Functional analysis of subelliptic operators on lie groups
[PB93-194793] p 1547 N94-18077

L(sub p)-regularity of subelliptic operators on Lie groups
[PB93-194785] p 1549 N94-18948

A priori estimates and existence of positive solutions of a superlinear polyharmonic equation
[REPT-93-12] p 1550 N94-19086

Existence of a maximal solution for quasimonotone elliptic systems
[REPT-93-30] p 1550 N94-19153

A comparison of iterative methods for a model coupled system of elliptic equations
[DE93-040482] p 1553 N94-19655

ELLIPTIC FUNCTIONS

Feasibility of a wind-ellipse criterion in a vortex advisory system for Schiphol Airport
[NLR-TP-91384-U] p 1315 N94-17733

Programmable linear phase digital filters
[AD-A270413] p 1404 N94-18709

A priori estimates and existence of positive solutions of a superlinear polyharmonic equation
[REPT-93-12] p 1550 N94-19086

ELLIPTICAL ORBITS

Schroedinger's hope
[AD-A270988] p 1581 N94-19772

EMBEDDED COMPUTER SYSTEMS

Embedded Computer Performance Measurement (ECPM). Advanced avionics subsystems and technology multiprocessor ECPM software documentation
[AD-A269921] p 1320 N94-18658

A research program in empirical computer science
[NASA-CR-194069] p 1530 N94-19429

EMBRITTLEMENT

Embrittlement of surface mount solder joints by hot solder-dipped, gold-plated leads
[DE93-017659] p 1358 N94-18003

Effects of irradiation temperature on embrittlement of nuclear pressure vessel steels
[DE93-015428] p 1359 N94-18245

Low-aluminum-content iron-aluminum alloys
[DE93-017862] p 1365 N94-19274

EMISSION

Land-use related sources of CO2, CH4 and N2O: Current global emissions and projections for the period 1990-2100
[PB93-194819] p 1475 N94-18949

EMISSION SPECTRA

Analysis of neon soft x ray spectra from short-pulse laser-produced plasmas
[DE93-014420] p 1582 N94-17708

Rapid analysis of mixed waste samples via the optical emission from laser initiated microplasmas
[DE93-014563] p 1582 N94-17727

Observations of comets with the IUE
[NASA-CR-193652] p 1624 N94-17843

Spectral radiance measurements on a bluff body stabilized flame: Characterization of the IR signature
[PB93-195899] p 1347 N94-18081

Imaging and blackbody emission spectra of hot particulates generated during laser ablation
[DE93-015818] p 1439 N94-18724

Determination of nitrogen to carbon abundance ratios from transition layer emission lines
[NASA-CR-191921] p 1622 N94-19421

Spectrophotometry of emission-line stars in the magellanic clouds
[NASA-CR-194082] p 1628 N94-19425

Ultraviolet observations of clusters of Wolf-Rayet stars in the SBm3 galaxy NGC 4214 and Ultraviolet and optical observations of LINER's
[NASA-CR-194307] p 1622 N94-19431

Spectrally and temporally resolved laser emission from vertical cavity surface emitting lasers
[DE93-019410] p 1442 N94-19563

EMISSIVITY

Development of a multi-point two-color pyrometer for tube and wall temperature and emissivity measurement at the CFFF
[DE93-014716] p 1429 N94-18207

EMITTANCE

Measuring emittance using beam position monitors
[DE93-014470] p 1434 N94-17709

Simulation of emittance dilution in electron storage ring from Compton backscattering
[DE93-017611] p 1386 N94-18503

Longitudinal beam dynamics with RF noise
[DE93-018649] p 1574 N94-18994

Induction accelerator development for heavy ion fusion
[DE93-019228] p 1591 N94-19479

Transverse beam combiner for ILSE
[DE93-019239] p 1591 N94-19559

Total hemispherical emittance of Niobium-1 percent zirconium fuel cladding for the SP-100 space reactor
[AD-A270456] p 1576 N94-19589

EMITTERS

Quantum optoelectronics technical digest, 1993. Voolume 8: Postconference edition
[AD-A268209] p 1576 N94-17887

RF vacuum microelectronics
[AD-A269454] p 1396 N94-18284

Field emitter array RF amplifier development project, phase 1, option 1
[AD-A268687] p 1396 N94-18293
EMPLOYMENT
Computing professionals: Changing needs for the 1990's
[B-030] p 1515 N94-19401
ENCAPSULATING
Polymerizable lipids in the development of controlled release carriers
[AD-D015789] p 1368 N94-17982
ENDOCRINOLOGY
Space research on organs and tissues
p 1503 N94-19214
ENERGETIC PARTICLES
Dense energetic compounds of C, H, N, and O atoms. 3: 5-(4-nitro-(1,2,5) oxadiazolyl)-5H-(1,2,3) triazolo (4,5-c)(1,2,5) oxadiazole
[AD-A268715] p 1338 N94-18314
The LET spectrum and its uncertainty during the CRRES mission
[AD-A269977] p 1630 N94-18676
Solar flares and magnetospheric particles: Investigations based upon the ONR-602 and ONR-604 experiments
[AD-A269495] p 1629 N94-18705
Advanced fusion diagnostics
[DE93-040085] p 1589 N94-19133
High rate resistive plate chambers: An inexpensive, fast, large area detector of energetic charged particles for accelerator and non-accelerator applications
[DE93-018664] p 1572 N94-19545
RAPID: The imaging energetic particle spectrometer on Cluster p 1329 N94-19633
ENERGY CONSERVATION
Safeguarding our energy future
[DE93-016001] p 1466 N94-18109
Energy Efficiency and Renewable Energy Program
[DE93-017936] p 1468 N94-18986
ENERGY CONSUMPTION
Techniques for low consumption circuits
p 1428 N94-18032
Evaluation of the consumption of electronic clocks
p 1408 N94-18033
Seasonal variability of wind electric potential in the US
[DE93-018182] p 1493 N94-19051
ENERGY CONVERSION
Energy Conversion and Storage Program
[DE93-018602] p 1469 N94-19098
ENERGY CONVERSION EFFICIENCY
Simplified processing for 23 percent-efficient silicon concentrator solar cells
[DE93-015018] p 1464 N94-17787
Performance mapping of the STM4-120 kinematic Stirling engine using a statistical design of experiments method
[DE93-015132] p 1464 N94-17798
Fin-efficiency calculation for condensation in the presence of noncondensable gases
[DE93-017684] p 1409 N94-18004
Feasibility survey of thermoelectric conversion technology using semiconductors
[DE93-520882] p 1595 N94-18105
First on-sun test of NaK pool-boiler solar receiver
[DE93-015003] p 1466 N94-18208
Tunable synchronously pumped intracavity two-stage optical frequency upconversion
[AD-A269105] p 1438 N94-18250
Silicon concentrator solar cell research
[DE93-018489] p 1468 N94-19015
Defect behavior of polycrystalline solar cell silicon
[DE93-018490] p 1468 N94-19016
ENERGY DISSIPATION
Evaluation of the consumption of electronic clocks
p 1408 N94-18033
Conductive garments to prevent Radio-Frequency (RF) burns
[AD-D015832] p 1512 N94-18730
Conversion of ADC pulse heights into MIP units: NUMASS test data, September 1991
[USIP-93-03] p 1432 N94-18848
EXANA: A program for analysing extended energy loss fine structures, EXELFS spectra
[USIP-92-01] p 1525 N94-19145
Atomic resolution electron energy loss spectroscopy in the scanning transmission electron microscope
[DE93-015334] p 1352 N94-19239
Contribution to the study of the additional losses in coil elements used in static converters
[ECL-92-60] p 1406 N94-19297
Energy loss measurement of cosmic ray muons
[KFK-5158] p 1631 N94-19504
ENERGY DISTRIBUTION
Chemical dynamics in time and energy space
[DE93-018595] p 1350 N94-19097
ENERGY GAPS (SOLID STATE)
Fundamental properties and device applications of Ge(x)Si(1-x)/Si superlattices (supplemental)
[AD-A269212] p 1600 N94-18884
Studies of deep levels in high resistivity silicon detectors irradiated by high fluence fast neutrons using a thermally stimulated current spectrometer
[DE93-016133] p 1602 N94-19258
ENERGY LEVELS
Proof of the feasibility of coherent and incoherent schemes for pumping a gamma ray laser
[AD-A269173] p 1440 N94-18880
Studies of deep levels in high resistivity silicon detectors irradiated by high fluence fast neutrons using a thermally stimulated current spectrometer
[DE93-016133] p 1602 N94-19258
Unimolecular photodissociation dynamics of ketene (CH2CO): The singlet/triplet branching ratio and experimental observation of the vibrational level thresholds of the transition-state
[DE93-019252] p 1352 N94-19304
ENERGY METHODS
A free energy simulation method based study of interfacial segregation
[DE93-019462] p 1364 N94-19032
ENERGY POLICY
Visibility impairment assessment: Importance of using theoretically derived optical characterizations
[DE93-017147] p 1470 N94-17749
Cost effective energy strategies for the reduction of CO2 emissions in the United States: Country report for ETSAP Annex 4
[DE93-016842] p 1472 N94-17852
Safeguarding our energy future
[DE93-016001] p 1466 N94-18109
Trends in Information Management at Department of Energy Headquarters
[DE93-017197] p 1615 N94-18496
National Program Plan Fuel Cells in Transportation
[DE93-017557] p 1469 N94-19346
ENERGY REQUIREMENTS
Regenerative fuel cells for High Altitude Long Endurance Solar Powered Aircraft
[DE93-016991] p 1465 N94-17853
Techniques for low consumption circuits
p 1428 N94-18032
Ultra low power CMOS technology
p 1401 N94-18373
ENERGY SPECTRA
On the difference caused by CP violation in the energy spectra of pions in K(sup (+-))(yields)(pi)(+-)(pi)(+-)(pi)-+ decays
[DE93-624828] p 1564 N94-17687
Investigation of the relative abundance of heavy versus light nuclei in primary cosmic rays using underground muon bundles
[DE93-017601] p 1630 N94-17818
EXANA: A program for analysing extended energy loss fine structures, EXELFS spectra
[USIP-92-01] p 1525 N94-19145
Measurement of the energy of horizontal cosmic ray muons
[KFK-5163] p 1631 N94-19505
ENERGY STORAGE
Regenerative fuel cells for High Altitude Long Endurance Solar Powered Aircraft
[DE93-016991] p 1465 N94-17853
Energy Conversion and Storage Program
[DE93-018602] p 1469 N94-19098
Pulsed power supply for Nova Upgrade
[DE93-019626] p 1441 N94-19307
ENERGY TECHNOLOGY
Cost effective energy strategies for the reduction of CO2 emissions in the United States: Country report for ETSAP Annex 4
[DE93-016842] p 1472 N94-17852
Fuel cell systems program plan, fiscal year 1993
[DE93-017828] p 1466 N94-18103
Safeguarding our energy future
[DE93-016001] p 1466 N94-18109
An evolving infrastructure for scientific computing and the integration of new graphics technology
[DE93-017164] p 1520 N94-18133
Workshop on Innovation in Materials Processing and Manufacture: Exploratory Concepts for Energy Applications
[DE93-017674] p 1467 N94-18478
Trends in Information Management at Department of Energy Headquarters
[DE93-017197] p 1615 N94-18496
EIA publications directory, 1992
[DE93-016833] p 1617 N94-18983
Energy Efficiency and Renewable Energy Program
[DE93-017936] p 1468 N94-18986
Energy Conversion and Storage Program
[DE93-018602] p 1469 N94-19098
ENERGY TRANSFER
Thermodynamic theory of exergy analysis
[PB93-187847] p 1607 N94-18120
Experimental and theoretical investigation of surface chemistry induced by direct and indirect electronic excitation
[AD-A268846] p 1348 N94-18221
Proton transfer dynamics and cluster ion fragmentation in phenol/ammonia cLusters
[AD-A269133] p 1348 N94-18256
Temperature, kinetic energy, and rotational temperature dependences for the reactions of Ar(+)(2)P3/2 with O2 and CO
[AD-A268974] p 1567 N94-18526
The use of chopper spectrometers for cold-to-epithermal neutron scattering at IPNS
[DE93-017798] p 1598 N94-18531
Full Boltzmann discrete spectral wave model, implementation and nondimensional tests
[AD-A269885] p 1498 N94-18685
ISTP Global Geospace Science. Energy transfer in geospace
[NASA-TM-109239] p 1620 N94-18851
Shock propagation in crustal rock
[AD-A270148] p 1485 N94-18899
Advanced fusion diagnostics
[DE93-040085] p 1589 N94-19133
Excited atomic bromine energy transfer and quenching mechanisms
[AD-A270672] p 1572 N94-19607
Theoretical studies of turbulence and anomalous transport in toroidal confinement devices
[DE93-040684] p 1592 N94-19656
ENGINE DESIGN
Overview of STOVL aircraft propulsion research offtakes and vertical lift systems
[NASA-TM-106387] p 1321 N94-19353
ENGINE PARTS
Studies of dynamic contact of ceramics and alloys for advanced heat engines
[DE93-016366] p 1368 N94-18110
ENGINE TESTS
Technology test bed
[NASA-TM-109354] p 1322 N94-18953
ENGINEERING
Mathematical sciences, technology, and economic competitiveness
[LC-91-60253] p 1514 N94-19478
A foundation for the 21st Century: A progressive framework for the National Science Foundation. Report of the National Science Board Commission on the future of the National Science Foundation
[NSB-92-196] p 1611 N94-19618
Guide to programs, fiscal year 1993
[NSF-92-78] p 1633 N94-19620
ENGINEERING MANAGEMENT
EDMS: Engineering data management system. User's reference
[PB93-187391] p 1614 N94-18119
ENGINEERS
Magnetic Fusion Energy Technology Fellowship: Report on survey of institutional coordinators
[DE93-014646] p 1583 N94-17739
ENTHALPY
Techniques for the estimation of Heats of Explosion (HEX) using thermochemical codes
[AD-A268584] p 1609 N94-18310
ENTRAPMENT
Resonance Raman and photophysical studies of transition metal complexes in solution and entrapped in zeolites
[DE93-019892] p 1363 N94-19019
ENTROPY
Thermodynamics of computation and information distance
[DE93-012730] p 1517 N94-17812
Evolution of r-process elements in the hot supernova bubble
[DE93-017169] p 1624 N94-17897
FEEST: A method for tabulating equation of state and opacity tables
[DE93-017965] p 1347 N94-18092
Structure, thermodynamics, and dynamical properties of supercooled liquids
[DE93-788387] p 1607 N94-18211
Regenerator optimization for Stirling cycle refrigeration
[DE93-018468] p 1380 N94-18818
ENVIRONMENT EFFECTS
Air pollution effects field research facility. 3: UV-B exposure and monitoring system
[DE93-013098] p 1470 N94-17773
Single STAGE Rocket Technology (SSRT) DC-X test program environmental assessment
[AD-A265940] p 1337 N94-17879

Overview of physical oceanographic measurements taken during the Mount Mitchell cruise to ROPME sea area
[DE93-018460] p 1497 N94-18494
Electromagnetic environmental effects compendium
[AD-A270441] p 1387 N94-18512
Compilation of 1992 annual reports of the navy ELF communications system ecological monitoring program. Volume 3: Tabs G - I
[AD-A269727] p 1388 N94-18741
Effects of the Mount Pinatubo eruption on solar insolation: Four case studies
[DE93-018454] p 1475 N94-18817
Penetrating radiation environment and effects study
[AD-A270126] p 1485 N94-18874
Ecological and environmental impacts of construction in the coastal zone
[AD-A269196] p 1475 N94-18881
The ecological and environmental impacts of manmade marshes
[AD-A269213] p 1475 N94-18885
Environmental Research Program
[DE93-019101] p 1477 N94-19105
National Program Plan Fuel Cells in Transportation
[DE93-017557] p 1469 N94-19346
Calamity weather: Environmental calamities and meteorology p 1495 N94-19703

ENVIRONMENT MANAGEMENT
Setting the global thermostat with an exhaustible tradeable permit system
[DE93-012911] p 1472 N94-17891
Environmental restoration and waste management five-year plan, fiscal years 1994-1998. Volume 3: Public concerns
[DOE/S-00097P-VOL-3] p 1475 N94-18835

ENVIRONMENT MODELS
Land-use related sources of CO2, CH4 and N2O: Current global emissions and projections for the period 1990-2100
[PB93-194819] p 1475 N94-18949

ENVIRONMENT POLLUTION
Improving the biodegradative capacity of subsurface bacteria
[DE93-013171] p 1501 N94-18051

ENVIRONMENT PROTECTION
Development and evaluation of alternative radioanalytical methods, including mass spectrometry for marine materials
[DE93-625117] p 1345 N94-17691
Title 1 implementation: Status report on nonattainment areas
[DE93-017677] p 1471 N94-17777
The carbon dioxide emissions game: Playing the net
[DE93-017670] p 1471 N94-17821
A comparison of wet and dry scrubbing systems for control of metals and dioxin/furan emissions from incinerators
[DE93-017446] p 1474 N94-18502
New applications for high average power beams
[DE93-018845] p 1439 N94-18522
Advances in passive-remote and extractive Fourier transform infrared systems
[DE93-017402] p 1478 N94-19241

ENVIRONMENTAL CHEMISTRY
Energy efficiency and the environment: Innovative ways to improve air quality in the Los Angeles Basin
[DE93-016964] p 1473 N94-18050
Program descriptions
[NSF-92-123] p 1531 N94-19619

ENVIRONMENTAL CONTROL
An emulator for testing HVAC-control and energy management systems
[VTT-TIED-1337] p 1444 N94-17974
Lunar base Controlled Ecological Life Support System (LCELSS): Preliminary conceptual design study
[NASA-CR-188479] p 1511 N94-18484
Environmental control and life support
[ESA-PSS-03-40-ISSUE-1] p 1513 N94-19442

ENVIRONMENTAL ENGINEERING
Program descriptions
[NSF-92-123] p 1531 N94-19619

ENVIRONMENTAL MONITORING
Air pollution effects field research facility. 3: UV-B exposure and monitoring system
[DE93-013098] p 1470 N94-17773
Screening analysis for chlorine-free alternative refrigerants to replace R-22 in air conditioning applications
[DE93-015920] p 1367 N94-17847
Pantex Plant Meteorological Monitoring Program
[DE93-018495] p 1493 N94-19127
Penetrometer compatible, fiber-optic sensor for continuous monitoring of chlorinated hydrocarbons: Field test results
[DE93-017974] p 1352 N94-19266
Fiber optic Raman spectrograph for in situ environmental monitoring
[DE93-019466] p 1478 N94-19305
Report of the Experts Meeting on Reference Climatological Stations (RCS) and National Climate Data Catalogues (NCC)
[WMO-TD-535] p 1494 N94-19312

ENVIRONMENTAL QUALITY
Environmental restoration and waste management five-year plan, fiscal years 1994-1998. Volume 3: Public concerns
[DOE/S-00097P-VOL-3] p 1475 N94-18835

ENVIRONMENTAL SURVEYS
Compilation of 1992 annual reports of the navy ELF communications system ecological monitoring program, volume 2
[AD-A269726] p 1388 N94-18751
Development and characterization of adiabatic shear prone tungsten heavy alloys
[AD-A270477] p 1366 N94-19673

ENVIRONMENTAL TESTS
NSWCWODET participation in Space Shuttle mission STS-46
[AD-A268875] p 1332 N94-18321
Analysis of bolted and bonded composite
[AD-A267792] p 1453 N94-18382
Laboratory test and evaluation report of the essex model 60C-0037-2 molecular sieve oxygen generating system
[AD-A269967] p 1445 N94-18778
LDEF update
[NASA-TM-109352] p 1334 N94-18921
Materials flight experiment carrier capability and future flight experiments on Hitchhiker-M carrier program
p 1326 N94-19175
Limited Duration of Candidate Materials Exposure Experiment (LDCE): A Complex Autonomous Payload (CAP) using a Get Away Special (GAS) canister
p 1326 N94-19176

ENZYME ACTIVITY
Improving the biodegradative capacity of subsurface bacteria
[DE93-013171] p 1501 N94-18051
Microbial degradation of poly-b-esters: A mechanistic study, cellulose acetate biodegradability
[AD-A271368] p 1374 N94-19586

ENZYMES
Polymerizable lipids in the development of controlled release carriers
[AD-D015789] p 1368 N94-17982
The c-jun gene expression in human cells exposed to either ionizing radiation or hydrogen peroxide
[DE93-017436] p 1502 N94-18476
Bienzyme sensors based on electrically wired peroxidase
[AD-A271364] p 1374 N94-19585
Microbial degradation of poly-b-esters: A mechanistic study, cellulose acetate biodegradability
[AD-A271368] p 1374 N94-19586

EPHEMERIDES
Absolute positioning by collecting Global Positioning System (GPS) data along short baselines
[AD-A271324] p 1317 N94-19572

EPIDEMIOLOGY
US Army aviation epidemiology data register: Prevalence of refractive error among US aircrew members
[AD-A269550] p 1505 N94-18289

EPIDERMIS
Evaluation of the nickel release by horological products p 1367 N94-18009

EPITAXY
Gallium arsenide-based ternary compounds and multi-band-gap solar cell research
[DE93-010049] p 1467 N94-18483
Growth of structures for integrated optoelectronic devices
[AD-A269014] p 1598 N94-18527
Integration of ferroelectric/semiconductor thin films for SLM and photorefractive applications
[AD-A268645] p 1598 N94-18633
Joint services electronics program
[AD-A269383] p 1403 N94-18638
Growth of epitaxial semiconductor alloys and superlattices with continuously variable composition by pulsed-laser ablation
[DE93-018726] p 1601 N94-18998

EPOXY COMPOUNDS
Remote cure monitoring of polymeric resins by laser Raman spectroscopy
[DE93-016445] p 1369 N94-18112

EPOXY MATRIX COMPOSITES
Evaluation of the production-grade class 4 flextensional transducer shell
[AD-A268796] p 1340 N94-18201
Mechanical properties and impact damage resistance of composites fabricated by low cost, vacuum assisted, resin transfer molding
[AD-A270361] p 1342 N94-18702

EPOXY RESINS
Remote cure monitoring of polymeric resins by laser Raman spectroscopy
[DE93-016445] p 1369 N94-18112
Mechanical properties and impact damage resistance of composites fabricated by low cost, vacuum assisted, resin transfer molding
[AD-A270361] p 1342 N94-18702
Bienzyme sensors based on electrically wired peroxidase
[AD-A271364] p 1374 N94-19585

EQUATIONS OF MOTION
Effects of transverse coupling on transverse beam size, simulation and measurements
[DE93-017804] p 1574 N94-18972
ISAC: A tool for aeroservoelastic modeling and analysis
[NASA-TM-109031] p 1321 N94-19316

EQUATIONS OF STATE
Direct Monte Carlo simulation of the chemical equilibrium composition of detonation products
[DE93-014559] p 1376 N94-17751
A new multiphase equation of state for iron
[DE93-017629] p 1357 N94-17819
FEEST: A method for tabulating equation of state and opacity tables
[DE93-017965] p 1347 N94-18092
Heavy-ion collisions and the nuclear equation of state
[DE93-019263] p 1566 N94-18104
Toward a characterization of the debris cloud created in a hypervelocity impact on a thin plate
[AD-A269190] p 1455 N94-18864
Sandia equation of state data base: Seslan file
[DE93-018693] p 1618 N94-19101

EQUATORIAL REGIONS
Internal instability of nonparallel flow on an equatorial beta-plane
[AD-A268927] p 1490 N94-18486
The activities of equatorial anticyclones of the Western Pacific and the South China Sea and their effects on the tracks of typhoon movement
[AD-A269954] p 1492 N94-18675
The effects of magnetic storm phases on f-layer irregularities from auroral to equatorial latitudes
[AD-A267388] p 1486 N94-19008

EQUATORS
Internal instability of nonparallel flow on an equatorial beta-plane
[AD-A268927] p 1490 N94-18486

EQUIVALENCE
An extension of Wolovich's definition of equivalence of linear systems
[MATHS-REPT-A-183] p 1547 N94-18069
Equivalence and reduction of hidden Markov models
[AD-A270762] p 1560 N94-19768

EQUIVALENT CIRCUITS
Synchrotron beam-loading stability with a higher RF harmonic
[DE93-014549] p 1573 N94-17726

EROSION
Using the Tritium Plasma Experiment to evaluate ITER PFC safety
[DE93-016614] p 1582 N94-17713
Thermal analysis of coatings and substrate materials during a disruption in fusion reactors
[DE93-017688] p 1588 N94-18971

ERROR ANALYSIS
The Earth radiation budget experiment: Overview of data-processing and error sources
[KNMI-TR-146] p 1481 N94-18142
Error propagation equations and tables for estimating the uncertainty in high-speed wind tunnel test results
[DE93-018685] p 1311 N94-18275
An empirical evaluation of five circular error probable estimation techniques and a method for improving them
[AD-A266528] p 1556 N94-18397
A comparison of single-station backazimuth estimates with regional event locations in the Central Appalachians
[AD-A269897] p 1483 N94-18690
Validation of a-posteriori error estimators by numerical approach
[AD-A269493] p 1549 N94-18697
A finite element scheme for shock capturing
[AD-A270182] p 1417 N94-18755
Correction of longitudinal errors in accelerators for heavy-ion fusion
[DE93-018656] p 1575 N94-19106
A parallel hashed oct-tree N-body algorithm
[DE93-012654] p 1526 N94-19205
Sensitivity and uncertainty analysis of Markov reward models
[MEMO-INF-92-89] p 1559 N94-19386

Refinement of unit cell parameters by least-squares: Comments on an old technique and the development of a new computer program
[AD-A270610] p 1531 N94-19590

ERROR CORRECTING CODES
Multichannel error correction code decoder
[NASA-TM-106331] p 1333 N94-19313

ERROR DETECTION CODES
An efficient implementation of error-valued semantics on imperative machines
[DE93-014658] p 1516 N94-17740

ERRORS
An efficient implementation of error-valued semantics on imperative machines
[DE93-014658] p 1516 N94-17740
Verification of 3I retrievals vis-a-vis radiosonde observations
[KNMI-TR-150] p 1488 N94-17924
An analytical approach to error localization by using information derived from error signature
[REPT-93-023] p 1518 N94-17960
The Earth radiation budget experiment: Overview of data-processing and error sources
[KNMI-TR-146] p 1481 N94-18142
Technology, design, simulation, and evaluation for SEP-hardened circuits p 1399 N94-18352
Analytic approximations of an integral in remote sensing
[AD-A270085] p 1463 N94-18800
Statistical learning theory and algorithms
[AD-A270209] p 1523 N94-18901

ESSENTIALLY NON-OSCILLATORY SCHEMES
Computational Fluid Dynamics
[VKI-LS-1993-04] p 1412 N94-18557
High order non-oscillatory schemes for the compressible Euler equations p 1412 N94-18558
ENO schemes on unstructured meshes
p 1412 N94-18561

ESTIMATING
Joint stiffness estimation based on force sensor measurements in industrial manipulators
[REPT-92-053] p 1443 N94-17937
Flight test techniques for aircraft parameter estimation in ground effect
[AD-A270058] p 1318 N94-18795
Spectral analysis on the canonical autoregressive decomposition
[AD-A270083] p 1549 N94-18798
Estimating the oceanic sound speed environmental for long-range acoustic propagation
[AD-A270231] p 1499 N94-18903

ESTUARIES
ADCIRC: An advanced three-dimensional circulation model for shelves, coasts, and estuaries. Report 3: Development of a tidal constituent database for the western North Atlantic and Gulf of Mexico
[AD-A268685] p 1497 N94-18455
Ecological and environmental impacts of construction in the coastal zone
[AD-A269196] p 1475 N94-18881

ETA-MESONS
Eta-nucleon interaction and nuclear production of eta mesons
[DE93-018469] p 1571 N94-19259

ETCHING
High- and low-temperature bonding techniques for microstructures
[DE93-017173] p 1595 N94-17992
Photovoltaic concentrator initiative: Concentrator cell development
[DE93-018505] p 1466 N94-18335

ETHANE
Conversion of ethane and of propane to higher olefin hydrocarbons
[DE93-015282] p 1347 N94-18194

EUCLIDEAN GEOMETRY
An annealing approach to multi-facility location problems in euclidean spaces
[REPT-93-022] p 1547 N94-17928
A geometric algorithm for the Euclidean 1-center problem
[REPT-93-001] p 1519 N94-17975

EULER EQUATIONS OF MOTION
High-lift system analysis method using unstructured meshes p 1307 N94-18426
High order non-oscillatory schemes for the compressible Euler equations p 1412 N94-18558
A multigrid acceleration technique for computing steady solutions to the equations of compressible flow
p 1412 N94-18559
ENO schemes on unstructured meshes
p 1412 N94-18561
Multidimensional wave decompositions for the Euler equations p 1413 N94-18562
Variational approaches to CFD: Applications to potential Euler and Navier-Stokes equations
p 1413 N94-18565
UUGM code development
[AD-A269945] p 1416 N94-18671
On positivity preserving finite volume schemes for compressible Euler equations
[NASA-CR-191534] p 1551 N94-19317
Three dimensional network generation and Euler calculation for a wing fuselage canard configuration
[MBB-LME-211-S-PUB-511-A] p 1319 N94-19500

EULER-LAGRANGE EQUATION
Fluid-structure-interaction analyses of reactor vessel using improved hybrid Lagrangian Eulerian code ALICE-II
[DE93-015536] p 1409 N94-18248

EURECA (ESA)
Superfluid Helium On-Orbit Transfer (SHOOT) flight demonstration p 1327 N94-19185

EUROPE
Eastern Europe: A climatological study
[AD-A269200] p 1493 N94-18883

EUROPEAN AIRBUS
High-lift design for large civil aircraft
p 1310 N94-18445

EUROPEAN SPACE AGENCY
Report on the activities of Space Science Department, 1990 - mid 1992
[ESA-SP-1161] p 1633 N94-19404
Rationale for the power standard
[ESA-PSS-02-10-VOL-2-ISSUE-] p 1338 N94-19516

EUTECTIC COMPOSITES
Field emission cathode and vacuum microelectronic microwave amplifier development
[AD-A269526] p 1403 N94-18639

EUTECTICS
Wetting behavior of alternative solder alloys
[DE93-016730] p 1359 N94-18127

EVALUATION
The stability and utility of the ESPRIT project, MUSiC, performance-based indicators of usability and tools: An evaluation of the usability of the NPL iSDX telephone system
[NPL-DITC-213/92] p 1613 N94-17925

EVAPORATION
Finite element modeling of evaporation and condensation during sol-gel film and fiber formation
[DE93-017655] p 1345 N94-17820
Temperature lowering in cryogenic chemical-synthesis techniques and system
[DE93-018348] p 1562 N94-18810

EVAPORATORS
Performance mapping of the STM4-120 kinematic Stirling engine using a statistical design of experiments method
[DE93-015132] p 1464 N94-17798

EXCIMER LASERS
Mechanical properties of excimer laser modified titanium surfaces
[DE93-012663] p 1358 N94-17875
Excimer laser induced permanent electrical conductivity and nanostructures in polymers
[DE93-015965] p 1368 N94-17946
Interaction of intense lasers and relativistic electron beams with solids, gases and plasmas
[AD-A269655] p 1439 N94-18737

EXCITATION
Observations of MeV electrons and scattered light from intense, subpicosecond laser-plasma interactions
[DE93-017153] p 1435 N94-17855
Response of transmission line systems to pulse excitation by radiation and injection methods
[DE93-015112] p 1384 N94-18210
Metal Film Surface Plasmon Resonance (MFSPR) fibre couplers
[AD-A268871] p 1579 N94-18635
Search for resonant electron transfer and double excitation in Kr(sup 34+) + H2 collisions
[DE93-018776] p 1569 N94-18999
Electron impact polarization and correlation properties of the inert gases
[DE93-018358] p 1570 N94-19125

EXCITONS
Polaron tunneling in high-temperature superconductors
[DE93-016880] p 1593 N94-17754
Quantum optoelectronics technical digest, 1993. Voolume 8: Postconference edition
[AD-A268209] p 1576 N94-17887
Molecular nonlinear optical susceptibilities in condensed phases
[AD-A270200] p 1568 N94-18784

EXCRETION
Nuclear Medicine Program
[DE93-013896] p 1504 N94-17699

EXERCISE PHYSIOLOGY
Road march performance of special operations soldiers carrying various loads and load distributions
[AD-A269198] p 1512 N94-18882

EXHAUST EMISSION
Visibility impairment assessment: Importance of using theoretically derived optical characterizations
[DE93-017147] p 1470 N94-17749
Title 1 implementation: Status report on nonattainment areas
[DE93-017677] p 1471 N94-17777
Data collection plan for phase 2 Alternative Fuels Bus Data Collection Program
[DE93-010047] p 1378 N94-18913

EXHAUST GASES
Title 1 implementation: Status report on nonattainment areas
[DE93-017677] p 1471 N94-17777
Low power arcjet system spacecraft impacts
[NASA-TM-106307] p 1336 N94-17856
Review of short-term, high-level exposure to metals: Antimony, barium, and cadmium
[AD-A268896] p 1505 N94-18392
Ultraviolet plume instrument calibration and sensor assessment
[AD-A269687] p 1337 N94-18574
Data collection plan for phase 2 Alternative Fuels Bus Data Collection Program
[DE93-010047] p 1378 N94-18913

EXOBIOLOGY
Aerospace medicine and biology: A continuing bibliography with indexes (supplement 382)
[NASA-SP-7011(382)] p 1507 N94-18936
Aerospace medicine and biology: A continuing bibliography with indexes (supplement 381)
[NASA-SP-7011(381)] p 1507 N94-19069
Space Life Sciences Research: The Importance of Long-Term Space Experiments
[NASA-TM-4502] p 1502 N94-19210
The rationale for fundamental research in space biology: Introduction and background p 1502 N94-19211
Opportunities and questions for the fundamental biological sciences in space p 1502 N94-19212

EXOS-C SATELLITE
Global zones of particle precipitation as observed EXOS-C
[AD-A268758] p 1481 N94-18467

EXPEDITIONS
Ozone hole
[NASA-TM-109368] p 1476 N94-18960

EXPERIMENT DESIGN
Performance mapping of the STM4-120 kinematic Stirling engine using a statistical design of experiments method
[DE93-015132] p 1464 N94-17798
Characterization of the Facility for Atmospheric Corrosion Testing (FACT) at Sandia
[DE93-018510] p 1474 N94-18521
Vane optimization for maximum efficiency using Design Of Experiments (DOX)
[AD-A270270] p 1320 N94-18907
The first flight of the QUESTS GAS payload G-521
p 1325 N94-19170
Shell designs
[AD-A270656] p 1460 N94-19606

EXPERIMENTATION
Efficient domain-independent experimentation
[AD-A269530] p 1557 N94-18640

EXPERT SYSTEMS
The organizational preparation of existing relational databases for the integration of expert systems
[AD-A268823] p 1614 N94-18191
System dynamics and computer modeling expertise. A conceptual structure research inquiry
[AD-A269860] p 1560 N94-18410
Automatic documentation generation: The interaction of text and examples
[AD-A269670] p 1616 N94-18570
Optimizing wind turbine control system parameters
[DE93-018861] p 1469 N94-19036
JPRS report: Central Eurasia. Aviation and cosmonautics, no. 1, January 1993
[JPRS-UAC-93-007] p 1632 N94-19147
An innovative neural manufacturing concept
[DE93-017212] p 1527 N94-19238

EXPLOSIONS
Instrumented experiments aboard the frigate WOLF. Wolf 2: Measurement results of the 5.5 kg TNT in the crew aft sleeping compartment
[PML-1992-12] p 1451 N94-17931
Scaling laws for diffraction loading by air blast
[PML-1991-54] p 1452 N94-17941
A probability method of fracture mechanics analysis for HFIR vessel
[DE93-015510] p 1453 N94-18246

Analysis of regional bodywave phases from earthquakes in western China, part 2
[AD-A270125] p 1485 N94-18873
Air blast measurements at 20 and 40 km distance from detonating 10 and 20 ton high explosive charges
[PB93-195949] p 1419 N94-19068
Round robin experiments on the Explosive Components Water Gap Test (ECWGT)
[PML-1992-69] p 1378 N94-19445

EXPLOSIVES
Modeling shock initiation in Composition B
[DE93-016544] p 1376 N94-18095
The use of post detonation analysis of stable isotope ratios to determine the type and production process of the explosive involved
[DE93-018497] p 1378 N94-19242
Round robin experiments on the Explosive Components Water Gap Test (ECWGT)
[PML-1992-69] p 1378 N94-19445

EXPONENTIAL FUNCTIONS
Exponential characteristic spatial quadrature for discrete ordinates neutral particle transport in two-dimensional cartesian coordinates
[AD-A270458] p 1554 N94-19671

EXPOSURE
Air pollution effects field research facility. 3: UV-B exposure and monitoring system
[DE93-013098] p 1470 N94-17773
Effects of a high-energy food supplement on cold-induced thermogenesis
[AD-A269301] p 1504 N94-17823
Using controlled daylight exposure and sleep timing in the prevention of shift lag during night operations
[AD-A269304] p 1504 N94-17824
A study of the effects of high power pulsed 2450 MHz microwaves, ELF modulated microwaves, and ELF fields on human lymphocytes and selected cell lines
[AD-A269070] p 1505 N94-18294
NSWCWODET participation in Space Shuttle mission STS-46
[AD-A268875] p 1332 N94-18321
Review of short-term, high-level exposure to metals: Antimony, barium, and cadmium
[AD-A268896] p 1505 N94-18392

EXTERNAL TANKS
Robotics
[NASA-TM-109351] p 1332 N94-18920

EXTERNALLY BLOWN FLAPS
Design and test of a low jitter metal to metal contact solid dielectric switch
[DE93-016957] p 1394 N94-17755
Navier-Stokes simulation of flow field around a blown-flap high-lift system p 1307 N94-18429

EXTINCTION
Optical properties of redispersed iron fibers measured at 94 GHz
[AD-A269739] p 1342 N94-18756

EXTRAPOLATION
Radiosity algorithms using higher order finite element methods
[DE93-018098] p 1531 N94-19548

EXTRATERRESTRIAL RADIATION
Update on parts SEE susceptibility from heavy ions
[AD-A268735] p 1596 N94-18316

EXTREME ULTRAVIOLET RADIATION
UVSTAR: An imaging spectrograph with telescope for the Shuttle Hitchhiker-M platform p 1326 N94-19178

EXTREMELY LOW FREQUENCIES
A study of the effects of high power pulsed 2450 MHz microwaves, ELF modulated microwaves, and ELF fields on human lymphocytes and selected cell lines
[AD-A269070] p 1505 N94-18294
Compilation of 1992 annual reports of the Navy ELF communications system ecological monitoring program, volume 1
[AD-A269569] p 1386 N94-18473
Compilation of 1992 annual reports of the navy ELF communications system ecological monitoring program. Volume 3: Tabs G - I
[AD-A269727] p 1388 N94-18741
Compilation of 1992 annual reports of the navy ELF communications system ecological monitoring program, volume 2
[AD-A269726] p 1388 N94-18751

EXTREMELY LOW RADIO FREQUENCIES
Compilation of 1992 annual reports of the Navy ELF communications system ecological monitoring program, volume 1
[AD-A269569] p 1386 N94-18473
Compilation of 1992 annual reports of the navy ELF communications system ecological monitoring program. Volume 3: Tabs G - I
[AD-A269727] p 1388 N94-18741
Compilation of 1992 annual reports of the navy ELF communications system ecological monitoring program, volume 2
[AD-A269726] p 1388 N94-18751

EXTRUDING
Summary of work on coatings and claddings for fossil energy applications
[DE93-017005] p 1367 N94-17881
Ageing in Processed Polymers: Programme, summary, and abstracts discussion meeting
[AD-A268931] p 1370 N94-18448

EYE MOVEMENTS
FY 1991 AASERT: Spatio-temporal making in human vision and its application to image coding
[AD-A268795] p 1505 N94-18190
Stochastic models of attention and search
[AD-A268622] p 1508 N94-18292

F

F REGION
RADARC HF ionospheric prediction program for OTH radar
[AD-A269557] p 1385 N94-18291
The effects of magnetic storm phases on f-layer irregularities from auroral to equatorial latitudes
[AD-A267388] p 1486 N94-19008
A physical model for one-dimension and time-dependent ionosphere. Part 1: Description of the model
[DE93-627958] p 1486 N94-19255

F-16 AIRCRAFT
Numerical prediction of transition of the F-16 wing at supersonic speeds
[NASA-CR-194407] p 1312 N94-19433

F-18 AIRCRAFT
Results of a joint Navy/Air Force operational test to evaluate USAF Integrated Maintenance Information Systems (IMIS), Interactive Electronic Technical Manual (IETM) technology applied to the F/A-18 aircraft
[AD-A271322] p 1619 N94-19571

FABRICATION
Ultra-shallow box-like profiles fabricated by pulsed UV-laser doping process
[DE93-017221] p 1437 N94-18083
Photovoltaic concentrator initiative: Concentrator cell development
[DE93-018505] p 1466 N94-18335
High-efficiency silicon concentrator cell commercialization
[DE93-018491] p 1467 N94-18409
Fabrication and microstructural development of Ag-clad TlBa2Ca2Cu3O(x) tapes
[DE93-017407] p 1597 N94-18500
Design and fabrication of a Multichannel Adaptive Optical Processor (MADOP)
[AD-A270004] p 1579 N94-18668
ARPA/CSTO rapid VLSI implementation
[AD-A269170] p 1403 N94-18695
VLSI for high-speed digital signal processing
[AD-A270406] p 1404 N94-18706
Fabrication process for cantilever beam micromechanical switches
[AD-A269716] p 1404 N94-18749
Integrated circuits: Resistless processing simplifies production and cuts costs
[DE93-018069] p 1405 N94-18941
Polycrystalline thin-film cadmium telluride solar cells fabricated by electrodeposition
[DE93-018201] p 1468 N94-18944
Fabrication and characterization of high-T(sub c) tapes and coils made from Ag-clad Bi-2223 superconductors
[DE93-018615] p 1601 N94-18993
MODIL cryocooler producibility demonstration project results
[DE93-017981] p 1335 N94-19275
Manufacturing technology
[DE93-019580] p 1381 N94-19480

FABRY-PEROT INTERFEROMETERS
A technique for measuring winds in the lower atmosphere using incoherent Doppler lidar
[DE93-017163] p 1488 N94-17758

FACE CENTERED CUBIC LATTICES
High dose effects in neutron irradiated face-centered cubic metals
[DE93-017671] p 1364 N94-19043
Role of pressure in the study of fullerenes
[DE93-018839] p 1602 N94-19340

FACSIMILE COMMUNICATION
Color test chart for facsimile
[AD-A269754] p 1387 N94-18721

FACTOR ANALYSIS
Shell designs
[AD-A270656] p 1460 N94-19606

FAILURE
Factors which affect fatigue strength of fasteners
[DE93-017272] p 1453 N94-18084
The application of nondestructive techniques to the testing of a wind turbine blade
[DE93-016731] p 1447 N94-18128
Analytical and experimental evaluation of joining silicon nitride to metal and silicon carbide to metal for advanced heat engine applications
[DE93-018128] p 1446 N94-19291

FAILURE ANALYSIS
Inelastic deformation and damage at high temperature
[DE93-018155] p 1448 N94-17814
Mechanical response comparison of gun propellants evaluated under equivalent time-temperature conditions
[AD-A270479] p 1378 N94-19674

FAILURE MODES
Fundamental research in nonlinear random vibration for aerospace applications
[AD-A268929] p 1454 N94-18487
The microstructural mechanism of electromigration failure in narrow interconnects of Al alloys
[DE93-018598] p 1365 N94-19282
Analytical and experimental evaluation of joining silicon nitride to metal and silicon carbide to metal for advanced heat engine applications
[DE93-018128] p 1446 N94-19291

FALLOUT
Inclusion of a three-dimensional washout coefficient in ADPIC
[DE93-018499] p 1476 N94-19038

FAR FIELDS
Wideband electromagnetic scattering/analysis program: Far zone electromagnetic scattering from complex shapes using geometrical theory of diffraction
[AD-A268790] p 1384 N94-18187
Computational aero-acoustics as a branch of turbulence research p 1411 N94-18552

FAR INFRARED RADIATION
A tunable compact high power far-infrared grating free-electron laser
[AD-A269875] p 1440 N94-18771
Final construction and operation of a continuous far-infrared free-electron laser for scientific applications
[AD-A269248] p 1440 N94-18912

FAR ULTRAVIOLET RADIATION
Chemical dynamics in time and energy space
[DE93-018595] p 1350 N94-19097
The 1982 to 1992 decade of research on the vacuum ultraviolet ring at National Synchrotron Light Source
[DE93-019469] p 1603 N94-19564

FARADAY EFFECT
An ultraviolet faraday rotator glass
[AD-D015879] p 1371 N94-18529

FAST FOURIER TRANSFORMATIONS
Introduction to wavelets
[AD-A268465] p 1389 N94-18801
Nontraditional windows in spectral analysis
[AD-A271336] p 1553 N94-19583
Investigations of a coherent vector radar technique for the observation of the atmosphere near 10 GHz
[KFK-5068] p 1494 N94-19616

FAST NEUTRONS
Effects of irradiation temperature on Charpy and tensile properties of high-copper, low upper-shelf, submerged-arc welds
[DE93-017858] p 1445 N94-19047
Studies of deep levels in high resistivity silicon detectors irradiated by high fluence fast neutrons using a thermally stimulated current spectrometer
[DE93-016133] p 1602 N94-19258

FASTENERS
Factors which affect fatigue strength of fasteners
[DE93-017272] p 1453 N94-18084

FASTING
Effects of a high-energy food supplement on cold-induced thermogenesis
[AD-A269301] p 1504 N94-17823

FATIGUE (MATERIALS)
Mathematical modelling of bonded fibre-composite repairs to aircraft
[AD-A268732] p 1341 N94-18327
Composites: Materials of the future
[AD-A268945] p 1341 N94-18450
The 6th Japan-U.S. conference on composite materials
[AD-A268535] p 1341 N94-18630
Fatigue technology assessment and strategies for fatigue avoidance in marine structures. Appendices
[AD-A269053] p 1455 N94-18716
JPRS report: Science and technology. Central Eurasia: Materials science
[JPRS-UMS-93-002] p 1339 N94-18833
Optimizing wind turbine control system parameters
[DE93-018861] p 1469 N94-19036

Fatigue crack initiation in riveted lap joints and in pressurized fuselages
[LR-725] p 1461 N94-19669
Microstructure and texture control of fatigue in hydrogen and marine environments
[AD-A271277] p 1344 N94-19744

FATIGUE LIFE
Spectrum fatigue testing of T-shaped tension clips
[FFA-TN-1992-22] p 1452 N94-17970
Microstructurally based thermomechanical fatigue lifetime model of solder joints for electronic applications
[DE93-016508] p 1452 N94-17995
FAROW: A tool for fatigue and reliability of wind turbines
[DE93-017639] p 1465 N94-18001
Development of the microstructure based stochastic life prediction models
[AD-A269880] p 1454 N94-18683
Development of the microstructure based stochastic life prediction models
[AD-A270453] p 1455 N94-18714
Development of the microstructure based stochastic life prediction model
[AD-A269742] p 1361 N94-18742
Design for cyclic loading endurance of composites
[NASA-TM-106407] p 1457 N94-19351
A review of aeronautical fatigue investigations in Sweden during the period May 1991 to April 1993
[FFA-TN-1993-22] p 1457 N94-19358
Microstructure and texture control of fatigue in hydrogen and marine environments
[AD-A271277] p 1344 N94-19744

FATIGUE TESTS
Inelastic deformation and damage at high temperature
[DE93-018155] p 1448 N94-17814
Spectrum fatigue testing of T-shaped tension clips
[FFA-TN-1992-22] p 1452 N94-17970
Factors which affect fatigue strength of fasteners
[DE93-017272] p 1453 N94-18084
Mechanism-dependent fractal character of fracture surfaces in high strength and toughness ASTM A723 steels
[AD-A268956] p 1360 N94-18542
New test method to determine modulus of elasticity of rocket grain material
[AD-A269758] p 1377 N94-18758
A review of aeronautical fatigue investigations in Sweden during the period May 1991 to April 1993
[FFA-TN-1993-22] p 1457 N94-19358
Fatigue crack initiation in riveted lap joints and in pressurized fuselages
[LR-725] p 1461 N94-19669

FATTY ACIDS
Nuclear Medicine Program
[DE93-013896] p 1504 N94-17699

FAULT DETECTION
An analytical approach to error localization by using information derived from error signature
[REPT-93-023] p 1518 N94-17960
Measurement selection for parametric IC fault diagnosis p 1399 N94-18356
Pulse mode VLSI asynchronous circuits
p 1402 N94-18377
On-line test methods of microprocessor based systems
[ETN-93-95008] p 1530 N94-19498
Applications of neural networks in fault detection of rotating machinery
[AD-A270755] p 1448 N94-19766

FAULT TOLERANCE
An efficient implementation of error-valued semantics on imperative machines
[DE93-014658] p 1516 N94-17740
Synthesis techniques and analysis tool for on-chip fault-tolerance
[AD-A269148] p 1521 N94-18259
Fault tolerant sequential circuits using sequence invariant state machines p 1398 N94-18344
Efficient transparent optimistic rollback recovery for distributed application programs
[AD-A268981] p 1522 N94-18696
A general theory of signal integration for fault-tolerant dynamic distributed sensor networks
[AD-A270316] p 1534 N94-18699
Radiation hardened microprocessor for small payloads
p 1327 N94-19184
A research program in empirical computer science
[NASA-CR-194069] p 1530 N94-19429
Fault-tolerance and complexity
[TR-450] p 1530 N94-19483
Computer security. Evolutions 1987 to 1992: Trends and perspectives
[RR-905-I] p 1532 N94-19713
Algorithms and architectures for high speed signal processing
[AD-A271000] p 1392 N94-19736

FAULT TREES
Optimal safety system design using fault tree analysis
[MATHS-REPT-A-187] p 1529 N94-19382

FEASIBILITY
Regenerative fuel cells for High Altitude Long Endurance Solar Powered Aircraft
[DE93-016991] p 1465 N94-17853
A survey on technical problems in designing high-speed rotors with developing materials
[DE93-788519] p 1444 N94-18159

FEASIBILITY ANALYSIS
Safety approaches for high power modular laser operation
[DE93-017213] p 1435 N94-17759
Development of alternatives to lead-bearing solders
[DE93-016509] p 1357 N94-17862
Space debris detection
[AD-A269254] p 1334 N94-18264
Proof of the feasibility of coherent and incoherent schemes for pumping a gamma ray laser
[AD-A269173] p 1440 N94-18880
NPAC distributed-parallel system feasibility study
[AD-A270972] p 1539 N94-19790
Feasibility study for a measuring system velocity projectile
[FEL-91-A368] p 1434 N94-19797

FEDERAL BUDGETS
Current information technology resource requirements of the federal government: Fiscal year 1994
p 1612 N94-17756
The 1994 NASA authorization, volume 2
[GPO-71-510] p 1620 N94-18842
A foundation for the 21st Century: A progressive framework for the National Science Foundation. Report of the National Science Board Commission on the future of the National Science Foundation
[NSB-92-196] p 1611 N94-19618

FEEDBACK
Deadbeat control by measurement feedback: A two sided approach
[REPT-93-20] p 1542 N94-19091
Analysis and design of robust decentralized controllers for nonlinear systems
[DE93-019224] p 1543 N94-19302
Discrete-time infinity control problem with measurement feedback
[PB93-197523] p 1543 N94-19329
Stabilization of time-delay systems: An overview of the algebraic approach
[PB93-191989] p 1553 N94-19556

FEEDBACK CONTROL
KINETIC: A system code for analyzing Nuclear thermal propulsion rocket engine transients
[DE93-016825] p 1337 N94-17884
Efficient dynamic modeling of manipulators containing closed kinematic loops
[REPT-92-083] p 1444 N94-17940
Introduction to Quantitative Feedback Theory (QFT) technique p 1545 N94-18241
Deadbeat control by measurement feedback: A two sided approach
[REPT-93-20] p 1542 N94-19091
The fixed, finite-order L(sup 2)-optimal control of infinite-dimensional time-varying discrete-time systems
[REPT-93-23] p 1542 N94-19138
The digital linear quadratic control problem for Pritchard-Salamon systems
[REPT-93-27] p 1542 N94-19142
Laser guide star measurements at Lawrence Livermore National Laboratory
[DE93-018081] p 1441 N94-19251
Discrete-time infinity control problem with measurement feedback
[PB93-197523] p 1543 N94-19329
Congestion/flow control and routing in data networks: A control-theoretic approach
[AD-A271121] p 1392 N94-19737

FEEDFORWARD CONTROL
Explorations of the practical issues of learning prediction-control tasks using temporal difference learning methods
[AD-A270836] p 1544 N94-19599

FERMI LIQUIDS
Lectures of Fermi liquid theory
[DE93-016630] p 1592 N94-17714

FERMI SURFACES
High energy resolution ARPES measurements of the normal and superconducting states of Bi2Sr2CaCu2O(8 + delta)
[DE93-018294] p 1599 N94-18804

FERMI-DIRAC STATISTICS
IR materials producibility
[AD-A268849] p 1577 N94-18223

FERMIONS
Cabibbo mixing in superstring derived standard-like models
[DE93-624814] p 1607 N94-17953
Four-fermion interactions
[DE93-629905] p 1566 N94-18199
Crossover from BCS to Bose superconductivity: A functional integral approach
[DE93-019503] p 1604 N94-19566

FERRIMAGNETIC MATERIALS
Comparison of ferrite materials for pulse applications
[DE93-017224] p 1574 N94-18497

FERRIMAGNETISM
Comparison of ferrite materials for pulse applications
[DE93-017224] p 1574 N94-18497

FERRIMAGNETS
Comparison of ferrite materials for pulse applications
[DE93-017224] p 1574 N94-18497

FERRITES
Comparison of ferrite materials for pulse applications
[DE93-017224] p 1574 N94-18497

FERRITIC STAINLESS STEELS
Helium-induced weld degradation of HT-9 steel
[DE93-015981] p 1358 N94-17915
Study of mechanical behavior and internal structure of ferritic nanocrystalline material
[DE93-019264] p 1596 N94-18184

FERROELECTRICITY
Spatial light modulators and applications: Summaries of papers presented at the Spatial Light Modulators and Applications Topical Meeting
[AD-A269452] p 1577 N94-18283
Integration of ferroelectric/semiconductor thin films for SLM and photorefractive applications
[AD-A268645] p 1598 N94-18633
Office of Naval Research Publications/Patents /Presentations/Honors report, 1 October 1992 - 30 September 1993
[AD-A270037] p 1632 N94-18791

FERROMAGNETIC MATERIALS
Corroboration of magnetic forces in US Maglev design
[DE93-014918] p 1443 N94-17785
Self-organized criticality and the Barkhausen effect in amorphous and polycrystalline metals
[AD-A269817] p 1361 N94-18735
Polarized optical emission due to decay or recombination of spin-polarized injected carriers
[AD-D015907] p 1408 N94-19763

FERROMAGNETIC RESONANCE
Some superhigh-frequency and magnetic properties of chemically precipitated films
[AD-A266195] p 1351 N94-19110
Nonlinear dynamics and instabilities in ferromagnetic resonance experiments: Examinations of spheres from yttrium iron garnet in coincidence area of the first Suhl instabilities
[ETN-93-95072] p 1604 N94-19612

FERROMAGNETISM
Ising model on tangled chain. Part 2: Magnetization and susceptibility
[DE93-628794] p 1607 N94-18174

FERROUS METALS
Damping in ferrous shape memory alloys
[AD-A271009] p 1366 N94-19775

FIBER COMPOSITES
The calculation methods of a cracked plastic composite laminate: A literature survey
[VTT-TIED-1362] p 1339 N94-17958
Strength optimization of C/Al metal matrix composites produced from prepregs
[DLR-FB-92-39] p 1340 N94-18122
A comprehensive study of matrix fracture mechanisms in fiber-reinforced ceramic matrix composites
[AD-A268809] p 1340 N94-18205
Mathematical modelling of bonded fibre-composite repairs to aircraft
[AD-A268732] p 1341 N94-18327
Mechanical properties of fiber-reinforced YBa2Cu3O(x) and Bi2Sr2CaCu2O(x) bars
[DE93-017689] p 1454 N94-18479
Bibliography on ceramic matrix composites and reinforcing whiskers, platelets, and fibers, 1970-1990
[AD-A270139] p 1371 N94-18750
Delamination in composite materials as observed using an optical fiber strain gage
[AD-A270803] p 1344 N94-19662
Residual strength predictions for fibre metal laminates: The R-curves approach
[LR-717] p 1344 N94-19666

FIBER OPTICS
Variable wide band fiber optic delay line
[AD-D015848] p 1576 N94-17716
Suppression of backscatter and stray reflection induced phase noise in Michelson interferometers
[AD-D015809] p 1382 N94-17902

Advanced optical fiber communication systems
[AD-A269120] p 1577 N94-18254
Applications of nonlinear optic effects in new specialty fibers
[AD-A268890] p 1578 N94-18457
Competitive dynamics and self-organization in photorefractive systems
[AD-A269663] p 1430 N94-18569
Investigation of a fiber optic frequency shifter and optical isolator
[AD-A269820] p 1579 N94-18738
Apparatus and method for varying a Bragg wavelength of a Bragg grating formed in an optical fiber
[AD-D015876] p 1579 N94-18743
Improved optical pseudospark switch
[AD-D015821] p 1580 N94-18947
Evaluation of fiber optic performance in the ACRR
[DE93-018515] p 1580 N94-18970
Penetrometer compatible, fiber-optic sensor for continuous monitoring of chlorinated hydrocarbons: Field test results
[DE93-017974] p 1352 N94-19266
Fiber optic Raman spectrograph for in situ environmental monitoring
[DE93-019466] p 1478 N94-19305
Optoelectronic packaging: A review
[DE93-040059] p 1515 N94-19535

FIBER STRENGTH
Strength optimization of C/Al metal matrix composites produced from prepregs
[DLR-FB-92-39] p 1340 N94-18122

FIBERS
Dispersion effects on millimeter wavelength attenuation efficiencies for a variety of fibers
[AD-A268992] p 1386 N94-18454
Optical properties of redispersed iron fibers measured at 94 GHz
[AD-A269739] p 1342 N94-18756

FIELD COILS
Limits on m = 2, n = 1 error field induced locked mode instability in TPX with typical sources of poloidal field coil error field and a proto type correction coil, C-coil
[DE93-014408] p 1582 N94-17702

FIELD EFFECT TRANSISTORS
Optically controlled active impedance element and filters employing the same
[AD-D015863] p 1396 N94-18062
New dynamic FET logic and serial memory circuits for VLSI GaAs technology p 1397 N94-18339
DC and small-signal physical models for the AlGaAs/GaAs high electron mobility transistor
p 1401 N94-18370
Kinetic aspects of lattice mismatch in molecular beam epitaxial growth on planar and patterned substrates
[AD-A270424] p 1597 N94-18506
Joint services electronics program
[AD-A269383] p 1403 N94-18638
Spice modeling of a FET-switched induction accelerator cell
[DE93-018662] p 1575 N94-18996
Quasi-optical transponder using FET's and patch antennas
[AD-A271339] p 1407 N94-19584
Design of power electronics for TVC EMA systems
[NASA-CR-193839] p 1407 N94-19642
Nanofabrication by focused ion beam
[AD-A271290] p 1345 N94-19746

FIELD EMISSION
Field emission cathode and vacuum microelectronic microwave amplifier development
[AD-A269526] p 1403 N94-18639

FIELD OF VIEW
Directional regions in Geographic Information Systems (GIS)
[AD-A268536] p 1462 N94-18309
SeaTrack: Ground station orbit prediction and planning software for sea-viewing satellites
[NASA-RP-1331] p 1532 N94-19761

FIELD THEORY (PHYSICS)
On a conformal perfect fluid in the classical vacuum
[DE93-624797] p 1480 N94-17682
Infinite Grassmannian and moduli space of G-bundles
[DE93-624798] p 1545 N94-17683
Renormalizations in supersymmetric and nonsupersymmetric non-abelian Chern-Simons field theories with matter
[DE93-626646] p 1593 N94-17748
A general solution of the BV-master equation and BRST field theories
[DE93-626622] p 1561 N94-18171
Impulsive moving mirror model and impulsive differential equations in Banach space
[DE93-629867] p 1549 N94-18197
Four-fermion interactions
[DE93-629905] p 1566 N94-18199
Impulsive moving mirror model and the stability of linear homogeneous differential equations with impulse effect in a Banach space
[DE93-629906] p 1549 N94-18200
Phase structure of (phi(4))(sub 3) field theory at finite temperature
[DE93-629907] p 1608 N94-18267
Modelling force-field effects on turbulence
p 1414 N94-18581
Numerical modelling of fringing fields and their use for complex permittivity measurements at high frequencies
[AD-A270198] p 1388 N94-18782

FIGHTER AIRCRAFT
Metals 2000
[DE93-016761] p 1355 N94-17752
Comparison between swept and delta canards on a model of a combat aircraft
[AD-A269561] p 1317 N94-17826
An experimental investigation of the optimum slat setting on a combat aircraft model p 1308 N94-18431
An experimental investigation of attachment-line transition on the slat of a combat aircraft model
p 1308 N94-18432
Close-coupled oscillating canard effects on post-stall lift enhancement
[AD-A268938] p 1321 N94-18541
A comparison of air force data systems
[AD-A269691] p 1616 N94-18575
Procedures and design data for the formulation of aircraft configurations
[AD-A270150] p 1318 N94-18779
JPRS report: Central Eurasia. Aviation and cosmonautics, no. 10, October 1992
[JPRS-UAC-93-004] p 1632 N94-19149
Research and design activities and the economic balance of MBB
[ETN-93-94909] p 1310 N94-19383
An investigation of fighter aircraft agility
[NASA-CR-194608] p 1318 N94-19448

FILE MAINTENANCE (COMPUTERS)
CAVEMAN: Configuration and version management
[DE93-018066] p 1524 N94-19048
Integrity checking in deductive databases: An exposition
[PB93-191724] p 1619 N94-19709

FILLERS
Environmental degradation of Alloy 600 and welded filler metal EN82 in an elevated temperature aqueous environment
[DE93-018049] p 1363 N94-18940

FILM CONDENSATION
Film condensation in a shock wave
[MPIS-22/1992] p 1422 N94-19509

FILM COOLING
Analysis of film cooling in rocket nozzles
[NASA-CR-194674] p 1338 N94-19438

FILM THICKNESS
Film condensation in a shock wave
[MPIS-22/1992] p 1422 N94-19509

FILTRATION
Aerosol filtration with steel fiber filters
[DE93-016990] p 1380 N94-18710

FINANCIAL MANAGEMENT
Technology benefits model user manual, version 01.00.04
[AD-A270637] p 1620 N94-19777

FINE STRUCTURE
Dynamic behaviors of fragments ejected from the surface of carbon materials by laser ablation
[DE93-788620] p 1438 N94-18161
Potential dependent structural changes of underpotentially deposited copper on an iodine treated platinum surface determined in situ by surface EXAFS and its polarization dependence
[AD-A269890] p 1360 N94-18687
EXANA: A program for analysing extended energy loss fine structures, EXELFS spectra
[USIP-92-01] p 1525 N94-19145
The effects of initial conditions on the 3-D topology of temporally evolving wakes (ARI on 3-D bluff body wakes)
[AD-A271008] p 1423 N94-19774

FINITE DIFFERENCE THEORY
A one dimensional numerical model, with an application to the vertical distribution of dissolved oxygen in the ocean
[DE93-018481] p 1495 N94-17779
FEM/SINDA: Combining the strengths of NASTRAN, SINDA, I-DEAS, and PATRAN for thermal and structural analysis p 1449 N94-17831
Comments on computational underwater acoustics
[DE93-013789] p 1562 N94-17873
The rise of accuracy for the multichannel scattering problem solving
[DE93-630145] p 1608 N94-18253
The longitudinal free vibrations of a fixed-free two-phase elastic bar
[AD-A268768] p 1453 N94-18387
An algebraic turbulence model for turbomachinery
p 1411 N94-18554
DYNLET1 model formulation and user's guide
[AD-A269843] p 1498 N94-18723
HEMP 3D: A finite difference program for calculating elastic-plastic flow, appendix B
[AD-A269171] p 1418 N94-18878
Finite difference program for calculating hydride bed wall temperature profiles
[DE93-019272] p 1523 N94-19005
Comments on computational underwater acoustics
[DE93-019880] p 1563 N94-19270
Pseudo-compressibility methods for the incompressible flow equations
[NASA-CR-191533] p 1551 N94-19315
Improved approximations applied to the S(sub N) even-parity equation
[DE93-016467] p 1551 N94-19343
Numerical simulation of viscous flows in chemical nonequilibrium
[MBB-LME-211-S-PUB-506] p 1421 N94-19497

FINITE ELEMENT METHOD
Atlas of formability: HAYNES 556
[AD-A268354] p 1356 N94-17768
Atlas of formability: HAYNES 188
[AD-A268355] p 1356 N94-17769
Atlas of formability: Permalloy - 80 flow stress curves
[AD-A268263] p 1356 N94-17801
Atlas of formability: Nickelvac C-276
[AD-A268264] p 1357 N94-17802
Atlas of formability: ALLVAC 718
[AD-A268304] p 1357 N94-17804
Finite element modeling of evaporation and condensation during sol-gel film and fiber formation
[DE93-017655] p 1345 N94-17820
The Twenty-First NASTRAN (R) Users' Colloquium
[NASA-CP-3203] p 1449 N94-17827
FEM/SINDA: Combining the strengths of NASTRAN, SINDA, I-DEAS, and PATRAN for thermal and structural analysis p 1449 N94-17831
The role of NASTRAN in the preliminary design cycle
p 1450 N94-17835
Eigenvalue routines in NASTRAN: A comparison with the Block Lanczos method p 1450 N94-17838
Comments on computational underwater acoustics
[DE93-013789] p 1562 N94-17873
The respectiveness of response in a bar under static and transient loads
[VTT-TIED-1377] p 1452 N94-17959
Computational strategies for composite structures
[PB93-195097] p 1452 N94-18079
SAND contact in DYNA3D
[DE93-016451] p 1340 N94-18113
Preliminary structural design: Defining the design space
[AD-A268898] p 1317 N94-18227
A finite strain ring dynamical model for pneumatic tires
[AD-A269286] p 1444 N94-18266
Computational Fluid Dynamics
[VKI-LS-1993-04] p 1412 N94-18557
Implementation of a nonisothermal unified inelastic-strain theory into ADINA6.0 for a titanium alloy: User guide
[AD-A269927] p 1360 N94-18660
Parallel and vector adaptations of the underwater finite element parabolic equation model
[AD-A269990] p 1563 N94-18678
Pressureless densification of ceramic matrix composites
[AD-A269137] p 1371 N94-18691
Validation of a-posteriori error estimators by numerical approach
[AD-A269493] p 1549 N94-18697
Development of a finite element method program for the analysis of laminated composite plates using first-order shear deformation theory
[AD-A270318] p 1342 N94-18700
A finite element scheme for shock capturing
[AD-A270182] p 1417 N94-18755
Knowledge sources for an intelligent MCM analyzer
[AD-A269224] p 1542 N94-18887
A numerical analysis of crack growth in brittle microcracking composites
[DE93-011562] p 1343 N94-18914
Dynamic characterization of a lightweight, highly maneuverable spacecraft using modal and finite element analyses
[DE93-018095] p 1335 N94-18942
A general-purpose contact detection algorithm for nonlinear structural analysis codes
[DE93-018507] p 1455 N94-19039
A constitutive theory for rigid polyurethane foam
[DE93-011596] p 1372 N94-19059

A massively parallel adaptive finite element method with dynamic load balancing [DE93-012844] p 1536 N94-19161
Comments on computational underwater acoustics [DE93-019880] p 1563 N94-19270
Computational mechanics of composite materials [PB93-195782] p 1343 N94-19281
Are bilinear quadrilaterals better than linear triangles? [DE93-019223] p 1551 N94-19301
Refining a triangulation of a planar straight-line graph to eliminate large angles [DE93-016510] p 1528 N94-19344
Numerical simulations of turbulent buoyant flows by finite element method: Application to the study of strongly heated or cooled stratified flow [ECL-92-28] p 1421 N94-19399
On the numerical analysis of nonlinear Galerkin methods: Spectral approximation and finite elements [ETN-93-94900] p 1552 N94-19407
Directions for computational mechanics in automotive crashworthiness p 1459 N94-19472
Current capabilities for simulating the extreme distortion of thin structures subjected to severe impacts p 1459 N94-19474
Crashdynamics with DYNA3D: Capabilities and research directions p 1460 N94-19475
Transient dynamics capability at Sandia National Laboratories p 1460 N94-19476
Radiosity algorithms using higher order finite element methods [DE93-018098] p 1531 N94-19548
ADAS implementation of a panel method for the prediction of aerodynamic loads [LR-723] p 1313 N94-19667
Implementation of parallel algorithms [AD-A271035] p 1539 N94-19682

FINITE VOLUME METHOD
Investigation of a matrix-model for the artificial dissipation in a cell vertex finite volume scheme for solving the Navier-Stokes equations [DLR-FB-92-33] p 1409 N94-18076
Navier-Stokes computations of turbulent flow around high-lift configurations p 1306 N94-18420
Prediction of the high-lift performance of multi-element aerofoils using an unstructured Navier-Stokes solver p 1307 N94-18427
Numerical calculations of high lift flows using structured and unstructured methods p 1307 N94-18428
Numerical investigation of complex, transitional, and chemically reacting flows p 1411 N94-18550
Computational Fluid Dynamics [VKI-LS-1993-04] p 1412 N94-18557
ENO schemes on unstructured meshes p 1412 N94-18561
Compact advection schemes on unstructured grids p 1413 N94-18564
Inclusion of second-moment closures into finite-volume solvers p 1415 N94-18588
Numerical implementation and performance of Reynolds-stress closures in finite-volume computations of recirculating and strongly swirling flows p 1415 N94-18589
STREMR: Numerical model for depth-averaged incompressible flow [AD-A269949] p 1417 N94-18672
Multigrid for a groundwater flow problem [REPT-93-29] p 1420 N94-19144
On positivity preserving finite volume schemes for compressible Euler equations [NASA-CR-191534] p 1551 N94-19317
On the numerical approximation of nonlinear hyperbolic problems: Application to the dynamics of compressible gas [ETN-93-95020] p 1420 N94-19365
Three dimensional network generation and Euler calculation for a wing fuselage canard configuration [MBB-LME-211-S-PUB-511-A] p 1319 N94-19500

FINNED BODIES
Parabolized Navier-Stokes computation of surface heat transfer characteristics for supersonic and hypersonic KE projectiles [AD-A268858] p 1410 N94-18391

FINS
Fin-efficiency calculation for condensation in the presence of noncondensable gases [DE93-017684] p 1409 N94-18004
Correlation of incoming boundary layer pitot pressure fluctuations with the unsteadiness of fin-induced shock wave turbulent boundary layer interactions [AD-A270059] p 1417 N94-18796

FIRE PREVENTION
The fire resistance of profiled thin steel sheet structures [VTT-TIED-1320] p 1380 N94-19373

FIREBEE 2 TARGET DRONE AIRCRAFT
An application of parameter estimation to the stability and control of the BQM-147 unmanned aerial vehicle [AD-A268741] p 1321 N94-18401

FIRES
Aircraft fire sentry. Volume 1: Summary [AD-A270087] p 1315 N94-18822
Aircraft fire sentry. Volume 2: Appendices A, B, C and D [AD-A270088] p 1315 N94-18823
Temperature of aircraft cargo flame exposure during accidents involving fuel spills [DE93-019633] p 1381 N94-19539

FISSION
Heavy ion nuclear physics research [DE93-018862] p 1565 N94-17776
LAHET calculations for accelerator neutron production [DE93-016518] p 1570 N94-19120

FLAME PROPAGATION
Transport phenomena and interfacial kinetics in multiphase combustion systems [AD-A270202] p 1349 N94-18785
Experimental study of flame front interactions [ECL-91-40] p 1353 N94-19376

FLAME SPECTROSCOPY
Spectral radiance measurements on a bluff body stabilized flame: Characterization of the IR signature [PB93-195899] p 1347 N94-18081

FLAME TEMPERATURE
Temperature of aircraft cargo flame exposure during accidents involving fuel spills [DE93-019633] p 1381 N94-19539

FLAMES
Spectral radiance measurements on a bluff body stabilized flame: Characterization of the IR signature [PB93-195899] p 1347 N94-18081
Temperature of aircraft cargo flame exposure during accidents involving fuel spills [DE93-019633] p 1381 N94-19539

FLAMMABILITY
The fire resistance of profiled thin steel sheet structures [VTT-TIED-1320] p 1380 N94-19373

FLASHOVER
Plasma-puff initiation of high Coulomb transfer switches [NASA-CR-193186] p 1591 N94-19441

FLAT SURFACES
Surface second harmonic generation studies of stepped Ag(111) electrode surfaces [AD-A265205] p 1594 N94-17876
Electro-optics display research, test, and evaluation laboratory program [AD-A270947] p 1408 N94-19751

FLEET BALLISTIC MISSILES
A Sandia Technology Bulletin: Testing technology, July 1993 [DE93-040197] p 1633 N94-19537

FLIGHT CHARACTERISTICS
An investigation of fighter aircraft agility [NASA-CR-194608] p 1318 N94-19448

FLIGHT CLOTHING
Analysis of seating and restraint limitations restricting total body weight for aircrew and passengers on US Army helicopters [AD-A269117] p 1511 N94-18296

FLIGHT CONDITIONS
Integrated Terminal Weather System (ITWS) [AD-A269884] p 1492 N94-18684

FLIGHT CONTROL
Non-linear flight dynamics p 1319 N94-18240
Introduction to Quantitative Feedback Theory (QFT) technique p 1545 N94-18241
A wind tunnel model control surface actuator interface [AD-A268729] p 1322 N94-18324
High lift and the forward swept wing p 1308 N94-18436
Flight test techniques for aircraft parameter estimation in ground effect [AD-A270058] p 1318 N94-18795
X-29: Research aircraft [NASA-TM-109370] p 1318 N94-18962

FLIGHT CREWS
Aircrew life support, AFSC 122X0(1T1X1) [AD-A268998] p 1511 N94-18394
Revision and verification of a seven-point workload estimate scale [AD-A269194] p 1511 N94-18412
A multivariate anthropometric method for crew station design [AD-A270652] p 1513 N94-19531

FLIGHT HAZARDS
Estimation of wake vortex advection and decay using meteorological sensors and aircraft data [AD-A270763] p 1316 N94-19661

FLIGHT OPERATIONS
Terminal area forecasts, FY 1993-2005 [AD-A269855] p 1316 N94-18336

FLIGHT PATHS
About the accuracy of an image-based navigation system during the runway approach [DLR-MITT-93-01] p 1316 N94-18146
Application of the A* algorithm to aircraft trajectory generation [AD-A268728] p 1317 N94-18315
VMC left turn curved approaches, test results — (visual meteorological conditions) [AD-A269476] p 1316 N94-18728
Estimation of wake vortex advection and decay using meteorological sensors and aircraft data [AD-A270763] p 1316 N94-19661

FLIGHT SAFETY
Analysis of seating and restraint limitations restricting total body weight for aircrew and passengers on US Army helicopters [AD-A269117] p 1511 N94-18296

FLIGHT SIMULATION
Modeling and new equipment definition for the vibration isolation box equipment system [NASA-CR-193185] p 1379 N94-17763

FLIGHT TESTS
Flight demonstration of image fix-taking with SAR [DE93-016499] p 1382 N94-17861
About the accuracy of an image-based navigation system during the runway approach [DLR-MITT-93-01] p 1316 N94-18146
An application of parameter estimation to the stability and control of the BQM-147 unmanned aerial vehicle [AD-A268741] p 1321 N94-18401
Revision and verification of a seven-point workload estimate scale [AD-A269194] p 1511 N94-18412
In-flight pressure distributions and skin-friction measurements on a subsonic transport high-lift wing section p 1308 N94-18435
Design, development, and flight evaluation of the Boeing YC-14 USB powered lift aircraft p 1310 N94-18444
VMC left turn curved approaches, test results — (visual meteorological conditions) [AD-A269476] p 1316 N94-18728
Flight test techniques for aircraft parameter estimation in ground effect [AD-A270058] p 1318 N94-18795
Attitude sensor package p 1325 N94-19172
Utilization of Shuttle small payload accommodations in the DOD Space Test Program p 1326 N94-19180
Superfluid Helium On-Orbit Transfer (SHOOT) flight demonstration p 1327 N94-19185

FLIGHT TRAINING
Integrated measurement of crew resource management and technical flying skills [AD-A270512] p 1510 N94-19677

FLIP-FLOPS
Evaluation of laser diode based optical switches for optical processors [AD-A270949] p 1581 N94-19602

FLIR DETECTORS
AN/APS-137 Forward Looking Airborne Radar (FLAR) evaluation Spring 1992 experiment [AD-A268899] p 1384 N94-18228

FLOW CHARACTERISTICS
Atlas of formability: NICKELVAC K-500 [AD-A268351] p 1356 N94-17772
Atlas of formability: Haynes 230 [AD-A268325] p 1356 N94-17788
Study of multi-phase flow characteristics in an MHD power train [DE93-018570] p 1586 N94-18272
Experimental investigation of flow around a multielement airfoil p 1305 N94-18417
In-flight pressure distributions and skin-friction measurements on a subsonic transport high-lift wing section p 1308 N94-18435
A fast computing method for the flow over high-lift wings p 1308 N94-18437
Turbulence modelling challenges posed by complex flows p 1415 N94-18592

FLOW CHARTS
A one dimensional numerical model, with an application to the vertical distribution of dissolved oxygen in the ocean [DE93-018481] p 1495 N94-17779
Modelling software for structure metrics [MEMO-INF-93-13] p 1526 N94-19200

FLOW DISTRIBUTION
WBNGRID, a program for generation of C-H and C-O topology grids around wing/body/nacelle configurations: User's guide [FFA-TN-1992-09] p 1311 N94-17721

Analysis of pultrusion processing for long fiber reinforced thermoplastic composite system [NASA-CR-194504] p 1339 N94-17766

CFD investigations of the hypersonic double delta wing greta: Sanger project no. 3.2 [FFA-TN-1992-42] p 1311 N94-17919

Exchange front stability in packed-column chromatography [DE93-017526] p 1346 N94-17997

Advanced in macrostatistical hydrodynamics [DE93-018479] p 1410 N94-18270

Efficient simulation of incompressible viscous flow over multi-element airfoils p 1306 N94-18421

Navier-Stokes simulation of flow field around a blown-flap high-lift system p 1307 N94-18429

Preliminary design of a water cooled avionics cooling rack [AD-A268826] p 1320 N94-18536

Analysis of supersonic flows using k-epsilon model and the RPLUS code: Progress towards high speed combustor analysis p 1411 N94-18551

Computational Fluid Dynamics (CFD) research branch technical briefs [AD-A269698] p 1417 N94-18739

Some parametric flow analyses of a particle bed fuel element [DE93-018440] p 1337 N94-18830

Experimental investigation of turbulent Prandtl number and Reynolds analogy in transitional and post-transitional boundary layers [AD-A270092] p 1418 N94-18867

Numerical simulation of turbulent mixing and combustion near the inlet of a burner [DE93-017960] p 1350 N94-18987

Time domain calculations of the second-order drift force on a floating two-dimensional object in current and waves [REPT-93-13] p 1419 N94-19087

Interferometric investigations of compressible dynamic stall over a transiently pitching airfoil [NASA-TM-109380] p 1312 N94-19119

Survey on the application of a 3D general purpose wind-tunnel research model [LR-713] p 1323 N94-19372

Semi-span model testing in the National Transonic Facility [NASA-CR-194479] p 1312 N94-19388

Numerical simulation of viscous flows in chemical nonequilibrium [MBB-LME-211-S-PUB-506] p 1421 N94-19497

Mathematical modeling of the free surface hydrodynamic and of transport in suspensions of non cohesive sediments: Aid to the interpretation of spatial images [ETN-93-95011] p 1421 N94-19502

Theoretical examination of the flow around a cylinder with a low dimensional Galerkin process [MPIS-25/1992] p 1422 N94-19525

The effects of initial conditions on the 3-D topology of temporally evolving wakes (ARI on 3-D bluff body wakes) [AD-A271008] p 1423 N94-19774

FLOW EQUATIONS

Research activities at the Center for Modeling of Turbulence and Transition p 1410 N94-18546

An introduction to second moment closure p 1414 N94-18580

Modelling force-field effects on turbulence p 1414 N94-18581

A new form of second-moment closure p 1414 N94-18582

Second-moment closure: Present... and future? p 1414 N94-18584

Contribution to the modelling of near-wall turbulence p 1414 N94-18585

Inclusion of second-moment closures into finite-volume solvers p 1415 N94-18588

Application of second-moment closure in complex flows p 1415 N94-18590

Turbulence modelling challenges posed by complex flows p 1415 N94-18592

Examples of turbulence model applications p 1415 N94-18593

Direct and large eddy simulation of turbulence: Summary of the state of the art 1993 p 1416 N94-18594

Large-eddy simulation of turbulent diffusion in stably stratified shear flow p 1416 N94-18595

Viscosity in the edge of tokamak plasmas [DE93-018039] p 1588 N94-18988

Pseudo-compressibility methods for the incompressible flow equations [NASA-CR-191533] p 1551 N94-19315

FLOW MEASUREMENT

In-flight pressure distributions and skin-friction measurements on a subsonic transport high-lift wing section p 1308 N94-18435

A review of hot-wire technique in compressible flows [LR-724] p 1423 N94-19668

FLOW RESISTANCE

A simple description of flow instability with application to a packed bed [DE93-017492] p 1420 N94-19345

FLOW STABILITY

A simple description of flow instability with application to a packed bed [DE93-017492] p 1420 N94-19345

Stability measurements of Rayleigh-Benard convection near the critical state using a spectral model [MPIS-15/1992] p 1422 N94-19520

Theoretical examination of the flow around a cylinder with a low dimensional Galerkin process [MPIS-25/1992] p 1422 N94-19525

Locally adaptive remeshing scheme for calculating fluid instabilities [DE93-019577] p 1422 N94-19568

FLOW VELOCITY

Exchange front stability in packed-column chromatography [DE93-017526] p 1346 N94-17997

Time domain calculations of the second-order drift force on a floating two-dimensional object in current and waves [REPT-93-13] p 1419 N94-19087

FLOW VISUALIZATION

Scaling laws for diffraction loading by air blast [PML-1991-54] p 1452 N94-17941

Interferometer stations at the Air Force Aeroballistic Research Facility [AD-A268776] p 1322 N94-18330

A computational and experimental investigation of incompressible oscillatory airfoil flow and flutter problems [AD-A268748] p 1311 N94-18402

Computational techniques for high-speed flows with viscous and chemical effects p 1412 N94-18560

Flow volumes for interactive vector field visualization [DE93-017102] p 1418 N94-18888

Airflow research [NASA-TM-109372] p 1312 N94-18964

Experimental study of flame front interactions [ECL-91-40] p 1353 N94-19376

Visualization of turbulent flow with particles [REPT-93-31] p 1423 N94-19645

FLUE GASES

Environmental Research Program [DE93-019101] p 1477 N94-19105

FLUENCE

Studies of deep levels in high resistivity silicon detectors irradiated by high fluence fast neutrons using a thermally stimulated current spectrometer [DE93-016133] p 1602 N94-19258

FLUID DYNAMICS

Atlas of formability: Haynes 230 [AD-A268325] p 1356 N94-17788

Numerical simulation of fluid dynamics and combustion for ram accelerator projectile/obturator interaction [AD-A269715] p 1320 N94-18748

Mathematical problems in combustion [AD-A270147] p 1349 N94-18776

Flow volumes for interactive vector field visualization [DE93-017102] p 1418 N94-18888

Characterization of fluid physics effects on cardiovascular response to microgravity (G-572) p 1323 N94-19163

A new approach to the study of the turbulence layer [NASA-CR-194546] p 1487 N94-19397

Visualization of turbulent flow with particles [REPT-93-31] p 1423 N94-19645

FLUID FILLED SHELLS

Fluid-structure-interaction analyses of reactor vessel using improved hybrid Lagrangian Eulerian code ALICE-II [DE93-015536] p 1409 N94-18248

FLUID FILMS

Contribution to the study of a symmetric film flow (with or without tensio-active elements) [ECL-93-13] p 1421 N94-19461

FLUID FLOW

Advanced in macrostatistical hydrodynamics [DE93-018479] p 1410 N94-18270

Data acquisition in aerodynamic research p 1431 N94-18644

Recent developments in fast response aerodynamic probe technology p 1431 N94-18645

Static pressure measurements for near isentropic flows using laser induced iodine fluorescence p 1431 N94-18646

Application of infrared thermography in fluid mechanics p 1431 N94-18649

DYNLET1 model formulation and user's guide [AD-A269843] p 1498 N94-18723

Efficiency of fiber dispersion [AD-A269740] p 1342 N94-18757

Flow volumes for interactive vector field visualization [DE93-017102] p 1418 N94-18888

Modeling of the formation of microporosity in alloys [DE93-017733] p 1364 N94-19044

An investigation of low Marangoni number fluid flow in a cold corner [AD-A271317] p 1422 N94-19569

FLUID JETS

Combustion instability phenomena of importance to liquid propellant engines [AD-A268800] p 1348 N94-18389

FLUID MANAGEMENT

Superfluid Helium On-Orbit Transfer (SHOOT) flight demonstration p 1327 N94-19185

FLUID MECHANICS

An overview of the SAFSIM computer program [DE93-017657] p 1519 N94-18002

Measurement Techniques [VKI-LS-1993-05] p 1430 N94-18643

Application of infrared thermography in fluid mechanics p 1431 N94-18649

Some parametric flow analyses of a particle bed fuel element [DE93-018440] p 1337 N94-18830

Group-invariant solutions of hydrodynamics and radiation hydrodynamics [DE93-018373] p 1423 N94-19604

FLUID POWER

Fluid dynamometer having fluid characteristic power absorption adjustment capability [AD-D015820] p 1424 N94-17904

FLUIDS

Stress pulse phenomena [DE93-019064] p 1456 N94-19078

FLUORESCENCE

SeaSoar CTD, fluorescence and scalar irradiance data from RRS Charles Darwin Cruises 58/59, NE Atlantic, Vivaldi 1991 [IOS-299-1992] p 1496 N94-18066

Detection of single molecules in microspheres [DE93-017776] p 1567 N94-18493

Final report on subcontract B076260 — borate synthesis [DE93-019501] p 1604 N94-19565

FLUORIDES

Calculation of the LiF-CeF3-BeF2 and LiF-PuF3-BeF2 ternary phase diagrams [DE93-017437] p 1360 N94-18501

An ultraviolet faraday rotator glass [AD-D015879] p 1371 N94-18529

FLUOROPOLYMERS

Polymer films with enhanced dielectric properties [AD-A271148] p 1375 N94-19740

FLUTTER

A computational and experimental investigation of incompressible oscillatory airfoil flow and flutter problems [AD-A268748] p 1311 N94-18402

Navier-Stokes, dynamics and aeroelastic computations for vortical flows, buffet and flutter applications [NASA-CR-194520] p 1313 N94-19621

FLUTTER ANALYSIS

A computational and experimental investigation of incompressible oscillatory airfoil flow and flutter problems [AD-A268748] p 1311 N94-18402

FLYING PERSONNEL

US Army aviation epidemiology data register: Prevalence of refractive error among US aircrew members [AD-A269550] p 1505 N94-18289

FOAMS

The Aerocapacitor: A carbon aerogel based supercapacitor [DE93-016537] p 1395 N94-17849

Summary report for supercritical carbon dioxide extraction and carbonization of Resorcinol-Formaldehyde (RF) foams [DE93-016924] p 1346 N94-17987

Shock-loading response of advanced materials [DE93-018344] p 1455 N94-19033

FOCUSING

Conical geometry for sagittal focusing as applied to x rays from synchrotrons [DE93-017238] p 1593 N94-17760

Alternating-phase focusing with amplitude modulation [DE93-018618] p 1574 N94-18273

FOG

Station climatic summaries: North America. Volume 1: The contiguous United States [AD-A269567] p 1490 N94-18303

FOKKER AIRCRAFT

Forty years of high-lift R/D: An aircraft manufacturer's experience p 1309 N94-18441

FOKKER-PLANCK EQUATION
Halo formation in mismatched, space-charge-dominated beams
[DE93-018581] p 1574 N94-18934

FOLDING STRUCTURES
Activities of the Center for Space Construction
[NASA-CR-193717] p 1335 N94-19371

FOOD INTAKE
Effects of a high-energy food supplement on cold-induced thermogenesis
[AD-A269301] p 1504 N94-17823

FOOD PROCESSING
FT-NIR spectroscopy in quantitative and qualitative measurements of cereal products
[VTT-TIED-1331] p 1346 N94-17973
Lunar base Controlled Ecological Life Support System (LCELSS): Preliminary conceptual design study
[NASA-CR-188479] p 1511 N94-18484

FOOD PRODUCTION (IN SPACE)
Lunar base Controlled Ecological Life Support System (LCELSS): Preliminary conceptual design study
[NASA-CR-188479] p 1511 N94-18484

FOOTPRINTS
Footprint size of a helicopter-borne electromagnetic induction sounding system versus antenna altitude
[AD-A270468] p 1463 N94-19672

FORCE DISTRIBUTION
Error propagation equations and tables for estimating the uncertainty in high-speed wind tunnel test results
[DE93-018685] p 1311 N94-18275

FORCED CONVECTION
Metal slurry droplet and spray combustion
[AD-A269648] p 1349 N94-18736

FORCED VIBRATION
Transformation of energy and momentum due to Landau damping in space
[DE93-624921] p 1581 N94-17689
Axial response of differently excited anchored viscous liquid bridges in zero-gravity
[LRT-WE-9-FB-1-1992] p 1379 N94-19489

FORECASTING
Terminal area forecasts, FY 1993-2005
[AD-A269855] p 1316 N94-18336
New techniques for contrail forecasting
[AD-A269686] p 1490 N94-18573
Directory of Energy Information Administration Models 1993
[DE93-016987] p 1616 N94-18707

FORESTS
Assessing impacts of climate change on forests: The state of biological modeling
[DE93-015916] p 1471 N94-17790

FORM FACTORS
Radiosity algorithms using higher order finite element methods
[DE93-018098] p 1531 N94-19548

FORMALDEHYDE
Summary report for supercritical carbon dioxide extraction and carbonization of Resorcinol-Formaldehyde (RF) foams
[DE93-016924] p 1346 N94-17987
Nonlinear optical properties of molecules
[AD-A270199] p 1567 N94-18783

FORMALISM
Multistack languages and grammars
[REPT-93-018] p 1518 N94-17926
Formal hardware verification of digital circuits
p 1401 N94-18367
Axiomatization, declarative semantics and operational semantics of passive and active updates in logic databases
[PB93-195956] p 1618 N94-19067

FORMAT
Vectorized presentation-level services for scientific distributed applications
[DE93-018091] p 1537 N94-19253

FORSTERITE
Tetravalent chromium (Cr(4+)) as laser-active ion for tunable solid-state lasers
[NASA-CR-194529] p 1441 N94-19369
Tetravalent chromium (Cr(4+)) as laser-active ion for tunable solid-state lasers
[NASA-CR-194528] p 1441 N94-19394

FORTRAN
High performance Fortran: An overview
[DE93-017181] p 1519 N94-18072

FORWARD SCATTERING
Statistical description of the bistatic radar cross section distributions for a right circular cylinder
[AD-A270001] p 1387 N94-18666
Forward scattering of a pulsed continuous wave signal through laminar and turbulent thermal plumes
[AD-A271210] p 1564 N94-19723

FOSSIL FUELS
Fifteenth Symposium on Biotechnology for Fuels and Chemicals: Program and Abstracts
[DE93-010005] p 1376 N94-18045
Directory of Energy Information Administration Models 1993
[DE93-016987] p 1616 N94-18707

FOUR-WAVE MIXING
Advanced optical fiber communication systems
[AD-A269120] p 1577 N94-18254
Novel nonlinear laser diagnostic techniques
[AD-A270968] p 1442 N94-19788

FOURIER ANALYSIS
Application of Fourier-based features for classification of synthetic aperture radar imagery
[AD-A270450] p 1387 N94-18513
The Fourier analysis technique and epsilon-pseudo-eigenvalues
[DE93-018805] p 1551 N94-19337

FOURIER TRANSFORMATION
An improved distributed arithmetic architecture
p 1398 N94-18349
Analysis of deposit precursors in jet fuels using Fourier transform infrared spectroscopy
[AD-A269035] p 1377 N94-18489
Application of wavelet transform techniques to spread spectrum demodulation and jamming
[AD-A267389] p 1389 N94-19009
Integrated test plan for the demonstration of a commercial Fourier Transform Infrared instrument
[DE93-018518] p 1433 N94-19041
Advances in passive-remote and extractive Fourier transform infrared systems
[DE93-017402] p 1478 N94-19241
Nontraditional windows in spectral analysis
[AD-A271336] p 1553 N94-19583

FOVEA
FY 1991 AASERT: Spatio-temporal making in human vision and its application to image coding
[AD-A268795] p 1505 N94-18190

FRACTALS
Application of fractal methods to estimate the aerosol-optical depth for atmospheric correction of high resolution satellite data
[DLR-FB-93-04] p 1480 N94-18088
JSEP fellowship: Fractal noise processes
[AD-A268841] p 1557 N94-18540
Mechanism-dependent fractal character of fracture surfaces in high strength and toughness ASTM A723 steels
[AD-A268956] p 1360 N94-18542

FRACTIONATION
Factors that control the stable carbon isotopic composition of methane produced in an anoxic marine sediment p 1477 N94-19235

FRACTURE MECHANICS
Inelastic deformation and damage at high temperature
[DE93-018155] p 1448 N94-17814
The calculation methods of a cracked plastic composite laminate: A literature survey
[VTT-TIED-1362] p 1339 N94-17958
Development and application of specially-focused ultrasonic transducers to location and sizing of defects in 75 mm- to 127 mm-thick austenitic stainless steel weld metals
[DE93-015975] p 1453 N94-18108
The Hall-Petch relationship and mechanisms of fracture in B2 compounds
[DE93-018887] p 1359 N94-18182
A comprehensive study of matrix fracture mechanisms in fiber-reinforced ceramic matrix composites
[AD-A268809] p 1340 N94-18205
A probability method of fracture mechanics analysis for HFIR vessel
[DE93-015510] p 1453 N94-18246
Steep geometric grating for use in moire interferometry
[AD-A268759] p 1453 N94-18328
Fundamental research in nonlinear random vibration for aerospace applications
[AD-A268929] p 1454 N94-18487
Fundamental concepts relating local atomic arrangements, deformation, and fracture of intermetallic alloys
[AD-A268745] p 1361 N94-18788
A numerical analysis of crack growth in brittle microcracking composites
[DE93-011562] p 1343 N94-18914
Stress pulse phenomena
[DE93-019064] p 1456 N94-19078
Interfacial cracks in plates: A three-dimensional numerical investigation p 1456 N94-19116
Computational mechanics of composite materials
[PB93-195782] p 1343 N94-19281
Micromechanics of interfaces in metal matrix composites
[AD-A271012] p 1345 N94-19776

FRACTURE STRENGTH
Interpretation of warm prestress-induced fracture toughness based on crack-tip constraint
[DE93-015967] p 1451 N94-17913
Mechanism-dependent fractal character of fracture surfaces in high strength and toughness ASTM A723 steels
[AD-A268956] p 1360 N94-18542
Fatigue technology assessment and strategies for fatigue avoidance in marine structures. Appendices
[AD-A269053] p 1455 N94-18716
Nondestructive inspection of graphite-epoxy laminates for heat damage using DRIFT and LPF spectroscopies
[DE93-017228] p 1343 N94-18761
Thermal stresses in the microchannel heatsink cooled by liquid nitrogen
[DE93-018660] p 1418 N94-18995
Micromechanics of interfaces in metal matrix composites
[AD-A271012] p 1345 N94-19776

FRACTURES (MATERIALS)
The application of nondestructive techniques to the testing of a wind turbine blade
[DE93-016731] p 1447 N94-18128
The 6th Japan-U.S. conference on composite materials
[AD-A268535] p 1341 N94-18630
Simulation of dynamic material response with the PAGOSA code
[DE93-018285] p 1460 N94-19603

FRACTURING
Computational strategies for composite structures
[PB93-195097] p 1452 N94-18079
The Hall-Petch relationship and mechanisms of fracture in B2 compounds
[DE93-018887] p 1359 N94-18182
A comprehensive study of matrix fracture mechanisms in fiber-reinforced ceramic matrix composites
[AD-A268809] p 1340 N94-18205
Experimental investigation of wave and fracture phenomena in impacted ceramics: Experiments on sapphire
[AD-A270040] p 1372 N94-18792
Interfacial cracks in plates: A three-dimensional numerical investigation p 1456 N94-19116
Analytical and experimental evaluation of joining silicon nitride to metal and silicon carbide to metal for advanced heat engine applications
[DE93-018128] p 1446 N94-19291
Simulation of dynamic material response with the PAGOSA code
[DE93-018285] p 1460 N94-19603

FRAGMENTATION
Proton transfer dynamics and cluster ion fragmentation in phenol/ammonia cLusters
[AD-A269133] p 1348 N94-18256

FRAGMENTS
Dynamic behaviors of fragments ejected from the surface of carbon materials by laser ablation
[DE93-788620] p 1438 N94-18161

FREE CONVECTION
A new approach to the study of the turbulence layer
[NASA-CR-194546] p 1487 N94-19397

FREE ELECTRON LASERS
Measuring emittance using beam position monitors
[DE93-014470] p 1434 N94-17709
Experiments in sideband suppression on the Los Alamos National Laboratory Free-Electron Laser
[DE93-014466] p 1435 N94-17724
Designs for optical components related to the Los Alamos free-electron laser
[DE93-016617] p 1436 N94-17865
Three-dimensional simulation analysis of the first sections of a standing-wave free-electron laser two-beam accelerator
[DE93-016977] p 1436 N94-17869
A superconducting short period undulator for a harmonic generation FEL experiment
[DE93-017581] p 1436 N94-17998
Design of a tunable 4-MW free electron maser for heating fusion plasmas
[DE93-017172] p 1437 N94-18134
FEL experiment with a focusing wiggler
[DE93-788586] p 1438 N94-18160
Simulation of emittance dilution in electron storage ring from Compton backscattering
[DE93-017611] p 1386 N94-18503
Magnetic field measurements of a superconducting undulator for a Harmonic Generation FEL experiment at the NSLS
[DE93-017621] p 1438 N94-18504
New applications for high average power beams
[DE93-018845] p 1439 N94-18522

Designs for a 10.6 micrometer electromagnetic wiggler Free-Electron Laser (FEL)
[AD-A269695] p 1439 N94-18576
Interaction of intense lasers and relativistic electron beams with solids, gases and plasmas
[AD-A269655] p 1439 N94-18737
A tunable compact high power far-infrared grating free-electron laser
[AD-A269875] p 1440 N94-18771
Final construction and operation of a continuous far-infrared free-electron laser for scientific applications
[AD-A269248] p 1440 N94-18912
Laser powered beam conditioner for free-electron lasers and synchrotrons
[DE93-017821] p 1441 N94-18974
Coherence and linewidth studies of a 4-nm high power FEL
[DE93-018533] p 1441 N94-19030
Experiments on nonlinear absorption of ECH waves in MTX and a comparison with theory
[DE93-019158] p 1589 N94-19074
Electron cyclotron resonance heating in the microwave tokamak experiment
[DE93-018083] p 1590 N94-19289
Compact free electron lasers for medical applications
[AD-A271272] p 1442 N94-19729
A study of the amplification of laser and VLF waves using a simple pendulum model
[AD-A270857] p 1442 N94-19770

FREE ELECTRONS
Upper atmospheric effects of the HF Active Auroral Research Program Ionospheric Research Instrument (HAARP IRI)
[AD-A268948] p 1481 N94-18451

FREE ENERGY
FEEST: A method for tabulating equation of state and opacity tables
[DE93-017965] p 1347 N94-18092
A free energy simulation method based study of interfacial segregation
[DE93-019462] p 1364 N94-19032
On neutral plasma oscillations
[DE93-040319] p 1590 N94-19194

FREE FALL
Free fall liquid column dynamics in a droptower
[LRT-WE-9-FB-6-1992] p 1379 N94-19491

FREE FLOW
Experimental investigation of turbulent Prandtl number and Reynolds analogy in transitional and post-transitional boundary layers
[AD-A270092] p 1418 N94-18867

FREE JETS
Static pressure measurements for near isentropic flows using laser induced iodine fluorescence
p 1431 N94-18646

FREE RADICALS
Photodissociation studies of polyatomic free radicals
[AD-A270084] p 1350 N94-18799

FREE VIBRATION
Transformation of energy and momentum due to Landau damping in space
[DE93-624921] p 1581 N94-17689
The longitudinal free vibrations of a fixed-free two-phase elastic bar
[AD-A268768] p 1453 N94-18387
Free fall liquid column dynamics in a droptower
[LRT-WE-9-FB-6-1992] p 1379 N94-19491

FREEZE DRYING
Evaluation of dried storage of platelets for transfusion: Physiologic integrity and hemostatic functionality
[AD-A270756] p 1507 N94-19593

FREEZING
Shrinkage void formation and its effect on freeze and thaw processes of lithium and lithium-fluoride for space applications
[DE93-019303] p 1338 N94-19128

FREON
Velocity measurements in a boundary layer with a density gradient
[DE93-019627] p 1422 N94-19515

FREQUENCIES
FY 1991 AASERT: Spatio-temporal making in human vision and its application to image coding
[AD-A268795] p 1505 N94-18190

FREQUENCY ANALYZERS
A RFI measurement system for field sites
[AD-A269340] p 1385 N94-18301

FREQUENCY CONTROL
Experiments in sideband suppression on the Los Alamos National Laboratory Free-Electron Laser
[DE93-014466] p 1435 N94-17724
Synchrotron beam-loading stability with a higher RF harmonic
[DE93-014549] p 1573 N94-17726
Military applications of high-accuracy frequency standards and clocks
[AD-A269303] p 1430 N94-18299
The gyrotron backward-wave-oscillator experiment — final progress report
[AD-A268982] p 1403 N94-18452

FREQUENCY CONVERTERS
Tunable synchronously pumped intracavity two-stage optical frequency upconversion
[AD-A269105] p 1438 N94-18250
Investigation of a fiber optic frequency shifter and optical isolator
[AD-A269820] p 1579 N94-18738
Contribution to the study of the additional losses in coil elements used in static converters
[ECL-92-60] p 1406 N94-19297

FREQUENCY DIVISION MULTIPLE ACCESS
Application of wavelet transform techniques to spread spectrum demodulation and jamming
[AD-A267389] p 1389 N94-19009

FREQUENCY DIVISION MULTIPLEXING
VHF air/ground communications for air traffic control. Volume 1: A decision tree approach to system innovations
[AD-A268485] p 1316 N94-18384

FREQUENCY HOPPING
Efficient simulation of DEDS by means of standard clock techniques: Queueing and integrated radio network examples
[AD-A269878] p 1432 N94-18681
Application of wavelet transform techniques to spread spectrum demodulation and jamming
[AD-A267389] p 1389 N94-19009

FREQUENCY MODULATION
A superconducting short period undulator for a harmonic generation FEL experiment
[DE93-017581] p 1436 N94-17998
Magnetostatic waves-based integrated optic bragg cell modules with applications to RF signal processing
[AD-A269115] p 1577 N94-18295
Resolution in radar mapping
[AD-A269730] p 1462 N94-18753

FREQUENCY RANGES
A RFI measurement system for field sites
[AD-A269340] p 1385 N94-18301
An application of parameter estimation to the stability and control of the BQM-147 unmanned aerial vehicle
[AD-A268741] p 1321 N94-18401
Broadband IF matching for quasioptical mixers
[MPE-PREPRINT-240] p 1390 N94-19416
Meteor burst communications improvement study
[AD-A270866] p 1393 N94-19793

FREQUENCY RESPONSE
Simulation of the ALS longitudinal multibunch feedback system
[DE93-019227] p 1575 N94-19152

FREQUENCY SHIFT
Magnetostatic waves-based integrated optic bragg cell modules with applications to RF signal processing
[AD-A269115] p 1577 N94-18295
Investigation of a fiber optic frequency shifter and optical isolator
[AD-A269820] p 1579 N94-18738

FREQUENCY SHIFT KEYING
Nontraditional windows in spectral analysis
[AD-A271336] p 1553 N94-19583

FREQUENCY STANDARDS
Development of atomic standards at the Neuchatel Observatory p 1428 N94-18038
Military applications of high-accuracy frequency standards and clocks
[AD-A269303] p 1430 N94-18299
Optical frequency division using an optical parametric oscillator
[AD-A270847] p 1581 N94-19578

FRESNEL LENSES
Photovoltaic concentrator initiative: Concentrator cell development
[DE93-018505] p 1466 N94-18335

FRICTION
Studies of dynamic contact of ceramics and alloys for advanced heat engines
[DE93-016366] p 1368 N94-18110
Atomic-scale friction measurements using friction force microscopy. Part 1: General principles and new measurement techniques
[AD-A270749] p 1446 N94-19678
Microtribology of magnetic media
[AD-A271209] p 1407 N94-19722
Examinations of the friction behavior in nonstationary flow processes in pipes
[MITT-7] p 1423 N94-19730
Surface species in tribology
[AD-A270970] p 1446 N94-19754
Atomic-scale friction measurements using friction force microscopy. Part 2: Application to magnetic media
[AD-A270759] p 1447 N94-19767

FRICTION DRAG
The effect of fine surface riblets on the flow around an inclined axially symmetrical body
[MPIS-105/1993] p 1420 N94-19356

FRICTION FACTOR
Heterogeneous slip and rupture models of the San Andreas fault zone based upon three-dimensional earthquake tomography
[DE93-015037] p 1480 N94-17898

FRICTION MEASUREMENT
Atomic-scale friction measurements using friction force microscopy. Part 1: General principles and new measurement techniques
[AD-A270749] p 1446 N94-19678
Atomic-scale friction measurements using friction force microscopy. Part 2: Application to magnetic media
[AD-A270759] p 1447 N94-19767

FUEL CELL POWER PLANTS
Molten carbonate fuel cell networks: Principles, analysis, and performance
[DE93-000281] p 1468 N94-18925

FUEL CELLS
Oxygen reduction at a stabilized zirconia interface with Y(1-x)Ca(x)MnO3 or La(1-x)Sr(x)MnO3 cathode materials
[DE93-015681] p 1593 N94-17747
Fuel cell systems program plan, fiscal year 1993
[DE93-017828] p 1466 N94-18103
Molten carbonate fuel cell networks: Principles, analysis, and performance
[DE93-000281] p 1468 N94-18925
National Program Plan Fuel Cells in Transportation
[DE93-017557] p 1469 N94-19346

FUEL COMBUSTION
Organic carbonyl compounds in Albuquerque, New Mexico, air: A preliminary study of the effects of oxygenated fuel use
[DE93-017748] p 1476 N94-19045

FUEL CONSUMPTION
Evaluation of aftermarket LPG conversion kits in light-duty vehicle applications
[DE93-010035] p 1377 N94-18617
Constant-thrust orbit-raising transfer charts
[AD-A269088] p 1334 N94-18718

FUEL FLOW
Some parametric flow analyses of a particle bed fuel element
[DE93-018440] p 1337 N94-18830

FUEL PRODUCTION
Photobiotechnology: Application of photosynthesis to the production of renewable fuels and chemicals
[DE93-015522] p 1466 N94-18247

FUEL SPRAYS
A coupled implicit solution method for turbulent spray combustion in propulsion systems p 1411 N94-18549

FUEL SYSTEMS
Evaluation of aftermarket LPG conversion kits in light-duty vehicle applications
[DE93-010035] p 1377 N94-18617

FUELS
Energy Efficiency and Renewable Energy Program
[DE93-017936] p 1468 N94-18986
A Sandia Technology Bulletin: Testing technology, July 1993
[DE93-040197] p 1633 N94-19537
A study of the effect of hydrocarbon structure on the induction of male rat nephropathy and metabolic structure
[AD-A270969] p 1504 N94-19789

FULL SCALE TESTS
The GARTEUR high lift research programme
p 1307 N94-18430

FULLERENES
Vibrational and electronic properties of clusters and ultrathin films
[DE93-012291] p 1367 N94-17678
Novel catalysts for methane activation
[DE93-040630] p 1349 N94-18532
Role of pressure in the study of fullerenes
[DE93-018839] p 1602 N94-19340
Effects of pressure on the orientational ordering and phase transitions in solid C(60) and C(70)
[DE93-018858] p 1603 N94-19347

FUNCTIONAL DESIGN SPECIFICATIONS
TDRS press release
[NASA-TM-109373] p 1335 N94-18965
Conceptual design of a sodium sulfur cell for US electric van batteries
[DE93-018683] p 1405 N94-19035
On the automation of object-oriented requirements analysis
[AD-A270673] p 1532 N94-19782

FUNCTIONS (MATHEMATICS)
Bits and relative order from residues, space efficiently
[TR-464] p 1530 N94-19482
FURANS
A comparison of wet and dry scrubbing systems for control of metals and dioxin/furan emissions from incinerators
[DE93-017446] p 1474 N94-18502
FURNACES
MUZO flight experience with the programmable multizone furnace p 1324 N94-19167
FUSELAGES
Metals 2000
[DE93-016761] p 1355 N94-17752
Vertical drop test of a Metro 3 aircraft
[AD-A270032] p 1318 N94-18789
Fatigue crack initiation in riveted lap joints and in pressurized fuselages
[LR-725] p 1461 N94-19669
FUSION REACTORS
Arc detection and protection in high-power antenna systems
[DE93-013272] p 1382 N94-17695
ITER EDA design confinement capability
[DE93-013729] p 1582 N94-17697
Laboratory microfusion capability study
[DE93-014373] p 1583 N94-17912
Report of the 1991 Workshop on Particle-Material Interactions for Fusion Research
[DE93-788393] p 1573 N94-18156
A survey on technical problems in designing high-speed rotors with developing materials
[DE93-788519] p 1444 N94-18159
Parametric analysis of the ARIES-3D-He-3 tokamak reactor
[DE93-018293] p 1587 N94-18803
Thermal analysis of coatings and substrate materials during a disruption in fusion reactors
[DE93-017688] p 1588 N94-18971
Review Committee report on the conceptual design of the tokamak physics experiment
[DE93-018408] p 1588 N94-19012
Beryllium processing technology review for applications in plasma-facing components
[DE93-018396] p 1363 N94-19028
Thermo-hydraulic analysis of superconducting toroidal-field magnets for the Tokamak Physics Experiment
[DE93-018096] p 1590 N94-19269
FUSION WELDING
Microstructural analysis of solid-state resistance welds
[DE93-017295] p 1443 N94-17761
FUZZY SETS
Fuzzy almost linear spaces
[DE93-624772] p 1545 N94-17680
Fuzzy hypergraphs and fuzzy intersection graphs
[AD-A270303] p 1549 N94-18815
FUZZY SYSTEMS
Fuzzy almost linear spaces
[DE93-624772] p 1545 N94-17680
Automatic tuning of an integral fuzzy controller
[REPT-93-006] p 1383 N94-17932
Fuzzy control of magnetic bearings
p 1399 N94-18357
Optimizing wind turbine control system parameters
[DE93-018861] p 1469 N94-19036

G

GADOLINIUM
Photoemission studies of Zn, Co, and Gd substituted YBa2Cu3O(7-delta)
[DE93-017403] p 1597 N94-18498
GALACTIC COSMIC RAYS
The LET spectrum and its uncertainty during the CRRES mission
[AD-A269977] p 1630 N94-18676
GALACTIC EVOLUTION
Space and time as outcome of decoherence in an expanding universe
[DE93-016199] p 1624 N94-18047
The universe at moderate redshift
[NASA-CR-193771] p 1627 N94-19093
GALACTIC NUCLEI
The 0.15 seconds near-infrared imaging of the central parsec of the galaxy
[MPE-PREPRINT-239] p 1621 N94-19415
GALAXIES
Pulse-timing studies of x ray pulsars
[NASA-CR-193778] p 1621 N94-18611
GALERKIN METHOD
A massively parallel adaptive finite element method with dynamic load balancing
[DE93-012844] p 1536 N94-19161
On the numerical analysis of nonlinear Galerkin methods: Spectral approximation and finite elements
[ETN-93-94900] p 1552 N94-19407
Stability measurements of Rayleigh-Benard convection near the critical state using a spectral model
[MPIS-15/1992] p 1422 N94-19520
Theoretical examination of the flow around a cylinder with a low dimensional Galerkin process
[MPIS-25/1992] p 1422 N94-19525
GALILEO PROJECT
Magellan, Galileo, and Ulysses
[NASA-TM-109362] p 1628 N94-18958
GALILEO SPACECRAFT
Magellan, Galileo, and Ulysses
[NASA-TM-109362] p 1628 N94-18958
GALLIUM ARSENIDES
Reorientation of misfit dislocations during annealing in InGaAs/GaAs(001) interfaces
[DE93-015046] p 1592 N94-17741
Defects in GaAs bulk crystals and multi-layers caused by In diffusion
[DE93-016968] p 1595 N94-18054
Nitridation of GaAs(100) by laser-induced decomposition of HN3
[AD-A269147] p 1438 N94-18258
New dynamic FET logic and serial memory circuits for VLSI GaAs technology p 1397 N94-18339
Gallium arsenide-based ternary compounds and multi-band-gap solar cell research
[DE93-010049] p 1467 N94-18483
Kinetic aspects of lattice mismatch in molecular beam epitaxial growth on planar and patterned substrates
[AD-A270424] p 1597 N94-18506
Growth of structures for integrated optoelectronic devices
[AD-A269014] p 1598 N94-18527
Design and simulation of a gallium-arsenide second order sigma-delta analog to digital converter
[AD-A269494] p 1404 N94-18701
High efficiency low cost monolithic module for SARSAT distress beacons
[NASA-CR-194234] p 1315 N94-18852
Study of GaAs substrates by ambient temperature photoluminescence imagery
[ECL-92-61] p 1603 N94-19357
Quasi-optical transponder using FET's and patch antennas
[AD-A271339] p 1407 N94-19584
Isolation mechanisms in III-V devices
[AD-A271197] p 1605 N94-19717
Single source precursors for the OMCVD of 3/5 compound semiconductors
[AD-A271147] p 1606 N94-19739
GALLIUM PHOSPHIDES
Gallium arsenide-based ternary compounds and multi-band-gap solar cell research
[DE93-010049] p 1467 N94-18483
GAME THEORY
Mathematical communications, volume 27, numbers 1 and 2, 1992. List and abstracts of memoranda published in the period July - December 1991
[PB93-191997] p 1553 N94-19557
GAMMA RAY ASTRONOMY
Telescope for x ray and gamma ray studies in astrophysics p 1324 N94-19166
GAMMA RAY BURSTS
The GAMCIT gamma ray burst detector
p 1324 N94-19168
GAMMA RAY LASERS
Proof of the feasibility of coherent and incoherent schemes for pumping a gamma ray laser
[AD-A269173] p 1440 N94-18880
GAMMA RAY OBSERVATORY
EGRET Mission and Data Analysis
[MPE-PREPRINT-223] p 1622 N94-19462
EGRET observations of 3 C 273
p 1623 N94-19464
GAMMA RAY SPECTROMETERS
Detection of a long-duration solar gamma-ray flare on Jun. 11, 1991 with EGRET on Compton-GRO
p 1623 N94-19463
GAMMA RAY TELESCOPES
Telescope for x ray and gamma ray studies in astrophysics p 1324 N94-19166
GAMMA RAYS
Crystal optics of high energy gamma-beams
[DE93-630228] p 1577 N94-18217
Evaluation of fiber optic performance in the ACRR
[DE93-018515] p 1580 N94-18970
Gamma scattering in condensed matter with high intensity Moessbauer radiation
[DE93-019461] p 1601 N94-19031
New room temperature high resolution solid-state detector (CdZnTe) for hard x rays and gamma rays
p 1324 N94-19165
The GAMCIT gamma ray burst detector
p 1324 N94-19168
GARMENTS
Conductive garments to prevent Radio-Frequency (RF) burns
[AD-D015832] p 1512 N94-18730
GAS ANALYSIS
Solid-state, resistive hydrogen sensors for safety monitoring
[DE93-017769] p 1424 N94-17778
A mobile remote sensing laboratory for water vapor, trace gas, aerosol, and wind speed measurements
[DE93-017158] p 1489 N94-18132
Global three dimensional model of tropospheric trace gases chemistry and transport
[AERONAUTICA-ACTA-A-370-199]
p 1479 N94-19518
GAS CHROMATOGRAPHY
Exchange front stability in packed-column chromatography
[DE93-017526] p 1346 N94-17997
GAS DETECTORS
Synoptic ocean prediction experiment. EN216 CTD section data report
[AD-A268903] p 1497 N94-18230
GAS DISSOCIATION
Experimental study of interactions of highly charged ions with atoms at keV energies
[DE93-040222] p 1571 N94-19257
GAS DYNAMICS
Wave structure induced by fluid dynamic limits in the Broadwell model
[AD-A268512] p 1410 N94-18385
Two-dimensional boundary surfaces for axi-symmetric external transonic flows
[AD-A269678] p 1312 N94-18571
UUGM code development
[AD-A269945] p 1416 N94-18671
On positivity preserving finite volume schemes for compressible Euler equations
[NASA-CR-191534] p 1551 N94-19317
GAS EVOLUTION
Modeling of the formation of microporosity in alloys
[DE93-017733] p 1364 N94-19044
GAS FLOW
Wave structure induced by fluid dynamic limits in the Broadwell model
[AD-A268512] p 1410 N94-18385
Regenerator optimization for Stirling cycle refrigeration
[DE93-018468] p 1380 N94-18818
A simple description of flow instability with application to a packed bed
[DE93-017492] p 1420 N94-19345
Collaborative research on combustion diagnostics and modeling between Rolls-Royce, Inc. and the United States Air Force Wright Laboratory
[AD-A270660] p 1354 N94-19778
GAS GIANT PLANETS
Planetary plasma waves
[NASA-CR-194295] p 1629 N94-19094
GAS JETS
Analysis of neon soft x ray spectra from short-pulse laser-produced plasmas
[DE93-014420] p 1582 N94-17708
Computational aero-acoustics as a branch of turbulence research p 1411 N94-18552
GAS LASERS
Proof of the feasibility of coherent and incoherent schemes for pumping a gamma ray laser
[AD-A269173] p 1440 N94-18880
Foil support structure for large electron guns
[DE93-018478] p 1322 N94-18890
GAS TEMPERATURE
Considerations for the use of the modified line reversal technique for gas temperature measurement
[DE93-015752] p 1576 N94-17857
Temperature lowering in cryogenic chemical-synthesis techniques and system
[DE93-018348] p 1562 N94-18810
GAS TRANSPORT
A preliminary model for crack-tip hydrogen transport
[NPL-DMM(A)-84] p 1451 N94-17899
Ratio of specimen thickness to detection area for reliable hydrogen permeation measurement
[NPL-DMM(A)-103] p 1451 N94-17929
GAS TUNGSTEN ARC WELDING
Technique to eliminate helium induced weld cracking in stainless steels
[DE93-015982] p 1357 N94-17859
Helium-induced weld degradation of HT-9 steel
[DE93-015981] p 1358 N94-17915
GAS TURBINE ENGINES
SAND contact in DYNA3D
[DE93-016451] p 1340 N94-18113

GAS TURBINES
Report to Congress: Comprehensive Program Plan for Advanced Turbine Systems [DE93-016718] p 1467 N94-18475
Vane optimization for maximum efficiency using Design Of Experiments (DOX) [AD-A270270] p 1320 N94-18907
Collaborative research on combustion diagnostics and modeling between Rolls-Royce, Inc. and the United States Air Force Wright Laboratory [AD-A270660] p 1354 N94-19778

GAS VISCOSITY
A simple description of flow instability with application to a packed bed [DE93-017492] p 1420 N94-19345

GAS-GAS INTERACTIONS
Experimental study of flame front interactions [ECL-91-40] p 1353 N94-19376

GAS-LIQUID INTERACTIONS
Condensed gases under winter conditions: A study for the rescue services [FOA-C-40305-4.5] p 1473 N94-18139

GAS-SOLID INTERACTIONS
Scaling laws for diamond chemical vapor deposition. Diamond surface chemistry [AD-A269874] p 1599 N94-18745

GASDYNAMIC LASERS
Electrically excited CO-lasers with gas dynamic cooling [DLR-FB-93-08] p 1437 N94-18061

GASEOUS DIFFUSION
Faulted structure of the bottom simulating reflector on the Blake Ridge, western North Atlantic [AD-A271289] p 1500 N94-19745

GASES
Suitability of infrared spectroscopy for remote sensing of tropospheric trace gases [KFK-5183] p 1479 N94-19507

GATES (CIRCUITS)
Single phase dynamic CMOS PLA using charge sharing technique p 1397 N94-18341
An SEU immune logic family p 1398 N94-18342
A tunable CMOS constant current source p 1401 N94-18369
Canonical multi-valued input Reed-Muller trees and forms p 1401 N94-18375
Evaluation of laser diode based optical switches for optical processors [AD-A270949] p 1581 N94-19602

GAUGE INVARIANCE
Avoiding degenerate coframes in an affine gauge approach to quantum gravity [DE93-013146] p 1607 N94-17892
Gauge coupling unification in superstring derived standard-like models [DE93-624801] p 1607 N94-17950
Gauge unification of fundamental forces: The story of success [DE93-624813] p 1383 N94-17952
A general solution of the BV-master equation and BRST field theories [DE93-628622] p 1561 N94-18171

GAUGE THEORY
Renormalizations in supersymmetric and nonsupersymmetric non-abelian Chern-Simons field theories with matter [DE93-626646] p 1593 N94-17748
Gauge coupling unification in superstring derived standard-like models [DE93-624801] p 1607 N94-17950
Gauge unification of fundamental forces: The story of success [DE93-624813] p 1383 N94-17952
Cabibbo mixing in superstring derived standard-like models [DE93-624814] p 1607 N94-17953
A general solution of the BV-master equation and BRST field theories [DE93-628622] p 1561 N94-18171
A multi-thread approach to coalescing small transfers generated by portable tool sets [DE93-012128] p 1525 N94-19186
Investigations in gauge theories, topological solitons, and string theories [DE93-015029] p 1609 N94-19250

GEAR TEETH
Tooth form design supporting system in module design p 1428 N94-18036
Gear sound levels with various tooth contact ratios and forms [NASA-TM-106432] p 1446 N94-19318

GEARS
Gear train behavior analyzer using laser beam scanning for watch movement p 1427 N94-18028
Gear sound levels with various tooth contact ratios and forms [NASA-TM-106432] p 1446 N94-19318

GELS
Studies on gel electrolyte based on nitrile-butadiene copolymers [AD-A269450] p 1370 N94-18282

GENE EXPRESSION
The c-jun gene expression in human cells exposed to either ionizing radiation or hydrogen peroxide [DE93-017436] p 1502 N94-18476
Life: Origin and evolution on Earth--How can we escape? p 1503 N94-19217

GENERAL AVIATION AIRCRAFT
Terminal area forecasts, FY 1993-2005 [AD-A269855] p 1316 N94-18336

GENES
Life: Origin and evolution on Earth--How can we escape? p 1503 N94-19217

GENETIC ALGORITHMS
Optimal design of binary phase-only filters using genetic algorithms [AD-A268737] p 1396 N94-18278
Training product unit neural networks with genetic algorithms p 1399 N94-18354

GENETIC CODE
The rationale for fundamental research in space biology: Introduction and background p 1502 N94-19211

GENETICS
Systolic array IC for genetic computation p 1400 N94-18361
Life: Origin and evolution on Earth--How can we escape? p 1503 N94-19217

GEODESIC LINES
(1,1)-geodesic maps into Grassmann manifolds [DE93-624799] p 1545 N94-17684
Unbounded components in parameter space of rational maps [DE93-628621] p 1548 N94-18170

GEODESY
(1,1)-geodesic maps into Grassmann manifolds [DE93-624799] p 1545 N94-17684
Belgian Royal Observatory Communications, Series A, No. 104, Geophysics Series No. 175 [COMMUNICATIONS-SER-A-104] p 1482 N94-18622
What can gravimetry contribute to recent and current tectonics in Belgium? p 1482 N94-18626
Current positioning possibilities by spatial techniques and the Royal Oservatory of Belgium program p 1483 N94-18627
Instrumentation developed at the Royal Observatory of Belgium for measuring slow displacements of the Earth p 1483 N94-18628
Research on Earth's rotation and the effect of atmospheric pressure on vertical deformation and sea level variability [NASA-CR-194300] p 1484 N94-18838
Gravity and the geoid in the Nepal Himalaya [NASA-CR-194166] p 1463 N94-19430
The interpretation of crustal dynamics data in terms of plate motions and regional deformation near plate boundaries [NASA-CR-194302] p 1487 N94-19432

GEODETIC SATELLITES
What can gravimetry contribute to recent and current tectonics in Belgium? p 1482 N94-18626

GEODETIC SURVEYS
Gravity and the geoid in the Nepal Himalaya [NASA-CR-194166] p 1463 N94-19430

GEODYNAMICS
Heterogeneous slip and rupture models of the San Andreas fault zone based upon three-dimensional earthquake tomography [DE93-015037] p 1480 N94-17898
Research on Earth's rotation and the effect of atmospheric pressure on vertical deformation and sea level variability [NASA-CR-194300] p 1484 N94-18838
Analysis of regional deformation and strain accumulation data adjacent to the San Andreas fault [NASA-CR-194072] p 1487 N94-19428
The interpretation of crustal dynamics data in terms of plate motions and regional deformation near plate boundaries [NASA-CR-194302] p 1487 N94-19432

GEOGRAPHIC INFORMATION SYSTEMS
Energy efficiency and the environment: Innovative ways to improve air quality in the Los Angeles Basin [DE93-016964] p 1473 N94-18050
Application of ARC/INFO to regional scale hydrogeologic modeling [DE93-015673] p 1461 N94-18107
Directional regions in Geographic Information Systems (GIS) [AD-A268536] p 1462 N94-18309
Working visit to the University of L'Aquila, Italy [FEL-93-B020] p 1618 N94-19452

GEOGRAPHY
Directional regions in Geographic Information Systems (GIS) [AD-A268536] p 1462 N94-18309
Eastern Europe: A climatological study [AD-A269200] p 1493 N94-18883

GEOIDS
What can gravimetry contribute to recent and current tectonics in Belgium? p 1482 N94-18626
Research on Earth's rotation and the effect of atmospheric pressure on vertical deformation and sea level variability [NASA-CR-194300] p 1484 N94-18838

GEOLOGICAL FAULTS
Historical seismicity of Hainaut, Flanders and Artois p 1482 N94-18623
Current (1985-1988) seismic activity in Belgium: Comparison with historical and instrumental seismic data p 1482 N94-18624
Macroseismic study of the Dour (Belgium) earthquakes of 22 March 1987 and of Gulpen (Belgium) 17 October 1988 p 1482 N94-18625
The interpretation of crustal dynamics data in terms of plate motions and regional deformation near plate boundaries [NASA-CR-194302] p 1487 N94-19432
Faulted structure of the bottom simulating reflector on the Blake Ridge, western North Atlantic [AD-A271289] p 1500 N94-19745

GEOLOGY
Technologies for assessing the geologic and geomorphic history of coasts [AD-A268780] p 1496 N94-18215
High resolution geological site characterization utilizing ground motion data [AD-A268926] p 1481 N94-18485
JPRS report: Science and technology. Central Eurasia: Earth Sciences [JPRS-UES-93-004] p 1461 N94-19209

GEOMAGNETIC LATITUDE
The effects of magnetic storm phases on f-layer irregularities from auroral to equatorial latitudes [AD-A267388] p 1486 N94-19008

GEOMAGNETISM
Global zones of particle precipitation as observed EXOS-C [AD-A268758] p 1481 N94-18467
ISTP Global Geospace Science. Energy transfer in geospace [NASA-TM-109239] p 1620 N94-18851
Contributions from geomagnetic inverse theory to the study of hydromagnetic conditions near the core-mantle boundary [NASA-CR-194303] p 1484 N94-18853
Activities of the Indian Institute of Geomagnetism p 1484 N94-18854

GEOMETRICAL OPTICS
The interpretation of optical caustics in the presence of dynamic non-uniform crack-tip motion histories: A study based on a higher order transient crack-tip expansion [SM91-12] p 1456 N94-19130

GEOMETRICAL THEORY OF DIFFRACTION
Wideband electromagnetic scattering/analysis program: Far zone electromagnetic scattering from complex shapes using geometrical theory of diffraction [AD-A268790] p 1384 N94-18187

GEOMORPHOLOGY
Technologies for assessing the geologic and geomorphic history of coasts [AD-A268780] p 1496 N94-18215
Mechanical modeling of the growth of salt structures [DE93-015342] p 1596 N94-18243
Macroseismic study of the Dour (Belgium) earthquakes of 22 March 1987 and of Gulpen (Belgium) 17 October 1988 p 1482 N94-18625
Applications of Quaternary stratigraphic, soil-geomorphic, and quantitative geomorphic analyses to the evaluation of tectonic activity and landscape evolution in the Upper Coastal Plain, South Carolina [DE93-016269] p 1484 N94-18725

GEOPHYSICS
Rapid geophysical surveyor [DE93-016637] p 1461 N94-17851
Geography and meteorological studies in the Far East [DE93-013563] p 1461 N94-17893
Belgian Royal Observatory Communications, Series A, No. 104, Geophysics Series No. 175 [COMMUNICATIONS-SER-A-104] p 1482 N94-18622
Current positioning possibilities by spatial techniques and the Royal Oservatory of Belgium program p 1483 N94-18627
Instrumentation developed at the Royal Observatory of Belgium for measuring slow displacements of the Earth p 1483 N94-18628

Center of Excellence in Theoretical Geoplasma Research
[AD-A270210] p 1588 N94-18902
Using computerized tomography to determine ionospheric structures
[DE93-018903] p 1485 N94-19001
Institute of Geophysics and Planetary Physics, 1992
[DE93-019209] p 1627 N94-19077

GEOSTROPHIC WIND
Some potential errors in satellite wind estimates using the geostrophic approximation and the thermal wind
[AD-A269784] p 1491 N94-18599
Moist wind relationships p 1492 N94-18607

GEOSYNCHRONOUS ORBITS
Broadband RF spectrum from electrostatic discharges on spacecraft
[AD-A269543] p 1385 N94-18287
JPRS report: Science and technology. Central Eurasia: Space
[JPRS-USP-93-004] p 1323 N94-19146

GEOTECHNICAL ENGINEERING
Centrifuge modeling of explosion-induced craters in unsaturated sand
[AD-A270194] p 1417 N94-18780
Research activities, Faculty of Civil Engineering, Delft University of Technology, 1990 - 1991
[PB93-195022] p 1380 N94-19254

GEOTEMPERATURE
Geothermal activity near Clearlake, California
[DE93-016627] p 1485 N94-18894

GERMAN SPACE PROGRAM
Research and design activities and the economic balance of MBB
[ETN-93-94909] p 1310 N94-19383

GERMANIUM
MUZO flight experience with the programmable multizone furnace p 1324 N94-19167

GERMANIUM ALLOYS
The low-temperature specific heat of CeCu2Ge2 at 0 and 9.5 kbar
[DE93-014914] p 1360 N94-18398
Fundamental properties and device applications of Ge(x)Si(1-x)/Si superlattices (supplemental)
[AD-A269212] p 1600 N94-18884

GET AWAY SPECIALS (STS)
The 1993 Shuttle Small Payloads Symposium
[NASA-CP-3233] p 1323 N94-19162
California Student Get Away Special Payload GAS-450 p 1324 N94-19164
MUZO flight experience with the programmable multizone furnace p 1324 N94-19167
The GAMCIT gamma ray burst detector p 1324 N94-19168
Static Computer Memory Integrity Testing (SCMIT): An experiment flown on STS-40 as part of GAS payload G-616 p 1325 N94-19169
The first flight of the QUESTS GAS payload G-521 p 1325 N94-19170
Attitude sensor package p 1325 N94-19172
Space Applications Industrial Laser System (SAILS) p 1325 N94-19173
A high resolution ultraviolet Shuttle glow spectrograph p 1325 N94-19174
Materials flight experiment carrier capability and future flight experiments on Hitchhiker-M carrier program p 1326 N94-19175
Limited Duration of Candidate Materials Exposure Experiment (LDCE): A Complex Autonomous Payload (CAP) using a Get Away Special (GAS) canister p 1326 N94-19176
Kennedy Space Center processing of Shuttle small payloads p 1326 N94-19177
Utilization of Shuttle small payload accommodations in the DOD Space Test Program p 1326 N94-19180
Your GAS experiment and the media or why does that other can get all of the publicity? p 1327 N94-19182
Superfluid Helium On-Orbit Transfer (SHOOT) flight demonstration p 1327 N94-19185

GIANT STARS
Determination of nitrogen to carbon abundance ratios from transition layer emission lines
[NASA-CR-191921] p 1622 N94-19421

GIMBALS
Analysis and design of robust decentralized controllers for nonlinear systems
[DE93-019224] p 1543 N94-19302

GINGA SATELLITE
Pulse-timing studies of x ray pulsars
[NASA-CR-193776] p 1621 N94-18611

GLACIERS
Research on Earth's rotation and the effect of atmospheric pressure on vertical deformation and sea level variability
[NASA-CR-194300] p 1484 N94-18838

GLASS
Performance of the Amorphous Materials Diffractometer GLAD at IPNS
[DE93-017746] p 1430 N94-18481
An ultraviolet faraday rotator glass
[AD-D015879] p 1371 N94-18529
High performance YBCO films
[AD-A269090] p 1599 N94-18719
Radiation induced darkening of the optical elements in the Startracker camera
[DE93-018907] p 1433 N94-19004

GLASS LASERS
Pulsed power supply for Nova Upgrade
[DE93-019626] p 1441 N94-19307

GLASS TRANSITION TEMPERATURE
Nondestructive inspection of graphite-epoxy laminates for heat damage using DRIFT and LPF spectroscopies
[DE93-017228] p 1343 N94-18761

GLINT
Marine-modified LOWTRAN: The contribution of sun glint
[AD-A269547] p 1500 N94-19762

GLOBAL AIR POLLUTION
Setting the global thermostat with an exhaustible tradeable permit system
[DE93-012911] p 1472 N94-17891

GLOBAL POSITIONING SYSTEM
Flight demonstration of image fix-taking with SAR
[DE93-018499] p 1382 N94-17861
On the use of differential GPS for automatic approach and landing of space and aircraft
[DLR-MITT-93-05] p 1316 N94-17921
Missile antenna pattern coordinate system and data formats
[AD-A269153] p 1385 N94-18260
Current positioning possibilities by spatial techniques and the Royal Oservatory of Belgium program p 1483 N94-18627
Absolute positioning by collecting Global Positioning System (GPS) data along short baselines
[AD-A271324] p 1317 N94-19572

GLOBAL WARMING
Biophysical characterization and surface radiation balance
[NASA-CR-194659] p 1470 N94-17762
Setting the global thermostat with an exhaustible tradeable permit system
[DE93-012911] p 1472 N94-17891
Cloud CCN feedback
[DE93-016878] p 1472 N94-17985
Infrared cross sections and global warming potentials of 10 alternative hydrohalocarbons
[AERONAUTICA-ACTA-A-371-199] p 1479 N94-19521

GLYCERIDES
Nuclear Medicine Program
[DE93-013896] p 1504 N94-17699

GOGGLES
Human integration evaluation of three helmet systems
[AD-A271320] p 1513 N94-19570

GOLD ALLOYS
Accelerated tests on the tarnish resistance of gold alloys p 1367 N94-18008
Gold-copper-zinc coatings as an alternative to gold-copper-cadmium p 1367 N94-18012

GOLD COATINGS
Superhardness effect in Au/Ni multilayers
[DE93-016444] p 1357 N94-17860
Embrittlement of surface mount solder joints by hot solder-dipped, gold-plated leads
[DE93-017659] p 1358 N94-18003

GOODNESS OF FIT
EDF tests for normality in linear models after a Box-Cox transformation
[AD-A269068] p 1557 N94-18517

GOVERNMENT PROCUREMENT
Naval aviation: Consider all alternatives before proceeding with the F/A-18E/F
[AD-A269302] p 1305 N94-18279

GOVERNMENT/INDUSTRY RELATIONS
White House technology reinvestment project: Briefing and transcripts
[PB93-169829] p 1611 N94-18090

GOVERNMENTS
Trends in Information Management at Department of Energy Headquarters
[DE93-017197] p 1615 N94-18496

GRADIENTS
Velocity measurements in a boundary layer with a density gradient
[DE93-019627] p 1422 N94-19515

GRAIN BOUNDARIES
The Hall-Petch relationship and mechanisms of fracture in B2 compounds
[DE93-018887] p 1359 N94-18182
Synthesis and study of high-T(sub c) superconducting electronic materials
[AD-A268851] p 1402 N94-18390
A free energy simulation method based study of interfacial segregation
[DE93-019462] p 1364 N94-19032
The effect of composition on the mechanism of continuous recrystallization and superplastic response of aluminum-scandium alloys
[DE93-018594] p 1365 N94-19280
The microstructural mechanism of electromigration failure in narrow interconnects of Al alloys
[DE93-018598] p 1365 N94-19282

GRAIN SIZE
Modeling microstructural evolution and the mechanical response of superplastic materials
[DE93-014417] p 1355 N94-17711
Tensile properties of as-cast iron-aluminide alloys
[DE93-017852] p 1363 N94-18975

GRAINS
Tunneling spectroscopy of ultrasmall clusters and grains
[AD-A268840] p 1598 N94-18539

GRAINS (FOOD)
FT-NIR spectroscopy in quantitative and qualitative measurements of cereal products
[VTT-TIED-1331] p 1346 N94-17973

GRAMMARS
Multistack languages and grammars
[REPT-93-018] p 1518 N94-17926
Attribute evaluation during generalized parsing
[MEMO-INF-92-85] p 1526 N94-19224
Stochastic grammars: Theory and applications
[MEMO-INF-93-19] p 1528 N94-19262

GRAND UNIFIED THEORY
Neutrino masses in superstring derived standard-like models
[DE93-624802] p 1565 N94-17951
Gauge unification of fundamental forces: The story of success
[DE93-624813] p 1383 N94-17952

GRAPH THEORY
An annealing approach to multi-facility location problems in euclidean spaces
[REPT-93-022] p 1547 N94-17928
Exact cost flow problems in acyclic networks
[REPT-93-030] p 1520 N94-18138
Fuzzy hypergraphs and fuzzy intersection graphs
[AD-A270303] p 1549 N94-18815
Refining a triangulation of a planar straight-line graph to eliminate large angles
[DE93-016510] p 1528 N94-19344
A perfection-preserving operation
[RR-911-I] p 1552 N94-19393
Neighbourhood-perfect line graphs
[RR-915-I] p 1552 N94-19395
The complexity of the optimal spanning hypertree problem
[TR-471] p 1561 N94-19481
Mathematical communications, volume 27, numbers 1 and 2, 1992. List and abstracts of memoranda published in the period July - December 1991
[PB93-191997] p 1553 N94-19557
Updated contributions to the Twente Workshop of Hamiltonian Graph Theory
[PB93-195568] p 1553 N94-19605
Updated Contributions to the Twente Workshop on Hamiltonian Graph Theory
[MEMO-1076] p 1554 N94-19683
On Hamilton-connectedness of Cayley graphs p 1554 N94-19684
On Hamiltonian properties of 2-tough graphs p 1554 N94-19685
Toughness and the cycle structure of graphs p 1554 N94-19686
The Hopping Lemma p 1554 N94-19687
Cycles containing all vertices of maximum degree p 1554 N94-19688
Long paths and cycles in tough graphs p 1554 N94-19689
The complete closure of a graph p 1555 N94-19690
Twenty odd statements in Twente p 1555 N94-19691
Generalized closures of graphs p 1555 N94-19692
Two problems related to results of Chvatal-Erdoes p 1555 N94-19693
Concerning the circumference of certain families of graphs p 1555 N94-19694
Ore-type conditions for cycles through specified vertices p 1555 N94-19695
Hamilton cycles in path-tough graphs p 1555 N94-19696
Cubic graphs containing k vertex-disjoint subgraphs of given cyclomatic number p 1555 N94-19697

Finding the strong components in a directed graph [PB93-187342] p 1555 N94-19708

GRAPHICAL USER INTERFACE

EDMS: Engineering data management system. User's reference [PB93-187391] p 1614 N94-18119

Three-dimensional cloud visualization based on satellite imagery [AD-A269318] p 1490 N94-18300

Why are human-computer interfaces difficult to design and implement? [AD-A268843] p 1514 N94-18317

Software distribution using xnetlib [DE93-018278] p 1523 N94-18989

How to apply the IEEE standards to software testing [DE93-018514] p 1527 N94-19245

GRAPHITE

Physico chemical and mechanic approach of lubricating properties of graphite + additive powders [ECL-93-02] p 1373 N94-19405

GRAPHITE-EPOXY COMPOSITES

Nondestructive inspection of graphite-epoxy laminates for heat damage using DRIFT and LPF spectroscopies [DE93-017228] p 1343 N94-18761

Characterization of vapor plume species and deposition residues resulting from pulsed laser ablation of a graphite/epoxy composite [AD-A270101] p 1343 N94-18869

A comparative evaluation of in-plane shear test methods for laminated graphite-epoxy composites [NASA-CR-193808] p 1456 N94-19095

GRAPHS (CHARTS)

Location of the absolute barycenter of a graph [REPT-93-027] p 1547 N94-17962

Exact cost flow problems in acyclic networks [REPT-93-030] p 1520 N94-18138

Annealing algorithms for multiresource absolute location problems on graph [REPT-93-028] p 1520 N94-18145

Color palette considerations for digital map displays [AD-A269991] p 1462 N94-18679

Fuzzy hypergraphs and fuzzy intersection graphs [AD-A270303] p 1549 N94-18815

A perfection-preserving operation [RR-911-I] p 1552 N94-19393

Neighbourhood-perfect line graphs [RR-915-I] p 1552 N94-19395

Updated Contributions to the Twente Workshop on Hamiltonian Graph Theory [MEMO-1076] p 1554 N94-19683

On Hamilton-connectedness of Cayley graphs p 1554 N94-19684

Long paths and cycles in tough graphs p 1554 N94-19689

Generalized closures of graphs p 1555 N94-19692

GRATINGS (SPECTRA)

Developmental testing of a prototype all-reflection Michelson interferometer [AD-A269064] p 1430 N94-18406

Apparatus and method for varying a Bragg wavelength of a Bragg grating formed in an optical fiber [AD-D015876] p 1579 N94-18743

A tunable compact high power far-infrared grating free-electron laser [AD-A269875] p 1440 N94-18771

GRAVIMETERS

What can gravimetry contribute to recent and current tectonics in Belgium? p 1482 N94-18626

Instrumentation developed at the Royal Observatory of Belgium for measuring slow displacements of the Earth p 1483 N94-18628

GRAVITATION

Avoiding degenerate coframes in an affine gauge approach to quantum gravity [DE93-013146] p 1607 N94-17892

Space and time as outcome of decoherence in an expanding universe [DE93-016199] p 1624 N94-18047

Extensions of 2D gravity [DE93-018525] p 1485 N94-18929

GRAVITATIONAL COLLAPSE

Weak neutral currents and collapse initiated supernova [DE93-018652] p 1627 N94-19284

GRAVITATIONAL EFFECTS

Opportunities and questions for the fundamental biological sciences in space p 1502 N94-19212

Space research with intact organisms: The role of Space Station Freedom p 1502 N94-19213

Space research on organs and tissues p 1503 N94-19214

A scientific role for Space Station Freedom: Research at the cellular level p 1503 N94-19215

Microgravity research in plant biological systems: Realizing the potential of molecular biology p 1503 N94-19216

Life: Origin and evolution on Earth--How can we escape? p 1503 N94-19217

Gravity and the geoid in the Nepal Himalaya [NASA-CR-194166] p 1463 N94-19430

GRAVITATIONAL FIELDS

On a conformal perfect fluid in the classical vacuum [DE93-624797] p 1480 N94-17682

About symmetry of the gravitational action [DE93-629955] p 1608 N94-18252

The application of front tracking to the simulation of shock refractions and shock accelerated interface mixing [DE93-018342] p 1419 N94-19025

JPRS report: Science and technology. Central Eurasia: Space [JPRS-USP-93-004] p 1323 N94-19146

GRAVITATIONAL PHYSIOLOGY

Characterization of fluid physics effects on cardiovascular response to microgravity (G-572) p 1323 N94-19163

Space research on organs and tissues p 1503 N94-19214

A scientific role for Space Station Freedom: Research at the cellular level p 1503 N94-19215

GRAVITY WAVES

Internal instability of nonparallel flow on an equatorial beta-plane [AD-A268927] p 1490 N94-18486

Constraints on crustal structure from long period pressure and displacement measurements on the deep seafloor [AD-A269931] p 1498 N94-18663

On the use of semi-Lagrangian methods for accurate predictions of gravity waves [DM-61] p 1562 N94-18859

GRAY SCALE

Progress in edge detection [RR-914-I] p 1529 N94-19396

GRAZING INCIDENCE

Single-transverse-mode, narrow-bandwidth pulsed tunable dye laser with hollow circular intracavity dielectric waveguide [AD-A270022] p 1439 N94-18614

GREASES

Study on radiation-induced deterioration of grease at high temperature, 3 [DE93-788368] p 1369 N94-18220

GREEN'S FUNCTIONS

Path integrals on warped product manifolds [DE93-629859] p 1561 N94-18151

Three dimensional multipole decomposition of fields [DE93-018530] p 1389 N94-19053

An investigation of low Marangoni number fluid flow in a cold corner [AD-A271317] p 1422 N94-19569

Acoustic propagation modeling using MATLAB [AD-A270905] p 1564 N94-19750

GREENHOUSE EFFECT

Monitoring the response of the upper troposphere/lower stratosphere to a greenhouse gas scenario [DE93-014509] p 1470 N94-17710

Assessing impacts of climate change on forests: The state of biological modeling [DE93-015916] p 1471 N94-17790

The carbon dioxide emissions game: Playing the net [DE93-017670] p 1471 N94-17821

Geography and meteorological studies in the Far East [DE93-013563] p 1461 N94-17893

Land-use related sources of CO2, CH4 and N2O: Current global emissions and projections for the period 1990-2100 [PB93-194819] p 1475 N94-18949

Kinetics programs for simulation of tropospheric photochemistry on the global scale [DE93-019035] p 1476 N94-19104

Valuation of temporary and future greenhouse gas reductions [DE93-018876] p 1478 N94-19319

GRID GENERATION (MATHEMATICS)

WBNGRID, a program for generation of C-H and C-O topology grids around wing/body/nacelle configurations: User's guide [FFA-TN-1992-09] p 1311 N94-17721

Finite element modeling of evaporation and condensation during sol-gel film and fiber formation [DE93-017655] p 1345 N94-17820

Advances and applications of ABCI [DE93-016971] p 1383 N94-18055

GREPOS: A GENESIS database repositioning program [DE93-018517] p 1614 N94-18164

Calculation of maximum and high lift characteristics of multi element aerofoils p 1305 N94-18419

Navier-Stokes calculations on multi-element airfoils using a chimera-based solver p 1306 N94-18422

High-lift system analysis method using unstructured meshes p 1307 N94-18426

UUGM code development [AD-A269945] p 1416 N94-18671

Computational Fluid Dynamics (CFD) research branch technical briefs [AD-A269698] p 1417 N94-18739

Multigrid methods for flow transition in three-dimensional boundary layers with surface roughness [NASA-CR-4540] p 1417 N94-18843

3D composite grids using Bezier curves and surfaces in component adaptive methods [AD-A269188] p 1549 N94-18863

A particle method for history-dependent materials [DE93-018696] p 1456 N94-19060

GENSHELL: A genesis database 2D to 3D shell transformation program [DE93-018694] p 1525 N94-19102

Content based-grid node selection for vector field visualization [REPT-93-35] p 1525 N94-19155

Are bilinear quadrilaterals better than linear triangles? [DE93-019223] p 1551 N94-19301

Adaptive methods for nonlinear structural dynamics and crashworthiness analysis p 1458 N94-19466

Transient dynamics capability at Sandia National Laboratories p 1460 N94-19476

Three dimensional network generation and Euler calculation for a wing fuselage canard configuration [MBB-LME-211-S-PUB-511-A] p 1319 N94-19500

Locally adaptive remeshing scheme for calculating fluid instabilities [DE93-019577] p 1422 N94-19568

GRINDING (MATERIAL REMOVAL)

Synchrotron/crystal sample preparation [NASA-CR-193837] p 1603 N94-19513

GROSS NATIONAL PRODUCT

The 1992 annual report on scientific programs: A broad research program on the sciences of complexity [DE93-018151] p 1561 N94-18178

GROUND BASED CONTROL

JPRS report: Central Eurasia. Aviation and cosmonautics, no. 10, October 1992 [JPRS-UAC-93-004] p 1632 N94-19149

GROUND EFFECT (AERODYNAMICS)

Wake structure and aerodynamic behavior of high lift aircraft configurations during unsteady maneuvers in ground effect p 1309 N94-18439

Lift and pitching moment induced on jet STOVL aircraft hovering in ground effect [AD-A269700] p 1317 N94-18577

Lift and pitching moment induced on jet STOVL aircraft by the ground vortex [AD-A269816] p 1318 N94-18733

Flight test techniques for aircraft parameter estimation in ground effect [AD-A270058] p 1318 N94-18795

GROUND EFFECT (COMMUNICATIONS)

RADARC HF ionospheric prediction program for OTH radar [AD-A269557] p 1385 N94-18291

GROUND STATE

Crossed molecular beam studies of atmospheric chemical reaction dynamics [DE93-019246] p 1478 N94-19303

GROUND STATIONS

The use of velocity spectra for stacking receiver functions with application to IRIS/IDA stations OBNINSK (OBN) and ARTI (ARU), Russia [AD-A269087] p 1483 N94-18717

ASTRO-1 to explore invisible universe [NASA-TM-109360] p 1336 N94-18956

SeaTrack: Ground station orbit prediction and planning software for sea-viewing satellites [NASA-RP-1331] p 1532 N94-19761

GROUND SUPPORT EQUIPMENT

Kennedy Space Center processing of Shuttle small payloads p 1326 N94-19177

Cluster: Mission, Payload, and Supporting Activities [ESA-SP-1159] p 1328 N94-19622

The Cluster spacecraft p 1330 N94-19635

Cluster ground segment and mission operations p 1330 N94-19636

GROUND TRACKS

Application of the A* algorithm to aircraft trajectory generation [AD-A268728] p 1317 N94-18315

GROUND TRUTH

CTD and XBT data collected on ERS-1 validation cruise RRS Charles Darwin Cruise 62A, Iceland-Faeroes region [IOS-294-1992] p 1461 N94-18063

GROUND WATER

A Bayesian approach to contaminant plume delineation [DE93-012909] p 1472 N94-17890

Application of ARC/INFO to regional scale hydrogeologic modeling
[DE93-015673] p 1461 N94-18107
Multigrid for a groundwater flow problem
[REPT-93-29] p 1420 N94-19144
Penetrometer compatible, fiber-optic sensor for continuous monitoring of chlorinated hydrocarbons: Field test results
[DE93-017974] p 1352 N94-19266

GROUND WIND
Wind products for use in coastal wave and surge models
[AD-A269753] p 1497 N94-18414
Application of an atmospheric dispersion model to simulated pollutant releases in the Colorado Front range
[DE93-017118] p 1480 N94-19732

GROUP DYNAMICS
Putting knowledge to use: The acquisition and transfer of knowledge in situated problem solving environments
[AD-A269746] p 1509 N94-18744

GROUP THEORY
Infinite Grassmannian and moduli space of G-bundles
[DE93-624798] p 1545 N94-17683
Deformed traces and covariant quantum algebras for quantum groups GL(sub qp)(2) and GL(sub qp)(1/1)
[DE93-629862] p 1561 N94-18153
Group-invariant solutions of hydrodynamics and radiation hydrodynamics
[DE93-018373] p 1423 N94-19604

GROUP VELOCITY
Surface wave group velocity tomography of East Asia, part 1
[AD-A270100] p 1484 N94-18868

GUIDANCE (MOTION)
Overview of research in progress at the Center of Excellence
[NASA-CR-194329] p 1618 N94-19256

GULF STREAM
Synoptic ocean prediction experiment. EN216 CTD section data report
[AD-A268903] p 1497 N94-18230
Preparation of data assimilation and model evaluation experiment data sets
[AD-A269996] p 1498 N94-18665
Modeling of current features in Gulf Stream SAR imagery
[AD-A270734] p 1499 N94-19609

GUN PROPELLANTS
Mechanical response comparison of gun propellants evaluated under equivalent time-temperature conditions
[AD-A270479] p 1378 N94-19674

GUSTS
Shape of wind gusts at a 130m tower at Wilhelmshaven (Germany)
[BER-BAND-B3] p 1494 N94-19503

GYROMAGNETISM
The anomalous magnetic moment of the muon
[DE93-018932] p 1572 N94-19320

H

H II REGIONS
The molecular environment of S106 IR
[MPE-PREPRINT-241] p 1622 N94-19417
ROSAT and IRAS observations
[MPE-PREPRINT-231] p 1623 N94-19526
IRAS galaxies observed in the ROSAT survey: Starbursts or central activity p 1623 N94-19528

H LINES
Unified NLTE model atmospheres including spherical extension and stellar winds, 4: Improved line transfer and wind contamination of H, He profiles
[MPA-905] p 1624 N94-17736

H-INFINITY CONTROL
Discrete-time infinity control problem with measurement feedback
[PB93-197523] p 1543 N94-19329
A learning autopilot for automatically controlled robust regulation
[ETN-93-95075] p 1321 N94-19711

HABITATS
Assessing impacts of climate change on forests: The state of biological modeling
[DE93-015916] p 1471 N94-17790

HADRONS
On the difference caused by CP violation in the energy spectra of pions in K(sup (+-))(yields)(pi)(+-)(pi)(+-)(pi)-+ decays
[DE93-624828] p 1564 N94-17687
Energy loss measurement of cosmic ray muons
[KFK-5158] p 1631 N94-19504
Measurements of cosmic ray muons with multi-wire proportional chambers with a prototype setup for KASCADE
[KFK-5173] p 1631 N94-19506

HALL EFFECT
IR materials producibility
[AD-A268849] p 1577 N94-18223
Growth of structures for integrated optoelectronic devices
[AD-A269014] p 1598 N94-18527

HALOS
Halo formation in mismatched, space-charge-dominated beams
[DE93-018581] p 1574 N94-18934

HAMILTONIAN FUNCTIONS
Exact solution of the generalized time-dependent Jaynes-Cummings Hamiltonian
[DE93-624773] p 1546 N94-17811
Some remarks on integrable Hamiltonian systems with two degrees of freedom
[DE93-624766] p 1546 N94-17815
Vortex methods and statistics
[DE93-016974] p 1556 N94-17886
Variable time-step integration for intense field effects
[DE93-013296] p 1382 N94-17909
A zeta function approach to the semiclassical quantization of maps
[DE93-624774] p 1547 N94-17949
Path integrals on warped product manifolds
[DE93-629859] p 1561 N94-18151
Impulsive moving mirror model in a Schroedinger picture with impulse effect in a Banach space
[DE93-629864] p 1561 N94-18155
Phase structure of (phi(4))(sub 3) field theory at finite temperature
[DE93-629907] p 1608 N94-18267
Contact 3-manifolds, integrable Hamiltonian systems and exotic symplectic structures in R(sup 4)
[DE93-624767] p 1551 N94-19248
Updated contributions to the Twente Workshop of Hamiltonian Graph Theory
[PB93-195568] p 1553 N94-19605

HAND (ANATOMY)
Synchronisation of cold induced vasodilation at various locations of one hand
[IZF-1992-B3] p 1504 N94-17966

HARBORS
The ecological and environmental impacts of manmade marshes
[AD-A269213] p 1475 N94-18885

HARDNESS
Mechanical properties of excimer laser modified titanium surfaces
[DE93-012663] p 1358 N94-17875
Impact strength and indentation hardness of high-strength ceramics
[DE93-018833] p 1373 N94-19338
Picoindentation hardness measurements using atomic force microscopy
[AD-A270877] p 1604 N94-19579

HARDNESS TESTS
Picoindentation hardness measurements using atomic force microscopy
[AD-A270877] p 1604 N94-19579

HARDWARE
A programmable systolic trigger processor for FERA-bus data
[USIP-92-04] p 1405 N94-19292
FASTBUS simulation models in VHDL
[USIP-92-07] p 1515 N94-19295
The universal BitBus node
[DIGEL-1993-1] p 1515 N94-19799

HARMONIC ANALYSIS
Method for extracting tidal and inertial motion from ARGOS ice buoys applied to the Barents Sea during CEAREX
[PB93-190213] p 1499 N94-19063

HARMONIC EXCITATION
Dynamics of short-pulse excitation, ionization and harmonic conversion
[DE93-017220] p 1436 N94-17996
Low frequency acoustics of laminated composite axisymmetric structures
[DRA-TM(USGR)-93302] p 1344 N94-19391
Axial response of differently excited anchored viscous liquid bridges in zero-gravity
[LRT-WE-9-FB-1-1992] p 1379 N94-19489

HARMONIC FUNCTIONS
A priori estimates and existence of positive solutions of a superlinear polyharmonic equation
[REPT-93-12] p 1550 N94-19086

HARMONIC GENERATIONS
Observations of MeV electrons and scattered light from intense, subpicosecond laser-plasma interactions
[DE93-017153] p 1435 N94-17855
Surface second harmonic generation studies of stepped Ag(111) electrode surfaces
[AD-A265205] p 1594 N94-17876
A superconducting short period undulator for a harmonic generation FEL experiment
[DE93-017581] p 1436 N94-17998
Magnetic field measurements of a superconducting undulator for a Harmonic Generation FEL experiment at the NSLS
[DE93-017621] p 1438 N94-18504
Relaxation of polar orientational order in nonlinear optical polymers by second harmonic generation
[AD-A269059] p 1370 N94-18515
Harmonic generation at high intensities
[DE93-018632] p 1572 N94-19283
Optical frequency doubling at adsorbates of silver(110) surface
[ETN-93-94837] p 1603 N94-19355

HARMONIC OSCILLATION
Synchrotron beam-loading stability with a higher RF harmonic
[DE93-014549] p 1573 N94-17726
A computational and experimental investigation of incompressible oscillatory airfoil flow and flutter problems
[AD-A268748] p 1311 N94-18402

HARMONIC OSCILLATORS
On paragrassmann differential calculus
[DE93-628594] p 1548 N94-18169
Thermodynamic q-distributions that aren't
[DE93-017385] p 1609 N94-19121

HARMONICS
Optical design for photonics. Organization of the 1993 Photonics Science Topical Meetings. Technical digest series, volume 9
[AD-A269027] p 1578 N94-18396
Theory of electromagnetic waves propagating in nonlinear anisotropic optical materials
[AD-A269305] p 1386 N94-18469
Effects of harmonics on EMI/RFI filters operating under nonlinear loading conditions
[AD-A269559] p 1388 N94-18769

HARNESSES
Army Cockpit Delethalization Program (CDP)
[AD-A268990] p 1512 N94-18765

HASTELLOY (TRADEMARK)
Atlas of formability: Hastelloy C-22
[AD-A268324] p 1356 N94-17796

HAZARDS
SUNRAYCE 1993: Working safely with lead-acid batteries and photovoltaic power systems
[DE93-016553] p 1464 N94-17712
Calamity weather: Environmental calamities and meteorology p 1495 N94-19703

HAZE
Analysis of meteorological conditions during AGASP-4: 30 March - 23 April 1992
[PB93-190205] p 1489 N94-18126

HEALTH
Review of short-term, high-level exposure to metals: Antimony, barium, and cadmium
[AD-A268896] p 1505 N94-18392
The urban perspectives of acid rain
[DE93-018881] p 1474 N94-18523

HEAO 2
The Einstein Observatory catalog of IPC x ray sources. Volume 4E: Right ascension range 08h 00m to 11h 59m
[NASA-TM-108401-VOL-4E] p 1625 N94-18612
The Einstein Observatory catalog of IPC x ray sources. Volume 5E: Right ascension range 12h 00m to 15h 59m
[NASA-TM-108401-VOL-5E] p 1625 N94-18613
The Einstein Observatory catalog of IPC x ray sources. Volume 6E: Right ascension range 16h 00m to 19h 59m
[NASA-TM-108401-VOL-6E] p 1625 N94-18615
The Einstein Observatory catalog of IPC x ray sources. Volume 7E: Right ascension range 20h 00m to 23h 59m
[NASA-TM-108401-VOL-7E] p 1625 N94-18618
The Einstein Observatory catalog of IPC x ray sources. Volume 1E: Documentation
[NASA-TM-108401-VOL-1E] p 1626 N94-18619
The Einstein Observatory catalog of IPC x ray sources. Volume 2E: Right ascension range 00h 00m to 03h 59m
[NASA-TM-108401-VOL-2E] p 1626 N94-18620
The Einstein Observatory catalog of IPC x ray sources. Volume 3E: Right ascension range 04h 00m to 07h 59m
[NASA-TM-108401-VOL-3E] p 1626 N94-18621

HEARING
The effects of reverberant impulse noise (blast waves) on hearing: Parametric studies
[AD-A269242] p 1506 N94-18911

HEART FUNCTION
Characterization of fluid physics effects on cardiovascular response to microgravity (G-572)
p 1323 N94-19163

HEART RATE
Metabolic changes and hemodynamic dysfunction following hypothermic shock
[AD-A269780] p 1506 N94-18598

Evaluation of physiological and psychological impairment of human performance in cold stressed subjects
[AD-A268637] p 1506 N94-18632

Characterization of fluid physics effects on cardiovascular response to microgravity (G-572)
p 1323 N94-19163

HEAT AFFECTED ZONE

Technique to eliminate helium induced weld cracking in stainless steels
[DE93-015982] p 1357 N94-17859

Thermal insulation of wet shielded metal arc welds
[AD-A268697] p 1445 N94-18465

Cutting and drilling studies using high power visible lasers
[DE93-019149] p 1441 N94-19294

HEAT BALANCE

Effects of a high-energy food supplement on cold-induced thermogenesis
[AD-A269301] p 1504 N94-17823

Thermodynamic theory of exergy analysis
[PB93-187847] p 1607 N94-18120

HEAT ENGINES

Studies of dynamic contact of ceramics and alloys for advanced heat engines
[DE93-016366] p 1368 N94-18110

Analytical and experimental evaluation of joining silicon nitride to metal and silicon carbide to metal for advanced heat engine applications
[DE93-018128] p 1446 N94-19291

Ceramic technology project data base
[DE93-019360] p 1374 N94-19561

HEAT EXCHANGERS

Malone refrigeration
[DE93-014468] p 1379 N94-17725

Fin-efficiency calculation for condensation in the presence of noncondensable gases
[DE93-017684] p 1409 N94-18004

The 7th International Cryocooler Conference
[AD-A268451] p 1379 N94-18147

HEAT FLUX

Surface fluxes important to cloud development
[DE93-016633] p 1488 N94-17715

Filamentation, current profiles and transport in a tokamak
[DE93-016768] p 1584 N94-17948

Transport in the self-organized relaxed state of ion temperature gradient instability
[DE93-016769] p 1584 N94-17983

Boundary layer heat budgets from wind profiler/RASS data: A feasibility study
[DE93-013187] p 1489 N94-18052

The vertical distribution of heating in the tropical atmosphere
[AD-A270452] p 1490 N94-18514

Liquid crystal heat transfer measurements
p 1432 N94-18653

Scaling laws for diamond chemical vapor deposition. 2: Atomic hydrogen transport
[AD-A269842] p 1371 N94-18740

Radiative divertor modeling studies
[DE93-018092] p 1590 N94-19290

Examinations of converging cylindrically symmetric second sound propagation in He2
[MPIS-9/1992] p 1564 N94-19715

HEAT OF FORMATION

A free energy simulation method based study of interfacial segregation
[DE93-019462] p 1364 N94-19032

HEAT OF FUSION

Melt spinning study
[NASA-CR-193823] p 1380 N94-19423

HEAT PIPES

Performance mapping of the STM4-120 kinematic Stirling engine using a statistical design of experiments method
[DE93-015132] p 1464 N94-17798

Development of a cryogenic heat pipe
[DE93-018448] p 1417 N94-18831

HEAT PUMPS

Thermodynamic theory of exergy analysis
[PB93-187847] p 1607 N94-18120

Adsorption analysis of ammonia in an aqueous solution
[DE93-019512] p 1353 N94-19552

HEAT RESISTANT ALLOYS

Metals 2000
[DE93-016761] p 1355 N94-17752

Atlas of formability: HAYNES 556
[AD-A268354] p 1356 N94-17768

Atlas of formability: HAYNES 188
[AD-A268355] p 1356 N94-17769

Atlas of formability: INCONEL 718
[AD-A268350] p 1356 N94-17789

Environmental effects on intermetallic compounds: A guide to the literature
[AD-A269587] p 1359 N94-18306

Developing and understanding the high temperature behavior of niobium aluminides and niobium aluminide composites
[AD-A268874] p 1341 N94-18636

Effects of shock loading on a solid-solution strengthened superalloy
[DE93-018345] p 1362 N94-18809

Analytical and experimental evaluation of joining silicon nitride to metal and silicon carbide to metal for advanced heat engine applications
[DE93-018128] p 1446 N94-19291

Incology 908 database report: On process-structure-property relationship
[DE93-017616] p 1366 N94-19546

HEAT SINKS

Diamond brazed to a metal
[AD-D015877] p 1371 N94-18746

Development of a cryogenic heat pipe
[DE93-018448] p 1417 N94-18831

Thermal stresses in the microchannel heatsink cooled by liquid nitrogen
[DE93-018660] p 1418 N94-18995

HEAT SOURCES

Ultrasonic technique for inspection of GPHS capsule girth weld integrity
[DE93-040072] p 1448 N94-19189

HEAT STORAGE

Regenerator optimization for Stirling cycle refrigeration
[DE93-018468] p 1380 N94-18818

HEAT TRANSFER

Heat load analysis on the cable-in-conduit with central core conductor for the TF coil Rebut layer design
[DE93-013783] p 1395 N94-17872

KINETIC: A system code for analyzing Nuclear thermal propulsion rocket engine transients
[DE93-016825] p 1337 N94-17884

Thermodynamic theory of exergy analysis
[PB93-187847] p 1607 N94-18120

Workshop on Computational Turbulence Modeling
[NASA-TM-109266] p 1410 N94-18545

Forecast model applications of retrieved three dimensional liquid water fields p 1492 N94-18606

Liquid crystal heat transfer measurements
p 1432 N94-18653

The application of liquid crystal techniques to determine heat transfer rates p 1432 N94-18654

Regenerator optimization for Stirling cycle refrigeration
[DE93-018468] p 1380 N94-18818

Potassium-Rankine power conversion subsystem modeling for nuclear electric propulsion
[NASA-CR-191134] p 1468 N94-18821

Some parametric flow analyses of a particle bed fuel element
[DE93-018440] p 1337 N94-18830

The quantum dynamics of electronically nonadiabatic chemical reactions
[NASA-CR-194309] p 1568 N94-18837

Effect of internal heating during hot compression testing on the stress-strain behavior and hot working characteristics of alloy 304L
[DE93-012701] p 1362 N94-18917

Evaluation of fiber optic performance in the ACRR
[DE93-018515] p 1580 N94-18970

Modeling of the formation of microporosity in alloys
[DE93-017733] p 1364 N94-19044

Numerical solutions for a flow with mixed convection in a vertical geometry
[DE93-011592] p 1419 N94-19058

Two-dimensional turbulent nonstationary superfluid counterflows: Numerical simulations, qualitative effects
[MPIS-23/1992] p 1422 N94-19510

Proceedings: International Symposium on Thermal Engineering and Science for Cold Regions
[AD-A270636] p 1487 N94-19529

Adsorption analysis of ammonia in an aqueous solution
[DE93-019512] p 1353 N94-19552

HEAT TRANSFER COEFFICIENTS

Parabolized Navier-Stokes computation of surface heat transfer characteristics for supersonic and hypersonic KE projectiles
[AD-A268858] p 1410 N94-18391

Heat transfer quantitative characterization: Passive and active methods p 1431 N94-18650

HEAT TRANSMISSION

On higher dimensional Ermakov systems: Canonical reductions
[MATHS-REPT-A-182] p 1548 N94-18140

Thermal insulation of wet shielded metal arc welds
[AD-A268697] p 1445 N94-18465

Some parametric flow analyses of a particle bed fuel element
[DE93-018440] p 1337 N94-18830

Geothermal activity near Clearlake, California
[DE93-016627] p 1485 N94-18894

Radiative divertor modeling studies
[DE93-018092] p 1590 N94-19290

HEAT TREATMENT

Charpy impact toughness of martensitic steels irradiated in FFTF: Effect of heat treatment
[DE93-015960] p 1450 N94-17848

Structural stability of 1100 C heated Pd/k during absorption cycling in protium
[DE93-016270] p 1346 N94-18048

Study of mechanical behavior and internal structure of ferritic nanocrystalline material
[DE93-019264] p 1596 N94-18184

Fabrication and microstructural development of Ag-clad TlBa2Ca2Cu3O(x) tapes
[DE93-017407] p 1597 N94-18500

Process relationship as influenced by carbonization rate
[AD-A269680] p 1341 N94-18572

Beryllium processing technology review for applications in plasma-facing components
[DE93-018396] p 1363 N94-19028

Fabrication, properties, and microstructures of high (Tc) tapes and coils made from Ag-clad Bi-2223 superconductor
[DE93-017405] p 1602 N94-19122

HEATING

Process for applying high application-temperature coating to heat-sensitive aluminum alloys
[AD-D015823] p 1368 N94-17905

Thermophysical properties
[DE93-040219] p 1351 N94-19134

HEATING EQUIPMENT

An emulator for testing HVAC-control and energy management systems
[VTT-TIED-1337] p 1444 N94-17974

Energy Efficiency and Renewable Energy Program
[DE93-017936] p 1468 N94-18986

Tehachapi solar thermal system
[DE93-018443] p 1468 N94-19014

HEAVY ELEMENTS

Development and characterization of adiabatic shear prone tungsten heavy alloys
[AD-A270477] p 1366 N94-19673

HEAVY IONS

Correlated charge-changing ion-atom collisions
[DE93-018717] p 1564 N94-17775

Heavy ion nuclear physics research
[DE93-018862] p 1565 N94-17776

Meson production in relativistic heavy-ion collisions at AGS energies
[DE93-016871] p 1565 N94-17984

Heavy-ion collisions and the nuclear equation of state
[DE93-019263] p 1566 N94-18104

Update on parts SEE susceptibility from heavy ions
[AD-A268735] p 1596 N94-18316

Heavy Ion Fusion Injector Program
[DE93-018706] p 1575 N94-18997

Task A: Yale Accelerator Users Group (YAUG)
[DE93-018417] p 1570 N94-19029

Overview of WARP: A particle code for heavy ion fusion
[DE93-018637] p 1588 N94-19034

The study of the phase structure of hadronic matter by searching for the deconfined quark-gluon phase transition using 2 TeV (bar-p)-p collisions, and by searching for critical phenomena in an exclusive study of multifragmentation using 1 GeV/nucleon heavy ion collisions
[DE93-018925] p 1570 N94-19103

Correction of longitudinal errors in accelerators for heavy-ion fusion
[DE93-018656] p 1575 N94-19106

Simulation of transient effects in the heavy ion fusion injectors
[DE93-018658] p 1575 N94-19107

Induction accelerator development for heavy ion fusion
[DE93-019228] p 1591 N94-19479

Transverse beam combiner for ILSE
[DE93-019239] p 1591 N94-19559

The ILSE Experimental Program
[DE93-019247] p 1576 N94-19560

HEAVY LIFT LAUNCH VEHICLES

Shuttle-C, the future is now
[NASA-TM-109355] p 1332 N94-18954

HEAVY NUCLEI

Investigation of the relative abundance of heavy versus light nuclei in primary cosmic rays using underground muon bundles
[DE93-017601] p 1630 N94-17818

Evolution of r-process elements in the hot supernova bubble
[DE93-017169] p 1624 N94-17897

HELICAL ANTENNAS
Plasma production by helicon waves
[DE93-788396] p 1586 N94-18213
HELICOPTER CONTROL
VMC left turn curved approaches, test results — (visual meteorological conditions)
[AD-A269476] p 1316 N94-18728
The dynamic stability of the helicopter
[LR-772] p 1321 N94-19615
HELIOSPHERE
Radial evolution of the solar wind turbulence with application to charged particle transport
[NASA-CR-194081] p 1629 N94-19427
HELIOSTATS
Testing and evaluation of large-area heliostats for solar thermal applications
[DE93-018509] p 1467 N94-18520
HELIPORTS
VMC left turn curved approaches, test results — (visual meteorological conditions)
[AD-A269476] p 1316 N94-18728
HELIUM
Technique to eliminate helium induced weld cracking in stainless steels
[DE93-015982] p 1357 N94-17859
Helium-induced weld degradation of HT-9 steel
[DE93-015981] p 1358 N94-17915
Dependence of helium transport on plasma current and ELM frequency in H-mode discharges in D3-D
[DE93-016986] p 1585 N94-18058
Low-energy continuum-electron emission at 0 degrees from O(q+) + He collisions
[DE93-018777] p 1570 N94-19108
Relativistic configuration interaction calculation of the correlation energies of heliumlike ions
[DE93-018093] p 1571 N94-19201
Overlay welding irradiated stainless steel
[DE93-018767] p 1446 N94-19334
Design verification and acceptance tests of the ASST-A helium refrigeration system
[DE93-019746] p 1381 N94-19540
HELIUM ISOTOPES
Parametric analysis of the ARIES-3D-He-3 tokamak reactor
[DE93-018293] p 1587 N94-18803
Future energy source — Mining Helium-3 on the moon
[NASA-TM-109363] p 1628 N94-18959
Helium isotopic abundance variation in nature
[DE93-019050] p 1487 N94-19477
HELMET MOUNTED DISPLAYS
Human integration evaluation of three helmet systems
[AD-A271320] p 1513 N94-19570
HELMETS
Human integration evaluation of three helmet systems
[AD-A271320] p 1513 N94-19570
HELMHOLTZ EQUATIONS
A new multiphase equation of state for iron
[DE93-017629] p 1357 N94-17819
HEMODYNAMIC RESPONSES
Metabolic changes and hemodynamic dysfunction following hypothermic shock
[AD-A269780] p 1506 N94-18598
HEPTANES
Film condensation in a shock wave
[MPIS-22/1992] p 1422 N94-19509
HERMES MANNED SPACEPLANE
Phasing strategies of the Hermes type space shuttle: Its optimization considering the thrust failures
[LAAS-93242] p 1544 N94-19361
HERMETIC SEALS
Analysis of high contact resistances associated with hermetic and lightning arrestor connectors
[DE93-014850] p 1395 N94-17783
HETEROCYCLIC COMPOUNDS
Royal Society of Chemistry, Heterocyclic Chemistry Group, Lakeland Heterocyclic Symposium
[AD-A270374] p 1338 N94-18703
HETEROJUNCTIONS
Reorientation of misfit dislocations during annealing in InGaAs/GaAs(001) interfaces
[DE93-015046] p 1592 N94-17741
Fundamental properties and device applications of Ge(x)Si(1-x)/Si superlattices (supplemental)
[AD-A269212] p 1600 N94-18884
HEURISTIC METHODS
Restricting query relaxation through user constraints
[DE93-017413] p 1612 N94-17870
Heuristics from nature for hard combinatorial optimization problems
[REPT-93-025] p 1547 N94-17961
Efficient domain-independent experimentation
[AD-A269530] p 1557 N94-18640
HIERARCHIES
Defense Technical Information Center thesaurus
[AD-A268855] p 1615 N94-18319
Scale sensitivity in the multiplicative AHP and SMART
[REPT-93-37] p 1611 N94-19157
Context-related scaling of human judgement in the multiplicative AHP, SMART and ELECTRE
[REPT-93-38] p 1611 N94-19158
Serial pattern complexity: Irregularity and hierarchy
[PB93-191914] p 1509 N94-19348
HIGH ALTITUDE
Regenerative fuel cells for High Altitude Long Endurance Solar Powered Aircraft
[DE93-016991] p 1465 N94-17853
HIGH DEFINITION TELEVISION
VLSI architectures for geometrical mapping problems in high-definition image processing
p 1398 N94-18345
HIGH ELECTRON MOBILITY TRANSISTORS
DC and small-signal physical models for the AlGaAs/GaAs high electron mobility transistor
p 1401 N94-18370
HIGH ENERGY INTERACTIONS
Activities report of the Rutherford Appleton Laboratory
[ETN-93-94555] p 1631 N94-17968
Research in particle physics
[DE93-040875] p 1567 N94-18534
Institute for Nuclear Theory
[DE93-017369] p 1568 N94-18824
Related investigations on the physics of high energy emission from active galactic nuclei
[NASA-CR-193615] p 1630 N94-18836
Experimental research in high energy physics
[DE93-011912] p 1574 N94-18916
Investigation of physical structures and interactions at high energy
[DE93-014444] p 1574 N94-18927
High energy physics at Tufts University
[DE93-018299] p 1575 N94-19023
Task A: Yale Accelerator Users Group (YAUG)
[DE93-018417] p 1570 N94-19029
High energy physics program. Task A: Experiment and theory. Task B: Numerical simulation
[DE93-018140] p 1575 N94-19050
LAHET calculations for accelerator neutron production
[DE93-016518] p 1570 N94-19120
Research in high energy physics
[DE93-018031] p 1575 N94-19287
High rate resistive plate chambers: An inexpensive, fast, large area detector of energetic charged particles for accelerator and non-accelerator applications
[DE93-018664] p 1572 N94-19545
HIGH FLUX BEAM REACTORS
Neutron-induced collision cascade mixing in Nb/V superlattices
[DE93-018575] p 1600 N94-18933
HIGH FLUX ISOTOPE REACTORS
A probability method of fracture mechanics analysis for HFIR vessel
[DE93-015510] p 1453 N94-18246
HIGH FREQUENCIES
Calibration of a high frequency monostatic acoustic echosounder
[AD-A268901] p 1481 N94-18229
Upper atmospheric effects of the HF Active Auroral Research Program Ionospheric Research Instrument (HAARP IRI)
[AD-A268948] p 1481 N94-18451
Morphology and characteristics of disturbed HF skywave channels
[AD-A269755] p 1388 N94-18722
Numerical modelling of fringing fields and their use for complex permittivity measurements at high frequencies
[AD-A270198] p 1388 N94-18782
Improved HF data network simulator, volume 1
[AD-A270953] p 1393 N94-19752
Improved HF data network simulator, software user's manual, volume 2
[AD-A270954] p 1393 N94-19753
HIGH LEVEL LANGUAGES
EXPECT: Intelligent support for knowledge base refinement
[AD-A269602] p 1612 N94-17745
HIGH PASS FILTERS
Monolithic low noise preamplifier for piezoelectric sensors
[AD-D015860] p 1563 N94-18734
HIGH POWER LASERS
New applications for high average power beams
[DE93-018845] p 1439 N94-18522
Interaction of intense lasers and relativistic electron beams with solids, gases and plasmas
[AD-A269655] p 1439 N94-18737
LLE Review
[DE93-017618] p 1602 N94-19123
Cutting and drilling studies using high power visible lasers
[DE93-019149] p 1441 N94-19294
MOCVD-grown InGaAsP heterostructure diode lasers
[AD-A270848] p 1606 N94-19769
HIGH PRESSURE
Studies on high pressure and unsteady flame phenomena: Revision
[AD-A269138] p 1348 N94-18257
High pressure metallization of Mott Insulators: Magnetic, structural and electronic properties
[DE93-018295] p 1404 N94-18805
Dynamical behavior of tantalum
[DE93-017877] p 1362 N94-18919
Institute of Geophysics and Planetary Physics, 1992
[DE93-019209] p 1627 N94-19077
HIGH RESOLUTION
CTD oxygen, tracer and nutrient data from RRS Charles Darwin Cruises 58/59 in the NE Atlantic as part of Vivaldi 1991
[IOS-296-1992] p 1496 N94-18065
High resolution geological site characterization utilizing ground motion data
[AD-A268926] p 1481 N94-18485
Development of parallel architectures for sensor array processing, volume 1
[AD-A270426] p 1534 N94-18507
High spatial resolution, range gated, underwater imaging method and apparatus
[AD-D015882] p 1430 N94-18530
Three-dimensional high-resolution seismic profiling on the New Jersey outer continental shelf
[AD-A269835] p 1498 N94-18600
Color test chart for facsimile
[AD-A269754] p 1387 N94-18721
Photodetector array having high pixel density
[AD-D015859] p 1432 N94-18731
New room temperature high resolution solid-state detector (CdZnTe) for hard x rays and gamma rays
p 1324 N94-19165
A high resolution ultraviolet Shuttle glow spectrograph
p 1325 N94-19174
High resolution transmission electron microscopy of mesoporous MCM-41 type materials
[AD-A271271] p 1354 N94-19728
HIGH REYNOLDS NUMBER
High Reynolds number configuration development of a high-lift airfoil p 1306 N94-18424
Two-equation models for high-Reynolds-number flow
p 1415 N94-18586
HIGH SPEED CAMERAS
High speed 512X512 camera system
[DE93-015871] p 1430 N94-18235
An RS-170 to 700 frame per second CCD camera
[DE93-018367] p 1432 N94-18828
HIGH SPEED PHOTOGRAPHY
An RS-170 to 700 frame per second CCD camera
[DE93-018367] p 1432 N94-18828
HIGH STRENGTH ALLOYS
Atlas of formability: HAYNES 556
[AD-A268354] p 1356 N94-17768
Atlas of formability: HAYNES 188
[AD-A268355] p 1356 N94-17769
Atlas of formability: NICKELVAC K-500
[AD-A268351] p 1356 N94-17772
HIGH STRENGTH STEELS
Summary of work on coatings and claddings for fossil energy applications
[DE93-017005] p 1367 N94-17881
Factors which affect fatigue strength of fasteners
[DE93-017272] p 1453 N94-18084
Initiation and growth of microcracks in high strength steel butt welds
[AD-A268751] p 1454 N94-18466
Mechanism-dependent fractal character of fracture surfaces in high strength and toughness ASTM A723 steels
[AD-A268956] p 1360 N94-18542
JPRS report: Science and technology. Central Eurasia: Materials science
[JPRS-UMS-93-002] p 1339 N94-18833
Microstructure and texture control of fatigue in hydrogen and marine environments
[AD-A271277] p 1344 N94-19744
HIGH TEMPERATURE
Atlas of formability: Ultimet
[AD-A268352] p 1355 N94-17767
Atlas of formability: HAYNES 556
[AD-A268354] p 1356 N94-17768
Atlas of formability: HAYNES 188
[AD-A268355] p 1356 N94-17769
Atlas of formability: NICKELVAC K-500
[AD-A268351] p 1356 N94-17772
Atlas of formability: Haynes 230
[AD-A268325] p 1356 N94-17788
Atlas of formability: INCONEL 718
[AD-A268350] p 1356 N94-17789
Atlas of formability: Hastelloy C-22
[AD-A268324] p 1356 N94-17796

Atlas of formability: Permalloy - 80 flow stress curves
[AD-A268263] p 1356 N94-17801
Atlas of formability: Nickelvac C-276
[AD-A268264] p 1357 N94-17802
Atlas of formability: Ti-6Al-4V ELI
[AD-A268300] p 1357 N94-17803
Atlas of formability: ALLVAC 718
[AD-A268304] p 1357 N94-17804
Atlas of formability: Waspaloy
[AD-A268323] p 1593 N94-17805
Study on radiation-induced deterioration of grease at high temperature, 3
[DE93-788368] p 1369 N94-18220
Environmental effects on intermetallic compounds: A guide to the literature
[AD-A269587] p 1359 N94-18306
High temperature strain measurement with a resistance strain gage
[NASA-CR-194441] p 1434 N94-19314
High temperature co-axial winding transformers
[NASA-CR-194580] p 1407 N94-19643

HIGH TEMPERATURE ENVIRONMENTS
Environmental degradation of Alloy 600 and welded filler metal EN82 in an elevated temperature aqueous environment
[DE93-018049] p 1363 N94-18940

HIGH TEMPERATURE PLASMAS
Active neutral particle diagnostics for high temperature plasma
[DE93-788457] p 1586 N94-18214

HIGH TEMPERATURE SUPERCONDUCTORS
Polaron tunneling in high-temperature superconductors
[DE93-016880] p 1593 N94-17754
Phase separation and superconductivity in La2CuO(4 + delta): Effects of oxygen diffusion
[DE93-016610] p 1594 N94-17907
Performance evaluations of demountable electrical connections
[DE93-017399] p 1396 N94-18135
Synthesis and study of high-T(sub c) superconducting electronic materials
[AD-A268851] p 1402 N94-18390
Fabrication and microstructural development of Ag-clad TlBa2Ca2Cu3O(x) tapes
[DE93-017407] p 1597 N94-18500
The use of chopper spectrometers for cold-to-epithermal neutron scattering at IPNS
[DE93-017798] p 1598 N94-18531
X ray studies of microstructures in semiconductor and superconducting materials
[DE93-040690] p 1601 N94-19056
Institute of Geophysics and Planetary Physics, 1992
[DE93-019209] p 1627 N94-19077
Superconducting flux flow devices, digital circuits and memories
[DE93-019072] p 1405 N94-19079
Fabrication, properties, and microstructures of high (Tc) tapes and coils made from Ag-clad Bi-2223 superconductor
[DE93-017405] p 1602 N94-19122
LLE Review
[DE93-017618] p 1602 N94-19123
Role of pressure in the study of fullerenes
[DE93-018839] p 1602 N94-19340
Crossover from BCS to Bose superconductivity: A functional integral approach
[DE93-019503] p 1604 N94-19566

HILBERT SPACE
On relation between Berry phase and one-dimensional models with long-range 1/r(sup 2)-interaction
[DE93-624967] p 1592 N94-17690
Space and time as outcome of decoherence in an expanding universe
[DE93-016199] p 1624 N94-18047
The fixed, finite-order L(sup 2)-optimal control of infinite-dimensional time-varying discrete-time systems
[REPT-93-23] p 1542 N94-19138
The digital linear quadratic control problem for Pritchard-Salamon systems
[REPT-93-27] p 1542 N94-19142

HINGES
Plastic mechanism analysis of T-joints in RHS subject to combined bending and concentrated force
[PB93-195774] p 1456 N94-19061

HIPPOCAMPUS
Extrathalamic modulation of cortical function
[AD-A270869] p 1507 N94-19783

HISTOLOGY
The effects of reverberant impulse noise (blast waves) on hearing: Parametric studies
[AD-A269242] p 1506 N94-18911

HISTORIES
Historical seismicity of Hainaut, Flanders and Artois
p 1482 N94-18623
X-29: Research aircraft
[NASA-TM-109370] p 1318 N94-18962
Apollo 11: 20th anniversary
[NASA-TM-109364] p 1323 N94-18979
Langley's 50th year
[NASA-TM-109365] p 1632 N94-18980
Essential shift: Scientific revolution in the 20th century
[AD-A270810] p 1610 N94-19663

HODOSCOPES
Precision machining and polishing of scintillating crystals for large calorimeters and hodoscopes
[DE93-018663] p 1381 N94-19544

HOLDERS
A radial transmission line material measurement apparatus
[DE93-018508] p 1394 N94-17780

HOLE GEOMETRY (MECHANICS)
High resolution transmission electron microscopy of mesoporous MCM-41 type materials
[AD-A271271] p 1354 N94-19728

HOLES (ELECTRON DEFICIENCIES)
Photo-induced and electrooptic properties of (Pb,La)(Zr,Ti)O3 films
[DE93-017496] p 1371 N94-18519
Molecular nonlinear optical susceptibilities in condensed phases
[AD-A270200] p 1568 N94-18784

HOLLOW CATHODES
Plasma contactor development for Space Station
[NASA-TM-106425] p 1587 N94-18861

HOLOGRAPHY
Optical computing. Organization of the 1993 Photonics Science Topical Meetings. Technical digest series, volume 7
[AD-A269025] p 1578 N94-18332
Competitive dynamics and self-organization in photorefractive systems
[AD-A269663] p 1430 N94-18569
Operational parameters of an opto-electronic neural network employing fixed planar holographic interconnects
[DE93-018795] p 1433 N94-19000
The performance and survivability of dichromated poly (vinyl alcohol) holograms for space based photonic applications
[AD-A270974] p 1434 N94-19791

HOMOGENEOUS TURBULENCE
Theoretical study and modelling of homogeneous turbulence under rotation for implantation in a code for solving Navier-Stokes equations
[ECL-93-05] p 1420 N94-19381

HOMOMORPHISMS
Thermal wave image processing for characterization of subsurface of flaws in materials
[DE93-019024] p 1344 N94-19551

HOMOPOLAR GENERATORS
Pulsed power supply for Nova Upgrade
[DE93-019626] p 1441 N94-19307

HONEYCOMB STRUCTURES
SAND contact in DYNA3D
[DE93-016451] p 1340 N94-18113
Aerodynamic characteristics of a helicopter rotor airfoil as affected by simulated ballistic damage
[AD-A269206] p 1311 N94-18413

HOT ISOSTATIC PRESSING
The intelligent processing of materials
[AD-A269250] p 1362 N94-18923

HOT STARS
Spectrophotometry of emission-line stars in the magellanic clouds
[NASA-CR-194082] p 1628 N94-19425

HOT WORKING
Effect of internal heating during hot compression testing on the stress-strain behavior and hot working characteristics of alloy 304L
[DE93-012701] p 1362 N94-18917

HOT-WIRE ANEMOMETERS
A review of hot-wire technique in compressible flows
[LR-724] p 1423 N94-19668

HOVERING
Lift and pitching moment induced on jet STOVL aircraft hovering in ground effect
[AD-A269700] p 1317 N94-18577

HOVERING STABILITY
The dynamic stability of the helicopter
[LR-772] p 1321 N94-19615

HTPB PROPELLANTS
Strained ring energetic binders
[AD-A269056] p 1377 N94-18491

HUBBLE SPACE TELESCOPE
Hubble Space Telescope
[NASA-TM-109359] p 1621 N94-19072

HUBS
Blade and hub loads of ballistically damaged helicopter rotors
[AD-A270663] p 1319 N94-19781

HUGONIOT EQUATION OF STATE
Impact strength and indentation hardness of high-strength ceramics
[DE93-018833] p 1373 N94-19338

HUMAN BEINGS
Somatosensory responsiveness in behaving monkeys and human subjects
[AD-A268924] p 1501 N94-18231
A comparison of polygraphic and actigraphic monitoring of sleep using a 5-channel programmable-sensitivity actigraph
[AD-A270731] p 1507 N94-19608

HUMAN BODY
A multivariate anthropometric method for crew station design
[AD-A270652] p 1513 N94-19531

HUMAN FACTORS ENGINEERING
The stability and utility of the ESPRIT project, MUSiC, performance-based indicators of usability and tools: An evaluation of the usability of the NPL iSDX telephone system
[NPL-DITC-213/92] p 1613 N94-17925
Analysis of seating and restraint limitations restricting total body weight for aircrew and passengers on US Army helicopters
[AD-A269117] p 1511 N94-18296
Why are human-computer interfaces difficult to design and implement?
[AD-A268843] p 1514 N94-18317
Revision and verification of a seven-point workload estimate scale
[AD-A269194] p 1511 N94-18412
Towards versatile and practical knowledge acquisition
[AD-A269596] p 1615 N94-18464
Human Transportation System (HTS) study: Executive summary
[NASA-TM-104780] p 1332 N94-18669
Human Transportation System (HTS) study, volume 1
[NASA-TM-104779] p 1332 N94-18670
Research on man-machine productivity in aviation at Human Engineering Institute of Hangzhou University
[AD-A269952] p 1512 N94-18673
Generating object descriptions: Intergrating examples with text
[AD-A269992] p 1522 N94-18680
Army Cockpit Delethalization Program (CDP)
[AD-A268990] p 1512 N94-18765
A user task analysis for command and control systems and its use in human-computer interaction research
[AD-A269877] p 1512 N94-18774
Interdisciplinary training in life science (FY 1991 ASSERT)
[AD-A269220] p 1512 N94-18886
The FAA Technical Center Human Factors Laboratory information guide
[AD-A269343] p 1513 N94-18992
A multivariate anthropometric method for crew station design
[AD-A270652] p 1513 N94-19531
Human integration evaluation of three helmet systems
[AD-A271320] p 1513 N94-19570
Integrated measurement of crew resource management and technical flying skills
[AD-A270512] p 1510 N94-19677
FAA airborne data link human factors research plan
[AD-A271006] p 1514 N94-19773

HUMAN FACTORS LABORATORIES
The FAA Technical Center Human Factors Laboratory information guide
[AD-A269343] p 1513 N94-18992

HUMAN PERFORMANCE
The clocks and the perception of time in the 18th century society p 1424 N94-18007
Human reliability analysis application guide
[DE93-015361] p 1511 N94-18244
Stochastic models of attention and search
[AD-A268622] p 1508 N94-18292
Cognitive limitations in coordination in hierarchical information processing structures
[AD-A268825] p 1616 N94-18535
Evaluation of physiological and psychological impairment of human performance in cold stressed subjects
[AD-A268637] p 1506 N94-18632
Road march performance of special operations soldiers carrying various loads and load distributions
[AD-A269198] p 1512 N94-18882
The FAA Technical Center Human Factors Laboratory information guide
[AD-A269343] p 1513 N94-18992
Effects of practice in selecting and executing keypressing sequences
[IZF-1992-B-10] p 1509 N94-19420
A forthcoming key press can be selected while earlier ones are executed
[IZF-1993-B-2] p 1509 N94-19422

Pilot studies on object motion perception during linear self-motion after long duration centrifugation of human subjects
[IZF-1993-B-3] p 1510 N94-19439
Effects of location cuing on redundant target processing
[IZF-1993-B-1] p 1510 N94-19443
The brain electrical activity in different G situations
[AERONAUTICA-ACTA-A-372-199] p 1507 N94-19523

HUMIDITY
Radiosonde data collected on the ERS-1 validation cruise RRS Charles Darwin Cruise 62A, Iceland Faeroes region
[IOS-297-1992] p 1461 N94-18137
Station climatic summaries: North America. Volume 1: The contiguous United States
[AD-A269567] p 1490 N94-18303
Station climatic summaries, North America. Volume 2: Alaska, Canada and Greenland
[AD-A269793] p 1493 N94-18732

HYDRATES
Ground movements associated with gas hydrate production
[DE93-019887] p 1486 N94-19018
Faulted structure of the bottom simulating reflector on the Blake Ridge, western North Atlantic
[AD-A271289] p 1500 N94-19745

HYDRAULIC SHOCK
A finite element scheme for shock capturing
[AD-A270182] p 1417 N94-18755

HYDRAULICS
KINETIC: A system code for analyzing Nuclear thermal propulsion rocket engine transients
[DE93-016825] p 1337 N94-17884

HYDROCARBON COMBUSTION
Numerical simulation of fluid dynamics and combustion for ram accelerator projectile/obturator interaction
[AD-A269715] p 1320 N94-18748

HYDROCARBONS
Catalytic hydrocarbon reactions over supported metals
[DE93-018168] p 1345 N94-17808
Strained ring energetic binders
[AD-A269056] p 1377 N94-18491
Novel catalysts for methane activation
[DE93-040630] p 1349 N94-18532
A study of the effect of hydrocarbon structure on the induction of male rat nephropathy and metabolic structure
[AD-A270969] p 1504 N94-19789

HYDROCRACKING
Control of catalytic hydrotreating selectivity with ammonia
[DE93-041223] p 1354 N94-19660

HYDRODYNAMIC EQUATIONS
Group-invariant solutions of hydrodynamics and radiation hydrodynamics
[DE93-018373] p 1423 N94-19604

HYDRODYNAMICS
Vortex methods and statistics
[DE93-016974] p 1556 N94-17886
Impact modeling with smooth particle hydrodynamics
[DE93-016561] p 1451 N94-17906
Modeling shock initiation in Composition B
[DE93-016544] p 1376 N94-18095
Advanced in macrostatistical hydrodynamics
[DE93-018479] p 1410 N94-18270
Hydrodynamic instability modeling for ICF
[DE93-018634] p 1587 N94-18274
Wind products for use in coastal wave and surge models
[AD-A269753] p 1497 N94-18414
ADCIRC: An advanced three-dimensional circulation model for shelves, coasts, and estuaries. Report 3: Development of a tidal constituent database for the western North Atlantic and Gulf of Mexico
[AD-A268685] p 1497 N94-18455
DYNLET1 model formulation and user's guide
[AD-A269843] p 1498 N94-18723
Langley's 50th year
[NASA-TM-109365] p 1632 N94-18980
Sandia equation of state data base: Seslan file
[DE93-018693] p 1618 N94-19101
Smooth particle hydrodynamics: The SPHINX and SPHC codes
[DE93-014358] p 1457 N94-19207
Mathematical modeling of the free surface hydrodynamic and of transport in suspensions of non cohesive sediments: Aid to the interpretation of spatial images
[ETN-93-95011] p 1421 N94-19502
Locally adaptive remeshing scheme for calculating fluid instabilities
[DE93-019577] p 1422 N94-19568
Group-invariant solutions of hydrodynamics and radiation hydrodynamics
[DE93-018373] p 1423 N94-19604

HYDROGEN
Solid-state, resistive hydrogen sensors for safety monitoring
[DE93-017769] p 1424 N94-17778
Comparison of the modeling solutions with the hydrogen discharge data
[DE93-015115] p 1565 N94-17797
A preliminary model for crack-tip hydrogen transport
[NPL-DMM(A)-84] p 1451 N94-17899
Electron stripping cross sections for light impurity ions in colliding with atomic hydrogens relevant to fusion research
[DE93-788476] p 1566 N94-18158
Synthesis of higher alcohols from carbon monoxide and hydrogen in a slurry reactor
[DE93-015086] p 1347 N94-18209
Dense energetic compounds of C, H, N, and O atoms. 3: 5-(4-nitro-(1,2,5) oxadiazolyl)-5H-(1,2,3) triazolo (4,5-c)(1,2,5) oxadiazole
[AD-A268715] p 1338 N94-18314
Scaling laws for diamond chemical vapor deposition. 2: Atomic hydrogen transport
[AD-A269842] p 1371 N94-18740
Calculation of molecular excitation rates
[NASA-CR-193782] p 1571 N94-19236
Testing of protective coatings in hydrogen
[DE93-040326] p 1375 N94-19651

HYDROGEN ATOMS
Ratio of specimen thickness to detection area for reliable hydrogen permeation measurement
[NPL-DMM(A)-103] p 1451 N94-17929
A hydrogen atom in the curved space. Expansion over free solutions on the three-dimensional sphere
[DE93-629868] p 1549 N94-18198

HYDROGEN EMBRITTLEMENT
Environmental effects on intermetallic compounds: A guide to the literature
[AD-A269587] p 1359 N94-18306
Overlay welding irradiated stainless steel
[DE93-018767] p 1446 N94-19334

HYDROGEN IONS
Comparison of the modeling solutions with the hydrogen discharge data
[DE93-015115] p 1565 N94-17797

HYDROGEN ISOTOPES
Exchange front stability in packed-column chromatography
[DE93-017526] p 1346 N94-17997

HYDROGEN PEROXIDE
The c-jun gene expression in human cells exposed to either ionizing radiation or hydrogen peroxide
[DE93-017436] p 1502 N94-18476
Bienzyme sensors based on electrically wired peroxidase
[AD-A271364] p 1374 N94-19585

HYDROGEN PRODUCTION
Photobiotechnology: Application of photosynthesis to the production of renewable fuels and chemicals
[DE93-015522] p 1466 N94-18247

HYDROGENATION
Studies on gel electrolyte based on nitrile-butadiene copolymers
[AD-A269450] p 1370 N94-18282
Novel catalysts for methane activation
[DE93-040630] p 1349 N94-18532
Control of catalytic hydrotreating selectivity with ammonia
[DE93-041223] p 1354 N94-19660

HYDROLOGY
Application of ARC/INFO to regional scale hydrogeologic modeling
[DE93-015673] p 1461 N94-18107
A survey of current approaches to modelling of hydrological time-series with respect to climate variability and change
[WMO/TD-534] p 1463 N94-19435

HYDROLOGY MODELS
Application of ARC/INFO to regional scale hydrogeologic modeling
[DE93-015673] p 1461 N94-18107

HYDROLYSIS
Hydrolysis reaction and positronium decay in silica gels
[AD-A270028] p 1371 N94-18713

HYDROMECHANICS
Research activities, Faculty of Civil Engineering, Delft University of Technology, 1990 - 1991
[PB93-195022] p 1380 N94-19254

HYDROPHONES
Design of a general purpose and autonomous transmitter and receiver system for underwater acoustic experiments at sea
[AD-A269268] p 1495 N94-17822

HYDROSTATIC PRESSURE
Continuum modeling of materials that can undergo martensitic phase transitions
[AD-A268767] p 1360 N94-18386
Transducers and method for making same
[AD-D015949] p 1408 N94-19759

HYDROSTATICS
Stability measurements of Rayleigh-Benard convection near the critical state using a spectral model
[MPIS-15/1992] p 1422 N94-19520

HYDROTHERMAL STRESS ANALYSIS
Design for cyclic loading endurance of composites
[NASA-TM-106407] p 1457 N94-19351

HYDROTHERMAL SYSTEMS
Geothermal activity near Clearlake, California
[DE93-016627] p 1485 N94-18894

HYPERBOLIC DIFFERENTIAL EQUATIONS
Numerical methods for one-dimensional hyperbolic conservation laws
[PB93-194801] p 1547 N94-18078
High order non-oscillatory schemes for the compressible Euler equations p 1412 N94-18558
On the numerical approximation of nonlinear hyperbolic problems: Application to the dynamics of compressible gas
[ETN-93-95020] p 1420 N94-19365

HYPERBOLIC FUNCTIONS
About structurally stable generating mechanism for invariant hyperbolic sets
[DE93-629858] p 1561 N94-18150
Introduction to spectral methods for hyperbolic system of conservation laws p 1413 N94-18567

HYPERCUBE MULTIPROCESSORS
Optimal eigenvalue computation on distributed-memory MIMD multiprocessors
[DE93-018337] p 1535 N94-18808
A massively parallel adaptive finite element method with dynamic load balancing
[DE93-012844] p 1536 N94-19161
Experience in implementing a parallel file system
[DE93-012840] p 1536 N94-19188

HYPERPLANES
Maximal hypersurfaces in asymptotically stationary spacetimes
[MPA-708] p 1621 N94-18141

HYPERSONIC AIRCRAFT
Metals 2000
[DE93-016761] p 1355 N94-17752

HYPERSONIC FLOW
CFD investigations of the hypersonic double delta wing greta: Sanger project no. 3.2
[FFA-TN-1992-42] p 1311 N94-17919
Synthesis of the Workshop on Hypersonic Flows for Reentry Problems
[INRIA-RR-1721] p 1311 N94-17957
Parabolized Navier-Stokes computation of surface heat transfer characteristics for supersonic and hypersonic KE projectiles
[AD-A268858] p 1410 N94-18391
Computational Fluid Dynamics (CFD) research branch technical briefs
[AD-A269698] p 1417 N94-18739
Numerical simulation of viscous flows in chemical nonequilibrium
[MBB-LME-211-S-PUB-506] p 1421 N94-19497

HYPERSONIC HEAT TRANSFER
Parabolized Navier-Stokes computation of surface heat transfer characteristics for supersonic and hypersonic KE projectiles
[AD-A268858] p 1410 N94-18391

HYPERSONIC INLETS
A comparative study of turbulence models in predicting hypersonic inlet flows p 1314 N94-18553

HYPERSONIC REENTRY
Synthesis of the Workshop on Hypersonic Flows for Reentry Problems
[INRIA-RR-1721] p 1311 N94-17957

HYPERSONIC WIND TUNNELS
Error propagation equations and tables for estimating the uncertainty in high-speed wind tunnel test results
[DE93-018685] p 1311 N94-18275

HYPERSONICS
Parabolized Navier-Stokes computation of surface heat transfer characteristics for supersonic and hypersonic KE projectiles
[AD-A268858] p 1410 N94-18391

HYPERSPACES
Maximal hypersurfaces in asymptotically stationary spacetimes
[MPA-708] p 1621 N94-18141

HYPERTHERMIA
Cellular and molecular level responses after radiofrequency radiation exposure, alone or in combination with x rays or chemicals
[AD-A268189] p 1501 N94-17729

HYPERVELOCITY GUNS
Numerical simulation of fluid dynamics and combustion for ram accelerator projectile/obturator interaction
[AD-A269715] p 1320 N94-18748

HYPERVELOCITY IMPACT
Impact modeling with smooth particle hydrodynamics
[DE93-016561] p 1451 N94-17906
Effect of phase change in a debris cloud on a backwall structure
[DE93-017506] p 1358 N94-18100
Toward a characterization of the debris cloud created in a hypervelocity impact on a thin plate
[AD-A269190] p 1455 N94-18864
Smooth particle hydrodynamics: The SPHINX and SPHC codes
[DE93-014358] p 1457 N94-19207

HYPERVELOCITY PROJECTILES
Parabolized Navier-Stokes computation of surface heat transfer characteristics for supersonic and hypersonic KE projectiles
[AD-A268858] p 1410 N94-18391
Numerical simulation of fluid dynamics and combustion for ram accelerator projectile/obturator interaction
[AD-A269715] p 1320 N94-18748
Toward a characterization of the debris cloud created in a hypervelocity impact on a thin plate
[AD-A269190] p 1455 N94-18864
Shock compression properties of silicon carbide
[DE93-019927] p 1373 N94-19271

HYPOTHALAMUS
Intracellular physiology of the rat suprachiasmatic nucleus: Electrical properties, neurotransmission and effects of neuromodulators
[AD-A268829] p 1505 N94-18538

HYPOTHERMIA
Metabolic changes and hemodynamic dysfunction following hypothermic shock
[AD-A269780] p 1506 N94-18598

HYPOTHESES
Somatosensory responsiveness in behaving monkeys and human subjects
[AD-A268924] p 1501 N94-18231
The role of chemical inhibition of gap junctional intercellular communication in toxicology
[AD-A269251] p 1502 N94-18924
A refinement for nonmonotonic logic
[REPT-93-21] p 1542 N94-19092

HYSTERESIS
Shock propagation in crustal rock
[AD-A270148] p 1485 N94-18899

I

IBM COMPUTERS
Early experiences with the IBM SP-1
[DE93-018398] p 1535 N94-19010

ICE
Condensed gases under winter conditions: A study for the rescue services
[FOA-C-40305-4.5] p 1473 N94-18139
Arctic ice studies
[AD-A268608] p 1497 N94-18277
Search for lunar water ice in cometary impact craters
[AD-A270130] p 1627 N94-18877

ICE CLOUDS
Airborne studies of ocean-particle-cloud interactions in the Arctic
[AD-A270752] p 1479 N94-19575

ICE FORMATION
Atlas of SSM/I satellite ice concentration interpolated to operational ice model domains of the Arctic for 1992
[AD-A270306] p 1499 N94-18727
Proceedings: International Symposium on Thermal Engineering and Science for Cold Regions
[AD-A270636] p 1487 N94-19529
Airborne studies of ocean-particle-cloud interactions in the Arctic
[AD-A270752] p 1479 N94-19575

ICE MAPPING
Modifications of airborne oceanographic lidar for the long range P-3 missions
[NASA-CR-194682] p 1499 N94-18819

ICE REPORTING
Atlas of SSM/I satellite ice concentration interpolated to operational ice model domains of the Arctic for 1992
[AD-A270306] p 1499 N94-18727
Footprint size of a helicopter-borne electromagnetic induction sounding system versus antenna altitude
[AD-A270468] p 1463 N94-19672

IDEAL FLUIDS
On a conformal perfect fluid in the classical vacuum
[DE93-624797] p 1480 N94-17682

IFF SYSTEMS (IDENTIFICATION)
Military applications of high-accuracy frequency standards and clocks
[AD-A269303] p 1430 N94-18299

ILLUMINATING
Research on man-machine productivity in aviation at Human Engineering Institute of Hangzhou University
[AD-A269952] p 1512 N94-18673

IMAGE ANALYSIS
A non-homogeneous, spatio-temporal, wavelet multiresolution analysis and its application to the analysis of motion
[AD-A270621] p 1538 N94-19534

IMAGE CLASSIFICATION
Application of Fourier-based features for classification of synthetic aperture radar imagery
[AD-A270450] p 1387 N94-18513

IMAGE FILTERS
Applications of motion estimation in image processing
[FEL-92-B356] p 1580 N94-19455

IMAGE MOTION COMPENSATION
The accuracy of monostatic and bistatic radar imaging by range-Doppler-processing with and without motion compensation
[DLR-FB-93-07] p 1384 N94-18071

IMAGE PROCESSING
Data fusion through simulated annealing of registered range and reflectance images
[DE93-015910] p 1612 N94-17858
An object-oriented environment for computer vision and pattern recognition
[DE93-017098] p 1517 N94-17867
Application of fractal methods to estimate the aerosol-optical depth for atmospheric correction of high resolution satellite data
[DLR-FB-93-04] p 1480 N94-18088
Texture splats for 3D vector and scalar field visualization
[DE93-017104] p 1520 N94-18130
Development and application of local 3-D x ray CT reconstruction software for imaging critical regions in large ceramic turbine rotors
[DE93-015159] p 1369 N94-18166
The spatial variance of ionospherically-induced phase errors in SAR imagery
[DE93-015643] p 1385 N94-18232
Evaluation of a liquid crystal spatial light modulator capable of amplitude- and phase-modulating modes
[AD-A269252] p 1577 N94-18262
Space debris detection
[AD-A269254] p 1334 N94-18264
VLSI architectures for geometrical mapping problems in high-definition image processing
p 1398 N94-18345
An analog retina model for detecting dim moving objects against a bright moving background
p 1399 N94-18350
Image reconstruction from interferometer data
[AD-A268463] p 1578 N94-18383
Application of Fourier-based features for classification of synthetic aperture radar imagery
[AD-A270450] p 1387 N94-18513
Portable parallel ray tracing algorithms
[AD-A268984] p 1522 N94-18698
Introduction to wavelets
[AD-A268465] p 1389 N94-18801
Quantification of volume flaw sizes in ceramics by image processing of 3D x ray tomographic data sets
[DE93-018573] p 1372 N94-18932
Three dimensional ultrasonic imaging: An aging aircraft nondestructive inspection tool
[DE93-018088] p 1448 N94-19252
Overview of research in progress at the Center of Excellence
[NASA-CR-194329] p 1618 N94-19256
Cesar user library
[FFI-93/7021] p 1529 N94-19378
Development of ISY data set, part 2
[NASDA-CNT-930006-PT-2] p 1463 N94-19384
Applications of motion estimation in image processing
[FEL-92-B356] p 1580 N94-19455
A non-homogeneous, spatio-temporal, wavelet multiresolution analysis and its application to the analysis of motion
[AD-A270621] p 1538 N94-19534
Earth Penetration Radar Imaging System (EPRIS)
[DE93-019890] p 1391 N94-19542
Thermal wave image processing for characterization of subsurface of flaws in materials
[DE93-019024] p 1344 N94-19551
Signal processing algorithms for heterogeneous architectures
[AD-A271248] p 1392 N94-19724

IMAGE RECONSTRUCTION
Development and application of local 3-D x ray CT reconstruction software for imaging critical regions in large ceramic turbine rotors
[DE93-015159] p 1369 N94-18166
Image reconstruction from interferometer data
[AD-A268463] p 1578 N94-18383
Super-resolution of multi-pixel and sub-pixel images for the SDI
[AD-A268537] p 1462 N94-18631
Overview of research in progress at the Center of Excellence
[NASA-CR-194329] p 1618 N94-19256

IMAGE RESOLUTION
Super-resolution of multi-pixel and sub-pixel images for the SDI
[AD-A268537] p 1462 N94-18631
Color test chart for facsimile
[AD-A269754] p 1387 N94-18721
Overview of research in progress at the Center of Excellence
[NASA-CR-194329] p 1618 N94-19256

IMAGING RADAR
Laser imaging radar system
[AD-A270436] p 1387 N94-18510
Solution of the Poisson equation with application to radar imaging
[PB93-195865] p 1389 N94-18950

IMAGING SPECTROMETERS
UVSTAR: An imaging spectrograph with telescope for the Shuttle Hitchhiker-M platform p 1326 N94-19178
RAPID: The imaging energetic particle spectrometer on Cluster p 1329 N94-19633

IMAGING TECHNIQUES
Development of short pulse soft x ray lasers
[DE93-017150] p 1437 N94-18131
UVPI imaging from the LACE satellite: The Nihka rocket plume
[AD-A268456] p 1334 N94-18149
Development and application of local 3-D x ray CT reconstruction software for imaging critical regions in large ceramic turbine rotors
[DE93-015159] p 1369 N94-18166
Tomographic mathematical ideas applied to radar detection
[AD-A268789] p 1384 N94-18186
Image reconstruction from interferometer data
[AD-A268463] p 1578 N94-18383
Application of Fourier-based features for classification of synthetic aperture radar imagery
[AD-A270450] p 1387 N94-18513
High spatial resolution, range gated, underwater imaging method and apparatus
[AD-D015882] p 1430 N94-18530
Super-resolution of multi-pixel and sub-pixel images for the SDI
[AD-A268537] p 1462 N94-18631
Soft X Ray Projection Lithography. Organization of the 1993 photonics science optical meetings
[AD-A269159] p 1579 N94-18693
Imaging and blackbody emission spectra of hot particulates generated during laser ablation
[DE93-015818] p 1439 N94-18724
Nondestructive inspection of graphite-epoxy laminates for heat damage using DRIFT and LPF spectroscopies
[DE93-017228] p 1343 N94-18761
Engineering research, development and technology thrust area report, FY92
[DE93-016334] p 1632 N94-18856
Visualization for applications in shock physics
[DE93-012849] p 1418 N94-18918
UVSTAR: An imaging spectrograph with telescope for the Shuttle Hitchhiker-M platform p 1326 N94-19178
Study of GaAs substrates by ambient temperature photoluminescence imagery
[ECL-92-61] p 1603 N94-19357
Multimodal image correlation applied to computer aided pedicular screwing
[ETN-93-95018] p 1528 N94-19363
Description of an infrared zoomcollimator
[FEL-93-A034] p 1580 N94-19424
Applications of motion estimation in image processing
[FEL-92-B356] p 1580 N94-19455
A Sandia Technology Bulletin: Testing technology, July 1993
[DE93-040197] p 1633 N94-19537
Earth Penetration Radar Imaging System (EPRIS)
[DE93-019890] p 1391 N94-19542
Center-of-Excellence: Microlaser microscope
[DE93-040688] p 1442 N94-19658
UVPI imaging from the LACE satellite: The Strypi rocket plume
[AD-A270967] p 1335 N94-19787

IMMUNE SYSTEMS
A scientific role for Space Station Freedom: Research at the cellular level p 1503 N94-19215

IMPACT

Three-dimensional shock wave physics simulations with MIMD PAGOSA on massively parallel computers
[DE93-011682] p 1455 N94-18829

IMPACT ACCELERATION

Efficiency and biofidelity of occupant simulations
p 1459 N94-19473

IMPACT DAMAGE

Lattice damage in ion-implanted compound semiconductors and its effect on electrical activation
[DE93-015907] p 1593 N94-17845

Mechanical properties and impact damage resistance of composites fabricated by low cost, vacuum assisted, resin transfer molding
[AD-A270361] p 1342 N94-18702

Experimental investigation of wave and fracture phenomena in impacted ceramics: Experiments on sapphire
[AD-A270040] p 1372 N94-18792

Numerical simulation of vehicle crashworthiness and occupant protection p 1459 N94-19471

Blade and hub loads of ballistically damaged helicopter rotors
[AD-A270663] p 1319 N94-19781

IMPACT LOADS

Measurement and analysis of three 1.5-GPa shock-wave profiles in copper
[DE93-016559] p 1451 N94-17864

Vertical drop test of a Metro 3 aircraft
[AD-A270032] p 1318 N94-18789

Experimental investigation of wave and fracture phenomena in impacted ceramics: Experiments on sapphire
[AD-A270040] p 1372 N94-18792

Toward a characterization of the debris cloud created in a hypervelocity impact on a thin plate
[AD-A269190] p 1455 N94-18864

Computational mechanics of composite materials
[PB93-195782] p 1343 N94-19281

Simulation of the impact of a plastic flyer on an aluminum block using the hydrocode AUTODYNE
[PML-1992-26] p 1458 N94-19444

Impact analysis of composite aircraft structures
p 1458 N94-19468

Explicit solution techniques for impact with contact constraints p 1459 N94-19470

Current capabilities for simulating the extreme distortion of thin structures subjected to severe impacts
p 1459 N94-19474

IMPACT PREDICTION

Impact response of composite laminates: A guide to closed form solutions
[FFA-TN-1992-33] p 1339 N94-17971

Missile antenna pattern coordinate system and data formats
[AD-A269153] p 1385 N94-18260

IMPACT RESISTANCE

Mechanical properties and impact damage resistance of composites fabricated by low cost, vacuum assisted, resin transfer molding
[AD-A270361] p 1342 N94-18702

IMPACT STRENGTH

Effect of phase change in a debris cloud on a backwall structure
[DE93-017506] p 1358 N94-18100

Impact strength and indentation hardness of high-strength ceramics
[DE93-018833] p 1373 N94-19338

The influence of the target strength model on computed perforation
[DE93-018659] p 1460 N94-19543

IMPACT TESTS

Measurement and analysis of three 1.5-GPa shock-wave profiles in copper
[DE93-016559] p 1451 N94-17864

Impact modeling with smooth particle hydrodynamics
[DE93-016561] p 1451 N94-17906

Vertical drop test of a Metro 3 aircraft
[AD-A270032] p 1318 N94-18789

Dynamical behavior of tantalum
[DE93-017877] p 1362 N94-18919

Composite impact dynamics research at NASA LaRC: A review p 1458 N94-19467

The influence of the target strength model on computed perforation
[DE93-018659] p 1460 N94-19543

IMPEDANCE

Impedence calculation with recursive folding
[ETN-93-95049] p 1406 N94-19387

IMPEDANCE MEASUREMENT

A radial transmission line material measurement apparatus
[DE93-018508] p 1394 N94-17780

IMPINGEMENT

Lift and pitching moment induced on jet STOVL aircraft hovering in ground effect
[AD-A269700] p 1317 N94-18577

IMPLOSIONS

Hydrodynamic instability modeling for ICF
[DE93-018634] p 1587 N94-18274

IMPREGNATING

Process relationship as influenced by carbonization rate
[AD-A269680] p 1341 N94-18572

IMPULSES

Asymptotic behaviour of the solutions of Schroedinger equation with impulse effect in a Banach space
[DE93-629865] p 1548 N94-18195

Impulsive moving mirror model and the stability of Schroedinger equation with impulse effect in a Banach space
[DE93-629866] p 1548 N94-18196

Impulsive moving mirror model and the stability of linear homogeneous differential equations with impulse effect in a Banach space
[DE93-629906] p 1549 N94-18200

IMPURITIES

Electron stripping cross sections for light impurity ions in colliding with atomic hydrogens relevant to fusion research
[DE93-788476] p 1566 N94-18158

Defect behavior of polycrystalline solar cell silicon
[DE93-018490] p 1468 N94-19016

X ray studies of microstructures in semiconductor and superconducting materials
[DE93-040690] p 1601 N94-19056

IN SITU MEASUREMENT

CTD and XBT data collected on ERS-1 validation cruise RRS Charles Darwin Cruise 62A, Iceland-Faeroes region
[IOS-234-1992] p 1461 N94-18063

In-situ growth monitoring of molecular beam epitaxy processes
[AD-A269287] p 1598 N94-18616

IN-FLIGHT MONITORING

In-flight pressure distributions and skin-friction measurements on a subsonic transport high-lift wing section p 1308 N94-18435

INCINERATORS

On-line monitoring of incinerator emissions
[DE93-017406] p 1474 N94-18499

A comparison of wet and dry scrubbing systems for control of metals and dioxin/furan emissions from incinerators
[DE93-017446] p 1474 N94-18502

INCLUSIONS

Pressureless densification of ceramic matrix composites
[AD-A269137] p 1371 N94-18691

Office of Naval Research Publications/Patents /Presentations/Honors report, 1 October 1992 - 30 September 1993
[AD-A270037] p 1632 N94-18791

INCOMPRESSIBILITY

AEOLUS-IT MHD simulation code based on a toroidally incompressible plasma model
[DE93-788461] p 1586 N94-18157

INCOMPRESSIBLE FLOW

A computational and experimental investigation of incompressible oscillatory airfoil flow and flutter problems
[AD-A268748] p 1311 N94-18402

Efficient simulation of incompressible viscous flow over multi-element airfoils p 1306 N94-18421

A viscous-inviscid solver for high-lift incompressible flows over multi-element airfoils at deep separation conditions p 1306 N94-18425

STREMR: Numerical model for depth-averaged incompressible flow
[AD-A269949] p 1417 N94-18672

Numerical solutions for a flow with mixed convection in a vertical geometry
[DE93-011592] p 1419 N94-19058

Pseudo-compressibility methods for the incompressible flow equations
[NASA-CR-191533] p 1551 N94-19315

Numerical investigation of the incompressible flow around a wing with a fixed spoiler
[ISL-R-109/91] p 1313 N94-19524

Theoretical examination of the flow around a cylinder with a low dimensional Galerkin process
[MPIS-25/1992] p 1422 N94-19525

INCONEL (TRADEMARK)

Atlas of formability: INCONEL 718
[AD-A268350] p 1356 N94-17789

Assessment of an improved multiaxial strength theory based on creep-rupture data for Inconel 600
[DE93-015929] p 1356 N94-17791

Summary of work on coatings and claddings for fossil energy applications
[DE93-017005] p 1367 N94-17881

Environmental degradation of Alloy 600 and welded filler metal EN82 in an elevated temperature aqueous environment
[DE93-018049] p 1363 N94-18940

INDENTATION

Superhardness effect in Au/Ni multilayers
[DE93-016444] p 1357 N94-17860

Impact strength and indentation hardness of high-strength ceramics
[DE93-018833] p 1373 N94-19338

Picoindentation hardness measurements using atomic force microscopy
[AD-A270877] p 1604 N94-19579

INDEPENDENT VARIABLES

Flight test techniques for aircraft parameter estimation in ground effect
[AD-A270058] p 1318 N94-18795

INDEXES (DOCUMENTATION)

Summaries of FY 1993 research in the chemical sciences
[DE93-011855] p 1632 N94-18915

Aeronautical engineering: A continuing bibliography with indexes (supplement 297)
[NASA-SP-7037(297)] p 1310 N94-18937

EIA publications directory, 1992
[DE93-016833] p 1617 N94-18983

Aeronautical engineering: A continuing bibliography with indexes (supplement 296)
[NASA-SP-7037(296)] p 1310 N94-19070

INDIAN SPACE PROGRAM

Activities of the Indian Institute of Geomagnetism
p 1484 N94-18854

INDIUM

Defects in GaAs bulk crystals and multi-layers caused by In diffusion
[DE93-016968] p 1595 N94-18054

INDIUM ARSENIDES

Reorientation of misfit dislocations during annealing in InGaAs/GaAs(001) interfaces
[DE93-015046] p 1592 N94-17741

Defects in GaAs bulk crystals and multi-layers caused by In diffusion
[DE93-016968] p 1595 N94-18054

INDIUM PHOSPHIDES

Construction of a scanning tunneling microscope in liquid media: Studies of the preparation of the graphite surface and the chemical cleaning of indium phosphide
[ECL-92-25] p 1353 N94-19406

INDOOR AIR POLLUTION

Indoor environment program
[DE93-018601] p 1513 N94-18935

INDUCED DRAG

A study of the influence of a delta wing geometry on the induced drag at transonic speed (M=0.55) and high angles of attack
[FFA-TN-1992-14] p 1311 N94-17722

INDUCTANCE

High temperature co-axial winding transformers
[NASA-CR-194580] p 1407 N94-19643

INDUCTION (MATHEMATICS)

A refinement for nonmonotonic logic
[REPT-93-21] p 1542 N94-19092

INDUSTRIAL AREAS

The Mexico City 1991 lidar measurements campaign
[DE93-019960] p 1478 N94-19272

INDUSTRIAL WASTES

Kinetic studies of electrochemical generation of Ag(II) ion and catalytic oxidation of selected organics
[DE93-016601] p 1352 N94-19240

INDUSTRIES

Implementation of electronic data interchange in the department of defense: Lessons learned from private industry
[AD-A269532] p 1534 N94-18768

Manufacturing technology
[DE93-019580] p 1381 N94-19480

Program descriptions
[NSF-92-123] p 1531 N94-19619

INELASTIC SCATTERING

Polaron tunneling in high-temperature superconductors
[DE93-016880] p 1593 N94-17754

The rise of accuracy for the multichannel scattering problem solving
[DE93-630145] p 1608 N94-18253

Investigation of physical structures and interactions at high energy
[DE93-014444] p 1574 N94-18927

Solid-state dynamics in novel semiconductor nanostructures
[AD-A271249] p 1605 N94-19725

INEQUALITIES
L(sub p)-regularity of subelliptic operators on Lie groups
[PB93-194785] p 1549 N94-18948
INERTIAL CONFINEMENT FUSION
Laboratory microfusion capability study
[DE93-014373] p 1583 N94-17912
Overview of WARP: A particle code for heavy ion fusion
[DE93-018637] p 1588 N94-19034
INERTIAL NAVIGATION
On the use of differential GPS for automatic approach and landing of space and aircraft
[DLR-MITT-93-05] p 1316 N94-17921
INFLUENCE COEFFICIENT
FNAS/summer faculty fellowship research continuation program. Task 6: Integrated model development for liquid fueled rocket propulsion systems. Task 9: Aspects of model-based rocket engine condition monitoring and control
[NASA-CR-194574] p 1338 N94-19706
INFORMATION
Intentionally Short Range Communications (ISRC)
[AD-A268788] p 1384 N94-18216
Competitive dynamics and self-organization in photorefractive systems
[AD-A269663] p 1430 N94-18569
INFORMATION DISSEMINATION
Metadata compiled and distributed by the Carbon Dioxide Information Analysis Center for global climate change and greenhouse gas-related data bases
[DE93-015338] p 1473 N94-18167
FEDIX on-line information service: Design, develop, test, and implement an on-line research and education information service
[DE93-018818] p 1614 N94-18181
Bibliography of scientific publications of the Naval Biodynamics Laboratory, 1980 - 1992
[AD-A268886] p 1505 N94-18226
Handbook for users
[AD-A268726] p 1615 N94-18323
INFORMATION MANAGEMENT
OSSA Information Systems Program
[NASA-TM-108774] p 1612 N94-17737
Current information technology resource requirements of the federal government: Fiscal year 1994
p 1612 N94-17756
Carbon Dioxide Information Analysis Center: FY 1992 activities
[DE93-013845] p 1471 N94-17774
Information technology resources assessment
[DE93-015276] p 1613 N94-17894
The organizational preparation of existing relational databases for the integration of expert systems
[AD-A268823] p 1614 N94-18191
Trends in Information Management at Department of Energy Headquarters
[DE93-017197] p 1615 N94-18496
Emerging technologies planning guide, 1993 edition — information systems technology
[DE93-017196] p 1616 N94-18689
Application of new technologies in the virtual library: Seminars in Turkey, Portugal, and Spain
[NASA-TM-109718] p 1611 N94-19131
Secure open systems: An investigation
[FEL-91-B293] p 1619 N94-19454
Models and building blocks for secure open systems
[FEL-92-B365] p 1619 N94-19457
Learning about the Internet bibliography and beginner's guide
[AD-A268847] p 1532 N94-19707
INFORMATION PROCESSING (BIOLOGY)
The identification of the computational significance of key neurobiological characteristics found in a number of telencephalic brain regions
[AD-A269374] p 1505 N94-18407
Effects of practice in selecting and executing keypressing sequences
[IZF-1992-B-10] p 1509 N94-19420
Cognitive ability and whole-body rotation
[IZF-1993-B-4] p 1510 N94-19440
Effects of location cuing on redundant target processing
[IZF-1993-B-1] p 1510 N94-19443
Modeling of driver behavior: Information perception, rule and control strategies in experiments and simulations
[ETN-93-95053] p 1510 N94-19649
Extrathalamic modulation of cortical function
[AD-A270869] p 1507 N94-19783
INFORMATION RETRIEVAL
Restricting query relaxation through user constraints
[DE93-017413] p 1612 N94-17870
Defense Technical Information Center thesaurus
[AD-A268855] p 1615 N94-18319
Handbook for users
[AD-A268726] p 1615 N94-18323
Retrieving and integrating data from multiple information sources
[AD-A269588] p 1615 N94-18461
On masking effect
[AD-A269593] p 1541 N94-18462
Learning database abstractions for query reformulation
[AD-A269531] p 1616 N94-18641
Department of Defense Gateway Information System (DGIS) users' guide
[AD-A270140] p 1617 N94-18752
Networked MS windows 3.1 based classified document control system (CDOCS)
[DE93-017880] p 1617 N94-18984
Application of new technologies in the virtual library: Seminars in Turkey, Portugal, and Spain
[NASA-TM-109718] p 1611 N94-19131
Working visit to the University of L'Aquila, Italy
[FEL-93-B020] p 1618 N94-19452
INFORMATION SYSTEMS
OSSA Information Systems Program
[NASA-TM-108774] p 1612 N94-17737
Current information technology resource requirements of the federal government: Fiscal year 1994
p 1612 N94-17756
Carbon Dioxide Information Analysis Center: FY 1992 activities
[DE93-013845] p 1471 N94-17774
Information technology resources assessment
[DE93-015276] p 1613 N94-17894
An environment for requirement reuse
[REPT-92-082] p 1613 N94-17939
Navigation in hypermedia applications: Modelling and semantics
[REPT-93-034] p 1520 N94-18136
Metadata compiled and distributed by the Carbon Dioxide Information Analysis Center for global climate change and greenhouse gas-related data bases
[DE93-015338] p 1473 N94-18167
FEDIX on-line information service: Design, develop, test, and implement an on-line research and education information service
[DE93-018818] p 1614 N94-18181
The organizational preparation of existing relational databases for the integration of expert systems
[AD-A268823] p 1614 N94-18191
Handbook for users
[AD-A268726] p 1615 N94-18323
Retrieving and integrating data from multiple information sources
[AD-A269588] p 1615 N94-18461
Trends in Information Management at Department of Energy Headquarters
[DE93-017197] p 1615 N94-18496
Automatic documentation generation: The interaction of text and examples
[AD-A269670] p 1616 N94-18570
A comparison of air force data systems
[AD-A269691] p 1616 N94-18575
Generating object descriptions: Intergrating examples with text
[AD-A269992] p 1522 N94-18680
Integrated Terminal Weather System (ITWS)
[AD-A269884] p 1492 N94-18684
Emerging technologies planning guide, 1993 edition — information systems technology
[DE93-017196] p 1616 N94-18689
A general theory of signal integration for fault-tolerant dynamic distributed sensor networks
[AD-A270316] p 1534 N94-18699
Department of Defense Gateway Information System (DGIS) users' guide
[AD-A270140] p 1617 N94-18752
Computer/information security design approaches for Complex 21/Reconfiguration facilities
[DE93-018547] p 1535 N94-18930
Networked MS windows 3.1 based classified document control system (CDOCS)
[DE93-017880] p 1617 N94-18984
Software distribution using xnetlib
[DE93-018278] p 1523 N94-18989
Application of new technologies in the virtual library: Seminars in Turkey, Portugal, and Spain
[NASA-TM-109718] p 1611 N94-19131
Feasibility study in linguistically motivated object-oriented conceptual design of information systems
[PB93-197754] p 1618 N94-19331
Secure open systems: An investigation of current standardisation efforts for security in open systems
[FEL-92-B225] p 1618 N94-19450
Models and building blocks for secure open systems
[FEL-92-B365] p 1619 N94-19457
Results of a joint Navy/Air Force operational test to evaluate USAF Integrated Maintenance Information Systems (IMIS), Interactive Electronic Technical Manual (IETM) technology applied to the F/A-18 aircraft
[AD-A271322] p 1619 N94-19571
Systems engineering for Air Force C3I systems
[AD-A270482] p 1391 N94-19676
Software reuse: Major issues need to be resolved before benefits can be achieved. Report to the Chairman, Subcommittee on Defense, Committee on Appropriations, House of Representatives
[GAO/IMTEC-93-16] p 1532 N94-19716
A real-time spoken-language system for interactive problem-solving, combining linguistic and statistical technology for improved spoken language understanding
[AD-A270901] p 1392 N94-19749
Automated processing of military messages according to ADatP-3
[FEL-92-A044] p 1393 N94-19798
INFORMATION THEORY
Thermodynamics of computation and information distance
[DE93-012730] p 1517 N94-17812
Efficient domain-independent experimentation
[AD-A269530] p 1557 N94-18640
INFORMATION TRANSFER
Interactive Collaborative Environments (ICE) in the design to manufacturing process
[DE93-014994] p 1518 N94-17944
NASA aeronautics: Protecting sensitive technology. Report to Congressional requesters
[GAO/NSIAD-93-201] p 1617 N94-18848
INFRARED ABSORPTION
Vibrational dynamics in photoinduced electron transfer
[DE93-040874] p 1567 N94-18533
Infrared cross sections and global warming potentials of 10 alternative hydrohalocarbons
[AERONAUTICA-ACTA-A-371-199]
p 1479 N94-19521
INFRARED ASTRONOMY
Related investigations on the physics of high energy emission from active galactic nuclei
[NASA-CR-193615] p 1630 N94-18836
IRAS high resolution studies and modeling of closely interacting galaxies. Galaxy collisions: Infrared observations and analysis of numerical models. UV spectroscopy of massive young stellar populations in interacting galaxies
[NASA-CR-194483] p 1627 N94-19218
The 0.15 seconds near-infrared imaging of the central parsec of the galaxy
[MPE-PREPRINT-239] p 1621 N94-19415
INFRARED ASTRONOMY SATELLITE
ROSAT and IRAS observations
[MPE-PREPRINT-231] p 1623 N94-19526
INFRARED DETECTORS
Infrared detection with high-(Tc bolometers and response of Nb tunnel junctions to picosecond voltage pulses
[DE93-016963] p 1595 N94-17989
Perspective and future possibilities
p 1431 N94-18651
Description of an infrared zoomcollimator
[FEL-93-A034] p 1580 N94-19424
INFRARED IMAGERY
Measurement Techniques
[VKI-LS-1993-05] p 1430 N94-18643
Fundamentals of infrared thermography
p 1431 N94-18648
Application of infrared thermography in fluid mechanics p 1431 N94-18649
Perspective and future possibilities
p 1431 N94-18651
Infrared thermography p 1432 N94-18652
Thermal wave image processing for characterization of subsurface of flaws in materials
[DE93-019024] p 1344 N94-19551
Electro-optics display research, test, and evaluation laboratory program
[AD-A270947] p 1408 N94-19751
INFRARED INSTRUMENTS
Integrated test plan for the demonstration of a commercial Fourier Transform Infrared instrument
[DE93-018518] p 1433 N94-19041
Advances in passive-remote and extractive Fourier transform infrared systems
[DE93-017402] p 1478 N94-19241
INFRARED LASERS
Removing CFC's from the atmosphere with lasers: A second look
[DE93-017516] p 1473 N94-18101
A tunable compact high power far-infrared grating free-electron laser
[AD-A269875] p 1440 N94-18771

INFRARED RADIATION
IR materials producibility
[AD-A268849] p 1577 N94-18223
Vibrational dynamics in photoinduced electron transfer
[DE93-040874] p 1567 N94-18533
Surface modification of sapphire for IR window application
[DE93-019168] p 1602 N94-19075
INFRARED RADIOMETERS
Infrared thermography p 1432 N94-18652
INFRARED SCANNERS
Fundamentals of infrared thermography
p 1431 N94-18648
INFRARED SIGNATURES
Spectral radiance measurements on a bluff body stabilized flame: Characterization of the IR signature
[PB93-195899] p 1347 N94-18081
INFRARED SOURCES (ASTRONOMY)
ROSAT X ray observation of the 30 Dor giant HII region p 1623 N94-19527
INFRARED SPECTRA
Metallization and charge-transfer gap closure of transition-metal iodides under pressure
[DE93-040301] p 1353 N94-19538
The application of jet spray and ion beam contamination removal techniques to samples from the LDEF spacecraft
[AD-A270973] p 1354 N94-19755
INFRARED SPECTROMETERS
FT-NIR spectroscopy in quantitative and qualitative measurements of cereal products
[VTT-TIED-1331] p 1346 N94-17973
Spectral radiance measurements on a bluff body stabilized flame: Characterization of the IR signature
[PB93-195899] p 1347 N94-18081
On-line monitoring of incinerator emissions
[DE93-017406] p 1474 N94-18499
Integrated test plan for the demonstration of a commercial Fourier Transform Infrared instrument
[DE93-018518] p 1433 N94-19041
Transcutaneous Analyte Measuring Methods (TAMM)
[AD-A271387] p 1408 N94-19756
INFRARED SPECTROSCOPY
FT-NIR spectroscopy in quantitative and qualitative measurements of cereal products
[VTT-TIED-1331] p 1346 N94-17973
Analysis of deposit precursors in jet fuels using Fourier transform infrared spectroscopy
[AD-A269035] p 1377 N94-18489
Advances in passive-remote and extractive Fourier transform infrared systems
[DE93-017402] p 1478 N94-19241
Suitability of infrared spectroscopy for remote sensing of tropospheric trace gases
[KFK-5183] p 1479 N94-19507
INFRARED WINDOWS
Surface modification of sapphire for IR window application
[DE93-019168] p 1602 N94-19075
INGOTS
Commercialization effort in support of electroslag-casting technology
[DE93-017988] p 1366 N94-19733
INHIBITORS
The c-jun gene expression in human cells exposed to either ionizing radiation or hydrogen peroxide
[DE93-017436] p 1502 N94-18476
INJECTION MOLDING
Ageing in Processed Polymers: Programme, summary, and abstracts discussion meeting
[AD-A268931] p 1370 N94-18448
INJECTORS
Compound-lens injector for a 19-MeV, 700-kA electron beam
[DE93-013752] p 1573 N94-17698
Combustion instability phenomena of importance to liquid propellant engines
[AD-A268800] p 1348 N94-18389
Heavy Ion Fusion Injector Program
[DE93-018706] p 1575 N94-18997
INLET FLOW
Defining the normal turbine inflow within a wind park environment
[DE93-010032] p 1489 N94-18046
Workshop on Computational Turbulence Modeling
[NASA-TM-109266] p 1410 N94-18545
A comparative study of turbulence models in predicting hypersonic inlet flows p 1314 N94-18553
Several examples where turbulence models fail in inlet flow field analysis p 1412 N94-18556
MHD integrated topping cycle project
[DE93-040520] p 1588 N94-18978
INLET TEMPERATURE
Potassium-Rankine power conversion subsystem modeling for nuclear electric propulsion
[NASA-CR-191134] p 1468 N94-18821
INORGANIC CHEMISTRY
Molecular and polymeric ceramic precursors
[DE93-040364] p 1372 N94-18891
Research program activities of the ORNL Analytical Chemistry Division
[DE93-017938] p 1339 N94-19117
INORGANIC COMPOUNDS
Advanced civil engineering materials based on inorganic polymers
[AD-A270837] p 1374 N94-19600
INPUT/OUTPUT ROUTINES
Control of nonlinear systems
[AD-A270141] p 1542 N94-18898
Protocol service decomposition for high-performance networking
[AD-A270613] p 1538 N94-19533
INSOLATION
Effects of the Mount Pinatubo eruption on solar insolation: Four case studies
[DE93-018454] p 1475 N94-18817
INSPECTION
Aircrew life support, AFSC 122X0(1T1X1)
[AD-A268998] p 1511 N94-18394
Three dimensional ultrasonic imaging: An aging aircraft nondestructive inspection tool
[DE93-018088] p 1448 N94-19252
INSTALLING
Evaluation of aftermarket LPG conversion kits in light-duty vehicle applications
[DE93-010035] p 1377 N94-18617
INSTRUCTORS
Undergraduate course and curriculum development program and calculus and the bridge to calculus program: 1992 awards
[NSF-93-24] p 1610 N94-19446
INSTRUMENT COMPENSATION
Aspects of the calibration and processing of the CRRES fluxgate magnetometer data
[AD-A270127] p 1432 N94-18875
Construction and evaluation of an environmental chamber for calibration of temperature and pressure sensors for laser interferometers emperature and pressure sensors for laser interferometers)
[PB93-197838] p 1322 N94-19332
Software quality in test and measurment equipment
[PB93-197846] p 1528 N94-19333
INSTRUMENT ERRORS
Some potential errors in satellite wind estimates using the geostrophic approximation and the thermal wind
[AD-A269784] p 1491 N94-18599
High temperature strain measurement with a resistance strain gage
[NASA-CR-194441] p 1434 N94-19314
INSTRUMENT LANDING SYSTEMS
JPRS report: Central Eurasia. Aviation and cosmonautics, no. 12, December 1992
[JPRS-UAC-93-006] p 1632 N94-19148
INSULATORS
Experimental and theoretical investigation of surface chemistry induced by direct and indirect electronic excitation
[AD-A268846] p 1348 N94-18221
High pressure metallization of Mott Insulators: Magnetic, structural and electronic properties
[DE93-018295] p 1404 N94-18805
Pressure induced metallization of the Mott Insulator 6(sub 2)
[DE93-018296] p 1600 N94-18969
INTEGRAL EQUATIONS
Structure, thermodynamics, and dynamical properties of supercooled liquids
[DE93-788387] p 1607 N94-18211
Crossover from BCS to Bose superconductivity: A functional integral approach
[DE93-019503] p 1604 N94-19566
INTEGRAL TRANSFORMATIONS
Path integrals on warped product manifolds
[DE93-629859] p 1561 N94-18151
INTEGRATED CIRCUITS
Aerogels for microelectronic applications: Fast, inexpensive, and light as air
[DE93-017170] p 1395 N94-17882
Techniques for low consumption circuits
p 1428 N94-18032
Evaluation of the consumption of electronic clocks
p 1408 N94-18033
Automatic soldering for watch circuit components
p 1428 N94-18037
SPROC: A multiple-processor DSP IC
p 1398 N94-18347
Technology, design, simulation, and evaluation for SEP-hardened circuits p 1399 N94-18352
Systolic array IC for genetic computation
p 1400 N94-18361
A new variable testability measure
p 1400 N94-18364
Controlling state explosion during automatic verification of delay-insensitive and delay-constrained VLSI systems using the POM verifier p 1400 N94-18365
Formal verification of an MMU and MMU cache
p 1400 N94-18366
Formal hardware verification of digital circuits
p 1401 N94-18367
High accuracy switched-current circuits using an improved dynamic mirror p 1401 N94-18368
VHDL simulation with access to transistor models
p 1402 N94-18381
The LET spectrum and its uncertainty during the CRRES mission
[AD-A269977] p 1630 N94-18676
Monolithic low noise preamplifier for piezoelectric sensors
[AD-D015860] p 1563 N94-18734
Fabrication process for cantilever beam micromechanical switches
[AD-A269716] p 1404 N94-18749
High efficiency low cost monolithic module for SARSAT distress beacons
[NASA-CR-194234] p 1315 N94-18852
Integrated circuits: Resistless processing simplifies production and cuts costs
[DE93-018069] p 1405 N94-18941
Thermal stresses in the microchannel heatsink cooled by liquid nitrogen
[DE93-018660] p 1418 N94-18995
Silicon MCM substrates for integration of 3-5 photonic devices and CMOS IC's
[DE93-017894] p 1405 N94-19112
A Sandia Technology Bulletin: Testing technology, July 1993
[DE93-040197] p 1633 N94-19537
Tribological studies of silicon for magnetic recording applications (Invited)
[AD-A270878] p 1447 N94-19784
INTELLIGIBILITY
A real-time spoken-language system for interactive problem-solving, combining linguistic and statistical technology for improved spoken language understanding
[AD-A270901] p 1392 N94-19749
INTERACTING GALAXIES
IRAS high resolution studies and modeling of closely interacting galaxies. Galaxy collisions: Infrared observations and analysis of numerical models. UV spectroscopy of massive young stellar populations in interacting galaxies
[NASA-CR-194483] p 1627 N94-19218
INTERACTIVE CONTROL
A user task analysis for command and control systems and its use in human-computer interaction research
[AD-A269877] p 1512 N94-18774
Interactive Production Line (IPL) p 1495 N94-19704
INTERATOMIC FORCES
Atomic-scale friction and microfriction of graphite and diamond using friction force microscopy
[AD-A270952] p 1605 N94-19679
INTERCEPTION
Predicted structural response of the lightweight-interceptor technology demonstration vehicle
[DE93-014676] p 1333 N94-17782
Intentionally Short Range Communications (ISRC)
[AD-A268788] p 1384 N94-18216
INTERCONTINENTAL BALLISTIC MISSILES
An empirical evaluation of five circular error probable estimation techniques and a method for improving them
[AD-A266528] p 1556 N94-18397
INTERFACE STABILITY
The 6th Japan-U.S. conference on composite materials
[AD-A268535] p 1341 N94-18630
The application of front tracking to the simulation of shock refractions and shock accelerated interface mixing
[DE93-018342] p 1419 N94-19025
INTERFACES
Reorientation of misfit dislocations during annealing in InGaAs/GaAs(001) interfaces
[DE93-015046] p 1592 N94-17741
Microstructure of the interfacial zone around aggregate particles in concrete
[PB93-195790] p 1380 N94-19322
INTERFACIAL TENSION
Finite element modeling of evaporation and condensation during sol-gel film and fiber formation
[DE93-017655] p 1345 N94-17820
Contribution to the study of a symmetric film flow (with or without tensio-active elements)
[ECL-93-13] p 1421 N94-19461
Axial response of differently excited anchored viscous liquid bridges in zero-gravity
[LRT-WE-9-FB-1-1992] p 1379 N94-19489

Transient response of a viscous and anchored liquid bridge to an axial pulse
[LRT-WE-9-FB-7-1992] p 1379 N94-19492

An investigation of low Marangoni number fluid flow in a cold corner
[AD-A271317] p 1422 N94-19569

INTERFEROMETERS

Portable, solid state, fiber optic coupled Doppler interferometer system for detonation and shock diagnostics
[DE93-013917] p 1423 N94-17700

Monitoring the response of the upper troposphere/lower stratosphere to a greenhouse gas scenario
[DE93-014509] p 1470 N94-17710

Interferometer stations at the Air Force Aeroballistic Research Facility
[AD-A268776] p 1322 N94-18330

Image reconstruction from interferometer data
[AD-A268463] p 1578 N94-18383

Behavior of the particle transport coefficients near the density limit in MTX
[DE93-019108] p 1591 N94-19311

INTERFEROMETRY

Development and test of readout electronics for optical quadrature signals
[DLR-MITT-92-11] p 1395 N94-17920

Interferometer stations at the Air Force Aeroballistic Research Facility
[AD-A268776] p 1322 N94-18330

Interferometric investigations of compressible dynamic stall over a transiently pitching airfoil
[NASA-TM-109380] p 1312 N94-19119

Shock compression properties of silicon carbide
[DE93-019927] p 1373 N94-19271

Film condensation in a shock wave
[MPIS-22/1992] p 1422 N94-19509

INTERGALACTIC MEDIA

The universe at moderate redshift
[NASA-CR-193771] p 1627 N94-19093

INTERGRANULAR CORROSION

Environmentally assisted cracking of nickel anode substrates in Li/SOCl2 cells: An engineering approach
[DE93-015130] p 1405 N94-18928

INTERLAYERS

Molecular dynamics modeling of the mechanical behavior of metallic multilayers
[DE93-017972] p 1365 N94-19263

INTERMEDIATE FREQUENCIES

A radial transmission line material measurement apparatus
[DE93-018508] p 1394 N94-17780

Broadband IF matching for quasioptical mixers
[MPE-PREPRINT-240] p 1390 N94-19416

INTERMETALLICS

Magnetic properties of single-crystalline UCu3Al2
[DE93-016607] p 1593 N94-17744

Summary of work on coatings and claddings for fossil energy applications
[DE93-017005] p 1367 N94-17881

The Hall-Petch relationship and mechanisms of fracture in B2 compounds
[DE93-018887] p 1359 N94-18182

Environmental effects on intermetallic compounds: A guide to the literature
[AD-A269587] p 1359 N94-18306

Solderability perservative coatings: Electroless tin versus organic azoles
[DE93-017634] p 1370 N94-18477

Developing and understanding the high temperature behavior of niobium aluminides and niobium aluminide composites
[AD-A268874] p 1341 N94-18636

Fundamental concepts relating local atomic arrangements, deformation, and fracture of intermetallic alloys
[AD-A268745] p 1361 N94-18788

Morphology, deformation, and defect structures of TiCr2 in Ti-Cr alloys
[DE93-018332] p 1361 N94-18807

Development of ductile Fe3Al-based aluminides
[DE93-017865] p 1362 N94-18938

Tensile properties of as-cast iron-aluminide alloys
[DE93-017852] p 1363 N94-18975

Shock-loading response of advanced materials
[DE93-018344] p 1455 N94-19033

Magnetic and crystallographic structures in UTX intermetallic compounds
[DE93-018291] p 1605 N94-19735

INTERMITTENCY

Singularities and symmetries of nonlinear ordinary and partial differential equations
[DE93-040083] p 1550 N94-19190

INTERMOLECULAR FORCES

Femtosecond Fourier-transform spectroscopy of low-frequency intermolecular motions in weakly interacting liquids
[DE93-017312] p 1566 N94-18085

Calculation of molecular excitation rates
[NASA-CR-193782] p 1571 N94-19236

INTERNAL COMBUSTION ENGINES

Evaluation of aftermarket LPG conversion kits in light-duty vehicle applications
[DE93-010035] p 1377 N94-18617

INTERNAL ENERGY

Techniques for the estimation of Heats of Explosion (HEX) using thermochemical codes
[AD-A268584] p 1609 N94-18310

Chemical dynamics in time and energy space
[DE93-018595] p 1350 N94-19097

INTERNAL PRESSURE

Compatibility of refrigerants and lubricants with motor materials, volume 1
[DE93-040216] p 1350 N94-18895

INTERNAL WAVES

Acoustic travel time perturbations due to an internal tide and internal wave field in the Barents Sea
[AD-A270879] p 1499 N94-19580

INTERPLANETARY DUST

Structuration processes in protoplanetary accretion disks
[MPE-243] p 1628 N94-19519

INTERPLANETARY MAGNETIC FIELDS

Radial evolution of the solar wind turbulence with application to charged particle transport
[NASA-CR-194081] p 1629 N94-19427

INTERPOLATION

Preparation of data assimilation and model evaluation experiment data sets
[AD-A269996] p 1498 N94-18665

Solar radiation in Saudi Arabia
[AD-A269970] p 1493 N94-18781

Smooth particle hydrodynamics: The SPHINX and SPHC codes
[DE93-014358] p 1457 N94-19207

Radiosity algorithms using higher order finite element methods
[DE93-018098] p 1531 N94-19548

INTERPROCESSOR COMMUNICATION

A fast adaptive convex hull algorithm on two-dimensional processor arrays with a reconfigurable BUS system
p 1402 N94-18380

The p4 Linda: A portable implementation of Linda
[DE93-017752] p 1535 N94-19046

A multi-thread approach to coalescing small transfers generated by portable tool sets
[DE93-012128] p 1525 N94-19186

Message passing in PUMA
[DE93-012841] p 1537 N94-19206

Wide-address spaces: Exploring the design space
[MEMO-INF-92-77] p 1537 N94-19219

Specification and verification of a dynamic leader election protocol in a broadcast network
[MEMO-INF-93-05] p 1558 N94-19228

Specifying and proving communication closedness in protocols
[MEMO-INF-93-23] p 1390 N94-19267

Action systems and action refinement in the development of parallel systems: An algebraic approach
[MEMO-INF-93-14] p 1538 N94-19296

Congestion/flow control and routing in data networks: A control-theoretic approach
[AD-A271121] p 1392 N94-19737

INTERSECTIONS

Fuzzy hypergraphs and fuzzy intersection graphs
[AD-A270303] p 1549 N94-18815

INTERSTELLAR EXTINCTION

Dust in the Small Magellanic Cloud
[NASA-CR-193344] p 1624 N94-17764

INTERSTELLAR MATTER

Calculation of molecular excitation rates
[NASA-CR-193782] p 1571 N94-19236

INTERSTITIALS

Selective electrochemical wafer thinning for silicon characterization
[DE93-015083] p 1592 N94-17742

INVARIANCE

On a conformal perfect fluid in the classical vacuum
[DE93-624797] p 1480 N94-17682

About structurally stable generating mechanism for invariant hyperbolic sets
[DE93-629858] p 1561 N94-18150

Deformed traces and covariant quantum algebras for quantum groups GL(sub qp)(2) and GL(sub qp)(1/1)
[DE93-629862] p 1561 N94-18153

Four-fermion interactions
[DE93-629905] p 1566 N94-18199

Fault tolerant sequential circuits using sequence invariant state machines p 1398 N94-18344

T violating neutron spin rotation asymmetry
[DE93-018470] p 1570 N94-19126

Decomposition invariance of generalized steady-state of a 1-D diffusion system
[REPT-93-26] p 1550 N94-19141

Group-invariant solutions of hydrodynamics and radiation hydrodynamics
[DE93-018373] p 1423 N94-19604

INVENTIONS

The mystery of the perpetual motion clock of Geiser and Son p 1427 N94-18027

INVENTORY MANAGEMENT

Inventory management plan for a research and development local area network
[DE93-018381] p 1617 N94-19026

INVERSE SCATTERING

Fast iterative solution of sparsely sampled seismic inverse problems
[REPT-93-16] p 1486 N94-19081

Inverse scattering of surface waves: A new look at surface consistency
[REPT-93-25] p 1486 N94-19140

An iterative inverse scattering method for the removal of scattered surface waves
[REPT-93-18] p 1488 N94-19644

INVERTERS

Design of power electronics for TVC EMA systems
[NASA-CR-193839] p 1407 N94-19642

INVISCID FLOW

The aero-mechanical design of a novel Fowler flap mechanism p 1309 N94-18443

Internal instability of nonparallel flow on an equatorial beta-plane
[AD-A268927] p 1490 N94-18486

Cell vertex methods for steady inviscid flow
p 1413 N94-18563

Two-dimensional boundary surfaces for axi-symmetric external transonic flows
[AD-A269678] p 1312 N94-18571

Stress pulse phenomena
[DE93-019064] p 1456 N94-19078

Pseudo-compressibility methods for the incompressible flow equations
[NASA-CR-191533] p 1551 N94-19315

IODIDES

Analysis of HgI2 and PbI2 crystals and detectors by Particle-Induced X Ray Emission (PIXE) and Ion Backscattering Spectroscopy (IBS)
[DE93-017168] p 1594 N94-17896

Metallization and charge-transfer gap closure of transition-metal iodides under pressure
[DE93-040301] p 1353 N94-19538

IODINE

Potential dependent structural changes of underpotentially deposited copper on an iodine treated platinum surface determined in situ by surface EXAFS and its polarization dependence
[AD-A269890] p 1360 N94-18687

ION ACCELERATORS

Alternating-phase focusing with amplitude modulation
[DE93-018618] p 1574 N94-18273

Spice modeling of a FET-switched induction accelerator cell
[DE93-018662] p 1575 N94-18996

Correction of longitudinal errors in accelerators for heavy-ion fusion
[DE93-018656] p 1575 N94-19106

Simulation of transient effects in the heavy ion fusion injectors
[DE93-018658] p 1575 N94-19107

Induction accelerator development for heavy ion fusion
[DE93-019228] p 1591 N94-19479

The ILSE Experimental Program
[DE93-019247] p 1576 N94-19560

ION BEAMS

Active neutral particle diagnostics for high temperature plasma
[DE93-788457] p 1586 N94-18214

Deep ion implantation into manganin to modify its pressure and electrothermocharacteristics
[DE93-630229] p 1359 N94-18218

New applications for high average power beams
[DE93-018845] p 1439 N94-18522

Optical properties of oxide coatings prepared by ion-assisted deposition
[AD-A270024] p 1599 N94-18711

Spice modeling of a FET-switched induction accelerator cell
[DE93-018662] p 1575 N94-18996

Overview of WARP: A particle code for heavy ion fusion
[DE93-018637] p 1588 N94-19034

Simulation of transient effects in the heavy ion fusion injectors
[DE93-018658] p 1575 N94-19107

Studies of clusters [DE93-018961] p 1572 N94-19309

Induction accelerator development for heavy ion fusion [DE93-019228] p 1591 N94-19479

Ionized-cluster beam/partially ionized beam deposition of electro-optical and nonlinear optical organic materials and device development [AD-A270832] p 1604 N94-19596

Active spacecraft potential control: An ion emitter experiment for Cluster p 1330 N94-19634

The deposition of electro-optic films on semiconductors [AD-A270823] p 1605 N94-19664

Nanofabrication by focused ion beam [AD-A271290] p 1345 N94-19746

The application of jet spray and ion beam contamination removal techniques to samples from the LDEF spacecraft [AD-A270973] p 1354 N94-19755

ION CONCENTRATION

Comparison of the modeling solutions with the hydrogen discharge data [DE93-015115] p 1565 N94-17797

ION CURRENTS

Studies on gel electrolyte based on nitrile-butadiene copolymers [AD-A269450] p 1370 N94-18282

Optical properties of oxide coatings prepared by ion-assisted deposition [AD-A270024] p 1599 N94-18711

ION CYCLOTRON RADIATION

New applications for high average power beams [DE93-018845] p 1439 N94-18522

Advanced fusion diagnostics [DE93-040085] p 1589 N94-19133

ION DISTRIBUTION

The Cluster Ion Spectroscopy experiment p 1329 N94-19631

ION EXCHANGING

Kinetic studies of electrochemical generation of Ag(II) ion and catalytic oxidation of selected organics [DE93-016601] p 1352 N94-19240

ION IMPLANTATION

Interdisciplinary research on wear of materials [AD-A268190] p 1443 N94-17730

Lattice damage in ion-implanted compound semiconductors and its effect on electrical activation [DE93-015907] p 1593 N94-17845

Metal-nanocluster composites made by ion implantation: A novel third-order nonlinear material [DE93-015908] p 1339 N94-17846

Deep ion implantation into manganin to modify its pressure and electrothermocharacteristics [DE93-630229] p 1359 N94-18218

Surface modification of sapphire for IR window application [DE93-019168] p 1602 N94-19075

Binding of copper to nanocavity surfaces in silicon [DE93-019073] p 1364 N94-19080

Nanofabrication by focused ion beam [AD-A271290] p 1345 N94-19746

ION MOTION

Ion mobility and transport barriers in the tokamak plasmas [DE93-040320] p 1587 N94-18524

Nanofabrication by focused ion beam [AD-A271290] p 1345 N94-19746

ION SCATTERING

Analysis of HgI2 and PbI2 crystals and detectors by Particle-Induced X Ray Emission (PIXE) and Ion Backscattering Spectroscopy (IBS) [DE93-017168] p 1594 N94-17896

ION SOURCES

Simulation of transient effects in the heavy ion fusion injectors [DE93-018658] p 1575 N94-19107

Studies of clusters [DE93-018961] p 1572 N94-19309

ION TEMPERATURE

Transport in the self-organized relaxed state of ion temperature gradient instability [DE93-016769] p 1584 N94-17983

Active neutral particle diagnostics for high temperature plasma [DE93-788457] p 1586 N94-18214

IONIC COLLISIONS

Meson production in relativistic heavy-ion collisions at AGS energies [DE93-016871] p 1565 N94-17984

Heavy-ion collisions and the nuclear equation of state [DE93-019263] p 1566 N94-18104

Task A: Yale Accelerator Users Group (YAUG) [DE93-018417] p 1570 N94-19029

The study of the phase structure of hadronic matter by searching for the deconfined quark-gluon phase transition using 2 TeV (bar-p)-p collisions, and by searching for critical phenomena in an exclusive study of multifragmentation using 1 GeV/nucleon heavy ion collisions [DE93-018925] p 1570 N94-19103

Advanced fusion diagnostics [DE93-040085] p 1589 N94-19133

Studies of clusters [DE93-018961] p 1572 N94-19309

IONIC DIFFUSION

Gamma scattering in condensed matter with high intensity Moessbauer radiation [DE93-019461] p 1601 N94-19031

Microstructure of the interfacial zone around aggregate particles in concrete [PB93-195790] p 1380 N94-19322

IONIC MOBILITY

Ion mobility and transport barriers in the tokamak plasmas [DE93-040320] p 1587 N94-18524

IONIC REACTIONS

The Fourteenth Symposium on Molecular Beams [AD-A268721] p 1568 N94-18787

IONIZATION

Correlated charge-changing ion-atom collisions [DE93-018717] p 1564 N94-17775

Investigation of the relative abundance of heavy versus light nuclei in primary cosmic rays using underground muon bundles [DE93-017601] p 1630 N94-17818

Radio wave propagation in structured ionization for satellite and radar applications [AD-A268457] p 1382 N94-17844

Dynamics of short-pulse excitation, ionization and harmonic conversion [DE93-017220] p 1436 N94-17996

Electron stripping cross sections for light impurity ions in colliding with atomic hydrogens relevant to fusion research [DE93-788476] p 1566 N94-18158

Penetrating radiation environment and effects study [AD-A270126] p 1485 N94-18874

Experimental study of interactions of highly charged ions with atoms at keV energies [DE93-040222] p 1571 N94-19257

IONIZATION CHAMBERS

Energy loss measurement of cosmic ray muons [KFK-5158] p 1631 N94-19504

Measurement of the energy of horizontal cosmic ray muons [KFK-5163] p 1631 N94-19505

Measurements of cosmic ray muons with multi-wire proportional chambers with a prototype setup for KASCADE [KFK-5173] p 1631 N94-19506

IONIZATION CROSS SECTIONS

Electron stripping cross sections for light impurity ions in colliding with atomic hydrogens relevant to fusion research [DE93-788476] p 1566 N94-18158

IONIZATION POTENTIALS

Conversion of ADC pulse heights into MIP units: NUMASS test data, September 1991 [USIP-93-03] p 1432 N94-18846

Active spacecraft potential control: An ion emitter experiment for Cluster p 1330 N94-19634

IONIZING RADIATION

Cellular and molecular level responses after radiofrequency radiation exposure, alone or in combination with x rays or chemicals [AD-A268189] p 1501 N94-17729

The c-jun gene expression in human cells exposed to either ionizing radiation or hydrogen peroxide [DE93-017436] p 1502 N94-18476

The performance and survivability of dichromated poly (vinyl alcohol) holograms for space based photonic applications [AD-A270974] p 1434 N94-19791

IONOSPHERIC DISTURBANCES

The spatial variance of ionospherically-induced phase errors in SAR imagery [DE93-015643] p 1385 N94-18232

Studies of enhanced radar backscatter [AD-A269544] p 1385 N94-18288

RADARC HF ionospheric prediction program for OTH radar [AD-A269557] p 1385 N94-18291

Morphology and characteristics of disturbed HF skywave channels [AD-A269755] p 1388 N94-18722

Center of Excellence in Theoretical Geoplasma Research [AD-A270210] p 1588 N94-18902

IONOSPHERIC ELECTRON DENSITY

Using computerized tomography to determine ionospheric structures [DE93-018903] p 1485 N94-19001

Using computerized tomography to determine ionospheric structures [DE93-018904] p 1485 N94-19002

IONOSPHERIC PROPAGATION

RADARC HF ionospheric prediction program for OTH radar [AD-A269557] p 1385 N94-18291

Morphology and characteristics of disturbed HF skywave channels [AD-A269755] p 1388 N94-18722

Using computerized tomography to determine ionospheric structures [DE93-018904] p 1485 N94-19002

Improved HF data network simulator, volume 1 [AD-A270953] p 1393 N94-19752

Improved HF data network simulator, software user's manual, volume 2 [AD-A270954] p 1393 N94-19753

IONOSPHERIC SOUNDING

Using computerized tomography to determine ionospheric structures [DE93-018904] p 1485 N94-19002

IONS

Correlated charge-changing ion-atom collisions [DE93-018717] p 1564 N94-17775

Proton transfer dynamics and cluster ion fragmentation in phenol/ammonia cLusters [AD-A269133] p 1348 N94-18256

Photodissociation dynamics of cluster ions [AD-A270296] p 1568 N94-18814

Relativistic configuration interaction calculation of the correlation energies of heliumlike ions [DE93-018093] p 1571 N94-19201

IRON

A new multiphase equation of state for iron [DE93-017629] p 1357 N94-17819

Optical properties of redispersed iron fibers measured at 94 GHz [AD-A269739] p 1342 N94-18756

IRON ALLOYS

Summary of work on coatings and claddings for fossil energy applications [DE93-017005] p 1367 N94-17881

Development of ductile Fe3Al-based aluminides [DE93-017865] p 1362 N94-18938

Tensile properties of as-cast iron-aluminide alloys [DE93-017852] p 1363 N94-18975

Low-aluminum-content iron-aluminum alloys [DE93-017862] p 1365 N94-19274

Bibliography on silicides [AD-A270516] p 1374 N94-19532

Incology 908 database report: On process-structure-property relationship [DE93-017616] p 1366 N94-19546

Commercialization effort in support of electroslag-casting technology [DE93-017988] p 1366 N94-19733

IRON METEORITES

Dynamical behavior of octahedrite from the Henbury meteorite [DE93-018834] p 1627 N94-19339

IRRADIANCE

Considerations for the use of the modified line reversal technique for gas temperature measurement [DE93-015752] p 1576 N94-17857

SeaSoar CTD, fluorescence and scalar irradiance data from RRS Charles Darwin Cruises 58/59, NE Atlantic, Vivaldi 1991 [IOS-299-1992] p 1496 N94-18066

Solar radiation in Saudi Arabia [AD-A269970] p 1493 N94-18781

Scientific studies in association with the Shuttle Solar Backscatter Ultraviolet (SSBUV) project [NASA-CR-193404] p 1630 N94-19437

IRRADIATION

PVDF measurement of soft x ray induced shock and filter debris impulse [DE93-017633] p 1382 N94-17806

Characteristics and pulsed radiation response of non-ideal quartz shock stress gauges [DE93-017628] p 1424 N94-17999

Time-resolved probing of electron thermal conduction in femtosecond-laser-pulse-produced plasmas [DE93-016996] p 1585 N94-18129

Deep ion implantation into manganin to modify its pressure and electrothermocharacteristics [DE93-630229] p 1359 N94-18218

Ultrasonic process for destruction of chlorinated organic compounds in aqueous solution [DE93-015551] p 1348 N94-18249

Neutron-induced collision cascade mixing in Nb/V superlattices
[DE93-018575] p 1600 N94-18933
Effects of irradiation temperature on Charpy and tensile properties of high-copper, low upper-shelf, submerged-arc welds
[DE93-017858] p 1445 N94-19047
Studies of deep levels in high resistivity silicon detectors irradiated by high fluence fast neutrons using a thermally stimulated current spectrometer
[DE93-016133] p 1602 N94-19258
Overlay welding irradiated stainless steel
[DE93-018767] p 1446 N94-19334

IRREVERSIBLE PROCESSES
Non Linear Dynamics and Chaos
[AGARD-LS-191] p 1607 N94-18236

ISCHEMIA
Cerebral ischemia and reperfusion injury: A brief review
[AD-A270480] p 1507 N94-19675

ISENTROPIC PROCESSES
Static pressure measurements for near isentropic flows using laser induced iodine fluorescence
p 1431 N94-18646

ISING MODEL
Ising model on tangled chain. Part 2: Magnetization and susceptibility
[DE93-628794] p 1607 N94-18174

ISOLATION
Isolation mechanisms in III-V devices
[AD-A271197] p 1605 N94-19717

ISOLATORS
Investigation of a fiber optic frequency shifter and optical isolator
[AD-A269820] p 1579 N94-18738

ISOMERS
An ab initio study of the weakly bonded CO-Cl2 complex
[AD-A269000] p 1349 N94-18395

ISOMORPHISM
A reduction of the globalization and U(1)-covering
[DE93-624769] p 1546 N94-17817

ISOTHERMAL FLOW
Contribution to the study of a symmetric film flow (with or without tensio-active elements)
[ECL-93-13] p 1421 N94-19461

ISOTHERMS
Geothermal activity near Clearlake, California
[DE93-016627] p 1485 N94-18894

ISOTOPE EFFECT
A carbon isotope mass balance for an anoxic marine sediment: Isotopic signatures of diagenesis
p 1477 N94-19232

ISOTOPE SEPARATION
The copper-pumped dye laser system at Lawrence Livermore National Laboratory
[DE93-014429] p 1435 N94-17723
Safety approaches for high power modular laser operation
[DE93-017213] p 1435 N94-17759
Exchange front stability in packed-column chromatography
[DE93-017526] p 1346 N94-17997

ISOTOPES
The use of post detonation analysis of stable isotope ratios to determine the type and production process of the explosive involved
[DE93-018497] p 1378 N94-19242

ISOTOPIC SPIN
Eta-nucleon interaction and nuclear production of eta mesons
[DE93-018469] p 1571 N94-19259

ISOTROPIC MEDIA
Waveguide and resonator perturbation techniques for measuring chirality and non-reciprocity of biisotropic materials
[PB93-187243] p 1384 N94-18116
Acoustic propagation modeling using MATLAB
[AD-A270905] p 1564 N94-19750

ISOTROPY
Formulation and identification of the anisotropic laws for thin sheets drawing
[ECL-92-55] p 1365 N94-19400

ITERATION
A least-squares computational tool kit
[DE93-018400] p 1557 N94-19011
Interior-point methodology for linear programming: Duality, sensitivity analysis and computational aspects
[REPT-93-28] p 1525 N94-19143
An iterative inverse scattering method for the removal of scattered surface waves
[REPT-93-18] p 1488 N94-19644

ITERATIVE SOLUTION
Parallel inverse iteration with reorthogonalization
[DE93-012867] p 1533 N94-17693
An annealing approach to multi-facility location problems in euclidean spaces
[REPT-93-022] p 1547 N94-17928
Introduction to spectral methods: Application to the Stokes problem p 1413 N94-18566
Optimal eigenvalue computation on distributed-memory MIMD multiprocessors
[DE93-018337] p 1535 N94-18808
Solution of the Poisson equation with application to radar imaging
[PB93-195865] p 1389 N94-18950
Fast iterative solution of sparsely sampled seismic inverse problems
[REPT-93-16] p 1486 N94-19081
New insights in GMRES-like methods with variable preconditioners
[REPT-93-10] p 1524 N94-19084
Multigrid for a groundwater flow problem
[REPT-93-29] p 1420 N94-19144
The Fourier analysis technique and epsilon-pseudo-eigenvalues
[DE93-018805] p 1551 N94-19337
A comparison of iterative methods for a model coupled system of elliptic equations
[DE93-040482] p 1553 N94-19655

J

J-85 ENGINE
The J85 cost/benefit engine study
[AD-A269280] p 1320 N94-18333

JAMMERS
Design and fabrication of a Multichannel Adaptive Optical Processor (MADOP)
[AD-A270004] p 1579 N94-18668

JAMMING
Design and fabrication of a Multichannel Adaptive Optical Processor (MADOP)
[AD-A270004] p 1579 N94-18668
Communication in the presence of unknown interference
[AD-A271146] p 1392 N94-19738

JAPAN
Survey of ceramic machining in Japan
[DE93-018277] p 1372 N94-18946

JET AIRCRAFT
Naval aviation: Consider all alternatives before proceeding with the F/A-18E/F
[AD-A269302] p 1305 N94-18279
Close-coupled oscillating canard effects on post-stall lift enhancement
[AD-A268938] p 1321 N94-18541
Lift and pitching moment induced on jet STOVL aircraft hovering in ground effect
[AD-A269700] p 1317 N94-18577
Lift and pitching moment induced on jet STOVL aircraft by the ground vortex
[AD-A269816] p 1318 N94-18733

JET AIRCRAFT NOISE
Supersonic jets from bevelled rectangular nozzles
[NASA-TM-106403] p 1313 N94-19484

JET BLAST EFFECTS
Lift and pitching moment induced on jet STOVL aircraft by the ground vortex
[AD-A269816] p 1318 N94-18733

JET ENGINE FUELS
Analysis of deposit precursors in jet fuels using Fourier transform infrared spectroscopy
[AD-A269035] p 1377 N94-18489

JET FLOW
Applications of the program UIFLOW-2D to the numerical simulation of axisymmetric flows
[AD-A268731] p 1410 N94-18326

JET IMPINGEMENT
Combustion instability phenomena of importance to liquid propellant engines
[AD-A268800] p 1348 N94-18389

JET MIXING FLOW
Supersonic jets from bevelled rectangular nozzles
[NASA-TM-106403] p 1313 N94-19484

JET PROPULSION
Overview of STOVL aircraft propulsion research offtakes and vertical lift systems
[NASA-TM-106387] p 1321 N94-19353

JET PUMPS
Efficiency of fiber dispersion
[AD-A269740] p 1342 N94-18757

JET STREAMS (METEOROLOGY)
Organized track system: Air ways above the ocean
p 1495 N94-19702

JOINTS (JUNCTIONS)
Joint stiffness estimation based on force sensor measurements in industrial manipulators
[REPT-92-053] p 1443 N94-17937
Plastic mechanism analysis of T-joints in RHS subject to combined bending and concentrated force
[PB93-195774] p 1456 N94-19061

JOSEPHSON JUNCTIONS
On relation between Berry phase and one-dimensional models with long-range 1/r(sup 2)-interaction
[DE93-624967] p 1592 N94-17690
Thin film studies of the proximity Josephson effect
[AD-A270129] p 1600 N94-18876

JUDGMENTS
Scale sensitivity in the multiplicative AHP and SMART
[REPT-93-37] p 1611 N94-19157
Context-related scaling of human judgement in the multiplicative AHP, SMART and ELECTRE
[REPT-93-38] p 1611 N94-19158

JUNCTION DIODES
Theoretical and experimental studies of quantum wells
[AD-A271180] p 1606 N94-19741

JUNCTION TRANSISTORS
Embrittlement of surface mount solder joints by hot solder-dipped, gold-plated leads
[DE93-017659] p 1358 N94-18003

K

K STARS
The 0.15 seconds near-infrared imaging of the central parsec of the galaxy
[MPE-PREPRINT-239] p 1621 N94-19415

K-EPSILON TURBULENCE MODEL
Research on two equation models
p 1411 N94-18547
Analysis of supersonic flows using k-epsilon model and the RPLUS code: Progress towards high speed combustor analysis p 1411 N94-18551
Two-equation models for high-Reynolds-number flow
p 1415 N94-18586
Two-equation models for low-Reynolds-number variants p 1415 N94-18587
Examples of turbulence model applications
p 1415 N94-18593
STREMR: Numerical model for depth-averaged incompressible flow
[AD-A269949] p 1417 N94-18672
Examinations of the friction behavior in nonstationary flow processes in pipes
[MITT-7] p 1423 N94-19730

KALMAN FILTERS
Flight demonstration of image fix-taking with SAR
[DE93-016499] p 1382 N94-17861
Tracking with time-delayed data in multisensor systems
[AD-A271334] p 1391 N94-19582

KAMACITE
Dynamical behavior of octahedrite from the Henbury meteorite
[DE93-018834] p 1627 N94-19339

KAON PRODUCTION
Meson production in relativistic heavy-ion collisions at AGS energies
[DE93-016871] p 1565 N94-17984

KAONS
On the difference caused by CP violation in the energy spectra of pions in K(sup (+-))(yields)(pi)(+-)(pi)(+-)(pi)-+ decays
[DE93-624828] p 1564 N94-17687

KERNEL FUNCTIONS
Smooth particle hydrodynamics: The SPHINX and SPHC codes
[DE93-014358] p 1457 N94-19207

KETENES
Unimolecular photodissociation dynamics of ketene (CH2CO): The singlet/triplet branching ratio and experimental observation of the vibrational level thresholds of the transition-state
[DE93-019252] p 1352 N94-19304

KEVLAR (TRADEMARK)
Thermal wave image processing for characterization of subsurface of flaws in materials
[DE93-019024] p 1344 N94-19551

KINEMATICS
Performance mapping of the STM4-120 kinematic Stirling engine using a statistical design of experiments method
[DE93-015132] p 1464 N94-17798
Efficient dynamic modeling of manipulators containing closed kinematic loops
[REPT-92-083] p 1444 N94-17940
Neutrino mass
[DE93-018467] p 1567 N94-18269
Direct kinematics solution architectures for industrial robot manipulators: Bit-serial versus parallel
p 1399 N94-18358

KINETIC ENERGY
Transformation of energy and momentum due to Landau damping in space
[DE93-624921] p 1581 N94-17689
Understanding curved detonation waves
[DE93-014581] p 1408 N94-17728
Temperature, kinetic energy, and rotational temperature dependences for the reactions of Ar(+)(2)P3/2 with O2 and CO
[AD-A268974] p 1567 N94-18526
Chemical dynamics in time and energy space
[DE93-018595] p 1350 N94-19097
KLYSTRONS
Plasma klystron amplifier
[AD-D015819] p 1395 N94-17903
KNOWLEDGE BASED SYSTEMS
Employing knowledge resources in a new text planner architecture
[AD-A269669] p 1518 N94-17732
EXPECT: Intelligent support for knowledge base refinement
[AD-A269602] p 1612 N94-17745
Bias in planning and explanation-based learning
[AD-A269608] p 1610 N94-17746
Distributed reasoning and planning
[AD-A268682] p 1540 N94-18399
Towards versatile and practical knowledge acquisition
[AD-A269596] p 1615 N94-18464
Putting knowledge to use: The acquisition and transfer of knowledge in situated problem solving environments
[AD-A269746] p 1509 N94-18744
On the automation of object-oriented requirements analysis
[AD-A270673] p 1532 N94-19782
KNOWLEDGE BASES (ARTIFICIAL INTELLIGENCE)
Retrieving and integrating data from multiple information sources
[AD-A269588] p 1615 N94-18461
PRACTICAL: Planning and resource allocation in C2-domains with time critical algorithms
[FEL-93-B029] p 1544 N94-19458
KNOWLEDGE REPRESENTATION
A method for cognitive task analysis
[IZF-1992-B5] p 1508 N94-17967
Towards versatile and practical knowledge acquisition
[AD-A269596] p 1615 N94-18464
Statistical probabilities for planning
[TR-474] p 1559 N94-19511
KOLMOGOROV THEORY
Thermodynamics of computation and information distance
[DE93-012730] p 1517 N94-17812
KONDO EFFECT
Realistic theories of heavy electron and other strongly correlated materials
[DE93-010350] p 1571 N94-19204
KORTEWEG-DEVRIES EQUATION
A method for solving the KDV equation and some numerical experiments
[DE93-624726] p 1550 N94-19246
KRYPTON FLUORIDE LASERS
Foil support structure for large electron guns
[DE93-018478] p 1322 N94-18890
Modelling ideal gas fluorides laser plasmas
[ETN-93-95073] p 1592 N94-19613
KURTOSIS
Moments of ambient Doppler spectra
[DE93-017948] p 1390 N94-19114

L

LABORATORIES
Computer/information security design approaches for Complex 21/Reconfiguration facilities
[DE93-018547] p 1535 N94-18930
A Sandia Technology Bulletin: Testing technology, July 1993
[DE93-040197] p 1633 N94-19537
Design verification and acceptance tests of the ASST-A helium refrigeration system
[DE93-019746] p 1381 N94-19540
LAGRANGE MULTIPLIERS
Efficient dynamic modeling of manipulators containing closed kinematic loops
[REPT-92-083] p 1444 N94-17940
LAGRANGIAN FUNCTION
Multidimensional geometric quantization and U(1)-covering
[DE93-624770] p 1546 N94-17795
Vortex methods and statistics
[DE93-016974] p 1556 N94-17886
Impact modeling with smooth particle hydrodynamics
[DE93-016561] p 1451 N94-17906
Phase structure of (phi(4))(sub 3) field theory at finite temperature
[DE93-629907] p 1608 N94-18267
Cooperative control of multiple space manipulators
[AD-A270291] p 1445 N94-18813
LAMB WAVES
Ultrasonic technique for inspection of GPHS capsule girth weld integrity
[DE93-040072] p 1448 N94-19189
LAMINAR BOUNDARY LAYER
Studies on high pressure and unsteady flame phenomena: Revision
[AD-A269138] p 1348 N94-18257
LAMINAR FLOW
Studies on high pressure and unsteady flame phenomena: Revision
[AD-A269138] p 1348 N94-18257
Transport phenomena and interfacial kinetics in multiphase combustion systems
[AD-A270202] p 1349 N94-18785
Airflow research
[NASA-TM-109372] p 1312 N94-18964
Numerical solutions for a flow with mixed convection in a vertical geometry
[DE93-011592] p 1419 N94-19058
Numerical prediction of transition of the F-16 wing at supersonic speeds
[NASA-CR-194407] p 1312 N94-19433
Forward scattering of a pulsed continuous wave signal through laminar and turbulent thermal plumes
[AD-A271210] p 1564 N94-19723
LAMINAR WAKES
Theoretical examination of the flow around a cylinder with a low dimensional Galerkin process
[MPIS-25/1992] p 1422 N94-19525
LAMINATES
The calculation methods of a cracked plastic composite laminate: A literature survey
[VTT-TIED-1362] p 1339 N94-17958
Impact response of composite laminates: A guide to closed form solutions
[FFA-TN-1992-33] p 1339 N94-17971
Process for preparing thermoplastic composites
[AD-D015864] p 1339 N94-18074
Development of a finite element method program for the analysis of laminated composite plates using first-order shear deformation theory
[AD-A270318] p 1342 N94-18700
Mechanical properties and impact damage resistance of composites fabricated by low cost, vacuum assisted, resin transfer molding
[AD-A270361] p 1342 N94-18702
Nondestructive inspection of graphite-epoxy laminates for heat damage using DRIFT and LPF spectroscopies
[DE93-017228] p 1343 N94-18761
Mechanical-property changes of structural composite materials after low-temperature proton irradiation: Implications for use in SSC magnet systems
[DE93-016735] p 1343 N94-18763
Shock-loading response of advanced materials
[DE93-018344] p 1455 N94-19033
A comparative evaluation of in-plane shear test methods for laminated graphite-epoxy composites
[NASA-CR-193808] p 1456 N94-19095
Low frequency acoustics of laminated composite axisymmetric structures
[DRA-TM(USGR)-93302] p 1344 N94-19391
Delamination in composite materials as observed using an optical fiber strain gage
[AD-A270803] p 1344 N94-19662
Residual strength predictions for fibre metal laminates: The R-curves approach
[LR-717] p 1344 N94-19666
LAND USE
Land-use related sources of CO2, CH4 and N2O: Current global emissions and projections for the period 1990-2100
[PB93-194819] p 1475 N94-18949
LANDAU DAMPING
Transformation of energy and momentum due to Landau damping in space
[DE93-624921] p 1581 N94-17689
LANDAU-GINZBURG EQUATIONS
Numerical experiments on the Ginzburg-Landau equations
[DE93-019504] p 1604 N94-19567
LANGEVIN FORMULA
Vortex methods and statistics
[DE93-016974] p 1556 N94-17886
LANGUAGE PROGRAMMING
FASTBUS simulation models in VHDL
[USIP-92-07] p 1515 N94-19295
LANGUAGES
A simple calculus of finite probabilistic processes
[MEMO-INF-93-08] p 1558 N94-19195
LANTHANUM COMPOUNDS
Photo-induced and electrooptic properties of (Pb,La)(Zr,Ti)O3 films
[DE93-017496] p 1371 N94-18519
An ultraviolet faraday rotator glass
[AD-D015879] p 1371 N94-18529
LANTHANUM OXIDES
Phase separation and superconductivity in La2CuO(4 + delta): Effects of oxygen diffusion
[DE93-016610] p 1594 N94-17907
Specific heat of La(1.875-x)Nd(x)Sr(0.125)CuO4: Magnetic and structural transitions
[DE93-016978] p 1600 N94-18968
LAP JOINTS
Fatigue crack initiation in riveted lap joints and in pressurized fuselages
[LR-725] p 1461 N94-19669
LAPLACE EQUATION
A hydrogen atom in the curved space. Expansion over free solutions on the three-dimensional sphere
[DE93-629868] p 1549 N94-18198
ISAC: A tool for aeroservoelastic modeling and analysis
[NASA-TM-109031] p 1321 N94-19316
LARGE SCALE INTEGRATION
Development of analog watch with minute repeater
p 1429 N94-18043
Radiation hardened microprocessor for small payloads
p 1327 N94-19184
LARGE SPACE STRUCTURES
Design considerations for remotely operated welding in space: Task definition and visual weld monitoring experiment
[AD-A268752] p 1445 N94-18634
LARMOR RADIUS
Profile stabilization of tilt mode in a field reversed configuration
[DE93-016770] p 1583 N94-17753
Generalized energy principle for flute perturbations in axisymmetric mirror machines
[DE93-019399] p 1589 N94-19037
LASER ABLATION
Mechanical properties of excimer laser modified titanium surfaces
[DE93-012663] p 1358 N94-17875
Excimer laser induced permanent electrical conductivity and nanostructures in polymers
[DE93-015965] p 1368 N94-17946
Production of dense vapor targets for laser-plasma interaction studies with intense, ultra-short pulses
[DE93-017175] p 1584 N94-17993
Dynamic behaviors of fragments ejected from the surface of carbon materials by laser ablation
[DE93-768620] p 1438 N94-18161
Imaging and blackbody emission spectra of hot particulates generated during laser ablation
[DE93-015818] p 1439 N94-18724
Characterization of vapor plume species and deposition residues resulting from pulsed laser ablation of a graphite/epoxy composite
[AD-A270101] p 1343 N94-18869
Advances in laser cooling
[AD-A270152] p 1440 N94-18900
Growth of epitaxial semiconductor alloys and superlattices with continuously variable composition by pulsed-laser ablation
[DE93-018726] p 1601 N94-18998
LASER APPLICATIONS
Polarized thin films from dye-substituted polymers containing hydrophobically terminated stilbazolium radicals
[AD-D015873] p 1367 N94-17706
CO2 laser with modulated losses: Theoretical models and experiments in the chaotic regime
[DE93-624901] p 1435 N94-17771
Gear train behavior analyzer using laser beam scanning for watch movement p 1427 N94-18028
Matrix- and substrate-assisted laser desorption for fast DNA sequencing
[DE93-015332] p 1501 N94-18242
Nitridation of GaAs(100) by laser-induced decomposition of HN3
[AD-A269147] p 1438 N94-18258
Hydrodynamic instability modeling for ICF
[DE93-018634] p 1587 N94-18274
New applications for high average power beams
[DE93-018845] p 1439 N94-18522
Nondestructive inspection of graphite-epoxy laminates for heat damage using DRIFT and LPF spectroscopies
[DE93-017228] p 1343 N94-18761
The Fourteenth Symposium on Molecular Beams
[AD-A268721] p 1568 N94-18787
Impact of shorter wavelengths on optical quality for laws
[NASA-CR-193873] p 1579 N94-18858

Advances in laser cooling
[AD-A270152] p 1440 N94-18900
Space Applications Industrial Laser System (SAILS)
p 1325 N94-19173
SPNDL: A concept for a small satellite Doppler lidar wind sounder p 1327 N94-19181
Laser guide star measurements at Lawrence Livermore National Laboratory
[DE93-018081] p 1441 N94-19251
Manufacturing technology
[DE93-019580] p 1381 N94-19480
A Sandia Technology Bulletin: Testing technology, July 1993
[DE93-040197] p 1633 N94-19537
MOCVD-grown InGaAsP heterostructure diode lasers
[AD-A270848] p 1606 N94-19769
A study of the amplification of laser and VLF waves using a simple pendulum model
[AD-A270857] p 1442 N94-19770
Novel nonlinear laser diagnostic techniques
[AD-A270968] p 1442 N94-19788

LASER BEAMS
X-ray laser oscillator-amplifier experiments
[DE93-017165] p 1436 N94-17868
Mechanical properties of excimer laser modified titanium surfaces
[DE93-012663] p 1358 N94-17875
Laser induced damage testing: Equipment and techniques
[DE93-017143] p 1437 N94-18060
Calibration of a high frequency monostatic acoustic echosounder
[AD-A268901] p 1481 N94-18229
Phase conjugation and beam combination using stimulated brillouin scattering
[AD-A269899] p 1439 N94-18656
The efficiency of continuous output of some titanium-doped gem-crystal lasers has exceeded 1 W
[AD-A269953] p 1439 N94-18674
Laser powered beam conditioner for free-electron lasers and synchrotrons
[DE93-017821] p 1441 N94-18974
Harmonic generation at high intensities
[DE93-018632] p 1572 N94-19283
RF phase stabilization for RF photocathode gun through electro-optical monitoring
[DE93-019059] p 1406 N94-19310
First and second order Stokes generation by SRS in methane: Influence of rep-rate, beam quality and astigmatism
[FEL-92-A125] p 1441 N94-19426
Manufacturing technology
[DE93-019580] p 1381 N94-19480
Spectrally and temporally resolved laser emission from vertical cavity surface emitting lasers
[DE93-019410] p 1442 N94-19563
Novel nonlinear laser diagnostic techniques
[AD-A270968] p 1442 N94-19788

LASER CAVITIES
Homoclinic crises in a model for the CO2 laser
[DE93-624900] p 1436 N94-17954
Tunable synchronously pumped intracavity two-stage optical frequency upconversion
[AD-A269105] p 1438 N94-18250
Tunable ytterbium-doped solid state laser
[AD-D015878] p 1440 N94-18747
Tetravalent chromium (Cr(4+)) as laser-active ion for tunable solid-state lasers
[NASA-CR-194529] p 1441 N94-19369
Spectrally and temporally resolved laser emission from vertical cavity surface emitting lasers
[DE93-019410] p 1442 N94-19563
MOCVD-grown InGaAsP heterostructure diode lasers
[AD-A270848] p 1606 N94-19769

LASER CUTTING
Laser materials processing applications at Lawrence Livermore National Laboratory
[DE93-017976] p 1437 N94-18093
Space Applications Industrial Laser System (SAILS)
p 1325 N94-19173
Cutting and drilling studies using high power visible lasers
[DE93-019149] p 1441 N94-19294

LASER DAMAGE
Laser induced damage testing: Equipment and techniques
[DE93-017143] p 1437 N94-18060
Proof of the feasibility of coherent and incoherent schemes for pumping a gamma ray laser
[AD-A269173] p 1440 N94-18880

LASER DRILLING
Laser materials processing applications at Lawrence Livermore National Laboratory
[DE93-017976] p 1437 N94-18093
Cutting and drilling studies using high power visible lasers
[DE93-019149] p 1441 N94-19294

LASER FUSION
LLE Review
[DE93-017618] p 1602 N94-19123

LASER GUIDANCE
Laser guide star measurements at Lawrence Livermore National Laboratory
[DE93-018081] p 1441 N94-19251

LASER HEATING
Characterization of short pulse laser-produced plasmas at the Lawrence Livermore National Laboratory ultra short-pulse laser
[DE93-017191] p 1585 N94-18082
Growth of epitaxial semiconductor alloys and superlattices with continuously variable composition by pulsed-laser ablation
[DE93-018726] p 1601 N94-18998

LASER INDUCED FLUORESCENCE
Static pressure measurements for near isentropic flows using laser induced iodine fluorescence
p 1431 N94-18646
Modifications of airborne oceanographic lidar for the long range P-3 missions
[NASA-CR-194682] p 1499 N94-18819
Feasibility study: Monodisperse polymer particles containing laser-excitable dyes
[NASA-CR-194280] p 1373 N94-19402

LASER INTERFEROMETRY
Portable, solid state, fiber optic coupled Doppler interferometer system for detonation and shock diagnostics
[DE93-013917] p 1423 N94-17700
Construction and evaluation of an environmental chamber for calibration of temperature and pressure sensors for laser interferometers emperature and pressure sensors for laser interferometers)
[PB93-197838] p 1322 N94-19332

LASER MATERIALS
Laser materials processing applications at Lawrence Livermore National Laboratory
[DE93-017976] p 1437 N94-18093
Space Applications Industrial Laser System (SAILS)
p 1325 N94-19173
Tetravalent chromium (Cr(4+)) as laser-active ion for tunable solid-state lasers
[NASA-CR-194529] p 1441 N94-19369
Final report on subcontract B076260 — borate synthesis
[DE93-019501] p 1604 N94-19565

LASER MICROSCOPY
Center-of-Excellence: Microlaser microscope
[DE93-040688] p 1442 N94-19658

LASER MODE LOCKING
Tetravalent chromium (Cr(4+)) as laser-active ion for tunable solid-state lasers
[NASA-CR-194528] p 1441 N94-19394

LASER OUTPUTS
The copper-pumped dye laser system at Lawrence Livermore National Laboratory
[DE93-014429] p 1435 N94-17723
Experiments in sideband suppression on the Los Alamos National Laboratory Free-Electron Laser
[DE93-014466] p 1435 N94-17724
Observations of MeV electrons and scattered light from intense, subpicosecond laser-plasma interactions
[DE93-017153] p 1435 N94-17855
X-ray laser oscillator-amplifier experiments
[DE93-017165] p 1436 N94-17868
Excimer laser induced permanent electrical conductivity and nanostructures in polymers
[DE93-015965] p 1368 N94-17946
Dynamics of short-pulse excitation, ionization and harmonic conversion
[DE93-017220] p 1436 N94-17996
Removing CFC's from the atmosphere with lasers: A second look
[DE93-017516] p 1473 N94-18101
Absorption and x ray measurements from ultra-intense laser-plasma interactions
[DE93-016538] p 1585 N94-18115
High spatial resolution, range gated, underwater imaging method and apparatus
[AD-D015882] p 1430 N94-18530
Phase conjugation and beam combination using stimulated brillouin scattering
[AD-A269899] p 1439 N94-18656
The efficiency of continuous output of some titanium-doped gem-crystal lasers has exceeded 1 W
[AD-A269953] p 1439 N94-18674
Multi-terrawatt, 100 fsec laser system using flashlamp-pumped, dye-converted Ti:sapphire as an amplifier
[DE93-017190] p 1440 N94-18889
Final construction and operation of a continuous far-infrared free-electron laser for scientific applications
[AD-A269248] p 1440 N94-18912
LLE Review
[DE93-017618] p 1602 N94-19123
Harmonic generation at high intensities
[DE93-018632] p 1572 N94-19283
Spectrally and temporally resolved laser emission from vertical cavity surface emitting lasers
[DE93-019410] p 1442 N94-19563

LASER PLASMA INTERACTIONS
Observations of MeV electrons and scattered light from intense, subpicosecond laser-plasma interactions
[DE93-017153] p 1435 N94-17855
Production of dense vapor targets for laser-plasma interaction studies with intense, ultra-short pulses
[DE93-017175] p 1584 N94-17993
Characterization of short pulse laser-produced plasmas at the Lawrence Livermore National Laboratory ultra short-pulse laser
[DE93-017191] p 1585 N94-18082
Absorption and x ray measurements from ultra-intense laser-plasma interactions
[DE93-016538] p 1585 N94-18115
Time-resolved probing of electron thermal conduction in femtosecond-laser-pulse-produced plasmas
[DE93-016996] p 1585 N94-18129
Nonlinear Thomson scattering of intense laser pulse from beams and plasmas
[AD-A269556] p 1438 N94-18460
Interaction of intense lasers and relativistic electron beams with solids, gases and plasmas
[AD-A269655] p 1439 N94-18737

LASER PLASMAS
Analysis of neon soft x ray spectra from short-pulse laser-produced plasmas
[DE93-014420] p 1582 N94-17708
Rapid analysis of mixed waste samples via the optical emission from laser initiated microplasmas
[DE93-014563] p 1582 N94-17727
Development of short pulse soft x ray lasers
[DE93-017150] p 1437 N94-18131
Enhanced acceleration in a self-modulated-laser wakefield accelerator
[AD-A268452] p 1586 N94-18148
Dynamic behaviors of fragments ejected from the surface of carbon materials by laser ablation
[DE93-788620] p 1438 N94-18161
Nonlinear Thomson scattering of intense laser pulse from beams and plasmas
[AD-A269556] p 1438 N94-18460
Interaction of intense lasers and relativistic electron beams with solids, gases and plasmas
[AD-A269655] p 1439 N94-18737
Development of robust multilayer optics for use in high-peak power radiation environments
[DE93-018557] p 1580 N94-18931
Modelling ideal gas fluorides laser plasmas
[ETN-93-95073] p 1592 N94-19613

LASER PUMPING
The copper-pumped dye laser system at Lawrence Livermore National Laboratory
[DE93-014429] p 1435 N94-17723
Tunable synchronously pumped intracavity two-stage optical frequency upconversion
[AD-A269105] p 1438 N94-18250
Proof of the feasibility of coherent and incoherent schemes for pumping a gamma ray laser
[AD-A269173] p 1440 N94-18880
Multi-terrawatt, 100 fsec laser system using flashlamp-pumped, dye-converted Ti:sapphire as an amplifier
[DE93-017190] p 1440 N94-18889
Tetravalent chromium (Cr(4+)) as laser-active ion for tunable solid-state lasers
[NASA-CR-194528] p 1441 N94-19394

LASER RANGE FINDERS
Laser imaging radar system
[AD-A270436] p 1387 N94-18510

LASER SPECTROSCOPY
Rapid analysis of mixed waste samples via the optical emission from laser initiated microplasmas
[DE93-014563] p 1582 N94-17727
Remote cure monitoring of polymeric resins by laser Raman spectroscopy
[DE93-016445] p 1369 N94-18112
Matrix- and substrate-assisted laser desorption for fast DNA sequencing
[DE93-015332] p 1501 N94-18242
Modifications of airborne oceanographic lidar for the long range P-3 missions
[NASA-CR-194682] p 1499 N94-18819
The A((2)pi(sub u))-X((2)pi(sub g)) system of Br2(+) studied by velocity modulation spectroscopy
[USIP-93-04] p 1569 N94-18847

LASER STABILITY
Homoclinic crises in a model for the CO2 laser
[DE93-624900] p 1436 N94-17954
LASER TARGET INTERACTIONS
Process and quality on-line control in laser welding
p 1426 N94-18020
Interaction of intense lasers and relativistic electron beams with solids, gases and plasmas
[AD-A269655] p 1439 N94-18737
LLE Review
[DE93-017616] p 1602 N94-19123
LASER TARGETS
Observations of MeV electrons and scattered light from intense, subpicosecond laser-plasma interactions
[DE93-017153] p 1435 N94-17855
Production of dense vapor targets for laser-plasma interaction studies with intense, ultra-short pulses
[DE93-017175] p 1584 N94-17993
Absorption and x ray measurements from ultra-intense laser-plasma interactions
[DE93-016538] p 1585 N94-18115
Hydrodynamic instability modeling for ICF
[DE93-018634] p 1587 N94-18274
Growth of epitaxial semiconductor alloys and superlattices with continuously variable composition by pulsed-laser ablation
[DE93-018726] p 1601 N94-18998
LASER WEAPONS
Legacy of the X Ray Laser Program
[DE93-019550] p 1442 N94-19554
LASER WELDING
Process and quality on-line control in laser welding
p 1426 N94-18020
Modeling of single-crystal laser-weld microstructures
[DE93-017853] p 1445 N94-18976
Space Applications Industrial Laser System (SAILS)
p 1325 N94-19173
Prediction of non-equilibrium solidification modes in austenitic stainless steel laser welds
[DE93-018457] p 1364 N94-19203
LASERS
The efficiency of continuous output of some titanium-doped gem-crystal lasers has exceeded 1 W
[AD-A269953] p 1439 N94-18674
Advances in laser cooling
[AD-A270152] p 1440 N94-18900
LATERAL STABILITY
An application of parameter estimation to the stability and control of the BQM-147 unmanned aerial vehicle
[AD-A268741] p 1321 N94-18401
The dynamic stability of the helicopter
[LR-772] p 1321 N94-19615
LATTICE PARAMETERS
Molecular structure of low temperature form of triaminoguanidinium nitrate (TAGN)
[AD-A270409] p 1377 N94-18708
A free energy simulation method based study of interfacial segregation
[DE93-019462] p 1364 N94-19032
Preparation and characterisation of the compound Tl(0.65) Bi(0.35) Ca(0.8) Sr(1.7) Cu2 O(y) using oxalate coprecipitation and analytical CBED and an initial preparation of Bi2Ca(n-1) Sr2Cu(n) O(4+2n) for n=5
[DE93-625470] p 1602 N94-19277
LATTICE VIBRATIONS
Effect of oxygen concentration and ordering on vanadium-oxygen alloy vibrational spectra
[DE93-627003] p 1355 N94-17692
LAY-UP
Process relationship as influenced by carbonization rate
[AD-A269680] p 1341 N94-18572
LEAD (METAL)
Development of alternatives to lead-bearing solders
[DE93-016509] p 1357 N94-17862
LEAD ACID BATTERIES
SUNRAYCE 1993: Working safely with lead-acid batteries and photovoltaic power systems
[DE93-016553] p 1464 N94-17712
LEAD ALLOYS
Development of alternatives to lead-bearing solders
[DE93-016509] p 1357 N94-17862
LEAD COMPOUNDS
The electromechanical properties of tetragonal BaTiO3 and PbTiO3 single crystals
[DE93-019008] p 1603 N94-19550
LEAD ZIRCONATE TITANATES
Photo-induced and electrooptic properties of (Pb,La)(Zr,Ti)O3 films
[DE93-017496] p 1371 N94-18519
LEADING EDGE FLAPS
High-lift design for large civil aircraft
p 1310 N94-18445
LEADING EDGE SLATS
Where is high-lift today? A review of past UK research programmes p 1305 N94-18416
Experimental investigation of flow around a multielement airfoil p 1305 N94-18417
Numerical solution of the Navier-Stokes equations for high-lift configurations on structured composite grids
p 1306 N94-18423
High Reynolds number configuration development of a high-lift airfoil p 1306 N94-18424
A viscous-inviscid solver for high-lift incompressible flows over multi-element airfoils at deep separation conditions p 1306 N94-18425
Navier-Stokes simulation of flow field around a blown-flap high-lift system p 1307 N94-18429
An experimental investigation of the optimum slat setting on a combat aircraft model p 1308 N94-18431
An experimental investigation of attachment-line transition on the slat of a combat aircraft model
p 1308 N94-18432
Viscous phenomena affecting high-lift systems and suggestions for future CFD development
p 1308 N94-18433
Forty years of high-lift R/D: An aircraft manufacturer's experience p 1309 N94-18441
High-lift design for large civil aircraft
p 1310 N94-18445
High lift systems for transport aircraft with advanced airfoils p 1310 N94-18446
LEADING EDGES
A study of the influence of a delta wing geometry on the induced drag at transonic speed (M=0.55) and high angles of attack
[FFA-TN-1992-14] p 1311 N94-17722
Calculation of maximum and high lift characteristics of multi element aerofoils p 1305 N94-18419
LEAKAGE
Mutrometre: Construction for fast water proof measurements under low pressure and air suppression
p 1427 N94-18031
LEARNING
Generating object descriptions: Intergrating examples with text
[AD-A269992] p 1522 N94-18680
Putting knowledge to use: The acquisition and transfer of knowledge in situated problem solving environments
[AD-A269746] p 1509 N94-18744
A refinement for nonmonotonic logic
[REPT-93-21] p 1542 N94-19092
Computer-assisted instruction and natural language systems
[MEMO-INF-92-86] p 1527 N94-19225
LEARNING THEORY
Efficient domain-independent experimentation
[AD-A269530] p 1557 N94-18640
Statistical learning theory and algorithms
[AD-A270209] p 1523 N94-18901
First results with utile distinction memory for reinforcement learning
[TR-446] p 1610 N94-19485
LEAST SQUARES METHOD
Strategies for testing form assessment software
[NPL-DITC-211/92] p 1518 N94-17930
A least-squares computational tool kit
[DE93-018400] p 1557 N94-19011
A method for finding the periodic solution of autonomous ordinary differential equations
[DE93-624725] p 1550 N94-19244
Refinement of unit cell parameters by least-squares: Comments on an old technique and the development of a new computer program
[AD-A270610] p 1531 N94-19590
LEAVES
Photosynthetic responses to the environment, volume 8
[AD-A269584] p 1502 N94-18305
LENGTH
On the Michelson-Morley experiment
[DE93-629908] p 1608 N94-18268
The influence of the target strength model on computed perforation
[DE93-018659] p 1460 N94-19543
LENNARD-JONES POTENTIAL
Phenomenological explanation of elastic anomalies in superlattices
[DE93-017475] p 1594 N94-17871
A numerical study of hybrid optimization methods for the molecular conformation problems
[DE93-017898] p 1569 N94-18985
LENSES
Compound-lens injector for a 19-MeV, 700-kA electron beam
[DE93-013752] p 1573 N94-17698
Radiation induced darkening of the optical elements in the Startracker camera
[DE93-018907] p 1433 N94-19004
LENTICULAR BODIES
Similarity solutions for gravity-dominated spreading of a lens of organic contaminant
[REPT-93-24] p 1420 N94-19139
LEPTONS
Gauge unification of fundamental forces: The story of success
[DE93-624813] p 1383 N94-17952
LEVITATION
Six degree of freedom fine motion positioning stage based on magnetic levitation
[DE93-017651] p 1446 N94-19547
LIAPUNOV FUNCTIONS
Fast-training algorithm for hidden-layer forward-feed neural networks
[AD-A269253] p 1540 N94-18263
The optimal projection equations for finite-dimensional fixed-order H2-optimal control of infinite-dimensional discrete-time systems
[REPT-93-11] p 1542 N94-19085
The fixed, finite-order L(sup 2)-optimal control of infinite-dimensional time-varying discrete-time systems
[REPT-93-23] p 1542 N94-19138
LIBRARIES
Application of new technologies in the virtual library: Seminars in Turkey, Portugal, and Spain
[NASA-TM-109718] p 1611 N94-19131
Cesar user library
[FFI-93/7021] p 1529 N94-19378
CVL: A C vector library manual. Version 2
[AD-A270614] p 1531 N94-19592
LIBRATION
Molecular structure of low temperature form of triaminoguanidinium nitrate (TAGN)
[AD-A270409] p 1377 N94-18708
LICENSING
Setting the global thermostat with an exhaustible tradeable permit system
[DE93-012911] p 1472 N94-17891
LIE GROUPS
Further on the current algebra of WZNW models at and away from criticality
[DE93-624809] p 1545 N94-17686
Multidimensional geometric quantization and U(1)-covering
[DE93-624770] p 1546 N94-17795
Finite-dimensional singletons of the quantum anti de Sitter algebra
[DE93-624771] p 1546 N94-17810
A reduction of the globalization and U(1)-covering
[DE93-624769] p 1546 N94-17817
Functional analysis of subelliptic operators on lie groups
[PB93-194793] p 1547 N94-18077
Paragrassmann analysis and quantum groups
[DE93-628593] p 1561 N94-18168
On paragrassmann differential calculus
[DE93-628594] p 1548 N94-18169
On a possible algebra morphism of U(sub q)(osp1/2) onto the deformed oscillator algebra W(sub q)(N)
[DE93-629857] p 1548 N94-18176
About symmetry of the gravitational action
[DE93-629955] p 1608 N94-18252
Extensions of 2D gravity
[DE93-018525] p 1485 N94-18929
L(sub p)-regularity of subelliptic operators on Lie groups
[PB93-194785] p 1549 N94-18948
Group-invariant solutions of hydrodynamics and radiation hydrodynamics
[DE93-018373] p 1423 N94-19604
Production and test of pseudo random elements
[ETN-93-95070] p 1559 N94-19610
LIFE RAFTS
AN/APS-137 Forward Looking Airborne Radar (FLAR) evaluation Spring 1992 experiment
[AD-A268899] p 1384 N94-18228
LIFE SCIENCES
Interdisciplinary training in life science (FY 1991 ASSERT)
[AD-A269220] p 1512 N94-18886
Aerospace medicine and biology: A continuing bibliography with indexes (supplement 382)
[NASA-SP-7011(382)] p 1507 N94-18936
Aerospace medicine and biology: A continuing bibliography with indexes (supplement 381)
[NASA-SP-7011(381)] p 1507 N94-19069
Guide to programs, fiscal year 1993
[NSF-92-78] p 1633 N94-19620
LIFE SUPPORT SYSTEMS
Analysis of seating and restraint limitations restricting total body weight for aircrew and passengers on US Army helicopters
[AD-A269117] p 1511 N94-18296
Aircrew life support, AFSC 122X0(1T1X1)
[AD-A268998] p 1511 N94-18394

Aerospace medicine and biology: A continuing bibliography with indexes (supplement 382)
[NASA-SP-7011(382)] p 1507 N94-18936

Aerospace medicine and biology: A continuing bibliography with indexes (supplement 381)
[NASA-SP-7011(381)] p 1507 N94-19069

Environmental control and life support
[ESA-PSS-03-40-ISSUE-1] p 1513 N94-19442

LIFT

High-Lift System Aerodynamics
[AGARD-CP-515] p 1305 N94-18415

Calculation of maximum and high lift characteristics of multi element aerofoils p 1305 N94-18419

Navier-Stokes computations of turbulent flow around high-lift configurations p 1306 N94-18420

Efficient simulation of incompressible viscous flow over multi-element airfoils p 1306 N94-18421

High Reynolds number configuration development of a high-lift airfoil p 1306 N94-18424

Numerical calculations of high lift flows using structured and unstructured methods p 1307 N94-18428

Navier-Stokes simulation of flow field around a blown-flap high-lift system p 1307 N94-18429

An experimental investigation of the optimum slat setting on a combat aircraft model p 1308 N94-18431

Viscous phenomena affecting high-lift systems and suggestions for future CFD development
p 1308 N94-18433

A study of the use of half-models in high-lift wind-tunnel testing p 1308 N94-18434

High lift and the forward swept wing
p 1308 N94-18436

Wake structure and aerodynamic behavior of high lift aircraft configurations during unsteady maneuvers in ground effect p 1309 N94-18439

Viscous-inviscid calculation of high-lift separated compressible flows over airfoils and wings
p 1309 N94-18440

Forty years of high-lift R/D: An aircraft manufacturer's experience p 1309 N94-18441

High-lift research: Application to the design of the ATR72 flap p 1309 N94-18442

High-lift design for large civil aircraft
p 1310 N94-18445

High lift systems for transport aircraft with advanced airfoils p 1310 N94-18446

Lift and pitching moment induced on jet STOVL aircraft by the ground vortex
[AD-A269816] p 1318 N94-18733

LIFT DEVICES

Lift enhancement device
[AD-D015868] p 1317 N94-17704

High-Lift System Aerodynamics
[AGARD-CP-515] p 1305 N94-18415

Where is high-lift today? A review of past UK research programmes p 1305 N94-18416

A design procedure for slotted flaps
p 1305 N94-18418

Navier-Stokes computations of turbulent flow around high-lift configurations p 1306 N94-18420

Navier-Stokes calculations on multi-element airfoils using a chimera-based solver p 1306 N94-18422

Numerical solution of the Navier-Stokes equations for high-lift configurations on structured composite grids
p 1306 N94-18423

High Reynolds number configuration development of a high-lift airfoil p 1306 N94-18424

A viscous-inviscid solver for high-lift incompressible flows over multi-element airfoils at deep separation conditions p 1306 N94-18425

High-lift system analysis method using unstructured meshes p 1307 N94-18426

Prediction of the high-lift performance of multi-element aerofoils using an unstructured Navier-Stokes solver
p 1307 N94-18427

Numerical calculations of high lift flows using structured and unstructured methods p 1307 N94-18428

Navier-Stokes simulation of flow field around a blown-flap high-lift system p 1307 N94-18429

The GARTEUR high lift research programme
p 1307 N94-18430

An experimental investigation of the optimum slat setting on a combat aircraft model p 1308 N94-18431

An experimental investigation of attachment-line transition on the slat of a combat aircraft model
p 1308 N94-18432

Viscous phenomena affecting high-lift systems and suggestions for future CFD development
p 1308 N94-18433

In-flight pressure distributions and skin-friction measurements on a subsonic transport high-lift wing section p 1308 N94-18435

High lift and the forward swept wing
p 1308 N94-18436

A fast computing method for the flow over high-lift wings p 1308 N94-18437

Calculation of multielement airfoils and wings at high lift p 1309 N94-18438

Wake structure and aerodynamic behavior of high lift aircraft configurations during unsteady maneuvers in ground effect p 1309 N94-18439

Forty years of high-lift R/D: An aircraft manufacturer's experience p 1309 N94-18441

High-lift research: Application to the design of the ATR72 flap p 1309 N94-18442

The aero-mechanical design of a novel Fowler flap mechanism p 1309 N94-18443

High-lift design for large civil aircraft
p 1310 N94-18445

High lift systems for transport aircraft with advanced airfoils p 1310 N94-18446

Choice and optimization of a high-lift system for an advanced amphibious aircraft p 1310 N94-18447

LIGANDS

Oligomer and mixed-metal compounds, potential multielectron transfer catalysts
[DE93-019592] p 1350 N94-19017

LIGHT (VISIBLE RADIATION)

Using controlled daylight exposure and sleep timing in the prevention of shift lag during night operations
[AD-A269304] p 1504 N94-17824

Rosat and optical observations of two X-ray transients: MX 0836-42 and GS 0834-430
[MPE-PREPRINT-237] p 1622 N94-19451

LIGHT AMPLIFIERS

X-ray laser oscillator-amplifier experiments
[DE93-017165] p 1436 N94-17868

Integrated photonics research volume 10. Conference edition
[AD-A269298] p 1577 N94-18298

Applications of nonlinear optic effects in new specialty fibers
[AD-A268890] p 1578 N94-18457

Quantum Optoelectronics. Organization of the 1993 photonics science topical meetings. Technical digest series, volume 8
[AD-A269026] p 1578 N94-18488

Advanced Solid-State Lasers/Compact Blue-Green Lasers. 1993 technical digest series. Volume 2: Organization of the 1993 photonics science topical meetings
[AD-A269058] p 1438 N94-18492

Photonics in Switching: Organization of the 1993 photonics science topical meetings. Technical digest
[AD-A269024] p 1578 N94-18528

Integrated Photonics Research: Post-deadline papers
[AD-A269232] p 1609 N94-18908

Pulsed power supply for Nova Upgrade
[DE93-019626] p 1441 N94-19307

A study of the amplification of laser and VLF waves using a simple pendulum model
[AD-A270857] p 1442 N94-19770

LIGHT BEAMS

High spatial resolution, range gated, underwater imaging method and apparatus
[AD-D015882] p 1430 N94-18530

Direct solar pumping of semiconductor lasers: A feasibility study
[NASA-CR-193760] p 1440 N94-18834

LIGHT CURVE

Computational astrophysics: Pulsating stars
[DE93-018369] p 1627 N94-18857

Detection of a long-duration solar gamma-ray flare on Jun. 11, 1991 with EGRET on Compton-GRO
p 1623 N94-19463

LIGHT EMISSION

Extending bandwidth of optical emitters using active matching technique
[AD-D015875] p 1394 N94-17707

Rapid analysis of mixed waste samples via the optical emission from laser initiated microplasmas
[DE93-014563] p 1582 N94-17727

Compact free electron lasers for medical applications
[AD-A271272] p 1442 N94-19729

Polarized optical emission due to decay or recombination of spin-polarized injected carriers
[AD-D015907] p 1408 N94-19763

LIGHT EMITTING DIODES

Extending bandwidth of optical emitters using active matching technique
[AD-D015875] p 1394 N94-17707

Polarized optical emission due to decay or recombination of spin-polarized injected carriers
[AD-D015907] p 1408 N94-19763

LIGHT IONS

Electron stripping cross sections for light impurity ions in colliding with atomic hydrogens relevant to fusion research
[DE93-788476] p 1566 N94-18158

LIGHT MODULATION

CO2 laser with modulated losses: Theoretical models and experiments in the chaotic regime
[DE93-624901] p 1435 N94-17771

Evaluation of a liquid crystal spatial light modulator capable of amplitude- and phase-modulating modes
[AD-A269252] p 1577 N94-18262

Spatial light modulators and applications: Summaries of papers presented at the Spatial Light Modulators and Applications Topical Meeting
[AD-A269452] p 1577 N94-18283

Kinetic aspects of lattice mismatch in molecular beam epitaxial growth on planar and patterned substrates
[AD-A270424] p 1597 N94-18506

Photonics in Switching: Organization of the 1993 photonics science topical meetings. Technical digest
[AD-A269024] p 1578 N94-18528

Integration of ferroelectric/semiconductor thin films for SLM and photorefractive applications
[AD-A268645] p 1598 N94-18633

Photodetector array having high pixel density
[AD-D015859] p 1432 N94-18731

Direct solar pumping of semiconductor lasers: A feasibility study
[NASA-CR-193760] p 1440 N94-18834

LIGHT SCATTERING

Elastic properties of a polyimide film determined by Brillouin scattering and mechanical techniques
[DE93-017404] p 1368 N94-18098

High spatial resolution, range gated, underwater imaging method and apparatus
[AD-D015882] p 1430 N94-18530

Millimeter wave reflectivity measurement system
[AD-A270008] p 1387 N94-18601

Effects of the Mount Pinatubo eruption on solar insolation: Four case studies
[DE93-018454] p 1475 N94-18817

LIGHT SOURCES

Developmental testing of a prototype all-reflection Michelson interferometer
[AD-A269064] p 1430 N94-18406

Magnetic field measurements of a superconducting undulator for a Harmonic Generation FEL experiment at the NSLS
[DE93-017621] p 1438 N94-18504

Simulation of the ALS longitudinal multibunch feedback system
[DE93-019227] p 1575 N94-19152

Study of coupled-bunch collective effects in the ALS
[DE93-019236] p 1575 N94-19558

The 1982 to 1992 decade of research on the vacuum ultraviolet ring at National Synchrotron Light Source
[DE93-019469] p 1603 N94-19564

LIGHT TRANSMISSION

An ultraviolet faraday rotator glass
[AD-D015879] p 1371 N94-18529

LIGHTNING

Analysis of high contact resistances associated with hermetic and lightning arrestor connectors
[DE93-014850] p 1395 N94-17783

Studies of enhanced radar backscatter
[AD-A269544] p 1385 N94-18288

LIKELIHOOD RATIO

Generalized multichannel signal detection
[AD-A271385] p 1391 N94-19587

LINE CURRENT

Response of transmission line systems to pulse excitation by radiation and injection methods
[DE93-015112] p 1384 N94-18210

LINE SPECTRA

Unified NLTE model atmospheres including spherical extension and stellar winds, 4: Improved line transfer and wind contamination of H, He profiles
[MPA-905] p 1624 N94-17736

Detection of accreting gas toward HD 45677: A newly recognized, Herbig Be proto-planetary system
[NASA-CR-189312] p 1621 N94-19288

Suitability of infrared spectroscopy for remote sensing of tropospheric trace gases
[KFK-5183] p 1479 N94-19507

LINEAR ACCELERATORS

Advanced methods for the computation of particle beam transport and the computation of electromagnetic fields and beam-cavity interactions
[DE93-018160] p 1573 N94-17807

Alternating-phase focusing with amplitude modulation
[DE93-018618] p 1574 N94-18273

Experimental research in high energy physics
[DE93-011912] p 1574 N94-18916

Spice modeling of a FET-switched induction accelerator cell
[DE93-018662] p 1575 N94-18996

Induction accelerator development for heavy ion fusion
[DE93-019228] p 1591 N94-19479

Transverse beam combiner for ILSE
[DE93-019239] p 1591 N94-19559
The ILSE Experimental Program
[DE93-019247] p 1576 N94-19560

LINEAR ENERGY TRANSFER (LET)
The LET spectrum and its uncertainty during the CRRES mission
[AD-A269977] p 1630 N94-18676

LINEAR EQUATIONS
EDF tests for normality in linear models after a Box-Cox transformation
[AD-A269068] p 1557 N94-18517
Implementation of the turn function method in KIVA-F90
[DE93-018394] p 1419 N94-19027

LINEAR PREDICTION
Linear parameter identification methods for ARMA models with periodic coefficients
[REPT-92-070] p 1556 N94-17938

LINEAR PROGRAMMING
Planning under uncertainty solving large-scale stochastic linear programs
[DE93-013920] p 1516 N94-17701
A model and an execution mechanism for active data bases
[ETN-93-94404] p 1614 N94-17979
A teaching tool for linear programming
[AD-A270240] p 1523 N94-18905
The theory of linear programming: Skew symmetric self-dual problems and the central path
[REPT-93-15] p 1524 N94-19089
Interior-point methodology for linear programming: Duality, sensitivity analysis and computational aspects
[REPT-93-28] p 1525 N94-19143
A polynomial primal-dual Dikin-type algorithm for linear programming
[REPT-93-36] p 1525 N94-19156

LINEAR QUADRATIC GAUSSIAN CONTROL
On comparison and extensions of control methods for narrow-band disturbance rejection
[REPT-93-015] p 1540 N94-17922

LINEAR QUADRATIC REGULATOR
The digital linear quadratic control problem for Pritchard-Salamon systems
[REPT-93-27] p 1542 N94-19142
Digital control of Pritchard-Salamon systems
[REPT-93-33] p 1543 N94-19286

LINEAR SYSTEMS
A modified direct preconditioner for indefinite symmetric Toeplitz systems
[DE93-015234] p 1516 N94-17800
A noniterative improvement of Guyan reduction
p 1449 N94-17833
An extension of Wolovich's definition of equivalence of linear systems
[MATHS-REPT-A-183] p 1547 N94-18069
Advances in the identification of transfer function models using Prony analysis
[DE93-017980] p 1548 N94-18094
Generalization of optimal control theory: Linear and nonlinear structures
[PB93-188621] p 1540 N94-18125
An ab initio study of the weakly bonded CO-Cl2 complex
[AD-A269000] p 1349 N94-18395
A multigrid acceleration technique for computing steady solutions to the equations of compressible flow
p 1412 N94-18559
New insights in GMRES-like methods with variable preconditioners
[REPT-93-10] p 1524 N94-19084
Deadbeat control by measurement feedback: A two sided approach
[REPT-93-20] p 1542 N94-19091
Stabilization of time-delay systems: An overview of the algebraic approach
[PB93-191989] p 1553 N94-19556

LINEAR TRANSFORMATIONS
Enumerative geometry of Del Pezzo Surfaces
[DE93-624768] p 1546 N94-17816
A parallel and pipelined architecture for estimation of direction of arrival using a bilinear transformation method, volume 3
[AD-A270137] p 1389 N94-18897

LINEARIZATION
Continuum modeling of materials that can undergo martensitic phase transitions
[AD-A268767] p 1360 N94-18386
Nonlinear disturbance decoupling and linearization: A partial interpretation of integral feedback
[PB93-197515] p 1543 N94-19328

LINGUISTICS
A real-time spoken-language system for interactive problem-solving, combining linguistic and statistical technology for improved spoken language understanding
[AD-A270901] p 1392 N94-19749

LININGS
Studies of dynamic contact of ceramics and alloys for advanced heat engines
[DE93-016366] p 1368 N94-18110

LIPIDS
Polymerizable lipids in the development of controlled release carriers
[AD-D015789] p 1368 N94-17982
Morphology of polymerized membranes on an amorphous substrate at molecular resolution by AFM
[AD-A268760] p 1370 N94-18403

LIQUEFIED GASES
Structure, thermodynamics, and dynamical properties of supercooled liquids
[DE93-788387] p 1607 N94-18211
Evaluation of aftermarket LPG conversion kits in light-duty vehicle applications
[DE93-010035] p 1377 N94-18617

LIQUID BRIDGES
Axial response of differently excited anchored viscous liquid bridges in zero-gravity
[LRT-WE-9-FB-1-1992] p 1379 N94-19489
Free fall liquid column dynamics in a droptower
[LRT-WE-9-FB-6-1992] p 1379 N94-19491
Transient response of a viscous and anchored liquid bridge to an axial pulse
[LRT-WE-9-FB-7-1992] p 1379 N94-19492

LIQUID COOLING
Preliminary design of a water cooled avionics cooling rack
[AD-A268826] p 1320 N94-18536
A laboratory model of a cooled continental shelf
[AD-A270862] p 1500 N94-19792

LIQUID CRYSTALS
Electrically controlled liquid-crystal heat valve
[AD-D015872] p 1443 N94-17705
Molecular composites from liquid crystalline polymers and liquid crystalline thermosets
[DE93-016608] p 1368 N94-18096
Evaluation of a liquid crystal spatial light modulator capable of amplitude- and phase-modulating modes
[AD-A269252] p 1577 N94-18262
Spatial light modulators and applications: Summaries of papers presented at the Spatial Light Modulators and Applications Topical Meeting
[AD-A269452] p 1577 N94-18283
Measurement Techniques
[VKI-LS-1993-05] p 1430 N94-18643
Liquid crystal heat transfer measurements
p 1432 N94-18653
The application of liquid crystal techniques to determine heat transfer rates p 1432 N94-18654
Polymer technology publication. Series no. 14, 1993
[PB93-195964] p 1372 N94-19052

LIQUID FLOW
Contribution to the study of a symmetric film flow (with or without tensio-active elements)
[ECL-93-13] p 1421 N94-19461

LIQUID HELIUM
Superfluid Helium On-Orbit Transfer (SHOOT) flight demonstration p 1327 N94-19185
Two-dimensional turbulent nonstationary superfluid counterflows: Numerical simulations, qualitative effects
[MPIS-23/1992] p 1422 N94-19510

LIQUID HELIUM 2
Examinations of converging cylindrically symmetric second sound propagation in He2
[MPIS-9/1992] p 1564 N94-19715

LIQUID INJECTION
Combustion instability phenomena of importance to liquid propellant engines
[AD-A268800] p 1348 N94-18389

LIQUID LASERS
Proof of the feasibility of coherent and incoherent schemes for pumping a gamma ray laser
[AD-A269173] p 1440 N94-18880

LIQUID METALS
First on-sun test of NaK pool-boiler solar receiver
[DE93-015003] p 1466 N94-18208
Structure, thermodynamics, and dynamical properties of supercooled liquids
[DE93-788387] p 1607 N94-18211
Metal slurry droplet and spray combustion
[AD-A269648] p 1349 N94-18736
Bench-scale screening tests for a boiling sodium-potassium alloy solar receiver
[DE93-018512] p 1469 N94-19040

LIQUID NITROGEN
Temperature lowering in cryogenic chemical-synthesis techniques and system
[DE93-018348] p 1562 N94-18810
Thermal stresses in the microchannel heatsink cooled by liquid nitrogen
[DE93-018660] p 1418 N94-18995

LIQUID PHASE SINTERING
Recent advances in high density tungsten composite processing
[AD-A270764] p 1344 N94-19576

LIQUID PHASES
A new multiphase equation of state for iron
[DE93-017629] p 1357 N94-17819
Molecular nonlinear optical susceptibilities in condensed phases
[AD-A270200] p 1568 N94-18784

LIQUID PROPELLANT ROCKET ENGINES
Combustion instability phenomena of importance to liquid propellant engines
[AD-A268800] p 1348 N94-18389

LIQUID-GAS MIXTURES
Measurement of viscosity, density, and gas solubility of refrigerant blends in selected synthetic lubricants
[DE93-040221] p 1350 N94-18977
Film condensation in a shock wave
[MPIS-22/1992] p 1422 N94-19509

LIQUID-LIQUID INTERFACES
The application of front tracking to the simulation of shock refractions and shock accelerated interface mixing
[DE93-018342] p 1419 N94-19025
Multigrid for a groundwater flow problem
[REPT-93-29] p 1420 N94-19144

LIQUID-SOLID INTERFACES
Axial response of differently excited anchored viscous liquid bridges in zero-gravity
[LRT-WE-9-FB-1-1992] p 1379 N94-19489

LIQUIDS
Structure, thermodynamics, and dynamical properties of supercooled liquids
[DE93-788387] p 1607 N94-18211
Performance of the Amorphous Materials Diffractometer GLAD at IPNS
[DE93-017746] p 1430 N94-18481

LISP (PROGRAMMING LANGUAGE)
OORA Automated Knowledge System (OAKS) code, appendix C
[AD-A270709] p 1531 N94-19573

LITHIUM
Shrinkage void formation and its effect on freeze and thaw processes of lithium and lithium-fluoride for space applications
[DE93-019303] p 1338 N94-19128

LITHIUM ALLOYS
Phase separation and ordering process in Al-Li alloys studied by small-angle neutron scattering and neutron diffraction
[DE93-016750] p 1358 N94-17947

LITHIUM FLUORIDES
Calculation of the LiF-CeF3-BeF2 and LiF-PuF3-BeF2 ternary phase diagrams
[DE93-017437] p 1360 N94-18501
Shrinkage void formation and its effect on freeze and thaw processes of lithium and lithium-fluoride for space applications
[DE93-019303] p 1338 N94-19128

LITHIUM NIOBATES
IR materials producibility
[AD-A268849] p 1577 N94-18223
Investigation of a fiber optic frequency shifter and optical isolator
[AD-A269820] p 1579 N94-18738

LITHIUM SULFUR BATTERIES
The ANL electric vehicle battery R&D program for DOE-EHP
[DE93-017414] p 1394 N94-17750

LITHOGRAPHY
Quantum Optoelectronics. Organization of the 1993 photonics science topical meetings. Technical digest series, volume 8
[AD-A269026] p 1578 N94-18488
Advanced Solid-State Lasers/Compact Blue-Green Lasers. 1993 technical digest series. Volume 2: Organization of the 1993 photonics science topical meetings
[AD-A269058] p 1438 N94-18492
RF vacuum microelectronics
[AD-A270003] p 1403 N94-18667
Soft X Ray Projection Lithography. Organization of the 1993 photonics science optical meetings
[AD-A269159] p 1579 N94-18693
Operational parameters of an opto-electronic neural network employing fixed planar holographic interconnects
[DE93-018795] p 1433 N94-19000
The 1982 to 1992 decade of research on the vacuum ultraviolet ring at National Synchrotron Light Source
[DE93-019469] p 1603 N94-19564
Nanofabrication by focused ion beam
[AD-A271290] p 1345 N94-19746

LIVER
Space research on organs and tissues p 1503 N94-19214

LOAD DISTRIBUTION (FORCES)
The role of NASTRAN in the preliminary design cycle p 1450 N94-17835
Road march performance of special operations soldiers carrying various loads and load distributions [AD-A269198] p 1512 N94-18882

LOADING OPERATIONS
Fatigue technology assessment and strategies for fatigue avoidance in marine structures. Appendices [AD-A269053] p 1455 N94-18716
ASTRO-1 to explore invisible universe [NASA-TM-109360] p 1336 N94-18956

LOADS (FORCES)
Heat load analysis on the cable-in-conduit with central core conductor for the TF coil Rebut layer design [DE93-013783] p 1395 N94-17872
The respectiveness of response in a bar under static and transient loads [VTT-TIED-1377] p 1452 N94-17959
Road march performance of special operations soldiers carrying various loads and load distributions [AD-A269198] p 1512 N94-18882
Plastic mechanism analysis of T-joints in RHS subject to combined bending and concentrated force [PB93-195774] p 1456 N94-19061

LOCAL AREA NETWORKS
Advanced optical fiber communication systems [AD-A269120] p 1577 N94-18254
Inventory management plan for a research and development local area network [DE93-018381] p 1617 N94-19026
A highly concurrent medium access control strategy for high speed multiwavelength networks using transceivers with limited tunability [MEMO-INF-93-07] p 1390 N94-19230

LOCAL THERMODYNAMIC EQUILIBRIUM
Configuration interaction in LTE spectra of heavy elements [DE93-017166] p 1584 N94-17990

LOGIC
Useful lambda notation [PB93-191856] p 1524 N94-19066
Axiomatization, declarative semantics and operational semantics of passive and active updates in logic databases [PB93-195956] p 1618 N94-19067

LOGIC CIRCUITS
New dynamic FET logic and serial memory circuits for VLSI GaAs technology p 1397 N94-18339
Automated ILA design for synchronous sequential circuits p 1397 N94-18340
Single phase dynamic CMOS PLA using charge sharing technique p 1397 N94-18341
An SEU immune logic family p 1398 N94-18342
Cellular logic array for computation of squares p 1398 N94-18343
Fault tolerant sequential circuits using sequence invariant state machines p 1398 N94-18344
Formal specification of a high speed CMOS correlator p 1401 N94-18371
Ultra low power CMOS technology p 1401 N94-18373
Canonical multi-valued input Reed-Muller trees and forms p 1401 N94-18375
Asynchronous sequential circuit design using pass transistor iterative logic arrays p 1402 N94-18376
Pulse mode VLSI asynchronous circuits p 1402 N94-18377
Improved self arbitrated VLSI asynchronous circuits p 1402 N94-18378
A special purpose silicon compiler for designing supercomputing VLSI systems p 1402 N94-18379
On timing faults in digital logic circuits [AD-A268714] p 1402 N94-18400
Naval research reviews. Mixing enhancement for air-breathing propulsion. Non-axisymmetric jets increase mixing, volume 44 and volume 45 [AD-A268966] p 1521 N94-18543
An RS-170 to 700 frame per second CCD camera [DE93-018367] p 1432 N94-18828
Motorola MC68040 high-speed design using Altera EPM5000 erasable programmable logic devices [DE93-017635] p 1523 N94-19006
Superconducting flux flow devices, digital circuits and memories [DE93-019072] p 1405 N94-19079
Evaluation of laser diode based optical switches for optical processors [AD-A270949] p 1581 N94-19602

LOGIC DESIGN
Weakened negative introspection in autoepistemic reasoning [PB93-187375] p 1520 N94-18118
A verification logic representation of indeterministic signal states p 1401 N94-18372
Ultra low power CMOS technology p 1401 N94-18373
Canonical multi-valued input Reed-Muller trees and forms p 1401 N94-18375
Asynchronous sequential circuit design using pass transistor iterative logic arrays p 1402 N94-18376
Pulse mode VLSI asynchronous circuits p 1402 N94-18377
Improved self arbitrated VLSI asynchronous circuits p 1402 N94-18378
A special purpose silicon compiler for designing supercomputing VLSI systems p 1402 N94-18379
VHDL simulation with access to transistor models p 1402 N94-18381
Naval research reviews. Mixing enhancement for air-breathing propulsion. Non-axisymmetric jets increase mixing, volume 44 and volume 45 [AD-A268966] p 1521 N94-18543

LOGIC PROGRAMMING
Weakened negative introspection in autoepistemic reasoning [PB93-187375] p 1520 N94-18118
A verification logic representation of indeterministic signal states p 1401 N94-18372
Ultra low power CMOS technology p 1401 N94-18373
Asynchronous rendezvous in the presence of backtracking [PB93-197739] p 1524 N94-19062
Axiomatization, declarative semantics and operational semantics of passive and active updates in logic databases [PB93-195956] p 1618 N94-19067
Integrity checking in deductive databases: An exposition [PB93-191724] p 1619 N94-19709

LOGICAL ELEMENTS
New automatic deduction techniques in first order finite and infinite polyvalent logic [ETN-93-95003] p 1528 N94-19359

LOGISTICS
A comparison of air force data systems [AD-A269691] p 1616 N94-18575

LONG DURATION EXPOSURE FACILITY
LDEF update [NASA-TM-109352] p 1334 N94-18921
The application of jet spray and ion beam contamination removal techniques to samples from the LDEF spacecraft [AD-A270973] p 1354 N94-19755

LONG RANGE WEATHER FORECASTING
JPRS report: Science and technology. Central Eurasia: Earth Sciences [JPRS-UES-93-004] p 1461 N94-19209

LONGITUDINAL STABILITY
The dynamic stability of the helicopter [LR-772] p 1321 N94-19615

LONGITUDINAL WAVES
Correction of longitudinal errors in accelerators for heavy-ion fusion [DE93-018656] p 1575 N94-19106
The electromechanical properties of tetragonal BaTiO3 and PbTiO3 single crystals [DE93-019008] p 1603 N94-19550

LOOP ANTENNAS
Arc detection and protection in high-power antenna systems [DE93-013272] p 1382 N94-17695

LORENTZ CONTRACTION
On the Michelson-Morley experiment [DE93-629908] p 1608 N94-18268

LORENTZ TRANSFORMATIONS
On the Michelson-Morley experiment [DE93-629908] p 1608 N94-18268

LOSSES
Regenerator optimization for Stirling cycle refrigeration [DE93-018468] p 1380 N94-18818
Bounds for expected loss in Bayesian decision theory with imprecise prior probabilities [PB93-197507] p 1558 N94-19327

LOVE WAVES
High resolution geological site characterization utilizing ground motion data [AD-A268926] p 1481 N94-18485
Surface wave group velocity tomography of East Asia, part 1 [AD-A270100] p 1484 N94-18868

LOW ASPECT RATIO WINGS
An experimental investigation of the optimum slat setting on a combat aircraft model p 1308 N94-18431

LOW COST
Laser materials processing applications at Lawrence Livermore National Laboratory [DE93-017976] p 1437 N94-18093
A rugged, low-cost advanced data acquisition system for field test projects [DE93-010041] p 1615 N94-18334
Optoelectronic packaging: A review [DE93-040059] p 1515 N94-19535
High rate resistive plate chambers: An inexpensive, fast, large area detector of energetic charged particles for accelerator and non-accelerator applications [DE93-018664] p 1572 N94-19545

LOW FREQUENCIES
Low frequency acoustics of laminated composite axisymmetric structures [DRA-TM(USGR)-93302] p 1344 N94-19391
Measurements of ocean surface and bottom backscattering strengths in the northwestern Atlantic Ocean [AD-A270893] p 1500 N94-19786

LOW GRAVITY MANUFACTURING
The first flight of the QUESTS GAS payload G-521 p 1325 N94-19170

LOW NOISE
High resolution SQUID magnetometry for non-destructive evaluation [AD-A268884] p 1447 N94-18225
Low-noise oscillators for airborne radar applications, revision 1 [AD-A269372] p 1403 N94-18471
Monolithic low noise preamplifier for piezoelectric sensors [AD-D015860] p 1563 N94-18734

LOW REYNOLDS NUMBER
Two-equation models for low-Reynolds-number variants p 1415 N94-18587
Theoretical examination of the flow around a cylinder with a low dimensional Galerkin process [MPIS-25/1992] p 1422 N94-19525

LOW TEMPERATURE
Molecular structure of low temperature form of triaminoguanidinium nitrate (TAGN) [AD-A270409] p 1377 N94-18708
Ground movements associated with gas hydrate production [DE93-019887] p 1486 N94-19018
Isolation mechanisms in III-V devices [AD-A271197] p 1605 N94-19717

LOW TEMPERATURE ENVIRONMENTS
Search for lunar water ice in cometary impact craters [AD-A270130] p 1627 N94-18877
Proceedings: International Symposium on Thermal Engineering and Science for Cold Regions [AD-A270636] p 1487 N94-19529

LOW TEMPERATURE PHYSICS
Realistic theories of heavy electron and other strongly correlated materials [DE93-010350] p 1571 N94-19204

LUBRICANTS
Compatibility of refrigerants and lubricants with motor materials, volume 1 [DE93-040216] p 1350 N94-18895
Compatibility of refrigerants and lubricants with motor materials, volume 2 [DE93-040217] p 1350 N94-18896
Measurement of viscosity, density, and gas solubility of refrigerant blends in selected synthetic lubricants [DE93-040221] p 1350 N94-18977
Accelerated screening methods for determining chemical and thermal stability of refrigerant-lubricant mixtures. Part 1: Method assessment [DE93-040215] p 1351 N94-19136
Compatibility of refrigerants and lubricants with motor materials, volume 3 [DE93-040218] p 1352 N94-19191
Surface species in tribology [AD-A270970] p 1446 N94-19754

LUBRICATION
Interdisciplinary research on wear of materials [AD-A268190] p 1443 N94-17730

LUMINOSITY
Search for top quark with D0 detector [DE93-040170] p 1572 N94-19536

LUMPED PARAMETER SYSTEMS
Improved approximations applied to the S(sub N) even-parity equation [DE93-016467] p 1551 N94-19343

LUNAR BASES
Lunar base Controlled Ecological Life Support System (LCELSS): Preliminary conceptual design study [NASA-CR-188479] p 1511 N94-18484
Space transfer concepts and analyses for exploration missions [NASA-CR-193876] p 1332 N94-18820
Space exploration initiative [NASA-TM-109366] p 1323 N94-18981

LUNAR CRATERS
Working group for planetary system nomenclature [NASA-CR-194406] p 1626 N94-18841

Search for lunar water ice in cometary impact craters
[AD-A270130] p 1627 N94-18877

LUNAR ENVIRONMENT
Space transfer concepts and analyses for exploration missions
[NASA-CR-193876] p 1332 N94-18820

LUNAR EXCAVATION EQUIPMENT
Future energy source — Mining Helium-3 on the moon
[NASA-TM-109363] p 1628 N94-18959

LUNAR LANDING
Apollo 11: 20th anniversary
[NASA-TM-109364] p 1323 N94-18979

LUNAR MINING
Future energy source — Mining Helium-3 on the moon
[NASA-TM-109363] p 1628 N94-18959

LUNAR RESOURCES
Search for lunar water ice in cometary impact craters
[AD-A270130] p 1627 N94-18877
Future energy source — Mining Helium-3 on the moon
[NASA-TM-109363] p 1628 N94-18959

LUNAR SURFACE
Search for lunar water ice in cometary impact craters
[AD-A270130] p 1627 N94-18877

LUNAR SURFACE VEHICLES
Activities of the Center for Space Construction
[NASA-CR-193717] p 1335 N94-19371

LYMPHOCYTES
A study of the effects of high power pulsed 2450 MHz microwaves, ELF modulated microwaves, and ELF fields on human lymphocytes and selected cell lines
[AD-A269070] p 1505 N94-18294

M

M STARS
The 0.15 seconds near-infrared imaging of the central parsec of the galaxy
[MPE-PREPRINT-239] p 1621 N94-19415
Stellar coronae at the end of the main sequence: A Rosat survey of the late M dwarfs
[NASA-CR-194700] p 1628 N94-19794

MACH NUMBER
Error propagation equations and tables for estimating the uncertainty in high-speed wind tunnel test results
[DE93-016685] p 1311 N94-18275
A comparative study of turbulence models in predicting hypersonic inlet flows p 1314 N94-18553
Acoustic intensity measurements in the presence of low Mach number flow
[AD-A269995] p 1562 N94-18664

MACHINE LEARNING
Bias in planning and explanation-based learning
[AD-A269608] p 1610 N94-17746
Application of the network discriminant function to learning
[AD-A268793] p 1540 N94-18189
Dialog-Based Learning (DBL) for adaptive interface agents and programming-by-demonstrations systems
[AD-A269154] p 1540 N94-18261
Fast-training algorithm for hidden-layer forward-feed neural networks
[AD-A269253] p 1540 N94-18263
On masking effect
[AD-A269593] p 1541 N94-18462
Towards versatile and practical knowledge acquisition
[AD-A269596] p 1615 N94-18464
Geometrical pattern learning
[DE93-017641] p 1542 N94-19007
A refinement for nonmonotonic logic
[REPT-93-21] p 1542 N94-19092
Learning control of large-scale systems
[MATHS-REPT-A-186] p 1544 N94-19408
Explorations of the practical issues of learning prediction-control tasks using temporal difference learning methods
[AD-A270636] p 1544 N94-19599
VLSI implementation of neuromorphic learning networks
[AD-A270825] p 1407 N94-19665

MACHINE TOOLS
Measuring machines for digitalizing and measuring complex surfaces, models and matrices
[CRIF-MC-97] p 1444 N94-17963
Present evolution of tools management
[CRIF-MC-102] p 1444 N94-17964
The machine reception: A business of experts
[CRIF-MC-94] p 1611 N94-17980
A rational design change methodology based on experimental and analytical modal analysis
[DE93-018537] p 1521 N94-18271
Survey of ceramic machining in Japan
[DE93-018277] p 1372 N94-18946

MACHINERY
Applications of neural networks in fault detection of rotating machinery
[AD-A270755] p 1448 N94-19766

MACHINING
Electrostatic micrometers: Recent developments and perspectives of uses in clock and watch making
p 1425 N94-18014
Survey of ceramic machining in Japan
[DE93-018277] p 1372 N94-18946
Precision machining and polishing of scintillating crystals for large calorimeters and hodoscopes
[DE93-018663] p 1381 N94-19544

MAGELLAN PROJECT (NASA)
Magellan, Galileo, and Ulysses
[NASA-TM-109362] p 1628 N94-18958

MAGELLAN SPACECRAFT (NASA)
Magellan, Galileo, and Ulysses
[NASA-TM-109362] p 1628 N94-18958

MAGELLANIC CLOUDS
Dust in the Small Magellanic Cloud
[NASA-CR-193344] p 1624 N94-17764
Spectrophotometry of emission-line stars in the magellanic clouds
[NASA-CR-194082] p 1628 N94-19425
IRAS galaxies observed in the ROSAT survey: Starbursts or central activity p 1623 N94-19528

MAGNESIUM COMPOUNDS
Advanced civil engineering materials based on inorganic polymers
[AD-A270837] p 1374 N94-19600

MAGNET COILS
Nonparaxial MHD stabilizers for an axisymmetric magnetic mirror
[DE93-017996] p 1587 N94-18505
Contribution to the study of the additional losses in coil elements used in static converters
[ECL-92-60] p 1406 N94-19297

MAGNETIC ANOMALIES
Research in particle physics
[DE93-040875] p 1567 N94-18534

MAGNETIC BEARINGS
Fuzzy control of magnetic bearings
p 1399 N94-18357

MAGNETIC COILS
Fabrication, properties, and microstructures of high (Tc) tapes and coils made from Ag-clad Bi-2223 superconductor
[DE93-017405] p 1602 N94-19122

MAGNETIC COOLING
The 7th International Cryocooler Conference
[AD-A268451] p 1379 N94-18147

MAGNETIC DIPOLES
Toroidal solenoids in the electromagnetic field and Aharonov-Casher effect
[DE93-629861] p 1566 N94-18152
Convection algorithms for magnetospheric particles
[AD-A270103] p 1493 N94-18871

MAGNETIC DISKS
Static Computer Memory Integrity Testing (SCMIT): An experiment flown on STS-40 as part of GAS payload G-616 p 1325 N94-19169
Picoindentation hardness measurements using atomic force microscopy
[AD-A270877] p 1604 N94-19579
Microtribology of magnetic media
[AD-A271209] p 1407 N94-19722
Atomic-scale friction measurements using friction force microscopy. Part 2: Application to magnetic media
[AD-A270759] p 1447 N94-19767
Tribological studies of silicon for magnetic recording applications (Invited)
[AD-A270878] p 1447 N94-19784

MAGNETIC ENERGY STORAGE
Analysis of superconducting magnetic energy storage applications at a proposed wind farm site near Browning, Montana
[DE93-018793] p 1466 N94-18276

MAGNETIC FIELD CONFIGURATIONS
Profile stabilization of tilt mode in a field reversed configuration
[DE93-016770] p 1583 N94-17753
Filamentary magnetohydrodynamic plasmas
[DE93-015616] p 1583 N94-17945
Toroidal solenoids in the electromagnetic field and Aharonov-Casher effect
[DE93-629861] p 1566 N94-18152
Finite beta plasma equilibrium in toroidally linked mirrors
[DE93-040318] p 1590 N94-19193
Magnetic and crystallographic structures in UTX intermetallic compounds
[DE93-018291] p 1605 N94-19735

MAGNETIC FIELD RECONNECTION
Resonant absorption of Alfven waves near a neutral point
[DE93-628761] p 1586 N94-18172

MAGNETIC FIELDS
The phase mixing of shear Alfven waves
[DE93-624920] p 1581 N94-17688
Limits on m = 2, n = 1 error field induced locked mode instability in TPX with typical sources of poloidal field coil error field and a proto type correction coil, C-coil
[DE93-014408] p 1582 N94-17702
Corroboration of magnetic forces in US Maglev design
[DE93-014918] p 1443 N94-17785
Rapid geophysical surveyor
[DE93-016637] p 1461 N94-17851
Synthesis and study of high-T(sub c) superconducting electronic materials
[AD-A268851] p 1402 N94-18390
Comparison of ferrite materials for pulse applications
[DE93-017224] p 1574 N94-18497
Magnetic field measurements of a superconducting undulator for a Harmonic Generation FEL experiment at the NSLS
[DE93-017621] p 1438 N94-18504
Numerical modelling of fringing fields and their use for complex permittivity measurements at high frequencies
[AD-A270198] p 1388 N94-18782
Convection algorithms for magnetospheric particles
[AD-A270103] p 1493 N94-18871
Fabrication and characterization of high-T(sub c) tapes and coils made from Ag-clad Bi-2223 superconductors
[DE93-018615] p 1601 N94-18993
Three dimensional multipole decomposition of fields
[DE93-018530] p 1389 N94-19053
The Cluster magnetic field investigation: Scientific objectives and instrumentation p 1329 N94-19629
The Electron Drift Instrument for Cluster
p 1329 N94-19630
Transient skin effect in a massive cylinder by eccentric location of exciting conduction bands
[ETN-93-95048] p 1391 N94-19646

MAGNETIC FILMS
Picoindentation hardness measurements using atomic force microscopy
[AD-A270877] p 1604 N94-19579
Magnetic Ultrathin Films: Multilayers and Surfaces, Interfaces, and Characterization, volume 313
[AD-A271402] p 1375 N94-19758

MAGNETIC FLUX
Microwave scattering from TAE modes
[DE93-018170] p 1583 N94-17809
Superconducting flux flow devices, digital circuits and memories
[DE93-019072] p 1405 N94-19079

MAGNETIC INDUCTION
Footprint size of a helicopter-borne electromagnetic induction sounding system versus antenna altitude
[AD-A270468] p 1463 N94-19672

MAGNETIC MATERIALS
Magnetic Ultrathin Films: Multilayers and Surfaces, Interfaces, and Characterization, volume 313
[AD-A271402] p 1375 N94-19758

MAGNETIC MEASUREMENT
High resolution SQUID magnetometry for non-destructive evaluation
[AD-A268884] p 1447 N94-18225
Magnetic field measurements of a superconducting undulator for a Harmonic Generation FEL experiment at the NSLS
[DE93-017621] p 1438 N94-18504

MAGNETIC MIRRORS
Nonparaxial MHD stabilizers for an axisymmetric magnetic mirror
[DE93-017996] p 1587 N94-18505
Generalized energy principle for flute perturbations in axisymmetric mirror machines
[DE93-019399] p 1589 N94-19037
Finite beta plasma equilibrium in toroidally linked mirrors
[DE93-040318] p 1590 N94-19193

MAGNETIC MOMENTS
Electric measurement of Lavet motors
p 1408 N94-18022
Toroidal solenoids in the electromagnetic field and Aharonov-Casher effect
[DE93-629861] p 1566 N94-18152
Research in particle physics
[DE93-040875] p 1567 N94-18534
The anomalous magnetic moment of the muon
[DE93-018932] p 1572 N94-19320
Magnetic and crystallographic structures in UTX intermetallic compounds
[DE93-018291] p 1605 N94-19735

MAGNETIC PERMEABILITY
High resolution SQUID magnetometry for non-destructive evaluation
[AD-A268884] p 1447 N94-18225
Realistic theories of heavy electron and other strongly correlated materials
[DE93-010350] p 1571 N94-19204
MAGNETIC PROPERTIES
Magnetic properties of single-crystalline UCu3Al2
[DE93-016607] p 1593 N94-17744
Spin-integrated and spin-dependent photoelectron diffraction
[DE93-016546] p 1565 N94-17850
Comparison of ferrite materials for pulse applications
[DE93-017224] p 1574 N94-18497
High pressure metallization of Mott Insulators: Magnetic, structural and electronic properties
[DE93-018295] p 1404 N94-18805
Superconductivity and magnetism in niobium doped YBa2Cu3O7 related high-(Tc) ceramics
[DE93-018086] p 1601 N94-19049
Some superhigh-frequency and magnetic properties of chemically precipitated films
[AD-A266195] p 1351 N94-19110
Magnetic Ultrathin Films: Multilayers and Surfaces, Interfaces, and Characterization, volume 313
[AD-A271402] p 1375 N94-19758
MAGNETIC RECORDING
Tribological studies of silicon for magnetic recording applications (Invited)
[AD-A270878] p 1447 N94-19784
MAGNETIC RELAXATION
Filamentation, current profiles and transport in a tokamak
[DE93-016768] p 1584 N94-17948
Relaxation of polar orientational order in nonlinear optical polymers by second harmonic generation
[AD-A269059] p 1370 N94-18515
MAGNETIC STORMS
Penetrating radiation environment and effects study
[AD-A270126] p 1485 N94-18874
The effects of magnetic storm phases on f-layer irregularities from auroral to equatorial latitudes
[AD-A267388] p 1486 N94-19008
MAGNETIC SURVEYS
Rapid geophysical surveyor
[DE93-016637] p 1461 N94-17851
MAGNETIC SUSPENSION
Corroboration of magnetic forces in US Maglev design
[DE93-014918] p 1443 N94-17785
Six degree of freedom fine motion positioning stage based on magnetic levitation
[DE93-017651] p 1446 N94-19547
MAGNETIC TAPES
Contribution to the tribological study of magnetic-tape head contact
[ECL-92-57] p 1434 N94-19414
Microtribology of magnetic media
[AD-A271209] p 1407 N94-19722
Atomic-scale friction measurements using friction force microscopy. Part 2: Application to magnetic media
[AD-A270759] p 1447 N94-19767
MAGNETIZATION
Magnetic properties of single-crystalline UCu3Al2
[DE93-016607] p 1593 N94-17744
Ising model on tangled chain. Part 2: Magnetization and susceptibility
[DE93-628794] p 1607 N94-18174
MAGNETO-OPTICS
Magnetic Ultrathin Films: Multilayers and Surfaces, Interfaces, and Characterization, volume 313
[AD-A271402] p 1375 N94-19758
MAGNETOHYDRODYNAMIC FLOW
Profile stabilization of tilt mode in a field reversed configuration
[DE93-016770] p 1583 N94-17753
Viscosity in the edge of tokamak plasmas
[DE93-018039] p 1588 N94-18988
Radiative divertor modeling studies
[DE93-018092] p 1590 N94-19290
MAGNETOHYDRODYNAMIC GENERATORS
Development of a multi-point two-color pyrometer for tube and wall temperature and emissivity measurement at the CFFF
[DE93-014716] p 1429 N94-18207
Study of multi-phase flow characteristics in an MHD power train
[DE93-018570] p 1586 N94-18272
MHD integrated topping cycle project
[DE93-040520] p 1588 N94-18978
MHD Integrated Topping Cycle Project
[DE93-040521] p 1589 N94-19055
MAGNETOHYDRODYNAMIC STABILITY
Transformation of energy and momentum due to Landau damping in space
[DE93-624921] p 1581 N94-17689
Limits on m = 2, n = 1 error field induced locked mode instability in TPX with typical sources of poloidal field coil error field and a proto type correction coil, C-coil
[DE93-014408] p 1582 N94-17702
Self-regulated shear flow turbulence in confined plasmas
[DE93-015823] p 1583 N94-17743
Profile stabilization of tilt mode in a field reversed configuration
[DE93-016770] p 1583 N94-17753
Plasma properties research: Task 3
[DE93-017087] p 1583 N94-17854
Filamentary magnetohydrodynamic plasmas
[DE93-015616] p 1583 N94-17945
AEOLUS-IT MHD simulation code based on a toroidally incompressible plasma model
[DE93-788461] p 1586 N94-18157
Resonant absorption of Alfven waves near a neutral point
[DE93-628761] p 1586 N94-18172
Hydrodynamic instability modeling for ICF
[DE93-018634] p 1587 N94-18274
Nonparaxial MHD stabilizers for an axisymmetric magnetic mirror
[DE93-017996] p 1587 N94-18505
Generalized energy principle for flute perturbations in axisymmetric mirror machines
[DE93-019399] p 1589 N94-19037
On neutral plasma oscillations
[DE93-040319] p 1590 N94-19194
MAGNETOHYDRODYNAMIC WAVES
The phase mixing of shear Alfven waves
[DE93-624920] p 1581 N94-17688
Profile stabilization of tilt mode in a field reversed configuration
[DE93-016770] p 1583 N94-17753
Microwave scattering from TAE modes
[DE93-018170] p 1583 N94-17809
MAGNETOHYDRODYNAMICS
Profile stabilization of tilt mode in a field reversed configuration
[DE93-016770] p 1583 N94-17753
Filamentary magnetohydrodynamic plasmas
[DE93-015616] p 1583 N94-17945
Coupled MHD and transport analysis of improved confinement D3-D discharges
[DE93-016985] p 1585 N94-18057
AEOLUS-IT MHD simulation code based on a toroidally incompressible plasma model
[DE93-788461] p 1586 N94-18157
Study of multi-phase flow characteristics in an MHD power train
[DE93-018570] p 1586 N94-18272
Hydrodynamic instability modeling for ICF
[DE93-018634] p 1587 N94-18274
Nonparaxial MHD stabilizers for an axisymmetric magnetic mirror
[DE93-017996] p 1587 N94-18505
Contributions from geomagnetic inverse theory to the study of hydromagnetic conditions near the core-mantle boundary
[NASA-CR-194303] p 1484 N94-18853
MHD technology transfer, integration and review committee
[DE93-040519] p 1588 N94-18892
Viscosity in the edge of tokamak plasmas
[DE93-018039] p 1588 N94-18988
Generalized energy principle for flute perturbations in axisymmetric mirror machines
[DE93-019399] p 1589 N94-19037
MAGNETOMETERS
High resolution SQUID magnetometry for non-destructive evaluation
[AD-A268884] p 1447 N94-18225
Experience with custom processors in space flight applications p 1336 N94-18338
Aspects of the calibration and processing of the CRRES fluxgate magnetometer data
[AD-A270127] p 1432 N94-18875
STAFF (Spatio-Temporal Analysis of Field Fluctuations) experiment for the Cluster mission p 1328 N94-19625
The Cluster magnetic field investigation: Scientific objectives and instrumentation p 1329 N94-19629
MAGNETOPAUSE
Penetrating radiation environment and effects study
[AD-A270126] p 1485 N94-18874
MAGNETOSTATICS
Magnetostatic waves-based integrated optic bragg cell modules with applications to RF signal processing
[AD-A269115] p 1577 N94-18295
Three dimensional multipole decomposition of fields
[DE93-018530] p 1389 N94-19053
MAGNETOSTRICTION
Magnetostrictive actuators for human sensory feedback
[AD-A269266] p 1511 N94-17841
MAGNONS
Lectures of Fermi liquid theory
[DE93-016630] p 1592 N94-17714
Polaron tunneling in high-temperature superconductors
[DE93-016880] p 1593 N94-17754
Nonlinear dynamics and instabilities in ferromagnetic resonance experiments: Examinations of spheres from yttrium iron garnet in coincidence area of the first Suhl instabilities
[ETN-93-95072] p 1604 N94-19612
MAIN SEQUENCE STARS
Stellar coronae at the end of the main sequence: A Rosat survey of the late M dwarfs
[NASA-CR-194700] p 1628 N94-19794
MAINTENANCE
SUNRAYCE 1993: Working safely with lead-acid batteries and photovoltaic power systems
[DE93-016553] p 1464 N94-17712
Restoration of an 18th century English clock
p 1427 N94-18026
Aircrew life support, AFSC 122X0(1T1X1)
[AD-A268998] p 1511 N94-18394
A case study in software maintenance
[AD-A269923] p 1521 N94-18659
Tehachapi solar thermal system
[DE93-018443] p 1468 N94-19014
Downsizing a database platform for increased performance and decreased costs
[DE93-018687] p 1618 N94-19099
MALES
Effects of a high-energy food supplement on cold-induced thermogenesis
[AD-A269301] p 1504 N94-17823
MAN MACHINE SYSTEMS
Research on man-machine productivity in aviation at Human Engineering Institute of Hangzhou University
[AD-A269952] p 1512 N94-18673
Aerospace medicine and biology: A continuing bibliography with indexes (supplement 382)
[NASA-SP-7011(382)] p 1507 N94-18936
Aerospace medicine and biology: A continuing bibliography with indexes (supplement 381)
[NASA-SP-7011(381)] p 1507 N94-19069
Human-machine interfaces
[AD-A270730] p 1513 N94-19764
MAN-COMPUTER INTERFACE
Current development in selected stress and thermal analysis software interfaces with PRO-ENGINEER
[DE93-014935] p 1518 N94-17943
Interactive Collaborative Environments (ICE) in the design to manufacturing process
[DE93-014994] p 1518 N94-17944
Dialog-Based Learning (DBL) for adaptive interface agents and programming-by-demonstrations systems
[AD-A269154] p 1540 N94-18261
Why are human-computer interfaces difficult to design and implement?
[AD-A268843] p 1514 N94-18317
CONTACT: An Air Force technical report on military satellite control technology
[AD-A269375] p 1334 N94-18408
Distributed Computing Design System (DCDS)
[AD-A270435] p 1534 N94-18509
Automatic documentation generation: The interaction of text and examples
[AD-A269670] p 1616 N94-18570
A case study in software maintenance
[AD-A269923] p 1521 N94-18659
Generating object descriptions: Intergrating examples with text
[AD-A269992] p 1522 N94-18680
A user task analysis for command and control systems and its use in human-computer interaction research
[AD-A269877] p 1512 N94-18774
Working visit to the University of L'Aquila, Italy
[FEL-93-B020] p 1618 N94-19452
Results of a joint Navy/Air Force operational test to evaluate USAF Integrated Maintenance Information Systems (IMIS), Interactive Electronic Technical Manual (IETM) technology applied to the F/A-18 aircraft
[AD-A271322] p 1619 N94-19571
MANAGEMENT INFORMATION SYSTEMS
EDMS: Engineering data management system. User's reference
[PB93-187391] p 1614 N94-18119
Corporate Information Management (CIM) report on the simulation processes, version 2.0
[AD-A269119] p 1617 N94-18770
Denver TMA assessment
[NASA-CR-4554] p 1315 N94-18844
Results of a joint Navy/Air Force operational test to evaluate USAF Integrated Maintenance Information Systems (IMIS), Interactive Electronic Technical Manual (IETM) technology applied to the F/A-18 aircraft
[AD-A271322] p 1619 N94-19571

A comparison Air Force data systems --- Comments on IDA Paper P-2863
[AD-A270662] p 1619 N94-19780

MANAGEMENT METHODS
Present evolution of tools management
[CRIF-MC-102] p 1444 N94-17964
Quality, management, and the interplay of self-assessment, process assessments, and performance-based observations
[DE93-018787] p 1448 N94-19336

MANAGEMENT PLANNING
Current information technology resource requirements of the federal government: Fiscal year 1994
p 1612 N94-17756
Safeguarding our energy future
[DE93-016001] p 1466 N94-18109
The organizational preparation of existing relational databases for the integration of expert systems
[AD-A268823] p 1614 N94-18191
Environmental restoration and waste management five-year plan, fiscal years 1994-1998. Volume 3: Public concerns
[DOE/S-00097P-VOL-3] p 1475 N94-18835
Computing professionals: Changing needs for the 1990's
[B-030] p 1515 N94-19401
Strategic plan, 1991: A strategy for leadership in space through excellence in space science and applications
[NASA-TM-109256] p 1611 N94-19434

MANAGEMENT SYSTEMS
Carbon Dioxide Information Analysis Center: FY 1992 activities
[DE93-013845] p 1471 N94-17774
User's manual of Tokamak Simulation Code
[DE93-788388] p 1586 N94-18212
Reference model for project support environments, version 1.0
[AD-A269110] p 1520 N94-18251
The J85 cost/benefit engine study
[AD-A269280] p 1320 N94-18333

MANEUVERABILITY
Predicted structural response of the lightweight-interceptor technology demonstration vehicle
[DE93-014676] p 1333 N94-17782
An investigation of fighter aircraft agility
[NASA-CR-194608] p 1318 N94-19448

MANEUVERABLE SPACECRAFT
Dynamic characterization of a lightweight, highly maneuverable spacecraft using modal and finite element analyses
[DE93-018095] p 1335 N94-18942

MANGANESE ALLOYS
Bibliography on silicides
[AD-A270516] p 1374 N94-19532

MANGANIN (TRADEMARK)
Deep ion implantation into manganin to modify its pressure and electrothermocharacteristics
[DE93-630229] p 1359 N94-18218

MANIFOLDS (MATHEMATICS)
(1,1)-geodesic maps into Grassmann manifolds
[DE93-624799] p 1545 N94-17684
Groups on transformations in Finslerian spaces
[DE93-624765] p 1606 N94-17794
Some remarks on integrable Hamiltonian systems with two degrees of freedom
[DE93-624766] p 1546 N94-17815
A reduction of the globalization and U(1)-covering
[DE93-624769] p 1546 N94-17817
About structurally stable generating mechanism for invariant hyperbolic sets
[DE93-629858] p 1561 N94-18150
Path integrals on warped product manifolds
[DE93-629859] p 1561 N94-18151

MANIPULATORS
Joint stiffness estimation based on force sensor measurements in industrial manipulators
[REPT-92-053] p 1443 N94-17937
Efficient dynamic modeling of manipulators containing closed kinematic loops
[REPT-92-083] p 1444 N94-17940
Direct kinematics solution architectures for industrial robot manipulators: Bit-serial versus parallel
p 1399 N94-18358
In-situ growth monitoring of molecular beam epitaxy processes
[AD-A269287] p 1598 N94-18616
Cooperative control of multiple space manipulators
[AD-A270291] p 1445 N94-18813
Adaptive path planning: Algorithm and analysis
[DE93-008348] p 1523 N94-18926

MANNED MARS MISSIONS
Space exploration initiative
[NASA-TM-109366] p 1323 N94-18981

MANNED SPACE FLIGHT
Human Transportation System (HTS) study: Executive summary
[NASA-TM-104780] p 1332 N94-18669
Human Transportation System (HTS) study, volume 1
[NASA-TM-104779] p 1332 N94-18670
Return to space
[NASA-TM-109356] p 1332 N94-18955

MANUALS
Results of a joint Navy/Air Force operational test to evaluate USAF Integrated Maintenance Information Systems (IMIS), Interactive Electronic Technical Manual (IETM) technology applied to the F/A-18 aircraft
[AD-A271322] p 1619 N94-19571

MANUFACTURING
Factors which affect fatigue strength of fasteners
[DE93-017272] p 1453 N94-18084
Autonomous neural network controllers for adaptive material handling
[AD-A268908] p 1540 N94-18331
Performance of defect-tolerant set-associative cache memories p 1398 N94-18346
High-efficiency silicon concentrator cell commercialization
[DE93-018491] p 1467 N94-18409
Workshop on Innovation in Materials Processing and Manufacture: Exploratory Concepts for Energy Applications
[DE93-017674] p 1467 N94-18478
New applications for high average power beams
[DE93-018845] p 1439 N94-18522
Materials processing and manufacturing technologies for diamond substrates multichip modules
[AD-A268989] p 1599 N94-18764
Integrated circuits: Resistless processing simplifies production and cuts costs
[DE93-018069] p 1405 N94-18941
Conceptual design of a sodium sulfur cell for US electric van batteries
[DE93-018683] p 1405 N94-19035
MODIL cryocooler producibility demonstration project results
[DE93-017981] p 1335 N94-19275
Manufacturing technology
[DE93-019580] p 1381 N94-19480
Incology 908 database report: On process-structure-property relationship
[DE93-017616] p 1366 N94-19546
Shell designs
[AD-A270656] p 1460 N94-19606
Program descriptions
[NSF-92-123] p 1531 N94-19619
Amorphous silicon batch process cost analysis
[DE93-018203] p 1470 N94-19760

MANY BODY PROBLEM
The physics of cellular automata and coherence and chaos in classical many-body dynamical systems
[DE93-018021] p 1561 N94-18177
A parallel hashed oct-tree N-body algorithm
[DE93-012654] p 1526 N94-19205

MAPPING
CTD oxygen, tracer and nutrient data from RRS Charles Darwin Cruises 58/59 in the NE Atlantic as part of Vivaldi 1991
[IOS-296-1992] p 1496 N94-18065
SeaSoar CTD, fluorescence and scalar irradiance data from RRS Charles Darwin Cruises 58/59, NE Atlantic, Vivaldi 1991
[IOS-299-1992] p 1496 N94-18066
Resolution in radar mapping
[AD-A269730] p 1462 N94-18753

MAPS
The Navy tessellated spheroid map projection system: A comprehensive definition
[AD-A269989] p 1462 N94-18677
Color palette considerations for digital map displays
[AD-A269991] p 1462 N94-18679

MARANGONI CONVECTION
An investigation of low Marangoni number fluid flow in a cold corner
[AD-A271317] p 1422 N94-19569

MARINE CHEMISTRY
Faulted structure of the bottom simulating reflector on the Blake Ridge, western North Atlantic
[AD-A271289] p 1500 N94-19745

MARINE ENVIRONMENTS
Development and evaluation of alternative radioanalytical methods, including mass spectrometry for marine materials
[DE93-625117] p 1345 N94-17691
Coastal Ocean Modeling Workshop
[AD-A268955] p 1497 N94-18393
Work plan for the Marine Aerosol Properties and the Thermal Imager Performance Trial (MAPTIP)
[AD-A270026] p 1483 N94-18712
Estimating the oceanic sound speed environmental for long-range acoustic propagation
[AD-A270231] p 1499 N94-18903
Microstructure and texture control of fatigue in hydrogen and marine environments
[AD-A271277] p 1344 N94-19744
Marine-modified LOWTRAN: The contribution of sun glint
[AD-A269547] p 1500 N94-19762

MARINE METEOROLOGY
Ship-produced cloud line of 13 July 1991
[DE93-016879] p 1472 N94-17986
Rapid oceanic cyclogenesis studies
[AD-A269258] p 1490 N94-18265
The activities of equatorial anticyclones of the Western Pacific and the South China Sea and their effects on the tracks of typhoon movement
[AD-A269954] p 1492 N94-18675
Work plan for the Marine Aerosol Properties and the Thermal Imager Performance Trial (MAPTIP)
[AD-A270026] p 1483 N94-18712

MARINE TECHNOLOGY
Fatigue technology assessment and strategies for fatigue avoidance in marine structures. Appendices
[AD-A269053] p 1455 N94-18716

MARKET RESEARCH
Directory of Energy Information Administration Models 1993
[DE93-016987] p 1616 N94-18707

MARKING
A tight lower bound for on-line monotonic list labeling
[TR-478] p 1531 N94-19508

MARKOV CHAINS
Bayesian analysis of ARMA processes: Complete sampling based inference under full likelihoods
[AD-A269168] p 1557 N94-18694
Adaptive uniformization: Technical details
[MEMO-INF-93-22] p 1558 N94-19265
Tandem queues with deterministic service times
[PB93-197465] p 1543 N94-19324
Adaptive uniformization
[MEMO-INF-92-88] p 1558 N94-19385
Finding optimal policies for Markov decision chains: A unifying framework for mean-variance-tradeoffs
[PB93-191930] p 1559 N94-19555
Production and test of pseudo random elements
[ETN-93-95070] p 1559 N94-19610

MARKOV PROCESSES
Longitudinal beam dynamics with RF noise
[DE93-018649] p 1574 N94-18994
Excursion theory of a finite set via resolvents
[REPT-93-19] p 1557 N94-19090
Excursions of stochastic processes, Cox-point processes, entrance behavior and resolvents
[PB93-197291] p 1558 N94-19323
Compensation approach for three or more dimensional random walks
[PB93-197499] p 1543 N94-19326
Sensitivity and uncertainty analysis of Markov reward models
[MEMO-INF-92-89] p 1559 N94-19386
Equivalence and reduction of hidden Markov models
[AD-A270762] p 1560 N94-19768

MARS (PLANET)
Space transfer concepts and analyses for exploration missions
[NASA-CR-193876] p 1332 N94-18820
Spacework 17: O'Leary's Mars
[NASA-TM-109374] p 1629 N94-18966

MARS SURFACE
Working group for planetary system nomenclature
[NASA-CR-194406] p 1626 N94-18841
JPRS report: Science and technology. Central Eurasia: Space
[JPRS-USP-93-004] p 1323 N94-19146

MARSHLANDS
The ecological and environmental impacts of manmade marshes
[AD-A269213] p 1475 N94-18885

MARTENSITE
Continuum modeling of materials that can undergo martensitic phase transitions
[AD-A268767] p 1360 N94-18386

MARTENSITIC TRANSFORMATION
Omega phase formation in shock-loaded zirconium
[DE93-018343] p 1595 N94-18162
Continuum modeling of materials that can undergo martensitic phase transitions
[AD-A268767] p 1360 N94-18386
The longitudinal free vibrations of a fixed-free two-phase elastic bar
[AD-A268768] p 1453 N94-18387
The temperature at the phase boundary during quasi-static motions of a two-phase thermoelastic bar
[AD-A268769] p 1596 N94-18388

Damping in ferrous shape memory alloys
[AD-A271009] p 1366 N94-19775

MASERS

Design of a tunable 4-MW free electron maser for heating fusion plasmas
[DE93-017172] p 1437 N94-18134
Proof of the feasibility of coherent and incoherent schemes for pumping a gamma ray laser
[AD-A269173] p 1440 N94-18880

MASKING

On masking effect
[AD-A269593] p 1541 N94-18462

MASKS

RF vacuum microelectronics
[AD-A270003] p 1403 N94-18667

MASS

Neutrino mass
[DE93-018467] p 1567 N94-18269

MASS BALANCE

A carbon isotope mass balance for an anoxic marine sediment: Isotopic signatures of diagenesis
p 1477 N94-19232

MASS FLOW

Vane optimization for maximum efficiency using Design Of Experiments (DOX)
[AD-A270270] p 1320 N94-18907
Mathematical modeling of the free surface hydrodynamic and of transport in suspensions of non cohesive sediments: Aid to the interpretation of spatial images
[ETN-93-95011] p 1421 N94-19502

MASS SPECTRA

Crossed molecular beam studies of atmospheric chemical reaction dynamics
[DE93-019246] p 1478 N94-19303
Studies of clusters
[DE93-018961] p 1572 N94-19309
Evaluation of mass spectra for a verification database
[PML-1993-12] p 1619 N94-19453

MASS SPECTROMETERS

The minimum detection limits of RDX and TNT deposited on various surfaces as determined by ion mobility spectroscopy
[DE93-018521] p 1378 N94-19042
Novel mass spectrometric instrument for gaseous and particulate characterization and monitoring
[DE93-019992] p 1433 N94-19054
Crossed molecular beam studies of atmospheric chemical reaction dynamics
[DE93-019246] p 1478 N94-19303

MASS SPECTROSCOPY

Development and evaluation of alternative radioanalytical methods, including mass spectrometry for marine materials
[DE93-625117] p 1345 N94-17691
Detonation reaction steps frozen by free expansion and analyzed by mass spectrometry
[DE93-012734] p 1376 N94-17813
Matrix- and substrate-assisted laser desorption for fast DNA sequencing
[DE93-015332] p 1501 N94-18242
Flame structure studies of a lean 20-torr H2/N2O/Ar flame employing molecular beam mass spectrometry
[AD-A268889] p 1349 N94-18456
Novel mass spectrometric instrument for gaseous and particulate characterization and monitoring
[DE93-019992] p 1433 N94-19054
Research program activities of the ORNL Analytical Chemistry Division
[DE93-017938] p 1339 N94-19117
Evaluation of mass spectra for a verification database
[PML-1993-12] p 1619 N94-19453

MASS TRANSFER

Pulse-timing studies of x ray pulsars
[NASA-CR-193778] p 1621 N94-18611
Adsorption analysis of ammonia in an aqueous solution
[DE93-019512] p 1353 N94-19552
Supercritical thermodynamics of sulfur and nitrogen species
[DE93-041221] p 1610 N94-19670

MASSIVE STARS

Detection of accreting gas toward HD 45677: A newly recognized, Herbig Be proto-planetary system
[NASA-CR-189312] p 1621 N94-19288

MASSIVELY PARALLEL PROCESSORS

PARX, kernel of a system for massively parallel computers: Control of communication between processes
[ETN-93-94353] p 1533 N94-17976
A fast adaptive convex hull algorithm on two-dimensional processor arrays with a reconfigurable BUS system
p 1402 N94-18380
Three-dimensional shock wave physics simulations with MIMD PAGOSA on massively parallel computers
[DE93-011682] p 1455 N94-18829
A massively parallel adaptive finite element method with dynamic load balancing
[DE93-012844] p 1536 N94-19161
Experience in implementing a parallel file system
[DE93-012840] p 1536 N94-19188
MIMD massively parallel methods for engineering and science problems
[DE93-019409] p 1531 N94-19562

MATERIALS HANDLING

Autonomous neural network controllers for adaptive material handling
[AD-A268908] p 1540 N94-18331
Workshop on Innovation in Materials Processing and Manufacture: Exploratory Concepts for Energy Applications
[DE93-017674] p 1467 N94-18478
Coordination of software-development activities among sites that are geographically separated
[DE93-019201] p 1524 N94-19076

MATERIALS RECOVERY

Mechanically refuelable zinc/air electric vehicle cells
[DE93-016446] p 1394 N94-17770

MATERIALS SCIENCE

Workshop on Innovation in Materials Processing and Manufacture: Exploratory Concepts for Energy Applications
[DE93-017674] p 1467 N94-18478
Contribution to the identification of nonlinear behavior laws in material mechanics
[ECL-92-36] p 1458 N94-19411

MATERIALS TESTS

Evaluation of materials proposed for the construction of the Plasma Electrode Pockels Cell (PEPC) on beamlet
[DE93-016952] p 1584 N94-17988
Limited Duration of Candidate Materials Exposure Experiment (LDCE): A Complex Autonomous Payload (CAP) using a Get Away Special (GAS) canister
p 1326 N94-19176

MATHEMATICAL LOGIC

Using semantic information for processing negation and disjunction in logic programs
[DE93-017412] p 1614 N94-18099
Verification of VLSI designs p 1400 N94-18363
A refinement for nonmonotonic logic
[REPT-93-21] p 1542 N94-19092
Technical development of a theory of programs
[ETN-93-95058] p 1532 N94-19652

MATHEMATICAL MODELS

On the Debye-Huckel's theory
[DE93-624789] p 1561 N94-17681
Further on the current algebra of WZNW models at and away from criticality
[DE93-624809] p 1545 N94-17686
Direct Monte Carlo simulation of the chemical equilibrium composition of detonation products
[DE93-014559] p 1376 N94-17751
Modeling and new equipment definition for the vibration isolation box equipment system
[NASA-CR-193185] p 1379 N94-17763
Dust in the Small Magellanic Cloud
[NASA-CR-193344] p 1624 N94-17764
CO2 laser with modulated losses: Theoretical models and experiments in the chaotic regime
[DE93-624901] p 1435 N94-17771
Air pollution effects field research facility. 3: UV-B exposure and monitoring system
[DE93-013098] p 1470 N94-17773
A one dimensional numerical model, with an application to the vertical distribution of dissolved oxygen in the ocean
[DE93-018481] p 1495 N94-17779
A radial transmission line material measurement apparatus
[DE93-018508] p 1394 N94-17780
A new multiphase equation of state for iron
[DE93-017629] p 1357 N94-17819
Considerations for the use of the modified line reversal technique for gas temperature measurement
[DE93-015752] p 1576 N94-17857
The value of windpower: An investigation using a qualified production cost model
[DE93-010043] p 1465 N94-17888
A preliminary model for crack-tip hydrogen transport
[NPL-DMM(A)-84] p 1451 N94-17899
On comparison and extensions of control methods for narrow-band disturbance rejection
[REPT-93-015] p 1540 N94-17922
Ratio of specimen thickness to detection area for reliable hydrogen permeation measurement
[NPL-DMM(A)-103] p 1451 N94-17929
TANGO: A notation for describing advanced transaction models
[REPT-93-014] p 1613 N94-17936
Linear parameter identification methods for ARMA models with periodic coefficients
[REPT-92-070] p 1556 N94-17938
Efficient dynamic modeling of manipulators containing closed kinematic loops
[REPT-92-083] p 1444 N94-17940
Kinetic growth of random-like and ballistic-like deposition models
[DE93-624946] p 1595 N94-17956
Format.m: A usage manual. Towards an efficient symbolic-numeric environment: Extending Mathematica's format rules
[MATHS-REPT-A-185] p 1547 N94-17969
Impact response of composite laminates: A guide to closed form solutions
[FFA-TN-1992-33] p 1339 N94-17971
A free boundary eigenvaue problem
[IPP-6/310] p 1584 N94-17981
Summary report for supercritical carbon dioxide extraction and carbonization of Resorcinol-Formaldehyde (RF) foams
[DE93-016924] p 1346 N94-17987
Limitations on the fidelity of 100 fs pulses produced by chirped pulse amplification
[DE93-017167] p 1396 N94-17991
Computational strategies for composite structures
[PB93-195097] p 1452 N94-18079
Cut and paste based modeling with boundary features
[PB93-187250] p 1520 N94-18117
Navigation in hypermedia applications: Modelling and semantics
[REPT-93-034] p 1520 N94-18136
The physics of cellular automata and coherence and chaos in classical many-body dynamical systems
[DE93-018021] p 1561 N94-18177
Non-linear flight dynamics p 1319 N94-18240
Mechanical modeling of the growth of salt structures
[DE93-015342] p 1596 N94-18243
A rational design change methodology based on experimental and analytical modal analysis
[DE93-018537] p 1521 N94-18271
Hydrodynamic instability modeling for ICF
[DE93-018634] p 1567 N94-18274
Bayesian model choice: Asymptotics and exact calculations
[AD-A269067] p 1557 N94-18516
Microwave (SSM/I) Estimates of the Precipitation Rate to Improve Numerical Atmospheric Model Forecasts
[NASA-CR-193566] p 1491 N94-18602
Diabatic forcing and initialization with assimilation of cloud and rain water in a forecast model: Methodology
p 1491 N94-18603
Moist wind relationships p 1492 N94-18607
Initialization and assimilation of cloud and rainwater in a regional model p 1492 N94-18608
Full Boltzmann discrete spectral wave model, implementation and nondimensional tests
[AD-A269885] p 1498 N94-18685
Soft X Ray Projection Lithography. Organization of the 1993 photonics science optical meetings
[AD-A269159] p 1579 N94-18693
Bayesian analysis of ARMA processes: Complete sampling based inference under full likelihoods
[AD-A269168] p 1557 N94-18694
Directory of Energy Information Administration Models 1993
[DE93-016987] p 1616 N94-18707
Constant-thrust orbit-raising transfer charts
[AD-A269088] p 1334 N94-18718
Solar radiation in Saudi Arabia
[AD-A269970] p 1493 N94-18781
Numerical modelling of fringing fields and their use for complex permittivity measurements at high frequencies
[AD-A270198] p 1388 N94-18782
Knowledge sources for an intelligent MCM analyzer
[AD-A269224] p 1542 N94-18887
Flow volumes for interactive vector field visualization
[DE93-017102] p 1418 N94-18888
BACKSCATTER.FOR: A program to calculate the backscattering strength of an inhomogeneous seabed
[AD-A269235] p 1499 N94-18910
The intelligent processing of materials
[AD-A269250] p 1362 N94-18923
Dynamic characterization of a lightweight, highly maneuverable spacecraft using modal and finite element analyses
[DE93-018095] p 1335 N94-18942
Viscosity in the edge of tokamak plasmas
[DE93-018039] p 1588 N94-18988
A least-squares computational tool kit
[DE93-018400] p 1557 N94-19011
Modeling of the formation of microporosity in alloys
[DE93-017733] p 1364 N94-19044
Plastic mechanism analysis of T-joints in RHS subject to combined bending and concentrated force
[PB93-195774] p 1456 N94-19061

Deterministic growth-dispersal models and branching random walk
[REPT-93-14] p 1550 N94-19088
Similarity solutions for gravity-dominated spreading of a lens of organic contaminant
[REPT-93-24] p 1420 N94-19139
Inverse scattering of surface waves: A new look at surface consistency
[REPT-93-25] p 1486 N94-19140
Modelling software for structure metrics
[MEMO-INF-93-13] p 1526 N94-19200
Molecular dynamics modeling of the mechanical behavior of metallic multilayers
[DE93-017972] p 1365 N94-19263
A unified performability evaluation framework for computer and communication systems
[MEMO-INF-93-21] p 1537 N94-19264
Adaptive uniformization: Technical details
[MEMO-INF-93-22] p 1558 N94-19265
Design for cyclic loading endurance of composites
[NASA-TM-106407] p 1457 N94-19351
Modelization, numerical simulation and optimal control of NET tokamak plasma configuration evolution for the future generation of fusion reactors
[ETN-93-95019] p 1591 N94-19364
Tetravalent chromium (Cr(4+)) as laser-active ion for tunable solid-state lasers
[NASA-CR-194529] p 1441 N94-19369
Numerical analysis of pressure meter tests: Application of parameter identification of soils behavior
[ECL-92-52] p 1487 N94-19380
Contribution to the modelling and the identification of nonlinear mechanical systems
[ECL-92-32] p 1529 N94-19409
Contribution to the identification of nonlinear behavior laws in material mechanics
[ECL-92-36] p 1458 N94-19411
Numerical prediction of transition of the F-16 wing at supersonic speeds
[NASA-CR-194407] p 1312 N94-19433
Contribution to the study of a symmetric film flow (with or without tensio-active elements)
[ECL-93-13] p 1421 N94-19461
Computational Methods for Crashworthiness
[NASA-CP-3223] p 1458 N94-19465
Impact analysis of composite aircraft structures
p 1458 N94-19468
Development and use of computational techniques in Army Aviation research and development programs for crash resistant helicopter technology
p 1459 N94-19469
Explicit solution techniques for impact with contact constraints p 1459 N94-19470
Mathematical sciences, technology, and economic competitiveness
[LC-91-60253] p 1514 N94-19478
Structuration processes in protoplanetary accretion disks
[MPE-243] p 1628 N94-19519
Stability measurements of Rayleigh-Benard convection near the critical state using a spectral model
[MPIS-15/1992] p 1422 N94-19520
Methods for description and control of dynamical systems and their application
[MPIS-17/1992] p 1553 N94-19522
An iterative inverse scattering method for the removal of scattered surface waves
[REPT-93-18] p 1488 N94-19644
Modeling of driver behavior: Information perception, rule and control strategies in experiments and simulations
[ETN-93-95053] p 1510 N94-19649
Remote sensing of Earth terrain
[NASA-CR-194598] p 1464 N94-19681
Updated Contributions to the Twente Workshop on Hamiltonian Graph Theory
[MEMO-1076] p 1554 N94-19683
On Hamilton-connectedness of Cayley graphs
p 1554 N94-19684
Toughness and the cycle structure of graphs
p 1554 N94-19686
The Hopping Lemma p 1554 N94-19687
Cycles containing all vertices of maximum degree
p 1554 N94-19688
Long paths and cycles in tough graphs
p 1554 N94-19689
The complete closure of a graph
p 1555 N94-19690
Twenty odd statements in Twente
p 1555 N94-19691
Generalized closures of graphs p 1555 N94-19692
Two problems related to results of Chvatal-Erdoes
p 1555 N94-19693
Concerning the circumference of certain families of graphs p 1555 N94-19694
Ore-type conditions for cycles through specified vertices p 1555 N94-19695
Hamilton cycles in path-tough graphs
p 1555 N94-19696
Cubic graphs containing k vertex-disjoint subgraphs of given cyclomatic number p 1555 N94-19697
Reports of the 1992 Synoptic Symposium
[KNMI-TR-151] p 1494 N94-19698
HIRLAM p 1494 N94-19699
The WAQUA/CSM-16 model p 1494 N94-19700
The wave forecasting model NEDWAM
p 1495 N94-19701
Amorphous silicon batch process cost analysis
[DE93-018203] p 1470 N94-19760
Equivalence and reduction of hidden Markov models
[AD-A270762] p 1560 N94-19768
A study of the amplification of laser and VLF waves using a simple pendulum model
[AD-A270857] p 1442 N94-19770

MATHEMATICS
Guide to programs, fiscal year 1993
[NSF-92-78] p 1633 N94-19620

MATRICES (MATHEMATICS)
Proposal for a numerical array library
[DE93-015017] p 1516 N94-17786
Differential geometry of CR-submanifolds of a normal almost para contact manifold
[DE93-624764] p 1545 N94-17793
A modified direct preconditioner for indefinite symmetric Toeplitz systems
[DE93-015234] p 1516 N94-17800
A zeta function approach to the semiclassical quantization of maps
[DE93-624774] p 1547 N94-17949
Deformed traces and covariant quantum algebras for quantum groups GL(sub qp)(2) and GL(sub qp)(1/1)
[DE93-629862] p 1561 N94-18153
Phase space representations and quantum probability theory
[DE93-629863] p 1556 N94-18154
Paragrassmann analysis and quantum groups
[DE93-628593] p 1561 N94-18168
On paragrassmann differential calculus
[DE93-628594] p 1548 N94-18169
A multigrid acceleration technique for computing steady solutions to the equations of compressible flow
p 1412 N94-18559
A parallel and pipelined architecture for estimation of direction of arrival using a bilinear transformation method, volume 3
[AD-A270137] p 1389 N94-18897
New insights in GMRES-like methods with variable preconditioners
[REPT-93-10] p 1524 N94-19084
PUMMA: Parallel Universal Matrix Multiplication Algorithms on distributed memory concurrent computers
[DE93-019163] p 1538 N94-19299
The Fourier analysis technique and epsilon-pseudo-eigenvalues
[DE93-018805] p 1551 N94-19337
A comparison of iterative methods for a model coupled system of elliptic equations
[DE93-040482] p 1553 N94-19655
On the computation of versal family of matrices
[RR-892-M] p 1532 N94-19712
Geometric contact for curves and surfaces
[RR-893-M] p 1556 N94-19731

MATRIX MATERIALS
A comprehensive study of matrix fracture mechanisms in fiber-reinforced ceramic matrix composites
[AD-A268809] p 1340 N94-18205
Process relationship as influenced by carbonization rate
[AD-A269680] p 1341 N94-18572
Bibliography on ceramic matrix composites and reinforcing whiskers, platelets, and fibers, 1970-1990
[AD-A270139] p 1371 N94-18750
Experiments and analysis of lateral piezoresistance gauges
[DE93-017874] p 1433 N94-19111

MATRIX METHODS
Improved omit set displacement recoveries in dynamic analysis p 1449 N94-17829
A noniterative improvement of Guyan reduction
p 1449 N94-17833
A methodology to model physical contact between structural components in NASTRAN
p 1450 N94-17836
The respectiveness of response in a bar under static and transient loads
[VTT-TIED-1377] p 1452 N94-17959
Fast-training algorithm for hidden-layer forward-feed neural networks
[AD-A269253] p 1540 N94-18263

MATRIX THEORY
On the computation of versal family of matrices
[RR-892-M] p 1532 N94-19712

MAXIMA
Cycles containing all vertices of maximum degree
p 1554 N94-19688
Concerning the circumference of certain families of graphs p 1555 N94-19694

MAXIMUM ENTROPY METHOD
Exact solution of the generalized time-dependent Jaynes-Cummings Hamiltonian
[DE93-624773] p 1546 N94-17811

MAXIMUM LIKELIHOOD ESTIMATES
EDF tests for normality in linear models after a Box-Cox transformation
[AD-A269068] p 1557 N94-18517
Spectral analysis on the canonical autoregressive decomposition
[AD-A270083] p 1549 N94-18798
Generalized regression trees: Function estimation via recursive partitioning and maximum likelihood
[AD-A271259] p 1560 N94-19726

MAXIMUM PRINCIPLE
Existence of a maximal solution for quasimonotone elliptic systems
[REPT-93-30] p 1550 N94-19153

MAXWELL EQUATION
Advances and applications of ABCI
[DE93-016971] p 1383 N94-18055
Current-potential characteristics of electrochemical systems
[DE93-040303] p 1352 N94-19192

MAXWELL-BOLTZMANN DENSITY FUNCTION
Modelling ideal gas fluorides laser plasmas
[ETN-93-95073] p 1592 N94-19613

MEAN FREE PATH
Wave structure induced by fluid dynamic limits in the Broadwell model
[AD-A268512] p 1410 N94-18385

MEAN SQUARE VALUES
An empirical evaluation of five circular error probable estimation techniques and a method for improving them
[AD-A266528] p 1556 N94-18397
Tracking with time-delayed data in multisensor systems
[AD-A271334] p 1391 N94-19582

MEASURE AND INTEGRATION
Numerical methods for molecular dynamics
[DE93-018321] p 1566 N94-18179

MEASURING INSTRUMENTS
A radial transmission line material measurement apparatus
[DE93-018508] p 1394 N94-17780
Verification of VALISYS cad based CMM software at LLNL
[DE93-013854] p 1517 N94-17911
Measuring machines for digitalizing and measuring complex surfaces, models and matrices
[CRIF-MC-97] p 1444 N94-17963
Simulation of quartz resonators p 1426 N94-18021
Laser induced damage testing: Equipment and techniques
[DE93-017143] p 1437 N94-18060
C-band PARC manual
[FEL-92-B159] p 1383 N94-18070
Belgian Royal Observatory Communications, Series A, No. 104, Geophysics Series No. 175
[COMMUNICATIONS-SER-A-104] p 1482 N94-18622
Recent developments in fast response aerodynamic probe technology p 1431 N94-18645
Experiments and analysis of lateral piezoresistance gauges
[DE93-017874] p 1433 N94-19111
Pantex Plant Meteorological Monitoring Program
[DE93-018495] p 1493 N94-19127
Software quality in test and measurment equipment
[PB93-197846] p 1528 N94-19333
Six degree of freedom fine motion positioning stage based on magnetic levitation
[DE93-017651] p 1446 N94-19547
A comparison of polygraphic and actigraphic monitoring of sleep using a 5-channel programmable-sensitivity actigraph
[AD-A270731] p 1507 N94-19608
The Electron Drift Instrument for Cluster
p 1329 N94-19630
The Cluster Ion Spectroscopy experiment
p 1329 N94-19631

MECHANICAL ENGINEERING
Research activities, Faculty of Civil Engineering, Delft University of Technology, 1990 - 1991
[PB93-195022] p 1380 N94-19254
Program descriptions
[NSF-92-123] p 1531 N94-19619

MECHANICAL MEASUREMENT
Omega phase formation in shock-loaded zirconium
[DE93-018343] p 1595 N94-18162

MECHANICAL PROPERTIES
Metals 2000 [DE93-016761] p 1355 N94-17752
Microstructural analysis of solid-state resistance welds [DE93-017295] p 1443 N94-17761
Atlas of formability: ALLVAC 718 [AD-A268304] p 1357 N94-17804
Measurement and analysis of three 1.5-GPa shock-wave profiles in copper [DE93-016559] p 1451 N94-17864
Mechanical properties of excimer laser modified titanium surfaces [DE93-012663] p 1358 N94-17875
Impact modeling with smooth particle hydrodynamics [DE93-016561] p 1451 N94-17906
Ceramic films and interfaces: Chemical and mechanical properties [DE93-018416] p 1369 N94-18163
Study of mechanical behavior and internal structure of ferritic nanocrystalline material [DE93-019264] p 1596 N94-18184
Mechanical properties of fiber-reinforced YBa2Cu3O(x) and Bi2Sr2CaCu2O(x) bars [DE93-017689] p 1454 N94-18479
Carbon/carbon composites coated with SiC by chemical vapor deposition [AD-A269934] p 1341 N94-18544
Pressureless densification of ceramic matrix composites [AD-A269137] p 1371 N94-18691
Mechanical properties and impact damage resistance of composites fabricated by low cost, vacuum assisted, resin transfer molding [AD-A270361] p 1342 N94-18702
Mechanical-property changes of structural composite materials after low-temperature proton irradiation: Implications for use in SSC magnet systems [DE93-016735] p 1343 N94-18763
Intelligent materials systems and structures. Part 4: The influence of thermomechanical loading on the life of shape memory alloys [PB93-195923] p 1363 N94-18952
High dose effects in neutron irradiated face-centered cubic metals [DE93-017671] p 1364 N94-19043
Polymer technology publication. Series no. 14, 1993 [PB93-195964] p 1372 N94-19052
Molecular dynamics modeling of the mechanical behavior of metallic multilayers [DE93-017972] p 1365 N94-19263
Low-aluminum-content iron-aluminum alloys [DE93-017862] p 1365 N94-19274
Microstructure of the interfacial zone around aggregate particles in concrete [PB93-195790] p 1380 N94-19322
Ni-Al2O3 solid state binding: Elaboration, state of thermal constraints, mechanical behavior [ECL-92-31] p 1366 N94-19436
New aircraft materials and structures [MBB-LME-202-S-PUB-502-A] p 1319 N94-19496
Incology 908 database report: On process-structure-property relationship [DE93-017616] p 1366 N94-19546
Ceramic technology project data base [DE93-019360] p 1374 N94-19561
Picoindentation hardness measurements using atomic force microscopy [AD-A270877] p 1604 N94-19579
Advanced civil engineering materials based on inorganic polymers [AD-A270837] p 1374 N94-19600
Simulation of dynamic material response with the PAGOSA code [DE93-018285] p 1460 N94-19603
Structure and properties of polycarbonate alloys [ETN-93-95071] p 1375 N94-19611
Commercialization effort in support of electroslag-casting technology [DE93-017988] p 1366 N94-19733

MECHANICAL SHOCK
A finite element scheme for shock capturing [AD-A270182] p 1417 N94-18755

MEDIA
Your GAS experiment and the media or why does that other can get all of the publicity? p 1327 N94-19182

MEDICAL ELECTRONICS
Transcutaneous Analyte Measuring Methods (TAMM) [AD-A271387] p 1408 N94-19756

MEDICAL EQUIPMENT
Legacy of the X Ray Laser Program [DE93-019550] p 1442 N94-19554
Transcutaneous Analyte Measuring Methods (TAMM) [AD-A271387] p 1408 N94-19756

MELT SPINNING
Melt spinning study [NASA-CR-193823] p 1380 N94-19423

MELTING
Low-aluminum-content iron-aluminum alloys [DE93-017862] p 1365 N94-19274
Proceedings: International Symposium on Thermal Engineering and Science for Cold Regions [AD-A270636] p 1487 N94-19529

MELTING POINTS
Studies on gel electrolyte based on nitrile-butadiene copolymers [AD-A269450] p 1370 N94-18282

MELTS (CRYSTAL GROWTH)
Polymer technology publication. Series no. 14, 1993 [PB93-195964] p 1372 N94-19052

MEMBRANE STRUCTURES
Cellular and molecular level responses after radiofrequency radiation exposure, alone or in combination with x rays or chemicals [AD-A268189] p 1501 N94-17729
Benchmarking the QUAD4/TRIA3 element p 1450 N94-17837

MEMBRANES
Morphology of polymerized membranes on an amorphous substrate at molecular resolution by AFM [AD-A268760] p 1370 N94-18403
Intracellular physiology of the rat suprachiasmatic nucleus: Electrical properties, neurotransmission and effects of neuromodulators [AD-A268829] p 1505 N94-18538
Molten carbonate fuel cell networks: Principles, analysis, and performance [DE93-000281] p 1468 N94-18925

MEMORY
Cortical substrate of haptic representation [AD-A269583] p 1508 N94-18304
The identification of the computational significance of key neurobiological characteristics found in a number of telencephalic brain regions [AD-A269374] p 1505 N94-18407
Comparing performance on implicit memory tests [AD-A269900] p 1508 N94-18657
Visual perception of features and objects [AD-A269879] p 1508 N94-18682
First results with utile distinction memory for reinforcement learning [TR-446] p 1610 N94-19485

MEMORY (COMPUTERS)
Superconducting/semiconducting hybrids and advance memory concepts for superconducting electronics [AD-A268679] p 1397 N94-18312
An SEU immune logic family p 1398 N94-18342
Performance of defect-tolerant set-associative cache memories p 1398 N94-18346
An improved distributed arithmetic architecture p 1398 N94-18349
Low power signal processing research at Stanford p 1393 N94-18351
Technology, design, simulation, and evaluation for SEP-hardened circuits p 1399 N94-18352
Formal verification of an MMU and MMU cache p 1400 N94-18366
A programming paradigm for distributed-memory computers [DE93-018336] p 1524 N94-19024
Performance and scalability aspects of directory-based cache coherence in shared-memory multiprocessors [DE93-016442] p 1536 N94-19115
Static Computer Memory Integrity Testing (SCMIT): An experiment flown on STS-40 as part of GAS payload G-616 p 1325 N94-19169
Radiation hardened microprocessor for small payloads p 1327 N94-19184
Wide-address spaces: Exploring the design space [MEMO-INF-92-77] p 1537 N94-19219
Toward a high performance distributed memory climate model [DE93-019156] p 1494 N94-19298
PUMMA: Parallel Universal Matrix Multiplication Algorithms on distributed memory concurrent computers [DE93-019163] p 1538 N94-19299
Data-Machine Independence (DMI) [DE93-018008] p 1539 N94-19734

MENISCI
Finite element modeling of evaporation and condensation during sol-gel film and fiber formation [DE93-017655] p 1345 N94-17820

MENTAL PERFORMANCE
A method for cognitive task analysis [IZF-1992-B5] p 1508 N94-17967
Cognitive limitations in coordination in hierarchical information processing structures [AD-A268825] p 1616 N94-18535
Comparing performance on implicit memory tests [AD-A269900] p 1508 N94-18657
Research on man-machine productivity in aviation at Human Engineering Institute of Hangzhou University [AD-A269952] p 1512 N94-18673
Cognitive ability and whole-body rotation [IZF-1993-B-4] p 1510 N94-19440

MERCURY CADMIUM TELLURIDES
IR materials producibility [AD-A268849] p 1577 N94-18223

MESON-NUCLEON INTERACTIONS
Unitary (pi)(pi)N model of N* excitations in (pi)N and (gamma)N reactions [DE93-017422] p 1568 N94-18826
Eta-nucleon interaction and nuclear production of eta mesons [DE93-018469] p 1571 N94-19259

MESONS
Gauge unification of fundamental forces: The story of success [DE93-624813] p 1383 N94-17952
Beauty without charm in B-meson decays [PREPRINT-732] p 1565 N94-17972
Unitary (pi)(pi)N model of N* excitations in (pi)N and (gamma)N reactions [DE93-017422] p 1568 N94-18826
Investigation of physical structures and interactions at high energy [DE93-014444] p 1574 N94-18927

MESOSCALE PHENOMENA
The vertical distribution of heating in the tropical atmosphere [AD-A270452] p 1490 N94-18514
Diabatic forcing and initialization with assimilation of cloud and rain water in a forecast model: Methodology p 1491 N94-18603
Moist wind relationships p 1492 N94-18607
Initialization and assimilation of cloud and rainwater in a regional model p 1492 N94-18608
Preparation of data assimilation and model evaluation experiment data sets [AD-A269996] p 1498 N94-18665
JPRS report: Science and technology. Central Eurasia: Earth Sciences [JPRS-UES-93-004] p 1481 N94-19209

MESOSPHERE
Internal instability of nonparallel flow on an equatorial beta-plane [AD-A268927] p 1490 N94-18486

MESSAGE PROCESSING
Embedded Computer Performance Measurement (ECPM). Advanced avionics subsystems and technology multiprocessor ECPM software documentation [AD-A269921] p 1320 N94-18658
Efficient transparent optimistic rollback recovery for distributed application programs [AD-A268981] p 1522 N94-18696
Corporate Information Management (CIM) report on the simulation processes, version 2.0 [AD-A269119] p 1617 N94-18770
Experience in implementing a parallel file system [DE93-012840] p 1536 N94-19188
Message passing in PUMA [DE93-012841] p 1537 N94-19206
Abstracting inter-object communications using composition filters [MEMO-INF-92-78] p 1528 N94-19220
Automated processing of military messages according to ADatP-3 [FEL-92-A044] p 1393 N94-19798

MESSAGES
Securing electronic mail: The risks and future of electronic mail [DE93-017187] p 1383 N94-17994
Message passing in PUMA [DE93-012841] p 1537 N94-19206

METABOLISM
Metabolic changes and hemodynamic dysfunction following hypothermic shock [AD-A269780] p 1506 N94-18598
Microgravity research in plant biological systems: Realizing the potential of molecular biology p 1503 N94-19216
A study of the effect of hydrocarbon structure on the induction of male rat nephropathy and metabolic structure [AD-A270969] p 1504 N94-19789

METABOLITES
Nuclear Medicine Program [DE93-013896] p 1504 N94-17699

METAL AIR BATTERIES
Mechanically refuelable zinc/air electric vehicle cells [DE93-016446] p 1394 N94-17770

METAL BONDING
Metal/ceramic interfaces: Relationships between structure and chemistry [AD-A268792] p 1369 N94-18188
High performance YBCO films [AD-A269090] p 1599 N94-18719

Joining and Adhesion of Advanced Inorganic Materials Symposium
[AD-A269748] p 1342 N94-18720
Binding of copper to nanocavity surfaces in silicon
[DE93-019073] p 1364 N94-19080

METAL COATINGS
Thermal analysis of coatings and substrate materials during a disruption in fusion reactors
[DE93-017688] p 1588 N94-18971

METAL COMBUSTION
Metal slurry droplet and spray combustion
[AD-A269648] p 1349 N94-18736

METAL CRYSTALS
Photorefractive tungsten bronze crystals for optical computing
[AD-A268859] p 1596 N94-18320
The effect of crystallographic orientation on the performance of single crystal tungsten subscale penetrators
[AD-A268988] p 1597 N94-18468

METAL FATIGUE
Factors which affect fatigue strength of fasteners
[DE93-017272] p 1453 N94-18084
Development of the microstructure based stochastic life prediction models
[AD-A269880] p 1454 N94-18683
Fatigue resistant Ti3Al composites
[AD-A270305] p 1341 N94-18692
Development of the microstructure based stochastic life prediction model
[AD-A269742] p 1361 N94-18742
Intelligent materials systems and structures. Part 4: The influence of thermomechanical loading on the life of shape memory alloys
[PB93-195923] p 1363 N94-18952

METAL FIBERS
Aerosol filtration with steel fiber filters
[DE93-016990] p 1380 N94-18710

METAL FILMS
Superhardness effect in Au/Ni multilayers
[DE93-016444] p 1357 N94-17860
Infrared detection with high-(Tc bolometers and response of Nb tunnel junctions to picosecond voltage pulses
[DE93-016963] p 1595 N94-17989
Metal Film Surface Plasmon Resonance (MFSPR) fibre couplers
[AD-A268871] p 1579 N94-18635

METAL FUELS
Aluminum powder/water reaction ignited by electrical pulsed power
[AD-A269223] p 1376 N94-17840

METAL HYDRIDES
Structural stability of 1100 C heated Pd/k during absorption cycling in protium
[DE93-016270] p 1346 N94-18048

METAL IONS
Modified aequorin shows increased bioluminescence activity
[AD-A268774] p 1347 N94-18185
Novel electrochemical materials prepared by sol-gel chemistry
[AD-A269060] p 1578 N94-18405
Kinetic studies of electrochemical generation of Ag(II) ion and catalytic oxidation of selected organics
[DE93-016601] p 1352 N94-19240
Tetravalent chromium (Cr(4+)) as laser-active ion for tunable solid-state lasers
[NASA-CR-194529] p 1441 N94-19369

METAL JOINTS
Wetting behavior of alternative solder alloys
[DE93-016730] p 1359 N94-18127

METAL MATRIX COMPOSITES
Metals 2000
[DE93-016761] p 1355 N94-17752
Strength optimization of C/Al metal matrix composites produced from prepregs
[DLR-FB-92-39] p 1340 N94-18122
NSWCWODET participation in Space Shuttle mission STS-46
[AD-A268875] p 1332 N94-18321
Fatigue resistant Ti3Al composites
[AD-A270305] p 1341 N94-18692
Wettability and reaction kinetics in metal matrix composites
[AD-A270377] p 1342 N94-18704
Bibliography on ceramic matrix composites and reinforcing whiskers, platelets, and fibers, 1970-1990
[AD-A270139] p 1371 N94-18750
The applications of modified metals in the construction industry
[VTT-TIED-1329] p 1365 N94-19374
Residual strength predictions for fibre metal laminates: The R-curves approach
[LR-717] p 1344 N94-19666
Damage accumulation in advanced metal matrix composites under thermal cycling/creep loadings
[AD-A271207] p 1344 N94-19720
Micromechanics of interfaces in metal matrix composites
[AD-A271012] p 1345 N94-19776

METAL OXIDE SEMICONDUCTORS
Development of analog watch with minute repeater
p 1429 N94-18043
ARPA/CSTO rapid VLSI implementation
[AD-A269170] p 1403 N94-18695
Design of power electronics for TVC EMA systems
[NASA-CR-193839] p 1407 N94-19642

METAL OXIDES
Catalytic hydrocarbon reactions over supported metals
[DE93-018168] p 1345 N94-17808
Surface phases and their influence on metal-oxide interfaces
[DE93-019931] p 1601 N94-19020
Electrocatalysts for oxygen electrodes
[DE93-040446] p 1354 N94-19653

METAL PARTICLES
Metal slurry droplet and spray combustion
[AD-A269648] p 1349 N94-18736
Atomic-scale friction measurements using friction force microscopy. Part 2: Application to magnetic media
[AD-A270759] p 1447 N94-19767

METAL PLATES
Metallurgical evaluation of SRAM 2/SRAM A program mer base plates
[DE93-018689] p 1364 N94-19100
The fire resistance of profiled thin steel sheet structures
[VTT-TIED-1320] p 1380 N94-19373

METAL POWDER
Aluminum powder/water reaction ignited by electrical pulsed power
[AD-A269223] p 1376 N94-17840
Field emission cathode and vacuum microelectronic microwave amplifier development
[AD-A269526] p 1403 N94-18639

METAL PROPELLANTS
Aluminum powder/water reaction ignited by electrical pulsed power
[AD-A269223] p 1376 N94-17840

METAL SHEETS
The fire resistance of profiled thin steel sheet structures
[VTT-TIED-1320] p 1380 N94-19373
Formulation and identification of the anisotropic laws for thin sheets drawing
[ECL-92-55] p 1365 N94-19400

METAL SURFACES
Mechanical properties of excimer laser modified titanium surfaces
[DE93-012663] p 1358 N94-17875
Process for applying high application-temperature coating to heat-sensitive aluminum alloys
[AD-D015823] p 1368 N94-17905
Surface phases and their influence on metal-oxide interfaces
[DE93-019931] p 1601 N94-19020
Binding of copper to nanocavity surfaces in silicon
[DE93-019073] p 1364 N94-19080
Surface species in tribology
[AD-A270970] p 1446 N94-19754

METAL VAPOR LASERS
The copper-pumped dye laser system at Lawrence Livermore National Laboratory
[DE93-014429] p 1435 N94-17723
Safety approaches for high power modular laser operation
[DE93-017213] p 1435 N94-17759
Laser materials processing applications at Lawrence Livermore National Laboratory
[DE93-017976] p 1437 N94-18093
Cutting and drilling studies using high power visible lasers
[DE93-019149] p 1441 N94-19294

METAL VAPORS
Bench-scale screening tests for a boiling sodium-potassium alloy solar receiver
[DE93-018512] p 1469 N94-19040

METAL WORKING
Atlas of formability: Ultimet
[AD-A268352] p 1355 N94-17767
Atlas of formability: HAYNES 556
[AD-A268354] p 1356 N94-17768
Atlas of formability: HAYNES 188
[AD-A268355] p 1356 N94-17769
Atlas of formability: NICKELVAC K-500
[AD-A268351] p 1356 N94-17772
Atlas of formability: Haynes 230
[AD-A268325] p 1356 N94-17788
Atlas of formability: INCONEL 718
[AD-A268350] p 1356 N94-17789
Atlas of formability: Hastelloy C-22
[AD-A268324] p 1356 N94-17796
Atlas of formability: Permalloy - 80 flow stress curves
[AD-A268263] p 1356 N94-17801
Atlas of formability: Nickelvac C-276
[AD-A268264] p 1357 N94-17802
Atlas of formability: Ti-6Al-4V ELI
[AD-A268300] p 1357 N94-17803
Atlas of formability: ALLVAC 718
[AD-A268304] p 1357 N94-17804
Atlas of formability: Waspaloy
[AD-A268323] p 1593 N94-17805
Formulation and identification of the anisotropic laws for thin sheets drawing
[ECL-92-55] p 1365 N94-19400

METAL-GAS SYSTEMS
Effect of oxygen concentration and ordering on vanadium-oxygen alloy vibrational spectra
[DE93-627003] p 1355 N94-17692
Report of the 1991 Workshop on Particle-Material Interactions for Fusion Research
[DE93-788393] p 1573 N94-18156

METAL-METAL BONDING
Beryllium processing technology review for applications in plasma-facing components
[DE93-018396] p 1363 N94-19028

METALLIZING
Development of large-area monolithically integrated silicon-film photovoltaic modules
[DE93-010037] p 1464 N94-17731
RF vacuum microelectronics
[AD-A270003] p 1403 N94-18667
High pressure metallization of Mott Insulators: Magnetic, structural and electronic properties
[DE93-018295] p 1404 N94-18805
Pressure induced metallization of the Mott Insulator 6(sub 2)
[DE93-018296] p 1600 N94-18969
Metallization and charge-transfer gap closure of transition-metal iodides under pressure
[DE93-040301] p 1353 N94-19538

METALLOGRAPHY
Microstructural analysis of solid-state resistance welds
[DE93-017295] p 1443 N94-17761
Dynamical behavior of octahedrite from the Henbury meteorite
[DE93-018834] p 1627 N94-19339

METALORGANIC CHEMICAL VAPOR DEPOSITION
Growth of structures for integrated optoelectronic devices
[AD-A269014] p 1598 N94-18527
Single source precursors for the OMCVD of 3/5 compound semiconductors
[AD-A271147] p 1606 N94-19739
MOCVD-grown InGaAsP heterostructure diode lasers
[AD-A270848] p 1606 N94-19769

METALS
Metals 2000
[DE93-016761] p 1355 N94-17752
Lightweight materials for transportation: Program plan
[DE93-017381] p 1340 N94-18087
A review of the stages of work hardening
[DE93-016456] p 1359 N94-18114
Modified aequorin shows increased bioluminescence activity
[AD-A268774] p 1347 N94-18185
A comparison of wet and dry scrubbing systems for control of metals and dioxin/furan emissions from incinerators
[DE93-017446] p 1474 N94-18502
Self-organized criticality and the Barkhausen effect in amorphous and polycrystalline metals
[AD-A269817] p 1361 N94-18735
Diamond brazed to a metal
[AD-D015877] p 1371 N94-18746
High dose effects in neutron irradiated face-centered cubic metals
[DE93-017671] p 1364 N94-19043
An ab initio Monte Carlo study of low energy positron and electron implantation in elemental metals and multilayers
[DE93-019847] p 1603 N94-19541

METASTABLE STATE
The microstructural mechanism of electromigration failure in narrow interconnects of Al alloys
[DE93-018598] p 1365 N94-19282

METATHESIS
Strained ring energetic binders
[AD-A269056] p 1377 N94-18491

METEOR TRAILS
Meteor burst communications improvement study
[AD-A270866] p 1393 N94-19793

METEORITE COLLISIONS
Search for lunar water ice in cometary impact craters
[AD-A270130] p 1627 N94-18877

METEORITIC COMPOSITION
Dynamical behavior of octahedrite from the Henbury meteorite
[DE93-018834] p 1627 N94-19339
METEOROID SHOWERS
Meteor burst communications improvement study
[AD-A270866] p 1393 N94-19793
METEOROLOGICAL INSTRUMENTS
A rugged, low-cost advanced data acquisition system for field test projects
[DE93-010041] p 1615 N94-18334
METEOROLOGICAL PARAMETERS
Cloudiest year study: An analysis of the 3DNEPH and RTNEPH databases
[AD-A269403] p 1490 N94-18281
Eastern Europe: A climatological study
[AD-A269200] p 1493 N94-18883
Protocol for computation of surface boundary layer parameters used to determine soil moisture flux from meteorological data collected at LLNL, 1992-1993
[DE93-018906] p 1463 N94-19003
Pantex Plant Meteorological Monitoring Program
[DE93-018495] p 1493 N94-19127
Report of the Experts Meeting on Reference Climatological Stations (RCS) and National Climate Data Catalogues (NCC)
[WMO-TD-535] p 1494 N94-19312
Interactive Production Line (IPL) p 1495 N94-19704
METEOROLOGICAL RADAR
A technique for measuring winds in the lower atmosphere using incoherent Doppler lidar
[DE93-017163] p 1488 N94-17758
Boundary layer heat budgets from wind profiler/RASS data: A feasibility study
[DE93-013187] p 1489 N94-18052
SPNDL: A concept for a small satellite Doppler lidar wind sounder p 1327 N94-19181
Investigations of a coherent vector radar technique for the observation of the atmosphere near 10 GHz
[KFK-5068] p 1494 N94-19616
METEOROLOGICAL SATELLITES
Some potential errors in satellite wind estimates using the geostrophic approximation and the thermal wind
[AD-A269784] p 1491 N94-18599
SERCAA cloud analysis integration: Design concepts and interaction with cloud forecast models
[AD-A269104] p 1492 N94-18637
METEOROLOGICAL SERVICES
Integrated Terminal Weather System (ITWS)
[AD-A269884] p 1492 N94-18684
Organized track system: Air ways above the ocean
p 1495 N94-19702
Calamity weather: Environmental calamities and meteorology p 1495 N94-19703
Report of the Second CLICOM Experts Meeting
[WCDMP-19] p 1495 N94-19705
METEOROLOGY
Geography and meteorological studies in the Far East
[DE93-013563] p 1461 N94-17893
Cloud CCN feedback
[DE93-016878] p 1472 N94-17985
Overview of physical oceanographic measurements taken during the Mount Mitchell cruise to ROPME sea area
[DE93-018460] p 1497 N94-18494
An investigation of warm-cloud microphysics using a multi-component cloud model: Interactive effects of the aerosol spectrum
[AD-A270273] p 1493 N94-18812
Eastern Europe: A climatological study
[AD-A269200] p 1493 N94-18883
Pantex Plant Meteorological Monitoring Program
[DE93-018495] p 1493 N94-19127
A survey of current approaches to modelling of hydrological time-series with respect to climate variability and change
[WMO/TD-534] p 1463 N94-19435
Shape of wind gusts at a 130m tower at Wilhelmshaven (Germany)
[BER-BAND-B3] p 1494 N94-19503
Reports of the 1992 Synoptic Symposium
[KNMI-TR-151] p 1494 N94-19698
HIRLAM p 1494 N94-19699
The WAQUA/CSM-16 model p 1494 N94-19700
The wave forecasting model NEDWAM
p 1495 N94-19701
Calamity weather: Environmental calamities and meteorology p 1495 N94-19703
Interactive Production Line (IPL) p 1495 N94-19704
METHANATION
Novel catalysts for methane activation
[DE93-040630] p 1349 N94-18532
The carbon isotope biogeochemistry of (epsilon)CO2 production in a methanogenic marine sediment
p 1477 N94-19233
The carbon isotope biogeochemistry of methane production in anoxic sediments. 1: Field observations
p 1477 N94-19234
Factors that control the stable carbon isotopic composition of methane produced in an anoxic marine sediment p 1477 N94-19235
METHANE
Titanium carbon-hydrogen layers on decorative surfaces p 1375 N94-18010
Fundamental studies of the mechanism of catalytic reactions with catalysts effective in the gasification of carbon solids and the oxidative coupling of methane
[DE93-015262] p 1347 N94-18193
Novel catalysts for methane activation
[DE93-040630] p 1349 N94-18532
Growth, characterization and device development in monocrystalline diamond films
[AD-A270074] p 1599 N94-18797
CDIAC catalog of numeric data and computer model packages
[DE93-017675] p 1475 N94-18832
Land-use related sources of CO2, CH4 and N2O: Current global emissions and projections for the period 1990-2100
[PB93-194819] p 1475 N94-18949
The CAESAR project: Experimental and modeling investigations of methane reforming in a catalytically enhanced solar absorption receiver on a parabolic dish
[DE93-040203] p 1469 N94-19109
Selective methane oxidation over promoted oxide catalysts
[DE93-040002] p 1351 N94-19132
Selective methane oxidation over promoted oxide catalysts
[DE93-040001] p 1351 N94-19150
Carbon Isotope Biogeochemistry of Methane from Anoxic Sediments
[NASA-CR-194620] p 1477 N94-19231
Analysis of satellite-derived ozone and water vapor measurements
[NASA-CR-193810] p 1486 N94-19237
Faulted structure of the bottom simulating reflector on the Blake Ridge, western North Atlantic
[AD-A271289] p 1500 N94-19745
METHYL COMPOUNDS
Photodissociation studies of polyatomic free radicals
[AD-A270084] p 1350 N94-18799
METRIC SPACE
Differential geometry of CR-submanifolds of a normal almost para contact manifold
[DE93-624764] p 1545 N94-17793
Geometrical pattern learning
[DE93-017641] p 1542 N94-19007
Excursion theory of a finite set via resolvents
[REPT-93-19] p 1557 N94-19090
METROLOGY
Soft X Ray Projection Lithography. Organization of the 1993 photonics science optical meetings
[AD-A269159] p 1579 N94-18693
MEXICO
The Mexico City 1991 lidar measurements campaign
[DE93-019960] p 1478 N94-19272
MICA
The direct synthesis of organic and organometallic-containing MICA-type aluminosilicates
[DE93-019001] p 1373 N94-19321
MICHELSON INTERFEROMETERS
Suppression of backscatter and stray reflection induced phase noise in Michelson interferometers
[AD-D015809] p 1382 N94-17902
On the Michelson-Morley experiment
[DE93-629908] p 1608 N94-18268
Developmental testing of a prototype all-reflection Michelson interferometer
[AD-A269064] p 1430 N94-18406
MICROANALYSIS
Detection of single molecules in microspheres
[DE93-017776] p 1567 N94-18493
Atomic resolution electron energy loss spectroscopy in the scanning transmission electron microscope
[DE93-015334] p 1352 N94-19239
MICROCHANNELS
High- and low-temperature bonding techniques for microstructures
[DE93-017173] p 1595 N94-17992
Active neutral particle diagnostics for high temperature plasma
[DE93-788457] p 1586 N94-18214
Thermal stresses in the microchannel heatsink cooled by liquid nitrogen
[DE93-018660] p 1418 N94-18995
MICROCRACKS
Helium-induced weld degradation of HT-9 steel
[DE93-015981] p 1358 N94-17915
Initiation and growth of microcracks in high strength steel butt welds
[AD-A268751] p 1454 N94-18466
Process relationship as influenced by carbonization rate
[AD-A269680] p 1341 N94-18572
A numerical analysis of crack growth in brittle microcracking composites
[DE93-011562] p 1343 N94-18914
MICROELECTRONICS
Aerogels for microelectronic applications: Fast, inexpensive, and light as air
[DE93-017170] p 1395 N94-17882
Silicon micro-actuator p 1408 N94-18017
RF vacuum microelectronics
[AD-A269454] p 1396 N94-18284
Update on parts SEE susceptibility from heavy ions
[AD-A268735] p 1596 N94-18316
Field emission cathode and vacuum microelectronic microwave amplifier development
[AD-A269526] p 1403 N94-18639
RF vacuum microelectronics
[AD-A270003] p 1403 N94-18667
Engineering research, development and technology thrust area report, FY92
[DE93-016334] p 1632 N94-18856
Integrated circuits: Resistless processing simplifies production and cuts costs
[DE93-018069] p 1405 N94-18941
Optoelectronic packaging: A review
[DE93-040059] p 1515 N94-19535
Simulation of the behavior of micro-electronic capacitive pressure sensors
[LAAS-93190] p 1434 N94-19659
MICROGRAVITY
Spacelab 3
[NASA-TM-108750] p 1323 N94-18849
Characterization of fluid physics effects on cardiovascular response to microgravity (G-572)
p 1323 N94-19163
MUZO flight experience with the programmable multizone furnace p 1324 N94-19167
Space Applications Industrial Laser System (SAILS)
p 1325 N94-19173
Space Life Sciences Research: The Importance of Long-Term Space Experiments
[NASA-TM-4502] p 1502 N94-19210
Space research on organs and tissues
p 1503 N94-19214
A scientific role for Space Station Freedom: Research at the cellular level p 1503 N94-19215
Microgravity research in plant biological systems: Realizing the potential of molecular biology
p 1503 N94-19216
Life: Origin and evolution on Earth--How can we escape? p 1503 N94-19217
MICROGRAVITY APPLICATIONS
The first flight of the QUESTS GAS payload G-521
p 1325 N94-19170
MICROHARDNESS
Superhardness effect in Au/Ni multilayers
[DE93-016444] p 1357 N94-17860
Developing and understanding the high temperature behavior of niobium aluminides and niobium aluminide composites
[AD-A268874] p 1341 N94-18636
MICROINSTRUMENTATION
High- and low-temperature bonding techniques for microstructures
[DE93-017173] p 1595 N94-17992
MICROMACHINING
Fabrication process for cantilever beam micromechanical switches
[AD-A269716] p 1404 N94-18749
Cutting and drilling studies using high power visible lasers
[DE93-019149] p 1441 N94-19294
MICROMECHANICS
Fabrication process for cantilever beam micromechanical switches
[AD-A269716] p 1404 N94-18749
The intelligent processing of materials
[AD-A269250] p 1362 N94-18923
Computational mechanics of composite materials
[PB93-195782] p 1343 N94-19281
Subcritical crack growth in continuous-fiber reinforced ceramic composites
[DE93-018784] p 1343 N94-19335
Micromechanics of interfaces in metal matrix composites
[AD-A271012] p 1345 N94-19776
MICROMETERS
Proceedings of the 4th European Congress on Chronometry
[ETN-93-94633] p 1424 N94-18006

Development of ultrasonic motor and application to silent alarm analog quartz watch p 1425 N94-18016
MICROMOTORS
Electrostatic micrometers: Recent developments and perspectives of uses in clock and watch making p 1425 N94-18014
Piezo-electric motor: Perspectives and miniaturization p 1408 N94-18015
Silicon micro-actuator p 1408 N94-18017
Simulation of a quartz-clockwork p 1426 N94-18019
Electric measurement of Lavet motors p 1408 N94-18022
New current reduction system for watches with integrated current regulation motors p 1428 N94-18034
Some variation in the movement base of the ETA 251 series p 1428 N94-18035
MICROORGANISMS
Improving the biodegradative capacity of subsurface bacteria
[DE93-013171] p 1501 N94-18051
Microbial degradation of poly-b-esters: A mechanistic study, cellulose acetate biodegradability
[AD-A271368] p 1374 N94-19586
MICROPARTICLES
Detection of single molecules in microspheres
[DE93-017776] p 1567 N94-18493
Feasibility study: Monodisperse polymer particles containing laser-excitable dyes
[NASA-CR-194280] p 1373 N94-19402
MICROPHONES
Acoustic intensity measurements in the presence of low Mach number flow
[AD-A269995] p 1562 N94-18664
MICROPLASMAS
Rapid analysis of mixed waste samples via the optical emission from laser initiated microplasmas
[DE93-014563] p 1582 N94-17727
MICROPOROSITY
Modeling of the formation of microporosity in alloys
[DE93-017733] p 1364 N94-19044
MICROPROCESSORS
Some variation in the movement base of the ETA 251 series p 1428 N94-18035
Experience with custom processors in space flight applications p 1336 N94-18338
Simplified microprocessor design for VLSI control applications p 1400 N94-18359
Verification of VLSI designs p 1400 N94-18363
VLSI for high-speed digital signal processing
[AD-A270406] p 1404 N94-18706
Motorola MC68040 high-speed design using Altera EPM5000 erasable programmable logic devices
[DE93-017635] p 1523 N94-19006
VPU(tm) demonstration mission vicinity processor unit(tm) overview p 1325 N94-19171
Radiation hardened microprocessor for small payloads p 1327 N94-19184
On-line test methods of microprocessor based systems
[ETN-93-95006] p 1530 N94-19496
MICROSCOPES
Center-of-Excellence: Microlaser microscope
[DE93-040686] p 1442 N94-19658
Atomic-scale friction measurements using friction force microscopy. Part 2: Application to magnetic media
[AD-A270759] p 1447 N94-19767
MICROSCOPY
Morphology of polymerized membranes on an amorphous substrate at molecular resolution by AFM
[AD-A268760] p 1370 N94-18403
Tunneling microscopy of semiconductors
[AD-A270232] p 1600 N94-18904
Picoindentation hardness measurements using atomic force microscopy
[AD-A270877] p 1604 N94-19579
Atomic-scale friction measurements using friction force microscopy. Part 1: General principles and new measurement techniques
[AD-A270749] p 1446 N94-19678
Atomic-scale friction and microfriction of graphite and diamond using friction force microscopy
[AD-A270952] p 1605 N94-19679
Atomic-scale friction measurements using friction force microscopy. Part 2: Application to magnetic media
[AD-A270759] p 1447 N94-19767
MICROSEISMS
Macroseismic study of the Dour (Belgium) earthquakes of 22 March 1987 and of Gulpen (Belgium) 17 October 1988 p 1482 N94-18625
MICROSTRUCTURE
Modeling microstructural evolution and the mechanical response of superplastic materials
[DE93-014417] p 1355 N94-17711
Microstructural analysis of solid-state resistance welds
[DE93-017295] p 1443 N94-17761
Atlas of formability: Ultimet
[AD-A268352] p 1355 N94-17767
Atlas of formability: HAYNES 556
[AD-A268354] p 1356 N94-17768
Atlas of formability: HAYNES 188
[AD-A268355] p 1356 N94-17769
Atlas of formability: NICKELVAC K-500
[AD-A268351] p 1356 N94-17772
Atlas of formability: Nickelvac C-276
[AD-A268264] p 1357 N94-17802
Plastic anisotropy in MoSi2 single crystals
[DE93-012650] p 1594 N94-17874
Mechanical properties of excimer laser modified titanium surfaces
[DE93-012663] p 1358 N94-17875
High- and low-temperature bonding techniques for microstructures
[DE93-017173] p 1595 N94-17992
Microstructurally based thermomechanical fatigue lifetime model of solder joints for electronic applications
[DE93-016508] p 1452 N94-17995
Embrittlement of surface mount solder joints by hot solder-dipped, gold-plated leads
[DE93-017659] p 1358 N94-18003
Omega phase formation in shock-loaded zirconium
[DE93-018343] p 1595 N94-18162
Advanced in macrostatistical hydrodynamics
[DE93-018479] p 1410 N94-18270
Several fundamental issues in the mechanics of inelastic behavior
[AD-A269455] p 1453 N94-18285
Nanostructured materials: Mind over matter
[DE93-017690] p 1597 N94-18480
Fabrication and microstructural development of Ag-clad TIBa2Ca2Cu3O(x) tapes
[DE93-017407] p 1597 N94-18500
Research on stable, high-efficiency amorphous silicon multijunction modules
[DE93-010046] p 1467 N94-18518
Developing and understanding the high temperature behavior of niobium aluminides and niobium aluminide composites
[AD-A268874] p 1341 N94-18636
Development of the microstructure based stochastic life prediction models
[AD-A269880] p 1454 N94-18683
Development of the microstructure based stochastic life prediction models
[AD-A270453] p 1455 N94-18714
Development of the microstructure based stochastic life prediction model
[AD-A269742] p 1361 N94-18742
Fundamental concepts relating local atomic arrangements, deformation, and fracture of intermetallic alloys
[AD-A268745] p 1361 N94-18788
High pressure metallization of Mott Insulators: Magnetic, structural and electronic properties
[DE93-018295] p 1404 N94-18805
Morphology, deformation, and defect structures of TiCr2 in Ti-Cr alloys
[DE93-018332] p 1361 N94-18807
Effects of shock loading on a solid-solution strengthened superalloy
[DE93-018345] p 1362 N94-18809
Development of ductile Fe3Al-based aluminides
[DE93-017865] p 1362 N94-18938
Tensile properties of as-cast iron-aluminide alloys
[DE93-017852] p 1363 N94-18975
Modeling of single-crystal laser-weld microstructures
[DE93-017853] p 1445 N94-18976
Fabrication and characterization of high-T(sub c) tapes and coils made from Ag-clad Bi-2223 superconductors
[DE93-018615] p 1601 N94-18993
High dose effects in neutron irradiated face-centered cubic metals
[DE93-017671] p 1364 N94-19043
X ray studies of microstructures in semiconductor and superconducting materials
[DE93-040690] p 1601 N94-19056
Metallurgical evaluation of SRAM 2/SRAM A programmer base plates
[DE93-018689] p 1364 N94-19100
Fabrication, properties, and microstructures of high (Tc) tapes and coils made from Ag-clad Bi-2223 superconductor
[DE93-017405] p 1602 N94-19122
The microstructural mechanism of electromigration failure in narrow interconnects of Al alloys
[DE93-018598] p 1365 N94-19282
Analytical and experimental evaluation of joining silicon nitride to metal and silicon carbide to metal for advanced heat engine applications
[DE93-018128] p 1446 N94-19291
Cutting and drilling studies using high power visible lasers
[DE93-019149] p 1441 N94-19294
Microstructure of the interfacial zone around aggregate particles in concrete
[PB93-195790] p 1380 N94-19322
Dynamical behavior of octahedrite from the Henbury meteorite
[DE93-018834] p 1627 N94-19339
Role of pressure in the study of fullerenes
[DE93-018839] p 1602 N94-19340
Melt spinning study
[NASA-CR-193823] p 1380 N94-19423
Microstructure and texture control of fatigue in hydrogen and marine environments
[AD-A271277] p 1344 N94-19744
Damping in ferrous shape memory alloys
[AD-A271009] p 1366 N94-19775
MICROWAVE AMPLIFIERS
Plasma klystron amplifier
[AD-D015819] p 1395 N94-17903
Field emission cathode and vacuum microelectronic microwave amplifier development
[AD-A269526] p 1403 N94-18639
MICROWAVE ANTENNAS
Design and fabrication of a Multichannel Adaptive Optical Processor (MADOP)
[AD-A270004] p 1579 N94-18668
MICROWAVE ATTENUATION
Dispersion effects on millimeter wavelength attenuation efficiencies for a variety of fibers
[AD-A268992] p 1386 N94-18454
MICROWAVE CIRCUITS
High efficiency low cost monolithic module for SARSAT distress beacons
[NASA-CR-194234] p 1315 N94-18852
MICROWAVE EQUIPMENT
Engineering research, development and technology thrust area report, FY92
[DE93-016334] p 1632 N94-18856
MICROWAVE IMAGERY
Packaging, deployment, and panel design concepts for a truss-stiffened 7-panel precision deployable reflector with feed boom
[NASA-TM-109000] p 1333 N94-17765
Microwave (SSM/I) Estimates of the Precipitation Rate to Improve Numerical Atmospheric Model Forecasts
[NASA-CR-193566] p 1491 N94-18602
Physical retrieval of precipitation water contents from Special Sensor Microwave/Imager (SSM/I) data. Part 1: A cloud ensemble/radiative parameterization for sensor response (report version) p 1491 N94-18604
Physical retrieval of precipitation water contents from Special Sensor Microwave/Imager (SSM/I) data. Part 2: Retrieval method and applications (report version) p 1491 N94-18605
Atlas of SSM/I satellite ice concentration interpolated to operational ice model domains of the Arctic for 1992
[AD-A270306] p 1499 N94-18727
MICROWAVE OSCILLATORS
Optically controlled active impedance element and filters employing the same
[AD-D015863] p 1396 N94-18062
The gyrotron backward-wave-oscillator experiment --- final progress report
[AD-A268982] p 1403 N94-18452
MICROWAVE RADIOMETERS
Physical retrieval of precipitation water contents from Special Sensor Microwave/Imager (SSM/I) data. Part 1: A cloud ensemble/radiative parameterization for sensor response (report version) p 1491 N94-18604
MICROWAVE SCATTERING
Microwave scattering from TAE modes
[DE93-018170] p 1583 N94-17809
The split-step algorithm for microwave propagation modeling above a conducting surface
[FEL-92-A430] p 1390 N94-19447
Theoretical and experimental research on coherent microwave backscatter from the ocean
[AD-A271276] p 1500 N94-19743
MICROWAVE SENSORS
Physical retrieval of precipitation water contents from Special Sensor Microwave/Imager (SSM/I) data. Part 1: A cloud ensemble/radiative parameterization for sensor response (report version) p 1491 N94-18604
MICROWAVE SIGNATURES
The split-step algorithm for microwave propagation modeling above a conducting surface
[FEL-92-A430] p 1390 N94-19447
A comparison between several computer codes for calculations on microwave propagation
[FEL-92-A435] p 1390 N94-19449
MICROWAVE TRANSMISSION
The split-step algorithm for microwave propagation modeling above a conducting surface
[FEL-92-A430] p 1390 N94-19447

A comparison between several computer codes for calculations on microwave propagation
[FEL-92-A435] p 1390 N94-19449

MICROWAVES

Design of a tunable 4-MW free electron maser for heating fusion plasmas
[DE93-017172] p 1437 N94-18134

A study of the effects of high power pulsed 2450 MHz microwaves, ELF modulated microwaves, and ELF fields on human lymphocytes and selected cell lines
[AD-A269070] p 1505 N94-18294

High-power microwave breakdown of dielectric interfaces
[AD-A268844] p 1397 N94-18318

The gyrotron backward-wave-oscillator experiment --- final progress report
[AD-A268982] p 1403 N94-18452

General geometry PIC for MIMD computers
[AD-A269085] p 1534 N94-18767

Electron cyclotron resonance heating in the microwave tokamak experiment
[DE93-018083] p 1590 N94-19289

Optical frequency division using an optical parametric oscillator
[AD-A270847] p 1581 N94-19578

Quasi-optical transponder using FET's and patch antennas
[AD-A271339] p 1407 N94-19584

MID-OCEAN RIDGES

Faulted structure of the bottom simulating reflector on the Blake Ridge, western North Atlantic
[AD-A271289] p 1500 N94-19745

MIDAIR COLLISIONS

Aircraft accident report: Midair collision, Mitsubishi MU-2B-60, N74FB, and PIPER PA-32-301, N82419, Greenwood Municipal Airport, Greenwood, Indiana, 11 September 1992
[PB93-910406] p 1315 N94-19352

MIDDLE ATMOSPHERE

Analysis of satellite-derived ozone and water vapor measurements
[NASA-CR-193810] p 1486 N94-19237

MIE SCATTERING

Remote sensing of Earth terrain
[NASA-CR-194598] p 1464 N94-19681

MILITARY AIRCRAFT

Naval aviation: Consider all alternatives before proceeding with the F/A-18E/F
[AD-A269302] p 1305 N94-18279

JPRS report: Central Eurasia. Aviation and cosmonautics, no. 12, December 1992
[JPRS-UAC-93-006] p 1632 N94-19148

JPRS report: Central Eurasia: Aviation and cosmonautics, no. 11, November 1992
[JPRS-UAC-93-005] p 1632 N94-19208

MILITARY HELICOPTERS

Army Cockpit Delethalization Program (CDP)
[AD-A268990] p 1512 N94-18765

Research and design activities and the economic balance of MBB
[ETN-93-94909] p 1310 N94-19383

MILITARY OPERATIONS

Coastal Ocean Modeling Workshop
[AD-A268955] p 1497 N94-18393

A comparison of air force data systems
[AD-A269691] p 1616 N94-18575

Road march performance of special operations soldiers carrying various loads and load distributions
[AD-A269198] p 1512 N94-18882

Coordination of software-development activities among sites that are geographically separated
[DE93-019201] p 1524 N94-19076

MILITARY TECHNOLOGY

Military applications of high-accuracy frequency standards and clocks
[AD-A269303] p 1430 N94-18299

An investigation of methods for updating ionospheric scintillation models using topside in-situ plasma density measurements
[AD-A269872] p 1483 N94-18655

Utilization of Shuttle small payload accommodations in the DOD Space Test Program p 1326 N94-19180

MILKY WAY GALAXY

The 0.15 seconds near-infrared imaging of the central parsec of the galaxy
[MPE-PREPRINT-239] p 1621 N94-19415

MILLIMETER WAVES

Dispersion effects on millimeter wavelength attenuation efficiencies for a variety of fibers
[AD-A268992] p 1386 N94-18454

Millimeter wave reflectivity measurement system
[AD-A270008] p 1387 N94-18601

Optical properties of redispersed iron fibers measured at 94 GHz
[AD-A269739] p 1342 N94-18756

Environmental characterization for target acquisition. Report 3: New concepts for evaluating low-grazing angle radar measurements
[AD-A269956] p 1388 N94-18777

Quasi-optical transponder using FET's and patch antennas
[AD-A271339] p 1407 N94-19584

Experimental and theoretical investigation of broadband high-power windows for millimeter waves
[KFK-5157] p 1391 N94-19617

MIMD (COMPUTERS)

Distributed memory parallel computers and computational fluid dynamics p 1413 N94-18568

General geometry PIC for MIMD computers
[AD-A269085] p 1534 N94-18767

Optimal eigenvalue computation on distributed-memory MIMD multiprocessors
[DE93-018337] p 1535 N94-18808

Three-dimensional shock wave physics simulations with MIMD PAGOSA on massively parallel computers
[DE93-011682] p 1455 N94-18829

A massively parallel adaptive finite element method with dynamic load balancing
[DE93-012844] p 1536 N94-19161

MIMD massively parallel methods for engineering and science problems
[DE93-019409] p 1531 N94-19562

MINE DETECTORS

Constructing a reference event list for ARCESS
[AD-A269288] p 1481 N94-18297

MINERAL DEPOSITS

Mechanical modeling of the growth of salt structures
[DE93-015342] p 1596 N94-18243

MINERAL METABOLISM

Space research on organs and tissues
p 1503 N94-19214

MINERALS

In situ observation of radiation induced amorphization of crystals with apatite structure
[DE93-018450] p 1599 N94-18816

MINES (ORDNANCE)

Earth Penetration Radar Imaging System (EPRIS)
[DE93-019890] p 1391 N94-19542

MINIATURIZATION

Piezo-electric motor: Perspectives and miniaturization
p 1408 N94-18015

MINKOWSKI SPACE

Impulsive moving mirror model in a Schroedinger picture with impulse effect in a Banach space
[DE93-629864] p 1561 N94-18155

Impulsive moving mirror model and the stability of linear homogeneous differential equations with impulse effect in a Banach space
[DE93-629906] p 1549 N94-18200

MINORITY CARRIERS

Development of large-area monolithically integrated silicon-film photovoltaic modules
[DE93-010037] p 1464 N94-17731

Defect behavior of polycrystalline solar cell silicon
[DE93-018490] p 1468 N94-19016

MIR SPACE STATION

A stereoscopic vision system with applications to automated docking and tracking
[AD-A270754] p 1333 N94-19765

MIRRORS

Profile stabilization of tilt mode in a field reversed configuration
[DE93-016770] p 1583 N94-17753

Impulsive moving mirror model and the stability of Schroedinger equation with impulse effect in a Banach space
[DE93-629866] p 1548 N94-18196

Impulsive moving mirror model and impulsive differential equations in Banach space
[DE93-629867] p 1549 N94-18197

Impulsive moving mirror model and the stability of linear homogeneous differential equations with impulse effect in a Banach space
[DE93-629906] p 1549 N94-18200

Developmental testing of a prototype all-reflection Michelson interferometer
[AD-A269064] p 1430 N94-18406

Testing and evaluation of large-area heliostats for solar thermal applications
[DE93-018509] p 1467 N94-18520

Development of robust multilayer optics for use in high-peak power radiation environments
[DE93-018557] p 1580 N94-18931

Tetravalent chromium (Cr(4+)) as laser-active ion for tunable solid-state lasers
[NASA-CR-194529] p 1441 N94-19369

Synchrotron/crystal sample preparation
[NASA-CR-193837] p 1603 N94-19513

MISS DISTANCE

An empirical evaluation of five circular error probable estimation techniques and a method for improving them
[AD-A266528] p 1556 N94-18397

MISSILE ANTENNAS

Missile antenna pattern coordinate system and data formats
[AD-A269153] p 1385 N94-18260

MISSILE CONTROL

Military applications of high-accuracy frequency standards and clocks
[AD-A269303] p 1430 N94-18299

MISSILE DEFENSE

Corporate Information Management (CIM) report on the simulation processes, version 2.0
[AD-A269119] p 1617 N94-18770

MISSILE DETECTION

Super-resolution of multi-pixel and sub-pixel images for the SDI
[AD-A268537] p 1462 N94-18631

MISSILE STRUCTURES

Metals 2000
[DE93-016761] p 1355 N94-17752

MISSILE TRACKING

UVPI imaging from the LACE satellite: The Nihka rocket plume
[AD-A268456] p 1334 N94-18149

Super-resolution of multi-pixel and sub-pixel images for the SDI
[AD-A268537] p 1462 N94-18631

UVPI imaging from the LACE satellite: The Strypi rocket plume
[AD-A270967] p 1335 N94-19787

NPAC distributed-parallel system feasibility study
[AD-A270972] p 1539 N94-19790

MISSILE TRAJECTORIES

Missile antenna pattern coordinate system and data formats
[AD-A269153] p 1385 N94-18260

MISSILES

Missile antenna pattern coordinate system and data formats
[AD-A269153] p 1385 N94-18260

Two-dimensional boundary surfaces for axi-symmetric external transonic flows
[AD-A269678] p 1312 N94-18571

Dynamic response analysis of composite structural members during missile launch
[AD-A270023] p 1332 N94-18760

MISSION PLANNING

Human Transportation System (HTS) study: Executive summary
[NASA-TM-104780] p 1332 N94-18669

Human Transportation System (HTS) study, volume 1
[NASA-TM-104779] p 1332 N94-18670

The Navy tessellated spheroid map projection system: A comprehensive definition
[AD-A269989] p 1462 N94-18677

Spacelab 3
[NASA-TM-108750] p 1323 N94-18849

Cluster ground segment and mission operations
p 1330 N94-19636

The Cluster Joint Science Operations Centre
p 1331 N94-19639

MIXED OXIDES

Fabrication and microstructural development of Ag-clad TlBa2Ca2Cu3O(x) tapes
[DE93-017407] p 1597 N94-18500

MIXING

Analysis of supersonic flows using k-epsilon model and the RPLUS code: Progress towards high speed combustor analysis p 1411 N94-18551

MIXING CIRCUITS

Broadband IF matching for quasioptical mixers
[MPE-PREPRINT-240] p 1390 N94-19416

Quasi-optical transponder using FET's and patch antennas
[AD-A271339] p 1407 N94-19584

MIXING LAYERS (FLUIDS)

Studies on high pressure and unsteady flame phenomena: Revision
[AD-A269138] p 1348 N94-18257

The application of front tracking to the simulation of shock refractions and shock accelerated interface mixing
[DE93-018342] p 1419 N94-19025

The effects of initial conditions on the 3-D topology of temporally evolving wakes (ARI on 3-D bluff body wakes)
[AD-A271008] p 1423 N94-19774

MIXING LENGTH FLOW THEORY

On memory effects in turbulence
[DLR-FB-93-03] p 1409 N94-18124

MNEMONICS

Comparing performance on implicit memory tests
[AD-A269900] p 1508 N94-18657

MOBILITY
In situ observation of radiation induced amorphization of crystals with apatite structure
[DE93-018450] p 1599 N94-18816
MODAL RESPONSE
Improved omit set displacement recoveries in dynamic analysis p 1449 N94-17829
Dynamic characterization of a lightweight, highly maneuverable spacecraft using modal and finite element analyses
[DE93-018095] p 1335 N94-18942
MODULATION
Plasma klystron amplifier
[AD-D015819] p 1395 N94-17903
Advanced optical fiber communication systems
[AD-A269120] p 1577 N94-18254
Extrathalamic modulation of cortical function
[AD-A270869] p 1507 N94-19783
MODULATORS
Spatial light modulators and applications: Summaries of papers presented at the Spatial Light Modulators and Applications Topical Meeting
[AD-A269452] p 1577 N94-18283
High efficiency low cost monolithic module for SARSAT distress beacons
[NASA-CR-194234] p 1315 N94-18852
Spice modeling of a FET-switched induction accelerator cell
[DE93-018662] p 1575 N94-18996
MODULES
Research on stable, high-efficiency amorphous silicon multijunction modules
[DE93-010046] p 1467 N94-18518
Knowledge sources for an intelligent MCM analyzer
[AD-A269224] p 1542 N94-18887
MODULUS OF ELASTICITY
New test method to determine modulus of elasticity of rocket grain material
[AD-A269758] p 1377 N94-18758
Elastic properties of amorphous thin films studied by Rayleigh waves
[DE93-018375] p 1372 N94-19202
Molecular dynamics modeling of the mechanical behavior of metallic multilayers
[DE93-017972] p 1365 N94-19263
MOIRE EFFECTS
Steep geometric grating for use in moire interferometry
[AD-A268759] p 1453 N94-18328
MOIRE FRINGES
Steep geometric grating for use in moire interferometry
[AD-A268759] p 1453 N94-18328
MOIRE INTERFEROMETRY
Steep geometric grating for use in moire interferometry
[AD-A268759] p 1453 N94-18328
A comparative evaluation of in-plane shear test methods for laminated graphite-epoxy composites
[NASA-CR-193808] p 1456 N94-19095
MOISTURE CONTENT
Microwave (SSM/I) Estimates of the Precipitation Rate to Improve Numerical Atmospheric Model Forecasts
[NASA-CR-193566] p 1491 N94-18602
Physical retrieval of precipitation water contents from Special Sensor Microwave/Imager (SSM/I) data. Part 1: A cloud ensemble/radiative parameterization for sensor response (report version) p 1491 N94-18604
Physical retrieval of precipitation water contents from Special Sensor Microwave/Imager (SSM/I) data. Part 2: Retrieval method and applications (report version)
p 1491 N94-18605
Forecast model applications of retrieved three dimensional liquid water fields p 1492 N94-18606
MOLECULAR BEAM EPITAXY
Kinetic aspects of lattice mismatch in molecular beam epitaxial growth on planar and patterned substrates
[AD-A270424] p 1597 N94-18506
In-situ growth monitoring of molecular beam epitaxy processes
[AD-A269287] p 1598 N94-18616
Isolation mechanisms in III-V devices
[AD-A271197] p 1605 N94-19717
MOLECULAR BEAMS
Metal/ceramic interfaces: Relationships between structure and chemistry
[AD-A268792] p 1369 N94-18188
Flame structure studies of a lean 20-torr H2/N2O/Ar flame employing molecular beam mass spectrometry
[AD-A268889] p 1349 N94-18456
The Fourteenth Symposium on Molecular Beams
[AD-A268721] p 1568 N94-18787
Crossed molecular beam studies of atmospheric chemical reaction dynamics
[DE93-019246] p 1478 N94-19303
MOLECULAR BIOLOGY
The role of chemical inhibition of gap junctional intercellular communication in toxicology
[AD-A269251] p 1502 N94-18924
Microgravity research in plant biological systems: Realizing the potential of molecular biology
p 1503 N94-19216
MOLECULAR CLOUDS
The molecular environment of S106 IR
[MPE-PREPRINT-241] p 1622 N94-19417
MOLECULAR COLLISIONS
Femtosecond Fourier-transform spectroscopy of low-frequency intermolecular motions in weakly interacting liquids
[DE93-017312] p 1566 N94-18085
The quantum dynamics of electronically nonadiabatic chemical reactions
[NASA-CR-194309] p 1568 N94-18837
Calculation of molecular excitation rates
[NASA-CR-193782] p 1571 N94-19236
MOLECULAR DIFFUSION
Defects in GaAs bulk crystals and multi-layers caused by In diffusion
[DE93-016968] p 1595 N94-18054
MOLECULAR ELECTRONICS
Photosynthetic reaction centers as active molecular electronic components, phase 1
[AD-A271388] p 1503 N94-19757
MOLECULAR ENERGY LEVELS
The A((2)pi(sub u))-X((2)pi(sub g)) system of Br2(+) studied by velocity modulation spectroscopy
[USIP-93-04] p 1569 N94-18847
MOLECULAR EXCITATION
Experimental and theoretical investigation of surface chemistry induced by direct and indirect electronic excitation
[AD-A268846] p 1348 N94-18221
Vibrational dynamics in photoinduced electron transfer
[DE93-040874] p 1567 N94-18533
Nonlinear optical properties of molecules
[AD-A270199] p 1567 N94-18783
Calculation of molecular excitation rates
[NASA-CR-193782] p 1571 N94-19236
Unimolecular photodissociation dynamics of ketene (CH2CO): The singlet/triplet branching ratio and experimental observation of the vibrational level thresholds of the transition-state
[DE93-019252] p 1352 N94-19304
MOLECULAR GASES
Molecular and polymeric ceramic precursors
[DE93-040364] p 1372 N94-18891
MOLECULAR INTERACTIONS
Femtosecond Fourier-transform spectroscopy of low-frequency intermolecular motions in weakly interacting liquids
[DE93-017312] p 1566 N94-18085
The Fourteenth Symposium on Molecular Beams
[AD-A268721] p 1568 N94-18787
Supercritical thermodynamics of sulfur and nitrogen species
[DE93-041221] p 1610 N94-19670
MOLECULAR IONS
The Fourteenth Symposium on Molecular Beams
[AD-A268721] p 1568 N94-18787
The A((2)pi(sub u))-X((2)pi(sub g)) system of Br2(+) studied by velocity modulation spectroscopy
[USIP-93-04] p 1569 N94-18847
MOLECULAR OSCILLATIONS
Proton transfer dynamics and cluster ion fragmentation in phenol/ammonia cLusters
[AD-A269133] p 1348 N94-18256
MOLECULAR PHYSICS
Molecular dynamics modeling of the mechanical behavior of metallic multilayers
[DE93-017972] p 1365 N94-19263
MOLECULAR RELAXATION
Computational techniques for high-speed flows with viscous and chemical effects p 1412 N94-18560
Hydrolysis reaction and positronium decay in silica gels
[AD-A270028] p 1371 N94-18713
MOLECULAR STRUCTURE
X ray absorption spectroscopic studies of the active sites of nickel- and copper-containing metalloproteins
[DE93-017142] p 1347 N94-18059
Numerical methods for molecular dynamics
[DE93-018321] p 1566 N94-18179
Metal/ceramic interfaces: Relationships between structure and chemistry
[AD-A268792] p 1369 N94-18188
Morphology of polymerized membranes on an amorphous substrate at molecular resolution by AFM
[AD-A268760] p 1370 N94-18403
Mesoepitaxy: A universal route to oriented materials
[AD-A270437] p 1598 N94-18511
Molecular structure of low temperature form of triaminoguanidinium nitrate (TAGN)
[AD-A270409] p 1377 N94-18708
A numerical study of hybrid optimization methods for the molecular conformation problems
[DE93-017898] p 1569 N94-18985
Structure-property relationships in radical-cation (electron-donor molecule) and anion-based (including fullerides) organic superconductors and their use in the design of new materials
[DE93-018617] p 1601 N94-19022
Polymer films with enhanced dielectric properties
[AD-A271148] p 1375 N94-19740
Cooperative formation of inorganic-organic interfaces in the synthesis of silicate mesostructures
[AD-A271196] p 1375 N94-19742
MOLECULAR THEORY
Calculation of molecular excitation rates
[NASA-CR-193782] p 1571 N94-19236
MOLECULES
Experimental and theoretical investigation of surface chemistry induced by direct and indirect electronic excitation
[AD-A268846] p 1348 N94-18221
Detection of single molecules in microspheres
[DE93-017776] p 1567 N94-18493
MOLYBDENUM
Plastic anisotropy in MoSi2 single crystals
[DE93-012650] p 1594 N94-17874
MOLYBDENUM ALLOYS
Atlas of formability: Ultimet
[AD-A268352] p 1355 N94-17767
Bibliography on silicides
[AD-A270516] p 1374 N94-19532
MOMENT DISTRIBUTION
Error propagation equations and tables for estimating the uncertainty in high-speed wind tunnel test results
[DE93-018685] p 1311 N94-18275
MOMENTS OF INERTIA
Friction drive position transducer
[AD-D015851] p 1424 N94-17717
MOMENTUM TRANSFER
Transformation of energy and momentum due to Landau damping in space
[DE93-624921] p 1581 N94-17689
MONITORS
Measuring emittance using beam position monitors
[DE93-014470] p 1434 N94-17709
Solid-state, resistive hydrogen sensors for safety monitoring
[DE93-017769] p 1424 N94-17778
VPU(tm) demonstration mission vicinity processor unit(tm) overview p 1325 N94-19171
MONKEYS
Somatosensory responsiveness in behaving monkeys and human subjects
[AD-A268924] p 1501 N94-18231
Extrathalamic modulation of cortical function
[AD-A270869] p 1507 N94-19783
MONOCHROMATIZATION
Conical geometry for sagittal focusing as applied to x rays from synchrotrons
[DE93-017238] p 1593 N94-17760
MONOMOLECULAR FILMS
Nanofabrication by focused ion beam
[AD-A271290] p 1345 N94-19746
MONOTONE FUNCTIONS
Existence of a maximal solution for quasimonotone elliptic systems
[REPT-93-30] p 1550 N94-19153
Using geometric techniques to improve dynamic programming algorithms for the economic lot-sizing problem and extensions
[PB93-197556] p 1528 N94-19330
MONTE CARLO METHOD
Planning under uncertainty solving large-scale stochastic linear programs
[DE93-013920] p 1516 N94-17701
Direct Monte Carlo simulation of the chemical equilibrium composition of detonation products
[DE93-014559] p 1376 N94-17751
Heavy ion nuclear physics research
[DE93-018862] p 1565 N94-17776
Investigation of the relative abundance of heavy versus light nuclei in primary cosmic rays using underground muon bundles
[DE93-017601] p 1630 N94-17818
Criticality benchmark comparisons leading to cross-section upgrades
[DE93-017184] p 1556 N94-18073
Recent studies of short-range order in alloys: The Cowley theory revisited
[DE93-016416] p 1358 N94-18111
Diffusion in ordered alloys
[AD-A268232] p 1359 N94-18322

Simulation of emittance dilution in electron storage ring from Compton backscattering
[DE93-017611] p 1386 N94-18503
Bayesian model choice: Asymptotics and exact calculations
[AD-A269067] p 1557 N94-18516
Bayesian analysis of ARMA processes: Complete sampling based inference under full likelihoods
[AD-A269168] p 1557 N94-18694
Polarimetric statistics of electromagnetic waves scattered by distributed targets
[PB93-195907] p 1389 N94-18951
The PAPAGENO Partonic Monte-Carlo Program
[DE93-018524] p 1571 N94-19247
Single sided tomography of extremely large dense objects
[DE93-017993] p 1580 N94-19268
Sensitivity and uncertainty analysis of Markov reward models
[MEMO-INF-92-89] p 1559 N94-19386
An ab initio Monte Carlo study of low energy positron and electron implantation in elemental metals and multilayers
[DE93-019847] p 1603 N94-19541
Uncertainty versus interindividual variability
[DE93-018105] p 1559 N94-19549

MORPHOLOGY
Morphology of polymerized membranes on an amorphous substrate at molecular resolution by AFM
[AD-A268760] p 1370 N94-18403
Morphology, deformation, and defect structures of TiCr2 in Ti-Cr alloys
[DE93-018332] p 1361 N94-18807
A scientific role for Space Station Freedom: Research at the cellular level p 1503 N94-19215

MOSSBAUER EFFECT
Pressure induced metallization of the Mott Insulator 6(sub 2)
[DE93-018296] p 1600 N94-18969
Gamma scattering in condensed matter with high intensity Moessbauer radiation
[DE93-019461] p 1601 N94-19031

MOTION PERCEPTION
Overview of research in progress at the Center of Excellence
[NASA-CR-194329] p 1618 N94-19256
Pilot studies on object motion perception during linear self-motion after long duration centrifugation of human subjects
[IZF-1993-B-3] p 1510 N94-19439
Applications of motion estimation in image processing
[FEL-92-B356] p 1580 N94-19455
A non-homogeneous, spatio-temporal, wavelet multiresolution analysis and its application to the analysis of motion
[AD-A270621] p 1538 N94-19534

MOTION SICKNESS
The brain electrical activity in different G situations
[AERONAUTICA-ACTA-A-372-199]
p 1507 N94-19523

MOUNTAINS
The Mexico City 1991 lidar measurements campaign
[DE93-019960] p 1478 N94-19272

MOVING TARGET INDICATORS
Low-noise oscillators for airborne radar applications, revision 1
[AD-A269372] p 1403 N94-18471

MULTICHANNEL COMMUNICATION
Multichannel error correction code decoder
[NASA-TM-106331] p 1333 N94-19313

MULTIGRID METHODS
Numerical calculations of high lift flows using structured and unstructured methods p 1307 N94-18428
A multigrid acceleration technique for computing steady solutions to the equations of compressible flow
p 1412 N94-18559
Computational techniques for high-speed flows with viscous and chemical effects p 1412 N94-18560
Multigrid methods for flow transition in three-dimensional boundary layers with surface roughness
[NASA-CR-4540] p 1417 N94-18843
3D composite grids using Bezier curves and surfaces in component adaptive methods
[AD-A269188] p 1549 N94-18863
Multigrid for a groundwater flow problem
[REPT-93-29] p 1420 N94-19144

MULTIMEDIA
Information technology resources assessment
[DE93-015276] p 1613 N94-17894
Pegasus project description
[MEMO-INF-92-75] p 1536 N94-19159
Pegasus: Operating system support for distributed multimedia systems
[MEMO-INF-92-76] p 1536 N94-19160

MULTIPATH TRANSMISSION
Design and fabrication of a Multichannel Adaptive Optical Processor (MADOP)
[AD-A270004] p 1579 N94-18668
Generalized multichannel signal detection
[AD-A271385] p 1391 N94-19587

MULTIPHASE FLOW
Study of multi-phase flow characteristics in an MHD power train
[DE93-018570] p 1586 N94-18272
Transport phenomena and interfacial kinetics in multiphase combustion systems
[AD-A270202] p 1349 N94-18785

MULTIPHOTON ABSORPTION
Removing CFC's from the atmosphere with lasers: A second look
[DE93-017516] p 1473 N94-18101
Harmonic generation at high intensities
[DE93-018632] p 1572 N94-19283

MULTIPLE ACCESS
Communication in the presence of unknown interference
[AD-A271146] p 1392 N94-19738

MULTIPLEXING
VHF air/ground communications for air traffic control: A decision tree approach to system innovations, volume 2
[AD-A268632] p 1386 N94-18495
Specifying and proving communication closedness in protocols
[MEMO-INF-93-23] p 1390 N94-19267
Tandem queues with deterministic service times
[PB93-197465] p 1543 N94-19324

MULTIPOLES
Three dimensional multipole decomposition of fields
[DE93-018530] p 1389 N94-19053

MULTIPROCESSING (COMPUTERS)
SPROC: A multiple-processor DSP IC
p 1398 N94-18347
High-performance multiprocessor architecture for a 3-D lattice gas model p 1400 N94-18362
Parallelization of the Air Force Space Command (AFSPACECOM) satellite motion models
[AD-A269327] p 1334 N94-18470
A programming paradigm for distributed-memory computers
[DE93-018336] p 1524 N94-19024
The p4 Linda: A portable implementation of Linda
[DE93-017752] p 1535 N94-19046
Performance and scalability aspects of directory-based cache coherence in shared-memory multiprocessors
[DE93-016442] p 1536 N94-19115
Pegasus project description
[MEMO-INF-92-75] p 1536 N94-19159
Pegasus: Operating system support for distributed multimedia systems
[MEMO-INF-92-76] p 1536 N94-19160
Wide-address spaces: Exploring the design space
[MEMO-INF-92-77] p 1537 N94-19219
A multi-level data-flow architecture for signal and data processing applications
[DE93-041272] p 1539 N94-19588

MULTIPROGRAMMING
The p4 Linda: A portable implementation of Linda
[DE93-017752] p 1535 N94-19046

MULTISENSOR APPLICATIONS
Operator performance in pattern matching as a function of reference material structure
[AD-A269889] p 1509 N94-18686
Tracking with time-delayed data in multisensor systems
[AD-A271334] p 1391 N94-19582

MULTISTATIC RADAR
The accuracy of monostatic and bistatic radar imaging by range-Doppler-processing with and without motion compensation
[DLR-FB-93-07] p 1384 N94-18071
Statistical description of the bistatic radar cross section distributions for a right circular cylinder
[AD-A270001] p 1387 N94-18666

MULTIVARIABLE CONTROL
Active control of a multivariable system by way of polynomial neural networks: Computer simulation evaluations and laboratory experimental results
[AD-A270033] p 1541 N94-18790

MULTIVARIATE STATISTICAL ANALYSIS
Multivariate wavelet representations and approximations
[AD-A269350] p 1546 N94-17825
Active control of a multivariable system by way of polynomial neural networks: Computer simulation evaluations and laboratory experimental results
[AD-A270033] p 1541 N94-18790
A multivariate anthropometric method for crew station design
[AD-A270652] p 1513 N94-19531

MUONS
Investigation of the relative abundance of heavy versus light nuclei in primary cosmic rays using underground muon bundles
[DE93-017601] p 1630 N94-17818
Investigation of physical structures and interactions at high energy
[DE93-014444] p 1574 N94-18927
SSC detector muon sub-system beam tests
[DE93-018415] p 1569 N94-19013
The anomalous magnetic moment of the muon
[DE93-018932] p 1572 N94-19320
Energy loss measurement of cosmic ray muons
[KFK-5158] p 1631 N94-19504
Measurement of the energy of horizontal cosmic ray muons
[KFK-5163] p 1631 N94-19505
Measurements of cosmic ray muons with multi-wire proportional chambers with a prototype setup for KASCADE
[KFK-5173] p 1631 N94-19506
High rate resistive plate chambers: An inexpensive, fast, large area detector of energetic charged particles for accelerator and non-accelerator applications
[DE93-018664] p 1572 N94-19545

MUSCLES
Control of shoulder muscles during goal directed movements
[PB93-195139] p 1504 N94-18080
Space research on organs and tissues
p 1503 N94-19214

MUSCULAR FUNCTION
Evaluation of physiological and psychological impairment of human performance in cold stressed subjects
[AD-A268637] p 1506 N94-18632

MUSCULOSKELETAL SYSTEM
In vivo animal models of body composition in aging
[DE93-012527] p 1501 N94-17889

MUSEUMS
Pathfinder: Shuttle exhibit
[NASA-TM-109357] p 1333 N94-19071

MUSIC
Analysis, representation and processing of the instrumental gesture: Application to keyboard instruments
[ETN-93-94402] p 1519 N94-17977

N

N-TYPE SEMICONDUCTORS
Selective electrochemical wafer thinning for silicon characterization
[DE93-015083] p 1592 N94-17742
Silicon concentrator solar cell research
[DE93-018489] p 1468 N94-19015

NARROWBAND
On comparison and extensions of control methods for narrow-band disturbance rejection
[REPT-93-015] p 1540 N94-17922

NASA PROGRAMS
OSSA Information Systems Program
[NASA-TM-108774] p 1612 N94-17737
The 1994 NASA authorization, volume 2
[GPO-71-510] p 1620 N94-18842
National Boy Scout Jamboree
[NASA-TM-109367] p 1610 N94-18982
California Student Get Away Special Payload GAS-450
p 1324 N94-19164
The GAMCIT gamma ray burst detector
p 1324 N94-19168
The first flight of the QUESTS GAS payload G-521
p 1325 N94-19170
Marshall Space Flight Center 1989 annual chronology of events
[NASA-TM-109381] p 1633 N94-19486

NASA SPACE PROGRAMS
Human Transportation System (HTS) study: Executive summary
[NASA-TM-104780] p 1332 N94-18669
Human Transportation System (HTS) study, volume 1
[NASA-TM-104779] p 1332 N94-18670

NASTRAN
Design optimization studies using COSMIC NASTRAN
p 1450 N94-17834
The role of NASTRAN in the preliminary design cycle
p 1450 N94-17835
Benchmarking the QUAD4/TRIA3 element
p 1450 N94-17837

NATIONAL AIRSPACE SYSTEM
The FAA Technical Center Human Factors Laboratory information guide
[AD-A269343] p 1513 N94-18992

NATURAL GAS
Report to Congress: Comprehensive Program Plan for Advanced Turbine Systems
[DE93-016718] p 1467 N94-18475
EIA publications directory, 1992
[DE93-016833] p 1617 N94-18983
NATURAL LANGUAGE (COMPUTERS)
Employing knowledge resources in a new text planner architecture
[AD-A269669] p 1516 N94-17732
EXPECT: Intelligent support for knowledge base refinement
[AD-A269602] p 1612 N94-17745
Intelligent help facilities: Generating natural language descriptions with examples
[AD-A269555] p 1521 N94-18290
Automatic documentation generation: The interaction of text and examples
[AD-A269670] p 1616 N94-18570
Generating object descriptions: Intergrating examples with text
[AD-A269992] p 1522 N94-18680
Computer-assisted instruction and natural language systems
[MEMO-INF-92-86] p 1527 N94-19225
NATURAL LANGUAGE PROCESSING
Automatic documentation generation: The interaction of text and examples
[AD-A269670] p 1616 N94-18570
Feasibility study in linguistically motivated object-oriented conceptual design of information systems
[PB93-197754] p 1618 N94-19331
Non-well-foundedness and type freeness can unify the interpretation of functional application
[PB93-191849] p 1560 N94-19710
A real-time spoken-language system for interactive problem-solving, combining linguistic and statistical technology for improved spoken language understanding
[AD-A270901] p 1392 N94-19749
NAUTICAL CHARTS
The Navy tessellated spheroid map projection system: A comprehensive definition
[AD-A269989] p 1462 N94-18677
NAVIER-STOKES EQUATION
Finite element modeling of evaporation and condensation during sol-gel film and fiber formation
[DE93-017655] p 1345 N94-17820
Investigation of a matrix-model for the artificial dissipation in a cell vertex finite volume scheme for solving the Navier-Stokes equations
[DLR-FB-92-33] p 1409 N94-18076
Parabolized Navier-Stokes computation of surface heat transfer characteristics for supersonic and hypersonic KE projectiles
[AD-A268856] p 1410 N94-18391
Navier-Stokes computations of turbulent flow around high-lift configurations p 1306 N94-18420
Efficient simulation of incompressible viscous flow over multi-element airfoils p 1306 N94-18421
Navier-Stokes calculations on multi-element airfoils using a chimera-based solver p 1306 N94-18422
Numerical solution of the Navier-Stokes equations for high-lift configurations on structured composite grids
p 1306 N94-18423
Prediction of the high-lift performance of multi-element aerofoils using an unstructured Navier-Stokes solver
p 1307 N94-18427
Numerical calculations of high lift flows using structured and unstructured methods p 1307 N94-18428
Navier-Stokes simulation of flow field around a blown-flap high-lift system p 1307 N94-18429
An algebraic turbulence model for turbomachinery
p 1411 N94-18554
Variational approaches to CFD: Applications to potential Euler and Navier-Stokes equations
p 1413 N94-18565
Introduction to spectral methods: Application to the Stokes problem p 1413 N94-18566
An introduction to the modelling of turbulence
p 1414 N94-18579
Turbulence modeling for compressible flows and implementation in Navier-Stokes solvers
p 1416 N94-18597
Theoretical study and modelling of homogeneous turbulence under rotation for implantation in a code for solving Navier-Stokes equations
[ECL-93-05] p 1420 N94-19381
On the numerical analysis of nonlinear Galerkin methods: Spectral approximation and finite elements
[ETN-93-94900] p 1552 N94-19407
Numerical prediction of transition of the F-16 wing at supersonic speeds
[NASA-CR-194407] p 1312 N94-19433
Numerical investigation of the incompressible flow around a wing with a fixed spoiler
[ISL-R-109/91] p 1313 N94-19524
Navier-Stokes, dynamics and aeroelastic computations for vortical flows, buffet and flutter applications
[NASA-CR-194520] p 1313 N94-19621
NAVIGATION
Military applications of high-accuracy frequency standards and clocks
[AD-A269303] p 1430 N94-18299
NAVY
Coastal Ocean Modeling Workshop
[AD-A268955] p 1497 N94-18393
The Navy tessellated spheroid map projection system: A comprehensive definition
[AD-A269989] p 1462 N94-18677
Compilation of 1992 annual reports of the navy ELF communications system ecological monitoring program, volume 2
[AD-A269726] p 1388 N94-18751
NEAR INFRARED RADIATION
The 0.15 seconds near-infrared imaging of the central parsec of the galaxy
[MPE-PREPRINT-239] p 1621 N94-19415
NEAR WAKES
The effects of initial conditions on the 3-D topology of temporally evolving wakes (ARI on 3-D bluff body wakes)
[AD-A271008] p 1423 N94-19774
NEARSHORE WATER
Wind products for use in coastal wave and surge models
[AD-A269753] p 1497 N94-18414
NEEL TEMPERATURE
The low-temperature specific heat of CeCu2Ge2 at 0 and 9.5 kbar
[DE93-014914] p 1360 N94-18398
NEGATIVE ELECTRON AFFINITY
Characterization of diamond film nucleation and growth surface
[AD-A269400] p 1597 N94-18459
NEGATIVE FEEDBACK
The Lever oscillator for use in high resistance resonator applications
[DE93-017652] p 1404 N94-18827
NEGATIVE IONS
Oligomer and mixed-metal compounds, potential multielectron transfer catalysts
[DE93-013592] p 1350 N94-19017
NEODYMIUM LASERS
Analysis of neon soft x ray spectra from short-pulse laser-produced plasmas
[DE93-014420] p 1582 N94-17708
Pulsed power supply for Nova Upgrade
[DE93-019626] p 1441 N94-19307
NEON
Analysis of neon soft x ray spectra from short-pulse laser-produced plasmas
[DE93-014420] p 1582 N94-17708
NEPHANALYSIS
Cloudiest year study: An analysis of the 3DNEPH and RTNEPH databases
[AD-A269403] p 1490 N94-18281
SERCAA cloud analysis integration: Design concepts and interaction with cloud forecast models
[AD-A269104] p 1492 N94-18637
NEPTUNE (PLANET)
Detailed analysis of low energy plasma data under the Voyager Uranus data analysis program
[NASA-CR-193668] p 1628 N94-17842
Working group for planetary system nomenclature
[NASA-CR-194406] p 1626 N94-18841
Voyager's last encounter
[NASA-TM-109361] p 1628 N94-18957
NEPTUNE ATMOSPHERE
Voyager's last encounter
[NASA-TM-109361] p 1628 N94-18957
NEPTUNE SATELLITES
Voyager's last encounter
[NASA-TM-109361] p 1628 N94-18957
NERVES
Coupled neural-dendritic processes: Cooperative stochastic effects and the analysis of spike trains
[AD-A270041] p 1506 N94-18793
NETHERLANDS
Reports of the 1992 Synoptic Symposium
[KNMI-TR-151] p 1494 N94-19698
The WAQUA/CSM-16 model p 1494 N94-19700
NETWORK ANALYSIS
APLAC: An object-oriented analog circuit simulator and design tool. 6.1 reference manual
[PB93-187193] p 1396 N94-18091
Exact cost flow problems in acyclic networks
[REPT-93-030] p 1520 N94-18138
Specification and analysis of a high speed transport protocol
[AD-A268941] p 1386 N94-18449
Naval research reviews. Mixing enhancement for air-breathing propulsion. Non-axisymmetric jets increase mixing, volume 44 and volume 45
[AD-A268966] p 1521 N94-18543
Improved HF data network simulator, volume 1
[AD-A270953] p 1393 N94-19752
Improved HF data network simulator, software user's manual, volume 2
[AD-A270954] p 1393 N94-19753
NETWORK CONTROL
Models and building blocks for secure open systems
[FEL-92-B365] p 1619 N94-19457
Protocol service decomposition for high-performance networking
[AD-A270613] p 1538 N94-19533
Congestion/flow control and routing in data networks: A control-theoretic approach
[AD-A271121] p 1392 N94-19737
NEURAL NETS
An object-oriented environment for computer vision and pattern recognition
[DE93-017098] p 1517 N94-17867
Neural networks to classify speaker independent isolated words recorded in radio car environments
[REPT-93-013] p 1383 N94-17935
Application of the network discriminant function to learning
[AD-A268793] p 1540 N94-18189
Proceedings of the 3rd Workshop on Balloon-Borne Experiments with Superconducting Magnet Spectrometers
[DE93-788362] p 1630 N94-18219
Optical associative processors and directed graphs
[AD-A268881] p 1615 N94-18224
Preliminary structural design: Defining the design space
[AD-A268898] p 1317 N94-18227
Fast-training algorithm for hidden-layer forward-feed neural networks
[AD-A269253] p 1540 N94-18263
Cortical substrate of haptic representation
[AD-A269583] p 1508 N94-18304
Autonomous neural network controllers for adaptive material handling
[AD-A268908] p 1540 N94-18331
Optical computing. Organization of the 1993 Photonics Science Topical Meetings. Technical digest series, volume 7
[AD-A269025] p 1578 N94-18332
Low power signal processing research at Stanford
p 1393 N94-18351
Pulse-firing winner-take-all networks
p 1399 N94-18353
Training product unit neural networks with genetic algorithms p 1399 N94-18354
VLSI synthesis of digital application specific neural networks p 1399 N94-18355
Measurement selection for parametric IC fault diagnosis p 1399 N94-18356
The identification of the computational significance of key neurobiological characteristics found in a number of telencephalic brain regions
[AD-A269374] p 1505 N94-18407
Joint services electronics program
[AD-A269383] p 1403 N94-18638
Interaction of intense lasers and relativistic electron beams with solids, gases and plasmas
[AD-A269655] p 1439 N94-18737
Neutral networks: An NRL perspective
[AD-A269122] p 1541 N94-18773
Active control of a multivariable system by way of polynomial neural networks: Computer simulation evaluations and laboratory experimental results
[AD-A270033] p 1541 N94-18790
Coupled neural-dendritic processes: Cooperative stochastic effects and the analysis of spike trains
[AD-A270041] p 1506 N94-18793
Operational parameters of an opto-electronic neural network employing fixed planar holographic interconnects
[DE93-018795] p 1433 N94-19000
An innovative neural manufacturing concept
[DE93-017212] p 1527 N94-19238
Use of shape memory alloys in the robust control of smart structures
[AD-A270827] p 1366 N94-19594
Explorations of the practical issues of learning prediction-control tasks using temporal difference learning methods
[AD-A270836] p 1544 N94-19599
VLSI implementation of neuromorphic learning networks
[AD-A270825] p 1407 N94-19665

Transcutaneous Analyte Measuring Methods (TAMM)
[AD-A271387] p 1408 N94-19756
Applications of neural networks in fault detection of rotating machinery
[AD-A270755] p 1448 N94-19766

NEUROLOGY
Cortical substrate of haptic representation
[AD-A269583] p 1508 N94-18304
Strategies for enhancing catecholamine-mediated neurotransmission
[NASA-CR-193807] p 1506 N94-18862
Interdisciplinary training in life science (FY 1991 ASSERT)
[AD-A269220] p 1512 N94-18886

NEURONS
Somatosensory responsiveness in behaving monkeys and human subjects
[AD-A268924] p 1501 N94-18231
Cortical substrate of haptic representation
[AD-A269583] p 1508 N94-18304
Intracellular physiology of the rat suprachiasmatic nucleus: Electrical properties, neurotransmission and effects of neuromodulators
[AD-A268829] p 1505 N94-18538
Operational parameters of an opto-electronic neural network employing fixed planar holographic interconnects
[DE93-018795] p 1433 N94-19000

NEUROPHYSIOLOGY
Localization of figure background segregation mechanisms in primate visual cortex
[PB93-187961] p 1508 N94-18121
Somatosensory responsiveness in behaving monkeys and human subjects
[AD-A268924] p 1501 N94-18231
Cortical substrate of haptic representation
[AD-A269583] p 1508 N94-18304
Intracellular physiology of the rat suprachiasmatic nucleus: Electrical properties, neurotransmission and effects of neuromodulators
[AD-A268829] p 1505 N94-18538
Strategies for enhancing catecholamine-mediated neurotransmission
[NASA-CR-193807] p 1506 N94-18862

NEUROTRANSMITTERS
Intracellular physiology of the rat suprachiasmatic nucleus: Electrical properties, neurotransmission and effects of neuromodulators
[AD-A268829] p 1505 N94-18538
Strategies for enhancing catecholamine-mediated neurotransmission
[NASA-CR-193807] p 1506 N94-18862

NEUTRAL BEAMS
Active neutral particle diagnostics for high temperature plasma
[DE93-788457] p 1586 N94-18214

NEUTRAL CURRENTS
Weak neutral currents and collapse initiated supernova
[DE93-018652] p 1627 N94-19284

NEUTRAL GASES
Radiative divertor modeling studies
[DE93-018092] p 1590 N94-19290

NEUTRAL PARTICLES
Active neutral particle diagnostics for high temperature plasma
[DE93-788457] p 1586 N94-18214
Exponential characteristic spatial quadrature for discrete ordinates neutral particle transport in two-dimensional cartesian coordinates
[AD-A270458] p 1554 N94-19671

NEUTRINO BEAMS
High energy physics at Tufts University
[DE93-018299] p 1575 N94-19023

NEUTRINOS
Neutrino masses in superstring derived standard-like models
[DE93-624802] p 1565 N94-17951
Neutrino mass
[DE93-018467] p 1567 N94-18269
Inverse neutrinoless double (beta)-decay at the NLC?
[DE93-017397] p 1568 N94-18825
Investigation of physical structures and interactions at high energy
[DE93-014444] p 1574 N94-18927
Weak neutral currents and collapse initiated supernova
[DE93-018652] p 1627 N94-19284

NEUTRON ACTIVATION ANALYSIS
Development and evaluation of alternative radioanalytical methods, including mass spectrometry for marine materials
[DE93-625117] p 1345 N94-17691

NEUTRON COUNTERS
Heavy ion nuclear physics research
[DE93-018862] p 1565 N94-17776
LAHET calculations for accelerator neutron production
[DE93-016518] p 1570 N94-19120
Thermal neutron multiplicity measurements using the pyrochemical multiplicity counter at Lawrence Livermore National Laboratory
[DE93-018538] p 1571 N94-19278

NEUTRON CROSS SECTIONS
Criticality benchmark comparisons leading to cross-section upgrades
[DE93-017184] p 1556 N94-18073
Computer codes for checking, plotting and processing of neutron cross-section covariance data and their application
[DE93-018459] p 1570 N94-19129

NEUTRON DIFFRACTION
Phase separation and ordering process in Al-Li alloys studied by small-angle neutron scattering and neutron diffraction
[DE93-016750] p 1358 N94-17947
Performance of the Amorphous Materials Diffractometer GLAD at IPNS
[DE93-017746] p 1430 N94-18481

NEUTRON DISTRIBUTION
Thermal neutron multiplicity measurements using the pyrochemical multiplicity counter at Lawrence Livermore National Laboratory
[DE93-018538] p 1571 N94-19278

NEUTRON IRRADIATION
Charpy impact toughness of martensitic steels irradiated in FFTF: Effect of heat treatment
[DE93-015960] p 1450 N94-17848
Effects of irradiation temperature on embrittlement of nuclear pressure vessel steels
[DE93-015428] p 1359 N94-18245
Evaluation of fiber optic performance in the ACRR
[DE93-018515] p 1580 N94-18970
High dose effects in neutron irradiated face-centered cubic metals
[DE93-017671] p 1364 N94-19043

NEUTRON SCATTERING
Polaron tunneling in high-temperature superconductors
[DE93-016880] p 1593 N94-17754
Phase transitions and neutron scattering
[DE93-016748] p 1594 N94-17866
Phase separation and ordering process in Al-Li alloys studied by small-angle neutron scattering and neutron diffraction
[DE93-016750] p 1358 N94-17947
The use of chopper spectrometers for cold-to-epithermal neutron scattering at IPNS
[DE93-017798] p 1598 N94-18531
T violating neutron spin rotation asymmetry
[DE93-018470] p 1570 N94-19126

NEUTRON SOURCES
Heavy ion nuclear physics research
[DE93-018862] p 1565 N94-17776
The use of chopper spectrometers for cold-to-epithermal neutron scattering at IPNS
[DE93-017798] p 1598 N94-18531
Generalized energy principle for flute perturbations in axisymmetric mirror machines
[DE93-019399] p 1589 N94-19037
LAHET calculations for accelerator neutron production
[DE93-016518] p 1570 N94-19120

NEUTRON SPECTRA
LAHET calculations for accelerator neutron production
[DE93-016518] p 1570 N94-19120

NEUTRON SPECTROMETERS
Phase transitions and neutron scattering
[DE93-016748] p 1594 N94-17866
The use of chopper spectrometers for cold-to-epithermal neutron scattering at IPNS
[DE93-017798] p 1598 N94-18531

NEUTRON STARS
Evolution of r-process elements in the hot supernova bubble
[DE93-017169] p 1624 N94-17897

NEUTRONS
Heavy ion nuclear physics research
[DE93-018862] p 1565 N94-17776
Characteristics and pulsed radiation response of non-ideal quartz shock stress gauges
[DE93-017628] p 1424 N94-17999
Neutron-induced collision cascade mixing in Nb/V superlattices
[DE93-018575] p 1600 N94-18933
LAHET calculations for accelerator neutron production
[DE93-016518] p 1570 N94-19120
T violating neutron spin rotation asymmetry
[DE93-018470] p 1570 N94-19126

NEWTON THEORY
Essential shift: Scientific revolution in the 20th century
[AD-A270810] p 1610 N94-19663

NICKEL
X ray absorption spectroscopic studies of the active sites of nickel- and copper-containing metalloproteins
[DE93-017142] p 1347 N94-18059
Environmentally assisted cracking of nickel anode substrates in Li/SOCl2 cells: An engineering approach
[DE93-015130] p 1405 N94-18928
Molecular dynamics modeling of the mechanical behavior of metallic multilayers
[DE93-017972] p 1365 N94-19263
Ni-Al2O3 solid state binding: Elaboration, state of thermal constraints, mechanical behavior
[ECL-92-31] p 1366 N94-19436

NICKEL ALLOYS
Atlas of formability: Ultimet
[AD-A268352] p 1355 N94-17767
Atlas of formability: HAYNES 556
[AD-A268354] p 1356 N94-17768
Atlas of formability: HAYNES 188
[AD-A268355] p 1356 N94-17769
Atlas of formability: NICKELVAC K-500
[AD-A268351] p 1356 N94-17772
Atlas of formability: Haynes 230
[AD-A268325] p 1356 N94-17788
Atlas of formability: Nickelvac C-276
[AD-A268264] p 1357 N94-17802
Atlas of formability: ALLVAC 718
[AD-A268304] p 1357 N94-17804
Summary of work on coatings and claddings for fossil energy applications
[DE93-017005] p 1367 N94-17881
Evaluation of the nickel release by horological products p 1367 N94-18009
Diffusion in ordered alloys
[AD-A268232] p 1359 N94-18322
Effects of shock loading on a solid-solution strengthened superalloy
[DE93-018345] p 1382 N94-18809
Environmental degradation of Alloy 600 and welded filler metal EN82 in an elevated temperature aqueous environment
[DE93-018049] p 1363 N94-18940
Intelligent materials systems and structures. Part 4: The influence of thermomechanical loading on the life of shape memory alloys
[PB93-195923] p 1363 N94-18952
Bibliography on silicides
[AD-A270516] p 1374 N94-19532
Incology 908 database report: On process-structure-property relationship
[DE93-017616] p 1366 N94-19546

NICKEL COATINGS
Superhardness effect in Au/Ni multilayers
[DE93-016444] p 1357 N94-17860

NIGHT VISION
Human integration evaluation of three helmet systems
[AD-A271320] p 1513 N94-19570
Electro-optics display research, test, and evaluation laboratory program
[AD-A270947] p 1408 N94-19751

NIOBIUM
Superconductivity and magnetism in niobium doped YBa2Cu3O7 related high-(Tc) ceramics
[DE93-018086] p 1601 N94-19049
Total hemispherical emittance of Niobium-1 percent zirconium fuel cladding for the SP-100 space reactor
[AD-A270456] p 1576 N94-19589

NIOBIUM ALLOYS
Developing and understanding the high temperature behavior of niobium aluminides and niobium aluminide composites
[AD-A268874] p 1341 N94-18636
Bibliography on silicides
[AD-A270516] p 1374 N94-19532

NITRIDES
Nitridation of GaAs(100) by laser-induced decomposition of HN3
[AD-A269147] p 1438 N94-18258

NITRIDING
Nitridation of GaAs(100) by laser-induced decomposition of HN3
[AD-A269147] p 1438 N94-18258

NITROGEN
Dense energetic compounds of C, H, N, and O atoms. 3: 5-(4-nitro-(1,2,5) oxadiazolyl)-5H-(1,2,3) triazolo (4,5-c)(1,2,5) oxadiazole
[AD-A268715] p 1338 N94-18314
Determination of nitrogen to carbon abundance ratios from transition layer emission lines
[NASA-CR-191921] p 1622 N94-19421

NITROGEN COMPOUNDS
Molecular and polymeric ceramic precursors
[DE93-040364] p 1372 N94-18891
Supercritical thermodynamics of sulfur and nitrogen species
[DE93-041221] p 1610 N94-19670

NITROGEN OXIDES
Title 1 implementation: Status report on nonattainment areas
[DE93-017677] p 1471 N94-17777
Land-use related sources of CO2, CH4 and N2O: Current global emissions and projections for the period 1990-2100
[PB93-194819] p 1475 N94-18949
NITROGEN 15
NMR studies of enriched species at interfaces
[AD-A264703] p 1367 N94-17878
NITROUS OXIDES
Analysis of satellite-derived ozone and water vapor measurements
[NASA-CR-193810] p 1486 N94-19237
NOAA SATELLITES
Scientific studies in association with the Shuttle Solar Backscatter Ultraviolet (SSBUV) project
[NASA-CR-193404] p 1630 N94-19437
NOISE (SOUND)
Active control of periodic noise with time-varying frequency
[REPT-93-012] p 1562 N94-17934
Parallel and vector adaptations of the underwater finite element parabolic equation model
[AD-A269990] p 1563 N94-18678
Analysis of data from Columbia Point Arena Ocean-Bottom Seismic Station (OBSS)
[AD-A271263] p 1500 N94-19727
A register of underwater acoustic test facilities in the US, Canada, and the United Kingdom
[AD-A270884] p 1500 N94-19785
Noise measurements on two types of airplanes used for spraying in agriculture
[LR-706] p 1319 N94-19796
NOISE GENERATORS
Acoustic intensity measurements in the presence of low Mach number flow
[AD-A269995] p 1562 N94-18664
NOISE MEASUREMENT
Gear sound levels with various tooth contact ratios and forms
[NASA-TM-106432] p 1446 N94-19318
Noise measurements on two types of airplanes used for spraying in agriculture
[LR-706] p 1319 N94-19796
NOISE POLLUTION
Transport policy options for reducing noise at airports; Hamburg airport taken as an example
[DLR-FB-92-40] p 1322 N94-18123
NOISE REDUCTION
Suppression of backscatter and stray reflection induced phase noise in Michelson interferometers
[AD-D015809] p 1382 N94-17902
Transport policy options for reducing noise at airports; Hamburg airport taken as an example
[DLR-FB-92-40] p 1322 N94-18123
Inverse scattering of surface waves: A new look at surface consistency
[REPT-93-25] p 1486 N94-19140
Gear sound levels with various tooth contact ratios and forms
[NASA-TM-106432] p 1446 N94-19318
Applications of motion estimation in image processing
[FEL-92-B356] p 1580 N94-19455
Supersonic jets from bevelled rectangular nozzles
[NASA-TM-106403] p 1313 N94-19484
NOMENCLATURES
Working group for planetary system nomenclature
[NASA-CR-194406] p 1626 N94-18841
NONADIABATIC CONDITIONS
Polaron tunneling in high-temperature superconductors
[DE93-016880] p 1593 N94-17754
The quantum dynamics of electronically nonadiabatic chemical reactions
[NASA-CR-194309] p 1568 N94-18837
NONCONDENSABLE GASES
Fin-efficiency calculation for condensation in the presence of noncondensable gases
[DE93-017684] p 1409 N94-18004
NONDESTRUCTIVE TESTS
The application of nondestructive techniques to the testing of a wind turbine blade
[DE93-016731] p 1447 N94-18128
High resolution SQUID magnetometry for non-destructive evaluation
[AD-A268884] p 1447 N94-18225
Nondestructive inspection of graphite-epoxy laminates for heat damage using DRIFT and LPF spectroscopies
[DE93-017228] p 1343 N94-18761
Metallurgical evaluation of SRAM 2/SRAM A program mer base plates
[DE93-018689] p 1364 N94-19100
Ultrasonic technique for inspection of GPHS capsule girth weld integrity
[DE93-040072] p 1448 N94-19189
Three dimensional ultrasonic imaging: An aging aircraft nondestructive inspection tool
[DE93-018088] p 1448 N94-19252
Materials characterization of propellants using ultrasonics
[NASA-CR-193877] p 1378 N94-19494
New aircraft materials and structures
[MBB-LME-202-S-PUB-502-A] p 1319 N94-19496
Thermal wave image processing for characterization of subsurface of flaws in materials
[DE93-019024] p 1344 N94-19551
NONEQUILIBRIUM THERMODYNAMICS
Numerical simulation of viscous flows in chemical nonequilibrium
[MBB-LME-211-S-PUB-506] p 1421 N94-19497
Essential shift: Scientific revolution in the 20th century
[AD-A270810] p 1610 N94-19663
NONINTRUSIVE MEASUREMENT
Studies on high pressure and unsteady flame phenomena: Revision
[AD-A269138] p 1348 N94-18257
Earth Penetration Radar Imaging System (EPRIS)
[DE93-019890] p 1391 N94-19542
NONLINEAR EQUATIONS
SAND contact in DYNA3D
[DE93-016451] p 1340 N94-18113
On higher dimensional Ermakov systems: Canonical reductions
[MATHS-REPT-A-182] p 1548 N94-18140
ASYS: a computer algebra package for analysis of nonlinear algebraic equations systems
[DE93-629819] p 1548 N94-18175
On the numerical analysis of nonlinear Galerkin methods: Spectral approximation and finite elements
[ETN-93-94900] p 1552 N94-19407
NONLINEAR FEEDBACK
Nonlinear disturbance decoupling and linearization: A partial interpretation of integral feedback
[PB93-197515] p 1543 N94-19328
NONLINEAR OPTICS
Polaron tunneling in high-temperature superconductors
[DE93-016880] p 1593 N94-17754
Metal-nanocluster composites made by ion implantation: A novel third-order nonlinear material
[DE93-015908] p 1339 N94-17846
Development of short pulse soft x ray lasers
[DE93-017150] p 1437 N94-18131
IR materials producibility
[AD-A268849] p 1577 N94-18223
Tunable synchronously pumped intracavity two-stage optical frequency upconversion
[AD-A269105] p 1438 N94-18250
Integrated photonics research volume 10. Conference edition
[AD-A269298] p 1577 N94-18298
Applications of nonlinear optic effects in new specialty fibers
[AD-A268890] p 1578 N94-18457
Theory of electromagnetic waves propagating in nonlinear anisotropic optical materials
[AD-A269305] p 1386 N94-18469
Quantum Optoelectronics. Organization of the 1993 photonics science topical meetings. Technical digest series, volume 8
[AD-A269026] p 1578 N94-18488
Advanced Solid-State Lasers/Compact Blue-Green Lasers. 1993 technical digest series. Volume 2: Organization of the 1993 photonics science topical meetings
[AD-A269058] p 1438 N94-18492
Relaxation of polar orientational order in nonlinear optical polymers by second harmonic generation
[AD-A269059] p 1370 N94-18515
Photonics in Switching: Organization of the 1993 photonics science topical meetings. Technical digest
[AD-A269024] p 1578 N94-18528
Phase conjugation and beam combination using stimulated brillouin scattering
[AD-A269899] p 1439 N94-18656
Nonlinear optical properties of molecules
[AD-A270199] p 1567 N94-18783
Molecular nonlinear optical susceptibilities in condensed phases
[AD-A270200] p 1568 N94-18784
Consortium for materials development in space
[NASA-CR-194411] p 1379 N94-18840
Final report on subcontract B076260 — borate synthesis
[DE93-019501] p 1604 N94-19565
Electro-optic beam steering using non-linear organic materials
[AD-A270809] p 1374 N94-19577
Ionized-cluster beam/partially ionized beam deposition of electro-optical and nonlinear optical organic materials and device development
[AD-A270832] p 1604 N94-19596
Optical switch evaluation support
[AD-A270948] p 1581 N94-19601
NONLINEAR PROGRAMMING
Design optimization studies using COSMIC NASTRAN
p 1450 N94-17834
NONLINEAR SYSTEMS
Modelling chaotic vibrations using NASTRAN
p 1449 N94-17830
Generalization of optimal control theory: Linear and nonlinear structures
[PB93-188621] p 1540 N94-18125
On higher dimensional Ermakov systems: Canonical reductions
[MATHS-REPT-A-182] p 1548 N94-18140
Non Linear Dynamics and Chaos
[AGARD-LS-191] p 1607 N94-18236
Stability analysis through bifurcation theory, 1
p 1608 N94-18238
Non-linear flight dynamics p 1319 N94-18240
An ab initio study of the weakly bonded CO-Cl2 complex
[AD-A269000] p 1349 N94-18395
Fundamental research in nonlinear random vibration for aerospace applications
[AD-A268929] p 1454 N94-18487
Competitive dynamics and self-organization in photorefractive systems
[AD-A269663] p 1430 N94-18569
Phase-space description of plasma waves: Linear and nonlinear theory
[IRF-SR-211] p 1587 N94-18860
Control of nonlinear systems
[AD-A270141] p 1542 N94-18898
Statistical learning theory and algorithms
[AD-A270209] p 1523 N94-18901
The intelligent processing of materials
[AD-A269250] p 1362 N94-18923
Analysis and design of robust decentralized controllers for nonlinear systems
[DE93-019224] p 1543 N94-19302
Nonlinear disturbance decoupling and linearization: A partial interpretation of integral feedback
[PB93-197515] p 1543 N94-19328
Time dependent identification of nonlinear structures
[ECL-92-64] p 1457 N94-19403
Contribution to the modelling and the identification of nonlinear mechanical systems
[ECL-92-32] p 1529 N94-19409
Contribution to the identification of nonlinear behavior laws in material mechanics
[ECL-92-36] p 1458 N94-19411
NONLINEARITY
The 1992 annual report on scientific programs: A broad research program on the sciences of complexity
[DE93-018151] p 1561 N94-18178
Nonlinear Thomson scattering of intense laser pulse from beams and plasmas
[AD-A269556] p 1438 N94-18460
Fundamental research in nonlinear random vibration for aerospace applications
[AD-A268929] p 1454 N94-18487
Multidimensional wave decompositions for the Euler equations p 1413 N94-18562
Effects of harmonics on EMI/RFI filters operating under nonlinear loading conditions
[AD-A269559] p 1388 N94-18769
Active control of a multivariable system by way of polynomial neural networks: Computer simulation evaluations and laboratory experimental results
[AD-A270033] p 1541 N94-18790
Application of differential sensitivity theory to continuum mechanics
[DE93-012732] p 1609 N94-19187
Singularities and symmetries of nonlinear ordinary and partial differential equations
[DE93-040083] p 1550 N94-19190
Analysis and design of robust decentralized controllers for nonlinear systems
[DE93-019224] p 1543 N94-19302
Time dependent identification of nonlinear structures
[ECL-92-64] p 1457 N94-19403
A comparison of iterative methods for a model coupled system of elliptic equations
[DE93-040482] p 1553 N94-19655
Theoretical studies of turbulence and anomalous transport in toroidal confinement devices
[DE93-040684] p 1592 N94-19656
NONUNIFORM FLOW
Internal instability of nonparallel flow on an equatorial beta-plane
[AD-A268927] p 1490 N94-18486

NONUNIFORMITY
Some problems in the rheological characterisation of composite rocket propellants
[AD-A268806] p 1376 N94-18203

NORMAL DENSITY FUNCTIONS
An empirical evaluation of five circular error probable estimation techniques and a method for improving them
[AD-A266528] p 1556 N94-18397

NORMALITY
EDF tests for normality in linear models after a Box-Cox transformation
[AD-A269068] p 1557 N94-18517

NORMALIZING (STATISTICS)
EDF tests for normality in linear models after a Box-Cox transformation
[AD-A269068] p 1557 N94-18517

NOVA LASER SYSTEM
Evaluation of materials proposed for the construction of the Plasma Electrode Pockels Cell (PEPC) on beamlet
[DE93-016952] p 1584 N94-17988

NOZZLE FLOW
Adaptations to micropep and rocket to allow performance evaluation of multiple grain and/or airbreathing motors
[AD-A268798] p 1337 N94-18202
Workshop on Computational Turbulence Modeling
[NASA-TM-109266] p 1410 N94-18545
High order non-oscillatory schemes for the compressible Euler equations p 1412 N94-18558

NOZZLE GEOMETRY
Study of multi-phase flow characteristics in an MHD power train
[DE93-018570] p 1586 N94-18272
Supersonic jets from bevelled rectangular nozzles
[NASA-TM-106403] p 1313 N94-19484

NOZZLE WALLS
Analysis of film cooling in rocket nozzles
[NASA-CR-194674] p 1338 N94-19438

NUCLEAR BINDING ENERGY
Effect of oxygen concentration and ordering on vanadium-oxygen alloy vibrational spectra
[DE93-627003] p 1355 N94-17692
Binding of copper to nanocavity surfaces in silicon
[DE93-019073] p 1364 N94-19080

NUCLEAR ELECTRIC POWER GENERATION
Directory of Energy Information Administration Models 1993
[DE93-016987] p 1616 N94-18707

NUCLEAR ELECTRIC PROPULSION
Critical technologies for reactors used in nuclear electric propulsion
[DE93-017685] p 1337 N94-17908
Potassium-Rankine power conversion subsystem modeling for nuclear electric propulsion
[NASA-CR-191134] p 1468 N94-18821

NUCLEAR FUELS
EIA publications directory, 1992
[DE93-016833] p 1617 N94-18983
Total hemispherical emittance of Niobium-1 percent zirconium fuel cladding for the SP-100 space reactor
[AD-A270456] p 1576 N94-19589

NUCLEAR FUSION
Magnetic Fusion Energy Technology Fellowship: Report on survey of institutional coordinators
[DE93-014646] p 1583 N94-17739
Plasma properties research: Task 3
[DE93-017087] p 1583 N94-17854
Evolution of r-process elements in the hot supernova bubble
[DE93-017169] p 1624 N94-17897
Electron stripping cross sections for light impurity ions in colliding with atomic hydrogens relevant to fusion research
[DE93-788476] p 1566 N94-18158
Institute of Geophysics and Planetary Physics, 1992
[DE93-019209] p 1627 N94-19077
Transverse beam combiner for ILSE
[DE93-019239] p 1591 N94-19559

NUCLEAR INTERACTIONS
Heavy-ion collisions and the nuclear equation of state
[DE93-019263] p 1566 N94-18104

NUCLEAR MAGNETIC RESONANCE
NMR studies of enriched species at interfaces
[AD-A264703] p 1367 N94-17878
Advanced in macrostatistical hydrodynamics
[DE93-018479] p 1410 N94-18270

NUCLEAR MEDICINE
Nuclear Medicine Program
[DE93-013896] p 1504 N94-17699

NUCLEAR MODELS
Investigation of the relative abundance of heavy versus light nuclei in primary cosmic rays using underground muon bundles
[DE93-017601] p 1630 N94-17818

NUCLEAR PHYSICS
Heavy ion nuclear physics research
[DE93-018862] p 1565 N94-17776
Activities report of the Rutherford Appleton Laboratory
[ETN-93-94555] p 1631 N94-17968
Institute for Nuclear Theory
[DE93-017369] p 1568 N94-18824

NUCLEAR PROPULSION
Mission needs and system commonality for space nuclear power and propulsion
[DE93-016557] p 1337 N94-17863
KINETIC: A system code for analyzing Nuclear thermal propulsion rocket engine transients
[DE93-016825] p 1337 N94-17884

NUCLEAR QUADRUPOLE RESONANCE
Phase separation and superconductivity in La2CuO(4 + delta): Effects of oxygen diffusion
[DE93-016610] p 1594 N94-17907

NUCLEAR REACTIONS
Evolution of r-process elements in the hot supernova bubble
[DE93-017169] p 1624 N94-17897
T violating neutron spin rotation asymmetry
[DE93-018470] p 1570 N94-19126

NUCLEAR REACTORS
Fluid-structure-interaction analyses of reactor vessel using improved hybrid Lagrangian Eulerian code ALICE-II
[DE93-015536] p 1409 N94-18248

NUCLEAR RESEARCH
Magnetic Fusion Energy Technology Fellowship: Report on survey of institutional coordinators
[DE93-014646] p 1583 N94-17739

NUCLEAR STRUCTURE
Institute for Nuclear Theory
[DE93-017369] p 1568 N94-18824

NUCLEAR WEAPONS
Computer/information security design approaches for Complex 21/Reconfiguration facilities
[DE93-018547] p 1535 N94-18930

NUCLEATION
Characterization of diamond film nucleation and growth surface
[AD-A269400] p 1597 N94-18459
Growth, characterization and device development in monocrystalline diamond films
[AD-A270074] p 1599 N94-18797
A numerical analysis of crack growth in brittle microcracking composites
[DE93-011562] p 1343 N94-18914
Surface phases and their influence on metal-oxide interfaces
[DE93-019931] p 1601 N94-19020
Melt spinning study
[NASA-CR-193823] p 1380 N94-19423

NUCLEI (NUCLEAR PHYSICS)
Eta-nucleon interaction and nuclear production of eta mesons
[DE93-018469] p 1571 N94-19259

NUCLEONS
Unitary (pi)(pi)N model of N* excitations in (pi)N and (gamma)N reactions
[DE93-017422] p 1568 N94-18826
Eta-nucleon interaction and nuclear production of eta mesons
[DE93-018469] p 1571 N94-19259

NUMERICAL ANALYSIS
The calculation methods of a cracked plastic composite laminate: A literature survey
[VTT-TIED-1362] p 1339 N94-17958
Format.m: A usage manual. Towards an efficient symbolic-numeric environment: Extending Mathematica's format rules
[MATHS-REPT-A-185] p 1547 N94-17969
Numerical methods for one-dimensional hyperbolic conservation laws
[PB93-194801] p 1547 N94-18078
Numerical methods for molecular dynamics
[DE93-018321] p 1566 N94-18179
Numerical and symbolic signal representation and processing
[AD-A270271] p 1389 N94-18811
A numerical study of hybrid optimization methods for the molecular conformation problems
[DE93-017898] p 1569 N94-18985
Using geometric techniques to improve dynamic programming algorithms for the economic lot-sizing problem and extensions
[PB93-197556] p 1528 N94-19330
Numerical analysis of proximal methods: Decomposition and parallelization
[ETN-93-95017] p 1552 N94-19362
Numerical experiments on the Ginzburg-Landau equations
[DE93-019504] p 1604 N94-19567

NUMERICAL CONTROL
Experience with custom processors in space flight applications p 1336 N94-18338
Simplified microprocessor design for VLSI control applications p 1400 N94-18359
Optimizing wind turbine control system parameters
[DE93-018861] p 1469 N94-19036
Analysis and design of robust decentralized controllers for nonlinear systems
[DE93-019224] p 1543 N94-19302

NUMERICAL FLOW VISUALIZATION
Infrared thermography p 1432 N94-18652
3D composite grids using Bezier curves and surfaces in component adaptive methods
[AD-A269188] p 1549 N94-18863
Content based-grid node selection for vector field visualization
[REPT-93-35] p 1525 N94-19155

NUMERICAL INTEGRATION
Numerical integration of structural elements in NIKE3D and DYNA3D
[DE93-016325] p 1452 N94-18049
Calculation of turbulent boundary layer wall pressure spectra
[AD-A269549] p 1416 N94-18642
Implementation of a nonisothermal unified inelastic-strain theory into ADINA6.0 for a titanium alloy: User guide
[AD-A269927] p 1360 N94-18660

NUMERICAL STABILITY
A modified direct preconditioner for indefinite symmetric Toeplitz systems
[DE93-015234] p 1516 N94-17800
Robustness and efficiency of generalized predictive control algorithms with guaranteed stability
[MATHS-REPT-A-190] p 1530 N94-19412

NUMERICAL WEATHER FORECASTING
Microwave (SSM/I) Estimates of the Precipitation Rate to Improve Numerical Atmospheric Model Forecasts
[NASA-CR-193566] p 1491 N94-18602
Diabatic forcing and initialization with assimilation of cloud and rain water in a forecast model: Methodology
p 1491 N94-18603
Physical retrieval of precipitation water contents from Special Sensor Microwave/Imager (SSM/I) data. Part 2: Retrieval method and applications (report version)
p 1491 N94-18605
Forecast model applications of retrieved three dimensional liquid water fields p 1492 N94-18606
Moist wind relationships p 1492 N94-18607
Initialization and assimilation of cloud and rainwater in a regional model p 1492 N94-18608
SERCAA cloud analysis integration: Design concepts and interaction with cloud forecast models
[AD-A269104] p 1492 N94-18637
On the use of semi-Lagrangian methods for accurate predictions of gravity waves
[DM-61] p 1562 N94-18859
Toward a high performance distributed memory climate model
[DE93-019156] p 1494 N94-19298
Reports of the 1992 Synoptic Symposium
[KNMI-TR-151] p 1494 N94-19698
HIRLAM p 1494 N94-19699
The WAQUA/CSM-16 model p 1494 N94-19700
The wave forecasting model NEDWAM
p 1495 N94-19701

O

O RING SEALS
Effect of temperature and O-ring gland finish on sealing ability of Viton V747-75
[NASA-TP-3391] p 1368 N94-18075

OBJECT-ORIENTED PROGRAMMING
Proposal for a numerical array library
[DE93-015017] p 1516 N94-17786
An object-oriented environment for computer vision and pattern recognition
[DE93-017098] p 1517 N94-17867
A structured approach for modeling, analyzing and simulating real-time control systems
[REPT-93-044] p 1539 N94-17916
An environment for requirement reuse
[REPT-92-082] p 1613 N94-17939
Object-oriented extension of a relational DBMS
[ETN-93-94403] p 1519 N94-17978
The development of a course sequence in real-time systems design
[AD-A269459] p 1522 N94-18726
NASA Electronic Library System (NELS) optimization
[NASA-CR-193688] p 1617 N94-18839
Software engineering for effective utilization of parallel processing computing system
[AD-A269191] p 1535 N94-18865

Asynchronous rendezvous in the presence of backtracking
[PB93-197739] p 1524 N94-19062
Abstracting inter-object communications using composition filters
[MEMO-INF-92-76] p 1526 N94-19220
DataTypeLog: A deductive object oriented query language
[MEMO-INF-92-79] p 1526 N94-19221
The TM typing rules
[MEMO-INF-92-80] p 1526 N94-19222
The TM manual version 1.3 working document
[MEMO-INF-93-06] p 1527 N94-19229
Feasibility study in linguistically motivated object-oriented conceptual design of information systems
[PB93-197754] p 1618 N94-19331
Advanced software development workstation: Object-oriented methodologies and applications for flight planning and mission operations
[NASA-CR-193706] p 1513 N94-19349
Managing persistent objects: From the programming language to the system
[ETN-93-95021] p 1529 N94-19368
Contribution to applications systems design MOSAIC method in the Aristote project
[ETN-93-95022] p 1529 N94-19370
OORA Automated Knowledge System (OAKS) code, appendix C
[AD-A270709] p 1531 N94-19573
Computer security. Evolutions 1987 to 1992: Trends and perspectives
[RR-905-I] p 1532 N94-19713
On the automation of object-oriented requirements analysis
[AD-A270673] p 1532 N94-19782

OCCUPATION

Interdisciplinary training in life science (FY 1991 ASSERT)
[AD-A269220] p 1512 N94-18886

OCCUPATIONAL DISEASES

Review of short-term, high-level exposure to metals: Antimony, barium, and cadmium
[AD-A268896] p 1505 N94-18392

OCEAN BOTTOM

Constraints on crustal structure from long period pressure and displacement measurements on the deep seafloor
[AD-A269931] p 1498 N94-18663
BACKSCATTER.FOR: A program to calculate the backscattering strength of an inhomogeneous seabed
[AD-A269235] p 1499 N94-18910
The interpretation of crustal dynamics data in terms of plate motions and regional deformation near plate boundaries
[NASA-CR-194302] p 1487 N94-19432
Analysis of data from Columbia Point Arena Ocean-Bottom Seismic Station (OBSS)
[AD-A271263] p 1500 N94-19727
Faulted structure of the bottom simulating reflector on the Blake Ridge, western North Atlantic
[AD-A271289] p 1500 N94-19745
Seismic studies of the geologic structure and physical properties of the seabed
[AD-A270895] p 1500 N94-19747
Measurements of ocean surface and bottom backscattering strengths in the northwestern Atlantic Ocean
[AD-A270893] p 1500 N94-19786
A laboratory model of a cooled continental shelf
[AD-A270862] p 1500 N94-19792

OCEAN CURRENTS

Wind products for use in coastal wave and surge models
[AD-A269753] p 1497 N94-18414
ADCIRC: An advanced three-dimensional circulation model for shelves, coasts, and estuaries. Report 3: Development of a tidal constituent database for the western North Atlantic and Gulf of Mexico
[AD-A268685] p 1497 N94-18455
Acoustic travel time perturbations due to an internal tide and internal wave field in the Barents Sea
[AD-A270879] p 1499 N94-19580

OCEAN DATA ACQUISITIONS SYSTEMS

CTD and XBT data collected on ERS-1 validation cruise RRS Charles Darwin Cruise 62A, Iceland-Faeroes region
[IOS-294-1992] p 1461 N94-18063
CTD oxygen, tracer and nutrient data from RRS Charles Darwin Cruises 58/59 in the NE Atlantic as part of Vivaldi 1991
[IOS-296-1992] p 1496 N94-18065
SeaSoar CTD, fluorescence and scalar irradiance data from RRS Charles Darwin Cruises 58/59, NE Atlantic, Vivaldi 1991
[IOS-299-1992] p 1496 N94-18066
Modifications of airborne oceanographic lidar for the long range P-3 missions
[NASA-CR-194682] p 1499 N94-18819
Method for extracting tidal and inertial motion from ARGOS ice buoys applied to the Barents Sea during CEAREX
[PB93-190213] p 1499 N94-19063

OCEAN MODELS

The performance of drag relations in the WAQUA storm surge model
[KNMI-TR-149] p 1496 N94-17923
Coastal Ocean Modeling Workshop
[AD-A268955] p 1497 N94-18393
ADCIRC: An advanced three-dimensional circulation model for shelves, coasts, and estuaries. Report 3: Development of a tidal constituent database for the western North Atlantic and Gulf of Mexico
[AD-A268685] p 1497 N94-18455
Preparation of data assimilation and model evaluation experiment data sets
[AD-A269996] p 1498 N94-18665
Work plan for the Marine Aerosol Properties and the Thermal Imager Performance Trial (MAPTIP)
[AD-A270026] p 1483 N94-18712
DYNLET1 model formulation and user's guide
[AD-A269843] p 1498 N94-18723
Connection machine software conversion of a Navy oceans model
[AD-A269876] p 1535 N94-18772
Estimating the oceanic sound speed environmental for long-range acoustic propagation
[AD-A270231] p 1499 N94-18903
Modeling of current features in Gulf Stream SAR imagery
[AD-A270734] p 1499 N94-19609
A laboratory model of a cooled continental shelf
[AD-A270862] p 1500 N94-19792

OCEAN SURFACE

Rapid oceanic cyclogenesis studies
[AD-A269258] p 1490 N94-18265
Wind products for use in coastal wave and surge models
[AD-A269753] p 1497 N94-18414
Full Boltzmann discrete spectral wave model, implementation and nondimensional tests
[AD-A269885] p 1498 N94-18685
Development of ISY data set, part 2
[NASDA-CNT-930006-PT-2] p 1463 N94-19384
The split-step algorithm for microwave propagation modeling above a conducting surface
[FEL-92-A430] p 1390 N94-19447
Acoustic travel time perturbations due to an internal tide and internal wave field in the Barents Sea
[AD-A270879] p 1499 N94-19580
Modeling of current features in Gulf Stream SAR imagery
[AD-A270734] p 1499 N94-19609
Remote sensing of Earth terrain
[NASA-CR-194598] p 1464 N94-19681
Theoretical and experimental research on coherent microwave backscatter from the ocean
[AD-A271276] p 1500 N94-19743
Measurements of ocean surface and bottom backscattering strengths in the northwestern Atlantic Ocean
[AD-A270893] p 1500 N94-19786

OCEAN TEMPERATURE

CTD and XBT data collected on ERS-1 validation cruise RRS Charles Darwin Cruise 62A, Iceland-Faeroes region
[IOS-294-1992] p 1461 N94-18063
SeaSoar and CTD sections across the Iceland-Faeroes Front and Faeroe Shetland Channel, August 1990
[IOS-295-1992] p 1496 N94-18064
An atlas of bathy-thermograph temperature cross-sections for Coral and Tasman Sea transects from 1960 to 1987
[AD-A268775] p 1497 N94-18329

OCEANOGRAPHIC PARAMETERS

Development and evaluation of alternative radioanalytical methods, including mass spectrometry for marine materials
[DE93-625117] p 1345 N94-17691
SeaSoar and CTD sections across the Iceland-Faeroes Front and Faeroe Shetland Channel, August 1990
[IOS-295-1992] p 1496 N94-18064
CTD oxygen, tracer and nutrient data from RRS Charles Darwin Cruises 58/59 in the NE Atlantic as part of Vivaldi 1991
[IOS-296-1992] p 1496 N94-18065

OCEANOGRAPHY

Development and evaluation of alternative radioanalytical methods, including mass spectrometry for marine materials
[DE93-625117] p 1345 N94-17691
A one dimensional numerical model, with an application to the vertical distribution of dissolved oxygen in the ocean
[DE93-018481] p 1495 N94-17779
Technologies for assessing the geologic and geomorphic history of coasts
[AD-A268780] p 1496 N94-18215
Synoptic ocean prediction experiment. EN216 CTD section data report
[AD-A268903] p 1497 N94-18230
An atlas of bathy-thermograph temperature cross-sections for Coral and Tasman Sea transects from 1960 to 1987
[AD-A268775] p 1497 N94-18329
Overview of physical oceanographic measurements taken during the Mount Mitchell cruise to ROPME sea area
[DE93-018460] p 1497 N94-18494
Preparation of data assimilation and model evaluation experiment data sets
[AD-A269996] p 1498 N94-18665
Atlas of SSM/I satellite ice concentration interpolated to operational ice model domains of the Arctic for 1992
[AD-A270306] p 1499 N94-18727
Estimating the oceanic sound speed environmental for long-range acoustic propagation
[AD-A270231] p 1499 N94-18903

OCEANS

A one dimensional numerical model, with an application to the vertical distribution of dissolved oxygen in the ocean
[DE93-018481] p 1495 N94-17779
Comments on computational underwater acoustics
[DE93-013789] p 1562 N94-17873
Synoptic ocean prediction experiment. EN216 CTD section data report
[AD-A268903] p 1497 N94-18230

OFF-ON CONTROL

Increasing mission reliability using open-loop control
[AD-A271208] p 1545 N94-19721

OIL ADDITIVES

Surface species in tribology
[AD-A270970] p 1446 N94-19754

OIL POLLUTION

Oil spreading in surface waters with an ice cover
[PB93-190767] p 1476 N94-19064

OIL SLICKS

Overview of physical oceanographic measurements taken during the Mount Mitchell cruise to ROPME sea area
[DE93-018460] p 1497 N94-18494
Oil spreading in surface waters with an ice cover
[PB93-190767] p 1476 N94-19064

OILS

Compatibility of refrigerants and lubricants with motor materials, volume 1
[DE93-040216] p 1350 N94-18895

OLIGOMERS

Nonlinear optical properties of molecules
[AD-A270199] p 1567 N94-18783
Oligomer and mixed-metal compounds, potential multielectron transfer catalysts
[DE93-019592] p 1350 N94-19017
Cooperative formation of inorganic-organic interfaces in the synthesis of silicate mesostructures
[AD-A271196] p 1375 N94-19742

ON-LINE PROGRAMMING

High precision on-line standard arithmetic operators: Design and implementation
[ETN-93-95006] p 1552 N94-19487

ON-LINE SYSTEMS

FEDIX on-line information service: Design, develop, test, and implement an on-line research and education information service
[DE93-018818] p 1614 N94-18181
Intelligent help facilities: Generating natural language descriptions with examples
[AD-A269555] p 1521 N94-18290
Handbook for users
[AD-A268726] p 1615 N94-18323
On-line monitoring of incinerator emissions
[DE93-017406] p 1474 N94-18499
Automatic documentation generation: The interaction of text and examples
[AD-A269670] p 1616 N94-18570
Software distribution using xnetlib
[DE93-018278] p 1523 N94-18989
On-line test methods of microprocessor based systems
[ETN-93-95008] p 1530 N94-19498

ONBOARD DATA PROCESSING

VPU(tm) demonstration mission vicinity processor unit(tm) overview p 1325 N94-19171
Multichannel error correction code decoder
[NASA-TM-106331] p 1333 N94-19313

OPACITY
FEEST: A method for tabulating equation of state and opacity tables
[DE93-017965] p 1347 N94-18092
OPERATING COSTS
Optimizing wind turbine control system parameters
[DE93-018861] p 1469 N94-19036
Downsizing a database platform for increased performance and decreased costs
[DE93-018687] p 1618 N94-19099
OPERATING SYSTEMS (COMPUTERS)
PARX: Architecture of an operating system for parallel machines
[ETN-93-94401] p 1533 N94-18068
Embedded Computer Performance Measurement (ECPM). Advanced avionics subsystems and technology multiprocessor ECPM software documentation
[AD-A269921] p 1320 N94-18658
Control of nonlinear systems
[AD-A270141] p 1542 N94-18898
Pegasus project description
[MEMO-INF-92-75] p 1536 N94-19159
Pegasus: Operating system support for distributed multimedia systems
[MEMO-INF-92-76] p 1536 N94-19160
Experience in implementing a parallel file system
[DE93-012840] p 1536 N94-19188
ACOS: A performance based approach to build a parallel complex object server
[MEMO-INF-93-11] p 1537 N94-19198
Message passing in PUMA
[DE93-012841] p 1537 N94-19206
Wide-address spaces: Exploring the design space
[MEMO-INF-92-77] p 1537 N94-19219
Service without servers
[AD-A270612] p 1515 N94-19591
OPERATING TEMPERATURE
Development of a cryogenic heat pipe
[DE93-018448] p 1417 N94-18831
OPERATIONS RESEARCH
Contribution to the analysis of tableaus based decision methods
[ETN-93-94355] p 1560 N94-18067
Polling systems: Moment stability of station times and central limit theorems
[PB93-191955] p 1560 N94-18990
OPERATOR PERFORMANCE
Operator performance in pattern matching as a function of reference material structure
[AD-A269889] p 1509 N94-18686
OPERATORS (MATHEMATICS)
Functional analysis of subelliptic operators on lie groups
[PB93-194793] p 1547 N94-18077
L(sub p)-regularity of subelliptic operators on Lie groups
[PB93-194785] p 1549 N94-18948
Numerical analysis of proximal methods: Decomposition and parallelization
[ETN-93-95017] p 1552 N94-19362
High precision on-line standard arithmetic operators: Design and implementation
[ETN-93-95006] p 1552 N94-19487
Computation of large numbers and VLSI: Application to GCD, to stretched GCD and at euclidian distance
[ETN-93-95009] p 1552 N94-19499
OPTICAL ACTIVITY
Kinetic aspects of lattice mismatch in molecular beam epitaxial growth on planar and patterned substrates
[AD-A270424] p 1597 N94-18506
OPTICAL COMMUNICATION
Intentionally Short Range Communications (ISRC)
[AD-A268788] p 1384 N94-18216
Advanced optical fiber communication systems
[AD-A269120] p 1577 N94-18254
Integrated photonics research volume 10. Conference edition
[AD-A269298] p 1577 N94-18298
Competitive dynamics and self-organization in photorefractive systems
[AD-A269663] p 1430 N94-18569
Integrated Photonics Research: Post-deadline papers
[AD-A269232] p 1609 N94-18908
A highly concurrent medium access control strategy for high speed multiwavelength networks using transceivers with limited tunability
[MEMO-INF-93-07] p 1390 N94-19230
Optical frequency division using an optical parametric oscillator
[AD-A270847] p 1581 N94-19578
Experimental examinations of semiconductor laser amplifiers for optical communication technology
[ETN-93-95050] p 1442 N94-19647
OPTICAL COMPUTERS
Coherent transient systems evaluation
[AD-A268808] p 1576 N94-18204
Optical associative processors and directed graphs
[AD-A268881] p 1615 N94-18224
Optical computing. Organization of the 1993 Photonics Science Topical Meetings. Technical digest series, volume 7
[AD-A269025] p 1578 N94-18332
Advanced Solid-State Lasers/Compact Blue-Green Lasers. 1993 technical digest series. Volume 2: Organization of the 1993 photonics science topical meetings
[AD-A269058] p 1438 N94-18492
Design and fabrication of a Multichannel Adaptive Optical Processor (MADOP)
[AD-A270004] p 1579 N94-18668
OPTICAL CORRELATORS
Coherent transient systems evaluation
[AD-A268808] p 1576 N94-18204
Evaluation of a liquid crystal spatial light modulator capable of amplitude- and phase-modulating modes
[AD-A269252] p 1577 N94-18262
Optimal design of binary phase-only filters using genetic algorithms
[AD-A268737] p 1396 N94-18278
OPTICAL COUNTERMEASURES
Millimeter wave reflectivity measurement system
[AD-A270008] p 1387 N94-18601
OPTICAL COUPLING
Optical computing. Organization of the 1993 Photonics Science Topical Meetings. Technical digest series, volume 7
[AD-A269025] p 1578 N94-18332
Phase conjugation and beam combination using stimulated brillouin scattering
[AD-A269899] p 1439 N94-18656
OPTICAL DATA PROCESSING
Examination of metrics and assumptions used in correlation filter design
[DE93-017636] p 1576 N94-18000
Evaluation of a liquid crystal spatial light modulator capable of amplitude- and phase-modulating modes
[AD-A269252] p 1577 N94-18262
Optimal design of binary phase-only filters using genetic algorithms
[AD-A268737] p 1396 N94-18278
Integrated photonics research volume 10. Conference edition
[AD-A269298] p 1577 N94-18298
Photorefractive tungsten bronze crystals for optical computing
[AD-A268859] p 1596 N94-18320
Optical computing. Organization of the 1993 Photonics Science Topical Meetings. Technical digest series, volume 7
[AD-A269025] p 1578 N94-18332
Quantum Optoelectronics. Organization of the 1993 photonics science topical meetings. Technical digest series, volume 8
[AD-A269026] p 1578 N94-18488
Photonics in Switching: Organization of the 1993 photonics science topical meetings. Technical digest
[AD-A269024] p 1578 N94-18528
Design and fabrication of a Multichannel Adaptive Optical Processor (MADOP)
[AD-A270004] p 1579 N94-18668
Integrated Photonics Research: Post-deadline papers
[AD-A269232] p 1609 N94-18908
Ultrafast Electronics and Optoelectronics: Summaries of papers. Technical digest conference edition
[AD-A269233] p 1405 N94-18909
Evaluation of laser diode based optical switches for optical processors
[AD-A270949] p 1581 N94-19602
OPTICAL DISKS
Photorefractive tungsten bronze crystals for optical computing
[AD-A268859] p 1596 N94-18320
OPTICAL EMISSION SPECTROSCOPY
Imaging and blackbody emission spectra of hot particulates generated during laser ablation
[DE93-015818] p 1439 N94-18724
OPTICAL EQUIPMENT
Experiments in sideband suppression on the Los Alamos National Laboratory Free-Electron Laser
[DE93-014466] p 1435 N94-17724
Considerations for the use of the modified line reversal technique for gas temperature measurement
[DE93-015752] p 1576 N94-17857
Designs for optical components related to the Los Alamos free-electron laser
[DE93-016617] p 1436 N94-17865
Calibration of a high frequency monostatic acoustic echosounder
[AD-A268901] p 1481 N94-18229
Evaluation of a liquid crystal spatial light modulator capable of amplitude- and phase-modulating modes
[AD-A269252] p 1577 N94-18262
Photorefractive receiver study
[AD-A269352] p 1577 N94-18302
Optical design for photonics. Organization of the 1993 Photonics Science Topical Meetings. Technical digest series, volume 9
[AD-A269027] p 1578 N94-18396
Quantum Optoelectronics. Organization of the 1993 photonics science topical meetings. Technical digest series, volume 8
[AD-A269026] p 1578 N94-18488
Advanced Solid-State Lasers/Compact Blue-Green Lasers. 1993 technical digest series. Volume 2: Organization of the 1993 photonics science topical meetings
[AD-A269058] p 1438 N94-18492
Liquid sound speeds at pressure from the optical analyzer technique
[DE93-018362] p 1563 N94-19151
Optical frequency division using an optical parametric oscillator
[AD-A270847] p 1581 N94-19578
OPTICAL FIBERS
Laser induced damage testing: Equipment and techniques
[DE93-017143] p 1437 N94-18060
Advanced optical fiber communication systems
[AD-A269120] p 1577 N94-18254
Applications of nonlinear optic effects in new specialty fibers
[AD-A268890] p 1578 N94-18457
Metal Film Surface Plasmon Resonance (MFSPR) fibre couplers
[AD-A268871] p 1579 N94-18635
Apparatus and method for varying a Bragg wavelength of a Bragg grating formed in an optical fiber
[AD-D015876] p 1579 N94-18743
Evaluation of fiber optic performance in the ACRR
[DE93-018515] p 1580 N94-18970
Penetrometer compatible, fiber-optic sensor for continuous monitoring of chlorinated hydrocarbons: Field test results
[DE93-017974] p 1352 N94-19266
Delamination in composite materials as observed using an optical fiber strain gage
[AD-A270803] p 1344 N94-19662
OPTICAL FILTERS
Experiments in sideband suppression on the Los Alamos National Laboratory Free-Electron Laser
[DE93-014466] p 1435 N94-17724
Optimal design of binary phase-only filters using genetic algorithms
[AD-A268737] p 1396 N94-18278
Integrated Photonics Research: Post-deadline papers
[AD-A269232] p 1609 N94-18908
OPTICAL HETERODYNING
Photorefractive receiver study
[AD-A269352] p 1577 N94-18302
Impact of shorter wavelengths on optical quality for laws
[NASA-CR-193873] p 1579 N94-18858
OPTICAL MATERIALS
IR materials producibility
[AD-A268849] p 1577 N94-18223
Spatial light modulators and applications: Summaries of papers presented at the Spatial Light Modulators and Applications Topical Meeting
[AD-A269452] p 1577 N94-18283
Novel electrochemical materials prepared by sol-gel chemistry
[AD-A269060] p 1578 N94-18405
Theory of electromagnetic waves propagating in nonlinear anisotropic optical materials
[AD-A269305] p 1386 N94-18469
Relaxation of polar orientational order in nonlinear optical polymers by second harmonic generation
[AD-A269059] p 1370 N94-18515
Consortium for materials development in space
[NASA-CR-194411] p 1379 N94-18840
Radiation induced darkening of the optical elements in the Startracker camera
[DE93-018907] p 1433 N94-19004
Surface modification of sapphire for IR window application
[DE93-019168] p 1602 N94-19075
Ionized-cluster beam/partially ionized beam deposition of electro-optical and nonlinear optical organic materials and device development
[AD-A270832] p 1604 N94-19596
Optical switch evaluation support
[AD-A270948] p 1581 N94-19601
OPTICAL MEASUREMENT
Gear train behavior analyzer using laser beam scanning for watch movement p 1427 N94-18028
Space debris detection
[AD-A269254] p 1334 N94-18264

Survey of collision avoidance and ranging sensors for mobile robots, revision 1
[AD-A269846] p 1541 N94-18474
Pressure sensitive paint technique
p 1431 N94-18647
Optical switch evaluation support
[AD-A270948] p 1581 N94-19601
OPTICAL MEASURING INSTRUMENTS
Portable, solid state, fiber optic coupled Doppler interferometer system for detonation and shock diagnostics
[DE93-013917] p 1423 N94-17700
Survey of collision avoidance and ranging sensors for mobile robots, revision 1
[AD-A269846] p 1541 N94-18474
Crossed molecular beam studies of atmospheric chemical reaction dynamics
[DE93-019246] p 1478 N94-19303
OPTICAL MEMORY (DATA STORAGE)
Coherent transient systems evaluation
[AD-A268808] p 1576 N94-18204
Photo-induced and electrooptic properties of (Pb,La)(Zr,Ti)O3 films
[DE93-017496] p 1371 N94-18519
OPTICAL PROPERTIES
Dust in the Small Magellanic Cloud
[NASA-CR-193344] p 1624 N94-17764
Metal-nanocluster composites made by ion implantation: A novel third-order nonlinear material
[DE93-015908] p 1339 N94-17846
Considerations for the use of the modified line reversal technique for gas temperature measurement
[DE93-015752] p 1576 N94-17857
Photorefractive tungsten bronze crystals for optical computing
[AD-A268859] p 1596 N94-18320
Kinetic aspects of lattice mismatch in molecular beam epitaxial growth on planar and patterned substrates
[AD-A270424] p 1597 N94-18506
Research on stable, high-efficiency amorphous silicon multijunction modules
[DE93-010046] p 1467 N94-18518
An ultraviolet faraday rotator glass
[AD-D015879] p 1371 N94-18529
Optical and transport properties of metallic and semiconductor nanostructures
[AD-A270009] p 1598 N94-18609
In-situ growth monitoring of molecular beam epitaxy processes
[AD-A269287] p 1598 N94-18616
Integration of ferroelectric/semiconductor thin films for SLM and photorefractive applications
[AD-A268645] p 1598 N94-18633
Optical properties of oxide coatings prepared by ion-assisted deposition
[AD-A270024] p 1599 N94-18711
Optical properties of redispersed iron fibers measured at 94 GHz
[AD-A269739] p 1342 N94-18756
Nonlinear optical properties of molecules
[AD-A270199] p 1567 N94-18783
Development of robust multilayer optics for use in high-peak power radiation environments
[DE93-018557] p 1580 N94-18931
Evaluation of fiber optic performance in the ACRR
[DE93-018515] p 1580 N94-18970
Surface modification of sapphire for IR window application
[DE93-019168] p 1602 N94-19075
Feasibility study: Monodisperse polymer particles containing laser-excitable dyes
[NASA-CR-194280] p 1373 N94-19402
Refinement of unit cell parameters by least-squares: Comments on an old technique and the development of a new computer program
[AD-A270610] p 1531 N94-19590
Ionized-cluster beam/partially ionized beam deposition of electro-optical and nonlinear optical organic materials and device development
[AD-A270832] p 1604 N94-19596
The deposition of electro-optic films on semiconductors
[AD-A270823] p 1605 N94-19664
OPTICAL PUMPING
Problems related to stimulated electromagnetic emissions, strong turbulence and ionospheric modification
[IRF-SR-212] p 1480 N94-17720
Pulsed power supply for Nova Upgrade
[DE93-019626] p 1441 N94-19307
OPTICAL RADAR
A technique for measuring winds in the lower atmosphere using incoherent Doppler lidar
[DE93-017163] p 1488 N94-17758
Data fusion through simulated annealing of registered range and reflectance images
[DE93-015910] p 1612 N94-17858
Laser imaging radar system
[AD-A270436] p 1387 N94-18510
Modifications of airborne oceanographic lidar for the long range P-3 missions
[NASA-CR-194682] p 1499 N94-18819
Impact of shorter wavelengths on optical quality for laws
[NASA-CR-193873] p 1579 N94-18858
SPNDL: A concept for a small satellite Doppler lidar wind sounder p 1327 N94-19181
The Mexico City 1991 lidar measurements campaign
[DE93-019960] p 1478 N94-19272
OPTICAL REFLECTION
Photodetector array having high pixel density
[AD-D015859] p 1432 N94-18731
OPTICAL RELAY SYSTEMS
Designs for optical components related to the Los Alamos free-electron laser
[DE93-016617] p 1436 N94-17865
OPTICAL RESONANCE
Feasibility study: Monodisperse polymer particles containing laser-excitable dyes
[NASA-CR-194280] p 1373 N94-19402
OPTICAL SCANNERS
High rate resistive plate chambers: An inexpensive, fast, large area detector of energetic charged particles for accelerator and non-accelerator applications
[DE93-018664] p 1572 N94-19545
OPTICAL SWITCHING
Evaluation of materials proposed for the construction of the Plasma Electrode Pockels Cell (PEPC) on beamlet
[DE93-016952] p 1584 N94-17988
Integrated photonics research volume 10. Conference edition
[AD-A269298] p 1577 N94-18298
Quantum Optoelectronics. Organization of the 1993 photonics science topical meetings. Technical digest series, volume 8
[AD-A269026] p 1578 N94-18488
Photonics in Switching: Organization of the 1993 photonics science topical meetings. Technical digest
[AD-A269024] p 1578 N94-18528
Ultrafast Electronics and Optoelectronics: Summaries of papers. Technical digest conference edition
[AD-A269233] p 1405 N94-18909
Improved optical pseudospark switch
[AD-D015821] p 1580 N94-18947
Optical switch evaluation support
[AD-A270948] p 1581 N94-19601
Evaluation of laser diode based optical switches for optical processors
[AD-A270949] p 1581 N94-19602
OPTICAL THICKNESS
Application of fractal methods to estimate the aerosol-optical depth for atmospheric correction of high resolution satellite data
[DLR-FB-93-04] p 1480 N94-18088
OPTICAL WAVEGUIDES
Magnetostatic waves-based integrated optic bragg cell modules with applications to RF signal processing
[AD-A269115] p 1577 N94-18295
High-power microwave breakdown of dielectric interfaces
[AD-A268844] p 1397 N94-18318
Optical design for photonics. Organization of the 1993 Photonics Science Topical Meetings. Technical digest series, volume 9
[AD-A269027] p 1578 N94-18396
Photonics in Switching: Organization of the 1993 photonics science topical meetings. Technical digest
[AD-A269024] p 1578 N94-18528
A tunable compact high power far-infrared grating free-electron laser
[AD-A269875] p 1440 N94-18771
Integrated Photonics Research: Post-deadline papers
[AD-A269232] p 1609 N94-18908
OPTICS
Quantum optoelectronics technical digest, 1993. Voolume 8: Postconference edition
[AD-A268209] p 1576 N94-17887
OPTIMAL CONTROL
Generalization of optimal control theory: Linear and nonlinear structures
[PB93-188621] p 1540 N94-18125
Parallel optimization algorithms and their implementation in VLSI design p 1401 N94-18374
Optimizing wind turbine control system parameters
[DE93-018861] p 1469 N94-19036
The optimal projection equations for finite-dimensional fixed-order H2-optimal control of infinite-dimensional discrete-time systems
[REPT-93-11] p 1542 N94-19085
The fixed, finite-order L(sup 2)-optimal control of infinite-dimensional time-varying discrete-time systems
[REPT-93-23] p 1542 N94-19138
Digital control of Pritchard-Salamon systems
[REPT-93-33] p 1543 N94-19286
Analysis and design of robust decentralized controllers for nonlinear systems
[DE93-019224] p 1543 N94-19302
Phasing strategies of the Hermes type space shuttle: Its optimization considering the thrust failures
[LAAS-93242] p 1544 N94-19361
Modeling of driver behavior: Information perception, rule and control strategies in experiments and simulations
[ETN-93-95053] p 1510 N94-19649
OPTIMIZATION
Applications of an algebraic Monge property
[DE93-016869] p 1546 N94-17885
Heuristics from nature for hard combinatorial optimization problems
[REPT-93-025] p 1547 N94-17961
The optimal numerical algorithm for processing of phase coded time signals for radio-clocks
p 1426 N94-18018
New current reduction system for watches with integrated current regulation motors
p 1428 N94-18034
A study of the automatic generating system. 3: Improvement of the total system performance
p 1429 N94-18040
Preliminary structural design: Defining the design space
[AD-A268898] p 1317 N94-18227
Learning database abstractions for query reformulation
[AD-A269531] p 1616 N94-18641
A numerical study of hybrid optimization methods for the molecular conformation problems
[DE93-017898] p 1569 N94-18985
Numerical analysis of proximal methods: Decomposition and parallelization
[ETN-93-95017] p 1552 N94-19362
Optimal safety system design using fault tree analysis
[MATHS-REPT-A-187] p 1529 N94-19382
On network representation of the solutions in combinatorial optimization
[RR-910-I] p 1552 N94-19392
Reanalysis of structure models
[ECL-93-07] p 1458 N94-19460
The complexity of the optimal spanning hypertree problem
[TR-471] p 1561 N94-19481
Finding optimal policies for Markov decision chains: A unifying framework for mean-variance-tradeoffs
[PB93-191930] p 1559 N94-19555
Shell designs
[AD-A270656] p 1460 N94-19606
OPTOELECTRONIC DEVICES
Optically controlled active impedance element and filters employing the same
[AD-D015863] p 1396 N94-18062
Growth of structures for integrated optoelectronic devices
[AD-A269014] p 1598 N94-18527
Joint services electronics program
[AD-A269383] p 1403 N94-18638
Photodetector array having high pixel density
[AD-D015859] p 1432 N94-18731
Attitude sensor package p 1325 N94-19172
Electro-optic beam steering using non-linear organic materials
[AD-A270809] p 1374 N94-19577
Experimental examinations of semiconductor laser amplifiers for optical communication technology
[ETN-93-95050] p 1442 N94-19647
Feasibility study for a measuring system velocity projectile
[FEL-91-A368] p 1434 N94-19797
ORBIT CALCULATION
SeaTrack: Ground station orbit prediction and planning software for sea-viewing satellites
[NASA-RP-1331] p 1532 N94-19761
ORBITAL ASSEMBLY
Designing Space Station
[NASA-TM-109353] p 1334 N94-18922
Shuttle-C, the future is now
[NASA-TM-109355] p 1332 N94-18954
Space Applications Industrial Laser System (SAILS)
p 1325 N94-19173
ORBITAL ELEMENTS
SeaTrack: Ground station orbit prediction and planning software for sea-viewing satellites
[NASA-RP-1331] p 1532 N94-19761
ORBITAL MANEUVERING VEHICLES
Shuttle-C, the future is now
[NASA-TM-109355] p 1332 N94-18954

ORBITAL MECHANICS
The Cluster orbit and mission scenario
p 1330 N94-19637
ORBITAL RENDEZVOUS
Phasing strategies of the Hermes type space shuttle: Its optimization considering the thrust failures
[LAAS-93242] p 1544 N94-19361
ORBITAL SERVICING
Superfluid Helium On-Orbit Transfer (SHOOT) flight demonstration p 1327 N94-19185
ORDER-DISORDER TRANSFORMATIONS
Effect of oxygen concentration and ordering on vanadium-oxygen alloy vibrational spectra
[DE93-627003] p 1355 N94-17692
Surface phases and their influence on metal-oxide interfaces
[DE93-019931] p 1601 N94-19020
A free energy simulation method based study of interfacial segregation
[DE93-019462] p 1364 N94-19032
ORDNANCE
Earth Penetration Radar Imaging System (EPRIS)
[DE93-019890] p 1391 N94-19542
ORGANIC CHEMISTRY
Royal Society of Chemistry, Heterocyclic Chemistry Group, Lakeland Heterocyclic Symposium
[AD-A270374] p 1338 N94-18703
Research program activities of the ORNL Analytical Chemistry Division
[DE93-017938] p 1339 N94-19117
ORGANIC COMPOUNDS
Title 1 implementation: Status report on nonattainment areas
[DE93-017677] p 1471 N94-17777
Indoor environment program
[DE93-018601] p 1513 N94-18935
Organic carbonyl compounds in Albuquerque, New Mexico, air: A preliminary study of the effects of oxygenated fuel use
[DE93-017748] p 1476 N94-19045
Kinetic studies of electrochemical generation of Ag(II) ion and catalytic oxidation of selected organics
[DE93-016601] p 1352 N94-19240
ORGANIC LIQUIDS
Similarity solutions for gravity-dominated spreading of a lens of organic contaminant
[REPT-93-24] p 1420 N94-19139
ORGANIC MATERIALS
Process relationship as influenced by carbonization rate
[AD-A269680] p 1341 N94-18572
Ionized-cluster beam/partially ionized beam deposition of electro-optical and nonlinear optical organic materials and device development
[AD-A270832] p 1604 N94-19596
ORGANIC SEMICONDUCTORS
Studies of interactions between conducting polymer and organic vapors: Applications to chemical sensing
[DE93-015694] p 1369 N94-18233
ORGANIC SUPERCONDUCTORS
Structure-property relationships in radical-cation (electron-donor molecule) and anion-based (including fullerides) organic superconductors and their use in the design of new materials
[DE93-018617] p 1601 N94-19022
ORGANISMS
Space research with intact organisms: The role of Space Station Freedom p 1502 N94-19213
ORGANIZATIONS
Trends in Information Management at Department of Energy Headquarters
[DE93-017197] p 1615 N94-18496
Quality, management, and the interplay of self-assessment, process assessments, and performance-based observations
[DE93-018787] p 1448 N94-19336
ORGANOMETALLIC COMPOUNDS
X ray absorption spectroscopic studies of the active sites of nickel- and copper-containing metalloproteins
[DE93-017142] p 1347 N94-18059
Molecular and polymeric ceramic precursors
[DE93-040364] p 1372 N94-18891
The direct synthesis of organic and organometallic-containing MICA-type aluminosilicates
[DE93-019001] p 1373 N94-19321
ORIENTATION
Effects of pressure on the orientational ordering and phase transitions in solid C(60) and C(70)
[DE93-018858] p 1603 N94-19347
OROGRAPHY
Effect of spatial resolution on the simulation of regional precipitation in China in a global climate model
[DE93-013433] p 1489 N94-18053
ORTHOGONAL FUNCTIONS
Canonical multi-valued input Reed-Muller trees and forms p 1401 N94-18375
ORTHOGONALITY
Parallel inverse iteration with reorthogonalization
[DE93-012867] p 1533 N94-17693
On polynomials orthogonal with respect to an inner product involving differences (the general case)
[REPT-93-32] p 1551 N94-19285
OSCILLATING FLOW
ENO schemes on unstructured meshes
p 1412 N94-18561
OSCILLATIONS
Decoherence and recoherence of beam in phase space
[DE93-014885] p 1573 N94-17784
FY 1991 AASERT: Spatio-temporal making in human vision and its application to image coding
[AD-A268795] p 1505 N94-18190
Neutrino mass
[DE93-018467] p 1567 N94-18269
Close-coupled oscillating canard effects on post-stall lift enhancement
[AD-A268938] p 1321 N94-18541
OSCILLATORS
X-ray laser oscillator-amplifier experiments
[DE93-017165] p 1436 N94-17868
On a possible algebra morphism of U(sub q)(osp1/2) onto the deformed oscillator algebra W(sub q)(N)
[DE93-629857] p 1548 N94-18176
High-power microwave breakdown of dielectric interfaces
[AD-A268844] p 1397 N94-18318
Designs for a 10.6 micrometer electromagnetic wiggler Free-Electron Laser (FEL)
[AD-A269695] p 1439 N94-18576
The Lever oscillator for use in high resistance resonator applications
[DE93-017652] p 1404 N94-18827
Contribution to the modelling and the identification of nonlinear mechanical systems
[ECL-92-32] p 1529 N94-19409
Optical frequency division using an optical parametric oscillator
[AD-A270847] p 1581 N94-19578
OVER-THE-HORIZON RADAR
RADARC HF ionospheric prediction program for OTH radar
[AD-A269557] p 1385 N94-18291
OVERPRESSURE
Air blast measurements at 20 and 40 km distance from detonating 10 and 20 ton high explosive charges
[PB93-195949] p 1419 N94-19068
OXIDASE
Bienzyme sensors based on electrically wired peroxidase
[AD-A271364] p 1374 N94-19585
OXIDATION
Catalytic hydrocarbon reactions over supported metals
[DE93-018168] p 1345 N94-17808
Fundamental studies of the mechanism of catalytic reactions with catalysts effective in the gasification of carbon solids and the oxidative coupling of methane
[DE93-015262] p 1347 N94-18193
Environmental effects on intermetallic compounds: A guide to the literature
[AD-A269587] p 1359 N94-18306
Analysis of deposit precursors in jet fuels using Fourier transform infrared spectroscopy
[AD-A269035] p 1377 N94-18489
Surface phases and their influence on metal-oxide interfaces
[DE93-019931] p 1601 N94-19020
Selective methane oxidation over promoted oxide catalysts
[DE93-040002] p 1351 N94-19132
Selective methane oxidation over promoted oxide catalysts
[DE93-040001] p 1351 N94-19150
Factors that control the stable carbon isotopic composition of methane produced in an anoxic marine sediment p 1477 N94-19235
OXIDATION RESISTANCE
Environmental effects on intermetallic compounds: A guide to the literature
[AD-A269587] p 1359 N94-18306
Carbon/carbon composites coated with SiC by chemical vapor deposition
[AD-A269934] p 1341 N94-18544
OXIDATION-REDUCTION REACTIONS
Oxygen reduction at a stabilized zirconia interface with Y(1-x)Ca(x)MnO3 or La(1-x)Sr(x)MnO3 cathode materials
[DE93-015681] p 1593 N94-17747
Applications of scanning tunneling microscopy to electrochemistry
[AD-A269129] p 1348 N94-18255
Kinetic studies of electrochemical generation of Ag(II) ion and catalytic oxidation of selected organics
[DE93-016601] p 1352 N94-19240
Bienzyme sensors based on electrically wired peroxidase
[AD-A271364] p 1374 N94-19585
OXIDE FILMS
Surface phases and their influence on metal-oxide interfaces
[DE93-019931] p 1601 N94-19020
Optical switch evaluation support
[AD-A270948] p 1581 N94-19601
Nanofabrication by focused ion beam
[AD-A271290] p 1345 N94-19746
OXIDES
Office of Naval Research Publications/Patents /Presentations/Honors report, 1 October 1992 - 30 September 1993
[AD-A270037] p 1632 N94-18791
Selective methane oxidation over promoted oxide catalysts
[DE93-040002] p 1351 N94-19132
Selective methane oxidation over promoted oxide catalysts
[DE93-040001] p 1351 N94-19150
OXYGEN
Effect of oxygen concentration and ordering on vanadium-oxygen alloy vibrational spectra
[DE93-627003] p 1355 N94-17692
Selective electrochemical wafer thinning for silicon characterization
[DE93-015083] p 1592 N94-17742
Oxygen reduction at a stabilized zirconia interface with Y(1-x)Ca(x)MnO3 or La(1-x)Sr(x)MnO3 cathode materials
[DE93-015681] p 1593 N94-17747
A one dimensional numerical model, with an application to the vertical distribution of dissolved oxygen in the ocean
[DE93-018481] p 1495 N94-17779
Phase separation and superconductivity in La2CuO(4 + delta): Effects of oxygen diffusion
[DE93-016610] p 1594 N94-17907
Dense energetic compounds of C, H, N, and O atoms. 3: 5-(4-nitro-(1,2,5) oxadiazolyl)-5H-(1,2,3) triazolo (4,5-c)(1,2,5) oxadiazole
[AD-A268715] p 1338 N94-18314
Temperature, kinetic energy, and rotational temperature dependences for the reactions of Ar(+)(2)P3/2 with O2 and CO
[AD-A268974] p 1567 N94-18526
Electrocatalysts for oxygen electrodes
[DE93-040446] p 1354 N94-19653
OXYGEN ANALYZERS
CTD oxygen, tracer and nutrient data from RRS Charles Darwin Cruises 58/59 in the NE Atlantic as part of Vivaldi 1991
[IOS-296-1992] p 1496 N94-18065
OXYGEN ATOMS
Effect of oxygen concentration and ordering on vanadium-oxygen alloy vibrational spectra
[DE93-627003] p 1355 N94-17692
NSWCWODET participation in Space Shuttle mission STS-46
[AD-A268875] p 1332 N94-18321
OXYGEN IONS
Low-energy continuum-electron emission at 0 degrees from O(q+) + He collisions
[DE93-018777] p 1570 N94-19108
OXYGEN SPECTRA
Effect of oxygen concentration and ordering on vanadium-oxygen alloy vibrational spectra
[DE93-627003] p 1355 N94-17692
OXYGEN SUPPLY EQUIPMENT
Laboratory test and evaluation report of the essex model 60C-0037-2 molecular sieve oxygen generating system
[AD-A269967] p 1445 N94-18778
OXYGENATION
Organic carbonyl compounds in Albuquerque, New Mexico, air: A preliminary study of the effects of oxygenated fuel use
[DE93-017748] p 1476 N94-19045
OZONE
Air pollution effects field research facility. 3: UV-B exposure and monitoring system
[DE93-013098] p 1470 N94-17773
Title 1 implementation: Status report on nonattainment areas
[DE93-017677] p 1471 N94-17777
Screening analysis for chlorine-free alternative refrigerants to replace R-22 in air conditioning applications
[DE93-015920] p 1367 N94-17847
Analysis of meteorological conditions during AGASP-4: 30 March - 23 April 1992
[PB93-190205] p 1489 N94-18126
Upper atmospheric effects of the HF Active Auroral Research Program Ionospheric Research Instrument (HAARP IRI)
[AD-A268948] p 1481 N94-18451

October 1979-1989 Southern Hemisphere total ozone as seen by TOMS
[NASA-TM-109375] p 1476 N94-18967
Spatiotemporal variability of non-urban ozone concentrations over the eastern United States and its potential replication by satellite data
[PB93-191326] p 1476 N94-19065
Analysis of satellite-derived ozone and water vapor measurements
[NASA-CR-193810] p 1486 N94-19237
Crossed molecular beam studies of atmospheric chemical reaction dynamics
[DE93-019246] p 1478 N94-19303

OZONE DEPLETION
Removing CFC's from the atmosphere with lasers: A second look
[DE93-017516] p 1473 N94-18101
Upper atmospheric effects of the HF Active Auroral Research Program Ionospheric Research Instrument (HAARP IRI)
[AD-A268948] p 1481 N94-18451
Ozone hole
[NASA-TM-109368] p 1476 N94-18960

OZONOSPHERE
Air pollution effects field research facility. 3: UV-B exposure and monitoring system
[DE93-013098] p 1470 N94-17773
Removing CFC's from the atmosphere with lasers: A second look
[DE93-017516] p 1473 N94-18101
Upper atmospheric effects of the HF Active Auroral Research Program Ionospheric Research Instrument (HAARP IRI)
[AD-A268948] p 1481 N94-18451

P

P WAVES
A comparison of single-station backazimuth estimates with regional event locations in the Central Appalachians
[AD-A269697] p 1483 N94-18690

P-N JUNCTIONS
Gallium arsenide-based ternary compounds and multi-band-gap solar cell research
[DE93-010049] p 1467 N94-18483
Defect behavior of polycrystalline solar cell silicon
[DE93-018490] p 1468 N94-19016
MOCVD-grown InGaAsP heterostructure diode lasers
[AD-A270848] p 1606 N94-19769

P-TYPE SEMICONDUCTORS
Selective electrochemical wafer thinning for silicon characterization
[DE93-015083] p 1592 N94-17742

PACIFIC OCEAN
Spectral analysis of synoptic time scale disturbances over the tropical eastern Pacific during summer 1989, 1990 and 1991
[AD-A268821] p 1490 N94-18206

PACKING DENSITY
Equipment for investigation of cryogenic compaction of nanosize silicon nitride powders
[DE93-018740] p 1340 N94-18180
Molecular dynamics modeling of the mechanical behavior of metallic multilayers
[DE93-017972] p 1365 N94-19263

PAINTS
Pressure sensitive paint technique
p 1431 N94-18647

PAIR PRODUCTION
Crystal optics of high energy gamma-beams
[DE93-630228] p 1577 N94-18217

PALEONTOLOGY
Technologies for assessing the geologic and geomorphic history of coasts
[AD-A268780] p 1496 N94-18215

PALLADIUM
Study of mechanical behavior and internal structure of ferritic nanocrystalline material
[DE93-019264] p 1596 N94-18184

PALLADIUM ALLOYS
Realistic theories of heavy electron and other strongly correlated materials
[DE93-010350] p 1571 N94-19204

PALLADIUM COMPOUNDS
Structural stability of 1100 C heated Pd/k during absorption cycling in protium
[DE93-016270] p 1346 N94-18048

PANCREAS
Nuclear Medicine Program
[DE93-013896] p 1504 N94-17699

PANEL METHOD (FLUID DYNAMICS)
A computational and experimental investigation of incompressible oscillatory airfoil flow and flutter problems
[AD-A268748] p 1311 N94-18402
ADAS implementation of a panel method for the prediction of aerodynamic loads
[LR-723] p 1313 N94-19667

PANELS
Packaging, deployment, and panel design concepts for a truss-stiffened 7-panel precision deployable reflector with feed boom
[NASA-TM-109000] p 1333 N94-17765

PARABOLIC REFLECTORS
Packaging, deployment, and panel design concepts for a truss-stiffened 7-panel precision deployable reflector with feed boom
[NASA-TM-109000] p 1333 N94-17765
The CAESAR project: Experimental and modeling investigations of methane reforming in a catalytically enhanced solar absorption receiver on a parabolic dish
[DE93-040203] p 1469 N94-19109

PARALLEL COMPUTERS
Optical computing. Organization of the 1993 Photonics Science Topical Meetings. Technical digest series, volume 7
[AD-A269025] p 1578 N94-18332
Case studies of software development tools for parallel architectures
[AD-A269193] p 1535 N94-18866
Early experiences with the IBM SP-1
[DE93-018398] p 1535 N94-19010
MIMD massively parallel methods for engineering and science problems
[DE93-019409] p 1531 N94-19562

PARALLEL FLOW
Heat load analysis on the cable-in-conduit with central core conductor for the TF coil Rebut layer design
[DE93-013783] p 1395 N94-17872

PARALLEL PLATES
Anomalous dielectric properties of carbon-black filled elastomers
[AD-A269378] p 1370 N94-18280

PARALLEL PROCESSING (COMPUTERS)
Parallel inverse iteration with reorthogonalization
[DE93-012867] p 1533 N94-17693
An efficient implementation of error-valued semantics on imperative machines
[DE93-014658] p 1516 N94-17740
PARX, kernel of a system for massively parallel computers: Control of communication between processes
[ETN-93-94353] p 1533 N94-17976
PARX: Architecture of an operating system for parallel machines
[ETN-93-94401] p 1533 N94-18068
High performance Fortran: An overview
[DE93-017181] p 1519 N94-18072
An evolving infrastructure for scientific computing and the integration of new graphics technology
[DE93-017164] p 1520 N94-18133
Parallel optimization algorithms and their implementation in VLSI design p 1401 N94-18374
A fast adaptive convex hull algorithm on two-dimensional processor arrays with a reconfigurable BUS system
p 1402 N94-18380
Parallelization of the Air Force Space Command (AFSPACECOM) satellite motion models
[AD-A269327] p 1334 N94-18470
The evolution of the PVM concurrent computing system
[DE93-017764] p 1534 N94-18482
Development of parallel architectures for sensor array processing. Volume 2: A parallel architecture for broad-band direction-of-arrival estimation
[AD-A270427] p 1534 N94-18508
Distributed memory parallel computers and computational fluid dynamics p 1413 N94-18568
Parallel and vector adaptations of the underwater finite element parabolic equation model
[AD-A269990] p 1563 N94-18678
Connection machine software conversion of a Navy oceans model
[AD-A269876] p 1535 N94-18772
Neutral networks: An NRL perspective
[AD-A269122] p 1541 N94-18773
Software engineering for effective utilization of parallel processing computing system
[AD-A269191] p 1535 N94-18865
Case studies of software development tools for parallel architectures
[AD-A269193] p 1535 N94-18866
A parallel and pipelined architecture for estimation of direction of arrival using a bilinear transformation method, volume 3
[AD-A270137] p 1389 N94-18897
Early experiences with the IBM SP-1
[DE93-018398] p 1535 N94-19010
Implementation of the turn function method in KIVA-F90
[DE93-018394] p 1419 N94-19027
The p4 Linda: A portable implementation of Linda
[DE93-017752] p 1535 N94-19046
Performance and scalability aspects of directory-based cache coherence in shared-memory multiprocessors
[DE93-016442] p 1536 N94-19115
A massively parallel adaptive finite element method with dynamic load balancing
[DE93-012844] p 1536 N94-19161
A multi-thread approach to coalescing small transfers generated by portable tool sets
[DE93-012128] p 1525 N94-19186
Experience in implementing a parallel file system
[DE93-012840] p 1536 N94-19188
ACOS: A performance based approach to build a parallel complex object server
[MEMO-INF-93-11] p 1537 N94-19198
A parallel hashed oct-tree N-body algorithm
[DE93-012654] p 1526 N94-19205
Message passing in PUMA
[DE93-012841] p 1537 N94-19206
Action systems and action refinement in the development of parallel systems: An algebraic approach
[MEMO-INF-93-14] p 1538 N94-19296
PUMMA: Parallel Universal Matrix Multiplication Algorithms on distributed memory concurrent computers
[DE93-019163] p 1538 N94-19299
Process allocation on distributed memory parallel architectures
[ETN-93-95004] p 1538 N94-19514
MIMD massively parallel methods for engineering and science problems
[DE93-019409] p 1531 N94-19562
CVL: A C vector library manual. Version 2
[AD-A270614] p 1531 N94-19592
Simulation of dynamic material response with the PAGOSA code
[DE93-018285] p 1460 N94-19603
Systolic design with asynchronous controls for digital-signal processing
[AD-A270976] p 1392 N94-19680
Implementation of parallel algorithms
[AD-A271035] p 1539 N94-19682
NPAC distributed-parallel system feasibility study
[AD-A270972] p 1539 N94-19790

PARALLEL PROGRAMMING
PARX: Architecture of an operating system for parallel machines
[ETN-93-94401] p 1533 N94-18068
High performance Fortran: An overview
[DE93-017181] p 1519 N94-18072
The evolution of the PVM concurrent computing system
[DE93-017764] p 1534 N94-18482
Software engineering for effective utilization of parallel processing computing system
[AD-A269191] p 1535 N94-18865
Asynchronous rendezvous in the presence of backtracking
[PB93-197739] p 1524 N94-19062
Performance and scalability aspects of directory-based cache coherence in shared-memory multiprocessors
[DE93-016442] p 1536 N94-19115
An annotated bibliography on parallel parsing: Updated version
[MEMO-INF-92-84] p 1537 N94-19223
Heap construction in the parallel comparison tree model
[TR-409] p 1536 N94-19512

PARAMETER IDENTIFICATION
Linear parameter identification methods for ARMA models with periodic coefficients
[REPT-92-070] p 1556 N94-17938
Comparative examinations of several field oriented position control structures for asynchronous servomotors with a multitransputer system
[ETN-93-95051] p 1406 N94-19390
Contribution to the identification of nonlinear behavior laws in material mechanics
[ECL-92-36] p 1458 N94-19411
Methods for description and control of dynamical systems and their application
[MPIS-17/1992] p 1553 N94-19522
A learning autopilot for automatically controlled robust regulation
[ETN-93-95075] p 1321 N94-19711
Algorithms and architectures for high speed signal processing
[AD-A271000] p 1392 N94-19736

PARAMETRIC AMPLIFIERS
Optical frequency division using an optical parametric oscillator
[AD-A270847] p 1581 N94-19578

PARITY
On the difference caused by CP violation in the energy spectra of pions in K(sup (+-))(yields)(pi)(+-)(pi)(+-)(pi)-+ decays
[DE93-624828] p 1564 N94-17687
Improved approximations applied to the S(sub N) even-parity equation
[DE93-016467] p 1551 N94-19343

PARSING ALGORITHMS
An annotated bibliography on parallel parsing: Updated version
[MEMO-INF-92-84] p 1537 N94-19223
Attribute evaluation during generalized parsing
[MEMO-INF-92-85] p 1526 N94-19224
Non-well-foundedness and type freeness can unify the interpretation of functional application
[PB93-191849] p 1560 N94-19710

PARTIAL DIFFERENTIAL EQUATIONS
Numerical methods for one-dimensional hyperbolic conservation laws
[PB93-194801] p 1547 N94-18078
Introduction to spectral methods: Application to the Stokes problem p 1413 N94-18566
3D composite grids using Bezier curves and surfaces in component adaptive methods
[AD-A269188] p 1549 N94-18863
Application of differential sensitivity theory to continuum mechanics
[DE93-012732] p 1609 N94-19187
Singularities and symmetries of nonlinear ordinary and partial differential equations
[DE93-040083] p 1550 N94-19190
Group-invariant solutions of hydrodynamics and radiation hydrodynamics
[DE93-018373] p 1423 N94-19604

PARTIAL PRESSURE
Control of catalytic hydrotreating selectivity with ammonia
[DE93-041223] p 1354 N94-19660

PARTICLE ACCELERATION
Enhanced acceleration in a self-modulated-laser wakefield accelerator
[AD-A268452] p 1586 N94-18148

PARTICLE ACCELERATOR TARGETS
Compound-lens injector for a 19-MeV, 700-kA electron beam
[DE93-013752] p 1573 N94-17698
Overview of WARP: A particle code for heavy ion fusion
[DE93-018637] p 1588 N94-19034
High energy physics program. Task A: Experiment and theory. Task B: Numerical simulation
[DE93-018140] p 1575 N94-19050
Induction accelerator development for heavy ion fusion
[DE93-019228] p 1591 N94-19479

PARTICLE ACCELERATORS
The design of the MAD Design Program
[DE93-013343] p 1539 N94-17696
Enhanced acceleration in a self-modulated-laser wakefield accelerator
[AD-A268452] p 1586 N94-18148
Halo formation in mismatched, space-charge-dominated beams
[DE93-018581] p 1574 N94-18934
High energy physics at Tufts University
[DE93-018299] p 1575 N94-19023

PARTICLE BEAMS
The Intense Slow Positron Source concept: A theoretical perspective on a proposed INEL Facility
[DE93-013675] p 1564 N94-17738
Advanced methods for the computation of particle beam transport and the computation of electromagnetic fields and beam-cavity interactions
[DE93-018160] p 1573 N94-17807
The Fourteenth Symposium on Molecular Beams
[AD-A268721] p 1568 N94-18787
SSC detector muon sub-system beam tests
[DE93-018415] p 1569 N94-19013
Simulation of the ALS longitudinal multibunch feedback system
[DE93-019227] p 1575 N94-19152
Transverse beam combiner for ILSE
[DE93-019239] p 1591 N94-19559

PARTICLE COLLISIONS
Correlated charge-changing ion-atom collisions
[DE93-018717] p 1564 N94-17775
High-performance multiprocessor architecture for a 3-D lattice gas model p 1400 N94-18362
Research in particle physics
[DE93-040875] p 1567 N94-18534
A bit serial first level calorimeter trigger for an LHC detector
[USIP-92-08] p 1574 N94-18845
Neutron-induced collision cascade mixing in Nb/V superlattices
[DE93-018575] p 1600 N94-18933
Search for resonant electron transfer and double excitation in Kr(sup 34+) + H2 collisions
[DE93-018776] p 1569 N94-18999
High energy physics at Tufts University
[DE93-018299] p 1575 N94-19023
Electron impact polarization and correlation properties of the inert gases
[DE93-018358] p 1570 N94-19125
Experimental study of interactions of highly charged ions with atoms at keV energies
[DE93-040222] p 1571 N94-19257

PARTICLE EMISSION
The Intense Slow Positron Source concept: A theoretical perspective on a proposed INEL Facility
[DE93-013675] p 1564 N94-17738

PARTICLE ENERGY
Convection algorithms for magnetospheric particles
[AD-A270103] p 1493 N94-18871
Advanced fusion diagnostics
[DE93-040085] p 1589 N94-19133
An ab initio Monte Carlo study of low energy positron and electron implantation in elemental metals and multilayers
[DE93-019847] p 1603 N94-19541

PARTICLE FLUX DENSITY
Filamentation, current profiles and transport in a tokamak
[DE93-016768] p 1584 N94-17948

PARTICLE IN CELL TECHNIQUE
General geometry PIC for MIMD computers
[AD-A269085] p 1534 N94-18767
A particle method for history-dependent materials
[DE93-018696] p 1456 N94-19060

PARTICLE INTERACTIONS
Variable time-step integration for intense field effects
[DE93-013296] p 1382 N94-17909
Report of the 1991 Workshop on Particle-Material Interactions for Fusion Research
[DE93-788393] p 1573 N94-18156
Technology, design, simulation, and evaluation for SEP-hardened circuits p 1399 N94-18352
Charmonium physics from (bar p)p interactions
[DE93-017809] p 1569 N94-18973
Task A: Yale Accelerator Users Group (YAUG)
[DE93-018417] p 1570 N94-19029

PARTICLE MASS
Cabibbo mixing in superstring derived standard-like models
[DE93-624814] p 1607 N94-17953

PARTICLE MOTION
High-performance multiprocessor architecture for a 3-D lattice gas model p 1400 N94-18362
Effects of transverse coupling on transverse beam size, simulation and measurements
[DE93-017804] p 1574 N94-18972
Visualization of turbulent flow with particles
[REPT-93-31] p 1423 N94-19645

PARTICLE PRECIPITATION
Global zones of particle precipitation as observed EXOS-C
[AD-A268758] p 1481 N94-18467

PARTICLE PRODUCTION
Beauty without charm in B-meson decays
[PREPRINT-732] p 1565 N94-17972
Experimental consequences of supersymmetry
[DE93-018270] p 1569 N94-18945
Task A: Yale Accelerator Users Group (YAUG)
[DE93-018417] p 1570 N94-19029
Extraction of Z(prime) coupling data from Z(prime) (yields) jj at the LHC and SSC
[DE93-018576] p 1570 N94-19096
Eta-nucleon interaction and nuclear production of eta mesons
[DE93-018469] p 1571 N94-19259

PARTICLE SPIN
Measuring the sea quark polarization
[DE93-015792] p 1566 N94-18234
Research activity on particle spin systems and related problems
[AD-A269456] p 1562 N94-18286

PARTICLE THEORY
Research in particle physics
[DE93-040875] p 1567 N94-18534
High energy physics program. Task A: Experiment and theory. Task B: Numerical simulation
[DE93-018140] p 1575 N94-19050
Electrokinetic transport of heterogeneous particles in suspensions
[NASA-CR-194478] p 1353 N94-19367

PARTICLE TRACKS
Measurements of cosmic ray muons with multi-wire proportional chambers with a prototype setup for KASCADE
[KFK-5173] p 1631 N94-19506

PARTICLE TRAJECTORIES
Experimental research in high energy physics
[DE93-011912] p 1574 N94-18916
Electrokinetic transport of heterogeneous particles in suspensions
[NASA-CR-194478] p 1353 N94-19367

PARTICULATE SAMPLING
Novel mass spectrometric instrument for gaseous and particulate characterization and monitoring
[DE93-019992] p 1433 N94-19054

PARTICULATES
Title 1 implementation: Status report on nonattainment areas
[DE93-017677] p 1471 N94-17777
Imaging and blackbody emission spectra of hot particulates generated during laser ablation
[DE93-015818] p 1439 N94-18724

PARTITIONS (MATHEMATICS)
An efficient implementation of error-valued semantics on imperative machines
[DE93-014658] p 1516 N94-17740
Software engineering for effective utilization of parallel processing computing system
[AD-A269191] p 1535 N94-18865
Decomposition invariance of generalized steady-state of a 1-D diffusion system
[REPT-93-26] p 1550 N94-19141

PARTONS
Measuring the sea quark polarization
[DE93-015792] p 1566 N94-18234
Investigation of physical structures and interactions at high energy
[DE93-014444] p 1574 N94-18927
The PAPAGENO Partonic Monte-Carlo Program
[DE93-018524] p 1571 N94-19247

PATENTS
Numerical and symbolic signal representation and processing
[AD-A270271] p 1389 N94-18811

PATTERN RECOGNITION
An object-oriented environment for computer vision and pattern recognition
[DE93-017098] p 1517 N94-17867
Examination of metrics and assumptions used in correlation filter design
[DE93-017636] p 1576 N94-18000
Application of the network discriminant function to learning
[AD-A268793] p 1540 N94-18189
Optical associative processors and directed graphs
[AD-A268881] p 1615 N94-18224
Evaluation of a liquid crystal spatial light modulator capable of amplitude- and phase-modulating modes
[AD-A269252] p 1577 N94-18262
Optimal design of binary phase-only filters using genetic algorithms
[AD-A268737] p 1396 N94-18278
Constructing a reference event list for ARCESS
[AD-A269288] p 1481 N94-18297
Psychophysical analyses of perceptual representations
[AD-A268711] p 1508 N94-18313
Visual perception of features and objects
[AD-A269879] p 1508 N94-18682
Operator performance in pattern matching as a function of reference material structure
[AD-A269889] p 1509 N94-18686
Neutral networks: An NRL perspective
[AD-A269122] p 1541 N94-18773
Geometrical pattern learning
[DE93-017641] p 1542 N94-19007
Serial pattern complexity: Irregularity and hierarchy
[PB93-191914] p 1509 N94-19348
A non-homogeneous, spatio-temporal, wavelet multiresolution analysis and its application to the analysis of motion
[AD-A270621] p 1538 N94-19534
Transcutaneous Analyte Measuring Methods (TAMM)
[AD-A271387] p 1408 N94-19756
A stereoscopic vision system with applications to automated docking and tracking
[AD-A270754] p 1333 N94-19765
Applications of neural networks in fault detection of rotating machinery
[AD-A270755] p 1448 N94-19766
Equivalence and reduction of hidden Markov models
[AD-A270762] p 1560 N94-19768

PAYLOAD CONTROL
Superfluid Helium On-Orbit Transfer (SHOOT) flight demonstration p 1327 N94-19185
The Cluster Joint Science Operations Centre
p 1331 N94-19639

PAYLOAD INTEGRATION

The first flight of the QUESTS GAS payload G-521
p 1325 N94-19170

Kennedy Space Center processing of Shuttle small payloads
p 1326 N94-19177

PAYLOADS

Cooperative control of multiple space manipulators
[AD-A270291] p 1445 N94-18813

The star identification, pointing and tracking system of UVSTAR, an attached payload instrument system for the Shuttle Hitchhiker-M platform
p 1326 N94-19179

Cluster: Mission, Payload, and Supporting Activities
[ESA-SP-1159] p 1328 N94-19622

PEARSON DISTRIBUTIONS

Synchronisation of cold induced vasodilation at various locations of one hand
[IZF-1992-B3] p 1504 N94-17966

PENDULUMS

A study of the amplification of laser and VLF waves using a simple pendulum model
[AD-A270857] p 1442 N94-19770

PENETRATION

SAND contact in DYNA3D
[DE93-016451] p 1340 N94-18113

The effect of crystallographic orientation on the performance of single crystal tungsten subscale penetrators
[AD-A268988] p 1597 N94-18468

Three-dimensional shock wave physics simulations with MIMD PAGOSA on massively parallel computers
[DE93-011682] p 1455 N94-18829

Earth Penetration Radar Imaging System (EPRIS)
[DE93-019690] p 1391 N94-19542

The influence of the target strength model on computed perforation
[DE93-018659] p 1460 N94-19543

PENETROMETERS

Penetrometer compatible, fiber-optic sensor for continuous monitoring of chlorinated hydrocarbons: Field test results
[DE93-017974] p 1352 N94-19266

PERFORMANCE PREDICTION

Take-off performance monitoring system algorithm and display development
[NLR-TP-91395-U] p 1317 N94-17734

A study of the automatic generating system. 3: Improvement of the total system performance
p 1429 N94-18040

RADARC HF ionospheric prediction program for OTH radar
[AD-A269557] p 1385 N94-18291

Prediction of the high-lift performance of multi-element aerofoils using an unstructured Navier-Stokes solver
p 1307 N94-18427

Turbulence modeling in aircraft icing
p 1412 N94-18555

Toward a high performance distributed memory climate model
[DE93-019156] p 1494 N94-19298

FNAS/summer faculty fellowship research continuation program. Task 6: Integrated model development for liquid fueled rocket propulsion systems. Task 9: Aspects of model-based rocket engine condition monitoring and control
[NASA-CR-194574] p 1338 N94-19706

PERFORMANCE TESTS

The stability and utility of the ESPRIT project, MUSiC, performance-based indicators of usability and tools: An evaluation of the usability of the NPL iSDX telephone system
[NPL-DITC-213/92] p 1613 N94-17925

Electric measurement of Lavet motors
p 1408 N94-18022

Reliability control for wrist watches and their casements
p 1427 N94-18030

Studies of dynamic contact of ceramics and alloys for advanced heat engines
[DE93-016366] p 1368 N94-18110

Performance evaluations of demountable electrical connections
[DE93-017399] p 1396 N94-18135

Adaptations to micropep and rocket to allow performance evaluation of multiple grain and/or airbreathing motors
[AD-A268798] p 1337 N94-18202

First on-sun test of NaK pool-boiler solar receiver
[DE93-015003] p 1466 N94-18208

Magnetic field measurements of a superconducting undulator for a Harmonic Generation FEL experiment at the NSLS
[DE93-017621] p 1438 N94-18504

Research on stable, high-efficiency amorphous silicon multijunction modules
[DE93-010046] p 1467 N94-18518

Testing and evaluation of large-area heliostats for solar thermal applications
[DE93-018509] p 1467 N94-18520

Characterization of the Facility for Atmospheric Corrosion Testing (FACT) at Sandia
[DE93-018510] p 1474 N94-18521

Evaluation of aftermarket LPG conversion kits in light-duty vehicle applications
[DE93-010035] p 1377 N94-18617

Building a joint-service classification research roadmap: Criterion-related issues
[AD-A269735] p 1512 N94-18754

Laboratory test and evaluation report of the essex model 60C-0037-2 molecular sieve oxygen generating system
[AD-A269967] p 1445 N94-18778

Technology test bed
[NASA-TM-109354] p 1322 N94-18953

Metallurgical evaluation of SRAM 2/SRAM A program mer base plates
[DE93-018689] p 1364 N94-19100

Development of a quartz digital accelerometer for environmental sensing and navigation applications
[DE93-018503] p 1433 N94-19243

On-line test methods of microprocessor based systems
[ETN-93-95008] p 1530 N94-19498

Design verification and acceptance tests of the ASST-A helium refrigeration system
[DE93-019746] p 1381 N94-19540

Human integration evaluation of three helmet systems
[AD-A271320] p 1513 N94-19570

Electro-optics display research, test, and evaluation laboratory program
[AD-A270947] p 1408 N94-19751

PERIOD DOUBLING

Bifurcation theory: Chaos and patterns
p 1607 N94-18237

PERIODIC VARIATIONS

Observations of comets with the IUE
[NASA-CR-193652] p 1624 N94-17843

Active control of periodic noise with time-varying frequency
[REPT-93-012] p 1562 N94-17934

Global zones of particle precipitation as observed EXOS-C
[AD-A268758] p 1481 N94-18467

PERMAFROST

Ground movements associated with gas hydrate production
[DE93-019887] p 1486 N94-19018

Proceedings: International Symposium on Thermal Engineering and Science for Cold Regions
[AD-A270636] p 1487 N94-19529

PERMALLOYS (TRADEMARK)

Atlas of formability: Permalloy - 80 flow stress curves
[AD-A268263] p 1356 N94-17801

PERMEABILITY

Aerosol filtration with steel fiber filters
[DE93-016990] p 1380 N94-18710

PERMITTIVITY

Numerical modelling of fringing fields and their use for complex permittivity measurements at high frequencies
[AD-A270198] p 1388 N94-18782

Polymer films with enhanced dielectric properties
[AD-A271148] p 1375 N94-19740

Theoretical and experimental studies of quantum wells
[AD-A271180] p 1606 N94-19741

PERMUTATIONS

Heap construction in the parallel comparison tree model
[TR-409] p 1538 N94-19512

PERSIAN GULF

Overview of physical oceanographic measurements taken during the Mount Mitchell cruise to ROPME sea area
[DE93-018460] p 1497 N94-18494

PERSONAL COMPUTERS

Systolic array IC for genetic computation
p 1400 N94-18361

Downsizing a database platform for increased performance and decreased costs
[DE93-018687] p 1618 N94-19099

PERSONNEL

Human reliability analysis application guide
[DE93-015361] p 1511 N94-18244

Building a joint-service classification research roadmap: Criterion-related issues
[AD-A269735] p 1512 N94-18754

Road march performance of special operations soldiers carrying various loads and load distributions
[AD-A269198] p 1512 N94-18882

PERSONNEL DEVELOPMENT

Building a joint-service classification research roadmap: Criterion-related issues
[AD-A269735] p 1512 N94-18754

PERSONNEL MANAGEMENT

Using controlled daylight exposure and sleep timing in the prevention of shift lag during night operations
[AD-A269304] p 1504 N94-17824

Computing professionals: Changing needs for the 1990's
[B-030] p 1515 N94-19401

PERSONNEL SELECTION

Computing professionals: Changing needs for the 1990's
[B-030] p 1515 N94-19401

PERTURBATION

Further on the current algebra of WZNW models at and away from criticality
[DE93-624809] p 1545 N94-17686

Exchange front stability in packed-column chromatography
[DE93-017526] p 1346 N94-17997

Fundamental research in nonlinear random vibration for aerospace applications
[AD-A268929] p 1454 N94-18487

Resonance Raman and photophysical studies of transition metal complexes in solution and entrapped in zeolites
[DE93-019892] p 1363 N94-19019

PERTURBATION THEORY

Waveguide and resonator perturbation techniques for measuring chirality and non-reciprocity of biisotropic materials
[PB93-187243] p 1384 N94-18116

PERVEANCE

Novel electron beam cathode
[AD-A270106] p 1404 N94-18872

PETRI NETS

TANGO: A notation for describing advanced transaction models
[REPT-93-014] p 1613 N94-17936

Sensitivity and uncertainty analysis of Markov reward models
[MEMO-INF-92-89] p 1559 N94-19386

PHASE CHANGE MATERIALS

Shrinkage void formation and its effect on freeze and thaw processes of lithium and lithium-fluoride for space applications
[DE93-019303] p 1338 N94-19128

PHASE CONJUGATION

Phase conjugation and beam combination using stimulated brillouin scattering
[AD-A269899] p 1439 N94-18656

PHASE DIAGRAMS

A new multiphase equation of state for iron
[DE93-017629] p 1357 N94-17819

Calculation of the LiF-CeF3-BeF2 and LiF-PuF3-BeF2 ternary phase diagrams
[DE93-017437] p 1360 N94-18501

Realistic theories of heavy electron and other strongly correlated materials
[DE93-010350] p 1571 N94-19204

PHASE ERROR

The spatial variance of ionospherically-induced phase errors in SAR imagery
[DE93-015643] p 1385 N94-18232

PHASE LOCKED SYSTEMS

Phase conjugation and beam combination using stimulated brillouin scattering
[AD-A269899] p 1439 N94-18656

A method for eliminating skew introduced by non-uniform buffer delay and wire lengths in clock distribution trees
[AD-A270649] p 1544 N94-19530

Optical frequency division using an optical parametric oscillator
[AD-A270847] p 1581 N94-19578

PHASE MODULATION

The optimal numerical algorithm for processing of phase coded time signals for radio-clocks
p 1426 N94-18018

Evaluation of a liquid crystal spatial light modulator capable of amplitude- and phase-modulating modes
[AD-A269252] p 1577 N94-18262

Alternating-phase focusing with amplitude modulation
[DE93-018618] p 1574 N94-18273

Nanostructured materials: Mind over matter
[DE93-017690] p 1597 N94-18480

Resolution in radar mapping
[AD-A269730] p 1462 N94-18753

Integrated Photonics Research: Post-deadline papers
[AD-A269232] p 1609 N94-18908

PHASE SEPARATION (MATERIALS)

Phase separation and superconductivity in La2CuO(4 + delta): Effects of oxygen diffusion
[DE93-016610] p 1594 N94-17907

Phase separation and ordering process in Al-Li alloys studied by small-angle neutron scattering and neutron diffraction
[DE93-016750] p 1358 N94-17947

PHASE SHIFT

Arc detection and protection in high-power antenna systems
[DE93-013272] p 1382 N94-17695

Development and test of readout electronics for optical quadrature signals
[DLR-MITT-92-11] p 1395 N94-17920

PHASE STABILITY (MATERIALS)

Bench-scale screening tests for a boiling sodium-potassium alloy solar receiver
[DE93-018512] p 1469 N94-19040

Fabrication, properties, and microstructures of high (Tc) tapes and coils made from Ag-clad Bi-2223 superconductor
[DE93-017405] p 1602 N94-19122

Prediction of non-equilibrium solidification modes in austenitic stainless steel laser welds
[DE93-018457] p 1364 N94-19203

PHASE TRANSFORMATIONS

On relation between Berry phase and one-dimensional models with long-range 1/r(sup 2)-interaction
[DE93-624967] p 1592 N94-17690

A new multiphase equation of state for iron
[DE93-017629] p 1357 N94-17819

Phase transitions and neutron scattering
[DE93-016748] p 1594 N94-17866

Structure, thermodynamics, and dynamical properties of supercooled liquids
[DE93-788387] p 1607 N94-18211

Phase structure of (phi(4))(sub 3) field theory at finite temperature
[DE93-629907] p 1608 N94-18267

Research activity on particle spin systems and related problems
[AD-A269456] p 1562 N94-18286

Competitive dynamics and self-organization in photorefractive systems
[AD-A269663] p 1430 N94-18569

Ionic and molecular environments in heterogeneous electrocatalysis: Studies by radioactive labeling and LEED/AUGER spectroscopy
[AD-A268850] p 1567 N94-18766

Deformation mechanisms in a Laves phase
[DE93-018331] p 1361 N94-18806

Toward a characterization of the debris cloud created in a hypervelocity impact on a thin plate
[AD-A269190] p 1455 N94-18864

Pressure induced metallization of the Mott Insulator 6(sub 2)
[DE93-018296] p 1600 N94-18969

A free energy simulation method based study of interfacial segregation
[DE93-019462] p 1364 N94-19032

The study of the phase structure of hadronic matter by searching for the deconfined quark-gluon phase transition using 2 TeV (bar-p)-p collisions, and by searching for critical phenomena in an exclusive study of multifragmentation using 1 GeV/nucleon heavy ion collisions
[DE93-018925] p 1570 N94-19103

Prediction of non-equilibrium solidification modes in austenitic stainless steel laser welds
[DE93-018457] p 1364 N94-19203

Effects of pressure on the orientational ordering and phase transitions in solid C(60) and C(70)
[DE93-018858] p 1603 N94-19347

Optical frequency doubling at adsorbates of silver(110) surface
[ETN-93-94837] p 1603 N94-19355

Melt spinning study
[NASA-CR-193823] p 1380 N94-19423

Metallization and charge-transfer gap closure of transition-metal iodides under pressure
[DE93-040301] p 1353 N94-19538

High resolution transmission electron microscopy of mesoporous MCM-41 type materials
[AD-A271271] p 1354 N94-19728

Cooperative formation of inorganic-organic interfaces in the synthesis of silicate mesostructures
[AD-A271196] p 1375 N94-19742

PHASE VELOCITY

The phase mixing of shear Alfven waves
[DE93-624920] p 1581 N94-17688

Modeling and new equipment definition for the vibration isolation box equipment system
[NASA-CR-193185] p 1379 N94-17763

PHASE-SPACE INTEGRAL

Phase space representations and quantum probability theory
[DE93-629863] p 1556 N94-18154

PHASED ARRAYS

Power compensators for phased operation of antenna arrays on JET and D3-D
[DE93-013208] p 1581 N94-17694

PHENOLS

Proton transfer dynamics and cluster ion fragmentation in phenol/ammonia cLusters
[AD-A269133] p 1348 N94-18256

PHENOMENOLOGY

Phenomenological explanation of elastic anomalies in superlattices
[DE93-017475] p 1594 N94-17871

Institute for Nuclear Theory
[DE93-017369] p 1568 N94-18824

PHONONS

Polaron tunneling in high-temperature superconductors
[DE93-016880] p 1593 N94-17754

Suppressed electron-phonon scattering in superlattices
[AD-A270834] p 1604 N94-19597

Solid-state dynamics in novel semiconductor nanostructures
[AD-A271249] p 1605 N94-19725

PHOSPHATES

An ultraviolet faraday rotator glass
[AD-D015879] p 1371 N94-18529

Advanced civil engineering materials based on inorganic polymers
[AD-A270837] p 1374 N94-19600

PHOTOCATHODES

RF phase stabilization for RF photocathode gun through electro-optical monitoring
[DE93-019059] p 1406 N94-19310

PHOTOCHEMICAL REACTIONS

Pulse radiolytic studies of electron transfer processes and applications to solar photochemistry
[DE93-018715] p 1464 N94-17781

Energy efficiency and the environment: Innovative ways to improve air quality in the Los Angeles Basin
[DE93-016964] p 1473 N94-18050

Research at the Notre Dame Radiation Laboratory
[DE93-018716] p 1566 N94-18165

Experimental and theoretical investigation of surface chemistry induced by direct and indirect electronic excitation
[AD-A268846] p 1348 N94-18221

Photo-induced and electrooptic properties of (Pb,La)(Zr,Ti)O3 films
[DE93-017496] p 1371 N94-18519

Vibrational dynamics in photoinduced electron transfer
[DE93-040874] p 1567 N94-18533

Photodissociation studies of polyatomic free radicals
[AD-A270084] p 1350 N94-18799

Summaries of FY 1993 research in the chemical sciences
[DE93-011855] p 1632 N94-18915

Oligomer and mixed-metal compounds, potential multielectron transfer catalysts
[DE93-019592] p 1350 N94-19017

Resonance Raman and photophysical studies of transition metal complexes in solution and entrapped in zeolites
[DE93-019892] p 1363 N94-19019

Kinetics programs for simulation of tropospheric photochemistry on the global scale
[DE93-019035] p 1476 N94-19104

The Mexico City 1991 lidar measurements campaign
[DE93-019960] p 1478 N94-19272

PHOTOCONDUCTORS

Photodetector array having high pixel density
[AD-D015859] p 1432 N94-18731

PHOTODISSOCIATION

Removing CFC's from the atmosphere with lasers: A second look
[DE93-017516] p 1473 N94-18101

Photodissociation studies of polyatomic free radicals
[AD-A270084] p 1350 N94-18799

Photodissociation dynamics of cluster ions
[AD-A270296] p 1568 N94-18814

Unimolecular photodissociation dynamics of ketene (CH2CO): The singlet/triplet branching ratio and experimental observation of the vibrational level thresholds of the transition-state
[DE93-019252] p 1352 N94-19304

Ultraviolet absorption cross-sections of some carbonyl compounds and their temperature dependence
[AERONAUTICA-ACTA-A-368-199]
p 1353 N94-19456

Temperature dependence of ultraviolet absorption cross-sections of alternative hydrochlorofluorocarbons
[AERONAUTICA-ACTA-A-369-199]
p 1353 N94-19459

PHOTOELECTRIC EMISSION

Dynamics of short-pulse excitation, ionization and harmonic conversion
[DE93-017220] p 1436 N94-17996

Photoemission studies of Zn, Co, and Gd substituted YBa2Cu3O(7-delta)
[DE93-017403] p 1597 N94-18498

PHOTOELECTRON SPECTROSCOPY

Guidelines for the expression of uncertainties in surface chemical analysis by Auger Electron Spectroscopy (AES) and X ray Photoelectron Spectroscopy (XPS)
[NPL-DMM(A)-99] p 1346 N94-17900

PHOTOELECTRONS

Spin-integrated and spin-dependent photoelectron diffraction
[DE93-016546] p 1565 N94-17850

Dynamics of short-pulse excitation, ionization and harmonic conversion
[DE93-017220] p 1436 N94-17996

PHOTOEXCITATION

Direct solar pumping of semiconductor lasers: A feasibility study
[NASA-CR-193760] p 1440 N94-18834

PHOTOGRAPHIC FILM

The performance and survivability of dichromated poly (vinyl alcohol) holograms for space based photonic applications
[AD-A270974] p 1434 N94-19791

PHOTOGRAPHS

Image blur
[DE93-017944] p 1580 N94-19113

PHOTOGRAPHY

High speed 512X512 camera system
[DE93-015871] p 1430 N94-18235

Image blur
[DE93-017944] p 1580 N94-19113

PHOTOIONIZATION

Production of dense vapor targets for laser-plasma interaction studies with intense, ultra-short pulses
[DE93-017175] p 1584 N94-17993

Dynamics of short-pulse excitation, ionization and harmonic conversion
[DE93-017220] p 1436 N94-17996

A physical model for one-dimension and time-dependent ionosphere. Part 1: Description of the model
[DE93-627958] p 1486 N94-19255

Harmonic generation at high intensities
[DE93-018632] p 1572 N94-19283

Ultraviolet observations of clusters of Wolf-Rayet stars in the SBm3 galaxy NGC 4214 and Ultraviolet and optical observations of LINER's
[NASA-CR-194307] p 1622 N94-19431

PHOTOLITHOGRAPHY

Field emission cathode and vacuum microelectronic microwave amplifier development
[AD-A269526] p 1403 N94-18639

PHOTOLUMINESCENCE

Pressure sensitive paint technique
p 1431 N94-18647

Study of GaAs substrates by ambient temperature photoluminescence imagery
[ECL-92-61] p 1603 N94-19357

PHOTOLYSIS

Pulse radiolytic studies of electron transfer processes and applications to solar photochemistry
[DE93-018715] p 1464 N94-17781

Nitridation of GaAs(100) by laser-induced decomposition of HN3
[AD-A269147] p 1438 N94-18258

Vibrational dynamics in photoinduced electron transfer
[DE93-040874] p 1567 N94-18533

Unimolecular photodissociation dynamics of ketene (CH2CO): The singlet/triplet branching ratio and experimental observation of the vibrational level thresholds of the transition-state
[DE93-019252] p 1352 N94-19304

Excited atomic bromine energy transfer and quenching mechanisms
[AD-A270672] p 1572 N94-19607

PHOTOMETERS

An analog retina model for detecting dim moving objects against a bright moving background
p 1399 N94-18350

Photodetector array having high pixel density
[AD-D015859] p 1432 N94-18731

Radiation induced darkening of the optical elements in the Startracker camera
[DE93-018907] p 1433 N94-19004

PHOTOMETRY

Laser guide star measurements at Lawrence Livermore National Laboratory
[DE93-018081] p 1441 N94-19251

PHOTON-ELECTRON INTERACTION

Studies of clusters
[DE93-018961] p 1572 N94-19309

PHOTONICS

Integrated photonics research volume 10. Conference edition
[AD-A269298] p 1577 N94-18298

Optical computing. Organization of the 1993 Photonics Science Topical Meetings. Technical digest series, volume 7
[AD-A269025] p 1578 N94-18332

Optical design for photonics. Organization of the 1993 Photonics Science Topical Meetings. Technical digest series, volume 9
[AD-A269027] p 1578 N94-18396

Quantum Optoelectronics. Organization of the 1993 photonics science topical meetings. Technical digest series, volume 8
[AD-A269026] p 1578 N94-18488

Advanced Solid-State Lasers/Compact Blue-Green Lasers. 1993 technical digest series. Volume 2: Organization of the 1993 photonics science topical meetings
[AD-A269058] p 1438 N94-18492

Photonics in Switching: Organization of the 1993 photonics science topical meetings. Technical digest
[AD-A269024] p 1578 N94-18528

Soft X Ray Projection Lithography. Organization of the 1993 photonics science optical meetings
[AD-A269159] p 1579 N94-18693

Integrated Photonics Research: Post-deadline papers
[AD-A269232] p 1609 N94-18908

Ultrafast Electronics and Optoelectronics: Summaries of papers. Technical digest conference edition
[AD-A269233] p 1405 N94-18909

Silicon MCM substrates for integration of 3-5 photonic devices and CMOS IC's
[DE93-017894] p 1405 N94-19112

Optoelectronic packaging: A review
[DE93-040059] p 1515 N94-19535

Novel nonlinear laser diagnostic techniques
[AD-A270968] p 1442 N94-19788

The performance and survivability of dichromated poly (vinyl alcohol) holograms for space based photonic applications
[AD-A270974] p 1434 N94-19791

PHOTONS

Space and time as outcome of decoherence in an expanding universe
[DE93-016199] p 1624 N94-18047

Criticality benchmark comparisons leading to cross-section upgrades
[DE93-017184] p 1556 N94-18073

Coherent transient systems evaluation
[AD-A268808] p 1576 N94-18204

Experimental and theoretical investigation of surface chemistry induced by direct and indirect electronic excitation
[AD-A268846] p 1348 N94-18221

Simulation of emittance dilution in electron storage ring from Compton backscattering
[DE93-017611] p 1386 N94-18503

Investigation of physical structures and interactions at high energy
[DE93-014444] p 1574 N94-18927

The study of the phase structure of hadronic matter by searching for the deconfined quark-gluon phase transition using 2 TeV (bar-p)-p collisions, and by searching for critical phenomena in an exclusive study of multifragmentation using 1 GeV/nucleon heavy ion collisions
[DE93-018925] p 1570 N94-19103

Harmonic generation at high intensities
[DE93-018632] p 1572 N94-19283

PHOTOPRODUCTION

Investigation of physical structures and interactions at high energy
[DE93-014444] p 1574 N94-18927

Research in high energy physics
[DE93-018031] p 1575 N94-19287

PHOTOSENSITIVITY

Photo-induced and electrooptic properties of (Pb,La)(Zr,Ti)O3 films
[DE93-017496] p 1371 N94-18519

PHOTOSPHERE

Spectrophotometry of emission-line stars in the magellanic clouds
[NASA-CR-194082] p 1628 N94-19425

PHOTOSYNTHESIS

Photobiotechnology: Application of photosynthesis to the production of renewable fuels and chemicals
[DE93-015522] p 1466 N94-18247

Photosynthetic responses to the environment, volume 8
[AD-A269584] p 1502 N94-18305

Photosynthetic reaction centers as active molecular electronic components, phase 1
[AD-A271368] p 1503 N94-19757

PHOTOTHERMAL CONVERSION

First on-sun test of NaK pool-boiler solar receiver
[DE93-015003] p 1466 N94-18208

Tehachapi solar thermal system
[DE93-018443] p 1468 N94-19014

Examination of charge carriers dynamics in silicon and silicon solar cells with photoinduced laser beam deflection
[ETN-93-95060] p 1470 N94-19654

PHOTOVOLTAIC CELLS

SUNRAYCE 1993: Working safely with lead-acid batteries and photovoltaic power systems
[DE93-016553] p 1464 N94-17712

Development of large-area monolithically integrated silicon-film photovoltaic modules
[DE93-010037] p 1464 N94-17731

Research on stable, high-efficiency amorphous silicon multijunction modules
[DE93-010046] p 1467 N94-18518

PHOTOVOLTAIC CONVERSION

Gallium arsenide-based ternary compounds and multi-band-gap solar cell research
[DE93-010049] p 1467 N94-18483

PHYSICAL CHEMISTRY

Energy Conversion and Storage Program
[DE93-018602] p 1469 N94-19098

Physical chemical studies of conducting polymers fundamental and applied
[AD-A270728] p 1374 N94-19574

PHYSICAL PROPERTIES

A new multiphase equation of state for iron
[DE93-017629] p 1357 N94-17819

PHYSICAL SCIENCES

Guide to programs, fiscal year 1993
[NSF-92-78] p 1633 N94-19620

PHYSICS

The 1982 to 1992 decade of research on the vacuum ultraviolet ring at National Synchrotron Light Source
[DE93-019469] p 1603 N94-19564

PHYSIOLOGICAL EFFECTS

Using controlled daylight exposure and sleep timing in the prevention of shift lag during night operations
[AD-A269304] p 1504 N94-17824

Bibliography of scientific publications of the Naval Biodynamics Laboratory, 1980 - 1992
[AD-A268886] p 1505 N94-18226

Compilation of 1992 annual reports of the navy ELF communications system ecological monitoring program. Volume 3: Tabs G - I
[AD-A269727] p 1388 N94-18741

Space research with intact organisms: The role of Space Station Freedom p 1502 N94-19213

Space research on organs and tissues
p 1503 N94-19214

Microgravity research in plant biological systems: Realizing the potential of molecular biology
p 1503 N94-19216

Life: Origin and evolution on Earth--How can we escape? p 1503 N94-19217

PHYSIOLOGICAL FACTORS

JPRS report: Central Eurasia: Aviation and cosmonautics, no. 11, November 1992
[JPRS-UAC-93-005] p 1632 N94-19208

PHYSIOLOGICAL RESPONSES

Evaluation of physiological and psychological impairment of human performance in cold stressed subjects
[AD-A268637] p 1506 N94-18632

Compilation of 1992 annual reports of the navy ELF communications system ecological monitoring program, volume 2
[AD-A269726] p 1388 N94-18751

Characterization of fluid physics effects on cardiovascular response to microgravity (G-572)
p 1323 N94-19163

A scientific role for Space Station Freedom: Research at the cellular level p 1503 N94-19215

Microgravity research in plant biological systems: Realizing the potential of molecular biology
p 1503 N94-19216

PHYSIOLOGY

Using controlled daylight exposure and sleep timing in the prevention of shift lag during night operations
[AD-A269304] p 1504 N94-17824

Evaluation of dried storage of platelets for transfusion: Physiologic integrity and hemostatic functionality
[AD-A270756] p 1507 N94-19593

PICOSECOND PULSES

Tetravalent chromium (Cr(4+)) as laser-active ion for tunable solid-state lasers
[NASA-CR-194528] p 1441 N94-19394

PIEZOELECTRIC CERAMICS

Modeling and characterization of mechanoelectric conversion piezoelectric generators through dynamical or quasi static uniaxial stress
[ISAL-92-0097] p 1406 N94-19490

PIEZOELECTRIC GAGES

Application of piezoelectric stress gauges to the measurement of fast-rise-time multimegampere electric currents
[DE93-017625] p 1429 N94-18102

PIEZOELECTRIC TRANSDUCERS

Application of piezoelectric stress gauges to the measurement of fast-rise-time multimegampere electric currents
[DE93-017625] p 1429 N94-18102

Monolithic low noise preamplifier for piezoelectric sensors
[AD-D015860] p 1563 N94-18734

PIEZOELECTRICITY

PVDF measurement of soft x ray induced shock and filter debris impulse
[DE93-017633] p 1382 N94-17806

Piezo-electric motor: Perspectives and miniaturization
p 1408 N94-18015

Application of piezoelectric stress gauges to the measurement of fast-rise-time multimegampere electric currents
[DE93-017625] p 1429 N94-18102

Office of Naval Research Publications/Patents /Presentations/Honors report, 1 October 1992 - 30 September 1993
[AD-A270037] p 1632 N94-18791

Experiments and analysis of lateral piezoresistance gauges
[DE93-017874] p 1433 N94-19111

Modeling and characterization of mechanoelectric conversion piezoelectric generators through dynamical or quasi static uniaxial stress
[ISAL-92-0097] p 1406 N94-19490

The electromechanical properties of tetragonal BaTiO3 and PbTiO3 single crystals
[DE93-019008] p 1603 N94-19550

PIGMENTS

Polyurethane self-priming topcoats
[AD-D015870] p 1367 N94-17719

PILOT PERFORMANCE

Research on man-machine productivity in aviation at Human Engineering Institute of Hangzhou University
[AD-A269952] p 1512 N94-18673

VMC left turn curved approaches, test results --- (visual meteorological conditions)
[AD-A269476] p 1316 N94-18728

Integrated measurement of crew resource management and technical flying skills
[AD-A270512] p 1510 N94-19677

PINCH EFFECT

Plasma-puff initiation of high Coulomb transfer switches
[NASA-CR-193186] p 1591 N94-19441

PIONS

On the difference caused by CP violation in the energy spectra of pions in K(sup (+-))(yields)(pi)(+-)(pi)(+-)(pi)-+ decays
[DE93-624828] p 1564 N94-17687

Meson production in relativistic heavy-ion collisions at AGS energies
[DE93-016871] p 1565 N94-17984

PIPE FLOW

Examinations of the friction behavior in nonstationary flow processes in pipes
[MITT-7] p 1423 N94-19730

PIPELINING (COMPUTERS)

Cesar user library
[FFI-93/7021] p 1529 N94-19378

PIPES (TUBES)

Summary of work on coatings and claddings for fossil energy applications
[DE93-017005] p 1367 N94-17881

Wideband electromagnetic scattering/analysis program: Far zone electromagnetic scattering from complex shapes using geometrical theory of diffraction
[AD-A268790] p 1384 N94-18187

PISTONS

Studies of dynamic contact of ceramics and alloys for advanced heat engines
[DE93-016366] p 1368 N94-18110

Acoustic propagation modeling using MATLAB
[AD-A270905] p 1564 N94-19750

PITCHING MOMENTS

Comparison between swept and delta canards on a model of a combat aircraft
[AD-A269561] p 1317 N94-17826

Aerodynamic characteristics of a helicopter rotor airfoil as affected by simulated ballistic damage
[AD-A269206] p 1311 N94-18413

Lift and pitching moment induced on jet STOVL aircraft hovering in ground effect
[AD-A269700] p 1317 N94-18577

Lift and pitching moment induced on jet STOVL aircraft by the ground vortex
[AD-A269816] p 1318 N94-18733

PIXELS

Color palette considerations for digital map displays
[AD-A269991] p 1462 N94-18679

Photodetector array having high pixel density
[AD-D015859] p 1432 N94-18731

PLANE STRAIN
Numerical analysis of pressure meter tests: Application of parameter identification of soils behavior
[ECL-92-52] p 1487 N94-19380
PLANE STRESS
Interfacial cracks in plates: A three-dimensional numerical investigation p 1456 N94-19116
Formulation and identification of the anisotropic laws for thin sheets drawing
[ECL-92-55] p 1365 N94-19400
PLANE WAVES
Development of parallel architectures for sensor array processing, volume 1
[AD-A270426] p 1534 N94-18507
A parallel and pipelined architecture for estimation of direction of arrival using a bilinear transformation method, volume 3
[AD-A270137] p 1389 N94-18897
Transmission of acoustic waves through strongly heterogeneous, two-dimensional velocity models
[REPT-93-09] p 1563 N94-19083
PLANETARY BOUNDARY LAYER
A new approach to the study of the turbulence layer
[NASA-CR-194546] p 1487 N94-19397
PLANETARY CRUSTS
JPRS report: Science and technology. Central Eurasia: Space
[JPRS-USP-93-004] p 1323 N94-19146
PLANETARY EVOLUTION
Applications of Quaternary stratigraphic, soil-geomorphic, and quantitative geomorphic analyses to the evaluation of tectonic activity and landscape evolution in the Upper Coastal Plain, South Carolina
[DE93-016269] p 1484 N94-18725
PLANETARY GEOLOGY
Applications of Quaternary stratigraphic, soil-geomorphic, and quantitative geomorphic analyses to the evaluation of tectonic activity and landscape evolution in the Upper Coastal Plain, South Carolina
[DE93-016269] p 1484 N94-18725
Magellan, Galileo, and Ulysses
[NASA-TM-109362] p 1628 N94-18958
JPRS report: Science and technology. Central Eurasia: Space
[JPRS-USP-93-004] p 1323 N94-19146
PLANETARY RINGS
Voyager's last encounter
[NASA-TM-109361] p 1628 N94-18957
PLANETARY STRUCTURE
The use of velocity spectra for stacking receiver functions with application to IRIS/IDA stations OBNINSK (OBN) and ARTI (ARU), Russia
[AD-A269087] p 1483 N94-18717
PLANETARY WAVES
Planetary plasma waves
[NASA-CR-194295] p 1629 N94-19094
PLANNING
Bias in planning and explanation-based learning
[AD-A269608] p 1610 N94-17746
PRACTICAL: Planning and resource allocation in C2-domains with time critical algorithms
[FEL-93-B029] p 1544 N94-19458
Statistical probabilities for planning
[TR-474] p 1559 N94-19511
PLANTING
The carbon dioxide emissions game: Playing the net
[DE93-017670] p 1471 N94-17821
PLANTS (BOTANY)
Photosynthetic responses to the environment, volume 8
[AD-A269584] p 1502 N94-18305
Compilation of 1992 annual reports of the Navy ELF communications system ecological monitoring program, volume 1
[AD-A269569] p 1386 N94-18473
Compilation of 1992 annual reports of the navy ELF communications system ecological monitoring program, volume 2
[AD-A269726] p 1388 N94-18751
Microgravity research in plant biological systems: Realizing the potential of molecular biology
p 1503 N94-19216
PLASMA ACCELERATION
Observations of MeV electrons and scattered light from intense, subpicosecond laser-plasma interactions
[DE93-017153] p 1435 N94-17855
PLASMA ANTENNAS
Plasma production by helicon waves
[DE93-788396] p 1586 N94-18213
PLASMA CONTROL
ITER EDA design confinement capability
[DE93-013729] p 1582 N94-17697
Limits on m = 2, n = 1 error field induced locked mode instability in TPX with typical sources of poloidal field coil error field and a proto type correction coil, C-coil
[DE93-014408] p 1582 N94-17702
Self-regulated shear flow turbulence in confined plasmas
[DE93-015823] p 1583 N94-17743
Analysis of the ITER H-mode confinement database
[DE93-016984] p 1585 N94-18056
Coupled MHD and transport analysis of improved confinement D3-D discharges
[DE93-016985] p 1585 N94-18057
Dependence of helium transport on plasma current and ELM frequency in H-mode discharges in D3-D
[DE93-016986] p 1585 N94-18058
Application of piezoelectric stress gauges to the measurement of fast-rise-time multimegampere electric currents
[DE93-017625] p 1429 N94-18102
Ion mobility and transport barriers in the tokamak plasmas
[DE93-040320] p 1587 N94-18524
Materials processing and manufacturing technologies for diamond substrates multichip modules
[AD-A268989] p 1599 N94-18764
Lower hybrid counter current drive for edge current density modification in D3-D
[DE93-019157] p 1589 N94-19073
Modelization, numerical simulation and optimal control of NET tokamak plasma configuration evolution for the future generation of fusion reactors
[ETN-93-95019] p 1591 N94-19364
Transverse beam combiner for ILSE
[DE93-019239] p 1591 N94-19559
Theoretical studies of turbulence and anomalous transport in toroidal confinement devices
[DE93-040684] p 1592 N94-19656
PLASMA CURRENTS
Detailed analysis of low energy plasma data under the Voyager Uranus data analysis program
[NASA-CR-193668] p 1628 N94-17842
Filamentary magnetohydrodynamic plasmas
[DE93-015616] p 1583 N94-17945
Coupled MHD and transport analysis of improved confinement D3-D discharges
[DE93-016985] p 1585 N94-18057
Dependence of helium transport on plasma current and ELM frequency in H-mode discharges in D3-D
[DE93-016986] p 1585 N94-18058
Lower hybrid counter current drive for edge current density modification in D3-D
[DE93-019157] p 1589 N94-19073
Electron cyclotron resonance heating in the microwave tokamak experiment
[DE93-018083] p 1590 N94-19289
Modelization, numerical simulation and optimal control of NET tokamak plasma configuration evolution for the future generation of fusion reactors
[ETN-93-95019] p 1591 N94-19364
PLASMA DENSITY
Characterization of short pulse laser-produced plasmas at the Lawrence Livermore National Laboratory ultra short-pulse laser
[DE93-017191] p 1585 N94-18082
Plasma production by helicon waves
[DE93-788396] p 1586 N94-18213
An investigation of methods for updating ionospheric scintillation models using topside in-situ plasma density measurements
[AD-A269872] p 1483 N94-18655
Phase-space description of plasma waves: Linear and nonlinear theory
[IRF-SR-211] p 1587 N94-18860
The spherical probe Electric Field and Wave Experiment for the Cluster mission p 1328 N94-19624
WHISPER: A sounder and high-frequency wave analyser experiment p 1328 N94-19626
PLASMA DIAGNOSTICS
Analysis of neon soft x ray spectra from short-pulse laser-produced plasmas
[DE93-014420] p 1582 N94-17708
Application of piezoelectric stress gauges to the measurement of fast-rise-time multimegampere electric currents
[DE93-017625] p 1429 N94-18102
Time-resolved probing of electron thermal conduction in femtosecond-laser-pulse-produced plasmas
[DE93-016996] p 1585 N94-18129
Development of short pulse soft x ray lasers
[DE93-017150] p 1437 N94-18131
Active neutral particle diagnostics for high temperature plasma
[DE93-788457] p 1586 N94-18214
Experiments on nonlinear absorption of ECH waves in MTX and a comparison with theory
[DE93-019158] p 1589 N94-19074
Electron cyclotron resonance heating in the microwave tokamak experiment
[DE93-018083] p 1590 N94-19289
PLASMA DRIFT
Convection algorithms for magnetospheric particles
[AD-A270103] p 1493 N94-18871
PLASMA DYNAMICS
Filamentary magnetohydrodynamic plasmas
[DE93-015616] p 1583 N94-17945
Ion mobility and transport barriers in the tokamak plasmas
[DE93-040320] p 1587 N94-18524
RAPID: The imaging energetic particle spectrometer on Cluster p 1329 N94-19633
PLASMA ELECTRODES
Evaluation of materials proposed for the construction of the Plasma Electrode Pockels Cell (PEPC) on beamlet
[DE93-016952] p 1584 N94-17988
PLASMA EQUILIBRIUM
Profile stabilization of tilt mode in a field reversed configuration
[DE93-016770] p 1583 N94-17753
A free boundary eigenvaue problem
[IPP-6/310] p 1584 N94-17981
Nonparaxial MHD stabilizers for an axisymmetric magnetic mirror
[DE93-017996] p 1587 N94-18505
Finite beta plasma equilibrium in toroidally linked mirrors
[DE93-040318] p 1590 N94-19193
On neutral plasma oscillations
[DE93-040319] p 1590 N94-19194
PLASMA ETCHING
Field emission cathode and vacuum microelectronic microwave amplifier development
[AD-A269526] p 1403 N94-18639
PLASMA HEATING
Power compensators for phased operation of antenna arrays on JET and D3-D
[DE93-013208] p 1581 N94-17694
Arc detection and protection in high-power antenna systems
[DE93-013272] p 1382 N94-17695
ITER EDA design confinement capability
[DE93-013729] p 1582 N94-17697
Design of a tunable 4-MW free electron maser for heating fusion plasmas
[DE93-017172] p 1437 N94-18134
Plasma production by helicon waves
[DE93-788396] p 1586 N94-18213
Experiments on nonlinear absorption of ECH waves in MTX and a comparison with theory
[DE93-019158] p 1589 N94-19074
ICRF direct electron heating experiments in TFTR
[DE93-017857] p 1590 N94-19273
Electron cyclotron resonance heating in the microwave tokamak experiment
[DE93-018083] p 1590 N94-19289
PLASMA INTERACTIONS
Plasma contactor development for Space Station
[NASA-TM-106425] p 1587 N94-18861
The study of the phase structure of hadronic matter by searching for the deconfined quark-gluon phase transition using 2 TeV (bar-p)-p collisions, and by searching for critical phenomena in an exclusive study of multifragmentation using 1 GeV/nucleon heavy ion collisions
[DE93-018925] p 1570 N94-19103
PLASMA LAYERS
Time-resolved probing of electron thermal conduction in femtosecond-laser-pulse-produced plasmas
[DE93-016996] p 1585 N94-18129
Radiative divertor modeling studies
[DE93-018092] p 1590 N94-19290
Behavior of the particle transport coefficients near the density limit in MTX
[DE93-019108] p 1591 N94-19311
PLASMA OSCILLATIONS
On neutral plasma oscillations
[DE93-040319] p 1590 N94-19194
PLASMA PHYSICS
Problems related to stimulated electromagnetic emissions, strong turbulence and ionospheric modification
[IRF-SR-212] p 1480 N94-17720
Self-regulated shear flow turbulence in confined plasmas
[DE93-015823] p 1583 N94-17743
Plasma properties research: Task 3
[DE93-017087] p 1583 N94-17854
Center of Excellence in Theoretical Geoplasma Research
[AD-A270210] p 1588 N94-18902
Review Committee report on the conceptual design of the tokamak physics experiment
[DE93-018408] p 1588 N94-19012

Generalized energy principle for flute perturbations in axisymmetric mirror machines
[DE93-019399] p 1589 N94-19037

PLASMA PINCH
Plasma-puff initiation of high Coulomb transfer switches
[NASA-CR-193186] p 1591 N94-19441

PLASMA POTENTIALS
Plasma contactor development for Space Station
[NASA-TM-106425] p 1587 N94-18861

PLASMA PRESSURE
Finite beta plasma equilibrium in toroidally linked mirrors
[DE93-040318] p 1590 N94-19193

PLASMA RADIATION
Application of piezoelectric stress gauges to the measurement of fast-rise-time multimegampere electric currents
[DE93-017625] p 1429 N94-18102
Substrate temperature measurement and control during thermal plasma CVD
[DE93-040305] p 1433 N94-19135

PLASMA RESONANCE
Resonant absorption of Alfven waves near a neutral point
[DE93-628761] p 1586 N94-18172

PLASMA SHEATHS
Detailed analysis of low energy plasma data under the Voyager Uranus data analysis program
[NASA-CR-193668] p 1628 N94-17842

PLASMA SPECTRA
Detailed analysis of low energy plasma data under the Voyager Uranus data analysis program
[NASA-CR-193668] p 1628 N94-17842

PLASMA TEMPERATURE
Characterization of short pulse laser-produced plasmas at the Lawrence Livermore National Laboratory ultra short-pulse laser
[DE93-017191] p 1585 N94-18082

PLASMA TURBULENCE
Problems related to stimulated electromagnetic emissions, strong turbulence and ionospheric modification
[IRF-SR-212] p 1480 N94-17720
Behavior of the particle transport coefficients near the density limit in MTX
[DE93-019108] p 1591 N94-19311
Radial evolution of the solar wind turbulence with application to charged particle transport
[NASA-CR-194081] p 1629 N94-19427
The Wave Experiment Consortium
p 1328 N94-19623
Theoretical studies of turbulence and anomalous transport in toroidal confinement devices
[DE93-040684] p 1592 N94-19656

PLASMA WAVES
The phase mixing of shear Alfven waves
[DE93-624920] p 1581 N94-17688
Transformation of energy and momentum due to Landau damping in space
[DE93-624921] p 1581 N94-17689
Resonant absorption of Alfven waves near a neutral point
[DE93-628761] p 1586 N94-18172
Plasma production by helicon waves
[DE93-788396] p 1586 N94-18213
Phase-space description of plasma waves: Linear and nonlinear theory
[IRF-SR-211] p 1587 N94-18860
Planetary plasma waves
[NASA-CR-194295] p 1629 N94-19094
On neutral plasma oscillations
[DE93-040319] p 1590 N94-19194
The Wave Experiment Consortium
p 1328 N94-19623
The spherical probe Electric Field and Wave Experiment for the Cluster mission p 1328 N94-19624
WHISPER: A sounder and high-frequency wave analyser experiment p 1328 N94-19626
The wideband plasma wave investigation
p 1328 N94-19627
Implementation of the digital wave-processing experiment p 1329 N94-19628

PLASMA-ELECTROMAGNETIC INTERACTION
Limits on m = 2, n = 1 error field induced locked mode instability in TPX with typical sources of poloidal field coil error field and a proto type correction coil, C-coil
[DE93-014408] p 1582 N94-17702
Wake field in electron-positron plasmas
[DE93-624929] p 1584 N94-17955
Resonant absorption of Alfven waves near a neutral point
[DE93-628761] p 1586 N94-18172
Studies of enhanced radar backscatter
[AD-A269544] p 1385 N94-18288

PLASMA-PARTICLE INTERACTIONS
Advanced fusion diagnostics
[DE93-040085] p 1589 N94-19133

PLASMAS (PHYSICS)
Observations of MeV electrons and scattered light from intense, subpicosecond laser-plasma interactions
[DE93-017153] p 1435 N94-17855
Configuration interaction in LTE spectra of heavy elements
[DE93-017166] p 1584 N94-17990
Analysis of the ITER H-mode confinement database
[DE93-016984] p 1585 N94-18056
Coupled MHD and transport analysis of improved confinement D3-D discharges
[DE93-016985] p 1585 N94-18057
Dependence of helium transport on plasma current and ELM frequency in H-mode discharges in D3-D
[DE93-016986] p 1585 N94-18058
Characterization of short pulse laser-produced plasmas at the Lawrence Livermore National Laboratory ultra short-pulse laser
[DE93-017191] p 1585 N94-18082
AEOLUS-IT MHD simulation code based on a toroidally incompressible plasma model
[DE93-788461] p 1586 N94-18157
RF vacuum microelectronics
[AD-A269454] p 1396 N94-18284
Nonparaxial MHD stabilizers for an axisymmetric magnetic mirror
[DE93-017996] p 1587 N94-18505
Center of Excellence in Theoretical Geoplasma Research
[AD-A270210] p 1588 N94-18902
Viscosity in the edge of tokamak plasmas
[DE93-018039] p 1588 N94-18988
Experiments on nonlinear absorption of ECH waves in MTX and a comparison with theory
[DE93-019158] p 1589 N94-19074
Radiative divertor modeling studies
[DE93-018092] p 1590 N94-19290
Manufacturing technology
[DE93-019580] p 1381 N94-19480

PLASMONS
Experimental and theoretical investigation of surface chemistry induced by direct and indirect electronic excitation
[AD-A268846] p 1348 N94-18221
Metal Film Surface Plasmon Resonance (MFSPR) fibre couplers
[AD-A268871] p 1579 N94-18635

PLASTIC AIRCRAFT STRUCTURES
New aircraft materials and structures
[MBB-LME-202-S-PUB-502-A] p 1319 N94-19496

PLASTIC ANISOTROPY
Plastic anisotropy in MoSi2 single crystals
[DE93-012650] p 1594 N94-17874

PLASTIC DEFORMATION
Modeling microstructural evolution and the mechanical response of superplastic materials
[DE93-014417] p 1355 N94-17711
A benchmark bending test of a thick specimen. Part 1: Experiments
[AD-A268730] p 1360 N94-18325
Dislocation-drag contribution to high-rate plastic deformation in shock-loaded tantalum
[DE93-018286] p 1361 N94-18802
Deformation mechanisms in a Laves phase
[DE93-018331] p 1361 N94-18806
Influence of peak pressure and temperature on the shock-loading response of tantalum
[DE93-018561] p 1457 N94-19279
The effect of composition on the mechanism of continuous recrystallization and superplastic response of aluminum-scandium alloys
[DE93-018594] p 1365 N94-19280
Ni-Al2O3 solid state binding: Elaboration, state of thermal constraints, mechanical behavior
[ECL-92-31] p 1366 N94-19436
Current capabilities for simulating the extreme distortion of thin structures subjected to severe impacts
p 1459 N94-19474
Crashdynamics with DYNA3D: Capabilities and research directions p 1460 N94-19475

PLASTIC FLOW
Interdisciplinary research on wear of materials
[AD-A268190] p 1443 N94-17730
Dislocation-drag contribution to high-rate plastic deformation in shock-loaded tantalum
[DE93-018286] p 1361 N94-18802
HEMP 3D: A finite difference program for calculating elastic-plastic flow, appendix B
[AD-A269171] p 1418 N94-18878

PLASTIC PROPERTIES
Computational strategies for composite structures
[PB93-195097] p 1452 N94-18079
Several fundamental issues in the mechanics of inelastic behavior
[AD-A269455] p 1453 N94-18285
HEMP 3D: A finite difference program for calculating elastic-plastic flow, appendix B
[AD-A269171] p 1418 N94-18878
A constitutive theory for rigid polyurethane foam
[DE93-011596] p 1372 N94-19059
Plastic mechanism analysis of T-joints in RHS subject to combined bending and concentrated force
[PB93-195774] p 1456 N94-19061
Formulation and identification of the anisotropic laws for thin sheets drawing
[ECL-92-55] p 1365 N94-19400

PLASTICS
Sputtered TiN coatings in plastic
p 1367 N94-18011
Ageing in Processed Polymers: Programme, summary, and abstracts discussion meeting
[AD-A268931] p 1370 N94-18448
Simulation of the impact of a plastic flyer on an aluminum block using the hydrocode AUTODYNE
[PML-1992-26] p 1458 N94-19444

PLATELETS
Evaluation of dried storage of platelets for transfusion: Physiologic integrity and hemostatic functionality
[AD-A270756] p 1507 N94-19593

PLATES (STRUCTURAL MEMBERS)
Development of a finite element method program for the analysis of laminated composite plates using first-order shear deformation theory
[AD-A270318] p 1342 N94-18700

PLATES (TECTONICS)
Current (1985-1988) seismic activity in Belgium: Comparison with historical and instrumental seismic data
p 1482 N94-18624
What can gravimetry contribute to recent and current tectonics in Belgium? p 1482 N94-18626

PLATINUM
Potential dependent structural changes of underpotentially deposited copper on an iodine treated platinum surface determined in situ by surface EXAFS and its polarization dependence
[AD-A269890] p 1360 N94-18687

PLOTTING
Computer codes for checking, plotting and processing of neutron cross-section covariance data and their application
[DE93-018459] p 1570 N94-19129

PLUMES
Low power arcjet system spacecraft impacts
[NASA-TM-106307] p 1336 N94-17856
A Bayesian approach to contaminant plume delineation
[DE93-012909] p 1472 N94-17890
UVPI imaging from the LACE satellite: The Nihka rocket plume
[AD-A268456] p 1334 N94-18149
Characterization of vapor plume species and deposition residues resulting from pulsed laser ablation of a graphite/epoxy composite
[AD-A270101] p 1343 N94-18869
Forward scattering of a pulsed continuous wave signal through laminar and turbulent thermal plumes
[AD-A271210] p 1564 N94-19723
UVPI imaging from the LACE satellite: The Strypi rocket plume
[AD-A270967] p 1335 N94-19787

PLUTONIUM FLUORIDES
Calculation of the LiF-CeF3-BeF2 and LiF-PuF3-BeF2 ternary phase diagrams
[DE93-017437] p 1360 N94-18501

PNEUMATIC EQUIPMENT
Friction drive position transducer
[AD-D015851] p 1424 N94-17717
A finite strain ring dynamical model for pneumatic tires
[AD-A269286] p 1444 N94-18266
Study and modeling of compressible flows of flapper nozzle type potentiometric systems
[ETN-93-95012] p 1421 N94-19495

POINT DEFECTS
Lattice damage in ion-implanted compound semiconductors and its effect on electrical activation
[DE93-015907] p 1593 N94-17845

POINTING CONTROL SYSTEMS
The star identification, pointing and tracking system of UVSTAR, an attached payload instrument system for the Shuttle Hitchhiker-M platform p 1326 N94-19179

POINTS (MATHEMATICS)
Interior-point methodology for linear programming: Duality, sensitivity analysis and computational aspects
[REPT-93-28] p 1525 N94-19143

POISSON DENSITY FUNCTIONS
JSEP fellowship: Fractal noise processes
[AD-A268841] p 1557 N94-18540

POISSON EQUATION
Calculation of turbulent boundary layer wall pressure spectra
[AD-A269549] p 1416 N94-18642
Solution of the Poisson equation with application to radar imaging
[PB93-195865] p 1389 N94-18950

POLARIMETRY
Polarimetric statistics of electromagnetic waves scattered by distributed targets
[PB93-195907] p 1389 N94-18951

POLARIZATION
Polarized thin films from dye-substituted polymers containing hydrophobically terminated stilbazolium radicals
[AD-D015873] p 1367 N94-17706

POLARIZATION (CHARGE SEPARATION)
Relaxation of polar orientational order in nonlinear optical polymers by second harmonic generation
[AD-A269059] p 1370 N94-18515

POLARIZATION (SPIN ALIGNMENT)
Measuring the sea quark polarization
[DE93-015792] p 1566 N94-18234

POLARIZATION (WAVES)
Crystal optics of high energy gamma-beams
[DE93-630228] p 1577 N94-18217
Potential dependent structural changes of underpotentially deposited copper on an iodine treated platinum surface determined in situ by surface EXAFS and its polarization dependence
[AD-A269890] p 1360 N94-18687
A comparison of single-station backazimuth estimates with regional event locations in the Central Appalachians
[AD-A269897] p 1483 N94-18690
Polarimetric statistics of electromagnetic waves scattered by distributed targets
[PB93-195907] p 1389 N94-18951

POLARIZATION CHARACTERISTICS
Potential dependent structural changes of underpotentially deposited copper on an iodine treated platinum surface determined in situ by surface EXAFS and its polarization dependence
[AD-A269890] p 1360 N94-18687

POLARIZED LIGHT
Polarized optical emission due to decay or recombination of spin-polarized injected carriers
[AD-D015907] p 1408 N94-19763

POLARIZERS
Mesoepitaxy: A universal route to oriented materials
[AD-A270437] p 1598 N94-18511

POLARONS
Polaron tunneling in high-temperature superconductors
[DE93-016880] p 1593 N94-17754

POLICIES
Setting the global thermostat with an exhaustible tradeable permit system
[DE93-012911] p 1472 N94-17891
Coastal Ocean Modeling Workshop
[AD-A268955] p 1497 N94-18393
Land-use related sources of CO2, CH4 and N2O: Current global emissions and projections for the period 1990-2100
[PB93-194819] p 1475 N94-18949
Finding optimal policies for Markov decision chains: A unifying framework for mean-variance-tradeoffs
[PB93-191930] p 1559 N94-19555

POLISHING
Surface modification of sapphire for IR window application
[DE93-019168] p 1602 N94-19075
Synchrotron/crystal sample preparation
[NASA-CR-193837] p 1603 N94-19513
Precision machining and polishing of scintillating crystals for large calorimeters and hodoscopes
[DE93-018663] p 1381 N94-19544

POLLUTION CONTROL
Title 1 implementation: Status report on nonattainment areas
[DE93-017677] p 1471 N94-17777
The carbon dioxide emissions game: Playing the net
[DE93-017670] p 1471 N94-17821
Cost effective energy strategies for the reduction of CO2 emissions in the United States: Country report for ETSAP Annex 4
[DE93-016842] p 1472 N94-17852
A comparison of wet and dry scrubbing systems for control of metals and dioxin/furan emissions from incinerators
[DE93-017446] p 1474 N94-18502
Land-use related sources of CO2, CH4 and N2O: Current global emissions and projections for the period 1990-2100
[PB93-194819] p 1475 N94-18949
Organic carbonyl compounds in Albuquerque, New Mexico, air: A preliminary study of the effects of oxygenated fuel use
[DE93-017748] p 1476 N94-19045
Valuation of temporary and future greenhouse gas reductions
[DE93-018876] p 1478 N94-19319

POLLUTION MONITORING
On-line monitoring of incinerator emissions
[DE93-017406] p 1474 N94-18499
Organic carbonyl compounds in Albuquerque, New Mexico, air: A preliminary study of the effects of oxygenated fuel use
[DE93-017748] p 1476 N94-19045
Novel mass spectrometric instrument for gaseous and particulate characterization and monitoring
[DE93-019992] p 1433 N94-19054
Spatiotemporal variability of non-urban ozone concentrations over the eastern United States and its potential replication by satellite data
[PB93-191328] p 1476 N94-19065
Advances in passive-remote and extractive Fourier transform infrared systems
[DE93-017402] p 1478 N94-19241

POLLUTION TRANSPORT
A review of wind field models for atmospheric transport
[DE93-016085] p 1488 N94-17895
International Symposium on the Ecological Effects of Arctic Airborne Contaminants --- abstracts
[AD-A269955] p 1475 N94-18775
Inclusion of a three-dimensional washout coefficient in ADPIC
[DE93-018499] p 1476 N94-19038
Application of an atmospheric dispersion model to simulated pollutant releases in the Colorado Front range
[DE93-017118] p 1480 N94-19732

POLYAMIDE RESINS
Mechanical properties and impact damage resistance of composites fabricated by low cost, vacuum assisted, resin transfer molding
[AD-A270361] p 1342 N94-18702

POLYATOMIC MOLECULES
Photodissociation studies of polyatomic free radicals
[AD-A270084] p 1350 N94-18799

POLYCARBONATES
Structure and properties of polycarbonate alloys
[ETN-93-95071] p 1375 N94-19611

POLYCRYSTALS
Development of large-area monolithically integrated silicon-film photovoltaic modules
[DE93-010037] p 1464 N94-17731
Phase separation and ordering process in Al-Li alloys studied by small-angle neutron scattering and neutron diffraction
[DE93-016750] p 1358 N94-17947
Self-organized criticality and the Barkhausen effect in amorphous and polycrystalline metals
[AD-A269817] p 1361 N94-18735
Growth, characterization and device development in monocrystalline diamond films
[AD-A270074] p 1599 N94-18797
Polycrystalline thin-film cadmium telluride solar cells fabricated by electrodeposition
[DE93-018201] p 1468 N94-18944
Defect behavior of polycrystalline solar cell silicon
[DE93-018490] p 1468 N94-19016
Tribological studies of silicon for magnetic recording applications (Invited)
[AD-A270878] p 1447 N94-19784

POLYESTER RESINS
Polymer technology publication. Series no. 14, 1993
[PB93-195964] p 1372 N94-19052

POLYESTERS
Mechanical properties and impact damage resistance of composites fabricated by low cost, vacuum assisted, resin transfer molding
[AD-A270361] p 1342 N94-18702

POLYETHYLENES
Computer simulation of macromolecular crystals and their defects
[DE93-015213] p 1596 N94-18192
Mesoepitaxy: A universal route to oriented materials
[AD-A270437] p 1598 N94-18511

POLYIMIDES
Excimer laser induced permanent electrical conductivity and nanostructures in polymers
[DE93-015965] p 1368 N94-17946
Elastic properties of a polyimide film determined by Brillouin scattering and mechanical techniques
[DE93-017404] p 1368 N94-18098

POLYMER BLENDS
Polymer technology publication. Series no. 14, 1993
[PB93-195964] p 1372 N94-19052
Structure and properties of polycarbonate alloys
[ETN-93-95071] p 1375 N94-19611
Polymer films with enhanced dielectric properties
[AD-A271148] p 1375 N94-19740

POLYMER CHEMISTRY
Royal Society of Chemistry, Heterocyclic Chemistry Group, Lakeland Heterocyclic Symposium
[AD-A270374] p 1338 N94-18703
Molecular and polymeric ceramic precursors
[DE93-040364] p 1372 N94-18891
Physical chemical studies of conducting polymers fundamental and applied
[AD-A270728] p 1374 N94-19574

POLYMER MATRIX COMPOSITES
Molecular composites from liquid crystalline polymers and liquid crystalline thermosets
[DE93-016608] p 1368 N94-18096
Nondestructive inspection of graphite-epoxy laminates for heat damage using DRIFT and LPF spectroscopies
[DE93-017228] p 1343 N94-18761

POLYMERIC FILMS
Polarized thin films from dye-substituted polymers containing hydrophobically terminated stilbazolium radicals
[AD-D015873] p 1367 N94-17706
Elastic properties of a polyimide film determined by Brillouin scattering and mechanical techniques
[DE93-017404] p 1368 N94-18098
Polymer films with enhanced dielectric properties
[AD-A271148] p 1375 N94-19740

POLYMERIZATION
Detonation reaction steps frozen by free expansion and analyzed by mass spectrometry
[DE93-012734] p 1376 N94-17813
Polymerizable lipids in the development of controlled release carriers
[AD-D015789] p 1368 N94-17982
Morphology of polymerized membranes on an amorphous substrate at molecular resolution by AFM
[AD-A268760] p 1370 N94-18403
Strained ring energetic binders
[AD-A269056] p 1377 N94-18491
Cooperative formation of inorganic-organic interfaces in the synthesis of silicate mesostructures
[AD-A271196] p 1375 N94-19742

POLYMERS
NMR studies of enriched species at interfaces
[AD-A264703] p 1367 N94-17878
Mechanical-property changes of structural composite materials after low-temperature proton irradiation: Implications for use in SSC magnet systems
[DE93-016735] p 1343 N94-18763

POLYMETHYL METHACRYLATE
Structure and properties of polycarbonate alloys
[ETN-93-95071] p 1375 N94-19611

POLYNOMIALS
An extension of Wolovich's definition of equivalence of linear systems
[MATHS-REPT-A-183] p 1547 N94-18069
Introduction to spectral methods: Application to the Stokes problem p 1413 N94-18566
Active control of a multivariable system by way of polynomial neural networks: Computer simulation evaluations and laboratory experimental results
[AD-A270033] p 1541 N94-18790
Difference equations for generalized Meixner polynomials
[REPT-93-17] p 1550 N94-19082
A polynomial primal-dual Dikin-type algorithm for linear programming
[REPT-93-36] p 1525 N94-19156
On polynomials orthogonal with respect to an inner product involving differences (the general case)
[REPT-93-32] p 1551 N94-19285
Notes on multi-step ahead prediction based on the principle of concatenation
[MATHS-REPT-A-189] p 1544 N94-19410

POLYPEPTIDES
Polaron tunneling in high-temperature superconductors
[DE93-016880] p 1593 N94-17754

POLYTETRAFLUOROETHYLENE
Mesoepitaxy: A universal route to oriented materials
[AD-A270437] p 1598 N94-18511

POLYTOPES
Finding optimal policies for Markov decision chains: A unifying framework for mean-variance-tradeoffs
[PB93-191930] p 1559 N94-19555

POLYURETHANE FOAM
A constitutive theory for rigid polyurethane foam
[DE93-011596] p 1372 N94-19059

POLYURETHANE RESINS
Polyurethane self-priming topcoats
[AD-D015870] p 1367 N94-17719

POLYVINYL ALCOHOL
The performance and survivability of dichromated poly (vinyl alcohol) holograms for space based photonic applications
[AD-A270974] p 1434 N94-19791

POLYVINYL FLUORIDE
PVDF measurement of soft x ray induced shock and filter debris impulse
[DE93-017633] p 1382 N94-17806

POPULATIONS
Uncertainty versus interindividual variability
[DE93-018105] p 1559 N94-19549

POROSITY
Process relationship as influenced by carbonization rate
[AD-A269680] p 1341 N94-18572
Hydrolysis reaction and positronium decay in silica gels
[AD-A270028] p 1371 N94-18713
Development of the microstructure based stochastic life prediction model
[AD-A269742] p 1361 N94-18742
Numerical simulation of fluid dynamics and combustion for ram accelerator projectile/obturator interaction
[AD-A269715] p 1320 N94-18748
Modeling of the formation of microporosity in alloys
[DE93-017733] p 1364 N94-19044
Microstructure of the interfacial zone around aggregate particles in concrete
[PB93-195790] p 1380 N94-19322
High resolution transmission electron microscopy of mesoporous MCM-41 type materials
[AD-A271271] p 1354 N94-19728

POROUS MATERIALS
The Aerocapacitor: A carbon aerogel based supercapacitor
[DE93-016537] p 1395 N94-17849
Characterization of short pulse laser-produced plasmas at the Lawrence Livermore National Laboratory ultra short-pulse laser
[DE93-017191] p 1585 N94-18082

PORPHYRINS
Pulse radiolytic studies of electron transfer processes and applications to solar photochemistry
[DE93-018715] p 1464 N94-17781

PORTABLE EQUIPMENT
Portable, solid state, fiber optic coupled Doppler interferometer system for detonation and shock diagnostics
[DE93-013917] p 1423 N94-17700
The First International Conference on PCTE
[FEL-92-A134] p 1518 N94-17965

POSITION (LOCATION)
Intentionally Short Range Communications (ISRC)
[AD-A268788] p 1384 N94-18216
Constructing a reference event list for ARCESS
[AD-A269288] p 1481 N94-18297
Historical seismicity of Hainaut, Flanders and Artois
p 1482 N94-18623
A program for passively tracking a target using an array of sensors
[DE93-019554] p 1390 N94-19306

POSITION ERRORS
Limits on m = 2, n = 1 error field induced locked mode instability in TPX with typical sources of poloidal field coil error field and a proto type correction coil, C-coil
[DE93-014408] p 1582 N94-17702
Flight demonstration of image fix-taking with SAR
[DE93-016499] p 1382 N94-17861
About the accuracy of an image-based navigation system during the runway approach
[DLR-MITT-93-01] p 1316 N94-18146

POSITIONING
Six degree of freedom fine motion positioning stage based on magnetic levitation
[DE93-017651] p 1446 N94-19547
Absolute positioning by collecting Global Positioning System (GPS) data along short baselines
[AD-A271324] p 1317 N94-19572

POSITIVE IONS
Novel electrochemical materials prepared by sol-gel chemistry
[AD-A269060] p 1578 N94-18405

POSITRONIUM
Hydrolysis reaction and positronium decay in silica gels
[AD-A270028] p 1371 N94-18713

POSITRONS
The Intense Slow Positron Source concept: A theoretical perspective on a proposed INEL Facility
[DE93-013675] p 1564 N94-17738
An ab initio Monte Carlo study of low energy positron and electron implantation in elemental metals and multilayers
[DE93-019647] p 1603 N94-19541

POTASSIUM
Potassium-Rankine power conversion subsystem modeling for nuclear electric propulsion
[NASA-CR-191134] p 1468 N94-18821

POTASSIUM ALLOYS
First on-sun test of NaK pool-boiler solar receiver
[DE93-015003] p 1466 N94-18208
Bench-scale screening tests for a boiling sodium-potassium alloy solar receiver
[DE93-018512] p 1469 N94-19040

POTENTIAL ENERGY
Seasonal variability of wind electric potential in the US
[DE93-018182] p 1493 N94-19051

POWDER (PARTICLES)
Process for applying high application-temperature coating to heat-sensitive aluminum alloys
[AD-D015823] p 1368 N94-17905
Equipment for investigation of cryogenic compaction of nanosize silicon nitride powders
[DE93-018740] p 1340 N94-18180
Fabrication and microstructural development of Ag-clad TlBa2Ca2Cu3O(x) tapes
[DE93-017407] p 1597 N94-18500
Fabrication and characterization of high-T(sub c) tapes and coils made from Ag-clad Bi-2223 superconductors
[DE93-018615] p 1601 N94-18993

POWDERED ALUMINUM
Aluminum powder/water reaction ignited by electrical pulsed power
[AD-A269223] p 1376 N94-17840

POWER AMPLIFIERS
High efficiency low cost monolithic module for SARSAT distress beacons
[NASA-CR-194234] p 1315 N94-18852
Simulation of the ALS longitudinal multibunch feedback system
[DE93-019227] p 1575 N94-19152

POWER CONDITIONING
Analysis of superconducting magnetic energy storage applications at a proposed wind farm site near Browning, Montana
[DE93-018793] p 1466 N94-18276

POWER CONVERTERS
Potassium-Rankine power conversion subsystem modeling for nuclear electric propulsion
[NASA-CR-191134] p 1468 N94-18821

POWER EFFICIENCY
Fuel cell systems program plan, fiscal year 1993
[DE93-017828] p 1466 N94-18103
National Program Plan Fuel Cells in Transportation
[DE93-017557] p 1469 N94-19346

POWER LINES
Response of transmission line systems to pulse excitation by radiation and injection methods
[DE93-015112] p 1384 N94-18210
Effects of harmonics on EMI/RFI filters operating under nonlinear loading conditions
[AD-A269559] p 1388 N94-18769

POWER SPECTRA
Self-organized criticality and the Barkhausen effect in amorphous and polycrystalline metals
[AD-A269817] p 1361 N94-18735

POWER SUPPLY CIRCUITS
Techniques for low consumption circuits
p 1428 N94-18032
A study of the automatic generating system. 3: Improvement of the total system performance
p 1429 N94-18040
Design of power electronics for TVC EMA systems
[NASA-CR-193839] p 1407 N94-19642

POWER TRANSMISSION
Fluid dynamometer having fluid characteristic power absorption adjustment capability
[AD-D015820] p 1424 N94-17904

POWERED LIFT AIRCRAFT
Design, development, and flight evaluation of the Boeing YC-14 USB powered lift aircraft p 1310 N94-18444

PRANDTL NUMBER
Experimental investigation of turbulent Prandtl number and Reynolds analogy in transitional and post-transitional boundary layers
[AD-A270092] p 1418 N94-18867

PREAMPLIFIERS
A RFI measurement system for field sites
[AD-A269340] p 1385 N94-18301
Monolithic low noise preamplifier for piezoelectric sensors
[AD-D015860] p 1563 N94-18734

PRECIPITATION (CHEMISTRY)
Some superhigh-frequency and magnetic properties of chemically precipitated films
[AD-A266195] p 1351 N94-19110

PRECIPITATION (METEOROLOGY)
Effect of spatial resolution on the simulation of regional precipitation in China in a global climate model
[DE93-013433] p 1489 N94-18053
Station climatic summaries: North America. Volume 1: The contiguous United States
[AD-A269567] p 1490 N94-18303
Global zones of particle precipitation as observed EXOS-C
[AD-A268758] p 1481 N94-18467
Station climatic summaries, North America. Volume 2: Alaska, Canada and Greenland
[AD-A269793] p 1493 N94-18732
Investigations of a coherent vector radar technique for the observation of the atmosphere near 10 GHz
[KFK-5068] p 1494 N94-19616

PRECIPITATION HARDENING
Morphology, deformation, and defect structures of TiCr2 in Ti-Cr alloys
[DE93-018332] p 1361 N94-18807

PRECONDITIONING
Pseudo-compressibility methods for the incompressible flow equations
[NASA-CR-191533] p 1551 N94-19315

PREDICATE CALCULUS
Useful lambda notation
[PB93-191856] p 1524 N94-19066

PREDICTION ANALYSIS TECHNIQUES
Recirculation in forward roll coating
[VKI-TM-48] p 1409 N94-17901
The performance of drag relations in the WAQUA storm surge model
[KNMI-TR-149] p 1496 N94-17923
Development of the microstructure based stochastic life prediction models
[AD-A269880] p 1454 N94-18683
Development of the microstructure based stochastic life prediction models
[AD-A270453] p 1455 N94-18714
On the use of semi-Lagrangian methods for accurate predictions of gravity waves
[DM-61] p 1562 N94-18859
Adsorption analysis of ammonia in an aqueous solution
[DE93-019512] p 1353 N94-19552

PREDICTIONS
Development of the microstructure based stochastic life prediction model
[AD-A269742] p 1361 N94-18742
Statistical learning theory and algorithms
[AD-A270209] p 1523 N94-18901

PREFLIGHT OPERATIONS
Kennedy Space Center processing of Shuttle small payloads p 1326 N94-19177

PREFORMS
Process relationship as influenced by carbonization rate
[AD-A269680] p 1341 N94-18572
Transducers and method for making same
[AD-D015949] p 1408 N94-19759

PREMIXED FLAMES
Studies on high pressure and unsteady flame phenomena: Revision
[AD-A269138] p 1348 N94-18257
Flame structure studies of a lean 20-torr H2/N2O/Ar flame employing molecular beam mass spectrometry
[AD-A268889] p 1349 N94-18456
Mathematical problems in combustion
[AD-A270147] p 1349 N94-18776

PREMIXING
Studies on high pressure and unsteady flame phenomena: Revision
[AD-A269138] p 1348 N94-18257
Research activity on particle spin systems and related problems
[AD-A269456] p 1562 N94-18286
Metal slurry droplet and spray combustion
[AD-A269648] p 1349 N94-18736

PREPOLYMERS
Single source precursors for the OMCVD of 3/5 compound semiconductors
[AD-A271147] p 1606 N94-19739

PREPREGS
Process for preparing thermoplastic composites
[AD-D015864] p 1339 N94-18074

PRESSURE DEPENDENCE
The low-temperature specific heat of CeCu2Ge2 at 0 and 9.5 kbar
[DE93-014914] p 1360 N94-18398
Role of pressure in the study of fullerenes
[DE93-018839] p 1602 N94-19340
Effects of pressure on the orientational ordering and phase transitions in solid C(60) and C(70)
[DE93-018858] p 1603 N94-19347
Metallization and charge-transfer gap closure of transition-metal iodides under pressure
[DE93-040301] p 1353 N94-19538

PRESSURE DISTRIBUTION
Recirculation in forward roll coating
[VKI-TM-48] p 1409 N94-17901

In-flight pressure distributions and skin-friction measurements on a subsonic transport high-lift wing section p 1308 N94-18435
Preliminary design of a water cooled avionics cooling rack
[AD-A268826] p 1320 N94-18536
A comparative study of turbulence models in predicting hypersonic inlet flows p 1314 N94-18553
Finite beta plasma equilibrium in toroidally linked mirrors
[DE93-040318] p 1590 N94-19193
Semi-span model testing in the National Transonic Facility
[NASA-CR-194479] p 1312 N94-19388
Numerical investigation of the incompressible flow around a wing with a fixed spoiler
[ISL-R-109/91] p 1313 N94-19524

PRESSURE EFFECTS
The low-temperature specific heat of CeCu2Ge2 at 0 and 9.5 kbar
[DE93-014914] p 1360 N94-18398
Growth, characterization and device development in monocrystalline diamond films
[AD-A270074] p 1599 N94-18797
Research on Earth's rotation and the effect of atmospheric pressure on vertical deformation and sea level variability
[NASA-CR-194300] p 1484 N94-18838
Influence of peak pressure and temperature on the shock-loading response of tantalum
[DE93-018561] p 1457 N94-19279
Role of pressure in the study of fullerenes
[DE93-018839] p 1602 N94-19340
Effects of pressure on the orientational ordering and phase transitions in solid C(60) and C(70)
[DE93-018858] p 1603 N94-19347
Pressure and temperature effects on the kinetics and quality of diamond films
[AD-A270876] p 1606 N94-19771

PRESSURE MEASUREMENT
Instrumented experiments aboard the frigate WOLF. Wolf 2: Measurement results of the 5.5 kg TNT in the crew aft sleeping compartment
[PML-1992-12] p 1451 N94-17931
Measurement Techniques
[VKI-LS-1993-05] p 1430 N94-18643
Static pressure measurements for near isentropic flows using laser induced iodine fluorescence
p 1431 N94-18646
Pressure sensitive paint technique
p 1431 N94-18647
Construction and evaluation of an environmental chamber for calibration of temperature and pressure sensors for laser interferometers emperature and pressure sensors for laser interferometers)
[PB93-197838] p 1322 N94-19332
Numerical analysis of pressure meter tests: Application of parameter identification of soils behavior
[ECL-92-52] p 1487 N94-19380

PRESSURE OSCILLATIONS
Calculation of turbulent boundary layer wall pressure spectra
[AD-A269549] p 1416 N94-18642
Correlation of incoming boundary layer pitot pressure fluctuations with the unsteadiness of fin-induced shock wave turbulent boundary layer interactions
[AD-A270059] p 1417 N94-18796
Relation between the fluctuating wall pressure and the turbulent structure of a boundary layer on a cylinder in axial flow
[AD-A270242] p 1418 N94-18906

PRESSURE PULSES
A probability method of fracture mechanics analysis for HFIR vessel
[DE93-015510] p 1453 N94-18246
Stress pulse phenomena
[DE93-019064] p 1456 N94-19078

PRESSURE RATIO
Vane optimization for maximum efficiency using Design Of Experiments (DOX)
[AD-A270270] p 1320 N94-18907

PRESSURE REDUCTION
Temperature lowering in cryogenic chemical-synthesis techniques and system
[DE93-018348] p 1562 N94-18810

PRESSURE SENSORS
Calculation of turbulent boundary layer wall pressure spectra
[AD-A269549] p 1416 N94-18642
Recent developments in fast response aerodynamic probe technology p 1431 N94-18645
Construction and evaluation of an environmental chamber for calibration of temperature and pressure sensors for laser interferometers emperature and pressure sensors for laser interferometers)
[PB93-197838] p 1322 N94-19332
Simulation of the behavior of micro-electronic capacitive pressure sensors
[LAAS-93190] p 1434 N94-19659

PRESSURE VESSELS
Effects of irradiation temperature on embrittlement of nuclear pressure vessel steels
[DE93-015428] p 1359 N94-18245
A probability method of fracture mechanics analysis for HFIR vessel
[DE93-015510] p 1453 N94-18246
Fluid-structure-interaction analyses of reactor vessel using improved hybrid Lagrangian Eulerian code ALICE-II
[DE93-015536] p 1409 N94-18248
Mechanism-dependent fractal character of fracture surfaces in high strength and toughness ASTM A723 steels
[AD-A268956] p 1360 N94-18542
Effects of irradiation temperature on Charpy and tensile properties of high-copper, low upper-shelf, submerged-arc welds
[DE93-017858] p 1445 N94-19047

PRESSURIZING
A finite strain ring dynamical model for pneumatic tires
[AD-A269286] p 1444 N94-18266

PRESTRESSING
Interpretation of warm prestress-induced fracture toughness based on crack-tip constraint
[DE93-015967] p 1451 N94-17913

PRETREATMENT
The c-jun gene expression in human cells exposed to either ionizing radiation or hydrogen peroxide
[DE93-017436] p 1502 N94-18476

PRIMARY COSMIC RAYS
Investigation of the relative abundance of heavy versus light nuclei in primary cosmic rays using underground muon bundles
[DE93-017601] p 1630 N94-17818
Measurement of the energy of horizontal cosmic ray muons
[KFK-5163] p 1631 N94-19505

PRIMATES
Localization of figure background segregation mechanisms in primate visual cortex
[PB93-187961] p 1508 N94-18121
Cortical substrate of haptic representation
[AD-A269583] p 1508 N94-18304

PRINCIPAL COMPONENTS ANALYSIS
Spatiotemporal variability of non-urban ozone concentrations over the eastern United States and its potential replication by satellite data
[PB93-191328] p 1476 N94-19065

PRINTED CIRCUITS
Development of alternatives to lead-bearing solders
[DE93-016509] p 1357 N94-17862
Solderability perservative coatings: Electroless tin versus organic azoles
[DE93-017634] p 1370 N94-18477

PRISMS
Metal Film Surface Plasmon Resonance (MFSPR) fibre couplers
[AD-A268871] p 1579 N94-18635

PRIVACY
Securing electronic mail: The risks and future of electronic mail
[DE93-017187] p 1383 N94-17994

PROBABILITY DENSITY FUNCTIONS
A Bayesian approach to contaminant plume delineation
[DE93-012909] p 1472 N94-17890
Polarimetric statistics of electromagnetic waves scattered by distributed targets
[PB93-195907] p 1389 N94-18951

PROBABILITY DISTRIBUTION FUNCTIONS
EDF tests for normality in linear models after a Box-Cox transformation
[AD-A269068] p 1557 N94-18517
Learning control of large-scale systems
[MATHS-REPT-A-186] p 1544 N94-19408

PROBABILITY THEORY
Kinetic growth of random-like and ballistic-like deposition models
[DE93-624946] p 1595 N94-17956
An empirical evaluation of five circular error probable estimation techniques and a method for improving them
[AD-A266528] p 1556 N94-18397
Software reliability: Estimation and prediction
[AD-A268895] p 1521 N94-18458
The rank of the present excursion
[REPT-93-22] p 1558 N94-19137
A simple calculus of finite probabilistic processes
[MEMO-INF-93-08] p 1558 N94-19195
Bahadur-Kiefer theorem beyond the largest observation
[PB93-197473] p 1558 N94-19325
Bounds for expected loss in Bayesian decision theory with imprecise prior probabilities
[PB93-197507] p 1558 N94-19327
A language of finite probabilistic processes and its interleaving semantics
[MEMO-INF-93-24] p 1558 N94-19354
Adaptive uniformization
[MEMO-INF-92-88] p 1558 N94-19385
Fault-tolerance and complexity
[TR-450] p 1530 N94-19483
Statistical probabilities for planning
[TR-474] p 1559 N94-19511
Uncertainty versus interindividual variability
[DE93-018105] p 1559 N94-19549
Problems in probability, statistics and reliability
[AD-A270830] p 1559 N94-19595
Equivalence and reduction of hidden Markov models
[AD-A270762] p 1560 N94-19768

PROBLEM SOLVING
A method for cognitive task analysis
[IZF-1992-B5] p 1508 N94-17967
Why are human-computer interfaces difficult to design and implement?
[AD-A268843] p 1514 N94-18317
On masking effect
[AD-A269593] p 1541 N94-18462
Towards versatile and practical knowledge acquisition
[AD-A269596] p 1615 N94-18464
Efficient domain-independent experimentation
[AD-A269530] p 1557 N94-18640
Putting knowledge to use: The acquisition and transfer of knowledge in situated problem solving environments
[AD-A269746] p 1509 N94-18744
Automatically generating abstractions for planning
[AD-A269772] p 1541 N94-18759
Neutral networks: An NRL perspective
[AD-A269122] p 1541 N94-18773
Adaptive uniformization
[MEMO-INF-92-88] p 1558 N94-19385
Problems in probability, statistics and reliability
[AD-A270830] p 1559 N94-19595
A real-time spoken-language system for interactive problem-solving, combining linguistic and statistical technology for improved spoken language understanding
[AD-A270901] p 1392 N94-19749

PROCEDURES
Safety-routines and guidelines for work in the clean room at the Epitek-Laboratory, Kjeller (Norway)
[FFI-93/7012] p 1322 N94-17735

PROCESS CONTROL (INDUSTRY)
A structured approach for modeling, analyzing and simulating real-time control systems
[REPT-93-044] p 1539 N94-17916
The intelligent processing of materials
[AD-A269250] p 1362 N94-18923

PROCUREMENT
An evolutionary approach to space launch commercialization
[AD-A269861] p 1331 N94-18411

PROCUREMENT MANAGEMENT
Implementation of electronic data interchange in the department of defense: Lessons learned from private industry
[AD-A269532] p 1534 N94-18768

PRODUCT DEVELOPMENT
Cut and paste based modeling with boundary features
[PB93-187250] p 1520 N94-18117
Reference model for project support environments, version 1.0
[AD-A269110] p 1520 N94-18251
Engineering research, development and technology thrust area report, FY92
[DE93-016334] p 1632 N94-18856
Technology benefits model user manual, version 01.00.04
[AD-A270637] p 1620 N94-19777

PRODUCTION COSTS
Integrated circuits: Resistless processing simplifies production and cuts costs
[DE93-018069] p 1405 N94-18941

PRODUCTION ENGINEERING
The intelligent processing of materials
[AD-A269250] p 1362 N94-18923
Integrated circuits: Resistless processing simplifies production and cuts costs
[DE93-018069] p 1405 N94-18941
MODIL cryocooler producibility demonstration project results
[DE93-017981] p 1335 N94-19275

PROGRAM VERIFICATION (COMPUTERS)
Verification of VALISYS cad based CMM software at LLNL
[DE93-013854] p 1517 N94-17911
A verification logic representation of indeterministic signal states p 1401 N94-18372

A case study in software maintenance
[AD-A269923] p 1521 N94-18659
UUGM code development
[AD-A269945] p 1416 N94-18671
Initial Graphics Exchange Specification (IGES)
[AD-A270049] p 1522 N94-18794
How to apply the IEEE standards to software testing
[DE93-018514] p 1527 N94-19245
Software quality in test and measurment equipment
[PB93-197846] p 1528 N94-19333
A research program in empirical computer science
[NASA-CR-194069] p 1530 N94-19429
On-line test methods of microprocessor based systems
[ETN-93-95008] p 1530 N94-19498

PROGRAMMABLE LOGIC DEVICES
Motorola MC68040 high-speed design using Altera EPM5000 erasable programmable logic devices
[DE93-017635] p 1523 N94-19006

PROGRAMMERS
A case study in software maintenance
[AD-A269923] p 1521 N94-18659
The development of a course sequence in real-time systems design
[AD-A269459] p 1522 N94-18726
Performance and scalability aspects of directory-based cache coherence in shared-memory multiprocessors
[DE93-016442] p 1536 N94-19115
Computing professionals: Changing needs for the 1990's
[B-030] p 1515 N94-19401

PROGRAMMING ENVIRONMENTS
An object-oriented environment for computer vision and pattern recognition
[DE93-017098] p 1517 N94-17867
Reference model for project support environments, version 1.0
[AD-A269110] p 1520 N94-18251
The evolution of the PVM concurrent computing system
[DE93-017764] p 1534 N94-18482
Software engineering for effective utilization of parallel processing computing system
[AD-A269191] p 1535 N94-18865
Case studies of software development tools for parallel architectures
[AD-A269193] p 1535 N94-18866
Early experiences with the IBM SP-1
[DE93-018398] p 1535 N94-19010
Cesar user library
[FFI-93/7021] p 1529 N94-19378

PROGRAMMING LANGUAGES
PostScript: A study in conformity
[NPL-DITC-214/93] p 1517 N94-17917
Multistack languages and grammars
[REPT-93-018] p 1518 N94-17926
TANGO: A notation for describing advanced transaction models
[REPT-93-014] p 1613 N94-17936
PARX: Architecture of an operating system for parallel machines
[ETN-93-94401] p 1533 N94-18068
APLAC: An object-oriented analog circuit simulator and design tool. 6.1 reference manual
[PB93-187193] p 1396 N94-18091
Portable parallel ray tracing algorithms
[AD-A268984] p 1522 N94-18698
Connection machine software conversion of a Navy oceans model
[AD-A269876] p 1535 N94-18772
Software engineering for effective utilization of parallel processing computing system
[AD-A269191] p 1535 N94-18865
A teaching tool for linear programming
[AD-A270240] p 1523 N94-18905
Asynchronous rendezvous in the presence of backtracking
[PB93-197739] p 1524 N94-19062
DataTypeLog: A deductive object oriented query language
[MEMO-INF-92-79] p 1526 N94-19221
The TM typing rules
[MEMO-INF-92-80] p 1526 N94-19222
The TM manual version 1.3 working document
[MEMO-INF-93-06] p 1527 N94-19229
Advances in architectural concepts to support distributed systems design
[MEMO-INF-93-17] p 1527 N94-19261
Stochastic grammars: Theory and applications
[MEMO-INF-93-19] p 1528 N94-19262
A language of finite probabilistic processes and its interleaving semantics
[MEMO-INF-93-24] p 1558 N94-19354

PROJECT MANAGEMENT
Lightweight materials for transportation: Program plan
[DE93-017381] p 1340 N94-18087
Safeguarding our energy future
[DE93-016001] p 1466 N94-18109
Reference model for project support environments, version 1.0
[AD-A269110] p 1520 N94-18251
Knowledge sources for an intelligent MCM analyzer
[AD-A269224] p 1542 N94-18887
Review Committee report on the conceptual design of the tokamak physics experiment
[DE93-018408] p 1588 N94-19012
Pantex Plant Meteorological Monitoring Program
[DE93-018495] p 1493 N94-19127

PROJECT PLANNING
Lightweight materials for transportation: Program plan
[DE93-017381] p 1340 N94-18087
Report to Congress: Comprehensive Program Plan for Advanced Turbine Systems
[DE93-016718] p 1467 N94-18475
Automatically generating abstractions for planning
[AD-A269772] p 1541 N94-18759

PROJECTILES
Feasibility study for a measuring system velocity projectile
[FEL-91-A368] p 1434 N94-19797

PROJECTIVE GEOMETRY
VLSI architectures for geometrical mapping problems in high-definition image processing
p 1398 N94-18345

PROLATE SPHEROIDS
Mathematical problems in combustion
[AD-A270147] p 1349 N94-18776

PRONY SERIES
Advances in the identification of transfer function models using Prony analysis
[DE93-017980] p 1548 N94-18094

PROPANE
Conversion of ethane and of propane to higher olefin hydrocarbons
[DE93-015282] p 1347 N94-18194
Evaluation of aftermarket LPG conversion kits in light-duty vehicle applications
[DE93-010035] p 1377 N94-18617

PROPELLANT BINDERS
Strained ring energetic binders
[AD-A269056] p 1377 N94-18491

PROPELLANT COMBUSTION
Aluminum powder/water reaction ignited by electrical pulsed power
[AD-A269223] p 1376 N94-17840

PROPELLANT GRAINS
New test method to determine modulus of elasticity of rocket grain material
[AD-A269758] p 1377 N94-18758

PROPELLANT SPRAYS
Combustion instability phenomena of importance to liquid propellant engines
[AD-A268800] p 1348 N94-18389
A coupled implicit solution method for turbulent spray combustion in propulsion systems p 1411 N94-18549

PROPELLANTS
Shock compression properties of silicon carbide
[DE93-019927] p 1373 N94-19271

PROPORTIONAL COUNTERS
Measurements of cosmic ray muons with multi-wire proportional chambers with a prototype setup for KASCADE
[KFK-5173] p 1631 N94-19506

PROPULSION
KINETIC: A system code for analyzing Nuclear thermal propulsion rocket engine transients
[DE93-016825] p 1337 N94-17884

PROPULSION SYSTEM CONFIGURATIONS
The ANL electric vehicle battery R&D program for DOE-EHP
[DE93-017414] p 1394 N94-17750
Mission needs and system commonality for space nuclear power and propulsion
[DE93-016557] p 1337 N94-17863
National Program Plan Fuel Cells in Transportation
[DE93-017557] p 1469 N94-19346
Overview of STOVL aircraft propulsion research offtakes and vertical lift systems
[NASA-TM-106387] p 1321 N94-19353

PROPULSION SYSTEM PERFORMANCE
The ANL electric vehicle battery R&D program for DOE-EHP
[DE93-017414] p 1394 N94-17750
Mission needs and system commonality for space nuclear power and propulsion
[DE93-016557] p 1337 N94-17863
Adaptations to micropep and rocket to allow performance evaluation of multiple grain and/or airbreathing motors
[AD-A268798] p 1337 N94-18202
Evaluation of aftermarket LPG conversion kits in light-duty vehicle applications
[DE93-010035] p 1377 N94-18617
Technology test bed
[NASA-TM-109354] p 1322 N94-18953
National Program Plan Fuel Cells in Transportation
[DE93-017557] p 1469 N94-19346

PROPULSIVE EFFICIENCY
Fuel cell systems program plan, fiscal year 1993
[DE93-017828] p 1466 N94-18103
National Program Plan Fuel Cells in Transportation
[DE93-017557] p 1469 N94-19346

PROTECTION
The effect of surface treatment and gaseous rust protection paper on the atmospheric corrosion stability of aluminium alloy
[DE93-623326] p 1355 N94-17679

PROTECTIVE CLOTHING
Conductive garments to prevent Radio-Frequency (RF) burns
[AD-D015832] p 1512 N94-18730
Aerospace medicine and biology: A continuing bibliography with indexes (supplement 382)
[NASA-SP-7011(382)] p 1507 N94-18936
Aerospace medicine and biology: A continuing bibliography with indexes (supplement 381)
[NASA-SP-7011(381)] p 1507 N94-19069

PROTECTIVE COATINGS
Titanium carbon-hydrogen layers on decorative surfaces p 1375 N94-18010
Sputtered TiN coatings in plastic
p 1367 N94-18011
Gold-copper-zinc coatings as an alternative to gold-copper-cadmium p 1367 N94-18012
NSWCWODET participation in Space Shuttle mission STS-46
[AD-A268875] p 1332 N94-18321
Solderability perservative coatings: Electroless tin versus organic azoles
[DE93-017634] p 1370 N94-18477
Carbon/carbon composites coated with SiC by chemical vapor deposition
[AD-A269934] p 1341 N94-18544
Joining and Adhesion of Advanced Inorganic Materials Symposium
[AD-A269748] p 1342 N94-18720
JPRS report: Science and technology. Central Eurasia: Materials science
[JPRS-UMS-93-002] p 1339 N94-18833
Thermal analysis of coatings and substrate materials during a disruption in fusion reactors
[DE93-017688] p 1588 N94-18971
Contribution to the tribological study of magnetic-tape head contact
[ECL-92-57] p 1434 N94-19414
Testing of protective coatings in hydrogen
[DE93-040326] p 1375 N94-19651
Tribological studies of silicon for magnetic recording applications (Invited)
[AD-A270878] p 1447 N94-19784

PROTEIN METABOLISM
Space research on organs and tissues
p 1503 N94-19214

PROTEIN SYNTHESIS
Cellular and molecular level responses after radiofrequency radiation exposure, alone or in combination with x rays or chemicals
[AD-A268189] p 1501 N94-17729

PROTEINS
In vivo animal models of body composition in aging
[DE93-012527] p 1501 N94-17889
X ray absorption spectroscopic studies of the active sites of nickel- and copper-containing metalloproteins
[DE93-017142] p 1347 N94-18059
The c-jun gene expression in human cells exposed to either ionizing radiation or hydrogen peroxide
[DE93-017436] p 1502 N94-18476

PROTOCOL (COMPUTERS)
PARX: Architecture of an operating system for parallel machines
[ETN-93-94401] p 1533 N94-18068
Specification and analysis of a high speed transport protocol
[AD-A268941] p 1386 N94-18449
On asynchronous testing
[MEMO-INF-93-03] p 1543 N94-19226
Specification and verification of a dynamic leader election protocol in a broadcast network
[MEMO-INF-93-05] p 1558 N94-19228
Vectorized presentation-level services for scientific distributed applications
[DE93-018091] p 1537 N94-19253
Specifying and proving communication closedness in protocols
[MEMO-INF-93-23] p 1390 N94-19267

Protocol service decomposition for high-performance networking
[AD-A270613] p 1538 N94-19533
Learning about the Internet bibliography and beginner's guide
[AD-A268847] p 1532 N94-19707

PROTON BEAMS
Effects of transverse coupling on transverse beam size, simulation and measurements
[DE93-017804] p 1574 N94-18972

PROTON IRRADIATION
Mechanical-property changes of structural composite materials after low-temperature proton irradiation: Implications for use in SSC magnet systems
[DE93-016735] p 1343 N94-18763

PROTON-PROTON REACTIONS
The PAPAGENO Partonic Monte-Carlo Program
[DE93-018524] p 1571 N94-19247

PROTONS
Proton transfer dynamics and cluster ion fragmentation in phenol/ammonia cLusters
[AD-A269133] p 1348 N94-18256
Global zones of particle precipitation as observed EXOS-C
[AD-A268758] p 1481 N94-18467
Charmonium physics from (bar p)p interactions
[DE93-017809] p 1569 N94-18973

PROTOPLANETS
Structuration processes in protoplanetary accretion disks
[MPE-243] p 1628 N94-19519

PROTOSTARS
The molecular environment of S106 IR
[MPE-PREPRINT-241] p 1622 N94-19417

PROTOTYPES
Developmental testing of a prototype all-reflection Michelson interferometer
[AD-A269064] p 1430 N94-18406
Tunneling spectroscopy of ultrasmall clusters and grains
[AD-A268840] p 1598 N94-18539
ARPA/CSTO rapid VLSI implementation
[AD-A269170] p 1403 N94-18695
Computer-Aided Prototyping System (CAPS) within the software acquisition process. A case study
[AD-A268705] p 1522 N94-18786
Fiber optic Raman spectrograph for in situ environmental monitoring
[DE93-019466] p 1478 N94-19305

PROVING
Verification of 3I retrievals vis-a-vis radiosonde observations
[KNMI-TR-150] p 1488 N94-17924

PROXIMITY EFFECT (ELECTRICITY)
Thin film studies of the proximity Josephson effect
[AD-A270129] p 1600 N94-18876

PSEUDORANDOM SEQUENCES
Production and test of pseudo random elements
[ETN-93-95070] p 1559 N94-19610

PSYCHOLOGY
Interdisciplinary training in life science (FY 1991 ASSERT)
[AD-A269220] p 1512 N94-18886

PSYCHOMOTOR PERFORMANCE
Evaluation of physiological and psychological impairment of human performance in cold stressed subjects
[AD-A268637] p 1506 N94-18632
Effects of practice in selecting and executing keypressing sequences
[IZF-1992-B-10] p 1509 N94-19420
A forthcoming key press can be selected while earlier ones are executed
[IZF-1993-B-2] p 1509 N94-19422

PSYCHOPHYSICS
Context-related scaling of human judgement in the multiplicative AHP, SMART and ELECTRE
[REPT-93-38] p 1611 N94-19158

PSYCHOPHYSIOLOGY
Psychophysical analyses of perceptual representations
[AD-A268711] p 1508 N94-18313

PUBLIC HEALTH
International Symposium on the Ecological Effects of Arctic Airborne Contaminants — abstracts
[AD-A269955] p 1475 N94-18775

PULLING
Analysis of pultrusion processing for long fiber reinforced thermoplastic composite system
[NASA-CR-194504] p 1339 N94-17766

PULSARS
Pulse-timing studies of x ray pulsars
[NASA-CR-193778] p 1621 N94-18611
Eclipsing cataclysmic variables. Deep eclipses in H0928+501. YY Draconis, the whirling dervish. New x ray pulsar candidates from HEAO-1
[NASA-CR-194027] p 1621 N94-18855
Computational astrophysics: Pulsating stars
[DE93-018369] p 1627 N94-18857

PULSE AMPLITUDE
Conversion of ADC pulse heights into MIP units: NUMASS test data, September 1991
[USIP-93-03] p 1432 N94-18846

PULSE COMMUNICATION
VHF air/ground communications for air traffic control. Volume 1: A decision tree approach to system innovations
[AD-A268485] p 1316 N94-18384
Initial Graphics Exchange Specification (IGES)
[AD-A270049] p 1522 N94-18794

PULSE COMPRESSION
Resolution in radar mapping
[AD-A269730] p 1462 N94-18753

PULSE DURATION
Development of short pulse soft x ray lasers
[DE93-017150] p 1437 N94-18131
Resolution in radar mapping
[AD-A269730] p 1462 N94-18753
Spice modeling of a FET-switched induction accelerator cell
[DE93-018662] p 1575 N94-18996

PULSE DURATION MODULATION
Design of power electronics for TVC EMA systems
[NASA-CR-193839] p 1407 N94-19642

PULSE HEATING
Experiments on nonlinear absorption of ECH waves in MTX and a comparison with theory
[DE93-019158] p 1589 N94-19074

PULSE MODULATION
Enhanced acceleration in a self-modulated-laser wakefield accelerator
[AD-A268452] p 1586 N94-18148

PULSE RADAR
The accuracy of monostatic and bistatic radar imaging by range-Doppler-processing with and without motion compensation
[DLR-FB-93-07] p 1384 N94-18071
Missile antenna pattern coordinate system and data formats
[AD-A269153] p 1385 N94-18260

PULSE RATE
Spice modeling of a FET-switched induction accelerator cell
[DE93-018662] p 1575 N94-18996

PULSE REPETITION RATE
First and second order Stokes generation by SRS in methane: Influence of rep-rate, beam quality and astigmatism
[FEL-92-A125] p 1441 N94-19426

PULSED LASER DEPOSITION
Imaging and blackbody emission spectra of hot particulates generated during laser ablation
[DE93-015818] p 1439 N94-18724

PULSED LASERS
The copper-pumped dye laser system at Lawrence Livermore National Laboratory
[DE93-014429] p 1435 N94-17723
Pulse radiolytic studies of electron transfer processes and applications to solar photochemistry
[DE93-018715] p 1464 N94-17781
Observations of MeV electrons and scattered light from intense, subpicosecond laser-plasma interactions
[DE93-017153] p 1435 N94-17855
Pulsed LASER for testing silicon strip detectors
[DE93-017816] p 1436 N94-17883
Limitations on the fidelity of 100 fs pulses produced by chirped pulse amplification
[DE93-017167] p 1396 N94-17991
Production of dense vapor targets for laser-plasma interaction studies with intense, ultra-short pulses
[DE93-017175] p 1584 N94-17993
Dynamics of short-pulse excitation, ionization and harmonic conversion
[DE93-017220] p 1436 N94-17996
Ultra-shallow box-like profiles fabricated by pulsed UV-laser doping process
[DE93-017221] p 1437 N94-18083
Development of short pulse soft x ray lasers
[DE93-017150] p 1437 N94-18131
Enhanced acceleration in a self-modulated-laser wakefield accelerator
[AD-A268452] p 1586 N94-18148
Integrated photonics research volume 10. Conference edition
[AD-A269298] p 1577 N94-18298
Nonlinear Thomson scattering of intense laser pulse from beams and plasmas
[AD-A269556] p 1438 N94-18460
Quantum Optoelectronics. Organization of the 1993 photonics science topical meetings. Technical digest series, volume 8
[AD-A269026] p 1578 N94-18488
Advanced Solid-State Lasers/Compact Blue-Green Lasers. 1993 technical digest series. Volume 2: Organization of the 1993 photonics science topical meetings
[AD-A269058] p 1438 N94-18492
Photonics in Switching: Organization of the 1993 photonics science topical meetings. Technical digest
[AD-A269024] p 1578 N94-18528
High spatial resolution, range gated, underwater imaging method and apparatus
[AD-D015882] p 1430 N94-18530
Single-transverse-mode, narrow-bandwidth pulsed tunable dye laser with hollow circular intracavity dielectric waveguide
[AD-A270022] p 1439 N94-18614
Characterization of vapor plume species and deposition residues resulting from pulsed laser ablation of a graphite/epoxy composite
[AD-A270101] p 1343 N94-18869
Multi-terrawatt, 100 fsec laser system using flashlamp-pumped, dye-converted Ti:sapphire as an amplifier
[DE93-017190] p 1440 N94-18889
Ultrafast Electronics and Optoelectronics: Summaries of papers. Technical digest conference edition
[AD-A269233] p 1405 N94-18909
Growth of epitaxial semiconductor alloys and superlattices with continuously variable composition by pulsed-laser ablation
[DE93-018726] p 1601 N94-18998
Electron cyclotron resonance heating in the microwave tokamak experiment
[DE93-018083] p 1590 N94-19289
Tetravalent chromium (Cr(4+)) as laser-active ion for tunable solid-state lasers
[NASA-CR-194528] p 1441 N94-19394
Spectrally and temporally resolved laser emission from vertical cavity surface emitting lasers
[DE93-019410] p 1442 N94-19563

PULSED RADIATION
Characteristics and pulsed radiation response of non-ideal quartz shock stress gauges
[DE93-017628] p 1424 N94-17999
A study of the effects of high power pulsed 2450 MHz microwaves, ELF modulated microwaves, and ELF fields on human lymphocytes and selected cell lines
[AD-A269070] p 1505 N94-18294
First and second order Stokes generation by SRS in methane: Influence of rep-rate, beam quality and astigmatism
[FEL-92-A125] p 1441 N94-19426

PULTRUSION
Analysis of pultrusion processing for long fiber reinforced thermoplastic composite system
[NASA-CR-194504] p 1339 N94-17766

PYRIDINES
The direct synthesis of organic and organometallic-containing MICA-type aluminosilicates
[DE93-019001] p 1373 N94-19321

PYROLYSIS
Characterization of vapor plume species and deposition residues resulting from pulsed laser ablation of a graphite/epoxy composite
[AD-A270101] p 1343 N94-18869
Molecular and polymeric ceramic precursors
[DE93-040364] p 1372 N94-18891
Accelerated screening methods for determining chemical and thermal stability of refrigerant-lubricant mixtures. Part 1: Method assessment
[DE93-040215] p 1351 N94-19136

PYROLYTIC GRAPHITE
Tunneling spectroscopy of ultrasmall clusters and grains
[AD-A268840] p 1598 N94-18539
Atomic-scale friction and microfriction of graphite and diamond using friction force microscopy
[AD-A270952] p 1605 N94-19679

PYROMETERS
Development of a multi-point two-color pyrometer for tube and wall temperature and emissivity measurement at the CFFF
[DE93-014716] p 1429 N94-18207

Q

QUADRATURE PHASE SHIFT KEYING
Development and test of readout electronics for optical quadrature signals
[DLR-MITT-92-11] p 1395 N94-17920

QUADRATURES
Exponential characteristic spatial quadrature for discrete ordinates neutral particle transport in two-dimensional cartesian coordinates
[AD-A270458] p 1554 N94-19671

QUADRUPOLES
Heavy Ion Fusion Injector Program
[DE93-018706] p 1575 N94-18997
QUALITY CONTROL
Verification of VALISYS cad based CMM software at LLNL
[DE93-013854] p 1517 N94-17911
Process and quality on-line control in laser welding
p 1426 N94-18020
Testing and evaluation of large-area heliostats for solar thermal applications
[DE93-018509] p 1467 N94-18520
Metallurgical evaluation of SRAM 2/SRAM A program mer base plates
[DE93-018689] p 1364 N94-19100
Image blur
[DE93-017944] p 1580 N94-19113
Pantex Plant Meteorological Monitoring Program
[DE93-018495] p 1493 N94-19127
Incology 908 database report: On process-structure-property relationship
[DE93-017616] p 1366 N94-19546
QUANTILES
Bahadur-Kiefer theorem beyond the largest observation
[PB93-197473] p 1558 N94-19325
QUANTITATIVE ANALYSIS
Analysis of deposit precursors in jet fuels using Fourier transform infrared spectroscopy
[AD-A269035] p 1377 N94-18489
Integrated test plan for the demonstration of a commercial Fourier Transform Infrared instrument
[DE93-018518] p 1433 N94-19041
Novel mass spectrometric instrument for gaseous and particulate characterization and monitoring
[DE93-019992] p 1433 N94-19054
QUANTUM CHROMODYNAMICS
Measuring the sea quark polarization
[DE93-015792] p 1566 N94-18234
Institute for Nuclear Theory
[DE93-017369] p 1568 N94-18824
Charmonium physics from (bar p)p interactions
[DE93-017809] p 1569 N94-18973
Investigations in gauge theories, topological solitons, and string theories
[DE93-015029] p 1609 N94-19250
QUANTUM EFFICIENCY
Simplified processing for 23 percent-efficient silicon concentrator solar cells
[DE93-015018] p 1464 N94-17787
QUANTUM ELECTRODYNAMICS
Quantum optoelectronics technical digest, 1993. Voolume 8: Postconference edition
[AD-A268209] p 1576 N94-17887
Detection of single molecules in microspheres
[DE93-017776] p 1567 N94-18493
Relativistic configuration interaction calculation of the correlation energies of heliumlike ions
[DE93-018093] p 1571 N94-19201
QUANTUM ELECTRONICS
Spatial light modulators and applications: Summaries of papers presented at the Spatial Light Modulators and Applications Topical Meeting
[AD-A269452] p 1577 N94-18283
Quantum Optoelectronics. Organization of the 1993 photonics science topical meetings. Technical digest series, volume 8
[AD-A269026] p 1578 N94-18488
Advanced Solid-State Lasers/Compact Blue-Green Lasers. 1993 technical digest series. Volume 2: Organization of the 1993 photonics science topical meetings
[AD-A269058] p 1438 N94-18492
Photonics in Switching: Organization of the 1993 photonics science topical meetings. Technical digest
[AD-A269024] p 1578 N94-18528
Joint services electronics program
[AD-A269383] p 1403 N94-18638
Ultrafast Electronics and Optoelectronics: Summaries of papers. Technical digest conference edition
[AD-A269233] p 1405 N94-18909
Theoretical and experimental studies of quantum wells
[AD-A271180] p 1606 N94-19741
QUANTUM MECHANICS
Tensorial structure of a q-deformed sp(4,R) superalgebra
[DE93-624806] p 1545 N94-17685
On relation between Berry phase and one-dimensional models with long-range 1/r(sup 2)-interaction
[DE93-624967] p 1592 N94-17690
A zeta function approach to the semiclassical quantization of maps
[DE93-624774] p 1547 N94-17949
Space and time as outcome of decoherence in an expanding universe
[DE93-016199] p 1624 N94-18047
Advanced Solid-State Lasers/Compact Blue-Green Lasers. 1993 technical digest series. Volume 2: Organization of the 1993 photonics science topical meetings
[AD-A269058] p 1438 N94-18492
Space and time from quantum mechanics
[DE93-015263] p 1609 N94-18629
The quantum dynamics of electronically nonadiabatic chemical reactions
[NASA-CR-194309] p 1568 N94-18837
QUANTUM THEORY
On a conformal perfect fluid in the classical vacuum
[DE93-624797] p 1480 N94-17682
Infinite Grassmannian and moduli space of G-bundles
[DE93-624798] p 1545 N94-17683
International Centre for Theoretical Physics, Trieste Scientific activities in 1991
[DE93-624757] p 1606 N94-17792
Avoiding degenerate coframes in an affine gauge approach to quantum gravity
[DE93-013146] p 1607 N94-17892
Phase space representations and quantum probability theory
[DE93-629863] p 1556 N94-18154
Four-fermion interactions
[DE93-629905] p 1566 N94-18199
Optical and transport properties of metallic and semiconductor nanostructures
[AD-A270009] p 1598 N94-18609
Space and time from quantum mechanics
[DE93-015263] p 1609 N94-18629
Investigations in gauge theories, topological solitons, and string theories
[DE93-015029] p 1609 N94-19250
Essential shift: Scientific revolution in the 20th century
[AD-A270810] p 1610 N94-19663
Schroedinger's hope
[AD-A270988] p 1581 N94-19772
QUANTUM WELL LASERS
Quantum optoelectronics technical digest, 1993. Voolume 8: Postconference edition
[AD-A268209] p 1576 N94-17887
Direct solar pumping of semiconductor lasers: A feasibility study
[NASA-CR-193760] p 1440 N94-18834
QUANTUM WELLS
Kinetic aspects of lattice mismatch in molecular beam epitaxial growth on planar and patterned substrates
[AD-A270424] p 1597 N94-18506
Fundamental properties and device applications of Ge(x)Si(1-x)/Si superlattices (supplemental)
[AD-A269212] p 1600 N94-18884
Suppressed electron-phonon scattering in superlattices
[AD-A270834] p 1604 N94-19597
Solid-state dynamics in novel semiconductor nanostructures
[AD-A271249] p 1605 N94-19725
Theoretical and experimental studies of quantum wells
[AD-A271180] p 1606 N94-19741
QUARK MODELS
Search for top quark with D0 detector
[DE93-040170] p 1572 N94-19536
QUARKS
Beauty without charm in B-meson decays
[PREPRINT-732] p 1565 N94-17972
Measuring the sea quark polarization
[DE93-015792] p 1566 N94-18234
Charmonium physics from (bar p)p interactions
[DE93-017809] p 1569 N94-18973
Search for top quark with D0 detector
[DE93-040170] p 1572 N94-19536
QUARTIC EQUATIONS
Enumerative geometry of Del Pezzo Surfaces
[DE93-624768] p 1546 N94-17816
QUARTZ
The Lever oscillator for use in high resistance resonator applications
[DE93-017652] p 1404 N94-18827
Development of a quartz digital accelerometer for environmental sensing and navigation applications
[DE93-018503] p 1433 N94-19243
QUARTZ CRYSTALS
Proceedings of the 4th European Congress on Chronometry
[ETN-93-94633] p 1424 N94-18006
Simulation of a quartz-clockwork
p 1426 N94-18019
Simulation of quartz resonators p 1426 N94-18021
Quartz analog watch with perpetual calendar
p 1429 N94-18042
QUASARS
EGRET Mission and Data Analysis
[MPE-PREPRINT-223] p 1622 N94-19462
EGRET observations of 3 C 273
p 1623 N94-19464
QUASI-STEADY STATES
The temperature at the phase boundary during quasi-static motions of a two-phase thermoelastic bar
[AD-A268769] p 1596 N94-18388
QUENCHING (COOLING)
Ageing in Processed Polymers: Programme, summary, and abstracts discussion meeting
[AD-A268931] p 1370 N94-18448
QUERY LANGUAGES
EDMS: Engineering data management system. User's reference
[PB93-187391] p 1614 N94-18119
Learning database abstractions for query reformulation
[AD-A269531] p 1616 N94-18641
DataTypeLog: A deductive object oriented query language
[MEMO-INF-92-79] p 1526 N94-19221
Working visit to the University of L'Aquila, Italy
[FEL-93-B020] p 1618 N94-19452
QUEUEING THEORY
Efficient simulation of DEDS by means of standard clock techniques: Queueing and integrated radio network examples
[AD-A269878] p 1432 N94-18681
Polling systems: Moment stability of station times and central limit theorems
[PB93-191955] p 1560 N94-18990
On asynchronous testing
[MEMO-INF-93-03] p 1543 N94-19226
Tandem queues with deterministic service times
[PB93-197465] p 1543 N94-19324
Compensation approach for three or more dimensional random walks
[PB93-197499] p 1543 N94-19326
Control of integrated voice/data multi-hop radio networks via reduced-load approximations
[AD-A270661] p 1393 N94-19779

R

RADAR ANTENNAS
C-band PARC manual
[FEL-92-B159] p 1383 N94-18070
Modeling a Yagi array antenna for VHF radar use
[AD-A268973] p 1387 N94-18525
RADAR APPROACH CONTROL
Terminal area forecasts, FY 1993-2005
[AD-A269855] p 1316 N94-18336
RADAR BEACONS
Missile antenna pattern coordinate system and data formats
[AD-A269153] p 1385 N94-18260
RADAR BEAMS
Resolution in radar mapping
[AD-A269730] p 1462 N94-18753
RADAR CROSS SECTIONS
Statistical description of the bistatic radar cross section distributions for a right circular cylinder
[AD-A270001] p 1387 N94-18666
RADAR DATA
Environmental characterization for target acquisition. Report 3: New concepts for evaluating low-grazing angle radar measurements
[AD-A269956] p 1388 N94-18777
Polarimetric statistics of electromagnetic waves scattered by distributed targets
[PB93-195907] p 1389 N94-18951
Moments of ambient Doppler spectra
[DE93-017948] p 1390 N94-19114
RADAR DETECTION
Tomographic mathematical ideas applied to radar detection
[AD-A268789] p 1384 N94-18186
Space debris detection
[AD-A269254] p 1334 N94-18264
Low-noise oscillators for airborne radar applications, revision 1
[AD-A269372] p 1403 N94-18471
A comparison between several computer codes for calculations on microwave propagation
[FEL-92-A435] p 1390 N94-19449
Earth Penetration Radar Imaging System (EPRIS)
[DE93-019890] p 1391 N94-19542
RADAR EQUIPMENT
Space debris detection
[AD-A269254] p 1334 N94-18264
RADAR IMAGERY
The accuracy of monostatic and bistatic radar imaging by range-Doppler-processing with and without motion compensation
[DLR-FB-93-07] p 1384 N94-18071
Tomographic mathematical ideas applied to radar detection
[AD-A268789] p 1384 N94-18186

The spatial variance of ionospherically-induced phase errors in SAR imagery
[DE93-015643] p 1385 N94-18232
Laser imaging radar system
[AD-A270436] p 1387 N94-18510
Application of Fourier-based features for classification of synthetic aperture radar imagery
[AD-A270450] p 1387 N94-18513
Resolution in radar mapping
[AD-A269730] p 1462 N94-18753
Solution of the Poisson equation with application to radar imaging
[PB93-195865] p 1389 N94-18950
Modeling of current features in Gulf Stream SAR imagery
[AD-A270734] p 1499 N94-19609
Remote sensing of Earth terrain
[NASA-CR-194598] p 1464 N94-19681
SeaTrack: Ground station orbit prediction and planning software for sea-viewing satellites
[NASA-RP-1331] p 1532 N94-19761

RADAR MAPS
Resolution in radar mapping
[AD-A269730] p 1462 N94-18753

RADAR MEASUREMENT
Flight demonstration of image fix-taking with SAR
[DE93-016499] p 1382 N94-17861
Environmental characterization for target acquisition. Report 3: New concepts for evaluating low-grazing angle radar measurements
[AD-A269956] p 1388 N94-18777
The Mexico City 1991 lidar measurements campaign
[DE93-019960] p 1478 N94-19272
Investigations of a coherent vector radar technique for the observation of the atmosphere near 10 GHz
[KFK-5068] p 1494 N94-19616

RADAR SCATTERING
The split-step algorithm for microwave propagation modeling above a conducting surface
[FEL-92-A430] p 1390 N94-19447
A comparison between several computer codes for calculations on microwave propagation
[FEL-92-A435] p 1390 N94-19449

RADAR SIGNATURES
Environmental characterization for target acquisition. Report 3: New concepts for evaluating low-grazing angle radar measurements
[AD-A269956] p 1388 N94-18777

RADAR TARGETS
The accuracy of monostatic and bistatic radar imaging by range-Doppler-processing with and without motion compensation
[DLR-FB-93-07] p 1384 N94-18071
Millimeter wave reflectivity measurement system
[AD-A270008] p 1387 N94-18601

RADAR TRACKING
Range safety transponder catalog
[AD-A270882] p 1323 N94-19581

RADIAL DISTRIBUTION
A radial transmission line material measurement apparatus
[DE93-018508] p 1394 N94-17780

RADIANCE
Spectral radiance measurements on a bluff body stabilized flame: Characterization of the IR signature
[PB93-195899] p 1347 N94-18081
Work plan for the Marine Aerosol Properties and the Thermal Imager Performance Trial (MAPTIP)
[AD-A270026] p 1483 N94-18712
Cutting and drilling studies using high power visible lasers
[DE93-019149] p 1441 N94-19294
Scientific studies in association with the Shuttle Solar Backscatter Ultraviolet (SSBUV) project
[NASA-CR-193404] p 1630 N94-19437
Marine-modified LOWTRAN: The contribution of sun glint
[AD-A269547] p 1500 N94-19762

RADIANT FLUX DENSITY
High temperature co-axial winding transformers
[NASA-CR-194580] p 1407 N94-19643
UVPI imaging from the LACE satellite: The Strypi rocket plume
[AD-A270967] p 1335 N94-19787

RADIATION ABSORPTION
Work plan for the Marine Aerosol Properties and the Thermal Imager Performance Trial (MAPTIP)
[AD-A270026] p 1483 N94-18712
Evaluation of fiber optic performance in the ACRR
[DE93-018515] p 1580 N94-18970
Radiation induced darkening of the optical elements in the Startracker camera
[DE93-018907] p 1433 N94-19004

RADIATION BELTS
Penetrating radiation environment and effects study
[AD-A270126] p 1485 N94-18874

RADIATION CHEMISTRY
Research at the Notre Dame Radiation Laboratory
[DE93-018716] p 1566 N94-18165
Summaries of FY 1993 research in the chemical sciences
[DE93-011855] p 1632 N94-18915

RADIATION COUNTERS
A bit serial first level calorimeter trigger for an LHC detector
[USIP-92-08] p 1574 N94-18845
Research in high energy physics
[DE93-018031] p 1575 N94-19287
A programmable systolic trigger processor for FERA-bus data
[USIP-92-04] p 1405 N94-19292
Search for top quark with D0 detector
[DE93-040170] p 1572 N94-19536

RADIATION DAMAGE
Report of the 1991 Workshop on Particle-Material Interactions for Fusion Research
[DE93-788393] p 1573 N94-18156
Studies of deep levels in high resistivity silicon detectors irradiated by high fluence fast neutrons using a thermally stimulated current spectrometer
[DE93-016133] p 1602 N94-19258

RADIATION DETECTORS
New room temperature high resolution solid-state detector (CdZnTe) for hard x rays and gamma rays
p 1324 N94-19165
The GAMCIT gamma ray burst detector
p 1324 N94-19168
High rate resistive plate chambers: An inexpensive, fast, large area detector of energetic charged particles for accelerator and non-accelerator applications
[DE93-018664] p 1572 N94-19545

RADIATION DOSAGE
Cellular and molecular level responses after radiofrequency radiation exposure, alone or in combination with x rays or chemicals
[AD-A268189] p 1501 N94-17729
High dose effects in neutron irradiated face-centered cubic metals
[DE93-017671] p 1364 N94-19043
Effect of EMP fields on cell membrane potentials
[DE93-015819] p 1503 N94-19341

RADIATION EFFECTS
Air pollution effects field research facility. 3: UV-B exposure and monitoring system
[DE93-013098] p 1470 N94-17773
PVDF measurement of soft x ray induced shock and filter debris impulse
[DE93-017633] p 1382 N94-17806
Using controlled daylight exposure and sleep timing in the prevention of shift lag during night operations
[AD-A269304] p 1504 N94-17824
Charpy impact toughness of martensitic steels irradiated in FFTF: Effect of heat treatment
[DE93-015960] p 1450 N94-17848
Characteristics and pulsed radiation response of non-ideal quartz shock stress gauges
[DE93-017628] p 1424 N94-17999
Report of the 1991 Workshop on Particle-Material Interactions for Fusion Research
[DE93-788393] p 1573 N94-18156
Study on radiation-induced deterioration of grease at high temperature, 3
[DE93-788368] p 1369 N94-18220
Effects of irradiation temperature on embrittlement of nuclear pressure vessel steels
[DE93-015428] p 1359 N94-18245
A study of the effects of high power pulsed 2450 MHz microwaves, ELF modulated microwaves, and ELF fields on human lymphocytes and selected cell lines
[AD-A269070] p 1505 N94-18294
Experience with custom processors in space flight applications p 1336 N94-18338
Upper atmospheric effects of the HF Active Auroral Research Program Ionospheric Research Instrument (HAARP IRI)
[AD-A268948] p 1481 N94-18451
Compilation of 1992 annual reports of the Navy ELF communications system ecological monitoring program, volume 1
[AD-A269569] p 1386 N94-18473
The c-jun gene expression in human cells exposed to either ionizing radiation or hydrogen peroxide
[DE93-017436] p 1502 N94-18476
Electromagnetic environmental effects compendium
[AD-A270441] p 1387 N94-18512
The LET spectrum and its uncertainty during the CRRES mission
[AD-A269977] p 1630 N94-18676
Mechanical-property changes of structural composite materials after low-temperature proton irradiation: Implications for use in SSC magnet systems
[DE93-016735] p 1343 N94-18763
Penetrating radiation environment and effects study
[AD-A270126] p 1485 N94-18874
Development of robust multilayer optics for use in high-peak power radiation environments
[DE93-018557] p 1580 N94-18931
Neutron-induced collision cascade mixing in Nb/V superlattices
[DE93-018575] p 1600 N94-18933
Evaluation of fiber optic performance in the ACRR
[DE93-018515] p 1580 N94-18970
Radiation induced darkening of the optical elements in the Startracker camera
[DE93-018907] p 1433 N94-19004
High dose effects in neutron irradiated face-centered cubic metals
[DE93-017671] p 1364 N94-19043
Effects of irradiation temperature on Charpy and tensile properties of high-copper, low upper-shelf, submerged-arc welds
[DE93-017858] p 1445 N94-19047
Static Computer Memory Integrity Testing (SCMIT): An experiment flown on STS-40 as part of GAS payload G-616 p 1325 N94-19169
Overlay welding irradiated stainless steel
[DE93-018767] p 1446 N94-19334
Effect of EMP fields on cell membrane potentials
[DE93-015819] p 1503 N94-19341
The performance and survivability of dichromated poly (vinyl alcohol) holograms for space based photonic applications
[AD-A270974] p 1434 N94-19791

RADIATION HARDENING
Technology, design, simulation, and evaluation for SEP-hardened circuits p 1399 N94-18352
Radiation hardened microprocessor for small payloads
p 1327 N94-19184

RADIATION INJURIES
Conductive garments to prevent Radio-Frequency (RF) burns
[AD-D015832] p 1512 N94-18730

RADIATION MEASUREMENT
Development and evaluation of alternative radioanalytical methods, including mass spectrometry for marine materials
[DE93-625117] p 1345 N94-17691
Planetary plasma waves
[NASA-CR-194295] p 1629 N94-19094

RADIATION SHIELDING
Exponential characteristic spatial quadrature for discrete ordinates neutral particle transport in two-dimensional cartesian coordinates
[AD-A270458] p 1554 N94-19671

RADIATION SOURCES
Conical geometry for sagittal focusing as applied to x rays from synchrotrons
[DE93-017238] p 1593 N94-17760
General geometry PIC for MIMD computers
[AD-A269085] p 1534 N94-18767
Harmonic generation at high intensities
[DE93-018632] p 1572 N94-19283

RADIATION SPECTRA
Development of robust multilayer optics for use in high-peak power radiation environments
[DE93-018557] p 1580 N94-18931
EGRET Mission and Data Analysis
[MPE-PREPRINT-223] p 1622 N94-19462
Suitability of infrared spectroscopy for remote sensing of tropospheric trace gases
[KFK-5183] p 1479 N94-19507

RADIATION TOLERANCE
Experience with custom processors in space flight applications p 1336 N94-18338
Radiation hardened microprocessor for small payloads
p 1327 N94-19184

RADIATIVE HEAT TRANSFER
Heat transfer quantitative characterization: Passive and active methods p 1431 N94-18650
Total hemispherical emittance of Niobium-1 percent zirconium fuel cladding for the SP-100 space reactor
[AD-A270456] p 1576 N94-19589

RADIATIVE TRANSFER
The vertical distribution of heating in the tropical atmosphere
[AD-A270452] p 1490 N94-18514
Physical retrieval of precipitation water contents from Special Sensor Microwave/Imager (SSM/I) data. Part 1: A cloud ensemble/radiative parameterization for sensor response (report version) p 1491 N94-18604
Computational astrophysics: Pulsating stars
[DE93-018369] p 1627 N94-18857
Radiosity algorithms using higher order finite element methods
[DE93-018098] p 1531 N94-19548
Remote sensing of Earth terrain
[NASA-CR-194598] p 1464 N94-19681

RADIO ANTENNAS
Meteor burst communications improvement study
[AD-A270866] p 1393 N94-19793
RADIO BEACONS
High efficiency low cost monolithic module for SARSAT distress beacons
[NASA-CR-194234] p 1315 N94-18852
RADIO COMMUNICATION
Swatch Pager p 1428 N94-18039
Control of integrated voice/data multi-hop radio networks via reduced-load approximations
[AD-A270661] p 1393 N94-19779
RADIO EQUIPMENT
Radio wave propagation in structured ionization for satellite and radar applications
[AD-A268457] p 1382 N94-17844
Intentionally Short Range Communications (ISRC)
[AD-A268788] p 1384 N94-18216
Efficient simulation of DEDS by means of standard clock techniques: Queueing and integrated radio network examples
[AD-A269878] p 1432 N94-18681
Control of integrated voice/data multi-hop radio networks via reduced-load approximations
[AD-A270661] p 1393 N94-19779
RADIO FREQUENCIES
Power compensators for phased operation of antenna arrays on JET and D3-D
[DE93-013208] p 1581 N94-17694
Synchrotron beam-loading stability with a higher RF harmonic
[DE93-014549] p 1573 N94-17726
RF vacuum microelectronics
[AD-A269454] p 1396 N94-18284
Broadband RF spectrum from electrostatic discharges on spacecraft
[AD-A269543] p 1385 N94-18287
Field emitter array RF amplifier development project, phase 1, option 1
[AD-A268687] p 1396 N94-18293
Magnetostatic waves-based integrated optic bragg cell modules with applications to RF signal processing
[AD-A269115] p 1577 N94-18295
Millimeter wave reflectivity measurement system
[AD-A270008] p 1387 N94-18601
RF vacuum microelectronics
[AD-A270003] p 1403 N94-18667
Conductive garments to prevent Radio-Frequency (RF) burns
[AD-D015832] p 1512 N94-18730
Experiments on nonlinear absorption of ECH waves in MTX and a comparison with theory
[DE93-019158] p 1589 N94-19074
Advanced fusion diagnostics
[DE93-040085] p 1589 N94-19133
RF phase stabilization for RF photocathode gun through electro-optical monitoring
[DE93-019059] p 1406 N94-19310
Study of coupled-bunch collective effects in the ALS
[DE93-019236] p 1575 N94-19558
RADIO FREQUENCY HEATING
ICRF direct electron heating experiments in TFTR
[DE93-017857] p 1590 N94-19273
RADIO FREQUENCY INTERFERENCE
Studies of enhanced radar backscatter
[AD-A269544] p 1385 N94-18288
A RFI measurement system for field sites
[AD-A269340] p 1385 N94-18301
Communication in the presence of unknown interference
[AD-A271146] p 1392 N94-19738
RADIO METEORS
Meteor burst communications improvement study
[AD-A270866] p 1393 N94-19793
RADIO RECEIVERS
Swatch Pager p 1428 N94-18039
RADIO SIGNALS
A RFI measurement system for field sites
[AD-A269340] p 1385 N94-18301
RADIO TRANSMISSION
Radio wave propagation in structured ionization for satellite and radar applications
[AD-A268457] p 1382 N94-17844
Studies of enhanced radar backscatter
[AD-A269544] p 1385 N94-18288
Morphology and characteristics of disturbed HF skywave channels
[AD-A269755] p 1388 N94-18722
Compilation of 1992 annual reports of the navy ELF communications system ecological monitoring program. Volume 3: Tabs G - I
[AD-A269727] p 1388 N94-18741
Compilation of 1992 annual reports of the navy ELF communications system ecological monitoring program, volume 2
[AD-A269726] p 1388 N94-18751
Quasi-optical transponder using FET's and patch antennas
[AD-A271339] p 1407 N94-19584
Communication in the presence of unknown interference
[AD-A271146] p 1392 N94-19738
Meteor burst communications improvement study
[AD-A270866] p 1393 N94-19793
RADIO TRANSMITTERS
The optimal numerical algorithm for processing of phase coded time signals for radio-clocks
p 1426 N94-18018
Compilation of 1992 annual reports of the Navy ELF communications system ecological monitoring program, volume 1
[AD-A269569] p 1386 N94-18473
Aircraft fire sentry. Volume 1: Summary
[AD-A270087] p 1315 N94-18822
Aircraft fire sentry. Volume 2: Appendices A, B, C and D
[AD-A270088] p 1315 N94-18823
RADIO WAVES
Radio wave propagation in structured ionization for satellite and radar applications
[AD-A268457] p 1382 N94-17844
Studies of enhanced radar backscatter
[AD-A269544] p 1385 N94-18288
RADIOACTIVE CONTAMINANTS
A review of wind field models for atmospheric transport
[DE93-016085] p 1488 N94-17895
Inclusion of a three-dimensional washout coefficient in ADPIC
[DE93-018499] p 1476 N94-19038
RADIOACTIVE DECAY
Investigation of the relative abundance of heavy versus light nuclei in primary cosmic rays using underground muon bundles
[DE93-017601] p 1630 N94-17818
Beauty without charm in B-meson decays
[PREPRINT-732] p 1565 N94-17972
Neutrino mass
[DE93-018467] p 1567 N94-18269
Research in particle physics
[DE93-040875] p 1567 N94-18534
Inverse neutrinoless double (beta)-decay at the NLC?
[DE93-017397] p 1568 N94-18825
Experimental research in high energy physics
[DE93-011912] p 1574 N94-18916
High energy physics at Tufts University
[DE93-018299] p 1575 N94-19023
RADIOACTIVE ISOTOPES
Development and evaluation of alternative radioanalytical methods, including mass spectrometry for marine materials
[DE93-625117] p 1345 N94-17691
Gamma scattering in condensed matter with high intensity Moessbauer radiation
[DE93-019461] p 1601 N94-19031
Studies of clusters
[DE93-018961] p 1572 N94-19309
RADIOACTIVE WASTES
Rapid analysis of mixed waste samples via the optical emission from laser initiated microplasmas
[DE93-014563] p 1582 N94-17727
Rapid geophysical surveyor
[DE93-016637] p 1461 N94-17851
RADIOACTIVITY
Development and evaluation of alternative radioanalytical methods, including mass spectrometry for marine materials
[DE93-625117] p 1345 N94-17691
RADIOCHEMISTRY
Ionic and molecular environments in heterogeneous electrocatalysis: Studies by radioactive labeling and LEED/AUGER spectroscopy
[AD-A268850] p 1567 N94-18766
Research program activities of the ORNL Analytical Chemistry Division
[DE93-017938] p 1339 N94-19117
RADIOGRAPHY
Single sided tomography of extremely large dense objects
[DE93-017993] p 1580 N94-19268
RADIOLOGY
Development and evaluation of alternative radioanalytical methods, including mass spectrometry for marine materials
[DE93-625117] p 1345 N94-17691
RADIOLYSIS
Pulse radiolytic studies of electron transfer processes and applications to solar photochemistry
[DE93-018715] p 1464 N94-17781
The effects of radiolysis on the corrosion and stress corrosion behavior of 316 stainless steels
[DE93-019933] p 1363 N94-19021
RADIOMETERS
The Earth radiation budget experiment: Overview of data-processing and error sources
[KNMI-TR-146] p 1481 N94-18142
Broadband IF matching for quasioptical mixers
[MPE-PREPRINT-240] p 1390 N94-19416
RADIOSONDES
Verification of 3I retrievals vis-a-vis radiosonde observations
[KNMI-TR-150] p 1488 N94-17924
Radiosonde data collected on the ERS-1 validation cruise RRS Charles Darwin Cruise 62A, Iceland Faeroes region
[IOS-297-1992] p 1461 N94-18137
RADON
Indoor environment program
[DE93-018601] p 1513 N94-18935
RAIN
Initialization and assimilation of cloud and rainwater in a regional model p 1492 N94-18608
Inclusion of a three-dimensional washout coefficient in ADPIC
[DE93-018499] p 1476 N94-19038
RAMAN SPECTRA
Applications of nonlinear optic effects in new specialty fibers
[AD-A268890] p 1578 N94-18457
Resonance Raman and photophysical studies of transition metal complexes in solution and entrapped in zeolites
[DE93-019892] p 1363 N94-19019
First and second order Stokes generation by SRS in methane: Influence of rep-rate, beam quality and astigmatism
[FEL-92-A125] p 1441 N94-19426
RAMAN SPECTROSCOPY
Femtosecond Fourier-transform spectroscopy of low-frequency intermolecular motions in weakly interacting liquids
[DE93-017312] p 1566 N94-18085
Remote cure monitoring of polymeric resins by laser Raman spectroscopy
[DE93-016445] p 1369 N94-18112
Fiber optic Raman spectrograph for in situ environmental monitoring
[DE93-019466] p 1478 N94-19305
RAMJET ENGINES
Numerical simulation of fluid dynamics and combustion for ram accelerator projectile/obturator interaction
[AD-A269715] p 1320 N94-18748
RANDOM ACCESS
VHF air/ground communications for air traffic control. Volume 1: A decision tree approach to system innovations
[AD-A268485] p 1316 N94-18384
Communication in the presence of unknown interference
[AD-A271146] p 1392 N94-19738
RANDOM ACCESS MEMORY
Performance of defect-tolerant set-associative cache memories p 1398 N94-18346
VLSI for high-speed digital signal processing
[AD-A270406] p 1404 N94-18706
RANDOM ERRORS
An extended Reed Solomon decoder design
p 1398 N94-18348
RANDOM NOISE
Fundamental research in nonlinear random vibration for aerospace applications
[AD-A268929] p 1454 N94-18487
JSEP fellowship: Fractal noise processes
[AD-A268841] p 1557 N94-18540
Analytic approximations of an integral in remote sensing
[AD-A270085] p 1463 N94-18800
RANDOM NUMBERS
Production and test of pseudo random elements
[ETN-93-95070] p 1559 N94-19610
RANDOM PROCESSES
Non Linear Dynamics and Chaos
[AGARD-LS-191] p 1607 N94-18236
Generalized multichannel signal detection
[AD-A271385] p 1391 N94-19587
RANDOM VARIABLES
Bahadur-Kiefer theorem beyond the largest observation
[PB93-197473] p 1558 N94-19325
Sensitivity and uncertainty analysis of Markov reward models
[MEMO-INF-92-89] p 1559 N94-19386
RANDOM VIBRATION
Low-noise oscillators for airborne radar applications, revision 1
[AD-A269372] p 1403 N94-18471

Fundamental research in nonlinear random vibration for aerospace applications
[AD-A268929] p 1454 N94-18487

RANDOM WALK
Deterministic growth-dispersal models and branching random walk
[REPT-93-14] p 1550 N94-19088
Compensation approach for three or more dimensional random walks
[PB93-197499] p 1543 N94-19326

RANGE SAFETY
Range safety transponder catalog
[AD-A270882] p 1323 N94-19581

RANGEFINDING
Data fusion through simulated annealing of registered range and reflectance images
[DE93-015910] p 1612 N94-17858
Flight demonstration of image fix-taking with SAR
[DE93-016499] p 1382 N94-17861
Survey of collision avoidance and ranging sensors for mobile robots, revision 1
[AD-A269846] p 1541 N94-18474
Absolute positioning by collecting Global Positioning System (GPS) data along short baselines
[AD-A271324] p 1317 N94-19572

RANK TESTS
The rank of the present excursion
[REPT-93-22] p 1558 N94-19137

RANKINE CYCLE
Potassium-Rankine power conversion subsystem modeling for nuclear electric propulsion
[NASA-CR-191134] p 1468 N94-18821

RAPID QUENCHING (METALLURGY)
Melt spinning study
[NASA-CR-193823] p 1380 N94-19423
Recent advances in high density tungsten composite processing
[AD-A270764] p 1344 N94-19576

RARE EARTH ALLOYS
Bibliography on silicides
[AD-A270516] p 1374 N94-19532

RARE GASES
Structure, thermodynamics, and dynamical properties of supercooled liquids
[DE93-788387] p 1607 N94-18211
Excited atomic bromine energy transfer and quenching mechanisms
[AD-A270672] p 1572 N94-19607

RATES (PER TIME)
Template based low data rate speech encoder
[AD-A270900] p 1392 N94-19748

RATS
Intracellular physiology of the rat suprachiasmatic nucleus: Electrical properties, neurotransmission and effects of neuromodulators
[AD-A268829] p 1505 N94-18538
A study of the effect of hydrocarbon structure on the induction of male rat nephropathy and metabolic structure
[AD-A270969] p 1504 N94-19789

RAY TRACING
Portable parallel ray tracing algorithms
[AD-A268984] p 1522 N94-18698

RAYLEIGH NUMBER
Stability measurements of Rayleigh-Benard convection near the critical state using a spectral model
[MPIS-15/1992] p 1422 N94-19520

RAYLEIGH WAVES
High resolution geological site characterization utilizing ground motion data
[AD-A268926] p 1481 N94-18485
Experimental investigation of wave and fracture phenomena in impacted ceramics: Experiments on sapphire
[AD-A270040] p 1372 N94-18792
Surface wave group velocity tomography of East Asia, part 1
[AD-A270100] p 1484 N94-18868
Elastic properties of amorphous thin films studied by Rayleigh waves
[DE93-018375] p 1372 N94-19202

RAYLEIGH-BENARD CONVECTION
Stability measurements of Rayleigh-Benard convection near the critical state using a spectral model
[MPIS-15/1992] p 1422 N94-19520

RDX
The minimum detection limits of RDX and TNT deposited on various surfaces as determined by ion mobility spectroscopy
[DE93-018521] p 1378 N94-19042

REACTING FLOW
Chemical reactions in turbulent mixing flows
[AD-A269377] p 1410 N94-18472
A coupled implicit solution method for turbulent spray combustion in propulsion systems p 1411 N94-18549
Numerical investigation of complex, transitional, and chemically reacting flows p 1411 N94-18550
Analysis of supersonic flows using k-epsilon model and the RPLUS code: Progress towards high speed combustor analysis p 1411 N94-18551
Numerical simulation of turbulent mixing and combustion near the inlet of a burner
[DE93-017960] p 1350 N94-18987
Numerical simulation of viscous flows in chemical nonequilibrium
[MBB-LME-211-S-PUB-506] p 1421 N94-19497

REACTION KINETICS
Fundamental studies of the mechanism of catalytic reactions with catalysts effective in the gasification of carbon solids and the oxidative coupling of methane
[DE93-015262] p 1347 N94-18193
Applications of scanning tunneling microscopy to electrochemistry
[AD-A269129] p 1348 N94-18255
Temperature, kinetic energy, and rotational temperature dependences for the reactions of Ar(+)(2)P3/2 with O2 and CO
[AD-A268974] p 1567 N94-18526
Numerical investigation of complex, transitional, and chemically reacting flows p 1411 N94-18550
Wettability and reaction kinetics in metal matrix composites
[AD-A270377] p 1342 N94-18704
Transport phenomena and interfacial kinetics in multiphase combustion systems
[AD-A270202] p 1349 N94-18785
The Fourteenth Symposium on Molecular Beams
[AD-A268721] p 1568 N94-18787
LX-17 chemical kinetic material model for Chemical TOPAZ2D
[DE93-014363] p 1377 N94-18893
Surface phases and their influence on metal-oxide interfaces
[DE93-019931] p 1601 N94-19020
Chemical dynamics in time and energy space
[DE93-018595] p 1350 N94-19097
Kinetics programs for simulation of tropospheric photochemistry on the global scale
[DE93-019035] p 1476 N94-19104
Environmental Research Program
[DE93-019101] p 1477 N94-19105
Single source precursors for the OMCVD of 3/5 compound semiconductors
[AD-A271147] p 1606 N94-19739
Pressure and temperature effects on the kinetics and quality of diamond films
[AD-A270876] p 1606 N94-19771
Collaborative research on combustion diagnostics and modeling between Rolls-Royce, Inc. and the United States Air Force Wright Laboratory
[AD-A270660] p 1354 N94-19778

REACTION PRODUCTS
Penetrometer compatible, fiber-optic sensor for continuous monitoring of chlorinated hydrocarbons: Field test results
[DE93-017974] p 1352 N94-19266

REACTIVITY
Temperature, kinetic energy, and rotational temperature dependences for the reactions of Ar(+)(2)P3/2 with O2 and CO
[AD-A268974] p 1567 N94-18526
Photodissociation dynamics of cluster ions
[AD-A270296] p 1566 N94-18814

REACTOR DESIGN
Laboratory microfusion capability study
[DE93-014373] p 1583 N94-17912
Review Committee report on the conceptual design of the tokamak physics experiment
[DE93-018408] p 1588 N94-19012
Thermo-hydraulic analysis of superconducting toroidal-field magnets for the Tokamak Physics Experiment
[DE93-018096] p 1590 N94-19269

REACTOR MATERIALS
Using the Tritium Plasma Experiment to evaluate ITER PFC safety
[DE93-016614] p 1582 N94-17713
Report of the 1991 Workshop on Particle-Material Interactions for Fusion Research
[DE93-788393] p 1573 N94-18156
Effects of irradiation temperature on embrittlement of nuclear pressure vessel steels
[DE93-015428] p 1359 N94-18245
A probability method of fracture mechanics analysis for HFIR vessel
[DE93-015510] p 1453 N94-18246
Thermal analysis of coatings and substrate materials during a disruption in fusion reactors
[DE93-017688] p 1588 N94-18971
The effects of radiolysis on the corrosion and stress corrosion behavior of 316 stainless steels
[DE93-019933] p 1363 N94-19021
Beryllium processing technology review for applications in plasma-facing components
[DE93-018396] p 1363 N94-19028
Overlay welding irradiated stainless steel
[DE93-018767] p 1446 N94-19334

REACTOR SAFETY
Using the Tritium Plasma Experiment to evaluate ITER PFC safety
[DE93-016614] p 1582 N94-17713
Safety approaches for high power modular laser operation
[DE93-017213] p 1435 N94-17759
A probability method of fracture mechanics analysis for HFIR vessel
[DE93-015510] p 1453 N94-18246
Fluid-structure-interaction analyses of reactor vessel using improved hybrid Lagrangian Eulerian code ALICE-II
[DE93-015536] p 1409 N94-18248
Review Committee report on the conceptual design of the tokamak physics experiment
[DE93-018408] p 1588 N94-19012

REACTOR TECHNOLOGY
Beryllium processing technology review for applications in plasma-facing components
[DE93-018396] p 1363 N94-19028

READOUT
Development and test of readout electronics for optical quadrature signals
[DLR-MITT-92-11] p 1395 N94-17920

REAL TIME OPERATION
Magnetostrictive actuators for human sensory feedback
[AD-A269266] p 1511 N94-17841
An object-oriented environment for computer vision and pattern recognition
[DE93-017098] p 1517 N94-17867
A structured approach for modeling, analyzing and simulating real-time control systems
[REPT-93-044] p 1539 N94-17916
Single phase dynamic CMOS PLA using charge sharing technique p 1397 N94-18341
VHF air/ground communications for air traffic control: A decision tree approach to system innovations, volume 2
[AD-A268632] p 1386 N94-18495
Distributed Computing Design System (DCDS)
[AD-A270435] p 1534 N94-18509
SERCAA cloud analysis integration: Design concepts and interaction with cloud forecast models
[AD-A269104] p 1492 N94-18637
The development of a course sequence in real-time systems design
[AD-A269459] p 1522 N94-18726
Atlas of SSM/I satellite ice concentration interpolated to operational ice model domains of the Arctic for 1992
[AD-A270306] p 1499 N94-18727
ControlShell: A real-time software framework
[AD-A269172] p 1523 N94-18879
Adaptive path planning: Algorithm and analysis
[DE93-008348] p 1523 N94-18926
Template based low data rate speech encoder
[AD-A270900] p 1392 N94-19748
A real-time spoken-language system for interactive problem-solving, combining linguistic and statistical technology for improved spoken language understanding
[AD-A270901] p 1392 N94-19749
Improved HF data network simulator, software user's manual, volume 2
[AD-A270954] p 1393 N94-19753

RECEIVERS
Development of a selective volumetric receiver for central receiver systems: Investigation of parameters and exergetic evaluation
[DLR-FB-93-05] p 1465 N94-18089
Advanced optical fiber communication systems
[AD-A269120] p 1577 N94-18254
Photorefractive receiver study
[AD-A269352] p 1577 N94-18302
Testing and evaluation of large-area heliostats for solar thermal applications
[DE93-018509] p 1467 N94-18520
The use of velocity spectra for stacking receiver functions with application to IRIS/IDA stations OBNINSK (OBN) and ARTI (ARU), Russia
[AD-A269087] p 1483 N94-18717
Quasi-optical transponder using FET's and patch antennas
[AD-A271339] p 1407 N94-19584

RECEPTORS (PHYSIOLOGY)
Modified aequorin shows increased bioluminescence activity
[AD-A268774] p 1347 N94-18185

Intracellular physiology of the rat suprachiasmatic nucleus: Electrical properties, neurotransmission and effects of neuromodulators
[AD-A268829] p 1505 N94-18538

RECIRCULATIVE FLUID FLOW

Recirculation in forward roll coating
[VKI-TM-48] p 1409 N94-17901

RECLAMATION

Rapid geophysical surveyor
[DE93-016637] p 1461 N94-17851

RECOIL IONS

Experimental study of interactions of highly charged ions with atoms at keV energies
[DE93-040222] p 1571 N94-19257

RECOMBINATION REACTIONS

A physical model for one-dimension and time-dependent ionosphere. Part 1: Description of the model
[DE93-627958] p 1486 N94-19255

RECOMMENDATIONS

Guidelines for the expression of uncertainties in surface chemical analysis by Auger Electron Spectroscopy (AES) and X ray Photoelectron Spectroscopy (XPS)
[NPL-DMM(A)-99] p 1346 N94-17900

RECONSTRUCTION

ENO schemes on unstructured meshes
p 1412 N94-18561

RECORDING HEADS

Contribution to the tribological study of magnetic-tape head contact
[ECL-92-57] p 1434 N94-19414

RECORDS MANAGEMENT

Document control and conduct of operations
[DE93-016555] p 1613 N94-17880

Networked MS windows 3.1 based classified document control system (CDOCS)
[DE93-017880] p 1617 N94-18984

A comparison Air Force data systems — Comments on IDA Paper P-2863
[AD-A270662] p 1619 N94-19780

RECRYSTALLIZATION

Atlas of formability: Nickelvac C-276
[AD-A268264] p 1357 N94-17802

Atlas of formability: ALLVAC 718
[AD-A268304] p 1357 N94-17804

The effect of composition on the mechanism of continuous recrystallization and superplastic response of aluminum-scandium alloys
[DE93-018594] p 1365 N94-19280

RECTANGULAR WINGS

Viscous-inviscid calculation of high-lift separated compressible flows over airfoils and wings
p 1309 N94-18440

RECURSIVE FUNCTIONS

Using geometric techniques to improve dynamic programming algorithms for the economic lot-sizing problem and extensions
[PB93-197556] p 1528 N94-19330

Time dependent identification of nonlinear structures
[ECL-92-64] p 1457 N94-19403

Notes on multi-step ahead prediction based on the principle of concatenation
[MATHS-REPT-A-189] p 1544 N94-19410

RED SHIFT

The universe at moderate redshift
[NASA-CR-193771] p 1627 N94-19093

REDUCTION (CHEMISTRY)

Oxygen reduction at a stabilized zirconia interface with Y(1-x)Ca(x)MnO3 or La(1-x)Sr(x)MnO3 cathode materials
[DE93-015681] p 1593 N94-17747

REDUNDANCY

Computation of large numbers and VLSI: Application to GCD, to stretched GCD and at euclidian distance
[ETN-93-95009] p 1552 N94-19499

REDUNDANCY ENCODING

Fault tolerant sequential circuits using sequence invariant state machines p 1398 N94-18344

REDUNDANT COMPONENTS

Synthesis techniques and analysis tool for on-chip fault-tolerance
[AD-A269148] p 1521 N94-18259

REED-SOLOMON CODES

An extended Reed Solomon decoder design
p 1398 N94-18348

REENTRY TRAJECTORIES

START user manual version 2.1
[LR-726] p 1335 N94-19614

REFLECTANCE

Data fusion through simulated annealing of registered range and reflectance images
[DE93-015910] p 1612 N94-17858

Time-resolved probing of electron thermal conduction in femtosecond-laser-pulse-produced plasmas
[DE93-016996] p 1585 N94-18129

Studies of enhanced radar backscatter
[AD-A269544] p 1385 N94-18288

Testing and evaluation of large-area heliostats for solar thermal applications
[DE93-018509] p 1467 N94-18520

Millimeter wave reflectivity measurement system
[AD-A270008] p 1387 N94-18601

REFRACTION

Using computerized tomography to determine ionospheric structures
[DE93-018904] p 1485 N94-19002

REFRACTIVITY

Photorefractive receiver study
[AD-A269352] p 1577 N94-18302

Apparatus and method for varying a Bragg wavelength of a Bragg grating formed in an optical fiber
[AD-D015876] p 1579 N94-18743

A comparison between several computer codes for calculations on microwave propagation
[FEL-92-A435] p 1390 N94-19449

Optical switch evaluation support
[AD-A270948] p 1581 N94-19601

REFRACTORY MATERIALS

Plastic anisotropy in MoSi2 single crystals
[DE93-012650] p 1594 N94-17874

The 6th Japan-U.S. conference on composite materials
[AD-A268535] p 1341 N94-18630

Developing and understanding the high temperature behavior of niobium aluminides and niobium aluminide composites
[AD-A268874] p 1341 N94-18636

REFRACTORY METAL ALLOYS

Fundamental concepts relating local atomic arrangements, deformation, and fracture of intermetallic alloys
[AD-A268745] p 1361 N94-18788

REFRIGERANTS

Malone refrigeration
[DE93-014468] p 1379 N94-17725

Compatibility of refrigerants and lubricants with motor materials, volume 1
[DE93-040216] p 1350 N94-18895

Compatibility of refrigerants and lubricants with motor materials, volume 2
[DE93-040217] p 1350 N94-18896

Measurement of viscosity, density, and gas solubility of refrigerant blends in selected synthetic lubricants
[DE93-040221] p 1350 N94-18977

Thermophysical properties
[DE93-040219] p 1351 N94-19134

Accelerated screening methods for determining chemical and thermal stability of refrigerant-lubricant mixtures. Part 1: Method assessment
[DE93-040215] p 1351 N94-19136

Compatibility of refrigerants and lubricants with motor materials, volume 3
[DE93-040218] p 1352 N94-19181

REFRIGERATING

Malone refrigeration
[DE93-014468] p 1379 N94-17725

The 7th International Cryocooler Conference
[AD-A268451] p 1379 N94-18147

Regenerator optimization for Stirling cycle refrigeration
[DE93-018468] p 1380 N94-18818

Design verification and acceptance tests of the ASST-A helium refrigeration system
[DE93-019746] p 1381 N94-19540

REFRIGERATORS

The 7th International Cryocooler Conference
[AD-A268451] p 1379 N94-18147

Design verification and acceptance tests of the ASST-A helium refrigeration system
[DE93-019746] p 1381 N94-19540

REFUELING

Mechanically refuelable zinc/air electric vehicle cells
[DE93-016446] p 1394 N94-17770

REGENERATIVE FUEL CELLS

Regenerative fuel cells for High Altitude Long Endurance Solar Powered Aircraft
[DE93-016991] p 1465 N94-17853

REGENERATORS

The 7th International Cryocooler Conference
[AD-A268451] p 1379 N94-18147

Regenerator optimization for Stirling cycle refrigeration
[DE93-018468] p 1380 N94-18818

REGIONS

Eastern Europe: A climatological study
[AD-A269200] p 1493 N94-18883

REGRESSION ANALYSIS

Linear parameter identification methods for ARMA models with periodic coefficients
[REPT-92-070] p 1556 N94-17938

EDF tests for normality in linear models after a Box-Cox transformation
[AD-A269068] p 1557 N94-18517

Modeling of driver behavior: Information perception, rule and control strategies in experiments and simulations
[ETN-93-95053] p 1510 N94-19649

Generalized regression trees: Function estimation via recursive partitioning and maximum likelihood
[AD-A271259] p 1560 N94-19726

REGULARITY

Serial pattern complexity: Irregularity and hierarchy
[PB93-191914] p 1509 N94-19348

REGULATIONS

Safeguarding our energy future
[DE93-016001] p 1466 N94-18109

Airport activity statistics of certificated route air carriers, 1992
[AD-A269042] p 1315 N94-18490

REINFORCED PLASTICS

The calculation methods of a cracked plastic composite laminate: A literature survey
[VTT-TIED-1362] p 1339 N94-17958

REINFORCING FIBERS

A comprehensive study of matrix fracture mechanisms in fiber-reinforced ceramic matrix composites
[AD-A268809] p 1340 N94-18205

Bibliography on ceramic matrix composites and reinforcing whiskers, platelets, and fibers, 1970-1990
[AD-A270139] p 1371 N94-18750

RELATIVISTIC EFFECTS

Acoustic travel time perturbations due to an internal tide and internal wave field in the Barents Sea
[AD-A270879] p 1499 N94-19580

RELATIVISTIC ELECTRON BEAMS

Interaction of intense lasers and relativistic electron beams with solids, gases and plasmas
[AD-A269655] p 1439 N94-18737

RELATIVISTIC PARTICLES

Meson production in relativistic heavy-ion collisions at AGS energies
[DE93-016871] p 1565 N94-17984

Relativistic configuration interaction calculation of the correlation energies of heliumlike ions
[DE93-018093] p 1571 N94-19201

RELATIVISTIC PLASMAS

Enhanced acceleration in a self-modulated-laser wakefield accelerator
[AD-A268452] p 1586 N94-18148

RELATIVISTIC THEORY

Meson production in relativistic heavy-ion collisions at AGS energies
[DE93-016871] p 1565 N94-17984

RELATIVITY

Maximal hypersurfaces in asymptotically stationary spacetimes
[MPA-708] p 1621 N94-18141

RELAXATION METHOD (MATHEMATICS)

Shop problems with two machines and time lags
[REPT-93-020] p 1518 N94-17927

RELAXATION TIME

Relaxation of polar orientational order in nonlinear optical polymers by second harmonic generation
[AD-A269059] p 1370 N94-18515

RELIABILITY

Development of a new concept diver's watch
p 1429 N94-18041

Laser materials processing applications at Lawrence Livermore National Laboratory
[DE93-017976] p 1437 N94-18093

Performance evaluations of demountable electrical connections
[DE93-017399] p 1396 N94-18135

Problems in probability, statistics and reliability
[AD-A270830] p 1559 N94-19595

Increasing mission reliability using open-loop control
[AD-A271208] p 1545 N94-19721

RELIABILITY ANALYSIS

FAROW: A tool for fatigue and reliability of wind turbines
[DE93-017639] p 1465 N94-18001

Human reliability analysis application guide
[DE93-015361] p 1511 N94-18244

Software reliability: Estimation and prediction
[AD-A268895] p 1521 N94-18458

Knowledge sources for an intelligent MCM analyzer
[AD-A269224] p 1542 N94-18887

RELIABILITY ENGINEERING

Reliability control for wrist watches and their casements p 1427 N94-18030

Mutrometre: Construction for fast water proof measurements under low pressure and air suppression
p 1427 N94-18031

REMOTE CONTROL

Magnetostrictive actuators for human sensory feedback
[AD-A269266] p 1511 N94-17841

A wind tunnel model control surface actuator interface
[AD-A268729] p 1322 N94-18324

Design considerations for remotely operated welding in space: Task definition and visual weld monitoring experiment
[AD-A268752] p 1445 N94-18634
VPU(tm) demonstration mission vicinity processor unit(tm) overview p 1325 N94-19171

REMOTE MANIPULATOR SYSTEM
Robotics
[NASA-TM-109351] p 1332 N94-18920

REMOTE SENSING
Packaging, deployment, and panel design concepts for a truss-stiffened 7-panel precision deployable reflector with feed boom
[NASA-TM-109000] p 1333 N94-17765
A mobile remote sensing laboratory for water vapor, trace gas, aerosol, and wind speed measurements
[DE93-017158] p 1489 N94-18132
Arctic ice studies
[AD-A268608] p 1497 N94-18277
A RFI measurement system for field sites
[AD-A269340] p 1385 N94-18301
Microwave (SSM/I) Estimates of the Precipitation Rate to Improve Numerical Atmospheric Model Forecasts
[NASA-CR-193566] p 1491 N94-18602
Physical retrieval of precipitation water contents from Special Sensor Microwave/Imager (SSM/I) data. Part 1: A cloud ensemble/radiative parameterization for sensor response (report version) p 1491 N94-18604
Physical retrieval of precipitation water contents from Special Sensor Microwave/Imager (SSM/I) data. Part 2: Retrieval method and applications (report version)
p 1491 N94-18605
Forecast model applications of retrieved three dimensional liquid water fields p 1492 N94-18606
Current positioning possibilities by spatial techniques and the Royal Oservatory of Belgium program
p 1483 N94-18627
Atlas of SSM/I satellite ice concentration interpolated to operational ice model domains of the Arctic for 1992
[AD-A270306] p 1499 N94-18727
Analytic approximations of an integral in remote sensing
[AD-A270085] p 1463 N94-18800
Engineering research, development and technology thrust area report, FY92
[DE93-016334] p 1632 N94-18856
Spatiotemporal variability of non-urban ozone concentrations over the eastern United States and its potential replication by satellite data
[PB93-191328] p 1476 N94-19065
Development of ISY data set, part 2
[NASDA-CNT-930006-PT-2] p 1463 N94-19384
Suitability of infrared spectroscopy for remote sensing of tropospheric trace gases
[KFK-5183] p 1479 N94-19507
Airborne studies of ocean-particle-cloud interactions in the Arctic
[AD-A270752] p 1479 N94-19575
Footprint size of a helicopter-borne electromagnetic induction sounding system versus antenna altitude
[AD-A270468] p 1463 N94-19672
Remote sensing of Earth terrain
[NASA-CR-194598] p 1464 N94-19681

RENDEZVOUS TRAJECTORIES
Automated rendezvous and capture demonstration study
[NASA-CR-192587] p 1331 N94-19366

RENORMALIZATION GROUP METHODS
Renormalizations in supersymmetric and nonsupersymmetric non-abelian Chern-Simons field theories with matter
[DE93-626646] p 1593 N94-17748

REPEATERS
Development of analog watch with minute repeater
p 1429 N94-18043

REPORTS
Activities report of the Rutherford Appleton Laboratory
[ETN-93-94555] p 1631 N94-17968

REPRODUCTION (BIOLOGY)
Opportunities and questions for the fundamental biological sciences in space p 1502 N94-19212

REPRODUCTION (COPYING)
Color test chart for facsimile
[AD-A269754] p 1387 N94-18721

REPUBLIC OF SOUTH AFRICA
The South African Astronomical Observatory
[SAAO-17] p 1623 N94-19657

REQUIREMENTS
An environment for requirement reuse
[REPT-92-082] p 1613 N94-17939
Secure open systems: An investigation of current standardisation efforts for security in open systems
[FEL-92-B225] p 1618 N94-19450

RESCUE OPERATIONS
AN/APS-137 Forward Looking Airborne Radar (FLAR) evaluation Spring 1992 experiment
[AD-A268899] p 1384 N94-18228

RESEARCH
White House technology reinvestment project: Briefing and transcripts
[PB93-169829] p 1611 N94-18090
Research activities, Faculty of Civil Engineering, Delft University of Technology, 1990 - 1991
[PB93-195022] p 1380 N94-19254
A foundation for the 21st Century: A progressive framework for the National Science Foundation. Report of the National Science Board Commission on the future of the National Science Foundation
[NSB-92-196] p 1611 N94-19618

RESEARCH AIRCRAFT
Ozone hole
[NASA-TM-109368] p 1476 N94-18960
X-29: Research aircraft
[NASA-TM-109370] p 1316 N94-18962
The world's largest wind tunnel
[NASA-TM-109371] p 1322 N94-18963

RESEARCH AND DEVELOPMENT
The ANL electric vehicle battery R&D program for DOE-EHP
[DE93-017414] p 1394 N94-17750
Activities report of the Rutherford Appleton Laboratory
[ETN-93-94555] p 1631 N94-17968
Lightweight materials for transportation: Program plan
[DE93-017381] p 1340 N94-18087
White House technology reinvestment project: Briefing and transcripts
[PB93-169829] p 1611 N94-18090
Trends in Information Management at Department of Energy Headquarters
[DE93-017197] p 1615 N94-18496
The 1994 NASA authorization, volume 2
[GPO-71-510] p 1620 N94-18842
The FAA Technical Center Human Factors Laboratory information guide
[AD-A269343] p 1513 N94-18992
Research and design activities and the economic balance of MBB
[ETN-93-94909] p 1310 N94-19383
Report on the activities of Space Science Department, 1990 - mid 1992
[ESA-SP-1161] p 1633 N94-19404
Program descriptions
[NSF-92-123] p 1531 N94-19619

RESEARCH FACILITIES
Activities report of the Rutherford Appleton Laboratory
[ETN-93-94555] p 1631 N94-17968
The world's most powerful computer
[NASA-TM-109369] p 1514 N94-18961
The world's largest wind tunnel
[NASA-TM-109371] p 1322 N94-18963
The FAA Technical Center Human Factors Laboratory information guide
[AD-A269343] p 1513 N94-18992

RESEARCH MANAGEMENT
Activities report of the Rutherford Appleton Laboratory
[ETN-93-94555] p 1631 N94-17968
A foundation for the 21st Century: A progressive framework for the National Science Foundation. Report of the National Science Board Commission on the future of the National Science Foundation
[NSB-92-196] p 1611 N94-19618

RESEARCH PROJECTS
Research at the Notre Dame Radiation Laboratory
[DE93-018716] p 1566 N94-18165
Where is high-lift today? A review of past UK research programmes p 1305 N94-18416
The GARTEUR high lift research programme
p 1307 N94-18430
Langley's 50th year
[NASA-TM-109365] p 1632 N94-18980
Report on the activities of Space Science Department, 1990 - mid 1992
[ESA-SP-1161] p 1633 N94-19404
Guide to programs, fiscal year 1993
[NSF-92-78] p 1633 N94-19620

RESIDUAL STRENGTH
Residual strength predictions for fibre metal laminates: The R-curves approach
[LR-717] p 1344 N94-19666

RESIDUAL STRESS
Residual strain measurement on the production-grade class 4 flextensional transducer shell
[AD-A268828] p 1430 N94-18537
Fatigue resistant Ti3Al composites
[AD-A270305] p 1341 N94-18692
Analytical and experimental evaluation of joining silicon nitride to metal and silicon carbide to metal for advanced heat engine applications
[DE93-018128] p 1446 N94-19291
Ni-Al2O3 solid state binding: Elaboration, state of thermal constraints, mechanical behavior
[ECL-92-31] p 1366 N94-19436

RESIDUES
Analysis of deposit precursors in jet fuels using Fourier transform infrared spectroscopy
[AD-A269035] p 1377 N94-18489
The use of post detonation analysis of stable isotope ratios to determine the type and production process of the explosive involved
[DE93-018497] p 1378 N94-19242
Bits and relative order from residues, space efficiently
[TR-464] p 1530 N94-19482

RESILIENCE
Filamentation, current profiles and transport in a tokamak
[DE93-016768] p 1584 N94-17948

RESIN MATRIX COMPOSITES
Analysis of pultrusion processing for long fiber reinforced thermoplastic composite system
[NASA-CR-194504] p 1339 N94-17766

RESIN TRANSFER MOLDING
Mechanical properties and impact damage resistance of composites fabricated by low cost, vacuum assisted, resin transfer molding
[AD-A270361] p 1342 N94-18702

RESONANCE
Metal Film Surface Plasmon Resonance (MFSPR) fibre couplers
[AD-A268871] p 1579 N94-18635
Resonance Raman and photophysical studies of transition metal complexes in solution and entrapped in zeolites
[DE93-019892] p 1363 N94-19019
Contribution to the modelling and the identification of nonlinear mechanical systems
[ECL-92-32] p 1529 N94-19409

RESONANCE LINES
Electron impact excitation of copper atoms
[DE93-017995] p 1363 N94-18939

RESONANCE PROBES
WHISPER: A sounder and high-frequency wave analyser experiment p 1328 N94-19626

RESONANT FREQUENCIES
Predicted structural response of the lightweight-interceptor technology demonstration vehicle
[DE93-014676] p 1333 N94-17782
The Lever oscillator for use in high resistance resonator applications
[DE93-017652] p 1404 N94-18827
Free fall liquid column dynamics in a droptower
[LRT-WE-9-FB-6-1992] p 1379 N94-19491
Transient response of a viscous and anchored liquid bridge to an axial pulse
[LRT-WE-9-FB-7-1992] p 1379 N94-19492

RESONANT TUNNELING
Metal Film Surface Plasmon Resonance (MFSPR) fibre couplers
[AD-A268871] p 1579 N94-18635
Theoretical and experimental studies of quantum wells
[AD-A271180] p 1606 N94-19741

RESONANT VIBRATION
Time dependent identification of nonlinear structures
[ECL-92-64] p 1457 N94-19403
Blade and hub loads of ballistically damaged helicopter rotors
[AD-A270663] p 1319 N94-19781

RESONATORS
Simulation of quartz resonators p 1426 N94-18021
The Lever oscillator for use in high resistance resonator applications
[DE93-017652] p 1404 N94-18827

RESOURCE ALLOCATION
An annealing approach to multi-facility location problems in euclidean spaces
[REPT-93-022] p 1547 N94-17928
Annealing algorithms for multiresource absolute location problems on graph
[REPT-93-028] p 1520 N94-18145
PRACTICAL: Planning and resource allocation in C2-domains with time critical algorithms
[FEL-93-B029] p 1544 N94-19458

RESOURCES MANAGEMENT
Trends in Information Management at Department of Energy Headquarters
[DE93-017197] p 1615 N94-18496
The ecological and environmental impacts of manmade marshes
[AD-A269213] p 1475 N94-18885
Integrated measurement of crew resource management and technical flying skills
[AD-A270512] p 1510 N94-19677

RESPIRATORY RATE

Evaluation of physiological and psychological impairment of human performance in cold stressed subjects
[AD-A268637] p 1506 N94-18632

RESPONSE TIME (COMPUTERS)

Conception and analysis of numerical parallel algorithms: Realization on the Connection Machine
[ETN-93-95005] p 1531 N94-19517

RESTORATION

Restoration of an 18th century English clock
p 1427 N94-18026

Environmental restoration and waste management five-year plan, fiscal years 1994-1998. Volume 3: Public concerns
[DOE/S-00097P-VOL-3] p 1475 N94-18835

Fiber optic Raman spectrograph for in situ environmental monitoring
[DE93-019466] p 1478 N94-19305

RETENTION (PSYCHOLOGY)

Comparing performance on implicit memory tests
[AD-A269900] p 1508 N94-18657

RETINA

Localization of figure background segregation mechanisms in primate visual cortex
[PB93-187961] p 1508 N94-18121

An analog retina model for detecting dim moving objects against a bright moving background
p 1399 N94-18350

REVERSE FIELD PINCH

Profile stabilization of tilt mode in a field reversed configuration
[DE93-016770] p 1583 N94-17753

REYNOLDS NUMBER

Error propagation equations and tables for estimating the uncertainty in high-speed wind tunnel test results
[DE93-018685] p 1311 N94-18275

An experimental investigation of attachment-line transition on the slat of a combat aircraft model
p 1308 N94-18432

Semi-span model testing in the National Transonic Facility
[NASA-CR-194479] p 1312 N94-19388

Numerical prediction of transition of the F-16 wing at supersonic speeds
[NASA-CR-194407] p 1312 N94-19433

Numerical investigation of the incompressible flow around a wing with a fixed spoiler
[ISL-R-109/91] p 1313 N94-19524

An investigation of low Marangoni number fluid flow in a cold corner
[AD-A271317] p 1422 N94-19569

REYNOLDS STRESS

Self-regulated shear flow turbulence in confined plasmas
[DE93-015823] p 1583 N94-17743

On memory effects in turbulence
[DLR-FB-93-03] p 1409 N94-18124

Assessment and development of second order turbulence models p 1411 N94-18548

Numerical implementation and performance of Reynolds-stress closures in finite-volume computations of recirculating and strongly swirling flows
p 1415 N94-18589

Modelling engineering flows with Reynolds stress turbulence closure p 1415 N94-18591

RHEOLOGY

Some problems in the rheological characterisation of composite rocket propellants
[AD-A268806] p 1376 N94-18203

Numerical analysis of pressure meter tests: Application of parameter identification of soils behavior
[ECL-92-52] p 1487 N94-19380

RHEOMETERS

Some problems in the rheological characterisation of composite rocket propellants
[AD-A268806] p 1376 N94-18203

RIBLETS

The effect of fine surface riblets on the flow around an inclined axially symmetrical body
[MPIS-105/1993] p 1420 N94-19356

RICCATI EQUATION

The optimal projection equations for finite-dimensional fixed-order H2-optimal control of infinite-dimensional discrete-time systems
[REPT-93-11] p 1542 N94-19085

The fixed, finite-order L(sup 2)-optimal control of infinite-dimensional time-varying discrete-time systems
[REPT-93-23] p 1542 N94-19138

Discrete-time infinity control problem with measurement feedback
[PB93-197523] p 1543 N94-19329

RIEMANN MANIFOLD

Differential geometry of CR-submanifolds of a normal almost para contact manifold
[DE93-624764] p 1545 N94-17793

Unbounded components in parameter space of rational maps
[DE93-628621] p 1546 N94-18170

Contact 3-manifolds, integrable Hamiltonian systems and exotic symplectic structures in R(sup 4)
[DE93-624767] p 1551 N94-19248

RIGID STRUCTURES

Crashdynamics with DYNA3D: Capabilities and research directions p 1460 N94-19475

RING CURRENTS

Penetrating radiation environment and effects study
[AD-A270126] p 1485 N94-18874

RINGS (MATHEMATICS)

Stabilization of time-delay systems: An overview of the algebraic approach
[PB93-191989] p 1553 N94-19556

RISK

Indoor environment program
[DE93-018601] p 1513 N94-18935

Uncertainty versus interindividual variability
[DE93-018105] p 1559 N94-19549

RIVERS

The ecological and environmental impacts of manmade marshes
[AD-A269213] p 1475 N94-18885

RIVETED JOINTS

Fatigue crack initiation in riveted lap joints and in pressurized fuselages
[LR-725] p 1461 N94-19669

ROBOT CONTROL

Efficient dynamic modeling of manipulators containing closed kinematic loops
[REPT-92-083] p 1444 N94-17940

Autonomous neural network controllers for adaptive material handling
[AD-A268908] p 1540 N94-18331

Flexible integration of path-planning capabilities
[AD-A269594] p 1541 N94-18463

MART: An overview of the Mobile Autonomous Robot Twente project
[MEMO-INF-93-12] p 1543 N94-19199

Robot navigation in unknown terrains: Introductory survey of non-heuristic algorithms
[DE93-019221] p 1316 N94-19300

ROBOT DYNAMICS

Joint stiffness estimation based on force sensor measurements in industrial manipulators
[REPT-92-053] p 1443 N94-17937

Direct kinematics solution architectures for industrial robot manipulators: Bit-serial versus parallel
p 1399 N94-18358

Survey of collision avoidance and ranging sensors for mobile robots, revision 1
[AD-A269846] p 1541 N94-18474

ROBOT SENSORS

MART: An overview of the Mobile Autonomous Robot Twente project
[MEMO-INF-93-12] p 1543 N94-19199

Automated rendezvous and capture demonstration study
[NASA-CR-192587] p 1331 N94-19366

ROBOTICS

Magnetostrictive actuators for human sensory feedback
[AD-A269266] p 1511 N94-17841

Joint stiffness estimation based on force sensor measurements in industrial manipulators
[REPT-92-053] p 1443 N94-17937

Autonomous neural network controllers for adaptive material handling
[AD-A268908] p 1540 N94-18331

Survey of collision avoidance and ranging sensors for mobile robots, revision 1
[AD-A269846] p 1541 N94-18474

Robotics
[NASA-TM-109351] p 1332 N94-18920

ROBOTS

An object-oriented environment for computer vision and pattern recognition
[DE93-017098] p 1517 N94-17867

Joint stiffness estimation based on force sensor measurements in industrial manipulators
[REPT-92-053] p 1443 N94-17937

Flexible integration of path-planning capabilities
[AD-A269594] p 1541 N94-18463

Survey of collision avoidance and ranging sensors for mobile robots, revision 1
[AD-A269846] p 1541 N94-18474

Robotics
[NASA-TM-109351] p 1332 N94-18920

Adaptive path planning: Algorithm and analysis
[DE93-008348] p 1523 N94-18926

Geometrical pattern learning
[DE93-017641] p 1542 N94-19007

MART: An overview of the Mobile Autonomous Robot Twente project
[MEMO-INF-93-12] p 1543 N94-19199

Robot navigation in unknown terrains: Introductory survey of non-heuristic algorithms
[DE93-019221] p 1316 N94-19300

ROBUSTNESS (MATHEMATICS)

An overview of the SAFSIM computer program
[DE93-017657] p 1519 N94-18002

Non Linear Dynamics and Chaos
[AGARD-LS-191] p 1607 N94-18236

Robustness and efficiency of generalized predictive control algorithms with guaranteed stability
[MATHS-REPT-A-190] p 1530 N94-19412

Fault-tolerance and complexity
[TR-450] p 1530 N94-19483

Use of shape memory alloys in the robust control of smart structures
[AD-A270827] p 1366 N94-19594

A learning autopilot for automatically controlled robust regulation
[ETN-93-95075] p 1321 N94-19711

A real-time spoken-language system for interactive problem-solving, combining linguistic and statistical technology for improved spoken language understanding
[AD-A270901] p 1392 N94-19749

ROCK MECHANICS

Ground movements associated with gas hydrate production
[DE93-019887] p 1486 N94-19018

ROCKET ENGINE CONTROL

FNAS/summer faculty fellowship research continuation program. Task 6: Integrated model development for liquid fueled rocket propulsion systems. Task 9: Aspects of model-based rocket engine condition monitoring and control
[NASA-CR-194574] p 1338 N94-19706

ROCKET ENGINES

KINETIC: A system code for analyzing Nuclear thermal propulsion rocket engine transients
[DE93-016825] p 1337 N94-17884

Adaptations to micropep and rocket to allow performance evaluation of multiple grain and/or airbreathing motors
[AD-A268798] p 1337 N94-18202

ROCKET EXHAUST

UVPI imaging from the LACE satellite: The Nihka rocket plume
[AD-A268456] p 1334 N94-18149

Ultraviolet plume instrument calibration and sensor assessment
[AD-A269687] p 1337 N94-18574

JPRS report: Science and technology. Central Eurasia: Earth Sciences
[JPRS-UES-93-004] p 1461 N94-19209

ROCKET NOZZLES

Analysis of film cooling in rocket nozzles
[NASA-CR-194674] p 1338 N94-19438

ROCKET OXIDIZERS

Aluminum powder/water reaction ignited by electrical pulsed power
[AD-A269223] p 1376 N94-17840

ROCKET PROPELLANTS

Some problems in the rheological characterisation of composite rocket propellants
[AD-A268806] p 1376 N94-18203

New test method to determine modulus of elasticity of rocket grain material
[AD-A269758] p 1377 N94-18758

ROCKWELL HARDNESS

Thermal insulation of wet shielded metal arc welds
[AD-A268697] p 1445 N94-18465

RODS

A finite strain ring dynamical model for pneumatic tires
[AD-A269286] p 1444 N94-18266

The influence of the target strength model on computed perforation
[DE93-018659] p 1460 N94-19543

ROLLING CONTACT LOADS

Measuring methods for evaluation of dynamic tyre properties
[ETN-93-95054] p 1381 N94-19650

ROOM TEMPERATURE

New room temperature high resolution solid-state detector (CdZnTe) for hard x rays and gamma rays
p 1324 N94-19165

ROSAT MISSION

Rosat and optical observations of two X-ray transients: MX 0836-42 and GS 0834-430
[MPE-PREPRINT-237] p 1622 N94-19451

ROSAT and IRAS observations
[MPE-PREPRINT-231] p 1623 N94-19526

ROSAT X ray observation of the 30 Dor giant HII region p 1623 N94-19527

IRAS galaxies observed in the ROSAT survey: Starbursts or central activity p 1623 N94-19528

Particle induced background by Roentgen satellites
[MPE-242] p 1631 N94-19714
Stellar coronae at the end of the main sequence: A Rosat survey of the late M dwarfs
[NASA-CR-194700] p 1628 N94-19794

ROTARY WINGS
Aerodynamic characteristics of a helicopter rotor airfoil as affected by simulated ballistic damage
[AD-A269206] p 1311 N94-18413
Blade and hub loads of ballistically damaged helicopter rotors
[AD-A270663] p 1319 N94-19781

ROTATING BODIES
Applications of neural networks in fault detection of rotating machinery
[AD-A270755] p 1448 N94-19766

ROTATING SHAFTS
Fluid dynamometer having fluid characteristic power absorption adjustment capability
[AD-D015820] p 1424 N94-17904

ROTATION
Theoretical study and modelling of homogeneous turbulence under rotation for implantation in a code for solving Navier-Stokes equations
[ECL-93-05] p 1420 N94-19381
Cognitive ability and whole-body rotation
[IZF-1993-B-4] p 1510 N94-19440

ROTORS
A survey on technical problems in designing high-speed rotors with developing materials
[DE93-788519] p 1444 N94-18159
Some problems in the rheological characterisation of composite rocket propellants
[AD-A268806] p 1376 N94-18203

ROUTES
Airport activity statistics of certificated route air carriers, 1992
[AD-A269042] p 1315 N94-18490

RULES
Better termination analysis for active databases
[REPT-93-026] p 1614 N94-18144

RUNGE-KUTTA METHOD
Numerical calculations of high lift flows using structured and unstructured methods p 1307 N94-18428
An algebraic turbulence model for turbomachinery
p 1411 N94-18554

RURAL AREAS
Spatiotemporal variability of non-urban ozone concentrations over the eastern United States and its potential replication by satellite data
[PB93-191328] p 1476 N94-19065

S

S MATRIX THEORY
Polarimetric statistics of electromagnetic waves scattered by distributed targets
[PB93-195907] p 1389 N94-18951

S WAVES
The phase mixing of shear Alfven waves
[DE93-624920] p 1581 N94-17688
Constraints on crustal structure from long period pressure and displacement measurements on the deep seafloor
[AD-A269931] p 1498 N94-18663
Seismic studies of the geologic structure and physical properties of the seabed
[AD-A270895] p 1500 N94-19747

S-N DIAGRAMS
Factors which affect fatigue strength of fasteners
[DE93-017272] p 1453 N94-18084

SAFETY
SUNRAYCE 1993: Working safely with lead-acid batteries and photovoltaic power systems
[DE93-016553] p 1464 N94-17712
Safety-routines and guidelines for work in the clean room at the Epitek-Laboratory, Kjeller (Norway)
[FFI-93/7012] p 1322 N94-17735
Laboratory test and evaluation report of the essex model 60C-0037-2 molecular sieve oxygen generating system
[AD-A269967] p 1445 N94-18778

SAFETY DEVICES
Solid-state, resistive hydrogen sensors for safety monitoring
[DE93-017769] p 1424 N94-17778
Army Cockpit Delethalization Program (CDP)
[AD-A268990] p 1512 N94-18765
Plasma contactor development for Space Station
[NASA-TM-106425] p 1587 N94-18861

SAFETY MANAGEMENT
Safety approaches for high power modular laser operation
[DE93-017213] p 1435 N94-17759
Human reliability analysis application guide
[DE93-015361] p 1511 N94-18244

SALINITY
CTD and XBT data collected on ERS-1 validation cruise RRS Charles Darwin Cruise 62A, Iceland-Faeroes region
[IOS-294-1992] p 1461 N94-18063
SeaSoar and CTD sections across the Iceland-Faeroes Front and Faeroe Shetland Channel, August 1990
[IOS-295-1992] p 1496 N94-18064
SeaSoar CTD, fluorescence and scalar irradiance data from RRS Charles Darwin Cruises 58/59, NE Atlantic, Vivaldi 1991
[IOS-299-1992] p 1496 N94-18066
Synoptic ocean prediction experiment. EN216 CTD section data report
[AD-A268903] p 1497 N94-18230
Overview of physical oceanographic measurements taken during the Mount Mitchell cruise to ROPME sea area
[DE93-018460] p 1497 N94-18494

SALTS
Mechanical modeling of the growth of salt structures
[DE93-015342] p 1596 N94-18243

SAMPLED DATA SYSTEMS
High accuracy switched-current circuits using an improved dynamic mirror p 1401 N94-18368

SAMPLERS
Novel mass spectrometric instrument for gaseous and particulate characterization and monitoring
[DE93-019992] p 1433 N94-19054

SAMPLES
Practical reporting times for environmental samples
[DE93-013461] p 1472 N94-17910

SAMPLING
Practical reporting times for environmental samples
[DE93-013461] p 1472 N94-17910
Bayesian analysis of ARMA processes: Complete sampling based inference under full likelihoods
[AD-A269168] p 1557 N94-18694
Ultrafast Electronics and Optoelectronics: Summaries of papers. Technical digest conference edition
[AD-A269233] p 1405 N94-18909

SAN ANDREAS FAULT
Heterogeneous slip and rupture models of the San Andreas fault zone based upon three-dimensional earthquake tomography
[DE93-015037] p 1480 N94-17898
Analysis of regional deformation and strain accumulation data adjacent to the San Andreas fault
[NASA-CR-194072] p 1487 N94-19428

SANDS
Centrifuge modeling of explosion-induced craters in unsaturated sand
[AD-A270194] p 1417 N94-18780

SANDWICH STRUCTURES
Packaging, deployment, and panel design concepts for a truss-stiffened 7-panel precision deployable reflector with feed boom
[NASA-TM-109000] p 1333 N94-17765

SANITATION
Research activities, Faculty of Civil Engineering, Delft University of Technology, 1990 - 1991
[PB93-195022] p 1380 N94-19254

SAPPHIRE
Experimental investigation of wave and fracture phenomena in impacted ceramics: Experiments on sapphire
[AD-A270040] p 1372 N94-18792
Multi-terrawatt, 100 fsec laser system using flashlamp-pumped, dye-converted Ti:sapphire as an amplifier
[DE93-017190] p 1440 N94-18889
Surface modification of sapphire for IR window application
[DE93-019168] p 1602 N94-19075

SARSAT
High efficiency low cost monolithic module for SARSAT distress beacons
[NASA-CR-194234] p 1315 N94-18852

SATELLITE ANTENNAS
Missile antenna pattern coordinate system and data formats
[AD-A269153] p 1385 N94-18260

SATELLITE ATTITUDE CONTROL
The star identification, pointing and tracking system of UVSTAR, an attached payload instrument system for the Shuttle Hitchhiker-M platform p 1326 N94-19179

SATELLITE COMMUNICATION
Radio wave propagation in structured ionization for satellite and radar applications
[AD-A268457] p 1382 N94-17844
Direct solar pumping of semiconductor lasers: A feasibility study
[NASA-CR-193760] p 1440 N94-18834

SATELLITE CONTROL
CONTACT: An Air Force technical report on military satellite control technology
[AD-A269375] p 1334 N94-18408
Corporate Information Management (CIM) report on the simulation processes, version 2.0
[AD-A269119] p 1617 N94-18770

SATELLITE IMAGERY
Ship-produced cloud line of 13 July 1991
[DE93-016879] p 1472 N94-17986
Application of fractal methods to estimate the aerosol-optical depth for atmospheric correction of high resolution satellite data
[DLR-FB-93-04] p 1480 N94-18088
Three-dimensional cloud visualization based on satellite imagery
[AD-A269318] p 1490 N94-18300
The Navy tessellated spheroid map projection system: A comprehensive definition
[AD-A269989] p 1462 N94-18677
Ozone hole
[NASA-TM-109368] p 1476 N94-18960
Mathematical modeling of the free surface hydrodynamic and of transport in suspensions of non cohesive sediments: Aid to the interpretation of spatial images
[ETN-93-95011] p 1421 N94-19502

SATELLITE INSTRUMENTS
Experience with custom processors in space flight applications p 1336 N94-18338
Ultraviolet plume instrument calibration and sensor assessment
[AD-A269687] p 1337 N94-18574

SATELLITE NETWORKS
CONTACT: An Air Force technical report on military satellite control technology
[AD-A269375] p 1334 N94-18408

SATELLITE OBSERVATION
Current positioning possibilities by spatial techniques and the Royal Oservatory of Belgium program
p 1483 N94-18627
Modifications of airborne oceanographic lidar for the long range P-3 missions
[NASA-CR-194682] p 1499 N94-18819
Development of ISY data set, part 2
[NASDA-CNT-930006-PT-2] p 1463 N94-19384
SeaTrack: Ground station orbit prediction and planning software for sea-viewing satellites
[NASA-RP-1331] p 1532 N94-19761

SATELLITE SOUNDING
Verification of 3I retrievals vis-a-vis radiosonde observations
[KNMI-TR-150] p 1488 N94-17924
Some potential errors in satellite wind estimates using the geostrophic approximation and the thermal wind
[AD-A269784] p 1491 N94-18599

SATELLITE TRACKING
CONTACT: An Air Force technical report on military satellite control technology
[AD-A269375] p 1334 N94-18408
Parallelization of the Air Force Space Command (AFSPACECOM) satellite motion models
[AD-A269327] p 1334 N94-18470

SATELLITE-BORNE PHOTOGRAPHY
JPRS report: Central Eurasia. Aviation and cosmonautics, no. 1, January 1993
[JPRS-UAC-93-007] p 1632 N94-19147

SATURN 5 LAUNCH VEHICLES
Technology test bed
[NASA-TM-109354] p 1322 N94-18953

SCALARS
On a conformal perfect fluid in the classical vacuum
[DE93-624797] p 1480 N94-17682
Texture splats for 3D vector and scalar field visualization
[DE93-017104] p 1520 N94-18130

SCALE EFFECT
An experimental investigation of attachment-line transition on the slat of a combat aircraft model
p 1308 N94-18432

SCALE MODELS
The application of nondestructive techniques to the testing of a wind turbine blade
[DE93-016731] p 1447 N94-18128
A study of the use of half-models in high-lift wind-tunnel testing p 1308 N94-18434

SCALING LAWS
Scaling laws for diffraction loading by air blast
[PML-1991-54] p 1452 N94-17941
Analysis of the ITER H-mode confinement database
[DE93-016984] p 1585 N94-18056
Scaling laws for diamond chemical vapor deposition. 2: Atomic hydrogen transport
[AD-A269842] p 1371 N94-18740
Scaling laws for diamond chemical vapor deposition. Diamond surface chemistry
[AD-A269874] p 1599 N94-18745
Centrifuge modeling of explosion-induced craters in unsaturated sand
[AD-A270194] p 1417 N94-18780

SCANNING ELECTRON MICROSCOPY
Applications of scanning tunneling microscopy to electrochemistry
[AD-A269129] p 1348 N94-18255
Thin film studies of the proximity Josephson effect
[AD-A270129] p 1600 N94-18876
Atomic resolution electron energy loss spectroscopy in the scanning transmission electron microscope
[DE93-015334] p 1352 N94-19239
Microtribology of magnetic media
[AD-A271209] p 1407 N94-19722
SCANNING TUNNELING MICROSCOPY
Applications of scanning tunneling microscopy to electrochemistry
[AD-A269129] p 1348 N94-18255
Tunneling spectroscopy of ultrasmall clusters and grains
[AD-A268840] p 1598 N94-18539
Thin film studies of the proximity Josephson effect
[AD-A270129] p 1600 N94-18876
SCATTER PROPAGATION
BACKSCATTER.FOR: A program to calculate the backscattering strength of an inhomogeneous seabed
[AD-A269235] p 1499 N94-18910
SCATTERING
Optical properties of redispersed iron fibers measured at 94 GHz
[AD-A269738] p 1342 N94-18756
Analytic approximations of an integral in remote sensing
[AD-A270085] p 1463 N94-18800
Research in high energy physics
[DE93-018031] p 1575 N94-19287
SCATTERING AMPLITUDE
Lectures of Fermi liquid theory
[DE93-016630] p 1592 N94-17714
First and second order Stokes generation by SRS in methane: Influence of rep-rate, beam quality and astigmatism
[FEL-92-A125] p 1441 N94-19426
SCATTERING COEFFICIENTS
Analysis of meteorological conditions during AGASP-4: 30 March - 23 April 1992
[PB93-190205] p 1489 N94-18126
SCATTERING CROSS SECTIONS
Criticality benchmark comparisons leading to cross-section upgrades
[DE93-017184] p 1556 N94-18073
SCATTERING FUNCTIONS
Forward scattering of a pulsed continuous wave signal through laminar and turbulent thermal plumes
[AD-A271210] p 1564 N94-19723
SCATTEROMETERS
Theoretical and experimental research on coherent microwave backscatter from the ocean
[AD-A271276] p 1500 N94-19743
SCHEDULES
Using controlled daylight exposure and sleep timing in the prevention of shift lag during night operations
[AD-A269304] p 1504 N94-17824
SCHEDULING
Shop problems with two machines and time lags
[REPT-93-020] p 1518 N94-17927
PRACTICAL: Planning and resource allocation in C2-domains with time critical algorithms
[FEL-93-B029] p 1544 N94-19458
SCHOOLS
Undergraduate origins of recent science and engineering doctorate recipients
[NSF-92-332] p 1610 N94-19389
Undergraduate course and curriculum development program and calculus and the bridge to calculus program: 1992 awards
[NSF-93-24] p 1610 N94-19446
SCHROEDINGER EQUATION
Variable time-step integration for intense field effects
[DE93-013296] p 1382 N94-17909
Impulsive moving mirror model in a Schroedinger picture with impulse effect in a Banach space
[DE93-629864] p 1561 N94-18155
Asymptotic behaviour of the solutions of Schroedinger equation with impulse effect in a Banach space
[DE93-629865] p 1548 N94-18195
Impulsive moving mirror model and the stability of Schroedinger equation with impulse effect in a Banach space
[DE93-629866] p 1548 N94-18196
Impulsive moving mirror model and impulsive differential equations in Banach space
[DE93-629867] p 1549 N94-18197
A hydrogen atom in the curved space. Expansion over free solutions on the three-dimensional sphere
[DE93-629868] p 1549 N94-18198
The rise of accuracy for the multichannel scattering problem solving
[DE93-630145] p 1608 N94-18253
Schroedinger's hope
[AD-A270988] p 1581 N94-19772
SCIENCE
A foundation for the 21st Century: A progressive framework for the National Science Foundation. Report of the National Science Board Commission on the future of the National Science Foundation
[NSB-92-196] p 1611 N94-19618
SCIENTIFIC SATELLITES
Space debris detection
[AD-A269254] p 1334 N94-18264
SCIENTIFIC VISUALIZATION
Texture splats for 3D vector and scalar field visualization
[DE93-017104] p 1520 N94-18130
An evolving infrastructure for scientific computing and the integration of new graphics technology
[DE93-017164] p 1520 N94-18133
Three-dimensional cloud visualization based on satellite imagery
[AD-A269318] p 1490 N94-18300
VHDL simulation with access to transistor models
p 1402 N94-18381
3D composite grids using Bezier curves and surfaces in component adaptive methods
[AD-A269188] p 1549 N94-18863
A visualization environment for supercomputing-based applications in computational mechanics
[DE93-015024] p 1537 N94-19249
Volume rendering of 3D scalar and vector fields at Lawrence Livermore National Laboratory
[DE93-018000] p 1528 N94-19276
SCIENTISTS
Magnetic Fusion Energy Technology Fellowship: Report on survey of institutional coordinators
[DE93-014646] p 1583 N94-17739
Origins of solar activity. First year report, AASERT grant
[AD-A268848] p 1629 N94-18222
Computing professionals: Changing needs for the 1990's
[B-030] p 1515 N94-19401
SCINTILLATION
Radio wave propagation in structured ionization for satellite and radar applications
[AD-A268457] p 1382 N94-17844
An investigation of methods for updating ionospheric scintillation models using topside in-situ plasma density measurements
[AD-A269872] p 1483 N94-18655
Precision machining and polishing of scintillating crystals for large calorimeters and hodoscopes
[DE93-018663] p 1381 N94-19544
SCINTILLATION COUNTERS
An investigation of methods for updating ionospheric scintillation models using topside in-situ plasma density measurements
[AD-A269872] p 1483 N94-18655
Conversion of ADC pulse heights into MIP units: NUMASS test data, September 1991
[USIP-93-03] p 1432 N94-18846
SSC detector muon sub-system beam tests
[DE93-018415] p 1569 N94-19013
New room temperature high resolution solid-state detector (CdZnTe) for hard x rays and gamma rays
p 1324 N94-19165
Telescope for x ray and gamma ray studies in astrophysics p 1324 N94-19166
SEA FLOOR SPREADING
Constraints on crustal structure from long period pressure and displacement measurements on the deep seafloor
[AD-A269931] p 1498 N94-18663
SEA ICE
Atlas of SSM/I satellite ice concentration interpolated to operational ice model domains of the Arctic for 1992
[AD-A270306] p 1499 N94-18727
Method for extracting tidal and inertial motion from ARGOS ice buoys applied to the Barents Sea during CEAREX
[PB93-190213] p 1499 N94-19063
Oil spreading in surface waters with an ice cover
[PB93-190767] p 1476 N94-19064
Airborne studies of ocean-particle-cloud interactions in the Arctic
[AD-A270752] p 1479 N94-19575
SEA LEVEL
Research on Earth's rotation and the effect of atmospheric pressure on vertical deformation and sea level variability
[NASA-CR-194300] p 1484 N94-18838
The WAQUA/CSM-16 model p 1494 N94-19700
SEA SURFACE TEMPERATURE
Effect of spatial resolution on the simulation of regional precipitation in China in a global climate model
[DE93-013433] p 1489 N94-18053
SeaSoar CTD, fluorescence and scalar irradiance data from RRS Charles Darwin Cruises 58/59, NE Atlantic, Vivaldi 1991
[IOS-299-1992] p 1496 N94-18066
SEALING
Joining and Adhesion of Advanced Inorganic Materials Symposium
[AD-A269748] p 1342 N94-18720
SEARCH PROFILES
Software Toolkit for Analysis Research (STAR)
[DE93-017368] p 1519 N94-18086
SEARCHING
Finding the strong components in a directed graph
[PB93-187342] p 1555 N94-19708
SEAS
An atlas of bathy-thermograph temperature cross-sections for Coral and Tasman Sea transects from 1960 to 1987
[AD-A268775] p 1497 N94-18329
Overview of physical oceanographic measurements taken during the Mount Mitchell cruise to ROPME sea area
[DE93-018460] p 1497 N94-18494
SeaTrack: Ground station orbit prediction and planning software for sea-viewing satellites
[NASA-RP-1331] p 1532 N94-19761
SEASONS
CTD oxygen, tracer and nutrient data from RRS Charles Darwin Cruises 58/59 in the NE Atlantic as part of Vivaldi 1991
[IOS-296-1992] p 1496 N94-18065
SEAT BELTS
Numerical simulation of vehicle crashworthiness and occupant protection p 1459 N94-19471
Efficiency and biofidelity of occupant simulations
p 1459 N94-19473
SEATS
Analysis of seating and restraint limitations restricting total body weight for aircrew and passengers on US Army helicopters
[AD-A269117] p 1511 N94-18296
Army Cockpit Delethalization Program (CDP)
[AD-A268990] p 1512 N94-18765
SECONDARY FLOW
STREMR: Numerical model for depth-averaged incompressible flow
[AD-A269949] p 1417 N94-18672
SECONDARY ION MASS SPECTROMETRY
Ultra-shallow box-like profiles fabricated by pulsed UV-laser doping process
[DE93-017221] p 1437 N94-18083
Research program activities of the ORNL Analytical Chemistry Division
[DE93-017938] p 1339 N94-19117
SECURITY
Automated assistance for detecting malicious code
[DE93-018106] p 1523 N94-18943
SEDIMENT TRANSPORT
Mathematical modeling of the free surface hydrodynamic and of transport in suspensions of non cohesive sediments: Aid to the interpretation of spatial images
[ETN-93-95011] p 1421 N94-19502
SEDIMENTARY ROCKS
Shock propagation in crustal rock
[AD-A270148] p 1485 N94-18899
SEDIMENTS
Three-dimensional high-resolution seismic profiling on the New Jersey outer continental shelf
[AD-A269835] p 1498 N94-18600
Carbon Isotope Biogeochemistry of Methane from Anoxic Sediments
[NASA-CR-194620] p 1477 N94-19231
A carbon isotope mass balance for an anoxic marine sediment: Isotopic signatures of diagenesis
p 1477 N94-19232
The carbon isotope biogeochemistry of (epsilon)CO2 production in a methanogenic marine sediment
p 1477 N94-19233
The carbon isotope biogeochemistry of methane production in anoxic sediments. 1: Field observations
p 1477 N94-19234
Factors that control the stable carbon isotopic composition of methane produced in an anoxic marine sediment p 1477 N94-19235
Gravity and the geoid in the Nepal Himalaya
[NASA-CR-194166] p 1463 N94-19430
Mathematical modeling of the free surface hydrodynamic and of transport in suspensions of non cohesive sediments: Aid to the interpretation of spatial images
[ETN-93-95011] p 1421 N94-19502
Faulted structure of the bottom simulating reflector on the Blake Ridge, western North Atlantic
[AD-A271289] p 1500 N94-19745

SEISMIC ENERGY

Analysis of regional bodywave phases from earthquakes in western China, part 2
[AD-A270125] p 1485 N94-18873

SEISMIC WAVES

Generalized seismic analysis p 1449 N94-17832

A comparison of single-station backazimuth estimates with regional event locations in the Central Appalachians
[AD-A269897] p 1483 N94-18690

Wave propagation near explosive sources
[AD-A270102] p 1418 N94-18870

Analysis of regional bodywave phases from earthquakes in western China, part 2
[AD-A270125] p 1485 N94-18873

Fast iterative solution of sparsely sampled seismic inverse problems
[REPT-93-16] p 1486 N94-19081

Transmission of acoustic waves through strongly heterogeneous, two-dimensional velocity models
[REPT-93-09] p 1563 N94-19083

Inverse scattering of surface waves: A new look at surface consistency
[REPT-93-25] p 1486 N94-19140

An iterative inverse scattering method for the removal of scattered surface waves
[REPT-93-18] p 1488 N94-19644

Analysis of data from Columbia Point Arena Ocean-Bottom Seismic Station (OBSS)
[AD-A271263] p 1500 N94-19727

SEISMOGRAMS

Analysis of regional bodywave phases from earthquakes in western China, part 2
[AD-A270125] p 1485 N94-18873

SEISMOGRAPHS

Analysis of regional bodywave phases from earthquakes in western China, part 2
[AD-A270125] p 1485 N94-18873

SEISMOLOGY

Generalized seismic analysis p 1449 N94-17832

Constructing a reference event list for ARCESS
[AD-A269288] p 1481 N94-18297

High resolution geological site characterization utilizing ground motion data
[AD-A268926] p 1481 N94-18485

Belgian Royal Observatory Communications, Series A, No. 104, Geophysics Series No. 175
[COMMUNICATIONS-SER-A-104] p 1482 N94-18622

Historical seismicity of Hainaut, Flanders and Artois
p 1482 N94-18623

Current (1985-1988) seismic activity in Belgium: Comparison with historical and instrumental seismic data
p 1482 N94-18624

Macroseismic study of the Dour (Belgium) earthquakes of 22 March 1987 and of Gulpen (Belgium) 17 October 1988 p 1482 N94-18625

Current positioning possibilities by spatial techniques and the Royal Oservatory of Belgium program
p 1483 N94-18627

The use of velocity spectra for stacking receiver functions with application to IRIS/IDA stations OBNINSK (OBN) and ARTI (ARU), Russia
[AD-A269087] p 1483 N94-18717

Analysis of regional deformation and strain accumulation data adjacent to the San Andreas fault
[NASA-CR-194072] p 1487 N94-19428

The interpretation of crustal dynamics data in terms of plate motions and regional deformation near plate boundaries
[NASA-CR-194302] p 1487 N94-19432

Seismic studies of the geologic structure and physical properties of the seabed
[AD-A270895] p 1500 N94-19747

SELECTIVE DISSEMINATION OF INFORMATION

NASA aeronautics: Protecting sensitive technology. Report to Congressional requesters
[GAO/NSIAD-93-201] p 1617 N94-18848

Inventory management plan for a research and development local area network
[DE93-018381] p 1617 N94-19026

Secure open systems: An investigation of current standardisation efforts for security in open systems
[FEL-92-B225] p 1618 N94-19450

Secure open systems: An investigation
[FEL-91-B293] p 1619 N94-19454

Computer security. Evolutions 1987 to 1992: Trends and perspectives
[RR-905-I] p 1532 N94-19713

SELECTIVE SURFACES

Development of a selective volumetric receiver for central receiver systems: Investigation of parameters and exergetic evaluation
[DLR-FB-93-05] p 1465 N94-18089

SELECTIVITY

Stimulus-driven capture and attentional set: Selective search for color and visual abrupt onsets
[IZF-1992-B-9] p 1509 N94-19419

SELF CONSISTENT FIELDS

Polaron tunneling in high-temperature superconductors
[DE93-016880] p 1593 N94-17754

Overview of WARP: A particle code for heavy ion fusion
[DE93-018637] p 1588 N94-19034

SELF FOCUSING

Singularities and symmetries of nonlinear ordinary and partial differential equations
[DE93-040083] p 1550 N94-19190

SELF ORGANIZING SYSTEMS

Application of the network discriminant function to learning
[AD-A268793] p 1540 N94-18189

Competitive dynamics and self-organization in photorefractive systems
[AD-A269663] p 1430 N94-18569

SELF OSCILLATION

Quasi-optical transponder using FET's and patch antennas
[AD-A271339] p 1407 N94-19584

SEMANTICS

Using semantic information for processing negation and disjunction in logic programs
[DE93-017412] p 1614 N94-18099

Navigation in hypermedia applications: Modelling and semantics
[REPT-93-034] p 1520 N94-18136

Asynchronous rendezvous in the presence of backtracking
[PB93-197739] p 1524 N94-19062

Axiomatization, declarative semantics and operational semantics of passive and active updates in logic databases
[PB93-195956] p 1618 N94-19067

The TM typing rules
[MEMO-INF-92-80] p 1526 N94-19222

Attribute evaluation during generalized parsing
[MEMO-INF-92-85] p 1526 N94-19224

Action systems and action refinement in the development of parallel systems: An algebraic approach
[MEMO-INF-93-14] p 1538 N94-19296

A language of finite probabilistic processes and its interleaving semantics
[MEMO-INF-93-24] p 1558 N94-19354

Non-well-foundedness and type freeness can unify the interpretation of functional application
[PB93-191849] p 1560 N94-19710

Semantic models for distributed data base management. Part 2: Development of an integral meta-model for data modeling and data base modeling
[REPT-93-08-PT-2] p 1620 N94-19795

SEMICONDUCTOR DEVICES

Joint services electronics program
[AD-A269383] p 1403 N94-18638

Recent developments in fast response aerodynamic probe technology p 1431 N94-18645

Optoelectronic packaging: A review
[DE93-040059] p 1515 N94-19535

A comparison of iterative methods for a model coupled system of elliptic equations
[DE93-040482] p 1553 N94-19655

SEMICONDUCTOR DIODES

Laser imaging radar system
[AD-A270436] p 1387 N94-18510

SEMICONDUCTOR JUNCTIONS

Ultra-shallow box-like profiles fabricated by pulsed UV-laser doping process
[DE93-017221] p 1437 N94-18083

SEMICONDUCTOR LASERS

Pulsed LASER for testing silicon strip detectors
[DE93-017816] p 1436 N94-17883

Advanced optical fiber communication systems
[AD-A269120] p 1577 N94-18254

Laser imaging radar system
[AD-A270436] p 1387 N94-18510

Ultrafast Electronics and Optoelectronics: Summaries of papers. Technical digest conference edition
[AD-A269233] p 1405 N94-18909

Evaluation of laser diode based optical switches for optical processors
[AD-A270949] p 1581 N94-19602

Experimental examinations of semiconductor laser amplifiers for optical communication technology
[ETN-93-95050] p 1442 N94-19647

SEMICONDUCTORS (MATERIALS)

Design and test of a low jitter metal to metal contact solid dielectric switch
[DE93-016957] p 1394 N94-17755

Lattice damage in ion-implanted compound semiconductors and its effect on electrical activation
[DE93-015907] p 1593 N94-17845

Feasibility survey of thermoelectric conversion technology using semiconductors
[DE93-520882] p 1595 N94-18105

Experimental and theoretical investigation of surface chemistry induced by direct and indirect electronic excitation
[AD-A268846] p 1348 N94-18221

Superconducting/semiconducting hybrids and advance memory concepts for superconducting electronics
[AD-A268679] p 1397 N94-18312

Gallium arsenide-based ternary compounds and multi-band-gap solar cell research
[DE93-010049] p 1467 N94-18483

Optical and transport properties of metallic and semiconductor nanostructures
[AD-A270009] p 1598 N94-18609

In-situ growth monitoring of molecular beam epitaxy processes
[AD-A269287] p 1598 N94-18616

Integration of ferroelectric/semiconductor thin films for SLM and photorefractive applications
[AD-A268645] p 1598 N94-18633

Joint services electronics program
[AD-A269383] p 1403 N94-18638

Photodetector array having high pixel density
[AD-D015859] p 1432 N94-18731

Tunneling microscopy of semiconductors
[AD-A270232] p 1600 N94-18904

Ultrafast Electronics and Optoelectronics: Summaries of papers. Technical digest conference edition
[AD-A269233] p 1405 N94-18909

Growth of epitaxial semiconductor alloys and superlattices with continuously variable composition by pulsed-laser ablation
[DE93-018726] p 1601 N94-18998

X ray studies of microstructures in semiconductor and superconducting materials
[DE93-040690] p 1601 N94-19056

Radiation hardened microprocessor for small payloads
p 1327 N94-19184

A comparison of iterative methods for a model coupled system of elliptic equations
[DE93-040482] p 1553 N94-19655

The deposition of electro-optic films on semiconductors
[AD-A270823] p 1605 N94-19664

Solid-state dynamics in novel semiconductor nanostructures
[AD-A271249] p 1605 N94-19725

Single source precursors for the OMCVD of 3/5 compound semiconductors
[AD-A271147] p 1606 N94-19739

Nanofabrication by focused ion beam
[AD-A271290] p 1345 N94-19746

Polarized optical emission due to decay or recombination of spin-polarized injected carriers
[AD-D015907] p 1408 N94-19763

MOCVD-grown InGaAsP heterostructure diode lasers
[AD-A270848] p 1606 N94-19769

SEMISPAN MODELS

Semi-span model testing in the National Transonic Facility
[NASA-CR-194479] p 1312 N94-19388

SENSITIVITY

Scale sensitivity in the multiplicative AHP and SMART
[REPT-93-37] p 1611 N94-19157

Round robin experiments on the Explosive Components Water Gap Test (ECWGT)
[PML-1992-69] p 1378 N94-19445

SENSORS

Solid-state, resistive hydrogen sensors for safety monitoring
[DE93-017769] p 1424 N94-17778

SENSORY FEEDBACK

Magnetostrictive actuators for human sensory feedback
[AD-A269266] p 1511 N94-17841

SENSORY PERCEPTION

The clocks and the perception of time in the 18th century society p 1424 N94-18007

About time p 1426 N94-18024

Somatosensory responsiveness in behaving monkeys and human subjects
[AD-A268924] p 1501 N94-18231

Comparing performance on implicit memory tests
[AD-A269900] p 1508 N94-18657

SENSORY STIMULATION

Effects of practice in selecting and executing keypressing sequences
[IZF-1992-B-10] p 1509 N94-19420

SENTENCES

Non-well-foundedness and type freeness can unify the interpretation of functional application
[PB93-191849] p 1560 N94-19710

SEPARATED FLOW

Numerical solution of the Navier-Stokes equations for high-lift configurations on structured composite grids
p 1306 N94-18423

A viscous-inviscid solver for high-lift incompressible flows over multi-element airfoils at deep separation conditions p 1306 N94-18425
Viscous-inviscid calculation of high-lift separated compressible flows over airfoils and wings
p 1309 N94-18440
Correlation of incoming boundary layer pitot pressure fluctuations with the unsteadiness of fin-induced shock wave turbulent boundary layer interactions
[AD-A270059] p 1417 N94-18796
Interferometric investigations of compressible dynamic stall over a transiently pitching airfoil
[NASA-TM-109380] p 1312 N94-19119

SEQUENCING
Shop problems with two machines and time lags
[REPT-93-020] p 1518 N94-17927
Matrix- and substrate-assisted laser desorption for fast DNA sequencing
[DE93-015332] p 1501 N94-18242

SEQUENTIAL CONTROL
Motorola MC68040 high-speed design using Altera EPM5000 erasable programmable logic devices
[DE93-017635] p 1523 N94-19006

SERIES (MATHEMATICS)
Time dependent identification of nonlinear structures
[ECL-92-64] p 1457 N94-19403

SERIES EXPANSION
Decomposition invariance of generalized steady-state of a 1-D diffusion system
[REPT-93-26] p 1550 N94-19141

SEROTONIN
Strategies for enhancing catecholamine-mediated neurotransmission
[NASA-CR-193807] p 1506 N94-18862

SERVOCONTROL
Increasing mission reliability using open-loop control
[AD-A271208] p 1545 N94-19721

SERVOMECHANISMS
Design of power electronics for TVC EMA systems
[NASA-CR-193839] p 1407 N94-19642

SERVOMOTORS
Increasing mission reliability using open-loop control
[AD-A271208] p 1545 N94-19721

SET THEORY
Fuzzy almost linear spaces
[DE93-624772] p 1545 N94-17680
Performance of defect-tolerant set-associative cache memories p 1398 N94-18346
Fuzzy hypergraphs and fuzzy intersection graphs
[AD-A270303] p 1549 N94-18815
Excursion theory of a finite set via resolvents
[REPT-93-19] p 1557 N94-19090
Excursions of stochastic processes, Cox-point processes, entrance behavior and resolvents
[PB93-197291] p 1558 N94-19323
On network representation of the solutions in combinatorial optimization
[RR-910-I] p 1552 N94-19392
A perfection-preserving operation
[RR-911-I] p 1552 N94-19393
Neighbourhood-perfect line graphs
[RR-915-I] p 1552 N94-19395
On Hamilton-connectedness of Cayley graphs
p 1554 N94-19684
On Hamiltonian properties of 2-tough graphs
p 1554 N94-19685
Toughness and the cycle structure of graphs
p 1554 N94-19686
The Hopping Lemma p 1554 N94-19687
Two problems related to results of Chvatal-Erdoes
p 1555 N94-19693
Non-well-foundedness and type freeness can unify the interpretation of functional application
[PB93-191849] p 1560 N94-19710

SH WAVES
High resolution geological site characterization utilizing ground motion data
[AD-A268926] p 1481 N94-18485

SHAFTS (MACHINE ELEMENTS)
Friction drive position transducer
[AD-D015851] p 1424 N94-17717

SHALLOW WATER
Comments on computational underwater acoustics
[DE93-013789] p 1562 N94-17873
DYNLET1 model formulation and user's guide
[AD-A269843] p 1498 N94-18723
A finite element scheme for shock capturing
[AD-A270182] p 1417 N94-18755
Seismic studies of the geologic structure and physical properties of the seabed
[AD-A270895] p 1500 N94-19747

SHAPE MEMORY ALLOYS
Intelligent materials systems and structures. Part 4: The influence of thermomechanical loading on the life of shape memory alloys
[PB93-195923] p 1363 N94-18952
The applications of modified metals in the construction industry
[VTT-TIED-1329] p 1365 N94-19374
Use of shape memory alloys in the robust control of smart structures
[AD-A270827] p 1366 N94-19594
Damping in ferrous shape memory alloys
[AD-A271009] p 1366 N94-19775

SHAPED CHARGES
Instrumented experiments aboard the frigate WOLF. Wolf 2: Measurement results of the 5.5 kg TNT in the crew aft sleeping compartment
[PML-1992-12] p 1451 N94-17931

SHAPES
Wideband electromagnetic scattering/analysis program: Far zone electromagnetic scattering from complex shapes using geometrical theory of diffraction
[AD-A268790] p 1384 N94-18187

SHEAR FLOW
Self-regulated shear flow turbulence in confined plasmas
[DE93-015823] p 1583 N94-17743
On memory effects in turbulence
[DLR-FB-93-03] p 1409 N94-18124
Research on two equation models
p 1411 N94-18547
Large-eddy simulation of turbulent diffusion in stably stratified shear flow p 1416 N94-18595
Research and training activities of the Joint Institute for Aeronautics and Acoustics
[NASA-CR-194742] p 1421 N94-19493
The effects of initial conditions on the 3-D topology of temporally evolving wakes (ARI on 3-D bluff body wakes)
[AD-A271008] p 1423 N94-19774

SHEAR LAYERS
Chemical reactions in turbulent mixing flows
[AD-A269377] p 1410 N94-18472

SHEAR PROPERTIES
Numerical integration of structural elements in NIKE3D and DYNA3D
[DE93-016325] p 1452 N94-18049
Chemical reactions in turbulent mixing flows
[AD-A269377] p 1410 N94-18472
Development of a finite element method program for the analysis of laminated composite plates using first-order shear deformation theory
[AD-A270318] p 1342 N94-18700
Elastic properties of amorphous thin films studied by Rayleigh waves
[DE93-018375] p 1372 N94-19202
Development and characterization of adiabatic shear prone tungsten heavy alloys
[AD-A270477] p 1366 N94-19673

SHEAR STRENGTH
Evaluation of the production-grade class 4 flextensional transducer shell
[AD-A268796] p 1340 N94-18201

SHEAR STRESS
Dislocation-drag contribution to high-rate plastic deformation in shock-loaded tantalum
[DE93-018286] p 1361 N94-18802
Stress pulse phenomena
[DE93-019064] p 1456 N94-19078
A comparative evaluation of in-plane shear test methods for laminated graphite-epoxy composites
[NASA-CR-193808] p 1456 N94-19095
Development of engineering models for calculation of failure loads and defect states of steel concrete beams and plates
[ETN-93-95052] p 1460 N94-19648
Collaborative research on combustion diagnostics and modeling between Rolls-Royce, Inc. and the United States Air Force Wright Laboratory
[AD-A270660] p 1354 N94-19778

SHELL THEORY
Numerical integration of structural elements in NIKE3D and DYNA3D
[DE93-016325] p 1452 N94-18049

SHELLS (STRUCTURAL FORMS)
Evaluation of the production-grade class 4 flextensional transducer shell
[AD-A268796] p 1340 N94-18201
Residual strain measurement on the production-grade class 4 flextensional transducer shell
[AD-A268828] p 1430 N94-18537

SHIPS
Instrumented experiments aboard the frigate WOLF. Wolf 2: Measurement results of the 5.5 kg TNT in the crew aft sleeping compartment
[PML-1992-12] p 1451 N94-17931
Ship-produced cloud line of 13 July 1991
[DE93-016879] p 1472 N94-17986

SHIVERING
Evaluation of physiological and psychological impairment of human performance in cold stressed subjects
[AD-A268637] p 1506 N94-18632

SHOCK FRONTS
Velocity measurements in a boundary layer with a density gradient
[DE93-019627] p 1422 N94-19515

SHOCK LOADS
Omega phase formation in shock-loaded zirconium
[DE93-018343] p 1595 N94-18162
Dislocation-drag contribution to high-rate plastic deformation in shock-loaded tantalum
[DE93-018286] p 1361 N94-18802
Effects of shock loading on a solid-solution strengthened superalloy
[DE93-018345] p 1362 N94-18809
Toward a characterization of the debris cloud created in a hypervelocity impact on a thin plate
[AD-A269190] p 1455 N94-18864
Shock-loading response of advanced materials
[DE93-018344] p 1455 N94-19033
Shock compression properties of silicon carbide
[DE93-019927] p 1373 N94-19271
Influence of peak pressure and temperature on the shock-loading response of tantalum
[DE93-018561] p 1457 N94-19279
Simulation of the impact of a plastic flyer on an aluminum block using the hydrocode AUTODYNE
[PML-1992-26] p 1458 N94-19444

SHOCK TUBES
Film condensation in a shock wave
[MPIS-22/1992] p 1422 N94-19509

SHOCK WAVE PROFILES
Measurement and analysis of three 1.5-GPa shock-wave profiles in copper
[DE93-016559] p 1451 N94-17864
Wave structure induced by fluid dynamic limits in the Broadwell model
[AD-A268512] p 1410 N94-18385

SHOCK WAVES
PVDF measurement of soft x ray induced shock and filter debris impulse
[DE93-017633] p 1382 N94-17806
A new multiphase equation of state for iron
[DE93-017629] p 1357 N94-17819
Measurement and analysis of three 1.5-GPa shock-wave profiles in copper
[DE93-016559] p 1451 N94-17864
Modeling shock initiation in Composition B
[DE93-016544] p 1376 N94-18095
Wave structure induced by fluid dynamic limits in the Broadwell model
[AD-A268512] p 1410 N94-18385
Introduction to spectral methods for hyperbolic system of conservation laws p 1413 N94-18567
Correlation of incoming boundary layer pitot pressure fluctuations with the unsteadiness of fin-induced shock wave turbulent boundary layer interactions
[AD-A270059] p 1417 N94-18796
Three-dimensional shock wave physics simulations with MIMD PAGOSA on massively parallel computers
[DE93-011682] p 1455 N94-18829
Shock propagation in crustal rock
[AD-A270148] p 1485 N94-18899
The effects of reverberant impulse noise (blast waves) on hearing: Parametric studies
[AD-A269242] p 1506 N94-18911
Visualization for applications in shock physics
[DE93-012849] p 1418 N94-18918
The application of front tracking to the simulation of shock refractions and shock accelerated interface mixing
[DE93-018342] p 1419 N94-19025
Shock-loading response of advanced materials
[DE93-018344] p 1455 N94-19033
Air blast measurements at 20 and 40 km distance from detonating 10 and 20 ton high explosive charges
[PB93-195949] p 1419 N94-19068
Experiments and analysis of lateral piezoresistance gauges
[DE93-017874] p 1433 N94-19111
Liquid sound speeds at pressure from the optical analyzer technique
[DE93-018362] p 1563 N94-19151
Impact strength and indentation hardness of high-strength ceramics
[DE93-018833] p 1373 N94-19338
Simulation of the impact of a plastic flyer on an aluminum block using the hydrocode AUTODYNE
[PML-1992-26] p 1458 N94-19444
Velocity measurements in a boundary layer with a density gradient
[DE93-019627] p 1422 N94-19515

Locally adaptive remeshing scheme for calculating fluid instabilities
[DE93-019577] p 1422 N94-19568

SHORELINES
Ecological and environmental impacts of construction in the coastal zone
[AD-A269196] p 1475 N94-18881

SHORT CIRCUITS
Impedence calculation with recursive folding
[ETN-93-95049] p 1406 N94-19387

SHORT TAKEOFF AIRCRAFT
Design, development, and flight evaluation of the Boeing YC-14 USB powered lift aircraft p 1310 N94-18444
Lift and pitching moment induced on jet STOVL aircraft by the ground vortex
[AD-A269816] p 1318 N94-18733

SHOT NOISE
JSEP fellowship: Fractal noise processes
[AD-A268841] p 1557 N94-18540

SHOULDERS
Control of shoulder muscles during goal directed movements
[PB93-195139] p 1504 N94-18080

SHRINKAGE
Shrinkage void formation and its effect on freeze and thaw processes of lithium and lithium-fluoride for space applications
[DE93-019303] p 1338 N94-19128

SHUTTLE DERIVED VEHICLES
Shuttle-C, the future is now
[NASA-TM-109355] p 1332 N94-18954

SIDEBANDS
Experiments in sideband suppression on the Los Alamos National Laboratory Free-Electron Laser
[DE93-014466] p 1435 N94-17724

SIDELOBES
Nontraditional windows in spectral analysis
[AD-A271336] p 1553 N94-19583

SIGNAL ANALYSIS
A non-homogeneous, spatio-temporal, wavelet multiresolution analysis and its application to the analysis of motion
[AD-A270621] p 1538 N94-19534

SIGNAL ANALYZERS
Coherent transient systems evaluation
[AD-A268808] p 1576 N94-18204
Widget: A data acquisition system for a balloon borne Si particle calorimeter
[DE93-624668] p 1630 N94-18762

SIGNAL DETECTION
A RFI measurement system for field sites
[AD-A269340] p 1385 N94-18301
Wavelet transform for time-frequency analysis of the vibrational signature and its application
[AD-A269928] p 1454 N94-18661
Generalized multichannel signal detection
[AD-A271385] p 1391 N94-19587

SIGNAL DETECTORS
Monolithic low noise preamplifier for piezoelectric sensors
[AD-D015860] p 1563 N94-18734

SIGNAL ENCODING
Friction drive position transducer
[AD-D015851] p 1424 N94-17717

SIGNAL FADING
Radio wave propagation in structured ionization for satellite and radar applications
[AD-A268457] p 1382 N94-17844

SIGNAL FLOW GRAPHS
SPROC: A multiple-processor DSP IC
p 1398 N94-18347

SIGNAL MEASUREMENT
Variable wide band fiber optic delay line
[AD-D015848] p 1576 N94-17716

SIGNAL PROCESSING
Design of a general purpose and autonomous transmitter and receiver system for underwater acoustic experiments at sea
[AD-A269268] p 1495 N94-17822
Development and test of readout electronics for optical quadrature signals
[DLR-MITT-92-11] p 1395 N94-17920
Neural networks to classify speaker independent isolated words recorded in radio car environments
[REPT-93-013] p 1383 N94-17935
Analysis, representation and processing of the instrumental gesture: Application to keyboard instruments
[ETN-93-94402] p 1519 N94-17977
Coherent transient systems evaluation
[AD-A268808] p 1576 N94-18204
Magnetostatic waves-based integrated optic bragg cell modules with applications to RF signal processing
[AD-A269115] p 1577 N94-18295
Single phase dynamic CMOS PLA using charge sharing technique p 1397 N94-18341
SPROC: A multiple-processor DSP IC
p 1398 N94-18347
An improved distributed arithmetic architecture
p 1398 N94-18349
Low power signal processing research at Stanford
p 1393 N94-18351
High accuracy switched-current circuits using an improved dynamic mirror p 1401 N94-18368
A verification logic representation of indeterministic signal states p 1401 N94-18372
On timing faults in digital logic circuits
[AD-A268714] p 1402 N94-18400
The identification of the computational significance of key neurobiological characteristics found in a number of telencephalic brain regions
[AD-A269374] p 1505 N94-18407
Development of parallel architectures for sensor array processing, volume 1
[AD-A270426] p 1534 N94-18507
Development of parallel architectures for sensor array processing. Volume 2: A parallel architecture for broad-band direction-of-arrival estimation
[AD-A270427] p 1534 N94-18508
Data acquisition in aerodynamic research
p 1431 N94-18644
A general theory of signal integration for fault-tolerant dynamic distributed sensor networks
[AD-A270316] p 1534 N94-18699
VLSI for high-speed digital signal processing
[AD-A270406] p 1404 N94-18706
Programmable linear phase digital filters
[AD-A270413] p 1404 N94-18709
Monolithic low noise preamplifier for piezoelectric sensors
[AD-D015860] p 1563 N94-18734
Widget: A data acquisition system for a balloon borne Si particle calorimeter
[DE93-624668] p 1630 N94-18762
Neutral networks: An NRL perspective
[AD-A269122] p 1541 N94-18773
Spectral analysis on the canonical autoregressive decomposition
[AD-A270083] p 1549 N94-18798
Analytic approximations of an integral in remote sensing
[AD-A270085] p 1463 N94-18800
Introduction to wavelets
[AD-A268465] p 1389 N94-18801
Numerical and symbolic signal representation and processing
[AD-A270271] p 1389 N94-18811
A parallel and pipelined architecture for estimation of direction of arrival using a bilinear transformation method, volume 3
[AD-A270137] p 1389 N94-18897
Solution of the Poisson equation with application to radar imaging
[PB93-195865] p 1389 N94-18950
MIMD massively parallel methods for engineering and science problems
[DE93-019409] p 1531 N94-19562
Generalized multichannel signal detection
[AD-A271385] p 1391 N94-19587
A multi-level data-flow architecture for signal and data processing applications
[DE93-041272] p 1539 N94-19588
Systolic design with asynchronous controls for digital-signal processing
[AD-A270976] p 1392 N94-19680
Signal processing algorithms for heterogeneous architectures
[AD-A271248] p 1392 N94-19724
Algorithms and architectures for high speed signal processing
[AD-A271000] p 1392 N94-19736
Transcutaneous Analyte Measuring Methods (TAMM)
[AD-A271387] p 1408 N94-19756

SIGNAL RECEPTION
Photorefractive receiver study
[AD-A269352] p 1577 N94-18302

SIGNAL TO NOISE RATIOS
Laser imaging radar system
[AD-A270436] p 1387 N94-18510
A comparison of single-station backazimuth estimates with regional event locations in the Central Appalachians
[AD-A269897] p 1483 N94-18690
The use of velocity spectra for stacking receiver functions with application to IRIS/IDA stations OBNINSK (OBN) and ARTI (ARU), Russia
[AD-A269087] p 1483 N94-18717
Nontraditional windows in spectral analysis
[AD-A271336] p 1553 N94-19583
Transcutaneous Analyte Measuring Methods (TAMM)
[AD-A271387] p 1408 N94-19756
Feasibility study for a measuring system velocity projectile
[FEL-91-A368] p 1434 N94-19797

SIGNAL TRANSMISSION
Design of a general purpose and autonomous transmitter and receiver system for underwater acoustic experiments at sea
[AD-A269268] p 1495 N94-17822
Swatch Pager p 1428 N94-18039
A method for eliminating skew introduced by non-uniform buffer delay and wire lengths in clock distribution trees
[AD-A270649] p 1544 N94-19530

SIGNATURE ANALYSIS
An analytical approach to error localization by using information derived from error signature
[REPT-93-023] p 1518 N94-17960
Wavelet transform for time-frequency analysis of the vibrational signature and its application
[AD-A269928] p 1454 N94-18661
Environmental characterization for target acquisition. Report 3: New concepts for evaluating low-grazing angle radar measurements
[AD-A269956] p 1388 N94-18777

SIGNS AND SYMPTOMS
Using controlled daylight exposure and sleep timing in the prevention of shift lag during night operations
[AD-A269304] p 1504 N94-17824
Cerebral ischemia and reperfusion injury: A brief review
[AD-A270480] p 1507 N94-19675

SILANES
NMR studies of enriched species at interfaces
[AD-A264703] p 1367 N94-17878

SILICA GEL
Hydrolysis reaction and positronium decay in silica gels
[AD-A270028] p 1371 N94-18713

SILICA GLASS
Laser induced damage testing: Equipment and techniques
[DE93-017143] p 1437 N94-18060

SILICATES
Cooperative formation of inorganic-organic interfaces in the synthesis of silicate mesostructures
[AD-A271196] p 1375 N94-19742

SILICIDES
Plastic anisotropy in MoSi2 single crystals
[DE93-012650] p 1594 N94-17874
Bibliography on silicides
[AD-A270516] p 1374 N94-19532

SILICON
Selective electrochemical wafer thinning for silicon characterization
[DE93-015083] p 1592 N94-17742
Simplified processing for 23 percent-efficient silicon concentrator solar cells
[DE93-015018] p 1464 N94-17787
Pulsed LASER for testing silicon strip detectors
[DE93-017816] p 1436 N94-17883
Electron mobility in high resistivity silicon
[REPT-93-007] p 1565 N94-17933
High- and low-temperature bonding techniques for microstructures
[DE93-017173] p 1595 N94-17992
Electrostatic micrometers: Recent developments and perspectives of uses in clock and watch making
p 1425 N94-18014
Silicon micro-actuator p 1408 N94-18017
High-efficiency silicon concentrator cell commercialization
[DE93-018491] p 1467 N94-18409
Research on stable, high-efficiency amorphous silicon multijunction modules
[DE93-010046] p 1467 N94-18518
Thermal stresses in the microchannel heatsink cooled by liquid nitrogen
[DE93-018660] p 1418 N94-18995
Binding of copper to nanocavity surfaces in silicon
[DE93-019073] p 1364 N94-19080
Silicon MCM substrates for integration of 3-5 photonic devices and CMOS IC's
[DE93-017894] p 1405 N94-19112
Studies of deep levels in high resistivity silicon detectors irradiated by high fluence fast neutrons using a thermally stimulated current spectrometer
[DE93-016133] p 1602 N94-19258
Picoindentation hardness measurements using atomic force microscopy
[AD-A270877] p 1604 N94-19579
Examination of charge carriers dynamics in silicon and silicon solar cells with photoinduced laser beam deflection
[ETN-93-95060] p 1470 N94-19654

SILICON ALLOYS
Research on stable, high-efficiency amorphous silicon multijunction modules
[DE93-010046] p 1467 N94-18518
Fundamental properties and device applications of Ge(x)Si(1-x)/Si superlattices (supplemental)
[AD-A269212] p 1600 N94-18884
SILICON CARBIDES
Carbon/carbon composites coated with SiC by chemical vapor deposition
[AD-A269934] p 1341 N94-18544
Shock compression properties of silicon carbide
[DE93-019927] p 1373 N94-19271
Analytical and experimental evaluation of joining silicon nitride to metal and silicon carbide to metal for advanced heat engine applications
[DE93-018128] p 1446 N94-19291
SILICON CONTROLLED RECTIFIERS
Design of power electronics for TVC EMA systems
[NASA-CR-193839] p 1407 N94-19642
SILICON DIOXIDE
Catalytic hydrocarbon reactions over supported metals
[DE93-018168] p 1345 N94-17808
Aerogels for microelectronic applications: Fast, inexpensive, and light as air
[DE93-017170] p 1395 N94-17882
Optical properties of oxide coatings prepared by ion-assisted deposition
[AD-A270024] p 1599 N94-18711
High resolution transmission electron microscopy of mesoporous MCM-41 type materials
[AD-A271271] p 1354 N94-19728
SILICON FILMS
Development of large-area monolithically integrated silicon-film photovoltaic modules
[DE93-010037] p 1464 N94-17731
SILICON NITRIDES
Equipment for investigation of cryogenic compaction of nanosize silicon nitride powders
[DE93-018740] p 1340 N94-18180
Analytical and experimental evaluation of joining silicon nitride to metal and silicon carbide to metal for advanced heat engine applications
[DE93-018128] p 1446 N94-19291
Atomic-scale friction and microfriction of graphite and diamond using friction force microscopy
[AD-A270952] p 1605 N94-19679
SILICON RADIATION DETECTORS
Experimental research in high energy physics
[DE93-011912] p 1574 N94-18916
SILVER
Surface second harmonic generation studies of stepped Ag(111) electrode surfaces
[AD-A265205] p 1594 N94-17876
Optical frequency doubling at adsorbates of silver(110) surface
[ETN-93-94837] p 1603 N94-19355
SIMD (COMPUTERS)
Parallel optimization algorithms and their implementation in VLSI design p 1401 N94-18374
Distributed memory parallel computers and computational fluid dynamics p 1413 N94-18568
Conception and analysis of numerical parallel algorithms: Realization on the Connection Machine
[ETN-93-95005] p 1531 N94-19517
SIMILARITY THEOREM
Similarity solutions for gravity-dominated spreading of a lens of organic contaminant
[REPT-93-24] p 1420 N94-19139
SIMPLEX METHOD
Parallel optimization algorithms and their implementation in VLSI design p 1401 N94-18374
A teaching tool for linear programming
[AD-A270240] p 1523 N94-18905
SIMULATED ANNEALING
Data fusion through simulated annealing of registered range and reflectance images
[DE93-015910] p 1612 N94-17858
SIMULATION
Efficient simulation of DEDS by means of standard clock techniques: Queueing and integrated radio network examples
[AD-A269878] p 1432 N94-18681
Efficiency and biofidelity of occupant simulations
p 1459 N94-19473
SIMULATORS
An overview of the SAFSIM computer program
[DE93-017657] p 1519 N94-18002
New applications for high average power beams
[DE93-018845] p 1439 N94-18522
Improved HF data network simulator, volume 1
[AD-A270953] p 1393 N94-19752
Improved HF data network simulator, software user's manual, volume 2
[AD-A270954] p 1393 N94-19753
SINE WAVES
Active control of periodic noise with time-varying frequency
[REPT-93-012] p 1562 N94-17934
Spectral analysis on the canonical autoregressive decomposition
[AD-A270083] p 1549 N94-18798
SINGLE CRYSTALS
Magnetic properties of single-crystalline UCu3Al2
[DE93-016607] p 1593 N94-17744
Plastic anisotropy in MoSi2 single crystals
[DE93-012650] p 1594 N94-17874
Recent studies of short-range order in alloys: The Cowley theory revisited
[DE93-016416] p 1358 N94-18111
Nitridation of GaAs(100) by laser-induced decomposition of HN3
[AD-A269147] p 1438 N94-18258
Photorefractive tungsten bronze crystals for optical computing
[AD-A268859] p 1596 N94-18320
The effect of crystallographic orientation on the performance of single crystal tungsten subscale penetrators
[AD-A268988] p 1597 N94-18468
Ionic and molecular environments in heterogeneous electrocatalysis: Studies by radioactive labeling and LEED/AUGER spectroscopy
[AD-A268850] p 1567 N94-18766
Experimental investigation of wave and fracture phenomena in impacted ceramics: Experiments on sapphire
[AD-A270040] p 1372 N94-18792
Growth, characterization and device development in monocrystalline diamond films
[AD-A270074] p 1599 N94-18797
Modeling of single-crystal laser-weld microstructures
[DE93-017853] p 1445 N94-18976
Surface phases and their influence on metal-oxide interfaces
[DE93-019931] p 1601 N94-19020
The electromechanical properties of tetragonal BaTiO3 and PbTiO3 single crystals
[DE93-019008] p 1603 N94-19550
Final report on subcontract B076260 — borate synthesis
[DE93-019501] p 1604 N94-19565
SINGLE EVENT UPSETS
Experience with custom processors in space flight applications p 1336 N94-18338
An SEU immune logic family p 1398 N94-18342
Technology, design, simulation, and evaluation for SEP-hardened circuits p 1399 N94-18352
The LET spectrum and its uncertainty during the CRRES mission
[AD-A269977] p 1630 N94-18676
Static Computer Memory Integrity Testing (SCMIT): An experiment flown on STS-40 as part of GAS payload G-616 p 1325 N94-19169
SINGLE STAGE ROCKET VEHICLES
Single STAGE Rocket Technology (SSRT) DC-X test program environmental assessment
[AD-A265940] p 1337 N94-17879
SINGULARITY (MATHEMATICS)
Finite-dimensional singletons of the quantum anti de Sitter algebra
[DE93-624771] p 1546 N94-17810
Some remarks on integrable Hamiltonian systems with two degrees of freedom
[DE93-624766] p 1546 N94-17815
Singularities and symmetries of nonlinear ordinary and partial differential equations
[DE93-040083] p 1550 N94-19190
Bits and relative order from residues, space efficiently
[TR-464] p 1530 N94-19482
SINTERING
Pressureless densification of ceramic matrix composites
[AD-A269137] p 1371 N94-18691
Manufacturing technology
[DE93-019580] p 1381 N94-19480
SIS (SUPERCONDUCTORS)
Infrared detection with high-(Tc bolometers and response of Nb tunnel junctions to picosecond voltage pulses
[DE93-016963] p 1595 N94-17989
SIZE DISTRIBUTION
Dispersion effects on millimeter wavelength attenuation efficiencies for a variety of fibers
[AD-A268992] p 1386 N94-18454
Hydrolysis reaction and positronium decay in silica gels
[AD-A270028] p 1371 N94-18713
Development of the microstructure based stochastic life prediction models
[AD-A270453] p 1455 N94-18714
SKEWNESS
The theory of linear programming: Skew symmetric self-dual problems and the central path
[REPT-93-15] p 1524 N94-19089
SKIN FRICTION
In-flight pressure distributions and skin-friction measurements on a subsonic transport high-lift wing section p 1308 N94-18435
SKIN RESISTANCE
Transient skin effect in a massive cylinder by eccentric location of exciting conduction bands
[ETN-93-95048] p 1391 N94-19646
SKIN TEMPERATURE (BIOLOGY)
Effects of a high-energy food supplement on cold-induced thermogenesis
[AD-A269301] p 1504 N94-17823
Synchronisation of cold induced vasodilation at various locations of one hand
[IZF-1992-B3] p 1504 N94-17966
SKY WAVES
Morphology and characteristics of disturbed HF skywave channels
[AD-A269755] p 1388 N94-18722
SLEEP
Using controlled daylight exposure and sleep timing in the prevention of shift lag during night operations
[AD-A269304] p 1504 N94-17824
A comparison of polygraphic and actigraphic monitoring of sleep using a 5-channel programmable-sensitivity actigraph
[AD-A270731] p 1507 N94-19608
SLIDING
Heterogeneous slip and rupture models of the San Andreas fault zone based upon three-dimensional earthquake tomography
[DE93-015037] p 1480 N94-17898
Fatigue resistant Ti3Al composites
[AD-A270305] p 1341 N94-18692
SLIDING FRICTION
Interdisciplinary research on wear of materials
[AD-A268190] p 1443 N94-17730
Atomic-scale friction and microfriction of graphite and diamond using friction force microscopy
[AD-A270952] p 1605 N94-19679
Tribological studies of silicon for magnetic recording applications (Invited)
[AD-A270878] p 1447 N94-19784
SLOTS
High-Lift System Aerodynamics
[AGARD-CP-515] p 1305 N94-18415
SLUMPING
A review and evaluation of the ADAM 2.1 dispersion model
[AD-A269896] p 1474 N94-18688
SLURRIES
Advanced in macrostatistical hydrodynamics
[DE93-018479] p 1410 N94-18270
Metal slurry droplet and spray combustion
[AD-A269648] p 1349 N94-18736
SMART STRUCTURES
The 6th Japan-U.S. conference on composite materials
[AD-A268535] p 1341 N94-18630
Use of shape memory alloys in the robust control of smart structures
[AD-A270827] p 1366 N94-19594
SMOG
Energy efficiency and the environment: Innovative ways to improve air quality in the Los Angeles Basin
[DE93-016964] p 1473 N94-18050
SMOOTHING
A time-frequency smoothing algorithm for cyclic spectral analysis
[DE93-016634] p 1519 N94-18097
SNOW
Condensed gases under winter conditions: A study for the rescue services
[FOA-C-40305-4.5] p 1473 N94-18139
SOBOLEV SPACE
On polynomials orthogonal with respect to an inner product involving differences (the general case)
[REPT-93-32] p 1551 N94-19285
SOCIAL FACTORS
The clocks and the perception of time in the 18th century society p 1424 N94-18007
SODIUM
First on-sun test of NaK pool-boiler solar receiver
[DE93-015003] p 1466 N94-18208
Developmental testing of a prototype all-reflection Michelson interferometer
[AD-A269064] p 1430 N94-18406
SODIUM ALLOYS
Bench-scale screening tests for a boiling sodium-potassium alloy solar receiver
[DE93-018512] p 1469 N94-19040

SODIUM SULFUR BATTERIES
Conceptual design of a sodium sulfur cell for US electric van batteries
[DE93-018683] p 1405 N94-19035

SOFTWARE ENGINEERING
The design of the MAD Design Program
[DE93-013343] p 1539 N94-17696
The First International Conference on PCTE
[FEL-92-A134] p 1518 N94-17965
Format.m: A usage manual. Towards an efficient symbolic-numeric environment: Extending Mathematica's format rules
[MATHS-REPT-A-185] p 1547 N94-17969
Reference model for project support environments, version 1.0
[AD-A269110] p 1520 N94-18251
Teaching a computer simulation course with Ada
[AD-A267901] p 1521 N94-18308
Why are human-computer interfaces difficult to design and implement?
[AD-A268843] p 1514 N94-18317
VLSI synthesis of digital application specific neural networks p 1399 N94-18355
The CMU masters in software engineering core curriculum
[AD-A268983] p 1521 N94-18453
The evolution of the PVM concurrent computing system
[DE93-017764] p 1534 N94-18482
UUGM code development
[AD-A269945] p 1416 N94-18671
The development of a course sequence in real-time systems design
[AD-A269459] p 1522 N94-18726
Case studies of software development tools for parallel architectures
[AD-A269193] p 1535 N94-18866
ControlShell: A real-time software framework
[AD-A269172] p 1523 N94-18879
Modelling software for structure metrics
[MEMO-INF-93-13] p 1526 N94-19200
How to apply the IEEE standards to software testing
[DE93-018514] p 1527 N94-19245
Advanced software development workstation: Object-oriented methodologies and applications for flight planning and mission operations
[NASA-CR-193706] p 1513 N94-19349
A multi-level data-flow architecture for signal and data processing applications
[DE93-041272] p 1539 N94-19588
Technical development of a theory of programs
[ETN-93-95058] p 1532 N94-19652
Report of the Second CLICOM Experts Meeting
[WCDMP-19] p 1495 N94-19705
Software reuse: Major issues need to be resolved before benefits can be achieved. Report to the Chairman, Subcommittee on Defense, Committee on Appropriations, House of Representatives
[GAO/IMTEC-93-16] p 1532 N94-19716
Technology benefits model user manual, version 01.00.04
[AD-A270637] p 1620 N94-19777

SOFTWARE RELIABILITY
An efficient implementation of error-valued semantics on imperative machines
[DE93-014658] p 1516 N94-17740
Software reliability: Estimation and prediction
[AD-A268895] p 1521 N94-18458
Software quality in test and measurment equipment
[PB93-197846] p 1528 N94-19333

SOFTWARE REUSE
An environment for requirement reuse
[REPT-92-082] p 1613 N94-17939
High performance Fortran: An overview
[DE93-017181] p 1519 N94-18072
Software reuse: Major issues need to be resolved before benefits can be achieved. Report to the Chairman, Subcommittee on Defense, Committee on Appropriations, House of Representatives
[GAO/IMTEC-93-16] p 1532 N94-19716

SOFTWARE TOOLS
A structured approach for modeling, analyzing and simulating real-time control systems
[REPT-93-044] p 1539 N94-17916
An environment for requirement reuse
[REPT-92-082] p 1613 N94-17939
The First International Conference on PCTE
[FEL-92-A134] p 1518 N94-17965
Software Toolkit for Analysis Research (STAR)
[DE93-017368] p 1519 N94-18086
Cut and paste based modeling with boundary features
[PB93-187250] p 1520 N94-18117
Dialog-Based Learning (DBL) for adaptive interface agents and programming-by-demonstrations systems
[AD-A269154] p 1540 N94-18261
A special purpose silicon compiler for designing supercomputing VLSI systems p 1402 N94-18379
VHDL simulation with access to transistor models
p 1402 N94-18381
CONTACT: An Air Force technical report on military satellite control technology
[AD-A269375] p 1334 N94-18408
Embedded Computer Performance Measurement (ECPM). Advanced avionics subsystems and technology multiprocessor ECPM software documentation
[AD-A269921] p 1320 N94-18658
A case study in software maintenance
[AD-A269923] p 1521 N94-18659
NASA Electronic Library System (NELS) optimization
[NASA-CR-193688] p 1617 N94-18839
3D composite grids using Bezier curves and surfaces in component adaptive methods
[AD-A269188] p 1549 N94-18863
Case studies of software development tools for parallel architectures
[AD-A269193] p 1535 N94-18866
Early experiences with the IBM SP-1
[DE93-018398] p 1535 N94-19010
A least-squares computational tool kit
[DE93-018400] p 1557 N94-19011
A programming paradigm for distributed-memory computers
[DE93-018336] p 1524 N94-19024
CAVEMAN: Configuration and version management
[DE93-018066] p 1524 N94-19048
An ORACLE CASE history: Experiences with ORACLE CASE tools
[DE93-010827] p 1617 N94-19057
Computer codes for checking, plotting and processing of neutron cross-section covariance data and their application
[DE93-018459] p 1570 N94-19129
A multi-thread approach to coalescing small transfers generated by portable tool sets
[DE93-012128] p 1525 N94-19186
Vectorized presentation-level services for scientific distributed applications
[DE93-018091] p 1537 N94-19253
European network for the numerical simulation of space plasmas p 1331 N94-19641
Report of the Second CLICOM Experts Meeting
[WCDMP-19] p 1495 N94-19705
Data-Machine Independence (DMI)
[DE93-018008] p 1539 N94-19734
Technology benefits model user manual, version 01.00.04
[AD-A270637] p 1620 N94-19777

SOIL EROSION
Three-dimensional high-resolution seismic profiling on the New Jersey outer continental shelf
[AD-A269835] p 1498 N94-18600
Gravity and the geoid in the Nepal Himalaya
[NASA-CR-194166] p 1463 N94-19430

SOIL MECHANICS
Centrifuge modeling of explosion-induced craters in unsaturated sand
[AD-A270194] p 1417 N94-18780
Numerical analysis of pressure meter tests: Application of parameter identification of soils behavior
[ECL-92-52] p 1487 N94-19380
Proceedings: International Symposium on Thermal Engineering and Science for Cold Regions
[AD-A270636] p 1487 N94-19529

SOIL MOISTURE
Protocol for computation of surface boundary layer parameters used to determine soil moisture flux from meteorological data collected at LLNL, 1992-1993
[DE93-018906] p 1463 N94-19003

SOILS
Rapid geophysical surveyor
[DE93-016637] p 1461 N94-17851
Applications of Quaternary stratigraphic, soil-geomorphic, and quantitative geomorphic analyses to the evaluation of tectonic activity and landscape evolution in the Upper Coastal Plain, South Carolina
[DE93-016269] p 1484 N94-18725

SOL-GEL PROCESSES
Finite element modeling of evaporation and condensation during sol-gel film and fiber formation
[DE93-017655] p 1345 N94-17820
Novel electrochemical materials prepared by sol-gel chemistry
[AD-A269060] p 1578 N94-18405
Photo-induced and electrooptic properties of (Pb,La)(Zr,Ti)O3 films
[DE93-017496] p 1371 N94-18519
Hydrolysis reaction and positronium decay in silica gels
[AD-A270028] p 1371 N94-18713

SOLAR ACTIVITY
Origins of solar activity. First year report, AASERT grant
[AD-A268848] p 1629 N94-18222

SOLAR ATMOSPHERE
The solar optical telescope
[NASA-TM-109240] p 1621 N94-18850

SOLAR CELLS
Development of large-area monolithically integrated silicon-film photovoltaic modules
[DE93-010037] p 1464 N94-17731
Simplified processing for 23 percent-efficient silicon concentrator solar cells
[DE93-015018] p 1464 N94-17787
Photovoltaic concentrator initiative: Concentrator cell development
[DE93-018505] p 1466 N94-18335
High-efficiency silicon concentrator cell commercialization
[DE93-018491] p 1467 N94-18409
Gallium arsenide-based ternary compounds and multi-band-gap solar cell research
[DE93-010049] p 1467 N94-18483
Research on stable, high-efficiency amorphous silicon multijunction modules
[DE93-010046] p 1467 N94-18518
Polycrystalline thin-film cadmium telluride solar cells fabricated by electrodeposition
[DE93-018201] p 1468 N94-18944
Silicon concentrator solar cell research
[DE93-018489] p 1468 N94-19015
Defect behavior of polycrystalline solar cell silicon
[DE93-018490] p 1468 N94-19016
A Sandia Technology Bulletin: Testing technology, July 1993
[DE93-040197] p 1633 N94-19537
Examination of charge carriers dynamics in silicon and silicon solar cells with photoinduced laser beam deflection
[ETN-93-95060] p 1470 N94-19654
Amorphous silicon batch process cost analysis
[DE93-018203] p 1470 N94-19760

SOLAR COLLECTORS
Development of a selective volumetric receiver for central receiver systems: Investigation of parameters and exergetic evaluation
[DLR-FB-93-05] p 1465 N94-18089
First on-sun test of NaK pool-boiler solar receiver
[DE93-015003] p 1466 N94-18208
Photovoltaic concentrator initiative: Concentrator cell development
[DE93-018505] p 1466 N94-18335
High-efficiency silicon concentrator cell commercialization
[DE93-018491] p 1467 N94-18409
Testing and evaluation of large-area heliostats for solar thermal applications
[DE93-018509] p 1467 N94-18520
Tehachapi solar thermal system
[DE93-018443] p 1468 N94-19014
Bench-scale screening tests for a boiling sodium-potassium alloy solar receiver
[DE93-018512] p 1469 N94-19040
The CAESAR project: Experimental and modeling investigations of methane reforming in a catalytically enhanced solar absorption receiver on a parabolic dish
[DE93-040203] p 1469 N94-19109

SOLAR CORPUSCULAR RADIATION
Solar flares and magnetospheric particles: Investigations based upon the ONR-602 and ONR-604 experiments
[AD-A269495] p 1629 N94-18705

SOLAR DYNAMIC POWER SYSTEMS
Performance mapping of the STM4-120 kinematic Stirling engine using a statistical design of experiments method
[DE93-015132] p 1464 N94-17798

SOLAR ENERGY
Solar radiation in Saudi Arabia
[AD-A269970] p 1493 N94-18781
Effects of the Mount Pinatubo eruption on solar insolation: Four case studies
[DE93-018454] p 1475 N94-18817
EIA publications directory, 1992
[DE93-016833] p 1617 N94-18983

SOLAR ENERGY CONVERSION
Pulse radiolytic studies of electron transfer processes and applications to solar photochemistry
[DE93-018715] p 1464 N94-17781
S/EV 1992: Solar and Electric Vehicles. Volume 1: Proceedings
[DE93-015762] p 1445 N94-18307
Research on stable, high-efficiency amorphous silicon multijunction modules
[DE93-010046] p 1467 N94-18518
Silicon concentrator solar cell research
[DE93-018489] p 1468 N94-19015

SOLAR FLARES
Solar flares and magnetospheric particles: Investigations based upon the ONR-602 and ONR-604 experiments
[AD-A269495] p 1629 N94-18705
The solar optical telescope
[NASA-TM-109240] p 1621 N94-18850
EGRET Mission and Data Analysis
[MPE-PREPRINT-223] p 1622 N94-19462
Detection of a long-duration solar gamma-ray flare on Jun. 11, 1991 with EGRET on Compton-GRO
p 1623 N94-19463

SOLAR FLUX
The Sudbury Neutrino Observatory and the solar neutrino problem
[DE93-018528] p 1629 N94-19260

SOLAR GENERATORS
First on-sun test of NaK pool-boiler solar receiver
[DE93-015003] p 1466 N94-18208

SOLAR HEATING
Tehachapi solar thermal system
[DE93-018443] p 1468 N94-19014

SOLAR NEUTRINOS
Neutrino mass
[DE93-018467] p 1567 N94-18269
The Sudbury Neutrino Observatory and the solar neutrino problem
[DE93-018528] p 1629 N94-19260

SOLAR OPTICAL TELESCOPE
The solar optical telescope
[NASA-TM-109240] p 1621 N94-18850

SOLAR OSCILLATIONS
The Sudbury Neutrino Observatory and the solar neutrino problem
[DE93-018528] p 1629 N94-19260

SOLAR PHYSICS
Origins of solar activity. First year report, AASERT grant
[AD-A268848] p 1629 N94-18222
The solar optical telescope
[NASA-TM-109240] p 1621 N94-18850
The Sudbury Neutrino Observatory and the solar neutrino problem
[DE93-018528] p 1629 N94-19260

SOLAR POWERED AIRCRAFT
Regenerative fuel cells for High Altitude Long Endurance Solar Powered Aircraft
[DE93-016991] p 1465 N94-17853

SOLAR PROPULSION
S/EV 1992: Solar and Electric Vehicles. Volume 1: Proceedings
[DE93-015762] p 1445 N94-18307

SOLAR RADIATION
Pulse radiolytic studies of electron transfer processes and applications to solar photochemistry
[DE93-018715] p 1464 N94-17781
Global zones of particle precipitation as observed EXOS-C
[AD-A268758] p 1481 N94-18467
Solar radiation in Saudi Arabia
[AD-A269970] p 1493 N94-18781
Effects of the Mount Pinatubo eruption on solar insolation: Four case studies
[DE93-018454] p 1475 N94-18817
Marine-modified LOWTRAN: The contribution of sun glint
[AD-A269547] p 1500 N94-19762

SOLAR REFLECTORS
Development of a selective volumetric receiver for central receiver systems: Investigation of parameters and exergetic evaluation
[DLR-FB-93-05] p 1465 N94-18089

SOLAR SPECTRA
Tunable ytterbium-doped solid state laser
[AD-D015878] p 1440 N94-18747

SOLAR TERRESTRIAL INTERACTIONS
ISTP Global Geospace Science. Energy transfer in geospace
[NASA-TM-109239] p 1620 N94-18851
The Wave Experiment Consortium
p 1328 N94-19623

SOLAR WIND
ISTP Global Geospace Science. Energy transfer in geospace
[NASA-TM-109239] p 1620 N94-18851
Radial evolution of the solar wind turbulence with application to charged particle transport
[NASA-CR-194081] p 1629 N94-19427

SOLAR-PUMPED LASERS
Direct solar pumping of semiconductor lasers: A feasibility study
[NASA-CR-193760] p 1440 N94-18834

SOLDERED JOINTS
Microstructurally based thermomechanical fatigue lifetime model of solder joints for electronic applications
[DE93-016506] p 1452 N94-17995
Embrittlement of surface mount solder joints by hot solder-dipped, gold-plated leads
[DE93-017659] p 1358 N94-18003
Wetting behavior of alternative solder alloys
[DE93-016730] p 1359 N94-18127
Reducing inadvertent alloying of metal/ceramic brazes
[DE93-009842] p 1373 N94-19308

SOLDERING
Development of alternatives to lead-bearing solders
[DE93-016509] p 1357 N94-17862
Automatic soldering for watch circuit components
p 1428 N94-18037
Solderability perservative coatings: Electroless tin versus organic azoles
[DE93-017634] p 1370 N94-18477

SOLDERS
Development of alternatives to lead-bearing solders
[DE93-016509] p 1357 N94-17862
Wetting behavior of alternative solder alloys
[DE93-016730] p 1359 N94-18127
Solderability perservative coatings: Electroless tin versus organic azoles
[DE93-017634] p 1370 N94-18477

SOLENOIDS
Toroidal solenoids in the electromagnetic field and Aharonov-Casher effect
[DE93-629861] p 1566 N94-18152
Generalized energy principle for flute perturbations in axisymmetric mirror machines
[DE93-019399] p 1589 N94-19037

SOLID ELECTROLYTES
Mixed polymer electrolyte and mixed polymer electrolyte battery
[AD-D015856] p 1394 N94-17718
Oxygen reduction at a stabilized zirconia interface with Y(1-x)Ca(x)MnO3 or La(1-x)Sr(x)MnO3 cathode materials
[DE93-015681] p 1593 N94-17747
Fuel cell systems program plan, fiscal year 1993
[DE93-017828] p 1466 N94-18103
Novel electrochemical materials prepared by sol-gel chemistry
[AD-A269060] p 1578 N94-18405

SOLID LUBRICANTS
Titanium carbon-hydrogen layers on decorative surfaces p 1375 N94-18010
Physico chemical and mechanic approach of lubricating properties of graphite + additive powders
[ECL-93-02] p 1373 N94-19405

SOLID MECHANICS
HEMP 3D: A finite difference program for calculating elastic-plastic flow, appendix B
[AD-A269171] p 1418 N94-18878

SOLID PHASES
A new multiphase equation of state for iron
[DE93-017629] p 1357 N94-17819
Deformation mechanisms in a Laves phase
[DE93-018331] p 1361 N94-18806
Morphology, deformation, and defect structures of TiCr2 in Ti-Cr alloys
[DE93-018332] p 1361 N94-18807

SOLID ROCKET PROPELLANTS
Adaptations to micropep and rocket to allow performance evaluation of multiple grain and/or airbreathing motors
[AD-A268798] p 1337 N94-18202
Materials characterization of propellants using ultrasonics
[NASA-CR-193877] p 1378 N94-19494

SOLID SOLUTIONS
Effects of shock loading on a solid-solution strengthened superalloy
[DE93-018345] p 1362 N94-18809

SOLID STATE
Polaron tunneling in high-temperature superconductors
[DE93-016880] p 1593 N94-17754
Microstructural analysis of solid-state resistance welds
[DE93-017295] p 1443 N94-17761
Solid State Sciences Committee Forum
[AD-A270454] p 1342 N94-18715
Solid-state dynamics in novel semiconductor nanostructures
[AD-A271249] p 1605 N94-19725

SOLID STATE DEVICES
Portable, solid state, fiber optic coupled Doppler interferometer system for detonation and shock diagnostics
[DE93-013917] p 1423 N94-17700
Solid-state, resistive hydrogen sensors for safety monitoring
[DE93-017769] p 1424 N94-17778
New room temperature high resolution solid-state detector (CdZnTe) for hard x rays and gamma rays
p 1324 N94-19165

SOLID STATE LASERS
Integrated photonics research volume 10. Conference edition
[AD-A269298] p 1577 N94-18298
Quantum Optoelectronics. Organization of the 1993 photonics science topical meetings. Technical digest series, volume 8
[AD-A269026] p 1578 N94-18488
Advanced Solid-State Lasers/Compact Blue-Green Lasers. 1993 technical digest series. Volume 2: Organization of the 1993 photonics science topical meetings
[AD-A269058] p 1438 N94-18492
Photonics in Switching: Organization of the 1993 photonics science topical meetings. Technical digest
[AD-A269024] p 1578 N94-18528
Tunable ytterbium-doped solid state laser
[AD-D015878] p 1440 N94-18747
Impact of shorter wavelengths on optical quality for laws
[NASA-CR-193873] p 1579 N94-18858
Proof of the feasibility of coherent and incoherent schemes for pumping a gamma ray laser
[AD-A269173] p 1440 N94-18880
Tetravalent chromium (Cr(4+)) as laser-active ion for tunable solid-state lasers
[NASA-CR-194529] p 1441 N94-19369
Tetravalent chromium (Cr(4+)) as laser-active ion for tunable solid-state lasers
[NASA-CR-194528] p 1441 N94-19394
Center-of-Excellence: Microlaser microscope
[DE93-040688] p 1442 N94-19658

SOLID STATE PHYSICS
Solid State Sciences Committee Forum
[AD-A270454] p 1342 N94-18715

SOLID SURFACES
NMR studies of enriched species at interfaces
[AD-A264703] p 1367 N94-17878

SOLID SUSPENSIONS
Advanced in macrostatistical hydrodynamics
[DE93-018479] p 1410 N94-18270

SOLID-SOLID INTERFACES
Experimental contribution to the contact between two bodies and the effect of roughness
[ECL-91-41] p 1451 N94-17918
Micromechanics of interfaces in metal matrix composites
[AD-A271012] p 1345 N94-19776

SOLIDIFICATION
Prediction of non-equilibrium solidification modes in austenitic stainless steel laser welds
[DE93-018457] p 1364 N94-19203
Recent advances in high density tungsten composite processing
[AD-A270764] p 1344 N94-19576

SOLIDS
Interaction of intense lasers and relativistic electron beams with solids, gases and plasmas
[AD-A269655] p 1439 N94-18737
Stress pulse phenomena
[DE93-019064] p 1456 N94-19078

SOLITARY WAVES
A method for solving the KDV equation and some numerical experiments
[DE93-624726] p 1550 N94-19246
Investigations in gauge theories, topological solitons, and string theories
[DE93-015029] p 1609 N94-19250

SOLUBILITY
Molecular composites from liquid crystalline polymers and liquid crystalline thermosets
[DE93-016608] p 1368 N94-18096
Measurement of viscosity, density, and gas solubility of refrigerant blends in selected synthetic lubricants
[DE93-040221] p 1350 N94-18977

SOLUTES
The effect of composition on the mechanism of continuous recrystallization and superplastic response of aluminum-scandium alloys
[DE93-018594] p 1365 N94-19280
Melt spinning study
[NASA-CR-193823] p 1380 N94-19423

SOLVATION
Femtosecond Fourier-transform spectroscopy of low-frequency intermolecular motions in weakly interacting liquids
[DE93-017312] p 1566 N94-18085

SOLVENT EXTRACTION
Summary report for supercritical carbon dioxide extraction and carbonization of Resorcinol-Formaldehyde (RF) foams
[DE93-016924] p 1346 N94-17987

SOLVENTS
Densities and viscosities of ternary ammonia/water fluids
[DE93-015966] p 1351 N94-19118

SONAR
Processing and analysis of SeaMARC 2 data: Fieberling guyot; raw phase experiment in Norwegian-Greenland Sea
[AD-A269930] p 1498 N94-18662
A register of underwater acoustic test facilities in the US, Canada, and the United Kingdom
[AD-A270884] p 1500 N94-19785
SOOT
Novel catalysts for methane activation
[DE93-040630] p 1349 N94-18532
SOS (SEMICONDUCTORS)
Radiation hardened microprocessor for small payloads
p 1327 N94-19184
SOUND FIELDS
Acoustic intensity measurements in the presence of low Mach number flow
[AD-A269995] p 1562 N94-18664
SOUND GENERATORS
Acoustic propagation modeling using MATLAB
[AD-A270905] p 1564 N94-19750
SOUND LOCALIZATION
Human-machine interfaces
[AD-A270730] p 1513 N94-19764
SOUND PRESSURE
Transducers and method for making same
[AD-D015949] p 1408 N94-19759
SOUND PROPAGATION
Ultrasonic technique for inspection of GPHS capsule girth weld integrity
[DE93-040072] p 1448 N94-19189
Numerical simulation of acoustic waves propagation in turbulent media
[ECL-92-37] p 1563 N94-19413
Examinations of converging cylindrically symmetric second sound propagation in He2
[MPIS-9/1992] p 1564 N94-19715
SOUND WAVES
Comments on computational underwater acoustics
[DE93-013789] p 1562 N94-17873
Low-noise oscillators for airborne radar applications, revision 1
[AD-A269372] p 1403 N94-18471
Acoustic intensity measurements in the presence of low Mach number flow
[AD-A269995] p 1562 N94-18664
Estimating the oceanic sound speed environmental for long-range acoustic propagation
[AD-A270231] p 1499 N94-18903
Elastic properties of amorphous thin films studied by Rayleigh waves
[DE93-018375] p 1372 N94-19202
Comments on computational underwater acoustics
[DE93-019880] p 1563 N94-19270
Low frequency acoustics of laminated composite axisymmetric structures
[DRA-TM(USGR)-93302] p 1344 N94-19391
Numerical simulation of acoustic waves propagation in turbulent media
[ECL-92-37] p 1563 N94-19413
The electromechanical properties of tetragonal BaTiO3 and PbTiO3 single crystals
[DE93-019008] p 1603 N94-19550
Acoustic travel time perturbations due to an internal tide and internal wave field in the Barents Sea
[AD-A270879] p 1499 N94-19580
Seismic studies of the geologic structure and physical properties of the seabed
[AD-A270895] p 1500 N94-19747
Acoustic propagation modeling using MATLAB
[AD-A270905] p 1564 N94-19750
SOUNDING ROCKETS
UVPI imaging from the LACE satellite: The Nihka rocket plume
[AD-A268456] p 1334 N94-18149
SOUTH CAROLINA
Applications of Quaternary stratigraphic, soil-geomorphic, and quantitative geomorphic analyses to the evaluation of tectonic activity and landscape evolution in the Upper Coastal Plain, South Carolina
[DE93-016269] p 1484 N94-18725
SPACE CHARGE
Nonlinear Thomson scattering of intense laser pulse from beams and plasmas
[AD-A269556] p 1438 N94-18460
Halo formation in mismatched, space-charge-dominated beams
[DE93-018581] p 1574 N94-18934
Correction of longitudinal errors in accelerators for heavy-ion fusion
[DE93-018656] p 1575 N94-19106
Induction accelerator development for heavy ion fusion
[DE93-019228] p 1591 N94-19479
SPACE COMMERCIALIZATION
An evolutionary approach to space launch commercialization
[AD-A269861] p 1331 N94-18411
Future energy source --- Mining Helium-3 on the moon
[NASA-TM-109363] p 1628 N94-18959
SPACE DEBRIS
Space debris detection
[AD-A269254] p 1334 N94-18264
Proceedings of the 11th Space Surveillance Workshop
[AD-A269477] p 1462 N94-18729
SPACE EXPLORATION
Space transfer concepts and analyses for exploration missions
[NASA-CR-193876] p 1332 N94-18820
Shuttle-C, the future is now
[NASA-TM-109355] p 1332 N94-18954
Magellan, Galileo, and Ulysses
[NASA-TM-109362] p 1628 N94-18958
Spacework 17: O'Leary's Mars
[NASA-TM-109374] p 1629 N94-18966
Space exploration initiative
[NASA-TM-109366] p 1323 N94-18981
SPACE HABITATS
Space transfer concepts and analyses for exploration missions
[NASA-CR-193876] p 1332 N94-18820
SPACE INDUSTRIALIZATION
Consortium for materials development in space
[NASA-CR-194411] p 1379 N94-18840
SPACE LABORATORIES
Consortium for materials development in space
[NASA-CR-194411] p 1379 N94-18840
Opportunities and questions for the fundamental biological sciences in space p 1502 N94-19212
SPACE MANUFACTURING
Activities of the Center for Space Construction
[NASA-CR-193717] p 1335 N94-19371
SPACE MISSIONS
Mission needs and system commonality for space nuclear power and propulsion
[DE93-016557] p 1337 N94-17863
Human Transportation System (HTS) study: Executive summary
[NASA-TM-104780] p 1332 N94-18669
Human Transportation System (HTS) study, volume 1
[NASA-TM-104779] p 1332 N94-18670
Report on the activities of Space Science Department, 1990 - mid 1992
[ESA-SP-1161] p 1633 N94-19404
SPACE NAVIGATION
Radiation induced darkening of the optical elements in the Startracker camera
[DE93-018907] p 1433 N94-19004
SPACE OBSERVATIONS (FROM EARTH)
Hubble Space Telescope
[NASA-TM-109359] p 1621 N94-19072
Co-ordination of ground-based observations with Cluster p 1331 N94-19640
SPACE PERCEPTION
Psychophysical analyses of perceptual representations
[AD-A268711] p 1508 N94-18313
Modeling of driver behavior: Information perception, rule and control strategies in experiments and simulations
[ETN-93-95053] p 1510 N94-19649
SPACE PLASMAS
Correlated charge-changing ion-atom collisions
[DE93-018717] p 1564 N94-17775
Detailed analysis of low energy plasma data under the Voyager Uranus data analysis program
[NASA-CR-193668] p 1628 N94-17842
Plasma properties research: Task 3
[DE93-017087] p 1583 N94-17854
An investigation of methods for updating ionospheric scintillation models using topside in-situ plasma density measurements
[AD-A269872] p 1483 N94-18655
Plasma contactor development for Space Station
[NASA-TM-106425] p 1587 N94-18861
Convection algorithms for magnetospheric particles
[AD-A270103] p 1493 N94-18871
Cluster: Mission, Payload, and Supporting Activities
[ESA-SP-1159] p 1328 N94-19622
The Cluster Ion Spectroscopy experiment
p 1329 N94-19631
PEACE: A Plasma Electron and Current Experiment
p 1329 N94-19632
European network for the numerical simulation of space plasmas p 1331 N94-19641
SPACE PLATFORMS
ISOBUS: A new versatile spacecraft platform using Shuttle small payloads p 1327 N94-19183
Activities of the Center for Space Construction
[NASA-CR-193717] p 1335 N94-19371
SPACE POWER REACTORS
Mission needs and system commonality for space nuclear power and propulsion
[DE93-016557] p 1337 N94-17863
Total hemispherical emittance of Niobium-1 percent zirconium fuel cladding for the SP-100 space reactor
[AD-A270456] p 1576 N94-19589
SPACE PROBES
Predicted structural response of the lightweight-interceptor technology demonstration vehicle
[DE93-014676] p 1333 N94-17782
SPACE PROCESSING
The first flight of the QUESTS GAS payload G-521
p 1325 N94-19170
Space Applications Industrial Laser System (SAILS)
p 1325 N94-19173
SPACE RENDEZVOUS
Automated rendezvous and capture demonstration study
[NASA-CR-192587] p 1331 N94-19366
SPACE SHUTTLE BOOSTERS
Effect of temperature and O-ring gland finish on sealing ability of Viton V747-75
[NASA-TP-3391] p 1368 N94-18075
SPACE SHUTTLE MAIN ENGINE
Technology test bed
[NASA-TM-109354] p 1322 N94-18953
FNAS/summer faculty fellowship research continuation program. Task 6: Integrated model development for liquid fueled rocket propulsion systems. Task 9: Aspects of model-based rocket engine condition monitoring and control
[NASA-CR-194574] p 1338 N94-19706
SPACE SHUTTLE MISSIONS
Return to space
[NASA-TM-109356] p 1332 N94-18955
Your GAS experiment and the media or why does that other can get all of the publicity? p 1327 N94-19182
SPACE SHUTTLE ORBITERS
Pathfinder: Shuttle exhibit
[NASA-TM-109357] p 1333 N94-19071
A high resolution ultraviolet Shuttle glow spectrograph
p 1325 N94-19174
Kennedy Space Center processing of Shuttle small payloads p 1326 N94-19177
Utilization of Shuttle small payload accommodations in the DOD Space Test Program p 1326 N94-19180
SPACE SHUTTLE PAYLOADS
LDEF update
[NASA-TM-109352] p 1334 N94-18921
The 1993 Shuttle Small Payloads Symposium
[NASA-CP-3233] p 1323 N94-19162
VPU(tm) demonstration mission vicinity processor unit(tm) overview p 1325 N94-19171
Space Applications Industrial Laser System (SAILS)
p 1325 N94-19173
Kennedy Space Center processing of Shuttle small payloads p 1326 N94-19177
Utilization of Shuttle small payload accommodations in the DOD Space Test Program p 1326 N94-19180
ISOBUS: A new versatile spacecraft platform using Shuttle small payloads p 1327 N94-19183
Radiation hardened microprocessor for small payloads
p 1327 N94-19184
Superfluid Helium On-Orbit Transfer (SHOOT) flight demonstration p 1327 N94-19185
SPACE SHUTTLES
Robotics
[NASA-TM-109351] p 1332 N94-18920
Langley's 50th year
[NASA-TM-109365] p 1632 N94-18980
A stereoscopic vision system with applications to automated docking and tracking
[AD-A270754] p 1333 N94-19765
SPACE STATION FREEDOM
Designing Space Station
[NASA-TM-109353] p 1334 N94-18922
Space exploration initiative
[NASA-TM-109366] p 1323 N94-18981
Space Applications Industrial Laser System (SAILS)
p 1325 N94-19173
Space research with intact organisms: The role of Space Station Freedom p 1502 N94-19213
Strategic plan, 1991: A strategy for leadership in space through excellence in space science and applications
[NASA-TM-109256] p 1611 N94-19434
SPACE STATION POWER SUPPLIES
Plasma contactor development for Space Station
[NASA-TM-106425] p 1587 N94-18861
SPACE STATIONS
The 1994 NASA authorization, volume 2
[GPO-71-510] p 1620 N94-18842
Plasma contactor development for Space Station
[NASA-TM-106425] p 1587 N94-18861
Shuttle-C, the future is now
[NASA-TM-109355] p 1332 N94-18954

SPACE SURVEILLANCE (GROUND BASED)
Super-resolution of multi-pixel and sub-pixel images for the SDI [AD-A268537] p 1462 N94-18631
Proceedings of the 11th Space Surveillance Workshop [AD-A269477] p 1462 N94-18729

SPACE SURVEILLANCE (SPACEBORNE)
UVPI imaging from the LACE satellite: The Nihka rocket plume [AD-A268456] p 1334 N94-18149
Proceedings of the 11th Space Surveillance Workshop [AD-A269477] p 1462 N94-18729

SPACE TRANSPORTATION
Human Transportation System (HTS) study: Executive summary [NASA-TM-104780] p 1332 N94-18669
Human Transportation System (HTS) study, volume 1 [NASA-TM-104779] p 1332 N94-18670

SPACE TRANSPORTATION SYSTEM
The 1994 NASA authorization, volume 2 [GPO-71-510] p 1620 N94-18842

SPACE TRANSPORTATION SYSTEM FLIGHTS
Return to space [NASA-TM-109356] p 1332 N94-18955

SPACE-TIME FUNCTIONS
Space and time as outcome of decoherence in an expanding universe [DE93-016199] p 1624 N94-18047
Impulsive moving mirror model in a Schroedinger picture with impulse effect in a Banach space [DE93-629864] p 1561 N94-18155
Space and time from quantum mechanics [DE93-015263] p 1609 N94-18629

SPACEBORNE ASTRONOMY
The Einstein Observatory catalog of IPC x ray sources. Volume 4E: Right ascension range 08h 00m to 11h 59m [NASA-TM-108401-VOL-4E] p 1625 N94-18612
The Einstein Observatory catalog of IPC x ray sources. Volume 5E: Right ascension range 12h 00m to 15h 59m [NASA-TM-108401-VOL-5E] p 1625 N94-18613
The Einstein Observatory catalog of IPC x ray sources. Volume 6E: Right ascension range 16h 00m to 19h 59m [NASA-TM-108401-VOL-6E] p 1625 N94-18615
The Einstein Observatory catalog of IPC x ray sources. Volume 7E: Right ascension range 20h 00m to 23h 59m [NASA-TM-108401-VOL-7E] p 1625 N94-18618
The Einstein Observatory catalog of IPC x ray sources. Volume 1E: Documentation [NASA-TM-108401-VOL-1E] p 1626 N94-18619
The Einstein Observatory catalog of IPC x ray sources. Volume 2E: Right ascension range 00h 00m to 03h 59m [NASA-TM-108401-VOL-2E] p 1626 N94-18620
The Einstein Observatory catalog of IPC x ray sources. Volume 3E: Right ascension range 04h 00m to 07h 59m [NASA-TM-108401-VOL-3E] p 1626 N94-18621
ASTRO-1 to explore invisible universe [NASA-TM-109360] p 1336 N94-18956
The star identification, pointing and tracking system of UVSTAR, an attached payload instrument system for the Shuttle Hitchhiker-M platform p 1326 N94-19179
Particle induced background by Roentgen satellites [MPE-242] p 1631 N94-19714

SPACEBORNE EXPERIMENTS
Consortium for materials development in space [NASA-CR-194411] p 1379 N94-18840
Spacelab 3 [NASA-TM-108750] p 1323 N94-18849
California Student Get Away Special Payload GAS-450 p 1324 N94-19164
MUZO flight experience with the programmable multizone furnace p 1324 N94-19167
Static Computer Memory Integrity Testing (SCMIT): An experiment flown on STS-40 as part of GAS payload G-616 p 1325 N94-19169
The first flight of the QUESTS GAS payload G-521 p 1325 N94-19170
VPU(tm) demonstration mission vicinity processor unit(tm) overview p 1325 N94-19171
Materials flight experiment carrier capability and future flight experiments on Hitchhiker-M carrier program p 1326 N94-19175
Limited Duration of Candidate Materials Exposure Experiment (LDCE): A Complex Autonomous Payload (CAP) using a Get Away Special (GAS) canister p 1326 N94-19176
Utilization of Shuttle small payload accommodations in the DOD Space Test Program p 1326 N94-19180
Your GAS experiment and the media or why does that other can get all of the publicity? p 1327 N94-19182
Space Life Sciences Research: The Importance of Long-Term Space Experiments [NASA-TM-4502] p 1502 N94-19210

SPACEBORNE LASERS
Direct solar pumping of semiconductor lasers: A feasibility study [NASA-CR-193760] p 1440 N94-18834
SPNDL: A concept for a small satellite Doppler lidar wind sounder p 1327 N94-19181

SPACEBORNE TELESCOPES
ASTRO-1 to explore invisible universe [NASA-TM-109360] p 1336 N94-18956
UVSTAR: An imaging spectrograph with telescope for the Shuttle Hitchhiker-M platform p 1326 N94-19178
The star identification, pointing and tracking system of UVSTAR, an attached payload instrument system for the Shuttle Hitchhiker-M platform p 1326 N94-19179

SPACECRAFT ANTENNAS
Missile antenna pattern coordinate system and data formats [AD-A269153] p 1385 N94-18260

SPACECRAFT CHARGING
Broadband RF spectrum from electrostatic discharges on spacecraft [AD-A269543] p 1385 N94-18287
Active spacecraft potential control: An ion emitter experiment for Cluster p 1330 N94-19634

SPACECRAFT CONFIGURATIONS
ISOBUS: A new versatile spacecraft platform using Shuttle small payloads p 1327 N94-19183

SPACECRAFT CONSTRUCTION MATERIALS
Low power arcjet system spacecraft impacts [NASA-TM-106307] p 1336 N94-17856
Consortium for materials development in space [NASA-CR-194411] p 1379 N94-18840
Materials flight experiment carrier capability and future flight experiments on Hitchhiker-M carrier program p 1326 N94-19175
Limited Duration of Candidate Materials Exposure Experiment (LDCE): A Complex Autonomous Payload (CAP) using a Get Away Special (GAS) canister p 1326 N94-19176

SPACECRAFT CONTAMINATION
Low power arcjet system spacecraft impacts [NASA-TM-106307] p 1336 N94-17856
The application of jet spray and ion beam contamination removal techniques to samples from the LDEF spacecraft [AD-A270973] p 1354 N94-19755

SPACECRAFT CONTROL
Cooperative control of multiple space manipulators [AD-A270291] p 1445 N94-18813
Phasing strategies of the Hermes type space shuttle: Its optimization considering the thrust failures [LAAS-93242] p 1544 N94-19361
Automated rendezvous and capture demonstration study [NASA-CR-192587] p 1331 N94-19366
Activities of the Center for Space Construction [NASA-CR-193717] p 1335 N94-19371

SPACECRAFT DESIGN
Designing Space Station [NASA-TM-109353] p 1334 N94-18922
Shuttle-C, the future is now [NASA-TM-109355] p 1332 N94-18954
ISOBUS: A new versatile spacecraft platform using Shuttle small payloads p 1327 N94-19183
Activities of the Center for Space Construction [NASA-CR-193717] p 1335 N94-19371
Cluster: Mission, Payload, and Supporting Activities [ESA-SP-1159] p 1328 N94-19622
The Cluster spacecraft p 1330 N94-19635

SPACECRAFT DOCKING
Automated rendezvous and capture demonstration study [NASA-CR-192587] p 1331 N94-19366
A stereoscopic vision system with applications to automated docking and tracking [AD-A270754] p 1333 N94-19765

SPACECRAFT ENVIRONMENTS
Environmental control and life support [ESA-PSS-03-40-ISSUE-1] p 1513 N94-19442

SPACECRAFT GLOW
A high resolution ultraviolet Shuttle glow spectrograph p 1325 N94-19174

SPACECRAFT LANDING
Single STAGE Rocket Technology (SSRT) DC-X test program environmental assessment [AD-A265940] p 1337 N94-17879

SPACECRAFT LAUNCHING
Single STAGE Rocket Technology (SSRT) DC-X test program environmental assessment [AD-A265940] p 1337 N94-17879
An evolutionary approach to space launch commercialization [AD-A269861] p 1331 N94-18411

SPACECRAFT MAINTENANCE
Robotics [NASA-TM-109351] p 1332 N94-18920

SPACECRAFT MANEUVERS
Constant-thrust orbit-raising transfer charts [AD-A269088] p 1334 N94-18718

SPACECRAFT MOTION
Dynamic characterization of a lightweight, highly maneuverable spacecraft using modal and finite element analyses [DE93-018095] p 1335 N94-18942

SPACECRAFT ORBITS
The Cluster orbit and mission scenario p 1330 N94-19637

SPACECRAFT POWER SUPPLIES
Mission needs and system commonality for space nuclear power and propulsion [DE93-016557] p 1337 N94-17863
Ultrasonic technique for inspection of GPHS capsule girth weld integrity [DE93-040072] p 1448 N94-19189
Rationale for the power standard [ESA-PSS-02-10-VOL-2-ISSUE-] p 1338 N94-19516

SPACECRAFT PROPULSION
Mission needs and system commonality for space nuclear power and propulsion [DE93-016557] p 1337 N94-17863
Critical technologies for reactors used in nuclear electric propulsion [DE93-017685] p 1337 N94-17908
Technology test bed [NASA-TM-109354] p 1322 N94-18953

SPACECRAFT RECOVERY
LDEF update [NASA-TM-109352] p 1334 N94-18921

SPACECRAFT STRUCTURES
Design considerations for remotely operated welding in space: Task definition and visual weld monitoring experiment [AD-A268752] p 1445 N94-18634
Activities of the Center for Space Construction [NASA-CR-193717] p 1335 N94-19371

SPACECRAFT TRAJECTORIES
Parallelization of the Air Force Space Command (AFSPACECOM) satellite motion models [AD-A269327] p 1334 N94-18470
Constant-thrust orbit-raising transfer charts [AD-A269088] p 1334 N94-18718
START user manual version 2.1 [LR-726] p 1335 N94-19614

SPACELAB
Spacelab 3 [NASA-TM-108750] p 1323 N94-18849

SPALLATION
Mechanical-property changes of structural composite materials after low-temperature proton irradiation: Implications for use in SSC magnet systems [DE93-016735] p 1343 N94-18763

SPARK IGNITION
Evaluation of aftermarket LPG conversion kits in light-duty vehicle applications [DE93-010035] p 1377 N94-18617

SPATIAL DISTRIBUTION
Observations of comets with the IUE [NASA-CR-193652] p 1624 N94-17843
A Bayesian approach to contaminant plume delineation [DE93-012909] p 1472 N94-17890
Efficiency of fiber dispersion [AD-A269740] p 1342 N94-18757
Spatiotemporal variability of non-urban ozone concentrations over the eastern United States and its potential replication by satellite data [PB93-191328] p 1476 N94-19065

SPATIAL FILTERING
Evaluation of a liquid crystal spatial light modulator capable of amplitude- and phase-modulating modes [AD-A269252] p 1577 N94-18262
Interferometer stations at the Air Force Aeroballistic Research Facility [AD-A268776] p 1322 N94-18330
A non-homogeneous, spatio-temporal, wavelet multiresolution analysis and its application to the analysis of motion [AD-A270621] p 1538 N94-19534

SPATIAL RESOLUTION
Effect of spatial resolution on the simulation of regional precipitation in China in a global climate model [DE93-013433] p 1489 N94-18053
The land component of the global climate system with adequate spatial resolution [DE93-018951] p 1474 N94-18183
High spatial resolution, range gated, underwater imaging method and apparatus [AD-D015882] p 1430 N94-18530
Description of an infrared zoomcollimator [FEL-93-A034] p 1580 N94-19424
Earth Penetration Radar Imaging System (EPRIS) [DE93-019890] p 1391 N94-19542

SPECIFIC HEAT
The low-temperature specific heat of CeCu2Ge2 at 0 and 9.5 kbar
[DE93-014914] p 1360 N94-18398
Specific heat of La(1.875-x)Nd(x)Sr(0.125)CuO4: Magnetic and structural transitions
[DE93-016978] p 1600 N94-18968
Thermophysical properties
[DE93-040219] p 1351 N94-19134
Realistic theories of heavy electron and other strongly correlated materials
[DE93-010350] p 1571 N94-19204
SPECIFICATIONS
PostScript: A study in conformity
[NPL-DITC-214/93] p 1517 N94-17917
The TM manual version 1.3 working document
[MEMO-INF-93-06] p 1527 N94-19229
SPECIMEN GEOMETRY
Interfacial cracks in plates: A three-dimensional numerical investigation p 1456 N94-19116
SPECTRA
A time-frequency smoothing algorithm for cyclic spectral analysis
[DE93-016634] p 1519 N94-18097
UVPI imaging from the LACE satellite: The Nihka rocket plume
[AD-A268456] p 1334 N94-18149
The LET spectrum and its uncertainty during the CRRES mission
[AD-A269977] p 1630 N94-18676
SPECTRAL CORRELATION
A time-frequency smoothing algorithm for cyclic spectral analysis
[DE93-016634] p 1519 N94-18097
SPECTRAL ENERGY DISTRIBUTION
Acoustic intensity measurements in the presence of low Mach number flow
[AD-A269995] p 1562 N94-18664
Relation between the fluctuating wall pressure and the turbulent structure of a boundary layer on a cylinder in axial flow
[AD-A270242] p 1418 N94-18906
EXANA: A program for analysing extended energy loss fine structures, EXELFS spectra
[USIP-92-01] p 1525 N94-19145
Structuration processes in protoplanetary accretion disks
[MPE-243] p 1628 N94-19519
SPECTRAL METHODS
Computational Fluid Dynamics
[VKI-LS-1993-04] p 1412 N94-18557
Introduction to spectral methods: Application to the Stokes problem p 1413 N94-18566
Introduction to spectral methods for hyperbolic system of conservation laws p 1413 N94-18567
On the numerical analysis of nonlinear Galerkin methods: Spectral approximation and finite elements
[ETN-93-94900] p 1552 N94-19407
Stability measurements of Rayleigh-Benard convection near the critical state using a spectral model
[MPIS-15/1992] p 1422 N94-19520
SPECTRAL RESOLUTION
Monitoring the response of the upper troposphere/lower stratosphere to a greenhouse gas scenario
[DE93-014509] p 1470 N94-17710
Detailed analysis of low energy plasma data under the Voyager Uranus data analysis program
[NASA-CR-193668] p 1628 N94-17842
New room temperature high resolution solid-state detector (CdZnTe) for hard x rays and gamma rays
p 1324 N94-19165
A high resolution ultraviolet Shuttle glow spectrograph
p 1325 N94-19174
SPECTRAL SIGNATURES
Materials processing and manufacturing technologies for diamond substrates multichip modules
[AD-A268989] p 1599 N94-18764
SPECTRAL THEORY
Full Boltzmann discrete spectral wave model, implementation and nondimensional tests
[AD-A269885] p 1498 N94-18685
SPECTROGRAPHS
UVSTAR: An imaging spectrograph with telescope for the Shuttle Hitchhiker-M platform p 1326 N94-19178
The star identification, pointing and tracking system of UVSTAR, an attached payload instrument system for the Shuttle Hitchhiker-M platform p 1326 N94-19179
Fiber optic Raman spectrograph for in situ environmental monitoring
[DE93-019466] p 1478 N94-19305
SPECTROMETERS
Designs for optical components related to the Los Alamos free-electron laser
[DE93-016617] p 1436 N94-17865
Proceedings of the 3rd Workshop on Balloon-Borne Experiments with Superconducting Magnet Spectrometers
[DE93-788362] p 1630 N94-18219
Fiber optic Raman spectrograph for in situ environmental monitoring
[DE93-019466] p 1478 N94-19305
Legacy of the X Ray Laser Program
[DE93-019550] p 1442 N94-19554
SPECTROSCOPIC ANALYSIS
Analysis of neon soft x ray spectra from short-pulse laser-produced plasmas
[DE93-014420] p 1582 N94-17708
Flame structure studies of a lean 20-torr H2/N2O/Ar flame employing molecular beam mass spectrometry
[AD-A268889] p 1349 N94-18456
Nondestructive inspection of graphite-epoxy laminates for heat damage using DRIFT and LPF spectroscopies
[DE93-017228] p 1343 N94-18761
The minimum detection limits of RDX and TNT deposited on various surfaces as determined by ion mobility spectroscopy
[DE93-018521] p 1378 N94-19042
Examination of charge carriers dynamics in silicon and silicon solar cells with photoinduced laser beam deflection
[ETN-93-95060] p 1470 N94-19654
The application of jet spray and ion beam contamination removal techniques to samples from the LDEF spacecraft
[AD-A270973] p 1354 N94-19755
Micromechanics of interfaces in metal matrix composites
[AD-A271012] p 1345 N94-19776
SPECTROSCOPY
Analysis of HgI2 and PbI2 crystals and detectors by Particle-Induced X Ray Emission (PIXE) and Ion Backscattering Spectroscopy (IBS)
[DE93-017168] p 1594 N94-17896
Tunneling spectroscopy of ultrasmall clusters and grains
[AD-A268840] p 1598 N94-18539
Photodissociation studies of polyatomic free radicals
[AD-A270084] p 1350 N94-18799
High pressure metallization of Mott Insulators: Magnetic, structural and electronic properties
[DE93-018295] p 1404 N94-18805
Nontraditional windows in spectral analysis
[AD-A271336] p 1553 N94-19583
The Cluster Ion Spectroscopy experiment
p 1329 N94-19631
SPECTRUM ANALYSIS
Rapid analysis of mixed waste samples via the optical emission from laser initiated microplasmas
[DE93-014563] p 1582 N94-17727
A time-frequency smoothing algorithm for cyclic spectral analysis
[DE93-016634] p 1519 N94-18097
Spectral analysis of synoptic time scale disturbances over the tropical eastern Pacific during summer 1989, 1990 and 1991
[AD-A268821] p 1490 N94-18206
Full Boltzmann discrete spectral wave model, implementation and nondimensional tests
[AD-A269885] p 1498 N94-18685
The use of velocity spectra for stacking receiver functions with application to IRIS/IDA stations OBNINSK (OBN) and ARTI (ARU), Russia
[AD-A269087] p 1483 N94-18717
Spectral analysis on the canonical autoregressive decomposition
[AD-A270083] p 1549 N94-18798
Advanced fusion diagnostics
[DE93-040085] p 1589 N94-19133
EXANA: A program for analysing extended energy loss fine structures, EXELFS spectra
[USIP-92-01] p 1525 N94-19145
New room temperature high resolution solid-state detector (CdZnTe) for hard x rays and gamma rays
p 1324 N94-19165
Detection of a long-duration solar gamma-ray flare on Jun. 11, 1991 with EGRET on Compton-GRO
p 1623 N94-19463
EGRET observations of 3 C 273
p 1623 N94-19464
Nontraditional windows in spectral analysis
[AD-A271336] p 1553 N94-19583
STAFF (Spatio-Temporal Analysis of Field Fluctuations) experiment for the Cluster mission p 1328 N94-19625
SPECULAR REFLECTION
Electro-optic beam steering using non-linear organic materials
[AD-A270809] p 1374 N94-19577
Marine-modified LOWTRAN: The contribution of sun glint
[AD-A269547] p 1500 N94-19762
SPEECH RECOGNITION
Neural networks to classify speaker independent isolated words recorded in radio car environments
[REPT-93-013] p 1383 N94-17935
Feasibility study in linguistically motivated object-oriented conceptual design of information systems
[PB93-197754] p 1618 N94-19331
A real-time spoken-language system for interactive problem-solving, combining linguistic and statistical technology for improved spoken language understanding
[AD-A270901] p 1392 N94-19749
SPENT FUELS
Development and characterization of adiabatic shear prone tungsten heavy alloys
[AD-A270477] p 1366 N94-19673
SPHERES
Geometrical pattern learning
[DE93-017641] p 1542 N94-19007
SPHERICAL HARMONICS
Asymptotic derivation of the modified time-dependent SP2 equations and numerical calculations
[DE93-016466] p 1551 N94-19342
SPHEROIDS
The Navy tessellated spheroid map projection system: A comprehensive definition
[AD-A269989] p 1462 N94-18677
Color palette considerations for digital map displays
[AD-A269991] p 1462 N94-18679
SPILLING
Condensed gases under winter conditions: A study for the rescue services
[FOA-C-40305-4.5] p 1473 N94-18139
SPIN
Phase space representations and quantum probability theory
[DE93-629863] p 1556 N94-18154
Nonlinear dynamics and instabilities in ferromagnetic resonance experiments: Examinations of spheres from yttrium iron garnet in coincidence area of the first Suhl instabilities
[ETN-93-95072] p 1604 N94-19612
SPIN DYNAMICS
T violating neutron spin rotation asymmetry
[DE93-018470] p 1570 N94-19126
SPIN REDUCTION
Aspects of the calibration and processing of the CRRES fluxgate magnetometer data
[AD-A270127] p 1432 N94-18875
SPIN-ORBIT INTERACTIONS
Spin-integrated and spin-dependent photoelectron diffraction
[DE93-016546] p 1565 N94-17850
Electron impact polarization and correlation properties of the inert gases
[DE93-018358] p 1570 N94-19125
SPINE
Multimodal image correlation applied to computer aided pedicular screwing
[ETN-93-95018] p 1528 N94-19363
SPIRAL ANTENNAS
Earth Penetration Radar Imaging System (EPRIS)
[DE93-019890] p 1391 N94-19542
SPLINE FUNCTIONS
Multivariate wavelet representations and approximations
[AD-A269350] p 1546 N94-17825
SPOILERS
High Reynolds number configuration development of a high-lift airfoil p 1306 N94-18424
Numerical investigation of the incompressible flow around a wing with a fixed spoiler
[ISL-R-109/91] p 1313 N94-19524
SPONTANEOUS EMISSION
Coherence and linewidth studies of a 4-nm high power FEL
[DE93-018533] p 1441 N94-19030
Novel nonlinear laser diagnostic techniques
[AD-A270968] p 1442 N94-19788
SPRAYED COATINGS
Thermal analysis of coatings and substrate materials during a disruption in fusion reactors
[DE93-017688] p 1588 N94-18971
SPRAYERS
Metal slurry droplet and spray combustion
[AD-A269648] p 1349 N94-18736
The application of jet spray and ion beam contamination removal techniques to samples from the LDEF spacecraft
[AD-A270973] p 1354 N94-19755
SPREAD SPECTRUM TRANSMISSION
Military applications of high-accuracy frequency standards and clocks
[AD-A269303] p 1430 N94-18299

Application of wavelet transform techniques to spread spectrum demodulation and jamming
[AD-A267389] p 1389 N94-19009

SPREADING
Oil spreading in surface waters with an ice cover
[PB93-190767] p 1476 N94-19064
Similarity solutions for gravity-dominated spreading of a lens of organic contaminant
[REPT-93-24] p 1420 N94-19139

SPUTTERING
Sputtered TiN coatings in plastic
p 1367 N94-18011
RF vacuum microelectronics
[AD-A270003] p 1403 N94-18667
The deposition of electro-optic films on semiconductors
[AD-A270823] p 1605 N94-19664

SQUARE WELLS
Acoustic propagation modeling using MATLAB
[AD-A270905] p 1564 N94-19750

SQUARES (MATHEMATICS)
Catalogue of simple perfect squared squares of orders 21 through 25
[PB93-191971] p 1550 N94-18991

SQUID (DETECTORS)
High resolution SQUID magnetometry for non-destructive evaluation
[AD-A268884] p 1447 N94-18225

STABILITY
Lectures of Fermi liquid theory
[DE93-016630] p 1592 N94-17714
Impulsive moving mirror model and the stability of linear homogeneous differential equations with impulse effect in a Banach space
[DE93-629906] p 1549 N94-18200
The microstructural mechanism of electromigration failure in narrow interconnects of Al alloys
[DE93-018598] p 1365 N94-19282
Electrocatalysts for oxygen electrodes
[DE93-040446] p 1354 N94-19653

STABILITY TESTS
A one dimensional numerical model, with an application to the vertical distribution of dissolved oxygen in the ocean
[DE93-018481] p 1495 N94-17779
Competitive dynamics and self-organization in photorefractive systems
[AD-A269663] p 1430 N94-18569

STABILIZATION
Stabilization of time-delay systems: An overview of the algebraic approach
[PB93-191989] p 1553 N94-19556

STABILIZERS (FLUID DYNAMICS)
Procedures and design data for the formulation of aircraft configurations
[AD-A270150] p 1318 N94-18779

STAGNATION TEMPERATURE
A comparative study of turbulence models in predicting hypersonic inlet flows p 1314 N94-18553

STAINLESS STEELS
Assessment of an improved multiaxial strength theory based on creep-rupture data for Inconel 600
[DE93-015929] p 1356 N94-17791
Summary of work on coatings and claddings for fossil energy applications
[DE93-017005] p 1367 N94-17881
Development and application of specially-focused ultrasonic transducers to location and sizing of defects in 75 mm- to 127 mm-thick austenitic stainless steel weld metals
[DE93-015975] p 1453 N94-18108
A probability method of fracture mechanics analysis for HFIR vessel
[DE93-015510] p 1453 N94-18246
Aerosol filtration with steel fiber filters
[DE93-016990] p 1380 N94-18710
Foil support structure for large electron guns
[DE93-018478] p 1322 N94-18890
Finite difference program for calculating hydride bed wall temperature profiles
[DE93-019272] p 1523 N94-19005
The effects of radiolysis on the corrosion and stress corrosion behavior of 316 stainless steels
[DE93-019933] p 1363 N94-19021
Overlay welding irradiated stainless steel
[DE93-018767] p 1446 N94-19334

STANDARD DEVIATION
Moments of ambient Doppler spectra
[DE93-017948] p 1390 N94-19114

STANDARDIZATION
PostScript: A study in conformity
[NPL-DITC-214/93] p 1517 N94-17917
Secure open systems: An investigation of current standardisation efforts for security in open systems
[FEL-92-B225] p 1618 N94-19450

STANDARDS
PostScript: A study in conformity
[NPL-DITC-214/93] p 1517 N94-17917
The stability and utility of the ESPRIT project, MUSiC, performance-based indicators of usability and tools: An evaluation of the usability of the NPL iSDX telephone system
[NPL-DITC-213/92] p 1613 N94-17925
About time p 1426 N94-18024
Rationale for the power standard
[ESA-PSS-02-10-VOL-2-ISSUE-] p 1338 N94-19516

STANDING WAVES
Three-dimensional simulation analysis of the first sections of a standing-wave free-electron laser two-beam accelerator
[DE93-016977] p 1436 N94-17869

STAR CLUSTERS
Ultraviolet observations of clusters of Wolf-Rayet stars in the SBm3 galaxy NGC 4214 and Ultraviolet and optical observations of LINER's
[NASA-CR-194307] p 1622 N94-19431

STAR DISTRIBUTION
The star identification, pointing and tracking system of UVSTAR, an attached payload instrument system for the Shuttle Hitchhiker-M platform p 1326 N94-19179

STAR TRACKERS
The star identification, pointing and tracking system of UVSTAR, an attached payload instrument system for the Shuttle Hitchhiker-M platform p 1326 N94-19179

STARBURST GALAXIES
ROSAT and IRAS observations
[MPE-PREPRINT-231] p 1623 N94-19526
ROSAT X ray observation of the 30 Dor giant HII region p 1623 N94-19527

STATE VECTORS
An extension of Wolovich's definition of equivalence of linear systems
[MATHS-REPT-A-183] p 1547 N94-18069
Space and time from quantum mechanics
[DE93-015263] p 1609 N94-18629

STATIC CHARACTERISTICS
Study and modeling of compressible flows of flapper nozzle type potentiometric systems
[ETN-93-95012] p 1421 N94-19495

STATIC LOADS
Implementation of mixed formulation elements in PC/NASTRAN p 1449 N94-17828
Spectrum fatigue testing of T-shaped tension clips
[FFA-TN-1992-22] p 1452 N94-17970

STATIC PRESSURE
Static pressure measurements for near isentropic flows using laser induced iodine fluorescence
p 1431 N94-18646
New test method to determine modulus of elasticity of rocket grain material
[AD-A269758] p 1377 N94-18758

STATIC TESTS
Static Computer Memory Integrity Testing (SCMIT): An experiment flown on STS-40 as part of GAS payload G-616 p 1325 N94-19169

STATISTICAL ANALYSIS
Planning under uncertainty solving large-scale stochastic linear programs
[DE93-013920] p 1516 N94-17701
Statistical intercomparison of global climate models: A common principal component approach with application to GCM data
[DE93-017951] p 1473 N94-18005
Putting knowledge to use: The acquisition and transfer of knowledge in situated problem solving environments
[AD-A269746] p 1509 N94-18744
Spectral analysis on the canonical autoregressive decomposition
[AD-A270083] p 1549 N94-18798
Statistical learning theory and algorithms
[AD-A270209] p 1523 N94-18901
Stochastic grammars: Theory and applications
[MEMO-INF-93-19] p 1528 N94-19262
Mathematical communications, volume 27, numbers 1 and 2, 1992. List and abstracts of memoranda published in the period July - December 1991
[PB93-191997] p 1553 N94-19557
A real-time spoken-language system for interactive problem-solving, combining linguistic and statistical technology for improved spoken language understanding
[AD-A270901] p 1392 N94-19749

STATISTICAL DECISION THEORY
Examination of metrics and assumptions used in correlation filter design
[DE93-017636] p 1576 N94-18000
Bounds for expected loss in Bayesian decision theory with imprecise prior probabilities
[PB93-197507] p 1558 N94-19327
Problems in probability, statistics and reliability
[AD-A270830] p 1559 N94-19595

STATISTICAL DISTRIBUTIONS
JSEP fellowship: Fractal noise processes
[AD-A268841] p 1557 N94-18540
Statistical description of the bistatic radar cross section distributions for a right circular cylinder
[AD-A270001] p 1387 N94-18666
Bahadur-Kiefer theorem beyond the largest observation
[PB93-197473] p 1558 N94-19325

STATISTICAL MECHANICS
Advanced in macrostatistical hydrodynamics
[DE93-018479] p 1410 N94-18270

STEADY FLOW
Cell vertex methods for steady inviscid flow
p 1413 N94-18563
Two-dimensional boundary surfaces for axi-symmetric external transonic flows
[AD-A269678] p 1312 N94-18571
Numerical solutions for a flow with mixed convection in a vertical geometry
[DE93-011592] p 1419 N94-19058

STEADY STATE
An overview of the SAFSIM computer program
[DE93-017657] p 1519 N94-18002
Decomposition invariance of generalized steady-state of a 1-D diffusion system
[REPT-93-26] p 1550 N94-19141
Excited atomic bromine energy transfer and quenching mechanisms
[AD-A270672] p 1572 N94-19607
Control of catalytic hydrotreating selectivity with ammonia
[DE93-041223] p 1354 N94-19660

STEEL STRUCTURES
The fire resistance of profiled thin steel sheet structures
[VTT-TIED-1320] p 1380 N94-19373

STEELS
Inelastic deformation and damage at high temperature
[DE93-018155] p 1448 N94-17814
Effects of irradiation temperature on embrittlement of nuclear pressure vessel steels
[DE93-015428] p 1359 N94-18245
The effect of crystallographic orientation on the performance of single crystal tungsten subscale penetrators
[AD-A268988] p 1597 N94-18468
Effects of irradiation temperature on Charpy and tensile properties of high-copper, low upper-shelf, submerged-arc welds
[DE93-017858] p 1445 N94-19047

STEEPEST DESCENT METHOD
Steepest descent method for set-valued locally accretive mappings
[DE93-628592] p 1548 N94-18106

STEERING
Electro-optic beam steering using non-linear organic materials
[AD-A270809] p 1374 N94-19577

STEFAN-BOLTZMANN LAW
Total hemispherical emittance of Niobium-1 percent zirconium fuel cladding for the SP-100 space reactor
[AD-A270456] p 1576 N94-19589

STELLAR ATMOSPHERES
Unified NLTE model atmospheres including spherical extension and stellar winds, 4: Improved line transfer and wind contamination of H, He profiles
[MPA-905] p 1624 N94-17736

STELLAR COMPOSITION
Determination of nitrogen to carbon abundance ratios from transition layer emission lines
[NASA-CR-191921] p 1622 N94-19421

STELLAR CORONAS
Stellar coronae at the end of the main sequence: A Rosat survey of the late M dwarfs
[NASA-CR-194700] p 1628 N94-19794

STELLAR ENVELOPES
Detection of accreting gas toward HD 45677: A newly recognized, Herbig Be proto-planetary system
[NASA-CR-189312] p 1621 N94-19288
The molecular environment of S106 IR
[MPE-PREPRINT-241] p 1622 N94-19417

STELLAR EVOLUTION
A new approach to the study of the turbulence layer
[NASA-CR-194546] p 1487 N94-19397
Structuration processes in protoplanetary accretion disks
[MPE-243] p 1628 N94-19519

STELLAR GRAVITATION
Structuration processes in protoplanetary accretion disks
[MPE-243] p 1628 N94-19519

STELLAR MASS ACCRETION
Detection of accreting gas toward HD 45677: A newly recognized, Herbig Be proto-planetary system
[NASA-CR-189312] p 1621 N94-19288

STELLAR MODELS
Computational astrophysics: Pulsating stars
[DE93-018369] p 1627 N94-18857
Structuration processes in protoplanetary accretion disks
[MPE-243] p 1628 N94-19519
STELLAR RADIATION
Computational astrophysics: Pulsating stars
[DE93-018369] p 1627 N94-18857
STELLAR ROTATION
Plasma properties research: Task 3
[DE93-017087] p 1583 N94-17854
Pulse-timing studies of x ray pulsars
[NASA-CR-193778] p 1621 N94-18611
STELLAR SPECTRA
Determination of nitrogen to carbon abundance ratios from transition layer emission lines
[NASA-CR-191921] p 1622 N94-19421
STELLAR STRUCTURE
A new approach to the study of the turbulence layer
[NASA-CR-194546] p 1487 N94-19397
STELLAR TEMPERATURE
Spectrophotometry of emission-line stars in the magellanic clouds
[NASA-CR-194082] p 1628 N94-19425
STELLAR WINDS
Unified NLTE model atmospheres including spherical extension and stellar winds, 4: Improved line transfer and wind contamination of H, He profiles
[MPA-905] p 1624 N94-17736
Spectrophotometry of emission-line stars in the magellanic clouds
[NASA-CR-194082] p 1628 N94-19425
STEPPING MOTORS
Control of torque in stepping motors of quartz watches and clocks p 1408 N94-18023
STEREOCHEMISTRY
Microbial degradation of poly-b-esters: A mechanistic study, cellulose acetate biodegradability
[AD-A271368] p 1374 N94-19586
STEREOSCOPIC VISION
A stereoscopic vision system with applications to automated docking and tracking
[AD-A270754] p 1333 N94-19765
STIFFENING
Compression strength of composite primary structural components
[NASA-CR-194562] p 1457 N94-19350
STIFFNESS
Packaging, deployment, and panel design concepts for a truss-stiffened 7-panel precision deployable reflector with feed boom
[NASA-TM-109000] p 1333 N94-17765
Analysis of high contact resistances associated with hermetic and lightning arrestor connectors
[DE93-014850] p 1395 N94-17783
Joint stiffness estimation based on force sensor measurements in industrial manipulators
[REPT-92-053] p 1443 N94-17937
Elastic properties of a polyimide film determined by Brillouin scattering and mechanical techniques
[DE93-017404] p 1368 N94-18098
A constitutive theory for rigid polyurethane foam
[DE93-011596] p 1372 N94-19059
STIMULATED EMISSION
Problems related to stimulated electromagnetic emissions, strong turbulence and ionospheric modification
[IRF-SR-212] p 1480 N94-17720
STIRLING CYCLE
Performance mapping of the STM4-120 kinematic Stirling engine using a statistical design of experiments method
[DE93-015132] p 1464 N94-17798
The 7th International Cryocooler Conference
[AD-A268451] p 1379 N94-18147
Regenerator optimization for Stirling cycle refrigeration
[DE93-018468] p 1380 N94-18818
STIRLING ENGINES
Performance mapping of the STM4-120 kinematic Stirling engine using a statistical design of experiments method
[DE93-015132] p 1464 N94-17798
STOCHASTIC PROCESSES
Planning under uncertainty solving large-scale stochastic linear programs
[DE93-013920] p 1516 N94-17701
Data fusion through simulated annealing of registered range and reflectance images
[DE93-015910] p 1612 N94-17858
Stochastic models of attention and search
[AD-A268622] p 1508 N94-18292
JSEP fellowship: Fractal noise processes
[AD-A268841] p 1557 N94-18540
Development of the microstructure based stochastic life prediction models
[AD-A269880] p 1454 N94-18683
Development of the microstructure based stochastic life prediction model
[AD-A269742] p 1361 N94-18742
Coupled neural-dendritic processes: Cooperative stochastic effects and the analysis of spike trains
[AD-A270041] p 1506 N94-18793
Statistical learning theory and algorithms
[AD-A270209] p 1523 N94-18901
Adaptive path planning: Algorithm and analysis
[DE93-008348] p 1523 N94-18926
A numerical study of hybrid optimization methods for the molecular conformation problems
[DE93-017898] p 1569 N94-18985
A simple calculus of finite probabilistic processes
[MEMO-INF-93-08] p 1558 N94-19195
Stochastic grammars: Theory and applications
[MEMO-INF-93-19] p 1528 N94-19262
Excursions of stochastic processes, Cox-point processes, entrance behavior and resolvents
[PB93-197291] p 1558 N94-19323
The brain electrical activity in different G situations
[AERONAUTICA-ACTA-A-372-199]
p 1507 N94-19523
Equivalence and reduction of hidden Markov models
[AD-A270762] p 1560 N94-19768
STORAGE BATTERIES
Mechanically refuelable zinc/air electric vehicle cells
[DE93-016446] p 1394 N94-17770
STORAGE RINGS (PARTICLE ACCELERATORS)
Simulation of emittance dilution in electron storage ring from Compton backscattering
[DE93-017611] p 1386 N94-18503
Effects of transverse coupling on transverse beam size, simulation and measurements
[DE93-017804] p 1574 N94-18972
Simulation of the ALS longitudinal multibunch feedback system
[DE93-019227] p 1575 N94-19152
Study of coupled-bunch collective effects in the ALS
[DE93-019236] p 1575 N94-19558
STORAGE STABILITY
Practical reporting times for environmental samples
[DE93-013461] p 1472 N94-17910
STORM SURGES
The performance of drag relations in the WAQUA storm surge model
[KNMI-TR-149] p 1496 N94-17923
Wind products for use in coastal wave and surge models
[AD-A269753] p 1497 N94-18414
STORMS (METEOROLOGY)
Diabatic forcing and initialization with assimilation of cloud and rain water in a forecast model: Methodology
p 1491 N94-18603
STOVL AIRCRAFT
Lift and pitching moment induced on jet STOVL aircraft hovering in ground effect
[AD-A269700] p 1317 N94-18577
Lift and pitching moment induced on jet STOVL aircraft by the ground vortex
[AD-A269816] p 1318 N94-18733
Overview of STOVL aircraft propulsion research offtakes and vertical lift systems
[NASA-TM-106387] p 1321 N94-19353
STRAIN DISTRIBUTION
Spectrum fatigue testing of T-shaped tension clips
[FFA-TN-1992-22] p 1452 N94-17970
Analysis of regional deformation and strain accumulation data adjacent to the San Andreas fault
[NASA-CR-194072] p 1487 N94-19428
STRAIN GAGES
Characteristics and pulsed radiation response of non-ideal quartz shock stress gauges
[DE93-017628] p 1424 N94-17999
Residual strain measurement on the production-grade class 4 flextensional transducer shell
[AD-A268828] p 1430 N94-18537
A comparative evaluation of in-plane shear test methods for laminated graphite-epoxy composites
[NASA-CR-193808] p 1456 N94-19095
Experiments and analysis of lateral piezoresistance gauges
[DE93-017874] p 1433 N94-19111
High temperature strain measurement with a resistance strain gage
[NASA-CR-194441] p 1434 N94-19314
STRAIN HARDENING
A review of the stages of work hardening
[DE93-016456] p 1359 N94-18114
Effects of shock loading on a solid-solution strengthened superalloy
[DE93-018345] p 1362 N94-18809
STRAIN MEASUREMENT
Instrumented experiments aboard the frigate WOLF. Wolf 2: Measurement results of the 5.5 kg TNT in the crew aft sleeping compartment
[PML-1992-12] p 1451 N94-17931
Residual strain measurement on the production-grade class 4 flextensional transducer shell
[AD-A268828] p 1430 N94-18537
High temperature strain measurement with a resistance strain gage
[NASA-CR-194441] p 1434 N94-19314
Delamination in composite materials as observed using an optical fiber strain gage
[AD-A270803] p 1344 N94-19662
STRAIN RATE
Modeling microstructural evolution and the mechanical response of superplastic materials
[DE93-014417] p 1355 N94-17711
Atlas of formability: Ultimet
[AD-A268352] p 1355 N94-17767
Atlas of formability: HAYNES 556
[AD-A268354] p 1356 N94-17768
Atlas of formability: HAYNES 188
[AD-A268355] p 1356 N94-17769
Atlas of formability: NICKELVAC K-500
[AD-A268351] p 1356 N94-17772
Atlas of formability: INCONEL 718
[AD-A268350] p 1356 N94-17789
Atlas of formability: Hastelloy C-22
[AD-A268324] p 1356 N94-17796
Atlas of formability: Permalloy - 80 flow stress curves
[AD-A268263] p 1356 N94-17801
Atlas of formability: Nickelvac C-276
[AD-A268264] p 1357 N94-17802
Atlas of formability: Ti-6Al-4V ELI
[AD-A268300] p 1357 N94-17803
Atlas of formability: ALLVAC 718
[AD-A268304] p 1357 N94-17804
Atlas of formability: Waspaloy
[AD-A268323] p 1593 N94-17805
A review of the stages of work hardening
[DE93-016456] p 1359 N94-18114
Several fundamental issues in the mechanics of inelastic behavior
[AD-A269455] p 1453 N94-18265
Implementation of a nonisothermal unified inelastic-strain theory into ADINA6.0 for a titanium alloy: User guide
[AD-A269927] p 1360 N94-18660
Dislocation-drag contribution to high-rate plastic deformation in shock-loaded tantalum
[DE93-018286] p 1361 N94-18802
Effects of shock loading on a solid-solution strengthened superalloy
[DE93-018345] p 1362 N94-18809
Three-dimensional shock wave physics simulations with MIMD PAGOSA on massively parallel computers
[DE93-011682] p 1455 N94-18829
Effect of internal heating during hot compression testing on the stress-strain behavior and hot working characteristics of alloy 304L
[DE93-012701] p 1362 N94-18917
The effect of composition on the mechanism of continuous recrystallization and superplastic response of aluminum-scandium alloys
[DE93-018594] p 1365 N94-19280
Impact strength and indentation hardness of high-strength ceramics
[DE93-018833] p 1373 N94-19338
Dynamical behavior of octahedrite from the Henbury meteorite
[DE93-018834] p 1627 N94-19339
Mechanical response comparison of gun propellants evaluated under equivalent time-temperature conditions
[AD-A270479] p 1378 N94-19674
STRANGE ATTRACTORS
Homoclinic crises in a model for the CO2 laser
[DE93-624900] p 1436 N94-17954
The brain electrical activity in different G situations
[AERONAUTICA-ACTA-A-372-199]
p 1507 N94-19523
STRANGENESS
Institute for Nuclear Theory
[DE93-017369] p 1568 N94-18824
STRATEGY
A method for cognitive task analysis
[IZF-1992-B5] p 1508 N94-17967
STRATIFIED FLOW
Numerical simulations of turbulent buoyant flows by finite element method: Application to the study of strongly heated or cooled stratified flow
[ECL-92-28] p 1421 N94-19399
STRATIGRAPHY
Three-dimensional high-resolution seismic profiling on the New Jersey outer continental shelf
[AD-A269835] p 1498 N94-18600

Applications of Quaternary stratigraphic, soil-geomorphic, and quantitative geomorphic analyses to the evaluation of tectonic activity and landscape evolution in the Upper Coastal Plain, South Carolina
[DE93-016269] p 1484 N94-18725

STRATOSPHERE
Monitoring the response of the upper troposphere/lower stratosphere to a greenhouse gas scenario
[DE93-014509] p 1470 N94-17710
Screening analysis for chlorine-free alternative refrigerants to replace R-22 in air conditioning applications
[DE93-015920] p 1367 N94-17847
Ozone hole
[NASA-TM-109368] p 1476 N94-18960

STRATUS CLOUDS
Three-dimensional cloud visualization based on satellite imagery
[AD-A269318] p 1490 N94-18300

STREAM FUNCTIONS (FLUIDS)
Numerical investigation of the incompressible flow around a wing with a fixed spoiler
[ISL-R-109/91] p 1313 N94-19524

STRESS (PHYSIOLOGY)
Effects of a high-energy food supplement on cold-induced thermogenesis
[AD-A269301] p 1504 N94-17823
Road march performance of special operations soldiers carrying various loads and load distributions
[AD-A269198] p 1512 N94-18882

STRESS ANALYSIS
PVDF measurement of soft x ray induced shock and filter debris impulse
[DE93-017633] p 1382 N94-17806
Generalized seismic analysis p 1449 N94-17832
Current development in selected stress and thermal analysis software interfaces with PRO-ENGINEER
[DE93-014935] p 1518 N94-17943
Characteristics and pulsed radiation response of non-ideal quartz shock stress gauges
[DE93-017628] p 1424 N94-17999
Numerical integration of structural elements in NIKE3D and DYNA3D
[DE93-016325] p 1452 N94-18049
Steep geometric grating for use in moire interferometry
[AD-A268759] p 1453 N94-18328
The 6th Japan-U.S. conference on composite materials
[AD-A268535] p 1341 N94-18630
Fatigue technology assessment and strategies for fatigue avoidance in marine structures. Appendices
[AD-A269053] p 1455 N94-18716
A constitutive theory for rigid polyurethane foam
[DE93-011596] p 1372 N94-19059
Plastic mechanism analysis of T-joints in RHS subject to combined bending and concentrated force
[PB93-195774] p 1456 N94-19061
A comparative evaluation of in-plane shear test methods for laminated graphite-epoxy composites
[NASA-CR-193808] p 1456 N94-19095
Interfacial cracks in plates: A three-dimensional numerical investigation p 1456 N94-19116
The interpretation of optical caustics in the presence of dynamic non-uniform crack-tip motion histories: A study based on a higher order transient crack-tip expansion
[SM91-12] p 1456 N94-19130
Modeling and characterization of mechanoelectric conversion piezoelectric generators through dynamical or quasi static uniaxial stress
[ISAL-92-0097] p 1406 N94-19490

STRESS CONCENTRATION
Fatigue technology assessment and strategies for fatigue avoidance in marine structures. Appendices
[AD-A269053] p 1455 N94-18716

STRESS CORROSION
Environmentally assisted cracking of nickel anode substrates in Li/SOCl2 cells: An engineering approach
[DE93-015130] p 1405 N94-18928
The effects of radiolysis on the corrosion and stress corrosion behavior of 316 stainless steels
[DE93-019933] p 1363 N94-19021

STRESS CORROSION CRACKING
Environmental degradation of Alloy 600 and welded filler metal EN82 in an elevated temperature aqueous environment
[DE93-018049] p 1363 N94-18940

STRESS CYCLES
Defining the normal turbine inflow within a wind park environment
[DE93-010032] p 1489 N94-18046

STRESS DISTRIBUTION
Implementation of mixed formulation elements in PC/NASTRAN p 1449 N94-17828
Impact response of composite laminates: A guide to closed form solutions
[FFA-TN-1992-33] p 1339 N94-17971
Numerical integration of structural elements in NIKE3D and DYNA3D
[DE93-016325] p 1452 N94-18049
New test method to determine modulus of elasticity of rocket grain material
[AD-A269758] p 1377 N94-18758
A numerical analysis of crack growth in brittle microcracking composites
[DE93-011562] p 1343 N94-18914

STRESS INTENSITY FACTORS
Interfacial cracks in plates: A three-dimensional numerical investigation p 1456 N94-19116
The interpretation of optical caustics in the presence of dynamic non-uniform crack-tip motion histories: A study based on a higher order transient crack-tip expansion
[SM91-12] p 1456 N94-19130
Subcritical crack growth in continuous-fiber reinforced ceramic composites
[DE93-018784] p 1343 N94-19335
Residual strength predictions for fibre metal laminates: The R-curves approach
[LR-717] p 1344 N94-19666

STRESS MEASUREMENT
PVDF measurement of soft x ray induced shock and filter debris impulse
[DE93-017633] p 1382 N94-17806
Application of piezoelectric stress gauges to the measurement of fast-rise-time multimegampere electric currents
[DE93-017625] p 1429 N94-18102
A comparative evaluation of in-plane shear test methods for laminated graphite-epoxy composites
[NASA-CR-193808] p 1456 N94-19095

STRESS RELAXATION
Mechanical response comparison of gun propellants evaluated under equivalent time-temperature conditions
[AD-A270479] p 1378 N94-19674

STRESS TENSORS
On a conformal perfect fluid in the classical vacuum
[DE93-624797] p 1480 N94-17682
Assessment of an improved multiaxial strength theory based on creep-rupture data for Inconel 600
[DE93-015929] p 1356 N94-17791

STRESS-STRAIN RELATIONSHIPS
Modeling microstructural evolution and the mechanical response of superplastic materials
[DE93-014417] p 1355 N94-17711
Atlas of formability: Ultimet
[AD-A268352] p 1355 N94-17767
Atlas of formability: HAYNES 556
[AD-A268354] p 1356 N94-17768
Atlas of formability: HAYNES 188
[AD-A268355] p 1356 N94-17769
Atlas of formability: Nickelvac C-276
[AD-A268264] p 1357 N94-17802
Ceramic films and interfaces: Chemical and mechanical properties
[DE93-018416] p 1369 N94-18163
Evaluation of the production-grade class 4 flextensional transducer shell
[AD-A266796] p 1340 N94-18201
A finite strain ring dynamical model for pneumatic tires
[AD-A269286] p 1444 N94-18266
Residual strain measurement on the production-grade class 4 flextensional transducer shell
[AD-A268828] p 1430 N94-18537
Implementation of a nonisothermal unified inelastic-strain theory into ADINA6.0 for a titanium alloy: User guide
[AD-A269927] p 1360 N94-18660
Dislocation-drag contribution to high-rate plastic deformation in shock-loaded tantalum
[DE93-018286] p 1361 N94-18802
Wave propagation near explosive sources
[AD-A270102] p 1418 N94-18870
Effect of internal heating during hot compression testing on the stress-strain behavior and hot working characteristics of alloy 304L
[DE93-012701] p 1362 N94-18917
Experiments and analysis of lateral piezoresistance gauges
[DE93-017874] p 1433 N94-19111
Shock compression properties of silicon carbide
[DE93-019927] p 1373 N94-19271
A review of aeronautical fatigue investigations in Sweden during the period May 1991 to April 1993
[FFA-TN-1993-22] p 1457 N94-19358
Current capabilities for simulating the extreme distortion of thin structures subjected to severe impacts
p 1459 N94-19474
Development of engineering models for calculation of failure loads and defect states of steel concrete beams and plates
[ETN-93-95052] p 1460 N94-19648
Residual strength predictions for fibre metal laminates: The R-curves approach
[LR-717] p 1344 N94-19666

STRESSES
The respectiveness of response in a bar under static and transient loads
[VTT-TIED-1377] p 1452 N94-17959

STRING THEORY
Gauge coupling unification in superstring derived standard-like models
[DE93-624801] p 1607 N94-17950
Neutrino masses in superstring derived standard-like models
[DE93-624802] p 1565 N94-17951
Cabibbo mixing in superstring derived standard-like models
[DE93-624814] p 1607 N94-17953
Investigations in gauge theories, topological solitons, and string theories
[DE93-015029] p 1609 N94-19250

STROKE VOLUME
Characterization of fluid physics effects on cardiovascular response to microgravity (G-572)
p 1323 N94-19163

STRONTIUM OXIDES
Specific heat of La(1.875-x)Nd(x)Sr(0.125)CuO4: Magnetic and structural transitions
[DE93-016978] p 1600 N94-18968

STRONTIUM TITANATES
Phase transitions and neutron scattering
[DE93-016748] p 1594 N94-17866

STRUCTURAL ANALYSIS
The Twenty-First NASTRAN (R) Users' Colloquium
[NASA-CP-3203] p 1449 N94-17827
Implementation of mixed formulation elements in PC/NASTRAN p 1449 N94-17828
The respectiveness of response in a bar under static and transient loads
[VTT-TIED-1377] p 1452 N94-17959
Numerical integration of structural elements in NIKE3D and DYNA3D
[DE93-016325] p 1452 N94-18049
Computational strategies for composite structures
[PB93-195097] p 1452 N94-18079
Preliminary structural design: Defining the design space
[AD-A268898] p 1317 N94-18227
The 6th Japan-U.S. conference on composite materials
[AD-A268535] p 1341 N94-18630
Potential dependent structural changes of underpotentially deposited copper on an iodine treated platinum surface determined in situ by surface EXAFS and its polarization dependence
[AD-A269890] p 1360 N94-18687
Research activities, Faculty of Civil Engineering, Delft University of Technology, 1990 - 1991
[PB93-195022] p 1380 N94-19254
Preparation and characterisation of the compound Tl(0.65) Bi(0.35) Ca(0.8) Sr(1.7) Cu2 O(y) using oxalate coprecipitation and analytical CBED and an initial preparation of Bi2Ca(n-1) Sr2Cu(n) O(4+2n) for n=5
[DE93-625470] p 1602 N94-19277
Design for cyclic loading endurance of composites
[NASA-TM-106407] p 1457 N94-19351
Time dependent identification of nonlinear structures
[ECL-92-64] p 1457 N94-19403
Refinement of unit cell parameters by least-squares: Comments on an old technique and the development of a new computer program
[AD-A270610] p 1531 N94-19590

STRUCTURAL DESIGN
Design optimization studies using COSMIC NASTRAN
p 1450 N94-17834
Preliminary structural design: Defining the design space
[AD-A268898] p 1317 N94-18227
Centrifuge modeling of explosion-induced craters in unsaturated sand
[AD-A270194] p 1417 N94-18780
Optimizing wind turbine control system parameters
[DE93-018861] p 1469 N94-19036
Numerical simulation of vehicle crashworthiness and occupant protection p 1459 N94-19471

STRUCTURAL DESIGN CRITERIA
ADAS implementation of a panel method for the prediction of aerodynamic loads
[LR-723] p 1313 N94-19667

STRUCTURAL ENGINEERING
Scaling laws for diffraction loading by air blast
[PML-1991-54] p 1452 N94-17941

The ecological and environmental impacts of manmade marshes
[AD-A269213] p 1475 N94-18885

Research activities, Faculty of Civil Engineering, Delft University of Technology, 1990 - 1991
[PB93-195022] p 1380 N94-19254

STRUCTURAL FAILURE

Computational strategies for composite structures
[PB93-195097] p 1452 N94-18079

Fluid-structure-interaction analyses of reactor vessel using improved hybrid Lagrangian Eulerian code ALICE-II
[DE93-015536] p 1409 N94-18248

Fundamental research in nonlinear random vibration for aerospace applications
[AD-A268929] p 1454 N94-18487

Impact analysis of composite aircraft structures
p 1458 N94-19468

Delamination in composite materials as observed using an optical fiber strain gage
[AD-A270803] p 1344 N94-19662

STRUCTURAL MEMBERS

Dynamic response analysis of composite structural members during missile launch
[AD-A270023] p 1332 N94-18760

STRUCTURAL PROPERTIES (GEOLOGY)

Seismic studies of the geologic structure and physical properties of the seabed
[AD-A270895] p 1500 N94-19747

STRUCTURAL RELIABILITY

FAROW: A tool for fatigue and reliability of wind turbines
[DE93-017639] p 1465 N94-18001

STRUCTURAL STABILITY

Structural stability of 1100 C heated Pd/k during absorption cycling in protium
[DE93-016270] p 1346 N94-18048

About structurally stable generating mechanism for invariant hyperbolic sets
[DE93-629858] p 1561 N94-18150

STRUCTURAL VIBRATION

Modelling chaotic vibrations using NASTRAN
p 1449 N94-17830

Generalization of optimal control theory: Linear and nonlinear structures
[PB93-188621] p 1540 N94-18125

The effects of initial conditions and control time on optimal actuator placement by way of a max-min genetic algorithm
[DE93-017640] p 1525 N94-19124

STRUCTURAL WEIGHT

Regenerative fuel cells for High Altitude Long Endurance Solar Powered Aircraft
[DE93-016991] p 1465 N94-17853

STUDENTS

Magnetic Fusion Energy Technology Fellowship: Report on survey of institutional coordinators
[DE93-014646] p 1583 N94-17739

Joint services electronics program
[AD-A269383] p 1403 N94-18638

National Boy Scout Jamboree
[NASA-TM-109367] p 1610 N94-18982

California Student Get Away Special Payload GAS-450
p 1324 N94-19164

Undergraduate origins of recent science and engineering doctorate recipients
[NSF-92-332] p 1610 N94-19389

Undergraduate course and curriculum development program and calculus and the bridge to calculus program: 1992 awards
[NSF-93-24] p 1610 N94-19446

SUBROUTINE LIBRARIES (COMPUTERS)

Cesar user library
[FFI-93/7021] p 1529 N94-19378

SUBROUTINES

Radio wave propagation in structured ionization for satellite and radar applications
[AD-A268457] p 1382 N94-17844

SUBSIDENCE

Ground movements associated with gas hydrate production
[DE93-019887] p 1486 N94-19018

SUBSONIC FLOW

A fast computing method for the flow over high-lift wings p 1308 N94-18437

SUBSTITUTES

Development of alternatives to lead-bearing solders
[DE93-016509] p 1357 N94-17862

SUBSTRATES

Metal-nanocluster composites made by ion implantation: A novel third-order nonlinear material
[DE93-015908] p 1339 N94-17846

Characterization of diamond film nucleation and growth surface
[AD-A269400] p 1597 N94-18459

Kinetic aspects of lattice mismatch in molecular beam epitaxial growth on planar and patterned substrates
[AD-A270424] p 1597 N94-18506

Diamond brazed to a metal
[AD-D015877] p 1371 N94-18746

Growth, characterization and device development in monocrystalline diamond films
[AD-A270074] p 1599 N94-18797

Thermal analysis of coatings and substrate materials during a disruption in fusion reactors
[DE93-017688] p 1588 N94-18971

The minimum detection limits of RDX and TNT deposited on various surfaces as determined by ion mobility spectroscopy
[DE93-018521] p 1378 N94-19042

Silicon MCM substrates for integration of 3-5 photonic devices and CMOS IC's
[DE93-017894] p 1405 N94-19112

The microstructural mechanism of electromigration failure in narrow interconnects of Al alloys
[DE93-018598] p 1365 N94-19282

Study of GaAs substrates by ambient temperature photoluminescence imagery
[ECL-92-61] p 1603 N94-19357

Testing of protective coatings in hydrogen
[DE93-040326] p 1375 N94-19651

SUBURBAN AREAS

Spatiotemporal variability of non-urban ozone concentrations over the eastern United States and its potential replication by satellite data
[PB93-191328] p 1476 N94-19065

SUHL EFFECT

Nonlinear dynamics and instabilities in ferromagnetic resonance experiments: Examinations of spheres from yttrium iron garnet in coincidence area of the first Suhl instabilities
[ETN-93-95072] p 1604 N94-19612

SULFATES

The global atmospheric sulfur cycle: An evaluation of model predictions and observations
[CM-81] p 1479 N94-19379

SULFIDES

The global atmospheric sulfur cycle: An evaluation of model predictions and observations
[CM-81] p 1479 N94-19379

SULFUR

The d(exp 3)delta-a(exp 3)delta and b(exp 3)phi-a(exp 3)delta systems of ZrS, Part 2: Appendix, list of wavenumbers
[USIP-92-05] p 1602 N94-19293

SULFUR COMPOUNDS

Supercritical thermodynamics of sulfur and nitrogen species
[DE93-041221] p 1610 N94-19670

SULFUR DIOXIDES

Condensed gases under winter conditions: A study for the rescue services
[FOA-C-40305-4.5] p 1473 N94-18139

Photodissociation studies of polyatomic free radicals
[AD-A270084] p 1350 N94-18799

Effects of the Mount Pinatubo eruption on solar insolation: Four case studies
[DE93-018454] p 1475 N94-18817

The global atmospheric sulfur cycle: An evaluation of model predictions and observations
[CM-81] p 1479 N94-19379

SULFUR FLUORIDES

Application of an atmospheric dispersion model to simulated pollutant releases in the Colorado Front range
[DE93-017118] p 1480 N94-19732

SULFUR OXIDES

Photodissociation studies of polyatomic free radicals
[AD-A270084] p 1350 N94-18799

SUMMARIES

Summaries of FY 1993 research in the chemical sciences
[DE93-011855] p 1632 N94-18915

SUMMER

Spectral analysis of synoptic time scale disturbances over the tropical eastern Pacific during summer 1989, 1990 and 1991
[AD-A268821] p 1490 N94-18206

SUPERCOMPUTERS

Introductory user's guide to the ARL supercomputer facility at Aberdeen Proving Ground
[AD-A265204] p 1514 N94-17877

An evolving infrastructure for scientific computing and the integration of new graphics technology
[DE93-017164] p 1520 N94-18133

A special purpose silicon compiler for designing supercomputing VLSI systems p 1402 N94-18379

Visualization for applications in shock physics
[DE93-012849] p 1418 N94-18918

The world's most powerful computer
[NASA-TM-109369] p 1514 N94-18961

SUPERCONDUCTING DEVICES

Superconducting flux flow devices, digital circuits and memories
[DE93-019072] p 1405 N94-19079

SUPERCONDUCTING FILMS

Synthesis and study of high-T(sub c) superconducting electronic materials
[AD-A268851] p 1402 N94-18390

Fabrication and microstructural development of Ag-clad TlBa2Ca2Cu3O(x) tapes
[DE93-017407] p 1597 N94-18500

High performance YBCO films
[AD-A269090] p 1599 N94-18719

Fabrication and characterization of high-T(sub c) tapes and coils made from Ag-clad Bi-2223 superconductors
[DE93-018615] p 1601 N94-18993

LLE Review
[DE93-017618] p 1602 N94-19123

SUPERCONDUCTING MAGNETS

Corroboration of magnetic forces in US Maglev design
[DE93-014918] p 1443 N94-17785

A superconducting short period undulator for a harmonic generation FEL experiment
[DE93-017581] p 1436 N94-17998

Development and application of specially-focused ultrasonic transducers to location and sizing of defects in 75 mm- to 127 mm-thick austenitic stainless steel weld metals
[DE93-015975] p 1453 N94-18108

Proceedings of the 3rd Workshop on Balloon-Borne Experiments with Superconducting Magnet Spectrometers
[DE93-788362] p 1630 N94-18219

Analysis of superconducting magnetic energy storage applications at a proposed wind farm site near Browning, Montana
[DE93-018793] p 1466 N94-18276

Magnetic field measurements of a superconducting undulator for a Harmonic Generation FEL experiment at the NSLS
[DE93-017621] p 1438 N94-18504

Fabrication and characterization of high-T(sub c) tapes and coils made from Ag-clad Bi-2223 superconductors
[DE93-018615] p 1601 N94-18993

Thermo-hydraulic analysis of superconducting toroidal-field magnets for the Tokamak Physics Experiment
[DE93-018096] p 1590 N94-19269

Incology 908 database report: On process-structure-property relationship
[DE93-017616] p 1366 N94-19546

SUPERCONDUCTING SUPER COLLIDER

Mechanical-property changes of structural composite materials after low-temperature proton irradiation: Implications for use in SSC magnet systems
[DE93-016735] p 1343 N94-18763

Experimental research in high energy physics
[DE93-011912] p 1574 N94-18916

Investigation of physical structures and interactions at high energy
[DE93-014444] p 1574 N94-18927

Longitudinal beam dynamics with RF noise
[DE93-018649] p 1574 N94-18994

SSC detector muon sub-system beam tests
[DE93-018415] p 1569 N94-19013

High energy physics program. Task A: Experiment and theory. Task B: Numerical simulation
[DE93-018140] p 1575 N94-19050

Extraction of Z(prime) coupling data from Z(prime) (yields) jj at the LHC and SSC
[DE93-018576] p 1570 N94-19096

Design verification and acceptance tests of the ASST-A helium refrigeration system
[DE93-019746] p 1381 N94-19540

High rate resistive plate chambers: An inexpensive, fast, large area detector of energetic charged particles for accelerator and non-accelerator applications
[DE93-018664] p 1572 N94-19545

SUPERCONDUCTIVITY

Phase separation and superconductivity in La2CuO(4 + delta): Effects of oxygen diffusion
[DE93-016610] p 1594 N94-17907

Report of the 1991 Workshop on Particle-Material Interactions for Fusion Research
[DE93-788393] p 1573 N94-18156

Superconducting/semiconducting hybrids and advance memory concepts for superconducting electronics
[AD-A268679] p 1397 N94-18312

High energy resolution ARPES measurements of the normal and superconducting states of Bi2Sr2CaCu2O(8 + delta)
[DE93-018294] p 1599 N94-18804

Specific heat of La(1.875-x)Nd(x)Sr(0.125)CuO4: Magnetic and structural transitions
[DE93-016978] p 1600 N94-18968

Superconductivity and magnetism in niobium doped YBa2Cu3O7 related high-(Tc) ceramics [DE93-018086] p 1601 N94-19049

Fabrication, properties, and microstructures of high (Tc) tapes and coils made from Ag-clad Bi-2223 superconductor [DE93-017405] p 1602 N94-19122

Crossover from BCS to Bose superconductivity: A functional integral approach [DE93-019503] p 1604 N94-19566

Numerical experiments on the Ginzburg-Landau equations [DE93-019504] p 1604 N94-19567

SUPERCONDUCTORS

Superconducting/semiconducting hybrids and advance memory concepts for superconducting electronics [AD-A268679] p 1397 N94-18312

The low-temperature specific heat of CeCu2Ge2 at 0 and 9.5 kbar [DE93-014914] p 1360 N94-18398

Thin film studies of the proximity Josephson effect [AD-A270129] p 1600 N94-18876

Ultrafast Electronics and Optoelectronics: Summaries of papers. Technical digest conference edition [AD-A269233] p 1405 N94-18909

Dimensional crossover in the torque in a layered superconductor [DE93-019544] p 1407 N94-19553

SUPERCRITICAL AIRFOILS

Navier-Stokes simulation of flow field around a blown-flap high-lift system p 1307 N94-18429

SUPERCRITICAL FLUIDS

Supercritical thermodynamics of sulfur and nitrogen species [DE93-041221] p 1610 N94-19670

SUPERCRITICAL WINGS

High lift and the forward swept wing p 1308 N94-18436

SUPERFLUIDITY

The 7th International Cryocooler Conference [AD-A268451] p 1379 N94-18147

Superfluid Helium On-Orbit Transfer (SHOOT) flight demonstration p 1327 N94-19185

Two-dimensional turbulent nonstationary superfluid counterflows: Numerical simulations, qualitative effects [MPIS-23/1992] p 1422 N94-19510

Examinations of converging cylindrically symmetric second sound propagation in He2 [MPIS-9/1992] p 1564 N94-19715

SUPERGIANT STARS

Determination of nitrogen to carbon abundance ratios from transition layer emission lines [NASA-CR-191921] p 1622 N94-19421

SUPERHIGH FREQUENCIES

Numerical modelling of fringing fields and their use for complex permittivity measurements at high frequencies [AD-A270198] p 1388 N94-18782

Some superhigh-frequency and magnetic properties of chemically precipitated films [AD-A266195] p 1351 N94-19110

SUPERLATTICES

Superhardness effect in Au/Ni multilayers [DE93-016444] p 1357 N94-17860

Phenomenological explanation of elastic anomalies in superlattices [DE93-017475] p 1594 N94-17871

Fundamental properties and device applications of Ge(x)Si(1-x)/Si superlattices (supplemental) [AD-A269212] p 1600 N94-18884

Neutron-induced collision cascade mixing in Nb/V superlattices [DE93-018575] p 1600 N94-18933

Growth of epitaxial semiconductor alloys and superlattices with continuously variable composition by pulsed-laser ablation [DE93-018726] p 1601 N94-18998

Suppressed electron-phonon scattering in superlattices [AD-A270834] p 1604 N94-19597

SUPERNOVAE

Evolution of r-process elements in the hot supernova bubble [DE93-017169] p 1624 N94-17897

Weak neutral currents and collapse initiated supernova [DE93-018652] p 1627 N94-19284

SUPERPLASTICITY

Modeling microstructural evolution and the mechanical response of superplastic materials [DE93-014417] p 1355 N94-17711

Ceramic films and interfaces: Chemical and mechanical properties [DE93-018416] p 1369 N94-18163

The effect of composition on the mechanism of continuous recrystallization and superplastic response of aluminum-scandium alloys [DE93-018594] p 1365 N94-19280

SUPERSATURATION

Film condensation in a shock wave [MPIS-22/1992] p 1422 N94-19509

SUPERSONIC BOUNDARY LAYERS

Studies on high pressure and unsteady flame phenomena: Revision [AD-A269138] p 1348 N94-18257

SUPERSONIC COMBUSTION

Studies on high pressure and unsteady flame phenomena: Revision [AD-A269138] p 1348 N94-18257

Numerical simulation of fluid dynamics and combustion for ram accelerator projectile/obturator interaction [AD-A269715] p 1320 N94-18748

SUPERSONIC COMBUSTION RAMJET ENGINES

Analysis of supersonic flows using k-epsilon model and the RPLUS code: Progress towards high speed combustor analysis p 1411 N94-18551

SUPERSONIC FLOW

Analysis of supersonic flows using k-epsilon model and the RPLUS code: Progress towards high speed combustor analysis p 1411 N94-18551

SUPERSONIC JET FLOW

Computational aero-acoustics as a branch of turbulence research p 1411 N94-18552

Unimolecular photodissociation dynamics of ketene (CH2CO): The singlet/triplet branching ratio and experimental observation of the vibrational level thresholds of the transition-state [DE93-019252] p 1352 N94-19304

Supersonic jets from bevelled rectangular nozzles [NASA-TM-106403] p 1313 N94-19484

SUPERSONIC NOZZLES

Electrically excited CO-lasers with gas dynamic cooling [DLR-FB-93-08] p 1437 N94-18061

MHD integrated topping cycle project [DE93-040520] p 1588 N94-18978

MHD Integrated Topping Cycle Project [DE93-040521] p 1589 N94-19055

SUPERSONIC SPEED

Numerical prediction of transition of the F-16 wing at supersonic speeds [NASA-CR-194407] p 1312 N94-19433

SUPERSONIC WIND TUNNELS

Error propagation equations and tables for estimating the uncertainty in high-speed wind tunnel test results [DE93-018685] p 1311 N94-18275

SUPERSYMMETRY

Tensorial structure of a q-deformed sp(4,R) superalgebra [DE93-624808] p 1545 N94-17685

Renormalizations in supersymmetric and nonsupersymmetric non-abelian Chern-Simons field theories with matter [DE93-626646] p 1593 N94-17748

Paragrassmann analysis and quantum groups [DE93-628593] p 1561 N94-18168

Experimental consequences of supersymmetry [DE93-018270] p 1569 N94-18945

SUPPORT SYSTEMS

Reference model for project support environments, version 1.0 [AD-A269110] p 1520 N94-18251

Lunar base Controlled Ecological Life Support System (LCELSS): Preliminary conceptual design study [NASA-CR-188479] p 1511 N94-18484

SURFACE DEFECTS

Defects in GaAs bulk crystals and multi-layers caused by In diffusion [DE93-016968] p 1595 N94-18054

Surface modification of sapphire for IR window application [DE93-019168] p 1602 N94-19075

SURFACE DIFFUSION

Tunneling microscopy of semiconductors [AD-A270232] p 1600 N94-18904

SURFACE DISTORTION

Measuring machines for digitalizing and measuring complex surfaces, models and matrices [CRIF-MC-97] p 1444 N94-17963

A benchmark bending test of a thick specimen. Part 1: Experiments [AD-A268730] p 1360 N94-18325

SURFACE EMITTING LASERS

Spectrally and temporally resolved laser emission from vertical cavity surface emitting lasers [DE93-019410] p 1442 N94-19563

SURFACE FINISHING

Titanium carbon-hydrogen layers on decorative surfaces p 1375 N94-18010

Effect of temperature and O-ring gland finish on sealing ability of Viton V747-75 [NASA-TP-3391] p 1368 N94-18075

Soft X Ray Projection Lithography. Organization of the 1993 photonics science optical meetings [AD-A269159] p 1579 N94-18693

Synchrotron/crystal sample preparation [NASA-CR-193837] p 1603 N94-19513

Precision machining and polishing of scintillating crystals for large calorimeters and hodoscopes [DE93-018663] p 1381 N94-19544

SURFACE GEOMETRY

Morphology of polymerized membranes on an amorphous substrate at molecular resolution by AFM [AD-A268760] p 1370 N94-18403

SURFACE LAYERS

Mechanical properties of excimer laser modified titanium surfaces [DE93-012663] p 1358 N94-17875

Time-resolved probing of electron thermal conduction in femtosecond-laser-pulse-produced plasmas [DE93-016996] p 1585 N94-18129

SURFACE NAVIGATION

Survey of collision avoidance and ranging sensors for mobile robots, revision 1 [AD-A269846] p 1541 N94-18474

SURFACE PROPERTIES

Friction drive position transducer [AD-D015851] p 1424 N94-17717

A radial transmission line material measurement apparatus [DE93-018508] p 1394 N94-17780

Mechanical properties of excimer laser modified titanium surfaces [DE93-012663] p 1358 N94-17875

Surface second harmonic generation studies of stepped Ag(111) electrode surfaces [AD-A265205] p 1594 N94-17876

Accelerated tests on the tarnish resistance of gold alloys p 1367 N94-18008

Energy efficiency and the environment: Innovative ways to improve air quality in the Los Angeles Basin [DE93-016964] p 1473 N94-18050

Working group for planetary system nomenclature [NASA-CR-194406] p 1626 N94-18841

Surface modification of sapphire for IR window application [DE93-019168] p 1602 N94-19075

SURFACE REACTIONS

Interdisciplinary research on wear of materials [AD-A268190] p 1443 N94-17730

Kinetic growth of random-like and ballistic-like deposition models [DE93-624946] p 1595 N94-17956

Accelerated tests on the tarnish resistance of gold alloys p 1367 N94-18008

Report of the 1991 Workshop on Particle-Material Interactions for Fusion Research [DE93-788393] p 1573 N94-18156

The land component of the global climate system with adequate spatial resolution [DE93-018951] p 1474 N94-18183

Experimental and theoretical investigation of surface chemistry induced by direct and indirect electronic excitation [AD-A268846] p 1348 N94-18221

Hydrolysis reaction and positronium decay in silica gels [AD-A270028] p 1371 N94-18713

Scaling laws for diamond chemical vapor deposition. Diamond surface chemistry [AD-A269874] p 1599 N94-18745

Ionic and molecular environments in heterogeneous electrocatalysis: Studies by radioactive labeling and LEED/AUGER spectroscopy [AD A268850] p 1567 N94-18766

Surface species in tribology [AD-A270970] p 1446 N94-19754

SURFACE ROUGHNESS

Experimental contribution to the contact between two bodies and the effect of roughness [ECL-91-41] p 1451 N94-17918

Turbulence modeling in aircraft icing p 1412 N94-18555

Multigrid methods for flow transition in three-dimensional boundary layers with surface roughness [NASA-CR-4540] p 1417 N94-18843

Synchrotron/crystal sample preparation [NASA-CR-193837] p 1603 N94-19513

Precision machining and polishing of scintillating crystals for large calorimeters and hodoscopes [DE93-018663] p 1381 N94-19544

Comparative evaluation of Kirchhoff, perturbation, and full wave methods for rough surface scattering [AD-A271198] p 1392 N94-19718

Atomic-scale friction measurements using friction force microscopy. Part 2: Application to magnetic media
[AD-A270759] p 1447 N94-19767

SURFACE TEMPERATURE
Development of a multi-point two-color pyrometer for tube and wall temperature and emissivity measurement at the CFFF
[DE93-014716] p 1429 N94-18207
The application of liquid crystal techniques to determine heat transfer rates p 1432 N94-18654

SURFACE TREATMENT
The effect of surface treatment and gaseous rust protection paper on the atmospheric corrosion stability of aluminium alloy
[DE93-623326] p 1355 N94-17679
Cutting and drilling studies using high power visible lasers
[DE93-019149] p 1441 N94-19294

SURFACE WATER
Oil spreading in surface waters with an ice cover
[PB93-190767] p 1476 N94-19064
Mathematical modeling of the free surface hydrodynamic and of transport in suspensions of non cohesive sediments: Aid to the interpretation of spatial images
[ETN-93-95011] p 1421 N94-19502

SURFACE WAVES
The phase mixing of shear Alfven waves
[DE93-624920] p 1581 N94-17688
Resonant absorption of Alfven waves near a neutral point
[DE93-628761] p 1586 N94-18172
High resolution geological site characterization utilizing ground motion data
[AD-A268926] p 1481 N94-18485
Constraints on crustal structure from long period pressure and displacement measurements on the deep seafloor
[AD-A269931] p 1498 N94-18663
Surface wave group velocity tomography of East Asia, part 1
[AD-A270100] p 1484 N94-18868
Inverse scattering of surface waves: A new look at surface consistency
[REPT-93-25] p 1486 N94-19140
An iterative inverse scattering method for the removal of scattered surface waves
[REPT-93-18] p 1488 N94-19644

SURFACTANTS
Cooperative formation of inorganic-organic interfaces in the synthesis of silicate mesostructures
[AD-A271196] p 1375 N94-19742

SURGERY
Multimodal image correlation applied to computer aided pedicular screwing
[ETN-93-95018] p 1528 N94-19363

SURVEILLANCE
Military applications of high-accuracy frequency standards and clocks
[AD-A269303] p 1430 N94-18299

SURVEILLANCE RADAR
Military applications of high-accuracy frequency standards and clocks
[AD-A269303] p 1430 N94-18299

SURVEYS
Magnetic Fusion Energy Technology Fellowship: Report on survey of institutional coordinators
[DE93-014646] p 1583 N94-17739
Rapid geophysical surveyor
[DE93-016637] p 1461 N94-17851
A survey on technical problems in designing high-speed rotors with developing materials
[DE93-788519] p 1444 N94-18159
Aircrew life support, AFSC 122X0(1T1X1)
[AD-A268998] p 1511 N94-18394
Survey of collision avoidance and ranging sensors for mobile robots, revision 1
[AD-A269846] p 1541 N94-18474
Commercialization effort in support of electroslag-casting technology
[DE93-017988] p 1366 N94-19733

SUSPENSIONS
Electrokinetic transport of heterogeneous particles in suspensions
[NASA-CR-194478] p 1353 N94-19367

SWEPT FORWARD WINGS
High lift and the forward swept wing
p 1308 N94-18436
X-29: Research aircraft
[NASA-TM-109370] p 1318 N94-18962

SWEPT WINGS
Comparison between swept and delta canards on a model of a combat aircraft
[AD-A269561] p 1317 N94-17826
Viscous-inviscid calculation of high-lift separated compressible flows over airfoils and wings
p 1309 N94-18440
Numerical prediction of transition of the F-16 wing at supersonic speeds
[NASA-CR-194407] p 1312 N94-19433

SWEPTBACK WINGS
An experimental investigation of the optimum slat setting on a combat aircraft model p 1308 N94-18431
An experimental investigation of attachment-line transition on the slat of a combat aircraft model
p 1308 N94-18432

SWIRLING
Collaborative research on combustion diagnostics and modeling between Rolls-Royce, Inc. and the United States Air Force Wright Laboratory
[AD-A270660] p 1354 N94-19778

SWITCHES
Fabrication process for cantilever beam micromechanical switches
[AD-A269716] p 1404 N94-18749
Improved optical pseudospark switch
[AD-D015821] p 1580 N94-18947

SWITCHING
Plasma-puff initiation of high Coulomb transfer switches
[NASA-CR-193186] p 1591 N94-19441

SWITCHING CIRCUITS
Pulsed LASER for testing silicon strip detectors
[DE93-017816] p 1436 N94-17883
Training product unit neural networks with genetic algorithms p 1399 N94-18354
Asynchronous sequential circuit design using pass transistor iterative logic arrays p 1402 N94-18376
Pulse mode VLSI asynchronous circuits
p 1402 N94-18377
Improved self arbitrated VLSI asynchronous circuits
p 1402 N94-18378
Compensation approach for three or more dimensional random walks
[PB93-197499] p 1543 N94-19326
Evaluation of laser diode based optical switches for optical processors
[AD-A270949] p 1581 N94-19602

SYMMETRY
On the difference caused by CP violation in the energy spectra of pions in K(sup (+-))(yields)(pi)(+-)(pi)(+-)(pi)-+ decays
[DE93-624828] p 1564 N94-17687
Beauty without charm in B-meson decays
[PREPRINT-732] p 1565 N94-17972
Deformed traces and covariant quantum algebras for quantum groups GL(sub qp)(2) and GL(sub qp)(1/1)
[DE93-629862] p 1561 N94-18153
About symmetry of the gravitational action
[DE93-629955] p 1608 N94-18252
The theory of linear programming: Skew symmetric self-dual problems and the central path
[REPT-93-15] p 1524 N94-19089

SYNAPSES
The identification of the computational significance of key neurobiological characteristics found in a number of telencephalic brain regions
[AD-A269374] p 1505 N94-18407

SYNCHRONISM
On asynchronous testing
[MEMO-INF-93-03] p 1543 N94-19226
Systolic design with asynchronous controls for digital-signal processing
[AD-A270976] p 1392 N94-19680

SYNCHROTRON RADIATION
Conical geometry for sagittal focusing as applied to x rays from synchrotrons
[DE93-017238] p 1593 N94-17760
Nonlinear Thomson scattering of intense laser pulse from beams and plasmas
[AD-A269556] p 1438 N94-18460
A tunable compact high power far-infrared grating free-electron laser
[AD-A269875] p 1440 N94-18771
Simulation of the ALS longitudinal multibunch feedback system
[DE93-019227] p 1575 N94-19152
Study of coupled-bunch collective effects in the ALS
[DE93-019236] p 1575 N94-19558

SYNCHROTRONS
Synchrotron beam-loading stability with a higher RF harmonic
[DE93-014549] p 1573 N94-17726
Conical geometry for sagittal focusing as applied to x rays from synchrotrons
[DE93-017238] p 1593 N94-17760
Magnetic field measurements of a superconducting undulator for a Harmonic Generation FEL experiment at the NSLS
[DE93-017621] p 1438 N94-18504
Laser powered beam conditioner for free-electron lasers and synchrotrons
[DE93-017821] p 1441 N94-18974
The 1982 to 1992 decade of research on the vacuum ultraviolet ring at National Synchrotron Light Source
[DE93-019469] p 1603 N94-19564

SYNOPTIC METEOROLOGY
Spectral analysis of synoptic time scale disturbances over the tropical eastern Pacific during summer 1989, 1990 and 1991
[AD-A268821] p 1490 N94-18206
Reports of the 1992 Synoptic Symposium
[KNMI-TR-151] p 1494 N94-19698

SYNTAX
Proposal for a numerical array library
[DE93-015017] p 1516 N94-17786
Better termination analysis for active databases
[REPT-93-026] p 1614 N94-18144
Attribute evaluation during generalized parsing
[MEMO-INF-92-85] p 1526 N94-19224
Feasibility study in linguistically motivated object-oriented conceptual design of information systems
[PB93-197754] p 1618 N94-19331

SYNTHESIS (CHEMISTRY)
Modified aequorin shows increased bioluminescence activity
[AD-A268774] p 1347 N94-18185
Conversion of ethane and of propane to higher olefin hydrocarbons
[DE93-015282] p 1347 N94-18194
Synthesis of higher alcohols from carbon monoxide and hydrogen in a slurry reactor
[DE93-015086] p 1347 N94-18209
Nanostructured materials: Mind over matter
[DE93-017690] p 1597 N94-18480
Royal Society of Chemistry, Heterocyclic Chemistry Group, Lakeland Heterocyclic Symposium
[AD-A270374] p 1338 N94-18703
Temperature lowering in cryogenic chemical-synthesis techniques and system
[DE93-018348] p 1562 N94-18810
Molecular and polymeric ceramic precursors
[DE93-040364] p 1372 N94-18891
Final report on subcontract B076260 — borate synthesis
[DE93-019501] p 1604 N94-19565
Isolation mechanisms in III-V devices
[AD-A271197] p 1605 N94-19717

SYNTHETIC APERTURE RADAR
Flight demonstration of image fix-taking with SAR
[DE93-016499] p 1382 N94-17861
Tomographic mathematical ideas applied to radar detection
[AD-A268789] p 1384 N94-18186
AN/APS-137 Forward Looking Airborne Radar (FLAR) evaluation Spring 1992 experiment
[AD-A268899] p 1384 N94-18228
The spatial variance of ionospherically-induced phase errors in SAR imagery
[DE93-015643] p 1385 N94-18232
Arctic ice studies
[AD-A268608] p 1497 N94-18277
Application of Fourier-based features for classification of synthetic aperture radar imagery
[AD-A270450] p 1387 N94-18513
Resolution in radar mapping
[AD-A269730] p 1462 N94-18753
Modeling of current features in Gulf Stream SAR imagery
[AD-A270734] p 1499 N94-19609
Theoretical and experimental research on coherent microwave backscatter from the ocean
[AD-A271276] p 1500 N94-19743

SYNTHETIC FUELS
Fifteenth Symposium on Biotechnology for Fuels and Chemicals: Program and Abstracts
[DE93-010005] p 1376 N94-18045
Data collection plan for phase 2 Alternative Fuels Bus Data Collection Program
[DE93-010047] p 1378 N94-18913

SYSTEM EFFECTIVENESS
Denver TMA assessment
[NASA-CR-4554] p 1315 N94-18844
Molten carbonate fuel cell networks: Principles, analysis, and performance
[DE93-000281] p 1468 N94-18925

SYSTEM FAILURES
Workshop on multifactor aging mechanisms and models
[AD-A268668] p 1397 N94-18311
On timing faults in digital logic circuits
[AD-A268714] p 1402 N94-18400

SYSTEM IDENTIFICATION
Advances in the identification of transfer function models using Prony analysis
[DE93-017980] p 1548 N94-18094

SYSTEMS ANALYSIS
TANGO: A notation for describing advanced transaction models
[REPT-93-014] p 1613 N94-17936
An overview of the SAFSIM computer program
[DE93-017657] p 1519 N94-18002
Specification and analysis of a high speed transport protocol
[AD-A268941] p 1386 N94-18449
Deadbeat control by measurement feedback: A two sided approach
[REPT-93-20] p 1542 N94-19091
Scale sensitivity in the multiplicative AHP and SMART
[REPT-93-37] p 1611 N94-19157
Context-related scaling of human judgement in the multiplicative AHP, SMART and ELECTRE
[REPT-93-38] p 1611 N94-19158
Goal-driven LOTOS execution
[MEMO-INF-93-04] p 1527 N94-19227
A unified performability evaluation framework for computer and communication systems
[MEMO-INF-93-21] p 1537 N94-19264
Optimal safety system design using fault tree analysis
[MATHS-REPT-A-187] p 1529 N94-19382

SYSTEMS ENGINEERING
Reference model for project support environments, version 1.0
[AD-A269110] p 1520 N94-18251
VHDL simulation with access to transistor models
p 1402 N94-18381
Lunar base Controlled Ecological Life Support System (LCELSS): Preliminary conceptual design study
[NASA-CR-188479] p 1511 N94-18484
Integrated Terminal Weather System (ITWS)
[AD-A269684] p 1492 N94-18684
Operator performance in pattern matching as a function of reference material structure
[AD-A269889] p 1509 N94-18686
The development of a course sequence in real-time systems design
[AD-A269459] p 1522 N94-18726
MHD Integrated Topping Cycle Project
[DE93-040521] p 1589 N94-19055
Pegasus: Operating system support for distributed multimedia systems
[MEMO-INF-92-76] p 1536 N94-19160
The Cluster spacecraft p 1330 N94-19635
Systems engineering for Air Force C3I systems
[AD-A270482] p 1391 N94-19676

SYSTEMS INTEGRATION
On the use of differential GPS for automatic approach and landing of space and aircraft
[DLR-MITT-93-05] p 1316 N94-17921
Coordination of software-development activities among sites that are geographically separated
[DE93-019201] p 1524 N94-19076
Problem of control in an integral vision system: Use of a multi-agent system
[ETN-93-95007] p 1530 N94-19488

SYSTEMS MANAGEMENT
The organizational preparation of existing relational databases for the integration of expert systems
[AD-A268823] p 1614 N94-18191
Report of the Second CLICOM Experts Meeting
[WCDMP-19] p 1495 N94-19705

SYSTEMS SIMULATION
Goal-driven LOTOS execution
[MEMO-INF-93-04] p 1527 N94-19227
Sensitivity and uncertainty analysis of Markov reward models
[MEMO-INF-92-89] p 1559 N94-19386
Automated qualitative modeling of dynamic physical systems
[AD-A270835] p 1422 N94-19598

SYSTEMS STABILITY
Control of nonlinear systems
[AD-A270141] p 1542 N94-18898

SYSTOLIC ARRAYS
Systolic array IC for genetic computation
p 1400 N94-18361
A bit serial first level calorimeter trigger for an LHC detector
[USIP-92-08] p 1574 N94-18845
A programmable systolic trigger processor for FERA-bus data
[USIP-92-04] p 1405 N94-19292
Systolic design with asynchronous controls for digital-signal processing
[AD-A270976] p 1392 N94-19680

T

TABLES (DATA)
Station climatic summaries, North America. Volume 2: Alaska, Canada and Greenland
[AD-A269793] p 1493 N94-18732
Solar radiation in Saudi Arabia
[AD-A269970] p 1493 N94-18781

TABS (CONTROL SURFACES)
Compilation of 1992 annual reports of the navy ELF communications system ecological monitoring program. Volume 3: Tabs G - I
[AD-A269727] p 1388 N94-18741

TABULATION PROCESSES
FEEST: A method for tabulating equation of state and opacity tables
[DE93-017965] p 1347 N94-18092

TAGN
Molecular structure of low temperature form of triaminoguanidinium nitrate (TAGN)
[AD-A270409] p 1377 N94-18708

TAKEOFF
Wake structure and aerodynamic behavior of high lift aircraft configurations during unsteady maneuvers in ground effect p 1309 N94-18439
Procedures and design data for the formulation of aircraft configurations
[AD-A270150] p 1318 N94-18779

TAKEOFF RUNS
Take-off performance monitoring system algorithm and display development
[NLR-TP-91395-U] p 1317 N94-17734

TANTALUM
Dislocation-drag contribution to high-rate plastic deformation in shock-loaded tantalum
[DE93-018286] p 1361 N94-18802
Dynamical behavior of tantalum
[DE93-017877] p 1362 N94-18919
Influence of peak pressure and temperature on the shock-loading response of tantalum
[DE93-018561] p 1457 N94-19279

TARGET ACQUISITION
AN/APS-137 Forward Looking Airborne Radar (FLAR) evaluation Spring 1992 experiment
[AD-A268899] p 1384 N94-18228
Environmental characterization for target acquisition. Report 3: New concepts for evaluating low-grazing angle radar measurements
[AD-A269956] p 1388 N94-18777
The star identification, pointing and tracking system of UVSTAR, an attached payload instrument system for the Shuttle Hitchhiker-M platform p 1326 N94-19179

TARGET RECOGNITION
An analog retina model for detecting dim moving objects against a bright moving background
p 1399 N94-18350
Operator performance in pattern matching as a function of reference material structure
[AD-A269889] p 1509 N94-18686
Environmental characterization for target acquisition. Report 3: New concepts for evaluating low-grazing angle radar measurements
[AD-A269956] p 1388 N94-18777
Applications of motion estimation in image processing
[FEL-92-B356] p 1580 N94-19455
A non-homogeneous, spatio-temporal, wavelet multiresolution analysis and its application to the analysis of motion
[AD-A270621] p 1538 N94-19534
Tracking with time-delayed data in multisensor systems
[AD-A271334] p 1391 N94-19582

TARGETS
Hydrodynamic instability modeling for ICF
[DE93-018634] p 1587 N94-18274
A program for passively tracking a target using an array of sensors
[DE93-019554] p 1390 N94-19306
Effects of location cuing on redundant target processing
[IZF-1993-B-1] p 1510 N94-19443

TASK PLANNING (ROBOTICS)
Efficient domain-independent experimentation
[AD-A269530] p 1557 N94-18640

TASKS
Building a joint-service classification research roadmap: Criterion-related issues
[AD-A269735] p 1512 N94-18754

TATB
The use of post detonation analysis of stable isotope ratios to determine the type and production process of the explosive involved
[DE93-018497] p 1378 N94-19242

TAYLOR SERIES
A finite strain ring dynamical model for pneumatic tires
[AD-A269286] p 1444 N94-18266
Error propagation equations and tables for estimating the uncertainty in high-speed wind tunnel test results
[DE93-018685] p 1311 N94-18275

TDR SATELLITES
TDRS press release
[NASA-TM-109373] p 1335 N94-18965

TEACHING MACHINES
Computer-assisted instruction and natural language systems
[MEMO-INF-92-86] p 1527 N94-19225

TEAMS
Cognitive limitations in coordination in hierarchical information processing structures
[AD-A268825] p 1616 N94-18535

TEARING MODES (PLASMAS)
Resonant absorption of Alfven waves near a neutral point
[DE93-628761] p 1586 N94-18172

TECHNOLOGICAL FORECASTING
Emerging technologies planning guide, 1993 edition — information systems technology
[DE93-017196] p 1616 N94-18689

TECHNOLOGIES
Solid State Sciences Committee Forum
[AD-A270454] p 1342 N94-18715
Program descriptions
[NSF-92-123] p 1531 N94-19619

TECHNOLOGY ASSESSMENT
Metals 2000
[DE93-016761] p 1355 N94-17752
Cost effective energy strategies for the reduction of CO2 emissions in the United States: Country report for ETSAP Annex 4
[DE93-016842] p 1472 N94-17852
Information technology resources assessment
[DE93-015276] p 1613 N94-17894
Critical technologies for reactors used in nuclear electric propulsion
[DE93-017685] p 1337 N94-17909
Laboratory microfusion capability study
[DE93-014373] p 1583 N94-17912
The stability and utility of the ESPRIT project, MUSIC, performance-based indicators of usability and tools: An evaluation of the usability of the NPL iSDX telephone system
[NPL-DITC-213/92] p 1613 N94-17925
The perspectives in application of hot casting technology for ceramic parts of timekeeping devices
p 1375 N94-18013
Safeguarding our energy future
[DE93-016001] p 1466 N94-18109
Workshop on Innovation in Materials Processing and Manufacture: Exploratory Concepts for Energy Applications
[DE93-017674] p 1467 N94-18478
Fatigue technology assessment and strategies for fatigue avoidance in marine structures. Appendices
[AD-A269053] p 1455 N94-18716
Survey of ceramic machining in Japan
[DE93-018277] p 1372 N94-18946

TECHNOLOGY TRANSFER
Interactive Collaborative Environments (ICE) in the design to manufacturing process
[DE93-014994] p 1518 N94-17944
Lightweight materials for transportation: Program plan
[DE93-017381] p 1340 N94-18087
White House technology reinvestment project: Briefing and transcripts
[PB93-169829] p 1611 N94-18090
New applications for high average power beams
[DE93-018845] p 1439 N94-18522
Solid State Sciences Committee Forum
[AD-A270454] p 1342 N94-18715
MHD technology transfer, integration and review committee
[DE93-040519] p 1588 N94-18892
Silicon concentrator solar cell research
[DE93-018489] p 1468 N94-19015
The applications of modified metals in the construction industry
[VTT-TIED-1329] p 1365 N94-19374
Manufacturing technology
[DE93-019580] p 1381 N94-19480

TECHNOLOGY UTILIZATION
Current information technology resource requirements of the federal government: Fiscal year 1994
p 1612 N94-17756
Lightweight materials for transportation: Program plan
[DE93-017381] p 1340 N94-18087
Safeguarding our energy future
[DE93-016001] p 1466 N94-18109

Engineering research, development and technology thrust area report, FY92
[DE93-016334] p 1632 N94-18856

Beryllium processing technology review for applications in plasma-facing components
[DE93-018396] p 1363 N94-19028

Application of new technologies in the virtual library: Seminars in Turkey, Portugal, and Spain
[NASA-TM-109718] p 1611 N94-19131

Space Applications Industrial Laser System (SAILS)
p 1325 N94-19173

The applications of modified metals in the construction industry
[VTT-TIED-1329] p 1365 N94-19374

Legacy of the X Ray Laser Program
[DE93-019550] p 1442 N94-19554

Commercialization effort in support of electroslag-casting technology
[DE93-017988] p 1366 N94-19733

TECTONICS

Belgian Royal Observatory Communications, Series A, No. 104, Geophysics Series No. 175
[COMMUNICATIONS-SER-A-104] p 1482 N94-18622

Current (1985-1988) seismic activity in Belgium: Comparison with historical and instrumental seismic data
p 1482 N94-18624

What can gravimetry contribute to recent and current tectonics in Belgium? p 1482 N94-18626

Applications of Quaternary stratigraphic, soil-geomorphic, and quantitative geomorphic analyses to the evaluation of tectonic activity and landscape evolution in the Upper Coastal Plain, South Carolina
[DE93-016269] p 1484 N94-18725

The interpretation of crustal dynamics data in terms of plate motions and regional deformation near plate boundaries
[NASA-CR-194302] p 1487 N94-19432

TELECOMMUNICATION

The stability and utility of the ESPRIT project, MUSiC, performance-based indicators of usability and tools: An evaluation of the usability of the NPL iSDX telephone system
[NPL-DITC-213/92] p 1613 N94-17925

Broadband RF spectrum from electrostatic discharges on spacecraft
[AD-A269543] p 1385 N94-18287

CONTACT: An Air Force technical report on military satellite control technology
[AD-A269375] p 1334 N94-18408

Morphology and characteristics of disturbed HF skywave channels
[AD-A269755] p 1388 N94-18722

Compilation of 1992 annual reports of the navy ELF communications system ecological monitoring program. Volume 3: Tabs G - I
[AD-A269727] p 1388 N94-18741

Optoelectronic packaging: A review
[DE93-040059] p 1515 N94-19535

Program descriptions
[NSF-92-123] p 1531 N94-19619

TELECONFERENCING

Information technology resources assessment
[DE93-015276] p 1613 N94-17894

TELEMETRY

Missile antenna pattern coordinate system and data formats
[AD-A269153] p 1385 N94-18260

A rugged, low-cost advanced data acquisition system for field test projects
[DE93-010041] p 1615 N94-18334

TELEOPERATORS

Magnetostrictive actuators for human sensory feedback
[AD-A269266] p 1511 N94-17841

TELEROBOTICS

Magnetostrictive actuators for human sensory feedback
[AD-A269266] p 1511 N94-17841

TELESCOPES

Origins of solar activity. First year report, AASERT grant
[AD-A268848] p 1629 N94-18222

Calibration of a high frequency monostatic acoustic echosounder
[AD-A268901] p 1481 N94-18229

Space debris detection
[AD-A269254] p 1334 N94-18264

Laser guide star measurements at Lawrence Livermore National Laboratory
[DE93-018081] p 1441 N94-19251

TEMPERATURE

The temperature at the phase boundary during quasi-static motions of a two-phase thermoelastic bar
[AD-A268769] p 1596 N94-18388

TEMPERATURE CONTROL

Substrate temperature measurement and control during thermal plasma CVD
[DE93-040305] p 1433 N94-19135

TEMPERATURE DEPENDENCE

Phase transitions and neutron scattering
[DE93-016748] p 1594 N94-17866

Pulsed LASER for testing silicon strip detectors
[DE93-017816] p 1436 N94-17883

Fin-efficiency calculation for condensation in the presence of noncondensable gases
[DE93-017684] p 1409 N94-18004

Effect of phase change in a debris cloud on a backwall structure
[DE93-017506] p 1358 N94-18100

Relaxation of polar orientational order in nonlinear optical polymers by second harmonic generation
[AD-A269059] p 1370 N94-18515

In-situ growth monitoring of molecular beam epitaxy processes
[AD-A269287] p 1598 N94-18616

In situ observation of radiation induced amorphization of crystals with apatite structure
[DE93-018450] p 1599 N94-18816

Densities and viscosities of ternary ammonia/water fluids
[DE93-015966] p 1351 N94-19118

Thermodynamic q-distributions that aren't
[DE93-017385] p 1609 N94-19121

Selective methane oxidation over promoted oxide catalysts
[DE93-040002] p 1351 N94-19132

Thermophysical properties
[DE93-040219] p 1351 N94-19134

Selective methane oxidation over promoted oxide catalysts
[DE93-040001] p 1351 N94-19150

A simple description of flow instability with application to a packed bed
[DE93-017492] p 1420 N94-19345

Ultraviolet absorption cross-sections of some carbonyl compounds and their temperature dependence
[AERONAUTICA-ACTA-A-368-199]
p 1353 N94-19456

Temperature of aircraft cargo flame exposure during accidents involving fuel spills
[DE93-019633] p 1381 N94-19539

Excited atomic bromine energy transfer and quenching mechanisms
[AD-A270672] p 1572 N94-19607

Testing of protective coatings in hydrogen
[DE93-040326] p 1375 N94-19651

TEMPERATURE DISTRIBUTION

Mixture distributions in climatological research
[DE93-014125] p 1488 N94-17942

Development of a selective volumetric receiver for central receiver systems: Investigation of parameters and exergetic evaluation
[DLR-FB-93-05] p 1465 N94-18089

Spectral analysis of synoptic time scale disturbances over the tropical eastern Pacific during summer 1989, 1990 and 1991
[AD-A268821] p 1490 N94-18206

Application of infrared thermography in fluid mechanics p 1431 N94-18649

Liquid crystal heat transfer measurements
p 1432 N94-18653

TEMPERATURE EFFECTS

Modeling microstructural evolution and the mechanical response of superplastic materials
[DE93-014417] p 1355 N94-17711

Atlas of formability: Ultimet
[AD-A268352] p 1355 N94-17767

Atlas of formability: HAYNES 556
[AD-A268354] p 1356 N94-17768

Atlas of formability: HAYNES 188
[AD-A268355] p 1356 N94-17769

Atlas of formability: NICKELVAC K-500
[AD-A268351] p 1356 N94-17772

Atlas of formability: Haynes 230
[AD-A268325] p 1356 N94-17788

Atlas of formability: INCONEL 718
[AD-A268350] p 1356 N94-17789

Atlas of formability: Hastelloy C-22
[AD-A268324] p 1356 N94-17796

Atlas of formability: Permalloy - 80 flow stress curves
[AD-A268263] p 1356 N94-17801

Atlas of formability: Nickelvac C-276
[AD-A268264] p 1357 N94-17802

Atlas of formability: Ti-6Al-4V ELI
[AD-A268300] p 1357 N94-17803

Atlas of formability: ALLVAC 718
[AD-A268304] p 1357 N94-17804

Atlas of formability: Waspaloy
[AD-A268323] p 1593 N94-17805

Charpy impact toughness of martensitic steels irradiated in FFTF: Effect of heat treatment
[DE93-015960] p 1450 N94-17848

Synchronisation of cold induced vasodilation at various locations of one hand
[IZF-1992-B3] p 1504 N94-17966

Fin-efficiency calculation for condensation in the presence of noncondensable gases
[DE93-017684] p 1409 N94-18004

Effect of temperature and O-ring gland finish on sealing ability of Viton V747-75
[NASA-TP-3391] p 1368 N94-18075

Effect of phase change in a debris cloud on a backwall structure
[DE93-017506] p 1358 N94-18100

Evaluation of physiological and psychological impairment of human performance in cold stressed subjects
[AD-A268637] p 1506 N94-18632

Work plan for the Marine Aerosol Properties and the Thermal Imager Performance Trial (MAPTIP)
[AD-A270026] p 1483 N94-18712

Nondestructive inspection of graphite-epoxy laminates for heat damage using DRIFT and LPF spectroscopies
[DE93-017228] p 1343 N94-18761

LX-17 chemical kinetic material model for Chemical TOPAZ2D
[DE93-014363] p 1377 N94-18893

Effect of internal heating during hot compression testing on the stress-strain behavior and hot working characteristics of alloy 304L
[DE93-012701] p 1362 N94-18917

Environmental degradation of Alloy 600 and welded filler metal EN82 in an elevated temperature aqueous environment
[DE93-018049] p 1363 N94-18940

Thermal stresses in the microchannel heatsink cooled by liquid nitrogen
[DE93-018660] p 1418 N94-18995

Effects of irradiation temperature on Charpy and tensile properties of high-copper, low upper-shelf, submerged-arc welds
[DE93-017858] p 1445 N94-19047

Densities and viscosities of ternary ammonia/water fluids
[DE93-015966] p 1351 N94-19118

Thermodynamic q-distributions that aren't
[DE93-017385] p 1609 N94-19121

Shrinkage void formation and its effect on freeze and thaw processes of lithium and lithium-fluoride for space applications
[DE93-019303] p 1338 N94-19128

Influence of peak pressure and temperature on the shock-loading response of tantalum
[DE93-018561] p 1457 N94-19279

Suppressed electron-phonon scattering in superlattices
[AD-A270834] p 1604 N94-19597

Pressure and temperature effects on the kinetics and quality of diamond films
[AD-A270876] p 1606 N94-19771

TEMPERATURE GRADIENTS

Transport in the self-organized relaxed state of ion temperature gradient instability
[DE93-016769] p 1584 N94-17983

Geothermal activity near Clearlake, California
[DE93-016627] p 1485 N94-18894

Finite difference program for calculating hydride bed wall temperature profiles
[DE93-019272] p 1523 N94-19005

A laboratory model of a cooled continental shelf
[AD-A270862] p 1500 N94-19792

TEMPERATURE MEASUREMENT

Considerations for the use of the modified line reversal technique for gas temperature measurement
[DE93-015752] p 1576 N94-17857

Mixture distributions in climatological research
[DE93-014125] p 1488 N94-17942

Boundary layer heat budgets from wind profiler/RASS data: A feasibility study
[DE93-013187] p 1489 N94-18052

Development of a multi-point two-color pyrometer for tube and wall temperature and emissivity measurement at the CFFF
[DE93-014716] p 1429 N94-18207

Flame structure studies of a lean 20-torr H2/N2O/Ar flame employing molecular beam mass spectrometry
[AD-A268889] p 1349 N94-18456

Fundamentals of infrared thermography
p 1431 N94-18648

Heat transfer quantitative characterization: Passive and active methods p 1431 N94-18650

Liquid crystal heat transfer measurements
p 1432 N94-18653

The application of liquid crystal techniques to determine heat transfer rates p 1432 N94-18654

Imaging and blackbody emission spectra of hot particulates generated during laser ablation
[DE93-015818] p 1439 N94-18724
Substrate temperature measurement and control during thermal plasma CVD
[DE93-040305] p 1433 N94-19135
Construction and evaluation of an environmental chamber for calibration of temperature and pressure sensors for laser interferometers emperature and pressure sensors for laser interferometers)
[PB93-197838] p 1322 N94-19332

TEMPERATURE MEASURING INSTRUMENTS
Construction and evaluation of an environmental chamber for calibration of temperature and pressure sensors for laser interferometers emperature and pressure sensors for laser interferometers)
[PB93-197838] p 1322 N94-19332

TEMPERATURE PROFILES
An atlas of bathy-thermograph temperature cross-sections for Coral and Tasman Sea transects from 1960 to 1987
[AD-A268775] p 1497 N94-18329
Flame structure studies of a lean 20-torr H2/N2O/Ar flame employing molecular beam mass spectrometry
[AD-A268889] p 1349 N94-18456
Finite difference program for calculating hydride bed wall temperature profiles
[DE93-019272] p 1523 N94-19005

TEMPERATURE SENSORS
Synoptic ocean prediction experiment. EN216 CTD section data report
[AD-A268903] p 1497 N94-18230
Description of an infrared zoomcollimator
[FEL-93-A034] p 1580 N94-19424

TEMPLATES
Developmental testing of a prototype all-reflection Michelson interferometer
[AD-A269064] p 1430 N94-18406
Template based low data rate speech encoder
[AD-A270900] p 1392 N94-19748

TEMPORAL DISTRIBUTION
Observations of comets with the IUE
[NASA-CR-193652] p 1624 N94-17843
Spatiotemporal variability of non-urban ozone concentrations over the eastern United States and its potential replication by satellite data
[PB93-191328] p 1476 N94-19065
Radial evolution of the solar wind turbulence with application to charged particle transport
[NASA-CR-194081] p 1629 N94-19427

TEMPORAL RESOLUTION
An RS-170 to 700 frame per second CCD camera
[DE93-018367] p 1432 N94-18828
Spectrally and temporally resolved laser emission from vertical cavity surface emitting lasers
[DE93-019410] p 1442 N94-19563

TENSILE PROPERTIES
The Hall-Petch relationship and mechanisms of fracture in B2 compounds
[DE93-018887] p 1359 N94-18182
Effects of irradiation temperature on embrittlement of nuclear pressure vessel steels
[DE93-015428] p 1359 N94-18245
Continuum modeling of materials that can undergo martensitic phase transitions
[AD-A268767] p 1360 N94-18386
Development of ductile Fe3Al-based aluminides
[DE93-017865] p 1362 N94-18938
Tensile properties of as-cast iron-aluminide alloys
[DE93-017852] p 1363 N94-18975
Effects of irradiation temperature on Charpy and tensile properties of high-copper, low upper-shelf, submerged-arc welds
[DE93-017858] p 1445 N94-19047

TENSILE STRESS
Assessment of an improved multiaxial strength theory based on creep-rupture data for Inconel 600
[DE93-015929] p 1356 N94-17791
Construction of a tension-torsion anisotropic brittle damage elastic model
[ECL-91-27] p 1457 N94-19375
Delamination in composite materials as observed using an optical fiber strain gage
[AD-A270803] p 1344 N94-19662

TENSILE TESTS
Effects of irradiation temperature on Charpy and tensile properties of high-copper, low upper-shelf, submerged-arc welds
[DE93-017858] p 1445 N94-19047

TENSORS
Tensorial structure of a q-deformed sp(4,R) superalgebra
[DE93-624808] p 1545 N94-17685

TERMINAL FACILITIES
Terminal area forecasts, FY 1993-2005
[AD-A269855] p 1316 N94-18336

TERMINOLOGY
Technical development of a theory of programs
[ETN-93-95058] p 1532 N94-19652

TERMS
Defense Technical Information Center thesaurus
[AD-A268855] p 1615 N94-18319

TERNARY ALLOYS
Magnetic properties of single-crystalline UCu3Al2
[DE93-016607] p 1593 N94-17744
Magnetic and crystallographic structures in UTX intermetallic compounds
[DE93-018291] p 1605 N94-19735

TERNARY SYSTEMS
Calculation of the LiF-CeF3-BeF2 and LiF-PuF3-BeF2 ternary phase diagrams
[DE93-017437] p 1360 N94-18501

TERRACES (LANDFORMS)
Applications of Quaternary stratigraphic, soil-geomorphic, and quantitative geomorphic analyses to the evaluation of tectonic activity and landscape evolution in the Upper Coastal Plain, South Carolina
[DE93-016269] p 1484 N94-18725

TERRAIN
Environmental characterization for target acquisition. Report 3: New concepts for evaluating low-grazing angle radar measurements
[AD-A269956] p 1388 N94-18777
Robot navigation in unknown terrains: Introductory survey of non-heuristic algorithms
[DE93-019221] p 1316 N94-19300
Remote sensing of Earth terrain
[NASA-CR-194598] p 1464 N94-19681

TERRESTRIAL PLANETS
Planetary plasma waves
[NASA-CR-194295] p 1629 N94-19094

TEST CHAMBERS
Acoustic intensity measurements in the presence of low Mach number flow
[AD-A269995] p 1562 N94-18664

TEST FACILITIES
High-efficiency silicon concentrator cell commercialization
[DE93-018491] p 1467 N94-18409
A register of underwater acoustic test facilities in the US, Canada, and the United Kingdom
[AD-A270884] p 1500 N94-19785

TEST FIRING
Technology test bed
[NASA-TM-109354] p 1322 N94-18953

TEST STANDS
Technology test bed
[NASA-TM-109354] p 1322 N94-18953

TEXTBOOKS
A teaching tool for linear programming
[AD-A270240] p 1523 N94-18905

TEXTS
Intelligent help facilities: Generating natural language descriptions with examples
[AD-A269555] p 1521 N94-18290
Automatic documentation generation: The interaction of text and examples
[AD-A269670] p 1616 N94-18570
Generating object descriptions: Intergrating examples with text
[AD-A269992] p 1522 N94-18680

THALLIUM
Fabrication and microstructural development of Ag-clad TlBa2Ca2Cu3O(x) tapes
[DE93-017407] p 1597 N94-18500
Preparation and characterisation of the compound Tl(0.65) Bi(0.35) Ca(0.8) Sr(1.7) Cu2 O(y) using oxalate coprecipitation and analytical CBED and an initial preparation of Bi2Ca(n-1) Sr2Cu(n) O(4+2n) for n=5
[DE93-625470] p 1602 N94-19277

THEOREM PROVING
Contribution to the analysis of tableaus based decision methods
[ETN-93-94355] p 1560 N94-18067
Formal hardware verification of digital circuits
p 1401 N94-18367
Updated Contributions to the Twente Workshop on Hamiltonian Graph Theory
[MEMO-1076] p 1554 N94-19683
On Hamilton-connectedness of Cayley graphs
p 1554 N94-19684
On Hamiltonian properties of 2-tough graphs
p 1554 N94-19685
The complete closure of a graph
p 1555 N94-19690
Twenty odd statements in Twente
p 1555 N94-19691
Generalized closures of graphs p 1555 N94-19692

THEOREMS
Polling systems: Moment stability of station times and central limit theorems
[PB93-191955] p 1560 N94-18990
Attribute evaluation during generalized parsing
[MEMO-INF-92-85] p 1526 N94-19224
Excursions of stochastic processes, Cox-point processes, entrance behavior and resolvents
[PB93-197291] p 1558 N94-19323
On Hamilton-connectedness of Cayley graphs
p 1554 N94-19684

THEORETICAL PHYSICS
On the difference caused by CP violation in the energy spectra of pions in K(sup (+-))(yields)(pi)(+-)(pi)(+-)(pi)-+ decays
[DE93-624828] p 1564 N94-17687
International Centre for Theoretical Physics, Trieste Scientific activities in 1991
[DE93-624757] p 1606 N94-17792
Center of Excellence in Theoretical Geoplasma Research
[AD-A270210] p 1588 N94-18902
Experimental research in high energy physics
[DE93-011912] p 1574 N94-18916
Extensions of 2D gravity
[DE93-018525] p 1485 N94-18929
Search for top quark with D0 detector
[DE93-040170] p 1572 N94-19536

THERMAL ANALYSIS
FEM/SINDA: Combining the strengths of NASTRAN, SINDA, I-DEAS, and PATRAN for thermal and structural analysis p 1449 N94-17831
Heat load analysis on the cable-in-conduit with central core conductor for the TF coil Rebut layer design
[DE93-013783] p 1395 N94-17872
Current development in selected stress and thermal analysis software interfaces with PRO-ENGINEER
[DE93-014935] p 1518 N94-17943
Infrared detection with high-(Tc bolometers and response of Nb tunnel junctions to picosecond voltage pulses
[DE93-016963] p 1595 N94-17989
Knowledge sources for an intelligent MCM analyzer
[AD-A269224] p 1542 N94-18887
Thermal analysis of coatings and substrate materials during a disruption in fusion reactors
[DE93-017688] p 1588 N94-18971
Accelerated screening methods for determining chemical and thermal stability of refrigerant-lubricant mixtures. Part 1: Method assessment
[DE93-040215] p 1351 N94-19136
Thermo-hydraulic analysis of superconducting toroidal-field magnets for the Tokamak Physics Experiment
[DE93-018096] p 1590 N94-19269
Effects of pressure on the orientational ordering and phase transitions in solid C(60) and C(70)
[DE93-018858] p 1603 N94-19347
Proceedings: International Symposium on Thermal Engineering and Science for Cold Regions
[AD-A270636] p 1487 N94-19529

THERMAL BOUNDARY LAYER
Experimental investigation of turbulent Prandtl number and Reynolds analogy in transitional and post-transitional boundary layers
[AD-A270092] p 1418 N94-18867

THERMAL CONDUCTIVITY
Coupled MHD and transport analysis of improved confinement D3-D discharges
[DE93-016985] p 1585 N94-18057
Development of a cryogenic heat pipe
[DE93-018448] p 1417 N94-18831

THERMAL CONTROL COATINGS
Robotics
[NASA-TM-109351] p 1332 N94-18920

THERMAL CYCLING TESTS
Microstructurally based thermomechanical fatigue lifetime model of solder joints for electronic applications
[DE93-016508] p 1452 N94-17995
Embrittlement of surface mount solder joints by hot solder-dipped, gold-plated leads
[DE93-017659] p 1358 N94-18003
Structural stability of 1100 C heated Pd/k during absorption cycling in protium
[DE93-016270] p 1346 N94-18048
Solderability perservative coatings: Electroless tin versus organic azoles
[DE93-017634] p 1370 N94-18477
Damage accumulation in advanced metal matrix composites under thermal cycling/creep loadings
[AD-A271207] p 1344 N94-19720

THERMAL DEGRADATION
Study on radiation-induced deterioration of grease at high temperature, 3
[DE93-788368] p 1369 N94-18220
Workshop on multifactor aging mechanisms and models
[AD-A268668] p 1397 N94-18311

THERMAL DIFFUSION
LX-17 chemical kinetic material model for Chemical TOPAZ2D
[DE93-014363] p 1377 N94-18893

THERMAL ENERGY
Techniques for the estimation of Heats of Explosion (HEX) using thermochemical codes
[AD-A268584] p 1609 N94-18310
Melt spinning study
[NASA-CR-193823] p 1380 N94-19423

THERMAL EXPANSION
Structural stability of 1100 C heated Pd/k during absorption cycling in protium
[DE93-016270] p 1346 N94-18048

THERMAL FATIGUE
Finite difference program for calculating hydride bed wall temperature profiles
[DE93-019272] p 1523 N94-19005

THERMAL INSULATION
Thermal insulation of wet shielded metal arc welds
[AD-A268697] p 1445 N94-18465

THERMAL MAPPING
Infrared thermography p 1432 N94-18652

THERMAL NEUTRONS
Criticality benchmark comparisons leading to cross-section upgrades
[DE93-017184] p 1556 N94-18073
Thermal neutron multiplicity measurements using the pyrochemical multiplicity counter at Lawrence Livermore National Laboratory
[DE93-018538] p 1571 N94-19278

THERMAL PLASMAS
Advanced fusion diagnostics
[DE93-040085] p 1589 N94-19133
Substrate temperature measurement and control during thermal plasma CVD
[DE93-040305] p 1433 N94-19135

THERMAL PROTECTION
LX-17 chemical kinetic material model for Chemical TOPAZ2D
[DE93-014363] p 1377 N94-18893

THERMAL RESISTANCE
Study on radiation-induced deterioration of grease at high temperature, 3
[DE93-788368] p 1369 N94-18220
The fire resistance of profiled thin steel sheet structures
[VTT-TIED-1320] p 1380 N94-19373

THERMAL STABILITY
Study on radiation-induced deterioration of grease at high temperature, 3
[DE93-788368] p 1369 N94-18220
Analysis of deposit precursors in jet fuels using Fourier transform infrared spectroscopy
[AD-A269035] p 1377 N94-18489
Strained ring energetic binders
[AD-A269056] p 1377 N94-18491
Accelerated screening methods for determining chemical and thermal stability of refrigerant-lubricant mixtures. Part 1: Method assessment
[DE93-040215] p 1351 N94-19136
Isolation mechanisms in III-V devices
[AD-A271197] p 1605 N94-19717

THERMAL STRESSES
Workshop on multifactor aging mechanisms and models
[AD-A268668] p 1397 N94-18311
Effect of internal heating during hot compression testing on the stress-strain behavior and hot working characteristics of alloy 304L
[DE93-012701] p 1362 N94-18917
Thermal stresses in the microchannel heatsink cooled by liquid nitrogen
[DE93-018660] p 1418 N94-18995

THERMOCHEMISTRY
Techniques for the estimation of Heats of Explosion (HEX) using thermochemical codes
[AD-A268584] p 1609 N94-18310

THERMOCOUPLES
Flame structure studies of a lean 20-torr H2/N2O/Ar flame employing molecular beam mass spectrometry
[AD-A268889] p 1349 N94-18456

THERMODYNAMIC CYCLES
Thermodynamic theory of exergy analysis
[PB93-187847] p 1607 N94-18120
Adsorption analysis of ammonia in an aqueous solution
[DE93-019512] p 1353 N94-19552

THERMODYNAMIC PROPERTIES
A new multiphase equation of state for iron
[DE93-017629] p 1357 N94-17819
Diffusion in ordered alloys
[AD-A268232] p 1359 N94-18322
Carbon/carbon composites coated with SiC by chemical vapor deposition
[AD-A269934] p 1341 N94-18544
Wettability and reaction kinetics in metal matrix composites
[AD-A270377] p 1342 N94-18704
Structure-property relationships in radical-cation (electron-donor molecule) and anion-based (including fullerides) organic superconductors and their use in the design of new materials
[DE93-018617] p 1601 N94-19022
A free energy simulation method based study of interfacial segregation
[DE93-019462] p 1364 N94-19032
Thermophysical properties
[DE93-040219] p 1351 N94-19134
Proceedings: International Symposium on Thermal Engineering and Science for Cold Regions
[AD-A270636] p 1487 N94-19529
Adsorption analysis of ammonia in an aqueous solution
[DE93-019512] p 1353 N94-19552
Supercritical thermodynamics of sulfur and nitrogen species
[DE93-041221] p 1610 N94-19670
Damage accumulation in advanced metal matrix composites under thermal cycling/creep loadings
[AD-A271207] p 1344 N94-19720
Pressure and temperature effects on the kinetics and quality of diamond films
[AD-A270876] p 1606 N94-19771

THERMODYNAMICS
Lectures of Fermi liquid theory
[DE93-016630] p 1592 N94-17714
Thermodynamics of computation and information distance
[DE93-012730] p 1517 N94-17812
Thermodynamic theory of exergy analysis
[PB93-187847] p 1607 N94-18120
Structure, thermodynamics, and dynamical properties of supercooled liquids
[DE93-788387] p 1607 N94-18211
The temperature at the phase boundary during quasi-static motions of a two-phase thermoelastic bar
[AD-A268769] p 1596 N94-18388
Competitive dynamics and self-organization in photorefractive systems
[AD-A269663] p 1430 N94-18569
Molten carbonate fuel cell networks: Principles, analysis, and performance
[DE93-000281] p 1468 N94-18925
Ground movements associated with gas hydrate production
[DE93-019887] p 1486 N94-19018
Energy Conversion and Storage Program
[DE93-018602] p 1469 N94-19098
Thermodynamic q-distributions that aren't
[DE93-017385] p 1609 N94-19121
Supercritical thermodynamics of sulfur and nitrogen species
[DE93-041221] p 1610 N94-19670

THERMOELASTICITY
The temperature at the phase boundary during quasi-static motions of a two-phase thermoelastic bar
[AD-A268769] p 1596 N94-18388

THERMOELECTRIC GENERATORS
Feasibility survey of thermoelectric conversion technology using semiconductors
[DE93-520882] p 1595 N94-18105
Ultrasonic technique for inspection of GPHS capsule girth weld integrity
[DE93-040072] p 1448 N94-19189

THERMOELECTRIC MATERIALS
Feasibility survey of thermoelectric conversion technology using semiconductors
[DE93-520882] p 1595 N94-18105

THERMOELECTRIC POWER GENERATION
Feasibility survey of thermoelectric conversion technology using semiconductors
[DE93-520882] p 1595 N94-18105

THERMOELECTRICITY
Deep ion implantation into manganin to modify its pressure and electrothermocharacteristics
[DE93-630229] p 1359 N94-18218

THERMOGRAPHY
Measurement Techniques
[VKI-LS-1993-05] p 1430 N94-18643
Fundamentals of infrared thermography
p 1431 N94-18648
Application of infrared thermography in fluid mechanics p 1431 N94-18649
Heat transfer quantitative characterization: Passive and active methods p 1431 N94-18650
Perspective and future possibilities
p 1431 N94-18651
Infrared thermography p 1432 N94-18652

THERMOMECHANICAL TREATMENT
Development of ductile Fe3Al-based aluminides
[DE93-017865] p 1362 N94-18938

THERMONUCLEAR REACTIONS
Generalized energy principle for flute perturbations in axisymmetric mirror machines
[DE93-019399] p 1589 N94-19037

THERMOPHORESIS
Transport phenomena and interfacial kinetics in multiphase combustion systems
[AD-A270202] p 1349 N94-18765

THERMOPHYSICAL PROPERTIES
Malone refrigeration
[DE93-014468] p 1379 N94-17725
Thermophysical properties
[DE93-040219] p 1351 N94-19134

THERMOPLASTIC RESINS
Analysis of pultrusion processing for long fiber reinforced thermoplastic composite system
[NASA-CR-194504] p 1339 N94-17766
Process for preparing thermoplastic composites
[AD-D015864] p 1339 N94-18074
Polymer technology publication. Series no. 14, 1993
[PB93-195964] p 1372 N94-19052

THERMOPLASTICITY
Analysis of pultrusion processing for long fiber reinforced thermoplastic composite system
[NASA-CR-194504] p 1339 N94-17766
Strained ring energetic binders
[AD-A269056] p 1377 N94-18491

THERMOREGULATION
Metabolic changes and hemodynamic dysfunction following hypothermic shock
[AD-A269780] p 1506 N94-18598

THERMOSETTING RESINS
Analysis of pultrusion processing for long fiber reinforced thermoplastic composite system
[NASA-CR-194504] p 1339 N94-17766
Molecular composites from liquid crystalline polymers and liquid crystalline thermosets
[DE93-016608] p 1368 N94-18096

THERMOSPHERE
A physical model for one-dimension and time-dependent ionosphere. Part 1: Description of the model
[DE93-627958] p 1486 N94-19255
Venus lower thermosphere studies
[NASA-CR-193546] p 1629 N94-19418

THESAURI
Defense Technical Information Center thesaurus
[AD-A268855] p 1615 N94-18319

THESES
Numerical and symbolic signal representation and processing
[AD-A270271] p 1389 N94-18811

THICKNESS
Development of the microstructure based stochastic life prediction model
[AD-A269742] p 1361 N94-18742
Foil support structure for large electron guns
[DE93-018478] p 1322 N94-18890

THIN FILMS
Vibrational and electronic properties of clusters and ultrathin films
[DE93-012291] p 1367 N94-17678
Polarized thin films from dye-substituted polymers containing hydrophobically terminated stilbazolium radicals
[AD-D015873] p 1367 N94-17706
Finite element modeling of evaporation and condensation during sol-gel film and fiber formation
[DE93-017655] p 1345 N94-17820
Superhardness effect in Au/Ni multilayers
[DE93-016444] p 1357 N94-17860
Experimental contribution to the contact between two bodies and the effect of roughness
[ECL-91-41] p 1451 N94-17918
Titanium carbon-hydrogen layers on decorative surfaces p 1375 N94-18010
Studies of interactions between conducting polymer and organic vapors: Applications to chemical sensing
[DE93-015694] p 1369 N94-18233
Synthesis and study of high-T(sub c) superconducting electronic materials
[AD-A268851] p 1402 N94-18390
Solderability perservative coatings: Electroless tin versus organic azoles
[DE93-017634] p 1370 N94-18477
Mesoepitaxy: A universal route to oriented materials
[AD-A270437] p 1598 N94-18511
Growth of structures for integrated optoelectronic devices
[AD-A269014] p 1598 N94-18527
In-situ growth monitoring of molecular beam epitaxy processes
[AD-A269287] p 1598 N94-18616
Integration of ferroelectric/semiconductor thin films for SLM and photorefractive applications
[AD-A268645] p 1598 N94-18633

Scaling laws for diamond chemical vapor deposition. Diamond surface chemistry
[AD-A269874] p 1599 N94-18745
Thin film studies of the proximity Josephson effect
[AD-A270129] p 1600 N94-18876
Polycrystalline thin-film cadmium telluride solar cells fabricated by electrodeposition
[DE93-018201] p 1468 N94-18944
Growth of epitaxial semiconductor alloys and superlattices with continuously variable composition by pulsed-laser ablation
[DE93-018726] p 1601 N94-18998
Some superhigh-frequency and magnetic properties of chemically precipitated films
[AD-A266195] p 1351 N94-19110
Elastic properties of amorphous thin films studied by Rayleigh waves
[DE93-018375] p 1372 N94-19202
The microstructural mechanism of electromigration failure in narrow interconnects of Al alloys
[DE93-018598] p 1365 N94-19282
Picoindentation hardness measurements using atomic force microscopy
[AD-A270877] p 1604 N94-19579
Ionized-cluster beam/partially ionized beam deposition of electro-optical and nonlinear optical organic materials and device development
[AD-A270832] p 1604 N94-19596
The deposition of electro-optic films on semiconductors
[AD-A270823] p 1605 N94-19664
Single source precursors for the OMCVD of 3/5 compound semiconductors
[AD-A271147] p 1606 N94-19739
Nanofabrication by focused ion beam
[AD-A271290] p 1345 N94-19746
Magnetic Ultrathin Films: Multilayers and Surfaces, Interfaces, and Characterization, volume 313
[AD-A271402] p 1375 N94-19758

THIN PLATES
Effect of phase change in a debris cloud on a backwall structure
[DE93-017506] p 1358 N94-18100
Toward a characterization of the debris cloud created in a hypervelocity impact on a thin plate
[AD-A269190] p 1455 N94-18864
Interfacial cracks in plates: A three-dimensional numerical investigation p 1456 N94-19116

THIN WALLED SHELLS
Current capabilities for simulating the extreme distortion of thin structures subjected to severe impacts
p 1459 N94-19474

THOMSON SCATTERING
Nonlinear Thomson scattering of intense laser pulse from beams and plasmas
[AD-A269556] p 1438 N94-18460

THREE DIMENSIONAL BOUNDARY LAYER
Viscous-inviscid calculation of high-lift separated compressible flows over airfoils and wings
p 1309 N94-18440
Multigrid methods for flow transition in three-dimensional boundary layers with surface roughness
[NASA-CR-4540] p 1417 N94-18843
The effect of fine surface riblets on the flow around an inclined axially symmetrical body
[MPIS-105/1993] p 1420 N94-19356

THREE DIMENSIONAL COMPOSITES
JPRS report: Science and technology. Central Eurasia: Materials science
[JPRS-UMS-93-002] p 1339 N94-18833

THREE DIMENSIONAL FLOW
Application of ARC/INFO to regional scale hydrogeologic modeling
[DE93-015673] p 1481 N94-18107
An algebraic turbulence model for turbomachinery
p 1411 N94-18554
Several examples where turbulence models fail in inlet flow field analysis p 1412 N94-18556
Theoretical examination of the flow around a cylinder with a low dimensional Galerkin process
[MPIS-25/1992] p 1422 N94-19525
Visualization of turbulent flow with particles
[REPT-93-31] p 1423 N94-19645

THREE DIMENSIONAL MODELS
Three-dimensional simulation analysis of the first sections of a standing-wave free-electron laser two-beam accelerator
[DE93-016977] p 1436 N94-17869
Texture splats for 3D vector and scalar field visualization
[DE93-017104] p 1520 N94-18130
High-performance multiprocessor architecture for a 3-D lattice gas model p 1400 N94-18362
The GARTEUR high lift research programme
p 1307 N94-18430
ADCIRC: An advanced three-dimensional circulation model for shelves, coasts, and estuaries. Report 3: Development of a tidal constituent database for the western North Atlantic and Gulf of Mexico
[AD-A268685] p 1497 N94-18455
3D composite grids using Bezier curves and surfaces in component adaptive methods
[AD-A269188] p 1549 N94-18863
Flow volumes for interactive vector field visualization
[DE93-017102] p 1418 N94-18888
Volume rendering of 3D scalar and vector fields at Lawrence Livermore National Laboratory
[DE93-018000] p 1528 N94-19276
Crossover from BCS to Bose superconductivity: A functional integral approach
[DE93-019503] p 1604 N94-19566

THRESHOLDS (PERCEPTION)
The effects of reverberant impulse noise (blast waves) on hearing: Parametric studies
[AD-A269242] p 1506 N94-18911

THRUST
Constant-thrust orbit-raising transfer charts
[AD-A269088] p 1334 N94-18718

THRUST CONTROL
Phasing strategies of the Hermes type space shuttle: Its optimization considering the thrust failures
[LAAS-93242] p 1544 N94-19361

THUNDERSTORMS
Station climatic summaries: North America. Volume 1: The contiguous United States
[AD-A269567] p 1490 N94-18303
Station climatic summaries, North America. Volume 2: Alaska, Canada and Greenland
[AD-A269793] p 1493 N94-18732

TIDES
ADCIRC: An advanced three-dimensional circulation model for shelves, coasts, and estuaries. Report 3: Development of a tidal constituent database for the western North Atlantic and Gulf of Mexico
[AD-A268685] p 1497 N94-18455
Method for extracting tidal and inertial motion from ARGOS ice buoys applied to the Barents Sea during CEAREX
[PB93-190213] p 1499 N94-19063

TILTMETERS
Instrumentation developed at the Royal Observatory of Belgium for measuring slow displacements of the Earth
p 1483 N94-18628

TIME
About time p 1426 N94-18024
Space and time from quantum mechanics
[DE93-015263] p 1609 N94-18629

TIME DEPENDENCE
Exact solution of the generalized time-dependent Jaynes-Cummings Hamiltonian
[DE93-624773] p 1546 N94-17811
Three-dimensional simulation analysis of the first sections of a standing-wave free-electron laser two-beam accelerator
[DE93-016977] p 1436 N94-17869
Variable time-step integration for intense field effects
[DE93-013296] p 1382 N94-17909
Practical reporting times for environmental samples
[DE93-013461] p 1472 N94-17910
The effects of initial conditions and control time on optimal actuator placement by way of a max-min genetic algorithm
[DE93-017640] p 1525 N94-19124
Asymptotic derivation of the modified time-dependent SP2 equations and numerical calculations
[DE93-016466] p 1551 N94-19342
Time dependent identification of nonlinear structures
[ECL-92-64] p 1457 N94-19403

TIME DIVISION MULTIPLEXING
VHF air/ground communications for air traffic control. Volume 1: A decision tree approach to system innovations
[AD-A268485] p 1316 N94-18384

TIME LAG
Shop problems with two machines and time lags
[REPT-93-020] p 1518 N94-17927
A method for eliminating skew introduced by non-uniform buffer delay and wire lengths in clock distribution trees
[AD-A270649] p 1544 N94-19530
Stabilization of time-delay systems: An overview of the algebraic approach
[PB93-191989] p 1553 N94-19556
Tracking with time-delayed data in multisensor systems
[AD-A271334] p 1391 N94-19582

TIME MARCHING
An algebraic turbulence model for turbomachinery
p 1411 N94-18554

TIME MEASUREMENT
Proceedings of the 4th European Congress on Chronometry
[ETN-93-94633] p 1424 N94-18006
The clocks and the perception of time in the 18th century society p 1424 N94-18007
About time p 1426 N94-18024
Marine chronometry in the Neuchatel mountains (Switzerland) p 1427 N94-18025
Restoration of an 18th century English clock
p 1427 N94-18026
Techniques for low consumption circuits
p 1428 N94-18032
Evaluation of the consumption of electronic clocks
p 1408 N94-18033
Development of atomic standards at the Neuchatel Observatory p 1428 N94-18038
Multifunction chronograph movement using a modular structure multimotor p 1429 N94-18044

TIME OF FLIGHT SPECTROMETERS
Detonation reaction steps frozen by free expansion and analyzed by mass spectrometry
[DE93-012734] p 1376 N94-17813
Matrix- and substrate-assisted laser desorption for fast DNA sequencing
[DE93-015332] p 1501 N94-18242
The study of the phase structure of hadronic matter by searching for the deconfined quark-gluon phase transition using 2 TeV (bar-p)-p collisions, and by searching for critical phenomena in an exclusive study of multifragmentation using 1 GeV/nucleon heavy ion collisions
[DE93-018925] p 1570 N94-19103

TIME OPTIMAL CONTROL
The effects of initial conditions and control time on optimal actuator placement by way of a max-min genetic algorithm
[DE93-017640] p 1525 N94-19124

TIME SERIES ANALYSIS
Linear parameter identification methods for ARMA models with periodic coefficients
[REPT-92-070] p 1556 N94-17938
Fast-training algorithm for hidden-layer forward-feed neural networks
[AD-A269253] p 1540 N94-18263
Spectral analysis on the canonical autoregressive decomposition
[AD-A270083] p 1549 N94-18798
A survey of current approaches to modelling of hydrological time-series with respect to climate variability and change
[WMO/TD-534] p 1463 N94-19435
Methods for description and control of dynamical systems and their application
[MPIS-17/1992] p 1553 N94-19522
Generalized multichannel signal detection
[AD-A271385] p 1391 N94-19587

TIME TEMPERATURE PARAMETER
FEM/SINDA: Combining the strengths of NASTRAN, SINDA, I-DEAS, and PATRAN for thermal and structural analysis p 1449 N94-17831
Mechanical response comparison of gun propellants evaluated under equivalent time-temperature conditions
[AD-A270479] p 1378 N94-19674

TIMING DEVICES
Proceedings of the 4th European Congress on Chronometry
[ETN-93-94633] p 1424 N94-18006
The clocks and the perception of time in the 18th century society p 1424 N94-18007
The perspectives in application of hot casting technology for ceramic parts of timekeeping devices
p 1375 N94-18013
The optimal numerical algorithm for processing of phase coded time signals for radio-clocks
p 1426 N94-18018
Marine chronometry in the Neuchatel mountains (Switzerland) p 1427 N94-18025
Restoration of an 18th century English clock
p 1427 N94-18026
The mystery of the perpetual motion clock of Geiser and Son p 1427 N94-18027
Gear train behavior analyzer using laser beam scanning for watch movement p 1427 N94-18028
Universal measurement device for electronic watches and small clocks p 1427 N94-18029
Reliability control for wrist watches and their casements p 1427 N94-18030
Mutrometre: Construction for fast water proof measurements under low pressure and air suppression
p 1427 N94-18031
Multifunction chronograph movement using a modular structure multimotor p 1429 N94-18044
Military applications of high-accuracy frequency standards and clocks
[AD-A269303] p 1430 N94-18299

TIN OXIDES
Solderability perservative coatings: Electroless tin versus organic azoles
[DE93-017634] p 1370 N94-18477
TIRES
A finite strain ring dynamical model for pneumatic tires
[AD-A269286] p 1444 N94-18266
Measuring methods for evaluation of dynamic tyre properties
[ETN-93-95054] p 1381 N94-19650
TITANATES
The electromechanical properties of tetragonal BaTiO3 and PbTiO3 single crystals
[DE93-019008] p 1603 N94-19550
TITANIA
Transport phenomena and interfacial kinetics in multiphase combustion systems
[AD-A270202] p 1349 N94-18785
TITANIUM
The efficiency of continuous output of some titanium-doped gem-crystal lasers has exceeded 1 W
[AD-A269953] p 1439 N94-18674
Multi-terrawatt, 100 fsec laser system using flashlamp-pumped, dye-converted Ti:sapphire as an amplifier
[DE93-017190] p 1440 N94-18889
TITANIUM ALLOYS
Atlas of formability: Ti-6Al-4V ELI
[AD-A268300] p 1357 N94-17803
Mechanical properties of excimer laser modified titanium surfaces
[DE93-012663] p 1358 N94-17875
Implementation of a nonisothermal unified inelastic-strain theory into ADINA6.0 for a titanium alloy: User guide
[AD-A269927] p 1360 N94-18660
Fatigue resistant Ti3Al composites
[AD-A270305] p 1341 N94-18692
Intelligent materials systems and structures. Part 4: The influence of thermomechanical loading on the life of shape memory alloys
[PB93-195923] p 1363 N94-18952
Bibliography on silicides
[AD-A270516] p 1374 N94-19532
Microstructure and texture control of fatigue in hydrogen and marine environments
[AD-A271277] p 1344 N94-19744
TITANIUM COMPOUNDS
Titanium carbon-hydrogen layers on decorative surfaces p 1375 N94-18010
TITANIUM NITRIDES
Sputtered TiN coatings in plastic
p 1367 N94-18011
TITANIUM OXIDES
Nanostructured materials: Mind over matter
[DE93-017690] p 1597 N94-18480
Optical properties of oxide coatings prepared by ion-assisted deposition
[AD-A270024] p 1599 N94-18711
TOKAMAK DEVICES
Power compensators for phased operation of antenna arrays on JET and D3-D
[DE93-013208] p 1581 N94-17694
Arc detection and protection in high-power antenna systems
[DE93-013272] p 1382 N94-17695
ITER EDA design confinement capability
[DE93-013729] p 1582 N94-17697
Limits on m = 2, n = 1 error field induced locked mode instability in TPX with typical sources of poloidal field coil error field and a proto type correction coil, C-coil
[DE93-014408] p 1582 N94-17702
Using the Tritium Plasma Experiment to evaluate ITER PFC safety
[DE93-016614] p 1582 N94-17713
Plasma properties research: Task 3
[DE93-017087] p 1583 N94-17854
Heat load analysis on the cable-in-conduit with central core conductor for the TF coil Rebut layer design
[DE93-013783] p 1395 N94-17872
Filamentation, current profiles and transport in a tokamak
[DE93-016768] p 1584 N94-17948
Transport in the self-organized relaxed state of ion temperature gradient instability
[DE93-016769] p 1584 N94-17983
Analysis of the ITER H-mode confinement database
[DE93-016984] p 1585 N94-18056
Dependence of helium transport on plasma current and ELM frequency in H-mode discharges in D3-D
[DE93-016986] p 1585 N94-18058
AEOLUS-IT MHD simulation code based on a toroidally incompressible plasma model
[DE93-788461] p 1586 N94-18157
User's manual of Tokamak Simulation Code
[DE93-788388] p 1586 N94-18212
Active neutral particle diagnostics for high temperature plasma
[DE93-788457] p 1586 N94-18214
Ion mobility and transport barriers in the tokamak plasmas
[DE93-040320] p 1587 N94-18524
Parametric analysis of the ARIES-3D-He-3 tokamak reactor
[DE93-018293] p 1587 N94-18803
Thermal analysis of coatings and substrate materials during a disruption in fusion reactors
[DE93-017688] p 1588 N94-18971
Viscosity in the edge of tokamak plasmas
[DE93-018039] p 1588 N94-18988
Review Committee report on the conceptual design of the tokamak physics experiment
[DE93-018408] p 1588 N94-19012
The effects of radiolysis on the corrosion and stress corrosion behavior of 316 stainless steels
[DE93-019933] p 1363 N94-19021
Lower hybrid counter current drive for edge current density modification in D3-D
[DE93-019157] p 1589 N94-19073
Experiments on nonlinear absorption of ECH waves in MTX and a comparison with theory
[DE93-019158] p 1589 N94-19074
Thermo-hydraulic analysis of superconducting toroidal-field magnets for the Tokamak Physics Experiment
[DE93-018096] p 1590 N94-19269
ICRF direct electron heating experiments in TFTR
[DE93-017857] p 1590 N94-19273
Electron cyclotron resonance heating in the microwave tokamak experiment
[DE93-018083] p 1590 N94-19289
Radiative divertor modeling studies
[DE93-018092] p 1590 N94-19290
Behavior of the particle transport coefficients near the density limit in MTX
[DE93-019108] p 1591 N94-19311
Modelization, numerical simulation and optimal control of NET tokamak plasma configuration evolution for the future generation of fusion reactors
[ETN-93-95019] p 1591 N94-19364
Theoretical studies of turbulence and anomalous transport in toroidal confinement devices
[DE93-040684] p 1592 N94-19656
TOMOGRAPHY
Tomographic mathematical ideas applied to radar detection
[AD-A268789] p 1384 N94-18186
Surface wave group velocity tomography of East Asia, part 1
[AD-A270100] p 1484 N94-18868
Single sided tomography of extremely large dense objects
[DE93-017993] p 1580 N94-19268
TOPOGRAPHY
Three-dimensional high-resolution seismic profiling on the New Jersey outer continental shelf
[AD-A269835] p 1498 N94-18600
JPRS report: Central Eurasia. Aviation and cosmonautics, no. 1, January 1993
[JPRS-UAC-93-007] p 1632 N94-19147
Measurements of ocean surface and bottom backscattering strengths in the northwestern Atlantic Ocean
[AD-A270893] p 1500 N94-19786
TOPOLOGY
WBNGRID, a program for generation of C-H and C-O topology grids around wing/body/nacelle configurations: User's guide
[FFA-TN-1992-09] p 1311 N94-17721
Working visit to the University of L'Aquila, Italy
[FEL-93-B020] p 1618 N94-19452
The effects of initial conditions on the 3-D topology of temporally evolving wakes (ARI on 3-D bluff body wakes)
[AD-A271008] p 1423 N94-19774
TOROIDAL PLASMAS
Limits on m = 2, n = 1 error field induced locked mode instability in TPX with typical sources of poloidal field coil error field and a proto type correction coil, C-coil
[DE93-014408] p 1582 N94-17702
Self-regulated shear flow turbulence in confined plasmas
[DE93-015823] p 1583 N94-17743
Transport in the self-organized relaxed state of ion temperature gradient instability
[DE93-016769] p 1584 N94-17983
Toroidal solenoids in the electromagnetic field and Aharonov-Casher effect
[DE93-629861] p 1566 N94-18152
User's manual of Tokamak Simulation Code
[DE93-788388] p 1586 N94-18212
Ion mobility and transport barriers in the tokamak plasmas
[DE93-040320] p 1587 N94-18524
Lower hybrid counter current drive for edge current density modification in D3-D
[DE93-019157] p 1589 N94-19073
Finite beta plasma equilibrium in toroidally linked mirrors
[DE93-040318] p 1590 N94-19193
Modelization, numerical simulation and optimal control of NET tokamak plasma configuration evolution for the future generation of fusion reactors
[ETN-93-95019] p 1591 N94-19364
Theoretical studies of turbulence and anomalous transport in toroidal confinement devices
[DE93-040684] p 1592 N94-19656
TORQUE
Tooth form design supporting system in module design p 1428 N94-18036
Cooperative control of multiple space manipulators
[AD-A270291] p 1445 N94-18813
Dimensional crossover in the torque in a layered superconductor
[DE93-019544] p 1407 N94-19553
TORQUEMETERS
Control of torque in stepping motors of quartz watches and clocks p 1408 N94-18023
TORSIONAL STRESS
Construction of a tension-torsion anisotropic brittle damage elastic model
[ECL-91-27] p 1457 N94-19375
TORUSES
Contact 3-manifolds, integrable Hamiltonian systems and exotic symplectic structures in R(sup 4)
[DE93-624767] p 1551 N94-19248
TOTAL OZONE MAPPING SPECTROMETER
October 1979-1989 Southern Hemisphere total ozone as seen by TOMS
[NASA-TM-109375] p 1476 N94-18967
TOTAL QUALITY MANAGEMENT
Document control and conduct of operations
[DE93-016555] p 1613 N94-17880
Quality, management, and the interplay of self-assessment, process assessments, and performance-based observations
[DE93-018787] p 1448 N94-19336
TOUCH
Cortical substrate of haptic representation
[AD-A269583] p 1508 N94-18304
Robot navigation in unknown terrains: Introductory survey of non-heuristic algorithms
[DE93-019221] p 1316 N94-19300
TOUGHNESS
Charpy impact toughness of martensitic steels irradiated in FFTF: Effect of heat treatment
[DE93-015960] p 1450 N94-17848
Mechanism-dependent fractal character of fracture surfaces in high strength and toughness ASTM A723 steels
[AD-A268956] p 1360 N94-18542
TOXIC HAZARDS
Review of short-term, high-level exposure to metals: Antimony, barium, and cadmium
[AD-A268896] p 1505 N94-18392
A review and evaluation of the ADAM 2.1 dispersion model
[AD-A269896] p 1474 N94-18688
TOXICITY
A review and evaluation of the ADAM 2.1 dispersion model
[AD-A269896] p 1474 N94-18688
The role of chemical inhibition of gap junctional intercellular communication in toxicology
[AD-A269251] p 1502 N94-18924
A study of the effect of hydrocarbon structure on the induction of male rat nephropathy and metabolic structure
[AD-A270969] p 1504 N94-19789
TOXICOLOGY
Review of short-term, high-level exposure to metals: Antimony, barium, and cadmium
[AD-A268896] p 1505 N94-18392
The role of chemical inhibition of gap junctional intercellular communication in toxicology
[AD-A269251] p 1502 N94-18924
TRACE CONTAMINANTS
A technique for measuring winds in the lower atmosphere using incoherent Doppler lidar
[DE93-017163] p 1488 N94-17758
Analysis of HgI2 and PbI2 crystals and detectors by Particle-Induced X Ray Emission (PIXE) and Ion Backscattering Spectroscopy (IBS)
[DE93-017168] p 1594 N94-17896
A mobile remote sensing laboratory for water vapor, trace gas, aerosol, and wind speed measurements
[DE93-017158] p 1489 N94-18132

CDIAC catalog of numeric data and computer model packages
[DE93-017675] p 1475 N94-18832
Suitability of infrared spectroscopy for remote sensing of tropospheric trace gases
[KFK-5183] p 1479 N94-19507
Application of an atmospheric dispersion model to simulated pollutant releases in the Colorado Front range
[DE93-017118] p 1480 N94-19732

TRACE ELEMENTS
Carbon Dioxide Information Analysis Center: FY 1992 activities
[DE93-013845] p 1471 N94-17774
Analysis of HgI2 and PbI2 crystals and detectors by Particle-Induced X Ray Emission (PIXE) and Ion Backscattering Spectroscopy (IBS)
[DE93-017168] p 1594 N94-17896
CDIAC catalog of numeric data and computer model packages
[DE93-017675] p 1475 N94-18832
Global three dimensional model of tropospheric trace gases chemistry and transport
[AERONAUTICA-ACTA-A-370-199] p 1479 N94-19518

TRACKING (POSITION)
Tracking with time-delayed data in multisensor systems
[AD-A271334] p 1391 N94-19582
A stereoscopic vision system with applications to automated docking and tracking
[AD-A270754] p 1333 N94-19765

TRACKING FILTERS
Tracking with time-delayed data in multisensor systems
[AD-A271334] p 1391 N94-19582

TRACTION
Continuum modeling of materials that can undergo martensitic phase transitions
[AD-A268767] p 1360 N94-18386
The longitudinal free vibrations of a fixed-free two-phase elastic bar
[AD-A268768] p 1453 N94-18387
The temperature at the phase boundary during quasi-static motions of a two-phase thermoelastic bar
[AD-A268769] p 1596 N94-18388

TRAILING EDGE FLAPS
Calculation of maximum and high lift characteristics of multi element aerofoils p 1305 N94-18419
Efficient simulation of incompressible viscous flow over multi-element airfoils p 1306 N94-18421
Navier-Stokes calculations on multi-element airfoils using a chimera-based solver p 1306 N94-18422
Numerical solution of the Navier-Stokes equations for high-lift configurations on structured composite grids p 1306 N94-18423
High Reynolds number configuration development of a high-lift airfoil p 1306 N94-18424
A viscous-inviscid solver for high-lift incompressible flows over multi-element airfoils at deep separation conditions p 1306 N94-18425
Prediction of the high-lift performance of multi-element aerofoils using an unstructured Navier-Stokes solver p 1307 N94-18427
Navier-Stokes simulation of flow field around a blown-flap high-lift system p 1307 N94-18429
An experimental investigation of the optimum slat setting on a combat aircraft model p 1308 N94-18431
An experimental investigation of attachment-line transition on the slat of a combat aircraft model p 1308 N94-18432
Viscous phenomena affecting high-lift systems and suggestions for future CFD development p 1308 N94-18433
In-flight pressure distributions and skin-friction measurements on a subsonic transport high-lift wing section p 1308 N94-18435
High lift and the forward swept wing p 1308 N94-18436
A fast computing method for the flow over high-lift wings p 1308 N94-18437
Calculation of multielement airfoils and wings at high lift p 1309 N94-18438
Forty years of high-lift R/D: An aircraft manufacturer's experience p 1309 N94-18441
High-lift research: Application to the design of the ATR72 flap p 1309 N94-18442
The aero-mechanical design of a novel Fowler flap mechanism p 1309 N94-18443
High-lift design for large civil aircraft p 1310 N94-18445
High lift systems for transport aircraft with advanced airfoils p 1310 N94-18446
Choice and optimization of a high-lift system for an advanced amphibious aircraft p 1310 N94-18447

TRAILING EDGES
Lift enhancement device
[AD-D015868] p 1317 N94-17704
A design procedure for slotted flaps p 1305 N94-18418

TRAINING ANALYSIS
Aircrew life support, AFSC 122X0(1T1X1)
[AD-A268998] p 1511 N94-18394

TRAJECTORIES
Application of the A* algorithm to aircraft trajectory generation
[AD-A268728] p 1317 N94-18315
Cooperative control of multiple space manipulators
[AD-A270291] p 1445 N94-18813

TRAJECTORY ANALYSIS
Flexible integration of path-planning capabilities
[AD-A269594] p 1541 N94-18463
Constant-thrust orbit-raising transfer charts
[AD-A269088] p 1334 N94-18718
Electrokinetic transport of heterogeneous particles in suspensions
[NASA-CR-194478] p 1353 N94-19367

TRAJECTORY CONTROL
An application of parameter estimation to the stability and control of the BQM-147 unmanned aerial vehicle
[AD-A268741] p 1321 N94-18401
ControlShell: A real-time software framework
[AD-A269172] p 1523 N94-18879

TRAJECTORY MEASUREMENT
About the accuracy of an image-based navigation system during the runway approach
[DLR-MITT-93-01] p 1316 N94-18146
Missile antenna pattern coordinate system and data formats
[AD-A269153] p 1385 N94-18260

TRAJECTORY OPTIMIZATION
Application of the A* algorithm to aircraft trajectory generation
[AD-A268728] p 1317 N94-18315
Flexible integration of path-planning capabilities
[AD-A269594] p 1541 N94-18463

TRAJECTORY PLANNING
Flexible integration of path-planning capabilities
[AD-A269594] p 1541 N94-18463
Adaptive path planning: Algorithm and analysis
[DE93-008348] p 1523 N94-18926

TRANSCONDUCTANCE
Field emitter array RF amplifier development project, phase 1, option 1
[AD-A268687] p 1396 N94-18293
DC and small-signal physical models for the AlGaAs/GaAs high electron mobility transistor p 1401 N94-18370

TRANSDUCERS
Evaluation of the production-grade class 4 flextensional transducer shell
[AD-A268796] p 1340 N94-18201
Residual strain measurement on the production-grade class 4 flextensional transducer shell
[AD-A268828] p 1430 N94-18537
Transducers and method for making same
[AD-D015949] p 1408 N94-19759

TRANSFER FUNCTIONS
Fast-training algorithm for hidden-layer forward-feed neural networks
[AD-A269253] p 1540 N94-18263
Acoustic propagation modeling using MATLAB
[AD-A270905] p 1564 N94-19750

TRANSFORMATIONS (MATHEMATICS)
Groups on transformations in Finslerian spaces
[DE93-624765] p 1606 N94-17794
A noniterative improvement of Guyan reduction p 1449 N94-17833
Avoiding degenerate coframes in an affine gauge approach to quantum gravity
[DE93-013146] p 1607 N94-17892
Deformed traces and covariant quantum algebras for quantum groups GL(sub qp)(2) and GL(sub qp)(1/1)
[DE93-629862] p 1561 N94-18153
On paragrassmann differential calculus
[DE93-628594] p 1548 N94-18169
A general solution of the BV-master equation and BRST field theories
[DE93-628622] p 1561 N94-18171
EDF tests for normality in linear models after a Box-Cox transformation
[AD-A269068] p 1557 N94-18517

TRANSFORMERS
Solid-state, resistive hydrogen sensors for safety monitoring
[DE93-017769] p 1424 N94-17778

TRANSFUSION
Evaluation of dried storage of platelets for transfusion: Physiologic integrity and hemostatic functionality
[AD-A270756] p 1507 N94-19593

TRANSIENT HEATING
Liquid crystal heat transfer measurements p 1432 N94-18653
A simple description of flow instability with application to a packed bed
[DE93-017492] p 1420 N94-19345

TRANSIENT LOADS
Transient response of a viscous and anchored liquid bridge to an axial pulse
[LRT-WE-9-FB-7-1992] p 1379 N94-19492

TRANSIENT RESPONSE
Transient response of a viscous and anchored liquid bridge to an axial pulse
[LRT-WE-9-FB-7-1992] p 1379 N94-19492
Methods for description and control of dynamical systems and their application
[MPIS-17/1992] p 1553 N94-19522
Simulation of the behavior of micro-electronic capacitive pressure sensors
[LAAS-93190] p 1434 N94-19659

TRANSISTOR LOGIC
Asynchronous sequential circuit design using pass transistor iterative logic arrays p 1402 N94-18376
Pulse mode VLSI asynchronous circuits p 1402 N94-18377
Improved self arbitrated VLSI asynchronous circuits p 1402 N94-18378
VHDL simulation with access to transistor models p 1402 N94-18381

TRANSISTORS
VLSI for high-speed digital signal processing
[AD-A270406] p 1404 N94-18706
Superconducting flux flow devices, digital circuits and memories
[DE93-019072] p 1405 N94-19079

TRANSITION FLOW
Research activities at the Center for Modeling of Turbulence and Transition p 1410 N94-18546
Numerical investigation of complex, transitional, and chemically reacting flows p 1411 N94-18550
Numerical prediction of transition of the F-16 wing at supersonic speeds
[NASA-CR-194407] p 1312 N94-19433

TRANSITION METALS
Pressure induced metallization of the Mott Insulator 6(sub 2)
[DE93-018296] p 1600 N94-18969
Resonance Raman and photophysical studies of transition metal complexes in solution and entrapped in zeolites
[DE93-019892] p 1363 N94-19019
Electrocatalysts for oxygen electrodes
[DE93-040446] p 1354 N94-19653

TRANSITION POINTS
Dynamical behavior of octahedrite from the Henbury meteorite
[DE93-018834] p 1627 N94-19339

TRANSITION TEMPERATURE
Phase separation and superconductivity in La2CuO(4 + delta): Effects of oxygen diffusion
[DE93-016610] p 1594 N94-17907
Role of pressure in the study of fullerenes
[DE93-018839] p 1602 N94-19340

TRANSMISSION EFFICIENCY
Tooth form design supporting system in module design p 1428 N94-18036

TRANSMISSION ELECTRON MICROSCOPY
Characterization of vapor plume species and deposition residues resulting from pulsed laser ablation of a graphite/epoxy composite
[AD-A270101] p 1343 N94-18869
High resolution transmission electron microscopy of mesoporous MCM-41 type materials
[AD-A271271] p 1354 N94-19728

TRANSMISSION LINES
Design and test of a low jitter metal to metal contact solid dielectric switch
[DE93-016957] p 1394 N94-17755
A radial transmission line material measurement apparatus
[DE93-018508] p 1394 N94-17780

TRANSMISSION RATE (COMMUNICATIONS)
Protocol service decomposition for high-performance networking
[AD-A270613] p 1538 N94-19533

TRANSMISSIVITY
Time-resolved probing of electron thermal conduction in femtosecond-laser-pulse-produced plasmas
[DE93-016996] p 1585 N94-18129

TRANSMITTER RECEIVERS
Design of a general purpose and autonomous transmitter and receiver system for underwater acoustic experiments at sea
[AD-A269268] p 1495 N94-17822

TRANSMITTERS

Extending bandwidth of optical emitters using active matching technique
[AD-D015875] p 1394 N94-17707

Intentionally Short Range Communications (ISRC)
[AD-A268788] p 1384 N94-18216

The asymptotic theory of the reflection and transmission of a pulsed electromagnetic beam field at a planar interface separating two dispersive media
[AD-A269033] p 1385 N94-18404

TRANSONIC FLOW

Two-dimensional boundary surfaces for axi-symmetric external transonic flows
[AD-A269678] p 1312 N94-18571

Navier-Stokes, dynamics and aeroelastic computations for vortical flows, buffet and flutter applications
[NASA-CR-194520] p 1313 N94-19621

TRANSONIC SPEED

A study of the influence of a delta wing geometry on the induced drag at transonic speed (M=0.55) and high angles of attack
[FFA-TN-1992-14] p 1311 N94-17722

TRANSONIC WIND TUNNELS

Error propagation equations and tables for estimating the uncertainty in high-speed wind tunnel test results
[DE93-018685] p 1311 N94-18275

TRANSPARENCE

Time-resolved probing of electron thermal conduction in femtosecond-laser-pulse-produced plasmas
[DE93-016996] p 1585 N94-18129

TRANSPONDERS

Range safety transponder catalog
[AD-A270882] p 1323 N94-19581

Quasi-optical transponder using FET's and patch antennas
[AD-A271339] p 1407 N94-19584

TRANSPORT AIRCRAFT

Metals 2000
[DE93-016761] p 1355 N94-17752

In-flight pressure distributions and skin-friction measurements on a subsonic transport high-lift wing section p 1308 N94-18435

High-lift design for large civil aircraft
p 1310 N94-18445

High lift systems for transport aircraft with advanced airfoils p 1310 N94-18446

Procedures and design data for the formulation of aircraft configurations
[AD-A270150] p 1318 N94-18779

TRANSPORT PROPERTIES

Electron mobility in high resistivity silicon
[REPT-93-007] p 1565 N94-17933

Dependence of helium transport on plasma current and ELM frequency in H-mode discharges in D3-D
[DE93-016986] p 1585 N94-18058

Assessment and development of second order turbulence models p 1411 N94-18548

Optical and transport properties of metallic and semiconductor nanostructures
[AD-A270009] p 1598 N94-18609

Scaling laws for diamond chemical vapor deposition. 2: Atomic hydrogen transport
[AD-A269842] p 1371 N94-18740

Transport phenomena and interfacial kinetics in multiphase combustion systems
[AD-A270202] p 1349 N94-18785

LAHET calculations for accelerator neutron production
[DE93-016518] p 1570 N94-19120

ICRF direct electron heating experiments in TFTR
[DE93-017857] p 1590 N94-19273

Behavior of the particle transport coefficients near the density limit in MTX
[DE93-019108] p 1591 N94-19311

Electrokinetic transport of heterogeneous particles in suspensions
[NASA-CR-194478] p 1353 N94-19367

Radial evolution of the solar wind turbulence with application to charged particle transport
[NASA-CR-194081] p 1629 N94-19427

Global three dimensional model of tropospheric trace gases chemistry and transport
[AERONAUTICA-ACTA-A-370-199]
p 1479 N94-19518

TRANSPORT THEORY

A preliminary model for crack-tip hydrogen transport
[NPL-DMM(A)-84] p 1451 N94-17899

Ratio of specimen thickness to detection area for reliable hydrogen permeation measurement
[NPL-DMM(A)-103] p 1451 N94-17929

Chemical reactions in turbulent mixing flows
[AD-A269377] p 1410 N94-18472

Asymptotic derivation of the modified time-dependent SP2 equations and numerical calculations
[DE93-016466] p 1551 N94-19342

Improved approximations applied to the S(sub N) even-parity equation
[DE93-016467] p 1551 N94-19343

Exponential characteristic spatial quadrature for discrete ordinates neutral particle transport in two-dimensional cartesian coordinates
[AD-A270458] p 1554 N94-19671

TRANSPORTATION

Research activities, Faculty of Civil Engineering, Delft University of Technology, 1990 - 1991
[PB93-195022] p 1380 N94-19254

National Program Plan Fuel Cells in Transportation
[DE93-017557] p 1469 N94-19346

TRANSPUTERS

Comparative examinations of several field oriented position control structures for asynchronous servomotors with a multitransputer system
[ETN-93-95051] p 1406 N94-19390

TRANSVERSE LOADS

Development of engineering models for calculation of failure loads and defect states of steel concrete beams and plates
[ETN-93-95052] p 1460 N94-19648

TRANSVERSE WAVES

The electromechanical properties of tetragonal BaTiO3 and PbTiO3 single crystals
[DE93-019008] p 1603 N94-19550

TREES (MATHEMATICS)

Contribution to the analysis of tableaus based decision methods
[ETN-93-94355] p 1560 N94-18067

A parallel hashed oct-tree N-body algorithm
[DE93-012654] p 1526 N94-19205

Compensation approach for three or more dimensional random walks
[PB93-197499] p 1543 N94-19326

The complexity of the optimal spanning hypertree problem
[TR-471] p 1561 N94-19481

Heap construction in the parallel comparison tree model
[TR-409] p 1538 N94-19512

Finding the strong components in a directed graph
[PB93-187342] p 1555 N94-19708

Generalized regression trees: Function estimation via recursive partitioning and maximum likelihood
[AD-A271259] p 1560 N94-19726

TREES (PLANTS)

The carbon dioxide emissions game: Playing the net
[DE93-017670] p 1471 N94-17821

TRENDS

Trends in Information Management at Department of Energy Headquarters
[DE93-017197] p 1615 N94-18496

TRESCA FLOW

Assessment of an improved multiaxial strength theory based on creep-rupture data for Inconel 600
[DE93-015929] p 1356 N94-17791

TRIANGLES

Are bilinear quadrilaterals better than linear triangles?
[DE93-019223] p 1551 N94-19301

TRIANGULATION

Refining a triangulation of a planar straight-line graph to eliminate large angles
[DE93-016510] p 1528 N94-19344

Numerical modelling of crystal growth
[AD-A271206] p 1605 N94-19719

TRIBOLOGY

Titanium carbon-hydrogen layers on decorative surfaces p 1375 N94-18010

Physico chemical and mechanic approach of lubricating properties of graphite + additive powders
[ECL-93-02] p 1373 N94-19405

Contribution to the tribological study of magnetic-tape head contact
[ECL-92-57] p 1434 N94-19414

Microtribology of magnetic media
[AD-A271209] p 1407 N94-19722

Surface species in tribology
[AD-A270970] p 1446 N94-19754

Atomic-scale friction measurements using friction force microscopy. Part 2: Application to magnetic media
[AD-A270759] p 1447 N94-19767

Tribological studies of silicon for magnetic recording applications (Invited)
[AD-A270878] p 1447 N94-19784

TRIBUTARIES

DYNLET1 model formulation and user's guide
[AD-A269843] p 1498 N94-18723

TRIGGER CIRCUITS

Design and test of a low jitter metal to metal contact solid dielectric switch
[DE93-016957] p 1394 N94-17755

A bit serial first level calorimeter trigger for an LHC detector
[USIP-92-08] p 1574 N94-18845

Improved optical pseudospark switch
[AD-D015821] p 1580 N94-18947

A programmable systolic trigger processor for FERA-bus data
[USIP-92-04] p 1405 N94-19292

TRINITROTOLUENE

Instrumented experiments aboard the frigate WOLF. Wolf 2: Measurement results of the 5.5 kg TNT in the crew aft sleeping compartment
[PML-1992-12] p 1451 N94-17931

The minimum detection limits of RDX and TNT deposited on various surfaces as determined by ion mobility spectroscopy
[DE93-018521] p 1378 N94-19042

TRITIUM

Using the Tritium Plasma Experiment to evaluate ITER PFC safety
[DE93-016614] p 1582 N94-17713

The rise of accuracy for the multichannel scattering problem solving
[DE93-630145] p 1608 N94-18253

Finite difference program for calculating hydride bed wall temperature profiles
[DE93-019272] p 1523 N94-19005

TRITON

Working group for planetary system nomenclature
[NASA-CR-194406] p 1626 N94-18841

TROPICAL REGIONS

Spectral analysis of synoptic time scale disturbances over the tropical eastern Pacific during summer 1989, 1990 and 1991
[AD-A268821] p 1490 N94-18206

Internal instability of nonparallel flow on an equatorial beta-plane
[AD-A268927] p 1490 N94-18486

TROPICAL STORMS

Forecast model applications of retrieved three dimensional liquid water fields p 1492 N94-18606

Moist wind relationships p 1492 N94-18607

TROPOSPHERE

Kinetics programs for simulation of tropospheric photochemistry on the global scale
[DE93-019035] p 1476 N94-19104

Analysis of satellite-derived ozone and water vapor measurements
[NASA-CR-193810] p 1486 N94-19237

The split-step algorithm for microwave propagation modeling above a conducting surface
[FEL-92-A430] p 1390 N94-19447

Suitability of infrared spectroscopy for remote sensing of tropospheric trace gases
[KFK-5183] p 1479 N94-19507

Global three dimensional model of tropospheric trace gases chemistry and transport
[AERONAUTICA-ACTA-A-370-199]
p 1479 N94-19518

TRUCKS

Lightweight materials for transportation: Program plan
[DE93-017381] p 1340 N94-18087

Conceptual design of a sodium sulfur cell for US electric van batteries
[DE93-018683] p 1405 N94-19035

TRYPTOPHAN

Strategies for enhancing catecholamine-mediated neurotransmission
[NASA-CR-193807] p 1506 N94-18862

TUNABLE LASERS

Variable wide band fiber optic delay line
[AD-D015848] p 1576 N94-17716

The copper-pumped dye laser system at Lawrence Livermore National Laboratory
[DE93-014429] p 1435 N94-17723

Design of a tunable 4-MW free electron maser for heating fusion plasmas
[DE93-017172] p 1437 N94-18134

Tunable synchronously pumped intracavity two-stage optical frequency upconversion
[AD-A269105] p 1438 N94-18250

Single-transverse-mode, narrow-bandwidth pulsed tunable dye laser with hollow circular intracavity dielectric waveguide
[AD-A270022] p 1439 N94-18614

Tunable ytterbium-doped solid state laser
[AD-D015878] p 1440 N94-18747

A tunable compact high power far-infrared grating free-electron laser
[AD-A269875] p 1440 N94-18771

Tetravalent chromium (Cr(4+)) as laser-active ion for tunable solid-state lasers
[NASA-CR-194529] p 1441 N94-19369

Tetravalent chromium (Cr(4+)) as laser-active ion for tunable solid-state lasers
[NASA-CR-194528] p 1441 N94-19394

TUNGSTEN
Photorefractive tungsten bronze crystals for optical computing
[AD-A268659] p 1596 N94-18320
The effect of crystallographic orientation on the performance of single crystal tungsten subscale penetrators
[AD-A268988] p 1597 N94-18468
Recent advances in high density tungsten composite processing
[AD-A270764] p 1344 N94-19576

TUNGSTEN ALLOYS
Atlas of formability: HAYNES 188
[AD-A268355] p 1356 N94-17769
Bibliography on silicides
[AD-A270516] p 1374 N94-19532
Recent advances in high density tungsten composite processing
[AD-A270764] p 1344 N94-19576
Development and characterization of adiabatic shear prone tungsten heavy alloys
[AD-A270477] p 1366 N94-19673

TUNGSTEN OXIDES
Optical switch evaluation support
[AD-A270948] p 1581 N94-19601

TUNING
Decoherence and recoherence of beam in phase space
[DE93-014885] p 1573 N94-17784
Automatic tuning of an integral fuzzy controller
[REPT-93-006] p 1383 N94-17932
Limitations on the fidelity of 100 fs pulses produced by chirped pulse amplification
[DE93-017167] p 1396 N94-17991
A tunable CMOS constant current source
p 1401 N94-18369
The gyrotron backward-wave-oscillator experiment — final progress report
[AD-A268982] p 1403 N94-18452

TUNNEL JUNCTIONS
Synthesis and study of high-T(sub c) superconducting electronic materials
[AD-A268851] p 1402 N94-18390

TURBIDITY
Solar radiation in Saudi Arabia
[AD-A269970] p 1493 N94-18781

TURBINE BLADES
Defining the normal turbine inflow within a wind park environment
[DE93-010032] p 1489 N94-18046
SAND contact in DYNA3D
[DE93-016451] p 1340 N94-18113
The application of nondestructive techniques to the testing of a wind turbine blade
[DE93-016731] p 1447 N94-18128

TURBINES
Potassium-Rankine power conversion subsystem modeling for nuclear electric propulsion
[NASA-CR-191134] p 1468 N94-18821

TURBOCOMPRESSORS
Vane optimization for maximum efficiency using Design Of Experiments (DOX)
[AD-A270270] p 1320 N94-18907

TURBOFAN ENGINES
New techniques for contrail forecasting
[AD-A269686] p 1490 N94-18573

TURBOFANS
Vane optimization for maximum efficiency using Design Of Experiments (DOX)
[AD-A270270] p 1320 N94-18907

TURBOMACHINERY
Workshop on Computational Turbulence Modeling
[NASA-TM-109266] p 1410 N94-18545
An algebraic turbulence model for turbomachinery
p 1411 N94-18554
Simulation of three dimensional unsteady viscous flows in turbomachines
[ECL-92-15] p 1420 N94-19398

TURBULENCE
Vortex methods and statistics
[DE93-016974] p 1556 N94-17886
Defining the normal turbine inflow within a wind park environment
[DE93-010032] p 1489 N94-18046
Workshop on Computational Turbulence Modeling
[NASA-TM-109266] p 1410 N94-18545
Research activities at the Center for Modeling of Turbulence and Transition p 1410 N94-18546
Research on two equation models
p 1411 N94-18547
Assessment and development of second order turbulence models p 1411 N94-18548
Computational aero-acoustics as a branch of turbulence research p 1411 N94-18552
Turbulence modeling in aircraft icing
p 1412 N94-18555
Several examples where turbulence models fail in inlet flow field analysis p 1412 N94-18556
STREMR: Numerical model for depth-averaged incompressible flow
[AD-A269949] p 1417 N94-18672
Correlation of incoming boundary layer pitot pressure fluctuations with the unsteadiness of fin-induced shock wave turbulent boundary layer interactions
[AD-A270059] p 1417 N94-18796
Experimental investigation of turbulent Prandtl number and Reynolds analogy in transitional and post-transitional boundary layers
[AD-A270092] p 1418 N94-18867
Relation between the fluctuating wall pressure and the turbulent structure of a boundary layer on a cylinder in axial flow
[AD-A270242] p 1418 N94-18906
Numerical simulation of turbulent mixing and combustion near the inlet of a burner
[DE93-017960] p 1350 N94-18987

TURBULENCE EFFECTS
Work plan for the Marine Aerosol Properties and the Thermal Imager Performance Trial (MAPTIP)
[AD-A270026] p 1483 N94-18712
Experimental investigation of turbulent Prandtl number and Reynolds analogy in transitional and post-transitional boundary layers
[AD-A270092] p 1418 N94-18867
Numerical simulation of acoustic waves propagation in turbulent media
[ECL-92-37] p 1563 N94-19413

TURBULENCE MODELS
Navier-Stokes calculations on multi-element airfoils using a chimera-based solver p 1306 N94-18422
Workshop on Computational Turbulence Modeling
[NASA-TM-109266] p 1410 N94-18545
Research activities at the Center for Modeling of Turbulence and Transition p 1410 N94-18546
Assessment and development of second order turbulence models p 1411 N94-18548
Numerical investigation of complex, transitional, and chemically reacting flows p 1411 N94-18550
Computational aero-acoustics as a branch of turbulence research p 1411 N94-18552
A comparative study of turbulence models in predicting hypersonic inlet flows p 1314 N94-18553
An algebraic turbulence model for turbomachinery
p 1411 N94-18554
Turbulence modeling in aircraft icing
p 1412 N94-18555
Several examples where turbulence models fail in inlet flow field analysis p 1412 N94-18556
Introduction to the Modeling of Turbulence
[VKI-LS-1993-02] p 1414 N94-18578
An introduction to the modelling of turbulence
p 1414 N94-18579
An introduction to second moment closure
p 1414 N94-18580
Modelling force-field effects on turbulence
p 1414 N94-18581
A new form of second-moment closure
p 1414 N94-18582
An introduction to single-point closure methodology
p 1414 N94-18583
Second-moment closure: Present... and future?
p 1414 N94-18584
Contribution to the modelling of near-wall turbulence
p 1414 N94-18585
Two-equation models for high-Reynolds-number flow
p 1415 N94-18586
Application of second-moment closure in complex flows p 1415 N94-18590
Modelling engineering flows with Reynolds stress turbulence closure p 1415 N94-18591
Turbulence modelling challenges posed by complex flows p 1415 N94-18592
Turbulence modeling for compressible flows and implementation in Navier-Stokes solvers
p 1416 N94-18597

TURBULENT BOUNDARY LAYER
Research on two equation models
p 1411 N94-18547
Calculation of turbulent boundary layer wall pressure spectra
[AD-A269549] p 1416 N94-18642
Correlation of incoming boundary layer pitot pressure fluctuations with the unsteadiness of fin-induced shock wave turbulent boundary layer interactions
[AD-A270059] p 1417 N94-18796
Relation between the fluctuating wall pressure and the turbulent structure of a boundary layer on a cylinder in axial flow
[AD-A270242] p 1418 N94-18906
A new approach to the study of the turbulence layer
[NASA-CR-194546] p 1487 N94-19397

TURBULENT COMBUSTION
Spectral radiance measurements on a bluff body stabilized flame: Characterization of the IR signature
[PB93-195899] p 1347 N94-18081
Research activity on particle spin systems and related problems
[AD-A269456] p 1562 N94-18286
A coupled implicit solution method for turbulent spray combustion in propulsion systems p 1411 N94-18549
Numerical simulation of turbulent mixing and combustion near the inlet of a burner
[DE93-017960] p 1350 N94-18987

TURBULENT FLOW
Defining the normal turbine inflow within a wind park environment
[DE93-010032] p 1489 N94-18046
On memory effects in turbulence
[DLR-FB-93-03] p 1409 N94-18124
Research activity on particle spin systems and related problems
[AD-A269456] p 1562 N94-18286
Applications of the program UIFLOW-2D to the numerical simulation of axisymmetric flows
[AD-A268731] p 1410 N94-18326
Navier-Stokes computations of turbulent flow around high-lift configurations p 1306 N94-18420
Dispersion effects on millimeter wavelength attenuation efficiencies for a variety of fibers
[AD-A268992] p 1386 N94-18454
Chemical reactions in turbulent mixing flows
[AD-A269377] p 1410 N94-18472
Workshop on Computational Turbulence Modeling
[NASA-TM-109266] p 1410 N94-18545
Research activities at the Center for Modeling of Turbulence and Transition p 1410 N94-18546
Research on two equation models
p 1411 N94-18547
Assessment and development of second order turbulence models p 1411 N94-18548
A coupled implicit solution method for turbulent spray combustion in propulsion systems p 1411 N94-18549
Numerical investigation of complex, transitional, and chemically reacting flows p 1411 N94-18550
Analysis of supersonic flows using k-epsilon model and the RPLUS code: Progress towards high speed combustor analysis p 1411 N94-18551
A comparative study of turbulence models in predicting hypersonic inlet flows p 1314 N94-18553
An algebraic turbulence model for turbomachinery
p 1411 N94-18554
Introduction to the Modeling of Turbulence
[VKI-LS-1993-02] p 1414 N94-18578
An introduction to the modelling of turbulence
p 1414 N94-18579
An introduction to single-point closure methodology
p 1414 N94-18583
Inclusion of second-moment closures into finite-volume solvers p 1415 N94-18588
Application of second-moment closure in complex flows p 1415 N94-18590
Modelling engineering flows with Reynolds stress turbulence closure p 1415 N94-18591
Turbulence modelling challenges posed by complex flows p 1415 N94-18592
Examples of turbulence model applications
p 1415 N94-18593
Large-eddy simulation of turbulent diffusion in stably stratified shear flow p 1416 N94-18595
Numerical simulation of turbulent convective flow over wavy terrain p 1416 N94-18596
STREMR: Numerical model for depth-averaged incompressible flow
[AD-A269949] p 1417 N94-18672
Computational Fluid Dynamics (CFD) research branch technical briefs
[AD-A269698] p 1417 N94-18739
Experimental investigation of turbulent Prandtl number and Reynolds analogy in transitional and post-transitional boundary layers
[AD-A270092] p 1418 N94-18867
Relation between the fluctuating wall pressure and the turbulent structure of a boundary layer on a cylinder in axial flow
[AD-A270242] p 1418 N94-18906
Numerical simulations of turbulent buoyant flows by finite element method: Application to the study of strongly heated or cooled stratified flow
[ECL-92-28] p 1421 N94-19399
Numerical prediction of transition of the F-16 wing at supersonic speeds
[NASA-CR-194407] p 1312 N94-19433
Two-dimensional turbulent nonstationary superfluid counterflows: Numerical simulations, qualitative effects
[MPIS-23/1992] p 1422 N94-19510
Visualization of turbulent flow with particles
[REPT-93-31] p 1423 N94-19645

A review of hot-wire technique in compressible flows
[LR-724] p 1423 N94-19668

Forward scattering of a pulsed continuous wave signal through laminar and turbulent thermal plumes
[AD-A271210] p 1564 N94-19723

Collaborative research on combustion diagnostics and modeling between Rolls-Royce, Inc. and the United States Air Force Wright Laboratory
[AD-A270660] p 1354 N94-19778

TURBULENT JETS

Combustion instability phenomena of importance to liquid propellant engines
[AD-A268800] p 1348 N94-18389

TURBULENT MIXING

Chemical reactions in turbulent mixing flows
[AD-A269377] p 1410 N94-18472

Numerical investigation of complex, transitional, and chemically reacting flows p 1411 N94-18550

Numerical simulation of turbulent mixing and combustion near the inlet of a burner
[DE93-017960] p 1350 N94-18987

TURBULENT WAKES

Applications of the program UIFLOW-2D to the numerical simulation of axisymmetric flows
[AD-A268731] p 1410 N94-18326

Theoretical examination of the flow around a cylinder with a low dimensional Galerkin process
[MPIS-25/1992] p 1422 N94-19525

TURING MACHINES

Reducing extended transition systems
[MEMO-INF-93-09] p 1526 N94-19196

TURNING FLIGHT

VMC left turn curved approaches, test results — (visual meteorological conditions)
[AD-A269476] p 1316 N94-18728

TVD SCHEMES

Computational Fluid Dynamics
[VKI-LS-1993-04] p 1412 N94-18557

Multidimensional wave decompositions for the Euler equations p 1413 N94-18562

TWO DIMENSIONAL BODIES

Two-dimensional boundary surfaces for axi-symmetric external transonic flows
[AD-A269678] p 1312 N94-18571

TWO DIMENSIONAL FLOW

Calculation of multielement airfoils and wings at high lift p 1309 N94-18438

Numerical solutions for a flow with mixed convection in a vertical geometry
[DE93-011592] p 1419 N94-19058

Multigrid for a groundwater flow problem
[REPT-93-29] p 1420 N94-19144

Two-dimensional turbulent nonstationary superfluid counterflows: Numerical simulations, qualitative effects
[MPIS-23/1992] p 1422 N94-19510

TWO DIMENSIONAL MODELS

Mechanical modeling of the growth of salt structures
[DE93-015342] p 1596 N94-18243

The GARTEUR high lift research programme
p 1307 N94-18430

ADCIRC: An advanced three-dimensional circulation model for shelves, coasts, and estuaries. Report 3: Development of a tidal constituent database for the western North Atlantic and Gulf of Mexico
[AD-A268685] p 1497 N94-18455

STREMR: Numerical model for depth-averaged incompressible flow
[AD-A269949] p 1417 N94-18672

Subcritical crack growth in continuous-fiber reinforced ceramic composites
[DE93-018784] p 1343 N94-19335

The influence of the target strength model on computed perforation
[DE93-018659] p 1460 N94-19543

TWO PHASE FLOW

Study of multi-phase flow characteristics in an MHD power train
[DE93-018570] p 1586 N94-18272

A coupled implicit solution method for turbulent spray combustion in propulsion systems p 1411 N94-18549

TYPHOONS

The activities of equatorial anticyclones of the Western Pacific and the South China Sea and their effects on the tracks of typhoon movement
[AD-A269954] p 1492 N94-18675

TYROSINE

Strategies for enhancing catecholamine-mediated neurotransmission
[NASA-CR-193807] p 1506 N94-18862

U

UH-60A HELICOPTER

Aerodynamic characteristics of a helicopter rotor airfoil as affected by simulated ballistic damage
[AD-A269206] p 1311 N94-18413

ULTRAHIGH FREQUENCIES

High efficiency low cost monolithic module for SARSAT distress beacons
[NASA-CR-194234] p 1315 N94-18852

ULTRAHIGH VACUUM

Thin film studies of the proximity Josephson effect
[AD-A270129] p 1600 N94-18876

ULTRASONIC FLAW DETECTION

Nondestructive inspection of graphite-epoxy laminates for heat damage using DRIFT and LPF spectroscopies
[DE93-017228] p 1343 N94-18761

Three dimensional ultrasonic imaging: An aging aircraft nondestructive inspection tool
[DE93-018088] p 1448 N94-19252

ULTRASONIC RADIATION

Development of ultrasonic motor and application to silent alarm analog quartz watch p 1425 N94-18016

Ultrasonic process for destruction of chlorinated organic compounds in aqueous solution
[DE93-015551] p 1348 N94-18249

ULTRASONIC TESTS

Development and application of specially-focused ultrasonic transducers to location and sizing of defects in 75 mm- to 127 mm-thick austenitic stainless steel weld metals
[DE93-015975] p 1453 N94-18108

Ultrasonic technique for inspection of GPHS capsule girth weld integrity
[DE93-040072] p 1448 N94-19189

Three dimensional ultrasonic imaging: An aging aircraft nondestructive inspection tool
[DE93-018088] p 1448 N94-19252

Materials characterization of propellants using ultrasonics
[NASA-CR-193877] p 1378 N94-19494

ULTRASONIC WAVE TRANSDUCERS

Development and application of specially-focused ultrasonic transducers to location and sizing of defects in 75 mm- to 127 mm-thick austenitic stainless steel weld metals
[DE93-015975] p 1453 N94-18108

ULTRAVIOLET ABSORPTION

Detection of accreting gas toward HD 45677: A newly recognized, Herbig Be proto-planetary system
[NASA-CR-189312] p 1621 N94-19288

Ultraviolet absorption cross-sections of some carbonyl compounds and their temperature dependence
[AERONAUTICA-ACTA-A-368-199]
p 1353 N94-19456

Temperature dependence of ultraviolet absorption cross-sections of alternative hydrochlorofluorocarbons
[AERONAUTICA-ACTA-A-369-199]
p 1353 N94-19459

ULTRAVIOLET ASTRONOMY

Determination of nitrogen to carbon abundance ratios from transition layer emission lines
[NASA-CR-191921] p 1622 N94-19421

Ultraviolet observations of clusters of Wolf-Rayet stars in the SBm3 galaxy NGC 4214 and Ultraviolet and optical observations of LINER's
[NASA-CR-194307] p 1622 N94-19431

ULTRAVIOLET DETECTORS

Ultraviolet plume instrument calibration and sensor assessment
[AD-A269687] p 1337 N94-18574

UVPI imaging from the LACE satellite: The Strypi rocket plume
[AD-A270967] p 1335 N94-19787

ULTRAVIOLET LASERS

Ultra-shallow box-like profiles fabricated by pulsed UV-laser doping process
[DE93-017221] p 1437 N94-18083

ULTRAVIOLET PHOTOGRAPHY

UVPI imaging from the LACE satellite: The Strypi rocket plume
[AD-A270967] p 1335 N94-19787

ULTRAVIOLET RADIATION

Air pollution effects field research facility. 3: UV-B exposure and monitoring system
[DE93-013098] p 1470 N94-17773

Photosynthetic responses to the environment, volume 8
[AD-A269584] p 1502 N94-18305

Ultraviolet plume instrument calibration and sensor assessment
[AD-A269687] p 1337 N94-18574

Improved optical pseudospark switch
[AD-D015821] p 1580 N94-18947

Scientific studies in association with the Shuttle Solar Backscatter Ultraviolet (SSBUV) project
[NASA-CR-193404] p 1630 N94-19437

ULTRAVIOLET SPECTRA

Air pollution effects field research facility. 3: UV-B exposure and monitoring system
[DE93-013098] p 1470 N94-17773

Determination of nitrogen to carbon abundance ratios from transition layer emission lines
[NASA-CR-191921] p 1622 N94-19421

Spectrophotometry of emission-line stars in the magellanic clouds
[NASA-CR-194082] p 1628 N94-19425

Ultraviolet observations of clusters of Wolf-Rayet stars in the SBm3 galaxy NGC 4214 and Ultraviolet and optical observations of LINER's
[NASA-CR-194307] p 1622 N94-19431

ULTRAVIOLET SPECTROMETERS

Chemical dynamics in time and energy space
[DE93-018595] p 1350 N94-19097

A high resolution ultraviolet Shuttle glow spectrograph
p 1325 N94-19174

ULTRAVIOLET SPECTROSCOPY

IRAS high resolution studies and modeling of closely interacting galaxies. Galaxy collisions: Infrared observations and analysis of numerical models. UV spectroscopy of massive young stellar populations in interacting galaxies
[NASA-CR-194483] p 1627 N94-19218

Novel nonlinear laser diagnostic techniques
[AD-A270968] p 1442 N94-19788

ULYSSES MISSION

Magellan, Galileo, and Ulysses
[NASA-TM-109362] p 1628 N94-18958

UNDAMPED OSCILLATIONS

Transformation of energy and momentum due to Landau damping in space
[DE93-624921] p 1581 N94-17689

UNDERGROUND EXPLOSIONS

A comparison of single-station backazimuth estimates with regional event locations in the Central Appalachians
[AD-A269897] p 1483 N94-18690

Centrifuge modeling of explosion-induced craters in unsaturated sand
[AD-A270194] p 1417 N94-18790

UNDERWATER ACOUSTICS

Design of a general purpose and autonomous transmitter and receiver system for underwater acoustic experiments at sea
[AD-A269268] p 1495 N94-17822

Comments on computational underwater acoustics
[DE93-013789] p 1562 N94-17873

Parallel and vector adaptations of the underwater finite element parabolic equation model
[AD-A269990] p 1563 N94-18678

Estimating the oceanic sound speed environmental for long-range acoustic propagation
[AD-A270231] p 1499 N94-18903

BACKSCATTER.FOR: A program to calculate the backscattering strength of an inhomogeneous seabed
[AD-A269235] p 1499 N94-18910

Liquid sound speeds at pressure from the optical analyzer technique
[DE93-018362] p 1563 N94-19151

Comments on computational underwater acoustics
[DE93-019880] p 1563 N94-19270

Acoustic travel time perturbations due to an internal tide and internal wave field in the Barents Sea
[AD-A270879] p 1499 N94-19580

Analysis of data from Columbia Point Arena Ocean-Bottom Seismic Station (OBSS)
[AD-A271263] p 1500 N94-19727

Seismic studies of the geologic structure and physical properties of the seabed
[AD-A270895] p 1500 N94-19747

A register of underwater acoustic test facilities in the US, Canada, and the United Kingdom
[AD-A270884] p 1500 N94-19785

UNDERWATER PHOTOGRAPHY

High spatial resolution, range gated, underwater imaging method and apparatus
[AD-D015882] p 1430 N94-18530

UNDERWATER STRUCTURES

Fatigue technology assessment and strategies for fatigue avoidance in marine structures. Appendices
[AD-A269053] p 1455 N94-18716

UNDERWATER TESTS

Mutrometre: Construction for fast water proof measurements under low pressure and air suppression
p 1427 N94-18031

A register of underwater acoustic test facilities in the US, Canada, and the United Kingdom
[AD-A270884] p 1500 N94-19785

UNDERWATER VEHICLES

Damping in ferrous shape memory alloys
[AD-A271009] p 1368 N94-19775

UNIFIED FIELD THEORY
Gauge coupling unification in superstring derived standard-like models
[DE93-624801] p 1607 N94-17950
UNITED KINGDOM
Where is high-lift today? A review of past UK research programmes p 1305 N94-18416
UNITED STATES
Current information technology resource requirements of the federal government: Fiscal year 1994
p 1612 N94-17756
Terminal area forecasts, FY 1993-2005
[AD-A269855] p 1316 N94-18336
Trends in Information Management at Department of Energy Headquarters
[DE93-017197] p 1615 N94-18496
Seasonal variability of wind electric potential in the US
[DE93-018182] p 1493 N94-19051
Spatiotemporal variability of non-urban ozone concentrations over the eastern United States and its potential replication by satellite data
[PB93-191328] p 1476 N94-19065
UNIVERSE
The universe at moderate redshift
[NASA-CR-193771] p 1627 N94-19093
UNIVERSITIES
California Student Get Away Special Payload GAS-450
p 1324 N94-19164
The GAMCIT gamma ray burst detector
p 1324 N94-19168
Undergraduate origins of recent science and engineering doctorate recipients
[NSF-92-332] p 1610 N94-19389
Undergraduate course and curriculum development program and calculus and the bridge to calculus program: 1992 awards
[NSF-93-24] p 1610 N94-19446
UNIVERSITY PROGRAM
The first flight of the QUESTS GAS payload G-521
p 1325 N94-19170
UNIX (OPERATING SYSTEM)
CAVEMAN: Configuration and version management
[DE93-018066] p 1524 N94-19048
Cesar user library
[FFI-93/7021] p 1529 N94-19378
Learning about the Internet bibliography and beginner's guide
[AD-A268847] p 1532 N94-19707
UNLOADING
Efficiency and biofidelity of occupant simulations
p 1459 N94-19473
UNSTEADY AERODYNAMICS
Comparison between swept and delta canards on a model of a combat aircraft
[AD-A269561] p 1317 N94-17826
ISAC: A tool for aeroservoelastic modeling and analysis
[NASA-TM-109031] p 1321 N94-19316
UNSTEADY FLOW
Numerical investigation of complex, transitional, and chemically reacting flows p 1411 N94-18550
Computational Fluid Dynamics
[VKI-LS-1993-04] p 1412 N94-18557
Interferometric investigations of compressible dynamic stall over a transiently pitching airfoil
[NASA-TM-109380] p 1312 N94-19119
A simple description of flow instability with application to a packed bed
[DE93-017492] p 1420 N94-19345
Simulation of three dimensional unsteady viscous flows in turbomachines
[ECL-92-15] p 1420 N94-19398
Examinations of the friction behavior in nonstationary flow processes in pipes
[MITT-7] p 1423 N94-19730
UPPER SURFACE BLOWING
Design, development, and flight evaluation of the Boeing YC-14 USB powered lift aircraft p 1310 N94-18444
UPWIND SCHEMES (MATHEMATICS)
Investigation of a matrix-model for the artificial dissipation in a cell vertex finite volume scheme for solving the Navier-Stokes equations
[DLR-FB-92-33] p 1409 N94-18076
Efficient simulation of incompressible viscous flow over multi-element airfoils p 1306 N94-18421
High-lift system analysis method using unstructured meshes p 1307 N94-18426
Three dimensional network generation and Euler calculation for a wing fuselage canard configuration
[MBB-LME-211-S-PUB-511-A] p 1319 N94-19500
URANIUM ALLOYS
Magnetic properties of single-crystalline UCu3Al2
[DE93-016607] p 1593 N94-17744
Realistic theories of heavy electron and other strongly correlated materials
[DE93-010350] p 1571 N94-19204
URANIUM COMPOUNDS
Magnetic and crystallographic structures in UTX intermetallic compounds
[DE93-018291] p 1605 N94-19735
URANIUM ISOTOPES
Safety approaches for high power modular laser operation
[DE93-017213] p 1435 N94-17759
URANUS (PLANET)
Detailed analysis of low energy plasma data under the Voyager Uranus data analysis program
[NASA-CR-193668] p 1628 N94-17842
URINE
Nuclear Medicine Program
[DE93-013896] p 1504 N94-17699
USER MANUALS (COMPUTER PROGRAMS)
WBNGRID, a program for generation of C-H and C-O topology grids around wing/body/nacelle configurations: User's guide
[FFA-TN-1992-09] p 1311 N94-17721
Introductory user's guide to the ARL supercomputer facility at Aberdeen Proving Ground
[AD-A265204] p 1514 N94-17877
Format.m: A usage manual. Towards an efficient symbolic-numeric environment: Extending Mathematica's format rules
[MATHS-REPT-A-185] p 1547 N94-17969
APLAC: An object-oriented analog circuit simulator and design tool. 6.1 reference manual
[PB93-187193] p 1396 N94-18091
User's manual of Tokamak Simulation Code
[DE93-788388] p 1586 N94-18212
Teaching a computer simulation course with Ada
[AD-A267901] p 1521 N94-18308
DYNLET1 model formulation and user's guide
[AD-A269843] p 1498 N94-18723
Department of Defense Gateway Information System (DGIS) users' guide
[AD-A270140] p 1617 N94-18752
CAVEMAN: Configuration and version management
[DE93-018066] p 1524 N94-19048
Cesar user library
[FFI-93/7021] p 1529 N94-19378
START user manual version 2.1
[LR-726] p 1335 N94-19614
Learning about the Internet bibliography and beginner's guide
[AD-A268847] p 1532 N94-19707
Improved HF data network simulator, software user's manual, volume 2
[AD-A270954] p 1393 N94-19753
Technology benefits model user manual, version 01.00.04
[AD-A270637] p 1620 N94-19777
USER REQUIREMENTS
The First International Conference on PCTE
[FEL-92-A134] p 1518 N94-17965
Computer/information security design approaches for Complex 21/Reconfiguration facilities
[DE93-018547] p 1535 N94-18930
Application of new technologies in the virtual library: Seminars in Turkey, Portugal, and Spain
[NASA-TM-109718] p 1611 N94-19131
UTILITIES
The value of windpower: An investigation using a qualified production cost model
[DE93-010043] p 1465 N94-17888
Directory of Energy Information Administration Models 1993
[DE93-016987] p 1616 N94-18707

V

VACUUM
On a conformal perfect fluid in the classical vacuum
[DE93-624797] p 1480 N94-17682
Impulsive moving mirror model in a Schroedinger picture with impulse effect in a Banach space
[DE93-629864] p 1561 N94-18155
Impulsive moving mirror model and the stability of Schroedinger equation with impulse effect in a Banach space
[DE93-629866] p 1548 N94-18196
RF vacuum microelectronics
[AD-A269454] p 1396 N94-18284
RF vacuum microelectronics
[AD-A270003] p 1403 N94-18667
VACUUM APPARATUS
Mechanical properties and impact damage resistance of composites fabricated by low cost, vacuum assisted, resin transfer molding
[AD-A270361] p 1342 N94-18702
VACUUM CHAMBERS
Detonation reaction steps frozen by free expansion and analyzed by mass spectrometry
[DE93-012734] p 1376 N94-17813
Process for preparing thermoplastic composites
[AD-D015864] p 1339 N94-18074
VACUUM PUMPS
A survey on technical problems in designing high-speed rotors with developing materials
[DE93-788519] p 1444 N94-18159
VACUUM SPECTROSCOPY
Chemical dynamics in time and energy space
[DE93-018595] p 1350 N94-19097
VACUUM SYSTEMS
Temperature lowering in cryogenic chemical-synthesis techniques and system
[DE93-018348] p 1562 N94-18810
VACUUM TUBE OSCILLATORS
Experimental and theoretical investigation of broadband high-power windows for millimeter waves
[KFK-5157] p 1391 N94-19617
VALENCE
Novel electrochemical materials prepared by sol-gel chemistry
[AD-A269060] p 1578 N94-18405
Characterization of diamond film nucleation and growth surface
[AD-A269400] p 1597 N94-18459
High pressure metallization of Mott Insulators: Magnetic, structural and electronic properties
[DE93-018295] p 1404 N94-18805
VALVES
Electrically controlled liquid-crystal heat valve
[AD-D015872] p 1443 N94-17705
VANADIUM ALLOYS
Effect of oxygen concentration and ordering on vanadium-oxygen alloy vibrational spectra
[DE93-627003] p 1355 N94-17692
Atlas of formability: Ti-6Al-4V ELI
[AD-A268300] p 1357 N94-17803
Bibliography on silicides
[AD-A270516] p 1374 N94-19532
VANADIUM OXIDES
Effect of oxygen concentration and ordering on vanadium-oxygen alloy vibrational spectra
[DE93-627003] p 1355 N94-17692
Nanostructured materials: Mind over matter
[DE93-017690] p 1597 N94-18480
VANES
Vane optimization for maximum efficiency using Design Of Experiments (DOX)
[AD-A270270] p 1320 N94-18907
VAPOR DEPOSITION
Gallium arsenide-based ternary compounds and multi-band-gap solar cell research
[DE93-010049] p 1467 N94-18483
Carbon/carbon composites coated with SiC by chemical vapor deposition
[AD-A269934] p 1341 N94-18544
Scaling laws for diamond chemical vapor deposition. 2: Atomic hydrogen transport
[AD-A269842] p 1371 N94-18740
Scaling laws for diamond chemical vapor deposition. Diamond surface chemistry
[AD-A269874] p 1599 N94-18745
Characterization of vapor plume species and deposition residues resulting from pulsed laser ablation of a graphite/epoxy composite
[AD-A270101] p 1343 N94-18869
Substrate temperature measurement and control during thermal plasma CVD
[DE93-040305] p 1433 N94-19135
The microstructural mechanism of electromigration failure in narrow interconnects of Al alloys
[DE93-018598] p 1365 N94-19282
Ionized-cluster beam/partially ionized beam deposition of electro-optical and nonlinear optical organic materials and device development
[AD-A270832] p 1604 N94-19596
Pressure and temperature effects on the kinetics and quality of diamond films
[AD-A270876] p 1606 N94-19771
VAPOR PHASES
Effect of phase change in a debris cloud on a backwall structure
[DE93-017506] p 1358 N94-18100
Photodissociation studies of polyatomic free radicals
[AD-A270084] p 1350 N94-18799
VAPOR PRESSURE
Studies on gel electrolyte based on nitrile-butadiene copolymers
[AD-A269450] p 1370 N94-18282
Station climatic summaries: North America. Volume 1: The contiguous United States
[AD-A269567] p 1490 N94-18303

Station climatic summaries, North America. Volume 2: Alaska, Canada and Greenland
[AD-A269793] p 1493 N94-18732

VAPORS
Studies of interactions between conducting polymer and organic vapors: Applications to chemical sensing
[DE93-015694] p 1369 N94-18233

VARIABILITY
A survey of current approaches to modelling of hydrological time-series with respect to climate variability and change
[WMO/TD-534] p 1463 N94-19435
Uncertainty versus interindividual variability
[DE93-018105] p 1559 N94-19549

VARIANCE (STATISTICS)
Polarimetric statistics of electromagnetic waves scattered by distributed targets
[PB93-195907] p 1389 N94-18951

VASODILATION
Synchronisation of cold induced vasodilation at various locations of one hand
[IZF-1992-B3] p 1504 N94-17966

VAX COMPUTERS
Heavy ion nuclear physics research
[DE93-018862] p 1565 N94-17776

VECTOR PROCESSING (COMPUTERS)
Cesar user library
[FFI-93/7021] p 1529 N94-19378
CVL: A C vector library manual. Version 2
[AD-A270614] p 1531 N94-19592

VECTOR QUANTIZATION
Color palette considerations for digital map displays
[AD-A269991] p 1462 N94-18679

VECTOR SPACES
Groups on transformations in Finslerian spaces
[DE93-624765] p 1606 N94-17794
Content based-grid node selection for vector field visualization
[REPT-93-35] p 1525 N94-19155

VECTORS (MATHEMATICS)
A modified direct preconditioner for indefinite symmetric Toeplitz systems
[DE93-015234] p 1516 N94-17800

VEGARD-KAPLAN BANDS
A high resolution ultraviolet Shuttle glow spectrograph
p 1325 N94-19174

VEGETATION
Surface fluxes important to cloud development
[DE93-016633] p 1488 N94-17715
Biophysical characterization and surface radiation balance
[NASA-CR-194659] p 1470 N94-17762

VEGETATION GROWTH
Assessing impacts of climate change on forests: The state of biological modeling
[DE93-015916] p 1471 N94-17790

VEHICLE WHEELS
Measuring methods for evaluation of dynamic tyre properties
[ETN-93-95054] p 1381 N94-19650

VELOCITY
The use of velocity spectra for stacking receiver functions with application to IRIS/IDA stations OBNINSK (OBN) and ARTI (ARU), Russia
[AD-A269087] p 1483 N94-18717

VELOCITY DISTRIBUTION
Moist wind relationships p 1492 N94-18607
Surface wave group velocity tomography of East Asia, part 1
[AD-A270100] p 1484 N94-18868
Analysis of regional bodywave phases from earthquakes in western China, part 2
[AD-A270125] p 1485 N94-18873
PEACE: A Plasma Electron and Current Experiment
p 1329 N94-19632
Numerical modelling of crystal growth
[AD-A271206] p 1605 N94-19719
Examinations of the friction behavior in nonstationary flow processes in pipes
[MITT-7] p 1423 N94-19730

VELOCITY MEASUREMENT
Portable, solid state, fiber optic coupled Doppler interferometer system for detonation and shock diagnostics
[DE93-013917] p 1423 N94-17700
A mobile remote sensing laboratory for water vapor, trace gas, aerosol, and wind speed measurements
[DE93-017158] p 1489 N94-18132
Materials characterization of propellants using ultrasonics
[NASA-CR-193877] p 1378 N94-19494
Velocity measurements in a boundary layer with a density gradient
[DE93-019627] p 1422 N94-19515
Feasibility study for a measuring system velocity projectile
[FEL-91-A368] p 1434 N94-19797

VELOCITY MODULATION
The A((2)pi(sub u))-X((2)pi(sub g)) system of Br2(+) studied by velocity modulation spectroscopy
[USIP-93-04] p 1569 N94-18847

VENTILATION
Indoor environment program
[DE93-018601] p 1513 N94-18935

VENUS (PLANET)
Working group for planetary system nomenclature
[NASA-CR-194406] p 1626 N94-18841

VENUS ATMOSPHERE
Venus lower thermosphere studies
[NASA-CR-193546] p 1629 N94-19418

VENUS SURFACE
Working group for planetary system nomenclature
[NASA-CR-194406] p 1626 N94-18841

VERTICAL DISTRIBUTION
A one dimensional numerical model, with an application to the vertical distribution of dissolved oxygen in the ocean
[DE93-018481] p 1495 N94-17779
The vertical distribution of heating in the tropical atmosphere
[AD-A270452] p 1490 N94-18514
Using computerized tomography to determine ionospheric structures
[DE93-018904] p 1485 N94-19002

VERTICAL LANDING
Single STAGE Rocket Technology (SSRT) DC-X test program environmental assessment
[AD-A265940] p 1337 N94-17879
Lift and pitching moment induced on jet STOVL aircraft hovering in ground effect
[AD-A269700] p 1317 N94-18577

VERTICAL MOTION
New techniques for contrail forecasting
[AD-A269686] p 1490 N94-18573

VERTICAL TAKEOFF
Single STAGE Rocket Technology (SSRT) DC-X test program environmental assessment
[AD-A265940] p 1337 N94-17879
Overview of STOVL aircraft propulsion research offtakes and vertical lift systems
[NASA-TM-106387] p 1321 N94-19353

VERY HIGH FREQUENCIES
VHF air/ground communications for air traffic control. Volume 1: A decision tree approach to system innovations
[AD-A268485] p 1316 N94-18384
VHF air/ground communications for air traffic control: A decision tree approach to system innovations, volume 2
[AD-A268632] p 1386 N94-18495

VERY LARGE SCALE INTEGRATION
Synthesis techniques and analysis tool for on-chip fault-tolerance
[AD-A269148] p 1521 N94-18259
The 1991 3rd NASA Symposium on VLSI Design
[NASA-CR-194589] p 1397 N94-18337
New dynamic FET logic and serial memory circuits for VLSI GaAs technology p 1397 N94-18339
Automated ILA design for synchronous sequential circuits p 1397 N94-18340
Single phase dynamic CMOS PLA using charge sharing technique p 1397 N94-18341
Cellular logic array for computation of squares
p 1398 N94-18343
Fault tolerant sequential circuits using sequence invariant state machines p 1398 N94-18344
VLSI architectures for geometrical mapping problems in high-definition image processing
p 1398 N94-18345
Low power signal processing research at Stanford
p 1393 N94-18351
Pulse-firing winner-take-all networks
p 1399 N94-18353
VLSI synthesis of digital application specific neural networks p 1399 N94-18355
Measurement selection for parametric IC fault diagnosis p 1399 N94-18356
Fuzzy control of magnetic bearings
p 1399 N94-18357
Direct kinematics solution architectures for industrial robot manipulators: Bit-serial versus parallel
p 1399 N94-18358
Simplified microprocessor design for VLSI control applications p 1400 N94-18359
A modified reconfigurable data path processor
p 1400 N94-18360
Systolic array IC for genetic computation
p 1400 N94-18361
High-performance multiprocessor architecture for a 3-D lattice gas model p 1400 N94-18362
Verification of VLSI designs p 1400 N94-18363
A new variable testability measure
p 1400 N94-18364
Controlling state explosion during automatic verification of delay-insensitive and delay-constrained VLSI systems using the POM verifier p 1400 N94-18365
Formal verification of an MMU and MMU cache
p 1400 N94-18366
Formal hardware verification of digital circuits
p 1401 N94-18367
A verification logic representation of indeterministic signal states p 1401 N94-18372
Parallel optimization algorithms and their implementation in VLSI design p 1401 N94-18374
Asynchronous sequential circuit design using pass transistor iterative logic arrays p 1402 N94-18376
Pulse mode VLSI asynchronous circuits
p 1402 N94-18377
Improved self arbitrated VLSI asynchronous circuits
p 1402 N94-18378
A special purpose silicon compiler for designing supercomputing VLSI systems p 1402 N94-18379
ARPA/CSTO rapid VLSI implementation
[AD-A269170] p 1403 N94-18695
VLSI for high-speed digital signal processing
[AD-A270406] p 1404 N94-18706
An innovative neural manufacturing concept
[DE93-017212] p 1527 N94-19238
FASTBUS simulation models in VHDL
[USIP-92-07] p 1515 N94-19295
High precision on-line standard arithmetic operators: Design and implementation
[ETN-93-95006] p 1552 N94-19487
Computation of large numbers and VLSI: Application to GCD, to stretched GCD and at euclidian distance
[ETN-93-95009] p 1552 N94-19499
Silicon compilation: From the circuit to the system
[ETN-93-95010] p 1406 N94-19501
VLSI implementation of neuromorphic learning networks
[AD-A270825] p 1407 N94-19665
Signal processing algorithms for heterogeneous architectures
[AD-A271248] p 1392 N94-19724

VERY LOW FREQUENCIES
A study of the amplification of laser and VLF waves using a simple pendulum model
[AD-A270857] p 1442 N94-19770

VESTIBULAR TESTS
Pilot studies on object motion perception during linear self-motion after long duration centrifugation of human subjects
[IZF-1993-B-3] p 1510 N94-19439

VIABILITY
Cellular and molecular level responses after radiofrequency radiation exposure, alone or in combination with x rays or chemicals
[AD-A268189] p 1501 N94-17729

VIBRATION
Vibrational and electronic properties of clusters and ultrathin films
[DE93-012291] p 1367 N94-17678
Design and test of a low jitter metal to metal contact solid dielectric switch
[DE93-016957] p 1394 N94-17755
Wavelet transform for time-frequency analysis of the vibrational signature and its application
[AD-A269928] p 1454 N94-18661
Unimolecular photodissociation dynamics of ketene (CH2CO): The singlet/triplet branching ratio and experimental observation of the vibrational level thresholds of the transition-state
[DE93-019252] p 1352 N94-19304

VIBRATION DAMPING
Generalization of optimal control theory: Linear and nonlinear structures
[PB93-188621] p 1540 N94-18125
The longitudinal free vibrations of a fixed-free two-phase elastic bar
[AD-A268768] p 1453 N94-18387
Analysis and design of robust decentralized controllers for nonlinear systems
[DE93-019224] p 1543 N94-19302

VIBRATION ISOLATORS
Modeling and new equipment definition for the vibration isolation box equipment system
[NASA-CR-193185] p 1379 N94-17763
Generalization of optimal control theory: Linear and nonlinear structures
[PB93-188621] p 1540 N94-18125

VIBRATION MODE
Predicted structural response of the lightweight-interceptor technology demonstration vehicle
[DE93-014676] p 1333 N94-17782

Comparison of the modeling solutions with the hydrogen discharge data
[DE93-015115] p 1565 N94-17797
Eigenvalue routines in NASTRAN: A comparison with the Block Lanczos method p 1450 N94-17838

VIBRATION TESTS
The 7th International Cryocooler Conference
[AD-A268451] p 1379 N94-18147

VIBRATIONAL SPECTRA
Effect of oxygen concentration and ordering on vanadium-oxygen alloy vibrational spectra
[DE93-627003] p 1355 N94-17692
An ab initio study of the weakly bonded CO-Cl2 complex
[AD-A269000] p 1349 N94-18395
Wavelet transform for time-frequency analysis of the vibrational signature and its application
[AD-A269928] p 1454 N94-18661

VIBRATIONAL STATES
Vibrational dynamics in photoinduced electron transfer
[DE93-040874] p 1567 N94-18533

VIDEO DATA
Pegasus project description
[MEMO-INF-92-75] p 1536 N94-19159
Pegasus: Operating system support for distributed multimedia systems
[MEMO-INF-92-76] p 1536 N94-19160

VIGNETTING
Considerations for the use of the modified line reversal technique for gas temperature measurement
[DE93-015752] p 1576 N94-17857

VISCOELASTICITY
A finite strain ring dynamical model for pneumatic tires
[AD-A269286] p 1444 N94-18266
Wave propagation near explosive sources
[AD-A270102] p 1418 N94-18870
Dynamical behavior of tantalum
[DE93-017877] p 1362 N94-18919

VISCOMETERS
Some problems in the rheological characterisation of composite rocket propellants
[AD-A268806] p 1376 N94-18203

VISCOMETRY
Advanced in macrostatistical hydrodynamics
[DE93-018479] p 1410 N94-18270

VISCOPLASTICITY
Inelastic deformation and damage at high temperature
[DE93-018155] p 1448 N94-17814

VISCOSITY
Investigation of a matrix-model for the artificial dissipation in a cell vertex finite volume scheme for solving the Navier-Stokes equations
[DLR-FB-92-33] p 1409 N94-18076
Some problems in the rheological characterisation of composite rocket propellants
[AD-A268806] p 1376 N94-18203
Advanced in macrostatistical hydrodynamics
[DE93-018479] p 1410 N94-18270
Measurement of viscosity, density, and gas solubility of refrigerant blends in selected synthetic lubricants
[DE93-040221] p 1350 N94-18977
Viscosity in the edge of tokamak plasmas
[DE93-018039] p 1588 N94-18968
Polymer technology publication. Series no. 14, 1993
[PB93-195964] p 1372 N94-19052
Densities and viscosities of ternary ammonia/water fluids
[DE93-015966] p 1351 N94-19116
Locally adaptive remeshing scheme for calculating fluid instabilities
[DE93-019577] p 1422 N94-19568

VISCOUS DAMPING
Time dependent identification of nonlinear structures
[ECL-92-64] p 1457 N94-19403

VISCOUS FLOW
Vortex methods and statistics
[DE93-016974] p 1556 N94-17886
Efficient simulation of incompressible viscous flow over multi-element airfoils p 1306 N94-18421
Viscous phenomena affecting high-lift systems and suggestions for future CFD development
p 1308 N94-18433
A fast computing method for the flow over high-lift wings p 1308 N94-18437
Computational techniques for high-speed flows with viscous and chemical effects p 1412 N94-18560
Simulation of three dimensional unsteady viscous flows in turbomachines
[ECL-92-15] p 1420 N94-19398
Transient response of a viscous and anchored liquid bridge to an axial pulse
[LRT-WE-9-FB-7-1992] p 1379 N94-19492
Numerical simulation of viscous flows in chemical nonequilibrium
[MBB-LME-211-S-PUB-506] p 1421 N94-19497
Theoretical examination of the flow around a cylinder with a low dimensional Galerkin process
[MPIS-25/1992] p 1422 N94-19525

VISCOUS FLUIDS
Axial response of differently excited anchored viscous liquid bridges in zero-gravity
[LRT-WE-9-FB-1-1992] p 1379 N94-19489
Free fall liquid column dynamics in a droptower
[LRT-WE-9-FB-6-1992] p 1379 N94-19491
Transient response of a viscous and anchored liquid bridge to an axial pulse
[LRT-WE-9-FB-7-1992] p 1379 N94-19492

VISIBILITY
Visibility impairment assessment: Importance of using theoretically derived optical characterizations
[DE93-017147] p 1470 N94-17749
Station climatic summaries: North America. Volume 1: The contiguous United States
[AD-A269567] p 1490 N94-18303
The urban perspectives of acid rain
[DE93-018881] p 1474 N94-18523
Station climatic summaries, North America. Volume 2: Alaska, Canada and Greenland
[AD-A269793] p 1493 N94-18732

VISIBLE SPECTRUM
Overview of research in progress at the Center of Excellence
[NASA-CR-194329] p 1618 N94-19256

VISION
Localization of figure background segregation mechanisms in primate visual cortex
[PB93-187961] p 1508 N94-18121
Effects of location cuing on redundant target processing
[IZF-1993-B-1] p 1510 N94-19443

VISUAL ACUITY
US Army aviation epidemiology data register: Prevalence of refractive error among US aircrew members
[AD-A269550] p 1505 N94-18289
Psychophysical analyses of perceptual representations
[AD-A268711] p 1508 N94-18313

VISUAL AIDS
Three-dimensional cloud visualization based on satellite imagery
[AD-A269318] p 1490 N94-18300

VISUAL DISCRIMINATION
Psychophysical analyses of perceptual representations
[AD-A268711] p 1508 N94-18313

VISUAL FIELDS
Stochastic models of attention and search
[AD-A268622] p 1508 N94-18292

VISUAL FLIGHT
VMC left turn curved approaches, test results --- (visual meteorological conditions)
[AD-A269476] p 1316 N94-18728

VISUAL OBSERVATION
Ultraviolet observations of clusters of Wolf-Rayet stars in the SBm3 galaxy NGC 4214 and Ultraviolet and optical observations of LINER's
[NASA-CR-194307] p 1622 N94-19431

VISUAL PERCEPTION
Localization of figure background segregation mechanisms in primate visual cortex
[PB93-187961] p 1508 N94-18121
Stochastic models of attention and search
[AD-A268622] p 1508 N94-18292
Visual perception of features and objects
[AD-A269879] p 1508 N94-18682
Interdisciplinary training in life science (FY 1991 ASSERT)
[AD-A269220] p 1512 N94-18886
Overview of research in progress at the Center of Excellence
[NASA-CR-194329] p 1618 N94-19256
Serial pattern complexity: Irregularity and hierarchy
[PB93-191914] p 1509 N94-19348
Stimulus-driven capture and attentional set: Selective search for color and visual abrupt onsets
[IZF-1992-B-9] p 1509 N94-19419
Pilot studies on object motion perception during linear self-motion after long duration centrifugation of human subjects
[IZF-1993-B-3] p 1510 N94-19439

VISUAL STIMULI
Localization of figure background segregation mechanisms in primate visual cortex
[PB93-187961] p 1508 N94-18121
Stimulus-driven capture and attentional set: Selective search for color and visual abrupt onsets
[IZF-1992-B-9] p 1509 N94-19419
Effects of location cuing on redundant target processing
[IZF-1993-B-1] p 1510 N94-19443

VISUAL TASKS
Stimulus-driven capture and attentional set: Selective search for color and visual abrupt onsets
[IZF-1992-B-9] p 1509 N94-19419

VITON RUBBER (TRADEMARK)
Effect of temperature and O-ring gland finish on sealing ability of Viton V747-75
[NASA-TP-3391] p 1368 N94-18075

VOICE COMMUNICATION
Template based low data rate speech encoder
[AD-A270900] p 1392 N94-19748
A real-time spoken-language system for interactive problem-solving, combining linguistic and statistical technology for improved spoken language understanding
[AD-A270901] p 1392 N94-19749
Improved HF data network simulator, volume 1
[AD-A270953] p 1393 N94-19752
Improved HF data network simulator, software user's manual, volume 2
[AD-A270954] p 1393 N94-19753
Control of integrated voice/data multi-hop radio networks via reduced-load approximations
[AD-A270661] p 1393 N94-19779

VOICE CONTROL
Feasibility study in linguistically motivated object-oriented conceptual design of information systems
[PB93-197754] p 1618 N94-19331

VOICE DATA PROCESSING
Template based low data rate speech encoder
[AD-A270900] p 1392 N94-19748
A real-time spoken-language system for interactive problem-solving, combining linguistic and statistical technology for improved spoken language understanding
[AD-A270901] p 1392 N94-19749

VOIDS
Evaluation of the production-grade class 4 flextensional transducer shell
[AD-A268796] p 1340 N94-18201
Binding of copper to nanocavity surfaces in silicon
[DE93-019073] p 1364 N94-19080
Shrinkage void formation and its effect on freeze and thaw processes of lithium and lithium-fluoride for space applications
[DE93-019303] p 1338 N94-19128

VOLCANOES
Effects of the Mount Pinatubo eruption on solar insolation: Four case studies
[DE93-018454] p 1475 N94-18817

VOLTAGE CONVERTERS (DC TO DC)
High temperature co-axial winding transformers
[NASA-CR-194580] p 1407 N94-19643

VOLTERRA EQUATIONS
Time dependent identification of nonlinear structures
[ECL-92-64] p 1457 N94-19403

VORTEX BREAKDOWN
Navier-Stokes, dynamics and aeroelastic computations for vortical flows, buffet and flutter applications
[NASA-CR-194520] p 1313 N94-19621

VORTEX GENERATORS
Several examples where turbulence models fail in inlet flow field analysis p 1412 N94-18556

VORTICES
Vortex methods and statistics
[DE93-016974] p 1556 N94-17886
Filamentary magnetohydrodynamic plasmas
[DE93-015616] p 1583 N94-17945
Wake structure and aerodynamic behavior of high lift aircraft configurations during unsteady maneuvers in ground effect p 1309 N94-18439
Close-coupled oscillating canard effects on post-stall lift enhancement
[AD-A268938] p 1321 N94-18541
Computational aero-acoustics as a branch of turbulence research p 1411 N94-18552
Several examples where turbulence models fail in inlet flow field analysis p 1412 N94-18556
Compact advection schemes on unstructured grids
p 1413 N94-18564
Lift and pitching moment induced on jet STOVL aircraft by the ground vortex
[AD-A269816] p 1318 N94-18733
Interferometric investigations of compressible dynamic stall over a transiently pitching airfoil
[NASA-TM-109380] p 1312 N94-19119
Research and training activities of the Joint Institute for Aeronautics and Acoustics
[NASA-CR-194742] p 1421 N94-19493
Three dimensional network generation and Euler calculation for a wing fuselage canard configuration
[MBB-LME-211-S-PUB-511-A] p 1319 N94-19500
Estimation of wake vortex advection and decay using meteorological sensors and aircraft data
[AD-A270763] p 1316 N94-19661

Examinations of converging cylindrically symmetric second sound propagation in He2
[MPIS-9/1992] p 1564 N94-19715

VORTICITY

Vortex methods and statistics
[DE93-016974] p 1556 N94-17886

Filamentary magnetohydrodynamic plasmas
[DE93-015616] p 1583 N94-17945

Research on two equation models
p 1411 N94-18547

Implementation of the turn function method in KIVA-F90
[DE93-018394] p 1419 N94-19027

Numerical modelling of crystal growth
[AD-A271206] p 1605 N94-19719

VORTICITY EQUATIONS

Cell vertex methods for steady inviscid flow
p 1413 N94-18563

Variational approaches to CFD: Applications to potential Euler and Navier-Stokes equations
p 1413 N94-18565

Implementation of the turn function method in KIVA-F90
[DE93-018394] p 1419 N94-19027

VOYAGER 2 SPACECRAFT

Voyager's last encounter
[NASA-TM-109361] p 1628 N94-18957

VSAT (NETWORK)

Multichannel error correction code decoder
[NASA-TM-106331] p 1333 N94-19313

W

WAFERS

Selective electrochemical wafer thinning for silicon characterization
[DE93-015083] p 1592 N94-17742

RF vacuum microelectronics
[AD-A269454] p 1396 N94-18284

Integrated circuits: Resistless processing simplifies production and cuts costs
[DE93-018069] p 1405 N94-18941

WAKES

Wake field in electron-positron plasmas
[DE93-624929] p 1584 N94-17955

Enhanced acceleration in a self-modulated-laser wakefield accelerator
[AD-A268452] p 1586 N94-18148

Wake structure and aerodynamic behavior of high lift aircraft configurations during unsteady maneuvers in ground effect p 1309 N94-18439

WALKING

Road march performance of special operations soldiers carrying various loads and load distributions
[AD-A269198] p 1512 N94-18882

WALL FLOW

Research on two equation models
p 1411 N94-18547

Contribution to the modelling of near-wall turbulence
p 1414 N94-18585

Relation between the fluctuating wall pressure and the turbulent structure of a boundary layer on a cylinder in axial flow
[AD-A270242] p 1418 N94-18906

WALL PRESSURE

Calculation of turbulent boundary layer wall pressure spectra
[AD-A269549] p 1416 N94-18642

Correlation of incoming boundary layer pitot pressure fluctuations with the unsteadiness of fin-induced shock wave turbulent boundary layer interactions
[AD-A270059] p 1417 N94-18796

Relation between the fluctuating wall pressure and the turbulent structure of a boundary layer on a cylinder in axial flow
[AD-A270242] p 1418 N94-18906

WALL TEMPERATURE

Development of a multi-point two-color pyrometer for tube and wall temperature and emissivity measurement at the CFFF
[DE93-014716] p 1429 N94-18207

Parabolized Navier-Stokes computation of surface heat transfer characteristics for supersonic and hypersonic KE projectiles
[AD-A268858] p 1410 N94-18391

Correlation of incoming boundary layer pitot pressure fluctuations with the unsteadiness of fin-induced shock wave turbulent boundary layer interactions
[AD-A270059] p 1417 N94-18796

Finite difference program for calculating hydride bed wall temperature profiles
[DE93-019272] p 1523 N94-19005

Analysis of film cooling in rocket nozzles
[NASA-CR-194674] p 1338 N94-19438

WALLS

Report of the 1991 Workshop on Particle-Material Interactions for Fusion Research
[DE93-788393] p 1573 N94-18156

Thermal analysis of coatings and substrate materials during a disruption in fusion reactors
[DE93-017688] p 1588 N94-18971

WARNING SYSTEMS

Development of ultrasonic motor and application to silent alarm analog quartz watch p 1425 N94-18016

Aircraft fire sentry. Volume 1: Summary
[AD-A270087] p 1315 N94-18822

Aircraft fire sentry. Volume 2: Appendices A, B, C and D
[AD-A270088] p 1315 N94-18823

WASHING

A comparison of wet and dry scrubbing systems for control of metals and dioxin/furan emissions from incinerators
[DE93-017446] p 1474 N94-18502

WASPALOY

Atlas of formability: Waspaloy
[AD-A268323] p 1593 N94-17805

WASTE DISPOSAL

Rapid geophysical surveyor
[DE93-016637] p 1461 N94-17851

Research activities, Faculty of Civil Engineering, Delft University of Technology, 1990 - 1991
[PB93-195022] p 1380 N94-19254

WASTE ENERGY UTILIZATION

Feasibility survey of thermoelectric conversion technology using semiconductors
[DE93-520882] p 1595 N94-18105

Molten carbonate fuel cell networks: Principles, analysis, and performance
[DE93-000281] p 1468 N94-18925

WASTE TREATMENT

Rapid geophysical surveyor
[DE93-016637] p 1461 N94-17851

Ultrasonic process for destruction of chlorinated organic compounds in aqueous solution
[DE93-015551] p 1348 N94-18249

WASTE WATER

Ultrasonic process for destruction of chlorinated organic compounds in aqueous solution
[DE93-015551] p 1348 N94-18249

WATER

Aluminum powder/water reaction ignited by electrical pulsed power
[AD-A269223] p 1376 N94-17840

Search for lunar water ice in cometary impact craters
[AD-A270130] p 1627 N94-18877

Calculation of molecular excitation rates
[NASA-CR-193782] p 1571 N94-19236

WATER CIRCULATION

Ecological and environmental impacts of construction in the coastal zone
[AD-A269196] p 1475 N94-18881

WATER CURRENTS

Overview of physical oceanographic measurements taken during the Mount Mitchell cruise to ROPME sea area
[DE93-018460] p 1497 N94-18494

Method for extracting tidal and inertial motion from ARGOS ice buoys applied to the Barents Sea during CEAREX
[PB93-190213] p 1499 N94-19063

Time domain calculations of the second-order drift force on a floating two-dimensional object in current and waves
[REPT-93-13] p 1419 N94-19087

WATER DEPTH

A laboratory model of a cooled continental shelf
[AD-A270862] p 1500 N94-19792

WATER FLOW

Preliminary design of a water cooled avionics cooling rack
[AD-A268826] p 1320 N94-18536

WATER HAMMER

Examinations of the friction behavior in nonstationary flow processes in pipes
[MITT-7] p 1423 N94-19730

WATER POLLUTION

Ecological and environmental impacts of construction in the coastal zone
[AD-A269196] p 1475 N94-18881

WATER TABLES

Application of ARC/INFO to regional scale hydrogeologic modeling
[DE93-015673] p 1461 N94-18107

Similarity solutions for gravity-dominated spreading of a lens of organic contaminant
[REPT-93-24] p 1420 N94-19139

WATER TUNNEL TESTS

The effect of fine surface riblets on the flow around an inclined axially symmetrical body
[MPIS-105/1993] p 1420 N94-19356

WATER VAPOR

Surface fluxes important to cloud development
[DE93-016633] p 1488 N94-17715

A mobile remote sensing laboratory for water vapor, trace gas, aerosol, and wind speed measurements
[DE93-017158] p 1489 N94-18132

Analysis of satellite-derived ozone and water vapor measurements
[NASA-CR-193810] p 1486 N94-19237

WATER WAVES

Design of a general purpose and autonomous transmitter and receiver system for underwater acoustic experiments at sea
[AD-A269268] p 1495 N94-17822

Wind products for use in coastal wave and surge models
[AD-A269753] p 1497 N94-18414

Full Boltzmann discrete spectral wave model, implementation and nondimensional tests
[AD-A269885] p 1498 N94-18685

Acoustic travel time perturbations due to an internal tide and internal wave field in the Barents Sea
[AD-A270879] p 1499 N94-19580

WATERPROOFING

Mutrometre: Construction for fast water proof measurements under low pressure and air suppression
p 1427 N94-18031

Development of a new concept diver's watch
p 1429 N94-18041

WATERWAYS

Overview of physical oceanographic measurements taken during the Mount Mitchell cruise to ROPME sea area
[DE93-018460] p 1497 N94-18494

DYNLET1 model formulation and user's guide
[AD-A269843] p 1498 N94-18723

Centrifuge modeling of explosion-induced craters in unsaturated sand
[AD-A270194] p 1417 N94-18780

The ecological and environmental impacts of manmade marshes
[AD-A269213] p 1475 N94-18885

WAVE AMPLIFICATION

A study of the amplification of laser and VLF waves using a simple pendulum model
[AD-A270857] p 1442 N94-19770

WAVE ATTENUATION

Seismic studies of the geologic structure and physical properties of the seabed
[AD-A270895] p 1500 N94-19747

WAVE DISPERSION

Transformation of energy and momentum due to Landau damping in space
[DE93-624921] p 1581 N94-17689

Phase-space description of plasma waves: Linear and nonlinear theory
[IRF-SR-211] p 1587 N94-18860

WAVE EQUATIONS

The phase mixing of shear Alfven waves
[DE93-624920] p 1581 N94-17688

On higher dimensional Ermakov systems: Canonical reductions
[MATHS-REPT-A-182] p 1548 N94-18140

Multidimensional wave decompositions for the Euler equations p 1413 N94-18562

Modeling of current features in Gulf Stream SAR imagery
[AD-A270734] p 1499 N94-19609

WAVE FUNCTIONS

A hydrogen atom in the curved space. Expansion over free solutions on the three-dimensional sphere
[DE93-629868] p 1549 N94-18198

WAVE GENERATION

Full Boltzmann discrete spectral wave model, implementation and nondimensional tests
[AD-A269885] p 1498 N94-18685

WAVE INTERACTION

Correlation of incoming boundary layer pitot pressure fluctuations with the unsteadiness of fin-induced shock wave turbulent boundary layer interactions
[AD-A270059] p 1417 N94-18796

A method for solving the KDV equation and some numerical experiments
[DE93-624726] p 1550 N94-19246

WAVE PACKETS

Schroedinger's hope
[AD-A270988] p 1581 N94-19772

WAVE PROPAGATION

Understanding curved detonation waves
[DE93-014581] p 1408 N94-17728

Microwave scattering from TAE modes
[DE93-018170] p 1583 N94-17809

Radio wave propagation in structured ionization for satellite and radar applications
[AD-A268457] p 1382 N94-17844
Comments on computational underwater acoustics
[DE93-013789] p 1562 N94-17873
Wake field in electron-positron plasmas
[DE93-624929] p 1584 N94-17955
Modeling shock initiation in Composition B
[DE93-016544] p 1376 N94-18095
Plasma production by helicon waves
[DE93-788396] p 1586 N94-18213
Crystal optics of high energy gamma-beams
[DE93-630228] p 1577 N94-18217
On the Michelson-Morley experiment
[DE93-629908] p 1608 N94-18268
Acoustic intensity measurements in the presence of low Mach number flow
[AD-A269995] p 1562 N94-18664
Wave propagation near explosive sources
[AD-A270102] p 1418 N94-18870
Shock propagation in crustal rock
[AD-A270148] p 1485 N94-18899
Estimating the oceanic sound speed environmental for long-range acoustic propagation
[AD-A270231] p 1499 N94-18903
Shock-loading response of advanced materials
[DE93-018344] p 1455 N94-19033
Stress pulse phenomena
[DE93-019064] p 1456 N94-19078
Transmission of acoustic waves through strongly heterogeneous, two-dimensional velocity models
[REPT-93-09] p 1563 N94-19083
Liquid sound speeds at pressure from the optical analyzer technique
[DE93-018362] p 1563 N94-19151
Comments on computational underwater acoustics
[DE93-019880] p 1563 N94-19270
Acoustic propagation modeling using MATLAB
[AD-A270905] p 1564 N94-19750

WAVE REFLECTION
Studies of enhanced radar backscatter
[AD-A269544] p 1385 N94-18288

WAVE SCATTERING
Millimeter wave reflectivity measurement system
[AD-A270008] p 1387 N94-18601
Fast iterative solution of sparsely sampled seismic inverse problems
[REPT-93-16] p 1486 N94-19081
Acoustic travel time perturbations due to an internal tide and internal wave field in the Barents Sea
[AD-A270679] p 1499 N94-19580

WAVE-PARTICLE INTERACTIONS
Implementation of the digital wave-processing experiment p 1329 N94-19628
A study of the amplification of laser and VLF waves using a simple pendulum model
[AD-A270857] p 1442 N94-19770

WAVEFORMS
The d(exp 3)delta-a(exp 3)delta and b(exp 3)phi-a(exp 3)delta systems of ZrS, Part 2: Appendix, list of wavenumbers
[USIP-92-05] p 1602 N94-19293
The wideband plasma wave investigation
p 1328 N94-19627

WAVEGUIDE WINDOWS
Experimental and theoretical investigation of broadband high-power windows for millimeter waves
[KFK-5157] p 1391 N94-19617

WAVEGUIDES
Comments on computational underwater acoustics
[DE93-013789] p 1562 N94-17873
Advances and applications of ABCI
[DE93-016971] p 1383 N94-18055
Waveguide and resonator perturbation techniques for measuring chirality and non-reciprocity of biisotropic materials
[PB93-187243] p 1384 N94-18116
Designs for a 10.6 micrometer electromagnetic wiggler Free-Electron Laser (FEL)
[AD-A269695] p 1439 N94-18576
Single-transverse-mode, narrow-bandwidth pulsed tunable dye laser with hollow circular intracavity dielectric waveguide
[AD-A270022] p 1439 N94-18614

WAVELENGTH DIVISION MULTIPLEXING
Advanced optical fiber communication systems
[AD-A269120] p 1577 N94-18254
Integrated Photonics Research: Post-deadline papers
[AD-A269232] p 1609 N94-18908

WAVELENGTHS
The A((2)pi(sub u))-X((2)pi(sub g)) system of Br2(+) studied by velocity modulation spectroscopy
[USIP-93-04] p 1569 N94-18847

The d(exp 3)delta-a(exp 3)delta and b(exp 3)phi-a(exp 3)delta systems of ZrS, Part 2: Appendix, list of wavenumbers
[USIP-92-05] p 1602 N94-19293

WAVELET ANALYSIS
Multivariate wavelet representations and approximations
[AD-A269350] p 1546 N94-17825
Wavelet transform for time-frequency analysis of the vibrational signature and its application
[AD-A269928] p 1454 N94-18661
Introduction to wavelets
[AD-A268465] p 1389 N94-18801
Application of wavelet transform techniques to spread spectrum demodulation and jamming
[AD-A267389] p 1389 N94-19009
A non-homogeneous, spatio-temporal, wavelet multiresolution analysis and its application to the analysis of motion
[AD-A270621] p 1538 N94-19534

WEAK INTERACTIONS (FIELD THEORY)
On the difference caused by CP violation in the energy spectra of pions in K(sup (+-))(yields)(pi)(+-)(pi)(+-)(pi)-+ decays
[DE93-624828] p 1564 N94-17687
Extraction of Z(prime) coupling data from Z(prime) (yields) jj at the LHC and SSC
[DE93-018576] p 1570 N94-19096

WEAPON SYSTEMS
Review of short-term, high-level exposure to metals: Antimony, barium, and cadmium
[AD-A268896] p 1505 N94-18392

WEAPONS
Temperature of aircraft cargo flame exposure during accidents involving fuel spills
[DE93-019633] p 1381 N94-19539

WEAR
Interdisciplinary research on wear of materials
[AD-A268190] p 1443 N94-17730
Effect of temperature and O-ring gland finish on sealing ability of Viton V747-75
[NASA-TP-3391] p 1368 N94-18075
Studies of dynamic contact of ceramics and alloys for advanced heat engines
[DE93-016366] p 1368 N94-18110
MHD integrated topping cycle project
[DE93-040520] p 1588 N94-18978
Contribution to the tribological study of magnetic-tape head contact
[ECL-92-57] p 1434 N94-19414
Atomic-scale friction measurements using friction force microscopy. Part 1: General principles and new measurement techniques
[AD-A270749] p 1446 N94-19678
Microtribology of magnetic media
[AD-A271209] p 1407 N94-19722
Tribological studies of silicon for magnetic recording applications (Invited)
[AD-A270878] p 1447 N94-19784

WEAR RESISTANCE
Joining and Adhesion of Advanced Inorganic Materials Symposium
[AD-A269748] p 1342 N94-18720

WEAR TESTS
Interdisciplinary research on wear of materials
[AD-A268190] p 1443 N94-17730

WEATHER
New techniques for contrail forecasting
[AD-A269686] p 1490 N94-18573
CDIAC catalog of numeric data and computer model packages
[DE93-017675] p 1475 N94-18832
Eastern Europe: A climatological study
[AD-A269200] p 1493 N94-18883

WEATHER FORECASTING
Rapid oceanic cyclogenesis studies
[AD-A269258] p 1490 N94-18265
Preparation of data assimilation and model evaluation experiment data sets
[AD-A269996] p 1498 N94-18665
Atlas of SSM/I satellite ice concentration interpolated to operational ice model domains of the Arctic for 1992
[AD-A270306] p 1499 N94-18727
Organized track system: Air ways above the ocean
p 1495 N94-19702
Calamity weather: Environmental calamities and meteorology p 1495 N94-19703

WEATHER STATIONS
Report of the Experts Meeting on Reference Climatological Stations (RCS) and National Climate Data Catalogues (NCC)
[WMO-TD-535] p 1494 N94-19312

WEIGHT (MASS)
SeaSoar and CTD sections across the Iceland-Faeroes Front and Faeroe Shetland Channel, August 1990
[IOS-295-1992] p 1496 N94-18064

WEIGHT ANALYSIS
Study on radiation-induced deterioration of grease at high temperature, 3
[DE93-788368] p 1369 N94-18220

WEIGHT MEASUREMENT
Testing of protective coatings in hydrogen
[DE93-040326] p 1375 N94-19651

WEIGHT REDUCTION
Regenerative fuel cells for High Altitude Long Endurance Solar Powered Aircraft
[DE93-016991] p 1465 N94-17853
Lightweight materials for transportation: Program plan
[DE93-017381] p 1340 N94-18087

WEIGHTING FUNCTIONS
Nontraditional windows in spectral analysis
[AD-A271336] p 1553 N94-19583

WEIGHTLESSNESS
Space research with intact organisms: The role of Space Station Freedom p 1502 N94-19213
Axial response of differently excited anchored viscous liquid bridges in zero-gravity
[LRT-WE-9-FB-1-1992] p 1379 N94-19489

WEIGHTLESSNESS SIMULATION
The brain electrical activity in different G situations
[AERONAUTICA-ACTA-A-372-199]
p 1507 N94-19523

WELD STRENGTH
Microstructural analysis of solid-state resistance welds
[DE93-017295] p 1443 N94-17761
Thermal insulation of wet shielded metal arc welds
[AD-A268697] p 1445 N94-18465

WELD TESTS
Initiation and growth of microcracks in high strength steel butt welds
[AD-A268751] p 1454 N94-18466

WELDABILITY
Technique to eliminate helium induced weld cracking in stainless steels
[DE93-015982] p 1357 N94-17859
Helium-induced weld degradation of HT-9 steel
[DE93-015981] p 1358 N94-17915

WELDED JOINTS
Microstructural analysis of solid-state resistance welds
[DE93-017295] p 1443 N94-17761
Helium-induced weld degradation of HT-9 steel
[DE93-015981] p 1358 N94-17915
Development and application of specially-focused ultrasonic transducers to location and sizing of defects in 75 mm- to 127 mm-thick austenitic stainless steel weld metals
[DE93-015975] p 1453 N94-18108
Initiation and growth of microcracks in high strength steel butt welds
[AD-A268751] p 1454 N94-18466
Environmental degradation of Alloy 600 and welded filler metal EN82 in an elevated temperature aqueous environment
[DE93-018049] p 1363 N94-18940
Modeling of single-crystal laser-weld microstructures
[DE93-017853] p 1445 N94-18976
Effects of irradiation temperature on Charpy and tensile properties of high-copper, low upper-shelf, submerged-arc welds
[DE93-017858] p 1445 N94-19047
Ultrasonic technique for inspection of GPHS capsule girth weld integrity
[DE93-040072] p 1448 N94-19189
Overlay welding irradiated stainless steel
[DE93-018767] p 1446 N94-19334

WELDING
Automatic soldering for watch circuit components
p 1428 N94-18037
Initiation and growth of microcracks in high strength steel butt welds
[AD-A268751] p 1454 N94-18466
Design considerations for remotely operated welding in space: Task definition and visual weld monitoring experiment
[AD-A268752] p 1445 N94-18634

WELDING MACHINES
Initiation and growth of microcracks in high strength steel butt welds
[AD-A268751] p 1454 N94-18466

WELLS
Penetrometer compatible, fiber-optic sensor for continuous monitoring of chlorinated hydrocarbons: Field test results
[DE93-017974] p 1352 N94-19266

WETLANDS
Ecological and environmental impacts of construction in the coastal zone
[AD-A269196] p 1475 N94-18881

WETTABILITY
Wetting behavior of alternative solder alloys
[DE93-016730] p 1359 N94-18127

Solderability perservative coatings: Electroless tin versus organic azoles
[DE93-017634] p 1370 N94-18477
Wettability and reaction kinetics in metal matrix composites
[AD-A270377] p 1342 N94-18704

WETTING
Wetting behavior of alternative solder alloys
[DE93-016730] p 1359 N94-18127

WHEAT
FT-NIR spectroscopy in quantitative and qualitative measurements of cereal products
[VTT-TIED-1331] p 1346 N94-17973

WHEELS
Friction drive position transducer
[AD-D015851] p 1424 N94-17717

WHISKER COMPOSITES
Bibliography on ceramic matrix composites and reinforcing whiskers, platelets, and fibers, 1970-1990
[AD-A270139] p 1371 N94-18750

WHITE DWARF STARS
Eclipsing cataclysmic variables. Deep eclipses in H0928+501. YY Draconis, the whirling dervish. New x ray pulsar candidates from HEAO-1
[NASA-CR-194027] p 1621 N94-18855

WHITE HOLES (ASTRONOMY)
Maximal hypersurfaces in asymptotically stationary spacetimes
[MPA-708] p 1621 N94-18141

WIGGLER MAGNETS
A superconducting short period undulator for a harmonic generation FEL experiment
[DE93-017581] p 1436 N94-17998
FEL experiment with a focusing wiggler
[DE93-788586] p 1438 N94-18160
Magnetic field measurements of a superconducting undulator for a Harmonic Generation FEL experiment at the NSLS
[DE93-017621] p 1438 N94-18504
Designs for a 10.6 micrometer electromagnetic wiggler Free-Electron Laser (FEL)
[AD-A269695] p 1439 N94-18576
Coherence and linewidth studies of a 4-nm high power FEL
[DE93-018533] p 1441 N94-19030
Compact free electron lasers for medical applications
[AD-A271272] p 1442 N94-19729

WILDLIFE
Assessing impacts of climate change on forests: The state of biological modeling
[DE93-015916] p 1471 N94-17790

WIND (METEOROLOGY)
Surface fluxes important to cloud development
[DE93-016633] p 1488 N94-17715
A review of wind field models for atmospheric transport
[DE93-016085] p 1488 N94-17895
A mobile remote sensing laboratory for water vapor, trace gas, aerosol, and wind speed measurements
[DE93-017158] p 1489 N94-18132
Spectral analysis of synoptic time scale disturbances over the tropical eastern Pacific during summer 1989, 1990 and 1991
[AD-A268821] p 1490 N94-18206
SPNDL: A concept for a small satellite Doppler lidar wind sounder p 1327 N94-19181

WIND DIRECTION
AN/APS-137 Forward Looking Airborne Radar (FLAR) evaluation Spring 1992 experiment
[AD-A268899] p 1384 N94-18228
Station climatic summaries: North America. Volume 1: The contiguous United States
[AD-A269567] p 1490 N94-18303
Station climatic summaries, North America. Volume 2: Alaska, Canada and Greenland
[AD-A269793] p 1493 N94-18732

WIND MEASUREMENT
Boundary layer heat budgets from wind profiler/RASS data: A feasibility study
[DE93-013187] p 1489 N94-18052
Some potential errors in satellite wind estimates using the geostrophic approximation and the thermal wind
[AD-A269784] p 1491 N94-18599
Impact of shorter wavelengths on optical quality for laws
[NASA-CR-193873] p 1579 N94-18858
SPNDL: A concept for a small satellite Doppler lidar wind sounder p 1327 N94-19181
Shape of wind gusts at a 130m tower at Wilhelmshaven (Germany)
[BER-BAND-B3] p 1494 N94-19503

WIND PROFILES
A review of wind field models for atmospheric transport
[DE93-016085] p 1488 N94-17895
SPNDL: A concept for a small satellite Doppler lidar wind sounder p 1327 N94-19181

WIND TUNNEL MODELS
A wind tunnel model control surface actuator interface
[AD-A268729] p 1322 N94-18324
A study of the use of half-models in high-lift wind-tunnel testing p 1308 N94-18434
High lift systems for transport aircraft with advanced airfoils p 1310 N94-18446
Survey on the application of a 3D general purpose wind-tunnel research model
[LR-713] p 1323 N94-19372

WIND TUNNEL TESTS
Aerodynamic characteristics of a helicopter rotor airfoil as affected by simulated ballistic damage
[AD-A269206] p 1311 N94-18413
Experimental investigation of flow around a multielement airfoil p 1305 N94-18417
High Reynolds number configuration development of a high-lift airfoil p 1306 N94-18424
The GARTEUR high lift research programme
p 1307 N94-18430
An experimental investigation of the optimum slat setting on a combat aircraft model p 1308 N94-18431
An experimental investigation of attachment-line transition on the slat of a combat aircraft model
p 1308 N94-18432
A study of the use of half-models in high-lift wind-tunnel testing p 1308 N94-18434
High-lift design for large civil aircraft
p 1310 N94-18445
High lift systems for transport aircraft with advanced airfoils p 1310 N94-18446
The world's largest wind tunnel
[NASA-TM-109371] p 1322 N94-18963

WIND TUNNELS
A wind tunnel model control surface actuator interface
[AD-A268729] p 1322 N94-18324
Perspective and future possibilities
p 1431 N94-18651
Acoustic intensity measurements in the presence of low Mach number flow
[AD-A269995] p 1562 N94-18664
The world's largest wind tunnel
[NASA-TM-109371] p 1322 N94-18963
Langley's 50th year
[NASA-TM-109365] p 1632 N94-18980

WIND TURBINES
The value of windpower: An investigation using a qualified production cost model
[DE93-010043] p 1465 N94-17888
FAROW: A tool for fatigue and reliability of wind turbines
[DE93-017639] p 1465 N94-18001
Defining the normal turbine inflow within a wind park environment
[DE93-010032] p 1489 N94-18046
The application of nondestructive techniques to the testing of a wind turbine blade
[DE93-016731] p 1447 N94-18128
Analysis of superconducting magnetic energy storage applications at a proposed wind farm site near Browning, Montana
[DE93-018793] p 1466 N94-18276
A rugged, low-cost advanced data acquisition system for field test projects
[DE93-010041] p 1615 N94-18334
Optimizing wind turbine control system parameters
[DE93-018861] p 1469 N94-19036

WIND VELOCITY
Feasibility of a wind-ellipse criterion in a vortex advisory system for Schiphol Airport
[NLR-TP-91384-U] p 1315 N94-17733
A technique for measuring winds in the lower atmosphere using incoherent Doppler lidar
[DE93-017163] p 1488 N94-17758
The value of windpower: An investigation using a qualified production cost model
[DE93-010043] p 1465 N94-17888
A review of wind field models for atmospheric transport
[DE93-016085] p 1488 N94-17895
A mobile remote sensing laboratory for water vapor, trace gas, aerosol, and wind speed measurements
[DE93-017158] p 1489 N94-18132
AN/APS-137 Forward Looking Airborne Radar (FLAR) evaluation Spring 1992 experiment
[AD-A268899] p 1384 N94-18228
Some potential errors in satellite wind estimates using the geostrophic approximation and the thermal wind
[AD-A269784] p 1491 N94-18599
Station climatic summaries, North America. Volume 2: Alaska, Canada and Greenland
[AD-A269793] p 1493 N94-18732
Moments of ambient Doppler spectra
[DE93-017948] p 1390 N94-19114

WIND VELOCITY MEASUREMENT
Shape of wind gusts at a 130m tower at Wilhelmshaven (Germany)
[BER-BAND-B3] p 1494 N94-19503

WINDING
High temperature co-axial winding transformers
[NASA-CR-194580] p 1407 N94-19643

WINDOWS (COMPUTER PROGRAMS)
Heavy ion nuclear physics research
[DE93-018862] p 1565 N94-17776
Why are human-computer interfaces difficult to design and implement?
[AD-A268843] p 1514 N94-18317

WINDPOWER UTILIZATION
The value of windpower: An investigation using a qualified production cost model
[DE93-010043] p 1465 N94-17888
Analysis of superconducting magnetic energy storage applications at a proposed wind farm site near Browning, Montana
[DE93-018793] p 1466 N94-18276
Optimizing wind turbine control system parameters
[DE93-018861] p 1469 N94-19036
Seasonal variability of wind electric potential in the US
[DE93-018182] p 1493 N94-19051

WINDPOWERED GENERATORS
The value of windpower: An investigation using a qualified production cost model
[DE93-010043] p 1465 N94-17888
Analysis of superconducting magnetic energy storage applications at a proposed wind farm site near Browning, Montana
[DE93-018793] p 1466 N94-18276

WINDSHIELDS
Explicit solution techniques for impact with contact constraints p 1459 N94-19470

WING FLAPS
High-Lift System Aerodynamics
[AGARD-CP-515] p 1305 N94-18415
Where is high-lift today? A review of past UK research programmes p 1305 N94-18416
Experimental investigation of flow around a multielement airfoil p 1305 N94-18417
A design procedure for slotted flaps
p 1305 N94-18418

WING OSCILLATIONS
Lift enhancement device
[AD-D015868] p 1317 N94-17704

WING SLOTS
A design procedure for slotted flaps
p 1305 N94-18418

WINGS
Lift enhancement device
[AD-D015868] p 1317 N94-17704
High-Lift System Aerodynamics
[AGARD-CP-515] p 1305 N94-18415
Prediction of the high-lift performance of multi-element aerofoils using an unstructured Navier-Stokes solver
p 1307 N94-18427
The GARTEUR high lift research programme
p 1307 N94-18430
Viscous phenomena affecting high-lift systems and suggestions for future CFD development
p 1308 N94-18433
In-flight pressure distributions and skin-friction measurements on a subsonic transport high-lift wing section p 1308 N94-18435
A fast computing method for the flow over high-lift wings p 1308 N94-18437
Calculation of multielement airfoils and wings at high lift p 1309 N94-18438
Forty years of high-lift R/D: An aircraft manufacturer's experience p 1309 N94-18441
High-lift research: Application to the design of the ATR72 flap p 1309 N94-18442
The aero-mechanical design of a novel Fowler flap mechanism p 1309 N94-18443
High lift systems for transport aircraft with advanced airfoils p 1310 N94-18446
Dynamic response analysis of composite structural members during missile launch
[AD-A270023] p 1332 N94-18760
Airflow research
[NASA-TM-109372] p 1312 N94-18964
Design for cyclic loading endurance of composites
[NASA-TM-106407] p 1457 N94-19351
Numerical investigation of the incompressible flow around a wing with a fixed spoiler
[ISL-R-109/91] p 1313 N94-19524

WIRELESS COMMUNICATION
Information technology resources assessment
[DE93-015276] p 1613 N94-17894

WOLF-RAYET STARS

Ultraviolet observations of clusters of Wolf-Rayet stars in the SBm3 galaxy NGC 4214 and Ultraviolet and optical observations of LINER's
[NASA-CR-194307] p 1622 N94-19431

WORDS (LANGUAGE)

Neural networks to classify speaker independent isolated words recorded in radio car environments
[REPT-93-013] p 1383 N94-17935

Feasibility study in linguistically motivated object-oriented conceptual design of information systems
[PB93-197754] p 1618 N94-19331

WORK HARDENING

A review of the stages of work hardening
[DE93-016456] p 1359 N94-18114

WORKING FLUIDS

Malone refrigeration
[DE93-014468] p 1379 N94-17725

WORKLOADS (PSYCHOPHYSIOLOGY)

Revision and verification of a seven-point workload estimate scale
[AD-A269194] p 1511 N94-18412

Integrated Terminal Weather System (ITWS)
[AD-A269884] p 1492 N94-18684

WORKSTATIONS

Advanced optical fiber communication systems
[AD-A269120] p 1577 N94-18254

Dialog-Based Learning (DBL) for adaptive interface agents and programming-by-demonstrations systems
[AD-A269154] p 1540 N94-18261

Cesar user library
[FFI-93/7021] p 1529 N94-19378

X

X RAY ABSORPTION

Dynamic behaviors of fragments ejected from the surface of carbon materials by laser ablation
[DE93-788620] p 1438 N94-18161

Potential dependent structural changes of underpotentially deposited copper on an iodine treated platinum surface determined in situ by surface EXAFS and its polarization dependence
[AD-A269890] p 1360 N94-18687

X RAY ANALYSIS

Analysis of HgI2 and PbI2 crystals and detectors by Particle-Induced X Ray Emission (PIXE) and Ion Backscattering Spectroscopy (IBS)
[DE93-017168] p 1594 N94-17896

Potential dependent structural changes of underpotentially deposited copper on an iodine treated platinum surface determined in situ by surface EXAFS and its polarization dependence
[AD-A269890] p 1360 N94-18687

Quantification of volume flaw sizes in ceramics by image processing of 3D x ray tomographic data sets
[DE93-018573] p 1372 N94-18932

X RAY ASTRONOMY

The Einstein Observatory catalog of IPC x ray sources. Volume 4E: Right ascension range 08h 00m to 11h 59m
[NASA-TM-108401-VOL-4E] p 1625 N94-18612

The Einstein Observatory catalog of IPC x ray sources. Volume 5E: Right ascension range 12h 00m to 15h 59m
[NASA-TM-108401-VOL-5E] p 1625 N94-18613

The Einstein Observatory catalog of IPC x ray sources. Volume 6E: Right ascension range 16h 00m to 19h 59m
[NASA-TM-108401-VOL-6E] p 1625 N94-18615

The Einstein Observatory catalog of IPC x ray sources. Volume 7E: Right ascension range 20h 00m to 23h 59m
[NASA-TM-108401-VOL-7E] p 1625 N94-18618

The Einstein Observatory catalog of IPC x ray sources. Volume 1E: Documentation
[NASA-TM-108401-VOL-1E] p 1626 N94-18619

The Einstein Observatory catalog of IPC x ray sources. Volume 2E: Right ascension range 00h 00m to 03h 59m
[NASA-TM-108401-VOL-2E] p 1626 N94-18620

The Einstein Observatory catalog of IPC x ray sources. Volume 3E: Right ascension range 04h 00m to 07h 59m
[NASA-TM-108401-VOL-3E] p 1626 N94-18621

Related investigations on the physics of high energy emission from active galactic nuclei
[NASA-CR-193615] p 1630 N94-18836

Telescope for x ray and gamma ray studies in astrophysics p 1324 N94-19166

Rosat and optical observations of two X-ray transients: MX 0836-42 and GS 0834-430
[MPE-PREPRINT-237] p 1622 N94-19451

IRAS galaxies observed in the ROSAT survey: Starbursts or central activity p 1623 N94-19528

Particle induced background by Roentgen satellites
[MPE-242] p 1631 N94-19714

Stellar coronae at the end of the main sequence: A Rosat survey of the late M dwarfs
[NASA-CR-194700] p 1628 N94-19794

X RAY BINARIES

Pulse-timing studies of x ray pulsars
[NASA-CR-193778] p 1621 N94-18611

X RAY DENSITY MEASUREMENT

Development and application of local 3-D x ray CT reconstruction software for imaging critical regions in large ceramic turbine rotors
[DE93-015159] p 1369 N94-18166

X RAY DIFFRACTION

High pressure metallization of Mott Insulators: Magnetic, structural and electronic properties
[DE93-018295] p 1404 N94-18805

Neutron-induced collision cascade mixing in Nb/V superlattices
[DE93-018575] p 1600 N94-18933

Refinement of unit cell parameters by least-squares: Comments on an old technique and the development of a new computer program
[AD-A270610] p 1531 N94-19590

Cooperative formation of inorganic-organic interfaces in the synthesis of silicate mesostructures
[AD-A271196] p 1375 N94-19742

X RAY FLUORESCENCE

In vivo animal models of body composition in aging
[DE93-012527] p 1501 N94-17889

X ray studies of microstructures in semiconductor and superconducting materials
[DE93-040690] p 1601 N94-19056

X RAY IMAGERY

Development and application of local 3-D x ray CT reconstruction software for imaging critical regions in large ceramic turbine rotors
[DE93-015159] p 1369 N94-18166

X RAY LASERS

Analysis of neon soft x ray spectra from short-pulse laser-produced plasmas
[DE93-014420] p 1582 N94-17708

X-ray laser oscillator-amplifier experiments
[DE93-017165] p 1436 N94-17868

Production of dense vapor targets for laser-plasma interaction studies with intense, ultra-short pulses
[DE93-017175] p 1584 N94-17993

Development of short pulse soft x ray lasers
[DE93-017150] p 1437 N94-18131

Optical design for photonics. Organization of the 1993 Photonics Science Topical Meetings. Technical digest series, volume 9
[AD-A269027] p 1578 N94-18396

Development of robust multilayer optics for use in high-peak power radiation environments
[DE93-018557] p 1580 N94-18931

Legacy of the X Ray Laser Program
[DE93-019550] p 1442 N94-19554

X RAY SCATTERING

Simulation of emittance dilution in electron storage ring from Compton backscattering
[DE93-017611] p 1386 N94-18503

X RAY SOURCES

Absorption and x ray measurements from ultra-intense laser-plasma interactions
[DE93-016538] p 1585 N94-18115

Pulse-timing studies of x ray pulsars
[NASA-CR-193778] p 1621 N94-18611

The Einstein Observatory catalog of IPC x ray sources. Volume 4E: Right ascension range 08h 00m to 11h 59m
[NASA-TM-108401-VOL-4E] p 1625 N94-18612

The Einstein Observatory catalog of IPC x ray sources. Volume 5E: Right ascension range 12h 00m to 15h 59m
[NASA-TM-108401-VOL-5E] p 1625 N94-18613

The Einstein Observatory catalog of IPC x ray sources. Volume 6E: Right ascension range 16h 00m to 19h 59m
[NASA-TM-108401-VOL-6E] p 1625 N94-18615

The Einstein Observatory catalog of IPC x ray sources. Volume 7E: Right ascension range 20h 00m to 23h 59m
[NASA-TM-108401-VOL-7E] p 1625 N94-18618

The Einstein Observatory catalog of IPC x ray sources. Volume 1E: Documentation
[NASA-TM-108401-VOL-1E] p 1626 N94-18619

The Einstein Observatory catalog of IPC x ray sources. Volume 2E: Right ascension range 00h 00m to 03h 59m
[NASA-TM-108401-VOL-2E] p 1626 N94-18620

The Einstein Observatory catalog of IPC x ray sources. Volume 3E: Right ascension range 04h 00m to 07h 59m
[NASA-TM-108401-VOL-3E] p 1626 N94-18621

Eclipsing cataclysmic variables. Deep eclipses in H0928+501. YY Draconis, the whirling dervish. New x ray pulsar candidates from HEAO-1
[NASA-CR-194027] p 1621 N94-18855

Rosat and optical observations of two X-ray transients: MX 0836-42 and GS 0834-430
[MPE-PREPRINT-237] p 1622 N94-19451

IRAS galaxies observed in the ROSAT survey: Starbursts or central activity p 1623 N94-19528

X RAY SPECTRA

Analysis of neon soft x ray spectra from short-pulse laser-produced plasmas
[DE93-014420] p 1582 N94-17708

X-ray laser oscillator-amplifier experiments
[DE93-017165] p 1436 N94-17868

Dynamic behaviors of fragments ejected from the surface of carbon materials by laser ablation
[DE93-788620] p 1438 N94-18161

Search for resonant electron transfer and double excitation in Kr(sup 34+) + H2 collisions
[DE93-018776] p 1569 N94-18999

X RAY SPECTROSCOPY

Guidelines for the expression of uncertainties in surface chemical analysis by Auger Electron Spectroscopy (AES) and X ray Photoelectron Spectroscopy (XPS)
[NPL-DMM(A)-99] p 1346 N94-17900

X ray absorption spectroscopic studies of the active sites of nickel- and copper-containing metalloproteins
[DE93-017142] p 1347 N94-18059

Absorption and x ray measurements from ultra-intense laser-plasma interactions
[DE93-016538] p 1585 N94-18115

X ray studies of microstructures in semiconductor and superconducting materials
[DE93-040690] p 1601 N94-19056

Legacy of the X Ray Laser Program
[DE93-019550] p 1442 N94-19554

X RAY TELESCOPES

Telescope for x ray and gamma ray studies in astrophysics p 1324 N94-19166

X RAYS

Conical geometry for sagittal focusing as applied to x rays from synchrotrons
[DE93-017238] p 1593 N94-17760

PVDF measurement of soft x ray induced shock and filter debris impulse
[DE93-017633] p 1382 N94-17806

Characteristics and pulsed radiation response of non-ideal quartz shock stress gauges
[DE93-017628] p 1424 N94-17999

Tomographic mathematical ideas applied to radar detection
[AD-A268789] p 1384 N94-18186

Soft X Ray Projection Lithography. Organization of the 1993 photonics science optical meetings
[AD-A269159] p 1579 N94-18693

Development of robust multilayer optics for use in high-peak power radiation environments
[DE93-018557] p 1580 N94-18931

Search for resonant electron transfer and double excitation in Kr(sup 34+) + H2 collisions
[DE93-018776] p 1569 N94-18999

New room temperature high resolution solid-state detector (CdZnTe) for hard x rays and gamma rays
p 1324 N94-19165

X-29 AIRCRAFT

High lift and the forward swept wing
p 1308 N94-18436

X-29: Research aircraft
[NASA-TM-109370] p 1318 N94-18962

XENON

Dynamics of short-pulse excitation, ionization and harmonic conversion
[DE93-017220] p 1436 N94-17996

Y

YAG LASERS

Space Applications Industrial Laser System (SAILS)
p 1325 N94-19173

YAGI ANTENNAS

Modeling a Yagi array antenna for VHF radar use
[AD-A268973] p 1387 N94-18525

YBCO SUPERCONDUCTORS

Infrared detection with high-(Tc bolometers and response of Nb tunnel junctions to picosecond voltage pulses
[DE93-016963] p 1595 N94-17989

Mechanical properties of fiber-reinforced YBa2Cu3O(x) and Bi2Sr2CaCu2O(x) bars
[DE93-017689] p 1454 N94-18479

Photoemission studies of Zn, Co, and Gd substituted YBa2Cu3O(7-delta)
[DE93-017403] p 1597 N94-18498

High performance YBCO films
[AD-A269090] p 1599 N94-18719

Imaging and blackbody emission spectra of hot particulates generated during laser ablation
[DE93-015818] p 1439 N94-18724

High energy resolution ARPES measurements of the normal and superconducting states of Bi2Sr2CaCu2O(8 + delta)
[DE93-018294] p 1599 N94-18804

Superconductivity and magnetism in niobium doped YBa2Cu3O7 related high-(Tc) ceramics
[DE93-018086] p 1601 N94-19049
YC-14 AIRCRAFT
Design, development, and flight evaluation of the Boeing YC-14 USB powered lift aircraft p 1310 N94-18444
YIELD STRENGTH
The Hall-Petch relationship and mechanisms of fracture in B2 compounds
[DE93-018887] p 1359 N94-18182
Dynamical behavior of tantalum
[DE93-017877] p 1362 N94-18919
Influence of peak pressure and temperature on the shock-loading response of tantalum
[DE93-018561] p 1457 N94-19279
Contribution to the identification of nonlinear behavior laws in material mechanics
[ECL-92-36] p 1458 N94-19411
YTTERBIUM
Tunable ytterbium-doped solid state laser
[AD-D015878] p 1440 N94-18747
YTTRIUM ALLOYS
Realistic theories of heavy electron and other strongly correlated materials
[DE93-010350] p 1571 N94-19204
YTTRIUM OXIDES
Nanostructured materials: Mind over matter
[DE93-017690] p 1597 N94-18480
YTTRIUM-IRON GARNET
Nonlinear dynamics and instabilities in ferromagnetic resonance experiments: Examinations of spheres from yttrium iron garnet in coincidence area of the first Suhl instabilities
[ETN-93-95072] p 1604 N94-19612

Z

ZEOLITES
Conversion of ethane and of propane to higher olefin hydrocarbons
[DE93-015282] p 1347 N94-18194
Resonance Raman and photophysical studies of transition metal complexes in solution and entrapped in zeolites
[DE93-019892] p 1363 N94-19019
ZINC
Photoemission studies of Zn, Co, and Gd substituted YBa2Cu3O(7-delta)
[DE93-017403] p 1597 N94-18498
ZINC ALLOYS
Gold-copper-zinc coatings as an alternative to gold-copper-cadmium p 1367 N94-18012
ZINC OXIDES
Nanostructured materials: Mind over matter
[DE93-017690] p 1597 N94-18480
Pressureless densification of ceramic matrix composites
[AD-A269137] p 1371 N94-18691
ZINC SULFIDES
Optical switch evaluation support
[AD-A270948] p 1581 N94-19601
ZINC TELLURIDES
New room temperature high resolution solid-state detector (CdZnTe) for hard x rays and gamma rays
p 1324 N94-19165
ZIRCONIUM
Omega phase formation in shock-loaded zirconium
[DE93-018343] p 1595 N94-18162
Total hemispherical emittance of Niobium-1 percent zirconium fuel cladding for the SP-100 space reactor
[AD-A270456] p 1576 N94-19589
ZIRCONIUM COMPOUNDS
The d(exp 3)delta-a(exp 3)delta and b(exp 3)phi-a(exp 3)delta systems of ZrS, Part 2: Appendix, list of wavenumbers
[USIP-92-05] p 1602 N94-19293
Advanced civil engineering materials based on inorganic polymers
[AD-A270837] p 1374 N94-19600
ZIRCONIUM OXIDES
Pressureless densification of ceramic matrix composites
[AD-A269137] p 1371 N94-18691
Optical properties of oxide coatings prepared by ion-assisted deposition
[AD-A270024] p 1599 N94-18711
ZOOM LENSES
Description of an infrared zoomcollimator
[FEL-93-A034] p 1580 N94-19424

PERSONAL AUTHOR INDEX

SCIENTIFIC AND TECHNICAL AEROSPACE REPORTS VOLUME 32 NUMBER 4

Typical Personal Author Index Listing

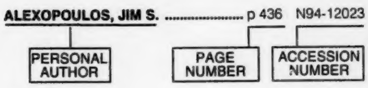

Listings in this index are arranged alphabetically by personal author. The page number helps you locate the citation in the abstract section. The accession number denotes the number by which the citation is identified.

A

AARONS, JULES p 1486 N94-19008
ABARE, A. C. p 1582 N94-17708
ABBOTT, JAMES R. p 1410 N94-18270
ABDALLA, M. C. B. p 1545 N94-17686
ABDULEZER, LOREN p 1325 N94-19171
ABE, TETSUYA p 1444 N94-18159
ABERLE, A. p 1468 N94-19015
ABGRALL, R. p 1412 N94-18561
ABGRALL, REMI p 1311 N94-17957
ABLES, E. p 1572 N94-19545
ABRAHAM, KUZHIKALAIL M. p 1394 N94-17718
ABRASHOFF, JAMES D. p 1564 N94-17738
ABRUNA, H. D. p 1360 N94-18687
ACETI, R. p 1325 N94-19172
ACEVEDO, D. p 1360 N94-18687
ACUNA, M. H. p 1329 N94-19629
ADAIR, R. K. p 1570 N94-19029
ADAMCZAK, DAVID W. p 1318 N94-18779
ADAMS, J. p 1375 N94-19651
ADAMS, J. R. p 1399 N94-18352
ADAMS, T. F. p 1460 N94-19603
ADAMS, WILLIAM M., JR. p 1321 N94-19316
ADAN, I. J. B. F. p 1543 N94-19326
AEBY, PIERRE-ANDRE p 1367 N94-18012
AFANASEV, G. N. p 1566 N94-18152
AGARWAL, V. K. p 1397 N94-18311
AGGSON, T. p 1328 N94-19624
AGRAWAL, SHREEKANT p 1306 N94-18422
AHLSTROM, D. J. p 1399 N94-18357
AHMAD, S. M. W. p 1383 N94-17952
AHRENS, E. T. p 1594 N94-17907
AHRENS, KLEMENS p 1406 N94-19387
AHRENS, THOMAS J. p 1485 N94-18899
AINSWORTH, R. W. p 1431 N94-18644
p 1431 N94-18645
AIZAWA, HITOMI p 1429 N94-18041
AKADA, TAMIO p 1369 N94-18220
AKHTER, N. p 1384 N94-18187
AKKERMAN, G. J. p 1542 N94-19092
AKSIT, MEHMET p 1526 N94-19220
AL-HASHEL, WALEED ISA p 1312 N94-18571
ALAHMAD, M. p 1398 N94-18344
ALAMGIR, MOHAMED p 1394 N94-17718
ALAVI, MANI p 1426 N94-18020
ALBANO, RICHARD K. p 1564 N94-17738
ALBERT, D. B. p 1477 N94-19235
ALBLAS, HENK p 1537 N94-19223
ALBRECHT, DIETER p 1395 N94-17920
ALBRIGHT, K. L. p 1432 N94-18828
ALDERSON, S. G. p 1461 N94-18063
p 1496 N94-18064
p 1496 N94-18065
p 1496 N94-18066
ALEEN, J. T. p 1496 N94-18064
ALEMDAROGLU, NAFIZ p 1305 N94-18417
ALESSO, H. P. p 1556 N94-18073
ALEXANDER, D. J. p 1450 N94-17848
ALEXANDER, DALE E. p 1600 N94-18933
ALEXANDRE, PIERRE p 1482 N94-18623
ALFANO, R. p 1339 N94-17846
ALFANO, ROBERT R. p 1441 N94-19369
p 1441 N94-19394
ALFANO, SALVATORE p 1334 N94-18718
ALFARO, R. A.M. p 1596 N94-18243
ALFREDSSON, V. p 1354 N94-19728
ALHO, K. p 1614 N94-18119
ALIAGA, J. p 1546 N94-17811
ALIPPI, C. p 1383 N94-17935
ALLEN, GREG p 1535 N94-18866
ALLEN, JAMES F. p 1559 N94-19511
ALLEN, S. L. p 1589 N94-19074
p 1590 N94-19289
p 1590 N94-19290
ALLEN, S. M. p 1361 N94-18806
p 1361 N94-18807
ALLEN, TOM p 1449 N94-17829
p 1450 N94-17839
ALLEYNE, H. SAINT C. p 1329 N94-19628
ALLISON, S. W. p 1355 N94-17752
ALLMAN, S. L. p 1501 N94-18242
ALLRED, D. p 1399 N94-18352
ALPERIN, M. J. p 1477 N94-19235
ALSOP, C. p 1329 N94-19632
ALSPACH, BRIAN p 1554 N94-19684
ALSPECTOR, JOSHUA p 1407 N94-19665
ALTMAN, E. p 1560 N94-18990
AMBROSE, K. R. p 1504 N94-17699
AMBROSIANO, J. J. p 1494 N94-19298
AMBROSY, U. p 1391 N94-19617
AMEIN, MICHAEL p 1498 N94-18723
AMES, GREGORY H. p 1576 N94-17716
AMES, LAWRENCE L. p 1511 N94-18412
AMMAR, H. H. p 1522 N94-18726
AMSTERDAM, JONATHAN p 1422 N94-19598
ANDERL, ROBERT A. p 1582 N94-17713
ANDERSON, BERNHARD H. p 1412 N94-18556
ANDERSON, C. J. p 1465 N94-17853
ANDERSON, D. p 1400 N94-18361
ANDERSON, DANA Z. p 1430 N94-18569
ANDERSON, DAVID P. p 1341 N94-18572
ANDERSON, JOHN L. p 1353 N94-19367
ANDERSON, MICHAEL D. p 1462 N94-18753
ANDERSON, NEAL G. p 1440 N94-18834
ANDERSON, PAUL B. p 1535 N94-18772
ANDERSON, R. C. p 1322 N94-18330
ANDERSON, TED p 1449 N94-17831
ANDERSON, W. E. p 1574 N94-18927
ANDERSON, WILLIAM E. p 1348 N94-18389
ANDERSON, WILLIAM W. p 1485 N94-18899
ANDERSSON, L. E. p 1389 N94-18950
ANDRAKA, C. E. p 1466 N94-18208
ANDREEV, A. V. p 1593 N94-17744
ANDREWS, HAROLD G., II p 1579 N94-18668
ANDREWS, J. D. p 1529 N94-19382
ANDREYEVA, O. G. p 1375 N94-18013
ANG, PHILIP p 1512 N94-18882
ANGELINI, RICHARD p 1514 N94-17877
ANNESE, C. E. p 1556 N94-18073
ANSTREICHER, KURT M. p 1525 N94-19154
ANTOLAK, A. J. p 1594 N94-17896
ANTONIADIS, DIMITRI A. p 1345 N94-19746
ANZAI, H. p 1451 N94-17899
AOUSTIN, C. p 1329 N94-19631
AOWELL, G. L. p 1343 N94-18761
AOYAMA, SHIGERU p 1428 N94-18036
p 1429 N94-18043
APPARAO, T. V. V. R. p 1381 N94-19540
APPELQUIST, G. p 1574 N94-18845
p 1405 N94-19292
p 1515 N94-19295
ARAKAWA, KAZUO p 1369 N94-18220
ARCHER, M. p 1523 N94-18943
ARCHULETA, F. L. p 1478 N94-19272
ARECCHI, F. T. p 1435 N94-17771
ARENS, YIGAL p 1615 N94-18461
ARLING, R. W. p 1446 N94-19547
ARMAN, B. p 1353 N94-19552
ARMAN, M. J. p 1403 N94-18452
ARMBRUSTER, ROBERT R. p 1616 N94-18535
ARMSTRONG, R. p 1481 N94-18451
ARMSTRONG, W. D. p 1344 N94-19720
ARNOLD, RICHARD D. p 1493 N94-18883
ARNOLD, S. p 1567 N94-18493
ARNONE, A. p 1551 N94-19315
ARSHAD, M. p 1545 N94-17680
ARTAKI, I. p 1370 N94-18477
ARTER, W. p 1534 N94-18767
ARTS, T. p 1432 N94-18654
ASEBORN, I. p 1419 N94-19068
ASHBY, M. R. p 1518 N94-17944
ASHER, M. p 1518 N94-17944
ASSINK, R. p 1602 N94-19340
ATHERTON, J. p 1584 N94-17988
ATTAWAY, S. W. p 1455 N94-19039
ATTAWAY, STEVEN W. p 1460 N94-19476
ATWOOD, KENNETH L. p 1394 N94-17703
AU, A. p 1374 N94-19577
AUCIELLO, ORLANDO H. p 1605 N94-19664
AUERKARI, PERTTI p 1365 N94-19374
AUTH, G. p 1343 N94-18761
AVDEEV, L. V. p 1593 N94-17748
AVERARDO, M. A. p 1310 N94-18447
AVERSA, F. p 1630 N94-18762
AVICOLA, K. p 1441 N94-19251
AVINASH, K. p 1584 N94-17955
AVRITZER, D. p 1546 N94-17816
AWALUDDIN, A. p 1373 N94-19321
AXELROD, T. S. p 1399 N94-18350
AXELSSON, S. p 1389 N94-18951
AZUMI, MASAFUMI p 1586 N94-18157

B

BABAN, FARZAD p 1377 N94-18758
BABBITT, WILLIAM R. p 1576 N94-18204
BABUSKA, I. p 1549 N94-18697
BACHMANN, CHIP p 1541 N94-18773
BACHMANN, KLAUS J. p 1605 N94-19664
BACKUS, GEORGE E. p 1484 N94-18853
BACON, J. L. p 1441 N94-19307
BADER, BERND p 1375 N94-18010
BAE, DOO-HWAN p 1535 N94-18865
BAER, H. p 1569 N94-18945
BAGENAL, FRANCES p 1628 N94-17842
BAGNOUD, PAUL p 1367 N94-18012
BAHAR, RAMDANE p 1487 N94-19380
BAHNSEN, A. p 1328 N94-19626
BAHOWICK, S. M. p 1333 N94-17782
BAILEY, ELIZABETH K. p 1616 N94-18575
p 1619 N94-19780
BAILEY, R. p 1307 N94-18428
BAINOV, D. D. p 1548 N94-18195
BAIPSYS, V. J. p 1450 N94-17835
BAKER, I. p 1359 N94-18182
BAKER, MARVIN C. p 1393 N94-19752
p 1393 N94-19753
BAKKER, J. A. p 1620 N94-19795
BAKKUM, E. A. p 1452 N94-17941
BAL, RENE p 1526 N94-19221
p 1526 N94-19222
BALACHANDRAN, U. p 1601 N94-18993
p 1602 N94-19122
BALAGEAS, D. L. p 1431 N94-18648
p 1431 N94-18649
p 1431 N94-18650
p 1431 N94-18651
BALASUBRAMANIAN, VIJAY p 1560 N94-19768
BALDINI, A. p 1602 N94-19258
BALDO, P. M. p 1600 N94-18933
BALDWIN, A. W. p 1318 N94-18779
BALDWIN, R. H. p 1365 N94-19274
BALLARD, B. W. p 1336 N94-18338
BALOGH, A. p 1329 N94-19629
BALSTERS, HERMAN p 1526 N94-19222
p 1527 N94-19229
BANDYOPADHYAY, B. P. p 1372 N94-18946
BANE, JOHN M., JR. p 1497 N94-18230
BANGERTER, R. O. p 1576 N94-19560
BANTER, BILLY D. p 1490 N94-18281
BAO, CHENG-LAN p 1492 N94-18675
BAR-SHALOM, A. p 1584 N94-17990

BARALIS, ELENA p 1614 N94-18144
BARANOWSKI, J. p 1595 N94-18054
BARB, FLORIN DAN p 1542 N94-19085
p 1542 N94-19138
p 1542 N94-19142
p 1543 N94-19286
BARBEE, T. W., JR. p 1580 N94-18931
BARCELOS, S. p 1579 N94-18635
BAREFIELD, J. E., II p 1582 N94-17727
BARKER, JEFFREY S. p 1485 N94-18873
BARLAG, SYLVIA p 1494 N94-19699
BARLETTA, R. p 1375 N94-19651
BARNARD, J. J. p 1575 N94-19106
BARNES, D. C. p 1583 N94-17753
BARNES, F. J. p 1488 N94-17715
BARNES, M. D. p 1567 N94-18493
BARNETT, A. M. p 1464 N94-17731
BARNHART, CRAIG M. p 1432 N94-18681
BARON, A. p 1309 N94-18439
BARRY, M. p 1399 N94-18352
BARSOUM, M. W. p 1340 N94-18205
BARTHELEMY, KENNETH E. p 1368 N94-17905
BARTHELME, NEAL p 1327 N94-19185
BARTHOD, DANIEL p 1421 N94-19461
BARTLIT, JOHN R. p 1582 N94-17713
BARTOLI, ALBERTO p 1537 N94-19219
BARTSCH, P. p 1306 N94-18420
BASORE, P. A. p 1464 N94-17787
BASS, E. A. p 1377 N94-18617
BATCHELOR, D. B. p 1590 N94-19273
BATES, J. L. p 1593 N94-17747
BATES, T. S. p 1479 N94-19379
BATHKE, C. G. p 1587 N94-18803
BATILL, STEPHEN M. p 1317 N94-18227
BATTAGLIA, V. S. p 1352 N94-19192
BATTAGLINI, F. p 1374 N94-19585
BATTAIOTTO, P. p 1630 N94-18762
BAUER, D. p 1554 N94-19685
p 1554 N94-19686
BAUER, F. p 1382 N94-17806
BAUER, HELMUT F. p 1379 N94-19489
p 1379 N94-19491
p 1379 N94-19492
BAUER, O. H. p 1329 N94-19630
BAUM, FRED p 1449 N94-17831
BAUMJOHANN, W. p 1329 N94-19630
BAVINCK, HERMAN p 1550 N94-19082
p 1551 N94-19285
BAXTER, KERSTIN p 1554 N94-19687
BAYNE, C. K. p 1472 N94-17910
BEAGLES, GRANT p 1399 N94-18355
BEASLEY, M. R. p 1397 N94-18312
BEAUDET, ROBERT A. p 1349 N94-18395
BECK, W. J. C. p 1580 N94-19455
BECKER, B. p 1418 N94-18888
p 1528 N94-19276
BECKER, K. p 1339 N94-17846
BECKER, S. M. p 1523 N94-19006
BECKERMAN, M. p 1612 N94-17858
BEDELL, K. S. p 1592 N94-17714
BEETS, A. L. p 1504 N94-17699
BEG, I. p 1545 N94-17680
BEIERKE, STEFAN p 1406 N94-19390
BEIN, W. W. p 1546 N94-17885
BEKEFI, GEORGE p 1442 N94-19729
BELAK, J. p 1365 N94-19263
BELASKAS, D. P. p 1476 N94-19064
BELCHER, JOHN W. p 1628 N94-17842
BELKACEMI, M. p 1328 N94-19625
BELLINZONA, R. p 1613 N94-17939
BELLO-MORA, M. p 1330 N94-19637
BELLONI, T. p 1622 N94-19451
BELYTSCHKO, TED p 1458 N94-19466
BEN-ZVI, I. p 1436 N94-17998
p 1438 N94-18504
p 1406 N94-19310
BENBOUTA, NAJAT p 1420 N94-19398
BENCH, G. S. p 1594 N94-17896
BENCHOUIKH, ABDELKRIM p 1365 N94-19400
BENDER, S. C. p 1435 N94-17724
p 1436 N94-17865
BENHARBIT, SAAD p 1420 N94-19365
BENICEWICZ, B. C. p 1368 N94-18096
BENMOHAMED, LOTFI p 1392 N94-19737
BENNAHMIAS, M. p 1601 N94-19049
BENNETT, C. H. p 1517 N94-17812
BENNETT, J. G. p 1521 N94-18271
BENNETT, JAMES A. p 1459 N94-19472
BENNETT, THOMAS E. p 1323 N94-19163
BENSEL, CAROLYN p 1512 N94-18882
BENSON, S. p 1453 N94-18108
p 1448 N94-19252
BENTLEY, J. p 1368 N94-17946
BENTON, R. D. p 1429 N94-18207
BERDING, M. A. p 1577 N94-18223
BEREZHIANI, V. I. p 1584 N94-17955
BERGER, R. C. p 1417 N94-18755
BERGERON, CLYDE J., JR. p 1463 N94-19672
BERGGREN, R. G. p 1445 N94-19047
BERGMAN, W. p 1380 N94-18710
BERGMANS, LODEWIJK p 1526 N94-19220
BERK, H. L. p 1590 N94-19193
BERKENBOSCH, A. C. p 1547 N94-18078
BERNARDES, JACK S. p 1580 N94-18947
BERNEY, JEAN-CLAUDE p 1428 N94-18035
BERNHARDT, A. F. p 1395 N94-17882
BERNSTEIN, E. R. p 1348 N94-18256
BERRY, RICHARD E. p 1499 N94-18819
BERSHAD, BRIAN N. p 1538 N94-19533
p 1515 N94-19591
BERTSCH, D. L. p 1623 N94-19463
p 1623 N94-19464
BERTSCH, G. p 1568 N94-18824
BEUTTENMULLER, R. p 1602 N94-19258
BEY, PAUL p 1541 N94-18773
BEYHOFF, STEFAN p 1322 N94-18123
BHARATRAM, G. p 1450 N94-17834
BHATIA, R. p 1349 N94-18736
BHATTACHARYYA, S. K. p 1337 N94-17908
BHUSHAN, BHARAT p 1604 N94-19579
p 1446 N94-19678
p 1605 N94-19679
p 1407 N94-19722
p 1447 N94-19767
p 1447 N94-19784
BIBLE, J. B. p 1325 N94-19173
BIEDERMAN, IRVING p 1508 N94-18313
BIENIULIS, M. Z. p 1489 N94-18126
BIESIADNY, THOMAS J. p 1321 N94-19353
BIFFLE, JOHNNY H. p 1460 N94-19476
BIGGERI, U. p 1602 N94-19258
BIGGERS, RAND R. p 1443 N94-17705
BIGNAMI, G. F. p 1622 N94-19451
BILHAM, ROGER p 1463 N94-19430
BINDEN, PETER J. p 1405 N94-19035
BINER, S. B. p 1343 N94-18914
BIONDO, A. C. p 1597 N94-18500
BIONTA, R. M. p 1572 N94-19545
BIRO, THOMAS p 1587 N94-18860
BISHOP, A. R. p 1593 N94-17754
BISHOP, D. M. p 1364 N94-19080
BISSINGER, H. p 1441 N94-19251
BJORDAL, HALVOR p 1529 N94-19378
BJORKMAN, K. S. p 1621 N94-19288
BLAAUBOER, DICK p 1495 N94-19704
BLACKBURN, DOUGLAS H. p 1371 N94-18529
BLACKWELL, SHERRI U. p 1513 N94-19570
BLAD, BLAINE L. p 1470 N94-17762
BLAIR, NEAL E. p 1477 N94-19231
p 1477 N94-19234
p 1477 N94-19235
BLAIR, WILLIAM D. p 1391 N94-19582
BLAIS, N. C. p 1376 N94-17813
BLAKELY, J. p 1601 N94-19020
BLANCHARD, NICOLAS p 1434 N94-19414
BLAND, M. p 1384 N94-18210
BLANKEN, HENK M. p 1537 N94-19198
BLAU, P. J. p 1372 N94-18946
BLELLOCH, GUY E. p 1531 N94-19592
BLIND, PASCAL p 1408 N94-18017
BLOCK, L. P. p 1328 N94-19624
BLOCK, M. p 1575 N94-19287
BLOM, ANDERS F. p 1457 N94-19358
BLONK, BASTIAN p 1486 N94-19140
p 1488 N94-19644
BLUM, E. p 1386 N94-18503
BLUM, FRANK D. p 1367 N94-17878
BLUMBERG, L. N. p 1386 N94-18503
BOATNER, L. A. p 1445 N94-18976
BOCIONEK, SIEGFRIED p 1540 N94-18261
BODE, ARTHUR P. p 1507 N94-19593
BODEN, T. A. p 1473 N94-18167
p 1475 N94-18832
BODETTE, D. E. p 1580 N94-18970
BODHAINE, B. A. p 1489 N94-18126
BOEHM-VITENSE, ERIKA p 1622 N94-19421
BOEHME, SUSAN E. p 1477 N94-19232
p 1477 N94-19233
p 1477 N94-19234
BOENSCH, F. D. p 1355 N94-17752
BOER, L. C. p 1510 N94-19440
BOERCKER, D. B. p 1365 N94-19263
BOFFADOSSI, M. p 1309 N94-18439
BOGEN, K. T. p 1559 N94-19549
BOGORAD, A. L. p 1336 N94-17856
BOHANNAN, BRUCE p 1628 N94-19425
BOHM, C. p 1574 N94-18845
p 1525 N94-19145
p 1405 N94-19292
BOHN, C. L. p 1574 N94-18934
BOISSIER, OLIVIER p 1530 N94-19488
BOKOR, JEFFREY p 1403 N94-18638
BOLDRINI, F. p 1325 N94-19172
BOLLER, T. p 1623 N94-19528
BOLTON, P. R. p 1584 N94-17993
BOMMARITO, G. M. p 1360 N94-18687
BONLIE, J. D. p 1440 N94-18889
BONOLI, P. T. p 1589 N94-19073
BOOKBINDER, J. A. p 1628 N94-19794
BORCHI, E. p 1602 N94-19258
BORNAND, ETIENNE p 1425 N94-18014
BOSCH, JAN p 1526 N94-19220
BOSE, ANIIMESH p 1366 N94-19673
BOSIA, G. p 1581 N94-17694
BOSLOUGH, M. B. p 1358 N94-18100
BOSQUED, J. M. p 1329 N94-19631
BOSTON, BRIAN p 1419 N94-19025
BOSTROEM, R. p 1328 N94-19624
BOTLO, M. p 1539 N94-19734
BOTTKOL, MATTHEW p 1382 N94-17861
BOUCHARDY, A.-M. p 1431 N94-18649
p 1431 N94-18651
BOUGHER, STEPHEN W. p 1629 N94-19418
BOUILLARD, J. X. p 1586 N94-18272
BOURAOUI, RACHID p 1552 N94-19499
BOURBON, FABIENNE p 1591 N94-19364
BOURGOIS, G. p 1413 N94-18564
BOUSSON, KOUAMANA p 1544 N94-19360
BOUWKAMP, C. J. p 1550 N94-18991
BOUWMAN, A. F. p 1475 N94-18949
BOUWS, EVERT p 1495 N94-19701
BOWDEN, CHARLES M. p 1540 N94-18263
BOWDEN, ROSEMARY p 1613 N94-17925
BOWEN, S. L. p 1487 N94-19529
BOWEN, STEPHEN G. p 1564 N94-19723
BOWERS, MICHAEL T. p 1568 N94-18814
BOXMA, O. J. p 1543 N94-19324
BOYD, JANICE D. p 1499 N94-18903
BOYER, JOSEPH H. p 1338 N94-18314
BOYLE, J. S. p 1473 N94-18005
p 1489 N94-18053
BOYNTON, PAUL E. p 1621 N94-18611
BRAATEN, E. p 1575 N94-19287
BRABERS, J. H. V. J. p 1593 N94-17744
BRACUTI, A. J. p 1377 N94-18708
BRADDY, D. p 1517 N94-17914
BRADLEY, E. L., III p 1365 N94-19280
BRADY, JOHN N. p 1503 N94-19215
BRAINARD, LEE A. p 1514 N94-17877
BRANDENBURG, J. E. p 1334 N94-18149
BRANDT, STEVE S. p 1627 N94-18877
BRANNON, P. J. p 1580 N94-18970
BRANSTETTER, M. L. p 1537 N94-19253
BRASE, J. p 1441 N94-19251
BRATOS, STEVEN M. p 1497 N94-18414
BRATT, N. p 1322 N94-19332
BRENNAN, T. M. p 1442 N94-19563
BRENNER, HOWARD p 1410 N94-18270
BREVEGLIERI, LUCA p 1518 N94-17926
BREWSTER, MARY J. p 1615 N94-18323
BRIGGS, STEVE J. p 1388 N94-18769
BRIMHALL, OWEN D. p 1511 N94-17841
BRINKER, C. J. p 1345 N94-17820
BRINKSMA, ED p 1543 N94-19226
p 1527 N94-19227
BRISSAUD, FREDERIC p 1529 N94-19370
BRITSCH, M. p 1306 N94-18420
BRIZUELA, E. p 1410 N94-18326
BROADFOOT, A. LYLE p 1326 N94-19178
p 1326 N94-19179
BROCKEL, KENNETH H. p 1387 N94-18512
BROCKMAN, F. J. p 1501 N94-18051
BRODERSEN, OLAF p 1409 N94-18076
BROERSMA, H. J. p 1553 N94-19605
p 1554 N94-19683
p 1554 N94-19685
p 1554 N94-19688
p 1554 N94-19689
BROOKS, E. D., III p 1536 N94-19115
BROUGHTON, JEREMEY p 1541 N94-18773
BROWN, A. p 1520 N94-18251
BROWN, ALAN p 1521 N94-18453
BROWN, ALAN W. p 1521 N94-18659
BROWN, D. H. p 1572 N94-19320
BROWN, DAVID H. p 1612 N94-17737
BROWN, DENICE p 1514 N94-17877
BROWN, J. C. p 1494 N94-19298
BROWN, J. D. p 1346 N94-17987
BROWN, PAUL W. p 1374 N94-19600
BROWN, S. A. p 1517 N94-17914
BROWN, S. B. p 1352 N94-19266
BROWN, W. D. p 1385 N94-18232
BROWNELL, K. C. p 1417 N94-18780
BROWNING, N. D. p 1352 N94-19239
BRUCE, C. W. p 1386 N94-18454
p 1342 N94-18756
p 1342 N94-18757
BRUCHEY, W. J. p 1597 N94-18468

BRUCKART, JAMES E. p 1445 N94-18778
BRUCKER, J. P. p 1322 N94-18890
BRUCKER, P. p 1546 N94-17885
BRUCKHART, JAMES E. p 1511 N94-18296
BRUECK, E. p 1593 N94-17744
BRUNEKREEF, JACOB p 1558 N94-19228
BRUZZI, M. p 1602 N94-19258
BU, Y. p 1438 N94-18258
BUCHHEIT, R. G. p 1405 N94-18928
BUCHHOLZ, D. p 1575 N94-19287
BUCHLIN, J.-M. p 1409 N94-17901
BUCK, M. E. p 1464 N94-17787
BUCK, R. p 1469 N94-19109
BUCKLES, W. E. p 1396 N94-18135
BUCKMASTER, JOHN p 1349 N94-18776
BUDEN, DAVID p 1337 N94-17863
BUDGE, K. G. p 1516 N94-17786
BUDWINE, C. M. p 1627 N94-19077
BUHL, M. R. p 1390 N94-19306
BUITELAAR, P. p 1618 N94-19331
BUKIET, B. G. p 1408 N94-17728
BULGADAEV, S. A. p 1592 N94-17690
BULLARD, THOMAS F. p 1484 N94-18725
BULSARA, A. R. p 1506 N94-18793
BUNTE, STEVEN W. p 1349 N94-18395
BURCHETT, S. N. p 1452 N94-17995
BURDICK, R. B. p 1335 N94-18942
BURES, M. p 1581 N94-17694
BURGER, A. p 1594 N94-17896
BURKE, EDMUND p 1324 N94-19164
BURKE, W. R. p 1328 N94-19622
BURNS, JAY p 1370 N94-18280
BURNS, K. L. p 1485 N94-18894
BURNS, R. J. p 1549 N94-18948
BURNS, THOMAS J. p 1536 N94-19534
BURR, J. p 1393 N94-18351
p 1401 N94-18373
BURR, T. p 1519 N94-18086
BURRELL, K. p 1585 N94-18058
BURROWS, LEROY T. p 1459 N94-19469
BUSCHOW, K. H. J. p 1593 N94-17744
BUSH, C. E. p 1590 N94-19273
BUSH, HAROLD G. p 1333 N94-17765
BUTLER, KETHRYN M. p 1316 N94-19661
BUTLER, RALPH M. p 1535 N94-19046
BUTLER, THOMAS G. p 1449 N94-17832
BUTZBACH, GUENTER DIETER p 1375 N94-19611
BYERS, J. A. p 1589 N94-19074
BYRD, D. A. p 1435 N94-17724
BYRD, DONALD A. p 1436 N94-17865
BYRD, J. p 1575 N94-19152
BYRD, J. M. p 1575 N94-19558

C

CABALA, R. p 1369 N94-18233
CABLE, G. D. p 1385 N94-18232
CABRAL, B. p 1528 N94-19276
CADWELL, K. L. p 1355 N94-17711
CAGLIOTI, VINCENZO p 1520 N94-18138
CAHN, R. W. p 1359 N94-18322
CAI, S. p 1468 N94-19015
CAIRNS, E. J. p 1469 N94-19098
CALDWELL, DOUGLASS R. p 1462 N94-18309
CALLAHAN, A. P. p 1504 N94-17699
CALLAHAN, D. A. p 1575 N94-19106
CALLAHAN, D. L. p 1368 N94-17946
CALLAHAN, DEBRA A. p 1588 N94-19034
CALLAN, GEARY p 1491 N94-18603
CAMELBEECK, T. p 1482 N94-18624
p 1482 N94-18625
CAMERON, K. p 1400 N94-18359
CAMERON, M. p 1599 N94-18816
CAMP, W. J. p 1531 N94-19562
CAMPBELL, D. L. p 1418 N94-18918
CAMPBELL, JOHN P. p 1512 N94-18754
CAMPI, MARCO p 1562 N94-17934
CANARIS, J. p 1398 N94-18342
p 1398 N94-18343
CANFIELD, P. C. p 1594 N94-17907
CANNIZZO, L. F. p 1377 N94-18491
CANNON, R. H., JR. p 1523 N94-18879
CANTWELL, BRIAN J. p 1423 N94-19774
CANU, P. p 1328 N94-19626
CAPANOGLU, CUNEYT C. p 1455 N94-18716
CAPBERN, P. p 1309 N94-18442
CAPLAN, M. p 1437 N94-18134
CAPONE, D. E. p 1416 N94-18642
CARAVEO, P. p 1622 N94-19451
CARDEN, HUEY D. p 1458 N94-19465
p 1458 N94-19467
CARDINAL, CATHERINE p 1424 N94-18007
CARDON, J. G. p 1334 N94-18149
p 1337 N94-18574
p 1335 N94-19787
CAREY, R. M. p 1572 N94-19320
CARIM, A. H. p 1342 N94-18720
CARLOMAGNO, G. M. p 1432 N94-18652
CARLSON, K. DOUGLAS p 1601 N94-19022
CARLSTEN, B. p 1434 N94-17709
CARNEY, D. p 1520 N94-18251
CARODISKEY, T. p 1453 N94-18108
CARPENTER, CHRISTOPHER D. p 1371 N94-18750
CARPENTER, G. p 1307 N94-18429
CARPENTER, G. S. p 1461 N94-17851
CARR, L. W. p 1312 N94-19119
CARRABBA, M. M. p 1478 N94-19305
CARRADO, K. A. p 1373 N94-19321
CARRERAS, B. A. p 1583 N94-17743
CARRUTHERS, GEORGE R. p 1325 N94-19174
CARSON, R. p 1405 N94-19112
CARSON, R. F. p 1515 N94-19535
CARTER, M. R. p 1436 N94-17868
CARTER, P. J. p 1329 N94-19632
CARTER, W. DALE, JR. p 1477 N94-19234
CARTWRIGHT, D. C. p 1570 N94-19125
CASASENT, DAVID p 1615 N94-18224
CASILLAS, M. p 1523 N94-18943
CASPARY, R. p 1360 N94-18398
CASPER, T. A. p 1589 N94-19074
p 1590 N94-19289
CASTNER, E. W., JR. p 1566 N94-18085
CASTOLDI, ANDREA p 1565 N94-17933
CASTRO, R. G. p 1363 N94-19028
CATS, GERARD p 1494 N94-19699
CAUGHMAN, J. B. O. p 1382 N94-17695
CAUSEY, RION A. p 1582 N94-17713
CAVADIAS, GEORGE S. p 1463 N94-19435
CAVESTRI, R. C. p 1350 N94-18977
CAVIRIS, NICHOLAS p 1432 N94-18731
CAYER, JAMES L. p 1424 N94-17717
CEBECI, TUNCER p 1309 N94-18438
CELATA, C. p 1591 N94-19559
CELATA, C. M. p 1576 N94-19560
CELLA, ALESSANDRO p 1305 N94-18418
CERDEIRA, H. A. p 1546 N94-17811
p 1436 N94-17954
CERDEIRA, HILDA A. p 1595 N94-17956
CERI, STEFANO p 1614 N94-18144
CERJAN, C. p 1382 N94-17909
CHA, KIMIN p 1407 N94-19584
CHA, Y. S. p 1396 N94-18135
CHABALOWSKI, CARY F. p 1349 N94-18395
CHAIKEN, JOSEPH p 1581 N94-19601
CHALKLEY, P. D. p 1341 N94-18327
CHAMBERS, SCOTT A. p 1375 N94-19758
CHAMIS, CHRISTOS C. p 1457 N94-19351
CHAN, S. K. p 1603 N94-19550
CHANDLER, G. T. p 1446 N94-19334
CHANDRASEKHARA, M. S. p 1312 N94-19119
CHANG, CHINLEY LEONARD p 1324 N94-19168
CHANG, DICK J. p 1377 N94-18758
CHANG, F. C. p 1364 N94-19044
CHANG, JIN-JIANG p 1550 N94-19244
p 1550 N94-19246
CHANG, S. L. p 1586 N94-18272
CHANG, SHIH-JUNG p 1453 N94-18246
CHANG, TOM p 1588 N94-18902
CHANG, Y. J. p 1566 N94-18085
CHANGKAKOTI, RUPAK p 1434 N94-19791
CHANTEUR, G. p 1331 N94-19641
CHAPMAN, MARTIN C. p 1483 N94-18690
CHAPMAN, S. p 1329 N94-19628
CHAPPERT, C. p 1375 N94-19758
CHARLIE, W. A. p 1417 N94-18780
CHARLSON, R. J. p 1479 N94-19379
CHARLTON, L. A. p 1583 N94-17743
CHATTERJEE, SIDDHARTHA p 1531 N94-19592
CHAUDHURY, PRABIR p 1356 N94-17788
p 1356 N94-17796
p 1357 N94-17803
CHAUDHURY, PRABIR K. p 1356 N94-17768
p 1356 N94-17769
p 1356 N94-17772
p 1356 N94-17789
p 1357 N94-17802
p 1357 N94-17804
p 1593 N94-17805
CHAUVEAU, P. p 1328 N94-19625
CHEE, CHIN Y. p 1615 N94-18461
CHEKANOVA, L. A. p 1351 N94-19110
CHEN, A. LI-CHUNG p 1353 N94-19538
CHEN, B. M. p 1543 N94-19329
CHEN, C. H. p 1501 N94-18242
CHEN, CHENG-HONG p 1316 N94-18384
p 1386 N94-18495
CHEN, GEMAI p 1557 N94-18517
CHEN, J. p 1398 N94-18348
CHEN, K. C. p 1361 N94-18807
CHEN, K.-H. p 1411 N94-18549
CHEN, MAU HSIUNG p 1571 N94-19201
CHEN, NAN p 1454 N94-18479
CHEN, PANG C. p 1523 N94-18926
CHEN, Q. p 1402 N94-18377
CHEN, VICTOR p 1541 N94-18773
CHEN, W. p 1602 N94-19258
CHEN, WEI p 1340 N94-18180
CHEN, Y. p 1592 N94-17741
CHEN, Y.-P. p 1604 N94-19597
CHEN, YU-JIUAN p 1575 N94-19107
CHEN, ZHEN p 1456 N94-19060
CHENETTE, D. L. p 1630 N94-18678
CHENG, A. p 1499 N94-18727
CHENG, KWOK-TSANG p 1571 N94-19201
CHERRY, DAVID R. p 1481 N94-18229
CHERTOK, M. p 1572 N94-19320
CHERUBINI, ALESSANDRA p 1518 N94-17926
CHESTER, R. p 1617 N94-19026
CHEW, G. F. p 1624 N94-18047
p 1609 N94-18629
CHHABILDAS, L. C. p 1358 N94-18100
p 1362 N94-18919
CHIANESE, ED p 1535 N94-18866
CHIAPPARO, A. p 1482 N94-18625
CHIDAMBARAM, MADHAN p 1535 N94-18865
CHIDUME, C. E. p 1548 N94-18106
CHIEN, PHILIP p 1327 N94-19182
CHIMA, RODRICK V. p 1411 N94-18554
CHIN, B. A. p 1357 N94-17859
p 1358 N94-17915
CHIN, THOMAS S. p 1385 N94-18287
CHIN, Y. H. p 1383 N94-18055
CHISHOLM, M. F. p 1352 N94-19239
CHISTYAKOV, N. S. p 1351 N94-19110
CHOI, JAE-YOUNG p 1538 N94-19299
CHOKANI, NDAONA p 1312 N94-19388
CHORIN, A. J. p 1556 N94-17886
CHOW, BRIAN G. p 1331 N94-18411
CHOW, R. p 1307 N94-18429
CHOWDHURY, T. p 1476 N94-19064
CHRISTENSEN, JENS HESSELBJERG
p 1489 N94-18143
CHRISTIAN-FREAR, T. L. p 1618 N94-19101
CHRISTIE, ALAN M. p 1521 N94-18659
CHRISTIE, S. J. p 1475 N94-18775
CHRUSCIEL, PIOTR T. p 1621 N94-18141
CHU, C. K. p 1550 N94-19190
CHU, C. Y. p 1454 N94-18479
CHU, K. p 1307 N94-18429
CHU, TAK-KIN p 1432 N94-18731
CHUBB, SCOTT R. p 1499 N94-19609
CHUDHURI, PROBAL p 1560 N94-19726
CHUPP, W. p 1576 N94-19560
CHUPP, W. W. p 1575 N94-18997
CHVILYOV, GENNADY p 1426 N94-18018
CIALONE, MARY A. p 1498 N94-18723
CIARLO, D. R. p 1595 N94-17992
CICCHELLI, WILLIAM M. p 1368 N94-17905
CIESLAK, W. R. p 1405 N94-18928
CIHANGIR, S. p 1436 N94-17883
CILKE, J. T. p 1315 N94-18822
p 1315 N94-18823
CIOFINI, M. p 1435 N94-17771
CITRINI, CLAUDIO p 1518 N94-17926
CLAMP, O. p 1572 N94-19545
CLARK, A. p 1604 N94-19597
CLARK, E. L. p 1311 N94-18275
CLARK, JAMES M. p 1318 N94-18795
CLARK, M. W. p 1569 N94-18999
p 1570 N94-19108
CLARKE, A. D. p 1479 N94-19379
CLARKE, R. p 1375 N94-19758
CLAUS, R. O. p 1355 N94-17752
CLERBAUX, C. p 1479 N94-19521
CLINE, D. D. p 1455 N94-18829
CLOUTMAN, L. D. p 1350 N94-18987
COATES, A. J. p 1329 N94-19632
COBB, J. W. p 1583 N94-17753
COCHRAN, DOUGLAS p 1389 N94-19009
COCHRAN, ROLAND C. p 1339 N94-18074
COFFEY, H. p 1443 N94-17785
COFIELD, DAVID p 1387 N94-18512
COGAN, JAMES p 1491 N94-18599
COGBURN, R. p 1574 N94-18994
COGGESHALL, S. V. p 1423 N94-19604
COGGIOLA, M. J. p 1433 N94-19054
COHEN, B. I. p 1589 N94-19074
COHEN, MICHAEL H. p 1392 N94-19749
COHEN, R. H. p 1589 N94-19074
COKER, A. J. p 1329 N94-19632
COLAVITA, A. p 1630 N94-18762
COLE, JOHN p 1514 N94-17877
COLELLA, DAVID p 1389 N94-18801
COLELLA, N. J. p 1465 N94-17853
COLEMAN, MONTE p 1514 N94-17877
COLGATE, S. A. p 1380 N94-18818
COLIN, R. p 1479 N94-19521

COLIN, STEPHANE p 1421 N94-19495
COLLART, F. R. p 1502 N94-18476
COLLIN, R. E. p 1392 N94-19718
COLLINS, C. B. p 1440 N94-18880
COLLINS, S. K. p 1613 N94-17880
COLLINS, TIMOTHY J. p 1333 N94-17765
COLORNI, A. p 1547 N94-17961
COLSTON, B. W., JR. p 1352 N94-19266
COLTON, J. S. p 1507 N94-19675
COLVIN, M. E. p 1399 N94-18350
COMPERATORE, CARLOS A. p 1504 N94-17824
CONCUS, P. p 1516 N94-17800
CONDER, A. p 1430 N94-18235
CONTOLINI, R. J. p 1395 N94-17882
COOK, GREG p 1449 N94-17829
COOK, WENDY p 1523 N94-18905
COOLEN, F. P. A. p 1558 N94-19327
COOPER, DAVID G. p 1371 N94-18529
COOPER, J. F. p 1394 N94-17770
COPPS, K. p 1549 N94-18697
CORDEIRO, P. G. p 1466 N94-18208
CORLETT, J. N. p 1575 N94-19558
CORNILLEAU-WEHRLIN, N. p 1328 N94-19625
p 1329 N94-19628
COSI, M. p 1325 N94-19172
COTE, P. J. p 1360 N94-18542
COTE, PAUL J. p 1361 N94-18735
COTTER, GLADYS A. p 1611 N94-19131
COTTER, J. E. p 1464 N94-17731
COULLET, P. p 1607 N94-18237
COUQUE, HERVE p 1366 N94-19673
COURTOIS, B. p 1532 N94-19713
COUSINEAU, K. L. p 1615 N94-18334
COWLEY, S. W. H. p 1329 N94-19629
COX, M. G. p 1518 N94-17930
COX, S. K. p 1470 N94-17710
COYLE, M. R. p 1435 N94-17724
CRAIG, GARY p 1539 N94-19790
CRAIG, M. J. p 1395 N94-17783
CRAINE, WILLIAM L. p 1549 N94-18815
CRANE, J. K. p 1582 N94-17708
CRAVEN, MIKE p 1481 N94-18485
CRAVEY, W. R. p 1575 N94-18996
CRAWFIS, R. p 1418 N94-18888
p 1528 N94-19276
CRAWFIS, R. A. p 1520 N94-18130
CRAWFORD, M. K. p 1600 N94-18968
CRAWFORD, MARK p 1397 N94-18318
CRAWFORD, R. p 1523 N94-18943
CRAWFORD, R. K. p 1430 N94-18481
CRAWFORD, S. p 1448 N94-19252
CRAXTON, R. S. p 1436 N94-17868
CREDLAND, J. p 1330 N94-19635
CREMERS, D. A. p 1582 N94-17727
CRESPIREGHIZZI, STEFANO p 1518 N94-17926
CRITES, R. C. p 1431 N94-18647
CRIVELLI, S. p 1535 N94-18808
p 1524 N94-19024
CROS, A. p 1329 N94-19631
CROSBY, E. p 1386 N94-18454
CROSIER, RONALD B. p 1460 N94-19606
CROWLEY, NANCY L. p 1531 N94-19573
p 1532 N94-19782
CROWLEY, W. P. p 1422 N94-19568
CRUMP, O. B. p 1423 N94-17700
CRUZ, G. E. p 1335 N94-19275
CSANAK, G. p 1570 N94-19125
CSILLAG, S. p 1525 N94-19145
CULETU, H. p 1480 N94-17682
CUMMINGS, RUSSELL M. p 1312 N94-19433
CUMPSON, P. J. p 1346 N94-17900
CUNNINGHAM, S. p 1496 N94-18065
CUNNINGHAM, S. A. p 1496 N94-18066
CURTIN, HOWARD R. p 1511 N94-17841
CURTIS, JOHN O. p 1388 N94-18777
CURTIT, DANIEL p 1427 N94-18026
CUSHMAN, R. M. p 1471 N94-17774
CYTRON, SHELDON p 1344 N94-19576
CZAJKOWSKI, C. p 1343 N94-18763
CZAJKOWSKI, EVA p 1326 N94-19180
CZICHOWSKY, W. p 1313 N94-19524

D

DAANEN, H. A. M. p 1504 N94-17966
DAGRACA, G. R. p 1495 N94-19702
DAI, X. p 1468 N94-19015
DAISEY, J. M. p 1513 N94-18935
DALDER, E. N. C. p 1453 N94-18108
DALE, V. H. p 1471 N94-17790
DALY, T. A. p 1472 N94-17891
DAMKROGER, B. K. p 1364 N94-19100
DANDOURAS, J. p 1329 N94-19631
DANDRIDGE, ANTHONY p 1382 N94-17902
DANILKIN, S. A. p 1355 N94-17692
DANNER, RUDOLF p 1631 N94-19714
DANNEVIK, W. P. p 1494 N94-19298
DAPKUNAS, S. J. p 1340 N94-18180
DARROW, C. p 1435 N94-17855
p 1585 N94-18115
DART, SUSAN p 1521 N94-18659
DARYOUSH, AFSHIN S. p 1394 N94-17707
DASILVA, L. B. p 1582 N94-17708
p 1437 N94-18131
p 1580 N94-18931
DAUGHERTY, M. A. p 1396 N94-18135
DAVID, D. C. p 1594 N94-17896
DAVID, S. A. p 1445 N94-18976
p 1364 N94-19203
DAVIES, P. N. H. p 1328 N94-19623
DAVIS, C. E. p 1403 N94-18452
DAVIS, C. G. p 1627 N94-18857
DAVIS, D. p 1410 N94-18326
p 1326 N94-19175
p 1326 N94-19176
DAVIS, J. M. p 1470 N94-17710
DAVIS, NOLAN R. p 1500 N94-19786
DAVIS, R. p 1398 N94-18347
DAVIS, ROBERT F. p 1599 N94-18797
DAVIS, S. J. p 1328 N94-19623
DAY, C. T. p 1514 N94-17799
DAYI, O. F. p 1561 N94-18171
DAYTON, DAVID C. p 1349 N94-18456
DAZEVEDO, E. F. p 1551 N94-19301
DEALLAUME, WILLIAM p 1387 N94-18512
DEB, KALYANMOY p 1396 N94-18278
DEBOER, F. R. p 1593 N94-17744
p 1605 N94-19735
DEBRUIJN, CISCO p 1494 N94-19699
DEBY, ROLF A. p 1526 N94-19222
p 1527 N94-19229
DECARLO, FRANCESCO p 1326 N94-19179
DECHAMBOUX, PASCAL p 1529 N94-19368
DECOCK, K. p 1307 N94-18426
DECONCHY, Y. p 1328 N94-19625
DECONINCK, H. p 1413 N94-18564
DECREAU, P. M. E. p 1328 N94-19626
DEETER, JOHN E. p 1621 N94-18611
DEFERAUDY, H. p 1328 N94-19626
DEFERRARI, HARRY p 1495 N94-17822
DEGRAAF, A. J. p 1543 N94-19199
DEGRAEVE, M. p 1507 N94-19523
DEJAGER, N. p 1434 N94-19797
DEJONG, A. p 1619 N94-19453
DEJONG, A. N. p 1580 N94-19424
DEJONG, E. G. p 1378 N94-19445
DEKKER, L. p 1550 N94-19141
DEKKERS, DAVID p 1391 N94-19587
DEKKING, F. M. p 1550 N94-19088
DEKONING, WILLEM L. p 1542 N94-19085
p 1542 N94-19138
p 1542 N94-19142
p 1543 N94-19286
DELAPORTE, B. p 1328 N94-19623
DELAURENTIS, J. p 1576 N94-18000
DELAYEN, J. R. p 1574 N94-18273
p 1574 N94-18934
DELEEUW, G. p 1483 N94-18712
DELEO, M. p 1310 N94-18447
DELESALLE, DENIS p 1531 N94-19517
DELLAMICO, MAURO p 1518 N94-17927
DEMETZ, K. p 1507 N94-19523
DEMIDENKO, SERGE p 1518 N94-17960
DEMIER, A. p 1307 N94-18428
DEMIRBILEK, ZEKI p 1497 N94-18414
DEMIRGIAN, J. C. p 1474 N94-18499
p 1478 N94-19241
DEMOUSTIER, C. p 1498 N94-18662
DEMUTH, D. E. p 1541 N94-18474
DENICOLAO, GIUSEPPE p 1540 N94-17922
DENIET, M. p 1393 N94-19798
DENLINGER, EDGAR J. p 1599 N94-18719
DENNEFELD, M. p 1623 N94-19528
DEPHILLIPS, M. P. p 1464 N94-17712
DEPONTE, SERGIO p 1305 N94-18418
DEROOIJ, NICO p 1425 N94-18014
DEROOY, WIM p 1494 N94-19699
DESAI, H. p 1496 N94-18064
DESAI, P. D. p 1374 N94-19532
DESAI, UPENDRA D. p 1324 N94-19165
p 1324 N94-19166
DESIDERI, JEAN-ANTOINE p 1311 N94-17957
DESLOVER, D. p 1489 N94-18132
DESLOVER, D. H. p 1488 N94-17758
DESONIER, L. M. p 1617 N94-18984
DESSAU, D. S. p 1599 N94-18804
DESTEESE, J. G. p 1466 N94-18276
DEVARY, J. L. p 1461 N94-18107
DEVERS, WAYNARD C. p 1616 N94-18575
p 1619 N94-19780
DEVINE, K. D. p 1536 N94-19161
DEVINK, E. P. p 1524 N94-19062
DEVREEZE, CHRIS C. p 1527 N94-19229
DEVRIES, HANS p 1494 N94-19700
DEVRIES, M. p 1355 N94-17752
DEVULDER, CHRISTOPHE p 1552 N94-19407
DEWINTER, D. p 1621 N94-19288
DEWIT, MARK W. p 1484 N94-18725
DEXTER, JAMES L. p 1371 N94-18529
DEY, D. K. p 1557 N94-18516
DEYOREO, J. p 1584 N94-17988
DHARANI, L. R. p 1371 N94-18691
DHONG, Y. B. p 1397 N94-18341
DHUY, C. W. p 1544 N94-19458
DIAMOND, P. H. p 1583 N94-17743
DICKERT, JOHN H. p 1615 N94-18319
DICKEY, F. p 1576 N94-18000
DICKINSON, R. E. p 1474 N94-18183
DIERICKX, L. p 1353 N94-19456
p 1353 N94-19459
DIETZ, PAUL F. p 1530 N94-19482
p 1531 N94-19508
p 1538 N94-19512
DIMBYLOW, T. p 1331 N94-19639
DIMOS, D. p 1371 N94-18519
DIMOTAKIS, PAUL E. p 1410 N94-18472
DINKEL, J. A. p 1574 N94-18497
DINNEL, SCOTT p 1497 N94-18393
DIPIRRO, MICHAEL p 1327 N94-19185
DIVAN, DEEPAKRAJ M. p 1407 N94-19643
DOAK, J. E. p 1519 N94-18086
DOBRANICH, D. p 1519 N94-18002
p 1337 N94-18830
p 1420 N94-19345
DOBREV, V. K. p 1546 N94-17810
DODSWORTH, S. J. p 1330 N94-19636
DOEHLER, HANS-ULLRICH p 1316 N94-18146
DOERNBRACK, A. p 1416 N94-18596
DOERR, R. p 1352 N94-19191
DOERR, ROBERT p 1350 N94-18895
p 1350 N94-18896
DOMINIK, CHET J. p 1306 N94-18424
DOMNING, E. E. p 1394 N94-17755
DONATO, J. M. p 1551 N94-19337
p 1553 N94-19655
DONG, TRAN DAO p 1546 N94-17817
DONGARRA, J. J. p 1523 N94-18989
p 1538 N94-19299
DONLAN, J. C. p 1496 N94-18066
DONLEY, L. I. p 1598 N94-18531
DONNELLY, M. K. p 1548 N94-18094
DORAN, L. p 1381 N94-19480
DORIGO, M. p 1547 N94-17961
DORSINVILLE, R. p 1339 N94-17846
DOTAN, I. p 1567 N94-18526
DOUGLAS, E. P. p 1368 N94-18096
DOWNING, DAVID R. p 1318 N94-19448
DOWNING, R. p 1569 N94-19013
DRAGO, RAYMOND J. p 1446 N94-19318
DRAGON, E. P. p 1437 N94-18093
p 1441 N94-19294
DRAGT, A. J. p 1573 N94-17807
DROUGGE, GEORG p 1311 N94-17722
DUBOIS, R. D. p 1570 N94-19108
DUCKWORTH, M. R. p 1572 N94-19320
DUDEK, F. E. p 1505 N94-18538
DUDEL, HELMUT P. p 1493 N94-18781
DUDLEY, V. E. p 1466 N94-18208
DUFF, J. p 1441 N94-19251
DUFFAIT, ROLAND p 1408 N94-18015
DUFRANE, K. F. p 1368 N94-18110
DUIJVESTIJN, A. J. W. p 1550 N94-18991
DUNFORD, C. p 1328 N94-19623
DUNFORD, C. M. p 1329 N94-19628
DUNFORD, E. p 1331 N94-19639
DUNG, NGUYEN TIEN p 1546 N94-17815
DUNKERTON, TIMOTHY J. p 1490 N94-18486
DUNLOP, M. W. p 1329 N94-19629
DUNN, M. L. p 1344 N94-19720
DUQUETTE, D. J. p 1363 N94-19021
DURKEE, P. A. p 1472 N94-17986
p 1479 N94-19379
DURLACH, NATHANIEL p 1513 N94-19764
DYBDAL, R. B. p 1385 N94-18301
DYER, K. M. p 1524 N94-19048
DYESS, JAMES W. p 1333 N94-17765
DYKSTRA, PHILLIP p 1514 N94-17877
DYMOND, LEE H. p 1616 N94-18575
p 1619 N94-19780
DZWILEWSKI, P. T. p 1315 N94-18822
p 1315 N94-18823

E

EARNSHAW, P. B. p 1308 N94-18434
EASTERLY, C. E. p 1503 N94-19341

EASTMAN, L. F. p 1604 N94-19597
EASTWOOD, J. W. p 1534 N94-18767
EATHER, ROBERT H. p 1334 N94-18264
EATON, JAMES C. p 1505 N94-18392
ECCLES, V. p 1481 N94-18451
ECKART, A. p 1621 N94-19415
ECKERT, C. A. p 1610 N94-19670
EDER, B. K. p 1476 N94-19065
EDER, D. p 1437 N94-18131
EDER, D. C. p 1584 N94-17993
p 1580 N94-18931
EDMONDS, J. A. p 1471 N94-17821
EDWARDS, GLEN R. p 1342 N94-18704
EDWARDS, N. T. p 1470 N94-17773
EECKMAN, F. H. p 1399 N94-18350
EERTINK, HENK p 1526 N94-19196
p 1527 N94-19227
EFIMOV, G. V. p 1608 N94-18267
EFRON, U. p 1374 N94-19577
EGGLESTON, B. p 1310 N94-18446
EHMER, HANSJOCHEN p 1322 N94-18123
EHRHARD, DAVID G. p 1387 N94-18513
EICHINGER, PETER p 1423 N94-19730
EICHINGER, W. E. p 1478 N94-19272
EIDELMAN, S. p 1416 N94-18671
EILERS, SUE p 1391 N94-19587
EINMAHL, J. H. J. p 1558 N94-19325
EKERDT, J. G. p 1345 N94-17808
EKERDT, JOHN G. p 1606 N94-19739
EL-GENK, M. S. p 1338 N94-19128
EL-RAHAIBY, SAID K. p 1371 N94-18750
ELDIN, A. G. p 1397 N94-18339
ELFVING, T. p 1389 N94-18950
ELIAS, LUIS R. p 1440 N94-18912
ELIASON, D. E. p 1495 N94-17779
ELIEANS, A. p 1524 N94-19062
ELLINGSON, W. A. p 1369 N94-18166
p 1372 N94-18932
ELLIOTT, D. L. p 1493 N94-19051
ELLIOTT, S. p 1476 N94-19104
ELLIS, CAROL p 1514 N94-17877
ELLIS, COLLEEN L. p 1320 N94-18536
ELLIS, MARY K. p 1522 N94-18786
ELLIS, N. p 1574 N94-18845
ELLISON, A. J. G. p 1430 N94-18481
ELLISON, J. A. p 1574 N94-18994
ELSMORE, TIMOTHY F. p 1507 N94-19608
ELTGROTH, P. G. p 1494 N94-19298
EMERSON, J. P. p 1360 N94-18398
EMMITT, G. D. p 1327 N94-19181
ENDERLE, CHRISTIAN p 1460 N94-19648
ENG, ANTHONY T. p 1367 N94-17719
ENGELBRECHT, J. R. p 1604 N94-19566
ENGELKE, R. P. p 1376 N94-17813
ENGELMANN, B. E. p 1452 N94-18049
p 1340 N94-18113
ENGELMANN, BRUCE E. p 1460 N94-19475
EPHREMIDES, ANTHONY p 1432 N94-18681
ERBES, GERHARD W. p 1562 N94-18859
ERDMANN, REINHARD p 1578 N94-18457
ERIKSSON, T. p 1419 N94-19068
ERNI, BRUNO p 1429 N94-18042
ERREDE, S. p 1569 N94-19013
ERSKINE, FRED T. p 1500 N94-19786
ESAREY, E. p 1586 N94-18148
ESAREY, ERIC p 1438 N94-18460
ESCHENBURG, J. H. p 1545 N94-17684
ESKER, BARBARA S. p 1321 N94-19353
ESTEROWITZ, LEON p 1440 N94-18747
EVANS, A. G. p 1341 N94-18450
EVANS, ALAN G. p 1317 N94-19572
EVANS, B. T. p 1463 N94-18800
EVANS, JAMES E. p 1492 N94-18684
EVERETT, H. R. p 1541 N94-18474
EWING, JOHN I. p 1500 N94-19747
EWING, R. C. p 1599 N94-18816
EXERTIER, FRANCOIS p 1519 N94-17978
EYLON, S. p 1575 N94-18997

F

FABY, E. Z. p 1617 N94-19057
p 1524 N94-19076
FAELTHAMMAR, C.-G. p 1328 N94-19624
FAIRFIELD, D. H. p 1329 N94-19629
FAIRFIELD, M. S. p 1419 N94-19027
FALCONE, R. W. p 1582 N94-17708
FALK, JOEL p 1439 N94-18656
FALLET, ESTELLE p 1427 N94-18025
FALTENS, A. p 1591 N94-19559
FANG, ZHENGXIU p 1599 N94-18711
FANN, G. I. p 1533 N94-17693
FARAGGI, A. E. p 1607 N94-17950
p 1565 N94-17951
p 1607 N94-17953
FARBER, P. S. p 1474 N94-18502
FARIS, GREGORY W. p 1442 N94-19788
FARLEY, J. W. p 1572 N94-19309
FARRARA, J. D. p 1494 N94-19298
FARRINGTON, GREGORY C. p 1578 N94-18405
FARROW, R. F. p 1375 N94-19758
FARTASH, A. p 1368 N94-18098
FATHY, ALY p 1599 N94-18719
FAUDREE, RALPH p 1555 N94-19690
FAVARON, ODILE p 1555 N94-19690
FAVRE, ERIC p 1429 N94-18042
FAWLEY, W. M. p 1441 N94-19030
FEELEY, J. J. p 1399 N94-18357
p 1401 N94-18374
FEHRINGER, M. p 1330 N94-19634
FEIJT, ARNOUT J. p 1481 N94-18142
FELDER, M. p 1613 N94-17936
FELDMAN, D. W. p 1435 N94-17724
FELDMAN, PAUL D. p 1624 N94-17843
FENNELL, J. F. p 1329 N94-19633
FENSTERMACHER, M. E. p 1589 N94-19073
p 1589 N94-19074
p 1590 N94-19289
FERGEAU, P. p 1328 N94-19626
FERRAN, M. D. p 1582 N94-17727
FERREIRAPIRES, LUIS p 1527 N94-19261
FERRETTI, GIANNI p 1443 N94-17937
p 1444 N94-17940
FERRISS, D. H. p 1451 N94-17899
p 1451 N94-17929
FERRON, J. R. p 1585 N94-18057
FERZIGER, JOEL H. p 1549 N94-18863
FESSENDEN, T. J. p 1575 N94-19106
FEURER, T. p 1368 N94-17946
FICHTEL, C. E. p 1623 N94-19464
FICHTEL, ED p 1434 N94-19314
FIELDS, DUDLEY p 1318 N94-18779
FIENUP, J. R. p 1578 N94-18383
FIEZ, T. p 1401 N94-18368
FIFER, ROBERT A. p 1609 N94-18310
FILIPPENKO, ALEXEI V. p 1622 N94-19431
FILIPPOV, A. T. p 1561 N94-18168
p 1548 N94-18169
FILLER, RAYMOND L. p 1403 N94-18471
FILLIUS, W. p 1329 N94-19630
FINKENTHAL, D. F. p 1585 N94-18058
FINNEY, J. M. p 1360 N94-18325
FISCHER, S. K. p 1367 N94-17847
FISCHLER, M. p 1525 N94-19186
FISH, G. I. p 1351 N94-19110
FISHER, A. p 1440 N94-18771
FISHER, B. p 1597 N94-18500
FISHER, I. A. p 1346 N94-18048
FISHER, R. A. p 1360 N94-18398
p 1600 N94-18968
FISHER, W. G. p 1343 N94-18761
FISK, Z. p 1594 N94-17907
FISZDON, W. p 1422 N94-19510
FITCHEL, C. E. p 1623 N94-19463
FLAHERTY, J. E. p 1536 N94-19161
FLAIG, A. p 1310 N94-18445
FLANDRIN, EVELYNE p 1555 N94-19690
FLEMING, K. J. p 1423 N94-17700
FLEMING, P. H. p 1424 N94-17778
FLEMING, T. A. p 1628 N94-19794
FLIFLET, ARNE W. p 1439 N94-18576
FLORAC, WILLIAM A. p 1616 N94-18575
p 1619 N94-19780
FLORES, R. p 1405 N94-19112
FLOYD, H. L. p 1381 N94-19480
FLYNN, GEORGE p 1571 N94-19236
FLYNN, GEORGE W. p 1557 N94-18540
FLYNN, M. p 1400 N94-18362
FOCKE, HORST p 1322 N94-18123
FOLEY, M. G. p 1461 N94-18107
FOLLSTAEDT, D. M. p 1364 N94-19080
FOLTZ, JOHN V. p 1332 N94-18321
FONG, K. W. p 1520 N94-18133
FOOTE, J. H. p 1589 N94-19074
p 1590 N94-19289
FOOTE, STEPHEN L. p 1507 N94-19783
FORBER, R. A. p 1374 N94-19577
FORBES, A. B. p 1518 N94-17930
FORMAN, W. p 1625 N94-18612
p 1625 N94-18613
p 1625 N94-18615
p 1625 N94-18618
p 1626 N94-18619
p 1626 N94-18620
p 1626 N94-18621
FORRESTER, T. N. p 1461 N94-18137
FOSTER, C. M. p 1603 N94-19550
FOURNIER, G. R. p 1463 N94-18600
FOXALL, W. p 1480 N94-17898
FRAEMAN, M. E. p 1336 N94-18338
FRANCO-FERREIRA, E. A. p 1446 N94-19334
FRANCOIS, M. p 1482 N94-18625
FRANK, R. N. p 1517 N94-17911
FRANK, WILLIAM M. p 1490 N94-18514
FRANKS, R. M. p 1335 N94-19275
FRANSEN, LAWRENCE p 1392 N94-19748
FRATNIK, F. p 1630 N94-18762
FRAZEL, ROBERT E. p 1500 N94-19792
FREAR, D. R. p 1452 N94-17995
FREDERICK, JOHN E. p 1630 N94-19437
FREDERICKSON, E. p 1590 N94-19273
FRENZEL, J. F. p 1398 N94-18346
p 1399 N94-18354
FREUND, L. B. p 1456 N94-19130
FRIBERG, STIG p 1578 N94-18405
FRIEDMAN, ALEX p 1588 N94-19034
FRIEDMAN, H. p 1441 N94-19251
FRIEDRICH, K. A. p 1594 N94-17876
FRITZ, J. N. p 1563 N94-19151
FRITZ, T. A. p 1329 N94-19633
FRITZ, WILLY p 1305 N94-18419
FROLOV, A. M. p 1577 N94-18217
FRY, H. A. p 1376 N94-17813
FTHENAKIS, V. M. p 1464 N94-17712
FU, CHI YUNG p 1527 N94-19238
FUCHS, B. A. p 1381 N94-19544
FUGINI, M. G. p 1613 N94-17939
FUJIKAWA, S. I. p 1358 N94-17947
FUJITA, HIROO p 1427 N94-18028
FULLER, ROBERT R. p 1443 N94-17705
FULLERTON, E. E. p 1594 N94-17871
FULLERTON, ERIC E. p 1600 N94-18933
FULTZ, B. p 1359 N94-18322
FURGER, M. p 1489 N94-18052
FURNISH, M. D. p 1362 N94-18919
p 1627 N94-19339
FURTAK, T. E. p 1468 N94-18944
FURUSAKA, M. p 1358 N94-17947
FURUTANI, TOSHIO p 1428 N94-18037
FURUYAMA, TOHRU p 1428 N94-18037
FUSINA, ROBERT A. p 1499 N94-19609

G

GAASTERLAND, T. p 1612 N94-17870
p 1614 N94-18099
GABLER, A. p 1624 N94-17736
GABLER, R. p 1624 N94-17736
GABRIEL, CAMELIA p 1388 N94-18782
GACS, P. p 1517 N94-17812
GAFFNEY, JEFFREY S. p 1476 N94-19045
GAILEY, P. C. p 1503 N94-19341
GAINES, E. E. p 1485 N94-18874
GAMBLES, J. W. p 1401 N94-18372
GANESAN, N. p 1449 N94-17833
GANESH, G. p 1400 N94-18360
GANGARAJ, S. K. p 1549 N94-18697
GANGSTAD, E. O. p 1475 N94-18881
p 1475 N94-18885
GANNI, V. p 1381 N94-19540
GAO, GUIZHONG p 1355 N94-17679
GARABEDIAN, CHRISTIAN p 1406 N94-19490
GARATE, E. p 1404 N94-18872
GARCIA, JOSEPH A. p 1312 N94-19433
GARCIA, L. p 1583 N94-17743
GARDNER, D. R. p 1455 N94-18829
GARDNER, H. p 1399 N94-18352
GARDNER, SHELDON p 1541 N94-18773
GARLAN, DAVID p 1521 N94-18453
GARLAND, MICHAEL J. p 1522 N94-18698
GARNER, F. A. p 1364 N94-19043
GARRITY, CHRIS p 1535 N94-18866
GARZOTTO, FRANCO p 1520 N94-18136
GATES, DARRIN p 1325 N94-19170
GAUDEL, M. C. p 1532 N94-19713
GAUDIOT, J. L. p 1539 N94-19588
GAUNCE, M. T. p 1332 N94-18669
p 1332 N94-18670
GAUSTAD, K. L. p 1466 N94-18276
GAUTHIER, A. p 1569 N94-19013
GAVEL, D. p 1441 N94-19251
GAYDOS, P. A. p 1368 N94-18110
GEE, J. M. p 1464 N94-17787
GEISER, URS p 1601 N94-19022
GELFAND, A. E. p 1557 N94-18694
GELFAND, ALAN E. p 1557 N94-18516
GELLMAN, ANDREW J. p 1446 N94-19754
GENZEL, R. p 1621 N94-19415
GEOHEGAN, D. B. p 1439 N94-18724
GEORGE, EDWARD J. p 1511 N94-18412
GEORGIEVA, A. p 1545 N94-17685
GERANIOTIS, EVAGGELOS p 1393 N94-19779
GERBERICH, WILLIAM W. p 1344 N94-19744
p 1345 N94-19776
GERDT, V. P. p 1548 N94-18175
GERSHMAN, VLADIMIR p 1394 N94-17707

GERZ, T. ..... p 1416 N94-18595
GETTERT, MICHAEL ..... p 1631 N94-19505
GETTRUST, J. F. ..... p 1500 N94-19745
GEYER, M. S. ..... p 1332 N94-18669
p 1332 N94-18670
GHEEN, G. ..... p 1576 N94-18000
GHIRAZINHOANTUNES, MARIA FRANCISCA
p 1614 N94-17979
GHOSH, V. J. ..... p 1603 N94-19541
GIAMPAPA, M. S. ..... p 1628 N94-19794
GIBBS, RICHARD ..... p 1382 N94-17861
GIBESON, L. ..... p 1384 N94-18216
GIBSON, J. ..... p 1402 N94-18381
GIBSON, KENNETH R. ..... p 1493 N94-18883
GIEST, G. A. ..... p 1534 N94-18482
GIFFORD, MICHAEL T. ..... p 1493 N94-18883
GIL, YOLANDA ..... p 1612 N94-17745
p 1615 N94-18464
p 1557 N94-18640
GILLOTAY, D. ..... p 1353 N94-19456
p 1353 N94-19459
GILP, B. F. ..... p 1374 N94-19532
GIOIA, I. M. ..... p 1625 N94-18612
p 1625 N94-18613
p 1625 N94-18615
p 1625 N94-18618
p 1626 N94-18619
p 1626 N94-18620
p 1626 N94-18621
GIVEN, H. ..... p 1483 N94-18717
GLASSMEIER, K. H. ..... p 1329 N94-19629
GLEIXNER, R. A. ..... p 1454 N94-18479
GLIEM, F. ..... p 1329 N94-19633
GLIMM, JAMES G. ..... p 1514 N94-19478
GLUCKSTERN, R. L. ..... p 1573 N94-17807
GMITRO, A. F. ..... p 1433 N94-19000
GOBBI, B. ..... p 1575 N94-19287
GOELZ, ULRICH ..... p 1391 N94-19646
GOETSCH, B. ..... p 1381 N94-19480
GOETTGENS, B. M. ..... p 1370 N94-18403
GOLDBERG, P. W. ..... p 1542 N94-19007
GOLDFINGER, R. C. ..... p 1590 N94-19273
GOLDSTEIN, G. ..... p 1472 N94-17852
GOLDSTEIN, J. C. ..... p 1435 N94-17724
GOLDSTEIN, W. ..... p 1584 N94-17990
p 1585 N94-18082
GOLTON, E. ..... p 1331 N94-19639
GONZALEZVALENZUELA, NESTOR A.
p 1533 N94-17976
GOODMAN, P. ..... p 1602 N94-19277
GOODMAN, SIMON ..... p 1480 N94-17720
GOODMAN, WESLEY L. ..... p 1306 N94-18424
GOODWIN, D. G. ..... p 1371 N94-18740
GOODWIN, DAVID G. ..... p 1599 N94-18745
GOODWIN, G. M. ..... p 1362 N94-18938
GOPALAN, K. ..... p 1344 N94-19551
GOPALSAMI, N. ..... p 1344 N94-19551
GORDAN, S. ..... p 1585 N94-18082
GORDON, H. M. ..... p 1370 N94-18477
GORDON, S. ..... p 1394 N94-17770
GORETTA, K. C. ..... p 1454 N94-18479
p 1597 N94-18500
GORR, LANNY ..... p 1387 N94-18512
GOUGH, M. P. ..... p 1328 N94-19623
p 1329 N94-19628
GOULDING, R. H. ..... p 1581 N94-17694
GOURLEY, P. L. ..... p 1442 N94-19563
GOUVEIA, F. ..... p 1463 N94-19003
GOWEN, R. A. ..... p 1329 N94-19632
GOWER, G. L. ..... p 1493 N94-19051
GRADY, C. A. ..... p 1621 N94-19288
GRADY, D. E. ..... p 1373 N94-19271
p 1373 N94-19338
GRAEBE, D. ..... p 1494 N94-19616
GRAFF, LINDA H. ..... p 1462 N94-18309
GRAHAM, ALAN L. ..... p 1410 N94-18270
GRANBOM, PER OLOF ..... p 1473 N94-18139
GRANGER, RICHARD ..... p 1505 N94-18407
GRANIER, C. ..... p 1479 N94-19521
GRANTSTEIN, V. L. ..... p 1439 N94-18737
GRARD, R. J. L. ..... p 1330 N94-19634
GRAS, J. ..... p 1479 N94-19379
GRAVES, D. W. ..... p 1577 N94-18302
GRAVES, J. ..... p 1341 N94-18692
GRAY, G. T., III ..... p 1595 N94-18162
p 1361 N94-18802
p 1362 N94-18809
p 1455 N94-19033
p 1457 N94-19279
p 1627 N94-19339
GRAY, M. G. ..... p 1584 N94-17983
GREEN, A. R. ..... p 1308 N94-18434
GREEN, M. A. ..... p 1468 N94-19015
GREENBAUM, E. ..... p 1466 N94-18247
GREENHALGH, SAMUEL ..... p 1317 N94-17704
GREENHOLT, C. J. ..... p 1474 N94-18521
GREENWOLL, J. I. ..... p 1424 N94-17999
GREGG, WATSON W. ..... p 1532 N94-19761
GREINER, N. R. ..... p 1376 N94-17813
GRETH, RICKY L. ..... p 1512 N94-18765
GRIBOVSKY, P. O. ..... p 1375 N94-18013
GRIFFITHS, G. ..... p 1496 N94-18065
p 1496 N94-18066
GRIFFITHS, M. ..... p 1496 N94-18065
GRIFFITHS, M. J. ..... p 1496 N94-18066
GRIFFITHS, S. K. ..... p 1346 N94-17997
GRIMSDITCH, M. ..... p 1594 N94-17871
p 1368 N94-18098
p 1603 N94-19550
GROENLAND, TOR-ARNE ..... p 1311 N94-17919
GROOMS, H. R. ..... p 1450 N94-17835
GROOT, J. S. ..... p 1383 N94-18070
GROOTHUIS, MICHIEL ..... p 1429 N94-18044
GROPP, W. ..... p 1535 N94-19010
GROSS, RICHARD A. ..... p 1374 N94-19586
GROSS, ROLF W. ..... p 1377 N94-18758
GROSSBECK, M. L. ..... p 1357 N94-17859
p 1358 N94-17915
GROSSE, IAN R. ..... p 1542 N94-18887
GROTCH, S. L. ..... p 1488 N94-17942
GROTE, DAVID P. ..... p 1588 N94-19034
GROTHAUS, MICHAEL G. ..... p 1580 N94-18947
GROVE, JOHN W. ..... p 1419 N94-19025
GRUBB, J. W. ..... p 1524 N94-19076
GRUBBS, R. H. ..... p 1377 N94-18491
GRUNBAUM, F. A. ..... p 1384 N94-18186
GRUNOW, PAUL ..... p 1470 N94-19654
GRUNSFELD, JOHN M. ..... p 1324 N94-19168
GRUVER, J. L. ..... p 1546 N94-17811
GU, CHUN ..... p 1597 N94-18498
GU, S. H. ..... p 1370 N94-18515
GUAN, H. W. ..... p 1370 N94-18515
GUERIN, YVES ..... p 1408 N94-18022
GUETHLEIN, G. ..... p 1584 N94-17993
GUETTLER, W. ..... p 1329 N94-19633
GUHA, S. ..... p 1467 N94-18518
GUICHETEAU, P. ..... p 1608 N94-18238
p 1608 N94-18239
p 1319 N94-18240
GUIDOS, BERNARD J. ..... p 1410 N94-18391
GUILINGER, T. R. ..... p 1474 N94-18521
GUINET, ALEXANDRE ..... p 1451 N94-17918
GULTEKIN, S. ..... p 1354 N94-19660
GUNASEKARAN, ANANTHAKRISHNAN
p 1338 N94-18314
GUO, H. ..... p 1433 N94-19135
GUO, X. ..... p 1398 N94-18349
GUPTA, D. ..... p 1359 N94-18322
GURNETT, D. A. ..... p 1328 N94-19627
GURNETT, DONALD A. ..... p 1629 N94-19094
GURROLA, H. ..... p 1483 N94-18717
GUSTAFSSON, G. ..... p 1328 N94-19624
GUYMER, T. H. ..... p 1461 N94-18137
GUZIK, T. G. ..... p 1630 N94-18676
p 1629 N94-18705

H

HAAN, S. W. ..... p 1587 N94-18274
HAAR, R. R. ..... p 1569 N94-18999
p 1570 N94-19108
HABER, IRVING ..... p 1588 N94-19034
HABETS, L. C. G. J. M. ..... p 1553 N94-19556
HACKEL, R. P. ..... p 1435 N94-17723
p 1437 N94-18093
HADDAD, MICHAEL E. ..... p 1326 N94-19177
HADDY, FRANCIS J. ..... p 1502 N94-19213
HAEGGKVIST, ROLAND ..... p 1555 N94-19691
HAERENDEL, G. ..... p 1329 N94-19630
HAFEZ, M. ..... p 1413 N94-18565
HAFIZI, B. ..... p 1440 N94-18771
HAGGAG, F. M. ..... p 1359 N94-18245
HAGIWARA, MIYUKI ..... p 1369 N94-18220
HAGLER, THOMAS ..... p 1326 N94-19180
HAGLUND, R. F., JR. ..... p 1339 N94-17846
HAHN, K. ..... p 1389 N94-19053
p 1591 N94-19559
HAINE, T. W. N. ..... p 1496 N94-18065
HAINES, JOHN R. ..... p 1582 N94-17713
HALBLEIB, J. A. ..... p 1573 N94-17698
HALDAR, P. ..... p 1601 N94-18993
p 1602 N94-19122
HALE, J. ..... p 1386 N94-18454
HALE, J. A. ..... p 1625 N94-18612
p 1625 N94-18613
p 1625 N94-18615
p 1625 N94-18618
p 1626 N94-18619
p 1626 N94-18620
p 1626 N94-18621
HALEY, JOSEPH L. ..... p 1511 N94-18296
HALL, R. B. ..... p 1464 N94-17731
HALL, ROBERT C. ..... p 1367 N94-17706
HALLING, A. M. ..... p 1574 N94-18972
HALOREN, R. ..... p 1386 N94-18454
HALPERN, M. E. ..... p 1317 N94-18315
HALSTEAD, THORA W. ..... p 1502 N94-19211
HALYO, E. ..... p 1607 N94-17953
HAMEED, S. ..... p 1489 N94-18053
HAMERNIK, ROGER P. ..... p 1506 N94-18911
HAMIL, THOMAS M. ..... p 1492 N94-18637
HAMILTON, L. J. ..... p 1497 N94-18329
HAMLEY, JOHN A. ..... p 1587 N94-18861
HAMMEL, P. C. ..... p 1594 N94-17907
HAMMER, C. ..... p 1478 N94-19241
HAMMONDS, J. P. ..... p 1598 N94-18531
HAMMONS, B. E. ..... p 1442 N94-19563
HAN, K. S. ..... p 1591 N94-19441
HAN, Q. Y. ..... p 1433 N94-19135
HANCOCK, B. K. ..... p 1329 N94-19632
HANCOCK, B. R. ..... p 1617 N94-19057
HANCOCK, G. J. ..... p 1456 N94-19061
HANCOCK, THOMAS ..... p 1325 N94-19169
HANDREN, R. T. ..... p 1435 N94-17759
HANEY, M. ..... p 1569 N94-19013
HANLY, M. P. ..... p 1468 N94-19016
HANSEN, L. V. ..... p 1603 N94-19347
HANSMA, H. G. ..... p 1370 N94-18403
HANSMA, P. K. ..... p 1370 N94-18403
HANSON, D. L. ..... p 1429 N94-18102
HANSON, KATHRYN L. ..... p 1484 N94-18725
HAPPEE, R. ..... p 1504 N94-18080
HARDIN, JAY D. ..... p 1308 N94-18435
HARDWICK, JONATHAN C. ..... p 1531 N94-19592
HARDY, B. C. ..... p 1308 N94-18432
p 1308 N94-18434
HARGROVE, R. S. ..... p 1437 N94-18093
p 1441 N94-19294
HARNDEN, F. R., JR. ..... p 1625 N94-18612
p 1625 N94-18613
p 1625 N94-18615
p 1625 N94-18618
p 1626 N94-18619
p 1626 N94-18620
p 1626 N94-18621
HARO, M. ..... p 1572 N94-19545
HARRIS, A. I. ..... p 1390 N94-19416
p 1622 N94-19417
HARRIS, D. E. ..... p 1625 N94-18612
p 1625 N94-18613
p 1625 N94-18615
p 1625 N94-18618
p 1626 N94-18619
p 1626 N94-18620
p 1626 N94-18621
HARRIS, STEPHEN J. ..... p 1606 N94-19771
HARSTAD, E. N. ..... p 1609 N94-19187
HARTMAN, R. C. ..... p 1623 N94-19463
p 1623 N94-19464
HARVEY, R. W. ..... p 1589 N94-19073
HARWOOD, KELLY ..... p 1315 N94-18844
HASINGER, G. ..... p 1622 N94-19451
HASRATIAN, A. S. ..... p 1555 N94-19692
p 1555 N94-19693
HASSANEIN, A. ..... p 1588 N94-18971
HASSENZAHL, W. V. ..... p 1590 N94-19269
HASSINEN, PAAVO ..... p 1365 N94-19374
HATA, SATOSHI ..... p 1444 N94-18159
HATFIELD, L. ..... p 1397 N94-18318
HAUER, J. F. ..... p 1548 N94-18094
HAUPTMAN, J. M. ..... p 1574 N94-18927
HAVELA, L. ..... p 1605 N94-19735
HAVERKORT, BOUDEWIJN R. ..... p 1537 N94-19264
p 1559 N94-19386
HAWKINS, S. A. ..... p 1575 N94-18996
HAXTON, W. ..... p 1568 N94-18824
HAYAKAWA, MOTOMU ..... p 1429 N94-18040
HAYES, J. R. ..... p 1336 N94-18338
HAYLYO, EDI ..... p 1565 N94-17951
HAYNES, T. E. ..... p 1593 N94-17845
HAYOT, F. ..... p 1561 N94-18177
HAYS, CYNTHIA J. ..... p 1470 N94-17762
HAYTON, G. E. ..... p 1547 N94-18069
HAZELTINE, R. D. ..... p 1587 N94-18524
HAZEN, E. S. ..... p 1572 N94-19320
HE, J. ..... p 1443 N94-17785
HE, K. X. ..... p 1373 N94-19402
HE, LIANZHU ..... p 1332 N94-18760
HEADRICK, J. M. ..... p 1385 N94-18291
HEARD, WALTER L., JR. ..... p 1333 N94-17765
HEARNE, G. ..... p 1404 N94-18805
HEBERLEIN, J. V. R. ..... p 1433 N94-19135
HEDEMANN, M. A. ..... p 1382 N94-17806
HEDMAN, SVEN G. ..... p 1311 N94-17721
HEDSTROM, G. ..... p 1562 N94-17873
p 1563 N94-19270
HEEGER, ALAN J. ..... p 1598 N94-18511

HEGEDUS, CHARLES R. p 1367 N94-17719
HEHL, F. W. p 1607 N94-17892
HEIKKINEN, D. W. p 1594 N94-17896
HEIKKINEN, M. A. p 1607 N94-18120
HEINEMANN, H. p 1347 N94-18193
p 1347 N94-18194
HEINRICHS, D. P. p 1556 N94-18073
HEINSTEIN, M. W. p 1455 N94-19039
p 1460 N94-19476
HEINTZENBERG, J. p 1479 N94-19379
HELLER, A. p 1374 N94-19585
HELMICKI, ARTHUR J. p 1338 N94-19706
HEMACHANDRA, LANE A. p 1530 N94-19483
HENAGER, C. H., JR. p 1343 N94-19335
HENDERSON, GIRARDEAU L. p 1443 N94-17705
HENDRICKS, J. T. p 1377 N94-18893
HENDRICKS, K. J. p 1403 N94-18452
p 1404 N94-18872
HENLEY, E. M. p 1568 N94-18824
HENNINGER, R. J. p 1609 N94-19187
HENSHAW, R. M. p 1336 N94-18338
HERBERT, G. A. p 1489 N94-18126
HERCZFELD, PETER R. p 1396 N94-18062
HERMAN, GERARD C. p 1486 N94-19081
p 1563 N94-19083
p 1486 N94-19140
p 1488 N94-19644
HERMAN, R. G. p 1351 N94-19132
p 1351 N94-19150
HERMANN, BRUCE R. p 1317 N94-19572
HERMANS, A. J. p 1419 N94-19087
HERNANDEZ, C. L. p 1359 N94-18127
HERNANDEZ, J. E. p 1517 N94-17867
HERRMANN, T. P. p 1453 N94-18084
HEWETT, D. W. p 1575 N94-19107
HEWITT, DON p 1539 N94-19790
HEYMA, P. M. p 1313 N94-19667
HIETALIA, V. M. p 1405 N94-19079
HIKIDA, KAZUO p 1444 N94-18159
HILBIG, R. p 1310 N94-18445
HILEMAN, M. S. p 1470 N94-17773
HILL, D. N. p 1403 N94-18639
p 1590 N94-19290
HILL, SUSAN T. p 1610 N94-19389
HILLIS, D. L. p 1585 N94-18058
HILLMYER, M. A. p 1377 N94-18491
HILLS, R. E. p 1622 N94-19417
HILTON, RICHARD D. p 1391 N94-19582
HIN, ANDREA J. S. p 1423 N94-19645
HINCHLIFFE, I. p 1571 N94-19247
HINDMAN, E. E. p 1472 N94-17986
HINEMAN, M. p 1348 N94-18256
HIRABAYASHI, TAKEO p 1444 N94-18159
HIROTOMI, JUN p 1425 N94-18016
HIRSCH, A. p 1570 N94-19103
HIRSCHON, A. S. p 1349 N94-18532
HIRST, DONALD J. p 1367 N94-17719
HISKES, J. R. p 1565 N94-17797
HIX, DEBORAH p 1512 N94-18774
HIXSON, R. S. p 1361 N94-18802
p 1563 N94-19151
HJELM, R. P., JR. p 1368 N94-18096
HLAVA, P. F. p 1373 N94-19308
HO, C. Y. p 1374 N94-19532
HO, HENJEN p 1456 N94-19095
HOADLEY, SHERWOOD TIFFANY
p 1321 N94-19316
HOAG, J. E. p 1536 N94-19115
HOBBS, PETER V. p 1479 N94-19575
HOCKNEY, R. W. p 1534 N94-18767
HOEHLER, T. M. p 1477 N94-19235
HOEHN, J. G. p 1602 N94-19122
HOEHN, J. G., JR. p 1601 N94-18993
HOEKSTRA, J. p 1399 N94-18352
HOENSELAERS, C. p 1548 N94-18140
HOF, D. E. p 1478 N94-19272
HOFFBAUER, B. p 1519 N94-18086
HOFFHEINS, B. S. p 1424 N94-17778
HOFFMAN, D. J. p 1581 N94-17694
p 1382 N94-17695
p 1590 N94-19273
HOFFMAN, RICHARD p 1506 N94-18632
HOFFMAN, ROSS p 1492 N94-18637
HOFMANN, D. J. p 1479 N94-19379
HOFMANN, R. p 1621 N94-19415
HOGAN, J. T. p 1585 N94-18058
HOGAN, R. E., JR. p 1469 N94-19109
HOISINGTON, CHARLES M. p 1532 N94-19761
HOLBACK, B. p 1328 N94-19624
HOLCOMB, FRANKLIN H. p 1388 N94-18769
HOLDEN, N. E. p 1487 N94-19477
HOLIAN, K. S. p 1460 N94-19603
HOLLADAY, J. S. p 1463 N94-19672
HOLLEY, S. p 1496 N94-18065
HOLLOWAY, D. A. p 1372 N94-18932
HOLLOWAY, D. L. p 1369 N94-18166
HOLLWURTEL, E. p 1494 N94-19503
HOLMES, R. p 1419 N94-19025
HOLMGREN, G. p 1328 N94-19624
HOLMSTROEM, H. p 1476 N94-19038
HOLTKAMP, D. B. p 1478 N94-19272
HOLTSLAG, BERT p 1494 N94-19699
HONG, K. C. p 1369 N94-18112
HOOPER, E. B. p 1589 N94-19074
p 1590 N94-19289
HOOPER, K. S. p 1571 N94-19278
HOOVER, JAMES M. p 1367 N94-17706
HOPKINS, D. p 1470 N94-17749
HORAN, D. M. p 1334 N94-18149
p 1337 N94-18574
p 1335 N94-19787
HORIO, M. p 1502 N94-18476
HOROWITZ, M. p 1397 N94-18312
HOROWITZ, STANLEY A. p 1616 N94-18575
p 1619 N94-19780
HORTON, J. p 1441 N94-19251
HORTON, L. L. p 1467 N94-18478
HORTON, W. p 1584 N94-17983
HORWATH, E. J. p 1597 N94-18468
HOSHINO, K. p 1590 N94-19289
HOSKING, F. M. p 1359 N94-18127
HOTALING, S. P. p 1354 N94-19755
HOTALING, STEVEN P. p 1434 N94-19791
HOU, S. Y. p 1405 N94-19079
HOU, T. H. p 1339 N94-17766
HOUPIS, CONSTANTINE H. p 1545 N94-18241
HOUSER, R. M. p 1467 N94-18520
HOVANDER, B. p 1405 N94-19292
HOVY, EDUARD p 1516 N94-17732
HOWELL, C. R. p 1365 N94-19274
HOWELL, J. A. p 1519 N94-18086
HOWLAND, JAMES W. p 1316 N94-18384
p 1386 N94-18495
HRUBESH, L. W. p 1395 N94-17882
HSU, CHUN-NAN p 1615 N94-18461
p 1616 N94-18641
HSU, MICHAEL M. p 1333 N94-19765
HU, J. p 1597 N94-18500
HUANG, CHANG-HUA p 1492 N94-18675
HUANG, H. S. p 1474 N94-18502
HUANG, HANN S. p 1348 N94-18249
HUANG, SHAOSONG p 1483 N94-18690
HUANG, XIN-YU p 1486 N94-19255
HUANG, Y. p 1559 N94-19555
HUBBARD, K. M. p 1358 N94-17875
HUBER, CARMEN I. p 1432 N94-18731
HUBER, M. C. E. p 1633 N94-19404
HUBER, MICHAEL R. p 1422 N94-19569
HUBER, TITO E. p 1432 N94-18731
HUBERMAN, E. p 1502 N94-18476
HUDDLESTON, R. L. p 1356 N94-17791
HUDSON, J. G. p 1472 N94-17985
p 1472 N94-17986
HUDSON, JEFFREY A. p 1513 N94-19531
HUDSON, TRACY D. p 1577 N94-18262
HUEBERT, B. p 1479 N94-19379
HUESTIS, DAVID L. p 1442 N94-19788
HUFF, R. L. p 1328 N94-19627
HUGHES, BRIAN L. p 1392 N94-19738
HUGHES, V. W. p 1572 N94-19320
HUGON-JEANNIN, YVES p 1563 N94-19413
HUIJBERTS, H. J. C. p 1543 N94-19328
HULL, J. R. p 1396 N94-18135
HUNTEMAN, W. J. p 1535 N94-18930
HUNTER, J. R. p 1440 N94-18889
HUNTER, JUDY F. p 1611 N94-19131
HUNTER, S. D. p 1623 N94-19463
p 1623 N94-19464
HUO, Q. p 1375 N94-19742
HURD, A. J. p 1345 N94-17820
HUTCHINGS, R. B. p 1451 N94-17929
HUTCHINSON, JACKY p 1631 N94-17968
HWANG, E. p 1474 N94-18499
p 1478 N94-19241
HWANG, I. G. p 1468 N94-19016
HWANG, I. S. p 1366 N94-19546

I

ICE, G. E. p 1593 N94-17760
IGARASHI, KIYOTAKA p 1429 N94-18043
IKEGAMI, TOMOMI p 1429 N94-18043
ILGISONIS, V. I. p 1590 N94-19193
IMHOF, W. L. p 1485 N94-18874
INFANGER, G. p 1516 N94-17701
INGLE, K. p 1617 N94-19026
INGOLD, G. p 1436 N94-17998
p 1438 N94-18504
INGRAM, A. E. p 1464 N94-17731
INUI, M. p 1520 N94-18117
IRELAND, P. T. p 1432 N94-18653
IRWIN, MARY J. p 1392 N94-19724
ISAEV, A. P. p 1561 N94-18153
p 1561 N94-18168
p 1548 N94-18169
ISBELL, CHARLES L. p 1544 N94-19599
ISHIDA, E. p 1437 N94-18083
ISHIZUKA, HIROSHI p 1438 N94-18160
ISMAY, DAVID K. p 1610 N94-19663
ISSEROW, SAUL p 1359 N94-18306
ITOH, TATSUO p 1407 N94-19584
IVANCIC, WILLIAM D. p 1333 N94-19313
IYENGAR, S. S. p 1534 N94-18699
p 1316 N94-19300
IYER, A. N. p 1601 N94-18993
p 1602 N94-19122
IZYGON, MICHEL p 1513 N94-19349

J

JACKSON, A. M. p 1370 N94-18477
JACKSON, BILL p 1555 N94-19694
JACKSON, DANIEL p 1521 N94-18453
JACOB, K. p 1308 N94-18437
JACOBS, I. p 1504 N94-17823
JACOBSON, J. p 1526 N94-19333
JACOBSON, L. A. p 1363 N94-19028
JAEGER, C. D. p 1535 N94-18930
JAEGER, E. F. p 1590 N94-19273
JAGIELSKI, M. p 1539 N94-19734
JAMALI, M. M. p 1534 N94-18507
p 1534 N94-18508
p 1389 N94-18897
JAMES, J. H. p 1344 N94-19391
JAMES, M. R. p 1341 N94-18692
JAMES, R. B. p 1594 N94-17896
JAMOUSSI, M. p 1400 N94-18364
JANG, P. R. p 1429 N94-18207
JANHUNEN, T. p 1520 N94-18118
JANKE, C. J. p 1343 N94-18761
JANKOWSKI, A. F. p 1357 N94-17860
JANSEN, B. p 1524 N94-19089
p 1525 N94-19143
p 1525 N94-19156
JANSEN, ROBERT W. p 1499 N94-19609
JANSON, D. J. p 1399 N94-18354
JANSSEN, LEO p 1611 N94-17980
JANSSEN, WIL p 1390 N94-19267
p 1538 N94-19296
JASPER, DONALD W. p 1306 N94-18422
JAYAPRAKASH, C. p 1561 N94-18177
JEANLOZ, R. p 1404 N94-18805
JEFFREY, JOSEPH p 1500 N94-19786
JEFFRIES, JAY B. p 1442 N94-19788
JELINEK, A. V. p 1386 N94-18454
p 1342 N94-18756
p 1342 N94-18757
JELLY, A. H. p 1308 N94-18434
JEMISON, WILLIAM D. p 1396 N94-18062
JENKINS, R. A. p 1472 N94-17910
JENSEN, C. C. p 1574 N94-18497
JENSEN, D. R. p 1483 N94-18712
JENSEN, L. p 1400 N94-18365
JEON, JAE-JIN p 1454 N94-18661
JERVIS, T. R. p 1358 N94-17875
JESSUP, E. R. p 1535 N94-18808
p 1524 N94-19024
JIN, WENXIONG p 1512 N94-18673
JOG, ANAGHA p 1542 N94-18887
JOHANSSON, M. E. p 1405 N94-19079
JOHANSSON, N. p 1322 N94-19332
JOHNSON, D. E. p 1382 N94-17806
JOHNSON, DAVID B. p 1522 N94-18696
JOHNSON, ERIC R. p 1457 N94-19350
JOHNSON, GREGORY A. p 1468 N94-18821
JOHNSON, J. N. p 1361 N94-18802
JOHNSON, LANE R. p 1418 N94-18870
JOHNSON, P. D. p 1401 N94-18375
JOHNSON, R. BARRY p 1603 N94-19513
JOHNSON, R. L. p 1472 N94-17890
JOHNSON, RAY O. p 1572 N94-19607
JOHNSON, RICHARD p 1512 N94-18882
JOHNSON, TERRY C. p 1503 N94-19215
JOHNSON, W. R. p 1571 N94-19201
JOHNSTON, G. W. p 1306 N94-18423
JOHNSTON, LESLIE J. p 1307 N94-18427
JOHNSTON, LESLIE W. p 1445 N94-18778
JOHNSTONE, A. D. p 1329 N94-19632
JOHNSTONE, WALTER p 1579 N94-18738
JOKINEN, H. p 1396 N94-18091
JONES, B. J. p 1534 N94-18699
JONES, C. p 1625 N94-18612
p 1625 N94-18613
p 1625 N94-18615
p 1625 N94-18618
p 1626 N94-18619
p 1626 N94-18620

p 1626 N94-18621
JONES, DAVID p 1378 N94-19494
JONES, K. p 1501 N94-17889
JONES, R. B. p 1501 N94-18242
JONES, R. H. p 1343 N94-19335
JONES, RICHARD A. p 1606 N94-19739
JONES, T. V. p 1432 N94-18653
JONKER, B. T. p 1375 N94-19758
JONKER, BEREND T. p 1408 N94-19763
JONSSON, J. p 1602 N94-19293
JOSOWICZ, M. p 1369 N94-18233
JOSTEN, N. E. p 1461 N94-17851
JOYCE, J. p 1401 N94-18367
JUDD, D. p 1591 N94-19559
JUNG, H. A. p 1554 N94-19688
p 1554 N94-19689
JUSKA, THOMAS p 1342 N94-18702

K

KAASSCHIETER, E. F. p 1547 N94-18078
KADOTA, K. p 1586 N94-18213
KAERKI, SATU p 1444 N94-17974
KAHN, MANFRED p 1408 N94-19759
KAILATH, THOMAS p 1392 N94-19736
KAISER, T. B. p 1590 N94-19290
KAJS, J. P. p 1441 N94-19307
KALLENBERG, L. C. M. p 1559 N94-19555
KALOKITIS, DAVID p 1599 N94-18719
KALTENBACH, H.-J. p 1416 N94-18595
KAMAKOTI, V. p 1402 N94-18379
KAMAREDDINE, F. p 1524 N94-19066
p 1560 N94-19710
KAMBAYASHI, SHAW p 1607 N94-18211
KAMIN, G. p 1437 N94-18134
KAMINSKA, B. p 1400 N94-18364
KANBACH, G. p 1623 N94-19463
p 1623 N94-19464
KANDIL, OSAMA A. p 1313 N94-19621
KANEFSKY, MORTON p 1439 N94-18656
KANG, S. p 1446 N94-19291
KANKKUNEN, A. p 1396 N94-18091
KANNE, W. R. p 1446 N94-19334
KANNE, W. R., JR. p 1443 N94-17761
KAO, C. Y. J. p 1476 N94-19104
KAO, Y. H. p 1601 N94-19056
KAPOOR, KAMLESH p 1314 N94-18553
KARAKASHIAN, T. p 1625 N94-18612
p 1625 N94-18613
p 1625 N94-18615
p 1625 N94-18618
p 1626 N94-18619
p 1626 N94-18620
p 1626 N94-18621
KARAMPETAKIS, N. P. p 1547 N94-18069
KARDAUN, O. p 1585 N94-18056
KARETI, S. p 1316 N94-19300
KARIM, MOHAMMAD A. p 1408 N94-19751
KARL, R. R., JR. p 1478 N94-19272
KARLINER, I. p 1569 N94-19013
KARLSSON, R. p 1389 N94-18950
KARS, PIM p 1526 N94-19196
KARTASHOV, G. B. p 1375 N94-18013
KARTHIKEYAN, B. p 1402 N94-18379
KASCHMITTER, J. L. p 1395 N94-17849
KASS, W. J. p 1433 N94-19243
KASUGA, MASAO p 1425 N94-18016
KATAJISTO, KATRI p 1444 N94-17974
KATOEN, JOOST-PIETER p 1558 N94-19228
KATRAGADDA, PRASANNA p 1542 N94-18887
KAUFFMAN, R. p 1351 N94-19136
KAUFMAN, GORDON p 1521 N94-18458
KAUTZ, D. D. p 1437 N94-18093
p 1441 N94-19294
KAWASAKI, SUNAO p 1438 N94-18160
KAWATA, MASAYUKI p 1425 N94-18016
KAYSER, R. F. p 1351 N94-19134
KAZAKOV, D. I. p 1593 N94-17748
KAZOVSKY, LEONID G. p 1577 N94-18254
KEAMPF, GEORGE L. p 1510 N94-19677
KEANE, C. J. p 1582 N94-17708
KEANE, D. p 1566 N94-18104
KEEFER, CHRISTOPHER W. p 1579 N94-18668
KEENAN, PATRICK J. p 1445 N94-18465
KEENE, A. P. p 1544 N94-19458
KEINAENEN, HEIKKI p 1339 N94-17958
KELLER, P. E. p 1433 N94-19000
KELLEY, D. F. p 1348 N94-18256
KELLEY, N. D. p 1489 N94-18046
KELLY, P. M. p 1519 N94-18086
KENKEREMATH, L. D. p 1471 N94-17777
KENNEDY, T. E. p 1329 N94-19632
KENNER, SCOTT p 1333 N94-17765
KENT, S. A. p 1322 N94-18324
KERCHEN, P. p 1523 N94-18943
KERGADALLAN, Y. p 1605 N94-19735
KERLEY, G. I. p 1357 N94-17819
p 1618 N94-19101
KERNEY, PAUL T. p 1320 N94-18907
KERNS, KEVIN J. p 1493 N94-18871
KERSEY, ALAN D. p 1382 N94-17902
p 1579 N94-18743
KERTIS, K. p 1617 N94-19026
KESZLER, D. A. p 1604 N94-19565
KETATA, MAHMOUD p 1457 N94-19375
KETSARIS, ALEXANDER p 1408 N94-18023
KEUNG, M. p 1354 N94-19728
KEY, SAMUEL W. p 1459 N94-19474
KEYES, B. L. P. p 1374 N94-19561
KHACHATRIAN, N. K. p 1555 N94-19692
p 1555 N94-19693
KHALIL, T. B. p 1459 N94-19472
KHUTORNOJ, N. V. p 1548 N94-18175
KIBBE, MARION P. p 1509 N94-18686
KIM, C. p 1408 N94-19759
KIM, CHOONGUN p 1365 N94-19282
KIM, D. p 1468 N94-18944
KIM, H. p 1446 N94-19291
KIM, HYUN S. p 1394 N94-17703
KIM, J. Y. p 1584 N94-17983
KIM, K. p 1398 N94-18345
p 1399 N94-18358
p 1446 N94-19291
KIM, KI C. p 1319 N94-19781
KIM, MICHAEL S. p 1388 N94-18769
KIM, S. K. p 1352 N94-19304
KIM, S.-W. p 1411 N94-18550
KIMURA, F. p 1520 N94-18117
KINCAID, J. R. p 1363 N94-19019
KING, D. M. p 1599 N94-18804
KING, N. S. P. p 1432 N94-18828
KINGON, ANGUS I. p 1605 N94-19664
KINI, ARAVINDA M. p 1601 N94-19022
KINNEY, R. p 1583 N94-17945
KINNUNEN, ARVO p 1346 N94-17973
KINSEY, DON W. p 1417 N94-18739
KIPP, M. E. p 1373 N94-19271
KIRAKOWSKI, JUREK p 1613 N94-17925
KIRBIE, H. C. p 1575 N94-18996
KIRCHNER, D. L. p 1328 N94-19627
KIRENSKIY, L. V. p 1351 N94-19110
KIRKENDALL, CLAY p 1382 N94-17902
KISHIMOTO, Y. p 1584 N94-17983
KJELL, G. p 1528 N94-19333
KLAMERUS, J. p 1527 N94-19245
KLEB, R. p 1598 N94-18531
KLEIN, J. E. p 1523 N94-19005
KLEIN, MAARTEN p 1537 N94-19198
KLEIN, STANLEY A. p 1505 N94-18190
KLEINTZ, MICHAEL p 1384 N94-18071
KLEM, D. p 1435 N94-17855
KLEM, D. E. p 1585 N94-18115
KLEM, J. F. p 1592 N94-17741
KLEMM, R. A. p 1407 N94-19553
KLENNER, JUERGEN p 1319 N94-19496
KLIER, K. p 1351 N94-19132
p 1351 N94-19150
KLIMENKO, K. G. p 1566 N94-18199
KLIMENKO, S. V. p 1561 N94-18150
KLINER, KRISTEN M. p 1341 N94-18572
KLINGER, DAVID W. p 1510 N94-19677
KLOOTSEMA, R. p 1428 N94-18032
KLUEH, R. L. p 1450 N94-17848
KMETYK, L. N. p 1358 N94-18100
KMOCH, KLAUS p 1381 N94-19650
KNAPIK, JOSEPH p 1512 N94-18882
KNAPP, DEIRDRE J. p 1512 N94-18754
KNAPP, F. F., JR. p 1504 N94-17699
KNIFFEN, D. A. p 1623 N94-19463
p 1623 N94-19464
KNIGHT, J. C. p 1530 N94-19429
KNIPP, PETER A. p 1598 N94-18609
KNOBLOCK, CRAIG A p 1616 N94-18641
KNOBLOCK, CRAIG A. p 1615 N94-18461
p 1541 N94-18759
KNOWLTON, DANIEL p 1511 N94-17841
KOBAYASHI, A. S. p 1453 N94-18328
KOBAYASHI, TAKAYUKI p 1438 N94-18160
KOCH, J. A. p 1437 N94-18131
p 1580 N94-18931
KOCKS, U. F. p 1359 N94-18114
KOEGLER, K. J. p 1433 N94-19041
KOHALMI, DIANE p 1320 N94-18658
KOHLER, S. M. p 1446 N94-19547
KOHONEN, REIJO p 1444 N94-17974
KOINKAR, VILAS N. p 1604 N94-19579
p 1407 N94-19722
p 1447 N94-19784
KOMM, DAVID S. p 1396 N94-18284
KONDRASHUK, I. N. p 1593 N94-17748
KONG, J. A. p 1464 N94-19681
KONOLIGE, KURT G. p 1540 N94-18399
KOONEN, A. M. J. p 1390 N94-19230
KOONS, HARRY C. p 1385 N94-18287
KOONTZ, T. E. p 1394 N94-17780
KORTAN, A. R. p 1602 N94-19340
KORTH, A. p 1329 N94-19633
KOSLOFF, R. p 1382 N94-17909
KOSOBUD, R. G. p 1472 N94-17891
KOSTADINOV, S. I. p 1548 N94-18195
p 1548 N94-18196
p 1549 N94-18200
KOSTER, M. P. p 1543 N94-19199
KOSTROUN, V. O. p 1571 N94-19257
KOTSCHENREUTHER, M. p 1584 N94-17983
KOTTAS, JAMES p 1540 N94-18331
KOTZIAN, M. p 1494 N94-19503
KOUVARITAKIS, B. p 1530 N94-19412
KOVACS, AUSTIN p 1463 N94-19672
KOVAL, LESLIE R. p 1366 N94-19594
KOWAL, E. p 1360 N94-18325
KOYMANS, RON p 1558 N94-19228
KRAKOWSKI, R. A. p 1587 N94-18803
KRALL, J. p 1586 N94-18148
KRAMER, G. D. p 1422 N94-19568
KRAMER, MARK T. p 1619 N94-19571
KRAMMER, JOHANN p 1319 N94-19496
KRANER, H. W. p 1602 N94-19258
KRAUSE, J. L. p 1436 N94-17996
p 1572 N94-19283
KRAUSS, ROBERT W. p 1502 N94-19211
KREMPL, E. p 1448 N94-17814
KRENELKA, T. p 1378 N94-18913
KRICK, M. S. p 1571 N94-19278
KRIEG, R. D. p 1372 N94-19059
KRIENEN, F. p 1572 N94-19320
KRIKORIAN, ABRAHAM D. p 1503 N94-19217
KRINSKY, S. p 1436 N94-17998
p 1438 N94-18504
KRISTIANSEN, M. p 1397 N94-18318
KROLL, N. p 1307 N94-18428
KROONENBERG, FRANK p 1495 N94-19703
KROUPA, JOSEPH L. p 1360 N94-18660
KRUM, DAVID M. p 1324 N94-19168
KUDRITZKI, R. P. p 1624 N94-17736
KUEHL, GARY p 1514 N94-17877
KUHL, A. L. p 1422 N94-19515
KUHN, HOWARD A. p 1356 N94-17801
KUHN, RICHARD E. p 1317 N94-18577
p 1318 N94-18733
KUJAK, S. p 1352 N94-19191
KUJAK, STEPHEN p 1350 N94-18895
p 1350 N94-18896
KUJALA, TIMO p 1452 N94-17959
KULANDER, K. C. p 1436 N94-17996
p 1572 N94-19283
KUMAR, B. p 1370 N94-18282
KUMAR, D. p 1375 N94-19742
KUMAR, R. S. p 1368 N94-18098
KUMAR, S. p 1545 N94-17683
KUMAR, S. S. p 1368 N94-18098
KUNKEL, BRUCE A. p 1474 N94-18688
KUNKEL, K. E. p 1488 N94-17715
KUPERSTEIN, MICHAEL p 1540 N94-18331
KURDIKOV, A. B. p 1561 N94-18168
p 1548 N94-18169
KURITA, GEN-ICHI p 1586 N94-18157
KURTZ, HENRY A. p 1567 N94-18783
KURZFELD, ANDY p 1631 N94-17968
KUSHNER, ALAN S. p 1458 N94-19468
KUSHNER, BRIAN G. p 1362 N94-18923
KUSUMAPUTRI-HORNIK, YUSTINA
p 1552 N94-19487
KWAK, DOCHAN p 1306 N94-18421
KWATRA, S. C. p 1534 N94-18507
p 1534 N94-18508
p 1389 N94-18897
KWOK, P. W. p 1623 N94-19463
p 1623 N94-19464
KWONG, MAN KAM p 1604 N94-19567

L

LAARHUIS, J. H. p 1390 N94-19230
LAASSIBI, ABDELJALIL p 1421 N94-19399
LACH, CYNTHIA L. p 1368 N94-18075
LACINA, J. p 1581 N94-17689
LACKNER, K. S. p 1408 N94-17728
LAFON, F. C. p 1412 N94-18561
LAHAYE, R. J. p 1582 N94-17702
LAI, C. A. p 1498 N94-18665
LAITILA, PAEIVI p 1444 N94-17974
LAMANI, BACHIR p 1458 N94-19411
LAMARQUE, CLAUDE-HENRI p 1529 N94-19409
LAMB, SUSAN A. p 1627 N94-19218
LAMBERT, C. R. p 1504 N94-17699

LAMBERT, KENNETH S. p 1532 N94-19761
LAMIE, EDWARD L. p 1521 N94-18308
LAMME, V. A. F. p 1508 N94-18121
LAMPINEN, M. J. p 1607 N94-18120
LANAGAN, M. T. p 1597 N94-18500
LANCASTER, P. p 1496 N94-18066
LANCE, N. p 1332 N94-18669
p 1332 N94-18670
LANDEN, O. L. p 1585 N94-18129
LANDMAN, WILLIAM H. p 1564 N94-17738
LANE, S. p 1435 N94-17855
p 1585 N94-18115
LANGDON, A. B. p 1575 N94-19106
LANGDON, A. BRUCE p 1588 N94-19034
LANGE, C. H. p 1465 N94-18001
LANGE, M. R. p 1577 N94-18302
LANGE, R. p 1480 N94-19732
LANGERAK, ROM p 1558 N94-19354
LANGLADE, CECILE p 1373 N94-19405
LANGLAND, R. T. p 1632 N94-18856
LANGNER, D. G. p 1571 N94-19278
LANGNER, J. p 1479 N94-19379
LANGUETSOBGNY, YVES BERTRAND
p 1533 N94-18068
LANKFORD, JAMES, JR. p 1366 N94-19673
LANNIN, J. S. p 1367 N94-17678
LANSKY, I. M. p 1589 N94-19037
LAO, L. L. p 1585 N94-18057
LAPOINTE, CLAUDE J. p 1514 N94-17877
LAPOINTE, KENNETH M. p 1424 N94-17717
LAPRIE, J. C. p 1532 N94-19713
LARBI, J. A. p 1380 N94-19322
LARRAURI, DIDIER p 1353 N94-19376
LARSEN, G. p 1380 N94-18710
LARSEN, JILL p 1371 N94-18750
LARSON, JAMES DANIEL p 1564 N94-17738
LARSON, ROBERT J. p 1496 N94-18215
LASEWICZ, VINCENT J., JR. p 1513 N94-18992
LASNIER, C. J. p 1589 N94-19074
p 1590 N94-19289
LATELLA, DIEGO p 1558 N94-19195
p 1558 N94-19354
LATOMBE, J. C. p 1523 N94-18879
LAU, P. p 1528 N94-19333
LAU, S. S. p 1593 N94-17845
LAUCHLE, G. C. p 1416 N94-18642
p 1562 N94-18664
LAUF, R. J. p 1424 N94-17778
LAULAINEN, N. p 1470 N94-17749
LAUNDER, B. E. p 1414 N94-18579
p 1414 N94-18580
p 1414 N94-18581
p 1414 N94-18582
p 1414 N94-18583
p 1414 N94-18584
p 1414 N94-18585
p 1415 N94-18586
p 1415 N94-18587
LAVID, JULIA p 1516 N94-17732
LAW, C. K. p 1348 N94-18257
LAWRENCE, ALBERT F. p 1503 N94-19757
LAWRENCE, R. J. p 1358 N94-18100
LAWSON, A. C. p 1605 N94-19735
LAZARETH, O. p 1337 N94-17884
LEACH, H. p 1496 N94-18065
p 1496 N94-18066
LEADORE, MICHAEL G. p 1378 N94-19674
LEAN, D. E. p 1305 N94-18416
LEBALLEUR, J. C. p 1306 N94-18425
p 1309 N94-18440
LEBLANC, S. P. p 1368 N94-17946
LEBRUN, M. J. p 1584 N94-17983
LECK, C. p 1479 N94-19379
LEDOUX, C. A. p 1500 N94-19785
LEDUC, S. K. p 1476 N94-19065
LEE, C. G. p 1378 N94-19242
LEE, E. p 1591 N94-19559
LEE, E. L. p 1376 N94-18095
LEE, F. p 1400 N94-18362
LEE, G. p 1401 N94-18374
LEE, J. p 1398 N94-18345
p 1399 N94-18358
p 1411 N94-18551
LEE, KANG M. p 1394 N94-17703
LEE, L. M. p 1382 N94-17806
LEE, MIN-CHANG p 1385 N94-18288
LEE, R. W. p 1582 N94-17708
LEE, SANG RYOOL p 1544 N94-19361
LEE, SOOWON p 1610 N94-17746
LEE, T. S. H. p 1568 N94-18826
LEE, W. M. p 1376 N94-17840
LEE, YEONG JOO p 1456 N94-19116
LEE, YUAN T. p 1568 N94-18787
LEEUWENBERG, E. L. J. p 1509 N94-19348
LEFEUVRE, F. p 1328 N94-19623
LEHEL, JENO p 1552 N94-19395
LEHMAN, S. K. p 1390 N94-19114
LEHMANN, STEPHAN p 1428 N94-18034
LEHN, G. p 1330 N94-19635
LEI, C. Y. p 1366 N94-19775
LEI, JIH-FEN p 1434 N94-19314
LEINO, TAPIO p 1380 N94-19373
LEISHMAN, J. G. p 1311 N94-18413
LEKSONO, MOELJANTO W. p 1598 N94-18527
LEMOINE, F. p 1431 N94-18646
LEMON, MARK W. p 1323 N94-19163
LENSKI, JOSEPH W., JR. p 1446 N94-19318
LENT, E. M. p 1556 N94-18073
LEONARD, ANTHONY p 1410 N94-18472
LEONARD, J. A. p 1381 N94-19480
LEPORCQ, B. p 1431 N94-18646
LEROU, R. J. L. p 1441 N94-19426
LESCHZINER, M. A. p 1415 N94-18586
p 1415 N94-18587
p 1415 N94-18588
p 1415 N94-18589
p 1415 N94-18590
p 1415 N94-18591
p 1415 N94-18592
LESKO, K. T. p 1629 N94-19260
LESLIE, IAN M. p 1536 N94-19159
p 1536 N94-19160
LESSARD, ROGER A. p 1434 N94-19791
LESUER, D. R. p 1355 N94-17711
LETRAN, T. p 1604 N94-19597
LEUNG, K. P. p 1406 N94-19310
LEVA, ALBERTO p 1539 N94-17916
LEVENSON, RUTH A. p 1487 N94-19397
LEVEQUE, M. p 1328 N94-19626
LEVETON, ALAN L. p 1535 N94-19046
LEVITT, K. p 1523 N94-18943
LEVITT, LARRY J. p 1493 N94-18781
LEVY, JOSEPH p 1560 N94-18067
LEWIS, NATHAN S. p 1348 N94-18255
LEWIS, NORMAN G. p 1503 N94-19216
LI, C. P. p 1412 N94-18560
LI, D. p 1436 N94-17998
LI, HAO p 1555 N94-19690
LI, M. p 1517 N94-17812
LI, Z. p 1540 N94-18125
p 1602 N94-19258
p 1603 N94-19550
LIANG, G. L. p 1596 N94-18192
LIAW, LESLIE D. G. p 1457 N94-19351
LIBBY, STUART I. p 1581 N94-19602
LICHTIN, D. A. p 1336 N94-17856
LICINA, JOSEPH R. p 1511 N94-18296
LIEB, ROBERT J. p 1378 N94-19674
LIEBERMAN, MICHAEL A. p 1403 N94-18638
LIKHAREV, K. p 1598 N94-18539
LILIENTAL-WEBER, Z. p 1592 N94-17741
p 1595 N94-18054
LIN, HUA T. p 1358 N94-17915
LIN, IE-HONG p 1393 N94-19779
LIN, M. C. p 1438 N94-18258
LIN, Y. C. p 1623 N94-19463
p 1623 N94-19464
LIN, Y. K. p 1454 N94-18487
LINCOLN, KENNETH A. p 1343 N94-18869
LINDEN, S. M. p 1370 N94-18282
LINDQUIST, W. p 1437 N94-18134
LINDQVIST, P.-A. p 1328 N94-19624
LINDSAY, GEOFFREY A. p 1367 N94-17706
LINDSLEY, NED J. p 1444 N94-18266
LING, J. p 1369 N94-18166
LISS, T. p 1569 N94-19013
LITTLEFIELD, R. J. p 1533 N94-17693
LIU, C. S. p 1439 N94-18737
LIU, C. T. p 1355 N94-17757
LIU, CHAOQUN p 1417 N94-18843
LIU, CHENG p 1456 N94-19130
LIU, H. p 1441 N94-18974
LIU, K. Z. p 1397 N94-18340
LIU, L. C. p 1571 N94-19259
LIU, M. N. p 1397 N94-18340
p 1402 N94-18376
LIU, R. p 1597 N94-18498
LIU, X. T. p 1565 N94-17776
LIU, YAPING p 1361 N94-18806
LIU, Z. p 1572 N94-19320
LIU, ZHINING p 1417 N94-18843
LIVI, S. p 1329 N94-19633
LIVINGSTON, J. D. p 1361 N94-18806
p 1361 N94-18807
LLOYD, W. R. p 1556 N94-18073
LO, WEN-DA p 1560 N94-19726
LOBO, J. p 1614 N94-18099
LOCATELLI, EVA p 1539 N94-17916
LOCKHART, RICHARD p 1557 N94-18517
LOCKOWANDT, CHRISTIAN p 1324 N94-19167
LOFTIS, J. P. p 1524 N94-19076
LOH, WEI-YIN p 1560 N94-19726
LOHR, D. A. p 1336 N94-18338
LOHRENZ, MAURA C. p 1462 N94-18677
p 1462 N94-18679
LOKEN, S. C. p 1613 N94-17894
LOMONOZOV, M. p 1552 N94-19392
LONDON, R. p 1437 N94-18131
LONDON, R. A. p 1436 N94-17868
LONG, A. E. p 1395 N94-17872
LONGHURST, GLEN R. p 1582 N94-17713
LONGO, J. M. A. p 1307 N94-18428
LONSDALE, P. F. p 1498 N94-18862
LONSINGER, HANS p 1319 N94-19496
LOONG, C. K. p 1598 N94-18531
LOOTSMA, F. A. p 1611 N94-19157
p 1611 N94-19158
LOPEZ, P. p 1590 N94-19289
LOPEZ, R. p 1380 N94-18710
LORANGE, RICHARD D. p 1323 N94-19163
LORITO, FABRIZIO p 1540 N94-17922
p 1562 N94-17934
LOTENS, W. A. p 1504 N94-17966
LOTH, KENNETH p 1324 N94-19167
LOTTES, S. A. p 1586 N94-18272
LOUER, JOHN W., III p 1493 N94-18883
LOURDIN, PIERRE p 1366 N94-19436
LOWE-MA, C. L. p 1531 N94-19590
LOWEN, STEVEN B. p 1557 N94-18540
LOWNDES, D. H. p 1601 N94-18998
LOWRY, R. K. p 1496 N94-18066
LOY, D. p 1602 N94-19340
LU, TOH-MING p 1604 N94-19596
LU, ZHENGGUO p 1439 N94-18614
LUBRANO, JEAN-LOUIS p 1420 N94-19381
LUCANIA, J. p 1343 N94-18761
LUCAS, D. L. p 1385 N94-18291
LUDEWIG, H. p 1337 N94-17884
LUDWIG, REINHOLD p 1442 N94-19647
LUEHR, H. p 1329 N94-19629
LUETTICH, R. A., JR. p 1497 N94-18455
LUEVANO, ANNETTA J. p 1454 N94-18683
p 1361 N94-18742
LUI, M. S. p 1344 N94-19720
LUIGJES, G. p 1515 N94-19799
LUNARDINI, V. J. p 1487 N94-19529
LUNDEEN, G. N. p 1499 N94-18727
LUSK, EWING L. p 1535 N94-19046
LYNCH, D. p 1436 N94-17998
LYNCH, GARY p 1505 N94-18407
LYNN, D. W. p 1398 N94-18349
LYNN, K. G. p 1603 N94-19541
LYON, R. E. p 1369 N94-18112

M

MA, C. C. p 1494 N94-19298
MABEY, D. G. p 1317 N94-17826
MACARIE, IOAN I. p 1530 N94-19482
MACCABE, A. B. p 1536 N94-19161
p 1536 N94-19188
MACCABE, ARTHUR B. p 1537 N94-19206
MACCACARO, T. p 1625 N94-18612
p 1625 N94-18613
p 1625 N94-18615
p 1625 N94-18618
p 1626 N94-18619
p 1626 N94-18620
p 1626 N94-18621
MACGOWAN, B. J. p 1437 N94-18131
p 1580 N94-18931
MACHADO, L. E. p 1570 N94-19125
MACHADO, LAWRENCE E. p 1320 N94-18333
MADAY, Y. p 1413 N94-18566
p 1413 N94-18567
MADHUKAR, A. p 1597 N94-18506
MADHUKAR, BURRA V. p 1502 N94-18924
MADYCH, WOLODYMYR p 1546 N94-17825
MAEDA, CHRIS p 1538 N94-19533
p 1515 N94-19591
MAELKKI, YRJOE p 1346 N94-17973
MAFFEZZONI, CLAUDIO p 1443 N94-17937
MAFFIOLI, F. p 1547 N94-17961
p 1547 N94-17962
MAFFIOLI, FRANCESCO p 1547 N94-17928
MAGALHAES, A. M. p 1624 N94-17764
MAGER, J. W. L. J. p 1518 N94-17965
MAGNANI, GIANANTONIO p 1443 N94-17937
MAGRUDER, R. H., III p 1339 N94-17846
MAGUIRE, M. C. p 1364 N94-19100
MAHURIN, ERIC W. p 1404 N94-18701
MAIER, ELISABETH A. p 1516 N94-17732
MAIMONI, A. p 1394 N94-17770
MAINETTI, LUCA p 1520 N94-18136
MAISHEEV, V. A. p 1577 N94-18217
MAJOR, PAUL A. p 1387 N94-18512
MAKDISI, Y. p 1566 N94-18234

MAKER, B. N. p 1452 N94-18049
MAKI, G. p 1400 N94-18360
p 1402 N94-18377
MAKI, G. K. p 1397 N94-18340
p 1402 N94-18376
MAKI, GARY K. p 1397 N94-18337
MAKIENKO, P. M. p 1548 N94-18170
MAKOWITZ, HENRY p 1564 N94-17738
MAKOWSKI, M. A. p 1590 N94-19289
MALARET, E. R. p 1334 N94-18149
p 1337 N94-18574
p 1335 N94-19787
MALGHAN, S. G. p 1340 N94-18180
MALHOTRA, R. p 1349 N94-18532
MALIK, R. P. p 1561 N94-18153
MALLET, MICHEL p 1311 N94-17957
MALLIKARJUN, M. p 1402 N94-18379
MALOY, S. A. p 1594 N94-17874
MALTBY, J. D. p 1340 N94-18201
p 1430 N94-18537
MANDEVILLE, P. p 1604 N94-19597
MANHEIMER, WALLACE M. p 1439 N94-18576
MANIEZZO, V. p 1547 N94-17961
MANIVANNAN, GURUSAMY p 1434 N94-19791
MANKBADI, REDA R. p 1411 N94-18552
MANNERSALO, K. p 1396 N94-18091
MANNING, P. A. p 1335 N94-18942
MANSFIELD, J. A. p 1381 N94-19539
MANTYLAE, M. p 1520 N94-18117
MANZELLA, DAVID H. p 1587 N94-18861
MAO, ZHUO-XIONG p 1474 N94-18499
p 1478 N94-19241
MARACAS, GEORGE N. p 1598 N94-18616
p 1605 N94-19717
MARCAZZAN, MARIO p 1305 N94-18418
MARCUSE, J. L. W. p 1472 N94-17852
MARDOYAN, L. G. p 1549 N94-18198
MAREDA, J. F. p 1537 N94-19249
MAREN, A. J. p 1506 N94-18793
MARGOLESE, D. p 1375 N94-19742
MARGON, BRUCE p 1630 N94-18836
MARHEFKA, R. J. p 1384 N94-18187
MARINAK, M. M. p 1590 N94-19289
p 1591 N94-19311
MARKERT, CLEMENT L. p 1503 N94-19217
MARRIOTT, JOHN p 1557 N94-18694
MARRONE, M. J. p 1382 N94-17902
MARSHALL, D. B. p 1341 N94-18692
MARTENS, C. S. p 1477 N94-19235
MARTENS, J. S. p 1405 N94-19079
MARTIN, BENEDIKT p 1367 N94-18011
MARTIN, DAVID A. p 1391 N94-19582
MARTIN, J. M. p 1475 N94-18775
MARTIN, JUTTA p 1367 N94-18011
MARTIN, L. J. p 1454 N94-18479
MARTIN, NATHANIEL G. p 1559 N94-19511
MARTIN, P. p 1328 N94-19626
MARTINELLI, G. p 1565 N94-17972
MARTINEZ, H. E. p 1562 N94-18810
MARTINEZ, K. R. p 1352 N94-19240
MARTINEZ, M. L. p 1569 N94-18985
MARTZ, C. p 1329 N94-19631
MASGONTY, J.-M. p 1428 N94-18032
MASON, KEVIN T. p 1505 N94-18289
MASSON, JEAN-JACQUES p 1340 N94-18122
MASUDA, YASUSHIRO p 1570 N94-19126
MATAYA, M. C. p 1362 N94-18917
MATHES, HERMANN-JOSEF p 1631 N94-19506
MATHEWS, G. J. p 1624 N94-17897
MATHEWS, J. R. p 1309 N94-18443
MATTHEWS, D. L. p 1437 N94-18131
MATTOX, J. R. p 1623 N94-19463
p 1623 N94-19464
MATULEWSKI, KENNETH p 1497 N94-18393
MAUDLIN, P. J. p 1609 N94-19187
MAUGER, G. J. p 1572 N94-19545
MAUW, SJOUKE p 1558 N94-19228
MAX, C. p 1441 N94-19251
MAX, N. p 1520 N94-18130
p 1418 N94-18888
p 1528 N94-19276
p 1531 N94-19548
MAY, G. B. p 1453 N94-18328
MAYER-HASSLEWANDER, H. A. p 1623 N94-19463
MAYER, S. T. p 1395 N94-17849
MAYES, J. S. p 1342 N94-18702
MAZIASZ, P. J. p 1363 N94-18975
MAZIER, BRUNO p 1528 N94-19363
MAZURE, MARIE-LAURENCE p 1556 N94-19731
MCANULTY, PETER p 1360 N94-18542
MCARDLE, JACK G. p 1321 N94-19353
MCATEE, AARON M. p 1337 N94-18202
MCAULEY, DEREK p 1536 N94-19159
p 1536 N94-19160
MCBANE, DOUGLAS G. p 1321 N94-18541
MCBRIDE, JOHN L. p 1490 N94-18514
MCCALL, BENJAMIN J. p 1324 N94-19168
MCCALLUM, R. ANDREW p 1610 N94-19485
MCCAMY, J. W. p 1601 N94-18998
MCCARRON, E. M., III p 1600 N94-18968
MCCARTY, ROBERT E. p 1459 N94-19470
MCCAY, T. D. p 1325 N94-19173
MCCORMICK, STEVE p 1417 N94-18843
MCCRACKEN, NANCY p 1539 N94-19790
MCCREA, J. D. p 1607 N94-17892
MCCUTCHEN, M. S. p 1347 N94-18209
MCDANIEL, AMOS p 1434 N94-19314
MCDONALD, J. F. p 1604 N94-19596
MCDONALD, T. E. p 1432 N94-18828
MCEVERS, J. A. p 1470 N94-17773
MCGAVRAN, L. p 1519 N94-18086
MCGHEE, ROBERT J. p 1306 N94-18424
MCGLAUN, M. p 1456 N94-19078
MCGUIRE, GARY E. p 1396 N94-18293
MCGUIRE, R. R. p 1378 N94-19242
MCGUIRE, ROBERT J. p 1318 N94-18789
MCHARGUE, C. J. p 1602 N94-19075
MCILWAIN, C. E. p 1329 N94-19630
MCINTOSH, ROBERT E. p 1500 N94-19743
MCKAMEY, C. G. p 1355 N94-17757
p 1362 N94-18938
p 1363 N94-18975
MCKEOWN, M. p 1603 N94-19541
MCKINLEY, B. J. p 1453 N94-18108
MCLEAN, EDGAR A. p 1430 N94-18530
MCMAHON, JOHN M. p 1440 N94-18747
MCMORROW, D. p 1566 N94-18085
MCNEAL, TOBY p 1562 N94-18664
MCNEESE, MICHAEL D. p 1509 N94-18744
MCNEIL, W. J. p 1432 N94-18875
MCNUTT, RALPH L., JR. p 1628 N94-17842
MCPHERSON, D. W. p 1504 N94-17699
MCQUEEN, R. G. p 1563 N94-19151
MCSWEENEY, J. D. p 1625 N94-18612
p 1625 N94-18613
p 1625 N94-18615
p 1625 N94-18618
p 1626 N94-18619
p 1626 N94-18620
p 1626 N94-18621
MCWETHY, G. p 1461 N94-18107
MCWILLIAMS, J. C. p 1583 N94-17945
MCWILLIAMS, R. p 1404 N94-18872
MEADOR, J. p 1399 N94-18356
MEADOR, JACK L. p 1399 N94-18353
MECHOSO, C. R. p 1494 N94-19298
MEDALE, J. L. p 1329 N94-19631
MEDERNACH, J. W. p 1592 N94-17742
MEERKOV, SEMYON M. p 1392 N94-19737
MEEUWISSEN, ADRIANUS M. H. p 1559 N94-19386
MEINDL, RICHARD S. p 1513 N94-19531
MEISEL, L. V. p 1360 N94-18542
MEISEL, LAWRENCE V. p 1361 N94-18735
MEISELMAN, HERBERT p 1512 N94-18882
MEISTER, PIERRE-ANDRE p 1428 N94-18039
MEJDANI, R. p 1607 N94-18174
MELINGER, J. S. p 1566 N94-18085
MELLO, F. J. p 1455 N94-19039
MELLO, J. E. p 1475 N94-18775
MELNGAILIS, JOHN p 1345 N94-19746
MELTZ, MARTIN L. p 1501 N94-17729
MELTZER, F. L. p 1613 N94-17880
MELZNER, F. p 1329 N94-19630
MENDILLO, MICHAEL p 1486 N94-19008
MENESES, G. D. p 1570 N94-19125
MENIKOFF, R. p 1408 N94-17728
MEREDITH, P. T. p 1308 N94-18433
MEREGHETTI, S. p 1622 N94-19451
MERMAGEN, TIMOTHY J. p 1404 N94-18749
MESARCH, MARK A. p 1470 N94-17762
MESSER, BURKHARD p 1532 N94-19652
METCALF, HAROLD J. p 1440 N94-18900
MEUCCI, R. p 1435 N94-17771
MEURS, E. J. A. p 1623 N94-19528
MEYER-SPASCHE, RITA p 1584 N94-17981
MEYER, A. p 1328 N94-19625
MEYER, D. G. p 1536 N94-19115
MEYER, J. J. C. p 1618 N94-19067
MEYERHOFER, D. D. p 1602 N94-19123
MEZA, J. C. p 1569 N94-18985
MICHEL, THIERRY p 1530 N94-19498
MICHIE, CRAIG p 1579 N94-18738
MIDDLETON, P. p 1470 N94-17749
MIELKE, E. W. p 1607 N94-17892
MIGLIONICO, CHARLES J. p 1343 N94-18869
MIKHALEV, V. L. p 1577 N94-18217
MILANOVICH, F. P. p 1352 N94-19266
MILHOLEN, WILLIAM E., II p 1312 N94-19388
MILLAR, ROBERT I. p 1316 N94-18384
p 1386 N94-18495
MILLER, A. H. p 1465 N94-17888
MILLER, CLARENCE A. p 1420 N94-19139
MILLER, D. p 1575 N94-19287
MILLER, D. J. p 1597 N94-18500
MILLER, GEORGE P. p 1482 N94-18610
MILLER, HARVEY I. p 1506 N94-18598
MILLER, J. P. p 1572 N94-19320
MILLER, K. p 1572 N94-19545
MILLER, L. p 1539 N94-19734
MILLER, M. M. p 1618 N94-19099
MILLER, P. p 1602 N94-19277
MILLER, P. J. p 1516 N94-17740
MILLER, R. L. p 1587 N94-18803
MILLER, R. W. p 1462 N94-18729
MILLER, W. F., JR. p 1551 N94-19342
p 1551 N94-19343
MILLIGAN, M. R. p 1465 N94-17888
MILLIMAN, JOHN D. p 1498 N94-18600
MILNE, A. p 1468 N94-19015
MILOSEVIC, M. p 1343 N94-18761
MILTON, J. E. p 1322 N94-18330
MINAEV, V. P. p 1355 N94-17692
MINICHINO, C. p 1632 N94-18856
MINJUN, LI p 1341 N94-18544
MINOR, BRYAN M. p 1554 N94-19671
MINOTTI, PATRICE p 1408 N94-18015
MINSAAS, DAG WILLY p 1322 N94-17735
MINSTER, J. B. p 1483 N94-18717
MIRIN, A. A. p 1494 N94-19298
MIRZADEH, S. p 1504 N94-17699
MISRA, R. B. p 1606 N94-17794
p 1383 N94-17952
MITCHELL, S. A. p 1528 N94-19344
MITCHELL, T. E. p 1594 N94-17874
MITIDIERI, ENZO p 1550 N94-19153
MITLITSKY, F. p 1465 N94-17853
MITTAL, VIBHU O. p 1516 N94-17732
p 1521 N94-18290
p 1616 N94-18570
p 1522 N94-18680
MIYASHITA, ATSUMI p 1438 N94-18161
MLADENOV, I. M. p 1561 N94-17681
MOBILIA, J. p 1485 N94-18874
MOCK, R. C. p 1573 N94-17698
MOEBIUS, E. p 1329 N94-19631
MOENE, TOON p 1494 N94-19699
MOERMAN, B. p 1528 N94-19330
MOHR, J. B. p 1468 N94-19016
MOHR, R. p 1426 N94-18021
MOIR, I. R. M. p 1308 N94-18431
MOLENAAR, J. p 1420 N94-19144
MONAHAN, JOHN H. p 1391 N94-19676
MONDY, LISA A. p 1410 N94-18270
MONNIER, A. p 1354 N94-19728
p 1375 N94-19742
MOODY, JOHN p 1523 N94-18901
MOOIJ, E. p 1335 N94-19614
MOON, DONALD L. p 1408 N94-19751
MOORE, GERALD T. p 1438 N94-18250
MOORE, R. E. p 1371 N94-18691
MOORE, R. GILBERT p 1327 N94-19183
MOORE, ROBERT C. p 1392 N94-19749
MORANG, ANDREW p 1496 N94-18215
MOREIRA-PAREDES, RAMIRO p 1553 N94-19583
MOREL, J. E. p 1551 N94-19342
p 1551 N94-19343
MORELLI, G. L. p 1437 N94-18060
MORENA, J. p 1343 N94-18763
MORENO, J. B. p 1466 N94-18208
p 1469 N94-19040
MOREY-HOLTON, EMILY p 1503 N94-19214
MORF, M. p 1400 N94-18362
MORI, T. T. p 1385 N94-18301
MOROI, DAVID S. p 1386 N94-18469
MOROSIN, B. p 1602 N94-19340
p 1603 N94-19347
MORRIS, C. E. p 1563 N94-19151
MORRIS, GEORGE V. p 1368 N94-17905
MORRIS, JEFFREY B. p 1609 N94-18310
MORRIS, M. E. p 1394 N94-17780
MORRIS, S. C. p 1472 N94-17852
MORRIS, W. L. p 1341 N94-18692
MORRISON, A. I. p 1461 N94-18063
MORRISON, P. J. p 1590 N94-19194
MORSE, D. H. p 1594 N94-17896
MORTON, JOHN p 1456 N94-19095
MORTON, R. p 1593 N94-17845
MOSES, K. G. p 1589 N94-19133
MOSIER, FRANCES L. p 1323 N94-19162
MOSKOWITZ, P. D. p 1464 N94-17712
MOSS, S. C. p 1358 N94-18111
MOSS, T. A. p 1466 N94-18208
p 1469 N94-19040
MOSSA, JOANN p 1496 N94-18215
MOTALLEBI, F. p 1423 N94-19668
MOTOWIDLO, L. R. p 1601 N94-18993
p 1602 N94-19122
MOYER, R. D. p 1394 N94-17780

MOYLAN, P. J. p 1546 N94-17810
MROWKA, S. p 1437 N94-13131
p 1580 N94-18931
MUELLER, JEAN-FRANCOIS p 1479 N94-19518
MUELLER, R. E. p 1325 N94-19173
MUELLER, RICHARD P. G. p 1461 N94-19669
MUELLERS, A. p 1329 N94-19633
MUGELE, R. M. p 1315 N94-18822
p 1315 N94-18823
MUIR, J. F. p 1469 N94-19109
MUKAMEL, SHAUL p 1568 N94-18784
MUKHEDKAR, D. p 1400 N94-18364
MULFORD, R. N. R. p 1360 N94-18501
MULLENDER, SAPE J. p 1536 N94-19159
p 1536 N94-19160
p 1537 N94-19219
MULLER, M. p 1577 N94-18223
MUNDT, C. p 1421 N94-19497
MURAKAMI, KOUICHI p 1438 N94-18161
MURAKAMI, M. p 1590 N94-19273
MURAKAMI, YOSHIO p 1444 N94-18159
MURPHY, D. p 1602 N94-19340
MURPHY, M. J. p 1376 N94-18095
MURR, LARRY E. p 1343 N94-18869
MURTHY, PAPPU L. N. p 1457 N94-19351
MURUGAVEL, P. p 1402 N94-18379
MUSGRAVE, K. p 1518 N94-17944
MUSIAL, W. p 1447 N94-18128
MUSMANN, G. p 1329 N94-19629
MUSTREDELEON, J. p 1593 N94-17754
MUSYOKI, S. p 1438 N94-18160
MYERS, B. p 1465 N94-17853
MYERS, BRAD A. p 1514 N94-18317
MYERS, J. D. p 1350 N94-19097
MYERS, S. M. p 1364 N94-19080
MYLLYMAEKI, JUKKI p 1380 N94-19373
MYRICK, M. L. p 1369 N94-18112
MYRICK, STEPHANIE A. p 1462 N94-18677

N

NAESLUND, E. p 1476 N94-19038
NAGAO, SHOUICHI p 1429 N94-18040
NAGASAWA, JUNJI p 1428 N94-18036
NAGASHIMA, TAKASHI p 1438 N94-18160
NAITOH, PAUL p 1507 N94-19608
NAKAMURA, YUKIHARU p 1586 N94-18212
NAKANISHI, HIROSHI p 1369 N94-18220
NAKAZAWA, S. p 1586 N94-18213
NAKOTTE, H. p 1593 N94-17744
p 1605 N94-19735
NAMIKI, RYOU p 1428 N94-18036
NANSTAD, R. K. p 1445 N94-19047
NAPPA, J. M. p 1328 N94-19625
NARASIMHAN, M. S. p 1545 N94-17683
NARAYANAN, S. p 1466 N94-18335
NARHEIM, B. T. p 1330 N94-19634
NARK, TED C. p 1310 N94-18444
NASH, WILLIAM O., JR. p 1448 N94-19766
NASTASI, M. p 1358 N94-17875
NAUGHTON, TIMOTHY D. p 1341 N94-18572
NAUMANN, HANS p 1395 N94-17920
NAUTA, J. M. p 1543 N94-19199
NAVE, S. E. p 1424 N94-17778
NEAU, E. L. p 1439 N94-18522
NECULAU, MIHAELA p 1510 N94-19649
NEDELKO, S. N. p 1608 N94-18267
NEDERPELT, R. p 1524 N94-19066
NEEMAN, Y. p 1607 N94-17892
NEIL, G. R. p 1441 N94-18974
NEILSEN, M. K. p 1372 N94-19059
NELMS, R. MARK p 1407 N94-19642
NELSON, AMY p 1587 N94-18861
NELSON, D. Z. p 1446 N94-19334
NELSON, RANDALL J. p 1501 N94-18231
NELSON, T. E. p 1306 N94-18423
NELSON, T. O. p 1562 N94-18810
NELSSON, C. p 1347 N94-18081
NEMANICH, ROBERT J. p 1597 N94-18459
NERON, M. p 1306 N94-18425
NESSETT, D. M. p 1537 N94-19253
NETA, P. p 1464 N94-17781
NEU, RICHARD W. p 1360 N94-18660
NEUMEIER, MARK E. p 1514 N94-19773
NEURGAONKAR, R. R. p 1598 N94-18633
NEURGAONKAR, RATNAKAR R. p 1596 N94-18320
NEUWALD, P. p 1422 N94-19515
NEVINS, W. M. p 1589 N94-19073
NEWBERGER, B. S. p 1574 N94-18994
NEWCOMB, JAMES E. p 1318 N94-18789
NEWPORT, JOHN p 1320 N94-18658
NEWTON, M. A. p 1575 N94-18996
NEXHIP, C. p 1602 N94-19277
NG, K. C. p 1567 N94-18493
NGUYEN, HIEN p 1495 N94-17822
NGUYEN, TIEN-DUNG p 1551 N94-19248
NICKOLS, D. K. p 1596 N94-18316
NIEDERAUER, G. M. p 1399 N94-18357
NIEDERER, J. p 1539 N94-17696
NIEMANN, R. C. p 1396 N94-18135
NIGRO, NATALIE A. p 1541 N94-18790
NIJHOLT, ANTON p 1537 N94-19223
NIJMEIJER, H. p 1543 N94-19328
NILSEN, J. p 1442 N94-19554
NILSON, R. H. p 1346 N94-17997
NISHINO, TOORU p 1586 N94-18212
NISSEN, M. R. p 1580 N94-19113
NISSINK, R. A. p 1393 N94-19798
NISSLEY, WILLIAM J. p 1318 N94-18789
NISTOR, S. V. p 1595 N94-18173
NITSCHE, W. p 1306 N94-18420
NIUTANEN, R. p 1396 N94-18091
NOACK, BERND R. p 1422 N94-19525
NOH, TAEWAN p 1551 N94-19343
NOID, D. W. p 1596 N94-18192
NOLL, ROBERT J. p 1579 N94-18858
NOLTE, RALPH p 1422 N94-19520
NOOR, AHMED K. p 1458 N94-19465
NORCI, LAURA p 1623 N94-19527
NORING, J. p 1394 N94-17770
NOVOTNY, DONALD W. p 1407 N94-19643
NOWLIN, SCOTT R. p 1417 N94-18796
NUSCA, MICHAEL J. p 1320 N94-18748
NUUTILA, E. p 1555 N94-19708

O

OAKES, R. p 1575 N94-19287
OBERNDORF, P. p 1520 N94-18251
OBERT, E. p 1309 N94-18441
OBRIEN, K. p 1384 N94-18228
OBRIEN, KEVEN p 1406 N94-19501
OBRIEN, M. E. p 1384 N94-18216
ODONNELL, T. p 1602 N94-19277
OEGELMAN, HAKKI B. p 1623 N94-19527
OELEN, W. p 1543 N94-19199
OFFEREINS, M. p 1527 N94-19225
OHALLORAN, T. p 1569 N94-19013
OHARA, F. M., JR. p 1475 N94-18832
OHARA, T. J. p 1374 N94-19585
OHLE, FRANK p 1553 N94-19522
OHLINGER, WAYNE L. p 1403 N94-18639
OHMORI, TOSHIO p 1427 N94-18028
OHMURO, MAKOTO p 1427 N94-18028
OHNUMA, SHOROKU p 1573 N94-17784
OHSAWA, HARUSHIGE p 1444 N94-18159
OHYANAGI, TAKASUMI p 1438 N94-18161
OKEEFE, THOMAS J. p 1366 N94-19594
OKIGAMI, TOMIO p 1429 N94-18043
OLARIU, S. p 1402 N94-18380
OLIGER, JOSEPH p 1549 N94-18863
OLIVIER, S. p 1441 N94-19251
OLLIS, C. W. p 1575 N94-18996
OLSEN, EDWARD p 1454 N94-18466
OLSEN, RICHARD G. p 1512 N94-18730
OLSON, DAVID L. p 1342 N94-18704
OLSON, H. p 1572 N94-19545
OLSON, ROBERT A. p 1387 N94-18510
OLSON, WILLIAM S. p 1491 N94-18602
p 1491 N94-18603
p 1491 N94-18604
p 1491 N94-18605
p 1492 N94-18606
p 1492 N94-18608
OLSSON, R. p 1523 N94-18943
OLSSON, ROBIN p 1339 N94-17971
OLSZOK, THOMAS p 1564 N94-19715
OMARA, MARIE T. p 1617 N94-18752
ONEIL, D. p 1446 N94-19291
ONSTOTT, R. G. p 1497 N94-18277
ONVLEE, J. R. N. p 1496 N94-17923
OPDENAKKER, RIEKS p 1537 N94-19223
p 1528 N94-19262
OPGENOORTH, H. p 1331 N94-19640
OPPENHEIM, ALAN V. p 1389 N94-18811
OREG, J. p 1584 N94-17990
OROURKE, P. J. p 1419 N94-19027
OSA, TAKASHI p 1429 N94-18043
OSBORNE, T. H. p 1585 N94-18057
OSHEA, P. G. p 1435 N94-17724
OSTERGAARD, JENS C. p 1387 N94-18525
OSTERHELD, A. p 1585 N94-18082
OSTERHELD, A. L. p 1436 N94-17868
OSTRIKER, JEREMIAH P. p 1627 N94-19093
OSTROM, SARA R. p 1334 N94-18470
OSTROWSKI, G. E. p 1598 N94-18531
OSWALD, FRED B. p 1446 N94-19318
OTT, EDWARD p 1439 N94-18737
OUALIBOUCH, MOULAY ES-SAID p 1552 N94-19362
OUDELUTTIGHUIS, PAUL p 1537 N94-19223
p 1526 N94-19224
OUGHSTON, KURT p 1385 N94-18404
OUILLON, SYLVAIN p 1421 N94-19502
OULD-KHOUNA, MOHAMED p 1406 N94-19297
OUYANG, J. p 1572 N94-19320
OVERBEEK, P. L. p 1618 N94-19450
p 1619 N94-19454
p 1619 N94-19457
OVERLAND, J. E. p 1499 N94-19063
OVERMYER, DONALD L. p 1601 N94-19022
OVSIEW, PHYLLIS L. p 1532 N94-19707
OWEN, TODD p 1382 N94-17861
OWENS, ROBERT M. p 1392 N94-19724
OWENS, T. p 1483 N94-18717
OWSLEY, P. p 1398 N94-18348

P

PADMAN, R. p 1622 N94-19417
PAGEN, M. J. p 1323 N94-19372
PALCHEFSKY, J. W. p 1336 N94-17856
PALEV, T. D. p 1548 N94-18176
PALMBERG, BJOERN p 1452 N94-17970
PANCE, A. p 1405 N94-19079
PANCHAL, C. B. p 1409 N94-18004
p 1353 N94-19552
PANDOL, C. L. p 1435 N94-17771
p 1436 N94-17954
PANKOVE, JACQUES I. p 1598 N94-18527
PANTALOS, GEORGE M. p 1323 N94-19163
PAOLINI, PAOLO p 1520 N94-18136
PAQUET, P. p 1483 N94-18627
PARASURAM, KANCHANA p 1539 N94-19790
PARATTE, LIONEL p 1425 N94-18014
PARIS, CECILE p 1521 N94-18290
p 1522 N94-18680
PARIS, CECILE L. p 1516 N94-17732
p 1612 N94-17745
p 1615 N94-18464
p 1616 N94-18570
PARK, J. K. p 1546 N94-17885
PARK, S. H. p 1468 N94-19016
PARKER, B. E., JR. p 1541 N94-18790
PARKER, G. p 1525 N94-19124
PARKER, MICHAEL A. p 1581 N94-19602
PARKS, D. R. p 1571 N94-19278
PARS, PIM p 1543 N94-19226
PASCH, H. L. p 1536 N94-19197
PASCHMANN, G. p 1329 N94-19630
PASTERNAK, M. P. p 1404 N94-18805
p 1600 N94-18969
PASTUKHOV, V. P. p 1590 N94-19193
PATT, FREDERICK S. p 1532 N94-19761
PATTERSON, E. L. p 1439 N94-18522
PATTERSON, F. G. p 1396 N94-17991
p 1440 N94-18889
PATTERSON, JOSEPH p 1621 N94-18855
PATTERSON, MICHAEL J. p 1587 N94-18861
PAUER, BRETT A. p 1342 N94-18700
PAUL, DIANE p 1320 N94-18658
PAULEY, PATRICIA M. p 1490 N94-18265
PAULRAJ, AROGYASWAMI p 1392 N94-19736
PAVLAKOS, C. J. p 1418 N94-18918
p 1537 N94-19249
PAXTON, A. H. p 1435 N94-17724
PAXTON, A. T. p 1577 N94-18223
PAYLOR, R. p 1496 N94-18065
PAYNE, P. p 1617 N94-19026
PEASE, C. H. p 1499 N94-19063
PECHENIK, A. p 1340 N94-18180
PECLAT, CHRISTIAN p 1408 N94-18022
PEDERSEN, A. p 1633 N94-19404
p 1330 N94-19634
PEDERSON, L. R. p 1593 N94-17747
PEKALA, R. W. p 1395 N94-17849
PENCIL, ERIC J. p 1336 N94-17856
PENDRICK, VALERIE p 1599 N94-18719
PENNYCOOK, S. J. p 1352 N94-19239
PEREZ, L. p 1337 N94-18574
PEREZ, M. R. p 1621 N94-19288
PERIAUX, JACQUES p 1311 N94-17957
PERKOWSKI, M. A. p 1401 N94-18375
PERNICI, B. p 1613 N94-17939
PEROTTO, J.-F. p 1428 N94-18032
PERRAUT, S. p 1328 N94-19625
PERRESSINI, D. L. p 1440 N94-18889
PERRIER, PIERRE p 1311 N94-17957
PERRY, D. L. p 1347 N94-18193
PERRY, M. D. p 1582 N94-17708
p 1435 N94-17855
p 1585 N94-18115
PERRY, MICHAEL A. p 1633 N94-19404
PERTHAME, BENOIT p 1551 N94-19317
PETERS, JEFFREY L. p 1490 N94-18573

PETERSEN, WENDELL C. .... p 1315 N94-18852
PETERSON, A. .... p 1393 N94-18351
p 1401 N94-18373
PETERSON, DAVID .... p 1393 N94-19793
PETHEL, SHAWN D. .... p 1540 N94-18263
PETITT, G. A. .... p 1565 N94-17776
PETRICEVIC, V. .... p 1441 N94-19369
p 1441 N94-19394
PETRICK, M. .... p 1586 N94-18272
PETROV, G. .... p 1561 N94-18155
p 1548 N94-18195
p 1548 N94-18196
p 1549 N94-18197
p 1549 N94-18200
PETSCHEK, A. G. .... p 1380 N94-18818
PETTY, C. C. .... p 1581 N94-17694
PETVIASHVILI, N. .... p 1583 N94-17945
PFAFF, MARK S. .... p 1512 N94-18765
PFAFF, R. .... p 1328 N94-19624
PFALZ, JOHN M. .... p 1320 N94-18333
PFENDER, E. .... p 1433 N94-19135
PHAM, CHUONG N. .... p 1443 N94-17705
PHANER, MAGALI .... p 1353 N94-19406
PHILLIPS, H. M. .... p 1368 N94-17946
PHILLIPS, N. E. .... p 1360 N94-18398
p 1600 N94-18968
PHILLIPS, ROBERT W. .... p 1502 N94-19213
PICANO, S. .... p 1536 N94-19115
PICAUT, JEAN .... p 1367 N94-18009
PICOZZA, P. .... p 1630 N94-18762
PIECHNA, J. .... p 1422 N94-19510
PIERMARINI, G. J. .... p 1340 N94-18180
PIETSCH, W. .... p 1622 N94-19451
PIFKO, ALLAN B. .... p 1458 N94-19468
PIGUET, C. .... p 1428 N94-18032
p 1408 N94-18033
PIGUET, JEAN-MICHEL .... p 1427 N94-18026
p 1427 N94-18027
PIIRA, KALEVI .... p 1444 N94-17974
PILKEY, WALTER D. .... p 1459 N94-19473
PINA, CESAR A. .... p 1403 N94-18695
PINEDA, JAIME A. .... p 1507 N94-19783
PINSKER, R. I. .... p 1581 N94-17694
PITCHER, E. J. .... p 1435 N94-17724
PITROF, STEPHEN M. .... p 1450 N94-17834
p 1450 N94-17837
PITTS, R. .... p 1519 N94-18086
PITZ-PAAL, ROBERT .... p 1465 N94-18089
PIURI, VINCENZO .... p 1518 N94-17960
PLACR, ARNOST .... p 1448 N94-19189
PLANO, V. L. .... p 1569 N94-18999
PLIMPTON, S. J. .... p 1531 N94-19562
PLUT, T. A. .... p 1405 N94-19079
POCOTTE, S. L. .... p 1507 N94-19675
POEL, MANNES .... p 1538 N94-19296
POEPPEL, R. B. .... p 1454 N94-18479
p 1597 N94-18500
POGOSYAN, G. S. .... p 1549 N94-18198
POIRIER, P. .... p 1384 N94-18216
POITEVIN, C. .... p 1482 N94-18626
POLAK, F. R. .... p 1315 N94-17733
POLLARD, R. T. .... p 1496 N94-18065
p 1496 N94-18066
POLUBARINOV, I. V. .... p 1556 N94-18154
POMILIA, A. .... p 1325 N94-19172
PONTAU, A. E. .... p 1594 N94-17896
POOLE, R. J. D. .... p 1310 N94-18446
POPP, CARL J. .... p 1476 N94-19045
PORCH, W. .... p 1488 N94-17715
PORCH, W. M. .... p 1472 N94-17986
PORKOLAB, M. .... p 1589 N94-19073
POSEY, P. G. .... p 1499 N94-18727
POST, FRITS H. .... p 1423 N94-19645
POTAPCZUK, MARK G. .... p 1412 N94-18555
POTTER, G. L. .... p 1489 N94-18053
POTTER, R. M. .... p 1485 N94-18894
POUKEY, J. W. .... p 1573 N94-17698
POULTER, G. A. .... p 1474 N94-18521
POUR, GILDA .... p 1535 N94-18865
POWELL, D. .... p 1532 N94-19713
POWELL, M. A. .... p 1464 N94-17798
POWERS, JOHN P. .... p 1564 N94-19750
PRABHAKAR, T. S. .... p 1402 N94-18379
PRABHU, ANNAPPA A. .... p 1450 N94-17836
PRADHAM, DHIRAJ K. .... p 1521 N94-18259
PRAEL, R. E. .... p 1570 N94-19120
PRANGSMA, G. J. .... p 1488 N94-17924
PRASHER, DOUGLAS C. .... p 1347 N94-18185
PRELLER, R. H. .... p 1499 N94-18727
PRENGER, F. C. .... p 1417 N94-18831
PREUSS, C. S. .... p 1355 N94-17711
PRIBYL, WILLIAM L. .... p 1617 N94-18839
PRICE, D. .... p 1585 N94-18082
PRICE, D. F. .... p 1396 N94-17991
p 1440 N94-18889
PRICE, D. L. .... p 1430 N94-18481
PRIMINI, F. A. .... p 1625 N94-18612
p 1625 N94-18613
p 1625 N94-18615
p 1625 N94-18618
p 1626 N94-18619
p 1626 N94-18620
p 1626 N94-18621
PRINS, H. J. .... p 1419 N94-19087
PRINSON, G. S. .... p 1385 N94-18291
PRIOR, M. H. .... p 1570 N94-19108
PRITCHARD, R. S. .... p 1499 N94-19063
PROBST, D. .... p 1400 N94-18365
PROKES, K. .... p 1593 N94-17744
PROMMEL, J. M. .... p 1519 N94-18086
PROTO, A. N. .... p 1546 N94-17811
PROTOPOPESCU, S. D. .... p 1572 N94-19536
PRZYSTUPA, M. A. .... p 1455 N94-18714
PRZYSTUPA, MAREK A. .... p 1454 N94-18683
p 1361 N94-18742
PUGH, A. C. .... p 1547 N94-18069
PULS, J. .... p 1624 N94-17736
PURANTO, A. .... p 1593 N94-17744
PURDY, G. M. .... p 1500 N94-19727
PURVIANCE, J. .... p 1398 N94-18348
PURVIANCE, J. E. .... p 1401 N94-18370
PUZYNIN, I. V. .... p 1608 N94-18253
PYNE, C. R. .... p 1317 N94-17826

Q

QIAN, WEN .... p 1498 N94-18665
QIU, X. Z. .... p 1436 N94-17998
QUADENS, O. .... p 1507 N94-19523
QUARARONE, JAMES R. .... p 1424 N94-17904
QUARTARONE, JAMES R. .... p 1368 N94-17905
QUATTLEBAUM, MARTIN .... p 1445 N94-18778
QUI, J. .... p 1574 N94-18927
QUICK, C. R., JR. .... p 1478 N94-19272
QUINN, JARUS W. .... p 1577 N94-18283
p 1577 N94-18298
p 1578 N94-18332
p 1578 N94-18396
p 1578 N94-18488
p 1438 N94-18492
p 1578 N94-18528
p 1579 N94-18693
p 1609 N94-18908
p 1405 N94-18909
QUINN, K. G. .... p 1472 N94-17891
QUINN, PATRICK J. .... p 1321 N94-18401

R

RABER, E. .... p 1378 N94-19242
RACICOT, RONALD L. .... p 1545 N94-19721
RACINE, GEORGES-ANDRE .... p 1425 N94-18014
RACKLEY, N. G. .... p 1518 N94-17944
RADESPIEL, R. .... p 1307 N94-18428
RADICELLA, S. M. .... p 1486 N94-19255
RADIUS, R. .... p 1426 N94-18021
RADMACHER, M. .... p 1370 N94-18403
RADOUSKY, H. B. .... p 1601 N94-19049
RAHAMAN, M. N. .... p 1371 N94-18691
RAHAMBININTSOA-KRAFFT, FARA
p 1603 N94-19357
RAINEY, THEODORE J. .... p 1619 N94-19571
RAJ, R. .... p 1369 N94-18163
RAMAN, GANESH .... p 1313 N94-19484
RAMANATHAN, A. .... p 1545 N94-17683
RAMONI, PIERRE .... p 1367 N94-18008
RAMSDELL, J. V., JR. .... p 1488 N94-17895
RAMSEY, J. M. .... p 1567 N94-18493
RAMSEY, P. .... p 1572 N94-19545
RAMSTEIN, CHRISTOPHE .... p 1519 N94-17977
RAND, J. A. .... p 1464 N94-17731
RANDALL, K. .... p 1570 N94-19108
RANDERIA, M. .... p 1604 N94-19566
RANDIN, JEAN-PAUL .... p 1367 N94-18008
RANDRIAMBOARISON, O. .... p 1328 N94-19626
RANGARAJAN, S. .... p 1402 N94-18379
RANTA, M. .... p 1520 N94-18117
RAO, N. S. V. .... p 1316 N94-19300
RAO, R. R. .... p 1345 N94-17820
RAO, VITTAL S. .... p 1366 N94-19594
RAPIDIS, P. .... p 1436 N94-17883
RAPP, D. .... p 1441 N94-19251
RAPPAZ, M. .... p 1445 N94-18976
RASHID, M. M. .... p 1452 N94-17995
RASMUSSEN, D. A. .... p 1590 N94-19273
RATHJE, R. .... p 1329 N94-19633
RATHZ, THOMAS .... p 1380 N94-19423
RATIER, PIERRE-NICOLAS .... p 1434 N94-19659
RATNER, ALBERT .... p 1324 N94-19168
RATOWSKY, R. P. .... p 1436 N94-17868
RAU, G. .... p 1432 N94-18654
RAUNIG, D. L. .... p 1384 N94-18228
RAUSCHER, H. M. .... p 1471 N94-17790
RAVISHANKER, N. .... p 1557 N94-18694
RAWLINSON, K. S. .... p 1464 N94-17798
p 1466 N94-18208
RAY, DOUGLAS S. .... p 1499 N94-19580
RAY, GLEN .... p 1324 N94-19164
RAY, J. R. .... p 1548 N94-18140
RAY, R. .... p 1569 N94-18973
RAY, U. .... p 1370 N94-18477
RAYMOND, WILLIAM H. .... p 1491 N94-18602
p 1491 N94-18603
p 1491 N94-18604
p 1492 N94-18606
p 1492 N94-18607
p 1492 N94-18608
RAZEGHI, M. .... p 1606 N94-19769
READ, J. F. .... p 1496 N94-18064
REARDON, JOHN .... p 1535 N94-18866
REAUGH, J. E. .... p 1460 N94-19543
REDD, LAWRENCE .... p 1337 N94-17863
REDDY, SUDHAKAR M. .... p 1402 N94-18400
REDMOND, J. .... p 1525 N94-19124
REED, CHARLES E. .... p 1615 N94-18323
REED, R. P. .... p 1424 N94-17999
REGINATO, L. L. .... p 1591 N94-19479
REHMANN, ALBERT J. .... p 1514 N94-19773
REHN, L. E. .... p 1600 N94-18933
REICHENBACH, H. .... p 1422 N94-19515
REID-MILLER, MARGARET .... p 1531 N94-19592
REIF, JOHN H. .... p 1539 N94-19682
REIFF, STEFAN .... p 1603 N94-19355
REIFSNIDER, K. L. .... p 1341 N94-18630
REIHANI, KAMRAN .... p 1392 N94-19680
REINER, R. H. .... p 1351 N94-19118
REINHARD, L. .... p 1358 N94-18111
REISS, HOWARD .... p 1374 N94-19574
REITIZE, D. H. .... p 1440 N94-18889
REJENT, J. A. .... p 1359 N94-18127
REME, H. .... p 1329 N94-19631
REMO, J. L. .... p 1627 N94-19339
RENAUD, JEAN-PIERRE .... p 1367 N94-18008
RENSINK, M. E. .... p 1590 N94-19290
RESING, J. A. C. .... p 1543 N94-19324
RESIO, DONALD T. .... p 1498 N94-18685
RESTUCCIO, JIM M. .... p 1360 N94-18386
p 1453 N94-18387
p 1596 N94-18388
REYES, A. P. .... p 1594 N94-17907
REYNERSON, CHARLES M. .... p 1445 N94-18634
REYNOLDS, JOHN R. .... p 1375 N94-19740
REYNOLDS, MICHAEL C. .... p 1514 N94-19773
REYNOLDS, R. M. .... p 1497 N94-18494
REZEAU, L. .... p 1328 N94-19625
RICE, EDWARD J. .... p 1313 N94-19484
RICHARDS, K. R. .... p 1471 N94-17821
p 1478 N94-19319
RICHARDSON, JOHN D. .... p 1628 N94-17842
RICHER, J. S. .... p 1622 N94-19417
RICHES, M. R. .... p 1461 N94-17893
RICHMOND, G. L. .... p 1594 N94-17876
RIDDLE, R. A. .... p 1418 N94-18995
RIDE, SALLY K. .... p 1438 N94-18460
RIDENOURE, REX W. .... p 1327 N94-19183
RIEDLER, W. .... p 1330 N94-19634
RIEDLINGER, LANCELOT M. .... p 1462 N94-18677
RIESEN, R. .... p 1536 N94-19188
RIESTER, PETER J. .... p 1311 N94-18402
RIGHINI, GIOVANNI .... p 1547 N94-17928
p 1547 N94-17961
p 1547 N94-17962
p 1519 N94-17975
p 1520 N94-18145
RIGNEY, D. A. .... p 1443 N94-17730
RILLEMA, D. P. .... p 1350 N94-19017
RIOS, A. .... p 1496 N94-18065
RISH, JEFF W., III .... p 1443 N94-17705
RISLEY, ALLAN D., JR. .... p 1430 N94-18406
RISSMANN, J. .... p 1494 N94-19503
RITSCHARD, R. .... p 1473 N94-18050
RIVIERE-BARBIER, FLORENCE . p 1481 N94-18297
RIZZO, T. G. .... p 1568 N94-18825
p 1570 N94-19096
ROARK, CHUCK .... p 1320 N94-18658
ROBB, C. .... p 1584 N94-17988
ROBE, R. Q. .... p 1384 N94-18228
ROBERT, J. M. .... p 1475 N94-18817
ROBERT, P. .... p 1328 N94-19625
ROBERTS, BERNARD .... p 1417 N94-18672
ROBERTS, D. .... p 1584 N94-17988
ROBERTS, L. .... p 1421 N94-19493
ROBERTS, R. S. .... p 1519 N94-18097
ROBERTSON, R. G. H. .... p 1567 N94-18269
ROBINETTE, KATHLEEN M. .... p 1513 N94-19570
ROBINO, C. V. .... p 1364 N94-19100

ROBINS, K. p 1438 N94-18504
ROBINSON, BRIAN A. p 1306 N94-18422
ROBINSON, D. N. p 1346 N94-17987
ROBINSON, D. W. p 1547 N94-18077
p 1549 N94-18948
ROBINSON, R. A. p 1593 N94-17744
p 1605 N94-19735
ROCCO, PAOLO p 1443 N94-17937
p 1444 N94-17940
ROD, BERNARD J. p 1404 N94-18749
RODACY, P. p 1378 N94-19042
RODI, W. p 1415 N94-18593
RODMAN, J. A. p 1614 N94-18181
RODRIGUEZ-CANABAL, J. p 1330 N94-19637
RODRIGUEZ, J. F. p 1360 N94-18687
ROE, PHILIP L. p 1413 N94-18564
ROEDIGER, HENRY, III p 1508 N94-18657
ROGERS, C. p 1548 N94-18140
ROGERS, L. C. p 1355 N94-17752
ROGERS, STUART E. p 1306 N94-18421
ROGNLIEN, T. D. p 1590 N94-19290
ROLLETT, A. D. p 1359 N94-18114
ROMANOVA, N. A. p 1375 N94-18013
ROME, J. p 1617 N94-19026
ROMERO, A. p 1539 N94-19734
ROMIJN, H. C. A. p 1434 N94-19797
ROMINE, M. F. p 1501 N94-18051
RONZHEIMER, A. p 1307 N94-18428
ROOS, C. p 1524 N94-19089
p 1525 N94-19143
p 1525 N94-19156
ROOSE, D. p 1413 N94-18568
ROSAKIS, A. J. p 1456 N94-19116
ROSAKIS, ARES J. p 1456 N94-19130
ROSCHE, HENRY, III p 1462 N94-18679
ROSE, A. p 1354 N94-19778
ROSE, B. p 1405 N94-19112
ROSE, E. A. p 1322 N94-18890
ROSEN, J. p 1575 N94-19287
ROSEN, WARREN A. p 1394 N94-17707
ROSENBLOOM, PAUL S. p 1610 N94-17746
p 1541 N94-18462
p 1541 N94-18463
ROSENTHAL, A. p 1468 N94-19014
ROSENTHAL, A. L. p 1475 N94-18817
ROSENTHAL, D. H. p 1471 N94-17821
ROSENZWEIG, EDWIN L. p 1339 N94-18074
ROSNER, DANIEL E. p 1349 N94-18785
ROSSIENSKY, M. p 1602 N94-19340
ROSSITER, J. A. p 1544 N94-19410
p 1530 N94-19412
ROSSOW, C.-C. p 1307 N94-18428
ROUSSIN, ROBERT W. p 1570 N94-19129
ROUTBORT, J. C. p 1454 N94-18479
ROUX, A. p 1328 N94-19623
p 1328 N94-19625
p 1329 N94-19628
p 1331 N94-19641
ROUZAUD, J. p 1329 N94-19631
ROWAN, T. H. p 1523 N94-18989
ROWE, M. M. p 1500 N94-19745
ROWE, W. R. p 1597 N94-18468
ROYBAL, L. G. p 1461 N94-17851
ROYBAL, ROBERT E. p 1343 N94-18869
RUAN, JU-AI p 1446 N94-19678
p 1605 N94-19679
p 1407 N94-19722
p 1447 N94-19767
RUBIN, J. B. p 1372 N94-19202
RUBY, D. S. p 1464 N94-17787
RUDECK, P. p 1399 N94-18352
RUDGYARD, MICHAEL A. p 1413 N94-18562
p 1413 N94-18563
RUDYAKOV, BORIS p 1426 N94-18018
RUEDENAUER, F. p 1330 N94-19634
RUFFINS, T. R. p 1464 N94-17731
RUHLE, M. p 1369 N94-18188
RUIJGROK, G. J. J. p 1319 N94-19796
RUIZ, A. C. p 1543 N94-19328
RUNYAN, J. E. p 1417 N94-18831
RUPAAL, A. S. p 1593 N94-17747
RUPERT, V. C. p 1422 N94-19568
RUSSELL, J. p 1579 N94-18635
RUSSELL, S. p 1434 N94-17709
RUSSO, V. p 1310 N94-18447
RUST, DAVID M. p 1629 N94-18222
RYAN, CLARENCE A. p 1503 N94-19216
RYAN, P. M. p 1581 N94-17694
RYERSON, F. J. p 1627 N94-19077
RYTER, F. p 1585 N94-18056
RYUTOV, D. D. p 1589 N94-19037
RYUTOV, DMITRI p 1587 N94-18505

S

SABERI, A. p 1543 N94-19329
SABIN, GLEN E. p 1344 N94-19662
SABOL, BRUCE M. p 1388 N94-18777
SACKSCHEWSKY, V. E. p 1362 N94-18917
SADEMELO, C. A. R. p 1604 N94-19566
SAGALOVSKY, L. p 1574 N94-18273
SAHA, NRIPEN K. p 1459 N94-19471
SAITO, AKIRA p 1555 N94-19695
SAKAMOTO, KEISHI p 1438 N94-18160
SAKAWA, Y. p 1586 N94-18213
SALKOLA, M. I. p 1593 N94-17754
SALMI, JAAKKO p 1365 N94-19374
SALMI, PEKKA p 1380 N94-19373
SALMON, J. K. p 1526 N94-19205
SALOTTI, MARC p 1529 N94-19396
SAMARA, G. A. p 1602 N94-19340
p 1603 N94-19347
SAMPSON, W. p 1438 N94-18504
SAMS, B. J. p 1621 N94-19415
SAMUEL, C. p 1619 N94-19571
SANCHEZ, JUAN M. p 1341 N94-18636
SAND, J. R. p 1367 N94-17847
SANDEL, BILL R. p 1326 N94-19178
p 1326 N94-19179
SANDERS, RICHARD p 1412 N94-18558
p 1412 N94-18559
SANDERS, WILLIAM H. p 1558 N94-19265
p 1558 N94-19385
SANDWEISS, J. p 1570 N94-19029
SANFORD, BEVERLY p 1315 N94-18844
SANFORD, T. W. L. p 1573 N94-17698
SANI, ROBERT L. p 1379 N94-17763
SANTARIUS, J. F. p 1587 N94-18803
SANTI, L. MICHAEL p 1338 N94-19706
SANTORO, ROBERT J. p 1348 N94-18389
SANTOSA, FADIL p 1549 N94-18798
SARKANY, J. p 1351 N94-19132
p 1351 N94-19150
SARKER, J. C. p 1401 N94-18370
SARMIENTO, CHARLES J. p 1336 N94-17856
p 1587 N94-18861
SARTORI, ENRICO p 1570 N94-19129
SARVER-VERHEY, TIMOTHY p 1587 N94-18861
SASSIN, MICHAEL p 1540 N94-18261
SASUGA, TUNEO p 1369 N94-18220
SATISH, V. p 1402 N94-18379
SATISH, VENKEEPURAM R. p 1535 N94-18865
SATO, T. p 1586 N94-18213
SATOH, TAKASHI p 1425 N94-18016
SATTERFIELD, C. N. p 1354 N94-19660
SAUERBREY, R. p 1368 N94-17946
SAUSA, ROSARIO C. p 1349 N94-18456
SAUVAUD, J. A. p 1329 N94-19631
SAVIDGE, DANA K. p 1497 N94-18230
SAYLOR, P. p 1516 N94-17800
SCATTOLINI, RICCARDO p 1539 N94-17916
p 1383 N94-17932
SCHAAFSTAL, A. M. p 1508 N94-17967
SCHAEFFER, HARRY G. p 1449 N94-17828
SCHAFER, K. J. p 1436 N94-17996
p 1572 N94-19283
SCHALLER, J. P. p 1377 N94-18491
SCHARENBERG, R. p 1570 N94-19103
SCHARLEMANN, E. T. p 1441 N94-19030
SCHEERER, KLAUS p 1375 N94-18010
SCHEFFER, CAREL L. p 1558 N94-19137
SCHEFFNER, NORMAN p 1497 N94-18455
SCHELLEKENS, J. C. J. p 1452 N94-18079
SCHELLMAN, H. p 1575 N94-19287
SCHETKY, L. M. p 1366 N94-19775
SCHIAVONI, NICOLA p 1383 N94-17932
SCHIDLOVSKY, G. p 1501 N94-17889
SCHIERMEYER, INGO p 1555 N94-19696
SCHINDLER, WERNER p 1559 N94-19610
SCHIPPER, D. p 1543 N94-19199
SCHIRBER, J. E. p 1594 N94-17907
p 1602 N94-19340
p 1603 N94-19347
SCHIRBER, JAMES E. p 1601 N94-19022
SCHISSEL, D. P. p 1585 N94-18056
SCHLAGER, KENNETH J. p 1408 N94-19756
SCHLUETER, JOHN A. p 1601 N94-19022
SCHLUTER, LARRY L. p 1469 N94-19036
SCHMEICHEL, E. p 1554 N94-19686
SCHMIDLI, PIERRE p 1429 N94-18042
SCHMIDT, E. p 1337 N94-17884
SCHMIDT, M. p 1570 N94-19029
SCHMIDT, R. p 1330 N94-19634
p 1330 N94-19637
p 1330 N94-19638
SCHMIDT, WALTER p 1395 N94-17920
SCHMITT, J. H. M. M. p 1628 N94-19794
SCHMOYER, D. D. p 1472 N94-17910
SCHNEIDER, D. p 1570 N94-19108
SCHNEIDER, JEAN-CLAUDE p 1427 N94-18030
SCHNEIDER, MICHAEL p 1420 N94-19356
SCHNEIDER, S. A. p 1523 N94-18879
SCHNELL, R. C. p 1489 N94-18126
SCHNUR, JOEL M. p 1368 N94-17982
SCHOENMAKERS, J. p 1558 N94-19323
SCHOENMAKERS, JOHN G. M. p 1557 N94-19090
SCHOENWALD, D. A. p 1543 N94-19302
SCHONBERG, WILLIAM P. p 1455 N94-18664
SCHOOF, L. A. p 1537 N94-19249
p 1460 N94-19476
SCHRAAGEN, J. M. C. p 1508 N94-17967
SCHREIBER, K.-J. p 1494 N94-19503
SCHREUR, BEN WICHERS p 1494 N94-19699
SCHREYER, H. L. p 1372 N94-19059
SCHREYER, HOWARD L. p 1456 N94-19060
SCHRIMSHER, ROBERT H. p 1505 N94-18289
SCHRODER, D. K. p 1468 N94-19016
SCHUBERT, E. T. p 1400 N94-18366
SCHUBERT, W. K. p 1464 N94-17787
SCHULLER, I. K. p 1594 N94-17871
p 1368 N94-18098
SCHULTE-LADBECK, R. E. p 1621 N94-19288
SCHULTZ, ARTHUR J. p 1601 N94-19022
SCHULZ, KAI p 1321 N94-19711
SCHULZ, WILLIAM p 1377 N94-18489
SCHULZE, J. p 1518 N94-17943
SCHUMANN, U. p 1416 N94-18594
p 1416 N94-18595
p 1416 N94-18596
SCHUNK, P. R. p 1345 N94-17820
SCHUSTER, K. F. p 1390 N94-19416
SCHUTH, F. p 1375 N94-19742
SCHWARTZ, D. S. p 1342 N94-18720
SCHWARTZ, H. R. p 1596 N94-18316
SCHWARTZ, M. N. p 1493 N94-19051
SCHWARTZKOPF, STEVEN H. p 1511 N94-18484
SCHWARZ, R. B. p 1372 N94-19202
SCHWING, J. p 1402 N94-18380
SCKOPKE, N. p 1329 N94-19630
SEAH, M. P. p 1346 N94-17900
SEAMEN, J. F. p 1429 N94-18102
SEARFUS, R. M. p 1399 N94-18350
SEAS, A. p 1441 N94-19369
p 1441 N94-19394
SECAN, JAMES A. p 1483 N94-18655
SECHOVSKY, V. p 1593 N94-17744
p 1605 N94-19735
SEEMANN, WILLIAM H., III p 1342 N94-18702
SEGER, C.-J. p 1401 N94-18367
SEGUCHI, TADAO p 1369 N94-18220
SEIDL, P. p 1591 N94-19559
SEIFERAS, JOEL I. p 1530 N94-19482
p 1531 N94-19508
SEIGAL, P. p 1405 N94-19112
SELDIN, J. H. p 1578 N94-18383
SELIN, B. p 1419 N94-19068
SELJEE, R. R. p 1619 N94-19709
SELLDEN, B. p 1405 N94-19292
SELLMAIER, F. p 1624 N94-17736
SELVERIAN, J. H. p 1446 N94-19291
SENE, F. X. p 1328 N94-19626
SENGUPTA, S. K. p 1473 N94-18005
SERVE, M. P. p 1504 N94-19789
SESSLER, A. M. p 1436 N94-17869
p 1441 N94-19030
SETHURAMAN, JAYARAM p 1559 N94-19595
SEVILLANO, EVELIO p 1599 N94-18764
SEVINK, AGUR G. J. p 1486 N94-19081
SEVRIN, A. p 1485 N94-18929
SHABALIN, E. P. p 1564 N94-17687
SHABBIR, AAMIR p 1411 N94-18548
SHABIR, M. p 1545 N94-17680
SHADWICK, B. A. p 1590 N94-19194
SHAFER, LARRY p 1535 N94-18866
SHAH, RAVI p 1327 N94-19184
SHAHID, M. H. p 1545 N94-17793
SHAMANNA, M. p 1398 N94-18343
SHANG, C. C. p 1437 N94-18134
SHANKARRAMAN, M. J. p 1402 N94-18379
SHANNON, S. C. p 1505 N94-18289
SHANNON, SAMUEL G. p 1511 N94-18296
SHARMA, A. p 1373 N94-19402
SHARP, D. H. p 1419 N94-19025
SHARP, JOSEPH C. p 1502 N94-19212
SHARP, M. KEITH p 1323 N94-19163
SHARP, W. M. p 1575 N94-19106
SHAW, G. M. p 1385 N94-18301
SHAW, M. C. p 1341 N94-18692
SHAW, M. S. p 1376 N94-17751
SHAY, THOMAS J. p 1497 N94-18230
SHEATHER, P. H. p 1329 N94-19632
SHEEHAN, J. p 1436 N94-17998
SHEERER, T. J. p 1449 N94-17830
SHEHEE, DAVID B. p 1377 N94-18489

SHELDON, P. ... p 1569 N94-19013
SHEN, HUI-CHIEN ... p 1523 N94-19006
SHEN, Z. X. ... p 1599 N94-18804
SHEPHERD, D. ... p 1621 N94-19288
SHEPHERD, R. ... p 1585 N94-18082
SHEPHERD, R. L. ... p 1396 N94-17991
p 1440 N94-18889
SHER, A. ... p 1577 N94-18223
SHERIDAN, P. J. ... p 1489 N94-18126
SHERRING, C. ... p 1470 N94-19760
SHI, JICONG ... p 1573 N94-17784
SHI, WEIMIN ... p 1316 N94-19300
SHIAO, MICHAEL C. ... p 1457 N94-19351
SHIH, H. J. ... p 1574 N94-18994
SHIH, TSAN-HSING ... p 1410 N94-18546
SHIHO, MAKOTO ... p 1438 N94-18160
SHIMKAVEG, G. M. ... p 1436 N94-17868
SHIN, UNCHEOL ... p 1551 N94-19342
SHIN, YOUNG S. ... p 1454 N94-18661
SHIPE, P. C. ... p 1524 N94-19076
SHIRAISHI, SHIGEYUKI ... p 1444 N94-18159
SHIRANE, G. ... p 1594 N94-17866
SHIRRON, PETER ... p 1327 N94-19185
SHOJI, T. ... p 1586 N94-18213
SHOPE, W. B. ... p 1512 N94-18765
SHOUJIN, SUN ... p 1341 N94-18544
SHREVE, K. P. ... p 1464 N94-17731
SHU, CHI-WANG ... p 1551 N94-19317
SHUCHMAN, R. A. ... p 1497 N94-18277
SHUEN, J.-S. ... p 1411 N94-18549
SHULTS, W. D. ... p 1339 N94-19117
SHUM, D. K. M. ... p 1451 N94-17913
SICURANZA, GIOVANNI ... p 1326 N94-19179
SIDIKMAN, K. ... p 1583 N94-17743
SIEGAL, M. P. ... p 1405 N94-19079
SIEGEL, MARK E. ... p 1560 N94-18410
SIEGEL, R. W. ... p 1597 N94-18480
SIERON, THOMAS R. ... p 1318 N94-18779
SIFERD, RAYMOND E. ... p 1404 N94-18701
SIGMON, T. W. ... p 1437 N94-18083
SIKKA, V. K. ... p 1355 N94-17757
p 1362 N94-18938
p 1363 N94-18975
p 1365 N94-19274
p 1366 N94-19733
SIKKEL, KLAAS ... p 1537 N94-19223
p 1526 N94-19224
SILBERGLITT, R. S. ... p 1342 N94-18720
SILVA, P. A. ... p 1342 N94-18756
SIMANDL, R. F. ... p 1346 N94-17987
SIMEONI, M. ... p 1383 N94-17935
SIMIATIS, V. ... p 1569 N94-19013
SIMMS, D. A. ... p 1615 N94-18334
SIMON, P. C. ... p 1353 N94-19456
p 1353 N94-19459
p 1479 N94-19521
SINCLAIR, C. ... p 1441 N94-18974
SINCLAIR, M. ... p 1442 N94-19563
SINGH, ALOK ... p 1368 N94-17982
SINGH, D. ... p 1454 N94-18479
SINGH, M. ... p 1335 N94-19787
SINTON, R. A. ... p 1467 N94-18409
SIPELSTEIN, JAY ... p 1531 N94-19592
SIRCAR, A. K. ... p 1370 N94-18282
SIRIGNANO, W. A. ... p 1349 N94-18736
SIRIWARDANE, H. J. ... p 1486 N94-19018
SISAKYAN, A. N. ... p 1549 N94-18198
SIU, DANIEL P. ... p 1315 N94-18852
SIVERS, E. A. ... p 1369 N94-18166
SJAARDEMA, G. D. ... p 1614 N94-18164
p 1525 N94-19102
p 1460 N94-19476
SKARITKA, J. ... p 1343 N94-18763
SKOCHKO, G. W. ... p 1453 N94-18084
SKOCYPEC, R. D. ... p 1469 N94-19109
SKYLLINGSTAD, E. D. ... p 1488 N94-17895
SLAUGHTER, D. ... p 1489 N94-18132
SLAUGHTER, D. R. ... p 1488 N94-17758
SLAUGHTER, G. ... p 1355 N94-17752
SLOWINSKI, B. ... p 1359 N94-18218
SMATHERS, H. W. ... p 1334 N94-18149
p 1337 N94-18574
p 1335 N94-19787
SMEDLEY, JAN M. ... p 1534 N94-18509
SMILANSKY, UZI ... p 1547 N94-17949
SMIRNOV, YU. S. ... p 1608 N94-18253
SMIRNOVA, V. V. ... p 1561 N94-18150
SMITH, CELIA M. ... p 1502 N94-18305
SMITH, CHARLES W. ... p 1629 N94-19427
SMITH, D. L. ... p 1557 N94-19011
SMITH, L. S. ... p 1596 N94-18316
SMITH, PAUL ... p 1598 N94-18511
SMITH, W. H. ... p 1352 N94-19240
SMOLENSKY, MARK W. ... p 1513 N94-18992
SMYRL, N. R. ... p 1343 N94-18761
SNAIL, LEO A. ... p 1371 N94-18746
SNARSKI, STEPHEN R. ... p 1418 N94-18906
SNEAD, C. L., JR. ... p 1343 N94-18763
SNEDDON, LARRY G. ... p 1372 N94-18891
SNOKE, J. A. ... p 1483 N94-18690
SNOW, WARREN W. ... p 1614 N94-18191
SNYDER, S. F. ... p 1493 N94-19127
SNYDER, T. C. ... p 1471 N94-17777
SNYDER, W. B., JR. ... p 1602 N94-19075
SOBAJIC, SRDJAN D. ... p 1324 N94-19168
SODA, TAKAO ... p 1369 N94-18220
SODERHOLM, L. ... p 1598 N94-18531
SOEGAARD, SVEIN-ERIK ... p 1529 N94-19378
SOFRONIOU, MARK ... p 1547 N94-17969
SOHIE, GUY R. ... p 1598 N94-18616
SOHN, H. ... p 1595 N94-18054
SOISALON-SOININEN, E. ... p 1555 N94-19708
SOJKA, JAN J. ... p 1323 N94-19163
SOKOLOSKI, M. M. ... p 1327 N94-19181
SOLI, G. ... p 1596 N94-18316
SOLOMON, L. ... p 1436 N94-17998
p 1438 N94-18504
SOLOMON, SEAN C. ... p 1487 N94-19432
SOMORJAI, G. A. ... p 1347 N94-18193
p 1347 N94-18194
SONG, SHIHONG ... p 1595 N94-18162
SONTAG, EDWARDO ... p 1542 N94-18898
SOOHOO, J. ... p 1384 N94-18210
SORANZO, RAMON ... p 1550 N94-19086
SORENSEN, N. R. ... p 1474 N94-18521
SORVANIEMI, JAANA ... p 1346 N94-17973
SOUGANIDIS, PANAGIOTIS E. ... p 1562 N94-18286
SOULAS, GEORGE C. ... p 1587 N94-18861
SOUTH, D. W. ... p 1472 N94-17891
SOUTHWOOD, D. J. ... p 1329 N94-19629
SOWERS, C. H. ... p 1600 N94-18933
SPAHR, J. A. ... p 1494 N94-19298
SPANNE, P. ... p 1501 N94-17889
SPARKS, C. J. ... p 1593 N94-17760
SPEARS, K. G. ... p 1567 N94-18533
SPENCER, ROBERT H. ... p 1446 N94-19318
SPENCER, T. A. ... p 1403 N94-18452
p 1404 N94-18872
SPERBER, K. R. ... p 1489 N94-18053
SPIEKSMA, F. ... p 1560 N94-18990
SPIELMAN, R. B. ... p 1429 N94-18102
SPILLANTINI, P. ... p 1602 N94-19258
SPRAGGE, M. ... p 1394 N94-17770
SPRANGLE, P. ... p 1586 N94-18148
p 1440 N94-18771
SPRANGLE, PHILLIP ... p 1438 N94-18460
SPRUIT, P. ... p 1618 N94-19067
SQUIRE, BRENDAN E. ... p 1445 N94-18778
SRIDHARAN, R ... p 1462 N94-18729
SROKOSZ, M. A. ... p 1461 N94-18063
SROLOVITZ, D. J. ... p 1364 N94-19032
ST.JOHN, H. ... p 1585 N94-18057
STACEY, W. M. ... p 1588 N94-18988
STAIR, PETER C. ... p 1348 N94-18221
STALIO, ROBERTO ... p 1326 N94-19178
p 1326 N94-19179
STALLARD, B. W. ... p 1589 N94-19074
STAMM, G. ... p 1422 N94-19510
STANBERRY, L. C. ... p 1537 N94-19253
STANEK, P. W. ... p 1363 N94-19028
STANFORD, JOHN L. ... p 1486 N94-19237
STARKS, PATRICK J. ... p 1470 N94-17762
START, D. ... p 1581 N94-17694
STASIEWICZ, K. ... p 1328 N94-19624
STEADMAN, S. G. ... p 1565 N94-17984
STEEVES, M. M. ... p 1366 N94-19546
STEGLICH, F. ... p 1360 N94-18398
STEIGER, W. ... p 1330 N94-19634
STEIN, CHARLES ... p 1343 N94-18869
STEIN, H. J. ... p 1592 N94-17742
STEIN, KARIN ... p 1592 N94-19613
STEINBERG, D. J. ... p 1362 N94-18919
STEINER, D. ... p 1363 N94-19021
STEINMAN, ROBERT M. ... p 1512 N94-18886
STELLINGWERF, R. F. ... p 1451 N94-17906
p 1457 N94-19207
STEPHENS, J. J. ... p 1373 N94-19308
STEPHENS, MICHAEL A. ... p 1557 N94-18517
STERER, E. ... p 1404 N94-18805
p 1600 N94-18969
STERZIK, MICHAEL F. ... p 1628 N94-19519
STEVENSON, J. O. ... p 1592 N94-17742
STEWART, AMYELIZABETH C. ... p 1324 N94-19165
STEWART, DORATHY A. ... p 1493 N94-18781
STEWART, R. ... p 1585 N94-18082
STEWART, R. E. ... p 1436 N94-17868
p 1584 N94-17993
STEWART, VEARL R. ... p 1317 N94-18577
p 1318 N94-18733
STEWART, W. F. ... p 1417 N94-18831
STIEVE, ALICE L. ... p 1484 N94-18725
STIFF, JAN S. ... p 1509 N94-18686
STINSON, M. C. ... p 1372 N94-18932
STIRLING, M. W. ... p 1496 N94-18066
STITZ, E. H. ... p 1541 N94-18474
STIX, T. H. ... p 1473 N94-18101
STOBIE, IAIN C. ... p 1541 N94-18463
STOILOVA, N. I. ... p 1548 N94-18176
STOLCIS, LUCA ... p 1307 N94-18427
STOLOVITCH, LAURENT ... p 1532 N94-19712
STONE, KEVIN L. ... p 1490 N94-18300
STONEMAN, ROBERT C. ... p 1440 N94-18747
STOORVOGEL, A. A. ... p 1543 N94-19329
STORCHAK, S. N. ... p 1561 N94-18151
STOSS, F. W. ... p 1471 N94-17774
p 1475 N94-18832
STOUDT, DAVID C. ... p 1580 N94-18947
STOUFFLET, BRUNO ... p 1311 N94-17957
STRACHAN, J. W. ... p 1467 N94-18520
STRADA, SILVIA ... p 1540 N94-17922
p 1556 N94-17938
STRAIN, JOHN ... p 1605 N94-19719
STRAW, TIMOTHY B. ... p 1563 N94-18734
STRELTSOV, V. N. ... p 1608 N94-18268
STRICKLER, D. ... p 1617 N94-19026
STRITTMATTER, R. B. ... p 1519 N94-18086
STRIZH, T. A. ... p 1549 N94-18198
STROSCIO, MICHAEL A. ... p 1605 N94-19725
STROTH, U. ... p 1585 N94-18056
STROUBOULIS, T. ... p 1549 N94-18697
STROUD, CARLOS ... p 1581 N94-19772
STRUBLE, DAVE ... p 1320 N94-18658
STRUIJS, ROBERT ... p 1413 N94-18564
STRUVE, K. W. ... p 1429 N94-18102
STUCKY, G. ... p 1354 N94-19728
STUMP, BRIAN W. ... p 1481 N94-18485
STUMPF, B. J. ... p 1363 N94-18939
STURGESS, KEITH A. ... p 1442 N94-19770
SU, YUAN-ZHI ... p 1486 N94-19255
SUGIHARA, MASAYOSHI ... p 1586 N94-18212
SUHR, STEVEN C. ... p 1549 N94-18863
SULSKY, DEBORAH ... p 1456 N94-19060
SUMIN, V. V. ... p 1355 N94-17692
SUMNER, A. ... p 1329 N94-19628
SUMPTER, B. G. ... p 1596 N94-18192
SUN, Q. ... p 1351 N94-19132
p 1351 N94-19150
SUNDARALINGAM, N. ... p 1630 N94-17818
SUNDERAM, V. S. ... p 1534 N94-18482
SUNG, CHI C. ... p 1540 N94-18263
SUO, ZHIGANG ... p 1632 N94-18791
SUPRIYADI, BAMBANG ... p 1458 N94-19460
SURIA, RAVINDRANATH ... p 1389 N94-18897
SUTHERLAND, H. J. ... p 1447 N94-18128
SUTTON, G. H. ... p 1500 N94-19727
SUZUKI, YUSUKE ... p 1316 N94-17921
SVANDRLIK, J. ... p 1375 N94-19651
SWANSON, PAUL D. ... p 1581 N94-19602
SWANSON, R. M. ... p 1467 N94-18409
SWART, R. J. ... p 1475 N94-18949
SWEENEY, F. J. ... p 1612 N94-17858
SWEERS, GUIDO ... p 1550 N94-19153
SWEGLE, J. W. ... p 1455 N94-19039
SWETT, WILLIAM C. ... p 1490 N94-18206
SWICORD, MAYS L. ... p 1505 N94-18294
SWIDER, W. ... p 1595 N94-18054
SWIFT, G. W. ... p 1379 N94-17725
SWIFT, RICHARD A. ... p 1317 N94-18227
SWINDEMAN, R. W. ... p 1367 N94-17881
SYN, C. K. ... p 1355 N94-17711
SZOKE, A. ... p 1585 N94-18129

T

TABAR, RAJA F. ... p 1534 N94-18508
TACCONI-GARMAN, L. E. ... p 1621 N94-19415
TACCONI, L. J. ... p 1390 N94-19416
TAFRESHI, M. A. ... p 1525 N94-19145
TAGHEZOUT, DAHO ... p 1408 N94-18022
TAJIMA, T. ... p 1583 N94-17753
p 1583 N94-17945
p 1584 N94-17983
TAJIMA, TOSHIKI ... p 1564 N94-17738
TAKAHASHI, MAYUKO ... p 1438 N94-18160
TAKAHASHI, S. ... p 1598 N94-18531
TAKEDA, TATSUOKI ... p 1586 N94-18157
TAKEMOTO, MIKIO ... p 1428 N94-18037
TAKLIF, A. G. ... p 1602 N94-19293
TALBI, EL-GHAZALI ... p 1538 N94-19514
TAMBE, MILIND ... p 1541 N94-18462
p 1541 N94-18463
TAMIR, DAVID ... p 1327 N94-19183
TAN, G. O. ... p 1347 N94-18059
TAN, SENG C. ... p 1453 N94-18382
TANAKA, SOUICHI ... p 1428 N94-18036
TANG, K. ... p 1501 N94-18242
TANG, XUEFEI ... p 1599 N94-18711

TANIS, J. A. p 1564 N94-17775
p 1569 N94-18999
p 1570 N94-19108
TARDY, H. L. p 1464 N94-17787
TATA, X. p 1569 N94-18945
TAUSANOVITCH, JEANETTE R. p 1579 N94-18858
TAWARA, H. p 1566 N94-18158
TAYA, M. p 1344 N94-19720
TAYLOR, B. G. p 1633 N94-19404
TAYLOR, J. B. p 1584 N94-17948
TAYLOR, R. D. p 1404 N94-18805
p 1600 N94-18969
TAYLOR, RONALD p 1342 N94-18715
TEDROW, PAUL M. p 1402 N94-18390
TEETERS, J. L. p 1399 N94-18350
TEEUW, WOUTER B. p 1537 N94-19198
TEICH, MALVIN C. p 1557 N94-18540
TELLIER, L. L. p 1478 N94-19272
TENTHIJEBOONKKAMP, J. H. M. p 1547 N94-18078
TENTYUKOV, M. N. p 1608 N94-18252
TEODORIDIS, VIRON p 1428 N94-18039
TERELST, A. F. M. p 1547 N94-18077
p 1549 N94-18948
TERLAKY, T. p 1524 N94-19089
p 1525 N94-19143
p 1525 N94-19156
TERRY, P. W. p 1592 N94-19656
TESKE, THOMAS p 1422 N94-19509
TETLOW, NICHOLAS p 1410 N94-18270
TETZLAFF, G. p 1494 N94-19503
THALER, BARRY p 1599 N94-18719
THALER, J. p 1569 N94-19013
THE, P. S. p 1621 N94-19288
THEEUWES, J. p 1509 N94-19419
p 1510 N94-19443
THEIHZEN, H. G. p 1494 N94-19698
THEISS, S. K. p 1600 N94-18904
THELEN, D. p 1401 N94-18369
THELEN, D. C. p 1399 N94-18354
THIBERT, J. J. p 1307 N94-18430
THISSEN, UWE p 1426 N94-18019
THOE, R. S. p 1580 N94-19268
THOMANN, PIERRE p 1428 N94-18038
THOMAS, G. H. p 1448 N94-19252
THOMAS, JOHN O. p 1578 N94-18405
THOMAS, LAWRENCE R. p 1323 N94-19162
THOMAS, T. R. p 1519 N94-18086
THOMASON, J. F. p 1385 N94-18291
THOMASON, JOHN E., III p 1576 N94-19589
THOMLINSON, J. G. p 1329 N94-19629
THOMPSON, DEBORAH L. p 1514 N94-17877
THOMPSON, EDWARD F. p 1497 N94-18414
THOMPSON, J. A. p 1329 N94-19628
THOMPSON, J. D. p 1594 N94-17907
THOMPSON, S. J. p 1585 N94-18057
THOREN, I. p 1528 N94-19333
THORNE, JAMES D. p 1334 N94-18718
THORPE, THOMAS P. p 1371 N94-18746
THOUVEREZ, FABRICE p 1457 N94-19403
THURSBY, GRAHAM p 1579 N94-18738
THURSTON, MIKE J. p 1342 N94-18757
TIEE, J. J. p 1478 N94-19272
TIENSUU, S. p 1363 N94-18952
TIESO, JOHN p 1617 N94-18770
TIGGES, C. P. p 1405 N94-19079
TILLEMA, H. G. p 1543 N94-19199
TILLMANN, R. W. p 1370 N94-18403
TINCKNELL, M. p 1570 N94-19103
TING, A. p 1586 N94-18148
TIPICI, HUSEYIN A. p 1386 N94-18449
TISCHLER, MARC E. p 1503 N94-19214
TISCHLER, V. A. p 1450 N94-17838
TIWARI, S. N. p 1339 N94-17766
TOBITA, KENJI p 1586 N94-18214
TOKMAKIAN, R. T. p 1461 N94-18063
TOLENDINO, L. F. p 1618 N94-19099
TOLOCZKO, M. B. p 1364 N94-19043
TOMA, L. S. p 1366 N94-19546
TOMAYKO, JIM p 1521 N94-18453
TONG, S. Y. p 1565 N94-17850
TONGUE, WILLIAM L. p 1556 N94-18397
TONKS, D. L. p 1451 N94-17864
p 1361 N94-18802
TONN, B. E. p 1474 N94-18523
TOPART, P. p 1369 N94-18233
TOPIWALA, PANKAJ N. p 1389 N94-18801
TORCZYNSKI, J. R. p 1419 N94-19058
TORKAR, K. p 1330 N94-19634
TORNOW, CARMEN p 1480 N94-18088
TORRI, V. p 1383 N94-17935
TRAMPUS, PAOLO p 1326 N94-19179
TRANQUADA, J. M. p 1358 N94-17947
TRAXLER, KATHLEEN M. p 1493 N94-18883
TREBES, J. E. p 1436 N94-17868
TREFNY, J. U. p 1468 N94-18944
TREISMAN, ANNE p 1508 N94-18682
TRENCHARD, MICHAEL E. p 1462 N94-18677
p 1462 N94-18679
TRETMANS, JAN p 1543 N94-19226
TRETYAKOV, S. A. p 1384 N94-18116
TREUMANN, R. p 1329 N94-19630
TREURNIET, W. p 1518 N94-17965
TREXLER, E. p 1470 N94-17749
TRIBUZY, R. p 1545 N94-17684
TRISCHBERGER, M. p 1325 N94-19172
TRITTSCHUH, JENNIFER E. p 1324 N94-19168
TROEIM, J. p 1330 N94-19634
TROSKO, JAMES E. p 1502 N94-18924
TROTIGNON, J. G. p 1328 N94-19626
TROTT, KEITH D. p 1387 N94-18601
TROUTMAN, R. p 1531 N94-19548
TRUBIAN, M. p 1547 N94-17961
TRUBIAN, MARCO p 1520 N94-18138
TRUDNOWSKI, D. J. p 1548 N94-18094
TRUETT, L. F. p 1617 N94-19057
p 1524 N94-19076
TRUHLAR, DONALD G. p 1568 N94-18837
TRUMMER, D. J. p 1333 N94-17782
TRUPPI, L. E. p 1476 N94-19065
TSACOYEANES, JAMES G. p 1579 N94-18858
TSAI, CHEN S. p 1577 N94-18295
TSAI, H. L. p 1364 N94-19044
TSANG, C. P. p 1397 N94-18341
TSAO, J. Y. p 1592 N94-17741
TSELEPIDAKIS, D. P. p 1414 N94-18585
TSO, W. p 1339 N94-17766
TSU, RAPHAEL p 1606 N94-19741
TSUNEMATSU, TOSHIHIDE p 1586 N94-18212
TSUNODA, TAKEO p 1429 N94-18041
TULLOCH, W. p 1489 N94-18132
TULLOCH, W. M. p 1488 N94-17758
TUNARE, J. p 1528 N94-19333
TURCO, R. P. p 1476 N94-19104
TURCOTTE, DONALD L. p 1487 N94-19428
TURET, P. p 1499 N94-19063
TURKEL, ELI p 1551 N94-19315
TURKO, B. T. p 1432 N94-18828
TURMAN, B. N. p 1439 N94-18522
TURNBULL, A. p 1451 N94-17899
p 1451 N94-17929
TURNER, J. A. p 1580 N94-18931
TURNER, ROBERT B. p 1534 N94-18768
TUSHKOV, B. P. p 1351 N94-19110
TUTTLE, B. A. p 1371 N94-18519
TUTTLE, JIM p 1327 N94-19185
TYSELL, LARS G. p 1311 N94-17721
TYSKIEWICZ, STACEN p 1462 N94-18679
TZAVARAS, ATHANASIOS E. p 1410 N94-18385

U

UBEROI, C. p 1581 N94-17688
p 1586 N94-18172
UCHIMA, M. p 1525 N94-19186
UCKAN, N. A. p 1582 N94-17697
UHM, HAN S. p 1395 N94-17903
UNDERWOOD, J. H. p 1580 N94-18931
UNDERWOOD, P. J. p 1325 N94-19172
UNGER, JOSEPH p 1631 N94-19504
UNGER, K. p 1354 N94-19728
UNRUH, AMY p 1610 N94-17746
UPADHYAY, C. S. p 1549 N94-18697
URSU, I. p 1595 N94-18173

V

VAALAND, PER ATLE p 1529 N94-19378
VACHON, WILLIAM A. p 1469 N94-19036
VAHALA, L. p 1583 N94-17809
VALANJU, P. M. p 1587 N94-18524
VALAREZO, WALTER O. p 1306 N94-18424
VALASEK, JOHN p 1318 N94-19448
VALCO, MARK J. p 1446 N94-19318
VALENZUELA, GASPER R. p 1499 N94-19609
VALLERAND, A. L. p 1504 N94-17823
VALTONEN, M. p 1396 N94-18091
VANDAM, C. P. p 1308 N94-18435
VANDEKASTEELE, R. M. p 1451 N94-17931
VANDEN, HEUVEL J. p 1553 N94-19605
VANDENBERG, K. G. p 1526 N94-19200
VANDENBERG, L. p 1594 N94-17896
VANDENBORN, G. J. p 1475 N94-18949
VANDENBROEK, P. M. p 1526 N94-19200
VANDENHEUVEL, J. p 1554 N94-19683
p 1554 N94-19685
p 1554 N94-19688
p 1554 N94-19689
VANDENHEUVEL, J. C. p 1441 N94-19426
VANDENHOUDT, GEERT p 1444 N94-17963
p 1611 N94-17980
VANDERHAVEN, J. p 1434 N94-19797
VANDERHELM, P. A. p 1509 N94-19348
VANDERIET, R. P. p 1618 N94-19331
VANDERSTEDE, FRANK p 1444 N94-17964
VANDERVALK, MARTIJN p 1537 N94-19219
VANDERWOUDE, J. W. p 1542 N94-19091
VANDRIESSCHE, R. p 1413 N94-18568
VANDROMME, D. p 1416 N94-18597
VANDUIJN, CORNELIS J. p 1420 N94-19139
VANEJIK, A. M. p 1483 N94-18712
VANES, J. T. p 1515 N94-19799
VANHAERINGEN, HENK p 1550 N94-19082
VANHALST, J. p 1432 N94-18654
VANHOESEL, C. P. M. p 1528 N94-19330
VANHOUTUM, G. J. p 1543 N94-19326
VANIER, P. E. p 1375 N94-19651
VANLIER, R. J. p 1509 N94-19348
VANMEIJGAARD, ERIK p 1489 N94-18143
VANMOORSEL, AAD P. A. p 1537 N94-19264
p 1558 N94-19265
p 1558 N94-19385
VANOOSTEROM, P. J. M. p 1618 N94-19452
VANPAASSEN, D. M. p 1319 N94-19796
VANPUTTEN, F. J. M. p 1441 N94-19426
VANRUYMBEKE, M. p 1483 N94-18628
VANSINDEREN, MARTEN p 1527 N94-19261
VANWALSUM, THEO p 1525 N94-19155
VANWOERKOM, L. D. p 1396 N94-17991
VARDULAKIS, A. I. p 1547 N94-18069
VASUDEVAN, A. K. p 1455 N94-18714
VAUGHAN, C. T. p 1455 N94-18829
VAUGHAN, K. H. p 1468 N94-18986
VAUGHAN, P. p 1331 N94-19639
VAWTER, G. A. p 1405 N94-19079
VAZ, M. p 1436 N94-17883
VEAL, B. W. p 1597 N94-18498
VECCHIO, K. S. p 1362 N94-18809
VEERS, P. S. p 1465 N94-18001
VELDMAN, H. J. p 1553 N94-19605
p 1554 N94-19683
p 1554 N94-19685
p 1554 N94-19688
p 1554 N94-19689
VELSKO, C. A. p 1378 N94-19242
VENABLE, D. D. p 1591 N94-19441
VENKATA, RAMANA G. p 1549 N94-18863
VENKATARAMAN, S. p 1630 N94-18762
VENKATASUBRAMANIAM, P. R. p 1402 N94-18379
VENKATESWARAN, N. p 1402 N94-18379
VENKATESWARLU, PUTCHA p 1373 N94-19402
VENKAYYA, VIPPERLA B. p 1450 N94-17834
p 1450 N94-17837
p 1450 N94-17838
VENTURINI, EUGENE L. p 1601 N94-19022
VERBEEK, H. J. p 1458 N94-19444
VERGHESE, S. p 1595 N94-17989
VERHAARD, LOUIS p 1543 N94-19226
VERHAGEN, T. L. A. p 1451 N94-17931
VERMEEREN, C. A. J. R. p 1344 N94-19666
VERMOT, MICHEL p 1427 N94-18029
VERNIKOS, JOAN p 1502 N94-19212
VERNON, S. p 1467 N94-18483
VERSPAY, SJACK J. L. H. p 1317 N94-17734
VERWEY, W. B. p 1509 N94-19420
p 1509 N94-19422
VESS, T. M. p 1369 N94-18112
VIAL, J.-P. p 1525 N94-19143
VIAL, JEAN-PHILIPPE p 1525 N94-19154
VIANCO, P. T. p 1358 N94-18003
p 1359 N94-18127
p 1370 N94-18477
p 1433 N94-19243
VIANCO, PAUL T. p 1357 N94-17862
VIENNEAU, ROBERT L. p 1391 N94-19587
VIG, JOHN R. p 1430 N94-18299
p 1403 N94-18471
VIGGIANO, A. A. p 1567 N94-18526
VIITANEN, A. J. p 1384 N94-18116
VIJGEN, PAUL M. H. W. p 1308 N94-18435
VIKDAL, L. N. p 1562 N94-18810
VILKNER, HANS p 1426 N94-18024
VILLARRUEL, C. A. p 1382 N94-17902
p 1579 N94-18743
VILSMEIER, JOSEF p 1319 N94-19496
VINITSKIJ, S. I. p 1549 N94-18198
p 1608 N94-18253
VISSERS, CHRIS A. p 1527 N94-19261
VISWANATHAN, S. p 1363 N94-18975
VITANYI, P. M. B. p 1517 N94-17812
VITEK, J. M. p 1445 N94-18976
p 1364 N94-19203
VITTITOE, C. N. p 1485 N94-19001
p 1485 N94-19002
VLANNES, N. p 1604 N94-19596
VOELS, S. A. p 1624 N94-17736
VOGEL, M. H. p 1390 N94-19447
p 1390 N94-19449

VOGELGESANG, OLIVER p 1319 N94-19500
VOKOS, S. p 1609 N94-19121
VOLIN, K. J. p 1430 N94-18481
VOLZ, STEVE p 1327 N94-19185
VONBUELOW, HARTWIG p 1437 N94-18061
VONGCHAVALITKUL, S. p 1540 N94-18125
VONKAENEL, V. p 1428 N94-18032
p 1408 N94-18033
VONMONTIGNY, C. p 1623 N94-19464
VOSS, D. E. p 1404 N94-18872
VOSS, H. D. p 1485 N94-18874
VOSS, HEINZ-JUERGEN p 1555 N94-19697
VREEKE, M. S. p 1374 N94-19585
VROUWENVELDER, A. C. W. M. p 1343 N94-19281
VUE, B. T. V. p 1585 N94-18129
VUI, TRAN p 1546 N94-17795
VUIK, KEES p 1524 N94-19084

W

WACHTER, E. A. p 1343 N94-18761
WACKERMAN, C. C. p 1497 N94-18277
WACLAWIK, RONALD E. p 1424 N94-17717
WADA, N. p 1468 N94-18944
WADE, M. R. p 1585 N94-18058
WADE, R. C. p 1523 N94-18989
WADE, T. p 1581 N94-17694
WAGELMANS, A. P. M. p 1528 N94-19330
WAGNER, LEONARD S. p 1388 N94-18722
WAGNER, PAUL K. p 1333 N94-19313
WAHR, JOHN p 1484 N94-18838
WAKITA, KEN p 1526 N94-19220
WAKSMAN, Z. p 1552 N94-19392
WALCHLI, LAWRENCE A. p 1308 N94-18436
WALD, ROBERT M. p 1621 N94-18141
WALDMAN, MARTY p 1324 N94-19164
WALKER, D. W. p 1538 N94-19299
WALKER, JOHN R., JR. p 1387 N94-18601
WALLIN, STEFAN p 1311 N94-17919
WALLING, R. p 1585 N94-18082
WALLING, R. S. p 1436 N94-17868
WALLS, A. p 1441 N94-19307
WALLS, BILL p 1449 N94-17829
WALLSTENIUS, BENGT p 1452 N94-17970
WALTER-SHEA, ELIZABETH A. p 1470 N94-17762
WANDELL, BRIAN A. p 1618 N94-19256
WANG, A. p 1468 N94-19015
WANG, A. S. p 1340 N94-18205
WANG, C. H. p 1370 N94-18515
WANG, C. Y. p 1409 N94-18248
WANG, CHANGBIAO p 1436 N94-17869
WANG, CHIN-AN p 1357 N94-17859
p 1358 N94-17915
WANG, F. X. p 1453 N94-18328
WANG, H. p 1602 N94-19340
WANG, H. HAU p 1601 N94-19022
WANG, JIAN p 1512 N94-18673
WANG, KANG L. p 1600 N94-18884
WANG, L. M. p 1599 N94-18816
WANG, TAI-SEN F. p 1573 N94-17726
WANG, TING p 1418 N94-18867
WANG, WEI p 1595 N94-17956
WANG, Z. p 1443 N94-17785
p 1432 N94-18653
WARD-THOMPSON, D. p 1622 N94-19417
WARD, DAVID G. p 1541 N94-18790
WARD, MICHAEL J. p 1579 N94-18668
WARHAUT, M. p 1330 N94-19636
p 1330 N94-19637
WARLITZER, VOLKER p 1322 N94-18123
WARNE, L. K. p 1394 N94-17780
WARNER, B. E. p 1435 N94-17723
p 1437 N94-18093
p 1441 N94-19294
WARNES, R. H. p 1451 N94-17864
WARREN, M. S. p 1526 N94-19205
WARREN, R. C. p 1376 N94-18203
WARREN, W. L. p 1371 N94-18519
WASHBURN, J. p 1592 N94-17741
WATANABE, AKIHIKO p 1438 N94-18160
WATSON, K. p 1596 N94-18316
WAYMAN, C. M. p 1366 N94-19775
WEAKLEY, CHRISTOPHER K. p 1334 N94-18408
WEAVER, W. D. p 1324 N94-19166
WEBB, G. L. p 1363 N94-18940
WEBB, R. H. p 1442 N94-19658
WEBB, SPAHR C. p 1498 N94-18663
WEBER, E. R. p 1595 N94-18054
WEBER, W. J. p 1599 N94-18816
WEEBER, S. A. p 1383 N94-17994
WEEKS, J. p 1527 N94-19245
WEERASURIYA, S. A. p 1476 N94-19064
WEERTMAN, J. R. p 1596 N94-18184
WEFEL, J. P. p 1630 N94-18676
WEFEL, JOHN P. p 1629 N94-18705
WEHNER, M. F. p 1494 N94-19298
WEI, RONG-MAO p 1492 N94-18675
WEIGAND, D. E. p 1405 N94-18928
WEINACHT, D. J. p 1521 N94-18271
WEINACHT, PAUL p 1410 N94-18391
WEINER, ANITA M. p 1606 N94-19771
WEINER, BRAD R. p 1350 N94-18799
WEINER, K. p 1405 N94-18941
WEINER, K. H. p 1437 N94-18083
WEINMANN, M. p 1426 N94-18021
WEISS, MARTIN p 1542 N94-19142
WEISS, ROSANNE M. p 1316 N94-18728
WEISS, W. p 1329 N94-19633
WEISSMAN, P. T. p 1370 N94-18282
WEITZ, ERIC p 1348 N94-18221
WELCH, D. O. p 1603 N94-19541
WELDON, W. F. p 1441 N94-19307
WELLINGER, ROGER p 1427 N94-18031
WENCHUAN, LIU p 1341 N94-18544
WENDT, J. R. p 1405 N94-19079
WENHAM, S. R. p 1468 N94-19015
WENNINK, HENK p 1526 N94-19196
WENZEL, K.-P. p 1633 N94-19404
WERLEY, K. A. p 1587 N94-18803
WERNER, P. p 1595 N94-18054
WERT, J. A. p 1361 N94-18788
WERTHEIM, A. H. p 1510 N94-19439
WERVE, M. E. p 1441 N94-19294
WESSELS, J. p 1543 N94-19326
WESSENDORF, K. O. p 1404 N94-18827
WEST, W. P. p 1585 N94-18058
WESTERINK, J. J. p 1497 N94-18455
WESTON, A. M. p 1376 N94-18095
WETZEL, GERALD p 1479 N94-19507
WETZEL, PAUL R. p 1320 N94-18333
WHEAT, S. R. p 1536 N94-19161
p 1536 N94-19188
WHEAT, STEPHEN R. p 1537 N94-19206
WHIPPLE, E. C. p 1329 N94-19630
WHIRLEY, R. G. p 1452 N94-18049
p 1340 N94-18113
WHIRLEY, ROBERT G. p 1460 N94-19475
WHISNANT, R. A. p 1470 N94-19760
WHITAKER, S. p 1398 N94-18343
p 1398 N94-18344
p 1400 N94-18360
WHITAKER, S. R. p 1397 N94-18340
p 1402 N94-18376
WHITE, BRIAN E. p 1316 N94-18384
p 1386 N94-18495
WHITE, C. J. p 1435 N94-17724
WHITE, C. W. p 1339 N94-17846
WHITE, R. H. p 1347 N94-18092
p 1433 N94-19004
WHITE, W. p 1585 N94-18082
p 1489 N94-18132
WHITE, W. E. p 1488 N94-17758
p 1396 N94-17991
p 1440 N94-18889
WHITEHEAD, J. A. p 1500 N94-19792
WHITEMAN, C. D. p 1489 N94-18052
WHITTEN, W. B. p 1567 N94-18493
WICHMANN, B. A. p 1517 N94-17917
WICKER, DEVERT p 1540 N94-18189
WICKS, P. J. p 1409 N94-17901
WIDOM, JENNIFER p 1614 N94-18144
WIECKOWSKI, ANDRZEJ p 1567 N94-18766
WIELOPOLSKI, L. p 1501 N94-17889
WIERINGA, R. p 1618 N94-19067
WIESE, GARRELT p 1604 N94-19612
WIESELTHIER, JEFFREY E. p 1432 N94-18681
WIKSWO, JOHN P. p 1447 N94-18225
WILDER, M. C. p 1312 N94-19119
WILKEN, B. p 1329 N94-19633
WILKINS, MARK L. p 1418 N94-18878
WILLETT, D. J. p 1448 N94-19336
WILLIAMS, A. E. p 1376 N94-18095
WILLIAMS, J. p 1602 N94-19340
WILLIAMS, JACK M. p 1601 N94-19022
WILLIAMS, M. C. p 1468 N94-18925
WILLIAMS, NEIL p 1495 N94-17822
WILLIAMS, R. L. p 1336 N94-18338
WILLIAMSON, D. L. p 1468 N94-18944
WILLIAMSON, P. R. p 1393 N94-18351
WILLIEMS, ROBERT p 1497 N94-18393
WILLSON, ALAN N., JR. p 1404 N94-18706
p 1404 N94-18709
WILS, E. p 1619 N94-19453
WILSON, J. R. p 1624 N94-17897
p 1590 N94-19273
p 1627 N94-19284
WILSON, K. p 1380 N94-18710
WILSON, R. B. p 1349 N94-18532
WILSON, WARREN J. p 1316 N94-18384
p 1386 N94-18495
WILTBERGER, N. LYN p 1306 N94-18421
WIMER, J. G. p 1468 N94-18925
WINDLEY, P. J. p 1400 N94-18363
p 1401 N94-18371
p 1401 N94-18372
WING, JEANNETTE p 1521 N94-18453
WINGATE, C. A. p 1451 N94-17906
p 1457 N94-19207
WINKLEMAN, B. C. p 1576 N94-17857
WINKLER, S. p 1372 N94-18792
WINTER, STELLAN p 1473 N94-18139
WINTERROWD, P. p 1402 N94-18378
WINTERS, KEL p 1399 N94-18355
WINTERSTEIN, S. R. p 1465 N94-18001
WIRTENSON, G. R. p 1433 N94-19004
WISCHOW, PERRY B. p 1462 N94-18677
WISE, M. p 1471 N94-17821
WISNIEWSKI, R. p 1359 N94-18218
WISSINGER, ALAN B. p 1579 N94-18858
WITTENBERG, H. p 1321 N94-19615
WITTIG, CURT p 1349 N94-18395
WITTIG, J. E. p 1339 N94-17846
WITTMERS, LORENTZ E. p 1506 N94-18632
WITTSCHEN, RICHARD L. p 1387 N94-18666
WITTWER, LEON A. p 1382 N94-17844
WNEK, G. E. p 1604 N94-19596
WOEHRLE, T. G. p 1335 N94-18942
WOHLGEMUTH, J. H. p 1466 N94-18335
WOLF, E. L. p 1600 N94-18876
WONG, M. K. W. p 1433 N94-19111
WONG, NGAI C. p 1581 N94-19578
WONG, R. L. p 1590 N94-19269
WONG, V. p 1584 N94-17983
WOODBURY, KEITH A. p 1338 N94-19438
WOODLE, M. p 1436 N94-17998
WOODLIFFE, R. D. p 1329 N94-19632
WOODRUFF, R. p 1399 N94-18352
WOODRUFF, STEWART J. p 1323 N94-19163
WOODWARD, D. S. p 1305 N94-18416
WOOLLISCROFT, L. J. C. p 1328 N94-19623
p 1329 N94-19628
p 1330 N94-19638
WOOSLEY, S. E. p 1624 N94-17897
WOPPOWA, STEFAN p 1409 N94-18124
WORKMAN, GARY L. p 1380 N94-19423
p 1378 N94-19494
WRIGHT, D. A. p 1600 N94-18968
WRIGHT, MICHAEL p 1633 N94-19486
WROBLEWSKI, D. p 1585 N94-18057
WU, A. p 1399 N94-18356
WU, C. T. p 1597 N94-18500
WU, FRANCIS T. p 1484 N94-18868
WU, HENRY M. p 1544 N94-19530
WU, JIANN M. p 1348 N94-18249
WU, M. H. p 1366 N94-19775
WU, Q. H. p 1544 N94-19408
WUEST, C. R. p 1381 N94-19544
p 1572 N94-19545
WUNDERLICH, B. p 1596 N94-18192
WURSTNER, S. K. p 1461 N94-18107
WURTMAN, RICHARD J. p 1506 N94-18862
WUTTIG, M. p 1366 N94-19775

X

XIAO, H. p 1587 N94-18524

Y

YAGI, TETSUYA p 1369 N94-18220
YAKUSAWA, NAOAKI p 1429 N94-18040
YALE, GARY E. p 1445 N94-18813
YAMAMOTO, AKIRA p 1630 N94-18219
YAMAMOTO, HARRY Y. p 1502 N94-18305
YAMDAGNI, N. p 1574 N94-18845
YANAGAWA, HIROSHI p 1427 N94-18028
YANG, CHING-CHING p 1560 N94-19726
YANG, J. N. p 1540 N94-18125
YANG, JAE-YOUNG p 1338 N94-19128
YANG, L. p 1339 N94-17846
p 1339 N94-17846
YANG, YUMIN p 1419 N94-19025
YANG, Z. p 1411 N94-18547
YANTIS, STEVEN p 1508 N94-18292
YAPA, P. D. p 1476 N94-19064
YASUMURA, S. p 1501 N94-17889
YATES, G. J. p 1432 N94-18828
YAU, STEPHEN S. p 1535 N94-18865
YAU, W. p 1595 N94-18054
YEAGER, E. p 1354 N94-19653
YEARBY, K. H. p 1329 N94-19628
YEN, J. p 1384 N94-18216
YIP, LONG P. p 1308 N94-18435
YODA, OSAMU p 1438 N94-18161
YONEZAWA, AKINORI p 1526 N94-19220

YOUNG, B. K. F. .... p 1436 N94-17868
YOUNG, MICHAEL A. .... p 1535 N94-18772
YOUNG, P. E. .... p 1584 N94-17993
YOUNGBLOOD, G. E. .... p 1593 N94-17747
YOUNGDAHL, C. A. .... p 1597 N94-18500
p 1601 N94-18993
p 1602 N94-19122
YU, L. H. .... p 1436 N94-17998
p 1438 N94-18504
p 1406 N94-19310
YU, S. .... p 1575 N94-18997
YUN, STEVEN P. .... p 1387 N94-18510
YUNN, B. .... p 1441 N94-18974

Z

ZABEL, NICOLAS .... p 1528 N94-19359
ZACHARIA, T. .... p 1445 N94-18976
ZACHOS, C. .... p 1609 N94-19121
ZACK, N. R. .... p 1535 N94-18930
ZACKRISSON, M. .... p 1569 N94-18847
ZAHARAKIS, K. E. .... p 1569 N94-18999
ZAHN, STEPHEN G. .... p 1493 N94-18812
ZALTASH, A. .... p 1351 N94-19118
ZAPOTOSKY, J. E. .... p 1386 N94-18473
p 1388 N94-18741
p 1388 N94-18751
ZARDA, P. RICHARD .... p 1449 N94-17831
ZARNSTORFF, M. C. .... p 1590 N94-19273
ZAUGG, T. J. .... p 1435 N94-17724
ZAWODZINSKI, C. .... p 1352 N94-19240
ZBASNIK, J. P. .... p 1590 N94-19269
ZEHNER, GREGORY F. .... p 1513 N94-19531
ZEISSE, C. R. .... p 1500 N94-19762
ZELKOWITZ, M. .... p 1520 N94-18251
ZEMIRLINE, A. .... p 1552 N94-19393
ZERDA, T. W. .... p 1371 N94-18713
ZHANG, J. .... p 1402 N94-18380
ZHANG, JIMIN .... p 1454 N94-18683
p 1361 N94-18742
ZHANG, JING-SONG .... p 1478 N94-19303
ZHANG, JU .... p 1531 N94-19508
ZHANG, LIN .... p 1476 N94-19045
ZHANG, Q.-P. .... p 1432 N94-18846
ZHANG, QIANG .... p 1419 N94-19025
ZHANG, SHUN-RONG .... p 1486 N94-19255
ZHANG, Y.-Z. .... p 1587 N94-18524
ZHANG, ZIYANG .... p 1565 N94-17776
ZHAO, DAN .... p 1356 N94-17768
p 1356 N94-17769
p 1356 N94-17772
p 1356 N94-17788
p 1356 N94-17789
p 1356 N94-17796
p 1357 N94-17802
p 1357 N94-17803
p 1357 N94-17804
p 1593 N94-17805
ZHAO, J. .... p 1468 N94-19015
ZHAO, PEILING .... p 1332 N94-18760
ZHAO, X. L. .... p 1456 N94-19061
ZHAO, X. P. .... p 1476 N94-19104
ZHAO, XING .... p 1574 N94-18845
ZHARKOV, A. YU. .... p 1548 N94-18175
ZHOU, JIANYING .... p 1439 N94-18614
ZHU, ZUXIANG .... p 1512 N94-18673
ZHUANG, Q. D. .... p 1433 N94-19135
ZHUR, R. A. .... p 1339 N94-17846
ZIJM, W. H. M. .... p 1543 N94-19326
ZIMAND, MARIUS .... p 1561 N94-19481
ZINGARELLI, ROBERT A. .... p 1563 N94-18678
ZINGG, D. W. .... p 1306 N94-18423
ZOCCO, T. G. .... p 1358 N94-17875
ZOSEL, M. E. .... p 1519 N94-18072
ZOWARKA, R. C. .... p 1441 N94-19307
ZUPPERO, ANTHONY .... p 1337 N94-17863
ZUREK, W. H. .... p 1517 N94-17812
ZWEIGLE, G. .... p 1401 N94-18368
ZWIERS, JOB .... p 1390 N94-19267
p 1538 N94-19296

CORPORATE SOURCE INDEX

SCIENTIFIC AND TECHNICAL AEROSPACE REPORTS VOLUME 32 NUMBER 4

Typical Corporate Source Index Listing

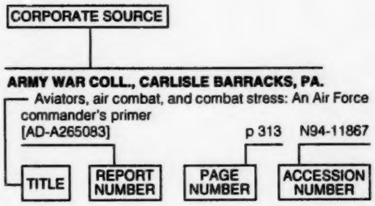
CORPORATE SOURCE
ARMY WAR COLL., CARLISLE BARRACKS, PA.
Aviators, air combat, and combat stress: An Air Force commander's primer
[AD-A265083] p 313 N94-11867
TITLE
REPORT NUMBER
PAGE NUMBER
ACCESSION NUMBER

Listings in this index are arranged alphabetically by corporate source. The title of the document provides the user with a brief description of the subject matter. The report number helps to indicate the type of document cited (e.g., NASA report, translation, NASA contractor report). The accession number denotes the number by which the citation is identified. The page number helps you locate the citation in the abstract section. The titles are arranged under each corporate source in ascending accession number order.

A

ACADEMY OF SCIENCES OF THE ARMENIAN SSR, ERIVAN.
Generalized closures of graphs p 1555 N94-19692
Two problems related to results of Chvatal-Erdoes
p 1555 N94-19693

ADMIRALTY RESEARCH ESTABLISHMENT, GOSPORT (ENGLAND).
Low frequency acoustics of laminated composite axisymmetric structures
[DRA-TM(USGR)-93302] p 1344 N94-19391

ADVISORY GROUP FOR AEROSPACE RESEARCH AND DEVELOPMENT, NEUILLY-SUR-SEINE (FRANCE).
Non Linear Dynamics and Chaos
[AGARD-LS-191] p 1607 N94-18236
High-Lift System Aerodynamics
[AGARD-CP-515] p 1305 N94-18415

AERONAUTICAL RESEARCH INST. OF SWEDEN, STOCKHOLM.
WBNGRID, a program for generation of C-H and C-O topology grids around wing/body/nacelle configurations: User's guide
[FFA-TN-1992-09] p 1311 N94-17721
A study of the influence of a delta wing geometry on the induced drag at transonic speed (M=0.55) and high angles of attack
[FFA-TN-1992-14] p 1311 N94-17722
CFD investigations of the hypersonic double delta wing greta: Sanger project no. 3.2
[FFA-TN-1992-42] p 1311 N94-17919
Spectrum fatigue testing of T-shaped tension clips
[FFA-TN-1992-22] p 1452 N94-17970
Impact response of composite laminates: A guide to closed form solutions
[FFA-TN-1992-33] p 1339 N94-17971
A review of aeronautical fatigue investigations in Sweden during the period May 1991 to April 1993
[FFA-TN-1993-22] p 1457 N94-19358

AERONAUTICAL RESEARCH LABS., MELBOURNE (AUSTRALIA).
Application of the A* algorithm to aircraft trajectory generation
[AD-A268728] p 1317 N94-18315
A wind tunnel model control surface actuator interface
[AD-A268729] p 1322 N94-18324
A benchmark bending test of a thick specimen. Part 1: Experiments
[AD-A268730] p 1360 N94-18325
Applications of the program UIFLOW-2D to the numerical simulation of axisymmetric flows
[AD-A268731] p 1410 N94-18326
Mathematical modelling of bonded fibre-composite repairs to aircraft
[AD-A268732] p 1341 N94-18327

AEROSPACE CORP., EL SEGUNDO, CA.
Broadband RF spectrum from electrostatic discharges on spacecraft
[AD-A269543] p 1385 N94-18287
A RFI measurement system for field sites
[AD-A269340] p 1385 N94-18301
Update on parts SEE susceptibility from heavy ions
[AD-A268735] p 1596 N94-18316
New test method to determine modulus of elasticity of rocket grain material
[AD-A269758] p 1377 N94-18758

AEROSPATIALE, TOULOUSE (FRANCE).
High-lift research: Application to the design of the ATR72 flap p 1309 N94-18442

AIR FORCE ENVIRONMENTAL TECHNICAL APPLICATIONS CENTER, SCOTT AFB, IL.
Cloudiest year study: An analysis of the 3DNEPH and RTNEPH databases
[AD-A269403] p 1490 N94-18281
Station climatic summaries: North America. Volume 1: The contiguous United States
[AD-A269567] p 1490 N94-18303
Station climatic summaries, North America. Volume 2: Alaska, Canada and Greenland
[AD-A269793] p 1493 N94-18732
Eastern Europe: A climatological study
[AD-A269200] p 1493 N94-18883

AIR FORCE FLIGHT TEST CENTER, EDWARDS AFB, CA.
Revision and verification of a seven-point workload estimate scale
[AD-A269194] p 1511 N94-18412

AIR FORCE INST. OF TECH., WRIGHT-PATTERSON AFB, OH.
Introduction to Quantitative Feedback Theory (QFT) technique p 1545 N94-18241
An empirical evaluation of five circular error probable estimation techniques and a method for improving them
[AD-A266528] p 1556 N94-18397
Application of Fourier-based features for classification of synthetic aperture radar imagery
[AD-A270450] p 1387 N94-18513
Carbon/carbon composites coated with SiC by chemical vapor deposition
[AD-A269934] p 1341 N94-18544
Single-transverse-mode, narrow-bandwidth pulsed tunable dye laser with hollow circular intracavity dielectric waveguide
[AD-A270022] p 1439 N94-18614
Research on man-machine productivity in aviation at Human Engineering Institute of Hangzhou University
[AD-A269952] p 1512 N94-18673
The efficiency of continuous output of some titanium-doped gem-crystal lasers has exceeded 1 W
[AD-A269953] p 1439 N94-18674
The activities of equatorial anticyclones of the Western Pacific and the South China Sea and their effects on the tracks of typhoon movement
[AD-A269954] p 1492 N94-18675
Development of a finite element method program for the analysis of laminated composite plates using first-order shear deformation theory
[AD-A270318] p 1342 N94-18700
Optical properties of oxide coatings prepared by ion-assisted deposition
[AD-A270024] p 1599 N94-18711
Dynamic response analysis of composite structural members during missile launch
[AD-A270023] p 1332 N94-18760
Flight test techniques for aircraft parameter estimation in ground effect
[AD-A270058] p 1318 N94-18795
Correlation of incoming boundary layer pitot pressure fluctuations with the unsteadiness of fin-induced shock wave turbulent boundary layer interactions
[AD-A270059] p 1417 N94-18796
An investigation of warm-cloud microphysics using a multi-component cloud model: Interactive effects of the aerosol spectrum
[AD-A270273] p 1493 N94-18812
Cooperative control of multiple space manipulators
[AD-A270291] p 1445 N94-18813
Fuzzy hypergraphs and fuzzy intersection graphs
[AD-A270303] p 1549 N94-18815
Search for lunar water ice in cometary impact craters
[AD-A270130] p 1627 N94-18877
A teaching tool for linear programming
[AD-A270240] p 1523 N94-18905
Some superhigh-frequency and magnetic properties of chemically precipitated films
[AD-A266195] p 1351 N94-19110
A non-homogeneous, spatio-temporal, wavelet multiresolution analysis and its application to the analysis of motion
[AD-A270621] p 1538 N94-19534
OORA Automated Knowledge System (OAKS) code, appendix C
[AD-A270709] p 1531 N94-19573
Total hemispherical emittance of Niobium-1 percent zirconium fuel cladding for the SP-100 space reactor
[AD-A270456] p 1576 N94-19589
Excited atomic bromine energy transfer and quenching mechanisms
[AD-A270672] p 1572 N94-19607
Exponential characteristic spatial quadrature for discrete ordinates neutral particle transport in two-dimensional cartesian coordinates
[AD-A270458] p 1554 N94-19671
On the automation of object-oriented requirements analysis
[AD-A270673] p 1532 N94-19782

AIR FORCE OCCUPATIONAL MEASUREMENT CENTER, RANDOLPH AFB, TX.
Aircrew life support, AFSC 122X0(1T1X1)
[AD-A268998] p 1511 N94-18394

AIR FORCE SYSTEMS COMMAND, VANDENBERG AFB, CA.
California Student Get Away Special Payload GAS-450
p 1324 N94-19164

AIR FORCE SYSTEMS COMMAND, WRIGHT-PATTERSON AFB, OH.
Putting knowledge to use: The acquisition and transfer of knowledge in situated problem solving environments
[AD-A269746] p 1509 N94-18744

AIR WEATHER SERVICE, SCOTT AFB, IL.
New techniques for contrail forecasting
[AD-A269686] p 1490 N94-18573

AKADEMIYA NAUK SSSR, NOVOSIBIRSK.
Generalized energy principle for flute perturbations in axisymmetric mirror machines
[DE93-019399] p 1589 N94-19037

ALABAMA AGRICULTURAL AND MECHANICAL COLL., NORMAL.
Feasibility study: Monodisperse polymer particles containing laser-excitable dyes
[NASA-CR-194280] p 1373 N94-19402

ALABAMA UNIV., HUNTSVILLE.
CRRES experiments, data collection, analysis and publication
[NASA-CR-192419] p 1482 N94-18610
Consortium for materials development in space
[NASA-CR-194411] p 1379 N94-18840
Toward a characterization of the debris cloud created in a hypervelocity impact on a thin plate
[AD-A269190] p 1455 N94-18864
Melt spinning study
[NASA-CR-193823] p 1380 N94-19423

Materials characterization of propellants using ultrasonics
[NASA-CR-193677] p 1378 N94-19494

Synchrotron/crystal sample preparation
[NASA-CR-193837] p 1603 N94-19513

FNAS/summer faculty fellowship research continuation program. Task 6: Integrated model development for liquid fueled rocket propulsion systems. Task 9: Aspects of model-based rocket engine condition monitoring and control
[NASA-CR-194574] p 1338 N94-19706

ALABAMA UNIV., TUSCALOOSA.

Analysis of film cooling in rocket nozzles
[NASA-CR-194674] p 1338 N94-19438

ALENIA AERONAUTICA, NAPLES (ITALY).

Choice and optimization of a high-lift system for an advanced amphibious aircraft p 1310 N94-18447

ALLIED-SIGNAL AEROSPACE CO., KANSAS CITY, MO.

Laser induced damage testing: Equipment and techniques
[DE93-017143] p 1437 N94-18060

AMERICAN SOCIETY OF MECHANICAL ENGINEERS, NEW YORK, NY.

Atomic-scale friction measurements using friction force microscopy. Part 1: General principles and new measurement techniques
[AD-A270749] p 1446 N94-19678

AMES LAB., IA.

A numerical analysis of crack growth in brittle microcracking composites
[DE93-011562] p 1343 N94-18914

Investigation of physical structures and interactions at high energy
[DE93-014444] p 1574 N94-18927

AMSTERDAM UNIV. (NETHERLANDS).

Localization of figure background segregation mechanisms in primate visual cortex
[PB93-187961] p 1508 N94-18121

ANALYTIC SCIENCES CORP., MIDWEST CITY, OK.

The J85 cost/benefit engine study
[AD-A269260] p 1320 N94-18333

ANSER ANALYTIC SERVICES, INC., ARLINGTON, VA.

Corporate Information Management (CIM) report on the simulation processes, version 2.0
[AD-A269119] p 1617 N94-18770

Utilization of Shuttle small payload accommodations in the DOD Space Test Program p 1326 N94-19180

ANTHROPOLOGY RESEARCH PROJECT, YELLOW SPRINGS, OH.

Human integration evaluation of three helmet systems
[AD-A271320] p 1513 N94-19570

APPLIED RESEARCH, INC., HUNTSVILLE, AL.

Automated rendezvous and capture demonstration study
[NASA-CR-192587] p 1331 N94-19366

APPLIED RESEARCH ASSOCIATES, INC., LAKEWOOD, CO.

Aircraft fire sentry. Volume 1: Summary
[AD-A270087] p 1315 N94-18822

Aircraft fire sentry. Volume 2: Appendices A, B, C and D
[AD-A270088] p 1315 N94-18823

APPLIED RESEARCH CORP., LANDOVER, MD.

Detection of accreting gas toward HD 45677: A newly recognized, Herbig Be proto-planetary system
[NASA-CR-189312] p 1621 N94-19288

APPLIED SCIENCE AND TECHNOLOGY, INC., WOBURN, MA.

Materials processing and manufacturing technologies for diamond substrates multichip modules
[AD-A268989] p 1599 N94-18764

ARGONNE NATIONAL LAB., IDAHO FALLS, ID.

Restricting query relaxation through user constraints
[DE93-017413] p 1612 N94-17870

Phenomenological explanation of elastic anomalies in superlattices
[DE93-017475] p 1594 N94-17871

ARGONNE NATIONAL LAB., IL.

The ANL electric vehicle battery R&D program for DOE-EHP
[DE93-017414] p 1394 N94-17750

Title 1 implementation: Status report on nonattainment areas
[DE93-017677] p 1471 N94-17777

Corroboration of magnetic forces in US Maglev design
[DE93-014918] p 1443 N94-17785

A Bayesian approach to contaminant plume delineation
[DE93-012909] p 1472 N94-17890

Setting the global thermostat with an exhaustible tradeable permit system
[DE93-012911] p 1472 N94-17891

Critical technologies for reactors used in nuclear electric propulsion
[DE93-017685] p 1337 N94-17908

Fin-efficiency calculation for condensation in the presence of noncondensable gases
[DE93-017684] p 1409 N94-18004

Elastic properties of a polyimide film determined by Brillouin scattering and mechanical techniques
[DE93-017404] p 1368 N94-18098

Using semantic information for processing negation and disjunction in logic programs
[DE93-017412] p 1614 N94-18099

Performance evaluations of demountable electrical connections
[DE93-017399] p 1396 N94-18135

Development and application of local 3-D x ray CT reconstruction software for imaging critical regions in large ceramic turbine rotors
[DE93-015159] p 1369 N94-18166

Fluid-structure-interaction analyses of reactor vessel using improved hybrid Lagrangian Eulerian code ALICE-II
[DE93-015536] p 1409 N94-18248

Ultrasonic process for destruction of chlorinated organic compounds in aqueous solution
[DE93-015551] p 1348 N94-18249

Study of multi-phase flow characteristics in an MHD power train
[DE93-018570] p 1586 N94-18272

Alternating-phase focusing with amplitude modulation
[DE93-018618] p 1574 N94-18273

The c-jun gene expression in human cells exposed to either ionizing radiation or hydrogen peroxide
[DE93-017436] p 1502 N94-18476

Mechanical properties of fiber-reinforced YBa2Cu3O(x) and Bi2Sr2CaCu2O(x) bars
[DE93-017689] p 1454 N94-18479

Nanostructured materials: Mind over matter
[DE93-017690] p 1597 N94-18480

Performance of the Amorphous Materials Diffractometer GLAD at IPNS
[DE93-017746] p 1430 N94-18481

Photoemission studies of Zn, Co, and Gd substituted YBa2Cu3O(7-delta)
[DE93-017403] p 1597 N94-18498

On-line monitoring of incinerator emissions
[DE93-017406] p 1474 N94-18499

Fabrication and microstructural development of Ag-clad TlBa2Ca2Cu3O(x) tapes
[DE93-017407] p 1597 N94-18500

A comparison of wet and dry scrubbing systems for control of metals and dioxin/furan emissions from incinerators
[DE93-017446] p 1474 N94-18502

The use of chopper spectrometers for cold-to-epithermal neutron scattering at IPNS
[DE93-017798] p 1598 N94-18531

Inverse neutrinoless double (beta)-decay at the NLC?
[DE93-017397] p 1568 N94-18825

Unitary (pi)(pi)N model of N* excitations in (pi)N and (gamma)N reactions
[DE93-017422] p 1568 N94-18826

Quantification of volume flaw sizes in ceramics by image processing of 3D x ray tomographic data sets
[DE93-018573] p 1372 N94-18932

Neutron-induced collision cascade mixing in Nb/V superlattices
[DE93-018575] p 1600 N94-18933

Halo formation in mismatched, space-charge-dominated beams
[DE93-018581] p 1574 N94-18934

Thermal analysis of coatings and substrate materials during a disruption in fusion reactors
[DE93-017688] p 1588 N94-18971

Fabrication and characterization of high-T(sub c) tapes and coils made from Ag-clad Bi-2223 superconductors
[DE93-018615] p 1601 N94-18993

Early experiences with the IBM SP-1
[DE93-018398] p 1535 N94-19010

A least-squares computational tool kit
[DE93-018400] p 1557 N94-19011

Structure-property relationships in radical-cation (electron-donor molecule) and anion-based (including fullerides) organic superconductors and their use in the design of new materials
[DE93-018617] p 1601 N94-19022

Modeling of the formation of microporosity in alloys
[DE93-017733] p 1364 N94-19044

Organic carbonyl compounds in Albuquerque, New Mexico, air: A preliminary study of the effects of oxygenated fuel use
[DE93-017748] p 1476 N94-19045

The p4 Linda: A portable implementation of Linda
[DE93-017752] p 1535 N94-19046

Extraction of Z(prime) coupling data from Z(prime) (yields) jj at the LHC and SSC
[DE93-018576] p 1570 N94-19096

Thermodynamic q-distributions that aren't
[DE93-017385] p 1609 N94-19121

Fabrication, properties, and microstructures of high (Tc) tapes and coils made from Ag-clad Bi-2223 superconductor
[DE93-017405] p 1602 N94-19122

Advances in passive-remote and extractive Fourier transform infrared systems
[DE93-017402] p 1478 N94-19241

Fiber optic Raman spectrograph for in situ environmental monitoring
[DE93-019466] p 1478 N94-19305

The direct synthesis of organic and organometallic-containing MICA-type aluminosilicates
[DE93-019001] p 1373 N94-19321

The electromechanical properties of tetragonal BaTiO3 and PbTiO3 single crystals
[DE93-019008] p 1603 N94-19550

Thermal wave image processing for characterization of subsurface of flaws in materials
[DE93-019024] p 1344 N94-19551

Adsorption analysis of ammonia in an aqueous solution
[DE93-019512] p 1353 N94-19552

Dimensional crossover in the torque in a layered superconductor
[DE93-019544] p 1407 N94-19553

Crossover from BCS to Bose superconductivity: A functional integral approach
[DE93-019503] p 1604 N94-19566

Numerical experiments on the Ginzburg-Landau equations
[DE93-019504] p 1604 N94-19567

ARIZONA STATE UNIV., TEMPE.

In-situ growth monitoring of molecular beam epitaxy processes
[AD-A269287] p 1598 N94-18616

Application of wavelet transform techniques to spread spectrum demodulation and jamming
[AD-A267389] p 1389 N94-19009

Isolation mechanisms in III-V devices
[AD-A271197] p 1605 N94-19717

ARIZONA UNIV., TUCSON.

The land component of the global climate system with adequate spatial resolution
[DE93-018951] p 1474 N94-18183

Space research on organs and tissues
p 1503 N94-19214

Venus lower thermosphere studies
[NASA-CR-193546] p 1629 N94-19418

ARKANSAS UNIV., PINE BLUFF.

Global zones of particle precipitation as observed EXOS-C
[AD-A268758] p 1481 N94-18467

ARMY AEROMEDICAL RESEARCH LAB., FORT RUCKER, AL.

Using controlled daylight exposure and sleep timing in the prevention of shift lag during night operations
[AD-A269304] p 1504 N94-17824

US Army aviation epidemiology data register: Prevalence of refractive error among US aircrew members
[AD-A269550] p 1505 N94-18289

Analysis of seating and restraint limitations restricting total body weight for aircrew and passengers on US Army helicopters
[AD-A269117] p 1511 N94-18296

Laboratory test and evaluation report of the essex model 60C-0037-2 molecular sieve oxygen generating system
[AD-A269967] p 1445 N94-18778

ARMY ARMAMENT RESEARCH, DEVELOPMENT AND ENGINEERING CENTER, PICATINNY ARSENAL, NJ.

Molecular structure of low temperature form of triaminoguanidinium nitrate (TAGN)
[AD-A270409] p 1377 N94-18708

Recent advances in high density tungsten composite processing
[AD-A270764] p 1344 N94-19576

ARMY ARMAMENT RESEARCH, DEVELOPMENT AND ENGINEERING CENTER, WATERVLIET, NY.

Mechanism-dependent fractal character of fracture surfaces in high strength and toughness ASTM A723 steels
[AD-A268956] p 1360 N94-18542

Self-organized criticality and the Barkhausen effect in amorphous and polycrystalline metals
[AD-A269817] p 1361 N94-18735

Increasing mission reliability using open-loop control
[AD-A271208] p 1545 N94-19721

ARMY AVIATION SYSTEMS COMMAND, FORT EUSTIS, VA.

Development and use of computational techniques in Army Aviation research and development programs for crash resistant helicopter technology
p 1459 N94-19469

ARMY COLD REGIONS RESEARCH AND ENGINEERING LAB., HANOVER, NH.
International Symposium on the Ecological Effects of Arctic Airborne Contaminants
[AD-A269955] p 1475 N94-18775
Proceedings: International Symposium on Thermal Engineering and Science for Cold Regions
[AD-A270636] p 1487 N94-19529
Footprint size of a helicopter-borne electromagnetic induction sounding system versus antenna altitude
[AD-A270468] p 1463 N94-19672

ARMY COMMUNICATIONS-ELECTRONICS COMMAND, FORT MONMOUTH, NJ.
Electromagnetic environmental effects compendium
[AD-A270441] p 1387 N94-18512

ARMY CONSTRUCTION ENGINEERING RESEARCH LAB., CHAMPAIGN, IL.
Effects of harmonics on EMI/RFI filters operating under nonlinear loading conditions
[AD-A269559] p 1388 N94-18769

ARMY ENGINEER WATERWAYS EXPERIMENT STATION, VICKSBURG, MS.
Technologies for assessing the geologic and geomorphic history of coasts
[AD-A268780] p 1496 N94-18215
STREMR: Numerical model for depth-averaged incompressible flow
[AD-A269949] p 1417 N94-18672
A finite element scheme for shock capturing
[AD-A270182] p 1417 N94-18755
Environmental characterization for target acquisition. Report 3: New concepts for evaluating low-grazing angle radar measurements
[AD-A269956] p 1388 N94-18777

ARMY LAB. COMMAND, FORT MONMOUTH, NJ.
Low-noise oscillators for airborne radar applications, revision 1
[AD-A269372] p 1403 N94-18471

ARMY MISSILE COMMAND, REDSTONE ARSENAL, AL.
Evaluation of a liquid crystal spatial light modulator capable of amplitude- and phase-modulating modes
[AD-A269252] p 1577 N94-18262
Fast-training algorithm for hidden-layer forward-feed neural networks
[AD-A269253] p 1540 N94-18263
Solar radiation in Saudi Arabia
[AD-A269970] p 1493 N94-18781

ARMY RESEARCH INST. OF ENVIRONMENTAL MEDICINE, NATICK, MA.
Road march performance of special operations soldiers carrying various loads and load distributions
[AD-A269198] p 1512 N94-18882

ARMY RESEARCH LAB., ABERDEEN PROVING GROUND, MD.
Introductory user's guide to the ARL supercomputer facility at Aberdeen Proving Ground
[AD-A265204] p 1514 N94-17877
Techniques for the estimation of Heats of Explosion (HEX) using thermochemical codes
[AD-A268584] p 1609 N94-18310
Parabolized Navier-Stokes computation of surface heat transfer characteristics for supersonic and hypersonic KE projectiles
[AD-A268858] p 1410 N94-18391
Flame structure studies of a lean 20-torr H2/N2O/Ar flame employing molecular beam mass spectrometry
[AD-A268889] p 1349 N94-18456
The effect of crystallographic orientation on the performance of single crystal tungsten subscale penetrators
[AD-A268988] p 1597 N94-18468
Numerical simulation of fluid dynamics and combustion for ram accelerator projectile/obturator interaction
[AD-A269715] p 1320 N94-18748
Mechanical response comparison of gun propellants evaluated under equivalent time-temperature conditions
[AD-A270479] p 1378 N94-19674
Blade and hub loads of ballistically damaged helicopter rotors
[AD-A270663] p 1319 N94-19781

ARMY RESEARCH LAB., ADELPHI, MD.
Some potential errors in satellite wind estimates using the geostrophic approximation and the thermal wind
[AD-A269784] p 1491 N94-18599
Fabrication process for cantilever beam micromechanical switches
[AD-A269716] p 1404 N94-18749

ARMY RESEARCH LAB., FORT MONMOUTH, NJ.
Military applications of high-accuracy frequency standards and clocks
[AD-A269303] p 1430 N94-18299

ARMY RESEARCH LAB., WATERTOWN, MA.
Environmental effects on intermetallic compounds: A guide to the literature
[AD-A269587] p 1359 N94-18306

ARMY RESEARCH LAB., WHITE SANDS MISSLE RANGE, NM.
Dispersion effects on millimeter wavelength attenuation efficiencies for a variety of fibers
[AD-A268992] p 1386 N94-18454
Optical properties of redispersed iron fibers measured at 94 GHz
[AD-A269739] p 1342 N94-18756
Efficiency of fiber dispersion
[AD-A269740] p 1342 N94-18757

ARMY TOPOGRAPHIC ENGINEERING CENTER, FORT BELVOIR, VA.
Directional regions in Geographic Information Systems (GIS)
[AD-A268536] p 1462 N94-18309

ASSISTANT SECRETARY OF DEFENSE (COMMUNICATIONS COMMAND CONTROL AND INTELLIGENCE), WASHINGTON, DC.
Corporate Information Management (CIM) report on the simulation processes, version 2.0
[AD-A269119] p 1617 N94-18770

ASTROPOWER, INC., NEWARK, DE.
Development of large-area monolithically integrated silicon-film photovoltaic modules
[DE93-010037] p 1464 N94-17731

ASULAB S.A., NEUCHATEL (SWITZERLAND).
Accelerated tests on the tarnish resistance of gold alloys p 1367 N94-18008
Electrostatic micrometers: Recent developments and perspectives of uses in clock and watch making
p 1425 N94-18014

ATMOSPHERIC AND ENVIRONMENTAL RESEARCH, INC., CAMBRIDGE, MA.
SERCAA cloud analysis integration: Design concepts and interaction with cloud forecast models
[AD-A269104] p 1492 N94-18637

AUBURN UNIV., AL.
Design of power electronics for TVC EMA systems
[NASA-CR-193839] p 1407 N94-19642

B

BALLISTIC MISSILE DEFENSE PROGRAM OFFICE, WASHINGTON, DC.
Single STAGE Rocket Technology (SSRT) DC-X test program environmental assessment
[AD-A265940] p 1337 N94-17879

BARRON ASSOCIATES, INC., STANDARDSVILLE, VA.
Active control of a multivariable system by way of polynomial neural networks: Computer simulation evaluations and laboratory experimental results
[AD-A270033] p 1541 N94-18790

BATTELLE COLUMBUS LABS., OH.
Studies of dynamic contact of ceramics and alloys for advanced heat engines
[DE93-016366] p 1368 N94-18110
Data collection plan for phase 2 Alternative Fuels Bus Data Collection Program
[DE93-010047] p 1378 N94-18913

BATTELLE MEMORIAL INST., COLUMBUS, OH.
Integrated measurement of crew resource management and technical flying skills
[AD-A270512] p 1510 N94-19677

BDM INTERNATIONAL, INC., MCLEAN, VA.
The intelligent processing of materials
[AD-A269250] p 1362 N94-18923

BELGIAN ROYAL OBSERVATORY, BRUSSELS.
Belgian Royal Observatory Communications, Series A, No. 104, Geophysics Series No. 175
[COMMUNICATIONS-SER-A-104] p 1482 N94-18622
Historical seismicity of Hainaut, Flanders and Artois
p 1482 N94-18623
Current (1985-1988) seismic activity in Belgium: Comparison with historical and instrumental seismic data
p 1482 N94-18624
What can gravimetry contribute to recent and current tectonics in Belgium? p 1482 N94-18626
Current positioning possibilities by spatial techniques and the Royal Oservatory of Belgium program
p 1483 N94-18627
Instrumentation developed at the Royal Observatory of Belgium for measuring slow displacements of the Earth
p 1483 N94-18628

BELL COMMUNICATIONS RESEARCH, INC., LIVINGSTON, NJ.
VLSI implementation of neuromorphic learning networks
[AD-A270825] p 1407 N94-19665

BIOLOGICAL COMPONENTS CORP., MENLO PARK, CA.
Photosynthetic reaction centers as active molecular electronic components, phase 1
[AD-A271388] p 1503 N94-19757

BIOTRONICS TECHNOLOGIES, INC., WAUKESHA, WI.
Transcutaneous Analyte Measuring Methods (TAMM)
[AD-A271387] p 1408 N94-19756

BOEING COMMERCIAL AIRPLANE CO., SEATTLE, WA.
Viscous phenomena affecting high-lift systems and suggestions for future CFD development
p 1308 N94-18433

BOEING DEFENSE AND SPACE GROUP, HUNTSVILLE, AL.
Space transfer concepts and analyses for exploration missions
[NASA-CR-193876] p 1332 N94-18820

BOEING DEFENSE AND SPACE GROUP, SEATTLE, WA.
Coherent transient systems evaluation
[AD-A268808] p 1576 N94-18204
Design, development, and flight evaluation of the Boeing YC-14 USB powered lift aircraft p 1310 N94-18444

BOSTON UNIV., MA.
Research in particle physics
[DE93-040875] p 1567 N94-18534
The effects of magnetic storm phases on f-layer irregularities from auroral to equatorial latitudes
[AD-A267388] p 1486 N94-19008

BRISTOL AEROSPACE LTD., WINNIPEG (MANITOBA).
The first flight of the QUESTS GAS payload G-521
p 1325 N94-19170

BRITISH COLUMBIA UNIV., VANCOUVER.
Formal hardware verification of digital circuits
p 1401 N94-18367

BROOKHAVEN NATIONAL LAB., UPTON, NY.
The design of the MAD Design Program
[DE93-013343] p 1539 N94-17696
SUNRAYCE 1993: Working safely with lead-acid batteries and photovoltaic power systems
[DE93-016553] p 1464 N94-17712
Cost effective energy strategies for the reduction of CO2 emissions in the United States: Country report for ETSAP Annex 4
[DE93-016842] p 1472 N94-17852
Phase transitions and neutron scattering
[DE93-016748] p 1594 N94-17866
KINETIC: A system code for analyzing Nuclear thermal propulsion rocket engine transients
[DE93-016825] p 1337 N94-17884
In vivo animal models of body composition in aging
[DE93-012527] p 1501 N94-17889
Phase separation and ordering process in Al-Li alloys studied by small-angle neutron scattering and neutron diffraction
[DE93-016750] p 1358 N94-17947
Meson production in relativistic heavy-ion collisions at AGS energies
[DE93-016871] p 1565 N94-17984
A superconducting short period undulator for a harmonic generation FEL experiment
[DE93-017581] p 1436 N94-17998
Femtosecond Fourier-transform spectroscopy of low-frequency intermolecular motions in weakly interacting liquids
[DE93-017312] p 1566 N94-18085
Measuring the sea quark polarization
[DE93-015792] p 1566 N94-18234
Overview of physical oceanographic measurements taken during the Mount Mitchell cruise to ROPME sea area
[DE93-018460] p 1497 N94-18494
Simulation of emittance dilution in electron storage ring from Compton backscattering
[DE93-017611] p 1386 N94-18503
Magnetic field measurements of a superconducting undulator for a Harmonic Generation FEL experiment at the NSLS
[DE93-017621] p 1438 N94-18504
Mechanical-property changes of structural composite materials after low-temperature proton irradiation: Implications for use in SSC magnet systems
[DE93-016735] p 1343 N94-18763
Studies of deep levels in high resistivity silicon detectors irradiated by high fluence fast neutrons using a thermally stimulated current spectrometer
[DE93-016133] p 1602 N94-19258
RF phase stabilization for RF photocathode gun through electro-optical monitoring
[DE93-019059] p 1406 N94-19310
Helium isotopic abundance variation in nature
[DE93-019050] p 1487 N94-19477
Search for top quark with D0 detector
[DE93-040170] p 1572 N94-19536
An ab initio Monte Carlo study of low energy positron and electron implantation in elemental metals and multilayers
[DE93-019847] p 1603 N94-19541
The 1982 to 1992 decade of research on the vacuum ultraviolet ring at National Synchrotron Light Source
[DE93-019469] p 1603 N94-19564

Testing of protective coatings in hydrogen
[DE93-040326] p 1375 N94-19651

BURNS (JAY) SCIENTIFIC CONSULTANTS, NORTH INDIATLANTIC, FL.
Anomalous dielectric properties of carbon-black filled elastomers
[AD-A269378] p 1370 N94-18280

BUTLER ANALYSES, TOWSON, MD.
Generalized seismic analysis p 1449 N94-17832

C

CALGARY UNIV. (ALBERTA).
New dynamic FET logic and serial memory circuits for VLSI GaAs technology p 1397 N94-18339

CALIFORNIA INST. OF TECH., PASADENA.
Applications of scanning tunneling microscopy to electrochemistry
[AD-A269129] p 1348 N94-18255
Continuum modeling of materials that can undergo martensitic phase transitions
[AD-A268767] p 1360 N94-18386
The longitudinal free vibrations of a fixed-free two-phase elastic bar
[AD-A268768] p 1453 N94-18387
The temperature at the phase boundary during quasi-static motions of a two-phase thermoelastic bar
[AD-A268769] p 1596 N94-18388
Chemical reactions in turbulent mixing flows
[AD-A269377] p 1410 N94-18472
Scaling laws for diamond chemical vapor deposition. 2: Atomic hydrogen transport
[AD-A269842] p 1371 N94-18740
Scaling laws for diamond chemical vapor deposition. Diamond surface chemistry
[AD-A269874] p 1599 N94-18745
Shock propagation in crustal rock
[AD-A270146] p 1485 N94-18899
Interfacial cracks in plates: A three-dimensional numerical investigation p 1456 N94-19116
The interpretation of optical caustics in the presence of dynamic non-uniform crack-tip motion histories: A study based on a higher order transient crack-tip expansion
[SM91-12] p 1456 N94-19130
The GAMCIT gamma ray burst detector
p 1324 N94-19168

CALIFORNIA POLYTECHNIC STATE UNIV., SAN LUIS OBISPO.
Numerical prediction of transition of the F-16 wing at supersonic speeds
[NASA-CR-194407] p 1312 N94-19433

CALIFORNIA STATE UNIV., LONG BEACH.
Calculation of multielement airfoils and wings at high lift p 1309 N94-18438

CALIFORNIA STATE UNIV., STANISLAUS.
Teaching a computer simulation course with Ada
[AD-A267901] p 1521 N94-18308

CALIFORNIA UNIV., BERKELEY.
Tomographic mathematical ideas applied to radar detection
[AD-A268789] p 1384 N94-18186
FY 1991 AASERT: Spatio-temporal making in human vision and its application to image coding
[AD-A268795] p 1505 N94-18190
Joint services electronics program
[AD-A269383] p 1403 N94-18638
Visual perception of features and objects
[AD-A269879] p 1508 N94-18682
The Fourteenth Symposium on Molecular Beams
[AD-A268721] p 1568 N94-18787
Wave propagation near explosive sources
[AD-A270102] p 1418 N94-18870
Ultraviolet observations of clusters of Wolf-Rayet stars in the SBm3 galaxy NGC 4214 and Ultraviolet and optical observations of LINER's
[NASA-CR-194307] p 1622 N94-19431

CALIFORNIA UNIV., BERKELEY. LAWRENCE BERKELEY LAB.
Reorientation of misfit dislocations during annealing in InGaAs/GaAs(001) interfaces
[DE93-015046] p 1592 N94-17741
RESQme studies for SDC regional computing centers
[DE93-015230] p 1514 N94-17799
A modified direct preconditioner for indefinite symmetric Toeplitz systems
[DE93-015234] p 1516 N94-17800
Three-dimensional simulation analysis of the first sections of a standing-wave free-electron laser two-beam accelerator
[DE93-016977] p 1436 N94-17869
Vortex methods and statistics
[DE93-016974] p 1556 N94-17886
Information technology resources assessment
[DE93-015276] p 1613 N94-17894
Heterogeneous slip and rupture models of the San Andreas fault zone based upon three-dimensional earthquake tomography
[DE93-015037] p 1480 N94-17898
Infrared detection with high-(Tc bolometers and response of Nb tunnel junctions to picosecond voltage pulses
[DE93-016963] p 1595 N94-17989
Energy efficiency and the environment: Innovative ways to improve air quality in the Los Angeles Basin
[DE93-016964] p 1473 N94-18050
Defects in GaAs bulk crystals and multi-layers caused by In diffusion
[DE93-016968] p 1595 N94-18054
Advances and applications of ABCI
[DE93-016971] p 1383 N94-18055
Fundamental studies of the mechanism of catalytic reactions with catalysts effective in the gasification of carbon solids and the oxidative coupling of methane
[DE93-015262] p 1347 N94-18193
Conversion of ethane and of propane to higher olefin hydrocarbons
[DE93-015282] p 1347 N94-18194
The low-temperature specific heat of CeCu2Ge2 at 0 and 9.5 kbar
[DE93-014914] p 1360 N94-18398
Space and time from quantum mechanics
[DE93-015263] p 1609 N94-18629
Extensions of 2D gravity
[DE93-018525] p 1485 N94-18929
Indoor environment program
[DE93-018601] p 1513 N94-18935
Specific heat of La(1.875-x)Nd(x)Sr(0.125)CuO4: Magnetic and structural transitions
[DE93-016978] p 1600 N94-18968
Heavy Ion Fusion Injector Program
[DE93-018706] p 1575 N94-18997
Coherence and linewidth studies of a 4-nm high power FEL
[DE93-018533] p 1441 N94-19030
Three dimensional multipole decomposition of fields
[DE93-018530] p 1389 N94-19053
Chemical dynamics in time and energy space
[DE93-018595] p 1350 N94-19097
Energy Conversion and Storage Program
[DE93-018602] p 1469 N94-19098
Environmental Research Program
[DE93-019101] p 1477 N94-19105
Simulation of the ALS longitudinal multibunch feedback system
[DE93-019227] p 1575 N94-19152
Current-potential characteristics of electrochemical systems
[DE93-040303] p 1352 N94-19192
The PAPAGENO Partonic Monte-Carlo Program
[DE93-018524] p 1571 N94-19247
The Sudbury Neutrino Observatory and the solar neutrino problem
[DE93-018528] p 1629 N94-19260
The microstructural mechanism of electromigration failure in narrow interconnects of Al alloys
[DE93-018598] p 1365 N94-19282
Crossed molecular beam studies of atmospheric chemical reaction dynamics
[DE93-019246] p 1478 N94-19303
Unimolecular photodissociation dynamics of ketene (CH2CO): The singlet/triplet branching ratio and experimental observation of the vibrational level thresholds of the transition-state
[DE93-019252] p 1352 N94-19304
Induction accelerator development for heavy ion fusion
[DE93-019228] p 1591 N94-19479
Metallization and charge-transfer gap closure of transition-metal iodides under pressure
[DE93-040301] p 1353 N94-19538
Study of coupled-bunch collective effects in the ALS
[DE93-019236] p 1575 N94-19558
Transverse beam combiner for ILSE
[DE93-019239] p 1591 N94-19559
The ILSE Experimental Program
[DE93-019247] p 1576 N94-19560
Electrocatalysts for oxygen electrodes
[DE93-040446] p 1354 N94-19653

CALIFORNIA UNIV., DAVIS.
Formal verification of an MMU and MMU cache
p 1400 N94-18366
Variational approaches to CFD: Applications to potential Euler and Navier-Stokes equations
p 1413 N94-18565

CALIFORNIA UNIV., IRVINE.
Generalization of optimal control theory: Linear and nonlinear structures
[PB93-188621] p 1540 N94-18125
Magnetostatic waves-based integrated optic bragg cell modules with applications to RF signal processing
[AD-A269115] p 1577 N94-18295
The identification of the computational significance of key neurobiological characteristics found in a number of telencephalic brain regions
[AD-A269374] p 1505 N94-18407
Metal slurry droplet and spray combustion
[AD-A269648] p 1349 N94-18736

CALIFORNIA UNIV., LOS ANGELES.
Cortical substrate of haptic representation
[AD-A269583] p 1508 N94-18304
Development of the microstructure based stochastic life prediction models
[AD-A269880] p 1454 N94-18683
VLSI for high-speed digital signal processing
[AD-A270406] p 1404 N94-18706
Programmable linear phase digital filters
[AD-A270413] p 1404 N94-18709
Development of the microstructure based stochastic life prediction models
[AD-A270453] p 1455 N94-18714
Development of the microstructure based stochastic life prediction model
[AD-A269742] p 1361 N94-18742
Fundamental properties and device applications of Ge(x)Si(1-x)/Si superlattices (supplemental)
[AD-A269212] p 1600 N94-18884
Physical chemical studies of conducting polymers fundamental and applied
[AD-A270728] p 1374 N94-19574
Quasi-optical transponder using FET's and patch antennas
[AD-A271339] p 1407 N94-19584

CALIFORNIA UNIV., SAN DIEGO, LA JOLLA.
The use of velocity spectra for stacking receiver functions with application to IRIS/IDA stations OBNINSK (OBN) and ARTI (ARU), Russia
[AD-A269087] p 1483 N94-18717
Extrathalamic modulation of cortical function
[AD-A270869] p 1507 N94-19783

CALIFORNIA UNIV., SANTA BARBARA.
Metal/ceramic interfaces: Relationships between structure and chemistry
[AD-A268792] p 1369 N94-18188
Morphology of polymerized membranes on an amorphous substrate at molecular resolution by AFM
[AD-A268760] p 1370 N94-18403
Composites: Materials of the future
[AD-A268945] p 1341 N94-18450
Mesoepitaxy: A universal route to oriented materials
[AD-A270437] p 1598 N94-18511
Office of Naval Research Publications/Patents /Presentations/Honors report, 1 October 1992 - 30 September 1993
[AD-A270037] p 1632 N94-18791
Photodissociation dynamics of cluster ions
[AD-A270296] p 1568 N94-18814
High resolution transmission electron microscopy of mesoporous MCM-41 type materials
[AD-A271271] p 1354 N94-19728
Cooperative formation of inorganic-organic interfaces in the synthesis of silicate mesostructures
[AD-A271196] p 1375 N94-19742

CALIFORNIA UNIV., SANTA CRUZ.
Experimental research in high energy physics
[DE93-011912] p 1574 N94-18916

CARNEGIE-MELLON UNIV., PITTSBURGH, PA.
Optical associative processors and directed graphs
[AD-A268881] p 1615 N94-18224
Dialog-Based Learning (DBL) for adaptive interface agents and programming-by-demonstrations systems
[AD-A269154] p 1540 N94-18261
Why are human-computer interfaces difficult to design and implement?
[AD-A268843] p 1514 N94-18317
The CMU masters in software engineering core curriculum
[AD-A268983] p 1521 N94-18453
A case study in software maintenance
[AD-A269923] p 1521 N94-18659
Efficient transparent optimistic rollback recovery for distributed application programs
[AD-A268981] p 1522 N94-18696
Portable parallel ray tracing algorithms
[AD-A268984] p 1522 N94-18698
Electrokinetic transport of heterogeneous particles in suspensions
[NASA-CR-194476] p 1353 N94-19367
Protocol service decomposition for high-performance networking
[AD-A270613] p 1538 N94-19533
Service without servers
[AD-A270612] p 1515 N94-19591
CVL: A C vector library manual. Version 2
[AD-A270614] p 1531 N94-19592

Surface species in tribology
[AD-A270970] p 1446 N94-19754

CASE WESTERN RESERVE UNIV., CLEVELAND, OH.

Materials flight experiment carrier capability and future flight experiments on Hitchhiker-M carrier program
p 1326 N94-19175

Limited Duration of Candidate Materials Exposure Experiment (LDCE): A Complex Autonomous Payload (CAP) using a Get Away Special (GAS) canister
p 1326 N94-19176

Comparative evaluation of Kirchhoff, perturbation, and full wave methods for rough surface scattering
[AD-A271198] p 1392 N94-19718

CCF S.A., LA CHAUX-DE-FONDS (SWITZERLAND).

Reliability control for wrist watches and their casements p 1427 N94-18030

CENTER FOR MATHEMATICS AND COMPUTER SCIENCE, AMSTERDAM (NETHERLANDS).

Tandem queues with deterministic service times
[PB93-197465] p 1543 N94-19324

CENTRE D'ETUDE SPATIALE DES RAYONNEMENTS, TOULOUSE (FRANCE).

The Cluster Ion Spectroscopy experiment
p 1329 N94-19631

CENTRE DE RECHERCHES SCIENTIFIQUES ET TECHNIQUES DE L'INDUSTRIE DES FABRICATIONS METALLIQUES, BRUSSELS (BELGIUM).

Measuring machines for digitalizing and measuring complex surfaces, models and matrices
[CRIF-MC-97] p 1444 N94-17963

Present evolution of tools management
[CRIF-MC-102] p 1444 N94-17964

The machine reception: A business of experts
[CRIF-MC-94] p 1611 N94-17980

CENTRE EUROPEEN RECHERCHE ET DE FORMATION ADVANCE EN CALCUL SCIENTIFIC, TOULOUSE (FRANCE).

Multidimensional wave decompositions for the Euler equations p 1413 N94-18562

Cell vertex methods for steady inviscid flow
p 1413 N94-18563

CENTRE HOSPITALIER UNIV. RANGUEIL, TOULOUSE (FRANCE).

Causal reasoning for model-based process supervisory control
[LAAS-93241] p 1544 N94-19360

CENTRE NATIONAL D'ETUDES DES TELECOMMUNICATIONS, ISSY-LES-MOULINEAUX (FRANCE).

STAFF (Spatio-Temporal Analysis of Field Fluctuations) experiment for the Cluster mission p 1328 N94-19625

European network for the numerical simulation of space plasmas p 1331 N94-19641

CENTRE NATIONAL D'ETUDES SPATIALES, TOULOUSE (FRANCE).

Computer security. Evolutions 1987 to 1992: Trends and perspectives
[RR-905-I] p 1532 N94-19713

CENTRE NATIONAL DE LA RECHERCHE SCIENTIFIQUE, ORLEANS (FRANCE).

The Wave Experiment Consortium
p 1328 N94-19623

WHISPER: A sounder and high-frequency wave analyser experiment p 1328 N94-19626

CENTRE TECHNIQUE DE L'INDUSTRIE HORLOGERE, BESANCON (FRANCE).

Evaluation of the nickel release by horological products p 1367 N94-18009

Piezo-electric motor: Perspectives and miniaturization
p 1408 N94-18015

Silicon micro-actuator p 1408 N94-18017

CESKOSLOVENSKA AKADEMIE VED, PRAGUE.

Transformation of energy and momentum due to Landau damping in space
[DE93-624921] p 1581 N94-17689

CHICAGO UNIV., IL.

Scientific studies in association with the Shuttle Solar Backscatter Ultraviolet (SSBUV) project
[NASA-CR-193404] p 1630 N94-19437

CHINA NUCLEAR INFORMATION CENTRE, BEIJING.

The effect of surface treatment and gaseous rust protection paper on the atmospheric corrosion stability of aluminium alloy
[DE93-623326] p 1355 N94-17679

CHRISTOPHER NEWPORT COLL., NEWPORT NEWS, VA.

Optical and transport properties of metallic and semiconductor nanostructures
[AD-A270009] p 1598 N94-18609

CHRONOMETER PRUFSTELLE STRALSUNG, GREIFSWALD (GERMANY).

About time p 1426 N94-18024

CHRYSLER TECHNOLOGIES AIRBORNE SYSTEMS, INC., WACO, TX.

Modelling chaotic vibrations using NASTRAN
p 1449 N94-17830

CITIZEN WATCH CO. LTD., TANASHI (JAPAN).

Gear train behavior analyzer using laser beam scanning for watch movement p 1427 N94-18028

Tooth form design supporting system in module design p 1428 N94-18036

Automatic soldering for watch circuit components
p 1428 N94-18037

Development of analog watch with minute repeater
p 1429 N94-18043

CITY COLL. OF THE CITY UNIV. OF NEW YORK, NY.

Tetravalent chromium (Cr(4+)) as laser-active ion for tunable solid-state lasers
[NASA-CR-194528] p 1441 N94-19394

CLARKSON UNIV., POTSDAM, NY.

Oil spreading in surface waters with an ice cover
[PB93-190767] p 1476 N94-19064

CLEMSON UNIV., SC.

Experimental investigation of turbulent Prandtl number and Reynolds analogy in transitional and post-transitional boundary layers
[AD-A270092] p 1418 N94-18867

COAST GUARD RESEARCH AND DEVELOPMENT CENTER, GROTON, CT.

AN/APS-137 Forward Looking Airborne Radar (FLAR) evaluation Spring 1992 experiment
[AD-A268899] p 1384 N94-18228

COASTAL ENGINEERING RESEARCH CENTER, VICKSBURG, MS.

Wind products for use in coastal wave and surge models
[AD-A269753] p 1497 N94-18414

ADCIRC: An advanced three-dimensional circulation model for shelves, coasts, and estuaries. Report 3: Development of a tidal constituent database for the western North Atlantic and Gulf of Mexico
[AD-A268685] p 1497 N94-18455

DYNLET1 model formulation and user's guide
[AD-A269843] p 1498 N94-18723

COLEMAN RESEARCH CORP., ORLANDO, FL.

Earth Penetration Radar Imaging System (EPRIS)
[DE93-019890] p 1391 N94-19542

COLORADO SCHOOL OF MINES, GOLDEN.

Wettability and reaction kinetics in metal matrix composites
[AD-A270377] p 1342 N94-18704

COLORADO STATE UNIV., FORT COLLINS.

Monitoring the response of the upper troposphere/lower stratosphere to a greenhouse gas scenario
[DE93-014509] p 1470 N94-17710

Proton transfer dynamics and cluster ion fragmentation in phenol/ammonia cLusters
[AD-A269133] p 1348 N94-18256

Intracellular physiology of the rat suprachiasmatic nucleus: Electrical properties, neurotransmission and effects of neuromodulators
[AD-A268829] p 1505 N94-18538

Centrifuge modeling of explosion-induced craters in unsaturated sand
[AD-A270194] p 1417 N94-18780

COLORADO UNIV., BOULDER.

Modeling and new equipment definition for the vibration isolation box equipment system
[NASA-CR-193185] p 1379 N94-17763

Growth of structures for integrated optoelectronic devices
[AD-A269014] p 1598 N94-18527

Competitive dynamics and self-organization in photorefractive systems
[AD-A269663] p 1430 N94-18569

Optimal eigenvalue computation on distributed-memory MIMD multiprocessors
[DE93-018337] p 1535 N94-18808

Research on Earth's rotation and the effect of atmospheric pressure on vertical deformation and sea level variability
[NASA-CR-194300] p 1484 N94-18838

A programming paradigm for distributed-memory computers
[DE93-018336] p 1524 N94-19024

Activities of the Center for Space Construction
[NASA-CR-193717] p 1335 N94-19371

Spectrophotometry of emission-line stars in the magellanic clouds
[NASA-CR-194082] p 1628 N94-19425

Gravity and the geoid in the Nepal Himalaya
[NASA-CR-194166] p 1463 N94-19430

COLUMBIA UNIV., NEW YORK, NY.

JSEP fellowship: Fractal noise processes
[AD-A268841] p 1557 N94-18540

Eclipsing cataclysmic variables. Deep eclipses in H0928+501. YY Draconis, the whirling dervish. New x ray pulsar candidates from HEAO-1
[NASA-CR-194027] p 1621 N94-18855

Singularities and symmetries of nonlinear ordinary and partial differential equations
[DE93-040083] p 1550 N94-19190

Calculation of molecular excitation rates
[NASA-CR-193782] p 1571 N94-19236

Tetravalent chromium (Cr(4+)) as laser-active ion for tunable solid-state lasers
[NASA-CR-194529] p 1441 N94-19369

COLUMBIA UNIV. TEACHERS COLL., NEW YORK, NY.

A new approach to the study of the turbulence layer
[NASA-CR-194546] p 1487 N94-19397

COMMITTEE ON SCIENCE, SPACE AND TECHNOLOGY (U.S. HOUSE).

The 1994 NASA authorization, volume 2
[GPO-71-510] p 1620 N94-18842

COMPUTER SOFTWARE MANAGEMENT AND INFORMATION CENTER, ATHENS, GA.

The Twenty-First NASTRAN (R) Users' Colloquium
[NASA-CP-3203] p 1449 N94-17827

COMPUTER TECHNOLOGY ASSOCIATES, INC., PLEASANTVILLE, NJ.

Denver TMA assessment
[NASA-CR-4554] p 1315 N94-18844

CONCORDIA UNIV., MONTREAL (QUEBEC).

Controlling state explosion during automatic verification of delay-insensitive and delay-constrained VLSI systems using the POM verifier p 1400 N94-18365

CONCURRENT TECHNOLOGIES CORP., JOHNSTOWN, PA.

Atlas of formability: Ultimet
[AD-A268352] p 1355 N94-17767

Atlas of formability: HAYNES 556
[AD-A268354] p 1356 N94-17768

Atlas of formability: HAYNES 188
[AD-A268355] p 1356 N94-17769

Atlas of formability: NICKELVAC K-500
[AD-A268351] p 1356 N94-17772

Atlas of formability: Haynes 230
[AD-A268325] p 1356 N94-17788

Atlas of formability: INCONEL 718
[AD-A268350] p 1356 N94-17789

Atlas of formability: Hastelloy C-22
[AD-A268324] p 1356 N94-17796

Atlas of formability: Permalloy - 80 flow stress curves
[AD-A268263] p 1356 N94-17801

Atlas of formability: Nickelvac C-276
[AD-A268264] p 1357 N94-17802

Atlas of formability: Ti-6Al-4V ELI
[AD-A268300] p 1357 N94-17803

Atlas of formability: ALLVAC 718
[AD-A268304] p 1357 N94-17804

Atlas of formability: Waspaloy
[AD-A268323] p 1593 N94-17805

CONNECTICUT UNIV., STORRS.

Multivariate wavelet representations and approximations
[AD-A269350] p 1546 N94-17825

CONSEILRAY S.A., LA CHAUX-DE-FONDS (SWITZERLAND).

Multifunction chronograph movement using a modular structure multimotor p 1429 N94-18044

CORNELL UNIV., ITHACA, NY.

Ceramic films and interfaces: Chemical and mechanical properties
[DE93-018416] p 1369 N94-18163

Potential dependent structural changes of underpotentially deposited copper on an iodine treated platinum surface determined in situ by surface EXAFS and its polarization dependence
[AD-A269890] p 1360 N94-18687

Surface phases and their influence on metal-oxide interfaces
[DE93-019931] p 1601 N94-19020

Experimental study of interactions of highly charged ions with atoms at keV energies
[DE93-040222] p 1571 N94-19257

Analysis of regional deformation and strain accumulation data adjacent to the San Andreas fault
[NASA-CR-194072] p 1487 N94-19428

Suppressed electron-phonon scattering in superlattices
[AD-A270834] p 1604 N94-19597

Evaluation of laser diode based optical switches for optical processors
[AD-A270949] p 1581 N94-19602

CORPS OF ENGINEERS, WASHINGTON, DC.

Ecological and environmental impacts of construction in the coastal zone
[AD-A269196] p 1475 N94-18881

The ecological and environmental impacts of manmade marshes
[AD-A269213] p 1475 N94-18885

D

DARTMOUTH COLL., HANOVER, NH.

The Hall-Petch relationship and mechanisms of fracture in B2 compounds
[DE93-018887] p 1359 N94-18182

DAVID SARNOFF RESEARCH CENTER, PRINCETON, NJ.

High performance YBCO films
[AD-A269090] p 1599 N94-18719

DAYTON UNIV., OH.

Studies on gel electrolyte based on nitrile-butadiene copolymers
[AD-A269450] p 1370 N94-18282

Implementation of a nonisothermal unified inelastic-strain theory into ADINA6.0 for a titanium alloy: User guide
[AD-A269927] p 1360 N94-18660

Electro-optics display research, test, and evaluation laboratory program
[AD-A270947] p 1408 N94-19751

DAYTON UNIV. RESEARCH INST., OH.

Accelerated screening methods for determining chemical and thermal stability of refrigerant-lubricant mixtures. Part 1: Method assessment
[DE93-040215] p 1351 N94-19136

DE HAVILLAND AIRCRAFT CO. OF CANADA LTD., DOWNSVIEW (ONTARIO).

High lift systems for transport aircraft with advanced airfoils p 1310 N94-18446

DEFENCE AND CIVIL INST. OF ENVIRONMENTAL MEDICINE, DOWNSVIEW (ONTARIO).

Effects of a high-energy food supplement on cold-induced thermogenesis
[AD-A269301] p 1504 N94-17823

DEFENCE RESEARCH AGENCY, BEDFORD (ENGLAND).

Comparison between swept and delta canards on a model of a combat aircraft
[AD-A269561] p 1317 N94-17826

DEFENCE RESEARCH AGENCY, FARNBOROUGH (ENGLAND).

Where is high-lift today? A review of past UK research programmes p 1305 N94-18416

An experimental investigation of the optimum slat setting on a combat aircraft model p 1308 N94-18431

An experimental investigation of attachment-line transition on the slat of a combat aircraft model
p 1308 N94-18432

A study of the use of half-models in high-lift wind-tunnel testing p 1308 N94-18434

DEFENCE RESEARCH ESTABLISHMENT ATLANTIC, DARTMOUTH (NOVA SCOTIA).

BACKSCATTER.FOR: A program to calculate the backscattering strength of an inhomogeneous seabed
[AD-A269235] p 1499 N94-18910

DEFENCE RESEARCH ESTABLISHMENT VALCARTIER (QUEBEC).

Analytic approximations of an integral in remote sensing
[AD-A270085] p 1463 N94-18800

DEFENSE ADVANCED RESEARCH PROJECTS AGENCY, ARLINGTON, VA.

White House technology reinvestment project: Briefing and transcripts
[PB93-169829] p 1611 N94-18090

DEFENSE NUCLEAR AGENCY, WASHINGTON, DC.

Radio wave propagation in structured ionization for satellite and radar applications
[AD-A268457] p 1382 N94-17844

DEFENSE TECHNICAL INFORMATION CENTER, ALEXANDRIA, VA.

Defense Technical Information Center thesaurus
[AD-A268855] p 1615 N94-18319

Handbook for users
[AD-A268726] p 1615 N94-18323

Department of Defense Gateway Information System (DGIS) users' guide
[AD-A270140] p 1617 N94-18752

Learning about the Internet bibliography and beginner's guide
[AD-A268847] p 1532 N94-19707

DELAWARE UNIV., NEWARK.

Spectral analysis on the canonical autoregressive decomposition
[AD-A270083] p 1549 N94-18798

Radial evolution of the solar wind turbulence with application to charged particle transport
[NASA-CR-194061] p 1629 N94-19427

DELTA INFORMATION SYSTEMS, INC., HORSHAM, PA.

Color test chart for facsimile
[AD-A269754] p 1387 N94-18721

DEPARTMENT OF ENERGY, OAK RIDGE, TN.

Summaries of FY 1993 research in the chemical sciences
[DE93-011855] p 1632 N94-18915

DEPARTMENT OF ENERGY, WASHINGTON, DC.

Fuel cell systems program plan, fiscal year 1993
[DE93-017828] p 1466 N94-18103

Safeguarding our energy future
[DE93-016001] p 1466 N94-18109

Report to Congress: Comprehensive Program Plan for Advanced Turbine Systems
[DE93-016718] p 1467 N94-18475

Trends in Information Management at Department of Energy Headquarters
[DE93-017197] p 1615 N94-18496

Emerging technologies planning guide, 1993 edition
[DE93-017196] p 1616 N94-18689

Environmental restoration and waste management five-year plan, fiscal years 1994-1998. Volume 3: Public concerns
[DOE/S-00097P-VOL-3] p 1475 N94-18835

Review Committee report on the conceptual design of the tokamak physics experiment
[DE93-018408] p 1588 N94-19012

National Program Plan Fuel Cells in Transportation
[DE93-017557] p 1469 N94-19346

DEPARTMENT OF THE NAVY, WASHINGTON, DC.

Precision digitally-controlled variable attenuation circuit
[AD-D015862] p 1394 N94-17703

Lift enhancement device
[AD-D015868] p 1317 N94-17704

Electrically controlled liquid-crystal heat valve
[AD-D015872] p 1443 N94-17705

Polarized thin films from dye-substituted polymers containing hydrophobically terminated stilbazolium radicals
[AD-D015873] p 1367 N94-17706

Extending bandwidth of optical emitters using active matching technique
[AD-D015875] p 1394 N94-17707

Variable wide band fiber optic delay line
[AD-D015848] p 1576 N94-17716

Friction drive position transducer
[AD-D015851] p 1424 N94-17717

Mixed polymer electrolyte and mixed polymer electrolyte battery
[AD-D015856] p 1394 N94-17718

Polyurethane self-priming topcoats
[AD-D015870] p 1367 N94-17719

Suppression of backscatter and stray reflection induced phase noise in Michelson interferometers
[AD-D015809] p 1382 N94-17902

Plasma klystron amplifier
[AD-D015819] p 1395 N94-17903

Fluid dynamometer having fluid characteristic power absorption adjustment capability
[AD-D015820] p 1424 N94-17904

Process for applying high application-temperature coating to heat-sensitive aluminum alloys
[AD-D015823] p 1368 N94-17905

Polymerizable lipids in the development of controlled release carriers
[AD-D015789] p 1368 N94-17982

Optically controlled active impedance element and filters employing the same
[AD-D015863] p 1396 N94-18062

Process for preparing thermoplastic composites
[AD-D015864] p 1339 N94-18074

An ultraviolet faraday rotator glass
[AD-D015879] p 1371 N94-18529

High spatial resolution, range gated, underwater imaging method and apparatus
[AD-D015882] p 1430 N94-18530

Conductive garments to prevent Radio-Frequency (RF) burns
[AD-D015832] p 1512 N94-18730

Photodetector array having high pixel density
[AD-D015859] p 1432 N94-18731

Monolithic low noise preamplifier for piezoelectric sensors
[AD-D015860] p 1563 N94-18734

Apparatus and method for varying a Bragg wavelength of a Bragg grating formed in an optical fiber
[AD-D015876] p 1579 N94-18743

Diamond brazed to a metal
[AD-D015877] p 1371 N94-18746

Tunable ytterbium-doped solid state laser
[AD-D015878] p 1440 N94-18747

Improved optical pseudospark switch
[AD-D015821] p 1580 N94-18947

Transducers and method for making same
[AD-D015949] p 1408 N94-19759

Polarized optical emission due to decay or recombination of spin-polarized injected carriers
[AD-D015907] p 1408 N94-19763

DEUTSCHE AIRBUS G.M.B.H., BREMEN (GERMANY).

High-lift design for large civil aircraft
p 1310 N94-18445

DEUTSCHE FORSCHUNGSANSTALT FUER LUFT- UND RAUMFAHRT, BERLIN (GERMANY).

Application of fractal methods to estimate the aerosol-optical depth for atmospheric correction of high resolution satellite data
[DLR-FB-93-04] p 1480 N94-18088

DEUTSCHE FORSCHUNGSANSTALT FUER LUFT- UND RAUMFAHRT, BRUNSWICK (GERMANY).

Development and test of readout electronics for optical quadrature signals
[DLR-MITT-92-11] p 1395 N94-17920

Investigation of a matrix-model for the artificial dissipation in a cell vertex finite volume scheme for solving the Navier-Stokes equations
[DLR-FB-92-33] p 1409 N94-18076

About the accuracy of an image-based navigation system during the runway approach
[DLR-MITT-93-01] p 1316 N94-18146

Numerical calculations of high lift flows using structured and unstructured methods p 1307 N94-18428

DEUTSCHE FORSCHUNGSANSTALT FUER LUFT- UND RAUMFAHRT, COLOGNE (GERMANY).

Development of a selective volumetric receiver for central receiver systems: Investigation of parameters and exergetic evaluation
[DLR-FB-93-05] p 1465 N94-18089

Strength optimization of C/Al metal matrix composites produced from prepregs
[DLR-FB-92-39] p 1340 N94-18122

Transport policy options for reducing noise at airports; Hamburg airport taken as an example
[DLR-FB-92-40] p 1322 N94-18123

DEUTSCHE FORSCHUNGSANSTALT FUER LUFT- UND RAUMFAHRT, GOETTINGEN (GERMANY).

On the use of differential GPS for automatic approach and landing of space and aircraft
[DLR-MITT-93-05] p 1316 N94-17921

On memory effects in turbulence
[DLR-FB-93-03] p 1409 N94-18124

DEUTSCHE FORSCHUNGSANSTALT FUER LUFT- UND RAUMFAHRT, OBERPFAFFENHOFEN (GERMANY).

The accuracy of monostatic and bistatic radar imaging by range-Doppler-processing with and without motion compensation
[DLR-FB-93-07] p 1384 N94-18071

Direct and large eddy simulation of turbulence: Summary of the state of the art 1993 p 1416 N94-18594

Large-eddy simulation of turbulent diffusion in stably stratified shear flow p 1416 N94-18595

Numerical simulation of turbulent convective flow over wavy terrain p 1416 N94-18596

DEUTSCHE FORSCHUNGSANSTALT FUER LUFT- UND RAUMFAHRT, STUTTGART (GERMANY).

Electrically excited CO-lasers with gas dynamic cooling
[DLR-FB-93-08] p 1437 N94-18061

DISTRICT OF COLUMBIA UNIV., WASHINGTON, DC.

System dynamics and computer modeling expertise. A conceptual structure research inquiry
[AD-A269860] p 1560 N94-18410

DORNIER LUFTFAHRT G.M.B.H., FRIEDRICHSHAFEN (GERMANY).

Calculation of maximum and high lift characteristics of multi element aerofoils p 1305 N94-18419

DREXEL UNIV., PHILADELPHIA, PA.

A comprehensive study of matrix fracture mechanisms in fiber-reinforced ceramic matrix composites
[AD-A268809] p 1340 N94-18205

DUKE UNIV., DURHAM, NC.

Implementation of parallel algorithms
[AD-A271035] p 1539 N94-19682

E

EARL AND WRIGHT, SAN FRANCISCO, CA.

Fatigue technology assessment and strategies for fatigue avoidance in marine structures. Appendices
[AD-A269053] p 1455 N94-18716

EARTH NEWS, TITUSVILLE, FL.

Your GAS experiment and the media or why does that other can get all of the publicity? p 1327 N94-19182

EAST CAROLINA UNIV., GREENVILLE, NC.

Evaluation of dried storage of platelets for transfusion: Physiologic integrity and hemostatic functionality
[AD-A270756] p 1507 N94-19593

ECODYNAMICS RESEARCH ASSOCIATES, INC., DENVER, CO.

Multigrid methods for flow transition in three-dimensional boundary layers with surface roughness
[NASA-CR-4540] p 1417 N94-18843

ECOLE CENTRALE DE LYON (FRANCE).

Experimental contribution to the contact between two bodies and the effect of roughness
[ECL-91-41] p 1451 N94-17918

Contribution to the study of the additional losses in coil elements used in static converters
[ECL-92-60] p 1406 N94-19297

Study of GaAs substrates by ambient temperature photoluminescence imagery
[ECL-92-61] p 1603 N94-19357

Construction of a tension-torsion anisotropic brittle damage elastic model
[ECL-91-27] p 1457 N94-19375

Experimental study of flame front interactions
[ECL-91-40] p 1353 N94-19376

Numerical analysis of pressure meter tests: Application of parameter identification of soils behavior
[ECL-92-52] p 1487 N94-19380

Theoretical study and modelling of homogeneous turbulence under rotation for implantation in a code for solving Navier-Stokes equations
[ECL-93-05] p 1420 N94-19381

Simulation of three dimensional unsteady viscous flows in turbomachines
[ECL-92-15] p 1420 N94-19398

Numerical simulations of turbulent buoyant flows by finite element method: Application to the study of strongly heated or cooled stratified flow
[ECL-92-28] p 1421 N94-19399

Formulation and identification of the anisotropic laws for thin sheets drawing
[ECL-92-55] p 1365 N94-19400

Time dependent identification of nonlinear structures
[ECL-92-64] p 1457 N94-19403

Physico chemical and mechanic approach of lubricating properties of graphite + additive powders
[ECL-93-02] p 1373 N94-19405

Construction of a scanning tunneling microscope in liquid media: Studies of the preparation of the graphite surface and the chemical cleaning of indium phosphide
[ECL-92-25] p 1353 N94-19406

On the numerical analysis of nonlinear Galerkin methods: Spectral approximation and finite elements
[ETN-93-94900] p 1552 N94-19407

Contribution to the modelling and the identification of nonlinear mechanical systems
[ECL-92-32] p 1529 N94-19409

Contribution to the identification of nonlinear behavior laws in material mechanics
[ECL-92-36] p 1458 N94-19411

Numerical simulation of acoustic waves propagation in turbulent media
[ECL-92-37] p 1563 N94-19413

Contribution to the tribological study of magnetic-tape head contact
[ECL-92-57] p 1434 N94-19414

Ni-Al2O3 solid state binding: Elaboration, state of thermal constraints, mechanical behavior
[ECL-92-31] p 1366 N94-19436

Reanalysis of structure models
[ECL-93-07] p 1458 N94-19460

Contribution to the study of a symmetric film flow (with or without tensio-active elements)
[ECL-93-13] p 1421 N94-19461

ECOLE D'INGENIEURS DU CANTON DE NEUCHATEL (SWITZERLAND).

Universal measurement device for electronic watches and small clocks p 1427 N94-18029

EDGERTON, GERMESHAUSEN AND GRIER, INC., IDAHO FALLS, ID.

The Intense Slow Positron Source concept: A theoretical perspective on a proposed INEL Facility
[DE93-013675] p 1564 N94-17738

Rapid geophysical surveyor
[DE93-016637] p 1461 N94-17851

EDGEWOOD ARSENAL, ABERDEEN PROVING GROUND, MD.

Shell designs
[AD-A270656] p 1460 N94-19606

EG AND G ENERGY MEASUREMENTS, INC., IDAHO FALLS.

Mission needs and system commonality for space nuclear power and propulsion
[DE93-016557] p 1337 N94-17863

Document control and conduct of operations
[DE93-016555] p 1613 N94-17880

EG AND G ROCKY FLATS, INC., GOLDEN, CO.

Effect of internal heating during hot compression testing on the stress-strain behavior and hot working characteristics of alloy 304L
[DE93-012701] p 1362 N94-18917

EIC, INC., NORWOOD, MA.

Fiber optic Raman spectrograph for in situ environmental monitoring
[DE93-019466] p 1478 N94-19305

EMORY UNIV., ATLANTA, GA.

Nitridation of GaAs(100) by laser-induced decomposition of HN3
[AD-A269147] p 1438 N94-18258

ENERGY INFORMATION ADMINISTRATION, WASHINGTON, DC.

Directory of Energy Information Administration Models 1993
[DE93-016987] p 1616 N94-18707

EIA publications directory, 1992
[DE93-016833] p 1617 N94-18983

ENVIRONMENTAL RESEARCH INST. OF MICHIGAN, ANN ARBOR.

Arctic ice studies
[AD-A268608] p 1497 N94-18277

Image reconstruction from interferometer data
[AD-A268463] p 1578 N94-18383

EPSON CORP., SUWA (JAPAN).

A study of the automatic generating system. 3: Improvement of the total system performance
p 1429 N94-18040

Development of a new concept diver's watch
p 1429 N94-18041

ETA S.A., GRENCHEN (SWITZERLAND).

Electric measurement of Lavet motors
p 1408 N94-18022

Swatch Pager p 1428 N94-18039

Quartz analog watch with perpetual calendar
p 1429 N94-18042

EUROPEAN SPACE AGENCY, PARIS (FRANCE).

Report on the activities of Space Science Department, 1990 - mid 1992
[ESA-SP-1161] p 1633 N94-19404

Cluster: Mission, Payload, and Supporting Activities
[ESA-SP-1159] p 1328 N94-19622

EUROPEAN SPACE AGENCY. EUROPEAN SPACE OPERATIONS CENTER, DARMSTADT (GERMANY).

Cluster ground segment and mission operations
p 1330 N94-19636

The Cluster orbit and mission scenario
p 1330 N94-19637

EUROPEAN SPACE AGENCY. EUROPEAN SPACE RESEARCH AND TECHNOLOGY CENTER, ESTEC, NOORDWIJK (NETHERLANDS).

Attitude sensor package p 1325 N94-19172

Environmental control and life support
[ESA-PSS-03-40-ISSUE-1] p 1513 N94-19442

Rationale for the power standard
[ESA-PSS-02-10-VOL-2-ISSUE-] p 1338 N94-19516

The Cluster spacecraft p 1330 N94-19635

The Cluster science data system: A distributed system to serve a wide international community
p 1330 N94-19638

EUROSIL G.M.B.H., ECHING (GERMANY).

New current reduction system for watches with integrated current regulation motors
p 1428 N94-18034

EVOLVING TECHNOLOGIES CORP., NEW YORK, NY.

VPU(tm) demonstration mission vicinity processor unit(tm) overview p 1325 N94-19171

F

FEDERAL AVIATION ADMINISTRATION, ATLANTIC CITY, NJ.

VMC left turn curved approaches, test results
[AD-A269476] p 1316 N94-18728

Vertical drop test of a Metro 3 aircraft
[AD-A270032] p 1318 N94-18789

The FAA Technical Center Human Factors Laboratory information guide
[AD-A269343] p 1513 N94-18992

FEDERAL AVIATION ADMINISTRATION, OKLAHOMA CITY, OK.

Advisory circular: Index of articles (materials, parts, processes, and appliances) certified under the technical standard order system
[AC-20-36S] p 1618 N94-19377

FEDERAL AVIATION ADMINISTRATION, WASHINGTON, DC.

Terminal area forecasts, FY 1993-2005
[AD-A269855] p 1316 N94-18336

Airport activity statistics of certificated route air carriers, 1992
[AD-A269042] p 1315 N94-18490

FEDERAL INFORMATION EXCHANGE, INC., GAITHERSBURG, MD.

FEDIX on-line information service: Design, develop, test, and implement an on-line research and education information service
[DE93-018818] p 1614 N94-18181

FERMI NATIONAL ACCELERATOR LAB., BATAVIA, IL.

Pulsed LASER for testing silicon strip detectors
[DE93-017816] p 1436 N94-17883

Comparison of ferrite materials for pulse applications
[DE93-017224] p 1574 N94-18497

Effects of transverse coupling on transverse beam size, simulation and measurements
[DE93-017804] p 1574 N94-18972

Charmonium physics from (bar p)p interactions
[DE93-017809] p 1569 N94-18973

A multi-thread approach to coalescing small transfers generated by portable tool sets
[DE93-012128] p 1525 N94-19186

FLORIDA ATLANTIC UNIV., BOCA RATON.

Fundamental research in nonlinear random vibration for aerospace applications
[AD-A268929] p 1454 N94-18487

FLORIDA INST. OF TECH., MELBOURNE.

Full Boltzmann discrete spectral wave model, implementation and nondimensional tests
[AD-A269885] p 1498 N94-18685

FLORIDA STATE UNIV., TALLAHASSEE.

Experimental consequences of supersymmetry
[DE93-018270] p 1569 N94-18945

High energy physics program. Task A: Experiment and theory. Task B: Numerical simulation
[DE93-018140] p 1575 N94-19050

Problems in probability, statistics and reliability
[AD-A270830] p 1559 N94-19595

FLORIDA UNIV., EGLIN AFB.

Interferometer stations at the Air Force Aeroballistic Research Facility
[AD-A268776] p 1322 N94-18330

FLORIDA UNIV., GAINESVILLE.

Several fundamental issues in the mechanics of inelastic behavior
[AD-A269455] p 1453 N94-18285

Software engineering for effective utilization of parallel processing computing system
[AD-A269191] p 1535 N94-18865

Polymer films with enhanced dielectric properties
[AD-A271148] p 1375 N94-19740

FOKKER B.V., SCHIPOL-OOST (NETHERLANDS).

Forty years of high-lift R/D: An aircraft manufacturer's experience p 1309 N94-18441

FOOD AND DRUG ADMINISTRATION, ROCKVILLE, MD.

A study of the effects of high power pulsed 2450 MHz microwaves, ELF modulated microwaves, and ELF fields on human lymphocytes and selected cell lines
[AD-A269070] p 1505 N94-18294

FORD MOTOR CO., DEARBORN, MI.

Numerical simulation of vehicle crashworthiness and occupant protection p 1459 N94-19471

FRAUNHOFER INST. FUER WERKSTOFFMECHANIK, FREIBURG (GERMANY).

Experimental investigation of wave and fracture phenomena in impacted ceramics: Experiments on sapphire
[AD-A270040] p 1372 N94-18792

FUSION PHYSICS AND TECHNOLOGIES, TORRANCE, CA.

Advanced fusion diagnostics
[DE93-040085] p 1589 N94-19133

G

GENERAL ACCOUNTING OFFICE, WASHINGTON, DC.

Naval aviation: Consider all alternatives before proceeding with the F/A-18E/F
[AD-A269302] p 1305 N94-18279

NASA aeronautics: Protecting sensitive technology. Report to Congressional requesters
[GAO/NSIAD-93-201] p 1617 N94-18848

Software reuse: Major issues need to be resolved before benefits can be achieved. Report to the Chairman, Subcommittee on Defense, Committee on Appropriations, House of Representatives
[GAO/IMTEC-93-16] p 1532 N94-19716

GENERAL ATOMIC CO., SAN DIEGO, CA.

Limits on m = 2, n = 1 error field induced locked mode instability in TPX with typical sources of poloidal field coil error field and a proto type correction coil, C-coil
[DE93-014408] p 1582 N94-17702

Analysis of the ITER H-mode confinement database
[DE93-016984] p 1585 N94-18056

Coupled MHD and transport analysis of improved confinement D3-D discharges
[DE93-016985] p 1585 N94-18057

Dependence of helium transport on plasma current and ELM frequency in H-mode discharges in D3-D
[DE93-016986] p 1585 N94-18058

GENERAL ELECTRIC CO., HOUSTON, TX.

A noniterative improvement of Guyan reduction
p 1449 N94-17833

A methodology to model physical contact between structural components in NASTRAN
p 1450 N94-17836

GENERAL ELECTRIC CO., SCHENECTADY, NY.
Factors which affect fatigue strength of fasteners
[DE93-017272] p 1453 N94-18084
GENERAL MOTORS CORP., WARREN, MI.
Directions for computational mechanics in automotive crashworthiness p 1459 N94-19472
GENERAL MOTORS RESEARCH LABS., WARREN, MI.
Pressure and temperature effects on the kinetics and quality of diamond films
[AD-A270876] p 1606 N94-19771
GENERAL SERVICES ADMINISTRATION, WASHINGTON, DC.
Current information technology resource requirements of the federal government: Fiscal year 1994
p 1612 N94-17756
GEO-CENTERS, INC., FREDERICK, MD.
Review of short-term, high-level exposure to metals: Antimony, barium, and cadmium
[AD-A268896] p 1505 N94-18392
GEORGE WASHINGTON UNIV., WASHINGTON, DC.
Space Life Sciences Research: The Importance of Long-Term Space Experiments
[NASA-TM-4502] p 1502 N94-19210
GEORGIA INST. OF TECH., ATLANTA.
Viscosity in the edge of tokamak plasmas
[DE93-018039] p 1588 N94-18988
Supercritical thermodynamics of sulfur and nitrogen species
[DE93-041221] p 1610 N94-19670
GEORGIA STATE UNIV., ATLANTA.
Heavy ion nuclear physics research
[DE93-018862] p 1565 N94-17776
GEORGIA TECH RESEARCH INST., ATLANTA.
Field emission cathode and vacuum microelectronic microwave amplifier development
[AD-A269526] p 1403 N94-18639
GOSUDARSTVENNYI KOMITET PO ISPOLZOVANIYU ATOMNOI ENERGII, OBNINSK (USSR).
Effect of oxygen concentration and ordering on vanadium-oxygen alloy vibrational spectra
[DE93-627003] p 1355 N94-17692
GOSUDARSTVENNYI KOMITET PO ISPOLZOVANIYU ATOMNOI ENERGII, SERPUKHOV (USSR).
About structurally stable generating mechanism for invariant hyperbolic sets
[DE93-629858] p 1561 N94-18150
Path integrals on warped product manifolds
[DE93-629859] p 1561 N94-18151
Four-fermion interactions
[DE93-629905] p 1566 N94-18199
Crystal optics of high energy gamma-beams
[DE93-630228] p 1577 N94-18217
GRENOBLE-1 UNIV. (FRANCE).
Object-oriented extension of a relational DBMS
[ETN-93-94403] p 1519 N94-17978
A model and an execution mechanism for active data bases
[ETN-93-94404] p 1614 N94-17979
Contribution to the analysis of tableaus based decision methods
[ETN-93-94355] p 1560 N94-18067
Numerical analysis of proximal methods: Decomposition and parallelization
[ETN-93-95017] p 1552 N94-19362
Multimodal image correlation applied to computer aided pedicular screwing
[ETN-93-95018] p 1528 N94-19363
Modelization, numerical simulation and optimal control of NET tokamak plasma configuration evolution for the future generation of fusion reactors
[ETN-93-95019] p 1591 N94-19364
On the numerical approximation of nonlinear hyperbolic problems: Application to the dynamics of compressible gas
[ETN-93-95020] p 1420 N94-19365
Managing persistent objects: From the programming language to the system
[ETN-93-95021] p 1529 N94-19368
Contribution to applications systems design MOSAIC method in the Aristote project
[ETN-93-95022] p 1529 N94-19370
On network representation of the solutions in combinatorial optimization
[RR-910-I] p 1552 N94-19392
A perfection-preserving operation
[RR-911-I] p 1552 N94-19393
Neighbourhood-perfect line graphs
[RR-915-I] p 1552 N94-19395
Progress in edge detection
[RR-914-I] p 1529 N94-19396
On the computation of versal family of matrices
[RR-892-M] p 1532 N94-19712
Geometric contact for curves and surfaces
[RR-893-M] p 1556 N94-19731
GRUMMAN AEROSPACE CORP., BETHPAGE, NY.
Navier-Stokes simulation of flow field around a blown-flap high-lift system p 1307 N94-18429
Impact analysis of composite aircraft structures
p 1458 N94-19468
GTE LABS., INC., WALTHAM, MA.
Analytical and experimental evaluation of joining silicon nitride to metal and silicon carbide to metal for advanced heat engine applications
[DE93-018128] p 1446 N94-19291

H

HAHN-SCHICKARD-INST. FUER MIKRO- UND INFORMATIONSTECHNIK, VILLINGEN-SCHWENNINGEN (GERMANY).
Process and quality on-line control in laser welding
p 1426 N94-18020
HAMPTON UNIV., VA.
Plasma-puff initiation of high Coulomb transfer switches
[NASA-CR-193186] p 1591 N94-19441
HANCOCK (THOMAS), HUNTSVILLE, AL.
Static Computer Memory Integrity Testing (SCMIT): An experiment flown on STS-40 as part of GAS payload G-616 p 1325 N94-19169
HARRIS CORP., MELBOURNE, FL.
Photorefractive receiver study
[AD-A269352] p 1577 N94-18302
Radiation hardened microprocessor for small payloads
p 1327 N94-19184
HARRIS CORP., ROCHESTER, NY.
Improved HF data network simulator, volume 1
[AD-A270953] p 1393 N94-19752
Improved HF data network simulator, software user's manual, volume 2
[AD-A270954] p 1393 N94-19753
HARVARD UNIV., CAMBRIDGE, MA.
Tunneling microscopy of semiconductors
[AD-A270232] p 1600 N94-18904
HAWAII UNIV., MANOA.
Photosynthetic responses to the environment, volume 8
[AD-A269584] p 1502 N94-18305
HELSINKI UNIV. OF TECHNOLOGY, ESPOO (FINLAND).
APLAC: An object-oriented analog circuit simulator and design tool. 6.1 reference manual
[PB93-187193] p 1396 N94-18091
Waveguide and resonator perturbation techniques for measuring chirality and non-reciprocity of biisotropic materials
[PB93-187243] p 1384 N94-18116
Cut and paste based modeling with boundary features
[PB93-187250] p 1520 N94-18117
Weakened negative introspection in autoepistemic reasoning
[PB93-187375] p 1520 N94-18118
EDMS: Engineering data management system. User's reference
[PB93-187391] p 1614 N94-18119
Thermodynamic theory of exergy analysis
[PB93-187647] p 1607 N94-18120
Polymer technology publication. Series no. 14, 1993
[PB93-195964] p 1372 N94-19052
Finding the strong components in a directed graph
[PB93-187342] p 1555 N94-19708
HEWLETT-PACKARD CO., CORVALLIS, OR.
SPROC: A multiple-processor DSP IC
p 1398 N94-18347
Systolic array IC for genetic computation
p 1400 N94-18361
HOUSTON UNIV., CLEAR LAKE, TX.
NASA Electronic Library System (NELS) optimization
[NASA-CR-193688] p 1617 N94-18839
Advanced software development workstation: Object-oriented methodologies and applications for flight planning and mission operations
[NASA-CR-193706] p 1513 N94-19349
HOUSTON UNIV., TX.
Decoherence and recoherence of beam in phase space
[DE93-014885] p 1573 N94-17784
Direct kinematics solution architectures for industrial robot manipulators: Bit-serial versus parallel
p 1399 N94-18358
High order non-oscillatory schemes for the compressible Euler equations p 1412 N94-18558
A multigrid acceleration technique for computing steady solutions to the equations of compressible flow
p 1412 N94-18559
HUGHES AIRCRAFT CO., TORRANCE, CA.
RF vacuum microelectronics
[AD-A269454] p 1396 N94-18284
HUGHES DANBURY OPTICAL SYSTEMS, INC., CT.
Impact of shorter wavelengths on optical quality for laws
[NASA-CR-193873] p 1579 N94-18858
HUGHES RESEARCH LABS., MALIBU, CA.
Electro-optic beam steering using non-linear organic materials
[AD-A270809] p 1374 N94-19577
HUMAN RESOURCES RESEARCH ORGANIZATION, ALEXANDRIA, VA.
Building a joint-service classification research roadmap: Criterion-related issues
[AD-A269735] p 1512 N94-18754

I

IDAHO UNIV., MOSCOW.
The 1991 3rd NASA Symposium on VLSI Design
[NASA-CR-194589] p 1397 N94-18337
Automated ILA design for synchronous sequential circuits p 1397 N94-18340
An SEU immune logic family p 1398 N94-18342
Cellular logic array for computation of squares
p 1398 N94-18343
Fault tolerant sequential circuits using sequence invariant state machines p 1398 N94-18344
Performance of defect-tolerant set-associative cache memories p 1398 N94-18346
An extended Reed Solomon decoder design
p 1398 N94-18348
An improved distributed arithmetic architecture
p 1398 N94-18349
Training product unit neural networks with genetic algorithms p 1399 N94-18354
Fuzzy control of magnetic bearings
p 1399 N94-18357
Simplified microprocessor design for VLSI control applications p 1400 N94-18359
A modified reconfigurable data path processor
p 1400 N94-18360
Verification of VLSI designs p 1400 N94-18363
A tunable CMOS constant current source
p 1401 N94-18369
DC and small-signal physical models for the AlGaAs/GaAs high electron mobility transistor
p 1401 N94-18370
Formal specification of a high speed CMOS correlator
p 1401 N94-18371
A verification logic representation of indeterministic signal states p 1401 N94-18372
Parallel optimization algorithms and their implementation in VLSI design p 1401 N94-18374
Asynchronous sequential circuit design using pass transistor iterative logic arrays p 1402 N94-18376
Pulse mode VLSI asynchronous circuits
p 1402 N94-18377
Improved self arbitrated VLSI asynchronous circuits
p 1402 N94-18378
VHDL simulation with access to transistor models
p 1402 N94-18381
IIT RESEARCH INST., CHICAGO, IL.
Compilation of 1992 annual reports of the Navy ELF communications system ecological monitoring program, volume 1
[AD-A269569] p 1386 N94-18473
Compilation of 1992 annual reports of the navy ELF communications system ecological monitoring program. Volume 3: Tabs G - I
[AD-A269727] p 1388 N94-18741
Compilation of 1992 annual reports of the navy ELF communications system ecological monitoring program, volume 2
[AD-A269726] p 1388 N94-18751
ILLINOIS UNIV., URBANA.
Numerical methods for molecular dynamics
[DE93-016321] p 1566 N94-18179
Optimal design of binary phase-only filters using genetic algorithms
[AD-A268737] p 1396 N94-18278
Ionic and molecular environments in heterogeneous electrocatalysis: Studies by radioactive labeling and LEED/AUGER spectroscopy
[AD-A268850] p 1567 N94-18766
Mathematical problems in combustion
[AD-A270147] p 1349 N94-18776
ILLINOIS UNIV., URBANA-CHAMPAIGN.
IRAS high resolution studies and modeling of closely interacting galaxies. Galaxy collisions: Infrared observations and analysis of numerical models. UV spectroscopy of massive young stellar populations in interacting galaxies
[NASA-CR-194483] p 1627 N94-19218

IMAGINATION RESOURCES, INC., DUBLIN, OH.
Measurement of viscosity, density, and gas solubility of refrigerant blends in selected synthetic lubricants
[DE93-040221] p 1350 N94-18977

INDIAN INST. OF GEOMAGNETISM, BOMBAY.
Activities of the Indian Institute of Geomagnetism
p 1484 N94-18854

INSTITUT D'AERONOMIE SPATIALE DE BELGIQUE, BRUSSELS.
Ultraviolet absorption cross-sections of some carbonyl compounds and their temperature dependence
[AERONAUTICA-ACTA-A-368-199] p 1353 N94-19456
Temperature dependence of ultraviolet absorption cross-sections of alternative hydrochlorofluorocarbons
[AERONAUTICA-ACTA-A-369-199] p 1353 N94-19459
Global three dimensional model of tropospheric trace gases chemistry and transport
[AERONAUTICA-ACTA-A-370-199] p 1479 N94-19518
Infrared cross sections and global warming potentials of 10 alternative hydrohalocarbons
[AERONAUTICA-ACTA-A-371-199] p 1479 N94-19521
The brain electrical activity in different G situations
[AERONAUTICA-ACTA-A-372-199] p 1507 N94-19523

INSTITUT DE MECANIQUE DES FLUIDES DE LILLE (FRANCE).
Static pressure measurements for near isentropic flows using laser induced iodine fluorescence
p 1431 N94-18646

INSTITUT FRANCO-ALLEMAND DE RECHERCHES, SAINT-LOUIS (FRANCE).
Numerical investigation of the incompressible flow around a wing with a fixed spoiler
[ISL-R-109/91] p 1313 N94-19524

INSTITUT FUER THEORETISCHE STROEMUNGSMECHANIK, GOETTINGEN (GERMANY).
A fast computing method for the flow over high-lift wings p 1308 N94-18437

INSTITUT FUER WELTRAUMFORSCHUNG, GRAZ (AUSTRIA).
Active spacecraft potential control: An ion emitter experiment for Cluster p 1330 N94-19634

INSTITUT NATIONAL DE RECHERCHE D'INFORMATIQUE ET D'AUTOMATIQUE, VALBONNE (FRANCE).
Synthesis of the Workshop on Hypersonic Flows for Reentry Problems
[INRIA-RR-1721] p 1311 N94-17957
ENO schemes on unstructured meshes
p 1412 N94-18561

INSTITUT NATIONAL DES SCIENCES APPLIQUEES DE LYON, VILLEURBANNE (FRANCE).
Modeling and characterization of mechanoelectric conversion piezoelectric generators through dynamical or quasi static uniaxial stress
[ISAL-92-0097] p 1406 N94-19490

INSTITUT NATIONAL POLYTECHNIQUE, GRENOBLE (FRANCE).
PARX, kernel of a system for massively parallel computers: Control of communication between processes
[ETN-93-94353] p 1533 N94-17976
Analysis, representation and processing of the instrumental gesture: Application to keyboard instruments
[ETN-93-94402] p 1519 N94-17977
PARX: Architecture of an operating system for parallel machines
[ETN-93-94401] p 1533 N94-18068
New automatic deduction techniques in first order finite and infinite polyvalent logic
[ETN-93-95003] p 1528 N94-19359
High precision on-line standard arithmetic operators: Design and implementation
[ETN-93-95006] p 1552 N94-19487
Problem of control in an integral vision system: Use of a multi-agent system
[ETN-93-95007] p 1530 N94-19488
On-line test methods of microprocessor based systems
[ETN-93-95008] p 1530 N94-19498
Computation of large numbers and VLSI: Application to GCD, to stretched GCD and at euclidian distance
[ETN-93-95009] p 1552 N94-19499
Silicon compilation: From the circuit to the system
[ETN-93-95010] p 1406 N94-19501
Process allocation on distributed memory parallel architectures
[ETN-93-95004] p 1538 N94-19514
Conception and analysis of numerical parallel algorithms: Realization on the Connection Machine
[ETN-93-95005] p 1531 N94-19517

INSTITUT NATIONAL POLYTECHNIQUE, TOULOUSE (FRANCE).
Study and modeling of compressible flows of flapper nozzle type potentiometric systems
[ETN-93-95012] p 1421 N94-19495
Mathematical modeling of the free surface hydrodynamic and of transport in suspensions of non cohesive sediments: Aid to the interpretation of spatial images
[ETN-93-95011] p 1421 N94-19502

INSTITUTE FOR COMPUTER APPLICATIONS IN SCIENCE AND ENGINEERING, HAMPTON, VA.
Pseudo-compressibility methods for the incompressible flow equations
[NASA-CR-191533] p 1551 N94-19315
On positivity preserving finite volume schemes for compressible Euler equations
[NASA-CR-191534] p 1551 N94-19317

INSTITUTE FOR DEFENSE ANALYSES, ALEXANDRIA, VA.
A comparison of air force data systems
[AD-A269691] p 1616 N94-18575
A comparison Air Force data systems
[AD-A270662] p 1619 N94-19780

INSTITUTE FOR PERCEPTION RVO-TNO, SOESTERBERG (NETHERLANDS).
Synchronisation of cold induced vasodilation at various locations of one hand
[IZF-1992-B3] p 1504 N94-17966
A method for cognitive task analysis
[IZF-1992-B5] p 1508 N94-17967
Stimulus-driven capture and attentional set: Selective search for color and visual abrupt onsets
[IZF-1992-B-9] p 1509 N94-19419
Effects of practice in selecting and executing keypressing sequences
[IZF-1992-B-10] p 1509 N94-19420
A forthcoming key press can be selected while earlier ones are executed
[IZF-1993-B-2] p 1509 N94-19422
Pilot studies on object motion perception during linear self-motion after long duration centrifugation of human subjects
[IZF-1993-B-3] p 1510 N94-19439
Cognitive ability and whole-body rotation
[IZF-1993-B-4] p 1510 N94-19440
Effects of location cuing on redundant target processing
[IZF-1993-B-1] p 1510 N94-19443

INSTITUTE OF OCEANOGRAPHIC SCIENCES, WORMLEY (ENGLAND).
CTD and XBT data collected on ERS-1 validation cruise RRS Charles Darwin Cruise 62A, Iceland-Faeroes region
[IOS-294-1992] p 1461 N94-18063
SeaSoar and CTD sections across the Iceland-Faeroes Front and Faeroe Shetland Channel, August 1990
[IOS-295-1992] p 1496 N94-18064
CTD oxygen, tracer and nutrient data from RRS Charles Darwin Cruises 58/59 in the NE Atlantic as part of Vivaldi 1991
[IOS-296-1992] p 1496 N94-18065
SeaSoar CTD, fluorescence and scalar irradiance data from RRS Charles Darwin Cruises 58/59, NE Atlantic, Vivaldi 1991
[IOS-299-1992] p 1496 N94-18066
Radiosonde data collected on the ERS-1 validation cruise RRS Charles Darwin Cruise 62A, Iceland Faeroes region
[IOS-297-1992] p 1461 N94-18137

INSTITUUT TNO VOOR BOUWMATERIALEN EN BOUWCONSTRUCTIES, DELFT (NETHERLANDS).
Computational mechanics of composite materials
[PB93-195782] p 1343 N94-19281
Microstructure of the interfacial zone around aggregate particles in concrete
[PB93-195790] p 1380 N94-19322

INTERMETRICS, INC., CAMBRIDGE, MA.
Case studies of software development tools for parallel architectures
[AD-A269193] p 1535 N94-18866

INTERNATIONAL ATOMIC ENERGY AGENCY, VIENNA (AUSTRIA).
Development and evaluation of alternative radioanalytical methods, including mass spectrometry for marine materials
[DE93-625117] p 1345 N94-17691
International Centre for Theoretical Physics, Trieste Scientific activities in 1991
[DE93-624757] p 1606 N94-17792

INTERNATIONAL CENTRE FOR THEORETICAL PHYSICS, TRIESTE (ITALY).
Fuzzy almost linear spaces
[DE93-624772] p 1545 N94-17680
On the Debye-Huckel's theory
[DE93-624789] p 1561 N94-17681
On a conformal perfect fluid in the classical vacuum
[DE93-624797] p 1480 N94-17682
Infinite Grassmannian and moduli space of G-bundles
[DE93-624798] p 1545 N94-17683
(1,1)-geodesic maps into Grassmann manifolds
[DE93-624799] p 1545 N94-17684
Tensorial structure of a q-deformed sp(4,R) superalgebra
[DE93-624808] p 1545 N94-17685
Further on the current algebra of WZNW models at and away from criticality
[DE93-624809] p 1545 N94-17686
On the difference caused by CP violation in the energy spectra of pions in K(sup (+-))(yields)(pi)(+-)(pi)(+-)(pi)-+ decays
[DE93-624828] p 1564 N94-17687
The phase mixing of shear Alfven waves
[DE93-624920] p 1581 N94-17688
On relation between Berry phase and one-dimensional models with long-range 1/r(sup 2)-interaction
[DE93-624967] p 1592 N94-17690
CO2 laser with modulated losses: Theoretical models and experiments in the chaotic regime
[DE93-624901] p 1435 N94-17771
Differential geometry of CR-submanifolds of a normal almost para contact manifold
[DE93-624764] p 1545 N94-17793
Groups on transformations in Finslerian spaces
[DE93-624765] p 1606 N94-17794
Multidimensional geometric quantization and U(1)-covering
[DE93-624770] p 1546 N94-17795
Finite-dimensional singletons of the quantum anti de Sitter algebra
[DE93-624771] p 1546 N94-17810
Exact solution of the generalized time-dependent Jaynes-Cummings Hamiltonian
[DE93-624773] p 1546 N94-17811
Some remarks on integrable Hamiltonian systems with two degrees of freedom
[DE93-624766] p 1546 N94-17815
Enumerative geometry of Del Pezzo Surfaces
[DE93-624768] p 1546 N94-17816
A reduction of the globalization and U(1)-covering
[DE93-624769] p 1546 N94-17817
Gauge unification of fundamental forces: The story of success
[DE93-624813] p 1383 N94-17952
Homoclinic crises in a model for the CO2 laser
[DE93-624900] p 1436 N94-17954
Wake field in electron-positron plasmas
[DE93-624929] p 1584 N94-17955
Kinetic growth of random-like and ballistic-like deposition models
[DE93-624946] p 1595 N94-17956
Steepest descent method for set-valued locally accretive mappings
[DE93-628592] p 1548 N94-18106
Unbounded components in parameter space of rational maps
[DE93-628621] p 1548 N94-18170
A general solution of the BV-master equation and BRST field theories
[DE93-628622] p 1561 N94-18171
Resonant absorption of Alfven waves near a neutral point
[DE93-628761] p 1586 N94-18172
Electron paramagnetic resonance of the ns(sup 1) centers in crystals
[DE93-628793] p 1595 N94-18173
Ising model on tangled chain. Part 2: Magnetization and susceptibility
[DE93-628794] p 1607 N94-18174
On a possible algebra morphism of U(sub q)(osp1/2) onto the deformed oscillator algebra W(sub q)(N)
[DE93-629857] p 1548 N94-18176
Widget: A data acquisition system for a balloon borne Si particle calorimeter
[DE93-624668] p 1630 N94-18762
A method for finding the periodic solution of autonomous ordinary differential equations
[DE93-624725] p 1550 N94-19244
A method for solving the KDV equation and some numerical experiments
[DE93-624726] p 1550 N94-19246
Contact 3-manifolds, integrable Hamiltonian systems and exotic symplectic structures in R(sup 4)
[DE93-624767] p 1551 N94-19248
A physical model for one-dimension and time-dependent ionosphere. Part 1: Description of the model
[DE93-627958] p 1486 N94-19255

INTERNATIONAL METEOROLOGICAL INST., STOCKHOLM (SWEDEN).
On the use of semi-Lagrangian methods for accurate predictions of gravity waves
[DM-61] p 1562 N94-18859
The global atmospheric sulfur cycle: An evaluation of model predictions and observations
[CM-81] p 1479 N94-19379

INTERSCIENCE, INC., TROY, NY.
Laboratory microfusion capability study
[DE93-014373] p 1583 N94-17912

IOWA STATE UNIV. OF SCIENCE AND TECHNOLOGY, AMES.
Analysis of satellite-derived ozone and water vapor measurements
[NASA-CR-193810] p 1486 N94-19237

IOWA UNIV., IOWA CITY.
On timing faults in digital logic circuits
[AD-A268714] p 1402 N94-18400
Planetary plasma waves
[NASA-CR-194295] p 1629 N94-19094
The wideband plasma wave investigation
p 1328 N94-19627

ITT AEROSPACE/OPTICAL DIV., FORT WAYNE, IN.
Meteor burst communications improvement study
[AD-A270866] p 1393 N94-19793

J

JAPAN ATOMIC ENERGY RESEARCH INST., TOKYO.
Report of the 1991 Workshop on Particle-Material Interactions for Fusion Research
[DE93-788393] p 1573 N94-18156
AEOLUS-IT MHD simulation code based on a toroidally incompressible plasma model
[DE93-788461] p 1586 N94-18157
A survey on technical problems in designing high-speed rotors with developing materials
[DE93-788519] p 1444 N94-18159
FEL experiment with a focusing wiggler
[DE93-788586] p 1438 N94-18160
Dynamic behaviors of fragments ejected from the surface of carbon materials by laser ablation
[DE93-788620] p 1438 N94-18161
Structure, thermodynamics, and dynamical properties of supercooled liquids
[DE93-788367] p 1607 N94-18211
User's manual of Tokamak Simulation Code
[DE93-788366] p 1586 N94-18212
Active neutral particle diagnostics for high temperature plasma
[DE93-788457] p 1586 N94-18214
Study on radiation-induced deterioration of grease at high temperature, 3
[DE93-788368] p 1369 N94-18220

JOHNS HOPKINS UNIV., BALTIMORE, MD.
Observations of comets with the IUE
[NASA-CR-193652] p 1624 N94-17843
Stochastic models of attention and search
[AD-A268622] p 1508 N94-18292
Communication in the presence of unknown interference
[AD-A271146] p 1392 N94-19738

JOHNS HOPKINS UNIV., LAUREL, MD.
Origins of solar activity. First year report, AASERT grant
[AD-A268848] p 1629 N94-18222
Experience with custom processors in space flight applications p 1336 N94-18338

JOINT INST. FOR NUCLEAR RESEARCH, DUBNA (USSR).
Renormalizations in supersymmetric and nonsupersymmetric non-abelian Chern-Simons field theories with matter
[DE93-626646] p 1593 N94-17748
Toroidal solenoids in the electromagnetic field and Aharonov-Casher effect
[DE93-629861] p 1566 N94-18152
Deformed traces and covariant quantum algebras for quantum groups GL(sub qp)(2) and GL(sub qp)(1/1)
[DE93-629862] p 1561 N94-18153
Phase space representations and quantum probability theory
[DE93-629863] p 1556 N94-18154
Impulsive moving mirror model in a Schroedinger picture with impulse effect in a Banach space
[DE93-629864] p 1561 N94-18155
Paragrassmann analysis and quantum groups
[DE93-628593] p 1561 N94-18168
On paragrassmann differential calculus
[DE93-628594] p 1548 N94-18169
ASYS: a computer algebra package for analysis of nonlinear algebraic equations systems
[DE93-629819] p 1548 N94-18175
Asymptotic behaviour of the solutions of Schroedinger equation with impulse effect in a Banach space
[DE93-629865] p 1548 N94-18195
Impulsive moving mirror model and the stability of Schroedinger equation with impulse effect in a Banach space
[DE93-629866] p 1548 N94-18196
Impulsive moving mirror model and impulsive differential equations in Banach space
[DE93-629867] p 1549 N94-18197
A hydrogen atom in the curved space. Expansion over free solutions on the three-dimensional sphere
[DE93-629868] p 1549 N94-18198
Impulsive moving mirror model and the stability of linear homogeneous differential equations with impulse effect in a Banach space
[DE93-629906] p 1549 N94-18200
Deep ion implantation into manganin to modify its pressure and electrothermocharacteristics
[DE93-630229] p 1359 N94-18218
About symmetry of the gravitational action
[DE93-629955] p 1608 N94-18252
The rise of accuracy for the multichannel scattering problem solving
[DE93-630145] p 1608 N94-18253
Phase structure of (phi(4))(sub 3) field theory at finite temperature
[DE93-629907] p 1608 N94-18267
On the Michelson-Morley experiment
[DE93-629908] p 1608 N94-18268

JOINT PUBLICATIONS RESEARCH SERVICE, ARLINGTON, VA.
JPRS report: Science and technology. Central Eurasia: Materials science
[JPRS-UMS-93-002] p 1339 N94-18833
JPRS report: Science and technology. Central Eurasia: Space
[JPRS-USP-93-004] p 1323 N94-19146
JPRS report: Central Eurasia. Aviation and cosmonautics, no. 1, January 1993
[JPRS-UAC-93-007] p 1632 N94-19147
JPRS report: Central Eurasia. Aviation and cosmonautics, no. 12, December 1992
[JPRS-UAC-93-006] p 1632 N94-19148
JPRS report: Central Eurasia. Aviation and cosmonautics, no. 10, October 1992
[JPRS-UAC-93-004] p 1632 N94-19149
JPRS report: Central Eurasia: Aviation and cosmonautics, no. 11, November 1992
[JPRS-UAC-93-005] p 1632 N94-19208
JPRS report: Science and technology. Central Eurasia: Earth Sciences
[JPRS-UES-93-004] p 1461 N94-19209

K

KAMAN SCIENCES CORP., UTICA, NY.
Generalized multichannel signal detection
[AD-A271385] p 1391 N94-19587

KANSAS STATE UNIV., MANHATTAN.
A scientific role for Space Station Freedom: Research at the cellular level p 1503 N94-19215

KANSAS UNIV. CENTER FOR RESEARCH, INC., LAWRENCE.
An investigation of fighter aircraft agility
[NASA-CR-194608] p 1318 N94-19448

KARLSRUHE UNIV. (GERMANY).
Examples of turbulence model applications
p 1415 N94-18593

KATHOLIEKE UNIV., NIJMEGEN (NETHERLANDS).
Serial pattern complexity: Irregularity and hierarchy
[PB93-191914] p 1509 N94-19348

KATHOLIEKE UNIV. TE LEUVEN (BELGIUM).
Distributed memory parallel computers and computational fluid dynamics p 1413 N94-18568

KENT STATE UNIV., OH.
Heavy-ion collisions and the nuclear equation of state
[DE93-019263] p 1566 N94-18104
Theory of electromagnetic waves propagating in nonlinear anisotropic optical materials
[AD-A269305] p 1386 N94-18469
A multivariate anthropometric method for crew station design
[AD-A270652] p 1513 N94-19531

KEO CONSULTANTS, BROOKLINE, MA.
Space debris detection
[AD-A269254] p 1334 N94-18264

KERNFORSCHUNGSZENTRUM G.M.B.H., KARLSRUHE (GERMANY).
Energy loss measurement of cosmic ray muons
[KFK-5158] p 1631 N94-19504
Measurement of the energy of horizontal cosmic ray muons
[KFK-5163] p 1631 N94-19505
Measurements of cosmic ray muons with multi-wire proportional chambers with a prototype setup for KASCADE
[KFK-5173] p 1631 N94-19506
Suitability of infrared spectroscopy for remote sensing of tropospheric trace gases
[KFK-5183] p 1479 N94-19507
Investigations of a coherent vector radar technique for the observation of the atmosphere near 10 GHz
[KFK-5068] p 1494 N94-19616
Experimental and theoretical investigation of broadband high-power windows for millimeter waves
[KFK-5157] p 1391 N94-19617

KEY ASSOCIATES, ALBUQUERQUE, NM.
Current capabilities for simulating the extreme distortion of thin structures subjected to severe impacts
p 1459 N94-19474

KINGS COLL., LONDON (ENGLAND).
Numerical modelling of fringing fields and their use for complex permittivity measurements at high frequencies
[AD-A270198] p 1388 N94-18782

KSA TECHNOLOGY, COLUMBUS, OH.
Lift and pitching moment induced on jet STOVL aircraft hovering in ground effect
[AD-A269700] p 1317 N94-18577
Lift and pitching moment induced on jet STOVL aircraft by the ground vortex
[AD-A269816] p 1318 N94-18733

L

LABORATOIRE D'AUTOMATIQUE ET D'ANALYSE DES SYSTEMES, TOULOUSE (FRANCE).
Causal reasoning for model-based process supervisory control
[LAAS-93241] p 1544 N94-19360
Phasing strategies of the Hermes type space shuttle: Its optimization considering the thrust failures
[LAAS-93242] p 1544 N94-19361
Simulation of the behavior of micro-electronic capacitive pressure sensors
[LAAS-93190] p 1434 N94-19659

LAWRENCE LIVERMORE NATIONAL LAB., CA.
Analysis of neon soft x ray spectra from short-pulse laser-produced plasmas
[DE93-014420] p 1582 N94-17708
Modeling microstructural evolution and the mechanical response of superplastic materials
[DE93-014417] p 1355 N94-17711
The copper-pumped dye laser system at Lawrence Livermore National Laboratory
[DE93-014429] p 1435 N94-17723
An efficient implementation of error-valued semantics on imperative machines
[DE93-014658] p 1516 N94-17740
Design and test of a low jitter metal to metal contact solid dielectric switch
[DE93-016957] p 1394 N94-17755
A technique for measuring winds in the lower atmosphere using incoherent Doppler lidar
[DE93-017163] p 1488 N94-17758
Safety approaches for high power modular laser operation
[DE93-017213] p 1435 N94-17759
Mechanically refuelable zinc/air electric vehicle cells
[DE93-016446] p 1394 N94-17770
A one dimensional numerical model, with an application to the vertical distribution of dissolved oxygen in the ocean
[DE93-018481] p 1495 N94-17779
Predicted structural response of the lightweight-interceptor technology demonstration vehicle
[DE93-014676] p 1333 N94-17782
Comparison of the modeling solutions with the hydrogen discharge data
[DE93-015115] p 1565 N94-17797
The Aerocapacitor: A carbon aerogel based supercapacitor
[DE93-016537] p 1395 N94-17849
Spin-integrated and spin-dependent photoelectron diffraction
[DE93-016546] p 1565 N94-17850
Regenerative fuel cells for High Altitude Long Endurance Solar Powered Aircraft
[DE93-016991] p 1465 N94-17853
Observations of MeV electrons and scattered light from intense, subpicosecond laser-plasma interactions
[DE93-017153] p 1435 N94-17855
Superhardness effect in Au/Ni multilayers
[DE93-016444] p 1357 N94-17860
An object-oriented environment for computer vision and pattern recognition
[DE93-017098] p 1517 N94-17867
X-ray laser oscillator-amplifier experiments
[DE93-017165] p 1436 N94-17868

Heat load analysis on the cable-in-conduit with central core conductor for the TF coil Rebut layer design
[DE93-013783] p 1395 N94-17872

Comments on computational underwater acoustics
[DE93-013789] p 1562 N94-17873

Aerogels for microelectronic applications: Fast, inexpensive, and light as air
[DE93-017170] p 1395 N94-17882

Analysis of HgI2 and PbI2 crystals and detectors by Particle-Induced X Ray Emission (PIXE) and Ion Backscattering Spectroscopy (IBS)
[DE93-017168] p 1594 N94-17896

Evolution of r-process elements in the hot supernova bubble
[DE93-017169] p 1624 N94-17897

Variable time-step integration for intense field effects
[DE93-013296] p 1382 N94-17909

Verification of VALISYS cad based CMM software at LLNL
[DE93-013854] p 1517 N94-17911

SX User's Manual for SX, version 2.0
[DE93-015971] p 1517 N94-17914

Mixture distributions in climatological research
[DE93-014125] p 1488 N94-17942

Evaluation of materials proposed for the construction of the Plasma Electrode Pockels Cell (PEPC) on beamlet
[DE93-016952] p 1584 N94-17988

Configuration interaction in LTE spectra of heavy elements
[DE93-017166] p 1584 N94-17990

Limitations on the fidelity of 100 fs pulses produced by chirped pulse amplification
[DE93-017167] p 1396 N94-17991

High- and low-temperature bonding techniques for microstructures
[DE93-017173] p 1595 N94-17992

Production of dense vapor targets for laser-plasma interaction studies with intense, ultra-short pulses
[DE93-017175] p 1584 N94-17993

Securing electronic mail: The risks and future of electronic mail
[DE93-017187] p 1383 N94-17994

Dynamics of short-pulse excitation, ionization and harmonic conversion
[DE93-017220] p 1436 N94-17996

Statistical intercomparison of global climate models: A common principal component approach with application to GCM data
[DE93-017951] p 1473 N94-18005

Space and time as outcome of decoherence in an expanding universe
[DE93-016199] p 1624 N94-18047

Numerical integration of structural elements in NIKE3D and DYNA3D
[DE93-016325] p 1452 N94-18049

Effect of spatial resolution on the simulation of regional precipitation in China in a global climate model
[DE93-013433] p 1489 N94-18053

High performance Fortran: An overview
[DE93-017181] p 1519 N94-18072

Criticality benchmark comparisons leading to cross-section upgrades
[DE93-017184] p 1556 N94-18073

Characterization of short pulse laser-produced plasmas at the Lawrence Livermore National Laboratory ultra short-pulse laser
[DE93-017191] p 1585 N94-18082

Ultra-shallow box-like profiles fabricated by pulsed UV-laser doping process
[DE93-017221] p 1437 N94-18083

FEEST: A method for tabulating equation of state and opacity tables
[DE93-017965] p 1347 N94-18092

Laser materials processing applications at Lawrence Livermore National Laboratory
[DE93-017976] p 1437 N94-18093

Modeling shock initiation in Composition B
[DE93-016544] p 1376 N94-18095

Development and application of specially-focused ultrasonic transducers to location and sizing of defects in 75 mm- to 127 mm-thick austenitic stainless steel weld metals
[DE93-015975] p 1453 N94-18108

Recent studies of short-range order in alloys: The Cowley theory revisited
[DE93-016416] p 1358 N94-18111

Remote cure monitoring of polymeric resins by laser Raman spectroscopy
[DE93-016445] p 1369 N94-18112

SAND contact in DYNA3D
[DE93-016451] p 1340 N94-18113

Absorption and x ray measurements from ultra-intense laser-plasma interactions
[DE93-016538] p 1585 N94-18115

Time-resolved probing of electron thermal conduction in femtosecond-laser-pulse-produced plasmas
[DE93-016996] p 1585 N94-18129

Texture splats for 3D vector and scalar field visualization
[DE93-017104] p 1520 N94-18130

Development of short pulse soft x ray lasers
[DE93-017150] p 1437 N94-18131

A mobile remote sensing laboratory for water vapor, trace gas, aerosol, and wind speed measurements
[DE93-017158] p 1489 N94-18132

An evolving infrastructure for scientific computing and the integration of new graphics technology
[DE93-017164] p 1520 N94-18133

Design of a tunable 4-MW free electron maser for heating fusion plasmas
[DE93-017172] p 1437 N94-18134

Response of transmission line systems to pulse excitation by radiation and injection methods
[DE93-015112] p 1384 N94-18210

High speed 512X512 camera system
[DE93-015871] p 1430 N94-18235

Hydrodynamic instability modeling for ICF
[DE93-018634] p 1587 N94-18274

An analog retina model for detecting dim moving objects against a bright moving background
p 1399 N94-18350

Nonparaxial MHD stabilizers for an axisymmetric magnetic mirror
[DE93-017996] p 1587 N94-18505

Aerosol filtration with steel fiber filters
[DE93-016990] p 1380 N94-18710

Engineering research, development and technology thrust area report, FY92
[DE93-016334] p 1632 N94-18856

HEMP 3D: A finite difference program for calculating elastic-plastic flow, appendix B
[AD-A269171] p 1418 N94-18878

Flow volumes for interactive vector field visualization
[DE93-017102] p 1418 N94-18888

Multi-terrawatt, 100 fsec laser system using flashlamp-pumped, dye-converted Ti:sapphire as an amplifier
[DE93-017190] p 1440 N94-18889

LX-17 chemical kinetic material model for Chemical TOPAZ2D
[DE93-014363] p 1377 N94-18893

Development of robust multilayer optics for use in high-peak power radiation environments
[DE93-018557] p 1580 N94-18931

Electron impact excitation of copper atoms
[DE93-017995] p 1363 N94-18939

Integrated circuits: Resistless processing simplifies production and cuts costs
[DE93-018069] p 1405 N94-18941

Dynamic characterization of a lightweight, highly maneuverable spacecraft using modal and finite element analyses
[DE93-018095] p 1335 N94-18942

Automated assistance for detecting malicious code
[DE93-018106] p 1523 N94-18943

Numerical simulation of turbulent mixing and combustion near the inlet of a burner
[DE93-017960] p 1350 N94-18987

Thermal stresses in the microchannel heatsink cooled by liquid nitrogen
[DE93-018660] p 1418 N94-18995

Spice modeling of a FET-switched induction accelerator cell
[DE93-018662] p 1575 N94-18996

Protocol for computation of surface boundary layer parameters used to determine soil moisture flux from meteorological data collected at LLNL, 1992-1993
[DE93-018906] p 1463 N94-19003

Radiation induced darkening of the optical elements in the Startracker camera
[DE93-018907] p 1433 N94-19004

Overview of WARP: A particle code for heavy ion fusion
[DE93-018637] p 1588 N94-19034

Inclusion of a three-dimensional washout coefficient in ADPIC
[DE93-018499] p 1476 N94-19038

CAVEMAN: Configuration and version management
[DE93-018066] p 1524 N94-19048

Superconductivity and magnetism in niobium doped YBa2Cu3O7 related high-(Tc) ceramics
[DE93-018086] p 1601 N94-19049

Lower hybrid counter current drive for edge current density modification in D3-D
[DE93-019157] p 1589 N94-19073

Experiments on nonlinear absorption of ECH waves in MTX and a comparison with theory
[DE93-019158] p 1589 N94-19074

Institute of Geophysics and Planetary Physics, 1992
[DE93-019209] p 1627 N94-19077

Correction of longitudinal errors in accelerators for heavy-ion fusion
[DE93-018656] p 1575 N94-19106

Simulation of transient effects in the heavy ion fusion injectors
[DE93-018658] p 1575 N94-19107

Moments of ambient Doppler spectra
[DE93-017948] p 1390 N94-19114

Performance and scalability aspects of directory-based cache coherence in shared-memory multiprocessors
[DE93-016442] p 1536 N94-19115

Relativistic configuration interaction calculation of the correlation energies of heliumlike ions
[DE93-018093] p 1571 N94-19201

An innovative neural manufacturing concept
[DE93-017212] p 1527 N94-19238

The use of post detonation analysis of stable isotope ratios to determine the type and production process of the explosive involved
[DE93-018497] p 1378 N94-19242

Laser guide star measurements at Lawrence Livermore National Laboratory
[DE93-018081] p 1441 N94-19251

Three dimensional ultrasonic imaging: An aging aircraft nondestructive inspection tool
[DE93-018088] p 1448 N94-19252

Vectorized presentation-level services for scientific distributed applications
[DE93-018091] p 1537 N94-19253

Molecular dynamics modeling of the mechanical behavior of metallic multilayers
[DE93-017972] p 1365 N94-19263

Penetrometer compatible, fiber-optic sensor for continuous monitoring of chlorinated hydrocarbons: Field test results
[DE93-017974] p 1352 N94-19266

Single sided tomography of extremely large dense objects
[DE93-017993] p 1580 N94-19268

Thermo-hydraulic analysis of superconducting toroidal-field magnets for the Tokamak Physics Experiment
[DE93-018096] p 1590 N94-19269

Comments on computational underwater acoustics
[DE93-019880] p 1563 N94-19270

MODIL cryocooler producibility demonstration project results
[DE93-017981] p 1335 N94-19275

Volume rendering of 3D scalar and vector fields at Lawrence Livermore National Laboratory
[DE93-018000] p 1528 N94-19276

The effect of composition on the mechanism of continuous recrystallization and superplastic response of aluminum-scandium alloys
[DE93-018594] p 1365 N94-19280

Harmonic generation at high intensities
[DE93-018632] p 1572 N94-19283

Weak neutral currents and collapse initiated supernova
[DE93-018652] p 1627 N94-19284

Electron cyclotron resonance heating in the microwave tokamak experiment
[DE93-018083] p 1590 N94-19289

Radiative divertor modeling studies
[DE93-018092] p 1590 N94-19290

Cutting and drilling studies using high power visible lasers
[DE93-019149] p 1441 N94-19294

Toward a high performance distributed memory climate model
[DE93-019156] p 1494 N94-19298

A program for passively tracking a target using an array of sensors
[DE93-019554] p 1390 N94-19306

Pulsed power supply for Nova Upgrade
[DE93-019626] p 1441 N94-19307

Behavior of the particle transport coefficients near the density limit in MTX
[DE93-019108] p 1591 N94-19311

Crashdynamics with DYNA3D: Capabilities and research directions p 1460 N94-19475

Velocity measurements in a boundary layer with a density gradient
[DE93-019627] p 1422 N94-19515

Temperature of aircraft cargo flame exposure during accidents involving fuel spills
[DE93-019633] p 1381 N94-19539

The influence of the target strength model on computed perforation
[DE93-018659] p 1460 N94-19543

Precision machining and polishing of scintillating crystals for large calorimeters and hodoscopes
[DE93-018663] p 1381 N94-19544

High rate resistive plate chambers: An inexpensive, fast, large area detector of energetic charged particles for accelerator and non-accelerator applications [DE93-018664] p 1572 N94-19545

Uncertainty versus interindividual variability [DE93-018105] p 1559 N94-19549

Legacy of the X Ray Laser Program [DE93-019550] p 1442 N94-19554

Final report on subcontract B076260 [DE93-019501] p 1604 N94-19565

Locally adaptive remeshing scheme for calculating fluid instabilities [DE93-019577] p 1422 N94-19568

Application of an atmospheric dispersion model to simulated pollutant releases in the Colorado Front range [DE93-017118] p 1480 N94-19732

LEHIGH UNIV., BETHLEHEM, PA.

Selective methane oxidation over promoted oxide catalysts [DE93-040002] p 1351 N94-19132

Selective methane oxidation over promoted oxide catalysts [DE93-040001] p 1351 N94-19150

LEIDEN UNIV. (NETHERLANDS).

Polling systems: Moment stability of station times and central limit theorems [PB93-191955] p 1560 N94-18990

Finding optimal policies for Markov decision chains: A unifying framework for mean-variance-tradeoffs [PB93-191930] p 1559 N94-19555

LIEGE UNIV. (BELGIUM).

Macroseismic study of the Dour (Belgium) earthquakes of 22 March 1987 and of Gulpen (Belgium) 17 October 1988 p 1482 N94-18625

LOCKHEED MISSILES AND SPACE CO., PALO ALTO, CA.

The LET spectrum and its uncertainty during the CRRES mission [AD-A269977] p 1630 N94-18676

Penetrating radiation environment and effects study [AD-A270126] p 1485 N94-18674

LOCKHEED MISSILES AND SPACE CO., SUNNYVALE, CA.

Lunar base Controlled Ecological Life Support System (LCELSS): Preliminary conceptual design study [NASA-CR-188479] p 1511 N94-18484

LOGISTICS MANAGEMENT ENGINEERING, INC., WARMINSTER, PA.

Army Cockpit Delethalization Program (CDP) [AD-A268990] p 1512 N94-18765

LONDON UNIV. (ENGLAND).

Concerning the circumference of certain families of graphs p 1555 N94-19694

LOS ALAMOS NATIONAL LAB., NM.

Measuring emittance using beam position monitors [DE93-014470] p 1434 N94-17709

Using the Tritium Plasma Experiment to evaluate ITER PFC safety [DE93-016614] p 1582 N94-17713

Lectures of Fermi liquid theory [DE93-016630] p 1592 N94-17714

Surface fluxes important to cloud development [DE93-016633] p 1488 N94-17715

Experiments in sideband suppression on the Los Alamos National Laboratory Free-Electron Laser [DE93-014466] p 1435 N94-17724

Malone refrigeration [DE93-014468] p 1379 N94-17725

Synchrotron beam-loading stability with a higher RF harmonic [DE93-014549] p 1573 N94-17726

Rapid analysis of mixed waste samples via the optical emission from laser initiated microplasmas [DE93-014563] p 1582 N94-17727

Understanding curved detonation waves [DE93-014581] p 1408 N94-17728

Magnetic properties of single-crystalline UCu3Al2 [DE93-016607] p 1593 N94-17744

Direct Monte Carlo simulation of the chemical equilibrium composition of detonation products [DE93-014559] p 1376 N94-17751

Polaron tunneling in high-temperature superconductors [DE93-016880] p 1593 N94-17754

Thermodynamics of computation and information distance [DE93-012730] p 1517 N94-17812

Detonation reaction steps frozen by free expansion and analyzed by mass spectrometry [DE93-012734] p 1376 N94-17813

Measurement and analysis of three 1.5-GPa shock-wave profiles in copper [DE93-016559] p 1451 N94-17864

Designs for optical components related to the Los Alamos free-electron laser [DE93-016617] p 1436 N94-17865

Plastic anisotropy in MoSi2 single crystals [DE93-012650] p 1594 N94-17874

Mechanical properties of excimer laser modified titanium surfaces [DE93-012663] p 1358 N94-17875

Impact modeling with smooth particle hydrodynamics [DE93-016561] p 1451 N94-17906

Phase separation and superconductivity in La2CuO(4 + delta): Effects of oxygen diffusion [DE93-016610] p 1594 N94-17907

Software Toolkit for Analysis Research (STAR) [DE93-017368] p 1519 N94-18086

Molecular composites from liquid crystalline polymers and liquid crystalline thermosets [DE93-016608] p 1368 N94-18096

A time-frequency smoothing algorithm for cyclic spectral analysis [DE93-016634] p 1519 N94-18097

A review of the stages of work hardening [DE93-016456] p 1359 N94-18114

Omega phase formation in shock-loaded zirconium [DE93-018343] p 1595 N94-18162

Neutrino mass [DE93-018467] p 1567 N94-18269

Advanced in macrostatistical hydrodynamics [DE93-018479] p 1410 N94-18270

A rational design change methodology based on experimental and analytical modal analysis [DE93-018537] p 1521 N94-18271

Calculation of the LiF-CeF3-BeF2 and LiF-PuF3-BeF2 ternary phase diagrams [DE93-017437] p 1360 N94-18501

Dislocation-drag contribution to high-rate plastic deformation in shock-loaded tantalum [DE93-018286] p 1361 N94-18802

Parametric analysis of the ARIES-3D-He-3 tokamak reactor [DE93-018293] p 1587 N94-18803

High energy resolution ARPES measurements of the normal and superconducting states of Bi2Sr2CaCu2O(8 + delta) [DE93-018294] p 1599 N94-18804

High pressure metallization of Mott Insulators: Magnetic, structural and electronic properties [DE93-018295] p 1404 N94-18805

Effects of shock loading on a solid-solution strengthened superalloy [DE93-018345] p 1362 N94-18809

Temperature lowering in cryogenic chemical-synthesis techniques and system [DE93-018348] p 1562 N94-18810

Regenerator optimization for Stirling cycle refrigeration [DE93-018468] p 1380 N94-18818

An RS-170 to 700 frame per second CCD camera [DE93-018367] p 1432 N94-18828

Development of a cryogenic heat pipe [DE93-018448] p 1417 N94-18831

Computational astrophysics: Pulsating stars [DE93-018369] p 1627 N94-18857

Foil support structure for large electron guns [DE93-018478] p 1322 N94-18890

Geothermal activity near Clearlake, California [DE93-016627] p 1485 N94-18894

Computer/information security design approaches for Complex 21/Reconfiguration facilities [DE93-018547] p 1535 N94-18930

Pressure induced metallization of the Mott Insulator 6(sub 2) [DE93-018296] p 1600 N94-18969

The application of front tracking to the simulation of shock refractions and shock accelerated interface mixing [DE93-018342] p 1419 N94-19025

Implementation of the turn function method in KIVA-F90 [DE93-018394] p 1419 N94-19027

Beryllium processing technology review for applications in plasma-facing components [DE93-018396] p 1363 N94-19028

Shock-loading response of advanced materials [DE93-018344] p 1455 N94-19033

Kinetics programs for simulation of tropospheric photochemistry on the global scale [DE93-019035] p 1476 N94-19104

LAHET calculations for accelerator neutron production [DE93-016518] p 1570 N94-19120

Electron impact polarization and correlation properties of the inert gases [DE93-018358] p 1570 N94-19125

T violating neutron spin rotation asymmetry [DE93-018470] p 1570 N94-19126

Shrinkage void formation and its effect on freeze and thaw processes of lithium and lithium-fluoride for space applications [DE93-019303] p 1338 N94-19128

Liquid sound speeds at pressure from the optical analyzer technique [DE93-018362] p 1563 N94-19151

Application of differential sensitivity theory to continuum mechanics [DE93-012732] p 1609 N94-19187

Elastic properties of amorphous thin films studied by Rayleigh waves [DE93-018375] p 1372 N94-19202

A parallel hashed oct-tree N-body algorithm [DE93-012654] p 1526 N94-19205

Smooth particle hydrodynamics: The SPHINX and SPHC codes [DE93-014358] p 1457 N94-19207

Kinetic studies of electrochemical generation of Ag(II) ion and catalytic oxidation of selected organics [DE93-016601] p 1352 N94-19240

Eta-nucleon interaction and nuclear production of eta mesons [DE93-018469] p 1571 N94-19259

The Mexico City 1991 lidar measurements campaign [DE93-019960] p 1478 N94-19272

Thermal neutron multiplicity measurements using the pyrochemical multiplicity counter at Lawrence Livermore National Laboratory [DE93-018538] p 1571 N94-19278

Influence of peak pressure and temperature on the shock-loading response of tantalum [DE93-018561] p 1457 N94-19279

Asymptotic derivation of the modified time-dependent SP2 equations and numerical calculations [DE93-016466] p 1551 N94-19342

Improved approximations applied to the S(sub N) even-parity equation [DE93-016467] p 1551 N94-19343

Simulation of dynamic material response with the PAGOSA code [DE93-018285] p 1460 N94-19603

Group-invariant solutions of hydrodynamics and radiation hydrodynamics [DE93-018373] p 1423 N94-19604

Magnetic and crystallographic structures in UTX intermetallic compounds [DE93-018291] p 1605 N94-19735

LOUGHBOROUGH UNIV. OF TECHNOLOGY (ENGLAND).

Format.m: A usage manual. Towards an efficient symbolic-numeric environment: Extending Mathematica's format rules [MATHS-REPT-A-185] p 1547 N94-17969

An extension of Wolovich's definition of equivalence of linear systems [MATHS-REPT-A-183] p 1547 N94-18069

On higher dimensional Ermakov systems: Canonical reductions [MATHS-REPT-A-182] p 1548 N94-18140

Optimal safety system design using fault tree analysis [MATHS-REPT-A-187] p 1529 N94-19382

Learning control of large-scale systems [MATHS-REPT-A-186] p 1544 N94-19408

Notes on multi-step ahead prediction based on the principle of concatenation [MATHS-REPT-A-189] p 1544 N94-19410

Robustness and efficiency of generalized predictive control algorithms with guaranteed stability [MATHS-REPT-A-190] p 1530 N94-19412

LOUISIANA STATE UNIV., BATON ROUGE.

A general theory of signal integration for fault-tolerant dynamic distributed sensor networks [AD-A270316] p 1534 N94-18699

Solar flares and magnetospheric particles: Investigations based upon the ONR-602 and ONR-604 experiments [AD-A269495] p 1629 N94-18705

LOUISIANA STATE UNIV., NEW ORLEANS.

Metabolic changes and hemodynamic dysfunction following hypothermic shock [AD-A269780] p 1506 N94-18598

LOUISVILLE UNIV., KY.

Implementation of mixed formulation elements in PC/NASTRAN p 1449 N94-17828

LOWELL UNIV., MA.

Modeling a Yagi array antenna for VHF radar use [AD-A268973] p 1387 N94-18525

M

MADRAS UNIV. (INDIA).

A special purpose silicon compiler for designing supercomputing VLSI systems p 1402 N94-18379

MANCHESTER COLL. OF SCIENCE AND TECHNOLOGY (ENGLAND).

Prediction of the high-lift performance of multi-element aerofoils using an unstructured Navier-Stokes solver p 1307 N94-18427

MANCHESTER UNIV. (ENGLAND).

An introduction to the modelling of turbulence
p 1414 N94-18579

An introduction to second moment closure
p 1414 N94-18580

Modelling force-field effects on turbulence
p 1414 N94-18581

A new form of second-moment closure
p 1414 N94-18582

An introduction to single-point closure methodology
p 1414 N94-18583

Second-moment closure: Present... and future?
p 1414 N94-18584

Contribution to the modelling of near-wall turbulence
p 1414 N94-18585

Two-equation models for high-Reynolds-number flow
p 1415 N94-18586

Two-equation models for low-Reynolds-number variants
p 1415 N94-18587

Inclusion of second-moment closures into finite-volume solvers
p 1415 N94-18588

Numerical implementation and performance of Reynolds-stress closures in finite-volume computations of recirculating and strongly swirling flows
p 1415 N94-18589

Application of second-moment closure in complex flows
p 1415 N94-18590

Modelling engineering flows with Reynolds stress turbulence closure
p 1415 N94-18591

Turbulence modelling challenges posed by complex flows
p 1415 N94-18592

MARQUETTE UNIV., MILWAUKEE, WI.

Resonance Raman and photophysical studies of transition metal complexes in solution and entrapped in zeolites
[DE93-019892] p 1363 N94-19019

MARTIN MARIETTA CORP., ORLANDO, FL.

FEM/SINDA: Combining the strengths of NASTRAN, SINDA, I-DEAS, and PATRAN for thermal and structufal analysis
p 1449 N94-17831

MARYLAND UNIV., COLLEGE PARK.

Advanced methods for the computation of particle beam transport and the computation of electromagnetic fields and beam-cavity interactions
[DE93-018160] p 1573 N94-17807

Aerodynamic characteristics of a helicopter rotor airfoil as affected by simulated ballistic damage
[AD-A269206] p 1311 N94-18413

Validation of a-posteriori error estimators by numerical approach
[AD-A269493] p 1549 N94-18697

Interaction of intense lasers and relativistic electron beams with solids, gases and plasmas
[AD-A269655] p 1439 N94-18737

Interdisciplinary training in life science (FY 1991 ASSERT)
[AD-A269220] p 1512 N94-18886

MASSACHUSETTS INST. OF TECH., CAMBRIDGE.

Detailed analysis of low energy plasma data under the Voyager Uranus data analysis program
[NASA-CR-193668] p 1628 N94-17842

Studies of enhanced radar backscatter
[AD-A269544] p 1385 N94-18288

Synthesis and study of high-T(sub c) superconducting electronic materials
[AD-A268851] p 1402 N94-18390

Software reliability: Estimation and prediction
[AD-A268895] p 1521 N94-18458

Thermal insulation of wet shielded metal arc welds
[AD-A268697] p 1445 N94-18465

Initiation and growth of microcracks in high strength steel butt welds
[AD-A268751] p 1454 N94-18466

Design considerations for remotely operated welding in space: Task definition and visual weld monitoring experiment
[AD-A268752] p 1445 N94-18634

Deformation mechanisms in a Laves phase
[DE93-018331] p 1361 N94-18806

Morphology, deformation, and defect structures of TiCr2 in Ti-Cr alloys
[DE93-018332] p 1361 N94-18807

Numerical and symbolic signal representation and processing
[AD-A270271] p 1389 N94-18811

Strategies for enhancing catecholamine-mediated neurotransmission
[NASA-CR-193807] p 1506 N94-18862

Center of Excellence in Theoretical Geoplasma Research
[AD-A270210] p 1588 N94-18902

The interpretation of crustal dynamics data in terms of plate motions and regional deformation near plate boundaries
[NASA-CR-194302] p 1487 N94-19432

A method for eliminating skew introduced by non-uniform buffer delay and wire lengths in clock distribution trees
[AD-A270649] p 1544 N94-19530

Incology 908 database report: On process-structure-property relationship
[DE93-017616] p 1366 N94-19546

Optical frequency division using an optical parametric oscillator
[AD-A270847] p 1581 N94-19578

Acoustic travel time perturbations due to an internal tide and internal wave field in the Barents Sea
[AD-A270879] p 1499 N94-19580

Automated qualitative modeling of dynamic physical systems
[AD-A270835] p 1422 N94-19598

Explorations of the practical issues of learning prediction-control tasks using temporal difference learning methods
[AD-A270836] p 1544 N94-19599

Control of catalytic hydrotreating selectivity with ammonia
[DE93-041223] p 1354 N94-19660

Remote sensing of Earth terrain
[NASA-CR-194598] p 1464 N94-19681

Forward scattering of a pulsed continuous wave signal through laminar and turbulent thermal plumes
[AD-A271210] p 1564 N94-19723

Compact free electron lasers for medical applications
[AD-A271272] p 1442 N94-19729

Nanofabrication by focused ion beam
[AD-A271290] p 1345 N94-19746

Human-machine interfaces
[AD-A270730] p 1513 N94-19764

Equivalence and reduction of hidden Markov models
[AD-A270762] p 1560 N94-19768

MASSACHUSETTS INST. OF TECH., LEXINGTON.

Integrated Terminal Weather System (ITWS)
[AD-A269884] p 1492 N94-18684

Proceedings of the 11th Space Surveillance Workshop
[AD-A269477] p 1462 N94-18729

Estimation of wake vortex advection and decay using meteorological sensors and aircraft data
[AD-A270763] p 1316 N94-19661

MASSACHUSETTS UNIV., AMHERST.

Direct solar pumping of semiconductor lasers: A feasibility study
[NASA-CR-193760] p 1440 N94-18834

Knowledge sources for an intelligent MCM analyzer
[AD-A269224] p 1542 N94-18887

Theoretical and experimental research on coherent microwave backscatter from the ocean
[AD-A271276] p 1500 N94-19743

MASSACHUSETTS UNIV., LOWELL.

Microbial degradation of poly-b-esters: A mechanistic study, cellulose acetate biodegradability
[AD-A271368] p 1374 N94-19586

MATERIALS RESEARCH LABS., ASCOT VALE (AUSTRALIA).

Some problems in the rheological characterisation of composite rocket propellants
[AD-A268806] p 1376 N94-18203

An atlas of bathy-thermograph temperature cross-sections for Coral and Tasman Sea transects from 1960 to 1987
[AD-A268775] p 1497 N94-18329

MATERIALS RESEARCH SOCIETY, PITTSBURG, PA.

Joining and Adhesion of Advanced Inorganic Materials Symposium
[AD-A269748] p 1342 N94-18720

Magnetic Ultrathin Films: Multilayers and Surfaces, Interfaces, and Characterization, volume 313
[AD-A271402] p 1375 N94-19758

MAX-PLANCK-INST. FUER AERONOMIE, KATLENBURG-LINDAU (GERMANY).

RAPID: The imaging energetic particle spectrometer on Cluster
p 1329 N94-19633

MAX-PLANCK-INST. FUER EXTRATERRESTRISCHE PHYSIK, GARCHING (GERMANY).

The Electron Drift Instrument for Cluster
p 1329 N94-19630

MAX-PLANCK-INST. FUER PHYSIK UND ASTROPHYSIK, GARCHING (GERMANY).

Unified NLTE model atmospheres including spherical extension and stellar winds, 4: Improved line transfer and wind contamination of H, He profiles
[MPA-905] p 1624 N94-17736

Maximal hypersurfaces in asymptotically stationary spacetimes
[MPA-708] p 1621 N94-18141

The 0.15 seconds near-infrared imaging of the central parsec of the galaxy
[MPE-PREPRINT-239] p 1621 N94-19415

Broadband IF matching for quasioptical mixers
[MPE-PREPRINT-240] p 1390 N94-19416

The molecular environment of S106 IR
[MPE-PREPRINT-241] p 1622 N94-19417

Rosat and optical observations of two X-ray transients: MX 0836-42 and GS 0834-430
[MPE-PREPRINT-237] p 1622 N94-19451

EGRET Mission and Data Analysis
[MPE-PREPRINT-223] p 1622 N94-19462

Structuration processes in protoplanetary accretion disks
[MPE-243] p 1628 N94-19519

ROSAT and IRAS observations
[MPE-PREPRINT-231] p 1623 N94-19526

ROSAT X ray observation of the 30 Dor giant HII region
p 1623 N94-19527

IRAS galaxies observed in the ROSAT survey: Starbursts or central activity
p 1623 N94-19528

Particle induced background by Roentgen satellites
[MPE-242] p 1631 N94-19714

Stellar coronae at the end of the main sequence: A Rosat survey of the late M dwarfs
[NASA-CR-194700] p 1628 N94-19794

MAX-PLANCK-INST. FUER PLASMAPHYSIK, MUNICH (GERMANY).

A free boundary eigenvaue problem
[IPP-6/310] p 1584 N94-17981

MAX-PLANCK-INST. FUER STROEMUNGSFORSCHUNG, GOETTINGEN (GERMANY).

The effect of fine surface riblets on the flow around an inclined axially symmetrical body
[MPIS-105/1993] p 1420 N94-19356

Film condensation in a shock wave
[MPIS-22/1992] p 1422 N94-19509

Two-dimensional turbulent nonstationary superfluid counterflows: Numerical simulations, qualitative effects
[MPIS-23/1992] p 1422 N94-19510

Stability measurements of Rayleigh-Benard convection near the critical state using a spectral model
[MPIS-15/1992] p 1422 N94-19520

Methods for description and control of dynamical systems and their application
[MPIS-17/1992] p 1553 N94-19522

Theoretical examination of the flow around a cylinder with a low dimensional Galerkin process
[MPIS-25/1992] p 1422 N94-19525

Examinations of converging cylindrically symmetric second sound propagation in He2
[MPIS-9/1992] p 1564 N94-19715

MCDONNELL AIRCRAFT CO., SAINT LOUIS, MO.

Navier-Stokes calculations on multi-element airfoils using a chimera-based solver
p 1306 N94-18422

MCDONNELL-DOUGLAS AEROSPACE, HUNTSVILLE, AL.

Improved omit set displacement recoveries in dynamic analysis
p 1449 N94-17829

MCDONNELL-DOUGLAS ASTRONAUTICS CO., SAINT LOUIS, MO.

Pressure sensitive paint technique
p 1431 N94-18647

MCDONNELL-DOUGLAS SPACE SYSTEMS CO., HUNTSVILLE, AL.

Automatic A-set selection for dynamics analysis
p 1450 N94-17839

MELBOURNE UNIV., PARKVILLE (AUSTRALIA).

Preparation and characterisation of the compound Tl(0.65) Bi(0.35) Ca(0.8) Sr(1.7) Cu2 O(y) using oxalate coprecipitation and analytical CBED and an initial preparation of Bi2Ca(n-1) Sr2Cu(n) O(4+2n) for n=5
[DE93-625470] p 1602 N94-19277

MEMPHIS STATE UNIV., TN.

Nonlinear optical properties of molecules
[AD-A270199] p 1567 N94-18783

The complete closure of a graph
p 1555 N94-19690

MEMRY TECHNOLOGIES, INC., NORWALK, CT.

Damping in ferrous shape memory alloys
[AD-A271009] p 1366 N94-19775

MESSERSCHMITT-BOELKOW-BLOHM G.M.B.H., MUNICH (GERMANY).

Research and design activities and the economic balance of MBB
[ETN-93-94909] p 1310 N94-19383

New aircraft materials and structures
[MBB-LME-202-S-PUB-502-A] p 1319 N94-19496

Numerical simulation of viscous flows in chemical nonequilibrium
[MBB-LME-211-S-PUB-506] p 1421 N94-19497

Three dimensional network generation and Euler calculation for a wing fuselage canard configuration
[MBB-LME-211-S-PUB-511-A] p 1319 N94-19500

METALS INFORMATION ANALYSIS CENTER, WEST LAFAYETTE, IN.

Bibliography on silicides
[AD-A270516] p 1374 N94-19532

METAUX PRECIEUX S.A. METALOR, NAUCHATEL (SWITZERLAND).

Gold-copper-zinc coatings as an alternative to gold-copper-cadmium
p 1367 N94-18012

MIAMI UNIV., FL.

Design of a general purpose and autonomous transmitter and receiver system for underwater acoustic experiments at sea
[AD-A269268] p 1495 N94-17822

MICHIGAN STATE UNIV., EAST LANSING.

The role of chemical inhibition of gap junctional intercellular communication in toxicology
[AD-A269251] p 1502 N94-18924

MICHIGAN UNIV., ANN ARBOR.

A free energy simulation method based study of interfacial segregation
[DE93-019462] p 1364 N94-19032

Congestion/flow control and routing in data networks: A control-theoretic approach
[AD-A271121] p 1392 N94-19737

MICROELECTRONICS CENTER OF NORTH CAROLINA, RESEARCH TRIANGLE PARK.

Field emitter array RF amplifier development project, phase 1, option 1
[AD-A268687] p 1396 N94-18293

MICROWAVE MONOLITHICS, INC., SIMI VALLEY, CA.

High efficiency low cost monolithic module for SARSAT distress beacons
[NASA-CR-194234] p 1315 N94-18852

MIDDLE EAST TECHNICAL UNIV., ANKARA (TURKEY).

Experimental investigation of flow around a multielement airfoil p 1305 N94-18417

MIDWEST RESEARCH INST., GOLDEN, CO.

Development of large-area monolithically integrated silicon-film photovoltaic modules
[DE93-010037] p 1464 N94-17731

The value of windpower: An investigation using a qualified production cost model
[DE93-010043] p 1465 N94-17888

Fifteenth Symposium on Biotechnology for Fuels and Chemicals: Program and Abstracts
[DE93-010005] p 1376 N94-18045

Defining the normal turbine inflow within a wind park environment
[DE93-010032] p 1489 N94-18046

A rugged, low-cost advanced data acquisition system for field test projects
[DE93-010041] p 1615 N94-18334

Gallium arsenide-based ternary compounds and multi-band-gap solar cell research
[DE93-010049] p 1467 N94-18483

Research on stable, high-efficiency amorphous silicon multijunction modules
[DE93-010046] p 1467 N94-18518

Evaluation of aftermarket LPG conversion kits in light-duty vehicle applications
[DE93-010035] p 1377 N94-18617

Data collection plan for phase 2 Alternative Fuels Bus Data Collection Program
[DE93-010047] p 1378 N94-18913

Polycrystalline thin-film cadmium telluride solar cells fabricated by electrodeposition
[DE93-018201] p 1468 N94-18944

Amorphous silicon batch process cost analysis
[DE93-018203] p 1470 N94-19760

MIDWEST SYSTEMS RESEARCH, INC., DAYTON, OH.

FAA airborne data link human factors research plan
[AD-A271006] p 1514 N94-19773

MINERALS, METALS AND MATERIALS SOCIETY, WARRENDALE, PA.

Diffusion in ordered alloys
[AD-A268232] p 1359 N94-18322

MINNESOTA UNIV., DULUTH.

Evaluation of physiological and psychological impairment of human performance in cold stressed subjects
[AD-A268637] p 1506 N94-18632

MINNESOTA UNIV., MINNEAPOLIS.

Psychophysical analyses of perceptual representations
[AD-A268711] p 1508 N94-18313

The quantum dynamics of electronically nonadiabatic chemical reactions
[NASA-CR-194309] p 1568 N94-18837

Substrate temperature measurement and control during thermal plasma CVD
[DE93-040305] p 1433 N94-19135

Microstructure and texture control of fatigue in hydrogen and marine environments
[AD-A271277] p 1344 N94-19744

Micromechanics of interfaces in metal matrix composites
[AD-A271012] p 1345 N94-19776

MISSION RESEARCH CORP., NASHUA, NH.

Upper atmospheric effects of the HF Active Auroral Research Program Ionospheric Research Instrument (HAARP IRI)
[AD-A268948] p 1481 N94-18451

MISSISSIPPI STATE UNIV., MISSISSIPPI STATE.

Development of a multi-point two-color pyrometer for tube and wall temperature and emissivity measurement at the CFFF
[DE93-014716] p 1429 N94-18207

MISSOURI UNIV., ROLLA.

NMR studies of enriched species at interfaces
[AD-A264703] p 1367 N94-17878

Pressureless densification of ceramic matrix composites
[AD-A269137] p 1371 N94-18691

Use of shape memory alloys in the robust control of smart structures
[AD-A270827] p 1366 N94-19594

MITRE CORP., BEDFORD, MA.

VHF air/ground communications for air traffic control. Volume 1: A decision tree approach to system innovations
[AD-A268485] p 1316 N94-18384

VHF air/ground communications for air traffic control: A decision tree approach to system innovations, volume 2
[AD-A268632] p 1386 N94-18495

Introduction to wavelets
[AD-A268465] p 1389 N94-18801

Systems engineering for Air Force C3I systems
[AD-A270482] p 1391 N94-19676

MONTANA STATE UNIV., BOZEMAN.

VLSI synthesis of digital application specific neural networks p 1399 N94-18355

MONTREAL UNIV. (QUEBEC).

A new variable testability measure
p 1400 N94-18364

MOREHEAD STATE UNIV., KY.

Workshop on multifactor aging mechanisms and models
[AD-A268668] p 1397 N94-18311

MORGANTOWN TECHNOLOGY CENTER, WV.

Molten carbonate fuel cell networks: Principles, analysis, and performance
[DE93-000281] p 1468 N94-18925

MULLARD SPACE SCIENCE LAB., DORKING (ENGLAND).

PEACE: A Plasma Electron and Current Experiment
p 1329 N94-19632

MUSEE INTERNATIONAL D'HOROLOGERIE, LA CHAUX-DE-FONDS (SWITZERLAND).

The clocks and the perception of time in the 18th century society p 1424 N94-18007

Marine chronometry in the Neuchatel mountains (Switzerland) p 1427 N94-18025

Restoration of an 18th century English clock
p 1427 N94-18026

The mystery of the perpetual motion clock of Geiser and Son p 1427 N94-18027

MUTRON S.A., BOUDRY (SWITZERLAND).

Mutrometre: Construction for fast water proof measurements under low pressure and air suppression
p 1427 N94-18031

N

NAGOYA UNIV. (JAPAN).

Plasma production by helicon waves
[DE93-788396] p 1586 N94-18213

NAPLES UNIV. (ITALY).

Infrared thermography p 1432 N94-18652

NATIONAAL INST. VOOR KERNFYSICA EN HOGE ENERGIEFYSICA, AMSTERDAM (NETHERLANDS).

The universal BitBus node
[DIGEL-1993-1] p 1515 N94-19799

NATIONAL ACADEMY OF SCIENCES - NATIONAL RESEARCH COUNCIL, WASHINGTON, DC.

Solid State Sciences Committee Forum
[AD-A270454] p 1342 N94-18715

Computing professionals: Changing needs for the 1990's
[B-030] p 1515 N94-19401

Mathematical sciences, technology, and economic competitiveness
[LC-91-60253] p 1514 N94-19478

NATIONAL AERONAUTICS AND SPACE ADMINISTRATION, WASHINGTON, DC.

OSSA Information Systems Program
[NASA-TM-108774] p 1612 N94-17737

ISTP Global Geospace Science. Energy transfer in geospace
[NASA-TM-109239] p 1620 N94-18851

Robotics
[NASA-TM-109351] p 1332 N94-18920

LDEF update
[NASA-TM-109352] p 1334 N94-18921

Designing Space Station
[NASA-TM-109353] p 1334 N94-18922

Aerospace medicine and biology: A continuing bibliography with indexes (supplement 382)
[NASA-SP-7011(382)] p 1507 N94-18936

Aeronautical engineering: A continuing bibliography with indexes (supplement 297)
[NASA-SP-7037(297)] p 1310 N94-18937

Return to space
[NASA-TM-109356] p 1332 N94-18955

Voyager's last encounter
[NASA-TM-109361] p 1628 N94-18957

Magellan, Galileo, and Ulysses
[NASA-TM-109362] p 1628 N94-18958

Future energy source
[NASA-TM-109363] p 1628 N94-18959

Ozone hole
[NASA-TM-109368] p 1476 N94-18960

The world's most powerful computer
[NASA-TM-109369] p 1514 N94-18961

X-29: Research aircraft
[NASA-TM-109370] p 1318 N94-18962

The world's largest wind tunnel
[NASA-TM-109371] p 1322 N94-18963

Airflow research
[NASA-TM-109372] p 1312 N94-18964

Apollo 11: 20th anniversary
[NASA-TM-109364] p 1323 N94-18979

Langley's 50th year
[NASA-TM-109365] p 1632 N94-18980

Space exploration initiative
[NASA-TM-109366] p 1323 N94-18981

Aerospace medicine and biology: A continuing bibliography with indexes (supplement 381)
[NASA-SP-7011(381)] p 1507 N94-19069

Aeronautical engineering: A continuing bibliography with indexes (supplement 296)
[NASA-SP-7037(296)] p 1310 N94-19070

Hubble Space Telescope
[NASA-TM-109359] p 1621 N94-19072

Application of new technologies in the virtual library: Seminars in Turkey, Portugal, and Spain
[NASA-TM-109718] p 1611 N94-19131

Space Life Sciences Research: The Importance of Long-Term Space Experiments
[NASA-TM-4502] p 1502 N94-19210

The rationale for fundamental research in space biology: Introduction and background p 1502 N94-19211

Space research with intact organisms: The role of Space Station Freedom p 1502 N94-19213

Strategic plan, 1991: A strategy for leadership in space through excellence in space science and applications
[NASA-TM-109256] p 1611 N94-19434

NATIONAL AERONAUTICS AND SPACE ADMINISTRATION. AMES RESEARCH CENTER, MOFFETT FIELD, CA.

Efficient simulation of incompressible viscous flow over multi-element airfoils p 1306 N94-18421

Interferometric investigations of compressible dynamic stall over a transiently pitching airfoil
[NASA-TM-109380] p 1312 N94-19119

Opportunities and questions for the fundamental biological sciences in space p 1502 N94-19212

NATIONAL AERONAUTICS AND SPACE ADMINISTRATION. GODDARD SPACE FLIGHT CENTER, GREENBELT, MD.

The solar optical telescope
[NASA-TM-109240] p 1621 N94-18850

TDRS press release
[NASA-TM-109373] p 1335 N94-18965

October 1979-1989 Southern Hemisphere total ozone as seen by TOMS
[NASA-TM-109375] p 1476 N94-18967

The 1993 Shuttle Small Payloads Symposium
[NASA-CP-3233] p 1323 N94-19162

New room temperature high resolution solid-state detector (CdZnTe) for hard x rays and gamma rays
p 1324 N94-19165

Telescope for x ray and gamma ray studies in astrophysics p 1324 N94-19166

Superfluid Helium On-Orbit Transfer (SHOOT) flight demonstration p 1327 N94-19185

Detection of a long-duration solar gamma-ray flare on Jun. 11, 1991 with EGRET on Compton-GRO
p 1623 N94-19463

EGRET observations of 3 C 273
p 1623 N94-19464

The spherical probe Electric Field and Wave Experiment for the Cluster mission p 1328 N94-19624

The Cluster magnetic field investigation: Scientific objectives and instrumentation p 1329 N94-19629

SeaTrack: Ground station orbit prediction and planning software for sea-viewing satellites
[NASA-RP-1331] p 1532 N94-19761

NATIONAL AERONAUTICS AND SPACE ADMINISTRATION. JOHN F. KENNEDY SPACE CENTER, COCOA BEACH, FL.

Kennedy Space Center processing of Shuttle small payloads p 1326 N94-19177

NATIONAL AERONAUTICS AND SPACE ADMINISTRATION. LYNDON B. JOHNSON SPACE CENTER, HOUSTON, TX.

Computational techniques for high-speed flows with viscous and chemical effects p 1412 N94-18560

Human Transportation System (HTS) study: Executive summary
[NASA-TM-104780] p 1332 N94-18669

Human Transportation System (HTS) study, volume 1
[NASA-TM-104779] p 1332 N94-18670

NATIONAL AERONAUTICS AND SPACE ADMINISTRATION. LANGLEY RESEARCH CENTER, HAMPTON, VA.

Packaging, deployment, and panel design concepts for a truss-stiffened 7-panel precision deployable reflector with feed boom
[NASA-TM-109000] p 1333 N94-17765

Effect of temperature and O-ring gland finish on sealing ability of Viton V747-75
[NASA-TP-3391] p 1368 N94-18075

High Reynolds number configuration development of a high-lift airfoil p 1306 N94-18424

In-flight pressure distributions and skin-friction measurements on a subsonic transport high-lift wing section p 1308 N94-18435

ISAC: A tool for aeroservoelastic modeling and analysis
[NASA-TM-109031] p 1321 N94-19316

Computational Methods for Crashworthiness
[NASA-CP-3223] p 1458 N94-19465

Composite impact dynamics research at NASA LaRC: A review p 1458 N94-19467

NATIONAL AERONAUTICS AND SPACE ADMINISTRATION. LEWIS RESEARCH CENTER, CLEVELAND, OH.

Low power arcjet system spacecraft impacts
[NASA-TM-106307] p 1336 N94-17856

Workshop on Computational Turbulence Modeling
[NASA-TM-109266] p 1410 N94-18545

Research activities at the Center for Modeling of Turbulence and Transition p 1410 N94-18546

Research on two equation models
p 1411 N94-18547

Assessment and development of second order turbulence models p 1411 N94-18548

Numerical investigation of complex, transitional, and chemically reacting flows p 1411 N94-18550

Computational aero-acoustics as a branch of turbulence research p 1411 N94-18552

A comparative study of turbulence models in predicting hypersonic inlet flows p 1314 N94-18553

An algebraic turbulence model for turbomachinery
p 1411 N94-18554

Turbulence modeling in aircraft icing
p 1412 N94-18555

Several examples where turbulence models fail in inlet flow field analysis p 1412 N94-18556

Plasma contactor development for Space Station
[NASA-TM-106425] p 1587 N94-18861

Spacework 17: O'Leary's Mars
[NASA-TM-109374] p 1629 N94-18966

Multichannel error correction code decoder
[NASA-TM-106331] p 1333 N94-19313

Gear sound levels with various tooth contact ratios and forms
[NASA-TM-106432] p 1446 N94-19318

Design for cyclic loading endurance of composites
[NASA-TM-106407] p 1457 N94-19351

Overview of STOVL aircraft propulsion research offtakes and vertical lift systems
[NASA-TM-106387] p 1321 N94-19353

Supersonic jets from bevelled rectangular nozzles
[NASA-TM-106403] p 1313 N94-19484

NATIONAL AERONAUTICS AND SPACE ADMINISTRATION. MARSHALL SPACE FLIGHT CENTER, HUNTSVILLE, AL.

The Einstein Observatory catalog of IPC x ray sources. Volume 4E: Right ascension range 08h 00m to 11h 59m
[NASA-TM-108401-VOL-4E] p 1625 N94-18612

The Einstein Observatory catalog of IPC x ray sources. Volume 5E: Right ascension range 12h 00m to 15h 59m
[NASA-TM-108401-VOL-5E] p 1625 N94-18613

The Einstein Observatory catalog of IPC x ray sources. Volume 6E: Right ascension range 16h 00m to 19h 59m
[NASA-TM-108401-VOL-6E] p 1625 N94-18615

The Einstein Observatory catalog of IPC x ray sources. Volume 7E: Right ascension range 20h 00m to 23h 59m
[NASA-TM-108401-VOL-7E] p 1625 N94-18618

The Einstein Observatory catalog of IPC x ray sources. Volume 1E: Documentation
[NASA-TM-108401-VOL-1E] p 1626 N94-18619

The Einstein Observatory catalog of IPC x ray sources. Volume 2E: Right ascension range 00h 00m to 03h 59m
[NASA-TM-108401-VOL-2E] p 1626 N94-18620

The Einstein Observatory catalog of IPC x ray sources. Volume 3E: Right ascension range 04h 00m to 07h 59m
[NASA-TM-108401-VOL-3E] p 1626 N94-18621

Spacelab 3
[NASA-TM-108750] p 1323 N94-18849

Technology test bed
[NASA-TM-109354] p 1322 N94-18953

Shuttle-C, the future is now
[NASA-TM-109355] p 1332 N94-18954

ASTRO-1 to explore invisible universe
[NASA-TM-109360] p 1336 N94-18956

National Boy Scout Jamboree
[NASA-TM-109367] p 1610 N94-18982

Pathfinder: Shuttle exhibit
[NASA-TM-109357] p 1333 N94-19071

Marshall Space Flight Center 1989 annual chronology of events
[NASA-TM-109381] p 1633 N94-19486

NATIONAL AEROSPACE LAB., AMSTERDAM (NETHERLANDS).

Feasibility of a wind-ellipse criterion in a vortex advisory system for Schiphol Airport
[NLR-TP-91384-U] p 1315 N94-17733

Take-off performance monitoring system algorithm and display development
[NLR-TP-91395-U] p 1317 N94-17734

High-lift system analysis method using unstructured meshes p 1307 N94-18426

NATIONAL CENTER FOR MFG. SCIENCES, ANN ARBOR, MI.

Development of alternatives to lead-bearing solders
[DE93-016509] p 1357 N94-17862

NATIONAL DEFENCE RESEARCH ESTABLISHMENT, UMEA (SWEDEN).

Condensed gases under winter conditions: A study for the rescue services
[FOA-C-40305-4.5] p 1473 N94-18139

NATIONAL INST. FOR FUSION SCIENCE, NAGOYA (JAPAN).

Electron stripping cross sections for light impurity ions in colliding with atomic hydrogens relevant to fusion research
[DE93-788476] p 1566 N94-18158

NATIONAL INST. OF STANDARDS AND TECHNOLOGY, GAITHERSBURG, MD.

Pulse radiolytic studies of electron transfer processes and applications to solar photochemistry
[DE93-018715] p 1464 N94-17781

Equipment for investigation of cryogenic compaction of nanosize silicon nitride powders
[DE93-018740] p 1340 N94-18180

Initial Graphics Exchange Specification (IGES)
[AD-A270049] p 1522 N94-18794

Thermophysical properties
[DE93-040219] p 1351 N94-19134

NATIONAL LAB. FOR HIGH ENERGY PHYSICS, TSUKUBA (JAPAN).

Proceedings of the 3rd Workshop on Balloon-Borne Experiments with Superconducting Magnet Spectrometers
[DE93-788362] p 1630 N94-18219

NATIONAL OCEANIC AND ATMOSPHERIC ADMINISTRATION, BOULDER, CO.

Analysis of meteorological conditions during AGASP-4: 30 March - 23 April 1992
[PB93-190205] p 1489 N94-18126

NATIONAL OCEANIC AND ATMOSPHERIC ADMINISTRATION, RESEARCH TRIANGLE PARK, NC.

Spatiotemporal variability of non-urban ozone concentrations over the eastern United States and its potential replication by satellite data
[PB93-191328] p 1476 N94-19065

NATIONAL OCEANIC AND ATMOSPHERIC ADMINISTRATION, SEATTLE, WA.

Method for extracting tidal and inertial motion from ARGOS ice buoys applied to the Barents Sea during CEAREX
[PB93-190213] p 1499 N94-19063

NATIONAL PHYSICAL LAB., TEDDINGTON (ENGLAND).

A preliminary model for crack-tip hydrogen transport
[NPL-DMM(A)-84] p 1451 N94-17899

Guidelines for the expression of uncertainties in surface chemical analysis by Auger Electron Spectroscopy (AES) and X ray Photoelectron Spectroscopy (XPS)
[NPL-DMM(A)-99] p 1346 N94-17900

PostScript: A study in conformity
[NPL-DITC-214/93] p 1517 N94-17917

The stability and utility of the ESPRIT project, MUSiC, performance-based indicators of usability and tools: An evaluation of the usability of the NPL iSDX telephone system
[NPL-DITC-213/92] p 1613 N94-17925

Ratio of specimen thickness to detection area for reliable hydrogen permeation measurement
[NPL-DMM(A)-103] p 1451 N94-17929

Strategies for testing form assessment software
[NPL-DITC-211/92] p 1518 N94-17930

NATIONAL SCIENCE FOUNDATION, WASHINGTON, DC.

Undergraduate origins of recent science and engineering doctorate recipients
[NSF-92-332] p 1610 N94-19389

Undergraduate course and curriculum development program and calculus and the bridge to calculus program: 1992 awards
[NSF-93-24] p 1610 N94-19446

A foundation for the 21st Century: A progressive framework for the National Science Foundation. Report of the National Science Board Commission on the future of the National Science Foundation
[NSB-92-196] p 1611 N94-19618

Program descriptions
[NSF-92-123] p 1531 N94-19619

Guide to programs, fiscal year 1993
[NSF-92-78] p 1633 N94-19620

NATIONAL TRANSPORTATION SAFETY BOARD, WASHINGTON, DC.

Aircraft accident report: Midair collision, Mitsubishi MU-2B-60, N74FB, and PIPER PA-32-301, N82419, Greenwood Municipal Airport, Greenwood, Indiana, 11 September 1992
[PB93-910406] p 1315 N94-19352

NAVAL ACADEMY, ANNAPOLIS, MD.

Delamination in composite materials as observed using an optical fiber strain gage
[AD-A270803] p 1344 N94-19662

Essential shift: Scientific revolution in the 20th century
[AD-A270810] p 1610 N94-19663

A stereoscopic vision system with applications to automated docking and tracking
[AD-A270754] p 1333 N94-19765

Applications of neural networks in fault detection of rotating machinery
[AD-A270755] p 1448 N94-19766

NAVAL AIR WARFARE CENTER, CHINA LAKE, CA.

Refinement of unit cell parameters by least-squares: Comments on an old technique and the development of a new computer program
[AD-A270610] p 1531 N94-19590

NAVAL AIR WARFARE CENTER, INDIANAPOLIS, IN.

Embedded Computer Performance Measurement (ECPM). Advanced avionics subsystems and technology multiprocessor ECPM software documentation
[AD-A269921] p 1320 N94-18658

NAVAL AIR WARFARE CENTER, WARMINSTER, PA.

Reference model for project support environments, version 1.0
[AD-A269110] p 1520 N94-18251

NAVAL BIODYNAMICS LAB., NEW ORLEANS, LA.

Bibliography of scientific publications of the Naval Biodynamics Laboratory, 1980 - 1992
[AD-A268886] p 1505 N94-18226

NAVAL COMMAND, CONTROL AND OCEAN SURVEILLANCE CENTER, SAN DIEGO, CA.

Evaluation of the production-grade class 4 flextensional transducer shell
[AD-A268796] p 1340 N94-18201

Intentionally Short Range Communications (ISRC)
[AD-A268788] p 1384 N94-18216

Survey of collision avoidance and ranging sensors for mobile robots, revision 1
[AD-A269846] p 1541 N94-18474

Residual strain measurement on the production-grade class 4 flextensional transducer shell
[AD-A268828] p 1430 N94-18537

Work plan for the Marine Aerosol Properties and the Thermal Imager Performance Trial (MAPTIP)
[AD-A270026] p 1483 N94-18712

Coupled neural-dendritic processes: Cooperative stochastic effects and the analysis of spike trains
[AD-A270041] p 1506 N94-18793

Marine-modified LOWTRAN: The contribution of sun glint
[AD-A269547] p 1500 N94-19762

NAVAL HEALTH RESEARCH CENTER, SAN DIEGO, CA.

A comparison of polygraphic and actigraphic monitoring of sleep using a 5-channel programmable-sensitivity actigraph
[AD-A270731] p 1507 N94-19608

NAVAL MEDICAL RESEARCH INST., BETHESDA, MD.

Cerebral ischemia and reperfusion injury: A brief review
[AD-A270480] p 1507 N94-19675

NAVAL POSTGRADUATE SCHOOL, MONTEREY, CA.

The organizational preparation of existing relational databases for the integration of expert systems
[AD-A268823] p 1614 N94-18191

Adaptations to micropep and rocket to allow performance evaluation of multiple grain and/or airbreathing motors
[AD-A268798] p 1337 N94-18202
Spectral analysis of synoptic time scale disturbances over the tropical eastern Pacific during summer 1989, 1990 and 1991
[AD-A268821] p 1490 N94-18206
Calibration of a high frequency monostatic acoustic echosounder
[AD-A268901] p 1481 N94-18229
Three-dimensional cloud visualization based on satellite imagery
[AD-A269318] p 1490 N94-18300
An application of parameter estimation to the stability and control of the BQM-147 unmanned aerial vehicle
[AD-A268741] p 1321 N94-18401
A computational and experimental investigation of incompressible oscillatory airfoil flow and flutter problems
[AD-A268748] p 1311 N94-18402
Developmental testing of a prototype all-reflection Michelson interferometer
[AD-A269064] p 1430 N94-18406
Specification and analysis of a high speed transport protocol
[AD-A268941] p 1386 N94-18449
Parallelization of the Air Force Space Command (AFSPACECOM) satellite motion models
[AD-A269327] p 1334 N94-18470
Cognitive limitations in coordination in hierarchical information processing structures
[AD-A268825] p 1616 N94-18535
Preliminary design of a water cooled avionics cooling rack
[AD-A268826] p 1320 N94-18536
Close-coupled oscillating canard effects on post-stall lift enhancement
[AD-A268938] p 1321 N94-18541
Two-dimensional boundary surfaces for axi-symmetric external transonic flows
[AD-A269678] p 1312 N94-18571
Wavelet transform for time-frequency analysis of the vibrational signature and its application
[AD-A269928] p 1454 N94-18661
Resolution in radar mapping
[AD-A269730] p 1462 N94-18753
Implementation of electronic data interchange in the department of defense: Lessons learned from private industry
[AD-A269532] p 1534 N94-18768
Computer-Aided Prototyping System (CAPS) within the software acquisition process. A case study
[AD-A268705] p 1522 N94-18786
An investigation of low Marangoni number fluid flow in a cold corner
[AD-A271317] p 1422 N94-19569
Nontraditional windows in spectral analysis
[AD-A271336] p 1553 N94-19583
Acoustic propagation modeling using MATLAB
[AD-A270905] p 1564 N94-19750
A study of the amplification of laser and VLF waves using a simple pendulum model
[AD-A270857] p 1442 N94-19770

NAVAL RESEARCH LAB., BAY SAINT LOUIS, MS.
The Navy tessellated spheroid map projection system: A comprehensive definition
[AD-A269989] p 1462 N94-18677
Parallel and vector adaptations of the underwater finite element parabolic equation model
[AD-A269990] p 1583 N94-18678
Color palette considerations for digital map displays
[AD-A269991] p 1462 N94-18679
Atlas of SSM/I satellite ice concentration interpolated to operational ice model domains of the Arctic for 1992
[AD-A270306] p 1499 N94-18727
Estimating the oceanic sound speed environmental for long-range acoustic propagation
[AD-A270231] p 1499 N94-18903
Faulted structure of the bottom simulating reflector on the Blake Ridge, western North Atlantic
[AD-A271289] p 1500 N94-19745

NAVAL RESEARCH LAB., WASHINGTON, DC.
Enhanced acceleration in a self-modulated-laser wakefield accelerator
[AD-A268452] p 1586 N94-18148
UVPI imaging from the LACE satellite: The Nihka rocket plume
[AD-A268456] p 1334 N94-18149
RADARC HF ionospheric prediction program for OTH radar
[AD-A269557] p 1385 N94-18291
Nonlinear Thomson scattering of intense laser pulse from beams and plasmas
[AD-A269556] p 1438 N94-18460
Ultraviolet plume instrument calibration and sensor assessment
[AD-A269687] p 1337 N94-18574
Designs for a 10.6 micrometer electromagnetic wiggler Free-Electron Laser (FEL)
[AD-A269695] p 1439 N94-18576
Efficient simulation of DEDS by means of standard clock techniques: Queueing and integrated radio network examples
[AD-A269878] p 1432 N94-18681
Morphology and characteristics of disturbed HF skywave channels
[AD-A269755] p 1388 N94-18722
A tunable compact high power far-infrared grating free-electron laser
[AD-A269875] p 1440 N94-18771
Connection machine software conversion of a Navy oceans model
[AD-A269876] p 1535 N94-18772
Neutral networks: An NRL perspective
[AD-A269122] p 1541 N94-18773
A user task analysis for command and control systems and its use in human-computer interaction research
[AD-A269877] p 1512 N94-18774
A high resolution ultraviolet Shuttle glow spectrograph
p 1325 N94-19174
Modeling of current features in Gulf Stream SAR imagery
[AD-A270734] p 1499 N94-19609
Template based low data rate speech encoder
[AD-A270900] p 1392 N94-19748
Control of integrated voice/data multi-hop radio networks via reduced-load approximations
[AD-A270661] p 1393 N94-19779
Measurements of ocean surface and bottom backscattering strengths in the northwestern Atlantic Ocean
[AD-A270893] p 1500 N94-19786
UVPI imaging from the LACE satellite: The Strypi rocket plume
[AD-A270967] p 1335 N94-19787

NAVAL SURFACE WARFARE CENTER, BETHESDA, MD.
Mechanical properties and impact damage resistance of composites fabricated by low cost, vacuum assisted, resin transfer molding
[AD-A270361] p 1342 N94-18702
Results of a joint Navy/Air Force operational test to evaluate USAF Integrated Maintenance Information Systems (IMIS), Interactive Electronic Technical Manual (IETM) technology applied to the F/A-18 aircraft
[AD-A271322] p 1619 N94-19571

NAVAL SURFACE WARFARE CENTER, DAHLGREN, VA.
NSWCWODET participation in Space Shuttle mission STS-46
[AD-A268875] p 1332 N94-18321
Absolute positioning by collecting Global Positioning System (GPS) data along short baselines
[AD-A271324] p 1317 N94-19572
Tracking with time-delayed data in multisensor systems
[AD-A271334] p 1391 N94-19582

NAVAL SURFACE WARFARE CENTER, SILVER SPRING, MD.
Aluminum powder/water reaction ignited by electrical pulsed power
[AD-A269223] p 1376 N94-17840

NAVAL UNDERSEA WARFARE CENTER, NEWPORT, RI.
Relation between the fluctuating wall pressure and the turbulent structure of a boundary layer on a cylinder in axial flow
[AD-A270242] p 1418 N94-18906
A register of underwater acoustic test facilities in the US, Canada, and the United Kingdom
[AD-A270884] p 1500 N94-19785

NAVAL WEAPONS CENTER, CHINA LAKE, CA.
Operator performance in pattern matching as a function of reference material structure
[AD-A269889] p 1509 N94-18686

NEBRASKA UNIV., LINCOLN.
Biophysical characterization and surface radiation balance
[NASA-CR-194659] p 1470 N94-17762
Relaxation of polar orientational order in nonlinear optical polymers by second harmonic generation
[AD-A269059] p 1370 N94-18515

NEVADA UNIV., LAS VEGAS.
Studies of clusters
[DE93-018961] p 1572 N94-19309

NEVADA UNIV., RENO.
Cloud CCN feedback
[DE93-016878] p 1472 N94-17985
Ship-produced cloud line of 13 July 1991
[DE93-016879] p 1472 N94-17986

NEW ENERGY AND INDUSTRIAL TECHNOLOGY DEVELOPMENT ORGANIZATION, TOKYO (JAPAN).
Feasibility survey of thermoelectric conversion technology using semiconductors
[DE93-520882] p 1595 N94-18105

NEW MEXICO STATE UNIV., LAS CRUCES.
Systolic design with asynchronous controls for digital-signal processing
[AD-A270976] p 1392 N94-19680

NEW MEXICO UNIV., ALBUQUERQUE.
Tunable synchronously pumped intracavity two-stage optical frequency upconversion
[AD-A269105] p 1438 N94-18250
Shrinkage void formation and its effect on freeze and thaw processes of lithium and lithium-fluoride for space applications
[DE93-019303] p 1338 N94-19128

NEW ORLEANS UNIV., LA.
Dense energetic compounds of C, H, N, and O atoms. 3: 5-(4-nitro-(1,2,5) oxadiazolyl)-5H-(1,2,3) triazolo (4,5-c)(1,2,5) oxadiazole
[AD-A268715] p 1338 N94-18314

NEW YORK UNIV., NEW YORK.
Plasma properties research: Task 3
[DE93-017087] p 1583 N94-17854

NICE UNIV. (FRANCE).
Bifurcation theory: Chaos and patterns
p 1607 N94-18237

NIHON UNIV., TOKYO (JAPAN).
Ore-type conditions for cycles through specified vertices p 1555 N94-19695

NOKIA RESEARCH CENTER, ESPOO (FINLAND).
APLAC: An object-oriented analog circuit simulator and design tool. 6.1 reference manual
[PB93-187193] p 1396 N94-18091

NORTH CAROLINA STATE UNIV., RALEIGH.
Synthesis of higher alcohols from carbon monoxide and hydrogen in a slurry reactor
[DE93-015086] p 1347 N94-18209
Characterization of diamond film nucleation and growth surface
[AD-A269400] p 1597 N94-18459
Growth, characterization and device development in monocrystalline diamond films
[AD-A270074] p 1599 N94-18797
Life: Origin and evolution on Earth--How can we escape? p 1503 N94-19217
Carbon Isotope Biogeochemistry of Methane from Anoxic Sediments
[NASA-CR-194620] p 1477 N94-19231
A carbon isotope mass balance for an anoxic marine sediment: Isotopic signatures of diagenesis
p 1477 N94-19232
The carbon isotope biogeochemistry of (epsilon)CO2 production in a methanogenic marine sediment
p 1477 N94-19233
The carbon isotope biogeochemistry of methane production in anoxic sediments. 1: Field observations
p 1477 N94-19234
Factors that control the stable carbon isotopic composition of methane produced in an anoxic marine sediment p 1477 N94-19235
Semi-span model testing in the National Transonic Facility
[NASA-CR-194479] p 1312 N94-19388
The deposition of electro-optic films on semiconductors
[AD-A270823] p 1605 N94-19664
Solid-state dynamics in novel semiconductor nanostructures
[AD-A271249] p 1605 N94-19725

NORTH CAROLINA UNIV., CHAPEL HILL.
Synoptic ocean prediction experiment. EN216 CTD section data report
[AD-A268903] p 1497 N94-18230
Theoretical and experimental studies of quantum wells
[AD-A271180] p 1606 N94-19741

NORTH CAROLINA UNIV., CHARLOTTE.
Oligomer and mixed-metal compounds, potential multielectron transfer catalysts
[DE93-019592] p 1350 N94-19017

NORTHEAST SUSTAINABLE ENERGY ASSOCIATION, GREENFIELD, MA.
S/EV 1992: Solar and Electric Vehicles. Volume 1: Proceedings
[DE93-015762] p 1445 N94-18307

NORTHWEST RESEARCH ASSOCIATES, INC., BELLEVUE, WA.
Internal instability of nonparallel flow on an equatorial beta-plane
[AD-A268927] p 1490 N94-18486
An investigation of methods for updating ionospheric scintillation models using topside in-situ plasma density measurements
[AD-A269872] p 1483 N94-18655

NORTHWESTERN UNIV., EVANSTON, IL.

Study of mechanical behavior and internal structure of ferritic nanocrystalline material
[DE93-019264] p 1596 N94-18184

Experimental and theoretical investigation of surface chemistry induced by direct and indirect electronic excitation
[AD-A268846] p 1348 N94-18221

Vibrational dynamics in photoinduced electron transfer
[DE93-040874] p 1567 N94-18533

Research in high energy physics
[DE93-018031] p 1575 N94-19287

Adaptive methods for nonlinear structural dynamics and crashworthiness analysis p 1458 N94-19466

MOCVD-grown InGaAsP heterostructure diode lasers
[AD-A270848] p 1606 N94-19769

NORWEGIAN DEFENCE RESEARCH ESTABLISHMENT, KJELLER.

Safety-routines and guidelines for work in the clean room at the Epitek-Laboratory, Kjeller (Norway)
[FFI-93/7012] p 1322 N94-17735

Cesar user library
[FFI-93/7021] p 1529 N94-19378

NOTRE DAME UNIV., IN.

Research at the Notre Dame Radiation Laboratory
[DE93-018716] p 1566 N94-18165

Preliminary structural design: Defining the design space
[AD-A268898] p 1317 N94-18227

O

OAK RIDGE INST. FOR SCIENCE AND EDUCATION, TN.

Magnetic Fusion Energy Technology Fellowship: Report on survey of institutional coordinators
[DE93-014646] p 1583 N94-17739

Excimer laser induced permanent electrical conductivity and nanostructures in polymers
[DE93-015965] p 1368 N94-17946

OAK RIDGE NATIONAL LAB., TN.

Power compensators for phased operation of antenna arrays on JET and D3-D
[DE93-013208] p 1581 N94-17694

Arc detection and protection in high-power antenna systems
[DE93-013272] p 1382 N94-17695

ITER EDA design confinement capability
[DE93-013729] p 1582 N94-17697

Nuclear Medicine Program
[DE93-013896] p 1504 N94-17699

Self-regulated shear flow turbulence in confined plasmas
[DE93-015823] p 1583 N94-17743

Metals 2000
[DE93-016761] p 1355 N94-17752

Alloy development of FeAl aluminide alloys for structural use in corrosive environments
[DE93-015100] p 1355 N94-17757

Conical geometry for sagittal focusing as applied to x rays from synchrotrons
[DE93-017238] p 1593 N94-17760

Air pollution effects field research facility. 3: UV-B exposure and monitoring system
[DE93-013098] p 1470 N94-17773

Carbon Dioxide Information Analysis Center: FY 1992 activities
[DE93-013845] p 1471 N94-17774

Solid-state, resistive hydrogen sensors for safety monitoring
[DE93-017769] p 1424 N94-17778

Assessing impacts of climate change on forests: The state of biological modeling
[DE93-015916] p 1471 N94-17790

Assessment of an improved multiaxial strength theory based on creep-rupture data for Inconel 600
[DE93-015929] p 1356 N94-17791

Lattice damage in ion-implanted compound semiconductors and its effect on electrical activation
[DE93-015907] p 1593 N94-17845

Metal-nanocluster composites made by ion implantation: A novel third-order nonlinear material
[DE93-015908] p 1339 N94-17846

Screening analysis for chlorine-free alternative refrigerants to replace R-22 in air conditioning applications
[DE93-015920] p 1367 N94-17847

Charpy impact toughness of martensitic steels irradiated in FFTF: Effect of heat treatment
[DE93-015960] p 1450 N94-17848

Data fusion through simulated annealing of registered range and reflectance images
[DE93-015910] p 1612 N94-17858

Technique to eliminate helium induced weld cracking in stainless steels
[DE93-015982] p 1357 N94-17859

Summary of work on coatings and claddings for fossil energy applications
[DE93-017005] p 1367 N94-17881

Practical reporting times for environmental samples
[DE93-013461] p 1472 N94-17910

Interpretation of warm prestress-induced fracture toughness based on crack-tip constraint
[DE93-015967] p 1451 N94-17913

Helium-induced weld degradation of HT-9 steel
[DE93-015981] p 1358 N94-17915

Excimer laser induced permanent electrical conductivity and nanostructures in polymers
[DE93-015965] p 1368 N94-17946

Lightweight materials for transportation: Program plan
[DE93-017381] p 1340 N94-18087

Studies of dynamic contact of ceramics and alloys for advanced heat engines
[DE93-016366] p 1368 N94-18110

Metadata compiled and distributed by the Carbon Dioxide Information Analysis Center for global climate change and greenhouse gas-related data bases
[DE93-015338] p 1473 N94-18167

Computer simulation of macromolecular crystals and their defects
[DE93-015213] p 1596 N94-18192

Matrix- and substrate-assisted laser desorption for fast DNA sequencing
[DE93-015332] p 1501 N94-18242

Human reliability analysis application guide
[DE93-015361] p 1511 N94-18244

Effects of irradiation temperature on embrittlement of nuclear pressure vessel steels
[DE93-015428] p 1359 N94-18245

A probability method of fracture mechanics analysis for HFIR vessel
[DE93-015510] p 1453 N94-18246

Photobiotechnology: Application of photosynthesis to the production of renewable fuels and chemicals
[DE93-015522] p 1466 N94-18247

Workshop on Innovation in Materials Processing and Manufacture: Exploratory Concepts for Energy Applications
[DE93-017674] p 1467 N94-18478

The evolution of the PVM concurrent computing system
[DE93-017764] p 1534 N94-18482

Detection of single molecules in microspheres
[DE93-017776] p 1567 N94-18493

The urban perspectives of acid rain
[DE93-018881] p 1474 N94-18523

Imaging and blackbody emission spectra of hot particulates generated during laser ablation
[DE93-015818] p 1439 N94-18724

CDIAC catalog of numeric data and computer model packages
[DE93-017675] p 1475 N94-18832

Development of ductile Fe3Al-based aluminides
[DE93-017865] p 1362 N94-18938

Survey of ceramic machining in Japan
[DE93-018277] p 1372 N94-18946

Tensile properties of as-cast iron-aluminide alloys
[DE93-017852] p 1363 N94-18975

Modeling of single-crystal laser-weld microstructures
[DE93-017853] p 1445 N94-18976

Energy Efficiency and Renewable Energy Program
[DE93-017936] p 1468 N94-18986

Software distribution using xnetlib
[DE93-018278] p 1523 N94-18989

Growth of epitaxial semiconductor alloys and superlattices with continuously variable composition by pulsed-laser ablation
[DE93-018726] p 1601 N94-18998

Inventory management plan for a research and development local area network
[DE93-018381] p 1617 N94-19026

Effects of irradiation temperature on Charpy and tensile properties of high-copper, low upper-shelf, submerged-arc welds
[DE93-017858] p 1445 N94-19047

An ORACLE CASE history: Experiences with ORACLE CASE tools
[DE93-010827] p 1617 N94-19057

Surface modification of sapphire for IR window application
[DE93-019168] p 1602 N94-19075

Coordination of software-development activities among sites that are geographically separated
[DE93-019201] p 1524 N94-19076

Research program activities of the ORNL Analytical Chemistry Division
[DE93-017938] p 1339 N94-19117

Densities and viscosities of ternary ammonia/water fluids
[DE93-015966] p 1351 N94-19118

Computer codes for checking, plotting and processing of neutron cross-section covariance data and their application
[DE93-018459] p 1570 N94-19129

Prediction of non-equilibrium solidification modes in austenitic stainless steel laser welds
[DE93-018457] p 1364 N94-19203

Atomic resolution electron energy loss spectroscopy in the scanning transmission electron microscope
[DE93-015334] p 1352 N94-19239

ICRF direct electron heating experiments in TFTR
[DE93-017857] p 1590 N94-19273

Low-aluminum-content iron-aluminum alloys
[DE93-017862] p 1365 N94-19274

Analytical and experimental evaluation of joining silicon nitride to metal and silicon carbide to metal for advanced heat engine applications
[DE93-018128] p 1446 N94-19291

PUMMA: Parallel Universal Matrix Multiplication Algorithms on distributed memory concurrent computers
[DE93-019163] p 1538 N94-19299

Robot navigation in unknown terrains: Introductory survey of non-heuristic algorithms
[DE93-019221] p 1316 N94-19300

Are bilinear quadrilaterals better than linear triangles?
[DE93-019223] p 1551 N94-19301

Analysis and design of robust decentralized controllers for nonlinear systems
[DE93-019224] p 1543 N94-19302

The Fourier analysis technique and epsilon-pseudo-eigenvalues
[DE93-018805] p 1551 N94-19337

Effect of EMP fields on cell membrane potentials
[DE93-015819] p 1503 N94-19341

Ceramic technology project data base
[DE93-019360] p 1374 N94-19561

A comparison of iterative methods for a model coupled system of elliptic equations
[DE93-040482] p 1553 N94-19655

Commercialization effort in support of electroslag-casting technology
[DE93-017988] p 1366 N94-19733

OAK RIDGE Y-12 PLANT, TN.

Summary report for supercritical carbon dioxide extraction and carbonization of Resorcinol-Formaldehyde (RF) foams
[DE93-016924] p 1346 N94-17987

Nondestructive inspection of graphite-epoxy laminates for heat damage using DRIFT and LPF spectroscopies
[DE93-017228] p 1343 N94-18761

OBSERVATOIRE CANTONAL, NEUCHATEL (SWITZERLAND).

Development of atomic standards at the Neuchatel Observatory p 1428 N94-18038

OFFICE NATIONAL D'ETUDES ET DE RECHERCHES AEROSPATIALES, PARIS (FRANCE).

Stability analysis through bifurcation theory, 1
p 1608 N94-18238

Stability analysis through bifurcation theory, 2
p 1608 N94-18239

Non-linear flight dynamics p 1319 N94-18240

A viscous-inviscid solver for high-lift incompressible flows over multi-element airfoils at deep separation conditions p 1306 N94-18425

The GARTEUR high lift research programme
p 1307 N94-18430

Viscous-inviscid calculation of high-lift separated compressible flows over airfoils and wings
p 1309 N94-18440

Fundamentals of infrared thermography
p 1431 N94-18648

Application of infrared thermography in fluid mechanics p 1431 N94-18649

Heat transfer quantitative characterization: Passive and active methods p 1431 N94-18650

Perspective and future possibilities
p 1431 N94-18651

OFFICE OF NAVAL RESEARCH, ARLINGTON, VA.

Naval research reviews. Mixing enhancement for air-breathing propulsion. Non-axisymmetric jets increase mixing, volume 44 and volume 45
[AD-A268966] p 1521 N94-18543

OFFICE OF NAVAL RESEARCH EUROPEAN OFFICE, FPO NEW YORK, NY.

Ageing in Processed Polymers: Programme, summary, and abstracts discussion meeting
[AD-A268931] p 1370 N94-18448

OHIO STATE UNIV., COLUMBUS.

Interdisciplinary research on wear of materials
[AD-A268190] p 1443 N94-17730

The physics of cellular automata and coherence and chaos in classical many-body dynamical systems
[DE93-018021] p 1561 N94-18177

Wideband electromagnetic scattering/analysis program: Far zone electromagnetic scattering from complex shapes using geometrical theory of diffraction
[AD-A268790] p 1384 N94-18187

Realistic theories of heavy electron and other strongly correlated materials
[DE93-010350] p 1571 N94-19204

Picoindentation hardness measurements using atomic force microscopy
[AD-A270877] p 1604 N94-19579

Atomic-scale friction and microfriction of graphite and diamond using friction force microscopy
[AD-A270952] p 1605 N94-19679

Microtribology of magnetic media
[AD-A271209] p 1407 N94-19722

Atomic-scale friction measurements using friction force microscopy. Part 2: Application to magnetic media
[AD-A270759] p 1447 N94-19767

Tribological studies of silicon for magnetic recording applications (Invited)
[AD-A270876] p 1447 N94-19784

OLD DOMINION UNIV., HAMPTON, VA.

A fast adaptive convex hull algorithm on two-dimensional processor arrays with a reconfigurable BUS system
p 1402 N94-18380

OLD DOMINION UNIV., NORFOLK, VA.

Analysis of pultrusion processing for long fiber reinforced thermoplastic composite system
[NASA-CR-194504] p 1339 N94-17766

Microwave scattering from TAE modes
[DE93-018170] p 1583 N94-17809

Navier-Stokes, dynamics and aeroelastic computations for vortical flows, buffet and flutter applications
[NASA-CR-194520] p 1313 N94-19621

OPTICAL SOCIETY OF AMERICA, WASHINGTON, DC.

Quantum optoelectronics technical digest, 1993. Voolume 8: Postconference edition
[AD-A268209] p 1576 N94-17887

Spatial light modulators and applications: Summaries of papers presented at the Spatial Light Modulators and Applications Topical Meeting
[AD-A269452] p 1577 N94-18283

Integrated photonics research volume 10. Conference edition
[AD-A269298] p 1577 N94-18298

Optical computing. Organization of the 1993 Photonics Science Topical Meetings. Technical digest series, volume 7
[AD-A269025] p 1578 N94-18332

Optical design for photonics. Organization of the 1993 Photonics Science Topical Meetings. Technical digest series, volume 9
[AD-A269027] p 1578 N94-18396

Quantum Optoelectronics. Organization of the 1993 photonics science topical meetings. Technical digest series, volume 8
[AD-A269026] p 1578 N94-18488

Advanced Solid-State Lasers/Compact Blue-Green Lasers. 1993 technical digest series. Volume 2: Organization of the 1993 photonics science topical meetings
[AD-A269058] p 1438 N94-18492

Photonics in Switching: Organization of the 1993 photonics science topical meetings. Technical digest
[AD-A269024] p 1578 N94-18528

Soft X Ray Projection Lithography. Organization of the 1993 photonics science optical meetings
[AD-A269159] p 1579 N94-18693

Integrated Photonics Research: Post-deadline papers
[AD-A269232] p 1609 N94-18908

Ultrafast Electronics and Optoelectronics: Summaries of papers. Technical digest conference edition
[AD-A269233] p 1405 N94-18909

OREGON UNIV., EUGENE.

Surface second harmonic generation studies of stepped Ag(111) electrode surfaces
[AD-A265205] p 1594 N94-17876

OXFORD UNIV. (ENGLAND).

Data acquisition in aerodynamic research
p 1431 N94-18644

Recent developments in fast response aerodynamic probe technology p 1431 N94-18645

Liquid crystal heat transfer measurements
p 1432 N94-18653

P

PACIFIC NORTHWEST LAB., RICHLAND, WA.

Parallel inverse iteration with reorthogonalization
[DE93-012867] p 1533 N94-17693

Oxygen reduction at a stabilized zirconia interface with Y(1-x)Ca(x)MnO3 or La(1-x)Sr(x)MnO3 cathode materials
[DE93-015681] p 1593 N94-17747

Visibility impairment assessment: Importance of using theoretically derived optical characterizations
[DE93-017147] p 1470 N94-17749

The carbon dioxide emissions game: Playing the net
[DE93-017670] p 1471 N94-17821

A review of wind field models for atmospheric transport
[DE93-016085] p 1488 N94-17895

Improving the biodegradative capacity of subsurface bacteria
[DE93-013171] p 1501 N94-18051

Boundary layer heat budgets from wind profiler/RASS data: A feasibility study
[DE93-013187] p 1489 N94-18052

Advances in the identification of transfer function models using Prony analysis
[DE93-017980] p 1548 N94-18094

Application of ARC/INFO to regional scale hydrogeologic modeling
[DE93-015673] p 1461 N94-18107

Studies of interactions between conducting polymer and organic vapors: Applications to chemical sensing
[DE93-015694] p 1369 N94-18233

Analysis of superconducting magnetic energy storage applications at a proposed wind farm site near Browning, Montana
[DE93-018793] p 1466 N94-18276

In situ observation of radiation induced amorphization of crystals with apatite structure
[DE93-018450] p 1599 N94-18816

Operational parameters of an opto-electronic neural network employing fixed planar holographic interconnects
[DE93-018795] p 1433 N94-19000

High dose effects in neutron irradiated face-centered cubic metals
[DE93-017671] p 1364 N94-19043

Seasonal variability of wind electric potential in the US
[DE93-018182] p 1493 N94-19051

Pantex Plant Meteorological Monitoring Program
[DE93-018495] p 1493 N94-19127

Valuation of temporary and future greenhouse gas reductions
[DE93-018876] p 1478 N94-19319

Subcritical crack growth in continuous-fiber reinforced ceramic composites
[DE93-018784] p 1343 N94-19335

Quality, management, and the interplay of self-assessment, process assessments, and performance-based observations
[DE93-018787] p 1448 N94-19336

PAEDAGOGISCHE HOCHSCHULE, DRESDEN (GERMANY).

Cubic graphs containing k vertex-disjoint subgraphs of given cyclomatic number p 1555 N94-19697

PARIS VI UNIV. (FRANCE).

Introduction to spectral methods: Application to the Stokes problem p 1413 N94-18566

Introduction to spectral methods for hyperbolic system of conservation laws p 1413 N94-18567

PENNSYLVANIA STATE UNIV., UNIVERSITY PARK.

Vibrational and electronic properties of clusters and ultrathin films
[DE93-012291] p 1367 N94-17678

Combustion instability phenomena of importance to liquid propellant engines
[AD-A268800] p 1348 N94-18389

The vertical distribution of heating in the tropical atmosphere
[AD-A270452] p 1490 N94-18514

Calculation of turbulent boundary layer wall pressure spectra
[AD-A269549] p 1416 N94-18642

Acoustic intensity measurements in the presence of low Mach number flow
[AD-A269995] p 1562 N94-18664

Advanced civil engineering materials based on inorganic polymers
[AD-A270837] p 1374 N94-19600

Signal processing algorithms for heterogeneous architectures
[AD-A271248] p 1392 N94-19724

PENNSYLVANIA UNIV., PHILADELPHIA.

Novel electrochemical materials prepared by sol-gel chemistry
[AD-A269060] p 1578 N94-18405

Molecular and polymeric ceramic precursors
[DE93-040364] p 1372 N94-18891

PHILLIPS LAB., EDWARDS AFB, CA.

Process relationship as influenced by carbonization rate
[AD-A269680] p 1341 N94-18572

PHILLIPS LAB., HANSCOM AFB, MA.

Temperature, kinetic energy, and rotational temperature dependences for the reactions of Ar(+)(2)P3/2 with O2 and CO
[AD-A268974] p 1567 N94-18526

A review and evaluation of the ADAM 2.1 dispersion model
[AD-A269896] p 1474 N94-18688

Convection algorithms for magnetospheric particles
[AD-A270103] p 1493 N94-18871

PHILLIPS LAB., KIRTLAND AFB, NM.

The 7th International Cryocooler Conference
[AD-A268451] p 1379 N94-18147

The gyrotron backward-wave-oscillator experiment
[AD-A268982] p 1403 N94-18452

Constant-thrust orbit-raising transfer charts
[AD-A269088] p 1334 N94-18718

Characterization of vapor plume species and deposition residues resulting from pulsed laser ablation of a graphite/epoxy composite
[AD-A270101] p 1343 N94-18869

Novel electron beam cathode
[AD-A270106] p 1404 N94-18872

PHYSICS AND ELECTRONICS LAB. TNO, THE HAGUE (NETHERLANDS).

The First International Conference on PCTE
[FEL-92-A134] p 1518 N94-17965

C-band PARC manual
[FEL-92-B159] p 1383 N94-18070

Description of an infrared zoomcollimator
[FEL-93-A034] p 1580 N94-19424

First and second order Stokes generation by SRS in methane: Influence of rep-rate, beam quality and astigmatism
[FEL-92-A125] p 1441 N94-19426

The split-step algorithm for microwave propagation modeling above a conducting surface
[FEL-92-A430] p 1390 N94-19447

A comparison between several computer codes for calculations on microwave propagation
[FEL-92-A435] p 1390 N94-19449

Secure open systems: An investigation of current standardisation efforts for security in open systems
[FEL-92-B225] p 1618 N94-19450

Working visit to the University of L'Aquila, Italy
[FEL-93-B020] p 1618 N94-19452

Secure open systems: An investigation
[FEL-91-B293] p 1619 N94-19454

Applications of motion estimation in image processing
[FEL-92-B356] p 1580 N94-19455

Models and building blocks for secure open systems
[FEL-92-B365] p 1619 N94-19457

PRACTICAL: Planning and resource allocation in C2-domains with time critical algorithms
[FEL-93-B029] p 1544 N94-19458

Feasibility study for a measuring system velocity projectile
[FEL-91-A368] p 1434 N94-19797

Automated processing of military messages according to ADatP-3
[FEL-92-A044] p 1393 N94-19798

PITTSBURGH UNIV., PA.

Phase conjugation and beam combination using stimulated brillouin scattering
[AD-A269899] p 1439 N94-18656

POLITECNICO DI MILANO (ITALY).

A structured approach for modeling, analyzing and simulating real-time control systems
[REPT-93-044] p 1539 N94-17916

On comparison and extensions of control methods for narrow-band disturbance rejection
[REPT-93-015] p 1540 N94-17922

Multistack languages and grammars
[REPT-93-018] p 1518 N94-17926

Shop problems with two machines and time lags
[REPT-93-020] p 1518 N94-17927

An annealing approach to multi-facility location problems in euclidean spaces
[REPT-93-022] p 1547 N94-17928

Automatic tuning of an integral fuzzy controller
[REPT-93-006] p 1383 N94-17932

Electron mobility in high resistivity silicon
[REPT-93-007] p 1565 N94-17933

Active control of periodic noise with time-varying frequency
[REPT-93-012] p 1562 N94-17934

Neural networks to classify speaker independent isolated words recorded in radio car environments
[REPT-93-013] p 1383 N94-17935

TANGO: A notation for describing advanced transaction models
[REPT-93-014] p 1613 N94-17936

Joint stiffness estimation based on force sensor measurements in industrial manipulators
[REPT-92-053] p 1443 N94-17937

Linear parameter identification methods for ARMA models with periodic coefficients
[REPT-92-070] p 1556 N94-17938
An environment for requirement reuse
[REPT-92-082] p 1613 N94-17939
Efficient dynamic modeling of manipulators containing closed kinematic loops
[REPT-92-083] p 1444 N94-17940
An analytical approach to error localization by using information derived from error signature
[REPT-93-023] p 1518 N94-17960
Heuristics from nature for hard combinatorial optimization problems
[REPT-93-025] p 1547 N94-17961
Location of the absolute barycenter of a graph
[REPT-93-027] p 1547 N94-17962
A geometric algorithm for the Euclidean 1-center problem
[REPT-93-001] p 1519 N94-17975
Navigation in hypermedia applications: Modelling and semantics
[REPT-93-034] p 1520 N94-18136
Exact cost flow problems in acyclic networks
[REPT-93-030] p 1520 N94-18138
Better termination analysis for active databases
[REPT-93-026] p 1614 N94-18144
Annealing algorithms for multiresource absolute location problems on graph
[REPT-93-028] p 1520 N94-18145
A design procedure for slotted flaps
p 1305 N94-18418
Wake structure and aerodynamic behavior of high lift aircraft configurations during unsteady maneuvers in ground effect p 1309 N94-18439

POLYTECHNIC UNIV., BROOKLYN, NY.
Thin film studies of the proximity Josephson effect
[AD-A270129] p 1600 N94-18876

PORTLAND STATE UNIV., OR.
Canonical multi-valued input Reed-Muller trees and forms p 1401 N94-18375

PRINCETON UNIV., NJ.
Removing CFC's from the atmosphere with lasers: A second look
[DE93-017516] p 1473 N94-18101
Studies on high pressure and unsteady flame phenomena: Revision
[AD-A269138] p 1348 N94-18257
Numerical modelling of crystal growth
[AD-A271206] p 1605 N94-19719

PRINCETON UNIV. OBSERVATORY, NJ.
The universe at moderate redshift
[NASA-CR-193771] p 1627 N94-19093

PRINS MAURITS LAB. TNO, RIJSWIJK (NETHERLANDS).
Instrumented experiments aboard the frigate WOLF. Wolf 2: Measurement results of the 5.5 kg TNT in the crew aft sleeping compartment
[PML-1992-12] p 1451 N94-17931
Scaling laws for diffraction loading by air blast
[PML-1991-54] p 1452 N94-17941
Simulation of the impact of a plastic flyer on an aluminum block using the hydrocode AUTODYNE
[PML-1992-26] p 1458 N94-19444
Round robin experiments on the Explosive Components Water Gap Test (ECWGT)
[PML-1992-69] p 1378 N94-19445
Evaluation of mass spectra for a verification database
[PML-1993-12] p 1619 N94-19453

PUERTO RICO UNIV., RIO PIEDRAS.
Photodissociation studies of polyatomic free radicals
[AD-A270084] p 1350 N94-18799

PURDUE UNIV., WEST LAFAYETTE, IN.
Bibliography on ceramic matrix composites and reinforcing whiskers, platelets, and fibers, 1970-1990
[AD-A270139] p 1371 N94-18750
Gamma scattering in condensed matter with high intensity Moessbauer radiation
[DE93-019461] p 1601 N94-19031
The study of the phase structure of hadronic matter by searching for the deconfined quark-gluon phase transition using 2 TeV (bar-p)-p collisions, and by searching for critical phenomena in an exclusive study of multifragmentation using 1 GeV/nucleon heavy ion collisions
[DE93-018925] p 1570 N94-19103

R

RADEX, INC., BEDFORD, MA.
Aspects of the calibration and processing of the CRRES fluxgate magnetometer data
[AD-A270127] p 1432 N94-18875

RAND CORP., SANTA MONICA, CA.
An evolutionary approach to space launch commercialization
[AD-A269861] p 1331 N94-18411

RANGE COMMANDERS COUNCIL, WHITE SANDS MISSILE RANGE, NM.
Missile antenna pattern coordinate system and data formats
[AD-A269153] p 1385 N94-18260
Range safety transponder catalog
[AD-A270882] p 1323 N94-19581

RAYTHEON CO., LEXINGTON, MA.
RF vacuum microelectronics
[AD-A270003] p 1403 N94-18667

REMOTE SENSING TECHNOLOGY CENTER, TOKYO (JAPAN).
Development of ISY data set, part 2
[NASDA-CNT-930006-PT-2] p 1463 N94-19384

RENSSELAER POLYTECHNIC INST., TROY, NY.
Inelastic deformation and damage at high temperature
[DE93-018155] p 1448 N94-17814
The effects of radiolysis on the corrosion and stress corrosion behavior of 316 stainless steels
[DE93-019933] p 1363 N94-19021
Ionized-cluster beam/partially ionized beam deposition of electro-optical and nonlinear optical organic materials and device development
[AD-A270832] p 1604 N94-19596

RESEARCH INST. OF NATIONAL DEFENCE, LINKOEPING (SWEDEN).
Spectral radiance measurements on a bluff body stabilized flame: Characterization of the IR signature
[PB93-195899] p 1347 N94-18081
Solution of the Poisson equation with application to radar imaging
[PB93-195865] p 1389 N94-18950
Polarimetric statistics of electromagnetic waves scattered by distributed targets
[PB93-195907] p 1389 N94-18951

RESEARCH INST. OF NATIONAL DEFENCE, STOCKHOLM (SWEDEN).
Intelligent materials systems and structures. Part 4: The influence of thermomechanical loading on the life of shape memory alloys
[PB93-195923] p 1363 N94-18952
Air blast measurements at 20 and 40 km distance from detonating 10 and 20 ton high explosive charges
[PB93-195949] p 1419 N94-19068

RESEARCH TRIANGLE INST., RESEARCH TRIANGLE PARK, NC.
Amorphous silicon batch process cost analysis
[DE93-018203] p 1470 N94-19760

RETINA FOUNDATION, BOSTON, MA.
Center-of-Excellence: Microlaser microscope
[DE93-040688] p 1442 N94-19658

RICE UNIV., HOUSTON, TX.
Comparing performance on implicit memory tests
[AD-A269900] p 1508 N94-18657

RIJKSINSTITUUT VOOR VOLKSGEZONDHEID EN MILIEUHYGIEENE, BILTHOVEN (NETHERLANDS).
Land-use related sources of CO2, CH4 and N2O: Current global emissions and projections for the period 1990-2100
[PB93-194819] p 1475 N94-18949

ROCHESTER UNIV., NY.
Molecular nonlinear optical susceptibilities in condensed phases
[AD-A270200] p 1568 N94-18784
LLE Review
[DE93-017618] p 1602 N94-19123
The complexity of the optimal spanning hypertree problem
[TR-471] p 1561 N94-19481
Bits and relative order from residues, space efficiently
[TR-464] p 1530 N94-19482
Fault-tolerance and complexity
[TR-450] p 1530 N94-19483
First results with utile distinction memory for reinforcement learning
[TR-446] p 1610 N94-19485
A tight lower bound for on-line monotonic list labeling
[TR-478] p 1531 N94-19508
Statistical probabilities for planning
[TR-474] p 1559 N94-19511
Heap construction in the parallel comparison tree model
[TR-409] p 1538 N94-19512
Schroedinger's hope
[AD-A270988] p 1581 N94-19772

ROCKWELL INTERNATIONAL CORP., CANOGA PARK, CA.
Potassium-Rankine power conversion subsystem modeling for nuclear electric propulsion
[NASA-CR-191134] p 1468 N94-18821

ROCKWELL INTERNATIONAL CORP., COCOA BEACH, FL.
ISOBUS: A new versatile spacecraft platform using Shuttle small payloads p 1327 N94-19183

ROCKWELL INTERNATIONAL CORP., DOWNEY, CA.
The role of NASTRAN in the preliminary design cycle
p 1450 N94-17835

ROCKWELL INTERNATIONAL SCIENCE CENTER, THOUSAND OAKS, CA.
Photorefractive tungsten bronze crystals for optical computing
[AD-A268859] p 1596 N94-18320
Integration of ferroelectric/semiconductor thin films for SLM and photorefractive applications
[AD-A268645] p 1598 N94-18633
Fatigue resistant Ti3Al composites
[AD-A270305] p 1341 N94-18692

ROLLS-ROYCE, INC., ATLANTA, GA.
Collaborative research on combustion diagnostics and modeling between Rolls-Royce, Inc. and the United States Air Force Wright Laboratory
[AD-A270660] p 1354 N94-19778

ROME LAB., GRIFFISS AFB, NY.
Applications of nonlinear optic effects in new specialty fibers
[AD-A268890] p 1578 N94-18457
Design and fabrication of a Multichannel Adaptive Optical Processor (MADOP)
[AD-A270004] p 1579 N94-18668
The application of jet spray and ion beam contamination removal techniques to samples from the LDEF spacecraft
[AD-A270973] p 1354 N94-19755
The performance and survivability of dichromated poly (vinyl alcohol) holograms for space based photonic applications
[AD-A270974] p 1434 N94-19791

ROME LAB., HANSCOM AFB, MA.
Statistical description of the bistatic radar cross section distributions for a right circular cylinder
[AD-A270001] p 1387 N94-18666

ROME UNIV. (ITALY).
Beauty without charm in B-meson decays
[PREPRINT-732] p 1565 N94-17972

ROUEN UNIV. (FRANCE).
Turbulence modeling for compressible flows and implementation in Navier-Stokes solvers
p 1416 N94-18597

ROYAL NETHERLANDS METEOROLOGICAL INST., DE BILT.
The performance of drag relations in the WAQUA storm surge model
[KNMI-TR-149] p 1496 N94-17923
Verification of 3I retrievals vis-a-vis radiosonde observations
[KNMI-TR-150] p 1488 N94-17924
The Earth radiation budget experiment: Overview of data-processing and error sources
[KNMI-TR-146] p 1481 N94-18142
On the construction of a regional atmospheric climate model
[KNMI-TR-147] p 1489 N94-18143
Reports of the 1992 Synoptic Symposium
[KNMI-TR-151] p 1494 N94-19698
HIRLAM p 1494 N94-19699
The WAQUA/CSM-16 model p 1494 N94-19700
The wave forecasting model NEDWAM
p 1495 N94-19701
Organized track system: Air ways above the ocean
p 1495 N94-19702
Calamity weather: Environmental calamities and meteorology p 1495 N94-19703
Interactive Production Line (IPL) p 1495 N94-19704

ROYAL SOCIETY, LONDON (ENGLAND).
Royal Society of Chemistry, Heterocyclic Chemistry Group, Lakeland Heterocyclic Symposium
[AD-A270374] p 1338 N94-18703

RUTGERS - THE STATE UNIV., NEW BRUNSWICK, NJ.
Control of nonlinear systems
[AD-A270141] p 1542 N94-18898

RUTHERFORD APPLETON LAB., CHILTON (ENGLAND).
The Cluster Joint Science Operations Centre
p 1331 N94-19639

RUTHERFORD HIGH ENERGY LAB., CHILTON (ENGLAND).
Activities report of the Rutherford Appleton Laboratory
[ETN-93-94555] p 1631 N94-17968

S

SAINT VINCENT COLL., LATROBE, PA.
Modifications of airborne oceanographic lidar for the long range P-3 missions
[NASA-CR-194882] p 1499 N94-18819

SANDIA NATIONAL LABS., ALBUQUERQUE, NM.

Compound-lens injector for a 19-MeV, 700-kA electron beam
[DE93-013752] p 1573 N94-17698

Portable, solid state, fiber optic coupled Doppler interferometer system for detonation and shock diagnostics
[DE93-013917] p 1423 N94-17700

Selective electrochemical wafer thinning for silicon characterization
[DE93-015083] p 1592 N94-17742

A radial transmission line material measurement apparatus
[DE93-018508] p 1394 N94-17780

Analysis of high contact resistances associated with hermetic and lightning arrestor connectors
[DE93-014850] p 1395 N94-17783

Proposal for a numerical array library
[DE93-015017] p 1516 N94-17786

Simplified processing for 23 percent-efficient silicon concentrator solar cells
[DE93-015018] p 1464 N94-17787

Performance mapping of the STM4-120 kinematic Stirling engine using a statistical design of experiments method
[DE93-015132] p 1464 N94-17798

PVDF measurement of soft x ray induced shock and filter debris impulse
[DE93-017633] p 1382 N94-17806

A new multiphase equation of state for iron
[DE93-017629] p 1357 N94-17819

Finite element modeling of evaporation and condensation during sol-gel film and fiber formation
[DE93-017655] p 1345 N94-17820

Flight demonstration of image fix-taking with SAR
[DE93-016499] p 1382 N94-17861

Development of alternatives to lead-bearing solders
[DE93-016509] p 1357 N94-17862

Applications of an algebraic Monge property
[DE93-016869] p 1546 N94-17885

Current development in selected stress and thermal analysis software interfaces with PRO-ENGINEER
[DE93-014935] p 1518 N94-17943

Interactive Collaborative Environments (ICE) in the design to manufacturing process
[DE93-014994] p 1518 N94-17944

Microstructurally based thermomechanical fatigue lifetime model of solder joints for electronic applications
[DE93-016508] p 1452 N94-17995

Characteristics and pulsed radiation response of non-ideal quartz shock stress gauges
[DE93-017628] p 1424 N94-17999

Examination of metrics and assumptions used in correlation filter design
[DE93-017636] p 1576 N94-18000

FAROW: A tool for fatigue and reliability of wind turbines
[DE93-017639] p 1465 N94-18001

An overview of the SAFSIM computer program
[DE93-017657] p 1519 N94-18002

Embrittlement of surface mount solder joints by hot solder-dipped, gold-plated leads
[DE93-017659] p 1358 N94-18003

Effect of phase change in a debris cloud on a backwall structure
[DE93-017506] p 1358 N94-18100

Application of piezoelectric stress gauges to the measurement of fast-rise-time multimegampere electric currents
[DE93-017625] p 1429 N94-18102

Wetting behavior of alternative solder alloys
[DE93-016730] p 1359 N94-18127

The application of nondestructive techniques to the testing of a wind turbine blade
[DE93-016731] p 1447 N94-18128

GREPOS: A GENESIS database repositioning program
[DE93-018517] p 1614 N94-18164

First on-sun test of NaK pool-boiler solar receiver
[DE93-015003] p 1466 N94-18208

The spatial variance of ionospherically-induced phase errors in SAR imagery
[DE93-015643] p 1385 N94-18232

Error propagation equations and tables for estimating the uncertainty in high-speed wind tunnel test results
[DE93-018685] p 1311 N94-18275

Photovoltaic concentrator initiative: Concentrator cell development
[DE93-018505] p 1466 N94-18335

High-efficiency silicon concentrator cell commercialization
[DE93-018491] p 1467 N94-18409

Solderability perservative coatings: Electroless tin versus organic azoles
[DE93-017634] p 1370 N94-18477

Photo-induced and electrooptic properties of (Pb,La)(Zr,Ti)O3 films
[DE93-017496] p 1371 N94-18519

Testing and evaluation of large-area heliostats for solar thermal applications
[DE93-018509] p 1467 N94-18520

Characterization of the Facility for Atmospheric Corrosion Testing (FACT) at Sandia
[DE93-018510] p 1474 N94-18521

New applications for high average power beams
[DE93-018845] p 1439 N94-18522

Effects of the Mount Pinatubo eruption on solar insolation: Four case studies
[DE93-018454] p 1475 N94-18817

The Lever oscillator for use in high resistance resonator applications
[DE93-017652] p 1404 N94-18827

Three-dimensional shock wave physics simulations with MIMD PAGOSA on massively parallel computers
[DE93-011682] p 1455 N94-18829

Some parametric flow analyses of a particle bed fuel element
[DE93-018440] p 1337 N94-18830

Visualization for applications in shock physics
[DE93-012849] p 1418 N94-18918

Dynamical behavior of tantalum
[DE93-017877] p 1362 N94-18919

Adaptive path planning: Algorithm and analysis
[DE93-008348] p 1523 N94-18926

Environmentally assisted cracking of nickel anode substrates in Li/SOCl2 cells: An engineering approach
[DE93-015130] p 1405 N94-18928

Evaluation of fiber optic performance in the ACRR
[DE93-018515] p 1580 N94-18970

Networked MS windows 3.1 based classified document control system (CDOCS)
[DE93-017880] p 1617 N94-18984

A numerical study of hybrid optimization methods for the molecular conformation problems
[DE93-017898] p 1569 N94-18985

Using computerized tomography to determine ionospheric structures
[DE93-018903] p 1485 N94-19001

Using computerized tomography to determine ionospheric structures
[DE93-018904] p 1485 N94-19002

Motorola MC68040 high-speed design using Altera EPM5000 erasable programmable logic devices
[DE93-017635] p 1523 N94-19006

Geometrical pattern learning
[DE93-017641] p 1542 N94-19007

Tehachapi solar thermal system
[DE93-018443] p 1468 N94-19014

Silicon concentrator solar cell research
[DE93-018489] p 1468 N94-19015

Defect behavior of polycrystalline solar cell silicon
[DE93-018490] p 1468 N94-19016

Conceptual design of a sodium sulfur cell for US electric van batteries
[DE93-018683] p 1405 N94-19035

Optimizing wind turbine control system parameters
[DE93-018861] p 1469 N94-19036

A general-purpose contact detection algorithm for nonlinear structural analysis codes
[DE93-018507] p 1455 N94-19039

Bench-scale screening tests for a boiling sodium-potassium alloy solar receiver
[DE93-018512] p 1469 N94-19040

The minimum detection limits of RDX and TNT deposited on various surfaces as determined by ion mobility spectroscopy
[DE93-018521] p 1378 N94-19042

Numerical solutions for a flow with mixed convection in a vertical geometry
[DE93-011592] p 1419 N94-19058

A constitutive theory for rigid polyurethane foam
[DE93-011596] p 1372 N94-19059

A particle method for history-dependent materials
[DE93-018696] p 1456 N94-19060

Stress pulse phenomena
[DE93-019064] p 1456 N94-19078

Superconducting flux flow devices, digital circuits and memories
[DE93-019072] p 1405 N94-19079

Binding of copper to nanocavity surfaces in silicon
[DE93-019073] p 1364 N94-19080

Downsizing a database platform for increased performance and decreased costs
[DE93-018687] p 1618 N94-19099

Metallurgical evaluation of SRAM 2/SRAM A program mer base plates
[DE93-018689] p 1364 N94-19100

Sandia equation of state data base: Seslan file
[DE93-018693] p 1618 N94-19101

GENSHELL: A genesis database 2D to 3D shell transformation program
[DE93-018694] p 1525 N94-19102

The CAESAR project: Experimental and modeling investigations of methane reforming in a catalytically enhanced solar absorption receiver on a parabolic dish
[DE93-040203] p 1469 N94-19109

Experiments and analysis of lateral piezoresistance gauges
[DE93-017874] p 1433 N94-19111

Silicon MCM substrates for integration of 3-5 photonic devices and CMOS IC's
[DE93-017894] p 1405 N94-19112

Image blur
[DE93-017944] p 1580 N94-19113

The effects of initial conditions and control time on optimal actuator placement by way of a max-min genetic algorithm
[DE93-017640] p 1525 N94-19124

A massively parallel adaptive finite element method with dynamic load balancing
[DE93-012844] p 1536 N94-19161

Experience in implementing a parallel file system
[DE93-012840] p 1536 N94-19188

Message passing in PUMA
[DE93-012841] p 1537 N94-19206

Development of a quartz digital accelerometer for environmental sensing and navigation applications
[DE93-018503] p 1433 N94-19243

How to apply the IEEE standards to software testing
[DE93-018514] p 1527 N94-19245

A visualization environment for supercomputing-based applications in computational mechanics
[DE93-015024] p 1537 N94-19249

Shock compression properties of silicon carbide
[DE93-019927] p 1373 N94-19271

Reducing inadvertent alloying of metal/ceramic brazes
[DE93-009842] p 1373 N94-19308

Impact strength and indentation hardness of high-strength ceramics
[DE93-018833] p 1373 N94-19338

Dynamical behavior of octahedrite from the Henbury meteorite
[DE93-018834] p 1627 N94-19339

Role of pressure in the study of fullerenes
[DE93-018839] p 1602 N94-19340

Refining a triangulation of a planar straight-line graph to eliminate large angles
[DE93-016510] p 1528 N94-19344

A simple description of flow instability with application to a packed bed
[DE93-017492] p 1420 N94-19345

Effects of pressure on the orientational ordering and phase transitions in solid C(60) and C(70)
[DE93-018858] p 1603 N94-19347

Transient dynamics capability at Sandia National Laboratories p 1460 N94-19476

Manufacturing technology
[DE93-019580] p 1381 N94-19480

Optoelectronic packaging: A review
[DE93-040059] p 1515 N94-19535

A Sandia Technology Bulletin: Testing technology, July 1993
[DE93-040197] p 1633 N94-19537

Six degree of freedom fine motion positioning stage based on magnetic levitation
[DE93-017651] p 1446 N94-19547

MIMD massively parallel methods for engineering and science problems
[DE93-019409] p 1531 N94-19562

Spectrally and temporally resolved laser emission from vertical cavity surface emitting lasers
[DE93-019410] p 1442 N94-19563

SANDIA NATIONAL LABS., LIVERMORE, CA.

Exchange front stability in packed-column chromatography
[DE93-017526] p 1346 N94-17997

SANTA FE INST., NM.

The 1992 annual report on scientific programs: A broad research program on the sciences of complexity
[DE93-018151] p 1561 N94-18178

SAO PAULO UNIV. (BRAZIL).

Dust in the Small Magellanic Cloud
[NASA-CR-193344] p 1624 N94-17764

SCHWARTZ ELECTRO-OPTICS, INC., ORLANDO, FL.

Laser imaging radar system
[AD-A270436] p 1387 N94-18510

SCIENCE APPLICATIONS INTERNATIONAL CORP., ARLINGTON, VA.

Constructing a reference event list for ARCESS
[AD-A269288] p 1481 N94-18297

SCIENCE APPLICATIONS INTERNATIONAL CORP., MCLEAN, VA.

UUGM code development
[AD-A269945] p 1416 N94-18671

SCIENTIFIC RESEARCH INST. OF INSTRUMENT AUTOMATION, MOSCOW (USSR).

The perspectives in application of hot casting technology for ceramic parts of timekeeping devices p 1375 N94-18013

The optimal numerical algorithm for processing of phase coded time signals for radio-clocks p 1426 N94-18018

Control of torque in stepping motors of quartz watches and clocks p 1408 N94-18023

SCRIPPS INSTITUTION OF OCEANOGRAPHY, LA JOLLA, CA.

Processing and analysis of SeaMARC 2 data: Fieberling guyot; raw phase experiment in Norwegian-Greenland Sea
[AD-A269930] p 1498 N94-18662

Constraints on crustal structure from long period pressure and displacement measurements on the deep seafloor
[AD-A269931] p 1498 N94-18663

Contributions from geomagnetic inverse theory to the study of hydromagnetic conditions near the core-mantle boundary
[NASA-CR-194303] p 1484 N94-18853

SEATTLE CITY LIGHT, WA.

Radiosity algorithms using higher order finite element methods
[DE93-018098] p 1531 N94-19548

SEIKO INSTRUMENTS, INC., MATSUDO (JAPAN).

Development of ultrasonic motor and application to silent alarm analog quartz watch p 1425 N94-18016

SHEFFIELD UNIV. (ENGLAND).

Implementation of the digital wave-processing experiment p 1329 N94-19628

SHORT BROS. AND HARLAND LTD., BELFAST (NORTHERN IRELAND).

The aero-mechanical design of a novel Fowler flap mechanism p 1309 N94-18443

SIMON FRASER UNIV., BURNABY (BRITISH COLUMBIA).

On Hamilton-connectedness of Cayley graphs p 1554 N94-19684

SIMPSON WEATHER ASSOCIATES, INC., CHARLOTTESVILLE, VA.

SPNDL: A concept for a small satellite Doppler lidar wind sounder p 1327 N94-19181

SOCIETE SUISSE DE CHRONOMETRIE, NEUCHATEL.

Proceedings of the 4th European Congress on Chronometry
[ETN-93-94633] p 1424 N94-18006

SOFTWARE PRODUCTIVITY CONSORTIUM, HERNDON, VA.

Technology benefits model user manual, version 01.00.04
[AD-A270637] p 1620 N94-19777

SOUTH AFRICAN ASTRONOMICAL OBSERVATORY, CAPE TOWN.

The South African Astronomical Observatory
[SAAO-17] p 1623 N94-19657

SOUTHAMPTON UNIV. (ENGLAND).

Metal Film Surface Plasmon Resonance (MFSPR) fibre couplers
[AD-A268871] p 1579 N94-18635

SOUTHEASTERN UNIV. RESEARCH ASSOCIATION, NEWPORT NEWS, VA.

Laser powered beam conditioner for free-electron lasers and synchrotrons
[DE93-017821] p 1441 N94-18974

SOUTHERN METHODIST UNIV., DALLAS, TX.

High resolution geological site characterization utilizing ground motion data
[AD-A268926] p 1481 N94-18485

SPACE AND MISSILE SYSTEMS ORGANIZATION, LOS ANGELES AIR FORCE STATION, CA.

CONTACT: An Air Force technical report on military satellite control technology
[AD-A269375] p 1334 N94-18408

SPIRE CORP., BEDFORD, MA.

Gallium arsenide-based ternary compounds and multi-band-gap solar cell research
[DE93-010049] p 1467 N94-18483

SRI INTERNATIONAL CORP., MENLO PARK, CA.

IR materials producibility
[AD-A268849] p 1577 N94-18223

Distributed reasoning and planning
[AD-A268682] p 1540 N94-18399

Novel catalysts for methane activation
[DE93-040630] p 1349 N94-18532

Novel mass spectrometric instrument for gaseous and particulate characterization and monitoring
[DE93-019992] p 1433 N94-19054

A real-time spoken-language system for interactive problem-solving, combining linguistic and statistical technology for improved spoken language understanding
[AD-A270901] p 1392 N94-19749

Novel nonlinear laser diagnostic techniques
[AD-A270968] p 1442 N94-19788

STANFORD RESEARCH INST., MENLO PARK, CA.

X ray absorption spectroscopic studies of the active sites of nickel- and copper-containing metalloproteins
[DE93-017142] p 1347 N94-18059

STANFORD UNIV., CA.

Planning under uncertainty solving large-scale stochastic linear programs
[DE93-013920] p 1516 N94-17701

Advanced optical fiber communication systems
[AD-A269120] p 1577 N94-18254

Superconducting/semiconducting hybrids and advance memory concepts for superconducting electronics
[AD-A268679] p 1397 N94-18312

Low power signal processing research at Stanford p 1393 N94-18351

High-performance multiprocessor architecture for a 3-D lattice gas model p 1400 N94-18362

Ultra low power CMOS technology p 1401 N94-18373

Bayesian model choice: Asymptotics and exact calculations
[AD-A269067] p 1557 N94-18516

EDF tests for normality in linear models after a Box-Cox transformation
[AD-A269068] p 1557 N94-18517

Bayesian analysis of ARMA processes: Complete sampling based inference under full likelihoods
[AD-A269168] p 1557 N94-18694

3D composite grids using Bezier curves and surfaces in component adaptive methods
[AD-A269188] p 1549 N94-18863

ControlShell: A real-time software framework
[AD-A269172] p 1523 N94-18879

Overview of research in progress at the Center of Excellence
[NASA-CR-194329] p 1618 N94-19256

Research and training activities of the Joint Institute for Aeronautics and Acoustics
[NASA-CR-194742] p 1421 N94-19493

Algorithms and architectures for high speed signal processing
[AD-A271000] p 1392 N94-19736

The effects of initial conditions on the 3-D topology of temporally evolving wakes (ARI on 3-D bluff body wakes)
[AD-A271008] p 1423 N94-19774

STATE UNIV. OF NEW YORK, ALBANY.

Geography and meteorological studies in the Far East
[DE93-013563] p 1461 N94-17893

STATE UNIV. OF NEW YORK, BINGHAMTON.

Surface wave group velocity tomography of East Asia, part 1
[AD-A270100] p 1484 N94-18868

Analysis of regional bodywave phases from earthquakes in western China, part 2
[AD-A270125] p 1485 N94-18873

STATE UNIV. OF NEW YORK, BUFFALO.

X ray studies of microstructures in semiconductor and superconducting materials
[DE93-040690] p 1601 N94-19056

STATE UNIV. OF NEW YORK, PLATTSBURGH.

The effects of reverberant impulse noise (blast waves) on hearing: Parametric studies
[AD-A269242] p 1506 N94-18911

STATE UNIV. OF NEW YORK, STONY BROOK.

Tunneling spectroscopy of ultrasmall clusters and grains
[AD-A268840] p 1598 N94-18539

Working group for planetary system nomenclature
[NASA-CR-194406] p 1626 N94-18841

Advances in laser cooling
[AD-A270152] p 1440 N94-18900

Discrete-time infinity control problem with measurement feedback
[PB93-197523] p 1543 N94-19329

STEVENS INST. OF TECH., HOBOKEN, NJ.

On Hamiltonian properties of 2-tough graphs p 1554 N94-19685

Toughness and the cycle structure of graphs p 1554 N94-19686

STOCKHOLM UNIV. (SWEDEN).

A bit serial first level calorimeter trigger for an LHC detector
[USIP-92-08] p 1574 N94-18845

Conversion of ADC pulse heights into MIP units: NUMASS test data, September 1991
[USIP-93-03] p 1432 N94-18846

The A((2)pi(sub u))-X((2)pi(sub g)) system of Br2(+) studied by velocity modulation spectroscopy
[USIP-93-04] p 1569 N94-18847

On the use of semi-Lagrangian methods for accurate predictions of gravity waves
[DM-61] p 1562 N94-18859

EXANA: A program for analysing extended energy loss fine structures, EXELFS spectra
[USIP-92-01] p 1525 N94-19145

A programmable systolic trigger processor for FERA-bus data
[USIP-92-04] p 1405 N94-19292

The d(exp 3)delta-a(exp 3)delta and b(exp 3)phi-a(exp 3)delta systems of ZrS, Part 2: Appendix, list of wavenumbers
[USIP-92-05] p 1602 N94-19293

FASTBUS simulation models in VHDL
[USIP-92-07] p 1515 N94-19295

The global atmospheric sulfur cycle: An evaluation of model predictions and observations
[CM-81] p 1479 N94-19379

STRATHCLYDE UNIV., GLASGOW (SCOTLAND).

Investigation of a fiber optic frequency shifter and optical isolator
[AD-A269820] p 1579 N94-18738

STUTTGART UNIV. (GERMANY).

Titanium carbon-hydrogen layers on decorative surfaces p 1375 N94-18010

Sputtered TiN coatings in plastic p 1367 N94-18011

Simulation of a quartz-clockwork p 1426 N94-18019

Simulation of quartz resonators p 1426 N94-18021

Examinations of the friction behavior in nonstationary flow processes in pipes
[MITT-7] p 1423 N94-19730

SUPERCONDUCTING SUPER COLLIDER LAB., DALLAS, TX.

VLSI architectures for geometrical mapping problems in high-definition image processing p 1398 N94-18345

Longitudinal beam dynamics with RF noise
[DE93-018649] p 1574 N94-18994

Design verification and acceptance tests of the ASST-A helium refrigeration system
[DE93-019746] p 1381 N94-19540

Data-Machine Independence (DMI)
[DE93-018008] p 1539 N94-19734

SVERDRUP TECHNOLOGY, INC., BROOK PARK, OH.

High temperature strain measurement with a resistance strain gage
[NASA-CR-194441] p 1434 N94-19314

SVERDRUP TECHNOLOGY, INC., CLEVELAND, OH.

Analysis of supersonic flows using k-epsilon model and the RPLUS code: Progress towards high speed combustor analysis p 1411 N94-18551

SWEDISH INST. FOR MATERIALS TESTING, BORAS.

Construction and evaluation of an environmental chamber for calibration of temperature and pressure sensors for laser interferometers emperature and pressure sensors for laser interferometers)
[PB93-197838] p 1322 N94-19332

Software quality in test and measurment equipment
[PB93-197846] p 1528 N94-19333

SWEDISH INST. OF SPACE PHYSICS, KIRUNA.

Problems related to stimulated electromagnetic emissions, strong turbulence and ionospheric modification
[IRF-SR-212] p 1480 N94-17720

Phase-space description of plasma waves: Linear and nonlinear theory
[IRF-SR-211] p 1587 N94-18860

SWEDISH INST. OF SPACE PHYSICS, UPPSALA.

Co-ordination of ground-based observations with Cluster p 1331 N94-19640

SWEDISH SPACE CORP., SOLNA.

MUZO flight experience with the programmable multizone furnace p 1324 N94-19167

SWISS CENTER FOR ELECTRONICS AND MICROTECHNOLOGY, INC., NEUCHATEL.

Techniques for low consumption circuits p 1428 N94-18032

Evaluation of the consumption of electronic clocks p 1408 N94-18033

SYDNEY UNIV. (AUSTRALIA).

Plastic mechanism analysis of T-joints in RHS subject to combined bending and concentrated force
[PB93-195774] p 1456 N94-19061

SYMBUS TECHNOLOGY, INC., WALTHAM, MA.

Autonomous neural network controllers for adaptive material handling
[AD-A268908] p 1540 N94-18331

SYRACUSE UNIV., NY.

Optical switch evaluation support
[AD-A270948] p 1581 N94-19601

NPAC distributed-parallel system feasibility study
[AD-A270972] p 1539 N94-19790

T

TECHNICAL RESEARCH ASSOCIATES, SALT LAKE CITY, UT.
Magnetostrictive actuators for human sensory feedback
[AD-A269266] p 1511 N94-17841

TECHNICAL RESEARCH CENTRE OF FINLAND, ESPOO.
The calculation methods of a cracked plastic composite laminate: A literature survey
[VTT-TIED-1362] p 1339 N94-17958
The respectiveness of response in a bar under static and transient loads
[VTT-TIED-1377] p 1452 N94-17959
FT-NIR spectroscopy in quantitative and qualitative measurements of cereal products
[VTT-TIED-1331] p 1346 N94-17973
An emulator for testing HVAC-control and energy management systems
[VTT-TIED-1337] p 1444 N94-17974
The fire resistance of profiled thin steel sheet structures
[VTT-TIED-1320] p 1380 N94-19373
The applications of modified metals in the construction industry
[VTT-TIED-1329] p 1365 N94-19374

TECHNISCHE HOCHSCHULE, AACHEN (GERMANY).
Hamilton cycles in path-tough graphs
p 1555 N94-19696

TECHNISCHE HOCHSCHULE, DARMSTADT (GERMANY).
Production and test of pseudo random elements
[ETN-93-95070] p 1559 N94-19610
Nonlinear dynamics and instabilities in ferromagnetic resonance experiments: Examinations of spheres from yttrium iron garnet in coincidence area of the first Suhl instabilities
[ETN-93-95072] p 1604 N94-19612
Modelling ideal gas fluorides laser plasmas
[ETN-93-95073] p 1592 N94-19613

TECHNISCHE UNIV., BERLIN (GERMANY).
Navier-Stokes computations of turbulent flow around high-lift configurations p 1306 N94-18420
Optical frequency doubling at adsorbates of silver(110) surface
[ETN-93-94837] p 1603 N94-19355
Impedence calculation with recursive folding
[ETN-93-95049] p 1406 N94-19387
Comparative examinations of several field oriented position control structures for asynchronous servomotors with a multitransputer system
[ETN-93-95051] p 1406 N94-19390
Structure and properties of polycarbonate alloys
[ETN-93-95071] p 1375 N94-19611
Transient skin effect in a massive cylinder by eccentric location of exciting conduction bands
[ETN-93-95048] p 1391 N94-19646
Experimental examinations of semiconductor laser amplifiers for optical communication technology
[ETN-93-95050] p 1442 N94-19647
Development of engineering models for calculation of failure loads and defect states of steel concrete beams and plates
[ETN-93-95052] p 1460 N94-19648
Modeling of driver behavior: Information perception, rule and control strategies in experiments and simulations
[ETN-93-95053] p 1510 N94-19649
Measuring methods for evaluation of dynamic tyre properties
[ETN-93-95054] p 1381 N94-19650
Technical development of a theory of programs
[ETN-93-95058] p 1532 N94-19652
Examination of charge carriers dynamics in silicon and silicon solar cells with photoinduced laser beam deflection
[ETN-93-95060] p 1470 N94-19654

TECHNISCHE UNIV., BRUNSWICK (GERMANY).
A learning autopilot for automatically controlled robust regulation
[ETN-93-95075] p 1321 N94-19711

TECHNISCHE UNIV., DELFT (NETHERLANDS).
Computational strategies for composite structures
[PB93-195097] p 1452 N94-18079
Control of shoulder muscles during goal directed movements
[PB93-195139] p 1504 N94-18080
Fast iterative solution of sparsely sampled seismic inverse problems
[REPT-93-16] p 1486 N94-19081
Difference equations for generalized Meixner polynomials
[REPT-93-17] p 1550 N94-19082
Transmission of acoustic waves through strongly heterogeneous, two-dimensional velocity models
[REPT-93-09] p 1563 N94-19083
New insights in GMRES-like methods with variable preconditioners
[REPT-93-10] p 1524 N94-19084
The optimal projection equations for finite-dimensional fixed-order H2-optimal control of infinite-dimensional discrete-time systems
[REPT-93-11] p 1542 N94-19085
A priori estimates and existence of positive solutions of a superlinear polyharmonic equation
[REPT-93-12] p 1550 N94-19086
Time domain calculations of the second-order drift force on a floating two-dimensional object in current and waves
[REPT-93-13] p 1419 N94-19087
Deterministic growth-dispersal models and branching random walk
[REPT-93-14] p 1550 N94-19088
The theory of linear programming: Skew symmetric self-dual problems and the central path
[REPT-93-15] p 1524 N94-19089
Excursion theory of a finite set via resolvents
[REPT-93-19] p 1557 N94-19090
Deadbeat control by measurement feedback: A two sided approach
[REPT-93-20] p 1542 N94-19091
A refinement for nonmonotonic logic
[REPT-93-21] p 1542 N94-19092
The rank of the present excursion
[REPT-93-22] p 1558 N94-19137
The fixed, finite-order L(sup 2)-optimal control of infinite-dimensional time-varying discrete-time systems
[REPT-93-23] p 1542 N94-19138
Similarity solutions for gravity-dominated spreading of a lens of organic contaminant
[REPT-93-24] p 1420 N94-19139
Inverse scattering of surface waves: A new look at surface consistency
[REPT-93-25] p 1486 N94-19140
Decomposition invariance of generalized steady-state of a 1-D diffusion system
[REPT-93-26] p 1550 N94-19141
The digital linear quadratic control problem for Pritchard-Salamon systems
[REPT-93-27] p 1542 N94-19142
Interior-point methodology for linear programming: Duality, sensitivity analysis and computational aspects
[REPT-93-28] p 1525 N94-19143
Multigrid for a groundwater flow problem
[REPT-93-29] p 1420 N94-19144
Existence of a maximal solution for quasimonotone elliptic systems
[REPT-93-30] p 1550 N94-19153
On the convergence of an unfeasible primal-dual interior-point method for convex programming
[REPT-93-34] p 1525 N94-19154
Content based-grid node selection for vector field visualization
[REPT-93-35] p 1525 N94-19155
A polynomial primal-dual Dikin-type algorithm for linear programming
[REPT-93-36] p 1525 N94-19156
Scale sensitivity in the multiplicative AHP and SMART
[REPT-93-37] p 1611 N94-19157
Context-related scaling of human judgement in the multiplicative AHP, SMART and ELECTRE
[REPT-93-38] p 1611 N94-19158
Research activities, Faculty of Civil Engineering, Delft University of Technology, 1990 - 1991
[PB93-195022] p 1380 N94-19254
Computational mechanics of composite materials
[PB93-195782] p 1343 N94-19281
On polynomials orthogonal with respect to an inner product involving differences (the general case)
[REPT-93-32] p 1551 N94-19285
Digital control of Pritchard-Salamon systems
[REPT-93-33] p 1543 N94-19286
Microstructure of the interfacial zone around aggregate particles in concrete
[PB93-195790] p 1380 N94-19322
Excursions of stochastic processes, Cox-point processes, entrance behavior and resolvents
[PB93-197291] p 1558 N94-19323
Survey on the application of a 3D general purpose wind-tunnel research model
[LR-713] p 1323 N94-19372
START user manual version 2.1
[LR-726] p 1335 N94-19614
The dynamic stability of the helicopter
[LR-772] p 1321 N94-19615
An iterative inverse scattering method for the removal of scattered surface waves
[REPT-93-18] p 1488 N94-19644
Visualization of turbulent flow with particles
[REPT-93-31] p 1423 N94-19645
Residual strength predictions for fibre metal laminates: The R-curves approach
[LR-717] p 1344 N94-19666
ADAS implementation of a panel method for the prediction of aerodynamic loads
[LR-723] p 1313 N94-19667
A review of hot-wire technique in compressible flows
[LR-724] p 1423 N94-19668
Fatigue crack initiation in riveted lap joints and in pressurized fuselages
[LR-725] p 1461 N94-19669
Semantic models for distributed data base management. Part 2: Development of an integral meta-model for data modeling and data base modeling
[REPT-93-08-PT-2] p 1620 N94-19795
Noise measurements on two types of airplanes used for spraying in agriculture
[LR-706] p 1319 N94-19796

TECHNISCHE UNIV., EINDHOVEN (NETHERLANDS).
Functional analysis of subelliptic operators on lie groups
[PB93-194793] p 1547 N94-18077
Numerical methods for one-dimensional hyperbolic conservation laws
[PB93-194801] p 1547 N94-18078
L(sub p)-regularity of subelliptic operators on Lie groups
[PB93-194785] p 1549 N94-18948
Catalogue of simple perfect squared squares of orders 21 through 25
[PB93-191971] p 1550 N94-18991
Useful lambda notation
[PB93-191856] p 1524 N94-19066
Tandem queues with deterministic service times
[PB93-197465] p 1543 N94-19324
Bahadur-Kiefer theorem beyond the largest observation
[PB93-197473] p 1558 N94-19325
Compensation approach for three or more dimensional random walks
[PB93-197499] p 1543 N94-19326
Bounds for expected loss in Bayesian decision theory with imprecise prior probabilities
[PB93-197507] p 1558 N94-19327
Nonlinear disturbance decoupling and linearization: A partial interpretation of integral feedback
[PB93-197515] p 1543 N94-19328
Discrete-time infinity control problem with measurement feedback
[PB93-197523] p 1543 N94-19329
Using geometric techniques to improve dynamic programming algorithms for the economic lot-sizing problem and extensions
[PB93-197556] p 1528 N94-19330
Stabilization of time-delay systems: An overview of the algebraic approach
[PB93-191989] p 1553 N94-19556
Integrity checking in deductive databases: An exposition
[PB93-191724] p 1619 N94-19709
Non-well-foundedness and type freeness can unify the interpretation of functional application
[PB93-191849] p 1560 N94-19710

TECHNISCHE UNIV., HANOVER (GERMANY).
Shape of wind gusts at a 130m tower at Wilhelmshaven (Germany)
[BER-BAND-B3] p 1494 N94-19503

TECHNISCHE UNIV., TWENTE (NETHERLANDS).
Nonlinear disturbance decoupling and linearization: A partial interpretation of integral feedback
[PB93-197515] p 1543 N94-19328
Mathematical communications, volume 27, numbers 1 and 2, 1992. List and abstracts of memoranda published in the period July - December 1991
[PB93-191997] p 1553 N94-19557
Updated contributions to the Twente Workshop of Hamiltonian Graph Theory
[PB93-195568] p 1553 N94-19605

TENNESSEE UNIV., MEMPHIS.
Somatosensory responsiveness in behaving monkeys and human subjects
[AD-A268924] p 1501 N94-18231

TENNESSEE UNIV., TULLAHOMA.
Considerations for the use of the modified line reversal technique for gas temperature measurement
[DE93-015752] p 1576 N94-17857
Space Applications Industrial Laser System (SAILS)
p 1325 N94-19173

TENNESSEE UNIV. SPACE INST., TULLAHOMA.
Space Applications Industrial Laser System (SAILS)
p 1325 N94-19173

TEXAS A&M UNIV., COLLEGE STATION.
Mechanical modeling of the growth of salt structures
[DE93-015342] p 1596 N94-18243

Synthesis techniques and analysis tool for on-chip fault-tolerance
[AD-A269148] p 1521 N94-18259

TEXAS CHRISTIAN UNIV., FORT WORTH.

Hydrolysis reaction and positronium decay in silica gels
[AD-A270028] p 1371 N94-18713

TEXAS TECHNOLOGICAL UNIV., LUBBOCK.

High-power microwave breakdown of dielectric interfaces
[AD-A268844] p 1397 N94-18318

TEXAS UNIV., AUSTIN.

Profile stabilization of tilt mode in a field reversed configuration
[DE93-016770] p 1583 N94-17753

Catalytic hydrocarbon reactions over supported metals
[DE93-018168] p 1345 N94-17808

Avoiding degenerate coframes in an affine gauge approach to quantum gravity
[DE93-013146] p 1607 N94-17892

Filamentary magnetohydrodynamic plasmas
[DE93-015616] p 1583 N94-17945

Filamentation, current profiles and transport in a tokamak
[DE93-016768] p 1584 N94-17948

Transport in the self-organized relaxed state of ion temperature gradient instability
[DE93-016769] p 1584 N94-17983

Ion mobility and transport barriers in the tokamak plasmas
[DE93-040320] p 1587 N94-18524

Developing and understanding the high temperature behavior of niobium aluminides and niobium aluminide composites
[AD-A268874] p 1341 N94-18636

Finite beta plasma equilibrium in toroidally linked mirrors
[DE93-040318] p 1590 N94-19193

On neutral plasma oscillations
[DE93-040319] p 1590 N94-19194

Pulsed power supply for Nova Upgrade
[DE93-019626] p 1441 N94-19307

Bienzyme sensors based on electrically wired peroxidase
[AD-A271364] p 1374 N94-19585

Single source precursors for the OMCVD of 3/5 compound semiconductors
[AD-A271147] p 1606 N94-19739

TEXAS UNIV. AT DALLAS, RICHARDSON.

Proof of the feasibility of coherent and incoherent schemes for pumping a gamma ray laser
[AD-A269173] p 1440 N94-18880

TEXAS UNIV. HEALTH SCIENCE CENTER, SAN ANTONIO.

Cellular and molecular level responses after radiofrequency radiation exposure, alone or in combination with x rays or chemicals
[AD-A268189] p 1501 N94-17729

THIOKOL CORP., BRIGHAM CITY, UT.

Strained ring energetic binders
[AD-A269056] p 1377 N94-18491

THOROUGHBRED CAE SOFTWARE, LOUISVILLE, KY.

Implementation of mixed formulation elements in PC/NASTRAN p 1449 N94-17828

TITAN SPECTRON DIV., TUSTIN, CA.

Super-resolution of multi-pixel and sub-pixel images for the SDI
[AD-A268537] p 1462 N94-18631

TOLEDO UNIV., OH.

Development of parallel architectures for sensor array processing, volume 1
[AD-A270426] p 1534 N94-18507

Development of parallel architectures for sensor array processing. Volume 2: A parallel architecture for broad-band direction-of-arrival estimation
[AD-A270427] p 1534 N94-18508

A coupled implicit solution method for turbulent spray combustion in propulsion systems p 1411 N94-18549

A parallel and pipelined architecture for estimation of direction of arrival using a bilinear transformation method, volume 3
[AD-A270137] p 1389 N94-18897

TORONTO UNIV., DOWNSVIEW (ONTARIO).

Numerical solution of the Navier-Stokes equations for high-lift configurations on structured composite grids
p 1306 N94-18423

TRANE CO., LACROSSE, WI.

Compatibility of refrigerants and lubricants with motor materials, volume 1
[DE93-040216] p 1350 N94-18895

Compatibility of refrigerants and lubricants with motor materials, volume 2
[DE93-040217] p 1350 N94-18896

Compatibility of refrigerants and lubricants with motor materials, volume 3
[DE93-040218] p 1352 N94-19191

TRIESTE UNIV. (ITALY).

UVSTAR: An imaging spectrograph with telescope for the Shuttle Hitchhiker-M platform p 1326 N94-19178

The star identification, pointing and tracking system of UVSTAR, an attached payload instrument system for the Shuttle Hitchhiker-M platform p 1326 N94-19179

TRW SPACE TECHNOLOGY LABS., REDONDO BEACH, CA.

MHD Integrated Topping Cycle Project
[DE93-040521] p 1589 N94-19055

TRW SYSTEMS GROUP, HUNTSVILLE, AL.

Distributed Computing Design System (DCDS)
[AD-A270435] p 1534 N94-18509

TRW SYSTEMS GROUP, REDONDO BEACH, CA.

MHD technology transfer, integration and review committee
[DE93-040519] p 1588 N94-18892

MHD integrated topping cycle project
[DE93-040520] p 1588 N94-18978

TUFTS UNIV., MEDFORD, MA.

Investigation of the relative abundance of heavy versus light nuclei in primary cosmic rays using underground muon bundles
[DE93-017601] p 1630 N94-17818

High energy physics at Tufts University
[DE93-018299] p 1575 N94-19023

U

UMEA UNIV. (SWEDEN).

Twenty odd statements in Twente
p 1555 N94-19691

UNITED KINGDOM ATOMIC ENERGY AUTHORITY, CULHAM (ENGLAND).

General geometry PIC for MIMD computers
[AD-A269085] p 1534 N94-18767

UNITED SOLAR SYSTEMS CORP., TROY, MI.

Research on stable, high-efficiency amorphous silicon multijunction modules
[DE93-010046] p 1467 N94-18518

UNITED TECHNOLOGIES CORP., COLORADO SPRINGS, CO.

Technology, design, simulation, and evaluation for SEP-hardened circuits p 1399 N94-18352

UNIVERSITAET DER BUNDESWEHR MUENCHEN, NEUBIBERG (GERMANY).

Axial response of differently excited anchored viscous liquid bridges in zero-gravity
[LRT-WE-9-FB-1-1992] p 1379 N94-19489

Free fall liquid column dynamics in a droptower
[LRT-WE-9-FB-6-1992] p 1379 N94-19491

Transient response of a viscous and anchored liquid bridge to an axial pulse
[LRT-WE-9-FB-7-1992] p 1379 N94-19492

UNIVERSITEIT TWENTE, ENSCHEDE (NETHERLANDS).

Pegasus project description
[MEMO-INF-92-75] p 1536 N94-19159

Pegasus: Operating system support for distributed multimedia systems
[MEMO-INF-92-76] p 1536 N94-19160

A simple calculus of finite probabilistic processes
[MEMO-INF-93-08] p 1558 N94-19195

Reducing extended transition systems
[MEMO-INF-93-09] p 1526 N94-19196

Simulation models of UCN, FDDI-2 and DQDB
[MEMO-INF-93-10] p 1536 N94-19197

ACOS: A performance based approach to build a parallel complex object server
[MEMO-INF-93-11] p 1537 N94-19198

MART: An overview of the Mobile Autonomous Robot Twente project
[MEMO-INF-93-12] p 1543 N94-19199

Modelling software for structure metrics
[MEMO-INF-93-13] p 1526 N94-19200

Wide-address spaces: Exploring the design space
[MEMO-INF-92-77] p 1537 N94-19219

Abstracting inter-object communications using composition filters
[MEMO-INF-92-78] p 1526 N94-19220

DataTypeLog: A deductive object oriented query language
[MEMO-INF-92-79] p 1526 N94-19221

The TM typing rules
[MEMO-INF-92-80] p 1526 N94-19222

An annotated bibliography on parallel parsing: Updated version
[MEMO-INF-92-84] p 1537 N94-19223

Attribute evaluation during generalized parsing
[MEMO-INF-92-85] p 1526 N94-19224

Computer-assisted instruction and natural language systems
[MEMO-INF-92-86] p 1527 N94-19225

On asynchronous testing
[MEMO-INF-93-03] p 1543 N94-19226

Goal-driven LOTOS execution
[MEMO-INF-93-04] p 1527 N94-19227

Specification and verification of a dynamic leader election protocol in a broadcast network
[MEMO-INF-93-05] p 1558 N94-19228

The TM manual version 1.3 working document
[MEMO-INF-93-06] p 1527 N94-19229

A highly concurrent medium access control strategy for high speed multiwavelength networks using transceivers with limited tunability
[MEMO-INF-93-07] p 1390 N94-19230

Advances in architectural concepts to support distributed systems design
[MEMO-INF-93-17] p 1527 N94-19261

Stochastic grammars: Theory and applications
[MEMO-INF-93-19] p 1528 N94-19262

A unified performability evaluation framework for computer and communication systems
[MEMO-INF-93-21] p 1537 N94-19264

Adaptive uniformization: Technical details
[MEMO-INF-93-22] p 1558 N94-19265

Specifying and proving communication closedness in protocols
[MEMO-INF-93-23] p 1390 N94-19267

Action systems and action refinement in the development of parallel systems: An algebraic approach
[MEMO-INF-93-14] p 1538 N94-19296

A language of finite probabilistic processes and its interleaving semantics
[MEMO-INF-93-24] p 1558 N94-19354

Adaptive uniformization
[MEMO-INF-92-88] p 1558 N94-19385

Sensitivity and uncertainty analysis of Markov reward models
[MEMO-INF-92-89] p 1559 N94-19386

Updated Contributions to the Twente Workshop on Hamiltonian Graph Theory
[MEMO-1076] p 1554 N94-19683

Cycles containing all vertices of maximum degree
p 1554 N94-19686

Long paths and cycles in tough graphs
p 1554 N94-19689

UNIVERSITY OF CENTRAL FLORIDA, ORLANDO.

Final construction and operation of a continuous far-infrared free-electron laser for scientific applications
[AD-A269248] p 1440 N94-18912

UNIVERSITY OF EASTERN KENTUCKY, RICHMOND.

Analysis of deposit precursors in jet fuels using Fourier transform infrared spectroscopy
[AD-A269035] p 1377 N94-18489

UNIVERSITY OF SOUTHERN CALIFORNIA, LOS ANGELES.

An ab initio study of the weakly bonded CO-Cl2 complex
[AD-A269000] p 1349 N94-18395

Kinetic aspects of lattice mismatch in molecular beam epitaxial growth on planar and patterned substrates
[AD-A270424] p 1597 N94-18506

A multi-level data-flow architecture for signal and data processing applications
[DE93-041272] p 1539 N94-19588

UNIVERSITY OF SOUTHERN CALIFORNIA, MARINA DEL REY.

Employing knowledge resources in a new text planner architecture
[AD-A269669] p 1516 N94-17732

EXPECT: Intelligent support for knowledge base refinement
[AD-A269602] p 1612 N94-17745

Bias in planning and explanation-based learning
[AD-A269608] p 1610 N94-17746

Intelligent help facilities: Generating natural language descriptions with examples
[AD-A269555] p 1521 N94-18290

Retrieving and integrating data from multiple information sources
[AD-A269588] p 1615 N94-18461

On masking effect
[AD-A269593] p 1541 N94-18462

Flexible integration of path-planning capabilities
[AD-A269594] p 1541 N94-18463

Towards versatile and practical knowledge acquisition
[AD-A269596] p 1615 N94-18464

Automatic documentation generation: The interaction of text and examples
[AD-A269670] p 1616 N94-18570

Learning database abstractions for query reformulation
[AD-A269531] p 1616 N94-18641

Generating object descriptions: Intergrating examples with text
[AD-A269992] p 1522 N94-18680

ARPA/CSTO rapid VLSI implementation
[AD-A269170] p 1403 N94-18695

Automatically generating abstractions for planning
[AD-A269772] p 1541 N94-18759

UNIVERSITY OF SOUTHERN MISSISSIPPI, BAY SAINT LOUIS.
Preparation of data assimilation and model evaluation experiment data sets [AD-A269996] p 1498 N94-18665
UNIVERSITY OF SOUTHERN MISSISSIPPI, LONG BEACH.
Coastal Ocean Modeling Workshop [AD-A268955] p 1497 N94-18393
UNIVERSITY OF WESTERN AUSTRALIA, NEDLANDS.
Single phase dynamic CMOS PLA using charge sharing technique p 1397 N94-18341
UNIVERSITY OF WESTERN MICHIGAN, KALAMAZOO.
Correlated charge-changing ion-atom collisions [DE93-018717] p 1564 N94-17775
Search for resonant electron transfer and double excitation in Kr(sup 34+) + H2 collisions [DE93-018776] p 1569 N94-18999
Low-energy continuum-electron emission at 0 degrees from O(q+) + He collisions [DE93-018777] p 1570 N94-19108
UTAH UNIV., SALT LAKE CITY.
Characterization of fluid physics effects on cardiovascular response to microgravity (G-572) p 1323 N94-19163

V

VALTRONIC S.A., LES CHARBONNIERES (SWITZERLAND).
Some variation in the movement base of the ETA 251 series p 1428 N94-18035
VANDERBILT UNIV., NASHVILLE, TN.
High resolution SQUID magnetometry for non-destructive evaluation [AD-A268384] p 1447 N94-18225
VERMONT UNIV., BURLINGTON.
The asymptotic theory of the reflection and transmission of a pulsed electromagnetic beam field at a planar interface separating two dispersive media [AD-A269033] p 1385 N94-18404
VIRGINIA POLYTECHNIC INST. AND STATE UNIV., BLACKSBURG.
The 6th Japan-U.S. conference on composite materials [AD-A268535] p 1341 N94-18630
A comparison of single-station backazimuth estimates with regional event locations in the Central Appalachians [AD-A269697] p 1483 N94-18690
A comparative evaluation of in-plane shear test methods for laminated graphite-epoxy composites [NASA-CR-193808] p 1456 N94-19095
Investigations in gauge theories, topological solitons, and string theories [DE93-015029] p 1609 N94-19250
Compression strength of composite primary structural components [NASA-CR-194562] p 1457 N94-19350
VIRGINIA UNIV., CHARLOTTESVILLE.
Fundamental concepts relating local atomic arrangements, deformation, and fracture of intermetallic alloys [AD-A268745] p 1361 N94-18788
A research program in empirical computer science [NASA-CR-194069] p 1530 N94-19429
Efficiency and biofidelity of occupant simulations p 1459 N94-19473
VON KARMAN INST. FOR FLUID DYNAMICS, RHODE-SAINT-GENESE (BELGIUM).
Recirculation in forward roll coating [VKI-TM-48] p 1409 N94-17901
Computational Fluid Dynamics [VKI-LS-1993-04] p 1412 N94-18557
Compact advection schemes on unstructured grids p 1413 N94-18564
Introduction to the Modeling of Turbulence [VKI-LS-1993-02] p 1414 N94-18578
Measurement Techniques [VKI-LS-1993-05] p 1430 N94-18643
The application of liquid crystal techniques to determine heat transfer rates p 1432 N94-18654
VRIJE UNIV., AMSTERDAM (NETHERLANDS).
Asynchronous rendezvous in the presence of backtracking [PB93-197739] p 1524 N94-19062
Axiomatization, declarative semantics and operational semantics of passive and active updates in logic databases [PB93-195956] p 1618 N94-19067
Feasibility study in linguistically motivated object-oriented conceptual design of information systems [PB93-197754] p 1618 N94-19331

W

WASHINGTON STATE UNIV., PULLMAN.
Pulse-firing winner-take-all networks p 1399 N94-18353
Measurement selection for parametric IC fault diagnosis p 1399 N94-18356
High accuracy switched-current circuits using an improved dynamic mirror p 1401 N94-18368
Microgravity research in plant biological systems: Realizing the potential of molecular biology p 1503 N94-19216
Discrete-time infinity control problem with measurement feedback [PB93-197523] p 1543 N94-19329
WASHINGTON UNIV., SEATTLE.
Steep geometric grating for use in moire interferometry [AD-A268759] p 1453 N94-18328
Pulse-timing studies of x ray pulsars [NASA-CR-193778] p 1621 N94-18611
Institute for Nuclear Theory [DE93-017369] p 1568 N94-18824
Related investigations on the physics of high energy emission from active galactic nuclei [NASA-CR-193615] p 1630 N94-18836
SSC detector muon sub-system beam tests [DE93-018415] p 1569 N94-19013
Determination of nitrogen to carbon abundance ratios from transition layer emission lines [NASA-CR-191921] p 1622 N94-19421
Airborne studies of ocean-particle-cloud interactions in the Arctic [AD-A270752] p 1479 N94-19575
Damage accumulation in advanced metal matrix composites under thermal cycling/creep loadings [AD-A271207] p 1344 N94-19720
WATERLOO UNIV. (ONTARIO).
The Hopping Lemma p 1554 N94-19687
WEIZMANN INST. OF SCIENCE, REHOVOTH (ISRAEL).
A zeta function approach to the semiclassical quantization of maps [DE93-624774] p 1547 N94-17949
Gauge coupling unification in superstring derived standard-like models [DE93-624801] p 1607 N94-17950
Neutrino masses in superstring derived standard-like models [DE93-624802] p 1565 N94-17951
Cabibbo mixing in superstring derived standard-like models [DE93-624814] p 1607 N94-17953
WEST VIRGINIA UNIV., MORGANTOWN.
The development of a course sequence in real-time systems design [AD-A269459] p 1522 N94-18726
Ground movements associated with gas hydrate production [DE93-019887] p 1486 N94-19018
WESTINGHOUSE ELECTRIC CORP., WEST MIFFLIN, PA.
Environmental degradation of Alloy 600 and welded filler metal EN82 in an elevated temperature aqueous environment [DE93-018049] p 1363 N94-18940
WESTINGHOUSE HANFORD CO., RICHLAND, WA.
Integrated test plan for the demonstration of a commercial Fourier Transform Infrared instrument [DE93-018518] p 1433 N94-19041
WESTINGHOUSE SAVANNAH RIVER CO., AIKEN, SC.
Microstructural analysis of solid-state resistance welds [DE93-017295] p 1443 N94-17761
Structural stability of 1100 C heated Pd/k during absorption cycling in protium [DE93-016270] p 1346 N94-18048
Applications of Quaternary stratigraphic, soil-geomorphic, and quantitative geomorphic analyses to the evaluation of tectonic activity and landscape evolution in the Upper Coastal Plain, South Carolina [DE93-016269] p 1484 N94-18725
Finite difference program for calculating hydride bed wall temperature profiles [DE93-019272] p 1523 N94-19005
Ultrasonic technique for inspection of GPHS capsule girth weld integrity [DE93-040072] p 1448 N94-19189
Overlay welding irradiated stainless steel [DE93-018767] p 1446 N94-19334
WISCONSIN UNIV., MADISON.
Rapid oceanic cyclogenesis studies [AD-A269258] p 1490 N94-18265
Research activity on particle spin systems and related problems [AD-A269456] p 1562 N94-18288
Wave structure induced by fluid dynamic limits in the Broadwell model [AD-A268512] p 1410 N94-18385
Microwave (SSM/I) Estimates of the Precipitation Rate to Improve Numerical Atmospheric Model Forecasts [NASA-CR-193566] p 1491 N94-18602
Diabatic forcing and initialization with assimilation of cloud and rain water in a forecast model: Methodology p 1491 N94-18603
Physical retrieval of precipitation water contents from Special Sensor Microwave/Imager (SSM/I) data. Part 1: A cloud ensemble/radiative parameterization for sensor response (report version) p 1491 N94-18604
Physical retrieval of precipitation water contents from Special Sensor Microwave/Imager (SSM/I) data. Part 2: Retrieval method and applications (report version) p 1491 N94-18605
Forecast model applications of retrieved three dimensional liquid water fields p 1492 N94-18606
Moist wind relationships p 1492 N94-18607
Initialization and assimilation of cloud and rainwater in a regional model p 1492 N94-18608
High temperature co-axial winding transformers [NASA-CR-194580] p 1407 N94-19643
Theoretical studies of turbulence and anomalous transport in toroidal confinement devices [DE93-040684] p 1592 N94-19656
Generalized regression trees: Function estimation via recursive partitioning and maximum likelihood [AD-A271259] p 1560 N94-19726
WOODS HOLE OCEANOGRAPHIC INST., MA.
Modified aequorin shows increased bioluminescence activity [AD-A268774] p 1347 N94-18185
Three-dimensional high-resolution seismic profiling on the New Jersey outer continental shelf [AD-A269835] p 1498 N94-18600
Analysis of data from Columbia Point Arena Ocean-Bottom Seismic Station (OBSS) [AD-A271263] p 1500 N94-19727
Seismic studies of the geologic structure and physical properties of the seabed [AD-A270895] p 1500 N94-19747
A laboratory model of a cooled continental shelf [AD-A270862] p 1500 N94-19792
WORLD METEOROLOGICAL ORGANIZATION, GENEVA (SWITZERLAND).
Report of the Experts Meeting on Reference Climatological Stations (RCS) and National Climate Data Catalogues (NCC) [WMO-TD-535] p 1494 N94-19312
A survey of current approaches to modelling of hydrological time-series with respect to climate variability and change [WMO/TD-534] p 1463 N94-19435
Report of the Second CLICOM Experts Meeting [WCDMP-19] p 1495 N94-19705
WRIGHT LAB., EGLIN AFB, FL.
Millimeter wave reflectivity measurement system [AD-A270008] p 1387 N94-18601
WRIGHT LAB., WRIGHT-PATTERSON AFB, OH.
Design optimization studies using COSMIC NASTRAN p 1450 N94-17834
Benchmarking the QUAD4/TRIA3 element p 1450 N94-17837
Eigenvalue routines in NASTRAN: A comparison with the Block Lanczos method p 1450 N94-17838
Application of the network discriminant function to learning [AD-A268793] p 1540 N94-18189
A finite strain ring dynamical model for pneumatic tires [AD-A269286] p 1444 N94-18266
High lift and the forward swept wing p 1308 N94-18436
Computational Fluid Dynamics (CFD) research branch technical briefs [AD-A269698] p 1417 N94-18739
Procedures and design data for the formulation of aircraft configurations [AD-A270150] p 1318 N94-18779
Vane optimization for maximum efficiency using Design Of Experiments (DOX) [AD-A270270] p 1320 N94-18907
Explicit solution techniques for impact with contact constraints p 1459 N94-19470
WRIGHT MATERIALS RESEARCH, BEAVERCREEK, OH.
Analysis of bolted and bonded composite [AD-A267792] p 1453 N94-18382
WRIGHT RESEARCH DEVELOPMENT CENTER, WRIGHT-PATTERSON AFB, OH.
Efficient domain-independent experimentation [AD-A269530] p 1557 N94-18640
WRIGHT STATE UNIV., DAYTON, OH.
Design and simulation of a gallium-arsenide second order sigma-delta analog to digital converter [AD-A269494] p 1404 N94-18701

A study of the effect of hydrocarbon structure on the induction of male rat nephropathy and metabolic structure
[AD-A270969] p 1504 N94-19789

WYMAN-GORDON CO., WORCESTER, MA.

Development and characterization of adiabatic shear prone tungsten heavy alloys
[AD-A270477] p 1366 N94-19673

Y

YALE UNIV., NEW HAVEN, CT.

Transport phenomena and interfacial kinetics in multiphase combustion systems
[AD-A270202] p 1349 N94-18785

Statistical learning theory and algorithms
[AD-A270209] p 1523 N94-18901

Task A: Yale Accelerator Users Group (YAUG)
[DE93-018417] p 1570 N94-19029

The anomalous magnetic moment of the muon
[DE93-018932] p 1572 N94-19320

CONTRACT NUMBER INDEX

SCIENTIFIC AND TECHNICAL AEROSPACE REPORTS VOLUME 32 NUMBER 4

Typical Contract Number Index Listing

AF PROJ. 2306 .... p 92 N94-11866

CONTRACT NUMBER | PAGE NUMBER | ACCESSION NUMBER

Listings in this index are arranged alphanumerically by contract number. Under each contract number the accession numbers denoting documents that have been produced as a result of research done under that contract are arranged in ascending order. The page number helps to locate the citation in the abstract section. The accession number denotes the number by which the citation is identified.

AF PROJ. LDFP .... p 1578 N94-18457
AF PROJ. X19-76 .... p 1520 N94-18251
AF PROJ. 1105 .... p 1379 N94-18147
AF PROJ. 2068 .... p 1387 N94-18601
AF PROJ. 2181 .... p 1334 N94-18718
AF PROJ. 2301 .... p 1403 N94-18452
p 1609 N94-18908
p 1405 N94-18909
AF PROJ. 2303 .... p 1567 N94-18526
AF PROJ. 2312 .... p 1502 N94-18924
AF PROJ. 2404 .... p 1417 N94-18739
AF PROJ. 2864 .... p 1341 N94-18572
AF PROJ. 4600 .... p 1387 N94-18666
p 1579 N94-18668
AF PROJ. 5581 .... p 1535 N94-18866
AF PROJ. 5636 .... p 1362 N94-18923
AF PROJ. 681B .... p 1320 N94-18907
AF PROJ. 7184 .... p 1509 N94-18744
AF PROJ. 7601 .... p 1493 N94-18871
AF PROJ. 7622 .... p 1384 N94-18187
AF-AFOSR-0010-90 .... p 1567 N94-18783
AF-AFOSR-0021-92 .... p 1568 N94-18814
AF-AFOSR-0024-91 .... p 1549 N94-18798
AF-AFOSR-0054-90 .... p 1568 N94-18784
AF-AFOSR-0070-90 .... p 1341 N94-18636
AF-AFOSR-0073-91 .... p 1454 N94-18487
AF-AFOSR-0081-91 .... p 1389 N94-19009
AF-AFOSR-0085-90 .... p 1588 N94-18902
AF-AFOSR-0090-93 .... p 1551 N94-19317
AF-AFOSR-0122-91 .... p 1388 N94-18782
AF-AFOSR-0130-90 .... p 1402 N94-18390
AF-AFOSR-0143-90 .... p 1361 N94-18788
AF-AFOSR-0165-90 .... p 1371 N94-18713
AF-AFOSR-0165-91 .... p 1605 N94-19719
AF-AFOSR-0170-91 .... p 1349 N94-18785
AF-AFOSR-0172-90 .... p 1340 N94-18205
AF-AFOSR-0176-89 .... p 1481 N94-18485
AF-AFOSR-0184-90 .... p 1597 N94-18506
AF-AFOSR-0200-90 .... p 1513 N94-19764
AF-AFOSR-0202-91 .... p 1386 N94-18469
AF-AFOSR-0206-91 .... p 1501 N94-17729
AF-AFOSR-0220-90 .... p 1349 N94-18776
AF-AFOSR-0245-91 .... p 1600 N94-18876
AF-AFOSR-0248-90 .... p 1600 N94-18904
AF-AFOSR-0250-90 .... p 1557 N94-18540
AF-AFOSR-0260-91 .... p 1397 N94-18318
AF-AFOSR-0267-90 .... p 1371 N94-18691
AF-AFOSR-0274-90 .... p 1508 N94-18313
AF-AFOSR-0278-89 .... p 1446 N94-19754
AF-AFOSR-0283-90 .... p 1598 N94-18511
AF-AFOSR-0286-90 .... p 1579 N94-18738
AF-AFOSR-0305-91 .... p 1440 N94-18900
AF-AFOSR-0311-90 .... p 1546 N94-17825
AF-AFOSR-0325-90 .... p 1507 N94-19783
AF-AFOSR-0330-91 .... p 1341 N94-18630
AF-AFOSR-0333-91 .... p 1501 N94-18231
AF-AFOSR-0336-91 .... p 1348 N94-18389
AF-AFOSR-0337-87 .... p 1447 N94-18225
AF-AFOSR-0346-91 .... p 1542 N94-18898
AF-AFOSR-0353-90 .... p 1579 N94-18635
AF-AFOSR-0355-90 .... p 1615 N94-18224
AF-AFOSR-0368-89 .... p 1567 N94-18766
AF-AFOSR-0370-90 .... p 1508 N94-18682
AF-AFOSR-0371-89 .... p 1521 N94-18458
AF-AFOSR-0377-91 .... p 1348 N94-18221
AF-AFOSR-0396-89 .... p 1504 N94-19789
AF-AFOSR-0405-89 .... p 1374 N94-19600
AF-AFOSR-0425-89 .... p 1374 N94-19574
ARO-MIPR-130-92 .... p 1312 N94-19119
ARPA ORDER 5636 .... p 1362 N94-18923
ARPA ORDER 6132 .... p 1403 N94-18695
ARPA ORDER 7330 .... p 1522 N94-18696
p 1538 N94-19533
p 1515 N94-19591
ARPA ORDER 7597 .... p 1514 N94-18317
p 1531 N94-19592
ARPA ORDER 8162 .... p 1403 N94-18667
ARPA ORDER 8557 .... p 1577 N94-18223
A3363 .... p 1400 N94-18365
A84/KL/147 .... p 1458 N94-19444
p 1378 N94-19445
A87/K/102 .... p 1518 N94-17965
A87/KL/055 .... p 1434 N94-19797
A88/KM/419 .... p 1451 N94-17931
A90/KM/666 .... p 1390 N94-19449
A91/KL/645 .... p 1393 N94-19798
A92/KM/662 .... p 1390 N94-19447
A93/D/402 .... p 1619 N94-19453
BMFT-0328787A .... p 1494 N94-19503
BMFT-50-QV-90955 .... p 1623 N94-19463
BMFT-50-90955 .... p 1623 N94-19464
CEC-SC1/900369 .... p 1307 N94-18427
DA PROJ. MR0-4101 .... p 1507 N94-19675
DA PROJ. RJ3-5-O-01 .... p 1563 N94-18678
DA PROJ. R03-5-B-03 .... p 1500 N94-19786
DA PROJ. 1L1-61102-AH-43 .... p 1349 N94-18395
p 1349 N94-18456
p 1378 N94-19674
DA PROJ. 1L1-61102-AN-43 .... p 1609 N94-18310
DA PROJ. 1L1-62211-A-47-A .... p 1446 N94-19318
DA PROJ. 1L1-62618-AH-80 .... p 1311 N94-18413
p 1597 N94-18468
DA PROJ. 1L1-62705-AH-94 .... p 1403 N94-18471
DA PROJ. 3M1-62787-A-878 .... p 1511 N94-18296
p 1505 N94-18392
DA PROJ. 3M1-62787-A-879 .... p 1505 N94-18289
DA PROJ. 3O1-62787-A-879 .... p 1506 N94-18632
DAAB07-91-D-B519 .... p 1617 N94-18770
DAAD05-92-C-0114 .... p 1311 N94-18413
DAAH04-93-C-0003 .... p 1503 N94-19757
DAAH04-93-G-0044 .... p 1606 N94-19769
DAAH04-93-G-0068 .... p 1407 N94-19584
DAAJ02-89-C-0017 .... p 1512 N94-18765
DAAL03-87-K-0118 .... p 1392 N94-19724
DAAL03-87-K-0121 .... p 1408 N94-19751
DAAL03-89-D-0003 .... p 1605 N94-19725
DAAL03-89-K-0038 .... p 1605 N94-19717
DAAL03-89-K-0130 .... p 1392 N94-19738
DAAL03-89-K-0164 .... p 1606 N94-19739
DAAL03-90-G-0053 .... p 1366 N94-19594
DAAL03-90-G-0067 .... p 1606 N94-19741
DAAL03-90-G-0082 .... p 1604 N94-19596
DAAL03-90-G-0083 .... p 1604 N94-19597
DAAL03-90-G-0094 .... p 1392 N94-19737
DAAL03-90-G-0103 .... p 1559 N94-19595
DAAL03-90-G-0108 .... p 1392 N94-19736
DAAL03-90-G-0122 .... p 1392 N94-19718
DAAL03-90-G-0128 .... p 1581 N94-19578
DAAL03-90-G-0149 .... p 1375 N94-19740
DAAL03-90-G-0211 .... p 1392 N94-19680
DAAL03-91-C-0027 .... p 1419 N94-19025
DAAL03-91-G-0123 .... p 1551 N94-19317
DAAL03-91-G-0222 .... p 1560 N94-19726
DAAL03-92-G-0111 .... p 1374 N94-19586
DAAL03-92-G-0147 .... p 1581 N94-19772
DAAL03-92-G-0185 .... p 1419 N94-19025
DAAL03-92-G-0217 .... p 1345 N94-19746
DAAL04-91-C-0065 .... p 1366 N94-19673
DABT63-91-C-0025 .... p 1516 N94-17732
p 1612 N94-17745
p 1521 N94-18290
p 1541 N94-18463
p 1615 N94-18464
p 1616 N94-18570
p 1522 N94-18680
DAJA45-90-C-0053 .... p 1372 N94-18792
DAJA45-93-M-0328 .... p 1338 N94-18703
DAMD17-88-C-8054 .... p 1506 N94-18632
DAMD17-91-C-1113 .... p 1506 N94-18911
DAMD17-93-C-3006 .... p 1505 N94-18392
DARPA ORDER 6775 .... p 1416 N94-18671
DARPA ORDER 7013 .... p 1407 N94-19665
DASG60-90-C-0092 .... p 1534 N94-18509
DCA100-91-C-0031 .... p 1387 N94-18721
DE-AC01-88MA-33222 .... p 1616 N94-18689
DE-AC01-91DP-00239 .... p 1583 N94-17912
DE-AC02-76CH-00016 .... p 1539 N94-17696
p 1464 N94-17712
p 1472 N94-17852
p 1594 N94-17866
p 1337 N94-17884
p 1501 N94-17889
p 1358 N94-17947
p 1565 N94-17984
p 1436 N94-17998
p 1566 N94-18085
p 1566 N94-18234
p 1386 N94-18503
p 1438 N94-18504
p 1343 N94-18763
p 1602 N94-19258
p 1406 N94-19310
p 1487 N94-19477
p 1572 N94-19536
p 1603 N94-19541
p 1603 N94-19564
p 1375 N94-19651
DE-AC02-76CH-03000 .... p 1436 N94-17883
p 1574 N94-18497
p 1574 N94-18972
p 1569 N94-18973
p 1525 N94-19186
DE-AC02-76CH-03073 .... p 1473 N94-18101
p 1590 N94-19273
DE-AC02-76ER-00038 .... p 1566 N94-18165
DE-AC02-79ET-10815 .... p 1576 N94-17857
DE-AC02-80ET-15601 .... p 1429 N94-18207
DE-AC02-83CH-10093 .... p 1464 N94-17731
p 1465 N94-17888
p 1376 N94-18045
p 1489 N94-18046
p 1615 N94-18334
p 1467 N94-18483
p 1467 N94-18518
p 1377 N94-18617
p 1378 N94-18913
p 1468 N94-18944
p 1470 N94-19760
DE-AC03-76SF-00098 .... p 1592 N94-17741
p 1514 N94-17799
p 1516 N94-17800
p 1436 N94-17869
p 1556 N94-17886
p 1613 N94-17894
p 1480 N94-17898
p 1595 N94-17989
p 1624 N94-18047
p 1473 N94-18050
p 1595 N94-18054
p 1383 N94-18055
p 1347 N94-18193
p 1347 N94-18194
p 1360 N94-18398
p 1609 N94-18629
p 1485 N94-18929
p 1513 N94-18935
p 1600 N94-18968
p 1575 N94-18997
p 1441 N94-19030
p 1389 N94-19053
p 1350 N94-19097
p 1469 N94-19098
p 1477 N94-19105
p 1575 N94-19152
p 1352 N94-19192
p 1571 N94-19247
p 1629 N94-19260

p 1365 N94-19280
p 1365 N94-19282
p 1478 N94-19303
p 1352 N94-19304
p 1591 N94-19479
p 1353 N94-19538
p 1575 N94-19558
p 1591 N94-19559
p 1576 N94-19560
p 1354 N94-19653
DE-AC03-76SF-00515 .... p 1347 N94-18059
DE-AC03-89ER-51114 .... p 1582 N94-17702
p 1585 N94-18056
p 1585 N94-18057
p 1585 N94-18058
DE-AC03-89ER-53277 .... p 1589 N94-19073
DE-AC04-76DP-00613 .... p 1437 N94-18060
DE-AC04-76DP-00789 .... p 1573 N94-17698
p 1423 N94-17700
p 1592 N94-17741
p 1592 N94-17742
p 1394 N94-17780
p 1395 N94-17783
p 1516 N94-17786
p 1464 N94-17787
p 1464 N94-17798
p 1382 N94-17806
p 1357 N94-17819
p 1345 N94-17820
p 1382 N94-17861
p 1357 N94-17862
p 1546 N94-17885
p 1594 N94-17896
p 1518 N94-17943
p 1518 N94-17944
p 1452 N94-17995
p 1424 N94-17999
p 1576 N94-18000
p 1465 N94-18001
p 1519 N94-18002
p 1358 N94-18003
p 1358 N94-18100
p 1429 N94-18102
p 1359 N94-18127
p 1447 N94-18128
p 1614 N94-18164
p 1466 N94-18206
p 1385 N94-18232
p 1410 N94-18270
p 1311 N94-18275
p 1466 N94-18335
p 1467 N94-18409
p 1370 N94-18477
p 1371 N94-18519
p 1467 N94-18520
p 1474 N94-18521
p 1439 N94-18522
p 1475 N94-18817
p 1404 N94-18827
p 1455 N94-18829
p 1337 N94-18830
p 1418 N94-18918
p 1362 N94-18919
p 1523 N94-18926
p 1405 N94-18928
p 1580 N94-18970
p 1617 N94-18984
p 1485 N94-19001
p 1485 N94-19002
p 1523 N94-19006
p 1542 N94-19007
p 1468 N94-19014
p 1468 N94-19015
p 1468 N94-19016
p 1601 N94-19022
p 1405 N94-19035
p 1469 N94-19036
p 1455 N94-19039
p 1469 N94-19040
p 1378 N94-19042
p 1419 N94-19058
p 1372 N94-19059
p 1456 N94-19060
p 1456 N94-19078
p 1405 N94-19079
p 1364 N94-19080
p 1618 N94-19099
p 1364 N94-19100
p 1618 N94-19101
p 1525 N94-19102
p 1469 N94-19109
p 1433 N94-19111
p 1405 N94-19112
p 1580 N94-19113
p 1525 N94-19124
p 1536 N94-19161
p 1536 N94-19188
p 1537 N94-19206
p 1433 N94-19243
p 1527 N94-19245
p 1537 N94-19249
p 1373 N94-19271
p 1373 N94-19308
p 1373 N94-19338
p 1627 N94-19339
p 1602 N94-19340
p 1528 N94-19344
p 1420 N94-19345
p 1603 N94-19347
p 1381 N94-19480
p 1515 N94-19535
p 1633 N94-19537
p 1446 N94-19547
p 1531 N94-19562
p 1442 N94-19563
DE-AC04-76DR-00789 .... p 1346 N94-17997
p 1569 N94-18985
DE-AC05-76OR-00033 .... p 1583 N94-17739
p 1358 N94-17915
p 1368 N94-17946
DE-AC05-84ER-40150 .... p 1441 N94-18974
DE-AC05-84OR-21400 .... p 1581 N94-17694
p 1382 N94-17695
p 1582 N94-17697
p 1504 N94-17699
p 1583 N94-17743
p 1355 N94-17752
p 1355 N94-17757
p 1593 N94-17760
p 1470 N94-17773
p 1471 N94-17774
p 1424 N94-17778
p 1471 N94-17790
p 1356 N94-17791
p 1593 N94-17845
p 1339 N94-17846
p 1367 N94-17847
p 1450 N94-17848
p 1612 N94-17858
p 1357 N94-17859
p 1367 N94-17881
p 1472 N94-17910
p 1451 N94-17913
p 1358 N94-17915
p 1368 N94-17946
p 1585 N94-18058
p 1340 N94-18087
p 1368 N94-18110
p 1473 N94-18167
p 1596 N94-18192
p 1501 N94-18242
p 1511 N94-18244
p 1359 N94-18245
p 1453 N94-18246
p 1466 N94-18247
p 1467 N94-18478
p 1534 N94-18482
p 1567 N94-18493
p 1497 N94-18494
p 1474 N94-18523
p 1439 N94-18724
p 1535 N94-18808
p 1475 N94-18832
p 1362 N94-18938
p 1372 N94-18946
p 1363 N94-18975
p 1445 N94-18976
p 1468 N94-18986
p 1523 N94-18989
p 1601 N94-18998
p 1617 N94-19026
p 1445 N94-19047
p 1617 N94-19057
p 1602 N94-19075
p 1524 N94-19076
p 1339 N94-19117
p 1351 N94-19118
p 1570 N94-19129
p 1364 N94-19203
p 1352 N94-19239
p 1590 N94-19273
p 1365 N94-19274
p 1446 N94-19291
p 1538 N94-19299
p 1316 N94-19300
p 1551 N94-19301
p 1543 N94-19302
p 1551 N94-19337
p 1503 N94-19341
p 1374 N94-19561
p 1553 N94-19655
p 1366 N94-19733
DE-AC05-84OS-21400 .... p 1346 N94-17987
p 1343 N94-18761
DE-AC06-76ER-01830 .... p 1599 N94-18816
DE-AC06-76RL-01830 .... p 1533 N94-17693
p 1593 N94-17747
p 1470 N94-17749
p 1471 N94-17821
p 1488 N94-17895
p 1501 N94-18051
p 1489 N94-18052
p 1548 N94-18094
p 1461 N94-18107
p 1369 N94-18233
p 1466 N94-18276
p 1433 N94-19000
p 1364 N94-19043
p 1493 N94-19051
p 1493 N94-19127
p 1478 N94-19319
p 1343 N94-19335
p 1448 N94-19336
DE-AC06-87RL-10930 .... p 1433 N94-19041
DE-AC07-76ID-01570 .... p 1582 N94-17713
p 1564 N94-17738
p 1461 N94-17851
p 1337 N94-17863
p 1613 N94-17880
DE-AC09-89SR-18035 .... p 1443 N94-17761
p 1424 N94-17778
p 1346 N94-18048
p 1484 N94-18725
p 1523 N94-19005
p 1448 N94-19189
p 1446 N94-19334
DE-AC11-89PN-38014 .... p 1363 N94-18940
DE-AC21-92MC-29116 .... p 1433 N94-19054
DE-AC22-87PC-90274 .... p 1588 N94-18892
p 1588 N94-18978
p 1589 N94-19055
DE-AC22-90PC-90043 .... p 1347 N94-18209
DE-AC22-92PC-92112 .... p 1349 N94-18532
DE-AC34-90DP-62349 .... p 1362 N94-18917
DE-AC35-89ER-40486 .... p 1574 N94-18994
p 1381 N94-19540
p 1539 N94-19734
DE-AI01-92EW-50616 .... p 1391 N94-19542
DE-AI05-83ER-13108 .... p 1464 N94-17781
DE-AI05-83ER-40112 .... p 1588 N94-19034
DE-AI05-92ER-54177 .... p 1588 N94-19034
DE-AI05-92OR-22041 .... p 1340 N94-18180
DE-AM03-76SF-00235 .... p 1569 N94-18945
DE-AS05-80ER-10713 .... p 1609 N94-19250
DE-AT03-86ER-40249 .... p 1574 N94-18916
DE-FC02-93ER-54186 .... p 1366 N94-19546
DE-FC03-85DP-40200 .... p 1602 N94-19123
DE-FC03-92SF-19460 .... p 1602 N94-19123
DE-FC08-90NV-10872 .... p 1572 N94-19309
DE-FG02-84ER-13190 .... p 1550 N94-19190
DE-FG02-84ER-45095 .... p 1367 N94-17678
DE-FG02-85ER-13433 .... p 1433 N94-19135
DE-FG02-85ER-45199 .... p 1601 N94-19031
DE-FG02-85ER-60314 .... p 1489 N94-18053
DE-FG02-86ER-13519 .... p 1571 N94-19257
DE-FG02-86ER-13566 .... p 1448 N94-17814
DE-FG02-86ER-13619 .... p 1363 N94-19019
DE-FG02-86ER-45229 .... p 1596 N94-18184
DE-FG02-86ER-53223 .... p 1583 N94-17854
DE-FG02-87ER-13732 .... p 1372 N94-18891
DE-FG02-87ER-13778 .... p 1564 N94-17775
p 1569 N94-18999
p 1570 N94-19108
DE-FG02-87ER-45283 .... p 1601 N94-19056
DE-FG02-87ER-45303 .... p 1369 N94-18163
DE-FG02-87ER-45311 .... p 1359 N94-18182
DE-FG02-87ER-45326 .... p 1571 N94-19204
DE-FG02-87ER-45328 .... p 1601 N94-19020
DE-FG02-88ER-13916 .... p 1561 N94-18177
DE-FG02-88ER-40412 .... p 1570 N94-19103
DE-FG02-88ER-45367 .... p 1364 N94-19032
DE-FG02-89ER-40531 .... p 1566 N94-18104
DE-FG02-89ER-52161 .... p 1363 N94-19021
DE-FG02-89ER-53291 .... p 1592 N94-19656
DE-FG02-90ER-25084 .... p 1419 N94-19025
DE-FG02-90ER-45426 .... p 1361 N94-18806
p 1361 N94-18807
DE-FG02-90ER-60970 .... p 1470 N94-17710
DE-FG02-91CE-23810 .... p 1350 N94-18895
p 1350 N94-18896
p 1350 N94-18977
p 1351 N94-19134
p 1351 N94-19136
p 1352 N94-19191
DE-FG02-91ER-14228 .... p 1567 N94-18533
DE-FG02-91ER-25099 .... p 1566 N94-18179
DE-FG02-91ER-40676 .... p 1567 N94-18534
DE-FG02-91ER-40684 .... p 1575 N94-19267

DE-FG02-91ER-61216 .... p 1474 N94-18183
DE-FG02-91ER-61229 .... p 1442 N94-19658
DE-FG02-92ER-25122 .... p 1535 N94-18808
p 1524 N94-19024
DE-FG02-92ER-40702 .... p 1630 N94-17818
p 1575 N94-19023
DE-FG02-92ER-40704 .... p 1570 N94-19029
p 1572 N94-19320
DE-FG02-92ER-40730 .... p 1574 N94-18927
DE-FG02-92ER-61369 .... p 1461 N94-17893
DE-FG03-84ER-45156 .... p 1593 N94-17845
DE-FG03-87ER-25043 .... p 1539 N94-19588
DE-FG03-89ER-04053 .... p 1349 N94-18395
DE-FG03-89ER-51116 .... p 1585 N94-18058
DE-FG03-90ER-54089 .... p 1589 N94-19133
DE-FG03-92ER-25116 .... p 1516 N94-17701
DE-FG03-93ER-40757 .... p 1607 N94-17892
DE-FG04-84ER-45099 .... p 1599 N94-18816
DE-FG05-80ET-53088 .... p 1583 N94-17753
p 1583 N94-17945
p 1584 N94-17948
p 1584 N94-17983
p 1587 N94-18524
p 1590 N94-19193
p 1590 N94-19194
DE-FG05-84ER-13263 .... p 1350 N94-19017
DE-FG05-84ER-40162 .... p 1565 N94-17776
DE-FG05-86ER-13604 .... p 1345 N94-17808
DE-FG05-86ER-45259 .... p 1601 N94-19022
DE-FG05-86ER-52139 .... p 1358 N94-17915
DE-FG05-87ER-13711 .... p 1596 N94-18243
DE-FG05-87ER-40319 .... p 1569 N94-18945
p 1575 N94-19050
DE-FG05-87ER-40374 .... p 1573 N94-17784
DE-FG05-87ER-52141 .... p 1588 N94-18988
DE-FG05-88ER-25054 .... p 1561 N94-18178
DE-FG05-89ER-75527 .... p 1614 N94-18181
DE-FG05-90ER-54093 .... p 1583 N94-17809
DE-FG05-91ER-54134 .... p 1357 N94-17859
DE-FG05-92ER-40748 .... p 1573 N94-17807
DE-FG06-90ER-40541 .... p 1569 N94-19013
DE-FG06-90ER-40561 .... p 1568 N94-18824
DE-FG06-91ER-40614 .... p 1609 N94-19121
DE-FG08-90ER-61012 .... p 1472 N94-17985
p 1472 N94-17986
DE-FG21-91MC-28080 .... p 1486 N94-19018
DE-FG21-92MC-29228 .... p 1351 N94-19132
p 1351 N94-19150
DE-FG22-89PC-89775 .... p 1354 N94-19660
DE-FG22-91PC-91287 .... p 1610 N94-19670
DE-FG41-92R1-10445 .... p 1445 N94-18307
DI-14-08-0001-G-1915 .... p 1476 N94-19064
DLA900-90-D-0304 .... p 1371 N94-18750
DLA900-90-D-0305 .... p 1374 N94-19532
DTCG23-88-C-20029 .... p 1455 N94-18716
DTFA01-91-Z-02036 .... p 1316 N94-19661
DTFA01-93-C-0001 .... p 1316 N94-18384
p 1386 N94-18495
DTFA03-89-C-00023 .... p 1315 N94-18844
FMV-82260-91-087-073-001 .... p 1311 N94-17722
FMV-82260-92-060-073-001 .... p 1311 N94-17722
FMV/FFL-82250-90-276-16-001 ... p 1452 N94-17970
FNSRS-12-24434.89 .... p 1525 N94-19154
FNSRS-12-34002.92 .... p 1525 N94-19143
F04701-88-C-0089 .... p 1385 N94-18287
p 1385 N94-18301
p 1596 N94-18316
p 1377 N94-18758
F08630-92-K-0017 .... p 1396 N94-18278
F08635-88-C-0067 .... p 1315 N94-18822
p 1315 N94-18823
F08635-88-C-0160 .... p 1322 N94-18330
F08635-90-C-0050 .... p 1387 N94-18510
F08635-90-C-0306 .... p 1417 N94-18780
F19628-90-C-0002 .... p 1492 N94-18684
p 1462 N94-18729
F19628-90-C-0003 .... p 1521 N94-18659
F19628-90-C-0072 .... p 1483 N94-18655
F19628-90-C-0101 .... p 1630 N94-18676
F19628-90-C-0103 .... p 1485 N94-18874
F19628-90-C-0118 .... p 1481 N94-18451
F19628-90-K-0039 .... p 1387 N94-18525
F19628-90-K-0042 .... p 1484 N94-18868
p 1485 N94-18873
F19628-90-K-0045 .... p 1483 N94-18717
F19628-90-K-0055 .... p 1418 N94-18870
F19628-91-C-0054 .... p 1334 N94-18264
F19628-92-C-0149 .... p 1492 N94-18637
F19628-92-K-0029 .... p 1483 N94-18690
F19628-93-C-0023 .... p 1432 N94-18875
F29601-87-C-0069 .... p 1403 N94-18695
F29601-89-K-0019 .... p 1439 N94-18656
F29601-92-C-0005 .... p 1481 N94-18297
F29601-92-C-0022 .... p 1438 N94-18250
F30602-88-D-0025 .... p 1539 N94-19790
F30602-89-C-0024 .... p 1393 N94-19793
F30602-89-C-0136 .... p 1393 N94-19752
p 1393 N94-19753
F30602-90-C-0023 .... p 1535 N94-18866
F30602-91-C-0045 .... p 1535 N94-18865
F30602-91-C-0081 .... p 1615 N94-18461
p 1616 N94-18641
p 1541 N94-18759
F30602-91-C-0129 .... p 1577 N94-18302
F30602-91-D-0001 .... p 1581 N94-19601
F30602-92-C-0010 .... p 1542 N94-18887
p 1559 N94-19511
F30602-92-C-0033 .... p 1391 N94-19587
F30602-92-C-0038 .... p 1581 N94-19602
F33615-85-C-0541 .... p 1513 N94-19531
F33615-87-C-2714 .... p 1377 N94-18489
F33615-89-C-0572 .... p 1513 N94-19570
F33615-89-C-3208 .... p 1317 N94-18227
F33615-89-C-3611 .... p 1317 N94-18577
p 1318 N94-18733
F33615-89-C-5643 .... p 1453 N94-18382
F33615-90-C-1465 .... p 1514 N94-18317
p 1557 N94-18640
p 1531 N94-19592
F33615-90-C-2036 .... p 1370 N94-18282
F33615-90-C-2092 .... p 1354 N94-19778
F33615-90-C-5928 .... p 1341 N94-18692
F33615-91-C-0015 .... p 1512 N94-18754
F33615-91-C-5606 .... p 1360 N94-18660
F33615-92-C-1056 .... p 1404 N94-18701
F33657-92-D-2055 .... p 1320 N94-18333
F41624-92-C-6005 .... p 1511 N94-17841
F49620-86-C-0036 .... p 1362 N94-18923
F49620-89-C-0070 .... p 1350 N94-18799
F49620-89-C-0071 .... p 1481 N94-18467
F49620-89-C-0087 .... p 1416 N94-18671
F49620-89-C-0107 .... p 1384 N94-18186
F49620-90-C-0029 .... p 1403 N94-18638
F49620-90-C-0042 .... p 1407 N94-19665
F49620-90-C-0044 .... p 1442 N94-19788
F49620-90-C-0076 .... p 1455 N94-18864
F49620-90-C-0084 .... p 1598 N94-18633
F49620-90-C-0089 .... p 1596 N94-18320
F49620-91-C-0031 .... p 1326 N94-19180
F49620-91-C-0068 .... p 1374 N94-19577
F49620-91-C-0088 .... p 1576 N94-18204
F49620-92-C-0033 .... p 1490 N94-18486
F49620-92-C-0035 .... p 1534 N94-18767
F49620-92-C-0284 .... p 1629 N94-18222
F49620-92-J-0143 .... p 1523 N94-18901
F49620-92-J-0170 .... p 1568 N94-18787
F49620-92-J-0186 .... p 1508 N94-18292
F49620-92-J-0206 .... p 1385 N94-18404
F49620-92-J-0227 .... p 1348 N94-18257
F49620-92-J-0260 .... p 1512 N94-18886
F49620-92-J-0290 .... p 1410 N94-18472
F49620-92-J-0293 .... p 1502 N94-18924
F49620-92-J-0297 .... p 1385 N94-18288
F49620-92-J-0358 .... p 1598 N94-18539
F49620-92-J-0359 .... p 1505 N94-18190
F49620-92-J-0367 .... p 1344 N94-19720
F49620-92-J-0402 .... p 1485 N94-18899
F49620-92-J-0417 .... p 1505 N94-18538
F49620-92-J-0437 .... p 1508 N94-18657
F49620-92-J-0455 .... p 1342 N94-18715
F49620-93-1-0181 .... p 1577 N94-18283
p 1577 N94-18298
p 1578 N94-18332
p 1578 N94-18396
p 1578 N94-18488
p 1438 N94-18492
p 1578 N94-18528
p 1579 N94-18693
GAS-RES-INST-5090-254-1993 .... p 1479 N94-19521
JPL-959193 .... p 1629 N94-19094
MAST-0050-C(PROFILE) .... p 1496 N94-17923
MDA903-89-C-0003 .... p 1616 N94-18575
p 1619 N94-19780
MDA903-90-C-0004 .... p 1331 N94-18411
MDA904-89-H-2008 .... p 1554 N94-19686
MDA972-90-C-0035 .... p 1522 N94-18696
p 1538 N94-19533
p 1515 N94-19591
MDA972-91-C-0028 .... p 1396 N94-18293
MDA972-91-C-0032 .... p 1403 N94-18667
MDA972-91-C-0034 .... p 1403 N94-18639
MDA972-92-C-0034 .... p 1396 N94-18284
MDA972-92-C-0053 .... p 1577 N94-18223
MDA972-92-J-1018 .... p 1620 N94-19777
MDA972-92-J-1019 .... p 1521 N94-18308
MDA972-92-J-1022 .... p 1522 N94-18726
MEF0040121 .... p 1400 N94-18365
MIPR-91MM1505 .... p 1507 N94-19608
MIPR-92-0004 .... p 1312 N94-19119
NAGW-112 .... p 1628 N94-19794
NAGW-1195 .... p 1325 N94-19173
NAGW-1197 .... p 1503 N94-19215
NAGW-1209 .... p 1628 N94-17842
NAGW-1388 .... p 1335 N94-19371
NAGW-1406 .... p 1398 N94-18342
p 1398 N94-18343
p 1398 N94-18346
p 1398 N94-18349
p 1400 N94-18360
p 1401 N94-18371
NAGW-1480 .... p 1628 N94-19794
NAGW-1617 .... p 1464 N94-19681
NAGW-1855 .... p 1491 N94-18602
p 1491 N94-18603
p 1491 N94-18604
p 1491 N94-18605
p 1492 N94-18606
p 1492 N94-18607
NAGW-1910 .... p 1393 N94-18351
p 1401 N94-18373
NAGW-2328 .... p 1503 N94-19215
NAGW-2704 .... p 1463 N94-19430
NAGW-3293 .... p 1397 N94-18337
NAGW-419 .... p 1393 N94-18351
p 1400 N94-18362
p 1401 N94-18373
NAGW-765 .... p 1627 N94-19093
NAGW-812 .... p 1379 N94-18840
NAGW-838 .... p 1477 N94-19231
NAG1-1053 .... p 1456 N94-19095
NAG1-1073 .... p 1530 N94-19429
NAG1-1145 .... p 1551 N94-19317
NAG1-1148 .... p 1440 N94-18834
NAG1-1210 .... p 1543 N94-19329
NAG1-1346 .... p 1441 N94-19369
p 1441 N94-19394
NAG1-363 .... p 1339 N94-17766
NAG1-537 .... p 1457 N94-19350
NAG1-648 .... p 1313 N94-19621
NAG1-970 .... p 1591 N94-19441
NAG2-210 .... p 1506 N94-18862
NAG2-553 .... p 1629 N94-19427
NAG2-679 .... p 1629 N94-19418
NAG3-1410 .... p 1379 N94-17763
NAG5-1043 .... p 1400 N94-18360
p 1401 N94-18370
NAG5-1060 .... p 1486 N94-19237
NAG5-1241 .... p 1627 N94-19218
NAG5-1255 .... p 1622 N94-19421
NAG5-1463 .... p 1624 N94-17764
NAG5-1740 .... p 1621 N94-19288
NAG5-1762 .... p 1470 N94-17762
NAG5-1783 .... p 1621 N94-19288
NAG5-1800 .... p 1622 N94-19431
NAG5-1958 .... p 1621 N94-18855
NAG5-485 .... p 1484 N94-18838
NAG5-689 .... p 1499 N94-18819
NAG5-814 .... p 1487 N94-19432
NAG5-818 .... p 1484 N94-18853
NAG5-833 .... p 1628 N94-19425
NAG5-860 .... p 1487 N94-19428
NAG5-873 .... p 1630 N94-19437
NAG8-212 .... p 1338 N94-19438
p 1338 N94-19706
NAG8-590 .... p 1630 N94-18836
NAG8-695 .... p 1621 N94-18611
NAG8-907 .... p 1373 N94-19402
NAG8-964 .... p 1353 N94-19367
NASA ORDER H-20752-D .... p 1579 N94-18858
NASA ORDER S-47197-E .... p 1329 N94-19633
NASW-4561 .... p 1612 N94-17737
NASW-4756 .... p 1621 N94-19288
NAS1-18605 .... p 1551 N94-19315
NAS1-19000 .... p 1308 N94-18435
NAS1-19299 .... p 1308 N94-18435
NAS1-19312 .... p 1417 N94-18843
NAS1-19480 .... p 1551 N94-19315
p 1551 N94-19317
NAS3-25266 .... p 1587 N94-18861
p 1434 N94-19314
p 1313 N94-19484
NAS3-25712 .... p 1315 N94-18852
NAS3-25808 .... p 1468 N94-18821
NAS5-32059 .... p 1621 N94-19288
NAS8-30751 .... p 1625 N94-18612
p 1625 N94-18613
p 1625 N94-18615
p 1625 N94-18618
p 1626 N94-18619
p 1626 N94-18620
p 1626 N94-18621
NAS8-37857 .... p 1332 N94-18820
NAS8-38609 .... p 1482 N94-18610
p 1380 N94-19423
p 1378 N94-19494
p 1603 N94-19513
NAS8-39131 .... p 1407 N94-19642
NAS8-39211 .... p 1331 N94-19366

NAS9-18069 p 1511 N94-18484
NCC1-163 p 1308 N94-18435
NCC1-169 p 1312 N94-19388
NCC1-99 p 1402 N94-18380
NCC2-250 p 1521 N94-18290
NCC2-307 p 1618 N94-19256
NCC2-526 p 1568 N94-18837
NCC2-55 p 1421 N94-19493
NCC2-588 p 1318 N94-19448
NCC2-754 p 1312 N94-19433
NCC3-261 p 1407 N94-19643
NCC5-45 p 1487 N94-19397
NCC5-46 p 1571 N94-19236
NCC9-16 p 1617 N94-18839
p 1513 N94-19349
NEC-91029 p 1540 N94-18125
NGT-70228 p 1312 N94-19433
NOP-8520587 p 1481 N94-18142
NR PROJ. RR0-1509 p 1393 N94-19779
NSF ATM-89-20508 p 1491 N94-18603
p 1491 N94-18604
p 1492 N94-18606
p 1492 N94-18607
NSF BCS-90-25010 p 1540 N94-18125
NSF CCR-88-20279 p 1549 N94-18697
NSF CCR-89-09667 p 1531 N94-19508
p 1538 N94-19512
NSF CCR-89-09996 p 1402 N94-18380
NSF CCR-89-57604 p 1561 N94-19481
p 1530 N94-19483
NSF CCR-91-21875 p 1535 N94-19046
NSF CDA-91-21558 p 1515 N94-19401
NSF DMS 90-57429 p 1419 N94-19025
NSF DMS 92-01581 p 1419 N94-19025
NSF DMS-89-04520 p 1554 N94-19686
NSF DMS-92-11820 p 1551 N94-19317
NSF INT-91-16781 p 1530 N94-19483
NSF IRI-89-03582 p 1610 N94-19485
NSF ISI-90-03087 p 1521 N94-18290
NSF MSS-90-24838 p 1456 N94-19116
NSF OCE-87-17141 p 1497 N94-18230
NSF OCE-87-17144 p 1497 N94-18230
NSG-5393 p 1624 N94-17843
NSG-7553 p 1626 N94-18841
NWO-R62-385 p 1558 N94-19265
p 1558 N94-19385
NWO-SIR13-1260 p 1558 N94-19265
p 1558 N94-19385
NWO-611-304-028 p 1524 N94-19089
p 1525 N94-19143
p 1525 N94-19156
N00014-81-C-0295 p 1497 N94-18277
N00014-82-K-0193 p 1559 N94-19511
N00014-84-K-0656 p 1360 N94-18687
N00014-87-J-1110 p 1515 N94-19401
N00014-87-J-1193 p 1453 N94-18285
N00014-88-K-0021 p 1490 N94-18265
N00014-88-K-0443 p 1500 N94-19743
N00014-89-C-0095 p 1540 N94-18399
N00014-89-C-0137 p 1541 N94-18790
N00014-89-J-1037 p 1500 N94-19792
N00014-89-J-1135 p 1349 N94-18736
N00014-89-J-1234 p 1443 N94-17730
N00014-89-J-1235 p 1438 N94-18258
N00014-89-J-1237 p 1348 N94-18256
N00014-89-J-1261 p 1594 N94-17876
N00014-89-J-1276 p 1453 N94-18328
N00014-89-J-1356 p 1495 N94-17822
N00014-89-J-1439 p 1418 N94-18906
N00014-89-J-1489 p 1389 N94-18811
N00014-89-J-1726 p 1344 N94-19744
N00014-89-J-1754 p 1486 N94-19008
N00014-89-J-1764 p 1369 N94-18188
N00014-89-J-1805 p 1508 N94-18304
N00014-89-J-1815 p 1549 N94-18863
N00014-89-J-3105 p 1418 N94-18867
N00014-89-J-3124 p 1506 N94-18598
N00014-89-J-3139 p 1544 N94-19599
N00014-89-J-3179 p 1505 N94-18407
N00014-89-K-0148 p 1498 N94-18600
N00014-89-K-0155 p 1610 N94-17746
N00014-90-C-0076 p 1366 N94-19775
N00014-90-C-0085 p 1392 N94-19749
N00014-90-C-0173 p 1462 N94-18631
N00014-90-C-0244 p 1578 N94-18383
N00014-90-C-0263 p 1377 N94-18491
N00014-90-J-1030 p 1549 N94-18697
N00014-90-J-1156 p 1578 N94-18405
N00014-90-J-1159 p 1354 N94-19728
p 1375 N94-19742
N00014-90-J-1340 p 1456 N94-19116
p 1456 N94-19130
N00014-90-J-1344 p 1549 N94-18863
N00014-90-J-1466 p 1629 N94-18705
N00014-90-J-1568 p 1497 N94-18230
N00014-90-J-1596 p 1497 N94-18230
N00014-90-J-1604 p 1599 N94-18797
N00014-90-J-1661 p 1338 N94-18314
N00014-90-J-1704 p 1347 N94-18165
N00014-90-J-1707 p 1597 N94-18459
N00014-90-J-1793 p 1402 N94-18400
N00014-90-J-1817 p 1500 N94-19747
N00014-90-J-1871 p 1360 N94-18386
p 1453 N94-18387
p 1596 N94-18388
N00014-90-J-1916 p 1500 N94-19727
N00014-90-J-1976 p 1423 N94-19774
N00014-90-J-4039 p 1577 N94-18295
N00014-90-J-4130 p 1442 N94-19729
N00014-90-J-4141 p 1600 N94-18884
N00014-90-K-2001 p 1440 N94-18880
N00014-90-K-2010 p 1439 N94-18737
N00014-91-C-0190 p 1408 N94-19756
N00014-91-C-0216 p 1599 N94-18719
N00014-91-C-0258 p 1540 N94-18331
N00014-91-C-2005 p 1327 N94-19184
N00014-91-F-0055 p 1405 N94-19079
N00014-91-J-1011 p 1534 N94-18507
p 1534 N94-18508
p 1389 N94-18897
N00014-91-J-1073 p 1498 N94-18662
N00014-91-J-1088 p 1498 N94-18663
N00014-91-J-1212 p 1430 N94-18569
N00014-91-J-1274 p 1367 N94-17878
N00014-91-J-1299 p 1454 N94-18683
p 1455 N94-18714
p 1361 N94-18742
N00014-91-J-1306 p 1534 N94-18699
N00014-91-J-1307 p 1605 N94-19664
N00014-91-J-1360 p 1560 N94-18410
N00014-91-J-1404 p 1521 N94-18259
N00014-91-J-1624 p 1541 N94-18463
N00014-91-J-1656 p 1374 N94-19585
N00014-91-J-1749 p 1598 N94-18527
N00014-91-J-1852 p 1404 N94-18706
N00014-91-J-1857 p 1577 N94-18254
N00014-91-J-1985 p 1539 N94-19682
N00014-91-J-4038 p 1422 N94-19598
p 1544 N94-19599
p 1560 N94-19768
N00014-92-J-1069 p 1490 N94-18514
N00014-92-J-1183 p 1348 N94-18255
N00014-92-J-1191 p 1479 N94-19575
N00014-92-J-1244 p 1507 N94-19593
N00014-92-J-1260 p 1370 N94-18403
N00014-92-J-1264 p 1557 N94-18516
p 1557 N94-18517
p 1557 N94-18694
N00014-92-J-1389 p 1342 N94-18704
N00014-92-J-1523 p 1502 N94-18305
N00014-92-J-1652 p 1341 N94-18450
N00014-92-J-1809 p 1523 N94-18879
N00014-92-J-1886 p 1397 N94-18312
N00014-92-J-1921 p 1359 N94-18322
N00014-92-J-1922 p 1397 N94-18311
N00014-92-J-1931 p 1598 N94-18616
N00014-92-J-1962 p 1345 N94-19776
N00014-92-J-4088 p 1440 N94-18912
N00014-92-J-4097 p 1544 N94-19530
N00014-92-J-4112 p 1498 N94-18665
N00014-92-K-2015 p 1541 N94-18462
N00014-93-C-0142 p 1392 N94-19749
N00014-93-C-2026 p 1599 N94-18764
N00014-93-I-0067 p 1407 N94-19722
N00014-93-I-0299 p 1342 N94-18720
N00014-93-I-1019 p 1404 N94-18709
N00014-93-1-0015 p 1562 N94-18286
N00014-93-1-0067 p 1604 N94-19579
p 1605 N94-19679
N00014-93-1-0110 p 1632 N94-18791
N00014-93-1-0140 p 1598 N94-18609
N00014-93-1-0365 p 1375 N94-19758
N00014-93-1-0472 p 1375 N94-19758
N00039-93-C-0001 p 1386 N94-18473
p 1388 N94-18741
p 1388 N94-18751
N00123-89-G-0580 p 1445 N94-18465
p 1454 N94-18466
p 1445 N94-18634
p 1499 N94-19580
p 1564 N94-19723
N00140-88-C-RC21 p 1355 N94-17767
p 1356 N94-17768
p 1356 N94-17769
p 1356 N94-17772
p 1356 N94-17788
p 1356 N94-17789
p 1356 N94-17796
p 1356 N94-17801
p 1357 N94-17802
p 1357 N94-17803
p 1357 N94-17804
p 1593 N94-17805
N62190-91-M-0526 p 1370 N94-18280
N68452-86-MP-6003 p 1463 N94-19672
OTKA-2116 p 1524 N94-19089
p 1525 N94-19143
p 1525 N94-19156
OTKA-2570 p 1552 N94-19395
RICIS PROJ. RB-07 p 1617 N94-18839
RICIS PROJ. SR-02 p 1513 N94-19349
RTOP 474-46-10 p 1587 N94-18861
RTOP 505-59-50-01 p 1417 N94-18843
RTOP 505-62-10 p 1446 N94-19318
RTOP 505-62-5B p 1434 N94-19314
RTOP 505-63-50-02 p 1368 N94-18075
RTOP 505-63-50-09 p 1458 N94-19465
RTOP 505-64-52-03 p 1321 N94-19316
RTOP 505-68-32 p 1321 N94-19353
RTOP 505-90-52-01 p 1551 N94-19315
p 1551 N94-19317
RTOP 506-42-31 p 1336 N94-17856
RTOP 506-43-41-02 p 1333 N94-17765
RTOP 506-72-21 p 1333 N94-19313
RTOP 510-02-12 p 1457 N94-19351
RTOP 537-02-22 p 1313 N94-19484
RTOP 593-72-00 p 1468 N94-18821
RTOP 906-11-01-01 p 1332 N94-18669
p 1332 N94-18670
SBIR-14.03-6642 p 1315 N94-18852
USGS-G-1915 p 1476 N94-19064
W-31-109-ENG-38 p 1394 N94-17750
p 1471 N94-17777
p 1443 N94-17785
p 1612 N94-17870
p 1594 N94-17871
p 1472 N94-17890
p 1472 N94-17891
p 1337 N94-17908
p 1409 N94-18004
p 1368 N94-18096
p 1368 N94-18098
p 1614 N94-18099
p 1396 N94-18135
p 1369 N94-18166
p 1409 N94-18248
p 1348 N94-18249
p 1586 N94-18272
p 1574 N94-18273
p 1445 N94-18307
p 1502 N94-18476
p 1454 N94-18479
p 1597 N94-18480
p 1430 N94-18481
p 1597 N94-18498
p 1474 N94-18499
p 1597 N94-18500
p 1474 N94-18502
p 1598 N94-18531
p 1568 N94-18825
p 1568 N94-18826
p 1372 N94-18932
p 1600 N94-18933
p 1574 N94-18934
p 1588 N94-18971
p 1601 N94-18993
p 1535 N94-19010
p 1557 N94-19011
p 1601 N94-19022
p 1364 N94-19044
p 1476 N94-19045
p 1535 N94-19046
p 1570 N94-19096
p 1609 N94-19121
p 1602 N94-19122
p 1478 N94-19241
p 1478 N94-19305
p 1373 N94-19321
p 1469 N94-19346
p 1603 N94-19550
p 1344 N94-19551
p 1353 N94-19552
p 1407 N94-19553
p 1604 N94-19566
p 1604 N94-19567
W-7405-ENG-36 p 1434 N94-17709
p 1582 N94-17713
p 1592 N94-17714
p 1488 N94-17715
p 1435 N94-17724
p 1379 N94-17725
p 1573 N94-17726
p 1582 N94-17727
p 1408 N94-17728
p 1593 N94-17744
p 1376 N94-17751
p 1593 N94-17754
p 1517 N94-17812

p 1376 N94-17813
p 1451 N94-17864
p 1436 N94-17865
p 1594 N94-17874
p 1358 N94-17875
p 1451 N94-17906
p 1594 N94-17907
p 1519 N94-18086
p 1368 N94-18096
p 1519 N94-18097
p 1595 N94-18162
p 1567 N94-18269
p 1410 N94-18270
p 1521 N94-18271
p 1360 N94-18501
p 1361 N94-18802
p 1587 N94-18803
p 1599 N94-18804
p 1404 N94-18805
p 1362 N94-18809
p 1562 N94-18810
p 1360 N94-18818
p 1432 N94-18828
p 1417 N94-18831
p 1627 N94-18857
p 1322 N94-18890
p 1485 N94-18894
p 1535 N94-18930
p 1600 N94-18969
p 1419 N94-19025
p 1419 N94-19027
p 1363 N94-19028
p 1455 N94-19033
p 1476 N94-19104
p 1570 N94-19120
p 1570 N94-19125
p 1570 N94-19126
p 1338 N94-19128
p 1563 N94-19151
p 1609 N94-19187
p 1372 N94-19202
p 1526 N94-19205
p 1457 N94-19207
p 1352 N94-19240
p 1571 N94-19259
p 1478 N94-19272
p 1571 N94-19278
p 1457 N94-19279
p 1551 N94-19342
p 1551 N94-19343
p 1460 N94-19603
p 1423 N94-19604
p 1605 N94-19735
W-7405-ENG-48 .... p 1582 N94-17708
p 1355 N94-17711
p 1435 N94-17723
p 1516 N94-17740
p 1394 N94-17755
p 1488 N94-17758
p 1435 N94-17759
p 1394 N94-17770
p 1495 N94-17779
p 1333 N94-17782
p 1565 N94-17797
p 1395 N94-17849
p 1565 N94-17850
p 1465 N94-17853
p 1435 N94-17855
p 1357 N94-17860
p 1517 N94-17867
p 1436 N94-17868
p 1395 N94-17872
p 1562 N94-17873
p 1395 N94-17882
p 1594 N94-17896
p 1624 N94-17897
p 1382 N94-17909
p 1517 N94-17911
p 1517 N94-17914
p 1488 N94-17942
p 1584 N94-17988
p 1584 N94-17990
p 1396 N94-17991
p 1595 N94-17992
p 1584 N94-17993
p 1383 N94-17994
p 1436 N94-17996
p 1473 N94-18005
p 1452 N94-18049
p 1489 N94-18053
p 1585 N94-18057
p 1519 N94-18072
p 1556 N94-18073
p 1585 N94-18082
p 1437 N94-18083
p 1347 N94-18092
p 1437 N94-18093
p 1376 N94-18095
p 1453 N94-18108
p 1358 N94-18111
p 1369 N94-18112
p 1340 N94-18113
p 1359 N94-18114
p 1585 N94-18115
p 1585 N94-18129
p 1520 N94-18130
p 1437 N94-18131
p 1489 N94-18132
p 1520 N94-18133
p 1437 N94-18134
p 1384 N94-18210
p 1430 N94-18235
p 1587 N94-18274
p 1399 N94-18350
p 1587 N94-18505
p 1380 N94-18710
p 1632 N94-18856
p 1418 N94-18888
p 1440 N94-18889
p 1377 N94-18893
p 1580 N94-18931
p 1363 N94-18939
p 1405 N94-18941
p 1335 N94-18942
p 1523 N94-18943
p 1350 N94-18987
p 1418 N94-18995
p 1575 N94-18996
p 1463 N94-19003
p 1433 N94-19004
p 1588 N94-19034
p 1589 N94-19037
p 1476 N94-19038
p 1524 N94-19048
p 1601 N94-19049
p 1589 N94-19073
p 1589 N94-19074
p 1627 N94-19077
p 1575 N94-19106
p 1575 N94-19107
p 1390 N94-19114
p 1536 N94-19115
p 1571 N94-19201
p 1527 N94-19238
p 1378 N94-19242
p 1441 N94-19251
p 1448 N94-19252
p 1537 N94-19253
p 1365 N94-19263
p 1352 N94-19266
p 1580 N94-19268
p 1590 N94-19269
p 1563 N94-19270
p 1335 N94-19275
p 1528 N94-19276
p 1572 N94-19283
p 1627 N94-19284
p 1590 N94-19289
p 1590 N94-19290
p 1441 N94-19294
p 1494 N94-19298
p 1390 N94-19306
p 1441 N94-19307
p 1591 N94-19311
p 1460 N94-19475
p 1422 N94-19515
p 1381 N94-19539
p 1460 N94-19543
p 1381 N94-19544
p 1572 N94-19545
p 1531 N94-19548
p 1559 N94-19549
p 1442 N94-19554
p 1604 N94-19565
p 1422 N94-19568
p 1480 N94-19732
W-7405-ENG-82 .... p 1343 N94-18914

REPORT NUMBER INDEX

SCIENTIFIC AND TECHNICAL AEROSPACE REPORTS VOLUME 32 NUMBER 4

Typical Report Number Index Listing

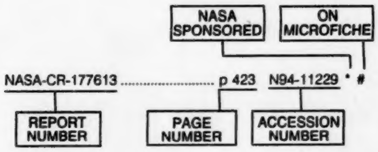

Listings in this index are arranged alphanumerically by report number. The accession number denotes the number by which the citation is identified. The page number helps to locate the citation in the abstract section. An asterisk (*) indicates that the item is a NASA report. A pound sign (#) indicates that the item is available on microfiche.

A-94009 .... p 1315 N94-18844 * #

AC-20-36S .... p 1618 N94-19377 #

AD-A260738 .... p 1615 N94-18323 #
AD-A264703 .... p 1367 N94-17878 #
AD-A265204 .... p 1514 N94-17877 #
AD-A265205 .... p 1594 N94-17876 #
AD-A265940 .... p 1337 N94-17879
AD-A266195 .... p 1351 N94-19110 #
AD-A266528 .... p 1556 N94-18397
AD-A267388 .... p 1486 N94-19008 #
AD-A267389 .... p 1389 N94-19009 #
AD-A267792 .... p 1453 N94-18382 #
AD-A267901 .... p 1521 N94-18308
AD-A268189 .... p 1501 N94-17729
AD-A268190 .... p 1443 N94-17730
AD-A268209 .... p 1576 N94-17887 #
AD-A268232 .... p 1359 N94-18322
AD-A268263 .... p 1356 N94-17801 #
AD-A268264 .... p 1357 N94-17802 #
AD-A268300 .... p 1357 N94-17803
AD-A268304 .... p 1357 N94-17804
AD-A268323 .... p 1593 N94-17805
AD-A268324 .... p 1356 N94-17798
AD-A268325 .... p 1356 N94-17788
AD-A268350 .... p 1356 N94-17789 #
AD-A268351 .... p 1356 N94-17772 #
AD-A268352 .... p 1355 N94-17767 #
AD-A268354 .... p 1356 N94-17768 #
AD-A268355 .... p 1356 N94-17769
AD-A268451 .... p 1379 N94-18147
AD-A268452 .... p 1586 N94-18148
AD-A268456 .... p 1334 N94-18149
AD-A266457 .... p 1382 N94-17844
AD-A268463 .... p 1578 N94-18383
AD-A268465 .... p 1389 N94-18801
AD-A268485 .... p 1316 N94-18384
AD-A268512 .... p 1410 N94-18385
AD-A268535 .... p 1341 N94-18630
AD-A268536 .... p 1462 N94-18309
AD-A268537 .... p 1462 N94-18631 #
AD-A268584 .... p 1609 N94-18310
AD-A268608 .... p 1497 N94-18277 #
AD-A268622 .... p 1508 N94-18292 #
AD-A268632 .... p 1386 N94-18495 #
AD-A268637 .... p 1506 N94-18632
AD-A268645 .... p 1598 N94-18633 #
AD-A268668 .... p 1397 N94-18311 #
AD-A268679 .... p 1397 N94-18312 #
AD-A268682 .... p 1540 N94-18399 #
AD-A268685 .... p 1497 N94-18455 #
AD-A268687 .... p 1396 N94-18293 #
AD-A268697 .... p 1445 N94-18465 #
AD-A268705 .... p 1522 N94-18786
AD-A268711 .... p 1508 N94-18313
AD-A268714 .... p 1402 N94-18400
AD-A268715 .... p 1338 N94-18314
AD-A268721 .... p 1568 N94-18787
AD-A268726 .... p 1615 N94-18323 #
AD-A268728 .... p 1317 N94-18315
AD-A268729 .... p 1322 N94-18324 #
AD-A268730 .... p 1360 N94-18325 #
AD-A268731 .... p 1410 N94-18326 #
AD-A268732 .... p 1341 N94-18327 #
AD-A268735 .... p 1596 N94-18316
AD-A268737 .... p 1396 N94-18278 #
AD-A268741 .... p 1321 N94-18401 #
AD-A268745 .... p 1361 N94-18788
AD-A268748 .... p 1311 N94-18402 #
AD-A268751 .... p 1454 N94-18466 #
AD-A268752 .... p 1445 N94-18634 #
AD-A268758 .... p 1481 N94-18467 #
AD-A268759 .... p 1453 N94-18328 #
AD-A268760 .... p 1370 N94-18403 #
AD-A268767 .... p 1360 N94-18386 #
AD-A268768 .... p 1453 N94-18387 #
AD-A268769 .... p 1596 N94-18388 #
AD-A268774 .... p 1347 N94-18185
AD-A268775 .... p 1497 N94-18329 #
AD-A268776 .... p 1322 N94-18330 #
AD-A268780 .... p 1496 N94-18215
AD-A268788 .... p 1384 N94-18216 #
AD-A268789 .... p 1384 N94-18186 #
AD-A268790 .... p 1384 N94-18187 #
AD-A268792 .... p 1369 N94-18188 #
AD-A268793 .... p 1540 N94-18189 #
AD-A268795 .... p 1505 N94-18190
AD-A268796 .... p 1340 N94-18201
AD-A268798 .... p 1337 N94-18202 #
AD-A268800 .... p 1348 N94-18389 #
AD-A268806 .... p 1376 N94-18203 #
AD-A268808 .... p 1576 N94-18204 #
AD-A268809 .... p 1340 N94-18205
AD-A268821 .... p 1490 N94-18206 #
AD-A268823 .... p 1614 N94-18191 #
AD-A268825 .... p 1616 N94-18535 #
AD-A268826 .... p 1320 N94-18536 #
AD-A268828 .... p 1430 N94-18537 #
AD-A268829 .... p 1505 N94-18538 #
AD-A268840 .... p 1598 N94-18539 #
AD-A268841 .... p 1557 N94-18540 #
AD-A268843 .... p 1514 N94-18317 #
AD-A268844 .... p 1397 N94-18318
AD-A268846 .... p 1348 N94-18221 #
AD-A268847 .... p 1532 N94-19707 #
AD-A268848 .... p 1629 N94-18222
AD-A268849 .... p 1577 N94-18223
AD-A268850 .... p 1567 N94-18766
AD-A268851 .... p 1402 N94-18390
AD-A268855 .... p 1615 N94-18319
AD-A268858 .... p 1410 N94-18391
AD-A268859 .... p 1596 N94-18320
AD-A268871 .... p 1579 N94-18635
AD-A268874 .... p 1341 N94-18636
AD-A268875 .... p 1332 N94-18321
AD-A268881 .... p 1615 N94-18224
AD-A268884 .... p 1447 N94-18225
AD-A268886 .... p 1505 N94-18226
AD-A268889 .... p 1349 N94-18456
AD-A268890 .... p 1578 N94-18457
AD-A268895 .... p 1521 N94-18458
AD-A268896 .... p 1505 N94-18392
AD-A268898 .... p 1317 N94-18227 #
AD-A268899 .... p 1384 N94-18228 #
AD-A268901 .... p 1481 N94-18229 #
AD-A268903 .... p 1497 N94-18230 #
AD-A268908 .... p 1540 N94-18331 #
AD-A268924 .... p 1501 N94-18231 #
AD-A268926 .... p 1481 N94-18485 #
AD-A268927 .... p 1490 N94-18486 #
AD-A268929 .... p 1454 N94-18487 #
AD-A268931 .... p 1370 N94-18448
AD-A268938 .... p 1321 N94-18541 #
AD-A268341 .... p 1386 N94-18449
AD-A268945 .... p 1341 N94-18450
AD-A268948 .... p 1481 N94-18451
AD-A268955 .... p 1497 N94-18393 #
AD-A268956 .... p 1360 N94-18542 #
AD-A268966 .... p 1521 N94-18543 #
AD-A268973 .... p 1387 N94-18525 #
AD-A268974 .... p 1567 N94-18526 #
AD-A268981 .... p 1522 N94-18696 #
AD-A268982 .... p 1403 N94-18452
AD-A268983 .... p 1521 N94-18453
AD-A268984 .... p 1522 N94-18698 #
AD-A268988 .... p 1597 N94-18468 #
AD-A268989 .... p 1599 N94-18764 #
AD-A268990 .... p 1512 N94-18765 #
AD-A268992 .... p 1386 N94-18454
AD-A268998 .... p 1511 N94-18394 #
AD-A269000 .... p 1349 N94-18395 #
AD-A269014 .... p 1598 N94-18527
AD-A269024 .... p 1578 N94-18528
AD-A269025 .... p 1578 N94-18332 #
AD-A269026 .... p 1578 N94-18488
AD-A269027 .... p 1578 N94-18396 #
AD-A269033 .... p 1385 N94-18404 #
AD-A269035 .... p 1377 N94-18489
AD-A269042 .... p 1315 N94-18490
AD-A269053 .... p 1455 N94-18716
AD-A269056 .... p 1377 N94-18491
AD-A269058 .... p 1438 N94-18492
AD-A269059 .... p 1370 N94-18515
AD-A269060 .... p 1578 N94-18405 #
AD-A269064 .... p 1430 N94-18406 #
AD-A269067 .... p 1557 N94-18516
AD-A269068 .... p 1557 N94-18517 #
AD-A269070 .... p 1505 N94-18294 #
AD-A269085 .... p 1534 N94-18767
AD-A269087 .... p 1483 N94-18717 #
AD-A269088 .... p 1334 N94-18718 #
AD-A269090 .... p 1599 N94-18719 #
AD-A269104 .... p 1492 N94-18637 #
AD-A269105 .... p 1438 N94-18250 #
AD-A269110 .... p 1520 N94-18251 #
AD-A269115 .... p 1577 N94-18295 #
AD-A269117 .... p 1511 N94-18296 #
AD-A269119 .... p 1617 N94-18770
AD-A269120 .... p 1577 N94-18254 #
AD-A269122 .... p 1541 N94-18773
AD-A269129 .... p 1348 N94-18255 #
AD-A269133 .... p 1348 N94-18256 #
AD-A269137 .... p 1371 N94-18691
AD-A269138 .... p 1348 N94-18257 #
AD-A269147 .... p 1438 N94-18258 #
AD-A269148 .... p 1521 N94-18259 #
AD-A269153 .... p 1385 N94-18260 #
AD-A269154 .... p 1540 N94-18261 #
AD-A269159 .... p 1579 N94-18693
AD-A269168 .... p 1557 N94-18694
AD-A269170 .... p 1403 N94-18695
AD-A269171 .... p 1418 N94-18878
AD-A269172 .... p 1523 N94-18879
AD-A269173 .... p 1440 N94-18880
AD-A269188 .... p 1549 N94-18863 #
AD-A269190 .... p 1455 N94-18864 #
AD-A269191 .... p 1535 N94-18865
AD-A269193 .... p 1535 N94-18866
AD-A269194 .... p 1511 N94-18412 #
AD-A269196 .... p 1475 N94-18881
AD-A269198 .... p 1512 N94-18882
AD-A269200 .... p 1493 N94-18883
AD-A269206 .... p 1311 N94-18413 #
AD-A269212 .... p 1600 N94-18884
AD-A269213 .... p 1475 N94-18885
AD-A269220 .... p 1512 N94-18886
AD-A269223 .... p 1376 N94-17840 #
AD-A269224 .... p 1542 N94-18887
AD-A269232 .... p 1609 N94-18908
AD-A269233 .... p 1405 N94-18909
AD-A269235 .... p 1499 N94-18910
AD-A269242 .... p 1506 N94-18911
AD-A269248 .... p 1440 N94-18912
AD-A269250 .... p 1362 N94-18923
AD-A269251 .... p 1502 N94-18924 #
AD-A269252 .... p 1577 N94-18262
AD-A269253 .... p 1540 N94-18263
AD-A269254 .... p 1334 N94-18264
AD-A269258 .... p 1490 N94-18265 #
AD-A269266 .... p 1511 N94-17841 #

AD-A269268 .... p 1495 N94-17822 #
AD-A269280 .... p 1320 N94-18333
AD-A269286 .... p 1444 N94-18266
AD-A269287 .... p 1598 N94-18616
AD-A269288 .... p 1481 N94-18297
AD-A269298 .... p 1577 N94-18298
AD-A269301 .... p 1504 N94-17823 #
AD-A269302 .... p 1305 N94-18279
AD-A269303 .... p 1430 N94-18299
AD-A269304 .... p 1504 N94-17824 #
AD-A269305 .... p 1386 N94-18469 #
AD-A269318 .... p 1490 N94-18300 #
AD-A269327 .... p 1334 N94-18470 #
AD-A269340 .... p 1385 N94-18301 #
AD-A269343 .... p 1513 N94-18992 #
AD-A269350 .... p 1546 N94-17825 #
AD-A269352 .... p 1577 N94-18302
AD-A269372 .... p 1403 N94-18471 #
AD-A269374 .... p 1505 N94-18407
AD-A269375 .... p 1334 N94-18408 #
AD-A269377 .... p 1410 N94-18472 #
AD-A269378 .... p 1370 N94-18280 #
AD-A269383 .... p 1403 N94-18638
AD-A269400 .... p 1597 N94-18459 #
AD-A269403 .... p 1490 N94-18281 #
AD-A269450 .... p 1370 N94-18282 #
AD-A269452 .... p 1577 N94-18283 #
AD-A269454 .... p 1396 N94-18284 #
AD-A269455 .... p 1453 N94-18285 #
AD-A269456 .... p 1562 N94-18286 #
AD-A269459 .... p 1522 N94-18726 #
AD-A269476 .... p 1316 N94-18728 #
AD-A269477 .... p 1462 N94-18729
AD-A269493 .... p 1549 N94-18697
AD-A269494 .... p 1404 N94-18701 #
AD-A269495 .... p 1629 N94-18705 #
AD-A269526 .... p 1403 N94-18639 #
AD-A269530 .... p 1557 N94-18640 #
AD-A269531 .... p 1616 N94-18641 #
AD-A269532 .... p 1534 N94-18768
AD-A269543 .... p 1385 N94-18287 #
AD-A269544 .... p 1385 N94-18288 #
AD-A269547 .... p 1500 N94-19762
AD-A269549 .... p 1416 N94-18642 #
AD-A269550 .... p 1505 N94-18289 #
AD-A269555 .... p 1521 N94-18290 *
AD-A269556 .... p 1438 N94-18460
AD-A269557 .... p 1385 N94-18291
AD-A269559 .... p 1388 N94-18769
AD-A269561 .... p 1317 N94-17826 #
AD-A269567 .... p 1490 N94-18303
AD-A269569 .... p 1386 N94-18473
AD-A269583 .... p 1508 N94-18304
AD-A269584 .... p 1502 N94-18305
AD-A269587 .... p 1359 N94-18306
AD-A269588 .... p 1615 N94-18461
AD-A269593 .... p 1541 N94-18462
AD-A269594 .... p 1541 N94-18463
AD-A269596 .... p 1615 N94-18464
AD-A269602 .... p 1612 N94-17745
AD-A269608 .... p 1610 N94-17746 #
AD-A269648 .... p 1349 N94-18736
AD-A269655 .... p 1439 N94-18737
AD-A269663 .... p 1430 N94-18569
AD-A269669 .... p 1516 N94-17732
AD-A269670 .... p 1616 N94-18570
AD-A269678 .... p 1312 N94-18571
AD-A269680 .... p 1341 N94-18572
AD-A269686 .... p 1490 N94-18573
AD-A269687 .... p 1337 N94-18574
AD-A269691 .... p 1616 N94-18575
AD-A269695 .... p 1439 N94-18576
AD-A269698 .... p 1417 N94-18739 #
AD-A269700 .... p 1317 N94-18577
AD-A269715 .... p 1320 N94-18748
AD-A269716 .... p 1404 N94-18749
AD-A269726 .... p 1388 N94-18751
AD-A269727 .... p 1388 N94-18741 #
AD-A269730 .... p 1462 N94-18753
AD-A269735 .... p 1512 N94-18754
AD-A269739 .... p 1342 N94-18756
AD-A269740 .... p 1342 N94-18757
AD-A269742 .... p 1361 N94-18742
AD-A269746 .... p 1509 N94-18744
AD-A269748 .... p 1342 N94-18720 #
AD-A269753 .... p 1497 N94-18414
AD-A269754 .... p 1387 N94-18721
AD-A269755 .... p 1388 N94-18722
AD-A269758 .... p 1377 N94-18758
AD-A269772 .... p 1541 N94-18759
AD-A269780 .... p 1506 N94-18598
AD-A269784 .... p 1491 N94-18599 #
AD-A269793 .... p 1493 N94-18732 #
AD-A269816 .... p 1318 N94-18733 #
AD-A269817 .... p 1361 N94-18735 #
AD-A269820 .... p 1579 N94-18738 #
AD-A269835 .... p 1498 N94-18600 #
AD-A269842 .... p 1371 N94-18740 #
AD-A269843 .... p 1498 N94-18723 #
AD-A269846 .... p 1541 N94-18474
AD-A269855 .... p 1316 N94-18336 #
AD-A269860 .... p 1560 N94-18410 #
AD-A269861 .... p 1331 N94-18411 #
AD-A269872 .... p 1483 N94-18655 #
AD-A269874 .... p 1599 N94-18745 #
AD-A269875 .... p 1440 N94-18771 #
AD-A269876 .... p 1535 N94-18772 #
AD-A269877 .... p 1512 N94-18774 #
AD-A269878 .... p 1432 N94-18681 #
AD-A269879 .... p 1508 N94-18682 #
AD-A269880 .... p 1454 N94-18683 #
AD-A269884 .... p 1492 N94-18684
AD-A269885 .... p 1498 N94-18685 #
AD-A269889 .... p 1509 N94-18686 #
AD-A269890 .... p 1360 N94-18687 #
AD-A269896 .... p 1474 N94-18688 #
AD-A269897 .... p 1483 N94-18690 #
AD-A269899 .... p 1439 N94-18656 #
AD-A269900 .... p 1508 N94-18657 #
AD-A269921 .... p 1320 N94-18658 #
AD-A269923 .... p 1521 N94-18659 #
AD-A269927 .... p 1360 N94-18660 #
AD-A269928 .... p 1454 N94-18661
AD-A269930 .... p 1498 N94-18662
AD-A269931 .... p 1498 N94-18663 #
AD-A269934 .... p 1341 N94-18544 #
AD-A269945 .... p 1416 N94-18671 #
AD-A269949 .... p 1417 N94-18672 #
AD-A269952 .... p 1512 N94-18673 #
AD-A269953 .... p 1439 N94-18674 #
AD-A269954 .... p 1492 N94-18675 #
AD-A269955 .... p 1475 N94-18775
AD-A269956 .... p 1388 N94-18777 #
AD-A269967 .... p 1445 N94-18778
AD-A269970 .... p 1493 N94-18781 #
AD-A269977 .... p 1630 N94-18676 #
AD-A269989 .... p 1462 N94-18677
AD-A269990 .... p 1563 N94-18678
AD-A269991 .... p 1462 N94-18679 #
AD-A269992 .... p 1522 N94-18680
AD-A269995 .... p 1562 N94-18664 #
AD-A269996 .... p 1498 N94-18665 #
AD-A270001 .... p 1387 N94-18666 #
AD-A270003 .... p 1403 N94-18667 #
AD-A270004 .... p 1579 N94-18668 #
AD-A270008 .... p 1387 N94-18601 #
AD-A270009 .... p 1598 N94-18609 #
AD-A270022 .... p 1439 N94-18614 #
AD-A270023 .... p 1332 N94-18760
AD-A270024 .... p 1599 N94-18711 #
AD-A270026 .... p 1483 N94-18712 #
AD-A270028 .... p 1371 N94-18713 #
AD-A270032 .... p 1318 N94-18789 #
AD-A270033 .... p 1541 N94-18790 #
AD-A270037 .... p 1632 N94-18791 #
AD-A270040 .... p 1372 N94-18792 #
AD-A270041 .... p 1506 N94-18793
AD-A270049 .... p 1522 N94-18794
AD-A270058 .... p 1318 N94-18795 #
AD-A270059 .... p 1417 N94-18796 #
AD-A270074 .... p 1599 N94-18797 #
AD-A270083 .... p 1549 N94-18798 #
AD-A270084 .... p 1350 N94-18799
AD-A270085 .... p 1463 N94-18800 #
AD-A270087 .... p 1315 N94-18822 #
AD-A270088 .... p 1315 N94-18823 #
AD-A270092 .... p 1418 N94-18867 #
AD-A270100 .... p 1484 N94-18868 #
AD-A270101 .... p 1343 N94-18869
AD-A270102 .... p 1418 N94-18870
AD-A270103 .... p 1493 N94-18871 #
AD-A270106 .... p 1404 N94-18872 #
AD-A270125 .... p 1485 N94-18873 #
AD-A270126 .... p 1485 N94-18874 #
AD-A270127 .... p 1432 N94-18875 #
AD-A270129 .... p 1600 N94-18876
AD-A270130 .... p 1627 N94-18877
AD-A270137 .... p 1389 N94-18897 #
AD-A270139 .... p 1371 N94-18750 #
AD-A270140 .... p 1617 N94-18752 #
AD-A270141 .... p 1542 N94-18898 #
AD-A270147 .... p 1349 N94-18776 #
AD-A270148 .... p 1485 N94-18899 #
AD-A270150 .... p 1318 N94-18779 #
AD-A270152 .... p 1440 N94-18900 #
AD-A270182 .... p 1417 N94-18755
AD-A270194 .... p 1417 N94-18780
AD-A270198 .... p 1388 N94-18782
AD-A270199 .... p 1567 N94-18783
AD-A270200 .... p 1568 N94-18784
AD-A270202 .... p 1349 N94-18785
AD-A270209 .... p 1523 N94-18901
AD-A270210 .... p 1588 N94-18902
AD-A270231 .... p 1499 N94-18903
AD-A270232 .... p 1600 N94-18904
AD-A270240 .... p 1523 N94-18905
AD-A270242 .... p 1418 N94-18906 #
AD-A270270 .... p 1320 N94-18907
AD-A270271 .... p 1389 N94-18811
AD-A270273 .... p 1493 N94-18812
AD-A270291 .... p 1445 N94-18813 #
AD-A270296 .... p 1568 N94-18814 #
AD-A270303 .... p 1549 N94-18815 #
AD-A270305 .... p 1341 N94-18692 #
AD-A270306 .... p 1499 N94-18727 #
AD-A270316 .... p 1534 N94-18699 #
AD-A270318 .... p 1342 N94-18700 #
AD-A270361 .... p 1342 N94-18702 #
AD-A270374 .... p 1338 N94-18703
AD-A270377 .... p 1342 N94-18704 #
AD-A270406 .... p 1404 N94-18706
AD-A270409 .... p 1377 N94-18708
AD-A270413 .... p 1404 N94-18709
AD-A270424 .... p 1597 N94-18506 #
AD-A270426 .... p 1534 N94-18507
AD-A270427 .... p 1534 N94-18508
AD-A270435 .... p 1534 N94-18509 #
AD-A270436 .... p 1387 N94-18510 #
AD-A270437 .... p 1598 N94-18511 #
AD-A270441 .... p 1387 N94-18512 #
AD-A270450 .... p 1387 N94-18513
AD-A270452 .... p 1490 N94-18514
AD-A270453 .... p 1455 N94-18714
AD-A270454 .... p 1342 N94-18715
AD-A270456 .... p 1576 N94-19589 #
AD-A270458 .... p 1554 N94-19671 #
AD-A270468 .... p 1463 N94-19672 #
AD-A270477 .... p 1366 N94-19673 #
AD-A270479 .... p 1378 N94-19674 #
AD-A270480 .... p 1507 N94-19675 #
AD-A270482 .... p 1391 N94-19676 #
AD-A270512 .... p 1510 N94-19677 #
AD-A270516 .... p 1374 N94-19532 #
AD-A270610 .... p 1531 N94-19590
AD-A270612 .... p 1515 N94-19591
AD-A270613 .... p 1538 N94-19533 #
AD-A270614 .... p 1531 N94-19592
AD-A270621 .... p 1538 N94-19534 #
AD-A270636 .... p 1487 N94-19529 #
AD-A270637 .... p 1620 N94-19777 #
AD-A270649 .... p 1544 N94-19530 #
AD-A270652 .... p 1513 N94-19531 #
AD-A270656 .... p 1460 N94-19606 #
AD-A270660 .... p 1354 N94-19778
AD-A270661 .... p 1393 N94-19779
AD-A270662 .... p 1619 N94-19780
AD-A270663 .... p 1319 N94-19781
AD-A270672 .... p 1572 N94-19607 #
AD-A270673 .... p 1532 N94-19782
AD-A270709 .... p 1531 N94-19573
AD-A270728 .... p 1374 N94-19574
AD-A270730 .... p 1513 N94-19764
AD-A270731 .... p 1507 N94-19608 #
AD-A270734 .... p 1499 N94-19609 #
AD-A270749 .... p 1446 N94-19678 #
AD-A270752 .... p 1479 N94-19575
AD-A270754 .... p 1333 N94-19765
AD-A270755 .... p 1448 N94-19766
AD-A270756 .... p 1507 N94-19593
AD-A270759 .... p 1447 N94-19767
AD-A270762 .... p 1560 N94-19768
AD-A270763 .... p 1316 N94-19661 #
AD-A270764 .... p 1344 N94-19576
AD-A270803 .... p 1344 N94-19662 #
AD-A270809 .... p 1374 N94-19577
AD-A270810 .... p 1610 N94-19663 #
AD-A270823 .... p 1605 N94-19664 #
AD-A270825 .... p 1407 N94-19665 #
AD-A270827 .... p 1366 N94-19594 #
AD-A270830 .... p 1559 N94-19595 #
AD-A270832 .... p 1604 N94-19596 #
AD-A270834 .... p 1604 N94-19597 #
AD-A270835 .... p 1422 N94-19598 #
AD-A270836 .... p 1544 N94-19599 #
AD-A270837 .... p 1374 N94-19600 #
AD-A270847 .... p 1581 N94-19578
AD-A270848 .... p 1606 N94-19769
AD-A270857 .... p 1442 N94-19770
AD-A270862 .... p 1500 N94-19792 #
AD-A270866 .... p 1393 N94-19793 #
AD-A270869 .... p 1507 N94-19783 #
AD-A270876 .... p 1606 N94-19771
AD-A270877 .... p 1604 N94-19579
AD-A270878 .... p 1447 N94-19784 #
AD-A270879 .... p 1499 N94-19580
AD-A270882 .... p 1323 N94-19581
AD-A270884 .... p 1500 N94-19785 #
AD-A270893 .... p 1500 N94-19786 #

AD-A270895 .... p 1500 N94-19747
AD-A270900 .... p 1392 N94-19748
AD-A270901 .... p 1392 N94-19749
AD-A270905 .... p 1564 N94-19750
AD-A270947 .... p 1408 N94-19751
AD-A270948 .... p 1581 N94-19601 #
AD-A270949 .... p 1581 N94-19602 #
AD-A270952 .... p 1605 N94-19679 #
AD-A270953 .... p 1393 N94-19752
AD-A270954 .... p 1393 N94-19753
AD-A270967 .... p 1335 N94-19787 #
AD-A270968 .... p 1442 N94-19788 #
AD-A270969 .... p 1504 N94-19789 #
AD-A270970 .... p 1446 N94-19754
AD-A270972 .... p 1539 N94-19790 #
AD-A270973 .... p 1354 N94-19755
AD-A270974 .... p 1434 N94-19791 #
AD-A270976 .... p 1392 N94-19680 #
AD-A270988 .... p 1581 N94-19772 #
AD-A271000 .... p 1392 N94-19736 #
AD-A271006 .... p 1514 N94-19773 #
AD-A271008 .... p 1423 N94-19774 #
AD-A271009 .... p 1366 N94-19775 #
AD-A271012 .... p 1345 N94-19776 #
AD-A271035 .... p 1539 N94-19682 #
AD-A271121 .... p 1392 N94-19737 #
AD-A271146 .... p 1392 N94-19738 #
AD-A271147 .... p 1606 N94-19739 #
AD-A271148 .... p 1375 N94-19740 #
AD-A271180 .... p 1606 N94-19741 #
AD-A271196 .... p 1375 N94-19742 #
AD-A271197 .... p 1605 N94-19717 #
AD-A271198 .... p 1392 N94-19718 #
AD-A271206 .... p 1605 N94-19719 #
AD-A271207 .... p 1344 N94-19720 #
AD-A271208 .... p 1545 N94-19721 #
AD-A271209 .... p 1407 N94-19722 #
AD-A271210 .... p 1564 N94-19723 #
AD-A271248 .... p 1392 N94-19724 #
AD-A271249 .... p 1605 N94-19725 #
AD-A271259 .... p 1560 N94-19726 #
AD-A271263 .... p 1500 N94-19727 #
AD-A271271 .... p 1354 N94-19728 #
AD-A271272 .... p 1442 N94-19729 #
AD-A271276 .... p 1500 N94-19743 #
AD-A271277 .... p 1344 N94-19744 #
AD-A271289 .... p 1500 N94-19745 #
AD-A271290 .... p 1345 N94-19746 #
AD-A271317 .... p 1422 N94-19569 #
AD-A271320 .... p 1513 N94-19570 #
AD-A271322 .... p 1619 N94-19571 #
AD-A271324 .... p 1317 N94-19572 #
AD-A271334 .... p 1391 N94-19582 #
AD-A271336 .... p 1553 N94-19583 #
AD-A271339 .... p 1407 N94-19584 #
AD-A271364 .... p 1374 N94-19585 #
AD-A271368 .... p 1374 N94-19586 #
AD-A271385 .... p 1391 N94-19587 #
AD-A271387 .... p 1408 N94-19756 #
AD-A271388 .... p 1503 N94-19757
AD-A271402 .... p 1375 N94-19758 #

AD-D015789 .... p 1368 N94-17982 #
AD-D015809 .... p 1382 N94-17902 #
AD-D015819 .... p 1395 N94-17903
AD-D015820 .... p 1424 N94-17904 #
AD-D015821 .... p 1580 N94-18947 #
AD-D015823 .... p 1368 N94-17905 #
AD-D015832 .... p 1512 N94-18730 #
AD-D015848 .... p 1576 N94-17716
AD-D015851 .... p 1424 N94-17717
AD-D015856 .... p 1394 N94-17718
AD-D015859 .... p 1432 N94-18731 #
AD-D015860 .... p 1563 N94-18734 #
AD-D015862 .... p 1394 N94-17703
AD-D015863 .... p 1396 N94-18062
AD-D015864 .... p 1339 N94-18074
AD-D015868 .... p 1317 N94-17704
AD-D015870 .... p 1367 N94-17719
AD-D015872 .... p 1443 N94-17705
AD-D015873 .... p 1367 N94-17706
AD-D015875 .... p 1394 N94-17707
AD-D015876 .... p 1579 N94-18743 #
AD-D015877 .... p 1371 N94-18746 #
AD-D015878 .... p 1440 N94-18747 #
AD-D015879 .... p 1371 N94-18529 #
AD-D015882 .... p 1430 N94-18530 #
AD-D015907 .... p 1408 N94-19763 #
AD-D015949 .... p 1408 N94-19759 #

AD-E201519 .... p 1379 N94-18147
AD-E201577 .... p 1567 N94-18526 #
AD-E201588 .... p 1403 N94-18452
AD-E201589 .... p 1334 N94-18718 #
AD-E201594 .... p 1439 N94-18656 #
AD-E201598 .... p 1484 N94-18868 #
AD-E201600 .... p 1483 N94-18690 #
AD-E201605 .... p 1474 N94-18688 #
AD-E201606 .... p 1485 N94-18873 #
AD-E201607 .... p 1630 N94-18676 #
AD-E201608 .... p 1485 N94-18874 #
AD-E201614 .... p 1432 N94-18875 #
AD-E201616 .... p 1404 N94-18872 #
AD-E201621 .... p 1418 N94-18870
AD-E201625 .... p 1343 N94-18869
AD-E501701 .... p 1619 N94-19780
AD-E952072 .... p 1577 N94-18262
AD-E952096 .... p 1540 N94-18263
AD-E952102 .... p 1493 N94-18781 #

AD-268794 .... p 1312 N94-19119 * #

AERONAUTICA-ACTA-A-368-1993 p 1353 N94-19456
AERONAUTICA-ACTA-A-369-1993 p 1353 N94-19459
AERONAUTICA-ACTA-A-370-1993 p 1479 N94-19518
AERONAUTICA-ACTA-A-371-1993 p 1479 N94-19521
AERONAUTICA-ACTA-A-372-1993 p 1507 N94-19523

AFCESA/ESL-TR-92-46 .... p 1417 N94-18780
AFCESA/ESL-TR-92-63-VOL-1 .... p 1315 N94-18822 #
AFCESA/ESL-TR-92-63-VOL-2 .... p 1315 N94-18823 #

AFFTC-TIM-93-01 .... p 1511 N94-18412 #

AFIT/CI/CIA-93-108 .... p 1387 N94-18513
AFIT/CI/CIA-93-138 .... p 1627 N94-18877
AFIT/CI/CIA-93-140 .... p 1493 N94-18812
AFIT/CI/CIA-93-143 .... p 1417 N94-18796 #
AFIT/CI/CIA-93-145 .... p 1318 N94-18795 #
AFIT/CI/CIA-93-146 .... p 1342 N94-18700 #
AFIT/CI/CIA-93-18D .... p 1549 N94-18815 #
AFIT/CI/CIA-93-20D .... p 1445 N94-18813 #

AFIT/DS/ENG/93-11 .... p 1532 N94-19782
AFIT/DS/ENG/93D-12 .... p 1538 N94-19534 #

AFIT/DS/ENP/93-05 .... p 1572 N94-19607 #
AFIT/DS/ENP/93-07 .... p 1554 N94-19671 #

AFIT/EN/TR/93-07-APP .... p 1531 N94-19573

AFIT/GNE/ENP/92D-1 .... p 1576 N94-19589 #

AFIT/GST/ENS/93M-13 .... p 1556 N94-18397

AFOSR-90-0010TR .... p 1567 N94-18783
AFOSR-93-0562TR .... p 1389 N94-19009 #
AFOSR-93-0586TR .... p 1501 N94-17729
AFOSR-93-0620TR .... p 1341 N94-18630
AFOSR-93-0623TR .... p 1385 N94-18404 #
AFOSR-93-0624TR .... p 1384 N94-18186 #
AFOSR-93-0626TR .... p 1508 N94-18313
AFOSR-93-0627TR .... p 1341 N94-18636
AFOSR-93-0629TR .... p 1508 N94-18292 #
AFOSR-93-0630TR .... p 1568 N94-18787
AFOSR-93-0634TR .... p 1598 N94-18539 #
AFOSR-93-0635TR .... p 1505 N94-18190
AFOSR-93-0636TR .... p 1629 N94-18222
AFOSR-93-0637TR .... p 1578 N94-18528
AFOSR-93-0638TR-VOL-8 .... p 1578 N94-18488
AFOSR-93-0640TR .... p 1405 N94-18909
AFOSR-93-0641TR .... p 1579 N94-18693
AFOSR-93-0643TR-VOL-7 .... p 1578 N94-18332 #
AFOSR-93-0644TR-VOL-9 .... p 1578 N94-18396 #
AFOSR-93-0645TR-VOL-2 .... p 1438 N94-18492
AFOSR-93-0646TR .... p 1577 N94-18298
AFOSR-93-0646TR .... p 1609 N94-18908
AFOSR-93-0647TR .... p 1577 N94-18283 #
AFOSR-93-0648TR .... p 1596 N94-18320
AFOSR-93-0649TR .... p 1576 N94-18204 #
AFOSR-93-0650TR .... p 1598 N94-18633 #
AFOSR-93-0652TR .... p 1481 N94-18485 #
AFOSR-93-0653TR .... p 1557 N94-18540 #
AFOSR-93-0654TR .... p 1361 N94-18788
AFOSR-93-0655TR .... p 1348 N94-18221 #
AFOSR-93-0656TR .... p 1567 N94-18766
AFOSR-93-0657TR .... p 1521 N94-18458
AFOSR-93-0658TR .... p 1402 N94-18390
AFOSR-93-0659TR .... p 1447 N94-18225
AFOSR-93-0660TR .... p 1615 N94-18224
AFOSR-93-0661TR .... p 1397 N94-18318
AFOSR-93-0664TR .... p 1340 N94-18205
AFOSR-93-0666TR .... p 1454 N94-18487 #
AFOSR-93-0667TR .... p 1348 N94-18389 #
AFOSR-93-0669TR .... p 1481 N94-18467 #
AFOSR-93-0670TR .... p 1490 N94-18486 #
AFOSR-93-0671TR .... p 1501 N94-18231 #
AFOSR-93-0672TR .... p 1348 N94-18257 #
AFOSR-93-0673TR .... p 1362 N94-18923
AFOSR-93-0675TR .... p 1502 N94-18924 #
AFOSR-93-0676TR .... p 1403 N94-18638
AFOSR-93-0677TR .... p 1512 N94-18886
AFOSR-93-0678TR .... p 1386 N94-18469 #
AFOSR-93-0679TR .... p 1410 N94-18472 #
AFOSR-93-0689TR .... p 1546 N94-17825 #
AFOSR-93-0690TR .... p 1385 N94-18288 #
AFOSR-93-0699TR .... p 1349 N94-18776 #
AFOSR-93-0701TR .... p 1523 N94-18901
AFOSR-93-0702TR .... p 1416 N94-18671 #
AFOSR-93-0703TR .... p 1350 N94-18799
AFOSR-93-0704TR .... p 1568 N94-18814 #
AFOSR-93-0705TR .... p 1549 N94-18798 #
AFOSR-93-0706TR .... p 1388 N94-18782
AFOSR-93-0708TR .... p 1568 N94-18784
AFOSR-93-0709TR .... p 1371 N94-18713 #
AFOSR-93-0712TR .... p 1349 N94-18785
AFOSR-93-0713TR .... p 1508 N94-18682 #
AFOSR-93-0714TR .... p 1508 N94-18657 #
AFOSR-93-0740TR .... p 1342 N94-18715
AFOSR-93-0741TR .... p 1485 N94-18899 #
AFOSR-93-0742TR .... p 1600 N94-18876
AFOSR-93-0743TR .... p 1600 N94-18904
AFOSR-93-0744TR .... p 1597 N94-18506 #
AFOSR-93-0745TR .... p 1440 N94-18900 #
AFOSR-93-0746TR .... p 1598 N94-18511 #
AFOSR-93-0747TR .... p 1542 N94-18898 #
AFOSR-93-0748TR .... p 1588 N94-18902
AFOSR-93-0751TR .... p 1504 N94-19789 #
AFOSR-93-0752TR .... p 1446 N94-19754
AFOSR-93-0754TR .... p 1407 N94-19665 #
AFOSR-93-0755TR .... p 1442 N94-19788 #
AFOSR-93-0756TR .... p 1374 N94-19577
AFOSR-93-0768TR .... p 1374 N94-19574
AFOSR-93-0769TR .... p 1513 N94-19764
AFOSR-93-0784TR .... p 1344 N94-19720 #
AFOSR-93-0784TR .... p 1507 N94-19783 #
AFOSR-93-0785TR .... p 1374 N94-19600 #
AFOSR-93-0786TR .... p 1605 N94-19719 #

AFPT-90-122-956 .... p 1511 N94-18394 #

AGARD-CP-515 .... p 1305 N94-18415 #

AGARD-LS-191 .... p 1607 N94-18236 #

AI-TR-1370 .... p 1560 N94-19768
AI-TR-1412 .... p 1422 N94-19598 #
AI-TR-1424 .... p 1544 N94-19599 #

AIAA PAPER 93-0211 .... p 1312 N94-19119 * #
AIAA PAPER 93-2392 .... p 1336 N94-17856 * #
AIAA PAPER 93-4865 .... p 1321 N94-19353 * #
AIAA PAPER 94-1025 .... p 1333 N94-19313 * #

AIM-1422 .... p 1544 N94-19530 #

AL-TR-1993-0028 .... p 1513 N94-19570 #
AL-TR-1993-0054 .... p 1513 N94-19531 #

AL/CF-TR-1993-0052 .... p 1509 N94-18744
AL/CF-TR-1993-0074 .... p 1511 N94-17841 #

AL/HR-TP-1993-0028 .... p 1512 N94-18754

AMSMI/TR-RD-WS-93-4 .... p 1577 N94-18262
AMSMI/TR-RD-WS-93-5 .... p 1540 N94-18263
AMSMI/TR-RD-WS-93-6 .... p 1493 N94-18781 #

ANL-HEP-CP-93-24 .... p 1568 N94-18825 #
ANL-HEP-CP-93-39 .... p 1609 N94-19121 #
ANL-HEP-CP-93-50 .... p 1570 N94-19096 #

ANL/CBM/CP-80231 .... p 1502 N94-18476 #

ANL/CHM/CP-79161 .... p 1373 N94-19321 #
ANL/CHM/CP-79705 .... p 1601 N94-19022 #

ANL/CMT-ACL/CP-77718 .... p 1474 N94-18499 #

ANL/CMT/CP-79698 .... p 1478 N94-19241 #

ANL/CMT/RP-80217 .... p 1394 N94-17750

ANL/EAIS/CP-79173 .... p 1472 N94-17890 #
ANL/EAIS/CP-79424 .... p 1472 N94-17891 #

ANL/EAIS/TM-98 .... p 1471 N94-17777 #

ANL/EP/CP-78372 .... p 1574 N94-18273 #
ANL/EP/CP-78375 .... p 1574 N94-18934 #
ANL/EP/CP-78902 .... p 1588 N94-18971 #
ANL/EP/CP-80316 .... p 1337 N94-17908 #

ANL/ER/CP-80321 .... p 1476 N94-19045 #

ANL/ES/CP-79581 .... p 1348 N94-18249 #
ANL/ES/CP-79714 .... p 1443 N94-17785 #
ANL/ES/CP-79722 .... p 1586 N94-18272 #

ANL/ES/CP-80045 .... p 1353 N94-19552 #
ANL/ES/CP-80079 .... p 1474 N94-18502 #
ANL/ES/CP-80354 .... p 1409 N94-18004 #

ANL/ET/CP-77180 .... p 1372 N94-18932 #
ANL/ET/CP-78473 .... p 1396 N94-18135
ANL/ET/CP-78557 .... p 1597 N94-18500 #
ANL/ET/CP-78558 .... p 1454 N94-18479 #
ANL/ET/CP-78721 .... p 1344 N94-19551 #
ANL/ET/CP-78882 .... p 1364 N94-19044 #
ANL/ET/CP-78928 .... p 1601 N94-18993

ANL/IPNS/CP-78912 .... p 1598 N94-18531 #

ANL/MCS-TM-177 .... p 1535 N94-19010 #

ANL/MCS/CP-80151 .... p 1614 N94-18099 #
ANL/MCS/CP-80152 .... p 1612 N94-17870 #
ANL/MCS/CP-80307 .... p 1535 N94-19046 #
ANL/MCS/CP-80513 .... p 1604 N94-19567 #

ANL/MCT/CP-76064 .... p 1369 N94-18166 #
ANL/MCT/CP-78646 .... p 1602 N94-19122 #

ANL/MSD/CP-78507 .... p 1603 N94-19550 #
ANL/MSD/CP-79154 .... p 1430 N94-18481 #
ANL/MSD/CP-79243 .... p 1600 N94-18933 #
ANL/MSD/CP-79538 .... p 1604 N94-19566 #
ANL/MSD/CP-79555 .... p 1407 N94-19553 #
ANL/MSD/CP-79602 .... p 1594 N94-17871 #
ANL/MSD/CP-79845 .... p 1597 N94-18480 #
ANL/MSD/CP-80248 .... p 1368 N94-18098 #
ANL/MSD/CP-80258 .... p 1597 N94-18498 #

ANL/NDM-128 .... p 1557 N94-19011 #

ANL/PHY/CP-80056 .... p 1568 N94-18826 #

ANL/RE/CP-77653 .... p 1409 N94-18248 #

ARAED-TR-93007 .... p 1344 N94-19576
ARAED-TR-93012 .... p 1377 N94-18708

ARCCB-TR-93024 .... p 1360 N94-18542 #
ARCCB-TR-93027 .... p 1361 N94-18735 #
ARCCB-TR-93030 .... p 1545 N94-19721 #

ARL-CR-60 .... p 1366 N94-19673 #
ARL-CR-66 .... p 1311 N94-18413 #

ARL-MR-112 .... p 1359 N94-18306
ARL-MR-36 .... p 1491 N94-18599 #
ARL-MR-89 .... p 1597 N94-18468 #
ARL-MR-96 .... p 1404 N94-18749

ARL-RR-6-PT-1 .... p 1360 N94-18325 #
ARL-RR-7 .... p 1341 N94-18327 #

ARL-TN-13 .... p 1322 N94-18324 #
ARL-TN-38 .... p 1410 N94-18326 #

ARL-TR-150 .... p 1514 N94-17877 #
ARL-TR-178 .... p 1349 N94-18395 #
ARL-TR-183 .... p 1349 N94-18456
ARL-TR-191 .... p 1410 N94-18391
ARL-TR-195 .... p 1609 N94-18310
ARL-TR-198 .... p 1320 N94-18748
ARL-TR-20 .... p 1317 N94-18315
ARL-TR-228 .... p 1378 N94-19674 #
ARL-TR-235 .... p 1319 N94-19781
ARL-TR-56 .... p 1342 N94-18757
ARL-TR-58 .... p 1386 N94-18454
ARL-TR-59 .... p 1342 N94-18756
ARL-TR-68 .... p 1430 N94-18299

ARL/PSU/TR-93-11 .... p 1562 N94-18664 #

ARO-23908.24-EL .... p 1392 N94-19724 #
ARO-25557.10-EL .... p 1408 N94-19751
ARO-26686.18-EL .... p 1605 N94-19717 #
ARO-26748.31-CH .... p 1606 N94-19739 #
ARO-26755.5-EL .... p 1604 N94-19597 #
ARO-27028.6-EL .... p 1392 N94-19738 #
ARO-27314.6-LS .... p 1374 N94-19586 #
ARO-27443.5-EL .... p 1606 N94-19741 #
ARO-27605.2-MS .... p 1604 N94-19596 #
ARO-27686.11-EG-SM .... p 1366 N94-19594 #
ARO-27808.4-CH .... p 1375 N94-19740 #
ARO-27834.1-EL .... p 1392 N94-19737 #
ARO-27868.28-MA .... p 1559 N94-19595 #
ARO-27911.4-GS .... p 1392 N94-19718 #
ARO-28060.25-MA .... p 1392 N94-19736 #
ARO-28176.9-MA-SAH .... p 1392 N94-19680 #
ARO-28187.1-EL .... p 1605 N94-19725 #
ARO-28679.13-MA .... p 1560 N94-19726 #
ARO-29631.2-EL .... p 1345 N94-19746 #
ARO-30367.27-PH-URI .... p 1581 N94-19772 #
ARO-30818.1-CH-SBI-PHASE-1 ... p 1503 N94-19757
ARO-30921.9-EL .... p 1407 N94-19584 #
ARO-31108.1-PH .... p 1606 N94-19769

ATC-201 .... p 1316 N94-19661 #
ATC-203 .... p 1492 N94-18684

AWS/TR-93/001 .... p 1490 N94-18573

B-030 .... p 1515 N94-19401 #
B-251542 .... p 1532 N94-19716 #

BER-BAND-B3 .... p 1494 N94-19503 #

BER-596-37 .... p 1338 N94-19438 * #

BINE-0017 .... p 1355 N94-17679

BN-1151 .... p 1549 N94-18697

BNL-48416 .... p 1464 N94-17712 #
BNL-48699 .... p 1337 N94-17884 #
BNL-48787 .... p 1501 N94-17889 #
BNL-48790 .... p 1539 N94-17696
BNL-48805 .... p 1603 N94-19564 #
BNL-48823 .... p 1603 N94-19541 #
BNL-48961 .... p 1472 N94-17852 #
BNL-49015 .... p 1566 N94-18234 #
BNL-49017 .... p 1602 N94-19258 #
BNL-49067 .... p 1343 N94-18763 #
BNL-49081 .... p 1358 N94-17947 #
BNL-49091 .... p 1565 N94-17984 #
BNL-49092 .... p 1594 N94-17866 #
BNL-49144 .... p 1436 N94-17998 #
BNL-49153 .... p 1438 N94-18504 #
BNL-49166 .... p 1386 N94-18503 #
BNL-49194 .... p 1497 N94-18494 #
BNL-49195 .... p 1566 N94-18085 #
BNL-49276 .... p 1406 N94-19310 #
BNL-49331 .... p 1487 N94-19477 #
BNL-49360 .... p 1572 N94-19536 #
BNL-49386 .... p 1375 N94-19651 #

BRL-IMR-970 .... p 1410 N94-18391

BR316760 .... p 1344 N94-19391 #

CAL-2117 .... p 1621 N94-18855 * #

CARDEROCKDIV-93/007 .... p 1619 N94-19571 #

CCL-TR-282 .... p 1536 N94-19160 #
CCL-TR-284 .... p 1536 N94-19159 #

CDNSWC/SSM-64-93/04 .... p 1342 N94-18702 #

CDP-871-041-A005 .... p 1512 N94-18765 #

CEBAF-PR-93-030 .... p 1441 N94-18974 #

CECOM-TR-93-5 .... p 1387 N94-18512 #

CERC-MP-93-7 .... p 1497 N94-18414

CERC-TR-92-6 .... p 1497 N94-18455 #

CERC-93-1 .... p 1498 N94-18685 #
CERC-93-3 .... p 1498 N94-18723 #
CERC-93-5 .... p 1496 N94-18215

CERL-TR-FE-93/22 .... p 1388 N94-18769

CGR/DC-08/93 .... p 1384 N94-18228 #

CIAC-SR-2 .... p 1371 N94-18750 #

CIT-64649 .... p 1485 N94-18899 #

CM-81 .... p 1479 N94-19379 #

CMS-TSR-94-2 .... p 1410 N94-18385

CMS-93-1 .... p 1497 N94-18230 #

CMU-CS-93-114 .... p 1531 N94-19592
CMU-CS-93-127 .... p 1522 N94-18696 #
CMU-CS-93-131 .... p 1538 N94-19533 #
CMU-CS-93-144 .... p 1515 N94-19591
CMU-CS-93-175 .... p 1540 N94-18261 #
CMU-CS-93-176 .... p 1522 N94-18698 #
CMU-CS-93-180 .... p 1521 N94-18453
CMU-CS-93-183 .... p 1514 N94-18317 #

CMU/SEI-93-TR-08 .... p 1521 N94-18659 #

CNIC-00601 .... p 1355 N94-17679

COMMUNICATIONS-SER-A-104 . p 1482 N94-18622 #

COMPUTING SCIENCE
NOTES-92/16 .... p 1619 N94-19709
COMPUTING SCIENCE
NOTES-92/21 .... p 1560 N94-19710

COMPUTING-SCIENCE-NOTES-92
/22 .... p 1524 N94-19066 #

CONF-8906428 .... p 1345 N94-17691
CONF-9201148-2 .... p 1489 N94-18053 #
CONF-9202174 .... p 1630 N94-18219 #
CONF-9203238-3 .... p 1382 N94-17909 #
CONF-9204244-1 .... p 1501 N94-17889 #
CONF-920673-18 .... p 1359 N94-18245 #
CONF-920673-20 .... p 1357 N94-17859 #
CONF-920673-21 .... p 1358 N94-17915 #
CONF-920673-22 .... p 1450 N94-17848 #
CONF-920673-23 .... p 1445 N94-19047 #
CONF-920799-8 .... p 1369 N94-18166 #
CONF-920817-1 .... p 1604 N94-19567 #
CONF-9208188-2 .... p 1572 N94-19283 #
CONF-920829-3 .... p 1564 N94-17738 #
CONF-920847-2 .... p 1569 N94-18973 #
CONF-920881-3 .... p 1472 N94-17986 #
CONF-920881-4 .... p 1472 N94-17985 #
CONF-920913-32 .... p 1590 N94-19289 #
CONF-9209239-7 .... p 1624 N94-17897
CONF-9209321-1 .... p 1569 N94-18945 #
CONF-9209372-1 .... p 1340 N94-18113 #
CONF-9209381-SUMM .... p 1474 N94-18523 #
CONF-920947-6 .... p 1597 N94-18480 #
CONF-920948-14 .... p 1569 N94-18999 #
CONF-920948-16 .... p 1570 N94-19108 #
CONF-9210173-7 .... p 1570 N94-19129 #
CONF-9210334-3 .... p 1488 N94-17942 #
CONF-9210362-VOL-1 .... p 1445 N94-18307 #
CONF-921049-10 .... p 1466 N94-18276 #
CONF-921077-4 .... p 1539 N94-17696
CONF-921109-5 .... p 1355 N94-17711 #
CONF-9211115-3 .... p 1473 N94-18167 #
CONF-9211134-2 .... p 1453 N94-18108 #
CONF-9211205-3 .... p 1361 N94-18806 #
CONF-9211205-4 .... p 1361 N94-18807 #
CONF-9211211-3 .... p 1584 N94-17990 #
CONF-9211237-1 .... p 1517 N94-17911 #
CONF-921131-14-APP-B .... p 1572 N94-19320 #
CONF-921232-2 .... p 1395 N94-17849 #
CONF-921233-3 .... p 1435 N94-17759 #
CONF-921256-6 .... p 1436 N94-17868
CONF-921256-7 .... p 1441 N94-19294 #
CONF-930103-41 .... p 1337 N94-17884 #
CONF-930103-42 .... p 1519 N94-18002 #
CONF-930103-43 .... p 1420 N94-19345 #
CONF-930105-1 .... p 1466 N94-18247 #
CONF-9301114-2 .... p 1358 N94-18111 #
CONF-9301117-1 .... p 1592 N94-17714 #
CONF-9301119-1 .... p 1436 N94-17996 #
CONF-9301123-1 .... p 1497 N94-18494 #
CONF-9301125-2 .... p 1456 N94-19078 #
CONF-930159-31 .... p 1435 N94-17724 #
CONF-930159-35 .... p 1435 N94-17723 #
CONF-930159-36 .... p 1582 N94-17708 #
CONF-930159-37 .... p 1501 N94-18242 #
CONF-930159-38 .... p 1339 N94-17846 #
CONF-930159-39 .... p 1368 N94-17946 #
CONF-930159-46 .... p 1584 N94-17993 #
CONF-930159-47 .... p 1435 N94-17855 #
CONF-930159-48 .... p 1437 N94-18131 #
CONF-930159-50 .... p 1585 N94-18115 #
CONF-930159-52 .... p 1585 N94-18082 #
CONF-930159-52 .... p 1437 N94-18093 #
CONF-930159-53 .... p 1567 N94-18493 #
CONF-930164-13 .... p 1372 N94-18932 #
CONF-930169-3 .... p 1629 N94-19260 #
CONF-930171-4 .... p 1441 N94-19251 #
CONF-930192-2 .... p 1396 N94-17991 #
CONF-930197-5 .... p 1565 N94-17984 #
CONF-930202-11 .... p 1364 N94-19203 #
CONF-9302103-3 .... p 1445 N94-18976 #
CONF-9302103-4 .... p 1601 N94-19049 #
CONF-9302120-2 .... p 1384 N94-18210 #
CONF-9302127-1 .... p 1471 N94-17790 #
CONF-9302135-1 .... p 1519 N94-18072 #
CONF-9302135-2 .... p 1534 N94-18482 #
CONF-930241-2 .... p 1335 N94-18942 #
CONF-930269-17 .... p 1588 N94-19034 #
CONF-930293-4 .... p 1627 N94-19284 #
CONF-930304-31 .... p 1365 N94-19263 #
CONF-9303122-3 .... p 1489 N94-18052 #
CONF-9303122-4 .... p 1488 N94-17715 #
CONF-9303126-7 .... p 1419 N94-19025 #
CONF-9303126-8 .... p 1587 N94-18274 #

CONF-9303153-1 .... p 1582 N94-17697
CONF-9303161-1 .... p 1594 N94-17874 #
CONF-9303190-2 .... p 1358 N94-17947 #
CONF-9303190-3 .... p 1594 N94-17866 #
CONF-9303193-1 .... p 1357 N94-17860 #
CONF-9303196-1 .... p 1437 N94-18083 #
CONF-9303198-2 .... p 1527 N94-19238 #
CONF-9303198-3 .... p 1395 N94-17882
CONF-9303198-4 .... p 1405 N94-18941 #
CONF-9303200-2 .... p 1409 N94-18004 #
CONF-9303207-1 .... p 1476 N94-19045 #
CONF-930331-10 .... p 1533 N94-17693
CONF-930331-13 .... p 1524 N94-19024 #
CONF-930331-14 .... p 1535 N94-18808 #
CONF-930346-2 .... p 1489 N94-18132 #
CONF-930346-3 .... p 1488 N94-17758 #
CONF-930363-7 .... p 1572 N94-19536 #
CONF-930364-6 .... p 1474 N94-18502 #
CONF-930367-7 .... p 1594 N94-17907 #
CONF-930367-8 .... p 1597 N94-18498 #
CONF-930372-12 .... p 1531 N94-19562 #
CONF-930389-20 .... p 1566 N94-18234 #
CONF-930405-19 .... p 1592 N94-17741 #
CONF-930405-1 .... p 1593 N94-17845 #
CONF-930405-29 .... p 1595 N94-18054 #
CONF-930405-30 .... p 1594 N94-17896
CONF-930405-31 .... p 1368 N94-18098 #
CONF-930405-32 .... p 1594 N94-17871 #
CONF-930405-33 .... p 1371 N94-18519 #
CONF-930405-33 .... p 1580 N94-18931 #
CONF-930405-34 .... p 1599 N94-18804 #
CONF-930405-35 .... p 1599 N94-18816 #
CONF-9304109-5 .... p 1461 N94-17851 #
CONF-9304112-22 .... p 1589 N94-19074 #
CONF-9304112-23 .... p 1589 N94-19073 #
CONF-9304112-6 .... p 1382 N94-17695
CONF-9304112-7 .... p 1581 N94-17694
CONF-9304125-2 .... p 1559 N94-19549 #
CONF-9304136-1 .... p 1358 N94-17875 #
CONF-9304144-10 .... p 1585 N94-18129 #
CONF-9304144-11 .... p 1601 N94-18998 #
CONF-9304144-7 .... p 1439 N94-18724 #
CONF-930415-1 .... p 1472 N94-17891 #
CONF-9304166-1 .... p 1359 N94-18114 #
CONF-9304167-1 .... p 1519 N94-18097 #
CONF-9304170-1 .... p 1343 N94-18761 #
CONF-9304172-1 .... p 1473 N94-18050 #
CONF-9304176-1 .... p 1520 N94-18133 #
CONF-9304177-1 .... p 1489 N94-18046 #
CONF-9304184-1 .... p 1485 N94-18929 #
CONF-930438-28 .... p 1343 N94-19335 #
CONF-930445-16 .... p 1612 N94-17858
CONF-930445-19 .... p 1580 N94-19268 #
CONF-930445-21 .... p 1335 N94-19275 #
CONF-930449-1 .... p 1568 N94-18825 #
CONF-930454-3 .... p 1502 N94-18476 #
CONF-930482-7 .... p 1501 N94-18051 #
CONF-930511-143 .... p 1573 N94-17784 #
CONF-930511-222 .... p 1383 N94-18055 #
CONF-930511-228 .... p 1436 N94-17869 #
CONF-930511-250 .... p 1436 N94-17998 #
CONF-930511-272 .... p 1438 N94-18504 #
CONF-930511-302 .... p 1386 N94-18503 #
CONF-930511-311 .... p 1574 N94-18972 #
CONF-930511-316 .... p 1441 N94-18974 #
CONF-930511-322 .... p 1389 N94-19053 #
CONF-930511-323 .... p 1441 N94-19030 #
CONF-930511-335 .... p 1575 N94-18997 #
CONF-930511-336 .... p 1575 N94-19107 #
CONF-930511-337 .... p 1575 N94-19106 #
CONF-930511-345 .... p 1574 N94-18934 #
CONF-930511-364 .... p 1575 N94-19152 #
CONF-930511-367 .... p 1574 N94-18273 #
CONF-930511-374 .... p 1575 N94-19558 #
CONF-930511-3 .... p 1573 N94-17698
CONF-930511-48 .... p 1434 N94-17709 #
CONF-930511-83 .... p 1573 N94-17726 #
CONF-9305124-3 .... p 1352 N94-19266 #
CONF-9305135-7 .... p 1363 N94-18975 #
CONF-9305135-8 .... p 1362 N94-18938 #
CONF-9305135-9 .... p 1365 N94-19274 #
CONF-9305136-11 .... p 1576 N94-19560 #
CONF-9305136-7 .... p 1591 N94-19559 #
CONF-9305136-8 .... p 1591 N94-19479 #
CONF-9305148-1 .... p 1571 N94-19259 #
CONF-9305151-8 .... p 1383 N94-17994 #
CONF-9305166-3 .... p 1380 N94-18710 #
CONF-9305170-3 .... p 1518 N94-17944 #
CONF-9305177-10 .... p 1598 N94-18531 #
CONF-9305177-8 .... p 1430 N94-18481 #
CONF-9305217-1 .... p 1385 N94-18232 #
CONF-9305220-1 .... p 1461 N94-18107 #
CONF-9305232-1 .... p 1369 N94-18112 #
CONF-9305235-3 .... p 1570 N94-19126 #
CONF-9305238 .... p 1376 N94-18045 #
CONF-9305241-2 .... p 1568 N94-18826 #
CONF-9305242-1 .... p 1612 N94-17870 #
CONF-9305269-1 .... p 1601 N94-19022 #
CONF-930537-84 .... p 1343 N94-18763 #
CONF-930537-94 .... p 1381 N94-19544 #
CONF-930537-96 .... p 1572 N94-19545 #
CONF-930538-3 .... p 1613 N94-17880 #
CONF-930538-4 .... p 1448 N94-19336 #
CONF-930540-4 .... p 1464 N94-17787 #
CONF-930550-4 .... p 1443 N94-17785 #
CONF-930571-19 .... p 1369 N94-18233 #
CONF-930571-20 .... p 1593 N94-17747 #
CONF-930571-22 .... p 1394 N94-17770 #
CONF-930571-23 .... p 1595 N94-17992 #
CONF-930571-24 .... p 1352 N94-19240 #
CONF-930571-26 .... p 1405 N94-19079 #
CONF-930572-8 .... p 1474 N94-18499 #
CONF-930572-9 .... p 1478 N94-19241 #
CONF-930586-6 .... p 1440 N94-18889 #
CONF-930586-7 .... p 1442 N94-19563 #
CONF-930601-25 .... p 1337 N94-17908 #
CONF-9306151-1 .... p 1614 N94-18099 #
CONF-9306155-1 .... p 1517 N94-17812 #
CONF-9306158-2 .... p 1472 N94-17890 #
CONF-930616-12 .... p 1574 N94-18497 #
CONF-930616-18 .... p 1322 N94-18890 #
CONF-930616-19 .... p 1575 N94-18996 #
CONF-930616-21 .... p 1439 N94-18522 #
CONF-9306166-1 .... p 1379 N94-17725 #
CONF-9306167-10 .... p 1451 N94-17864 #
CONF-9306173-1 .... p 1518 N94-17943 #
CONF-9306176-2 .... p 1570 N94-19096 #
CONF-9306176-4 .... p 1571 N94-19247 #
CONF-9306185-1 .... p 1382 N94-17861 #
CONF-9306187-1 .... p 1368 N94-18096 #
CONF-9306191-1 .... p 1582 N94-17713 #
CONF-9306194-1 .... p 1593 N94-17754 #
CONF-9306196-1 .... p 1556 N94-17886 #
CONF-9306203-1 .... p 1609 N94-19121 #
CONF-9306205-1 .... p 1404 N94-18827 #
CONF-9306214-1 .... p 1471 N94-17821 #
CONF-9306214-2 .... p 1478 N94-19319 #
CONF-9306216-1 .... p 1546 N94-17885 #
CONF-930626-13 .... p 1586 N94-18272 #
CONF-930626-1 .... p 1429 N94-18207 #
CONF-930626-9 .... p 1576 N94-17857
CONF-930647-5 .... p 1470 N94-17749 #
CONF-930652-1 .... p 1473 N94-18101
CONF-930663-3 .... p 1548 N94-18094 #
CONF-930672-1 .... p 1424 N94-17778 #
CONF-930675-5 .... p 1367 N94-17847 #
CONF-930676-10 .... p 1362 N94-18919 #
CONF-930676-13 .... p 1433 N94-19111 #
CONF-930676-14 .... p 1563 N94-19151 #
CONF-930676-15 .... p 1595 N94-18162 #
CONF-930676-16 .... p 1455 N94-19033 #
CONF-930676-17 .... p 1362 N94-18809 #
CONF-930676-26 .... p 1627 N94-19339 #
CONF-930676-27 .... p 1373 N94-19338 #
CONF-930676-29 .... p 1361 N94-18802 #
CONF-930676-30 .... p 1404 N94-18805 #
CONF-930676-31 .... p 1600 N94-18969 #
CONF-930676-32 .... p 1460 N94-19543 #
CONF-930676-33 .... p 1457 N94-19279 #
CONF-930676-35 .... p 1602 N94-19340 #
CONF-930676-37 .... p 1603 N94-19347 #
CONF-930676-3 .... p 1429 N94-18102 #
CONF-930676-4 .... p 1382 N94-17806 #
CONF-930676-6 .... p 1357 N94-17819 #
CONF-930676-7 .... p 1424 N94-17999 #
CONF-930676-8 .... p 1358 N94-18100 #
CONF-930695-1 .... p 1451 N94-17913 #
CONF-930702-34 .... p 1409 N94-18248 #
CONF-930702-42 .... p 1453 N94-18246 #
CONF-930702-44 .... p 1356 N94-17791 #
CONF-930703-10 .... p 1454 N94-18479 #
CONF-930703-12 .... p 1590 N94-19269
CONF-930703-13 .... p 1417 N94-18831 #
CONF-930703-15 .... p 1380 N94-18818 #
CONF-930703-17 .... p 1562 N94-18810 #
CONF-930703-27 .... p 1381 N94-19540 #
CONF-930703-6 .... p 1396 N94-18135
CONF-930703-7 .... p 1602 N94-19122 #
CONF-930703-8 .... p 1597 N94-18500 #
CONF-9307102-1 .... p 1451 N94-17906 #
CONF-9307107-1 .... p 1443 N94-17761 #
CONF-9307111-2 .... p 1494 N94-19298 #
CONF-9307111 .... p 1535 N94-19046 #
CONF-9307112-1-VUGRAPHS ..... p 1405 N94-19112 #
CONF-9307114-1 .... p 1567 N94-18269 #
CONF-9307116-1 .... p 1570 N94-19125 #
CONF-930712-1 .... p 1600 N94-18933 #
CONF-930712-4 .... p 1603 N94-19541 #
CONF-9307124-1 .... p 1364 N94-19080 #
CONF-9307125-1 .... p 1587 N94-18803 #
CONF-930713-13 .... p 1376 N94-17751 #
CONF-930713-15 .... p 1408 N94-17728 #
CONF-930713-16 .... p 1423 N94-17700 #
CONF-930713-19 .... p 1376 N94-18095 #
CONF-930713-7 .... p 1376 N94-17813 #
CONF-930720-13 .... p 1583 N94-17743 #
CONF-930720-14 .... p 1585 N94-18058 #
CONF-930720-15 .... p 1585 N94-18057 #
CONF-930720-16 .... p 1585 N94-18056 #
CONF-930720-17 .... p 1590 N94-19273 #
CONF-930720-18 .... p 1590 N94-19290 #
CONF-930722-14 .... p 1448 N94-19252 #
CONF-930722-15 .... p 1418 N94-18995 #
CONF-930722-17 .... p 1432 N94-18828 #
CONF-930722-20 .... p 1406 N94-19310 #
CONF-930722-22 .... p 1602 N94-19075 #
CONF-930722-5 .... p 1436 N94-17865 #
CONF-930722-8 .... p 1576 N94-18000 #
CONF-930722-9 .... p 1588 N94-18971 #
CONF-930726-1 .... p 1447 N94-18128 #
CONF-930726-2 .... p 1465 N94-17888 #
CONF-930726-3 .... p 1465 N94-18001 #
CONF-930726-4 .... p 1493 N94-19051 #
CONF-930726-5 .... p 1469 N94-19036 #
CONF-930741-4 .... p 1433 N94-19000 #
CONF-930749-16 .... p 1617 N94-18984 #
CONF-930749-39 .... p 1535 N94-18930 #
CONF-930749-45 .... p 1571 N94-19278 #
CONF-930755-3 .... p 1352 N94-19239 #
CONF-930765-3 .... p 1455 N94-18829 #
CONF-930788-5 .... p 1422 N94-19568 #
CONF-930792-1 .... p 1516 N94-17786 #
CONF-930796-1 .... p 1348 N94-18249 #
CONF-930796-3 .... p 1364 N94-19044 #
CONF-930801-11 .... p 1407 N94-19553 #
CONF-930801-4 .... p 1360 N94-18398 #
CONF-930801-6 .... p 1600 N94-18968 #
CONF-930801-8 .... p 1604 N94-19566 #
CONF-930802-6 .... p 1373 N94-19321 #
CONF-930804-11 .... p 1337 N94-17863 #
CONF-930804-12 .... p 1465 N94-17853 #
CONF-930804-15 .... p 1353 N94-19552 #
CONF-930804-5 .... p 1466 N94-18208 #
CONF-930804-6 .... p 1464 N94-17798 #
CONF-930810-5 .... p 1480 N94-19732 #
CONF-9308122-1 .... p 1601 N94-18993
CONF-9308126-1 .... p 1357 N94-17862 #
CONF-9308126-2 .... p 1370 N94-18477 #
CONF-9308126-3 .... p 1358 N94-18003 #
CONF-9308129-1 .... p 1536 N94-19115 #
CONF-9308138-1 .... p 1521 N94-18271 #
CONF-9308140-2 .... p 1372 N94-19202 #
CONF-9308141-1 .... p 1410 N94-18270 #
CONF-9308148-6 .... p 1487 N94-19477 #
CONF-930825-4 .... p 1363 N94-18940 #
CONF-930831-1 .... p 1566 N94-18085 #
CONF-930840-1 .... p 1446 N94-19547 #
CONF-930852-2 .... p 1603 N94-19550 #
CONF-930854-1 .... p 1344 N94-19551 #
CONF-930860-1 .... p 1593 N94-17744 #
CONF-930873-16 .... p 1582 N94-17727 #
CONF-930881-4 .... p 1531 N94-19548 #
CONF-930905-1 .... p 1605 N94-19735 #
CONF-930907-5 .... p 1556 N94-18073 #
CONF-9309124-1 .... p 1437 N94-18134 #
CONF-9309156-1 .... p 1345 N94-17820 #
CONF-9309175-1 .... p 1452 N94-17995 #
CONF-9309176-1 .... p 1571 N94-19201 #
CONF-9309176-2 .... p 1627 N94-18857 #
CONF-9309195-1 .... p 1359 N94-18127 #
CONF-9309201-1 .... p 1523 N94-19006 #
CONF-930928-1 .... p 1446 N94-19334 #
CONF-930978-1 .... p 1423 N94-19604 #
CONF-931009-1 .... p 1362 N94-18917 #
CONF-9310102-1 .... p 1484 N94-18725 #
CONF-9310131-1 .... p 1615 N94-18334 #
CONF-9310133-1 .... p 1364 N94-19043 #
CONF-931024-1 .... p 1405 N94-18928 #
CONF-931042-2 .... p 1485 N94-18894 #
CONF-931055-1 .... p 1523 N94-18926 #
CONF-931078-1 .... p 1343 N94-18914 #
CONF-931080-1 .... p 1418 N94-18918 #
CONF-931080-2 .... p 1418 N94-18888 #
CONF-931080-3 .... p 1520 N94-18130 #
CONF-931107-2 .... p 1602 N94-19258 #
CONF-931107-3 .... p 1503 N94-19341 #
CONF-931115-10 .... p 1537 N94-19253 #
CONF-931115-1 .... p 1525 N94-19186 #
CONF-931115-2 .... p 1536 N94-19161 #
CONF-931115-3 .... p 1526 N94-19205 #
CONF-931115-4 .... p 1536 N94-19188 #
CONF-931115-5 .... p 1537 N94-19206 #
CONF-931115-7 .... p 1537 N94-19249 #
CONF-931115-9 .... p 1528 N94-19276 #
CONF-931121-12 .... p 1525 N94-19124 #
CONF-931121-13 .... p 1460 N94-19603 #
CONF-931121-20 .... p 1515 N94-19535 #
CONF-931121-4 .... p 1372 N94-19059 #

CONF-931121-5 .... p 1419 N94-19058 #
CONF-931121-6 .... p 1609 N94-19187 #
CONF-931121-7 .... p 1457 N94-19207 #
CONF-931121-9 .... p 1351 N94-19118 #
CONF-931148-1 .... p 1617 N94-19057 #
CONF-931148-2 .... p 1524 N94-19076 #
CONF-931154-1 .... p 1373 N94-19308 #
CONF-931160-4 .... p 1570 N94-19120 #
CONF-931160-5 .... p 1551 N94-19343 #
CONF-931160-6 .... p 1551 N94-19342 #
CONF-931167-1-EXTD-ABST .... p 1528 N94-19344 #
CONF-931167-2-EXTD-ABST .... p 1542 N94-19007 #

CRIF-MC-102 .... p 1444 N94-17964 #
CRIF-MC-94 .... p 1611 N94-17980 #
CRIF-MC-97 .... p 1444 N94-17963 #

CRREL-SR-93-22 .... p 1487 N94-19529 #
CRREL-SR-93-23 .... p 1475 N94-18775

CRREL-93-12 .... p 1463 N94-19672 #

CU-CS-617-92 .... p 1535 N94-18808 #

CU-153-6505 .... p 1379 N94-17763 * #

DARPA-BAA-92-20 .... p 1599 N94-18764 #

DCIEM-93-36 .... p 1504 N94-17823 #

DDV-93-0004 .... p 1381 N94-19539 #

DE93-000281 .... p 1468 N94-18925 #
DE93-008348 .... p 1523 N94-18926 #
DE93-009842 .... p 1373 N94-19308 #
DE93-010005 .... p 1376 N94-18045 #
DE93-010032 .... p 1489 N94-18046 #
DE93-010035 .... p 1377 N94-18617 #
DE93-010037 .... p 1464 N94-17731 #
DE93-010041 .... p 1615 N94-18334 #
DE93-010043 .... p 1465 N94-17888 #
DE93-010046 .... p 1467 N94-18518 #
DE93-010047 .... p 1378 N94-18913 #
DE93-010049 .... p 1467 N94-18483 #
DE93-010350 .... p 1571 N94-19204 #
DE93-010827 .... p 1617 N94-19057 #
DE93-011562 .... p 1343 N94-18914 #
DE93-011592 .... p 1419 N94-19058 #
DE93-011596 .... p 1372 N94-19059 #
DE93-011682 .... p 1455 N94-18829 #
DE93-011855 .... p 1632 N94-18915 #
DE93-011912 .... p 1574 N94-18916 #
DE93-012128 .... p 1525 N94-19186 #
DE93-012291 .... p 1367 N94-17678 #
DE93-012527 .... p 1501 N94-17889 #
DE93-012650 .... p 1594 N94-17874 #
DE93-012654 .... p 1526 N94-19205 #
DE93-012663 .... p 1358 N94-17875 #
DE93-012701 .... p 1362 N94-18917 #
DE93-012730 .... p 1517 N94-17812 #
DE93-012732 .... p 1609 N94-19187 #
DE93-012734 .... p 1376 N94-17813 #
DE93-012840 .... p 1536 N94-19188 #
DE93-012841 .... p 1537 N94-19206 #
DE93-012844 .... p 1536 N94-19161 #
DE93-012849 .... p 1418 N94-18918 #
DE93-012867 .... p 1533 N94-17693
DE93-012909 .... p 1472 N94-17890 #
DE93-012911 .... p 1472 N94-17891 #
DE93-013098 .... p 1470 N94-17773 #
DE93-013146 .... p 1607 N94-17892 #
DE93-013171 .... p 1501 N94-18051 #
DE93-013187 .... p 1489 N94-18052 #
DE93-013208 .... p 1581 N94-17694
DE93-013272 .... p 1382 N94-17695
DE93-013296 .... p 1382 N94-17909 #
DE93-013343 .... p 1539 N94-17696
DE93-013433 .... p 1489 N94-18053 #
DE93-013461 .... p 1472 N94-17910 #
DE93-013563 .... p 1461 N94-17893 #
DE93-013675 .... p 1564 N94-17738 #
DE93-013729 .... p 1582 N94-17697
DE93-013752 .... p 1573 N94-17698
DE93-013783 .... p 1395 N94-17872
DE93-013789 .... p 1562 N94-17873
DE93-013845 .... p 1471 N94-17774 #
DE93-013854 .... p 1517 N94-17911 #
DE93-013896 .... p 1504 N94-17699 #
DE93-013917 .... p 1423 N94-17700 #
DE93-013920 .... p 1516 N94-17701 #
DE93-014125 .... p 1488 N94-17942 #
DE93-014358 .... p 1457 N94-19207 #
DE93-014363 .... p 1377 N94-18893 #
DE93-014373 .... p 1583 N94-17912 #
DE93-014408 .... p 1582 N94-17702 #
DE93-014417 .... p 1355 N94-17711 #
DE93-014420 .... p 1582 N94-17708 #
DE93-014429 .... p 1435 N94-17723 #
DE93-014444 .... p 1574 N94-18927 #
DE93-014466 .... p 1435 N94-17724 #
DE93-014468 .... p 1379 N94-17725 #
DE93-014470 .... p 1434 N94-17709 #
DE93-014509 .... p 1470 N94-17710 #
DE93-014549 .... p 1573 N94-17726 #
DE93-014559 .... p 1376 N94-17751 #
DE93-014563 .... p 1582 N94-17727 #
DE93-014581 .... p 1408 N94-17728 #
DE93-014646 .... p 1583 N94-17739 #
DE93-014658 .... p 1516 N94-17740 #
DE93-014676 .... p 1333 N94-17782 #
DE93-014716 .... p 1429 N94-18207 #
DE93-014850 .... p 1395 N94-17783 #
DE93-014885 .... p 1573 N94-17784 #
DE93-014914 .... p 1360 N94-18398 #
DE93-014918 .... p 1443 N94-17785 #
DE93-014935 .... p 1518 N94-17943 #
DE93-014994 .... p 1518 N94-17944 #
DE93-015003 .... p 1466 N94-18208 #
DE93-015017 .... p 1516 N94-17786 #
DE93-015018 .... p 1464 N94-17787 #
DE93-015024 .... p 1537 N94-19249 #
DE93-015029 .... p 1609 N94-19250 #
DE93-015037 .... p 1480 N94-17898 #
DE93-015046 .... p 1592 N94-17741 #
DE93-015083 .... p 1592 N94-17742 #
DE93-015086 .... p 1347 N94-18209 #
DE93-015100 .... p 1355 N94-17757 #
DE93-015112 .... p 1384 N94-18210 #
DE93-015115 .... p 1565 N94-17797 #
DE93-015130 .... p 1405 N94-18928 #
DE93-015132 .... p 1464 N94-17798 #
DE93-015159 .... p 1369 N94-18166 #
DE93-015213 .... p 1596 N94-18192 #
DE93-015230 .... p 1514 N94-17799 #
DE93-015234 .... p 1516 N94-17800 #
DE93-015262 .... p 1347 N94-18193 #
DE93-015263 .... p 1609 N94-18629 #
DE93-015276 .... p 1613 N94-17894 #
DE93-015282 .... p 1347 N94-18194 #
DE93-015332 .... p 1501 N94-18242 #
DE93-015334 .... p 1352 N94-19239 #
DE93-015338 .... p 1473 N94-18167 #
DE93-015342 .... p 1596 N94-18243 #
DE93-015361 .... p 1511 N94-18244 #
DE93-015428 .... p 1359 N94-18245 #
DE93-015510 .... p 1453 N94-18246 #
DE93-015522 .... p 1466 N94-18247 #
DE93-015536 .... p 1409 N94-18248 #
DE93-015551 .... p 1348 N94-18249 #
DE93-015616 .... p 1583 N94-17945 #
DE93-015643 .... p 1385 N94-18232 #
DE93-015673 .... p 1461 N94-18107 #
DE93-015681 .... p 1593 N94-17747 #
DE93-015694 .... p 1369 N94-18233 #
DE93-015752 .... p 1576 N94-17857
DE93-015762 .... p 1445 N94-18307 #
DE93-015792 .... p 1566 N94-18234 #
DE93-015818 .... p 1439 N94-18724 #
DE93-015819 .... p 1503 N94-19341 #
DE93-015823 .... p 1583 N94-17743 #
DE93-015871 .... p 1430 N94-18235 #
DE93-015907 .... p 1593 N94-17845 #
DE93-015908 .... p 1339 N94-17846 #
DE93-015910 .... p 1612 N94-17858
DE93-015916 .... p 1471 N94-17790 #
DE93-015920 .... p 1367 N94-17847 #
DE93-015929 .... p 1356 N94-17791 #
DE93-015960 .... p 1450 N94-17848 #
DE93-015965 .... p 1368 N94-17946 #
DE93-015966 .... p 1351 N94-19118 #
DE93-015967 .... p 1451 N94-17913 #
DE93-015971 .... p 1517 N94-17914 #
DE93-015975 .... p 1453 N94-18108 #
DE93-015981 .... p 1358 N94-17915 #
DE93-015982 .... p 1357 N94-17859 #
DE93-016001 .... p 1466 N94-18109 #
DE93-016085 .... p 1488 N94-17895 #
DE93-016133 .... p 1602 N94-19258 #
DE93-016199 .... p 1624 N94-18047 #
DE93-016269 .... p 1484 N94-18725 #
DE93-016270 .... p 1346 N94-18048 #
DE93-016325 .... p 1452 N94-18049 #
DE93-016334 .... p 1632 N94-18856 #
DE93-016366 .... p 1368 N94-18110
DE93-016416 .... p 1358 N94-18111 #
DE93-016442 .... p 1536 N94-19115 #
DE93-016444 .... p 1357 N94-17860 #
DE93-016445 .... p 1369 N94-18112 #
DE93-016446 .... p 1394 N94-17770 #
DE93-016451 .... p 1340 N94-18113 #
DE93-016456 .... p 1359 N94-18114 #
DE93-016466 .... p 1551 N94-19342 #
DE93-016467 .... p 1551 N94-19343 #
DE93-016499 .... p 1382 N94-17861 #
DE93-016508 .... p 1452 N94-17995 #
DE93-016509 .... p 1357 N94-17862 #
DE93-016510 .... p 1528 N94-19344 #
DE93-016518 .... p 1570 N94-19120 #
DE93-016537 .... p 1395 N94-17849 #
DE93-016538 .... p 1585 N94-18115 #
DE93-016544 .... p 1376 N94-18095 #
DE93-016546 .... p 1565 N94-17850 #
DE93-016553 .... p 1464 N94-17712 #
DE93-016555 .... p 1613 N94-17880 #
DE93-016557 .... p 1337 N94-17863 #
DE93-016559 .... p 1451 N94-17864 #
DE93-016561 .... p 1451 N94-17906 #
DE93-016601 .... p 1352 N94-19240 #
DE93-016607 .... p 1593 N94-17744 #
DE93-016608 .... p 1368 N94-18096 #
DE93-016610 .... p 1594 N94-17907 #
DE93-016614 .... p 1582 N94-17713 #
DE93-016617 .... p 1436 N94-17865 #
DE93-016627 .... p 1485 N94-18894 #
DE93-016630 .... p 1592 N94-17714 #
DE93-016633 .... p 1488 N94-17715 #
DE93-016634 .... p 1519 N94-18097 #
DE93-016637 .... p 1461 N94-17851 #
DE93-016718 .... p 1467 N94-18475 #
DE93-016730 .... p 1359 N94-18127 #
DE93-016731 .... p 1447 N94-18128 #
DE93-016735 .... p 1343 N94-18763 #
DE93-016748 .... p 1594 N94-17866 #
DE93-016750 .... p 1358 N94-17947 #
DE93-016761 .... p 1355 N94-17752 #
DE93-016768 .... p 1584 N94-17948 #
DE93-016769 .... p 1584 N94-17983 #
DE93-016770 .... p 1583 N94-17753 #
DE93-016825 .... p 1337 N94-17884 #
DE93-016833 .... p 1617 N94-18983 #
DE93-016842 .... p 1472 N94-17852 #
DE93-016869 .... p 1546 N94-17885 #
DE93-016871 .... p 1565 N94-17984 #
DE93-016878 .... p 1472 N94-17985 #
DE93-016879 .... p 1472 N94-17986 #
DE93-016880 .... p 1593 N94-17754 #
DE93-016924 .... p 1346 N94-17987 #
DE93-016952 .... p 1584 N94-17988 #
DE93-016957 .... p 1394 N94-17755 #
DE93-016963 .... p 1595 N94-17989 #
DE93-016964 .... p 1473 N94-18050 #
DE93-016968 .... p 1595 N94-18054 #
DE93-016971 .... p 1383 N94-18055 #
DE93-016974 .... p 1556 N94-17886 #
DE93-016977 .... p 1436 N94-17869 #
DE93-016978 .... p 1600 N94-18968 #
DE93-016984 .... p 1585 N94-18056 #
DE93-016985 .... p 1585 N94-18057 #
DE93-016986 .... p 1585 N94-18058 #
DE93-016987 .... p 1616 N94-18707 #
DE93-016990 .... p 1380 N94-18710 #
DE93-016991 .... p 1465 N94-17853 #
DE93-016996 .... p 1585 N94-18129 #
DE93-017005 .... p 1367 N94-17881 #
DE93-017087 .... p 1583 N94-17854 #
DE93-017098 .... p 1517 N94-17867
DE93-017102 .... p 1418 N94-18888 #
DE93-017104 .... p 1520 N94-18130 #
DE93-017118 .... p 1480 N94-19732 #
DE93-017142 .... p 1347 N94-18059 #
DE93-017143 .... p 1437 N94-18060 #
DE93-017147 .... p 1470 N94-17749 #
DE93-017150 .... p 1437 N94-18131 #
DE93-017153 .... p 1435 N94-17855 #
DE93-017158 .... p 1489 N94-18132 #
DE93-017163 .... p 1488 N94-17758 #
DE93-017164 .... p 1520 N94-18133 #
DE93-017165 .... p 1436 N94-17868
DE93-017166 .... p 1584 N94-17990 #
DE93-017167 .... p 1396 N94-17991 #
DE93-017168 .... p 1594 N94-17896
DE93-017169 .... p 1624 N94-17897
DE93-017170 .... p 1395 N94-17882
DE93-017172 .... p 1437 N94-18134 #
DE93-017173 .... p 1595 N94-17992 #
DE93-017175 .... p 1584 N94-17993 #
DE93-017181 .... p 1519 N94-18072 #
DE93-017184 .... p 1556 N94-18073 #
DE93-017187 .... p 1383 N94-17994 #
DE93-017190 .... p 1440 N94-18889 #
DE93-017191 .... p 1585 N94-18082 #
DE93-017196 .... p 1616 N94-18689 #
DE93-017197 .... p 1615 N94-18496 #
DE93-017212 .... p 1527 N94-19238 #
DE93-017213 .... p 1435 N94-17759 #
DE93-017220 .... p 1436 N94-17996 #
DE93-017221 .... p 1437 N94-18083 #
DE93-017224 .... p 1574 N94-18497 #

DE93-017228 .... p 1343 N94-18761 #
DE93-017238 .... p 1593 N94-17760 #
DE93-017272 .... p 1453 N94-18084 #
DE93-017295 .... p 1443 N94-17761 #
DE93-017312 .... p 1566 N94-18085 #
DE93-017368 .... p 1519 N94-18086 #
DE93-017369 .... p 1568 N94-18824 #
DE93-017381 .... p 1340 N94-18087 #
DE93-017385 .... p 1609 N94-19121 #
DE93-017397 .... p 1568 N94-18825 #
DE93-017399 .... p 1396 N94-18135
DE93-017402 .... p 1478 N94-19241 #
DE93-017403 .... p 1597 N94-18498 #
DE93-017404 .... p 1368 N94-18098 #
DE93-017405 .... p 1602 N94-19122 #
DE93-017406 .... p 1474 N94-18499 #
DE93-017407 .... p 1597 N94-18500 #
DE93-017412 .... p 1614 N94-18099 #
DE93-017413 .... p 1612 N94-17870 #
DE93-017414 .... p 1394 N94-17750
DE93-017422 .... p 1568 N94-18826 #
DE93-017436 .... p 1502 N94-18476 #
DE93-017437 .... p 1360 N94-18501 #
DE93-017446 .... p 1474 N94-18502 #
DE93-017475 .... p 1594 N94-17871 #
DE93-017492 .... p 1420 N94-19345 #
DE93-017496 .... p 1371 N94-18519 #
DE93-017506 .... p 1358 N94-18100 #
DE93-017516 .... p 1473 N94-18101
DE93-017526 .... p 1346 N94-17997 #
DE93-017557 .... p 1469 N94-19346 #
DE93-017581 .... p 1436 N94-17998 #
DE93-017601 .... p 1630 N94-17818 #
DE93-017611 .... p 1386 N94-18503 #
DE93-017616 .... p 1366 N94-19546 #
DE93-017618 .... p 1602 N94-19123 #
DE93-017621 .... p 1438 N94-18504 #
DE93-017625 .... p 1429 N94-18102 #
DE93-017628 .... p 1424 N94-17999 #
DE93-017629 .... p 1357 N94-17819 #
DE93-017633 .... p 1382 N94-17806 #
DE93-017634 .... p 1370 N94-18477 #
DE93-017635 .... p 1523 N94-19006 #
DE93-017636 .... p 1576 N94-18000 #
DE93-017639 .... p 1465 N94-18001 #
DE93-017640 .... p 1525 N94-19124 #
DE93-017641 .... p 1542 N94-19007 #
DE93-017651 .... p 1446 N94-19547 #
DE93-017652 .... p 1404 N94-18827 #
DE93-017655 .... p 1345 N94-17820 #
DE93-017657 .... p 1519 N94-18002 #
DE93-017659 .... p 1358 N94-18003 #
DE93-017670 .... p 1471 N94-17821 #
DE93-017671 .... p 1364 N94-19043 #
DE93-017674 .... p 1467 N94-18478 #
DE93-017675 .... p 1475 N94-18832 #
DE93-017677 .... p 1471 N94-17777 #
DE93-017684 .... p 1409 N94-18004 #
DE93-017685 .... p 1337 N94-17908 #
DE93-017688 .... p 1588 N94-18971 #
DE93-017689 .... p 1454 N94-18479 #
DE93-017690 .... p 1597 N94-18480 #
DE93-017733 .... p 1364 N94-19044 #
DE93-017746 .... p 1430 N94-18481 #
DE93-017748 .... p 1476 N94-19045 #
DE93-017752 .... p 1535 N94-19046 #
DE93-017764 .... p 1534 N94-18482 #
DE93-017769 .... p 1424 N94-17778 #
DE93-017776 .... p 1567 N94-18493 #
DE93-017798 .... p 1598 N94-18531 #
DE93-017804 .... p 1574 N94-18972 #
DE93-017809 .... p 1569 N94-18973 #
DE93-017816 .... p 1436 N94-17883
DE93-017821 .... p 1441 N94-18974 #
DE93-017828 .... p 1466 N94-18103
DE93-017852 .... p 1363 N94-18975 #
DE93-017853 .... p 1445 N94-18976 #
DE93-017857 .... p 1590 N94-19273 #
DE93-017858 .... p 1445 N94-19047 #
DE93-017862 .... p 1365 N94-19274 #
DE93-017865 .... p 1362 N94-18938 #
DE93-017874 .... p 1433 N94-19111 #
DE93-017877 .... p 1362 N94-18919 #
DE93-017880 .... p 1617 N94-18984 #
DE93-017894 .... p 1405 N94-19112 #
DE93-017898 .... p 1569 N94-18985 #
DE93-017936 .... p 1468 N94-18986 #
DE93-017938 .... p 1339 N94-19117 #
DE93-017944 .... p 1580 N94-19113 #
DE93-017948 .... p 1390 N94-19114 #
DE93-017951 .... p 1473 N94-18005 #
DE93-017960 .... p 1350 N94-18987 #
DE93-017965 .... p 1347 N94-18092 #
DE93-017972 .... p 1365 N94-19263 #
DE93-017974 .... p 1352 N94-19266 #
DE93-017976 .... p 1437 N94-18093 #
DE93-017980 .... p 1548 N94-18094 #
DE93-017981 .... p 1335 N94-19275 #
DE93-017988 .... p 1366 N94-19733 #
DE93-017993 .... p 1580 N94-19268 #
DE93-017995 .... p 1363 N94-18939 #
DE93-017996 .... p 1587 N94-18505 #
DE93-018000 .... p 1528 N94-19276 #
DE93-018008 .... p 1539 N94-19734 #
DE93-018021 .... p 1561 N94-18177 #
DE93-018031 .... p 1575 N94-19287 #
DE93-018039 .... p 1588 N94-18988 #
DE93-018049 .... p 1363 N94-18940 #
DE93-018066 .... p 1524 N94-19048 #
DE93-018069 .... p 1405 N94-18941 #
DE93-018081 .... p 1441 N94-19251 #
DE93-018083 .... p 1590 N94-19289 #
DE93-018086 .... p 1601 N94-19049 #
DE93-018088 .... p 1448 N94-19252 #
DE93-018091 .... p 1537 N94-19253 #
DE93-018092 .... p 1590 N94-19290 #
DE93-018093 .... p 1571 N94-19201 #
DE93-018095 .... p 1335 N94-18942 #
DE93-018096 .... p 1590 N94-19269
DE93-018098 .... p 1531 N94-19548 #
DE93-018105 .... p 1559 N94-19549 #
DE93-018106 .... p 1523 N94-18943 #
DE93-018128 .... p 1446 N94-19291 #
DE93-018140 .... p 1575 N94-19050 #
DE93-018151 .... p 1561 N94-18178 #
DE93-018155 .... p 1448 N94-17814 #
DE93-018160 .... p 1573 N94-17807 #
DE93-018168 .... p 1345 N94-17808 #
DE93-018170 .... p 1583 N94-17809 #
DE93-018182 .... p 1493 N94-19051 #
DE93-018201 .... p 1468 N94-18944 #
DE93-018203 .... p 1470 N94-19760 #
DE93-018270 .... p 1569 N94-18945 #
DE93-018277 .... p 1372 N94-18946 #
DE93-018278 .... p 1523 N94-18989 #
DE93-018285 .... p 1460 N94-19603 #
DE93-018286 .... p 1361 N94-18802 #
DE93-018291 .... p 1605 N94-19735 #
DE93-018293 .... p 1587 N94-18803 #
DE93-018294 .... p 1599 N94-18804 #
DE93-018295 .... p 1404 N94-18805 #
DE93-018296 .... p 1600 N94-18969 #
DE93-018299 .... p 1575 N94-19023 #
DE93-018321 .... p 1566 N94-18179 #
DE93-018331 .... p 1361 N94-18806 #
DE93-018332 .... p 1361 N94-18807 #
DE93-018336 .... p 1524 N94-19024 #
DE93-018337 .... p 1535 N94-18808 #
DE93-018342 .... p 1419 N94-19025 #
DE93-018343 .... p 1595 N94-18162 #
DE93-018344 .... p 1455 N94-19033 #
DE93-018345 .... p 1362 N94-18809 #
DE93-018348 .... p 1562 N94-18810 #
DE93-018358 .... p 1570 N94-19125 #
DE93-018362 .... p 1563 N94-19151 #
DE93-018367 .... p 1432 N94-18828 #
DE93-018369 .... p 1627 N94-18857 #
DE93-018373 .... p 1423 N94-19604 #
DE93-018375 .... p 1372 N94-19202 #
DE93-018381 .... p 1617 N94-19026 #
DE93-018394 .... p 1419 N94-19027 #
DE93-018396 .... p 1363 N94-19028 #
DE93-018398 .... p 1535 N94-19010 #
DE93-018400 .... p 1557 N94-19011 #
DE93-018408 .... p 1588 N94-19012 #
DE93-018415 .... p 1569 N94-19013 #
DE93-018416 .... p 1369 N94-18163 #
DE93-018417 .... p 1570 N94-19029 #
DE93-018440 .... p 1337 N94-18830 #
DE93-018443 .... p 1468 N94-19014 #
DE93-018448 .... p 1417 N94-18831 #
DE93-018450 .... p 1599 N94-18816 #
DE93-018454 .... p 1475 N94-18817 #
DE93-018457 .... p 1364 N94-19203 #
DE93-018459 .... p 1570 N94-19129 #
DE93-018460 .... p 1497 N94-18494 #
DE93-018467 .... p 1567 N94-18269 #
DE93-018468 .... p 1380 N94-18818 #
DE93-018469 .... p 1571 N94-19259 #
DE93-018470 .... p 1570 N94-19126 #
DE93-018478 .... p 1322 N94-18890 #
DE93-018479 .... p 1410 N94-18270 #
DE93-018481 .... p 1495 N94-17779 #
DE93-018489 .... p 1468 N94-19015 #
DE93-018490 .... p 1468 N94-19016 #
DE93-018491 .... p 1467 N94-18409 #
DE93-018495 .... p 1493 N94-19127 #
DE93-018497 .... p 1378 N94-19242 #
DE93-018499 .... p 1476 N94-19038 #
DE93-018503 .... p 1433 N94-19243 #
DE93-018505 .... p 1466 N94-18335 #
DE93-018507 .... p 1455 N94-19039 #
DE93-018508 .... p 1394 N94-17780 #
DE93-018509 .... p 1467 N94-18520 #
DE93-018510 .... p 1474 N94-18521 #
DE93-018512 .... p 1469 N94-19040 #
DE93-018514 .... p 1527 N94-19245 #
DE93-018515 .... p 1580 N94-18970
DE93-018517 .... p 1614 N94-18164 #
DE93-018518 .... p 1433 N94-19041 #
DE93-018521 .... p 1378 N94-19042 #
DE93-018524 .... p 1571 N94-19247 #
DE93-018525 .... p 1485 N94-18929 #
DE93-018528 .... p 1629 N94-19260 #
DE93-018530 .... p 1389 N94-19053 #
DE93-018533 .... p 1441 N94-19030 #
DE93-018537 .... p 1521 N94-18271 #
DE93-018538 .... p 1571 N94-19278 #
DE93-018547 .... p 1535 N94-18930 #
DE93-018557 .... p 1580 N94-18931 #
DE93-018561 .... p 1457 N94-19279 #
DE93-018570 .... p 1586 N94-18272 #
DE93-018573 .... p 1372 N94-18932 #
DE93-018575 .... p 1600 N94-18933 #
DE93-018576 .... p 1570 N94-19096 #
DE93-018581 .... p 1574 N94-18934 #
DE93-018594 .... p 1365 N94-19280 #
DE93-018595 .... p 1350 N94-19097 #
DE93-018598 .... p 1365 N94-19282 #
DE93-018601 .... p 1513 N94-18935 #
DE93-018602 .... p 1469 N94-19098 #
DE93-018615 .... p 1601 N94-18993
DE93-018617 .... p 1601 N94-19022 #
DE93-018618 .... p 1574 N94-18273 #
DE93-018632 .... p 1572 N94-19283 #
DE93-018634 .... p 1587 N94-18274 #
DE93-018637 .... p 1588 N94-19034 #
DE93-018649 .... p 1574 N94-18994 #
DE93-018652 .... p 1627 N94-19284 #
DE93-018656 .... p 1575 N94-19106 #
DE93-018658 .... p 1575 N94-19107 #
DE93-018659 .... p 1460 N94-19543 #
DE93-018660 .... p 1418 N94-18995 #
DE93-018662 .... p 1575 N94-18996 #
DE93-018663 .... p 1381 N94-19544 #
DE93-018664 .... p 1572 N94-19545 #
DE93-018683 .... p 1405 N94-19035 #
DE93-018685 .... p 1311 N94-18275 #
DE93-018687 .... p 1618 N94-19099 #
DE93-018689 .... p 1364 N94-19100 #
DE93-018693 .... p 1618 N94-19101 #
DE93-018694 .... p 1525 N94-19102 #
DE93-018696 .... p 1456 N94-19060 #
DE93-018706 .... p 1575 N94-18997 #
DE93-018715 .... p 1464 N94-17781 #
DE93-018716 .... p 1566 N94-18165 #
DE93-018717 .... p 1564 N94-17775 #
DE93-018726 .... p 1601 N94-18998 #
DE93-018740 .... p 1340 N94-18180 #
DE93-018767 .... p 1446 N94-19334 #
DE93-018776 .... p 1569 N94-18999 #
DE93-018777 .... p 1570 N94-19108 #
DE93-018784 .... p 1343 N94-19335 #
DE93-018787 .... p 1448 N94-19336 #
DE93-018793 .... p 1466 N94-18276 #
DE93-018795 .... p 1433 N94-19000 #
DE93-018805 .... p 1551 N94-19337 #
DE93-018818 .... p 1614 N94-18181 #
DE93-018833 .... p 1373 N94-19338 #
DE93-018834 .... p 1627 N94-19339 #
DE93-018839 .... p 1602 N94-19340 #
DE93-018845 .... p 1439 N94-18522 #
DE93-018858 .... p 1603 N94-19347 #
DE93-018861 .... p 1469 N94-19036 #
DE93-018862 .... p 1565 N94-17776 #
DE93-018876 .... p 1478 N94-19319 #
DE93-018881 .... p 1474 N94-18523 #
DE93-018887 .... p 1359 N94-18182 #
DE93-018903 .... p 1485 N94-19001 #
DE93-018904 .... p 1485 N94-19002 #
DE93-018906 .... p 1463 N94-19003 #
DE93-018907 .... p 1433 N94-19004 #
DE93-018925 .... p 1570 N94-19103 #
DE93-018932 .... p 1572 N94-19320 #
DE93-018951 .... p 1474 N94-18183 #
DE93-018961 .... p 1572 N94-19309 #
DE93-019001 .... p 1373 N94-19321 #
DE93-019008 .... p 1603 N94-19550 #
DE93-019024 .... p 1344 N94-19551 #
DE93-019035 .... p 1476 N94-19104 #
DE93-019050 .... p 1487 N94-19477 #
DE93-019059 .... p 1406 N94-19310 #
DE93-019064 .... p 1456 N94-19078 #
DE93-019072 .... p 1405 N94-19079 #
DE93-019073 .... p 1364 N94-19080 #
DE93-019101 .... p 1477 N94-19105 #
DE93-019108 .... p 1591 N94-19311 #
DE93-019149 .... p 1441 N94-19294 #

DE93-019156 .... p 1494 N94-19298 #
DE93-019157 .... p 1589 N94-19073 #
DE93-019158 .... p 1589 N94-19074 #
DE93-019163 .... p 1538 N94-19299 #
DE93-019168 .... p 1602 N94-19075 #
DE93-019201 .... p 1524 N94-19076 #
DE93-019209 .... p 1627 N94-19077 #
DE93-019221 .... p 1316 N94-19300 #
DE93-019223 .... p 1551 N94-19301 #
DE93-019224 .... p 1543 N94-19302 #
DE93-019227 .... p 1575 N94-19152 #
DE93-019228 .... p 1591 N94-19479 #
DE93-019236 .... p 1575 N94-19558 #
DE93-019239 .... p 1591 N94-19559 #
DE93-019246 .... p 1478 N94-19303 #
DE93-019247 .... p 1576 N94-19560 #
DE93-019252 .... p 1352 N94-19304 #
DE93-019263 .... p 1566 N94-18104 #
DE93-019264 .... p 1596 N94-18184 #
DE93-019272 .... p 1523 N94-19005 #
DE93-019303 .... p 1338 N94-19128 #
DE93-019360 .... p 1374 N94-19561 #
DE93-019399 .... p 1589 N94-19037 #
DE93-019409 .... p 1531 N94-19562 #
DE93-019410 .... p 1442 N94-19563 #
DE93-019461 .... p 1601 N94-19031 #
DE93-019462 .... p 1364 N94-19032 #
DE93-019466 .... p 1478 N94-19305 #
DE93-019469 .... p 1603 N94-19564 #
DE93-019501 .... p 1604 N94-19565 #
DE93-019503 .... p 1604 N94-19566 #
DE93-019504 .... p 1604 N94-19567 #
DE93-019512 .... p 1353 N94-19552 #
DE93-019544 .... p 1407 N94-19553 #
DE93-019550 .... p 1442 N94-19554 #
DE93-019554 .... p 1390 N94-19306 #
DE93-019577 .... p 1422 N94-19568 #
DE93-019580 .... p 1381 N94-19480 #
DE93-019585 .... p 1418 N94-18878
DE93-019592 .... p 1350 N94-19017 #
DE93-019626 .... p 1441 N94-19307 #
DE93-019627 .... p 1422 N94-19515 #
DE93-019633 .... p 1381 N94-19539 #
DE93-019746 .... p 1381 N94-19540 #
DE93-019847 .... p 1603 N94-19541 #
DE93-019880 .... p 1563 N94-19270 #
DE93-019887 .... p 1486 N94-19018 #
DE93-019890 .... p 1391 N94-19542 #
DE93-019892 .... p 1363 N94-19019 #
DE93-019927 .... p 1373 N94-19271 #
DE93-019931 .... p 1601 N94-19020 #
DE93-019933 .... p 1363 N94-19021 #
DE93-019960 .... p 1478 N94-19272 #
DE93-019992 .... p 1433 N94-19054 #
DE93-040001 .... p 1351 N94-19150 #
DE93-040002 .... p 1351 N94-19132 #
DE93-040059 .... p 1515 N94-19535 #
DE93-040072 .... p 1448 N94-19189 #
DE93-040083 .... p 1550 N94-19190 #
DE93-040085 .... p 1589 N94-19133 #
DE93-040170 .... p 1572 N94-19536 #
DE93-040197 .... p 1633 N94-19537 #
DE93-040203 .... p 1469 N94-19109 #
DE93-040215 .... p 1351 N94-19136 #
DE93-040216 .... p 1350 N94-18895 #
DE93-040217 .... p 1350 N94-18896 #
DE93-040218 .... p 1352 N94-19191 #
DE93-040219 .... p 1351 N94-19134 #
DE93-040221 .... p 1350 N94-18977 #
DE93-040222 .... p 1571 N94-19257 #
DE93-040301 .... p 1353 N94-19538 #
DE93-040303 .... p 1352 N94-19192 #
DE93-040305 .... p 1433 N94-19135 #
DE93-040316 .... p 1590 N94-19193 #
DE93-040319 .... p 1590 N94-19194 #
DE93-040320 .... p 1587 N94-18524 #
DE93-040326 .... p 1375 N94-19651 #
DE93-040364 .... p 1372 N94-18891 #
DE93-040446 .... p 1354 N94-19653 #
DE93-040482 .... p 1553 N94-19655 #
DE93-040519 .... p 1588 N94-18892 #
DE93-040520 .... p 1588 N94-18978 #
DE93-040521 .... p 1589 N94-19055
DE93-040630 .... p 1349 N94-18532 #
DE93-040684 .... p 1592 N94-19656 #
DE93-040688 .... p 1442 N94-19658 #
DE93-040690 .... p 1601 N94-19056
DE93-040874 .... p 1567 N94-18533 #
DE93-040875 .... p 1567 N94-18534 #
DE93-041221 .... p 1610 N94-19670 #
DE93-041223 .... p 1354 N94-19660 #
DE93-041272 .... p 1539 N94-19588 #
DE93-520882 .... p 1595 N94-18105 #
DE93-623326 .... p 1355 N94-17679
DE93-624668 .... p 1630 N94-18762 #
DE93-624725 .... p 1550 N94-19244 #
DE93-624726 .... p 1550 N94-19246 #
DE93-624757 .... p 1606 N94-17792 #
DE93-624764 .... p 1545 N94-17793 #
DE93-624765 .... p 1606 N94-17794 #
DE93-624766 .... p 1546 N94-17815 #
DE93-624767 .... p 1551 N94-19248 #
DE93-624768 .... p 1546 N94-17816
DE93-624769 .... p 1546 N94-17817
DE93-624770 .... p 1546 N94-17795 #
DE93-624771 .... p 1546 N94-17810
DE93-624772 .... p 1545 N94-17680 #
DE93-624773 .... p 1546 N94-17811
DE93-624774 .... p 1547 N94-17949
DE93-624789 .... p 1561 N94-17681 #
DE93-624797 .... p 1480 N94-17682 #
DE93-624798 .... p 1545 N94-17683 #
DE93-624799 .... p 1545 N94-17684 #
DE93-624801 .... p 1607 N94-17950
DE93-624802 .... p 1565 N94-17951
DE93-624808 .... p 1545 N94-17685 #
DE93-624809 .... p 1545 N94-17686 #
DE93-624813 .... p 1383 N94-17952
DE93-624814 .... p 1607 N94-17953
DE93-624828 .... p 1564 N94-17687 #
DE93-624900 .... p 1436 N94-17954
DE93-624901 .... p 1435 N94-17771
DE93-624920 .... p 1581 N94-17688 #
DE93-624921 .... p 1581 N94-17689 #
DE93-624929 .... p 1584 N94-17955
DE93-624946 .... p 1595 N94-17956 #
DE93-624967 .... p 1592 N94-17690
DE93-625117 .... p 1345 N94-17691
DE93-625470 .... p 1602 N94-19277
DE93-626646 .... p 1593 N94-17748 #
DE93-627003 .... p 1355 N94-17692
DE93-627958 .... p 1486 N94-19255
DE93-628592 .... p 1548 N94-18106
DE93-628593 .... p 1561 N94-18168
DE93-628594 .... p 1548 N94-18169
DE93-628621 .... p 1548 N94-18170
DE93-628622 .... p 1561 N94-18171
DE93-628761 .... p 1586 N94-18172
DE93-628793 .... p 1595 N94-18173
DE93-628794 .... p 1607 N94-18174
DE93-629819 .... p 1548 N94-18175
DE93-629857 .... p 1548 N94-18176
DE93-629858 .... p 1561 N94-18150
DE93-629859 .... p 1561 N94-18151
DE93-629861 .... p 1566 N94-18152
DE93-629862 .... p 1561 N94-18153
DE93-629863 .... p 1556 N94-18154
DE93-629864 .... p 1561 N94-18155
DE93-629865 .... p 1548 N94-18195
DE93-629866 .... p 1548 N94-18196
DE93-629867 .... p 1549 N94-18197
DE93-629868 .... p 1549 N94-18198
DE93-629905 .... p 1566 N94-18199
DE93-629906 .... p 1549 N94-18200
DE93-629907 .... p 1608 N94-18267
DE93-629908 .... p 1608 N94-18268
DE93-629955 .... p 1608 N94-18252
DE93-630145 .... p 1608 N94-18253
DE93-630228 .... p 1577 N94-18217
DE93-630229 .... p 1359 N94-18218
DE93-788362 .... p 1630 N94-18219 #
DE93-788368 .... p 1369 N94-18220 #
DE93-788387 .... p 1607 N94-18211 #
DE93-788388 .... p 1586 N94-18212 #
DE93-788393 .... p 1573 N94-18156
DE93-788396 .... p 1586 N94-18213 #
DE93-788457 .... p 1586 N94-18214
DE93-788461 .... p 1586 N94-18157
DE93-788476 .... p 1566 N94-18158
DE93-788519 .... p 1444 N94-18159
DE93-788586 .... p 1438 N94-18160
DE93-788620 .... p 1438 N94-18161

DIGEL-1993-1 .... p 1515 N94-19799 #

DLR-FB-92-33 .... p 1409 N94-18076 #
DLR-FB-92-39 .... p 1340 N94-18122 #
DLR-FB-92-40 .... p 1322 N94-18123 #
DLR-FB-93-03 .... p 1409 N94-18124
DLR-FB-93-04 .... p 1480 N94-18088 #
DLR-FB-93-05 .... p 1465 N94-18089
DLR-FB-93-07 .... p 1384 N94-18071 #
DLR-FB-93-08 .... p 1437 N94-18061 #

DLR-MITT-92-11 .... p 1395 N94-17920 #
DLR-MITT-93-01 .... p 1316 N94-18146 #
DLR-MITT-93-05 .... p 1316 N94-17921 #

DM-61 .... p 1562 N94-18859 #

DNA-IR-93-35 .... p 1382 N94-17844

DODA-AR-006-658 .... p 1322 N94-18324 #
DODA-AR-007-078 .... p 1317 N94-18315
DODA-AR-008-219 .... p 1497 N94-18329 #
DODA-AR-008-271 .... p 1376 N94-18203 #
DODA-AR-008-338 .... p 1410 N94-18326 #
DODA-AR-008-363-PT-1 .... p 1360 N94-18325 #
DODA-AR-008-365 .... p 1341 N94-18327 #

DOE-93017197 .... p 1615 N94-18496 #

DOE/CE-23810/10-PT-1 .... p 1351 N94-19136 #
DOE/CE-23810/13-VOL-1 .... p 1350 N94-18895 #
DOE/CE-23810/13-VOL-2 .... p 1350 N94-18896 #
DOE/CE-23810/13-VOL-3 .... p 1352 N94-19191 #
DOE/CE-23810/16 .... p 1351 N94-19134 #
DOE/CE-23810/20C .... p 1350 N94-18977 #

DOE/CH-9205 .... p 1478 N94-19305 #
DOE/CH-93019 .... p 1469 N94-19346 #

DOE/DP-0017 .... p 1583 N94-17912 #
DOE/DP-40200/251 .... p 1602 N94-19123 #

DOE/EIA-0149(92) .... p 1617 N94-18983 #
DOE/EIA-0293(93) .... p 1616 N94-18707 #

DOE/ER-00038/3626 .... p 1566 N94-18165 #
DOE/ER-0144-11 .... p 1632 N94-18915 #
DOE/ER-0592 .... p 1588 N94-19012 #
DOE/ER-10713/T5 .... p 1609 N94-19250 #
DOE/ER-13108/T8 .... p 1464 N94-17781 #
DOE/ER-13190/8 .... p 1550 N94-19190 #
DOE/ER-13263/T1 .... p 1350 N94-19017 #
DOE/ER-13433/5 .... p 1433 N94-19135 #
DOE/ER-13519/7 .... p 1571 N94-19257 #
DOE/ER-13566/6 .... p 1448 N94-17814 #
DOE/ER-13604/22 .... p 1345 N94-17808 #
DOE/ER-13619/7 .... p 1363 N94-19019 #
DOE/ER-13711/T3 .... p 1596 N94-18243 #
DOE/ER-13732/7 .... p 1372 N94-18891 #
DOE/ER-13778/6 .... p 1564 N94-17775 #
DOE/ER-13916/5 .... p 1561 N94-18177 #
DOE/ER-14228/2 .... p 1567 N94-18533 #
DOE/ER-25043/T1 .... p 1539 N94-19588 #
DOE/ER-25054/T1 .... p 1561 N94-18178 #
DOE/ER-25099/2 .... p 1566 N94-18179 #
DOE/ER-25122/4 .... p 1535 N94-18808 #
DOE/ER-25122/5 .... p 1524 N94-19024 #
DOE/ER-40150/227 .... p 1441 N94-18974 #
DOE/ER-40162/T6 .... p 1565 N94-17776 #
DOE/ER-40249/T1 .... p 1574 N94-18916 #
DOE/ER-40319/T3 .... p 1575 N94-19050 #
DOE/ER-40374/68 .... p 1573 N94-17784 #
DOE/ER-40412/6 .... p 1570 N94-19103 #
DOE/ER-40531/4 .... p 1566 N94-18104 #
DOE/ER-40541/1 .... p 1569 N94-19013 #
DOE/ER-40561/110-INT93 .... p 1568 N94-18824 #
DOE/ER-40676/T1 .... p 1567 N94-18534 #
DOE/ER-40684/3 .... p 1575 N94-19287 #
DOE/ER-40702/3 .... p 1630 N94-17818 #
DOE/ER-40702/4 .... p 1575 N94-19023 #
DOE/ER-40704/2-TASK-A .... p 1570 N94-19029 #
DOE/ER-40730/1 .... p 1574 N94-18927 #
DOE/ER-40748/1 .... p 1573 N94-17807 #
DOE/ER-40757/2 .... p 1607 N94-17892 #
DOE/ER-45095/7 .... p 1367 N94-17678 #
DOE/ER-45199/3 .... p 1601 N94-19031 #
DOE/ER-45229/33 .... p 1596 N94-18184 #
DOE/ER-45283/12 .... p 1601 N94-19056
DOE/ER-45303/3 .... p 1369 N94-18163 #
DOE/ER-45311/T2 .... p 1359 N94-18182 #
DOE/ER-45326/T3 .... p 1571 N94-19204 #
DOE/ER-45328/7 .... p 1601 N94-19020 #
DOE/ER-45367/5 .... p 1364 N94-19032 #
DOE/ER-52161/5 .... p 1363 N94-19021 #
DOE/ER-53223/207 .... p 1583 N94-17854 #
DOE/ER-53291/4 .... p 1592 N94-19656 #
DOE/ER-54089/2 .... p 1589 N94-19133 #
DOE/ER-54093/2 .... p 1583 N94-17809 #
DOE/ER-54186/T1 .... p 1366 N94-19546 #
DOE/ER-60970/T1 .... p 1470 N94-17710 #
DOE/ER-61216/2 .... p 1474 N94-18183 #
DOE/ER-61229/2 .... p 1442 N94-19658 #
DOE/ER-75527/5 .... p 1614 N94-18181 #

DOE/ET-10815/219 .... p 1576 N94-17857
DOE/ET-53088-606 .... p 1583 N94-17945 #
DOE/ET-53088/546 .... p 1590 N94-19194 #
DOE/ET-53088/608 .... p 1583 N94-17753 #
DOE/ET-53088/609 .... p 1587 N94-18524 #
DOE/ET-53088/612 .... p 1584 N94-17983 #
DOE/ET-53088/613 .... p 1584 N94-17948 #
DOE/ET-53088/616 .... p 1590 N94-19193 #

DOE/EW-50616/T13 .... p 1391 N94-19542 #

DOE/FE-0279 .... p 1467 N94-18475 #
DOE/FE-0280 .... p 1466 N94-18103
DOE/FE-0398 .... p 1466 N94-18109 #

DOE/FTR-93013563 .... p 1461 N94-17893 #

DOE/MA-33222/T1 .... p 1616 N94-18689 #

DOE/MC-28080/3381 .... p 1486 N94-19018 #
DOE/MC-29116/3406 .... p 1433 N94-19054 #
DOE/MC-29228/3407 .... p 1351 N94-19132 #
DOE/MC-29228/3408 .... p 1351 N94-19150 #

DOE/METC-93-4112 .... p 1468 N94-18925 #

DOE/NV-10872/T61 .... p 1572 N94-19309 #

DOE/OR-00033/T530 .... p 1583 N94-17739 #
DOE/OR-21400/T475 .... p 1596 N94-18192 #
DOE/OR-22041/1 .... p 1340 N94-18180 #

DOE/PC-89775/13 .... p 1354 N94-19660 #
DOE/PC-90043/T9 .... p 1347 N94-18209 #
DOE/PC-90274/T21 .... p 1589 N94-19055
DOE/PC-90274/T22 .... p 1588 N94-18978 #
DOE/PC-90274/T23 .... p 1588 N94-18892 #
DOE/PC-91287/9 .... p 1610 N94-19670 #
DOE/PC-92112/T2 .... p 1349 N94-18532 #

DOE/S-00097P-VOL-3 .... p 1475 N94-18835 #

DOT-VNTSC-FAA-93-6 .... p 1510 N94-19677 #

DOT/FAA/CT-TN92/46 .... p 1316 N94-18728 #
DOT/FAA/CT-TN93/15 .... p 1513 N94-18992 #
DOT/FAA/CT-TN93/5 .... p 1514 N94-19773 #

DOT/FAA/CT-93/1 .... p 1318 N94-18789 #

DOT/FAA/RD-93/16 .... p 1316 N94-19661 #
DOT/FAA/RD-93/26 .... p 1510 N94-19677 #
DOT/FAA/RD-93/27 .... p 1492 N94-18684

DRA-TM(USGR)-93302 .... p 1344 N94-19391 #

DRA-TM-AP-23 .... p 1317 N94-17826 #

DREA-TC-93/306 .... p 1499 N94-18910

DREV-R-4724/93 .... p 1463 N94-18800 #

DRIC-BR-318039 .... p 1317 N94-17826 #

DSPH-3-VOL-1 .... p 1534 N94-18507
DSPH-3-VOL-2 .... p 1534 N94-18508
DSPH-3-VOL-3 .... p 1389 N94-18897 #

DTIC-TR-93-26 .... p 1617 N94-18752 #

DTIC-TR/93-29 .... p 1615 N94-18319

DTIC/TR-93-33 .... p 1615 N94-18323 #
DTIC/TR-93-9 .... p 1615 N94-18323 #

DWA-1808 .... p 1598 N94-18616

E-8048 .... p 1336 N94-17856 * #
E-8092 .... p 1333 N94-19313 * #
E-8207 .... p 1321 N94-19353 * #
E-8239 .... p 1313 N94-19484 * #
E-8244 .... p 1457 N94-19351 * #
E-8267 .... p 1587 N94-18861 * #
E-8274 .... p 1446 N94-19318 * #
E-8300 .... p 1434 N94-19314 * #

ECL-91-27 .... p 1457 N94-19375 #
ECL-91-40 .... p 1353 N94-19376 #
ECL-91-41 .... p 1451 N94-17918 #
ECL-92-15 .... p 1420 N94-19398 #
ECL-92-25 .... p 1353 N94-19406 #
ECL-92-28 .... p 1421 N94-19399 #
ECL-92-31 .... p 1366 N94-19436 #
ECL-92-32 .... p 1529 N94-19409 #
ECL-92-36 .... p 1458 N94-19411 #
ECL-92-37 .... p 1563 N94-19413 #
ECL-92-52 .... p 1487 N94-19380 #
ECL-92-55 .... p 1365 N94-19400 #
ECL-92-57 .... p 1434 N94-19414 #
ECL-92-60 .... p 1406 N94-19297 #
ECL-92-61 .... p 1603 N94-19357 #
ECL-92-64 .... p 1457 N94-19403 #
ECL-93-02 .... p 1373 N94-19405 #
ECL-93-05 .... p 1420 N94-19381 #
ECL-93-07 .... p 1458 N94-19460 #
ECL-93-13 .... p 1421 N94-19461 #

EGG-M-92397 .... p 1564 N94-17738 #
EGG-M-92598 .... p 1461 N94-17851 #
EGG-M-92690 .... p 1613 N94-17880 #
EGG-M-93191 .... p 1337 N94-17863 #

EOARD-93-06 .... p 1579 N94-18738 #

EPA/600/A-93/079 .... p 1476 N94-19065 #

ERDEC-TR-104 .... p 1460 N94-19606 #

ERIM-154600-63-F .... p 1497 N94-18277 #
ERIM-232800-2-F .... p 1578 N94-18383

ERP-1109 .... p 1474 N94-18688 #
ERP-1127 .... p 1493 N94-18871 #

ES/CSET-16 .... p 1511 N94-18244 #

ESA-PSS-02-10-VOL-2-ISSUE-1 .. p 1338 N94-19516 #
ESA-PSS-03-40-ISSUE-1 .... p 1513 N94-19442 #

ESA-SP-1159 .... p 1328 N94-19622 #
ESA-SP-1161 .... p 1633 N94-19404 #

ESC-TR-93-185 .... p 1521 N94-18659 #
ESC-TR-93-249-VOL-2 .... p 1462 N94-18729

ESDC-3984 .... p 1471 N94-17774 #

ESG-220 .... p 1383 N94-18055 #
ESG-228 .... p 1575 N94-19558 #
ESG-229 .... p 1575 N94-19152 #

ETMWG-253-65 .... p 1385 N94-18260 #

ETN-93-94303-PT-2 .... p 1620 N94-19795 #
ETN-93-94353 .... p 1533 N94-17976
ETN-93-94355 .... p 1560 N94-18067 #
ETN-93-94370 .... p 1565 N94-17972 #
ETN-93-94401 .... p 1533 N94-18068
ETN-93-94402 .... p 1519 N94-17977 #
ETN-93-94403 .... p 1519 N94-17978 #
ETN-93-94404 .... p 1614 N94-17979
ETN-93-94423 .... p 1319 N94-19796 #
ETN-93-94431 .... p 1311 N94-17957 #
ETN-93-94441 .... p 1611 N94-17980 #
ETN-93-94442 .... p 1444 N94-17963 #
ETN-93-94443 .... p 1444 N94-17964 #
ETN-93-94445 .... p 1412 N94-18557 #
ETN-93-94447 .... p 1414 N94-18578 #
ETN-93-94469 .... p 1380 N94-19373 #
ETN-93-94471 .... p 1365 N94-19374 #
ETN-93-94472 .... p 1346 N94-17973 #
ETN-93-94473 .... p 1444 N94-17974 #
ETN-93-94478 .... p 1339 N94-17958 #
ETN-93-94479 .... p 1452 N94-17959 #
ETN-93-94491 .... p 1473 N94-18139 #
ETN-93-94493 .... p 1548 N94-18140 #
ETN-93-94494 .... p 1547 N94-18069 #
ETN-93-94505 .... p 1443 N94-17937
ETN-93-94506 .... p 1556 N94-17938
ETN-93-94508 .... p 1613 N94-17939
ETN-93-94509 .... p 1444 N94-17940
ETN-93-94510 .... p 1519 N94-17975
ETN-93-94513 .... p 1383 N94-17932
ETN-93-94514 .... p 1565 N94-17933
ETN-93-94516 .... p 1562 N94-17934
ETN-93-94517 .... p 1383 N94-17935
ETN-93-94518 .... p 1613 N94-17936
ETN-93-94519 .... p 1540 N94-17922
ETN-93-94520 .... p 1452 N94-17941
ETN-93-94521 .... p 1451 N94-17931
ETN-93-94522 .... p 1434 N94-19797
ETN-93-94523 .... p 1383 N94-18070
ETN-93-94524 .... p 1393 N94-19798
ETN-93-94525 .... p 1518 N94-17965
ETN-93-94526 .... p 1504 N94-17966
ETN-93-94527 .... p 1508 N94-17967
ETN-93-94529 .... p 1554 N94-19683 #
ETN-93-94531 .... p 1481 N94-18142
ETN-93-94532 .... p 1489 N94-18143
ETN-93-94534 .... p 1496 N94-17923
ETN-93-94535 .... p 1488 N94-17924
ETN-93-94536 .... p 1494 N94-19698
ETN-93-94546 .... p 1613 N94-17925
ETN-93-94555 .... p 1631 N94-17968 #
ETN-93-94556 .... p 1547 N94-17969 #
ETN-93-94557 .... p 1461 N94-18063 #
ETN-93-94558 .... p 1496 N94-18064 #
ETN-93-94559 .... p 1496 N94-18065 #
ETN-93-94560 .... p 1461 N94-18137
ETN-93-94562 .... p 1496 N94-18066 #
ETN-93-94570 .... p 1518 N94-17926
ETN-93-94571 .... p 1518 N94-17927
ETN-93-94572 .... p 1547 N94-17928
ETN-93-94573 .... p 1518 N94-17960
ETN-93-94574 .... p 1547 N94-17961
ETN-93-94575 .... p 1614 N94-18144
ETN-93-94576 .... p 1547 N94-17962
ETN-93-94577 .... p 1520 N94-18145
ETN-93-94578 .... p 1520 N94-18138
ETN-93-94580 .... p 1520 N94-18136
ETN-93-94581 .... p 1633 N94-19404 #
ETN-93-94585 .... p 1457 N94-19375 #
ETN-93-94586 .... p 1353 N94-19376 #
ETN-93-94587 .... p 1451 N94-17918 #
ETN-93-94588 .... p 1420 N94-19398 #
ETN-93-94589 .... p 1353 N94-19406 #
ETN-93-94590 .... p 1421 N94-19399 #
ETN-93-94591 .... p 1366 N94-19436 #
ETN-93-94592 .... p 1529 N94-19409 #
ETN-93-94593 .... p 1458 N94-19411 #
ETN-93-94594 .... p 1563 N94-19413 #
ETN-93-94600 .... p 1365 N94-19400 #
ETN-93-94601 .... p 1434 N94-19414 #
ETN-93-94612 .... p 1584 N94-17981
ETN-93-94614 .... p 1623 N94-19526
ETN-93-94622 .... p 1515 N94-19799 #
ETN-93-94626 .... p 1482 N94-18622 #
ETN-93-94628 .... p 1430 N94-18643 #
ETN-93-94633 .... p 1424 N94-18006 #
ETN-93-94636 .... p 1563 N94-19083 #
ETN-93-94637 .... p 1524 N94-19084 #
ETN-93-94638 .... p 1542 N94-19085 #
ETN-93-94639 .... p 1550 N94-19086 #
ETN-93-94640 .... p 1419 N94-19087 #
ETN-93-94641 .... p 1550 N94-19088 #
ETN-93-94642 .... p 1524 N94-19089 #
ETN-93-94643 .... p 1486 N94-19081 #
ETN-93-94644 .... p 1550 N94-19082 #
ETN-93-94645 .... p 1488 N94-19644
ETN-93-94646 .... p 1557 N94-19090 #
ETN-93-94647 .... p 1542 N94-19091 #
ETN-93-94648 .... p 1542 N94-19092 #
ETN-93-94649 .... p 1558 N94-19137 #
ETN-93-94650 .... p 1542 N94-19138 #
ETN-93-94651 .... p 1420 N94-19139 #
ETN-93-94652 .... p 1486 N94-19140 #
ETN-93-94653 .... p 1550 N94-19141 #
ETN-93-94654 .... p 1542 N94-19142 #
ETN-93-94655 .... p 1525 N94-19143 #
ETN-93-94656 .... p 1420 N94-19144 #
ETN-93-94657 .... p 1550 N94-19153 #
ETN-93-94658 .... p 1423 N94-19645
ETN-93-94659 .... p 1551 N94-19285 #
ETN-93-94661 .... p 1525 N94-19154 #
ETN-93-94662 .... p 1525 N94-19155 #
ETN-93-94663 .... p 1525 N94-19156 #
ETN-93-94664 .... p 1611 N94-19157 #
ETN-93-94665 .... p 1611 N94-19158 #
ETN-93-94666 .... p 1536 N94-19159 #
ETN-93-94667 .... p 1536 N94-19160 #
ETN-93-94668 .... p 1537 N94-19219 #
ETN-93-94669 .... p 1526 N94-19220 #
ETN-93-94670 .... p 1526 N94-19221 #
ETN-93-94671 .... p 1526 N94-19222 #
ETN-93-94672 .... p 1537 N94-19223 #
ETN-93-94673 .... p 1526 N94-19224 #
ETN-93-94674 .... p 1527 N94-19225 #
ETN-93-94675 .... p 1558 N94-19385 #
ETN-93-94676 .... p 1559 N94-19386 #
ETN-93-94677 .... p 1543 N94-19226 #
ETN-93-94678 .... p 1527 N94-19227 #
ETN-93-94679 .... p 1558 N94-19228 #
ETN-93-94680 .... p 1527 N94-19229 #
ETN-93-94681 .... p 1390 N94-19230 #
ETN-93-94682 .... p 1558 N94-19195 #
ETN-93-94683 .... p 1526 N94-19196 #
ETN-93-94684 .... p 1536 N94-19197 #
ETN-93-94685 .... p 1537 N94-19198 #
ETN-93-94686 .... p 1543 N94-19199 #
ETN-93-94687 .... p 1526 N94-19200 #
ETN-93-94688 .... p 1538 N94-19296 #
ETN-93-94690 .... p 1527 N94-19261 #
ETN-93-94692 .... p 1528 N94-19262 #
ETN-93-94693 .... p 1537 N94-19264 #
ETN-93-94694 .... p 1558 N94-19265 #
ETN-93-94695 .... p 1390 N94-19267 #
ETN-93-94696 .... p 1558 N94-19354 #
ETN-93-94782 .... p 1315 N94-17733
ETN-93-94783 .... p 1317 N94-17734
ETN-93-94837 .... p 1603 N94-19355 #
ETN-93-94838 .... p 1420 N94-19356 #
ETN-93-94840 .... p 1409 N94-17901 #
ETN-93-94844 .... p 1525 N94-19145 #
ETN-93-94847 .... p 1405 N94-19292 #
ETN-93-94848 .... p 1602 N94-19293 #
ETN-93-94849 .... p 1515 N94-19295 #
ETN-93-94850 .... p 1574 N94-18845 #
ETN-93-94851 .... p 1432 N94-18846 #
ETN-93-94852 .... p 1569 N94-18847 #

ETN-93-94853 .... p 1562 N94-18859 #
ETN-93-94854 .... p 1587 N94-18860 #
ETN-93-94855 .... p 1480 N94-17720
ETN-93-94856 .... p 1311 N94-17721
ETN-93-94857 .... p 1311 N94-17722
ETN-93-94858 .... p 1452 N94-17970 #
ETN-93-94859 .... p 1339 N94-17971
ETN-93-94860 .... p 1311 N94-17919 #
ETN-93-94863 .... p 1328 N94-19622 #
ETN-93-94865 .... p 1395 N94-17920 #
ETN-93-94866 .... p 1316 N94-18146 #
ETN-93-94867 .... p 1316 N94-17921 #
ETN-93-94869 .... p 1409 N94-18076 #
ETN-93-94871 .... p 1340 N94-18122 #
ETN-93-94872 .... p 1322 N94-18123 #
ETN-93-94873 .... p 1409 N94-18124
ETN-93-94874 .... p 1480 N94-18088 #
ETN-93-94875 .... p 1465 N94-18089
ETN-93-94876 .... p 1384 N94-18071 #
ETN-93-94877 .... p 1437 N94-18061 #
ETN-93-94880 .... p 1513 N94-19442 #
ETN-93-94882 .... p 1338 N94-19516 #
ETN-93-94883 .... p 1451 N94-17899
ETN-93-94884 .... p 1346 N94-17900
ETN-93-94886 .... p 1451 N94-17929
ETN-93-94887 .... p 1518 N94-17930
ETN-93-94888 .... p 1322 N94-17735
ETN-93-94890 .... p 1529 N94-19378 #
ETN-93-94892 .... p 1406 N94-19297 #
ETN-93-94893 .... p 1487 N94-19380 #
ETN-93-94894 .... p 1603 N94-19357 #
ETN-93-94895 .... p 1457 N94-19403 #
ETN-93-94896 .... p 1373 N94-19405 #
ETN-93-94897 .... p 1420 N94-19381 #
ETN-93-94898 .... p 1458 N94-19460 #
ETN-93-94899 .... p 1421 N94-19461 #
ETN-93-94900 .... p 1552 N94-19407 #
ETN-93-94901 .... p 1539 N94-17916
ETN-93-94904 .... p 1544 N94-19408 #
ETN-93-94905 .... p 1529 N94-19382 #
ETN-93-94907 .... p 1544 N94-19410 #
ETN-93-94908 .... p 1530 N94-19412 #
ETN-93-94909 .... p 1310 N94-19383 #
ETN-93-94910 .... p 1479 N94-19379 #
ETN-93-94911 .... p 1457 N94-19358 #
ETN-93-94912 .... p 1624 N94-17736
ETN-93-94915 .... p 1621 N94-18141
ETN-93-94917 .... p 1622 N94-19451
ETN-93-94919 .... p 1621 N94-19415
ETN-93-94920 .... p 1390 N94-19416
ETN-93-94921 .... p 1622 N94-19417
ETN-93-94924 .... p 1628 N94-19794 * #
ETN-93-94926 .... p 1509 N94-19419
ETN-93-94927 .... p 1509 N94-19420
ETN-93-94929 .... p 1509 N94-19422
ETN-93-94930 .... p 1510 N94-19439
ETN-93-94931 .... p 1510 N94-19440
ETN-93-94932 .... p 1510 N94-19443
ETN-93-94933 .... p 1458 N94-19444
ETN-93-94934 .... p 1378 N94-19445
ETN-93-94939 .... p 1619 N94-19453
ETN-93-94940 .... p 1619 N94-19454
ETN-93-94942 .... p 1580 N94-19424
ETN-93-94943 .... p 1441 N94-19426
ETN-93-94945 .... p 1390 N94-19447
ETN-93-94946 .... p 1390 N94-19449
ETN-93-94948 .... p 1618 N94-19450
ETN-93-94949 .... p 1580 N94-19455
ETN-93-94950 .... p 1619 N94-19457
ETN-93-94951 .... p 1618 N94-19452
ETN-93-94952 .... p 1544 N94-19458
ETN-93-94958 .... p 1517 N94-17917
ETN-93-94960 .... p 1353 N94-19456
ETN-93-94961 .... p 1353 N94-19459
ETN-93-94962 .... p 1479 N94-19518
ETN-93-94963 .... p 1479 N94-19521
ETN-93-94964 .... p 1507 N94-19523
ETN-93-94969 .... p 1344 N94-19391 #
ETN-93-94983 .... p 1532 N94-19712 #
ETN-93-94984 .... p 1556 N94-19731 #
ETN-93-94998 .... p 1552 N94-19392 #
ETN-93-94999 .... p 1552 N94-19393 #
ETN-93-95001 .... p 1552 N94-19395 #
ETN-93-95002 .... p 1529 N94-19396
ETN-93-95003 .... p 1528 N94-19359 #
ETN-93-95004 .... p 1538 N94-19514 #
ETN-93-95005 .... p 1531 N94-19517
ETN-93-95006 .... p 1552 N94-19487 #
ETN-93-95007 .... p 1530 N94-19488 #
ETN-93-95008 .... p 1530 N94-19498 #
ETN-93-95009 .... p 1552 N94-19499 #
ETN-93-95010 .... p 1406 N94-19501 #
ETN-93-95011 .... p 1421 N94-19502 #
ETN-93-95012 .... p 1421 N94-19495 #
ETN-93-95013 .... p 1406 N94-19490 #
ETN-93-95014 .... p 1434 N94-19659
ETN-93-95015 .... p 1544 N94-19360 #
ETN-93-95016 .... p 1544 N94-19361 #
ETN-93-95017 .... p 1552 N94-19362
ETN-93-95018 .... p 1528 N94-19363
ETN-93-95019 .... p 1591 N94-19364 #
ETN-93-95020 .... p 1420 N94-19365
ETN-93-95021 .... p 1529 N94-19368
ETN-93-95022 .... p 1529 N94-19370 #
ETN-93-95023 .... p 1532 N94-19713
ETN-93-95024 .... p 1323 N94-19372 #
ETN-93-95025 .... p 1344 N94-19666 #
ETN-93-95027 .... p 1313 N94-19667 #
ETN-93-95028 .... p 1423 N94-19668 #
ETN-93-95029 .... p 1461 N94-19669
ETN-93-95030 .... p 1335 N94-19614 #
ETN-93-95031 .... p 1321 N94-19615 #
ETN-93-95048 .... p 1391 N94-19646
ETN-93-95049 .... p 1406 N94-19387 #
ETN-93-95050 .... p 1442 N94-19647
ETN-93-95051 .... p 1406 N94-19390 #
ETN-93-95052 .... p 1460 N94-19648 #
ETN-93-95053 .... p 1510 N94-19649 #
ETN-93-95054 .... p 1381 N94-19650 #
ETN-93-95058 .... p 1532 N94-19652
ETN-93-95060 .... p 1470 N94-19654
ETN-93-95070 .... p 1559 N94-19610
ETN-93-95071 .... p 1375 N94-19611
ETN-93-95072 .... p 1604 N94-19612
ETN-93-95073 .... p 1592 N94-19613
ETN-93-95074 .... p 1423 N94-19730
ETN-93-95075 .... p 1321 N94-19711
ETN-93-95078 .... p 1494 N94-19616 #
ETN-93-95079 .... p 1391 N94-19617 #
ETN-93-95080 .... p 1631 N94-19504 #
ETN-93-95081 .... p 1631 N94-19505 #
ETN-93-95082 .... p 1631 N94-19506 #
ETN-93-95083 .... p 1479 N94-19507 #
ETN-93-95087 .... p 1379 N94-19489 #
ETN-93-95091 .... p 1379 N94-19491
ETN-93-95092 .... p 1379 N94-19492 #
ETN-93-95093 .... p 1319 N94-19496 #
ETN-93-95094 .... p 1421 N94-19497 #
ETN-93-95095 .... p 1319 N94-19500 #
ETN-93-95096 .... p 1494 N94-19503 #
ETN-93-95097 .... p 1631 N94-19714
ETN-93-95098 .... p 1628 N94-19519 #
ETN-93-95099 .... p 1564 N94-19715
ETN-93-95100 .... p 1422 N94-19520 #
ETN-93-95101 .... p 1553 N94-19522 #
ETN-93-95102 .... p 1422 N94-19509 #
ETN-93-95103 .... p 1422 N94-19510 #
ETN-93-95105 .... p 1422 N94-19525 #
ETN-93-95121 .... p 1313 N94-19524
ETN-94660 .... p 1543 N94-19286 #

EUT-92-WSK-02 .... p 1553 N94-19556
EUT-92-WSK-03 .... p 1550 N94-18991 #

FAA-APO-93-8 .... p 1315 N94-18490
FAA-APO-93-9 .... p 1316 N94-18336 #

FASTC-ID(RS)T-0041-93 .... p 1439 N94-18674 #
FASTC-ID(RS)T-0096-93 .... p 1492 N94-18675 #
FASTC-ID(RS)T-0098-93 .... p 1599 N94-18711 #
FASTC-ID(RS)T-0198-93 .... p 1439 N94-18614 #
FASTC-ID(RS)T-0201-93 .... p 1332 N94-18760
FASTC-ID(RS)T-0222-93 .... p 1341 N94-18544 #
FASTC-ID(RS)T-0851-92 .... p 1512 N94-18673 #

FASTC-IR(RS)T-0300-93 .... p 1351 N94-19110 #

FEI-2173 .... p 1355 N94-17692

FEL-91-A368 .... p 1434 N94-19797
FEL-91-B293 .... p 1619 N94-19454
FEL-92-A044 .... p 1393 N94-19798
FEL-92-A125 .... p 1441 N94-19426
FEL-92-A134 .... p 1518 N94-17965
FEL-92-A430 .... p 1390 N94-19447
FEL-92-A435 .... p 1390 N94-19449
FEL-92-B159 .... p 1383 N94-18070
FEL-92-B225 .... p 1618 N94-19450
FEL-92-B356 .... p 1580 N94-19455
FEL-92-B365 .... p 1619 N94-19457
FEL-93-A034 .... p 1580 N94-19424
FEL-93-B020 .... p 1618 N94-19452
FEL-93-B029 .... p 1544 N94-19458

FFA-TN-1992-09 .... p 1311 N94-17721
FFA-TN-1992-14 .... p 1311 N94-17722
FFA-TN-1992-22 .... p 1452 N94-17970 #
FFA-TN-1992-33 .... p 1339 N94-17971
FFA-TN-1992-42 .... p 1311 N94-17919 #
FFA-TN-1993-22 .... p 1457 N94-19358 #

FFI-93/7012 .... p 1322 N94-17735

FFI-93/7021 .... p 1529 N94-19378 #

FNAL-TM-1849 .... p 1436 N94-17883

FNAL/C-93/076 .... p 1525 N94-19186 #
FNAL/C-93/088 .... p 1569 N94-18973 #
FNAL/C-93/125 .... p 1574 N94-18972 #
FNAL/C-93/168 .... p 1574 N94-18497 #

FOA-C-20922-2.3 .... p 1419 N94-19068 #
FOA-C-20923-8.4-PT-4 .... p 1363 N94-18952 #
FOA-C-30656-3.3 .... p 1389 N94-18951 #
FOA-C-30683-3.3 .... p 1389 N94-18950 #
FOA-C-40305-4.5 .... p 1473 N94-18139 #

FOA-30694-8.3,3.1 .... p 1347 N94-18081 #

GA-A-21167 .... p 1582 N94-17702 #
GA-A-21305 .... p 1585 N94-18058 #
GA-A-21309 .... p 1585 N94-18057 #
GA-A-21310 .... p 1585 N94-18056 #

GAO/IMTEC-93-16 .... p 1532 N94-19716 #

GAO/NSIAD-93-144 .... p 1305 N94-18279
GAO/NSIAD-93-201 .... p 1617 N94-18848 #

GPO-71-510 .... p 1620 N94-18842 #

GRL/9301 .... p 1440 N94-18880

GTFR-108 .... p 1588 N94-18988 #

HAC/REF-J3338 .... p 1374 N94-19577

HIFAN-570 .... p 1441 N94-19030 #
HIFAN-571 .... p 1389 N94-19053 #
HIFAN-574 .... p 1575 N94-18997 #
HIFAN-579 .... p 1576 N94-19560 #
HIFAN-582 .... p 1591 N94-19559 #
HIFAN-584 .... p 1591 N94-19479 #

IAEA-CN-56/E-1-4 .... p 1590 N94-19289 #

IAEA-TECDOC-676 .... p 1606 N94-17792 #
IAEA-TECDOC-683 .... p 1345 N94-17691

IC-92/142 .... p 1592 N94-17690
IC-92/413 .... p 1545 N94-17793 #
IC-93/11 .... p 1606 N94-17794 #
IC-93/12 .... p 1383 N94-17952
IC-93/1 .... p 1550 N94-19244 #
IC-93/23 .... p 1480 N94-17682 #
IC-93/28 .... p 1545 N94-17683 #
IC-93/2 .... p 1550 N94-19246 #
IC-93/37 .... p 1546 N94-17815 #
IC-93/38 .... p 1551 N94-19248 #
IC-93/40 .... p 1545 N94-17684 #
IC-93/42 .... p 1595 N94-17956 #
IC-93/45-PT-1 .... p 1486 N94-19255
IC-93/48 .... p 1584 N94-17955
IC-93/50 .... p 1545 N94-17685 #
IC-93/53 .... p 1546 N94-17816
IC-93/54 .... p 1548 N94-18176
IC-93/55 .... p 1546 N94-17817
IC-93/56 .... p 1546 N94-17795 #
IC-93/57 .... p 1561 N94-17681 #
IC-93/58 .... p 1564 N94-17687 #
IC-93/59 .... p 1546 N94-17810
IC-93/61 .... p 1436 N94-17954
IC-93/62 .... p 1435 N94-17771
IC-93/64 .... p 1630 N94-18762 #
IC-93/68 .... p 1545 N94-17680 #
IC-93/69 .... p 1581 N94-17688 #
IC-93/70 .... p 1545 N94-17686 #
IC-93/76 .... p 1546 N94-17811
IC-93/84 .... p 1548 N94-18170
IC-93/86 .... p 1595 N94-18173
IC-93/89 .... p 1586 N94-18172
IC-93/90 .... p 1607 N94-18174
IC-93/94 .... p 1561 N94-18171
IC-93/97 .... p 1548 N94-18106

ICASE-93-66 .... p 1551 N94-19315 * #
ICASE-93-67 .... p 1551 N94-19317 * #

IDA-D-1400 .... p 1619 N94-19780

IDA-P-2863 .... p 1616 N94-18575

IDA/HQ-93-44150 .... p 1616 N94-18575
IDA/HQ-93-44315 .... p 1619 N94-19780

IEPC-93-246 .... p 1587 N94-18861 * #

IFSR-546 .... p 1590 N94-19194 #

IFSR-606 .... p 1583 N94-17945 #
IFSR-608 .... p 1583 N94-17753 #
IFSR-609 .... p 1587 N94-18524 #
IFSR-612 .... p 1584 N94-17983 #
IFSR-613 .... p 1584 N94-17948 #
IFSR-616 .... p 1590 N94-19193 #

IFVE-OMVT-91-131 .... p 1561 N94-18150

IFVE-OP-91-142 .... p 1577 N94-18217

IFVE-OTF-91-181 .... p 1566 N94-18199

IHEP-OTF-91-181 .... p 1566 N94-18199
IHEP-OTF-91-190 .... p 1561 N94-18151

IITRI-D06205-2-VOL-1 .... p 1386 N94-18473

IITRI-TR-D06205-2-VOL-2 .... p 1388 N94-18751
IITRI-TR-D06205-2-VOL-3 .... p 1388 N94-18741 #

INRIA-RR-1721 .... p 1311 N94-17957 #

IOS-294-1992 .... p 1461 N94-18063 #
IOS-295-1992 .... p 1496 N94-18064 #
IOS-296-1992 .... p 1496 N94-18065 #
IOS-297-1992 .... p 1461 N94-18137
IOS-299-1992 .... p 1496 N94-18066 #

IPP-6/310 .... p 1584 N94-17981

IPPCZ-325 .... p 1581 N94-17689 #

IR-291 .... p 1524 N94-19062 #
IR-293 .... p 1618 N94-19331
IR-294 .... p 1618 N94-19067 #

IRF-SR-211 .... p 1587 N94-18860 #
IRF-SR-212 .... p 1480 N94-17720

IRIG-STANDARD-253-93 .... p 1385 N94-18260 #

IS-M-747 .... p 1343 N94-18914 #

ISAL-92-0097 .... p 1406 N94-19490 #

ISBN 0-9583227-3-2 .... p 1623 N94-19657 #

ISBN-0-16-041532-2 .... p 1620 N94-18842 #
ISBN-0-16-042982-X .... p 1618 N94-19377 #
ISBN-0-309-04483-9 .... p 1514 N94-19478 #
ISBN-0-309-04790-0 .... p 1515 N94-19401 #
ISBN-3-92-362422-0 .... p 1494 N94-19503 #
ISBN-3-98-021306-4 .... p 1423 N94-19730
ISBN-9-03-692032-9 .... p 1494 N94-19698
ISBN-9-06-275887-8 .... p 1321 N94-19615 #
ISBN-9-29-092073-4 .... p 1328 N94-19622 #
ISBN-9-29-092081-5 .... p 1633 N94-19404 #
ISBN-90-369-2024-8 .... p 1481 N94-18142
ISBN-90-369-2026-4 .... p 1489 N94-18143
ISBN-90-369-2030-2 .... p 1496 N94-17923
ISBN-90-369-2031-0 .... p 1488 N94-17924
ISBN-90-370-0077-0 .... p 1504 N94-18080
ISBN-90-9005673-4 .... p 1452 N94-18079
ISBN-92-835-0714-2 .... p 1607 N94-18236 #
ISBN-92-835-0715-0 .... p 1305 N94-18415 #
ISBN-951-22-1282-X .... p 1520 N94-18117 #
ISBN-951-22-1344-3 .... p 1396 N94-18091 #
ISBN-951-22-1384-2 .... p 1372 N94-19052
ISBN-951-22-1407-5 .... p 1520 N94-18118 #
ISBN-951-22-1411-3 .... p 1384 N94-18116 #
ISBN-951-38-4053-0 .... p 1380 N94-19373 #
ISBN-951-38-4142-1 .... p 1365 N94-19374 #
ISBN-951-38-4144-8 .... p 1346 N94-17973 #
ISBN-951-38-4150-2 .... p 1444 N94-17974 #
ISBN-951-38-4175-8 .... p 1339 N94-17958 #
ISBN-951-38-4190-1 .... p 1452 N94-17959 #

ISI-RR-93-308 .... p 1615 N94-18461
ISI-RR-93-309 .... p 1616 N94-18641 #

ISI/RR-93-327 .... p 1522 N94-18680
ISI/RR-93-328 .... p 1516 N94-17732
ISI/RR-93-333 .... p 1616 N94-18570
ISI/RR-93-334 .... p 1521 N94-18290 *
ISI/RR-93-337 .... p 1557 N94-18640 #
ISI/RR-93-339 .... p 1612 N94-17745
ISI/RR-93-343 .... p 1615 N94-18464
ISI/RR-93-344 .... p 1541 N94-18759
ISI/RR-93-346 .... p 1610 N94-17746 #
ISI/RR-93-348 .... p 1541 N94-18463
ISI/RR-93-349 .... p 1541 N94-18462

ISL-R-109/91 .... p 1313 N94-19524

ITT-A/CD-33433A007 .... p 1393 N94-19793 #

IWM-T-8/93 .... p 1372 N94-18792 #

IZF-1992-B-10 .... p 1509 N94-19420
IZF-1992-B-9 .... p 1509 N94-19419
IZF-1992-B3 .... p 1504 N94-17966
IZF-1992-B5 .... p 1508 N94-17967
IZF-1993-B-1 .... p 1510 N94-19443
IZF-1993-B-2 .... p 1509 N94-19422
IZF-1993-B-3 .... p 1510 N94-19439
IZF-1993-B-4 .... p 1510 N94-19440

JAERI-M-92-092 .... p 1444 N94-18159
JAERI-M-92-109 .... p 1438 N94-18160
JAERI-M-92-134 .... p 1573 N94-18156
JAERI-M-92-173 .... p 1438 N94-18161
JAERI-M-92-176 .... p 1369 N94-18220 #
JAERI-M-92-181 .... p 1607 N94-18211 #
JAERI-M-92-189 .... p 1586 N94-18212 #
JAERI-M-92-214 .... p 1586 N94-18214
JAERI-M-93-004 .... p 1586 N94-18157

JINR-E-14-92-178 .... p 1359 N94-18218
JINR-E-2-91-544 .... p 1566 N94-18152
JINR-E-2-91-551 .... p 1561 N94-18153
JINR-E-2-91-579 .... p 1556 N94-18154
JINR-E-2-91-580 .... p 1608 N94-18252
JINR-E-2-92-171 .... p 1561 N94-18168
JINR-E-2-92-270 .... p 1593 N94-17748 #
JINR-E-2-92-272 .... p 1561 N94-18155
JINR-E-2-92-273 .... p 1549 N94-18200
JINR-E-2-92-274 .... p 1548 N94-18195
JINR-E-2-92-275 .... p 1548 N94-18196
JINR-E-2-92-276 .... p 1549 N94-18197
JINR-E-2-92-287 .... p 1608 N94-18267
JINR-E-5-92-392 .... p 1548 N94-18169

JINR-R-11-92-100 .... p 1548 N94-18175
JINR-R-11-92-126 .... p 1608 N94-18253
JINR-R-2-91-569 .... p 1608 N94-18268
JINR-R-2-92-302 .... p 1549 N94-18198

JPRS-UAC-93-004 .... p 1632 N94-19149 #
JPRS-UAC-93-005 .... p 1632 N94-19208 #
JPRS-UAC-93-006 .... p 1632 N94-19148 #
JPRS-UAC-93-007 .... p 1632 N94-19147 #

JPRS-UES-93-004 .... p 1461 N94-19209 #

JPRS-UMS-93-002 .... p 1339 N94-18833 #

JPRS-USP-93-004 .... p 1323 N94-19146 #

JTN-93-80460 .... p 1463 N94-19384 #

K-GAUO-00-030-102 .... p 1501 N94-17729

KCP-613-5080 .... p 1437 N94-18060 #

KEK-PROC-92-2 .... p 1630 N94-18219 #

KFK-5068 .... p 1494 N94-19616 #
KFK-5157 .... p 1391 N94-19617 #
KFK-5158 .... p 1631 N94-19504 #
KFK-5163 .... p 1631 N94-19505 #
KFK-5173 .... p 1631 N94-19506 #
KFK-5183 .... p 1479 N94-19507 #

KNMI-TR-146 .... p 1481 N94-18142
KNMI-TR-147 .... p 1489 N94-18143
KNMI-TR-149 .... p 1496 N94-17923
KNMI-TR-150 .... p 1488 N94-17924
KNMI-TR-151 .... p 1494 N94-19698

KSA-92-1 .... p 1318 N94-18733 #
KSA-92-2 .... p 1317 N94-18577

KU-FRL-831-7 .... p 1318 N94-19448 * #

L-17214 .... p 1368 N94-18075 * #
L-17284 .... p 1458 N94-19465 * #

LA-SUB-93-216 .... p 1338 N94-19128 #

LA-UR-93-1201 .... p 1358 N94-17875 #
LA-UR-93-1244 .... p 1526 N94-19205 #
LA-UR-93-1282 .... p 1594 N94-17874 #
LA-UR-93-1545 .... p 1376 N94-17813 #
LA-UR-93-1562 .... p 1609 N94-19187 #
LA-UR-93-1569 .... p 1517 N94-17812 #
LA-UR-93-1723 .... p 1408 N94-17728 #
LA-UR-93-1795 .... p 1582 N94-17727 #
LA-UR-93-1815 .... p 1376 N94-17751 #
LA-UR-93-1845 .... p 1573 N94-17726 #
LA-UR-93-1880 .... p 1434 N94-17709 #
LA-UR-93-1890 .... p 1379 N94-17725 #
LA-UR-93-1895 .... p 1435 N94-17724 #
LA-UR-93-1938 .... p 1457 N94-19207 #
LA-UR-93-1984 .... p 1519 N94-18097 #
LA-UR-93-1990 .... p 1488 N94-17715 #
LA-UR-93-2029 .... p 1592 N94-17714 #
LA-UR-93-2073 .... p 1485 N94-18894 #
LA-UR-93-2136 .... p 1436 N94-17865 #
LA-UR-93-2148 .... p 1582 N94-17713 #
LA-UR-93-2162 .... p 1594 N94-17907 #
LA-UR-93-2169 .... p 1368 N94-18096 #
LA-UR-93-2170 .... p 1593 N94-17744 #
LA-UR-93-2196 .... p 1352 N94-19240 #
LA-UR-93-2214 .... p 1457 N94-19279 #
LA-UR-93-2256 .... p 1451 N94-17906 #
LA-UR-93-2276 .... p 1451 N94-17864 #
LA-UR-93-2290 .... p 1362 N94-18809 #
LA-UR-93-2291 .... p 1455 N94-19033 #
LA-UR-93-2292 .... p 1595 N94-18162 #
LA-UR-93-2300 .... p 1551 N94-19343 #
LA-UR-93-2301 .... p 1551 N94-19342 #
LA-UR-93-2320 .... p 1593 N94-17754 #
LA-UR-93-2335 .... p 1419 N94-19025 #
LA-UR-93-2339 .... p 1359 N94-18114 #
LA-UR-93-2372 .... p 1562 N94-18810 #
LA-UR-93-2429 .... p 1570 N94-19120 #
LA-UR-93-2468 .... p 1563 N94-19151 #
LA-UR-93-2486 .... p 1570 N94-19125 #
LA-UR-93-2499 .... p 1372 N94-19202 #
LA-UR-93-2505 .... p 1423 N94-19604 #
LA-UR-93-2515 .... p 1417 N94-18831 #
LA-UR-93-2541 .... p 1627 N94-18857 #
LA-UR-93-2544 .... p 1432 N94-18828 #
LA-UR-93-2585 .... p 1535 N94-18930 #
LA-UR-93-2610 .... p 1571 N94-19278 #
LA-UR-93-2611 .... p 1521 N94-18271 #
LA-UR-93-2612 .... p 1410 N94-18270 #
LA-UR-93-2623 .... p 1322 N94-18890 #
LA-UR-93-2644 .... p 1570 N94-19126 #
LA-UR-93-2652 .... p 1571 N94-19259 #
LA-UR-93-2656 .... p 1380 N94-18818 #
LA-UR-93-2659 .... p 1567 N94-18269 #
LA-UR-93-2690 .... p 1600 N94-18969 #
LA-UR-93-2692 .... p 1404 N94-18805 #
LA-UR-93-2693 .... p 1599 N94-18804 #
LA-UR-93-2700 .... p 1587 N94-18803 #
LA-UR-93-2739 .... p 1605 N94-19735 #
LA-UR-93-2799 .... p 1361 N94-18802 #
LA-UR-93-2802 .... p 1460 N94-19603 #
LA-UR-93-2921 .... p 1478 N94-19272 #

LA-12536-MS .... p 1419 N94-19027 #
LA-12539-MS .... p 1476 N94-19104 #
LA-12545-MS .... p 1363 N94-19028 #
LA-12569 .... p 1360 N94-18501 #
LA-12617-MS .... p 1519 N94-18086 #

LAAS-92382 .... p 1532 N94-19713
LAAS-93190 .... p 1434 N94-19659
LAAS-93241 .... p 1544 N94-19360 #
LAAS-93242 .... p 1544 N94-19361 #

LBL-32852 .... p 1609 N94-18629 #
LBL-32857 .... p 1347 N94-18193 #
LBL-32858 .... p 1347 N94-18194 #
LBL-33027 .... p 1624 N94-18047 #
LBL-33167 .... p 1516 N94-17800 #
LBL-33256 .... p 1436 N94-17869 #
LBL-33268 .... p 1383 N94-18055 #
LBL-33270 .... p 1575 N94-19558 #
LBL-33271 .... p 1575 N94-19152 #
LBL-33285 .... p 1441 N94-19030 #
LBL-33286 .... p 1389 N94-19053 #
LBL-33289 .... p 1575 N94-18997 #
LBL-33442 .... p 1513 N94-18935 #
LBL-33444 .... p 1469 N94-19098 #
LBL-33445 .... p 1477 N94-19105 #
LBL-33540 .... p 1514 N94-17799 #
LBL-33700 .... p 1613 N94-17894 #
LBL-33725 .... p 1473 N94-18050 #
LBL-33800 .... p 1576 N94-19560 #
LBL-33803 .... p 1591 N94-19559 #
LBL-33805 .... p 1591 N94-19479 #
LBL-33814 .... p 1354 N94-19653 #
LBL-33984 .... p 1480 N94-17898 #
LBL-34028 .... p 1360 N94-18398 #
LBL-34030 .... p 1600 N94-18968 #
LBL-34070 .... p 1592 N94-17741 #
LBL-34091 .... p 1350 N94-19097 #
LBL-34124 .... p 1556 N94-17886 #
LBL-34143 .... p 1595 N94-18054 #
LBL-34171 .... p 1595 N94-17989 #
LBL-34189 .... p 1365 N94-19282 #
LBL-34240 .... p 1485 N94-18929 #
LBL-34241 .... p 1629 N94-19260 #
LBL-34251 .... p 1352 N94-19304 #
LBL-34291 .... p 1365 N94-19280 #
LBL-34297 .... p 1478 N94-19303 #

LBL-34372 .... p 1571 N94-19247 #
LBL-34386 .... p 1352 N94-19192 #
LBL-34400 .... p 1353 N94-19538 #

LC-91-60253 .... p 1514 N94-19478 #
LC-92-85596 .... p 1515 N94-19401 #

LMSC-F280196 .... p 1511 N94-18484 * #

LR-706 .... p 1319 N94-19796 #
LR-713 .... p 1323 N94-19372 #
LR-717 .... p 1344 N94-19666 #
LR-723 .... p 1313 N94-19667 #
LR-724 .... p 1423 N94-19668 #
LR-725 .... p 1461 N94-19669
LR-726 .... p 1335 N94-19614 #
LR-772 .... p 1321 N94-19615 #

LRI-786 .... p 1532 N94-19713

LRT-WE-9-FB-1-1992 .... p 1379 N94-19489 #
LRT-WE-9-FB-6-1992 .... p 1379 N94-19491
LRT-WE-9-FB-7-1992 .... p 1379 N94-19492 #

M-93-B0000032 .... p 1391 N94-19676 #

MAO-PR-92-01 .... p 1453 N94-18084 #

MATHS-REPT-A-182 .... p 1548 N94-18140 #
MATHS-REPT-A-183 .... p 1547 N94-18069 #
MATHS-REPT-A-185 .... p 1547 N94-17969 #
MATHS-REPT-A-186 .... p 1544 N94-19408 #
MATHS-REPT-A-187 .... p 1529 N94-19382 #
MATHS-REPT-A-189 .... p 1544 N94-19410 #
MATHS-REPT-A-190 .... p 1530 N94-19412 #

MBB-LME-202-S-PUB-502-A .... p 1319 N94-19496 #
MBB-LME-211-S-PUB-506 .... p 1421 N94-19497 #
MBB-LME-211-S-PUB-511-A .... p 1319 N94-19500 #

MEMO-COSOR-92-33 .... p 1543 N94-19324
MEMO-COSOR-92-34 .... p 1558 N94-19325
MEMO-COSOR-92-40 .... p 1558 N94-19327 #
MEMO-COSOR-92-41 .... p 1543 N94-19328
MEMO-COSOR-92-42 .... p 1543 N94-19329 * #
MEMO-COSOR-92-45 .... p 1528 N94-19330

MEMO-INF-92-75 .... p 1536 N94-19159 #
MEMO-INF-92-76 .... p 1536 N94-19160 #
MEMO-INF-92-77 .... p 1537 N94-19219 #
MEMO-INF-92-78 .... p 1526 N94-19220 #
MEMO-INF-92-79 .... p 1526 N94-19221 #
MEMO-INF-92-80 .... p 1526 N94-19222 #
MEMO-INF-92-84 .... p 1537 N94-19223 #
MEMO-INF-92-85 .... p 1526 N94-19224 #
MEMO-INF-92-86 .... p 1527 N94-19225 #
MEMO-INF-92-88 .... p 1558 N94-19385 #
MEMO-INF-92-89 .... p 1559 N94-19386 #
MEMO-INF-93-03 .... p 1543 N94-19226 #
MEMO-INF-93-04 .... p 1527 N94-19227 #
MEMO-INF-93-05 .... p 1558 N94-19228 #
MEMO-INF-93-06 .... p 1527 N94-19229 #
MEMO-INF-93-07 .... p 1390 N94-19230 #
MEMO-INF-93-08 .... p 1558 N94-19195 #
MEMO-INF-93-09 .... p 1526 N94-19196 #
MEMO-INF-93-10 .... p 1536 N94-19197 #
MEMO-INF-93-11 .... p 1537 N94-19198 #
MEMO-INF-93-12 .... p 1543 N94-19199 #
MEMO-INF-93-13 .... p 1526 N94-19200 #
MEMO-INF-93-14 .... p 1538 N94-19296 #
MEMO-INF-93-17 .... p 1527 N94-19261 #
MEMO-INF-93-19 .... p 1528 N94-19262 #
MEMO-INF-93-21 .... p 1537 N94-19264 #
MEMO-INF-93-22 .... p 1558 N94-19265 #
MEMO-INF-93-23 .... p 1390 N94-19267 #
MEMO-INF-93-24 .... p 1558 N94-19354 #

MEMO-1076 .... p 1553 N94-19605 #
MEMO-1076 .... p 1554 N94-19683 #

MHD-ITC-92-236 .... p 1589 N94-19055
MHD-ITC-93-017 .... p 1588 N94-18892 #
MHD-ITC-93-040 .... p 1588 N94-18978 #

MHR-19 .... p 1633 N94-19486 * #

MIAC-3 .... p 1374 N94-19532 #

MITT-7 .... p 1423 N94-19730

MPA-708 .... p 1621 N94-18141
MPA-905 .... p 1624 N94-17736

MPE-PREPRINT-223 .... p 1622 N94-19462 #
MPE-PREPRINT-231 .... p 1623 N94-19526
MPE-PREPRINT-237 .... p 1622 N94-19451
MPE-PREPRINT-239 .... p 1621 N94-19415
MPE-PREPRINT-240 .... p 1390 N94-19416
MPE-PREPRINT-241 .... p 1622 N94-19417
MPE-PREPRINT-247 .... p 1628 N94-19794 * #

MPE-242 .... p 1631 N94-19714
MPE-243 .... p 1628 N94-19519 #

MPIS-105/1993 .... p 1420 N94-19356 #
MPIS-15/1992 .... p 1422 N94-19520 #
MPIS-17/1992 .... p 1553 N94-19522 #
MPIS-22/1992 .... p 1422 N94-19509 #
MPIS-23/1992 .... p 1422 N94-19510 #
MPIS-25/1992 .... p 1422 N94-19525 #
MPIS-9/1992 .... p 1564 N94-19715

MPL-U-16/93 .... p 1498 N94-18662
MPL-U-22/93 .... p 1498 N94-18663 #

MRL-TN-620 .... p 1497 N94-18329 #
MRL-TN-642 .... p 1376 N94-18203 #

MT-CWR-093-019 .... p 1342 N94-18704 #

MTR-M-93B0000096-VOL-1 .... p 1316 N94-18384
MTR-M-93B0000096-VOL-2 .... p 1386 N94-18495 #

M93B0000076 .... p 1389 N94-18801

NAS 1.15:104779 .... p 1332 N94-18670 * #
NAS 1.15:104780 .... p 1332 N94-18669 * #
NAS 1.15:106307 .... p 1336 N94-17856 * #
NAS 1.15:106331 .... p 1333 N94-19313 * #
NAS 1.15:106387 .... p 1321 N94-19353 * #
NAS 1.15:106403 .... p 1313 N94-19484 * #
NAS 1.15:106407 .... p 1457 N94-19351 * #
NAS 1.15:106425 .... p 1587 N94-18861 * #
NAS 1.15:106432 .... p 1446 N94-19318 * #
NAS 1.15:108401-VOL-1E .... p 1626 N94-18619 * #
NAS 1.15:108401-VOL-2E .... p 1626 N94-18620 * #
NAS 1.15:108401-VOL-3E .... p 1626 N94-18621 * #
NAS 1.15:108401-VOL-4E .... p 1625 N94-18612 * #
NAS 1.15:108401-VOL-5E .... p 1625 N94-18613 * #
NAS 1.15:108401-VOL-6E .... p 1625 N94-18615 * #
NAS 1.15:108401-VOL-7E .... p 1625 N94-18618 * #
NAS 1.15:108750 .... p 1323 N94-18849 * #
NAS 1.15:108774 .... p 1612 N94-17737 * #
NAS 1.15:109000 .... p 1333 N94-17765 * #
NAS 1.15:109031 .... p 1321 N94-19316 * #
NAS 1.15:109239 .... p 1620 N94-18851 * #
NAS 1.15:109240 .... p 1621 N94-18850 * #
NAS 1.15:109256 .... p 1611 N94-19434 * #
NAS 1.15:109266 .... p 1410 N94-18545 * #
NAS 1.15:109380 .... p 1312 N94-19119 * #
NAS 1.15:109381 .... p 1633 N94-19486 * #
NAS 1.15:109718 .... p 1611 N94-19131 * #
NAS 1.15:4502 .... p 1502 N94-19210 * #
NAS 1.21:7011(381) .... p 1507 N94-19069 *
NAS 1.21:7011(382) .... p 1507 N94-18936 *
NAS 1.21:7037(296) .... p 1310 N94-19070 *
NAS 1.21:7037(297) .... p 1310 N94-18937 *
NAS 1.26:188479 .... p 1511 N94-18484 * #
NAS 1.26:189312 .... p 1621 N94-19288 * #
NAS 1.26:191134 .... p 1468 N94-18821 * #
NAS 1.26:191533 .... p 1551 N94-19315 * #
NAS 1.26:191534 .... p 1551 N94-19317 * #
NAS 1.26:191921 .... p 1622 N94-19421 * #
NAS 1.26:192419 .... p 1482 N94-18610 * #
NAS 1.26:192587 .... p 1331 N94-19366 * #
NAS 1.26:193185 .... p 1379 N94-17763 * #
NAS 1.26:193186 .... p 1591 N94-19441 * #
NAS 1.26:193344 .... p 1624 N94-17764 * #
NAS 1.26:193404 .... p 1630 N94-19437 * #
NAS 1.26:193546 .... p 1629 N94-19418 * #
NAS 1.26:193566 .... p 1491 N94-18602 * #
NAS 1.26:193615 .... p 1630 N94-18836 * #
NAS 1.26:193652 .... p 1624 N94-17843 * #
NAS 1.26:193668 .... p 1628 N94-17842 * #
NAS 1.26:193688 .... p 1617 N94-18839 * #
NAS 1.26:193706 .... p 1513 N94-19349 * #
NAS 1.26:193717 .... p 1335 N94-19371 * #
NAS 1.26:193760 .... p 1440 N94-18834 * #
NAS 1.26:193771 .... p 1627 N94-19093 * #
NAS 1.26:193778 .... p 1621 N94-18611 * #
NAS 1.26:193782 .... p 1571 N94-19236 * #
NAS 1.26:193807 .... p 1506 N94-18862 * #
NAS 1.26:193808 .... p 1456 N94-19095 * #
NAS 1.26:193810 .... p 1486 N94-19237 * #
NAS 1.26:193823 .... p 1380 N94-19423 * #
NAS 1.26:193837 .... p 1603 N94-19513 * #
NAS 1.26:193839 .... p 1407 N94-19642 * #
NAS 1.26:193873 .... p 1579 N94-18858 * #
NAS 1.26:193876 .... p 1332 N94-18820 * #
NAS 1.26:193877 .... p 1378 N94-19494 * #
NAS 1.26:194027 .... p 1621 N94-18855 * #
NAS 1.26:194069 .... p 1530 N94-19429 * #
NAS 1.26:194072 .... p 1487 N94-19428 * #
NAS 1.26:194081 .... p 1629 N94-19427 * #
NAS 1.26:194082 .... p 1628 N94-19425 * #
NAS 1.26:194166 .... p 1463 N94-19430 * #
NAS 1.26:194234 .... p 1315 N94-18852 * #
NAS 1.26:194280 .... p 1373 N94-19402 * #
NAS 1.26:194295 .... p 1629 N94-19094 * #
NAS 1.26:194300 .... p 1484 N94-18838 * #
NAS 1.26:194302 .... p 1487 N94-19432 * #
NAS 1.26:194303 .... p 1484 N94-18853 * #
NAS 1.26:194307 .... p 1622 N94-19431 * #
NAS 1.26:194309 .... p 1568 N94-18837 * #
NAS 1.26:194329 .... p 1618 N94-19256 * #
NAS 1.26:194406 .... p 1626 N94-18841 * #
NAS 1.26:194407 .... p 1312 N94-19433 * #
NAS 1.26:194411 .... p 1379 N94-18840 * #
NAS 1.26:194441 .... p 1434 N94-19314 * #
NAS 1.26:194478 .... p 1353 N94-19367 * #
NAS 1.26:194479 .... p 1312 N94-19388 * #
NAS 1.26:194483 .... p 1627 N94-19218 * #
NAS 1.26:194504 .... p 1339 N94-17766 * #
NAS 1.26:194520 .... p 1313 N94-19621 * #
NAS 1.26:194528 .... p 1441 N94-19394 * #
NAS 1.26:194529 .... p 1441 N94-19369 * #
NAS 1.26:194546 .... p 1487 N94-19397 * #
NAS 1.26:194562 .... p 1457 N94-19350 * #
NAS 1.26:194574 .... p 1338 N94-19706 * #
NAS 1.26:194580 .... p 1407 N94-19643 * #
NAS 1.26:194589 .... p 1397 N94-18337 * #
NAS 1.26:194598 .... p 1464 N94-19681 * #
NAS 1.26:194608 .... p 1318 N94-19448 * #
NAS 1.26:194620 .... p 1477 N94-19231 * #
NAS 1.26:194659 .... p 1470 N94-17762 * #
NAS 1.26:194674 .... p 1338 N94-19438 * #
NAS 1.26:194681 .... p 1543 N94-19329 * #
NAS 1.26:194682 .... p 1499 N94-18819 * #
NAS 1.26:194700 .... p 1628 N94-19794 * #
NAS 1.26:194742 .... p 1421 N94-19493 * #
NAS 1.26:4540 .... p 1417 N94-18843 * #
NAS 1.26:4554 .... p 1315 N94-18844 * #
NAS 1.55:3203 .... p 1449 N94-17827 * #
NAS 1.55:3223 .... p 1458 N94-19465 * #
NAS 1.55:3233 .... p 1323 N94-19162 * #
NAS 1.60:3391 .... p 1368 N94-18075 * #
NAS 1.61:1331 .... p 1532 N94-19761 * #

NASA-CP-3203 .... p 1449 N94-17827 * #
NASA-CP-3223 .... p 1458 N94-19465 * #
NASA-CP-3233 .... p 1323 N94-19162 * #

NASA-CR-188479 .... p 1511 N94-18484 * #
NASA-CR-189312 .... p 1621 N94-19288 * #
NASA-CR-191134 .... p 1468 N94-18821 * #
NASA-CR-191533 .... p 1551 N94-19315 * #
NASA-CR-191534 .... p 1551 N94-19317 * #
NASA-CR-191921 .... p 1622 N94-19421 * #
NASA-CR-192419 .... p 1482 N94-18610 * #
NASA-CR-192587 .... p 1331 N94-19366 * #
NASA-CR-193185 .... p 1379 N94-17763 * #
NASA-CR-193186 .... p 1591 N94-19441 * #
NASA-CR-193344 .... p 1624 N94-17764 * #
NASA-CR-193404 .... p 1630 N94-19437 * #
NASA-CR-193546 .... p 1629 N94-19418 * #
NASA-CR-193566 .... p 1491 N94-18602 * #
NASA-CR-193615 .... p 1630 N94-18836 * #
NASA-CR-193652 .... p 1624 N94-17843 * #
NASA-CR-193668 .... p 1628 N94-17842 * #
NASA-CR-193688 .... p 1617 N94-18839 * #
NASA-CR-193706 .... p 1513 N94-19349 * #
NASA-CR-193717 .... p 1335 N94-19371 * #
NASA-CR-193760 .... p 1440 N94-18834 * #
NASA-CR-193771 .... p 1627 N94-19093 * #
NASA-CR-193778 .... p 1621 N94-18611 * #
NASA-CR-193782 .... p 1571 N94-19236 * #
NASA-CR-193807 .... p 1506 N94-18862 * #
NASA-CR-193808 .... p 1456 N94-19095 * #
NASA-CR-193810 .... p 1486 N94-19237 * #
NASA-CR-193823 .... p 1380 N94-19423 * #
NASA-CR-193837 .... p 1603 N94-19513 * #
NASA-CR-193839 .... p 1407 N94-19642 * #
NASA-CR-193873 .... p 1579 N94-18858 * #
NASA-CR-193876 .... p 1332 N94-18820 * #
NASA-CR-193877 .... p 1378 N94-19494 * #
NASA-CR-194027 .... p 1621 N94-18855 * #
NASA-CR-194069 .... p 1530 N94-19429 * #
NASA-CR-194072 .... p 1487 N94-19428 * #
NASA-CR-194081 .... p 1629 N94-19427 * #
NASA-CR-194082 .... p 1628 N94-19425 * #
NASA-CR-194166 .... p 1463 N94-19430 * #
NASA-CR-194234 .... p 1315 N94-18852 * #
NASA-CR-194280 .... p 1373 N94-19402 * #
NASA-CR-194295 .... p 1629 N94-19094 * #
NASA-CR-194300 .... p 1484 N94-18838 * #
NASA-CR-194302 .... p 1487 N94-19432 * #
NASA-CR-194303 .... p 1484 N94-18853 * #
NASA-CR-194307 .... p 1622 N94-19431 * #

NASA-CR-194309 p 1568 N94-18837 * #
NASA-CR-194329 p 1618 N94-19256 * #
NASA-CR-194406 p 1626 N94-18841 * #
NASA-CR-194407 p 1312 N94-19433 * #
NASA-CR-194411 p 1379 N94-18840 * #
NASA-CR-194441 p 1434 N94-19314 * #
NASA-CR-194478 p 1353 N94-19367 * #
NASA-CR-194479 p 1312 N94-19388 * #
NASA-CR-194483 p 1627 N94-19218 * #
NASA-CR-194504 p 1339 N94-17766 * #
NASA-CR-194520 p 1313 N94-19621 * #
NASA-CR-194528 p 1441 N94-19394 * #
NASA-CR-194529 p 1441 N94-19369 * #
NASA-CR-194546 p 1487 N94-19397 * #
NASA-CR-194562 p 1457 N94-19350 * #
NASA-CR-194574 p 1338 N94-19706 * #
NASA-CR-194580 p 1407 N94-19643 * #
NASA-CR-194589 p 1397 N94-18337 * #
NASA-CR-194598 p 1464 N94-19681 * #
NASA-CR-194608 p 1318 N94-19448 * #
NASA-CR-194620 p 1477 N94-19231 * #
NASA-CR-194659 p 1470 N94-17762 * #
NASA-CR-194674 p 1338 N94-19438 * #
NASA-CR-194681 p 1543 N94-19329 * #
NASA-CR-194682 p 1499 N94-18819 * #
NASA-CR-194700 p 1628 N94-19794 * #
NASA-CR-194742 p 1421 N94-19493 * #
NASA-CR-4540 p 1417 N94-18843 * #
NASA-CR-4554 p 1315 N94-18844 * #

NASA-RP-1331 p 1532 N94-19761 * #

NASA-SP-7011(381) p 1507 N94-19069 *
NASA-SP-7011(382) p 1507 N94-18936 *
NASA-SP-7037(296) p 1310 N94-19070 *
NASA-SP-7037(297) p 1310 N94-18937 *

NASA-TM-104779 p 1332 N94-18670 * #
NASA-TM-104780 p 1332 N94-18669 * #
NASA-TM-106307 p 1336 N94-17856 * #
NASA-TM-106331 p 1333 N94-19313 * #
NASA-TM-106387 p 1321 N94-19353 * #
NASA-TM-106403 p 1313 N94-19484 * #
NASA-TM-106407 p 1457 N94-19351 * #
NASA-TM-106425 p 1587 N94-18861 * #
NASA-TM-106432 p 1446 N94-19318 * #
NASA-TM-108401-VOL-1E p 1626 N94-18619 * #
NASA-TM-108401-VOL-2E p 1626 N94-18620 * #
NASA-TM-108401-VOL-3E p 1626 N94-18621 * #
NASA-TM-108401-VOL-4E p 1625 N94-18612 * #
NASA-TM-108401-VOL-5E p 1625 N94-18613 * #
NASA-TM-108401-VOL-6E p 1625 N94-18615 * #
NASA-TM-108401-VOL-7E p 1625 N94-18618 * #
NASA-TM-108750 p 1323 N94-18849 * #
NASA-TM-108774 p 1612 N94-17737 * #
NASA-TM-109000 p 1333 N94-17765 * #
NASA-TM-109031 p 1321 N94-19316 * #
NASA-TM-109239 p 1620 N94-18851 * #
NASA-TM-109240 p 1621 N94-18850 * #
NASA-TM-109256 p 1611 N94-19434 * #
NASA-TM-109266 p 1410 N94-18545 * #
NASA-TM-109351 p 1332 N94-18920 *
NASA-TM-109352 p 1334 N94-18921 *
NASA-TM-109353 p 1334 N94-18922 *
NASA-TM-109354 p 1322 N94-18953 *
NASA-TM-109355 p 1332 N94-18954 *
NASA-TM-109356 p 1332 N94-18955 *
NASA-TM-109357 p 1333 N94-19071 *
NASA-TM-109359 p 1621 N94-19072 *
NASA-TM-109360 p 1336 N94-18956 *
NASA-TM-109361 p 1628 N94-18957 *
NASA-TM-109362 p 1628 N94-18958 *
NASA-TM-109363 p 1628 N94-18959 *
NASA-TM-109364 p 1323 N94-18979 *
NASA-TM-109365 p 1632 N94-18980 *
NASA-TM-109366 p 1323 N94-18981 *
NASA-TM-109367 p 1610 N94-18982 *
NASA-TM-109368 p 1476 N94-18960 *
NASA-TM-109369 p 1514 N94-18961 *
NASA-TM-109370 p 1318 N94-18962 *
NASA-TM-109371 p 1322 N94-18963 *
NASA-TM-109372 p 1312 N94-18964 *
NASA-TM-109373 p 1335 N94-18965 *
NASA-TM-109374 p 1629 N94-18966 *
NASA-TM-109375 p 1476 N94-18967 *
NASA-TM-109380 p 1312 N94-19119 * #
NASA-TM-109381 p 1633 N94-19486 * #
NASA-TM-109718 p 1611 N94-19131 * #
NASA-TM-4502 p 1502 N94-19210 * #

NASA-TP-3391 p 1368 N94-18075 * #

NASDA-CNT-930006-PT-2 p 1463 N94-19384 #

NAVY-CASE-74741 p 1408 N94-19763 #
NAVY-CASE-74904 p 1408 N94-19759 #

NAWC-WPNS-TP-8128 p 1531 N94-19590

NAWCADWAR-93023-70 p 1520 N94-18251 #

NAWCWPNS-TP-8145 p 1509 N94-18686 #

NBDL-93R001 p 1505 N94-18226

NCCOSC-TR-1604 p 1340 N94-18201

NCCOSC/RDT/E-1194-REV-1 p 1541 N94-18474

NCEER-92-0026 p 1540 N94-18125 #

NCS-TIB-92-10 p 1387 N94-18721

NDRL-3626 p 1566 N94-18165 #

NEDO-P-9212 p 1595 N94-18105 #

NIFS-DATA-17 p 1566 N94-18158

NIST-FIPS-PUB-177 p 1522 N94-18794

NLR-TP-91384-U p 1315 N94-17733
NLR-TP-91395-U p 1317 N94-17734

NMRI-93-55 p 1507 N94-19675 #

NOAA-TM-ERL-CMDL-5 p 1489 N94-18126 #

NOAA-TM-ERL-PMEL-99 p 1499 N94-19063 #

NONP-VT-94-198198 p 1332 N94-18920 *
NONP-VT-94-198199 p 1334 N94-18921 *
NONP-VT-94-198200 p 1334 N94-18922 *
NONP-VT-94-198201 p 1322 N94-18953 *
NONP-VT-94-198202 p 1332 N94-18954 *
NONP-VT-94-198203 p 1332 N94-18955 *
NONP-VT-94-198204 p 1333 N94-19071 *
NONP-VT-94-198206 p 1621 N94-19072 *
NONP-VT-94-198207 p 1336 N94-18956 *
NONP-VT-94-198208 p 1628 N94-18957 *
NONP-VT-94-198209 p 1628 N94-18958 *
NONP-VT-94-198210 p 1628 N94-18959 *
NONP-VT-94-198211 p 1323 N94-18979 *
NONP-VT-94-198212 p 1632 N94-18980 *
NONP-VT-94-198213 p 1323 N94-18981 *
NONP-VT-94-198214 p 1610 N94-18982 *
NONP-VT-94-198215 p 1476 N94-18960 *
NONP-VT-94-198216 p 1514 N94-18961 *
NONP-VT-94-198217 p 1318 N94-18962 *
NONP-VT-94-198218 p 1322 N94-18963 *
NONP-VT-94-198219 p 1312 N94-18964 *
NONP-VT-94-198220 p 1335 N94-18965 *
NONP-VT-94-198221 p 1629 N94-18966 *
NONP-VT-94-198222 p 1476 N94-18967 *

NPL-DITC-211/92 p 1518 N94-17930
NPL-DITC-213/92 p 1613 N94-17925
NPL-DITC-214/93 p 1517 N94-17917

NPL-DMM(A)-103 p 1451 N94-17929
NPL-DMM(A)-84 p 1451 N94-17899
NPL-DMM(A)-99 p 1346 N94-17900

NPS-EC-93-014 p 1564 N94-19750

NPS-ME-93-004 p 1454 N94-18661

NRAD-TR-1600 p 1384 N94-18216 #
NRAD-TR-1603 p 1430 N94-18537 #
NRAD-TR-1611 p 1500 N94-19762

NRAD/TD-2573 p 1483 N94-18712 #

NREL/CP-420-5466 p 1376 N94-18045 #

NREL/TP-411-5644 p 1470 N94-19760 #
NREL/TP-411-5654 p 1467 N94-18518 #
NREL/TP-413-5581 p 1464 N94-17731 #
NREL/TP-421-5264 p 1378 N94-18913 #
NREL/TP-421-5462 p 1377 N94-18617 #
NREL/TP-441-5730 p 1465 N94-17888 #
NREL/TP-442-5617 p 1615 N94-18334 #
NREL/TP-442-5619 p 1489 N94-18046 #
NREL/TP-451-5354 p 1467 N94-18483 #
NREL/TP-451-5652 p 1468 N94-18944 #

NRL-MR-7304 p 1370 N94-18280 #

NRL/FR/7142-93-9570 p 1500 N94-19786 #
NRL/FR/7181-93-9430 p 1563 N94-18678
NRL/FR/7441-92-9408 p 1462 N94-18677
NRL/FR/7441-92-9415 p 1462 N94-18679 #
NRL/FR/8105-93-9564 p 1337 N94-18574
NRL/FR/8121-93-9526 p 1335 N94-19787 #
NRL/FR/8121-93-9537 p 1334 N94-18149

NRL/JA/7321-93-0008 p 1500 N94-19745 #

NRL/MR/1003-93-7396 p 1541 N94-18773
NRL/MR/5309-93-7316 p 1385 N94-18291
NRL/MR/5520-93-7390 p 1393 N94-19779
NRL/MR/5521-93-7392 p 1432 N94-18681 #
NRL/MR/5530-93-7397 p 1512 N94-18774 #
NRL/MR/5531-93-7371 p 1392 N94-19748
NRL/MR/5554-93-7389 p 1388 N94-18722
NRL/MR/5581-93-7400 p 1535 N94-18772 #
NRL/MR/6790-93-7348 p 1586 N94-18148
NRL/MR/6790-93-7365 p 1438 N94-18460
NRL/MR/6790-93-7384 p 1440 N94-18771 #
NRL/MR/6793--93-7373 p 1439 N94-18576
NRL/MR/7234-93-7401 p 1499 N94-19609 #
NRL/MR/7322-93-7064 p 1499 N94-18727 #
NRL/MR/7332-93-7068 p 1499 N94-18903

NSB-92-196 p 1611 N94-19618 #

NSF-92-123 p 1531 N94-19619 #
NSF-92-332 p 1610 N94-19389 #
NSF-92-78 p 1633 N94-19620 #
NSF-93-24 p 1610 N94-19446 #

NSWCDD/TR-92/472 p 1332 N94-18321
NSWCDD/TR-93/108 p 1376 N94-17840 #
NSWCDD/TR-93/309 p 1317 N94-19572 #
NSWCDD/TR-93/351 p 1391 N94-19582 #

NTSB/AAR-93/05 p 1315 N94-19352 #

NUWC-NPT-TD-10184 p 1500 N94-19785 #

NUWC-NPT-TR-10223 p 1418 N94-18906 #

NWRA-CR-93-R096 p 1483 N94-18655 #
NWRA-CR-93-R103 p 1490 N94-18486 #

OCE/NRM/93-2 p 1475 N94-18885
OCE/NRM/93-3 p 1475 N94-18881

ODU/ICAM-93-103 p 1339 N94-17766 * #

ORNL-6749 p 1339 N94-19117 #
ORNL-6760 p 1467 N94-18478 #

ORNL/ATD-73 p 1355 N94-17752 #
ORNL/ATD-75 p 1340 N94-18087 #

ORNL/CDIAC-58 p 1471 N94-17774 #
ORNL/CDIAC-62 p 1475 N94-18832 #

ORNL/CON-368 p 1468 N94-18986 #

ORNL/M-2775 p 1374 N94-19561 #
ORNL/M-2881 p 1372 N94-18946 #
ORNL/M-2936-SUMM p 1474 N94-18523 #

ORNL/SUB-84-00216/2 p 1368 N94-18110
ORNL/SUB-90-SB047/2 p 1446 N94-19291 #

ORNL/TM-11607 p 1470 N94-17773 #
ORNL/TM-12181 p 1543 N94-19302 #
ORNL/TM-12199 p 1355 N94-17757 #
ORNL/TM-12252 p 1538 N94-19299 #
ORNL/TM-12316 p 1472 N94-17910 #
ORNL/TM-12318 p 1523 N94-18969 #
ORNL/TM-12327 p 1593 N94-17760 #
ORNL/TM-12341 p 1366 N94-19733 #
ORNL/TM-12343 p 1504 N94-17699 #
ORNL/TM-12347 p 1551 N94-19337 #
ORNL/TM-12367 p 1367 N94-17881 #
ORNL/TM-12388 p 1551 N94-19301 #
ORNL/TM-12408 p 1617 N94-19026 #
ORNL/TM-12410 p 1316 N94-19300 #
ORNL/TM-12447 p 1553 N94-19655 #

OUEL-1991/93 p 1530 N94-19412 #

PB93-169829 p 1611 N94-18090
PB93-187193 p 1396 N94-18091 #
PB93-187243 p 1384 N94-18116 #
PB93-187250 p 1520 N94-18117 #
PB93-187342 p 1555 N94-19708
PB93-187375 p 1520 N94-18118 #
PB93-187391 p 1614 N94-18119 #
PB93-187847 p 1607 N94-18120 #
PB93-187961 p 1508 N94-18121 #
PB93-188621 p 1540 N94-18125 #
PB93-190205 p 1489 N94-18126 #
PB93-190213 p 1499 N94-19063 #
PB93-190767 p 1476 N94-19064 #

PB93-191328 .... p 1476 N94-19065 #
PB93-191724 .... p 1619 N94-19709
PB93-191849 .... p 1560 N94-19710
PB93-191856 .... p 1524 N94-19066 #
PB93-191880 .... p 1489 N94-18143
PB93-191898 .... p 1481 N94-18142
PB93-191914 .... p 1509 N94-19348
PB93-191930 .... p 1559 N94-19555
PB93-191955 .... p 1560 N94-18990 #
PB93-191971 .... p 1550 N94-18991 #
PB93-191989 .... p 1553 N94-19556
PB93-191997 .... p 1553 N94-19557
PB93-194785 .... p 1549 N94-18948 #
PB93-194793 .... p 1547 N94-18077 #
PB93-194801 .... p 1547 N94-18078 #
PB93-194819 .... p 1475 N94-18949 #
PB93-195022 .... p 1380 N94-19254
PB93-195097 .... p 1452 N94-18079
PB93-195139 .... p 1504 N94-18080
PB93-195568 .... p 1553 N94-19605 #
PB93-195568 .... p 1554 N94-19683 #
PB93-195774 .... p 1456 N94-19061 #
PB93-195782 .... p 1343 N94-19281 #
PB93-195790 .... p 1380 N94-19322 #
PB93-195865 .... p 1389 N94-18950 #
PB93-195899 .... p 1347 N94-18081 #
PB93-195907 .... p 1389 N94-18951 #
PB93-195923 .... p 1363 N94-18952 #
PB93-195949 .... p 1419 N94-19068 #
PB93-195956 .... p 1618 N94-19067 #
PB93-195964 .... p 1372 N94-19052
PB93-197291 .... p 1558 N94-19323
PB93-197465 .... p 1543 N94-19324
PB93-197473 .... p 1558 N94-19325
PB93-197499 .... p 1543 N94-19326 #
PB93-197507 .... p 1558 N94-19327 #
PB93-197515 .... p 1543 N94-19328
PB93-197523 .... p 1543 N94-19329 * #
PB93-197556 .... p 1528 N94-19330
PB93-197739 .... p 1524 N94-19062 #
PB93-197754 .... p 1618 N94-19331
PB93-197838 .... p 1322 N94-19332 #
PB93-197846 .... p 1528 N94-19333 #
PB93-910406 .... p 1315 N94-19352 #

PEGASUS-PAPER-92-1 .... p 1536 N94-19159 #
PEGASUS-PAPER-92-2 .... p 1536 N94-19160 #
PEGASUS-PAPER-92-3 .... p 1537 N94-19219 #

PFC/RR-93-2 .... p 1366 N94-19546 #

PL-CP-93-1001-PT-4 .... p 1379 N94-18147

PL-TN-93-1025 .... p 1438 N94-18250 #

PL-TR-92-1075 .... p 1343 N94-18869
PL-TR-92-2245 .... p 1474 N94-18688 #
PL-TR-93-1007 .... p 1439 N94-18656 #
PL-TR-93-1010 .... p 1334 N94-18718 #
PL-TR-93-1011 .... p 1403 N94-18452
PL-TR-93-1024 .... p 1404 N94-18872 #
PL-TR-93-2058 .... p 1334 N94-18264
PL-TR-93-2069 .... p 1483 N94-18717 #
PL-TR-93-2100 .... p 1492 N94-18637 #
PL-TR-93-2102-PT-1 .... p 1484 N94-18868 #
PL-TR-93-2102-PT-2 .... p 1485 N94-18873 #
PL-TR-93-2111 .... p 1630 N94-18676 #
PL-TR-93-2118 .... p 1418 N94-18870
PL-TR-93-2122 .... p 1483 N94-18655 #
PL-TR-93-2124 .... p 1432 N94-18875 #
PL-TR-93-2126 .... p 1483 N94-18690 #
PL-TR-93-2147 .... p 1485 N94-18874 #
PL-TR-93-21502 .... p 1481 N94-18451
PL-TR-93-2152 .... p 1387 N94-18525 #
PL-TR-93-2163 .... p 1567 N94-18526 #
PL-TR-93-2183 .... p 1493 N94-18871 #

PML-1991-54 .... p 1452 N94-17941
PML-1992-12 .... p 1451 N94-17931
PML-1992-26 .... p 1458 N94-19444
PML-1992-69 .... p 1378 N94-19445
PML-1993-12 .... p 1619 N94-19453

PNL-SA-21235 .... p 1364 N94-19043 #
PNL-SA-21568 .... p 1470 N94-17749 #
PNL-SA-21637 .... p 1593 N94-17747 #
PNL-SA-21765 .... p 1501 N94-18051 #
PNL-SA-21790 .... p 1533 N94-17693
PNL-SA-21801 .... p 1369 N94-18233 #
PNL-SA-21852 .... p 1433 N94-19000 #
PNL-SA-21918 .... p 1489 N94-18052 #
PNL-SA-22018 .... p 1548 N94-18094 #
PNL-SA-22090 .... p 1493 N94-19051 #
PNL-SA-22371 .... p 1448 N94-19336 #
PNL-SA-22530 .... p 1461 N94-18107 #
PNL-SA-22609 .... p 1466 N94-18276 #
PNL-SA-22658 .... p 1471 N94-17821 #
PNL-SA-22659 .... p 1478 N94-19319 #
PNL-SA-22730 .... p 1599 N94-18816 #
PNL-SA-22777 .... p 1343 N94-19335 #

PNL-8744 .... p 1493 N94-19127 #

PNWD-2148-HEDR .... p 1488 N94-17895 #

PPL-2923 .... p 1473 N94-18101

PR-D15-0018-REV-A .... p 1579 N94-18858 * #

PREPRINT-732 .... p 1565 N94-17972 #

PSC-27 .... p 1586 N94-18213 #

PSL-93/49 .... p 1392 N94-19680 #

PSU/ARL-TR-93-10 .... p 1416 N94-18642 #

Q-144 .... p 1566 N94-18165 #

R-673 .... p 1456 N94-19061 #

R/D-6472-MS-01 .... p 1372 N94-18792 #
R/D-7107-CH-02 .... p 1338 N94-18703

RANA-92-13 .... p 1549 N94-18948 #
RANA-92-14 .... p 1547 N94-18077 #
RANA-92-15 .... p 1547 N94-18078 #

RAY/RD/S-4922 .... p 1403 N94-18667 #

REPT-141-05-FTR .... p 1541 N94-18790 #
REPT-724733-1 .... p 1384 N94-18187 #
REPT-91-NICI-05 .... p 1509 N94-19348
REPT-92-053 .... p 1443 N94-17937
REPT-92-070 .... p 1556 N94-17938
REPT-92-082 .... p 1613 N94-17939
REPT-92-083 .... p 1444 N94-17940
REPT-93-WA/NCA-26 .... p 1313 N94-19484 * #
REPT-93-001 .... p 1519 N94-17975
REPT-93-006 .... p 1383 N94-17932
REPT-93-007 .... p 1565 N94-17933
REPT-93-012 .... p 1562 N94-17934
REPT-93-013 .... p 1383 N94-17935
REPT-93-014 .... p 1613 N94-17936
REPT-93-015 .... p 1540 N94-17922
REPT-93-018 .... p 1518 N94-17926
REPT-93-020 .... p 1518 N94-17927
REPT-93-022 .... p 1547 N94-17928
REPT-93-023 .... p 1518 N94-17960
REPT-93-025 .... p 1547 N94-17961
REPT-93-026 .... p 1614 N94-18144
REPT-93-027 .... p 1547 N94-17962
REPT-93-028 .... p 1520 N94-18145
REPT-93-030 .... p 1520 N94-18138
REPT-93-034 .... p 1520 N94-18136
REPT-93-044 .... p 1539 N94-17916
REPT-93-08-PT-2 .... p 1620 N94-19795 #
REPT-93-09 .... p 1563 N94-19083 #
REPT-93-10 .... p 1524 N94-19084 #
REPT-93-11 .... p 1542 N94-19085 #
REPT-93-12 .... p 1550 N94-19086 #
REPT-93-13 .... p 1419 N94-19087 #
REPT-93-14 .... p 1550 N94-19088 #
REPT-93-15 .... p 1524 N94-19089 #
REPT-93-16 .... p 1486 N94-19081 #
REPT-93-17 .... p 1550 N94-19082 #
REPT-93-18 .... p 1488 N94-19644
REPT-93-19 .... p 1557 N94-19090 #
REPT-93-20 .... p 1542 N94-19091 #
REPT-93-21 .... p 1542 N94-19092 #
REPT-93-22 .... p 1558 N94-19137 #
REPT-93-23 .... p 1542 N94-19138 #
REPT-93-24 .... p 1420 N94-19139 #
REPT-93-25 .... p 1486 N94-19140 #
REPT-93-26 .... p 1550 N94-19141 #
REPT-93-27 .... p 1542 N94-19142 #
REPT-93-2881-06 .... p 1462 N94-18631 #
REPT-93-28 .... p 1525 N94-19143 #
REPT-93-29 .... p 1420 N94-19144 #
REPT-93-30 .... p 1550 N94-19153 #
REPT-93-31 .... p 1423 N94-19645
REPT-93-32 .... p 1551 N94-19285 #
REPT-93-33 .... p 1543 N94-19286 #
REPT-93-34 .... p 1525 N94-19154 #
REPT-93-35 .... p 1525 N94-19155 #
REPT-93-36 .... p 1525 N94-19156 #
REPT-93-37 .... p 1611 N94-19157 #
REPT-93-38 .... p 1611 N94-19158 #
REPT-93-3 .... p 1476 N94-19064 #
REPT-93B00119 .... p 1323 N94-19162 * #
REPT-94B00031 .... p 1532 N94-19761 * #

RFP-4739 .... p 1362 N94-18917 #

RIVM-222901004 .... p 1475 N94-18949 #

RL-TR-92-159 .... p 1387 N94-18666 #
RL-TR-92-333 .... p 1579 N94-18668 #
RL-TR-93-105 .... p 1578 N94-18457
RL-TR-93-109 .... p 1354 N94-19755
RL-TR-93-113 .... p 1535 N94-18865
RL-TR-93-114 .... p 1535 N94-18866
RL-TR-93-115 .... p 1577 N94-18302
RL-TR-93-123 .... p 1542 N94-18887
RL-TR-93-131 .... p 1434 N94-19791 #
RL-TR-93-134 .... p 1393 N94-19793 #
RL-TR-93-139-VOL-1 .... p 1393 N94-19752
RL-TR-93-139-VOL-2 .... p 1393 N94-19753
RL-TR-93-145 .... p 1581 N94-19602 #
RL-TR-93-149 .... p 1581 N94-19601 #
RL-TR-93-154 .... p 1391 N94-19587 #
RL-TR-93-164 .... p 1539 N94-19790 #

RR-892-M .... p 1532 N94-19712 #
RR-893-M .... p 1556 N94-19731 #
RR-905-I .... p 1532 N94-19713
RR-910-I .... p 1552 N94-19392 #
RR-911-I .... p 1552 N94-19393 #
RR-914-I .... p 1529 N94-19396
RR-915-I .... p 1552 N94-19395 #

RSG-308-84 .... p 1323 N94-19581
RSG-308-93 .... p 1323 N94-19581

RXR-930501 .... p 1432 N94-18875 #

S-739-VOL-1 .... p 1332 N94-18670 * #
S-740 .... p 1332 N94-18669 * #

SAAO-17 .... p 1623 N94-19657 #

SAIC-93/1152 .... p 1416 N94-18671 #

SAIC/CSS-STR-C93-03 .... p 1481 N94-18297

SAND-90-0566-REV .... p 1614 N94-18164 #
SAND-91-2764 .... p 1592 N94-17742 #
SAND-92-0229 .... p 1378 N94-19042 #
SAND-92-0535C .... p 1373 N94-19308 #
SAND-92-1094 .... p 1580 N94-18970
SAND-92-1381 .... p 1467 N94-18520 #
SAND-92-1832 .... p 1373 N94-19271 #
SAND-92-1864 .... p 1474 N94-18521 #
SAND-92-2117C .... p 1423 N94-17700 #
SAND-92-2131 .... p 1469 N94-19109 #
SAND-92-2141 .... p 1455 N94-19039 #
SAND-92-2221C .... p 1573 N94-17698
SAND-92-2253 .... p 1469 N94-19040 #
SAND-92-2257C .... p 1405 N94-19079 #
SAND-92-2259 .... p 1395 N94-17783 #
SAND-92-2487C .... p 1372 N94-19059 #
SAND-92-2521 .... p 1527 N94-19245 #
SAND-92-2701C .... p 1345 N94-17820 #
SAND-92-2759C .... p 1442 N94-19563 #
SAND-92-2788 .... p 1394 N94-17780 #
SAND-92-2808C .... p 1464 N94-17787 #
SAND-92-2825C .... p 1455 N94-18829 #
SAND-92-2844 .... p 1433 N94-19243 #
SAND-92-2869C .... p 1464 N94-17798 #
SAND-92-7007 .... p 1466 N94-18335 #
SAND-92-7331 .... p 1405 N94-19035 #
SAND-93-0082C .... p 1358 N94-18003 #
SAND-93-0145C .... p 1404 N94-18827 #
SAND-93-0183C .... p 1439 N94-18522 #
SAND-93-0186C .... p 1419 N94-19058 #
SAND-93-0208 .... p 1311 N94-18275 #
SAND-93-0225C .... p 1357 N94-17862 #
SAND-93-0242C .... p 1523 N94-18926 #
SAND-93-0244C .... p 1364 N94-19080 #
SAND-93-0251C .... p 1447 N94-18128 #
SAND-93-0376C .... p 1424 N94-17999 #
SAND-93-0388C .... p 1373 N94-19338 #
SAND-93-0390C .... p 1358 N94-18100 #
SAND-93-0391C .... p 1469 N94-19036 #
SAND-93-0424C .... p 1465 N94-18001 #
SAND-93-0425C .... p 1429 N94-18102 #
SAND-93-0427C .... p 1362 N94-18919 #
SAND-93-0457C .... p 1627 N94-19339 #
SAND-93-0529 .... p 1337 N94-18830 #
SAND-93-0541C .... p 1371 N94-18519 #
SAND-93-0587 .... p 1618 N94-19099 #
SAND-93-0644 .... p 1580 N94-19113 #
SAND-93-0743C .... p 1602 N94-19340 #
SAND-93-0763 .... p 1364 N94-19100 #
SAND-93-0779C .... p 1382 N94-17861 #
SAND-93-0809C .... p 1603 N94-19347 #
SAND-93-0875C .... p 1531 N94-19562 #
SAND-93-0882C .... p 1433 N94-19111 #

SAND-93-0916C .... p 1418 N94-18918 #
SAND-93-0917C .... p 1537 N94-19249 #
SAND-93-0934C .... p 1536 N94-19188 #
SAND-93-0935C .... p 1537 N94-19206 #
SAND-93-0936C .... p 1536 N94-19161 #
SAND-93-0976C .... p 1385 N94-18232 #
SAND-93-1063C .... p 1359 N94-18127 #
SAND-93-1083C .... p 1405 N94-18928 #
SAND-93-1181C .... p 1452 N94-17995 #
SAND-93-1206 .... p 1618 N94-19101 #
SAND-93-1207C .... p 1466 N94-18208 #
SAND-93-1215C .... p 1519 N94-18002 #
SAND-93-1263C .... p 1420 N94-19345 #
SAND-93-1278C .... p 1518 N94-17944 #
SAND-93-1283C .... p 1542 N94-19007 #
SAND-93-1327C .... p 1518 N94-17943 #
SAND-93-1349C .... p 1516 N94-17786 #
SAND-93-1373 .... p 1525 N94-19102 #
SAND-93-1388 .... p 1485 N94-19001 #
SAND-93-1389 .... p 1485 N94-19002 #
SAND-93-1392C .... p 1528 N94-19344 #
SAND-93-1393C .... p 1546 N94-17885 #
SAND-93-1414C .... p 1370 N94-18477 #
SAND-93-1455C .... p 1357 N94-17819 #
SAND-93-1491C .... p 1576 N94-18000 #
SAND-93-1495C .... p 1525 N94-19124 #
SAND-93-1518 .... p 1633 N94-19537 #
SAND-93-1539C .... p 1382 N94-17806 #
SAND-93-1597C .... p 1446 N94-19547 #
SAND-93-1598C .... p 1523 N94-19006 #
SAND-93-1661C .... p 1456 N94-19078 #
SAND-93-1672 .... p 1381 N94-19480 #
SAND-93-1701C .... p 1617 N94-18984 #
SAND-93-1773C .... p 1405 N94-19112 #
SAND-93-1990C .... p 1515 N94-19535 #
SAND-93-7000 .... p 1468 N94-19014 #
SAND-93-7031 .... p 1475 N94-18817 #
SAND-93-7044 .... p 1456 N94-19060 #
SAND-93-7049 .... p 1468 N94-19015 #
SAND-93-7051 .... p 1468 N94-19016 #
SAND-93-7055 .... p 1467 N94-18409 #
SAND-93-8233 .... p 1569 N94-18985 #
SAND-93-8503 .... p 1346 N94-17997 #

SC-71040-FR .... p 1598 N94-18633 #

SC71034.FRD .... p 1341 N94-18692 #
SC71041 .... p 1596 N94-18320

SER-GEOPHYS-175 .... p 1482 N94-18622 #

SESC-USPB-02-93 .... p 1481 N94-18467 #

SLAC/SSRL-0037 .... p 1347 N94-18059 #

SLCET-TR-91-26-REV-1 .... p 1403 N94-18471 #

SMC-TR-93-43 .... p 1596 N94-18316
SMC-TR-93-46 .... p 1385 N94-18301 #
SMC-TR-93-47 .... p 1385 N94-18287 #

SMU-G-11 .... p 1481 N94-18485 #

SM91-12 .... p 1456 N94-19130 #

SP-RAPP-1993:05 .... p 1322 N94-19332 #
SP-RAPP-1993:08 .... p 1528 N94-19333 #

SPC-93111-CMC .... p 1620 N94-19777 #

SR-1324-APP .... p 1455 N94-18716
SR-1 .... p 1492 N94-18637 #
SR-1 .... p 1483 N94-18690 #
SR-2 .... p 1630 N94-18676 #
SR-5 .... p 1387 N94-18525 #

SRI-MP-93-137 .... p 1442 N94-19788 #

SSCL-PREPRINT-488 .... p 1381 N94-19540 #

SSCL-578-REV-1 .... p 1574 N94-18994 #
SSCL-628 .... p 1539 N94-19734 #

SSRL-M-420 .... p 1347 N94-18059 #

STK-206-VOL-2 .... p 1462 N94-18729

SU-CLASSIC-93-32 .... p 1549 N94-18863 #

SU-SLAC-420 .... p 1347 N94-18059 #

SU-SOL-92-8 .... p 1516 N94-17701 #

SU-TR-470 .... p 1557 N94-18516
SU-TR-471 .... p 1557 N94-18694
SU-TR-472 .... p 1557 N94-18517 #

SWRI-06-4601 .... p 1366 N94-19673 #

TD-91-3972 .... p 1434 N94-19797
TD-92-0812 .... p 1393 N94-19798
TD-92-1518 .... p 1458 N94-19444
TD-92-1754 .... p 1441 N94-19426
TD-92-1906 .... p 1618 N94-19450
TD-92-2292 .... p 1509 N94-19419
TD-92-2293 .... p 1509 N94-19420
TD-92-3197 .... p 1510 N94-19443
TD-92-3202 .... p 1509 N94-19422
TD-92-3203 .... p 1510 N94-19439
TD-92-3675 .... p 1390 N94-19447
TD-92-3677 .... p 1390 N94-19449
TD-93-0292 .... p 1618 N94-19452
TD-93-0295 .... p 1580 N94-19424

TD91-2526 .... p 1451 N94-17931
TD91-2834 .... p 1452 N94-17941
TD91-3274 .... p 1619 N94-19454
TD92-0258 .... p 1504 N94-17966
TD92-1443 .... p 1383 N94-18070
TD92-1448 .... p 1518 N94-17965
TD92-2278 .... p 1508 N94-17967
TD92-2413 .... p 1378 N94-19445
TD92-3313 .... p 1619 N94-19457
TD92-3314 .... p 1580 N94-19455
TD92-3702 .... p 1619 N94-19453
TD93-0304 .... p 1544 N94-19458
TD93-0371 .... p 1510 N94-19440

TEC-R-196 .... p 1462 N94-18309

TIOS-92-33 .... p 1558 N94-19385 #
TIOS-92-34 .... p 1559 N94-19386 #
TIOS-93-01 .... p 1543 N94-19226 #
TIOS-93-02 .... p 1527 N94-19227 #
TIOS-93-03 .... p 1558 N94-19228 #
TIOS-93-04 .... p 1390 N94-19230 #
TIOS-93-05 .... p 1558 N94-19195 #
TIOS-93-06 .... p 1526 N94-19196 #
TIOS-93-07 .... p 1536 N94-19197 #
TIOS-93-09 .... p 1527 N94-19261 #
TIOS-93-12 .... p 1537 N94-19264 #
TIOS-93-13 .... p 1558 N94-19265 #
TIOS-93-14 .... p 1558 N94-19354 #

TKO-B94 .... p 1555 N94-19708

TKO-C58 .... p 1614 N94-18119 #

TR-0091(6940-05)-9 .... p 1596 N94-18316
TR-1/94 .... p 1498 N94-18665 #
TR-12 .... p 1360 N94-18386 #
TR-13 .... p 1596 N94-18388 #
TR-14 .... p 1453 N94-18387 #
TR-2/93 .... p 1497 N94-18393 #
TR-21-ONR .... p 1438 N94-18258 #
TR-33 .... p 1360 N94-18687 #
TR-3 .... p 1594 N94-17876 #
TR-4-ONR .... p 1370 N94-18403 #
TR-409 .... p 1538 N94-19512 #
TR-446 .... p 1610 N94-19485 #
TR-450 .... p 1530 N94-19483 #
TR-464 .... p 1530 N94-19482 #
TR-471 .... p 1561 N94-19481 #
TR-474 .... p 1559 N94-19511 #
TR-478 .... p 1531 N94-19508 #
TR-52 .... p 1338 N94-18314
TR-5 .... p 1546 N94-17825 #
TR-86 .... p 1348 N94-18256 #
TR-92(2930)-5 .... p 1385 N94-18301 #
TR-93(3935)-5 .... p 1377 N94-18758
TR-93(3940)-6 .... p 1385 N94-18287 #

TW-92-09 .... p 1560 N94-18990 #
TW-92-13 .... p 1559 N94-19555

U-OF-IOWA-93-7 .... p 1629 N94-19094 * #

UCB-PTH-93/21 .... p 1485 N94-18929 #

UCB/ERL-90/4 .... p 1403 N94-18638

UCLA-ENG-93-48 .... p 1407 N94-19584 #

UCRL-CR-103699 .... p 1604 N94-19565 #
UCRL-CR-112568 .... p 1587 N94-18505 #
UCRL-CR-112610 .... p 1441 N94-19307 #
UCRL-CR-113135 .... p 1589 N94-19037 #
UCRL-CR-113452 .... p 1363 N94-18939 #
UCRL-CR-113904 .... p 1422 N94-19515 #
UCRL-CR-114138 .... p 1565 N94-17850 #
UCRL-CR-114509 .... p 1381 N94-19539 #

UCRL-ID-111216 .... p 1430 N94-18235 #
UCRL-ID-111476 .... p 1452 N94-18049 #
UCRL-ID-111589 .... p 1395 N94-17872
UCRL-ID-112131 .... p 1333 N94-17782 #
UCRL-ID-112219 .... p 1584 N94-17988 #
UCRL-ID-112584 .... p 1517 N94-17867
UCRL-ID-112943 .... p 1350 N94-18987 #
UCRL-ID-113275 .... p 1378 N94-19242 #
UCRL-ID-113516 .... p 1463 N94-19003 #
UCRL-ID-113563 .... p 1377 N94-18893 #
UCRL-ID-113713 .... p 1433 N94-19004 #
UCRL-ID-113714 .... p 1347 N94-18092 #
UCRL-ID-113761 .... p 1390 N94-19114 #
UCRL-ID-113953-REV-1 .... p 1563 N94-19270 #
UCRL-ID-113953 .... p 1562 N94-17873
UCRL-ID-114054 .... p 1476 N94-19038 #
UCRL-ID-114222 .... p 1473 N94-18005 #
UCRL-ID-114259 .... p 1390 N94-19306 #
UCRL-ID-114993-APP-B .... p 1418 N94-18878

UCRL-JC-109884 .... p 1590 N94-19289 #
UCRL-JC-110128 .... p 1355 N94-17711 #
UCRL-JC-110927 .... p 1436 N94-17868
UCRL-JC-110987 .... p 1335 N94-18942 #
UCRL-JC-111151 .... p 1435 N94-17855 #
UCRL-JC-111263 .... p 1488 N94-17942 #
UCRL-JC-111378 .... p 1435 N94-17723 #
UCRL-JC-111481 .... p 1384 N94-18210 #
UCRL-JC-111560 .... p 1340 N94-18113 #
UCRL-JC-111577 .... p 1453 N94-18108 #
UCRL-JC-111591 .... p 1601 N94-19049 #
UCRL-JC-111666 .... p 1441 N94-19294 #
UCRL-JC-111835 .... p 1489 N94-18053 #
UCRL-JC-111856 .... p 1580 N94-19268 #
UCRL-JC-111934 .... p 1435 N94-17759 #
UCRL-JC-111975 .... p 1376 N94-18095 #
UCRL-JC-112020 .... p 1517 N94-17911 #
UCRL-JC-112157 .... p 1382 N94-17909 #
UCRL-JC-112167 .... p 1587 N94-18274 #
UCRL-JC-112182 .... p 1352 N94-19266 #
UCRL-JC-112189 .... p 1595 N94-17992 #
UCRL-JC-112216 .... p 1335 N94-19275 #
UCRL-JC-112225 .... p 1565 N94-17797 #
UCRL-JC-112246 .... p 1588 N94-19034 #
UCRL-JC-112344 .... p 1575 N94-19107 #
UCRL-JC-112347 .... p 1365 N94-19263 #
UCRL-JC-112377 .... p 1575 N94-19106 #
UCRL-JC-112422 .... p 1394 N94-17770 #
UCRL-JC-112438 .... p 1358 N94-18111 #
UCRL-JC-112511 .... p 1575 N94-18996 #
UCRL-JC-112573 .... p 1519 N94-18072 #
UCRL-JC-112604 .... p 1448 N94-19252 #
UCRL-JC-112652 .... p 1395 N94-17849 #
UCRL-JC-112686 .... p 1436 N94-17996 #
UCRL-JC-112762 .... p 1590 N94-19269
UCRL-JC-112824 .... p 1369 N94-18112 #
UCRL-JC-112831 .... p 1357 N94-17860 #
UCRL-JC-112934 .... p 1556 N94-18073 #
UCRL-JC-112950 .... p 1585 N94-18115 #
UCRL-JC-113033 .... p 1590 N94-19290 #
UCRL-JC-113039 .... p 1494 N94-19298 #
UCRL-JC-113138 .... p 1396 N94-17991 #
UCRL-JC-113151 .... p 1460 N94-19543 #
UCRL-JC-113165 .... p 1585 N94-18129 #
UCRL-JC-113173 .... p 1624 N94-17897
UCRL-JC-113177 .... p 1441 N94-19251 #
UCRL-JC-113179 .... p 1437 N94-18131 #
UCRL-JC-113221 .... p 1437 N94-18093 #
UCRL-JC-113264 .... p 1589 N94-19073 #
UCRL-JC-113265 .... p 1589 N94-19074 #
UCRL-JC-113269 .... p 1489 N94-18132 #
UCRL-JC-113274 .... p 1520 N94-18133 #
UCRL-JC-113302 .... p 1584 N94-17993 #
UCRL-JC-113310 .... p 1488 N94-17758 #
UCRL-JC-113319 .... p 1537 N94-19253 #
UCRL-JC-113355 .... p 1383 N94-17994 #
UCRL-JC-113469 .... p 1437 N94-18083 #
UCRL-JC-113485 .... p 1465 N94-17853 #
UCRL-JC-113498 .... p 1582 N94-17708 #
UCRL-JC-113527 .... p 1531 N94-19548 #
UCRL-JC-113547 .... p 1559 N94-19549 #
UCRL-JC-113579 .... p 1440 N94-18889 #
UCRL-JC-113607 .... p 1594 N94-17896
UCRL-JC-113619 .... p 1527 N94-19238 #
UCRL-JC-113625 .... p 1418 N94-18888 #
UCRL-JC-113626 .... p 1520 N94-18130 #
UCRL-JC-113639 .... p 1528 N94-19276 #
UCRL-JC-113642 .... p 1584 N94-17990 #
UCRL-JC-113645 .... p 1585 N94-18082 #
UCRL-JC-113650 .... p 1395 N94-17882
UCRL-JC-113651 .... p 1405 N94-18941 #
UCRL-JC-113747 .... p 1627 N94-19284 #
UCRL-JC-113768 .... p 1572 N94-19283 #
UCRL-JC-113814 .... p 1580 N94-18931 #
UCRL-JC-113854 .... p 1380 N94-18710 #
UCRL-JC-113858 .... p 1536 N94-19115 #
UCRL-JC-113874 .... p 1523 N94-18943 #

UCRL-JC-114014 p 1381 N94-19544 #
UCRL-JC-114015 p 1572 N94-19545 #
UCRL-JC-114098 p 1480 N94-19732 #
UCRL-JC-114326 p 1571 N94-19201 #
UCRL-JC-114422 p 1418 N94-18995 #
UCRL-JC-114531 p 1437 N94-18134 #
UCRL-JC-114801 p 1422 N94-19568 #

UCRL-LR-112757 p 1394 N94-17755 #
UCRL-LR-113559 p 1516 N94-17740 #
UCRL-LR-113984 p 1591 N94-19311 #
UCRL-LR-114552 p 1442 N94-19554 #

UCRL-MA-112315 p 1517 N94-17914 #
UCRL-MA-113603 p 1524 N94-19048 #
UCRL-MA-114027 p 1495 N94-17779 #

UCRL-53809-92 p 1627 N94-19077 #
UCRL-53868-92 p 1632 N94-18856 #

UDR-TR-92-120 p 1453 N94-18382 #

UIUCDCS-R-92-1782 p 1516 N94-17800 #

UM-P-92/102 p 1602 N94-19277

UMR-FDB-30 p 1367 N94-17878 #

US-PATENT-APPL-SN-023834 p 1368 N94-17982 #
US-PATENT-APPL-SN-037880 p 1424 N94-17904 #
US-PATENT-APPL-SN-038369 p 1368 N94-17905 #
US-PATENT-APPL-SN-045143 p 1563 N94-18734 #
US-PATENT-APPL-SN-053267 p 1371 N94-18529 #
US-PATENT-APPL-SN-058019 p 1382 N94-17902 #
US-PATENT-APPL-SN-056084 p 1580 N94-18947 #
US-PATENT-APPL-SN-064321 p 1395 N94-17903
US-PATENT-APPL-SN-076062 p 1512 N94-18730 #
US-PATENT-APPL-SN-076135 p 1408 N94-19759 #
US-PATENT-APPL-SN-077806 p 1432 N94-18731 #
US-PATENT-APPL-SN-083231 p 1408 N94-19763 #
US-PATENT-APPL-SN-083580 p 1430 N94-18530 #
US-PATENT-APPL-SN-083953 p 1579 N94-18743 #
US-PATENT-APPL-SN-099638 p 1440 N94-18747 #
US-PATENT-APPL-SN-099640 p 1371 N94-18746 #
US-PATENT-APPL-SN-623865 p 1367 N94-17706
US-PATENT-APPL-SN-676507 p 1394 N94-17718
US-PATENT-APPL-SN-701406 p 1367 N94-17719
US-PATENT-APPL-SN-759296 p 1394 N94-17707
US-PATENT-APPL-SN-783660 p 1424 N94-17717
US-PATENT-APPL-SN-786665 p 1394 N94-17703
US-PATENT-APPL-SN-830206 p 1317 N94-17704
US-PATENT-APPL-SN-844276 p 1339 N94-18074
US-PATENT-APPL-SN-888096 p 1443 N94-17705
US-PATENT-APPL-SN-905705 p 1576 N94-17716
US-PATENT-APPL-SN-989295 p 1396 N94-18062

US-PATENT-CLASS-33-773 p 1424 N94-17717
US-PATENT-CLASS-359-180 p 1394 N94-17707
US-PATENT-CLASS-524-204 p 1367 N94-17719

US-PATENT-5,166,009 p 1394 N94-17718
US-PATENT-5,208,842 p 1394 N94-17703
US-PATENT-5,210,807 p 1576 N94-17716
US-PATENT-5,214,525 p 1394 N94-17707
US-PATENT-5,220,731 p 1424 N94-17717
US-PATENT-5,222,548 p 1443 N94-17705
US-PATENT-5,225,285 p 1367 N94-17706
US-PATENT-5,226,618 p 1317 N94-17704
US-PATENT-5,229,665 p 1396 N94-18062
US-PATENT-5,236,646 p 1339 N94-18074

USAARL-93-23 p 1445 N94-18778
USAARL-93-24 p 1505 N94-18289 #
USAARL-93-25 p 1504 N94-17824 #
USAARL-93-26 p 1511 N94-18296 #

USAATCOM-TR-93-D-2 p 1512 N94-18765 #

USABRDL-TR-9303 p 1505 N94-18392

USAFETAC/DS-93/031-1 p 1490 N94-18303
USAFETAC/DS-93/031-2 p 1493 N94-18732 #

USAFETAC/PR-93/004 p 1490 N94-18281 #

USAFETAC/TN-93/004 p 1493 N94-18883

USARIEM-T-14-93 p 1512 N94-18882

USARL-MR-122 p 1446 N94-19318 * #

USGS/G-1915 p 1476 N94-19064 #

USIP-92-01 p 1525 N94-19145 #
USIP-92-04 p 1405 N94-19292 #
USIP-92-05 p 1602 N94-19293 #
USIP-92-07 p 1515 N94-19295 #
USIP-92-08 p 1574 N94-18845 #
USIP-93-03 p 1432 N94-18846 #
USIP-93-04 p 1569 N94-18847 #

USNA-TSPR-202 p 1610 N94-19663 #
USNA-TSPR-209 p 1344 N94-19662 #

UVA/525725/MSE93/101 p 1361 N94-18788
UVA/526334/CS91/101 p 1530 N94-19429 * #

UWA/DME/TR-93/73 p 1453 N94-18328 #

VKI-LS-1993-02 p 1414 N94-18578 #
VKI-LS-1993-04 p 1412 N94-18557 #
VKI-LS-1993-05 p 1430 N94-18643 #

VKI-TM-48 p 1409 N94-17901 #

VTT-TIED-1320 p 1380 N94-19373 #
VTT-TIED-1329 p 1365 N94-19374 #
VTT-TIED-1331 p 1346 N94-17973 #
VTT-TIED-1337 p 1444 N94-17974 #
VTT-TIED-1362 p 1339 N94-17958 #
VTT-TIED-1377 p 1452 N94-17959 #

WAPD-T-2989 p 1363 N94-18940 #

WCASP-23 p 1463 N94-19435 #

WCDMP-19 p 1495 N94-19705 #
WCDMP-23 p 1494 N94-19312 #

WES/TR/EL-93-9 p 1388 N94-18777 #

WES/TR/HL-REMR-HY-11 p 1417 N94-18672 #

WES/TR/HL-93-10 p 1506 N94-18598
WES/TR/HL-93-12 p 1417 N94-18755

WHC-SD-EN-TP-030 p 1433 N94-19041 #

WHOI-93-22 p 1500 N94-19792 #

WIS-PH-92-17 p 1607 N94-17950
WIS-PH-92-90 p 1547 N94-17949
WIS-PH-93-3 p 1607 N94-17953
WIS-PH-93-4 p 1565 N94-17951

WL-TR-92-4084 p 1453 N94-18382 #
WL-TR-92-7035 p 1322 N94-18330 #
WL-TR-93-1030 p 1384 N94-18187 #
WL-TR-93-1086 p 1540 N94-18189 #
WL-TR-93-2015 p 1377 N94-18489
WL-TR-93-2055 p 1320 N94-18907
WL-TR-93-2061 p 1354 N94-19778
WL-TR-93-2083 p 1370 N94-18282 #
WL-TR-93-3004 p 1317 N94-18227 #
WL-TR-93-30445 p 1318 N94-18733 #
WL-TR-93-3044 p 1317 N94-18577
WL-TR-93-3047 p 1417 N94-18739 #
WL-TR-93-3068 p 1318 N94-18779 #
WL-TR-93-3089 p 1444 N94-18266
WL-TR-93-4005 p 1360 N94-18660 #
WL-TR-93-4034 p 1341 N94-18692 #
WL-TR-93-5028 p 1404 N94-18701 #
WL-TR-93-7017 p 1396 N94-18278 #
WL-TR-93-7027 p 1387 N94-18601 #
WL-TR-93-7028 p 1455 N94-18864 #
WL-TR-93-7032 p 1387 N94-18510 #

WMO-TD-511 p 1495 N94-19705 #
WMO-TD-535 p 1494 N94-19312 #

WMO/TD-534 p 1463 N94-19435 #

WSRC-MS-93-008 p 1443 N94-17761 #
WSRC-MS-93-091 p 1446 N94-19334 #
WSRC-MS-93-361 p 1484 N94-18725 #

WSRC-RP-93-401 p 1346 N94-18048 #

WSRC-TR-92-501 p 1523 N94-19005 #
WSRC-TR-93-299 p 1448 N94-19189 #

Y-2461 p 1346 N94-17987 #

Y/DZ-1008/R1 p 1343 N94-18761 #

APPENDIX

NASA SCIENTIFIC AND TECHNICAL INFORMATION PROGRAM PRODUCTS AND SERVICES

The NASA Scientific and Technical Information (STI) Program provides for the collection and announcement of aerospace-related reports and literature obtained worldwide through agreements and exchanges. The result of the collection is the comprehensive NASA STI Database that covers aeronautics, space, and supporting disciplines.

The STI Database, documents generated or obtained by NASA, and products and services derived from or supporting the database are made available to the NASA research community and to the public. Descriptions and sources of these items are presented in the following pages.

Scientific and Technical Aerospace Reports (STAR) is an abstract journal, listing citations with abstracts for aerospace-related reports obtained from worldwide sources. *STAR* is issued on the first of each month, and announces current documents that have been entered into the NASA STI Database during the previous month. The reports are of the following types:

- NASA, NASA contractor, and NASA grantee reports;
- Reports issued by other U.S. Government agencies, domestic and foreign institutions, universities, and private firms;
- Translations in report form;
- NASA-owned patents and patent applications
- Other U.S. Government agency and foreign patents and patent applications
- Domestic and foreign dissertations and theses.

Journal, book, and conference literature, journal translations, and certain foreign dissertations having the same subject scope as *STAR* are announced in a companion journal, *NASA Open Volumes on Aerospace (NOVA). NOVA* is issued on the 15th of each month and is available from the NASA Center for AeroSpace Information, at the address below.

ELIGIBILITY AND REGISTRATION FOR NASA STI PRODUCTS AND SERVICES

Organizations of the type listed below that have registered with NASA can receive products and services.

- NASA offices and installations, contractors, subcontractors, grantees, and consultants;
- Other U.S. Government agencies and their contractors;
- Libraries in the United States that have arrangements with NASA to maintain collections of NASA documents for public reference;
- Other organizations in the United States having a need for NASA documents in work related to aeronautics and space research;
- Organizations abroad that have established reciprocal documents exchange arrangements with NASA.

The central service points—central points of document acquisition and control within qualified organizations—or individuals are eligible to register for NASA STI products and services. Domestic organizations or individuals may be eligible to receive various classes of NASA publications and services and should address their requests for registration or further information to:

ATTN: Registration Services
NASA Center for AeroSpace Information
800 Elkridge Landing Road
Linthicum Heights, MD 21090-2934
301-621-0390

Organizations abroad should direct requests to:

National Aeronautics and Space Administration
Scientific and Technical Information Program (JTT)
International STI Program
Washington, DC 20546-0001
USA
703-271-5640

SUBJECT SCOPE

The subject scope of *STAR* and *NOVA* includes all aspects of aeronautics and space research and development, supporting basic and applied research, and applications. Aerospace aspects of Earth resources, energy development, conservation, oceanography, environmental protection, urban transportation, and other topics of high national priority are also covered.

HOW TO USE *STAR* SUBJECT CATEGORIES

Abstracts in *STAR* are categorized by 10 major subject divisions that are divided further into 76 specific subject categories. The subject divisions and categories are listed in the Table of Contents together with a note for each that defines its scope and provides any cross-references. For example:

> **16 SPACE TRANSPORTATION**
>
> Includes passenger and cargo space transportation, e.g., shuttle operations; and space rescue techniques. For related information see also *03 Air Transportation and Safety* and *18 Spacecraft Design, Testing and Performance*. For space suits see *54 Man/System Technology and Life Support.*

CROSS-REFERENCES

Individual *STAR* abstracts are not ordinarily cross-referenced, except for certain conference reports or book translations that have had separate abstracts written for their component papers or chapters. Citations and abstracts of the components follow immediately after those of the parent document. When the subject content of a component differs sufficiently from the general content of the parent, a cross-reference citation also is printed at the end of the category to which it normally would have been assigned if it were independent.

DOCUMENTS ON MICROFICHE

Documents available on microfiche are designated by a pound sign (#) following the accession number.

LIMITED REPRODUCIBILITY

A note of limited reproducibility appears in the citation, if there are factors affecting the reproducibility of more than 20% of the document. These factors include faint or broken type, color photographs, black and white photographs, foldouts, dot matrix print, or some other factor that limits the reproducibility of the document. This notation also appears on the microfiche header.

COLOR COPIES

An increasing number of NASA scientific and technical reports are being produced with color graphs, charts, illustrations, and photographs. An indication that a document has color pages follows the source and pricing (SAP) information in the *STAR* citation.

Registered users of the NASA Scientific and Technical Information Program will receive ordered documents with color at no additional cost, as long as stock copies of the document are available. Otherwise, an additional fee of $2.00 per color page will be charged. The NASA Center for AeroSpace Information staff will contact registered users to determine individual user's needs.

Patents and patent applications owned by NASA are announced in *STAR* under appropriate subject categories and are referenced in the *STAR* indexes. In the Report Number Index, patents are indexed by the NASA Case Number, and the U.S. Patent Class. Patent applications are indexed by the NASA Case Number and the U.S. Patent Application Serial Number.

Printed copies of patents (which are not microfiched) are available for purchase from the U.S. Patent and Trademark Office.

When ordering patents, the U.S. Patent Number should be used, and payment must be remitted in advance, by money order or check payable to the Commissioner of Patents and Trademarks. Prepaid purchase coupons for ordering are also available from the U.S. Patent and Trademark Office.

NASA patent application specifications are sold in both paper copy and microfiche by the NASA Center for AeroSpace Information (CASI). The N accession number should be used in ordering either paper copy or microfiche from CASI.

The patents and patent applications announced in *STAR* are owned by NASA and are available for royalty-free licensing. Requests for licensing terms and further information should be addressed to:

National Aeronautics and Space Administration
Associate General Counsel for Intellectual Property
Code GP
Washington, DC 20546-0001

SOURCES FOR DOCUMENTS

One or more sources from which a document announced in *STAR* is available to the public is ordinarily given on the last line of the citation. The most commonly indicated sources and their acronyms or abbreviations are listed below, and their addresses are listed on page A-6. If the publication is available from a source other than those listed, the publisher and his address will be displayed on the availability line or in combination with the corporate source line.

Avail: CASI. Sold by the NASA Center for AeroSpace Information. Prices for hard copy (HC) and microfiche (MF) are indicated by a price code following the letters HC or MF in the *STAR* citation. Current values for the price codes are given in the tables on page A-7.

NOTE ON ORDERING DOCUMENTS: When ordering publications from CASI, use the N accession number or other report number. It is also advisable to cite the title and other bibliographic identification.

Avail: SOD (or GPO). Sold by the Superintendent of Documents, U.S. Government Printing Office, in hard copy.

Avail: BLL (formerly NLL): British Library Lending Division, Boston Spa, Wetherby, Yorkshire, England. Photocopies available from this organization at the price shown. (If none is given, inquiry should be addressed to the BLL.)

Avail: DOE Depository Libraries. Organizations in U.S. cities and abroad that maintain collections of Department of Energy reports, usually in microfiche form, are listed in *Energy Research Abstracts*. Services available from the DOE and its depositories are described in a booklet, *DOE Technical Information Center - Its Functions and Services* (TID-4660), which may be obtained without charge from the DOE Technical Information Center.

Avail: ESDU. Pricing information on specific data, computer programs, and details on Engineering Sciences Data Unit (ESDU) topic categories can be obtained from ESDU International Ltd. Requesters in North America should use the Virginia address while all other requesters should use the London address, both of which are on page A-6.

Avail: Fachinformationszentrum, Karlsruhe. Gesellschaft für wissenschaftlich-technische Information mbH 7514 Eggenstein-Leopoldshafen 2, Germany.

Avail: HMSO. Publications of Her Majesty's Stationery Office are sold in the U.S. by Pendragon

House, Inc. (PHI), Redwood City, CA. The U.S. price (including a service and mailing charge) is given, or a conversion table may be obtained from PHI.

Avail: Issuing Activity, or Corporate Author, or no indication of availability. Inquiries as to the availability of these documents should be addressed to the organization shown in the citation as the corporate author of the document.

Avail: NASA Public Document Rooms. Documents so indicated may be examined at or purchased from the National Aeronautics and Space Administration (JBD-4), Public Documents Room (Room 1H23), Washington, DC 20546-0001, or public document rooms located at NASA installations, and the NASA Pasadena Office at the Jet Propulsion Laboratory.

Avail: NTIS. Sold by the National Technical Information Service. Initially distributed microfiche under the NTIS SRIM (Selected Research in Microfiche) are available. For information concerning this service, consult the NTIS Subscription Section, Springfield, VA 22161.

Avail: Univ. Microfilms. Documents so indicated are dissertations selected from *Dissertation Abstracts* and are sold by University Microfilms as xerographic copy (HC) and microfilm. All requests should cite the author and the Order Number as they appear in the citation.

Avail: US Patent and Trademark Office. Sold by Commissioner of Patents and Trademarks, U.S. Patent and Trademark Office, at the standard price of $1.50 each, postage free. (See discussion of NASA patents and patent applications on page A-3.)

Avail: (US Sales Only). These foreign documents are available to users within the United States from the National Technical Information Service (NTIS). They are available to users outside the United States through the International Nuclear Information Service (INIS) representative in their country, or by applying directly to the issuing organization.

Avail: USGS. Originals of many reports from the U.S. Geological Survey, which may contain color illustrations, or otherwise may not have the quality of illustrations preserved in the microfiche or facsimile reproduction, may be examined by the public at the libraries of the USGS field offices whose addresses are listed on page A-6. The libraries may be queried concerning the availability of specific documents and the possible utilization of local copying services, such as color reproduction.

FEDERAL DEPOSITORY LIBRARY PROGRAM

In order to provide the general public with greater access to U.S. Government publications, Congress established the Federal Depository Library Program under the Government Printing Office (GPO), with 53 regional depositories responsible for permanent retention of material, inter-library loan, and reference services. At least one copy of nearly every NASA and NASA-sponsored publication, either in printed or microfiche format, is received and retained by the 53 regional depositories. A list of the regional GPO libraries, arranged alphabetically by state, appears on page A-8. These libraries are *not* sales outlets. A local library can contact a regional depository to help locate specific reports, or direct contact may be made by an individual.

PUBLIC COLLECTION OF NASA DOCUMENTS

An extensive collection of NASA and NASA-sponsored publications is maintained by the British Library Lending Division, Boston Spa, Wetherby, Yorkshire, England for public access. The British Library Lending Division also has available many of the non-NASA publications cited in *STAR*. European requesters may purchase facsimile copy or microfiche of NASA and NASA-sponsored documents, those identified by both the symbols # and * from ESA — Information Retrieval Service European Space Agency, 8-10 rue Mario-Nikis, 75738 CEDEX 15, France.

SUBMITTING DOCUMENTS

All users of this abstract service are urged to forward reports to be considered for announcement in *STAR*. This will aid NASA in its efforts to provide the fullest possible coverage of all scientific and technical publications that might support aeronautics and space research and development. If you have prepared relevant reports (other than those you will transmit to NASA, DOD, or DOE through the usual contract- or grant-reporting channels), please send them for consideration to the NASA Center for AeroSpace Information, 800 Elkridge Landing Road, Linthicum Heights, MD 21090-2934.

Reprints of journal articles, book chapters, and conference papers are also welcome. These will be considered for announcement in *STAR's* companion journal, *NOVA*.

You may specify a particular source to be included in a report announcement if you wish; otherwise the report will be placed on a public sale at the NASA Center for AeroSpace Information. Copyrighted publications will be announced but not distributed or sold.

PURCHASE OF *STAR*

STAR is publicly available on annual subscription from the NASA Center for AeroSpace Information (CASI) at $94.00/domestic, $117.00/foreign. Single copy prices: $33.00/domestic, $41.00/foreign.

An annual, cumulative *STAR Index* is also available at $54.00/domestic, $65.00/foreign.

STAR is available to registered users on annual subscription from the NASA Center for AeroSpace Information, ATTN: Registration Services, 800 Elkridge Landing Road, Linthicum Heights, MD 21090-2934.

ADDRESSES OF ORGANIZATIONS

British Library Lending Division
Boston Spa, Wetherby, Yorkshire
England

Commissioner of Patents and Trademarks
U.S. Patent and Trademark Office
Washington, DC 20231

Department of Energy
Technical Information Center
P.O. Box 62
Oak Ridge, TN 37830

European Space Agency-
Information Retrieval Service ESRIN
Via Galileo Galilei
00044 Frascati (Rome) Italy

Engineering Sciences Data Unit International
P.O. Box 1633
Manassas, VA 22110

Engineering Sciences Data Unit
International, Ltd.
251-259 Regent Street
London, W1R 7AD, England

Fachinformationszentrum Karlsruhe
Gesellschaft für wissenschaftlich-technische
Information mbH
7514 Eggenstein-Leopoldshafen 2, Germany

Her Majesty's Stationery Office
P.O. Box 569, S.E. 1
London, England

NASA Center for AeroSpace Information
800 Elkridge Landing Road
Linthicum Heights, MD 21090-2934

National Aeronautics and Space Administration
Scientific and Technical Information Program
(JTT)
Washington, DC 20546-0001

National Technical Information Service
5285 Port Royal Road
Springfield, VA 22161

Pendragon House, Inc.
899 Broadway Avenue
Redwood City, CA 94063

Superintendent of Documents
U.S. Government Printing Office
Washington, DC 20402

University Microfilms
A Xerox Company
300 North Zeeb Road
Ann Arbor, MI 48106

University Microfilms, Ltd.
Tylers Green
London, England

U.S. Geological Survey Library National Center
MS 950
12201 Sunrise Valley Drive
Reston, VA 22092

U.S. Geological Survey Library
2255 North Gemini Drive
Flagstaff, AZ 86001

U.S. Geological Survey
345 Middlefield Road
Menlo Park, CA 94025

U.S. Geological Survey Library
Box 25046
Denver Federal Center, MS914
Denver, CO 80225

CASI PRICE TABLES

(Effective August 1, 1993)

STANDARD PRICE DOCUMENTS

PRICE CODE	NORTH AMERICAN PRICE	FOREIGN PRICE
A01	$ 9.00	$ 18.00
A02	12.50	25.00
A03	17.50	35.00
A04-A05	19.50	39.00
A06-A09	27.00	54.00
A10-A13	36.50	73.00
A14-A17	44.50	89.00
A18-A21	52.00	104.00
A22-A25	61.00	122.00
A99	Call For Price	Call For Price

MICROFICHE

PRICE CODE	NORTH AMERICAN PRICE	FOREIGN PRICE
A01	$ 9.00	$ 18.00
A02	12.50	25.00
A03	17.50	35.00
A04	19.50	39.00
A06	27.00	54.00
A10	36.50	73.00

IMPORTANT NOTICE

CASI Shipping and Handling Charges
U.S.—ADD $3.00 per TOTAL ORDER
Canada and Mexico—ADD $3.50 per TOTAL ORDER
All Other Countries—ADD $7.50 per TOTAL ORDER
Does NOT apply to orders
requesting CASI RUSH HANDLING.
CASI accepts most credit/charge cards.

NASA Center for AeroSpace Information
800 Elkridge Landing Road
Linthicum Heights, MD 21090-2934
Telephone: (301) 621-0390
E-mail: help@sti.nasa.gov
Fax: (301) 621-0134

FEDERAL REGIONAL DEPOSITORY LIBRARIES

ALABAMA

AUBURN UNIV. AT MONTGOMERY LIBRARY
Documents Dept.
7300 University Dr.
Montgomery, AL 36117-3596
(205) 244-3650 Fax: (205) 244-0678

UNIV. OF ALABAMA
Amelia Gayle Gorgas Library
Govt. Documents
Box 870266
Tuscaloosa, AL 35487-0266
(205) 348-6046 Fax: (205) 348-8833

ARIZONA

DEPT. OF LIBRARY, ARCHIVES, AND PUBLIC RECORDS
Federal Documents
Third Floor State Capitol
1700 West Washington
Phoenix, AZ 85007
(602) 542-4121 Fax: (602) 542-4400, 542-4500

ARKANSAS

ARKANSAS STATE LIBRARY
State Library Services
One Capitol Mall
Little Rock, AR 72201
(501) 682-2869

CALIFORNIA

CALIFORNIA STATE LIBRARY
Govt. Publications Section
914 Capitol Mall - P.O. Box 942837
Sacramento, CA 94237-0001
(916) 322-4572 Fax: (916) 324-8120

COLORADO

UNIV. OF COLORADO - BOULDER
Norlin Library
Govt. Publications
Campus Box 184
Boulder, CO 83309-0184
(303) 492-8834 Fax: (303) 492-2185

DENVER PUBLIC LIBRARY
Govt. Publications Dept. BS/GPD
1357 Broadway
Denver, CO 80203
(303) 571-2135

CONNECTICUT

CONNECTICUT STATE LIBRARY
231 Capitol Avenue
Hartford, CT 06106
(203) 566-4971 Fax: (203) 566-3322

FLORIDA

UNIV. OF FLORIDA LIBRARIES
Documents Dept.
Library West
Gainesville, FL 32611-2048
(904) 392-0366 Fax: (904) 392-7251

GEORGIA

UNIV. OF GEORGIA LIBRARIES
Govt. Documents Dept.
Jackson Street
Athens, GA 30602
(404) 542-8949 Fax: (404) 542-6522

HAWAII

UNIV. OF HAWAII
Hamilton Library
Govt. Documents Collection
2550 The Mall
Honolulu, HI 96822
(808) 948-8230 Fax: (808) 956-5968

IDAHO

UNIV. OF IDAHO LIBRARY
Documents Section
Moscow, ID 83843
(208) 885-6344 Fax: (208) 885-6817

ILLINOIS

ILLINOIS STATE LIBRARY
Reference Dept.
300 South Second
Springfield, IL 62701-1796
(217) 782-7596 Fax: (217) 524-0041

INDIANA

INDIANA STATE LIBRARY
Serials/Documents Section
140 North Senate Avenue
Indianapolis, IN 46204
(317) 232-3678 Fax: (317) 232-3728

IOWA

UNIV. OF IOWA LIBRARIES
Govt. Publications Dept.
Washington & Madison Streets
Iowa City, IA 52242
(319) 335-5926 Fax: (319) 335-5830

KANSAS

UNIV. OF KANSAS
Govt. Documents & Map Library
6001 Malatt Hall
Lawrence, KS 66045-2800
(913) 864-4660 Fax: (913) 864-5380

KENTUCKY

UNIV. OF KENTUCKY LIBRARIES
Govt. Publications/Maps Dept.
Lexington, KY 40506-0039
(606) 257-3139 Fax: (606) 257-1563, 257-8379

LOUISIANA

LOUISIANA STATE UNIV.
Middleton Library
Govt. Documents Dept.
Baton Rouge, LA 70803
(504) 388-2570 Fax: (504) 388-6992

LOUISIANA TECHNICAL UNIV.
Prescott Memorial Library
Govt. Documents Dept.
305 Wisteria Street
Ruston, LA 71270-9985
(318) 257-4962 Fax: (318) 257-2447

MAINE

TRI-STATE DOCUMENTS DEPOS.
Raymond H. Fogler Library
Govt. Documents & Microforms Dept.
Univ. of Maine
Orono, ME 04469
(207) 581-1680

MARYLAND

UNIV. OF MARYLAND
Hornbake Library
Govt. Documents/Maps Unit
College Park, MD 20742
(301) 454-3034 Fax: (301) 454-4985

MASSACHUSETTS

BOSTON PUBLIC LIBRARY
Govt. Documents Dept.
666 Boylston Street
Boston, MA 02117
(617) 536-5400 ext. 226
Fax: (617) 267-8273, 267-8248

MICHIGAN

DETROIT PUBLIC LIBRARY
5201 Woodward Avenue
Detroit, MI 48202-4093
(313) 833-1440, 833-1409
Fax: (313) 833-5039

LIBRARY OF MICHIGAN
Govt. Documents Unit
P.O. Box 30007
Lansing, MI 48909
(517) 373-0640 Fax: (517) 373-3381

MINNESOTA

UNIV. OF MINNESOTA
Wilson Library
Govt. Publications Library
309 19th Avenue South
Minneapolis, MN 55455
(612) 624-5073 Fax: (612) 626-9353

MISSISSIPPI

UNIV. OF MISSISSIPPI
J.D. Williams Library
Federal Documents Dept.
106 Old Gym Bldg.
University, MS 38677
(601) 232-5857 Fax: (601) 232-5453

MISSOURI

UNIV. OF MISSOURI - COLUMBIA
Ellis Library
Govt. Documents
Columbia, MO 65201
(314) 882-6733 Fax: (314) 882-8044

MONTANA

UNIV. OF MONTANA
Maureen & Mike Mansfield Library
Documents Div.
Missoula, MT 59812-1195
(406)243-6700 Fax: (406) 243-2060

NEBRASKA

UNIV. OF NEBRASKA - LINCOLN
D.L. Love Memorial Library
Documents Dept.
Lincoln, NE 68588
(402) 472-2562

NEVADA

UNIV. OF NEVADA
Reno Library
Govt. Publications Dept.
Reno, NV 89557
(702) 784-6579 Fax: (702) 784-1751

NEW JERSEY

NEWARK PUBLIC LIBRARY
U.S. Documents Div.
5 Washington Street - P.O. Box 630
Newark, NJ 07101-0630
(201) 733-7812 Fax: (201) 733-5648

NEW MEXICO

UNIV. OF NEW MEXICO
General Library
Govt. Publications Dept.
Albuquerque, NM 87131-1466
(505) 277-5441 Fax: (505) 277-6019

NEW MEXICO STATE LIBRARY
325 Don Gaspar Avenue
Santa Fe, NM 87503
(505) 827-3826 Fax: (505) 827-3820

NEW YORK

NEW YORK STATE LIBRARY
Documents/Gift & Exchange Section
Federal Depository Program
Cultural Education Center
Albany, NY 12230
(518) 474-5563 Fax: (518) 474-5786

NORTH CAROLINA

UNIV. OF NORTH CAROLINA - CHAPEL HILL
CB#3912, Davis Library
BA/SS Dept. - Documents
Chapel Hill, NC 27599
(919) 962-1151 Fax: (919) 962-0484

NORTH DAKOTA

NORTH DAKOTA STATE UNIV. LIB.
Documents Office
Fargo, ND 58105
(701) 237-8886 Fax: (701) 237-7138
In cooperation with Univ. of North Dakota, Chester Fritz Library Grand Forks

OHIO

STATE LIBRARY OF OHIO
Documents Dept.
65 South Front Street
Columbus, OH 43266
(614) 644-7051 Fax: (614) 752-9178

OKLAHOMA

OKLAHOMA DEPT. OF LIBRARIES
U.S. Govt. Information Div.
200 NE 18th Street
Oklahoma City, OK 73105-3298
(405) 521-2502, ext. 252, 253
Fax: (405) 525-7804

OKLAHOMA STATE UNIV.
Edmon Low Library
Documents Dept.
Stillwater, OK 74078
(405) 744-6546 Fax: (405) 744-5183

OREGON

PORTLAND STATE UNIV.
Millar Library
934 SW Harrison - P.O. Box 1151
Portland, OR 97207
(503) 725-3673 Fax: (503) 725-4527

PENNSYLVANIA

STATE LIBRARY OF PENN.
Govt. Publications Section
Walnut St. & Commonwealth Ave. P.O. Box 1601
Harrisburg, PA 17105
(717) 787-3752

SOUTH CAROLINA

CLEMSON UNIV.
Cooper Library
Public Documents Unit
Clemson, SC 29634-3001
(803) 656-5174 Fax: (803) 656-3025
In cooperation with Univ. of South Carolina, Thomas Cooper Library, Columbia

TENNESSEE

MEMPHIS STATE UNIV. LIBRARIES
Govt. Documents
Memphis, TN 38152
(901) 678-2586 Fax: (901) 678-2511

TEXAS

TEXAS STATE LIBRARY
United States Documents
P.O. Box 12927 - 1201 Brazos
Austin, TX 78711
(512) 463-5455 Fax: (512) 463-5436

TEXAS TECH. UNIV. LIBRARY
Documents Dept.
Lubbock, TX 79409
(806) 742-2268 Fax: (806) 742-1920

UTAH

UTAH STATE UNIV.
Merrill Library & Learning Resources Center, UMC-3000
Documents Dept.
Logan, UT 84322-3000
(801) 750-2684 Fax: (801) 750-2677

VIRGINIA

UNIV. OF VIRGINIA
Aldermman Library
Govt. Documents
Charlottesville, VA 22903-2498
(804) 824-3133 Fax: (804) 924-4337

WASHINGTON

WASHINGTON STATE LIBRARY
Document Section
MS AJ-11
Olympia, WA 98504-0111
(206) 753-4027 Fax: (206) 753-3546

WEST VIRGINIA

WEST VIRGINIA UNIV. LIBRARY
Govt. Documents Section
P.O. Box 6069
Morgantown, WV 26506
(304) 293-3640

WISCONSIN

ST. HIST. SOC. OF WISCONSIN LIBRARY
Govt. Publications Section
816 State Street
Madison, WI 53706
(608) 262-2781 Fax: (608) 262-4711
In cooperation with Univ. of Wisconsin - Madison, Memorial Library

MILWAUKEE PUBLIC LIBRARY
Documents Div.
814 West Wisconsin Avenue
Milwaukee, WI 53233
(414) 278-2167 Fax: (414) 278-2137

•U.S. GOVERNMENT PRINTING OFFICE:1994-301-249/00003

POSTMASTER
Address Correction Requested
(Sections 137 and 159 Post Manual)

National Aeronautics and
Space Administration
Code JTT
Washington, DC 20546-0001

Official Business
Penalty for Private Use, $300

BULK RATE
POSTAGE & FEES PAID
NASA
PERMIT No. G-27

NASA

POSTMASTER: If Undeliverable (Section 158
Postal Manual) Do Not Return

Please circulate this publication to other colleagues within your organization.

NASA
STI PROGRAM
SCIENTIFIC &
TECHNICAL
INFORMATION